DEVELOPMENT AND MECHANISTIC STUDIES OF NI-CATALYZED ASYMMETRIC REDUCTIVE CROSS-COUPLING REACTIONS

Thesis by

Julie Lyn Hofstra

In Partial Fulfillment of the Requirements

for the Degree of

Doctor of Philosophy

CALIFORNIA INSTITUTE OF TECHNOLOGY

Pasadena, California

2019

(Defended April 26th, 2019)

Julie Lyn Hofstra

ORCID: 0000-0001-9558-4317

To the family and friends who not only
celebrated with me on the mountaintops,
but also walked with me through the valleys.
I wouldn't have finished without you.

ACKNOWLEDGEMENTS

When I started graduate school at Caltech five years ago, I already knew my time was going to be spent making a lot of carbon–carbon bonds; however, I did not anticipate how many close, strong friendships I would also form during my time here. I am truly grateful to have had such an enriching experience at Caltech, which never ceases to be a creative and collaborative atmosphere. I have had the pleasure to work amongst some extremely talented and caring people and I am thankful for all the support I received from friends and family which has been instrumental in seeing me through to the finish line. Caltech is a remarkable, close-knit community, and some of the friendships I have made during my time here I will undoubtedly take with me for the rest of my life.

First of all, I would like to thank my advisor, Prof. Sarah Reisman, for providing me the opportunity to join her laboratory. Sarah is dedicated to her students and challenges them to become better thinkers, writers, and scientists. I have benefited from her rigor and support over the years; it has grown me into the chemist I am today. Although I originally came to Caltech with an analytical/physical background, Sarah quickly recognized how my strengths could be useful in the context of organic chemistry and provided me with the opportunity to pioneer the laboratory's focused efforts in the realm of mechanistic studies on nickel catalysis. While being in her laboratory, I have also come to learn and appreciate her drive for natural product synthesis. This unique training environment has led me to develop skills I would not have obtained while working in a strictly methods group.

I would also like to thank the other members of my committee, Profs. Gregory Fu, Dennis Dougherty, and Brian Stoltz. Greg has never hesitated an opportunity to chat about nickel catalysis and provide his thoughts on some of my odd experimental results when I

came seeking advice. For all his insight into my research, I am truly grateful. Dennis has also been a valuable addition to my committee, especially with his expertise in physical organic chemistry. I remember buying his textbook when I was a senior in college and thought it was the best thing ever. When I came to Caltech and realized I would be taking his class, I was ecstatic; it was one of the highlights of my course experience here and helped propel me towards the field for my postdoctoral studies. Lastly, the ability to conduct research alongside Brian and his group has always made me feel at home on the third floor of Schlinger. I think it's a remarkable thing to be able to experience such close connections with students in his group; at times it felt like we were one big family.

I would also like to thank a number of Caltech staff and administration for all their support. Lynne Martinez and Veronica Triay work tremendously hard to keep the group running from an administrative position. Their warm, smiling faces have always been a pleasure to have around. I always enjoyed the simple moments of getting to chat and connect with Lynne in her office (or the elevator), and even though she has since retired, I am looking forward to seeing her again at our class graduation. I would also like to acknowledge all the hard work that Agnes Tong and Alison Ross have done for our department. They have worked hard to keep the graduate program running, from simple things such as scheduling seminar rooms to more complicated things like organizing recruitment. I would also like to thank Dr. Kate McAnulty and Prof. Doug Rees who have been advisors to me during my time on the Graduate Honor Council. I have appreciated Kate's periodic check-ins; she has always been there as an extra support when I needed it.

There are also numerous staff who deserve so much more than any words I can describe here. Dr. David VanderVelde does an amazing job keeping the NMR facility up

and running. It seems like one instrument or another is always having issues and Dave works endlessly to keep everything working. Without such an awesome facility, it would be exponentially more difficult to do the research that we do. I also owe a huge gratitude to Dr. Michael Takase and Mr. Lawrence Henling for all their hard work running the X-ray facility. It's not uncommon to get a phone call from Larry close to midnight following up on your late night requests, asking if your samples are ready to go. They work around the clock to make sure we get our structural data in a timely fashion. Mike and Larry have also been extremely patient with me and have taught me so much about structure solution over the past five years as I took on the inaugural "Reisman Lab X-ray Crystallography Liaison" group job. I have enjoyed getting to learn how to solve crystal structures and everything I know about X-ray crystallography I owe to them. I would also like to thank Dr. Angel Di Billo and Dr. Paul Oyala for their hard work running the EPR facilities. They have always been more than happy to help me run samples and teach me about EPR spectroscopy. It was not too uncommon to be sitting in the basement of Crellin while finding "interesting" peaks in my EPR samples; we often deduced that the lab glassware must simply be plagued with manganese. Finally, I would like to thank Dr. Mona Shahgholi and Naseem Torian for their hard work running our mass spectrometry facility. Whenever I had sensitive samples that needed to be run rather quickly, Mona was always accommodating to find time for me to get the data I needed.

I owe so much gratitude to Dr. Scott Virgil and Mrs. Silva Virgil. You hear so much about Scott in about every thesis defense that comes out of our organic laboratories. Scott truly does a phenomenal job maintaining the Caltech 3CS facility. He works tirelessly to keep instruments up and running, while always willing to provide students with feedback

on chemical conundrums. He does this even when juggling multiple things at once. Silva has been one of my closest friends I have had at Caltech. She has always had an open door and gets excited to have me stop by and tell her about all the things going on in my day. They are some of the kindest, most loving people I have met. I am going to miss seeing them so frequently but am looking forward to their visits in Utah.

I would also like to thank a number of people who contributed to my teaching experiences at Caltech. Dr. Jennifer Weaver and the directors in the Caltech Project for Effective Teaching (CPET) program have provided me with valuable feedback on my teaching portfolio as I worked to complete my Certificate of Practice in University Teaching. I am thankful to Ms. Jodi Marchesso and the high school chemistry teachers in the Pasadena Unified School District for their willingness to let me help on a year-long curricula redesign project during my first year of grad school. I would like to thank Prof. John Hanley at Pasadena City College who gave me the opportunity to come shadow his organic chemistry class for a semester and also guest lecture in his course. Lastly, I would like to thank my coworker, Dr. Carolyn Ladd, for taking on this huge undertaking of teaching Ch101 with me. It's been such a fun and rewarding (and sleepless) experience learning how to design and run our own course on natural products in medicine; Carolyn has been beyond supportive during the first few weeks of our course as I frantically wrapped up writing my thesis. I have really valued her continual encouragement and cheer. This experience has given me a lot more confidence in my teaching abilities which will be instrumental when I start my independent career.

Over the course of my graduate career, I have been privileged to work on a variety of collaborative projects with students in our group as well as with students at other

universities. I am indebted to Prof. Kendall Houk and his students Dr. Yunfang Yang and Dr. Xin Hong for their hard work running the geometry optimizations and energy calculations on our alkenylation reaction. Without them we could not have conducted some of our mechanistic studies. I am also grateful for the opportunity to work with Iris Guo and Prof. Matt Sigman on PHOX ligand parameterization. Iris is such a talented computational chemist and definitely put up with a lot of my excessive questions regarding MatLab and my confusion on how Python is not a coding language and has nothing to do with snakes. It was so fun to visit Matt's laboratory last February to learn how they conduct their research. Matt has been such a supportive semi-advisor throughout the past two years and I am excited to now have the opportunity to work for him in my postdoctoral studies.

I have also been fortunate to have worked alongside many fantastic coworkers during my time in the Reisman laboratory. I would like to particularly thank my project partners over the years; I think some of my greatest joys in grad school have been the opportunities I received to collaborate with my colleagues. Dr. Alan Cherney was my first mentor when I started in the laboratory back in 2014, and his willingness to give me feedback during my studies is something I have always appreciated. It has been an honor to be entrusted with the allylic silane project after he graduated. His insight into the alkenylation mechanism project has also always been a fun conversation starter. I would also like to thank Dr. Nathaniel Kadunce who also taught me so much about reductive cross-coupling during my first few years in grad school. I think one of the things I enjoyed most about being on Team Nickel was the openness in our group. Although everyone is usually working on their own project, the communication and feedback everyone gives each other makes it feel like you are part of something bigger.

I am thankful for a number of other project partners who have worked alongside me, including Dr. Naoyuki Suzuki, Alex Shimozono, and Raymond Turro. Naoyuki and Alex are such terrific scientists and work extremely hard with intense focus. I have learned a lot about dedication from both of them. Ray is also another gifted chemist; it has been refreshing to have a new set of eyes and hands take over the mechanism projects. I am confident that he will do well finishing up the work and I am excited to see what new chemistry everyone on Team Nickel will discover in the years to come.

Kelsey Poremba deserves a super special shout out. We both started on Team Nickel together during our first year and it has been incredible getting to work with her on various projects. We each came into the laboratory with a unique set of skills and I have been lucky to have learned so much from her. Kelsey can teach everyone a thing or two about organization (something I am still lacking) and is truly a reaction optimization queen.

I was also privileged to have the opportunity to mentor two fantastic undergraduate students, Ciara Ordner and Dana Gephart. It has been wonderful to watch them grow and develop careful, thoughtful approaches to their research. I am excited to see where their roads will take them and what accomplishments they achieve. In particular, Ciara came into the laboratory during a time when my graduate studies felt like a monotony, and working with her gave me a renewed sense of motivation. Ciara was a present reminder of what I was working towards in my teaching career, although it was definitely easy to mentor such an ambitious and thoughtful student. I think in the end, I learned more from Ciara than she learned from me and I am fortunate enough to also call her a close friend.

There are also a number of other close friends in the lab that have helped get me situated when I first started. I remember Dr. Lauren Chapman dropped what she was doing

and helped me clean out my entire fume hood and manifold for about three hours on my first day. She made an impression on me that lasted over the next few years as I got to know her more and more. Lauren was always so caring and her encouragement and friendship was something that helped get me through my first two years at Caltech. Dr. Haoxuan Wang, Dr. Kangway Chuang, and (especially) Dr. Matthew Hesse have taught me almost all I know about running reactions and laboratory techniques for which I am ever grateful. Matt was such a fun and spirited person to get to work alongside, both in the office and in the lab and for all his advice regarding chemistry I am forever grateful.

I have worked next to quite a few baymates during my time in the lab: Kevin Sokol, Dr. Kohei Takeuchi, and Nick Fastuca. Both Kevin and Kohei were such energetic young individuals who would always put a smile on my face. I have also thoroughly enjoyed working next to Nick for most of my time in the Reisman lab. We may not always be the best at keeping things clean and organized, but I think our work dynamic has been perfect. The two of us just seem to roll with all the things the other person does and it has been nice to work next to someone with such a calm and forgiving spirit, especially when my blue cobalt encrusted glassware often took over all the drying racks in our space. I am going to miss chatting with Nick about grad school life and Reisman lab softball strategies.

Dr. Denise Grünenfelder has been one of my closest friends in the lab here at Caltech. Denise is such a warm and loving person who will go out of her way to help out anyone who is in need with just about anything. She has always been a solid rock of advice during my time here and is one of the hardest working people I know. I am going to miss all of our mid-day coffee runs, crepe outings, and late night food adventures to the Habit

Burger. Even though Denise has now graduated and moved to Boston, I know her close friendship is something I will value for a long time to come.

There are so many other friends I have made in the lab, it would take me forever to talk about them all in length. Caitlin Laker has been such a close friend and someone I can talk to with just about anything. Sometimes the right people come into your life at the right time, and Caitlin was one of those people. Jordan Beck and Alice Wong, two of my classmates, are such intelligent synthetic chemists who know so much about chemistry. I am excited to see where their journeys take them in the years to come. Dr. Arthur Han is probably the most efficient and gifted chemist I know. I have appreciated all his feedback on government fellowship applications and definitely would not have accomplished all that I have without his advice. Some of my other close friends in the laboratory I am going to miss dearly: Dr. Chen Xu, Katie Chan, Dr. Justin Su, Dr. Suzie Stevenson, Dr. Nicholas Cowper, Sean Feng, Skyler Mendoza, Dr. Luke Hanna, Dr. Elliot Farney, Dr. Yasu Nakayama, Karli Holman, Travis DeLano, and Mike Maser. Thank you all for your friendships over the years and for making the lab such a fun place to be.

There are a number of people outside of Caltech to whom I owe much gratitude. My undergraduate advisors, Profs. Paula Hudson and Peter de Lijser, are the main reason I am finishing my graduate studies. When I first started at CSUF, I was on a path to become a high school chemistry teacher. However, it was the close mentorship I had in both of their research groups that drove me to continue my studies and pursue my Ph.D. Even when I thought I could not do something, they were there to encourage me every step of the way. I am thankful for all they taught me over the years and for their ability to keep in touch through lab alumni barbeques. I was lucky that Paula lived so close to Caltech and really

appreciated breakfast outings with her during my first few years of grad school. I would also like to thank Prof. Steve Buchwald for hosting me as a visiting undergraduate researcher the summer before my senior year of college. Working for Steve is what propelled me into studying organometallics for my Ph.D. dissertation work. While in the Buchwald lab, I was mentored by Dr. Thomas Barton, who is such a positive, caring person, and I have really appreciated all his support and encouragement over the years.

I am also appreciative of support from a number of friends here at Caltech and beyond. My two roommates, Elizabeth Goldstein and Rachel Ford, have enriched my life in ways I never imagined. I will always remember all the fun times we have shared, from cheesecake celebrations when finishing literally every exam in our first year, to the fun road trips and adventures we have had. Elizabeth has stuck with me as one of my closest friends since the very beginning and I will truly miss all of the fun adventures, food runs, and board game nights we have shared together. I think one of my favorite memories with her was going on our Sierra road trip a few years back. I somehow managed to get her to sleep in a tent and hike off-trail into the woods with me to find the Caltech Centennial Grove. I am looking forward to visiting her in Germany and maybe one day finally go on that Europe trip we dreamed of. I am also thankful for all my friends in the Caltech Volleyball Club: Reston Nash, Alex Phillips, Marianne Heida, Michelle Cua, Panagiotis Vergados, and so many others. I think this group is single handedly the most responsible for keeping me sane during my graduate studies. I am thankful for the time we get to play some serious volleyball together, but also for the friendships I have made and the times we have shared at barbeques, Congregation Ale House, and Hollywood Boulders rock climbing nights. I am going to miss them all so dearly. Finally, I would like to thank both

Rebecca Adamek, my best friend from college, and Nicholas Tay, a close friend from my time in the Buchwald lab. I don't get to see them as much as I would like, but their friendship has been much enjoyed along this journey.

I would also like to thank my family for all they have done to support me over the past five years. I am fortunate that they live close by and I could frequent trips home, often fed by their wonderful food and cooking which is something many of my coworkers on the third floor of Schlinger have come to experience around the holidays. My parents, Andrew and Patricia, have always poured so much love into me and for that I am forever grateful. I definitely would not have made it through grad school without all their love and support. I am also lucky to have such a wonderful and caring brother. I have watched James accomplish so many things in his life and he continues to be an inspiration to me.

Lastly, I would like to thank my partner, David Wahlman, for all his love and support, especially during the past few months while I was writing up and defending my thesis. He has been an extremely loving, selfless, and patient person and I have enjoyed getting to spend time with him and make the most of those few moments I have outside of the lab. Traveling home to see his family is always a wonderful time; I am thankful for Erik and Diana for welcoming me into their family. It is such a selfless act to uproot one's life for another, but I am looking forward to all the new adventures we will share and the memories we will make as we move to Salt Lake City.

ABSTRACT

Cross-coupling reactions have emerged as powerful methods to form carbon-carbon and carbon-heteroatom bonds in a vast array of synthetic contexts. Nickel-catalyzed reductive cross-coupling reactions have opened up a new mode of reactivity, allowing for the cross-coupling of bench-stable electrophiles as both coupling partners. Asymmetric variants, which use a chiral ligand, increase molecular complexity by introducing stereocenters with high levels of enantioselectivity. Application of this methodology to an array of electrophiles has led to the development of a number of transformations incorporating both C(sp^2)-hybridized electrophiles (aryl iodides, alkenyl bromides, and acyl chlorides) and C(sp^3)-hybridized electrophiles (benzyl chlorides and α-chloronitriles).

Herein we discuss our most recent efforts in the development and application of Ni-catalyzed asymmetric cross-coupling reactions with alkenyl electrophiles. First, the expansion of our previously developed methodology has allowed for bulky trimethylsilyl groups on the benzyl chloride electrophile, providing chiral allylic silane products in good yield and enantioselectivity. The utility of these products with both traditional and newly developed methodology is highlighted. Following this, we describe the development of reaction conditions that proceed with benzyl *N*-hydroxyphthalimide esters. This approach proceeds through a decarboxylative strategy, generates previously accessible radical intermediates, and proceeds with the use of a homogenous reductant. Our investigations into the mechanism on the cross-coupling of alkenyl bromides and benzyl chlorides is also disclosed, where we first identified the formation of alkenyl chloride and alkenyl iodide intermediates under the reaction conditions. This inspired us to develop a Ni-catalyzed alkenyl triflate halogenation in order to prepare alkenyl halide synthetic intermediates.

PUBLISHED CONTENT AND CONTRIBUTIONS

Portions of the work described herein were disclosed in the following communications:

1. Suzuki, N.[‡]; Hofstra, J. L[‡]; Poremba, K. E.; Reisman, S. E. *Org. Lett.* **2017**, *19*, 2150-2153. DOI: 10.1021/acs.orglett.7b00793. This article is available online at: https://pubs.acs.org/doi/abs/10.1021/acs.orglett.7b00793. Copyright © 2017 American Chemical Society

   J.L.H. contributed to the reaction development, conducted experiments, and participated in preparation of the supporting data and writing of the manuscript.

2. Hofstra, J. L; Cherney, A. H.; Ordner, C. M.; Reisman, S. E. *J. Am. Chem. Soc.* **2018**, *140*, 139-142. DOI: 10.1021/jacs.7b11707. This article is available online at: https://pubs.acs.org/doi/10.1021/jacs.7b11707. Copyright © 2018 American Chemical Society

   J.L.H. contributed to the reaction development, conducted experiments, and participated in preparation of the supporting data and writing of the manuscript.

TABLE OF CONTENTS

CHAPTER 1 ***1***

Emergence of C(sp^3) Ni-Catalyzed Reductive Cross-Couplings: From Achiral Catalysts to Asymmetric Variants

1.1 INTRODUCTION 1

1.2 CROSS-COUPLINGS WITH HALIDE ELECTROPHILES 7

1.2.1 Initial Developments in C(sp^2) Couplings 7

1.2.2 Electrochemical Methods 9

1.2.3 Hetereogeneous Metal Reductants 10

1.2.3.1 Unactivated Alkyl Electrophiles 10

1.2.3.2 Activated Alkyl Electrophiles 11

1.2.4 Soluble Organic Reductants 13

1.2.5 Metallaphotoredox Methods 15

1.3 CROSS-COUPLINGS WITH PSEUDOHALIDE ELECTROPHILES 18

1.3.1 Oxygen Electrophiles 18

1.3.2 Carboxylic Acid Derivatives 19

1.3.3 Epoxides and Aziridines 21

1.4 SYNTHETIC APPLICATIONS 23

1.4.1 Alkene Functionalization 24

1.4.2 Natural Product Synthesis 24

1.5 CONCLUSION 25

CHAPTER 2 ***35***

Synthesis and Utility of Chiral Allylic Silanes Prepared via Ni-Catalyzed Asymmetric Reductive Cross-Coupling

2.1 INTRODUCTION 35

2.2 REACTION OPTIMIZATION 39

2.2.1 Initial Reaction Hit 39

2.2.2 Solvents 40

2.2.3 Additives 40

2.2.4 Temperature 42

2.2.5 Electrophile Equivalents 43

2.2.6 CoPc Loading 44

2.2.7 Reaction Time 44

2.2.8 Optimization Summary and Controls 45

2.2.9 Scalability 46

2.2.10 Chiral Ligands 47

2.3 SUBSTRATE SCOPE 49

2.4 UTILITY OF CHIRAL ALLYLIC SILANES 53

2.4.1 Reduction of Allylic Silanes 53

2.4.2 Transposition Reactions 54

2.4.3 Hosomi-Sakurai Allylations 56

2.4.4 Synthesis of 2,3-Disubstituted Tetrahydrofurans 59

2.5 CONCLUSION 62

2.6 EXPERIMENTAL SECTION 62

2.6.1 Materials and Methods 62

2.6.2 Ni(II) Complex Preparation 64

2.6.3 Optimization of Reaction Parameters 66

2.6.4 Substrate Preparation 67

2.6.4.1 Chlorobenzyl Silane Electrophiles 67

2.6.4.2 Alkenyl Bromide Electrophiles 73

2.6.4.3 Oxygen-Based Electrophiles 91

2.6.5 Enantioselective Reductive Cross-Couplings 92

2.6.6 Derivatization of Enantioenriched Allylic Silanes 121

2.6.6.1 Products from Allylic Silanes 121

2.6.6.2 Synthesis of Standards 152

2.6.7 SFC and HPLC Traces of Racemic and Enantioenriched Products 158

2.7 REFERENCES 198

APPENDIX 1 ***204***

Spectra Relevant to Chapter 2

APPENDIX 2 ***424***

X-Ray Crystallography Reports Relevant to Chapter 2

CHAPTER 3 ***435***

Decarboxylative Asymmetric Ni-Catalyzed Cross-Coupling of Benzylic *N*-Hydroxyphthalimide Esters and Alkenyl Bromides

3.1 INTRODUCTION 435

3.2 REACTION OPTIMIZATION 439

3.2.1 Initial Hit with Additives 439

3.2.2 Activating Groups 440

3.2.3 Reductants 440

3.2.4 Halide Exchange 441

3.2.5 Temperature 442

3.2.6 Reductant Equivalents 443

3.2.7 Solvents 443

3.2.8 Optimization Controls 444

3.3 SUBSTRATE SCOPE 445

3.4 REACTION MECHANISM 451

3.5 CONCLUSION 453

3.6 EXPERIMENTAL SECTION 454

3.6.1 Materials and Methods 454

3.6.2 Ni(II) Complex Preparation 455

3.6.3 Large Scale Preparation of TDAE 457

3.6.4 Optimization of Reaction Parameters 459

3.6.5 Substrate Preparation 460

3.6.6 Enantioselective Reductive Cross-Couplings 473

3.6.7 GC-MS Traces of Radical Clock Products 497

3.6.8 SFC and HPLC Traces of Racemic and Enantioenriched Products 498

3.7 REFERENCES 526

APPENDIX 3 ***533***

Spectra Relevant to Chapter 3

APPENDIX 4 ***646***

X-Ray Crystallography Reports Relevant to Chapter 3

CHAPTER 4 ***651***

Mechanistic Investigations of Ni-Catalyzed Asymmetric Reductive Cross-Couplings with Alkenyl Bromide Electrophiles

4.1 INTRODUCTION 651

4.1.1 Recent Advances in Reductive Cross-Couplings 651

4.2 PROPOSED REACTION MECHANISMS 654

4.2.1 In Situ Organometallic Formation 655

4.2.2 Disproportionation/Transmetalation 656

4.2.3 Intermediate Reduction 657

4.2.4 Radical Chain 658

4.3 EXPERIMENTAL STUDIES: NICKEL COMPLEXES 659

4.3.1 Synthesis and Characterization of Ni(II) Complexes 659

4.3.2 UV-Vis Spectroscopy 662

4.3.3 Cyclic Voltammetry 663

4.3.4 EPR Spectroscopy 664

4.3.5 Oxidative Addition Complexes 666

4.3.6 Analysis of Ni(I) Intermediates 667

4.4 EXPERIMENTAL STUDIES: REACTION PROFILE 669

4.4.1 Stoichiometric Ni(0) Studies 669

4.4.2 Scalemic Ligand Study 671

4.4.3 Reaction Progress by ^{19}F NMR 672

4.4.4 Reaction Kinetics 673

4.4.4.1 Mn and Zn Reductants 674

4.4.4.2 Observation of Side Products 674

4.4.4.3 Nickel Loading 675

4.4.4.4 Electrophile Equivalents 677

4.4.4.5 Stirring Rate 678

4.4.5 Radical Clock Substrates 679

4.5 COMPUTATIONAL STUDIES 680

4.5.1 Generation of Ni(0) 681

4.5.2 First Oxidative Addition 682

4.5.3 Preference for Cross-Coupling 683

4.5.4 Competing Mechanisms during Second Oxidative Addition 684

4.5.5 Alternate Reduction 684

4.5.6 Radical Clock Substrate 686

4.5.7 Enantioinduction 686

4.6 CONCLUSIONS AND FUTURE DIRECTIONS 689

4.7 EXPERIMENTAL SECTION 691

4.7.1 Materials and Methods 691

4.7.2 Ni(II) Complex Preparation 693

4.7.3 Electronic Absorption 696

4.7.4 Cyclic Voltammetry 696

4.7.5 EPR Spectroscopy 697

4.7.6 Stoichiometric Ni(0) Studies 699

4.7.7 Scalemic Ligand Study 700

4.7.8 Analysis of Reaction by ^{19}F NMR 700

4.7.9 Kinetics Procedures, Standards, and GC-FID Fits 701

4.7.10 Radical Clock Experiments 708

4.8 REFERENCES 710

APPENDIX 5 ***713***

Spectra Relevant to Chapter 4

APPENDIX 6 ***716***

X-Ray Crystallography Reports Relevant to Chapter 4

CHAPTER 5 ***727***

Ni-Catalyzed Halogenation of Alkenyl Triflates

5.1 INTRODUCTION 727

5.2 REACTION OPTIMIZATION WITH NI(0) 731

5.2.1 Initial Hit 731

5.2.2 Solvents 732

5.2.3 Halide Source 733

5.2.4 Catalyst Loading 734

5.2.5 Concentration and Temperature 734

5.2.6 Other Alkenyl Electrophiles 735

5.3 SUBSTRATE SCOPE 736

5.4 MECHANISTIC INVESTIGATIONS 741

5.4.1 Kinetics 742
5.4.2 Radical Inhibitors 744
5.4.3 Investigating Catalyst Inhibition 745
5.4.4 EPR Spectroscopy 747
5.4.5 Crossover Experiments 748
5.4.6 Potential Reaction Mechanisms 751
5.5 EVALUATION OF NI(II) PRECATALYSTS 752
5.5.1 Optimization 752
5.5.2 Substrate Scope 755
5.6 CONCLUSION 756
5.7 EXPERIMENTAL SECTION 757
5.7.1 Materials and Methods 757
5.7.2 Optimization of Reaction Parameters 758
5.7.3 Substrate Preparation 759
5.7.3.1 Alkenyl Triflates 759
5.7.3.2 Alkenyl Nonaflates 774
5.7.4 Ni-Catalyzed Halogenation 778
5.7.5 Characterization of Reaction Products 780
5.7.6 Mechanistic Experiments 818
5.7.6.1 Radical Inhibitors 818
5.7.6.2 Kinetics 818
5.7.6.3 EPR Studies 819
5.7.6.4 Investigating Catalyst Death and Diene Formation 820

5.7.6.5 Crossover Experiments 821

5.7.6.6 Halide Competition Experiments 822

5.7.6.7 NMR Experiments 822

5.8 REFERENCES 823

APPENDIX 7 ***827***

Spectra Relevant to Chapter 5

APPENDIX 8 ***1024***

Phosphino(oxazoline) Ligand Parameterization for Asymmetric Ni-Catalyzed Reductive Cross-Coupling of Aryl Iodides and α-Chloronitriles

A8.1 INTRODUCTION 1024

A8.1.1 Origins of Stereoinduction 1025

A8.1.2 Asymmetric Reductive Cross-Couplings 1026

A8.1.3 Ligand Parameterization 1028

A8.2 PRELIMINARY RESULTS 1030

A8.2.1 Cross-Coupling of α-Chloronitriles and Aryl Iodides 1030

A8.2.2 Initial Data Set 1031

A8.3 EXPERIMENTAL RESULTS 1033

A8.3.1 Ligand Synthesis 1034

A8.3.2 Cyclic Voltammetry Studies 1036

A8.3.3 Iodobenzonitrile Aryl Electrophile 1038

A8.3.4 Pyrimidine Heteroaryl Iodide Electrophile 1040

A8.4 CONCLUSIONS AND FUTURE DIRECTIONS 1041

A8.5 EXPERIMENTAL SECTION 1042

A8.5.1 Materials and Methods 1042

A8.5.2 PHOX Ligand Synthesis 1043

A8.5.3 Cross-Coupling Reactions 1063

A8.6 REFERENCES 1064

ABOUT THE AUTHOR ***1067***

LIST OF ABBREVIATIONS

–	minus
%	percent
°	degrees
+	plus
<	less than
=	equals
>	greater than
~	approximately
λ	lambda (wavelength)
α	alpha
A	ampere or acid functional group
Å	angstrom(s)
$[\alpha]_D$	angle of optical rotation of plane-polarized light
Ac	acetyl
acac	acetylacetonate
AcOH	acetic acid
alk	alkyl
anal.	combustion elemental analysis
anti	opposite or same side
approx	approximately

aq	aqueous
Ar	aryl group
Ar^F	perfluorinated aryl group
atm	atmosphere(s)
AU	arbitrary units
AVG	average
β	beta
BDMAP	1,6-bis(dimethylamino)pyrene
BHT	2,6-di-*tert*-butyl-4-methylphenol ("butylated hydroxytoluene")
BiOX	bi(oxazoline)
Bn	benzyl
BnPHOX	benzyl phosphinooxazoline
Boc	*tert*-butoxycarbonyl
BOX	bis(oxazoline)
bp	boiling point
bpy	2,2'-bipyridine
br	broad
Bu	butyl
Bz	benzoyl
/C	supported on activated carbon charcoal
°C	degrees Celcius
^{13}C	carbon-13 isotope
c	concentration of sample for measurement of optical rotation

calc'd	calculated
CAM	cerium ammonium molybdate
Cbz	benzyloxycarbonyl
cis	on the same side
cm	centimeters
cm^{-1}	wavenumber(s)
CNB	1-chloro-2,4-dinitrobenzene
conv.	conversion
CoPc	cobalt(II) phthalocyanine
$CoPc_F$	perfluoroinated cobalt(II) phthalocyanine
COSY	homonuclear correlation spectroscopy
Cp	cyclopentyldienyl
CV	cyclic voltammetry
δ	chemical shift in ppm
D	deuterium
d	deutero or dextrorotatory
d	doublet
Δ	heat or difference
ΔG	change in Gibb's free energy
DBE	dibromoethane
DCM	dichloromethane
DEAD	diethyl azodicarboxylate

DEC	diethyl carbonate
DHA	dihydroanthracene
DIBAL	diisobutylaluminum hydride
diglyme	diethylene glycol dimethyl ether
DIPA	N-diisopropylamine
DIPEA	*N*,*N*-diisopropylethylamine
DMA	*N*,*N*-dimethylacetamide
DMAP	4-(dimethylamino)pyridine
DMBA	2,6-dimethylbenzoic acid
dme	1,2-dimethoxyethane
DMEDA	*N,N*′-dimethylethylenediamine
DMF	*N*,*N*-dimethylformamide
DMP	Dess-Martin periodinane
DMPU	1,3-dimethyl-3,4,5,6-tetrahydro-2(1H)-pyrimidinone
DMS	dimethylsulfide
DMSO	dimethylsulfoxide
dppf	1,1'-bis(diphenylphosphino)ferrocene
dpph	1,6-bis-(diphenylphosphino)hexane
dr	diastereomeric ratio
dtbbpy	4,4'-di-*tert*-butyl-2,2'-bipyridine
E	*trans* (entgegen) olefin geometry
e.g.	for example (Latin: *exempli gratia*)
E^+	electrophile

EA	elemental analysis
EDC	1-ethyl-3-(3-dimethylaminopropyl)carbodiimide
ee	enantiomeric excess
EI	electron impact
E_{pc}	cathodic peak potential
EPR	electron paramagnetic resonance
equiv	equivalent(s)
er	enantiomeric ratio
es	enantiospecificity
ESI	electrospray ionization
Et	ethyl
et al.	and others (Latin: *et alii*)
Et_2O	diethyl ether
Et_3N	triethylamine
etc	and the rest (Latin: *et cetera*)
EtOAc	ethyl acetate
EtOH	ethanol
^{19}F	fluorine-19 isotope
FAB	fast atom bombardment
Fc	ferrocene
Fc^+	ferrocenium cation
FDA	Food and Drug Administration
FID	flame ionization detector

FTIR	fourier transform infrared spectroscopy
G	gauss
g	gram(s)
g-value	dimensionless magnetic moment value
g/mL	grams per milliliter
GC	gas chromatography
GHz	gigahertz
^{1}H	proton
h	hour(s)
HAT	hydrogen atom transfer
Het	hetero
HMBC	heteronuclear multiple-bond correlation spectroscopy
HMDS	hexamethyldisilazide
HOAt	1-hydroxy-7-azabenzotriazole
HOMO	highest occupied molecular orbital
HPLC	high performance liquid chromatography
HRMS	high resolution mass spectrometry
HSQC	heteronuclear single quantum coherence spectroscopy
hυ	irradiation with light
Hz	hertz
i-Bu	*iso*-butyl
i-Bu_3Al	triisobutyl aluminum
i-Pr	isopropyl

i-Pr_2NH	diisopropyl amine
i-PrAc	isopropyl acetate
i-PrOH	isopropanol
i.e.	that is (Latin: *id est*)
in situ	in the reaction mixture
IPA	isopropanol
IR	infrared
J	coupling constant in Hz
K	Kelvin
k	rate constant
k_0	initial rate constant
k_c	equilibrium constant
kcal	kilocalorie(s)
kg	kilogram(s)
KO*t*-Bu	potassium tert-butoxide
L	liter
l	levorotatory
LC-MS	liquid chromatography–mass spectrometry
LDA	lithium diisopropylamide
LED	light emitting diode
ln	natural logarithm
log	logarithm
LRMS	low resolution mass spectrometry

LUMO	lowest unoccupied molecular orbital
m	multiplet or meter(s)
M	molar or molecular ion or metal
[M]	parent mass
m	*meta*
M^{-1}	inverse molarity
m.p.	melting point
m/z	mass-to-charge ratio
mA	milliamp(s)
*m*CPBA	*meta*-chloroperbenzoic acid
Me	methyl
MeCN	acetonitrile
$MeCO_2H$	acetic acid
MeI	methyl iodide
MeOH	methanol
mg	milligram(s)
mg/mL	milligrams per milliliter
MHz	megahertz
MIDA	methyliminodiacetic acid
min	minute(s)
μL	microliter(s)
mL	milliliter(s)
mL/min	milliliters per minute

mM	millimolar
mm	millimeter(s)
μm	micrometer(s)
mm Hg	millimeters mercury
mmol	millimole(s)
mol	mole(s)
mol %	mole percent
Ms	methanesulfonyl (mesyl)
MS	molecular sieves
MsCl	methanesulfonyl chloride
MSD	mass selective detector
^{14}N	nitrogen-14 isotope
n	number
n-Bu	*norm-butyl*
n-BuLi	*norm*-butyl lithium
n-Hex	*norm*-hexyl
n-Pr	*norm*-propyl
NaOTf	sodium triflate
NBS	*N*-bromosuccinimide
Nf	perfluorobutanesulfonyl
Nf-F	perfluorobutanesulfonyl fluoride
Nf_2O	perfluorobutanesulfonyl anhydride
NHP	*N*-hydroxyphthalimide

nm	nanometer(s)
NMP	*N*-methyl pyrrolidinone
NMR	nuclear magnetic resonance
Nu^-	nucleophile
o	*ortho*
^{31}P	phosphorus-31 isotope
p	*para*
p-TsOH	*para*-toluenesulfonic acid
Pc	phthalocyanine
PC	propylene carbonate
PcF	perfluorinated phthalocyanine
PDT	product
pH	hydrogen ion concentration in aqueous solution
Ph	phenyl
phen	1,10-phenanthroline
PhH	benzene
PhMe	toluene
PHOX	phosphinooxaozoline
Phth	phthalimide
Pin	pinacol
pm	picometer(s)
PMP	*para*-methoxyphenyl
ppm	parts per million

Pr	propyl
psi	pounds per square inch
py	pyridine
PyBOX	pyridine bis(oxazoline)
q	quartet
quant	quantitative
R	generic (alkyl) group
R	rectus
R^2	coefficient of determination
ref	reference
R_F	pefluorinated alkyl group
R_f	retention factor
RF	response factor
rpm	revolutions per minute
rr	regioisomeric ratio
rt	room temperature
σ	Hammett coefficient
s	singlet or seconds
S	sinister
sat.	saturated
SCE	saturated calomel electrode
SFC	supercritical fluid chromatography
STD	standard

syn	same side
T	temperature
t	triplet or time
t-Bu	*tert*-butyl
t-BuLi	tert-butyl lithium
taut.	tautomerize
TBA	tetra-n-butylammonium
TBABr	tetra-*n*-butylammonium bromide
TBACl	tetra-*n*-butylammonium chloride
TBACN	tetra-*n*-butylammonium cyanide
TBAF	tetra-*n*-butylammonium fluoride
TBAI	tetra-*n*-butylammonium iodide
TBAX	tetra-*n*-butylammonium salt
TBDPS	*tert*-butyldiphenylsilyl
TBDPSCl	tert-butyldiphenylsilyl chloride
TBS	*tert*-butyldimethylsilyl
TBSCl	*tert*-butyldimethylsilyl chloride
TDAE	tetrakis(dimethylamino)ethylene
TEA	triethylamine
temp	temperature
TEMPO	2,2,6,6-tetramethylpiperidine 1-oxyl
TEOA	triethanolamine
TES	triethylsilyl

Tf	trifluoromethanesulfonyl
Tf_2O	trifluoromethanesulfonic anhydride
TFA	trifluoroacetic acid
THF	tetrahydrofuran
TLC	thin layer chromatography
TMEDA	*N,N,N′,N′*-tetramethylethylenediamine
TMHD	2,2,6,6-tetramethyl-3,5-heptanedione
TMS	trimethylsilyl
TMSBr	trimethylsilyl bromide
TMSCl	trimethylsilyl chloride
TMSOTf	trimethylsilyl trifluoromethanesulfonate
TOF	time-of-flight
Tol	tolyl
TPP	tetraphenylporphyrin
tpy	2,2';6',2"-terpyridine
t_R	retention time
trans	on the opposite side
TS	transition state
Ts	*para*-toluenesulfonyl (tosyl)
TTF	tetrathiafulvalene
μ	micro
μL	microliter(s)
UV	ultraviolet

V	volt(s)
vide infra	see below
V_{max}	maximum rate
vs.	versus
W	watt(s)
w/	with
wt%	weight percent
X	anionic ligand or halide or chiral auxillary
X_{major}	fraction of mixture as major enantiomer
X_{minor}	fraction of mixture as minor enantiomer
Z	*cis* (zusammen) olefin geometry

Chapter 1

Emergence of C(sp^3) Ni-Catalyzed Reductive Cross-Couplings: From Achiral Catalysis to Asymmetric Variants

1.1 INTRODUCTION

Metal-catalyzed cross-coupling reactions have become one of the most utilized transformations in medicinal chemistry and in the synthesis of active pharmaceuticals.[1] In addition, these reactions have also found important use in the agrochemical industry and in the production of materials.[2–4] One can contend that the utility behind these methods is due to their simplicity; they allow one to reliably build complex molecules from simple building blocks through straightforward and strategic disconnections. The emergence of this field stemmed from seminal reports in the mid 19th century which describe the use of various metals to produce aryl homocoupling products. However, as reaction development continued and chemists sought ways to promote metal-catalyzed methods in the late 20th century, in particular to favor coupling of distinct partners to form cross-selective products,

Pd-catalyzed reactions were more widely developed in contrast to other metals.[5] Research in this newly formed area sought the optimization of conditions to access a wide variety of cross-couplings between nucleophiles and electrophiles, research that continues to be developed even today. In honor of important accomplishments in this area, in 2010 the Nobel Prize was awarded to Heck, Negishi, and Suzuki for their contributions to the development of Pd-catalyzed cross-coupling.

Although these reactions have shown utility in the generation of carbon–carbon and carbon–heteroatom bonds containing C(sp)- and C(sp^2)-hybridized centers, it has been challenging to expand the scope to include C(sp^3)-hybridized centers. Not only are C(sp^3)-hybridized products more difficult to synthesize due to facile β-hydride elimination during Pd-catalyzed cross-couplings, but the generation of C(sp^3)-hybridized centers introduces the opportunity to incorporate chirality into a molecule, and finding appropriate chiral ligands to set stereochemistry with high levels of enantioselectivity is often not trivial.

To address these challenges, the development of Ni-catalyzed cross-coupling reactions has garnered interest in the synthesis of molecules containing C(sp^3)-hybridized centers.[6–10] In contrast to Pd, Ni is less electronegative which promotes oxidative addition and mitigates β-hydride elimination; however, it is more challenging for Ni to undergo reductive elimination processes at comparable oxidation states (Figure 1.1). The intrinsic properties of Ni also allow for the access of putative 0, +1, +2, and +3 oxidation states of the metal center during the catalytic cycle, which can permit radical-type oxidative addition processes and enable access to new reaction mechanisms not traditionally seen in Pd catalysis. While these properties promote new modes of reactivity, it is often difficult to

harness and control reactive intermediates; therefore, the design of ligands to tune the reactivity of Ni is crucial to the success of reaction methods development.

Figure 1.1 *Properties of Ni and Pd.*

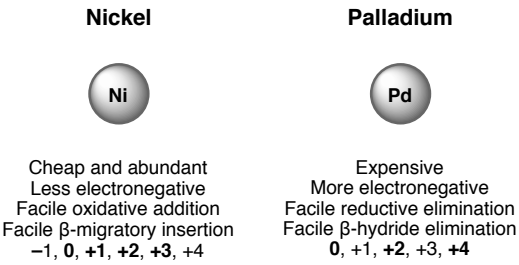

Towards this endeavor, a number of examples of stereoconvergent and stereospecific Ni-catalyzed cross-coupling reactions employing C(sp^3)-hybridized electrophiles have been developed (Figure 1.2). Fu and coworkers have reported numerous examples of stereoconvergent cross-couplings to set C(sp^3)-hybridized stereocenters through the coupling of racemic alkyl halide electrophiles and a variety of organometallic reagents (e.g., organozinc,[11–22] organoboron,[23–31] organosilicon,[32] organomagnesium,[33] organozirconium[34]) in the presence of a chiral Ni catalyst (Figure 1.2a). Doyle and coworkers expanded these methods to include the cross-coupling of quinolinium and pyridinium ions with organoboron reagents.[35] This stereoconvergent approach allows for the direct synthesis of complex chiral molecules from simple racemic coupling partners and eliminates the need for stoichiometric chiral auxiliaries. Furthermore, Jarvo and Watson have developed stereospecific examples using chiral electrophiles and achiral nickel catalysts, which have also enabled the synthesis of chiral products through stereoinvertive and stereoretentive approaches.[36–46] Despite their utility in cross-couplings reactions, C(sp^3)-hybridized organometallic reagents are difficult to prepare in high yield,

especially those that are chiral.[47] Overall, these traditional redox-neutral cross-coupling methods require the use of a nucleophile, typically an organometallic reagent, which can suffer from poor stability, air sensitivity, and limited commercial availability.

Figure 1.2 *Ni-catalyzed cross-couplings to form C(sp³)-hybridized stereocenters.*

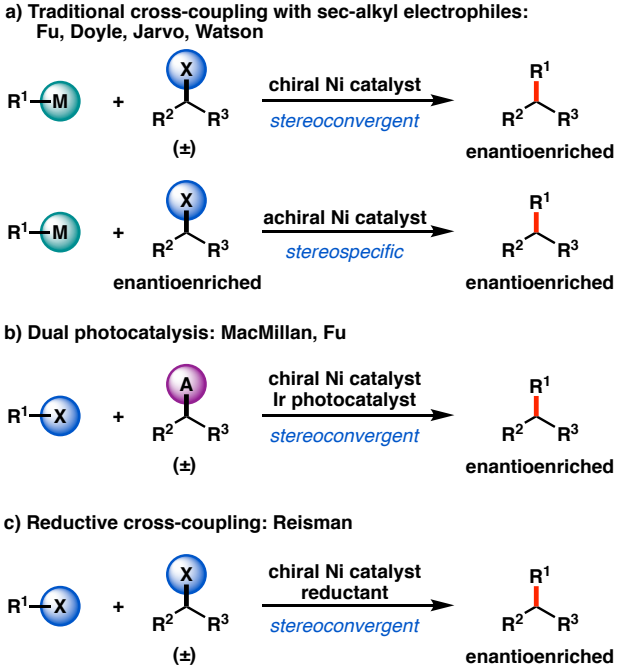

To complement these approaches, reactions that rely on synergistic Ni/photoredox (metallaphotoredox) catalysis[48,49] and Ni-catalyzed reductive cross-electrophile coupling[50–53] have recently been rendered enantioselective (Figure 1.2b–c).[54–60] Most Ni metallaphotoredox methods result from cross-coupling of bench stable carboxylic acids and halide electrophiles;[48,49,55,61–63] however, more recent approaches that generate reactive radical intermediates via C–H abstraction through hydrogen atom transfer (HAT) mechanisms have also been disclosed.[64,65] Typically, these reactions produce either achiral or racemic products; however, a singular example of an asymmetric Ni metallaphotoredox transformation has been developed by MacMillan, Fu, and coworkers (Figure 1.2b).[55]

A number of Ni-catalyzed asymmetric reductive cross-coupling reactions have also been pioneered, which has been the main focus in our laboratory's research surrounding Ni catalysis.[54,56–60] These methods allow inexpensive, bench stable electrophiles as both coupling partners and ultimately proceed with stereoconvergence when appropriate chiral ligands are used (Figure 1.2c). Mild reaction conditions are also employed, allowing methods to exhibit excellent functional group tolerance that would otherwise be incompatible with organometallic reagents. However, one of the major challenges of reductive cross-electrophile couplings, in contrast to conventional redox neutral methods, is the ability to achieve high levels of cross-selectivity. In order to differentiate between the two electrophiles, one can resort to extreme alterations to reagent stoichiometry; however, a more notable approach relies on distinguishing electrophiles via their hybridization which is typically employed by using one C(sp^2)-hybridized electrophile and one C(sp^3)-hybridized electrophile. If differently hybridized electrophiles can selectively react with distinct oxidation states of Ni in the catalytic cycle (e.g. radical type oxidative addition vs. polar mechanism), this could obviate the need for reagent excess and favor cross-selective products instead of homocoupling products.

In considering the mechanism of these transformations, Weix and coworkers have studied the related achiral reductive cross-coupling reaction between aryl iodides and alkyl iodides.[51,66] A few different mechanisms have been postulated and are discussed in greater detail in Chapter 4. A summary of their studies proposed the likelihood of a radical chain mechanism (Figure 1.3). The authors propose that C(sp^3)-hybridized electrophile may result in the formation of an alkyl radical intermediate, which when combined with a Ni(II)

complex—resulting from oxidative addition of the C(sp^2)-hybridized electrophile onto Ni(0)—forms a Ni(III) complex. Since reductive elimination from Ni(III) is much more favorable than from Ni(II), the desired cross-coupling product is obtained in good selectivity over the homocoupling products C(sp^2)–C(sp^2) and C(sp^3)–C(sp^3). The application of this reactivity towards method development focuses primarily on the ability to capitalize on the accessible odd oxidation states of Ni to generate and intercept secondary alkyl radicals.

Figure 1.3 *Proposed mechanism for reductive cross-couplings.*

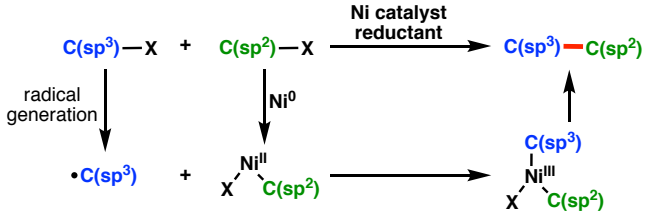

Herein, we discuss the development of Ni-catalyzed reductive cross-coupling reactions using C(sp^3)-hybridized electrophiles is discussed. Initial developments in achiral and racemic systems will be highlighted, and when appropriate, methods that detail developments of asymmetric variants will be discussed. We recognize that electrophiles are defined as electron pair acceptors; however, in the context of cross-coupling this is typically envisioned as an organic halide. As such, a majority of recent efforts in cross-electrophile coupling have been focused in this area. Nevertheless, a number of additional approaches have been developed using "pseudohalides" (i.e., tosylates, mesylates, epoxides, *N*-hydroxyphthalimide esters), which will also be discussed briefly.

1.2 CROSS-COUPLINGS WITH HALIDE ELECTROPHILES

1.2.1 Initial Developments in C(sp²) Couplings

Although this review focuses on the use of C(sp³)-hybridized electrophiles in cross-electrophile coupling, it would be remiss to exclude historical context highlighting initial discoveries regarding Ni-catalyzed reductive homocouplings with C(sp²)-hybridized electrophiles. These seminal investigations provided the necessary backround that led to the development of this area of research.

In the early 1970s, Semmelhack and coworkers reported the first homocoupling reactions of aryl iodides (**1**, **3**) in the presence of stoichiometric zerovalent Ni complexes (Figure 1.4).[67,68] These reactions proceeded either intermolecularly with $Ni(cod)_2$ or intramolecularly with $Ni(PPh_3)_4$ to afford biaryl products (**2**, **4**) in good yields. Notably, functional groups such as ketones, aldehydes, esters, and nitriles, which would typically interfere with organometallic intermediates, were tolerated in the cross-coupling reaction. In order to highlight its applicability, this method was demonstrated in the total synthesis of a natural product, alnusone (**5**), by a late stage aryl-aryl coupling (Figure 1.4c).[69,70]

Figure 1.4 *Aryl iodide homocoupling with stoichiometric Ni(0).*

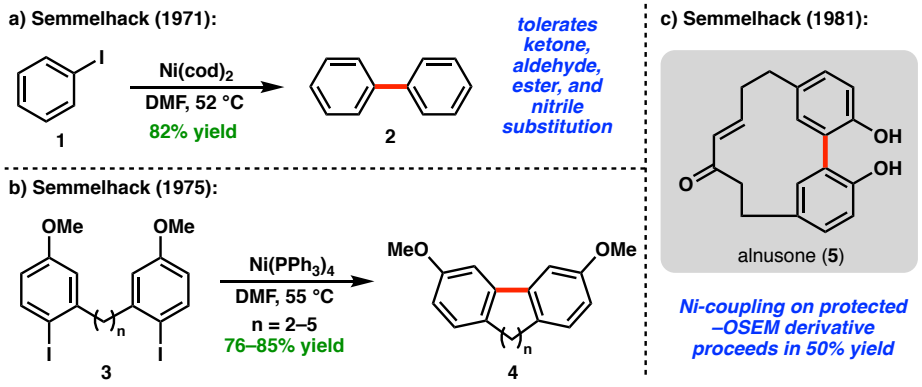

Following these initial reports, in 1974 Tolman and coworkers studied the kinetics of ligand dissociation from $Ni(PPh_3)_4$ and discovered that $Ni(PPh_3)_3$ was the active catalyst in the homocoupling transformation.[71] Kende and coworkers then identified a new method for the preparation of *in situ*-generated $Ni(PPh_3)_3$ via a Zn-mediated reduction of $NiCl_2(PPh_3)_2$ in the presence of PPh_3 (Figure 1.4a).[72] This approach alleviated the need for trialkyl- and dialkylalkoxyaluminum reducing agents which necessitate drybox conditions for the preparation of $Ni(PPh_3)_4$. The desired biaryl products (**7**) were then obtained following the treatment of the *in situ* generated, stoichiometric Ni(0) complex with a variety of aryl bromides (**6**). In 1977, Kumada and coworkers reported the first Ni-catalyzed version of the homodimerizaion reaction using a one-pot protocol (Figure 1.4b).[73] Only 2.5 mol % loading of the Ni catalyst was required, as stoichiometric use of Zn was sufficient to reduce the Ni catalyst *in situ* and promote efficient catalytic turnover. Yamishita and coworkers disclosed a similar transformation in 1986, albeit with the use of aryl triflates (**8**), demonstrating that other electrophiles besides halides can undergo reductive homocoupling processes (Figure 1.4c).[74]

Scheme 1.1 *Aryl iodide homocoupling by reduction of Ni(II) with Zn.*

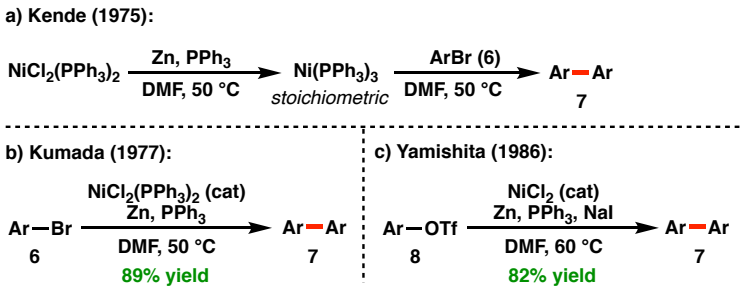

Following seminal studies on reductive homocouplings in the 1970s and 1980s, the 1990s and early 21st century saw the development of Ni-catalyzed cross-coupling methods.

However, due to the necessity to obtain cross-selective products over homocoupling products, the use of redox-neutral transformations between nucleophiles and electrophiles was more widely studied than reductive approaches.

1.2.2 Electrochemical Methods

Initial developments in Ni-catalyzed reductive cross-coupling focused on the use of electrochemical approaches using sacrificial metal anodes as the terminal reductant. A number of cross-electrophile couplings between C(sp^2)- and C(sp^3)-hybridized electrophiles with the use of a single-cell electrochemical setup were developed, most notably by Durandetti and coworkers (Figure 1.5).[75–81] The two electrophiles, an electrolyte, and the requisite Ni catalyst were dissolved in a solvent with high conductivity (e.g. MeCN, DMF), and upon passing current, the desired cross-coupling products were formed. In this setup, reduction processes occurred at the sacrificial metal anode, which dissolves over time as it becomes oxidized to metal cations. Reduction of Ni occurred at the inert cathode, which can then proceed to interact with electrophiles and promote the desired transformation in solution. Although electrochemical approaches were developed

Figure 1.5 *Ni-catalyzed electrochemical cross-electrophile couplings.*

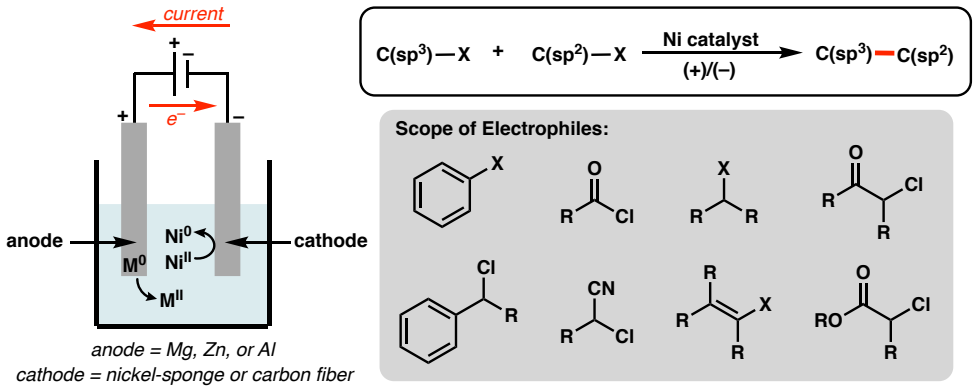

in the mid to late 1990s, the first Ni-catalyzed reductive cross-coupling reaction that used a chemical reductant (i.e. Zn dust) to turn over the catalyst was not reported until 2007.[82]

1.2.3 Heterogeneous Metal Reductants

1.2.3.1 Unactivated Alkyl Electrophiles

An abundant field of research in the development of Ni-catalyzed C(sp^3) cross-coupling has focused on the development of methods that use heterogeneous metal reductants such as Zn and Mn. One particular area concentrated efforts on the use of unactivated alkyl halides (**9**) as one of the coupling partners (Figure 1.6). Weix and coworkers were the first to demonstrate Ni-catalyzed cross-electrophile couplings with unactivated electrophiles,[50,53] and since then a plethora of coupling partners have been extensively investigated, predominantly by the Weix and Gong groups. These reactions form a variety of products (**10**–**15**) when used in cross-coupling reactions in conjunction

Figure 1.6 *Cross-electrophile couplings with unactivated alkyl halides.*

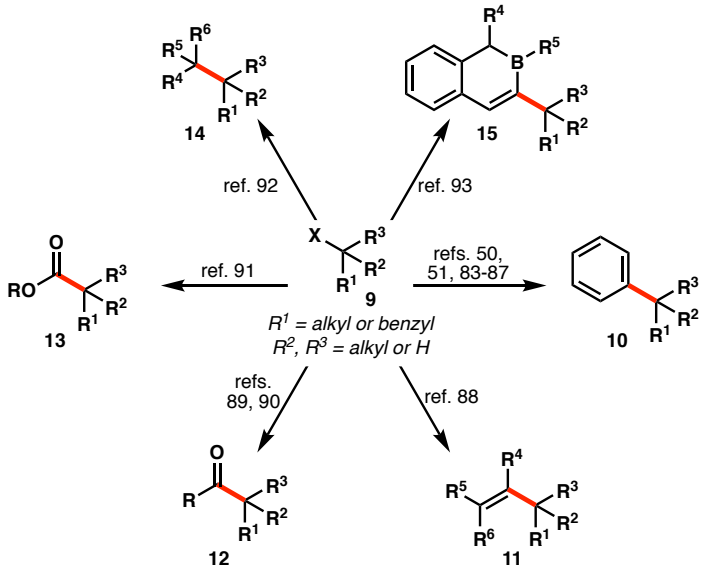

with aryl halides,[50,51,83–87] alkenyl halides,[88] acyl halides,[89,90] chloroformates,[91] alkyl halides,[92] and 3-bromo-azaborines.[93] While most ligands used in these transformations are achiral ligands (e.g. diamine, dtbbpy, phen), Gong and coworkers have demonstrated that PyBOX ligands are effective for alkyl–alkyl couplings,[92] albeit the products are reported as racemic mixtures. Future efforts in the development of asymmetric variants of these coupling reactions is necessary; however, given the unique sets of conditions that are already reported as the C(sp^2)-hybridized electrophile is altered, simply replacing achiral ligands with chiral substitutes is not pragmatic; reactions likely need to be entirely reoptimized to access good yield of analogous chiral products. As asymmetric cross-electrophile couplings all contain activated electrophiles, it is likely that matching the electronics of the catalyst to the lifetime of the alkyl radical is important, which is anticipated to be more challenging with shorter lived alkyl radical species.

1.2.3.2 Activated Alkyl Electrophiles

As alkyl radicals are generated on the C(sp^3)-hybridized electrophile following halide abstraction, any substituents present at the α-position will affect the stability and longevity of the generated intermediate. Following investigations using electrochemical methods to conduct cross-electrophile couplings, Durandetti and coworkers were the first to report the use of a chemical reductant (i.e. Mn) to obtain α-arylated ketone products from stabilized alkyl halide electrophiles.[82] Since then, a number of Ni-catalyzed reductive cross-couplings of alkyl halides containing radical stabilizing α-substituents have been developed (Scheme 1.2), including α-groups such as esters,[82] fluorinated alkanes,[94] ethers (glycosides),[95] and pinacol boronates.[96]

Scheme 1.2 *Cross-electrophile couplings with activated alkyl halides.*

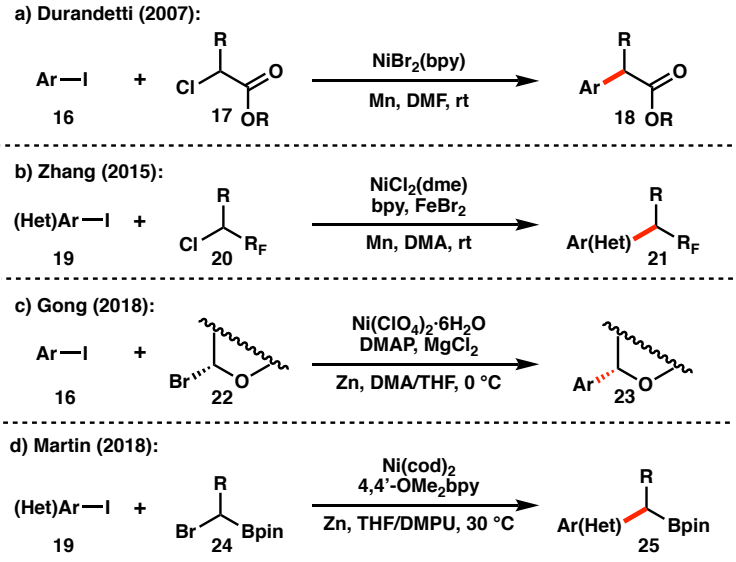

Our laboratory has focused on the development of asymmetric Ni-catalyzed cross-electrophile couplings using a broad scope of C(sp^2)-hybridized electrophiles (e.g. aryl iodides (**16**, **19**), alkenyl bromides (**29**), and acid chlorides (**26**)); however, diversifying the C(sp^3)-hybridized electrophile has proven challenging (Scheme 1.3). Thus far, the C(sp^3)-hybridized electrophiles require the use of a radical stabilizing functional group adjacent to the electrophilic carbon, which has afforded success when included as either an aromatic ring (**27**, **32**) or nitrile (**31**) moiety. To obtain high selectivity in the benzylic systems, the use of bis(oxazoline) (BOX) ligands **L1** or **L2**, or bi(oxazoline) (BiOX) ligand **L4**, provides the products in up to 98% enantiomeric excess (ee). With α-chloronitrile electrophiles, an electron-rich BnPHOX ligand **L3** was found to afford the best ee. Although there is some overlap in ligand selection (both alkenylation reactions use the same chiral BOX ligand **L2**), altering the identity of the electrophiles requires extensive screening operations to find the most appropriate ligand and reaction conditions.

Scheme 1.3 *Asymmetric cross-electrophile couplings with activated alkyl halides.*

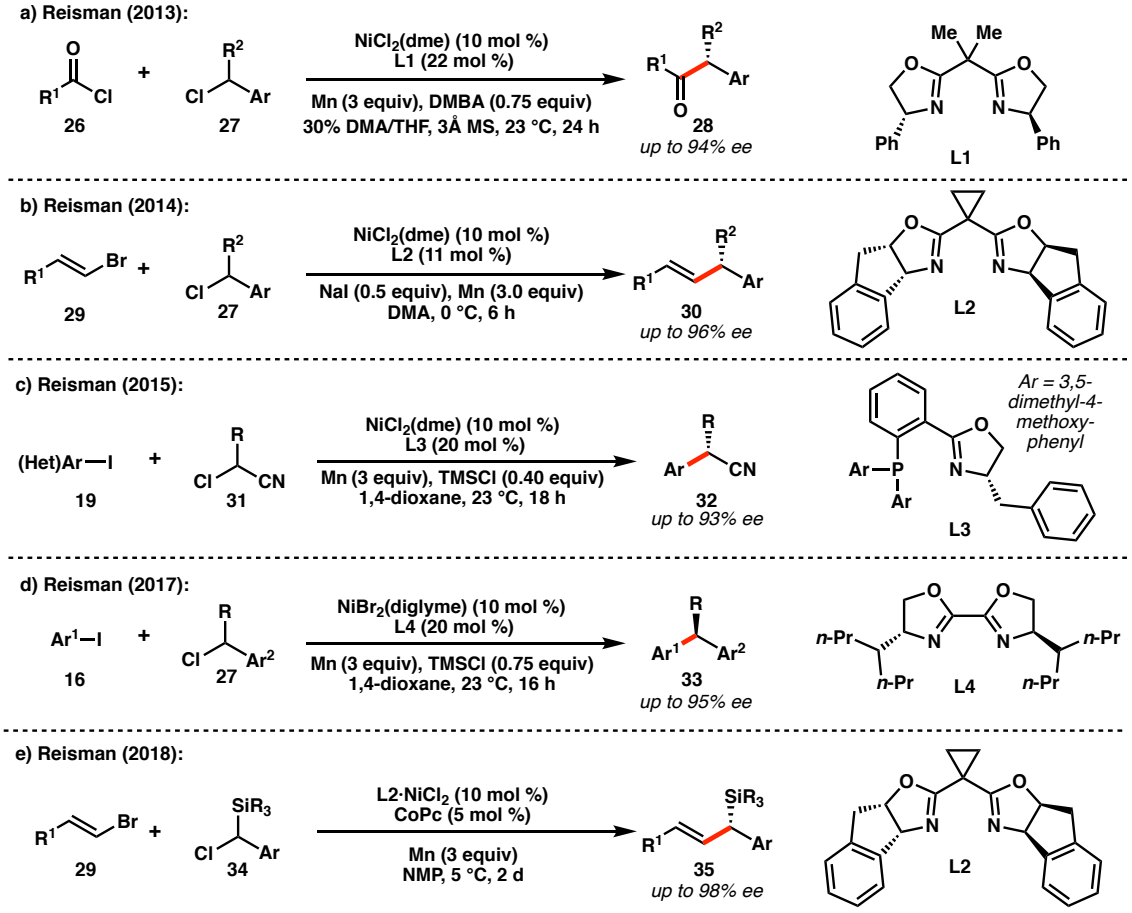

1.2.4 Soluble Organic Reductants

Although most cross-electrophile couplings use either Zn or Mn powder as the stoichiometric reductant, efforts to develop conditions using soluble organic reductants have also been investigated. Since metal reductants render reductive cross-couplings as heterogeneous mixtures, this requires special glassware setups for large scale applications due to capricious stirring effects.[97] While metals and metal complexes display a significant range of reduction potentials, synthetic organic reductants are significantly less reducing (Figure 1.7).[98] However, Murphy and coworkers have demonstrated the synthesis of "super

electron donors" **36** and **37**, which have similar reduction potentials to that of Zn and Mn, respectively.[99,100] These stronger organic reductants have yet to be used in cross-electrophile coupling but may find their use in future developments.

Figure 1.7 *Reduction potentials of metallic and organic reductants.*

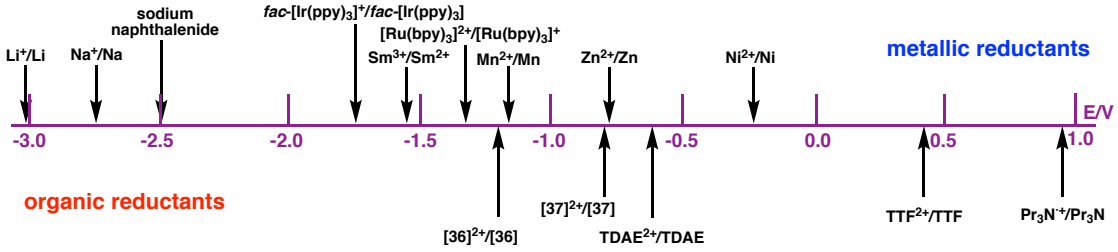

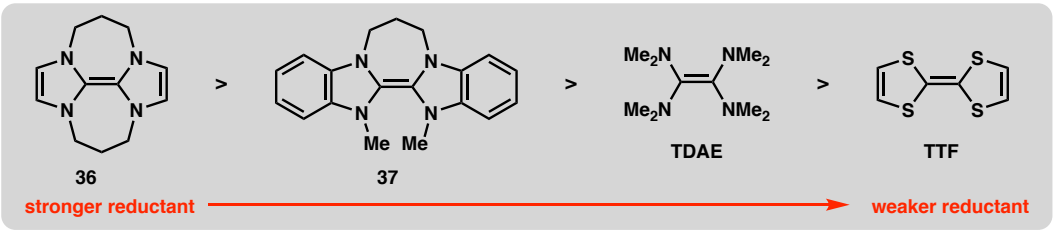

Weix and coworkers were able to demonstrate that tetrakis(*N*,*N*-dimethylamino)ethylene (TDAE) could be used as a soluble reductant in their initial report on the cross-coupling of aryl iodides and alkyl iodides: in comparison to an 88% yield when Mn was used, 57% yield of product **39** was formed with TDAE when 2 equivalents of alkyl iodide **38** was used (Figure 1.8).[50] Further optimization of conditions using benzylic chlorides (**40**) as the alkyl electrophile revealed that only 1.2 equivalents was necessary to promote good yields.[101] One notable advantage over the use of Zn reductants, besides the homogeneity of the reaction and elimination of deleterious side reactivity due to organozinc formation, is the broad applicability of a variety of solvents (Table 1.1). More environmentally friendly solvents such as acetonitrile (MeCN), propylene carbonate

Figure 1.8 *TDAE as a soluble reductant for cross-electrophile couplings.*

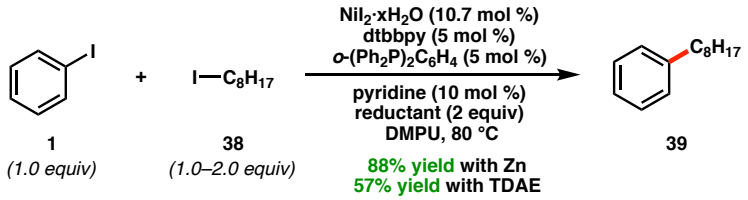

(PC), diethyl carbonate (DEC), isopropyl acetate (*i*-PrAc), and 2-methyl-tetrahydrofuran (2-Me-THF), which are widely adopted in the pharmaceutical industry, are effective in this transformation.[102] One drawback, however, is the limited availability for these organic reductants: TDAE is synthesized in three steps, each which possess sensitivity in the products or in reaction workup, and TDAE is still significantly more expensive compared to metal reductants.[59] Methods and detailed procedures to better prepare these reagents are necessary for better adoption in large scale applications.

Table 1.1. *Evaluation of solvents in aryl–benzyl coupling with TDAE.*

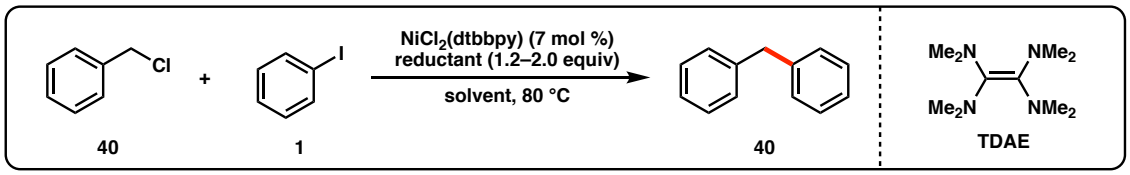

Entry	Solvent	Zn Yield (%)	TDAE yield (%)
1	DMA	82	79
2	MeCN	15	88
3	PC	58	>99
4	DEC	19	75
5	*i*-PrAc	53	79
6	2-Me-THF	51	76
7	PhMe	4	66
8	2-butanol	64	20

1.2.5 Metallaphotoredox Methods

Although most cross-coupling methods that use metallaphotoredox proceed through a redox neutral process, there have been a few seminal reports on reductive cross-couplings of two halide electrophiles.[103] In this approach, stoichiometric metal reductants

are replaced with alkyl amines[104–106] or silanols,[107–109] which become oxidized upon single electron transfer from the excited photoredox catalyst. Other metallaphotoredox examples that promote alkyl and aryl halide homocoupling[105,110] as well as alkyl halide carboxylation[111] with CO_2 have also been developed.

The first report of a Ni metallaphotoredox cross-electrophile coupling using an amine as the terminal reductant was reported by Li, Lei, and coworkers in 2016 (Scheme 1.4a).[104] Here, alkyl bromides and aryl bromides were cross-coupled in good yields; however, 5 equivalents of the alkyl bromide was required. This method uses trimethylamine (TEA) to oxidize the excited Ir^{III}* photocatalyst, which in turn reduces Ni in the catalytic cycle. In 2017, Vannucci and coworkers disclosed a similar cross-coupling which proceeds with a terpyridine ligated Ni catalyst and triethanolamine (TEOA) as the terminal reductant (Scheme 1.4b).[105] While an excess of one electrophile is still required, here the aryl halide, the authors found that when the aryl iodide was used, only 1.5

Scheme 1.4 *Metallaphotoredox methods using amine reductants.*

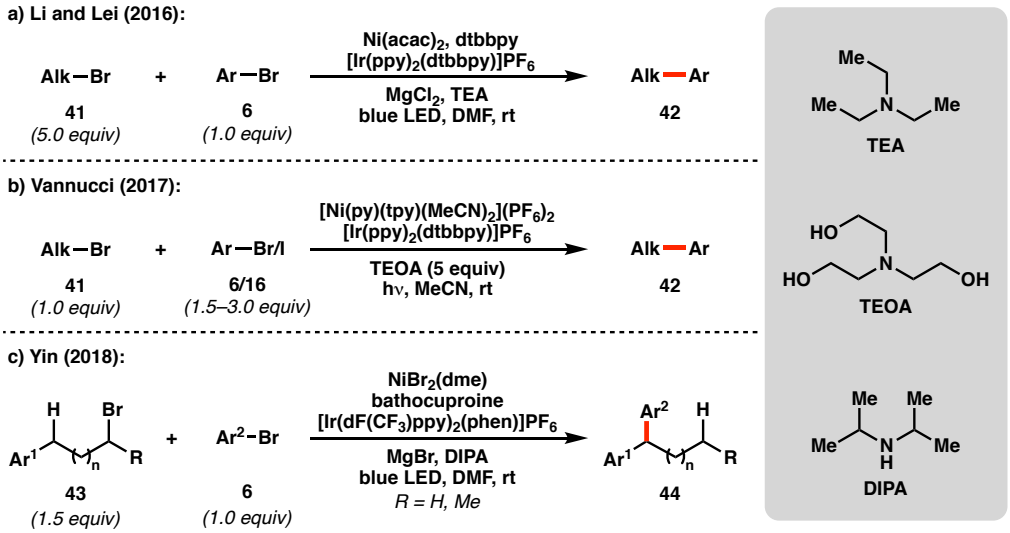

equivalents were necessary to obtain good product yields. Neither of these methods utilized alkyl bromides containing pendant aryl groups. In 2018, Yin and coworkers demonstrated that arylated alkyl bromide electrophiles (**43**) could be employed in metalllaphotoredox cross-coupling when dtbppy was used as a ligand (Scheme 1.4c).[106] When the bathocuproine was used, the 1,1-diarylalkane was instead isolated, indicating that a Ni-catalyzed chain walking mechanism was occurring, likely through iterative β-hydride elimination and subsequent β-migratory insertion. The formation of the branched coupling product is favored over the terminal coupling product due to the stability of the benzylic–Ni complex.

MacMillan and coworkers have well-established that metallaphotoredox catalysis can be used for redox neutral transformations between alkyl, alkenyl, alkynyl, or aryl halides with a plethora of carboxylic acids (and their derivatives). However, they recently expanded their efforts to apply metallaphotoredox to reductive cross-coupling (Scheme

Scheme 1.5 *Metallaphotoredox methods using silane and silanol reductants.*

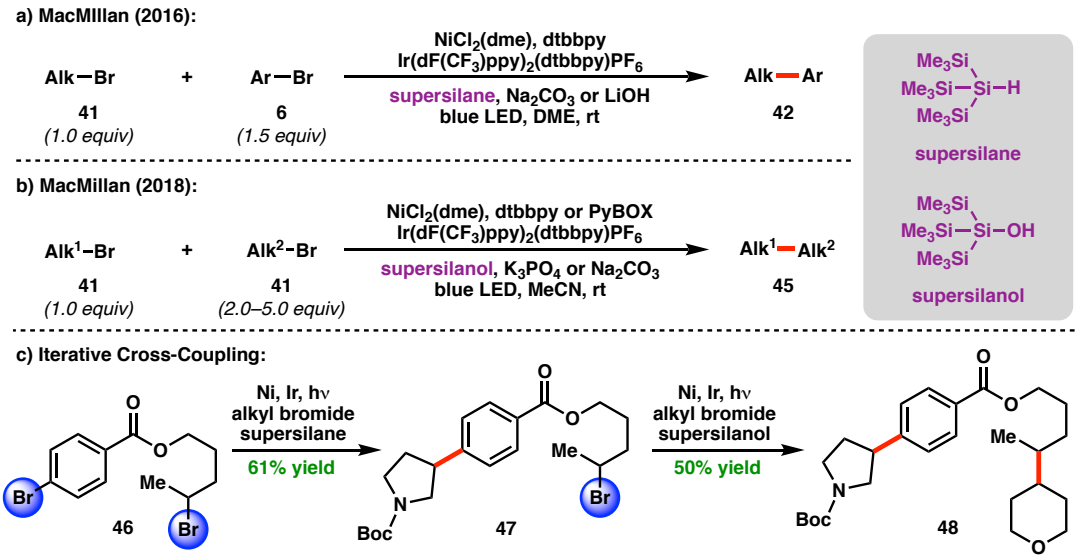

1.5).[107–109] Key to the reaction development was the identification of tris(trimethysilyl)silane (supersilane) and tris(trimethysilyl)silanol (supersilanol), which were found to be competent terminal reductants. While it is unsurprising that alkyl bromides and aryl iodides can be competent cross-coupling partners (Scheme 1.5a), the latter example depicts alkyl–alkyl couplings that produce high product yields when one electrophile is used in large excess (Scheme 1.5b). Both methods are compatible; an iterative cross-coupling approach demonstrated chemoselectivity for the aryl bromide over the alkyl bromide to form **47** (Scheme 1.5c). Subsequent alkylation afforded the bisfunctionalized product **48**.

While these transformations use achiral catalysts and provide racemic products, preliminary results using an achiral PyBOX ligand were reported. We envision that in time, asymmetric variants of metallophotoredox reductive cross-couplings will be developed and utilized in a variety of synthetic contexts.

1.3 CROSS-COUPLINGS WITH PSEUDOHALIDE ELECTROPHILES

1.3.1 Oxygen Electrophiles

Although organohalides represent the most broadly used and widely developed class of electrophiles employed in Ni-catalyzed reductive cross-couplings, other pseudohalides have also been utilized. One particular type is the use of oxygen-based electrophiles derived from alcohols, such as alkyl mesylates[60,112], alkyl tosylates[113], allylic acetates[86,114–117], and alkyl oxalates[118,119] (Scheme 1.6). Although recent reports have investigated the use of Lewis acid catalysis to activate allylic alcohols towards oxidative

addition,[120] typically activating groups are required for C–O bond insertion. As activated oxygen-based electrophiles are generally less reactive than their halide counterparts, the addition of co-catalysts to aid in radical generation processes has been used by Weix and coworkers (Scheme 1.6b).

Scheme 1.6 *Selected examples of reactions using oxygen-based electrophiles.*

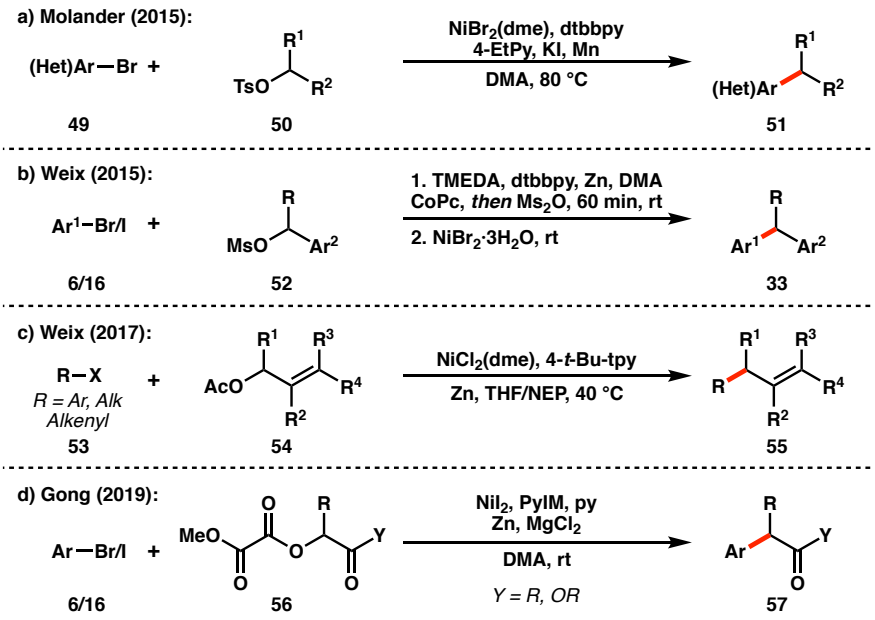

1.3.2 Carboxylic Acid Derivatives

The first cross-electrophile couplings using carboxylic acid derivatives (i.e. anhydrides) utilized these electrophiles as C(sp^2) coupling partners. As a follow-up to previous work,[121] Gong and coworkers were able to prepare unsymmetrical ketones via the cross-coupling of alkyl iodides (**58**) and alkyl carboxylic acids (**59**) in the presence of Boc_2O, which facilitates *in situ* anhydride formation, thus making the acid electrophile more prone to oxidative addition into the C–O bond (Figure 1.9).[122] Similar studies have been conducted by Liao and coworkers using symmetrical anhydrides and aryl iodides.[123]

Figure 1.9 *Synthesis of ketones from carboxylic acid derivatives.*

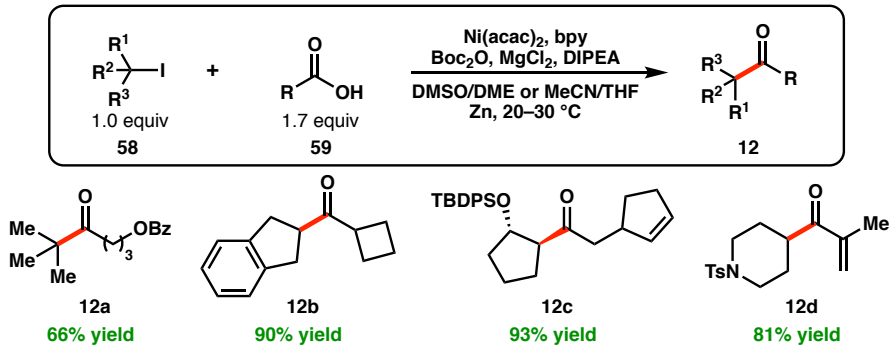

The use of alkyl carboxylic acids as C(sp^3) cross-coupling partners was ultimately envisioned via the formation of redox active ester derivatives such as *N*-hydroxyphthalimide (NHP) esters (Scheme 1.7). In 1988, Okada and Oda first demonstrated that the reduction of the phthalimide moiety induced decarboxylation to form alkyl radical species which could be intercepted by Michael acceptors.[124,125] More recently,

Scheme 1.7 *NHP esters derived from carboxylic acids as C(sp^3) electrophiles.*

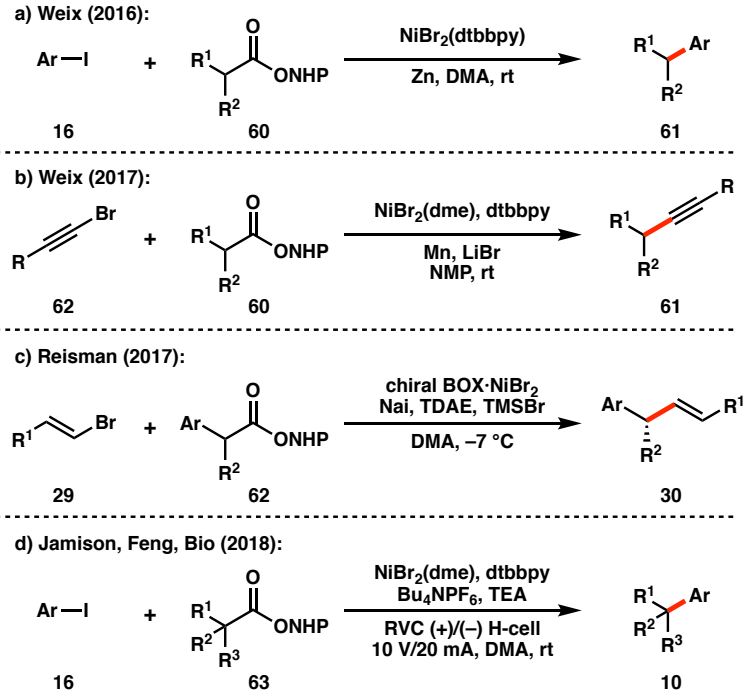

NHP esters have been utilized in Ni-catalyzed cross-electrophile couplings as alkyl radical precursors for arylation,[126,127] alkenylation,[59] and alkynylation reactions.[128] The first report of an enantioselective cross-coupling using NHP esters was demonstrated by Reisman and coworkers using a chiral BOX ligand.[59]

1.3.3 Epoxides and Aziridines

Ring opening reactions of epoxides and aziridines can provide an additional source of C(sp^3) alkyl radicals. Weix and coworkers demonstrated that epoxides (65) can be used in regiodivergent reductive cross-couplings to form either the branched or the linear coupling products depending on the mode of epoxide activation (Figure 1.10). Addition of NaI can lead to the formation of the branched alkyl radical (**67**) via the iodohydrin (**66**); in contrast, activation and ring-opening of the epoxide by titanocene complexes can result in the linear alkyl radical (**64**). This strategy was demonstrated in the Ni-catalyzed arylation of **65**, wherein iodide-mediated ring-opening afforded arylated product **69** and titanocene-mediated ring-opening afforded **70** as a 3.3:1 regiomeric ratio of isomers.[129]

Figure 1.10 *Ni-catalyzed cross-electrophile arylation of epoxides.*

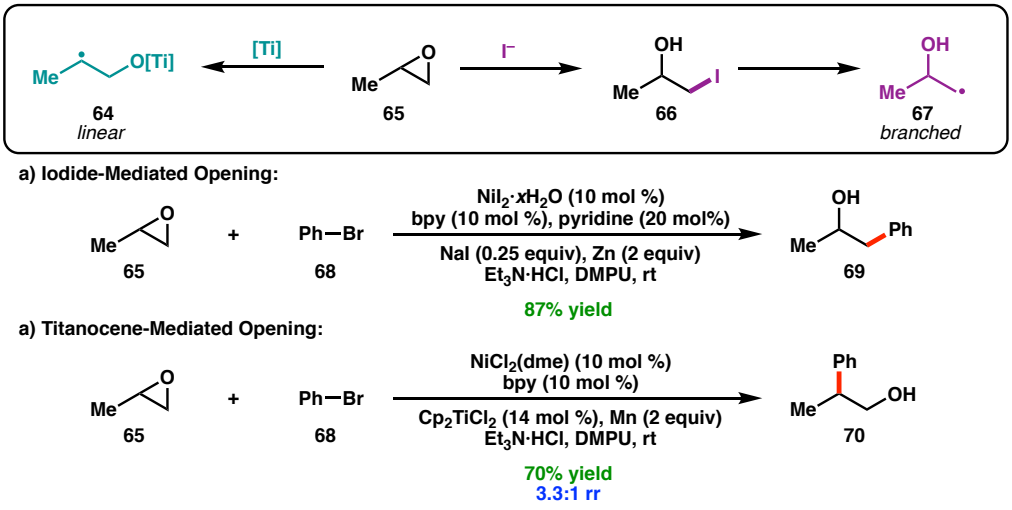

Following this study, Weix and coworkers showed that chiral titanocene complexes could be used to form enantioenriched products from *meso*-epoxides via a desymmeterization strategy (Figure 1.11).[130] The use of chiral titanocene catalyst **73** derived from (–)-menthone in the was able to provide arylated products following interception of the alkyl radical with the Ni catalyst. This method was applied towards 5-, 6-, and 7-membered cyclic epoxides to form the products (**72a**–**e**) in good yield with generally high levels of enantioselectivity.

Figure 1.11 *Enantioselective arylation of meso-epoxides.*

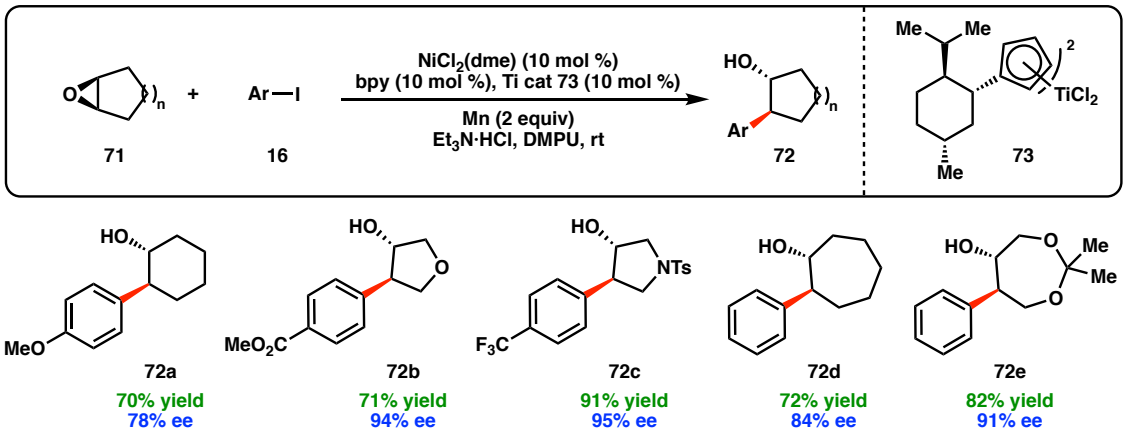

Doyle and coworkers recently reported an asymmetric Ni-catalyzed cross-coupling of styrenyl aziridines (**74**) with aryl iodides (**16**) using $NiCl_2$(dme) and BIOX ligand **L4**.[131] The diaryl alkane products (**75**) formed in this reaction provided the highest ee when a BIOX ligand containing 4-heptyl groups was used, although some products still suffered from lower ee due to arene substitution. Interestingly, **L4** is the same ligand developed in the Reisman group for the cross-coupling of benzyl chlorides and aryl iodides to form the same diaryl alkane products.[54] In collaboration with the Sigman laboratory, multivariate analysis using computationally-derived parameters of a series of BIOX ligands was

investigated. The obtained model depicts strong correlations between the predicted and measured $\Delta\Delta G^{\ddagger}$ when the ligand width, charge on the oxazoline N, and ligand polarizability are included. Interpretations suggest a long alkyl chain is best predicted. This study highlights the first approach at using ligand parameterization to provide rationale into observed enantioselectivity in asymmetric Ni-catalyzed reductive cross-couplings. We predict these types of studies can not only help explain the reaction mechanism, but also may be used to predict more selective ligands in the future.

Figure 1.12 *Enantioselective arylation of styrenyl aziridines.*

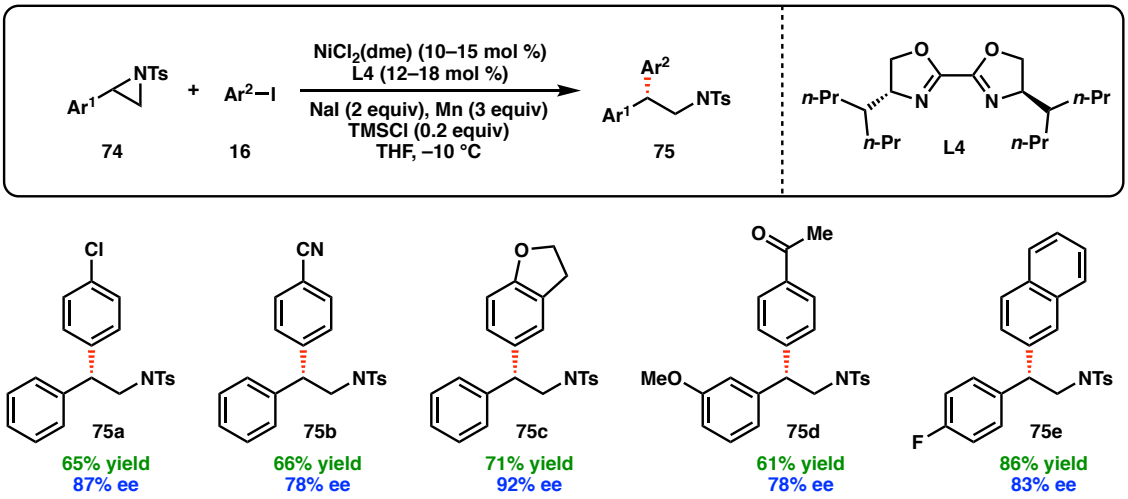

1.4 SYNTHETIC APPLICATIONS

A number of Ni-catalyzed cross-electrophile couplings between C(sp^2)–C(sp^3) and C(sp^3)–C(sp^3) centers have been developed. While advances in this methodology continue in both achiral and asymmetric regimes, other applications have recently emerged which include alkene functionalization and utility in the synthesis of natural products.

1.4.1 Alkene Functionalization

Recent developments have examined three-component couplings that incorporate an intermediate radical acceptor, thus joining together three fragments during the cross-electrophile coupling. Nevado and coworkers found that the use of $NiCl_2(Py)_4$ and dtbppy could successfully catalyze the dicarbofunctionalization reaction between terminal alkenes (**76**), aryl iodides (**16**), and alkyl iodides (**77**) with the use of TDAE as the terminal reductant (Scheme 1.8).[132] While the alkene scope is limited to Michael acceptors or activated allylic systems, this represents the first reductive variant of Ni-catalyzed dicarbofunctionalization. We envision that future advances in the field of Ni-catalyzed cross-electrophile couplings will continue efforts to intercept feedstock alkenes. Peng and coworkers have successfully demonstrated an intramolecular variant using an unactivated alkene system.[133] Tuning the electronic parameters of the catalyst will likely play an important role in tuning the lifetime of the alkyl radical.

Scheme 1.8 *Reductive dicarbofunctionalization of alkenes.*

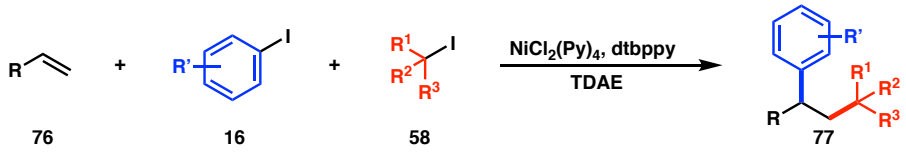

1.4.2 Natural Product Synthesis

Ni-catalyzed reductive cross-couplings have also found recent use in the synthesis of various natural products, including vitepyrroloid A (**78**),[134] podophyllotoxin (**79**),[135] and asperazine (**80**)[136] (Figure 1.13). These methods highlight the use of aryl–alkyl couplings and carbodifunctionalization strategies to access the natural products via key bond

disconnections. While asymmetric variants of cross-electrophile couplings have yet to be applied in natural product synthesis, we envision the continued development of new asymmetric methods will ultimately find its use in this synthetic context.

Figure 1.13 *Natural products synthesized via cross-electrophile couplings.*

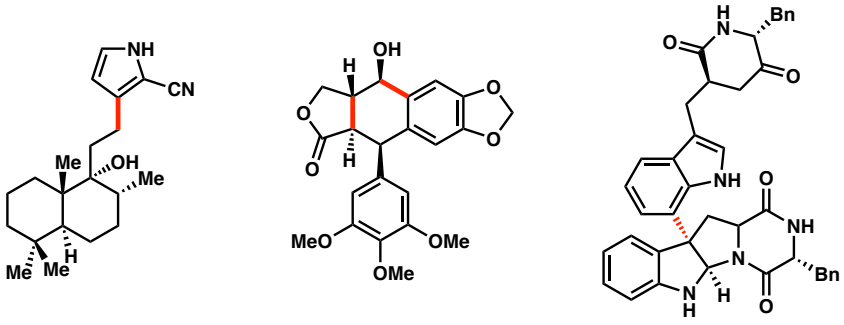

vitepyrroloid A **(78)** podophyllotoxin **(79)** asperazine **(80)**

1.5 CONCLUSION

In summary, Ni-catalyzed reductive cross-electrophile couplings using C(sp^3)-hybridized electrophiles is a diverse area of research with various applications in organic chemistry. These methods utilize a Ni catalyst to cross-couple bench-stable electrophiles in the presence of a terminal reductant. The ability to access alkyl radical intermediates allows for stereoconvergence to form enantioenriched products when chiral ligands are used, further expanding the utility of these transformations. The surge of new methods in this field has seen rapid development within the past decade and is likely to see numerous new modes of reactivity emerge in the years to come.

1.6 REFERENCES

(1) Brown, D. G.; Boström, J. *J. Med. Chem.* **2016**, *59*, 4443.

(2) Devendar, P.; Qu, R.-Y.; Kang, W.-M.; He, B.; Yang, G.-F. *J. Agric. Food Chem.* **2018**, *66*, 8914.

(3) Xu, S.; Kim, E. H.; Wei, A.; Negishi, E. *Sci. Technol. Adv. Mater.* **2014**, *15*, 044201.

(4) Ruiz-Castillo, P.; Buchwald, S. L. *Chem. Rev.* **2016**, *116*, 12564.

(5) Johansson Seechurn, C. C. C.; Kitching, M. O.; Colacot, T. J.; Snieckus, V. *Angew. Chem. Int. Ed.* **2012**, *51*, 5062.

(6) Jana, R.; Pathak, T. P.; Sigman, M. S. *Chem. Rev.* **2011**, *111*, 1417.

(7) Hu, X. *Chem. Sci.* **2011**, *2*, 1867.

(8) Tasker, S. Z.; Standley, E. A.; Jamison, T. F. *Nature* **2014**, *509*, 299.

(9) Ananikov, V. P. *ACS Catal.* **2015**, *5*, 1964.

(10) Netherton, M. R.; Fu, G. C. *Adv. Synth. Catal.* **2004**, *346*, 1525.

(11) Zhou, J.; Fu, G. C. *J. Am. Chem. Soc.* **2003**, *125*, 14726.

(12) Terao, J.; Todo, H.; Watanabe, H.; Ikumi, A.; Kambe, N. *Angew. Chem. Int. Ed.* **2004**, *43*, 6180.

(13) Fischer, C.; Fu, G. C. *J. Am. Chem. Soc.* **2005**, *127*, 4594.

(14) Arp, F. O.; Fu, G. C. *J. Am. Chem. Soc.* **2005**, *127*, 10482.

(15) Lundin, P. M.; Esquivias, J.; Fu, G. C. *Angew. Chem. Int. Ed.* **2009**, *48*, 154.

(16) Smith, S. W.; Fu, G. C. *J. Am. Chem. Soc.* **2008**, *130*, 12645.

(17) Do, H.-Q.; Chandrashekar, E. R. R.; Fu, G. C. *J. Am. Chem. Soc.* **2013**, *135*, 16288.

(18) Binder, J. T.; Cordier, C. J.; Fu, G. C. *J. Am. Chem. Soc.* **2012**, *134*, 17003.

(19) Liang, Y.; Fu, G. C. *J. Am. Chem. Soc.* **2014**, *136*, 5520.

(20) Choi, J.; Fu, G. C. *J. Am. Chem. Soc.* **2012**, *134*, 9102.

(21) Choi, J.; Martín-Gago, P.; Fu, G. C. *J. Am. Chem. Soc.* **2014**, *136*, 12161.

(22) Son, S.; Fu, G. C. *J. Am. Chem. Soc.* **2008**, *130*, 2756.

(23) Zhou, J.; Fu, G. C. *J. Am. Chem. Soc.* **2004**, *126*, 1340.

(24) González-Bobes, F.; Fu, G. C. *J. Am. Chem. Soc.* **2006**, *128*, 5360.

(25) Saito, B.; Fu, G. C. *J. Am. Chem. Soc.* **2007**, *129*, 9602.

(26) Saito, B.; Fu, G. C. *J. Am. Chem. Soc.* **2008**, *130*, 6694.

(27) Lundin, P. M.; Fu, G. C. *J. Am. Chem. Soc.* **2010**, *132*, 11027.

(28) Owston, N. A.; Fu, G. C. *J. Am. Chem. Soc.* **2010**, *132*, 11908.

(29) Lu, Z.; Wilsily, A.; Fu, G. C. *J. Am. Chem. Soc.* **2011**, *133*, 8154.

(30) Zultanski, S. L.; Fu, G. C. *J. Am. Chem. Soc.* **2011**, *133*, 15362.

(31) Cong, H.; Fu, G. C. *J. Am. Chem. Soc.* **2014**, *136*, 3788.

(32) Dai, X.; Strotman, N. A.; Fu, G. C. *J. Am. Chem. Soc.* **2008**, *130*, 3302.

(33) Lou, S.; Fu, G. C. *J. Am. Chem. Soc.* **2010**, *132*, 1264.

(34) Lou, S.; Fu, G. C. *J. Am. Chem. Soc.* **2010**, *132*, 5010.

(35) Shields, J. D.; Ahneman, D. T.; Graham, T. J. A.; Doyle, A. G. *Org. Lett.* **2014**, *16*, 142.

(36) Taylor, B. L. H.; Swift, E. C.; Waetzig, J. D.; Jarvo, E. R. *J. Am. Chem. Soc.* **2011**, *133*, 389.

(37) Greene, M. A.; Yonova, I. M.; Williams, F. J.; Jarvo, E. R. *Org. Lett.* **2012**, *14*, 4293.

(38) Yonova, I. M.; Johnson, A. G.; Osborne, C. A.; Moore, C. E.; Morrissette, N. S.; Jarvo, E. R. *Angew. Chem. Int. Ed.* **2014**, *53*, 2422.

(39) Zhou, Q.; Srinivas, H. D.; Dasgupta, S.; Watson, M. P. *J. Am. Chem. Soc.* **2013**, *135*, 3307.

(40) Tollefson, E. J.; Dawson, D. D.; Osborne, C. A.; Jarvo, E. R. *J. Am. Chem. Soc.* **2014**, *136*, 14951.

(41) Maity, P.; Shacklady-McAtee, D. M.; Yap, G. P. A.; Sirianni, E. R.; Watson, M. P. *J. Am. Chem. Soc.* **2013**, *135*, 280.

(42) Shacklady-McAtee, D. M.; Roberts, K. M.; Basch, C. H.; Song, Y.-G.; Watson, M. P. *Tetrahedron* **2014**, *70*, 4257.

(43) Taylor, B. L. H.; Harris, M. R.; Jarvo, E. R. *Angew. Chem. Int. Ed.* **2012**, *51*, 7790.

(44) Wisniewska, H. M.; Swift, E. C.; Jarvo, E. R. *J. Am. Chem. Soc.* **2013**, *135*, 9083.

(45) Harris, M. R.; Hanna, L. E.; Greene, M. A.; Moore, C. E.; Jarvo, E. R. *J. Am. Chem. Soc.* **2013**, *135*, 3303.

(46) Srinivas, H. D.; Zhou, Q.; Watson, M. P. *Org. Lett.* **2014**, *16*, 3596.

(47) Kalkofen, R.; Hoppe, D. *Synlett* **2006**, *12*, 1959.

(48) Zuo, Z.; Ahneman, D. T.; Chu, L.; Terrett, J. A.; Doyle, A. G.; MacMillan, D. W. C. *Science* **2014**, *345*, 437.

(49) Tellis, J. C.; Primer, D. N.; Molander, G. A. *Science* **2014**, *345*, 433.

(50) Everson, D. A.; Shrestha, R.; Weix, D. J. *J. Am. Chem. Soc.* **2010**, *132*, 920.

(51) Everson, D. A.; Jones, B. A.; Weix, D. J. *J. Am. Chem. Soc.* **2012**, *134*, 6146.

(52) Everson, D. A.; Weix, D. J. *J. Org. Chem.* **2014**, *79*, 4793.

(53) Weix, D. J. *Acc. Chem. Res.* **2015**, *48*, 1767.

(54) Poremba, K. E.; Kadunce, N. T.; Suzuki, N.; Cherney, A. H.; Reisman, S. E. *J. Am. Chem. Soc.* **2017**, *139*, 5684.

(55) Zuo, Z.; Cong, H.; Li, W.; Choi, J.; Fu, G. C.; MacMillan, D. W. C. *J. Am. Chem. Soc.* **2016**, *138*, 1832.

(56) Cherney, A. H.; Kadunce, N. T.; Reisman, S. E. *J. Am. Chem. Soc.* **2013**, *135*, 7442.

(57) Cherney, A. H.; Reisman, S. E. *J. Am. Chem. Soc.* **2014**, *136*, 14365.

(58) Kadunce, N. T.; Reisman, S. E. *J. Am. Chem. Soc.* **2015**, *137*, 10480.

(59) Suzuki, N.; Hofstra, J. L.; Poremba, K. E.; Reisman, S. E. *Org. Lett.* **2017**, *19*, 2150.

(60) Hofstra, J. L.; Cherney, A. H.; Ordner, C. M.; Reisman, S. E. *J. Am. Chem. Soc.* **2018**, *140*, 139.

(61) Till, N. A.; Smith, R. T.; MacMillan, D. W. C. *J. Am. Chem. Soc.* **2018**, *140*, 5701.

(62) Noble, A.; McCarver, S. J.; MacMillan, D. W. C. *J. Am. Chem. Soc.* **2015**, *137*, 624.

(63) Johnston, C. P.; Smith, R. T.; Allmendinger, S.; MacMillan, D. W. C. *Nature* **2016**, *536*, 322.

(64) Shaw, M. H.; Shurtleff, V. W.; Terrett, J. A.; Cuthbertson, J. D.; MacMillan, D. W. C. *Science* **2016**, *352*, 1304.

(65) Twilton, J.; Christensen, M.; DiRocco, D. A.; Ruck, R. T.; Davies, I. W.; MacMillan, D. W. C. *Angew. Chem. Int. Ed.* **2018**, *57*, 5369.

(66) Biswas, S.; Weix, D. J. *J. Am. Chem. Soc.* **2013**, *135*, 16192.

(67) Semmelhack, M. F.; Helquist, P. M.; Jones, L. D. *J. Am. Chem. Soc.* **1971**, *93*, 5908.

(68) Semmelhack, M. F.; Ryono, L. S. *J. Am. Chem. Soc.* **1975**, *97*, 3873.

(69) Semmelhack, M. F.; Helquist, P.; Jones, L. D.; Keller, L.; Mendelson, L.; Ryono, L. S.; Gorzynski Smith, J.; Stauffer, R. D. *J. Am. Chem. Soc.* **1981**, *103*, 6460.

(70) Nomura, M.; Tokoroyama, T.; Kubota, T. *J. Chem. Soc., Chem. Commun.* **1974**, *2*, 65.

(71) Tolman, C. A.; Seidel, W. C.; Gosser, L. W. *J. Am. Chem. Soc.* **1974**, *96*, 53.

(72) Kende, A. S.; Liebeskind, L. S.; Braitsch, D. M. *Tetrahedron Lett.* **1975**, *16*, 3375.

(73) Zembayashi, M.; Tamao, K.; Yoshida, J.; Kumada, M. *Tetrahedron Lett.* **1977**, *18*, 4089.

(74) Yamashita, J.; Inoue, Y.; Kondo, T.; Hashimoto, H. *Chem. Lett.* **1986**, *15*, 407.

(75) Conan, A.; Sibille, S. *J. Chem. Soc., Chem. Commun.* **1990**, 2.

(76) Marzouk, H.; Rollin, Y.; Folest, J. C.; Nédélec, J. Y.; Périchon, J. *J. Organomet. Chem.* **1989**, *369*, C47.

(77) Durandetti, M.; Nédélec, J.-Y.; Périchon, J. *J. Org. Chem.* **1996**, *61*, 1748.

(78) Durandetti, M.; Périchon, J.; Nédélec, J.-Y. *Tetrahedron Lett.* **1997**, *38*, 8683.

(79) Durandetti, M.; Périchon, J.; Nédélec, J.-Y. *J. Org. Chem.* **1997**, *62*, 7914.

(80) Durandetti, M.; Sibille, S.; Nédélec, J.-Y.; Périchon, J. *Synth. Commun.* **1994**, *24*, 145.

(81) Perkins, R. J.; Pedro, D. J.; Hansen, E. C. *Org. Lett.* **2017**, *19*, 3755.

(82) Durandetti, M.; Gosmini, C.; Périchon, J. *Tetrahedron* **2007**, *63*, 1146.

(83) Molander, G. A.; Traister, K. M.; O'Neill, B. T. *J. Org. Chem.* **2014**, *79*, 5771.

(84) Wang, X.; Ma, G.; Peng, Y.; Pitsch, C. E.; Moll, B. J.; Ly, T. D.; Wang, X.; Gong, H. *J. Am. Chem. Soc.* **2018**, *140*, 14490.

(85) Wang, X.; Wang, S.; Xue, W.; Gong, H. *J. Am. Chem. Soc.* **2015**, *137*, 11562.

(86) Wang, S.; Qian, Q.; Gong, H. *Org. Lett.* **2012**, *14*, 3352.

(87) Liu, X.; Yang, Z.; Li, Y.-M.; Yang, F.; Feng, L.; Wang, N.; Ma, D.; Chang, K.-J.; Shen, Y. *Tetrahedron* **2014**, *70*, 9522.

(88) Johnson, K. A.; Biswas, S.; Weix, D. J. *Chem. Eur. J.* **2016**, *22*, 7399.

(89) Wotal, A. C.; Weix, D. J. *Org. Lett.* **2012**, *14*, 1476.

(90) Wu, F.; Lu, W.; Qian, Q.; Ren, Q.; Gong, H. *Org. Lett.* **2012**, *14*, 3044.

(91) Zheng, M.; Xue, W.; Xue, T.; Gong, H. *Org. Lett.* **2016**, *18*, 6152.

(92) Yu, X.; Yang, T.; Wang, S.; Xu, H.; Gong, H. *Org. Lett.* **2011**, *13*, 2138.

(93) Molander, G. A.; Wisniewski, S. R.; Traister, K. M. *Org. Lett.* **2014**, *16*, 3692.

(94) Li, X.; Feng, Z.; Jiang, Z.-X.; Zhang, X. *Org. Lett.* **2015**, *17*, 5570.

(95) Liu, J.; Gong, H. *Org. Lett.* **2018**.

(96) Sun, S.-Z.; Martin, R. *Angew. Chem. Int. Ed.* **2018**, *57*, 3622.

(97) Wotal, A. C.; Batesky, D. C.; Weix, D. J. *Org. Syn.* **2016**, *93*, 50.

(98) Broggi, J.; Terme, T.; Vanelle, P. *Angew. Chem. Int. Ed.* **2014**, *53*, 384.

(99) Zhou, S.; Farwaha, H.; Murphy, J. A. *Chimia (Aarau)* **2012**, *66*, 418.

(100) Murphy, J. A. *J. Org. Chem.* **2014**, *79*, 3731.

(101) Anka-Lufford, L. L.; Huihui, K. M. M.; Gower, N. J.; Ackerman, L. K. G.; Weix, D. J. *Chem. Eur. J.* **2016**, *22*, 11564.

(102) Byrne, F. P.; Jin, S.; Paggiola, G.; Petchey, T. H. M.; Clark, J. H.; Farmer, T. J.; Hunt, A. J.; Robert McElroy, C.; Sherwood, J. *Sustain. Chem. Process.* **2016**, *4*, 7.

(103) Milligan, J. A.; Phelan, J. P.; Badir, S. O.; Molander, G. A. *Angew. Chem. Int. Ed.* **2019**.

(104) Duan, Z.; Li, W.; Lei, A. *Org. Lett.* **2016**, *18*, 4012.

(105) Paul, A.; Smith, M. D.; Vannucci, A. K. *J. Org. Chem.* **2017**, *82*, 1996.

(106) Peng, L.; Li, Z.; Yin, G. *Org. Lett.* **2018**, *20*, 1880.

(107) Zhang, P.; Le, C. "Chip"; MacMillan, D. W. C. *J. Am. Chem. Soc.* **2016**, *138*, 8084.

(108) Smith, R. T.; Zhang, X.; Rincón, J. A.; Agejas, J.; Mateos, C.; Barberis, M.; García-Cerrada, S.; de Frutos, O.; MacMillan, D. W. C. *J. Am. Chem. Soc.* **2018**, *140*, 17433.

(109) Bacauanu, V.; Cardinal, Sø.; Yamauchi, M.; Kondo, M.; Fernµndez, D. F.; Remy, R.; MacMillan, D. W. C. *Angew. Chem. Int. Ed.* **2018**, 6.

(110) Masuda, Y.; Ishida, N.; Murakami, M. *Eur. J. Org. Chem.* **2016**, *2016*, 5822.

(111) Meng, Q.-Y.; Wang, S.; König, B. *Angew. Chem. Int. Ed.* **2017**, *56*, 13426.

(112) Ackerman, L. K. G.; Anka-Lufford, L. L.; Naodovic, M.; Weix, D. J. *Chem. Sci.* **2015**, *6*, 1115.

(113) Molander, G. A.; Traister, K. M.; O'Neill, B. T. *J. Org. Chem.* **2015**, *80*, 2907.

(114) Anka-Lufford, L. L.; Prinsell, M. R.; Weix, D. J. *J. Org. Chem.* **2012**, *77*, 9989.

(115) Cui, X.; Wang, S.; Zhang, Y.; Deng, W.; Qian, Q.; Gong, H. *Org. Biomol. Chem.* **2013**, *11*, 3094.

(116) Prinsell, M. R.; Everson, D. A.; Weix, D. J. *Chem. Commun.* **2010**, *46*, 5743.

(117) Caputo, J. A.; Naodovic, M.; Weix, D. J. *Synlett* **2015**, *26*, 323.

(118) Gao, M.; Sun, D.; Gong, H. *Org. Lett.* **2019**, *21*, 1645.

(119) Ye, Y.; Chen, H.; Sessler, J. L.; Gong, H. *J. Am. Chem. Soc.* **2019**, *141*, 820.

(120) Jia, X.-G.; Guo, P.; Duan, J.; Shu, X.-Z. *Chem. Sci.* **2018**, *9*, 640.

(121) Yin, H.; Zhao, C.; You, H.; Lin, K.; Gong, H. *Chem. Commun.* **2012**, *48*, 7034.

(122) Zhao, C.; Jia, X.; Wang, X.; Gong, H. *J. Am. Chem. Soc.* **2014**, *136*, 17645.

(123) Chen, H.; Hu, L.; Ji, W.; Yao, L.; Liao, X. *ACS Catal.* **2018**, *8*, 10479.

(124) Okada, Keiji.; Okamoto, Kazushige.; Oda, Masaji. *J. Am. Chem. Soc.* **1988**, *110*, 8736.

(125) Okada, K.; Okamoto, K.; Morita, N.; Okubo, K.; Oda, M. *J. Am. Chem. Soc.* **1991**, *113*, 9401.

(126) Huihui, K. M. M.; Caputo, J. A.; Melchor, Z.; Olivares, A. M.; Spiewak, A. M.; Johnson, K. A.; DiBenedetto, T. A.; Kim, S.; Ackerman, L. K. G.; Weix, D. J. *J. Am. Chem. Soc.* **2016**, *138*, 5016.

(127) Li, H.; Breen, C. P.; Seo, H.; Jamison, T. F.; Fang, Y.-Q.; Bio, M. M. *Org. Lett.* **2018**, *20*, 1338.

(128) Huang, L.; Olivares, A. M.; Weix, D. J. *Angew. Chem. Int. Ed.* **2017**, *56*, 11901.

(129) Zhao, Y.; Weix, D. J. *J. Am. Chem. Soc.* **2014**, *136*, 48.

(130) Zhao, Y.; Weix, D. J. *J. Am. Chem. Soc.* **2015**, *137*, 3237.

(131) Woods, B. P.; Orlandi, M.; Huang, C.-Y.; Sigman, M. S.; Doyle, A. G. *J. Am. Chem. Soc.* **2017**, *139*, 5688.

(132) García-Domínguez, A.; Li, Z.; Nevado, C. *J. Am. Chem. Soc.* **2017**, *139*, 6835.

(133) Peng, Y.; Xiao, J.; Xu, X.-B.; Duan, S.-M.; Ren, L.; Shao, Y.-L.; Wang, Y.-W. *Org. Lett.* **2016**, *18*, 5170.

(134) Menger, M.; Lentz, D.; Christmann, M. *J. Org. Chem.* **2018**, *83*, 6793.

(135) Xiao, J.; Cong, X.-W.; Yang, G.-Z.; Wang, Y.-W.; Peng, Y. *Org. Lett.* **2018**, *20*, 1651.

(136) Luo, L.; Zhai, X.-Y.; Wang, Y.-W.; Peng, Y.; Gong, H. *Chem. Eur. J.* **2019**, *25*, 989.

Chapter 2

Synthesis and Utility of Chiral Allylic Silanes Prepared via Ni-Catalyzed Asymmetric Reductive Cross-Coupling[‡]

2.1 INTRODUCTION

The synthesis of chiral organosilanes has been an area of recent interest in organic chemistry.[1–3] Organosilanes are not only valuable organic materials with applications in medicinal chemistry[4–6] and materials science,[7] but they are also versatile reagents in organic synthesis.[8–11] In particular, chiral allylic silanes (**81**) engage in highly stereoselective reactions with a variety of electrophiles,[12–18] one example being the Hosomi-Sakurai reaction which is a powerful method for C–C bond constuction (Scheme

[‡] Portions of this chapter have been reproduced from the following communication: Hofstra, J. L.; Cherney, A. H.; Ordner, C. M.; Reisman, S. E. *J. Am. Chem. Soc.* **2018**, *140*, 139, DOI: 10.1021/jacs.7b11707, copyright 2018 American Chemical Society. The research presented in this chapter was completed in collaboration with Alan H. Cherney (graduate student), Ciara M. Ordner (undergraduate student), and Dana Gephart (undergraduate student) in the Reisman group.

2.1).[19–22] The reaction proceeds with excellent diastereoselectivity and transfer of chirality to provide the *syn* homoallylic alcohol (**82**) as the major diastereomer. The *trans* homoallylic alcohol (**83**) is formed as the minor diastereomer. This transformation has not only proven its utility in organic methodology but has also been useful in the total synthesis of natural products.[22–29]

Scheme 2.1 *Open transition state analysis for the Hosomi-Sakurai allylation.*

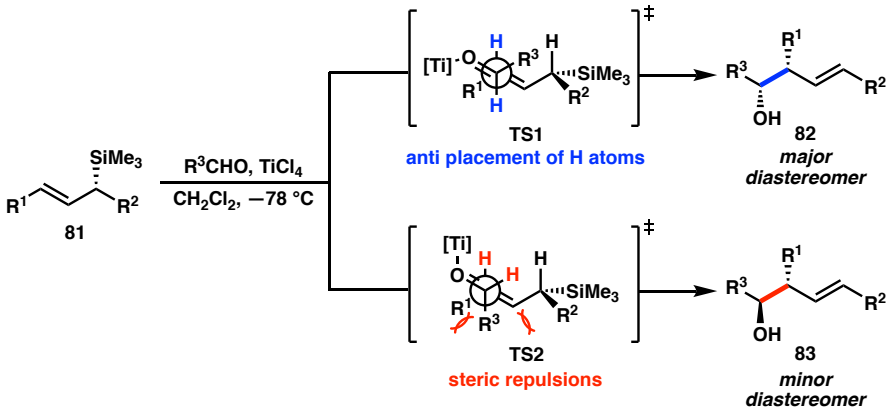

Despite the utility of chiral allylic silanes, the enantioselective preparation of these reagents often requires multistep sequences or the incorporation of specific functional groups to direct the formation of the C(sp^3)–Si bond. Chiral allylic silanes are most commonly prepared through diastereoselective or stereospecific transformations, which include Claisen rearrangement of vinyl silanes,[30,31] bis-silylation of allylic alcohols,[32] silylene insertion of allylic ethers,[33] and the alkenylation of 1,1-silaboronates.[34,35] In addition, several enantioselective transition metal-catalyzed reactions have been developed, which include the hydrosilylation of dienes,[36,37] the silylboration of allenes,[38] the insertion of metal carbenoids into Si–H bonds,[39,40] and conjugate addition[41,42] and allylic substitution[43] reactions. Notably, while metal-catalyzed cross-coupling methods for

C–Si bond formation have been developed in the racemic sense which allows straight-forward functional group interconversions (FGI), the ability to access chiral stereocenters through C–Si bond formation has yet to be envisioned.[44–49] In contrast, the use of Si-containing nucleophiles or electrophiles in asymmetric transition metal-catalyzed cross-coupling, in which the critical silicon-bearing C(sp^3)-hybridized stereogenic center is established in the C–C bond forming step, represents an alternative and highly modular approach to synthesize chiral allylic silanes (Figure 2.1).

Figure 2.1 *Disconnections to prepare alkyl silanes via cross-coupling.*

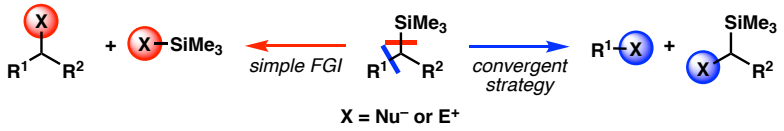

Indeed, the first synthesis of an enantioenriched chiral allylic silane was the Pd-catalyzed asymmetric cross-coupling between α-(trimethylsilyl)benzylmagnesium bromide (**84**) and alkenyl bromides (**83**) reported by Kumada, Hayashi, and coworkers in 1982; these results were followed up with a subsequent study in 1986 (Figure 2.2).[19,21] A variety of alkenyl bromides were evaluated, providing chiral allylic silane products containing alkyl and phenyl substituents (**85a**–**k**). While *Z*-alkenyl and cyclic alkenyl bromides (**85c**, **85e**, and **85k**) successfully provided the desired products, the ee was diminished compared to the use of *E*-alkenyl bromides. Additionally, the identity of the silane was critical to obtaining high ee: $SiEt_3$ > $SiMe_3$ = $SiMe_2Ph$ > $SiPh_3$ (**85g**, **85h**, **85f**, and **85i**). This method, however, employs Grignard reagents as coupling partners which are not stable to long-term storage and decrease the functional group compatibility of the reaction.

Figure 2.2 *Scope of Kumada's cross-coupling to synthesize chiral allyl silanes.*

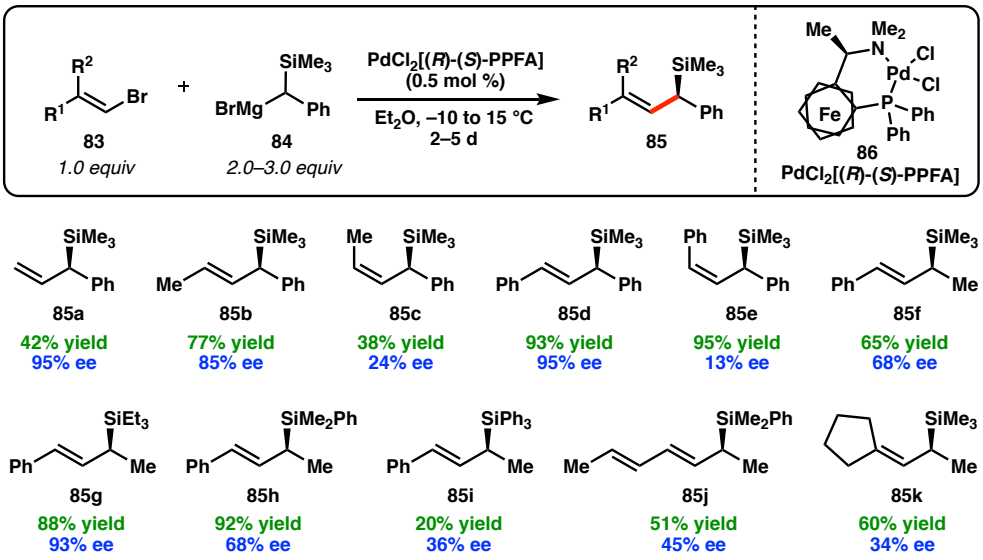

We envisioned that a Ni-catalyzed asymmetric reductive alkenylation would address the limitation of reagent stability and functional group compatibility, as the required (chlorobenzyl)silanes (**34**) are bench stable compounds and reductive cross-coupling reactions typically exhibit good functional group tolerance (Scheme 2.2).[50,51] Thus, a Ni-catalyzed reductive alkenylation could provide chiral allylic silanes that are not readily accessible by other methods. Herein we describe a Ni-catalyzed asymmetric reductive cross-coupling to directly prepare enantioenriched allylic silanes (**36**) from simple building blocks (**29** and **34**). The resulting chiral allylic silanes are shown to undergo a variety of post-coupling transformations that proceed with high levels of chirality transfer.

Scheme 2.2 *Ni-catalyzed reductive cross-coupling to synthesize chiral allyl silanes.*

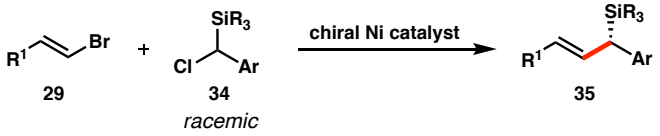

2.2 REACTION OPTIMIZATION EXPAND

2.2.1 Initial Reaction Hit

Our investigations began with the coupling between (*E*)-1-(2-bromovinyl)-4-methoxybenzene (**86**) and (chloro(phenyl)methyl)trimethylsilane (**87**) using $NiCl_2$(dme) and chiral bis(oxazoline) ligand **L2**, which was optimal in our previously developed enantioselective reductive alkenylation reaction (Figure 2.2).[50] When the reaction was conducted at 0 °C with *N,N*-dimethylacetamide (DMA) as the solvent, allylic silane **88c** was formed in a low amount (26% yield) but with a high level of enantioselectivity (98% ee). We hypothesized that the presence of the bulky trimethylsilyl group impeded the oxidative addition of **87** to the Ni catalyst. Indeed, a decrease in product yield was observed when the α-benzyl substituent increased in size (R = Me > *i*-Pr > $SiMe_3$). Evaluation of the reaction profile by ^{1}H NMR revealed full consumption of **87** and formation of benzyl homocoupling product as the major side product; alkenyl bromide **86** was recovered with minimal conversion to homocoupled diene. Although the yield of the cross-coupling

Figure 2.3 *Ni-catalyzed cross-coupling with various benzylic chlorides.*

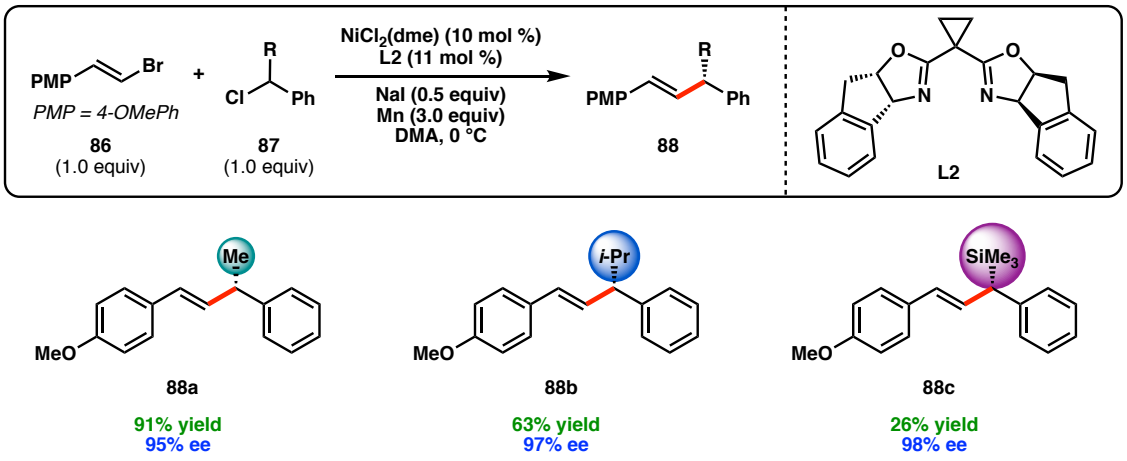

transformation remained to be optimized, the use of chiral bis(oxazoline) ligand **L2** showed remarkable enantioselectivity and was thus retained throughout the duration of reaction optimization. Optimization commenced to discover reaction conditions that mitigate benzyl homocoupling product to afford higher yields of the cross-coupled product (**88c**).

2.2.2 Solvents

A variety of solvents were evaluated in the cross-coupling reaction (Table 2.1) at room temperature (23 °C) in the absence of NaI. Amide solvents such as DMA and *N*-methyl-2-pyrrolidone (NMP) provided **88c** in comparable yields and enantioselectivities (entries 1–2). Dimethyl formamide (DMF) was also found to be a competent solvent in the reaction (entry 3), however both *N*,*N*′-dimethylpropyleneurea (DMPU) and tetrahydrofuran (THF) provided no product (entries 4–5). Further optimization studies were conducted in NMP as the solvent provided **88c** in the highest yield.

Table 2.1. *Evaluation of solvents.*

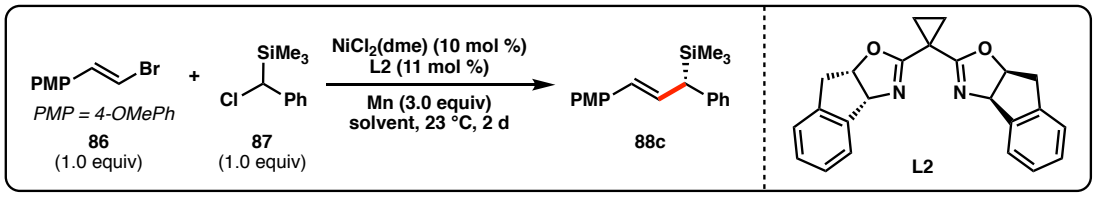

Entry	Solvent	yield (%)	ee (%)
1	DMA	20	94
2	NMP	23	94
3	DMF	12	90
4	DMPU	0	—
5	THF	0	—

2.2.3 Additives

A variety of additives were then evaluated (Table 2.2). While NaI proved to be an effective additive in our previous alkenylation reaction,[50] possibly through the formation

of reactive alkenyl iodide species, the use of NaI in the synthesis of **88c** did not appreciably improve the reaction yield (entry 2). However, the addition of cobalt(II) phthalocyanine (CoPc), a co-catalyst that also enables the Ni-catalyzed cross-coupling of benzyl mesylates by facilitating alkyl radical generation,[52] was found to significantly improve the yield of **88c** (entry 3). Kinetic studies by Kishi and coworkers found the addition of CoPc in Cr- and Fe-mediated haloallylations of aldehydes increased the reaction rate through the CoPc-mediated formation of catalytically active M-Br species.[53] When similar kinetic studies were conducted on the formation of **88c**, the reaction rate was instead found to decrease upon addition of CoPc. Given these results, we hypothesize that CoPc is used to mitigate benzyl homocoupling formation by sequestering reactive benzyl radical intermediates. This could result in an overall decrease in the rate of consumption of **87**. Therefore the addition of CoPc may be help moderate a mismatch in the rate of oxidative addition between the two electrophiles.

Other Co-containing co-catalysts were also evaluated. Interestingly, the perfluorinated CoPc co-catalyst ($CoPc_F$) did not improve the reaction (entry 4). A variety of other Co sources were also evaluated, many of which concomitantly diminished the ee and the reaction yield of **88c** (entries 5–10). A screen of Fe phthalocyanine and porphyrin co-catalysts were evaluated (entries 11–13), and both Fe(II)Pc and Fe(III)PcCl were found to improve the yield of **88c**. The use of $Fe(TMHD)_3$ provided **88c** in an essentially racemic form (entry 14). Taken together, it is likely that the co-catalyst phthalocyanine scaffold plays a more important role in improving the reaction yield compared to the identity of the coordinated metal center (Co vs. Fe).

Table 2.2. *Evaluation of Co and Fe co-catalysts.*

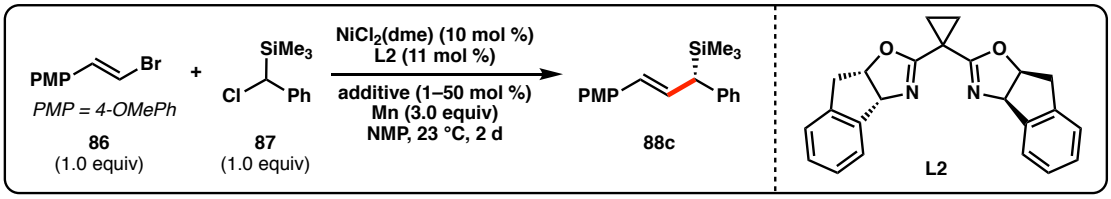

Entry	Additive	yield (%)	ee (%)
1	—	21	93
2	NaI (50 mol %)	24	94
3	CoPc (1 mol %)	38	96
4	$CoPc_F$ (1 mol %)	23	94
5	$CoCl_2$ (5 mol %)	3	57
6	$CoBr_2$ (5 mol %)	14	86
7	CoI_2 (5 mol %)	17	85

Entry	Additive	yield (%)	ee (%)
8	$Co(PPh_3)_2Cl_2$ (1 mol %)	7	31
9	$Co(acac)_2$ (1 mol%)	12	82
10	CoTPP (1 mol %)	17	88
11	Fe(II)Pc (1 mol %)	28	95
12	Fe(III)PcCl (1 mol %)	33	95
13	Hemin (1 mol %)	17	93
14	$Fe(TMHD)_3$ (1 mol %)	11	6

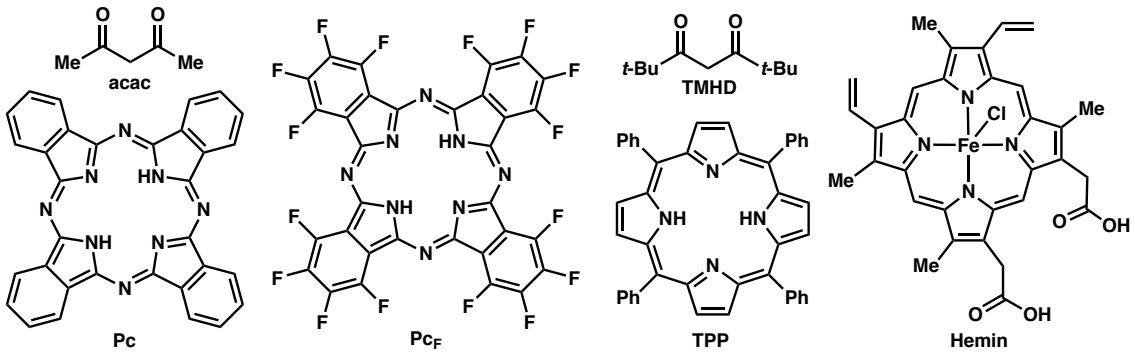

2.2.4 Temperature

In order to maximize our efforts to improve the yield of this transformation, we turned to the use of the Freeslate Core Module system housed within the Caltech Center for Catalysis and Chemical Synthesis. This equipment contained temperature regulated cold wells for reactions to be run at a variety of cryogenic temperatures while providing discrete rotary stirrers for each sample vial, a necessity to promote consistent stirring of heterogeneous reaction mixtures. During the course of reaction optimization, we discovered that decreasing the temperature improved the reaction yield (Table 2.3, entries 1–3), however achieving full conversion was inconsistent when conducted at 0 °C.

Therefore, in order to ensure complete conversion, the reaction was conducted at 5 °C which consistently provided full conversion for reactions run in the Freeslate system as well as in a benchtop cryocool system.

Table 2.3. *Evaluation of temperature.*

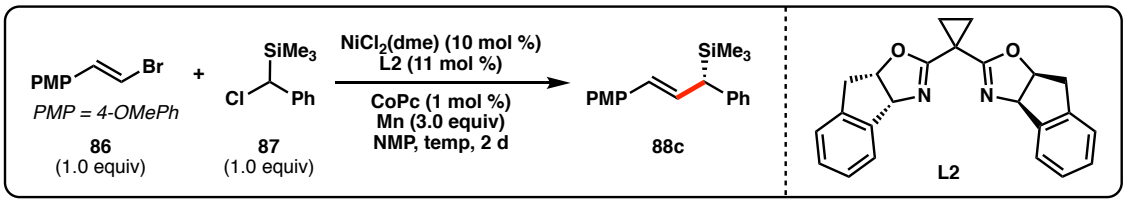

Entry	Temp	yield (%)	ee (%)
1	23 °C	33	96
2	10 °C	46	96
3	0 °C	58	94

2.2.5 Electrophile Equivalents

The electrophile ratio was then evaluated (Table 2.4) with the precomplexed **L2**·$NiCl_2$. The yield of **88c** increased when an excess of either electrophile was used, however excess alkenyl bromide improved the yield most significantly and without loss of enantioselectivity. In some cases, the use of 1.5 equivalents alkenyl bromide was sufficient to improve the reaction, however the use of 2.0 equivalents alkenyl bromide proved most

Table 2.4. *Evaluation of electrophile equivalents.*

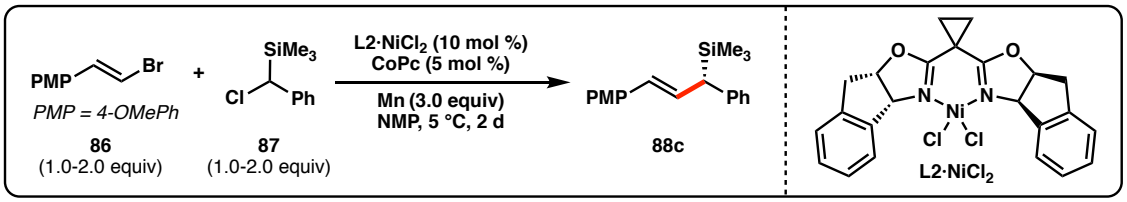

Entry	86 (equiv)	87 (equiv)	yield (%)	ee (%)
1	1.0	2.0	62	91
2	1.0	1.0	51	96
3	2.0	1.0	70	97

robust across a range of substrates (*vide infra*). Similarly, the use of the precomplex **L2**·$NiCl_2$ in place of $NiCl_2$(dme) and **L2** also proved most robust, particularly for low yielding substrates.

2.2.6 CoPc Loading

Evaluation of CoPc loading revealed that the yield of **88c** improved when 3 mol % CoPc was used, and no further increase was observed with 5 mol % or 10 mol % CoPc (Table 2.5, entries 2–5). The optimal amount of CoPc catalyst likely lies between 1 mol % and 3 mol % loading, however low loadings were difficult to weigh on small scale. The use of 5 mol % CoPc, which provided **88c** in 70% yield and 97% ee, was used to evaluate the reaction scope.

Table 2.5. *Evaluation of CoPc loading.*

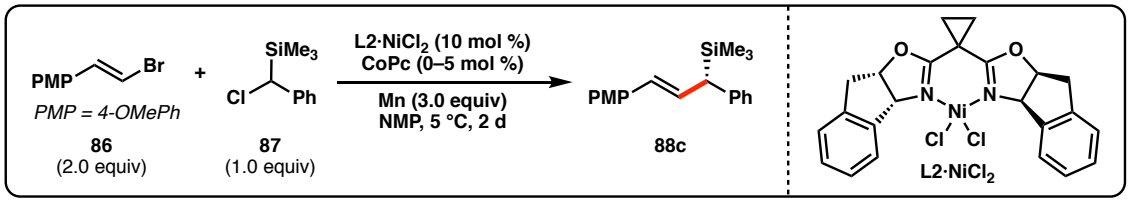

Entry	CoPc (mol %)	yield (%)	ee (%)
1	0	20	96
2	1	56	97
3	3	68	97
4	5	70	97
5	10	69	96

2.2.7 Reaction Time

While our previously developed alkenylation reaction was conducted for 6 hours at 0 °C,[50] the cross-coupling between **86** and **87** shows low conversion after 6 hours at 5 °C due to a lengthy induction period. We typically envision the induction period to be

due to the heterogeneous reduction of Ni(II) to the active nickel catalyst, possibly a Ni(0) species. The yield of **88c** was monitored for 2 days, which revealed that maximum conversion is reached after 24 hours (Figure 2.4). The yield of **88c** is then maintained between 24–48 hours, which demonstrates that no decomposition of **88c** occurs under the reaction conditions. In order to ensure full conversion during substrate scope evaluation, the cross-coupling reaction time was set for a total of 48 hours.

Figure 2.4 *Evaluation of reaction time.*

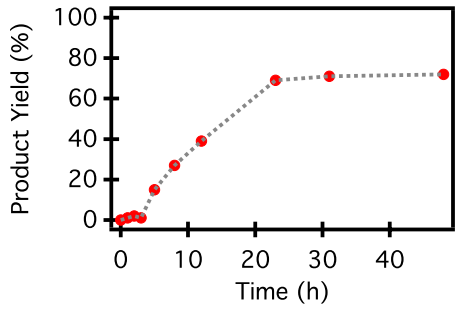

2.2.8 Optimization Summary and Controls

In summary, the cross-coupling between **86** and **87** was improved from our previous alkenylation conditions due to: 1) raising the temperature to 5 °C, 2) running the reaction for 2 days, 3) the addition of 5 mol % CoPc, and 4) increasing the alkenyl bromide to 2.0 equivalents. Control experiments confirmed that $NiCl_2$(dme), ligand, and Mn are all required to form **88c** (Table 2.6, entries 1–4), and other reductants such as Zn and tetrakis(*N*,*N*-dimethylamino)ethylene (TDAE) are deleterious to the yield and enantioselectivity (entries 5–6). While TDAE did afford 39% yield of **88c**, it is formed in only 2% ee. The cross-coupling of **86** and **87** with TDAE in the absence of CoPc shows no conversion (entry 7), indicating that the cross-coupling may be occurring on a reduced

CoPc complex when TDAE is used. The cross-coupling reactions are initially a deep blue upon addition of CoPc; however, upon reaction completion, the solution is a dark green color, indicating reduced CoPc.

Table 2.6. *Control experiments and evaluation of other reductants.*

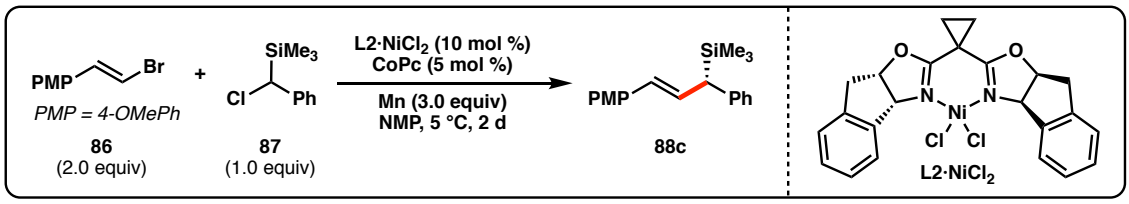

Entry	Deviation from Standard Conditions	yield (%)	ee (%)
1	—	70	97
2	no Mn	0	—
3	L2 (10 mol %), no L2·$NiCl_2$	0	—
4	$NiCl_2$(dme) (10 mol %), no L2·$NiCl_2$	13	—
5	Zn instead of Mn	22	85
6	TDAE instead of Mn	39	2
7	TDAE instead of Mn, no CoPc	0	—

2.2.9 Scalability

With the optimized conditions in hand, the scalability was investigated (Table 2.7). We were pleased to find that the cross-coupling could be set up in a variety of different

Table 2.7. *Evaluation of reaction scalability.*

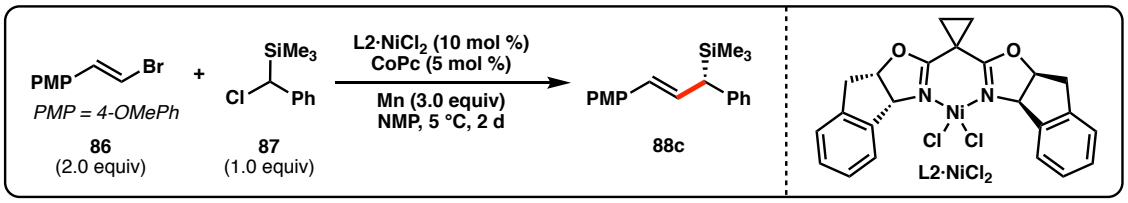

Entry	Scale (mmol)	Isolated Mass	Reaction Vessel	Setup	Cooling	yield (%)	ee (%)
1	0.2	42 mg	8 mL vial	glovebox	Freeslate	71	95
2	0.5	107 mg	20 mL vial	glovebox	Freeslate	72	96
3	0.5	104 mg	20 mL vial	glovebox	cryocool	70	98
4	0.5	114 mg	10 mL flask	glovebox	cryocool	77	97
5	1.0	211 mg	15 mL flask	bench top	cryocool	71	98
6	6.0	1.31 g	100 mL flask	glovebox	cryocool	74	97

glass containers and be cooled with a traditional laboratory cryocool (entries 3–5). The reaction could also be run directly on the benchtop using standard Schlenk techniques, alleviating the need for a glovebox (entry 5). Finally, we found that the reaction could be run on gram scale, providing an isolated 1.3 g of **88c** in 74% yield and 97% ee (entry 6).

2.2.10 Chiral Ligands

A variety of other chiral ligands were evaluated for the cross-coupling between **86** and **87**, either at room temperature with 1 mol % CoPc (Figure 2.5) or under the optimized reaction conditions (Figure 2.6). Although chiral BOX ligand **L6** provided **88c** in excellent enantioselectivity (90% ee) and in higher yield compared to **L2** at room temperature, upon cooling the reaction to 5 °C, **L2** provided a higher yield of **88c** compared to **L6**. Substitution at the *para* positon on the benzylic arene (**L7**) did not affect the ee of **88c**, however altering the cyclic linker to a cyclobutane (**L5**) or adding methyl groups to the

Figure 2.5 *Evaluation of chiral bidentate ligands at room temperature.*

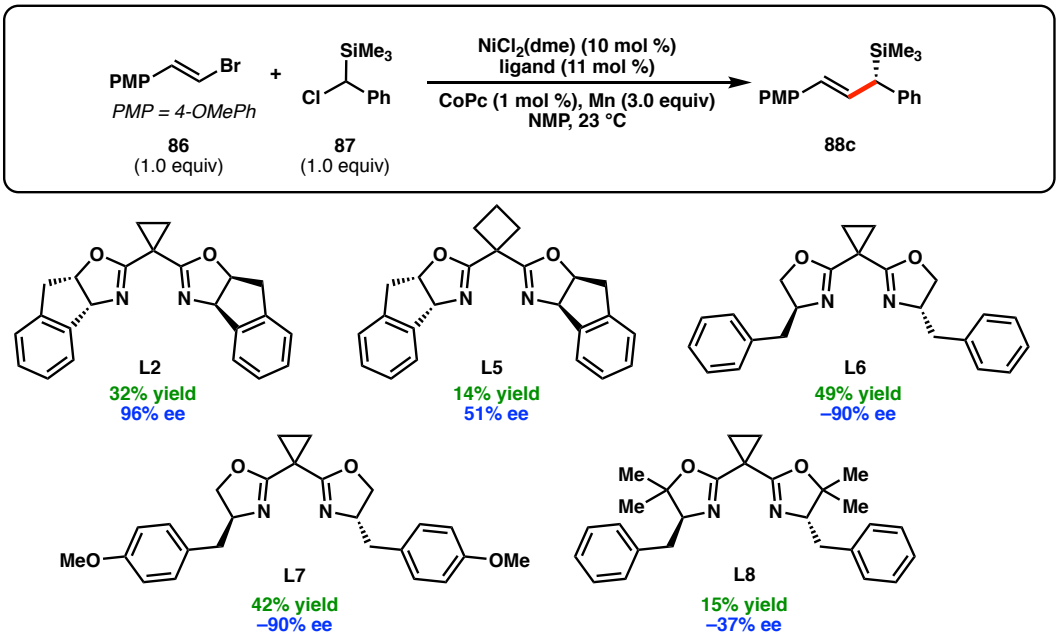

Figure 2.6 *Evaluation of chiral bidentate ligands at low temperature.*

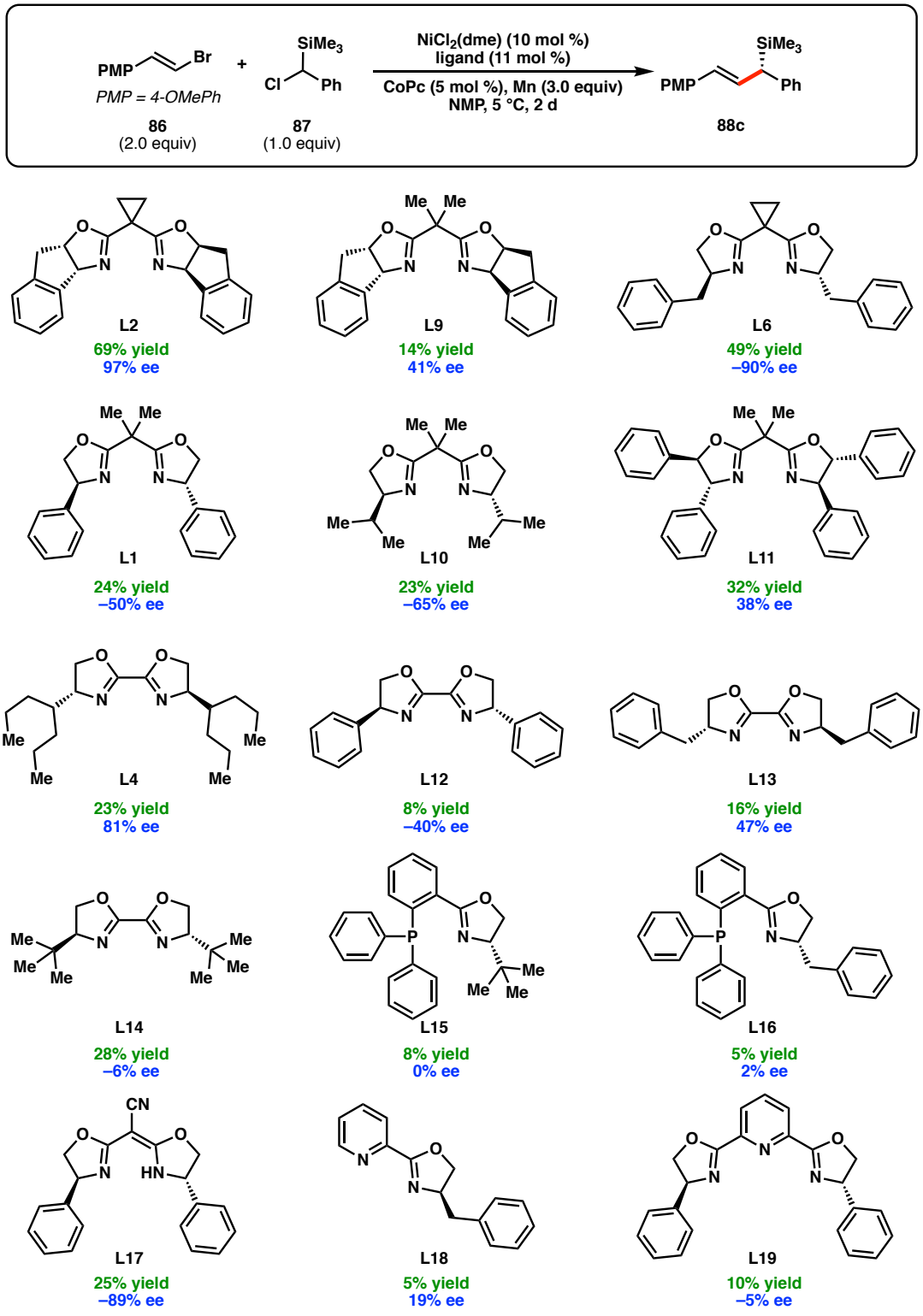

oxazoline (**L8**) diminished the ee. Taken together, these results suggest the bite angle of the oxazoline may contribute important factors in imparting enantioselectivity to **88c**.

A series of other ligand scaffolds were evaluated at 5 °C, and the desired allylic silane was also formed in excellent enantioselectivity when chiral BOX ligand **L6**, BiOx ligand **L4**, and CyanoBOX ligand **L17** were used (90%, 81%, and –89% ee, respectively) (Figure 2.6). Although these ligands provide **88c** in diminished yield, it is worthy to note other ligand scaffolds can be used to access **88c** with good ee. Other ligand scaffolds such as PHOX (**L15**, **L17**), PyOX (**L18**), and PyBOX (**L19**) do not perform well and provide **88c** in low yield.

2.3 SUBSTRATE SCOPE

With the optimized conditions in hand, the scope of the chlorobenzyl silane was investigated (Figure 2.6). Whereas strained silacyclobutane[54] **90a** was prepared in good yield and excellent ee, the corresponding triethylsilane **90c** was formed in poor yield, presumably due to increased steric encumbrance at Si. The dimethylphenyl silane **90b** could also be prepared, albeit in reduced yield. Substrates bearing either electron-withdrawing or electron-donating groups on the arene cross-coupled with universally high ee; however, in some cases the yield was diminished due to instability of the products (**90d**, **90f**). In these cases, special quenching protocols at low temperature were necessary to prevent product decomposition upon workup. While *m*-methoxy substitution provided **90g** in 81% yield, *p*-methoxy and *o*-methoxy substitution significantly decreased the yield of the cross-coupling products (**90h**, **90i**).

Figure 2.7 *Evaluation of chlorobenzyl silane scope.*

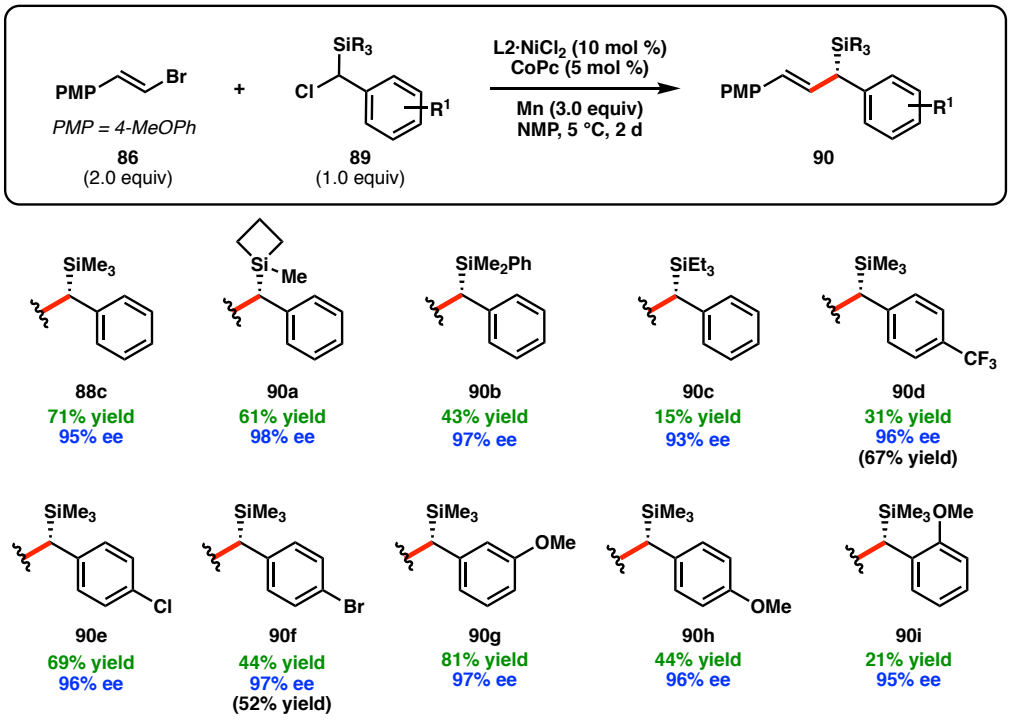

Reactions are conducted on 0.2 mmol scale under N_2. Isolated yields are provided; ee is determined by SFC using a chiral stationary phase. NMR yields of **90d** and **90f** versus an internal standard are provided in parentheses.

The reaction tolerates a diverse array of functional groups on the alkenyl bromide coupling partner (Figure 2.7), including aryl boronates (**91c**), esters (**91b**, **91j**), imides (**91m**), amides (**91n**), alkenyl silanes (**91o**), and alkyl halides (**91h**). For non-polar alkenyl bromide substrates, *m*-methoxy chlorobenzyl silane **89g** was used as the coupling partner to facilitate product purification (**91o**–**91u**). A number of alkyl-substituted alkenyl bromides performed comparably to styrenyl bromides. By changing which enantiomer of **L2**·$NiCl_2$ is employed, diastereomeric polyenes **90t** and **90u** were prepared, although the yield is decreased with the mismatched (3*S*,8*R*)-**L2**·$NiCl_2$ catalyst. Finally, alkenyl bromides bearing furan (**91q**), thiophene (**91r**), pyridine (**91k**), pyrimidine (**91l**), and indole (**91e**) heterocycles could be utilized, giving the corresponding allylic silanes in high ee.

Figure 2.8 *Evaluation of alkenyl bromide scope.*

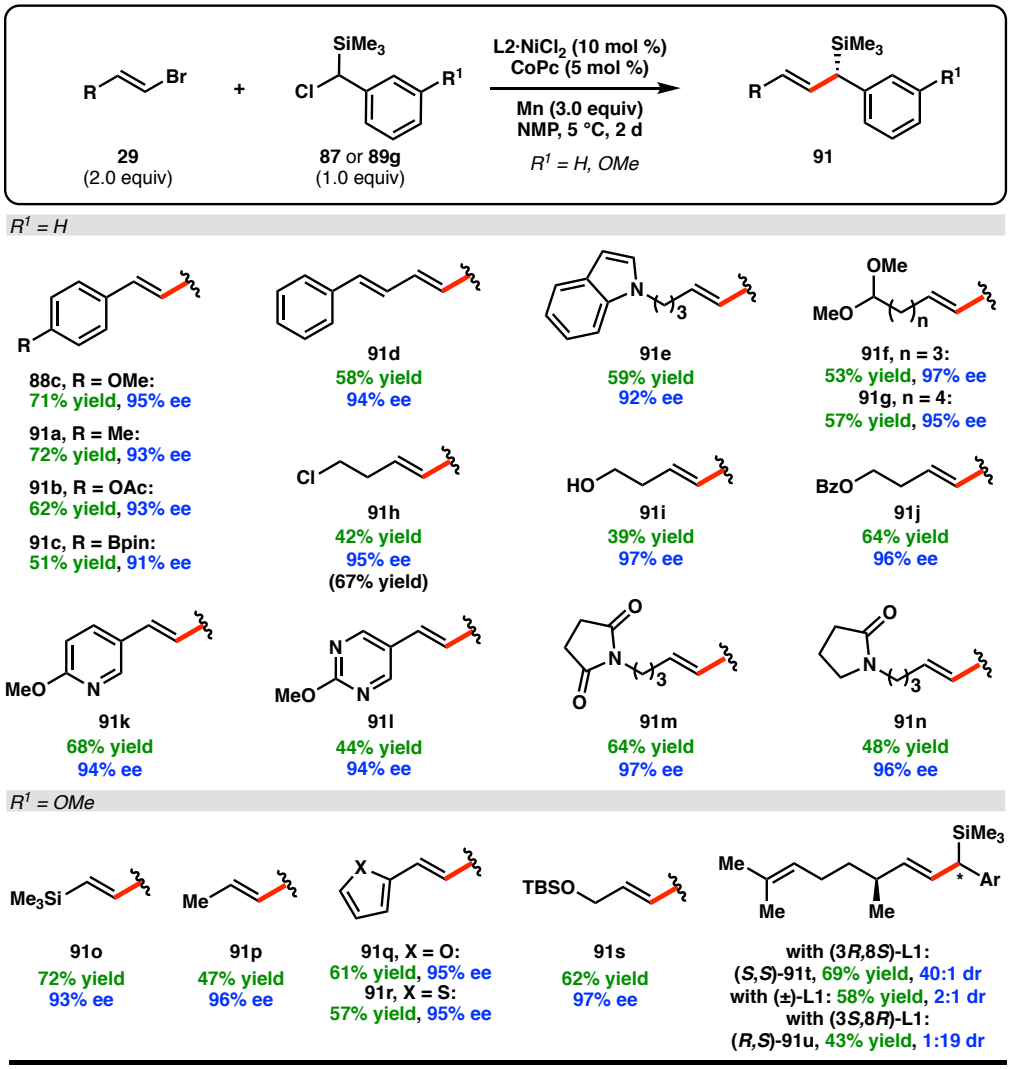

Reactions are conducted on 0.2 mmol scale under N_2. Isolated yields are provided; ee is determined by SFC or HPLC using a chiral stationary phase. NMR yield of **91h** versus an internal standard is provided in parentheses.

While a number of functional groups are tolerated under these conditions, geometric limitations do exist (Figure 2.9). For example, *Z*-alkenes (**92**) and tri- (**94**, **95**) and tetra-substituted (**93**) alkenyl bromides failed to react to produce the desired coupling products. Activated alkenyl halides (**95**, **97**) also fail in the reaction. The use of chlorobenzyl silane containing a free Si–OH group did not provide the desired product

Figure 2.9 *Limitations on the substrate scope.*

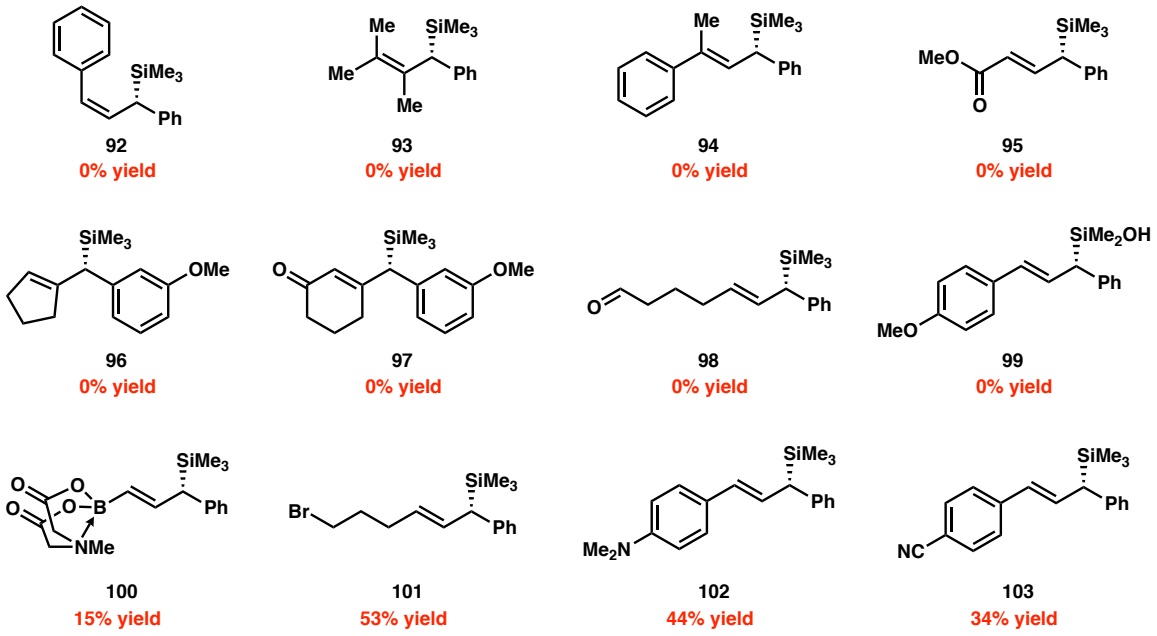

(**99**); rather, the cross-coupled desilylated product was obtained as a mixture of alkene regioisomers. Aldehyde functional groups (**98**) were not tolerated under the reaction conditions, however other functional groups such as MIDA boronates (**100**), alkyl bromides (**101**), dimethyl anilines (**102**), and nitriles (**103**) provided products albeit in low yields.

Although halide electrophiles were the primary focus of this study, oxygen-based electrophiles were also evaluated. We were pleased to find that mesylate **104** provided **88c** in 40% yield and 92% ee when conducted at 10 °C. The slight increase in temperature helped increase conversion of **104** compared to the reaction being run at 5 °C. However, starting material still remained in the reaction after 2 days, which contributed to the lower yield of **88c** (Scheme 2.3a). Attempts to improve the yield with excess **86** or upon addition of NaCl proved unfruitful. When the reaction was run in the absence of CoPc, **88c** was still

formed, albeit in reduced yields; this is in contrast to the cross-coupling of benzylic mesylates and aryl bromides conducted by Weix and coworkers which provide no product in the absence of CoPc. Enol triflate **105** also underwent cross-coupling to afford **91a** in 57% yield, again with excellent enantioselectivity (Scheme 2.3b). Although the yields were modest, we note that these reactions were conducted under conditions developed for the organic halides with minimal re-optimization.

Scheme 2.3 *Reactions with oxygen-based electrophiles.*

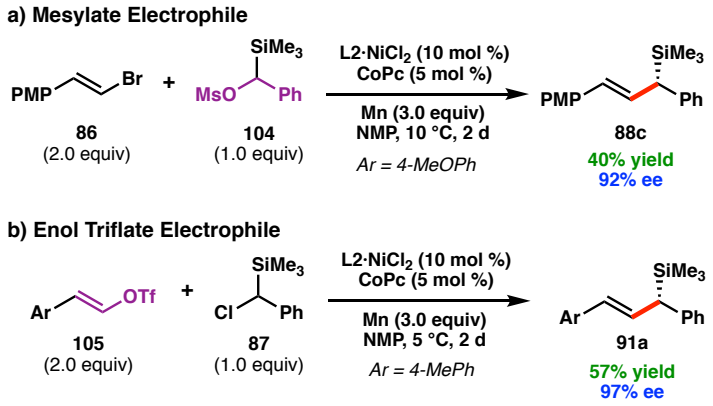

2.4 UTILITY OF CHIRAL ALLYLIC SILANES

The developed Ni-catalyzed cross-coupling reaction provides rapid access to functionalized chiral allylic silanes that are useful in a variety of synthetic contexts. A few transformations are highlighted in the following section to depict the use of these products as chiral starting materials, particularly for use in the construction of vicinal stereocenters.

2.4.1 Reduction of Allylic Silanes

Chiral alkyl silanes are commonly used as masked alcohols revealed via the Tamao–Fleming oxidation.[55–59] Oestreich and coworkers recently reported an elegant

chiral Ni-catalyzed cross-coupling between α-silyl alkyl iodides and alkyl zinc reagents using a chiral $NiCl_2$·PyBox catalyst generated in situ.[60] One advantage to this method is it does not rely on activated substrates (e.g. benzylic halides) to stabilize potential radical intermediates during the catalytic cycle, however the enantioselectivities of the products are somewhat diminished (60–92% ee). Chiral allylic silanes synthesized via our reductive cross-coupling can be converted into the corresponding alkyl silanes via hydrogenation. To demonstrate this, hydrogenation of **88c** with Pearlman's catalyst in the presence of H_2 provided alkyl silane **106** in 98% yield with only modest erosion of enantioselectivity (Scheme 2.4). The enantiospecificity (es) of this reaction is calculated to be 96% es.

Scheme 2.4 *Hydrogenation of chiral allyl silanes.*

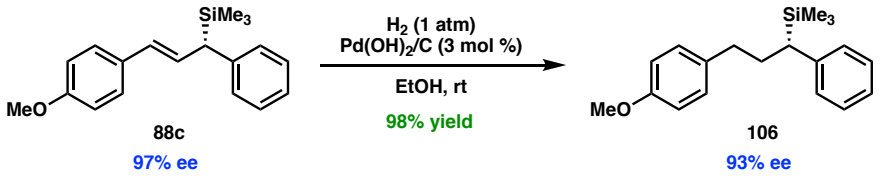

2.4.2 Transposition Reactions

Chiral allylic silanes can also undergo a variety of reactions to transpose the stereocenter and alkene moiety (Scheme 2.5). Gouverneur and coworkers demonstrated that allylic CF_3 products (**108**) can be synthesized from chiral allylic silanes (**107**) via photoredox catalysis with $Ru(bpy)_3Cl_2$ in the presence of Togni's reagent (Scheme 2.5a).[61] The reaction is proposed to proceed through stereospecific trifluoromethyl radical addition to the alkene, followed by elimination of the trimethylsilane. While the reaction proceeds in moderate yield, the stereochemical fidelity, however, is sub-optimal (74% es). In contrast, chiral allylic silanes (**109**) can undergo protodesilylation (Scheme 2.5b) or be

Scheme 2.5 *Transposition reactions of chiral allylic silanes.*

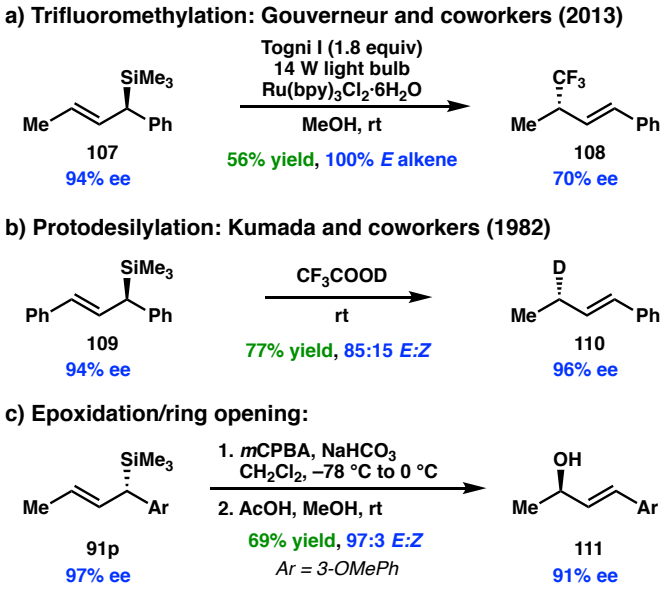

converted to chiral allylic alcohols (**111**) with higher levels of enantiospecificity (Scheme 2.5c). Hayashi and coworkers demonstrated that allylic silanes (**109**) can undergo stereospecific protodesilylation with deuterated acetic acid to form **110** with perfect enantiospecificity (Scheme 2.5b).[62] In a separate report, Hayashi and coworkers showed that epoxidation of the alkene in **91p** with *m*CPBA affords the chiral epoxide, which can undergo acid-catalyzed ring opening to afford the chiral allylic alcohol with only slight

Scheme 2.6 *Stereochemical outcome of chiral allylic silane epoxidation.*

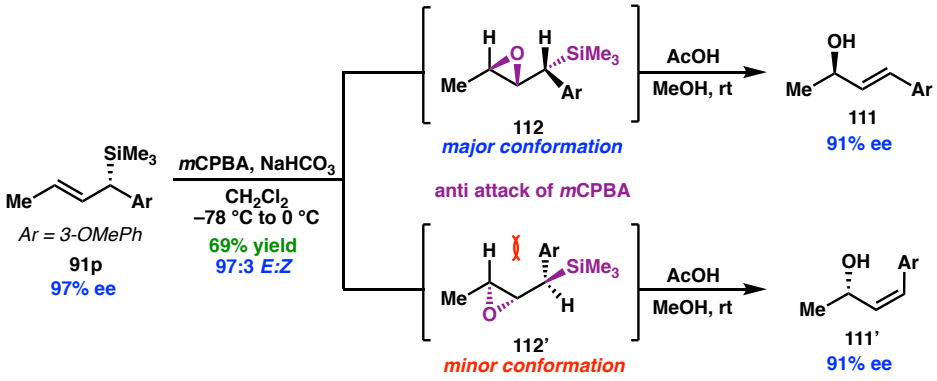

erosion of enantioselectivity. While Hayashi reports obtaining a 98% yield of **111** as an 81:19 mixture of *E*:*Z* isomers with 88% es when Ar = Ph,[63] in our hands, when Ar = 3-OMePh, **111** was obtained in 69% yield and 94% es as a 97:3 mixture of *E*:*Z* alkenes. The *E* and *Z* isomers are generated in opposite enantiomeric series due to anti-attack of *m*CPBA on the major and minor conformations of **112** during the epoxidation reaction (Scheme 2.6), which ultimately requires separation if oxidative cleavage of the alkene is planned.

2.4.3 Hosomi-Sakurai Allylations

Most notably, chiral allylic silanes are known for their ability to participate in Hosomi-Sakurai allylations with a wide variety of electrophiles.[9] These reactions can proceed in either an intermolecular or intramolecular manner to set vicinal stereocenters with excellent transfer of chirality. For example, chiral allylic silane **91p** can undergo an intermolecular Hosomi-Sakurai allylation with propanal and $TiCl_4$ to provide **113** in 75% yield as a single diastereomer and with no erosion of enantioselectivity (Scheme 2.7).[19,20] The resulting alcohol can be subsequently protected as the silyl ether and ozonolytic cleavage of the styrene provides primary alcohol **114** upon reduction with $NaBH_4$. In

Scheme 2.7 *Intermolecular Hosomi-Sakurai allylations.*

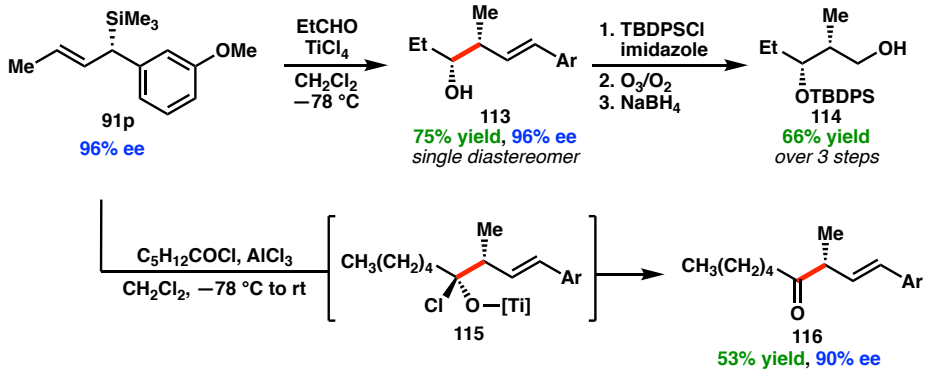

addition, allylation of **91p** with hexanoyl chloride in the presence of $AlCl_3$ directly affords the α-chiral ketone **116** without isomerization into conjugation. This reaction proceeds via displacement of the chloride from intermediate **115**, which leads to the formation of the ketone product.[19,64–68]

Chiral allylic silanes can also be used in intramolecular allylations. For example, allylic silanes **91f** and **91g**, which contain pendant acetals, undergo stereospecific $TiCl_4$-mediated intramolecular cyclization to form the 5- and 6-membered rings **117** and **118**, respectively (Figure 2.10). The observed absolute and relative stereochemistry is consistent with an *anti*-S_E' mode of addition to an oxocarbenium ion through a *syn*-clinal transition state, giving rise to the *trans*-substituted 5-membered ring and the *cis*-substituted 6-membered ring.[69] While these transition states support the stereochemical outcome, it is worthwhile to mention that mechanistic studies by Denmark and coworkers also suggest an S_N2-type mechanism may be consistent with the observed results.[70]

Figure 2.10 *Intramolecular Hosomi-Sakurai allylations.*

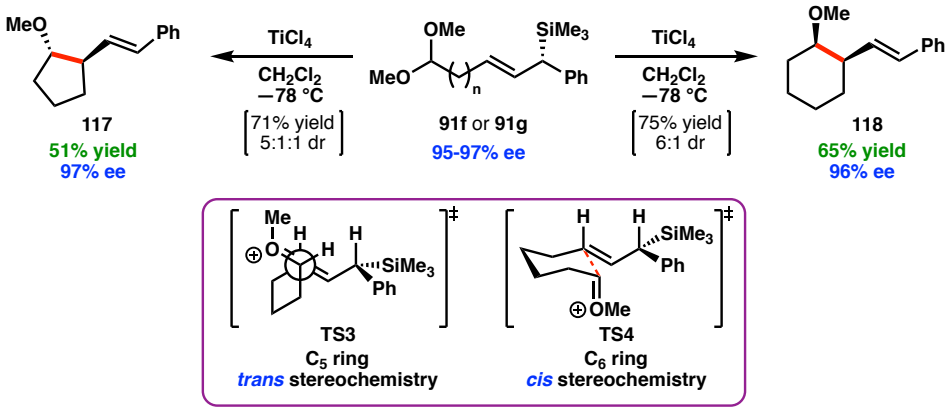

The utility of this method was further demonstrated in a concise enantioselective synthesis of (+)-tashiromine (Figure 2.11).[71,72] Sodium borohydride reduction of imide

91m at 0 °C provided aminal **120** in 99% yield as a 1:1 mixture of diastereomers.[73] The reaction temperature was critical for obtaining the desired aminal product; when the reduction was conducted at room temperature, further reduction of **120** afforded the ring-opened product **119**. Exposure of aminal **120** to neat formic acid[74] induced cyclization to form the fused bicycle in a 93% combined yield of a 3:1:1 mixture of isomers. The major isomer **121** was isolated in 57% yield and 97% ee. Finally, ozonolysis of the styrene and reduction of the amide provided (+)-tashiromine (**122**) in 68% yield over two steps.

Figure 2.11 *Total synthesis of (+)-tashiromine.*

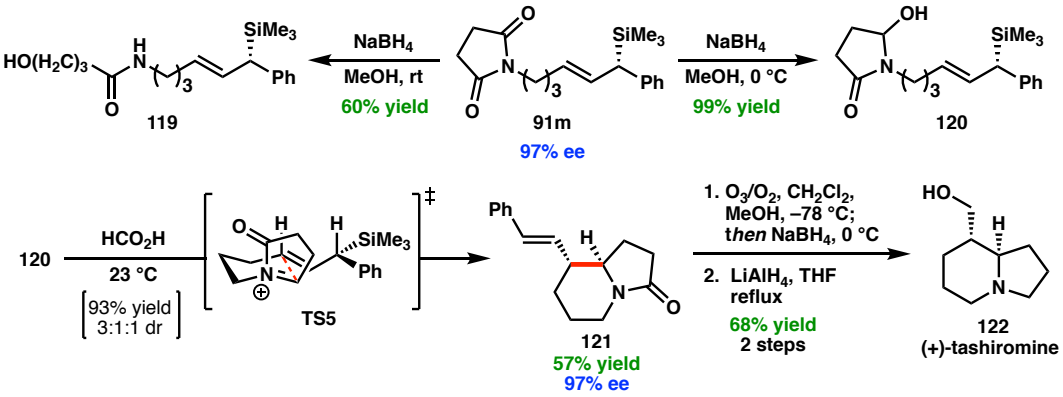

The selectivity of the acid-catalyzed cyclization of **120** was found to be dependent on the identity of the acid (Table 2.8). When trifluoroacetic acid was added to a solution of **120** in CH_2Cl_2 at room temperature, a 1.0:0.39:0.49 mixture of **121**:**121'**:**121''** was obtained (entry 1), providing the desired product **121** as 53% of the combined isomers. The addition of 4 Å molecular sieves had no effect on this ratio (entry 2). Both $TiCl_4$ and TMSOTf provided a poorer isomeric ratio, affording 44% and 48% of **121** as the major isomer, respectively (entries 3–4). The use of neat formic acid (HCO_2H) provided the best ratio of all acids tested; **121** was obtained as 68% of the total mixture. The absolute and

relative stereochemistry of the minor allylation isomers **121'** and **121''** were assigned based on literature precedent for the related glutarimide analog.[75]

Table 2.8. *Evaluation of acids in the intramolecular allylation of* ***120****.*

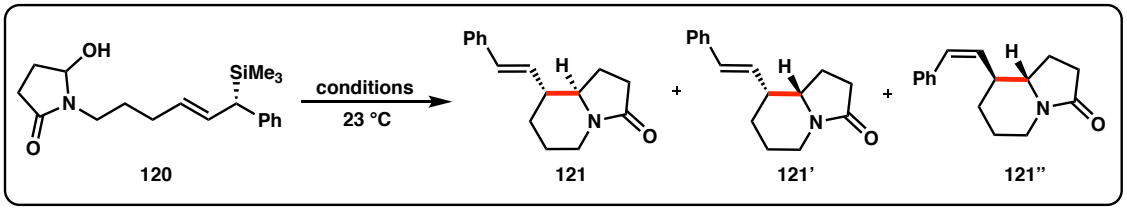

Entry	Conditions	121 :	121' :	121"	121 (%)
1	TFA, CH_2Cl_2	1.0	0.39	0.49	53
2	TFA, 4 Å MS, CH_2Cl_2	1.0	0.37	0.44	55
3	$TiCl_4$, 4 Å MS, CH_2Cl_2	1.0	0.62	0.64	44
4	TMSOTf, CH_2Cl_2	1.0	0.50	0.60	48
5	HCO_2H *(neat)*	1.0	0.30	0.17	68

2.4.4 Synthesis of 2,3-Disubstituted Tetrahydrofurans

Either the 2,3-*cis*- or 2,3-*trans*-disubstituted tetrahydrofurans can be prepared by Lewis acid-mediated cyclizations of alcohol **91i** or chloride **91h**, respectively; both proceed with excellent transfer of chirality (Scheme 2.8). Chiral allylic silane **91i** can undergo a Lewis acid-mediated condensation of acetaldehyde diethyl acetal onto the pendant alcohol to afford **123a**, therefore inducing an intramolecular allylation to set the *cis* stereochemical relationship across the tetrahydrofuran ring (Scheme 2.8a).[76] In contrast, $TiCl_4$-mediated intermolecular Hosomi-Sakurai allylation of **91h** with acetaldehyde proceeds smoothly (Scheme 2.8b). Upon completion, quenching the reaction with water affords the corresponding alcohol; however, addition of a strong base (KO*t*Bu) facilitates removal of Ti from the resulting alkoxide and induces intramolecular S_N2 cyclization to form the

tetrahydrofuran ring (**124a**). The stereochemistry from the intermolecular allylation translates to provide the *trans* stereochemical relationship across the tetrahydrofuran.

Scheme 2.8 *Synthesis of 2,3-disubstituted tetrahydrofurans.*

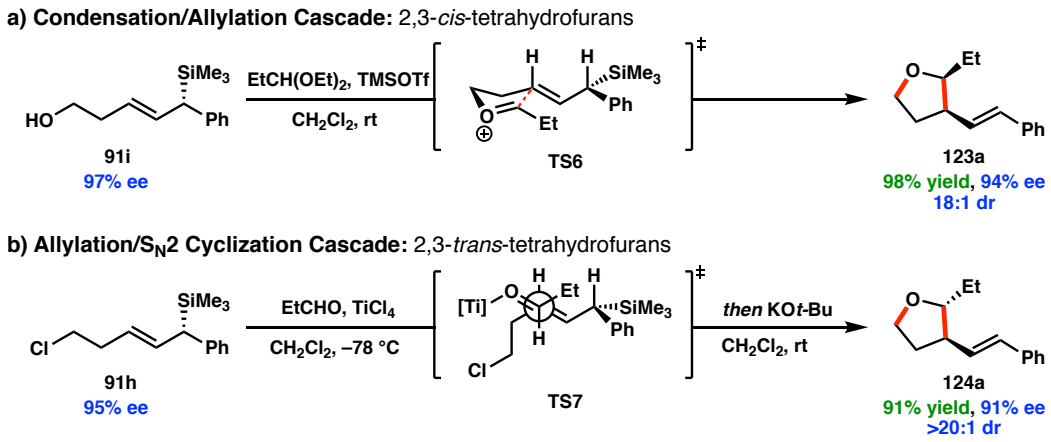

A series of aldehydes was then evaluated under these reaction conditions (Figure 2.10). A total of four product isomers are possible in both transformations: 1) *cis* tetrahydrofuran, *E* isomer, 2) *trans* tetrahydrofuran, *E* isomer, 3) *cis* tetrahydrofuran, *Z* isomer, and 4) *cis* tetrahydrofuran, *Z* isomer. Yields are reported for the combined mixture of isomers, and the major isomer as depicted is given as a percentage of the total mixture (representative purity). Excellent diastereoselectivity and *E:Z* ratio of the alkene moiety was observed in most cases, with the exception of decreased dr for **123b**, **123e**, **124d**, and **124e**. Interestingly, tetrahydrofuran **123e** was preferentially formed via S_N2 cyclization to afford the 5-membered heterocycle instead of the 6-membered heterocycle. While alkenes and alkyl chlorides are well-tolerated, the presence of benzyl ethers resulted in diminished dr for the *trans* tetrahydrofurans due to coordination to Ti.[75] While **124g** was formed in a poor 2:1 dr, the major isomer was still obtained as the *trans* product. However, **124f** was formed in a 1:3 ratio of *trans*:*cis*, demonstrating that the proximal benzyl ether can not only

erode dr, but also overturn inherent selectivity. In contrast, benzyl ethers were well-tolerated in the intramolecular allylation to form the *cis* tetrahydrofurans.

Figure 2.12 *Scope of the 2,3-disubstituted tetrahydrofurans.*

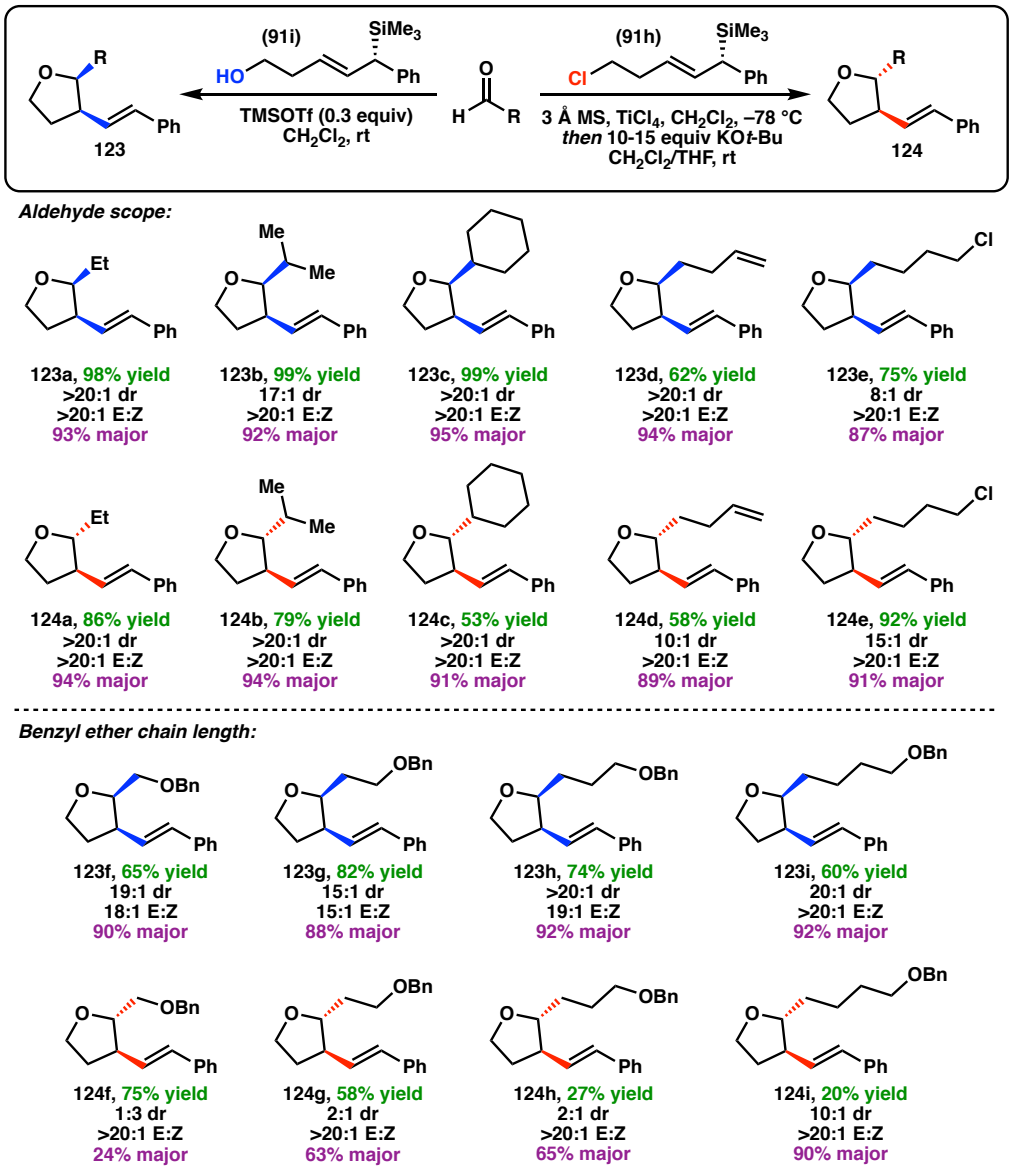

2.5 CONCLUSION

In summary, a highly enantioselective Ni-catalyzed cross-coupling reaction has been developed for the preparation of chiral allylic silanes. The reactions proceed under mild conditions and tolerate a variety of functional groups. The enantioenriched allylic silanes undergo several stereospecific transformations with high levels of chirality transfer, which we anticipate will prove useful in an array of synthetic contexts.

2.6 EXPERIMENTAL SECTION

2.6.1 Materials and Methods

Unless otherwise stated, reactions were performed under a N_2 atmosphere using freshly dried solvents. Tetrahydrofuran (THF), diethyl ether (Et_2O), methylene chloride (CH_2Cl_2), toluene (PhMe), hexane, and benzene (C_6H_6) were dried by passing through activated alumina columns. Triethylamine (Et_3N), diisopropylamine (*i*-Pr_2NH), and trimethylsilyl chloride (TMSCl) were distilled over calcium hydride prior to use. Anhydrous *N*,*N*'-dimethylacetamide (DMA) and anhydrous *N*-methylpyrrolidinone (NMP) were purchased from Aldrich and stored under N_2. Manganese powder (–325 mesh, 99.3%) was purchased from Alfa Aesar. Zinc dust (97.5%) was purchased from Strem. Unless otherwise stated, chemicals and reagents were used as received. All reactions were monitored by thin-layer chromatography using EMD/Merck silica gel 60 F254 pre-coated plates (0.25 mm) and were visualized by UV, CAM, or $KMnO_4$ staining. Flash column chromatography was performed as described by Still et al.[77] using silica gel (230-400 mesh, Silicycle) or 10% $AgNO_3$ doped silica gel (+230 mesh, Sigma Aldrich). Purified compounds were dried on

a high vacuum line (0.2 torr) to remove trace solvent. Optical rotations were measured on a Jasco P-2000 polarimeter using a 100 mm path-length cell at 589 nm. ^{1}H and ^{13}C NMR spectra were recorded on a Bruker Avance III HD with Prodigy cryoprobe (at 400 MHz and 101 MHz, respectively), a Varian 400 MR (at 400 MHz and 101 MHz, respectively), or a Varian Inova 500 (at 500 MHz and 126 MHz, respectively). ^{1}H and ^{19}F NMR spectra were also recorded on a Varian Inova 300 (at 300 MHz and 282 MHz, respectively). NMR data is reported relative to internal $CHCl_3$ (^{1}H, $\delta = 7.26$), $CDCl_3$ (^{13}C, $\delta = 77.0$), and C_6F_6 (^{19}F, $\delta = -164.9$). Data for ^{1}H NMR spectra are reported as follows: chemical shift (δ ppm) (multiplicity, coupling constant (Hz), integration). Multiplicity and qualifier abbreviations are as follows: s = singlet, d = doublet, t = triplet, q = quartet, m = multiplet, br = broad. IR spectra were recorded on a Perkin Elmer Paragon 1000 spectrometer and are reported in frequency of absorption (cm^{-1}). Analytical chiral SFC was performed with a Mettler SFC supercritical CO_2 analytical chromatography system (CO_2 = 1450 psi, column temperature = 40 °C) with Chiralcel AD-H, OD-H, AS-H, OB-H, and OJ-H columns (4.6 mm x 25 cm). Analytical chiral HPLC was performed with an Agilent 1100 Series HPLC with a Chiralcel OD-H column (4.6 mm x 25 cm, Daicel Chemical Industries, Ltd.). HRMS were acquired from the Caltech Mass Spectral Facility using fast-atom bombardment (FAB), electrospray ionization (ESI-TOF), or electron impact (EI). X-ray diffraction and elemental analysis (EA) were performed at the Caltech X-ray Crystal Facility.

2.6.2 Ni(II) Complex Preparation

Bis((3a*R*,8a*S*)-3a,8a-dihydro-8*H*-indeno[1,2-*d*]oxazol-2-yl)methane (L20)

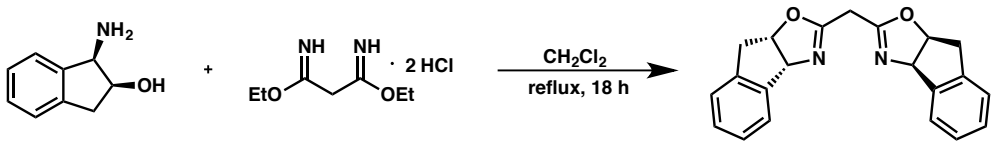

According to a procedure by Snyder and coworkers,[78] the (*1R*,*2S*)-(+)-cis-1-amino-2-indanol (4.70 g, 31.5 mmol, 2.1 equiv) and diethyl malonimidate dihydrochloride (3.47 g, 15 mmol, 1 equiv) were added to a flame-dried 1 L round bottom flask fitted with a reflux condenser and a magnetic stir bar, and put under an inert atmosphere (N_2). Then CH_2Cl_2 (360 mL) was added and the solution was heated at 45 °C for 18 hours. The reaction was cooled, and then quenched with water (690 mL). The layers were separated, the aqueous layer was extracted with CH_2Cl_2 (4 x 180 mL), and the combined organic layers were dried with $MgSO_4$, filtered, and concentrated. The crude material was purified by recrystallization from cooling hot ethanol to yield 3.30 g (67% yield) of **L20** as a white solid. Spectral data matched those reported in literature.[78]

(3a*R*,3a'*R*,8a*S*,8a'*S*)-2,2'-(Cyclopropane-1,1-diyl)bis(3a,8a-dihydro-8*H*-indeno[1,2-*d*]-oxazole) (L2)

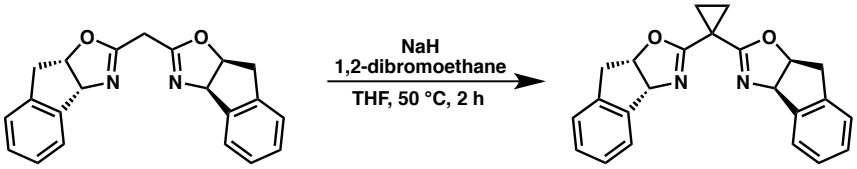

Following a procedure by Sibi and coworkers,[79] bis(oxazoline) **L20** (1.65 g, 5.0 mmol, 1 equiv) was added to a flame-dried 200 mL round bottom flask with a magnetic stir bar.

The flask was placed under inert atmosphere (N_2), THF (25 mL) was added, and the solution was cooled to 0 °C. Dry sodium hydride (60 wt % in mineral oil, 601 mg, 15 mmol, 3 equiv) was added in portions. **Note:** Wet NaH resulted in saponification of the oxazoline, which could be removed by column chromatography (silica, 10% MeOH/CH_2Cl_2). The solution was allowed to stir for 30 minutes before 1,2-dibromoethane (517 μL, 6 mmol, 1.2 equiv) was added dropwise over the course of 10 minutes. The reaction was then warmed to 50 °C and stirred for 2 hours. **Note:** Aliquots could be monitored by ^{1}H NMR to ensure complete conversion. The reaction was quenched with aqueous NH_4Cl (25 mL) and extracted with CH_2Cl_2 (2 x 85 mL). The combined organic layers were dried with Na_2SO_4, filtered, and concentrated under reduced pressure. The crude material was purified by recrystallization upon cooling from hot ethanol to yield 1.46 g (82% yield) of **L2** as a light tan solid. Spectral data matched those reported in the literature.[79]

Nickel(II) bis(chloride) (3a*R*,3a'*R*,8a*S*,8a'*S*)-2,2'-(cyclopropane-1,1-diyl)bis(3a,8a-dihydro-8*H*-indeno[1,2-*d*]oxazole) (L2·$NiCl_2$)

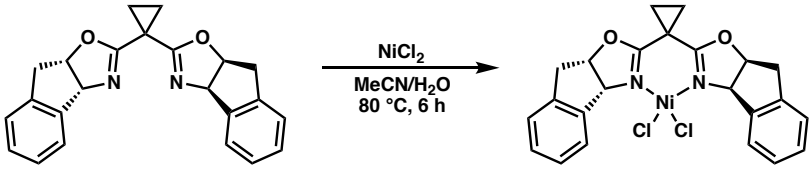

Adapted from a procedure by Evans and coworkers.[80] Bis(oxazoline) ligand **L2** (1.07 g, 3.0 mmol, 1 equiv) and anhydrous nickel(II) chloride (390 mg, 3.0 mmol, 1 equiv) were added to a round bottom flask equipped with a magnetic stirring rod and dissolved in a mixture of MeCN (65 mL) and water (0.75 mL). The solution was heated to 80 °C under

an N_2 atmosphere for 6 hours to afford a dark purple solution. The reaction was concentrated under reduced pressure and the obtained solid was dissolved in CH_2Cl_2, filtered through a plug of cotton, dispensed into four 20 mL scintillation vials, and recrystallized by vapor diffusion (CH_2Cl_2/pentane) to afford dark purple crystals suitable for X-ray diffraction. **Notes:** The **L2**·$NiCl_2$ complex can crystallize both as a monomeric species (purple solid, very common) or a trimeric species (orange solid, rare). The monomeric catalyst was used for the entirety of this manuscript, however a control reaction revealed that product **88c** was obtained in comparable yield and ee when the trimeric catalyst was used. To isolate **L2**·$NiCl_2$, the dichloromethane was decanted and the crystals were washed with hexane. The crystals were transferred by spatula to a new vial and crushed to provide a powder. The resulting complex was dried under vacuum to yield 1.3 g (89% yield) of **L2**·$NiCl_2$ as a purple solid. **m.p.** = >300 °C **^{1}H NMR (400 MHz, $CDCl_3$):** δ 94.87 (s, 2H), 47.79 (s, 2H), 20.23 (s, 2H), 11.77 (s, 4H), 11.51 (s, 2H), 10.45 (s, 2H), 5.34 (d, J = 119.5 Hz, 2H), 3.92 (s, 2H), -1.10 (s, 2H). **FTIR (NaCl, thin film, cm^{-1}):** 3611, 3306, 2835, 2214, 1836, 1651, 1479, 1461, 1442, 1367, 1312, 1274, 1247, 1224, 1172, 1154, 1114, 1009, 951, 911, 860, 835. **EA:** Anal. Calc'd. for **L1**·$NiCl_2$, $C_{23}H_{20}Cl_2N_2NiO_2$ (%): C, 56.84; H, 4.15; N, 5.76. Found: C, 56.24; H, 4.14; N, 5.63.

2.6.3 Optimization of Reaction Parameters

Ligand (0.011 mmol, 0.11 equiv), $NiCl_2$(dme) (0.010 mmol, 0.10 equiv), alkenyl bromide **86** (0.1-0.2 mmol, 1-2 equiv), Mn^0 (0.3 mmol, 3 equiv), and additive (if used, 0.005-0.05 mmol, 0.05-0.5 equiv, as specified) were charged to a vial on the benchtop. In some cases, **L2**·$NiCl_2$ complex (0.010 mmol, 0.10 equiv) was used in place of **L2** and $NiCl_2$(dme). The

vial was brought into a nitrogen-filled glovebox and charged with NMP (0.2 mL, 0.5 M) followed by a mixture of the chlorobenzyl silane (**87**, 20 μL, 0.1 mmol, 1 equiv) and dibenzyl ether (internal standard). The vials were sealed with Teflon caps and stirred at the specified reaction temperature at 250 rpm for 48 hours. The slurry was dissolved in 10% EtOAc/hexanes, loaded onto a silica plug in a glass pipet, and flushed with 8 mL of 10% EtOAc/hexanes into a 20 mL scintillation vial. The solution was concentrated under reduced pressure and analyzed by ^{1}H NMR to obtain the reaction yield. The product was purified by preparative TLC, dissolved in 10% EtOH/hexanes, and analyzed by SFC with chiral stationary phase to obtain the enantiomeric excess (% ee) of the reaction product.

2.6.4 Substrate Preparation

2.6.4.1 Chlorobenzyl Silane Electrophiles

General Procedure 1: Chlorobenzyl Silane Synthesis

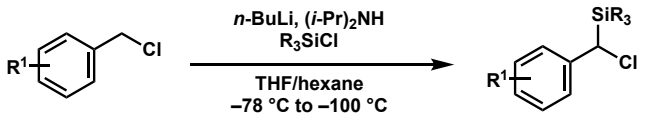

Adapted from a procedure by Hashmi and coworkers.[81] A flame-dried round bottom flask equipped with a magnetic stir bar was placed under inert atmosphere (N_2) and charged with diisopropylamine (2.8 mL, 20 mmol, 1.0 equiv) and THF (9 mL). The solution was cooled to –78 °C and stirred for 5 minutes. *n*-Butyllithium was added dropwise (8 mL, 2.5 M in hexane, 20 mmol, 1.0 equiv) and stirred for another 10 minutes, at which time the solution was diluted with hexane (9 mL) and cooled to –100 °C. A mixture of the benzyl chloride (20 mmol, 1.0 equiv) and silyl chloride (24 mmol, 1.2 equiv) in THF (9 mL) was added

dropwise over the course of 30 minutes via syringe or via cannula. The reaction was stirred for 20 minutes, then warmed to 0 °C and quenched with water (10 mL). The aqueous layer was extracted with ether (3 x 40 mL) and the combined organic layers were washed with 1 M HCl (20 mL), water (20 mL), then dried with $MgSO_4$, filtered, and concentrated under reduced pressure. The product was purified by column chromatography (silica, EtOAc/hexanes) and/or by distillation. For substrates **89c**, **89d**, **89f**, **89h**, and **89j** an inverse addition protocol was used, wherein lithium diisopropylamide (LDA) solution was added dropwise to the mixture of benzyl chloride and R_3SiCl. This procedure minimized the bis-silylated benzyl chloride.

(Chloro(phenyl)methyl)trimethylsilane (87)

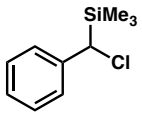

Prepared from (chloromethyl)benzene (11.5 mL, 100 mmol) and trimethylsilyl chloride (15.2 mL, 120 mmol) following General Procedure 1. The crude residue was purified by fractional distillation (0.25 Torr, 60 °C) to yield 14.9 g (75% yield) of **87** as a colorless oil. $\mathbf{R_f}$ = 0.61 (silica, hexane, UV). **^{1}H NMR (500 MHz, $CDCl_3$):** δ 7.35 – 7.31 (m, 2H), 7.29 – 7.26 (m, 2H), 7.25 – 7.21 (m, 1H), 4.37 (s, 1H), 0.12 (s, 9H). **^{13}C NMR (126 MHz, $CDCl_3$):** δ 140.3, 128.3, 127.0, 126.7, 53.1, -3.4. **FTIR (NaCl, thin film, cm^{-1}):** 3027, 2959, 1598, 1494, 1450, 1250, 1122, 1074, 912, 863, 844.**HRMS (EI, *m/z*):** calc'd for $C_{10}H_{15}ClSi$ $[M+\cdot]^+$: 198.0632; found: 198.0603.

1-(Chloro(phenyl)methyl)-1-methylsiletane (89a)

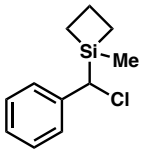

Prepared from (chloromethyl)benzene (1.15 mL, 10 mmol) and 1-chloro-1-methylsiletane (1.5 mL, 12 mmol) following General Procedure 1 using an

inverse addition protocol. The reaction was also stirred for 1 hour following the addition. The crude residue was purified by column chromatography (silica, hexane), followed by Kugelrohr distillation to yield 594 mg (28% yield) of **89a** as a colorless oil. $\mathbf{R_f}$ = 0.61 (silica, hexane, UV). **^{1}H NMR (500 MHz, $CDCl_3$):** δ 7.36 – 7.30 (m, 4H), 7.27 – 7.21 (m, 1H), 4.56 (s, 1H), 2.04 (dtt, *J* = 12.4, 10.2, 6.1 Hz, 1H), 1.90 (dtt, *J* = 12.7, 10.2, 6.8 Hz, 1H), 1.30 – 1.16 (m, 2H), 1.15 – 0.99 (m, 2H), 0.33 (s, 3H). **^{13}C NMR (126 MHz, $CDCl_3$):** δ 139.5, 128.5, 126.91, 126.86, 51.7, 17.6, 13.8, 13.5, -3.4. **FTIR (NaCl, thin film, cm^{-1}):** 2969, 2927, 1598, 1494, 1450, 1394, 1250, 1121, 1074, 874. **HRMS (EI, *m/z*):** calc'd for $C_{11}H_{15}ClSi$ $[M+\cdot]^+$: 210.0632; found: 210.0607.

(Chloro(phenyl)methyl)dimethyl(phenyl)silane (89b)

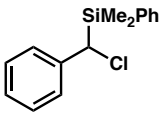

Prepared from (chloromethyl)benzene (2.3 mL, 20 mmol) and chlorodimethyl(phenyl)silane (3.7 mL, 22 mmol) following General Procedure 1 using an inverse addition protocol. The crude residue was purified by fractional distillation (0.25 Torr, 120-153 °C) to yield 2.72 g (52% yield) of **89b** as a light yellow oil. $\mathbf{R_f}$ = 0.22 (silica, hexane, UV). **^{1}H NMR (500 MHz, $CDCl_3$):** δ 7.44 – 7.39 (m, 3H), 7.37 – 7.32 (m, 2H), 7.27 – 7.22 (m, 2H), 7.22 – 7.17 (m, 1H), 7.13 – 7.08 (m, 2H), 4.51 (s, 1H), 0.48 (s, 3H), 0.38 (s, 3H). **^{13}C NMR (126 MHz, $CDCl_3$):** δ 139.7, 135.1, 134.53, 129.8, 128.1, 127.8, 127.3, 126.8, 52.4, -5.06, -5.07. **FTIR (NaCl, thin film, cm^{-1}):** 3070, 3026, 2961, 1494, 1450, 1428, 1250, 1117, 834. **HRMS (FAB, *m/z*):** calc'd for $C_{15}H_{17}ClSi$ $[M–Cl]^+$: 225.1100; found: 225.1104.

(Chloro(phenyl)methyl)triethylsilane (89c)

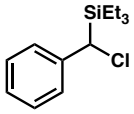

Prepared from (chloromethyl)benzene (2.3 mL, 20 mmol) and triethylsilyl chloride (4.0 mL, 24 mmol) following General Procedure 1. The crude residue was purified by Kugelrohr distillation to yield 3.5 g (73% yield) of **89c** as a light yellow oil. R_f = 0.71 (silica, hexane, UV). ^{1}H NMR (500 MHz, $CDCl_3$): δ 7.34 – 7.28 (m, 4H), 7.24 – 7.19 (m, 1H), 4.48 (s, 1H), 0.96 (t, *J* = 7.9 Hz, 9H), 0.77 – 0.59 (m, 6H). ^{13}C NMR (126 MHz, $CDCl_3$): δ 140.7, 128.4, 127.2, 126.7, 50.9, 7.4, 2.1. FTIR (NaCl, thin film, cm^{-1}): 2955, 2913, 2877, 1598, 1494, 1450, 1414, 1122, 1074, 1009. HRMS (FAB, *m/z*): calc'd for $C_{13}H_{21}ClSi$ $[M+H]^+$: 241.1179; found: 241.1189.

(Chloro(4-(trifluoromethyl)phenyl)methyl)trimethylsilane (89d)

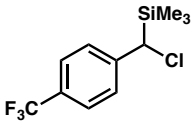

Prepared from 1-(chloromethyl)-4-(trifluoromethyl)benzene (3 mL, 20 mmol) and trimethylsilyl chloride (3 mL, 24 mmol) following General Procedure 1 using an inverse addition protocol. The reaction was also stirred for 1 hour following the addition. The crude residue was purified by fractional distillation (0.25 Torr, 65 °C) to yield 1.29 g (48% yield) of **89d** as a colorless oil. **R_f** = 0.58 (silica, hexane, UV). **^{1}H NMR (500 MHz, $CDCl_3$):** δ 7.58 (d, *J* = 8.2 Hz, 2H), 7.37 (d, *J* = 8.1 Hz, 2H), 4.39 (s, 1H), 0.11 (d, *J* = 0.7 Hz, 9H). **^{13}C NMR (126 MHz, $CDCl_3$):** δ 144.66 (q, J_{C-F} = 1.4 Hz), 128.84 (q, J_{C-F} = 32.5 Hz), 127.1, 125.30 (q, J_{C-F} = 3.8 Hz), 124.32 (q, J_{C-F} = 271.9 Hz), 52.3, -3.6. **^{19}F NMR (282 MHz, $CDCl_3$):** δ -65.6. **FTIR (NaCl, thin film, cm^{-1}):** 2962, 1618, 1415, 1327, 1253, 1166, 1127, 1106, 1069, 1018, 866, 849. **HRMS (FAB, *m/z*):** calc'd for $C_{11}H_{14}ClF_3Si$ $[M+H]^+$: 267.0584; found: 267.0572.

(Chloro(4-chlorophenyl)methyl)trimethylsilane (89e)

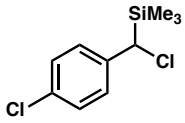

Prepared from 1-chloro-4-(chloromethyl)benzene (800 mg, 5 mmol) and trimethylsilyl chloride (0.76 mL, 6 mmol) following General Procedure 1. The crude residue was purified by column chromatography (silica, hexane) to yield 658 mg (57% yield) of **89e** as a colorless oil. $\mathbf{R_f}$ = 0.58 (silica, hexane, UV). **^{1}H NMR (500 MHz, $CDCl_3$):** δ 7.29 – 7.26 (m, 2H), 7.20 – 7.16 (m, 2H), 4.30 (s, 1H), 0.09 (s, 9H). **^{13}C NMR (126 MHz, $CDCl_3$):** δ 139.0, 132.3, 128.5, 128.3, 52.3, -3.5. **FTIR (NaCl, thin film, cm^{-1}):** 2959, 1490, 1404, 1251, 1122, 1093, 1014, 865, 846. **HRMS (EI, *m/z*):** calc'd for $C_{10}H_{14}Cl_2Si$ $[M+\cdot]^+$: 232.0242; found: 232.0270.

(Chloro(4-bromophenyl)methyl)trimethylsilane (89f)

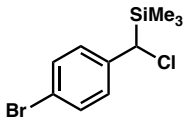

Prepared from 1-chloro-4-(bromomethyl)benzene (1.02 g, 5 mmol) and trimethylsilyl chloride (0.76 mL, 6 mmol) following General Procedure 1 using an inverse addition protocol. The crude residue was purified by fractional distillation (0.25 Torr, 85 °C) to yield 411.6 mg (30% yield) of **89f** as a colorless oil which solidified in the freezer. $\mathbf{R_f}$ = 0.58 (silica, hexane, UV). **m.p.** = 30-31 °C **^{1}H NMR (500 MHz, $CDCl_3$):** δ 7.45 – 7.40 (m, 2H), 7.14 – 7.09 (m, 2H), 4.28 (s, 1H), 0.08 (s, 9H). **^{13}C NMR (126 MHz, $CDCl_3$):** δ 139.5, 131.4, 128.6, 120.3, 52.3, -3.5. **FTIR (NaCl, thin film, cm^{-1}):** 2958, 1487, 1398, 1262, 1271, 1074, 1010, 864, 845, 829. **HRMS (EI, *m/z*):** calc'd for $C_{10}H_{14}BrClSi$ $[M+\cdot]^+$: 275.9737; found: 275.9760.

(Chloro(3-methoxyphenyl)methyl)trimethylsilane (89g)

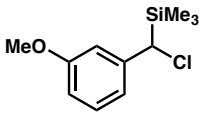

Prepared from 1-(chloromethyl)-3-methoxybenzene (2.9 mL, 20 mmol) and trimethylsilyl chloride (3.05 mL, 24 mmol) following General Procedure 1. The crude residue was purified by fractional distillation (0.25 Torr, 85 °C) to yield 1.2 g (27% yield) of **89g** as a colorless oil. $\mathbf{R}_f$ = 0.59 (silica, 10% EtOAc/ hexane, UV). **^{1}H NMR (500 MHz, $CDCl_3$):** δ 7.24 – 7.19 (m, 1H), 6.82 (ddq, *J* = 4.6, 2.4, 0.8 Hz, 2H), 6.76 (ddd, *J* = 8.2, 2.5, 1.0 Hz, 1H), 4.32 (s, 1H), 3.81 (s, 3H), 0.11 (s, 9H). **^{13}C NMR (126 MHz, $CDCl_3$):** δ 159.6, 141.9, 129.2, 119.5, 112.8, 112.1, 55.3, 53.0, -3.3. **FTIR (NaCl, thin film, cm^{-1}):** 3002, 2958, 1600, 1583, 1489, 1466, 1435, 1296, 1265, 1250, 1148, 1050, 882, 842. **HRMS (FAB, *m/z*):** calc'd for $C_{11}H_{17}ClOSi$ $[M+H]^+$: 229.0816; found: 229.0819.

(Chloro(4-methoxyphenyl)methyl)trimethylsilane (89h)

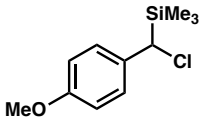

Prepared from 1-(chloromethyl)-4-methoxybenzene (2.7 mL, 20 mmol) and trimethylsilyl chloride (3.05 mL, 24 mmol) following General Procedure 1 using an inverse addition protocol. The reaction was also stirred for 1 hour following the addition. The crude residue was purified by fractional distillation (0.25 Torr, 85 °C) to yield 1.07 g (47% yield) of **89h** as a colorless oil which solidified in the freezer. Spectral data matched those reported in the literature.[81]

(Chloro(2-methoxyphenyl)methyl)trimethylsilane (89i)

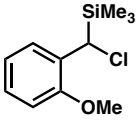

Prepared from 1-(chloromethyl)-2-methoxybenzene (700 μL, 5 mmol) and trimethylsilyl chloride (0.76 mL, 6 mmol) following General Procedure 1. The

crude residue was purified by column chromatography (silica, hexane to 10% Et_2O/hexane) to yield 633 mg (55% yield) of **89i** as a colorless oil. $\mathbf{R_f}$ = 0.67 (silica, 10% EtOAc/hexane, UV). **^{1}H NMR (500 MHz, $CDCl_3$):** δ 7.41 (dd, *J* = 7.6, 1.7 Hz, 1H), 7.18 (ddd, *J* = 8.2, 7.4, 1.7 Hz, 1H), 7.01 – 6.93 (m, 1H), 6.83 (dd, *J* = 8.2, 1.1 Hz, 1H), 4.98 (s, 1H), 3.81 (s, 3H), 0.09 (s, 9H). **^{13}C NMR (126 MHz, $CDCl_3$):** δ 155.5, 129.0, 128.8, 127.4, 120.7, 110.0, 55.3, 46.1, -3.3. **FTIR (NaCl, thin film, cm^{-1}):** 2958, 2837, 1598, 1585, 1488, 1464, 1438, 1289, 1245, 1101, 1051, 1030, 866, 842. **HRMS (EI, *m/z*):** calc'd for $C_{11}H_{17}ClOSi$ $[M+\cdot]^+$: 228.0737; found: 228.0738.

2.6.4.2 Alkenyl Bromide Electrophiles

General Procedure 2: Hydrozirconation/Bromination

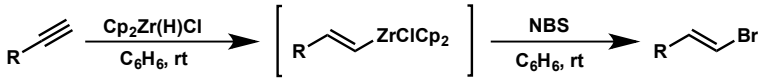

Adapted from a procedure by Zhou, Lin, and coworkers.[82] Schwartz's reagent (2.5 mmol, 1.25 equiv) was added to a flame-dried round bottom flask containing a magnetic stir bar in the glovebox and sealed under inert atmosphere (N_2). C_6H_6 (22 mL) was added via syringe, and the alkyne (2 mmol, 1 equiv) was added dropwise to the stirring mixture. The reaction was stirred for one hour and *N*-bromosuccinimide was added (2.5 mmol, 1.25 equiv). The reaction was stirred for one hour, and then diluted with Et_2O (150 mL). The solution was washed with brine and the organic layer was dried with Na_2SO_4, filtered, and concentrated under reduced pressure. The crude residue was dissolved in a 5% Et_2O/hexane solution, flushed through a silica plug, and concentrated to afford the desired product.

(*E*)-1-bromo-5-chloropent-1-ene (S2)

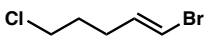

Prepared from 5-chloropent-1-yne (205 mg, 2 mmol, 1 equiv), Schwartz's reagent (645 mg, 2.5 mmol, 1.25 equiv), and N-bromosuccinimide (446 mg, 2.5 mmol, 1.25 equiv) following General Procedure 2. The crude residue was purified by filtration through a pad of silica (5% Et_2O/hexane) to yield 295 mg (80% yield) of **S2** as a colorless oil. Spectral data matched those reported in the literature.[83]

(*E*)-((5-bromopent-4-en-1-yl)oxy)(*tert*-butyl)dimethylsilane (S3)

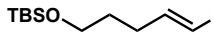

Prepared from *tert*-butyl(pent-4-yn-1-yloxy)dimethylsilane (3.95 g, 20 mmol, 1 equiv), Schwartz's reagent (7.2 g, 28 mmol, 1.4 equiv), and N-bromosuccinimide (5 g, 28 mmol, 1.4 equiv) following General Procedure 2. The crude residue was purified by filtration through a pad of silica (5% Et_2O/hexane) to yield 4.38 g (79% yield) of **S3** as a colorless oil. $\mathbf{R_f}$ = 0.38 (silica, hexane, $KMnO_4$). **^{1}H NMR (500 MHz, $CDCl_3$):** δ 6.18 (dt, *J* = 13.5, 7.3 Hz, 1H), 6.03 (dt, *J* = 13.5, 1.4 Hz, 1H), 3.61 (t, *J* = 6.2 Hz, 2H), 2.12 (qd, *J* = 7.3, 1.4 Hz, 2H), 1.65 – 1.57 (m, 2H), 0.90 (s, 9H), 0.05 (s, 6H). **^{13}C NMR (126 MHz, $CDCl_3$):** δ 137.9, 104.5, 62.1, 31.7, 29.5, 26.1, 18.5, -5.2. **FTIR (NaCl, thin film, cm^{-1}):** 2954, 2930, 2895, 2858, 1622, 1472, 1463, 1388, 1361, 1256, 1107, 1006, 937, 837. **HRMS (EI, m/z):** calc'd for $C_{11}H_{23}BrOSi$ $[M+H-H_2]^+$: 277.0623; found: 277.0608.

(*E*)-((6-bromohex-5-en-1-yl)oxy)(*tert*-butyl)dimethylsilane (S4)

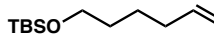

Prepared from *tert*-butyl(hex-5-yn-1-yloxy)dimethylsilane (2.5 g, 12 mmol, 1 equiv), Schwartz's reagent (4.4 g, 17.1 mmol, 1.45 equiv), and N-

bromosuccinimide (3.05 g, 17.1 mmol, 1.45 equiv) following General Procedure 2. The crude residue was purified by filtration through a pad of silica (5% Et_2O/hexane) to yield 2.5 g (72% yield) of **S4** as a colorless oil. $\mathbf{R_f}$ = 0.38 (silica, hexane, $KMnO_4$). **^{1}H NMR (500 MHz, $CDCl_3$):** δ 6.17 (dt, *J* = 13.8, 7.2 Hz, 1H), 6.02 (dt, *J* = 13.5, 1.2 Hz, 1H), 3.61 (t, *J* = 6.2 Hz, 2H), 2.07 (qd, *J* = 7.2, 1.4 Hz, 2H), 1.56 – 1.49 (m, 2H), 1.49 – 1.41 (m, 2H), 0.90 (d, *J* = 0.6 Hz, 9H), 0.06 (d, *J* = 0.6 Hz, 6H). **^{13}C NMR (126 MHz, $CDCl_3$):** δ 138.2, 104.4, 62.9, 32.9, 32.2, 26.1, 25.1, 18.5, -5.1. **FTIR (NaCl, thin film, cm^{-1}):** 2953, 2930, 2896, 2858, 1621, 1472, 1463, 1388, 1256, 1104, 1006, 938, 836, 812. **HRMS (FAB, *m/z*):** calc'd for $C_{12}H_{25}BrOSi$ $[M+H-H_2]^+$: 291.0780; found: 291.0773.

(*E*)-((7-bromohept-6-en-1-yl)oxy)(*tert*-butyl)dimethylsilane (S5)

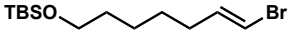

Prepared from *tert*-butyl(hept-6-yn-1-yloxy)dimethylsilane (2.27 g, 10 mmol, 1 equiv), Schwartz's reagent (3.6 g, 14 mmol, 1.4 equiv), and N-bromosuccinimide (2.5 g, 14 mmol, 1.4 equiv) following General Procedure 2. The crude residue was purified by filtration through a pad of silica (5% Et_2O/hexane) to yield 1.6 g (52% yield) of **S5** as a colorless oil. $\mathbf{R_f}$ = 0.28 (silica, hexane, $KMnO_4$). **^{1}H NMR (500 MHz, $CDCl_3$):** δ 6.16 (dt, *J* = 13.4, 7.3 Hz, 1H), 6.01 (dt, *J* = 13.4, 1.4 Hz, 1H), 3.60 (t, *J* = 6.5 Hz, 2H), 2.05 (qd, *J* = 7.2, 1.4 Hz, 2H), 1.55 – 1.48 (m, 2H), 1.46 – 1.38 (m, 2H), 1.38 – 1.30 (m, 2H), 0.90 (s, 9H), 0.05 (s, 6H). **^{13}C NMR (126 MHz, $CDCl_3$):** δ 138.3, 104.3, 63.2, 33.1, 32.7, 28.5, 26.1, 25.3, 18.5, -5.1. **FTIR (NaCl, thin film, cm^{-1}):** 1952, 2930, 2857, 1621, 1472, 1463, 1255, 1101, 938, 836. **HRMS (FAB, *m/z*):** calc'd for $C_{13}H_{27}BrOSi$ $[M+H-H_2]^+$: 305.0936; found: 305.0925.

(*E*)-1-(5-bromopent-4-en-1-yl)-1*H*-indole (29e)

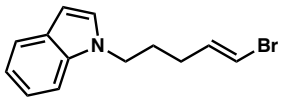

Prepared from 1-(pent-4-yn-1-yl)-1*H*-indole (356 mg, 2 mmol, 1 equiv), Schwartz's reagent (645 mg, 2.5 mmol, 1.25 equiv), and N-bromosuccinimide (451 mg, 2.5 mmol, 1.25 equiv) following General Procedure 2. The crude residue was purified by column chromatography (silica, 0 to 2% Et_2O/hexane) to yield 361 mg (52% yield) of **29e** as a colorless oil. Spectral data matched those reported in the literature.[84]

General Procedure 3: Silyl Ether Deprotection

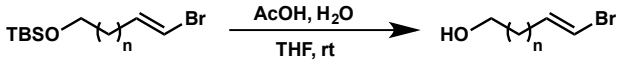

The alkenyl bromide (1.4 mmol, 1 equiv) was dissolved in a solution of acetic acid (3 mL), water (1 mL), and THF (1 mL) in a round bottom flask equipped with a magnetic stir bar, and stirred overnight at room temperature. The reaction was slowly added to a solution of $NaHCO_3$, extracted with Et_2O, dried with Na_2SO_4, filtered, and concentrated under reduced pressure. The crude material was purified by column chromatography (silica, Et_2O/hexanes).

(*E*)-5-bromopent-4-en-1-ol (S6)

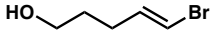

Prepared from **S3** (4.8 g, 15 mmol) following General Procedure 3. The crude residue was purified by column chromatography (silica, 30% Et_2O/hexane to 50% Et_2O/hexane) to yield 2.5 g (92% yield) of **S6** as a colorless oil. $\mathbf{R_f}$ = 0.64 (silica, 30% EtOAc/hexane, $KMnO_4$). **^{1}H NMR (500 MHz, $CDCl_3$):** δ 6.17 (dt, *J* = 13.5, 7.2 Hz, 1H), 6.05 (dt, *J* = 13.5, 1.4 Hz, 1H), 3.63 (t, *J* = 6.4 Hz, 2H), 2.14 (qd, *J* = 7.3, 1.4 Hz, 2H), 1.92

– 1.85 (m, 1H), 1.69 – 1.61 (m, 2H). **^{13}C NMR (126 MHz, $CDCl_3$):** δ 137.4, 104.8, 61.8, 31.5, 29.3. **FTIR (NaCl, thin film, cm^{-1}):** 3338, 2938, 2877, 1621, 1438, 1232, 1059, 940, 911. **HRMS (EI, *m/z*):** calc'd for C_5H_9BrO $[M+\cdot]^+$: 163.9837; found: 163.9846.

(*E*)-6-bromohex-5-en-1-ol (S7)

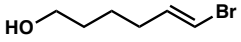

Prepared from **S4** (2.48 g, 8.5 mmol) following General Procedure 3. The crude residue was purified by column chromatography (silica, 30% Et_2O/hexane) to yield 1.15 g (76% yield) of **S7** as a colorless oil. $\mathbf{R_f}$ = 0.64 (silica, 30% EtOAc/hexane, $KMnO_4$). **^{1}H NMR (500 MHz, $CDCl_3$):** δ 6.17 (dt, *J* = 13.4, 7.2 Hz, 1H), 6.04 (dt, *J* = 13.5, 1.4 Hz, 1H), 3.65 (t, *J* = 6.4 Hz, 2H), 2.09 (qd, *J* = 7.2, 1.4 Hz, 2H), 1.63 – 1.55 (m, 2H), 1.54 – 1.45 (m, 2H), 1.27 (s, 1H). **^{13}C NMR (126 MHz, $CDCl_3$):** δ 137.9, 104.7, 62.7, 32.8, 32.1, 24.9. **FTIR (NaCl, thin film, cm^{-1}):** 3338, 2935, 2861, 1619, 1457, 1438, 1226, 1065, 943. **HRMS (EI, *m/z*):** calc'd for $C_6H_{11}BrO$ $[M+\cdot]^+$: 177.9993; found: 178.0008.

(*E*)-7-bromohept-6-en-1-ol (S8)

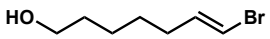

Prepared from **S5** (1.5 g, 5 mmol) following General Procedure 3. The crude residue was purified by column chromatography (silica, 30% Et_2O/hexane) to yield 684 mg (72% yield) of **S8** as a colorless oil. $\mathbf{R_f}$ = 0.73 (silica, 30% EtOAc/hexane, $KMnO_4$). **^{1}H NMR (500 MHz, $CDCl_3$):** δ 6.21 (dt, *J* = 13.5, 7.3 Hz, 1H), 6.06 (dt, *J* = 13.4, 1.4 Hz, 1H), 3.68 (t, *J* = 6.6 Hz, 2H), 2.11 (qd, *J* = 7.2, 1.4 Hz, 2H), 1.67 (s, 1H), 1.65 – 1.57 (m, 2H), 1.52 – 1.37 (m, 4H). **^{13}C NMR (126 MHz, $CDCl_3$):** δ 138.1, 104.4, 62.8, 33.0, 32.5, 28.5, 25.2. **FTIR (NaCl, thin film, cm^{-1}):** 3338, 2933, 2858, 1620, 1460, 1436,

1220, 1073, 1054, 935. **HRMS (FAB, *m/z*):** calc'd for $C_7H_{13}BrO$ $[M+H]^+$: 193.0223; found: 193.0228.

General Procedure 4: Aldehyde Formation

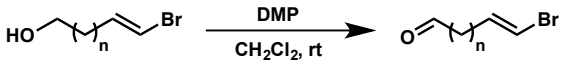

A flame-dried round bottom flask equipped with a magnetic stir bar was placed under inert atmosphere (N_2) and charged with the alcohol (4 mmol, 1 equiv). Anhydrous CH_2Cl_2 (24 mL) was added to the flask, followed by Dess-Martin periodinane (4.8 mmol, 1.2 equiv). The reaction was stirred at room temperature and monitored by TLC until it reached full conversion (approx. 2 hours). The reaction was quenched with aqueous $NaHCO_3$, extracted with Et_2O, dried with Na_2SO_4, filtered over a plug of silica with 50% Et_2O/hexane, and concentrated under reduced pressure to give the crude material.

(*E*)-6-bromohex-5-enal (S9)

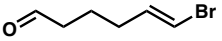

Prepared from **S7** (718 mg, 4 mmol) following General Procedure 4 to yield 689 mg (97% yield) of **S9** as a yellow oil. The crude residue was used in the next step without further purification. $\mathbf{R_f}$ = 0.24 (silica, 10% EtOAc/ hexane, $KMnO_4$). **^{1}H NMR (500 MHz, $CDCl_3$):** δ 9.76 (t, *J* = 1.5 Hz, 1H), 6.16 – 6.10 (m, 1H), 6.05 (dt, *J* = 13.5, 1.2 Hz, 1H), 2.46 (td, *J* = 7.2, 1.5 Hz, 2H), 2.09 (qd, *J* = 7.3, 1.2 Hz, 2H), 1.74 (p, *J* = 7.3 Hz, 2H). **^{13}C NMR (126 MHz, $CDCl_3$):** δ 201.9, 136.9, 105.5, 42.9, 32.2, 21.0. **FTIR (NaCl, thin film, cm^{-1}):** 2936, 2826, 2724, 1817, 1724, 1620, 1440, 1452, 1410, 1390, 1231, 1043, 945. **HRMS (FAB, *m/z*):** calc'd for C_6H_9BrO $[M+H]^+$: 176.9915; found: 176.9909.

(*E*)-7-bromohept-6-enal (S10)

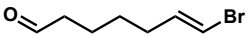

Prepared from **S8** (382 mg, 2 mmol) following General Procedure 4 to yield 413 mg (72% yield) of **S10** as a yellow oil. The crude residue was used in the next step without further purification. $\mathbf{R_f}$ = 0.28 (silica, 10% EtOAc/ hexane, $KMnO_4$). **^{1}H NMR (500 MHz, $CDCl_3$):** δ 9.76 (t, *J* = 1.6 Hz, 1H), 6.15 (dt, *J* = 13.5, 7.2 Hz, 1H), 6.03 (dt, *J* = 13.5, 1.3 Hz, 1H), 2.44 (td, *J* = 7.3, 1.6 Hz, 2H), 2.07 (qd, *J* = 7.3, 1.4 Hz, 2H), 1.68 – 1.59 (m, 2H), 1.47 – 1.39 (m, 2H). **^{13}C NMR (126 MHz, $CDCl_3$):** δ 202.4, 137.5, 104.8, 43.7, 32.8, 28.2, 21.4. **FTIR (NaCl, thin film, cm^{-1}):** 2934, 2722, 1724, 1620, 1459, 1390, 1224, 938. **HRMS (FAB, *m/z*):** calc'd for $C_7H_{11}BrO$ $[M+H]^+$: 191.0072; found: 191.0076.

General Procedure 5: Acetal Formation

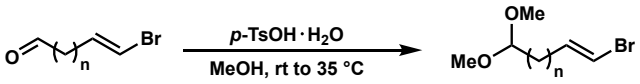

To a 20 mL scintillation vial equipped with a magnetic stir bar were added the aldehyde (2 mmol, 1 equiv), *p*-toluenesulfonic acid monohydrate (1 mmol, 0.5 equiv), and methanol (5.5 mL). The vial was sealed with a Teflon screw-cap, and stirred at 35 °C. The reaction was monitored by TLC until the reaction had reached full completion. The reaction was quenched with aqueous $NaHCO_3$, extracted with Et_2O, dried with $MgSO_4$, filtered, and concentrated under reduced pressure. The crude material was purified by column chromatography (silica, ether/hexanes). *Note: It is important to immediately quench the reaction upon removal from the stir plate. Hydrolysis of the product to the aldehyde proceeds upon standing at room temperature.*

(*E*)-1-bromo-6,6-dimethoxyhex-1-ene (29f)

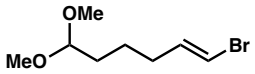

Prepared from **S9** (356 mg, 2 mmol) following General Procedure 5. The crude residue was purified by column chromatography (silica, 10% Et_2O/hexane to 30% Et_2O/hexane) to yield 410 mg (91% yield) of **29f** as a light yellow oil. $\mathbf{R}_f$ = 0.32 (silica, 10% EtOAc/hexane, $KMnO_4$). **^{1}H NMR (500 MHz, $CDCl_3$):** δ 6.15 (dt, *J* = 13.5, 7.2 Hz, 1H), 6.03 (dt, *J* = 13.5, 1.4 Hz, 1H), 4.35 (t, *J* = 5.6 Hz, 1H), 3.31 (s, 6H), 2.07 (qd, *J* = 7.3, 1.4 Hz, 2H), 1.63 – 1.57 (m, 2H), 1.50 – 1.42 (m, 2H). **^{13}C NMR (126 MHz, $CDCl_3$):** δ 137.8, 104.7, 104.3, 52.9, 32.8, 31.9, 23.7. **FTIR (NaCl, thin film, cm^{-1}):** 2949, 2830, 1440, 1621, 1458, 1439, 1386, 1193, 1162, 1128, 1071, 943. **HRMS (EI, *m/z*):** calc'd for $C_8H_{15}BrO_2$ $[M+H–H_2]^+$: 221.0177; found: 221.0172.

(*E*)-1-bromo-7,7-dimethoxyhept-1-ene (29g)

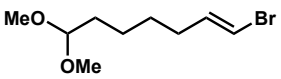

Prepared from **S10** (382 mg, 2 mmol) following General Procedure 5. The crude residue was purified by column chromatography (silica, 10% Et_2O/hexane to 30% Et_2O/hexane) to yield 421 mg (89% yield) of **29g** as a light yellow oil. $\mathbf{R}_f$ = 0.32 (silica, 10% EtOAc/hexane, $KMnO_4$). **^{1}H NMR (500 MHz, $CDCl_3$):** δ 6.21 (dt, *J* = 13.5, 7.2 Hz, 1H), 6.06 (dt, *J* = 13.5, 1.4 Hz, 1H), 4.40 (t, *J* = 5.7 Hz, 1H), 3.36 (s, 6H), 2.10 (qd, *J* = 7.2, 1.4 Hz, 2H), 1.68 – 1.61 (m, 2H), 1.52 – 1.36 (m, 4H). **^{13}C NMR (126 MHz, $CDCl_3$):** δ 138.0, 104.5, 104.4, 52.8, 33.0, 32.3, 28.6, 24.1. **FTIR (NaCl, thin film, cm^{-1}):** 2986, 2944, 2860, 2830, 1621, 1459, 1386, 1364, 1192, 1158, 1128, 1076, 1052, 937. **HRMS (EI, *m/z*):** calc'd for $C_9H_{17}BrO_2$ $[M+H–H_2]^+$: 235.0334; found: 235.0311.

General Procedure 6: Alkenyl Bromides from Aldehydes

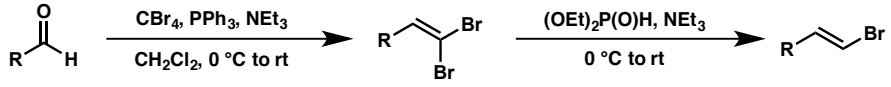

General Procedure 6, Part A: Following a procedure by Alexakis and coworkers,[85] a flame dried round bottom flask equipped with a magnetic stir bar was charged with tetrabromomethane (20 mmol, 2 equiv) and triphenylphosphine (40 mmol, 4 equiv) while under inert atmosphere (N_2). The flask was cooled to 0 °C and CH_2Cl_2 (30 mL) was added, followed by the triethylamine (10 mmol, 1 equiv). The aldehyde (10 mmol, 1 equiv) was dissolved in CH_2Cl_2 (5 mL) and added dropwise to the reaction mixture. The reaction was warmed to room temperature and stirred for 90 minutes. The reaction was removed from the stir plate and slowly added to a vigorously stirring solution of Et_2O (150 mL) and hexane (150 mL), filtered, and concentrated under reduced pressure. The crude residue was purified by column chromatography (silica, ether/hexanes) to afford the dibromoalkene.

5-(2,2-dibromovinyl)-2-methoxypyridine (S11)

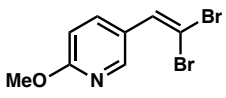

Prepared from 6-methoxynicotinaldehyde (1.36 g, 10 mmol) following General Procedure 6A. The crude residue was purified by column chromatography (silica, 1% Et_2O/hexane to 10% Et_2O/hexane) to yield 570 mg (20% yield) of **S11** as a yellow oil. $\mathbf{R_f}$ = 0.48 (silica, 10% EtOAc/hexane) **^{1}H NMR (500 MHz, $CDCl_3$):** δ 8.25 (dt, *J* = 2.4, 0.6 Hz, 1H), 7.90 (ddd, *J* = 8.7, 2.5, 0.6 Hz, 1H), 7.37 (q, *J* = 0.6 Hz, 1H), 6.74 (dt, *J* = 8.7, 0.5 Hz, 2H), 3.94 (s, 3H) **^{13}C NMR (126 MHz, $CDCl_3$):** δ 163.8, 147.6, 137.8, 133.5, 124.9, 110.7, 89.3, 53.8 **FTIR (NaCl, thin film, cm^{-1}):** 2982, 2946,

1603 1595, 1561, 1491, 1381, 1309, 1289, 1254, 1132, 1024, 1014, 867, 819 **HRMS (ESI-TOF, m/z):** calc'd for $C_8H_7NOBr_2$ $[M+H]^+$: 291.8973; found: 291.8967.

5-(2,2-dibromovinyl)-2-methoxypyrimidine (S12)

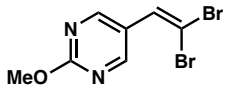

Prepared from 2-methoxypyrimidine-5-carbaldedyde (966 mg, 7 mmol) following General Procedure 6A. The crude residue was purified by column chromatography (silica, 30% Et_2O/hexane to 50% Et_2O/hexane) to yield 1.5 g (74% yield) of **S12** as a light yellow solid. $\mathbf{R_f}$ = 0.63 (silica, 25% EtOAc/ hexane, UV). **m.p.** = 62-63 °C **^{1}H NMR (500 MHz, $CDCl_3$):** δ 8.70 (d, *J* = 0.6 Hz, 2H), 7.33 (t, *J* = 0.6 Hz, 1H), 4.03 (s, 3H). **^{13}C NMR (126 MHz, $CDCl_3$):** δ 164.8, 158.7, 130.4, 123.8, 92.1, 55.4. **FTIR (NaCl, thin film, cm^{-1}):** 2991, 1589, 1549, 1524, 1473, 1412, 1391, 1338, 1291, 1233, 1046, 1028, 951, 812, 835. **HRMS (ESI-TOF, m/z):** calc'd for $C_7H_6N_2OBr_2$ $[M+H]^+$: 292.8920; found: 292.8950.

2-(2,2-dibromovinyl)furan (S13)

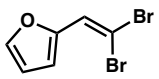

Prepared from furfural (1.9 g, 20 mmol) following General Procedure 6A. The crude residue was purified by column chromatography (silica, hexane) to yield 3.3 g (66% yield) of **S13** as a yellow oil. Spectral data matched those reported in the literature.[86]

General Procedure 6, Part B: The dibromoalkene (1.7 mmol, 1 equiv) and diethyl phosphite (5.1 mmol, 3 equiv) were added to a vial with a magnetic stirring rod and placed under an inert atmosphere (N_2). The solution was cooled to 0 °C and triethylamine (5.1 mmol, 3 equiv) was added dropwise. The reaction was warmed to room temperature and

stirred overnight. The reaction was quenched with water (5 mL) and extracted with CH_2Cl_2 (20 mL). The organic layer was washed with brine (5 mL), dried with Na_2SO_4, filtered, and concentrated under reduced pressure. The crude residue was purified by column chromatography (silica, ether/hexanes) to afford the vinyl bromide.

(*E*)-5-(2-bromovinyl)-2-methoxypyridine (29k)

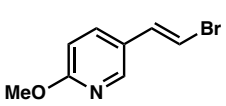

Prepared from **S11** (500 mg, 1.7 mmol) following General Procedure 6B. The crude residue was purified by column chromatography (silica, 2% Et_2O/hexane to 5% Et_2O/hexane) to yield 314 mg (86% yield, 96:4 *E*:*Z*) of **29k** as a white solid. $\mathbf{R_f}$ = 0.46 (silica, 10% EtOAc/hexane). **m.p.** = 53-56 °C **^{1}H NMR (500 MHz, $CDCl_3$):** δ 8.05 (d, *J* = 2.5 Hz, 1H), 7.54 (ddd, *J* = 8.7, 2.5, 0.4 Hz, 1H), 7.02 (dq, *J* = 14.0, 0.5 Hz, 1H), 6.70 (dt, *J* = 8.7, 0.6 Hz, 1H), 6.65 (d, *J* = 14.0 Hz, 1H), 3.93 (s, 3H). **^{13}C NMR (126 MHz, $CDCl_3$):** δ 164.0, 145.3, 135.3, 133.5, 125.5, 111.4, 105.5, 53.7. **FTIR (NaCl, thin film, cm^{-1}):** 3061, 2943, 1613, 1598, 1562, 1490, 1385, 1303, 1285, 1258, 1238, 1026, 1015, 947, 837. **HRMS (ESI-TOF, m/z):** calc'd for C_8H_8NOBr $[M+H]^+$: 213.9868; found: 213.9858.

(*E*)-5-(2-bromovinyl)-2-methoxypyrimidine (29l)

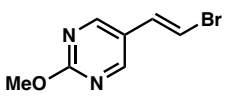

Prepared from **S12** (880 mg, 3 mmol) following General Procedure 6B. The crude residue was purified by column chromatography (silica, 5% Et_2O/hexane to 30% Et_2O/hexane) to yield 473 mg (73% yield, 97:3 *E*:*Z*) of **29l** as a white solid. $\mathbf{R_f}$ = 0.60 (silica, 25% EtOAc/ hexane, UV). **m.p.** = 89-90 °C **^{1}H NMR (500 MHz, $CDCl_3$):** δ 8.46 (s, 2H), 6.99 (dt, *J* = 14.2, 0.5 Hz, 1H), 6.79 (d, *J* = 14.2 Hz, 1H),

4.01 (d, J = 0.5 Hz, 3H). **^{13}C NMR (126 MHz, $CDCl_3$):** δ 165.2, 156.5, 130.2, 124.1, 107.7, 55.3. **FTIR (NaCl, thin film, cm^{-1}):** 3057, 2993, 1593, 1553, 1479, 1414, 1388, 1339, 1290, 1248, 1186, 1049, 1030, 951, 909, 803. **HRMS (ESI-TOF, m/z):** calc'd for $C_7H_7N_2OBr$ $[M+H]^+$: 214.9820; found: 214.9803.

(*E*)-2-(2-bromovinyl)furan (29q)

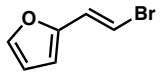

Prepared from **S13** (3.3 g, 13.1 mmol) following General Procedure 6B. The crude residue was purified by column chromatography (silica, hexane) to yield 400 mg (18% yield, *E* isomer) of **29q** as a yellow oil. **Note:** It is possible to separate the E and Z vinyl bromide isomers by column chromatography. The E isomer has a higher R_f than the Z isomer. Careful column separation eliminates the need for base mediated isomerization of the Z olefin, a lower yielding procedure (8% yield), typically employed in previous studies.[50] Spectral data matched those reported in the literature.[85]

Other Alkenyl Bromides

Alkenyl bromides **29o** and **29p** were purchased from commercial sources (Sigma Aldrich).

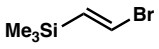

29o

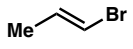

29p

Alkenyl bromides **86**, **29a**, **29c**, **29d**, **29i**, and **29j** were prepared according to literature procedures reported and referenced by Reisman and coworkers.[50]

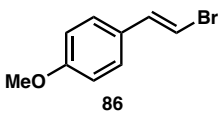

86

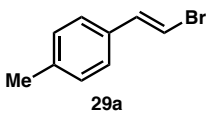

29a

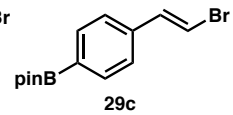

29c

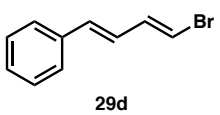

29d

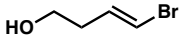

29i

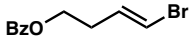

29j

Alkenyl bromide **29b** was prepared according to a literature procedure reported by Buchwald and coworkers.[87]

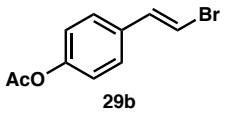

29b

Alkenyl bromide **29r** was prepared according to a literature procedure reported by Roy and coworkers.[88]

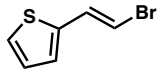

29r

(*E*)-1-bromo-4-chlorobut-1-ene (S14)

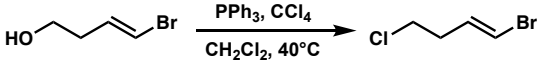

To a 10 mL round bottom flask equipped with a magnetic stir bar was added (*E*)-4-bromobut-3-en-1-ol (363 mg, 2.4 mmol, 1.0 equiv), PPh_3 (944 mg, 3.6 mmol, 1.5 equiv), CCl_4 (480 mL, 4.8 mmol, 2.0 equiv) and 2 mL of CH_2Cl_2. The reaction was stirred at overnight at 40 °C for 10 hours. After cooling to room temperature, the crude mixture was poured into pentane, filtered through a plug of silica gel with additional pentane, and concentrated under reduced pressure to afford 276 mg (68% yield) of **S14** as a colorless oil. $\mathbf{R_f}$ = 0.49 (silica, hexane, $KMnO_4$). **^{1}H NMR (500 MHz, $CDCl_3$):** δ 6.24 – 6.16 (m, 2H), 3.54 (t, *J* = 6.7 Hz, 2H), 2.57 – 2.47 (m, 2H). **^{13}C NMR (126 MHz, $CDCl_3$):** δ 133.7, 107.7, 43.0, 36.0. **FTIR (NaCl, thin film, cm^{-1}):** 3066, 2960, 1622, 1444, 1425, 1300, 1283, 1247, 1232, 1218, 937, 906. **HRMS (EI, *m/z*):** calc'd for C_4H_6BrCl $[M+\cdot]^+$: 169.9312; found: 169.9299.

(*E*)-1-bromo-5-iodopent-1-ene (S15)

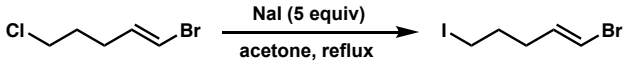

Alkyl chloride **S2** (1.96 g, 10.5 mmol, 1 equiv) and sodium iodide (7.49 g, 50 mmol, 5 equiv) were added to a 100 mL round bottom flask equipped with a magnetic stir bar and dissolved in 30 mL acetone. The reaction was refluxed overnight for 14 hours and then cooled to room temperature. Hexanes was added to the reaction to precipitate out the remaining NaI, and the mixture was filtered through a plug of silica gel with additional hexane. The solution was concentrated to obtain 2.47 g (90% yield) of **S15** as a yellow oil (*approximately 9% alkyl chloride remains*). $\mathbf{R_f}$ = 0.31 (silica, hexane, $KMNO_4$). **^{1}H NMR (500 MHz, $CDCl_3$):** δ 6.17 – 6.05 (m, 2H), 3.18 (t, *J* = 6.8 Hz, 2H), 2.18 (dddd, *J* = 7.4, 5.9, 4.3, 1.9 Hz, 2H), 1.91 (p, *J* = 6.7 Hz, 2H). **^{13}C NMR (126 MHz, $CDCl_3$):** δ 135.8, 105.9, 33.5, 31.9, 5.8. **FTIR (NaCl, thin film, cm^{-1}):** 2933, 2838, 1622, 1427, 1312, 1293, 1268, 1231, 1202, 1166, 936. **HRMS (FAB, *m/z*):** calc'd for C_5H_8BrI $[M+\cdot]^+$: 273.8854; found: 273.8862.

(*E*)-1-(5-bromopent-4-en-1-yl)pyrrolidine-2,5-dione (29m)

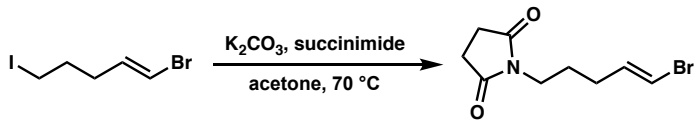

Alkyl iodide **S15** (275 mg, 1.0 mmol, 1.0 equiv), succinimide (99 mg, 1.0 mmol, 1.0 equiv), and K_2CO_3 (691 mg, 5.0 mmol, 5.0 equiv) were added to 20 mL scintillation vial equipped with a cross-shaped stir bar and dissolved in 3 mL of acetone. The vial was sealed with a Teflon cap and stirred at 70 °C for 4 hours. The reaction was cooled to room temperature,

quenched with H_2O, and extracted with EtOAc (2x). The combined organic layers were dried with Na_2SO_4, filtered, and concentrated under reduced pressure. The crude residue was purified by column chromatography (silica, hexane to 40% acetone/hexanes) to yield 169 mg (69% yield) of **29m** as a colorless oil. $\mathbf{R_f}$ = 0.47 (silica, 30% acetone/hexane, CAM). **^{1}H NMR (500 MHz, $CDCl_3$):** δ 6.13 (dt, *J* = 13.6, 6.8 Hz, 1H), 6.07 (dt, *J* = 13.5, 1.1 Hz, 1H), 3.51 (dd, *J* = 7.7, 6.7 Hz, 2H), 2.70 (s, 4H), 2.10 – 2.03 (m, 2H), 1.69 (p, *J* = 7.2 Hz, 2H). **^{13}C NMR (126 MHz, $CDCl_3$):** δ 177.4, 136.6, 105.4, 38.2, 30.5, 28.3, 26.4. **FTIR (NaCl, thin film, cm^{-1}):** 2941, 1774, 1697, 1621, 1438, 1402, 1343, 1250, 1206, 1151, 1104, 940, 820. **HRMS (FAB, *m/z*):** calc'd for $C_9H_{12}BrNO_2$ $[M+H]^+$: 246.0130; found: 246.0123.

(*E*)-1-(5-bromopent-4-en-1-yl)pyrrolidin-2-one (29n)

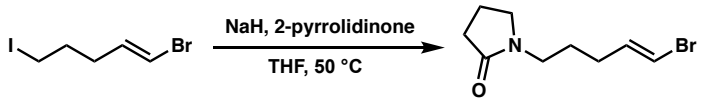

In the glovebox, sodium hydride (91 mg, 95% in mineral oil, 3.6 mmol, 1.2 equiv) was added to a flame-dried 50 mL round bottom flask equipped with a stir bar and sealed with a rubber septum. The flask was removed from the glovebox, 10 mL THF was added under an inert (N_2) atmosphere, and the solution was cooled to 0 °C. 2-pyrrolidinone (225 mg, 228 mL, 3.0 mmol, 1.0 equiv) was added dropwise and stirred for 10 minutes. Alkyl iodide **S15** (825 mg, 3.0 mmol, 1.0 equiv) was added and the reaction was heated to 50 °C and stirred for 15 hours. The reaction was cooled to room temperature, quenched with H_2O, and extracted with EtOAc (2x). The combined organic layers were dried with Na_2SO_4, filtered, and concentrated under reduced pressure. The crude residue was purified by

column chromatography (silica, hexane to 40% acetone/hexanes) to yield 476 mg (68% yield) of **29n** as a colorless oil. $\mathbf{R_f}$ = 0.31 (silica, 30% acetone/hexane, CAM). **^{1}H NMR (500 MHz, $CDCl_3$):** δ 6.12 (dt, *J* = 13.4, 7.1 Hz, 1H), 6.03 (dt, *J* = 13.5, 1.3 Hz, 1H), 3.36 – 3.31 (m, 2H), 3.25 (t, *J* = 7.2 Hz, 2H), 2.35 (t, *J* = 8.1 Hz, 2H), 2.06 – 1.95 (m, 4H), 1.64 – 1.56 (m, 2H). **^{13}C NMR (126 MHz, $CDCl_3$):** δ 175.1, 136.9, 105.1, 47.2, 41.9, 31.1, 30.4, 26.2, 17.9. **FTIR (NaCl, thin film, cm^{-1}):** 2928, 2863, 1682, 1620, 1494, 1462, 1426, 1287, 1262, 940. **HRMS (FAB, *m/z*):** calc'd for $C_9H_{14}BrNO$ $[M+H]^+$: 232.0337; found: 232.0333.

(*E*)-((3-bromoallyl)oxy)(*tert*-butyl)dimethylsilane (29s)

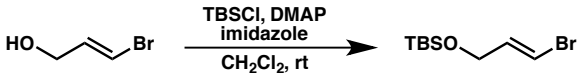

To a round bottom flask were added *tert*-butyldimethylsilyl chloride (514 mg, 3.3 mmol, 1.1 equiv), 4-dimethylaminopyridine (48 mg, 0.3 mmol, 0.1 equiv), imidazole (409 mg, 6 mmol, 2 equiv), and (*E*)-3-bromoprop-2-en-1-ol (411 mg, 3 mmol, 1 equiv) and the flask was placed under N_2. The solids were dissolved in CH_2Cl_2 (8 mL) and stirred overnight at room temperature. The reaction was quenched with aqueous NH_4Cl (3 mL), diluted with pentane (12 mL), and the layers were separated. The organic layer was washed with water (2 x 3 mL) and brine (3 mL), then dried with $MgSO_4$, filtered, and concentrated under reduced pressure. The crude material was purified by column chromatography (silica, pentane) to yield 684 mg of **29s** (91% yield) as a colorless oil. Spectral data matched those reported in the literature.[89]

(*S*,*E*)-1-bromo-3,7-dimethylocta-1,6-diene (29t)

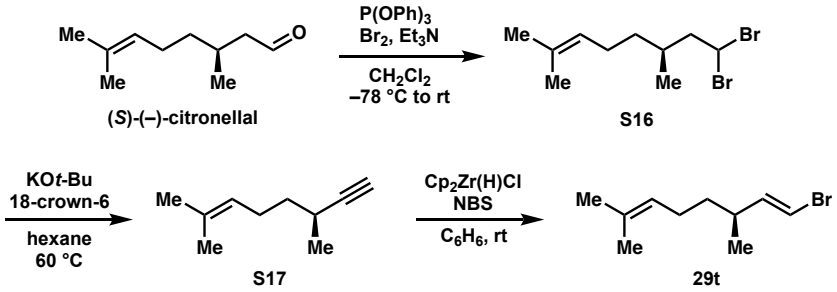

Similar to a route by Shenvi and co-workers,[90] the alkenyl bromide **29t** was prepared in three steps from enantiomerically pure (*S*)-(–)-citronellal.

Part A: Triphenylphosphite (9.8 mL, 37.5 mmol, 1.5 equiv) was added to a flame-dried 1 L flask with a magnetic stir bar and dissolved in anhydrous CH_2Cl_2 under an inert atmosphere (N_2). The flask was cooled to –78 °C and bromine (1.7 mL, 32.5 mmol, 1.3 equiv) and triethylamine (10.5 mL, 75 mmol, 3 equiv) were successively added dropwise. Citronellal (4.5 mL, 25 mmol, 1 equiv) was dissolved in CH_2Cl_2 (25 mL) and added dropwise. The reaction was warmed to room temperature and stirred for 2 hours then was concentrated under reduced pressure. Pentane was added to the crude residue and filtered through a pad of silica with pentane. The solution was concentrated under reduced pressure to yield 6.7 g (90% yield) of **S16** as a mixture of the dibromide and *cis*/*trans* vinyl bromide. The crude material was used in the next step without further purification. The ^{1}H NMR spectrum of the dibromide **S16** matches that reported in the literature.[90]

Part B: A flame-dried 500 mL round bottom flask with a magnetic stir bar was charged with potassium *tert*-butoxide (3.37 g, 30 mmol, 3 equiv) and sealed under inert atmosphere (N_2). Dry hexanes (250 mL) and 18-crown-6 (220 mg, 0.8 mmol, 0.08 equiv) were added

and the suspension was vigorously stirred. Dibromide **S16** (2.98 g, 10 mmol, 1 equiv) was added and the reaction was heated to 60 °C and refluxed for 8 hours. The reaction was quenched with water, extracted with hexane, and concentrated under reduced pressure. The crude material was filtered through a pad of silica with pentane to afford 1.15 g (85% yield) of **S17** as a mixture of the alkyne and vinyl bromide (>99% *E*-isomer). The crude material was used in the next step without further purification. The ^{1}H NMR spectra of **S17** matches that which is reported in the literature.[90]

Part C: Prepared from **S17** (1.15 g, 8.4 mmol, 1 equiv), Schwartz's reagent (2.7 g, 10.5 mmol, 1.25 equiv), and N-bromosuccinimide (1.87 g, 10.5 mmol, 1.25 equiv) following General Procedure 2. The crude residue was purified by column chromatography (silica, hexane) to yield 862 mg (47% yield, 95% pure) of **29t** as a colorless oil. $\mathbf{R_f}$ = 0.77 (silica, hexane, $KMnO_4$). $[\boldsymbol{\alpha}]_{\boldsymbol{D}}^{\mathbf{25}}$ = +54° (c = 1.0, $CHCl_3$). **^{1}H NMR (500 MHz, $CDCl_3$):** δ 6.06 (dd, *J* = 13.5, 8.1 Hz, 1H), 5.98 (dd, *J* = 13.6, 0.6 Hz, 1H), 5.06 (tdq, *J* = 7.2, 2.9, 1.5 Hz, 1H), 2.18 (ddt, *J* = 14.8, 13.6, 6.8 Hz, 1H), 1.96 (ddddd, *J* = 9.3, 8.2, 7.1, 2.1, 1.1 Hz, 2H), 1.69 (p, *J* = 1.5 Hz, 3H), 1.60 (d, *J* = 1.3 Hz, 3H), 1.37 – 1.30 (m, 2H), 1.01 (d, *J* = 6.8 Hz, 3H). **^{13}C NMR (126 MHz, $CDCl_3$):** δ 143.6, 131.8, 124.0, 103.2, 37.4, 36.4, 25.7, 25.6, 20.0, 17.8. **FTIR (NaCl, thin film, cm^{-1}):** 2964, 2926, 2916, 2871, 2853, 1618, 1458, 1376, 1278, 1206, 1108, 941. **HRMS (EI, m/z):** calc'd for $C_{10}H_{17}Br$ $[M+\cdot]^+$: 216.0514; found: 216.0510.

2.6.4.3 Oxygen-Based Electrophiles

Phenyl(trimethylsilyl)methyl methanesulfonate (104)

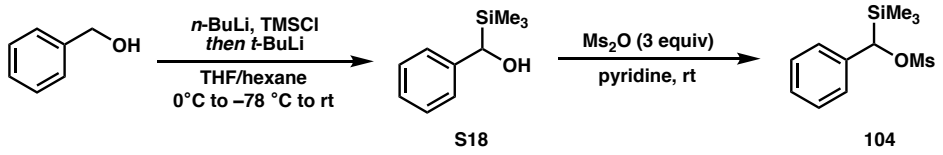

Part A: Adapted from a procedure by Maleczka and coworkers.[91] Benzyl alcohol (1 mL, 10 mmol, 1 equiv) was added to a flame-dried 200 mL round bottom flask and dissolved in 20 mL of THF. The reaction was cooled to 0 °C and *n*-BuLi (4.4. mL, 2.5 M in hexane, 11 mmol, 1.1 equiv) was added dropwise. The reaction was stirred for 15 min, then TMSCl (1.4 mL, 11.0 mmol, 1.1 equiv) was added dropwise and stirred for an additional 15 min. The flask was cooled to –78 °C and *t*-BuLi (7.5 mL, 1.7 M in pentane, 13.0 mmol, 1.3 equiv) was added dropwise. The reaction was warmed to room temperature and stirred for 1 hour. The reaction was quenched with sat. NH_4Cl (40 mL) and extracted with Et_2O (80 mL). The organic layer was washed with water (40 mL) and brine (40 mL), then dried with $MgSO_4$, filtered, and concentrated under reduced pressure. The crude material was purified by column chromatography (silica, 0 to 15% EtOAc/ hexane) to yield 1.3 g (73% yield) of **S188** as a colorless oil. Spectral data matched those reported in the literature.[91]

Part B: The benzyl alcohol **S18** (288 mg, 1.6 mmol, 1 equiv) was added to a 10 mL round bottom flask containing a magnetic stir bar and put under an inert atmosphere (N_2). Pyridine (1.0 mL) was added followed by methanesulfonic anhydride (442 mg, 2.5 mmol, 1.7 equiv). The reaction was stirred for 4 hours at room temperature, at which time an additional portion of methanesulfonic anhydride (1.3 equiv) was added, and the reaction

was stirred two more hours. The milky suspension was quenched with water (5 mL) and extracted with EtOAc (2 x 10 mL). The combined organic layers were washed with water (10 mL) and brine (2 x 10 mL), dried with $MgSO_4$, filtered, and concentrated under reduced pressure. The crude material was purified by column chromatography (florisil, 0 to 10% EtOAc/hexane) to yield 176 mg (43% yield) of **104** as a white solid. $\mathbf{R_f}$ = 0.19 (silica, 10% EtOAc/hexane, CAM). **m.p.** = 71-72 °C **^{1}H NMR (500 MHz, $CDCl_3$):** δ 7.38 – 7.33 (m, 2H), 7.28 – 7.24 (m, 1H), 7.23 – 7.19 (m, 2H), 5.38 (s, 1H), 2.66 (s, 3H), 0.09 (s, 9H). **^{13}C NMR (126 MHz, $CDCl_3$):** δ 137.8, 128.9, 127.5, 125.9, 81.0, 39.2, -4.0. **FTIR (NaCl, thin film, cm^{-1}):** 2959, 1357, 1251, 1174, 973, 933, 913, 864, 844, 827. **HRMS (FAB, *m/z*):** calc'd for $C_{11}H_{18}O_3SSi$ $[M+H-H_2]^+$: 257.0668; found: 257.0670.

(*E*)-4-methylstyryl trifluoromethanesulfonate (105)

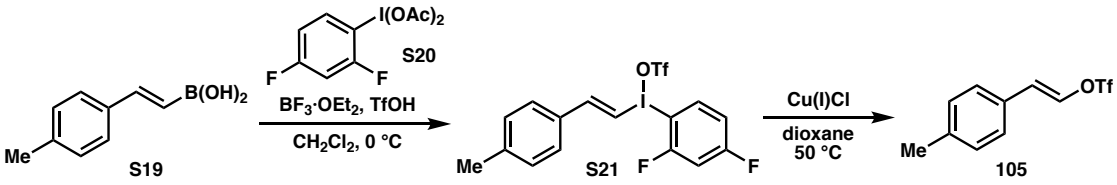

The alkenyl triflate was prepared from the corresponding alkenyl boronic acid according to a procedure by Sigman and coworkers.[92] Spectral data matched those reported in the literature.[92]

2.6.5 Enantioselective Reductive Cross-Couplings

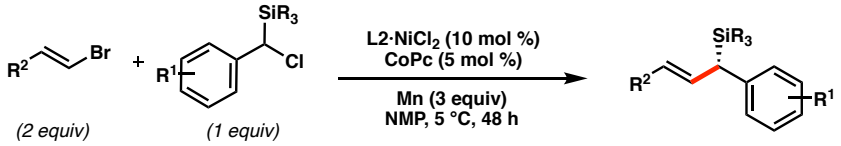

General Procedure 7: Reaction on 0.2 mmol scale.

On the bench-top, a 2 dram vial was equipped with a stir bar and the alkenyl bromide (0.4 mmol, 2 equiv), **L2**·$NiCl_2$ complex (9.7 mg, 0.02 mmol, 0.10 equiv), Mn powder (33.0 mg, 0.6 mmol, 3 equiv), and cobalt phthalocyanine (5.7 mg, 0.01 mmol, 0.05 equiv) were added. The vial was brought into a N_2-filled glovebox and the vial was charged with NMP (0.4 mL, 0.5 M) and the chlorobenzyl silane (0.2 mmol, 1 equiv). The vial was sealed with a Teflon cap and stirred at 250 rpm at 5 °C in a temperature-controlled well plate for 2 days. The crude reaction was brought out of the glove box, diluted with 2 mL H_2O, slowly quenched with 1 mL of 1 M HCl, and further diluted with water (10 mL). The aqueous layer was extracted with diethyl ether (3 x 20 mL) and the combined organic layers were washed with brine (15 mL), dried with $MgSO_4$, filtered, and concentrated under reduced pressure. The crude material was purified by column chromatography to afford the desired product. **Notes:** In order to efficiently remove the viscous contents from the vial, it is useful to fill the vial ¾ full with an extraction solvent, screw on the Teflon cap, and shake vigorously with the stir bar inside. Removal of blue CoPc stains from glassware was accomplished by scrubbing with Alconox soap solution. Removal of blue CoPc stains from stir bars was accomplished using conc. HNO_3.

Assignment of Absolute Stereochemistry

The absolute stereochemistry of **91c** was assigned by single crystal X-ray diffraction. The absolute stereochemistry of **S22** was assigned by comparing the optical rotation of the purified product to the literature value. All other chiral allylic silane products were assigned by analogy.

Characterization of Reaction Products

(*S*,*E*)-(3-(4-methoxyphenyl)-1-phenylallyl)trimethylsilane (88c)

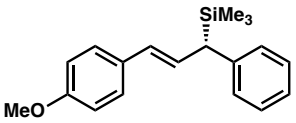

From (chloro(phenyl)methyl)trimethylsilane 87. Prepared from (*E*)-1-(2-bromovinyl)-4-methoxybenzene (**86**, 85.2 mg, 0.4 mmol) and (chloro(phenyl)methyl)trimethylsilane (**87**, 39.8 mg, 0.2 mmol) according to General Procedure 7. The crude residue was purified by column chromatography (silica, 0 to 2% Et_2O/hexane) to yield **88c** (42.4 mg, 71% yield) in 95% ee as a colorless oil. $\mathbf{R_f}$ = 0.61 (silica, 10% EtOAc/hexane, UV). **Chiral SFC:** (AD-H, 2.5 mL/min, 20% IPA in CO_2, λ = 280 nm): t_R (minor) = 3.0 min, t_R (major) = 3.9 min. $[\boldsymbol{\alpha}]_{\boldsymbol{D}}^{\mathbf{25}}$ = +27° (c = 1.0, $CHCl_3$). **^{1}H NMR (500 MHz, $CDCl_3$):** δ 7.36 – 7.29 (m, 4H), 7.21 – 7.13 (m, 3H), 6.91 – 6.84 (m, 2H), 6.49 (dd, *J* = 15.6, 9.9 Hz, 1H), 6.35 (d, *J* = 15.6 Hz, 1H), 3.82 (d, *J* = 0.5 Hz, 3H), 3.13 (d, *J* = 9.8 Hz, 1H), 0.05 (d, *J* = 0.6 Hz, 9H). **^{13}C NMR (126 MHz, $CDCl_3$):** δ 158.6, 142.7, 131.1, 128.5, 128.3, 127.7, 127.3, 127.0, 124.8, 114.0, 55.4, 43.8, -2.7. **FTIR (NaCl, thin film, cm^{-1}):** 3024, 2955, 2898, 1607, 1510, 1493, 1465, 1450, 1441, 1295, 1286, 1249, 1175, 1106, 1055, 1035, 963, 876, 861, 838. **HRMS (TOF-ESI, *m/z*):** calc'd for $C_{19}H_{24}OSi$ $[M+H]^+$: 297.1675; found: 297.1687.

From phenyl(trimethylsilyl)methyl methanesulfonate 104. Prepared from with (*E*)-1-(2-bromovinyl)-4-methoxybenzene (**87**, 85.2 mg, 0.4 mmol) and phenyl(trimethylsilyl)-methyl methanesulfonate (**104**, 51.7 mg, 0.2 mmol) according to General Procedure 7, but at 10 °C and with the addition of an internal standard. **Note:** The increased temperature provided slightly higher yield (~5%). The crude material was dissolved in 10% EtOAc/hexane and filtered through a pad of silica in place of the acidic aqueous workup.

The yield of **88c** was determined to be 40% yield by ^{1}H NMR, and the enantioselectivity was determined to be 92% ee following purification by preparative TLC.

Preparative Scale: Reaction on a 6.0 mmol scale:

On a bench-top to a 100 mL round bottom flask (with 24/40 joint) equipped with a medium-size egg-shaped stir bar was added alkenyl bromide **86** (2.56 g, 12 mmol, 2 equiv), **L2**·$NiCl_2$ (293 mg, 0.6 mmol, 0.10 equiv), Mn^0 powder (990 mg, 18 mmol, 3 equiv), and cobalt phthalocyanine (172 mg, 0.3 mmol, 0.05 equiv). Under an inert atmosphere in a glovebox, the flask was charged with NMP (12 mL, 0.5 M) followed by chlorobenzyl silane **L2** (1.19 g, 6 mmol, 1 equiv). The round bottom flask was sealed with an unpunctured large septum, wrapped with electrical tape, and brought out of the glovebox. The flask was stirred (at 450 rpm) at 5 °C in a bench-top cryocool by submerging it in an isopropanol bath cooled with a Thermo Scientific EK90 Immersion Cooler for 3 days. The reaction was diluted with 70 mL of water, slowly quenched with 30 mL of M HCl, and transferred to a separatory funnel with 100 mL water and 300 mL diethyl ether. The layers were separated and the aqueous layer was extracted with diethyl ether (2 x 400 mL). The combined organic layers were washed with brine, dried with $MgSO_4$, filtered, and concentrated under reduced pressure. The crude residue was purified by column chromatography (silica, 0 to 2% Et_2O/hexane) to yield **88c** (1.3 g, 74% yield) in 97% ee as a colorless oil.

Glovebox-free, Bench-top Setup:

On a bench-top to a 15 mL round bottom flask equipped with a small egg-shaped stir bar was added alkenyl bromide **86** (426 mg, 2.0 mmol, 2 equiv), **L2**·$NiCl_2$ (49 mg, 0.10 mmol,

0.10 equiv), Mn^0 powder (165 mg, 3.0 mmol, 3 equiv), and cobalt phthalocyanine (29 mg, 0.05 mmol, 0.05 equiv). The flask was sealed with a rubber septum and connected to a Schlenk line via a large gauge needle. The flask was evacuated and backfilled with N_2 (3 times). The NMP (2 mL, 0.5 M) and chlorobenzyl silane **87** (199 mg, 1.0 mmol, 1 equiv) were added via syringe. The N_2 needle was removed, the septum was sealed with electrical tape, and the reaction was stirred at 5 °C in a bench-top cryocool 2 days. The reaction was diluted (5 mL water + 5 mL of Et_2O) and stirred while quenched via slow addition of 1 M HCl (2 mL). The solution was transferred to a separatory funnel, diluted with additional water (35 mL) and Et_2O (35 mL), and the layers were separated. The aqueous layer was extracted with Et_2O (2 x 50 mL). The combined organic layers were dried with $MgSO_4$, filtered, and concentrated under reduced pressure. The crude residue was purified by column chromatography (silica, 0 to 30% PhMe/hexane) to yield **88c** (211 mg, 71% yield) in 98% ee as a colorless oil.

(*S*,*E*)-1-(3-(4-methoxyphenyl)-1-phenylallyl)-1-methylsiletane (90a)

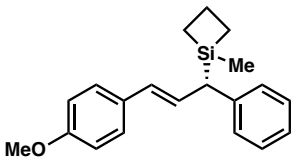

Prepared from (*E*)-1-(2-bromovinyl)-4-methoxybenzene (**86**, 85.2 mg, 0.4 mmol) and 1-(chloro(phenyl)methyl)-1-methylsiletane (**89a**, 42.2 mg, 0.2 mmol) according to General Procedure 7. The crude residue was purified by column chromatography (silica, 0 to 3% Et_2O/hexane) to yield **90a** (37.6 mg, 61% yield) in 98% ee as a colorless oil. $\mathbf{R_f}$ = 0.58 (silica, 10% EtOAc/hexane, UV). **Chiral SFC:** (AD-H, 2.5 mL/min, 20% IPA in CO_2, λ = 280 nm): t_R (minor) = 4.8 min, t_R (major) = 6.0 min. $[\alpha]_D^{25}$ = +41° (c = 1.0, $CHCl_3$). **^{1}H NMR (500 MHz, $CDCl_3$):** δ 7.37 – 7.30 (m, 4H), 7.25 – 7.20 (m, 2H), 7.20 – 7.15 (m,

1H), 6.90 – 6.85 (m, 2H), 6.52 (ddd, *J* = 15.7, 9.4, 1.0 Hz, 1H), 6.42 (d, *J* = 15.7 Hz, 1H), 3.82 (d, *J* = 0.9 Hz, 3H), 3.39 (d, *J* = 9.3 Hz, 1H), 2.11 – 1.91 (m, 2H), 1.25 – 1.13 (m, 2H), 1.10 – 0.97 (m, 2H), 0.25 (d, *J* = 0.9 Hz, 3H). **^{13}C NMR (126 MHz, $CDCl_3$):** δ 158.7, 141.7, 131.0, 128.7, 128.3, 127.3, 127.2, 127.1, 125.1, 114.1, 55.4, 43.1, 17.8, 13.9, 13.7, -2.9. **FTIR (NaCl, thin film, cm^{-1}):** 3023, 2960, 2929, 1607, 1510, 1491, 1450, 1293, 1429, 1175, 1118, 1074, 1035, 962, 867. **HRMS (TOF-ESI, *m/z*):** calc'd for $C_{20}H_{24}OSi$ $[M+H]^+$: 309.1675; found: 309.1667.

(*S*,*E*)-(3-(4-methoxyphenyl)-1-phenylallyl)dimethyl(phenyl)silane (90b)

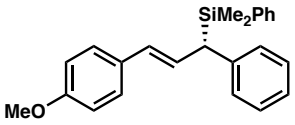

Prepared from (*E*)-1-(2-bromovinyl)-4-methoxybenzene (**86**, 85.2 mg, 0.4 mmol) and (chloro(phenyl)methyl)dimethyl-(phenyl)silane (**89b**, 52.2 mg, 0.2 mmol) according to General Procedure 7. The crude residue was purified by column chromatography (silica, 0 to 30% PhMe/hexane) to yield **90b** (30.7 mg, 43% yield) in 97% ee as a colorless oil. $\mathbf{R}_f$ = 0.48 (silica, 10% EtOAc/hexane, UV). **Chiral SFC:** (AD-H, 2.5 mL/min, 20% IPA in CO_2, λ = 280 nm): t_R (minor) = 3.7 min, t_R (major) = 4.2 min. $[\alpha]_D^{25}$ = +22° (c = 1.0, $CHCl_3$). **^{1}H NMR (500 MHz, $CDCl_3$):** δ 7.40 – 7.37 (m, 3H), 7.35 – 7.31 (m, 2H), 7.26 – 7.19 (m, 4H), 7.15 – 7.09 (m, 1H), 7.03 – 6.98 (m, 2H), 6.84 (d, *J* = 8.7 Hz, 2H), 6.37 (dd, *J* = 15.6, 9.7 Hz, 1H), 6.24 (d, *J* = 15.6 Hz, 1H), 3.82 (s, 3H), 3.29 (d, *J* = 9.7 Hz, 1H), 0.32 (s, 6H). **^{13}C NMR (126 MHz, $CDCl_3$):** δ 158.6, 142.0, 136.8, 134.5, 131.1, 129.3, 128.3, 128.1, 128.0, 127.6, 127.6, 127.0, 124.9, 114.0, 55.4, 43.4, -4.0, -4.5. **FTIR (NaCl, thin film, cm^{-1}):** 3024, 2956, 1606, 1510, 142, 1287, 1249, 1175, 1113, 1035, 831, 814. **HRMS (FAB, *m/z*):** calc'd for $C_{24}H_{26}OSi$ $[M+\cdot]^+$: 358.1753; found: 358.1749.

The reaction was also conducted on a larger reaction scale using alkenyl bromide **86** (1.70 g, 8.0 mmol), chlorobenzyl silane **86b** (1.044 g, 4.0 mmol), **L2**·$NiCl_2$ (194 mg, 0.4 mmol), Mn powder (660 mg, 12 mmol), and cobalt phthalocyanine (114 mg, 0.2 mmol) in 8 mL NMP. The reaction was stirred at 5 °C for 2 days and subsequently purified by column chromatography (silica, 0 to 30% PhMe/hexane) to yield **90b** (600 mg, 42% yield) in 97% ee as a yellow oil.

(*S*,*E*)-(3-(4-methoxyphenyl)-1-phenylallyl)triethylsilane (90c)

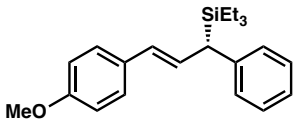

Prepared from (*E*)-1-(2-bromovinyl)-4-methoxybenzene (**86**, 85.2 mg, 0.4 mmol) and (chloro(phenyl)methyl)triethylsilane (**89c**, 48.2 mg, 0.2 mmol) according to General Procedure 7. The crude residue was purified by column chromatography (silica, 0 to 2% Et_2O/hexane) to yield **90c** (10.9 mg, 16% yield, 93% clean, contains 7% unidentified silyl isomer) in 93% ee as a colorless oil. The yield is adjusted accordingly to (16 x 0.93 = 15% yield). $\mathbf{R_f}$ = 0.61 (silica, 10% EtOAc/hexane, UV). **Chiral SFC:** (AD-H, 2.5 mL/min, 20% IPA in CO_2, λ = 280 nm): t_R (minor) = 3.0 min, t_R (major) = 3.5 min. $[\boldsymbol{\alpha}]_{\boldsymbol{D}}^{\mathbf{25}}$ = +73° (c = 0.3, $CHCl_3$). **^{1}H NMR (500 MHz, $CDCl_3$):** δ 7.30 – 7.23 (m, 4H), 7.19 – 7.15 (m, 2H), 7.14 – 7.09 (m, 1H), 6.86 – 6.81 (m, 2H), 6.47 (dd, *J* = 15.6, 10.0 Hz, 1H), 6.30 (d, *J* = 15.6 Hz, 1H), 3.80 (s, 3H), 3.25 (d, *J* = 10.0 Hz, 1H), 0.92 (t, *J* = 7.9 Hz, 9H), 0.61 – 0.56 (m, 6H). **^{13}C NMR (126 MHz, $CDCl_3$):** δ 158.6, 142.8, 131.2, 128.9, 128.5, 127.5, 127.1, 127.0, 124.8, 114.0, 55.4, 41.0, 7.6, 2.6. **FTIR (NaCl, thin film, cm^{-1}):** 3024, 2953, 2875, 1936, 2910, 1607, 1510, 1493, 1467, 1456, 1294, 1286, 1249, 115, 1036, 1010, 963. **HRMS (TOF-ESI, *m/z*):** calc'd for $C_{22}H_{30}OSi$ $[M+H–H_2]^+$: 337.1988; found: 337.1964.

(*S*,*E*)-(3-(4-methoxyphenyl)-1-(4-(trifluoromethyl)phenyl)allyl)trimethylsilane (90d)

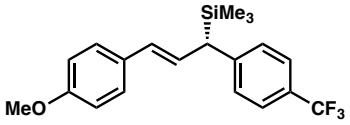

Prepared from (*E*)-1-(2-bromovinyl)-4-methoxybenzene (**86**, 85.2 mg, 0.4 mmol) and (chloro(4-trifluoromethyl-phenyl)methyl)-trimethylsilane (**89d**, 53.4 mg, 0.2 mmol) according to General Procedure 7. The crude material was dissolved in chilled (0 °C) 10% EtOAc/hexane while it was still cold, and filtered through a pad of silica in place of the acidic aqueous workup. **Note**: Complete decomposition of the product was observed when the crude reaction was warmed to room temperature and subjected to aqueous work up. The crude residue was purified by preparative TLC (silica, hexane to 20% toluene/hexane) to yield **90d** (22.5 mg, 31% yield) in 96% ee as a colorless oil. When the reaction was conducted with an internal standard, the yield was determined to be 67% yield by ^{1}H NMR. $\mathbf{R}_f$ = 0.56 (silica, 10% EtOAc/hexane). **Chiral SFC:** (AD-H, 2.5 mL/min, 20% IPA in CO_2, λ = 280 nm): t_R (minor) = 2.6 min, t_R (major) = 3.5 min. $[\alpha]_D^{25}$ = +25° (c = 1.0, $CHCl_3$). **^{1}H NMR (500 MHz, $CDCl_3$):** δ 7.53 (d, *J* = 7.8 Hz, 2H), 7.30 (d, *J* = 8.6 Hz, 2H), 7.24 (d, *J* = 7.9 Hz, 2H), 6.86 (d, *J* = 8.7 Hz, 2H), 6.43 (dd, *J* = 15.6, 9.7 Hz, 1H), 6.33 (d, *J* = 15.5 Hz, 1H), 3.81 (s, 3H), 3.19 (d, *J* = 9.7 Hz, 1H), 0.02 (s, 9H). **^{13}C NMR (126 MHz, $CDCl_3$):** δ 158.8, 147.2 (q, $J_{C\text{-}F}$ = 1.2 Hz), 130.7, 128.5, 127.3, 127.13 (q, $J_{C\text{-}F}$ = 32.2 Hz), 127.12, 126.9, 125.39 (q, $J_{C\text{-}F}$ = 3.8 Hz), 124.6 (q, $J_{C\text{-}F}$ = 271.5 Hz), 114.1, 55.4, 44.0, -2.8. **^{19}F NMR (282 MHz, $CDCl_3$):** δ -65.3. **FTIR (NaCl, thin film, cm^{-1}):** 2957, 2837, 1615, 1578, 1511, 1466, 1420, 1327, 1290, 1250, 1163, 1121, 1070, 1036, 1016, 962, 866, 846. **HRMS (FAB, *m/z*):** calc'd for $C_{20}H_{23}F_3OSi$ $[M+\cdot]^+$: 364.1470; found: 364.1480.

(*S*,*E*)-(1-(4-chlorophenyl)-3-(4-methoxyphenyl)allyl)trimethylsilane (90e)

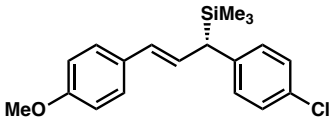

Prepared from (*E*)-1-(2-bromovinyl)-4-methoxybenzene (**86**, 85.2 mg, 0.4 mmol) and (chloro(4-chlorophenyl)methyl)-trimethylsilane (**89e**, 46.6 mg, 0.2 mmol) according to General Procedure 7. The crude residue was purified by column chromatography (silica, 0 to 2% Et_2O/hexane) to yield **90e** (45.7 mg, 69% yield) in 96% ee as a colorless oil. $\mathbf{R_f}$ = 0.58 (silica, 10% EtOAc/hexane, UV). **Chiral SFC:** (OJ-H, 2.5 mL/min, 10% IPA in CO_2, λ = 280 nm): t_R (major) = 5.0 min, t_R (minor) = 7.9 min. $[\boldsymbol{\alpha}]_D^{25}$ = +21° (c = 1.0, $CHCl_3$). **^{1}H NMR (500 MHz, $CDCl_3$):** δ 7.32 – 7.28 (m, 2H), 7.28 (s, 2H), 7.11 – 7.06 (m, 2H), 6.89 – 6.84 (m, 2H), 6.40 (dd, *J* = 15.5, 9.5 Hz, 1H), 6.32 (d, *J* = 15.6 Hz, 1H), 3.81 (s, 3H), 3.09 (d, *J* = 9.5 Hz, 1H), 0.03 (d, *J* = 0.5 Hz, 9H). **^{13}C NMR (126 MHz, $CDCl_3$):** δ 158.7, 141.3, 130.9, 130.3, 128.53, 128.52, 128.1, 127.5, 127.1, 114.06, 55.4, 43.2, -2.8. **FTIR (NaCl, thin film, cm^{-1}):** 3029, 2956, 1899, 2835, 1608, 1510, 1490, 1292, 1249, 1176, 1092, 1036, 1013, 963, 864, 841, 803. **HRMS (TOF-ESI, *m/z*):** calc'd for $C_{19}H_{23}ClOSi$ $[M+H-H_2]^+$: 329.1128; found: 329.1138.

(*S*,*E*)-(1-(4-bromophenyl)-3-(4-methoxyphenyl)allyl)trimethylsilane (90f)

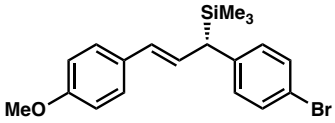

Prepared from (*E*)-1-(2-bromovinyl)-4-methoxybenzene (**86**, 85.2 mg, 0.4 mmol) and (chloro(4-bromophenyl)methyl)-trimethylsilane (**89f**, 55.5 mg, 0.2 mmol) according to General Procedure 7. The crude material was dissolved in chilled (0 °C) 10% EtOAc/hexane while it was still cold, and filtered through a pad of silica in place of the acidic aqueous workup. **Note:** Warming the reaction to room temperature and conducting an acidic workup resulted in unidentified side

products that could not be separated from the desired product by column chromatography. The crude residue was purified by column chromatography (silica, hexane to 20% toluene/hexane) to yield **90f** (32.7 mg, 44% yield) in 97% ee as a colorless oil. When the reaction was conducted with an internal standard, the yield was determined to be 52% yield by ^{1}H NMR analysis of the crude reaction mixture. $\mathbf{R}_f$ = 0.59 (silica, 10% EtOAc/hexane, UV). **Chiral SFC:** (AD-H, 2.5 mL/min, 20% IPA in CO_2, λ = 280 nm): t_R (minor) = 6.9 min, t_R (major) = 9.4 min. $[\boldsymbol{a}]_D^{25}$ = +15° (c = 1.0, $CHCl_3$). **^{1}H NMR (500 MHz, $CDCl_3$):** δ 7.39 (d, *J* = 8.5 Hz, 2H), 7.28 (d, *J* = 8.3 Hz, 2H), 7.01 (d, *J* = 8.2 Hz, 2H), 6.84 (d, *J* = 8.8 Hz, 2H), 6.37 (dd, *J* = 15.6, 9.5 Hz, 1H), 6.30 (d, *J* = 15.6 Hz, 1H), 3.81 (s, 3H), 3.06 (d, *J* = 9.4 Hz, 1H), 0.01 (s, 9H). **^{13}C NMR (126 MHz, $CDCl_3$):** δ 158.7, 141.8, 131.5, 130.9, 129.0, 128.1, 127.4, 127.1, 118.3, 114.1, 55.5, 43.2, -2.8. **FTIR (NaCl, thin film, cm^{-1}):** 3022, 2954, 1898, 1606, 1510, 1486, 1464, 1291, 1248, 1175, 1035, 1008, 962, 862, 840, 802. **HRMS (TOF-ESI, *m/z*):** calc'd for $C_{19}H_{23}BrOSi$ $[M+H-H_2]^+$: 373.0623; found: 373.0615.

(*S*,*E*)-(1-(3-methoxyphenyl)-3-(4-methoxyphenyl)allyl)trimethylsilane (90g)

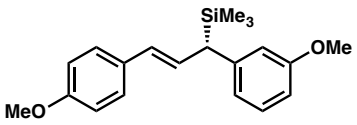

Prepared from (*E*)-1-(2-bromovinyl)-4-methoxybenzene (**86**, 85.2 mg, 0.4 mmol) and (chloro(3-methoxyphenyl)-methyl)-trimethylsilane (**89g**, 45.8 mg, 0.2 mmol) according to General Procedure 7. The crude residue was purified by column chromatography (silica, 0 to 3% Et_2O/hexane) to yield **90g** (53.0 mg, 81% yield) in 97% ee as a colorless oil. $\mathbf{R}_f$ = 0.45 (silica, 10% EtOAc/hexane, UV). **Chiral SFC:** (AD-H, 2.5 mL/min, 25% IPA in CO_2, λ = 280 nm): t_R (minor) = 2.8 min, t_R (major) = 3.7 min. $[\boldsymbol{a}]_D^{25}$ = +16° (c = 1.0, $CHCl_3$). **^{1}H NMR (500**

MHz, $CDCl_3$): δ 7.34 – 7.28 (m, 2H), 7.22 (t, *J* = 7.9 Hz, 1H), 6.88 – 6.84 (m, 2H), 6.79 – 6.74 (m, 1H), 6.74 – 6.68 (m, 2H), 6.45 (dd, *J* = 15.6, 9.8 Hz, 1H), 6.33 (d, *J* = 15.6 Hz, 1H), 3.82 (s, 3H), 3.81 (s, 3H), 3.10 (d, *J* = 9.8 Hz, 1H), 0.05 (s, 9H). **^{13}C NMR (126 MHz, $CDCl_3$):** δ 159.7, 158.6, 144.4, 131.1, 129.3, 128.1, 127.7, 127.0, 119.9, 114.0, 113.3, 109.7, 55.4, 55.2, 43.9, -2.6. **FTIR (NaCl, thin film, cm^{-1}):** 3000, 2955, 2834, 1607, 1579, 1510, 1464, 1438, 1299, 1287, 1248, 1174, 1148, 1038, 963, 838, 819. **HRMS (TOF-ESI, *m/z*):** calc'd for $C_{20}H_{26}O_2Si$ $[M+H-H_2]^+$: 325.1624; found: 325.1673.

(*S*,*E*)-(1,3-bis(4-methoxyphenyl)allyl)trimethylsilane (90h)

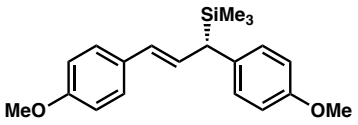

Prepared from (*E*)-1-(2-bromovinyl)-4-methoxybenzene (**86**, 85.2 mg, 0.4 mmol) and (chloro(4-methoxyphenyl)-methyl)-trimethylsilane (**89h**, 45.8 mg, 0.2 mmol) according to General Procedure 7. The crude residue was purified by preparative TLC (silica, 10% EtOAc/hexane) to yield **90h** (28.9 mg, 44% yield) in 96% ee as a colorless oil. $\mathbf{R_f}$ = 0.45 (silica, 10% EtOAc/hexane, UV). **Chiral SFC:** (AD-H, 2.5 mL/min, 20% IPA in CO_2, λ = 280 nm): t_R (minor) = 5.6 min, t_R (major) = 6.8 min. $[\alpha]_D^{25}$ = +21° (c = 1.0, $CHCl_3$). **^{1}H NMR (500 MHz, $CDCl_3$):** δ 7.31 – 7.26 (m, 2H), 7.10 – 7.05 (m, 2H), 6.88 – 6.83 (m, 4H), 6.41 (dd, *J* = 15.6, 9.6 Hz, 1H), 6.30 (d, *J* = 15.6 Hz, 1H), 3.81 (s, 3H), 3.80 (s, 3H), 3.05 (d, *J* = 9.6 Hz, 1H), 0.03 (s, 9H). **^{13}C NMR (126 MHz, $CDCl_3$):** δ 158.6, 157.1, 134.6, 131.2, 128.8, 128.2, 127.4, 127.0, 114.0, 113.9, 55.43, 55.37, 42.5, -2.6. **FTIR (NaCl, thin film, cm^{-1}):** 3000, 2954, 2834, 1608, 1509, 1464, 1441, 1297, 1289, 1248, 1175, 1036, 964, 863, 839. **HRMS (TOF-ESI, *m/z*):** calc'd for $C_{20}H_{26}O_2Si$ $[M+H-H_2]^+$: 325.1624; found: 325.1605.

(*S*,*E*)-(1-(2-methoxyphenyl)-3-(4-methoxyphenyl)allyl)trimethylsilane (90i)

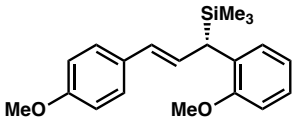

Prepared from (*E*)-1-(2-bromovinyl)-4-methoxybenzene (**86**, 85.2 mg, 0.4 mmol) and (chloro(2-methoxyphenyl)methyl)-trimethylsilane (**89i**, 45.8 mg, 0.2 mmol) according to General Procedure 7. The crude residue was purified by preparative TLC (silica, 10% EtOAc/hexane) to yield **90i** (13.4 mg, 21% yield) in 95% ee as a colorless oil. $\mathbf{R}_f$ = 0.52 (silica, 10% EtOAc/hexane, UV). **Chiral SFC:** (AD-H, 2.5 mL/min, 20% IPA in CO_2, λ = 280 nm): t_R (minor) = 2.5 min, t_R (major) = 3.5 min. $[\boldsymbol{a}]_D^{25}$ = +9° (c = 1.0, $CHCl_3$). **^{1}H NMR (500 MHz, $CDCl_3$):** δ 7.31 – 7.27 (m, 2H), 7.21 (dd, *J* = 7.6, 1.7 Hz, 1H), 7.10 (ddd, *J* = 8.0, 7.3, 1.7 Hz, 1H), 6.93 (td, *J* = 7.5, 1.2 Hz, 1H), 6.87 – 6.82 (m, 3H), 6.48 (ddd, *J* = 15.6, 10.0, 0.6 Hz, 1H), 6.33 (d, *J* = 15.6 Hz, 1H), 3.82 (s, 3H), 3.81 (s, 3H), 3.65 (d, *J* = 10.1 Hz, 1H), 0.00 (s, 9H). **^{13}C NMR (126 MHz, $CDCl_3$):** δ 158.5, 156.0, 131.4, 131.3, 128.5, 127.5, 127.0, 125.4, 120.6, 114.0, 110.4, 55.4, 55.2, 35.3, -2.6. **FTIR (NaCl, thin film, cm^{-1}):** 2951, 2901, 2834, 1608, 1510, 1490, 1464, 1439, 1289, 1246, 1174, 1032, 964, 837. **HRMS (FAB, *m/z*):** calc'd for $C_{20}H_{26}O_2Si$ $[M+H]^+$: 327.1780; found: 327.1795.

(*S*,*E*)-trimethyl(1-phenyl-3-(*p*-tolyl)allyl)silane (91a)

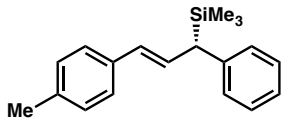

From (E)-1-(2-bromovinyl)-4-methylbenzene 86. Prepared from (*E*)-1-(2-bromovinyl)-4-methylbenzene (**29a**, 78.8 mg, 0.4 mmol) and (chloro(phenyl)methyl)trimethylsilane (**87**, 39.8 mg, 0.2 mmol) according to General Procedure 7. The crude residue was purified by column chromatography (silica, 0 to 3% Et_2O/hexane) to yield **91a** (40.5 mg, 72% yield) in 93% ee as a colorless oil. $\mathbf{R}_f$ = 0.24 (silica, hexane). **Chiral SFC:** (OJ-H, 2.5 mL/min, 7% IPA in CO_2, λ = 245 nm): t_R

(major) = 3.9 min, t_R (minor) = 9.5 min. $[\boldsymbol{a}]_D^{25}$ = +28° (c = 1.0, $CHCl_3$). **^{1}H NMR (500 MHz, $CDCl_3$):** δ 7.36 – 7.27 (m, 4H), 7.22 – 7.12 (m, 5H), 6.59 (dd, *J* = 15.6, 10.0 Hz, 1H), 6.38 (d, *J* = 15.6 Hz, 1H), 3.16 (d, *J* = 9.9 Hz, 1H), 2.37 (s, 3H), 0.06 (s, 9H). **^{13}C NMR (126 MHz, $CDCl_3$):** δ 142.6, 136.4, 135.5, 129.5, 129.3, 128.5, 128.1, 127.30, 125.9, 124.8, 43.9, 21.3, -2.7. **FTIR (NaCl, thin film, cm^{-1}):** 3023, 2955, 1639, 1595, 1512, 1496, 1450, 1248, 1211, 1183, 1106, 1077, 1056, 963, 905, 840. **HRMS (FAB, *m/z*):** calc'd for $C_{19}H_{24}Si$ $[M+\cdot]^+$: 280.1647; found: 280.1648.

From (E)-4-methylstyrenyl trifluoromethanesulfonate 105. Prepared from (*E*)-4-methylstyryl trifluoromethanesulfonate (**105**, 0.4 mmol, 2 equiv) and (chloro(phenyl)methyl)trimethylsilane (**87**, 39.8 mg, 0.2 mmol) according to General Procedure 7, but with the addition of an internal standard. The crude material was dissolved in 10% EtOAc/hexane and filtered through a pad of silica in place of the acidic aqueous workup. The yield of **91a** was determined to be 57% yield by ^{1}H NMR, and the enantioselectivity was determined to be 97% ee following purification by preparative TLC.

(*S*,*E*)-4-(3-phenyl-3-(trimethylsilyl)prop-1-en-1-yl)phenyl acetate (91b)

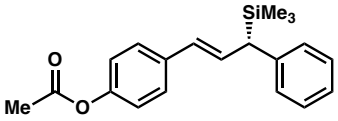

Prepared from (*E*)-4-(2-bromovinyl)phenyl acetate (**29b**, 96.4 mg, 0.4 mmol) and (chloro(phenyl)methyl)trimethylsilane (**87**, 39.8 mg, 0.2 mmol) according to General Procedure 7. The crude residue was purified by column chromatography (silica, 0 to 4% Et_2O/hexane) to yield **91b** (40.3 mg, 62% yield) in 93% ee as a colorless oil. $\mathbf{R}_f$ = 0.39 (silica, 10% EtOAc/hexane, UV). **Chiral SFC:** (AD-H, 2.5 mL/min, 20% IPA in CO_2, λ = 280 nm): t_R (minor) = 3.2 min, t_R (major) = 3.8 min.

$[\boldsymbol{\alpha}]_D^{25}$ = +18° (c = 1.0, $CHCl_3$). **^{1}H NMR (500 MHz, $CDCl_3$):** δ 7.39 – 7.35 (m, 2H), 7.30 (dd, *J* = 8.3, 7.1 Hz, 2H), 7.18 – 7.12 (m, 3H), 7.06 – 7.01 (m, 2H), 6.57 (dd, *J* = 15.6, 9.9 Hz, 1H), 6.36 (d, *J* = 15.6 Hz, 1H), 3.14 (d, *J* = 9.9 Hz, 1H), 2.31 (s, 3H), 0.03 (s, 9H). **^{13}C NMR (126 MHz, $CDCl_3$):** δ 169.7, 149.4, 142.3, 136.1, 130.9, 128.5, 127.3, 127.2, 126.8, 124.9, 121.7, 43.9, 21.3, -2.7. **FTIR (NaCl, thin film, cm^{-1}):** 3024, 2956, 1761, 1600, 1505, 1369, 1248, 1211, 1196, 1166, 1015, 910, 838. **HRMS (TOF-ESI, *m/z*):** calc'd for $C_{20}H_{24}O_2Si$ $[M+H-H_2]^+$: 323.1467; found: 323.1471.

(*S*,*E*)-trimethyl(1-phenyl-3-(4-(4,4,5,5-tetramethyl-1,3,2-dioxaborolan-2-yl)phenyl)-allyl)-silane (91c)

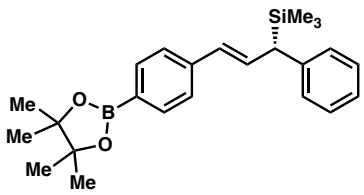

Prepared from (*E*)-1-(4-(2-bromovinyl)phenyl)-3,3,4,4-tetra-methylborolane (**29c**, 123.6 mg, 0.4 mmol) and (chloro(phenyl)-methyl)trimethylsilane (**87**, 39.8 mg, 0.2 mmol) according to General Procedure 7. The crude residue was purified by column chromatography (silica, 0 to 3% Et_2O/hexane) to yield **91c** (40.3 mg, 51% yield) in 91% ee as a white solid. Crystals of **91c** were grown by vapor diffusion (CH_2Cl_2, pentane) to provide colorless needles suitable for X-ray crystallography. $\mathbf{R_f}$ = 0.52 (silica, 10% EtOAc/hexane, UV). **m.p.** = 138-142 °C **Chiral SFC:** (AD-H, 2.5 mL/min, 20% IPA in CO_2, λ = 280 nm): t_R (minor) = 3.8 min, t_R (major) = 6.5 min. $[\boldsymbol{\alpha}]_D^{25}$ = +12° (c = 1.0, $CHCl_3$). **^{1}H NMR (500 MHz, $CDCl_3$):** δ 7.81 – 7.73 (m, 2H), 7.41 – 7.35 (m, 2H), 7.35 – 7.28 (m, 2H), 7.21 – 7.12 (m, 3H), 6.70 (dd, *J* = 15.6, 10.0 Hz, 1H), 6.39 (d, *J* = 15.6 Hz, 1H), 3.16 (d, *J* = 10.0 Hz, 1H), 1.36 (s, 12H), 0.03 (s, 9H). **^{13}C NMR (126 MHz, $CDCl_3$):** δ 142.2, 141.0, 135.2, 131.9, 128.5, 128.2, 127.3, 125.3, 124.9, 83.8, 44.2, 25.00, 24.97, -2.7. *(C*

bonded to boron not observed) **FTIR (NaCl, thin film, cm^{-1}):** 2976, 2955, 2915, 1607, 1398, 1361, 1321, 1268, 1248, 1144, 1091, 964, 860, 839. **HRMS (TOF-ESI, *m/z*):** calc'd for $C_{24}H_{33}BO_2Si$ $[M+H-H_2]^+$: 391.2265; found: 391.2242.

((*S*,2*E*,4*E*)-1,5-diphenylpenta-2,4-dien-1-yl)trimethylsilane (91d)

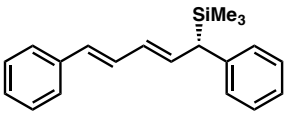

Prepared from ((1*E*,3*E*)-4-bromobuta-1,3-dien-1-yl)benzene (**29d**, 83.6 mg, 0.4 mmol) and (chloro(phenyl)methyl)-trimethylsilane (**87**, 39.8 mg, 0.2 mmol) according to General Procedure 7. The crude residue was purified by column chromatography (silica, hexane) to yield **91d** (33.7 mg, 58% yield) in 94% ee as a colorless oil. $\mathbf{R_f}$ = 0.73 (silica, 10% EtOAc/hexane, UV). **Chiral SFC:** (AD-H, 2.5 mL/min, 10% IPA in CO_2, λ = 280 nm): t_R (minor) = 6.1 min, t_R (major) = 7.6 min. $[\boldsymbol{a}]_{\boldsymbol{D}}^{\mathbf{25}}$ = +23° (c = 1.0, $CHCl_3$). **^{1}H NMR (500 MHz, $CDCl_3$):** δ 7.43 – 7.38 (m, 2H), 7.35 – 7.28 (m, 4H), 7.24 – 7.19 (m, 1H), 7.18 – 7.12 (m, 3H), 6.89 – 6.82 (m, 1H), 6.45 (d, *J* = 15.6 Hz, 1H), 6.28 – 6.18 (m, 2H), 3.12 – 3.07 (m, 1H), 0.03 (s, 9H). **^{13}C NMR (126 MHz, $CDCl_3$):** δ 142.2, 137.9, 135.2, 129.7, 129.5, 129.1, 128.7, 128.5, 127.3, 127.1, 126.1, 124.8, 44.1, -2.7. **FTIR (NaCl, thin film, cm^{-1}):** 3081, 3059, 3022, 2955, 1632, 1597, 1495, 1448, 1248, 1074, 1056, 986, 840. **HRMS (TOF-ESI, *m/z*):** calc'd for $C_{20}H_{24}Si$ $[M+H-H_2]^+$: 291.1569; found: 291.1566.

(*S*,*E*)-1-(6-phenyl-6-(trimethylsilyl)hex-4-en-1-yl)-1*H*-indole (91e)

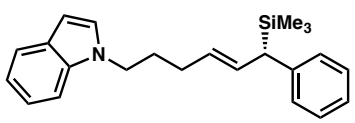

Prepared from (*E*)-1-(5-bromopent-4-en-1-yl)-1*H*-indole (**29e**, 105.7 mg, 0.4 mmol) and (chloro(phenyl)methyl)-trimethylsilane (**87**, 39.8 mg, 0.2 mmol) according to General Procedure 7. The crude

residue was purified by column chromatography (silica, 0 to 6% Et_2O/hexane) to yield **91e** (45.1 mg, 65% yield) in 92% ee as a faint blue oil (trace CoPc impurity). The ^{1}H NMR spectrum shows minor impurities in the aryl region, therefore the purity of **91e** was determined by quantitative NMR to be 90% pure. The yield is adjusted accordingly to (65 x 0.90 = 59% yield). $\mathbf{R}_f$ = 0.59 (silica, 10% EtOAc/hexane, UV). **Chiral SFC:** (OJ-H, 2.5 mL/min, 15% IPA in CO_2, λ = 280 nm): t_R (minor) = 7.7 min, t_R (major) = 10.0 min. $[\boldsymbol{a}]_D^{25}$ = +10° (c = 1.0, $CHCl_3$). **^{1}H NMR (500 MHz, $CDCl_3$):** δ 7.71 – 7.68 (m, 1H), 7.37 (dq, *J* = 8.1, 0.9 Hz, 1H), 7.34 – 7.29 (m, 2H), 7.27 – 7.23 (m, 1H), 7.18 – 7.11 (m, 5H), 6.55 (dd, *J* = 3.1, 0.8 Hz, 1H), 5.89 (ddt, *J* = 15.0, 9.9, 1.4 Hz, 1H), 5.48 – 5.41 (m, 1H), 4.16 (t, *J* = 7.1 Hz, 2H), 2.96 (d, *J* = 9.9 Hz, 1H), 2.16 – 2.09 (m, 2H), 2.00 – 1.93 (m, 2H), 0.02 (s, 9H). **^{13}C NMR (126 MHz, $CDCl_3$):** δ 142.9, 136.0, 130.8, 128.7, 128.4, 127.9, 127.5, 127.2, 124.7, 121.4, 121.0, 119.3, 109.5, 101.0, 45.8, 43.0, 30.4, 30.2, -2.8. **FTIR (NaCl, thin film, cm^{-1}):** 2955, 1597, 1511, 1464, 1316, 1247, 1083, 968, 839. **HRMS (FAB, *m/z*):** calc'd for $C_{23}H_{29}NSi$ $[M+H]^+$: 348.2148; found: 348.2162.

(*S*,*E*)-(7,7-dimethoxy-1-phenylhept-2-en-1-yl)trimethylsilane (91f)

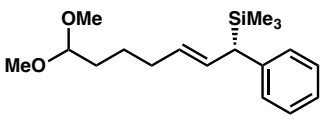

Prepared from (*E*)-1-bromo-6,6-dimethoxyhex-1-ene (**29f**, 89.2 mg, 0.4 mmol) and (chloro(phenyl)methyl)trimethylsilane (**87**, 39.8 mg, 0.2 mmol) according to General Procedure 7. The crude material was dissolved in Et_2O and filtered through a pad of silica in place of the acidic aqueous workup. The crude residue was purified by column chromatography (silica, 0 to 4% Et_2O/hexane) to yield **91f** (32.7 mg, 53% yield) in 97% ee as a colorless oil. $\mathbf{R}_f$ = 0.41 (silica, 10% EtOAc/hexane, CAM). **Chiral SFC:** (OJ-H, 2.5 mL/min, 1% IPA in CO_2, λ = 235 nm): t_R

(minor) = 6.1 min, t_R (major) = 6.7 min. $[\alpha]_D^{25}$ = +22° (c = 1.0, $CHCl_3$). **^{1}H NMR (500 MHz, $CDCl_3$):** δ 7.24 (ddd, *J* = 8.1, 7.2, 1.4 Hz, 2H), 7.11 – 7.04 (m, 3H), 5.80 (ddt, *J* = 15.0, 9.9, 1.4 Hz, 1H), 5.39 (dtd, *J* = 14.9, 6.8, 0.9 Hz, 1H), 4.37 (t, *J* = 5.7 Hz, 1H), 3.31 (s, 6H), 2.89 (d, *J* = 9.9 Hz, 1H), 2.07 (td, *J* = 7.4, 6.0 Hz, 2H), 1.64 – 1.58 (m, 2H), 1.48 – 1.39 (m, 2H), -0.04 (s, 9H). **^{13}C NMR (126 MHz, $CDCl_3$):** δ 143.2, 129.8, 128.7, 128.3, 127.2, 124.5, 104.6, 52.7, 42.9, 32.8, 32.1, 24.9, -2.8. **FTIR (NaCl, thin film, cm^{-1}):** 3024, 2951, 2898, 2829, 1598, 1493, 1450, 1385, 1248, 1128, 1070, 966, 839. **HRMS (FAB, *m/z*):** calc'd for $C_{18}H_{30}O_2Si$ $[M+H-H_2]^+$: 305.1937; found: 305.1940.

(*S*,*E*)-(8,8-dimethoxy-1-phenyloct-2-en-1-yl)trimethylsilane (91g)

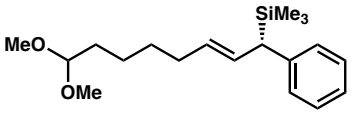

Prepared from (*E*)-1-bromo-7,7-dimethoxyhept-1-ene (**29g**, 94.9 mg, 0.4 mmol) and (chloro(phenyl)methyl)trimethylsilane (**87**, 39.8 mg, 0.2 mmol) according to General Procedure 7. The crude material was dissolved in Et_2O and filtered through a pad of silica in place of the acidic aqueous workup. The crude residue was purified by column chromatography (silica, 0 to 4% Et_2O/hexane) to yield **91g** (36.7 mg, 57% yield) in 95% ee as a colorless oil. $\mathbf{R}_f$ = 0.41 (silica, 10% EtOAc/hexane, CAM). **Chiral SFC:** (OJ-H, 2.5 mL/min, 1% IPA in CO_2, λ = 210 nm): t_R (minor) = 6.0 min, t_R (major) = 7.1 min. $[\alpha]_D^{25}$ = +18° (c = 1.0, $CHCl_3$). **^{1}H NMR (500 MHz, $CDCl_3$):** δ 7.31 – 7.25 (m, 2H), 7.15 – 7.07 (m, 3H), 5.82 (ddt, *J* = 15.0, 9.9, 1.3 Hz, 1H), 5.43 (dtd, *J* = 14.9, 6.8, 0.9 Hz, 1H), 4.39 (t, *J* = 5.7 Hz, 1H), 3.35 (s, 3H), 3.34 (s, 3H), 2.92 (d, *J* = 9.9 Hz, 1H), 2.15 – 2.04 (m, 2H), 1.69 – 1.60 (m, 2H), 1.49 – 1.35 (m, 4H), 0.00 (s, 9H). **^{13}C NMR (126 MHz, $CDCl_3$):** δ 143.2, 129.5, 129.0, 128.3, 127.2, 124.5, 104.6, 52.70, 52.65, 42.9, 32.8, 32.4, 29.8, 24.3, -2.9. **FTIR (NaCl, thin film, cm^{-}**

^{1}): 3024, 2948, 2859, 2829, 1597, 1493, 1450, 1248, 1127, 1079, 1054, 965, 839. **HRMS (FAB, *m/z*):** calc'd for $C_{19}H_{32}O_2Si$ $[M+\cdot]^+$: 320.2172; found: 320.2166.

(*S*,*E*)-(5-chloro-1-phenylpent-2-en-1-yl)trimethylsilane (91h)

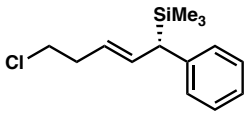

Prepared from (*E*)-1-bromo-4-chlorobut-1-ene (**29h**, 67.8 mg, 0.4 mmol) and (chloro(phenyl)methyl)trimethylsilane (**87**, 39.8 mg, 0.2 mmol) according to General Procedure 7. The crude residue was purified by column chromatography (silica, hexane) to yield **91h** (21.3 mg, 42% yield) in 95% ee as a colorless oil. When the reaction was conducted with an internal standard, the yield was determined to be 67% yield by ^{1}H NMR. $\mathbf{R_f}$ = 0.25 (silica, hexane, $KMnO_4$). **Chiral SFC:** (OD-H, 2.5 mL/min, 1% IPA in CO_2, λ = 210 nm): t_R (major) = 5.2 min, t_R (minor) = 5.9 min. $[\boldsymbol{\alpha}]_{\boldsymbol{D}}^{\mathbf{25}}$ = +25° (c = 1.0, $CHCl_3$). **^{1}H NMR (500 MHz, $CDCl_3$):** δ 7.29 – 7.23 (m, 2H), 7.13 – 7.09 (m, 1H), 7.09 – 7.05 (m, 2H), 5.94 (ddt, *J* = 15.1, 10.0, 1.3 Hz, 1H), 5.40 (dddd, *J* = 15.0, 7.4, 6.6, 1.0 Hz, 1H), 3.58 – 3.48 (m, 2H), 2.94 (d, *J* = 9.9 Hz, 1H), 2.59 – 2.46 (m, 2H), -0.02 (s, 9H). **^{13}C NMR (126 MHz, $CDCl_3$):** δ 142.6, 133.2, 128.4, 127.2, 124.7, 124.1, 44.8, 43.2, 36.2, -2.9. **FTIR (NaCl, thin film, cm^{-1}):** 3025, 2956, 2898, 159, 1494, 1450, 1248, 1081, 968, 840. **HRMS (FAB, *m/z*):** calc'd for $C_{14}H_{21}ClSi$ $[M+H]^+$: 253.1179; found: 253.1175.

The reaction was also conducted on a larger reaction scale using alkenyl bromide **29h** (3.39 g, 20.0 mmol), chlorobenzyl silane **87** (1.99 g, 10.0 mmol), **L2**·$NiCl_2$ (486 mg, 1.0 mmol), Mn powder (1.64 g, 30.0 mmol), and cobalt phthalocyanine (286 mg, 0.5 mmol) in 20 mL NMP. The reaction was stirred at 5 °C for 4 days and subsequently purified by column

chromatography (silica, hexane) to yield **91h** (1.11 g, 44% yield) in 97% ee as a colorless oil. The remaining mixed fractions were not further purified.

(*S*,*E*)-5-phenyl-5-(trimethylsilyl)pent-3-en-1-ol (91i)

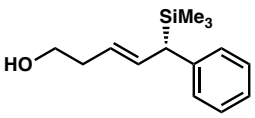

Prepared from (*E*)-4-bromobut-3-en-1-ol (**29i**, 60.4 mg, 0.4 mmol) and (chloro(phenyl)methyl)trimethylsilane (**87**, 39.8 mg, 0.2 mmol) according to General Procedure 7. The crude residue was purified by column chromatography (silica, 0 to 20% EtOAc/hexane) to yield **91i** (20.5 mg, 39% yield) in 97% ee as a faint blue oil (trace CoPc impurity). $\mathbf{R}_f$ = 0.54 (silica, 25% EtOAc/hexane, CAM). **Chiral SFC:** (OJ-H, 2.5 mL/min, 2% MeOH in CO_2, λ = 210 nm): t_R (major) = 6.5 min, t_R (minor) = 8.5 min. $[\boldsymbol{\alpha}]_D^{25}$ = +45° (c = 1.0, $CHCl_3$). **^{1}H NMR (500 MHz, $CDCl_3$):** δ 7.28 – 7.23 (m, 2H), 7.12 – 7.08 (m, 1H), 7.08 – 7.04 (m, 2H), 5.93 (ddt, *J* = 15.1, 10.0, 1.3 Hz, 1H), 5.37 (dtd, *J* = 15.0, 7.1, 0.9 Hz, 1H), 3.62 (t, *J* = 6.4 Hz, 2H), 2.94 (d, *J* = 9.9 Hz, 1H), 2.35 – 2.30 (m, 2H), 1.51 (s, 1H), -0.03 (s, 9H). **^{13}C NMR (126 MHz, $CDCl_3$):** δ 142.8, 133.2, 128.4, 127.2, 124.7, 124.5, 62.4, 43.3, 36.4, -2.9. **FTIR (NaCl, thin film, cm^{-1}):** 3340, 3024, 2954, 289, 1597, 1494, 1450, 1258, 1248, 1081, 1062, 1048, 1032, 967, 866, 839. **HRMS (FAB, *m/z*):** calc'd for $C_{14}H_{22}OSi$ $[M+H]^+$: 235.1518; found: 235.1528.

The reaction was also conducted on a larger reaction scale using alkenyl bromide **29i** (300 mg, 2.0 mmol), chlorobenzyl silane **87** (199 mg, 1.0 mmol), **L2**·$NiCl_2$ (49 mg, 0.1 mmol), Mn powder (165 mg, 3.0 mmol), and cobalt phthalocyanine (29 mg, 0.05 mmol) in 2 mL NMP. The reaction was stirred at 5 °C for 2 days and subsequently purified by column

chromatography (silica, 5 to 30% Et_2O/hexane) to yield **91i** (97 mg, 41% yield) in 97% ee as a faint blue oil.

(*S*,*E*)-5-phenyl-5-(trimethylsilyl)pent-3-en-1-yl benzoate (91j)

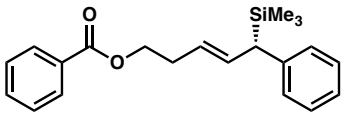

Prepared from (*E*)-4-bromobut-3-en-1-yl benzoate (**29j**, 102.0 mg, 0.4 mmol) and (chloro(phenyl)methyl)trimethylsilane (**87**, 39.8 mg, 0.2 mmol) according to General Procedure 7. The crude residue was purified by column chromatography (silica, 0 to 6% Et_2O/hexane) to yield **91j** (44.9 mg, 66% yield) in 96% ee as a colorless oil. The ^{1}H NMR spectrum shows minor impurities in the aryl region, therefore the purity of **91j** was determined by quantitative NMR to be 97% pure. The yield is adjusted accordingly to (66 x 0.97 = 64% yield). $\mathbf{R_f}$ = 0.52 (silica, 10% EtOAc/hexane, UV). **Chiral SFC:** (OJ-H, 2.5 mL/min, 10% IPA in CO_2, λ = 230 nm): t_R (major) = 3.1 min, t_R (minor) = 4.4 min. $[\boldsymbol{a}]_D^{25}$ = +15° (c = 1.0, $CHCl_3$). **^{1}H NMR (500 MHz, $CDCl_3$):** δ 8.08 – 8.04 (m, 2H), 7.60 – 7.55 (m, 1H), 7.47 – 7.42 (m, 2H), 7.31 – 7.25 (m, 2H), 7.16 – 7.12 (m, 1H), 7.12 – 7.07 (m, 2H), 6.00 (ddq, *J* = 15.1, 10.0, 1.2 Hz, 1H), 5.49 (dtt, *J* = 14.8, 6.9, 0.8 Hz, 1H), 4.38 (t, *J* = 6.6 Hz, 2H), 2.97 (d, *J* = 9.9 Hz, 1H), 2.56 (qd, *J* = 6.5, 1.1 Hz, 2H), -0.02 (d, *J* = 0.6 Hz, 9H). **^{13}C NMR (126 MHz, $CDCl_3$):** δ 166.6, 142.6, 132.8, 132.7, 130.4, 129.6, 128.3 (2C), 127.1, 124.6, 123.8, 64.7, 43.1, 32.4, -2.99. **FTIR (NaCl, thin film, cm^{-1}):** 2956, 1722, 1601, 1493, 1452, 1314, 1275, 1176, 1114, 1070, 1027, 967, 839. **HRMS (TOF-ESI, *m/z*):** calc'd for $C_{21}H_{26}O_2Si$ $[M+H]^+$: 339.1780; found: 339.1755.

(*S*,*E*)-2-methoxy-5-(3-phenyl-3-(trimethylsilyl)prop-1-en-1-yl)pyridine (91k)

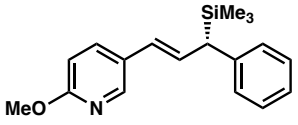

Prepared from (*E*)-5-(2-bromovinyl)-2-methoxypyridine (**29k**, 85.6 mg, 0.4 mmol) and (chloro(phenyl)methyl)trimethylsilane (**87**, 39.8 mg, 0.2 mmol) according to General Procedure 7. The crude residue was purified by column chromatography (silica, 0 to 4% Et_2O/hexane) to yield **91k** (40.6 mg, 68% yield) in 94% ee as a colorless oil. $\mathbf{R_f}$ = 0.45 (silica, 10% EtOAc/hexane, UV). **Chiral SFC:** (OB-H, 2.5 mL/min, 1% IPA in CO_2, λ = 280 nm): t_R (minor) = 7.8 min, t_R (major) = 9.4 min. $[\alpha]_D^{25}$ = +35° (c = 1.0, $CHCl_3$). **^{1}H NMR (500 MHz, $CDCl_3$):** δ 8.07 (dt, *J* = 2.6, 0.6 Hz, 1H), 7.64 (ddd, *J* = 8.6, 2.5, 0.5 Hz, 1H), 7.32 – 7.26 (m, 2H), 7.17 – 7.11 (m, 3H), 6.70 (dt, *J* = 8.6, 0.6 Hz, 1H), 6.48 (dd, *J* = 15.7, 9.9 Hz, 1H), 6.29 (d, *J* = 15.6 Hz, 1H), 3.93 (s, 3H), 3.12 (d, *J* = 9.9 Hz, 1H), 0.02 (s, 9H). **^{13}C NMR (126 MHz, $CDCl_3$):** δ 163.1, 144.7, 142.3, 135.3, 130.1, 128.5, 127.4, 127.2, 124.9, 124.2, 110.8, 53.6, 44.0, -2.7. **FTIR (NaCl, thin film, cm^{-1}):** 3022, 2951, 2899, 1600, 1567, 1492, 1384, 1287, 1249, 1028, 959, 838. **HRMS (FAB, *m/z*):** calc'd for $C_{18}H_{23}NOSi$ $[M+H]^+$: 298.1627; found: 298.1616.

(*S*,*E*)-2-methoxy-5-(3-phenyl-3-(trimethylsilyl)prop-1-en-1-yl)pyrimidine (91l)

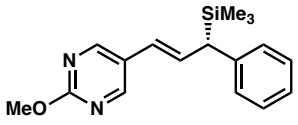

Prepared from (*E*)-5-(2-bromovinyl)-2-methoxypyrimidine (**29l**, 86.0 mg, 0.4 mmol) and (chloro(phenyl)methyl)trimethylsilane (**87**, 39.8 mg, 0.2 mmol) according to General Procedure 7. The crude residue was purified by column chromatography (silica, 0 to 20% Et_2O/hexane) to yield **91l** (26.2 mg, 44% yield) in 94% ee as a faint blue oil (trace CoPc impurity). $\mathbf{R_f}$ = 0.18 (silica, 10% EtOAc/hexane, UV). **Chiral SFC:** (OJ-H, 2.5 mL/min, 5% IPA in CO_2, λ = 254 nm): t_R

(minor) = 11.7 min, t_R (major) = 13.2 min. $[\alpha]_D^{25}$ = +34° (c = 1.0, $CHCl_3$). **^{1}H NMR (500 MHz, $CDCl_3$):** δ 8.47 (s, 2H), 7.32 – 7.27 (m, 2H), 7.17 – 7.10 (m, 3H), 6.56 (dd, *J* = 15.8, 9.9 Hz, 1H), 6.21 (d, *J* = 16.0 Hz, 1H), 4.00 (s, 3H), 3.12 (dd, *J* = 9.9, 1.0 Hz, 1H), 0.02 (s, 9H). **^{13}C NMR (126 MHz, $CDCl_3$):** δ 164.5, 156.2, 141.6, 132.6, 128.7, 127.2, 125.7, 125.1, 120.5, 55.0, 44.4, -2.7. **FTIR (NaCl, thin film, cm^{-1}):** 3023, 2956, 2899, 1593, 1553, 1473, 1410, 1330, 1248, 1047, 1030, 963, 840. **HRMS (FAB, *m/z*):** calc'd for $C_{17}H_{22}N_2OSi$ $[M+H]^+$: 299.1580; found: 299.1591.

(*S*,*E*)-1-(6-phenyl-6-(trimethylsilyl)hex-4-en-1-yl)pyrrolidine-2,5-dione (91m)

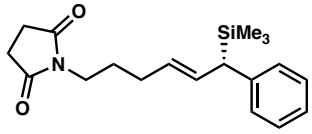

Prepared from (*E*)-1-(hex-4-en-1-yl)pyrrolidine-2,5-dione (**29m**, 98.4 mg, 0.4 mmol) and (chloro(phenyl)methyl)-trimethylsilane (**87**, 39.8 mg, 0.2 mmol) according to General Procedure 7. The crude residue was purified by column chromatography (silica, 0 to 30% acetone/hexane) to yield **91m** (42.0 mg, 64% yield) in 97% ee as a faint blue oil (trace CoPc impurity). $\mathbf{R_f}$ = 0.53 (silica, 30% acetone/hexane, CAM). **Chiral SFC:** (OJ-H, 2.5 mL/min, 5% IPA in CO_2, λ = 210 nm): t_R (minor) = 6.0 min, t_R (major) = 6.4 min. $[\alpha]_D^{25}$ = +15° (c = 1.0, $CHCl_3$). **^{1}H NMR (500 MHz, $CDCl_3$):** δ 7.23 (tt, *J* = 7.9, 1.8 Hz, 2H), 7.10 – 7.06 (m, 1H), 7.06 – 7.03 (m, 2H), 5.82 (ddt, *J* = 15.1, 10.0, 1.4 Hz, 1H), 5.36 (dtd, *J* = 15.1, 6.7, 0.9 Hz, 1H), 3.53 – 3.49 (m, 2H), 2.88 (d, *J* = 10.0 Hz, 1H), 2.63 (q, *J* = 1.4 Hz, 4H), 2.11 – 2.02 (m, 2H), 1.73 – 1.58 (m, 2H), -0.05 (s, 9H). **^{13}C NMR (126 MHz, $CDCl_3$):** δ 177.4, 143.0, 130.4, 128.3, 127.4, 127.2, 124.6, 43.0, 38.7, 30.2, 28.2, 27.7, -2.9. **FTIR (NaCl, thin film, cm^{-}**

[1]): 2950, 1774, 1703, 1437, 1402, 1369, 1344, 1248, 1158, 1129, 840. **HRMS (FAB, *m/z*):** calc'd for $C_{19}H_{27}NO_2Si$ $[M+H]^+$: 330.1889; found: 330.1880.

The reaction was also conducted on a larger reaction scale using alkenyl bromide **29m** (492 mg, 2.0 mmol), chlorobenzyl silane **87** (199 mg, 1.0 mmol), **L2**·$NiCl_2$ (49 mg, 0.1 mmol), Mn^0 powder (165 mg, 3.0 mmol), and cobalt phthalocyanine (29 mg, 0.05 mmol) in 2 mL NMP. The reaction was stirred at 5 °C for 4 days and subsequently purified by column chromatography (silica, 0 to 30% acetone/hexane) to yield **91m** (196 mg, 59% yield) in 97% ee as a faint blue oil.

(*S*,*E*)-1-(6-phenyl-6-(trimethylsilyl)hex-4-en-1-yl)pyrrolidin-2-one (91n)

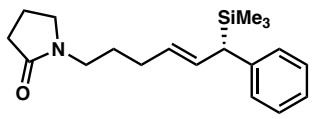

Prepared from (*E*)-1-(5-bromopent-4-en-1-yl)pyrrolidin-2-one (**29n**, 92.8 mg, 0.4 mmol) and (chloro(phenyl)methyl)-trimethylsilane (**87**, 39.8 mg, 0.2 mmol) according to General Procedure 7. The crude residue was purified by column chromatography (silica, 0 to 30% acetone/hexane) to yield **91n** (30.6 mg, 48% yield) in 96% ee as a faint blue oil (trace CoPc impurity). $\mathbf{R_f}$ = 0.44 (silica, 30% acetone/hexane, CAM). **Chiral SFC:** (OB-H, 2.5 mL/min, 5% IPA in CO_2, λ = 210 nm): t_R (major) = 6.4 min, t_R (minor) = 8.6 min. $[\boldsymbol{a}]_{\boldsymbol{D}}^{\mathbf{25}}$ = +26° (c = 0.5, $CHCl_3$). **^{1}H NMR (500 MHz, $CDCl_3$):** δ 7.26 – 7.21 (m, 2H), 7.11 – 7.06 (m, 1H), 7.06 – 7.03 (m, 2H), 5.81 (ddt, *J* = 15.1, 10.0, 1.4 Hz, 1H), 5.38 (dtd, *J* = 14.8, 6.8, 0.9 Hz, 1H), 3.39 – 3.33 (m, 2H), 3.28 (t, *J* = 7.4 Hz, 2H), 2.89 (d, *J* = 10.0 Hz, 1H), 2.37 (t, *J* = 8.1 Hz, 2H), 2.09 – 2.03 (m, 2H), 2.00 (ddd, *J* = 14.2, 8.1, 6.9 Hz, 2H), 1.59 (qt, *J* = 7.8, 3.4 Hz, 2H), -0.04 (s, 9H). **^{13}C NMR (126 MHz, $CDCl_3$):** δ 175.0, 143.1, 130.2, 128.4, 127.8, 127.2,

124.6, 47.3, 43.0, 42.4, 31.2, 30.3, 27.7, 18.0, -2.8. **FTIR (NaCl, thin film, cm^{-1}):** 2923, 2862, 1690, 1494, 1462, 1426, 1285, 1247, 839. **HRMS (FAB, *m/z*):** calc'd for $C_{19}H_{29}NOSi$ $[M+H]^+$: 316.2087; found: 316.2097.

(*S*,*E*)-(3-(3-methoxyphenyl)prop-1-ene-1,3-diyl)bis(trimethylsilane) (91o)

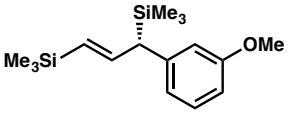

Prepared from (*E*)-(2-bromovinyl)trimethylsilane (**29o**, 71.7 mg, 0.4 mmol) and (chloro(3-methoxyphenyl)methyl)trimethylsilane (**89g**, 45.8 mg, 0.2 mmol) according to General Procedure 7. The crude residue was purified by column chromatography (silica, 0 to 15% toluene/hexane) to yield **91o** (42.0 mg, 72% yield) in 93% ee as a colorless oil. $\mathbf{R_f}$ = 0.69 (silica, 5% Et_2O/hexane, CAM). **Chiral HPLC:** (OD-H, 1.0 mL/min, hexane, λ = 230 nm): t_R (minor) = 4.5 min, t_R (major) = 4.8 min. $[\boldsymbol{\alpha}]_{\boldsymbol{D}}^{\mathbf{25}}$ = +26° (c = 1.0, $CHCl_3$). **^{1}H NMR (500 MHz, $CDCl_3$):** δ 7.20 (t, *J* = 7.9 Hz, 1H), 6.73 – 6.63 (m, 3H), 6.33 (dd, *J* = 18.3, 9.4 Hz, 1H), 5.57 (dd, *J* = 18.4, 1.1 Hz, 1H), 3.81 (s, 3H), 3.02 (dd, *J* = 9.3, 1.0 Hz, 1H), 0.08 (s, 9H), -0.02 (s, 9H). **^{13}C NMR (126 MHz, $CDCl_3$):** δ 159.7, 145.8, 144.0, 129.3, 127.8, 119.9, 113.3, 109.6, 55.2, 48.4, -0.9, -2.8. **FTIR (NaCl, thin film, cm^{-1}):** 2954, 2898, 2834, 1596, 1486, 1466, 1451, 1436, 1284, 1248, 1148, 1054, 988, 868, 838. **HRMS (EI, *m/z*):** calc'd for $C_{16}H_{28}OSi_2$ $[M+\cdot]^+$: 292.1679; found: 292.1690.

(*S*,*E*)-(1-(3-methoxyphenyl)but-2-en-1-yl)trimethylsilane (91p)

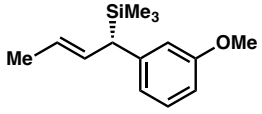

Prepared from (*E*)-1-bromoprop-1-ene (**29p**, 48.4 mg, 0.4 mmol) and (chloro(3-methoxyphenyl)methyl)trimethylsilane (**89g**, 45.8 mg, 0.2 mmol) according to General Procedure 7. The crude residue was purified by

column chromatography (silica, 0 to 10% toluene/hexane) to yield **91p** (22.1 mg, 47% yield) in 96% ee as a colorless oil. $\mathbf{R_f}$ = 0.63 (silica, 5% Et_2O/hexane, CAM). **Chiral SFC:** (OD-H, 2.5 mL/min, 3% IPA in CO_2, λ = 235 nm): t_R (major) = 3.4 min, t_R (minor) = 4.4 min. $[\boldsymbol{\alpha}]_D^{25}$ = +20° (c = 1.0, $CHCl_3$). **^{1}H NMR (500 MHz, $CDCl_3$):** δ 7.20 – 7.13 (m, 1H), 6.69 – 6.60 (m, 3H), 5.78 (ddq, *J* = 14.9, 10.0, 1.6 Hz, 1H), 5.41 (dqd, *J* = 15.0, 6.4, 0.9 Hz, 1H), 3.79 (s, 3H), 2.86 (d, *J* = 10.0 Hz, 1H), 1.70 (ddd, *J* = 6.4, 1.6, 0.6 Hz, 3H), -0.04 (s, 9H). **^{13}C NMR (126 MHz, $CDCl_3$):** δ 159.6, 145.0, 130.2, 129.2, 123.7, 119.9, 113.2, 109.6, 55.2, 43.1, 18.3, -2.8. **FTIR (NaCl, thin film, cm^{-1}):** 2956, 2917, 1598, 1579, 1487, 1436, 1290, 1258, 1247, 1149, 1050, 851, 838. **HRMS (TOF-ESI, *m/z*):** calc'd for $C_{14}H_{22}OSi$ $[M+H]^+$: 235.1518; found: 235.1498.

The reaction was also conducted with 1-bromoprop-1-ene (3:1 *cis* and *trans* mixture) (96.8 mg, 0.8 mmol, 4 equiv) and (chloro(3-methoxyphenyl)methyl)trimethylsilane (**89g**, 45.8 mg, 0.2 mmol) according to General Procedure 7. The crude residue was purified by column chromatography (silica, 0 to 20% toluene/hexane) to yield **91p** (12.5 mg, 27% yield) as a mixture of isomers (approx. 4 compounds, *E* allylic silane is the major product).

(*S*,*E*)-(3-(furan-2-yl)-1-(3-methoxyphenyl)allyl)trimethylsilane (91q)

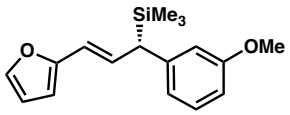

Prepared from (*E*)-2-(2-bromovinyl)furan (**29q**, 69.2 mg, 0.4 mmol) and (chloro(3-methoxyphenyl)methyl)trimethylsilane (**89g**, 45.8 mg, 0.2 mmol) according to General Procedure 7. The crude residue was purified by column chromatography (silica, 0 to 20% toluene/hexane) to yield **91q** (35.2 mg, 61% yield) in 95% ee as a yellow oil. $\mathbf{R_f}$ = 0.38 (silica, 5% Et_2O/hexane, UV). **Chiral SFC:**

(OJ-H, 2.5 mL/min, 1% IPA in CO_2, λ = 280 nm): t_R (minor) = 9.3 min, t_R (major) = 10.3 min. $[\boldsymbol{a}]_D^{25}$ = +13° (c = 1.0, $CHCl_3$). **^{1}H NMR (500 MHz, $CDCl_3$):** δ 7.31 (dd, *J* = 1.9, 0.7 Hz, 1H), 7.20 (td, *J* = 7.6, 1.0 Hz, 1H), 6.76 – 6.72 (m, 1H), 6.71 – 6.66 (m, 2H), 6.54 (dd, *J* = 15.6, 10.0 Hz, 1H), 6.35 (dd, *J* = 3.2, 1.8 Hz, 1H), 6.17 (dd, *J* = 15.6, 1.0 Hz, 1H), 6.10 (d, *J* = 3.2 Hz, 1H), 3.81 (s, 3H), 3.04 (d, *J* = 9.8 Hz, 1H), 0.03 (s, 9H). **^{13}C NMR (126 MHz, $CDCl_3$):** δ 159.7, 153.6, 143.9, 141.2, 129.43, 129.38, 120.0, 116.8, 113.4, 111.2, 109.9, 105.8, 55.3, 44.0, -2.6. **FTIR (NaCl, thin film, cm^{-1}):** 2956, 2899, 2835, 1598, 1580,1488, 1452, 1465, 1436, 1289, 1250, 1150, 1049, 1012, 960, 839. **HRMS (FAB, *m/z*):** calc'd for $C_{17}H_{22}O_2Si$ $[M+\cdot]^+$: 286.1389; found: 286.1377.

(*S*,*E*)-(1-(3-methoxyphenyl)-3-(thiophen-2-yl)allyl)trimethylsilane (91r)

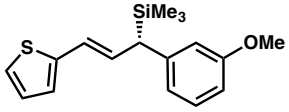

Prepared from (*E*)-2-(2-bromovinyl)thiophene (**29r**, 75.6 mg, 0.4 mmol) and (chloro(3-methoxyphenyl)methyl)trimethylsilane (**89g**, 45.8 mg, 0.2 mmol) according to General Procedure 7. The crude residue was purified by column chromatography (silica, 0 to 20% toluene/hexane) to yield **91r** (34.3 mg, 57% yield) in 95% ee as a yellow oil. $\mathbf{R}_f$ = 0.44 (silica, 5% Et_2O/hexane, UV). **Chiral SFC:** (OJ-H, 2.5 mL/min, 5% IPA in CO_2, λ = 280 nm): t_R (minor) = 4.4 min, t_R (major) = 5.5 min. $[\boldsymbol{a}]_D^{25}$ = +27° (c = 1.0, $CHCl_3$). **^{1}H NMR (500 MHz, $CDCl_3$):** δ 7.25 – 7.18 (m, 1H), 7.08 (dt, *J* = 5.1, 0.9 Hz, 1H), 6.94 (dd, *J* = 5.1, 3.5 Hz, 1H), 6.87 – 6.84 (m, 1H), 6.76 – 6.71 (m, 1H), 6.71 – 6.66 (m, 2H), 6.49 (d, *J* = 15.6 Hz, 1H), 6.42 (dd, *J* = 15.4, 9.2 Hz, 1H), 3.81 (s, 3H), 3.06 (d, *J* = 9.2 Hz, 1H), 0.04 (s, 9H). **^{13}C NMR (126 MHz, $CDCl_3$):** δ 159.7, 143.8, 143.4, 130.5, 129.4, 127.4, 124.0, 122.9, 121.5, 119.9, 113.4, 109.9, 55.3, 43.9, -2.6. **FTIR (NaCl, thin film, cm^{-1}):** 3021, 2998, 2954, 2834, 1604, 1598, 1580, 1488,

1465, 1451, 1435, 1288, 1258, 1248, 1148, 1048, 952, 838. **HRMS (FAB, *m/z*):** calc'd for $C_{17}H_{22}OSSi$ $[M+\cdot]^+$: 302.1161; found: 302.1168.

(*S*,*E*)-*tert*-butyl((4-(3-methoxyphenyl)-4-(trimethylsilyl)but-2-en-1-yl)oxy)dimethylsilane (91s)

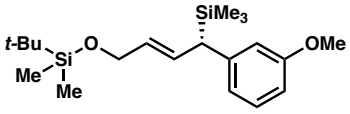

Prepared from (*E*)-((3-bromoallyl)oxy)(*tert*-butyl)dimethylsilane (**29s**, 100.5 mg, 0.4 mmol) and (chloro(3-methoxyphenyl)methyl)-trimethylsilane (**89g**, 45.8 mg, 0.2 mmol) according to General Procedure 7. The crude residue was purified by column chromatography (10% $AgNO_3$ on silica, 0 to 4% Et_2O/hexane) to yield **91s** (45.1 mg, 62% yield) in 97% ee as a colorless oil. $\mathbf{R_f}$ = 0.47 (silica, 5% Et_2O/hexane, CAM). **Chiral SFC:** (OD-H, 2.5 mL/min, 2% IPA in CO_2, λ = 210 nm): t_R (major) = 5.1 min, t_R (minor) = 7.4 min. $[\boldsymbol{\alpha}]_D^{25}$ = +14° (c = 1.0, $CHCl_3$). **^{1}H NMR (500 MHz, $CDCl_3$):** δ 7.17 (t, *J* = 7.9 Hz, 1H), 6.69 – 6.60 (m, 3H), 6.01 (ddt, *J* = 15.1, 9.9, 1.5 Hz, 1H), 5.52 (dtd, *J* = 15.0, 5.4, 1.0 Hz, 1H), 4.17 (dd, *J* = 5.4, 1.5 Hz, 2H), 3.79 (s, 3H), 2.93 (d, *J* = 9.9 Hz, 1H), 0.92 (s, 9H), 0.07 (s, 6H), -0.02 (s, 9H). **^{13}C NMR (126 MHz, $CDCl_3$):** δ 159.6, 144.3, 130.3, 129.2, 127.9, 119.9, 113.7, 109.8, 64.1, 55.2, 42.9, 26.1, 18.5, -2.8, -4.93, -4.95. **FTIR (NaCl, thin film, cm^{-1}):** 2955, 2930, 2896, 2857, 1599, 1580, 1488, 1464, 1249, 1149, 1031, 1102, 1050, 967, 837. **HRMS (FAB, *m/z*):** calc'd for $C_{20}H_{36}O_2Si_2$ $[M+H-H_2]^+$: 363.2176; found: 363.2193.

((4*S*,*E*)-1-(3-methoxyphenyl)-4,8-dimethylnona-2,7-dien-1-yl)trimethylsilane ((*rac*)-91tu)

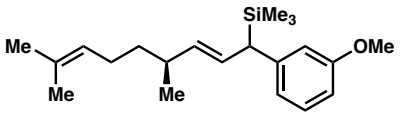

Prepared from (*S*,*E*)-1-bromo-3,7-dimethylocta-1,6-diene (**29t**, 86.9 mg, 0.4 mmol) and (chloro(3-methoxyphenyl)methyl)-trimethylsilane (**89g**, 45.8 mg, 0.2 mmol) according to General Procedure 7, with the exception of racemic **L2** (7.8 mg, 0.022 mmol) and $NiCl_2$(dme) (4.4 mg, 0.02 mmol) in place of (*3R*,*8S*)-**L2**·$NiCl_2$. The crude residue was purified by column chromatography (silica, 0 to 15% toluene/hexane) to yield **(***1-rac,4S***)-91tu** (38.3 mg, 58% yield) in 2:1 dr (determined by NMR analysis of the purified product) as a colorless oil. Spectral data for each diastereomer are reported below. $\mathbf{R}_f$ = 0.63 (silica, 5% Et_2O/hexane, CAM). $[\alpha]_D^{25}$ = +26° (c = 1.0, $CHCl_3$). **FTIR (NaCl, thin film, cm^{-1}):** 2958, 2913, 1598, 1580, 1487, 1451, 1436, 1258, 1248, 1148, 1048, 966, 837. **HRMS (FAB, *m/z*):** calc'd for $C_{21}H_{34}OSi$ $[M+H]^+$: 331.2457; found: 331.2455.

((1*S*,4*S*,*E*)-1-(3-methoxyphenyl)-4,8-dimethylnona-2,7-dien-1-yl)trimethylsilane ((*S*,*S*)-91t)

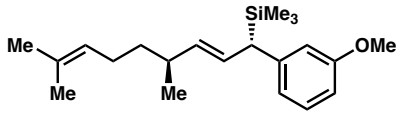

Prepared from (*S*,*E*)-1-bromo-3,7-dimethylocta-1,6-diene (**29t**, 86.9 mg, 0.4 mmol) and (chloro(3-methoxyphenyl)methyl)-trimethylsilane (**89g**, 45.8 mg, 0.2 mmol) according to General Procedure 7. The crude residue was purified by column chromatography (silica, 0 to 15% toluene/hexane) to yield (*1S*,*4S*)-**91t** (45.8 mg, 69% yield) in 40:1 dr (determined by NMR analysis of the purified product) as a colorless oil. $[\alpha]_D^{25}$ = +43° (c = 1.0, $CHCl_3$). **^{1}H NMR (500 MHz, $CDCl_3$):** δ 7.21 – 7.14 (m, 1H), 6.70 – 6.62 (m, 3H), 5.73 (ddd, *J* = 15.1, 10.0,

1.0 Hz, 1H), 5.26 (ddd, *J* = 15.0, 8.0, 0.9 Hz, 1H), 5.14 (tdq, *J* = 7.2, 2.9, 1.4 Hz, 1H), 3.80 (s, 3H), 2.87 (d, *J* = 9.9 Hz, 1H), 2.19 – 2.09 (m, 1H), 2.08 – 1.91 (m, 2H), 1.71 (q, *J* = 1.3 Hz, 3H), 1.62 (d, *J* = 1.3 Hz, 3H), 1.36 – 1.29 (m, 2H), 0.98 (d, *J* = 6.7 Hz, 3H), -0.02 (s, 9H). **^{13}C NMR (126 MHz, $CDCl_3$):** δ 159.6, 145.1, 135.3, 131.3, 129.2, 127.5, 124.9, 119.9, 113.2, 109.5, 55.2, 43.0, 37.6, 37.1, 26.2, 25.9, 21.3, 17.9, -2.7.

((1*R*,4*S*,*E*)-1-(3-methoxyphenyl)-4,8-dimethylnona-2,7-dien-1-yl)trimethylsilane ((*R*,*S*)-91u)

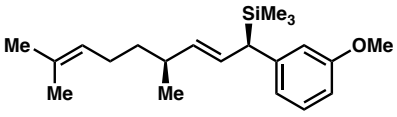

Prepared from (*S*,*E*)-1-bromo-3,7-dimethylocta-1,6-diene (**29t**, 86.9 mg, 0.4 mmol) and (chloro(3-methoxyphenyl)methyl)-trimethylsilane (**89g**, 45.8 mg, 0.2 mmol) according to General Procedure 7, with the exception of the (*3S,8R*)-**L2**·$NiCl_2$ catalyst (9.7 mg, 0.02 mmol) in place of the (*3R*,*8S*)-**L2**·$NiCl_2$ catalyst. The crude residue was purified by column chromatography (silica, 0 to 15% toluene/hexane) to yield (*1R*,*4S*)-**91u** (28.4 mg, 43% yield) in 1:19 dr (determined by NMR analysis of the purified product) as a colorless oil. $[\alpha]_D^{25}$ = –9° (c = 1.0, $CHCl_3$). **^{1}H NMR (500 MHz, $CDCl_3$):** δ 7.19 – 7.13 (m, 1H), 6.69 – 6.60 (m, 3H), 5.75 – 5.67 (m, 1H), 5.28 (ddd, *J* = 15.1, 7.7, 0.9 Hz, 1H), 5.08 (tdq, *J* = 7.2, 2.9, 1.5 Hz, 1H), 3.79 (s, 3H), 2.87 (d, *J* = 9.9 Hz, 1H), 2.18 – 2.08 (m, 1H), 1.98 – 1.90 (m, 2H), 1.67 (q, *J* = 1.3 Hz, 3H), 1.55 (d, *J* = 0.8 Hz, 3H), 1.33 – 1.25 (m, 2H), 1.00 (d, *J* = 6.7 Hz, 3H), -0.04 (s, 9H). **^{13}C NMR (126 MHz, $CDCl_3$):** δ 159.6, 145.1, 135.2, 131.3, 129.1, 127.3, 124.9, 119.9, 113.2, 109.5, 55.2, 42.9, 37.5, 36.7, 26.1, 25.9, 21.2, 17.8, -2.8.

(*S*,*E*)-trimethyl(1-phenylbut-2-en-1-yl)silane (S22)

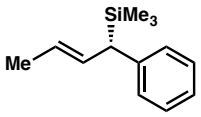

Prepared from (*E*)-1-bromoprop-1-ene (**29p**, 48.4 mg, 0.4 mmol) and (chloro(phenyl)methyl)trimethylsilane (**87**, 39.8 mg, 0.2 mmol) according to General Procedure 7. The reaction provided the desired product in 54% yield by ^{1}H NMR with an internal standard. The crude residue was purified by column chromatography (column 1 – silica, hexane and column 2 – 5% $AgNO_3$ doped silica, 1% Et_2O/hexane) to yield 7.5 mg (18% yield) of **S22** as a colorless oil. Spectral data matched those reported in the literature.[61]

The product was analyzed by optical rotation to give $[\boldsymbol{\alpha}]_{\boldsymbol{D}}^{\mathbf{25}}$ = +23° (c = 0.75, $CHCl_3$) and by comparison to a known literature value (R-isomer (94% ee), $[\boldsymbol{\alpha}]_{\boldsymbol{D}}^{\mathbf{25}}$ = –40.1° (c = 2.0, $CHCl_3$)) we have assigned our product as the S-isomer.[61]

2.6.6 Derivatization of Enantioenriched Allylic Silanes

2.6.6.1 Products from Allylic Silanes

(*S*)-(3-(4-methoxyphenyl)-1-phenylpropyl)trimethylsilane (106)

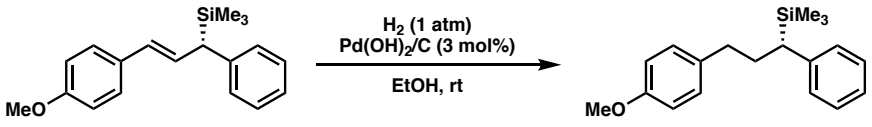

The allylic silane **88c** (267 mg, 0.9 mmol, 1.0 equiv, 97% ee) was added to a 10 mL round bottom flask and dissolved in 2 mL of EtOH. $Pd(OH)_2$/C (18 mg, 0.03 mmol, 0.03 equiv, 20% Pd on carbon) was added, the flask was sealed with a rubber septum, and the headspace was purged with H_2. The reaction stirred at room temperature for 2 hours under 1 atm of H_2, and was then removed from the stir plate and filtered over a plug of silica

while eluting with Et_2O. The solution was concentrated under reduced pressure to afford 262.9 mg (98% yield) of **106** in 93% ee as a colorless oil. $\mathbf{R}_f$ = 0.34 (silica, 10% EtOAc/hexane, UV). **Chiral SFC:** (AD-H, 2.5 mL/min, 5% IPA in CO_2, λ = 210 nm): t_R (minor) = 2.6 min, t_R (major) = 3.0 min. $[\alpha]_D^{25}$ = +4° (c = 1.0, $CHCl_3$). **^{1}H NMR (500 MHz, $CDCl_3$):** δ 7.35 – 7.30 (m, 2H), 7.20 – 7.15 (m, 1H), 7.09 (ddd, *J* = 15.9, 7.4, 1.8 Hz, 4H), 6.89 – 6.85 (m, 2H), 3.83 (s, 3H), 2.66 (ddd, *J* = 13.6, 9.3, 4.0 Hz, 1H), 2.41 (ddd, *J* = 13.5, 8.7, 7.2 Hz, 1H), 2.21 – 2.00 (m, 3H), -0.01 (s, 9H). **^{13}C NMR (126 MHz, $CDCl_3$):** δ 157.7, 143.4, 134.8, 129.5, 128.3, 127.9, 124.5, 113.8, 55.3, 36.5, 34.5, 31.7, -2.9. **FTIR (NaCl, thin film, cm^{-1}):** 2953, 2934, 1612, 1512, 1451, 1247, 1177, 1039, 858, 836. **HRMS (FAB, *m/z*):** calc'd for $C_{19}H_{26}OSi$ $[M+H]^+$: 299.1831; found: 299.1834.

(*R*,*E*)-4-(3-methoxyphenyl)but-3-en-2-ol (111)

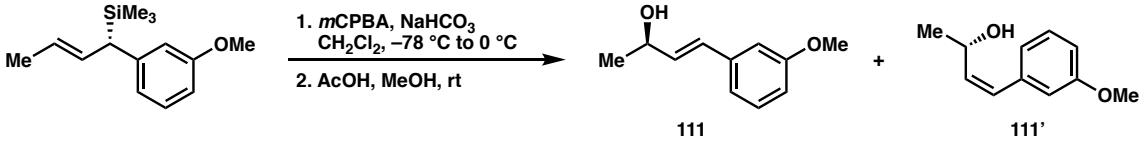

Similar to a procedure by Hayashi and coworkers,[63] the allylic silane **91p** (46.9 mg, 0.2 mmol, 1 equiv, 97% ee) and sodium bicarbonate (20 mg, 0.2 mmol, 1 equiv) were added to a 2 dram vial fitted with a magnetic stir bar and a septum. The vial was purged with N_2 and then 1.0 mL of CH_2Cl_2 was added. The mixture was cooled to –78 °C. A solution of *m*CPBA (54 mg, 77 wt%, 0.24 mmol, 1.2 equiv) in CH_2Cl_2 (1.0 mL) was added to the reaction. The vial was warmed to 0 °C and stirred for one hour, and then concentrated under reduced pressure. The crude residue was dissolved in MeOH (2.0 mL) and acetic acid (140 μL), and stirred at room temperature for 20 minutes, before being diluted with

Et_2O (0.2 mL), washed with 20% NaOH (10 mL) and water (10 mL), dried with $MgSO_4$, filtered, and concentrated under reduced pressure. The crude residue was purified by column chromatography (silica, 0 to 30% Et_2O/hexane) to yield 24.7 mg of **111**+**111'** (69% yield) as a 93:7 mixture of *E*:*Z* isomers (both in 91% ee) as a colorless oil. The stereochemistry of the alcohol is opposite for each *E*:*Z* isomer.[63] Absolute stereochemistry was assigned based on literature precedence.[63] $\mathbf{R}_f$ = 0.32 (silica, 30% EtOAc/hexane, UV). **Chiral SFC:** (OB-H, 2.5 mL/min, 10% IPA in CO_2, λ = 254 nm): *Z*-olefin, t_R (minor) = 2.8 min, t_R (major) = 3.3 min; *E*-olefin, t_R (minor) = 4.5 min, t_R (major) = 5.1 min. $[\boldsymbol{a}]_D^{25}$ = +14° (c = 1.0, $CHCl_3$). **FTIR (NaCl, thin film, cm^{-1}):** 3370, 2969, 2928, 2835, 1598, 1579, 1490, 1465, 1454, 1432, 1319, 1289, 1269, 1156, 1048, 970, 945, 868. **HRMS (FAB, *m/z*)**: calc'd for $C_{11}H_{14}O_2$ $[M+\cdot]^+$: 178.0994; found: 178.0999.

Major isomer (*R*-enantiomer, *E*-olefin): ^{1}H NMR (500 MHz, $CDCl_3$): δ 7.23 (t, *J* = 7.9 Hz, 1H), 6.97 (dt, *J* = 7.6, 1.2 Hz, 1H), 6.92 (dd, *J* = 2.6, 1.6 Hz, 1H), 6.80 (ddd, *J* = 8.3, 2.6, 0.9 Hz, 1H), 6.53 (dd, *J* = 15.9, 1.1 Hz, 1H), 6.26 (dd, *J* = 15.9, 6.4 Hz, 1H), 4.52 – 4.45 (m, 1H), 3.81 (s, 3H), 1.83 (s, 1H), 1.37 (d, *J* = 6.4 Hz, 3H). **^{13}C NMR (126 MHz, $CDCl_3$):** δ 159.9, 138.2, 134.0, 129.7, 129.3, 119.2, 113.4, 111.8, 69.0, 55.3, 23.5.

(3*R*,4*R*,*E*)-6-(3-methoxyphenyl)-4-methylhex-5-en-3-ol (113)

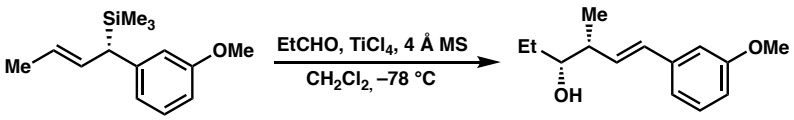

To a 2 dram vial equipped with a magnetic stir bar was added **91p** (46.9 mg, 0.2 mmol, 1 equiv, 97% ee) and 100 mg oven-dried 4 Å molecular sieves, and then placed under inert

atmosphere (Ar). The allylic silane was dissolved in 2.0 mL anhydrous CH_2Cl_2 (0.1 M) and the freshly distilled propionaldehyde (29 μL, 0.4 mmol, 2.0 equiv) was added via syringe. The reaction was cooled to –78 °C and stirred for 5 minutes, before the $TiCl_4$ (240 μL, 1.0 M in CH_2Cl_2, 0.24 mmol, 1.2 equiv) was added dropwise down the side of the vial. The reaction continued to stir at –78 °C for 10 minutes, before being quenched with H_2O (0.4 mL) at –78 °C and warmed to room temperature. The aqueous layer was extracted with Et_2O (3 x 20 mL), and the combined organic layers were dried with Na_2SO_4, filtered, and concentrated under reduced pressure. The crude material was purified by column chromatography (silica, 0 to 20% Et_2O/hexane) to yield 33.2 mg of **113** (75% yield) in 97% ee as a colorless oil. Absolute and relative stereochemistry was assigned based on literature precedence.[20] $\mathbf{R_f}$ = 0.48 (silica, 30% EtOAc/hexane, UV). **Chiral SFC:** (OB-H, 2.5 mL/min, 10% IPA in CO_2, λ = 254 nm): t_R (minor) = 4.8 min, t_R (major) = 6.2 min. $[\boldsymbol{\alpha}]_{\boldsymbol{D}}^{\mathbf{25}}$ = +47° (c = 1.0, $CHCl_3$). **^{1}H NMR (500 MHz, $CDCl_3$):** δ 7.22 (t, *J* = 7.9 Hz, 1H), 6.97 (ddt, *J* = 7.7, 1.5, 0.7 Hz, 1H), 6.91 (dd, *J* = 2.6, 1.6 Hz, 1H), 6.78 (ddd, *J* = 8.2, 2.6, 0.9 Hz, 1H), 6.41 (dt, *J* = 15.9, 0.7 Hz, 1H), 6.18 (dd, *J* = 15.9, 8.0 Hz, 1H), 3.82 (s, 3H), 3.49 (ddd, *J* = 8.9, 5.3, 3.7 Hz, 1H), 2.45 (dqdd, *J* = 8.0, 6.8, 5.3, 1.2 Hz, 1H), 1.62 (dqd, *J* = 13.9, 7.5, 3.8 Hz, 1H), 1.58 (s, 1H), 1.48 – 1.38 (m, 1H), 1.14 (d, *J* = 6.8 Hz, 3H), 1.00 (t, *J* = 7.4 Hz, 3H). **^{13}C NMR (126 MHz, $CDCl_3$):** δ 159.9, 139.0, 133.3, 130.3, 129.6, 118.9, 112.9, 111.5, 76.8, 55.3, 42.9, 27.3, 15.1, 10.5. **FTIR (NaCl, thin film, cm^{-1}):** 3401, 2962, 2935, 2875, 2835, 1599, 1579, 1489, 1464, 1457, 1433, 1375, 1318, 1289, 1264, 1157, 1048, 971. **HRMS (FAB, *m/z*):** calc'd for $C_{14}H_{20}O_2$ $[M+H]^+$: 221.1542; found: 221.1531.

tert-butyl(((3_R_,4_R_,_E_)-6-(3-methoxyphenyl)-4-methylhex-5-en-3-yl)oxy)diphenyl-silane (S23)

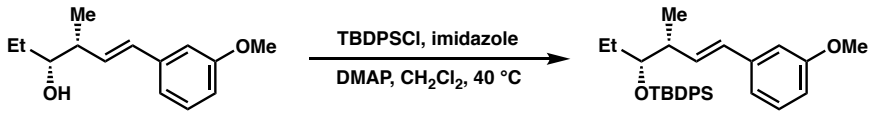

Alcohol **113** (24.2 mg, 0.11 mmol, 1 equiv) was added to a 20 mL scintillation vial equipped with a magnetic stir bar, placed under inert atmosphere (N_2), and dissolved in 2 mL CH_2Cl_2. The *tert*-butyldiphenylchlorosilane (TBDPSCl, 84 µL, 0.33 mmol, 3 equiv), imidazole (30 mg, 0.44 mmol, 4 equiv), and 4-dimethylaminopyridine (DMAP, 1.3 mg, 0.011 mmol, 0.10 equiv) were added, and the reaction was heated to 40 °C and stirred for 24 hours. The reaction was then cooled to room temperature, quenched with aq. NH_4Cl (20 mL), and extracted with pentane (3 x 20 ml). The combined organic layers were dried with $MgSO_4$, filtered, and concentrated under reduced pressure. The crude material was purified by column chromatography (silica, 0 to 3% Et_2O/hexane) to yield 47.6 mg of **S23** (97% yield) as a colorless oil. $\mathbf{R_f}$ = 0.42 (silica, 5% Et_2O/hexane, UV). $[\boldsymbol{a}]_D^{25}$ = +99° (c = 1.0, $CHCl_3$). **^{1}H NMR (500 MHz, $CDCl_3$):** δ 7.73 – 7.69 (m, 4H), 7.46 – 7.40 (m, 2H), 7.40 – 7.32 (m, 4H), 7.22 (t, *J* = 7.9 Hz, 1H), 6.90 (dt, *J* = 7.7, 1.2 Hz, 1H), 6.87 (dd, *J* = 2.6, 1.6 Hz, 1H), 6.78 (ddd, *J* = 8.2, 2.6, 0.9 Hz, 1H), 6.37 – 6.28 (m, 2H), 3.82 (s, 3H), 3.69 (ddd, *J* = 6.3, 5.4, 4.0 Hz, 1H), 2.55 – 2.47 (m, 1H), 1.57 – 1.41 (m, 2H), 1.10 (s, 9H), 1.09 (d, *J* = 6.9 Hz, 3H), 0.76 (t, *J* = 7.4 Hz, 3H). **^{13}C NMR (126 MHz, $CDCl_3$):** δ 159.8, 139.5, 136.22, 136.17, 134.9, 134.7, 134.4, 129.6, 129.53, 129.50, 129.0, 127.6, 127.5, 118.9, 112.7, 111.2, 78.6, 55.3, 41.1, 27.3, 27.0, 19.7, 14.6, 10.0, 1.2. **FTIR (NaCl, thin film, cm^{-1}):** 3071, 3048, 2963, 2932, 2857, 1598, 1579, 1488, 1464, 1428, 1377, 1288, 1265,

1192, 1157, 1110, 1049, 1018, 970, 821. **HRMS (FAB, *m/z*):** calc'd for $C_{30}H_{38}O_2Si$ $[M+H–H_2]^+$: 457.2563; found: 457.2556.

(2*R*,3*R*)-3-((*tert*-butyldiphenylsilyl)oxy)-2-methylpentan-1-ol (114)

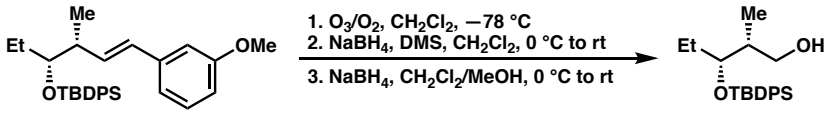

Alkene **S23** (45.9 mg, 0.1 mmol, 1 equiv) was dissolved in 10 mL of CH_2Cl_2 in a 25 mL round bottom flask, cooled to –78 °C, and O_2 was bubbled through the solution for 2 minutes. The ozone generator was turned on and a mixture of O_3/O_2 was bubbled through the reaction until the complete consumption of **S23** by TLC (*approx. 20 minutes, at which time the solution turned blue*). The ozone generator was turned off and N_2 was bubbled through the solution for 2 minutes. Sodium borohydride (75.6 mg, 2.0 mmol, 20 equiv) and dimethylsulfide (145 μL, 2.0 mmol, 20 equiv) were added, the reaction was stirred overnight at room temperature, then quenched with aq. NH_4Cl (10 mL) and extracted with Et_2O (3 x 10 mL). The combined organic layers were dried with $MgSO_4$, filtered, and concentrated. The crude material was dissolved in 5.0 mL of CH_2Cl_2 and 5.0 mL of MeOH, cooled to 0 °C, and sodium borohydride (37.8 mg, 1.0 mmol, 10 equiv) was added. The reaction was stirred at 0 °C and warmed to room temperature over the course of 3 hours. The reaction was quenched with aq. NH_4Cl (10 mL) and extracted with Et_2O (3 x 10 mL). The combined organic layers were dried with $MgSO_4$, filtered, and concentrated under reduced pressure. The crude residue was purified by column chromatography (silica, 0 to 25% Et_2O/hexane) to yield 24.4 mg of **114** (68% yield) as a colorless oil. $\mathbf{R}_f$ = 0.42 (silica, 20% EtOAc/hexane, UV/anisaldehyde (stains dark blue)). $[\alpha]_D^{25}$ = –8° (c = 1.0, $CHCl_3$). **^{1}H**

NMR (500 MHz, $CDCl_3$): δ 7.75 – 7.66 (m, 4H), 7.48 – 7.36 (m, 6H), 3.75 (ddd, *J* = 7.3, 6.1, 2.5 Hz, 1H), 3.66 (t, *J* = 9.3 Hz, 1H), 3.51 (dt, *J* = 10.3, 4.9 Hz, 1H), 1.95 – 1.87 (m, 1H), 1.86 (s, 1H), 1.59 – 1.45 (m, 2H), 1.07 (s, 9H), 0.86 (d, *J* = 7.0 Hz, 3H), 0.64 (t, *J* = 7.5 Hz, 3H). **^{13}C NMR (126 MHz, $CDCl_3$):** δ 136.1, 134.6, 133.8, 129.9, 129.7, 127.8, 127.6, 76.8, 66.1, 38.8, 27.2, 26.4, 19.6, 10.8, 10.6. **FTIR (NaCl, thin film, cm^{-1}):** 3372, 3071, 3049, 2964, 2932, 2857, 1472, 1427, 1389, 1361, 1110, 1050, 1021, 938, 821. **HRMS (FAB, *m/z*):** calc'd for $C_{22}H_{32}O_2Si$ $[M+H-H_2]^+$: 357.2250; found: 357.2258.

(*R*,*E*)-1-(3-methoxyphenyl)-3-methylnon-1-en-4-one (116)

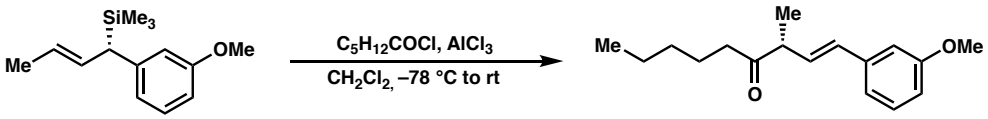

To a 2 dram vial equipped with a magnetic stir bar was added **91p** (46.9 mg, 0.2 mmol, 1 equiv, 97% ee) and then placed under inert atmosphere (N_2). Anhydrous CH_2Cl_2 (2.0 mL, 0.1 M) and cooled to –78 °C. Aluminum trichloride (32 mg, 0.24 mmol, 1.2 equiv) and hexanoyl chloride (42 μL, 0.3 mmol, 1.5 equiv) were added sequentially and stirred for 10 minutes. The dry ice/acetone bath was removed and the reaction was slowly warmed for 5 minutes until the reaction turned yellow-brown. The reaction was then quenched with H_2O (0.4 mL), and the aqueous layer was extracted with Et_2O (3 x 20 mL). The combined organic layers were dried with $MgSO_4$, filtered, and concentrated under reduced pressure. The crude material was purified by column chromatography (silica, 0 to 4% Et_2O/hexane) to yield 27.8 mg of **116** (53% yield) in 90% ee as a colorless oil. Absolute stereochemistry was assigned based on mechanistic precedence in the literature.[1969] $\mathbf{R}_f$ = 0.41 (silica, 10% EtOAc/hexane, UV). **Chiral SFC:** (OB-H, 2.5 mL/min, 5% IPA in CO_2, λ = 254 nm): t_R

(minor) = 7.1 min, t_R (major) = 8.9 min. $[\alpha]_D^{25}$ = –139° (c = 1.0, $CHCl_3$). **^{1}H NMR (500 MHz, $CDCl_3$):** δ 7.23 (dd, *J* = 8.1, 7.6 Hz, 1H), 6.97 – 6.94 (m, 1H), 6.91 – 6.89 (m, 1H), 6.79 (ddd, *J* = 8.2, 2.6, 0.9 Hz, 1H), 6.48 (dd, *J* = 15.8, 0.8 Hz, 1H), 6.16 (dd, *J* = 15.8, 8.7 Hz, 1H), 3.82 (s, 3H), 3.37 (dtd, *J* = 8.6, 6.9, 5.8 Hz, 1H), 2.59 – 2.44 (m, 2H), 1.61 – 1.54 (m, 2H), 1.35 – 1.21 (m, 7H), 0.88 (t, *J* = 7.1 Hz, 3H). **^{13}C NMR (126 MHz, $CDCl_3$):** δ 211.8, 159.9, 138.4, 131.9, 129.7, 129.6, 119.0, 113.4, 111.5, 55.3, 50.8, 41.1, 31.5, 23.5, 22.6, 16.5, 14.1. **FTIR (NaCl, thin film, cm^{-1}):** 2957, 2932, 2871, 1713, 1599, 1580, 1489, 1454, 1433, 1317, 1289, 1266, 1157, 1047, 970. **HRMS (FAB, *m/z*):** calc'd for $C_{17}H_{24}O_2$ $[M+H]^+$: 261.1855; found: 261.1844.

((*E*)-2-((1*R*,2*S*)-2-methoxycyclopentyl)vinyl)benzene (117)

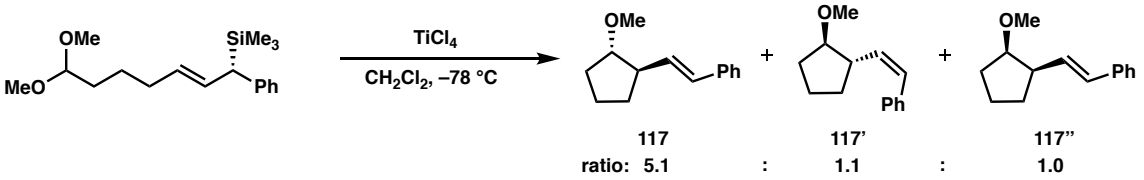

Allylic silane **91f** (23.3 mg, 0.076 mmol, 1 equiv, 97% ee) was added to a 2 dram vial equipped with a magnetic stir bar and placed under inert atmosphere (N_2). Anhydrous CH_2Cl_2 (2.0 mL, 0.038 M) was added and the reaction was cooled to –78 °C. $TiCl_4$ (91 µL, 1.0 M in CH_2Cl_2, 0.091 mmol, 1.2 equiv) was added dropwise down the side of the vial. The reaction continued to stir at –78 °C for 5 minutes, and then was quenched with H_2O (0.4 mL) at –78 °C and slowly warmed to room temperature. **Note:** If the reaction was warmed to room temperature before quenching with H_2O, the corresponding alkyl chloride was isolated. The aqueous layer was extracted with Et_2O (3 x 20 mL), and the combined organic layers were dried with $MgSO_4$, filtered, and concentrated under reduced pressure.

The crude material was purified by column chromatography (silica, 0 to 4% Et_2O/hexane) to yield 10.9 mg of **117**+**117'**+**117''** (71% yield) in 5.1:1.1:1.0 dr as determined by ^{1}H NMR analysis. The mixture of diastereomers was further purified by preparative TLC to isolate 7.8 mg (51% yield) of the major diastereomer (*E*-olefin, **117**) in 97% ee as a colorless oil, and 3.3 mg (21% yield) of a mixture of the minor diastereomers **117'**+**117''** in a 1.0:1.2 ratio as a colorless oil. Both diastereomers with the *E*-olefin (**117** and **117''**) were assigned based on comparison of ^{1}H NMR spectra to that of synthetically prepared standards. The absolute stereochemistry of **117** was assigned by optical rotation. The observed diastereoselectivity is consistent with the literature precedence on the intramolecular allylation of allylic silanes onto pendant aldehydes.[69]

Major diastereomer (*trans*-product, *E*-olefin, 117): R_f = 0.49 (silica, 10% EtOAc/hexane, UV). **Chiral SFC:** (OB-H, 2.5 mL/min, 5% IPA in CO_2, λ = 254 nm): t_R (minor) = 5.3 min, t_R (major) = 5.7 min. $[\boldsymbol{a}]_{\boldsymbol{D}}^{\mathbf{25}}$ = +80° ± 18° (c = 0.5, $CHCl_3$). **Note:** This optical rotation has a high standard deviation. **^{1}H NMR (500 MHz, $CDCl_3$):** δ 7.36 (dtd, *J* = 7.6, 1.6, 0.9 Hz, 2H), 7.29 (dd, *J* = 8.5, 6.9 Hz, 2H), 7.22 – 7.17 (m, 1H), 6.47 – 6.42 (m, 1H), 6.20 (dd, *J* = 15.8, 8.0 Hz, 1H), 3.62 – 3.57 (m, 1H), 3.35 (s, 3H), 2.70 – 2.63 (m, 1H), 2.02 – 1.90 (m, 2H), 1.81 – 1.65 (m, 3H), 1.55 – 1.46 (m, 1H). **^{13}C NMR (126 MHz, $CDCl_3$):** δ 137.7, 133.2, 129.5, 128.6, 127.1, 126.1, 88.0, 57.4, 49.5, 31.3, 30.9, 22.5. **FTIR (NaCl, thin film, cm^{-1}):** 3058, 3025, 2957, 2872, 2821, 1599, 1494, 1449, 1365, 1201, 1116, 964. **HRMS (FAB, *m/z*):** calc'd for $C_{14}H_{18}O$ $[M+\cdot]^+$: 202.1358; found: 202.1361.

Mixture of minor diastereomers (*trans*-product, *Z*-olefin, 117' + *cis*-product, *E*-olefin, 117''): R_f = 0.51 (silica, 10% EtOAc/hexane, UV). **^{1}H NMR (500 MHz, $CDCl_3$):** δ 7.40 – 7.27 (m, 9H), 7.25 – 7.16 (m, 2H), 6.46 – 6.39 (m, 3H), 5.56 (dd, *J* = 11.6, 10.3 Hz, 1H), 3.73 (td, *J* = 4.9, 2.7 Hz, 1H), 3.58 (dt, *J* = 6.5, 5.2 Hz, 1H), 3.30 (s, 3H), 3.29 (s, 3H), 3.12 – 3.04 (m, 1H), 2.68 – 2.60 (m, 1H), 2.02 – 1.90 (m, 2H), 1.89 – 1.78 (m, 5H), 1.78 – 1.60 (m, 6H), 1.47 – 1.38 (m, 1H). **^{13}C NMR (126 MHz, $CDCl_3$):** δ 138.0, 137.5, 135.7, 131.0, 129.9, 129.0, 128.9, 128.6, 128.3, 126.9, 126.8, 126.2, 88.9, 85.7, 57.3, 57.2, 48.5, 44.7, 32.0, 31.4, 30.8, 30.2, 29.9, 22.5, 22.2.

((*E*)-2-((1*R*,2*R*)-2-methoxycyclohexyl)vinyl)benzene (118)

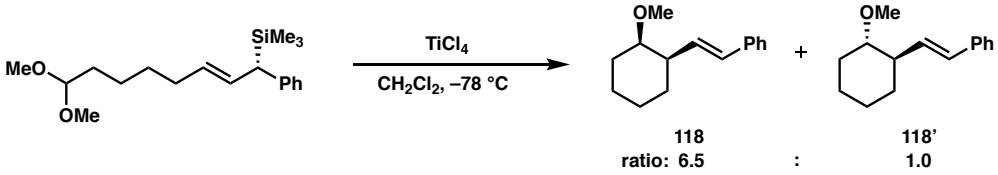

Allylic silane **91g** (28.0 mg, 0.087 mmol, 1 equiv, 95% ee) was added to a 2 dram vial equipped with a magnetic stir bar and placed under inert atmosphere (N_2) before 2.0 mL of anhydrous CH_2Cl_2 (0.044 M) was added and the reaction was cooled to –78 °C. $TiCl_4$ (104 µL, 1.0 M in CH_2Cl_2, 0.104 mmol, 1.2 equiv) was added dropwise down the side of the vial. The reaction was stirred at –78 °C for 5 minutes, and then was quenched with H_2O (0.4 mL) at –78 °C and slowly warmed to room temperature. The aqueous layer was extracted with Et_2O (3 x 20 mL), and the combined organic layers were dried with $MgSO_4$, filtered, and concentrated under reduced pressure. The crude material was purified by column chromatography (silica, 0 to 10% Et_2O/hexane) to yield 14.2 mg of **118**+**118'** (75% yield) in 6.5:1.0 dr as determined by ^{1}H NMR analysis. The mixture of diastereomers was

further purified by preparative TLC to isolate 12.3 mg (65% yield) of the major diastereomer (**118**) in 96% ee as a colorless oil, and 1.5 mg (8% yield) of the minor diastereomer (**118'**) in 96% ee as a colorless oil. The minor diastereomer (*trans*-product, **118'**) was assigned based on comparison of ^{1}H NMR spectra to that of a synthetically prepared standard; absolute stereochemistry was assigned by analogy (to the 5-membered ring product **117**). The absolute and relative stereochemistry of the major diastereomer (*cis*-product, **118**) was assigned by analogy (relative – to **118'**; absolute – to product **117**).

Major diastereomer (*cis*-product, 118): R_f = 0.58 (silica, 10% EtOAc/hexane, UV). **Chiral SFC:** (OB-H, 2.5 mL/min, 2% IPA in CO_2, λ = 280 nm): t_R (major) = 5.3 min, t_R (minor) = 8.4 min. $[\alpha]_D^{25}$ = –0.7° ± 0.7° (c = 1.0, $CHCl_3$). **Note:** This compound shows low optical rotation. **^{1}H NMR (500 MHz, $CDCl_3$):** δ 7.39 – 7.36 (m, 2H), 7.31 – 7.27 (m, 2H), 7.21 – 7.17 (m, 1H), 6.44 – 6.39 (m, 2H), 3.39 (dt, *J* = 6.0, 2.9 Hz, 1H), 3.33 (s, 3H), 2.51 – 2.45 (m, 1H), 1.95 – 1.86 (m, 1H), 1.75 (dtd, *J* = 13.2, 9.6, 3.8 Hz, 1H), 1.70 – 1.59 (m, 2H), 1.58 – 1.51 (m, 1H), 1.50 – 1.38 (m, 2H), 1.38 – 1.31 (m, 1H). **^{13}C NMR (126 MHz, $CDCl_3$):** δ 138.1, 132.7, 129.6, 128.5, 126.9, 126.2, 80.0, 56.5, 44.2, 28.23, 28.19, 24.3, 21.4. **FTIR (NaCl, thin film, cm^{-1}):** 3025, 2931, 2857, 2821, 1599, 1494, 1448, 1364, 1192, 1143, 1097, 1072, 966, 943. **HRMS (FAB, *m/z*):** calc'd for $C_{15}H_{20}O$ $[M+\cdot]^+$: 216.1514; found: 216.1509.

Minor diastereomer (*trans*-product, 118'): R_f = 0.52 (silica, 10% EtOAc/hexane, UV). **Chiral SFC:** (AD-H, 2.5 mL/min, 5% IPA in CO_2, λ = 280 nm): t_R (major) = 5.0 min, t_R (minor) = 6.1 min. $[\alpha]_D^{25}$ = +21° ± 8° (c = 0.1, $CHCl_3$). **Note:** This optical rotation has a

high standard deviation due to the low concentration value. **^{1}H NMR (500 MHz, $CDCl_3$):** δ 7.39 – 7.35 (m, 2H), 7.31 – 7.27 (m, 2H), 7.21 – 7.17 (m, 1H), 6.42 (d, *J* = 16.0 Hz, 1H), 6.27 (dd, *J* = 16.0, 7.5 Hz, 1H), 3.35 (s, 3H), 2.95 (td, *J* = 9.7, 4.0 Hz, 1H), 2.24 – 2.17 (m, 1H), 2.17 – 2.11 (m, 1H), 1.87 – 1.77 (m, 2H), 1.69 (tdd, *J* = 4.7, 3.1, 1.4 Hz, 1H), 1.32 – 1.19 (m, 4H). **^{13}C NMR (126 MHz, $CDCl_3$):** δ 138.1, 133.8, 129.4, 128.6, 126.9, 126.2, 83.3, 56.7, 47.3, 31.7, 30.8, 25.3, 24.7. **FTIR (NaCl, thin film, cm^{-1}):** 3025, 2928, 2856, 2820, 1600, 1493, 1448, 1361, 1190, 1123, 1100, 962. **HRMS (FAB, *m/z*):** calc'd for $C_{15}H_{20}O$ $[M+\cdot]^+$: 216.1514; found: 216.1519.

5-hydroxy-1-((*S*,*E*)-6-phenyl-6-(trimethylsilyl)hex-4-en-1-yl)pyrrolidin-2-one (120)

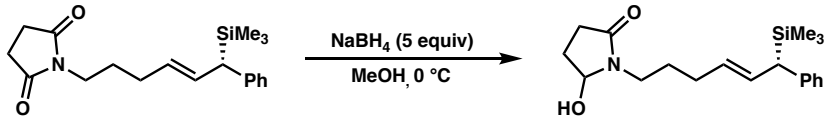

Similar to a procedure by Speckamp and coworkers,[73] allylic silane **91m** (49.9 mg, 0.15 mol, 1.0 equiv, 97% ee) was added to a 2 dram vial equipped with a magnetic stir bar, dissolved in 1 mL of MeOH, and cooled to 0 °C. Sodium borohydride (28.4 mg, 0.75 mmol, 5.0 equiv) was added and the reaction was stirred at 0 °C for 1 hour, then diluted with 4 mL Et_2O and quenched with 4 mL cold (0 °C) H_2O. The layers were separated and the aqueous layer was extracted with Et_2O (3 x 10 mL). The combined organic layers were dried with K_2CO_3, filtered, and concentrated under reduced pressure to afford 49.9 mg (99% yield, ~1:1 mixture of diastereomers) of **120** as a colorless oil. $\mathbf{R}_f$ = 0.26 (silica, 30% acetone/hexane, $KMnO_4$). $[\alpha]_D^{25}$ = +19° (c = 1.0, $CHCl_3$). **^{1}H NMR (500 MHz, $CDCl_3$):** δ 7.26 – 7.21 (m, 2H), 7.10 – 7.06 (m, 1H), 7.06 – 7.02 (m, 2H), 5.81 (dddd, *J* = 15.0, 10.0, 2.4, 1.3 Hz, 1H), 5.42 – 5.34 (m, 1H), 5.16 (s, 1H), 4.11 (s, 1H), 3.47 (dddd, *J* = 17.2, 8.8,

7.2, 3.8 Hz, 1H), 3.13 (ddt, *J* = 13.9, 8.9, 5.3 Hz, 1H), 2.88 (d, *J* = 10.0 Hz, 1H), 2.50 (dtdd, *J* = 12.4, 9.2, 7.0, 3.5 Hz, 1H), 2.31 – 2.19 (m, 2H), 2.05 (q, *J* = 7.2 Hz, 2H), 1.90 – 1.82 (m, 1H), 1.71 – 1.53 (m, 1H), -0.05 (s, 9H). **^{13}C NMR (126 MHz, $CDCl_3$):** δ (175.03, 175.02), 143.0, (130.17, 130.14), 128.3, (127.79, 127.76), 127.1, 124.6, (83.31, 83.29), (42.96, 42.93), (39.76, 39.72), (30.42, 30.40), (29.05, 29.02), 28.3, (27.95, 27.87), -2.9. **FTIR (NaCl, thin film, cm^{-1}):** 3333, 3024, 2954, 2866, 1668, 1652, 1493, 1464, 1422, 1262, 1247, 1072 968, 839. **HRMS (FAB, *m/z*):** calc'd for $C_{19}H_{29}NO_2Si$ $[M+H]^+$: 332.2046; found: 332.2023.

(8*R*,8a*R*)-8-((*E*)-styryl)hexahydroindolizin-3(2*H*)-one (121)

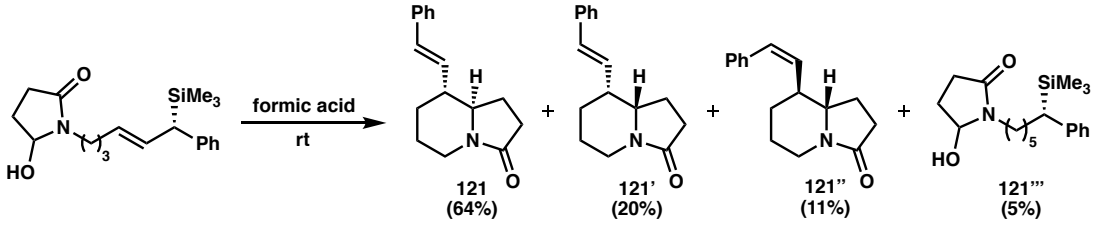

Similar to a procedure by Speckamp and coworkers,[74] allylic silane **120** (39.4 mg, 0.116 mol, 1.0 equiv) was added to a 2 dram vial equipped with a magnetic stir bar, dissolved in 1.5 mL of formic acid, and stirred at room temperature for 1 hour. The reaction was placed in a 50 °C water bath and concentrated under a gentle stream of N_2. The residue was dissolved in 10 mL CH_2Cl_2 and quenched with 6 mL aq. $NaHCO_3$. The aqueous layer was extracted with CH_2Cl_2 (3 x 10 mL). The combined organic layers were dried with K_2CO_3, filtered, and concentrated under reduced pressure to afford 28.6 mg (99% yield) of the crude mixture **121**+**121'**+**121''**+**121'''** (93% combined yield of allylation isomers **121**+**121'**+**121''**). The crude material was purified by column chromatography (silica, 14

cm diameter x 9 cm height, column repeated twice on mixed fractions, 5 to 40% acetone/hexanes) to afford 16.0 mg (57% yield) of the major diastereomer (*E*-olefin) **121** in 97% ee as a colorless oil. A portion of the minor diastereomer and *Z*-olefin were further purified by preparative TLC to remove the reduced alkene product (4.0 mg isolated). The absolute and relative stereochemistry of the minor allylation isomers **121'** and **121''** were assigned based on literature precedent for the related glutarimide analog.[75] **Major diastereomer (*E*-olefin, 121): R_f** = 0.18 (silica, 30% acetone/hexane, UV). **Chiral SFC:** (OD-H, 2.5 mL/min, 30% IPA in CO_2, λ = 254 nm): t_R (minor) = 4.4 min, t_R (major) = 4.8 min. $[\alpha]_D^{25}$ = +116° (c = 1.0, $CHCl_3$). **^{1}H NMR (400 MHz, $CDCl_3$):** δ 7.38 – 7.28 (m, 4H), 7.26 – 7.20 (m, 1H), 6.48 (d, *J* = 15.9 Hz, 1H), 6.01 (dd, *J* = 15.9, 8.1 Hz, 1H), 4.16 (ddt, *J* = 13.2, 4.5, 1.5 Hz, 1H), 3.24 (dt, *J* = 9.9, 7.2 Hz, 1H), 2.68 – 2.57 (m, 1H), 2.44 – 2.29 (m, 2H), 2.23 – 2.12 (m, 1H), 2.04 – 1.87 (m, 2H), 1.80 – 1.75 (m, 1H), 1.75 – 1.67 (m, 1H), 1.55 – 1.36 (m, 2H). **^{13}C NMR (101 MHz, $CDCl_3$):** δ 173.8, 137.1, 131.5, 130.0, 128.7, 127.6, 126.2, 61.1, 48.3, 39.9, 30.9, 30.4, 24.2, 23.9. **FTIR (NaCl, thin film, cm^{-1}):** 3025, 2932, 2854, 1683, 1493, 1436, 1421, 1370, 1315, 1295, 1267, 1143, 968. **HRMS (FAB, *m/z*):** calc'd for $C_{16}H_{19}NO$ $[M+H]^+$: 242.1545; found: 242.1520.

(8*S*,8a*R*)-8-(hydroxymethyl)hexahydroindolizin-3(2*H*)-one (S24)

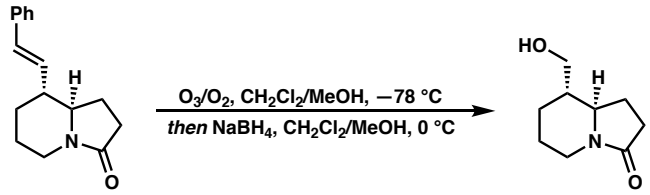

Alkene **121** (16.0 mg, 0.066 mmol, 1.0 equiv) was added to a 25 mL round bottom flask equipped with a stir bar and dissolved in 4 mL CH_2Cl_2 and 4 mL MeOH. The flask was

cooled to –78 °C and O_2 was bubbled through the solution for 2 minutes. The ozone generator was turned on and a mixture of O_3/O_2 was bubbled through the reaction (approx. 10 minutes, at which time the solution turned blue). The ozone generator was turned off and the headspace was purged with argon. Sodium borohydride (12.5 mg, 0.33 mmol, 5 equiv) was added. The reaction was warmed to 0 °C and continued to stir for 1 hour. The solution was quenched with 4 mL sat. NH_4Cl, diluted 4 mL H_2O, and the layers were separated. The aqueous layer was extracted with 20% MeOH/CH_2Cl_2 (5 x 15 mL). The combined organic layers were dried with Na_2SO_4, filtered, and concentrated under reduced pressure. The crude material was purified by column chromatography (silica, 0 to 10% MeOH/CH_2Cl_2) to afford 7.6 mg of **S24** (68% yield) as a white solid. The NMR spectra matched those previously reported in literature.[93] $\mathbf{R_f}$ = 0.11 (silica, 5% MeOH/CH_2Cl_2, CAM (*very faint*)). $[\alpha]_D^{25}$ = +63° (c = 0.5, $CHCl_3$). **^{1}H NMR (400 MHz, $CDCl_3$):** δ 4.12 (ddt, *J* = 13.3, 4.8, 1.8 Hz, 1H), 3.67 (dd, *J* = 10.9, 4.5 Hz, 1H), 3.58 (dd, *J* = 10.8, 5.4 Hz, 1H), 3.25 (dt, *J* = 10.0, 7.4 Hz, 1H), 2.63 – 2.50 (m, 1H), 2.39 – 2.24 (m, 3H), 1.93 (dqd, *J* = 12.8, 3.1, 1.6 Hz, 1H), 1.82 – 1.66 (m, 3H), 1.47 – 1.21 (m, 3H). **^{13}C NMR (101 MHz, $CDCl_3$):** δ 174.0, 64.5, 59.1, 46.1, 40.1, 30.7, 27.1, 24.7, 24.2. **FTIR (NaCl, thin film, cm^{-1}):** 3373, 2929, 2860, 1662, 1462, 1445, 1423, 1268, 1146, 1091, 1052. **HRMS (FAB, *m/z*):** calc'd for $C_{16}H_{19}NO_2$ $[M+H]^+$: 170.1181; found: 170.1184.

(+)-Tashiromine (122)

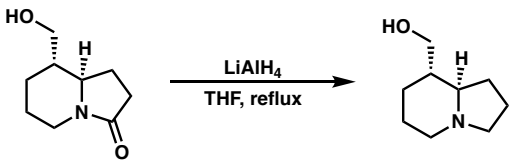

Amide **S24** (7.8 mg, 0.045 mol, 1.0 equiv) was added to a 2 dram vial equipped with a magnetic stir bar under an atmosphere of argon and dissolved in 0.5 mL of THF. The $LiAlH_4$ (45 µL, 0.045 mmol, 1.0 equiv, 1M in Et_2O) was added to the reaction at room temperature via syringe, which was then heated to 65 °C for 15 minutes. After cooling to room temperature, the reaction was quenched with 2 µL H_2O, 2 µL 15% NaOH, and 6 µL H_2O. The mixture was filtered through a plug of celite, eluted with additional THF, and concentrated under reduced pressure to afford 7.0 mg (99% yield) of **122** as a light yellow oil. The NMR spectra matched those previously reported in literature.[71,94] $[\boldsymbol{a}]_{\boldsymbol{D}}^{\mathbf{25}}$ = +29° (c = 0.5, $CHCl_3$). **^{1}H NMR (400 MHz, $CDCl_3$):** δ 3.64 (dd, *J* = 10.8, 4.6 Hz, 1H), 3.47 (dd, *J* = 10.8, 6.5 Hz, 1H), 3.13 – 2.99 (m, 2H), 2.06 (q, *J* = 9.1 Hz, 1H), 2.00 – 1.83 (m, 3H), 1.83 – 1.59 (m, 5H), 1.59 – 1.53 (m, 1H), 1.53 – 1.40 (m, 2H), 1.04 (tdd, *J* = 12.9, 11.7, 4.6 Hz, 1H). **^{13}C NMR (101 MHz, $CDCl_3$):** δ 66.5, 65.9, 54.3, 52.8, 44.8, 29.2, 27.7, 25.3, 20.9. **FTIR (NaCl, thin film, cm^{-1}):** 3392, 2930, 2876, 2794, 1671, 1461, 1445, 1385, 1331, 1279, 1217, 1186, 1165, 1123, 1091, 1050. HRMS (FAB, m/z): calc'd for $C_9H_{17}NO$ $[M+H]^+$: 156.1388; found: 156.1377.

The product was analyzed by optical rotation to give $[\boldsymbol{a}]_{\boldsymbol{D}}^{\mathbf{25}}$ = +29° (c = 0.5, $CHCl_3$), therefore the absolute configuration is assigned opposite of that which is reported in the Jacobsen paper $[\boldsymbol{a}]_{\boldsymbol{D}}^{\mathbf{25}}$ = –41° (c = 2.0, EtOH).[71]

Table 2.9. *Comparison of ^{1}H NMR spectroscopic data for natural and synthetic tashiromine (**122**).*

carbon number	**Natural tashiromine**[94] ^{1}H NMR, $CDCl_3$	**Jacobsen (–)-tashiromine**[71] ^{1}H NMR, $CDCl_3$	**Synthetic (+)-tashiromine** ^{1}H NMR, 400 MHz, $CDCl_3$
10	3.64 (dd, *J* = 10.0, 4.0 Hz, 1H)	3.63 (dd, *J* = 4.5, 10.5 Hz, 1H)	3.64 (dd, *J* = 10.8, 4.6 Hz, 1H)
10	3.48 (dd, *J* = 10.0, 6.0, 1H)	3.46 (dd, *J* = 7.0, 11.0 Hz, 1H)	3.47 (dd, *J* = 10.8, 6.5 Hz, 1H)
2,9	Not reported	3.03–3.10 (m, 2H),	3.13 – 2.99 (m, 2H)
9		2.05 (q, *J* = 9.0 Hz, 1H)	2.06 (q, *J* = 9.1 Hz, 1H)
2,4,7		1.43–1.97 (m, 11H)	2.00 – 1.83 (m, 3H)
8,3,10-OH			1.83 – 1.59 (m, 5H)
6			1.59 – 1.53 (m, 1H)
5,4			1.53 – 1.40 (m, 2H)
7		1.03 (qd, *J* = 5.0, 11.5 Hz, 1H)	1.04 (tdd, *J* = 12.9, 11.7, 4.6 Hz, 1H)

Table 2.10. *Comparison of ^{13}C NMR spectroscopic data for natural and synthetic tashiromine (**122**).*

carbon number	**Natural tashiromine**[94] ^{13}C NMR, $CDCl_3$	**Jacobsen (–)-tashiromine**[71] ^{13}C NMR, $CDCl_3$	**Synthetic (+)-tashiromine** ^{13}C NMR, 101 MHz, $CDCl_3$	**Δ** from isolation	**Δ** from Jacobsen
2	52.7	52.7	52.3	-0.4	0.4
3	25.2	25.1	25.3	0.1	-0.2
4	29.2	29.1	29.2	0.0	-0.1
5	44.7	44.6	44.8	0.1	-0.2
6	66.4	66.3	66.5	0.1	-0.2
7	27.6	27.6	27.7	0.1	-0.1
8	20.3	20.7	20.9	0.6	-0.2
9	54.2	54.2	54.3	0.1	-0.1
10	65.9	65.7	65.9	0.0	-0.2

Note: The reported ^{13}C line list in the Jacobsen report is incorrect due to copy/paste error from the synthesis of compound (+)-epilupinine, however the provided ^{13}C spectrum contains the correct ^{13}C peaks for (–)-tashiromine as reported.

Tashiromine (**122**) carbon numbering as reported by Ohmiya and coworkers.[94]

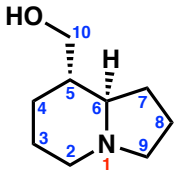

General Procedure 9: Condensation/Allylation for cis-2,3-tetrahydrofurans

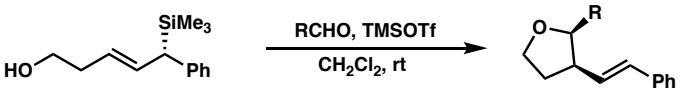

On a bench-top open to an atmosphere of air, the allylic silane (0.22 mmol, 1.1 equiv), aldehyde (0.2 mmol, 1.0 equiv) and CH_2Cl_2 (2 mL, 0.1M) were added to a 25 mL round bottom flask equipped with a stir bar. The TMSOTf (0.06 mmol, 0.03 equiv) was added to the flask and the reaction was allowed to stir at room temperature for 5 minutes before being diluted with CH_2Cl_2 (6 mL). Celite (500 mg) was added to the crude mixture and the solution was concentrated under reduced pressure. The resulting powder was then loaded onto a silica column and purified via column chromatography to yield the desired product.

(2*S*,3*R*)-2-ethyl-3-((*E*)-styryl)tetrahydrofuran (123a)

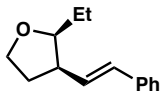

Prepared from (*S*,*E*)-5-phenyl-5-(trimethylsilyl)pent-3-en-1-ol (**91i**, 51.6 mg, 1.1 equiv, 0.22 mmol, 98% ee) and propionaldehyde (11.6 mg, 1.0 equiv, 0.2 mmol) according to General Procedure 9. The crude residue was purified by

column chromatography (silica, 0 to 5% Et_2O/hexanes) to yield 39.6 mg of **123a** (98% yield, >20:1 dr, >20:1 *E*:*Z*, 93% major isomer) as a colorless oil. $\mathbf{R_f}$ = 0.36 (silica, 10% EtOAc/hexane, UV). $[\boldsymbol{a}]_D^{25}$ = +28° (c = 1.0, $CHCl_3$). **^{1}H NMR (500 MHz, $CDCl_3$):** δ 7.39 – 7.34 (m, 2H), 7.34 – 7.27 (m, 2H), 7.25 – 7.19 (m, 1H), 6.41 (d, *J* = 15.8 Hz, 1H), 6.18 (dd, *J* = 15.8, 9.7 Hz, 1H), 4.05 (td, *J* = 8.3, 5.9 Hz, 1H), 3.86 – 3.73 (m, 2H), 2.95 (ddt, *J* = 12.5, 10.0, 5.2 Hz, 1H), 2.22 (dddd, *J* = 12.5, 8.4, 7.5, 5.9 Hz, 1H), 1.89 (dddd, *J* = 12.6, 8.1, 6.4, 4.7 Hz, 1H), 1.62 – 1.42 (m, 2H), 0.96 (t, *J* = 7.4 Hz, 3H). **^{13}C NMR (126 MHz, $CDCl_3$):** δ 137.5, 130.7, 129.7, 128.7, 127.3, 126.2, 126.2, 84.0, 66.6, 45.7, 32.9, 24.5, 10.9. **FTIR (NaCl, thin film, cm^{-1}):** 3026, 2964, 2934, 2874, 1494, 1463, 1450, 1359, 1101, 1063, 1033, 970, 750, 694.

(2*S*,3*R*)-2-isopropyl-3-((*E*)-styryl)tetrahydrofuran (123b)

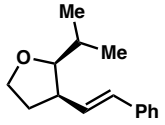

Prepared from (*S*,*E*)-5-phenyl-5-(trimethylsilyl)pent-3-en-1-ol (**91i**, 51.6 mg, 1.1 equiv, 0.22 mmol, 98% ee) and isobutylaldehyde (14.4 mg, 1.0 equiv, 0.2 mmol) according to General Procedure 9. The crude residue was purified by column chromatography (silica, 0 to 5% Et_2O/hexanes) to yield 44.0 mg of **123b** (99% yield, 17:1 dr, >20:1 *E*:*Z*, 92% major isomer) as a colorless oil. $\mathbf{R_f}$ = 0.45 (silica, 10% EtOAc/hexane, UV). $[\boldsymbol{a}]_D^{25}$ = +58° (c = 1.0, $CHCl_3$). **^{1}H NMR (400 MHz, $CDCl_3$):** δ 7.40 – 7.35 (m, 2H), 7.35 – 7.29 (m, 2H), 7.25 – 7.19 (m, 1H), 6.40 (s, 1H), 6.24 (dd, *J* = 15.8, 10.0 Hz, 1H), 4.06 (q, *J* = 8.0 Hz, 1H), 3.86 (ddd, *J* = 9.4, 8.4, 4.6 Hz, 1H), 3.33 (dd, *J* = 9.8, 4.5 Hz, 1H), 2.97 – 2.89 (m, 1H), 2.27 (ddt, *J* = 12.6, 9.4, 7.5 Hz, 1H), 1.88 (dddd, *J* = 12.5, 7.9, 4.6, 2.0 Hz, 1H), 1.81 – 1.70 (m, 1H), 1.05 (d, *J* = 6.5 Hz, 3H), 0.87 (d, *J* = 6.6 Hz, 3H). **^{13}C NMR (101 MHz, $CDCl_3$):** δ 137.5, 130.4, 129.6, 128.7, 127.2, 126.2, 88.8,

66.4, 45.0, 33.5, 29.5, 20.7, 18.9. **FTIR (NaCl, thin film, cm^{-1}):** 2958, 2872, 1494, 1450, 1388, 1066, 970, 754, 694.

(2*S*,3*R*)-2-cyclohexyl-3-((*E*)-styryl)tetrahydrofuran (123c)

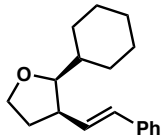

Prepared from (*S*,*E*)-5-phenyl-5-(trimethylsilyl)pent-3-en-1-ol (**91i**, 51.6 mg, 1.1 equiv, 0.22 mmol, 98% ee) and cyclohexanecarbaldehyde (22.4 mg, 1.0 equiv, 0.2 mmol) according to General Procedure 9. The crude residue was purified by column chromatography (silica, 0 to 5% Et_2O/hexanes) to yield 50.6 mg of **123c** (99% yield, >20:1 dr, >20:1 *E*:*Z*, 95% major isomer) as a colorless oil which crystallized upon standing. Crystals suitable for X-ray diffraction were grown from hexane upon standing in the freezer (–20 °C). $\mathbf{R_f}$ = 0.43 (silica, 10% EtOAc/hexane, UV). $[\boldsymbol{\alpha}]_D^{25}$ = +81° (c = 1.0, $CHCl_3$). **^{1}H NMR (400 MHz, $CDCl_3$):** δ 7.40 – 7.35 (m, 2H), 7.32 (dd, *J* = 8.5, 6.7 Hz, 2H), 7.26 – 7.20 (m, 1H), 6.41 (d, *J* = 15.8 Hz, 1H), 6.24 (dd, *J* = 15.9, 9.9 Hz, 1H), 4.04 (q, *J* = 8.0 Hz, 1H), 3.84 (ddd, *J* = 9.5, 8.4, 4.6 Hz, 1H), 3.39 (dd, *J* = 9.7, 4.5 Hz, 1H), 2.93 (dddd, *J* = 9.6, 6.8, 4.5, 1.9 Hz, 1H), 2.25 (ddt, *J* = 12.6, 9.4, 7.5 Hz, 1H), 2.08 – 1.99 (m, 1H), 1.87 (dddd, *J* = 12.5, 7.9, 4.6, 2.0 Hz, 1H), 1.77 – 1.68 (m, 2H), 1.68 – 1.60 (m, 2H), 1.48 (dddd, *J* = 13.2, 8.1, 7.0, 3.5 Hz, 1H), 1.32 – 1.12 (m, 3H), 1.05 (tdd, *J* = 12.5, 10.9, 3.5 Hz, 1H), 0.97 – 0.82 (m, 1H). **^{13}C NMR (101 MHz, $CDCl_3$):** δ 137.7, 130.4, 129.7, 128.6, 127.2, 126.2, 87.3, 66.2, 44.6, 38.9, 33.4, 31.0, 28.9, 26.6, 25.9, 25.8. **FTIR (NaCl, thin film, cm^{-1}):** 2924, 2851, 1492, 1449, 1062, 970, 884, 753, 693.

(2*S*,3*R*)-2-(but-3-en-1-yl)-3-((*E*)-styryl)tetrahydrofuran (123d)

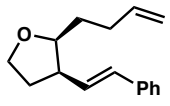

Prepared from (*S*,*E*)-5-phenyl-5-(trimethylsilyl)pent-3-en-1-ol (**91i**, 51.6 mg, 1.1 equiv, 0.22 mmol, 98% ee) and pent-4-enal (16.8 mg, 1.0 equiv, 0.2 mmol) according to General Procedure 9. The crude residue was purified by column chromatography (silica, 0 to 5% Et_2O/hexanes) to yield 28.4 mg of **123d** (62% yield, >20:1 dr, >20:1 *E*:*Z*, 94% major isomer) as a colorless oil. $\mathbf{R_f}$ = 0.43 (silica, 10% EtOAc/hexane, UV). $[\boldsymbol{a}]_D^{25}$ = +49° (c = 1.0, $CHCl_3$). **^{1}H NMR (400 MHz, $CDCl_3$):** δ 7.39 – 7.34 (m, 2H), 7.34 – 7.29 (m, 2H), 7.25 – 7.20 (m, 1H), 6.42 (d, *J* = 15.8 Hz, 1H), 6.17 (dd, *J* = 15.8, 9.6 Hz, 1H), 5.82 (ddt, *J* = 16.9, 10.2, 6.7 Hz, 1H), 5.06 – 4.92 (m, 2H), 4.05 (td, *J* = 8.3, 5.7 Hz, 1H), 3.90 – 3.78 (m, 2H), 3.01 – 2.91 (m, 1H), 2.28 – 2.17 (m, 2H), 2.17 – 2.05 (m, 1H), 1.89 (dddd, *J* = 12.8, 8.1, 6.6, 5.0 Hz, 1H), 1.67 – 1.48 (m, 2H). **^{13}C NMR (101 MHz, $CDCl_3$):** δ 138.6, 137.4, 130.7, 129.6, 128.7, 127.3, 126.2, 126.2, 114.8, 81.7, 67.0, 45.9, 32.9, 30.9, 30.8. **FTIR (NaCl, thin film, cm^{-1}):** 3026, 2974, 2937, 2871, 1640, 1449, 1066, 1051, 969, 911, 750, 694.

(2*S*,3*R*)-2-(4-chlorobutyl)-3-((*E*)-styryl)tetrahydrofuran (123e)

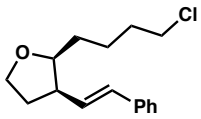

Prepared from (*S*,*E*)-5-phenyl-5-(trimethylsilyl)pent-3-en-1-ol (**91i**, 51.6 mg, 1.1 equiv, 0.22 mmol, 98% ee) and 5-chloropentanal (24.1 mg, 1.0 equiv, 0.2 mmol) according to General Procedure 9. The crude residue was purified by column chromatography (silica, 0 to 10% Et_2O/hexanes) to yield 39.9 mg of **123e** (75% yield, 8:1 dr, >20:1 *E*:*Z*, 87% major isomer) as a colorless oil. $\mathbf{R_f}$ = 0.27 (silica, 10% EtOAc/hexane, UV). $[\boldsymbol{a}]_D^{25}$ = +29° (c = 0.5, $CHCl_3$). **^{1}H NMR (400 MHz, $CDCl_3$):** δ 7.40 – 7.35 (m, 2H), 7.35 – 7.29 (m, 2H), 7.25 – 7.20 (m, 1H), 6.42 (d, *J* = 15.8 Hz, 1H), 6.16

(dd, *J* = 15.8, 9.6 Hz, 1H), 4.05 (td, *J* = 8.2, 5.8 Hz, 1H), 3.87 – 3.77 (m, 2H), 3.51 (t, *J* = 6.7 Hz, 2H), 2.95 (ddt, *J* = 10.1, 7.4, 5.3 Hz, 1H), 2.22 (dddd, *J* = 12.4, 8.4, 7.5, 5.8 Hz, 1H), 1.89 (dddd, *J* = 12.7, 8.1, 6.5, 4.8 Hz, 1H), 1.84 – 1.72 (m, 2H), 1.66 – 1.41 (m, 4H). **^{13}C NMR (101 MHz, $CDCl_3$):** δ 137.4, 130.9, 129.5, 128.7, 127.3, 126.2, 82.2, 66.7, 45.9, 45.1, 32.8, 32.7, 30.8, 24.1. **FTIR (NaCl, thin film, cm^{-1}):** 2934, 2867, 1493, 1449, 1073, 1043, 970, 752, 694.

(2*R*,3*R*)-2-((benzyloxy)methyl)-3-((*E*)-styryl)tetrahydrofuran (123f)

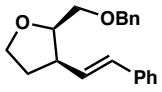

Prepared from (*S*,*E*)-5-phenyl-5-(trimethylsilyl)pent-3-en-1-ol (**91i**, 51.6 mg, 1.1 equiv, 0.22 mmol, 98% ee) and 2-(benzyloxy)acetaldehyde (30.0 mg, 1.0 equiv, 0.2 mmol) according to General Procedure 9. The crude residue was purified by column chromatography (silica, 0 to 15% Et_2O/hexanes) to yield 38.2 mg of **123f** (65% yield, 19:1 dr, 18:1 *E*:*Z*, 90% major isomer) as a colorless oil. $\mathbf{R_f}$ = 0.17 (silica, 10% EtOAc/hexane, UV). $[\alpha]_D^{25}$ = +29° (c = 1.0, $CHCl_3$). **^{1}H NMR (400 MHz, $CDCl_3$):** δ 7.38 – 7.21 (m, 10H), 6.45 (d, *J* = 15.8 Hz, 1H), 6.20 (dd, *J* = 15.8, 9.4 Hz, 1H), 4.55 (q, *J* = 12.1 Hz, 2H), 4.18 – 4.10 (m, 2H), 3.87 (q, *J* = 7.8 Hz, 1H), 3.59 – 3.50 (m, 2H), 3.09 (dq, *J* = 9.4, 6.9 Hz, 1H), 2.20 (dtd, *J* = 12.5, 7.6, 4.9 Hz, 1H), 1.98 (dtd, *J* = 12.3, 7.7, 6.4 Hz, 1H) **^{13}C NMR (101 MHz, $CDCl_3$):** δ 138.3, 137.3, 131.2, 128.8, 128.6, 128.4, 127.8, 127.6, 127.4, 126.2, 80.9, 73.6, 71.1, 67.8, 45.3, 32.9. **FTIR (NaCl, thin film, cm^{-1}):** 3027, 2919, 2861, 1495, 1451, 1361, 1076, 1027, 970, 748, 695.

(2*S*,3*R*)-2-(2-(benzyloxy)ethyl)-3-((*E*)-styryl)tetrahydrofuran (123g)

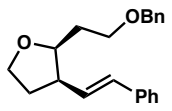

Prepared from (*S*,*E*)-5-phenyl-5-(trimethylsilyl)pent-3-en-1-ol (**91i**, 51.6 mg, 1.1 equiv, 0.22 mmol, 98% ee) and 3-(benzyloxy)propanal (32.8 mg, 1.0 equiv, 0.2 mmol) according to General Procedure 9. The crude residue was purified by column chromatography (silica, 0 to 15% Et_2O/hexanes) to yield 50.3 mg of **123g** (82% yield, 15:1 dr, 15:1 *E*:*Z*, 88% major isomer) as a colorless oil. $\mathbf{R_f}$ = 0.20 (silica, 10% EtOAc/hexane, UV). $[\boldsymbol{a}]_D^{25}$ = +49° (c = 1.0, $CHCl_3$). **^{1}H NMR (400 MHz, $CDCl_3$):** δ 7.39 – 7.20 (m, 10H), 6.40 (d, *J* = 15.8 Hz, 1H), 6.17 (dd, *J* = 15.8, 9.5 Hz, 1H), 4.57 – 4.48 (m, 2H), 4.10 – 4.02 (m, 2H), 3.83 (td, *J* = 8.3, 6.7 Hz, 1H), 3.62 (td, *J* = 6.7, 3.6 Hz, 2H), 2.97 (ddt, *J* = 9.6, 7.3, 5.5 Hz, 1H), 2.30 – 2.14 (m, 1H), 1.90 (dddd, *J* = 12.1, 8.2, 6.7, 5.1 Hz, 1H), 1.82 (q, *J* = 6.8 Hz, 2H). **^{13}C NMR (101 MHz, $CDCl_3$):** δ 138.6, 137.3, 131.0, 129.4, 128.6, 128.4, 127.8, 127.6, 127.3, 126.2, 79.2, 73.2, 68.0, 66.8, 45.9, 32.7, 31.9. **FTIR (NaCl, thin film, cm^{-1}):** 3027, 2927, 2946, 2861, 1495, 1453, 1363, 1092, 1028, 970, 750, 737, 696.

(2*S*,3*R*)-2-(3-(benzyloxy)propyl)-3-((*E*)-styryl)tetrahydrofuran (123h)

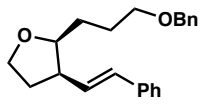

Prepared from (*S*,*E*)-5-phenyl-5-(trimethylsilyl)pent-3-en-1-ol (**91h**, 51.6 mg, 1.1 equiv, 0.22 mmol, 98% ee) and 4-(benzyloxy)butanal (35.6 mg, 1.0 equiv, 0.2 mmol) according to General Procedure 9. The crude residue was purified by column chromatography (silica, 0 to 15% Et_2O/hexanes) to yield 47.4 mg of **123h** (74% yield, >20:1 dr, 19:1 *E*:*Z*, 92% major isomer) as a colorless oil. $\mathbf{R_f}$ = 0.17 (silica, 10% EtOAc/hexane, UV). $[\boldsymbol{a}]_D^{25}$ = +33° (c = 1.0, $CHCl_3$). **^{1}H NMR (400 MHz, $CDCl_3$):** δ 7.43 – 7.20 (m, 10H), 6.43 (d, *J* = 15.8 Hz, 1H), 6.19 (dd, *J* = 15.8, 9.6 Hz, 1H), 4.49 (s, 2H),

4.06 (td, *J* = 8.3, 5.7 Hz, 1H), 3.92 – 3.78 (m, 2H), 3.49 (qt, *J* = 9.3, 6.4 Hz, 2H), 3.02 – 2.92 (m, 1H), 2.22 (dtd, *J* = 13.4, 7.9, 5.6 Hz, 1H), 1.96 – 1.85 (m, 1H), 1.85 – 1.76 (m, 1H), 1.76 – 1.65 (m, 1H), 1.58 (q, *J* = 7.1 Hz, 2H). **^{13}C NMR (101 MHz, $CDCl_3$):** δ 138.7, 137.4, 130.8, 129.6, 128.6, 128.4, 127.7, 127.5, 127.3, 126.2, 82.2, 72.8, 70.3, 66.7, 45.9, 32.8, 28.2, 26.9. **FTIR (NaCl, thin film, cm^{-1}):** 3027, 2934, 2855, 1495, 1452, 1362, 1100, 1073, 1028, 970, 749, 737, 696.

(2*S*,3*R*)-2-(4-(benzyloxy)butyl)-3-((*E*)-styryl)tetrahydrofuran (123i)

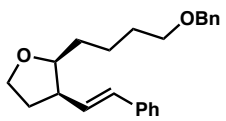

Prepared from (*S*,*E*)-5-phenyl-5-(trimethylsilyl)pent-3-en-1-ol (**91i**, 51.6 mg, 1.1 equiv, 0.22 mmol, 98% ee) and 5-(benzyloxy)pentanal (38.5 mg, 1.0 equiv, 0.2 mmol) according to General Procedure 9. The crude residue was purified by column chromatography (silica, 0 to 15% Et_2O/hexanes) to yield 40.1 mg of **123i** (60% yield, 20:1 dr, >20:1 *E*:*Z*, 92% major isomer) as a colorless oil. $\mathbf{R_f}$ = 0.23 (silica, 10% EtOAc/hexane, UV). $[\alpha]_D^{25}$ = +38° (c = 1.0, $CHCl_3$). **^{1}H NMR (400 MHz, $CDCl_3$):** δ 7.38 – 7.21 (m, 10H), 6.41 (d, *J* = 15.8 Hz, 1H), 6.17 (dd, *J* = 15.8, 9.6 Hz, 1H), 4.47 (s, 2H), 4.05 (td, *J* = 8.2, 5.8 Hz, 1H), 3.89 – 3.78 (m, 2H), 3.46 (t, *J* = 6.5 Hz, 2H), 2.99 – 2.88 (m, 1H), 2.22 (dddd, *J* = 12.5, 8.4, 7.5, 5.8 Hz, 1H), 1.88 (dddd, *J* = 12.7, 8.1, 6.4, 4.7 Hz, 1H), 1.69 – 1.39 (m, 6H). **^{13}C NMR (101 MHz, $CDCl_3$):** δ 138.8, 137.5, 130.7, 129.7, 128.7, 128.4, 127.7, 127.5, 127.3, 126.2, 82.4, 72.9, 70.4, 66.6, 45.9, 32.9, 31.3, 29.9, 23.3. **FTIR (NaCl, thin film, cm^{-1}):** 3027, 2936, 2860, 1495, 1452, 1361, 1102, 1073, 970, 750, 736, 696.

General Procedure 8: Allylation/Cyclization for trans-2,3-tetrahydrofurans

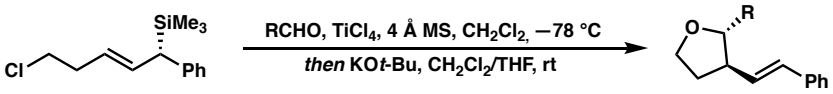

On a bench-top, a 10 mL round bottom flask equipped with a stir bar was sealed with a septum and electrical tape, then flame dried with a propane torch and backfilled with argon. Then 100 mg of oven-dried 3 Å molecular sieves were quickly added to the flask, which was subsequently evacuated and backfilled with argon. The allylic silane (0.22 mmol, 1.1 equiv), aldehyde (0.2 mmol, 1 equiv), and anhydrous CH_2Cl_2 (2.0 mL, 0.1 M) were added to the flask via syringe while under an Ar atmosphere. The reaction mixture was cooled to –78 °C and $TiCl_4$ solution (0.24 mmol, 1.2 equiv, 1 M in DCM) was added via syringe. After stirring for 10 minutes, anhydrous KOtBu solution (2 mmol, 10 equiv, 1 M in THF) was slowly added to the flask via syringe, the reaction was allowed to warm to room temperature, and continued to stir for 2 hours. The crude reaction was filtered through a plug of celite (approx. 4 cm in diameter and 1 cm thick), flushed with 50 mL of Et_2O, and concentrated under reduced pressure. The crude residue was purified by column chromatography to yield the desired product.

(2*R*,3*R*)-2-ethyl-3-((*E*)-styryl)tetrahydrofuran (124a)

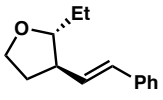

Prepared from (*S*,*E*)-(5-chloro-1-phenylpent-2-en-1-yl)trimethylsilane (**91h**, 55.6 mg, 1.1 equiv, 0.22 mmol, 98% ee) and propionaldehyde (14.4 µl, 1.0 equiv, 0.2 mmol) according to General Procedure 8. The crude residue was purified by column chromatography (silica, 0 to 5% Et_2O/hexanes) to yield 34.6 mg of **124a** (86% yield, >20:1 dr, >20:1 *E*:*Z*, 94% major isomer) as a colorless oil. $\mathbf{R}_f$ = 0.39 (silica, 10%

EtOAc/hexane, UV). $[\alpha]_D^{25}$ = +48° (c = 0.5, $CHCl_3$). **^{1}H NMR (500 MHz, $CDCl_3$):** δ 7.40 – 7.34 (m, 2H), 7.32 (ddd, *J* = 7.8, 6.7, 1.2 Hz, 2H), 7.25 – 7.20 (m, 1H), 6.45 (d, *J* = 15.8 Hz, 1H), 6.12 (dd, *J* = 15.8, 8.7 Hz, 1H), 3.92 (dd, *J* = 8.1, 5.9 Hz, 2H), 3.52 (td, *J* = 7.9, 4.1 Hz, 1H), 2.62 – 2.51 (m, 1H), 2.19 (ddt, *J* = 12.0, 8.1, 5.9 Hz, 1H), 1.89 (ddt, *J* = 12.4, 9.0, 8.1 Hz, 1H), 1.73 – 1.63 (m, 1H), 1.54 (dt, *J* = 13.9, 7.4 Hz, 1H), 1.01 (t, *J* = 7.4 Hz, 3H). **^{13}C NMR (126 MHz, $CDCl_3$):** δ 137.3, 131.0, 130.9, 128.7, 127.6, 126.2, 85.3, 67.3, 48.9, 33.9, 26.9, 10.8. **FTIR (NaCl, thin film, cm^{-1}):** 2964, 2932, 2875, 1493, 1450, 1116, 1020, 965, 746, 693.

(2*R*,3*R*)-2-isopropyl-3-((*E*)-styryl)tetrahydrofuran (124b)

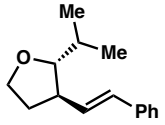

Prepared from (*S*,*E*)-(5-chloro-1-phenylpent-2-en-1-yl)trimethylsilane (**91h**, 55.6 mg, 1.1 equiv, 0.22 mmol, 98% ee) and isobutylaldehyde (18.2 µl, 1.0 equiv, 0.2 mmol) according to General Procedure 8. The crude residue was purified by column chromatography (silica, 0 to 5% Et_2O/hexanes) to yield 34.3 mg of **124b** (79% yield, >20:1 dr, >20:1 *E*:*Z*, 94% major isomer) as a colorless oil. $\mathbf{R}_f$ = 0.46 (silica, 10% EtOAc/hexane, UV). $[\alpha]_D^{25}$ = +46° (c = 1.0, $CHCl_3$). **^{1}H NMR (400 MHz, $CDCl_3$):** δ 7.39 – 7.28 (m, 4H), 7.25 – 7.19 (m, 1H), 6.43 (d, *J* = 15.8 Hz, 1H), 6.14 (dd, *J* = 15.8, 8.8 Hz, 1H), 3.93 – 3.83 (m, 2H), 3.45 (dd, *J* = 7.7, 5.5 Hz, 1H), 2.74 (p, *J* = 8.2 Hz, 1H), 2.16 (dddd, *J* = 12.0, 8.1, 6.6, 5.1 Hz, 1H), 1.92 – 1.77 (m, 2H), 0.98 (dd, *J* = 6.8, 1.0 Hz, 6H). **^{13}C NMR (101 MHz, $CDCl_3$):** δ 137.4, 132.1, 130.4, 128.7, 127.3, 126.1, 88.9, 67.5, 46.3, 34.6, 31.8, 19.7, 18.2. **FTIR (NaCl, thin film, cm^{-1}):** 3026, 2961, 2933, 2872, 1493, 1486, 1449, 1387, 1071, 1051, 965, 747, 693.

(2*R*,3*R*)-2-cyclohexyl-3-((*E*)-styryl)tetrahydrofuran (124c)

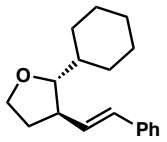

Prepared from (*S*,*E*)-(5-chloro-1-phenylpent-2-en-1-yl)trimethylsilane (**91h**, 55.6 mg, 1.1 equiv, 0.22 mmol, 98% ee) and cyclohexanecarbaldehyde (22.4 mg, 1.0 equiv, 0.2 mmol) according to General Procedure 8. The crude residue was purified by column chromatography (silica, 0 to 5% Et_2O/hexanes) to yield 27.1 mg of **124c** (53% yield, >20:1 dr, 20:1 *E*:*Z*, 91% major isomer) as a colorless oil. $\mathbf{R_f}$ = 0.42 (silica, 10% EtOAc/hexane, UV). $[\boldsymbol{a}]_D^{25}$ = +78° (c = 1.0, $CHCl_3$). **^{1}H NMR (400 MHz, $CDCl_3$):** δ 7.40 – 7.34 (m, 2H), 7.34 – 7.28 (m, 2H), 7.25 – 7.19 (m, 1H), 6.43 (d, *J* = 15.7 Hz, 1H), 6.13 (dd, *J* = 15.7, 8.8 Hz, 1H), 3.93 – 3.79 (m, 2H), 3.44 (dd, *J* = 7.6, 5.7 Hz, 1H), 2.78 (p, *J* = 8.2 Hz, 1H), 2.19 – 2.09 (m, 1H), 1.85 (dq, *J* = 12.3, 7.8 Hz, 2H), 1.79 – 1.69 (m, 3H), 1.68 – 1.61 (m, 1H), 1.49 (tdt, *J* = 11.7, 6.1, 3.3 Hz, 1H), 1.30 – 1.04 (m, 5H). **^{13}C NMR (101 MHz, $CDCl_3$):** δ 137.5, 132.1, 130.3, 128.7, 127.3, 126.1, 88.3, 67.4, 46.0, 41.9, 34.6, 30.1, 28.7, 26.7, 26.5, 26.3. **FTIR (NaCl, thin film, cm^{-1}):** 2925, 2852, 1492, 1449, 1085, 1066, 965, 887, 748, 694.

(2*R*,3*R*)-2-(but-3-en-1-yl)-3-((*E*)-styryl)tetrahydrofuran (124d)

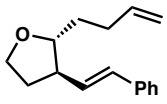

Prepared from (*S*,*E*)-(5-chloro-1-phenylpent-2-en-1-yl)trimethylsilane (**91h**, 55.6 mg, 1.1 equiv, 0.22 mmol, 98% ee) and pent-4-enal (16.8 mg, 1.0 equiv, 0.2 mmol) according to General Procedure 8. The crude residue was purified by column chromatography (silica, 0 to 5% Et_2O/hexanes) to yield 26.5 mg of **124d** (58% yield, 10:1 dr, >20:1 *E*:*Z*, 89% major isomer) as a colorless oil. $\mathbf{R_f}$ = 0.39 (silica, 10% EtOAc/hexane, UV). $[\boldsymbol{a}]_D^{25}$ = +69° (c = 1.0, $CHCl_3$). **^{1}H NMR (400 MHz, $CDCl_3$):** δ 7.40 – 7.35 (m, 2H), 7.35 – 7.28 (m, 2H), 7.26 – 7.20 (m, 1H), 6.46 (d, *J* = 15.7 Hz, 1H), 6.11

(dd, *J* = 15.8, 8.8 Hz, 1H), 5.84 (ddt, *J* = 16.8, 10.1, 6.6 Hz, 1H), 5.09 – 4.92 (m, 2H), 3.97 – 3.89 (m, 2H), 3.58 (td, *J* = 8.3, 3.7 Hz, 1H), 2.56 (p, *J* = 8.2 Hz, 1H), 2.35 – 2.10 (m, 3H), 1.89 (ddt, *J* = 12.3, 9.0, 8.1 Hz, 1H), 1.73 (dddd, *J* = 13.7, 10.0, 6.2, 3.7 Hz, 1H), 1.60 (dddd, *J* = 13.8, 9.7, 8.1, 5.3 Hz, 1H). **^{13}C NMR (101 MHz, $CDCl_3$):** δ 138.6, 137.3, 131.2, 130.6, 128.7, 127.4, 126.2, 114.7, 83.4, 67.3, 49.5, 33.9, 33.4, 30.8. **FTIR (NaCl, thin film, cm^{-1}):** 3026, 2974, 2931, 2868, 1640, 1493, 1449, 1071, 966, 911, 747, 693.

(2*R*,3*R*)-2-(4-chlorobutyl)-3-((*E*)-styryl)tetrahydrofuran (124e)

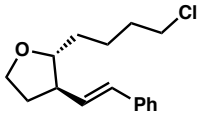

Prepared from (*S*,*E*)-(5-chloro-1-phenylpent-2-en-1-yl)trimethylsilane (**91h**, 55.6 mg, 1.1 equiv, 0.22 mmol, 98% ee) and 5-chloropentanal (24 µl, 1.0 equiv, 0.2 mmol) according to General Procedure 8. The crude residue was purified by column chromatography (silica, 0 to 6% Et_2O/hexanes) to yield 48.6 mg of **124e** (92% yield, 15:1 dr, >20:1 *E*:*Z*, 91% major isomer) as a colorless oil. $\mathbf{R_f}$ = 0.36 (silica, 10% EtOAc/hexane, UV). $[\alpha]_D^{25}$ = +64° (c = 1.0, $CHCl_3$). **^{1}H NMR (400 MHz, $CDCl_3$):** δ 7.40 – 7.28 (m, 4H), 7.25 – 7.20 (m, 1H), 6.46 (d, *J* = 15.8 Hz, 1H), 6.10 (dd, *J* = 15.7, 8.8 Hz, 1H), 3.95 – 3.88 (m, 2H), 3.59 – 3.50 (m, 3H), 2.60 – 2.49 (m, 1H), 2.20 (dddd, *J* = 12.0, 8.1, 6.4, 5.3 Hz, 1H), 1.94 – 1.85 (m, 1H), 1.85 – 1.75 (m, 2H), 1.70 – 1.62 (m, 2H), 1.57 – 1.47 (m, 2H). **^{13}C NMR (101 MHz, $CDCl_3$):** δ 137.2, 131.3, 130.5, 128.7, 127.4, 126.2, 83.7, 67.3, 49.4, 45.1, 33.8, 33.2, 32.8, 24.1. **FTIR (NaCl, thin film, cm^{-1}):** 2938, 2867, 1492, 1449, 1071, 1029, 1017, 966, 748, 693.

(2*S*,3*R*)-2-((benzyloxy)methyl)-3-((*E*)-styryl)tetrahydrofuran (124f)

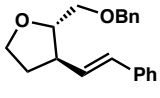

Prepared from (*S*,*E*)-(5-chloro-1-phenylpent-2-en-1-yl)trimethylsilane (**91h**, 55.6 mg, 1.1 equiv, 0.22 mmol, 98% ee) and 2-(benzyloxy)acetaldehyde (30.0 mg, 1.0 equiv, 0.2 mmol) according to General Procedure 8 with the exception that 2.0 equivalents $TiCl_4$ and 15.0 equivalents KOtBu were used in this procedure. The crude residue was purified by column chromatography (silica, 0 to 20% Et_2O/hexanes) to yield 44.2 mg of **124f** (75% yield, 1:3 dr (**Note:** trans is the minor diastereomer), >20:1 *E*:*Z*, 24% major isomer) as a yellow oil. $\mathbf{R_f}$ = 0.18 (silica, 10% EtOAc/hexane, UV). $[\boldsymbol{\alpha}]_D^{25}$ = +41° (c = 1.0, $CHCl_3$). **^{1}H NMR (400 MHz, $CDCl_3$): Note:** mixture of diastereomers, contains additional impurity: δ 7.39 – 7.16 (m, 10.00H), 6.50 – 6.34 (m, 0.74H), 6.25 – 6.07 (m, 0.75H), 4.68 – 4.46 (m, 1.88H), 4.18 – 4.03 (m, 1.36H), 4.01 – 3.92 (m, 0.42H), 3.92 – 3.79 (m, 0.94H), 3.66 (dd, *J* = 10.5, 2.9 Hz, 0.24H), 3.63 – 3.46 (m, 1.87H), 3.44 – 3.32 (m, 0.51H), 3.08 (dq, *J* = 9.4, 6.9 Hz, 0.57H), 2.80 (p, *J* = 8.5 Hz, 0.15H), 2.63 (dddt, *J* = 7.2, 4.3, 2.9, 1.4 Hz, 0.19H), 2.19 (dtd, *J* = 12.5, 7.6, 4.9 Hz, 0.74H), 2.03 – 1.85 (m, 0.83H). **^{13}C NMR (101 MHz, $CDCl_3$): Note:** mixture of diastereomers, contains additional impurity: δ 138.25, 137.19, 131.33, 131.07, 130.05, 128.74, 128.56, 128.51, 128.35, 128.33, 128.27, 127.73, 127.65, 127.56, 127.52, 127.37, 127.29, 126.16, 126.11, 80.81, 73.52, 70.99, 70.96, 67.93, 67.67, 45.23, 45.20, 36.24, 33.57, 32.81, 28.68, 27.59. **FTIR (NaCl, thin film, cm^{-1}):** 3027, 2973, 2930, 2866, 1495, 1452, 1364, 1197, 1092, 1028, 969, 748, 696.

(2*R*,3*R*)-2-(2-(benzyloxy)ethyl)-3-((*E*)-styryl)tetrahydrofuran (124g)

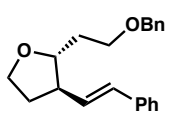

Prepared from (*S*,*E*)-(5-chloro-1-phenylpent-2-en-1-yl)trimethylsilane (**91h**, 55.6 mg, 1.1 equiv, 0.22 mmol, 98% ee) and 3-(benzyloxy)propanal (32.8 mg, 1.0 equiv, 0.2 mmol) according to General Procedure 8 with the exception that 2.0 equivalents $TiCl_4$ and 15.0 equivalents KOtBu were used in this procedure. The crude residue was purified by column chromatography (silica, 0 to 15% Et_2O/hexanes) to yield 35.7 mg of **124g** (58% yield, 2:1 dr, >20:1 *E*:*Z*, 63% major isomer) as a pale yellow oil. $\mathbf{R_f}$ = 0.18 (silica, 10% EtOAc/hexane, UV). $[\boldsymbol{\alpha}]_{\boldsymbol{D}}^{\mathbf{25}}$ = +38° (c = 1.0, $CHCl_3$). **^{1}H NMR (400 MHz, $CDCl_3$): Note:** mixture of diastereomers: δ 7.39 – 7.19 (m, 10H), 6.51 – 6.32 (m, 1H), 6.23 – 6.04 (m, 1H), 4.58 – 4.42 (m, 2H), 4.10 – 3.98 (m, 0.7H), 3.97 – 3.88 (m, 1.2H), 3.81 (td, *J* = 8.4, 6.7 Hz, 0.4H), 3.76 – 3.52 (m, 3H), 3.36 (t, *J* = 6.3 Hz, 0.3H), 3.01 – 2.90 (m, 0.3H), 2.59 (p, *J* = 8.4 Hz, 0.6H), 2.29 – 2.13 (m, 1H), 2.05 – 1.92 (m, 0.7H), 1.92 – 1.75 (m, 2.3H). **^{13}C NMR (101 MHz, $CDCl_3$): Note:** mixture of diastereomers: δ 138.63, 137.35, 137.25, 131.35, 131.08, 130.28, 129.46, 128.67, 128.47, 128.45, 127.83, 127.79, 127.64, 127.60, 127.41, 127.35, 126.22, 81.05, 79.21, 73.21, 73.18, 68.04, 67.91, 67.36, 66.80, 49.59, 45.97, 34.28, 33.76, 32.72, 31.95, 28.79, 27.71. **FTIR (NaCl, thin film, cm^{-1}):** 3027, 2969, 2930, 2865, 1495, 1453, 1363, 1198, 1099, 1028, 967, 748, 696.

(2*R*,3*R*)-2-(3-(benzyloxy)propyl)-3-((*E*)-styryl)tetrahydrofuran (124h)

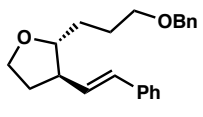

Prepared from (*S*,*E*)-(5-chloro-1-phenylpent-2-en-1-yl)trimethylsilane (**91h**, 55.6 mg, 1.1 equiv, 0.22 mmol, 98% ee) and 4-(benzyloxy)butanal (35.6 mg, 1.0 equiv, 0.2 mmol) according to General Procedure 8 with the exception that 2.0 equivalents $TiCl_4$ and 15.0 equivalents KOtBu were used in this procedure. The crude

residue was purified by column chromatography (silica, 0 to 20% Et_2O/hexanes) to yield 17.5 mg of **124h** (27% yield, 2:1 dr, >20:1 *E*:*Z*, 65% major isomer) as a yellow oil. $\mathbf{R_f}$ = 0.22 (silica, 10% EtOAc/hexane, UV). $[\boldsymbol{a}]_D^{25}$ = +13° (c = 1.0, $CHCl_3$). **^{1}H NMR (400 MHz, $CDCl_3$): Note:** mixture of diastereomers: δ 7.41 – 7.19 (m, 10.0H), 6.66 – 6.36 (m, 1H), 6.26 – 5.89 (m, 1H), 4.49 (d, *J* = 8.5 Hz, 2H), 4.04 (td, *J* = 8.2, 5.7 Hz, 0.4H), 3.97 – 3.88 (m, 1.4H), 3.88 – 3.70 (m, 0.7H), 3.59 (td, *J* = 8.2, 3.3 Hz, 0.7H), 3.55 – 3.41 (m, 2H), 3.02 – 2.89 (m, 0.3H), 2.56 (p, *J* = 8.5 Hz, 0.6H), 2.28 – 2.12 (m, 1H), 1.98 – 1.66 (m, 3.6H), 1.63 – 1.50 (m, 1.4H). **^{13}C NMR (101 MHz, $CDCl_3$): Note:** mixture of diastereomers: δ 138.75, 138.73, 137.45, 137.28, 131.17, 130.85, 130.60, 129.61, 128.68, 128.52, 128.44, 128.43, 128.37, 127.73, 127.71, 127.56, 127.40, 127.30, 126.24, 126.21, 83.78, 82.21, 72.90, 72.84, 72.79, 70.39, 70.30, 67.27, 66.70, 49.38, 45.96, 33.88, 32.84, 30.71, 28.19, 26.91, 26.77. **FTIR (NaCl, thin film, cm^{-1}):** 3060, 3027, 2933, 2857, 1495, 1453, 1363, 1203, 1100, 1073, 1028, 967, 747, 696.

(2*R*,3*R*)-2-(4-(benzyloxy)butyl)-3-((*E*)-styryl)tetrahydrofuran (124i)

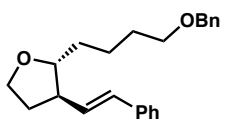

Prepared from (*S*,*E*)-(5-chloro-1-phenylpent-2-en-1-yl)trimethylsilane (**91h**, 55.6 mg, 1.1 equiv, 0.22 mmol, 98% ee) and 5-(benzyloxy)pentanal (38.5 mg, 1.0 equiv, 0.2 mmol) according to General Procedure 8 with the exception that 2.0 equivalents $TiCl_4$ and 15.0 equivalents KOtBu were used in this procedure. The crude residue was purified by column chromatography (silica, 0 to 15% Et_2O/hexanes) to yield 13.7 mg of **124i** (20% yield, 10:1 dr, >20:1 *E*:*Z*, 90% major isomer) as a colorless oil. $\mathbf{R_f}$ = 0.18 (silica, 10% EtOAc/hexane, UV). $[\boldsymbol{a}]_D^{25}$ = +48° (c = 1.0, $CHCl_3$). **^{1}H NMR (400 MHz, $CDCl_3$):** δ 7.39 – 7.12 (m, 10H), 6.44 (d, *J* = 15.7 Hz, 1H),

6.10 (dd, *J* = 15.8, 8.8 Hz, 1H), 4.48 (s, 2H), 3.90 (d, *J* = 8.1 Hz, 2H), 3.56 (td, *J* = 7.8, 3.3 Hz, 1H), 3.46 (td, *J* = 6.5, 2.8 Hz, 2H), 2.53 (p, *J* = 8.6 Hz, 1H), 2.19 (dddd, *J* = 12.0, 8.1, 6.5, 5.3 Hz, 1H), 1.93 – 1.82 (m, 1H), 1.69 – 1.45 (m, 6H). **^{13}C NMR (101 MHz, $CDCl_3$):** δ 138.8, 137.3, 131.1, 130.7, 128.7, 128.4, 127.7, 127.6, 127.4, 126.2, 84.0, 73.0, 70.5, 67.3, 49.4, 33.9, 33.9, 30.0, 23.3. **FTIR (NaCl, thin film, cm^{-1}):** 3027, 2935, 2860, 1495, 1454, 1363, 1102, 1028, 1017, 966, 747, 696.

2.6.6.2 Synthesis of Standards

(*trans*)-2-((*E*)-styryl)cyclopentan-1-ol (S25)

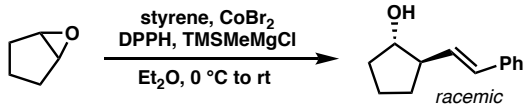

According to a procedure by Oshima and coworkers,[95] 1,6-bis(diphenylphosphino)hexane ligand (DPPH, 154 mg, 0.34 mmol, 0.085 equiv) was added to a round bottom flask equipped with a stir bar and pumped into the glovebox filled with an N_2 atmosphere. Cobalt(II) bromide (61 mg, 0.28 mmol, 0.07 equiv) was added, followed by 4 mL of Et_2O. The flask sealed with a septum, and stirred for 1 hour forming a green solution. The round bottom flask was removed from the glovebox and cooled to 0 °C. Cyclopentene oxide (524 µL, 6 mmol, 1.5 equiv), styrene (460 µL, 4 mmol, 1 equiv), and (trimethylsilyl)methyl-magnesium chloride (10 mL, 1 M in Et_2O, 10 mmol, 2.5 equiv) were added sequentially. The reaction was warmed to room temperature and stirred overnight, then quenched with aq. NH_4Cl and extracted with EtOAc (2 x 80 mL). The combined organic layers were dried with $MgSO_4$, filtered, and concentrated under reduced pressure. The crude material was

purified by column chromatography (silica, 0 to 30% EtOAc/hexane) to yield 325.6 mg of **S25** (43% yield) as a yellow oil. Spectral data matched those reported in the literature.[95]

((*E*)-2-((*trans*)-2-methoxycyclopentyl)vinyl)benzene (117)

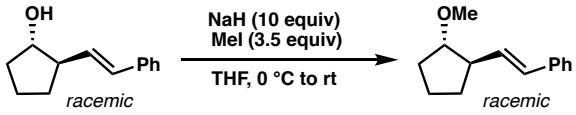

Alcohol **S25** (10.0 mg, 0.055 mmol, 1 equiv) was added to a 1 dram vial, dissolved in THF (0.55 mL), and cooled to 0 °C. Sodium hydride (22 mg, 60 wt% in mineral oil, 0.55 mmol, 10 equiv) and methyl iodide (10.5 µl, 0.165 mmol, 3 equiv) were subsequently added, and the reaction was stirred for 30 minutes at room temperature. The reaction was quenched with aq. NH_4Cl and extracted with Et_2O. The organic layer was dried with $MgSO_4$, filtered, and concentrated under reduced pressure. The crude material was purified by preparative TLC (silica, 10% EtOAc/hexane) to yield 8.3 mg of **117** (77% yield) as a colorless oil.

(*cis*)-2-((*E*)-styryl)cyclopentan-1-ol (S26)

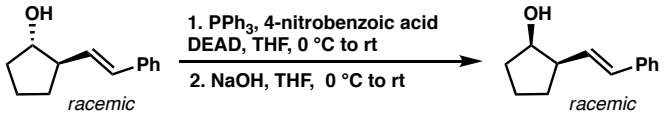

Alcohol **S25** (10.0 mg, 0.055 mmol, 1 equiv) was added to a 1 dram vial, sealed with a screw-cap septum, and purged with N_2 before 0.6 mL of THF, triphenylphosphine (57 mg, 0.21 mmol, 3.8 equiv), and 4-nitrobenzoic acid (38 mg, 0.23 mmol, 4.1 equiv) were added. The vial was cooled to 0 °C, diethyl azodicarboxylate (108 mg, 40 wt% in PhMe, 4.5 equiv) was added, and the reaction was stirred at room temperature overnight. The reaction was quenched with 2 mL of 1 M HCl and extracted with Et_2O (2 x 10 mL). The combined

organic layers were dried with $MgSO_4$, filtered, and concentrated under reduced pressure to afford the crude ester product, which was carried forward without further purification. The *para*-nitrobenzoate was then added to a 1 dram vial, dissolved in 0.7 mL THF, and cooled to 0 °C. Then 5% aqueous NaOH (0.6 mL) was added and the reaction was stirred at room temperature for 8 hours. The reaction was diluted with chloroform (5 mL) and washed with H_2O (5 mL), 1 M HCl (5 mL), and brine (5 mL). The organic layer was dried with $MgSO_4$, filtered, and concentrated under reduced pressure. The crude material was purified by preparative TLC (silica, 20% EtOAc/hexane) to yield 5.7 mg of **S26** (57% yield over 2 steps) as a colorless oil. $\mathbf{R_f}$ = 0.36 (silica, 20% EtOAc/hexane, UV). **^{1}H NMR (500 MHz, $CDCl_3$):** δ 7.40 – 7.37 (m, 2H), 7.33 – 7.29 (m, 2H), 7.24 – 7.19 (m, 1H), 6.54 – 6.49 (m, 1H), 6.36 (dd, *J* = 16.0, 7.4 Hz, 1H), 4.25 (td, *J* = 4.5, 2.1 Hz, 1H), 2.67 – 2.59 (m, 1H), 1.99 – 1.89 (m, 2H), 1.87 – 1.80 (m, 2H), 1.79 – 1.71 (m, 1H), 1.71 – 1.62 (m, 1H), 1.43 (s, 1H). **^{13}C NMR (126 MHz, $CDCl_3$):** δ 137.4, 132.0, 129.4, 128.7, 127.4, 126.2, 76.1, 49.5, 34.4, 28.5, 22.3. **FTIR (NaCl, thin film, cm^{-1}):** 3405, 3081, 3058, 3025, 2959, 1599, 1495, 1448, 1327, 1154, 1121, 1073, 1027, 968. **HRMS (FAB, *m/z*):** calc'd for $C_{13}H_{16}O$ $[M+H]^+$: 189.1279; found: 189.1272.

((*E*)-2-((*cis*)-2-methoxycyclopentyl)vinyl)benzene (117'')

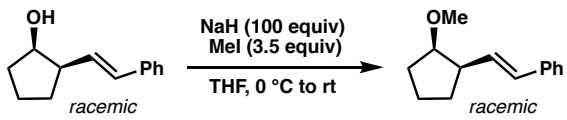

Alcohol **S26** (5.7 mg, 0.03 mmol, 1 equiv) was added to a 1 dram vial, dissolved in THF (0.5 mL), and cooled to 0 °C. Sodium hydride (120 mg, 60 wt% in mineral oil, 3.0 mmol,

100 equiv) and methyl iodide (7 µl, 0.105 mmol, 3.5 equiv) were subsequently added, and the reaction was stirred for 30 minutes at room temperature. The reaction was quenched with aq. NH_4Cl and extracted with Et_2O. The organic layer was dried with $MgSO_4$, filtered, and concentrated under reduced pressure. The crude material was purified by preparative TLC (silica, 10% EtOAc/hexane) to yield 2.5 mg of **117''** (41% yield) as a colorless oil. The ^{1}H NMR of the purified product matches the **minor** diastereomer **117''**. $\mathbf{R_f}$ = 0.49 (silica, 10% EtOAc/hexane, UV). **^{1}H NMR (500 MHz, $CDCl_3$):** δ 7.40 – 7.36 (m, 2H), 7.31 – 7.27 (m, 2H), 7.21 – 7.16 (m, 1H), 6.46 – 6.37 (m, 2H), 3.72 (tq, *J* = 4.8, 2.4 Hz, 1H), 3.30 (s, 3H), 2.67 – 2.60 (m, 1H), 1.88 – 1.77 (m, 4H), 1.77 – 1.67 (m, 1H), 1.66 – 1.59 (m, 1H). **^{13}C NMR (126 MHz, $CDCl_3$):** δ 138.0, 131.0, 129.9, 128.6, 126.9, 126.2, 85.7, 57.2, 48.5, 30.8, 30.2, 22.2. **FTIR (NaCl, thin film, cm^{-1}):** 3025, 2926, 2821, 1599, 1495, 1448, 1356, 1128, 1094, 1073, 965, 747. **HRMS (FAB, *m/z*)**: calc'd for $C_{14}H_{18}O$ $[M+\cdot]^+$: 202.1358; found: 202.1374.

(1*S*,2*R*)-2-((*E*)-styryl)cyclopentan-1-ol and (1*R*,2*S*)-2-((*E*)-styryl)cyclopentan-1-ol

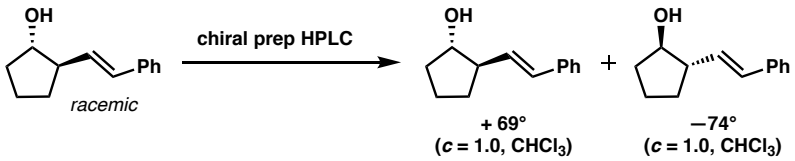

Approximately 60 mg of the racemic alcohol **S25** was separated via preparative HPLC using a chiral AD-H column and 20% isopropanol/hexane to provide 28 mg of the (+)-1*S*,2*R* enantiomer and 24 mg of the (–)-1*R*,2*S* enantiomer. The (+) enantiomer was measured to have an optical rotation of $[\boldsymbol{a}]_D^{25}$ = +69° (c = 1.0, $CHCl_3$) whereas the (–) enantiomer was measured to have an optical rotation of $[\boldsymbol{a}]_D^{25}$ = –74° (c = 1.0, $CHCl_3$). The

optical rotation of the (+) enantiomer has been previously reported in the literature, which allowed for the appropriate assignment of the two chiral products.[96]

((*E*)-2-((1*R*,2*S*)-2-methoxycyclopentyl)vinyl)benzene (117)

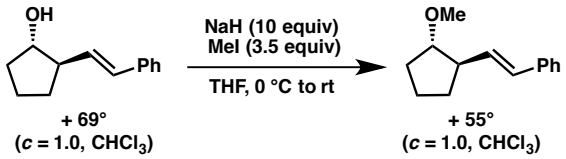

Enantioenriched alcohol **117** ($[\boldsymbol{a}]_D^{25}$ = +69°, 28 mg, 0.15 mmol, 1 equiv) was added to a 20 mL vial, dissolved in THF (2.5 mL), and cooled to 0 °C. Sodium hydride (60 mg, 60 wt% in mineral oil, 1.5 mmol, 10 equiv) and methyl iodide (35 µl, 0.53 mmol, 3.5 equiv) were subsequently added, and the reaction was allowed to stir for 2 hours at room temperature. The reaction was quenched with aq. NH_4Cl and extracted with Et_2O. The organic layer was dried with $MgSO_4$, filtered, and concentrated under reduced pressure. The crude material was purified by column chromatography (silica, hexane to 10% EtOAc/hexane) to yield 24 mg of **117** (80% yield) as a colorless oil. The enantiopure product was measured to have an optical rotation of $[\boldsymbol{a}]_D^{25}$ = +55° (c = 1.0, $CHCl_3$).

(*trans*)-2-((*E*)-styryl)cyclohexan-1-ol (S27)

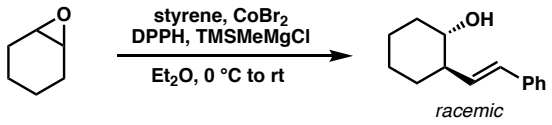

According to a procedure by Oshima and coworkers,[95] 1,6-bis(diphenylphosphino)hexane ligand (DPPH, 154 mg, 0.34 mmol, 0.085 equiv) was added to a round bottom flask equipped with a stir bar and pumped into the glovebox filled with an N_2 atmosphere.

Cobalt(II) bromide (61 mg, 0.28 mmol, 0.07 equiv) was added, dissolved in 4 mL of Et_2O, sealed with a septum, and stirred for 1 hour forming a green solution. The round bottom flask was removed from the glovebox and cooled to 0 °C before cyclohexene oxide (608 µL, 6 mmol, 1.5 equiv), styrene (460 µL, 4 mmol, 1 equiv), and (trimethylsilyl)methylmagnesium chloride (10 mL, 1 M in Et_2O, 10 mmol, 2.5 equiv) were added sequentially. The reaction was warmed to room temperature and stirred overnight, then quenched with aq. NH_4Cl and extracted with EtOAc (2 x 80 mL). The combined organic layers were dried with $MgSO_4$, filtered, and concentrated under reduced pressure. The crude material was purified by column chromatography (silica, 0 to 30% EtOAc/hexane) to yield 191 mg of **S27** (24% yield) as a yellow oil. Spectral data matched those reported in the literature.[97]

((*E*)-2-((*trans*)-2-methoxycyclohexyl)vinyl)benzene (118')

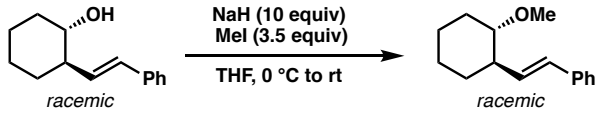

Alcohol **S27** (12.4 mg, 0.06 mmol, 1 equiv) was added to a 1 dram vial, dissolved in THF (1.0 mL), and cooled to 0 °C. Sodium hydride (240 mg, 60 wt% in mineral oil, 6.0 mmol, 100 equiv) and methyl iodide (14 µl, 0.210 mmol, 3.5 equiv) were subsequently added, and the reaction was allowed to stir for 30 minutes at room temperature. The reaction was quenched with aq. NH_4Cl and extracted with Et_2O. The organic layer was dried with $MgSO_4$, filtered, and concentrated under reduced pressure. The crude material was purified by preparative TLC (silica, 10% EtOAc/hexane) to yield 7.3 mg of **118'** (55% yield) as a colorless oil. The ^1H NMR of the purified product matches the **minor** diastereomer **118'**.

2.6.7 SFC and HPLC Traces of Racemic and Enantioenriched Products

88c (Figure 2.7): racemic

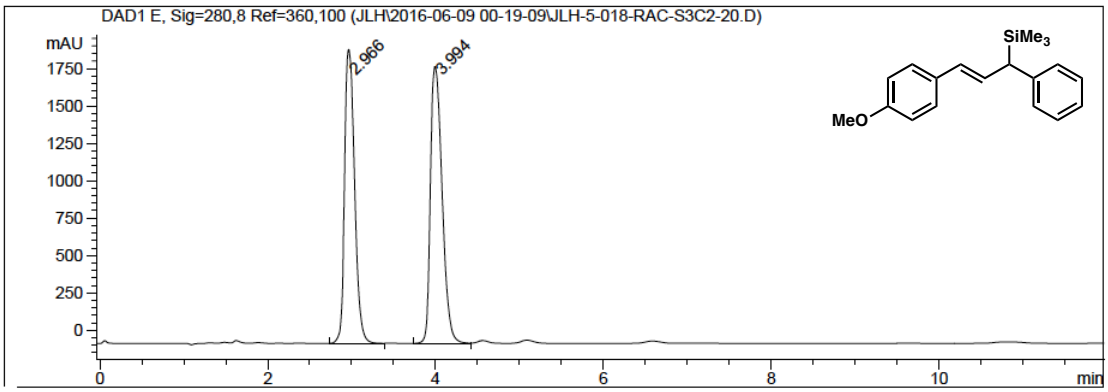

Peak #	RetTime [min]	Type	Width [min]	Area [mAU*s]	Height [mAU]	Area %
1	2.966	BV	0.1332	1.63275e4	1960.21167	47.6290
2	3.994	BV	0.1534	1.79530e4	1847.51770	52.3710

88c (Figure 2.7): enantioenriched, 95% ee

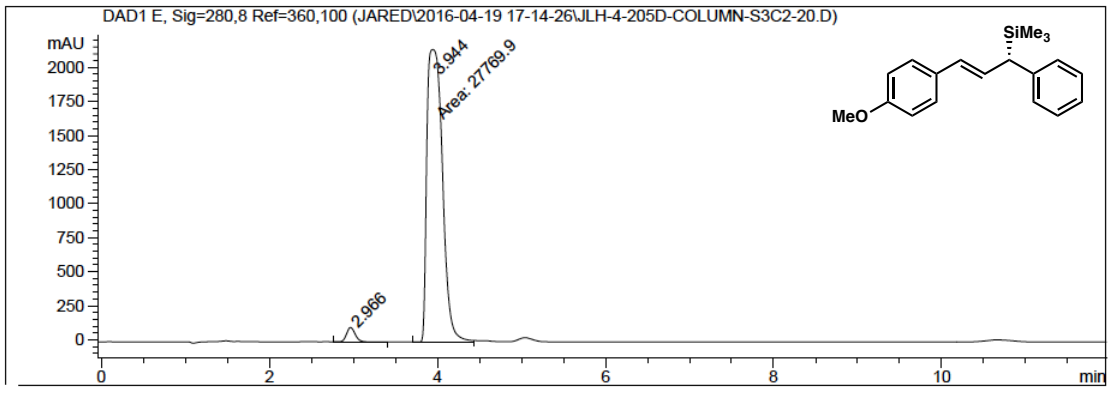

Peak #	RetTime [min]	Type	Width [min]	Area [mAU*s]	Height [mAU]	Area %
1	2.966	VB	0.1140	779.79077	105.83328	2.7313
2	3.944	MM	0.2154	2.77699e4	2149.07568	97.2687

90a (Figure 2.7): racemic

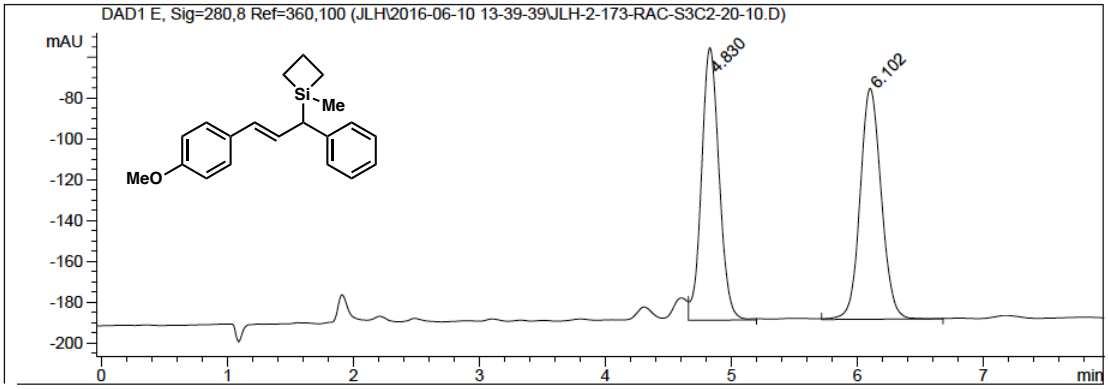

Peak #	RetTime [min]	Type	Width [min]	Area [mAU*s]	Height [mAU]	Area %
1	4.830	VB	0.1536	1297.76147	133.29198	49.5648
2	6.102	BB	0.1805	1320.54907	112.90835	50.4352

90a (Figure 2.7): enantioenriched, 98% ee

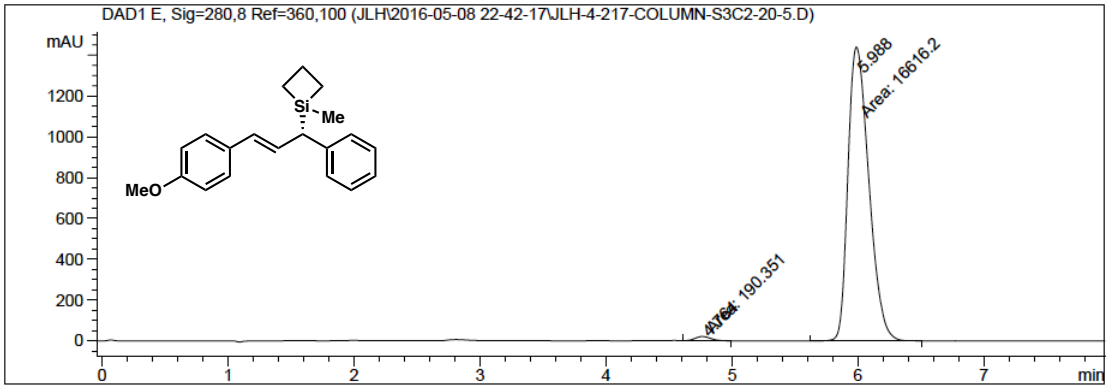

Peak #	RetTime [min]	Type	Width [min]	Area [mAU*s]	Height [mAU]	Area %
1	4.764	MM	0.1484	190.35126	21.37501	1.1326
2	5.988	MM	0.1922	1.66162e4	1440.68481	98.8674

90b (Figure 2.7): racemic

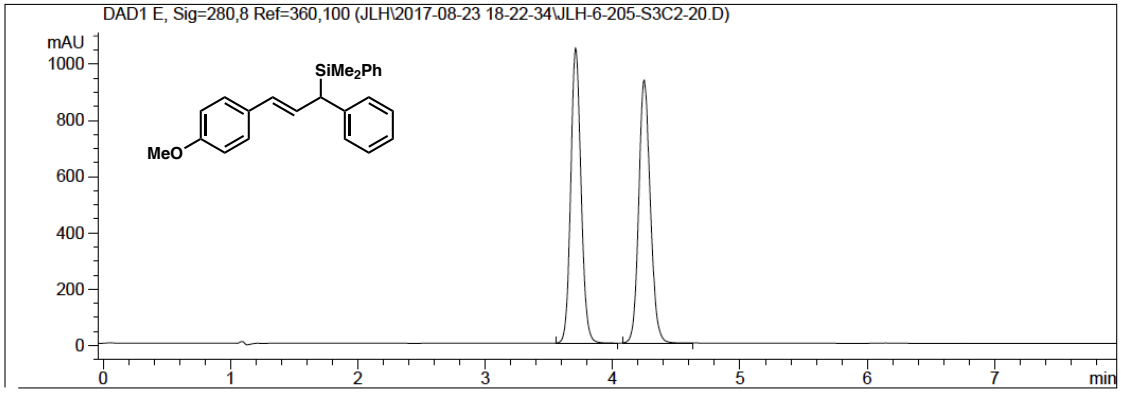

Peak #	RetTime [min]	Type	Width [min]	Area [mAU*s]	Height [mAU]	Area %
1	3.710	BB	0.0900	5919.53662	1045.89319	49.9092
2	4.248	BB	0.0985	5941.06885	930.83258	50.0908

90b (Figure 2.7): enantioenriched, 97% ee

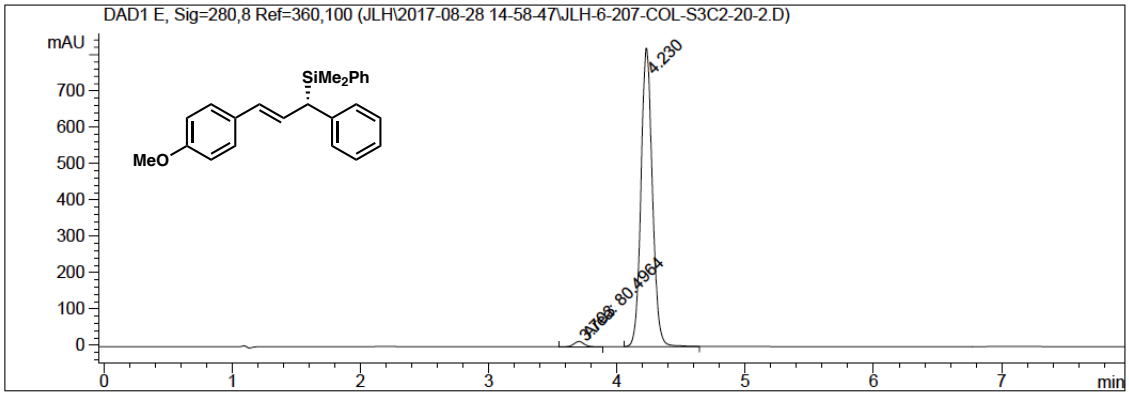

Peak #	RetTime [min]	Type	Width [min]	Area [mAU*s]	Height [mAU]	Area %
1	3.703	MM	0.0913	80.49639	14.69651	1.5530
2	4.230	BB	0.0965	5102.88428	821.41608	98.4470

90c (Figure 2.7): racemic

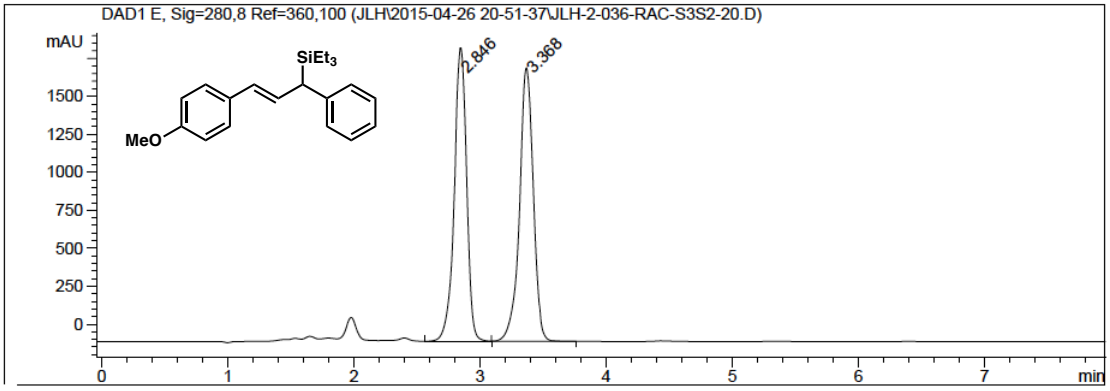

Peak #	RetTime [min]	Type	Width [min]	Area [mAU*s]	Height [mAU]	Area %
1	2.846	VV	0.1057	1.32271e4	1937.00806	49.0137
2	3.368	VB	0.1170	1.37594e4	1803.53308	50.9863

90c (Figure 2.7): enantioenriched, 93% ee

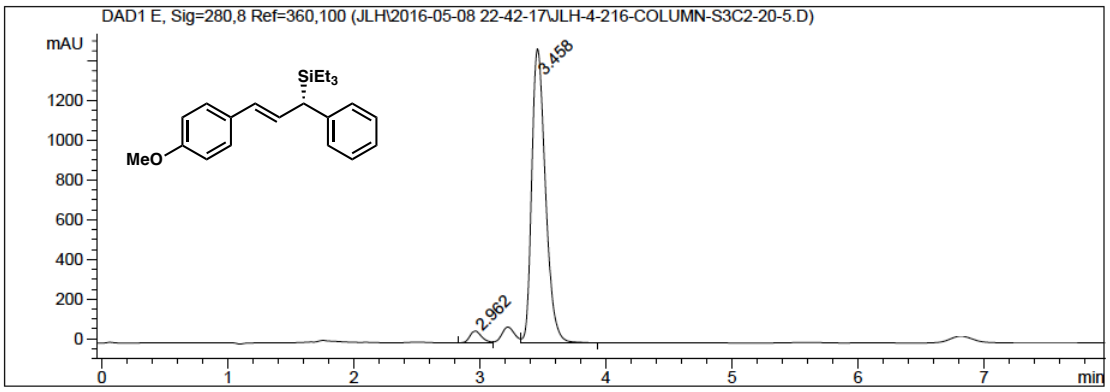

Peak #	RetTime [min]	Type	Width [min]	Area [mAU*s]	Height [mAU]	Area %
1	2.962	VV	0.0992	386.79767	59.99361	3.3328
2	3.458	VB	0.1164	1.12188e4	1481.32935	96.6672

90d (Figure 2.7): racemic

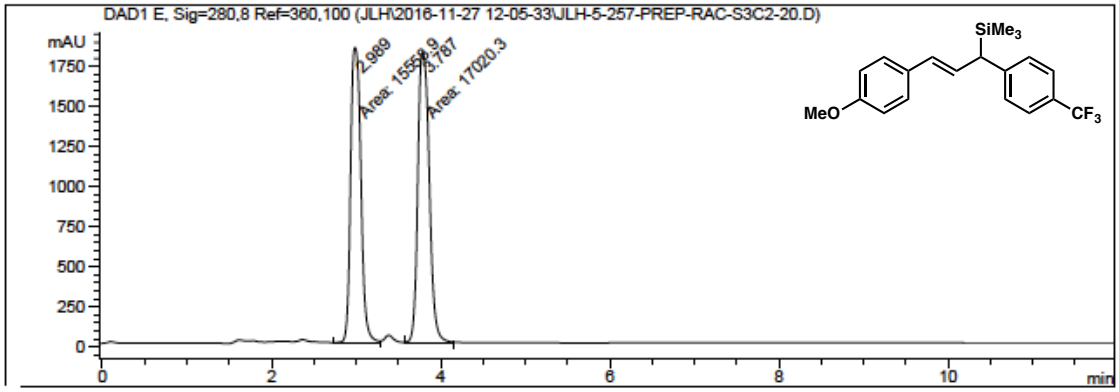

Peak #	RetTime [min]	Type	Width [min]	Area [mAU*s]	Height [mAU]	Area %
1	2.989	MM	0.1406	1.55589e4	1844.16211	47.7570
2	3.787	MM	0.1563	1.70203e4	1814.95007	52.2430

90d (Figure 2.7): enantioenriched, 96% ee

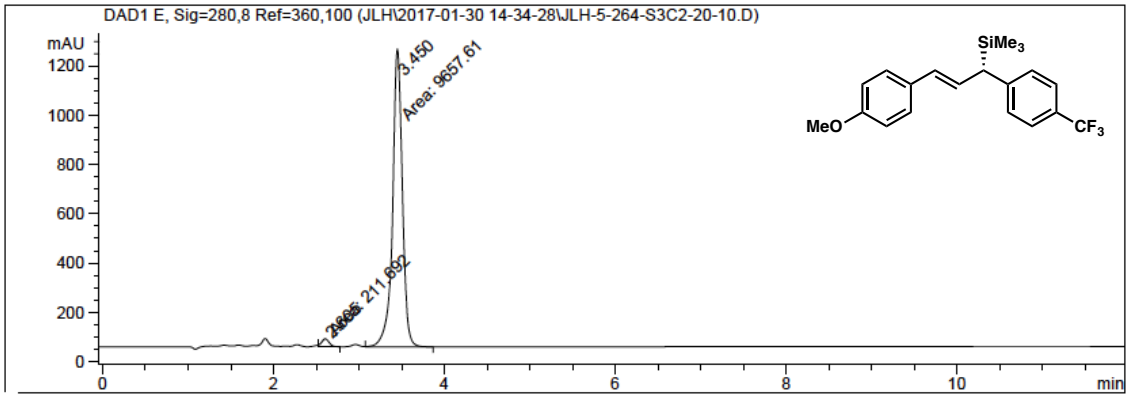

Peak #	RetTime [min]	Type	Width [min]	Area [mAU*s]	Height [mAU]	Area %
1	2.605	MM	0.1056	211.69177	33.39671	2.1450
2	3.450	MM	0.1330	9657.60938	1210.65833	97.8550

90e (Figure 2.7): racemic

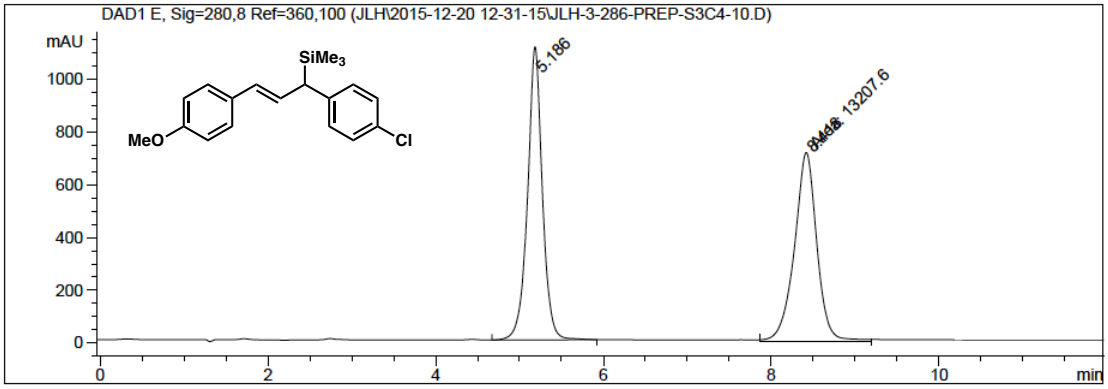

Peak #	RetTime [min]	Type	Width [min]	Area [mAU*s]	Height [mAU]	Area %
1	5.186	VB	0.1774	1.36628e4	1111.58838	50.8470
2	8.418	MM	0.3079	1.32076e4	714.82355	49.1530

90e (Figure 2.7): enantioenriched, 96% ee

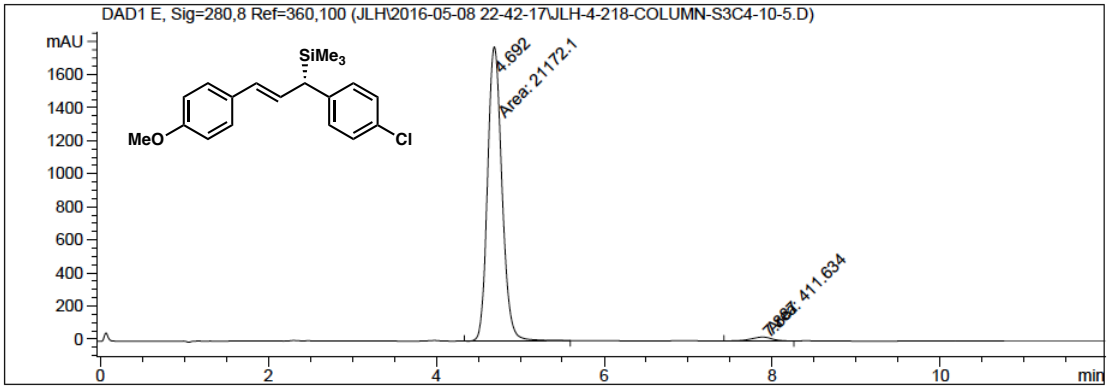

Peak #	RetTime [min]	Type	Width [min]	Area [mAU*s]	Height [mAU]	Area %
1	4.692	MM	0.1983	2.11721e4	1779.80176	98.0929
2	7.887	MM	0.2914	411.63358	23.54672	1.9071

90f (Figure 2.7): racemic

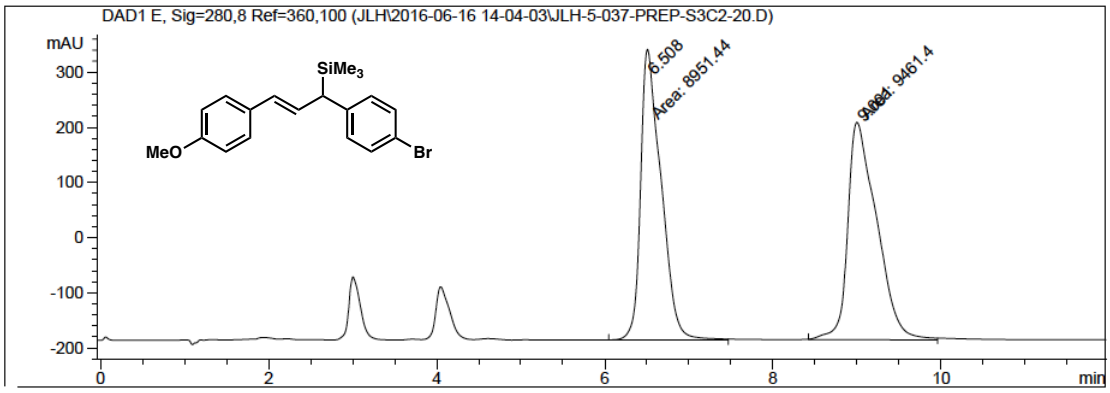

Peak #	RetTime [min]	Type	Width [min]	Area [mAU*s]	Height [mAU]	Area %
1	6.508	MM	0.2827	8951.43945	527.74286	48.6152
2	9.001	MM	0.3993	9461.40332	394.91501	51.3848

90f (Figure 2.7): enantioenriched, 97% ee

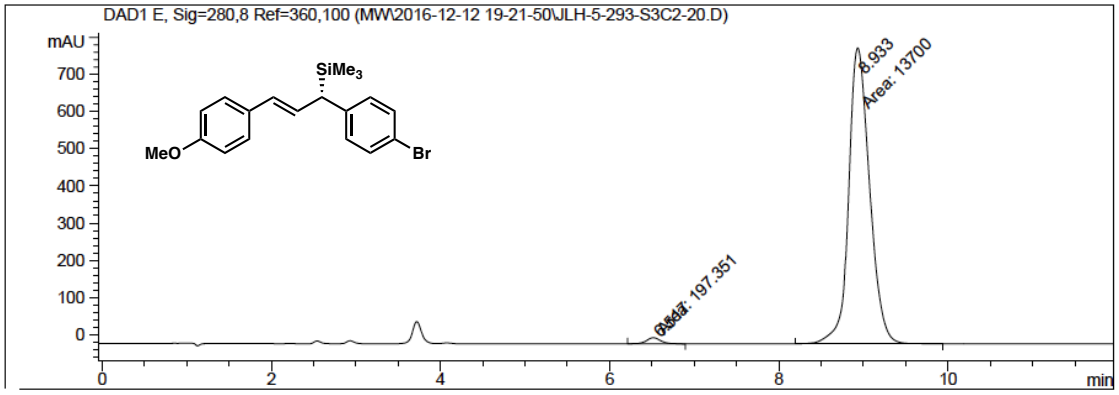

Peak #	RetTime [min]	Type	Width [min]	Area [mAU*s]	Height [mAU]	Area %
1	6.517	MM	0.1995	197.35112	16.48802	1.4201
2	8.933	MM	0.2865	1.37000e4	796.90198	98.5799

90g (Figure 2.7): racemic

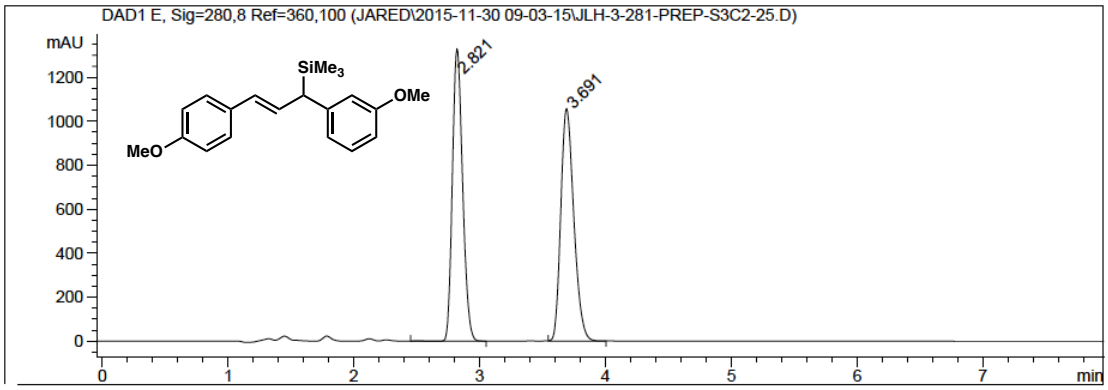

Peak #	RetTime [min]	Type	Width [min]	Area [mAU*s]	Height [mAU]	Area %
1	2.821	BB	0.0880	7524.96826	1330.39319	49.6931
2	3.691	BB	0.1120	7617.91406	1058.05420	50.3069

90g (Figure 2.7): enantioenriched, 97% ee

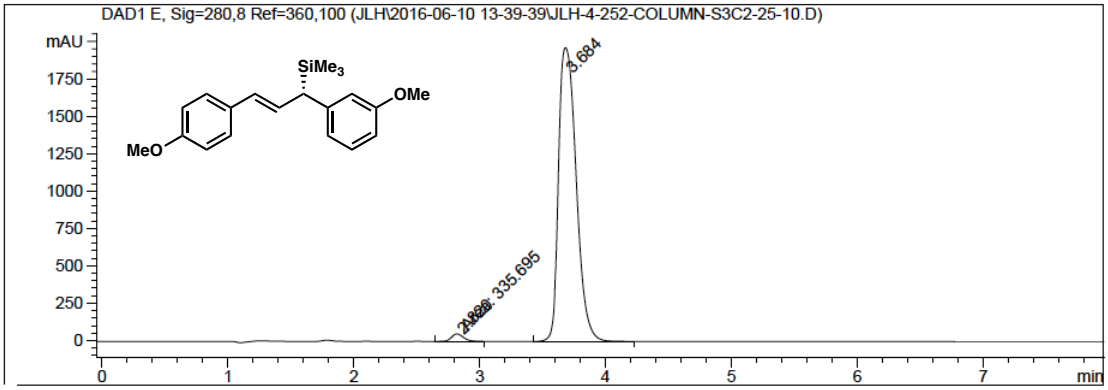

Peak #	RetTime [min]	Type	Width [min]	Area [mAU*s]	Height [mAU]	Area %
1	2.820	MM	0.1102	335.69470	50.78532	1.7209
2	3.684	BB	0.1578	1.91711e4	1964.58142	98.2791

90h (Figure 2.7): racemic

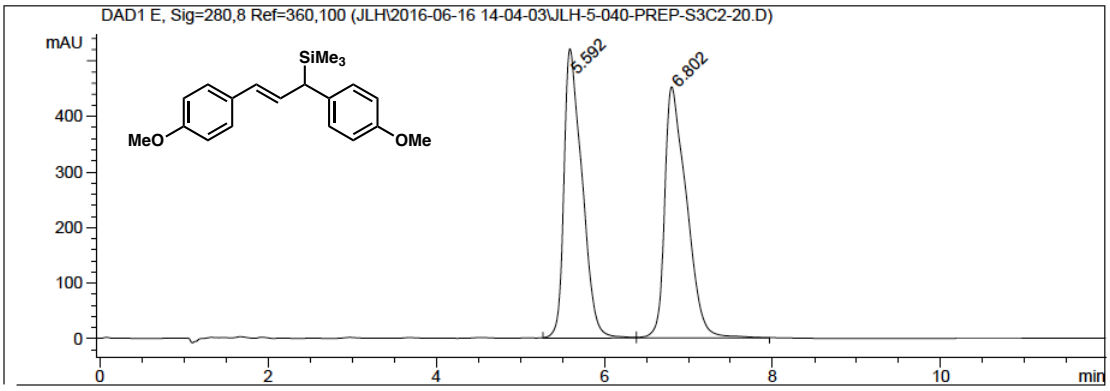

Peak #	RetTime [min]	Type	Width [min]	Area [mAU*s]	Height [mAU]	Area %
1	5.592	BV	0.2107	7794.18457	520.59595	48.8511
2	6.802	VB	0.2549	8160.78564	451.39059	51.1489

90h (Figure 2.7): enantioenriched, 96% ee

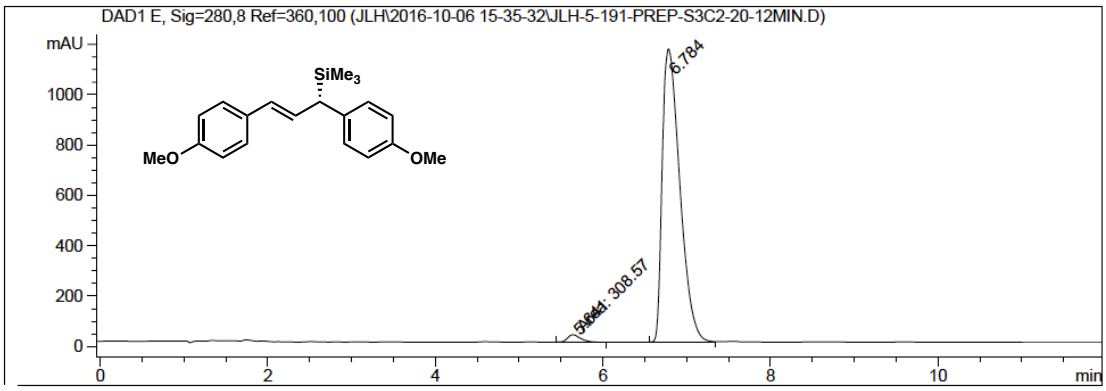

Peak #	RetTime [min]	Type	Width [min]	Area [mAU*s]	Height [mAU]	Area %
1	5.641	MM	0.1755	308.56979	29.30574	1.7776
2	6.784	BV	0.2270	1.70501e4	1163.17297	98.2224

90i (Figure 2.7): racemic

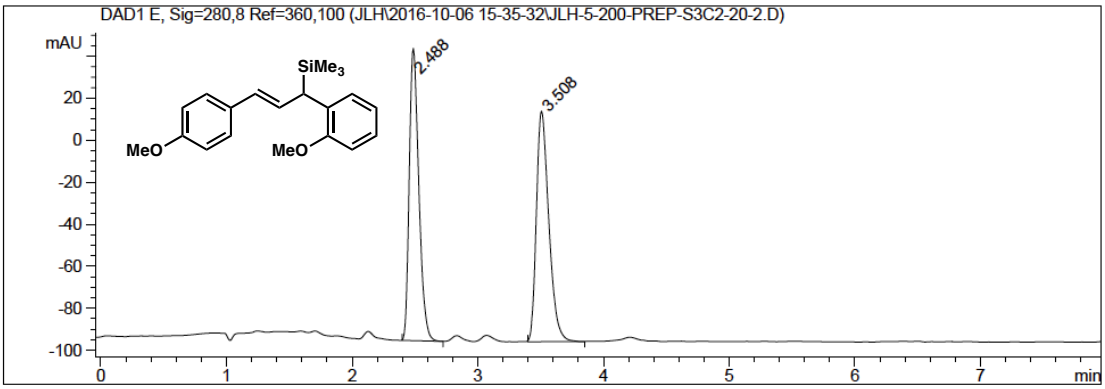

Peak #	RetTime [min]	Type	Width [min]	Area [mAU*s]	Height [mAU]	Area %
1	2.488	BV	0.0821	734.53345	137.91168	49.3425
2	3.508	BB	0.1042	754.10883	109.69971	50.6575

90i (Figure 2.7): enantioenriched, 95% ee

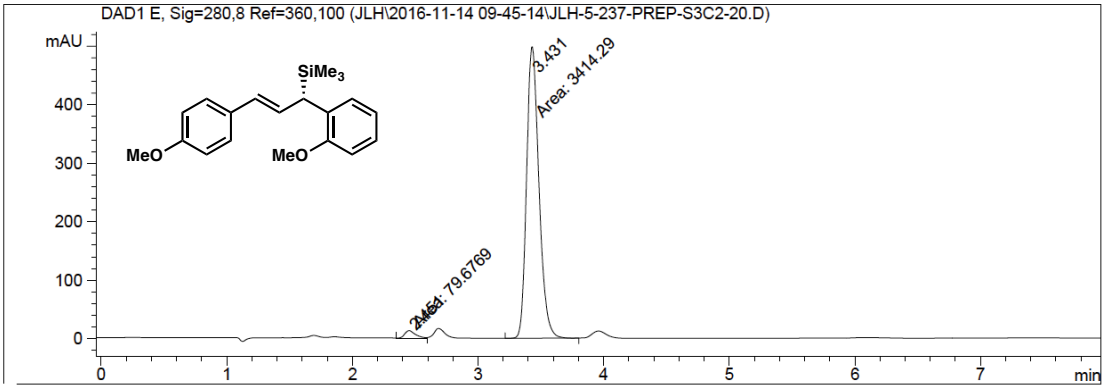

Peak #	RetTime [min]	Type	Width [min]	Area [mAU*s]	Height [mAU]	Area %
1	2.451	MM	0.1004	79.67693	13.23026	2.2804
2	3.431	MM	0.1137	3414.29102	500.48816	97.7196

91a (Figure 2.8): racemic

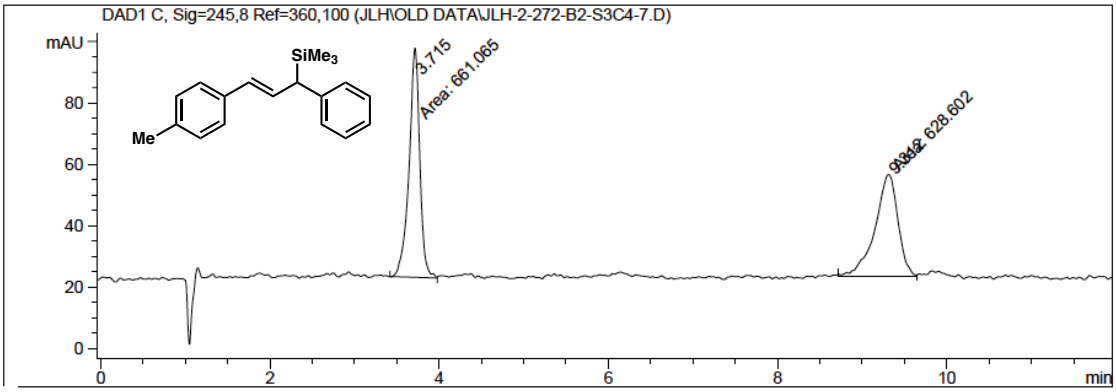

Peak #	RetTime [min]	Type	Width [min]	Area [mAU*s]	Height [mAU]	Area %
1	3.715	MM	0.1469	661.06458	74.99195	51.2586
2	9.312	MM	0.3153	628.60205	33.22607	48.7414

91a (Figure 2.8): enantioenriched, 93% ee

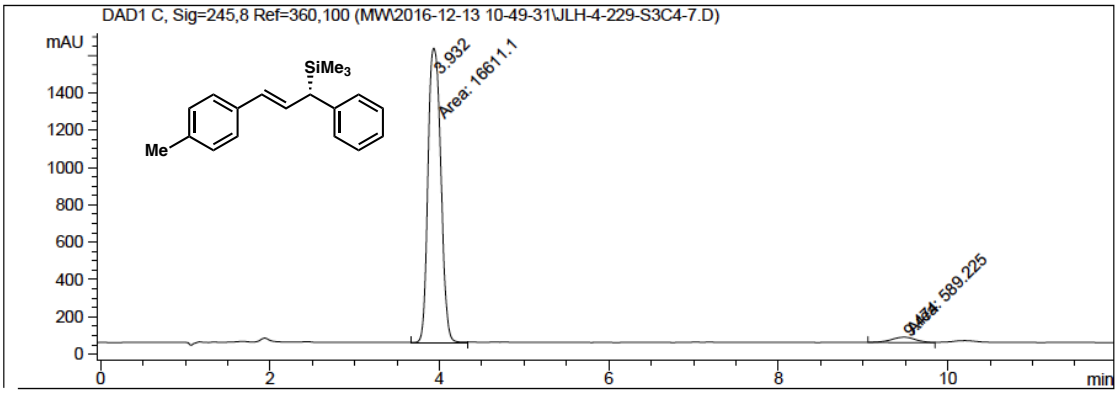

Peak #	RetTime [min]	Type	Width [min]	Area [mAU*s]	Height [mAU]	Area %
1	3.932	MM	0.1754	1.66111e4	1578.40051	96.5743
2	9.474	MM	0.3380	589.22534	29.05238	3.4257

91b (Figure 2.8): racemic

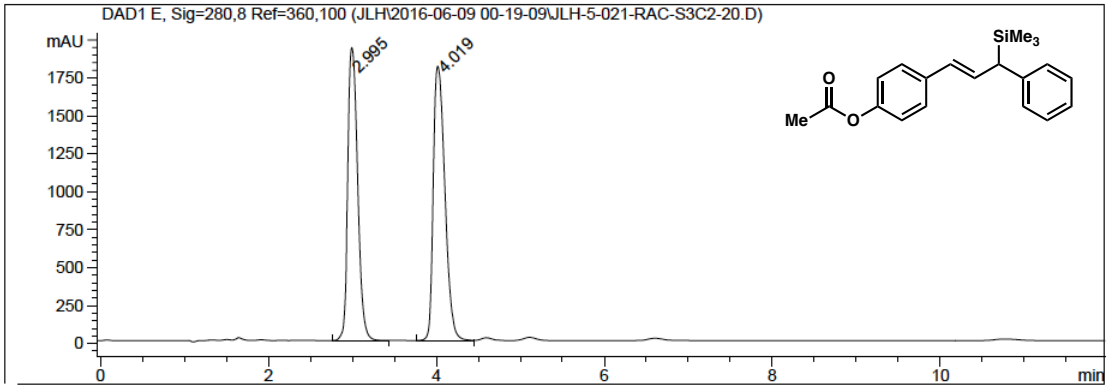

Peak #	RetTime [min]	Type	Width [min]	Area [mAU*s]	Height [mAU]	Area %
1	2.995	BV	0.1317	1.57998e4	1925.37463	47.5626
2	4.019	BV	0.1526	1.74192e4	1804.08923	52.4374

91b (Figure 2.8): enantioenriched, 93% ee

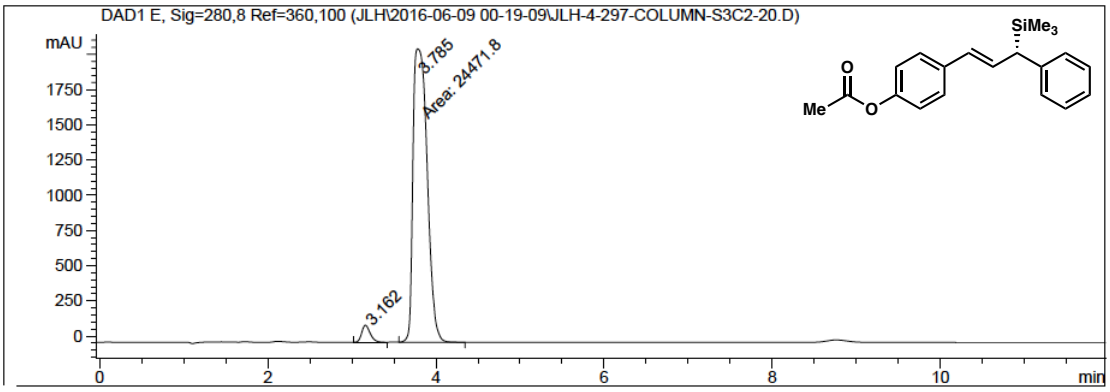

Peak #	RetTime [min]	Type	Width [min]	Area [mAU*s]	Height [mAU]	Area %
1	3.162	BB	0.1112	861.72925	120.86167	3.4015
2	3.785	MM	0.1958	2.44718e4	2083.04150	96.5985

91c (Figure 2.8): racemic

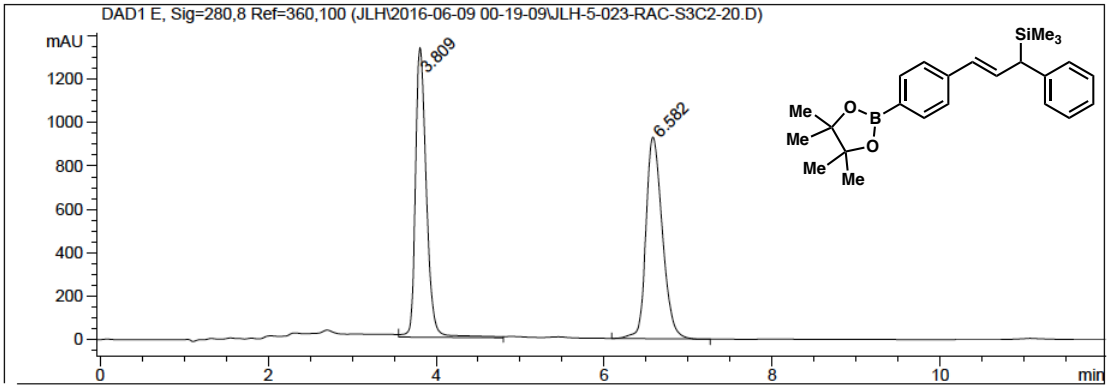

Peak #	RetTime [min]	Type	Width [min]	Area [mAU*s]	Height [mAU]	Area %
1	3.809	VV	0.1422	1.21206e4	1330.88916	48.9675
2	6.582	VB	0.2109	1.26317e4	927.68268	51.0325

91c (Figure 2.8): enantioenriched, 91% ee

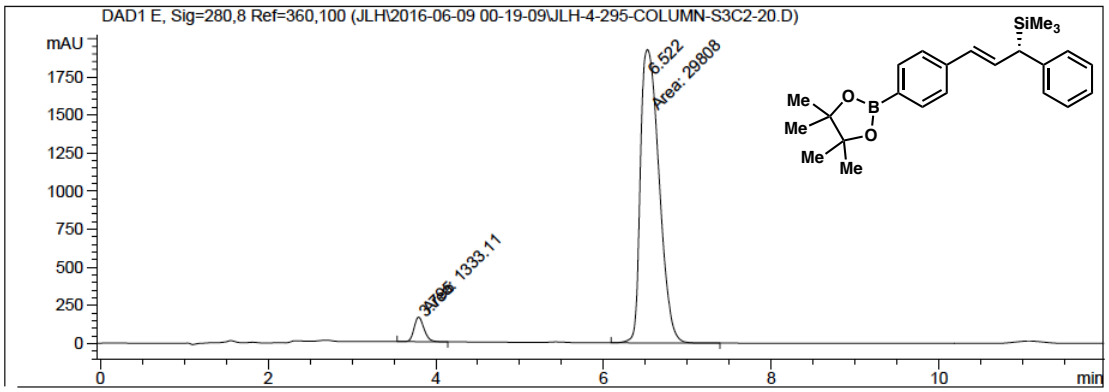

Peak #	RetTime [min]	Type	Width [min]	Area [mAU*s]	Height [mAU]	Area %
1	3.795	MM	0.1374	1333.10791	161.69827	4.2809
2	6.522	MM	0.2579	2.98080e4	1926.34448	95.7191

91d (Figure 2.8): racemic

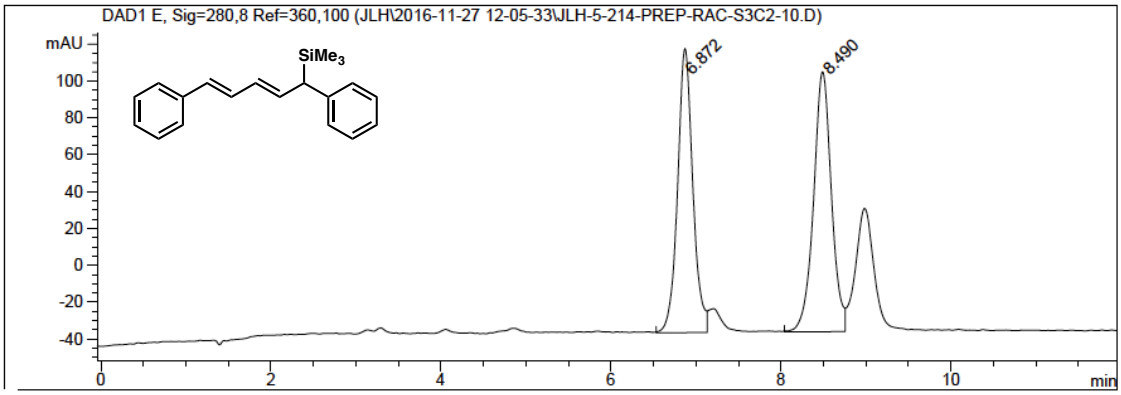

Peak #	RetTime [min]	Type	Width [min]	Area [mAU*s]	Height [mAU]	Area %
1	6.872	BV	0.1856	1922.17102	154.03583	48.2717
2	8.490	BV	0.2185	2059.81567	140.98209	51.7283

91d (Figure 2.8): enantioenriched, 94% ee

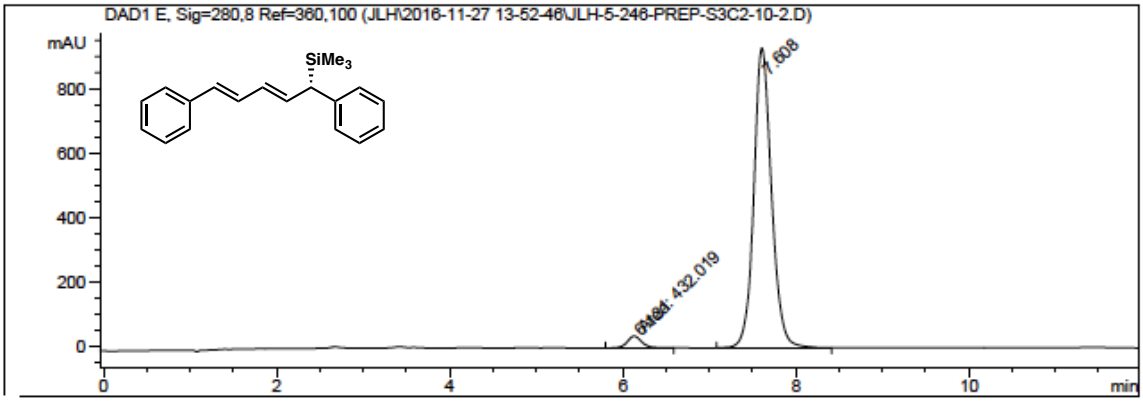

Peak #	RetTime [min]	Type	Width [min]	Area [mAU*s]	Height [mAU]	Area %
1	6.131	MM	0.1950	432.01929	36.92301	3.1471
2	7.608	BV	0.2189	1.32957e4	929.16394	96.8529

91e (Figure 2.8): racemic

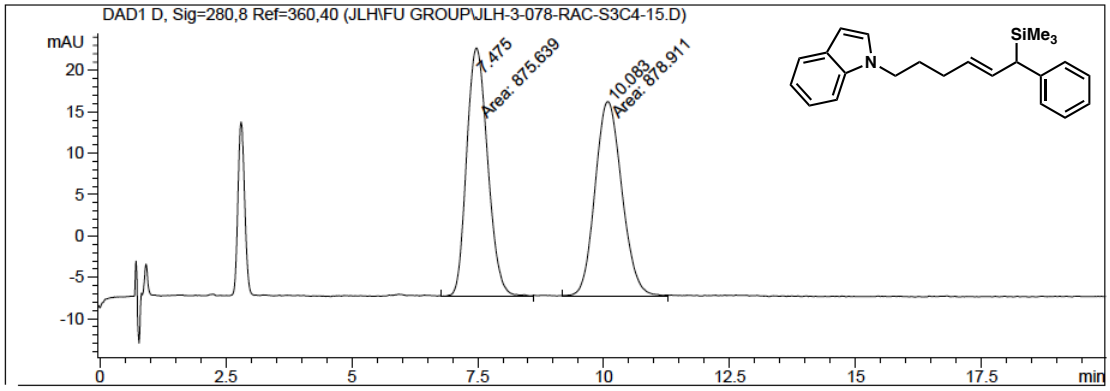

Peak #	RetTime [min]	Type	Width [min]	Area [mAU*s]	Height [mAU]	Area %
1	7.475	MM	0.4862	875.63855	30.01655	49.9068
2	10.083	MM	0.6219	878.91064	23.55369	50.0932

91e (Figure 2.8): enantioenriched, 92% ee

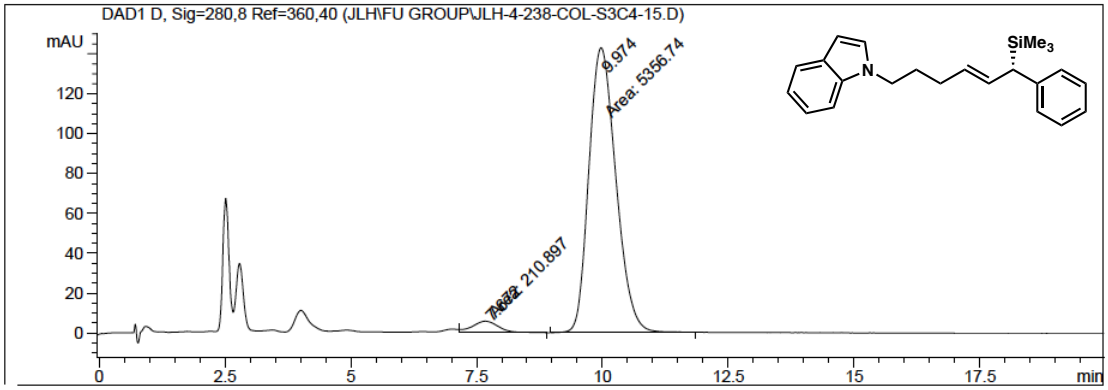

Peak #	RetTime [min]	Type	Width [min]	Area [mAU*s]	Height [mAU]	Area %
1	7.672	MM	0.6110	210.89684	5.75319	3.7879
2	9.974	MM	0.6244	5356.73975	142.97990	96.2121

91f (Figure 2.8): racemic

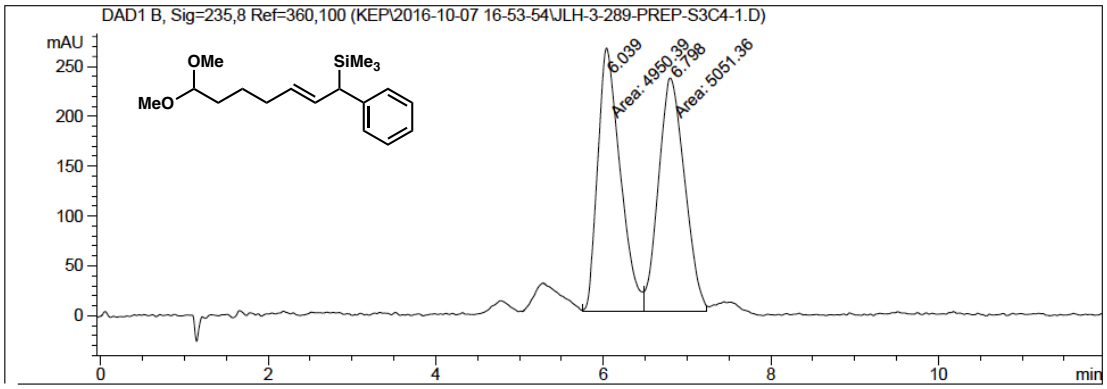

Peak #	RetTime [min]	Type	Width [min]	Area [mAU*s]	Height [mAU]	Area %
1	6.039	MM	0.3128	4950.39160	263.80368	49.4952
2	6.798	MM	0.3601	5051.36084	233.77972	50.5048

91f (Figure 2.8): enantioenriched, 97% ee

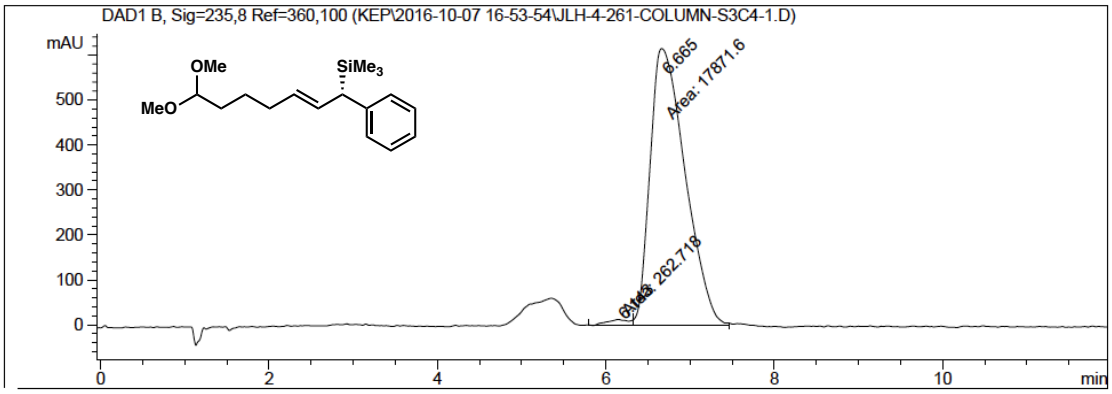

Peak #	RetTime [min]	Type	Width [min]	Area [mAU*s]	Height [mAU]	Area %
1	6.143	MM	0.3226	262.71774	13.57335	1.4487
2	6.665	MM	0.4833	1.78716e4	616.27795	98.5513

91g (Figure 2.8): racemic

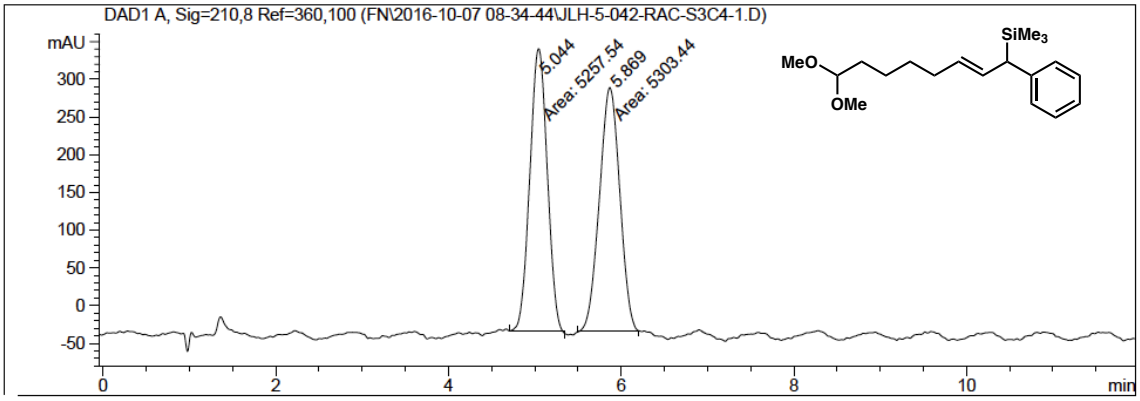

Peak #	RetTime [min]	Type	Width [min]	Area [mAU*s]	Height [mAU]	Area %
1	5.044	MM	0.2336	5257.54492	375.13754	49.7827
2	5.869	MM	0.2734	5303.44434	323.33304	50.2173

91g (Figure 2.8): enantioenriched, 95% ee

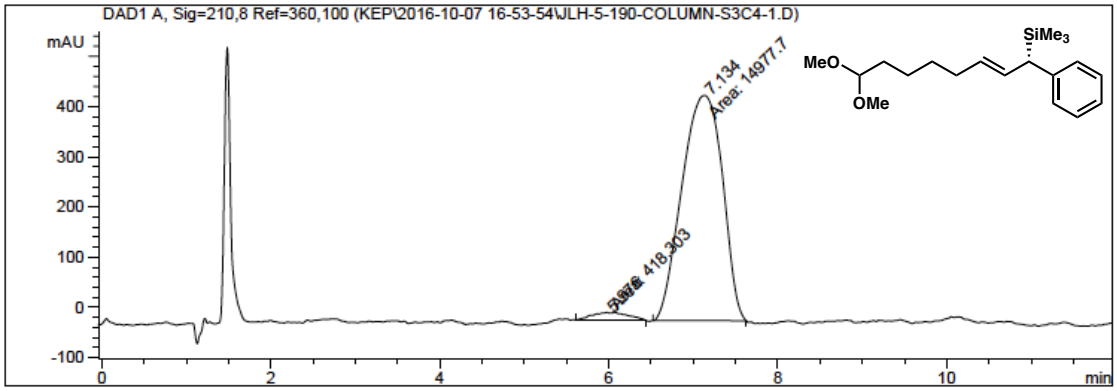

Peak #	RetTime [min]	Type	Width [min]	Area [mAU*s]	Height [mAU]	Area %
1	5.976	MM	0.4692	418.30276	14.85876	2.7170
2	7.134	MM	0.5565	1.49777e4	448.60516	97.2830

91h (Figure 2.8): racemic

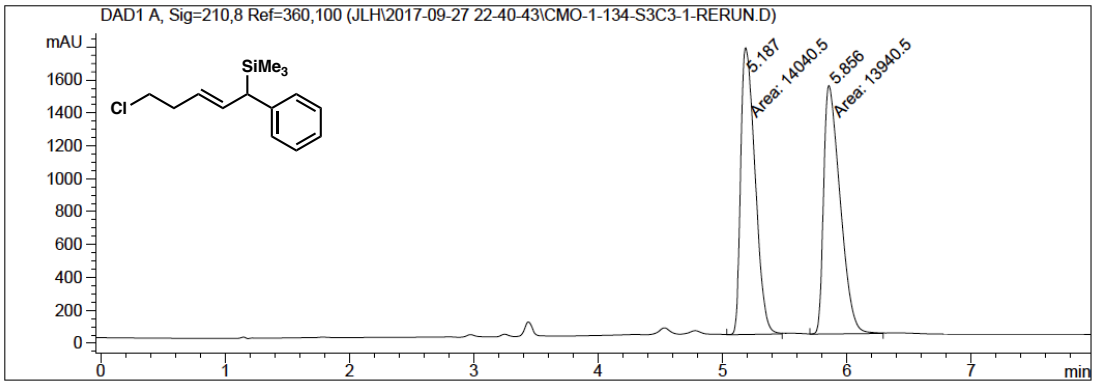

Peak #	RetTime [min]	Type	Width [min]	Area [mAU*s]	Height [mAU]	Area %
1	5.187	MM	0.1333	1.40405e4	1755.09863	50.1787
2	5.856	MM	0.1533	1.39405e4	1515.26782	49.8213

91h (Figure 2.8): enantioenriched, 95% ee

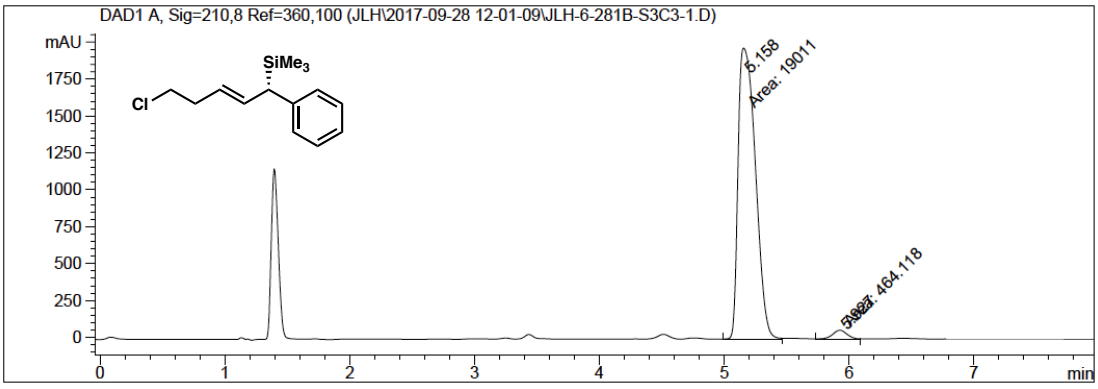

Peak #	RetTime [min]	Type	Width [min]	Area [mAU*s]	Height [mAU]	Area %
1	5.158	MM	0.1605	1.90110e4	1974.68127	97.6169
2	5.927	MM	0.1312	464.11768	58.96592	2.3831

91i (Figure 2.8): racemic

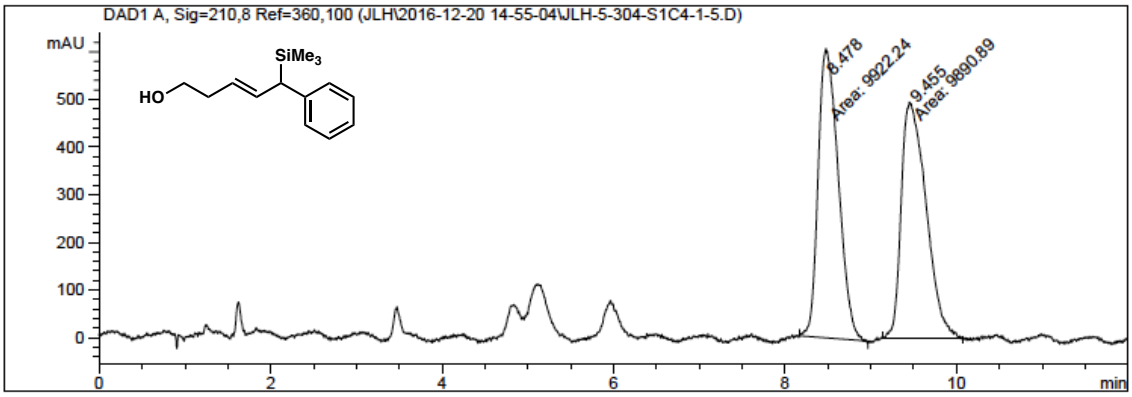

Peak #	RetTime [min]	Type	Width [min]	Area [mAU*s]	Height [mAU]	Area %
1	8.478	MM	0.2718	9922.24219	608.50598	50.0791
2	9.455	MM	0.3338	9890.89258	493.89984	49.9209

91i (Figure 2.8): enantioenriched, 97% ee

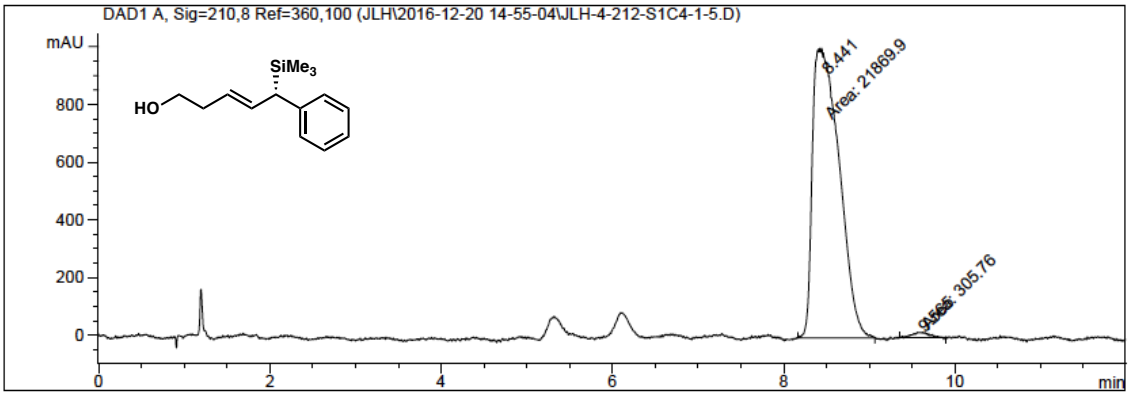

Peak #	RetTime [min]	Type	Width [min]	Area [mAU*s]	Height [mAU]	Area %
1	8.441	MM	0.3621	2.18699e4	1006.71216	98.6212
2	9.565	MM	0.2544	305.75977	20.02871	1.3788

91j (Figure 2.8): racemic

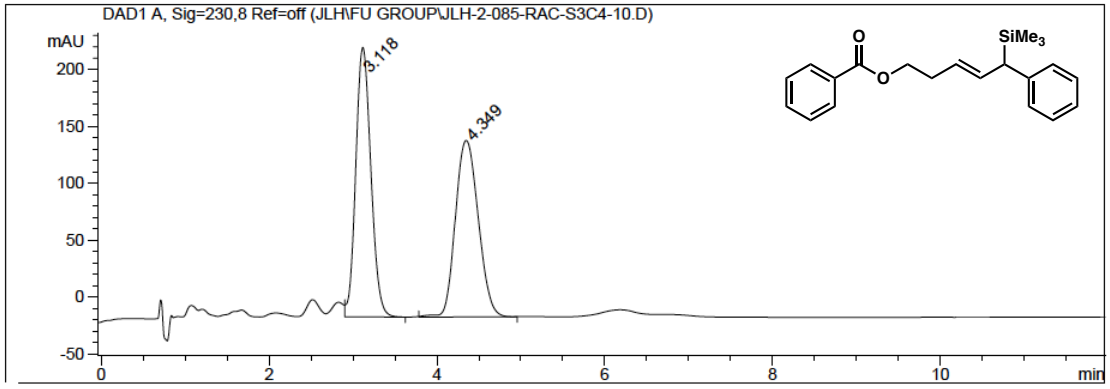

Peak #	RetTime [min]	Type	Width [min]	Area [mAU*s]	Height [mAU]	Area %
1	3.118	VB	0.1985	2974.74390	236.89671	50.2506
2	4.349	BB	0.3012	2945.07666	155.31581	49.7494

91j (Figure 2.8): enantioenriched, 96% ee

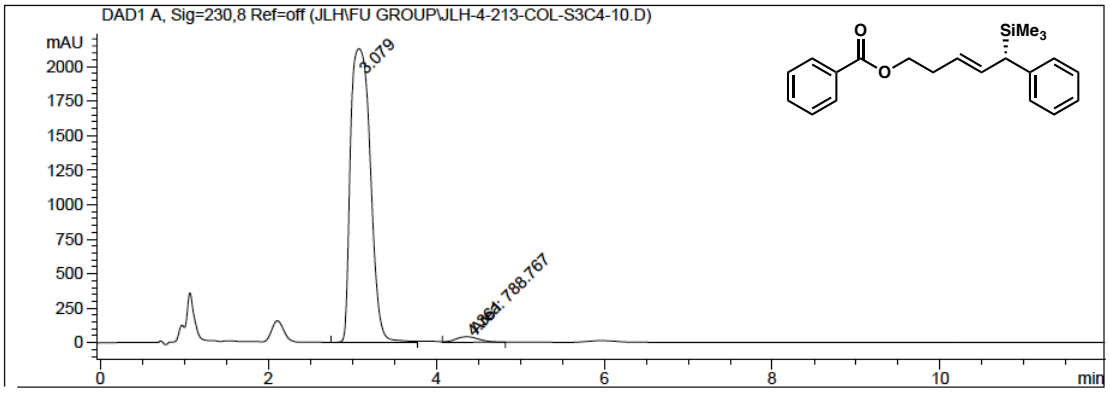

Peak #	RetTime [min]	Type	Width [min]	Area [mAU*s]	Height [mAU]	Area %
1	3.079	VV	0.2723	3.50735e4	2127.52100	97.8006
2	4.361	MM	0.3241	788.76727	40.55814	2.1994

91k (Figure 2.8): racemic

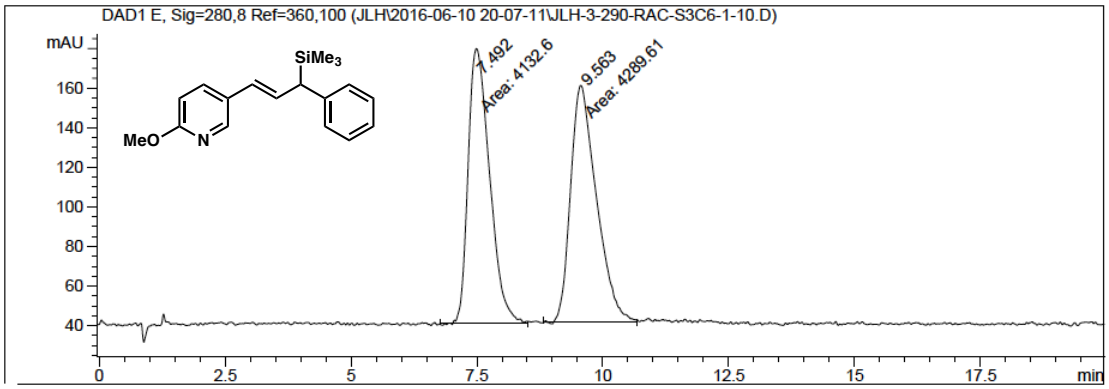

Peak #	RetTime [min]	Type	Width [min]	Area [mAU*s]	Height [mAU]	Area %
1	7.492	MM	0.4961	4132.59570	138.82385	49.0679
2	9.563	MM	0.5976	4289.60547	119.63455	50.9321

91k (Figure 2.8): enantioenriched, 94% ee

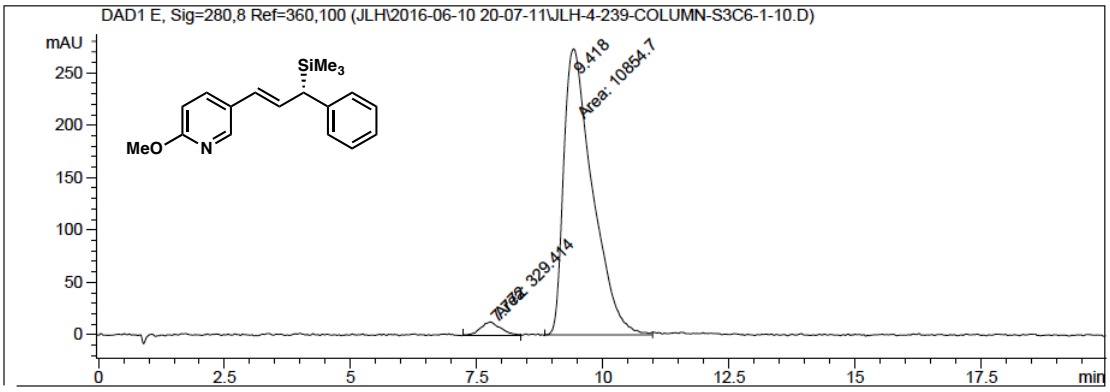

Peak #	RetTime [min]	Type	Width [min]	Area [mAU*s]	Height [mAU]	Area %
1	7.772	MM	0.4447	329.41449	12.34658	2.9454
2	9.418	MM	0.6623	1.08547e4	273.13736	97.0546

91l (Figure 2.8): racemic

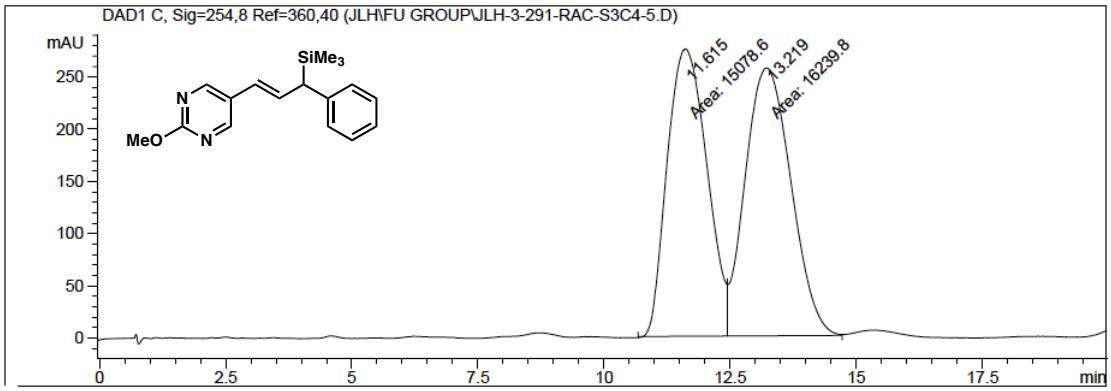

Peak #	RetTime [min]	Type	Width [min]	Area [mAU*s]	Height [mAU]	Area %
1	11.615	MF	0.9132	1.50786e4	275.19785	48.1463
2	13.219	FM	1.0553	1.62398e4	256.47855	51.8537

91l (Figure 2.8): enantioenriched, 94% ee

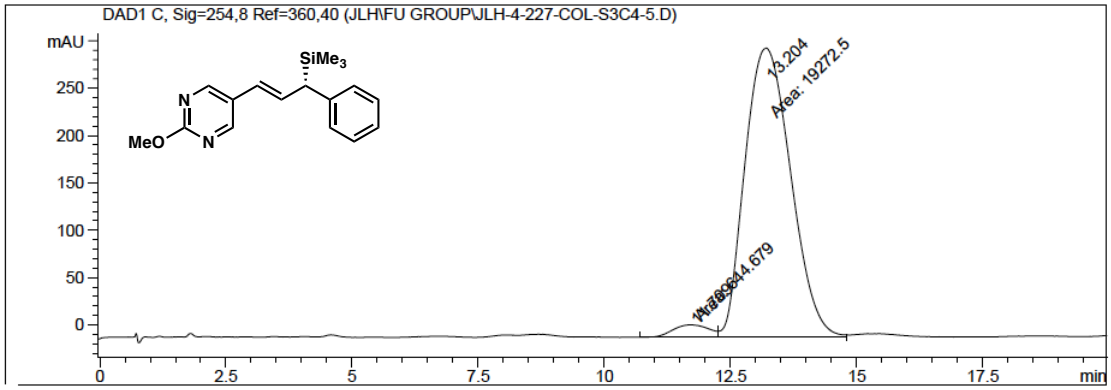

Peak #	RetTime [min]	Type	Width [min]	Area [mAU*s]	Height [mAU]	Area %
1	11.709	MF	0.8228	644.67889	13.05884	3.2368
2	13.204	FM	1.0519	1.92725e4	305.36429	96.7632

91m (Figure 2.8): racemic

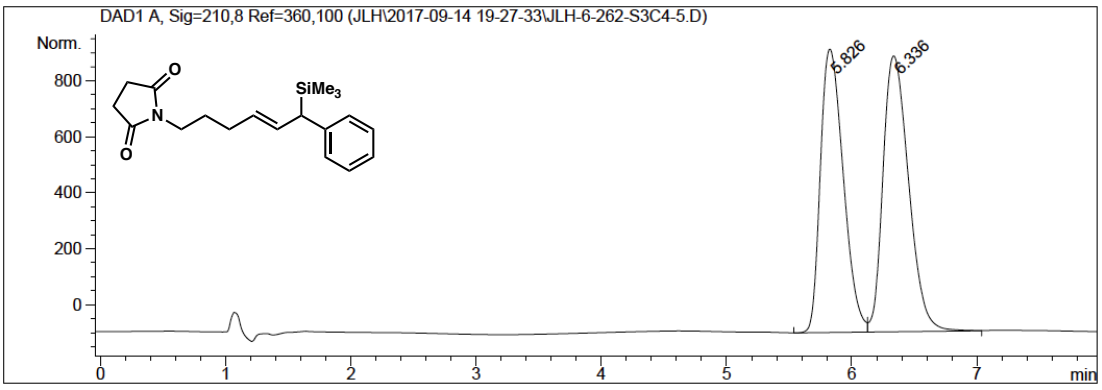

Peak #	RetTime [min]	Type	Width [min]	Area [mAU*s]	Height [mAU]	Area %
1	5.826	VV	0.2023	1.28826e4	1013.52417	47.7844
2	6.336	VB	0.2265	1.40773e4	986.41656	52.2156

91m (Figure 2.8): enantioenriched, 97% ee

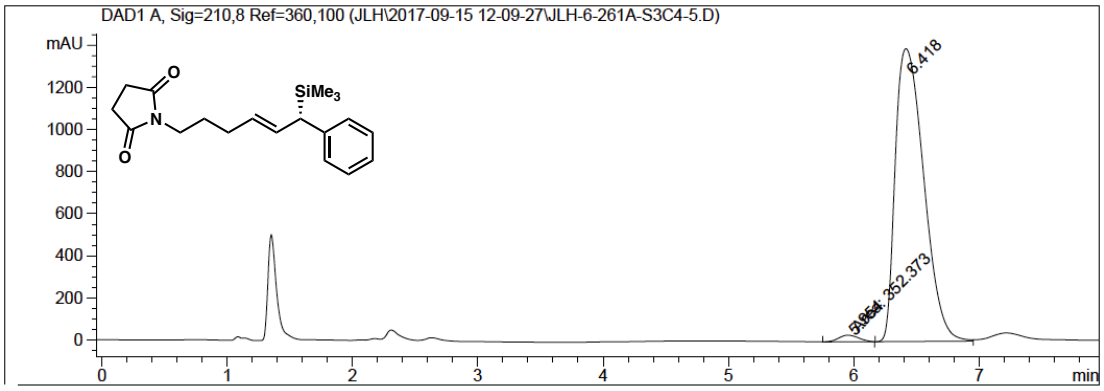

Peak #	RetTime [min]	Type	Width [min]	Area [mAU*s]	Height [mAU]	Area %
1	5.954	MM	0.1863	352.37341	31.52633	1.5768
2	6.418	VV	0.2565	2.19949e4	1390.66895	98.4232

91n (Figure 2.8): racemic

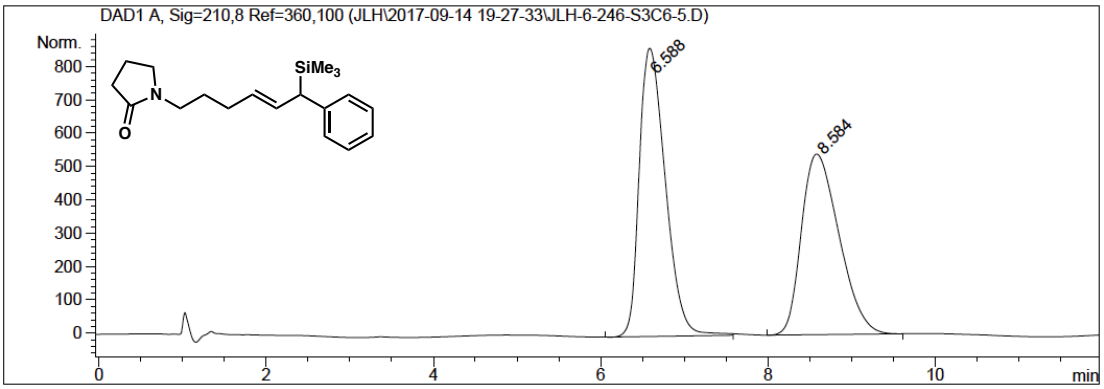

Peak #	RetTime [min]	Type	Width [min]	Area [mAU*s]	Height [mAU]	Area %
1	6.588	VB	0.3437	1.88022e4	864.66400	52.6067
2	8.584	BB	0.4907	1.69389e4	541.81793	47.3933

91n (Figure 2.8): enantioenriched, 96% ee

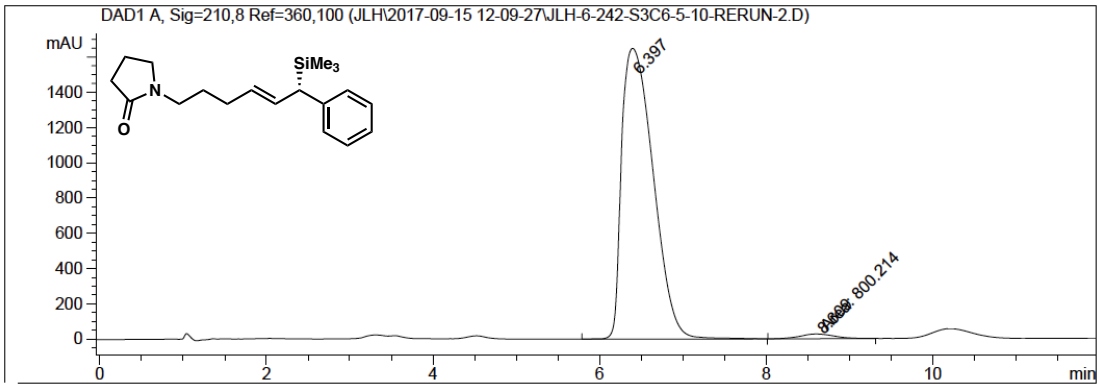

Peak #	RetTime [min]	Type	Width [min]	Area [mAU*s]	Height [mAU]	Area %
1	6.397	BV	0.4280	4.35448e4	1649.31226	98.1955
2	8.609	MM	0.4921	800.21442	27.09959	1.8045

91o (Figure 2.8): racemic

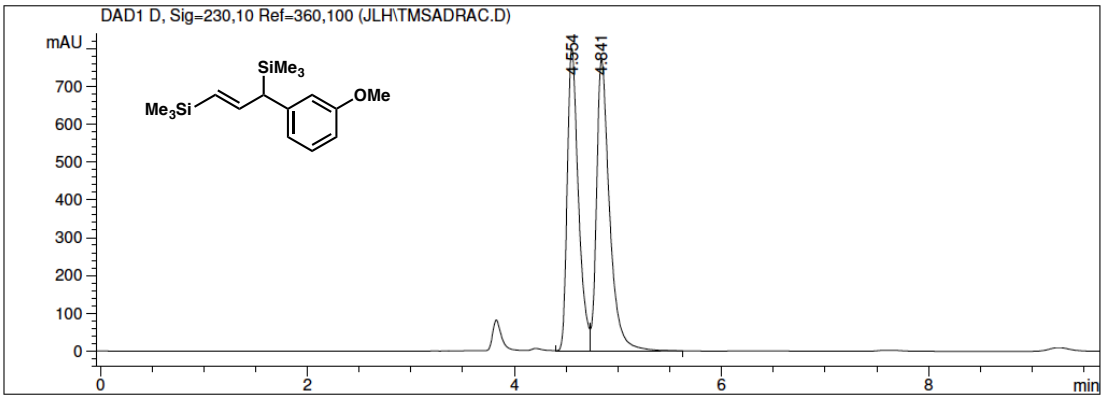

Peak #	RetTime [min]	Type	Width [min]	Area [mAU*s]	Height [mAU]	Area %
1	4.554	VV	0.1129	5969.46826	801.09521	46.9286
2	4.841	VB	0.1299	6750.85742	772.95972	53.0714

91o (Figure 2.8): enantioenriched, 93% ee

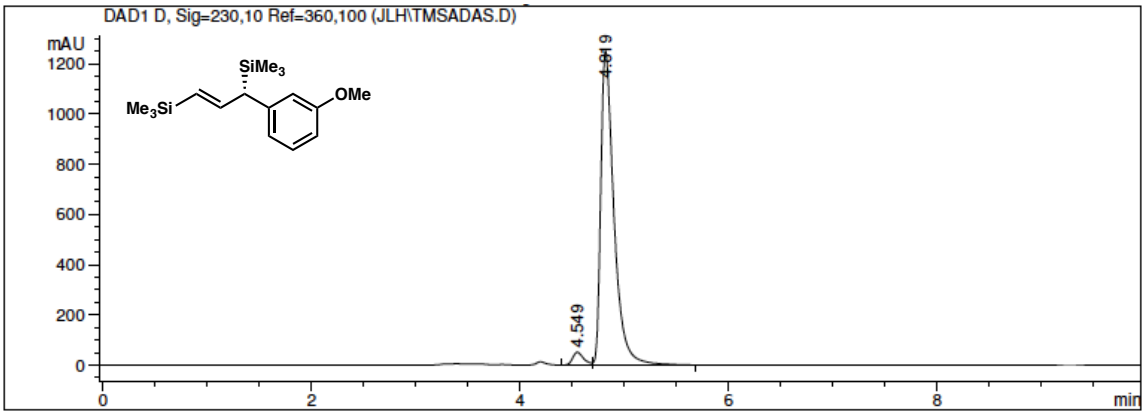

Peak #	RetTime [min]	Type	Width [min]	Area [mAU*s]	Height [mAU]	Area %
1	4.549	VV	0.1082	370.31830	51.32189	3.2662
2	4.819	VB	0.1323	1.09674e4	1251.31555	96.7338

91p (Figure 2.8): racemic

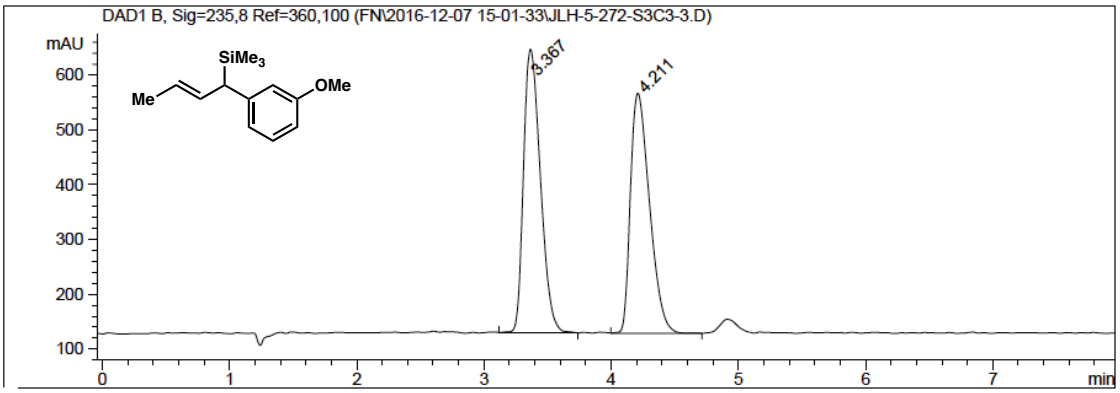

Peak #	RetTime [min]	Type	Width [min]	Area [mAU*s]	Height [mAU]	Area %
1	3.367	VV	0.1447	4823.06299	517.59222	51.3268
2	4.211	VV	0.1618	4573.71729	438.16852	48.6732

91p (Figure 2.8): enantioenriched, 96% ee

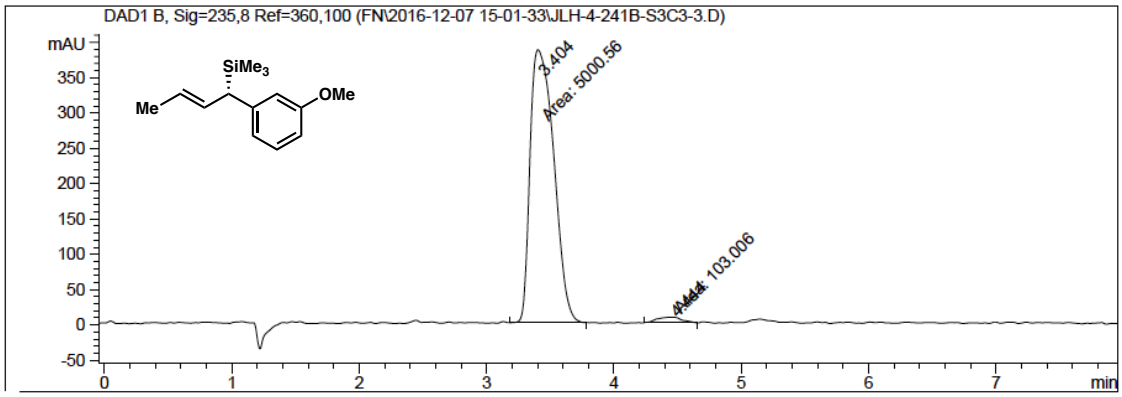

Peak #	RetTime [min]	Type	Width [min]	Area [mAU*s]	Height [mAU]	Area %
1	3.404	MM	0.2153	5000.55615	387.10941	97.9817
2	4.444	MM	0.2190	103.00621	7.83907	2.0183

91q (Figure 2.8): racemic

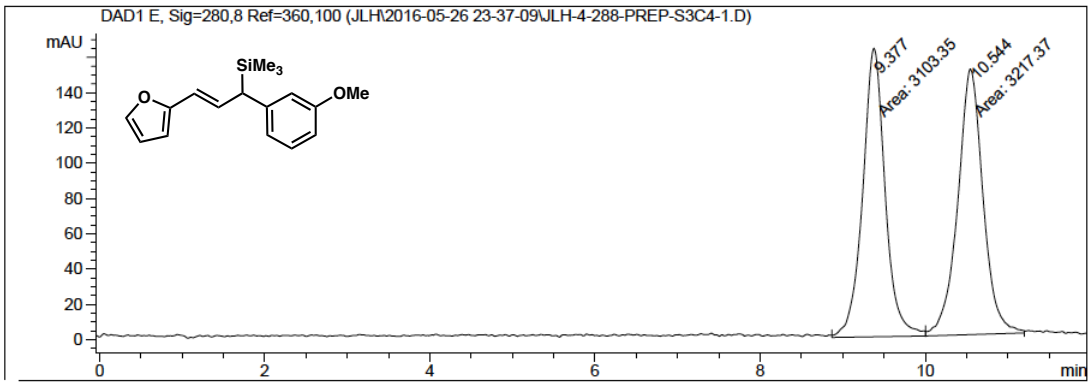

Peak #	RetTime [min]	Type	Width [min]	Area [mAU*s]	Height [mAU]	Area %
1	9.377	MM	0.3160	3103.34863	163.69301	49.0980
2	10.544	MM	0.3557	3217.37183	150.74971	50.9020

91q (Figure 2.8): enantioenriched, 95% ee

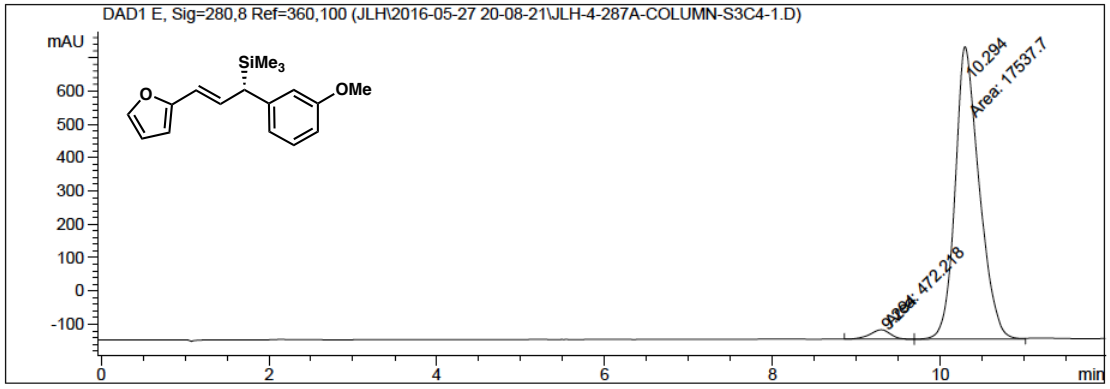

Peak #	RetTime [min]	Type	Width [min]	Area [mAU*s]	Height [mAU]	Area %
1	9.294	MM	0.2809	472.21768	28.02045	2.6220
2	10.294	MM	0.3330	1.75377e4	877.67529	97.3780

91r (Figure 2.8): racemic

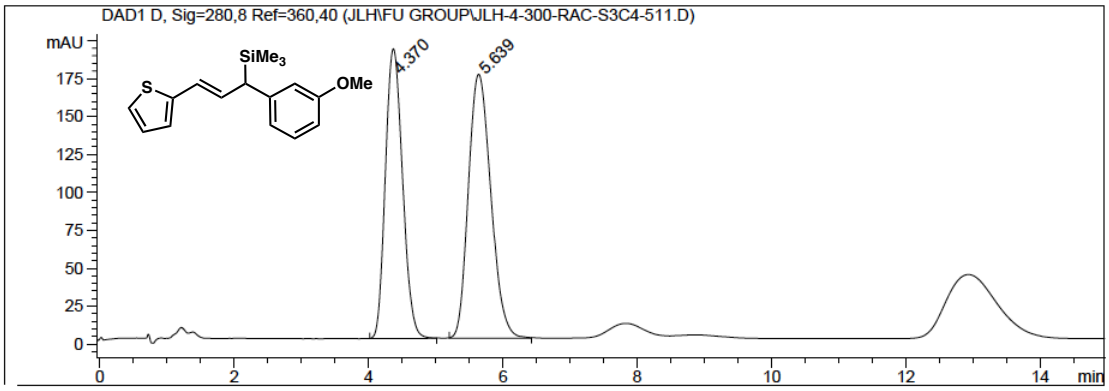

Peak #	RetTime [min]	Type	Width [min]	Area [mAU*s]	Height [mAU]	Area %
1	4.370	BB	0.2795	3393.40796	190.79709	45.5995
2	5.639	BB	0.3634	4048.35034	174.02675	54.4005

91r (Figure 2.8): enantioenriched, 95% ee

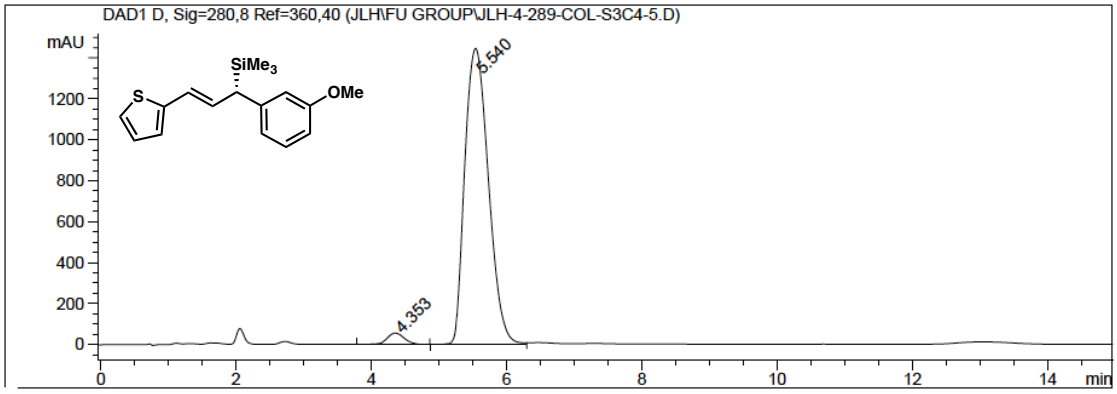

Peak #	RetTime [min]	Type	Width [min]	Area [mAU*s]	Height [mAU]	Area %
1	4.353	BV	0.2785	972.86749	54.97358	2.6947
2	5.540	VV	0.3956	3.51307e4	1445.08362	97.3053

91s (Figure 2.8): racemic

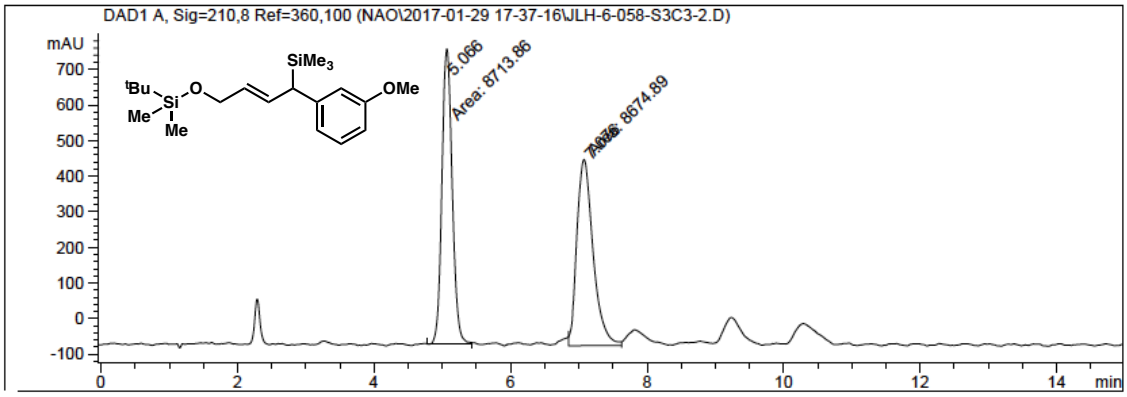

Peak #	RetTime [min]	Type	Width [min]	Area [mAU*s]	Height [mAU]	Area %
1	5.066	MM	0.1746	8713.86035	831.57080	50.1121
2	7.076	MM	0.2759	8674.88574	524.05389	49.8879

91s (Figure 2.8): enantioenriched, 97% ee

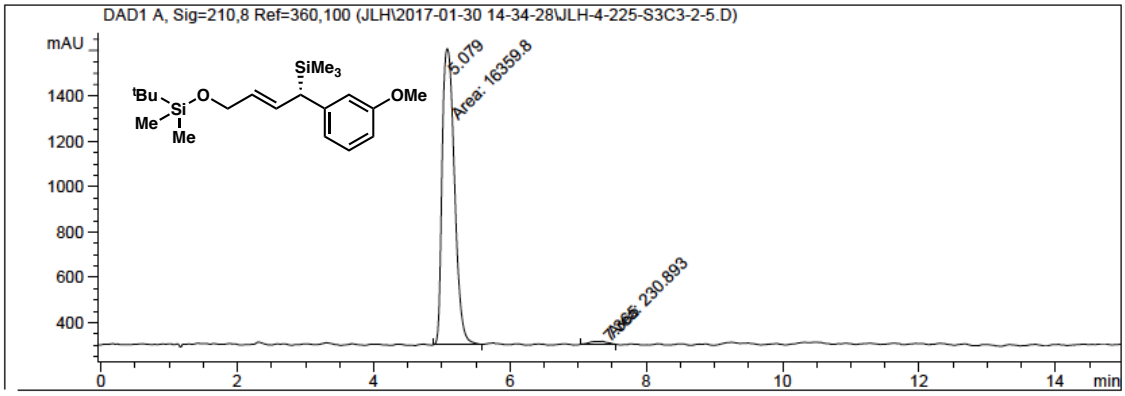

Peak #	RetTime [min]	Type	Width [min]	Area [mAU*s]	Height [mAU]	Area %
1	5.079	MM	0.2092	1.63598e4	1303.59607	98.6083
2	7.365	MM	0.2925	230.89261	13.15635	1.3917

106 (Scheme 2.4): racemic

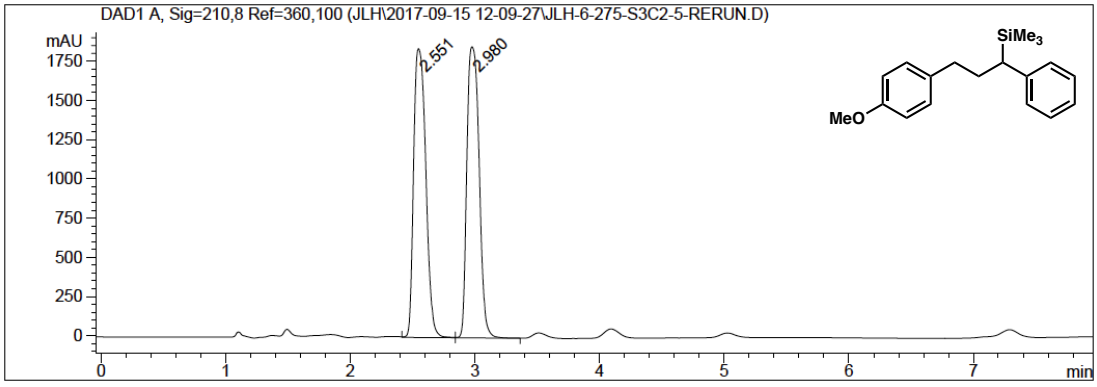

Peak #	RetTime [min]	Type	Width [min]	Area [mAU*s]	Height [mAU]	Area %
1	2.551	VV	0.1113	1.24955e4	1838.88037	49.5922
2	2.980	VV	0.1118	1.27010e4	1857.98621	50.4078

106 (Scheme 2.4): enantioenriched, 93% ee

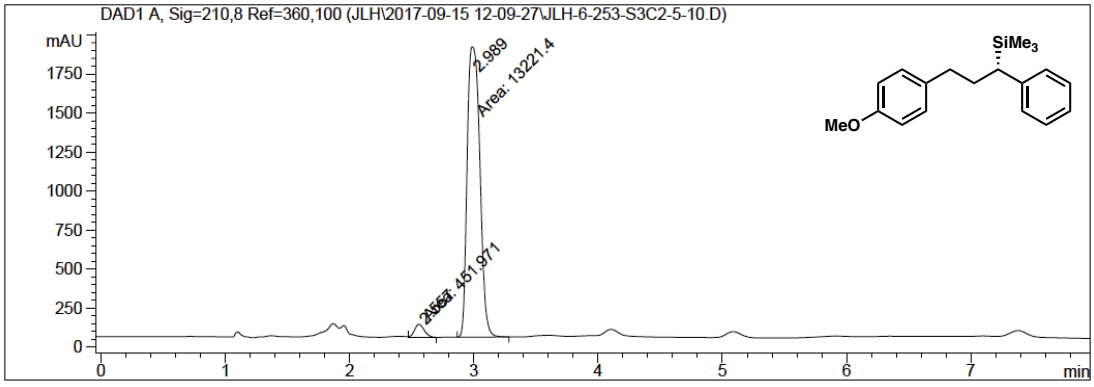

Peak #	RetTime [min]	Type	Width [min]	Area [mAU*s]	Height [mAU]	Area %
1	2.557	MM	0.0898	451.97076	83.84869	3.3055
2	2.989	MM	0.1184	1.32214e4	1860.47168	96.6945

111 (Scheme 2.6): racemic

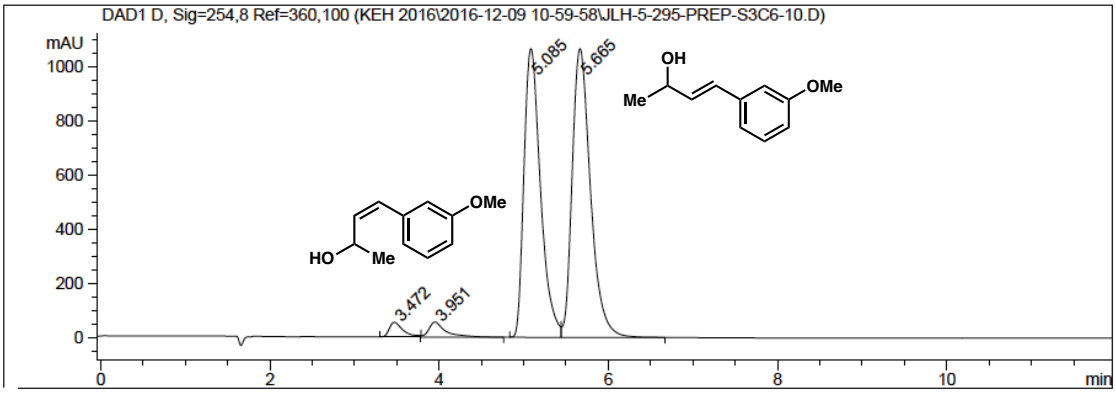

Peak #	RetTime [min]	Type	Width [min]	Area [mAU*s]	Height [mAU]	Area %
1	3.472	VV	0.1639	618.88599	54.74337	1.9391
2	3.951	VB	0.1983	774.84723	55.69344	2.4277
3	5.085	BV	0.2106	1.44659e4	1063.92664	45.3241
4	5.665	VB	0.2320	1.60569e4	1064.43738	50.3091

111 (Scheme 2.6): enantioenriched, both *E*/*Z*-isomers, 91% ee

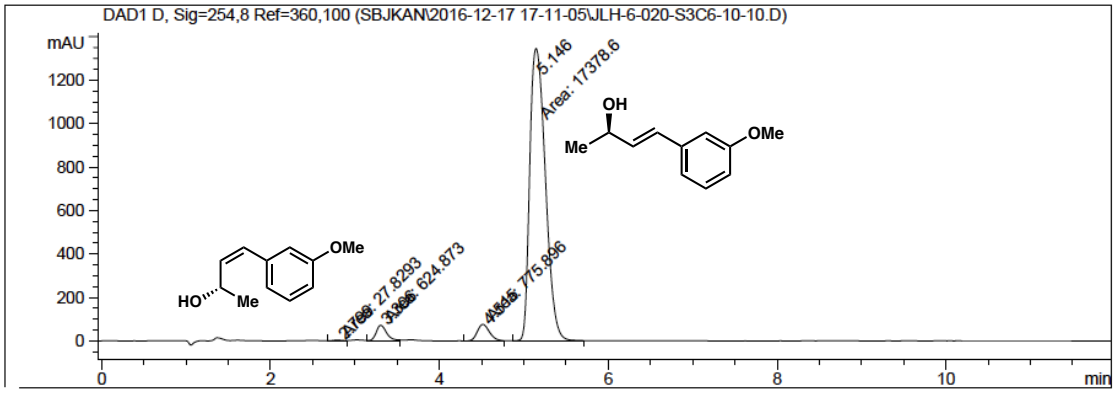

Peak #	RetTime [min]	Type	Width [min]	Area [mAU*s]	Height [mAU]	Area %
1	2.799	MM	0.1206	27.82935	3.84628	0.1480
2	3.306	MM	0.1454	624.87256	71.64183	3.3225
3	4.515	MM	0.1686	775.89587	76.70793	4.1255
4	5.146	MM	0.2151	1.73786e4	1346.51550	92.4040

113 (Scheme 2.7): racemic

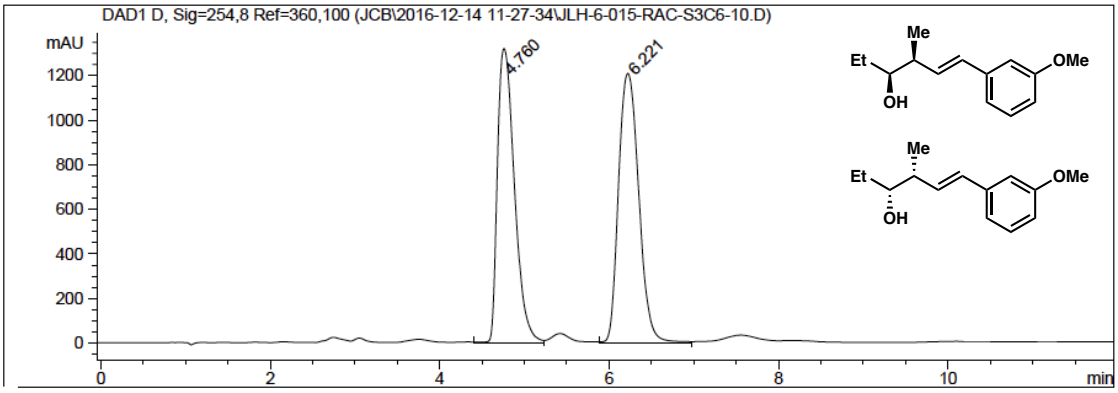

Peak #	RetTime [min]	Type	Width [min]	Area [mAU*s]	Height [mAU]	Area %
1	4.760	VV	0.2185	1.83661e4	1318.21326	47.8907
2	6.221	VV	0.2651	1.99840e4	1207.41687	52.1093

113 (Scheme 2.7): enantioenriched, 97% ee

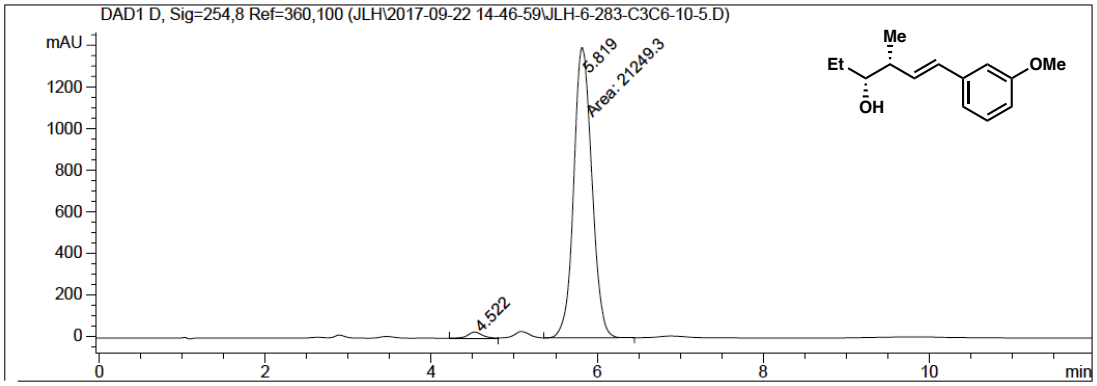

Peak #	RetTime [min]	Type	Width [min]	Area [mAU*s]	Height [mAU]	Area %
1	4.522	BV	0.1773	341.61523	29.02138	1.5822
2	5.819	MM	0.2530	2.12493e4	1399.80737	98.4178

116 (Scheme 2.7): racemic

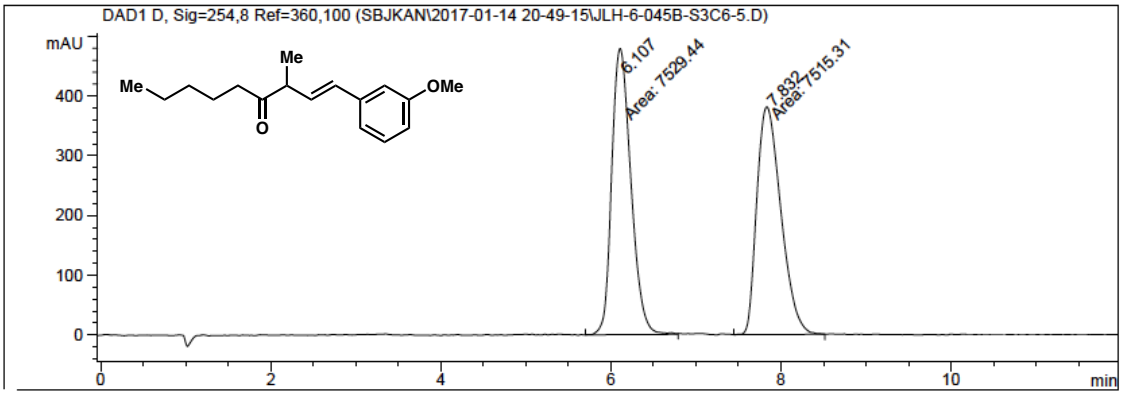

Peak #	RetTime [min]	Type	Width [min]	Area [mAU*s]	Height [mAU]	Area %
1	6.107	MM	0.2617	7529.43945	479.46429	50.0470
2	7.832	MM	0.3282	7515.30908	381.61700	49.9530

116 (Scheme 2.7): enantioenriched, 90% ee

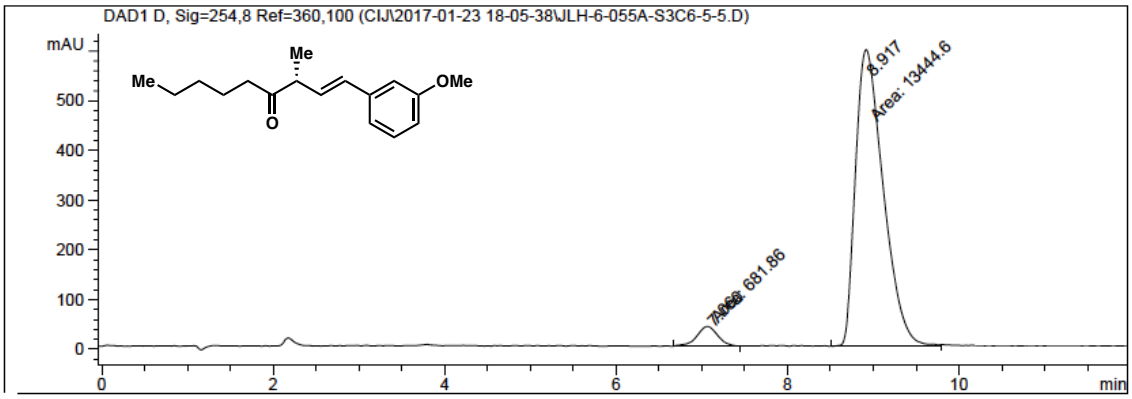

Peak #	RetTime [min]	Type	Width [min]	Area [mAU*s]	Height [mAU]	Area %
1	7.060	MM	0.2842	681.85974	39.98673	4.8268
2	8.917	MM	0.3756	1.34446e4	596.64233	95.1732

117 (Figure 2.10): racemic, *trans*-product

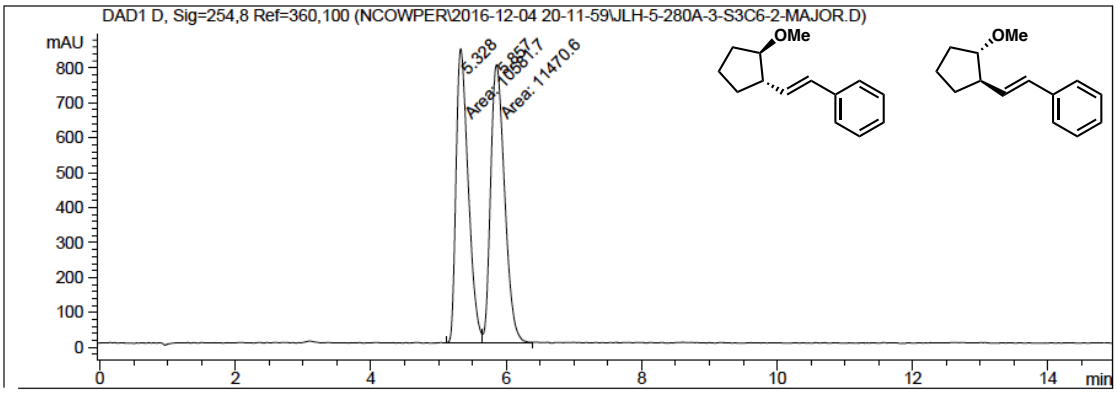

Peak #	RetTime [min]	Type	Width [min]	Area [mAU*s]	Height [mAU]	Area %
1	5.328	MM	0.2089	1.05817e4	844.24554	47.9846
2	5.857	MM	0.2395	1.14706e4	798.26849	52.0154

117 (Figure 2.10): enantioenriched, 97% ee

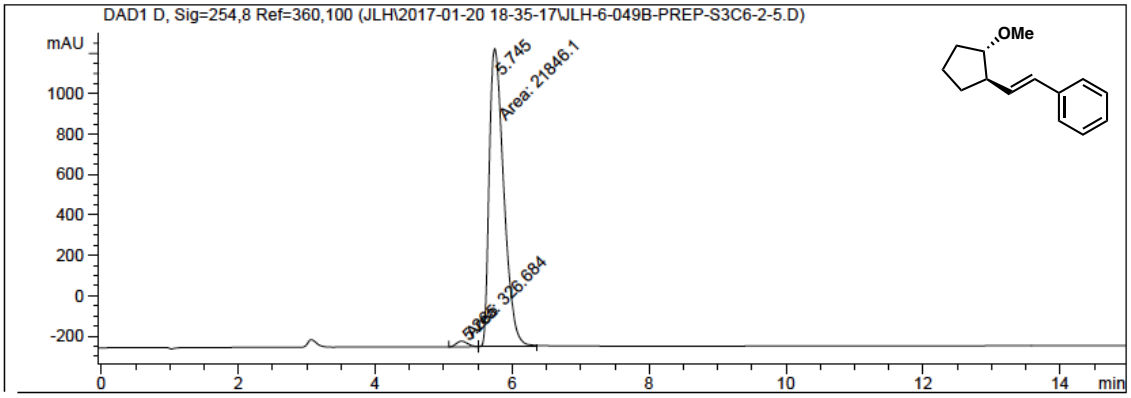

Peak #	RetTime [min]	Type	Width [min]	Area [mAU*s]	Height [mAU]	Area %
1	5.265	MM	0.1917	326.68356	28.39545	1.4734
2	5.745	MM	0.2466	2.18461e4	1476.56323	98.5266

118(Figure 2.10): racemic, *cis*-product

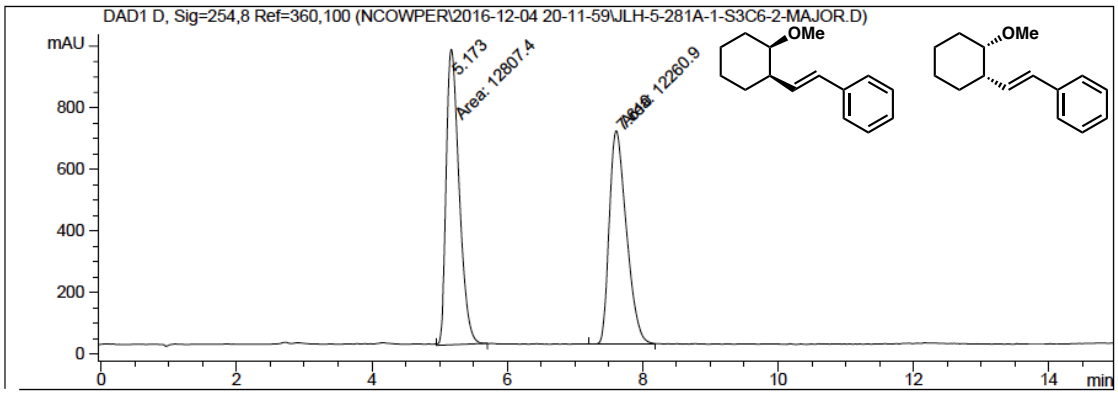

Peak #	RetTime [min]	Type	Width [min]	Area [mAU*s]	Height [mAU]	Area %
1	5.173	MM	0.2222	1.28074e4	960.75812	51.0900
2	7.610	MM	0.2944	1.22609e4	694.19666	48.9100

118 (Figure 2.10): enantioenriched, 96% ee

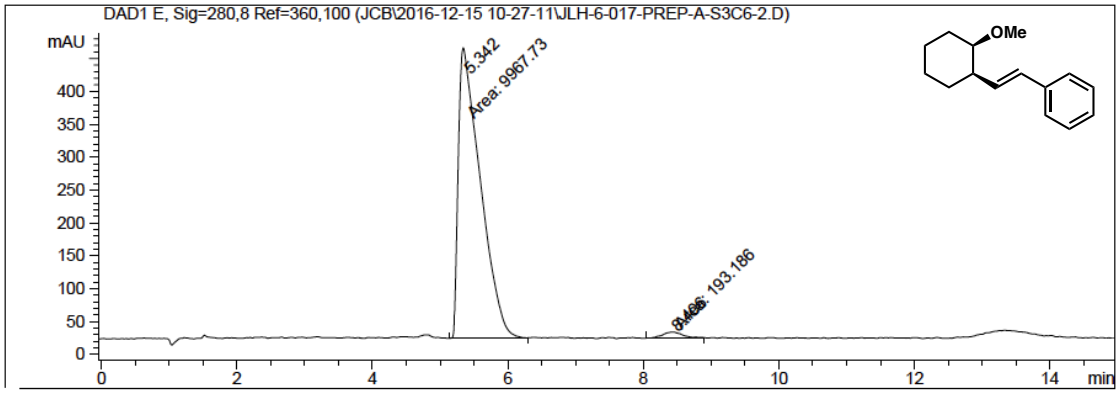

Peak #	RetTime [min]	Type	Width [min]	Area [mAU*s]	Height [mAU]	Area %
1	5.342	MM	0.3759	9967.73145	442.00150	98.0987
2	8.406	MM	0.3517	193.18593	9.15547	1.9013

118' (Figure 2.10): racemic, *trans*-product

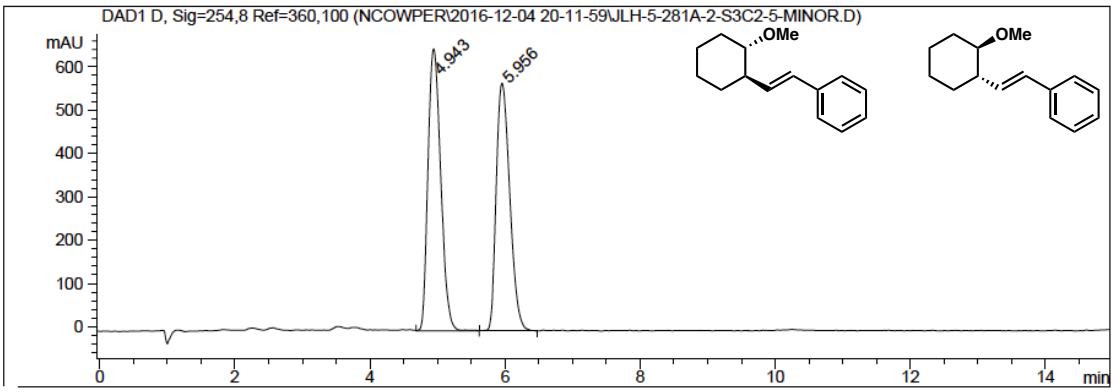

Peak #	RetTime [min]	Type	Width [min]	Area [mAU*s]	Height [mAU]	Area %
1	4.943	VV	0.2092	8538.20312	650.19324	51.7336
2	5.956	VV	0.2227	7965.97852	571.36676	48.2664

118' (Figure 2.10): enantioenriched, 96% ee

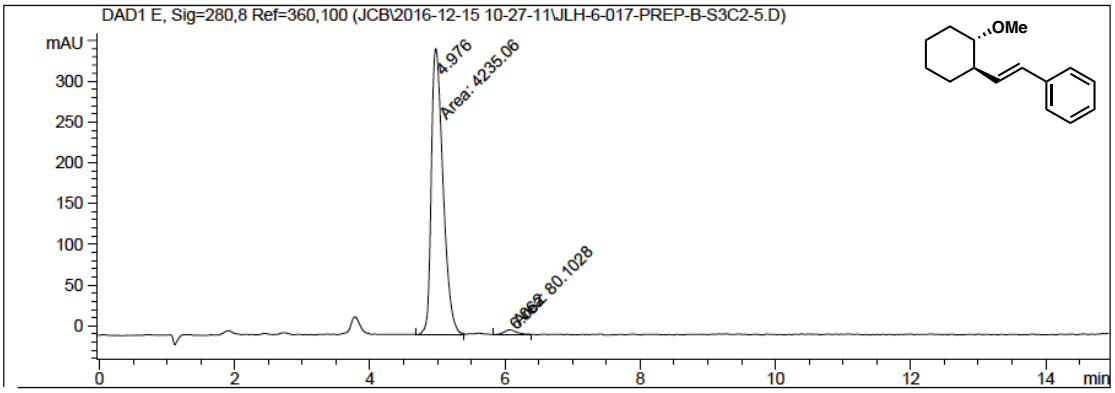

Peak #	RetTime [min]	Type	Width [min]	Area [mAU*s]	Height [mAU]	Area %
1	4.976	MM	0.2009	4235.05713	351.38831	98.1437
2	6.062	MM	0.2212	80.10277	6.03670	1.8563

121 (Figure 2.11): racemic

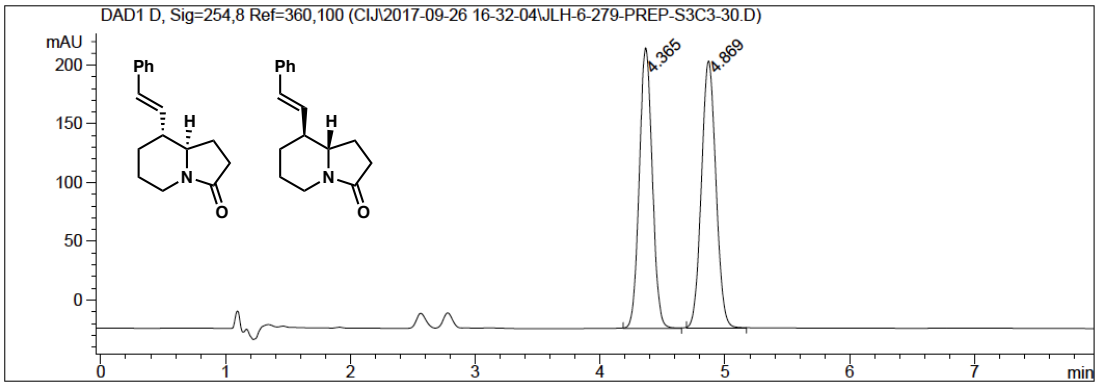

Peak #	RetTime [min]	Type	Width [min]	Area [mAU*s]	Height [mAU]	Area %
1	4.365	BB	0.1164	1725.97961	238.47392	48.3867
2	4.869	BB	0.1265	1841.07483	227.26039	51.6133

121 (Figure 2.11): enantioenriched, 97% ee

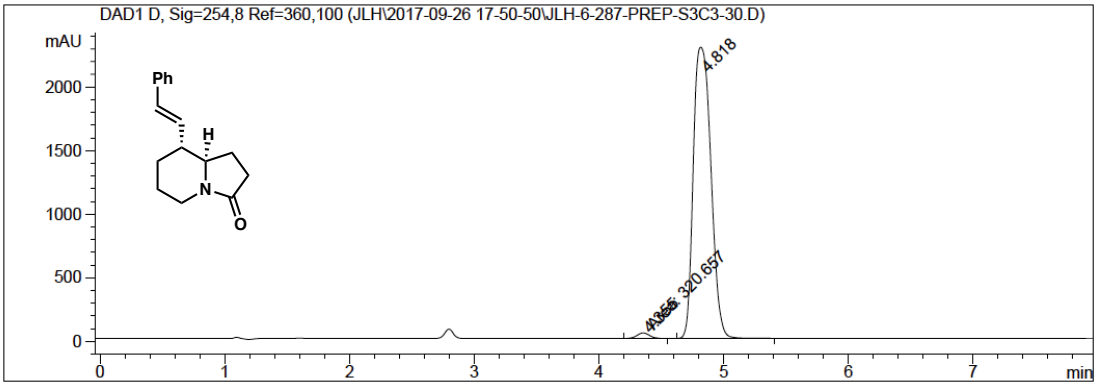

Peak #	RetTime [min]	Type	Width [min]	Area [mAU*s]	Height [mAU]	Area %
1	4.355	MM	0.1195	320.65738	44.71091	1.4017
2	4.818	BB	0.1586	2.25552e4	2295.60620	98.5983

123a (Scheme 2.8): racemic

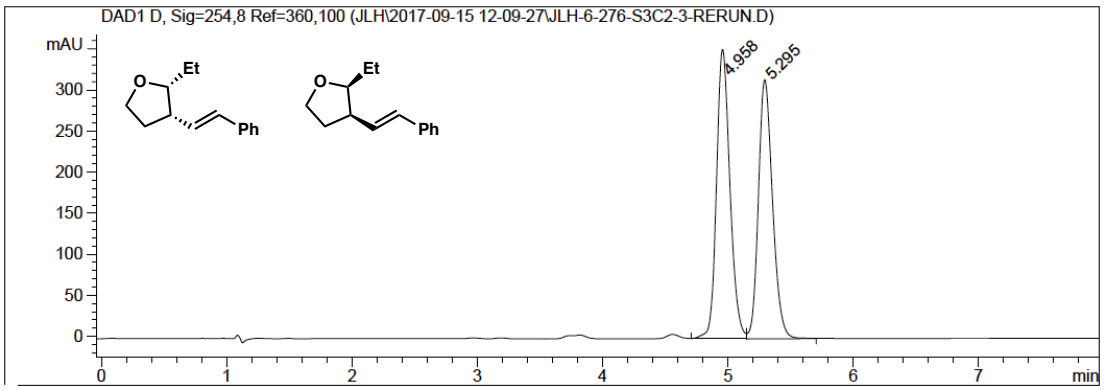

Peak #	RetTime [min]	Type	Width [min]	Area [mAU*s]	Height [mAU]	Area %
1	4.958	VV	0.1153	2631.88892	351.65015	51.5197
2	5.295	VB	0.1197	2476.61987	314.98431	48.4803

123a (Scheme 2.8): enantioenriched, 94% ee

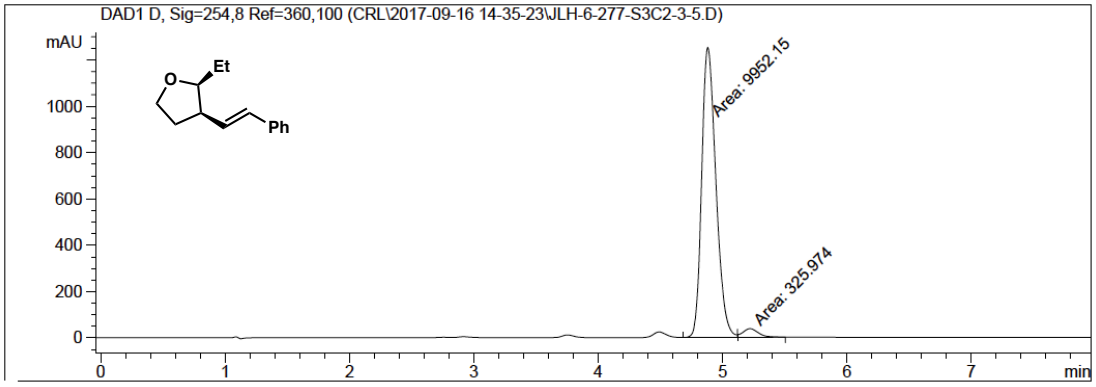

Peak #	RetTime [min]	Type	Width [min]	Area [mAU*s]	Height [mAU]	Area %
1	4.881	MM	0.1319	9952.15039	1257.06738	96.8285
2	5.220	MM	0.1437	325.97403	37.80476	3.1715

124a (Scheme 2.8): racemic (*OD-H column, separates diastereomers*), 20:1 dr

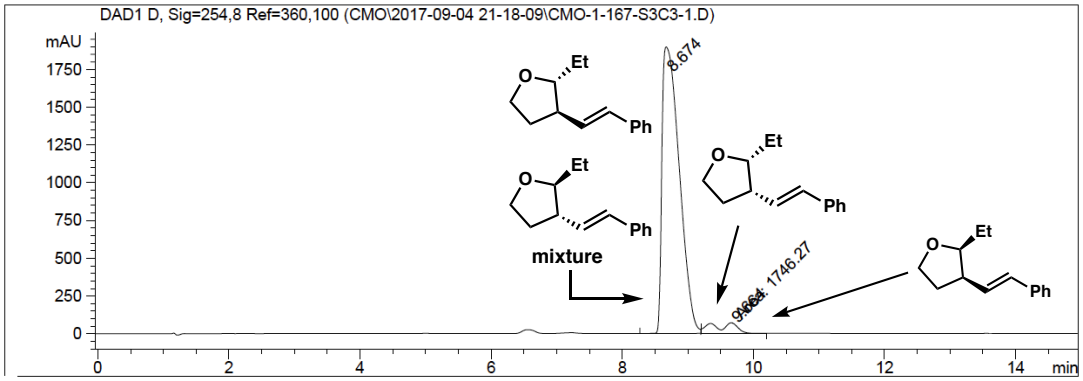

Peak #	RetTime [min]	Type	Width [min]	Area [mAU*s]	Height [mAU]	Area %
1	8.674	BV	0.2905	3.48916e4	1897.94568	95.2337
2	9.664	MM	0.4156	1746.26965	70.03025	4.7663

124a (Scheme 2.8): enantioenriched (*OD-H column, separates diastereomers*), 30:1 dr

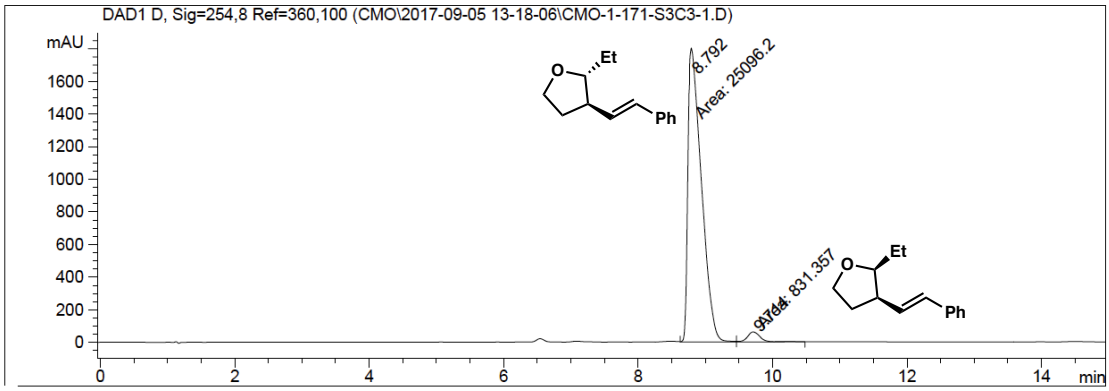

Peak #	RetTime [min]	Type	Width [min]	Area [mAU*s]	Height [mAU]	Area %
1	8.792	MM	0.2318	2.50962e4	1804.12939	96.7935
2	9.714	MM	0.2231	831.35657	62.09455	3.2065

124a (Scheme 2.8): racemic (*OB-H column, separates enantiomers*)

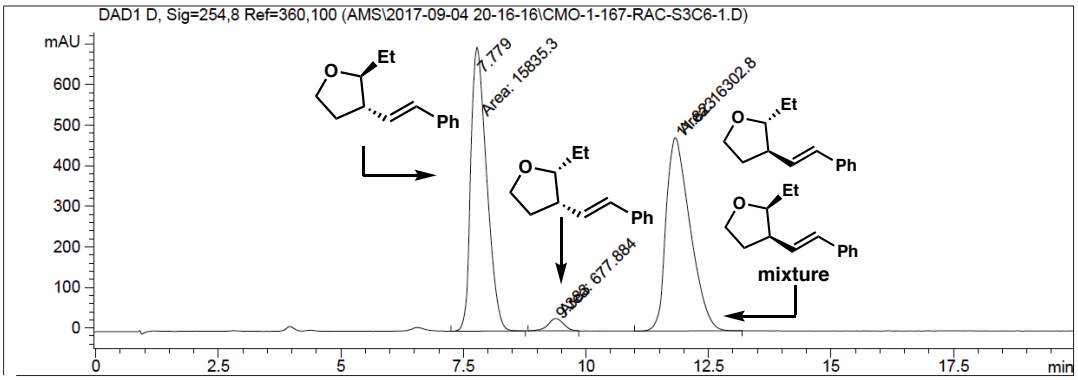

Peak #	RetTime [min]	Type	Width [min]	Area [mAU*s]	Height [mAU]	Area %
1	7.779	MM	0.3770	1.58353e4	700.04340	48.2548
2	9.383	MM	0.3664	677.88428	30.83868	2.0657
3	11.823	MM	0.5703	1.63028e4	476.39767	49.6795

124a (Scheme 2.8): enantioenriched (*OB-H column, separates enantiomers*), 91% ee

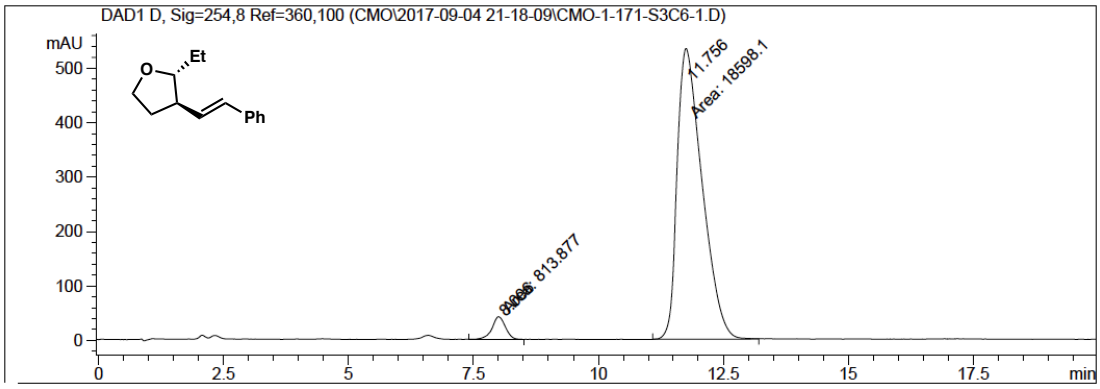

Peak #	RetTime [min]	Type	Width [min]	Area [mAU*s]	Height [mAU]	Area %
1	8.006	MM	0.3198	813.87683	42.41827	4.1927
2	11.756	MM	0.5799	1.85981e4	534.51337	95.8073

raw % ee = 95.8073 – 4.1927 = 91.61% ee
remove minor diastereomer: remove 3.2% of total area from peak 2 → new area = 17977
adjusted % ee = 95.6745 – 4.3255 = 91.35% ee

2.7 REFERENCES

(1) Chen, D.; Zhu, D.-X.; Xu, M.-H. *J. Am. Chem. Soc.* **2016**, *138*, 1498.

(2) Kan, S. B. J.; Lewis, R. D.; Chen, K.; Arnold, F. H. *Science* **2016**, *354*, 1048.

(3) Gribble, M. W.; Pirnot, M. T.; Bandar, J. S.; Liu, R. Y.; Buchwald, S. L. *J. Am. Chem. Soc.* **2017**, *139*, 2192.

(4) Showell, G. A.; Mills, J. S. *Drug Discov. Today* **2003**, *8*, 551.

(5) Min, G. K.; Hernández, D.; Skrydstrup, T. *Acc. Chem. Res.* **2013**, *46*, 457.

(6) Franz, A. K.; Wilson, S. O. *J. Med. Chem.* **2013**, *56*, 388.

(7) Auner, N.; Weis, J. *Organosilicon Chemistry V: From Molecules to Materials*; Wiley-VCH: Weinheim, Germany, 2004.

(8) Chan, T. H.; Wang, D. *Chem. Rev.* **1992**, *92*, 995.

(9) Masse, C. E.; Panek, J. S. *Chem. Rev.* **1995**, *95*, 1293.

(10) Fleming, I.; Barbero, A.; Walter, D. *Chem. Rev.* **1997**, *97*, 2063.

(11) Chabaud, L.; James, P.; Landais, Y. *Eur. J. Org. Chem.* **2004**, *2004*, 3173.

(12) Hosomi, A.; Sakurai, H. *Tetrahedron Lett.* **1976**, *16*, 1295.

(13) Hosomi, A.; Endo, M.; Sakurai, H. *Chem. Lett.* **1976**, *5*, 941.

(14) Kira, M.; Kobayashi, M.; Sakurai, H. *Tetrahedron Lett.* **1987**, *28*, 4081.

(15) Kira, M.; Sato, K.; Sakurai, H. *J. Am. Chem. Soc.* **1990**, *112*, 257.

(16) Chemler, S. R.; Roush, W. R. *J. Org. Chem.* **1998**, *63*, 3800.

(17) Berger, R.; Duff, K.; Leighton, J. L. *J. Am. Chem. Soc.* **2004**, *126*, 5686.

(18) Kim, H.; Ho, S.; Leighton, J. L. *J. Am. Chem. Soc.* **2011**, *133*, 6517.

(19) Hayashi, T.; Konishi, M.; Ito, H.; Kumada, M. *J. Am. Chem. Soc.* **1982**, *104*, 4962.

(20) Hayashi, T.; Konishi, M.; Kumada, M. *J. Am. Chem. Soc.* **1982**, *104*, 4963.

(21) Hayashi, T.; Konishi, M.; Okamoto, Y.; Kabeta, K.; Kumada, M. *J. Org. Chem.* **1986**, *51*, 3772.

(22) Jain, N. F.; Takenaka, N.; Panek, J. S. *J. Am. Chem. Soc.* **1996**, *118*, 12475.

(23) Park, P. K.; O'Malley, S. J.; Schmidt, D. R.; Leighton, J. L. *J. Am. Chem. Soc.* **2006**, *128*, 2796.

(24) Hu, T.; Takenaka, N.; Panek, J. S. *J. Am. Chem. Soc.* **1999**, *121*, 9229.

(25) Jain, N. F.; Panek, J. S. *Tetrahedron Lett.* **1997**, *38*, 1345.

(26) Arefolov, A.; Panek, J. S. *Org. Lett.* **2002**, *4*, 2397.

(27) Arefolov, A.; Panek, J. S. *J. Am. Chem. Soc.* **2005**, *127*, 5596.

(28) Wu, J.; Panek, J. S. *J. Org. Chem.* **2011**, *76*, 9900.

(29) Lee, J.; Panek, J. S. *Org. Lett.* **2011**, *13*, 502.

(30) Sparks, M. A.; Panek, J. S. *J. Org. Chem.* **1991**, *56*, 3431.

(31) Panek, J. S.; Clark, T. D. *J. Org. Chem.* **1992**, *57*, 4323.

(32) Suginome, M.; Matsumoto, A.; Ito, Y. *J. Am. Chem. Soc.* **1996**, *118*, 3061.

(33) Bourque, L. E.; Cleary, P. A.; Woerpel, K. A. *J. Am. Chem. Soc.* **2007**, *129*, 12602.

(34) Binanzer, M.; Fang, G. Y.; Aggarwal, V. K. *Angew. Chem. Int. Ed.* **2010**, *49*, 4264.

(35) Aggarwal, V. K.; Binanzer, M.; de Ceglie, M. C.; Gallanti, M.; Glasspoole, B. W.; Kendrick, S. J. F.; Sonawane, R. P.; Vázquez-Romero, A.; Webster, M. P. *Org. Lett.* **2011**, *13*, 1490.

(36) Hayashi, T.; Kabeta, K. *Tetrahedron Lett.* **1985**, *26*, 3023.

(37) Hayashi, T.; Han, J. W.; Takeda, A.; Tang, T.; Nohmi, K.; Mukaide, K.; Tsuji, H.; Uozumi, Y. *Adv. Synth. Catal.* **2001**, *343*, 279.

(38) Ohmura, T.; Taniguchi, H.; Suginome, M. *J. Am. Chem. Soc.* **2006**, *128*, 13682.

(39) Davies, H. M. L.; Hansen, T.; Rutberg, J.; Bruzinski, P. R. *Tetrahedron Lett.* **1997**, *38*, 1741.

(40) Wu, J.; Chen, Y.; Panek, J. S. *Org. Lett.* **2010**, *12*, 2112.

(41) Shintani, R.; Ichikawa, Y.; Hayashi, T.; Chen, J.; Nakao, Y.; Hiyama, T. *Org. Lett.* **2007**, *9*, 4643.

(42) Lee, K.; Wu, H.; Haeffner, F.; Hoveyda, A. H. *Organometallics* **2012**, *31*, 7823.

(43) Kacprzynski, M. A.; May, T. L.; Kazane, S. A.; Hoveyda, A. H. *Angew. Chem. Int. Ed.* **2007**, *46*, 4554.

(44) Bähr, S.; Xue, W.; Oestreich, M. *ACS Catal.* **2019**, *9*, 16.

(45) Xue, W.; Qu, Z.-W.; Grimme, S.; Oestreich, M. *J. Am. Chem. Soc.* **2016**, *138*, 14222.

(46) Xue, W.; Shishido, R.; Oestreich, M. *Angew. Chem. Int. Ed.* **2018**, *57*, 12141.

(47) Cinderella, A. P.; Vulovic, B.; Watson, D. A. *J. Am. Chem. Soc.* **2017**, *139*, 7741.

(48) Vulovic, B.; Cinderella, A. P.; Watson, D. A. *ACS Catal.* **2017**, *7*, 8113.

(49) Chu, C. K.; Liang, Y.; Fu, G. C. *J. Am. Chem. Soc.* **2016**, *138*, 6404.

(50) Cherney, A. H.; Reisman, S. E. *J. Am. Chem. Soc.* **2014**, *136*, 14365.

(51) Suzuki, N.; Hofstra, J. L.; Poremba, K. E.; Reisman, S. E. *Org. Lett.* **2017**, *19*, 2150.

(52) Ackerman, L. K. G.; Anka-Lufford, L. L.; Naodovic, M.; Weix, D. J. *Chem. Sci.* **2015**, *6*, 1115.

(53) Kurosu, M.; Lin, M.-H.; Kishi, Y. *J. Am. Chem. Soc.* **2004**, *126*, 12248.

(54) Matsumoto, K.; Oshima, K.; Utimoto, K. *J. Org. Chem.* **1994**, *59*, 7152.

(55) Tamao, K.; Ishida, N.; Tanaka, T.; Kumada, M. *Organometallics* **1983**, *2*, 1694.

(56) Fleming, I.; Terrett, N. K. *Tetrahedron Lett.* **1984**, *25*, 5103.

(57) Fleming, I.; Henning, R.; Plaut, H. *J. Chem. Soc., Chem. Commun.* **1984**, *0*, 29.

(58) Jones, G. R.; Landais, Y. *Tetrahedron* **1996**, *52*, 7599.

(59) Torigoe, T.; Ohmura, T.; Suginome, M. *J. Org. Chem.* **2017**, *82*, 2943.

(60) Yi, H.; Mao, W.; Oestreich, M. *Angew. Chem. Int. Ed.* **2019**, *58*, 3575.

(61) Mizuta, S.; Engle, K. M.; Verhoog, S.; Galicia-López, O.; O'Duill, M.; Médebielle, M.; Wheelhouse, K.; Rassias, G.; Thompson, A. L.; Gouverneur, V. *Org. Lett.* **2013**, *15*, 1250.

(62) Hayashi, T.; Ito, H.; Kumada, M. *Tetrahedron Lett.* **1982**, *23*, 4605.

(63) Hayashi, T.; Okamoto, Y.; Kabeta, K.; Hagihara, T.; Kumada, M. *J. Org. Chem.* **1984**, *49*, 4224.

(64) Ochiai, M.; Fujita, E. *Tetrahedron Lett.* **1980**, *21*, 4369.

(65) Hiroi, K.; Chen, L.-M. *J. Chem. Soc., Chem. Commun.* **1981**, *0*, 377.

(66) Hiyama, T.; Obayashi, M.; Mori, I.; Nozaki, H. *J. Org. Chem.* **1983**, *48*, 912.

(67) Kunio, H.; Sato, H.; Chen, L.-M.; Kotsuji, K. *Chem. Pharm. Bull.* **1987**, *35*, 1413.

(68) Mayr, H.; Gabriel, A. O.; Schumacher, R. *Liebigs Ann.* **1995**, *9*, 1583.

(69) Wu, J.; Pu, Y.; Panek, J. S. *J. Am. Chem. Soc.* **2012**, *134*, 18440.

(70) Denmark, S. E.; Willson, T. M. *J. Am. Chem. Soc.* **1989**, *111*, 3475.

(71) Park, Y.; Schindler, C. S.; Jacobsen, E. N. *J. Am. Chem. Soc.* **2016**, *138*, 14848.

(72) McElhinney, A. D.; Marsden, S. P. *Synlett* **2005**, *16*, 2528.

(73) Hubert, J. C.; Wijnberg, J. B. P. A.; Speckamp, W. N. *Tetrahedron* **1975**, *31*, 1437.

(74) Hiemstra, H.; Sno, M. H. A. M.; Vijn, R. J.; Speckamp, W. N. *J. Org. Chem.* **1985**, *50*, 4014.

(75) Judd, W. R.; Ban, S.; Aubé, J. *J. Am. Chem. Soc.* **2006**, *128*, 13736.

(76) Suginome, M.; Iwanami, T.; Ito, Y. *J. Org. Chem.* **1998**, *63*, 6096.

(77) Still, W. C.; Kahn, M.; Mitra, A. *J. Org. Chem.* **1978**, *43*, 2923.

(78) Snyder, S. A.; ElSohly, A. M.; Kontes, F. *Angew. Chem. Int. Ed.* **2010**, *49*, 9693.

(79) Sibi, M. P.; Liu, M. *Org. Lett.* **2000**, *2*, 3393.

(80) Evans, D. A.; Downey, C. W.; Hubbs, J. L. *J. Am. Chem. Soc.* **2003**, *125*, 8706.

(81) Manzano, R.; Rominger, F.; Hashmi, A. S. K. *Organometallics* **2013**, *32*, 2199.

(82) Li, D.-R.; Zhang, D.-H.; Sun, C.-Y.; Zhang, J.-W.; Yang, L.; Chen, J.; Liu, B.; Su, C.; Zhou, W.-S.; Lin, G.-Q. *Chem. Eur. J.* **2006**, *12*, 1185.

(83) Brown, H. C.; Larock, R. C.; Gupta, S. K.; Rajagopalan, S.; Bhat, N. G. *J. Org. Chem.* **1989**, *54*, 6079.

(84) Uehling, M. R.; Rucker, R. P.; Lalic, G. *J. Am. Chem. Soc.* **2014**, *136*, 8799.

(85) Müller, D.; Alexakis, A. *Chem. Eur. J.* **2013**, *19*, 15226.

(86) Roper, K. A.; Berry, M. B.; Ley, S. V. *Beilstein J. Org. Chem.* **2013**, *9*, 1781.

(87) Cheung, C. W.; Buchwald, S. L. *J. Org. Chem.* **2012**, *77*, 7526.

(88) Das, J. P.; Roy, S. *J. Org. Chem.* **2002**, *67*, 7861.

(89) Gallagher, W. P.; Maleczka, R. E. *J. Org. Chem.* **2005**, *70*, 841.

(90) Lu, H.-H.; Martinez, M. D.; Shenvi, R. A. *Nat. Chem.* **2015**, *7*, 604.

(91) Maleczka, Robert E.; Geng, F. *Org. Lett.* **1999**, *1*, 1111.

(92) Patel, H. H.; Sigman, M. S. *J. Am. Chem. Soc.* **2016**, *138*, 14226.

(93) Koley, D.; Krishna, Y.; Srinivas, K.; Khan, A. A.; Kant, R. *Angew. Chem. Int. Ed.* **2014**, *53*, 13196.

(94) Ohmiya, S.; Kubo, H.; Otomasu, H.; Saito, K.; Murakoshi, I. *Heterocycles* **1990**, *30*, 537.

(95) Ikeda, Y.; Yorimitsu, H.; Shinokubo, H.; Oshima, K. *Adv. Synth. Catal.* **2004**, *346*, 1631.

(96) Yoshida, T.; Yamauchi, S.; Tago, R.; Maruyama, M.; Akiyama, K.; Sugahara, T.; Kishida, T.; Koba, Y. *Biosci. Biotechnol. Biochem.* **2008**, *72*, 2342.

(97) Fernández-Mateos, A.; Encinas-Madrazo, S.; Herrero-Teijón, P.; González, R. R. *Eur. J. Org. Chem.* **2015**, 548.

Appendix 1

Spectra Relevant to Chapter 2:

Synthesis and Utility of Chiral Allylic Silanes Prepared

via Ni-Catalyzed Asymmetric Reductive Cross-Coupling

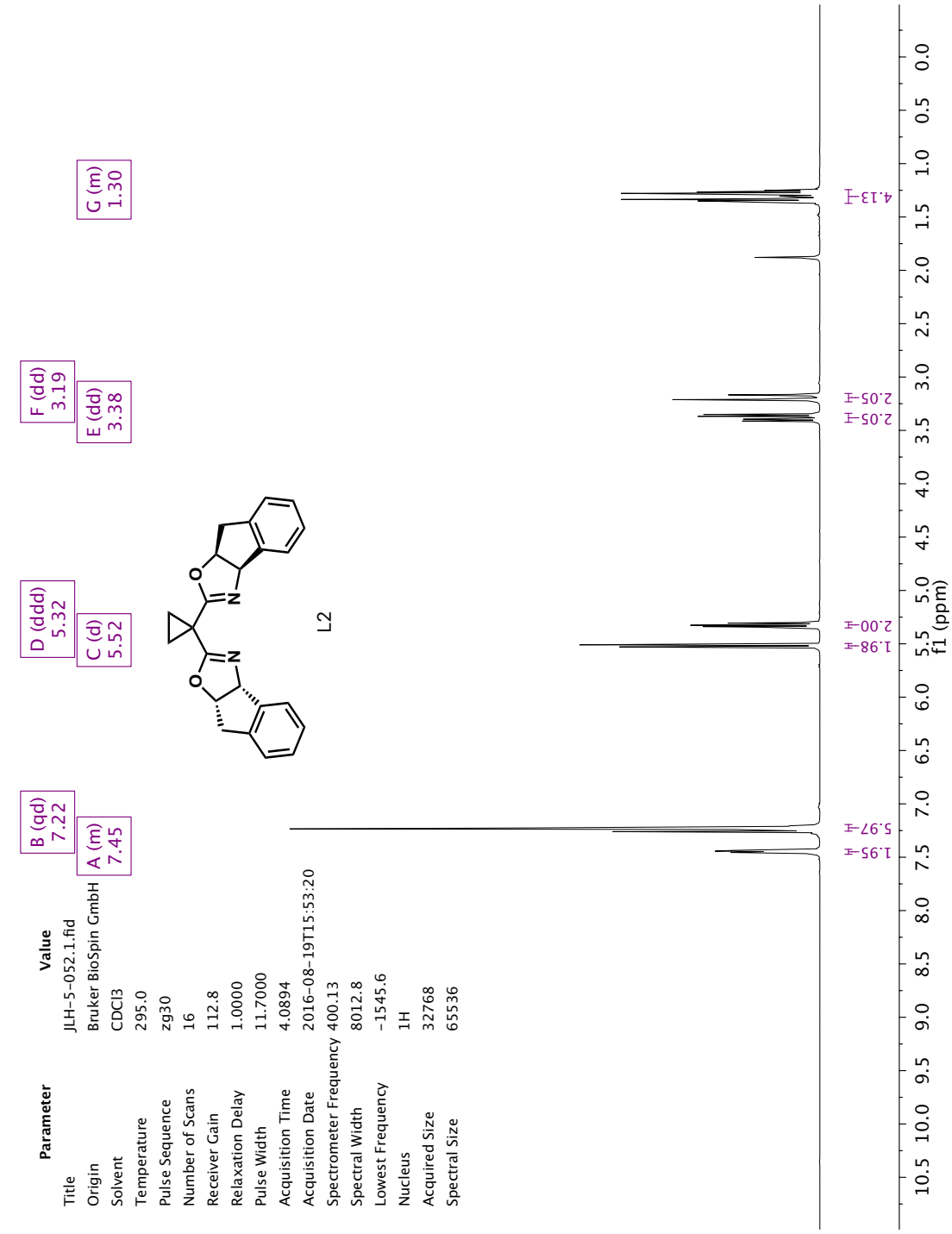
Parameter
Value
Title
JLH-5-052.1.fid
Origin
Bruker BioSpin GmbH
Solvent
CDCl3
Temperature
295.0
Pulse Sequence
zg30
Number of Scans
16
Receiver Gain
112.8
Relaxation Delay
1.0000
Pulse Width
11.7000
Acquisition Time
4.0894
Acquisition Date
2016-08-19T15:53:20
Spectrometer Frequency
400.13
Spectral Width
8012.8
Lowest Frequency
-1545.6
Nucleus
1H
Acquired Size
32768
Spectral Size
65536
B (qd)
7.22
A (m)
7.45
D (ddd)
5.32
C (d)
5.52
F (dd)
3.19
E (dd)
3.38
G (m)
1.30
L2
5.97
1.95
1.98
2.00
2.05
2.05
4.13
f1 (ppm)

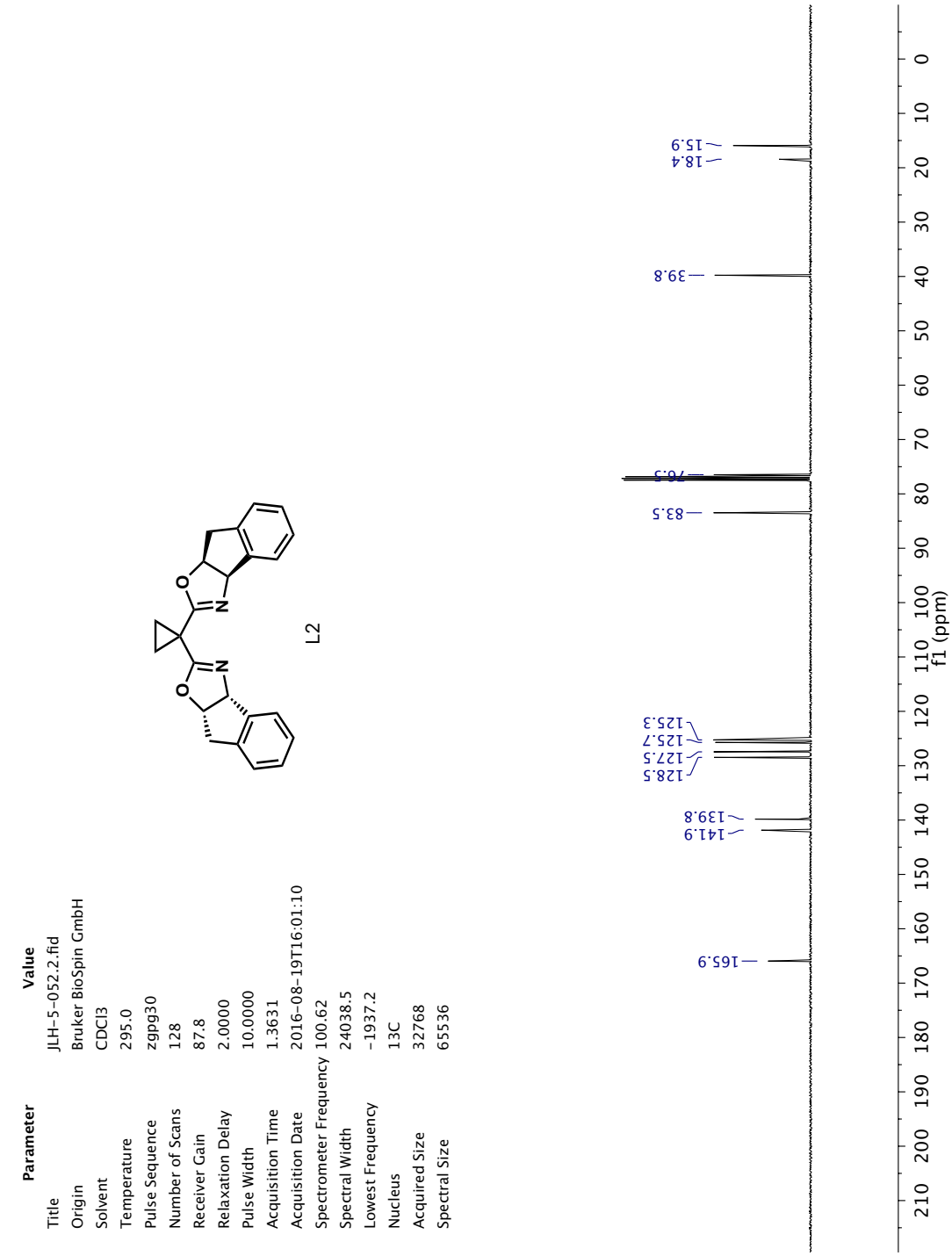
Parameter Value
Title JLH-5-052.2.fid
Origin Bruker BioSpin GmbH
Solvent CDCl3
Temperature 295.0
Pulse Sequence zgpg30
Number of Scans 128
Receiver Gain 87.8
Relaxation Delay 2.0000
Pulse Width 10.0000
Acquisition Time 1.3631
Acquisition Date 2016-08-19T16:01:10
Spectrometer Frequency 100.62
Spectral Width 24038.5
Lowest Frequency -1937.2
Nucleus 13C
Acquired Size 32768
Spectral Size 65536
L2
165.9
141.9
139.8
128.5
127.5
125.7
125.3
83.5
76.5
39.8
18.4
15.9
f1 (ppm)

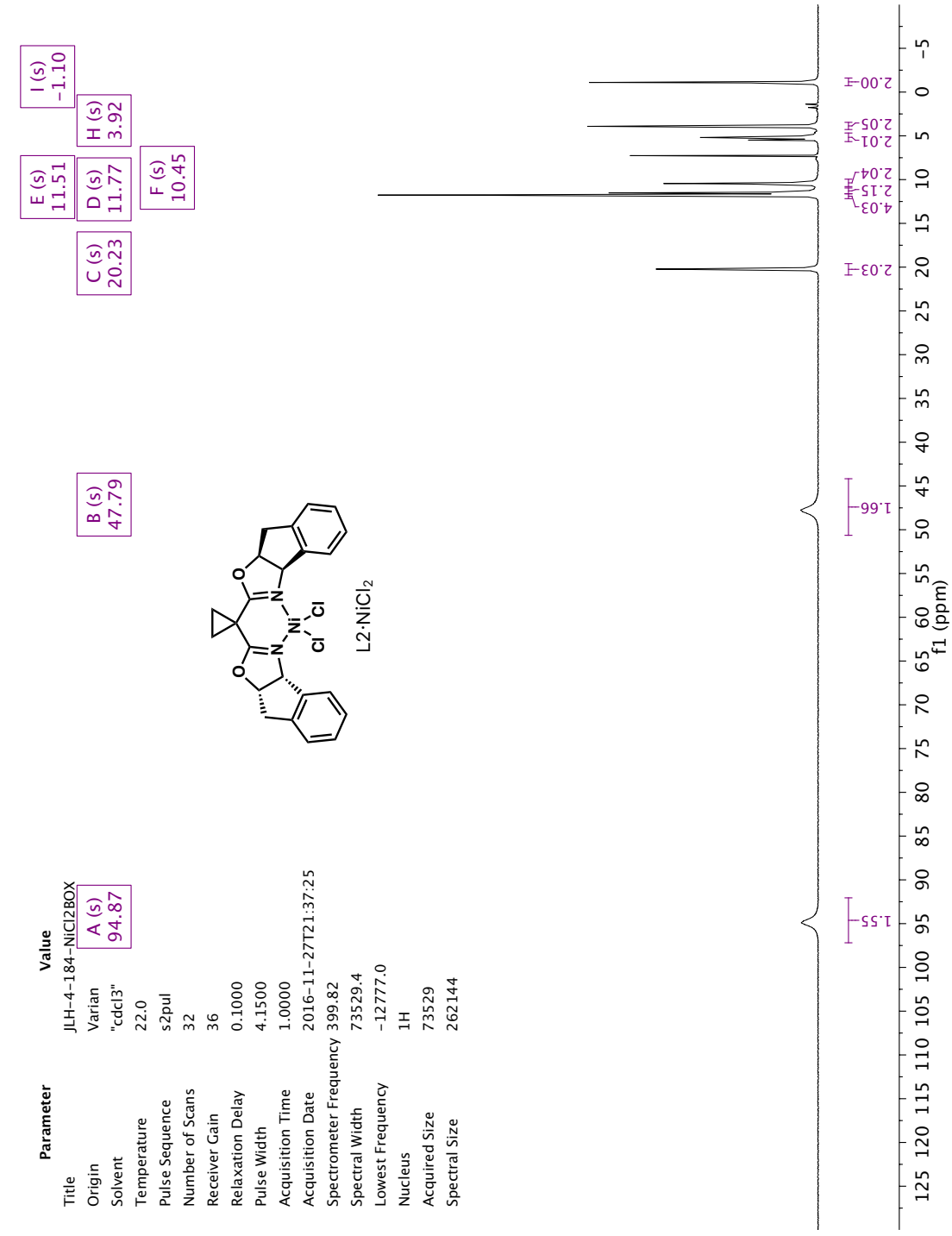
Parameter
Value
Title
JLH-4-184-NiCl2BOX
Origin
Varian
Solvent
"cdcl3"
Temperature
22.0
Pulse Sequence
s2pul
Number of Scans
32
Receiver Gain
36
Relaxation Delay
0.1000
Pulse Width
4.1500
Acquisition Time
1.0000
Acquisition Date
2016-11-27T21:37:25
Spectrometer Frequency
399.82
Spectral Width
73529.4
Lowest Frequency
-12777.0
Nucleus
1H
Acquired Size
73529
Spectral Size
262144
A (s) 94.87
B (s) 47.79
C (s) 20.23
D (s) 11.77
E (s) 11.51
F (s) 10.45
H (s) 3.92
I (s) -1.10
L2·NiCl2
1.55
1.66
2.03
4.03
2.15
2.04
2.01
2.05
2.00
f1 (ppm)

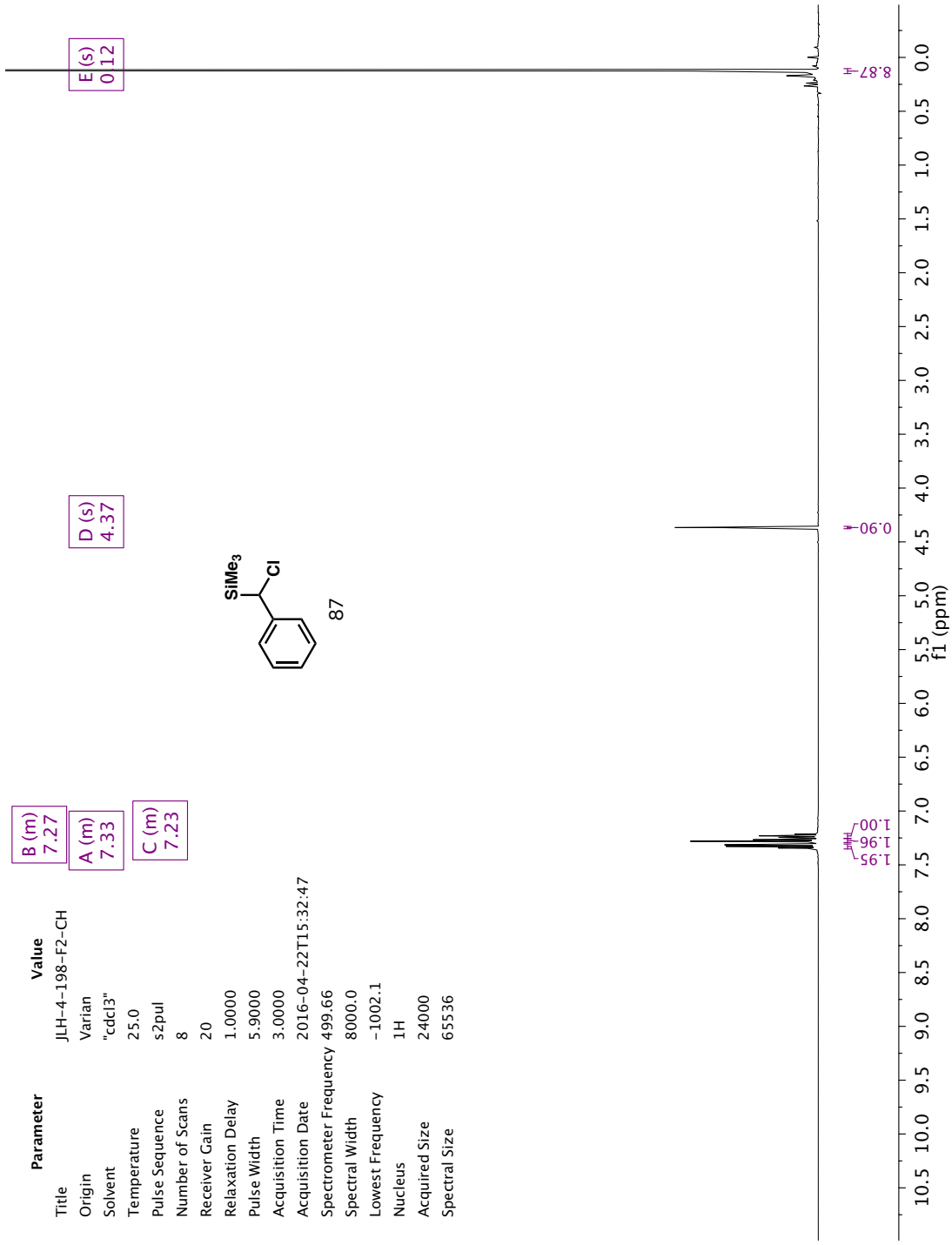

Parameter	Value
Title	JLH-4-198-F2-CH
Origin	Varian
Solvent	"cdcl3"
Temperature	25.0
Pulse Sequence	s2pul
Number of Scans	8
Receiver Gain	20
Relaxation Delay	1.0000
Pulse Width	5.9000
Acquisition Time	3.0000
Acquisition Date	2016-04-22T15:32:47
Spectrometer Frequency	499.66
Spectral Width	8000.0
Lowest Frequency	-1002.1
Nucleus	1H
Acquired Size	24000
Spectral Size	65536

Parameter	Value
Title	JLH-4-198-F2-CH
Origin	Varian
Solvent	"cdcl3"
Temperature	25.0
Pulse Sequence	s2pul
Number of Scans	256
Receiver Gain	30
Relaxation Delay	1.0000
Pulse Width	4.5000
Acquisition Time	1.0420
Acquisition Date	2016-04-22T15:33:35
Spectrometer Frequency	125.65
Spectral Width	31446.5
Lowest Frequency	-1903.0
Nucleus	13C
Acquired Size	32768
Spectral Size	65536

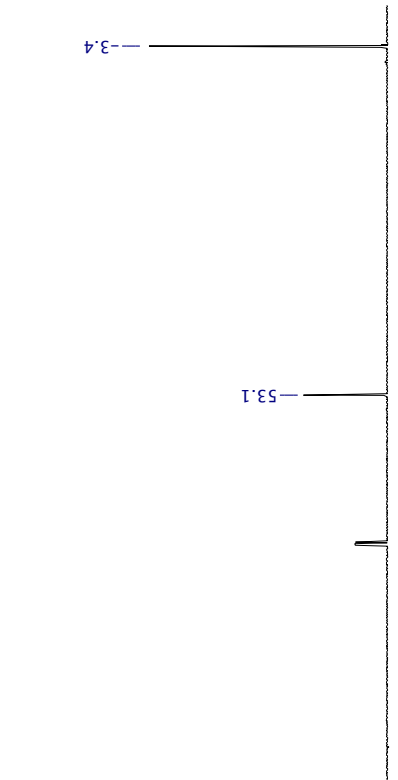

87

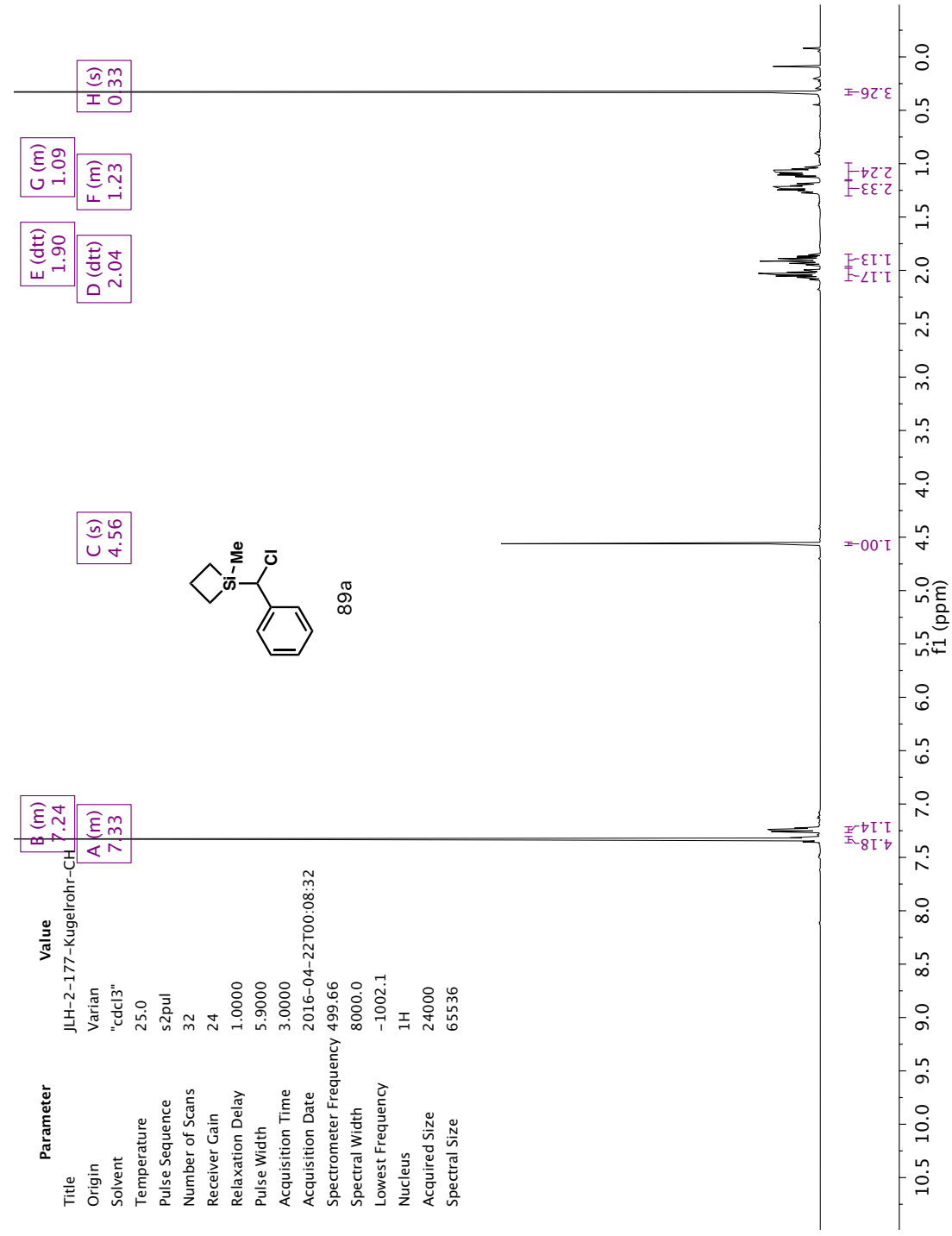
Parameter
Value
Title JLH-2-177-Kugelrohr-CH
Origin Varian
Solvent "cdcl3"
Temperature 25.0
Pulse Sequence s2pul
Number of Scans 32
Receiver Gain 24
Relaxation Delay 1.0000
Pulse Width 5.9000
Acquisition Time 3.0000
Acquisition Date 2016-04-22T00:08:32
Spectrometer Frequency 499.66
Spectral Width 8000.0
Lowest Frequency -1002.1
Nucleus 1H
Acquired Size 24000
Spectral Size 65536
B (m) 7.24
A (m) 7.33
C (s) 4.56
E (dtt) 1.90
D (dtt) 2.04
G (m) 1.09
F (m) 1.23
H (s) 0.33
Si
Me
Cl
89a
4.18
1.14
1.00
1.17
1.13
2.33
2.24
3.26
10.5 10.0 9.5 9.0 8.5 8.0 7.5 7.0 6.5 6.0 5.5 5.0 4.5 4.0 3.5 3.0 2.5 2.0 1.5 1.0 0.5 0.0
f1 (ppm)

Parameter	Value
Title	JLH-2-177-Kugelrohr-CH
Origin	Varian
Solvent	"cdcl3"
Temperature	25.0
Pulse Sequence	s2pul
Number of Scans	1000
Receiver Gain	30
Relaxation Delay	1.0000
Pulse Width	4.5000
Acquisition Time	1.0420
Acquisition Date	2016-04-22T00:10:56
Spectrometer Frequency	125.65
Spectral Width	31446.5
Lowest Frequency	-1903.0
Nucleus	13C
Acquired Size	32768
Spectral Size	65536

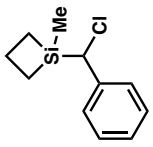

89a

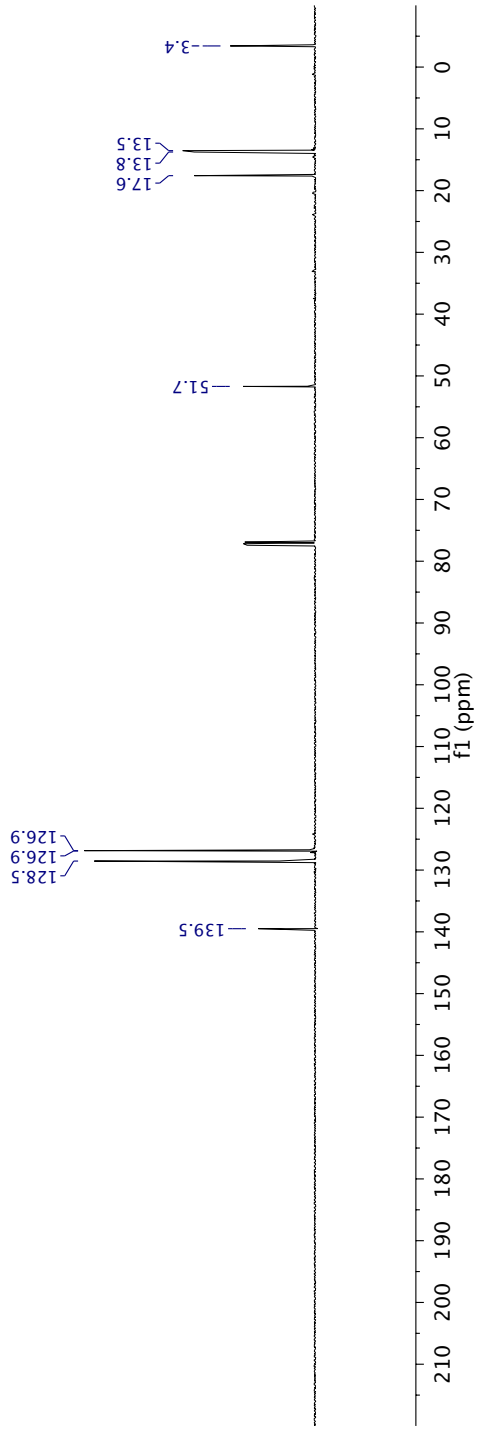

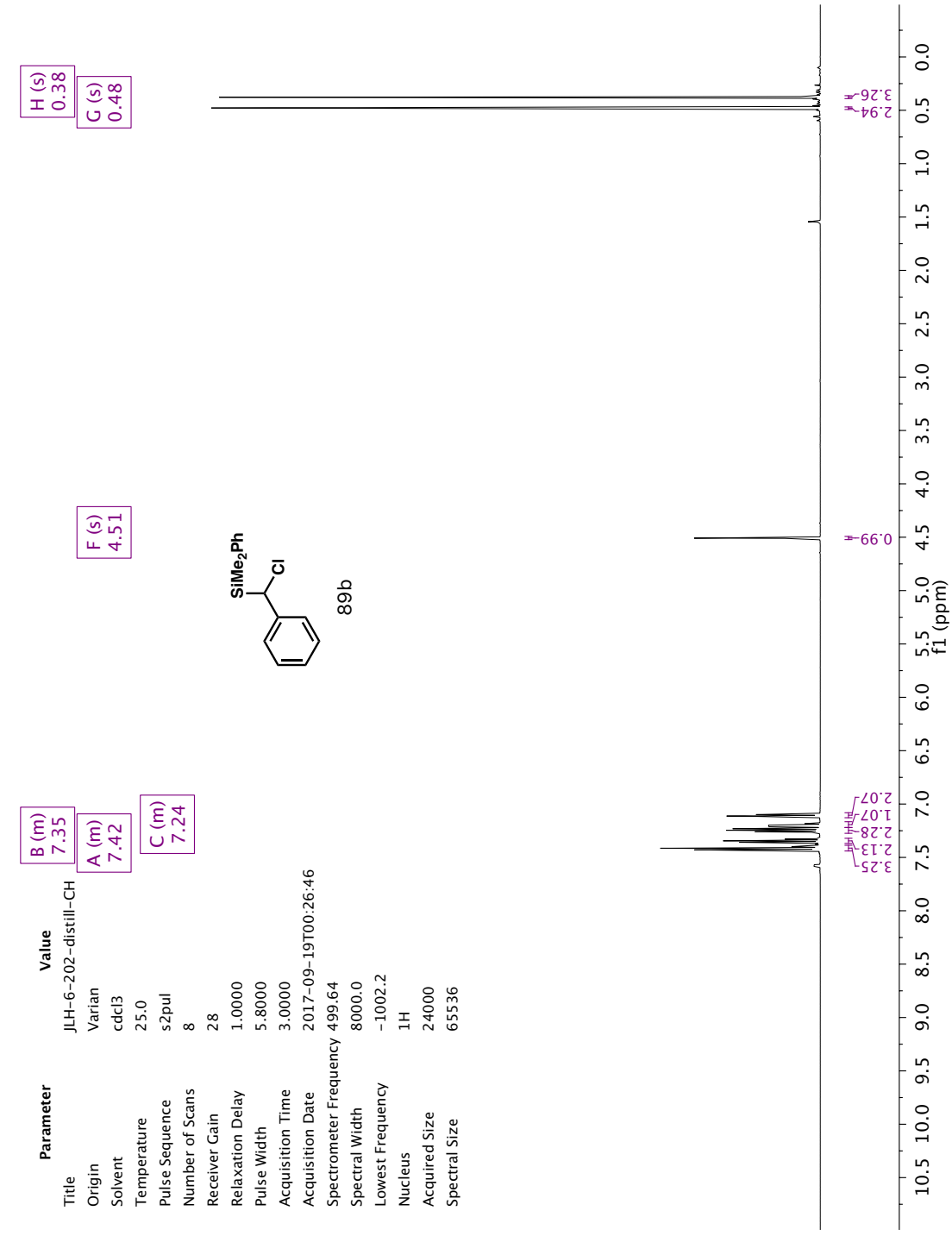
B (m) 7.35
A (m) 7.42
C (m) 7.24
F (s) 4.51
H (s) 0.38
G (s) 0.48
SiMe2Ph
Cl
89b
Parameter Value
Title JLH-6-202-distill-CH
Origin Varian
Solvent cdcl3
Temperature 25.0
Pulse Sequence s2pul
Number of Scans 8
Receiver Gain 28
Relaxation Delay 1.0000
Pulse Width 5.8000
Acquisition Time 3.0000
Acquisition Date 2017-09-19T00:26:46
Spectrometer Frequency 499.64
Spectral Width 8000.0
Lowest Frequency -1002.2
Nucleus 1H
Acquired Size 24000
Spectral Size 65536
3.25
2.13
2.28
1.07
2.07
0.99
2.94
3.26
f1 (ppm)

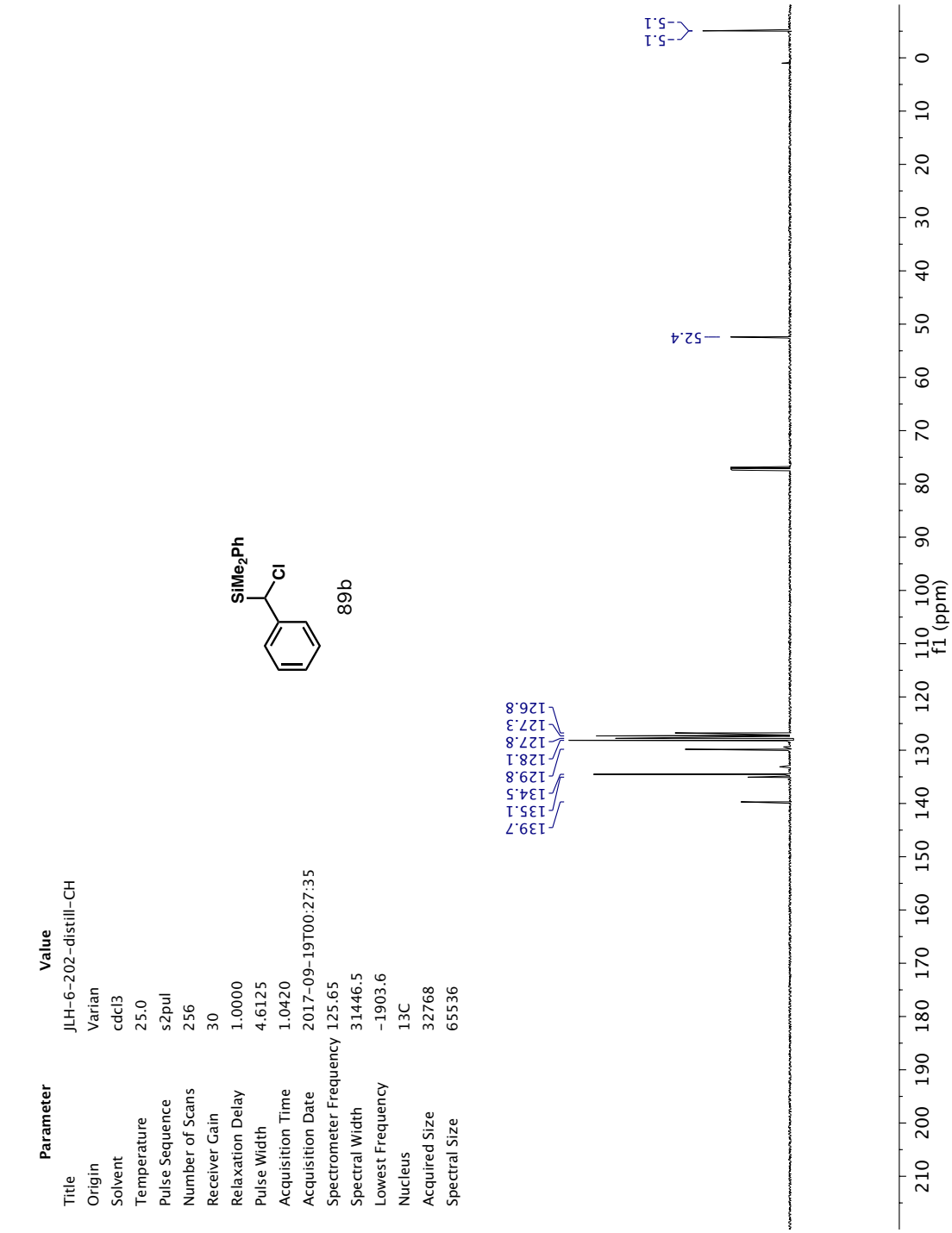

Parameter	Value
Title	JLH-6-202-distill-CH
Origin	Varian
Solvent	cdcl3
Temperature	25.0
Pulse Sequence	s2pul
Number of Scans	256
Receiver Gain	30
Relaxation Delay	1.0000
Pulse Width	4.6125
Acquisition Time	1.0420
Acquisition Date	2017-09-19T00:27:35
Spectrometer Frequency	125.65
Spectral Width	31446.5
Lowest Frequency	-1903.6
Nucleus	13C
Acquired Size	32768
Spectral Size	65536

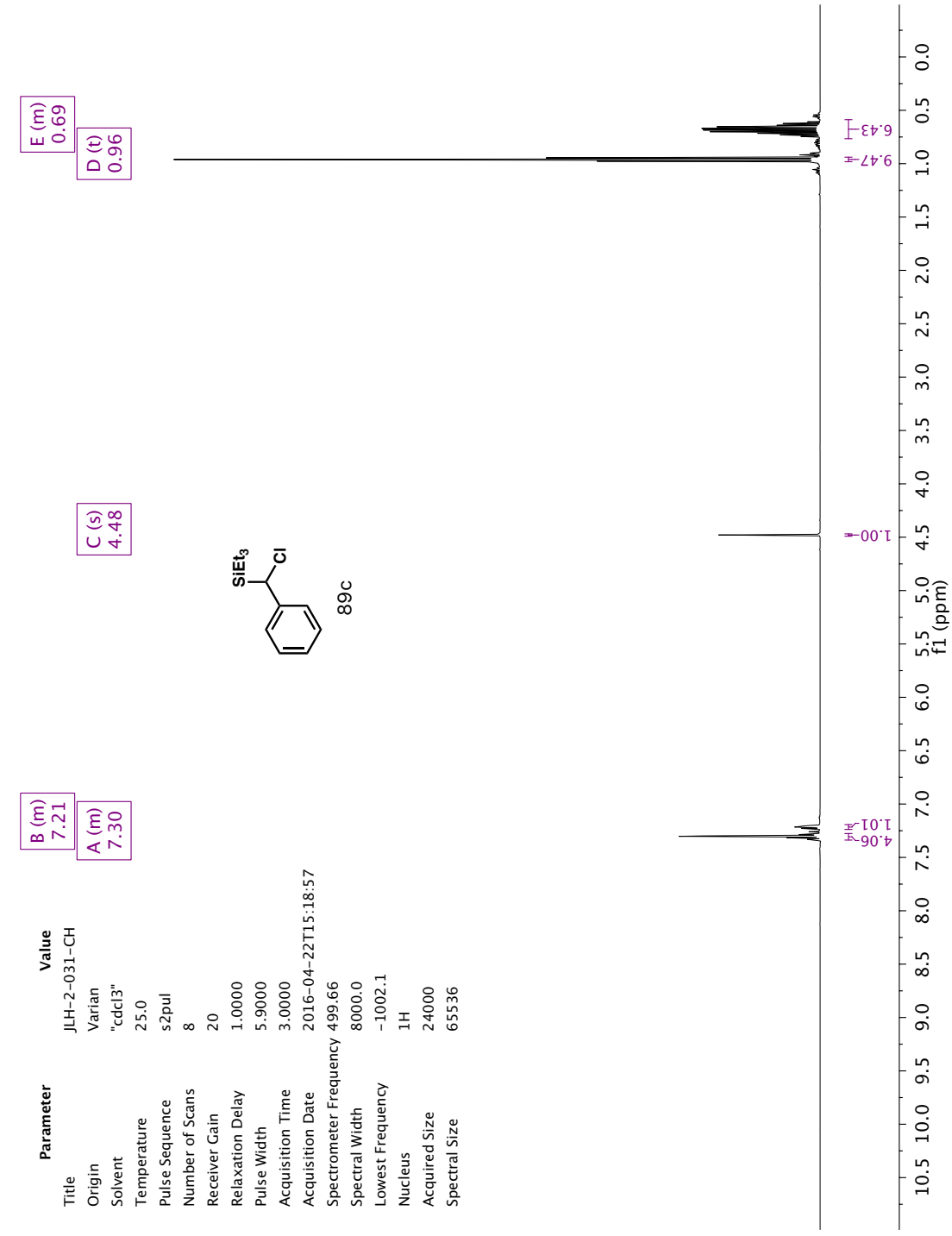

Parameter	Value
Title	JLH-2-031-CH
Origin	Varian
Solvent	"cdcl3"
Temperature	25.0
Pulse Sequence	s2pul
Number of Scans	8
Receiver Gain	20
Relaxation Delay	1.0000
Pulse Width	5.9000
Acquisition Time	3.0000
Acquisition Date	2016-04-22T15:18:57
Spectrometer Frequency	499.66
Spectral Width	8000.0
Lowest Frequency	-1002.1
Nucleus	1H
Acquired Size	24000
Spectral Size	65536

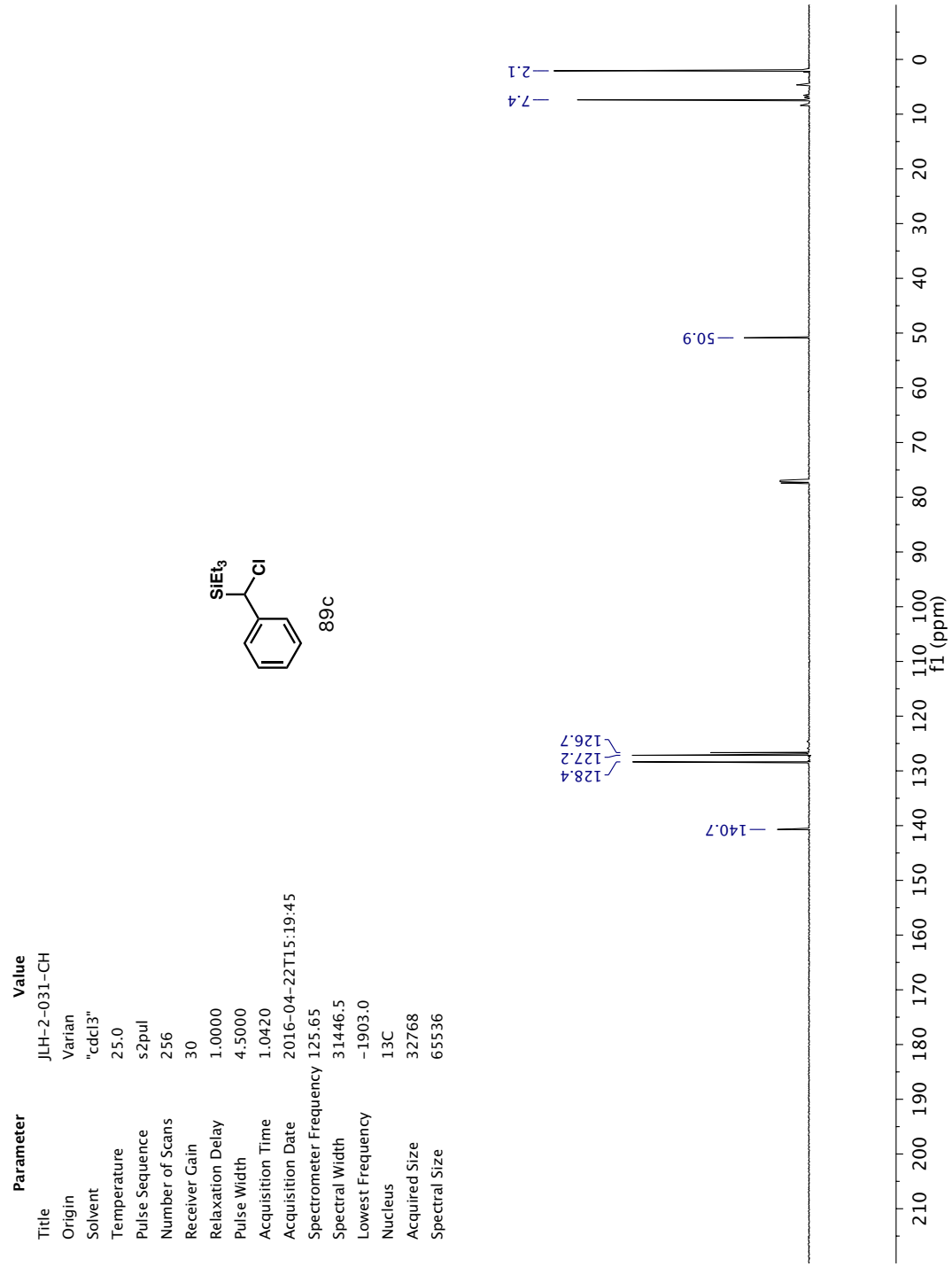

Parameter	Value
Title	JLH-2-031-CH
Origin	Varian
Solvent	"cdcl3"
Temperature	25.0
Pulse Sequence	s2pul
Number of Scans	256
Receiver Gain	30
Relaxation Delay	1.0000
Pulse Width	4.5000
Acquisition Time	1.0420
Acquisition Date	2016-04-22T15:19:45
Spectrometer Frequency	125.65
Spectral Width	31446.5
Lowest Frequency	-1903.0
Nucleus	13C
Acquired Size	32768
Spectral Size	65536

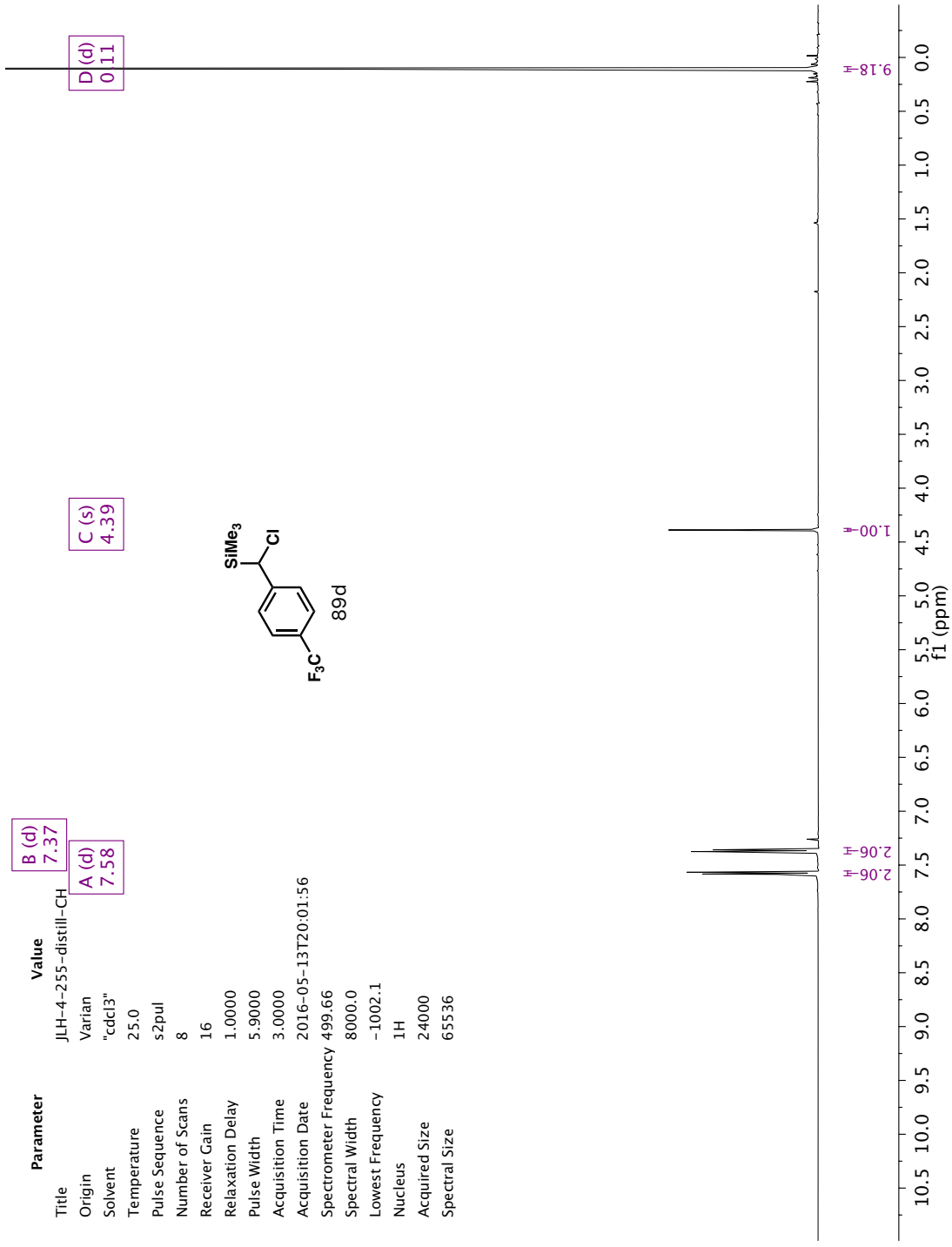
Parameter
Value
Title
JLH-4-255-distill-CH
Origin
Varian
Solvent
"cdcl3"
Temperature
25.0
Pulse Sequence
s2pul
Number of Scans
8
Receiver Gain
16
Relaxation Delay
1.0000
Pulse Width
5.9000
Acquisition Time
3.0000
Acquisition Date
2016-05-13T20:01:56
Spectrometer Frequency
499.66
Spectral Width
8000.0
Lowest Frequency
-1002.1
Nucleus
1H
Acquired Size
24000
Spectral Size
65536
B (d) 7.37
A (d) 7.58
C (s) 4.39
D (d) 0 11
SiMe3
Cl
F3C
89d
9.18
2.06
2.06
1.00
10.5 10.0 9.5 9.0 8.5 8.0 7.5 7.0 6.5 6.0 5.5 5.0 4.5 4.0 3.5 3.0 2.5 2.0 1.5 1.0 0.5 0.0
f1 (ppm)

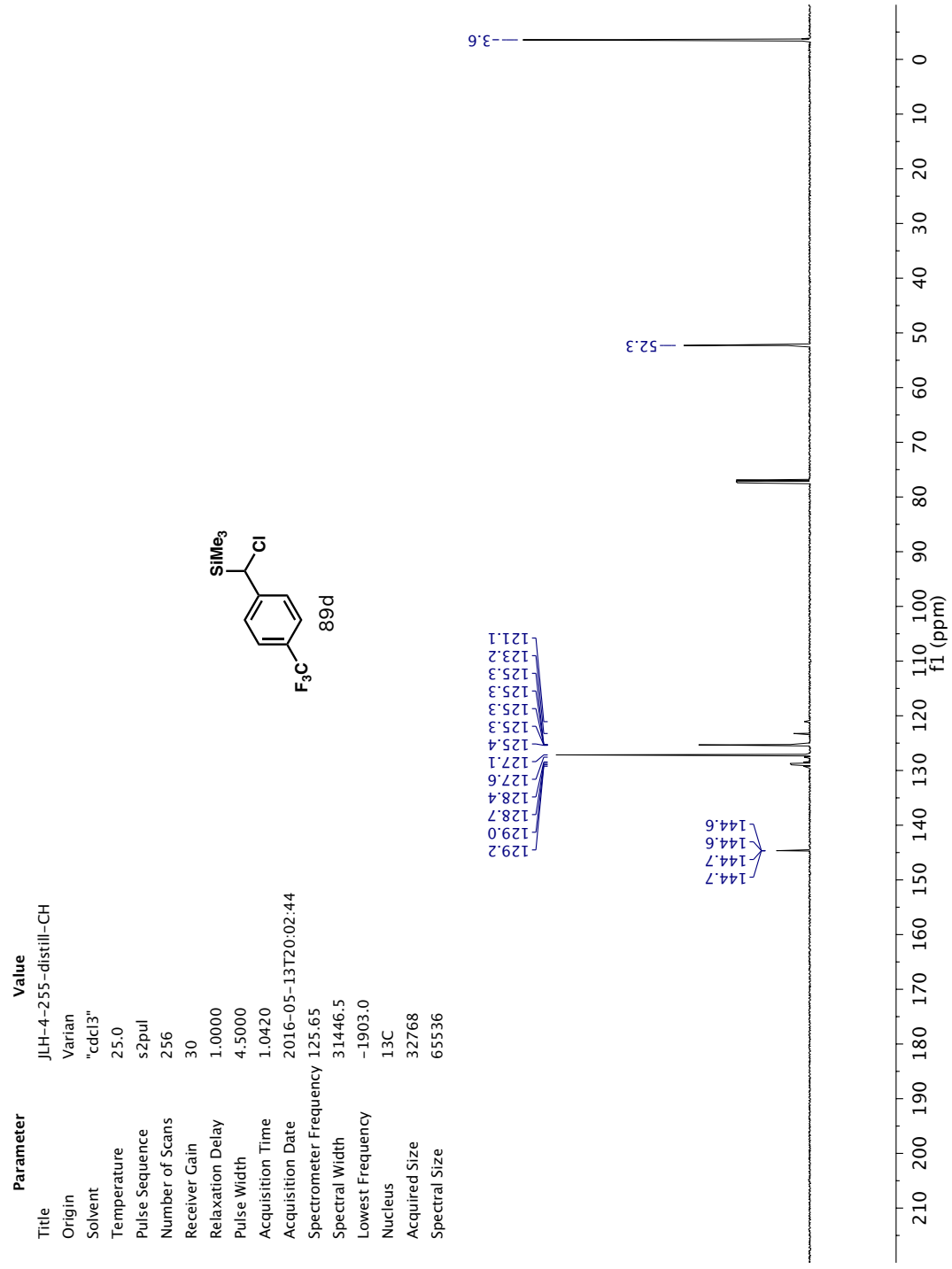

Parameter	Value
Title	JLH-4-255-distill-CH
Origin	Varian
Solvent	"cdcl3"
Temperature	25.0
Pulse Sequence	s2pul
Number of Scans	256
Receiver Gain	30
Relaxation Delay	1.0000
Pulse Width	4.5000
Acquisition Time	1.0420
Acquisition Date	2016-05-13T20:02:44
Spectrometer Frequency	125.65
Spectral Width	31446.5
Lowest Frequency	-1903.0
Nucleus	13C
Acquired Size	32768
Spectral Size	65536

Parameter	Value
Title	JLH-4-255-F-CH
Origin	Varian
Solvent	"cdcl3"
Temperature	25.0
Pulse Sequence	s2pul
Number of Scans	16
Receiver Gain	30
Relaxation Delay	1.0000
Pulse Width	6.3333
Acquisition Time	0.9856
Acquisition Date	2016-10-11T14:22:53
Spectrometer Frequency	282.34
Spectral Width	64935.1
Lowest Frequency	-56468.7
Nucleus	19F
Acquired Size	64000
Spectral Size	131072

Parameter	Value
Title	JLH-4-255-F-C6F6-CH
Origin	Varian
Solvent	"cdcl3"
Temperature	25.0
Pulse Sequence	s2pul
Number of Scans	16
Receiver Gain	30
Relaxation Delay	1.0000
Pulse Width	6.3333
Acquisition Time	0.9856
Acquisition Date	2016-10-11T14:27:04
Spectrometer Frequency	282.34
Spectral Width	64935.1
Lowest Frequency	-56468.7
Nucleus	19F
Acquired Size	64000
Spectral Size	131072

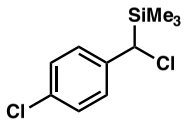

89d
with C_6F_6

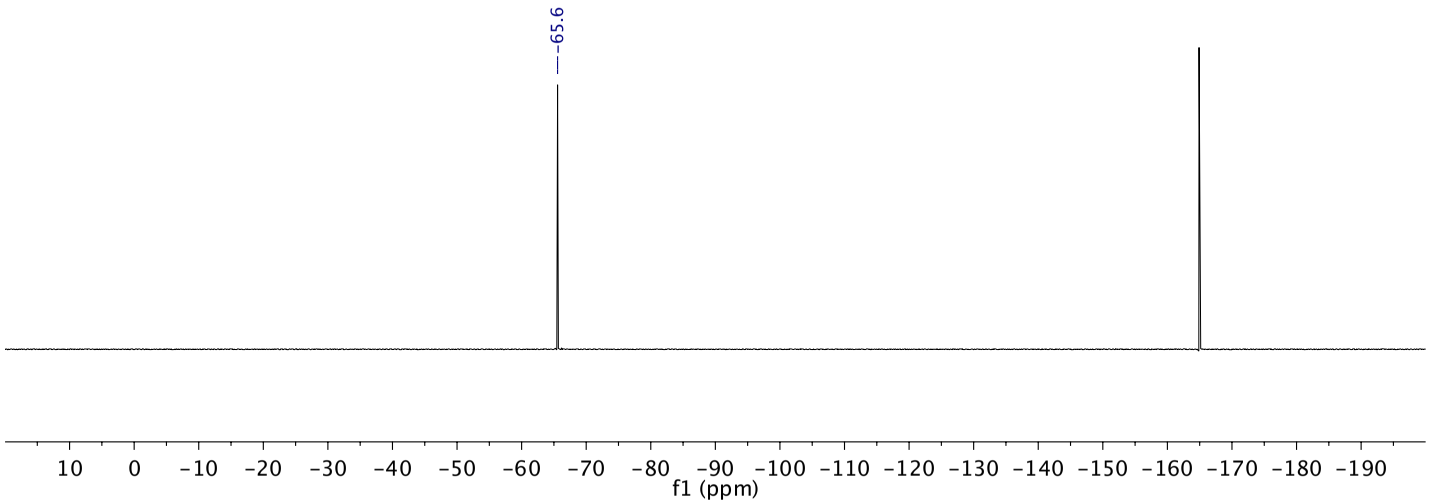

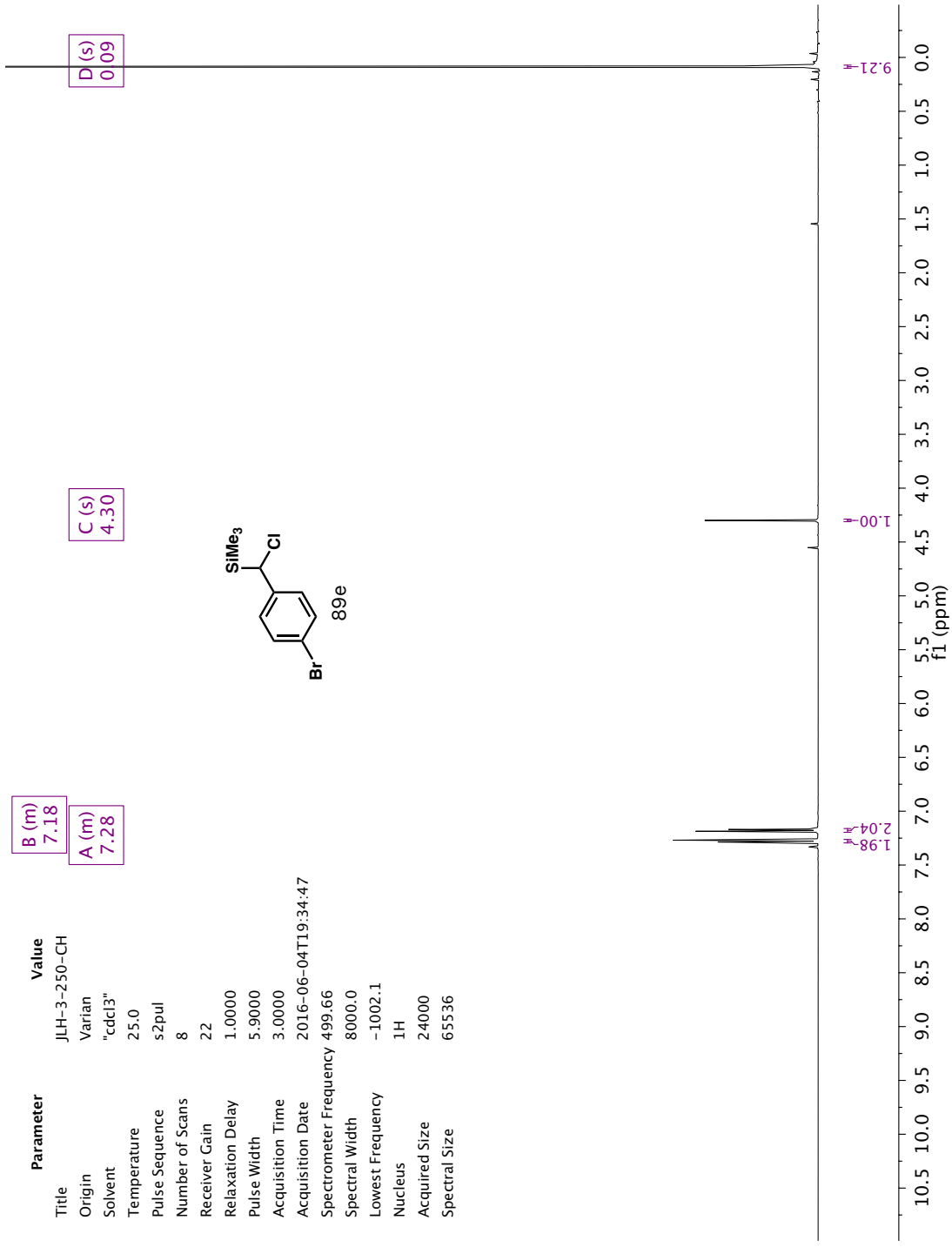
Parameter
Value
Title
JLH-3-250-CH
Origin
Varian
Solvent
"cdcl3"
Temperature
25.0
Pulse Sequence
s2pul
Number of Scans
8
Receiver Gain
22
Relaxation Delay
1.0000
Pulse Width
5.9000
Acquisition Time
3.0000
Acquisition Date
2016-06-04T19:34:47
Spectrometer Frequency
499.66
Spectral Width
8000.0
Lowest Frequency
-1002.1
Nucleus
1H
Acquired Size
24000
Spectral Size
65536
B (m) 7.18
A (m) 7.28
C (s) 4.30
D (s) 0.09
SiMe3
Cl
Br
89e
9.21
1.00
1.98
2.04
10.5 10.0 9.5 9.0 8.5 8.0 7.5 7.0 6.5 6.0 5.5 5.0 4.5 4.0 3.5 3.0 2.5 2.0 1.5 1.0 0.5 0.0
f1 (ppm)

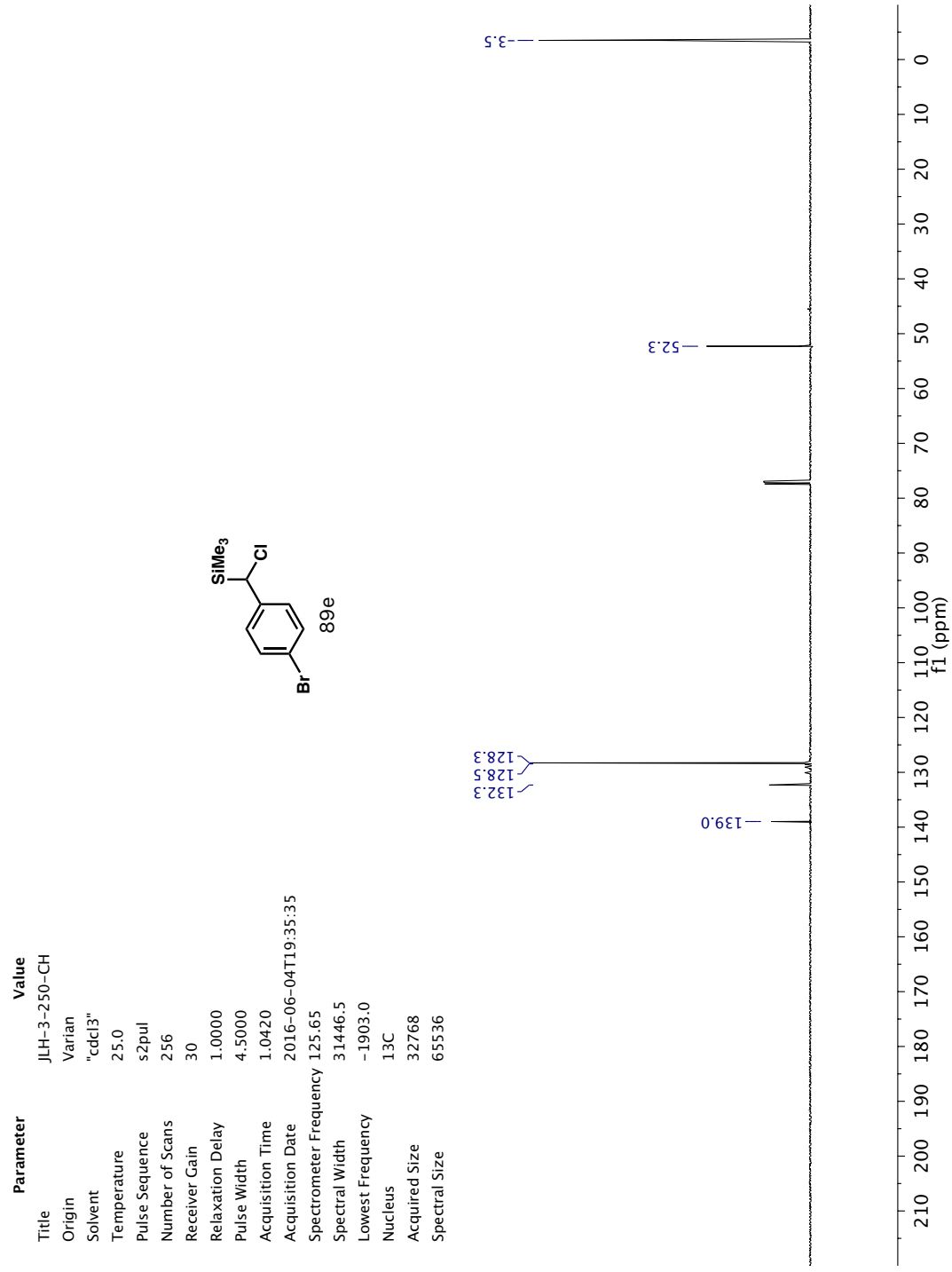

Parameter	Value
Title	JLH-3-250-CH
Origin	Varian
Solvent	"cdcl3"
Temperature	25.0
Pulse Sequence	s2pul
Number of Scans	256
Receiver Gain	30
Relaxation Delay	1.0000
Pulse Width	4.5000
Acquisition Time	1.0420
Acquisition Date	2016-06-04T19:35:35
Spectrometer Frequency	125.65
Spectral Width	31446.5
Lowest Frequency	-1903.0
Nucleus	13C
Acquired Size	32768
Spectral Size	65536

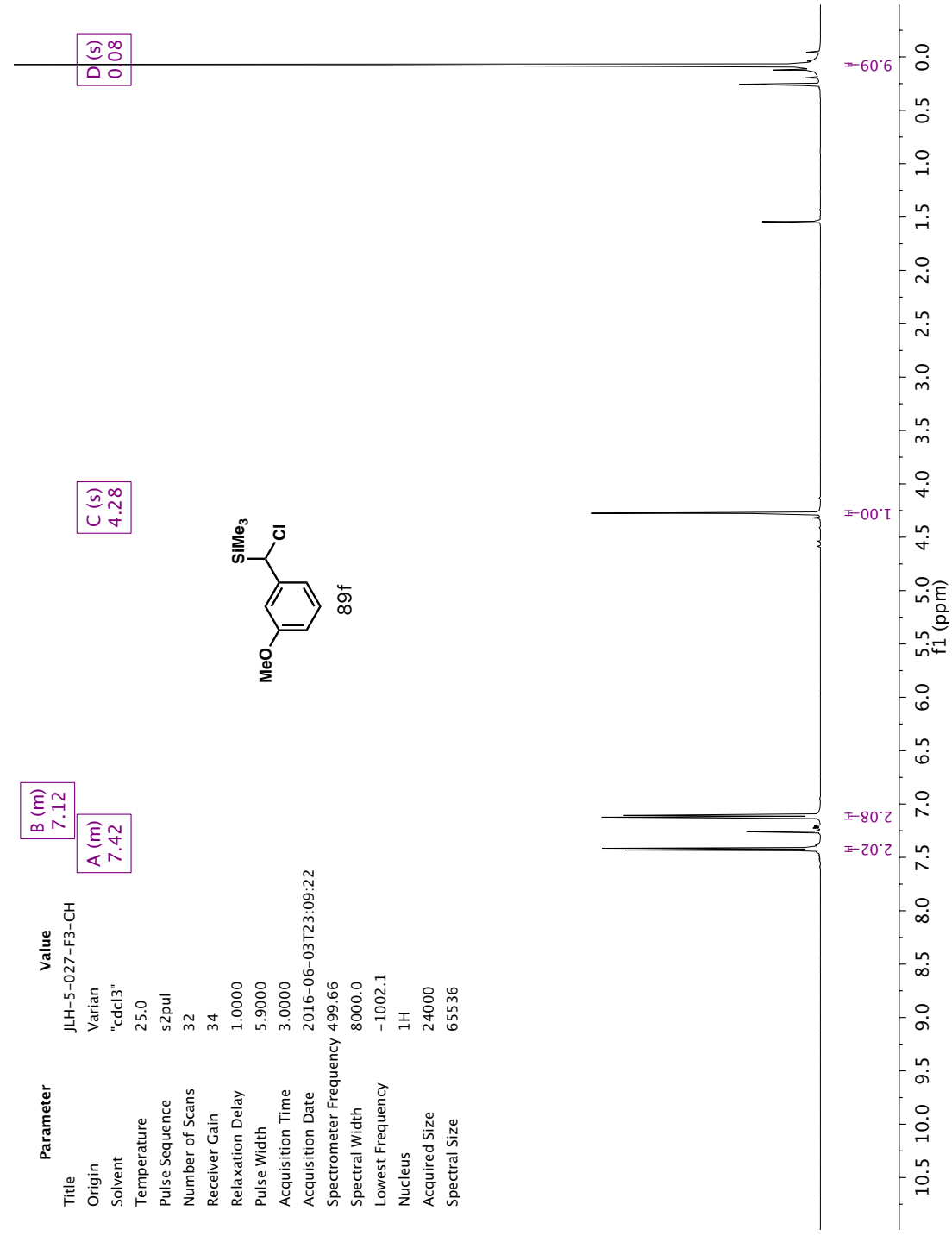
Parameter
Value
Title
JLH-5-027-F3-CH
Origin
Varian
Solvent
"cdcl3"
Temperature
25.0
Pulse Sequence
s2pul
Number of Scans
32
Receiver Gain
34
Relaxation Delay
1.0000
Pulse Width
5.9000
Acquisition Time
3.0000
Acquisition Date
2016-06-03T23:09:22
Spectrometer Frequency
499.66
Spectral Width
8000.0
Lowest Frequency
-1002.1
Nucleus
1H
Acquired Size
24000
Spectral Size
65536
B (m) 7.12
A (m) 7.42
C (s) 4.28
D (s) 0.08
SiMe3
Cl
MeO
89f
9.09
1.00
2.08
2.02
10.5 10.0 9.5 9.0 8.5 8.0 7.5 7.0 6.5 6.0 5.5 5.0 4.5 4.0 3.5 3.0 2.5 2.0 1.5 1.0 0.5 0.0
f1 (ppm)

Parameter	Value
Title	JLH-5-027-F3-CH
Origin	Varian
Solvent	"cdcl3"
Temperature	25.0
Pulse Sequence	s2pul
Number of Scans	1000
Receiver Gain	30
Relaxation Delay	1.0000
Pulse Width	4.5000
Acquisition Time	1.0420
Acquisition Date	2016-06-03T23:11:46
Spectrometer Frequency	125.65
Spectral Width	31446.5
Lowest Frequency	-1903.0
Nucleus	13C
Acquired Size	32768
Spectral Size	65536

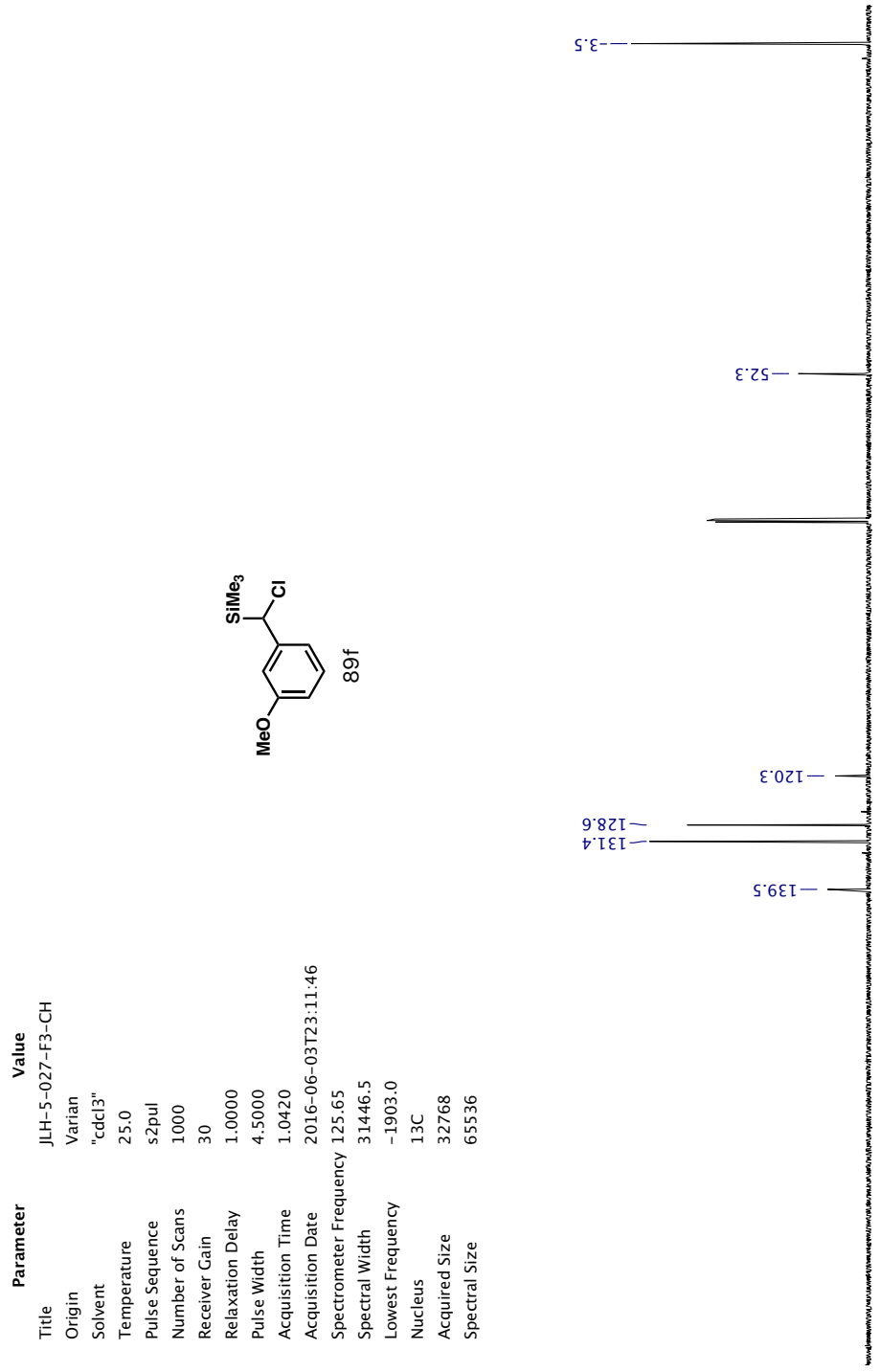

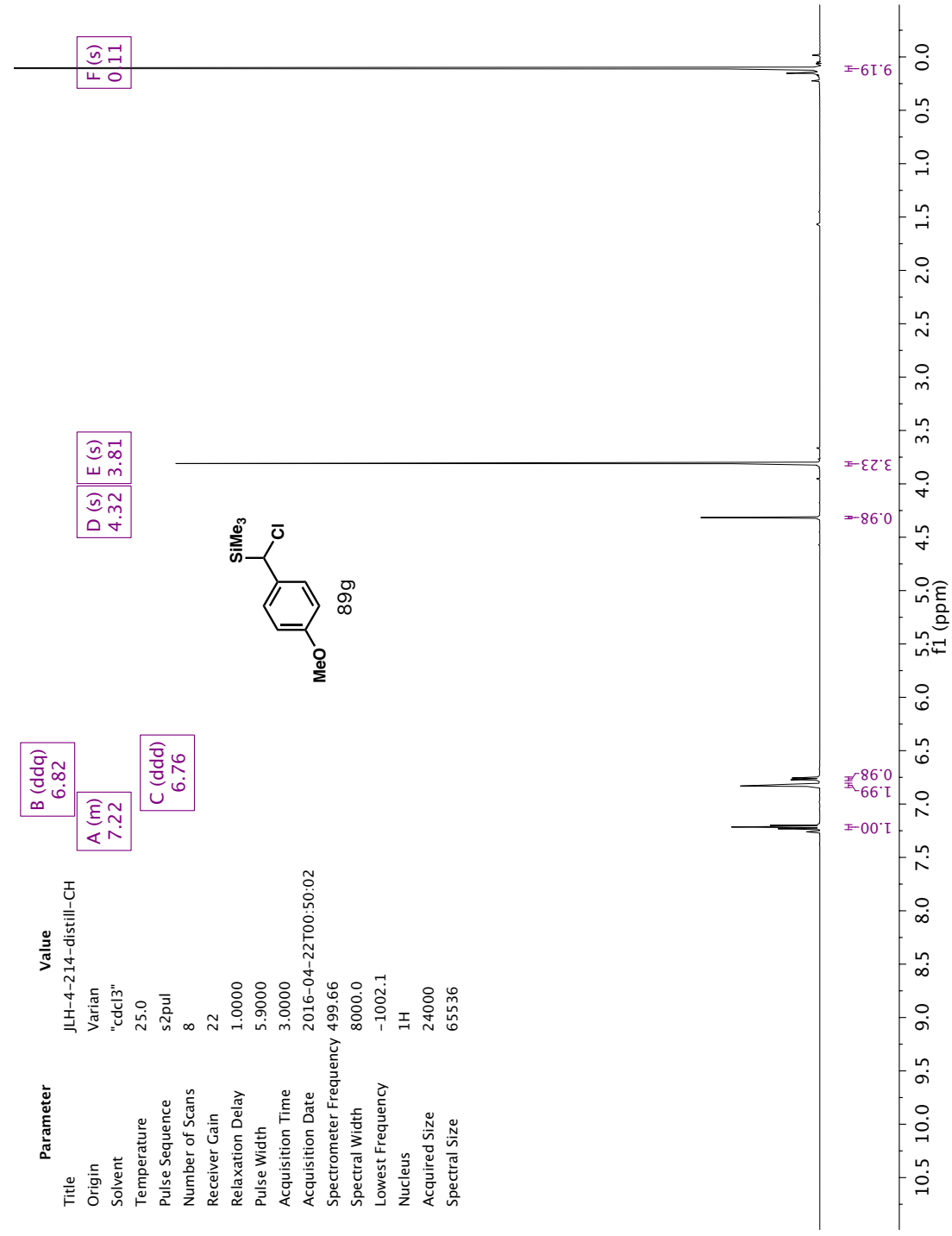
Parameter
Value
Title
JLH-4-214-distill-CH
Origin
Varian
Solvent
"cdcl3"
Temperature
25.0
Pulse Sequence
s2pul
Number of Scans
8
Receiver Gain
22
Relaxation Delay
1.0000
Pulse Width
5.9000
Acquisition Time
3.0000
Acquisition Date
2016-04-22T00:50:02
Spectrometer Frequency
499.66
Spectral Width
8000.0
Lowest Frequency
-1002.1
Nucleus
1H
Acquired Size
24000
Spectral Size
65536
B (ddq) 6.82
A (m) 7.22
C (ddd) 6.76
D (s) 4.32
E (s) 3.81
F (s) 9.11
SiMe3
Cl
MeO
89g
9.19
3.23
0.98
1.00
1.99
0.98
f1 (ppm)

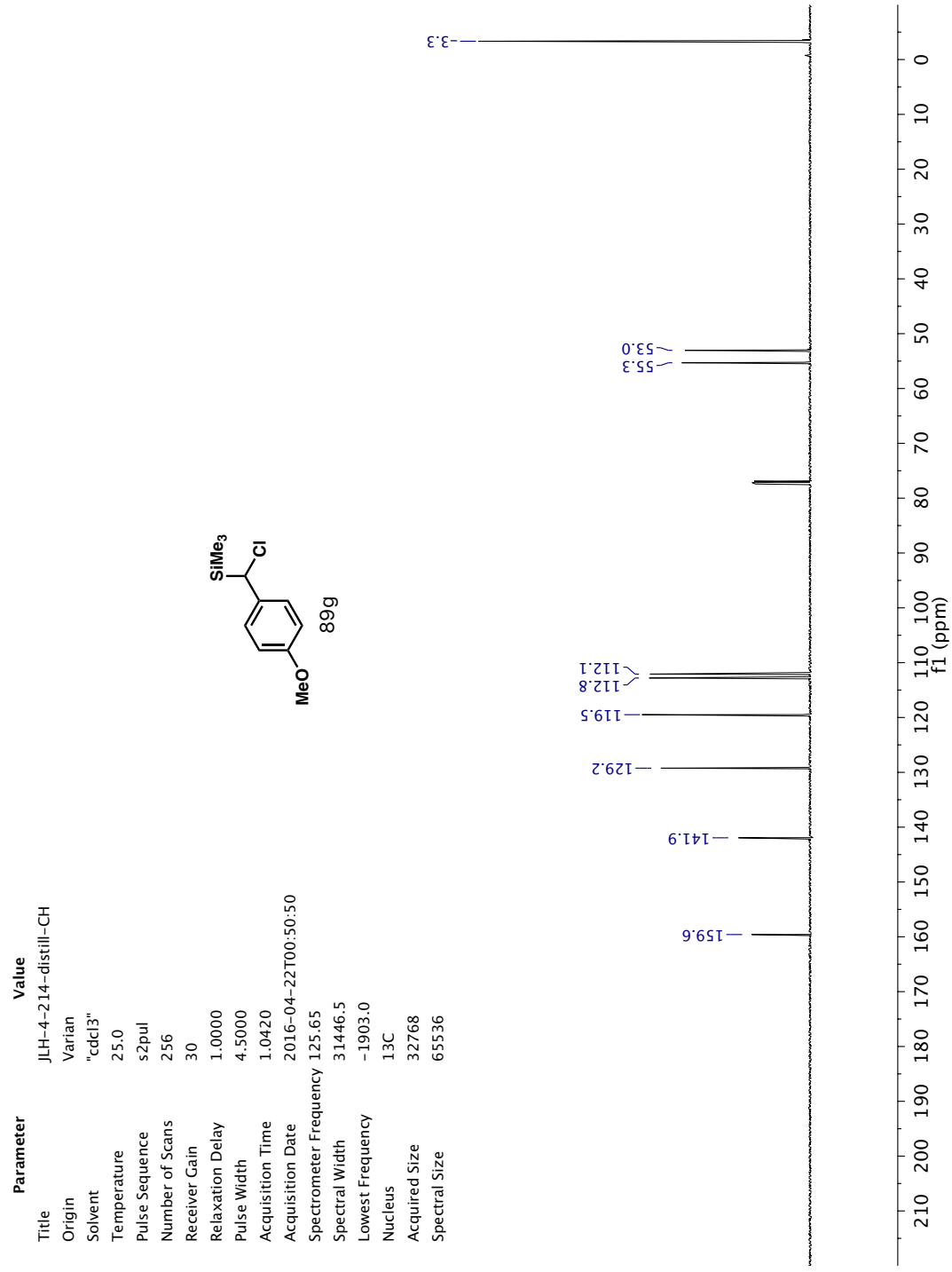
Parameter Value
Title JLH-4-214-distill-CH
Origin Varian
Solvent "cdcl3"
Temperature 25.0
Pulse Sequence s2pul
Number of Scans 256
Receiver Gain 30
Relaxation Delay 1.0000
Pulse Width 4.5000
Acquisition Time 1.0420
Acquisition Date 2016-04-22T00:50:50
Spectrometer Frequency 125.65
Spectral Width 31446.5
Lowest Frequency -1903.0
Nucleus 13C
Acquired Size 32768
Spectral Size 65536
SiMe3
Cl
MeO
89g
-3.3
53.0
55.3
112.1
112.8
119.5
129.2
141.9
159.6
f1 (ppm)

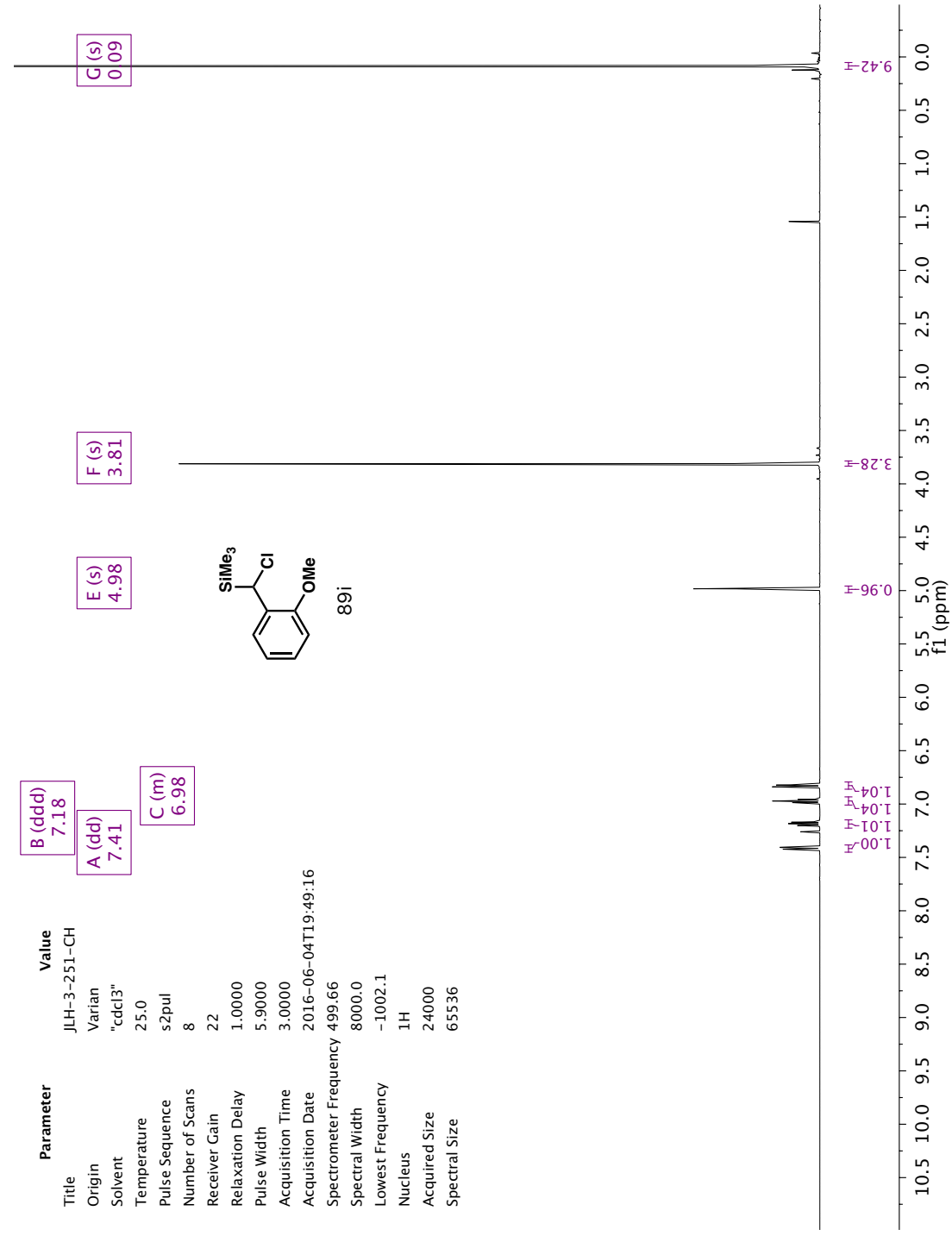
Parameter Value
Title JLH-3-251-CH
Origin Varian
Solvent "cdcl3"
Temperature 25.0
Pulse Sequence s2pul
Number of Scans 8
Receiver Gain 22
Relaxation Delay 1.0000
Pulse Width 5.9000
Acquisition Time 3.0000
Acquisition Date 2016-06-04T19:49:16
Spectrometer Frequency 499.66
Spectral Width 8000.0
Lowest Frequency -1002.1
Nucleus 1H
Acquired Size 24000
Spectral Size 65536
B (ddd) 7.18
A (dd) 7.41
C (m) 6.98
E (s) 4.98
F (s) 3.81
G (s) 0.09
SiMe3
Cl
OMe
89i
9.42
3.28
0.96
1.00
1.01
1.04
1.04
10.5 10.0 9.5 9.0 8.5 8.0 7.5 7.0 6.5 6.0 5.5 5.0 4.5 4.0 3.5 3.0 2.5 2.0 1.5 1.0 0.5 0.0
f1 (ppm)

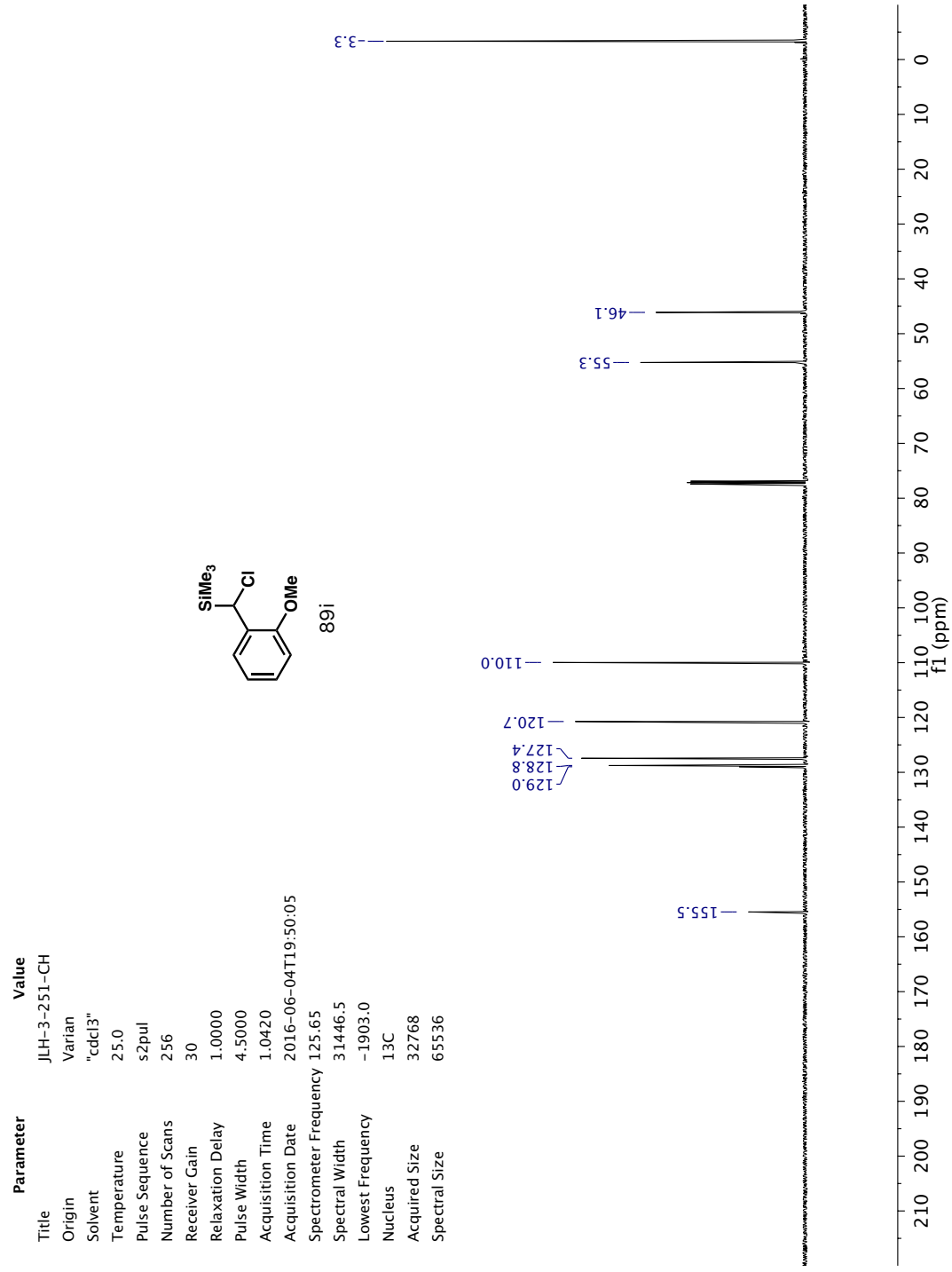
Parameter Value
Title JLH-3-251-CH
Origin Varian
Solvent "cdcl3"
Temperature 25.0
Pulse Sequence s2pul
Number of Scans 256
Receiver Gain 30
Relaxation Delay 1.0000
Pulse Width 4.5000
Acquisition Time 1.0420
Acquisition Date 2016-06-04T19:50:05
Spectrometer Frequency 125.65
Spectral Width 31446.5
Lowest Frequency -1903.0
Nucleus 13C
Acquired Size 32768
Spectral Size 65536
SiMe3
Cl
OMe
89i
-3.3
46.1
55.3
110.0
120.7
129.0
128.8
127.4
155.5
f1 (ppm)

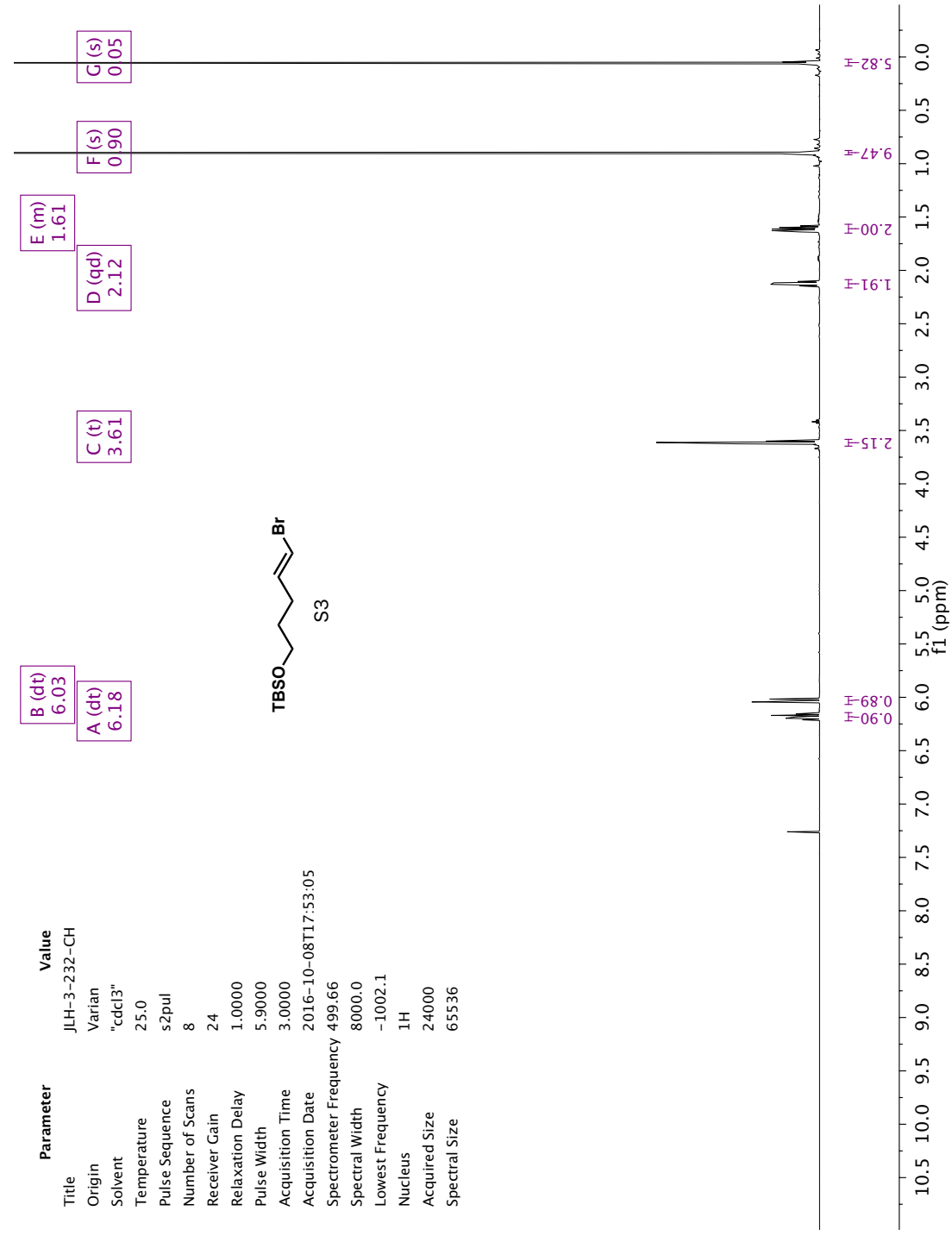

Parameter	Value
Title	JLH-3-232-CH
Origin	Varian
Solvent	"cdcl3"
Temperature	25.0
Pulse Sequence	s2pul
Number of Scans	8
Receiver Gain	24
Relaxation Delay	1.0000
Pulse Width	5.9000
Acquisition Time	3.0000
Acquisition Date	2016-10-08T17:53:05
Spectrometer Frequency	499.66
Spectral Width	8000.0
Lowest Frequency	-1002.1
Nucleus	1H
Acquired Size	24000
Spectral Size	65536

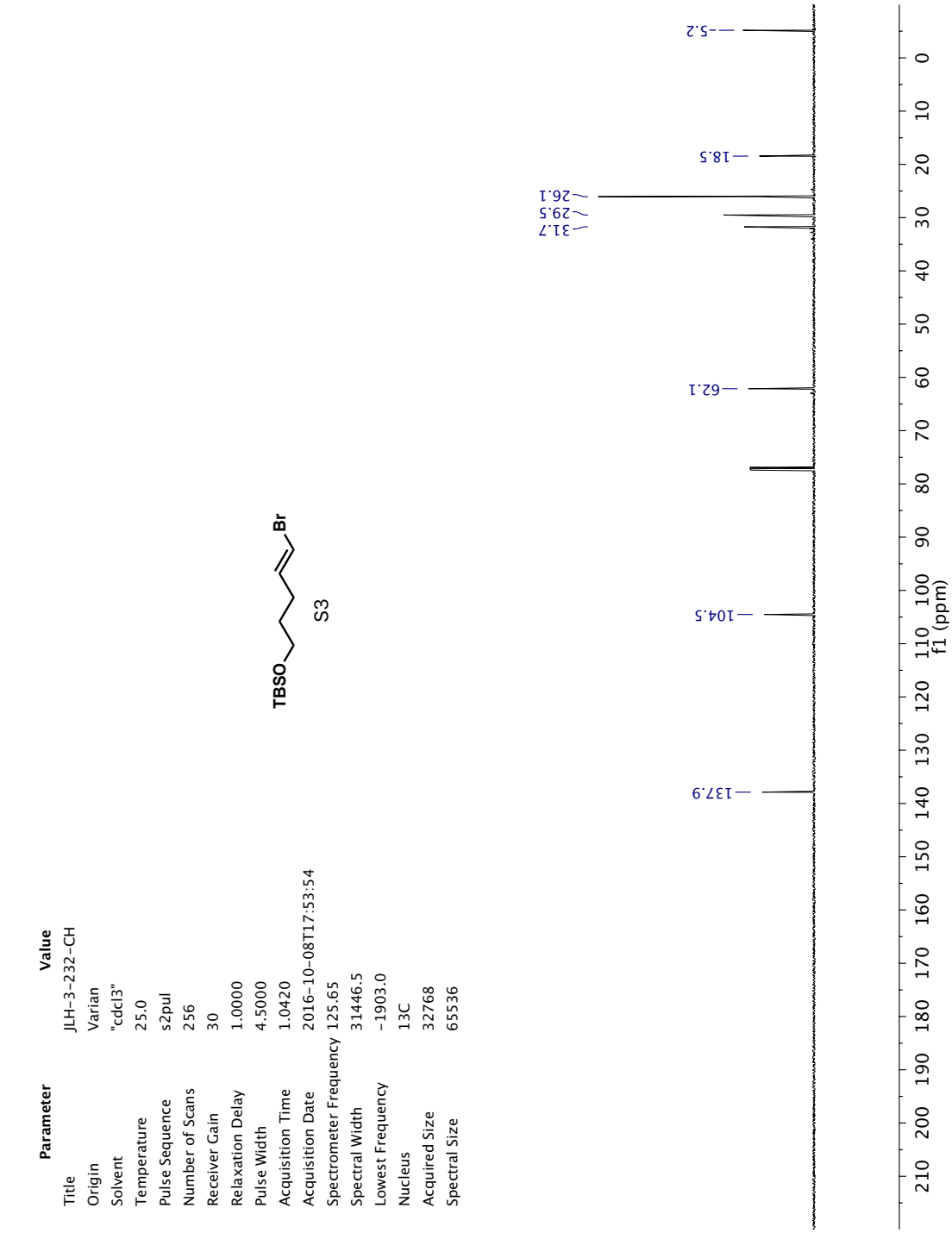
Parameter Value
Title JLH-3-232-CH
Origin Varian
Solvent "cdcl3"
Temperature 25.0
Pulse Sequence s2pul
Number of Scans 256
Receiver Gain 30
Relaxation Delay 1.0000
Pulse Width 4.5000
Acquisition Time 1.0420
Acquisition Date 2016-10-08T17:53:54
Spectrometer Frequency 125.65
Spectral Width 31446.5
Lowest Frequency -1903.0
Nucleus 13C
Acquired Size 32768
Spectral Size 65536
TBSO
Br
S3
137.9
104.5
62.1
31.7
29.5
26.1
18.5
-5.2
f1 (ppm)

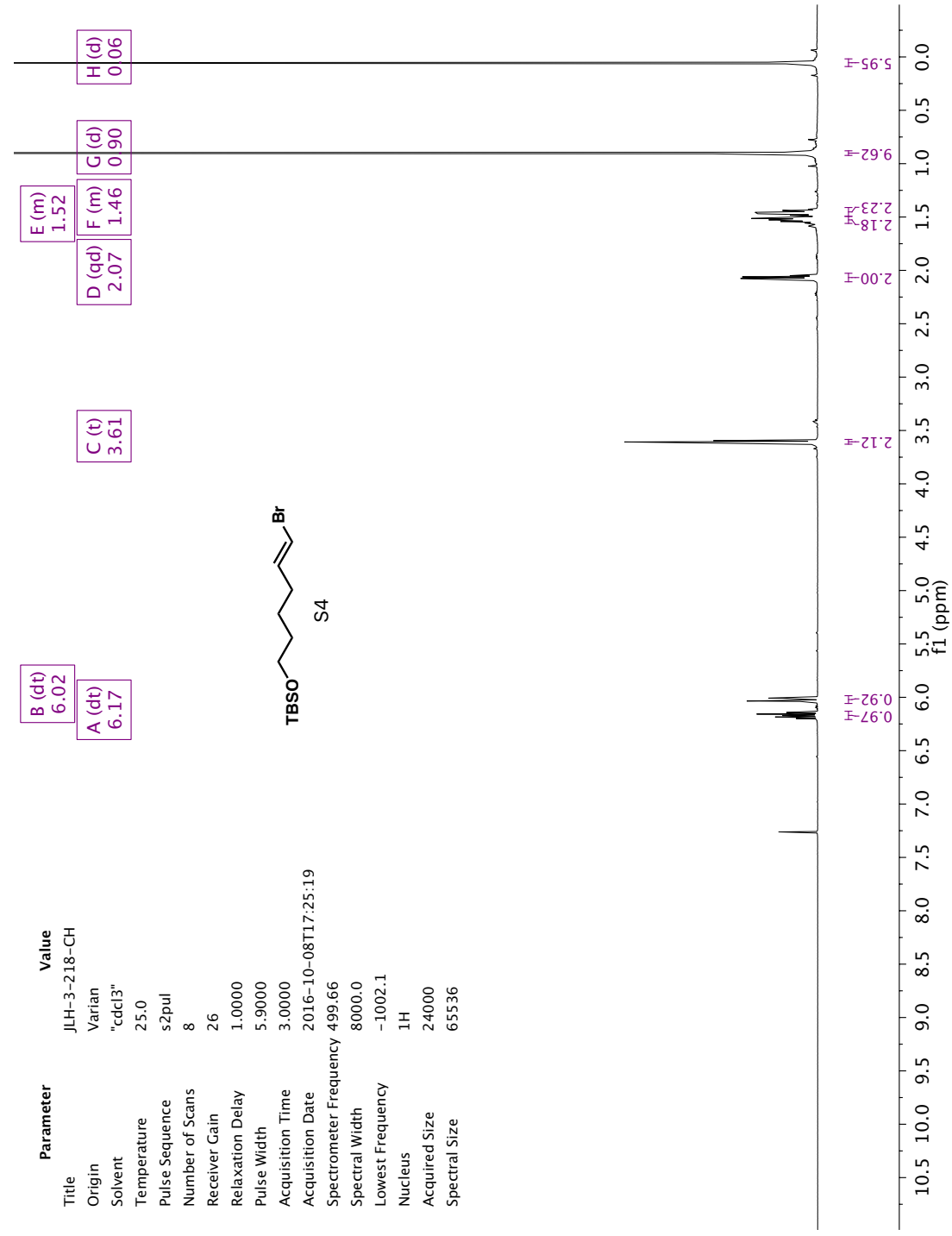
Parameter Value
Title JLH-3-218-CH
Origin Varian
Solvent "cdcl3"
Temperature 25.0
Pulse Sequence s2pul
Number of Scans 8
Receiver Gain 26
Relaxation Delay 1.0000
Pulse Width 5.9000
Acquisition Time 3.0000
Acquisition Date 2016-10-08T17:25:19
Spectrometer Frequency 499.66
Spectral Width 8000.0
Lowest Frequency -1002.1
Nucleus 1H
Acquired Size 24000
Spectral Size 65536
B (dt) 6.02
A (dt) 6.17
C (t) 3.61
D (qd) 2.07
E (m) 1.52
F (m) 1.46
G (d) 0.90
H (d) 0.06
TBSO
Br
S4
0.97
0.92
2.12
2.00
2.18
2.23
9.62
5.95
f1 (ppm)

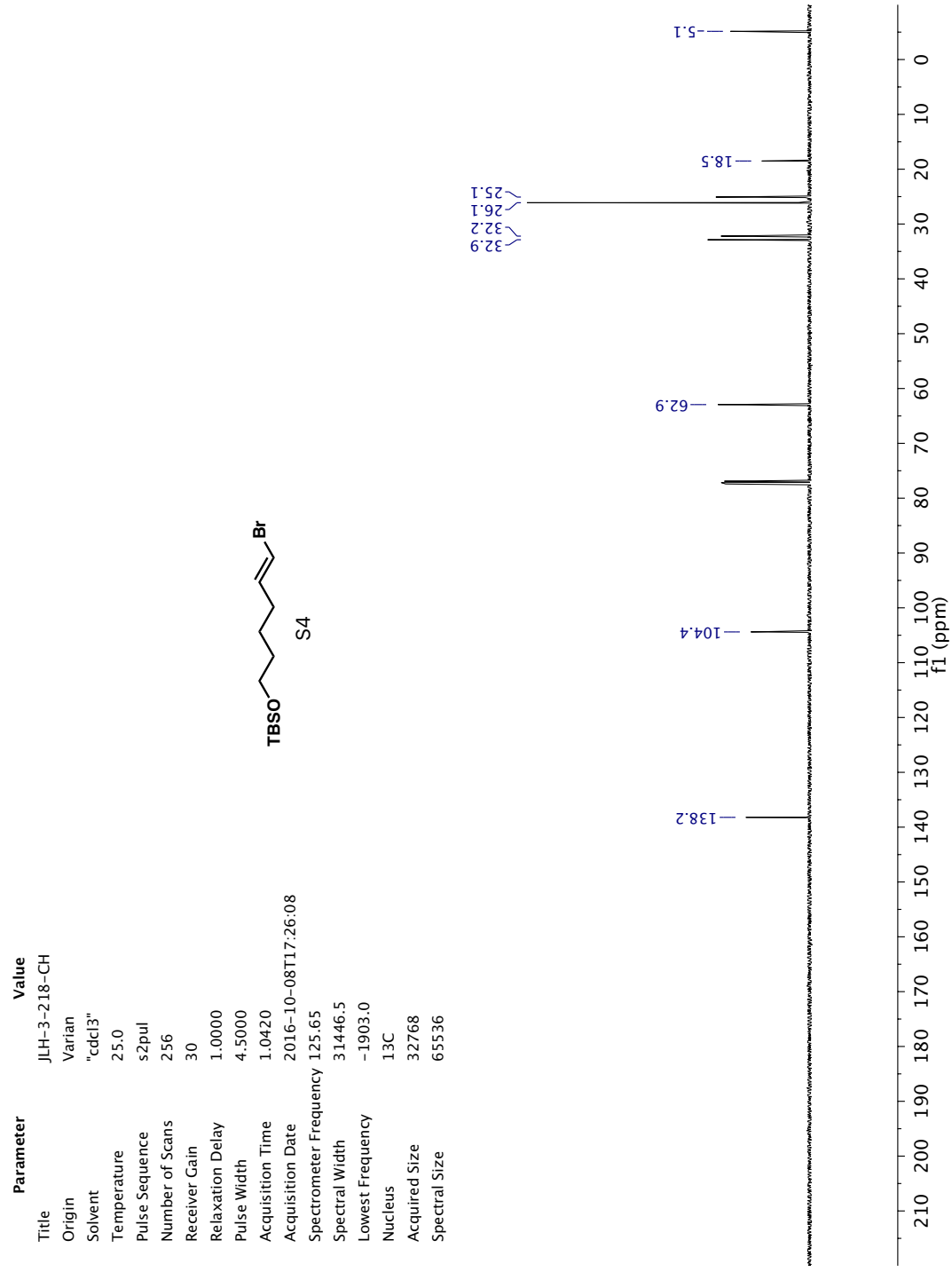
Parameter Value
Title JLH-3-218-CH
Origin Varian
Solvent "cdcl3"
Temperature 25.0
Pulse Sequence s2pul
Number of Scans 256
Receiver Gain 30
Relaxation Delay 1.0000
Pulse Width 4.5000
Acquisition Time 1.0420
Acquisition Date 2016-10-08T17:26:08
Spectrometer Frequency 125.65
Spectral Width 31446.5
Lowest Frequency -1903.0
Nucleus 13C
Acquired Size 32768
Spectral Size 65536
TBSO
Br
S4
138.2
104.4
62.9
32.9
32.2
26.1
25.1
18.5
-5.1
f1 (ppm)

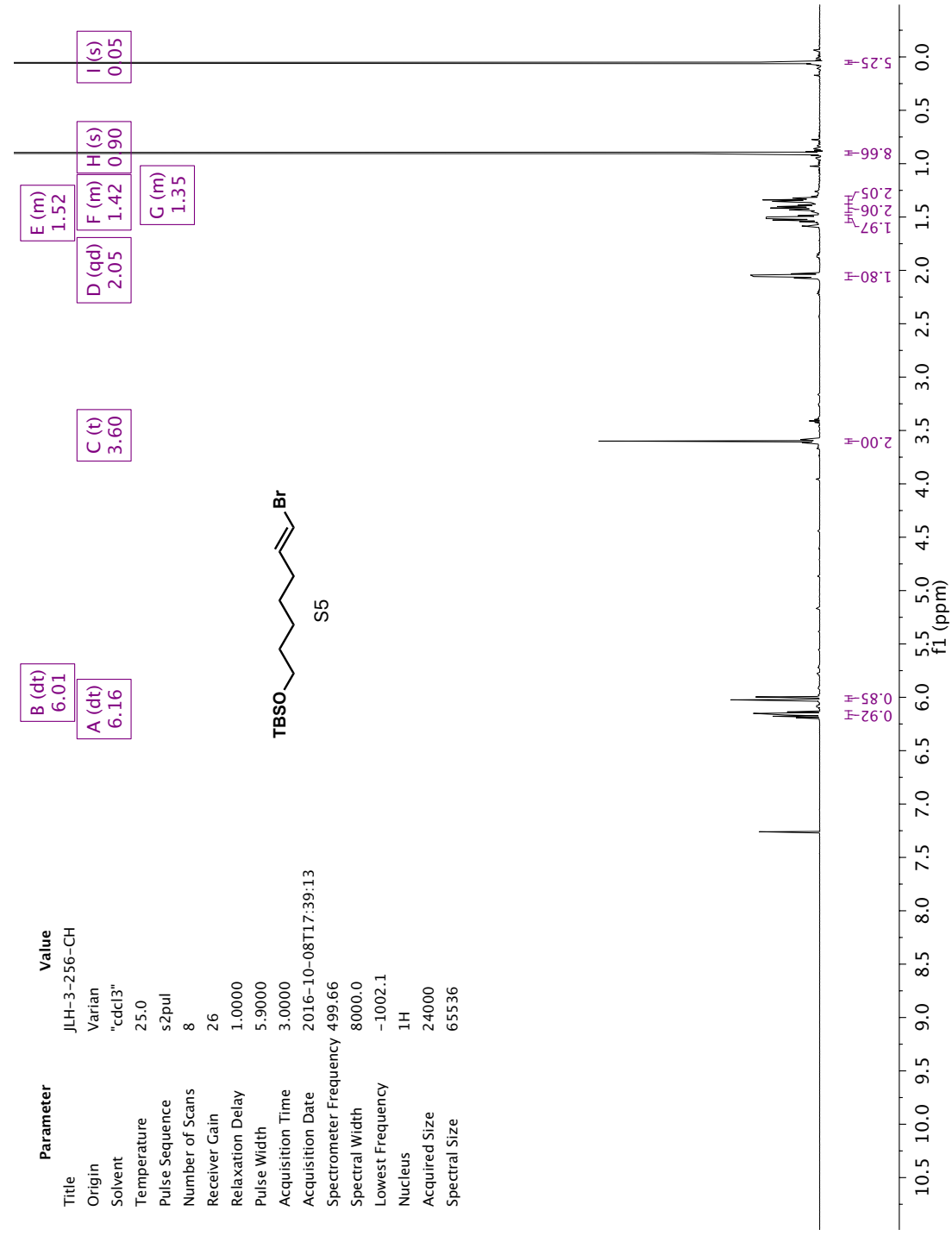
Parameter Value
Title JLH-3-256-CH
Origin Varian
Solvent "cdcl3"
Temperature 25.0
Pulse Sequence s2pul
Number of Scans 8
Receiver Gain 26
Relaxation Delay 1.0000
Pulse Width 5.9000
Acquisition Time 3.0000
Acquisition Date 2016-10-08T17:39:13
Spectrometer Frequency 499.66
Spectral Width 8000.0
Lowest Frequency -1002.1
Nucleus 1H
Acquired Size 24000
Spectral Size 65536
B (dt) 6.01
A (dt) 6.16
C (t) 3.60
E (m) 1.52
D (qd) 2.05
F (m) 1.42
G (m) 1.35
H (s) 0.90
I (s) 0.05
TBSO
Br
S5
0.92
0.85
2.00
1.80
1.97
2.06
2.05
8.66
5.25
f1 (ppm)

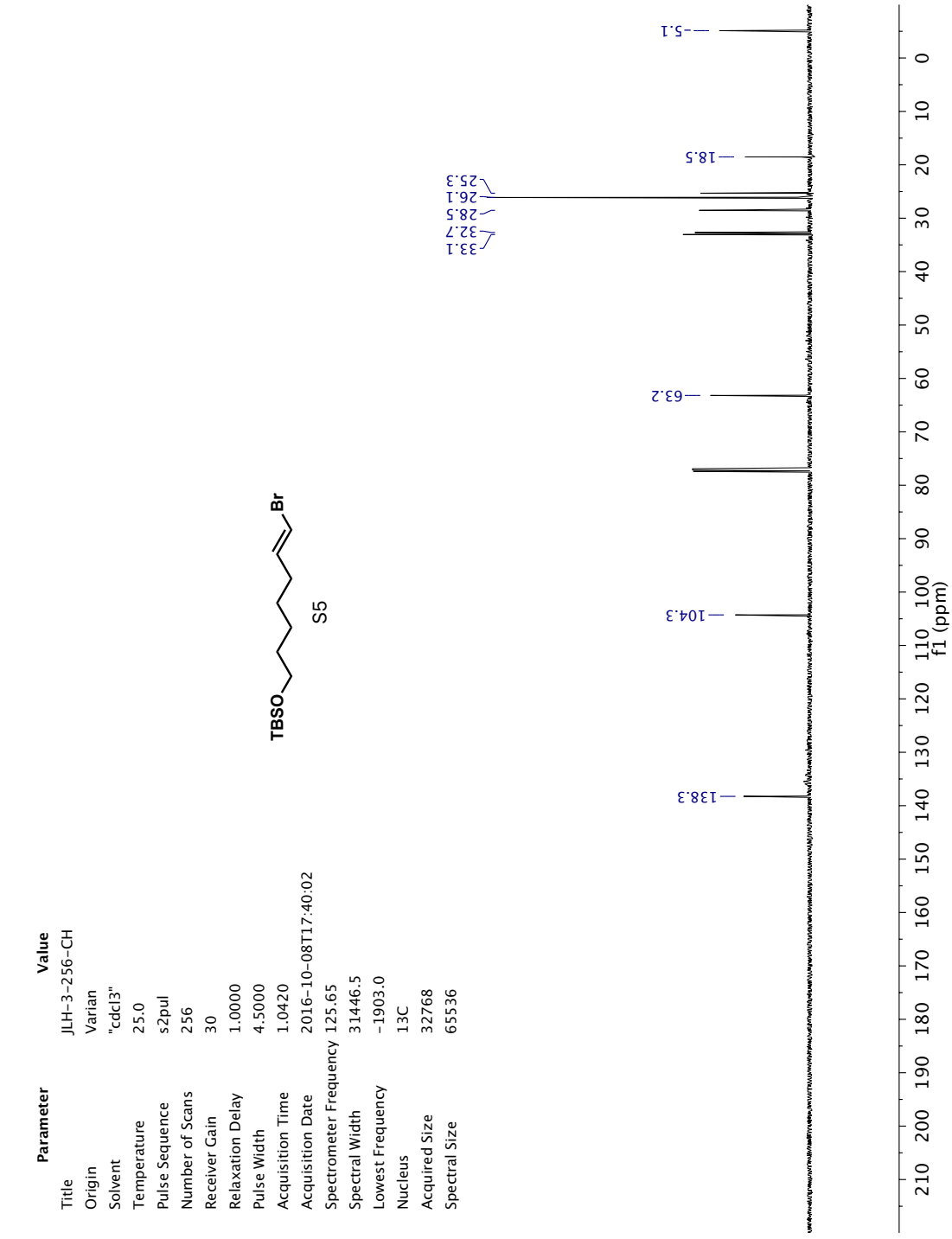
Parameter Value
Title JLH-3-256-CH
Origin Varian
Solvent "cdcl3"
Temperature 25.0
Pulse Sequence s2pul
Number of Scans 256
Receiver Gain 30
Relaxation Delay 1.0000
Pulse Width 4.5000
Acquisition Time 1.0420
Acquisition Date 2016-10-08T17:40:02
Spectrometer Frequency 125.65
Spectral Width 31446.5
Lowest Frequency -1903.0
Nucleus 13C
Acquired Size 32768
Spectral Size 65536
TBSO
Br
S5
138.3
104.3
63.2
33.1
32.7
28.5
26.1
25.3
18.5
-5.1
f1 (ppm)

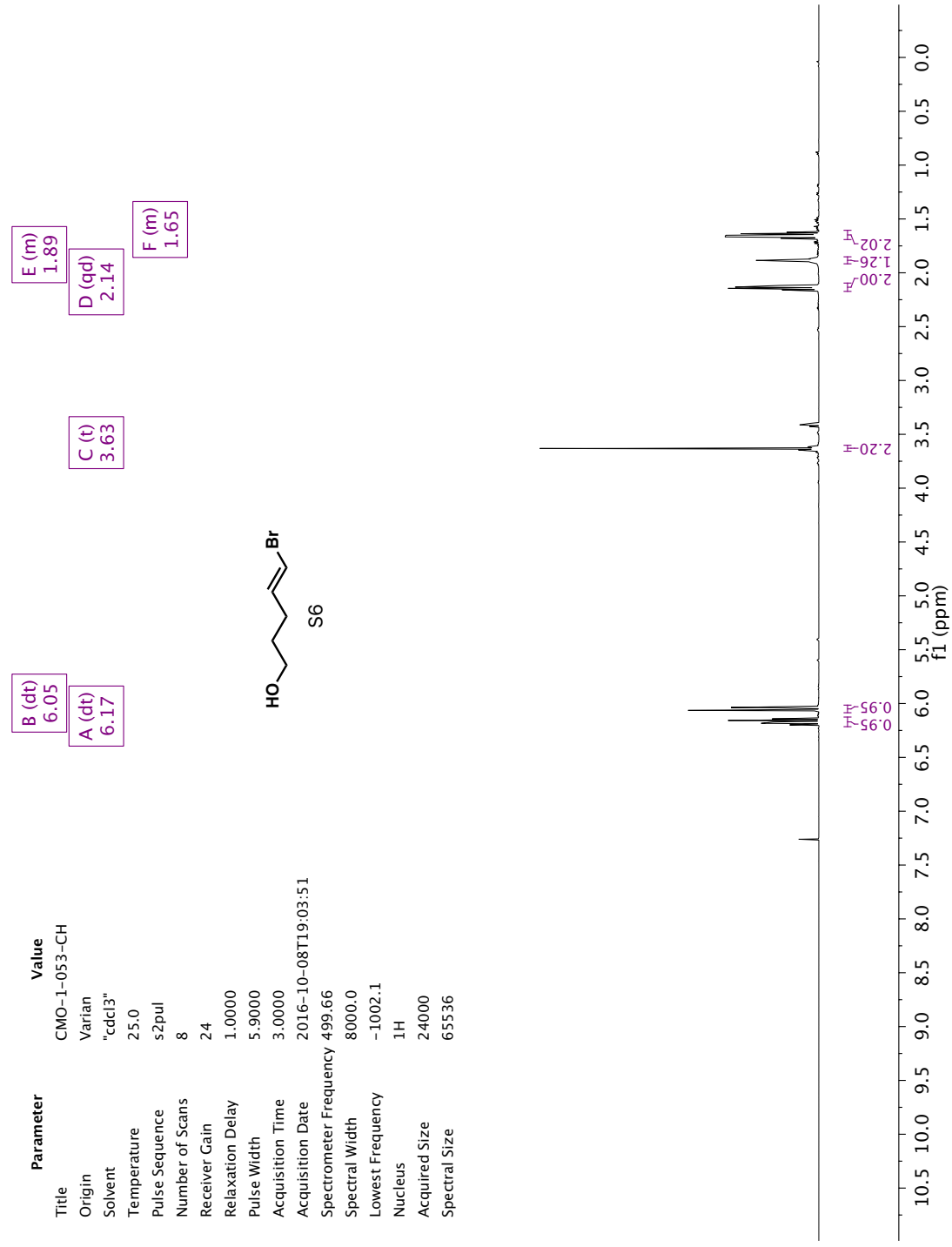
B (dt) 6.05
A (dt) 6.17
C (t) 3.63
E (m) 1.89
D (qd) 2.14
F (m) 1.65
HO
Br
S6
Parameter Value
Title CMO-1-053-CH
Origin Varian
Solvent "cdcl3"
Temperature 25.0
Pulse Sequence s2pul
Number of Scans 8
Receiver Gain 24
Relaxation Delay 1.0000
Pulse Width 5.9000
Acquisition Time 3.0000
Acquisition Date 2016-10-08T19:03:51
Spectrometer Frequency 499.66
Spectral Width 8000.0
Lowest Frequency -1002.1
Nucleus 1H
Acquired Size 24000
Spectral Size 65536
0.95
0.95
2.20
2.00
1.26
2.02
10.5 10.0 9.5 9.0 8.5 8.0 7.5 7.0 6.5 6.0 5.5 5.0 4.5 4.0 3.5 3.0 2.5 2.0 1.5 1.0 0.5 0.0
f1 (ppm)

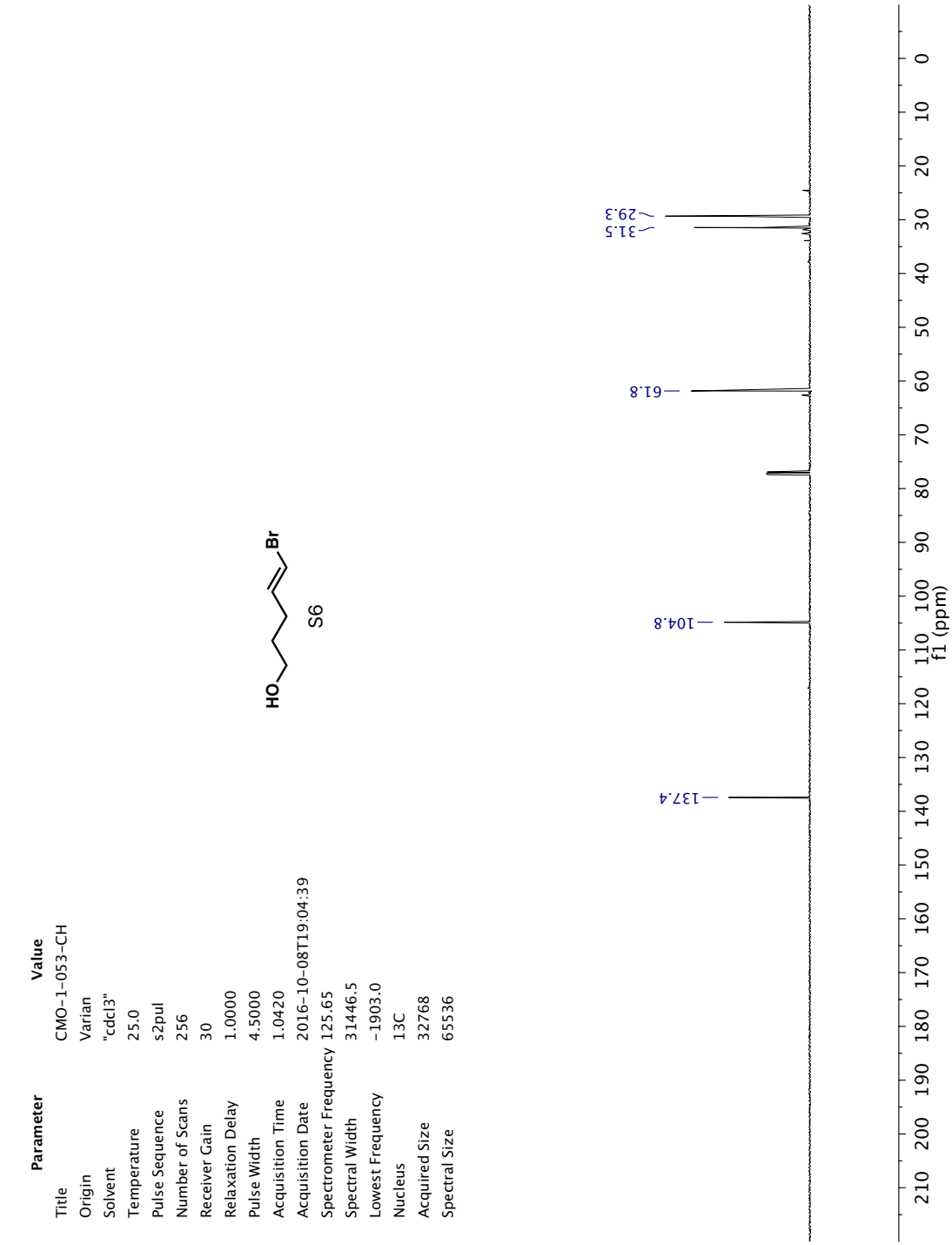
Parameter Value
Title CMO-1-053-CH
Origin Varian
Solvent "cdcl3"
Temperature 25.0
Pulse Sequence s2pul
Number of Scans 256
Receiver Gain 30
Relaxation Delay 1.0000
Pulse Width 4.5000
Acquisition Time 1.0420
Acquisition Date 2016-10-08T19:04:39
Spectrometer Frequency 125.65
Spectral Width 31446.5
Lowest Frequency -1903.0
Nucleus 13C
Acquired Size 32768
Spectral Size 65536
HO
Br
S6
137.4
104.8
61.8
31.5
29.3
f1 (ppm)

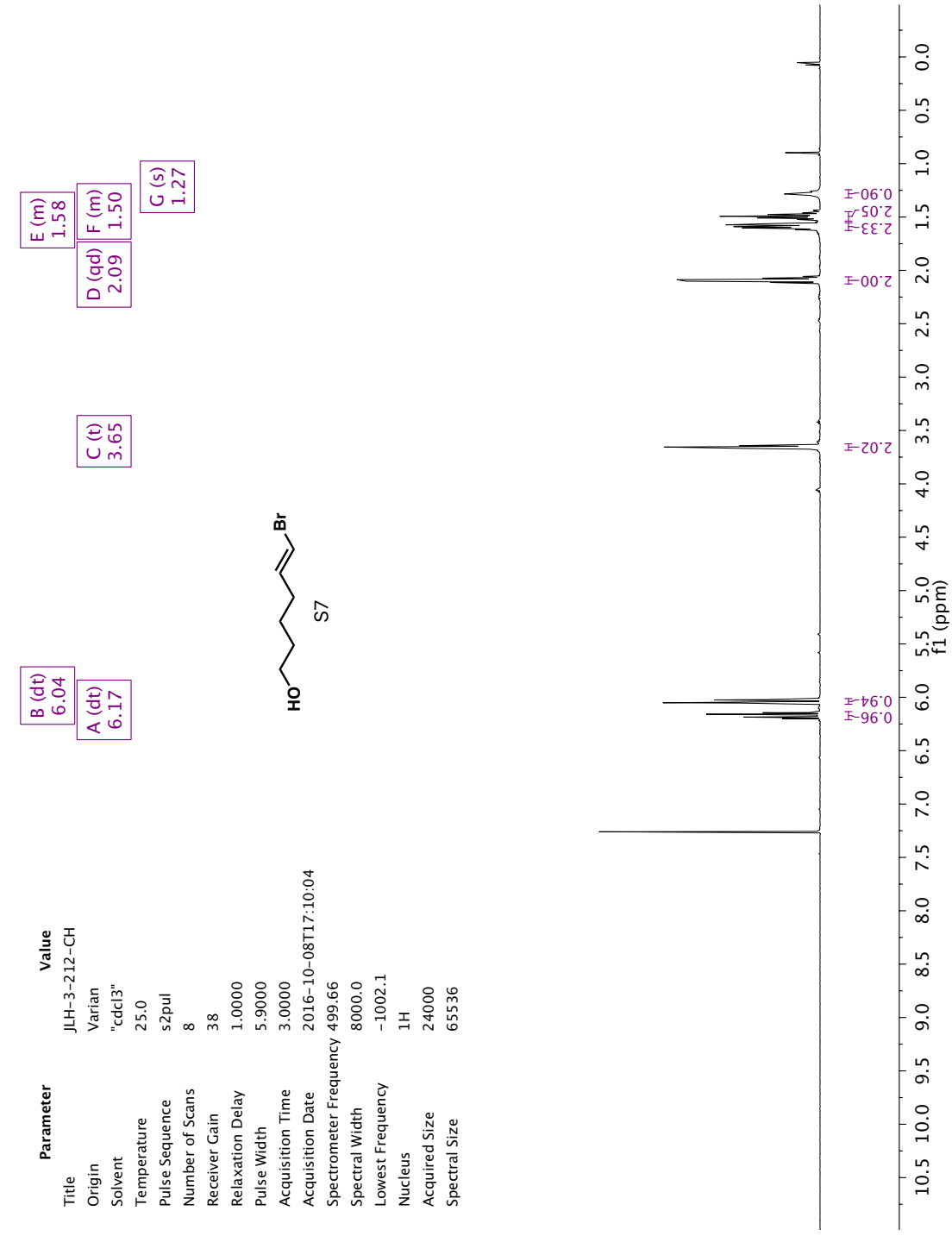

Parameter	Value
Title	JLH-3-212-CH
Origin	Varian
Solvent	"cdcl3"
Temperature	25.0
Pulse Sequence	s2pul
Number of Scans	8
Receiver Gain	38
Relaxation Delay	1.0000
Pulse Width	5.9000
Acquisition Time	3.0000
Acquisition Date	2016-10-08T17:10:04
Spectrometer Frequency	499.66
Spectral Width	8000.0
Lowest Frequency	-1002.1
Nucleus	1H
Acquired Size	24000
Spectral Size	65536

Parameter	Value
Title	JLH-3-212-CH
Origin	Varian
Solvent	"cdcl3"
Temperature	25.0
Pulse Sequence	s2pul
Number of Scans	256
Receiver Gain	30
Relaxation Delay	1.0000
Pulse Width	4.5000
Acquisition Time	1.0420
Acquisition Date	2016-10-08T17:10:53
Spectrometer Frequency	125.65
Spectral Width	31446.5
Lowest Frequency	-1903.0
Nucleus	13C
Acquired Size	32768
Spectral Size	65536

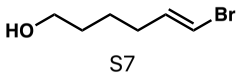

S7

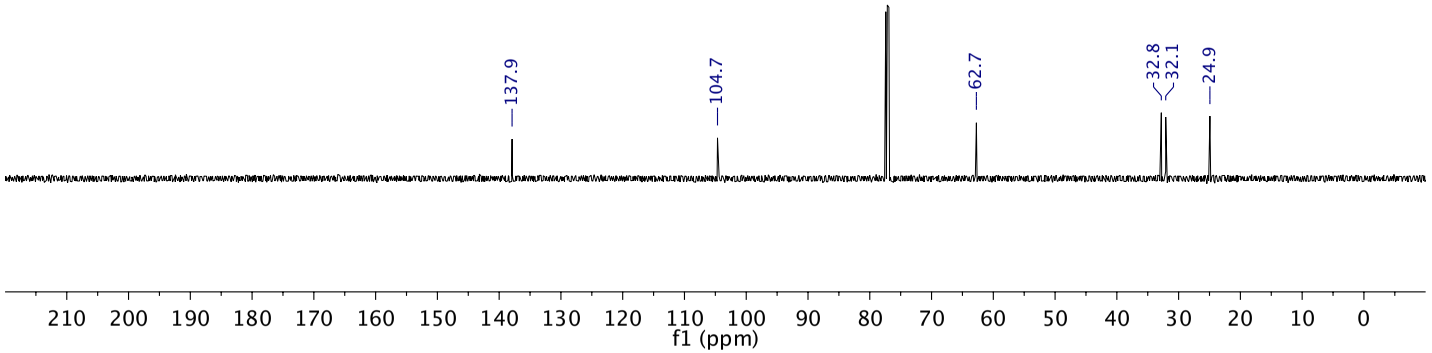

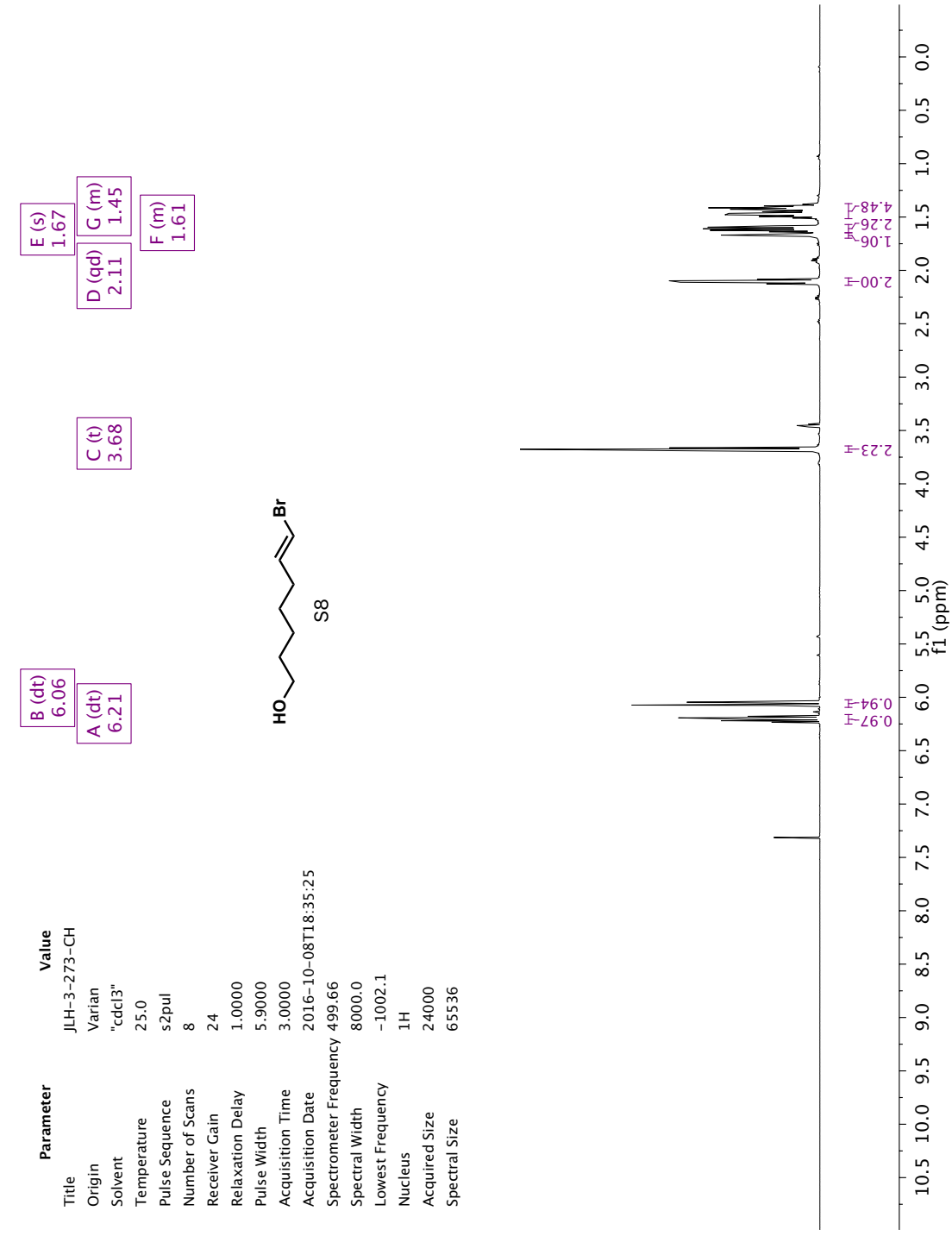

Parameter	Value
Title	JLH-3-273-CH
Origin	Varian
Solvent	"cdcl3"
Temperature	25.0
Pulse Sequence	s2pul
Number of Scans	8
Receiver Gain	24
Relaxation Delay	1.0000
Pulse Width	5.9000
Acquisition Time	3.0000
Acquisition Date	2016-10-08T18:35:25
Spectrometer Frequency	499.66
Spectral Width	8000.0
Lowest Frequency	-1002.1
Nucleus	1H
Acquired Size	24000
Spectral Size	65536

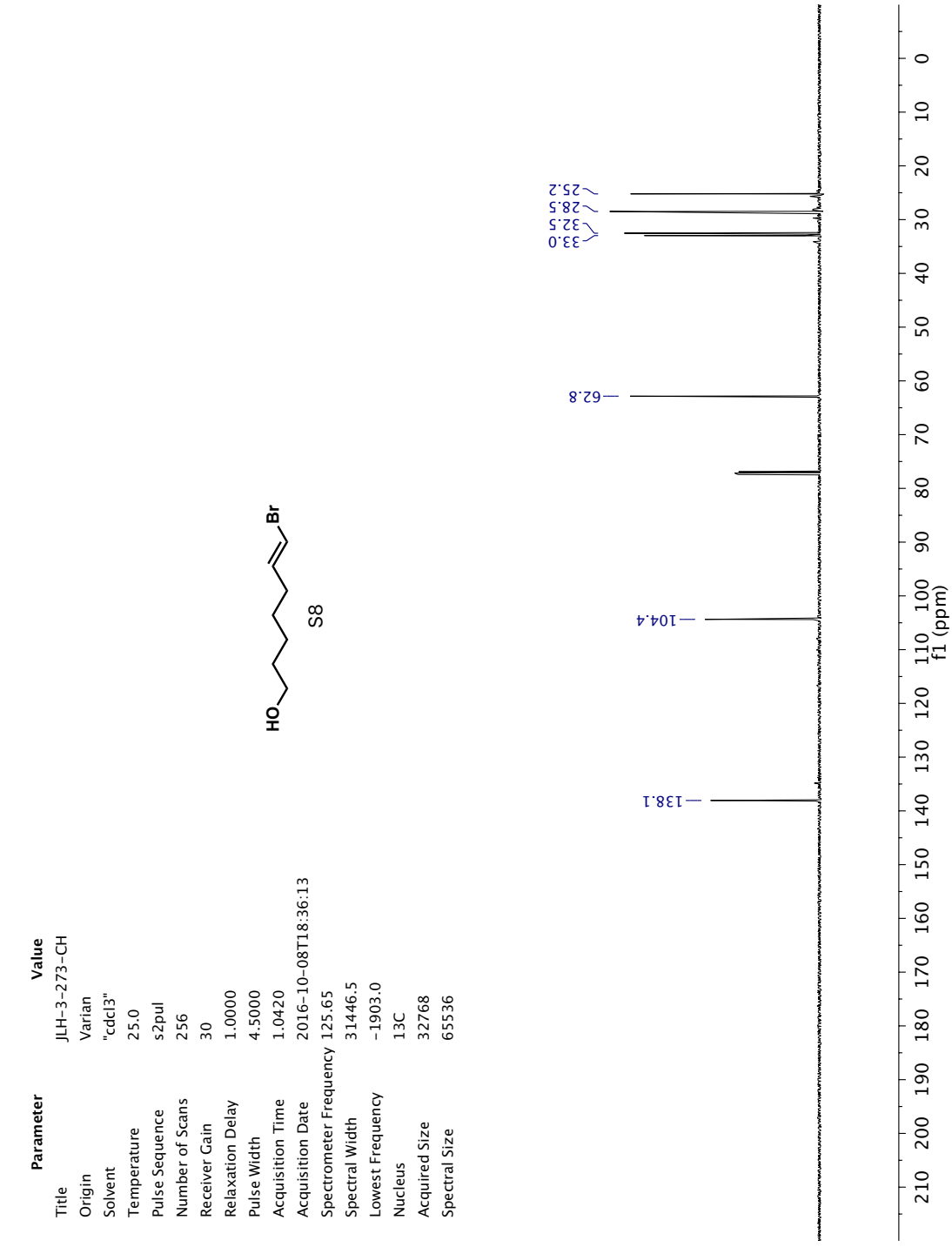
Parameter Value
Title JLH-3-273-CH
Origin Varian
Solvent "cdcl3"
Temperature 25.0
Pulse Sequence s2pul
Number of Scans 256
Receiver Gain 30
Relaxation Delay 1.0000
Pulse Width 4.5000
Acquisition Time 1.0420
Acquisition Date 2016-10-08T18:36:13
Spectrometer Frequency 125.65
Spectral Width 31446.5
Lowest Frequency -1903.0
Nucleus 13C
Acquired Size 32768
Spectral Size 65536
HO
Br
S8
138.1
104.4
62.8
33.0
32.5
28.5
25.2
f1 (ppm)

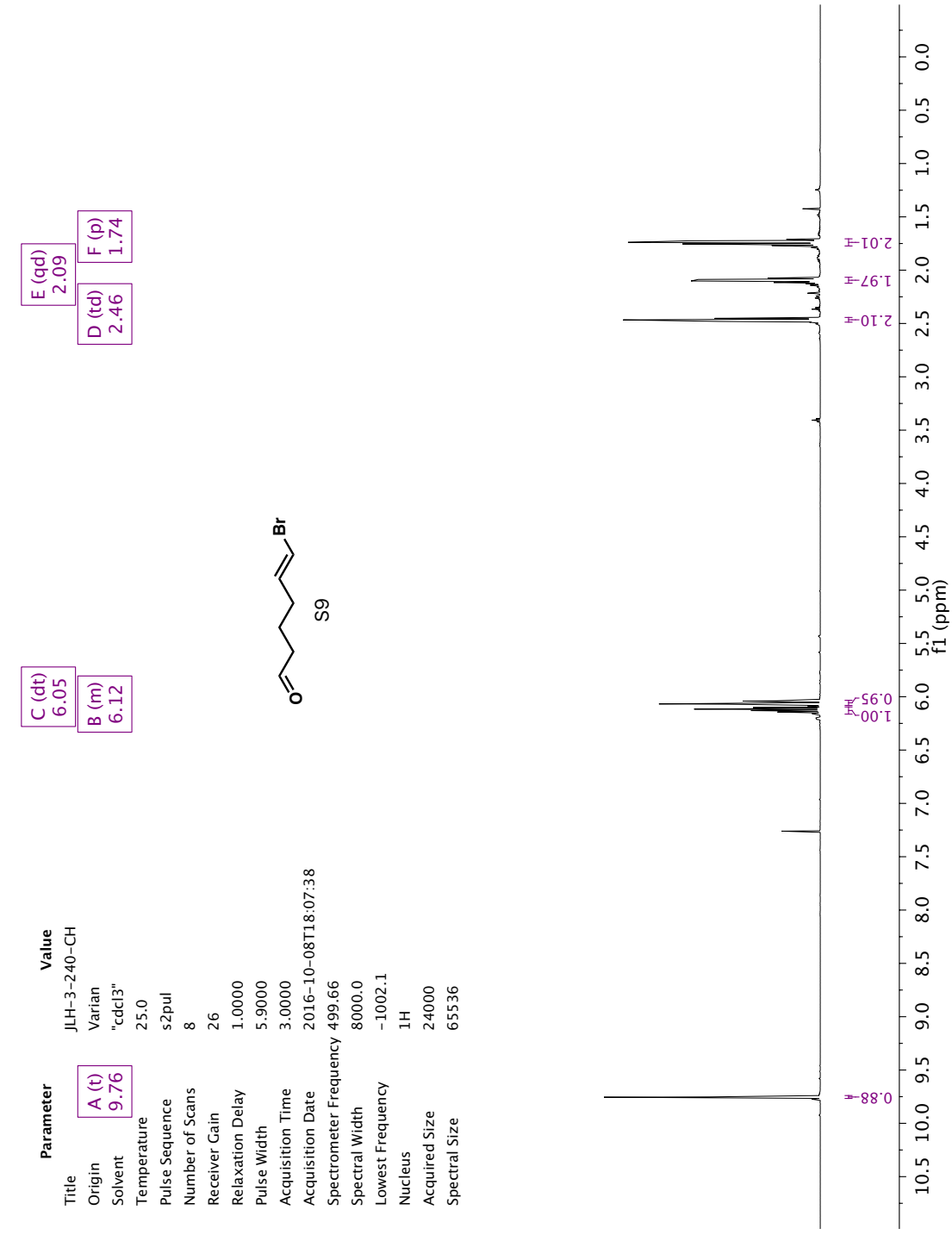
A (t) 9.76
B (m) 6.12
C (dt) 6.05
D (td) 2.46
E (qd) 2.09
F (p) 1.74
Br
O
S9
Parameter Value
Title JLH-3-240-CH
Origin Varian
Solvent "cdcl3"
Temperature 25.0
Pulse Sequence s2pul
Number of Scans 8
Receiver Gain 26
Relaxation Delay 1.0000
Pulse Width 5.9000
Acquisition Time 3.0000
Acquisition Date 2016-10-08T18:07:38
Spectrometer Frequency 499.66
Spectral Width 8000.0
Lowest Frequency -1002.1
Nucleus 1H
Acquired Size 24000
Spectral Size 65536
0.88
1.00
0.95
2.10
1.97
2.01
f1 (ppm)

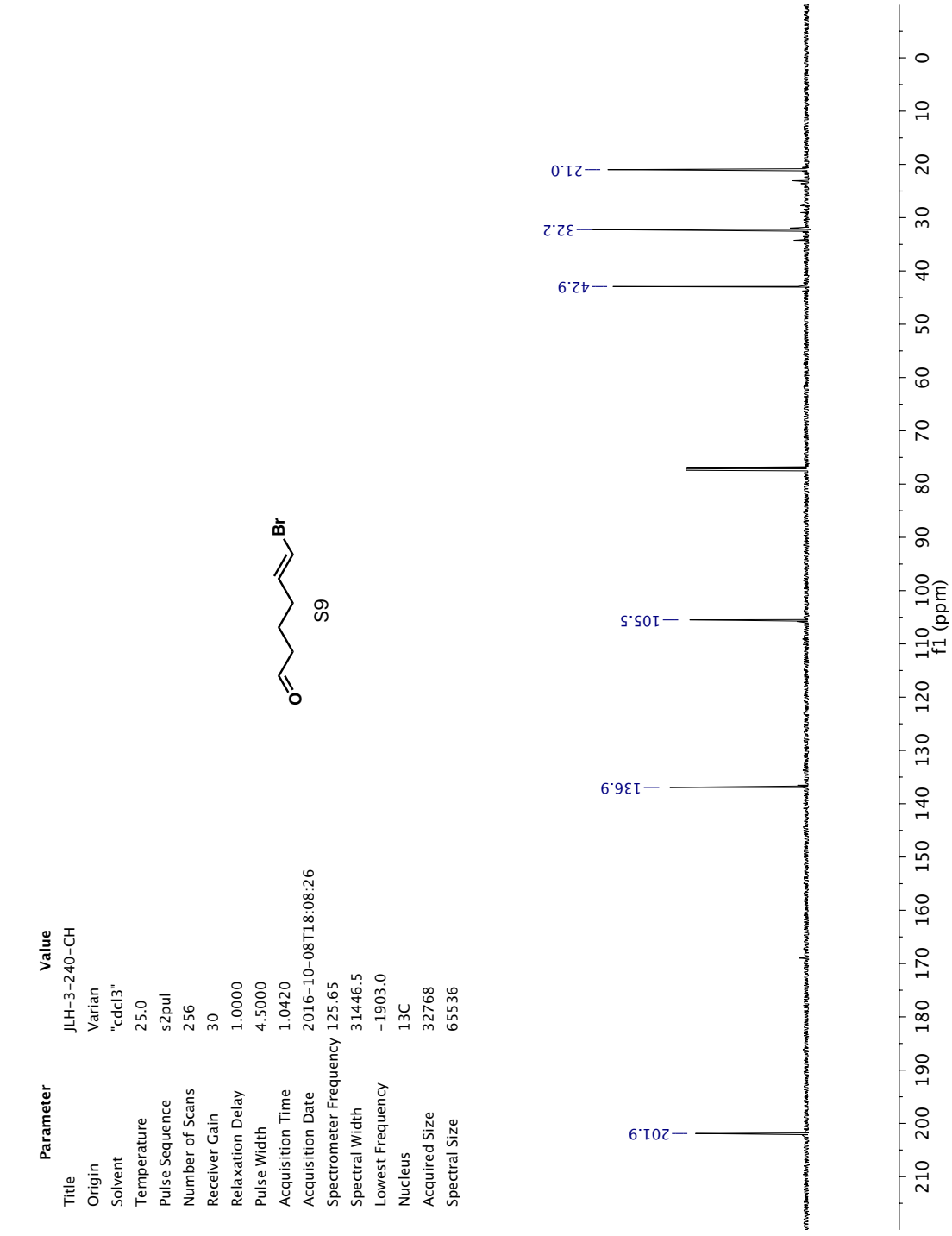
Parameter Value
Title JLH-3-240-CH
Origin Varian
Solvent "cdcl3"
Temperature 25.0
Pulse Sequence s2pul
Number of Scans 256
Receiver Gain 30
Relaxation Delay 1.0000
Pulse Width 4.5000
Acquisition Time 1.0420
Acquisition Date 2016-10-08T18:08:26
Spectrometer Frequency 125.65
Spectral Width 31446.5
Lowest Frequency -1903.0
Nucleus 13C
Acquired Size 32768
Spectral Size 65536
Br
O
S9
201.9
136.9
105.5
42.9
32.2
21.0
f1 (ppm)

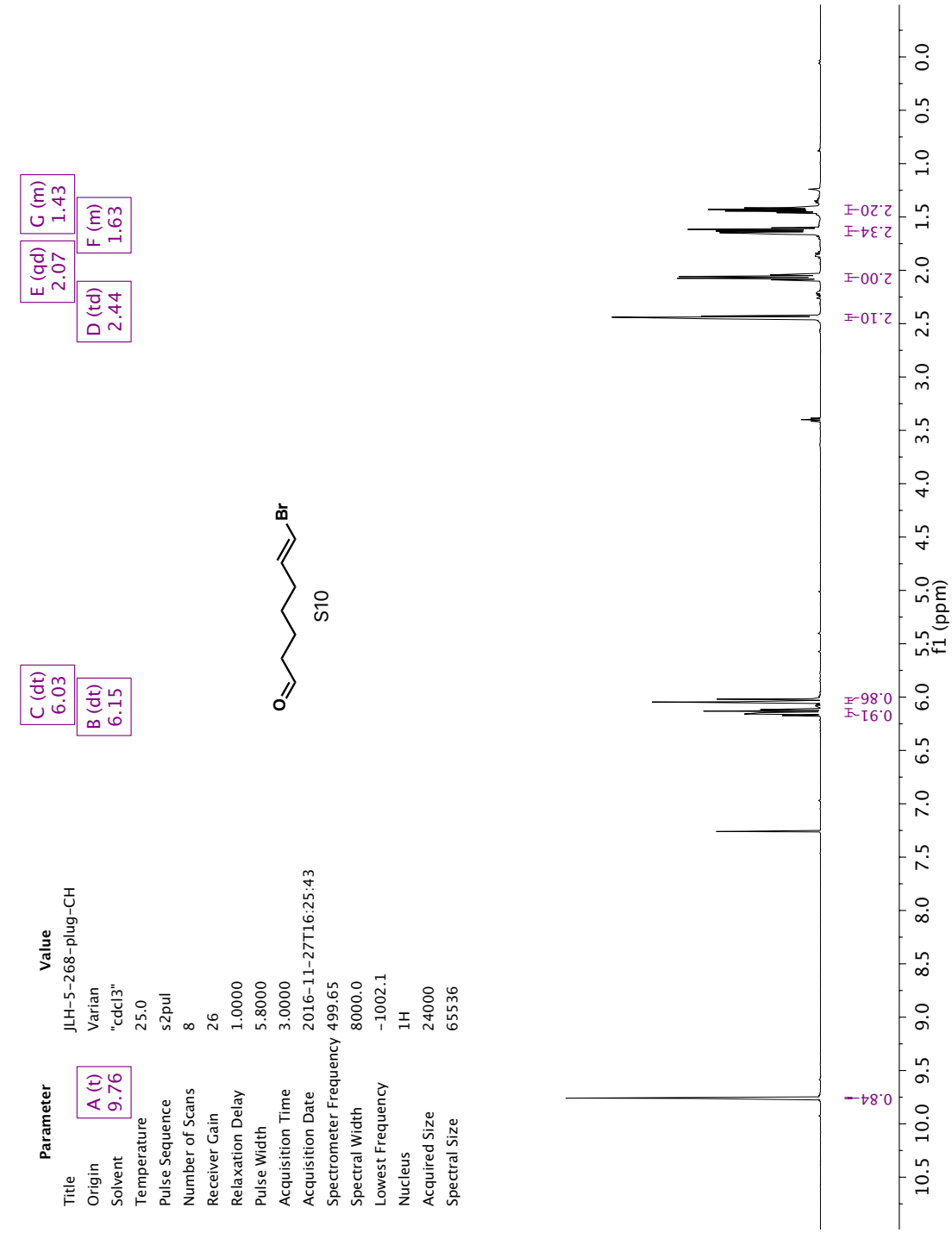
Parameter
Value
Title
JLH-5-268-plug-CH
Origin
Varian
Solvent
"cdcl3"
Temperature
25.0
Pulse Sequence
s2pul
Number of Scans
8
Receiver Gain
26
Relaxation Delay
1.0000
Pulse Width
5.8000
Acquisition Time
3.0000
Acquisition Date
2016-11-27T16:25:43
Spectrometer Frequency
499.65
Spectral Width
8000.0
Lowest Frequency
-1002.1
Nucleus
1H
Acquired Size
24000
Spectral Size
65536
A (t) 9.76
B (dt) 6.15
C (dt) 6.03
D (td) 2.44
E (qd) 2.07
F (m) 1.63
G (m) 1.43
O
Br
S10
0.84
0.91
0.86
2.10
2.00
2.34
2.20
f1 (ppm)

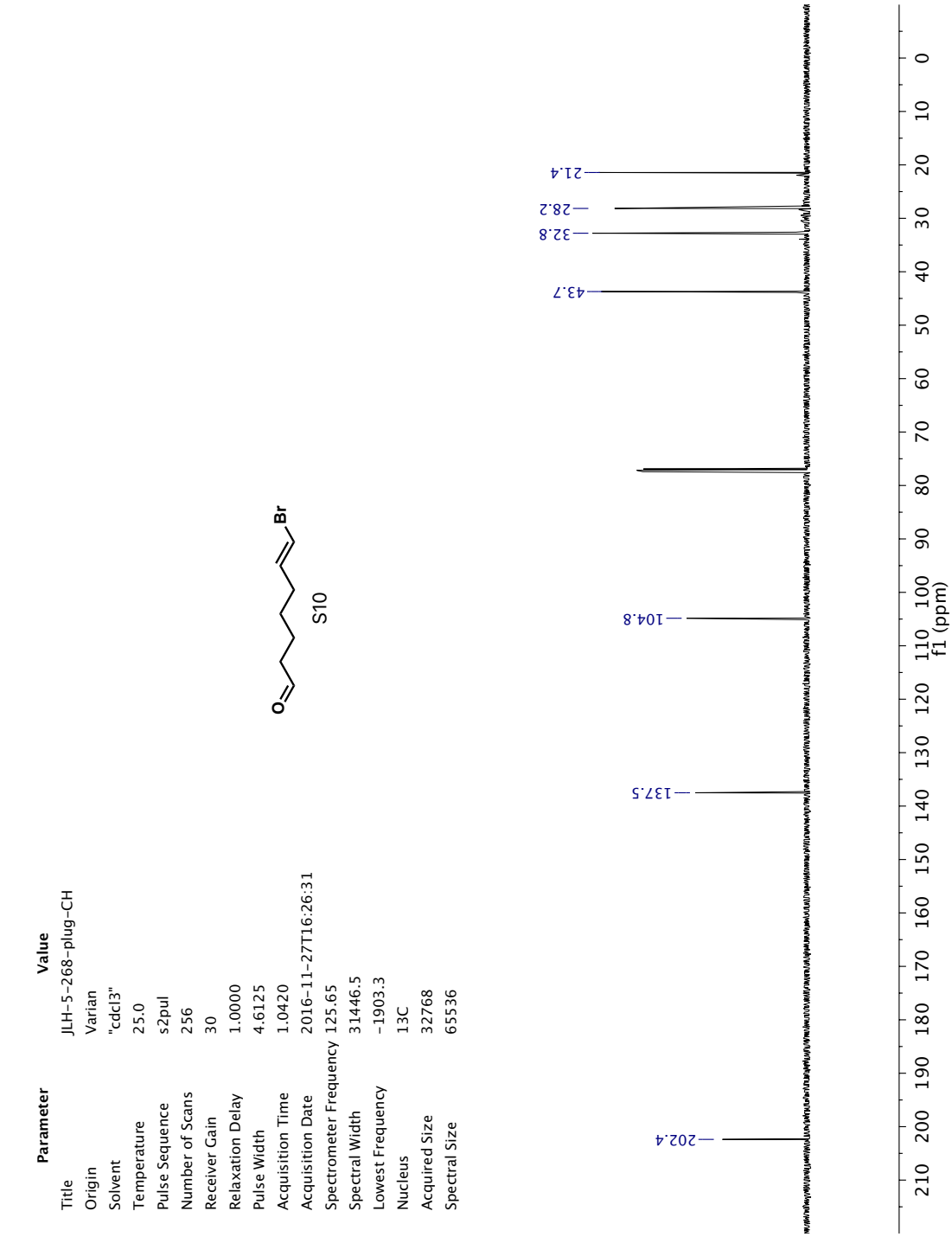
Parameter Value
Title JLH-5-268-plug-CH
Origin Varian
Solvent "cdcl3"
Temperature 25.0
Pulse Sequence s2pul
Number of Scans 256
Receiver Gain 30
Relaxation Delay 1.0000
Pulse Width 4.6125
Acquisition Time 1.0420
Acquisition Date 2016-11-27T16:26:31
Spectrometer Frequency 125.65
Spectral Width 31446.5
Lowest Frequency -1903.3
Nucleus 13C
Acquired Size 32768
Spectral Size 65536
Br
O
S10
202.4
137.5
104.8
43.7
32.8
28.2
21.4
f1 (ppm)

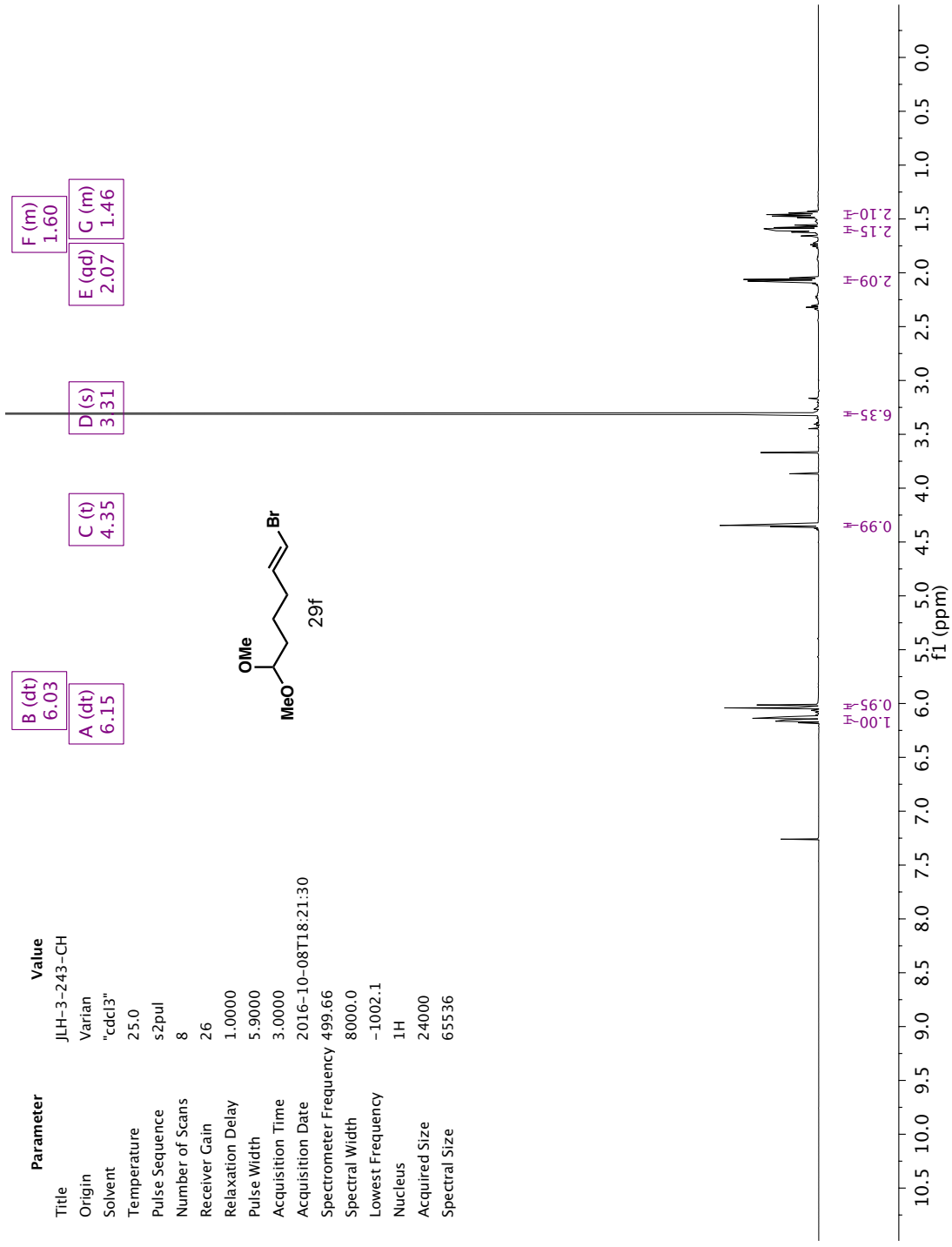

Parameter	Value
Title	JLH-3-243-CH
Origin	Varian
Solvent	"cdcl3"
Temperature	25.0
Pulse Sequence	s2pul
Number of Scans	8
Receiver Gain	26
Relaxation Delay	1.0000
Pulse Width	5.9000
Acquisition Time	3.0000
Acquisition Date	2016-10-08T18:21:30
Spectrometer Frequency	499.66
Spectral Width	8000.0
Lowest Frequency	-1002.1
Nucleus	1H
Acquired Size	24000
Spectral Size	65536

Parameter	Value
Title	JLH-3-243-CH
Origin	Varian
Solvent	"cdcl3"
Temperature	25.0
Pulse Sequence	s2pul
Number of Scans	256
Receiver Gain	30
Relaxation Delay	1.0000
Pulse Width	4.5000
Acquisition Time	1.0420
Acquisition Date	2016-10-08T18:22:18
Spectrometer Frequency	125.65
Spectral Width	31446.5
Lowest Frequency	-1903.0
Nucleus	13C
Acquired Size	32768
Spectral Size	65536

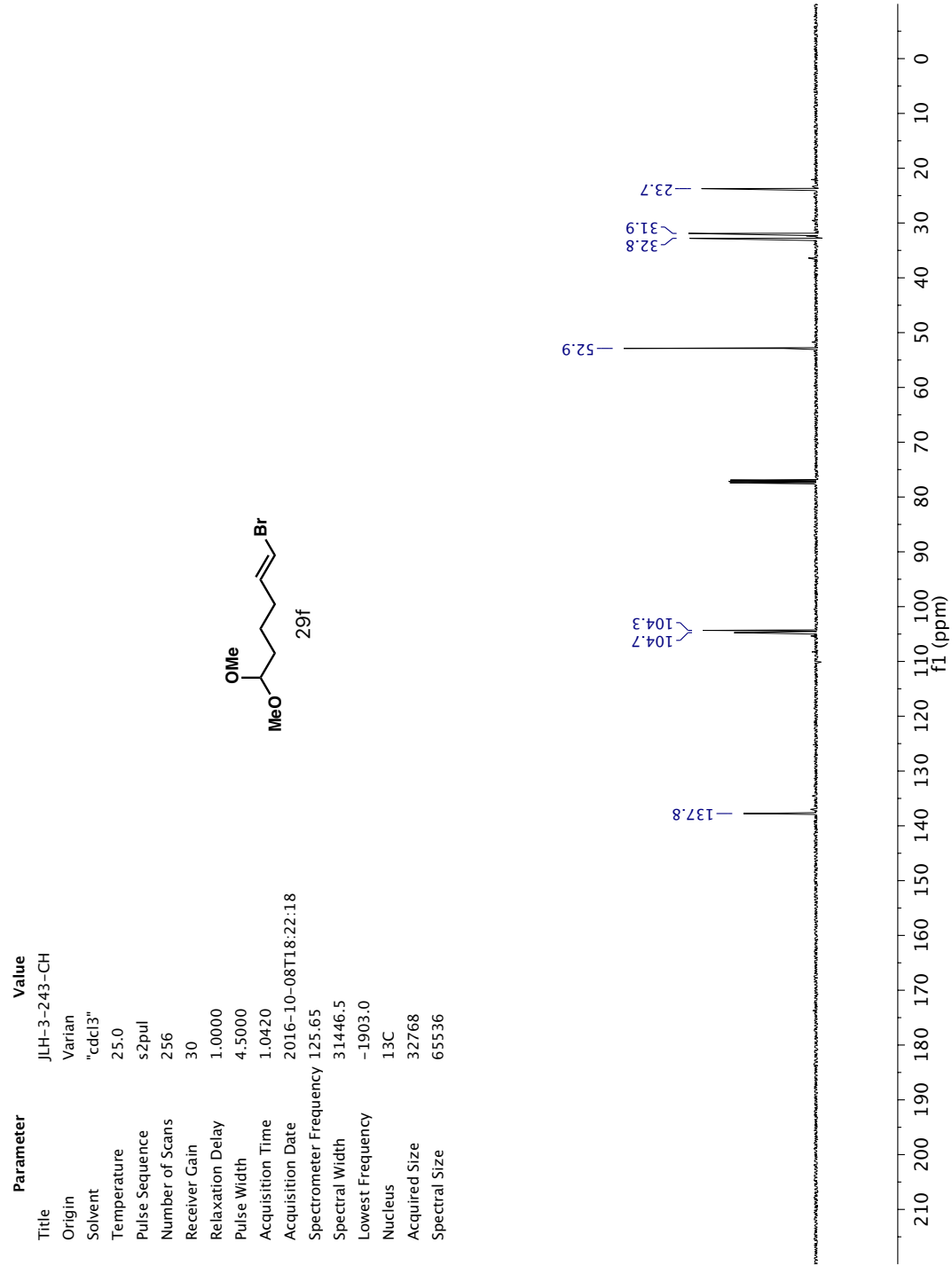

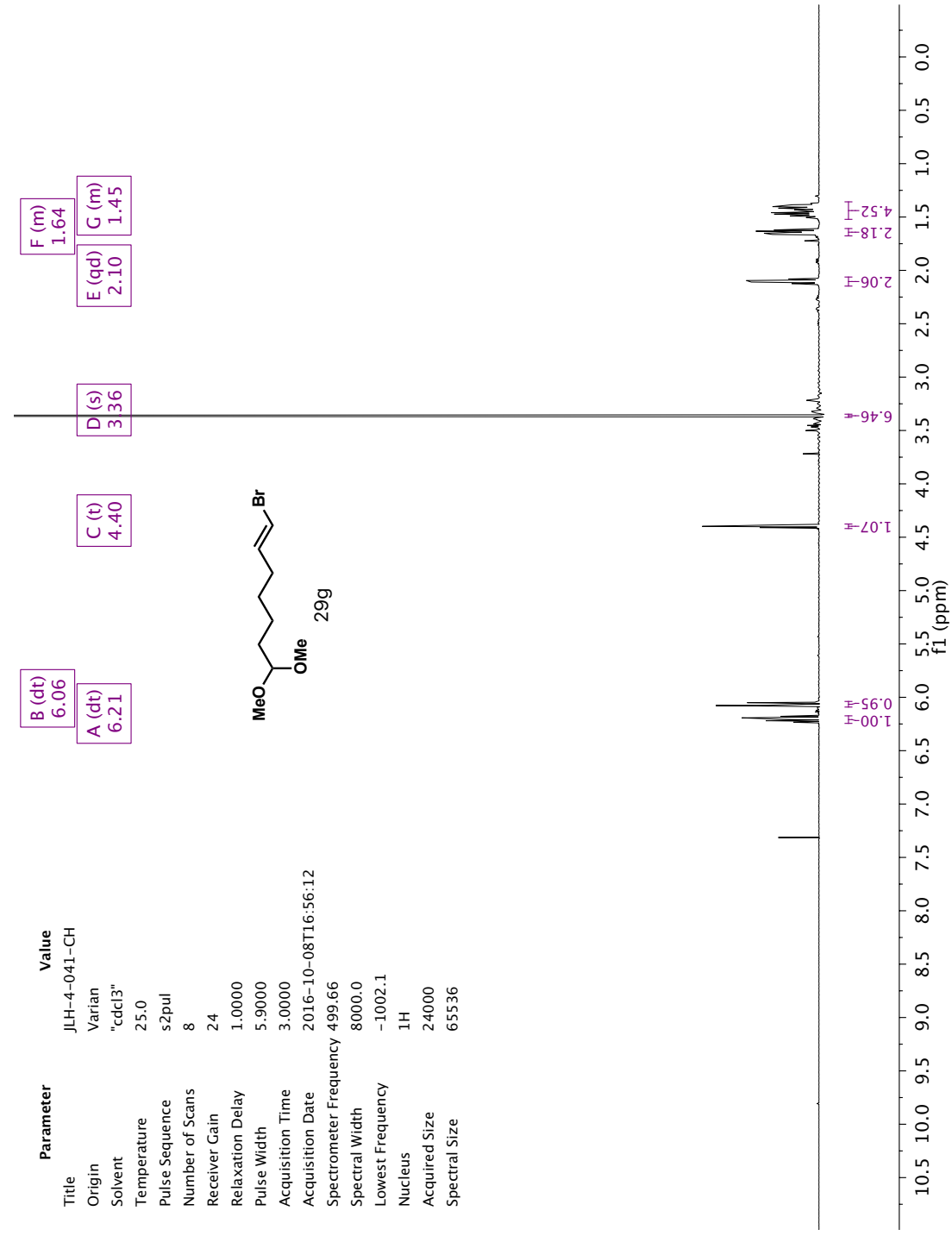
B (dt) 6.06
A (dt) 6.21
C (t) 4.40
D (s) 3.36
F (m) 1.64
E (qd) 2.10
G (m) 1.45
MeO
OMe
Br
29g
Parameter Value
Title JLH-4-041-CH
Origin Varian
Solvent "cdcl3"
Temperature 25.0
Pulse Sequence s2pul
Number of Scans 8
Receiver Gain 24
Relaxation Delay 1.0000
Pulse Width 5.9000
Acquisition Time 3.0000
Acquisition Date 2016-10-08T16:56:12
Spectrometer Frequency 499.66
Spectral Width 8000.0
Lowest Frequency -1002.1
Nucleus 1H
Acquired Size 24000
Spectral Size 65536
1.00
0.95
1.07
6.46
2.06
2.18
4.52
f1 (ppm)

Parameter	Value
Title	JLH-4-041-CH
Origin	Varian
Solvent	"cdcl3"
Temperature	25.0
Pulse Sequence	s2pul
Number of Scans	256
Receiver Gain	30
Relaxation Delay	1.0000
Pulse Width	4.5000
Acquisition Time	1.0420
Acquisition Date	2016-10-08T16:57:01
Spectrometer Frequency	125.65
Spectral Width	31446.5
Lowest Frequency	-1903.0
Nucleus	13C
Acquired Size	32768
Spectral Size	65536

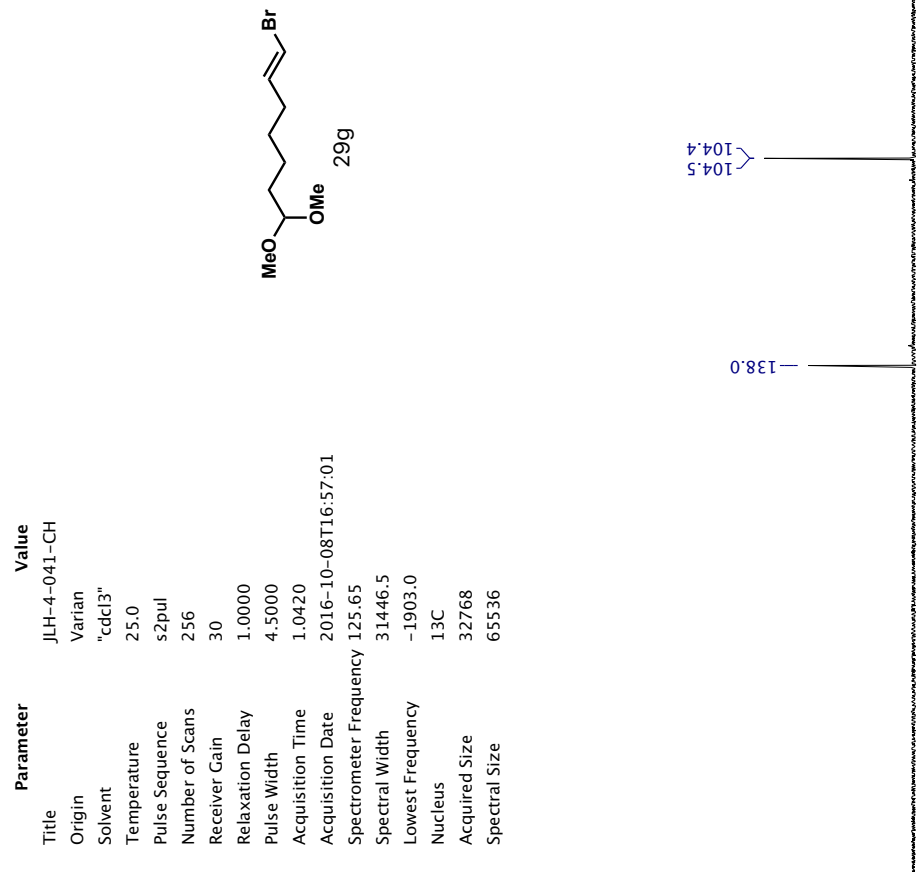

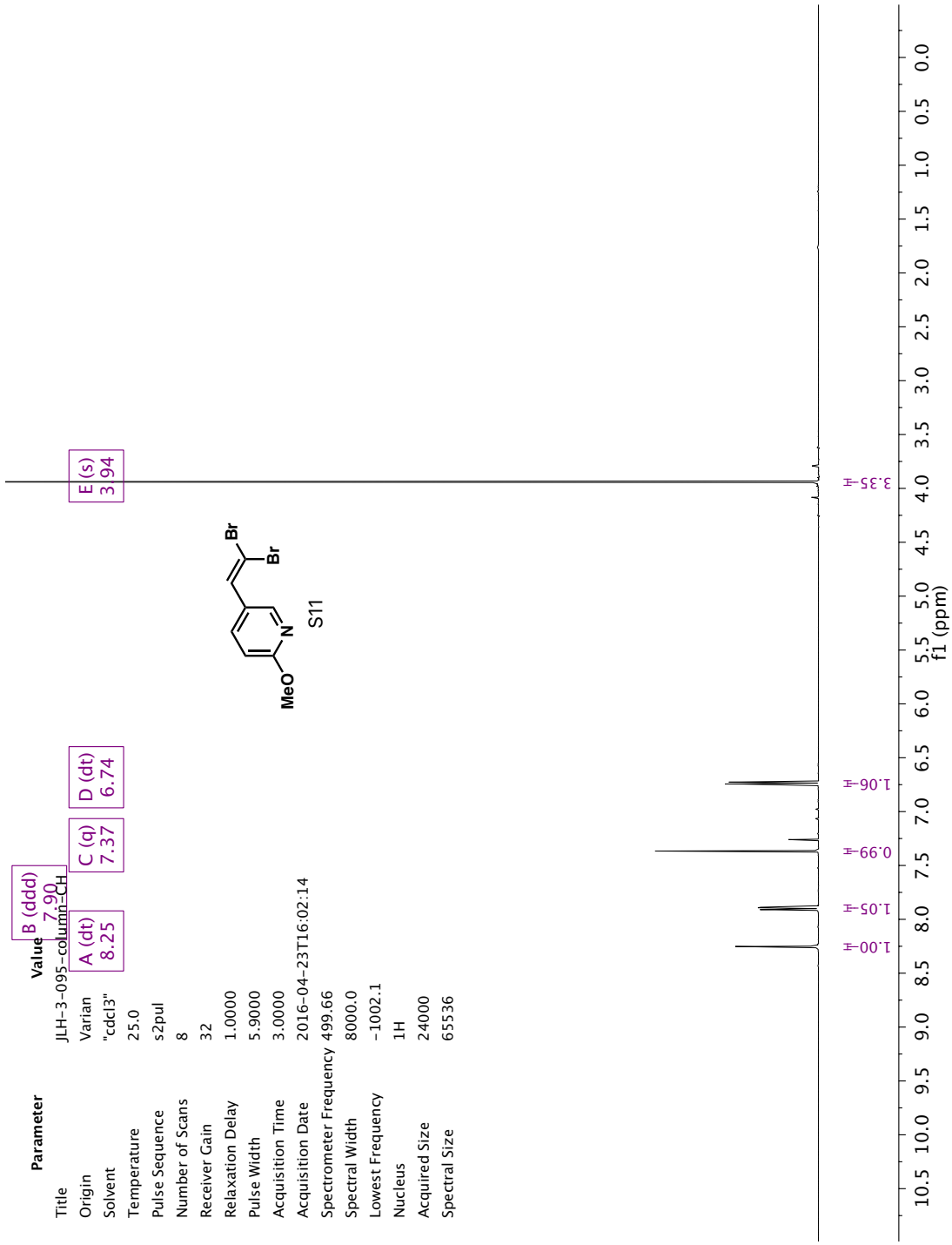
Parameter
Value
Title JLH-3-095-column-CH
Origin Varian
Solvent "cdcl3"
Temperature 25.0
Pulse Sequence s2pul
Number of Scans 8
Receiver Gain 32
Relaxation Delay 1.0000
Pulse Width 5.9000
Acquisition Time 3.0000
Acquisition Date 2016-04-23T16:02:14
Spectrometer Frequency 499.66
Spectral Width 8000.0
Lowest Frequency -1002.1
Nucleus 1H
Acquired Size 24000
Spectral Size 65536
B (ddd) 7.90
A (dt) 8.25
C (q) 7.37
D (dt) 6.74
E (s) 3.94
Br
Br
N
MeO
S11
1.00
1.05
0.99
1.06
3.35
10.5 10.0 9.5 9.0 8.5 8.0 7.5 7.0 6.5 6.0 5.5 5.0 4.5 4.0 3.5 3.0 2.5 2.0 1.5 1.0 0.5 0.0
f1 (ppm)

Parameter	Value
Title	JLH-3-095-column-CH
Origin	Varian
Solvent	"cdcl3"
Temperature	25.0
Pulse Sequence	s2pul
Number of Scans	256
Receiver Gain	30
Relaxation Delay	1.0000
Pulse Width	4.5000
Acquisition Time	1.0420
Acquisition Date	2016-04-23T16:03:02
Spectrometer Frequency	125.65
Spectral Width	31446.5
Lowest Frequency	-1874.1
Nucleus	13C
Acquired Size	32768
Spectral Size	65536

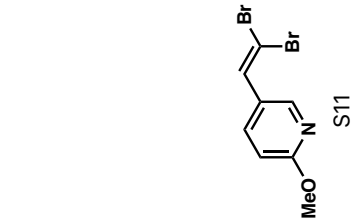

S11

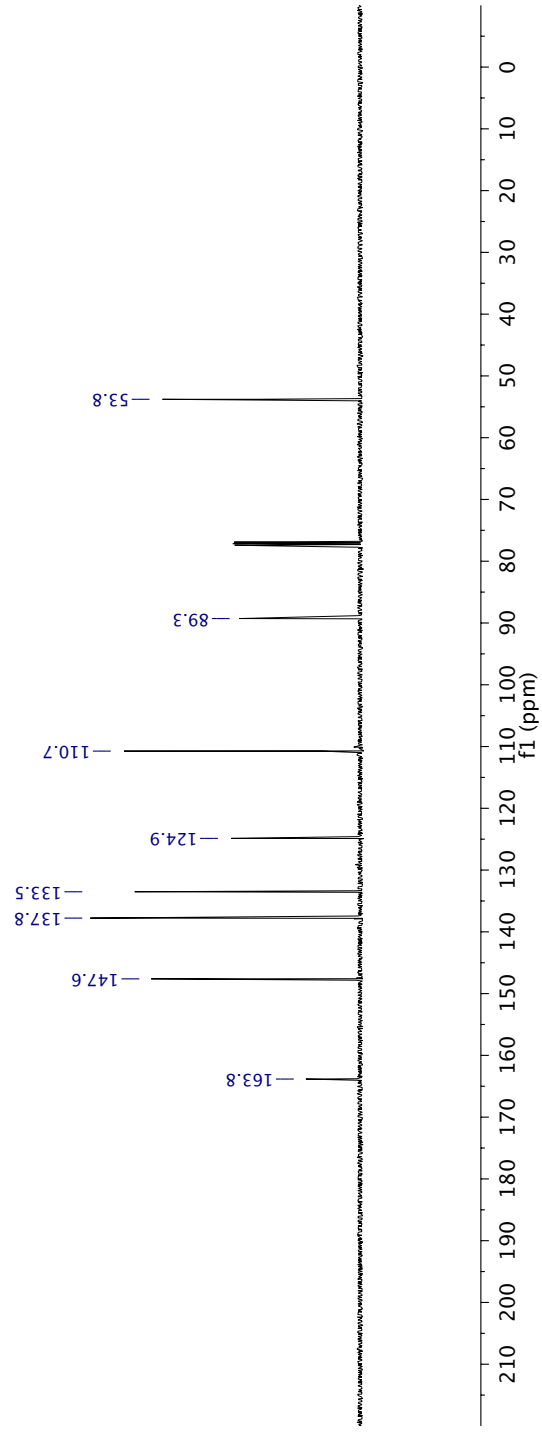

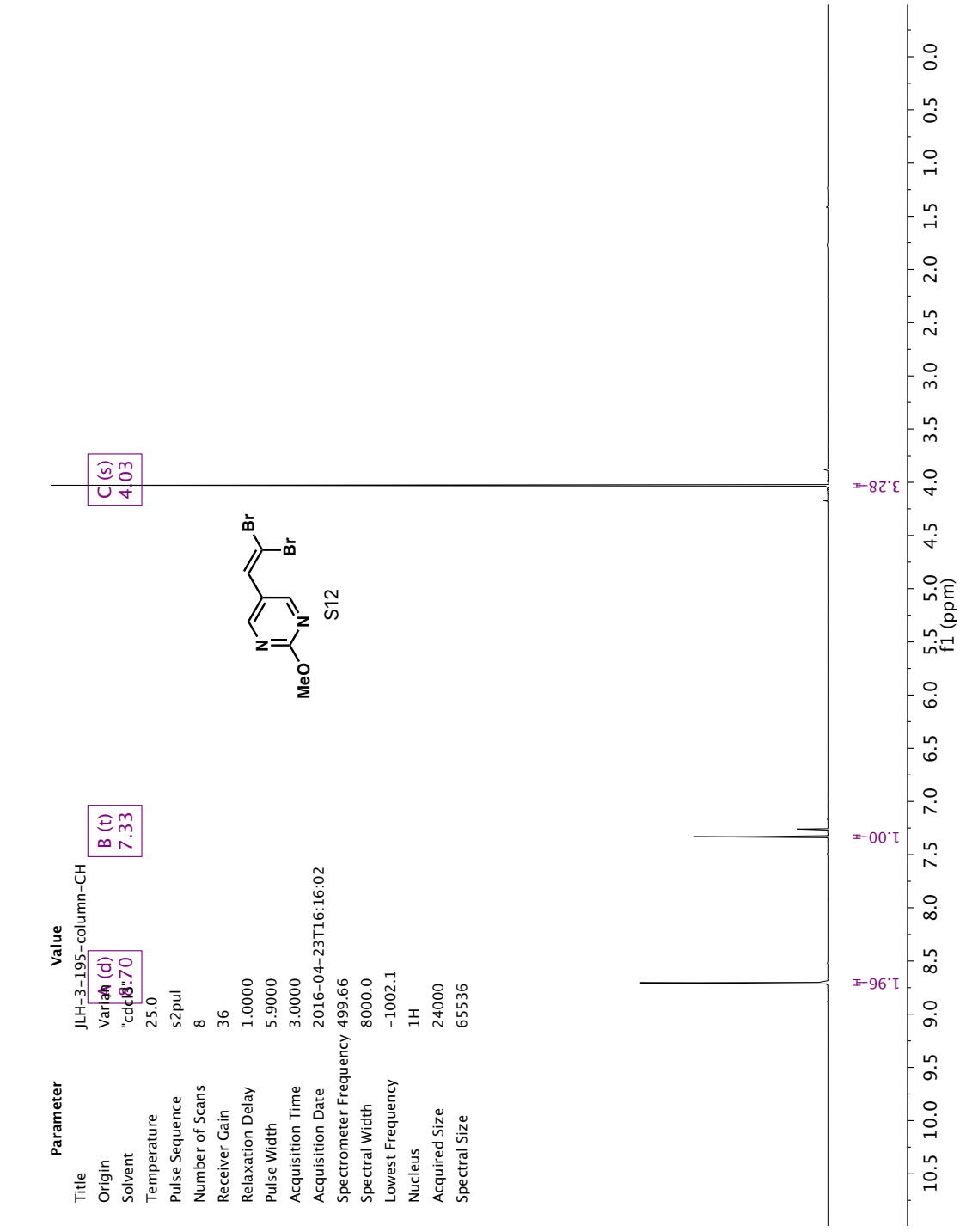
Parameter
Value
Title
JLH-3-195-column-CH
Origin
Varian
Solvent
"cdcl3"
Temperature
25.0
Pulse Sequence
s2pul
Number of Scans
8
Receiver Gain
36
Relaxation Delay
1.0000
Pulse Width
5.9000
Acquisition Time
3.0000
Acquisition Date
2016-04-23T16:16:02
Spectrometer Frequency
499.66
Spectral Width
8000.0
Lowest Frequency
-1002.1
Nucleus
1H
Acquired Size
24000
Spectral Size
65536
A (d)
8.70
B (t)
7.33
C (s)
4.03
Br
Br
N
N
MeO
S12
1.96
1.00
3.28
10.5 10.0 9.5 9.0 8.5 8.0 7.5 7.0 6.5 6.0 5.5 5.0 4.5 4.0 3.5 3.0 2.5 2.0 1.5 1.0 0.5 0.0
f1 (ppm)

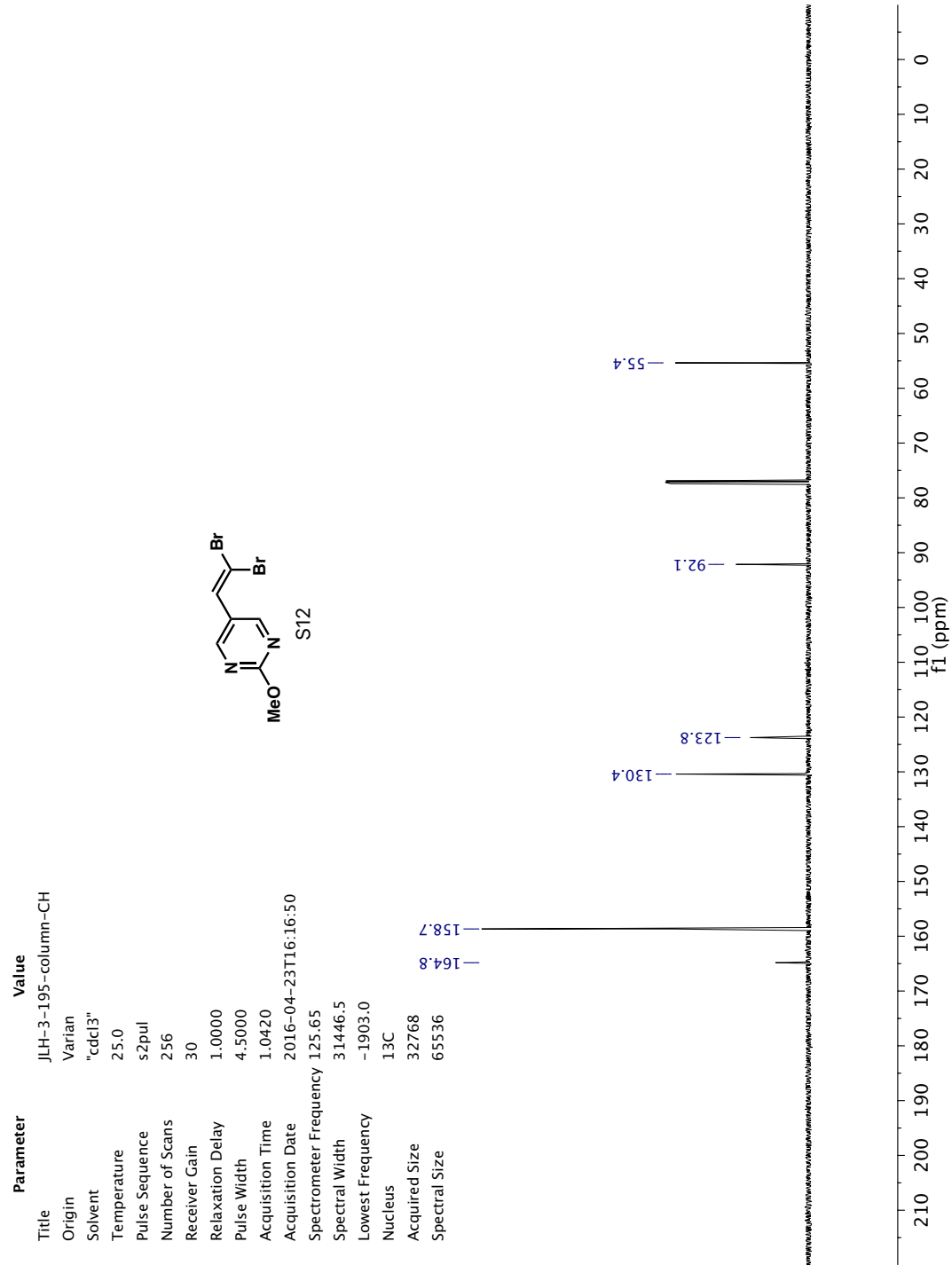
Parameter Value
Title JLH-3-195-column-CH
Origin Varian
Solvent "cdcl3"
Temperature 25.0
Pulse Sequence s2pul
Number of Scans 256
Receiver Gain 30
Relaxation Delay 1.0000
Pulse Width 4.5000
Acquisition Time 1.0420
Acquisition Date 2016-04-23T16:16:50
Spectrometer Frequency 125.65
Spectral Width 31446.5
Lowest Frequency -1903.0
Nucleus 13C
Acquired Size 32768
Spectral Size 65536
Br
Br
N
N
MeO
S12
158.7
164.8
130.4
123.8
92.1
55.4
f1 (ppm)

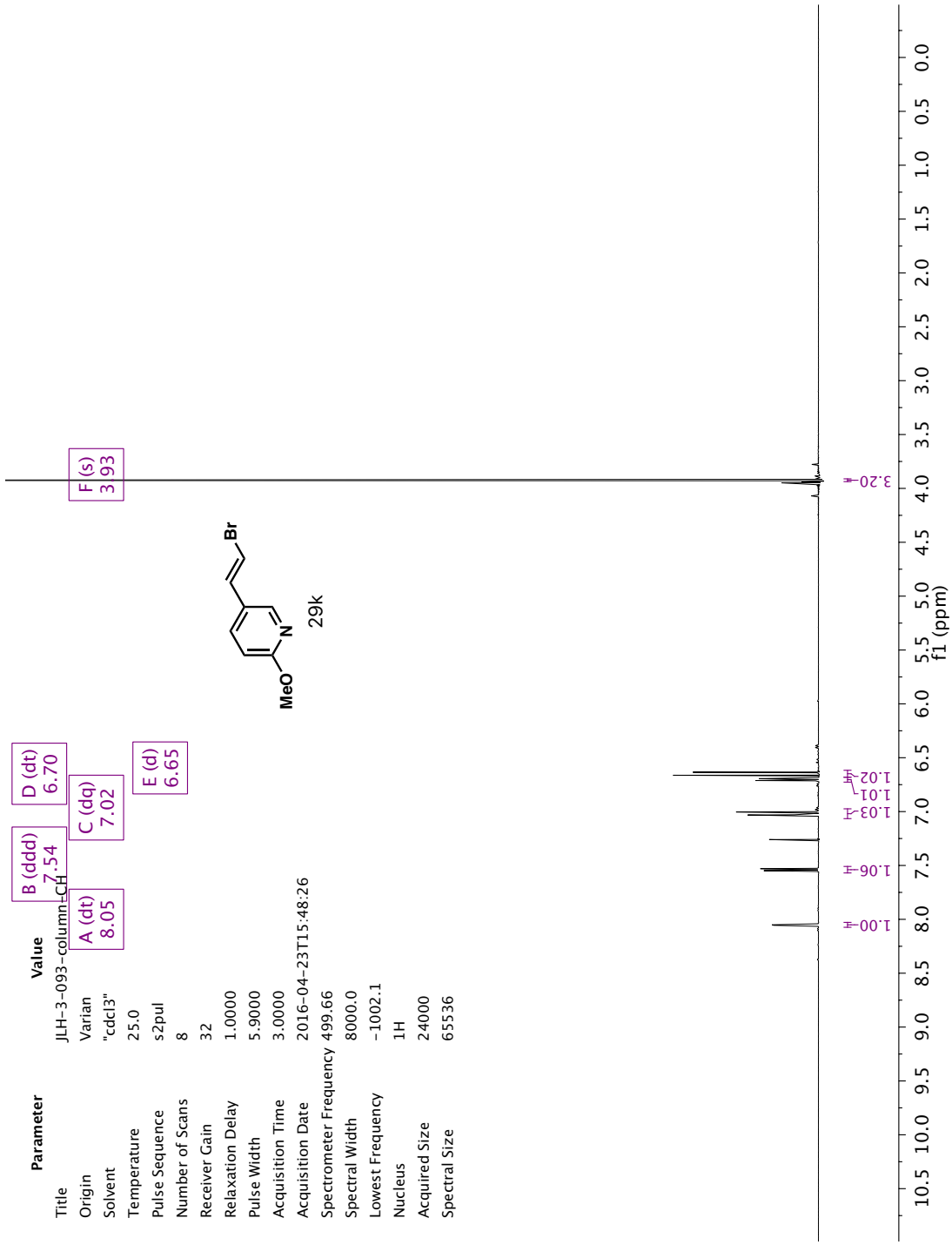
Parameter
Value
Title JLH-3-093-column-CH
Origin Varian
Solvent "cdcl3"
Temperature 25.0
Pulse Sequence s2pul
Number of Scans 8
Receiver Gain 32
Relaxation Delay 1.0000
Pulse Width 5.9000
Acquisition Time 3.0000
Acquisition Date 2016-04-23T15:48:26
Spectrometer Frequency 499.66
Spectral Width 8000.0
Lowest Frequency -1002.1
Nucleus 1H
Acquired Size 24000
Spectral Size 65536
B (ddd) 7.54
A (dt) 8.05
C (dq) 7.02
D (dt) 6.70
E (d) 6.65
F (s) 3.93
Br
MeO
N
29k
1.00
1.06
1.03
1.01
1.02
3.20
10.5 10.0 9.5 9.0 8.5 8.0 7.5 7.0 6.5 6.0 5.5 5.0 4.5 4.0 3.5 3.0 2.5 2.0 1.5 1.0 0.5 0.0
f1 (ppm)

Parameter	Value
Title	JLH-3-093-column-CH
Origin	Varian
Solvent	"cdcl3"
Temperature	25.0
Pulse Sequence	s2pul
Number of Scans	256
Receiver Gain	30
Relaxation Delay	1.0000
Pulse Width	4.5000
Acquisition Time	1.0420
Acquisition Date	2016-04-23T15:49:14
Spectrometer Frequency	125.65
Spectral Width	31446.5
Lowest Frequency	-1903.0
Nucleus	13C
Acquired Size	32768
Spectral Size	65536

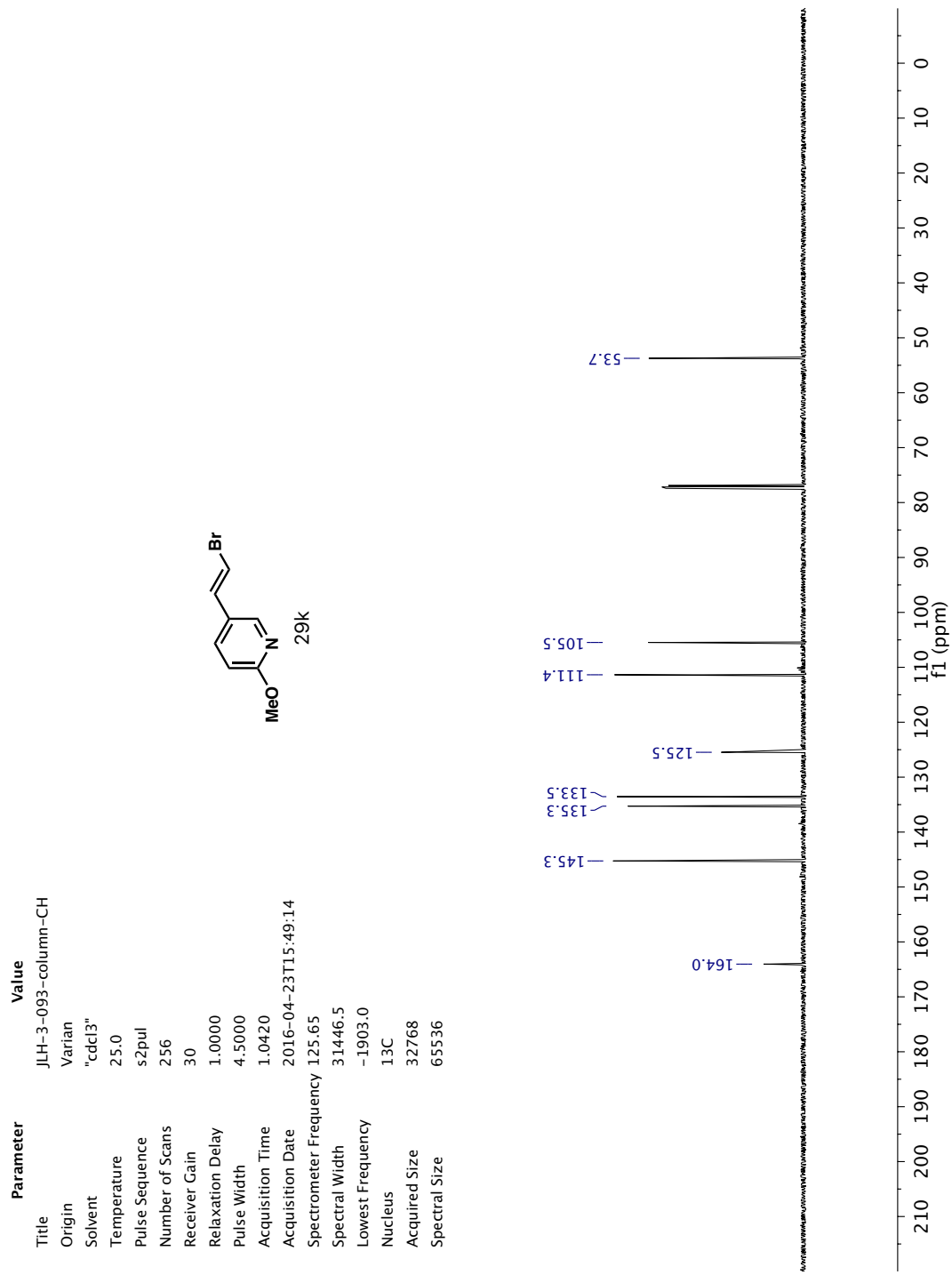

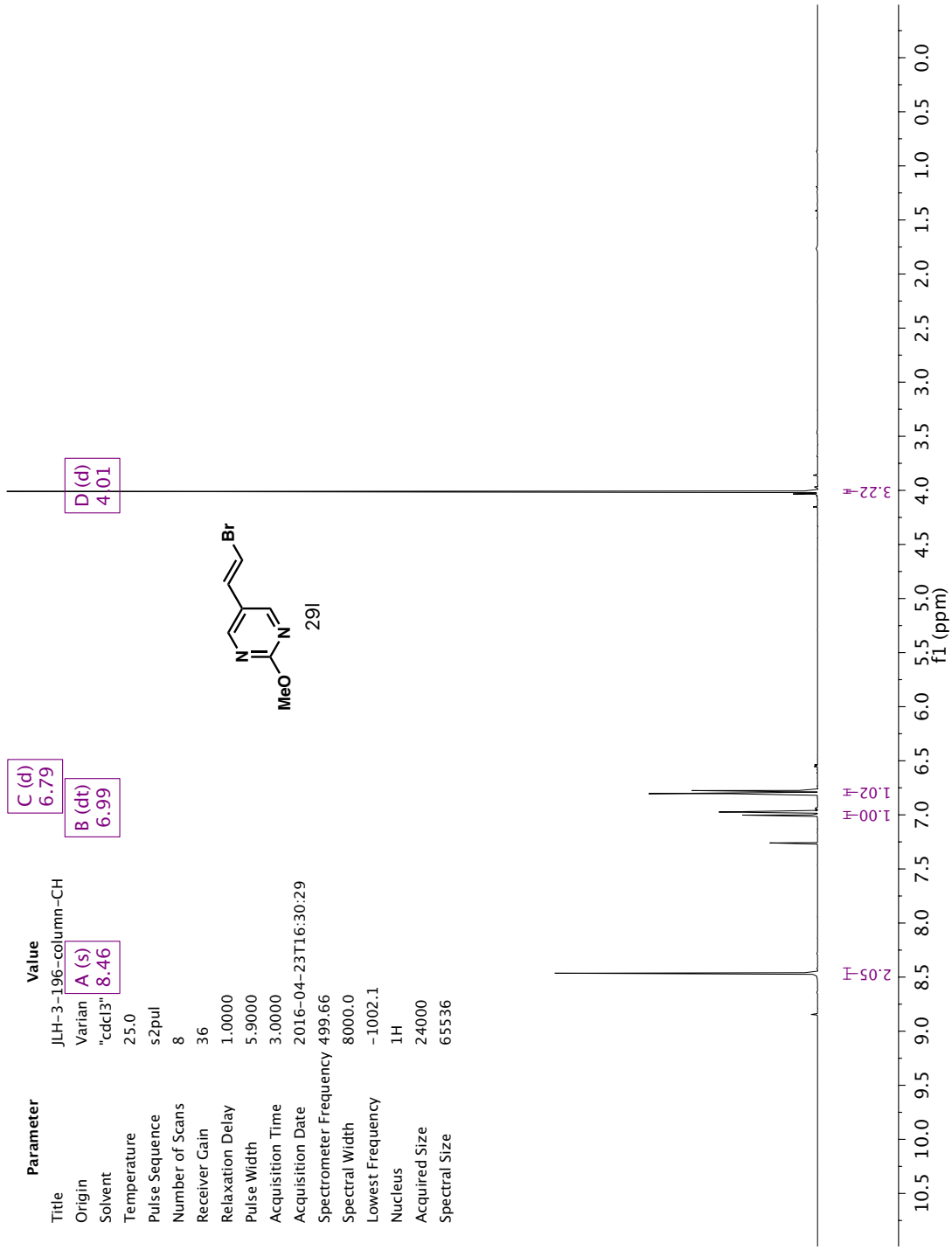
Parameter
Value
Title JLH-3-196-column-CH
Origin Varian
Solvent "cdcl3"
Temperature 25.0
Pulse Sequence s2pul
Number of Scans 8
Receiver Gain 36
Relaxation Delay 1.0000
Pulse Width 5.9000
Acquisition Time 3.0000
Acquisition Date 2016-04-23T16:30:29
Spectrometer Frequency 499.66
Spectral Width 8000.0
Lowest Frequency -1002.1
Nucleus 1H
Acquired Size 24000
Spectral Size 65536
A (s) 8.46
B (dt) 6.99
C (d) 6.79
D (d) 4.01
Br
N
N
MeO
29l
2.05
1.00
1.02
3.22
10.5 10.0 9.5 9.0 8.5 8.0 7.5 7.0 6.5 6.0 5.5 5.0 4.5 4.0 3.5 3.0 2.5 2.0 1.5 1.0 0.5 0.0
f1 (ppm)

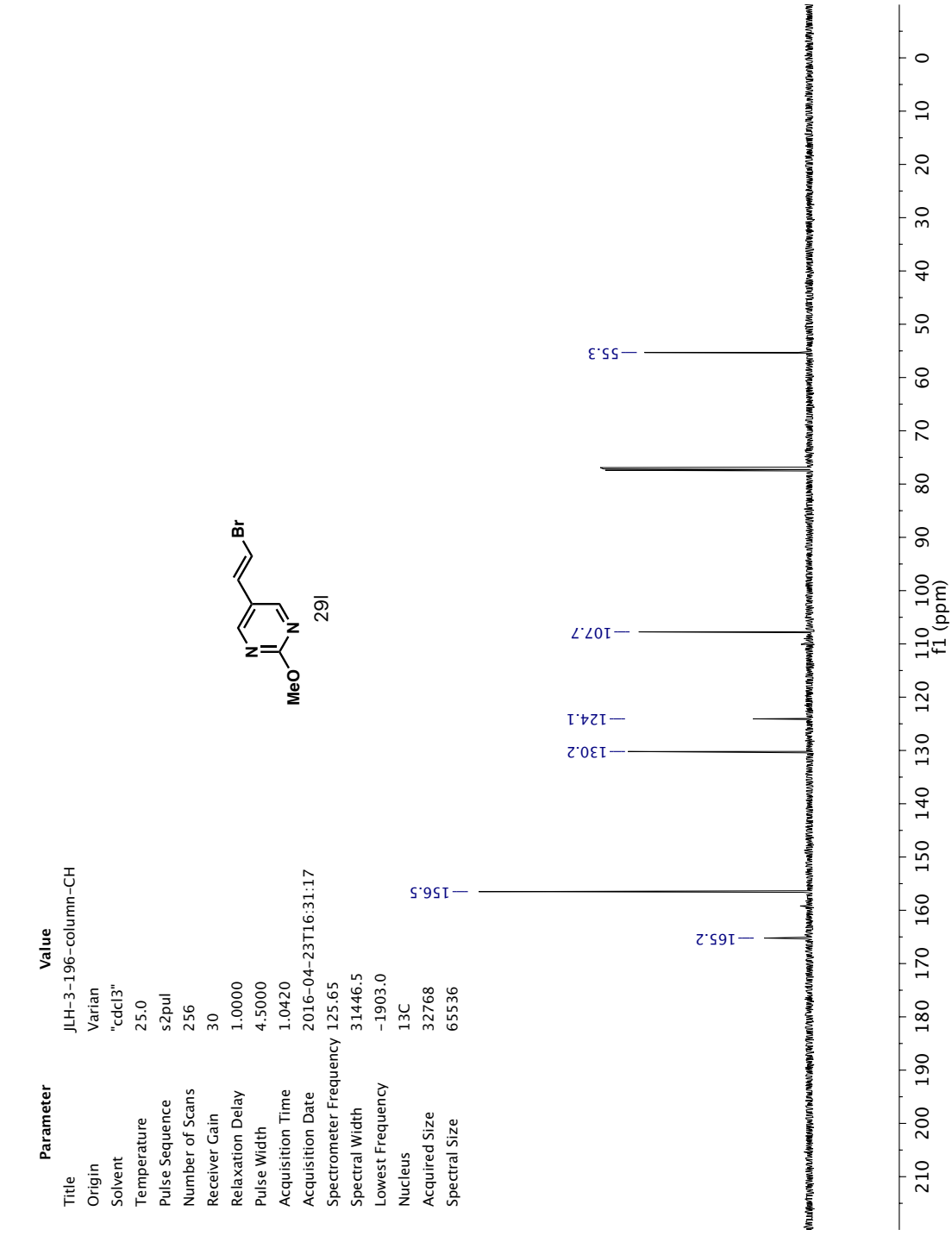
Parameter Value
Title JLH-3-196-column-CH
Origin Varian
Solvent "cdcl3"
Temperature 25.0
Pulse Sequence s2pul
Number of Scans 256
Receiver Gain 30
Relaxation Delay 1.0000
Pulse Width 4.5000
Acquisition Time 1.0420
Acquisition Date 2016-04-23T16:31:17
Spectrometer Frequency 125.65
Spectral Width 31446.5
Lowest Frequency -1903.0
Nucleus 13C
Acquired Size 32768
Spectral Size 65536
Br
N
N
MeO
29l
165.2
156.5
130.2
124.1
107.7
55.3
f1 (ppm)

Parameter	Value
Title	CMO-1-155-CH
Origin	Varian
Solvent	cdcl3
Temperature	25.0
Pulse Sequence	s2pul
Number of Scans	8
Receiver Gain	28
Relaxation Delay	1.0000
Pulse Width	5.8000
Acquisition Time	3.0000
Acquisition Date	2017-09-30T13:51:12
Spectrometer Frequency	499.64
Spectral Width	8000.0
Lowest Frequency	-1002.2
Nucleus	1H
Acquired Size	24000
Spectral Size	65536

A (m) 6.20

B (t) 3.54

C (m) 2.52

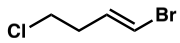

S14

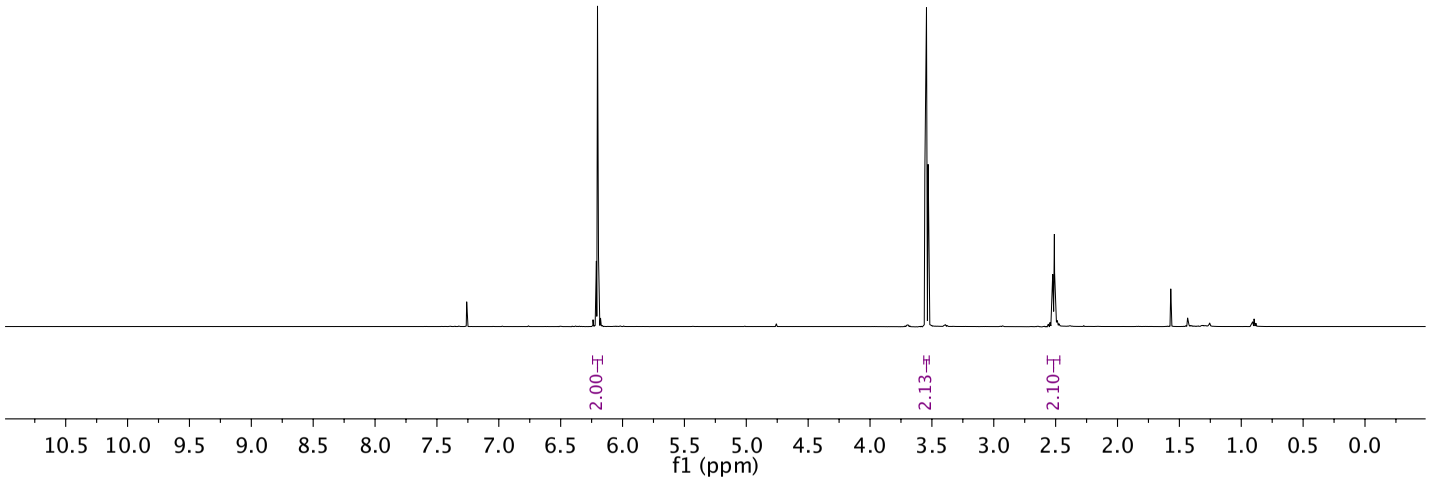

Parameter	Value
Title	CMO-1-155-CH
Origin	Varian
Solvent	cdcl3
Temperature	25.0
Pulse Sequence	s2pul
Number of Scans	256
Receiver Gain	30
Relaxation Delay	1.0000
Pulse Width	4.6125
Acquisition Time	1.0420
Acquisition Date	2017-09-30T13:52:01
Spectrometer Frequency	125.65
Spectral Width	31446.5
Lowest Frequency	-1903.6
Nucleus	13C
Acquired Size	32768
Spectral Size	65536

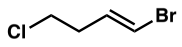

S14

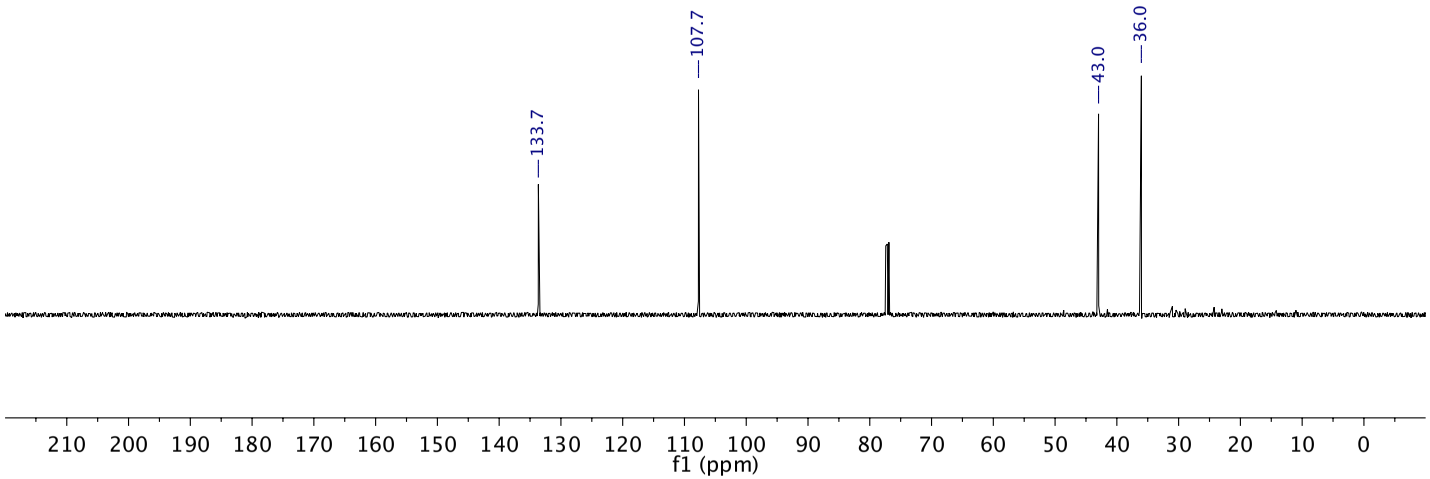

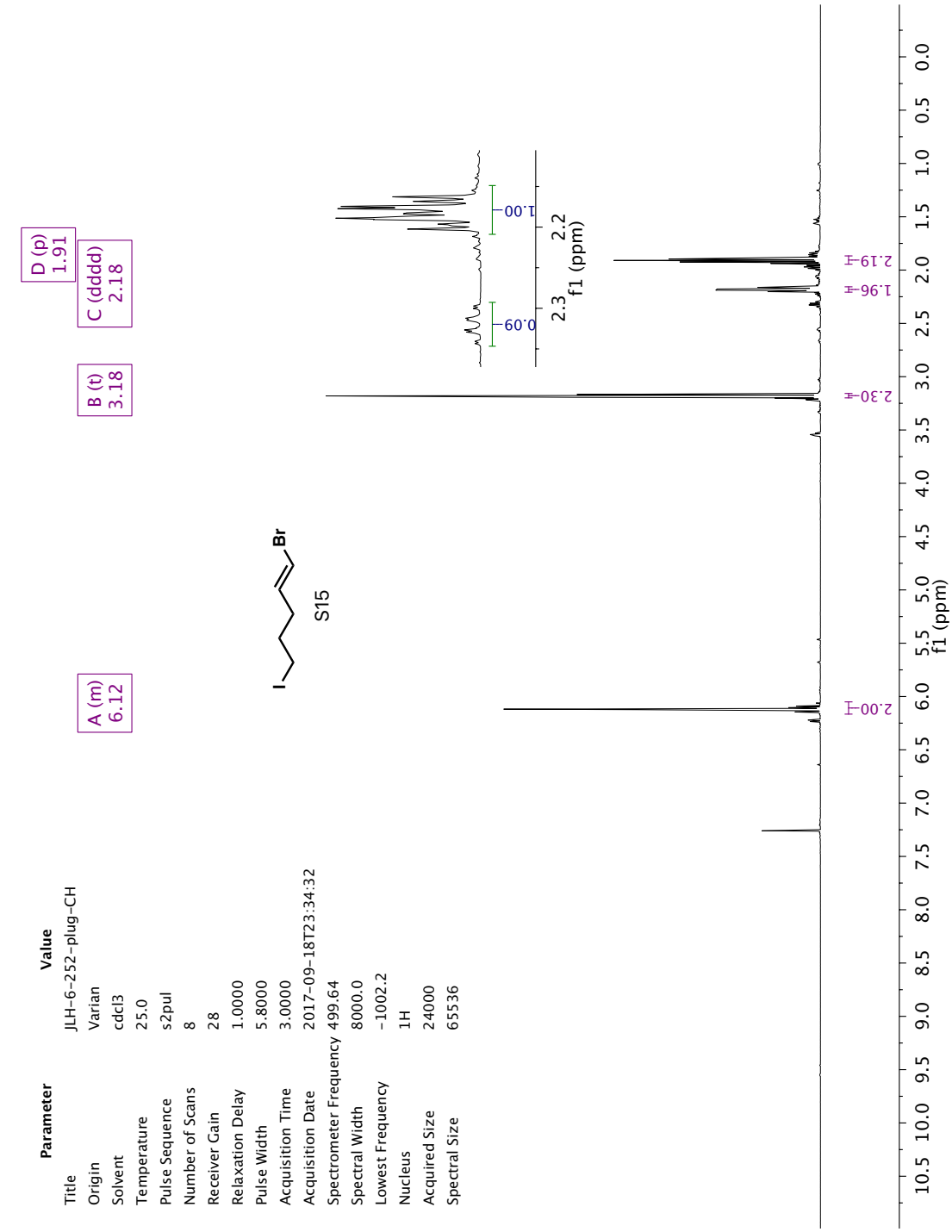
Parameter
Value
Title
JLH-6-252-plug-CH
Origin
Varian
Solvent
cdcl3
Temperature
25.0
Pulse Sequence
s2pul
Number of Scans
8
Receiver Gain
28
Relaxation Delay
1.0000
Pulse Width
5.8000
Acquisition Time
3.0000
Acquisition Date
2017-09-18T23:34:32
Spectrometer Frequency
499.64
Spectral Width
8000.0
Lowest Frequency
-1002.2
Nucleus
1H
Acquired Size
24000
Spectral Size
65536
A (m) 6.12
B (t) 3.18
C (dddd) 2.18
D (p) 1.91
I
Br
S15
2.00
2.30
1.96
2.19
1.00
0.60
2.3
2.2
f1 (ppm)
10.5 10.0 9.5 9.0 8.5 8.0 7.5 7.0 6.5 6.0 5.5 5.0 4.5 4.0 3.5 3.0 2.5 2.0 1.5 1.0 0.5 0.0
f1 (ppm)

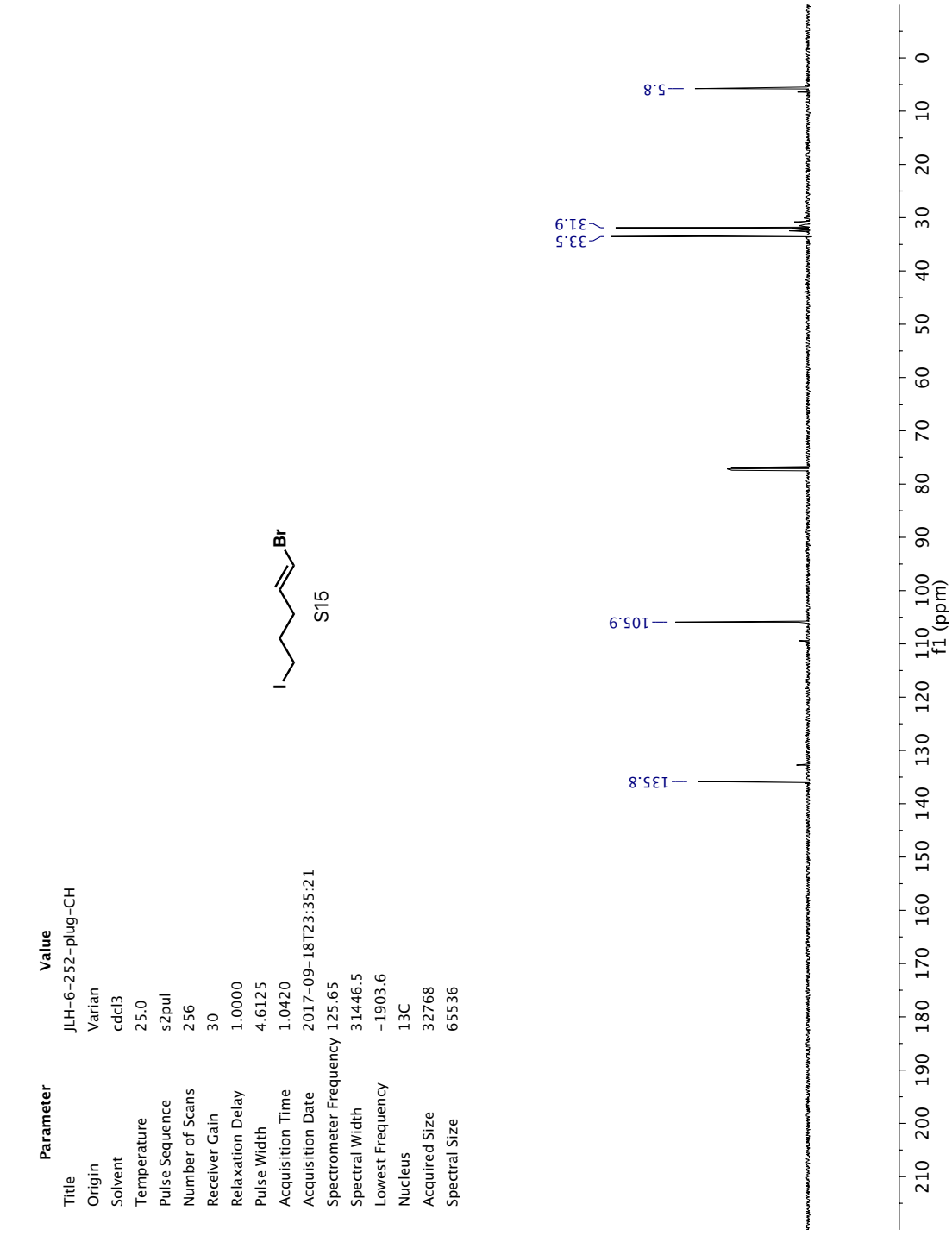
Parameter Value
Title JLH-6-252-plug-CH
Origin Varian
Solvent cdcl3
Temperature 25.0
Pulse Sequence s2pul
Number of Scans 256
Receiver Gain 30
Relaxation Delay 1.0000
Pulse Width 4.6125
Acquisition Time 1.0420
Acquisition Date 2017-09-18T23:35:21
Spectrometer Frequency 125.65
Spectral Width 31446.5
Lowest Frequency -1903.6
Nucleus 13C
Acquired Size 32768
Spectral Size 65536
Br
I
S15
135.8
105.9
33.5
31.9
5.8
210 200 190 180 170 160 150 140 130 120 110 100 90 80 70 60 50 40 30 20 10 0
f1 (ppm)

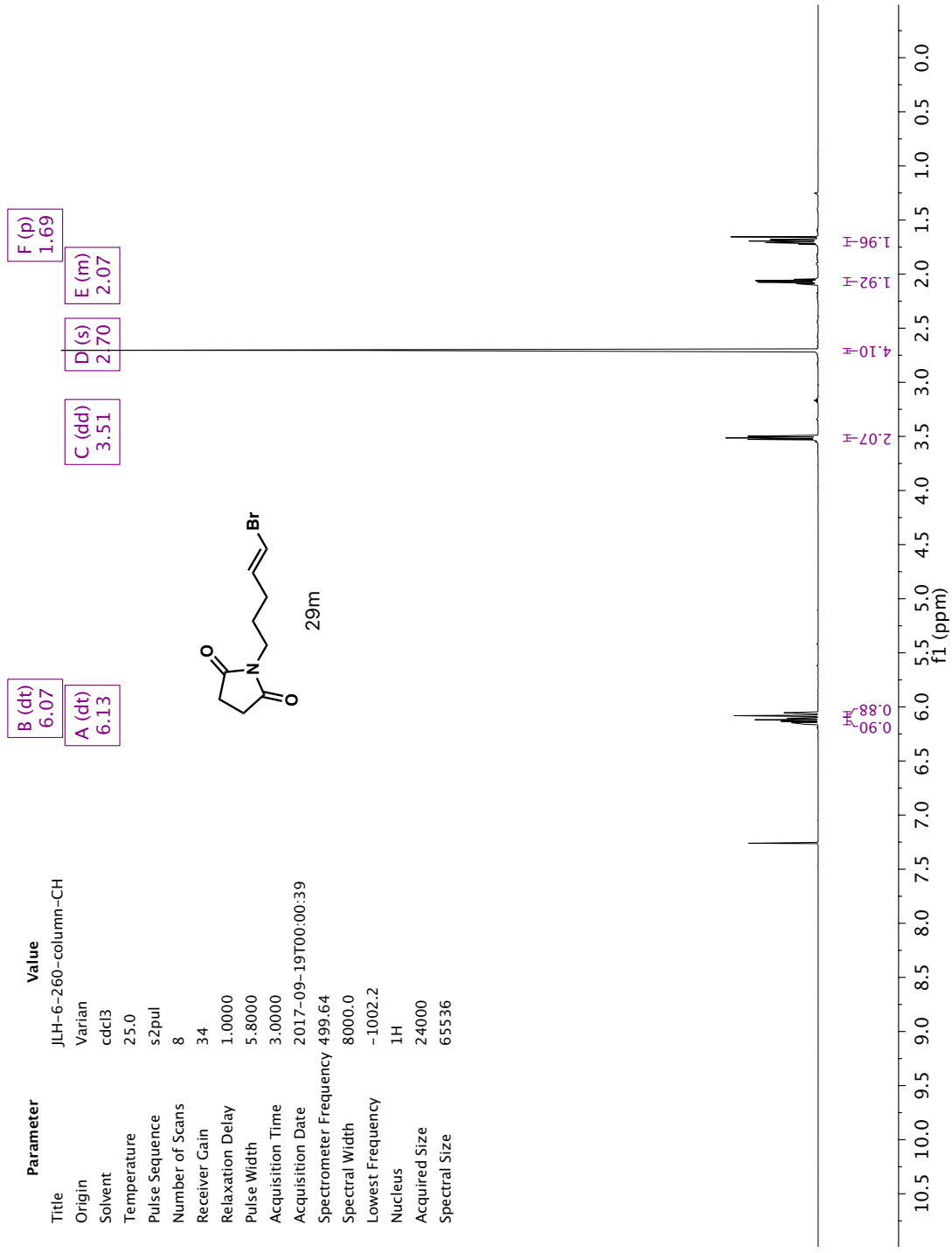
B (dt) 6.07
A (dt) 6.13
C (dd) 3.51
D (s) 2.70
E (m) 2.07
F (p) 1.69
Br
O
N
O
29m
Parameter Value
Title JLH-6-260-column-CH
Origin Varian
Solvent cdcl3
Temperature 25.0
Pulse Sequence s2pul
Number of Scans 8
Receiver Gain 34
Relaxation Delay 1.0000
Pulse Width 5.8000
Acquisition Time 3.0000
Acquisition Date 2017-09-19T00:00:39
Spectrometer Frequency 499.64
Spectral Width 8000.0
Lowest Frequency -1002.2
Nucleus 1H
Acquired Size 24000
Spectral Size 65536
0.90
0.88
2.07
4.10
1.92
1.96
10.5 10.0 9.5 9.0 8.5 8.0 7.5 7.0 6.5 6.0 5.5 5.0 4.5 4.0 3.5 3.0 2.5 2.0 1.5 1.0 0.5 0.0
f1 (ppm)

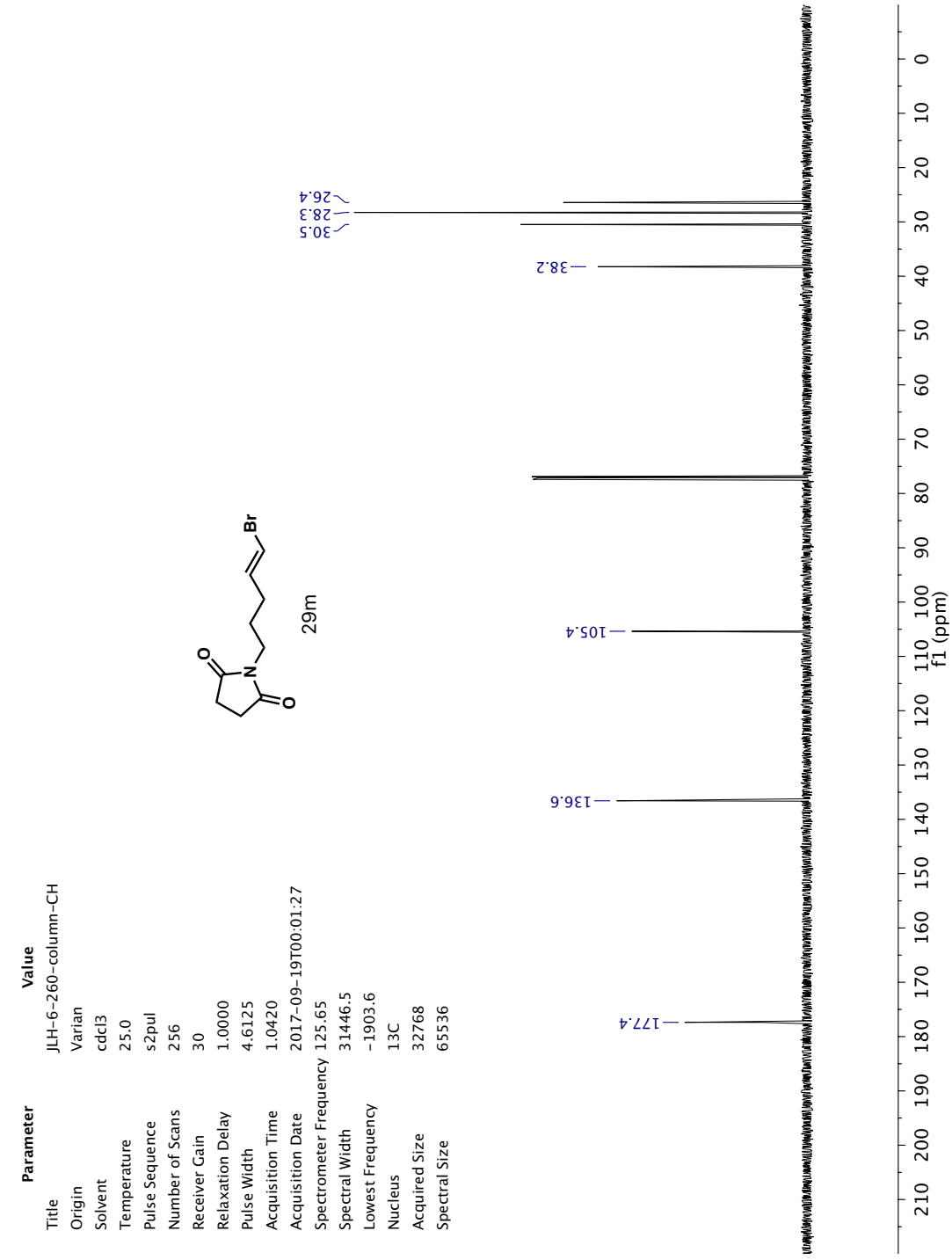
Parameter Value
Title JLH-6-260-column-CH
Origin Varian
Solvent cdcl3
Temperature 25.0
Pulse Sequence s2pul
Number of Scans 256
Receiver Gain 30
Relaxation Delay 1.0000
Pulse Width 4.6125
Acquisition Time 1.0420
Acquisition Date 2017-09-19T00:01:27
Spectrometer Frequency 125.65
Spectral Width 31446.5
Lowest Frequency -1903.6
Nucleus 13C
Acquired Size 32768
Spectral Size 65536
Br
O
N
O
29m
177.4
136.6
105.4
38.2
30.5
28.3
26.4
f1 (ppm)

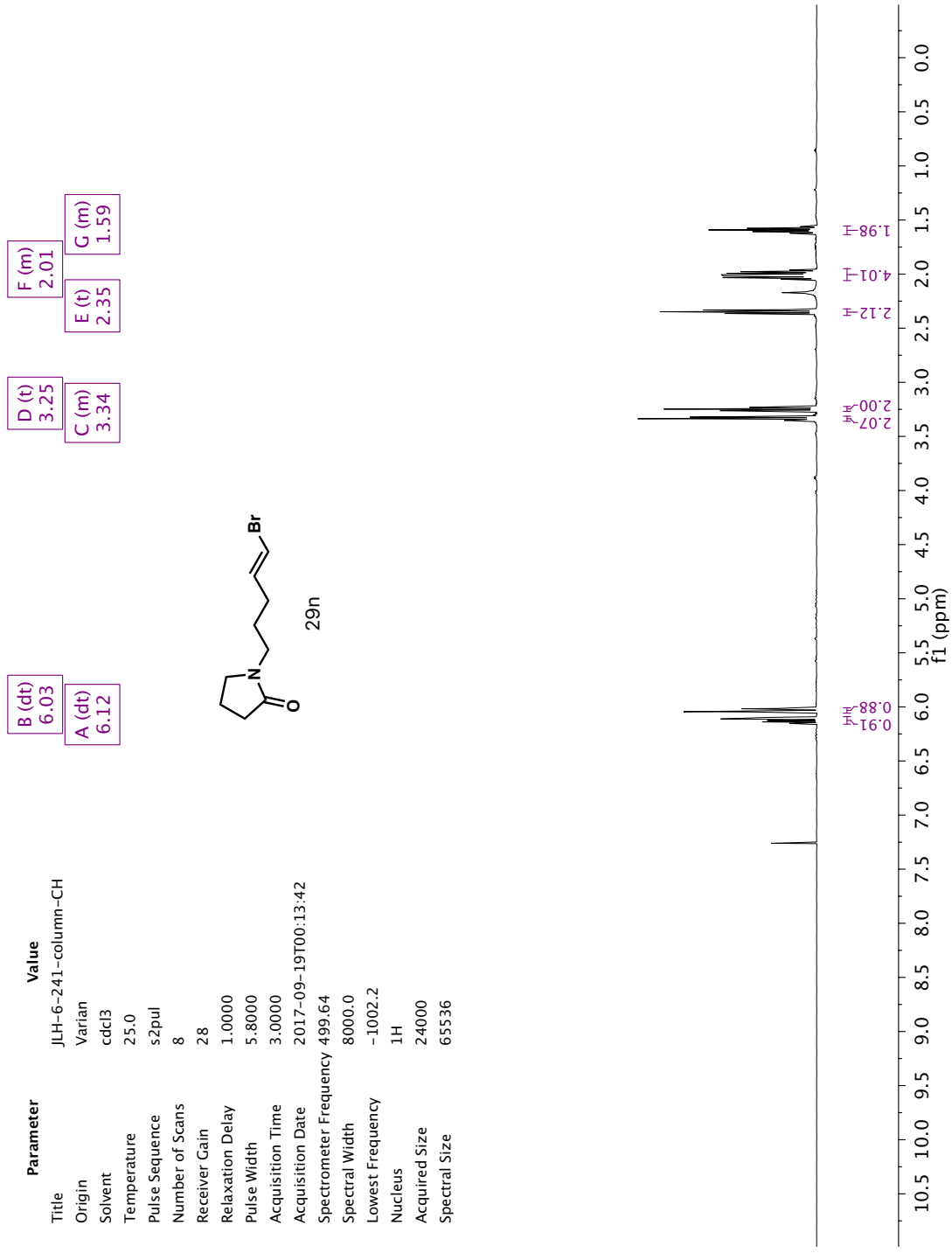
B (dt) 6.03
A (dt) 6.12
D (t) 3.25
C (m) 3.34
F (m) 2.01
E (t) 2.35
G (m) 1.59
Br
N
O
29n
Parameter Value
Title JLH-6-241-column-CH
Origin Varian
Solvent cdcl3
Temperature 25.0
Pulse Sequence s2pul
Number of Scans 8
Receiver Gain 28
Relaxation Delay 1.0000
Pulse Width 5.8000
Acquisition Time 3.0000
Acquisition Date 2017-09-19T00:13:42
Spectrometer Frequency 499.64
Spectral Width 8000.0
Lowest Frequency -1002.2
Nucleus 1H
Acquired Size 24000
Spectral Size 65536
0.91
0.88
2.07
2.00
2.12
4.01
1.98
10.5 10.0 9.5 9.0 8.5 8.0 7.5 7.0 6.5 6.0 5.5 5.0 4.5 4.0 3.5 3.0 2.5 2.0 1.5 1.0 0.5 0.0
f1 (ppm)

Parameter	Value
Title	JLH-6-241-column-CH
Origin	Varian
Solvent	cdcl3
Temperature	25.0
Pulse Sequence	s2pul
Number of Scans	256
Receiver Gain	30
Relaxation Delay	1.0000
Pulse Width	4.6125
Acquisition Time	1.0420
Acquisition Date	2017-09-19T00:14:31
Spectrometer Frequency	125.65
Spectral Width	31446.5
Lowest Frequency	-1903.6
Nucleus	13C
Acquired Size	32768
Spectral Size	65536

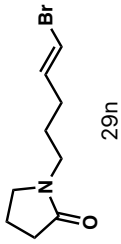

29n

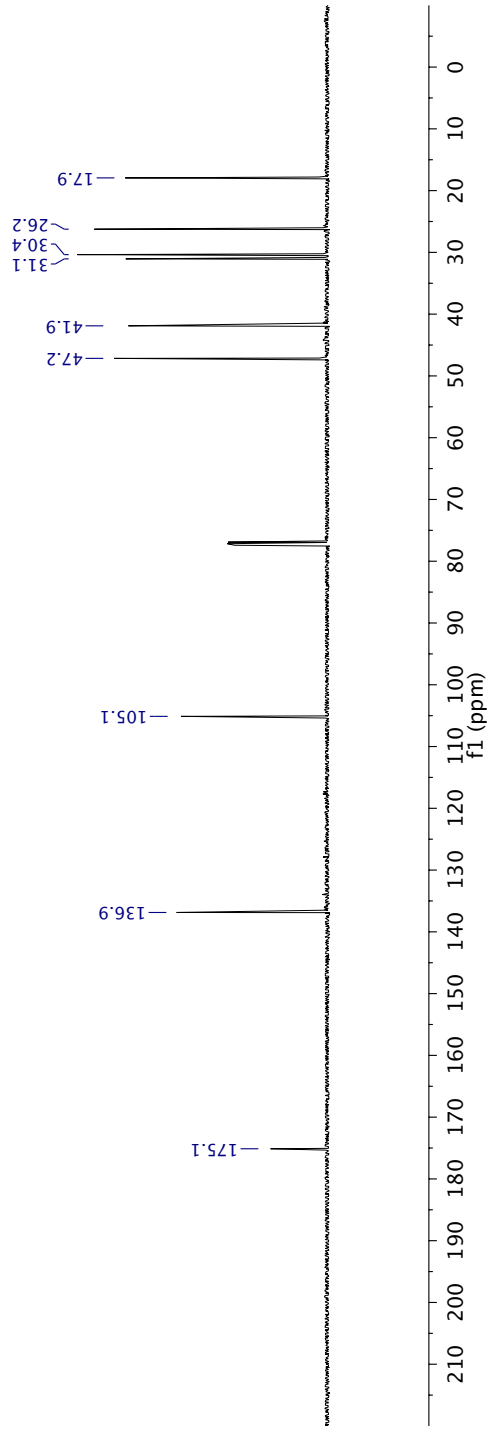

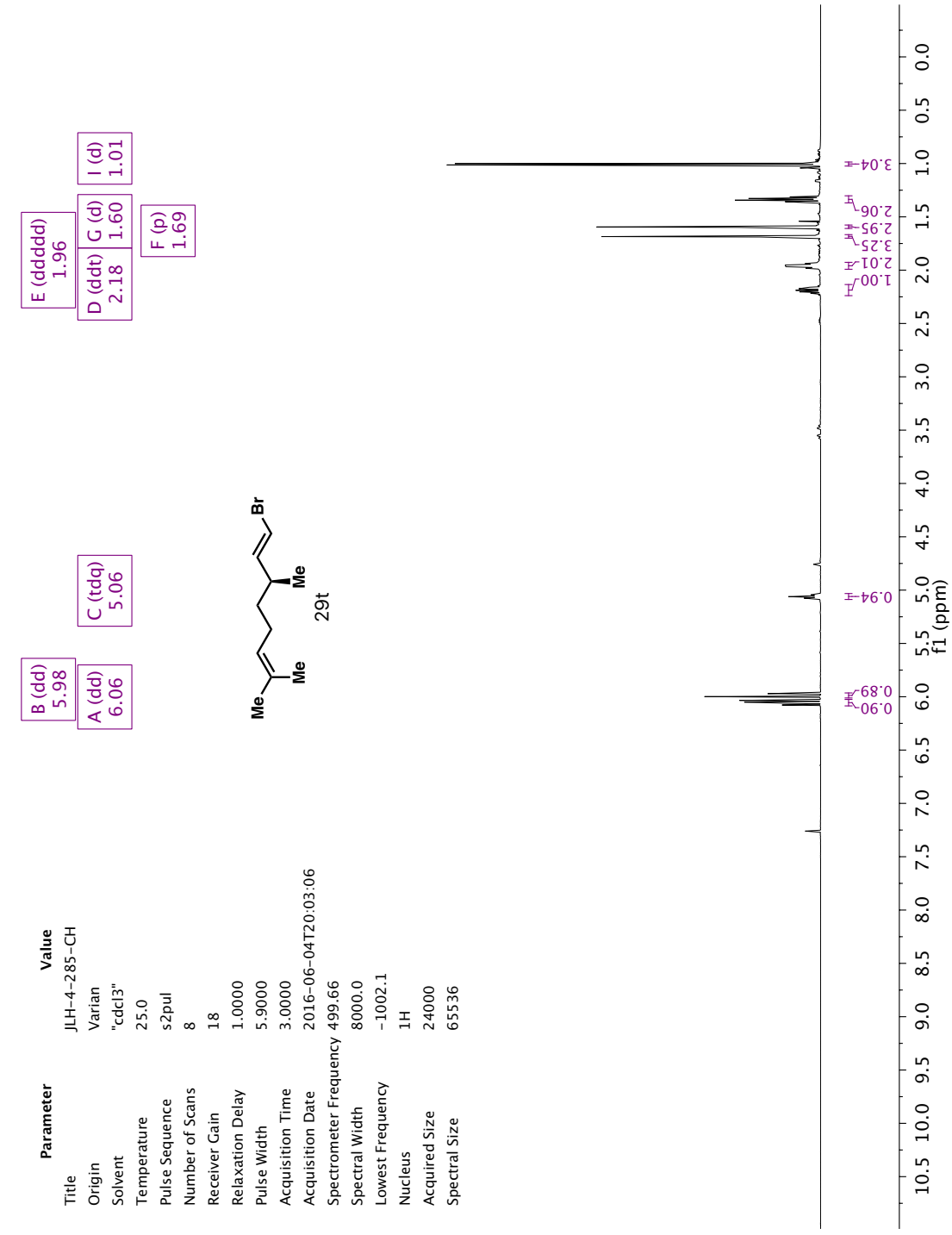
B (dd) 5.98
A (dd) 6.06
C (tdq) 5.06
E (ddddd) 1.96
D (ddt) 2.18
G (d) 1.60
I (d) 1.01
F (p) 1.69
Me
Me
Me
Br
29t
Parameter Value
Title JLH-4-285-CH
Origin Varian
Solvent "cdcl3"
Temperature 25.0
Pulse Sequence s2pul
Number of Scans 8
Receiver Gain 18
Relaxation Delay 1.0000
Pulse Width 5.9000
Acquisition Time 3.0000
Acquisition Date 2016-06-04T20:03:06
Spectrometer Frequency 499.66
Spectral Width 8000.0
Lowest Frequency -1002.1
Nucleus 1H
Acquired Size 24000
Spectral Size 65536
0.90
0.89
0.94
1.00
2.01
3.25
2.95
2.06
3.04
10.5 10.0 9.5 9.0 8.5 8.0 7.5 7.0 6.5 6.0 5.5 5.0 4.5 4.0 3.5 3.0 2.5 2.0 1.5 1.0 0.5 0.0
f1 (ppm)

Parameter	Value
Title	JLH-4-285-CH
Origin	Varian
Solvent	"cdcl3"
Temperature	25.0
Pulse Sequence	s2pul
Number of Scans	256
Receiver Gain	30
Relaxation Delay	1.0000
Pulse Width	4.5000
Acquisition Time	1.0420
Acquisition Date	2016-06-04T20:03:54
Spectrometer Frequency	125.65
Spectral Width	31446.5
Lowest Frequency	-1903.0
Nucleus	13C
Acquired Size	32768
Spectral Size	65536

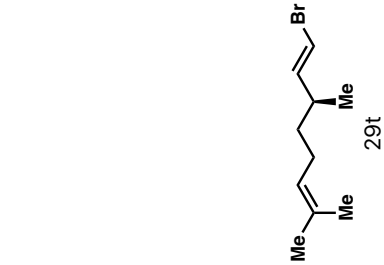

29t

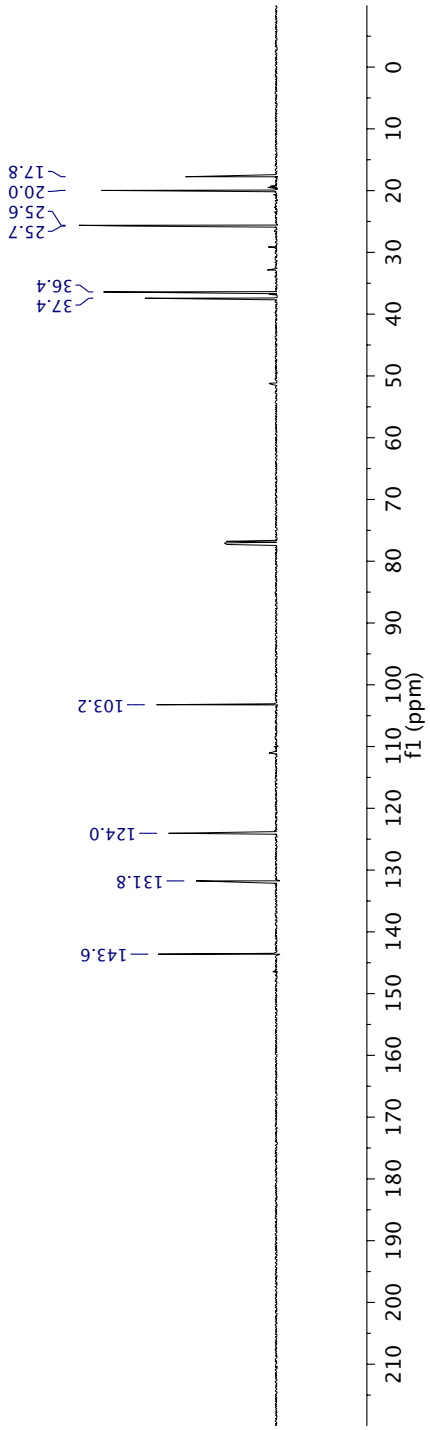

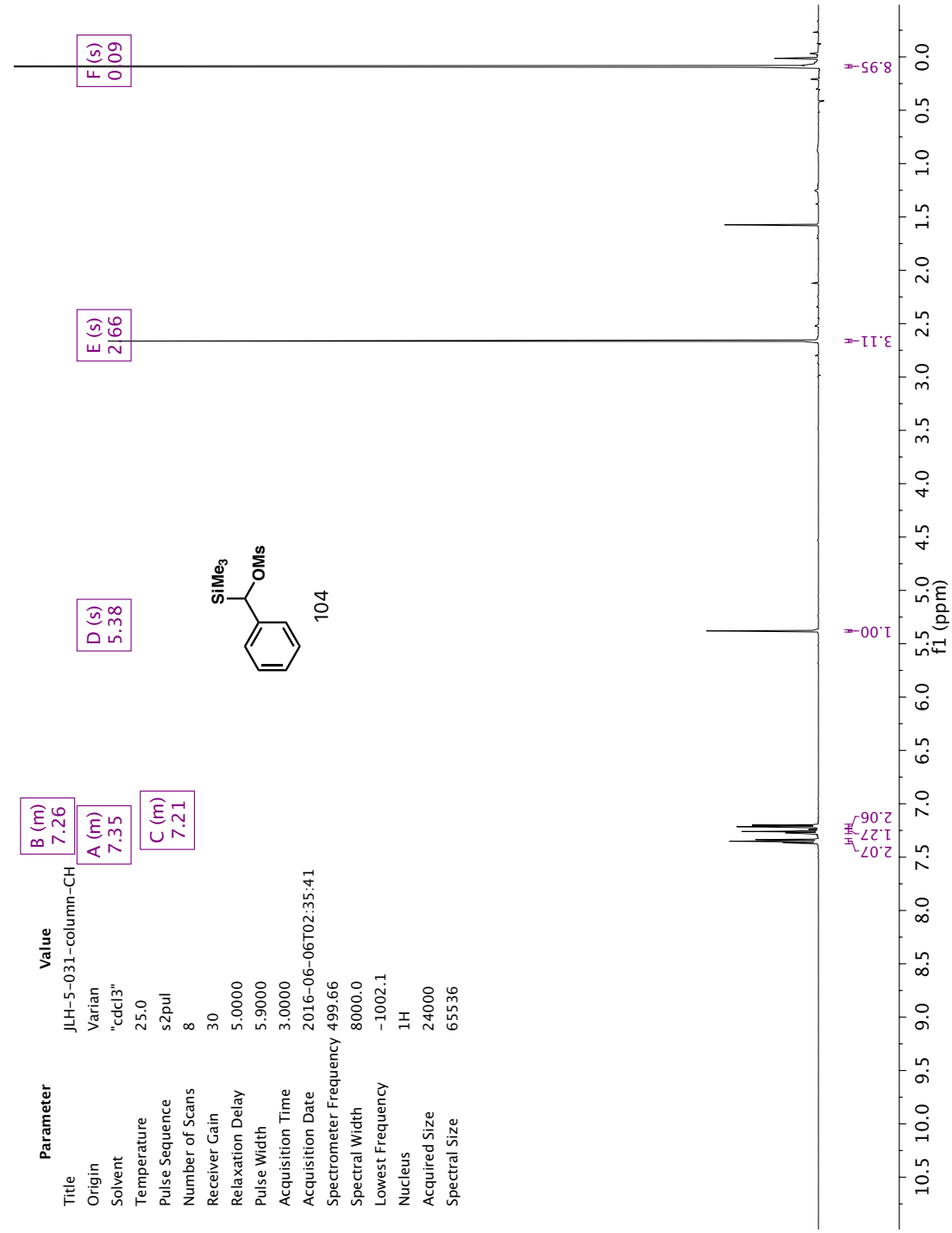
Parameter
Value
Title
JLH-5-031-column-CH
Origin
Varian
Solvent
"cdcl3"
Temperature
25.0
Pulse Sequence
s2pul
Number of Scans
8
Receiver Gain
30
Relaxation Delay
5.0000
Pulse Width
5.9000
Acquisition Time
3.0000
Acquisition Date
2016-06-06T02:35:41
Spectrometer Frequency
499.66
Spectral Width
8000.0
Lowest Frequency
-1002.1
Nucleus
1H
Acquired Size
24000
Spectral Size
65536
B (m) 7.26
A (m) 7.35
C (m) 7.21
D (s) 5.38
E (s) 2.66
F (s) 0.09
SiMe3
OMs
104
8.95
3.11
1.00
2.07
1.27
2.06
f1 (ppm)

Parameter	Value
Title	JLH-5-031-column-CH
Origin	Varian
Solvent	"cdcl3"
Temperature	25.0
Pulse Sequence	s2pul
Number of Scans	512
Receiver Gain	30
Relaxation Delay	1.0000
Pulse Width	4.5000
Acquisition Time	1.0420
Acquisition Date	2016-06-06T02:17:43
Spectrometer Frequency	125.65
Spectral Width	31446.5
Lowest Frequency	-1903.0
Nucleus	13C
Acquired Size	32768
Spectral Size	65536

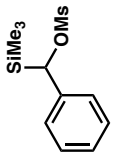

104

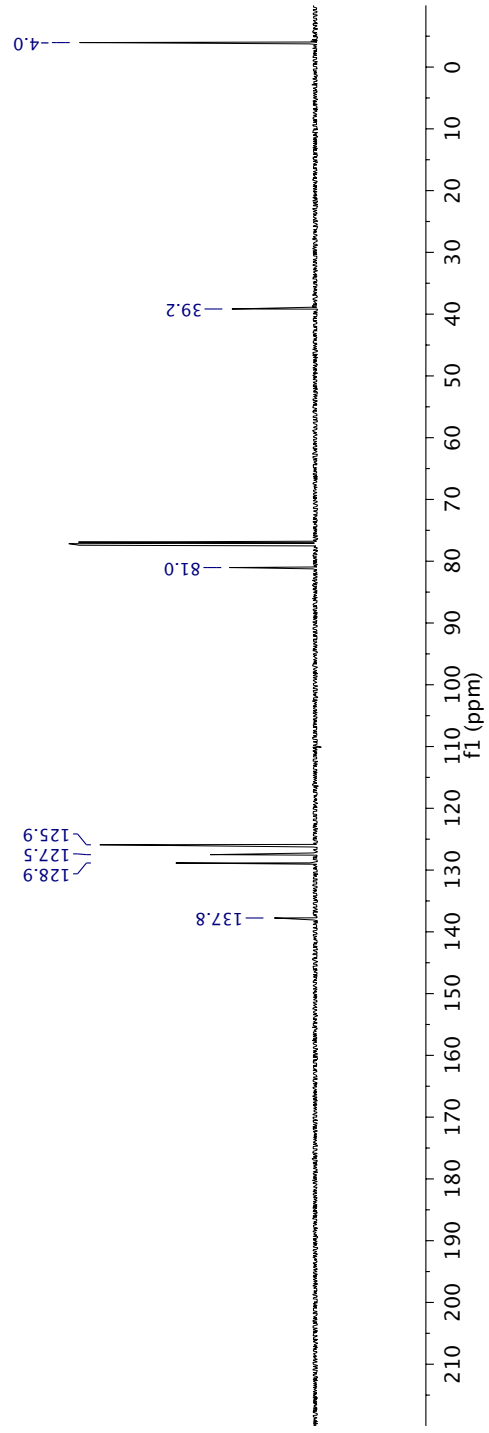

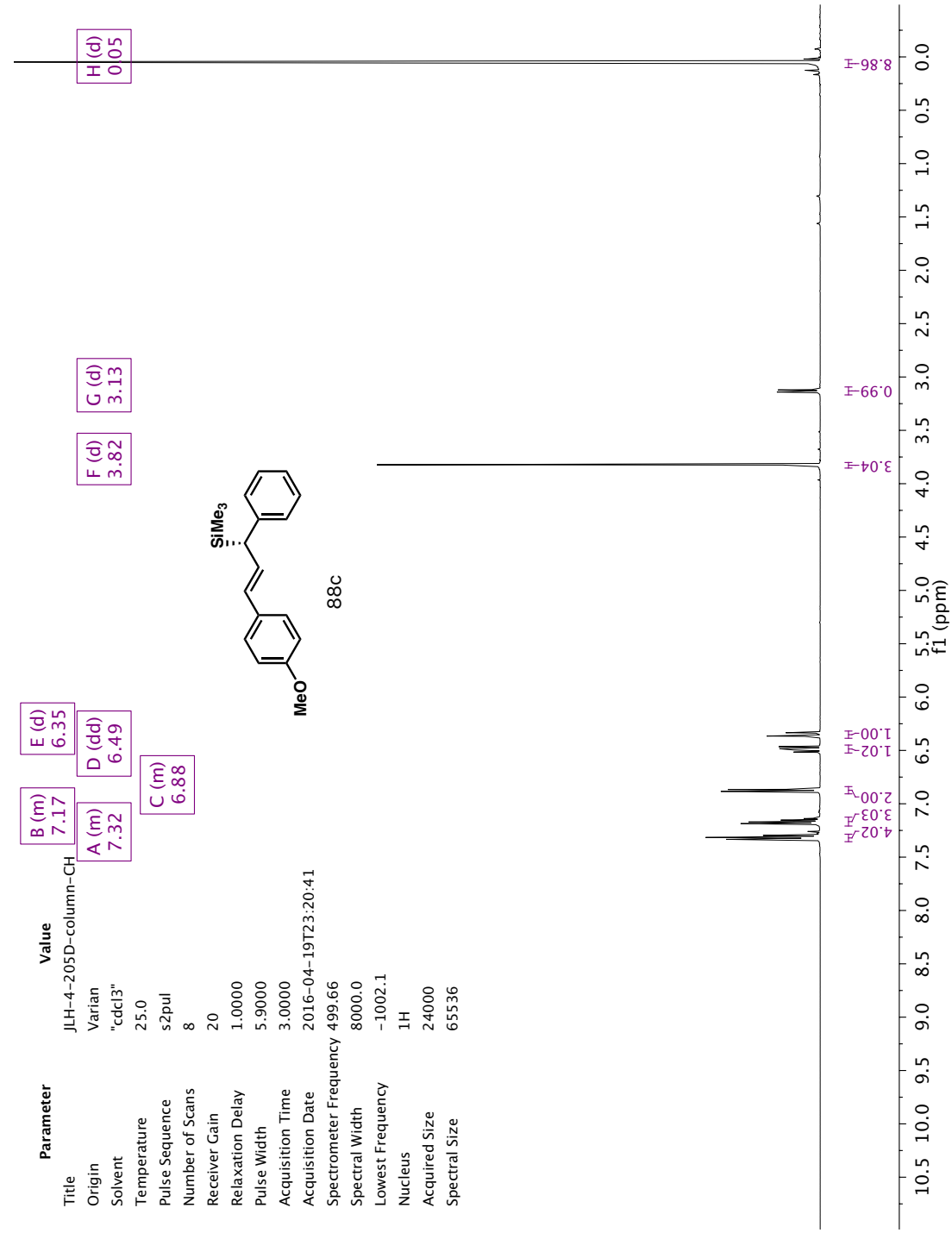
Parameter
Value
Title
JLH-4-205D-column-CH
Origin
Varian
Solvent
"cdcl3"
Temperature
25.0
Pulse Sequence
s2pul
Number of Scans
8
Receiver Gain
20
Relaxation Delay
1.0000
Pulse Width
5.9000
Acquisition Time
3.0000
Acquisition Date
2016-04-19T23:20:41
Spectrometer Frequency
499.66
Spectral Width
8000.0
Lowest Frequency
-1002.1
Nucleus
1H
Acquired Size
24000
Spectral Size
65536
A (m) 7.32
B (m) 7.17
C (m) 6.88
D (dd) 6.49
E (d) 6.35
F (d) 3.82
G (d) 3.13
H (d) 0.05
SiMe3
MeO
88c
8.86
3.04
0.99
1.02
1.00
2.00
3.03
4.02
f1 (ppm)

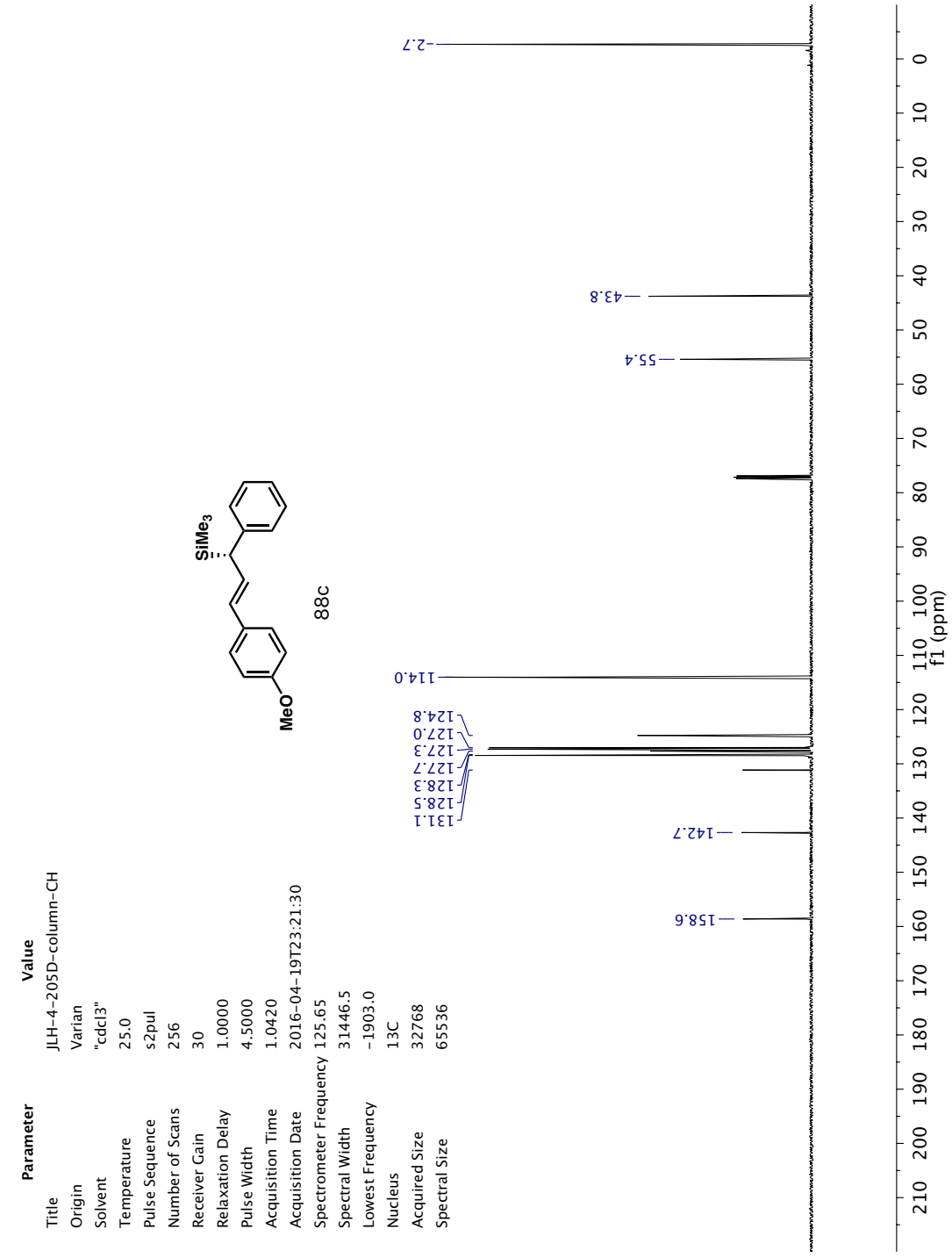

Parameter	Value
Title	JLH-4-205D-column-CH
Origin	Varian
Solvent	"cdcl3"
Temperature	25.0
Pulse Sequence	s2pul
Number of Scans	256
Receiver Gain	30
Relaxation Delay	1.0000
Pulse Width	4.5000
Acquisition Time	1.0420
Acquisition Date	2016-04-19T23:21:30
Spectrometer Frequency	125.65
Spectral Width	31446.5
Lowest Frequency	-1903.0
Nucleus	13C
Acquired Size	32768
Spectral Size	65536

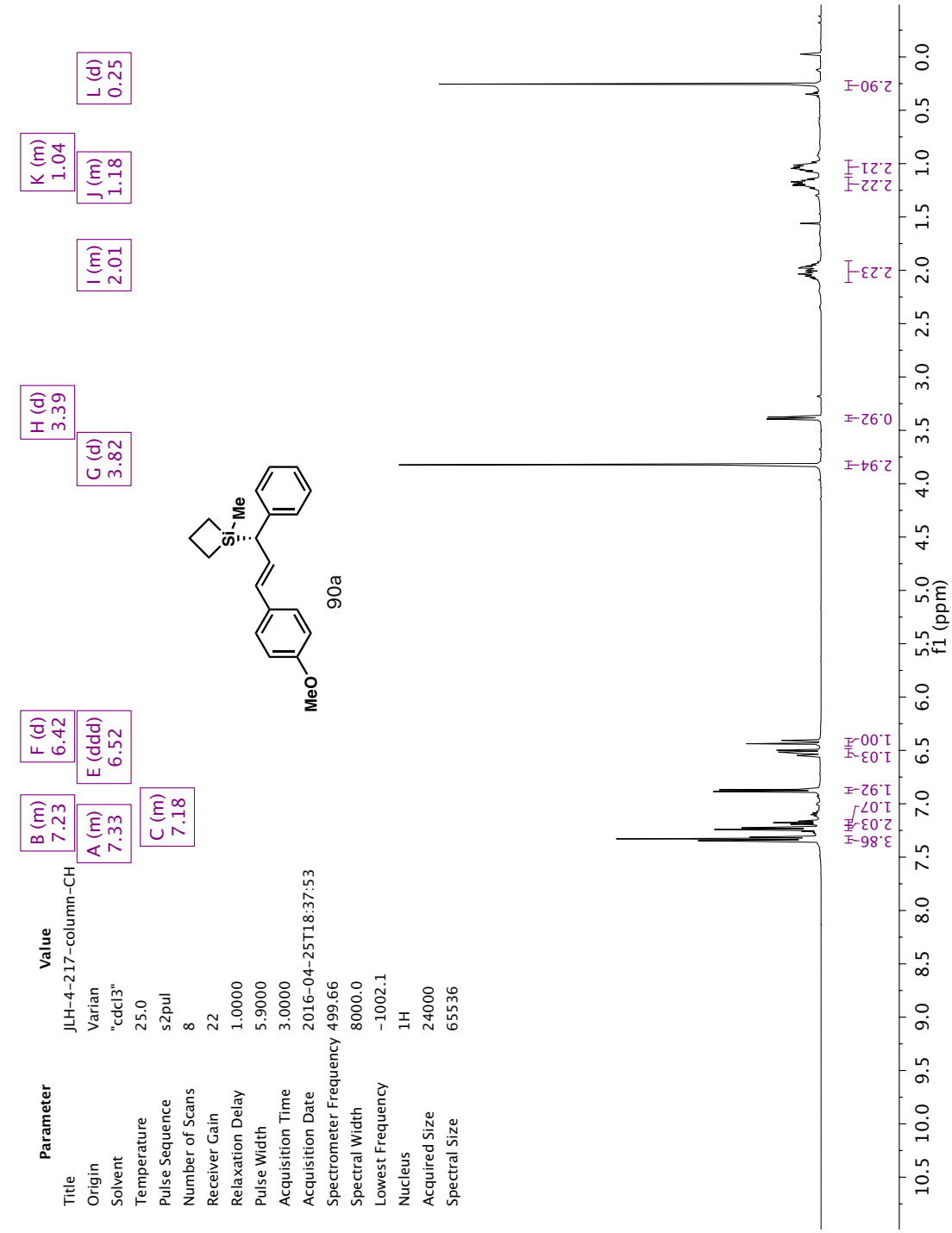
Parameter
Value
Title JLH-4-217-column-CH
Origin Varian
Solvent "cdcl3"
Temperature 25.0
Pulse Sequence s2pul
Number of Scans 8
Receiver Gain 22
Relaxation Delay 1.0000
Pulse Width 5.9000
Acquisition Time 3.0000
Acquisition Date 2016-04-25T18:37:53
Spectrometer Frequency 499.66
Spectral Width 8000.0
Lowest Frequency -1002.1
Nucleus 1H
Acquired Size 24000
Spectral Size 65536
B (m) 7.23
A (m) 7.33
C (m) 7.18
F (d) 6.42
E (ddd) 6.52
G (d) 3.82
H (d) 3.39
I (m) 2.01
J (m) 1.18
K (m) 1.04
L (d) 0.25
Si
Me
MeO
90a
3.86
2.03
1.07
1.92
1.03
1.00
2.94
0.92
2.23
2.22
2.21
2.90
f1 (ppm)

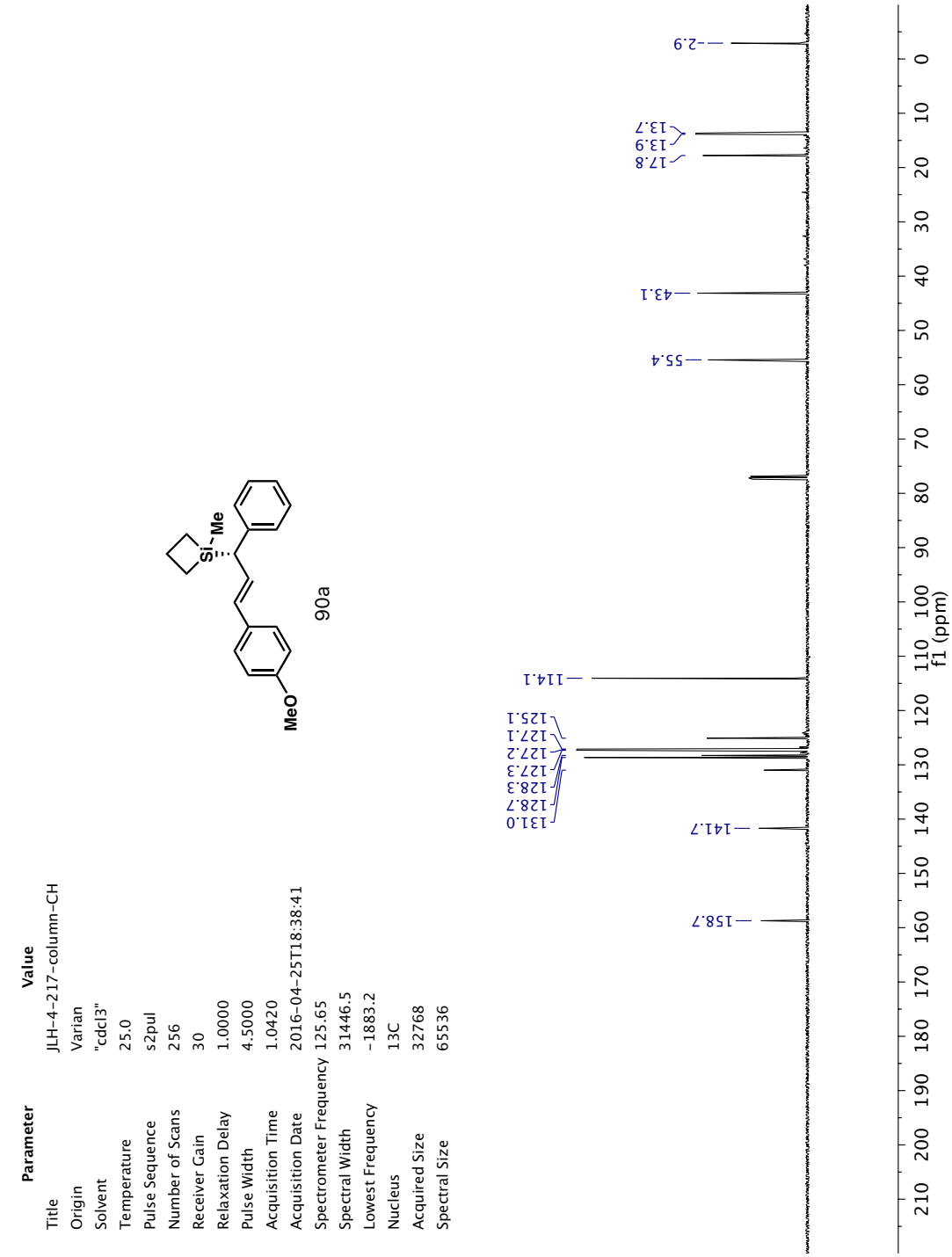
Parameter Value
Title JLH-4-217-column-CH
Origin Varian
Solvent "cdcl3"
Temperature 25.0
Pulse Sequence s2pul
Number of Scans 256
Receiver Gain 30
Relaxation Delay 1.0000
Pulse Width 4.5000
Acquisition Time 1.0420
Acquisition Date 2016-04-25T18:38:41
Spectrometer Frequency 125.65
Spectral Width 31446.5
Lowest Frequency -1883.2
Nucleus 13C
Acquired Size 32768
Spectral Size 65536
Si
Me
MeO
90a
158.7
141.7
131.0
128.7
128.3
127.3
127.2
127.1
125.1
114.1
55.4
43.1
17.8
13.9
13.7
2.9
f1 (ppm)

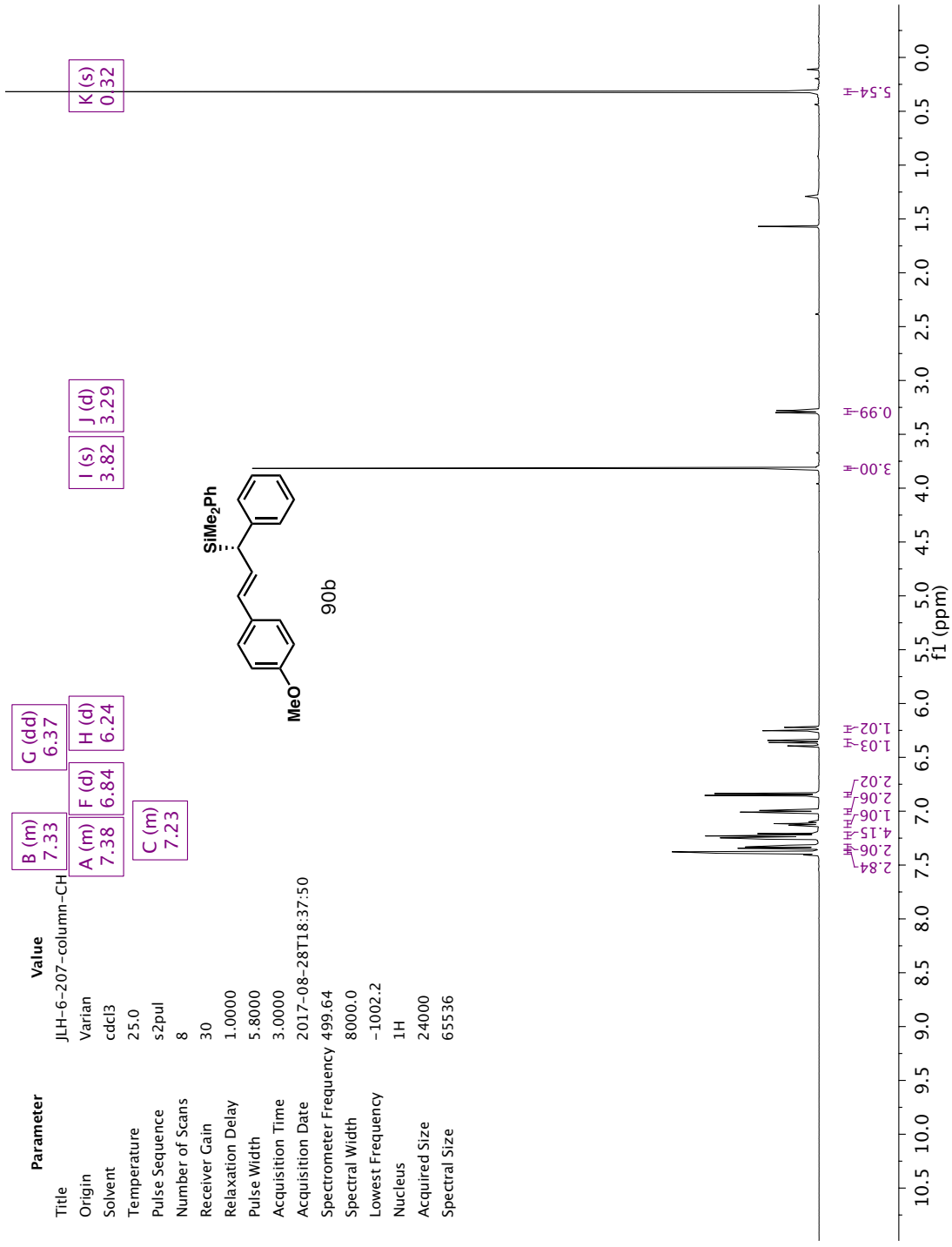
Parameter
Value
Title JLH-6-207-column-CH
Origin Varian
Solvent cdcl3
Temperature 25.0
Pulse Sequence s2pul
Number of Scans 8
Receiver Gain 30
Relaxation Delay 1.0000
Pulse Width 5.8000
Acquisition Time 3.0000
Acquisition Date 2017-08-28T18:37:50
Spectrometer Frequency 499.64
Spectral Width 8000.0
Lowest Frequency -1002.2
Nucleus 1H
Acquired Size 24000
Spectral Size 65536
B (m) 7.33
A (m) 7.38
G (dd) 6.37
F (d) 6.84
H (d) 6.24
C (m) 7.23
I (s) 3.82
J (d) 3.29
K (s) 0.32
SiMe2Ph
MeO
90b
5.54
0.99
3.00
1.02
1.03
2.02
2.06
1.06
4.15
2.06
2.84
f1 (ppm)

Parameter	Value
Title	JLH-6-207-column-CH
Origin	Varian
Solvent	cdcl3
Temperature	25.0
Pulse Sequence	s2pul
Number of Scans	256
Receiver Gain	30
Relaxation Delay	1.0000
Pulse Width	4.6125
Acquisition Time	1.0420
Acquisition Date	2017-08-28T18:38:39
Spectrometer Frequency	125.65
Spectral Width	31446.5
Lowest Frequency	-1903.6
Nucleus	13C
Acquired Size	32768
Spectral Size	65536

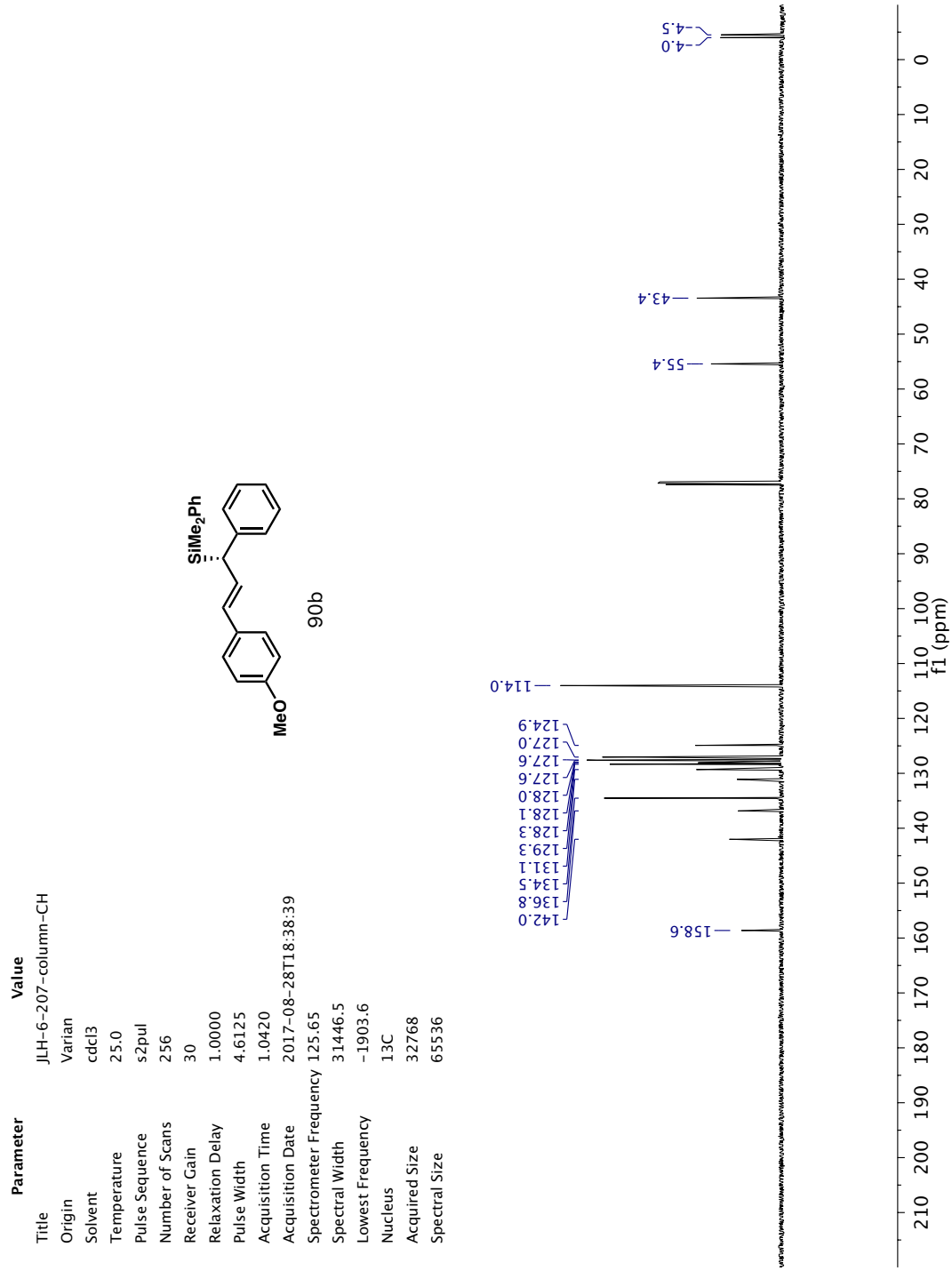

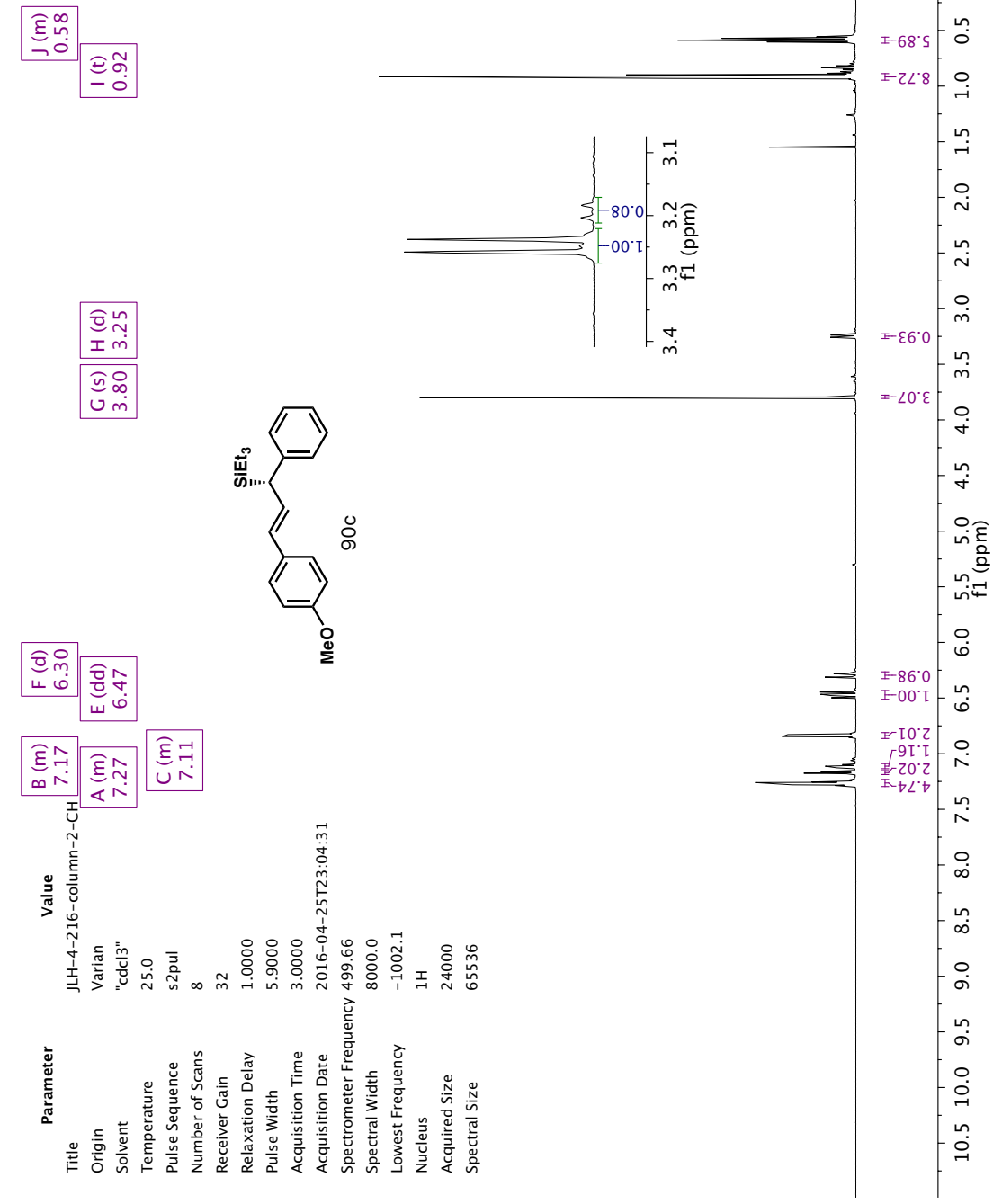
Parameter Value
Title JLH-4-216-column-2-CH
Origin Varian
Solvent "cdcl3"
Temperature 25.0
Pulse Sequence s2pul
Number of Scans 8
Receiver Gain 32
Relaxation Delay 1.0000
Pulse Width 5.9000
Acquisition Time 3.0000
Acquisition Date 2016-04-25T23:04:31
Spectrometer Frequency 499.66
Spectral Width 8000.0
Lowest Frequency -1002.1
Nucleus 1H
Acquired Size 24000
Spectral Size 65536
B (m) 7.17
A (m) 7.27
C (m) 7.11
F (d) 6.30
E (dd) 6.47
G (s) 3.80
H (d) 3.25
J (m) 0.58
I (t) 0.92
SiEt3
MeO
90c
4.74
2.02
1.16
2.01
1.00
0.98
3.07
0.93
8.72
5.89
0.08
1.00
f1 (ppm)

Parameter	Value
Title	JLH-4-216-column-2-CH
Origin	Varian
Solvent	"cdcl3"
Temperature	25.0
Pulse Sequence	s2pul
Number of Scans	512
Receiver Gain	30
Relaxation Delay	1.0000
Pulse Width	4.5000
Acquisition Time	1.0420
Acquisition Date	2016-04-25T23:05:19
Spectrometer Frequency	125.65
Spectral Width	31446.5
Lowest Frequency	-1903.0
Nucleus	13C
Acquired Size	32768
Spectral Size	65536

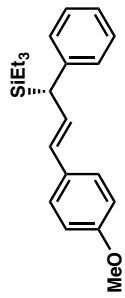

90c

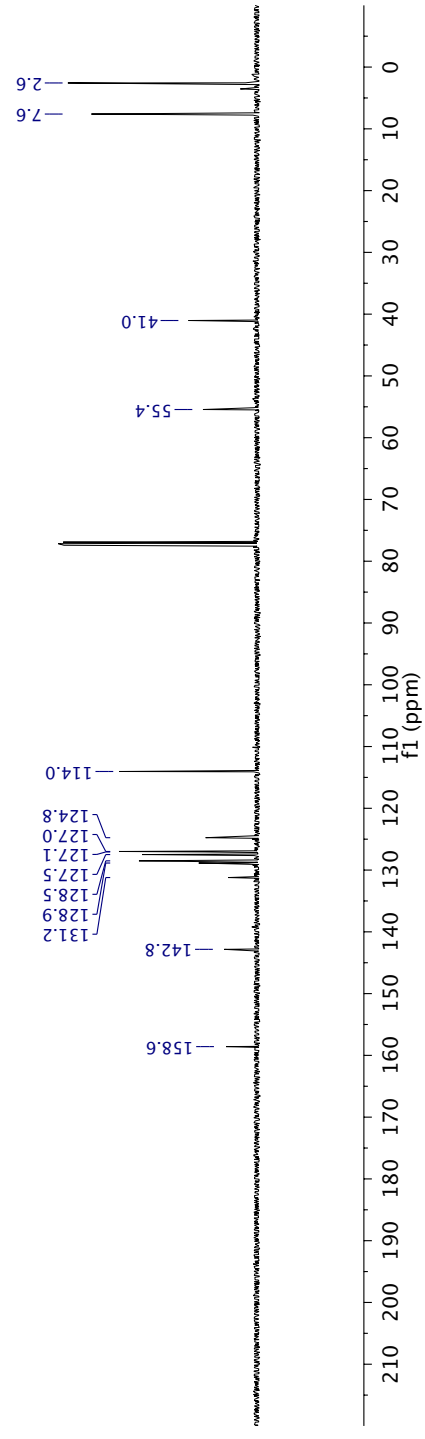

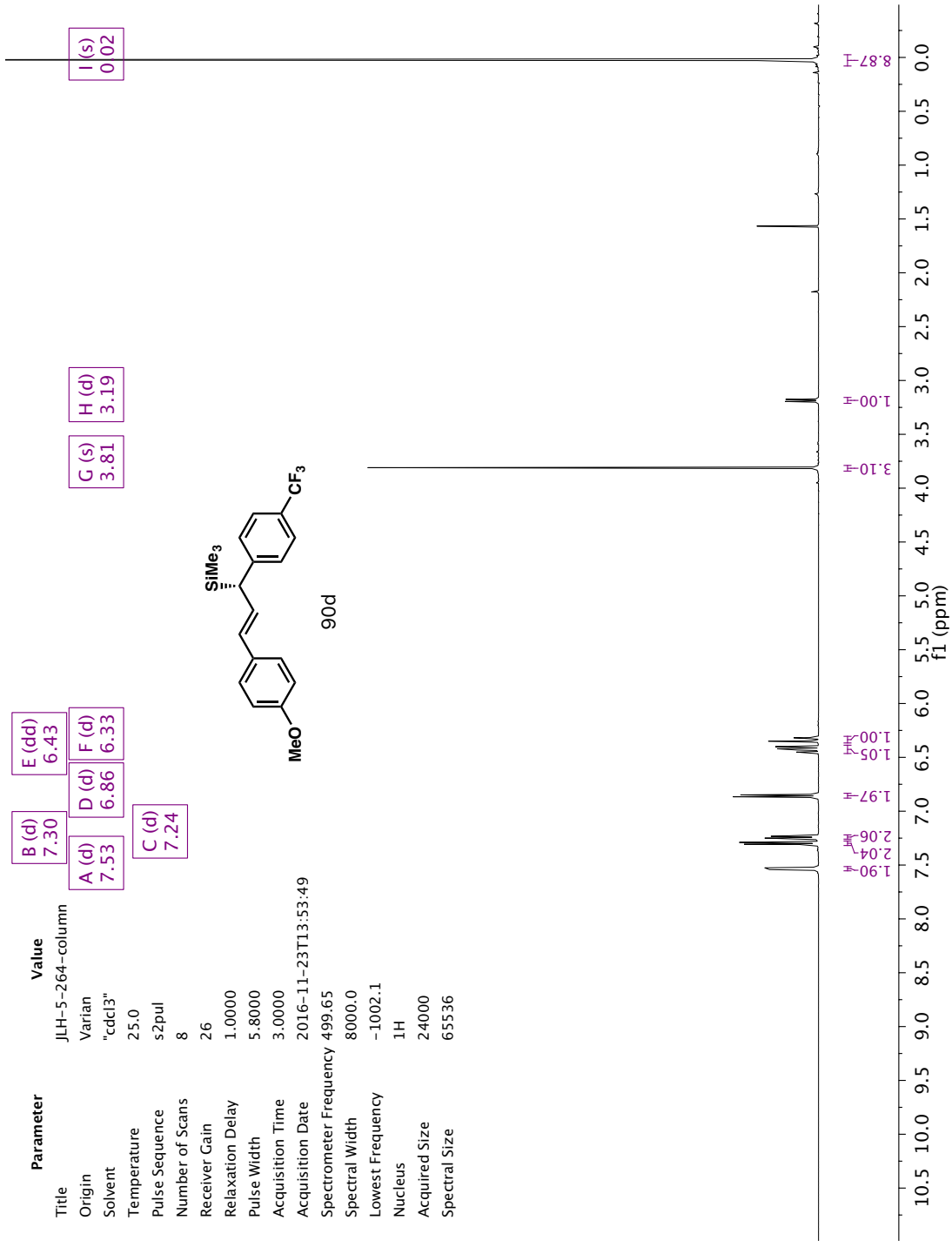
Parameter
Value
Title JLH-5-264-column
Origin Varian
Solvent "cdcl3"
Temperature 25.0
Pulse Sequence s2pul
Number of Scans 8
Receiver Gain 26
Relaxation Delay 1.0000
Pulse Width 5.8000
Acquisition Time 3.0000
Acquisition Date 2016-11-23T13:53:49
Spectrometer Frequency 499.65
Spectral Width 8000.0
Lowest Frequency -1002.1
Nucleus 1H
Acquired Size 24000
Spectral Size 65536
A (d) 7.53
B (d) 7.30
C (d) 7.24
D (d) 6.86
E (dd) 6.43
F (d) 6.33
G (s) 3.81
H (d) 3.19
I (s) 0.02
SiMe3
CF3
MeO
90d
8.87
3.10
1.00
1.90
2.04
2.06
1.97
1.05
1.00
f1 (ppm)

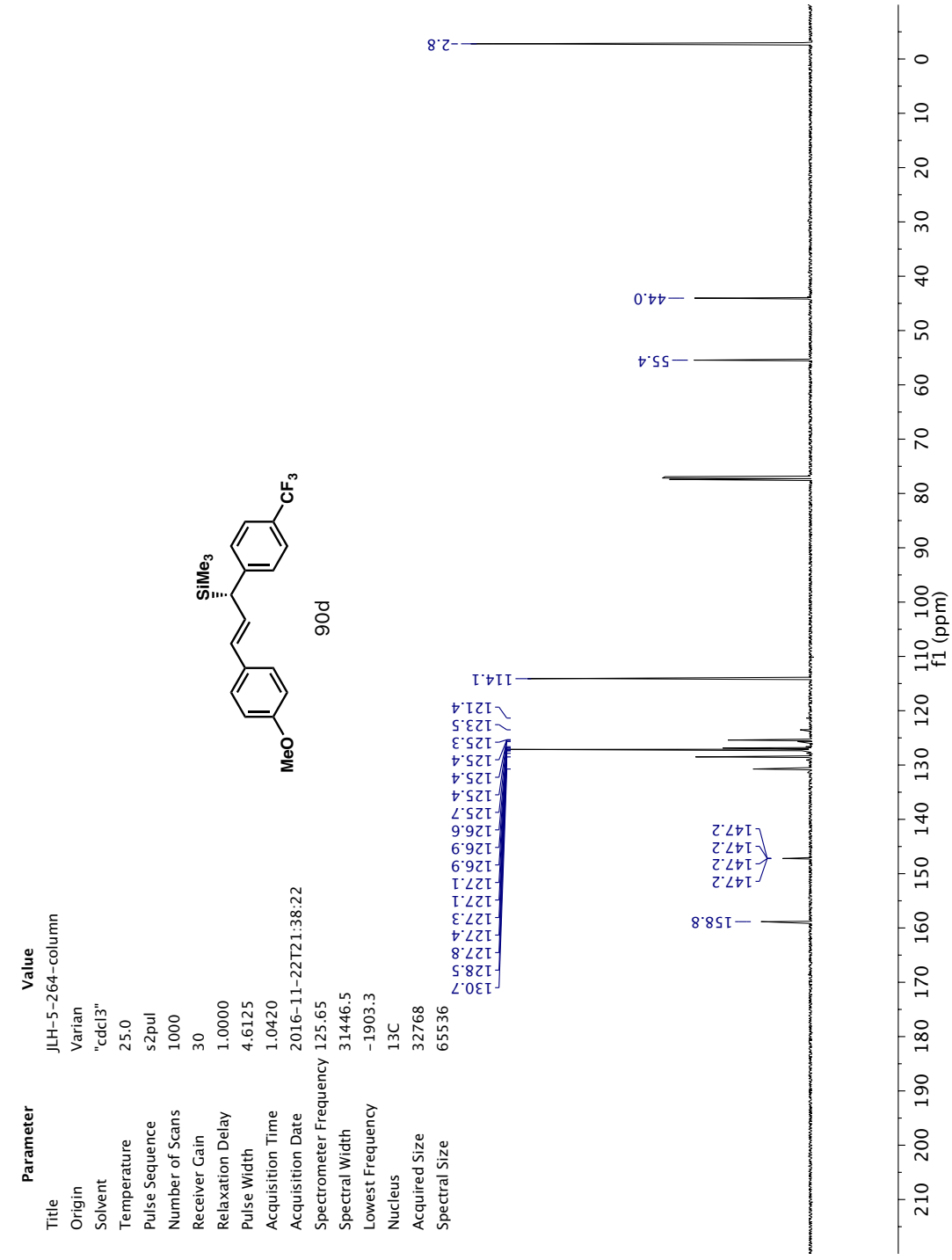
Parameter Value
Title JLH-5-264-column
Origin Varian
Solvent "cdcl3"
Temperature 25.0
Pulse Sequence s2pul
Number of Scans 1000
Receiver Gain 30
Relaxation Delay 1.0000
Pulse Width 4.6125
Acquisition Time 1.0420
Acquisition Date 2016-11-22T21:38:22
Spectrometer Frequency 125.65
Spectral Width 31446.5
Lowest Frequency -1903.3
Nucleus 13C
Acquired Size 32768
Spectral Size 65536
SiMe3
CF3
MeO
90d
-2.8
44.0
55.4
114.1
121.4
123.5
125.3
125.4
125.4
125.4
125.7
126.6
126.9
126.9
127.1
127.1
127.3
127.4
127.8
128.5
130.7
147.2
147.2
147.2
147.2
158.8
f1 (ppm)

Parameter	Value
Title	JLH-5-264-fluorine
Origin	Varian
Solvent	"cdcl3"
Temperature	25.0
Pulse Sequence	s2pul
Number of Scans	16
Receiver Gain	30
Relaxation Delay	1.0000
Pulse Width	6.3333
Acquisition Time	0.9856
Acquisition Date	2017-01-16T21:58:17
Spectrometer Frequency	282.34
Spectral Width	64935.1
Lowest Frequency	-56468.7
Nucleus	19F
Acquired Size	64000
Spectral Size	131072

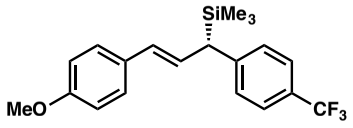

90d

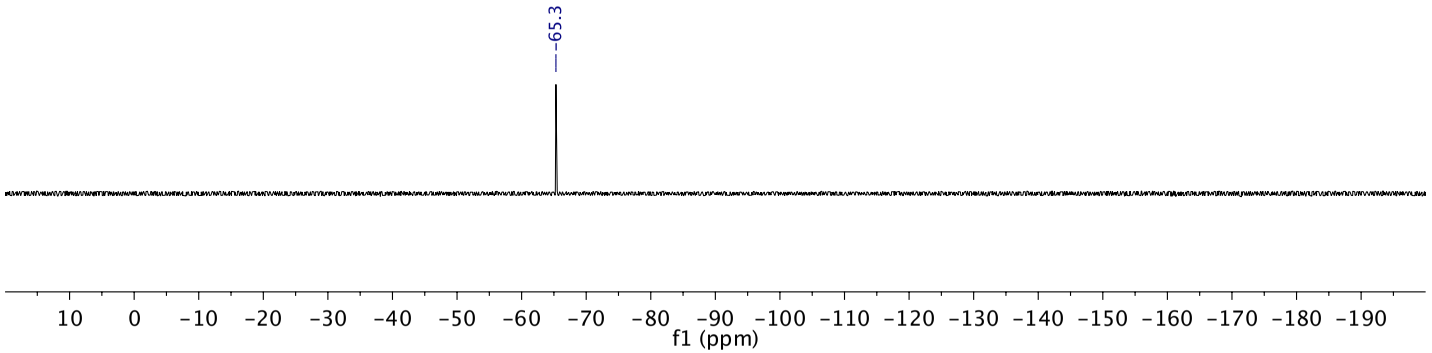

Parameter	Value
Title	JLH-5-264-fluorine-C6F6
Origin	Varian
Solvent	"cdcl3"
Temperature	25.0
Pulse Sequence	s2pul
Number of Scans	16
Receiver Gain	30
Relaxation Delay	1.0000
Pulse Width	6.3333
Acquisition Time	0.9856
Acquisition Date	2017-01-16T22:03:20
Spectrometer Frequency	282.34
Spectral Width	64935.1
Lowest Frequency	-56468.7
Nucleus	19F
Acquired Size	64000
Spectral Size	131072

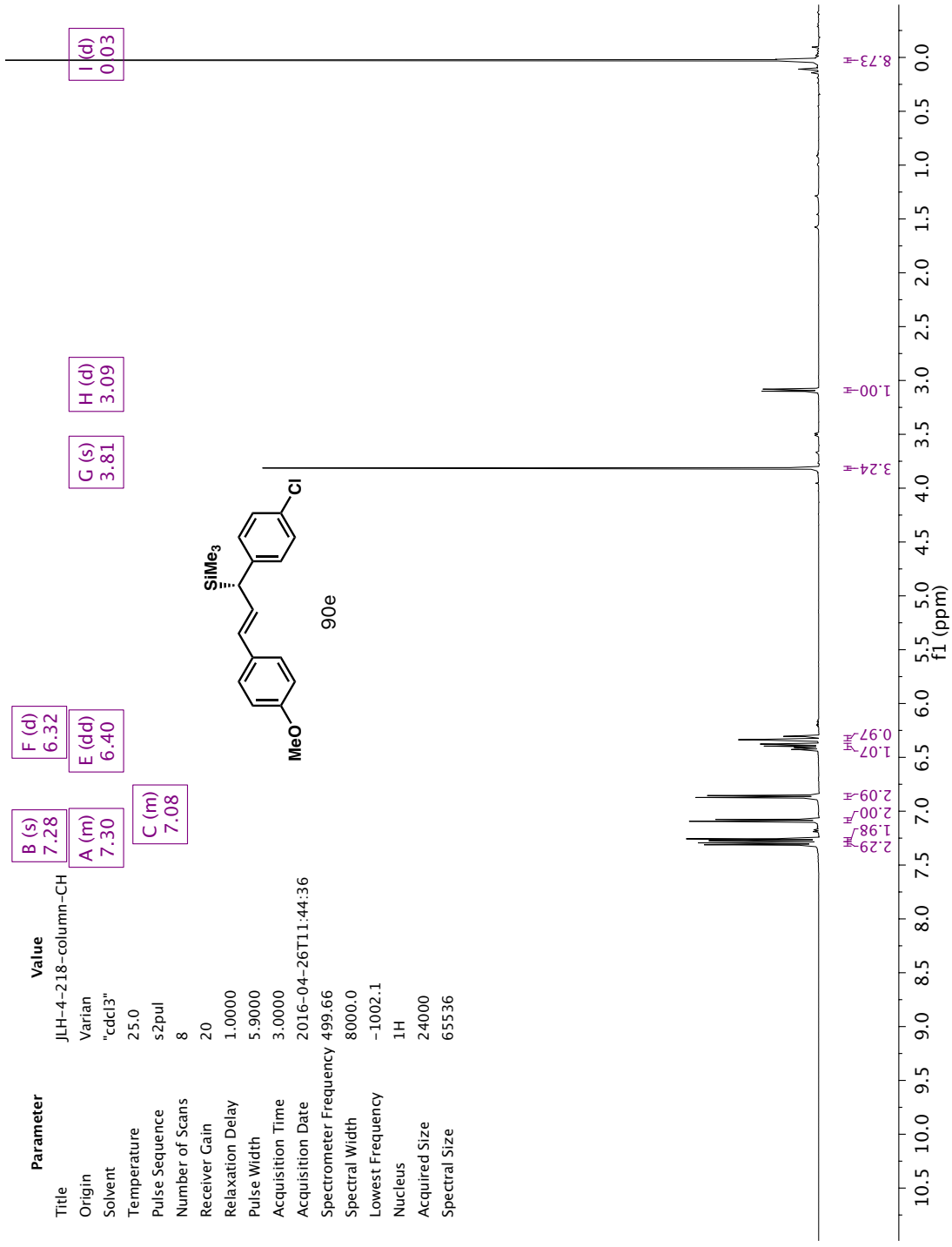

Parameter	Value
Title	JLH-4-218-column-CH
Origin	Varian
Solvent	"cdcl3"
Temperature	25.0
Pulse Sequence	s2pul
Number of Scans	8
Receiver Gain	20
Relaxation Delay	1.0000
Pulse Width	5.9000
Acquisition Time	3.0000
Acquisition Date	2016-04-26T11:44:36
Spectrometer Frequency	499.66
Spectral Width	8000.0
Lowest Frequency	-1002.1
Nucleus	1H
Acquired Size	24000
Spectral Size	65536

Parameter	Value
Title	JLH-4-218-column-CH
Origin	Varian
Solvent	"cdcl3"
Temperature	25.0
Pulse Sequence	s2pul
Number of Scans	256
Receiver Gain	30
Relaxation Delay	1.0000
Pulse Width	4.5000
Acquisition Time	1.0420
Acquisition Date	2016-04-26T11:45:24
Spectrometer Frequency	125.65
Spectral Width	31446.5
Lowest Frequency	-1903.0
Nucleus	13C
Acquired Size	32768
Spectral Size	65536

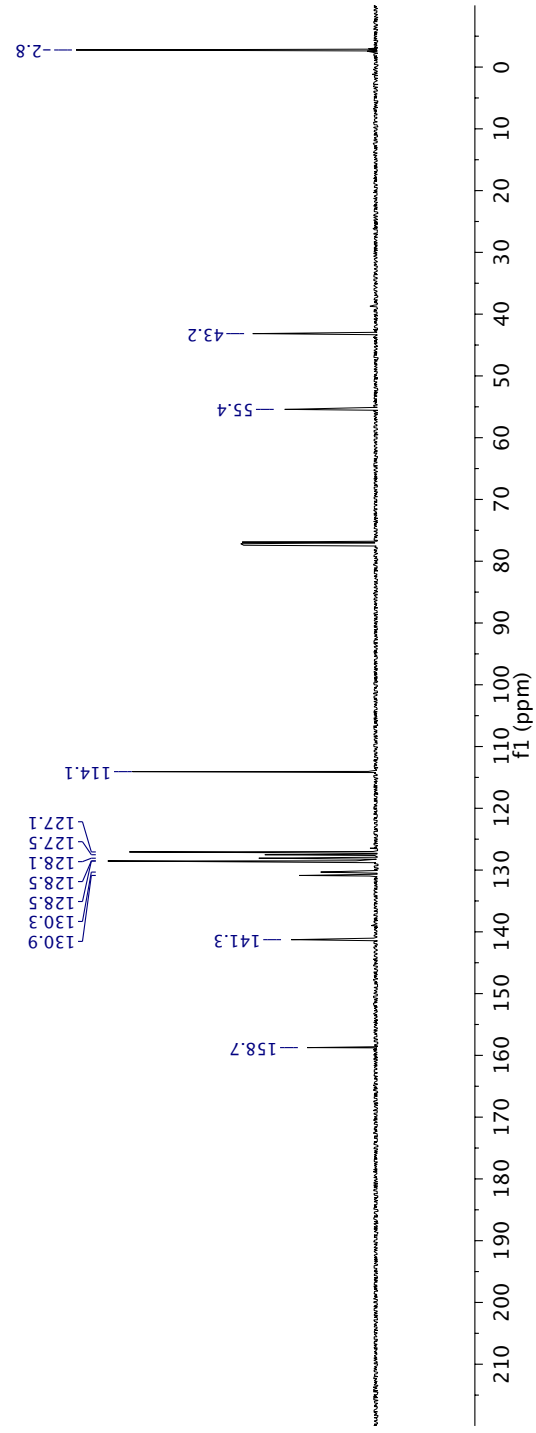

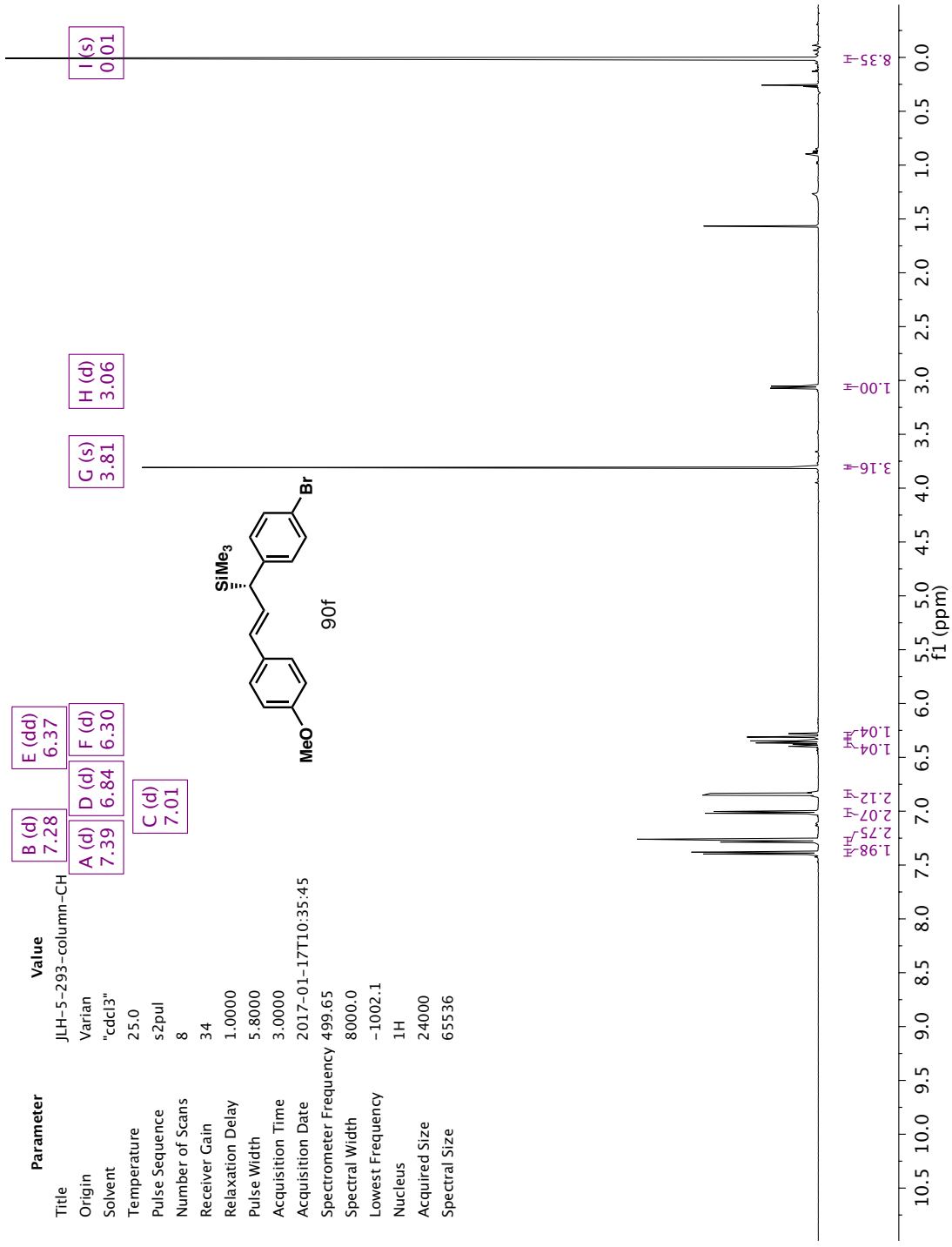
Parameter
Value
Title JLH-5-293-column-CH
Origin Varian
Solvent "cdcl3"
Temperature 25.0
Pulse Sequence s2pul
Number of Scans 8
Receiver Gain 34
Relaxation Delay 1.0000
Pulse Width 5.8000
Acquisition Time 3.0000
Acquisition Date 2017-01-17T10:35:45
Spectrometer Frequency 499.65
Spectral Width 8000.0
Lowest Frequency -1002.1
Nucleus 1H
Acquired Size 24000
Spectral Size 65536
A (d) 7.39
B (d) 7.28
C (d) 7.01
D (d) 6.84
E (dd) 6.37
F (d) 6.30
G (s) 3.81
H (d) 3.06
I (s) 0.01
SiMe3
Br
MeO
90f
8.35
3.16
1.00
1.04
2.12
2.07
2.75
1.98
f1 (ppm)

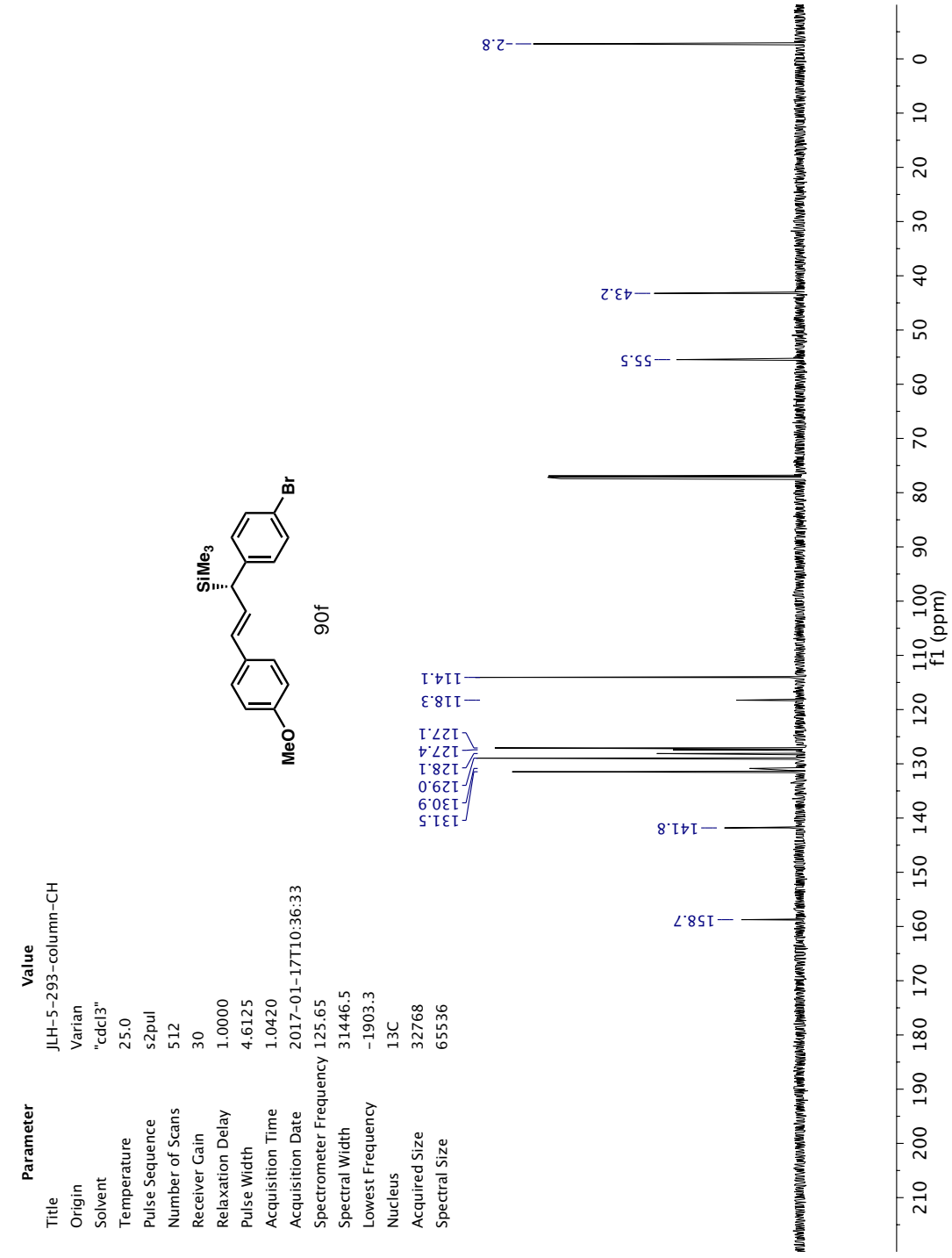
Parameter Value
Title JLH-5-293-column-CH
Origin Varian
Solvent "cdcl3"
Temperature 25.0
Pulse Sequence s2pul
Number of Scans 512
Receiver Gain 30
Relaxation Delay 1.0000
Pulse Width 4.6125
Acquisition Time 1.0420
Acquisition Date 2017-01-17T10:36:33
Spectrometer Frequency 125.65
Spectral Width 31446.5
Lowest Frequency -1903.3
Nucleus 13C
Acquired Size 32768
Spectral Size 65536
SiMe3
Br
MeO
90f
158.7
141.8
131.5
130.9
129.0
128.1
127.4
127.1
118.3
114.1
55.5
43.2
-2.8
f1 (ppm)

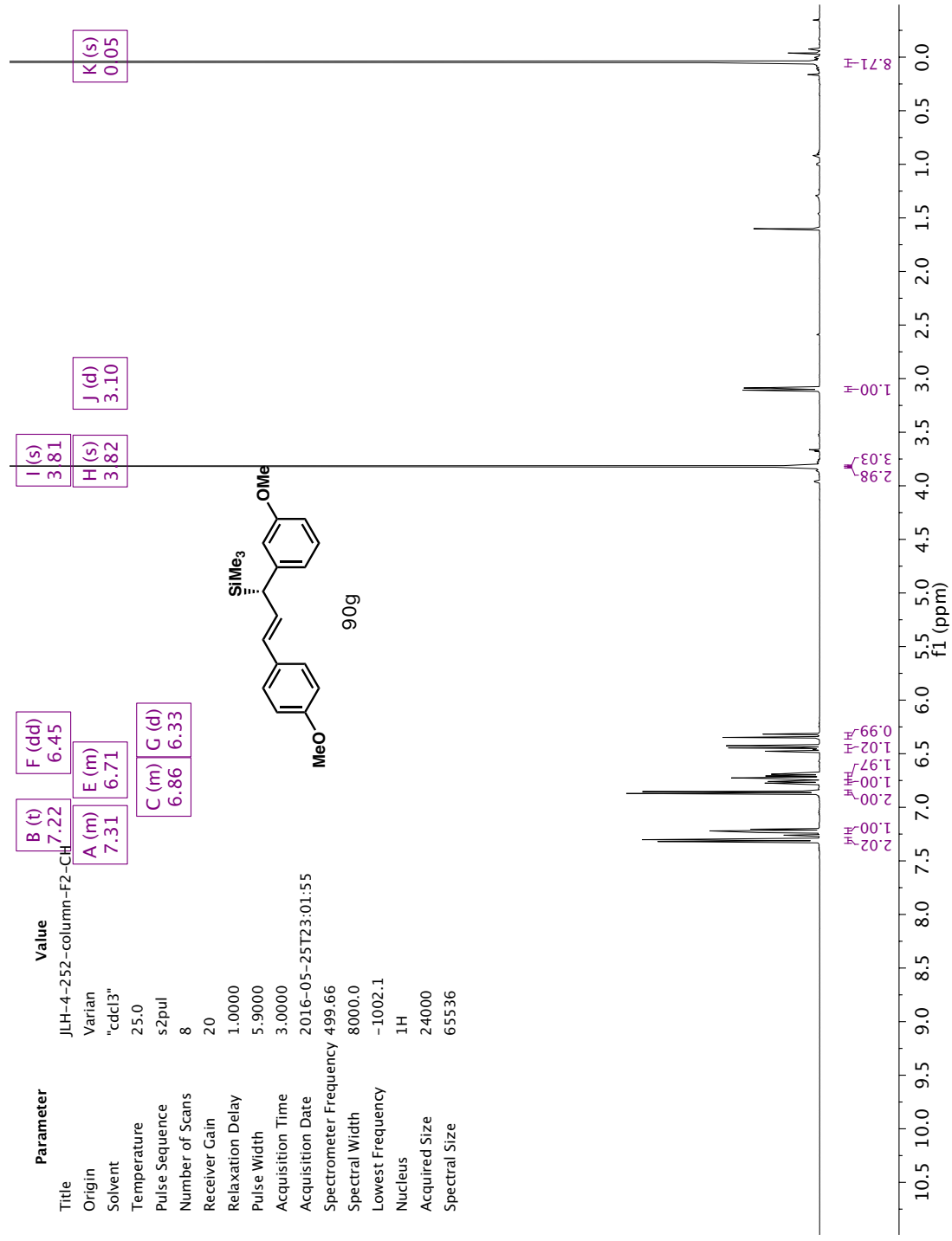
Parameter
Value
Title JLH-4-252-column-F2-CH
Origin Varian
Solvent "cdcl3"
Temperature 25.0
Pulse Sequence s2pul
Number of Scans 8
Receiver Gain 20
Relaxation Delay 1.0000
Pulse Width 5.9000
Acquisition Time 3.0000
Acquisition Date 2016-05-25T23:01:55
Spectrometer Frequency 499.66
Spectral Width 8000.0
Lowest Frequency -1002.1
Nucleus 1H
Acquired Size 24000
Spectral Size 65536
B (t) 7.22
A (m) 7.31
F (dd) 6.45
E (m) 6.71
C (m) 6.86
G (d) 6.33
I (s) 3.81
H (s) 3.82
J (d) 3.10
K (s) 0.05
SiMe3
OMe
MeO
90g
8.71
2.98
3.03
1.00
2.02
1.00
2.00
1.00
1.97
1.02
0.99
f1 (ppm)

Parameter	Value
Title	JLH-4-252-column-F2-CH
Origin	Varian
Solvent	"cdcl3"
Temperature	25.0
Pulse Sequence	s2pul
Number of Scans	256
Receiver Gain	30
Relaxation Delay	1.0000
Pulse Width	4.5000
Acquisition Time	1.0420
Acquisition Date	2016-05-25T23:02:43
Spectrometer Frequency	125.65
Spectral Width	31446.5
Lowest Frequency	-1903.0
Nucleus	13C
Acquired Size	32768
Spectral Size	65536

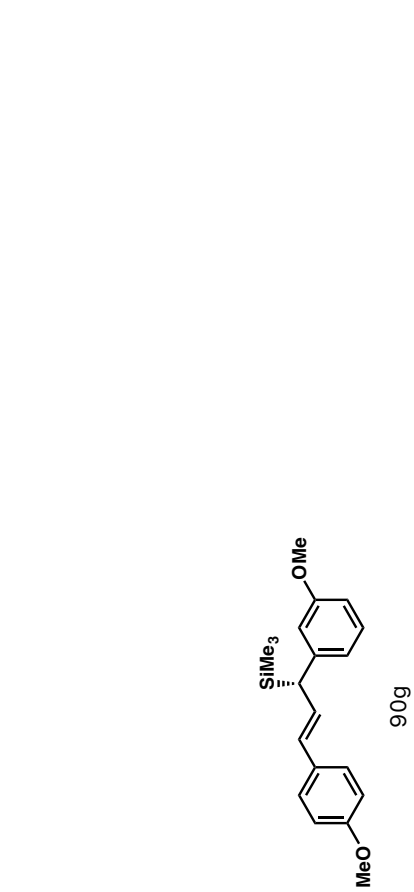

90g

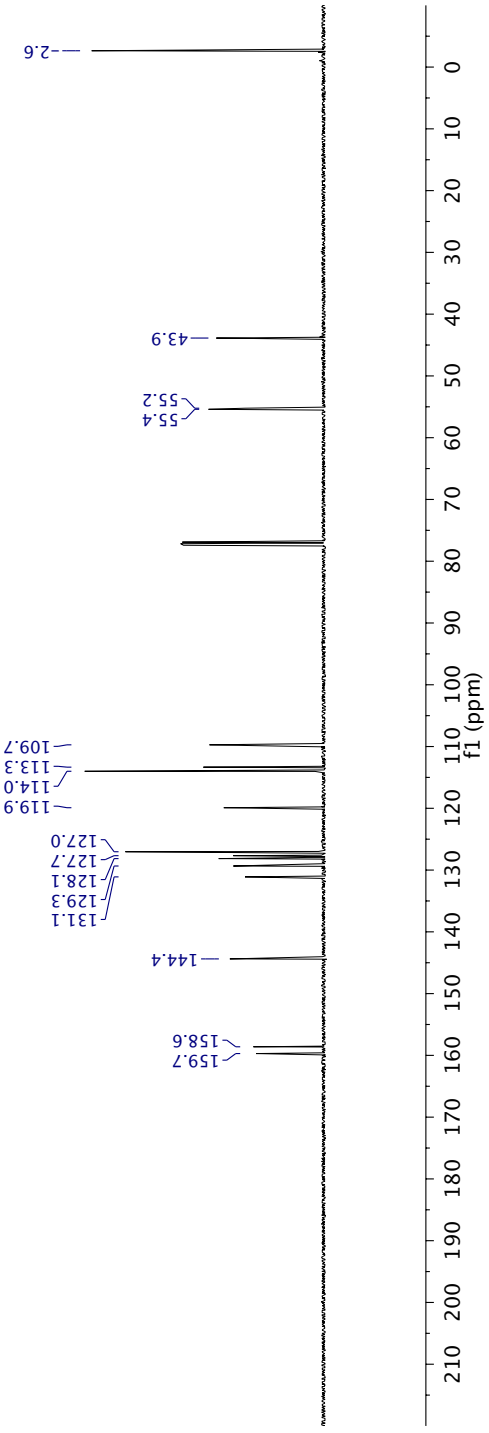

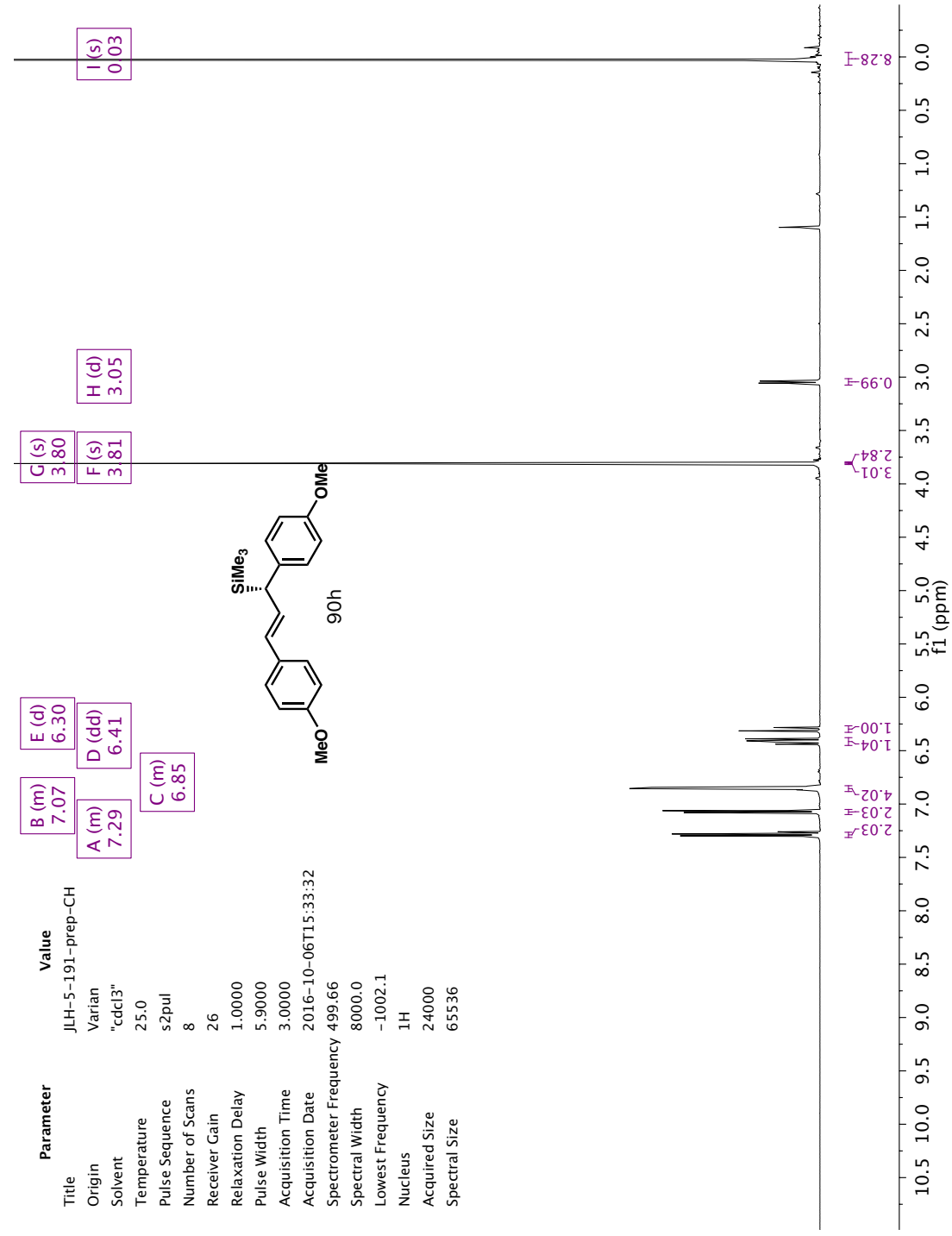
Parameter Value
Title JLH-5-191-prep-CH
Origin Varian
Solvent "cdcl3"
Temperature 25.0
Pulse Sequence s2pul
Number of Scans 8
Receiver Gain 26
Relaxation Delay 1.0000
Pulse Width 5.9000
Acquisition Time 3.0000
Acquisition Date 2016-10-06T15:33:32
Spectrometer Frequency 499.66
Spectral Width 8000.0
Lowest Frequency -1002.1
Nucleus 1H
Acquired Size 24000
Spectral Size 65536
A (m) 7.29
B (m) 7.07
C (m) 6.85
D (dd) 6.41
E (d) 6.30
F (s) 3.81
G (s) 3.80
H (d) 3.05
I (s) 0.03
SiMe3
OMe
MeO
90h
8.28
0.99
2.84
3.01
1.00
1.04
4.02
2.03
2.03
f1 (ppm)

Parameter	Value
Title	JLH-5-191-prep-CH
Origin	Varian
Solvent	"cdcl3"
Temperature	25.0
Pulse Sequence	s2pul
Number of Scans	256
Receiver Gain	30
Relaxation Delay	1.0000
Pulse Width	4.5000
Acquisition Time	1.0420
Acquisition Date	2016-10-06T15:34:21
Spectrometer Frequency	125.65
Spectral Width	31446.5
Lowest Frequency	-1903.0
Nucleus	13C
Acquired Size	32768
Spectral Size	65536

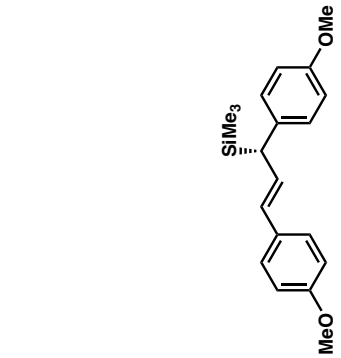

90h

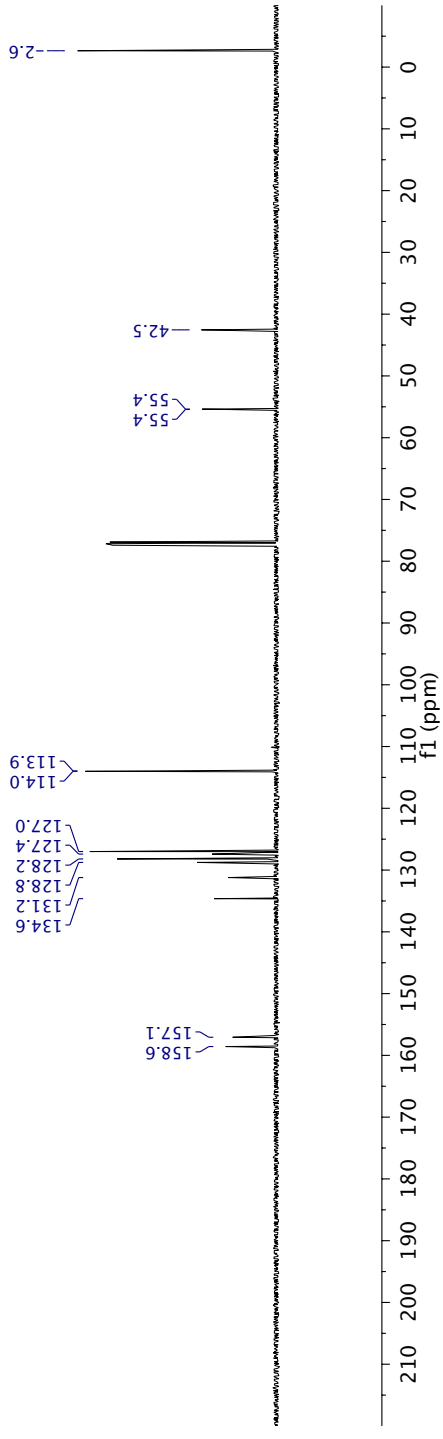

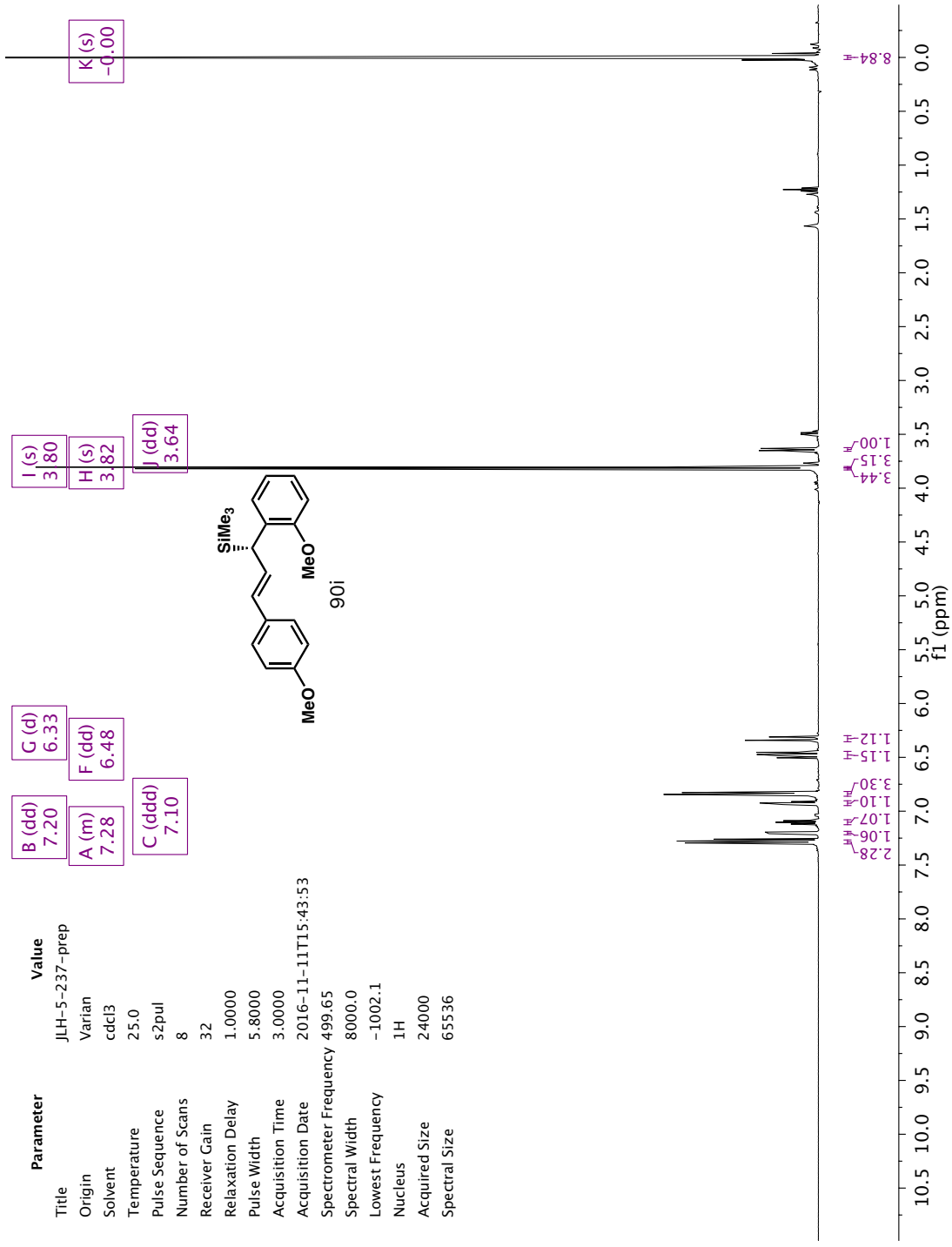

Parameter	Value
Title	JLH-5-237-prep
Origin	Varian
Solvent	cdcl3
Temperature	25.0
Pulse Sequence	s2pul
Number of Scans	8
Receiver Gain	32
Relaxation Delay	1.0000
Pulse Width	5.8000
Acquisition Time	3.0000
Acquisition Date	2016-11-11T15:43:53
Spectrometer Frequency	499.65
Spectral Width	8000.0
Lowest Frequency	-1002.1
Nucleus	1H
Acquired Size	24000
Spectral Size	65536

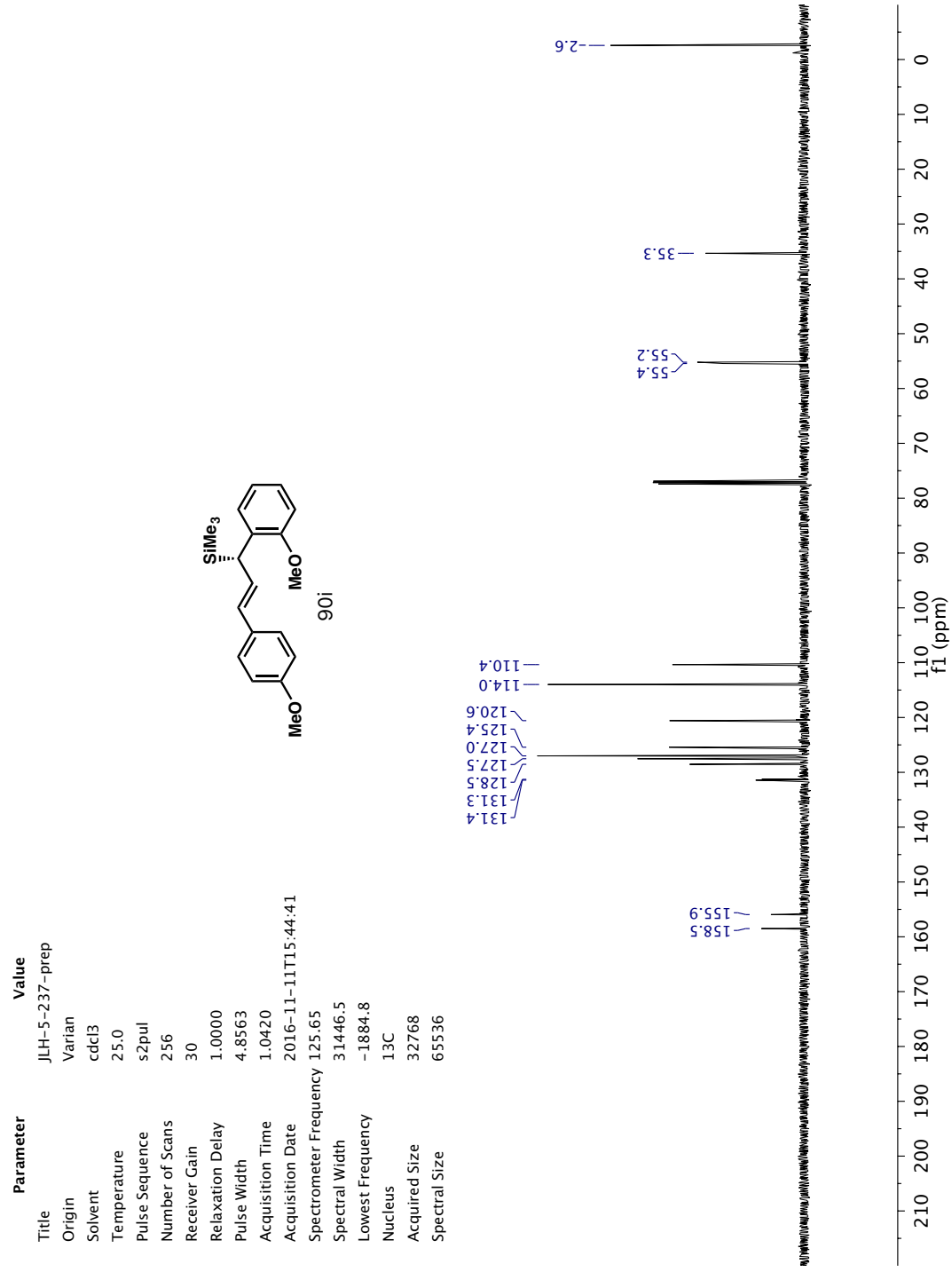
Parameter Value
Title JLH-5-237-prep
Origin Varian
Solvent cdcl3
Temperature 25.0
Pulse Sequence s2pul
Number of Scans 256
Receiver Gain 30
Relaxation Delay 1.0000
Pulse Width 4.8563
Acquisition Time 1.0420
Acquisition Date 2016-11-11T15:44:41
Spectrometer Frequency 125.65
Spectral Width 31446.5
Lowest Frequency -1884.8
Nucleus 13C
Acquired Size 32768
Spectral Size 65536
SiMe3
MeO
MeO
90i
-2.6
35.3
55.4
55.2
110.4
114.0
120.6
125.4
127.0
127.5
128.5
131.3
131.4
155.9
158.5
f1 (ppm)

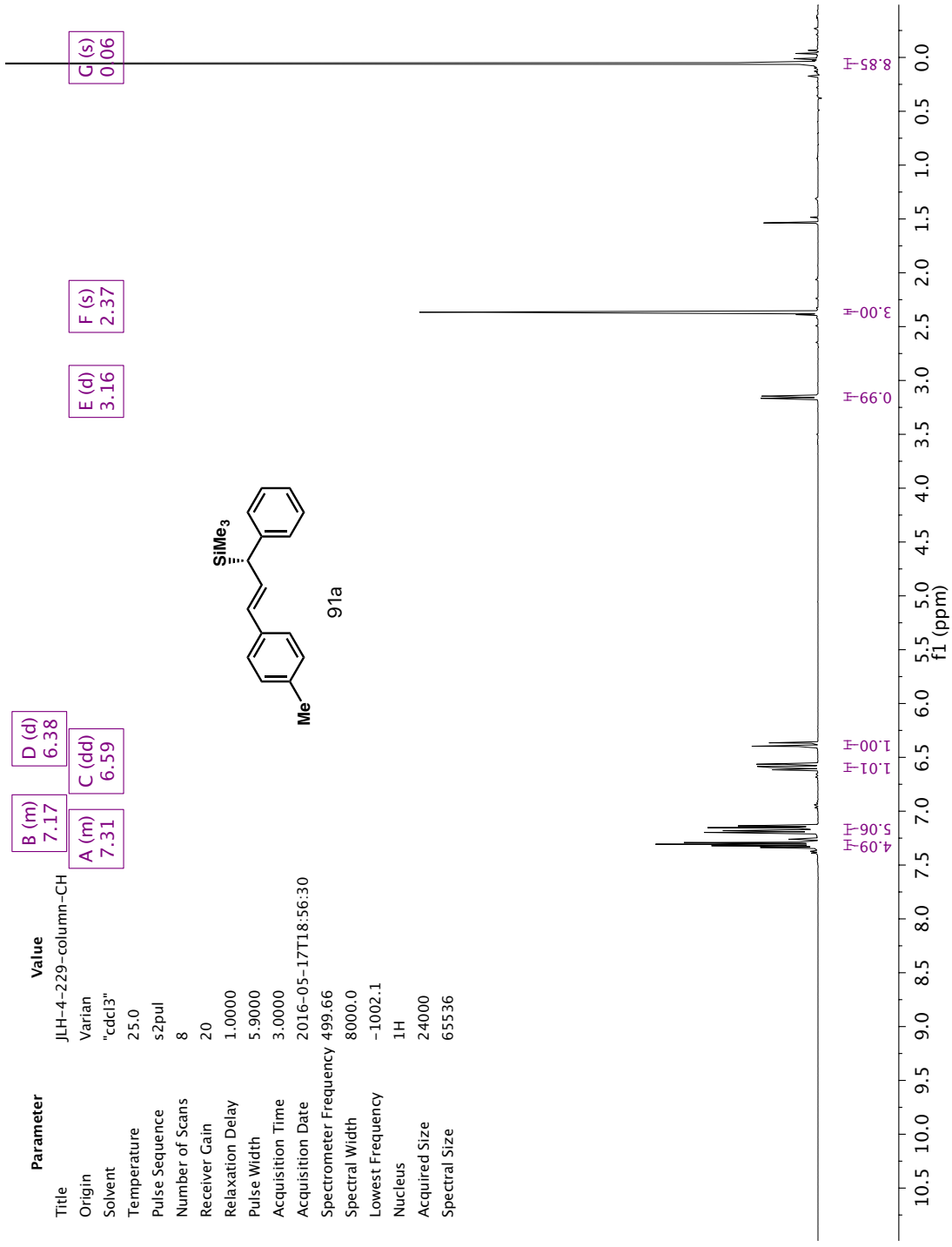
Parameter
Value
Title JLH-4-229-column-CH
Origin Varian
Solvent "cdcl3"
Temperature 25.0
Pulse Sequence s2pul
Number of Scans 8
Receiver Gain 20
Relaxation Delay 1.0000
Pulse Width 5.9000
Acquisition Time 3.0000
Acquisition Date 2016-05-17T18:56:30
Spectrometer Frequency 499.66
Spectral Width 8000.0
Lowest Frequency -1002.1
Nucleus 1H
Acquired Size 24000
Spectral Size 65536
A (m) 7.31
B (m) 7.17
C (dd) 6.59
D (d) 6.38
E (d) 3.16
F (s) 2.37
G (s) 0.06
SiMe3
Me
91a
8.85
3.00
0.99
1.00
1.01
5.06
4.09
f1 (ppm)

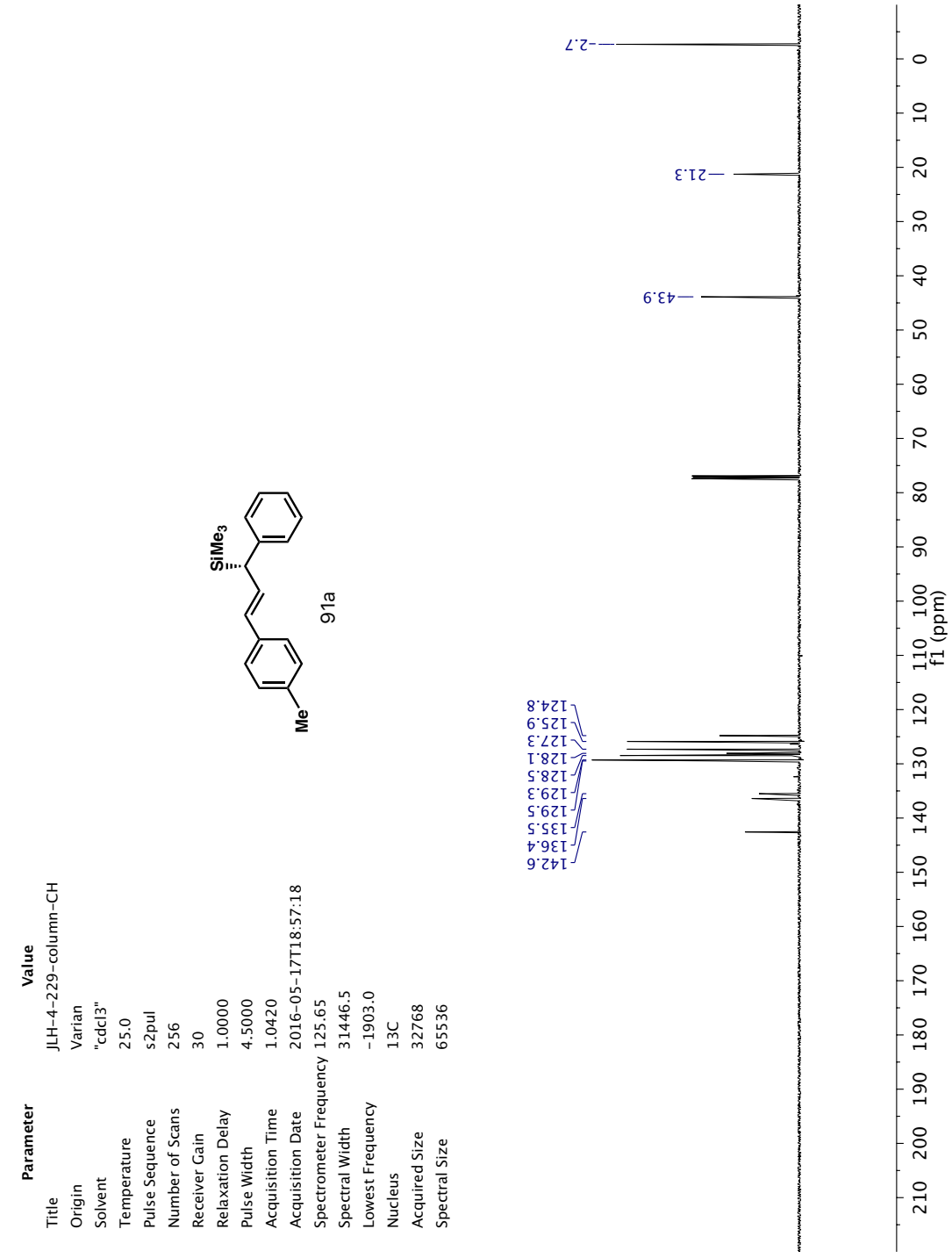
Parameter Value
Title JLH-4-229-column-CH
Origin Varian
Solvent "cdcl3"
Temperature 25.0
Pulse Sequence s2pul
Number of Scans 256
Receiver Gain 30
Relaxation Delay 1.0000
Pulse Width 4.5000
Acquisition Time 1.0420
Acquisition Date 2016-05-17T18:57:18
Spectrometer Frequency 125.65
Spectral Width 31446.5
Lowest Frequency -1903.0
Nucleus 13C
Acquired Size 32768
Spectral Size 65536
SiMe3
Me
91a
142.6
136.4
135.5
129.5
129.3
128.5
128.1
127.3
125.9
124.8
43.9
21.3
-2.7
f1 (ppm)

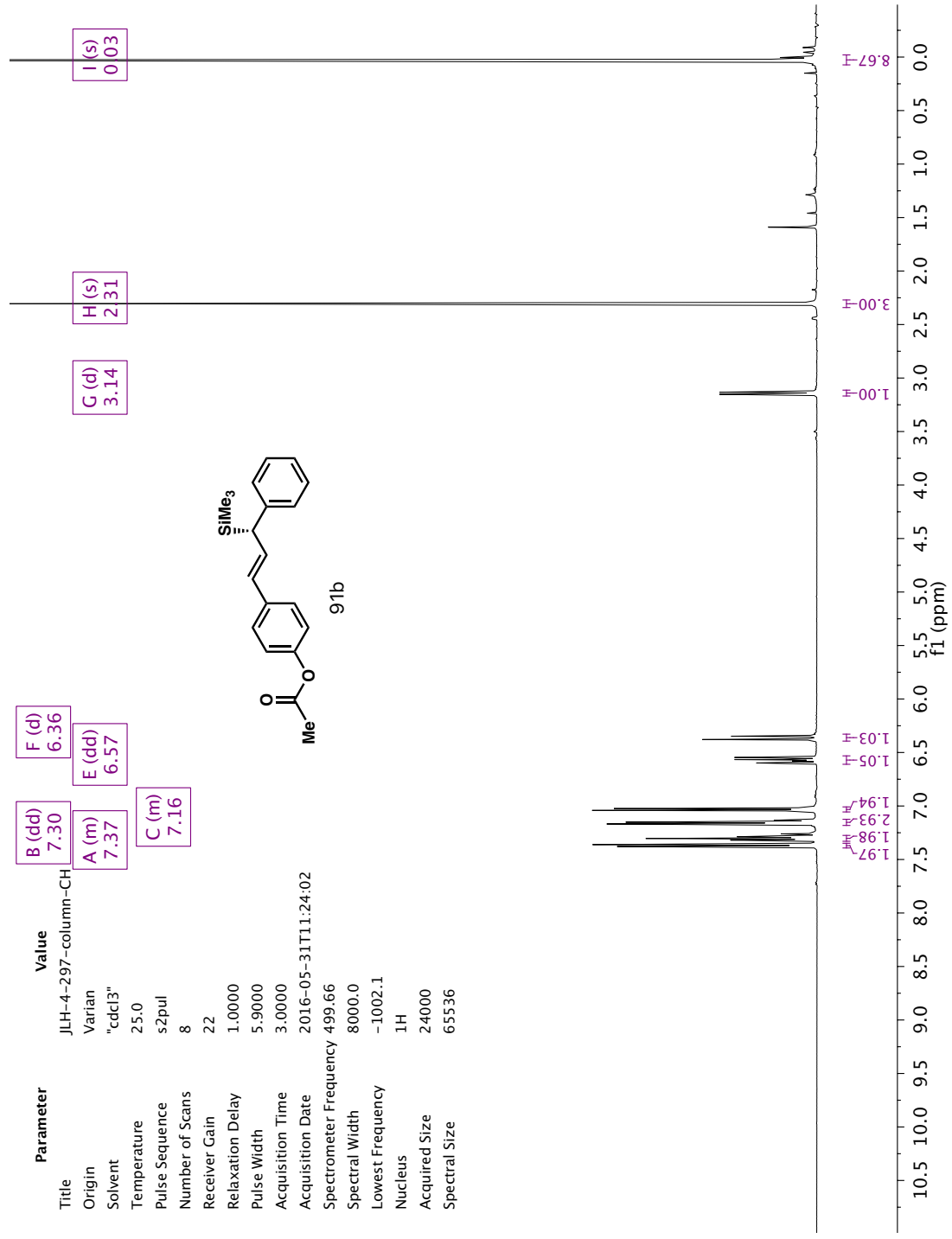
Parameter
Value
Title JLH-4-297-column-CH
Origin Varian
Solvent "cdcl3"
Temperature 25.0
Pulse Sequence s2pul
Number of Scans 8
Receiver Gain 22
Relaxation Delay 1.0000
Pulse Width 5.9000
Acquisition Time 3.0000
Acquisition Date 2016-05-31T11:24:02
Spectrometer Frequency 499.66
Spectral Width 8000.0
Lowest Frequency -1002.1
Nucleus 1H
Acquired Size 24000
Spectral Size 65536
B (dd) 7.30
A (m) 7.37
C (m) 7.16
F (d) 6.36
E (dd) 6.57
G (d) 3.14
H (s) 2.31
I (s) 0.03
SiMe3
Me
91b
8.67
3.00
1.00
1.03
1.05
1.94
2.93
1.98
1.97
f1 (ppm)

Parameter	Value
Title	JLH-4-297-column-CH
Origin	Varian
Solvent	"cdcl3"
Temperature	25.0
Pulse Sequence	s2pul
Number of Scans	256
Receiver Gain	30
Relaxation Delay	1.0000
Pulse Width	4.5000
Acquisition Time	1.0420
Acquisition Date	2016-05-31T11:25:03
Spectrometer Frequency	125.65
Spectral Width	31446.5
Lowest Frequency	-1903.0
Nucleus	13C
Acquired Size	32768
Spectral Size	65536

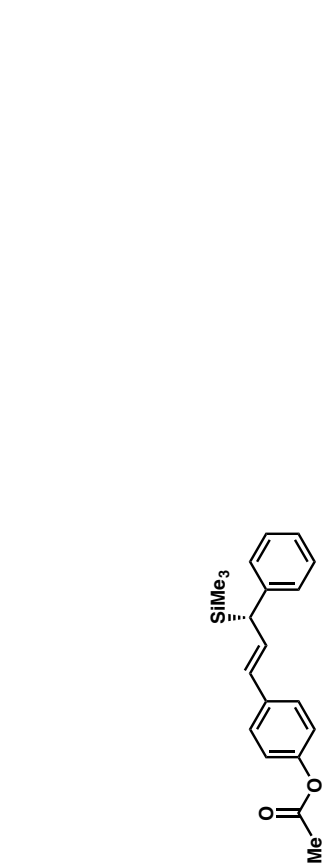

91b

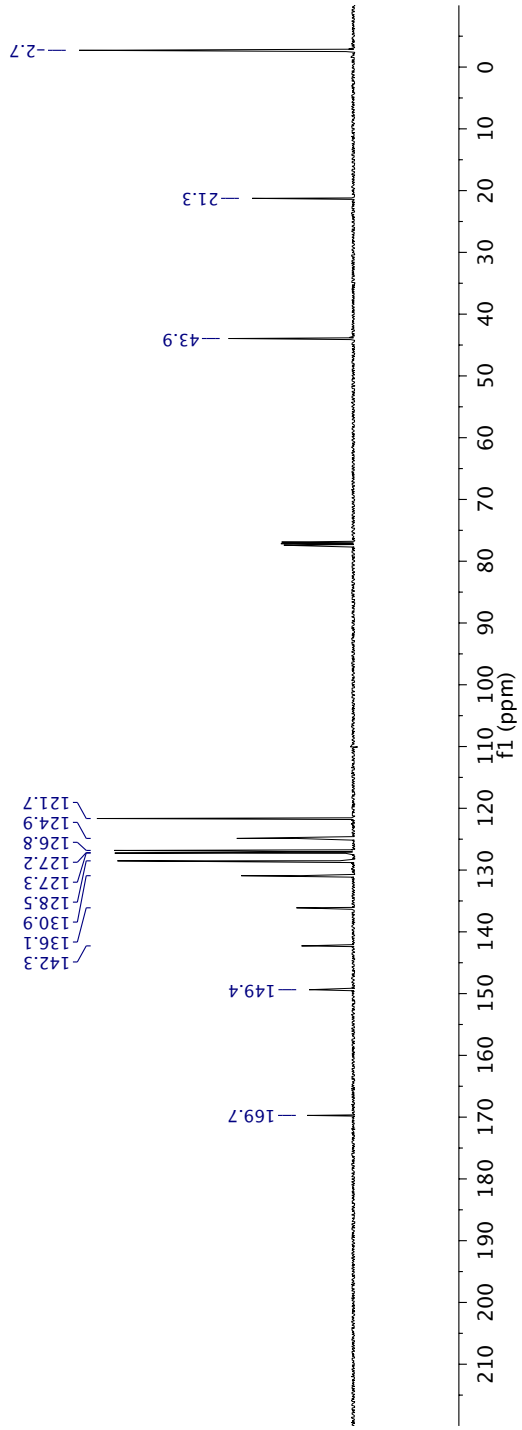

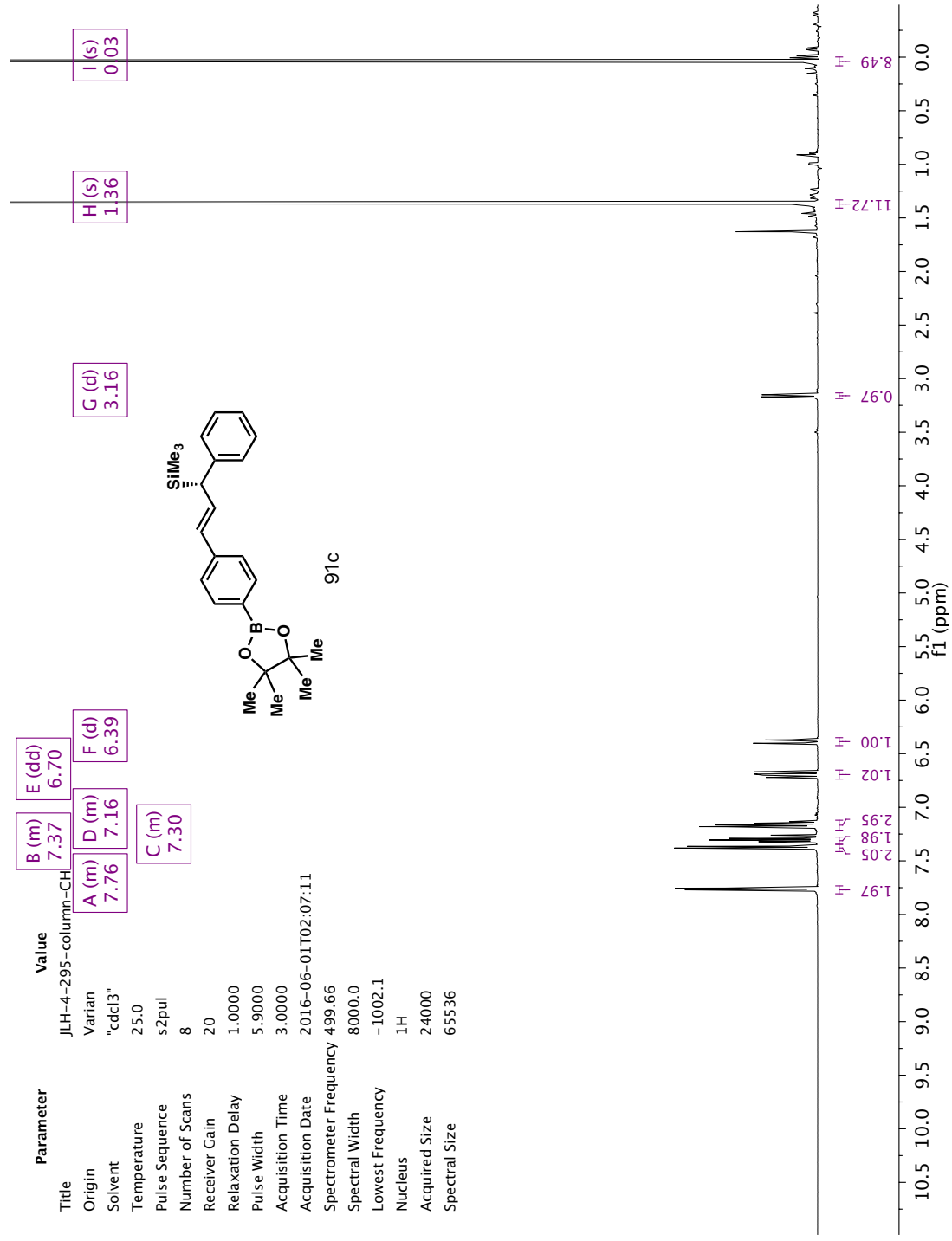
Parameter
Value
Title JLH-4-295-column-CH
Origin Varian
Solvent "cdcl3"
Temperature 25.0
Pulse Sequence s2pul
Number of Scans 8
Receiver Gain 20
Relaxation Delay 1.0000
Pulse Width 5.9000
Acquisition Time 3.0000
Acquisition Date 2016-06-01T02:07:11
Spectrometer Frequency 499.66
Spectral Width 8000.0
Lowest Frequency -1002.1
Nucleus 1H
Acquired Size 24000
Spectral Size 65536
A (m) 7.76
B (m) 7.37
C (m) 7.30
D (m) 7.16
E (dd) 6.70
F (d) 6.39
G (d) 3.16
H (s) 1.36
I (s) 0.03
SiMe3
Me
Me
Me
Me
91c
8.49
11.72
0.97
1.00
1.02
2.95
1.98
2.05
1.97
f1 (ppm)

Parameter	Value
Title	JLH-4-295-column-CH
Origin	Varian
Solvent	"cdcl3"
Temperature	25.0
Pulse Sequence	s2pul
Number of Scans	256
Receiver Gain	30
Relaxation Delay	1.0000
Pulse Width	4.5000
Acquisition Time	1.0420
Acquisition Date	2016-06-01T02:07:59
Spectrometer Frequency	125.65
Spectral Width	31446.5
Lowest Frequency	-1903.0
Nucleus	13C
Acquired Size	32768
Spectral Size	65536

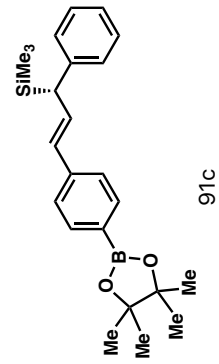

91c

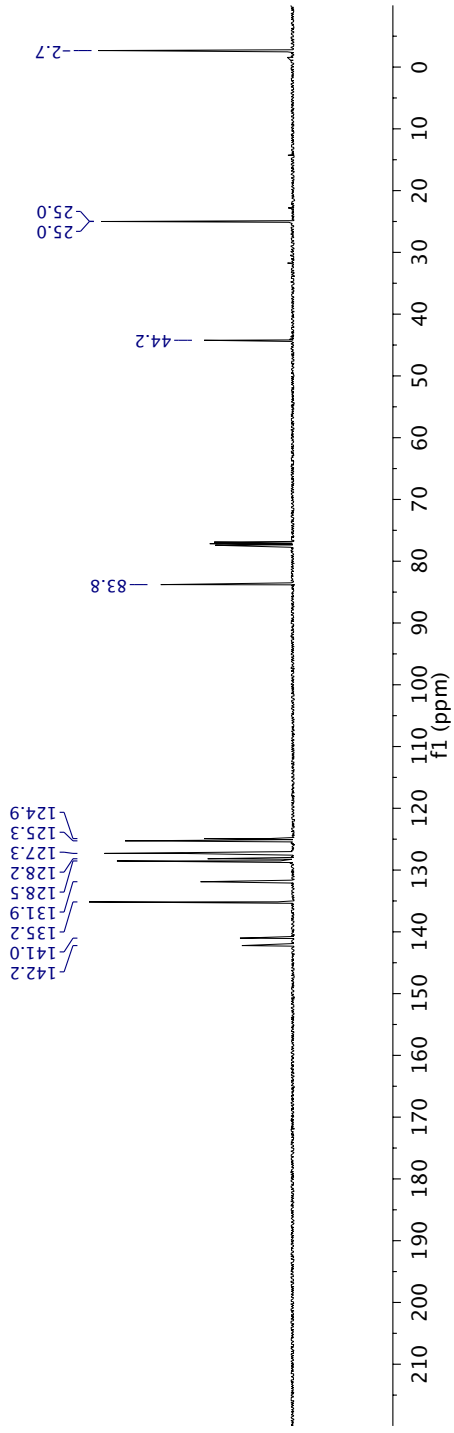

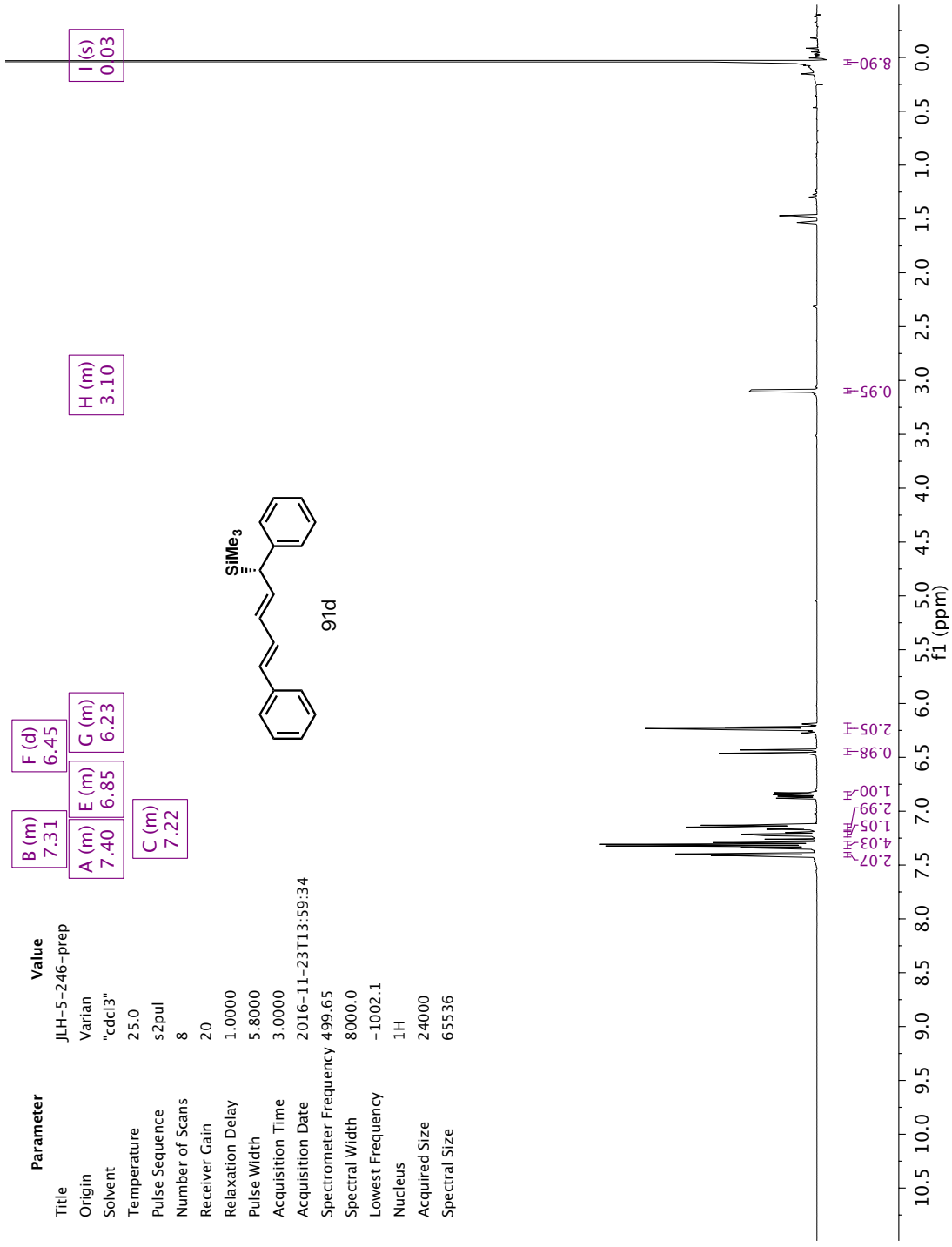

Parameter	Value
Title	JLH-5-246-prep
Origin	Varian
Solvent	"cdcl3"
Temperature	25.0
Pulse Sequence	s2pul
Number of Scans	8
Receiver Gain	20
Relaxation Delay	1.0000
Pulse Width	5.8000
Acquisition Time	3.0000
Acquisition Date	2016-11-23T13:59:34
Spectrometer Frequency	499.65
Spectral Width	8000.0
Lowest Frequency	-1002.1
Nucleus	1H
Acquired Size	24000
Spectral Size	65536

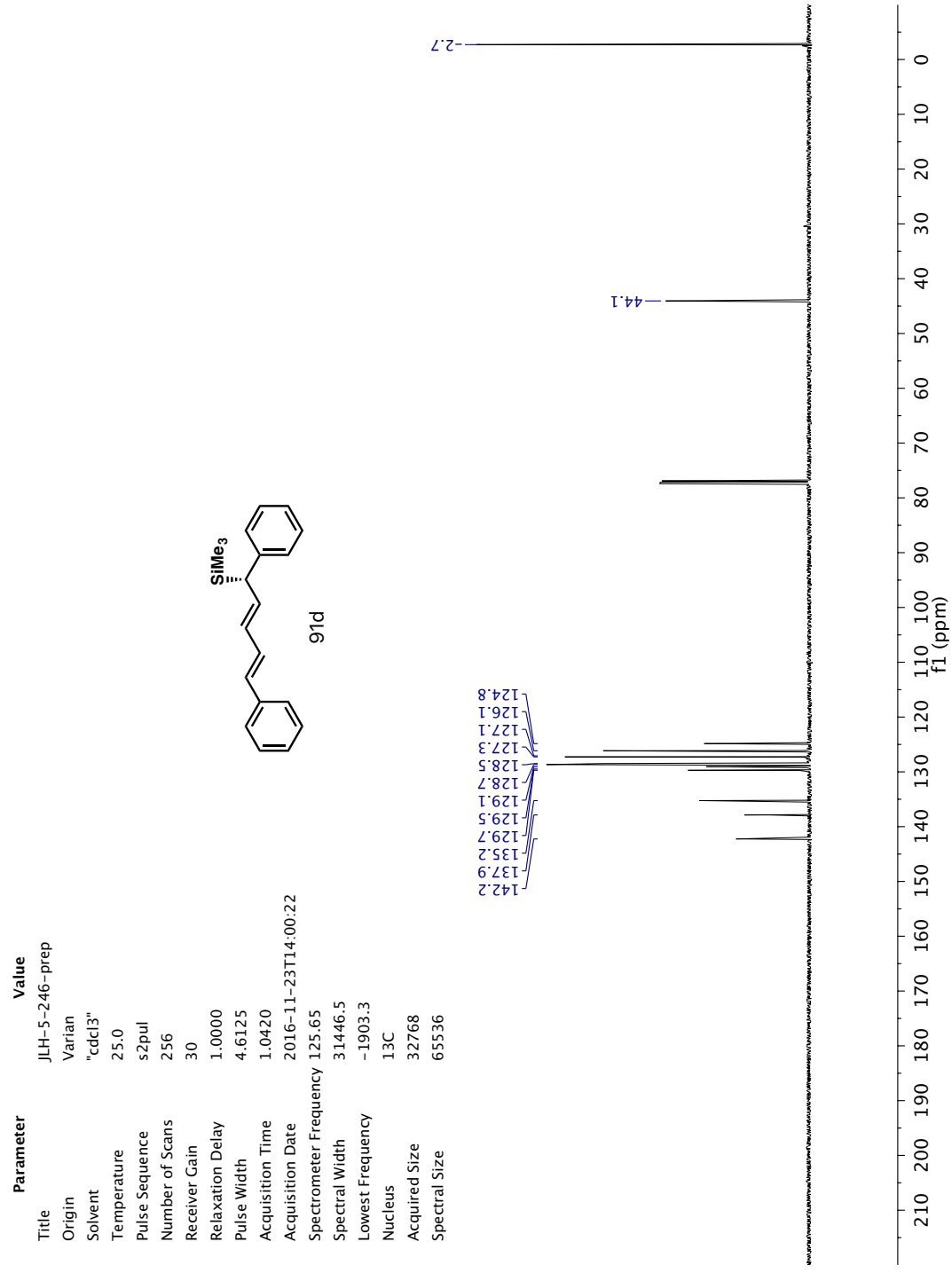

Parameter	Value
Title	JLH-5-246-prep
Origin	Varian
Solvent	"cdcl3"
Temperature	25.0
Pulse Sequence	s2pul
Number of Scans	256
Receiver Gain	30
Relaxation Delay	1.0000
Pulse Width	4.6125
Acquisition Time	1.0420
Acquisition Date	2016-11-23T14:00:22
Spectrometer Frequency	125.65
Spectral Width	31446.5
Lowest Frequency	-1903.3
Nucleus	13C
Acquired Size	32768
Spectral Size	65536

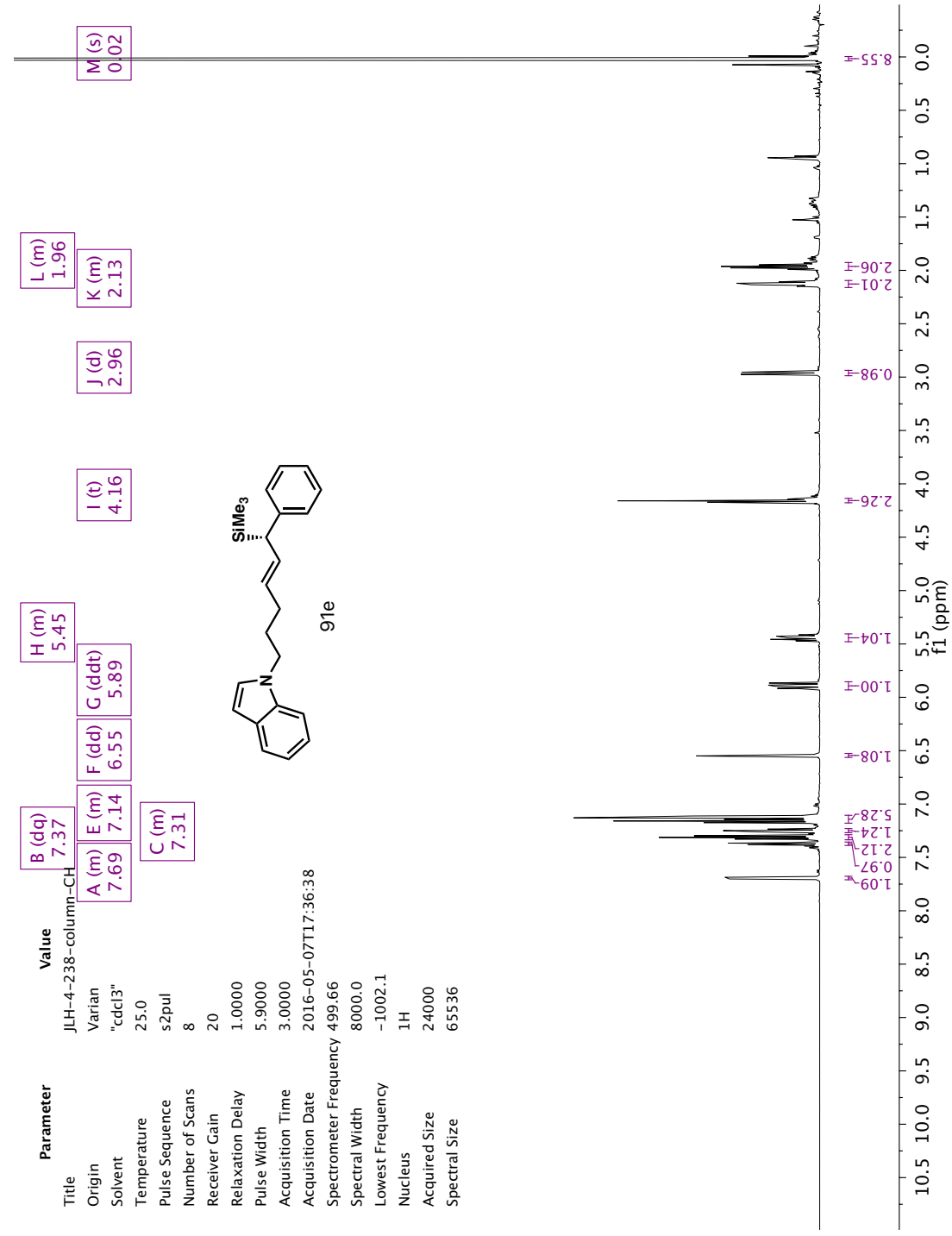
Parameter
Value
Title JLH-4-238-column-CH
Origin Varian
Solvent "cdcl3"
Temperature 25.0
Pulse Sequence s2pul
Number of Scans 8
Receiver Gain 20
Relaxation Delay 1.0000
Pulse Width 5.9000
Acquisition Time 3.0000
Acquisition Date 2016-05-07T17:36:38
Spectrometer Frequency 499.66
Spectral Width 8000.0
Lowest Frequency -1002.1
Nucleus 1H
Acquired Size 24000
Spectral Size 65536
A (m) 7.69
B (dq) 7.37
C (m) 7.31
E (m) 7.14
F (dd) 6.55
G (ddt) 5.89
H (m) 5.45
I (t) 4.16
J (d) 2.96
K (m) 2.13
L (m) 1.96
M (s) 0.02
SiMe3
N
91e
1.09
0.97
2.12
1.24
5.28
1.08
1.00
1.04
2.26
0.98
2.01
2.06
8.55
f1 (ppm)

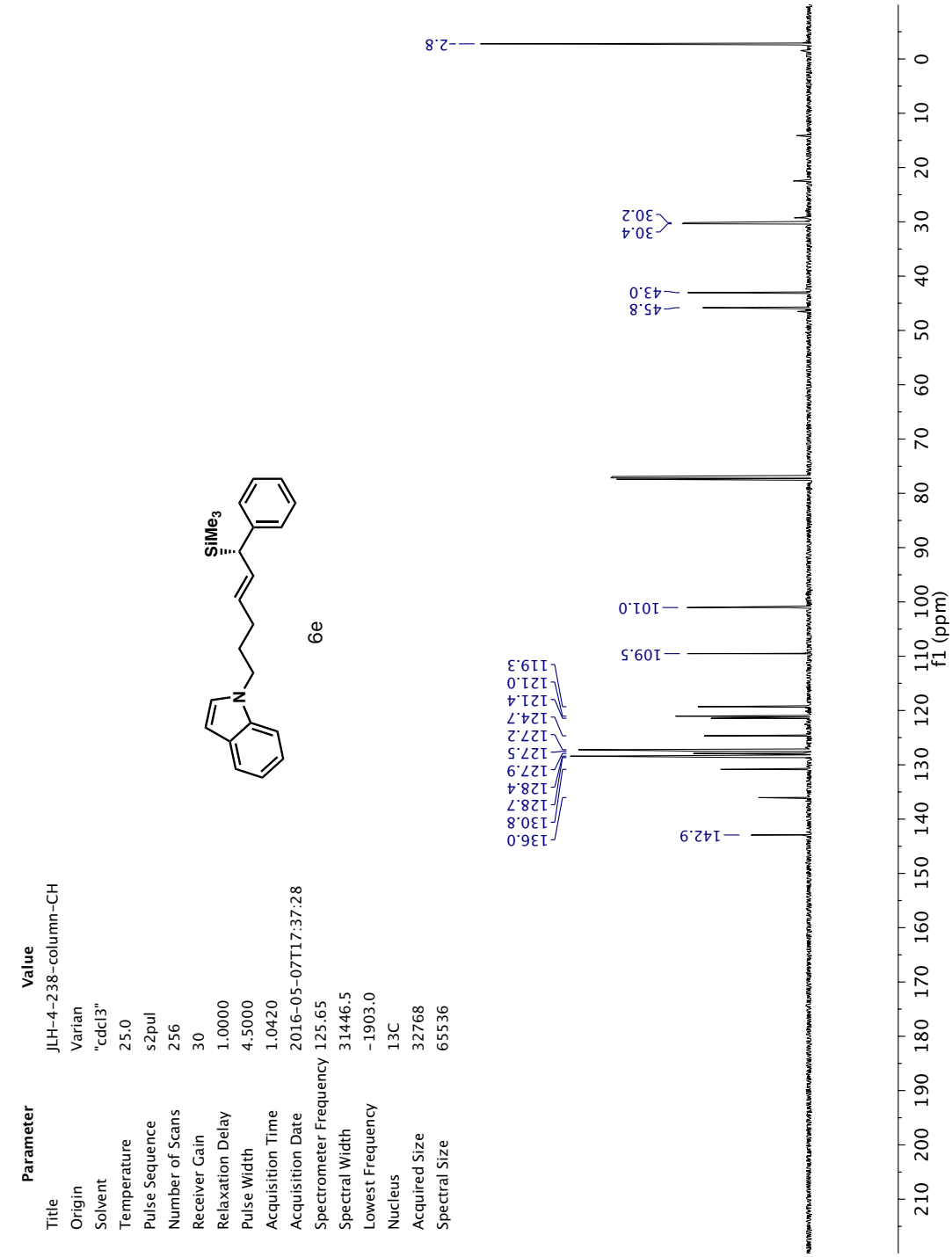
Parameter Value
Title JLH-4-238-column-CH
Origin Varian
Solvent "cdcl3"
Temperature 25.0
Pulse Sequence s2pul
Number of Scans 256
Receiver Gain 30
Relaxation Delay 1.0000
Pulse Width 4.5000
Acquisition Time 1.0420
Acquisition Date 2016-05-07T17:37:28
Spectrometer Frequency 125.65
Spectral Width 31446.5
Lowest Frequency -1903.0
Nucleus 13C
Acquired Size 32768
Spectral Size 65536
SiMe3
N
6e
-2.8
30.4
30.2
43.0
45.8
101.0
109.5
119.3
121.0
121.4
124.7
127.2
127.5
127.9
128.4
128.7
130.8
136.0
142.9
f1 (ppm)

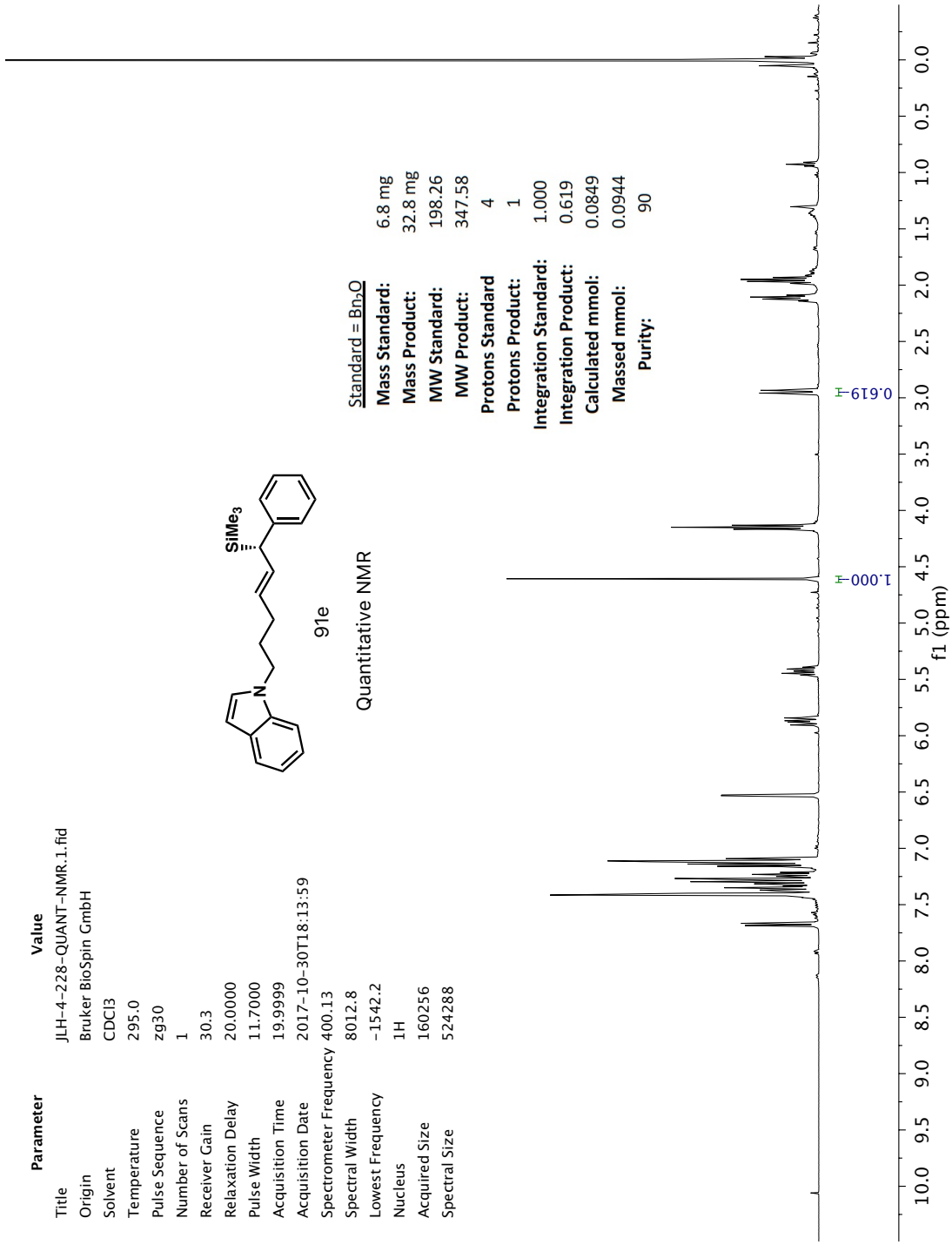
Parameter Value
Title JLH-4-228-QUANT-NMR.1.fid
Origin Bruker BioSpin GmbH
Solvent CDCl3
Temperature 295.0
Pulse Sequence zg30
Number of Scans 1
Receiver Gain 30.3
Relaxation Delay 20.0000
Pulse Width 11.7000
Acquisition Time 19.9999
Acquisition Date 2017-10-30T18:13:59
Spectrometer Frequency 400.13
Spectral Width 8012.8
Lowest Frequency -1542.2
Nucleus 1H
Acquired Size 160256
Spectral Size 524288
SiMe3
91e
Quantitative NMR
Standard = Bn2O
Mass Standard: 6.8 mg
Mass Product: 32.8 mg
MW Standard: 198.26
MW Product: 347.58
Protons Standard 4
Protons Product: 1
Integration Standard: 1.000
Integration Product: 0.619
Calculated mmol: 0.0849
Massed mmol: 0.0944
Purity: 90
1.000
0.619
f1 (ppm)

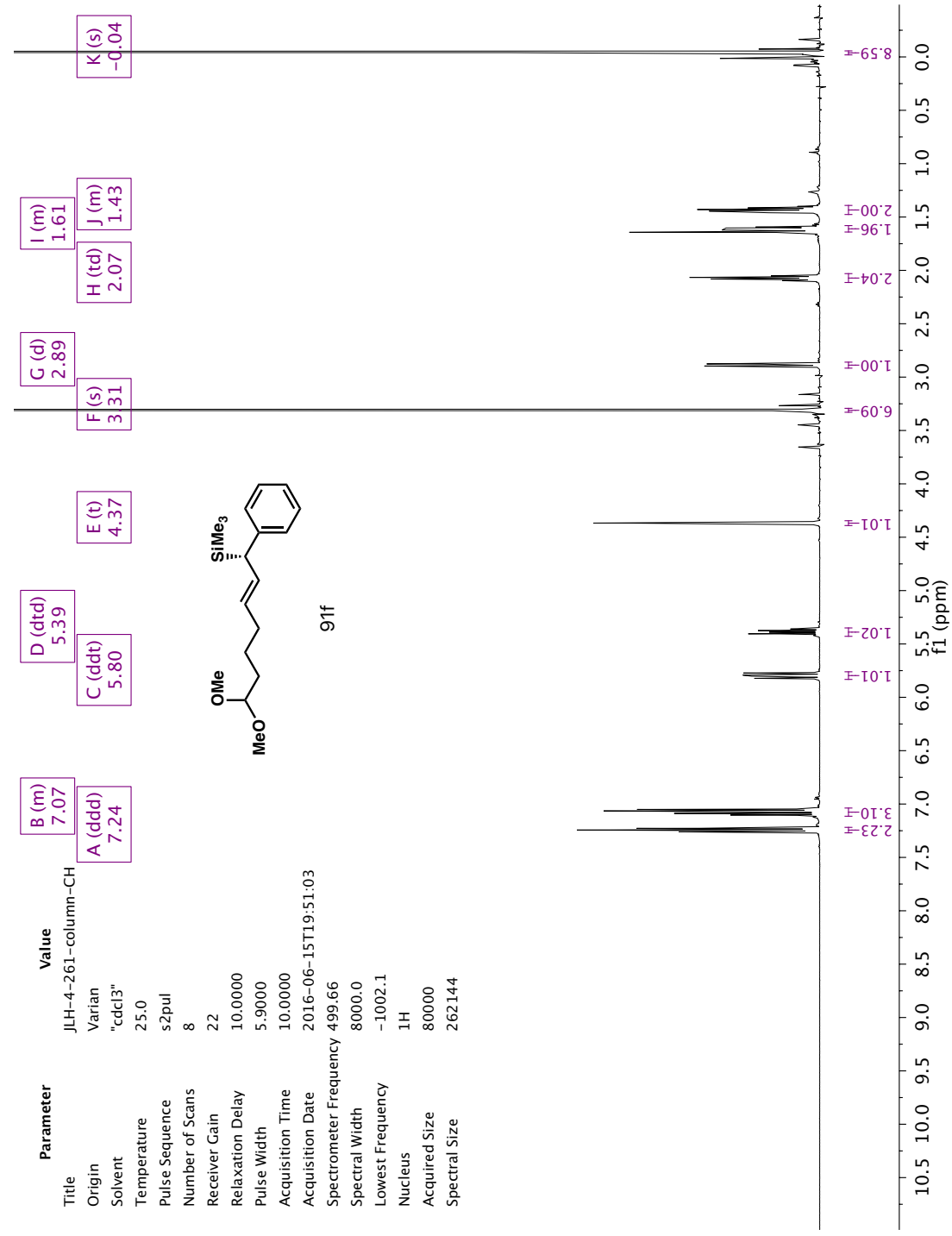
Parameter
Value
Title
JLH-4-261-column-CH
Origin
Varian
Solvent
"cdcl3"
Temperature
25.0
Pulse Sequence
s2pul
Number of Scans
8
Receiver Gain
22
Relaxation Delay
10.0000
Pulse Width
5.9000
Acquisition Time
10.0000
Acquisition Date
2016-06-15T19:51:03
Spectrometer Frequency
499.66
Spectral Width
8000.0
Lowest Frequency
-1002.1
Nucleus
1H
Acquired Size
80000
Spectral Size
262144
A (ddd) 7.24
B (m) 7.07
C (ddt) 5.80
D (dtd) 5.39
E (t) 4.37
F (s) 3.31
G (d) 2.89
H (td) 2.07
I (m) 1.61
J (m) 1.43
K (s) -0.04
OMe
MeO
SiMe3
91f
8.59
2.23
3.10
1.01
1.02
1.01
1.01
6.09
1.00
2.04
1.96
2.00
f1 (ppm)

Parameter	Value
Title	JLH-4-261-column-CH
Origin	Varian
Solvent	"cdcl3"
Temperature	25.0
Pulse Sequence	s2pul
Number of Scans	256
Receiver Gain	30
Relaxation Delay	1.0000
Pulse Width	4.5000
Acquisition Time	1.0420
Acquisition Date	2016-06-15T19:41:23
Spectrometer Frequency	125.65
Spectral Width	31446.5
Lowest Frequency	-1903.0
Nucleus	13C
Acquired Size	32768
Spectral Size	65536

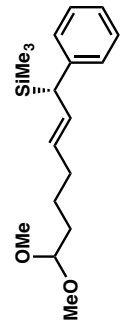

91f

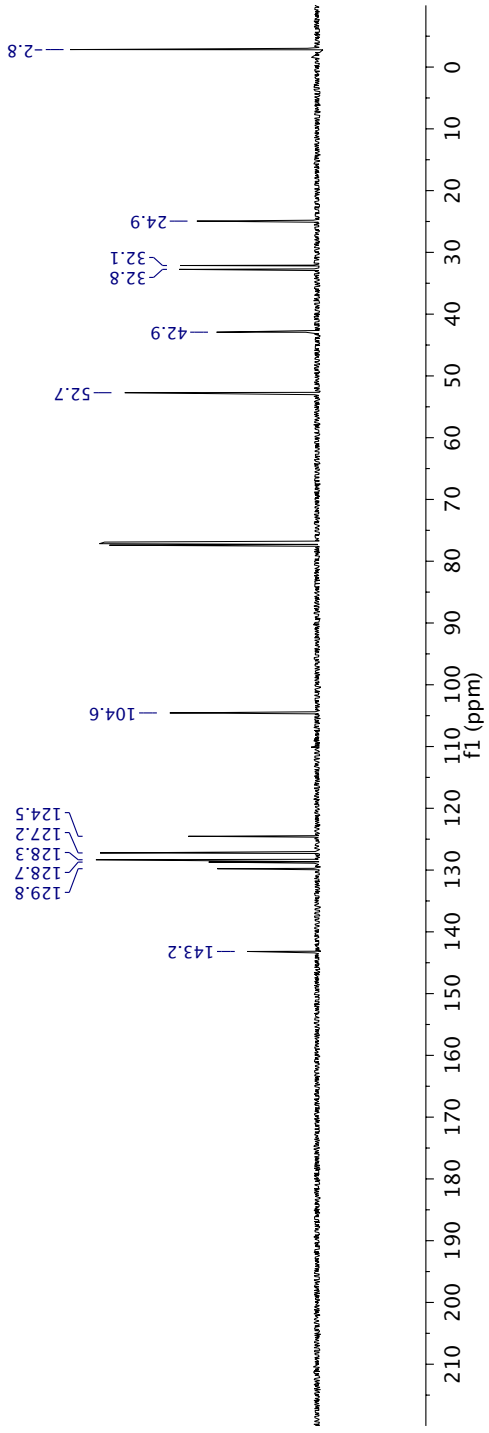

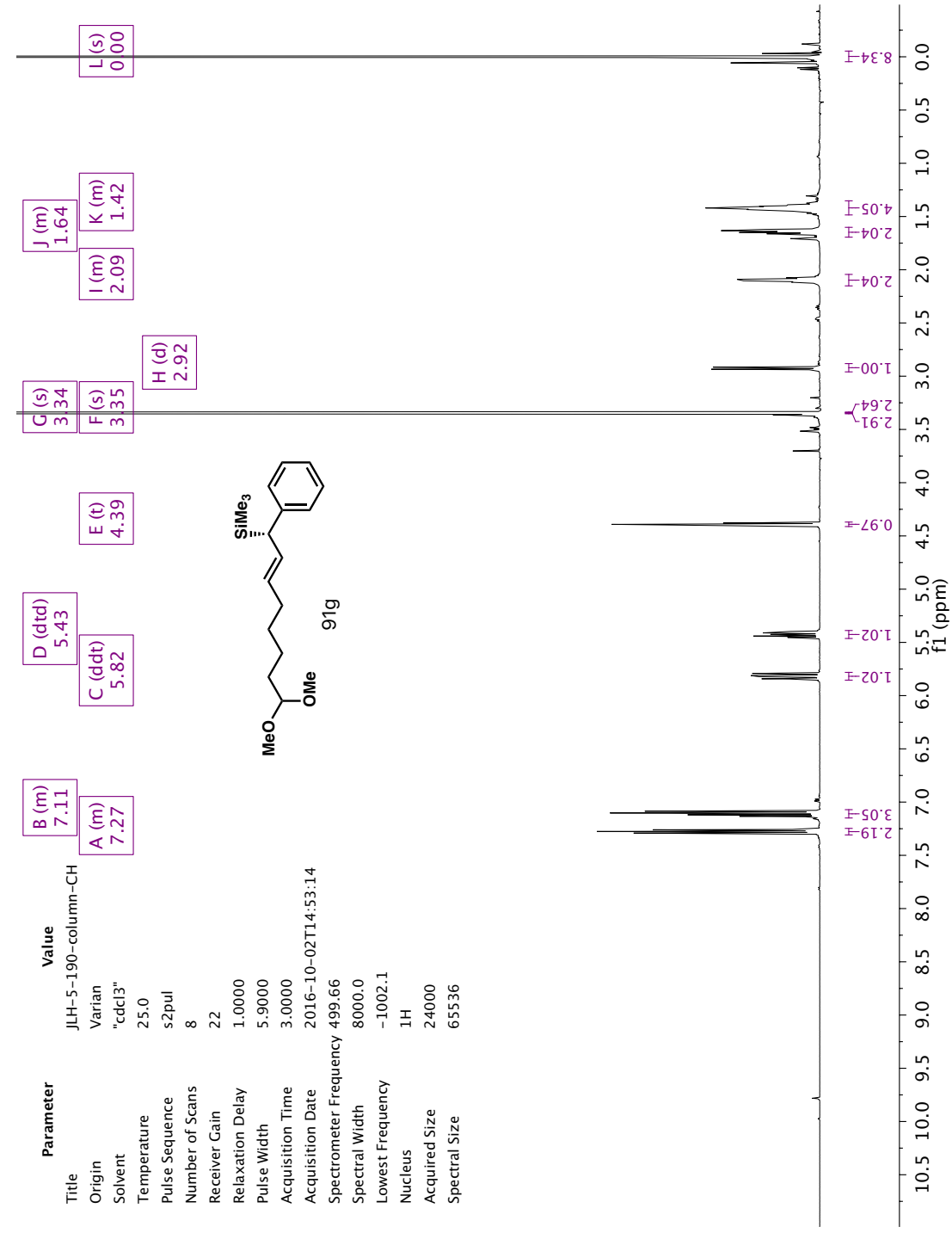
Parameter
Value
Title
JLH-5-190-column-CH
Origin
Varian
Solvent
"cdcl3"
Temperature
25.0
Pulse Sequence
s2pul
Number of Scans
8
Receiver Gain
22
Relaxation Delay
1.0000
Pulse Width
5.9000
Acquisition Time
3.0000
Acquisition Date
2016-10-02T14:53:14
Spectrometer Frequency
499.66
Spectral Width
8000.0
Lowest Frequency
-1002.1
Nucleus
1H
Acquired Size
24000
Spectral Size
65536
A (m) 7.27
B (m) 7.11
C (ddt) 5.82
D (dtd) 5.43
E (t) 4.39
F (s) 3.35
G (s) 3.34
H (d) 2.92
I (m) 2.09
J (m) 1.64
K (m) 1.42
L (s) 0.00
SiMe3
MeO
OMe
91g
8.34
4.05
2.04
2.04
1.00
2.91
2.64
0.97
1.02
1.02
3.05
2.19
f1 (ppm)

Parameter	Value
Title	JLH-5-190-column-CH
Origin	Varian
Solvent	"cdcl3"
Temperature	25.0
Pulse Sequence	s2pul
Number of Scans	256
Receiver Gain	30
Relaxation Delay	1.0000
Pulse Width	4.5000
Acquisition Time	1.0420
Acquisition Date	2016-10-02T14:54:02
Spectrometer Frequency	125.65
Spectral Width	31446.5
Lowest Frequency	-1903.0
Nucleus	13C
Acquired Size	32768
Spectral Size	65536

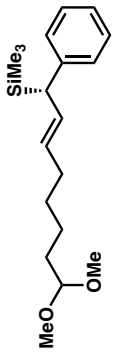

91g

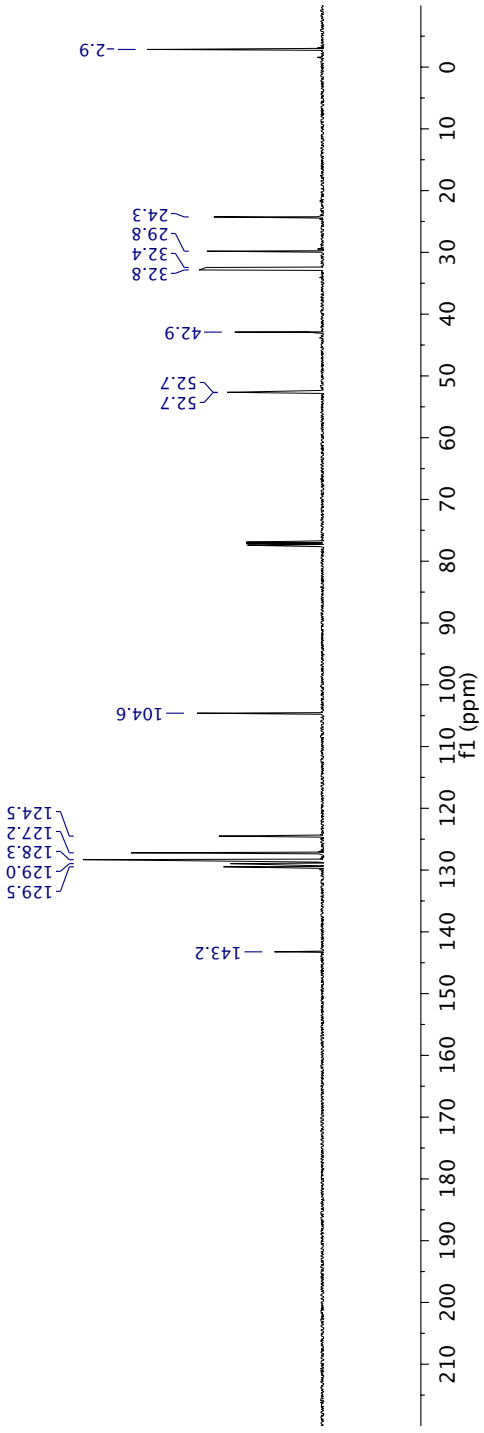

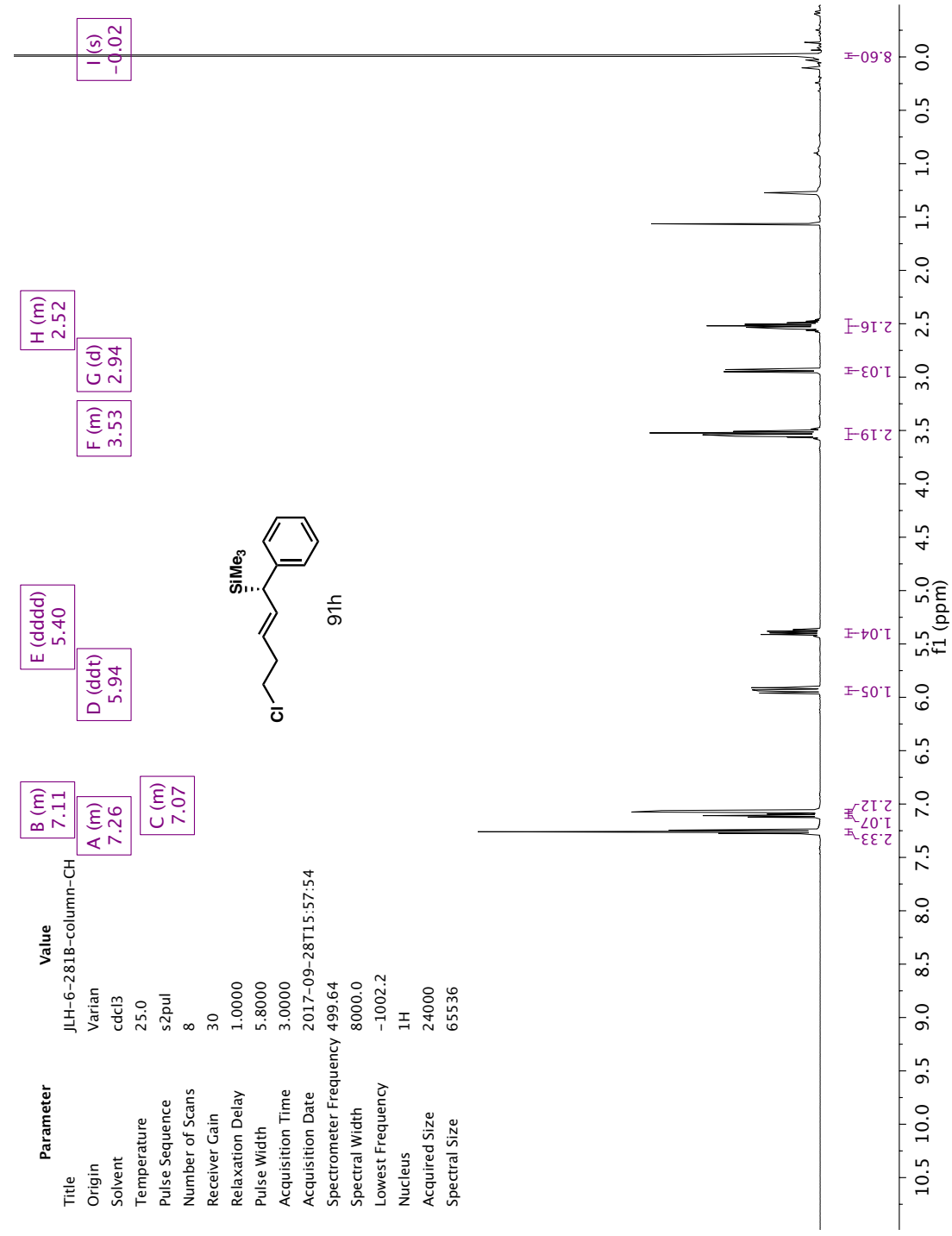
B (m) 7.11
A (m) 7.26
C (m) 7.07
E (dddd) 5.40
D (ddt) 5.94
F (m) 3.53
G (d) 2.94
H (m) 2.52
I (s) -0.02
SiMe3
Cl
91h
Parameter Value
Title JLH-6-281B-column-CH
Origin Varian
Solvent cdcl3
Temperature 25.0
Pulse Sequence s2pul
Number of Scans 8
Receiver Gain 30
Relaxation Delay 1.0000
Pulse Width 5.8000
Acquisition Time 3.0000
Acquisition Date 2017-09-28T15:57:54
Spectrometer Frequency 499.64
Spectral Width 8000.0
Lowest Frequency -1002.2
Nucleus 1H
Acquired Size 24000
Spectral Size 65536
2.33
1.07
2.12
1.05
1.04
2.19
1.03
2.16
8.60
f1 (ppm)

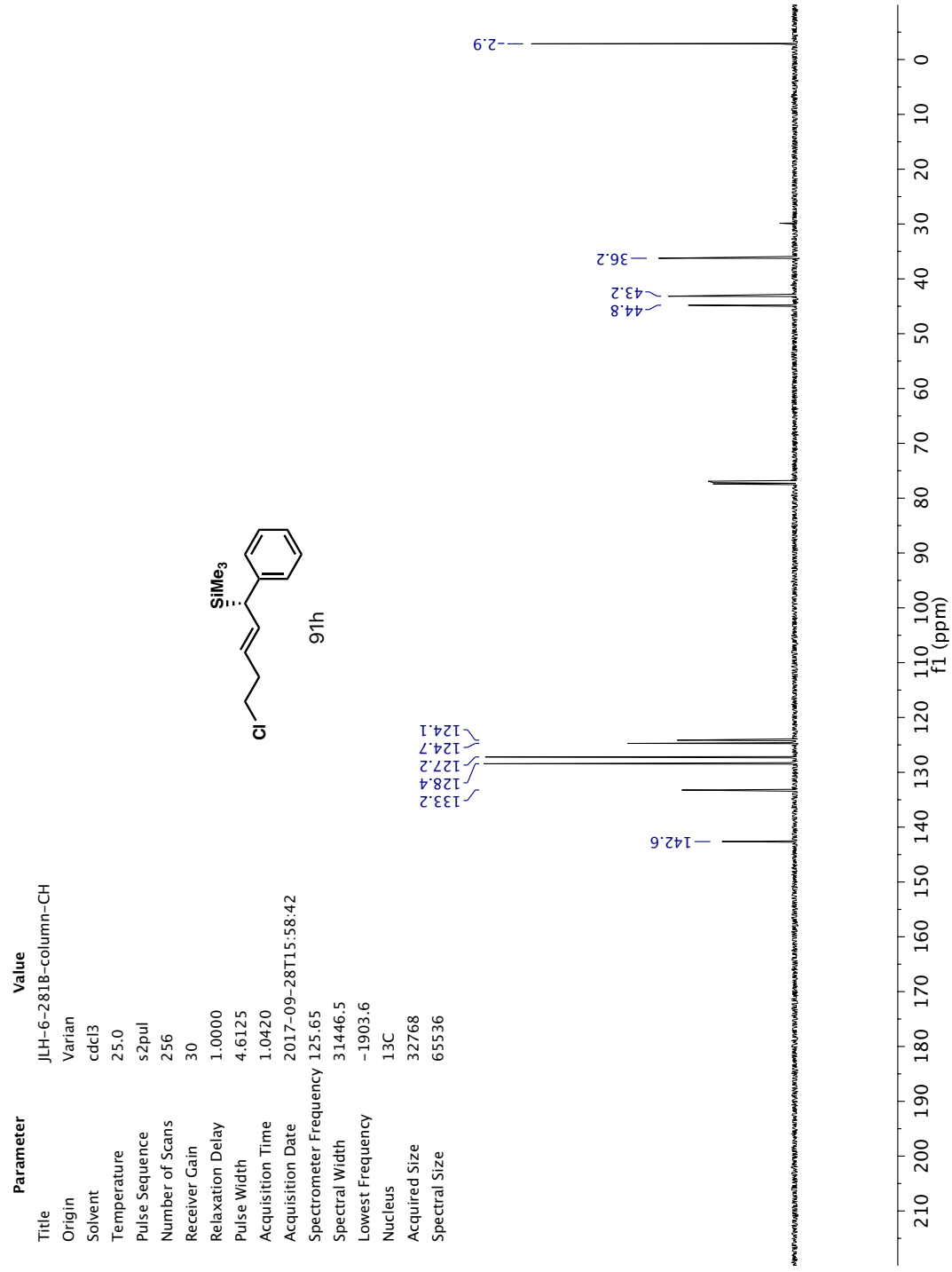
Parameter Value
Title JLH-6-281B-column-CH
Origin Varian
Solvent cdcl3
Temperature 25.0
Pulse Sequence s2pul
Number of Scans 256
Receiver Gain 30
Relaxation Delay 1.0000
Pulse Width 4.6125
Acquisition Time 1.0420
Acquisition Date 2017-09-28T15:58:42
Spectrometer Frequency 125.65
Spectral Width 31446.5
Lowest Frequency -1903.6
Nucleus 13C
Acquired Size 32768
Spectral Size 65536
SiMe3
Cl
91h
-2.9
36.2
43.2
44.8
124.1
124.7
127.2
128.4
133.2
142.6
f1 (ppm)

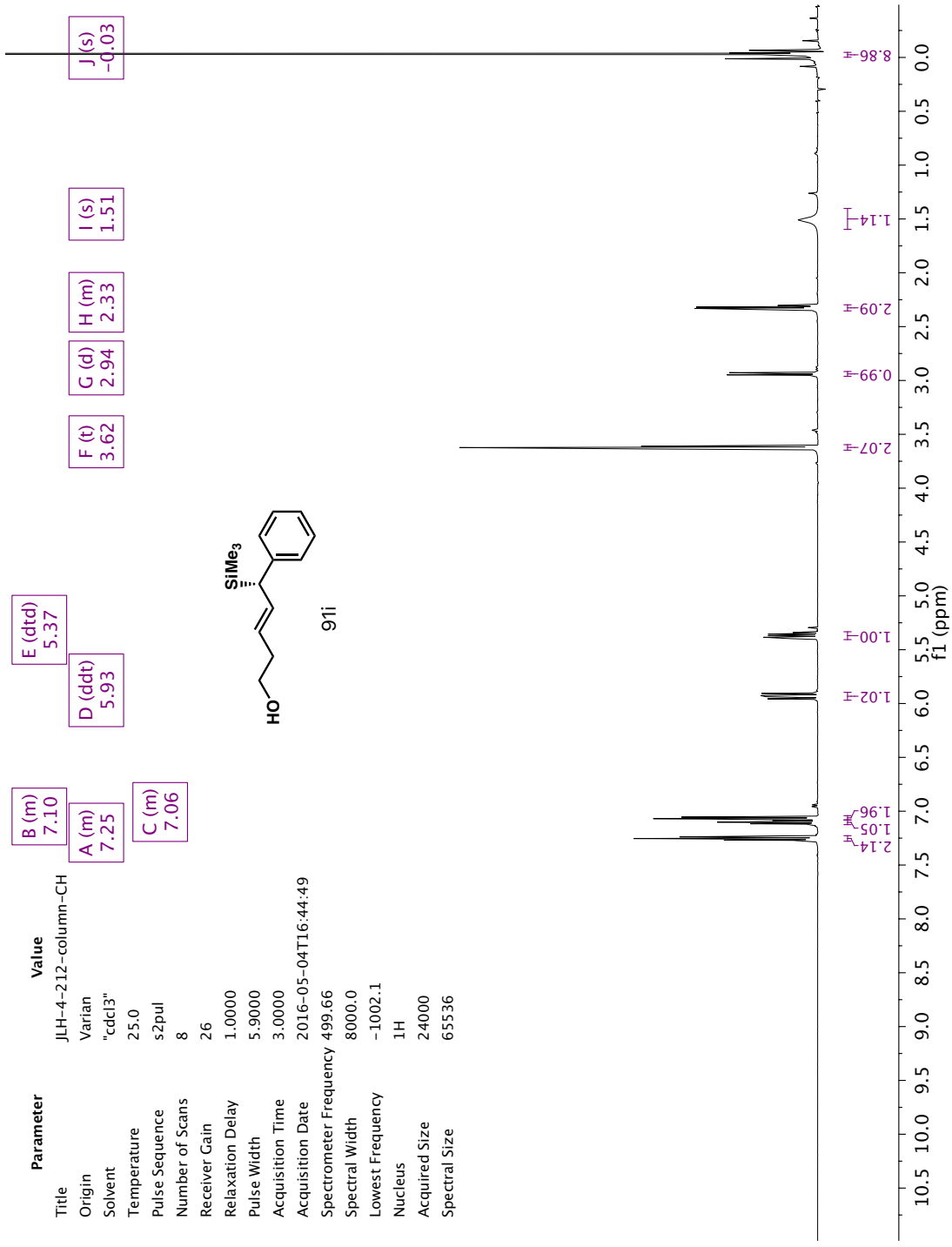
Parameter
Value
Title JLH-4-212-column-CH
Origin Varian
Solvent "cdcl3"
Temperature 25.0
Pulse Sequence s2pul
Number of Scans 8
Receiver Gain 26
Relaxation Delay 1.0000
Pulse Width 5.9000
Acquisition Time 3.0000
Acquisition Date 2016-05-04T16:44:49
Spectrometer Frequency 499.66
Spectral Width 8000.0
Lowest Frequency -1002.1
Nucleus 1H
Acquired Size 24000
Spectral Size 65536
B (m) 7.10
A (m) 7.25
C (m) 7.06
E (dtd) 5.37
D (ddt) 5.93
F (t) 3.62
G (d) 2.94
H (m) 2.33
I (s) 1.51
J (s) -0.03
SiMe3
HO
91i
8.86
1.14
2.09
0.99
2.07
1.00
1.02
2.14
1.05
1.96
10.5 10.0 9.5 9.0 8.5 8.0 7.5 7.0 6.5 6.0 5.5 5.0 4.5 4.0 3.5 3.0 2.5 2.0 1.5 1.0 0.5 0.0
f1 (ppm)

Parameter	Value
Title	JLH-4-212-column-CH
Origin	Varian
Solvent	"cdcl3"
Temperature	25.0
Pulse Sequence	s2pul
Number of Scans	256
Receiver Gain	30
Relaxation Delay	1.0000
Pulse Width	4.5000
Acquisition Time	1.0420
Acquisition Date	2016-05-04T16:45:37
Spectrometer Frequency	125.65
Spectral Width	31446.5
Lowest Frequency	-1903.0
Nucleus	13C
Acquired Size	32768
Spectral Size	65536

91i

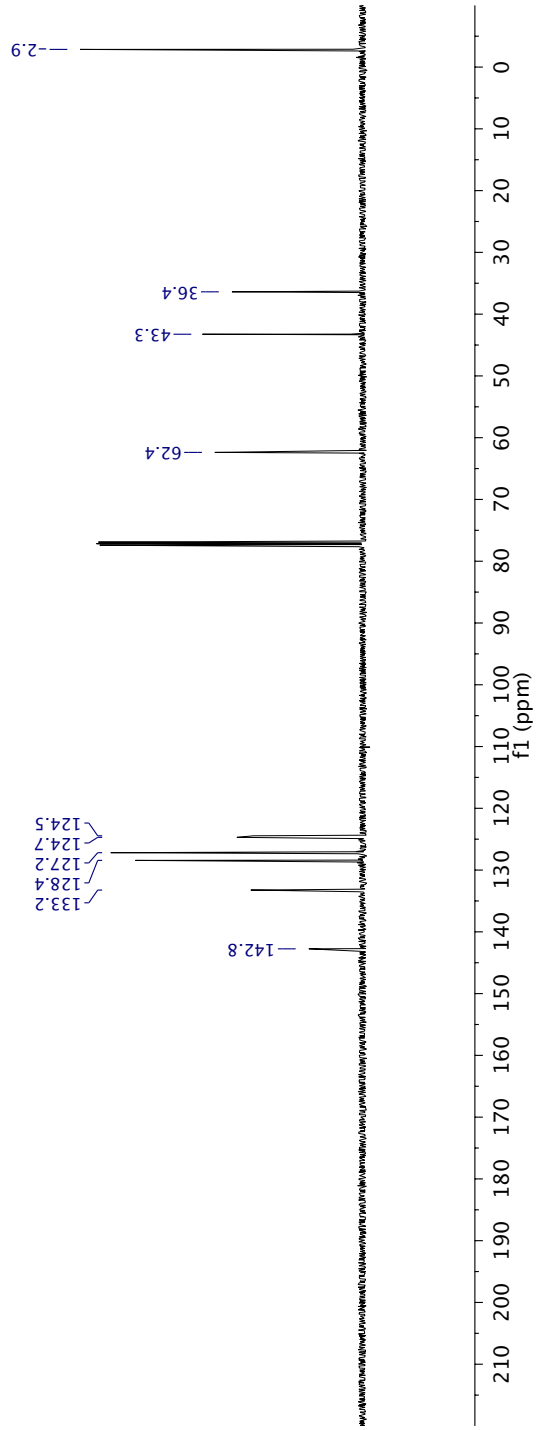

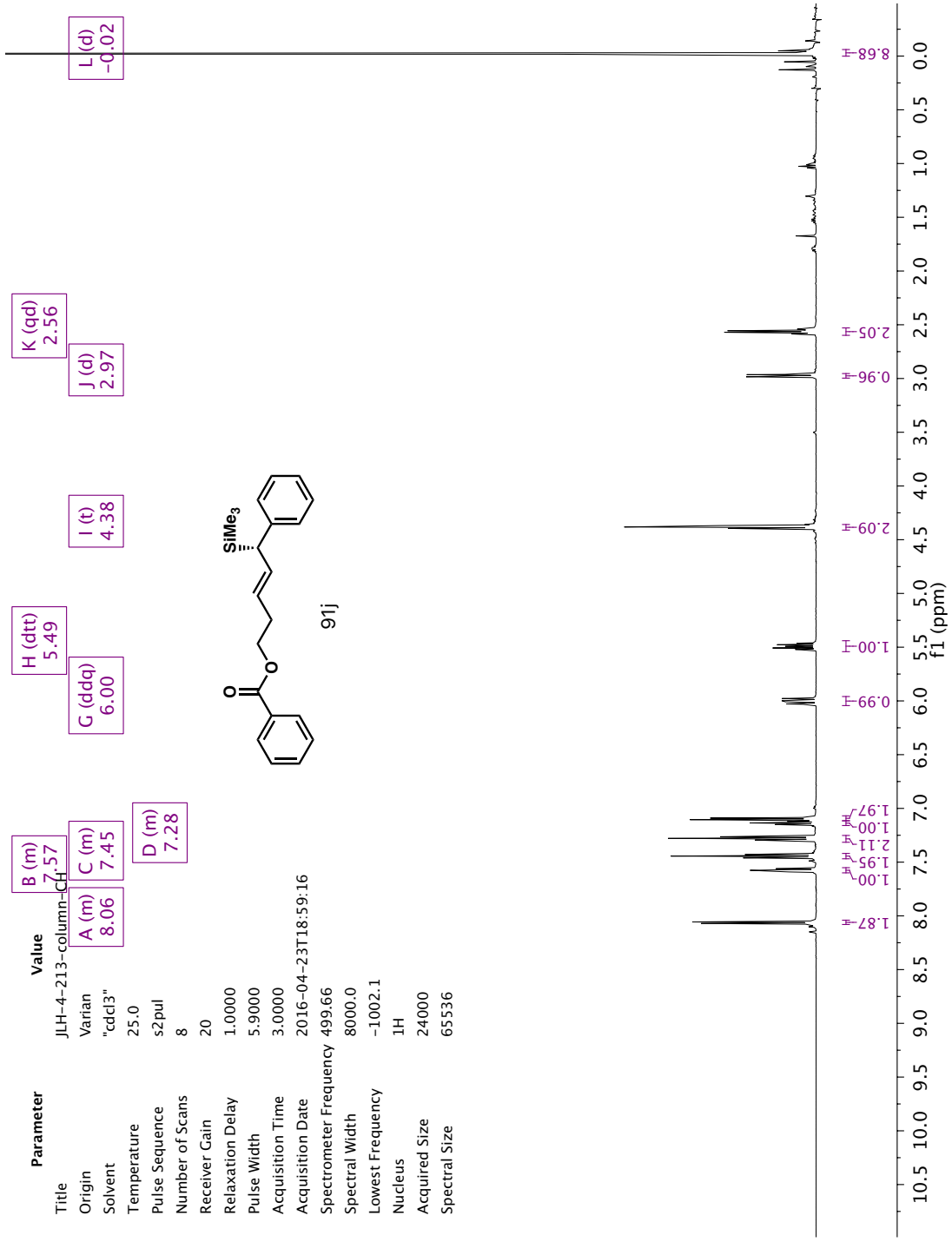

Parameter	Value
Title	JLH-4-213-column-CH
Origin	Varian
Solvent	"cdcl3"
Temperature	25.0
Pulse Sequence	s2pul
Number of Scans	8
Receiver Gain	20
Relaxation Delay	1.0000
Pulse Width	5.9000
Acquisition Time	3.0000
Acquisition Date	2016-04-23T18:59:16
Spectrometer Frequency	499.66
Spectral Width	8000.0
Lowest Frequency	-1002.1
Nucleus	1H
Acquired Size	24000
Spectral Size	65536

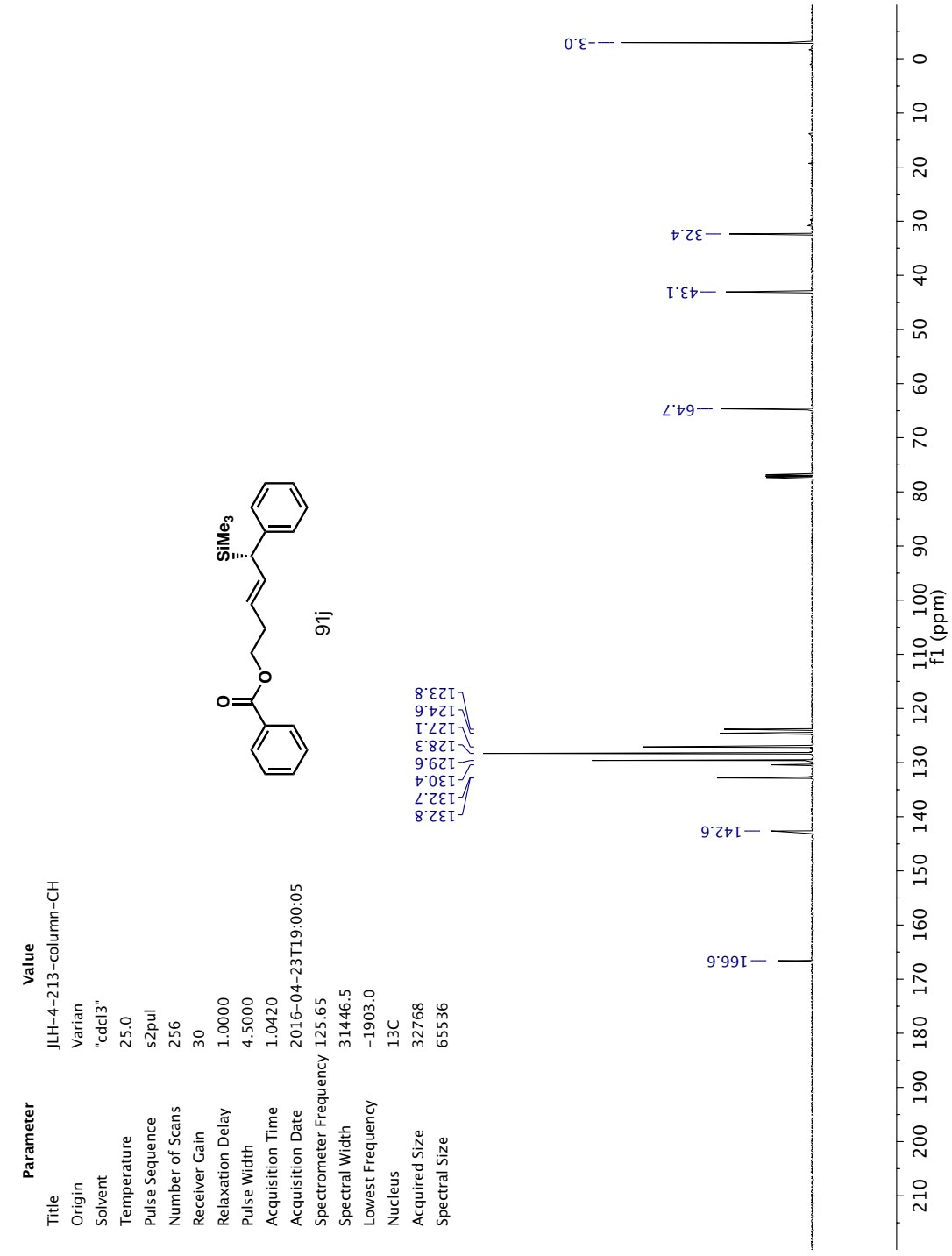
Parameter Value
Title JLH-4-213-column-CH
Origin Varian
Solvent "cdcl3"
Temperature 25.0
Pulse Sequence s2pul
Number of Scans 256
Receiver Gain 30
Relaxation Delay 1.0000
Pulse Width 4.5000
Acquisition Time 1.0420
Acquisition Date 2016-04-23T19:00:05
Spectrometer Frequency 125.65
Spectral Width 31446.5
Lowest Frequency -1903.0
Nucleus 13C
Acquired Size 32768
Spectral Size 65536
SiMe3
O
O
91j
132.8
132.7
130.4
129.6
128.3
127.1
124.6
123.8
166.6
142.6
64.7
43.1
32.4
-3.0
f1 (ppm)

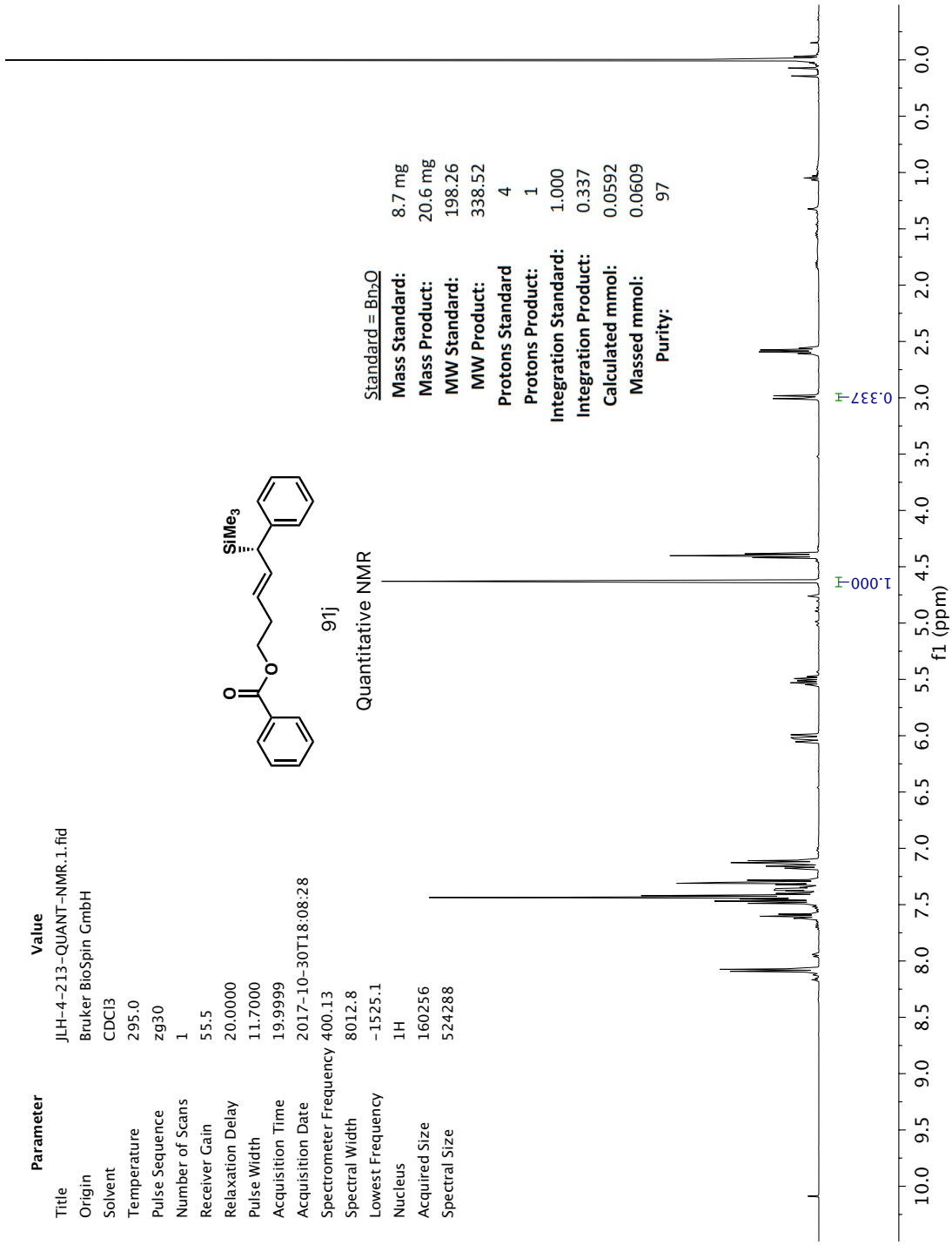
Parameter Value
Title JLH-4-213-QUANT-NMR.1.fid
Origin Bruker BioSpin GmbH
Solvent CDCl3
Temperature 295.0
Pulse Sequence zg30
Number of Scans 1
Receiver Gain 55.5
Relaxation Delay 20.0000
Pulse Width 11.7000
Acquisition Time 19.9999
Acquisition Date 2017-10-30T18:08:28
Spectrometer Frequency 400.13
Spectral Width 8012.8
Lowest Frequency -1525.1
Nucleus 1H
Acquired Size 160256
Spectral Size 524288
SiMe3
91j
Quantitative NMR
Standard = Bn2O
Mass Standard: 8.7 mg
Mass Product: 20.6 mg
MW Standard: 198.26
MW Product: 338.52
Protons Standard 4
Protons Product: 1
Integration Standard: 1.000
Integration Product: 0.337
Calculated mmol: 0.0592
Massed mmol: 0.0609
Purity: 97
1.000
0.337
10.0 9.5 9.0 8.5 8.0 7.5 7.0 6.5 6.0 5.5 5.0 4.5 4.0 3.5 3.0 2.5 2.0 1.5 1.0 0.5 0.0
f1 (ppm)

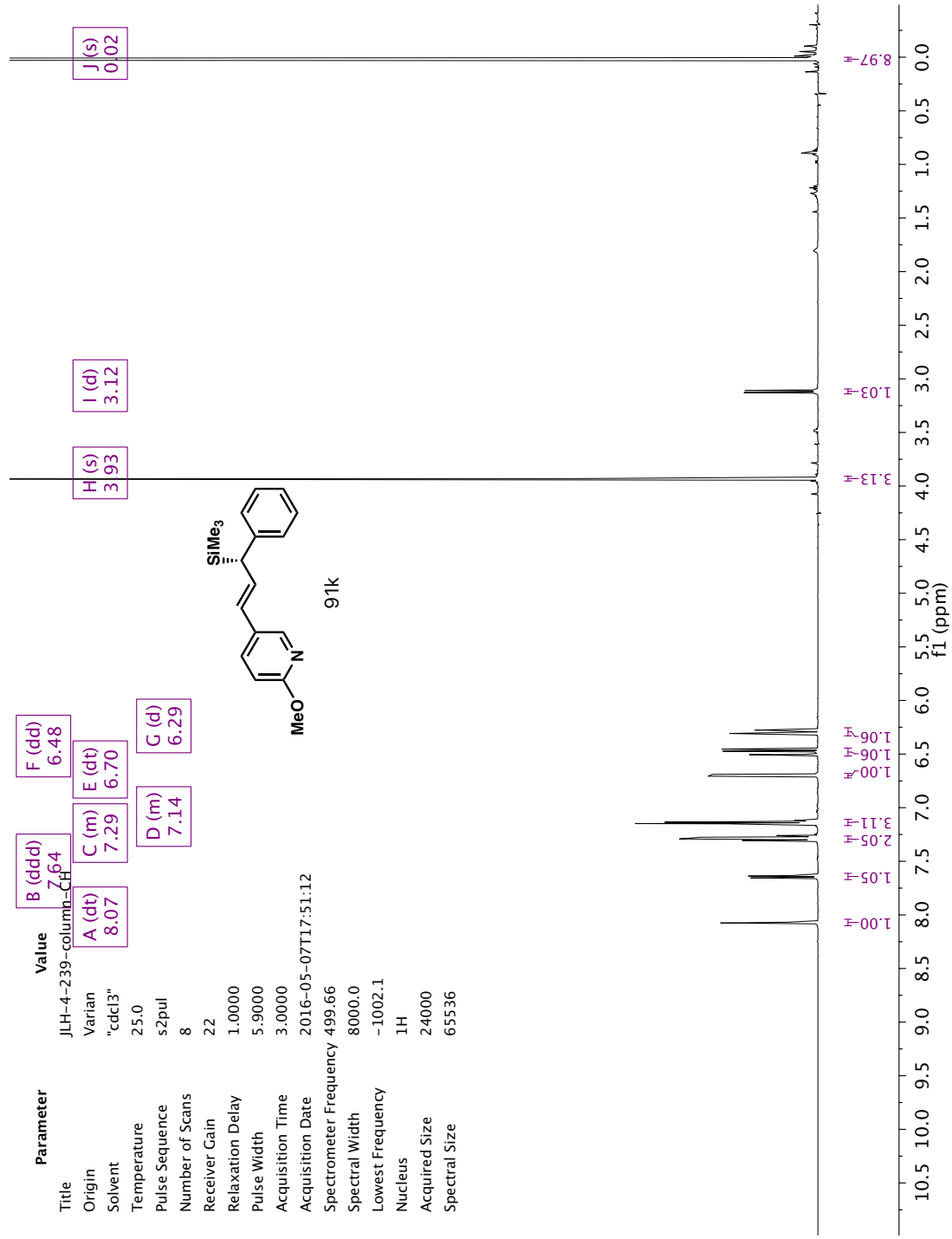
Parameter
Value
Title JLH-4-239-column-CH
Origin Varian
Solvent "cdcl3"
Temperature 25.0
Pulse Sequence s2pul
Number of Scans 8
Receiver Gain 22
Relaxation Delay 1.0000
Pulse Width 5.9000
Acquisition Time 3.0000
Acquisition Date 2016-05-07T17:51:12
Spectrometer Frequency 499.66
Spectral Width 8000.0
Lowest Frequency -1002.1
Nucleus 1H
Acquired Size 24000
Spectral Size 65536
B (ddd) 7.64
A (dt) 8.07
C (m) 7.29
D (m) 7.14
F (dd) 6.48
E (dt) 6.70
G (d) 6.29
H (s) 3.93
I (d) 3.12
J (s) 0.02
SiMe3
MeO
N
91k
1.00
1.05
2.05
3.11
1.00
1.06
1.06
3.13
1.03
8.97
f1 (ppm)

Parameter	Value
Title	JLH-4-239-column-CH
Origin	Varian
Solvent	"cdcl3"
Temperature	25.0
Pulse Sequence	s2pul
Number of Scans	256
Receiver Gain	30
Relaxation Delay	1.0000
Pulse Width	4.5000
Acquisition Time	1.0420
Acquisition Date	2016-05-07T17:52:01
Spectrometer Frequency	125.65
Spectral Width	31446.5
Lowest Frequency	-1903.0
Nucleus	13C
Acquired Size	32768
Spectral Size	65536

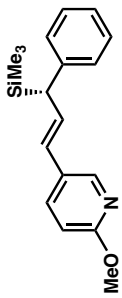

91k

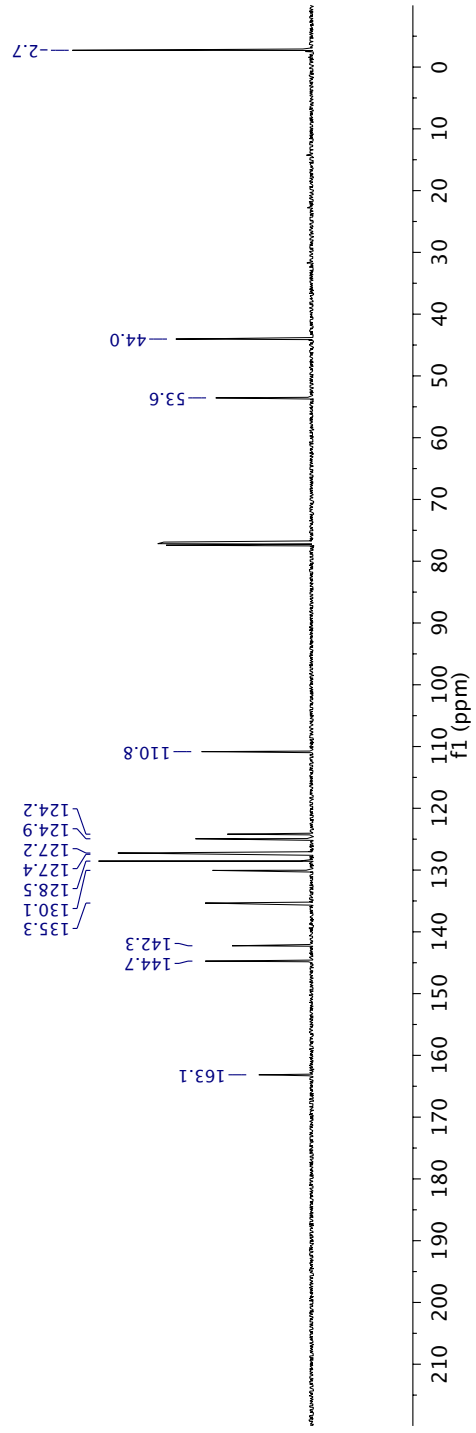

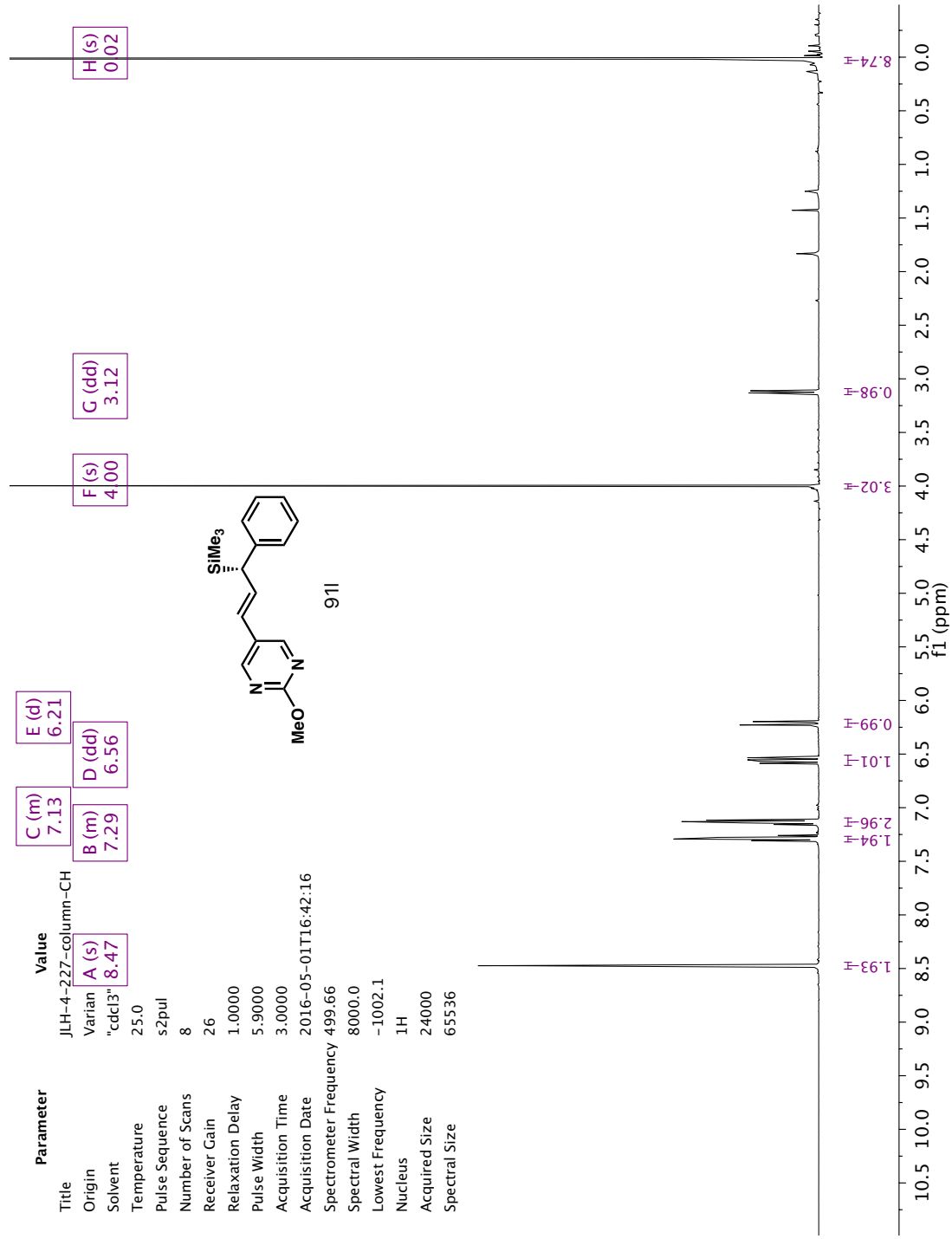
Parameter
Value
Title JLH-4-227-column-CH
Origin Varian
Solvent "cdcl3"
Temperature 25.0
Pulse Sequence s2pul
Number of Scans 8
Receiver Gain 26
Relaxation Delay 1.0000
Pulse Width 5.9000
Acquisition Time 3.0000
Acquisition Date 2016-05-01T16:42:16
Spectrometer Frequency 499.66
Spectral Width 8000.0
Lowest Frequency -1002.1
Nucleus 1H
Acquired Size 24000
Spectral Size 65536
A (s) 8.47
B (m) 7.29
C (m) 7.13
D (dd) 6.56
E (d) 6.21
F (s) 4.00
G (dd) 3.12
H (s) 0.02
SiMe3
MeO
N
N
91l
8.74
3.02
0.98
1.93
1.94
2.96
1.01
0.99
f1 (ppm)

Parameter	Value
Title	JLH-4-227-column-CH
Origin	Varian
Solvent	"cdcl3"
Temperature	25.0
Pulse Sequence	s2pul
Number of Scans	256
Receiver Gain	30
Relaxation Delay	1.0000
Pulse Width	4.5000
Acquisition Time	1.0420
Acquisition Date	2016-05-01T16:43:04
Spectrometer Frequency	125.65
Spectral Width	31446.5
Lowest Frequency	-1903.0
Nucleus	13C
Acquired Size	32768
Spectral Size	65536

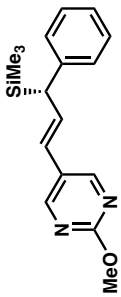

91l

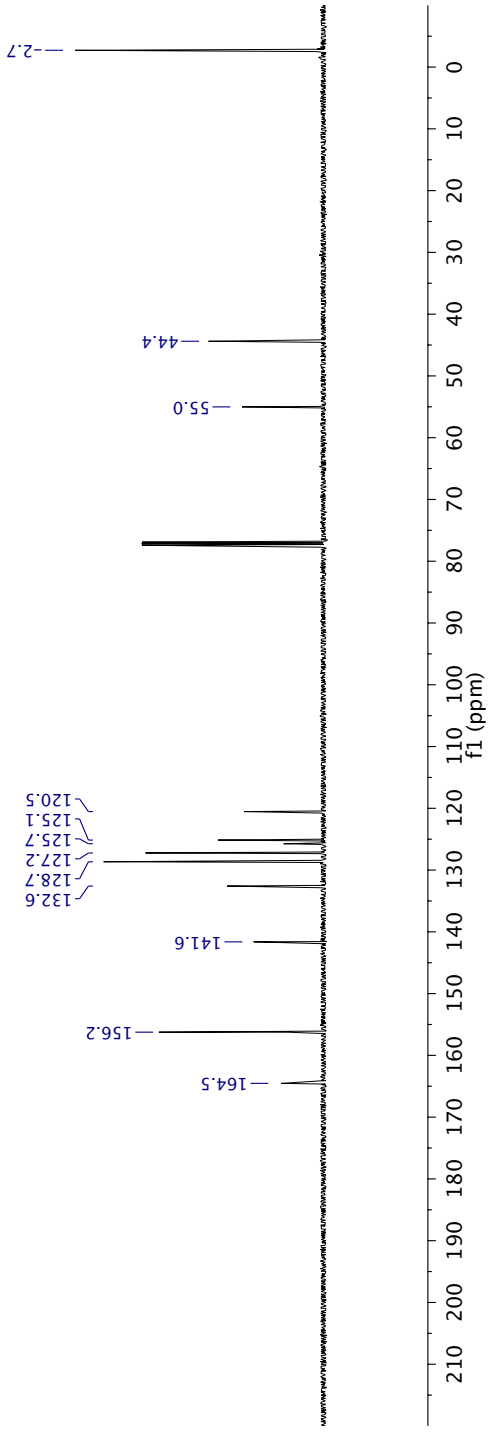

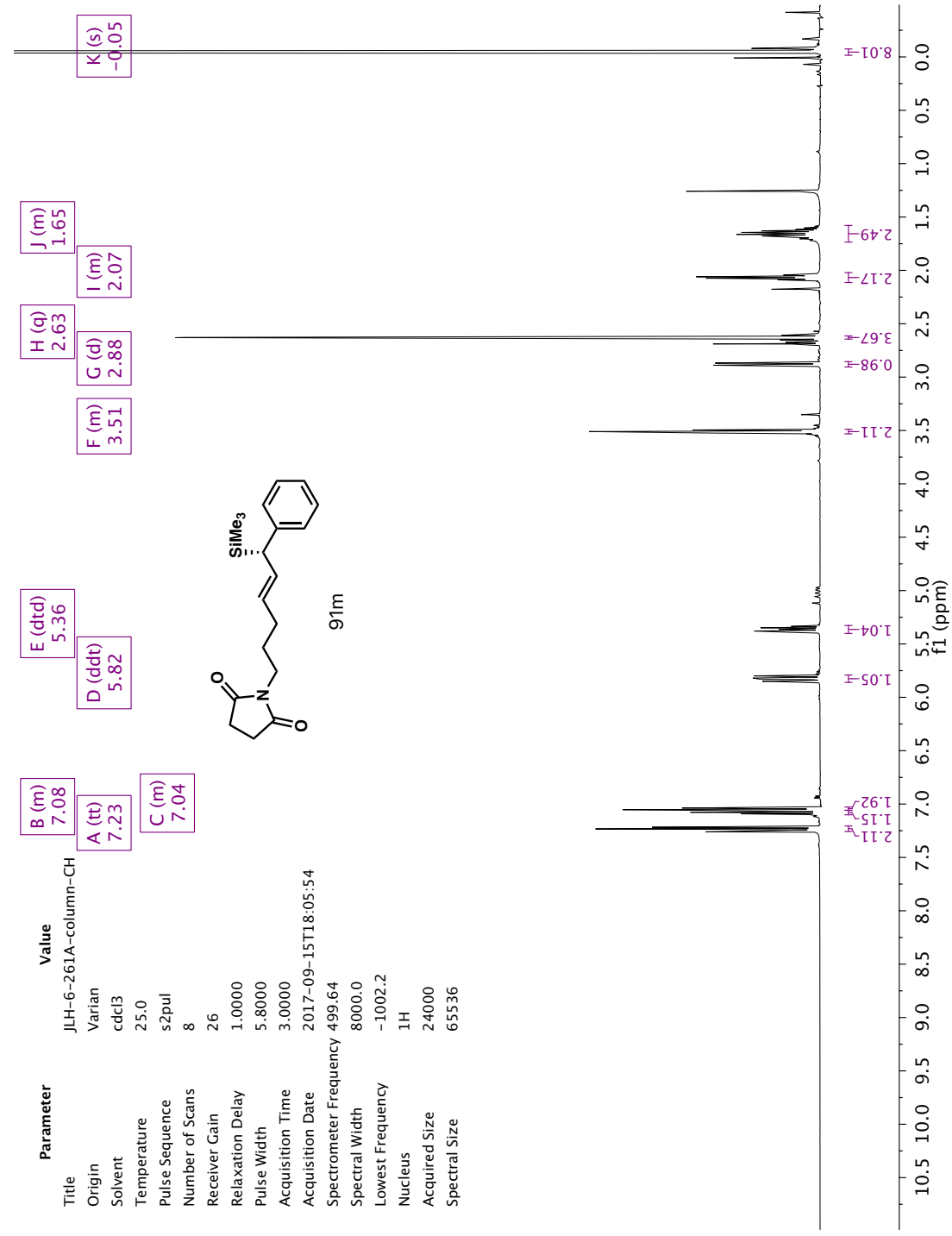

Parameter	Value
Title	JLH-6-261A-column-CH
Origin	Varian
Solvent	cdcl3
Temperature	25.0
Pulse Sequence	s2pul
Number of Scans	8
Receiver Gain	26
Relaxation Delay	1.0000
Pulse Width	5.8000
Acquisition Time	3.0000
Acquisition Date	2017-09-15T18:05:54
Spectrometer Frequency	499.64
Spectral Width	8000.0
Lowest Frequency	-1002.2
Nucleus	1H
Acquired Size	24000
Spectral Size	65536

Parameter	Value
Title	JLH-6-261A-column-CH
Origin	Varian
Solvent	cdcl3
Temperature	25.0
Pulse Sequence	s2pul
Number of Scans	256
Receiver Gain	30
Relaxation Delay	1.0000
Pulse Width	4.6125
Acquisition Time	1.0420
Acquisition Date	2017-09-15T18:06:42
Spectrometer Frequency	125.65
Spectral Width	31446.5
Lowest Frequency	-1903.6
Nucleus	13C
Acquired Size	32768
Spectral Size	65536

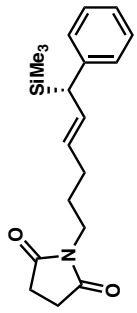

91m

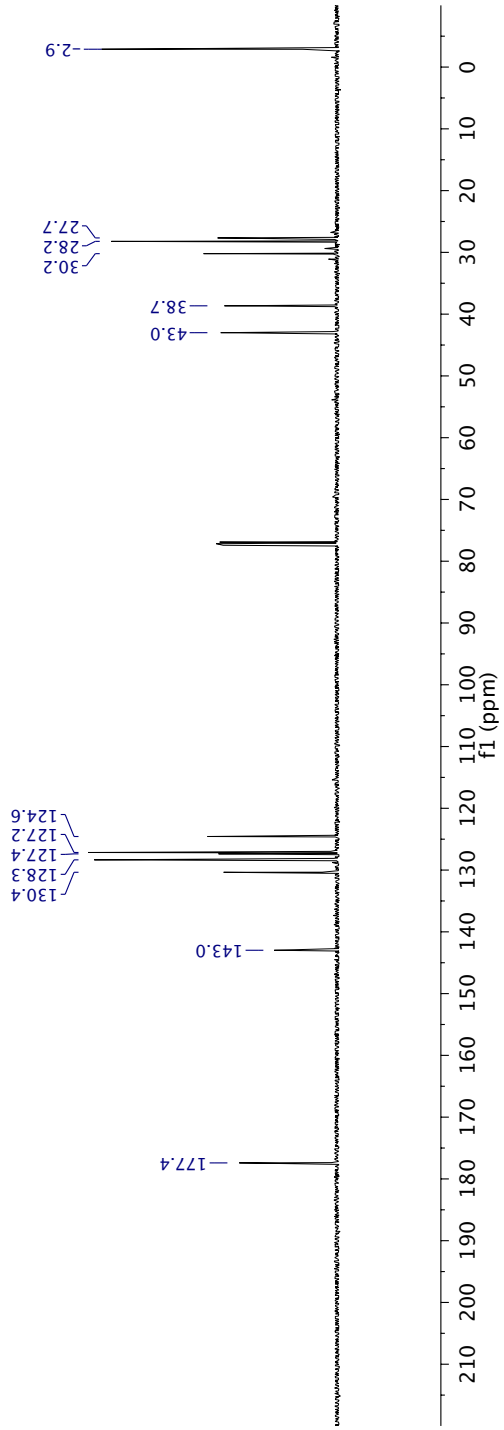

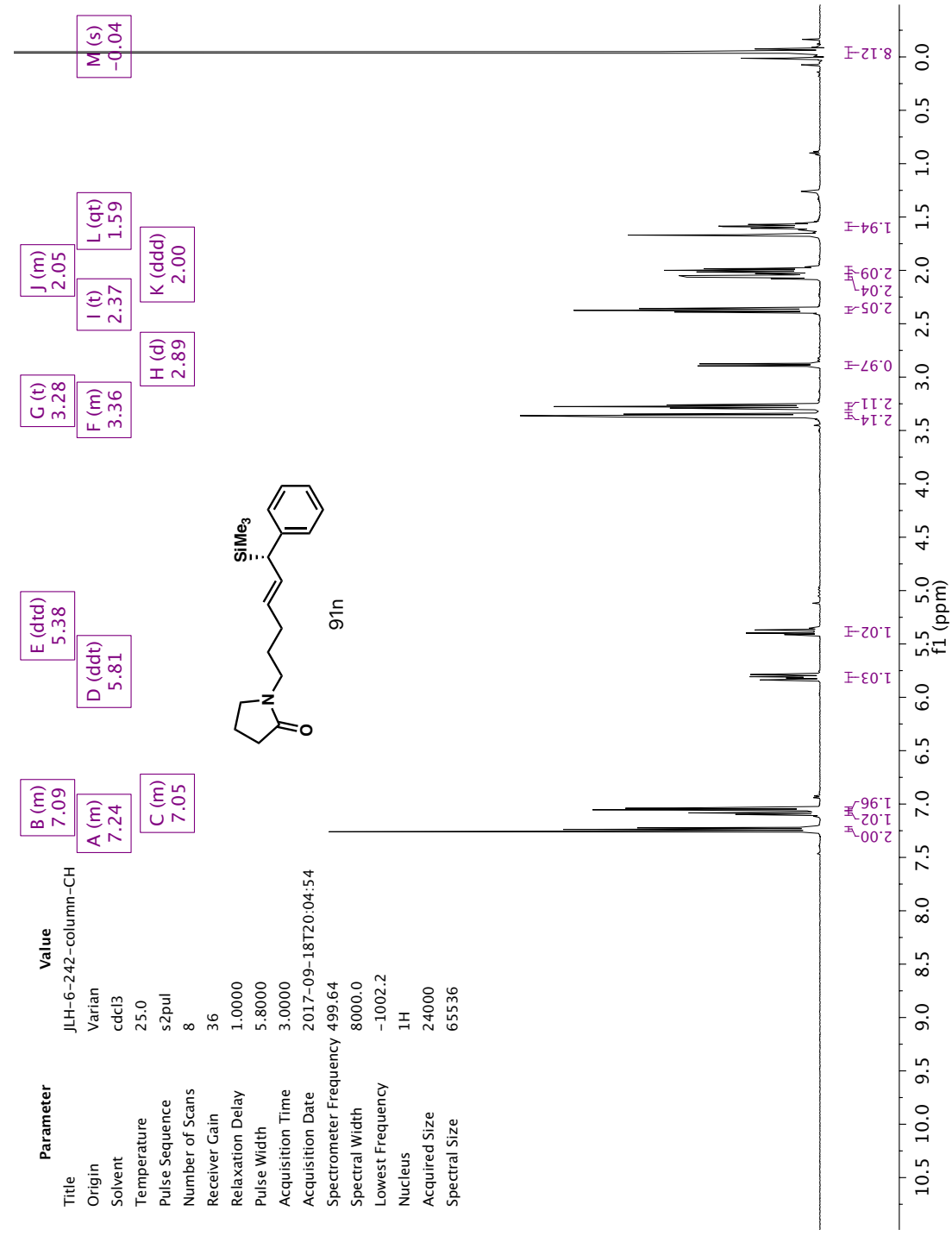
Parameter
Value
Title JLH-6-242-column-CH
Origin Varian
Solvent cdcl3
Temperature 25.0
Pulse Sequence s2pul
Number of Scans 8
Receiver Gain 36
Relaxation Delay 1.0000
Pulse Width 5.8000
Acquisition Time 3.0000
Acquisition Date 2017-09-18T20:04:54
Spectrometer Frequency 499.64
Spectral Width 8000.0
Lowest Frequency -1002.2
Nucleus 1H
Acquired Size 24000
Spectral Size 65536
B (m) 7.09
A (m) 7.24
C (m) 7.05
E (dtd) 5.38
D (ddt) 5.81
G (t) 3.28
F (m) 3.36
H (d) 2.89
J (m) 2.05
I (t) 2.37
K (ddd) 2.00
L (qt) 1.59
M (s) -0.04
SiMe3
N
O
91n
8.12
1.94
2.09
2.04
2.05
0.97
2.14
2.11
1.02
1.03
2.00
1.02
1.96
f1 (ppm)

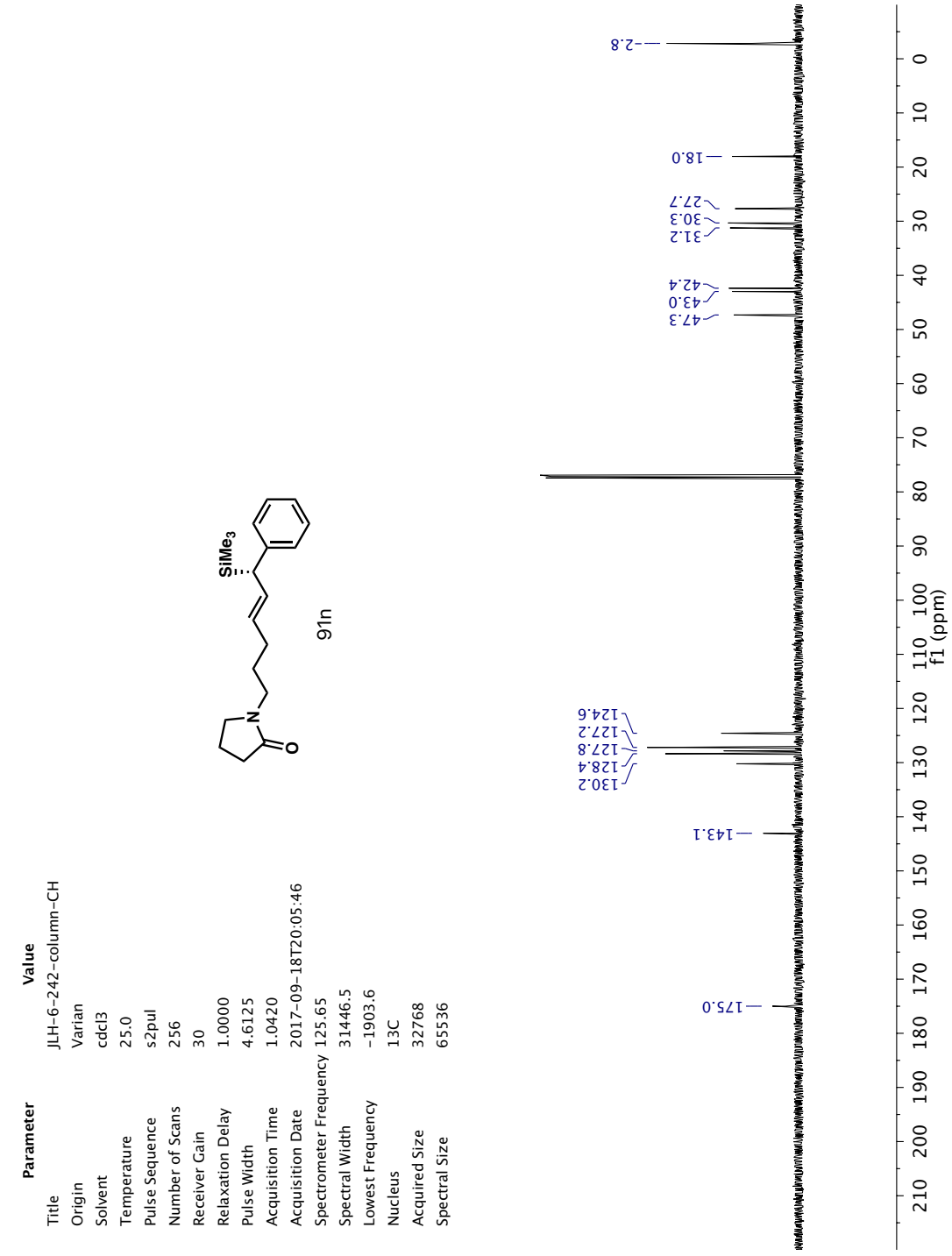
Parameter Value
Title JLH-6-242-column-CH
Origin Varian
Solvent cdcl3
Temperature 25.0
Pulse Sequence s2pul
Number of Scans 256
Receiver Gain 30
Relaxation Delay 1.0000
Pulse Width 4.6125
Acquisition Time 1.0420
Acquisition Date 2017-09-18T20:05:46
Spectrometer Frequency 125.65
Spectral Width 31446.5
Lowest Frequency -1903.6
Nucleus 13C
Acquired Size 32768
Spectral Size 65536
SiMe3
N
O
91n
175.0
143.1
130.2
128.4
127.8
127.2
124.6
47.3
43.0
42.4
31.2
30.3
27.7
18.0
-2.8
f1 (ppm)

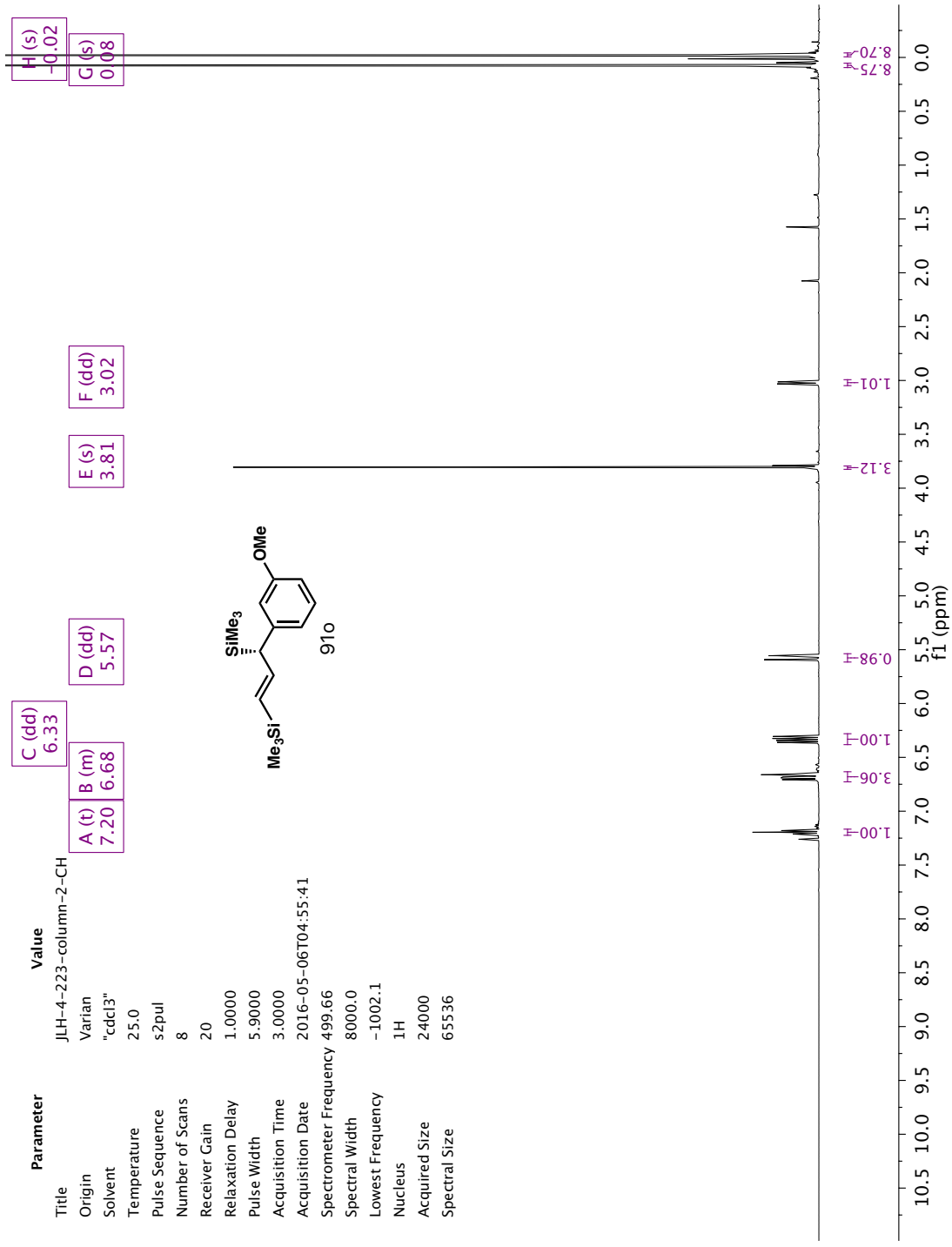
Parameter
Value
Title
JLH-4-223-column-2-CH
Origin
Varian
Solvent
"cdcl3"
Temperature
25.0
Pulse Sequence
s2pul
Number of Scans
8
Receiver Gain
20
Relaxation Delay
1.0000
Pulse Width
5.9000
Acquisition Time
3.0000
Acquisition Date
2016-05-06T04:55:41
Spectrometer Frequency
499.66
Spectral Width
8000.0
Lowest Frequency
-1002.1
Nucleus
1H
Acquired Size
24000
Spectral Size
65536
A (t) 7.20
B (m) 6.68
C (dd) 6.33
D (dd) 5.57
E (s) 3.81
F (dd) 3.02
G (s) 0.08
H (s) -0.02
SiMe3
OMe
Me3Si
91o
8.75
8.70
3.12
1.01
0.98
1.00
3.06
1.00
1.00
f1 (ppm)

Parameter	Value
Title	JLH-4-223-column-2-CH
Origin	Varian
Solvent	"cdcl3"
Temperature	25.0
Pulse Sequence	s2pul
Number of Scans	256
Receiver Gain	30
Relaxation Delay	1.0000
Pulse Width	4.5000
Acquisition Time	1.0420
Acquisition Date	2016-05-06T04:56:31
Spectrometer Frequency	125.65
Spectral Width	31446.5
Lowest Frequency	-1903.0
Nucleus	13C
Acquired Size	32768
Spectral Size	65536

91o

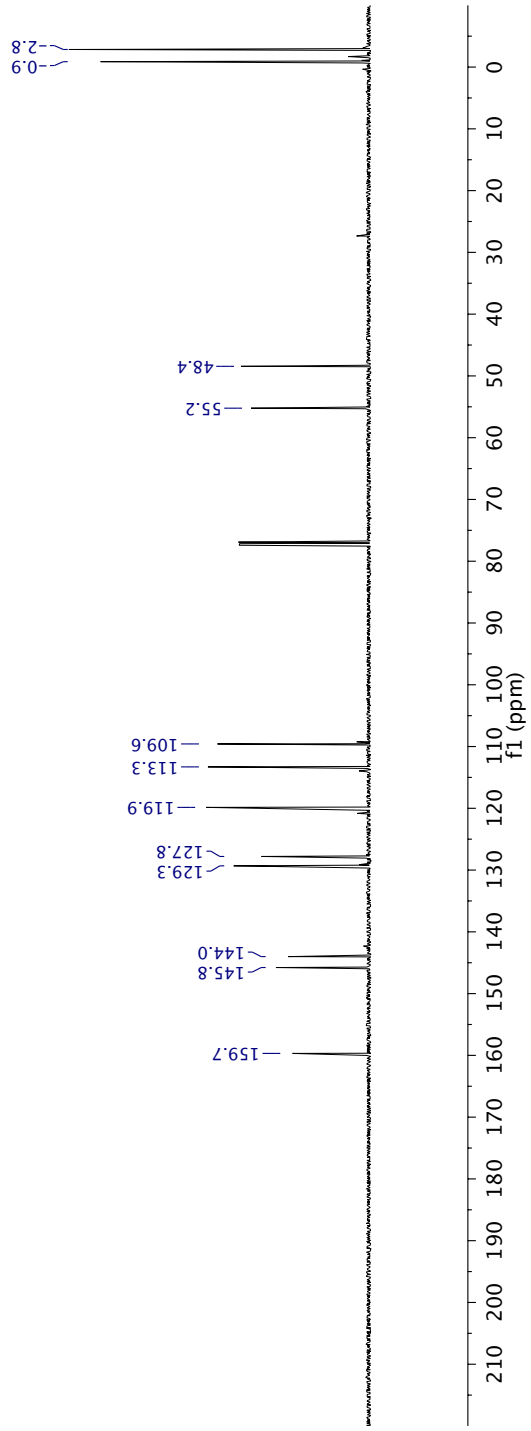

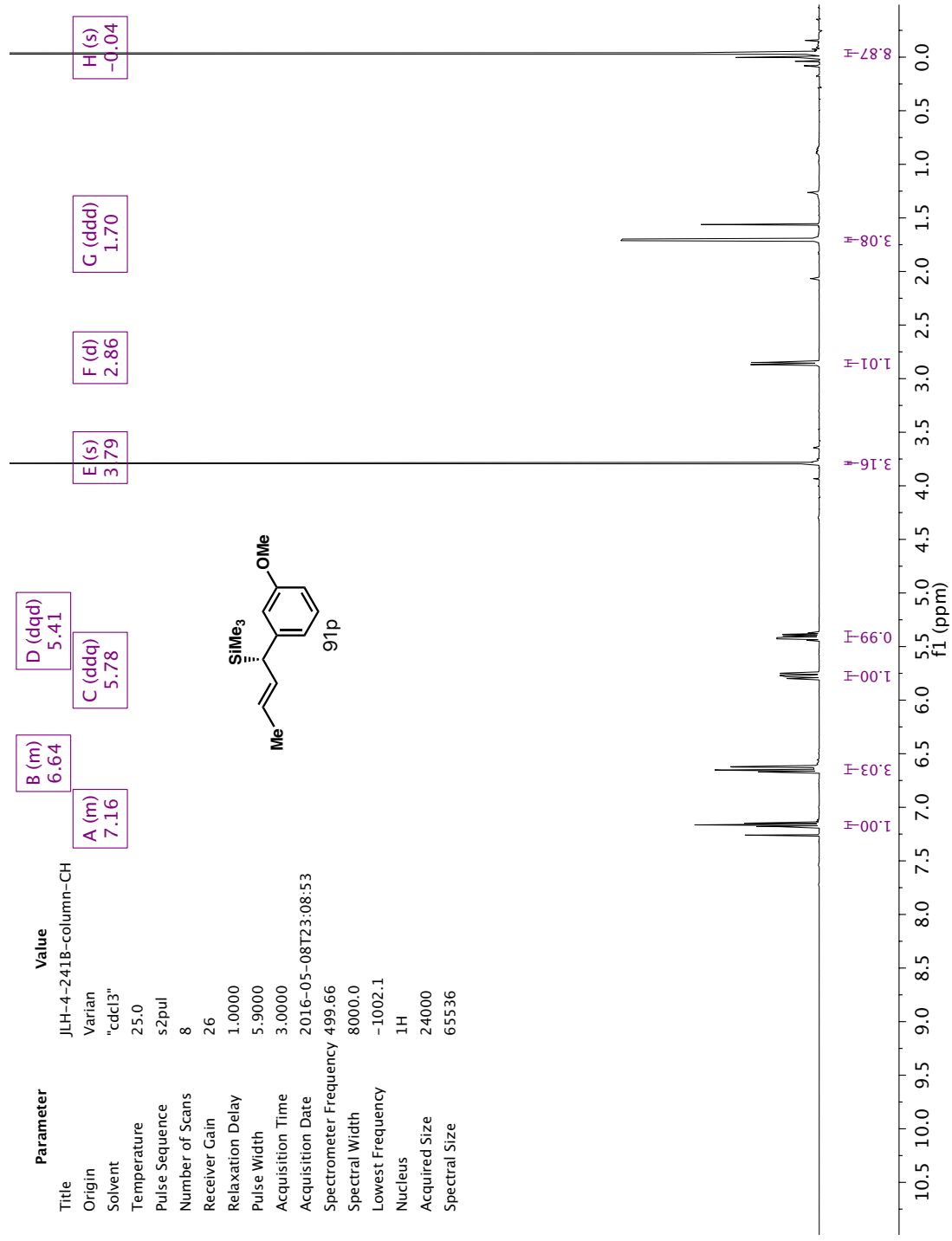

Parameter	Value
Title	JLH-4-241B-column-CH
Origin	Varian
Solvent	"cdcl3"
Temperature	25.0
Pulse Sequence	s2pul
Number of Scans	8
Receiver Gain	26
Relaxation Delay	1.0000
Pulse Width	5.9000
Acquisition Time	3.0000
Acquisition Date	2016-05-08T23:08:53
Spectrometer Frequency	499.66
Spectral Width	8000.0
Lowest Frequency	-1002.1
Nucleus	1H
Acquired Size	24000
Spectral Size	65536

Parameter	Value
Title	JLH-4-241B-column-CH
Origin	Varian
Solvent	"cdcl3"
Temperature	25.0
Pulse Sequence	s2pul
Number of Scans	256
Receiver Gain	30
Relaxation Delay	1.0000
Pulse Width	4.5000
Acquisition Time	1.0420
Acquisition Date	2016-05-08T23:09:41
Spectrometer Frequency	125.65
Spectral Width	31446.5
Lowest Frequency	-1903.0
Nucleus	13C
Acquired Size	32768
Spectral Size	65536

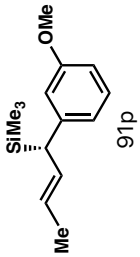

91p

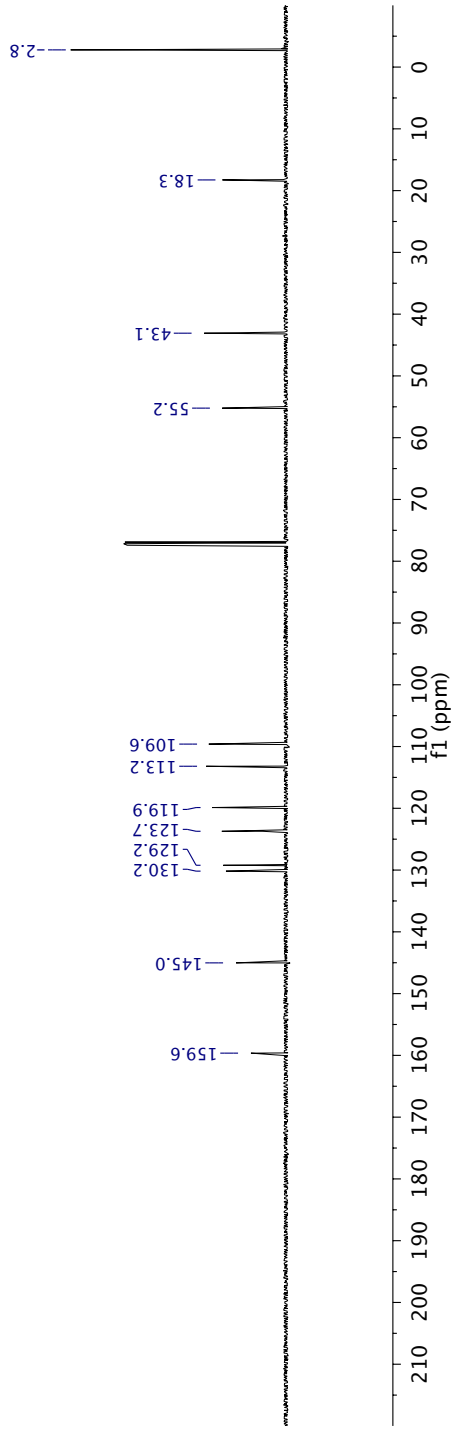

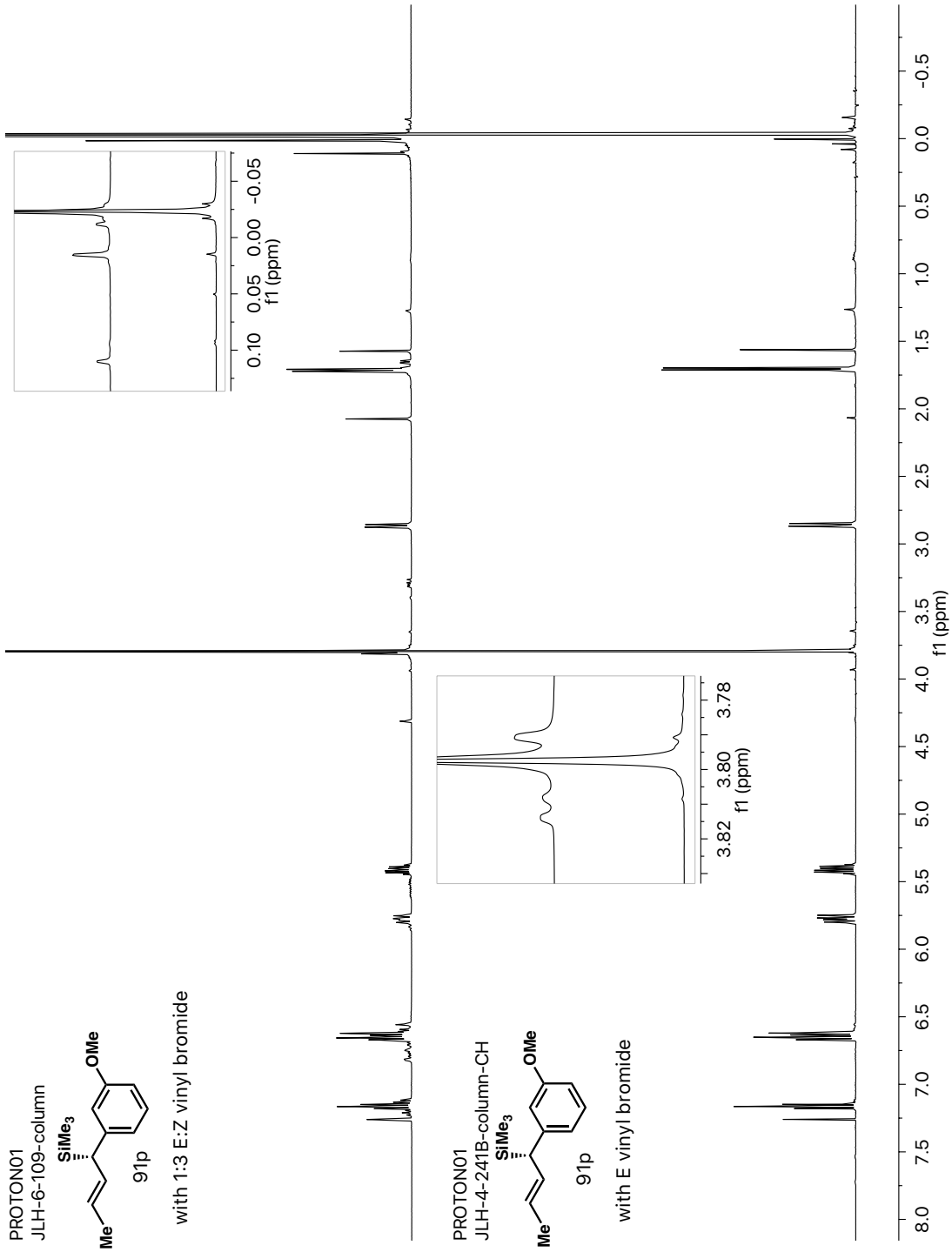
PROTON01
JLH-6-109-column
SiMe3
OMe
Me
91p
with 1:3 E:Z vinyl bromide
PROTON01
JLH-4-241B-column-CH
SiMe3
OMe
Me
91p
with E vinyl bromide
0.10 0.05 0.00 -0.05
f1 (ppm)
3.82 3.80 3.78
f1 (ppm)
8.0 7.5 7.0 6.5 6.0 5.5 5.0 4.5 4.0 3.5 3.0 2.5 2.0 1.5 1.0 0.5 0.0 -0.5
f1 (ppm)

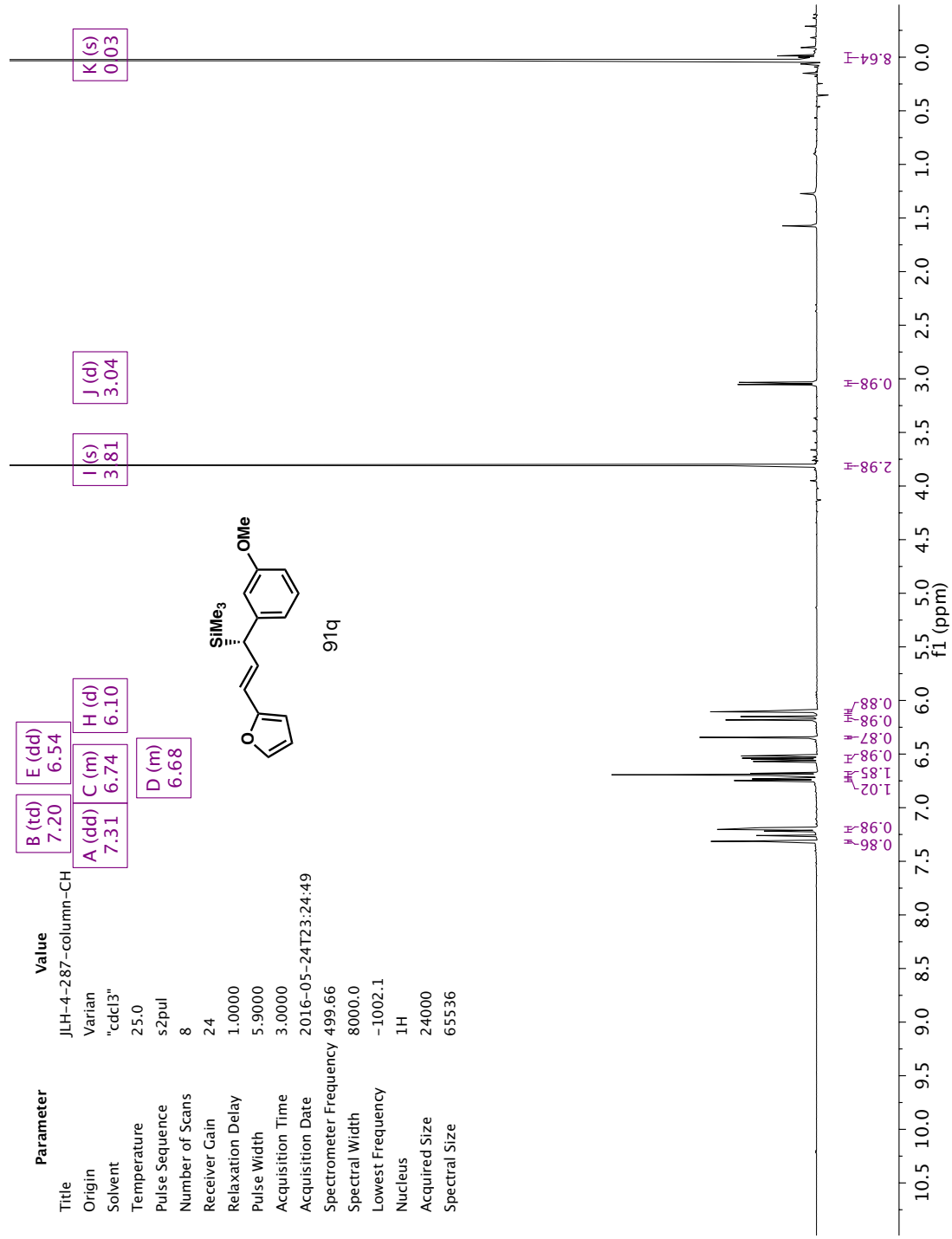
Parameter
Value
Title
JLH-4-287-column-CH
Origin
Varian
Solvent
"cdcl3"
Temperature
25.0
Pulse Sequence
s2pul
Number of Scans
8
Receiver Gain
24
Relaxation Delay
1.0000
Pulse Width
5.9000
Acquisition Time
3.0000
Acquisition Date
2016-05-24T23:24:49
Spectrometer Frequency
499.66
Spectral Width
8000.0
Lowest Frequency
-1002.1
Nucleus
1H
Acquired Size
24000
Spectral Size
65536
B (td) 7.20
E (dd) 6.54
A (dd) 7.31
C (m) 6.74
H (d) 6.10
D (m) 6.68
I (s) 3.81
J (d) 3.04
K (s) 0.03
SiMe3
OMe
O
91q
8.64
2.98
0.98
0.86
0.98
1.02
1.85
0.98
0.87
0.98
0.88
f1 (ppm)

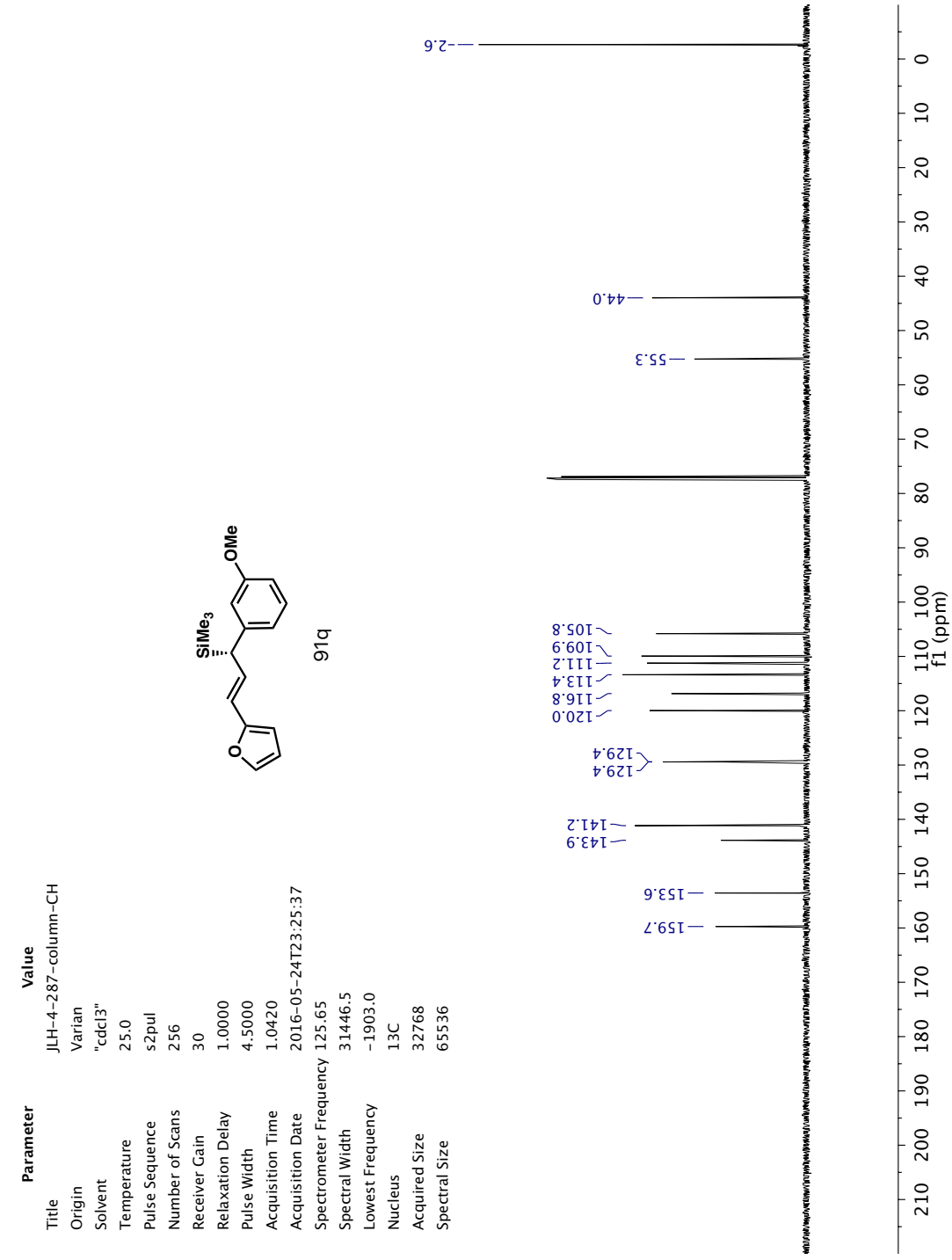
Parameter Value
Title JLH-4-287-column-CH
Origin Varian
Solvent "cdcl3"
Temperature 25.0
Pulse Sequence s2pul
Number of Scans 256
Receiver Gain 30
Relaxation Delay 1.0000
Pulse Width 4.5000
Acquisition Time 1.0420
Acquisition Date 2016-05-24T23:25:37
Spectrometer Frequency 125.65
Spectral Width 31446.5
Lowest Frequency -1903.0
Nucleus 13C
Acquired Size 32768
Spectral Size 65536
SiMe3
OMe
O
91q
-2.6
44.0
55.3
77.0
77.3
77.7
105.8
109.9
111.2
113.4
116.8
120.0
129.4
129.4
141.2
143.9
153.6
159.7
f1 (ppm)

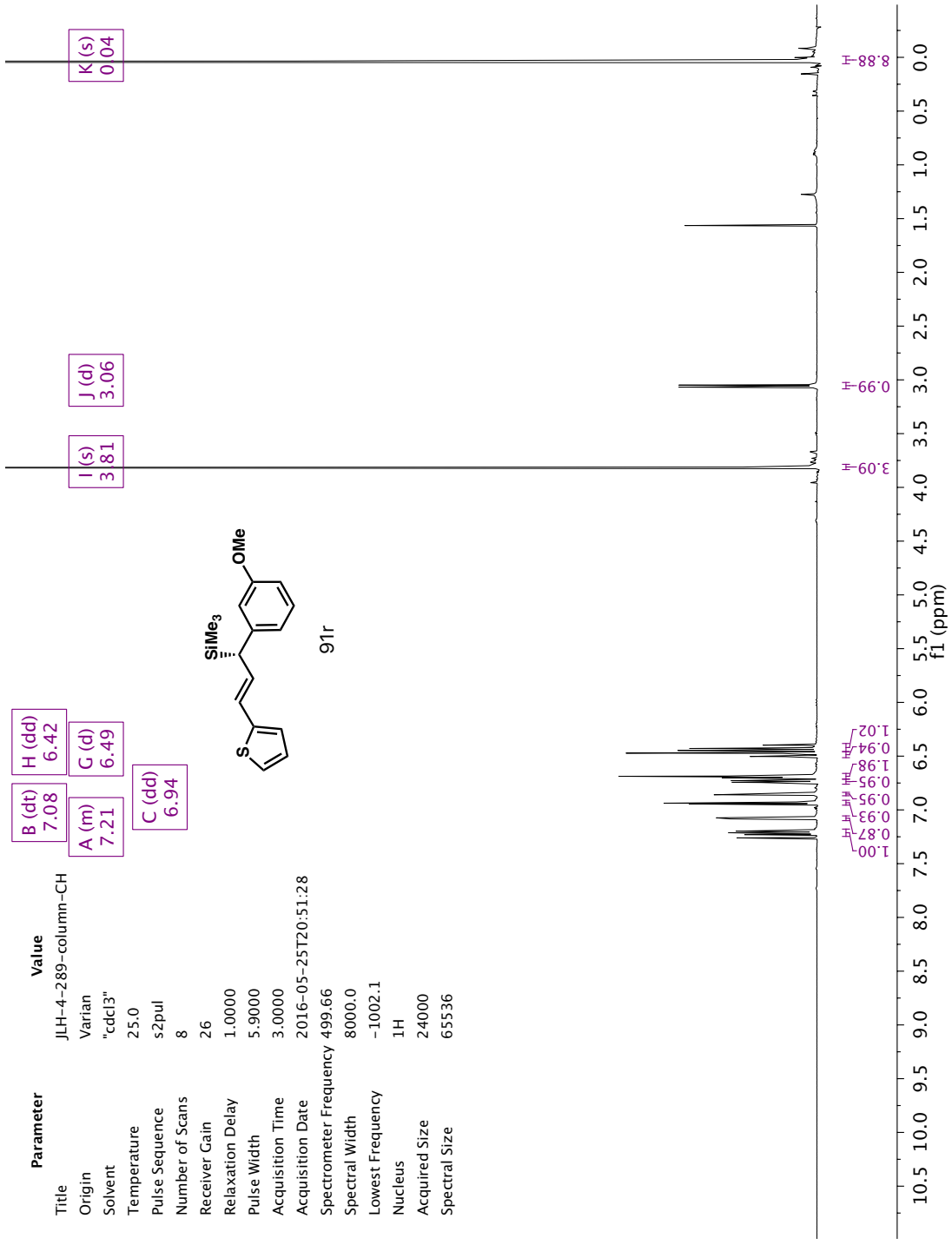
Parameter
Value
Title
JLH-4-289-column-CH
Origin
Varian
Solvent
"cdcl3"
Temperature
25.0
Pulse Sequence
s2pul
Number of Scans
8
Receiver Gain
26
Relaxation Delay
1.0000
Pulse Width
5.9000
Acquisition Time
3.0000
Acquisition Date
2016-05-25T20:51:28
Spectrometer Frequency
499.66
Spectral Width
8000.0
Lowest Frequency
-1002.1
Nucleus
1H
Acquired Size
24000
Spectral Size
65536
B (dt) 7.08
H (dd) 6.42
A (m) 7.21
G (d) 6.49
C (dd) 6.94
I (s) 3.81
J (d) 3.06
K (s) 0.04
SiMe3
OMe
S
91r
8.88
3.09
0.99
1.00
0.87
0.93
0.95
0.95
1.98
0.94
1.02
f1 (ppm)

Parameter	Value
Title	JLH-4-289-column-CH
Origin	Varian
Solvent	"cdcl3"
Temperature	25.0
Pulse Sequence	s2pul
Number of Scans	256
Receiver Gain	30
Relaxation Delay	1.0000
Pulse Width	4.5000
Acquisition Time	1.0420
Acquisition Date	2016-05-25T20:52:16
Spectrometer Frequency	125.65
Spectral Width	31446.5
Lowest Frequency	-1903.0
Nucleus	13C
Acquired Size	32768
Spectral Size	65536

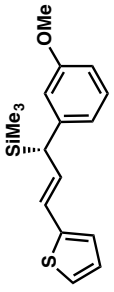

91r

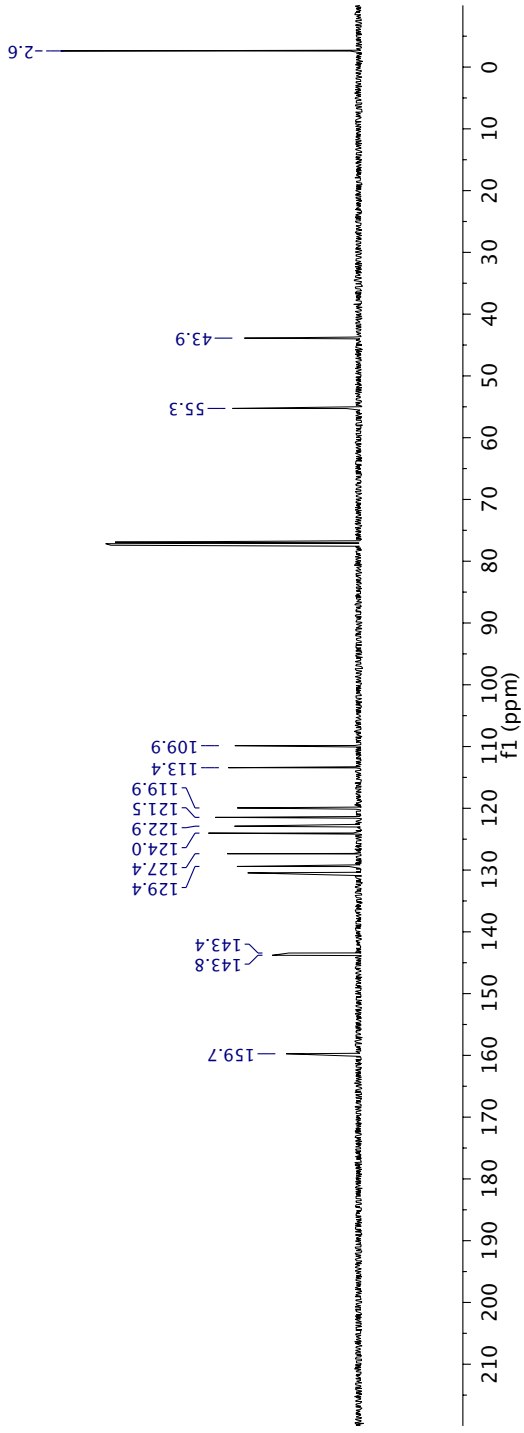

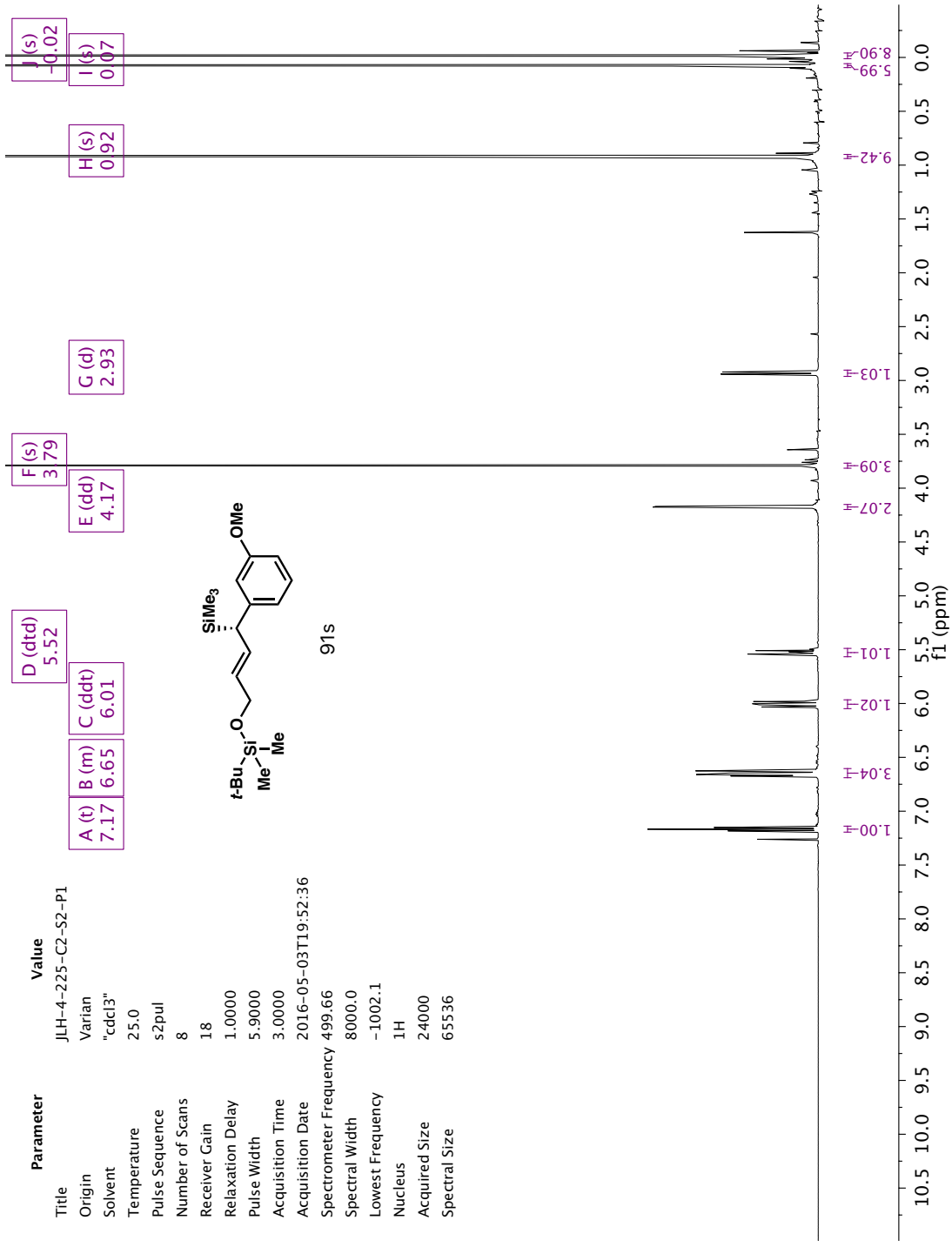
A (t) 7.17
B (m) 6.65
C (ddt) 6.01
D (dtd) 5.52
E (dd) 4.17
F (s) 3.79
G (d) 2.93
H (s) 0.92
I (s) 0.07
J (s) -0.02
SiMe3
OMe
t-Bu
Si
Me
Me
O
91s
Parameter Value
Title JLH-4-225-C2-S2-P1
Origin Varian
Solvent "cdcl3"
Temperature 25.0
Pulse Sequence s2pul
Number of Scans 8
Receiver Gain 18
Relaxation Delay 1.0000
Pulse Width 5.9000
Acquisition Time 3.0000
Acquisition Date 2016-05-03T19:52:36
Spectrometer Frequency 499.66
Spectral Width 8000.0
Lowest Frequency -1002.1
Nucleus 1H
Acquired Size 24000
Spectral Size 65536
1.00
3.04
1.02
1.01
2.07
3.09
1.03
9.42
5.99
8.90
f1 (ppm)

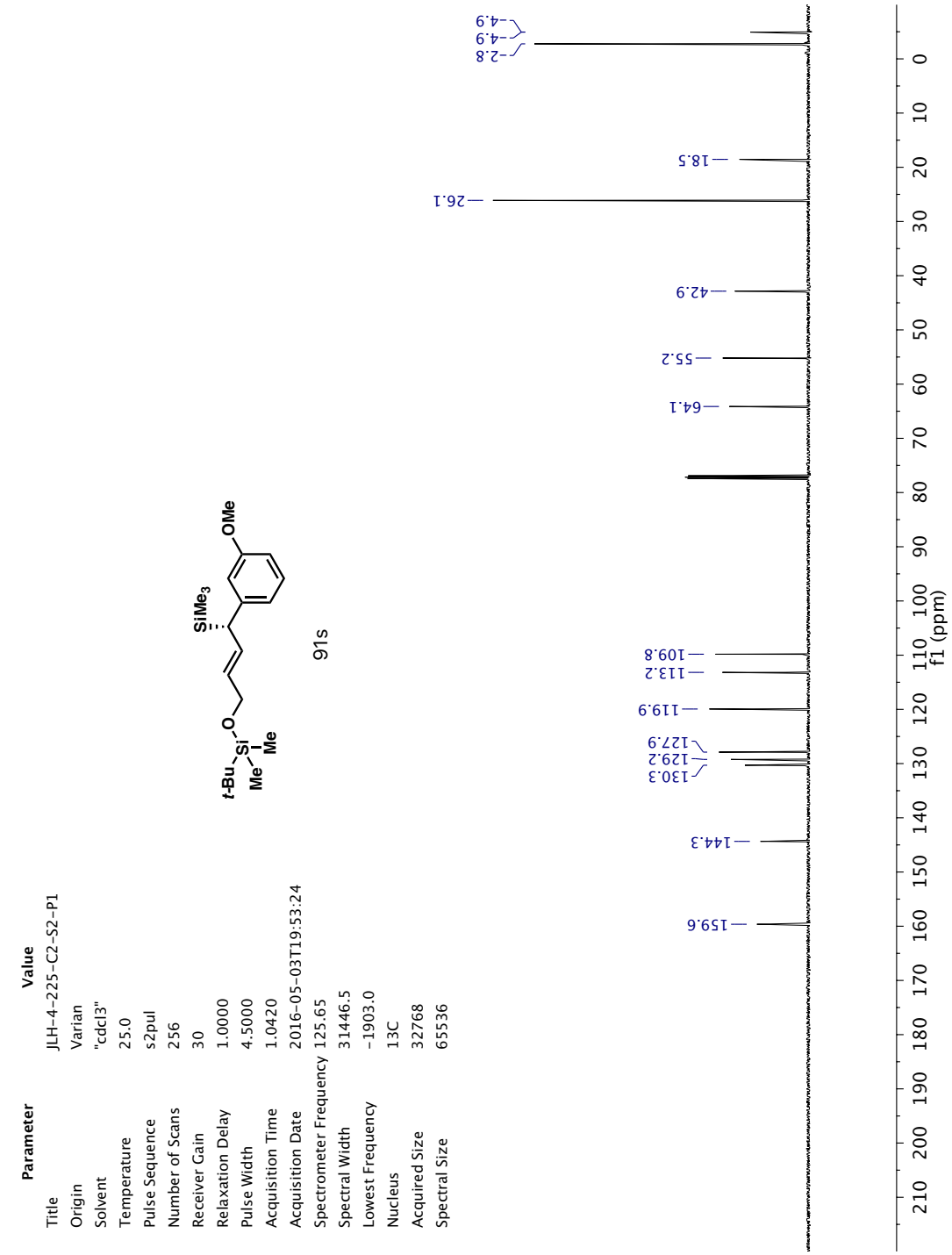
Parameter Value
Title JLH-4-225-C2-S2-P1
Origin Varian
Solvent "cdcl3"
Temperature 25.0
Pulse Sequence s2pul
Number of Scans 256
Receiver Gain 30
Relaxation Delay 1.0000
Pulse Width 4.5000
Acquisition Time 1.0420
Acquisition Date 2016-05-03T19:53:24
Spectrometer Frequency 125.65
Spectral Width 31446.5
Lowest Frequency -1903.0
Nucleus 13C
Acquired Size 32768
Spectral Size 65536
SiMe3
OMe
t-Bu
Si
Me
Me
O
91s
-2.8
-4.9
-4.9
18.5
26.1
42.9
55.2
64.1
109.8
113.2
119.9
127.9
129.2
130.3
144.3
159.6
f1 (ppm)

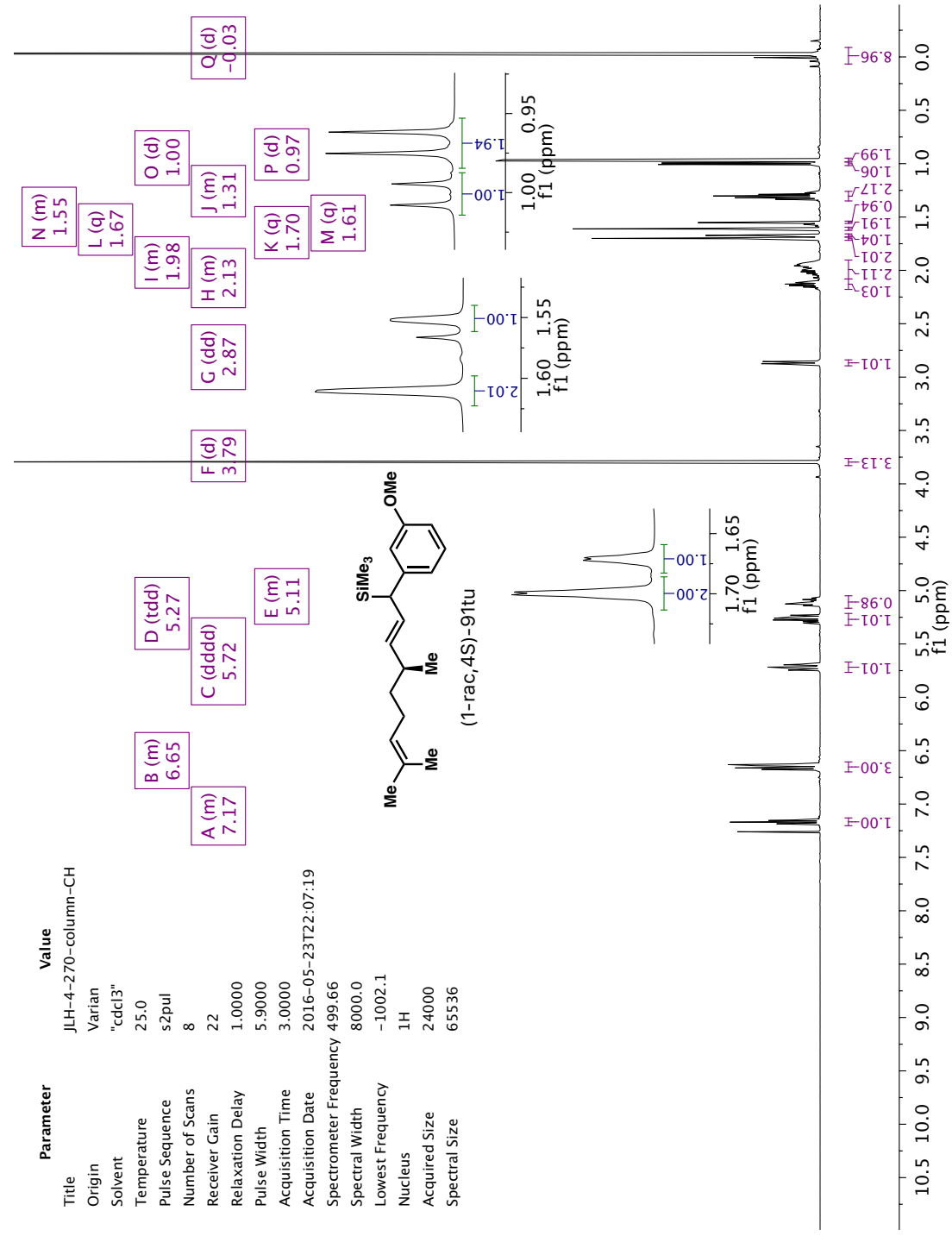
Parameter Value
Title JLH-4-270-column-CH
Origin Varian
Solvent "cdcl3"
Temperature 25.0
Pulse Sequence s2pul
Number of Scans 8
Receiver Gain 22
Relaxation Delay 1.0000
Pulse Width 5.9000
Acquisition Time 3.0000
Acquisition Date 2016-05-23T22:07:19
Spectrometer Frequency 499.66
Spectral Width 8000.0
Lowest Frequency -1002.1
Nucleus 1H
Acquired Size 24000
Spectral Size 65536
A (m) 7.17
B (m) 6.65
C (dddd) 5.72
D (tdd) 5.27
E (m) 5.11
F (d) 3.79
G (dd) 2.87
H (m) 2.13
I (m) 1.98
J (m) 1.31
K (q) 1.70
L (q) 1.67
M (q) 1.61
N (m) 1.55
O (d) 1.00
P (d) 0.97
Q (d) -0.03
SiMe3
OMe
Me
Me
Me
(1-rac,4S)-91tu
f1 (ppm)

Parameter	Value
Title	JLH-4-270-column-CH
Origin	Varian
Solvent	"cdcl3"
Temperature	25.0
Pulse Sequence	s2pul
Number of Scans	256
Receiver Gain	30
Relaxation Delay	1.0000
Pulse Width	4.5000
Acquisition Time	1.0420
Acquisition Date	2016-05-23T22:08:07
Spectrometer Frequency	125.65
Spectral Width	31446.5
Lowest Frequency	-1903.0
Nucleus	13C
Acquired Size	32768
Spectral Size	65536

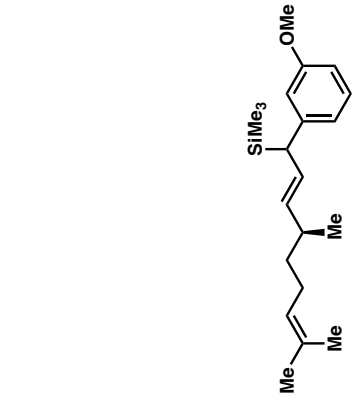

(1-rac,4S)-91tu

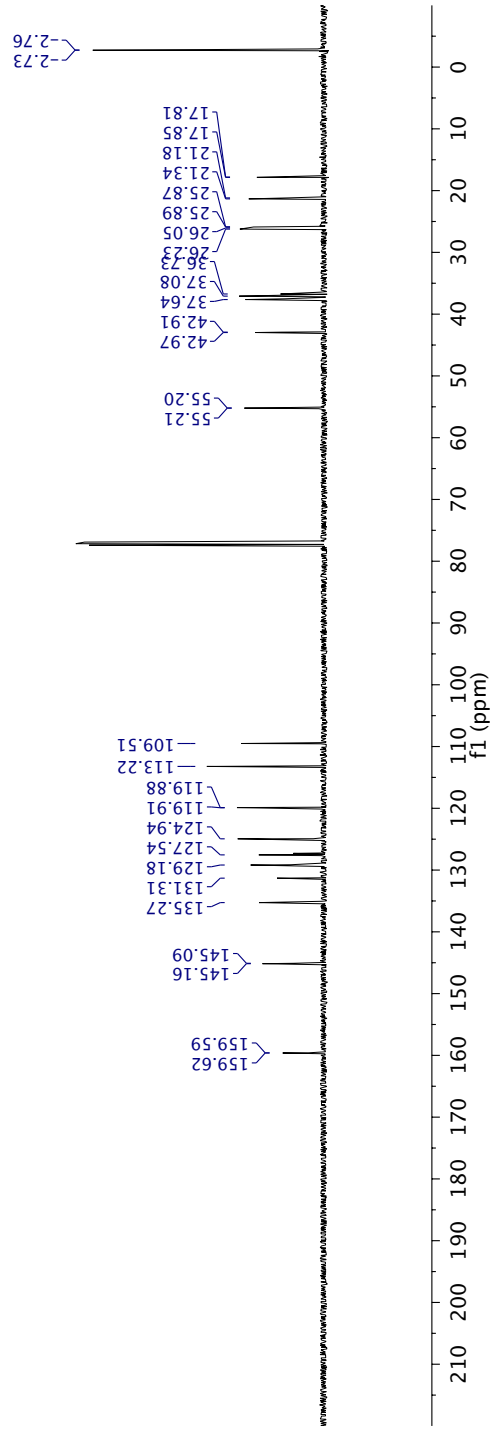

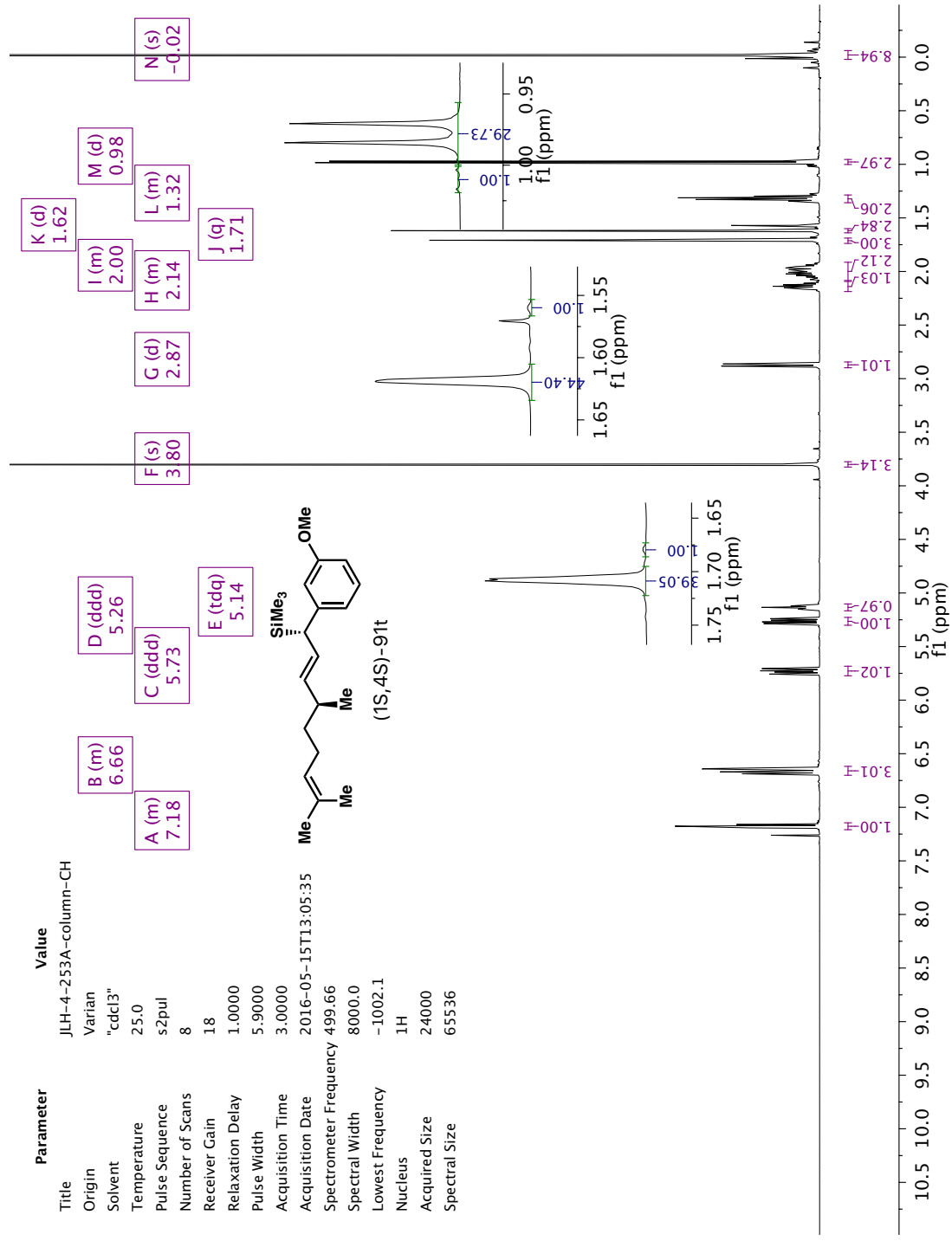
Parameter
Value
Title
JLH-4-253A-column-CH
Origin
Varian
Solvent
"cdcl3"
Temperature
25.0
Pulse Sequence
s2pul
Number of Scans
8
Receiver Gain
18
Relaxation Delay
1.0000
Pulse Width
5.9000
Acquisition Time
3.0000
Acquisition Date
2016-05-15T13:05:35
Spectrometer Frequency
499.66
Spectral Width
8000.0
Lowest Frequency
-1002.1
Nucleus
1H
Acquired Size
24000
Spectral Size
65536
A (m) 7.18
B (m) 6.66
C (ddd) 5.73
D (ddd) 5.26
E (tdq) 5.14
F (s) 3.80
G (d) 2.87
H (m) 2.14
I (m) 2.00
J (q) 1.71
K (d) 1.62
L (m) 1.32
M (d) 0.98
N (s) -0.02
SiMe3
OMe
Me
Me
Me
(1S,4S)-91t
f1 (ppm)

Parameter	Value
Title	JLH-4-253A-column-CH
Origin	Varian
Solvent	"cdcl3"
Temperature	25.0
Pulse Sequence	s2pul
Number of Scans	256
Receiver Gain	30
Relaxation Delay	1.0000
Pulse Width	4.5000
Acquisition Time	1.0420
Acquisition Date	2016-05-15T13:06:23
Spectrometer Frequency	125.65
Spectral Width	31446.5
Lowest Frequency	-1903.0
Nucleus	13C
Acquired Size	32768
Spectral Size	65536

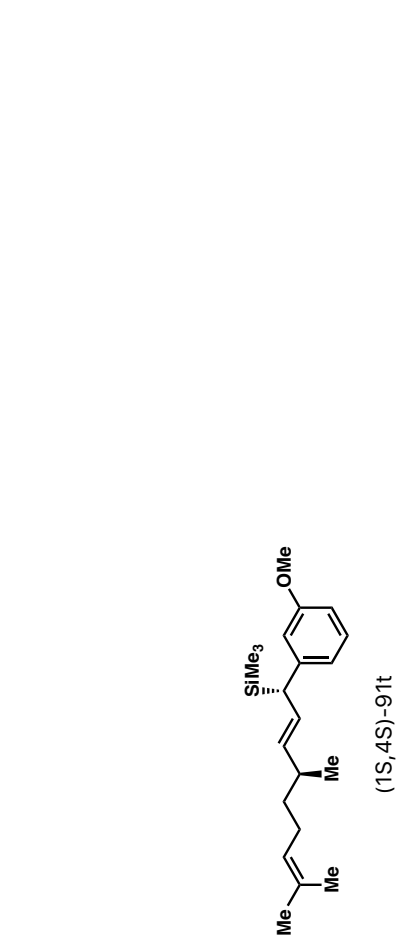

(1S,4S)-91t

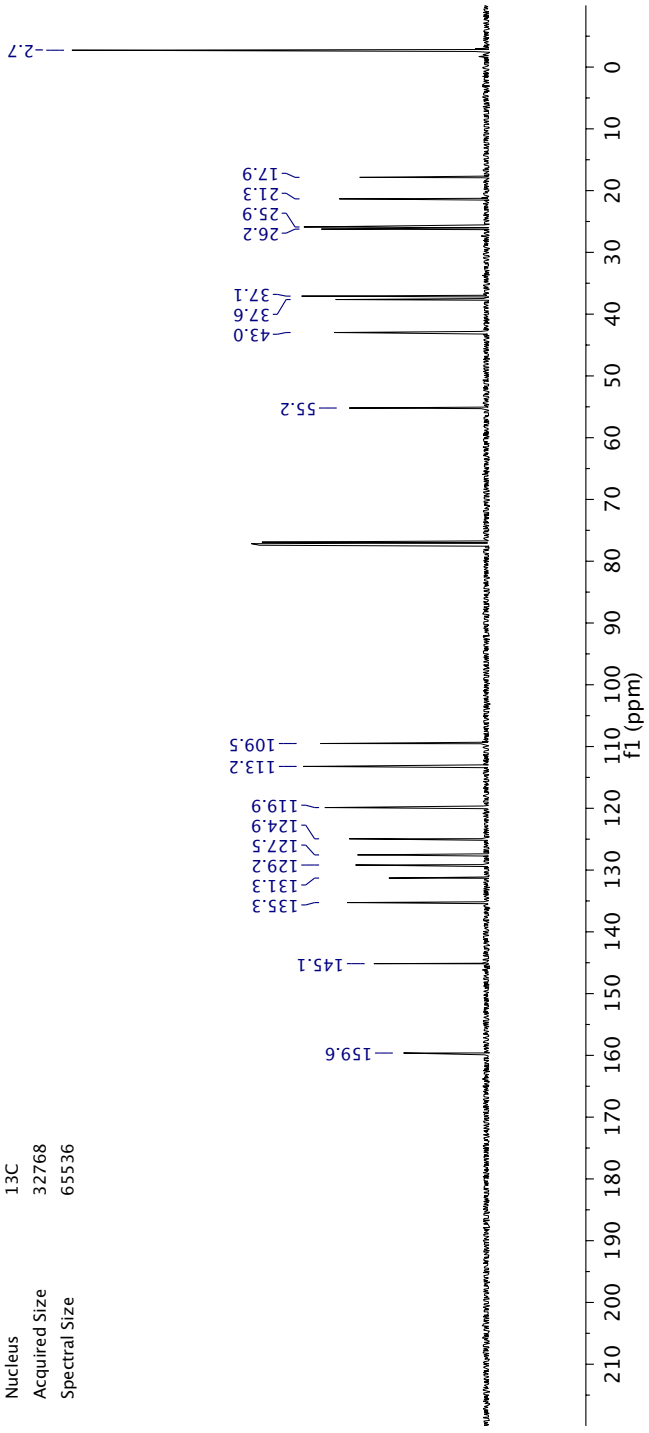

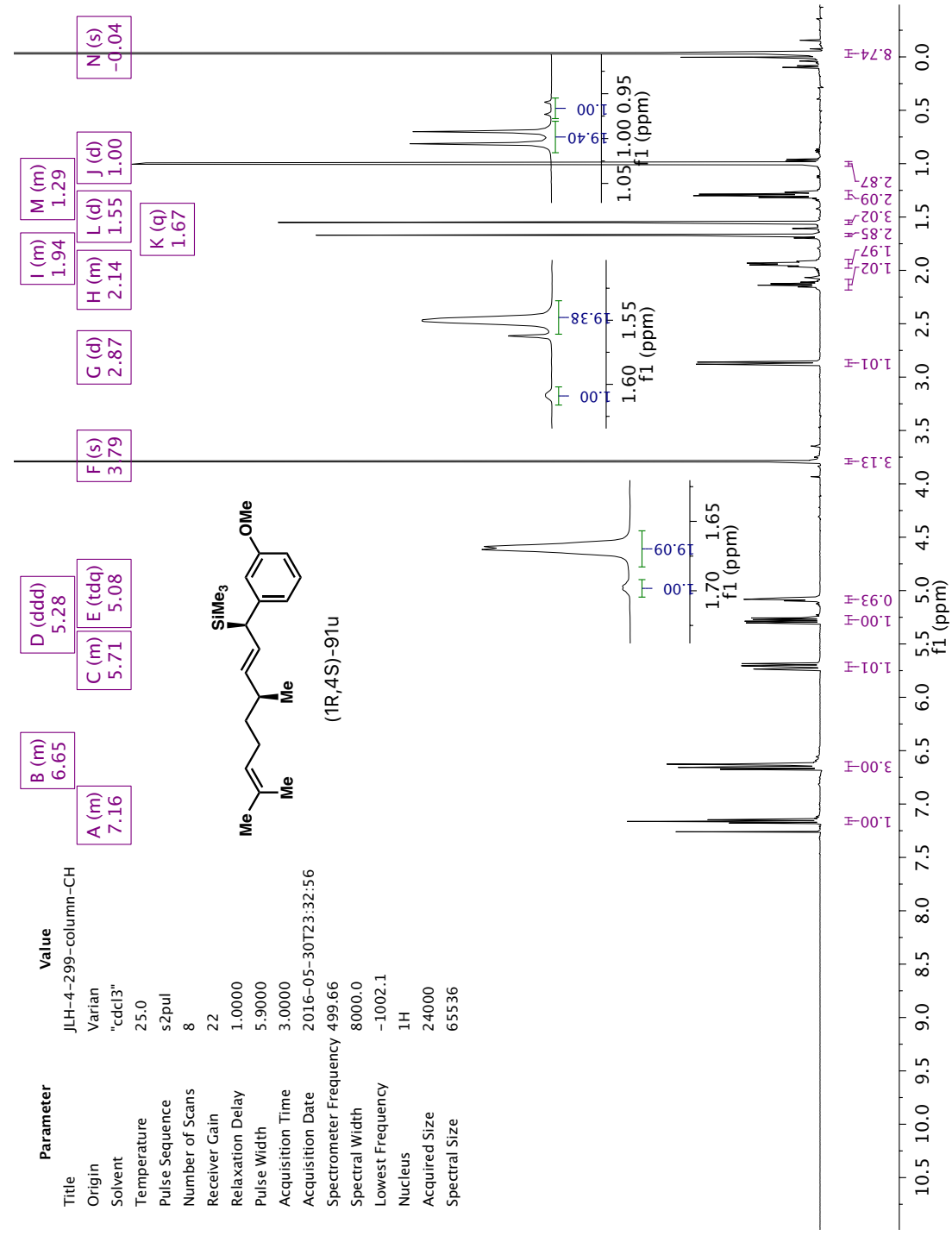
A (m) 7.16
B (m) 6.65
C (m) 5.71
D (ddd) 5.28
E (tdq) 5.08
F (s) 3.79
G (d) 2.87
H (m) 2.14
I (m) 1.94
J (d) 1.00
K (q) 1.67
L (d) 1.55
M (m) 1.29
N (s) -0.04
SiMe3
OMe
Me
Me
Me
(1R,4S)-91u
Parameter Value
Title JLH-4-299-column-CH
Origin Varian
Solvent "cdcl3"
Temperature 25.0
Pulse Sequence s2pul
Number of Scans 8
Receiver Gain 22
Relaxation Delay 1.0000
Pulse Width 5.9000
Acquisition Time 3.0000
Acquisition Date 2016-05-30T23:32:56
Spectrometer Frequency 499.66
Spectral Width 8000.0
Lowest Frequency -1002.1
Nucleus 1H
Acquired Size 24000
Spectral Size 65536
f1 (ppm)

Parameter	Value
Title	JLH-4-299-column-CH
Origin	Varian
Solvent	"cdcl3"
Temperature	25.0
Pulse Sequence	s2pul
Number of Scans	256
Receiver Gain	30
Relaxation Delay	1.0000
Pulse Width	4.5000
Acquisition Time	1.0420
Acquisition Date	2016-05-30T23:33:45
Spectrometer Frequency	125.65
Spectral Width	31446.5
Lowest Frequency	-1903.0
Nucleus	13C
Acquired Size	32768
Spectral Size	65536

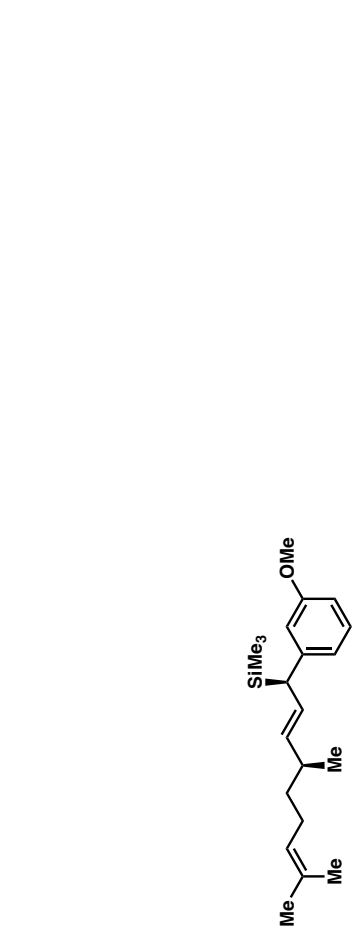

(1R,4S)-91u

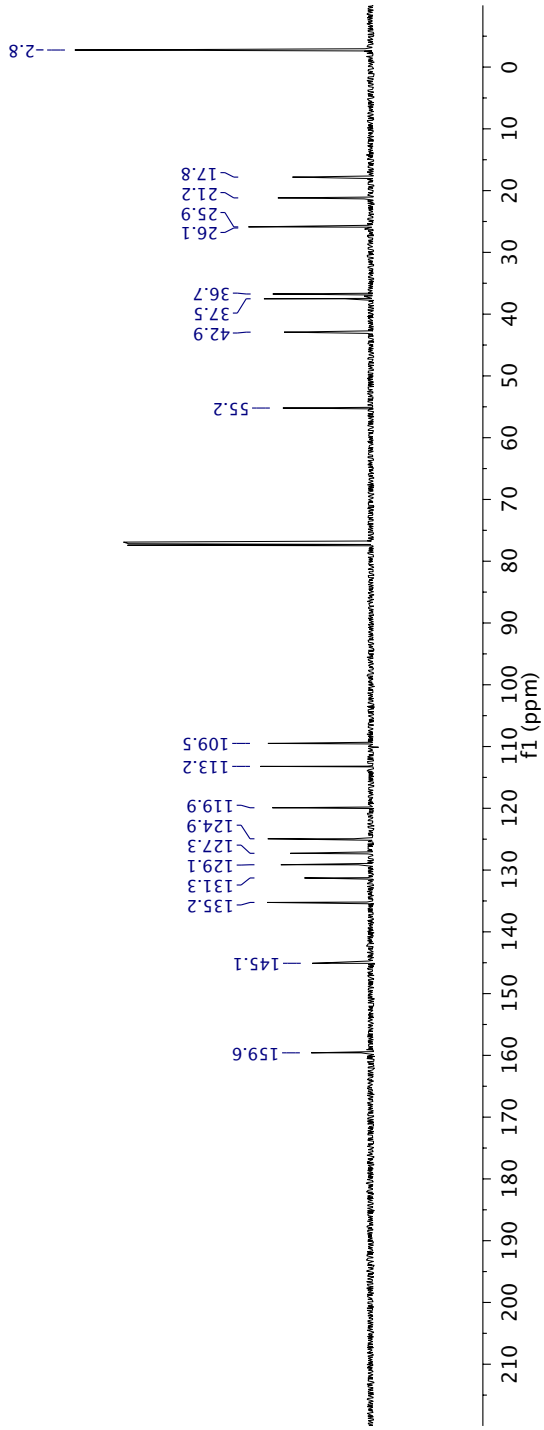

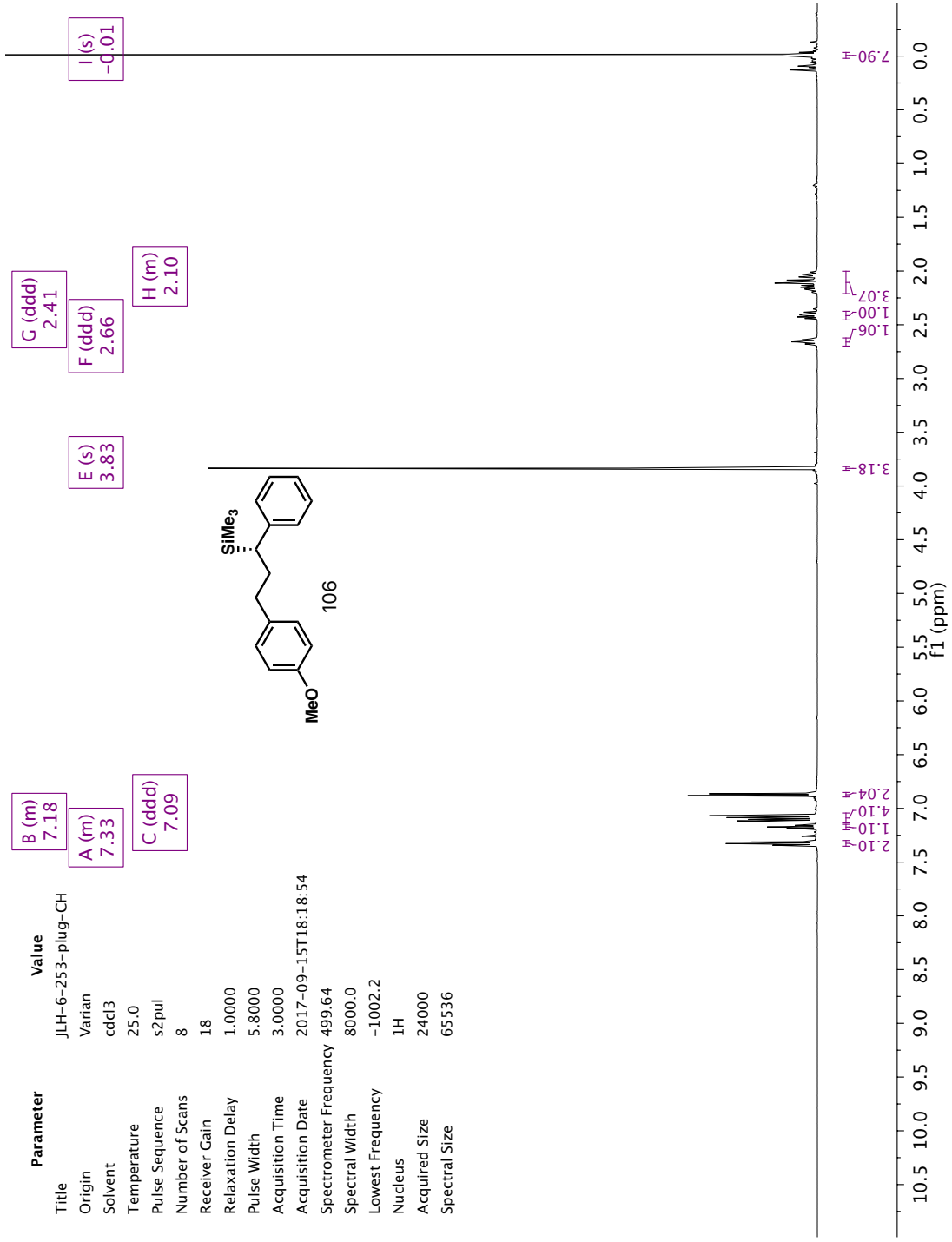
B (m) 7.18
A (m) 7.33
C (ddd) 7.09
E (s) 3.83
G (ddd) 2.41
F (ddd) 2.66
H (m) 2.10
I (s) −0.01
SiMe3
MeO
106
Parameter Value
Title JLH-6-253-plug-CH
Origin Varian
Solvent cdcl3
Temperature 25.0
Pulse Sequence s2pul
Number of Scans 8
Receiver Gain 18
Relaxation Delay 1.0000
Pulse Width 5.8000
Acquisition Time 3.0000
Acquisition Date 2017-09-15T18:18:54
Spectrometer Frequency 499.64
Spectral Width 8000.0
Lowest Frequency -1002.2
Nucleus 1H
Acquired Size 24000
Spectral Size 65536
2.10
1.10
4.10
2.04
3.18
1.06
1.00
3.07
7.90
f1 (ppm)

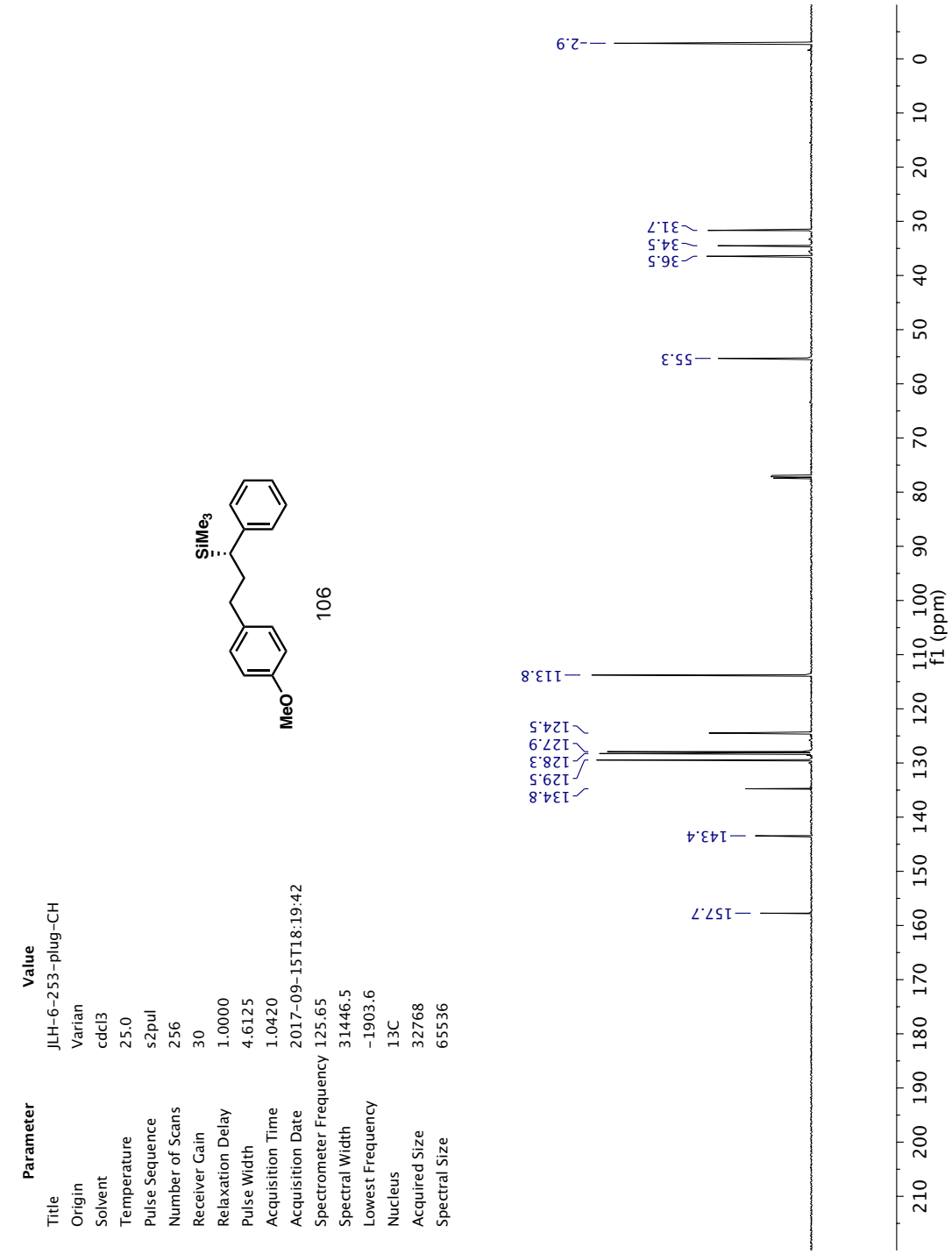

Parameter	Value
Title	JLH-6-253-plug-CH
Origin	Varian
Solvent	cdcl3
Temperature	25.0
Pulse Sequence	s2pul
Number of Scans	256
Receiver Gain	30
Relaxation Delay	1.0000
Pulse Width	4.6125
Acquisition Time	1.0420
Acquisition Date	2017-09-15T18:19:42
Spectrometer Frequency	125.65
Spectral Width	31446.5
Lowest Frequency	-1903.6
Nucleus	13C
Acquired Size	32768
Spectral Size	65536

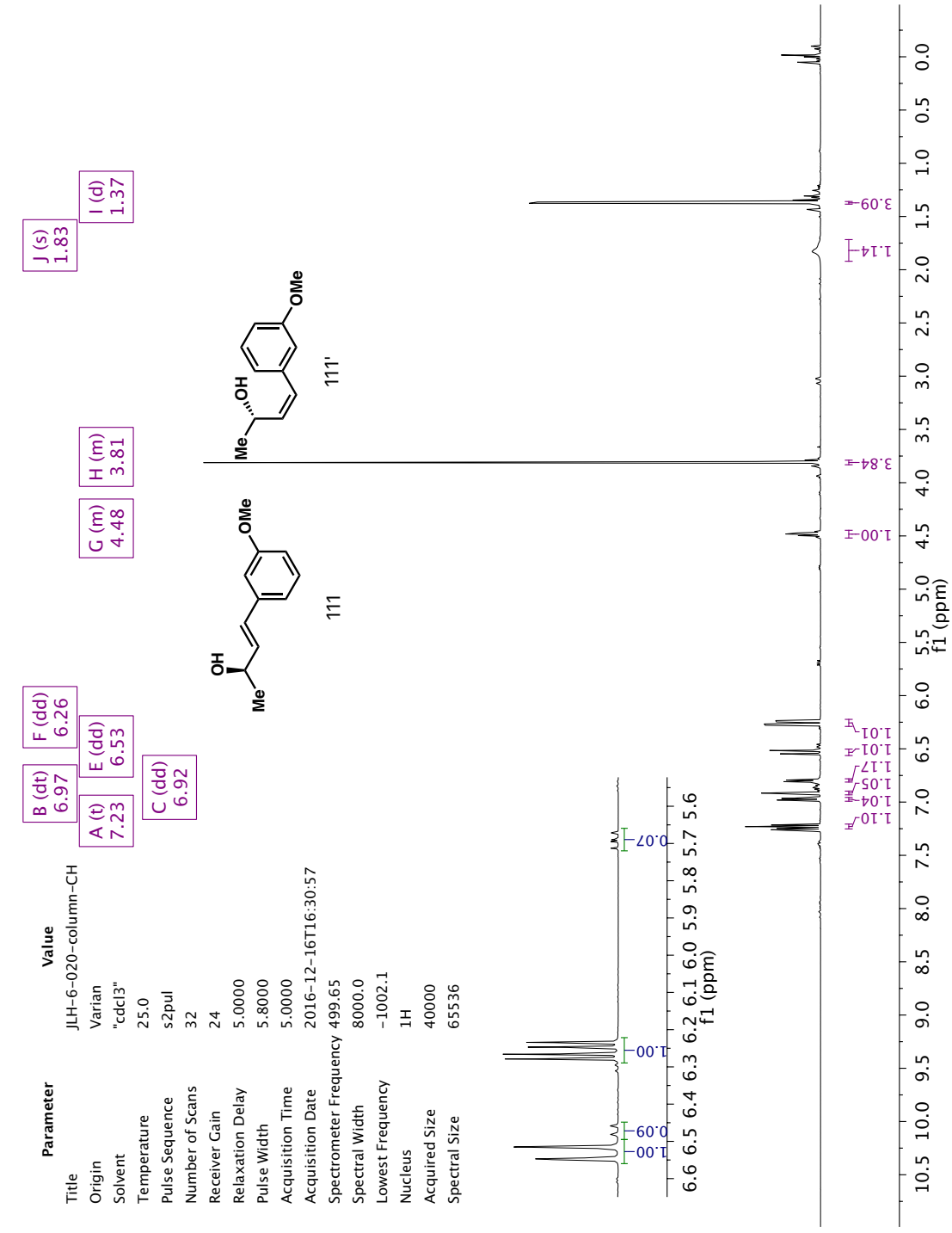
Parameter Value
Title JLH-6-020-column-CH
Origin Varian
Solvent "cdcl3"
Temperature 25.0
Pulse Sequence s2pul
Number of Scans 32
Receiver Gain 24
Relaxation Delay 5.0000
Pulse Width 5.8000
Acquisition Time 5.0000
Acquisition Date 2016-12-16T16:30:57
Spectrometer Frequency 499.65
Spectral Width 8000.0
Lowest Frequency -1002.1
Nucleus 1H
Acquired Size 40000
Spectral Size 65536
A (t) 7.23
B (dt) 6.97
C (dd) 6.92
E (dd) 6.53
F (dd) 6.26
G (m) 4.48
H (m) 3.81
I (d) 1.37
J (s) 1.83
111
111'
f1 (ppm)

Parameter	Value
Title	JLH-6-020-column-CH
Origin	Varian
Solvent	"cdcl3"
Temperature	25.0
Pulse Sequence	s2pul
Number of Scans	256
Receiver Gain	30
Relaxation Delay	1.0000
Pulse Width	4.6125
Acquisition Time	1.0420
Acquisition Date	2016-12-16T16:36:33
Spectrometer Frequency	125.65
Spectral Width	31446.5
Lowest Frequency	-1903.3
Nucleus	13C
Acquired Size	32768
Spectral Size	65536

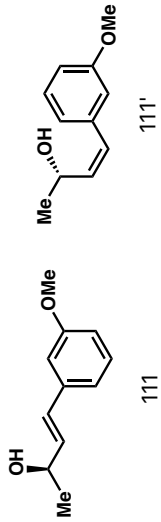

111

111'

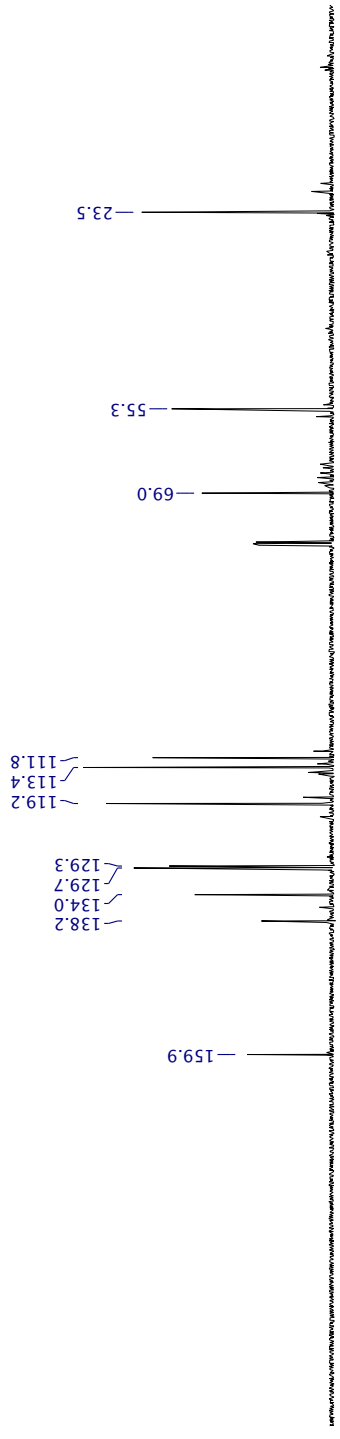

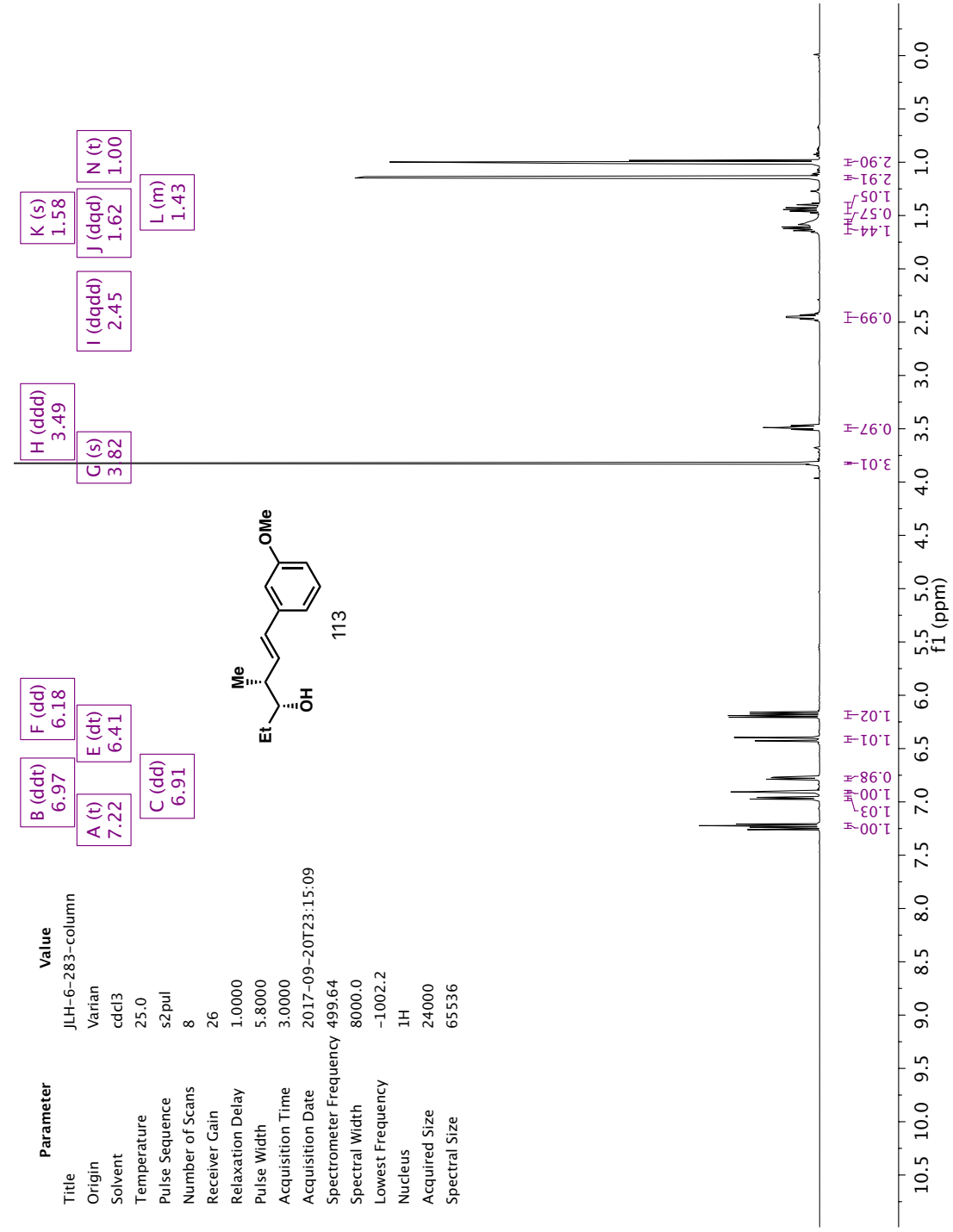
Parameter
Value
Title
JLH-6-283-column
Origin
Varian
Solvent
cdcl3
Temperature
25.0
Pulse Sequence
s2pul
Number of Scans
8
Receiver Gain
26
Relaxation Delay
1.0000
Pulse Width
5.8000
Acquisition Time
3.0000
Acquisition Date
2017-09-20T23:15:09
Spectrometer Frequency
499.64
Spectral Width
8000.0
Lowest Frequency
-1002.2
Nucleus
1H
Acquired Size
24000
Spectral Size
65536
B (ddt) 6.97
F (dd) 6.18
A (t) 7.22
E (dt) 6.41
C (dd) 6.91
Me
Et
OH
OMe
113
H (ddd) 3.49
G (s) 3.82
I (dqdd) 2.45
K (s) 1.58
J (dqd) 1.62
N (t) 1.00
L (m) 1.43
1.00
1.03
1.00
0.98
1.01
1.02
3.01
0.97
0.99
1.44
0.57
1.05
2.91
2.90
f1 (ppm)

Parameter	Value
Title	JLH-6-283-column
Origin	Varian
Solvent	cdcl3
Temperature	25.0
Pulse Sequence	s2pul
Number of Scans	256
Receiver Gain	30
Relaxation Delay	1.0000
Pulse Width	4.6125
Acquisition Time	1.0420
Acquisition Date	2017-09-20T23:15:57
Spectrometer Frequency	125.65
Spectral Width	31446.5
Lowest Frequency	-1903.6
Nucleus	13C
Acquired Size	32768
Spectral Size	65536

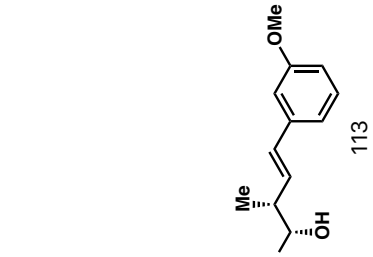

113

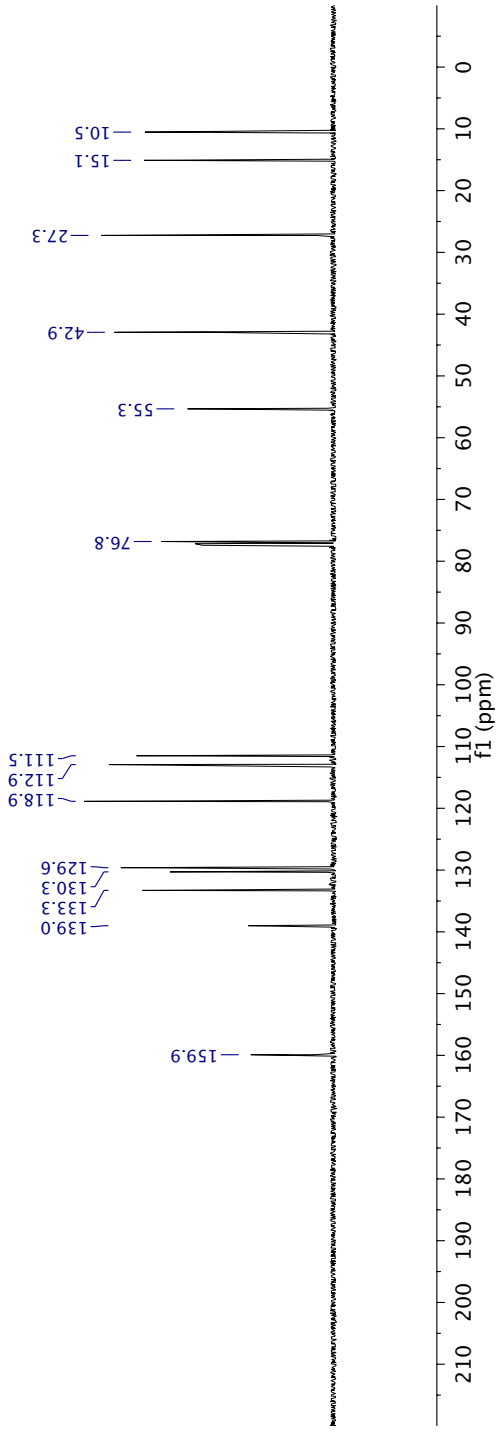

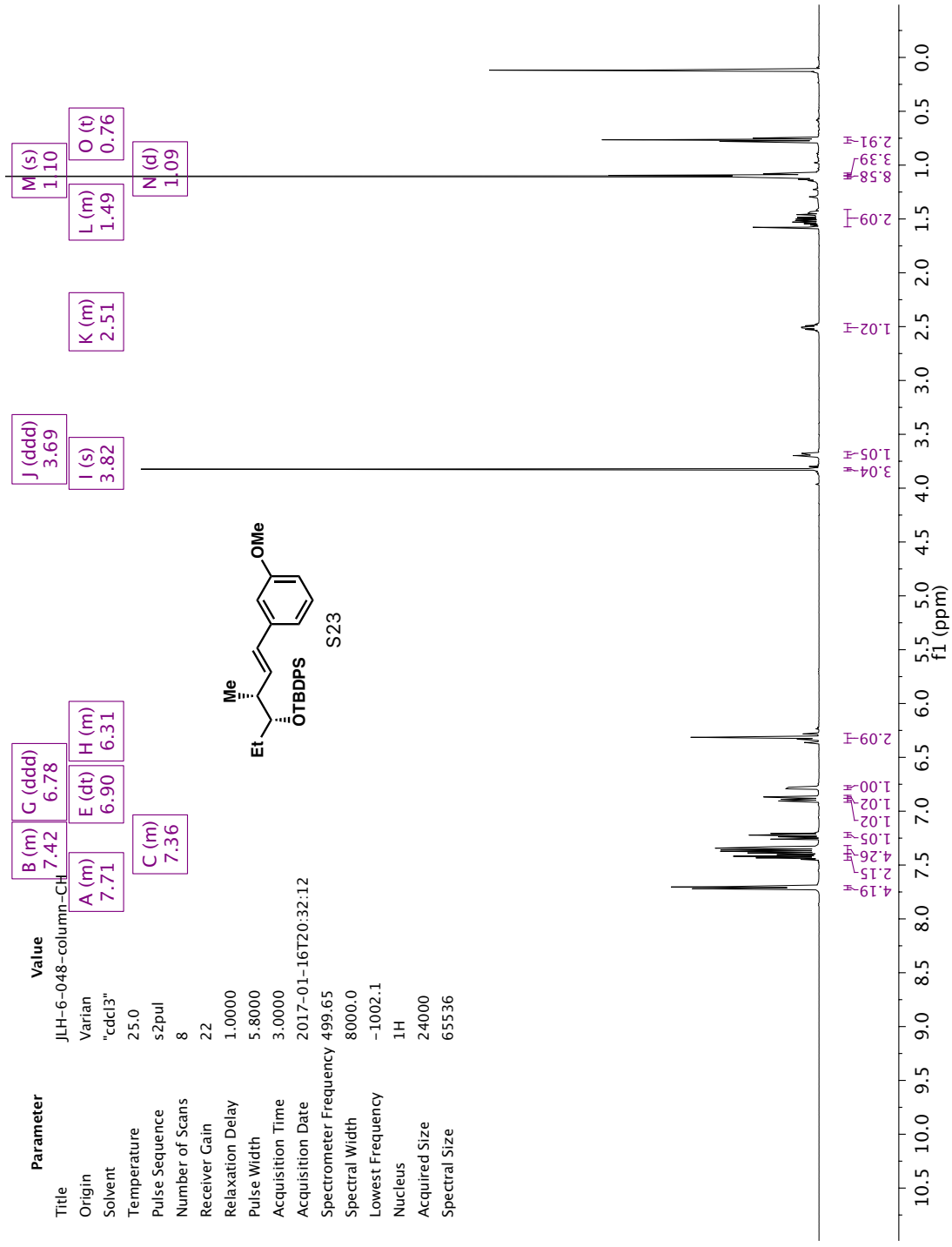
Parameter
Value
Title JLH-6-048-column-CH
Origin Varian
Solvent "cdcl3"
Temperature 25.0
Pulse Sequence s2pul
Number of Scans 8
Receiver Gain 22
Relaxation Delay 1.0000
Pulse Width 5.8000
Acquisition Time 3.0000
Acquisition Date 2017-01-16T20:32:12
Spectrometer Frequency 499.65
Spectral Width 8000.0
Lowest Frequency -1002.1
Nucleus 1H
Acquired Size 24000
Spectral Size 65536
B (m) 7.42
G (ddd) 6.78
A (m) 7.71
E (dt) 6.90
H (m) 6.31
C (m) 7.36
J (ddd) 3.69
I (s) 3.82
K (m) 2.51
M (s) 1.10
L (m) 1.49
O (t) 0.76
N (d) 1.09
Me
Et
OTBDPS
OMe
S23
4.19
2.15
4.26
1.05
1.02
1.02
1.00
2.09
1.05
3.04
1.02
2.09
8.58
3.39
2.91
10.5 10.0 9.5 9.0 8.5 8.0 7.5 7.0 6.5 6.0 5.5 5.0 4.5 4.0 3.5 3.0 2.5 2.0 1.5 1.0 0.5 0.0
f1 (ppm)

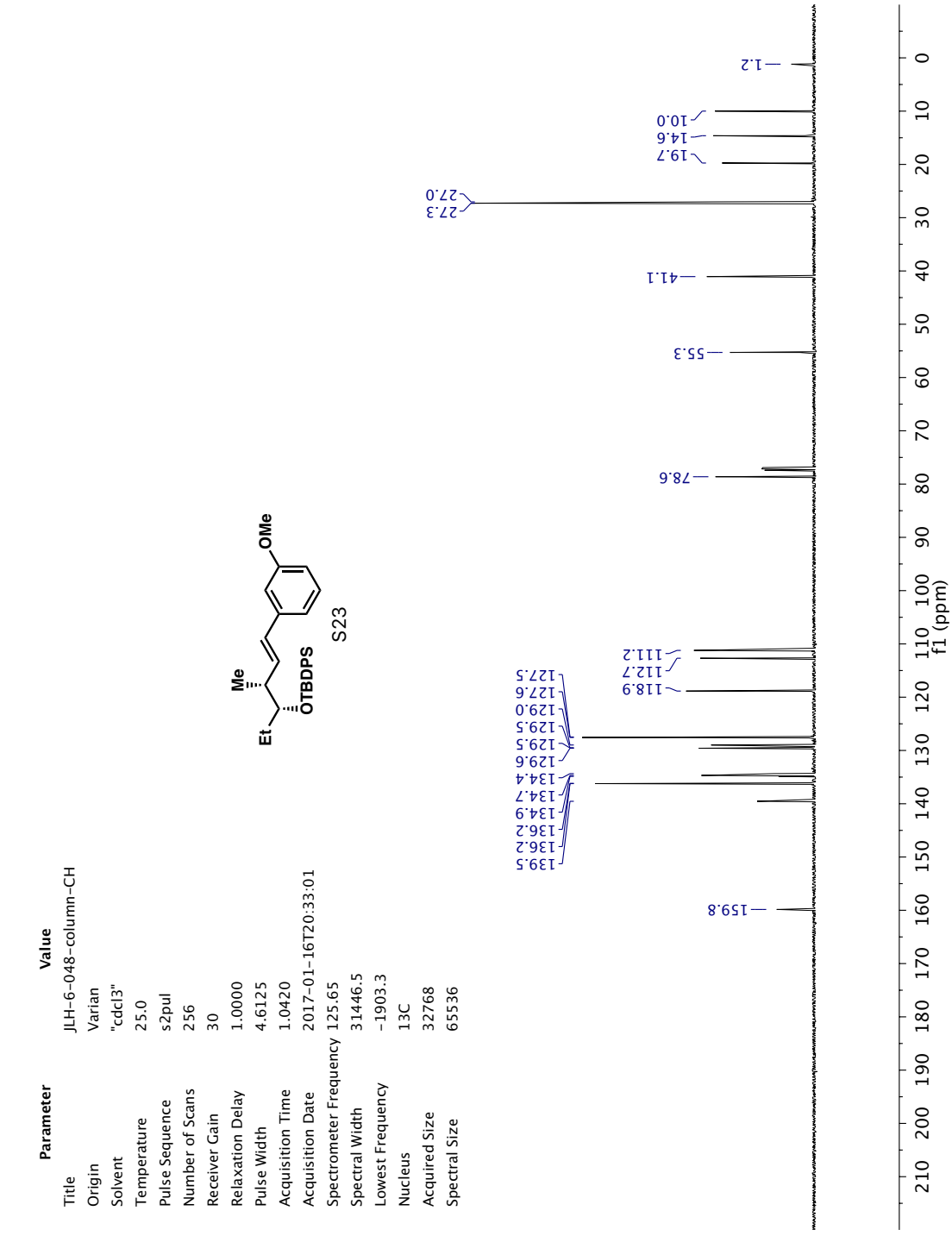
Parameter Value
Title JLH-6-048-column-CH
Origin Varian
Solvent "cdcl3"
Temperature 25.0
Pulse Sequence s2pul
Number of Scans 256
Receiver Gain 30
Relaxation Delay 1.0000
Pulse Width 4.6125
Acquisition Time 1.0420
Acquisition Date 2017-01-16T20:33:01
Spectrometer Frequency 125.65
Spectral Width 31446.5
Lowest Frequency -1903.3
Nucleus 13C
Acquired Size 32768
Spectral Size 65536
Me
Et
OTBDPS
OMe
S23
159.8
139.5
136.2
136.2
134.9
134.7
134.4
129.6
129.5
129.5
129.0
127.6
127.5
118.9
112.7
111.2
78.6
55.3
41.1
27.3
27.0
19.7
14.6
10.0
1.2
f1 (ppm)

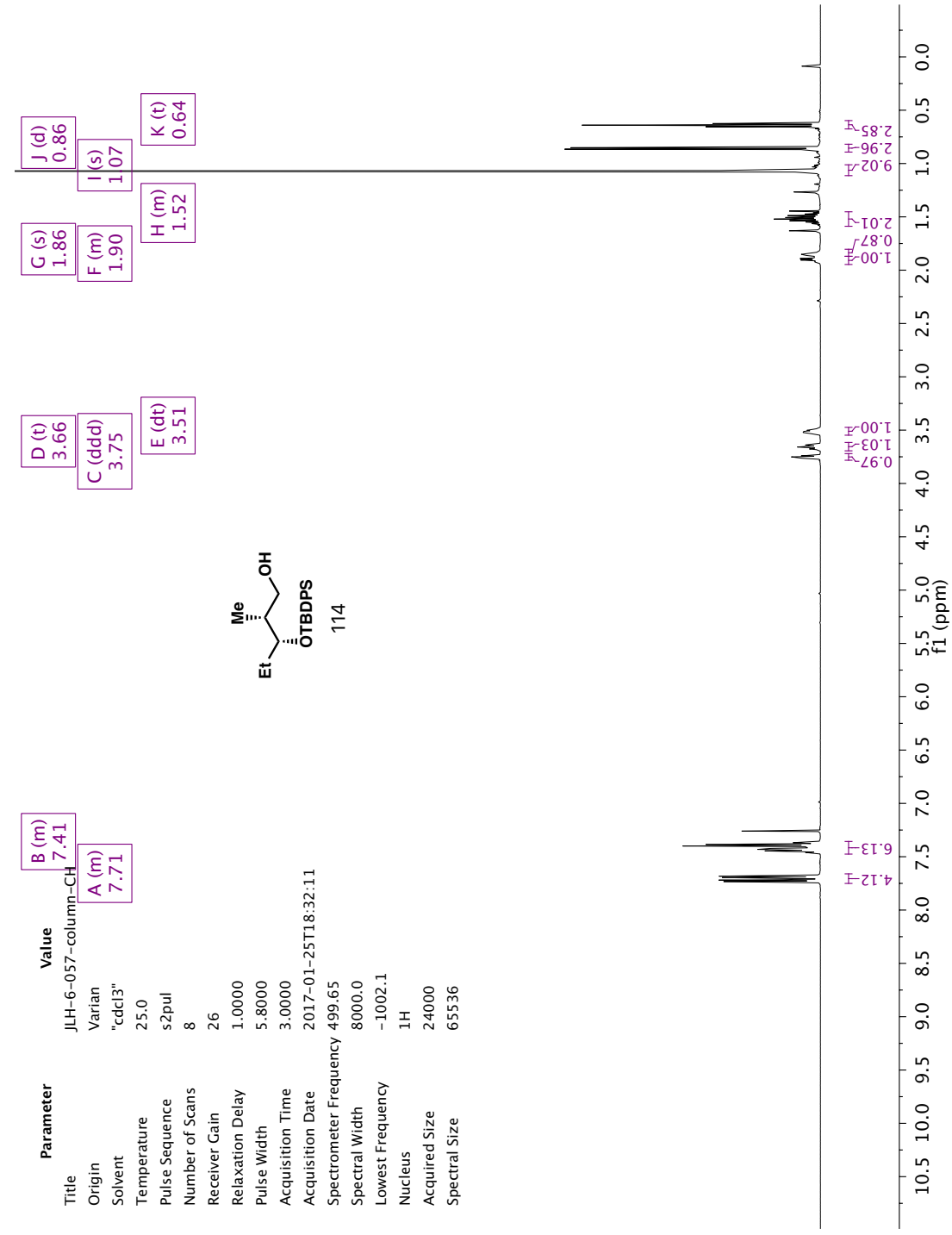
Parameter
Value
Title
JLH-6-057-column-CH
Origin
Varian
Solvent
"cdcl3"
Temperature
25.0
Pulse Sequence
s2pul
Number of Scans
8
Receiver Gain
26
Relaxation Delay
1.0000
Pulse Width
5.8000
Acquisition Time
3.0000
Acquisition Date
2017-01-25T18:32:11
Spectrometer Frequency
499.65
Spectral Width
8000.0
Lowest Frequency
-1002.1
Nucleus
1H
Acquired Size
24000
Spectral Size
65536
B (m) 7.41
A (m) 7.71
D (t) 3.66
C (ddd) 3.75
E (dt) 3.51
G (s) 1.86
F (m) 1.90
H (m) 1.52
J (d) 0.86
I (s) 1.07
K (t) 0.64
Me
OH
Et
OTBDPS
114
6.13
4.12
1.00
1.03
0.97
1.00
0.87
2.01
9.02
2.96
2.85
10.5 10.0 9.5 9.0 8.5 8.0 7.5 7.0 6.5 6.0 5.5 5.0 4.5 4.0 3.5 3.0 2.5 2.0 1.5 1.0 0.5 0.0
f1 (ppm)

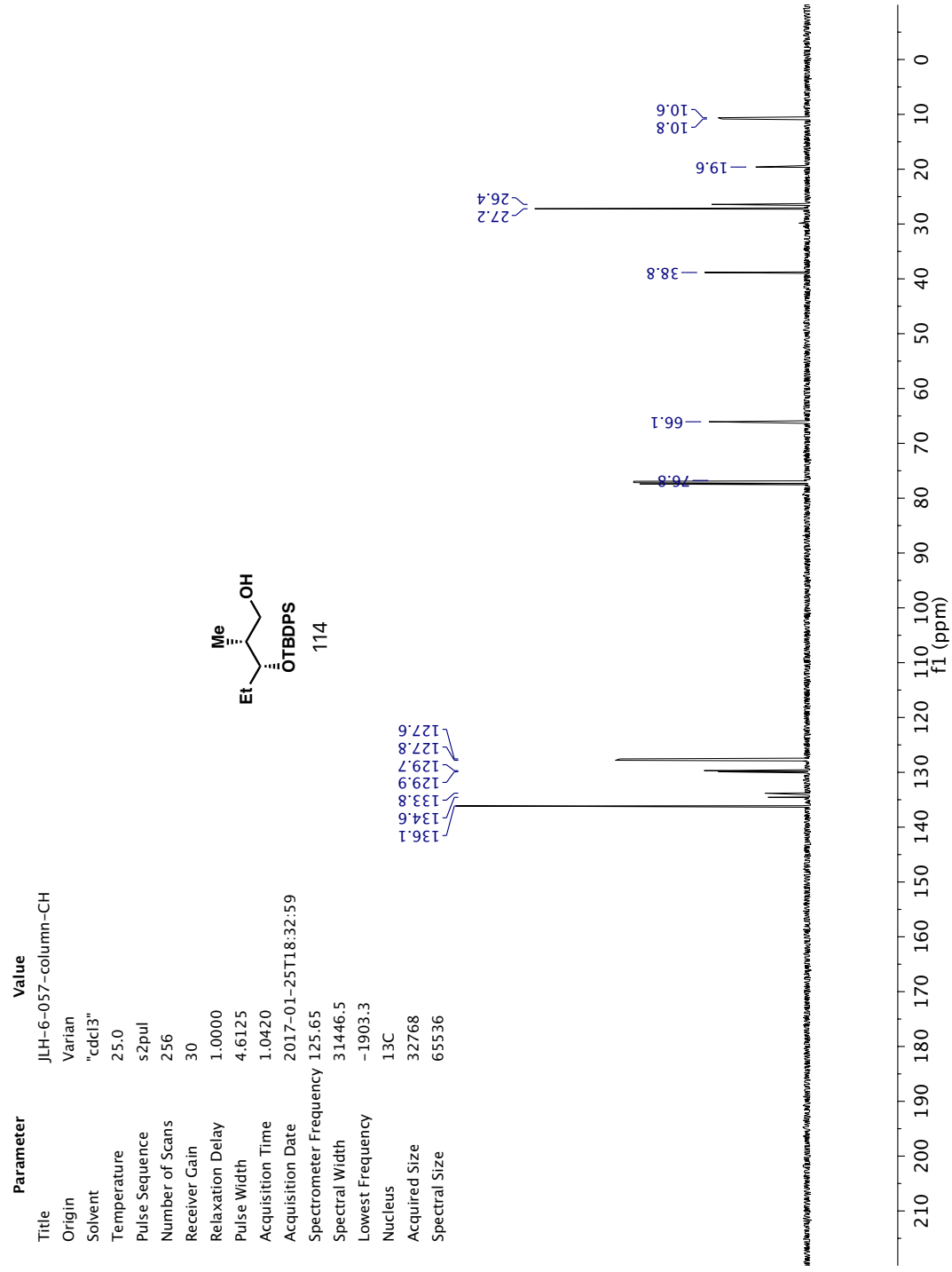
Parameter Value
Title JLH-6-057-column-CH
Origin Varian
Solvent "cdcl3"
Temperature 25.0
Pulse Sequence s2pul
Number of Scans 256
Receiver Gain 30
Relaxation Delay 1.0000
Pulse Width 4.6125
Acquisition Time 1.0420
Acquisition Date 2017-01-25T18:32:59
Spectrometer Frequency 125.65
Spectral Width 31446.5
Lowest Frequency -1903.3
Nucleus 13C
Acquired Size 32768
Spectral Size 65536
Me
OH
Et
OTBDPS
114
136.1
134.6
133.8
129.9
129.7
127.8
127.6
76.8
66.1
38.8
27.2
26.4
19.6
10.8
10.6
f1 (ppm)

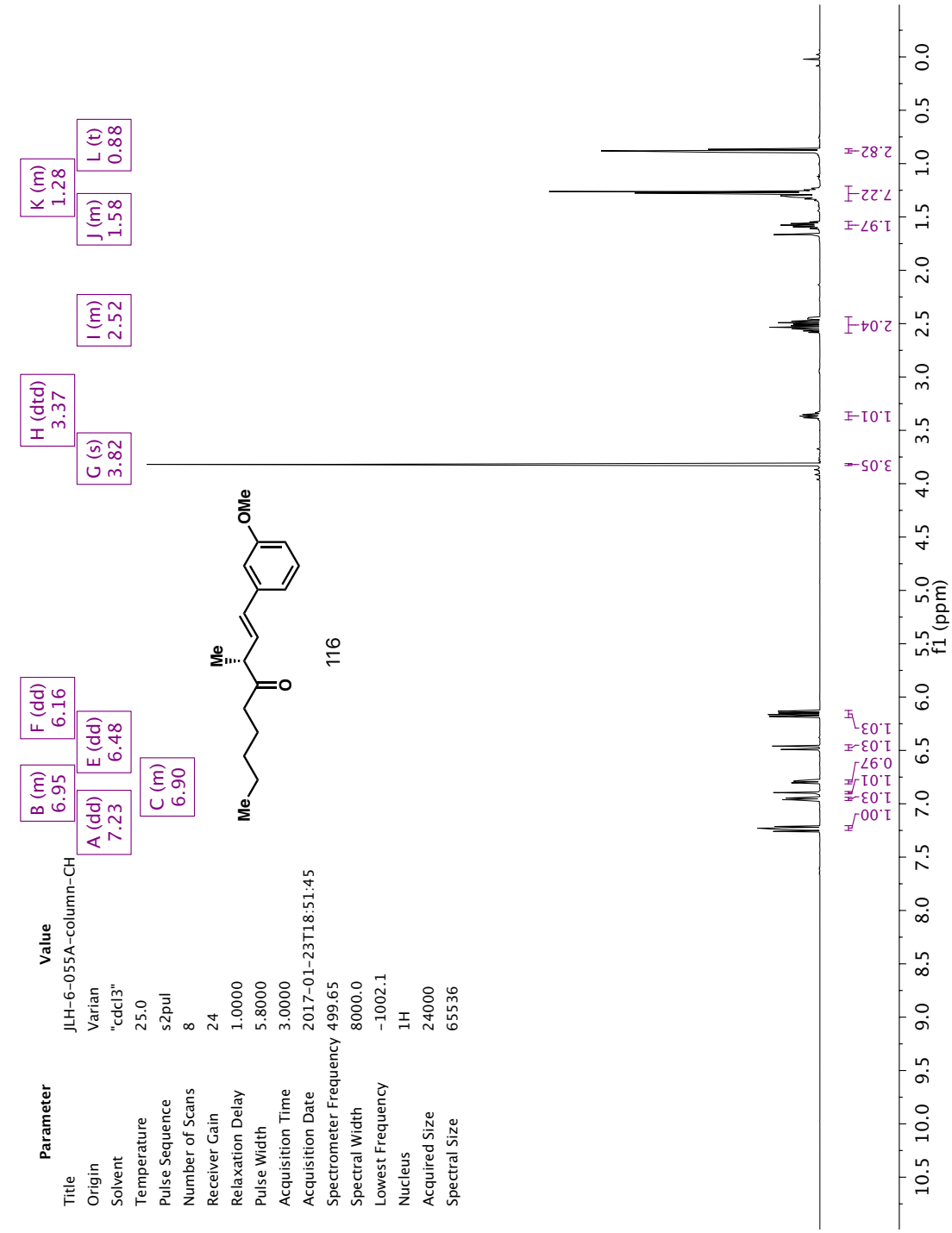
Parameter
Value
Title JLH-6-055A-column-CH
Origin Varian
Solvent "cdcl3"
Temperature 25.0
Pulse Sequence s2pul
Number of Scans 8
Receiver Gain 24
Relaxation Delay 1.0000
Pulse Width 5.8000
Acquisition Time 3.0000
Acquisition Date 2017-01-23T18:51:45
Spectrometer Frequency 499.65
Spectral Width 8000.0
Lowest Frequency -1002.1
Nucleus 1H
Acquired Size 24000
Spectral Size 65536
A (dd) 7.23
B (m) 6.95
C (m) 6.90
E (dd) 6.48
F (dd) 6.16
G (s) 3.82
H (dtd) 3.37
I (m) 2.52
J (m) 1.58
K (m) 1.28
L (t) 0.88
Me
Me
OMe
O
116
1.00
1.03
1.01
0.97
1.03
1.03
2.82
7.22
1.97
2.04
1.01
3.05
10.5 10.0 9.5 9.0 8.5 8.0 7.5 7.0 6.5 6.0 5.5 5.0 4.5 4.0 3.5 3.0 2.5 2.0 1.5 1.0 0.5 0.0
f1 (ppm)

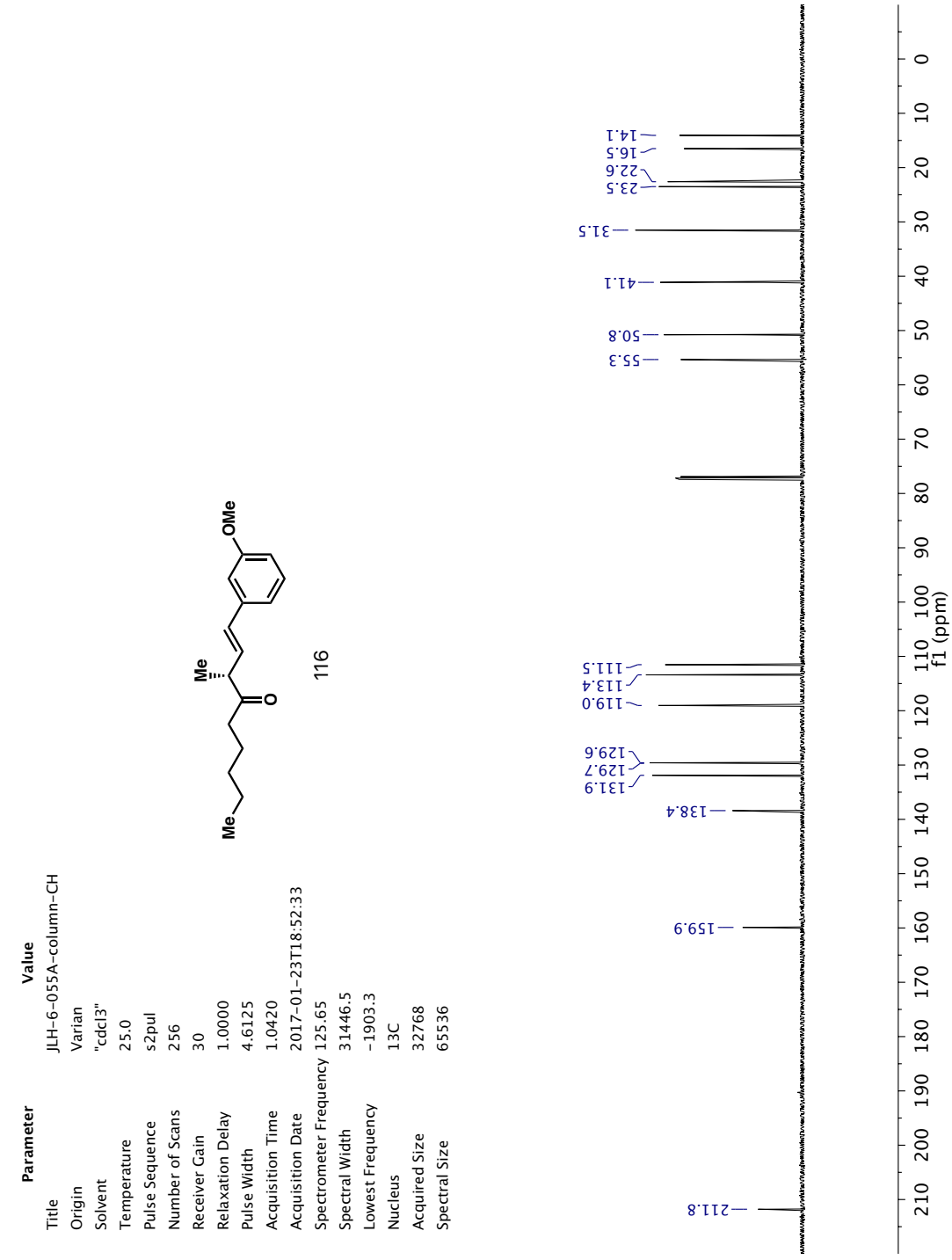

Parameter	Value
Title	JLH-6-055A-column-CH
Origin	Varian
Solvent	"cdcl3"
Temperature	25.0
Pulse Sequence	s2pul
Number of Scans	256
Receiver Gain	30
Relaxation Delay	1.0000
Pulse Width	4.6125
Acquisition Time	1.0420
Acquisition Date	2017-01-23T18:52:33
Spectrometer Frequency	125.65
Spectral Width	31446.5
Lowest Frequency	-1903.3
Nucleus	13C
Acquired Size	32768
Spectral Size	65536

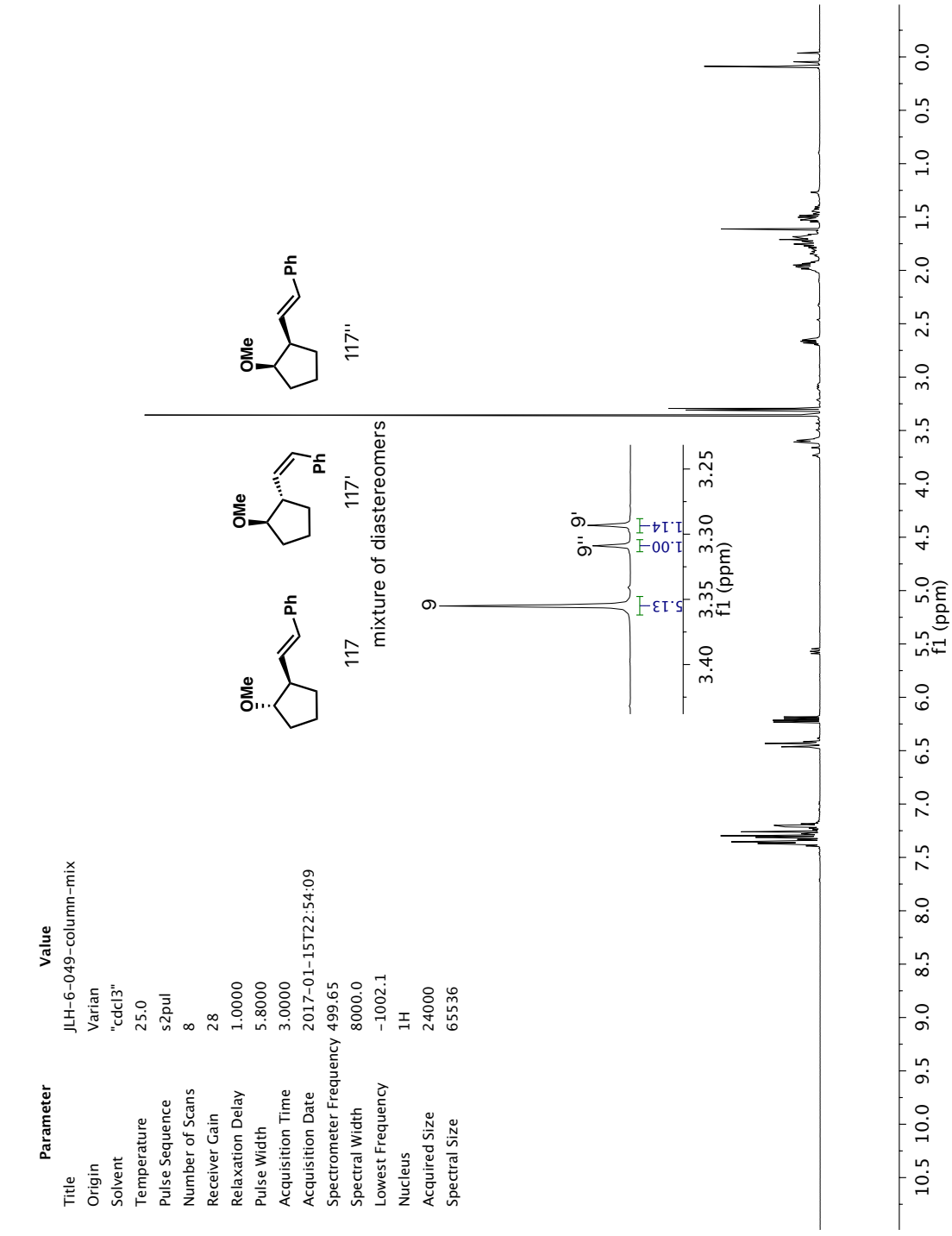
Parameter Value
Title JLH-6-049-column-mix
Origin Varian
Solvent "cdcl3"
Temperature 25.0
Pulse Sequence s2pul
Number of Scans 8
Receiver Gain 28
Relaxation Delay 1.0000
Pulse Width 5.8000
Acquisition Time 3.0000
Acquisition Date 2017-01-15T22:54:09
Spectrometer Frequency 499.65
Spectral Width 8000.0
Lowest Frequency -1002.1
Nucleus 1H
Acquired Size 24000
Spectral Size 65536
OMe
Ph
117
OMe
Ph
117'
OMe
Ph
117''
mixture of diastereomers
9
9''
9'
5.13
1.00
1.14
3.40 3.35 3.30 3.25
f1 (ppm)
10.5 10.0 9.5 9.0 8.5 8.0 7.5 7.0 6.5 6.0 5.5 5.0 4.5 4.0 3.5 3.0 2.5 2.0 1.5 1.0 0.5 0.0
f1 (ppm)

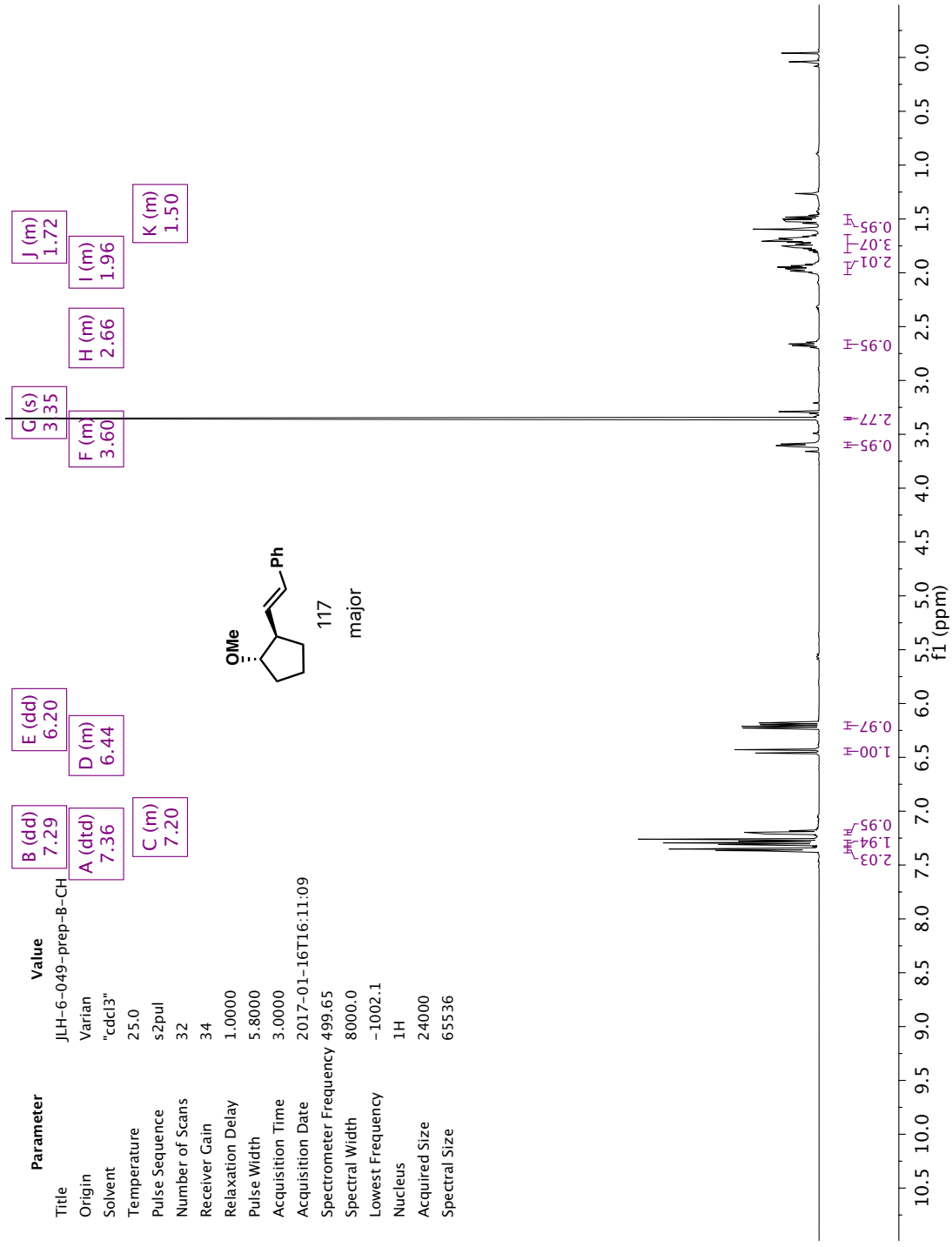
B (dd) 7.29
A (dtd) 7.36
C (m) 7.20
E (dd) 6.20
D (m) 6.44
G (s) 3.35
F (m) 3.60
H (m) 2.66
J (m) 1.72
I (m) 1.96
K (m) 1.50
OMe
Ph
117
major
Parameter Value
Title JLH-6-049-prep-B-CH
Origin Varian
Solvent "cdcl3"
Temperature 25.0
Pulse Sequence s2pul
Number of Scans 32
Receiver Gain 34
Relaxation Delay 1.0000
Pulse Width 5.8000
Acquisition Time 3.0000
Acquisition Date 2017-01-16T16:11:09
Spectrometer Frequency 499.65
Spectral Width 8000.0
Lowest Frequency -1002.1
Nucleus 1H
Acquired Size 24000
Spectral Size 65536
2.03
1.94
0.95
1.00
0.97
0.95
2.77
0.95
2.01
3.07
0.95
10.5 10.0 9.5 9.0 8.5 8.0 7.5 7.0 6.5 6.0 5.5 5.0 4.5 4.0 3.5 3.0 2.5 2.0 1.5 1.0 0.5 0.0
f1 (ppm)

Parameter	Value
Title	JLH-6-049-prep-B-CH
Origin	Varian
Solvent	"cdcl3"
Temperature	25.0
Pulse Sequence	s2pul
Number of Scans	1000
Receiver Gain	30
Relaxation Delay	1.0000
Pulse Width	4.6125
Acquisition Time	1.0420
Acquisition Date	2017-01-16T16:13:33
Spectrometer Frequency	125.65
Spectral Width	31446.5
Lowest Frequency	-1903.3
Nucleus	13C
Acquired Size	32768
Spectral Size	65536

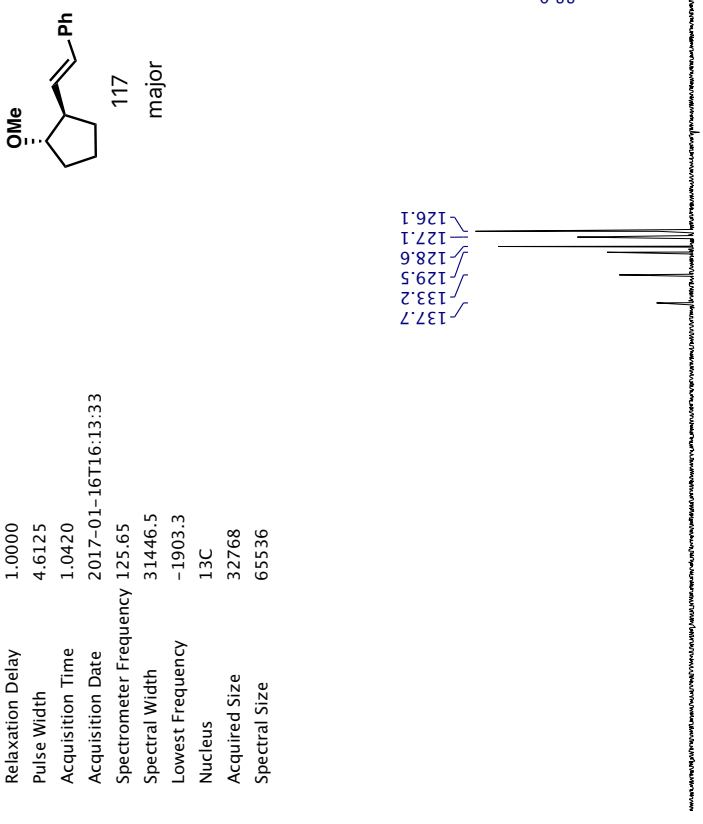

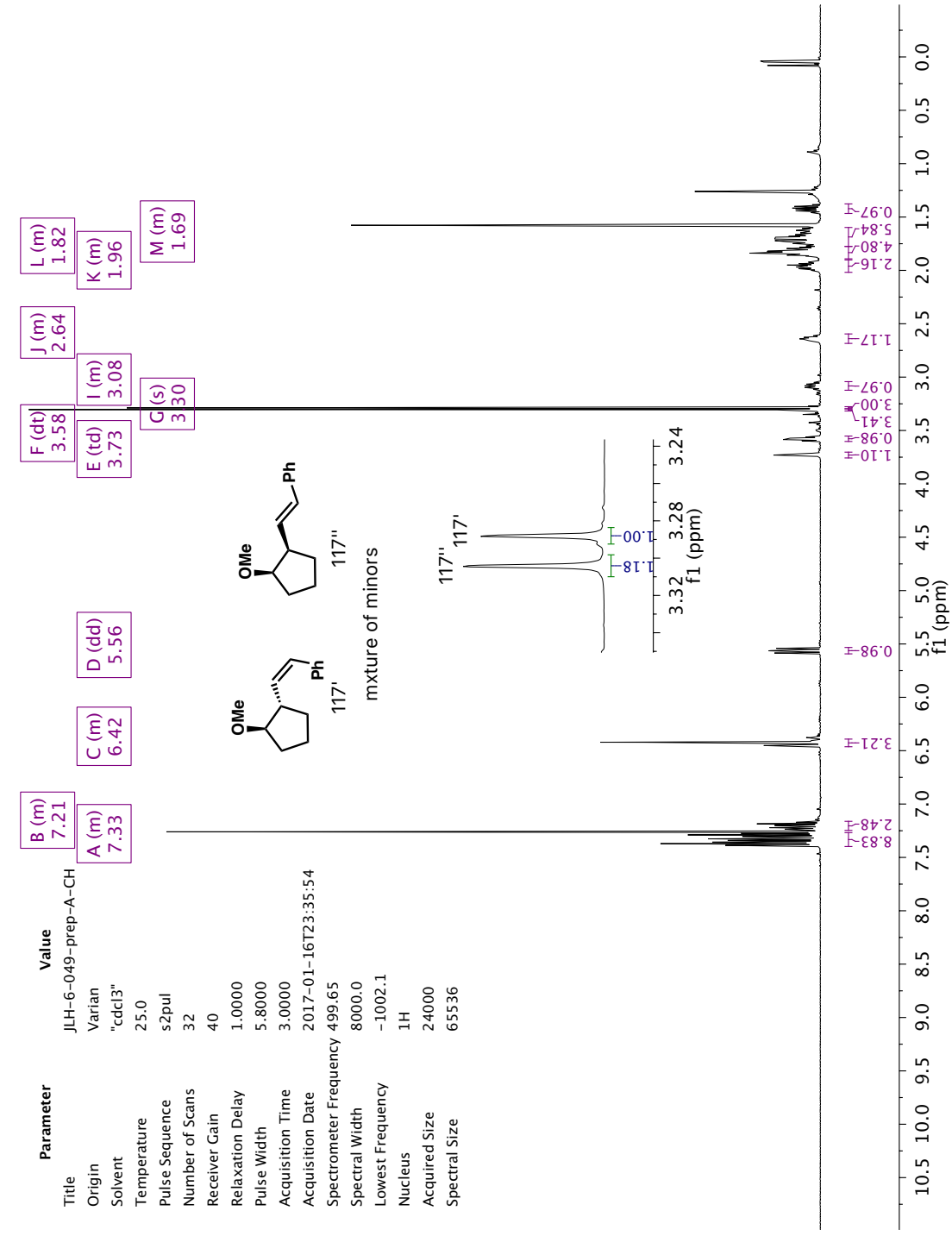
Parameter
Value
Title JLH-6-049-prep-A-CH
Origin Varian
Solvent "cdcl3"
Temperature 25.0
Pulse Sequence s2pul
Number of Scans 32
Receiver Gain 40
Relaxation Delay 1.0000
Pulse Width 5.8000
Acquisition Time 3.0000
Acquisition Date 2017-01-16T23:35:54
Spectrometer Frequency 499.65
Spectral Width 8000.0
Lowest Frequency -1002.1
Nucleus 1H
Acquired Size 24000
Spectral Size 65536
B (m) 7.21
A (m) 7.33
C (m) 6.42
D (dd) 5.56
F (dt) 3.58
E (td) 3.73
G (s) 3.30
I (m) 3.08
J (m) 2.64
L (m) 1.82
K (m) 1.96
M (m) 1.69
OMe
Ph
117'
OMe
Ph
117''
mxture of minors
117''
117'
1.00
1.18
3.32
3.28
3.24
f1 (ppm)
8.83
2.48
3.21
0.98
1.17
0.97
3.00
3.41
1.10
0.98
0.97
2.16
4.80
5.84
0.97
f1 (ppm)

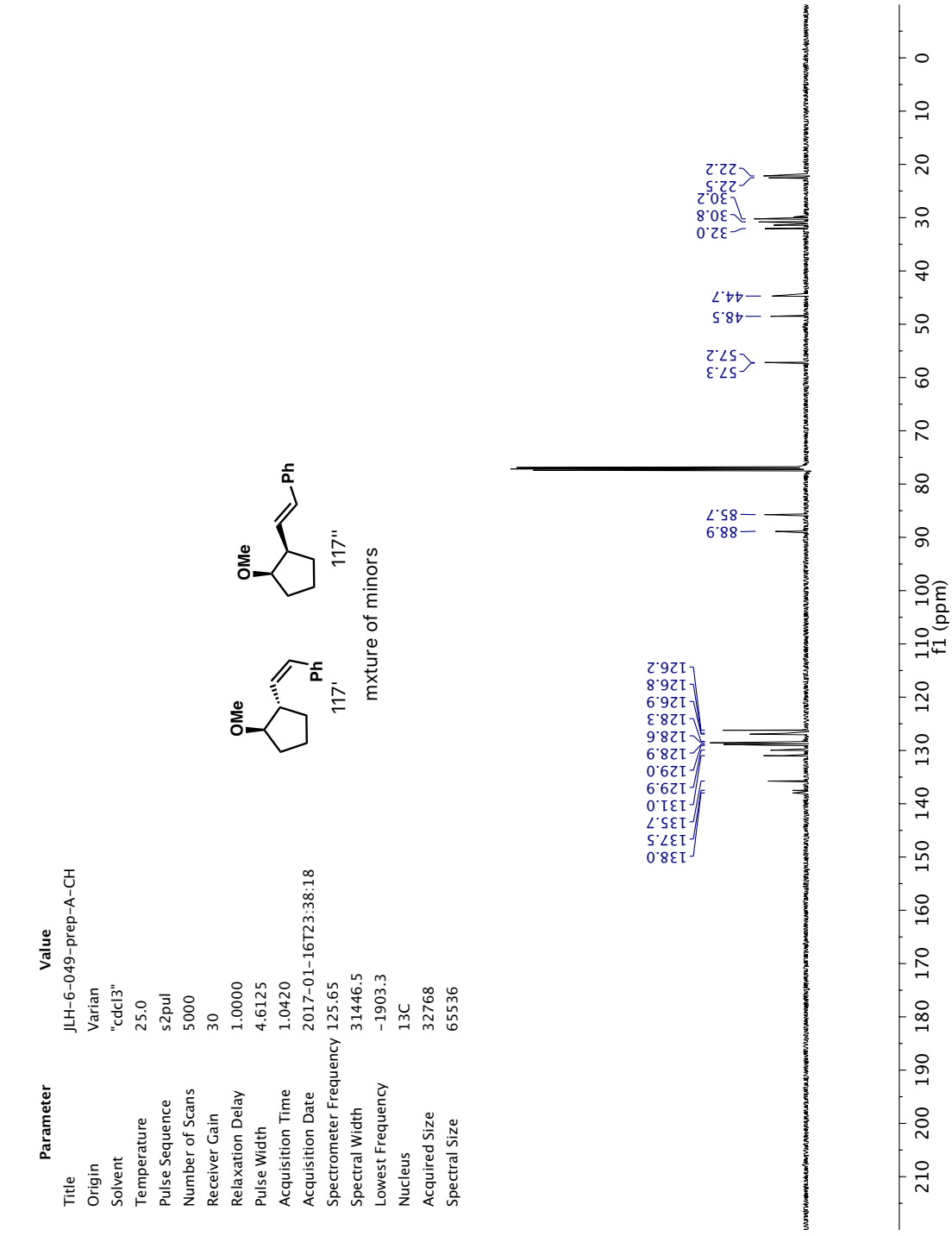
Parameter Value
Title JLH-6-049-prep-A-CH
Origin Varian
Solvent "cdcl3"
Temperature 25.0
Pulse Sequence s2pul
Number of Scans 5000
Receiver Gain 30
Relaxation Delay 1.0000
Pulse Width 4.6125
Acquisition Time 1.0420
Acquisition Date 2017-01-16T23:38:18
Spectrometer Frequency 125.65
Spectral Width 31446.5
Lowest Frequency -1903.3
Nucleus 13C
Acquired Size 32768
Spectral Size 65536
OMe
Ph
117'
OMe
Ph
117''
mxture of minors
138.0
137.5
135.7
131.0
129.9
129.0
128.9
128.6
128.3
126.9
126.8
126.2
88.9
85.7
57.3
57.2
48.5
44.7
32.0
30.8
30.2
22.5
22.2
210 200 190 180 170 160 150 140 130 120 110 100 90 80 70 60 50 40 30 20 10 0
f1 (ppm)

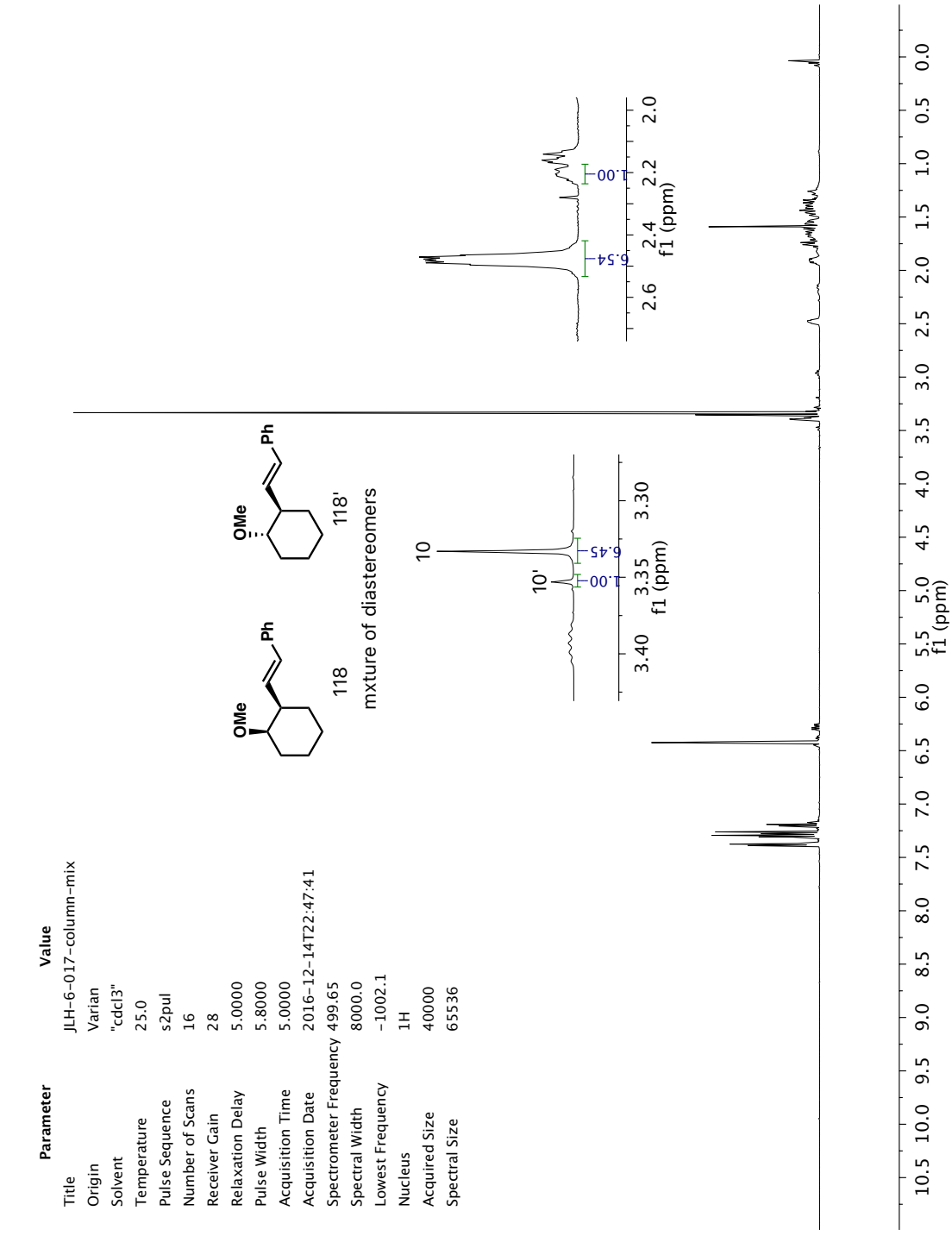
Parameter Value
Title JLH-6-017-column-mix
Origin Varian
Solvent "cdcl3"
Temperature 25.0
Pulse Sequence s2pul
Number of Scans 16
Receiver Gain 28
Relaxation Delay 5.0000
Pulse Width 5.8000
Acquisition Time 5.0000
Acquisition Date 2016-12-14T22:47:41
Spectrometer Frequency 499.65
Spectral Width 8000.0
Lowest Frequency -1002.1
Nucleus 1H
Acquired Size 40000
Spectral Size 65536
OMe
Ph
118
OMe
Ph
118'
mxture of diastereomers
10
10'
1.00
6.45
1.00
6.54
f1 (ppm)
f1 (ppm)
f1 (ppm)

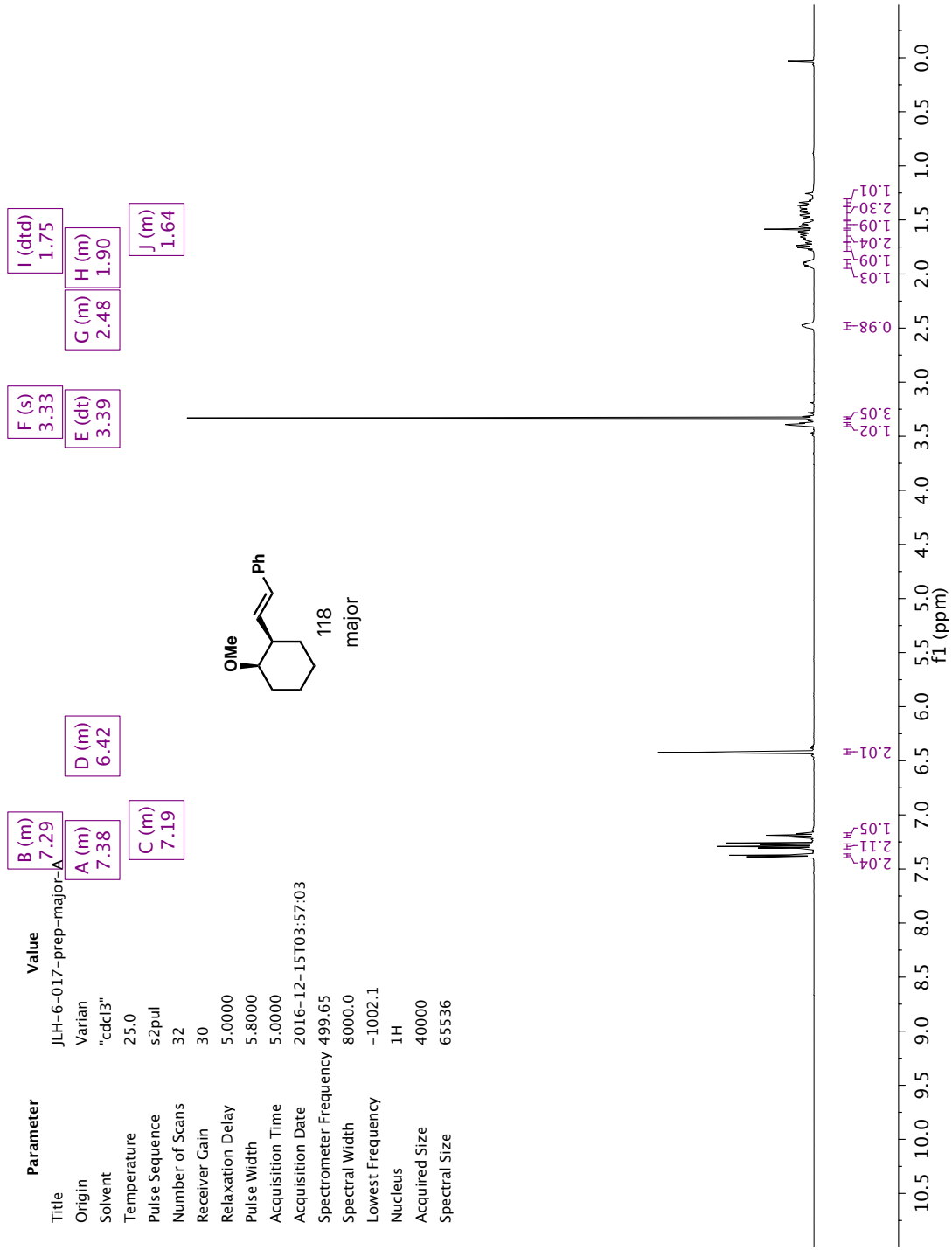
Parameter
Value
Title JLH-6-017-prep-major-A
Origin Varian
Solvent "cdcl3"
Temperature 25.0
Pulse Sequence s2pul
Number of Scans 32
Receiver Gain 30
Relaxation Delay 5.0000
Pulse Width 5.8000
Acquisition Time 5.0000
Acquisition Date 2016-12-15T03:57:03
Spectrometer Frequency 499.65
Spectral Width 8000.0
Lowest Frequency -1002.1
Nucleus 1H
Acquired Size 40000
Spectral Size 65536
B (m) 7.29
A (m) 7.38
C (m) 7.19
D (m) 6.42
F (s) 3.33
E (dt) 3.39
G (m) 2.48
H (m) 1.90
I (dtd) 1.75
J (m) 1.64
OMe
Ph
118
major
2.04
1.05
2.11
2.01
1.02
3.05
0.98
1.03
1.09
2.04
1.09
2.30
1.01
f1 (ppm)

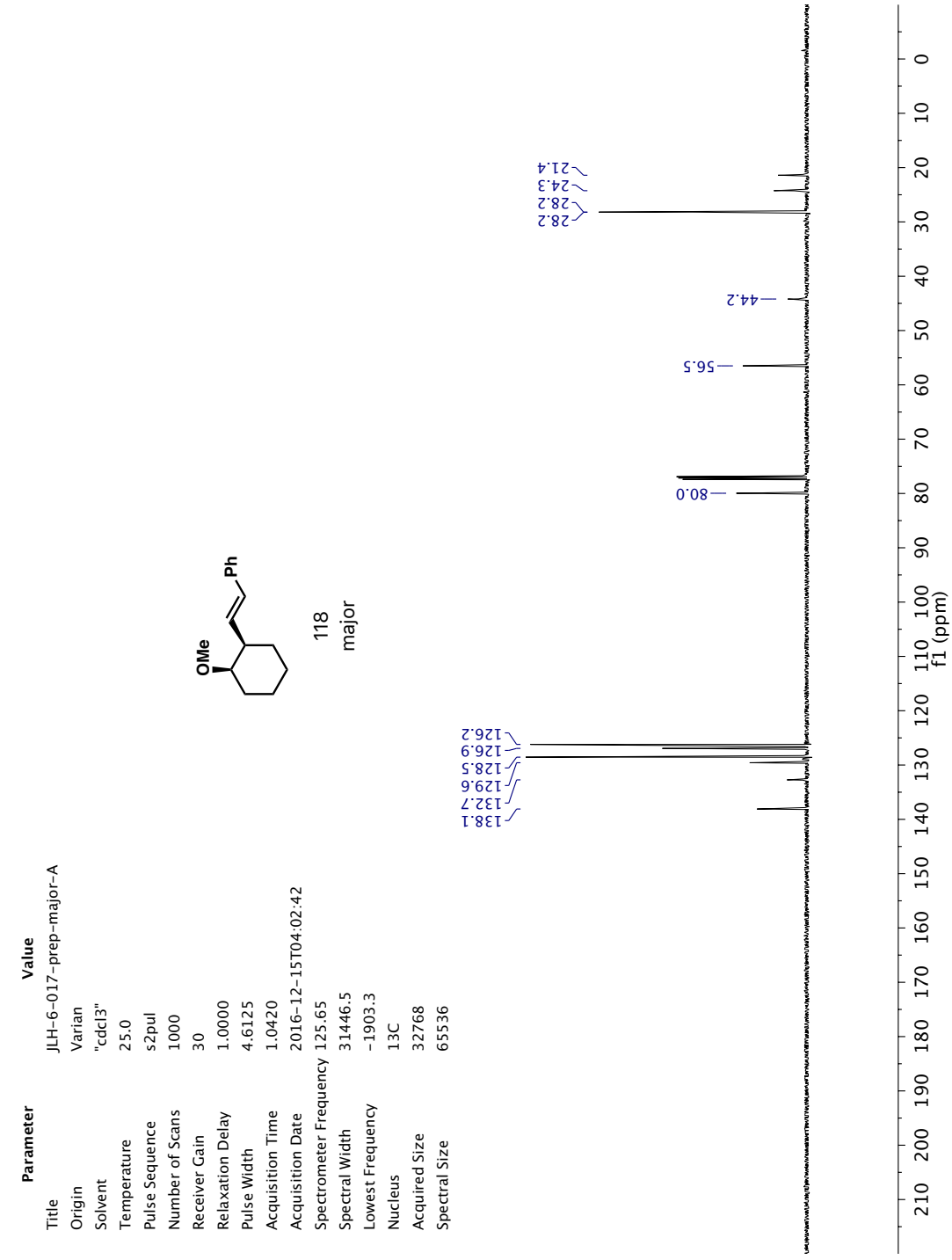
Parameter Value
Title JLH-6-017-prep-major-A
Origin Varian
Solvent "cdcl3"
Temperature 25.0
Pulse Sequence s2pul
Number of Scans 1000
Receiver Gain 30
Relaxation Delay 1.0000
Pulse Width 4.6125
Acquisition Time 1.0420
Acquisition Date 2016-12-15T04:02:42
Spectrometer Frequency 125.65
Spectral Width 31446.5
Lowest Frequency -1903.3
Nucleus 13C
Acquired Size 32768
Spectral Size 65536
OMe
Ph
118
major
138.1
132.7
129.6
128.5
126.9
126.2
80.0
56.5
44.2
28.2
28.2
24.3
21.4
f1 (ppm)

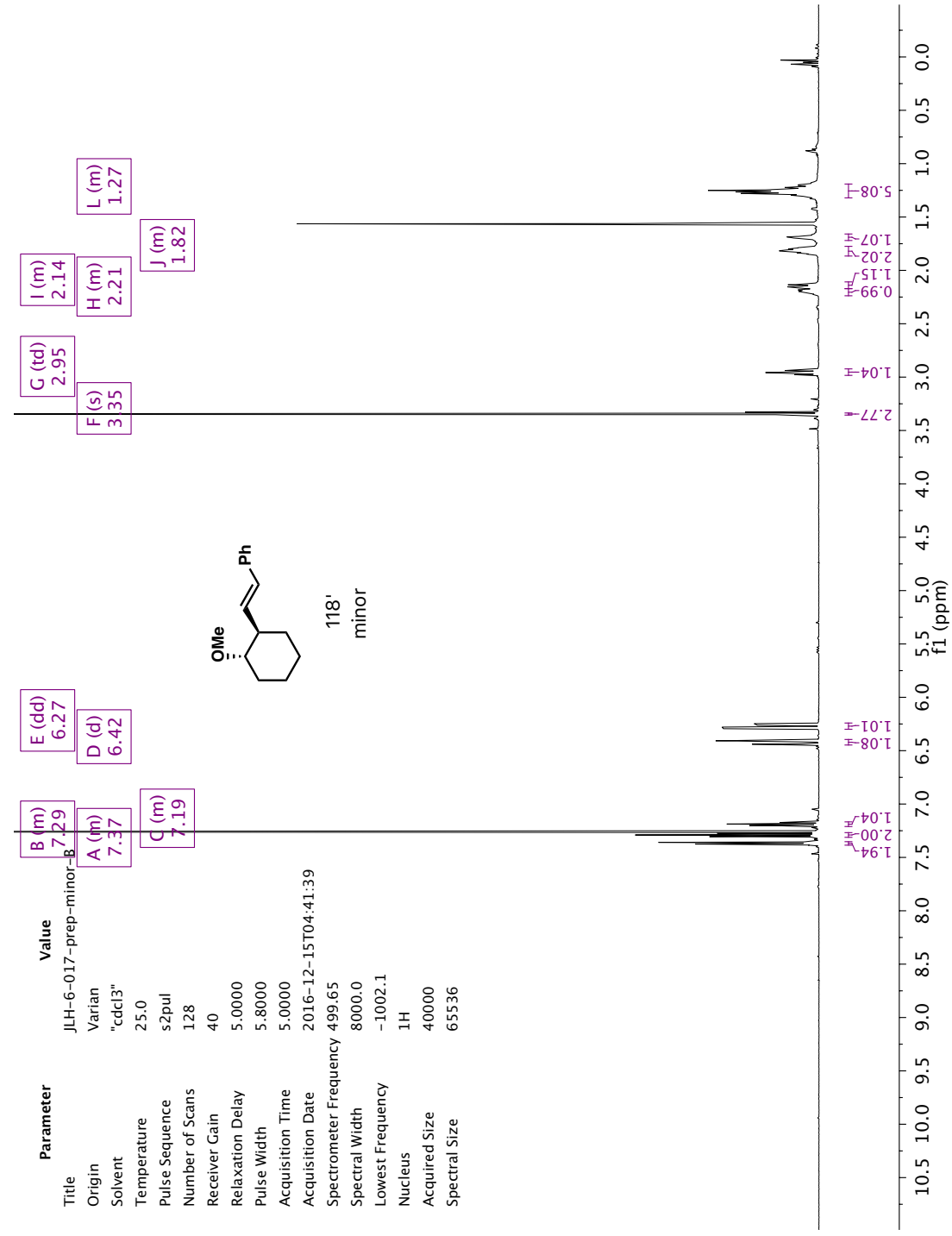
B (m) 7.29
A (m) 7.37
C (m) 7.19
E (dd) 6.27
D (d) 6.42
G (td) 2.95
F (s) 3.35
I (m) 2.14
H (m) 2.21
J (m) 1.82
L (m) 1.27
OMe
Ph
118'
minor
Parameter Value
Title JLH-6-017-prep-minor-B
Origin Varian
Solvent "cdcl3"
Temperature 25.0
Pulse Sequence s2pul
Number of Scans 128
Receiver Gain 40
Relaxation Delay 5.0000
Pulse Width 5.8000
Acquisition Time 5.0000
Acquisition Date 2016-12-15T04:41:39
Spectrometer Frequency 499.65
Spectral Width 8000.0
Lowest Frequency -1002.1
Nucleus 1H
Acquired Size 40000
Spectral Size 65536
1.94
2.00
1.04
1.08
1.01
2.77
1.04
0.99
1.15
2.02
1.07
5.08
f1 (ppm)

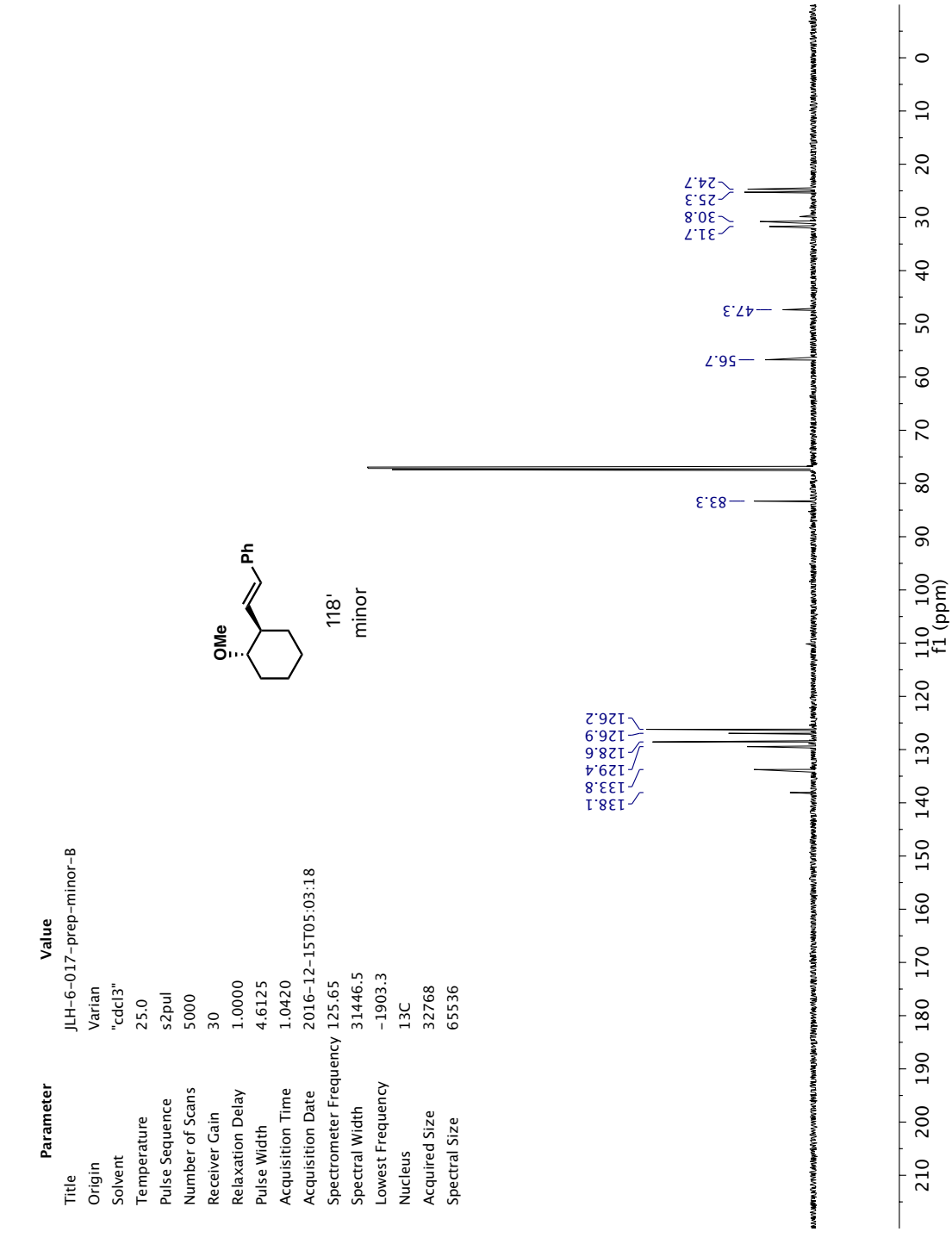
Parameter Value
Title JLH-6-017-prep-minor-B
Origin Varian
Solvent "cdcl3"
Temperature 25.0
Pulse Sequence s2pul
Number of Scans 5000
Receiver Gain 30
Relaxation Delay 1.0000
Pulse Width 4.6125
Acquisition Time 1.0420
Acquisition Date 2016-12-15T05:03:18
Spectrometer Frequency 125.65
Spectral Width 31446.5
Lowest Frequency -1903.3
Nucleus 13C
Acquired Size 32768
Spectral Size 65536
OMe
Ph
118'
minor
138.1
133.8
129.4
128.6
126.9
126.2
83.3
56.7
47.3
31.7
30.8
25.3
24.7
f1 (ppm)

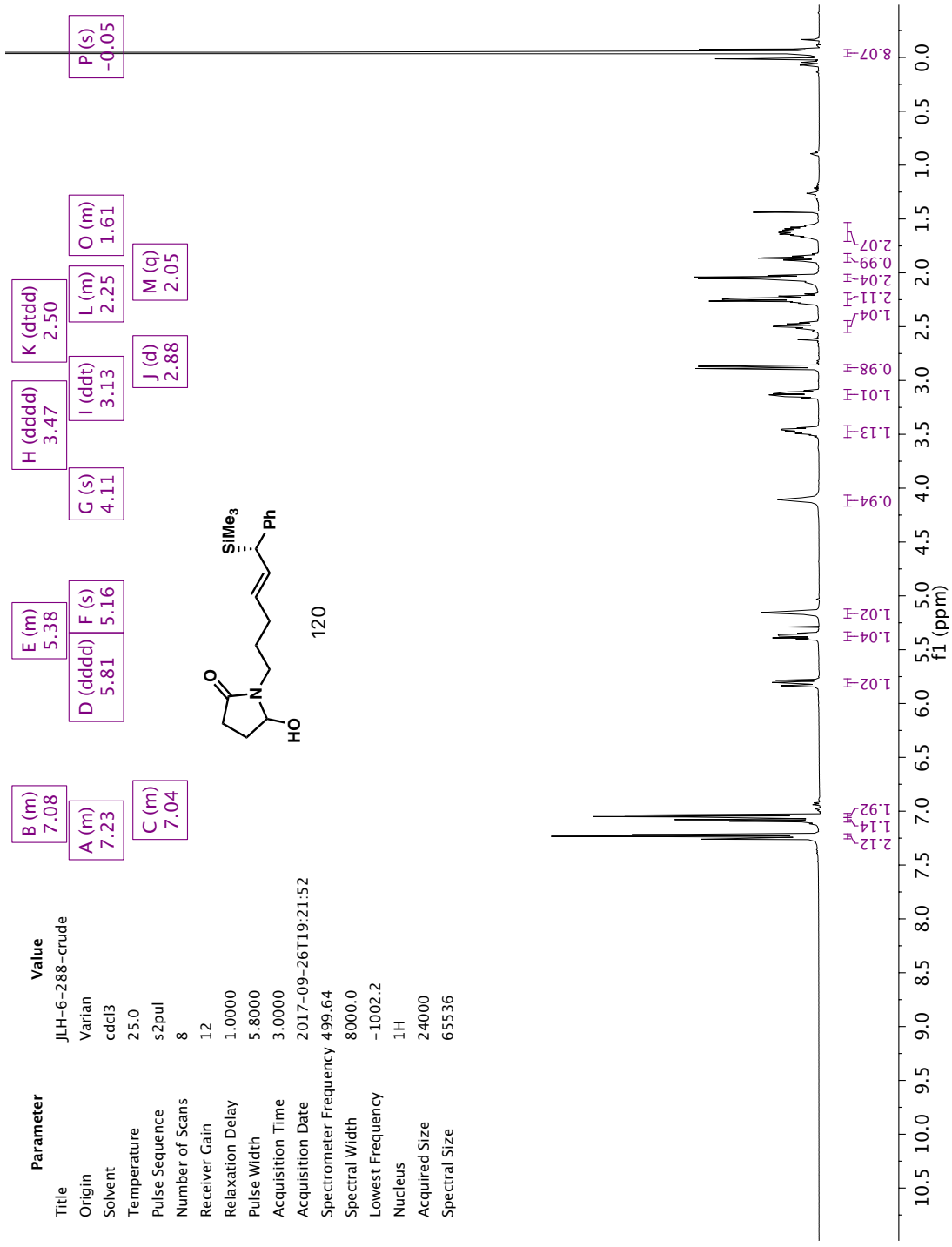
Parameter
Value
Title
JLH-6-288-crude
Origin
Varian
Solvent
cdcl3
Temperature
25.0
Pulse Sequence
s2pul
Number of Scans
8
Receiver Gain
12
Relaxation Delay
1.0000
Pulse Width
5.8000
Acquisition Time
3.0000
Acquisition Date
2017-09-26T19:21:52
Spectrometer Frequency
499.64
Spectral Width
8000.0
Lowest Frequency
-1002.2
Nucleus
1H
Acquired Size
24000
Spectral Size
65536
A (m) 7.23
B (m) 7.08
C (m) 7.04
D (dddd) 5.81
E (m) 5.38
F (s) 5.16
G (s) 4.11
H (dddd) 3.47
I (ddt) 3.13
J (d) 2.88
K (dtdd) 2.50
L (m) 2.25
M (q) 2.05
O (m) 1.61
P (s) -0.05
SiMe3
Ph
O
N
HO
120
f1 (ppm)

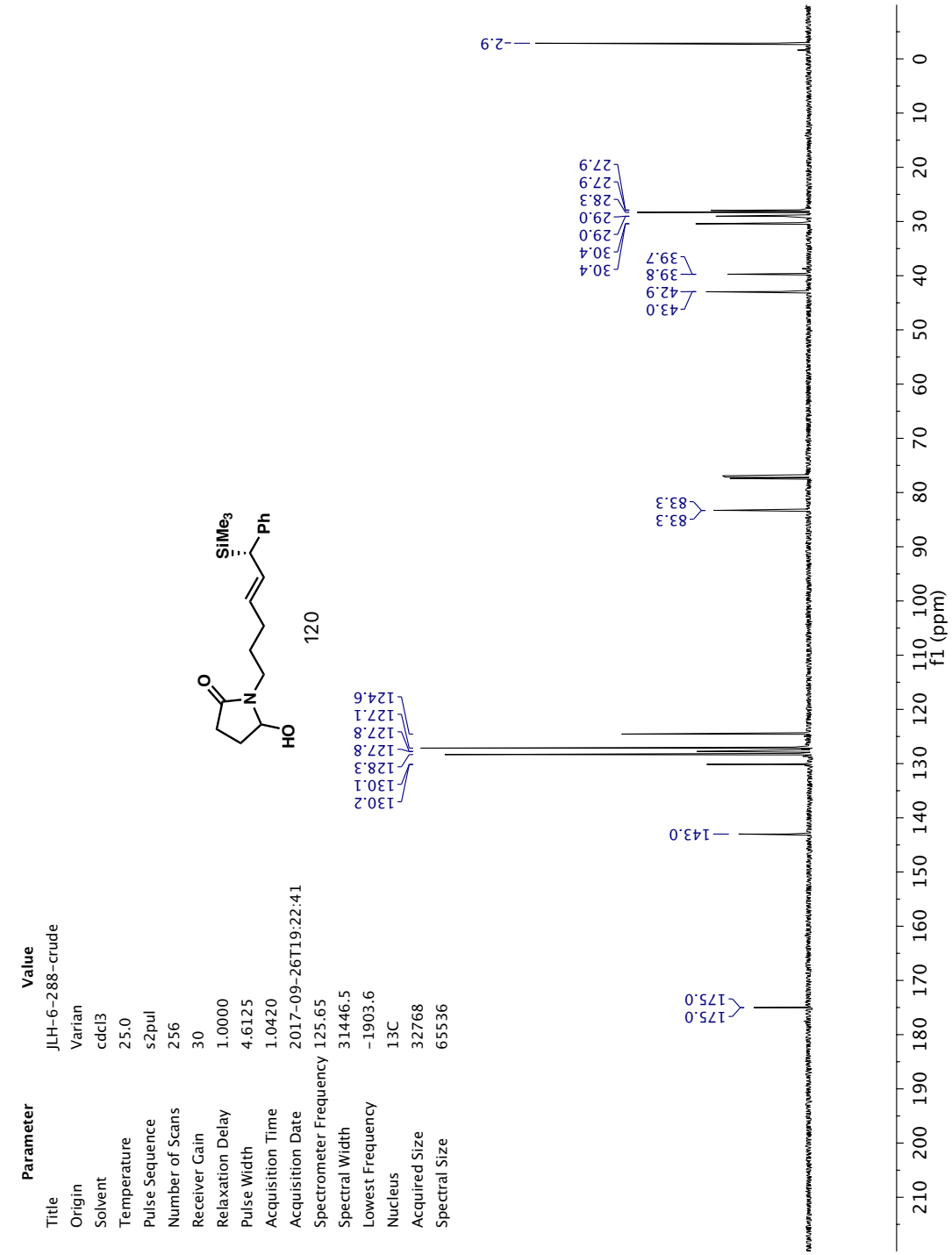
Parameter Value
Title JLH-6-288-crude
Origin Varian
Solvent cdcl3
Temperature 25.0
Pulse Sequence s2pul
Number of Scans 256
Receiver Gain 30
Relaxation Delay 1.0000
Pulse Width 4.6125
Acquisition Time 1.0420
Acquisition Date 2017-09-26T19:22:41
Spectrometer Frequency 125.65
Spectral Width 31446.5
Lowest Frequency -1903.6
Nucleus 13C
Acquired Size 32768
Spectral Size 65536
SiMe3
Ph
O
N
HO
120
175.0
175.0
143.0
130.2
130.1
128.3
127.8
127.8
127.1
124.6
83.3
83.3
43.0
42.9
39.8
39.7
30.4
30.4
29.0
29.0
28.3
27.9
27.9
-2.9
f1 (ppm)

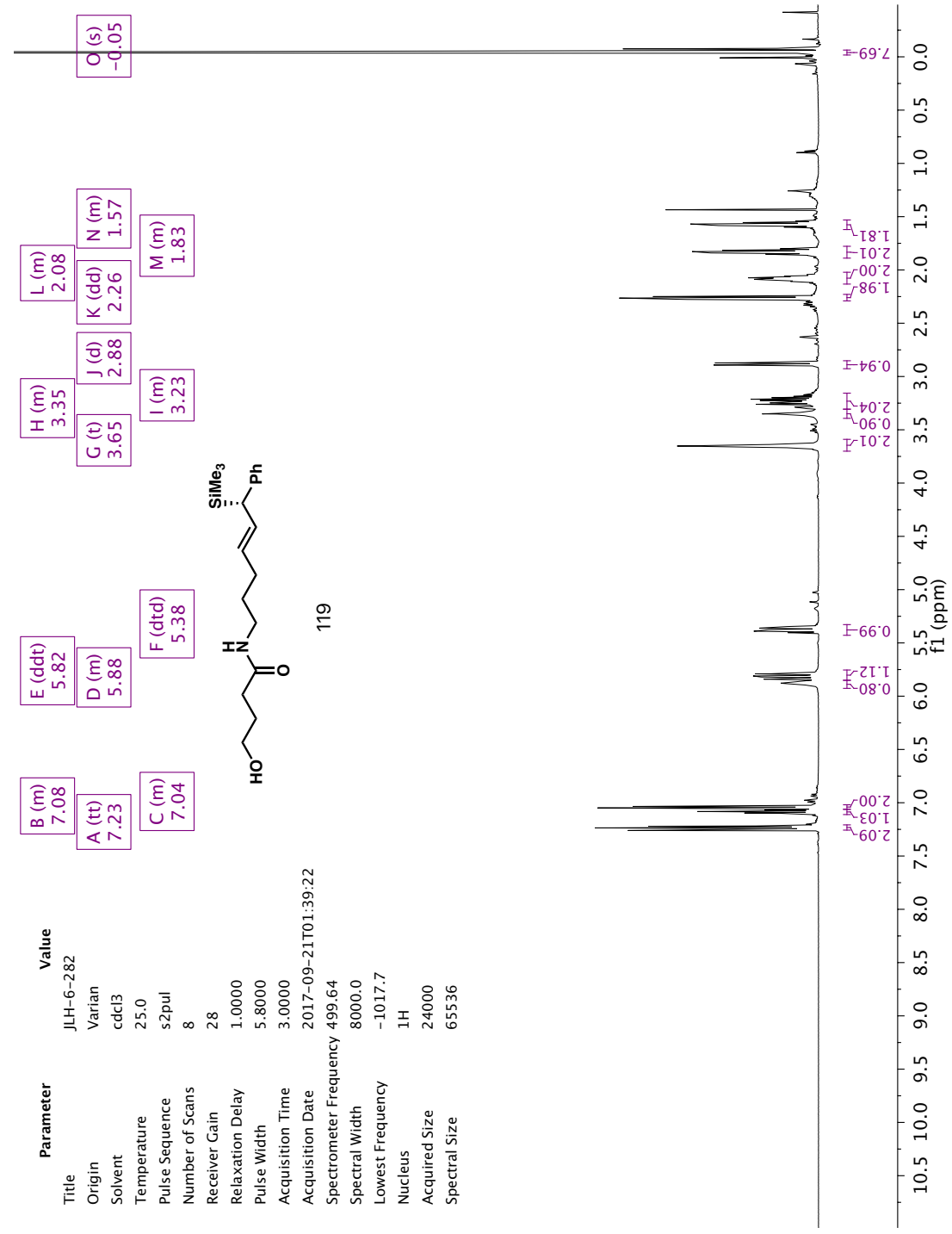
Parameter Value
Title JLH-6-282
Origin Varian
Solvent cdcl3
Temperature 25.0
Pulse Sequence s2pul
Number of Scans 8
Receiver Gain 28
Relaxation Delay 1.0000
Pulse Width 5.8000
Acquisition Time 3.0000
Acquisition Date 2017-09-21T01:39:22
Spectrometer Frequency 499.64
Spectral Width 8000.0
Lowest Frequency -1017.7
Nucleus 1H
Acquired Size 24000
Spectral Size 65536
B (m) 7.08
A (tt) 7.23
C (m) 7.04
E (ddt) 5.82
D (m) 5.88
F (dtd) 5.38
H (m) 3.35
G (t) 3.65
I (m) 3.23
J (d) 2.88
L (m) 2.08
K (dd) 2.26
M (m) 1.83
N (m) 1.57
O (s) -0.05
SiMe3
Ph
HO
H
N
O
119
2.09
1.03
2.00
0.80
1.12
0.99
2.01
0.90
2.04
0.94
1.98
2.00
2.01
1.81
7.69
10.5 10.0 9.5 9.0 8.5 8.0 7.5 7.0 6.5 6.0 5.5 5.0 4.5 4.0 3.5 3.0 2.5 2.0 1.5 1.0 0.5 0.0
f1 (ppm)

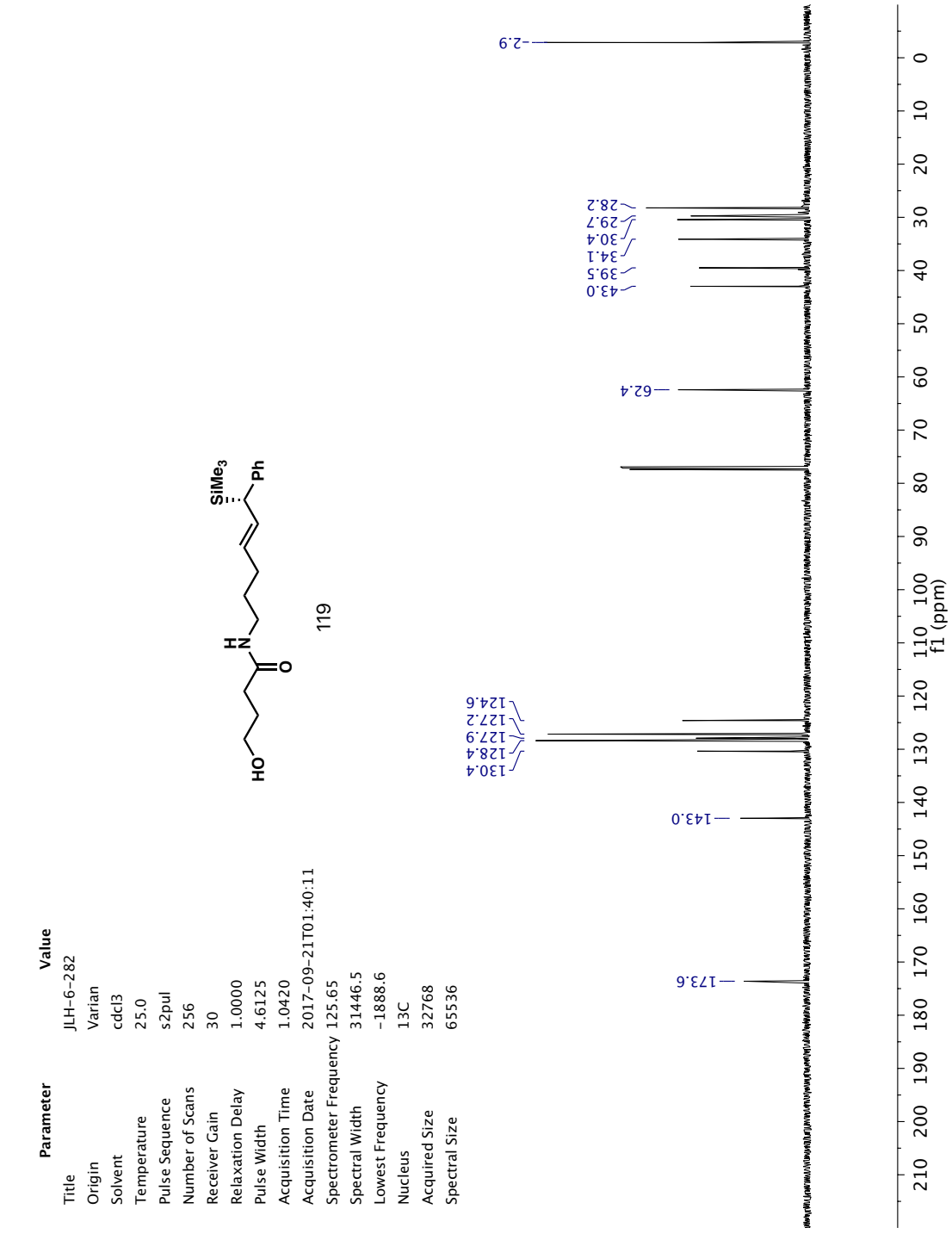
Parameter Value
Title JLH-6-282
Origin Varian
Solvent cdcl3
Temperature 25.0
Pulse Sequence s2pul
Number of Scans 256
Receiver Gain 30
Relaxation Delay 1.0000
Pulse Width 4.6125
Acquisition Time 1.0420
Acquisition Date 2017-09-21T01:40:11
Spectrometer Frequency 125.65
Spectral Width 31446.5
Lowest Frequency -1888.6
Nucleus 13C
Acquired Size 32768
Spectral Size 65536
SiMe3
Ph
H
N
O
HO
119
-2.9
28.2
29.7
30.4
34.1
39.5
43.0
62.4
130.4
128.4
127.9
127.2
124.6
143.0
173.6
f1 (ppm)

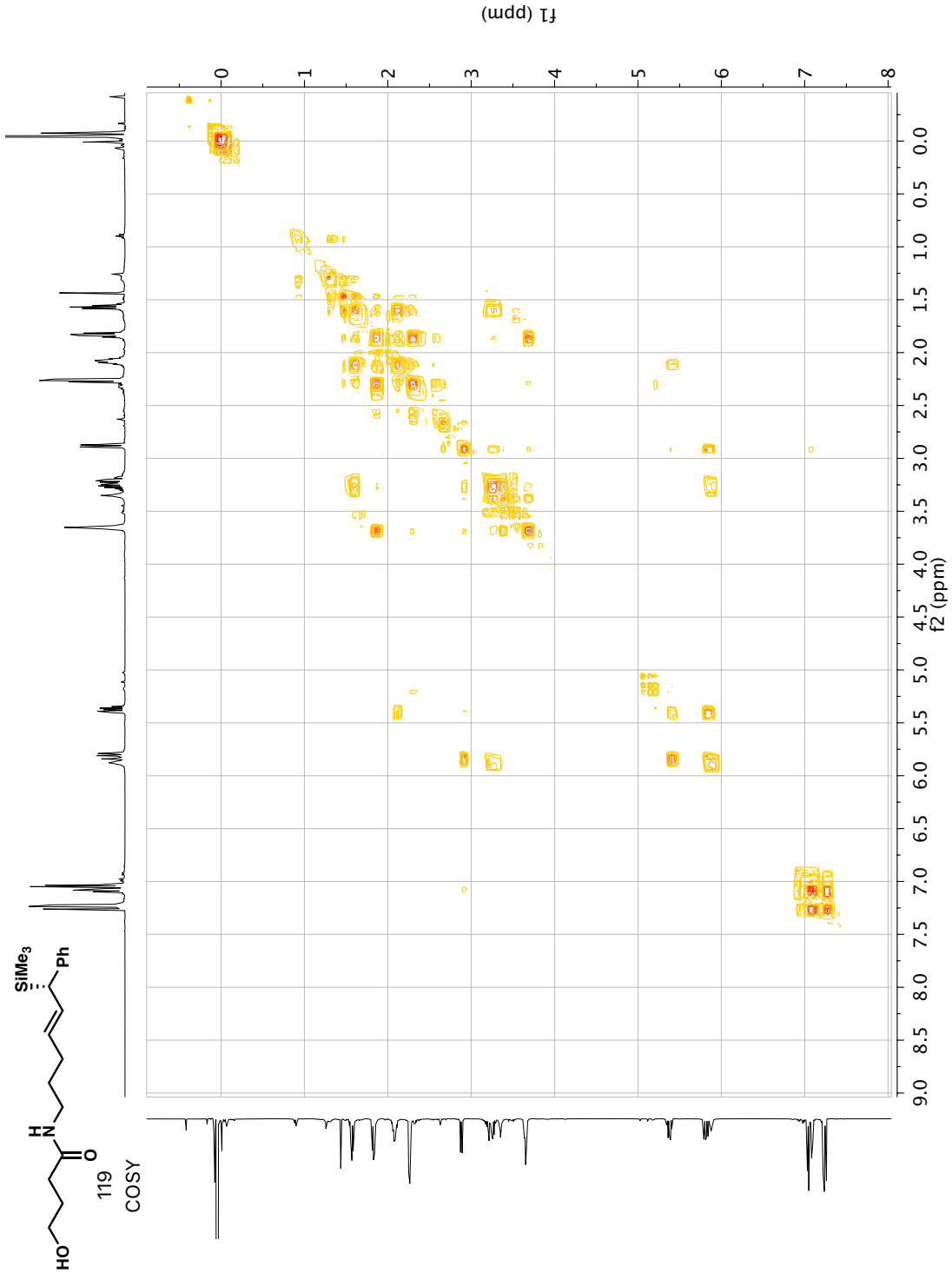
f1 (ppm)
f2 (ppm)
SiMe3
Ph
HO
119
COSY

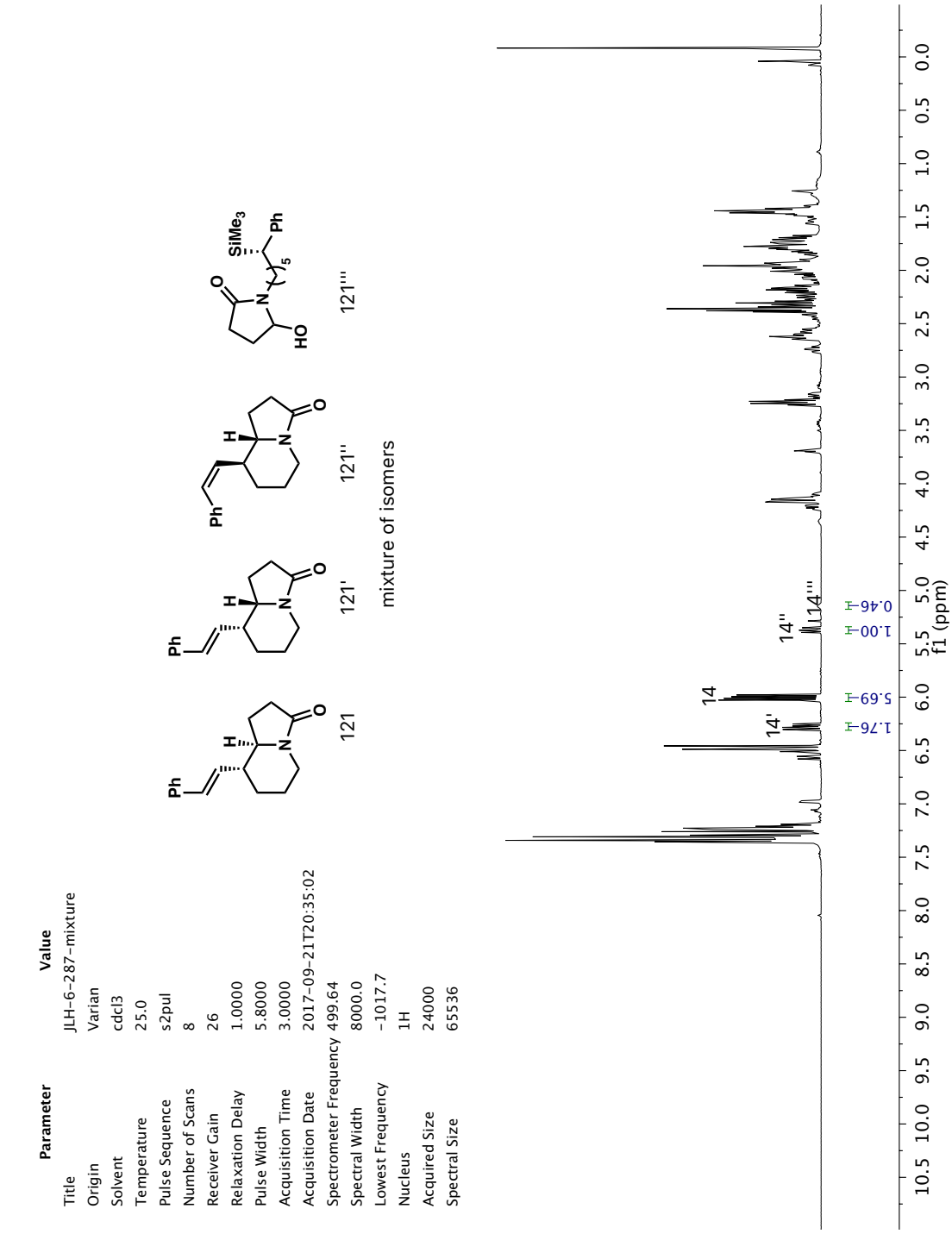
Parameter Value
Title JLH-6-287-mixture
Origin Varian
Solvent cdcl3
Temperature 25.0
Pulse Sequence s2pul
Number of Scans 8
Receiver Gain 26
Relaxation Delay 1.0000
Pulse Width 5.8000
Acquisition Time 3.0000
Acquisition Date 2017-09-21T20:35:02
Spectrometer Frequency 499.64
Spectral Width 8000.0
Lowest Frequency -1017.7
Nucleus 1H
Acquired Size 24000
Spectral Size 65536
121
121'
121''
121'''
mixture of isomers
14
14'
14''
14'''
1.76
5.69
1.00
0.46
f1 (ppm)

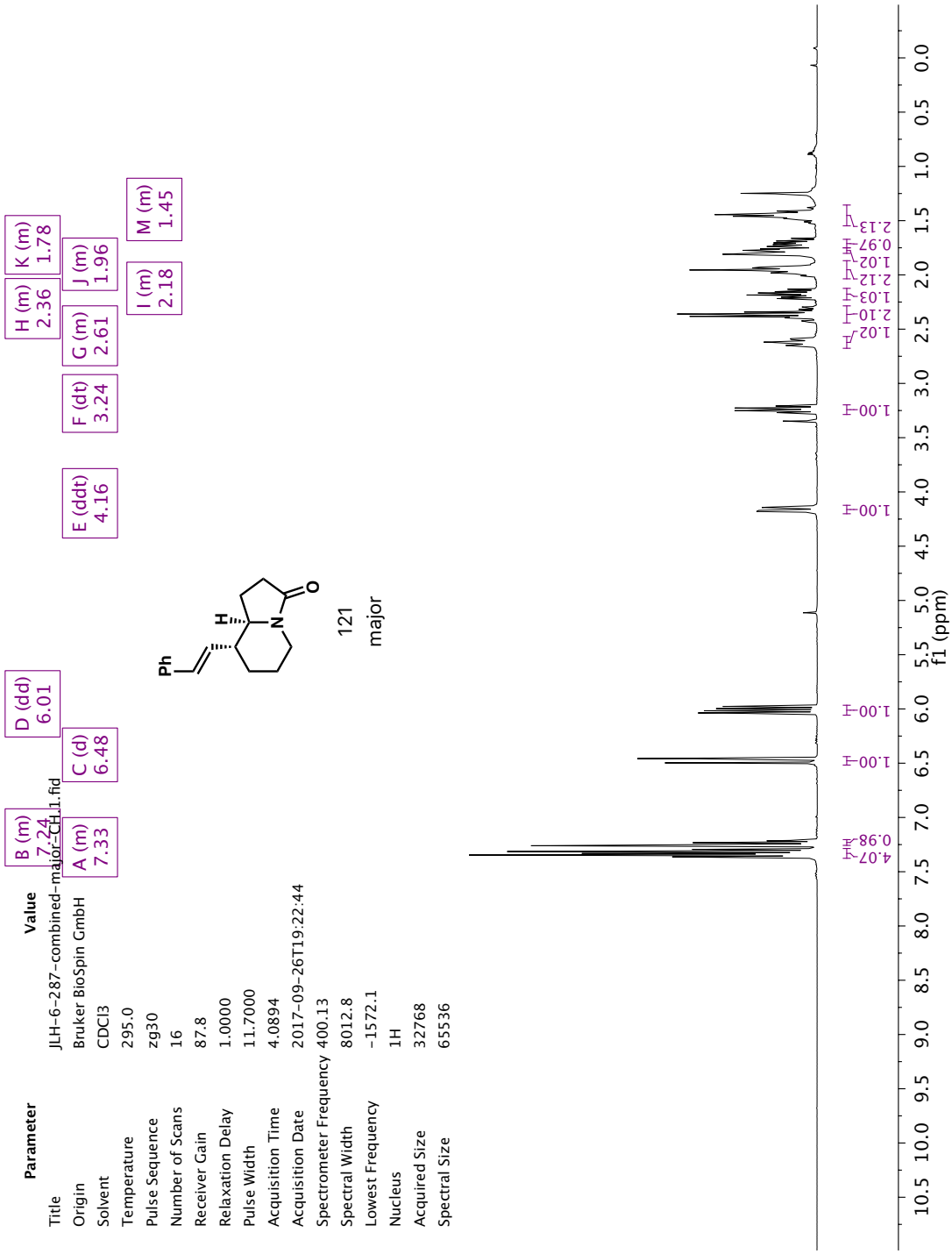
Parameter
Value
Title
JLH-6-287-combined-major-CH.1.fid
Origin
Bruker BioSpin GmbH
Solvent
CDCl3
Temperature
295.0
Pulse Sequence
zg30
Number of Scans
16
Receiver Gain
87.8
Relaxation Delay
1.0000
Pulse Width
11.7000
Acquisition Time
4.0894
Acquisition Date
2017-09-26T19:22:44
Spectrometer Frequency
400.13
Spectral Width
8012.8
Lowest Frequency
-1572.1
Nucleus
1H
Acquired Size
32768
Spectral Size
65536
B (m) 7.24
A (m) 7.33
D (dd) 6.01
C (d) 6.48
E (ddt) 4.16
F (dt) 3.24
G (m) 2.61
H (m) 2.36
J (m) 1.96
K (m) 1.78
I (m) 2.18
M (m) 1.45
Ph
H
N
O
121
major
4.07
0.98
1.00
1.00
1.00
1.00
1.02
2.10
1.03
2.12
1.02
0.97
2.13
10.5 10.0 9.5 9.0 8.5 8.0 7.5 7.0 6.5 6.0 5.5 5.0 4.5 4.0 3.5 3.0 2.5 2.0 1.5 1.0 0.5 0.0
f1 (ppm)

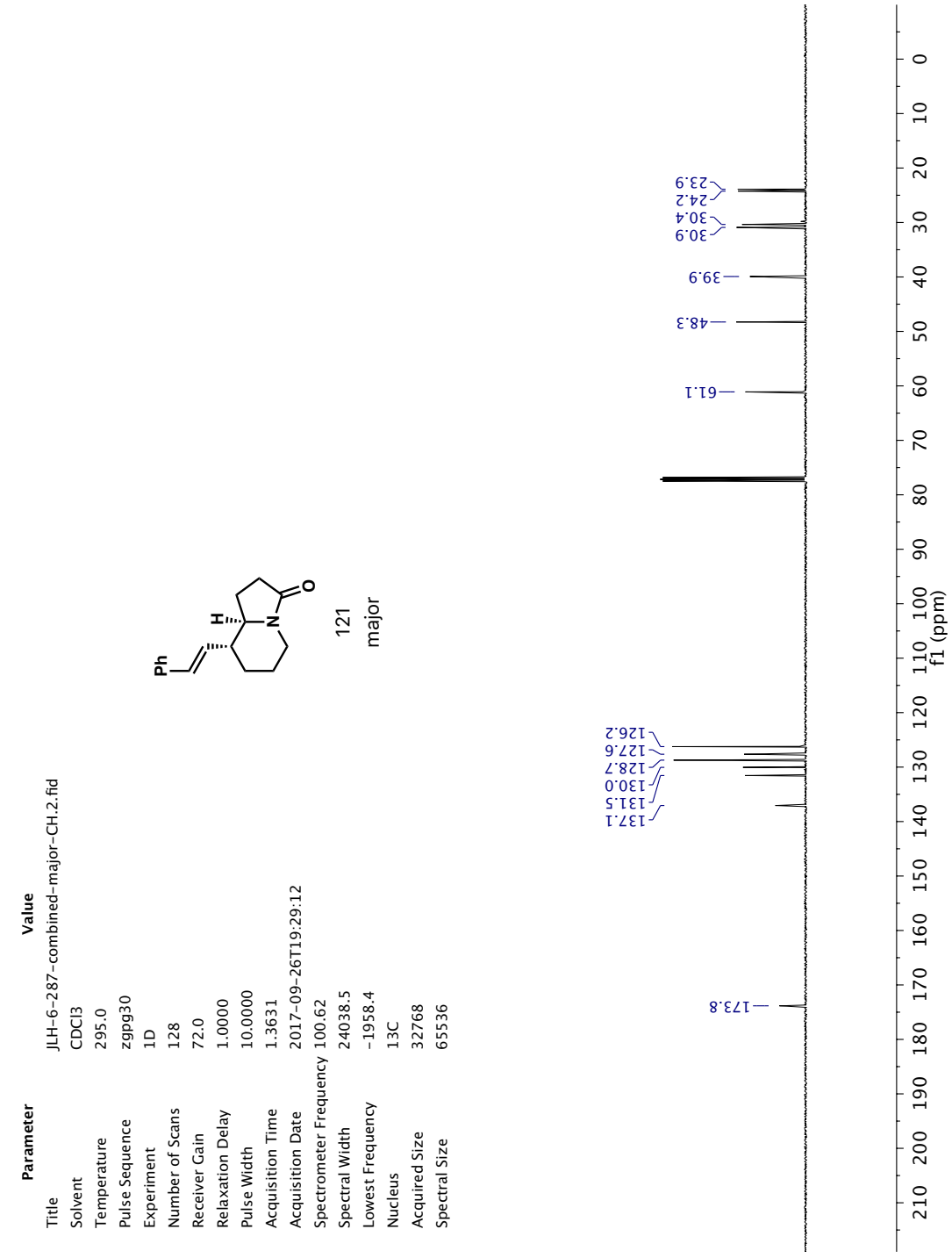
Parameter
Value
Title
JLH-6-287-combined-major-CH.2.fid
Solvent
CDCl3
Temperature
295.0
Pulse Sequence
zgpg30
Experiment
1D
Number of Scans
128
Receiver Gain
72.0
Relaxation Delay
1.0000
Pulse Width
10.0000
Acquisition Time
1.3631
Acquisition Date
2017-09-26T19:29:12
Spectrometer Frequency
100.62
Spectral Width
24038.5
Lowest Frequency
-1958.4
Nucleus
13C
Acquired Size
32768
Spectral Size
65536
Ph
H
N
O
121
major
173.8
137.1
131.5
130.0
128.7
127.6
126.2
61.1
48.3
39.9
30.9
30.4
24.2
23.9
f1 (ppm)


f1 (ppm)
0.5
1.0
1.5
2.0
2.5
3.0
3.5
4.0
4.5
5.0
5.5
6.0
6.5
7.0
7.5
f2 (ppm)
Ph
H
N
O
121
COSY

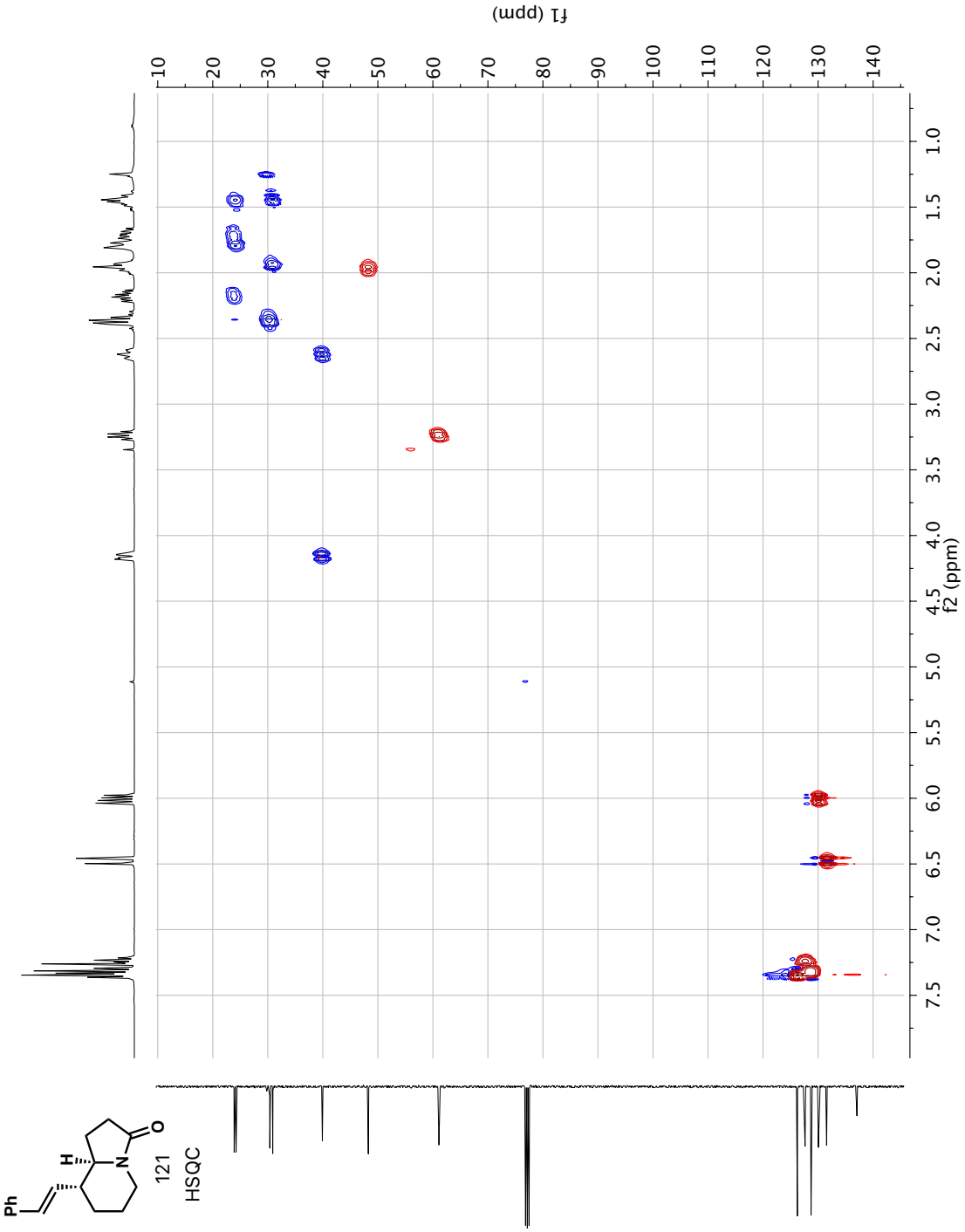
f1 (ppm)
10
20
30
40
50
60
70
80
90
100
110
120
130
140
f2 (ppm)
1.0
1.5
2.0
2.5
3.0
3.5
4.0
4.5
5.0
5.5
6.0
6.5
7.0
7.5
Ph
H
N
O
121
HSQC

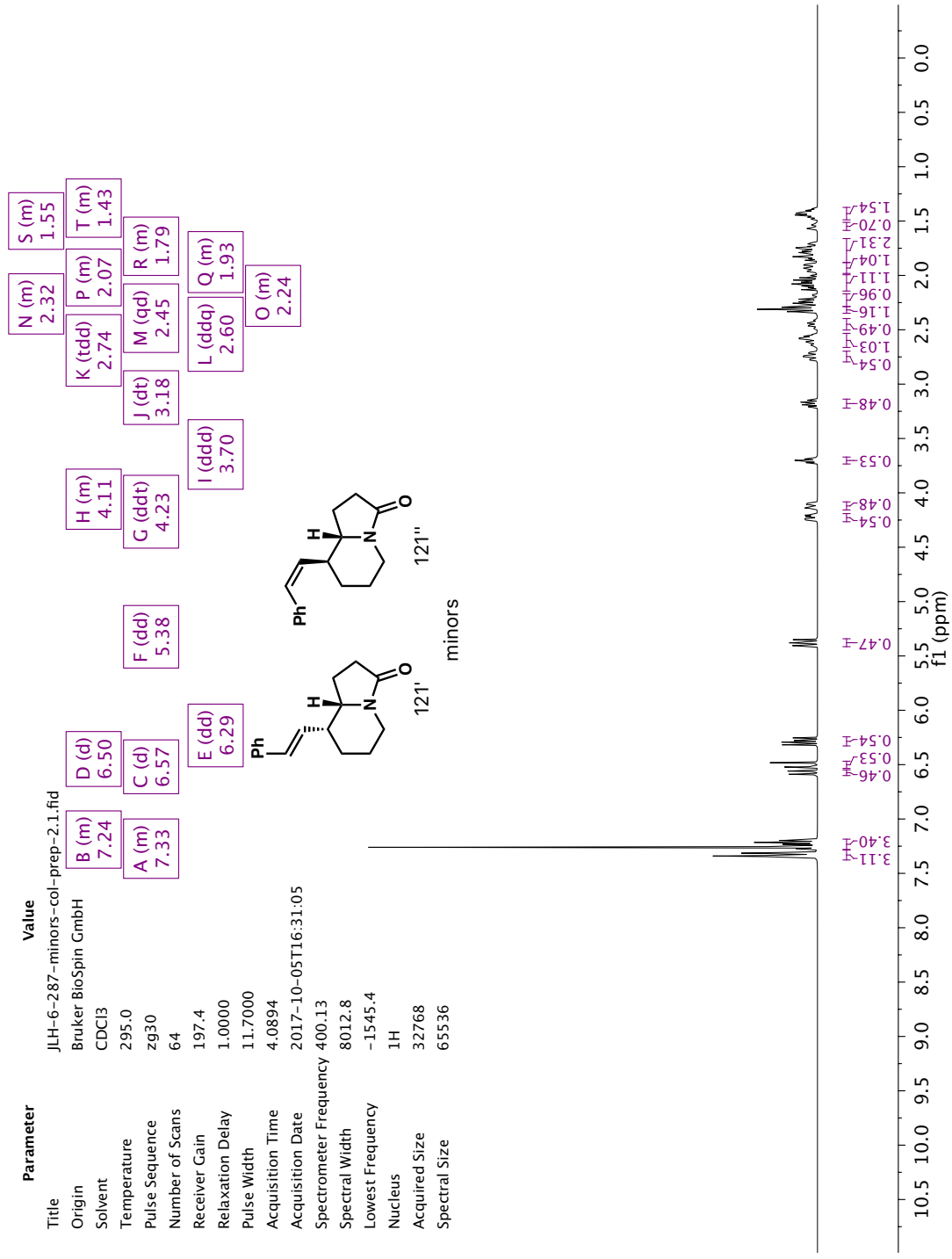
Parameter
Value
Title
JLH-6-287-minors-col-prep-2.1.fid
Origin
Bruker BioSpin GmbH
Solvent
CDCl3
Temperature
295.0
Pulse Sequence
zg30
Number of Scans
64
Receiver Gain
197.4
Relaxation Delay
1.0000
Pulse Width
11.7000
Acquisition Time
4.0894
Acquisition Date
2017-10-05T16:31:05
Spectrometer Frequency
400.13
Spectral Width
8012.8
Lowest Frequency
-1545.4
Nucleus
1H
Acquired Size
32768
Spectral Size
65536
B (m) 7.24
A (m) 7.33
D (d) 6.50
C (d) 6.57
E (dd) 6.29
F (dd) 5.38
H (m) 4.11
G (ddt) 4.23
I (ddd) 3.70
J (dt) 3.18
K (tdd) 2.74
M (qd) 2.45
L (ddq) 2.60
N (m) 2.32
P (m) 2.07
R (m) 1.79
Q (m) 1.93
O (m) 2.24
S (m) 1.55
T (m) 1.43
Ph
121'
121''
minors
3.11
3.40
0.46
0.53
0.54
0.47
0.54
0.48
0.53
0.48
0.54
1.03
0.49
1.16
0.96
1.11
1.04
2.31
0.70
1.54
f1 (ppm)

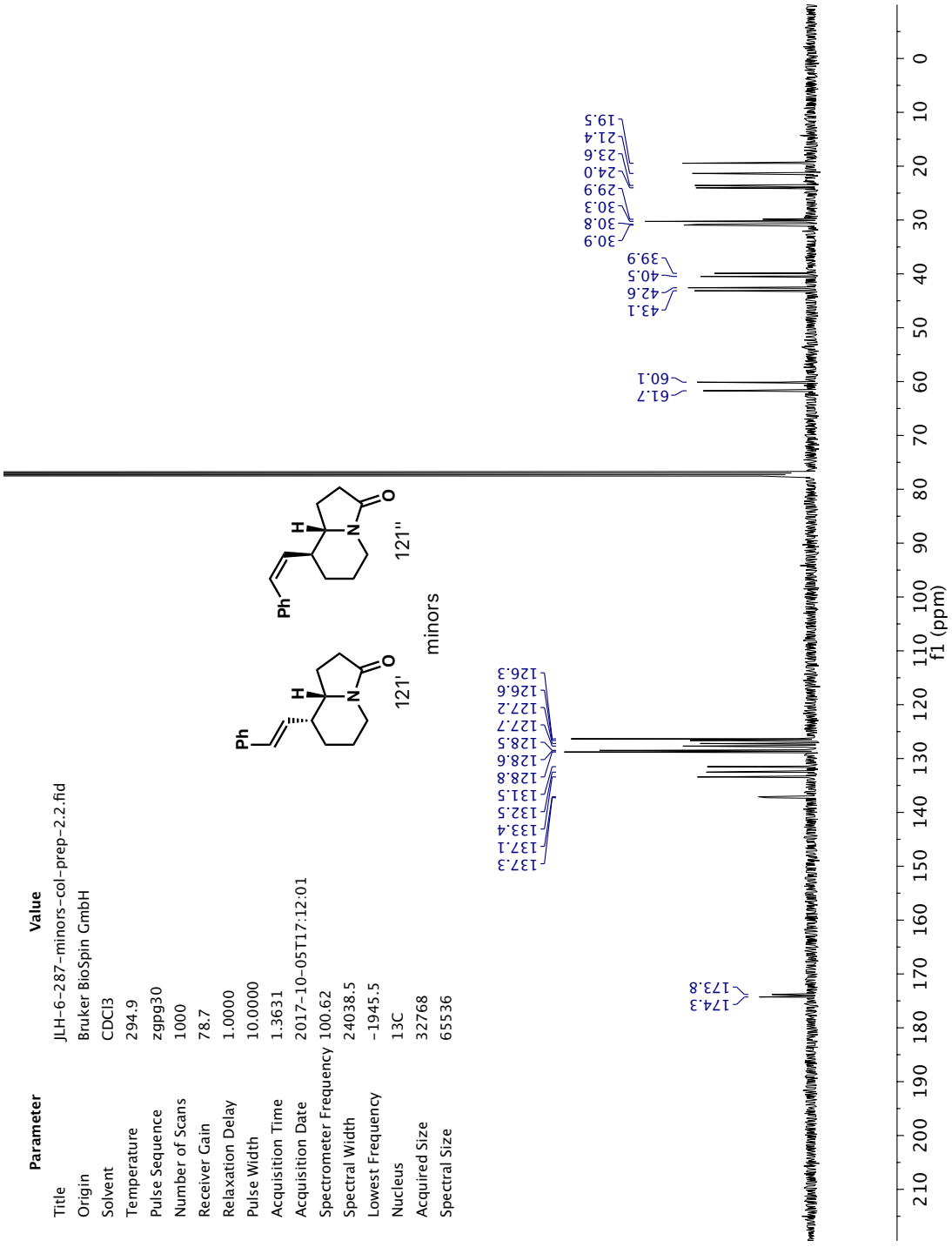
Parameter
Value
Title
JLH-6-287-minors-col-prep-2.2.fid
Origin
Bruker BioSpin GmbH
Solvent
CDCl3
Temperature
294.9
Pulse Sequence
zgpg30
Number of Scans
1000
Receiver Gain
78.7
Relaxation Delay
1.0000
Pulse Width
10.0000
Acquisition Time
1.3631
Acquisition Date
2017-10-05T17:12:01
Spectrometer Frequency
100.62
Spectral Width
24038.5
Lowest Frequency
-1945.5
Nucleus
13C
Acquired Size
32768
Spectral Size
65536
Ph
H
N
O
121'
minors
Ph
H
N
O
121''
174.3
173.8
137.3
137.1
133.4
132.5
131.5
128.8
128.6
128.5
127.7
127.2
126.6
126.3
61.7
60.1
43.1
42.6
40.5
39.9
30.9
30.8
30.3
29.9
24.0
23.6
21.4
19.5
f1 (ppm)

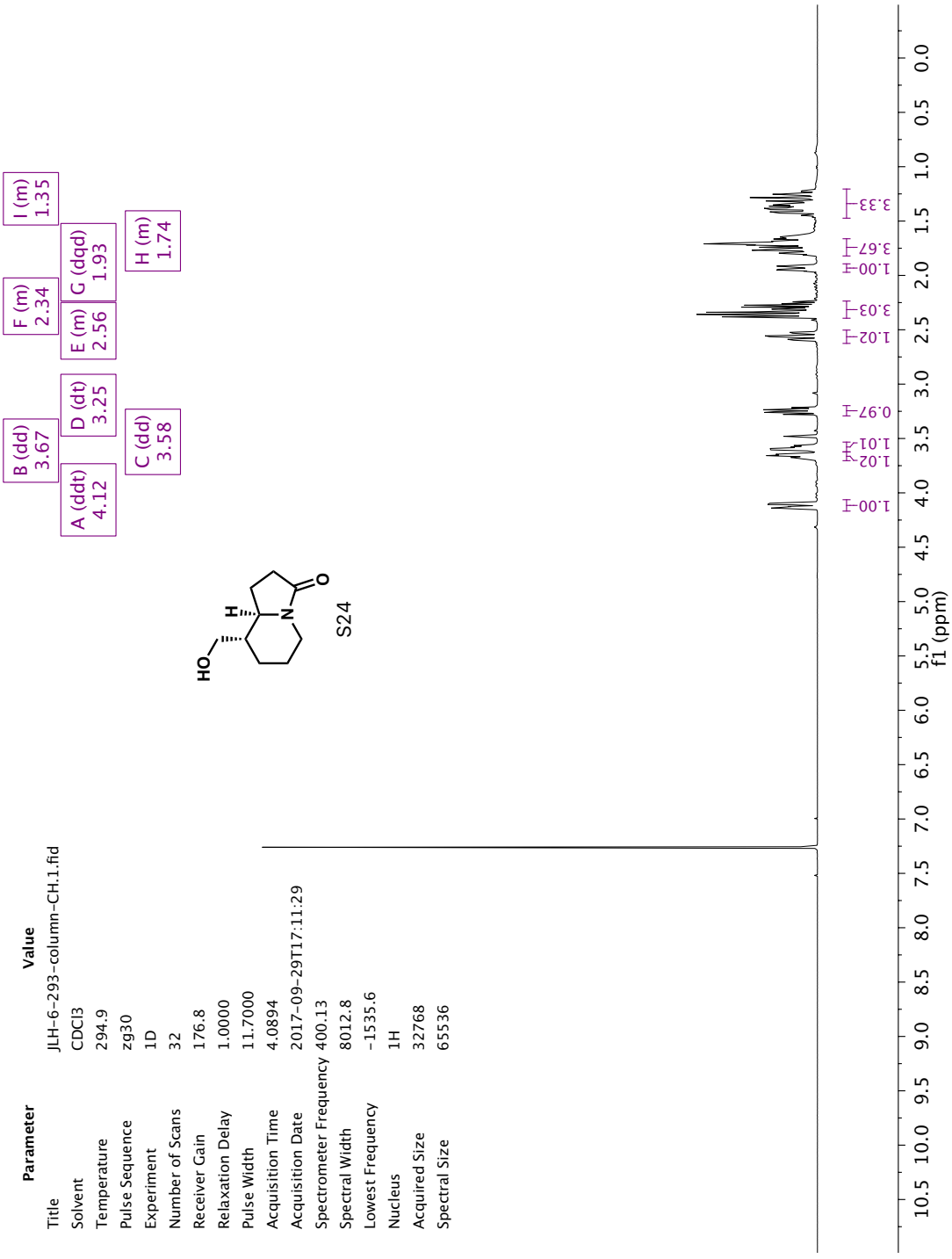

Parameter	Value
Title	JLH-6-293-column-CH.1.fid
Solvent	CDCl3
Temperature	294.9
Pulse Sequence	zg30
Experiment	1D
Number of Scans	32
Receiver Gain	176.8
Relaxation Delay	1.0000
Pulse Width	11.7000
Acquisition Time	4.0894
Acquisition Date	2017-09-29T17:11:29
Spectrometer Frequency	400.13
Spectral Width	8012.8
Lowest Frequency	-1535.6
Nucleus	1H
Acquired Size	32768
Spectral Size	65536

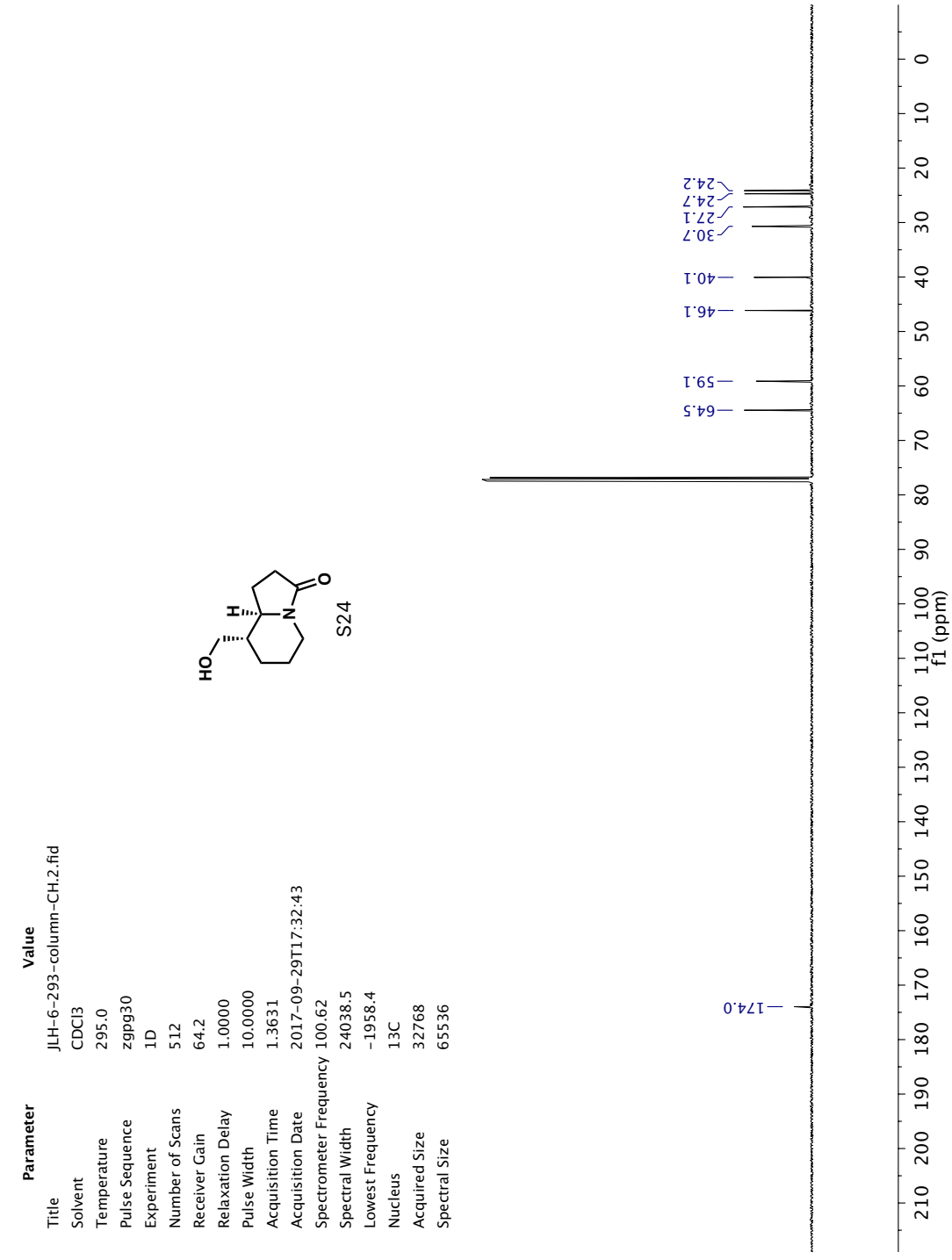
Parameter Value
Title JLH-6-293-column-CH.2.fid
Solvent CDCl3
Temperature 295.0
Pulse Sequence zgpg30
Experiment 1D
Number of Scans 512
Receiver Gain 64.2
Relaxation Delay 1.0000
Pulse Width 10.0000
Acquisition Time 1.3631
Acquisition Date 2017-09-29T17:32:43
Spectrometer Frequency 100.62
Spectral Width 24038.5
Lowest Frequency -1958.4
Nucleus 13C
Acquired Size 32768
Spectral Size 65536
HO
H
N
O
S24
174.0
64.5
59.1
46.1
40.1
30.7
27.1
24.7
24.2
f1 (ppm)

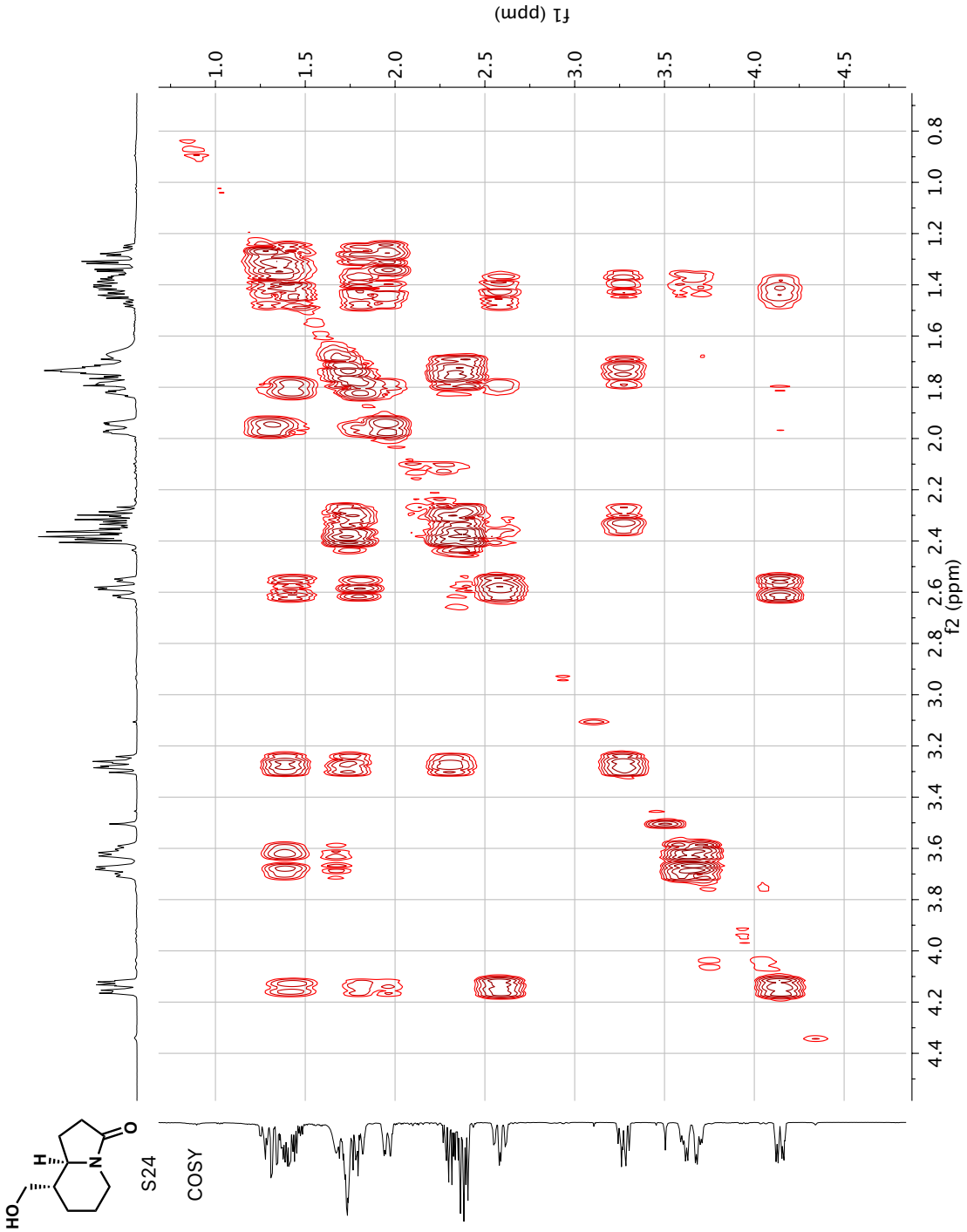
f1 (ppm)
1.0
1.5
2.0
2.5
3.0
3.5
4.0
4.5
f2 (ppm)
0.8
1.0
1.2
1.4
1.6
1.8
2.0
2.2
2.4
2.6
2.8
3.0
3.2
3.4
3.6
3.8
4.0
4.2
4.4
S24
COSY
HO
H
N
O

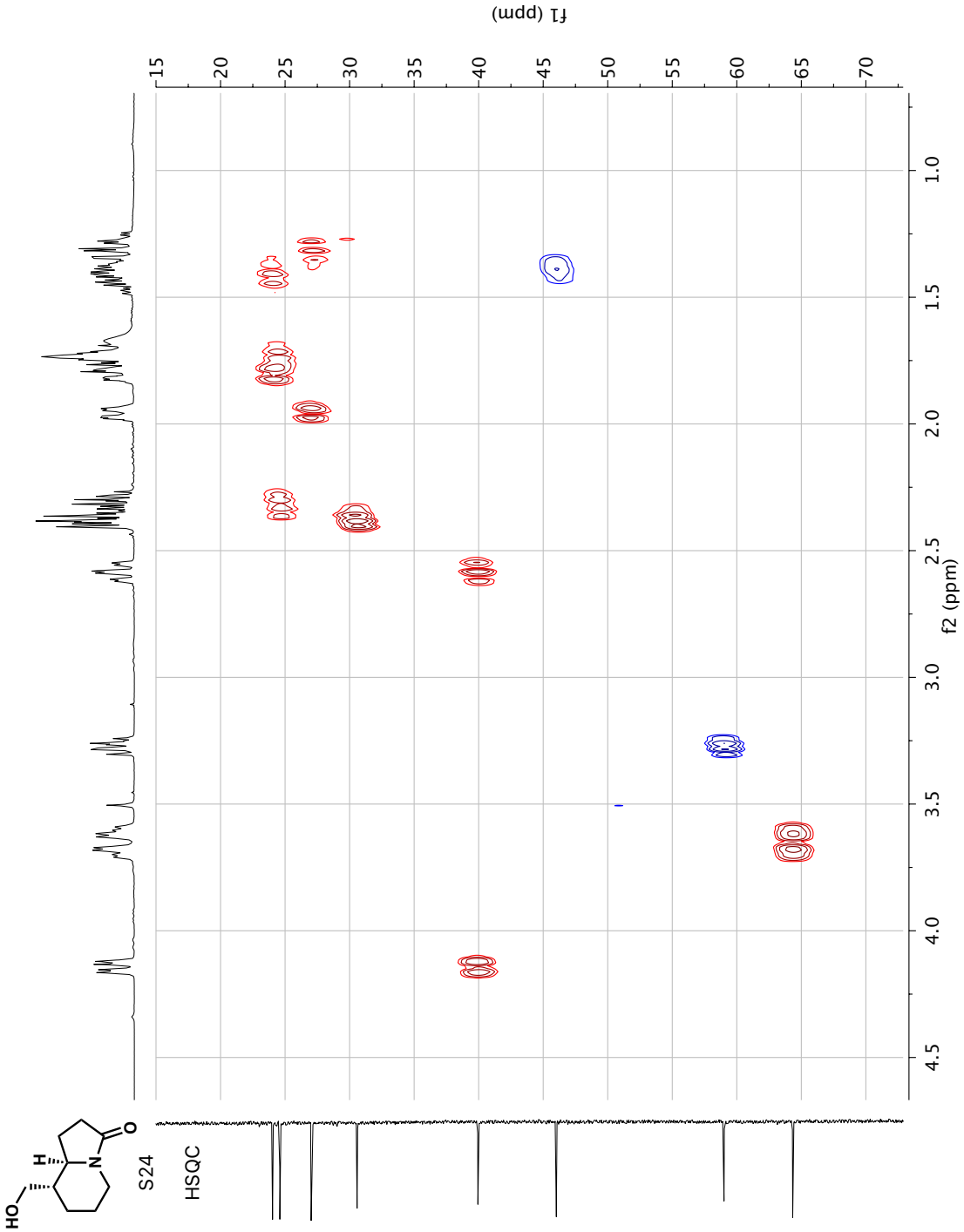
f1 (ppm)
15
20
25
30
35
40
45
50
55
60
65
70
f2 (ppm)
1.0
1.5
2.0
2.5
3.0
3.5
4.0
4.5
S24
HSQC
HO
H
N
O

Parameter	Value
Title	JLH-6-294-crude.1.fid
Solvent	CDCl3
Temperature	294.9
Pulse Sequence	zg30
Experiment	1D
Number of Scans	32
Receiver Gain	127.1
Relaxation Delay	1.0000
Pulse Width	11.7000
Acquisition Time	4.0894
Acquisition Date	2017-09-30T15:41:30
Spectrometer Frequency	400.13
Spectral Width	8012.8
Lowest Frequency	-1569.5
Nucleus	1H
Acquired Size	32768
Spectral Size	65536

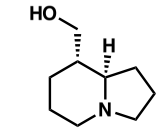

122

(+)-tashiromine

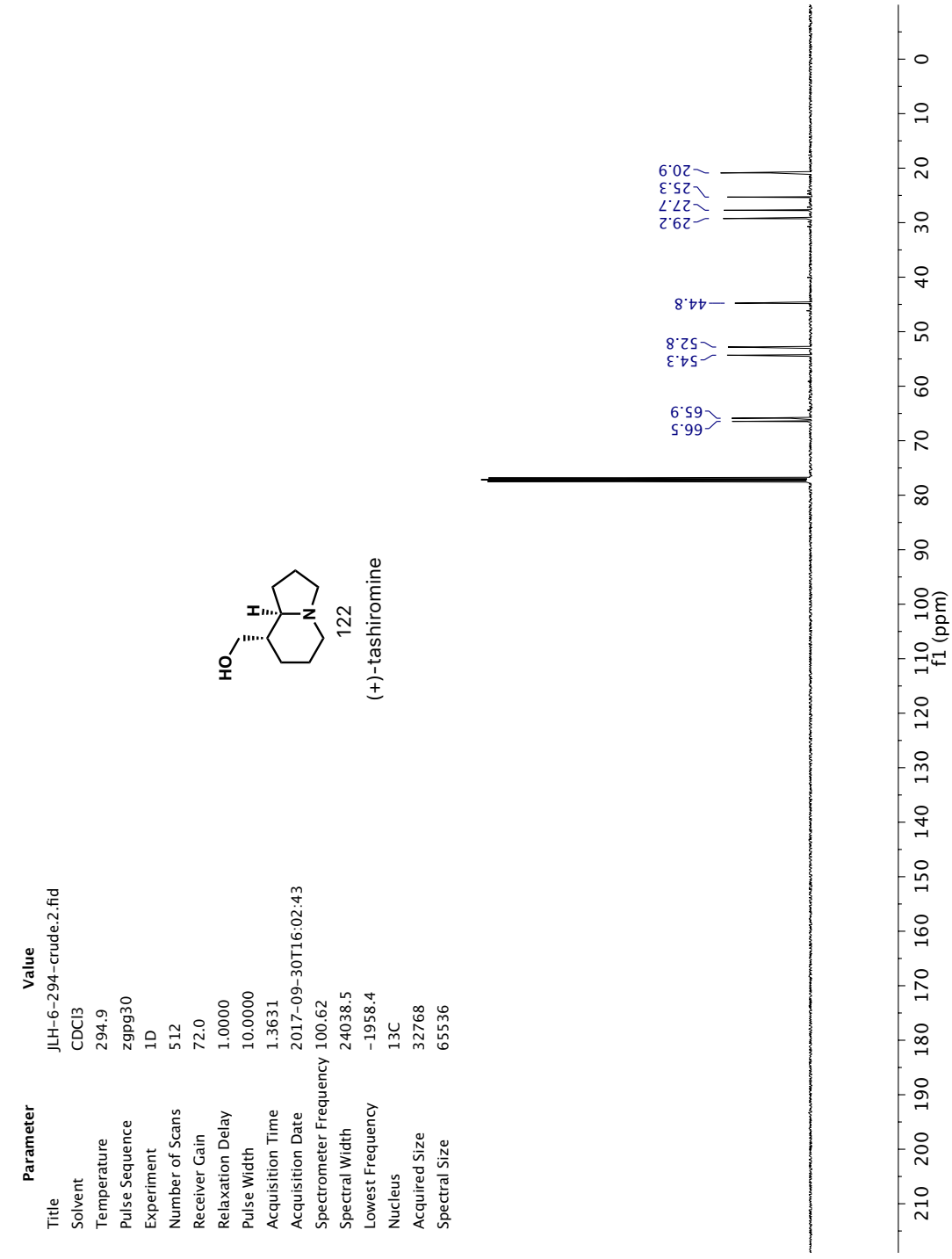
Parameter Value
Title JLH-6-294-crude.2.fid
Solvent CDCl3
Temperature 294.9
Pulse Sequence zgpg30
Experiment 1D
Number of Scans 512
Receiver Gain 72.0
Relaxation Delay 1.0000
Pulse Width 10.0000
Acquisition Time 1.3631
Acquisition Date 2017-09-30T16:02:43
Spectrometer Frequency 100.62
Spectral Width 24038.5
Lowest Frequency -1958.4
Nucleus 13C
Acquired Size 32768
Spectral Size 65536
HO
H
N
122
(+)-tashiromine
66.5
65.9
54.3
52.8
44.8
29.2
27.7
25.3
20.9
210 200 190 180 170 160 150 140 130 120 110 100 90 80 70 60 50 40 30 20 10 0
f1 (ppm)

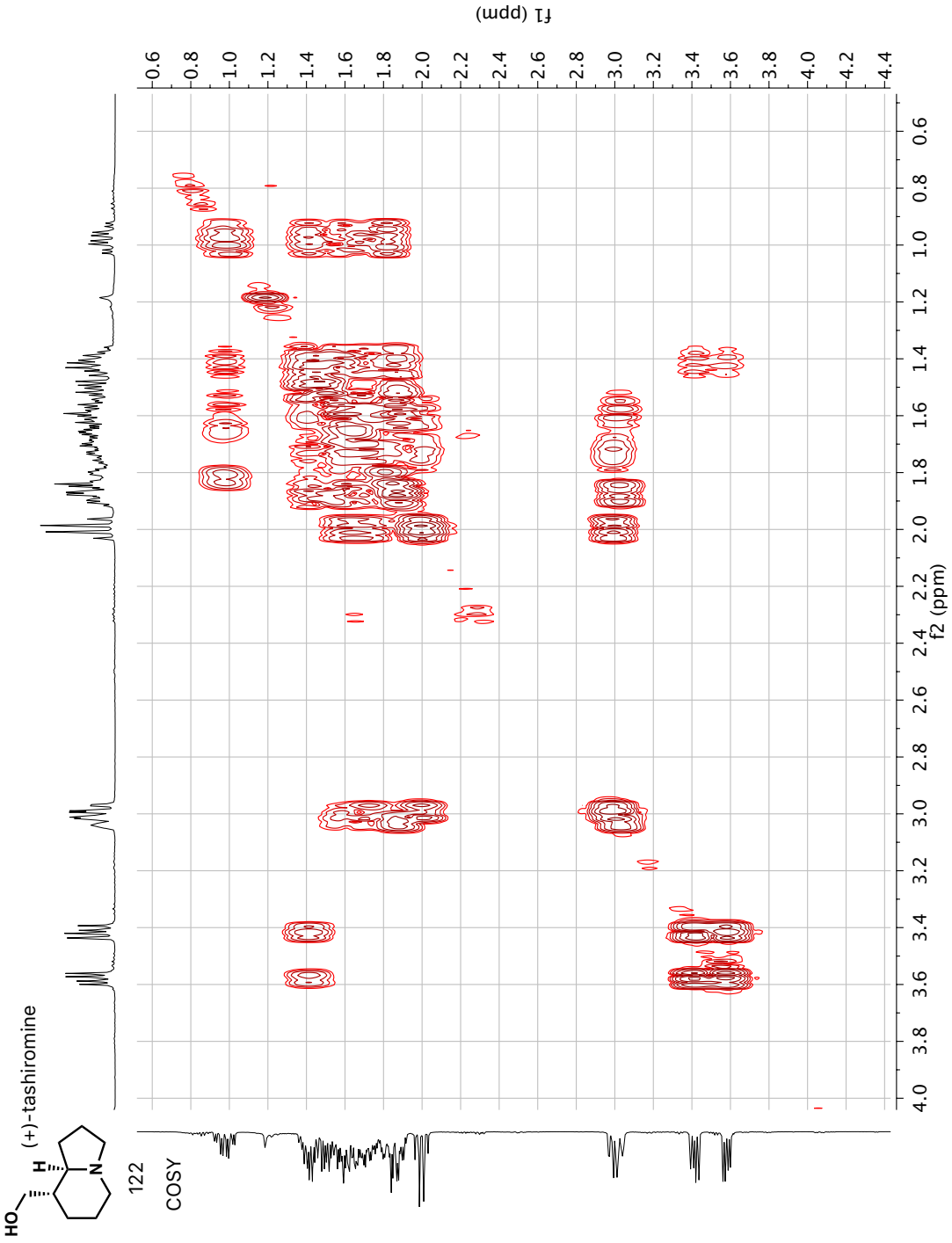
(+)-tashiromine
HO
H
N
122
COSY
f1 (ppm)
f2 (ppm)

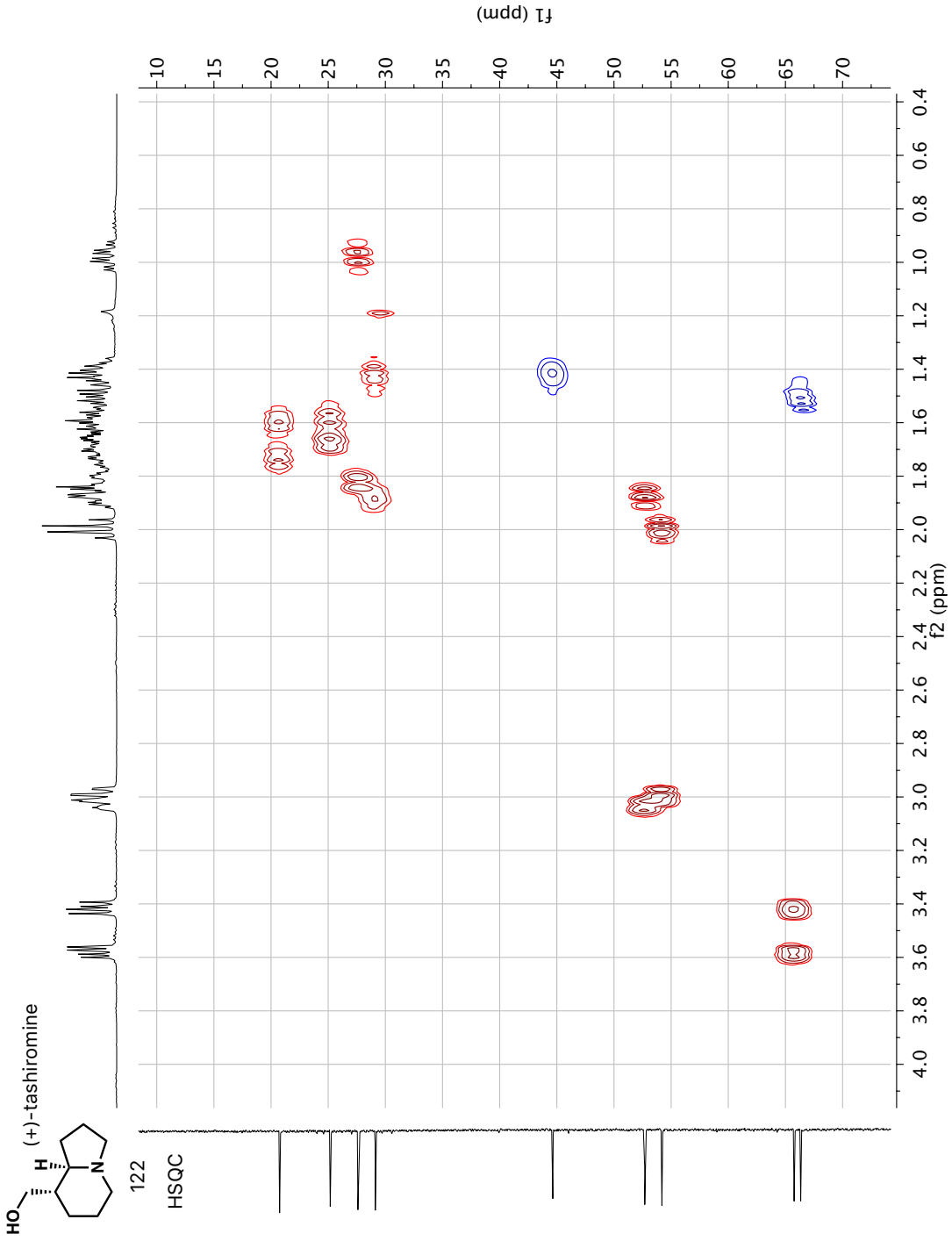
(+)-tashiromine
HO
H
N
122
HSQC
f1 (ppm)
f2 (ppm)

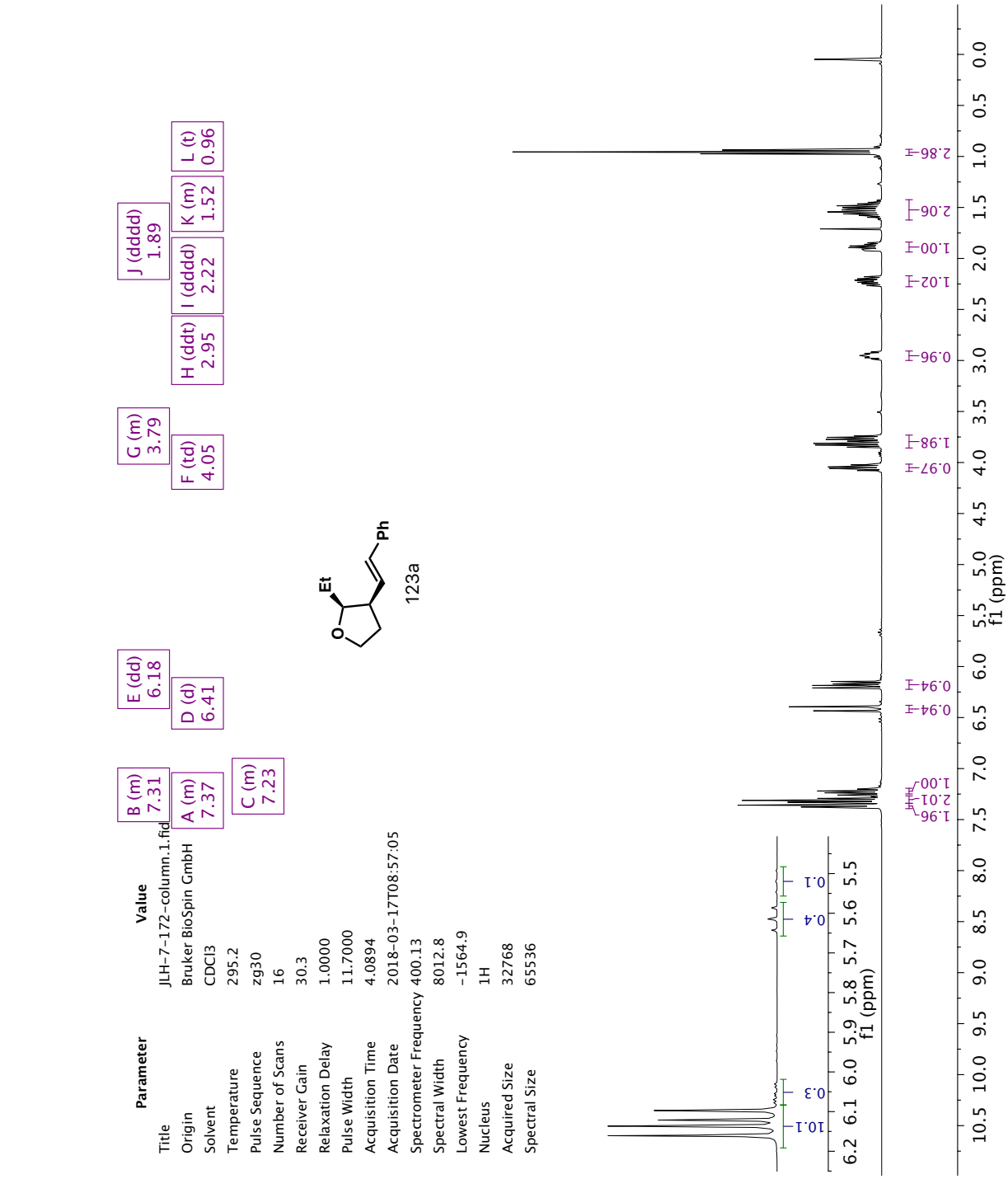
Parameter
Value
Title
JLH-7-172-column.1.fid
Origin
Bruker BioSpin GmbH
Solvent
CDCl3
Temperature
295.2
Pulse Sequence
zg30
Number of Scans
16
Receiver Gain
30.3
Relaxation Delay
1.0000
Pulse Width
11.7000
Acquisition Time
4.0894
Acquisition Date
2018-03-17T08:57:05
Spectrometer Frequency
400.13
Spectral Width
8012.8
Lowest Frequency
-1564.9
Nucleus
1H
Acquired Size
32768
Spectral Size
65536
B (m) 7.31
A (m) 7.37
C (m) 7.23
E (dd) 6.18
D (d) 6.41
G (m) 3.79
F (td) 4.05
J (dddd) 1.89
H (ddt) 2.95
I (dddd) 2.22
K (m) 1.52
L (t) 0.96
Et
Ph
O
123a
f1 (ppm)

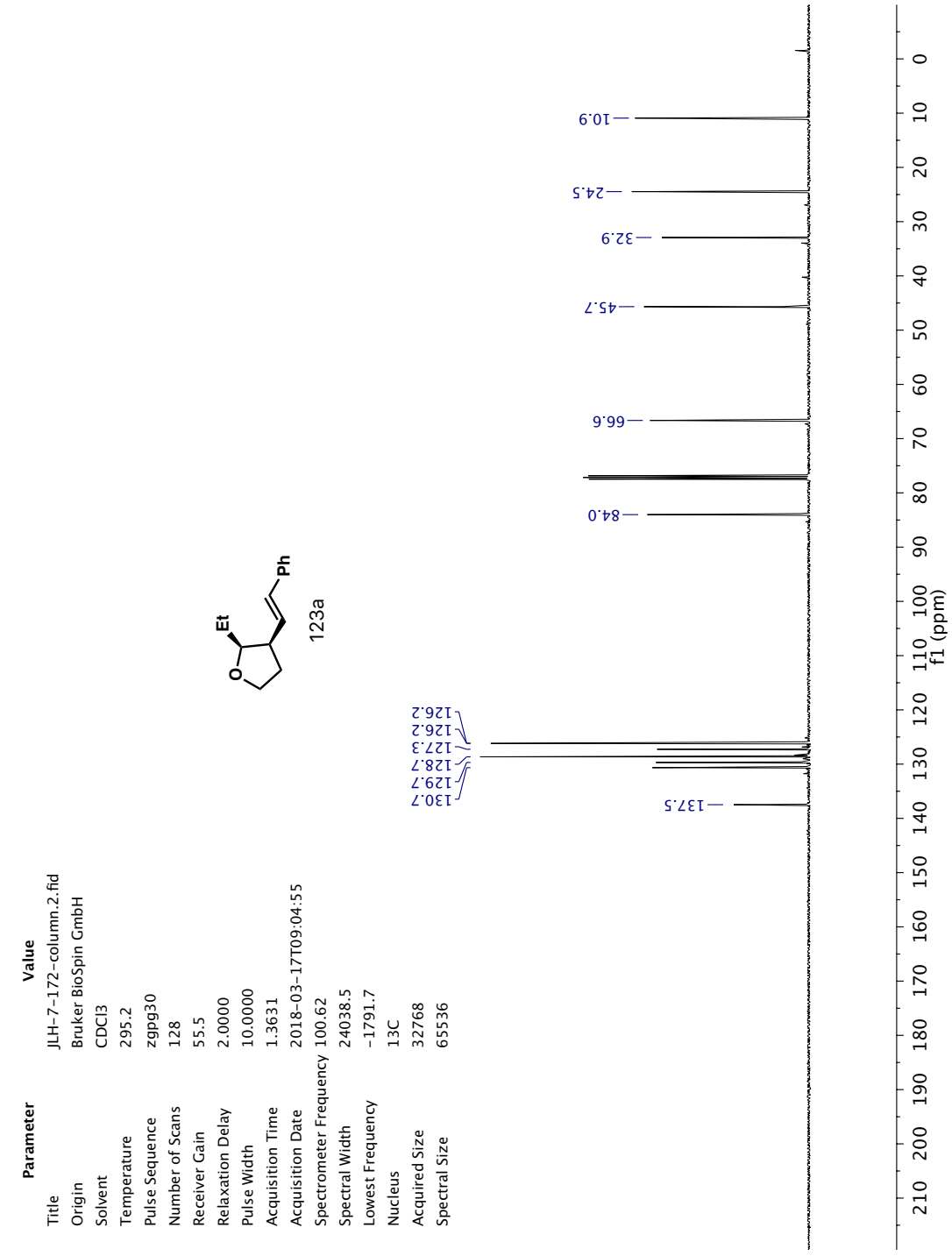
Parameter Value
Title JLH-7-172-column.2.fid
Origin Bruker BioSpin GmbH
Solvent CDCl3
Temperature 295.2
Pulse Sequence zgpg30
Number of Scans 128
Receiver Gain 55.5
Relaxation Delay 2.0000
Pulse Width 10.0000
Acquisition Time 1.3631
Acquisition Date 2018-03-17T09:04:55
Spectrometer Frequency 100.62
Spectral Width 24038.5
Lowest Frequency -1791.7
Nucleus 13C
Acquired Size 32768
Spectral Size 65536
Et
O
Ph
123a
10.9
24.5
32.9
45.7
66.6
84.0
126.2
126.2
127.3
128.7
129.7
130.7
137.5
f1 (ppm)

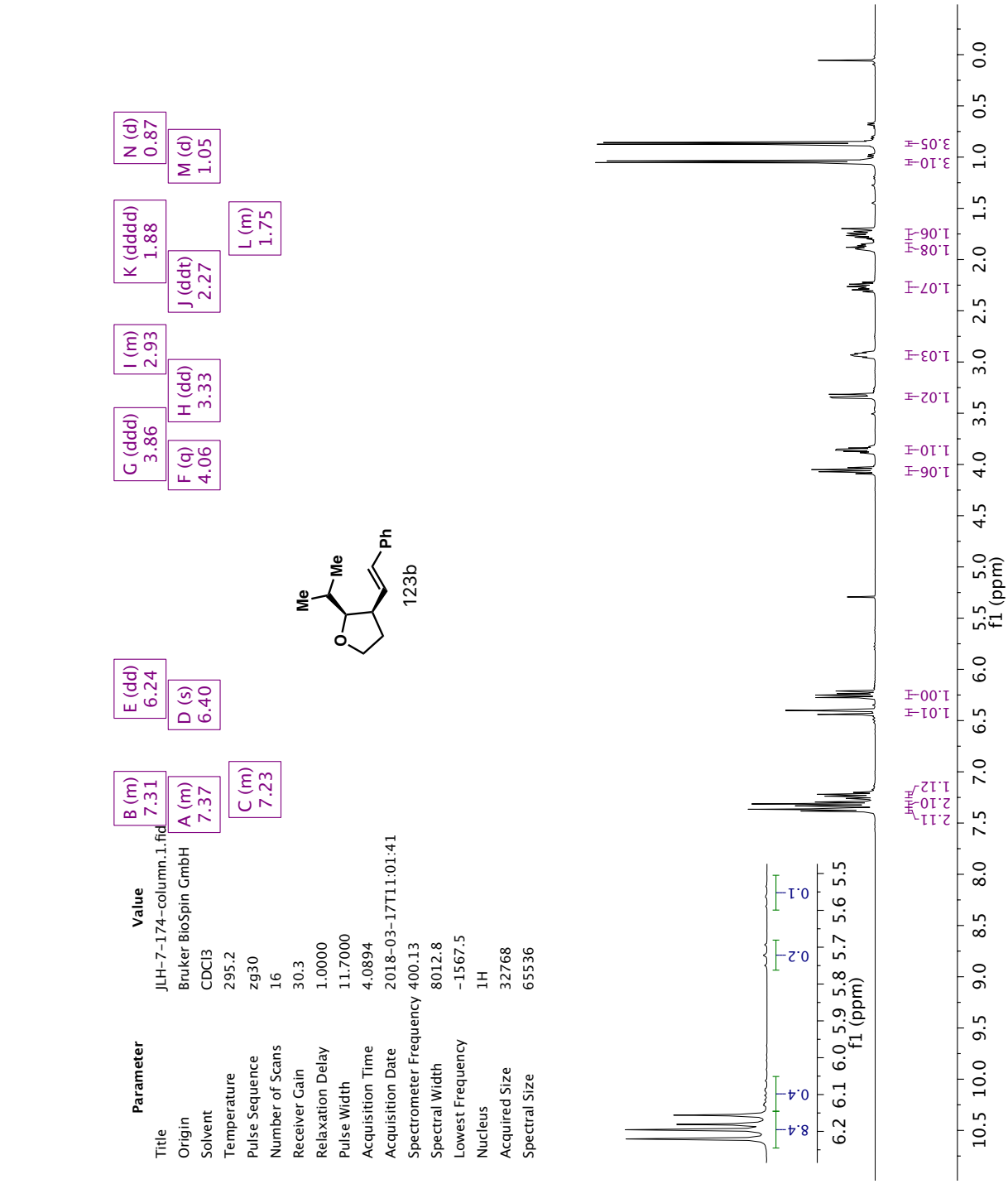
Parameter
Value
Title
JLH-7-174-column.1.fid
Origin
Bruker BioSpin GmbH
Solvent
CDCl3
Temperature
295.2
Pulse Sequence
zg30
Number of Scans
16
Receiver Gain
30.3
Relaxation Delay
1.0000
Pulse Width
11.7000
Acquisition Time
4.0894
Acquisition Date
2018-03-17T11:01:41
Spectrometer Frequency
400.13
Spectral Width
8012.8
Lowest Frequency
-1567.5
Nucleus
1H
Acquired Size
32768
Spectral Size
65536
B (m) 7.31
A (m) 7.37
C (m) 7.23
E (dd) 6.24
D (s) 6.40
G (ddd) 3.86
F (q) 4.06
H (dd) 3.33
I (m) 2.93
J (ddt) 2.27
K (dddd) 1.88
L (m) 1.75
M (d) 1.05
N (d) 0.87
Me
Me
O
Ph
123b
f1 (ppm)

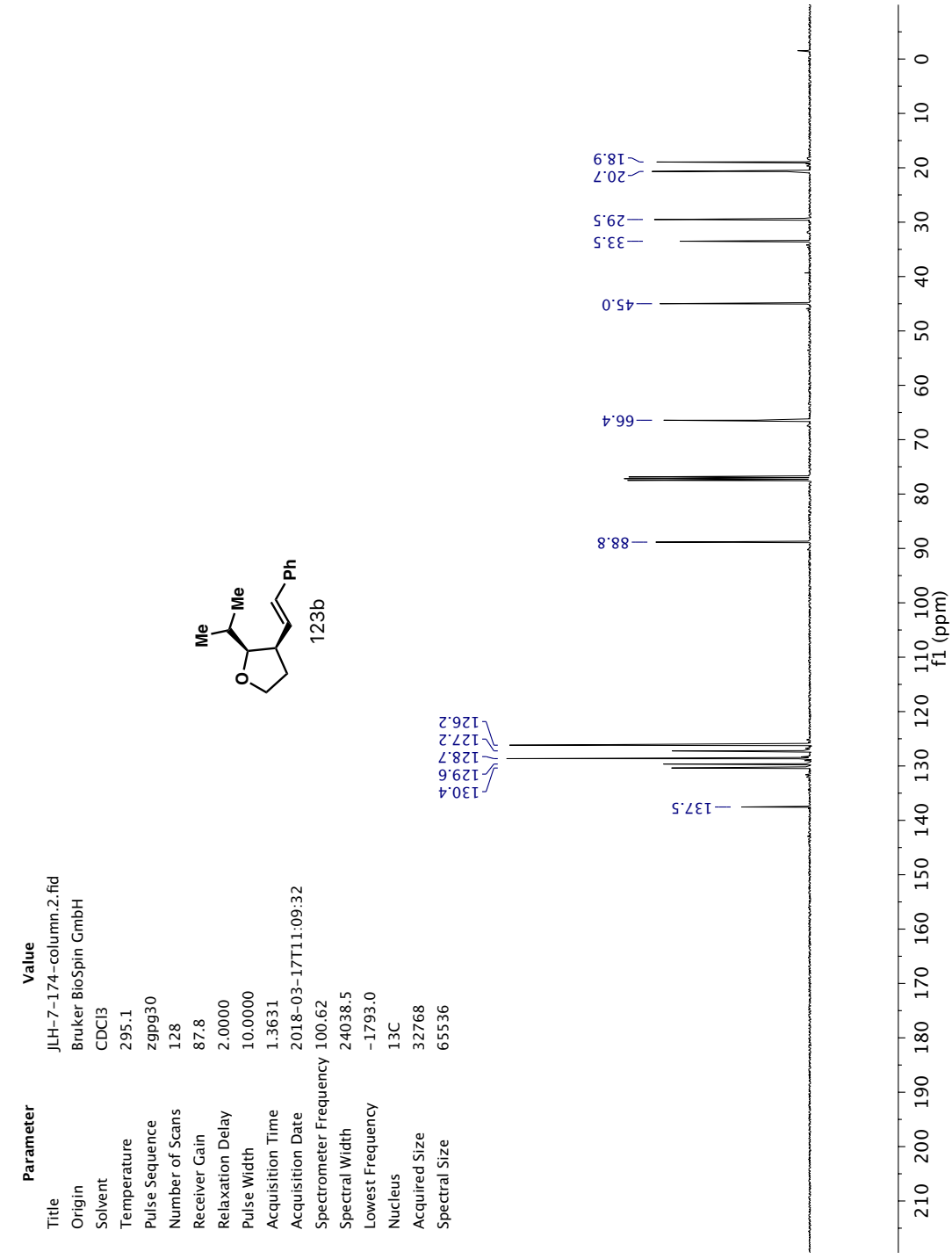
Parameter Value
Title JLH-7-174-column.2.fid
Origin Bruker BioSpin GmbH
Solvent CDCl3
Temperature 295.1
Pulse Sequence zgpg30
Number of Scans 128
Receiver Gain 87.8
Relaxation Delay 2.0000
Pulse Width 10.0000
Acquisition Time 1.3631
Acquisition Date 2018-03-17T11:09:32
Spectrometer Frequency 100.62
Spectral Width 24038.5
Lowest Frequency -1793.0
Nucleus 13C
Acquired Size 32768
Spectral Size 65536
Me
Me
Ph
O
123b
18.9
20.7
29.5
33.5
45.0
66.4
88.8
126.2
127.2
128.7
129.6
130.4
137.5
f1 (ppm)

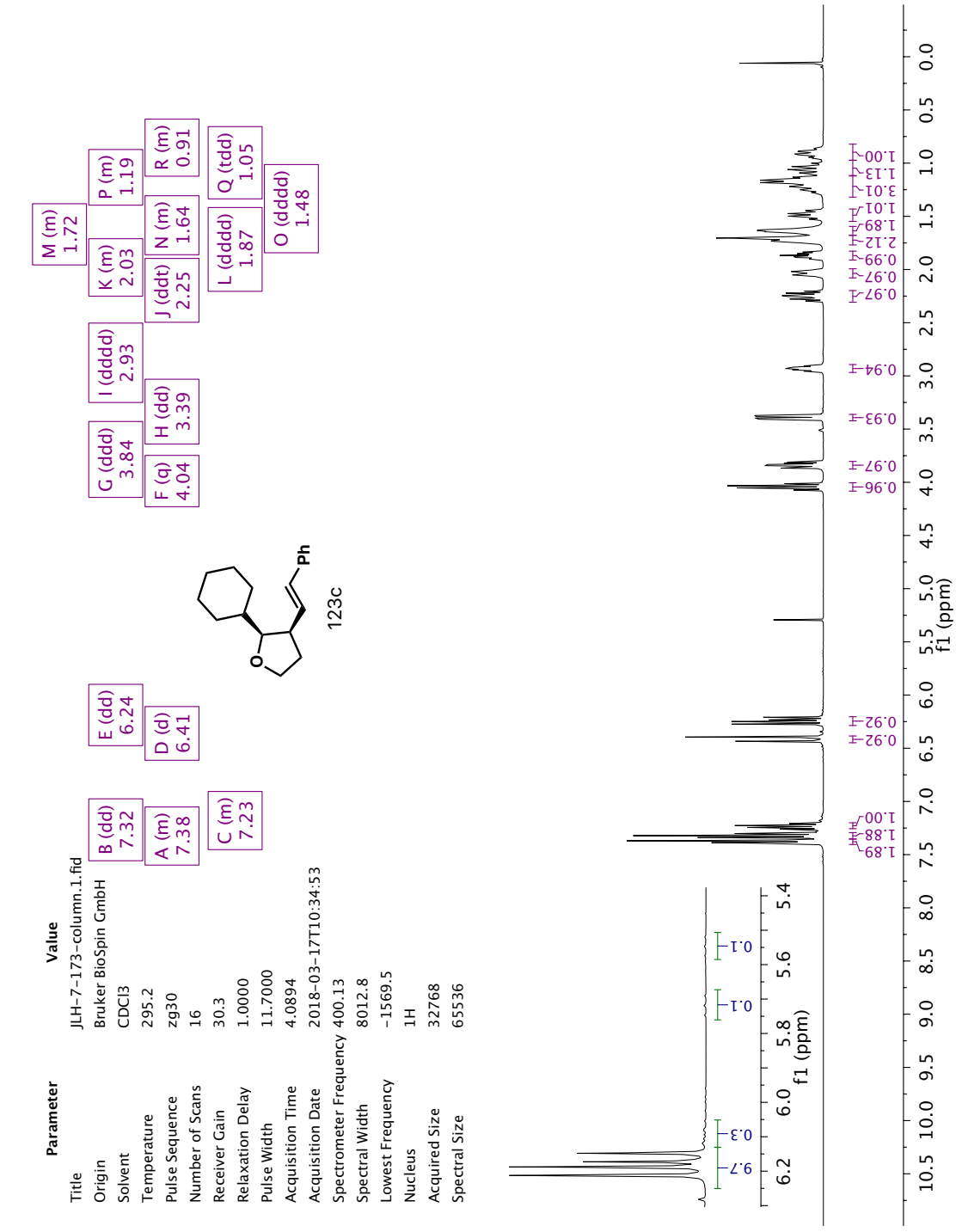
Parameter
Value
Title JLH-7-173-column.1.fid
Origin Bruker BioSpin GmbH
Solvent CDCl3
Temperature 295.2
Pulse Sequence zg30
Number of Scans 16
Receiver Gain 30.3
Relaxation Delay 1.0000
Pulse Width 11.7000
Acquisition Time 4.0894
Acquisition Date 2018-03-17T10:34:53
Spectrometer Frequency 400.13
Spectral Width 8012.8
Lowest Frequency -1569.5
Nucleus 1H
Acquired Size 32768
Spectral Size 65536
B (dd) 7.32
A (m) 7.38
C (m) 7.23
E (dd) 6.24
D (d) 6.41
G (ddd) 3.84
F (q) 4.04
H (dd) 3.39
I (dddd) 2.93
J (ddt) 2.25
K (m) 2.03
N (m) 1.64
M (m) 1.72
L (dddd) 1.87
P (m) 1.19
R (m) 0.91
Q (tdd) 1.05
O (dddd) 1.48
Ph
O
123c
f1 (ppm)

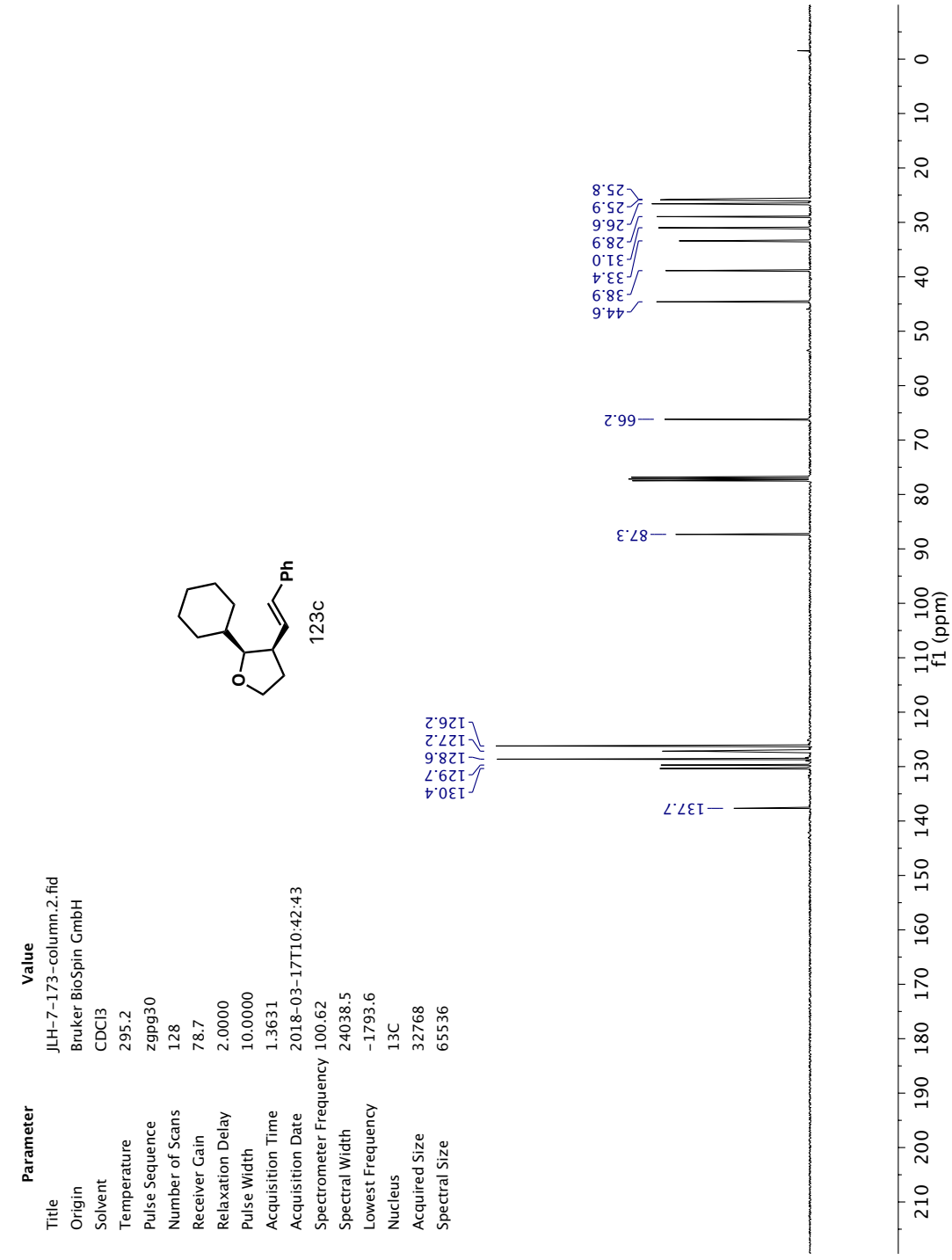
Parameter Value
Title JLH-7-173-column.2.fid
Origin Bruker BioSpin GmbH
Solvent CDCl3
Temperature 295.2
Pulse Sequence zgpg30
Number of Scans 128
Receiver Gain 78.7
Relaxation Delay 2.0000
Pulse Width 10.0000
Acquisition Time 1.3631
Acquisition Date 2018-03-17T10:42:43
Spectrometer Frequency 100.62
Spectral Width 24038.5
Lowest Frequency -1793.6
Nucleus 13C
Acquired Size 32768
Spectral Size 65536
Ph
O
123c
137.7
130.4
129.7
128.6
127.2
126.2
87.3
66.2
44.6
38.9
33.4
31.0
28.9
26.6
25.9
25.8
f1 (ppm)

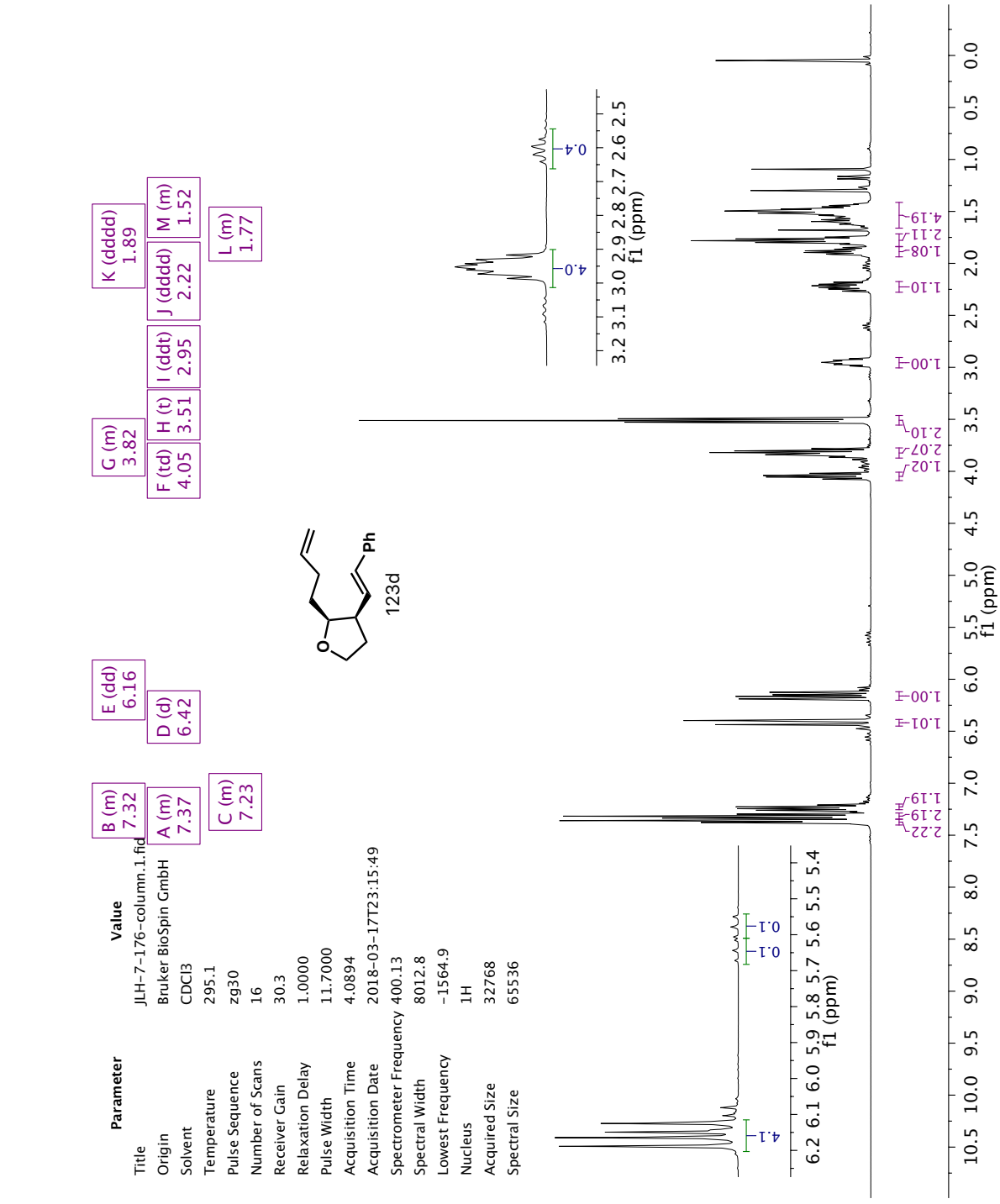
Parameter
Value
Title JLH-7-176-column.1.fid
Origin Bruker BioSpin GmbH
Solvent CDCl3
Temperature 295.1
Pulse Sequence zg30
Number of Scans 16
Receiver Gain 30.3
Relaxation Delay 1.0000
Pulse Width 11.7000
Acquisition Time 4.0894
Acquisition Date 2018-03-17T23:15:49
Spectrometer Frequency 400.13
Spectral Width 8012.8
Lowest Frequency -1564.9
Nucleus 1H
Acquired Size 32768
Spectral Size 65536
B (m) 7.32
A (m) 7.37
C (m) 7.23
E (dd) 6.16
D (d) 6.42
G (m) 3.82
F (td) 4.05
H (t) 3.51
I (ddt) 2.95
J (dddd) 2.22
K (ddddd) 1.89
L (m) 1.77
M (m) 1.52
O
Ph
123d
f1 (ppm)

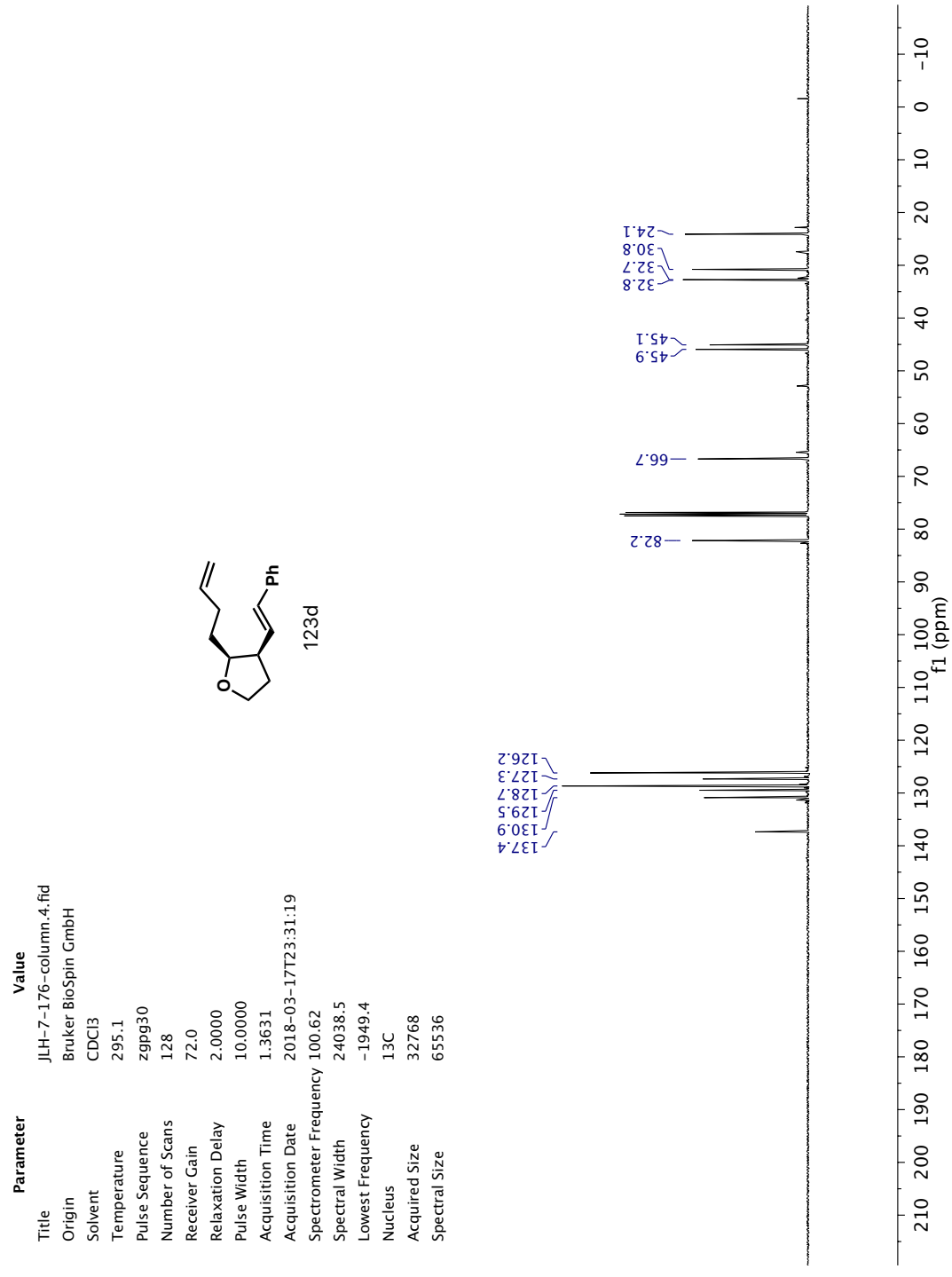
Parameter Value
Title JLH-7-176-column.4.fid
Origin Bruker BioSpin GmbH
Solvent CDCl3
Temperature 295.1
Pulse Sequence zgpg30
Number of Scans 128
Receiver Gain 72.0
Relaxation Delay 2.0000
Pulse Width 10.0000
Acquisition Time 1.3631
Acquisition Date 2018-03-17T23:31:19
Spectrometer Frequency 100.62
Spectral Width 24038.5
Lowest Frequency -1949.4
Nucleus 13C
Acquired Size 32768
Spectral Size 65536
Ph
O
123d
137.4
130.9
129.5
128.7
127.3
126.2
82.2
66.7
45.9
45.1
32.8
32.7
30.8
24.1
f1 (ppm)

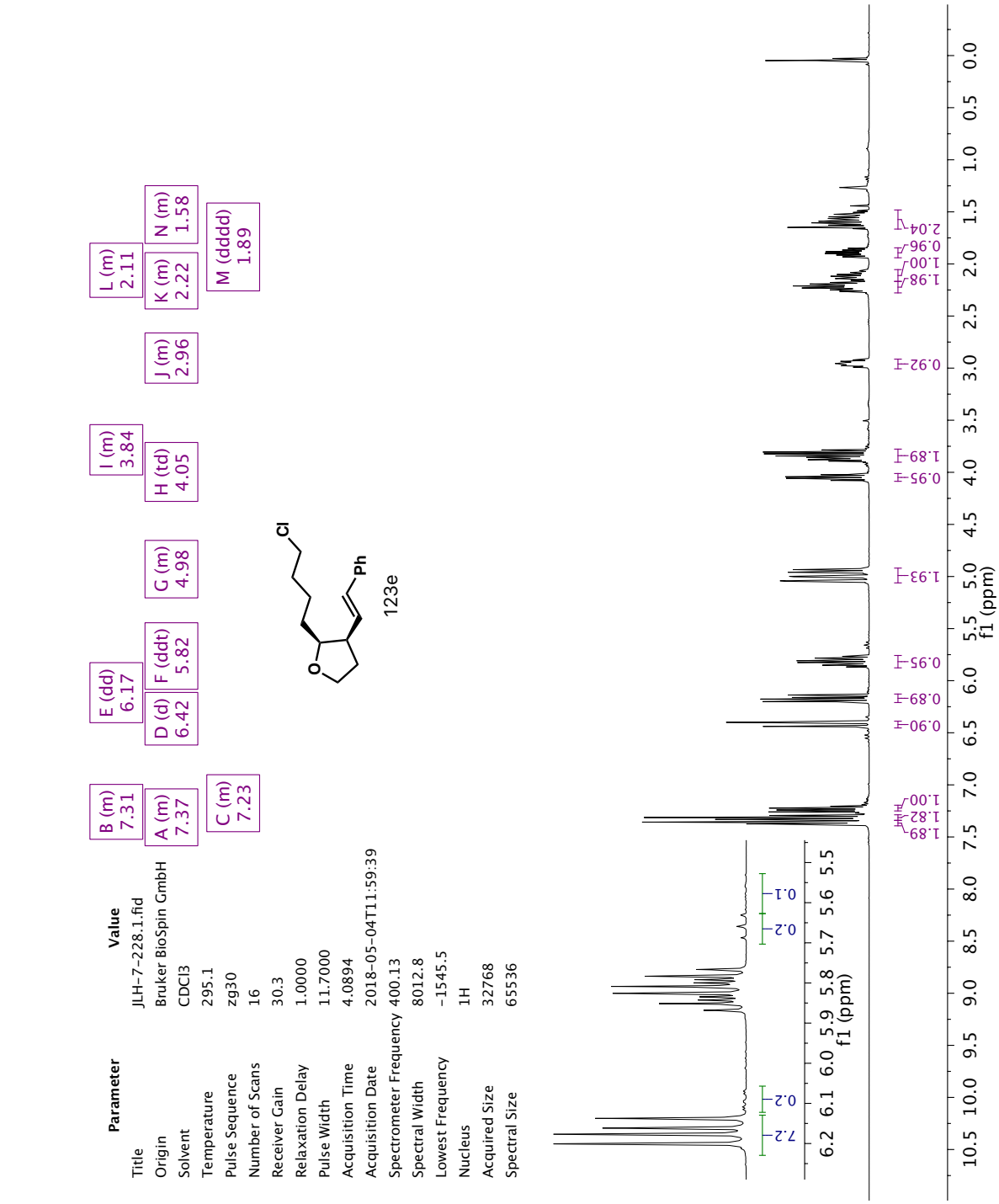

Parameter	Value
Title	JLH-7-228.1.fid
Origin	Bruker BioSpin GmbH
Solvent	CDCl3
Temperature	295.1
Pulse Sequence	zg30
Number of Scans	16
Receiver Gain	30.3
Relaxation Delay	1.0000
Pulse Width	11.7000
Acquisition Time	4.0894
Acquisition Date	2018-05-04T11:59:39
Spectrometer Frequency	400.13
Spectral Width	8012.8
Lowest Frequency	-1545.5
Nucleus	1H
Acquired Size	32768
Spectral Size	65536

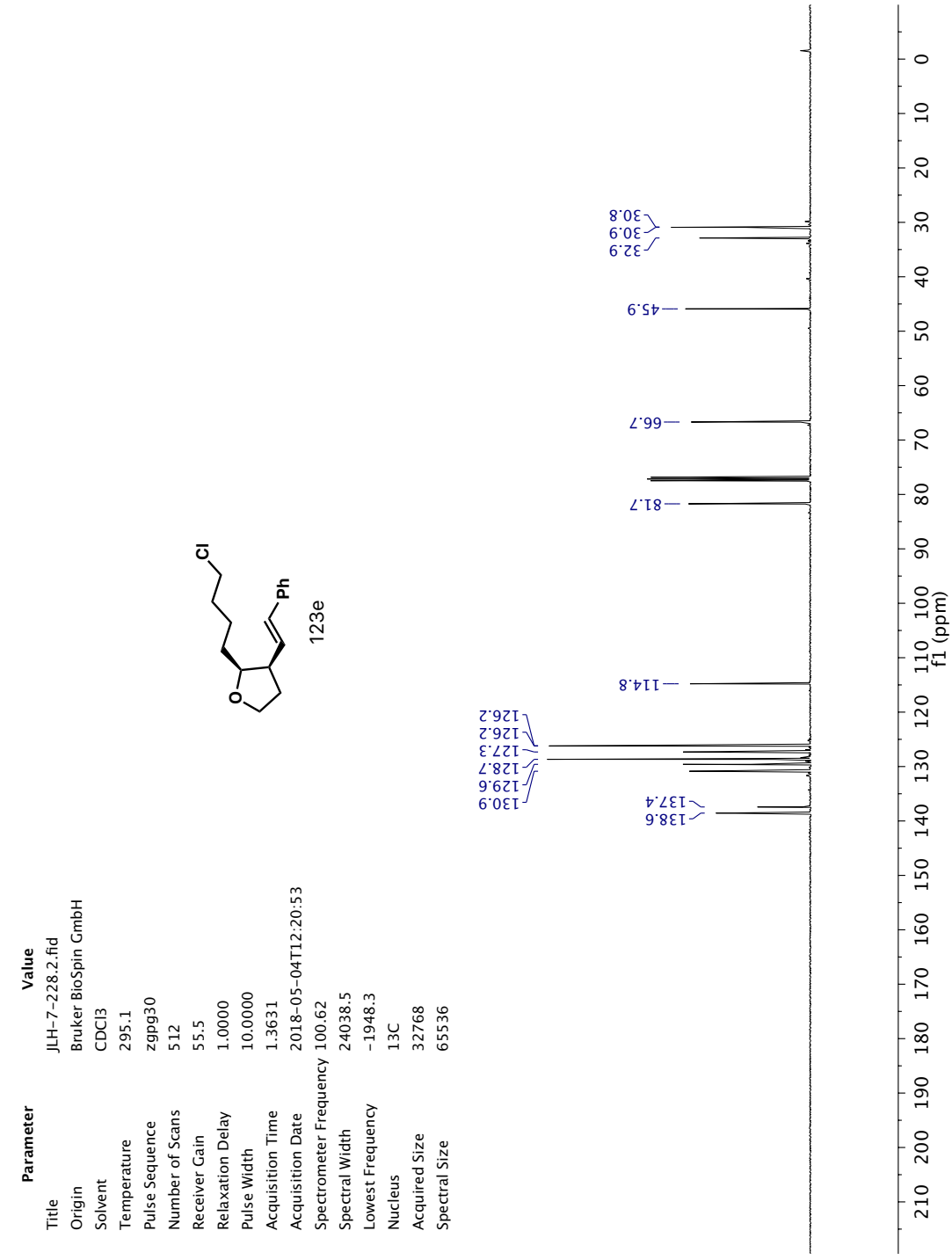

Parameter	Value
Title	JLH-7-228.2.fid
Origin	Bruker BioSpin GmbH
Solvent	CDCl3
Temperature	295.1
Pulse Sequence	zgpg30
Number of Scans	512
Receiver Gain	55.5
Relaxation Delay	1.0000
Pulse Width	10.0000
Acquisition Time	1.3631
Acquisition Date	2018-05-04T12:20:53
Spectrometer Frequency	100.62
Spectral Width	24038.5
Lowest Frequency	-1948.3
Nucleus	13C
Acquired Size	32768
Spectral Size	65536

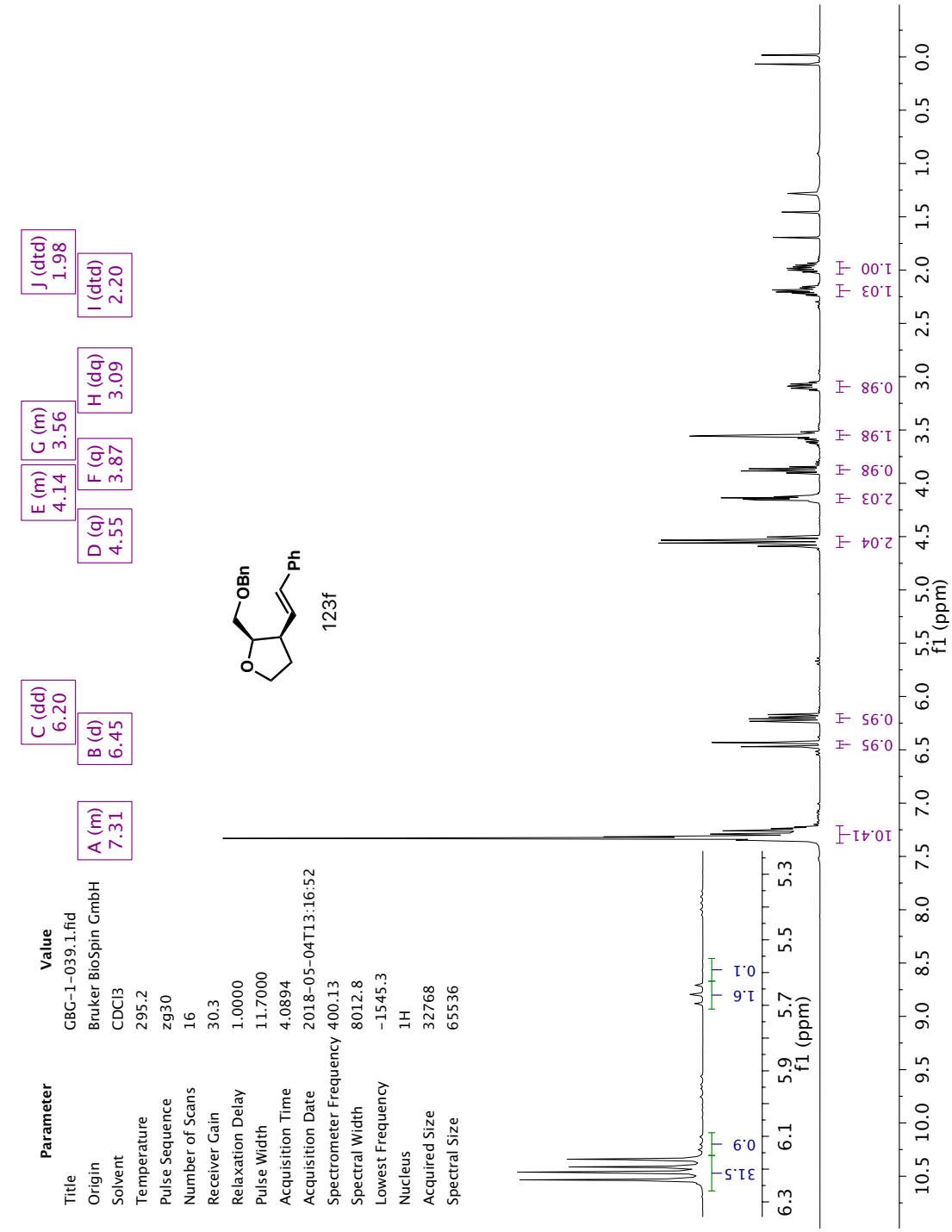
Parameter
Value
Title
GBG-1-039.1.fid
Origin
Bruker BioSpin GmbH
Solvent
CDCl3
Temperature
295.2
Pulse Sequence
zg30
Number of Scans
16
Receiver Gain
30.3
Relaxation Delay
1.0000
Pulse Width
11.7000
Acquisition Time
4.0894
Acquisition Date
2018-05-04T13:16:52
Spectrometer Frequency
400.13
Spectral Width
8012.8
Lowest Frequency
-1545.3
Nucleus
1H
Acquired Size
32768
Spectral Size
65536
A (m) 7.31
B (d) 6.45
C (dd) 6.20
D (q) 4.55
E (m) 4.14
F (q) 3.87
G (m) 3.56
H (dq) 3.09
I (dtd) 2.20
J (dtd) 1.98
OBn
Ph
O
123f
10.41
0.95
0.95
2.04
2.03
0.98
1.98
0.98
1.03
1.00
31.5
0.9
1.6
0.1
f1 (ppm)

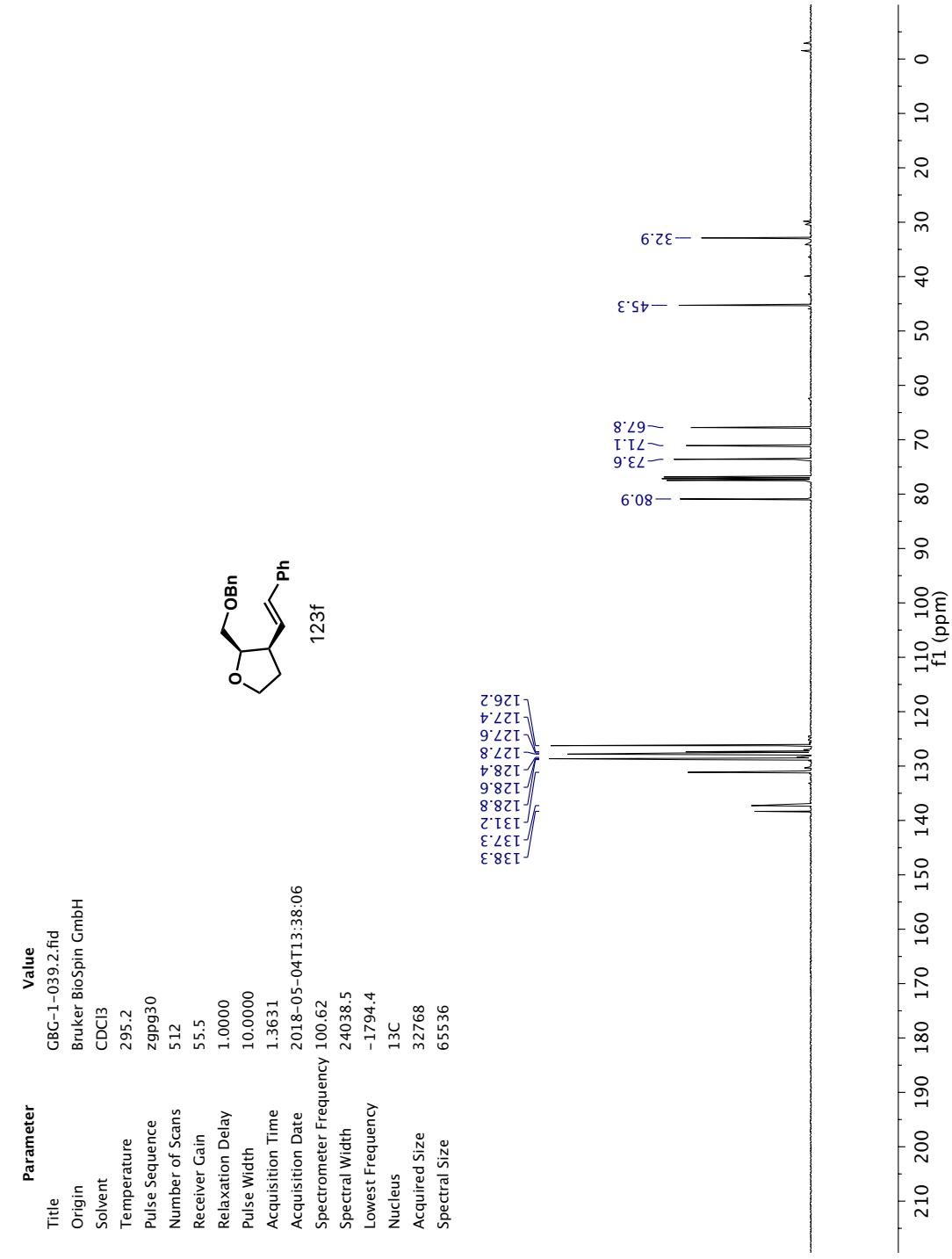
Parameter Value
Title GBG-1-039.2.fid
Origin Bruker BioSpin GmbH
Solvent CDCl3
Temperature 295.2
Pulse Sequence zgpg30
Number of Scans 512
Receiver Gain 55.5
Relaxation Delay 1.0000
Pulse Width 10.0000
Acquisition Time 1.3631
Acquisition Date 2018-05-04T13:38:06
Spectrometer Frequency 100.62
Spectral Width 24038.5
Lowest Frequency -1794.4
Nucleus 13C
Acquired Size 32768
Spectral Size 65536
OBn
Ph
O
123f
138.3
137.3
131.2
128.8
128.6
128.4
127.8
127.6
127.4
126.2
80.9
73.6
71.1
67.8
45.3
32.9
f1 (ppm)

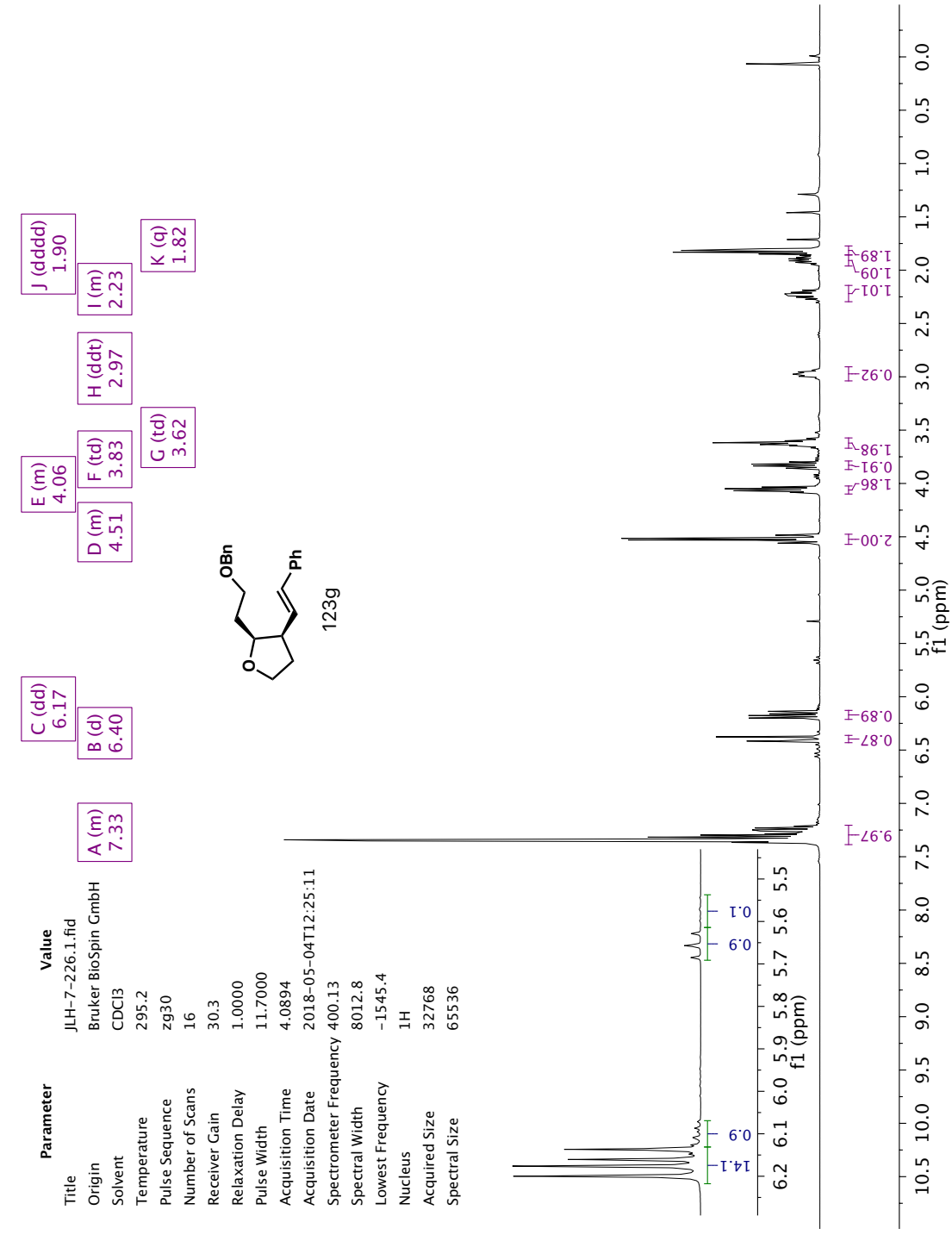
Parameter
Value
Title
JLH-7-226.1.fid
Origin
Bruker BioSpin GmbH
Solvent
CDCl3
Temperature
295.2
Pulse Sequence
zg30
Number of Scans
16
Receiver Gain
30.3
Relaxation Delay
1.0000
Pulse Width
11.7000
Acquisition Time
4.0894
Acquisition Date
2018-05-04T12:25:11
Spectrometer Frequency
400.13
Spectral Width
8012.8
Lowest Frequency
-1545.4
Nucleus
1H
Acquired Size
32768
Spectral Size
65536
A (m) 7.33
B (d) 6.40
C (dd) 6.17
D (m) 4.51
E (m) 4.06
F (td) 3.83
G (td) 3.62
H (ddt) 2.97
I (m) 2.23
J (dddd) 1.90
K (q) 1.82
OBn
Ph
O
123g
9.97
0.87
0.89
2.00
1.86
0.91
1.98
0.92
1.01
1.09
1.89
14.1
0.9
0.9
0.1
f1 (ppm)

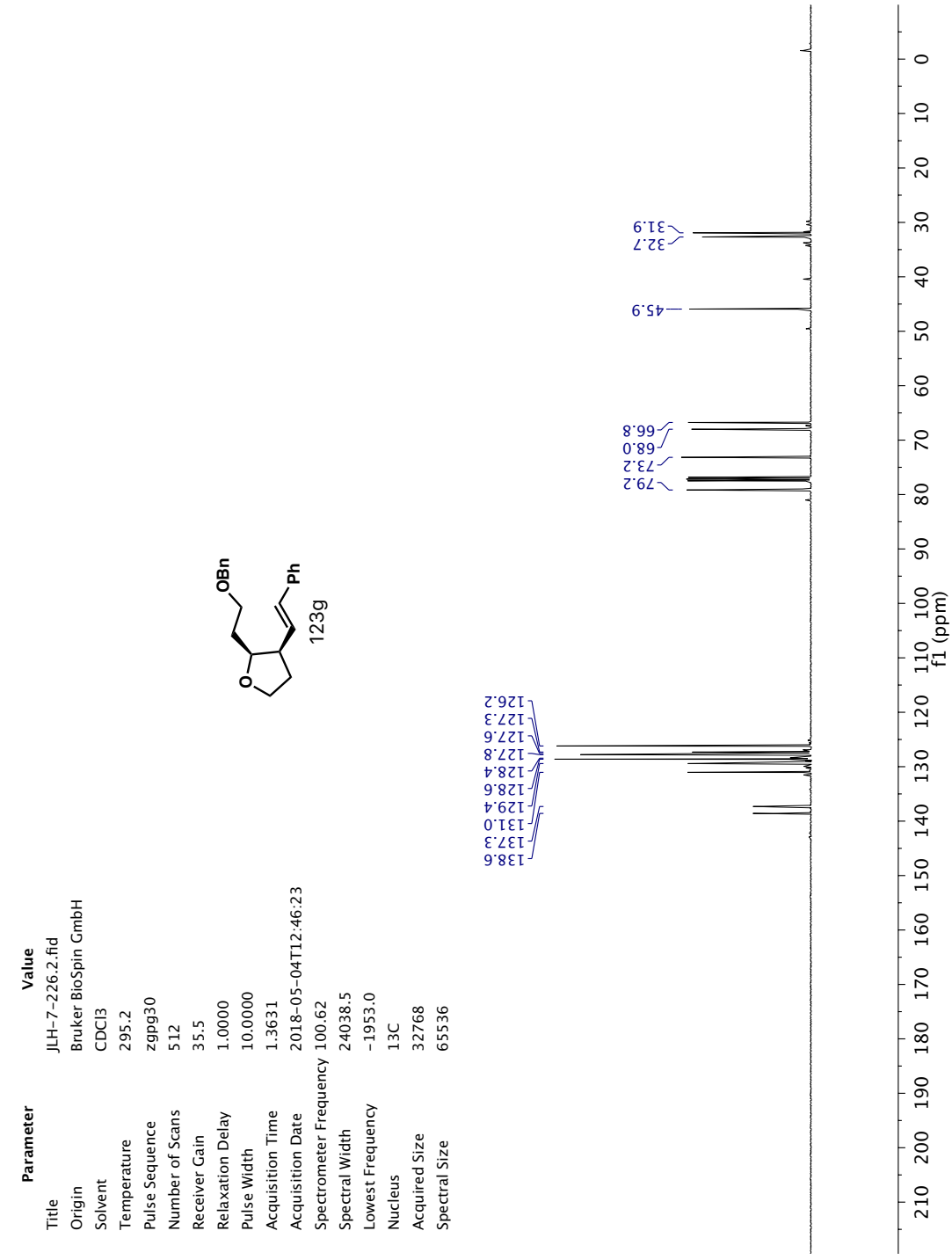
Parameter Value
Title JLH-7-226.2.fid
Origin Bruker BioSpin GmbH
Solvent CDCl3
Temperature 295.2
Pulse Sequence zgpg30
Number of Scans 512
Receiver Gain 35.5
Relaxation Delay 1.0000
Pulse Width 10.0000
Acquisition Time 1.3631
Acquisition Date 2018-05-04T12:46:23
Spectrometer Frequency 100.62
Spectral Width 24038.5
Lowest Frequency -1953.0
Nucleus 13C
Acquired Size 32768
Spectral Size 65536
OBn
Ph
O
123g
138.6
137.3
131.0
129.4
128.6
128.4
127.8
127.6
127.3
126.2
79.2
73.2
68.0
66.8
45.9
32.7
31.9
f1 (ppm)

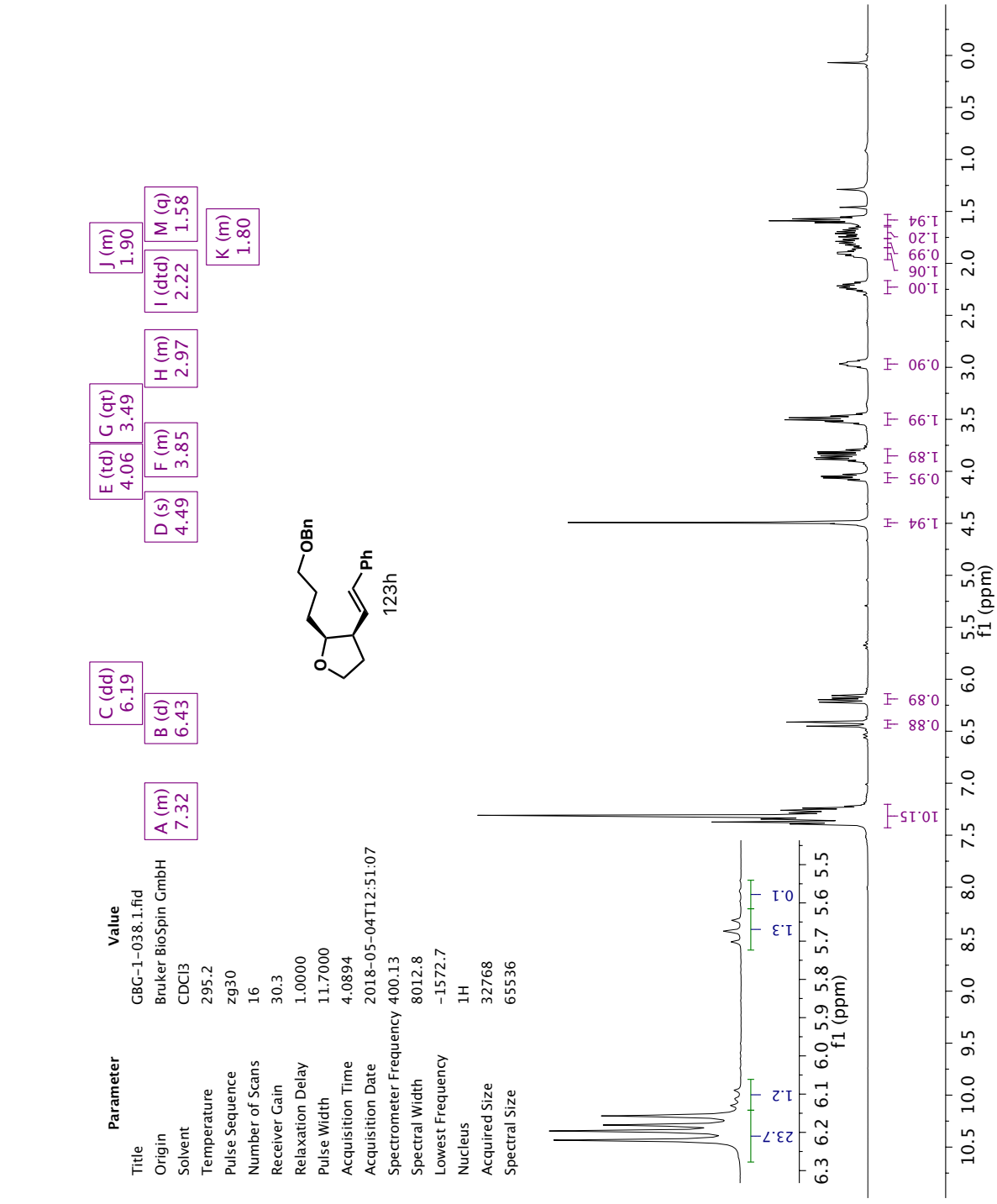
Parameter
Value
Title GBG-1-038.1.fid
Origin Bruker BioSpin GmbH
Solvent CDCl3
Temperature 295.2
Pulse Sequence zg30
Number of Scans 16
Receiver Gain 30.3
Relaxation Delay 1.0000
Pulse Width 11.7000
Acquisition Time 4.0894
Acquisition Date 2018-05-04T12:51:07
Spectrometer Frequency 400.13
Spectral Width 8012.8
Lowest Frequency -1572.7
Nucleus 1H
Acquired Size 32768
Spectral Size 65536
A (m) 7.32
B (d) 6.43
C (dd) 6.19
D (s) 4.49
E (td) 4.06
F (m) 3.85
G (qt) 3.49
H (m) 2.97
I (dtd) 2.22
J (m) 1.90
K (m) 1.80
M (q) 1.58
OBn
Ph
123h
f1 (ppm)

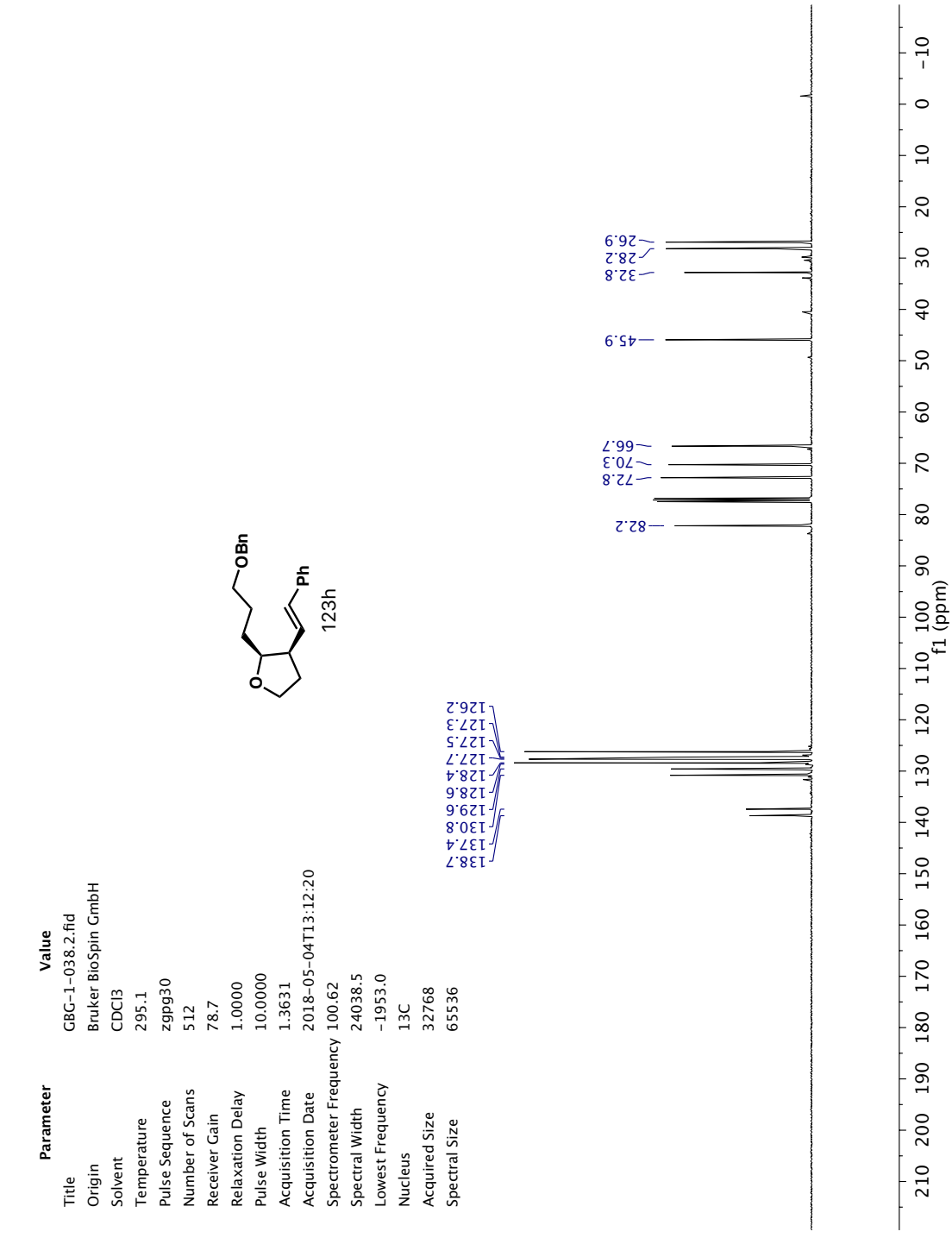
Parameter Value
Title GBG-1-038.2.fid
Origin Bruker BioSpin GmbH
Solvent CDCl3
Temperature 295.1
Pulse Sequence zgpg30
Number of Scans 512
Receiver Gain 78.7
Relaxation Delay 1.0000
Pulse Width 10.0000
Acquisition Time 1.3631
Acquisition Date 2018-05-04T13:12:20
Spectrometer Frequency 100.62
Spectral Width 24038.5
Lowest Frequency -1953.0
Nucleus 13C
Acquired Size 32768
Spectral Size 65536
OBn
Ph
O
123h
138.7
137.4
130.8
129.6
128.6
128.4
127.7
127.5
127.3
126.2
82.2
72.8
70.3
66.7
45.9
32.8
28.2
26.9
f1 (ppm)

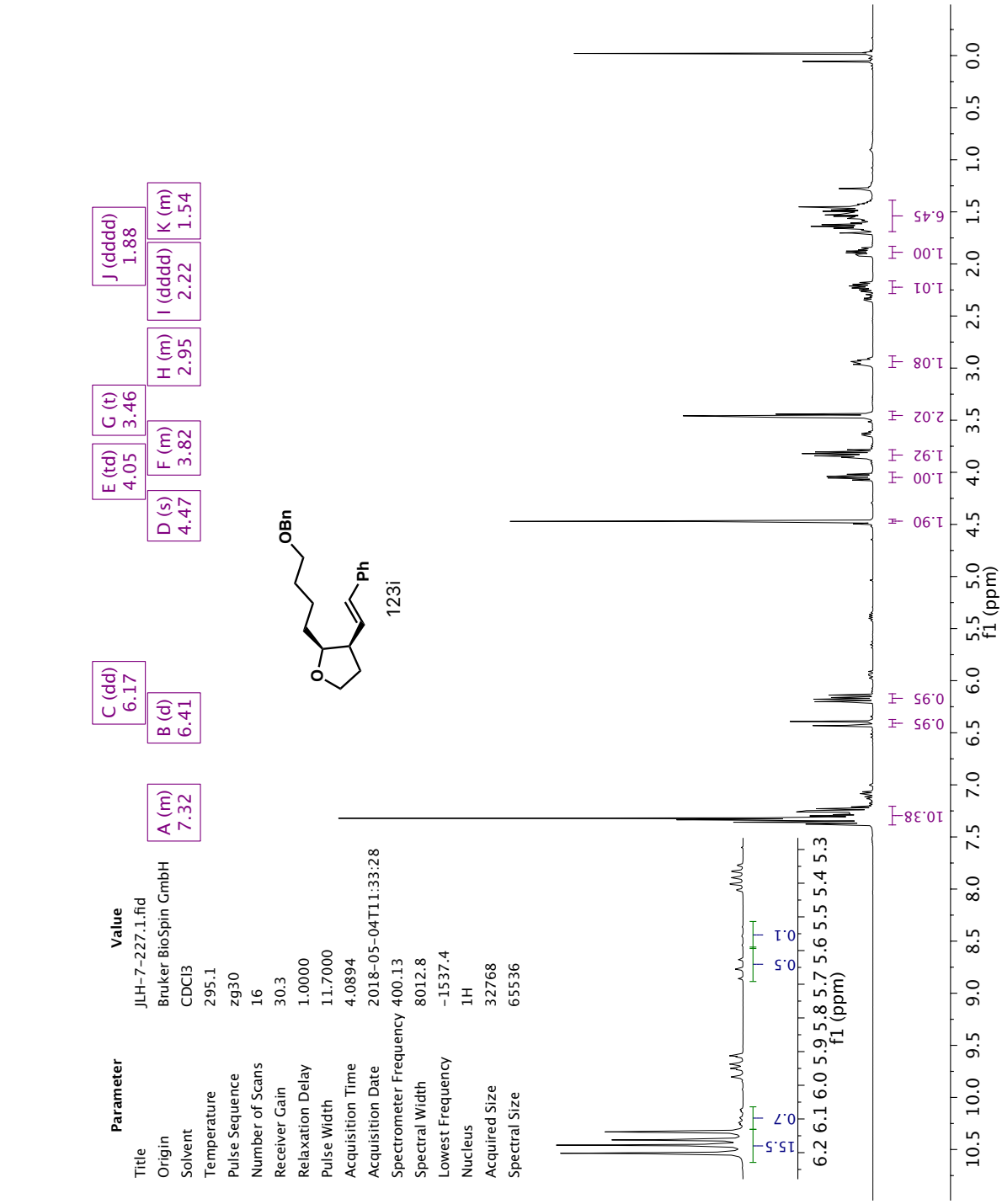
Parameter
Value
Title
JLH-7-227.1.fid
Origin
Bruker BioSpin GmbH
Solvent
CDCl3
Temperature
295.1
Pulse Sequence
zg30
Number of Scans
16
Receiver Gain
30.3
Relaxation Delay
1.0000
Pulse Width
11.7000
Acquisition Time
4.0894
Acquisition Date
2018-05-04T11:33:28
Spectrometer Frequency
400.13
Spectral Width
8012.8
Lowest Frequency
-1537.4
Nucleus
1H
Acquired Size
32768
Spectral Size
65536
A (m) 7.32
B (d) 6.41
C (dd) 6.17
D (s) 4.47
E (td) 4.05
F (m) 3.82
G (t) 3.46
H (m) 2.95
I (dddd) 2.22
J (dddd) 1.88
K (m) 1.54
OBn
Ph
O
123i
10.38
0.95
0.95
1.90
1.00
1.92
2.02
1.08
1.01
1.00
6.45
15.5
0.7
0.5
0.1
f1 (ppm)

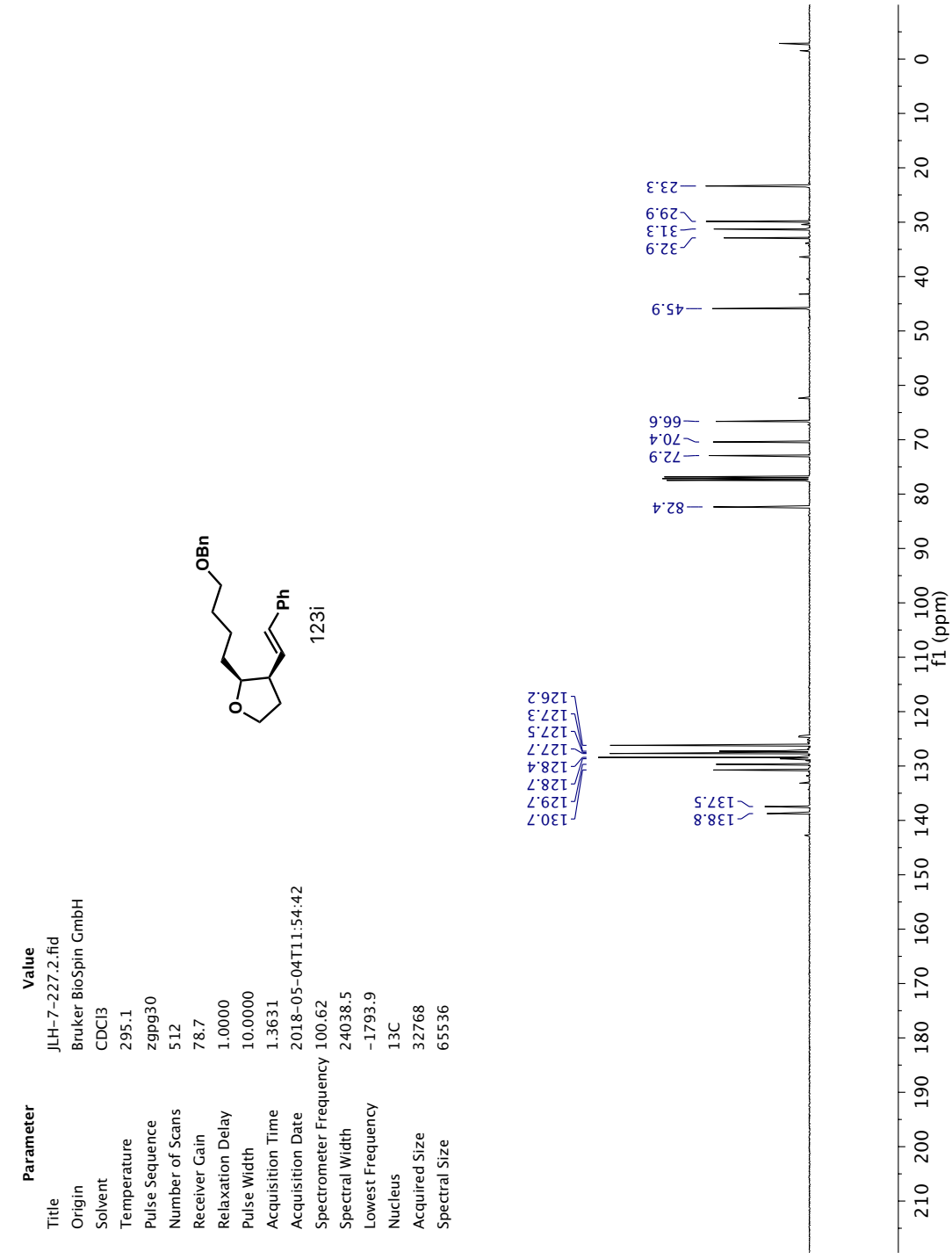
OBn
Ph
O
123i
Parameter Value
Title JLH-7-227.2.fid
Origin Bruker BioSpin GmbH
Solvent CDCl3
Temperature 295.1
Pulse Sequence zgpg30
Number of Scans 512
Receiver Gain 78.7
Relaxation Delay 1.0000
Pulse Width 10.0000
Acquisition Time 1.3631
Acquisition Date 2018-05-04T11:54:42
Spectrometer Frequency 100.62
Spectral Width 24038.5
Lowest Frequency -1793.9
Nucleus 13C
Acquired Size 32768
Spectral Size 65536
130.7
129.7
128.7
128.4
127.7
127.5
127.3
126.2
138.8
137.5
82.4
72.9
70.4
66.6
45.9
32.9
31.3
29.9
23.3
f1 (ppm)

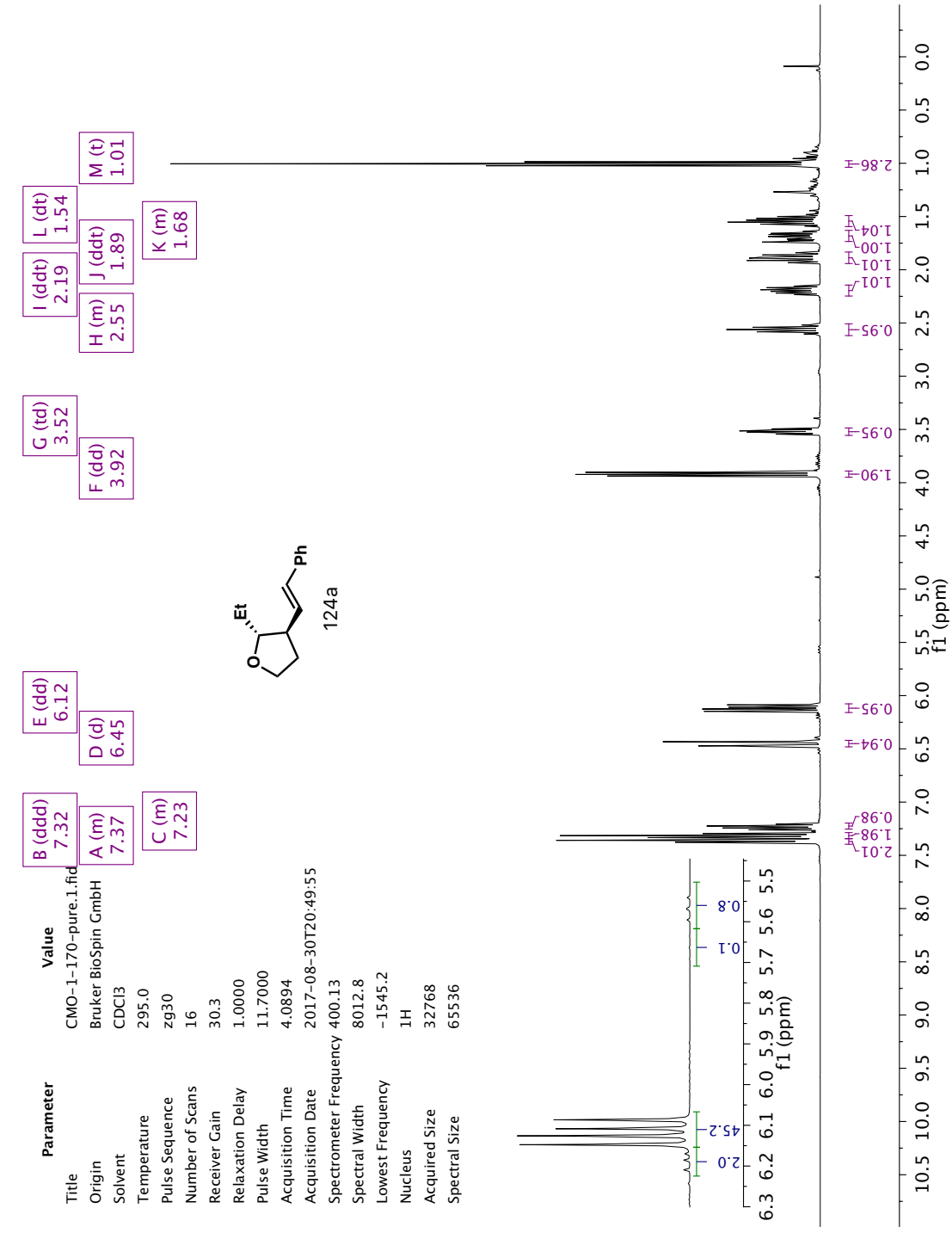
Parameter
Value
Title
CMO-1-170-pure.1.fid
Origin
Bruker BioSpin GmbH
Solvent
CDCl3
Temperature
295.0
Pulse Sequence
zg30
Number of Scans
16
Receiver Gain
30.3
Relaxation Delay
1.0000
Pulse Width
11.7000
Acquisition Time
4.0894
Acquisition Date
2017-08-30T20:49:55
Spectrometer Frequency
400.13
Spectral Width
8012.8
Lowest Frequency
-1545.2
Nucleus
1H
Acquired Size
32768
Spectral Size
65536
B (ddd) 7.32
A (m) 7.37
C (m) 7.23
E (dd) 6.12
D (d) 6.45
G (td) 3.52
F (dd) 3.92
I (ddt) 2.19
H (m) 2.55
J (ddt) 1.89
L (dt) 1.54
K (m) 1.68
M (t) 1.01
Et
Ph
O
124a
f1 (ppm)

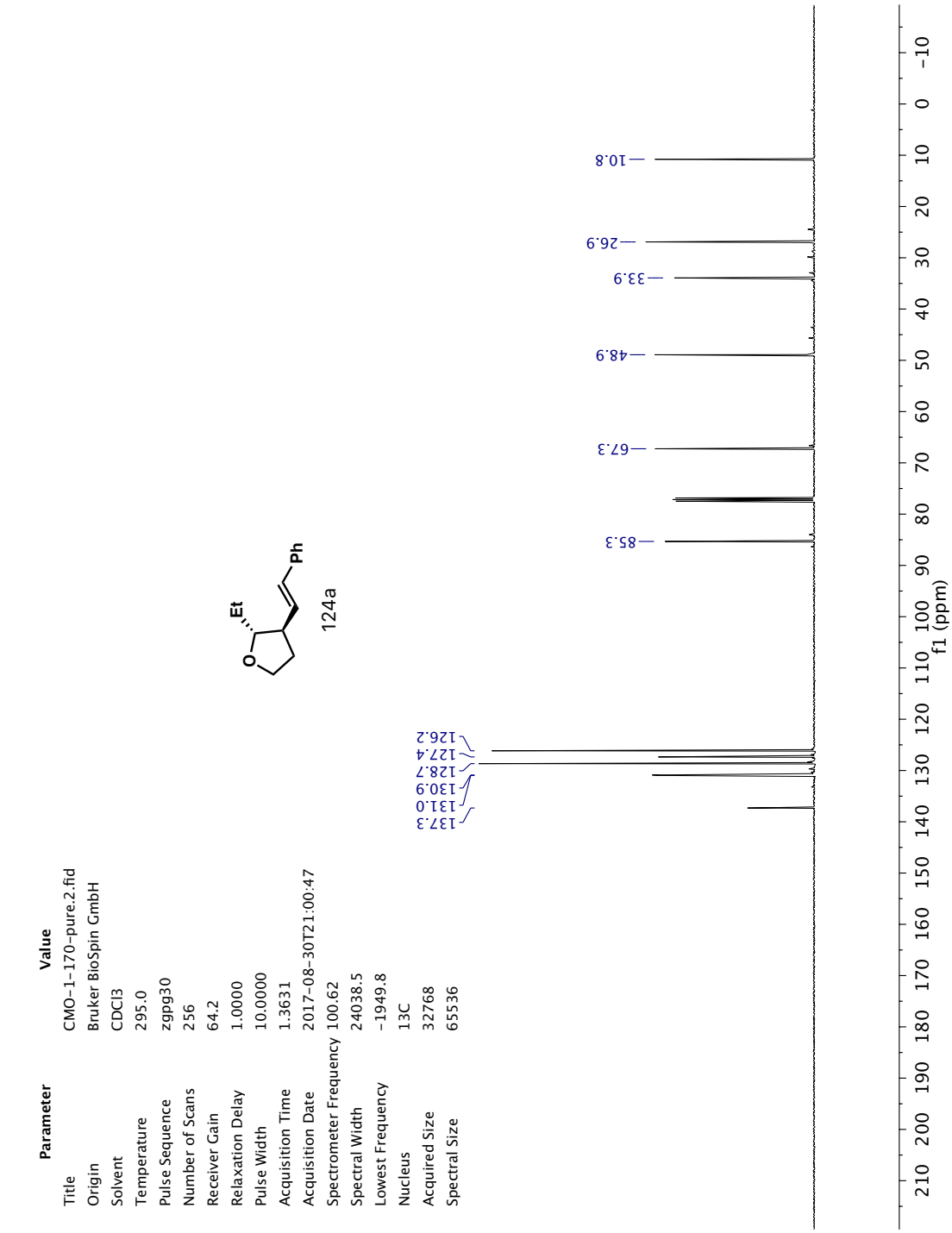
Parameter Value
Title CMO-1-170-pure.2.fid
Origin Bruker BioSpin GmbH
Solvent CDCl3
Temperature 295.0
Pulse Sequence zgpg30
Number of Scans 256
Receiver Gain 64.2
Relaxation Delay 1.0000
Pulse Width 10.0000
Acquisition Time 1.3631
Acquisition Date 2017-08-30T21:00:47
Spectrometer Frequency 100.62
Spectral Width 24038.5
Lowest Frequency -1949.8
Nucleus 13C
Acquired Size 32768
Spectral Size 65536
Et
O
Ph
124a
137.3
131.0
130.9
128.7
127.4
126.2
85.3
67.3
48.9
33.9
26.9
10.8
f1 (ppm)

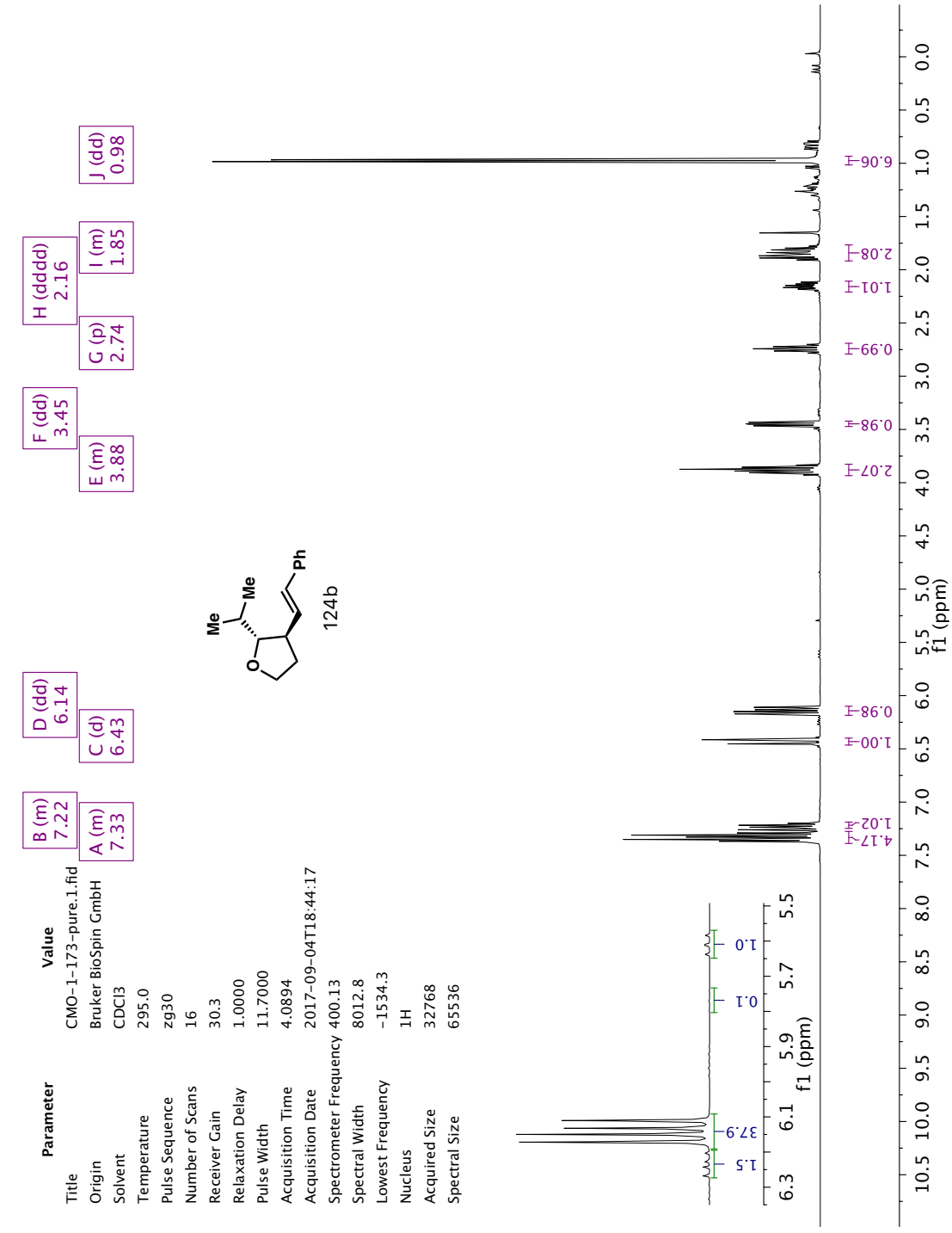
Parameter
Value
Title
CMO-1-173-pure.1.fid
Origin
Bruker BioSpin GmbH
Solvent
CDCl3
Temperature
295.0
Pulse Sequence
zg30
Number of Scans
16
Receiver Gain
30.3
Relaxation Delay
1.0000
Pulse Width
11.7000
Acquisition Time
4.0894
Acquisition Date
2017-09-04T18:44:17
Spectrometer Frequency
400.13
Spectral Width
8012.8
Lowest Frequency
-1534.3
Nucleus
1H
Acquired Size
32768
Spectral Size
65536
B (m) 7.22
A (m) 7.33
D (dd) 6.14
C (d) 6.43
F (dd) 3.45
E (m) 3.88
H (ddd) 2.16
G (p) 2.74
I (m) 1.85
J (dd) 0.98
Me
Me
Ph
O
124b
f1 (ppm)

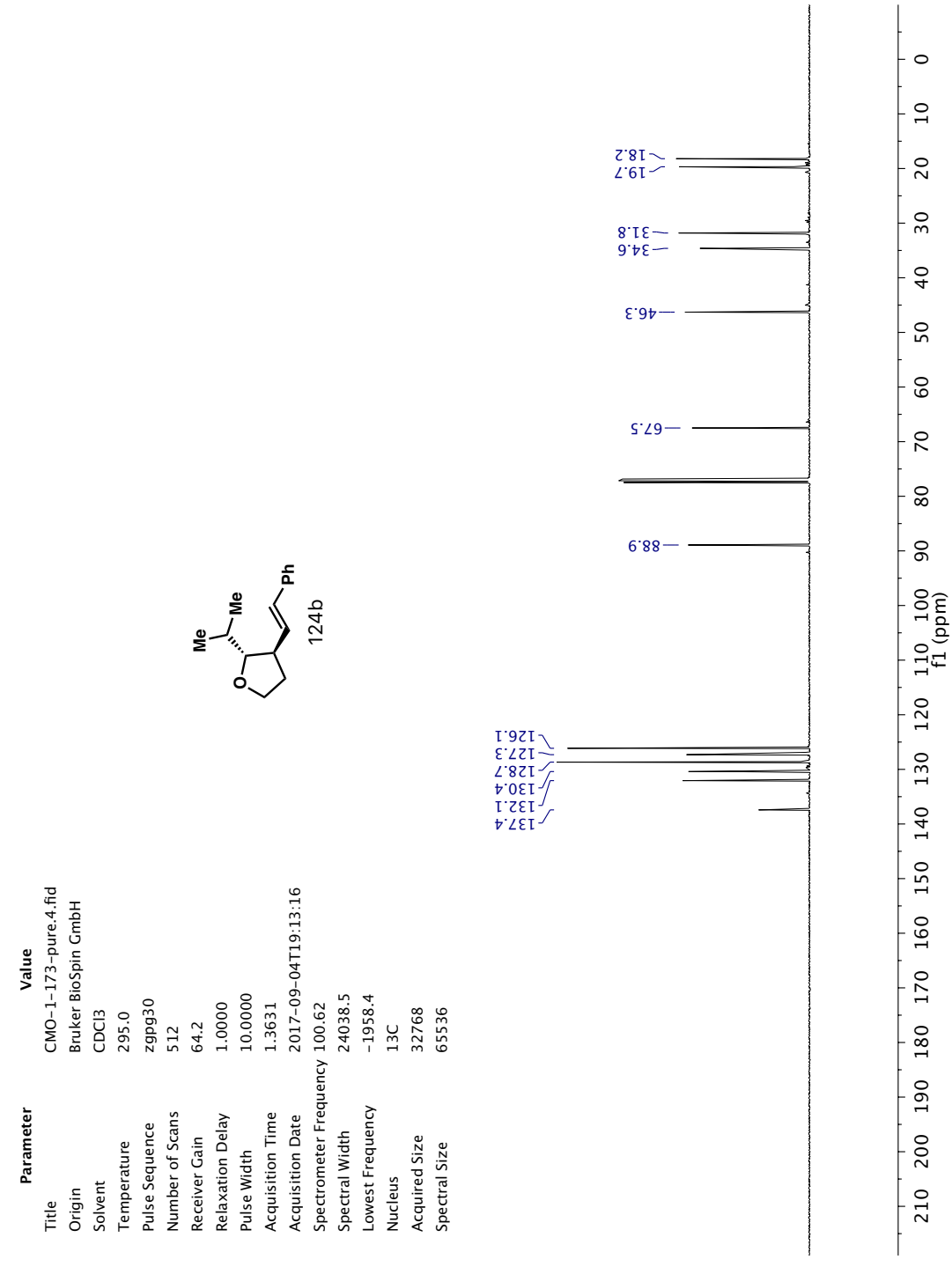

Parameter	Value
Title	CMO-1-173-pure.4.fid
Origin	Bruker BioSpin GmbH
Solvent	CDCl3
Temperature	295.0
Pulse Sequence	zgpg30
Number of Scans	512
Receiver Gain	64.2
Relaxation Delay	1.0000
Pulse Width	10.0000
Acquisition Time	1.3631
Acquisition Date	2017-09-04T19:13:16
Spectrometer Frequency	100.62
Spectral Width	24038.5
Lowest Frequency	-1958.4
Nucleus	13C
Acquired Size	32768
Spectral Size	65536

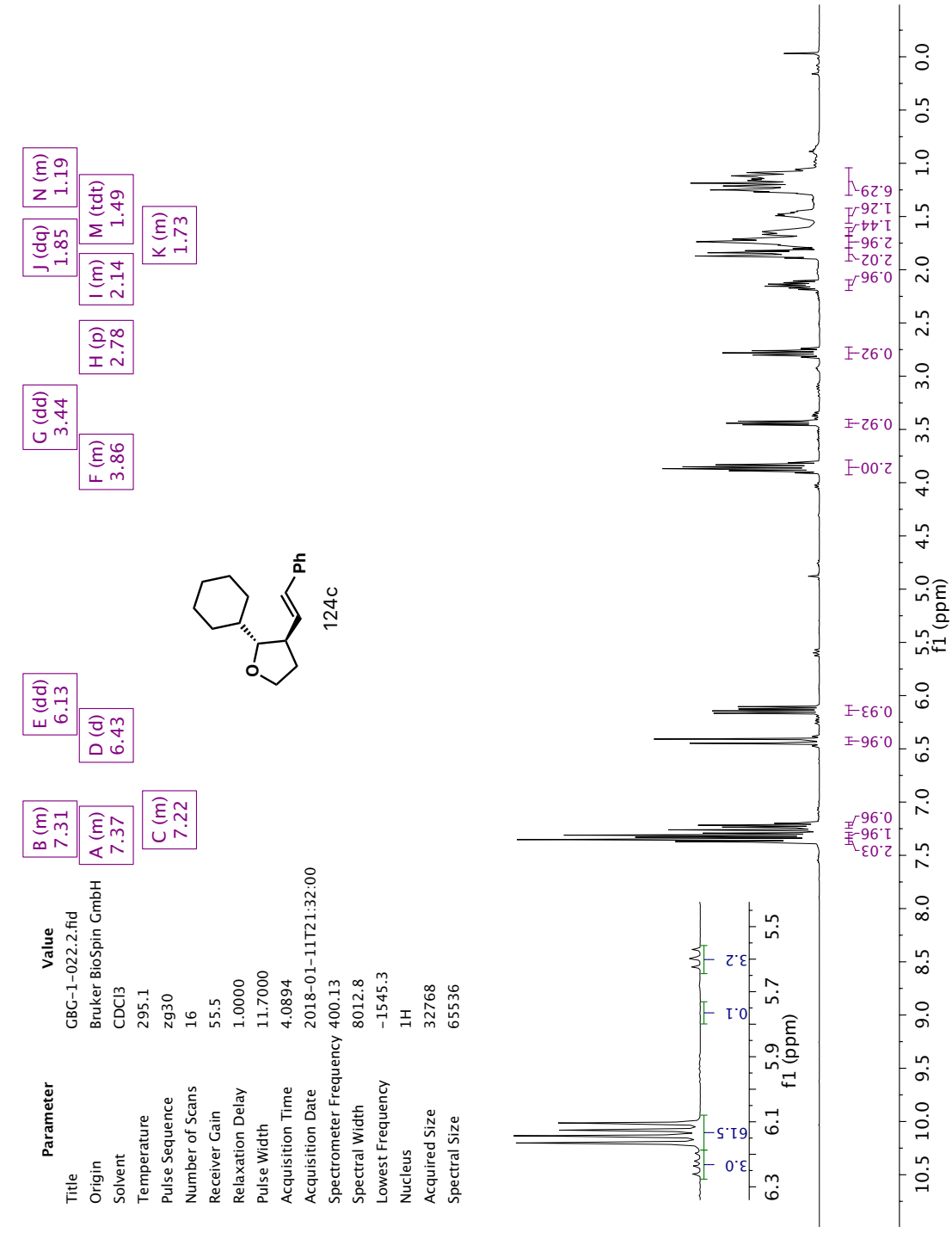
Parameter
Value
Title GBG-1-022.2.fid
Origin Bruker BioSpin GmbH
Solvent CDCl3
Temperature 295.1
Pulse Sequence zg30
Number of Scans 16
Receiver Gain 55.5
Relaxation Delay 1.0000
Pulse Width 11.7000
Acquisition Time 4.0894
Acquisition Date 2018-01-11T21:32:00
Spectrometer Frequency 400.13
Spectral Width 8012.8
Lowest Frequency -1545.3
Nucleus 1H
Acquired Size 32768
Spectral Size 65536
B (m) 7.31
A (m) 7.37
C (m) 7.22
E (dd) 6.13
D (d) 6.43
F (m) 3.86
G (dd) 3.44
H (p) 2.78
J (dq) 1.85
I (m) 2.14
M (tdt) 1.49
K (m) 1.73
N (m) 1.19
Ph
O
124c
f1 (ppm)

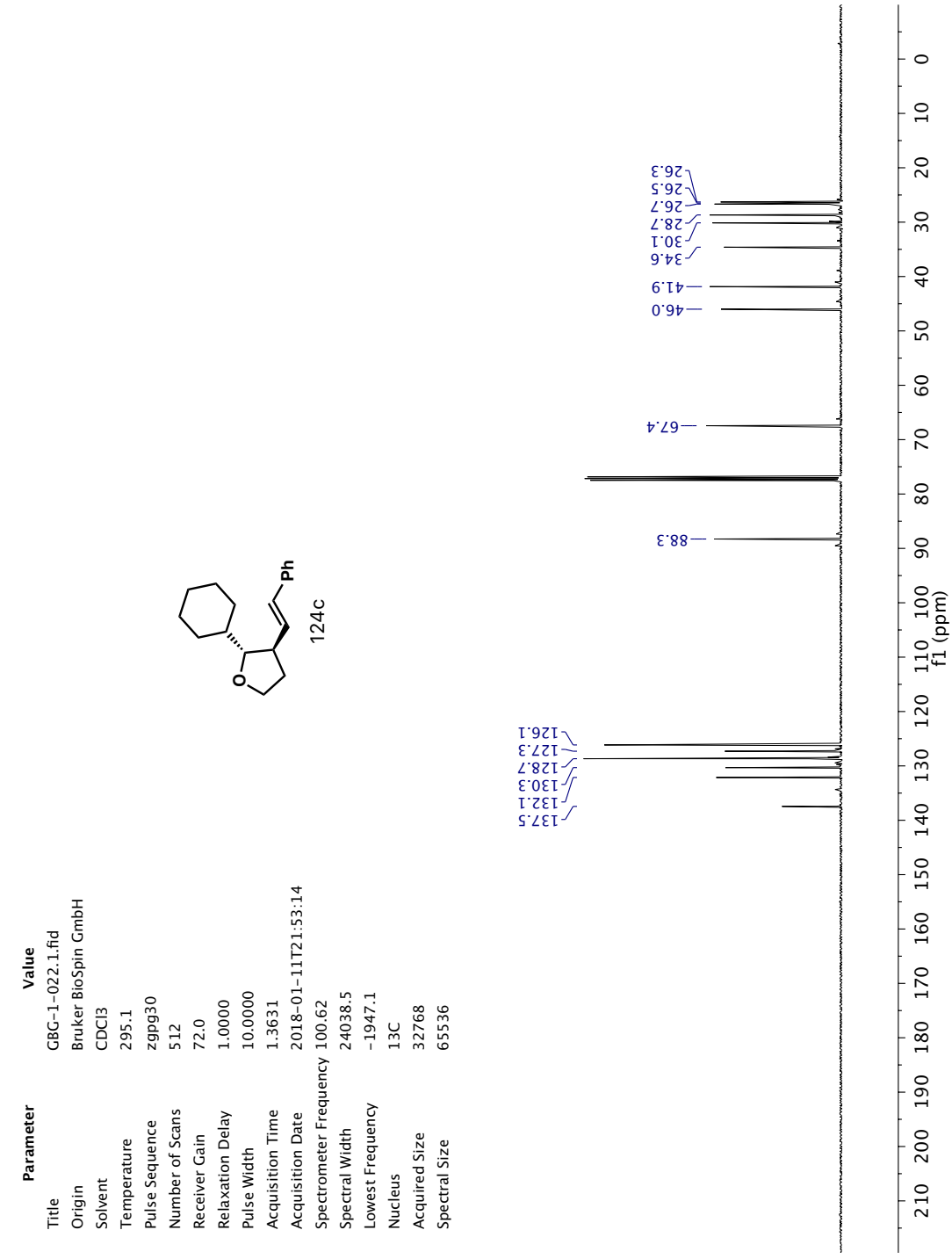
Parameter Value
Title GBG-1-022.1.fid
Origin Bruker BioSpin GmbH
Solvent CDCl3
Temperature 295.1
Pulse Sequence zgpg30
Number of Scans 512
Receiver Gain 72.0
Relaxation Delay 1.0000
Pulse Width 10.0000
Acquisition Time 1.3631
Acquisition Date 2018-01-11T21:53:14
Spectrometer Frequency 100.62
Spectral Width 24038.5
Lowest Frequency -1947.1
Nucleus 13C
Acquired Size 32768
Spectral Size 65536
Ph
O
124c
137.5
132.1
130.3
128.7
127.3
126.1
88.3
67.4
46.0
41.9
34.6
30.1
28.7
26.7
26.5
26.3
f1 (ppm)

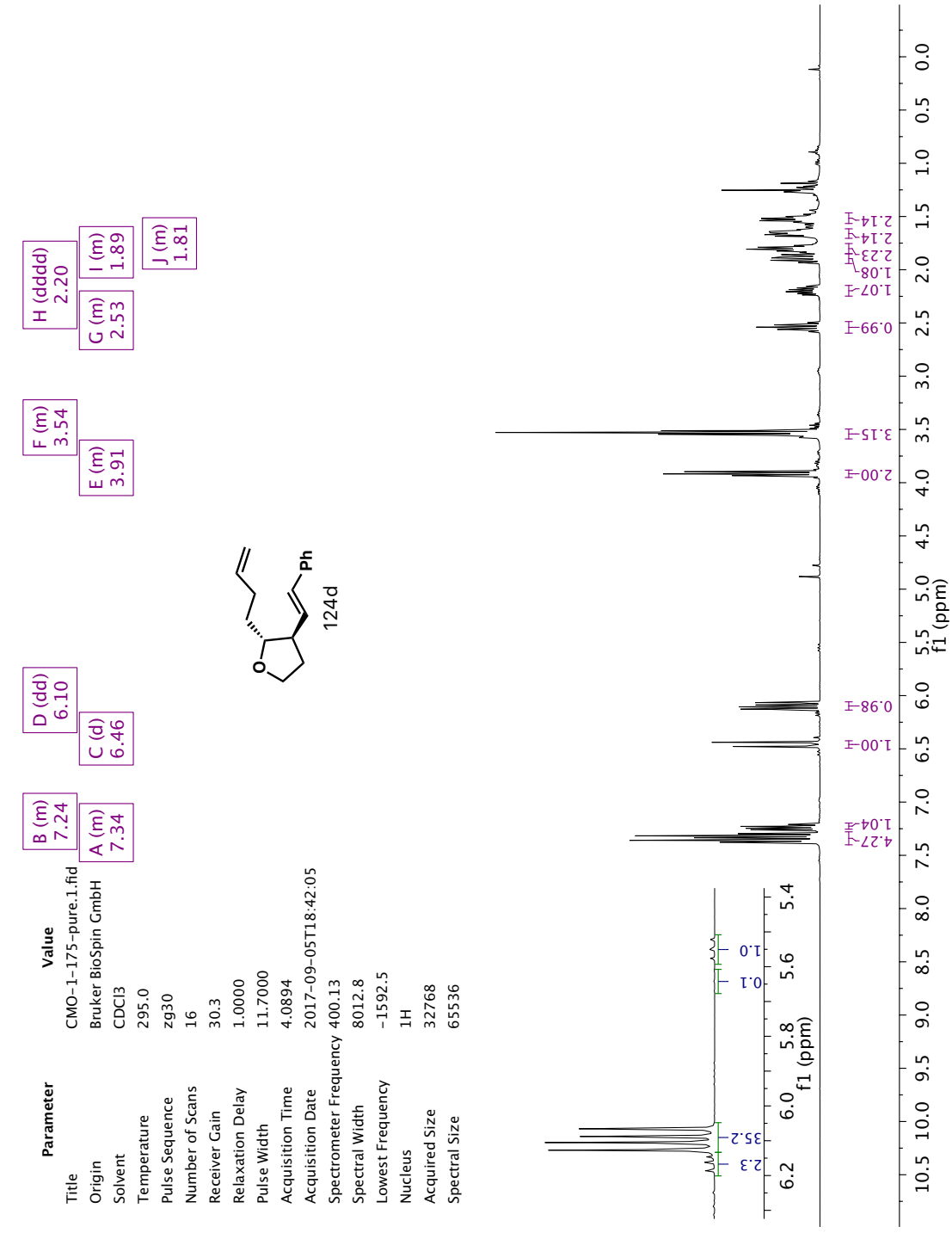
Parameter
Value
Title
CMO-1-175-pure.1.fid
Origin
Bruker BioSpin GmbH
Solvent
CDCl3
Temperature
295.0
Pulse Sequence
zg30
Number of Scans
16
Receiver Gain
30.3
Relaxation Delay
1.0000
Pulse Width
11.7000
Acquisition Time
4.0894
Acquisition Date
2017-09-05T18:42:05
Spectrometer Frequency
400.13
Spectral Width
8012.8
Lowest Frequency
-1592.5
Nucleus
1H
Acquired Size
32768
Spectral Size
65536
A (m) 7.34
B (m) 7.24
C (d) 6.46
D (dd) 6.10
E (m) 3.91
F (m) 3.54
G (m) 2.53
H (dddd) 2.20
I (m) 1.89
J (m) 1.81
Ph
124d
f1 (ppm)

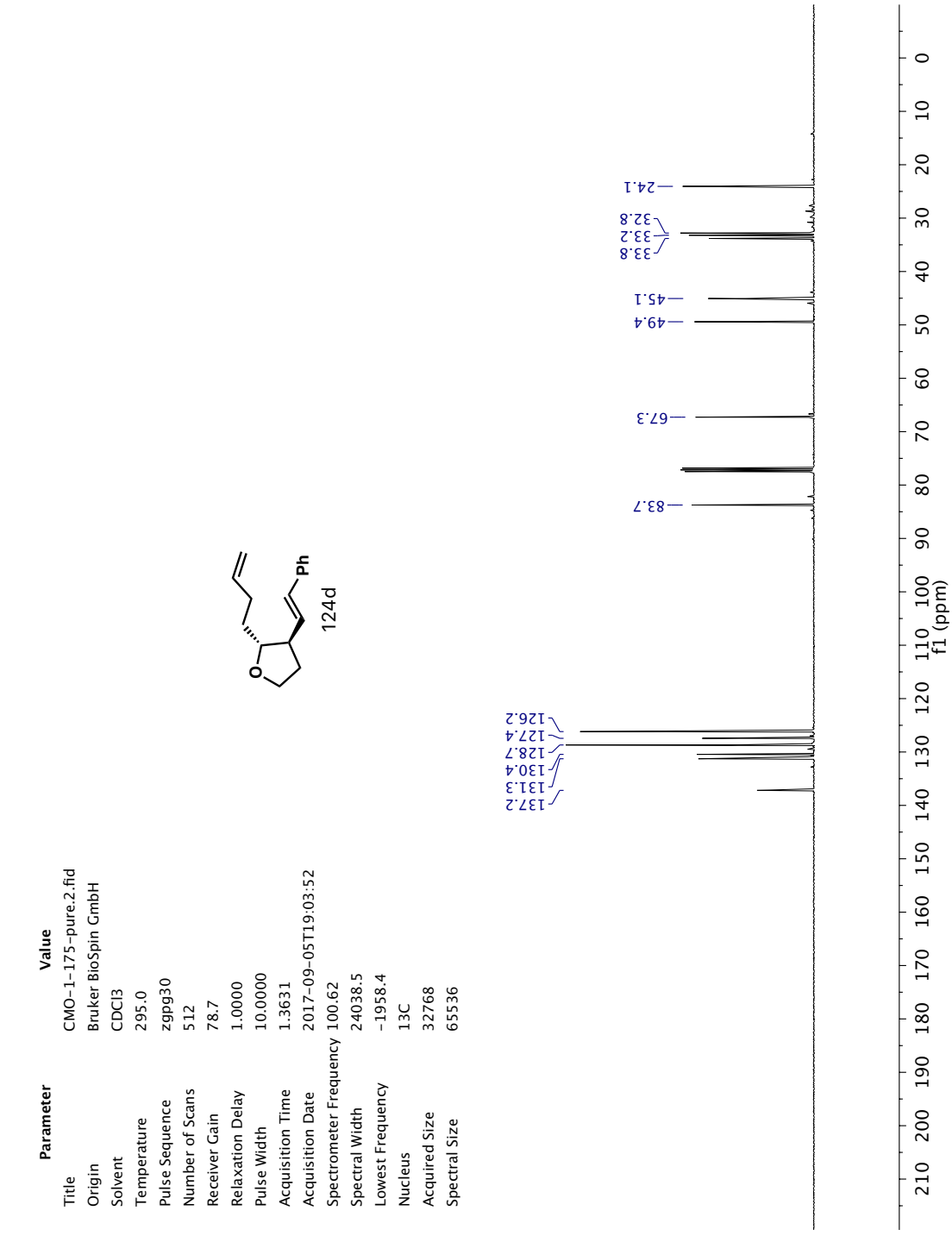
Parameter Value
Title CMO-1-175-pure.2.fid
Origin Bruker BioSpin GmbH
Solvent CDCl3
Temperature 295.0
Pulse Sequence zgpg30
Number of Scans 512
Receiver Gain 78.7
Relaxation Delay 1.0000
Pulse Width 10.0000
Acquisition Time 1.3631
Acquisition Date 2017-09-05T19:03:52
Spectrometer Frequency 100.62
Spectral Width 24038.5
Lowest Frequency -1958.4
Nucleus 13C
Acquired Size 32768
Spectral Size 65536
O
Ph
124d
137.2
131.3
130.4
128.7
127.4
126.2
83.7
67.3
49.4
45.1
33.8
33.2
32.8
24.1
f1 (ppm)

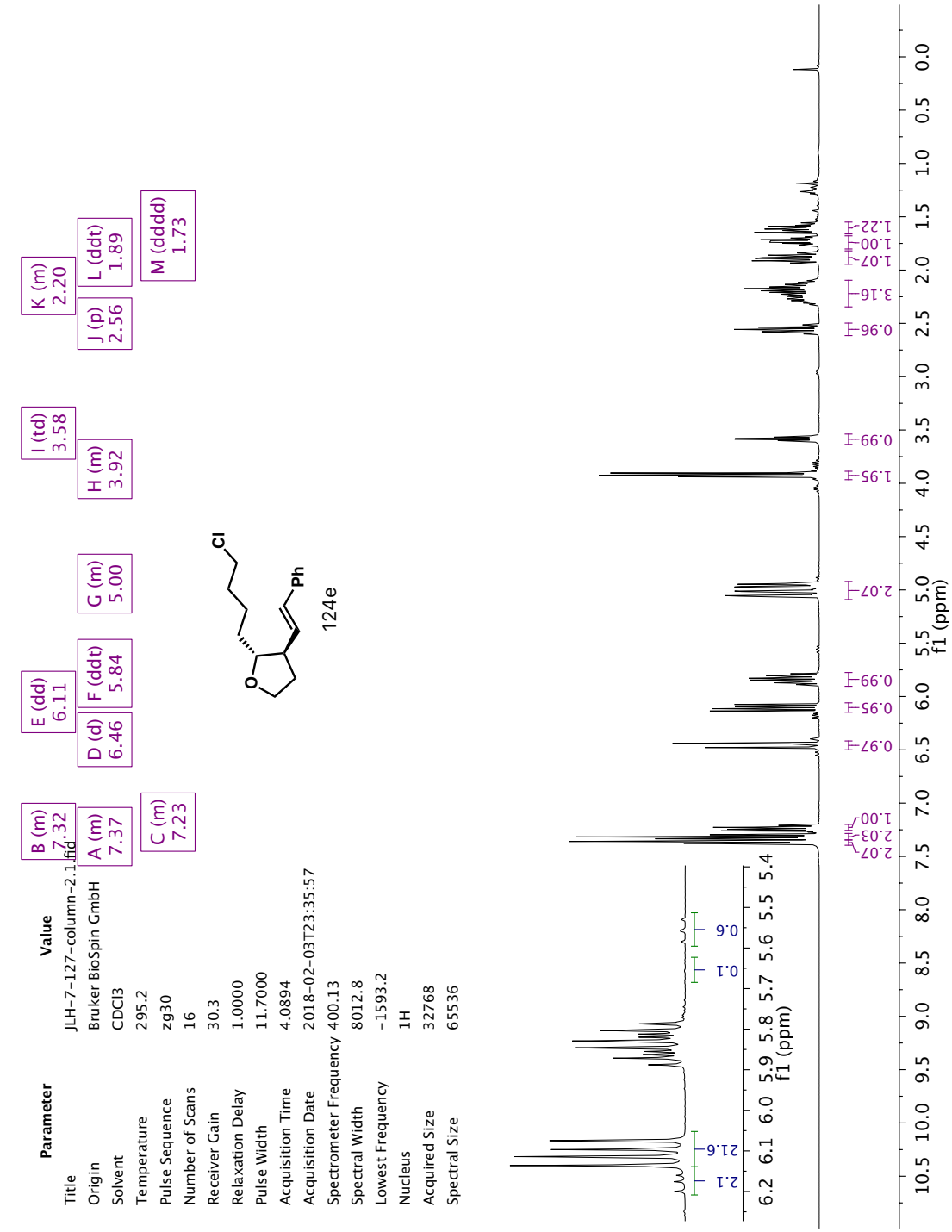
B (m) 7.32
A (m) 7.37
C (m) 7.23
D (d) 6.46
E (dd) 6.11
F (ddt) 5.84
G (m) 5.00
H (m) 3.92
I (td) 3.58
J (p) 2.56
K (m) 2.20
L (ddt) 1.89
M (dddd) 1.73
Cl
Ph
O
124e
Parameter Value
Title JLH-7-127-column-2.1.fid
Origin Bruker BioSpin GmbH
Solvent CDCl3
Temperature 295.2
Pulse Sequence zg30
Number of Scans 16
Receiver Gain 30.3
Relaxation Delay 1.0000
Pulse Width 11.7000
Acquisition Time 4.0894
Acquisition Date 2018-02-03T23:35:57
Spectrometer Frequency 400.13
Spectral Width 8012.8
Lowest Frequency -1593.2
Nucleus 1H
Acquired Size 32768
Spectral Size 65536
f1 (ppm)

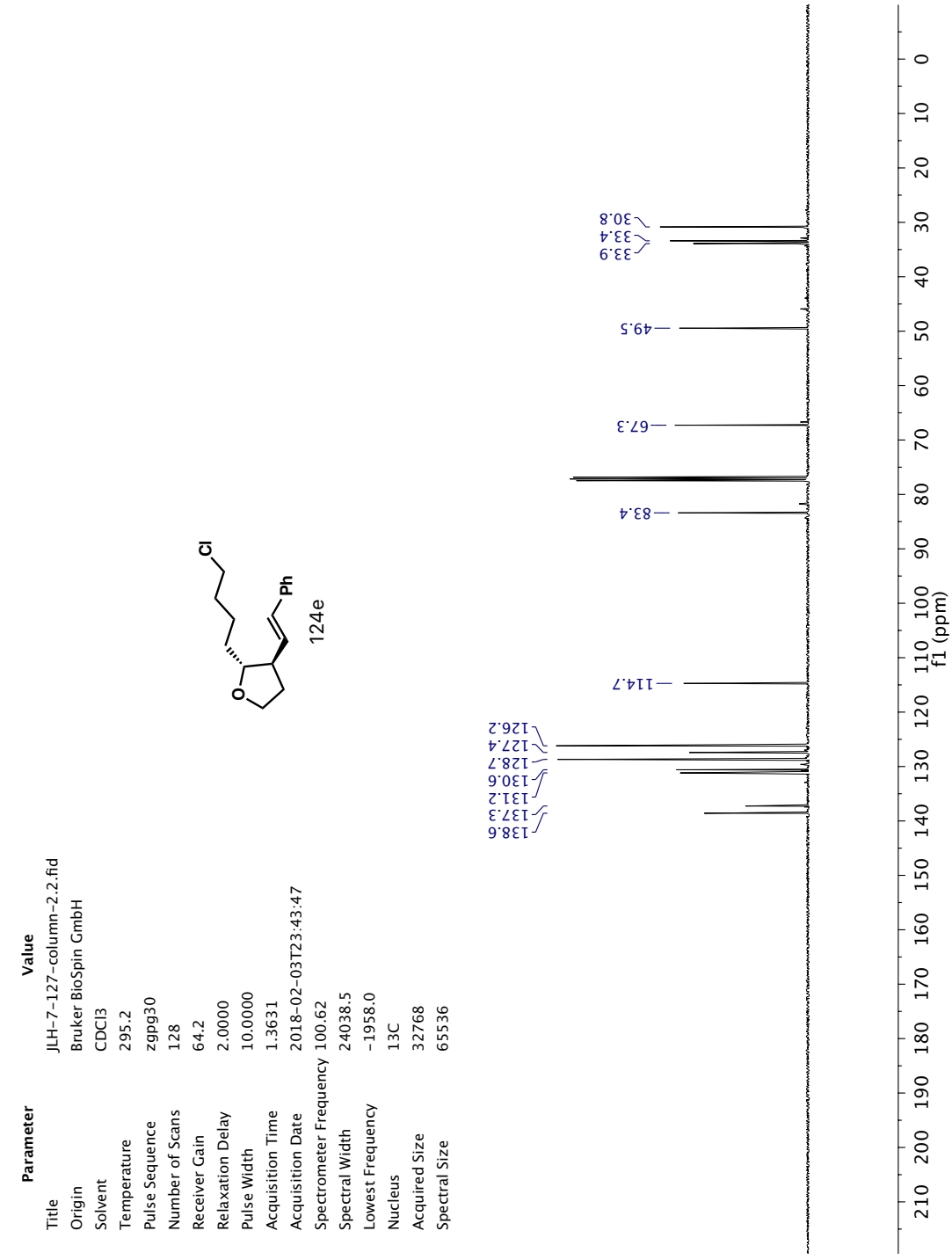
Cl
Ph
O
124e
Parameter Value
Title JLH-7-127-column-2.2.fid
Origin Bruker BioSpin GmbH
Solvent CDCl3
Temperature 295.2
Pulse Sequence zgpg30
Number of Scans 128
Receiver Gain 64.2
Relaxation Delay 2.0000
Pulse Width 10.0000
Acquisition Time 1.3631
Acquisition Date 2018-02-03T23:43:47
Spectrometer Frequency 100.62
Spectral Width 24038.5
Lowest Frequency -1958.0
Nucleus 13C
Acquired Size 32768
Spectral Size 65536
138.6
137.3
131.2
130.6
128.7
127.4
126.2
114.7
83.4
67.3
49.5
33.9
33.4
30.8
f1 (ppm)

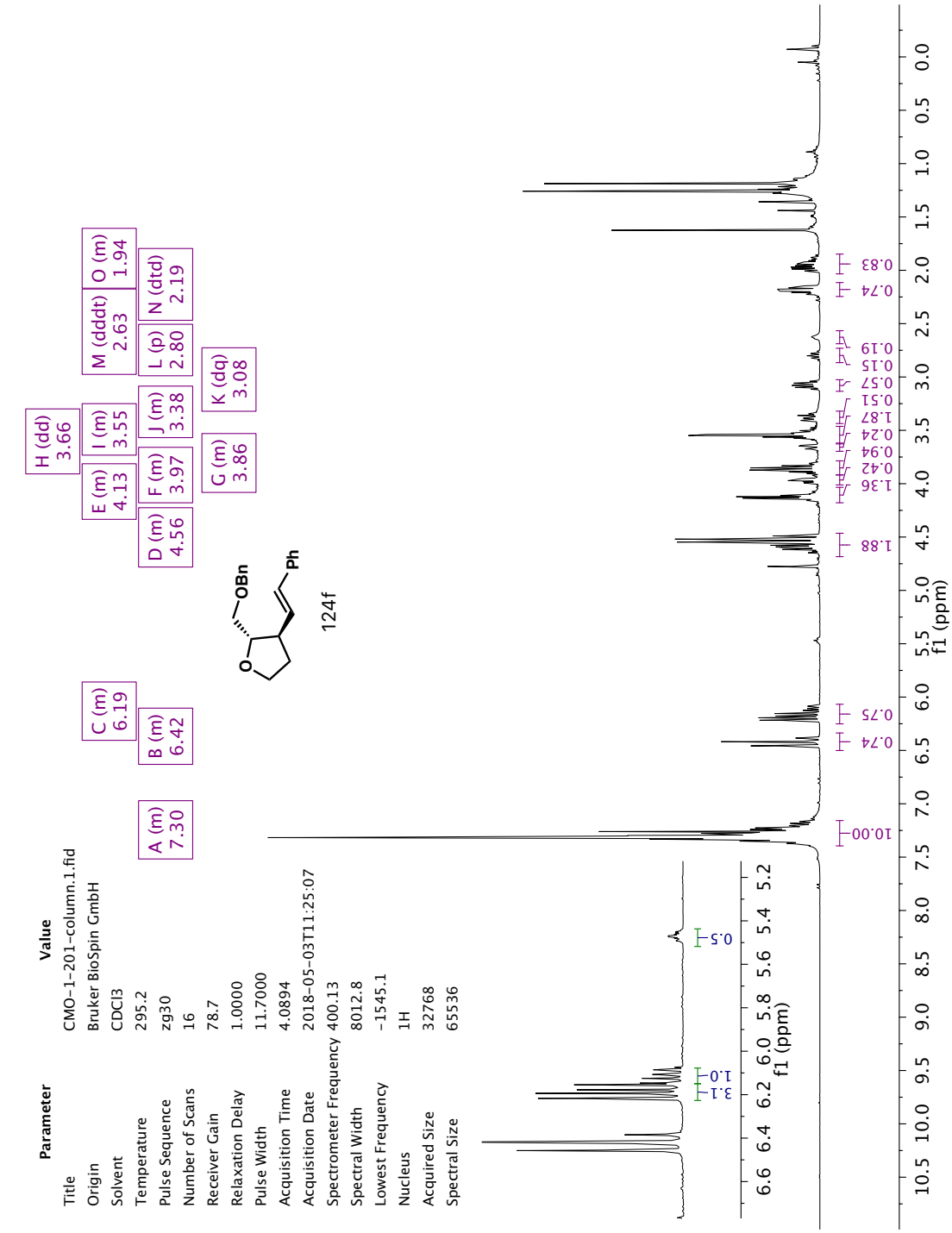
Parameter Value
Title CMO-1-201-column.1.fid
Origin Bruker BioSpin GmbH
Solvent CDCl3
Temperature 295.2
Pulse Sequence zg30
Number of Scans 16
Receiver Gain 78.7
Relaxation Delay 1.0000
Pulse Width 11.7000
Acquisition Time 4.0894
Acquisition Date 2018-05-03T11:25:07
Spectrometer Frequency 400.13
Spectral Width 8012.8
Lowest Frequency -1545.1
Nucleus 1H
Acquired Size 32768
Spectral Size 65536
A (m) 7.30
B (m) 6.42
C (m) 6.19
D (m) 4.56
E (m) 4.13
F (m) 3.97
G (m) 3.86
H (dd) 3.66
I (m) 3.55
J (m) 3.38
K (dq) 3.08
L (p) 2.80
M (dddt) 2.63
N (dtd) 2.19
O (m) 1.94
OBn
Ph
O
124f
10.00
0.74
0.75
1.88
1.36
0.42
0.94
0.24
1.87
0.51
0.57
0.15
0.19
0.74
0.83
0.5
1.0
3.1
f1 (ppm)

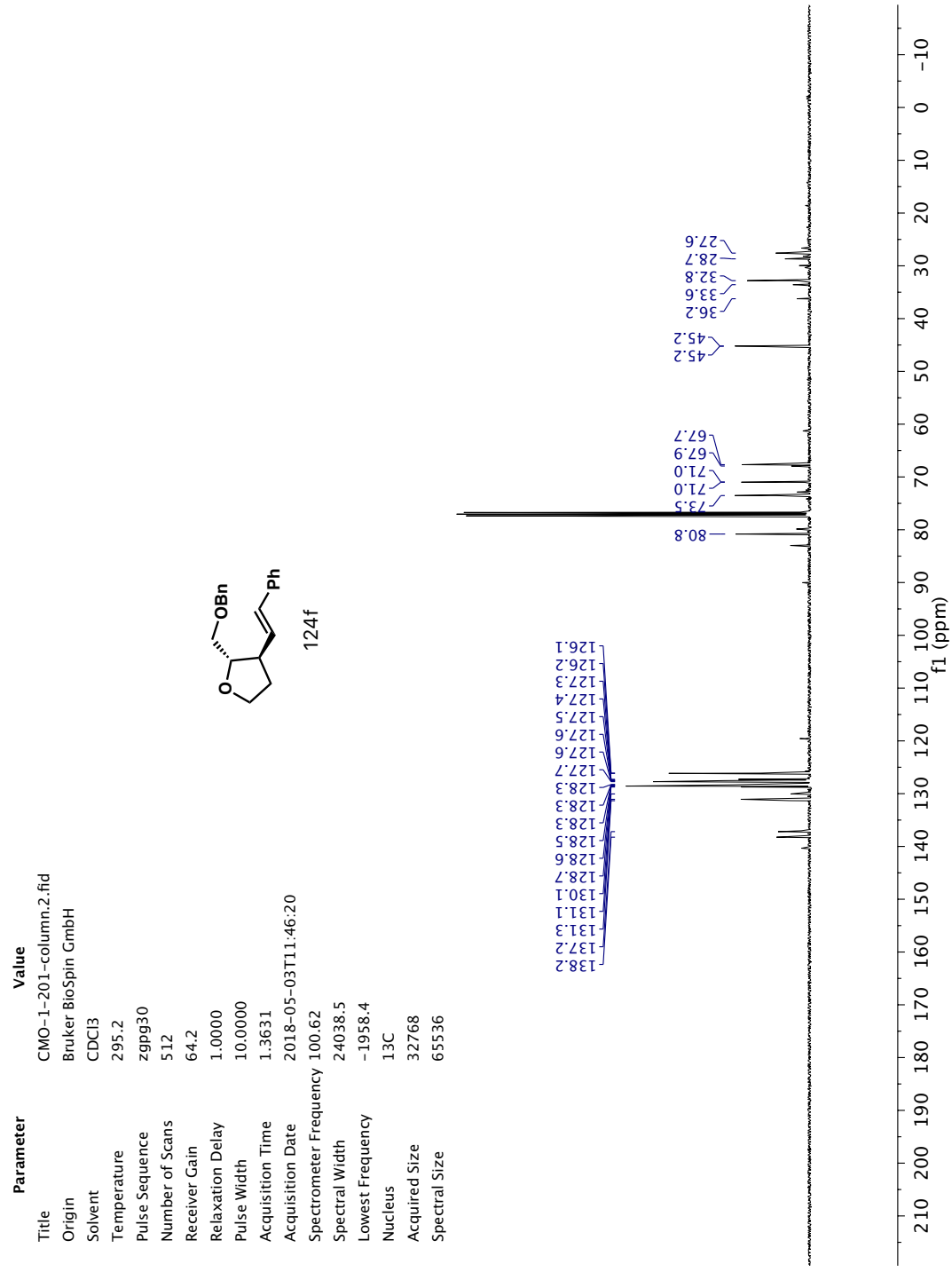
Parameter Value
Title CMO-1-201-column.2.fid
Origin Bruker BioSpin GmbH
Solvent CDCl3
Temperature 295.2
Pulse Sequence zgpg30
Number of Scans 512
Receiver Gain 64.2
Relaxation Delay 1.0000
Pulse Width 10.0000
Acquisition Time 1.3631
Acquisition Date 2018-05-03T11:46:20
Spectrometer Frequency 100.62
Spectral Width 24038.5
Lowest Frequency -1958.4
Nucleus 13C
Acquired Size 32768
Spectral Size 65536
OBn
Ph
O
124f
138.2
137.2
131.3
131.1
130.1
128.7
128.6
128.5
128.3
128.3
128.3
127.7
127.6
127.6
127.5
127.4
127.3
126.2
126.1
80.8
73.5
71.0
71.0
67.9
67.7
45.2
45.2
36.2
33.6
32.8
28.7
27.6
f1 (ppm)

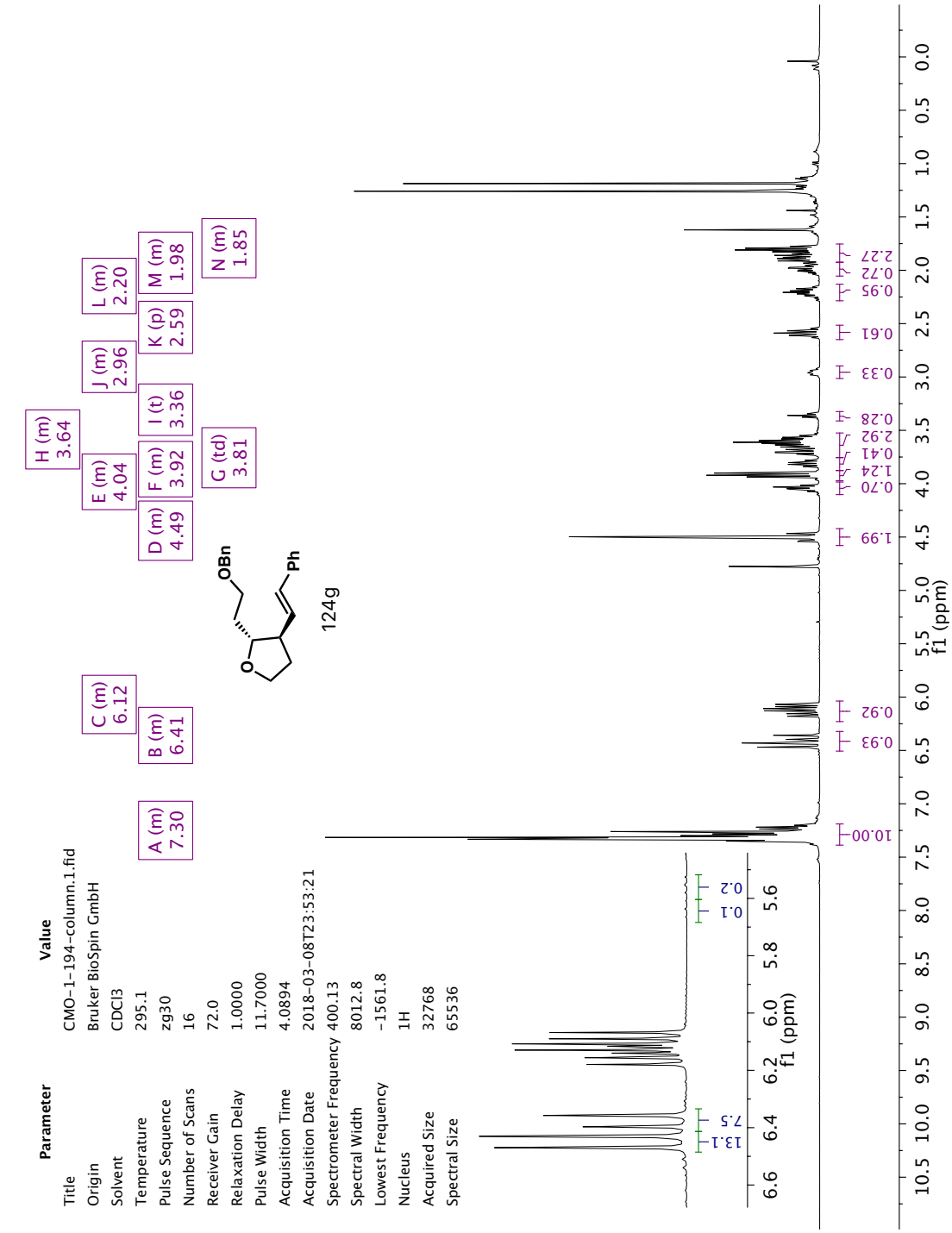
Parameter
Value
Title
CMO-1-194-column.1.fid
Origin
Bruker BioSpin GmbH
Solvent
CDCl3
Temperature
295.1
Pulse Sequence
zg30
Number of Scans
16
Receiver Gain
72.0
Relaxation Delay
1.0000
Pulse Width
11.7000
Acquisition Time
4.0894
Acquisition Date
2018-03-08T23:53:21
Spectrometer Frequency
400.13
Spectral Width
8012.8
Lowest Frequency
-1561.8
Nucleus
1H
Acquired Size
32768
Spectral Size
65536
A (m) 7.30
B (m) 6.41
C (m) 6.12
D (m) 4.49
E (m) 4.04
F (m) 3.92
G (td) 3.81
H (m) 3.64
I (t) 3.36
J (m) 2.96
K (p) 2.59
L (m) 2.20
M (m) 1.98
N (m) 1.85
OBn
Ph
O
124g
10.00
0.93
0.92
1.99
0.70
1.24
0.41
2.92
0.28
0.33
0.61
0.95
0.72
2.27
13.1
7.5
0.1
0.2
f1 (ppm)

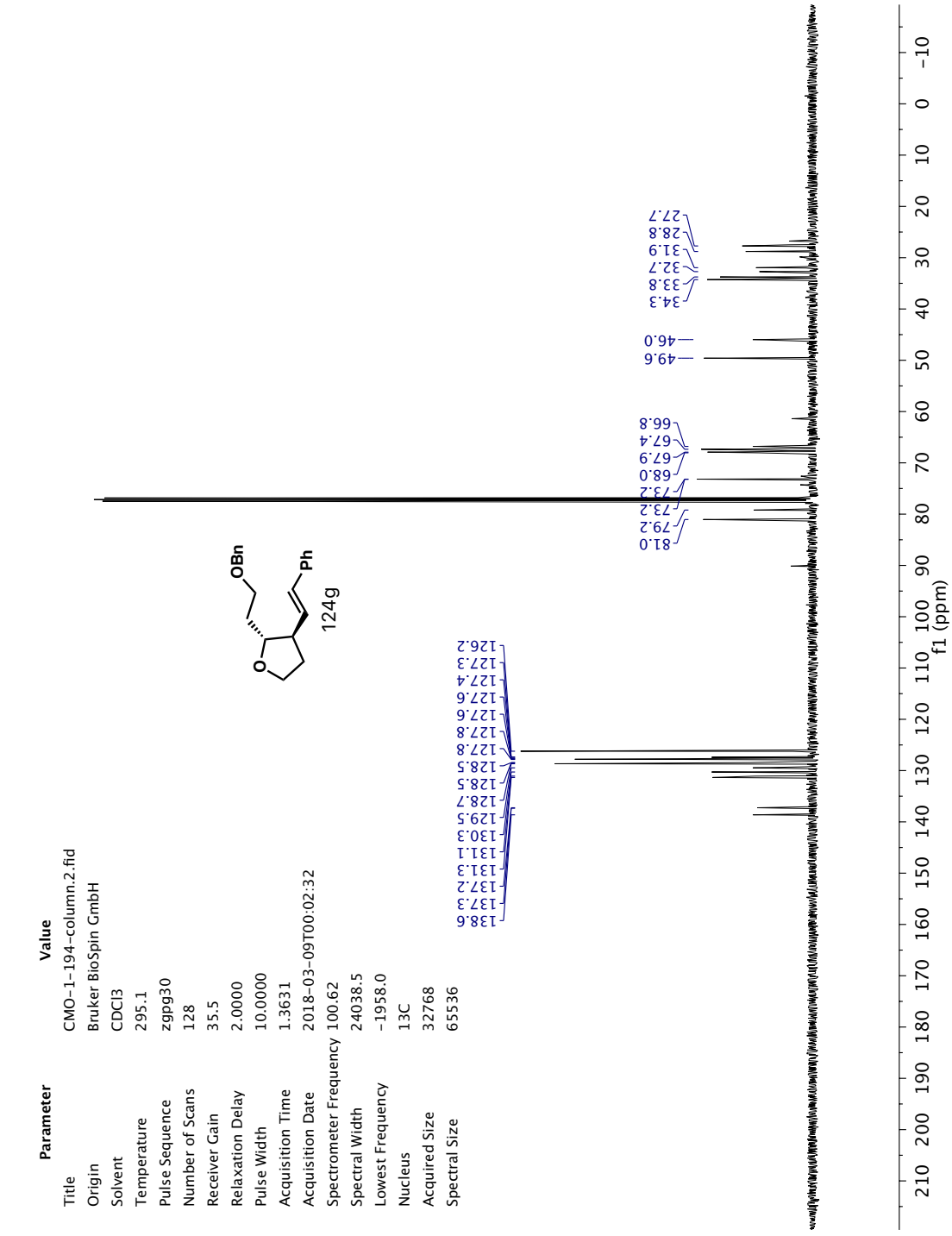
Parameter Value
Title CMO-1-194-column.2.fid
Origin Bruker BioSpin GmbH
Solvent CDCl3
Temperature 295.1
Pulse Sequence zgpg30
Number of Scans 128
Receiver Gain 35.5
Relaxation Delay 2.0000
Pulse Width 10.0000
Acquisition Time 1.3631
Acquisition Date 2018-03-09T00:02:32
Spectrometer Frequency 100.62
Spectral Width 24038.5
Lowest Frequency -1958.0
Nucleus 13C
Acquired Size 32768
Spectral Size 65536
OBn
Ph
O
124g
138.6
137.3
137.2
131.3
131.1
130.3
129.5
128.7
128.5
128.5
127.8
127.8
127.6
127.6
127.4
127.3
126.2
81.0
79.2
73.2
73.2
68.0
67.9
67.4
66.8
49.6
46.0
34.3
33.8
32.7
31.9
28.8
27.7
f1 (ppm)

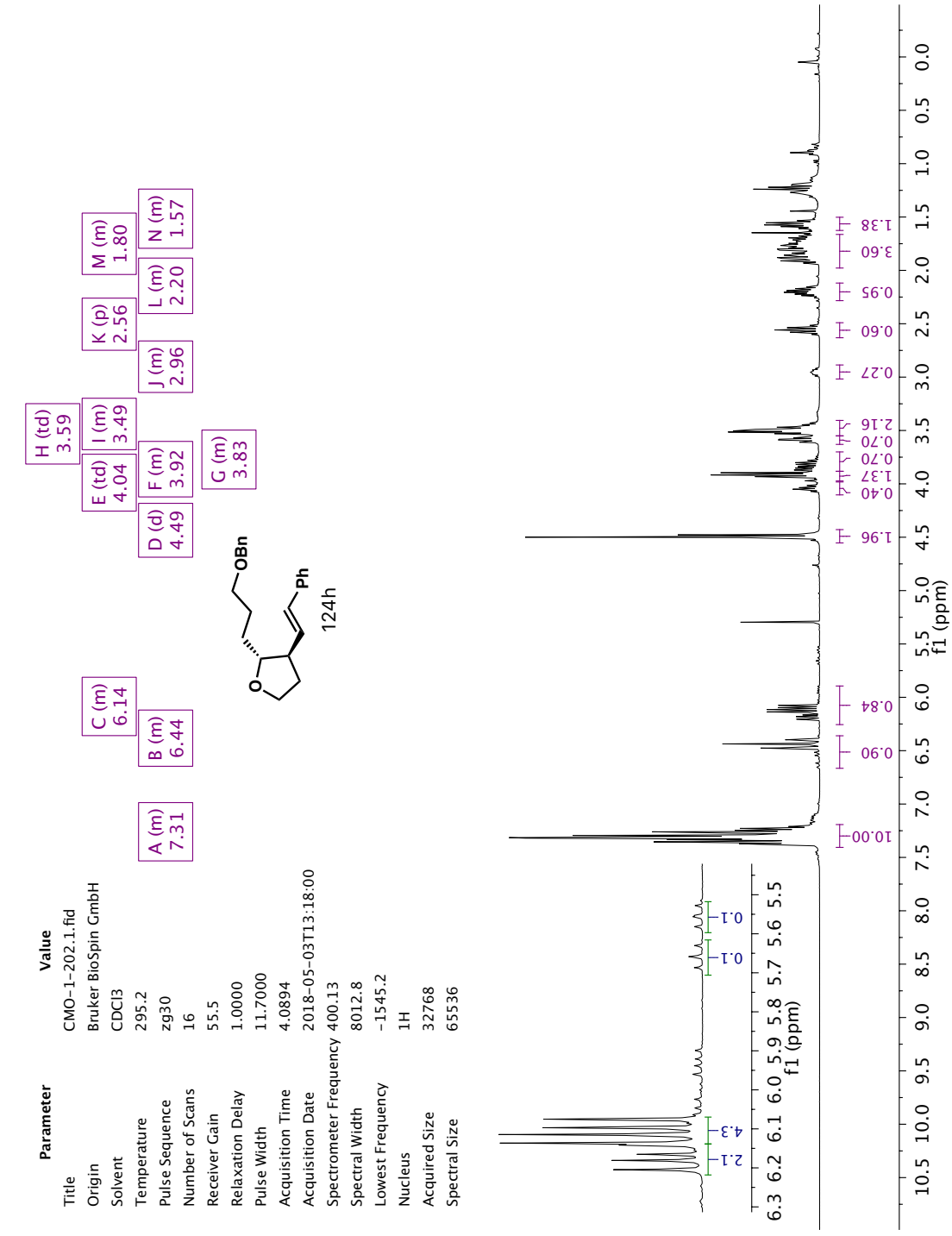
Parameter Value
Title CMO-1-202.1.fid
Origin Bruker BioSpin GmbH
Solvent CDCl3
Temperature 295.2
Pulse Sequence zg30
Number of Scans 16
Receiver Gain 55.5
Relaxation Delay 1.0000
Pulse Width 11.7000
Acquisition Time 4.0894
Acquisition Date 2018-05-03T13:18:00
Spectrometer Frequency 400.13
Spectral Width 8012.8
Lowest Frequency -1545.2
Nucleus 1H
Acquired Size 32768
Spectral Size 65536
A (m) 7.31
B (m) 6.44
C (m) 6.14
D (d) 4.49
E (td) 4.04
F (m) 3.92
G (m) 3.83
H (td) 3.59
I (m) 3.49
J (m) 2.96
K (p) 2.56
L (m) 2.20
M (m) 1.80
N (m) 1.57
OBn
Ph
O
124h
10.00
0.90
0.84
1.96
0.40
1.37
0.70
0.70
2.16
0.27
0.60
0.95
3.60
1.38
4.3
2.1
0.1
0.1
f1 (ppm)

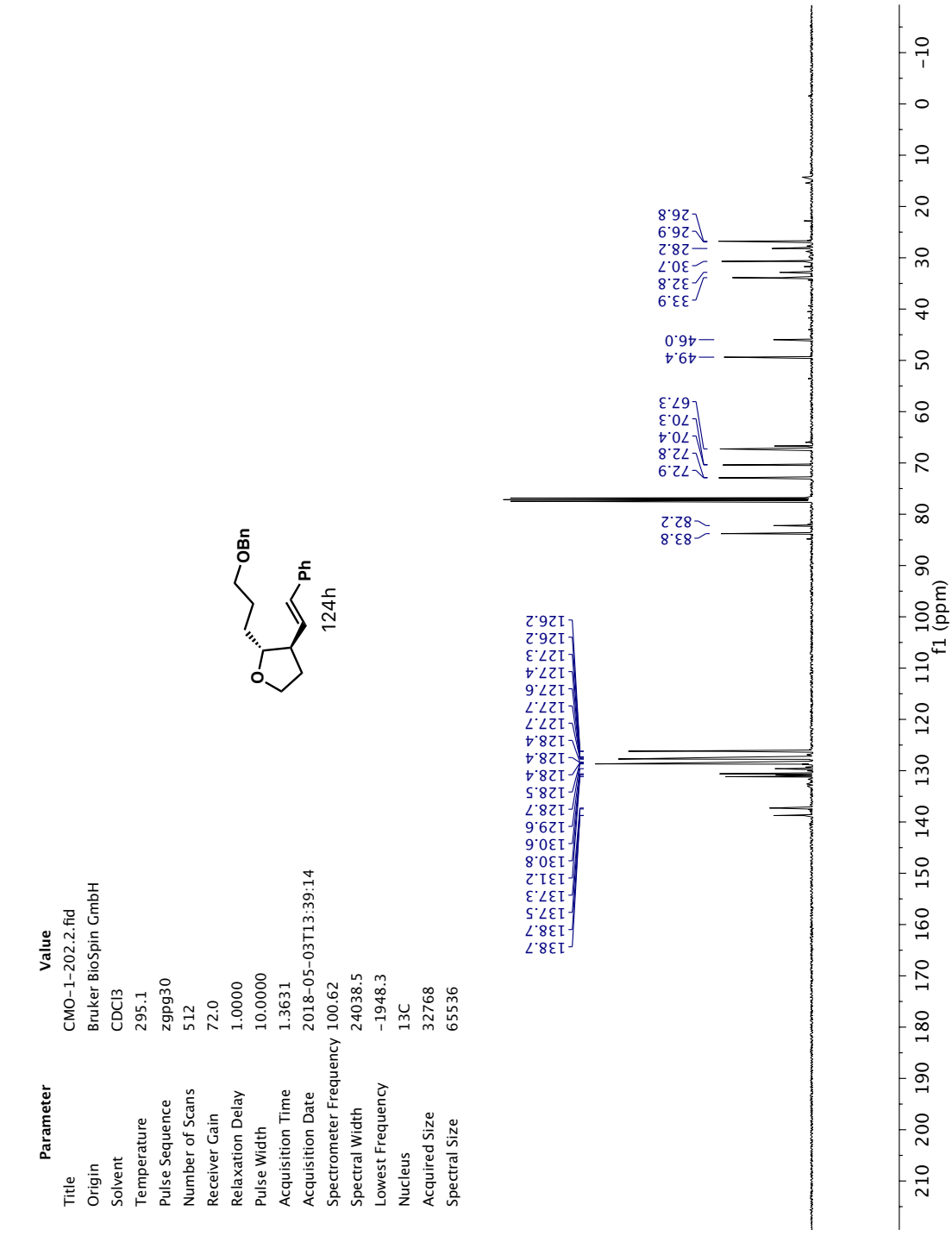
Parameter Value
Title CMO-1-202.2.fid
Origin Bruker BioSpin GmbH
Solvent CDCl3
Temperature 295.1
Pulse Sequence zgpg30
Number of Scans 512
Receiver Gain 72.0
Relaxation Delay 1.0000
Pulse Width 10.0000
Acquisition Time 1.3631
Acquisition Date 2018-05-03T13:39:14
Spectrometer Frequency 100.62
Spectral Width 24038.5
Lowest Frequency -1948.3
Nucleus 13C
Acquired Size 32768
Spectral Size 65536
OBn
Ph
O
124h
138.7
138.7
137.5
137.3
131.2
130.8
130.6
129.6
128.7
128.5
128.4
128.4
128.4
127.7
127.7
127.6
127.4
127.3
126.2
126.2
83.8
82.2
72.9
72.8
70.4
70.3
67.3
49.4
46.0
33.9
32.8
30.7
28.2
26.9
26.8
f1 (ppm)

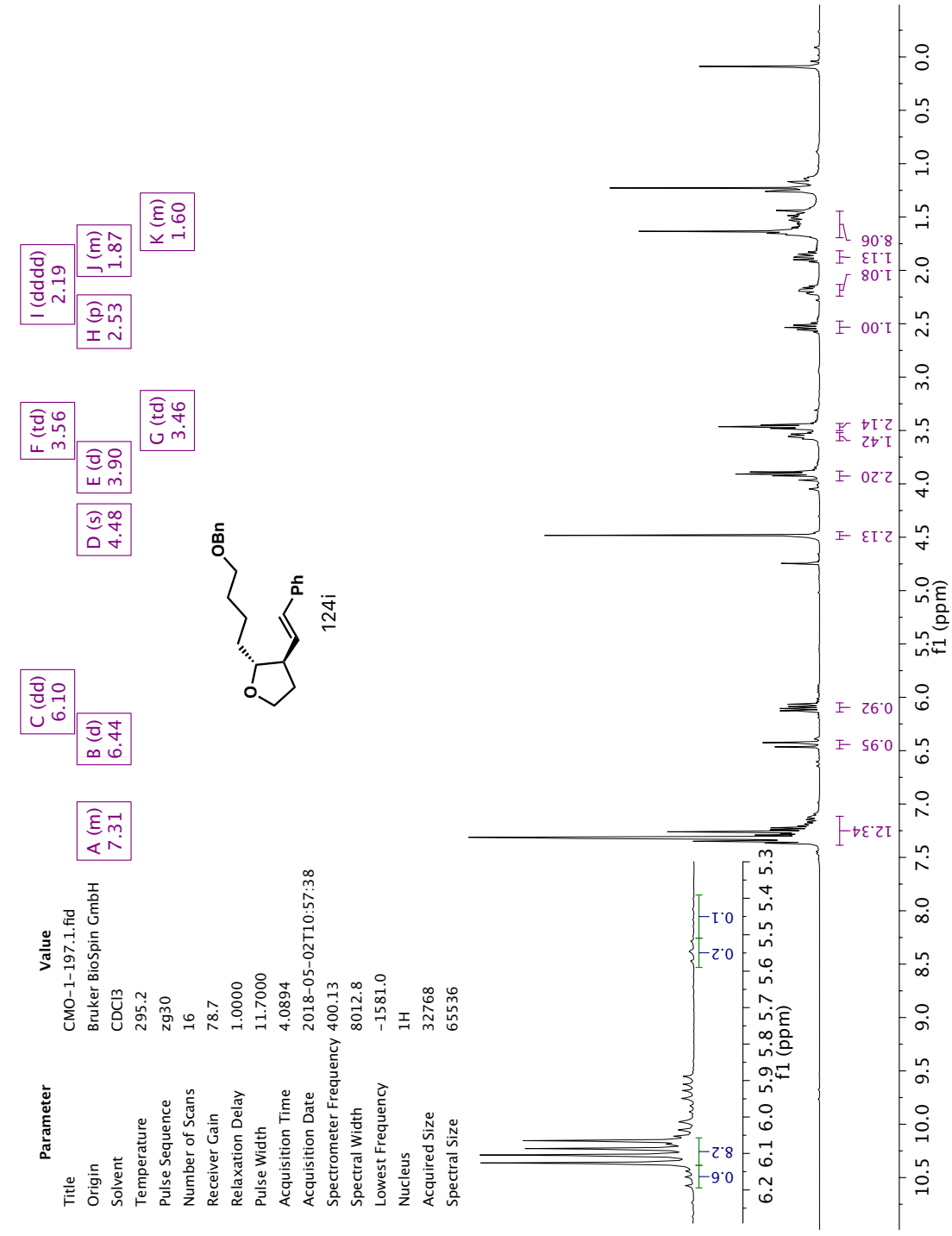
Parameter
Value
Title
CMO-1-197.1.fid
Origin
Bruker BioSpin GmbH
Solvent
CDCl3
Temperature
295.2
Pulse Sequence
zg30
Number of Scans
16
Receiver Gain
78.7
Relaxation Delay
1.0000
Pulse Width
11.7000
Acquisition Time
4.0894
Acquisition Date
2018-05-02T10:57:38
Spectrometer Frequency
400.13
Spectral Width
8012.8
Lowest Frequency
-1581.0
Nucleus
1H
Acquired Size
32768
Spectral Size
65536
A (m) 7.31
B (d) 6.44
C (dd) 6.10
D (s) 4.48
E (d) 3.90
F (td) 3.56
G (td) 3.46
H (p) 2.53
I (dddd) 2.19
J (m) 1.87
K (m) 1.60
OBn
Ph
O
124i
12.34
0.92
0.95
2.13
2.20
1.42
2.14
1.00
1.08
1.13
8.06
0.1
0.2
0.6
8.2
f1 (ppm)

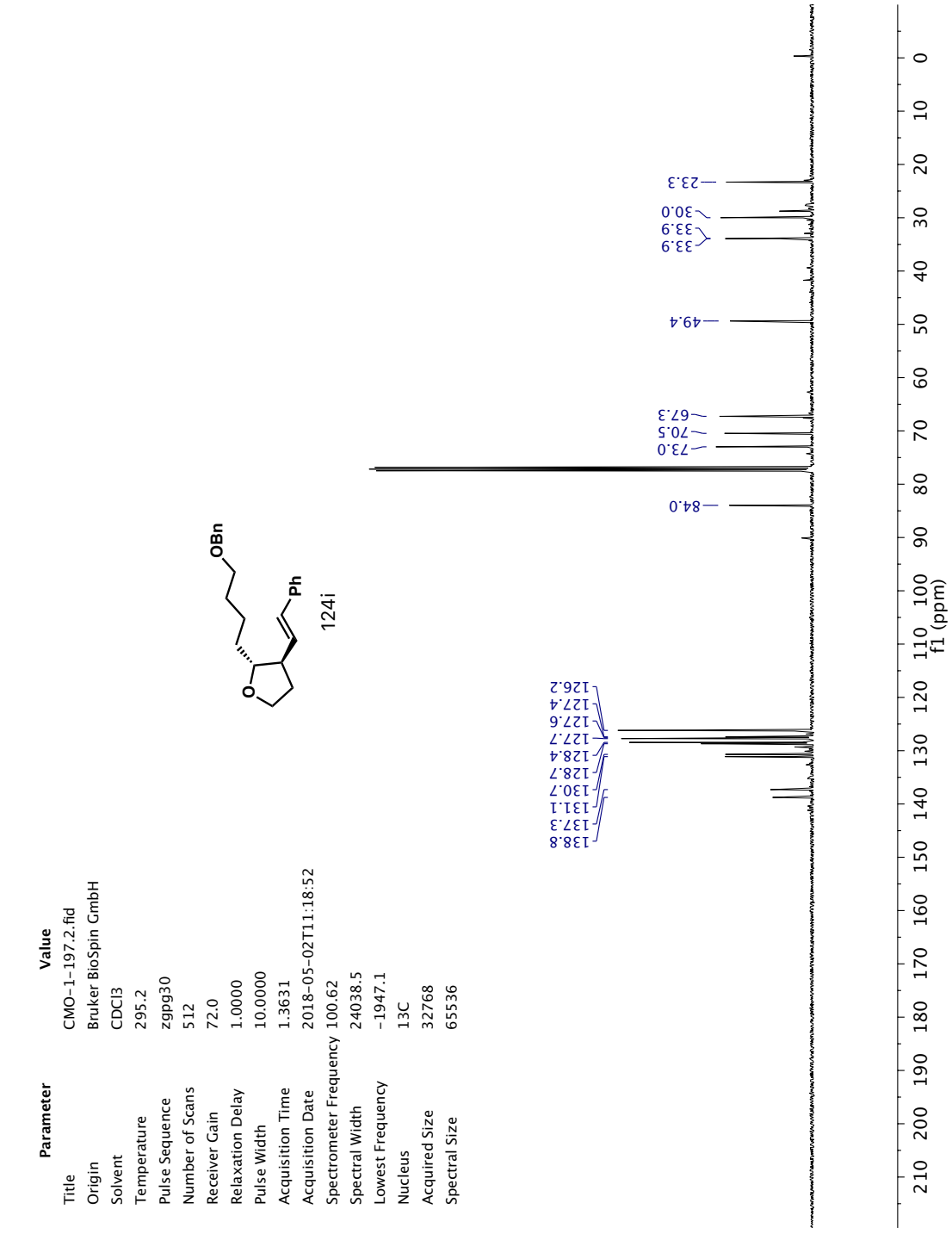
Parameter Value
Title CMO-1-197.2.fid
Origin Bruker BioSpin GmbH
Solvent CDCl3
Temperature 295.2
Pulse Sequence zgpg30
Number of Scans 512
Receiver Gain 72.0
Relaxation Delay 1.0000
Pulse Width 10.0000
Acquisition Time 1.3631
Acquisition Date 2018-05-02T11:18:52
Spectrometer Frequency 100.62
Spectral Width 24038.5
Lowest Frequency -1947.1
Nucleus 13C
Acquired Size 32768
Spectral Size 65536
OBn
Ph
O
124i
23.3
30.0
33.9
33.9
49.4
67.3
70.5
73.0
84.0
126.2
127.4
127.6
127.7
128.4
128.7
130.7
131.1
137.3
138.8
f1 (ppm)

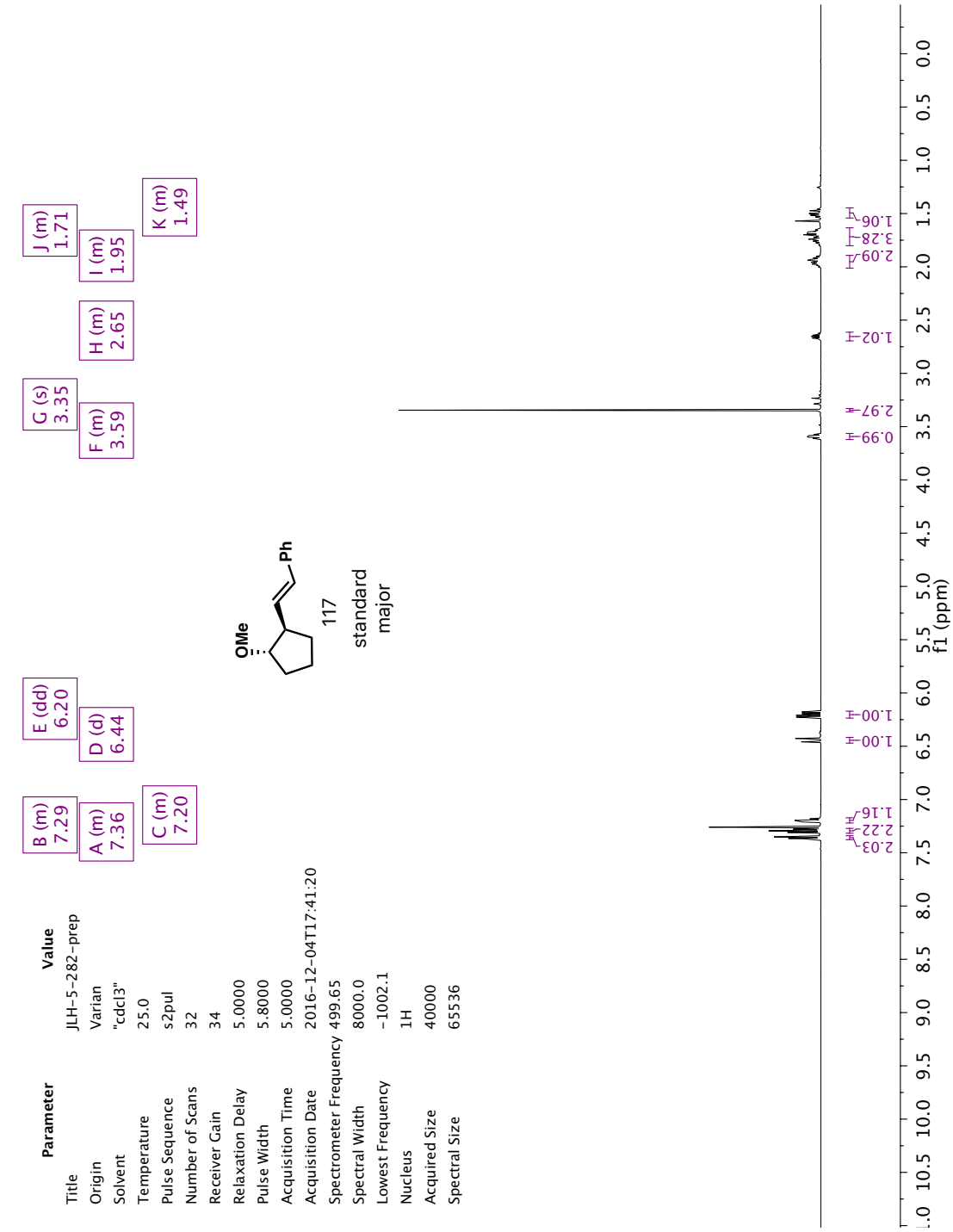
B (m) 7.29
A (m) 7.36
C (m) 7.20
E (dd) 6.20
D (d) 6.44
G (s) 3.35
F (m) 3.59
H (m) 2.65
J (m) 1.71
I (m) 1.95
K (m) 1.49
OMe
Ph
117
standard
major
Parameter Value
Title JLH-5-282-prep
Origin Varian
Solvent "cdcl3"
Temperature 25.0
Pulse Sequence s2pul
Number of Scans 32
Receiver Gain 34
Relaxation Delay 5.0000
Pulse Width 5.8000
Acquisition Time 5.0000
Acquisition Date 2016-12-04T17:41:20
Spectrometer Frequency 499.65
Spectral Width 8000.0
Lowest Frequency -1002.1
Nucleus 1H
Acquired Size 40000
Spectral Size 65536
2.03
2.22
1.16
1.00
1.00
2.97
0.99
1.02
2.09
3.28
1.06
f1 (ppm)

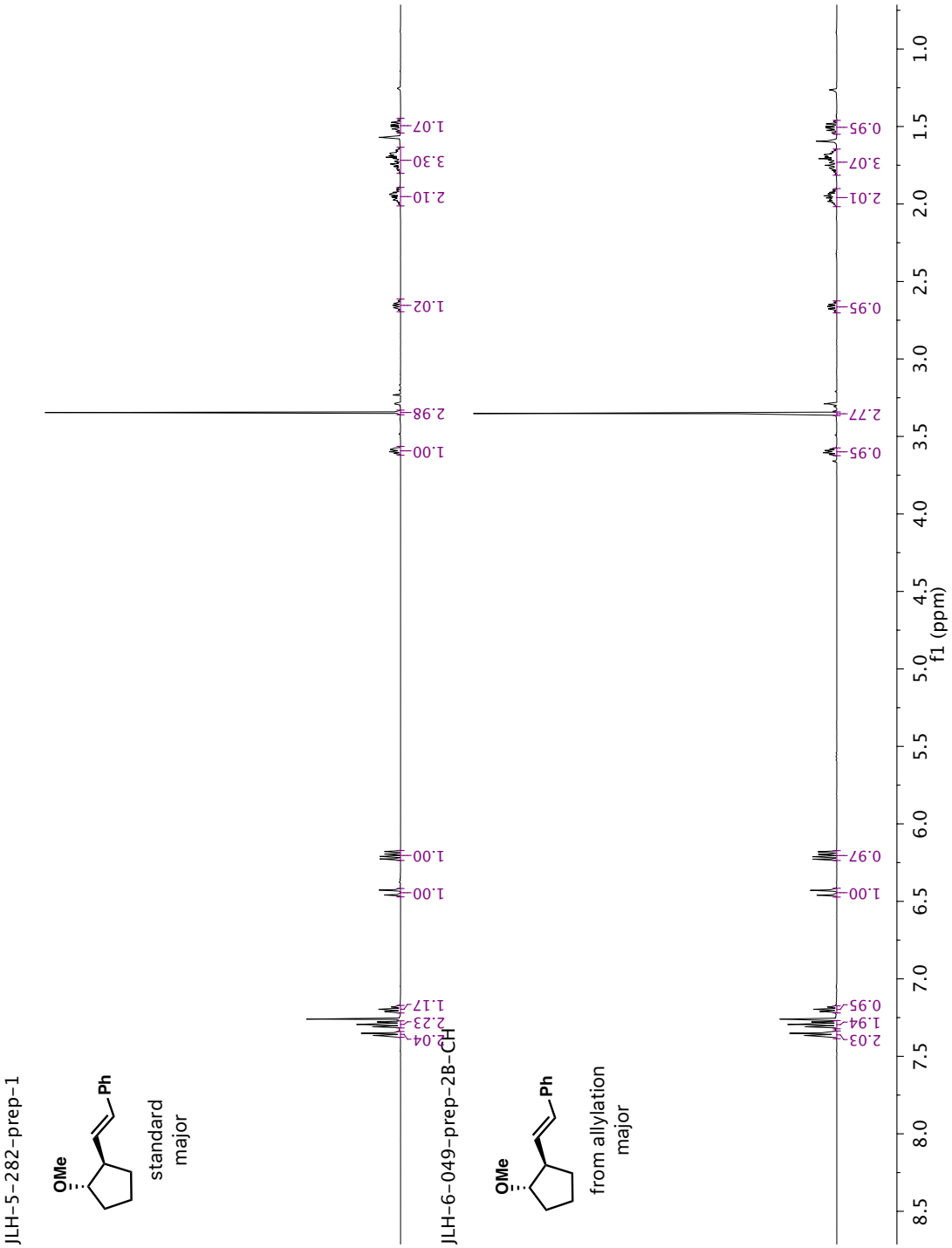
JLH-5-282-prep-1
OMe
Ph
standard
major
JLH-6-049-prep-2B-CH
1.07
3.30
2.10
1.02
2.98
1.00
1.00
1.00
1.17
2.23
2.04
OMe
Ph
from allylation
major
0.95
3.07
2.01
0.95
2.77
0.95
0.97
1.00
0.95
1.94
2.03
8.5
8.0
7.5
7.0
6.5
6.0
5.5
5.0
4.5
4.0
3.5
3.0
2.5
2.0
1.5
1.0
f1 (ppm)

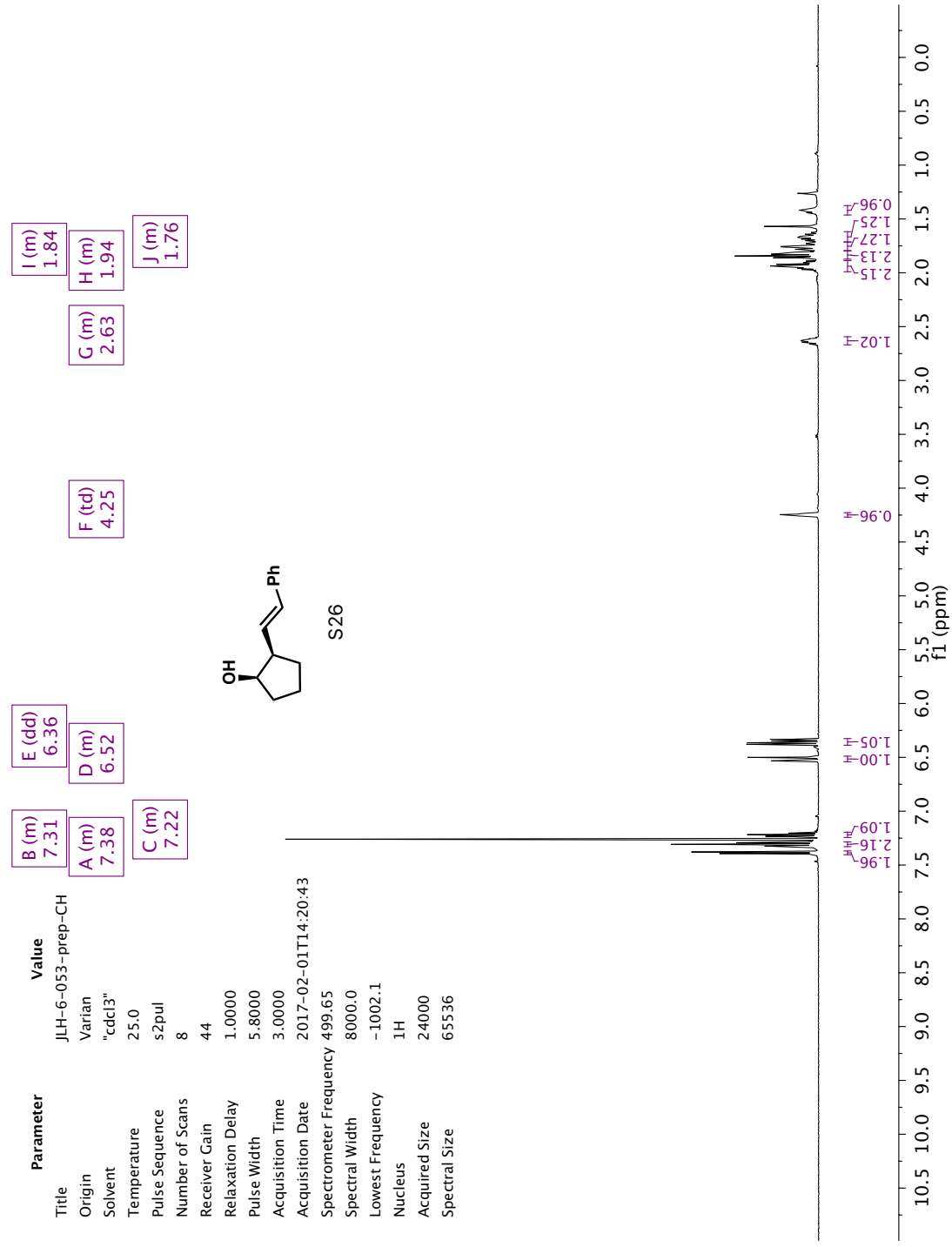
Parameter
Value
Title JLH-6-053-prep-CH
Origin Varian
Solvent "cdcl3"
Temperature 25.0
Pulse Sequence s2pul
Number of Scans 8
Receiver Gain 44
Relaxation Delay 1.0000
Pulse Width 5.8000
Acquisition Time 3.0000
Acquisition Date 2017-02-01T14:20:43
Spectrometer Frequency 499.65
Spectral Width 8000.0
Lowest Frequency -1002.1
Nucleus 1H
Acquired Size 24000
Spectral Size 65536
B (m) 7.31
A (m) 7.38
C (m) 7.22
E (dd) 6.36
D (m) 6.52
F (td) 4.25
G (m) 2.63
I (m) 1.84
H (m) 1.94
J (m) 1.76
OH
Ph
S26
1.96
2.16
1.09
1.00
1.05
0.96
1.02
2.15
2.13
1.27
1.25
0.96
10.5 10.0 9.5 9.0 8.5 8.0 7.5 7.0 6.5 6.0 5.5 5.0 4.5 4.0 3.5 3.0 2.5 2.0 1.5 1.0 0.5 0.0
f1 (ppm)

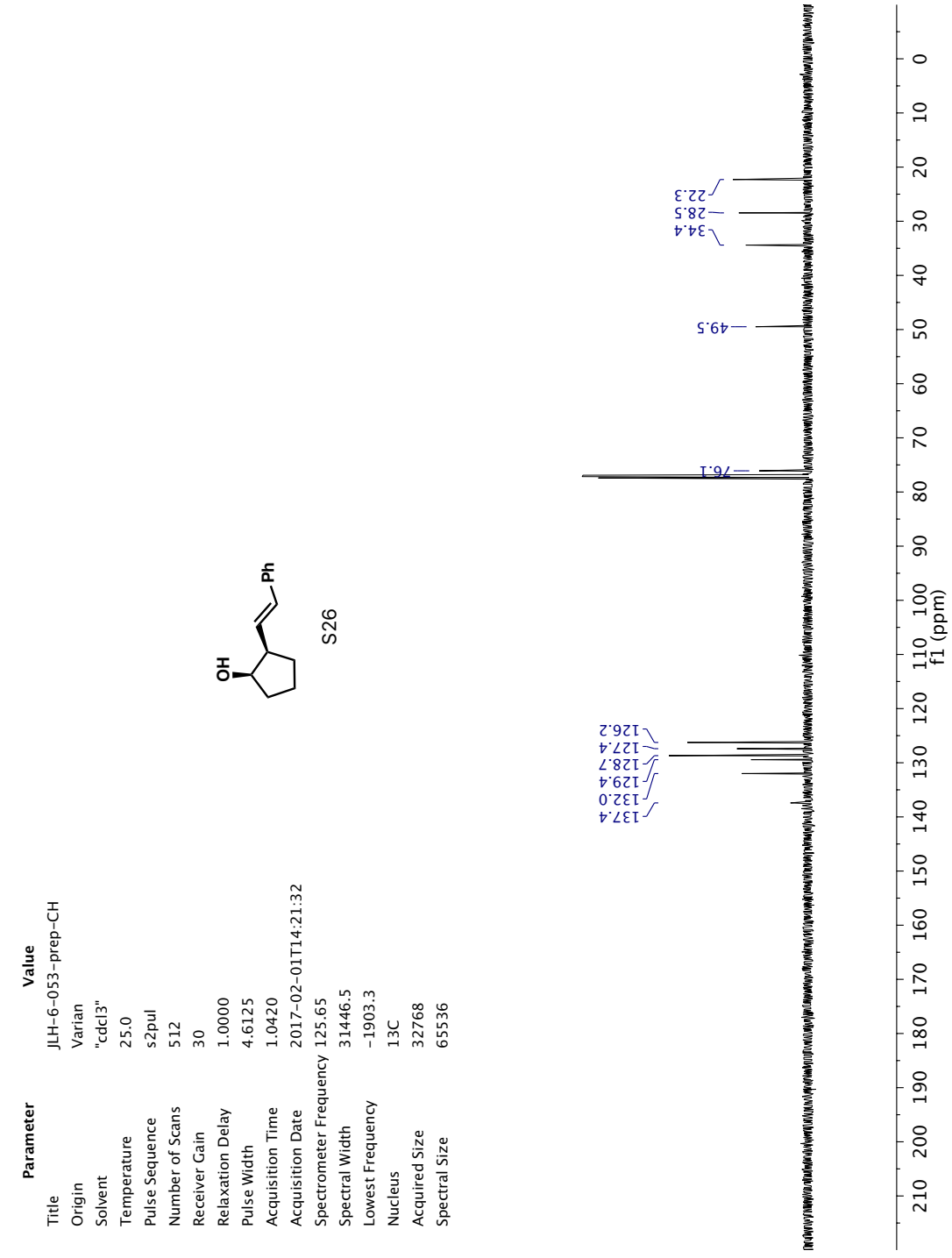
Parameter Value
Title JLH-6-053-prep-CH
Origin Varian
Solvent "cdcl3"
Temperature 25.0
Pulse Sequence s2pul
Number of Scans 512
Receiver Gain 30
Relaxation Delay 1.0000
Pulse Width 4.6125
Acquisition Time 1.0420
Acquisition Date 2017-02-01T14:21:32
Spectrometer Frequency 125.65
Spectral Width 31446.5
Lowest Frequency -1903.3
Nucleus 13C
Acquired Size 32768
Spectral Size 65536
OH
Ph
S26
137.4
132.0
129.4
128.7
127.4
126.2
76.1
49.5
34.4
28.5
22.3
f1 (ppm)

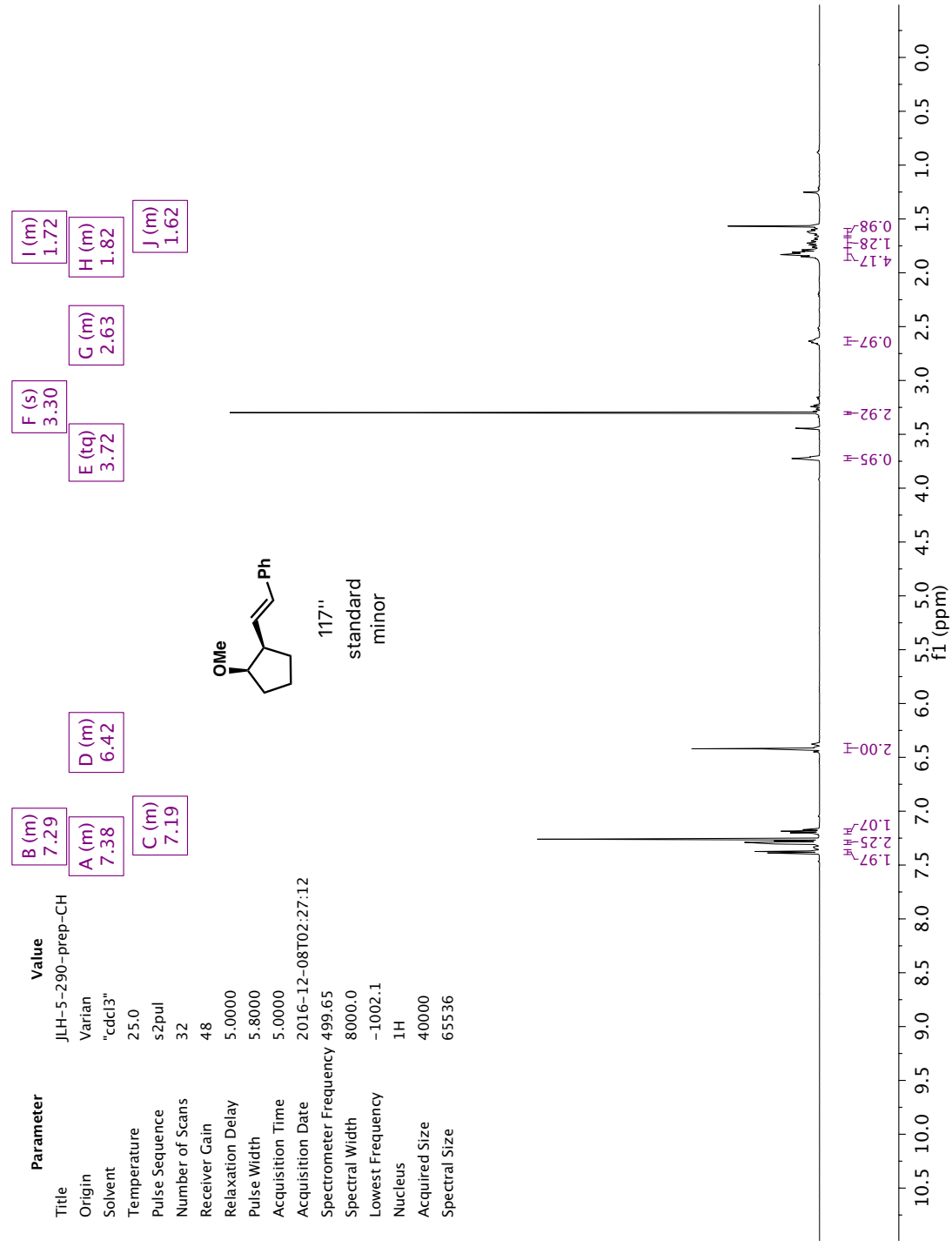
Parameter
Value
Title JLH-5-290-prep-CH
Origin Varian
Solvent "cdcl3"
Temperature 25.0
Pulse Sequence s2pul
Number of Scans 32
Receiver Gain 48
Relaxation Delay 5.0000
Pulse Width 5.8000
Acquisition Time 5.0000
Acquisition Date 2016-12-08T02:27:12
Spectrometer Frequency 499.65
Spectral Width 8000.0
Lowest Frequency -1002.1
Nucleus 1H
Acquired Size 40000
Spectral Size 65536
B (m) 7.29
A (m) 7.38
C (m) 7.19
D (m) 6.42
F (s) 3.30
E (tq) 3.72
G (m) 2.63
I (m) 1.72
H (m) 1.82
J (m) 1.62
OMe
Ph
117''
standard
minor
1.97
2.25
1.07
2.00
0.95
2.92
0.97
4.17
1.28
0.98
f1 (ppm)

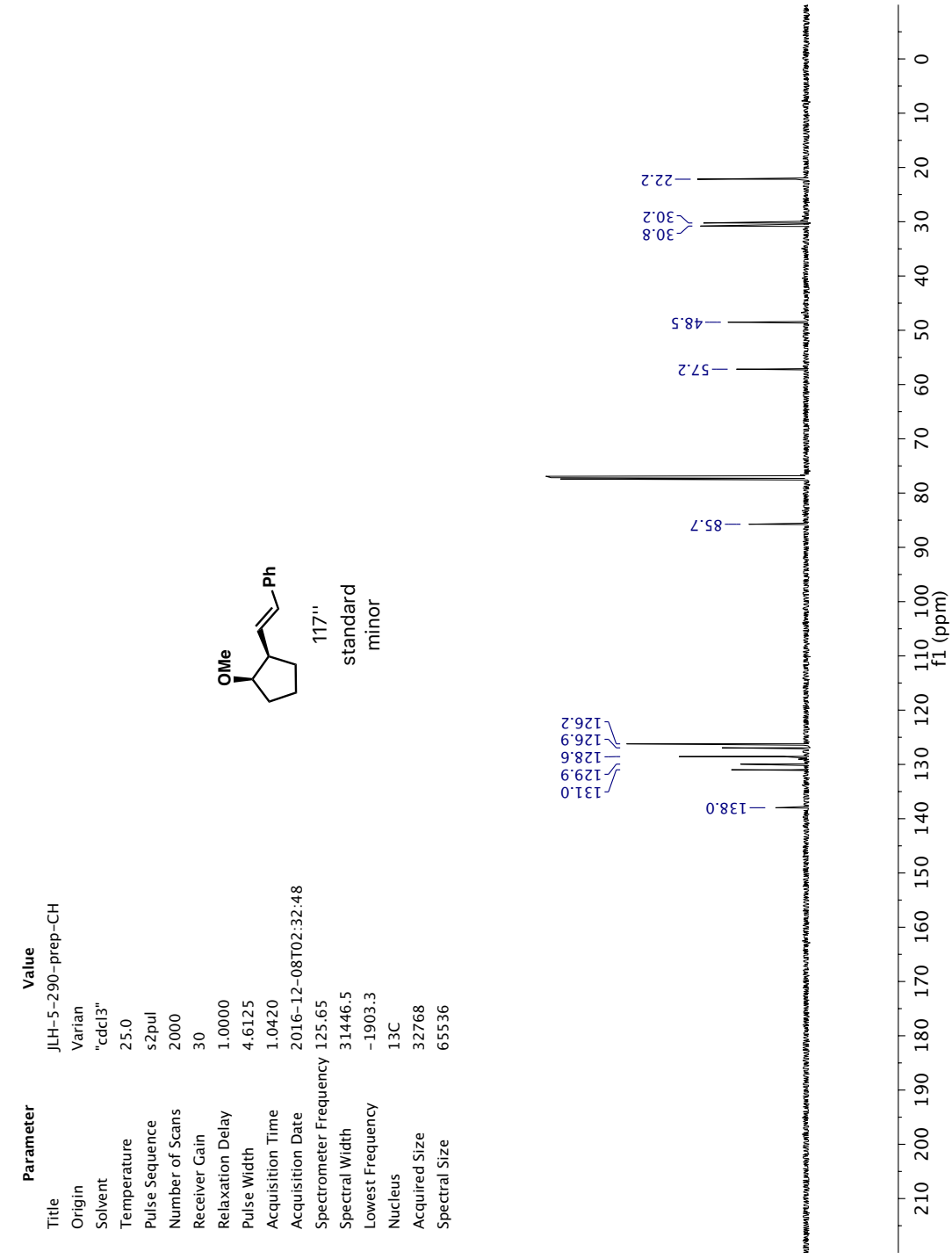

Parameter	Value
Title	JLH-5-290-prep-CH
Origin	Varian
Solvent	"cdcl3"
Temperature	25.0
Pulse Sequence	s2pul
Number of Scans	2000
Receiver Gain	30
Relaxation Delay	1.0000
Pulse Width	4.6125
Acquisition Time	1.0420
Acquisition Date	2016-12-08T02:32:48
Spectrometer Frequency	125.65
Spectral Width	31446.5
Lowest Frequency	-1903.3
Nucleus	13C
Acquired Size	32768
Spectral Size	65536

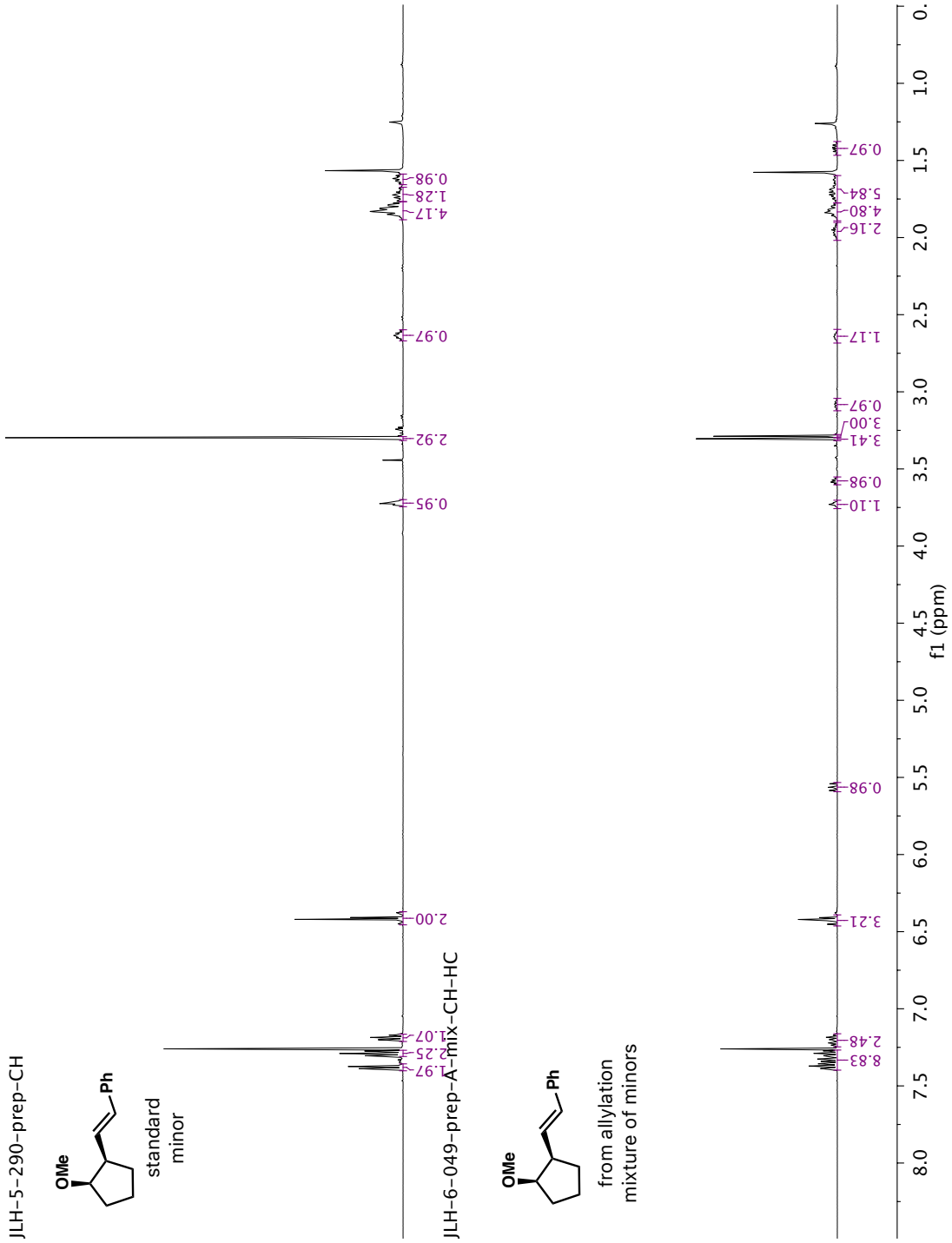
JLH-5-290-prep-CH
OMe
Ph
standard
minor
JLH-6-049-prep-A-mix-CH-HC
OMe
Ph
from allylation
mixture of minors
f1 (ppm)

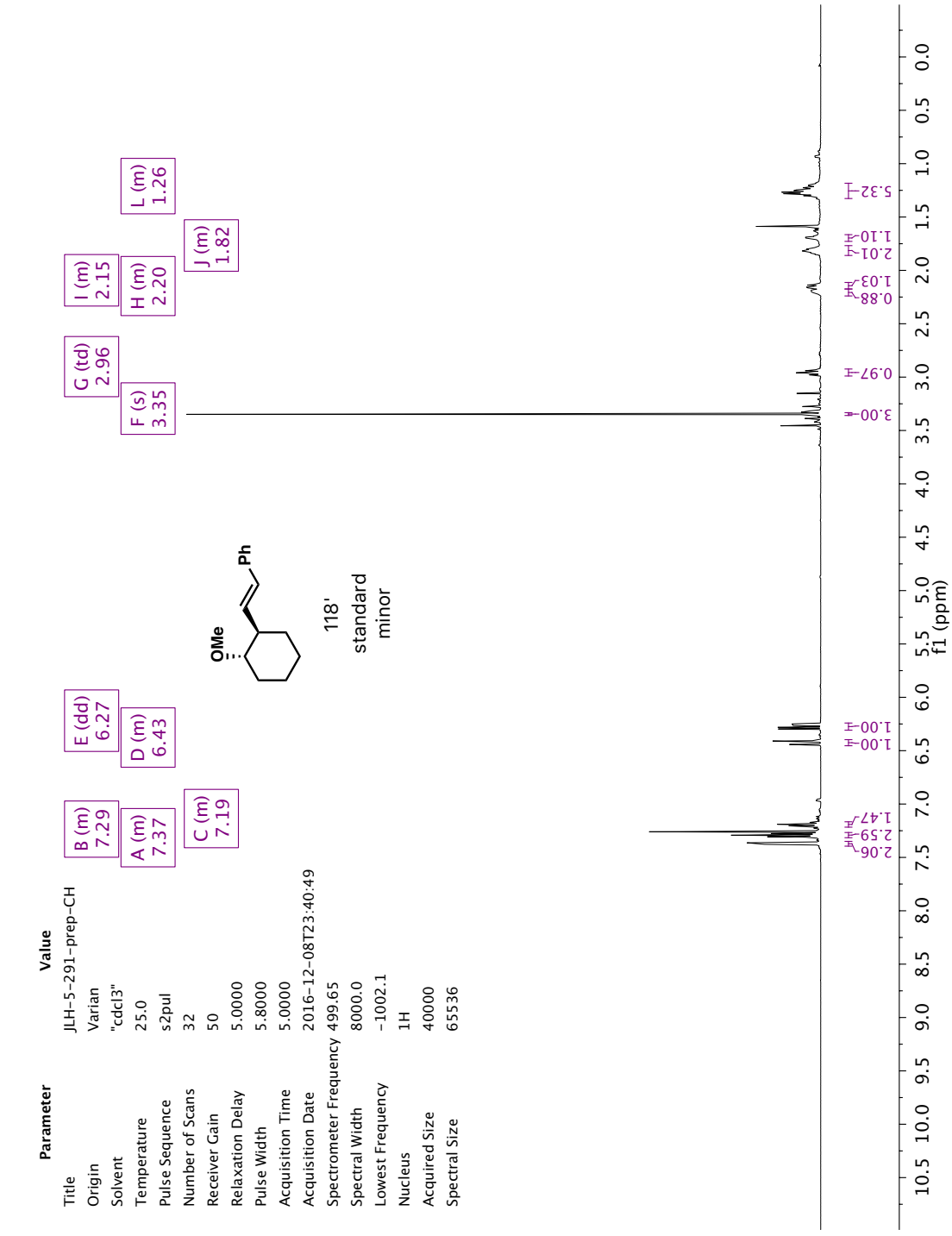
Parameter
Value
Title JLH-5-291-prep-CH
Origin Varian
Solvent "cdcl3"
Temperature 25.0
Pulse Sequence s2pul
Number of Scans 32
Receiver Gain 50
Relaxation Delay 5.0000
Pulse Width 5.8000
Acquisition Time 5.0000
Acquisition Date 2016-12-08T23:40:49
Spectrometer Frequency 499.65
Spectral Width 8000.0
Lowest Frequency -1002.1
Nucleus 1H
Acquired Size 40000
Spectral Size 65536
B (m) 7.29
A (m) 7.37
C (m) 7.19
E (dd) 6.27
D (m) 6.43
OMe
Ph
118'
standard
minor
F (s) 3.35
G (td) 2.96
I (m) 2.15
H (m) 2.20
J (m) 1.82
L (m) 1.26
2.06
2.59
1.47
1.00
1.00
3.00
0.97
0.88
1.03
2.01
1.10
5.32
10.5 10.0 9.5 9.0 8.5 8.0 7.5 7.0 6.5 6.0 5.5 5.0 4.5 4.0 3.5 3.0 2.5 2.0 1.5 1.0 0.5 0.0
f1 (ppm)

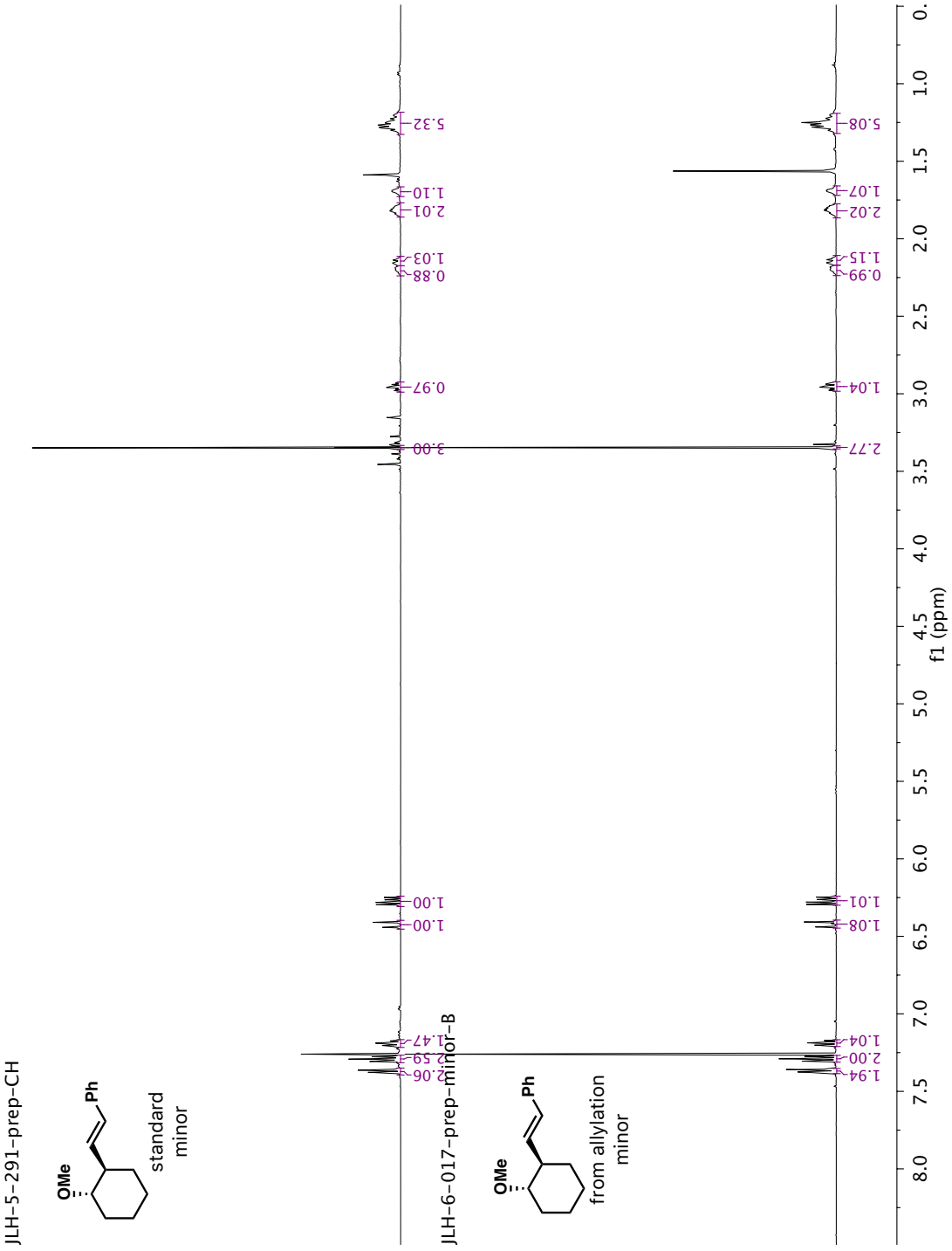
JLH-5-291-prep-CH
OMe
Ph
standard
minor
JLH-6-017-prep-minor-B
OMe
Ph
from allylation
minor
5.32
1.10
2.01
1.03
0.88
0.97
3.00
1.00
1.00
1.47
2.59
2.06
5.08
1.07
2.02
1.15
0.99
1.04
2.77
1.01
1.08
1.04
2.00
1.94
0.
1.0
1.5
2.0
2.5
3.0
3.5
4.0
4.5
5.0
5.5
6.0
6.5
7.0
7.5
8.0
f1 (ppm)

Appendix 2

X-Ray Crystallography Reports Relevant to Chapter 2:

Synthesis and Utility of Chiral Allylic Silanes Prepared

via Ni-Catalyzed Asymmetric Reductive Cross-Coupling

A2.1 STRUCTURAL DETERMINATION AND REFINEMENT DETAILS

Low-temperature diffraction data (ϕ- and ω-scans) were collected on a Bruker AXS D8 VENTURE KAPPA diffractometer coupled to a PHOTON 100 CMOS detector with Mo-$K\alpha$ radiation (λ = 0.71073 Å) or a PHOTON II CPAD detector with Cu-$K\alpha$ radiation (λ = 1.54178 Å) from an $I_\mu S$ HB micro-focused X-ray tube. All diffractometer manipulations, including data collection integration, and scaling were carried out using the Bruker APEXII software.[1] Absorption corrections were applied using SADABS.[2] The structure was solved by using intrinsic phasing using SHELXT[3] and refined against F^2 on all data by full-matrix least squares with SHELXL-2014[4] using established refinement techniques.[5] All non-hydrogen atoms were refined anisotropically. All hydrogen atoms were included in the model at geometrically calculated positions and refined using a riding model. The isotropic displacement parameters of all hydrogen atoms were fixed to 1.2 times the U value of the atoms they are linked to (1.5 times for methyl groups). Absolute configuration was determined by anomalous dispersion[6] and confirmed by Bayesian statistical analysis using the program PLATON.[7] Graphical representation of the structure with 50% probability thermal ellipsoids was generated using Mercury visualization software.

A2.2 CRYSTALLOGRAPHIC ANALYSIS OF L2·$NiCl_2$ (MONOMER)

A2.2.1 Special Refinement Details

Figure A2.1 *Rendering of Ni-complex* ***L2***·$NiCl_2$ *(monomer).*

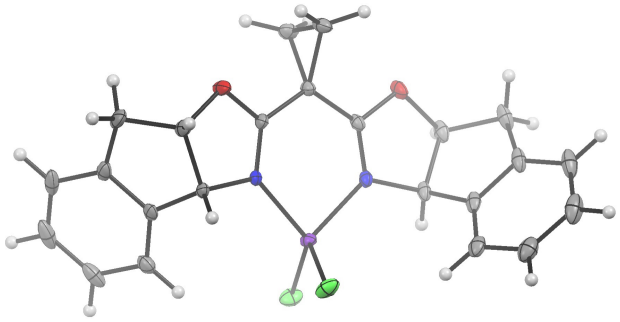

L2·$NiCl_2$ crystallizes in the orthorhombic space group $P2_12_12_1$ with one molecule in the asymmetric unit. Data was collected with Mo-$K\alpha$ radiation (λ = 0.71073 Å) at 100 K. Absolute configuration was determined by anomalous dispersion (Flack = 0.017(2)).[6]

A2.2.2 Crystallographic Tables

Table A2.1. *Crystal data and structure refinement for* ***L2***·$NiCl_2$ *(monomer).*

Identification code	P15028	
CCDC Number	1547485	
Empirical formula	$C_{23}H_{20}Cl_2N_2NiO_2$	
Formula weight	486.02	
Temperature	100 K	
Wavelength	0.71073 Å	
Crystal system	Orthorhombic	
Space group	$P2_12_12_1$	
Unit cell dimensions	a = 9.2189(2) Å	α = 90°
	b = 10.5914(3) Å	β = 90°
	c = 22.0654(6) Å	γ = 90°
Volume	2154.49(10) $Å^3$	
Z	4	
Density (calculated)	1.498 Mg/m^3	
Absorption coefficient	1.171 mm^{-1}	
F(000)	1000	
Crystal size	0.22 x 0.18 x 0.17 mm^3	
Theta range for data collection	2.394 to 43.426°	
Index ranges	-17<=h<=16, -20<=k<=20, -42<=l<=42	
Reflections collected	201119	
Independent reflections	16184 [R(int) = 0.0685]	
Completeness to theta = 25.000°	99.8 %	
Absorption correction	Semi-empirical from equivalents	
Max. and min. transmission	1.0000 and 0.9466	
Refinement method	Full-matrix least-squares on F^2	
Data / restraints / parameters	16184 / 0 / 271	
Goodness-of-fit on F^2	1.042	
Final R indices [I>2sigma(I)]	R1 = 0.0474, wR2 = 0.0700	
R indices (all data)	R1 = 0.0985, wR2 = 0.0785	
Absolute structure parameter	0.017(2)	
Extinction coefficient	n/a	
Largest diff. peak and hole	0.562 and -0.595 e.$Å^{-3}$	

A2.3 CRYSTALLOGRAPHIC ANALYSIS OF L2·$NiCl_2$ (TRIMER)

A2.3.1 Special Refinement Details

Figure A2.2 *Rendering of Ni-complex* ***L2***·$NiCl_2$ *(trimer).*

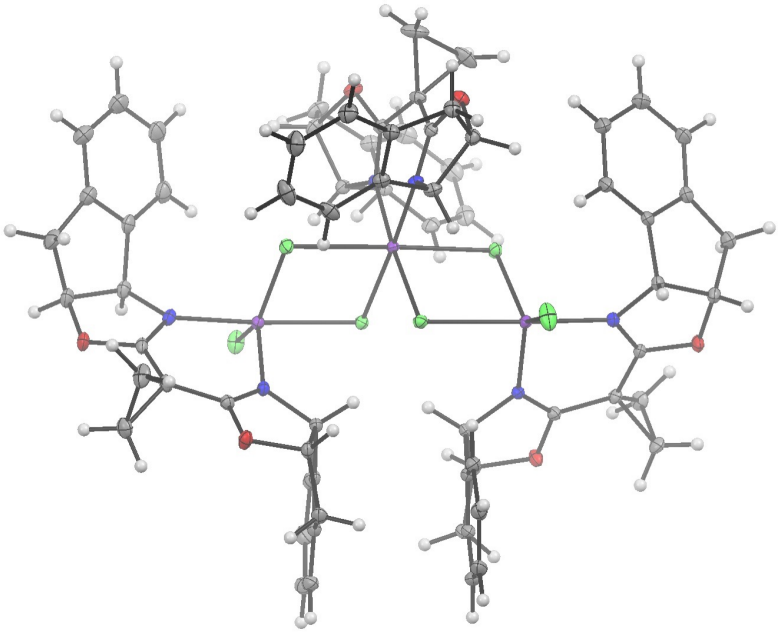

L2·$NiCl_2$ crystallizes in the monoclinic space group $P2_1$ with one molecule (consisting of three ligand·nickel subunits) in the asymmetric unit. Data was collected with Mo-$K\alpha$ radiation (λ = 0.71073 Å) at 100 K. The first solvent void was fully occupied by CH_2Cl_2. The second solvent void was occupied by either CH_2Cl_2 or MeCN with relative populations of 27% and 73%, respectively. Solvent is omitted for clarity in the graphical representation. Absolute configuration was determined by anomalous dispersion (Flack = 0.0162(19)).[6]

A2.3.2 Crystallographic Tables

Table A2.2. *Crystal data and structure refinement for* ***L2***·$NiCl_2$ *(trimer).*

Identification code	P16408	
CCDC Number	1547484	
Empirical formula	$C_{69}H_{60}Cl_6N_6Ni_3O_6$, 1.27($CH_2Cl_2$), 0.73($C_2H_3N$)	
Formula weight	1595.88	
Temperature	100 K	
Wavelength	0.71073 Å	
Crystal system	Monoclinic	
Space group	P 1 21 1	
Unit cell dimensions	a = 14.8277(18) Å	α = 90°
	b = 15.771(2) Å	β = 116.546(4)°
	c = 16.569(2) Å	γ = 90°
Volume	3466.1(8) $Å^3$	
Z	2	
Density (calculated)	1.529 Mg/m^3	
Absorption coefficient	1.194 mm^{-1}	
F(000)	1639	
Crystal size	0.30 x 0.30 x 0.15 mm^3	
Theta range for data collection	2.476 to 36.402°	
Index ranges	-24<=h<=24, -26<=k<=26, -27<=l<=27	
Reflections collected	214882	
Independent reflections	33574 [R(int) = 0.0487]	
Completeness to theta = 25.242°	99.9 %	
Absorption correction	Semi-empirical from equivalents	
Max. and min. transmission	0.7471 and 0.6863	
Refinement method	Full-matrix least-squares on F^2	
Data / restraints / parameters	33574 / 8 / 894	
Goodness-of-fit on F^2	1.022	
Final R indices [I>2sigma(I)]	R1 = 0.0388, wR2 = 0.0842	
R indices (all data)	R1 = 0.0541, wR2 = 0.0891	
Absolute structure parameter	0.0162(19)	
Extinction coefficient	n/a	
Largest diff. peak and hole	1.137 and -1.072 e.$Å^{-3}$	

A2.4 CRYSTALLOGRAPHIC ANALYSIS OF 91c

A2.4.1 Special Refinement Details

Figure A2.3 *Rendering of allylic silane* ***91c****.*

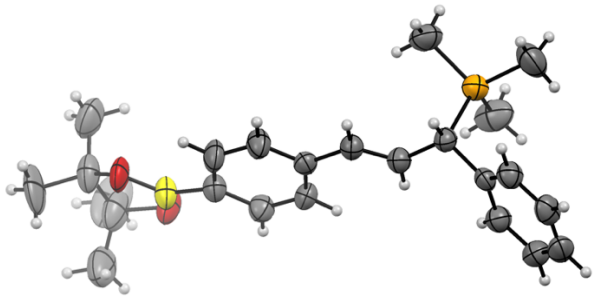

Compound **91c** crystallizes in the orthorhombic space group $P2_12_12_1$ with one molecule in the asymmetric unit. Data was collected with Mo-$K\alpha$ radiation (λ = 0.71073 Å) at 270 K. The structure exhibits significant positional disorder of the pinacol boronate ring, which was satisfactorily modeled over three positions with relative populations of 47%, 34%, and 19%. The 1,2 and 1,3 distances of this moiety were restrained to be equivalent and refined with both U_{ij} and enhanced rigid bond restraints. The absolute configuration was determined by anomalous dispersion (Flack = –0.02(6)); there was no discernible disorder of the chiral center of interest.[6]

A2.4.2 Crystallographic Tables

Table A2.3. *Crystal data and structure refinement for* ***91c****.*

Identification code	P16169	
CCDC Number	1547483	
Empirical formula	$C_{24}H_{33}BO_2Si$	
Formula weight	392.40	
Temperature	270 K	
Wavelength	0.71073 Å	
Crystal system	Orthorhombic	
Space group	$P2_12_12_1$	
Unit cell dimensions	a = 6.4080(3) Å	α = 90°
	b = 12.5679(5) Å	β = 90°
	c = 30.4781(13) Å	γ = 90°
Volume	2454.56(18) $Å^3$	
Z	4	
Density (calculated)	1.062 Mg/m^3	
Absorption coefficient	0.111 mm^{-1}	
F(000)	848	
Crystal size	0.18 x 0.13 x 0.06 mm^3	
Theta range for data collection	2.578 to 27.515°	
Index ranges	-8<=h<=8, -16<=k<=16, -39<=l<=39	
Reflections collected	31898	
Independent reflections	5646 [R(int) = 0.0848]	
Completeness to theta = 25.242°	99.9 %	
Absorption correction	Semi-empirical from equivalents	
Max. and min. transmission	0.7456 and 0.6970	
Refinement method	Full-matrix least-squares on F^2	
Data / restraints / parameters	5646 / 1045 / 421	
Goodness-of-fit on F^2	1.037	
Final R indices [I>2sigma(I)]	R1 = 0.0626, wR2 = 0.1005	
R indices (all data)	R1 = 0.1483, wR2 = 0.1207	
Absolute structure parameter	-0.02(6)	
Extinction coefficient	n/a	
Largest diff. peak and hole	0.141 and -0.193 $e.Å^{-3}$	

A2.5 CRYSTALLOGRAPHIC ANALYSIS OF 123c

A2.5.1 Special Refinement Details

Figure A2.4 *Rendering of tetrahydrofuran* ***123c****.*

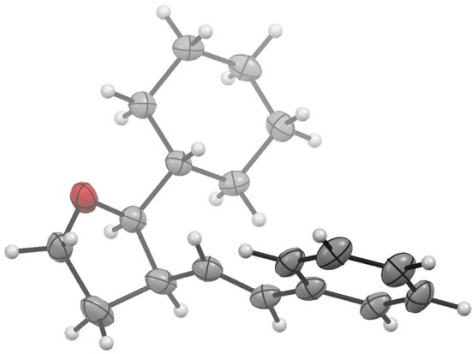

Compound **123c** crystallizes in the orthorhombic space group $P2_12_12_1$ with one molecule in the asymmetric unit. Data was collected with Cu-$K\alpha$ radiation (λ = 1.54178 Å) at 100 K. The secondary α-carbon in the tetrahydrofuran ring was disordered over two positions (68% and 32% occupancy). The disordered tetrahydrofuran ring is omitted for clarity. Absolute configuration was determined by anomalous dispersion (Flack = 0.12(18)).[6] Bayesian statistics further confirm the absolute stereochemistry: P2(true) = 1.000, P3(true) = 0.978, P3(rac-twin) = 0.022, and P3(false) = $0.1\text{x}10^{-7}$.[7]

A2.5.2 Crystallographic Tables

Table A2.4. *Crystal data and structure refinement for* ***123c****.*

Identification code	V18180	
Empirical formula	$C_{18}H_{24}O$	
Formula weight	256.37	
Temperature	100 K	
Wavelength	1.54178 Å	
Crystal system	Orthorhombic	
Space group	$P2_12_12_1$	
Unit cell dimensions	a = 5.8196(6) Å	α = 90°.
	b = 14.5241(14) Å	β = 90°.
	c = 17.675(2) Å	γ = 90°.
Volume	1494.0(3) $Å^3$	
Z	4	
Density (calculated)	1.140 Mg/m^3	
Absorption coefficient	0.519 mm^{-1}	
F(000)	560	
Crystal size	0.18 x 0.16 x 0.02 mm^3	
Theta range for data collection	3.939 to 81.258°.	
Index ranges	-5<=h<=6, -14<=k<=16, -22<=l<=13	
Reflections collected	9181	
Independent reflections	2267 [R(int) = 0.0409]	
Completeness to theta = 67.679°	83.4 %	
Absorption correction	Semi-empirical from equivalents	
Max. and min. transmission	1.0000 and 0.9028	
Refinement method	Full-matrix least-squares on F^2	
Data / restraints / parameters	2267 / 0 / 182	
Goodness-of-fit on F^2	1.083	
Final R indices [I>2sigma(I)]	R1 = 0.0399, wR2 = 0.1033	
R indices (all data)	R1 = 0.0441, wR2 = 0.1059	
Absolute structure parameter	0.12(18)	
Extinction coefficient	n/a	
Largest diff. peak and hole	0.232 and -0.104 $e.Å^{-3}$	

A2.6 REFERENCES

(1) *APEX2, Version 2 User Manual, M86-E01078, Bruker Analytical X-ray Systems*, Madison, WI, **2006**.

(2) Sheldrick, G.M. *SADABS (version 2008/1): Program for Absorption Correction for Data from Area Detector Frames*, University of Göttingen, **2008**.

(3) Sheldrick, G. *Acta Crystallogr., Sect. A: Found. Crystallogr*. **2008**, *64*, 112.

(4) Sheldrick, G. M. *Acta Crystallogr., Sect. C: Struct. Chem.* **2015**, *C71*, 3.

(5) Müller, P. *Crystallogr. Rev.* **2009**, *15*, 57.

(6) Parsons, S.; Flack, H. D.; Wagner, T. *Acta Crystallogr., Sect. B: Struct. Sci. Cryst. Eng. Mater.* **2013**, *B69*, 249.

(7) Spek, A. L. *Acta Crystallogr., Sect. D: Struct. Biol.* **2009**, *D65*, 148.

Chapter 3

Decarboxylative Asymmetric Ni-Catalyzed Cross-Coupling of Benzylic N-Hydroxyphthalimide Esters and Alkenyl Bromides‡

3.1 INTRODUCTION

Nickel catalyzed cross-coupling reactions have emerged as powerful methods to form $C(sp^3)$–$C(sp^2)$ and $C(sp^3)$–$C(sp^3)$ bonds.[1–5] Whereas pioneering investigations focused on the canonical cross-coupling of $C(sp^3)$ electrophiles with organometallic reagents—variants of the venerable Negishi,[6–13] Kumada,[14–18] and Suzuki,[19–23] reactions, among others—additional modes of alkyl cross-coupling using nickel catalysis have recently been disclosed. These include cross-electrophile "reductive" couplings that use an

‡Portions of this chapter have been reproduced from the following communication: Suzuki, N.†; Hofstra, J. L.†; Poremba, K. E.; Reisman, S. E. *Org. Lett.* **2017**, *19*, 2150–2153, DOI: 10.1021/acs.orglett.7b00793, copyright 2017 American Chemical Society. The research presented in this chapter was completed in collaboration with Naoyuki Suzuki (postdoctoral scholar) and Kelsey E. Poremba (graduate student) in the Reisman group.

exogenous, stoichiometric reductant to shuttle electrons to the nickel catalyst,[24–32] as well as cross-coupling reactions that rely on synergistic reactivity between nickel and photoredox co-catalysts.[33–40] Taken together, these reactions enable the cross-coupling of a broad range of C(sp^3) substrates, providing access to a variety of products.

Ni-catalyzed reductive cross-coupling reactions have proven particularly useful for the cross-coupling of secondary alkyl electrophiles, often affording chiral products as racemic mixtures.[24–30,32] Recognizing that the ability to render these transformations enantioselective would enhance their utility,[41,42] our laboratory has recently developed enantioselective Ni-catalyzed reductive cross-coupling reactions of both benzylic chlorides[43–45] and α-chloronitriles.[46] An important objective for further improving the synthetic usefulness of asymmetric reductive cross-coupling reactions is to develop reactions of new electrophile classes. Just as in conventional cross-coupling reactions, where different organometallic reagents (e.g. organozinc, organomagnesium, organoboron reagents, etc.) bring unique advantages to a specific synthetic scenario, the ability to cross-couple new electrophile classes broadens the tool box for strategic C–C bond formation. However, it can be challenging to apply conditions from previously developed reductive cross-coupling reactions to new electrophile classes, especially if there are changes to the mechanism by which the coupling partner undergoes oxidative addition. In particular, it can require tuning of either the ligand structure or the stoichiometric reductant (or both) in order to develop reactions that proceed both in good yield and enantioselectivity.

As part of our efforts to develop asymmetric cross-coupling reactions that employ a variety of C(sp^3) electrophiles, we became interested in the coupling of redox-active *N*-

hydroxyphthalimide (NHP) esters (**124**) which are readily prepared from the corresponding carboxylic acids.[47,48] In 1988, Okada and Oda demonstrated that NHP esters could undergo fragmentation to afford alkyl radicals via a photosensitized electron transfer mechanism (Figure 3.1). Irradiation of an alkyl NHP ester (**124**) with light (>350 nm) in the presence of 1,6-bis(dimethylamino)pyrene (BDMAP, **127**) provided the corresponding alkane (**125**) in good yield (88%). The reaction was proposed to proceed via excitation of BDMAP to the excited singlet state, followed by electron transfer to **124** to afford the NHP ester radical anion (**125**). Protonation of **125**, cleavage of the N–O bond, and extrusion of CO_2 produced alkyl radical **129**, which terminated via H atom abstraction. While an alternative sequence could occur via N–O bond cleavage prior to protonation, both operative mechanisms produce alkyl radical **129**, which could potentially engage in a variety of radical reactions.

Figure 3.1 *Mechanism of NHP ester fragmentation.*

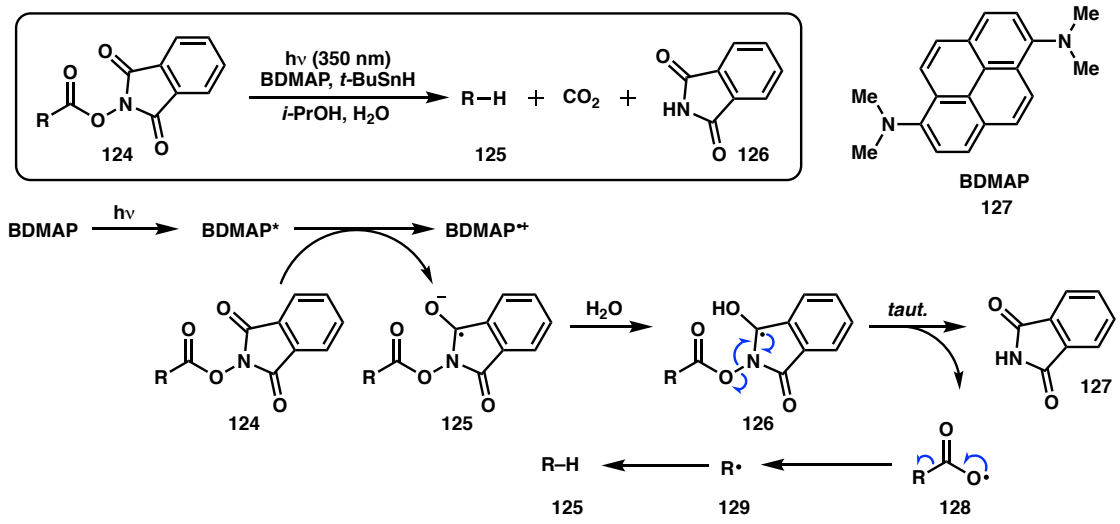

Alkyl radicals generated from NHP esters can be intercepted by metal catalysts and have recently been used in a variety of cross-coupling reactions.[49,50] For example, NHP esters have been demonstrated as C(sp^3) substrates for Ni-catalyzed Negishi,[51–57]

Suzuki,[55,58] and reductive[59–62] cross-coupling reactions to generate racemic products (Scheme 3.1a–c). Furthermore, NHP esters have also been shown to undergo other Ni-catalyzed reactions such as Giese additions,[63] radical additions to sulfinimies,[64] hydroalkylations,[65] and borylations[66]. Despite a breadth of reactivity, NHP esters have not been demonstrated as competent coupling partners in Ni-catalyzed *enantioselective* cross-coupling reactions. We recognized that the use of NHP esters might be advantageous for substrates in which the corresponding alkyl chlorides are unstable or challenging to prepare. Herein, we report the first Ni-catalyzed asymmetric cross-coupling reactions of NHP esters (Scheme 3.1d). These alkenylation reactions proceed under mild conditions using tetrakis(*N*,*N*-dimethylamino)ethylene (TDAE) as a homogenous reductant.

Scheme 3.1 *Selected examples of NHP esters in cross-coupling.*

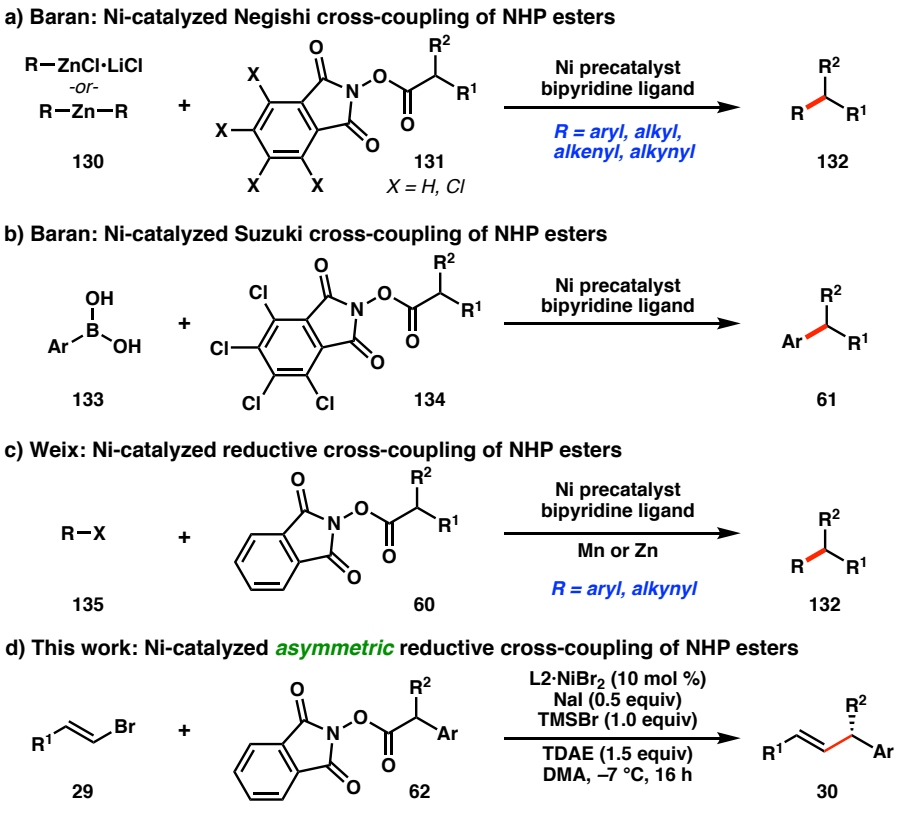

3.2 REACTION OPTIMIZATION

3.2.1 Initial Hit with Additives

Our efforts began with NHP ester **136**, which was prepared in one step from commercially available 2-phenylpropanoic acid. Subjection of NHP ester **136** and alkenyl bromide **86** to our optimal conditions developed for the reductive cross-coupling of alkenyl bromides and benzyl chlorides provided only trace quantities of product (Table 3.1, entry 1).[44] The use of Zn as a reductant did not improve the reaction (entry 2). We were pleased to find, however, that the addition of stoichiometric TMSCl, which has previously been used as a substoichiometric additive in Ni-catalyzed reductive cross-couplings,[46,67–69] provided the desired product **137** in low yield but with good enantioselectivity (90% ee) when Mn was used as the reductant (entries 3). It has been proposed that the role of TMSCl in reductive cross-couplings may activate the surface of the heterogeneous metal reductant, which is typically either Mn powder or Zn dust. The addition of 1,2-dibromoethane (DBE), which is typically used to activate Mg turnings in Grignard reagent formations,

Table 3.1. *Evaluation of reaction additives.*

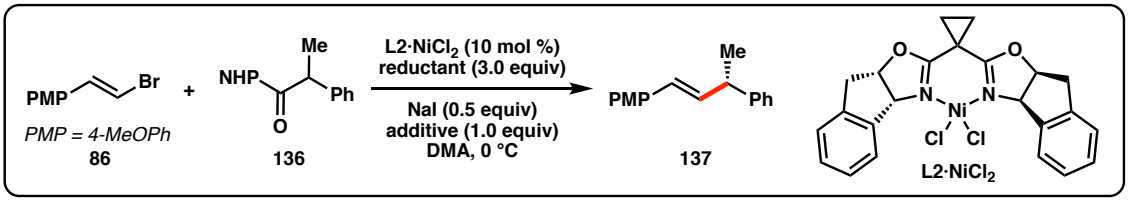

Entry	Reductant	Additive	yield (%)	ee (%)
1	Mn	—	trace	—
2	Zn	—	trace	—
3	Mn	TMSCl	27	90
4	Zn	TMSCl	38	64
5	Zn	DBE	trace	—

failed to provide **137** (entry 5). Given these results, we propose that alternatively, TMSCl may be used to sequester phthalimide anions, which would prevent recombination with Ni in the catalytic cycle if such a process is deleterious to the cross-coupling reaction.[52]

3.2.2 Activating Groups

A variety of other activated esters have previously been studied in decarboxylative cross-couplings.[52] Unfortunately, both the tetrachloro-*N*-hydroxyphthalimide ester (**138a**) and 1-hydroxy-7-azabenzotriazole (HOAt) ester (**138b**) failed to yield any cross-coupling product under the reaction conditions (Figure 3.2). Further optimization of the cross-coupling reaction was investigated with NHP ester **136**.

Figure 3.2 *Evaluation of activating groups.*

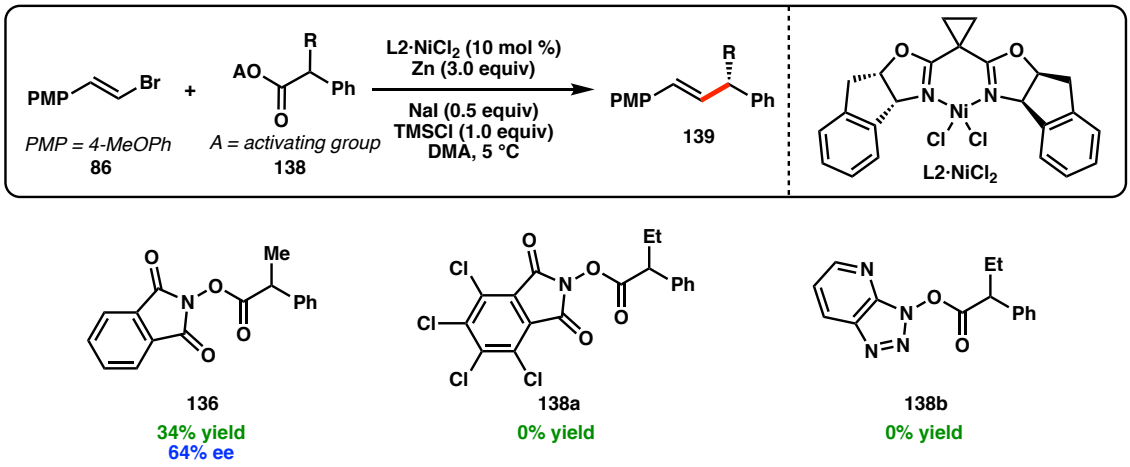

3.2.3 Reductants

While Zn and Mn reductants both showed reactivity to produce **137** when TMSCl was used as an additive, the enantioselectivity was diminished (64% and 90% ee, Table 3.2 entries 1–2) compared to the optimal conditions developed for the cross-coupling of alkenyl bromides and benzylic chlorides (96% ee with **L2**·$NiCl_2$).[44] During our

mechanistic investigations between alkenyl bromides and benzylic chlorides (*see Chapter 4*), we investigated the addition of TMSCl to activate Mn or Zn. While this led to increased reaction rates it also decreased the enantioselectivity of the cross-coupling product.[70] Therefore, we became interested in non-metal reductants to see if the combination of Mn/Zn and TMSCl was deleterious to ee; if so, this could allow us to still employ TDAE as an additive without diminishing enantioselectivity. As our previous reaction between alkenyl bromides and benzylic chlorides could be conducted using the organic reductant TDAE in 23% yield, an investigation of alternative homogenous reductants revealed that TDAE was a competent reductant and delivered **137** in 95% ee.[44,71,72] More notably, the use of TDAE also substantially increased the reactivity, thus providing **137** in 61% yield (entry 3).

Table 3.2. *Evaluation of reductants.*

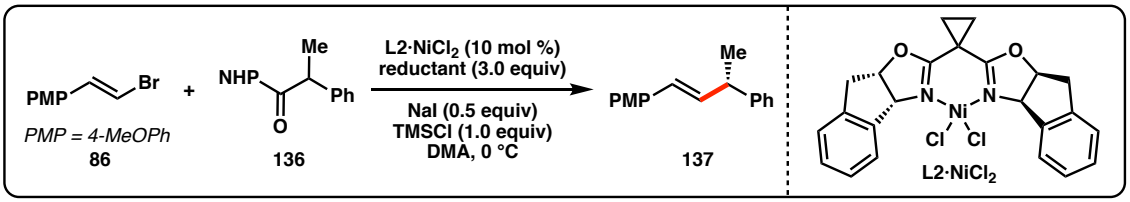

Entry	Reductant	yield (%)	ee (%)
1	Zn	38	64
2	Mn	27	90
3	TDAE	61	95

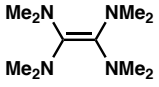

TDAE

3.2.4 Halide Exchange

Monitoring the reaction progress at room temperature determined that (*E*)-1-(2-chlorovinyl)-4-methoxybenzene (**140**) was forming and accumulating under the reaction conditions, presumably through a Ni-catalyzed halide exchange process.[73,74] Since alkenyl

chloride **140** does not readily engage in the cross-coupling reaction, we hypothesized that the yield of **137** could be improved by removing chloride from the reaction and thus preventing formation of this unproductive side product. Indeed, the use of TMSBr instead of TMSCl, and the use of **L2**·$NiBr_2$ as the catalyst, furnished product **137** in 75% yield and 92% ee (Table 3.3, entry 2).

Table 3.3. *Evaluation of halide exchange.*

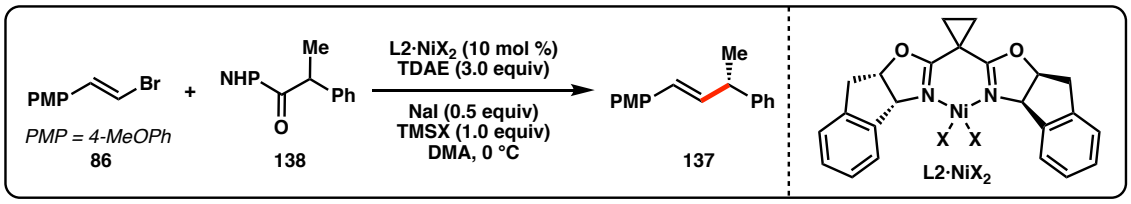

PMP = 4-MeOPh
86 **138** **137**

Entry	X	yield (%)	ee (%)
1	Cl	61	95
2	Br	75	92

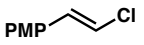

PMP = 4-MeOPh
140

3.2.5 Temperature

The reaction temperature was then evaluated (Table 3.4). By decreasing the reaction temperature to –7 °C, the yield was slightly improved, providing **137** in 79% yield and 93% ee (entry 3). We note that the melting point of TDAE is reported as 0 °C, however,

Table 3.4. *Evaluation of temperature.*

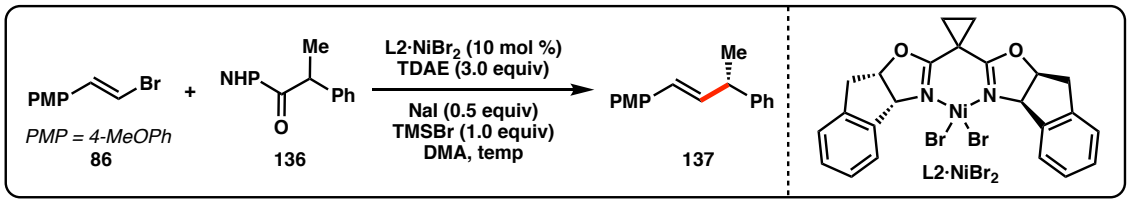

PMP = 4-MeOPh
86 **136** **137**

Entry	Temperature	yield (%)	ee (%)
1	5 °C	58	91
2	0 °C	75	92
3	–7 °C	79	93

the reaction remains homogenous down to a temperature of –7 °C. When the reaction was conducted at temperatures below –7 °C, solidification of TDAE was observed in the reaction mixture.

3.2.6 Reductant Equivalents

The quantity of reductant was then evaluated (Table 3.5). Typically, Mn reductants are used in extreme excess (2.0–3.0 equiv) in asymmetric Ni-catalyzed cross-coupling reactions, possibly due to the heterogenous nature of the reaction where the addition of Mn increases the reaction rate.[43,44,46,69,75] Excess reductant is needed in order to obtain good conversion. In this case, TDAE is a homogenous reductant, and we were pleased to find that lowering the amount to 1.5 equivalents provided **137** in comparable yield and ee (entries 1–2).[72]

Table 3.5. *Evaluation of reductant equivalents.*

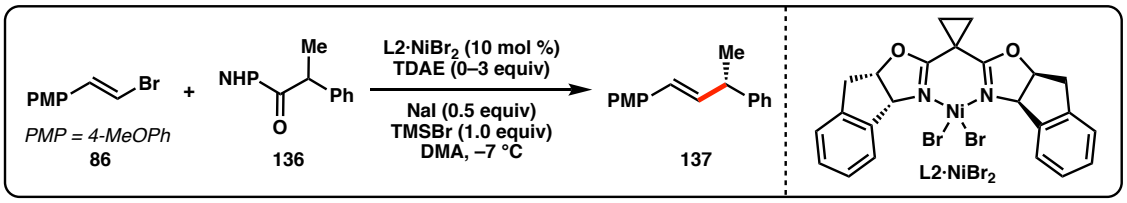

Entry	TDAE (equiv)	yield (%)	ee (%)
1	3.0	79	93
2	1.5	80	96

3.2.7 Solvents

Although *N*,*N'*-dimethylacetamide (DMA) as a solvent showed good levels of reactivity and enantioselectivity under the optimal conditions, other solvents were evaluated (Table 3.6). Weix and coworkers found that compared to Zn reductants, cross-coupling reactions of aryl iodides with benzylic chlorides with TDAE were more generally

robust in a variety of solvents.[72] For this alkenylation reaction, both acetonitrile (MeCN) and propylene carbonate were found to provide cross-coupled product **137** with excellent enantioselectivity, though in moderate yield (entries 2–3). Since the coordination sphere of these solvents are different, given these results we hypothesize that it is unlikely DMA is coordinated to Ni during the enantiodetermining step.

Table 3.6. *Evaluation of solvents.*

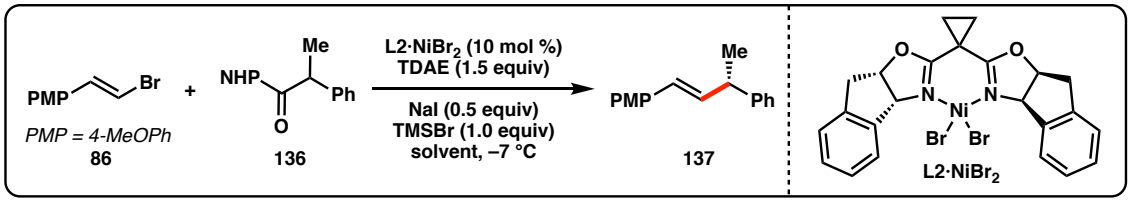

Entry	Solvent	yield (%)	ee (%)
1	DMA	80	96
2	MeCN	30	99
3	propylene carbonate	43	95

3.2.8 Optimization Controls

A variety of control reactions were conducted by running the optimal conditions but omitting various components of the reaction (Table 3.7). Without NaI, the yield of **137** was slightly reduced. In contrast to Ni-catalyzed cross-coupling of alkenyl bromides and benzyl chlorides where NaI additives may play a role in halide exchange and prevent the formation of alkenyl chloride,[44,73,74] the NaI additive in this transformation plays a different, yet unknown role. Without either TDAE or **L2**·$NiBr_2$ catalyst, no product was formed (entries 2–3). Running the reaction but omitting TMSBr confirmed that this additive remains crucial for obtaining high yields of **137** (entry 5).

Table 3.7. *Control reactions.*

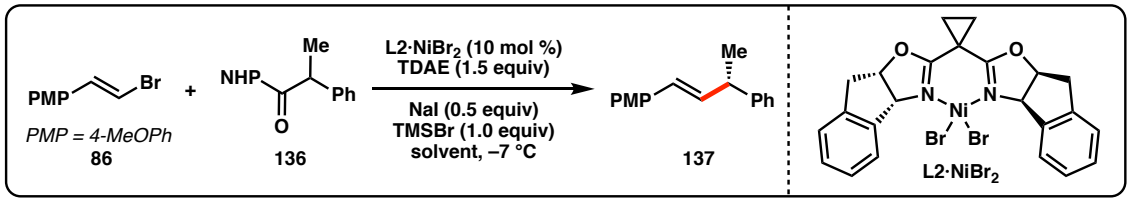

Entry	Deviation	yield (%)	ee (%)
1	—	80	96
2	no NaI	68	95
3	no TDAE	0	—
4	no L2·$NiBr_2$	0	—
5	no TMSBr	19	88

3.3 SUBSTRATE SCOPE

To demonstrate the scope of the reaction, a series of (*E*)-alkenyl bromides was cross-coupled with NHP ester **136**, providing the corresponding products (**140**) in uniformly good yield and high ee (Figure 3.3). The reaction exhibits good tolerance of Lewis basic functional groups: for example, dimethyl anilines (**140b**), nitriles (**140d**), and esters (**140e**, **140i**) could be incorporated into the substrate without detriment to the yield or enantioselectivity. A pyridine-containing alkenyl bromide also performed well, providing **140h** in 67% yield and 95% ee. In addition, alkyl-substituted alkenyl bromides reacted smoothly, providing the corresponding products in good yield and ee (**140i**–**140n**). An alkenyl bromide possessing a free alcohol coupled efficiently, although silylation occurred under the reaction conditions to give silyl ether **140l**. In order to obtain complete conversion for this substrate, 2 equivalents of TMSBr are used in the reaction. The silyl ether can easily be cleaved with a mild acid workup; in this case it was preserved in order

to facilitate purification. It is notable that alkenyl MIDA boronate **140m** and alkenyl silane **140n** could be prepared in 97% ee from commercially available vinyl bromides, which could be used as cross-coupling handles for further derivatization. To demonstrate that this method can be used preparatively, the coupling was conducted on 5.0 mmol scale, which delivered 918 mg (77% yield) of **137** in 91% ee.

Figure 3.3 *Scope of the alkenyl bromide coupling partner.*

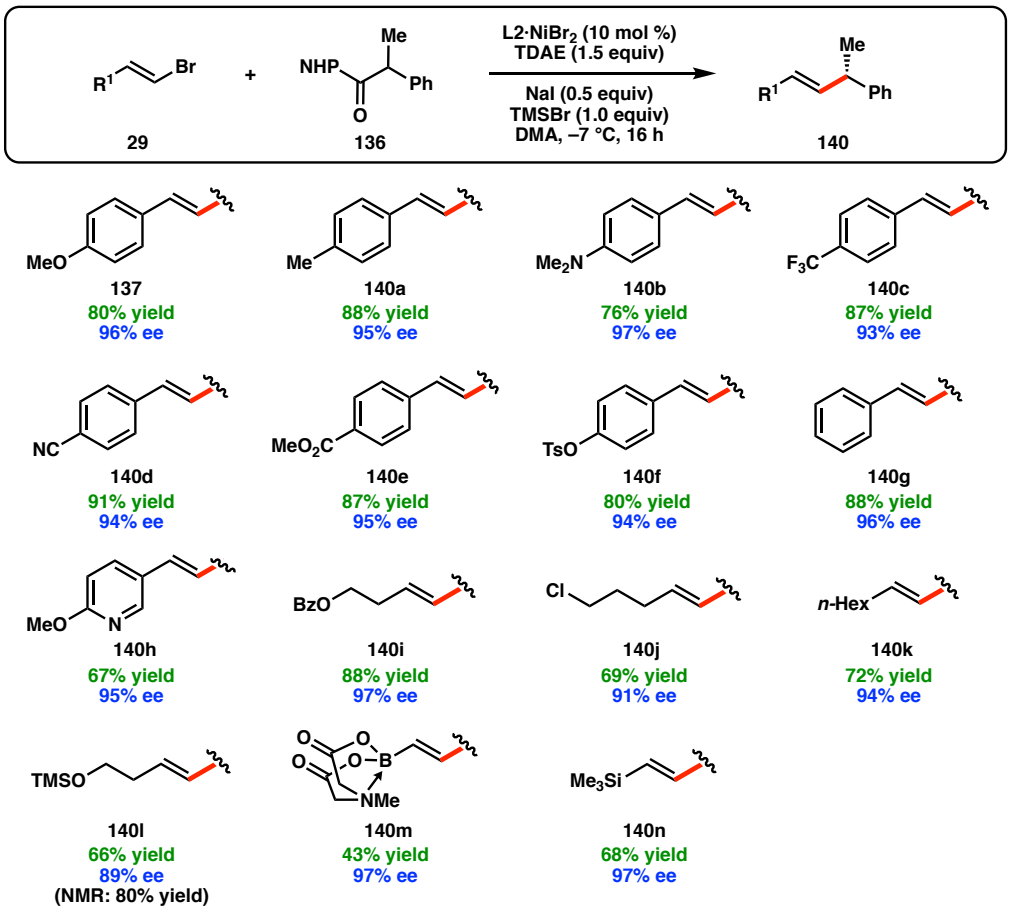

Reactions are conducted on 0.2 mmol scale under N_2. Isolated yields are provided; ee is determined by SFC using a chiral stationary phase. For **140f**, 1.5 equiv NHP ester was used. For **140l**, 2.0 equiv TMSBr was used; the alcohol is silylated under the reaction conditions. NMR yield of **140l** versus an internal standard is provided in parenthesis.

The reaction also exhibits broad scope for the NHP ester coupling partner, delivering good yields and high enantioselectivities for a range of substrates bearing substitution on

the arene or at the benzylic position (Figure 3.4). In certain cases (e.g. **141e–141f**), the NHP esters cross-coupled with improved yield relative to the corresponding benzyl chlorides (under the previously reported conditions).[44] For example, aryl dichloride **141f** could be prepared in 77% yield and 82% ee with the corresponding NHP ester; use of the benzyl chloride electrophile provided **141f** in 21% yield and 75% ee. Moreover, dimethyl aniline **141e** could be prepared in 66% yield and 94% ee; this compound could not be accessed via our previously reported benzylic chloride coupling due challenges in preparing and handling 4-(chloro(phenyl)methyl)-*N*,*N*-dimethylaniline under standard

Figure 3.4 *Scope of the NHP ester coupling partner.*

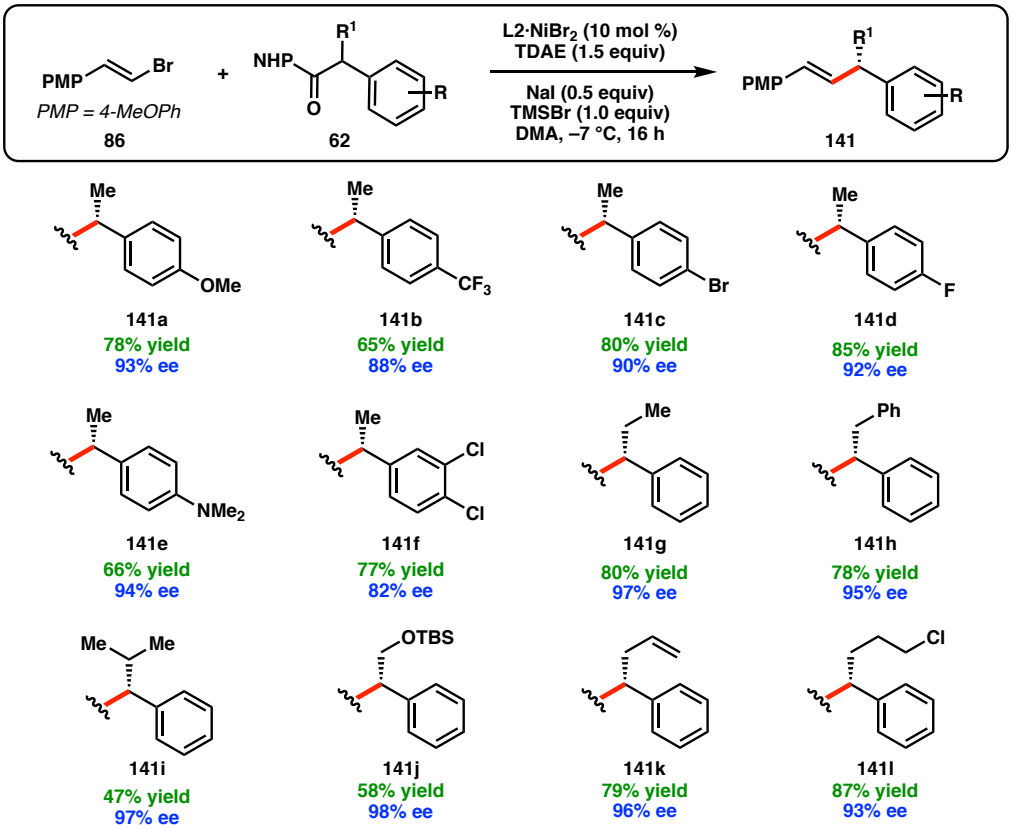

Reactions are conducted on 0.2 mmol scale under N_2. Isolated yields are provided; ee is determined by SFC using a chiral stationary phase.

conditions. Chlorination of the corresponding benzyl alcohol using either $SOCl_2$ or PPh_3/CCl_4 provided the desired benzyl chloride product, however the reaction profile was messy, and purification was ultimately unsuccessful. Higher substitution at the benzylic position was also tolerated (**141g–141l**), although the yield began to decrease with larger groups (e.g. *i*-Pr, **141i**). Notable products include those containing pendant functional groups at the benzylic position including a siloxy group (**141j**), alkene (**141k**), and alkyl chloride (**141l**). Perfect chemoselectivity for cross-coupling of the NHP ester over the primary alkyl chloride is observed.

Nevertheless, a few substrates were evaluated that provided the desired cross-coupling products in moderate to good yield, but with synthetically intractable ee (Figure 3.5). An alkenyl bromide containing an alkenyl fluoride motif provided **142** in 43% yield and 32% ee. Particular benzylic groups on the NHP ester fragment were also found to decrease enantioselectivity. Both trimethoxy **143** an *N*-methyl indole **144** could be prepared in moderate to good yield, however the products were formed in 71% ee and 75% ee, respectively.

Figure 3.5 *Products with poor enantioselectivity.*

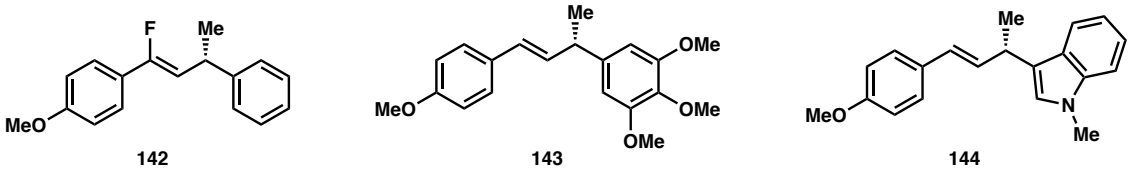

Although the primary focus of this study was the cross-coupling of NHP esters with alkyl substituents at the benzylic position, we also investigated substrates containing heteroatom substitution (Scheme 3.2). Reaction of α-methoxy ester **145** furnished allylic

ether **146** in good yield and ee. This highlights an advantage of the NHP ester for certain C(sp^3) electrophiles, as the corresponding α-chloroether substrate is unstable and difficult to work with.

Scheme 3.2 *Cross-coupling of α-methoxy NHP ester.*

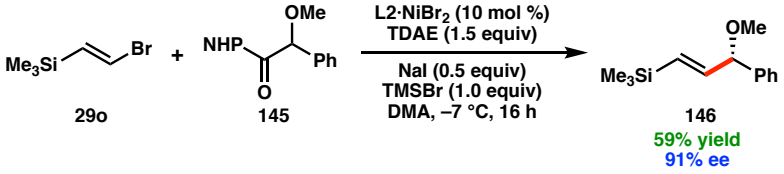

While alkyl benzylic substituents and α-methoxy NHP ester **145** were successful coupling partners, other substrates containing benzylic α-heteroatoms were not tolerated under the reaction conditions (Figure 3.6). For example, NHP esters containing dimethyl amines (**147**) as well as Boc protected amines (**148**, **149**) did not form the desired cross-coupling products. An NHP ester which would provide a tetrasubstituted center also did not form any desired product (**150**). A variety of non-benzylic substrates containing

Figure 3.6 *Unsuccessful chiral products.*

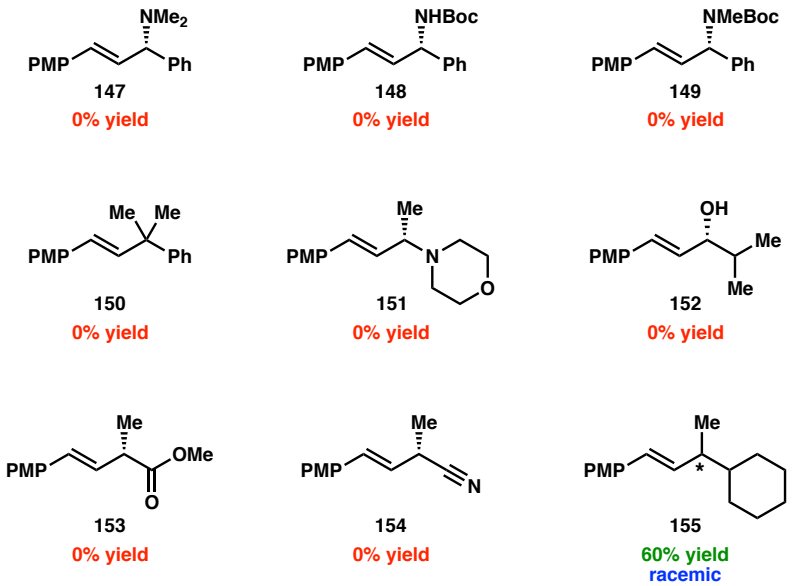

functional groups that could potentially stabilize an α-radical (**151**–**154**) did not form any desired cross-coupling product. However, a simple alkyl NHP ester did react to form the cyclohexyl substituted product **155** in 60% yield, albeit in racemic form.

Further investigations into the Ni-catalyzed cross coupling of cyclohexyl NHP ester **156** were conducted. Since **155** was formed as a racemate, we hypothesized that the cross-coupling reaction was not occurring on Ni, preventing the catalyst from imparting any enantioinduction. Running the reaction in the absence of **L2**·$NiBr_2$ demonstrated that styrenyl bromides successfully reacted to form the desired cross-coupled products (**155** and **157a**), however, alkyl substituted alkenyl bromides failed under these conditions (**157b** and **157d**) (Figure 3.7).

Figure 3.7 *Evaluation of alkenyl bromides in Ni-free cross-coupling.*

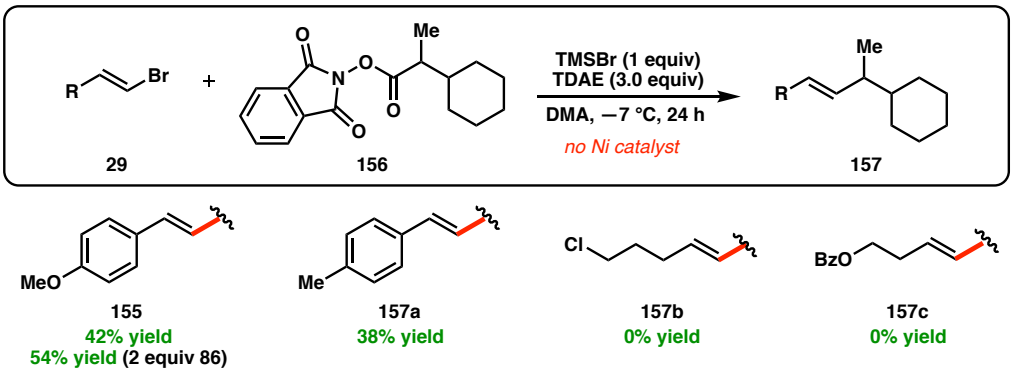

One possible mechanistic explanation for the observed results is depicted in Figure 3.8. Addition of alkyl radical **158** to alkenyl bromide **86** could form stabilized benzylic radical **159** when styrenyl bromides are used in the reaction. In contrast, an unstable alkyl radical would be generated if alkyl substituted alkenyl halides were used in this process. Radical elimination of the bromide could reform the styrene moiety and provide **155** in racemic form. The tuning of the reaction rate and the stability of the alkyl radical may

prove to be important in Ni-catalyzed cross-coupling reactions that proceed through cage escape processes. While additional studies into the reaction mechanism are required, these studies highlight the importance for appropriate substrate selection to avoid inherent background reactivity.

Figure 3.8 *Possible mechanism for Ni-free cross-coupling.*

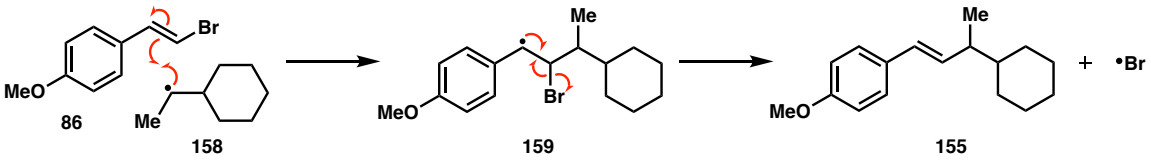

3.4 REACTION MECHANISM

To probe for the intermediacy of a radical species, NHP ester **160** was prepared and subjected to the standard cross-coupling conditions (Table 3.8, 10 mol % **L2**·$NiBr_2$). A 42% combined yield of the coupled products **161a–161c** was obtained. It has been shown that for phenyl substituted cyclopropyl carbonyl radicals, the ring opening is reversible and that the cyclopropane species is favored at lower temperatures (Figure 3.9).[76,77] The fact

Table 3.8. *Evaluation of Ni loading with cyclopropyl ring opening radical clock.*

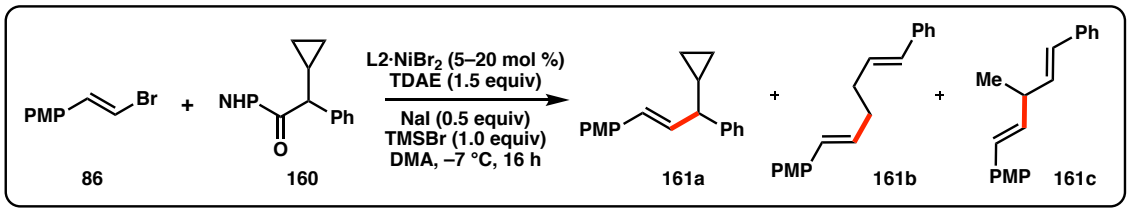

Entry	L2·$NiBr_2$ (mol %)	Total Yield (%)	161a :	161b :	161c
1	5	44	12%	85%	3%
2	10	42	15%	79%	6%
3	20	49	20%	69%	11%

that **161b** predominates, even though it derives from the minor equilibrium species, could indicate that the rate of radical recombination with nickel is sensitive to the steric profile of the radical. When the catalyst loading of **L2**·$NiBr_2$ was varied, the ratio of **161a** to total ring opened product (**161b** + **161c**) was found to increase at higher nickel concentrations (entries 2–3). This Ni-dependent behavior suggests that the mechanism proceeds through a cage-escaped radical, which at higher concentrations of **L2**·$NiBr_2$, can competitively recombine with nickel before undergoing ring scission; a radical-chain mechanism may be in effect.[70]

Figure 3.9 *Rate constants for cyclopropyl carbinyl radicals.*

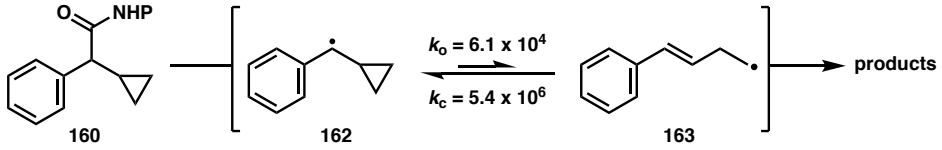

Further studies of the mechanism are ongoing; it is unclear at this time whether the absolute stereochemistry of the cross-coupling product is set during the oxidative addition or reductive elimination steps.[78] We do note, however, that the products are formed in similar ee when using either the NHP esters under the conditions reported here or the benzylic chloride using the conditions reported previously (Figure 3.10).[44] The enantioselectivities of **141** were converted into $\Delta\Delta G^{\ddagger}$ by using the reported er and the reaction temperature. A linear correlation is observed between $\Delta\Delta G^{\ddagger}$ values for the benzyl chlorides (Conditions A) vs. $\Delta\Delta G^{\ddagger}$ values for the NHP esters (Conditions B). This linear trendline ($y = 0.86x + 0.30$, $R^2 = 0.96$) suggests that both reactions proceed through the same stereochemistry-determining step.

Figure 3.10 *Evaluation of enantioselectivity for the benzylic chloride and benzylic NHP ester alkenylation reactions.*

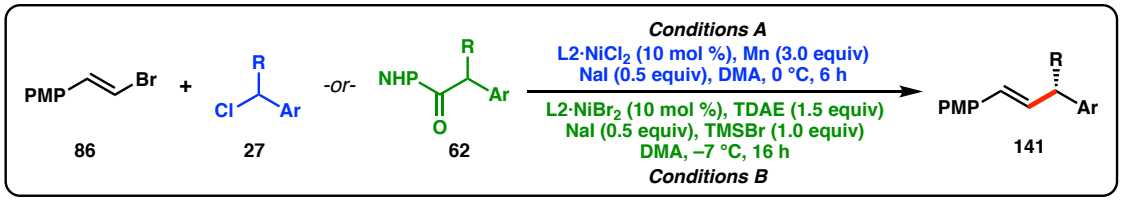

		Conditions:	A	B
Entry	Ar	R	ee(%)	ee(%)
1	Ph	Me	96	96
2	4-OMePh	Me	93	93
3	4-CF_3Ph	Me	87	88
4	4-BrPh	Me	90	90
5	4-FPh	Me	90	92
6	3,4-Cl_2Ph	Me	77	82
7	Ph	Et	97	97
8	Ph	Bn	92	95
9	Ph	*i*-Pr	97	97

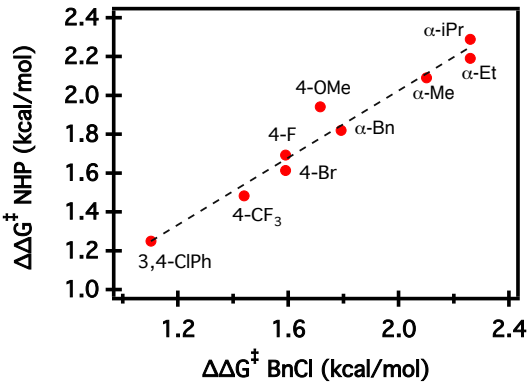

3.5 CONCLUSION

In summary, these results demonstrate that Ni-catalyzed reductive cross-coupling reactions of NHP esters can be rendered highly enantioselective, thus broadening the scope of C(sp^3) electrophiles available for asymmetric C–C bond formation. In contrast to the related reductive cross-couplings of benzyl chlorides,[44] optimal results were obtained when TDAE was used as the terminal reductant. A preliminary result demonstrated that these conditions could be used to cross-couple α-alkoxy NHP esters and other substrates for which the corresponding benzylic chloride could be difficult to prepare or unstable. The ability to use both NHP esters (this study) and benzylic chlorides in asymmetric reductive alkenylation reactions allows users to select from either electrophile depending on factors

such as commercial availability of the corresponding carboxylic acid or benzylic chloride starting material and improves the overall scope of this transformation. The further development of asymmetric cross-electrophile coupling reactions of NHP esters and other $C(sp^3)$ electrophiles is the focus of ongoing work in our laboratory.

3.6 EXPERIMENTAL SECTION

3.6.1 Materials and Methods

Unless otherwise stated, reactions were performed under a nitrogen atmosphere using freshly dried solvents. Tetrahydrofuran (THF), methylene chloride (CH_2Cl_2), diethyl ether (Et_2O), and toluene (PhMe) were dried by passing through activated alumina columns. Trimethylsilyl chloride (TMSCl) was distilled over calcium hydride. Trimethylsilyl bromide (TMSBr) and anhydrous dimethylacetamide (DMA) were purchased from Aldrich and stored in the glovebox. Manganese powder (–325 mesh, 99.3%) was purchased from Alfa Aesar. Zinc dust (97.5%) and nickel(II) chloride ($NiCl_2$) were purchased from Strem. Tetrakis(dimethylamino)ethylene (TDAE) was purchased from TCI and stored in the glovebox. Unless otherwise stated, chemicals were used as received. All reactions were monitored by thin-layer chromatography (TLC) using EMD/Merck silica gel 60 F254 pre-coated plates (0.25 mm) and were visualized by ultraviolet (UV) light or with cerium ammonium molybdate (CAM) staining. Flash column chromatography was performed as described by Still et al.[79] using silica gel (230-400 mesh) purchased from Silicycle or 10% $AgNO_3$ doped silica gel (+230 mesh) purchased from Sigma Aldrich. Optical rotations were measured on a Jasco P-2000 polarimeter using a 100 mm path-length cell at 589 nm.

^{1}H and ^{13}C NMR spectra were recorded on a Bruker Avance III HD with Prodigy cyroprobe (at 400 MHz and 101 MHz, respectively), a Varian 400 MR (at 400 MHz and 101 MHz, respectively), or a Varian Inova 500 (at 500 MHz and 126 MHz, respectively). ^{1}H and ^{19}F NMR spectra were also recorded on a Varian Inova 300 (at 300 MHz and 282 MHz, respectively). NMR data is reported relative to internal $CHCl_3$ (^{1}H, $\delta = 7.26$), $CDCl_3$ (^{13}C, $\delta = 77.1$), C_6F_6 (^{19}F, $\delta = -164.9$), $CH_3C_6D_5$ (^{1}H, $\delta = 2.09$), and $CD_3C_6D_5$ (^{13}C, $\delta = 20.4$). Data for ^{1}H NMR spectra are reported as follows: chemical shift (δ ppm) (multiplicity, coupling constant (Hz), integration). Multiplicity and qualifier abbreviations are as follows: s = singlet, d = doublet, t = triplet, q = quartet, m = multiplet. IR spectra were recorded on a Perkin Elmer Paragon 1000 spectrometer and are reported in frequency of absorption (cm^{-1}). Analytical chiral SFC was performed with a Mettler SFC supercritical CO_2 chromatography system with Chiralcel AD-H, OD-H, AS-H, OB-H, and OJ-H columns (4.6 mm x 25 cm). LRMS were obtained using an Aglient 1290 Infinity/6140 Quadrupole system (LC-MS) or an Agilent 7890A GC/5975C VL MSD system (GC-MS). HRMS were acquired from the Caltech Mass Spectral Facility using fast-atom bombardment (FAB), electrospray ionization (ESI-TOF), or electron impact (EI). X-ray diffraction and elemental analysis (EA) were performed at Caltech X-ray Crystal Facility.

3.6.2 Ni(II) Complex Preparation

For the synthesis of ligand **L2**, see Chapter 2.

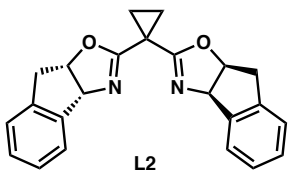

L2

Nickel(II) bis(bromide) (3a*R*,3a'*R*,8a*S*,8a'*S*)-2,2'-(cyclopropane-1,1-diyl)bis(3a,8a-dihydro-8*H*-indeno[1,2-*d*]oxazole) (L2·$NiBr_2$)

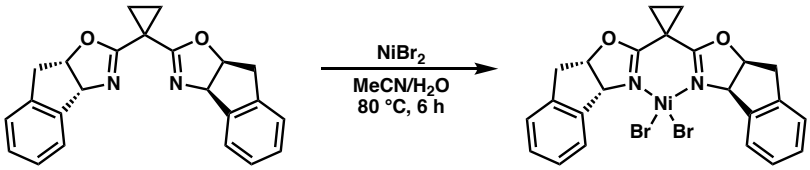

Similar to a procedure reported by Evans and coworkers,[80] the bis(oxazoline) ligand **L2** (1.07 g, 3.0 mmol, 1 equiv) and anhydrous nickel(II) bromide (655 mg, 3.0 mmol, 1 equiv) were added to a round bottom flask equipped with a magnetic stir bar and dissolved in a mixture of acetonitrile (CH_3CN, 65 mL) and water (0.75 mL). The solution was heated to 80 °C for 6 hours to afford a dark purple solution. The reaction was concentrated under reduced pressure and the obtained solid was saturated in CH_2Cl_2, filtered through a plug of cotton, dispensed into four 20 mL scintillation vials, and recrystallized by vapor diffusion (CH_2Cl_2/pentane) to afford dark purple crystals suitable for X-ray diffraction. For the isolation of **L2**·$NiBr_2$, the crystals were washed with hexane, which was added by pipet and subsequently removed. The crystals were removed with a spatula, transferred to a new vial, and crushed to provide a powder. The resulting complex was dried under vacuum to yield 1.6 g (91% yield) of **L2**·$NiBr_2$ as a purple solid. **m.p.** = >300 °C. **^{1}H NMR (400 MHz, $CDCl_3$):** δ 96.48 (s, 2H), 46.46 (s, 2H), 20.16 (d, *J* = 17.1 Hz, 2H), 11.67 – 10.85 (m, 6H), 10.55 (d, *J* = 16.6 Hz, 2H), 6.96 (s, 2H), 5.40 (s, 2H), -0.65 (s, 2H). **FTIR (NaCl, thin film, cm^{-1}):** 3333, 2222, 1660, 1479, 1461, 1444, 1427, 1312, 1247, 1227, 1214, 1120, 1010, 911, 859, 758, 728. **EA:** Anal. Calc'd. for **L2**·$NiBr_2$, $C_{23}H_{20}Br_2N_2NiO_2$ (%): C, 48.05; H, 3.51; N, 4.87. Found: C, 48.38; H, 3.54; N, 4.84.

3.6.3 Large Scale Preparation of TDAE

N,N,N',N'-tetramethylformamidinium chloride (S28)

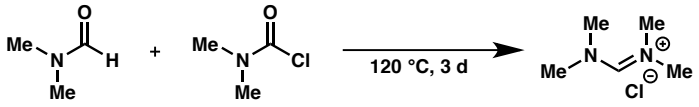

According to a procedure by Bestmann and coworkers,[81] the dimethylcarbamyl chloride (500 mmol, 46 mL, 1 equiv) and anhydrous dimethylformamide (DMF, 1 mol, 77 mL, 2 equiv) were added under an inert atmosphere (N_2) to a flame-dried 500 mL round bottom flask fitted with a reflux condenser and a magnetic stir bar. The solution was heated to 120 °C for 3 days, during which the reaction remained a homogeneous solution and turned dark brown in color. The reaction was removed from the stir plate and allowed to cool to room temperature, which initiated crystallization of the formamidinium chloride salt. Anhydrous diethyl ether (200 mL) was added to the crude reaction, swirled vigorously, quickly transferred to a fritted glass funnel, and filtered under a cone of argon gas. The crystals were quickly transferred to a round bottom flask and dried overnight under vacuum to yield 60.3 g (88% yield) of **S28** as a tan solid. The product is *extremely* hygroscopic, thus it was stored in the glovebox away from ambient moisture.

Tris(dimethylamino)methane (S29)

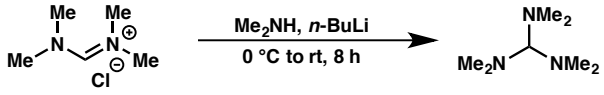

Similar to a procedure by Wasserman and coworkers,[82] anhydrous diethyl ether (500 mL) and dimethylamine (440 mL, 2 M in THF, 369 mmol, 2 equiv) were added under an inert atmosphere (N_2) to a flame-dried 2 L round bottom flask with a magnetic stir bar. The

reaction was cooled to –78 °C and *n*-butyllithium (*n*-BuLi, 210 mL, 2.5 M in hexane, 295 mmol, 1.2 equiv) was added via cannula under a stream of N_2, resulting in a pink homogenous solution. The reaction was warmed to room temperature and stirred for 30 min, forming a white slurry. The flask was cooled to 0 °C, **S28** (60.3 g, 246 mmol, 1 equiv) was quickly added, and the reaction was warmed to room temperature and stirred overnight for 8 h forming a light brown slurry. The flask was fitted with a distillation head and reflux condenser, and the solvent was distilled off into a 2 L receiving flask under ambient pressure. The flask was cooled and a new collection flask was added along with a vacuum regulator. The desired product was distilled out of the crude residue by slowly decreasing the pressure of the vacuum regulator to 1 mm Hg while increasing the oil bath temperature upwards of 100 °C. The liquid collected in the trap was THF, whereas the liquid collected in the receiving flask yielded 45.2 g (71% yield) of tris(dimethylamino)methane as a colorless oil. **^{1}H NMR (300 MHz, $CDCl_3$):** δ 3.02 (s, 1H), 2.29 (s, 18H). **^{13}C NMR (101 MHz, $CDCl_3$)**: δ 100.3, 41.3.

Tetrakis(dimethylamino)ethylene (TDAE)

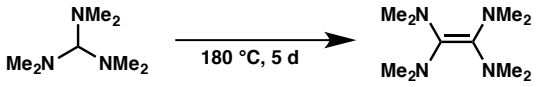

Similar to a procedure by Murphy and coworkers,[83] the tris(dimethylamino)methane was added to a 250 mL flame-dried round bottom flask fitted with a reflux condenser and a magnetic stir bar, and sparged with argon for 15 minutes. The reaction was heated to reflux for 5 days at 180 °C while being maintained under a steady stream of dry argon. The reaction was cooled to room temperature and remained under an argon atmosphere while

the flask was fitted with a distillation apparatus (also under an argon atmosphere). The product was purified via fractional distillation under reduced pressure with the aid of a Vigreux column. The remaining tris(dimethylamino)methane starting material was collected in the first fraction at 1 mm Hg and 30 °C as a colorless oil. When a yellow-green oil began to collect in the receiving flask, the fractions were exchanged and the desired product was collected at 1 mm Hg and 65 °C to yield 19.4 g (62% yield) of tetrakis(dimethylamino)ethylene as a yellow-green oil. Spectra matched those reported in literature[83] and also matched a sample of the commercially available material. The reagent was stored under inert atmosphere (N_2) in the glovebox. **^{1}H NMR (400 MHz, $C_6D_5CD_3$):** δ 2.57 (s, 24H). **^{13}C NMR (101 MHz, $C_6D_5CD_3$):** δ 131.5, 41.2.

3.6.4 Optimization of Reaction Parameters

On a bench-top to a 1 dram vial equipped with a stir bar was added alkenyl bromide **86** (43 mg, 0.2 mmol, 1 equiv), NHP ester **136** (59 mg, 0.2 mmol, 1 equiv), **L2**·$NiCl_2$ or **L2**·$NiBr_2$ (0.00–0.02 mmol, 0.00–0.10 equiv), reductant (if Mn or Zn, 0.6 mmol, 3 equiv), and sodium iodide (0.0–15.0 mg, 0.0–0.1 mmol, 0.0–0.5 equiv). Under an inert atmosphere in a glovebox, the vial was charged with DMA (0.2 mL, 1.0 M), the reagents were stirred until dissolved, and then cooled to the desired temperature. The reductant was then added (if tetrakis(dimethylamino)ethylene, TDAE, 0.3–0.6 mmol, 70–140 µl, 1.5–3 equiv). The reaction was stirred for 10 minutes before the trimethylsilyl chloride (TMSCl) or trimethylsilyl bromide (TMSBr) was added (0.0–0.2 mmol, 0–1 equiv). The vial was sealed with a screw cap and stirred for 16 hours. As the reaction proceeds, the TDAE salts begin

to precipitate, forming an orange slurry. The vial was removed from the glovebox and dibenzyl ether was added as an internal standard. The solution was quenched with aqueous HCl, extracted with Et_2O, dried with $MgSO_4$, and concentrated to afford the crude reaction mixture, which was analyzed by ^1H NMR and chiral phase SFC to provide the reaction yield and enantioselectivity of the desired product (**137**).

3.6.5 Substrate Preparation

General Procedure 1: NHP Ester Synthesis

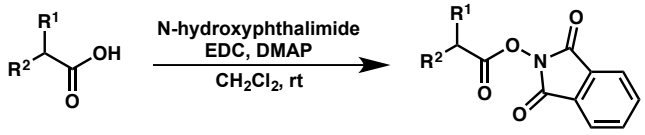

To a round bottom flask equipped with a magnetic stir bar was added the carboxylic acid (1.0 equiv), N-hydroxyphthalimide (1.0 equiv), and 4-dimethylaminopyridine (DMAP, 0.10 equiv). The reagents were dissolved in CH_2Cl_2 (0.2 M) and the N-(3-dimethylaminopropyl)-N-ethylcarbodiimide·HCl (EDC, 1.1 equiv) was added. The reaction continued to stir overnight at room temperature. The crude reaction was concentrated to afford a thick oil, which was purified by column chromatography (silica, EtOAc/hexane or CH_2Cl_2) to afford the desired product.

1,3-dioxoisoindolin-2-yl 2-phenylpropanoate (136)

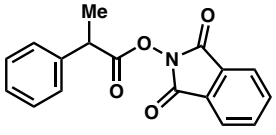

Prepared from 2-phenylpropanoic acid (5.0 g, 33.3 mmol) according to General Procedure 1. The crude residue was purified by filtering through a plug of silica with CH_2Cl_2 as the eluent to yield 8.7 g (88% yield) of **136** as a white solid. $\mathbf{R_f}$ = 0.28 (silica gel, 20% EtOAc/hexane, UV). **m.p.** = 62–64 °C. ^{1}**H**

NMR (400 MHz, $CDCl_3$): δ 7.85 (d, *J* = 5.5, 3.1 Hz, 2H), 7.76 (dd, *J* = 5.5, 3.1 Hz, 2H), 7.43 – 7.37 (m, 4H), 7.37 – 7.30 (m, 1H), 4.13 (q, *J* = 7.2 Hz, 1H), 1.68 (d, *J* = 7.2 Hz, 3H). **^{13}C NMR (101 MHz, $CDCl_3$):** δ 170.9, 161.9, 138.5, 134.9, 129.02, 128.98, 127.9, 127.7, 124.0, 43.1, 19.1. **FTIR (NaCl, thin film, cm^{-1}):** 1810, 1785, 1743, 1466, 1453, 1358, 1186, 1123, 1043, 1028, 877, 695. **HRMS (ESI-TOF, m/z):** calc'd for $C_{17}H_{13}NO_4$ $[M+H]^+$: 296.0923; found: 296.0903.

1,3-dioxoisoindolin-2-yl 2-(4-methoxyphenyl)propanoate (62a)

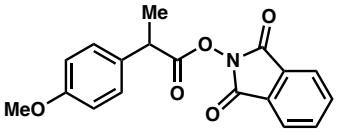

Prepared from 2-(4-methoxyphenyl)propanoic acid (500 mg, 2.77 mmol) according to General Procedure 1. The crude residue was purified by filtering through a plug of silica with 30% EtOAc/hexane as the eluent to yield 671 mg (74% yield) of **62a** as a white solid. **R_f** = 0.22 (silica gel, 20% EtOAc/hexane, UV). **m.p.** = 91–92 °C. **^{1}H NMR (400 MHz, $CDCl_3$):** δ 7.86 (dd, *J* = 5.5, 3.1 Hz, 2H), 7.77 (dd, 2H), 7.33 (d, *J* = 8.7 Hz, 2H), 6.92 (d, *J* = 8.8 Hz, 2H), 4.08 (q, *J* = 7.2 Hz, 1H), 3.81 (s, 3H), 1.65 (d, *J* = 7.2 Hz, 3H). **^{13}C NMR (101 MHz, $CDCl_3$):** δ 171.1, 162.0, 159.2, 134.9, 130.5, 129.0, 128.8, 124.0, 114.4, 55.4, 42.2, 19.2. **FTIR (NaCl, thin film, cm^{-1}):** 1810, 1784, 1743, 1611, 1513, 1467, 1371, 1249, 1185, 1123, 1045, 1033, 878, 832, 696. **HRMS (ESI-TOF, m/z):** calc'd for $C_{18}H_{15}NO_5$, $[M+H]^+$: 326.1028; found: 326.1022.

1,3-dioxoisoindolin-2-yl 2-(4-(trifluoromethyl)phenyl)propanoate (62b)

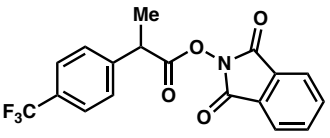

Prepared from 2-(4-(trifluoromethyl)phenyl)propanoic acid (200 mg, 0.92 mmol) according to General Procedure 1. The

crude residue was purified by filtering through a plug of silica with 30% EtOAc/hexane as the eluent to yield 290 mg (87% yield) of **62b** as a yellow solid. $\mathbf{R_f}$ = 0.28 (silica gel, 20% EtOAc/hexane, UV). **m.p.** = 76–77 °C. **^{1}H NMR (400 MHz, $CDCl_3$):** δ 7.87 (dd, *J* = 5.6, 3.2 Hz, 2H), 7.78 (dd, *J* = 5.5, 3.1 Hz, 2H), 7.66 (d, *J* = 7.8 Hz, 2H), 7.54 (d, *J* = 8.1 Hz, 2H), 4.19 (q, *J* = 7.2 Hz, 1H), 1.69 (d, *J* = 7.2 Hz, 3H). **^{13}C NMR (101 MHz, $CDCl_3$):** δ 170.3, 161.9, 142.4 (q, J_{C-F} = 1 Hz), 135.0, 130.2 (q, J_{C-F} = 33 Hz), 128.9, 128.2, 126.1 (q, J_{C-F} = 4 Hz). 124.14, 124.11 (q, J_{C-F} = 272 Hz), 43.0, 19.1. **^{19}F NMR (282 MHz, $CDCl_3$):** δ -65.8. **FTIR (NaCl, thin film, cm^{-1}):** 1813, 1788, 1746, 1620, 1468, 1421, 1359, 1326, 1186, 1168, 1125, 1079, 1067, 1048, 1017, 878, 842, 697. **HRMS (ESI-TOF, m/z):** calc'd for $C_{18}H_{12}F_3NO_4$ [M+H]+: 364.0797; found: 364.0815.

1,3-dioxoisoindolin-2-yl 2-(4-bromophenyl)propanoate (62c)

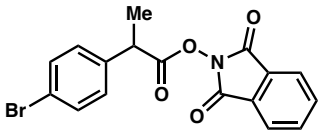

Prepared from 2-(4-bromophenyl)propanoic acid (1.0 g, 4.65 mmol) according to General Procedure 1. The crude residue was purified by filtering through a plug of silica with 20% EtOAc/hexane as the eluent to yield 511 mg (48% yield) of **62c** as a light yellow solid. $\mathbf{R_f}$ = 0.69 (silica gel, 20% EtOAc/hexane, UV). **m.p.** = 77–78 °C. **^{1}H NMR (400 MHz, $CDCl_3$):** δ 7.86 (dd, *J* = 5.5, 3.0 Hz, 2H), 7.80 – 7.75 (m, 2H), 7.52 (d, *J* = 8.5 Hz, 2H), 7.29 (d, *J* = 8.4 Hz, 2H), 4.08 (q, *J* = 7.2 Hz, 1H), 1.65 (d, *J* = 7.2 Hz, 3H). **^{13}C NMR (101 MHz, $CDCl_3$):** δ 170.5, 161.9, 137.4, 134.9, 132.2, 129.4, 129.0, 124.1, 122.0, 42.6, 19.0. **FTIR (NaCl, thin film, cm^{-1}):** 1811, 1786, 1742, 1489, 1467, 1369, 1186, 1133, 1078, 1046, 1010, 877, 696. **LRMS (API-ES, m/z):** calc'd for $C_{17}H_{12}BrNO_4$ $[M+H_2O]^+$: 391.0; found: 391.0.

1,3-dioxoisoindolin-2-yl 2-(4-fluorophenyl)propanoate (62d)

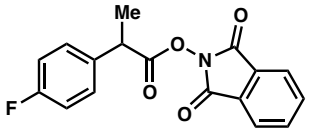

Prepared from 2-(4-fluorophenyl)propanoic acid (500 mg, 2.92 mmol) according to General Procedure 1. The crude residue was purified by filtering through a plug of silica with 20% EtOAc/hexane as the eluent to yield 590 mg (63% yield) of **62d** as a white solid. $\mathbf{R_f}$ = 0.35 (silica gel, 20% EtOAc/hexane, UV). **m.p.** = 108–110 °C. **^{1}H NMR (400 MHz, $CDCl_3$):** δ 7.86 (dd, *J* = 5.6, 3.1 Hz, 2H), 7.77 (dd, *J* = 5.5, 3.1 Hz, 2H), 7.41 – 7.35 (m, 2H), 7.12 – 7.05 (m, 2H), 4.11 (q, *J* = 7.2 Hz, 1H), 1.66 (d, *J* = 7.2 Hz, 3H). **^{13}C NMR (101 MHz, $CDCl_3$):** δ 170.78, 162.42 (d, $J_{C–F}$ = 246.4 Hz), 161.9, 134.9, 134.2 (d, $J_{C–F}$ = 3.3 Hz), 129.37 (d, $J_{C–F}$ = 8.3 Hz), 129.9, 124.1, 115.95 (d, $J_{C–F}$ = 21.5 Hz), 42.3, 19.2. **^{19}F NMR (282 MHz, $CDCl_3$):** δ -117.64 (tt, JF H = 8.4, 5.2 Hz). **FTIR (NaCl, thin film, cm^{-1}):** 1811, 1785, 1739, 1605, 1509, 1467, 1360, 1225, 1186, 1120, 1045, 1016, 959, 877, 837, 783, 696. **HRMS (FAB, m/z):** calc'd for $C_{17}H_{12}FNO_4$ $[M+H]^+$: 314.0823; found: 314.0859.

1,3-dioxoisoindolin-2-yl 2-(4-(dimethylamino)phenyl)propanoate (62e)

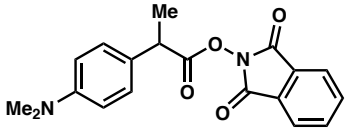

Prepared from 2-(4-(dimethylamino)phenyl)propanoic acid (392 mg, 2.02 mmol) according to General Procedure 1, with the exception of no DMAP. The crude residue was purified column chromatography (silica, 20 to 50% EtOAc/hexane) to yield 640 mg (94% yield) of **62e** as a yellow solid. $\mathbf{R_f}$ = 0.54 (silica gel, 50% EtOAc/hexane, UV). **m.p.** = 106–108 °C. **^{1}H NMR (400 MHz, $CDCl_3$):** δ 7.85 (dd, *J* = 5.6, 3.1 Hz, 2H), 7.76 (dd, *J* = 5.5, 3.1 Hz, 2H), 7.27 (d, *J* = 8.8 Hz, 2H), 6.75 (d, *J* = 8.8 Hz, 2H), 4.04 (q, *J* = 7.2 Hz, 1H), 2.95 (s, 6H), 1.64 (d, *J* = 7.2 Hz, 3H). **^{13}C NMR (101 MHz, $CDCl_3$):** δ 171.4, 162.1, 150.2, 134.8, 129.1, 128.3, 126.0, 124.0,

112.8, 42.1, 40.6, 19.2. **FTIR (NaCl, thin film, cm^{-1}):** 1809, 1784, 1743, 1615, 1523, 1467, 1356, 1186, 1134, 1081, 1044, 878, 819, 697. **HRMS (FAB, m/z):** calc'd for $C_{19}H_{18}N_2O_4$ $[M+\cdot]^+$: 338.1267; found: 338.1272.

1,3-dioxoisoindolin-2-yl 2-(3,4-dichlorophenyl)propanoate (62f)

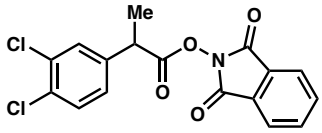

Prepared from 2-(3,4-dichlorophenyl)propanoic acid (231 mg, 1.05 mmol) according to General Procedure 1, with the exception of no DMAP. The crude residue was purified by column chromatography (silica, 0 to 15% EtOAc/hexane) to yield 241 mg (63% yield) of **62f** as a white solid. $\mathbf{R_f}$ = 0.35 (silica gel, 20% EtOAc/hexane, UV). **m.p.** = 103–105 °C. **^{1}H NMR (400 MHz, $CDCl_3$):** δ 7.87 (dd, *J* = 5.5, 3.1 Hz, 2H), 7.79 (dd, *J* = 5.5, 3.1 Hz, 2H), 7.52 (d, *J* = 2.2 Hz, 1H), 7.47 (d, *J* = 8.3 Hz, 1H), 7.26 (dd, *J* = 8.3, 2.2 Hz, 1H), 4.08 (q, *J* = 7.2 Hz, 1H), 1.66 (d, *J* = 7.2 Hz, 3H). **^{13}C NMR (101 MHz, $CDCl_3$):** δ 170.1, 161.9, 138.4, 135.0, 133.1, 132.2, 131.0, 129.9, 128.9, 127.1, 124.2, 42.3, 19.0. **FTIR (NaCl, thin film, cm^{-1}):** 2341, 2359, 1785, 1743, 1426, 1186, 1135, 1049, 962, 878, 696. **HRMS (FAB, m/z):** calc'd for $C_{17}H_{11}Cl_2NO_4$ $[M+H]^+$: 364.0143; found: 364.0131.

1,3-dioxoisoindolin-2-yl 2-phenylbutanoate (62g)

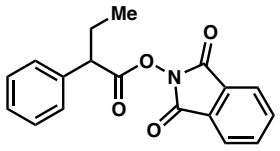

Prepared from 2-phenylbutanoic acid (5.0 g, 30.5 mmol) according to General Procedure 1. The crude residue was purified by column chromatography (silica, 20% EtOAc/hexane) to yield 8.1 g (86% yield) of **62g** as a white solid. $\mathbf{R_f}$ = 0.31 (silica gel, 20% EtOAc/hexane, UV). **m.p.** = 61–64 °C. **^{1}H NMR (400 MHz, $CDCl_3$):** δ 7.85 (dd, *J* = 5.6, 3.1 Hz, 2H), 7.76 (dd, *J* = 5.5, 3.1 Hz, 2H), 7.42

– 7.29 (m, 5H), 3.86 (t, J = 7.6 Hz, 1H), 2.31 – 2.18 (m, 1H), 2.03 – 1.90 (m, 1H), 1.04 (t, J = 7.4 Hz, 3H). **^{13}C NMR (101 MHz, $CDCl_3$):** δ 170.4, 162.0, 136.9, 134.8, 129.0, 128.9, 128.2, 128.0, 124.0, 50.5, 27.3, 12.0. **FTIR (NaCl, thin film, cm^{-1}):** 1811, 1786, 1744, 1467, 1455, 1360, 1186, 1128, 1080, 1058, 969, 877, 656. **HRMS (ESI-TOF, m/z):** calc'd for $C_{18}H_{15}NO_4$ $[M+H]^+$: 310.1079; found: 310.1061.

1,3-dioxoisoindolin-2-yl 2,3-diphenylpropanoate (62h)

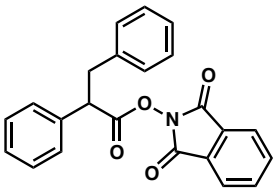

Prepared from 2,3-diphenylpropanoic acid (353 mg, 1.56 mmol) according to General Procedure 1. The crude residue was purified by column chromatography (silica, 20% EtOAc/hexane) to yield 542 mg (94% yield) of **62h** as a white solid. **R_f** = 0.28 (silica gel, 20% EtOAc/hexane, UV). **m.p.** = 116–119 °C. **^{1}H NMR (400 MHz, $CDCl_3$):** δ 7.85 (dd, J = 5.5, 3.0 Hz, 2H), 7.76 (dd, J = 5.5, 3.1 Hz, 2H), 7.41 – 7.20 (m, 8H), 7.15 – 7.10 (m, 2H), 4.23 (t, J = 7.6 Hz, 1H), 3.56 (dd, J = 13.9, 7.5 Hz, 1H), 3.19 (dd, J = 13.9, 7.8 Hz, 1H). **^{13}C NMR (101 MHz, $CDCl_3$):** δ 170.0, 161.8, 137.7, 136.4, 134.8, 129.2, 129.0, 128.9, 128.6, 128.3, 128.1, 126.9, 124.0, 50.9, 39.9. **FTIR (NaCl, thin film, cm^{-1}):** 3030, 1810, 1784, 1744, 1496, 1467, 1454, 1359, 1186, 1134, 1080, 1068, 972, 877, 736, 695. **HRMS (ESI-TOF, m/z):** calc'd for $C_{23}H_{17}NO_4$ $[M+H]^+$: 372.1236; found: 372.1236.

1,3-dioxoisoindolin-2-yl 3-methyl-2-phenylbutanoate (62i)

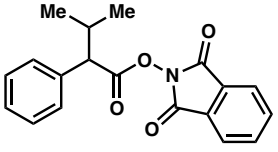

Prepared from 3-methyl-2-phenylbutanoic acid (300 mg, 1.68 mmol) according to General Procedure 1. The crude residue was purified by filtering through a plug of silica with 20% EtOAc/hexane as the eluent to yield

509 mg (93% yield) of **62i** as a white solid. $\mathbf{R_f}$ = 0.34 (silica gel, 20% EtOAc/hexane, UV). **m.p.** = 77–81 °C. **^{1}H NMR (400 MHz, $CDCl_3$):** δ 7.84 (dd, *J* = 5.6, 3.1 Hz, 2H), 7.76 (dd, *J* = 5.5, 3.1 Hz, 2H), 7.42 – 7.29 (m, 5H), 3.58 (d, *J* = 10.0 Hz, 1H), 2.51 – 2.37 (m, 1H), 1.23 (d, *J* = 6.6 Hz, 3H), 0.84 (d, *J* = 6.7 Hz, 3H). **^{13}C NMR (101 MHz, $CDCl_3$):** δ 170.2, 162.0, 136.1, 134.8, 129.0, 128.8, 128.7, 128.0, 124.0, 56.7, 32.6, 21.3, 20.3. **FTIR (NaCl, thin film, cm^{-1}):** 2966, 1811, 1786, 1745, 1468, 1455, 1375, 1311, 1186, 1132, 1080, 1060, 974, 889, 877, 786, 745, 696. **HRMS (ESI-TOF, m/z):** calc'd for $C_{19}H_{17}NO_4$ $[M+H]^+$: 324.1236; found: 324.1227.

1,3-dioxoisoindolin-2-yl 3-((*tert*-butyldimethylsilyl)oxy)-2-phenylpropanoate (62j)

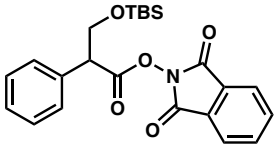

To a round bottom flask equipped with a stirring magnet was added tropic acid (830 mg, 5 mmol, 1 equiv), *tert*-butyldimethylsilyl chloride (1.1 g, 5.5 mmol, 1.1 equiv), dimethylaminopyridine (63 mg, 0.5 mmol, 0.1 equiv), and imidazole (682 mg, 10 mmol, 2 equiv). The reagents were dissolved in 15 mL of CH_2Cl_2 and stirred overnight at room temperature. The reaction was quenched with aq. NH_4Cl, extracted with Et_2O, dried with $MgSO_4$, filtered, and concentrated under reduced pressure to afford crude 3-((*tert*-butyldimethylsilyl)oxy)-2-phenylpropanoic acid. This crude material was used in the esterification step without purification, which was performed according to General Procedure 1. The crude residue was purified by column chromatography and dried under high vacuum (silica, 0 to 20% EtOAc/hexane) to yield 664 mg (31% yield) of **62j** as a colorless oil. $\mathbf{R_f}$ = 0.38 (silica gel, 20% EtOAc/hexane, UV). **^{1}H NMR (400 MHz, $CDCl_3$):** δ 7.86 (dd, *J* = 5.6, 3.1 Hz, 2H), 7.77 (dd, *J* = 5.5, 3.1 Hz, 2H), 7.43 – 7.31 (m, 5H), 4.28 – 4.18 (m, 2H), 3.93 (dd, *J* = 8.6,

4.4 Hz, 1H), 0.89 (s, 9H), 0.05 (s, 3H), 0.03 (s, 3H). **^{13}C NMR (101 MHz, $CDCl_3$):** δ 169.0, 161.8, 134.8, 134.1, 129.1, 129.0, 128.5, 128.3, 124.0, 65.3, 52.2, 25.9, 18.4, -5.4, -5.6. **FTIR (NaCl, thin film, cm^{-1}):** 2953, 2929, 2856, 1814, 1788, 1747, 1468, 1361, 1256, 1186, 1113, 1049, 1023, 877, 836, 780, 696. **HRMS (ESI-TOF, m/z):** calc'd for $C_{23}H_{27}NO_5Si$ $[M+H]^+$: 426.1737; found: 426.1708.

1,3-dioxoisoindolin-2-yl 2-phenylpent-4-enoate (62k)

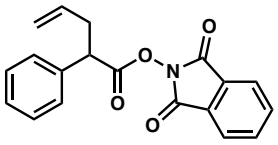

Prepared from 2-phenylpent-4-enoic acid (240 mg, 1.36 mmol) according to General Procedure 1. The crude residue was purified by column chromatography (silica, 0 to 20% EtOAc/hexane) to yield 295 mg (67% yield) of **62k** as a white solid. **R_f =** 0.31 (silica gel, 20% EtOAc/hexane, UV). **m.p. =** 68–69 °C. **^{1}H NMR (400 MHz, $CDCl_3$):** δ 7.85 (dd, *J* = 5.6, 3.1 Hz, 2H), 7.76 (dd, *J* = 5.5, 3.1 Hz, 2H), 7.42 – 7.31 (m, 5H), 5.81 (ddt, *J* = 17.1, 10.2, 6.9 Hz, 1H), 5.16 (dq, *J* = 17.1, 1.5 Hz, 1H), 5.14 – 5.09 (m, 1H), 4.04 (dd, *J* = 8.0, 7.2 Hz, 1H), 3.00 – 2.90 (m, 1H), 2.68 (dtt, *J* = 14.3, 7.1, 1.3 Hz, 1H). **^{13}C NMR (101 MHz, $CDCl_3$):** δ 169.9, 161.9, 136.4, 134.9, 134.0, 129.02, 128.99, 128.2, 128.1, 124.0, 118.3, 48.8, 37.9. **FTIR (NaCl, thin film, cm^{-1}):** 1811, 1785, 1743, 1467, 1359, 1186, 1133, 1080, 1068, 971, 877, 695. **HRMS (ESI-TOF, m/z):** calc'd for $C_{19}H_{15}NO_4$ $[M+H]^+$: 322.1079; found: 322.1063.

1,3-dioxoisoindolin-2-yl 5-chloro-2-phenylpentanoate (62l)

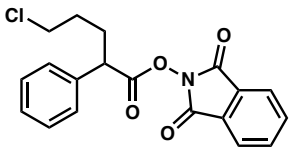

Prepared from 5-chloro-2-phenylpentanoic acid (1.01 g, 4.75 mmol) according to General Procedure 1. The crude residue was purified by filtering through a plug of silica with 20% EtOAc/hexane as the eluent to yield

977 mg (58% yield) of **62l** as a white solid. **R_f =** 0.25 (silica gel, 20% EtOAc/hexane, UV). **m.p. =** 96–99 °C. **^{1}H NMR (400 MHz, $CDCl_3$):** δ 7.85 (dd, *J* = 5.6, 3.1 Hz, 2H), 7.77 (dd, *J* = 5.5, 3.1 Hz, 2H), 7.42 – 7.31 (m, 5H), 3.97 (t, *J* = 7.7 Hz, 1H), 3.64 – 3.52 (m, 2H), 2.34 (dddd, *J* = 13.2, 10.4, 8.0, 5.1 Hz, 1H), 2.13 (dddd, *J* = 13.5, 10.3, 7.4, 5.5 Hz, 1H), 2.01 – 1.78 (m, 2H). **^{13}C NMR (101 MHz, $CDCl_3$):** δ 170.1, 161.9, 136.4, 134.9, 129.1, 129.0, 128.2, 128.1, 124.1, 48.2, 44.4, 31.2, 30.1. **FTIR (NaCl, thin film, cm^{-1}):** 2960, 1811, 1786, 1744, 1494, 1455, 1468, 1361, 1186, 1134, 1081, 1045, 965, 878, 697. **HRMS (FAB, m/z):** calc'd for $C_{19}H_{16}NO_4Cl$ $[M+H]^+$: 358.0846; found: 358.0872.

1,3-dioxoisoindolin-2-yl 2-methoxy-2-phenylacetate (145)

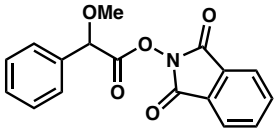

Prepared from 2-methoxy-2-phenylacetic acid (830 mg, 5.0 mmol) according to General Procedure 1. The crude residue was purified by column chromatography (silica, 10 to 30% EtOAc/hexane) to yield 1.16 g (74% yield) of **145** as a colorless oil. **Note:** This compound will slowly decompose (solidifies/hydrolyzes) under ambient conditions over extended periods (~1 month). **R_f =** 0.22 (silica gel, 20% EtOAc/hexane, UV). **^{1}H NMR (400 MHz, $CDCl_3$):** δ 7.83 (dd, *J* = 5.5, 3.1 Hz, 2H), 7.75 (dd, *J* = 5.5, 3.1 Hz, 2H), 7.60 – 7.52 (m, 2H), 7.50 – 7.37 (m, 3H), 5.19 (s, 1H), 3.56 (s, 3H). **^{13}C NMR (101 MHz, $CDCl_3$):** δ 167.4, 161.6, 134.9, 134.4, 129.6, 129.0, 128.8, 127.6, 124.1, 81.0, 58.0. **FTIR (NaCl, thin film, cm^{-1}):** 1818, 1789, 1745, 1468, 1359, 1186, 1079, 988, 969, 877, 696. **HRMS (ESI-TOF, m/z):** calc'd for $C_{17}H_{13}NO_5$ $[M+H]^+$: 312.0872; found: 312.0846.

1,3-dioxoisoindolin-2-yl 2-cyclopropyl-2-phenylacetate (160)

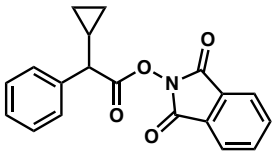

Prepared from 2-cyclopropyl-2-phenylacetic acid (50 mg, 0.28 mmol) according to General Procedure 1. The crude residue was purified by filtering through a plug of silica with 20% EtOAc/hexane as the eluent to yield 80 mg (89% yield) of **160** as a white solid. $\mathbf{R_f}$ **=** 0.39 (silica gel, 50% EtOAc/hexane, UV). **m.p. =** 92–93 °C. **^{1}H NMR (400 MHz, $CDCl_3$):** δ 7.87 (dd, *J* = 5.5, 3.0 Hz, 2H), 7.81 – 7.75 (m, 2H), 7.50 – 7.45 (m, 2H), 7.44 – 7.38 (m, 2H), 7.37 – 7.31 (m, 1H), 3.29 (d, *J* = 9.7 Hz, 1H), 1.53 (dtt, *J* = 9.7, 8.0, 4.9 Hz, 1H), 0.82 (dddd, *J* = 9.0, 8.1, 4.6, 2.9 Hz, 1H), 0.69 (dddd, *J* = 8.9, 8.0, 5.8, 4.8 Hz, 1H), 0.63 – 0.55 (m, 1H), 0.42 – 0.34 (m, 1H). **^{13}C NMR (101 MHz, $CDCl_3$):** δ 170.0, 162.0, 136.8, 134.9, 129.1, 128.9, 128.1, 128.0, 124.1, 53.4, 14.6, 4.91, 4.90. **FTIR (NaCl, thin film, cm^{-1}):** 1811, 1742, 1362, 1170, 1135, 1063, 974, 876. **HRMS (FAB, m/z):** calc'd for $C_{19}H_{15}NO_4$ $[M+H]^+$: 322.1079; found: 322.1065.

Alkenyl Bromide Synthesis

Alkenyl bromides **86**, **29a**, **29u**, **29j**, and **29i** were prepared according to procedures reported and referenced by Reisman and coworkers.[44]

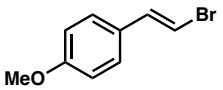

86

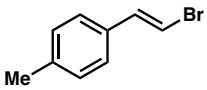

29a

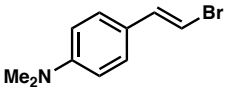

29u

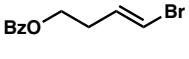

29j

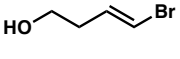

29i

Alkenyl bromides **29v**, **29w**, **29x**, **29y**, and **29k** were prepared according to General Procedure 2. Alkenyl bromides **29v** and **29x** were subjected to NaOH-mediated isomerization to afford geometrically pure *E*-isomer. Alkenyl bromides **29w**, **29y**, and **29k** were not subjected to NaOH-mediated isomerization;[84] alkenyl bromide **29w** decomposes

under these conditions therefore the substrate used in the cross-coupling reaction was a 93:7 E:Z ratio. The NMR spectra of **29v,**[44] **29w,**[85] and **29x**[86] matched those reported in literature. The characterization data for **29y** is reported below. For **29k**, see Chapter 2.

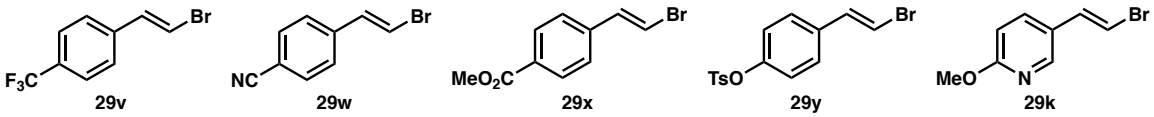

General Procedure 2: Alkenyl Bromides from Aldehydes

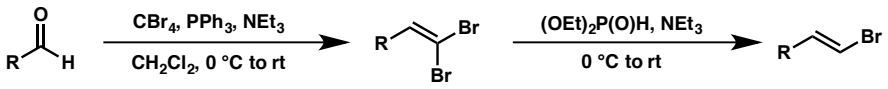

General Procedure 2, Part A: According to a procedure by Alexakis and coworkers,[84] a flame dried round bottom flask equipped with a magnetic stir bar was put under an inert atmosphere (N_2) and charged with the tetrabromomethane (20 mmol, 2 equiv) and triphenylphosphine (40 mmol, 4 equiv). The flask was cooled to 0 °C and then CH_2Cl_2 (30 mL) was added, followed by the triethylamine (10 mmol, 1 equiv). The aldehyde (10 mmol, 1 equiv) was dissolved in CH_2Cl_2 (5 mL) and added dropwise to the reaction mixture. The reaction was allowed to warm to room temperature and continued to stir for 90 minutes. The reaction was removed from the stir plate and slowly added to a vigorously stirring solution of Et_2O (150 mL) and hexane (150 mL), filtered through a plug of silica gel, and concentrated under reduced pressure to afford the desired dibromoalkene.

4-(2,2-dibromovinyl)phenyl 4-methylbenzenesulfonate (S30)

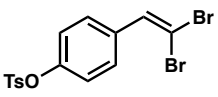

Prepared from 4-formylphenyl 4-methylbenzenesulfonate (5.14 g, 18.6 mmol) following General Procedure 2A. The crude residue was

purified by filtering through a plug of silica to yield 6.2 g (77% yield) of **S30** as a white solid. $\mathbf{R_f}$ = 0.38 (silica gel, 10% EtOAc/hexane). **m.p.** = 108–110 °C. **^{1}H NMR (400 MHz, $CDCl_3$):** δ 7.73 – 7.67 (m, 2H), 7.49 – 7.43 (m, 2H), 7.41 (s, 1H), 7.34 – 7.29 (m, 2H), 7.01 – 6.95 (m, 2H), 2.45 (s, 3H). **^{13}C NMR (101 MHz, $CDCl_3$):** δ 149.3, 145.7, 135.6, 134.2, 132.3, 129.9, 129.8, 128.6, 122.5, 90.8, 21.9. **FTIR (NaCl, thin film, cm^{-1})**: 3081, 3065, 1929, 1910, 1596, 1500, 1495, 1406, 1379, 1360, 1271, 1178, 1160, 1094, 1018, 877, 832, 914, 781, 732, 706, 698, 658. **HRMS (FAB, m/z)**: calc'd for $C_{15}H_{12}Br_2O_3S$ $[M+H]^+$: 432.8932; found: 432.8915.

General Procedure 2, Part B: The dibromoalkene (1.7 mmol, 1 equiv) and diethyl phosphite (5.1 mmol, 3 equiv) were added to a vial with a magnetic stirring rod and put under an inert atmosphere (N_2). The solution was cooled to 0 °C and the triethylamine (5.1 mmol, 3 equiv) was added dropwise. The reaction was warmed to room temperature and stirred overnight. The reaction was quenched with water (5 mL) and extracted with CH_2Cl_2 (20 mL). The organic layer was washed with brine (5 mL), dried with Na_2SO_4, filtered, and concentrated under reduced pressure. The crude residue was purified by column chromatography (silica, ether/hexanes) to afford the vinyl bromide.

(*E*)-4-(2-bromovinyl)phenyl 4-methylbenzenesulfonate (29y)

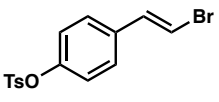

Prepared from **S30** (4.32 g, 10 mmol) following General Procedure 2B. The crude residue was purified by column chromatography (silica, 5% EtOAc/hexane to 20% EtOAc/hexane) to yield 2.75 g (78% yield, 90:10 E:Z) of **29y** as a white solid. $\mathbf{R_f}$ = 0.34 (silica gel, 10% EtOAc/hexane). **m.p.** = 90–93 °C. **^{1}H NMR (400**

MHz, $CDCl_3$): δ 7.72 – 7.67 (m, 2H), 7.34 – 7.28 (m, 2H), 7.23 – 7.17 (m, 2H), 7.03 (d, *J* = 14.0 Hz, 1H), 6.96 – 6.90 (m, 2H), 6.73 (d, *J* = 14.0 Hz, 1H), 2.44 (s, 3H). **^{13}C NMR (101 MHz, $CDCl_3$):** δ 149.3, 145.6, 135.9, 134.9, 132.3, 129.9, 128.6, 127.3, 122.9, 107.7, 21.9. **HRMS (FAB, m/z)**: calc'd for $C_{15}H_{13}BrO_3S$ $[M+\cdot]^+$: 353.9748; found: 353.9733.

Alkenyl bromide **29z** was prepared by a NaOH-mediated isomerization of commercially available β-bromostyrene as reported by Alexakis and coworkers.[84]

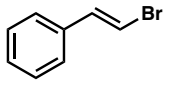

29z

Alkenyl bromide **S2** was prepared via a hydrozirconation/bromination sequence similar to a procedure reported by Zhou, Lin, and coworkers, which is reported in Chapter 2.[87] The NMR spectra matched those reported in literature.[88]

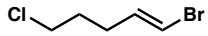

S2

Alkneyl bromide **29aa** was prepared according to a procedure reported by Wolfe and coworkers.[89]

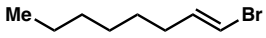

29aa

Alkneyl bromides **29ab** and **29o** were purchased from a commercial source (Sigma Aldrich).

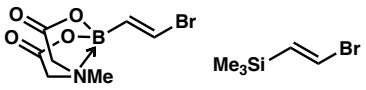

29ab **29o**

3.6.6 Enantioselective Reductive Cross-Couplings

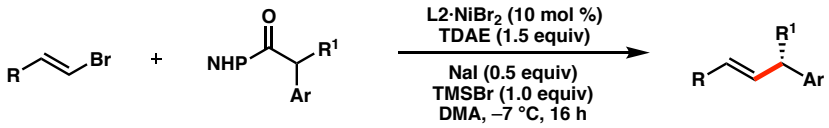

General Procedure 3: Reaction on 0.2 mmol scale.

On a bench-top, a 1 dram vial equipped with a stir bar was charged with the vinyl bromide (if air stable, 0.2 mmol, 1 equiv), NHP ester (0.2 mmol, 1 equiv), **L2**·$NiBr_2$ (11.5 mg, 0.02 mmol, 0.10 equiv), and sodium iodide (15.0 mg, 0.1 mmol, 0.5 equiv). The vial was then brought into the glovebox and charged with the vinyl bromide (if air sensitive, 0.2 mmol, 1 equiv) and DMA (0.2 mL, 1.0 M). The vial was then cooled to –7 °C and the reagents were stirred at 250 rpm until dissolved. **Note:** The recirculating Julabo LH45 chiller was set to –10 °C however an external thermometer in the glovebox read the temperature as –7 °C. The tetrakis(dimethylamino)ethylene (TDAE, 0.3 mmol, 70 μl, 1.5 equiv) was added and stirred for 10 minutes before the trimethylsilyl bromide (TMSBr, 0.2 mmol, 26 μL, 1 equiv) was added. The vial was sealed with a screw cap and stirred under nitrogen at –7 °C for 16 hours (overnight) in temperature controlled well plates in the glovebox. **Note:** Monitoring the reaction kinetics for product **137** revealed that the reaction went to >90% conversion after 1 hour, however we choose to run these reactions overnight to ensure full conversion. As the reaction proceeds, the TDAE salts begin to precipitate, forming an orange slurry. The crude reaction was quenched with 0.5 mL of 1 M HCl, diluted with water (5 mL), and extracted with diethyl ether (3 x 10 mL). **Note:** In order to efficiently remove all of the viscous reaction contents from the vial, we found it useful to fill the vial ¾ full with an extraction solvent (2.5 mL each time: first HCl/water, then Et_2O, water, Et_2O

3x), screw on a Teflon cap, and shake the vial vigorously with the stir bar still inside. The contents could then be easily poured into a separatory funnel. The combined organic layers were washed with brine (5 mL), dried with $MgSO_4$, filtered, and concentrated under reduced pressure. The crude residue was purified by column chromatography.

Assignment of Absolute Stereochemistry

The absolute stereochemistry of **137**, **140a**, and **140b** were assigned by comparing the optical rotation of the purified products to literature values. The optical rotation of products **137**, **140b–c**, **140i**, **141a**, **141c**, **141d**, **141g**, and **141h** correspond with those in reported in literature synthesized using the same chiral ligand **L2**.[44] Chiral products **140d–f**, **140h**, **140j–n**, **141b**, **141e**, **141f**, **141i–l**, and **146** were assigned by analogy.

Characterization of Reaction Products

(*S*,*E*)-1-methoxy-4-(3-phenylbut-1-en-1-yl)benzene (137)

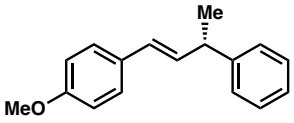

Prepared from (*E*)-1-(2-bromovinyl)-4-methoxybenzene (**86**, 43 mg, 0.2 mmol) and 1,3-dioxoisoindolin-2-yl 2-phenylpropanoate (**136**, 59 mg, 0.2 mmol) according to General Procedure 3. The crude residue was purified by column chromatography (silica gel, 10 to 20% toluene/hexane) to yield **137** (39 mg, 80% yield) in 96% ee as a colorless oil. Spectral data matched those reported in literature.[44] $\mathbf{R_f}$ = 0.59 (silica gel, 10% EtOAc/hexane, UV). **Chiral SFC**: (OB-H, 2.5 mL/min, 20% IPA in CO_2, λ = 254 nm): t_R (major) = 7.1 min, t_R (minor) = 8.4 min. $[\boldsymbol{\alpha}]_{\boldsymbol{D}}^{\mathbf{25}}$ = –34° (c = 1.0, $CHCl_3$). **^{1}H NMR (400 MHz, $CDCl_3$):** δ 7.37 – 7.27 (m, 6H), 7.25 – 7.20 (m, 1H), 6.85

(d, J = 8.8 Hz, 2H), 6.38 (d, J = 16.2 Hz, 1H), 6.27 (dd, J = 15.9, 6.7 Hz, 1H), 3.81 (s, 3H), 3.70 – 3.58 (m, 1H), 1.48 (d, J = 7.0 Hz, 3H). **^{13}C NMR (101 MHz, $CDCl_3$):** δ 158.9, 146.0, 133.3, 130.5, 128.6, 128.0, 127.42, 127.36, 126.3, 114.0, 55.4, 42.7, 21.5. The optical rotation of **137** generated in the presence of **L2**·$NiBr_2$ was measured as $[\boldsymbol{\alpha}]_{\boldsymbol{D}}^{\mathbf{25}}$ = –34° (c = 1.0, $CHCl_3$). Lit: $[\boldsymbol{\alpha}]_{\boldsymbol{D}}^{\mathbf{25}}$ = –16° (c = 1.28, $CHCl_3$, *S* enantiomer, 94% ee).[90] Based on the literature precedent, we assign our product as the *S* enantiomer.

Preparative Scale: Reaction on 5.0 mmol scale:

On a bench-top to a 25 mL round bottom flask equipped with a stir bar was added alkenyl bromide **86** (1.065 g, 5 mmol, 1 equiv), NHP ester **136** (1.476 g, 5 mmol, 1 equiv), **L2**·$NiBr_2$ (0.29 g, 0.5 mmol, 0.10 equiv), and sodium iodide (0.37 g, 2.5 mmol, 0.5 equiv). The flask was sealed with a rubber septum, purged with nitrogen, and the reagents were dissolved in DMA (5.0 mL, 1.0 M). The flask was cooled to –5 °C by submerging it in an isopropanol bath cooled with a Thermo Scientific EK90 Immersion Cooler. **Note:** TDAE will begin to freeze at temperatures below –8 °C with this setup. The TDAE (1.74 mL, 7.5 mmol, 1.5 equiv) was added and stirred for 10 minutes before the TMSBr (TMSBr, 0.66 mL, 5.0 mmol, 1 equiv) was added. The flask was stirred under a balloon of nitrogen at –5 °C for 16 hours. As the reaction proceeds, the TDAE salts begin to precipitate, forming an orange slurry. The crude reaction was quenched with 1 M HCl (30 mL), and extracted with diethyl ether (3 x 20 mL). The combined organic layers were washed with water (2 x 20 mL) and brine (20 mL), dried with $MgSO_4$, filtered, and concentrated under reduced pressure. The crude residue was purified by column chromatography (silica gel, 10 to 20% toluene/hexane) to yield **137** (918 mg, 77% yield) in 91% ee as a colorless oil.

(*S*,*E*)-1-methyl-4-(3-phenylbut-1-en-1-yl)benzene (140a)

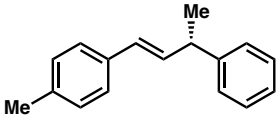

Prepared from (*E*)-1-(2-bromovinyl)-4-methylbenzene (**29a**, 39 mg, 0.2 mmol) and 1,3-dioxoisoindolin-2-yl 2-phenylpropanoate (**136**, 59 mg, 0.2 mmol) according to General Procedure 3. The crude residue was purified by column chromatography (10% $AgNO_3$ silica gel, 0 to 2% Et_2O/hexane) to yield **140a** (39 mg, 88% yield) in 95% ee as a colorless oil. Spectral data matched those reported in literature.[91] $\mathbf{R_f}$ = 0.26 (silica gel, hexane, UV). **Chiral SFC:** (OJ-H, 2.5 mL/min, 7% IPA in CO_2, λ = 254 nm): t_R (minor) = 8.0 min, t_R (major) = 10.0 min. $[\boldsymbol{\alpha}]_D^{25}$ = –41° (c = 1.0, $CHCl_3$). **^{1}H NMR (400 MHz, $CDCl_3$):** δ 7.41 – 7.30 (m, 6H), 7.30 – 7.24 (m, 1H), 7.16 (d, *J* = 8.0 Hz, 2H), 6.52 – 6.34 (m, 2H), 3.74 – 3.64 (m, 1H), 2.38 (s, 3H), 1.53 (d, *J* = 7.0 Hz, 3H). **^{13}C NMR (101 MHz, $CDCl_3$):** δ 145.9, 136.9, 134.9, 134.3, 129.3, 128.6, 128.5, 127.5, 126.3, 126.2, 42.7, 21.5, 21.3. The optical rotation of **140a** generated in the presence of **L2**·$NiBr_2$ was measured as $[\boldsymbol{\alpha}]_D^{25}$ = –41° (c = 1.0, $CHCl_3$). Lit: $[\boldsymbol{\alpha}]_D^{25}$ = +38.4° (c = 0.98, $CHCl_3$, *R* enantiomer, 91% ee).[90] Based on the literature precedent, we assign our product as the *S* enantiomer.

(*S*,*E*)-*N*,*N*-dimethyl-4-(3-phenylbut-1-en-1-yl)aniline (140b)

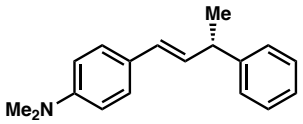

Prepared from (*E*)-4-(2-bromovinyl)-*N*,*N*-dimethylaniline (**29u**, 45 mg, 0.2 mmol) and 1,3-dioxoisoindolin-2-yl 2-phenyl-propanoate (**136**, 59 mg, 0.2 mmol) according to General Procedure 3. The crude residue was purified by column chromatography (silica gel, 5% Et_2O/hexane) to yield **140b** (38 mg, 76% yield) in 97% ee as a white solid. Spectral data matched those reported in literature.[44] $\mathbf{R_f}$ = 0.21 (silica gel, 5% Et_2O/hexane, UV). **m.p.** = 65–67 °C. **Chiral SFC:**

(OB-H, 2.5 mL/min, 35% IPA in CO_2, λ = 254 nm): t_R (major) = 6.0 min, t_R (minor) = 9.0 min. $[\boldsymbol{a}]_D^{25}$ = –56° (c = 1.0, $CHCl_3$). **^{1}H NMR (400 MHz, $CDCl_3$):** δ 7.40 – 7.29 (m, 6H), 7.29 – 7.23 (m, 1H), 6.73 (d, *J* = 8.8 Hz, 2H), 6.40 (d, *J* = 15.9 Hz, 1H), 6.24 (dd, *J* = 15.8, 6.8 Hz, 1H), 3.72 – 3.62 (m, 1H), 3.00 (s, 6H), 1.51 (d, *J* = 7.0 Hz, 3H). **^{13}C NMR (101 MHz, $CDCl_3$):** δ 149.9, 146.4, 131.2, 128.5, 128.4, 127.5, 127.1, 126.4, 126.1, 112.7, 42.7, 40.8, 21.6.

(*S*,*E*)-1-(3-phenylbut-1-en-1-yl)-4-(trifluoromethyl)benzene (140c)

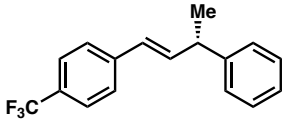

Prepared from (*E*)-1-(2-bromovinyl)-4-(trifluoromethyl)benzene (**29v**, 50 mg, 0.2 mmol) and 1,3-dioxoisoindolin-2-yl 2-phenylpropanoate (**136**, 59 mg, 0.2 mmol) according to General Procedure 3. The crude residue was purified by column chromatography (silica gel, hexane) to yield **140c** (48 mg, 87% yield) in 93% ee as a colorless oil. Spectral data matched those reported in literature.[44] **R_f** = 0.32 (silica gel, hexane, UV). **Chiral SFC:** (OJ-H, 2.5 mL/min, 3% IPA in CO_2, λ = 254 nm): t_R (minor) = 6.3 min, t_R (major) = 7.3 min. $[\boldsymbol{a}]_D^{25}$ = –27° (c = 1.0, $CHCl_3$). **^{1}H NMR (400 MHz, $CDCl_3$):** δ 7.56 (d, *J* = 8.6 Hz, 2H), 7.46 (d, *J* = 8.2 Hz, 2H), 7.40 – 7.33 (m, 2H), 7.33 – 7.23 (m, 3H), 6.52 (dd, *J* = 15.9, 6.2 Hz, 1H), 6.45 (d, *J* = 16.0 Hz, 1H), 3.74 – 3.64 (m, 1H), 1.51 (d, *J* = 7.0 Hz, 3H). **^{13}C NMR (101 MHz, $CDCl_3$):** δ 145.2, 141.2 (q, $J_{C\text{-}F}$ = 1 Hz), 138.1, 129.0 (q, $J_{C\text{-}F}$ = 32 Hz), 128.7, 127.5, 127.4, 126.6, 126.4, 125.6 (q, $J_{C\text{-}F}$ = 4 Hz), 124.4 (q, $J_{C\text{-}F}$ = 272 Hz), 42.8, 21.2. **^{19}F NMR (282 MHz, $CDCl_3$):** δ -65.6.

(*S*,*E*)-4-(3-phenylbut-1-en-1-yl)benzonitrile (140d)

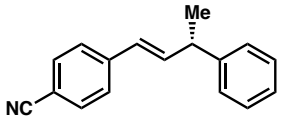

Prepared from methyl (*E*)-4-(2-bromovinyl)benzonitrile (**29w**, 42 mg, 0.2 mmol) and 1,3-dioxoisoindolin-2-yl 2-phenylpropanoate (**136**, 59 mg, 0.2 mmol) according to General Procedure 3. The crude residue was purified by column chromatography (silica gel, 0 to 3% Et_2O/hexane) to yield **140d** (42 mg, 91% yield) in 94% ee as a colorless oil. $\mathbf{R_f}$ = 0.42 (silica gel, 10% EtOAc/hexane, UV). **Chiral SFC**: (OB-H, 2.5 mL/min, 10% IPA in CO_2, λ = 254 nm): t_R (minor) = 9.5 min, t_R (major) = 10.1 min. $[\alpha]_D^{25}$ = –51° (c = 1.0, $CHCl_3$). **^{1}H NMR (400 MHz, $CDCl_3$):** δ 7.54 (d, *J* = 8.5 Hz, 2H), 7.40 (d, *J* = 8.3 Hz, 2H), 7.36 – 7.30 (m, 2H), 7.28 – 7.19 (m, 3H), 6.52 (dd, *J* = 15.9, 6.7 Hz, 1H), 6.40 (d, *J* = 16.0 Hz, 1H), 3.72 – 3.61 (m, 1H), 1.48 (d, *J* = 7.0 Hz, 3H). **^{13}C NMR (101 MHz, $CDCl_3$):** δ 144.7, 142.1, 139.5, 132.4, 128.7, 127.3, 127.2, 126.7, 126.6, 119.2, 110.2, 42.8, 21.0. **FTIR (NaCl, thin film, cm^{-1})**: 3027, 2967, 2872, 2225, 1646, 1604, 1504, 1493, 1452, 1412, 1176, 1013, 970, 866, 819, 763, 701. **HRMS (FAB, *m/z*)**: calc'd for $C_{17}H_{15}N$ $[M+H]^+$: 234.1283; found: 234.1265.

Methyl (*S*,*E*)-4-(3-phenylbut-1-en-1-yl)benzoate (140e)

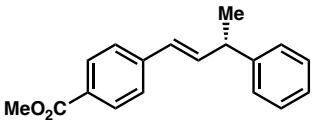

Prepared from methyl (*E*)-4-(2-bromovinyl)benzoate (**29x**, 48 mg, 0.2 mmol) and 1,3-dioxoisoindolin-2-yl 2-phenyl-propanoate (**136**, 59 mg, 0.2 mmol) according to General Procedure 3. The crude residue was purified by column chromatography (silica gel, 5% Et_2O/hexane) to yield **140e** (46 mg, 87% yield) in 95% ee as a colorless oil. $\mathbf{R_f}$ = 0.19 (silica gel, 5% Et_2O/hexane, UV). **Chiral SFC**: (OB-H, 2.5 mL/min, 20% IPA in CO_2, λ = 254 nm): t_R (minor) = 8.2 min, t_R (major) = 11.6 min. $[\alpha]_D^{25}$ = –44° (c = 1.0, $CHCl_3$). **^{1}H NMR (400 MHz, $CDCl_3$):** δ 7.96

(d, J = 8.4 Hz, 2H), 7.41 (d, J = 8.3 Hz, 2H), 7.37 – 7.30 (m, 2H), 7.30 – 7.20 (m, 3H), 6.53 (dd, J = 15.9, 6.5 Hz, 1H), 6.44 (d, J = 16.1 Hz, 1H), 3.91 (s, 3H), 3.72 – 3.62 (m, 1H), 1.49 (d, J = 7.0 Hz, 3H). **^{13}C NMR (101 MHz, $CDCl_3$):** δ 167.1, 145.2, 142.2, 138.2, 130.0, 128.7, 128.6, 127.9, 127.4, 126.5, 126.1, 52.2, 42.8, 21.2. **FTIR (NaCl, thin film, cm^{-1})**: 3025, 2963, 1718, 1605, 1492, 1433, 1411, 1276, 1177, 1108, 1015, 968, 759, 698. **LRMS (GC-MS, *m/z*)**: calc'd for $C_{18}H_{18}O_2$ $[M]^+$: 266.1; found: 266.1.

(*S*,*E*)-4-(3-phenylbut-1-en-1-yl)phenyl 4-methylbenzenesulfonate (140f)

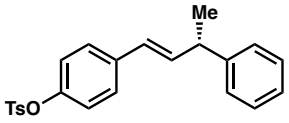

Prepared from (*E*)-4-(2-bromovinyl)phenyl 4-methyl-benzenesulfonate (**29y**, 71 mg, 0.2 mmol) and 1,3-dioxoisoindolin-2-yl 2-phenylpropanoate (**136**, 89 mg, 0.3 mmol) according to General Procedure 3 with the exception that 1.5 equiv NHP ester was used instead of 1.0 equiv. **Note:** The addition of excess NHP ester ensured full consumption of the vinyl bromide, which we found to be inseparable from the product when it remained in the crude reaction. The crude residue was purified by column chromatography (silica gel, hexane to 5% Et_2O/hexane) to yield **140f** (61 mg, 80% yield) in 94% ee as a colorless oil. $\mathbf{R_f}$ = 0.39 (silica gel, 10% EtOAc/hexane, UV). **Chiral SFC:** (OJ-H, 2.5 mL/min, 15% IPA in CO_2, λ = 254 nm): t_R (minor) = 12.2 min, t_R (major) = 13.7 min. $[\boldsymbol{\alpha}]_D^{25}$ = –24° (c = 1.0, $CHCl_3$). **^{1}H NMR (400 MHz, $CDCl_3$):** δ 7.70 (d, J = 8.4 Hz, 2H), 7.36 – 7.28 (m, 4H), 7.28 – 7.20 (m, 5H), 6.90 (d, J = 8.7 Hz, 2H), 6.39 – 6.30 (m, 2H), 3.69 – 3.58 (m, 1H), 2.45 (s, 3H), 1.46 (d, J = 7.0 Hz, 3H). **^{13}C NMR (101 MHz, $CDCl_3$):** δ 148.5, 145.4, 145.3, 136.7, 136.5, 132.4, 129.8, 128.6, 127.3, 127.2, 126.4, 122.5, 42.7, 21.8, 21.2. **FTIR (NaCl, thin film, cm^{-1})**: 3061, 3028, 2966, 2928, 2872, 1647, 1599, 1504, 1453, 1372, 1307, 1296, 1198, 1176,

1152, 1093, 1016, 969, 867, 841, 815, 763, 735, 700, 661. **HRMS (FAB, *m/z*)**: calc'd for $C_{23}H_{22}O_3S$ $[M+\cdot]^+$: 378.1290; found: 378.1283.

(*S*,*E*)-but-1-ene-1,3-diyldibenzene (140g)

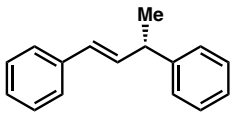

Prepared from (*E*)-(2-bromovinyl)benzene (**29z**, 37 mg, 0.2 mmol) and 1,3-dioxoisoindolin-2-yl 2-phenylpropanoate (**136**, 59 mg, 0.2 mmol) according to General Procedure 3. The crude residue was purified by column chromatography (silica gel, hexane) to yield **140g** (37 mg, 88% yield) in 96% ee as a colorless oil. $\mathbf{R_f}$ = 0.48 (silica gel, hexane, UV). **Chiral SFC**: (OJ-H, 2.5 mL/min, 5% IPA in CO_2, λ = 254 nm): t_R (minor) = 9.8 min, t_R (major) = 10.9 min. $[\boldsymbol{a}]_D^{25}$ = –35° (c = 1.0, $CHCl_3$). **^{1}H NMR (400 MHz, $CDCl_3$):** δ 7.43 – 7.29 (m, 8H), 7.29 – 7.21 (m, 2H), 6.51 – 6.38 (m, 2H), 3.73 – 3.65 (m, 1H), 1.52 (d, *J* = 7.0 Hz, 3H). **^{13}C NMR (101 MHz, $CDCl_3$):** δ 145.7, 137.7, 135.3, 128.6 (3C), 127.4, 127.2, 126.35, 126.27, 42.7, 21.4. **FTIR (NaCl, thin film, cm^{-1})**: 3080, 3058, 3024, 2964, 2928, 2871, 1599, 1492, 1448, 1371, 1010, 964, 742, 692. **HRMS (ESI-TOF, *m/z*)**: calc'd for $C_{16}H_{16}$ $[M–H_2+H]^+$: 207.1174; found: 207.1155. The optical rotation of **136** generated in the presence of **L2**·$NiBr_2$ was measured as $[\boldsymbol{a}]_D^{25}$ = –35° (c = 1.0, $CHCl_3$). Lit: $[\boldsymbol{a}]_D^{25}$ = –21.1° (c = 1.42, $CHCl_3$, *S* enantiomer, 95% ee).[92] Based on the literature precedent, we assign our product as the *S* enantiomer.

(*S*,*E*)-2-methoxy-5-(3-phenylbut-1-en-1-yl)pyridine (140h)

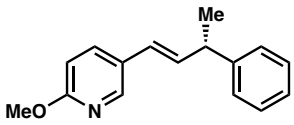

Prepared from (*E*)-5-(2-bromovinyl)-2-methoxypyridine (**29k**, 43 mg, 0.2 mmol) and 1,3-dioxoisoindolin-2-yl 2-phenyl-propanoate (**136**, 59 mg, 0.2 mmol) according to General Procedure 3. The crude residue

was purified by column chromatography (silica gel, 5% Et_2O/hexane) to yield **140h** (32 mg, 67% yield) in 95% ee as a colorless oil. $\mathbf{R_f}$ = 0.53 (silica gel, 10% EtOAc/hexane, UV). **Chiral SFC**: (OB-H, 2.5 mL/min, 15% IPA in CO_2, λ = 280 nm): t_R (major) = 5.0 min, t_R (minor) = 6.9 min. $[\alpha]_D^{25}$ = –33° (c = 1.0, $CHCl_3$). **^{1}H NMR (400 MHz, $CDCl_3$):** δ 8.06 (d, *J* = 2.4 Hz, 1H), 7.62 (dd, *J* = 8.7, 2.5 Hz, 1H), 7.35 – 7.28 (m, 2H), 7.28 – 7.18 (m, 3H), 6.67 (d, *J* = 8.6 Hz, 1H), 6.33 (d, *J* = 16.1 Hz, 1H), 6.26 (dd, *J* = 15.9, 6.3 Hz, 1H), 3.91 (s, 3H), 3.66 – 3.57 (m, 1H), 1.45 (d, *J* = 7.0 Hz, 3H). **^{13}C NMR (101 MHz, $CDCl_3$):** δ 163.4, 145.6, 145.3, 135.5, 134.7, 128.7, 127.4, 126.8, 126.4, 124.7, 110.9, 53.6, 42.8, 21.3. **FTIR (NaCl, thin film, cm^{-1})**: 2965, 1601, 1493, 1384, 1286, 1026, 962, 822, 762, 699. **HRMS (FAB, *m/z*)**: calc'd for $C_{16}H_{17}NO$ $[M+H]^+$: 240.1388; found: 240.1398.

(*S*,*E*)-5-phenylhex-3-en-1-yl benzoate (140i)

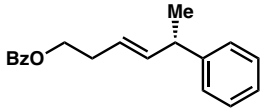

Prepared from (*E*)-4-bromobut-3-en-1-yl benzoate (**29j**, 51 mg, 0.2 mmol) and 1,3-dioxoisoindolin-2-yl 2-phenylpropanoate (**136**, 59 mg, 0.2 mmol) according to General Procedure 3. The crude residue was purified by column chromatography (silica gel, 5% Et_2O/hexane) to yield **140i** (49 mg, 88% yield) in 97% ee as a colorless oil. Spectral data matched those reported in literature.[44] $\mathbf{R_f}$ = 0.24 (silica gel, 5% Et_2O/hexane, UV). **Chiral SFC:** (OJ-H, 2.5 mL/min, 10% IPA in CO_2, λ = 254 nm): t_R (major) = 5.2 min, t_R (minor) = 6.1 min. $[\alpha]_D^{25}$ = +5° (c =1.0, $CHCl_3$). **^{1}H NMR (400 MHz, $CDCl_3$):** δ 8.04 – 8.00 (m, 2H), 7.59 – 7.53 (m, 1H), 7.46 – 7.40 (m, 2H), 7.29 – 7.23 (m, 2H), 7.22 – 7.15 (m, 3H), 5.77 (ddt, *J* = 15.4, 6.8, 1.3 Hz, 1H), 5.52 (dtd, *J* = 15.2, 6.8, 1.3 Hz, 1H), 4.36 (td, *J* = 6.7, 1.4 Hz, 2H), 3.50 – 3.42 (m, 1H), 2.54 – 2.46 (m, 2H), 1.35 (d, *J* = 7.0 Hz, 3H). **^{13}C NMR (101 MHz, $CDCl_3$):** δ 166.7, 146.0, 138.3, 133.0,

130.5, 129.7, 128.5, 128.4, 127.3, 126.2, 124.3, 64.4, 42.4, 32.2, 21.4.

(*S*,*E*)-(7-chlorohept-3-en-2-yl)benzene (140j)

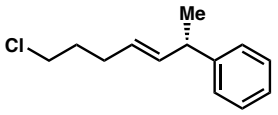

Prepared from (*E*)-1-bromo-5-chloropent-1-ene (**S2**, 37 mg, 0.2 mmol) and 1,3-dioxoisoindolin-2-yl 2-phenylpropanoate (**136**, 59 mg, 0.2 mmol) according to General Procedure 3. The crude residue was purified by column chromatography (silica gel, hexane) to yield **140j** (29 mg, 69% yield) in 91% ee as a colorless oil. $\mathbf{R}_f$ = 0.29 (silica gel, hexane, UV/CAM). **Chiral SFC:** (OD-H, 2.5 mL/min, 1% IPA in CO_2, λ = 210 nm): t_R (minor) = 5.4 min, t_R (major) = 6.0 min. $[\boldsymbol{\alpha}]_{\boldsymbol{D}}^{\mathbf{25}}$ = +9° (c =1.0, $CHCl_3$). **^{1}H NMR (400 MHz, $CDCl_3$):** δ 7.35 – 7.29 (m, 2H), 7.25 – 7.18 (m, 3H), 5.69 (ddt, *J* = 15.3, 6.8, 1.4 Hz, 1H), 5.43 (dtd, *J* = 15.1, 6.8, 1.1 Hz, 1H), 3.54 (t, *J* = 6.7 Hz, 2H), 3.50 – 3.40 (m, 1H), 2.23 – 2.16 (m, 2H), 1.90 – 1.82 (m, 2H), 1.36 (d, *J* = 7.0 Hz, 3H). **^{13}C NMR (101 MHz, $CDCl_3$):** δ 146.3, 136.7, 128.5, 127.24, 127.17, 126.1, 44.6, 42.4, 32.4, 29.7, 21.6. **FTIR (NaCl, thin film, cm^{-1})**: 3025, 2962, 2929, 2871, 1601, 1492, 1450, 1371, 1297, 1017, 969, 759, 698. **HRMS (FAB, *m/z*)**: calc'd for $C_{13}H_{17}Cl$ [M–H_2+H]$^+$: 207.0940; found: 207.0910.

(*S*,*E*)-dec-3-en-2-ylbenzene (140k)

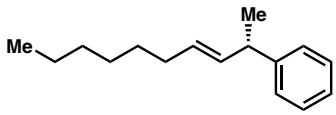

Prepared from (*E*)-1-bromooct-1-ene (**29aa**, 38 mg, 0.2 mmol) and 1,3-dioxoisoindolin-2-yl 2-phenylpropanoate (**136**, 59 mg, 0.2 mmol) according to General Procedure 3. The crude residue was purified by column chromatography (silica gel, hexane) to yield **140k** (31 mg, 72% yield) in 94% ee as a colorless oil. $\mathbf{R}_f$ = 0.59 (silica gel, hexane, UV/CAM). **Chiral SFC:** (OJ-H, 2.5 mL/min,

1% IPA in CO_2, λ = 210 nm): t_R (minor) = 3.9 min, t_R (major) = 4.5 min. $[\alpha]_D^{25}$ = +4° (c = 0.9, $CHCl_3$). **^{1}H NMR (400 MHz, $CDCl_3$):** δ 7.34 – 7.27 (m, 2H), 7.25 – 7.15 (m, 3H), 5.60 (ddt, *J* = 15.3, 6.6, 1.4 Hz, 1H), 5.46 (dtd, *J* = 15.1, 6.6, 1.2 Hz, 1H), 3.47 – 3.38 (m, 1H), 2.06 – 1.97 (m, 2H), 1.40 – 1.22 (m, 11H), 0.95 – 0.83 (m, 3H). **^{13}C NMR (101 MHz, $CDCl_3$):** δ 146.7, 135.0, 129.5, 128.4, 127.3, 126.0, 42.4, 32.7, 31.9, 29.6, 29.0, 22.8, 21.7, 14.3. **FTIR (NaCl, thin film, cm^{-1})**: 3025, 2959, 2925, 2854, 1492, 1451, 1371, 1016, 965, 758, 697. **LRMS (GC-MS, *m/z*)**: calc'd for $C_{16}H_{24}$ $[M]^+$: 216.2; found: 216.2.

(*S*,*E*)-trimethyl((5-phenylhex-3-en-1-yl)oxy)silane (140l)

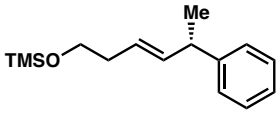

Prepared from (*E*)-4-bromobut-3-en-1-ol (**29i**, 30 mg, 0.2 mmol) and 1,3-dioxoisoindolin-2-yl 2-phenylpropanoate (**136**, 59 mg, 0.2 mmol) according to General Procedure 3 with the exception that 2.0 equiv TMSBr was used instead of 1.0 equiv. The reaction was quenched with water instead of 1 M HCl to prevent decomposition of the primary silyl ether. **Note:** An acidic workup yielded a mixture of the silyl ether and alcohol product, however the alcohol was inseparable from the phthalimide byproduct. The crude residue was purified by column chromatography (florisil, hexane to 1% Et_2O/hexane) to yield **140l** (33 mg, 66% yield) as a colorless oil. **Note:** The two enantiomers of the racemic silyl ether were inseparable by chiral SFC. **R_f** = 0.67 (silica gel, 10% EtOAc/hexane, UV/CAM). $[\alpha]_D^{25}$ = +6° (c = 1.0, $CHCl_3$). **^{1}H NMR (400 MHz, $CDCl_3$):** δ 7.35 – 7.28 (m, 2H), 7.25 – 7.17 (m, 3H), 5.69 (ddt, *J* = 15.4, 6.7, 1.3 Hz, 1H), 5.47 (dtd, *J* = 15.3, 6.9, 1.4 Hz, 1H), 3.61 (t, *J* = 7.0 Hz, 2H), 3.49 – 3.40 (m, 1H), 2.28 (qt, *J* = 7.0, 1.1 Hz, 2H), 1.36 (d, *J* = 7.1 Hz, 3H), 0.13 (s, 9H). **^{13}C NMR (101 MHz, $CDCl_3$):** δ 146.3, 137.3, 128.5, 127.3, 126.1, 125.4, 62.7, 42.5, 36.2, 21.5, -0.3.

FTIR (NaCl, thin film, cm^{-1}): 2961, 2930, 2902, 2863, 1602, 1493, 1452, 1382, 1251, 1094, 968, 940, 876, 841, 758, 748, 699. **HRMS (FAB, *m/z*)**: calc'd for $C_{15}H_{24}OSi$ $[M+H]^+$: 249.1675; found: 249.1684.

(*S*,*E*)-5-phenylhex-3-en-1-ol (S31)

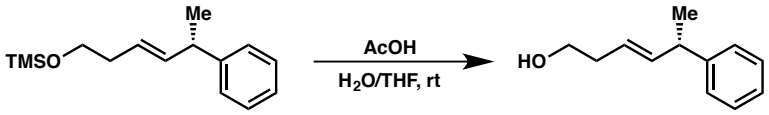

Deprotection of Silyl Ether: Silyl ether **140l** (33.0 mg, 0.132 mmol, 1 equiv) was dissolved in a solution of acetic acid (0.5 mL), water (0.5 mL), and THF (2.5 mL) in a 20 mL vial equipped with a magnetic stir bar and stirred at room temperature for 15 min. The reaction was slowly quenched with a solution of saturated $NaHCO_3$ until the pH was slightly basic (approx. 15 mL), extracted with Et_2O (3 x 10 mL), dried with $MgSO_4$, filtered, and concentrated under reduced pressure to yield **S31** (22.6 mg, 97% yield) in 89% ee as a colorless oil. Spectral data matched those reported in literature.[44] $\mathbf{R}_f$ = 0.11 (silica gel, 10% EtOAc/hexane, UV/CAM). **Chiral SFC:** (OB-H, 2.5 mL/min, 3% IPA in CO_2, λ = 210 nm): t_R (minor) = 6.9 min, t_R (major) = 7.5 min. $[\boldsymbol{a}]_{\boldsymbol{D}}^{\mathbf{25}}$ = +9° (c = 1.0, $CHCl_3$). **^{1}H NMR (400 MHz, $CDCl_3$):** δ 7.34 – 7.27 (m, 2H), 7.25 – 7.16 (m, 3H), 5.76 (ddt, *J* = 15.4, 6.7, 1.4 Hz, 1H), 5.45 (dtd, *J* = 15.3, 7.0, 1.4 Hz, 1H), 3.65 (t, *J* = 6.3 Hz, 2H), 3.52 – 3.42 (m, 1H), 2.30 (q, *J* = 6.3 Hz, 2H), 1.54 (s, 1H), 1.37 (d, *J* = 7.1 Hz, 3H). **^{13}C NMR (101 MHz, $CDCl_3$):** δ 146.1, 138.8, 128.6, 127.2, 126.2, 124.8, 62.2, 42.5, 36.0, 21.6.

(*S*,*E*)-6-methyl-2-(3-phenylbut-1-en-1-yl)-1,3,6,2-dioxazaborocane-4,8-dione (140m)

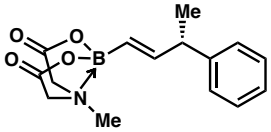

Prepared from *trans*-1-bromovinylboronic acid MIDA ester (**29ab**, 52 mg, 0.2 mmol) and 1,3-dioxoisoindolin-2-yl 2-phenylpropanoate (**136**, 59 mg, 0.2 mmol) according to General Procedure 3. The crude residue was purified by column chromatography (silica gel, 10% EtOAc/hexane to 100% EtOAc) to yield **140m** (25 mg, 43% yield) in 97% ee as a yellow solid. **Note:** The ^{1}H NMR contains two minor impurities that were identified as DMA and methyliminodiacetic acid. $\mathbf{R_f}$ = 0.35 (silica gel, EtOAc, UV/$KMnO_4$). **m.p.** = 144–146 °C. **Chiral SFC:** (OJ-H, 2.5 mL/min, 30% IPA in CO_2, λ = 210 nm): t_R (major) = 5.5 min, t_R (minor) = 10.2 min. $[\boldsymbol{\alpha}]_D^{25}$ = +0.5° ± 1.1° (c = 1.0, $CHCl_3$). **Note:** This compound shows low optical rotation. **^{1}H NMR (400 MHz, $CDCl_3$):** δ 7.32 – 7.23 (m, 2H), 7.21 – 7.13 (m, 3H), 6.32 (dd, *J* = 17.7, 6.4 Hz, 1H), 5.38 (dd, *J* = 17.7, 1.5 Hz, 1H), 3.92 (dd, *J* = 16.7, 4.5 Hz, 2H), 3.59 (dd, *J* = 16.8, 13.9 Hz, 2H), 3.54 – 3.46 (m, 1H), 2.69 (s, 3H), 1.36 (d, *J* = 7.0 Hz, 3H). **^{13}C NMR (101 MHz, $CDCl_3$):** δ 168.34, 168.27, 151.7, 145.3, 128.6, 127.4, 126.3, 61.53, 61.49, 47.0, 44.8, 20.8. **FTIR (NaCl, thin film, cm^{-1})**: 2963, 1762, 1636, 1492, 1338, 1290, 1246, 1193, 1154, 1126, 1090, 1025, 1007, 956, 867, 761, 702. **HRMS (FAB, *m/z*)**: calc'd for $C_{15}H_{18}BNO_4$ $[M+H]^+$: 288.1407; found: 288.1414.

(*S*,*E*)-trimethyl(3-phenylbut-1-en-1-yl)silane (140n)

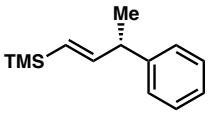

Prepared from (*E*)-(2-bromovinyl)trimethylsilane (**29o**, 36 mg, 0.2 mmol) and 1,3-dioxoisoindolin-2-yl 2-phenylpropanoate (**136**, 59 mg, 0.2 mmol) according to General Procedure 3. Alkenyl bromide **29o** is reported to be air

sensitive, and was added to the reaction while inside the glovebox. The crude residue was purified by column chromatography (silica gel, hexane) to yield **140n** (28 mg, 68% yield) in 97% ee as a colorless oil. $\mathbf{R_f}$ = 0.65 (silica gel, hexane, UV/CAM). **Chiral SFC:** (OJ-H, 2.5 mL/min, CO_2, λ = 210 nm): t_R (major) = 1.8 min, t_R (minor) = 2.0 min. $[\boldsymbol{a}]_D^{25}$ = –2.4° ± 0.2° (c = 0.9, $CHCl_3$). **^{1}H NMR (400 MHz, $CDCl_3$):** δ 7.35 – 7.28 (m, 2H), 7.24 – 7.18 (m, 3H), 6.19 (dd, *J* = 18.6, 5.9 Hz, 1H), 5.68 (dd, *J* = 18.6, 1.6 Hz, 1H), 3.52 – 3.44 (m, 1H), 1.36 (d, *J* = 7.0 Hz, 3H), 0.06 (s, 9H). **^{13}C NMR (101 MHz, $CDCl_3$):** δ 150.8, 145.8, 128.5, 128.1, 127.5, 126.2, 45.6, 20.9, -1.0. **FTIR (NaCl, thin film, cm^{-1})**: 3028, 2958, 1612, 1602, 1492, 1452, 1248, 1009, 987, 868, 837, 759, 698. **LRMS (GC-MS, *m/z*)**: calc'd for $C_{13}H_{20}Si$ $[M]^+$: 204.1; found: 204.1.

(*S*,*E*)-4,4'-(but-1-ene-1,3-diyl)bis(methoxybenzene) (141a)

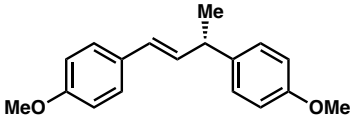

Prepared from (*E*)-1-(2-bromovinyl)-4-methoxybenzene (**86**, 43 mg, 0.2 mmol) and 1,3-dioxoisoindolin-2-yl 2-(4-methoxyphenyl)propanoate (**62a**, 65 mg, 0.2 mmol) according to General Procedure 3. The crude residue was purified by column chromatography (silica gel, 10% toluene/hexane then 10% Et_2O/hexane) to yield **141a** (42 mg, 78% yield) in 93% ee as a white solid. Spectral data matched those reported in literature.[44] $\mathbf{R_f}$ = 0.45 (silica gel, 10% EtOAc/hexane, UV). **m.p.** = 51–59 °C. **Chiral SFC**: (AD-H, 2.5 mL/min, 20% IPA in CO_2, λ = 235 nm): t_R (major) = 7.0 min, t_R (minor) = 8.5 min. $[\boldsymbol{a}]_D^{25}$ = –34° (c = 1.0, $CHCl_3$). **^{1}H NMR (400 MHz, $CDCl_3$)**: δ 7.32 (d, *J* = 8.7 Hz, 2H), 7.22 (d, *J* = 8.5 Hz, 2H), 6.89 (d, *J* = 8.8 Hz, 2H), 6.86 (d, *J* = 8.8 Hz, 2H), 6.37 (d, *J* = 16.0 Hz, 1H), 6.25 (dd, *J* = 15.9, 6.6 Hz, 1H), 3.82 (s, 3H), 3.81 (s, 3H), 3.65 – 3.55 (m, 1H), 1.46 (d, *J* = 7.0 Hz, 3H). **^{13}C NMR (101 MHz, $CDCl_3$):**

δ 158.9, 158.0, 138.1, 133.6, 130.5, 128.3, 127.7, 127.3, 114.0, 113.9, 55.4 (2C), 41.8, 21.6.

(*S*,*E*)-1-methoxy-4-(3-(4-(trifluoromethyl)phenyl)but-1-en-1-yl)benzene (141b)

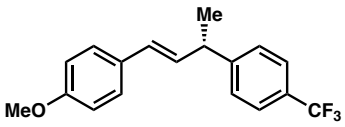

Prepared from (*E*)-1-(2-bromovinyl)-4-methoxybenzene (**86**, 43 mg, 0.2 mmol) and 1,3-dioxoisoindolin-2-yl 2-(4-(trifluoromethyl)phenyl)propanoate (**62b**, 73 mg, 0.2 mmol) according to General Procedure 3. The crude residue was purified by column chromatography (silica gel, 5% toluene/hexane) to yield **141b** (40 mg, 65% yield) in 88% ee as a white solid. $\mathbf{R_f}$ = 0.48 (silica gel, 10% EtOAc/hexane, UV). **m.p.** = 67–70 °C. **Chiral SFC**: (OB-H, 2.5 mL/min, 5% IPA in CO_2, λ = 254 nm): t_R (major) = 6.5 min, t_R (minor) = 7.5 min. $[\boldsymbol{\alpha}]_D^{25}$ = –39° (c = 1.0, $CHCl_3$). **^{1}H NMR (400 MHz, $CDCl_3$):** δ 7.58 (d, *J* = 8.1 Hz, 2H), 7.39 (d, *J* = 8.4 Hz, 2H), 7.30 (d, *J* = 8.7 Hz, 2H), 6.85 (d, *J* = 8.8 Hz, 2H), 6.38 (d, *J* = 16.0 Hz, 1H), 6.21 (dd, *J* = 15.9, 6.8 Hz, 1H), 3.81 (s, 3H), 3.73 – 3.64 (m, 1H), 1.48 (d, *J* = 7.0 Hz, 3H). **^{13}C NMR (101 MHz, $CDCl_3$):** δ 159.1, 150.1 (q, $J_{C\text{-}F}$ = 1.4 Hz), 132.0, 130.1, 128.8, 128.6 (q, $J_{C\text{-}F}$ = 32.3 Hz), 127.8, 127.4, 125.5 (q, $J_{C\text{-}F}$ = 3.8 Hz), 124.5 (q, $J_{C\text{-}F}$ = 271.9 Hz), 114.1, 55.4, 42.6, 21.3. **^{19}F NMR (282 MHz, $CDCl_3$):** δ -65.4. **FTIR (NaCl, thin film, cm^{-1})**: 2965, 1608, 1512, 1252, 1174, 1164, 1122, 1069, 1036, 1016, 967, 840, 818. **HRMS (EI, *m/z*)**: calc'd for $C_{18}H_{17}F_3O$ $[M+\cdot]^+$: 306.1232; found: 306.1241.

(*S*,*E*)-1-bromo-4-(4-(4-methoxyphenyl)but-3-en-2-yl)benzene (141c)

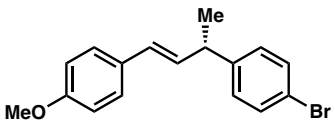

Prepared from (*E*)-1-(2-bromovinyl)-4-methoxybenzene (**86**, 43 mg, 0.2 mmol) and 1,3-dioxoisoindolin-2-yl 2-(4-

bromophenyl)propanoate (**62c**, 75 mg, 0.2 mmol) according to General Procedure 3. The crude residue was purified by column chromatography (silica gel, 5 to 10% toluene/hexane) to yield **141c** (51 mg, 80% yield) in 90% ee as a white solid. Spectral data matched those reported in literature.[44] $\mathbf{R_f}$ = 0.59 (silica gel, 10% EtOAc/hexane, UV). **m.p.** = 74–76 °C. **Chiral SFC**: (OB-H, 2.5 mL/min, 35% IPA in CO_2, λ = 254 nm): t_R (major) = 5.3 min, t_R (minor) = 8.5 min. $[\boldsymbol{a}]_D^{25}$ = –32° (c = 1.0, $CHCl_3$). **^{1}H NMR (400 MHz, $CDCl_3$):** δ 7.45 (d, *J* = 8.5 Hz, 2H), 7.30 (d, *J* = 8.6 Hz, 2H), 7.16 (d, *J* = 8.3 Hz, 2H), 6.86 (d, *J* = 8.8 Hz, 2H), 6.36 (d, *J* = 16.0 Hz, 1H), 6.20 (dd, *J* = 15.9, 6.7 Hz, 1H), 3.81 (s, 3H), 3.64 – 3.55 (m, 1H), 1.45 (d, *J* = 7.0 Hz, 3H). **^{13}C NMR (101 MHz, $CDCl_3$):** δ 159.0, 145.0, 132.5, 131.6, 130.2, 129.2, 128.4, 127.4, 120.0, 114.0, 55.4, 42.1, 21.3.

(*S*,*E*)-1-fluoro-4-(4-(4-methoxyphenyl)but-3-en-2-yl)benzene (141d)

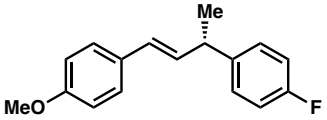

Prepared from (*E*)-1-(2-bromovinyl)-4-methoxybenzene (**86**, 43 mg, 0.2 mmol) and 1,3-dioxoisoindolin-2-yl 2-(4-fluorophenyl)propanoate (**62d**, 63 mg, 0.2 mmol) according to General Procedure 3. The crude residue was purified by column chromatography (silica gel, 5 to 30% toluene/hexane) to yield **141d** (44 mg, 85% yield) in 92% ee as a colorless oil. Spectral data matched those reported in literature.[44] $\mathbf{R_f}$ = 0.70 (silica gel, 10% EtOAc/hexane, UV). **Chiral SFC**: (OB-H, 2.5 mL/min, 15% IPA in CO_2, λ = 280 nm): t_R (major) = 5.9 min, t_R (minor) = 8.3 min. $[\boldsymbol{a}]_D^{25}$ = –29° (c = 1.0, $CHCl_3$). **^{1}H NMR (400 MHz, $CDCl_3$):** δ 7.34 – 7.28 (m, 2H), 7.28 – 7.20 (m, 2H), 7.06 – 6.98 (m, 2H), 6.89 – 6.83 (m, 2H), 6.40 – 6.32 (m, 1H), 6.23 (dd, *J* = 15.9, 6.7 Hz, 1H), 3.81 (s, 3H), 3.67 – 3.58 (m, 1H), 1.46 (d, *J* = 7.0 Hz, 3H). **^{13}C NMR (101 MHz, $CDCl_3$):** δ 161.5 (d, $J_{C\text{-}F}$ = 243.7 Hz), 159.0, 141.6 (d, $J_{C\text{-}F}$

= 3.1 Hz), 133.0, 130.3, 128.8 (d, $J_{C\text{-}F}$ = 7.8 Hz), 128.1, 127.4, 115.3 (d, $J_{C\text{-}F}$ = 21.2 Hz), 114.1, 55.4, 41.9, 21.6. **^{19}F NMR (282 MHz, $CDCl_3$):** δ -123.56 (tt, $J_{F\text{-}H}$ = 8.9, 5.4 Hz).

(*S*,*E*)-4-(4-(4-methoxyphenyl)but-3-en-2-yl)-*N*,*N*-dimethylaniline (141e)

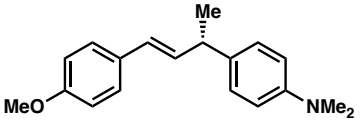

Prepared from (*E*)-1-(2-bromovinyl)-4-methoxybenzene (**89**, 43 mg, 0.2 mmol) and 1,3-dioxoisoindolin-2-yl 2-(4-(dimethylamino)phenyl)propanoate (**62e**, 68 mg, 0.2 mmol) according to General Procedure 3. The reaction was quenched with water instead of 1 M HCl. The crude residue was purified by column chromatography (silica gel, hexane to 10% Et_2O/hexane) to yield **141e** (37 mg, 66% yield) in 94% ee as a white solid. $\mathbf{R_f}$ = 0.28 (silica gel, 10% EtOAc/hexane, UV). **m.p.** = 72–75 °C. **Chiral SFC**: (AD-H, 2.5 mL/min, 20% IPA in CO_2, λ = 280 nm): t_R (major) = 8.2 min, t_R (minor) = 10.6 min. $[\boldsymbol{a}]_{\boldsymbol{D}}^{\mathbf{25}}$ = –29° (c = 1.1, $CHCl_3$). **^{1}H NMR (400 MHz, $CDCl_3$):** δ 7.29 (d, *J* = 8.7 Hz, 2H), 7.15 (d, *J* = 8.5 Hz, 2H), 6.83 (d, *J* = 8.8 Hz, 2H), 6.73 (d, *J* = 8.7 Hz, 2H), 6.34 (dd, *J* = 16.2, 0.8 Hz, 1H), 6.23 (dd, *J* = 15.9, 6.6 Hz, 1H), 3.80 (s, 3H), 3.58 – 3.50 (m, 1H), 2.93 (s, 6H), 1.42 (d, *J* = 7.1 Hz, 3H). **^{13}C NMR (101 MHz, $CDCl_3$):** δ 158.8, 149.3, 134.1, 130.7, 128.0, 127.3, 114.0, 113.1, 55.4, 41.6, 41.0, 21.5. **FTIR (NaCl, thin film, cm^{-1})**: 2958, 1608, 1518, 1509, 1456, 1341, 1249, 1173, 1034, 966, 948, 815. **HRMS (FAB, *m/z*)**: calc'd for $C_{19}H_{23}NO$ $[M+\cdot]^+$: 281.1780; found: 281.1774.

(*S*,*E*)-1,2-dichloro-4-(4-(4-methoxyphenyl)but-3-en-2-yl)benzene (141f)

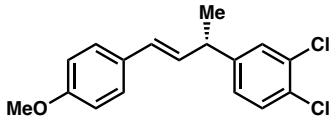

Prepared from (*E*)-1-(2-bromovinyl)-4-methoxybenzene (**86**, 43 mg, 0.2 mmol) and 1,3-dioxoisoindolin-2-yl 2-(3,4-

dichlorophenyl)propanoate (**62f**, 73 mg, 0.2 mmol) according to General Procedure 3. The crude residue was purified by column chromatography (silica gel, hexane to 5% Et_2O/hexane) to yield **141f** (48 mg, 77% yield) in 82% ee as a colorless oil. $\mathbf{R_f}$ = 0.51 (silica gel, 10% EtOAc/hexane, UV). **Chiral SFC**: (OB-H, 2.5 mL/min, 25% IPA in CO_2, λ = 280 nm): t_R (major) = 6.5 min, t_R (minor) = 9.0 min. $[\alpha]_D^{25}$ = –26° (c = 1.1, $CHCl_3$). **^{1}H NMR (400 MHz, $CDCl_3$):** δ 7.37 (d, *J* = 8.3 Hz, 1H), 7.35 (d, *J* = 2.1 Hz, 1H), 7.32 – 7.27 (m, 2H), 7.10 (ddd, *J* = 8.2, 2.1, 0.6 Hz, 1H), 6.87 – 6.82 (m, 2H), 6.35 (dd, *J* = 15.9, 1.3 Hz, 1H), 6.15 (dd, *J* = 15.9, 6.8 Hz, 1H), 3.81 (s, 3H), 3.62 – 3.53 (m, 1H), 1.43 (d, *J* = 7.0 Hz, 3H). **^{13}C NMR (101 MHz, $CDCl_3$):** δ 159.2, 146.3, 132.4, 131.7, 130.5, 130.1, 130.0, 129.4, 128.9, 127.4, 127.0, 114.1, 55.4, 41.9, 21.2. **FTIR (NaCl, thin film, cm^{-1})**: 2964, 1607, 1511, 1466, 1299, 1250, 1174, 1106, 1030, 967, 815. **HRMS (FAB, *m/z*)**: calc'd for $C_{17}H_{16}Cl_2O$ $[M+\cdot]^+$: 306.0578; found: 306.0582.

(*S*,*E*)-1-methoxy-4-(3-phenylpent-1-en-1-yl)benzene (141g)

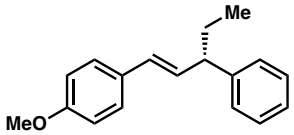

Prepared from (*E*)-1-(2-bromovinyl)-4-methoxybenzene (**86**, 43 mg, 0.2 mmol) and 1,3-dioxoisoindolin-2-yl 2-phenylbutanoate (**62g**, 62 mg, 0.2 mmol) according to General Procedure 3. The crude residue was purified by column chromatography (silica gel, 10 to 20% toluene/hexane) to yield **141g** (40 mg, 80% yield) in 97% ee as a colorless oil. Spectral data matched those reported in literature.[44] $\mathbf{R_f}$ = 0.59 (silica gel, 10% EtOAc/hexane, UV). **Chiral SFC:** (OB-H, 2.5 mL/min, 15% IPA in CO_2, λ = 254 nm): t_R (minor) = 8.0 min, t_R (major) = 9.9 min. $[\alpha]_D^{25}$ = –46° (c = 1.0, $CHCl_3$). **^{1}H NMR (400 MHz, $CDCl_3$):** δ 7.37 – 7.19 (m, 7H), 6.84 (d, *J* = 8.8 Hz, 2H), 6.37 (d, *J* = 15.8 Hz, 1H), 6.21 (dd, *J* = 15.8, 7.8 Hz, 1H), 3.80 (s, 3H), 3.35 – 3.26 (m,

1H), 1.90 – 1.78 (m, 2H), 0.93 (t, *J* = 7.4 Hz, 3H). **^{13}C NMR (101 MHz, $CDCl_3$):** δ 158.9, 144.9, 132.2, 130.6, 128.9, 128.6, 127.8, 127.3, 126.2, 114.0, 55.4, 51.1, 29.0, 12.5.

(*S*,*E*)-(4-(4-methoxyphenyl)but-3-ene-1,2-diyl)dibenzene (141h)

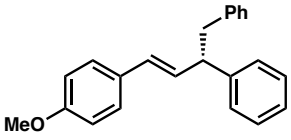

Prepared from (*E*)-1-(2-bromovinyl)-4-methoxybenzene (**86**, 43 mg, 0.2 mmol) and 1,3-dioxoisoindolin-2-yl 2,3-diphenylpropanoate (**62h**, 74 mg, 0.2 mmol) according to General Procedure 3. The crude residue was purified by column chromatography (silica gel, 10% toluene/hexane then 10% Et_2O/hexane) to yield **141h** (49 mg, 78% yield) in 95% ee as a white solid. Spectral data matched those reported in literature.[44] **R_f** = 0.48 (silica gel, 10% EtOAc/hexane, UV). **m.p.** = 72–73 °C. **Chiral SFC:** (AS-H, 2.5 mL/min, 10% IPA in CO_2, λ = 254 nm): t_R (minor) = 6.0 min, t_R (major) = 6.5 min. $[\alpha]_D^{25}$ = +19° (c = 1.0, $CHCl_3$). **^{1}H NMR (400 MHz, $CDCl_3$):** δ 7.34 – 7.13 (m, 10H), 7.10 (d, *J* = 8.8 Hz, 2H), 6.83 (d, *J* = 8.8 Hz, 2H), 6.30 (dd, *J* = 15.9, 6.3 Hz, 1H), 6.25 (d, *J* = 15.9 Hz, 1H), 3.80 (s, 3H), 3.78 – 3.67 (m, 1H), 3.19 – 3.06 (m, 2H). **^{13}C NMR (101 MHz, $CDCl_3$):** δ 158.9, 144.1, 140.2, 131.3, 130.4, 129.53, 129.49, 128.5, 128.2, 128.0, 127.4, 126.4, 126.0, 114.0, 55.4, 51.0, 42.9.

(*S*,*E*)-1-methoxy-4-(4-methyl-3-phenylpent-1-en-1-yl)benzene (141i)

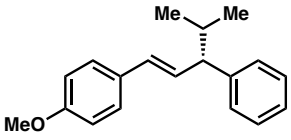

Prepared from (*E*)-1-(2-bromovinyl)-4-methoxybenzene (**86**, 43 mg, 0.2 mmol) and 1,3-dioxoisoindolin-2-yl 3-methyl-2-phenylbutanoate (**62i**, 65 mg, 0.2 mmol) according to General Procedure 3. The crude residue was purified by column chromatography (silica gel, 10 to 20% toluene/hexane) to yield **141i** (25 mg, 47% yield) in 97% ee as a white solid. **R_f** = 0.58 (silica gel, 10%

EtOAc/hexane, UV). **m.p.** = 67–68 °C. **Chiral SFC**: (AS-H, 2.5 mL/min, 10% IPA in CO_2, λ = 254 nm): t_R (minor) = 4.8 min, t_R (major) = 6.1 min. $[\boldsymbol{a}]_D^{25}$ = –39° (c = 1.0, $CHCl_3$). **^{1}H NMR (400 MHz, $CDCl_3$):** δ 7.34 – 7.28 (m, 4H), 7.26 – 7.17 (m, 3H), 6.84 (d, *J* = 8.8 Hz, 2H), 6.36 (d, *J* = 15.7 Hz, 1H), 6.26 (dd, *J* = 15.7, 8.8 Hz, 1H), 3.80 (s, 3H), 3.04 (t, *J* = 8.8 Hz, 1H), 2.14 – 1.96 (m, 1H), 1.02 (d, *J* = 6.7 Hz, 3H), 0.82 (d, *J* = 6.6 Hz, 3H). **^{13}C NMR (101 MHz, $CDCl_3$):** δ 158.9, 144.7, 131.2, 130.6, 129.8, 128.5, 128.1, 127.3, 126.1, 114.0, 57.8, 55.4, 33.4, 21.3, 21.1. **FTIR (NaCl, thin film, cm^{-1})**: 2953, 1600, 1509, 1450, 1251, 1027, 966, 838, 701. **LRMS (GC-MS, *m/z*)**: calc'd for $C_{19}H_{22}O$ $[M]^+$: 266.2; found: 266.1.

(*S*,*E*)-*tert*-butyl((4-(4-methoxyphenyl)-2-phenylbut-3-en-1-yl)oxy)dimethylsilane (141j)

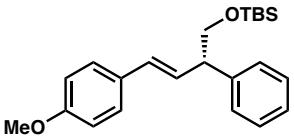

Prepared from (*E*)-1-(2-bromovinyl)-4-methoxybenzene (**86**, 43 mg, 0.2 mmol) and 1,3-dioxoisoindolin-2-yl 3-((*tert*-butyldimethylsilyl)oxy)-2-phenylpropanoate (**62j**, 74 mg, 0.2 mmol) according to General Procedure 3. The crude residue was purified by column chromatography (silica gel, 10% toluene/hexane then 10% Et_2O/hexane) to yield **141j** (43 mg, 58% yield) in 98% ee as a colorless oil. $\mathbf{R_f}$ = 0.55 (silica gel, 10% EtOAc/hexane, UV). **Chiral SFC**: (OJ-H, 2.5 mL/min, 10% IPA in CO_2, λ = 254 nm): t_R (major) = 3.4 min, t_R (minor) = 5.8 min. $[\boldsymbol{a}]_D^{25}$ = –14° (c = 1.0, $CHCl_3$). **^{1}H NMR (400 MHz, $CDCl_3$):** δ 7.39 – 7.29 (m, 6H), 7.28 – 7.23 (m, 1H), 6.87 (d, *J* = 8.8 Hz, 2H), 6.44 (d, *J* = 16.0 Hz, 1H), 6.34 (dd, *J* = 15.9, 7.2 Hz, 1H), 3.98 – 3.89 (m, 2H), 3.83 (s, 3H), 3.70 – 3.63 (m, 1H), 0.89 (s, 9H), 0.02 (s, 3H), 0.01 (s, 3H). **^{13}C NMR (101 MHz, $CDCl_3$):** δ 159.0, 142.3, 130.7, 130.5, 128.8, 128.45, 128.42,

127.4, 126.6, 114.0, 67.5, 55.4, 51.8, 26.0, 18.4, -5.2, -5.3. **FTIR (NaCl, thin film, cm^{-1})**: 2953, 2928, 2892, 2855, 1607, 1511, 1463, 1250, 1174, 1106, 1036, 836, 775, 699. **HRMS (FAB, *m/z*)**: calc'd for $C_{23}H_{32}O_2Si$ $[M–H_2+H]^+$: 367.2093; found: 367.2081.

(*S*,*E*)-1-methoxy-4-(3-phenylhexa-1,5-dien-1-yl)benzene (141k)

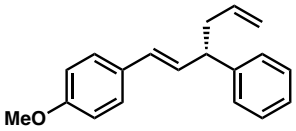

Prepared from (*E*)-1-(2-bromovinyl)-4-methoxybenzene (**86**, 43 mg, 0.2 mmol) and 1,3-dioxoisoindolin-2-yl 2-phenylpent-4-enoate (**62k**, 53 mg, 0.2 mmol) according to General Procedure 3. The crude residue was purified by column chromatography (silica gel, 5 to 20% toluene/hexane) to yield **141k** (42 mg, 79% yield) in 96% ee as a colorless oil. $\mathbf{R}_f$ = 0.55 (silica gel, 10% EtOAc/hexane, UV). **Chiral SFC**: (OJ-H, 2.5 mL/min, 10% IPA in CO_2, λ = 254 nm): t_R (minor) = 7.8 min, t_R (major) = 8.5 min. $[\alpha]_D^{25}$ = –19° (c =1.0, $CHCl_3$). **^{1}H NMR (400 MHz, $CDCl_3$):** δ 7.31 – 7.14 (m, 7H), 6.78 (d, *J* = 8.8 Hz, 2H), 6.30 (d, *J* = 15.9 Hz, 1H), 6.18 (dd, *J* = 15.8, 7.5 Hz, 1H), 5.73 (ddt, *J* = 17.1, 10.2, 6.9 Hz, 1H), 5.01 (ddt, *J* = 17.0, 2.0, 1.5 Hz, 1H), 4.95 (ddt, *J* = 10.2, 2.1, 1.0 Hz, 1H), 3.74 (s, 3H), 3.50 – 3.42 (m, 1H), 2.57 – 2.51 (m, 2H). **^{13}C NMR (101 MHz, $CDCl_3$):** δ 159.0, 144.2, 136.8, 131.5, 130.4, 129.2, 128.6, 127.8, 127.4, 126.4, 116.4, 114.0, 55.4, 49.1, 40.4. **FTIR (NaCl, thin film, cm^{-1})**: 3025, 2913, 2834, 1606, 1509, 1246, 1173, 1032, 963, 911, 756, 698. **HRMS (EI, *m/z*)**: calc'd for $C_{19}H_{20}O$ $[M+\cdot]^+$: 264.1514; found: 264.1521.

(*S*,*E*)-1-(6-chloro-3-phenylhex-1-en-1-yl)-4-methoxybenzene (141l)

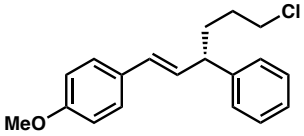

Prepared from (*E*)-1-(2-bromovinyl)-4-methoxybenzene (**86**, 43 mg, 0.2 mmol) and 1,3-dioxoisoindolin-2-yl 5-chloro-2-

phenylpentanoate (**62l**, 72 mg, 0.2 mmol) according to General Procedure 3. The crude residue was purified by column chromatography (silica gel, 5% Et_2O/hexane) to yield **141l** (52 mg, 87% yield) in 93% ee as a colorless oil. $\mathbf{R_f}$ = 0.53 (silica gel, 10% EtOAc/hexane, UV). **Chiral SFC**: (AS-H, 2.5 mL/min, 15% IPA in CO_2, λ = 254 nm): t_R (minor) = 3.7 min, t_R (major) = 4.7 min. $[\boldsymbol{a}]_D^{25}$ = –21° (c = 1.0, $CHCl_3$). **^{1}H NMR (400 MHz, $CDCl_3$):** δ 7.37 – 7.21 (m, 7H), 6.85 (d, *J* = 8.8 Hz, 2H), 6.38 (d, *J* = 15.8 Hz, 1H), 6.20 (dd, *J* = 15.8, 7.9 Hz, 1H), 3.81 (s, 3H), 3.56 (t, *J* = 6.5 Hz, 2H), 3.46 – 3.38 (m, 1H), 2.02 – 1.92 (m, 2H), 1.92 – 1.69 (m, 2H). **^{13}C NMR (101 MHz, $CDCl_3$):** δ 159.0, 144.2, 131.5, 130.2, 129.2, 128.7, 127.7, 127.4, 126.5, 114.0, 55.4, 48.7, 45.2, 33.2, 30.8. **FTIR (NaCl, thin film, cm^{-1})**: 2915, 1605, 1491, 1438, 1509, 1246, 1173, 1031, 964. **HRMS (FAB, *m/z*)**: calc'd for $C_{19}H_{21}ClO$ $[M+\cdot]^+$: 300.1281; found: 300.1274.

(*S*,*E*)-(3-methoxy-3-phenylprop-1-en-1-yl)trimethylsilane (146)

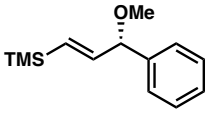

Prepared from (*E*)-(2-bromovinyl)trimethylsilane (**29o**, 36 mg, 0.2 mmol) and 1,3-dioxoisoindolin-2-yl 2-methoxy-2-phenylacetate (**145**, 62 mg, 0.2 mmol) according to General Procedure 3. The crude residue was purified by column chromatography (silica gel, 0 to 3% Et_2O/hexane) to yield **146** (26 mg, 59% yield) in 91% ee as a colorless oil. $\mathbf{R_f}$ = 0.62 (silica gel, 10% EtOAc/hexane, UV/CAM). **Chiral SFC:** (OD-H, 2.5 mL/min, 1% IPA in CO_2, λ = 210 nm): t_R (minor) = 2.6 min, t_R (major) = 5.9 min. $[\boldsymbol{a}]_D^{25}$ = +8° (c = 0.6, $CHCl_3$). **^{1}H NMR (400 MHz, $CDCl_3$):** δ 7.40 – 7.27 (m, 5H), 6.10 (dd, *J* = 18.6, 5.9 Hz, 1H), 5.93 (dd, *J* = 18.6, 1.2 Hz, 1H), 4.61 (d, *J* = 5.8 Hz, 1H), 3.32 (s, 3H), 0.07 (s, 9H). **^{13}C NMR (101 MHz, $CDCl_3$):** δ 145.7, 140.9, 131.9, 128.6, 127.7, 127.1, 86.6, 56.6, -1.2. **FTIR (NaCl, thin film, cm^{-1})**: 2955, 2820, 1453, 1248,

1100, 990, 863, 838, 760, 699. **HRMS (FAB, *m/z*)**: calc'd for $C_{13}H_{20}Osi$ $[M–H_2+H]^+$: 219.1205; found: 219.1191.

(*E*)-1-(3-cyclopropyl-3-phenylprop-1-en-1-yl)-4-methoxybenzene (161a)

1-methoxy-4-((1*E*,5*E*)-6-phenylhexa-1,5-dien-1-yl)benzene (161b)

1-methoxy-4-((1*E*,4*E*)-3-methyl-5-phenylpenta-1,4-dien-1-yl)benzene (161c)

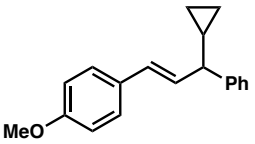

161a

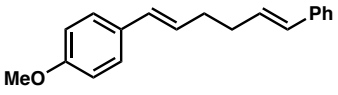

161b

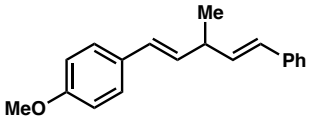

161c

Prepared from (*E*)-1-(2-bromovinyl)-4-methoxybenzene (**86**, 43 mg, 0.2 mmol) and 1,3-dioxoisoindolin-2-yl 2-cyclopropyl-2-phenylacetate (**160**, 64 mg, 0.2 mmol) according to General Procedure 3. The crude residue was purified by column chromatography (silica gel, hexane to 30% toluene/hexane) to yield a mixture of **161a–c** (22 mg, 42% yield) as a colorless oil. The reaction was repeated with 5 mol % and 20 mol % of **L2**·$NiBr_2$, yielding a mixture of **161a–c** in 44% and 49% yield, respectively. Three products are confirmed by GC-MS (extract ion *m/z* = 264). Distinct $^1H/^{13}C$ signals and coupling correlations are confirmed by ^1H, ^{13}C, COSY, HSQC, and HMBC NMR spectroscopy.

NMR data for **161a–c** with 20 mol % **L2**·$NiBr_2$:

^{1}H NMR (400 MHz, $CDCl_3$): δ 7.42 – 7.18 (m, 7H), 6.86 (dq, *J* = 8.9, 2.5 Hz, 2H), 6.49 – 6.36 (m, 1.8H), 6.34 – 6.08 (m, 1.82H), 3.81 (s, 3H), 3.20 (qt, *J* = 6.9, 1.3 Hz, 0.1H, *11c*), 2.76 (ddd, *J* = 8.6, 6.9, 1.2 Hz, 0.2H, *11a*), 2.49 – 2.31 (m, 2.8H, *11b*), 1.31 (d, *J* = 6.9 Hz, 0.3H, *11c*), 1.23 – 1.13 (m, 0.2H, *11a*), 0.68 (dddd, *J* = 9.1, 8.0, 5.3, 4.1 Hz, 0.2H, *11a*),

0.56 (dddd, J = 9.4, 8.0, 5.2, 4.1 Hz, 0.2H, *11a*), 0.40 – 0.31 (m, 0.2H, *11a*), 0.28 (dtd, J = 9.3, 5.2, 4.2 Hz, 0.2H, *11a*). **^{13}C NMR (101 MHz, $CDCl_3$):** δ 158.9, 158.8, 144.6, 137.9, 137.8, 134.7, 132.2, 131.2, 130.7, 130.5, 130.4, 130.3, 129.8, 129.0, 128.7, 128.6, 128.5, 128.3, 128.0, 127.9, 127.4, 127.3, 127.2, 127.1, 127.0, 126.4, 126.2, 126.1, 114.03, 114.02, 55.4, 53.2, 40.2, 33.2, 33.0, 20.5, 16.4, 4.9, 4.4. **FTIR (NaCl, thin film, cm^{-1})**: 3026, 2931, 2837, 1607, 1511, 1252, 1176, 1034, 966, 800, 692. **LRMS (GC-MS, *m/z*)**: calc'd for $C_{19}H_{20}O$ $[M]^+$: 264.2; found: 3 products, 264.1, 264.1, 264.2.

3.6.7 GC-MS Traces of Radical Clock Products

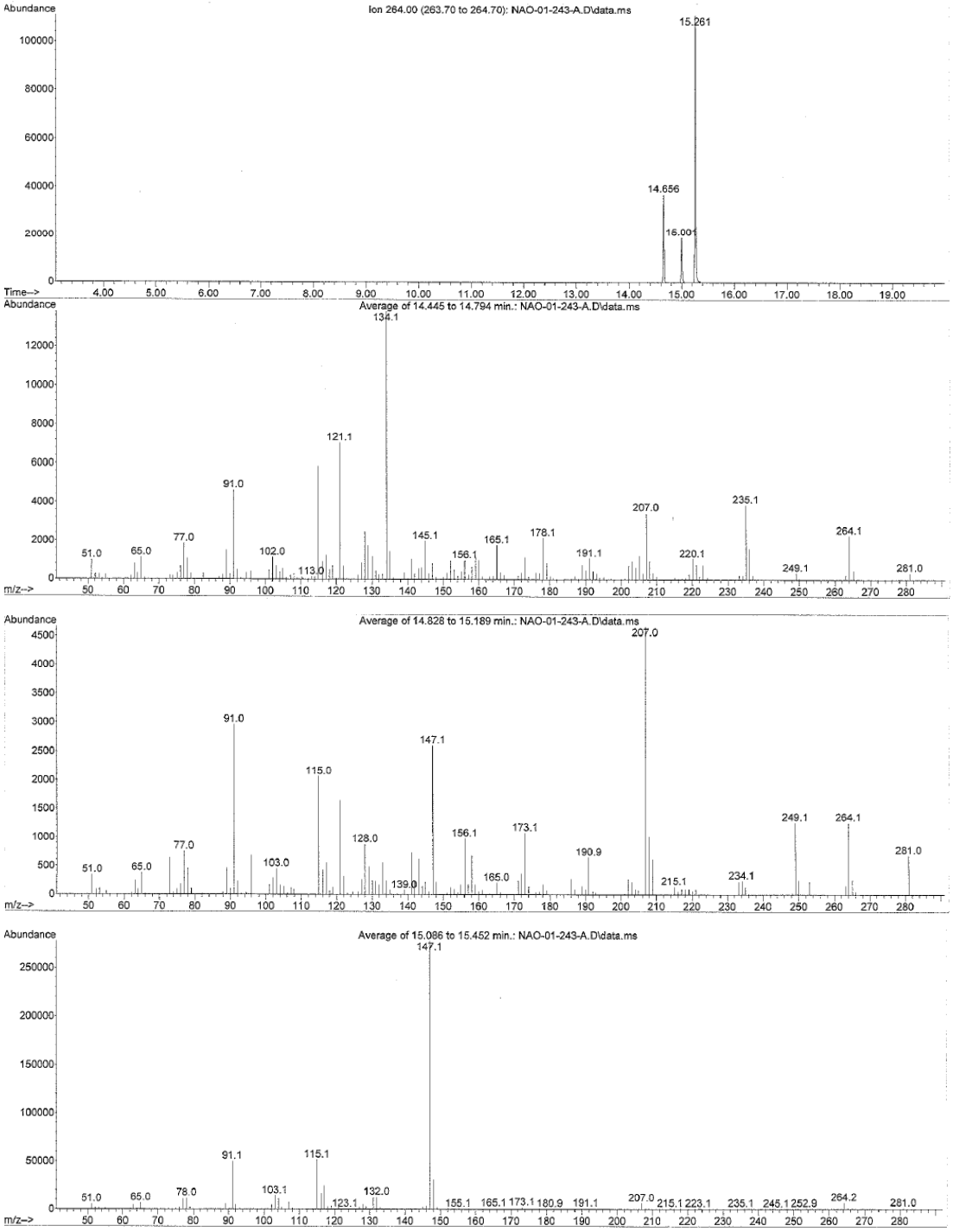

3.6.8 SFC and HPLC Traces of Racemic and Enantioenriched Products

137 (Figure 3.3): racemic

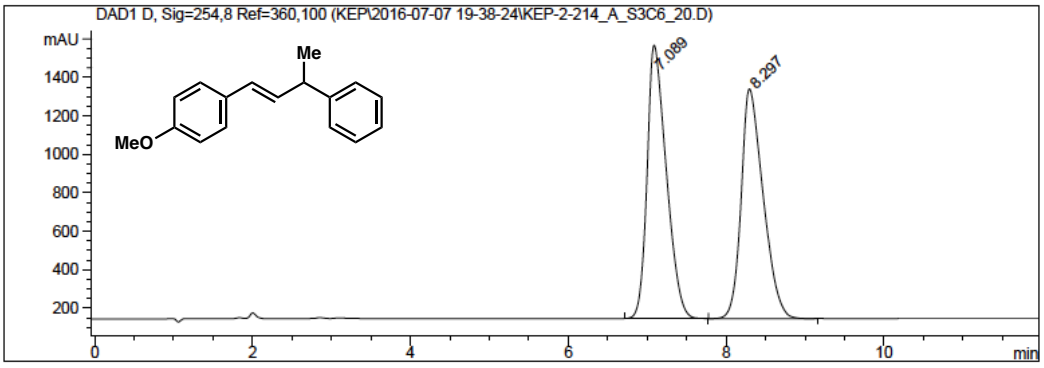

Peak #	RetTime [min]	Type	Width [min]	Area [mAU*s]	Height [mAU]	Area %
1	7.089	BV	0.2581	2.40965e4	1419.46216	50.9929
2	8.297	VB	0.2903	2.31582e4	1193.77161	49.0071

137 (Figure 3.3): enantioenriched, 96% ee

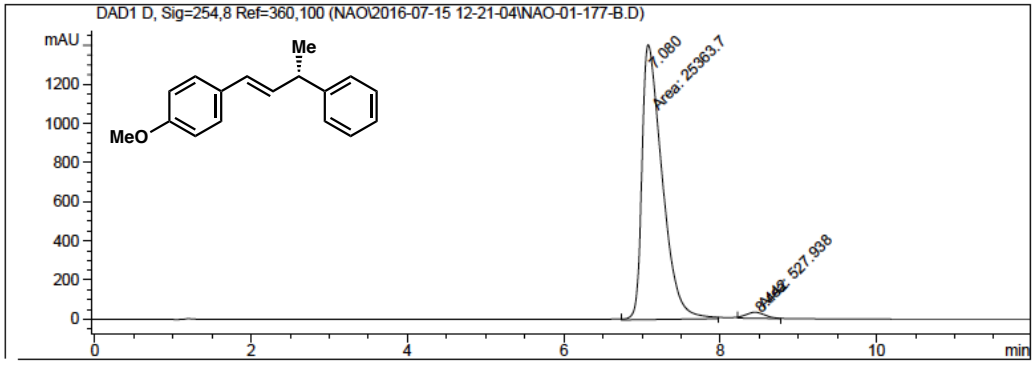

Peak #	RetTime [min]	Type	Width [min]	Area [mAU*s]	Height [mAU]	Area %
1	7.080	MM	0.3005	2.53637e4	1406.71533	97.9610
2	8.442	MM	0.2816	527.93842	31.25150	2.0390

140a (Figure 3.3): racemic

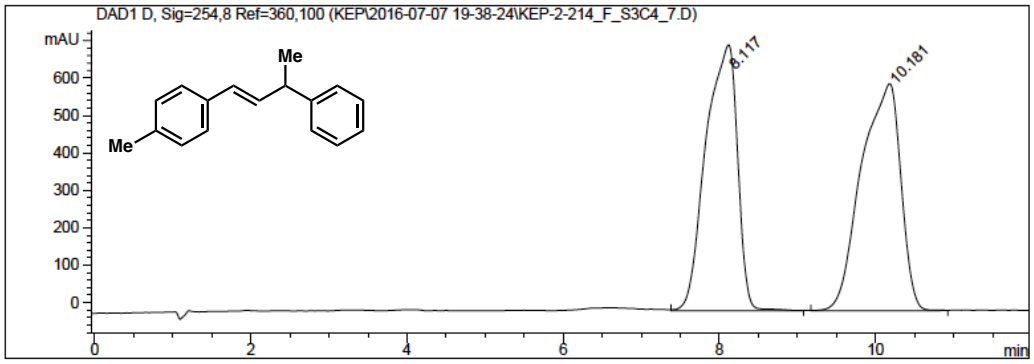

Peak #	RetTime [min]	Type	Width [min]	Area [mAU*s]	Height [mAU]	Area %
1	8.117	VB	0.3807	2.00095e4	710.31079	48.4555
2	10.181	BV	0.4692	2.12851e4	606.82129	51.5445

140a (Figure 3.3): enantioenriched, 95% ee

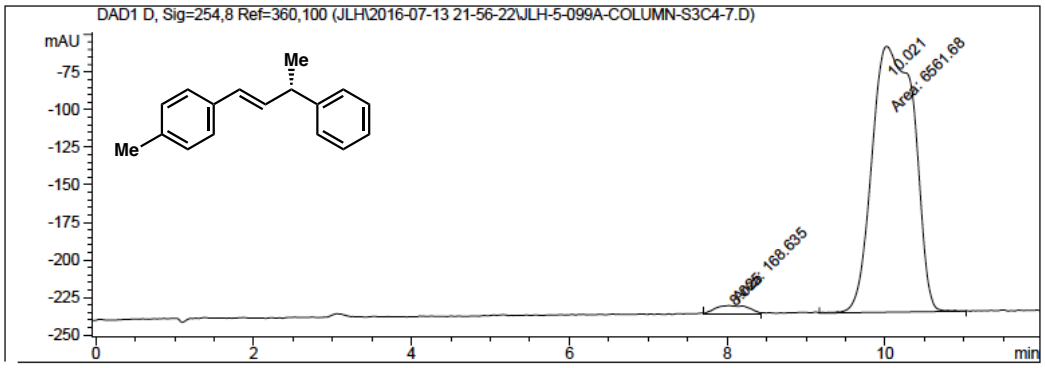

Peak #	RetTime [min]	Type	Width [min]	Area [mAU*s]	Height [mAU]	Area %
1	8.025	MM	0.4882	168.63531	5.75649	2.5056
2	10.021	MM	0.6182	6561.67920	176.91377	97.4944

140b (Figure 3.3): racemic

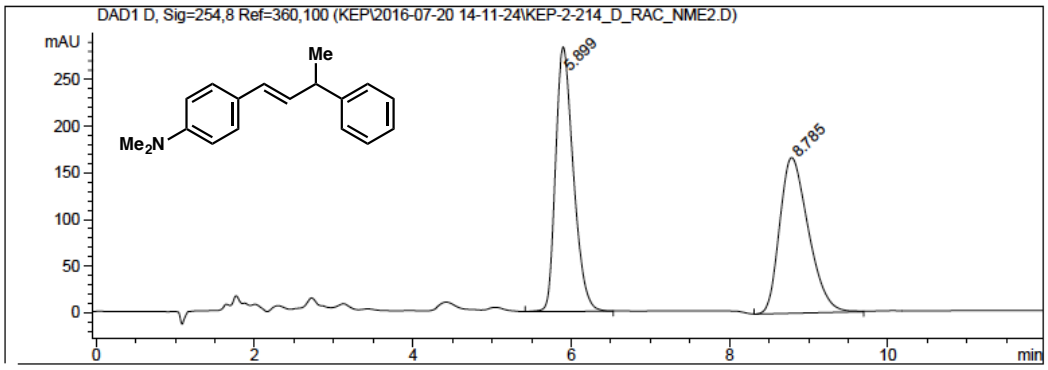

Peak #	RetTime [min]	Type	Width [min]	Area [mAU*s]	Height [mAU]	Area %
1	5.899	VB	0.2423	4429.97607	283.53226	51.2284
2	8.785	BB	0.3949	4217.52539	166.83267	48.7716

140b (Figure 3.3): enantioenriched, 97% ee

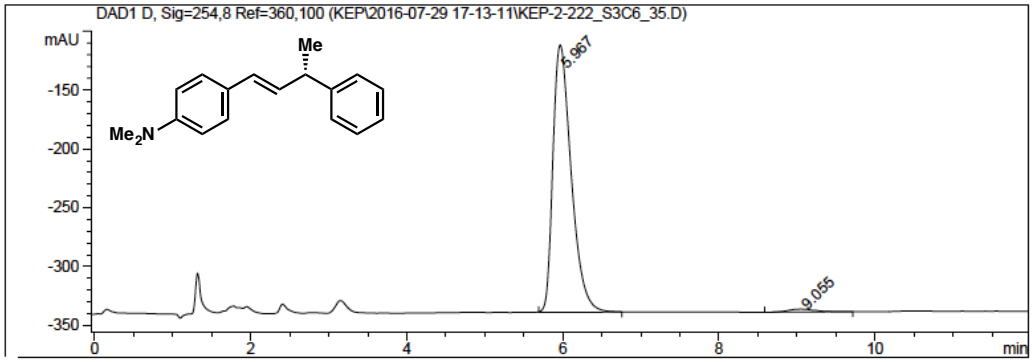

Peak #	RetTime [min]	Type	Width [min]	Area [mAU*s]	Height [mAU]	Area %
1	5.967	BB	0.2505	3707.96924	227.13380	98.4506
2	9.055	BB	0.2926	58.35402	2.46108	1.5494

140c (Figure 3.3): racemic

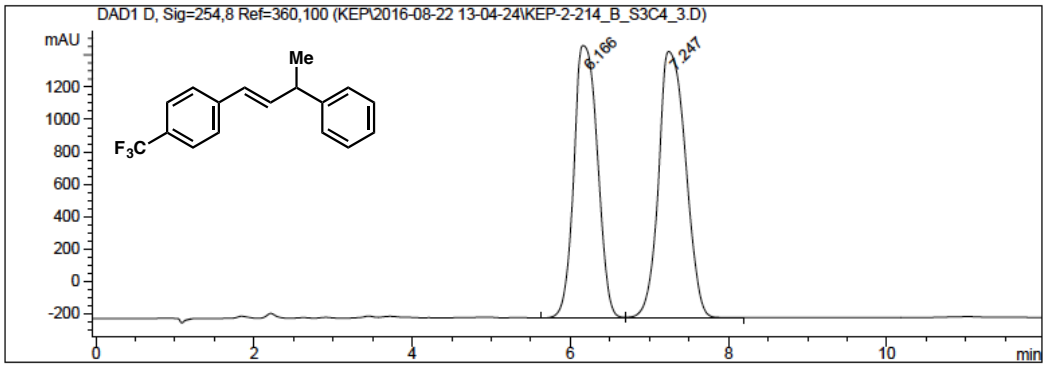

Peak #	RetTime [min]	Type	Width [min]	Area [mAU*s]	Height [mAU]	Area %
1	6.166	VV	0.3308	3.50747e4	1685.07422	47.1051
2	7.247	VB	0.3749	3.93858e4	1647.52795	52.8949

140c (Figure 3.3): enantioenriched, 93% ee

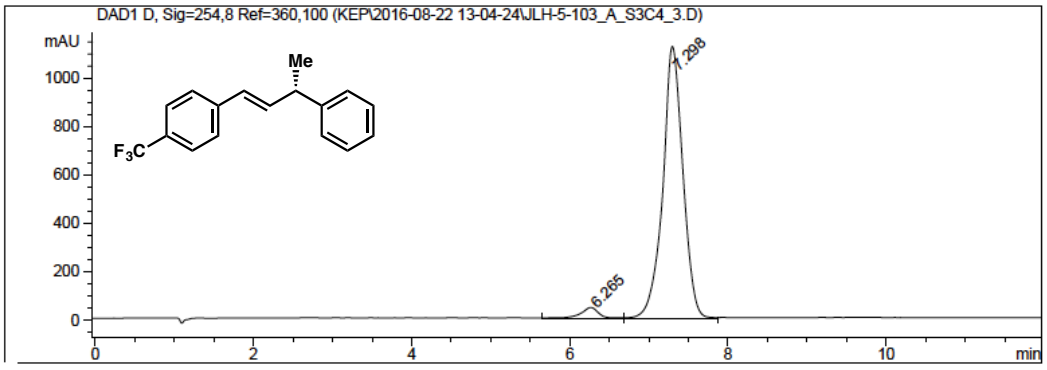

Peak #	RetTime [min]	Type	Width [min]	Area [mAU*s]	Height [mAU]	Area %
1	6.265	VV	0.2265	687.93018	43.98362	3.3472
2	7.298	VV	0.2624	1.98645e4	1122.81396	96.6528

140d (Figure 3.3): racemic

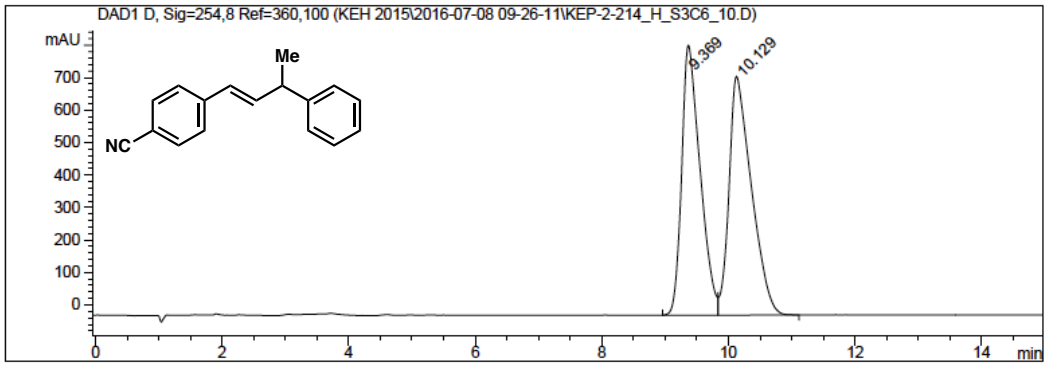

Peak #	RetTime [min]	Type	Width [min]	Area [mAU*s]	Height [mAU]	Area %
1	9.369	BV	0.2960	1.68057e4	830.62769	48.1897
2	10.129	VB	0.3508	1.80684e4	734.99915	51.8103

140d (Figure 3.3): enantioenriched, 94% ee

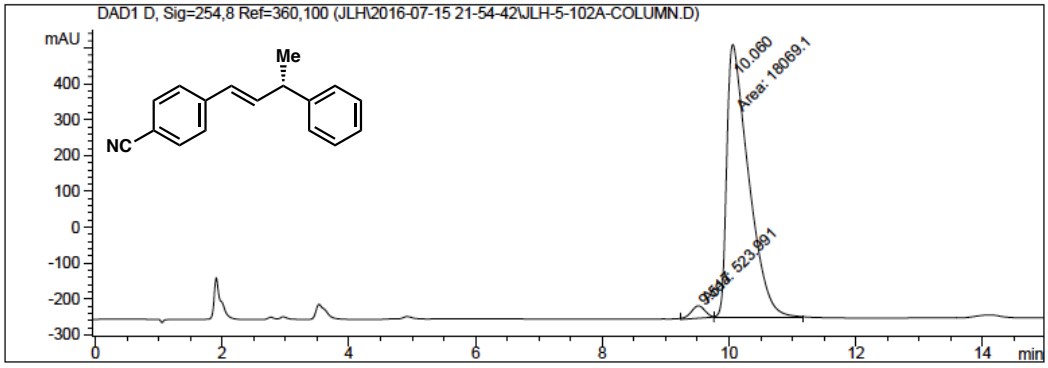

Peak #	RetTime [min]	Type	Width [min]	Area [mAU*s]	Height [mAU]	Area %
1	9.517	MM	0.2532	523.99091	34.49692	2.8182
2	10.060	MM	0.3962	1.80691e4	760.05249	97.1818

140e (Figure 3.3): racemic

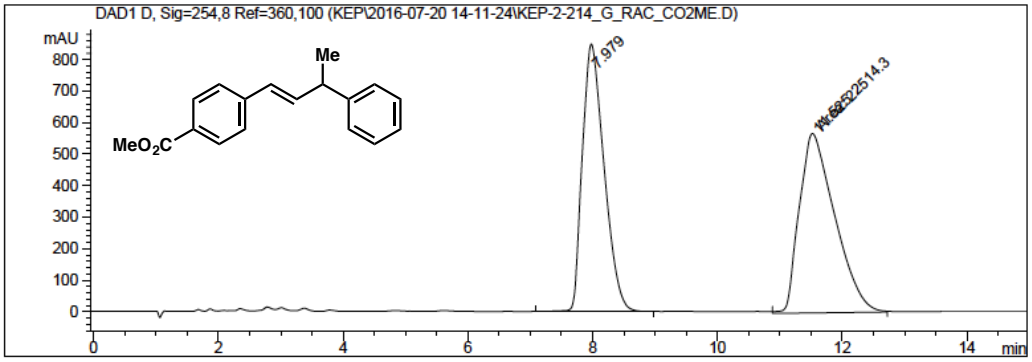

Peak #	RetTime [min]	Type	Width [min]	Area [mAU*s]	Height [mAU]	Area %
1	7.979	BB	0.3869	2.05724e4	848.34802	47.7466
2	11.525	MM	0.6592	2.25143e4	569.27423	52.2534

140e (Figure 3.3): enantioenriched, 95% ee

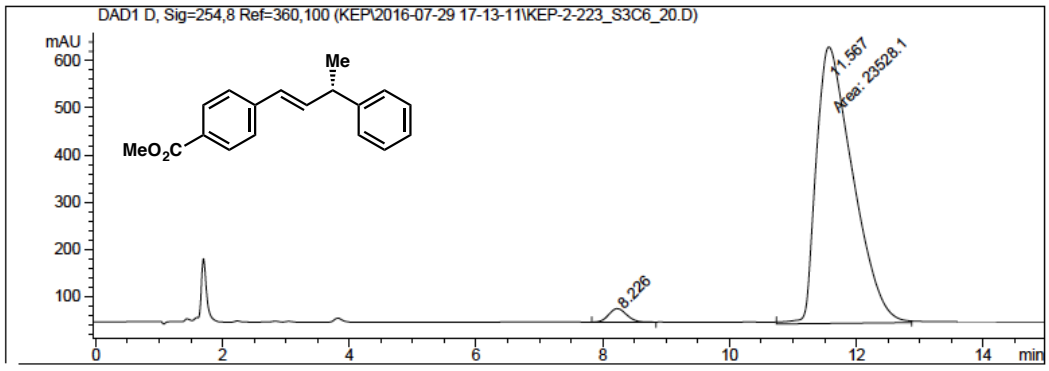

Peak #	RetTime [min]	Type	Width [min]	Area [mAU*s]	Height [mAU]	Area %
1	8.226	BB	0.3069	568.03058	28.69778	2.3574
2	11.567	MM	0.6679	2.35281e4	587.09686	97.6426

140f (Figure 3.3): racemic

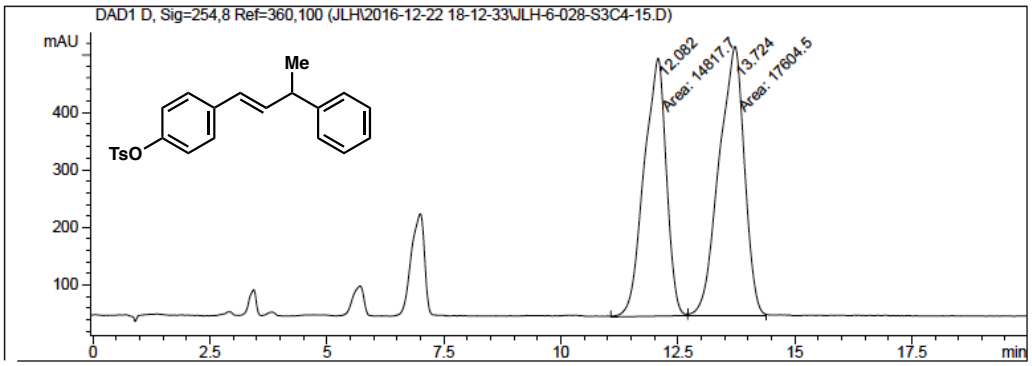

Peak #	RetTime [min]	Type	Width [min]	Area [mAU*s]	Height [mAU]	Area %
1	12.082	MM	0.5513	1.48177e4	447.97232	45.7023
2	13.724	MM	0.6275	1.76045e4	467.56030	54.2977

140f (Figure 3.3): enantioenriched, 94% ee

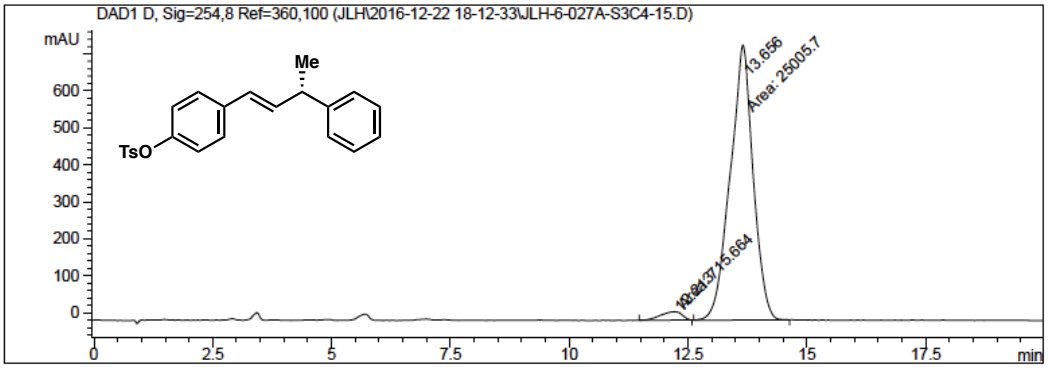

Peak #	RetTime [min]	Type	Width [min]	Area [mAU*s]	Height [mAU]	Area %
1	12.213	MM	0.5201	715.66412	22.93249	2.7824
2	13.656	MM	0.5598	2.50057e4	744.50916	97.2176

140g (Figure 3.3): racemic

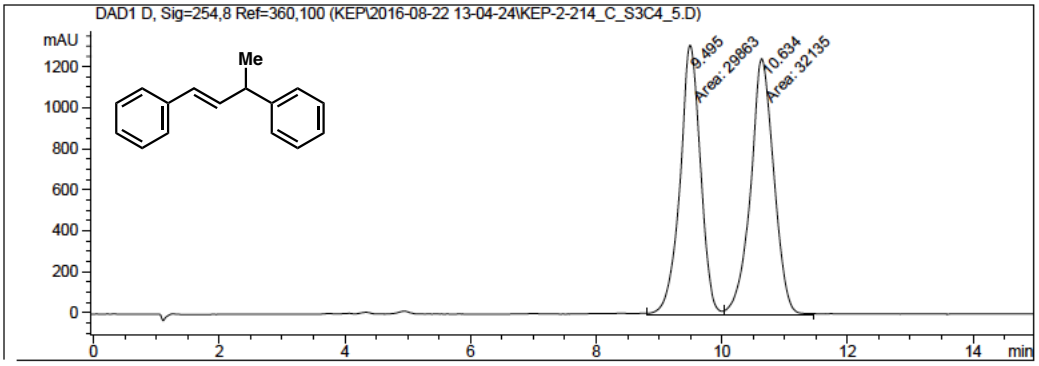

Peak #	RetTime [min]	Type	Width [min]	Area [mAU*s]	Height [mAU]	Area %
1	9.495	MM	0.3786	2.98630e4	1314.49744	48.1677
2	10.634	MM	0.4290	3.21350e4	1248.56421	51.8323

140g (Figure 3.3): enantioenriched, 96% ee

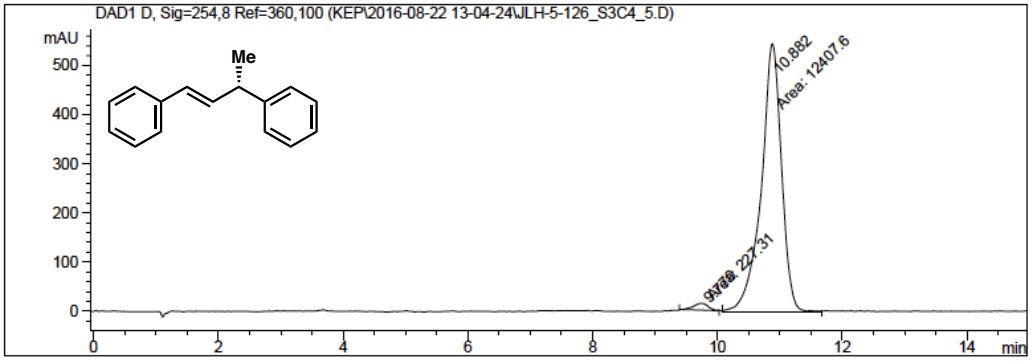

Peak #	RetTime [min]	Type	Width [min]	Area [mAU*s]	Height [mAU]	Area %
1	9.770	MM	0.2725	227.31046	13.90100	1.7991
2	10.882	MM	0.3782	1.24076e4	546.85577	98.2009

140h (Figure 3.3): racemic

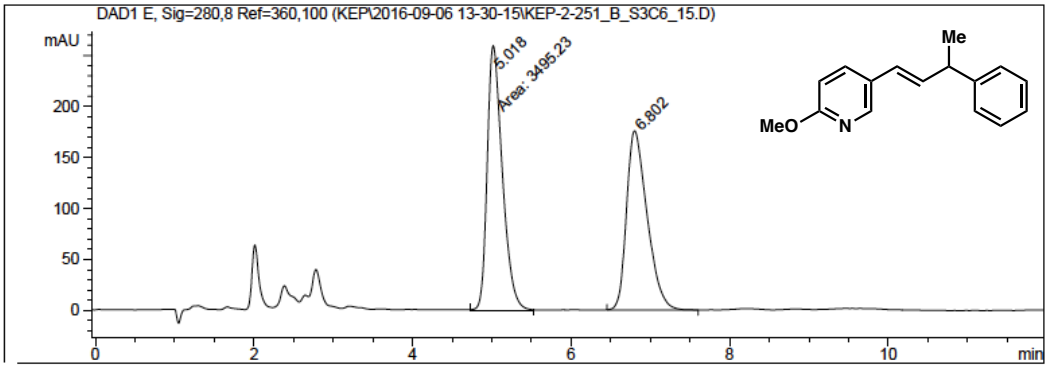

Peak #	RetTime [min]	Type	Width [min]	Area [mAU*s]	Height [mAU]	Area %
1	5.018	MM	0.2233	3495.22925	260.81982	52.4318
2	6.802	BB	0.2747	3171.01147	175.57878	47.5682

140h (Figure 3.3): enantioenriched, 95% ee

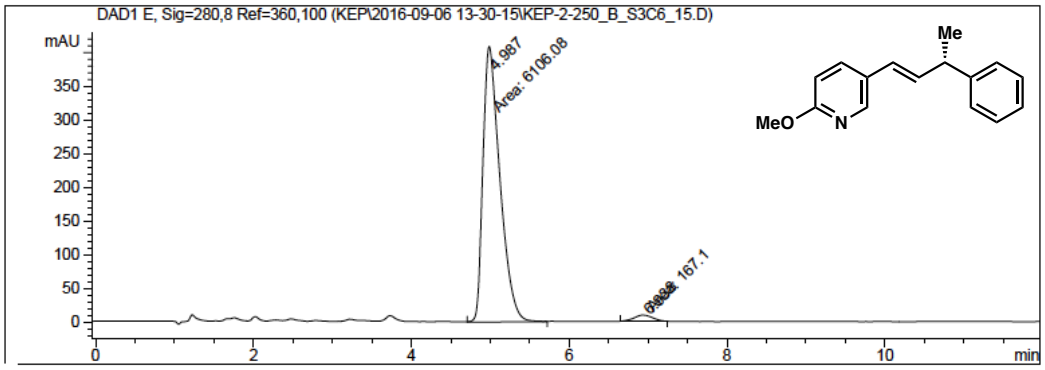

Peak #	RetTime [min]	Type	Width [min]	Area [mAU*s]	Height [mAU]	Area %
1	4.987	MM	0.2488	6106.07617	408.96854	97.3363
2	6.938	MM	0.2866	167.10007	9.71596	2.6637

140i (Figure 3.3): racemic

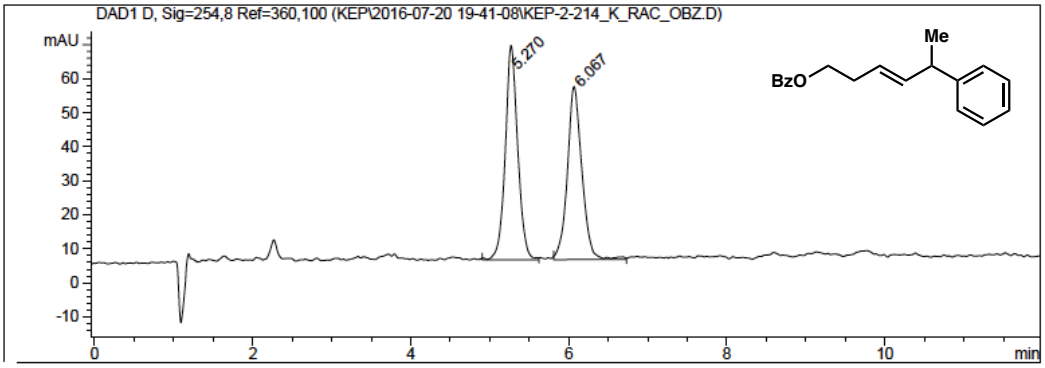

Peak #	RetTime [min]	Type	Width [min]	Area [mAU*s]	Height [mAU]	Area %
1	5.270	BB	0.1643	692.65100	62.99958	51.5795
2	6.067	BB	0.1892	650.22839	50.83070	48.4205

140i (Figure 3.3): enantioenriched, 97% ee

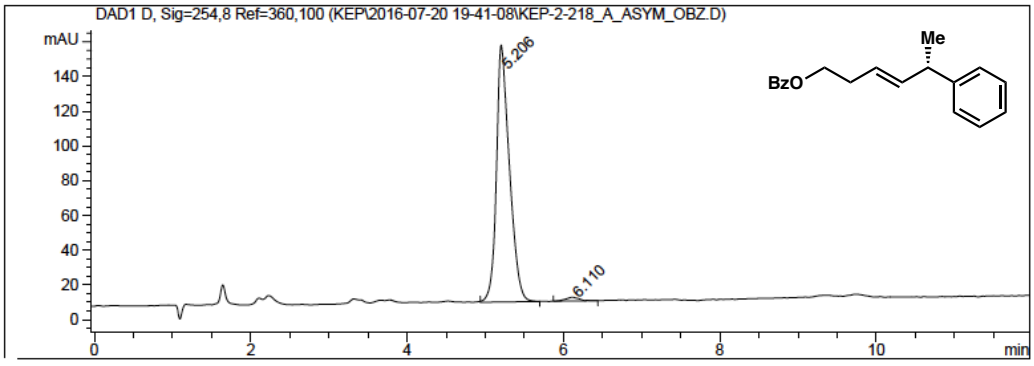

Peak #	RetTime [min]	Type	Width [min]	Area [mAU*s]	Height [mAU]	Area %
1	5.206	BB	0.1708	1710.15393	148.02460	98.4760
2	6.110	BB	0.1607	26.46575	2.19494	1.5240

140j (Figure 3.3): racemic

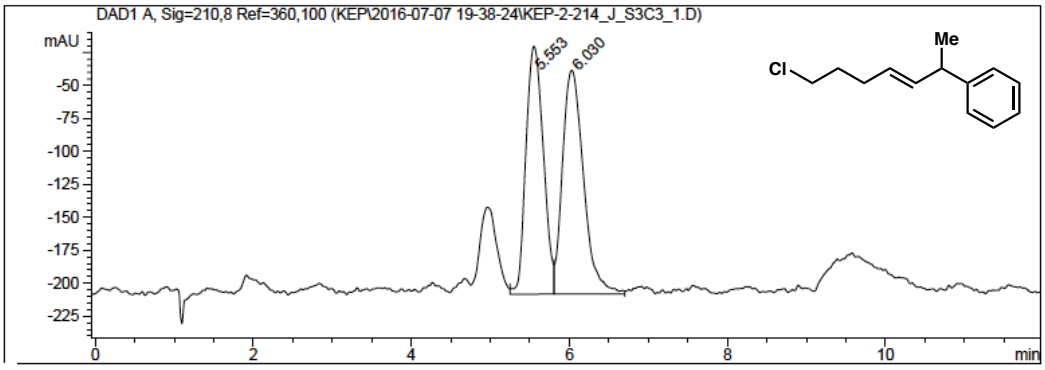

Peak #	RetTime [min]	Type	Width [min]	Area [mAU*s]	Height [mAU]	Area %
1	5.553	VV	0.2466	2879.10791	188.09062	47.7991
2	6.030	VV	0.2922	3144.24927	169.66949	52.2009

140j (Figure 3.3): enantioenriched, 91% ee

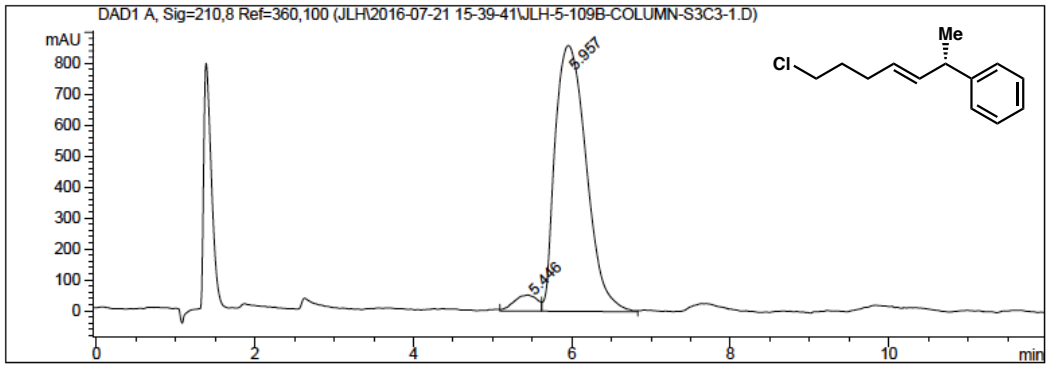

Peak #	RetTime [min]	Type	Width [min]	Area [mAU*s]	Height [mAU]	Area %
1	5.446	VV	0.2528	1053.08008	51.88251	4.2859
2	5.957	VV	0.4514	2.35179e4	858.91888	95.7141

140k (Figure 3.3): racemic

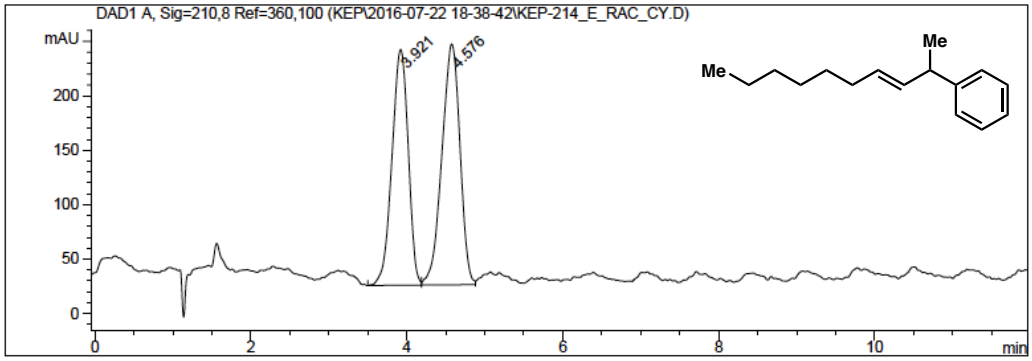

Peak #	RetTime [min]	Type	Width [min]	Area [mAU*s]	Height [mAU]	Area %
1	3.921	VV	0.2294	3145.27051	216.62386	46.8268
2	4.576	VV	0.2603	3571.54810	221.25337	53.1732

140k (Figure 3.3): enantioenriched, 94% ee

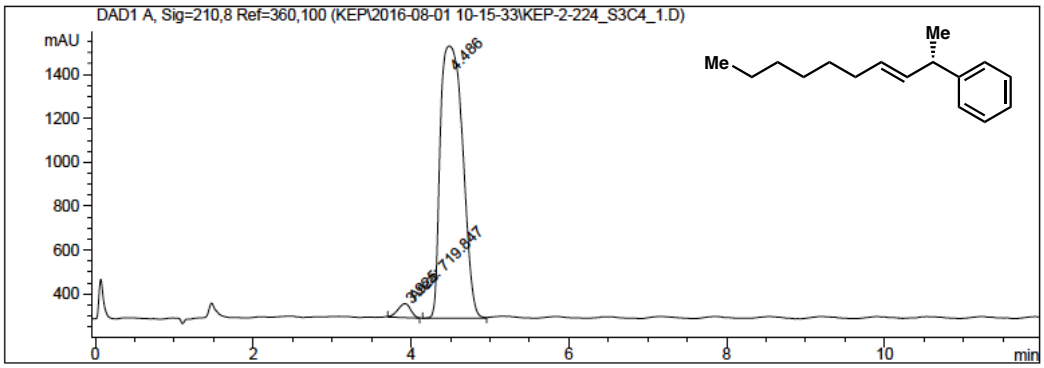

Peak #	RetTime [min]	Type	Width [min]	Area [mAU*s]	Height [mAU]	Area %
1	3.925	MM	0.1890	719.84717	63.47777	2.8630
2	4.486	VV	0.3261	2.44231e4	1238.09705	97.1370

S31 (de-silylated 140l, Figure 3.3): racemic

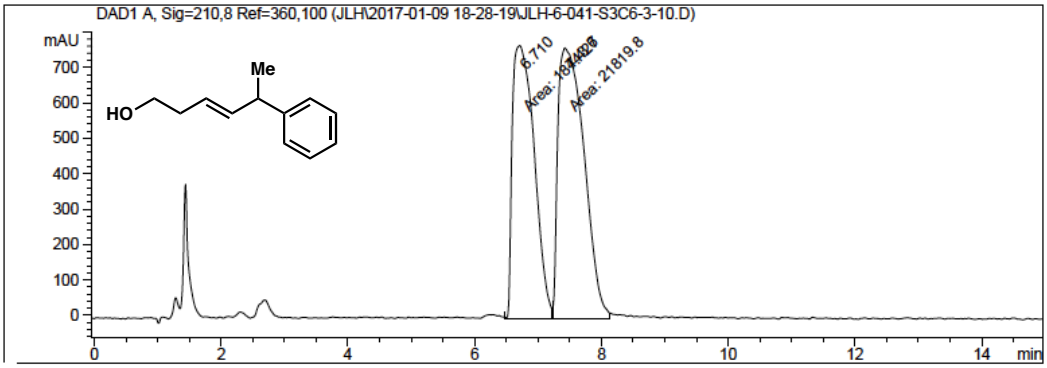

Peak #	RetTime [min]	Type	Width [min]	Area [mAU*s]	Height [mAU]	Area %
1	6.710	MM	0.3992	1.84436e4	770.06226	45.8074
2	7.427	MM	0.4761	2.18198e4	763.80591	54.1926

S31 (de-silylated 140l, Figure 3.3): enantioenriched, 89% ee

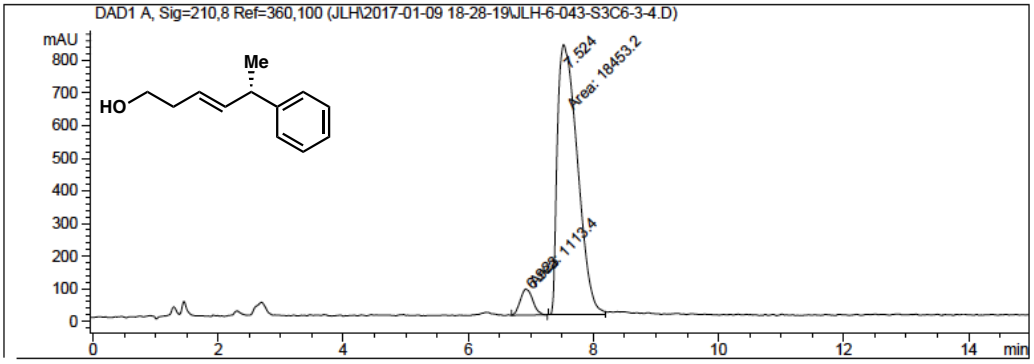

Peak #	RetTime [min]	Type	Width [min]	Area [mAU*s]	Height [mAU]	Area %
1	6.923	MM	0.2309	1113.40063	80.37251	5.6903
2	7.524	MM	0.3711	1.84532e4	828.86755	94.3097

140m (Figure 3.3): racemic

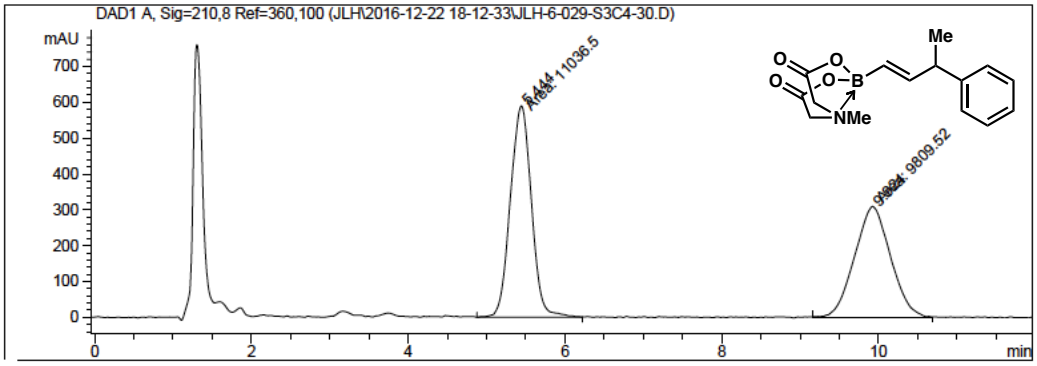

Peak #	RetTime [min]	Type	Width [min]	Area [mAU*s]	Height [mAU]	Area %
1	5.444	MM	0.3119	1.10365e4	589.78003	52.9429
2	9.924	MM	0.5290	9809.52246	309.03564	47.0571

140m (Figure 3.3): enantioenriched, 97% ee

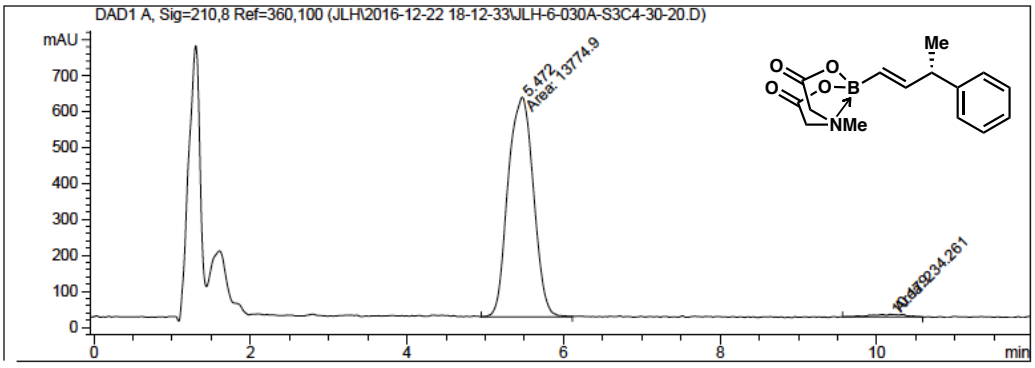

Peak #	RetTime [min]	Type	Width [min]	Area [mAU*s]	Height [mAU]	Area %
1	5.472	MM	0.3758	1.37749e4	610.96771	98.3278
2	10.179	MM	0.5146	234.26103	7.58734	1.6722

140n (Figure 3.3): racemic

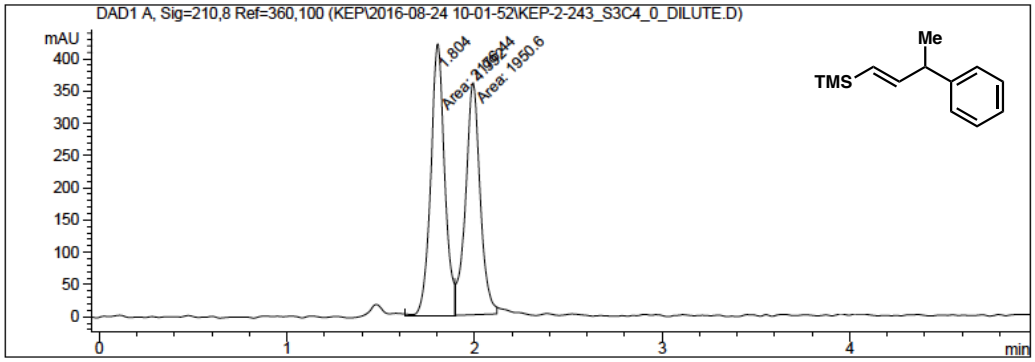

Peak #	RetTime [min]	Type	Width [min]	Area [mAU*s]	Height [mAU]	Area %
1	1.804	MM	0.0852	2176.43945	425.78909	52.7360
2	1.992	MM	0.0896	1950.60413	362.93353	47.2640

140n (Figure 3.3): enantioenriched, 97% ee

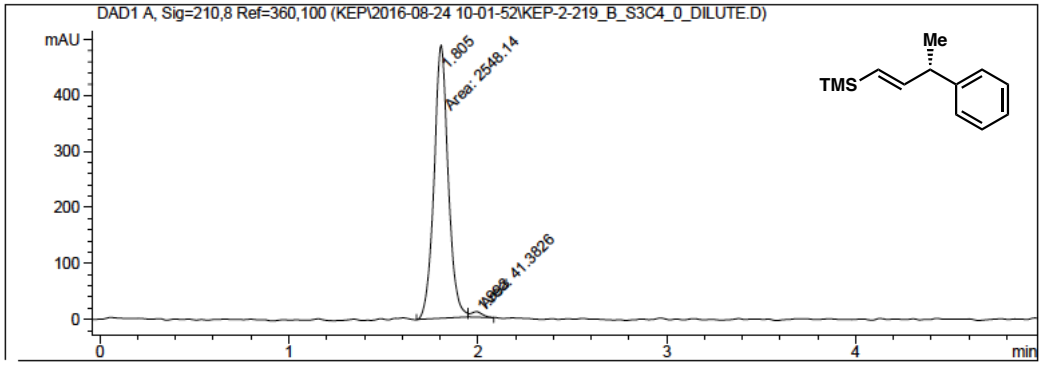

Peak #	RetTime [min]	Type	Width [min]	Area [mAU*s]	Height [mAU]	Area %
1	1.805	MM	0.0863	2548.14233	492.12225	98.4019
2	1.993	MM	0.0681	41.38256	10.12810	1.5981

141a (Figure 3.4): racemic

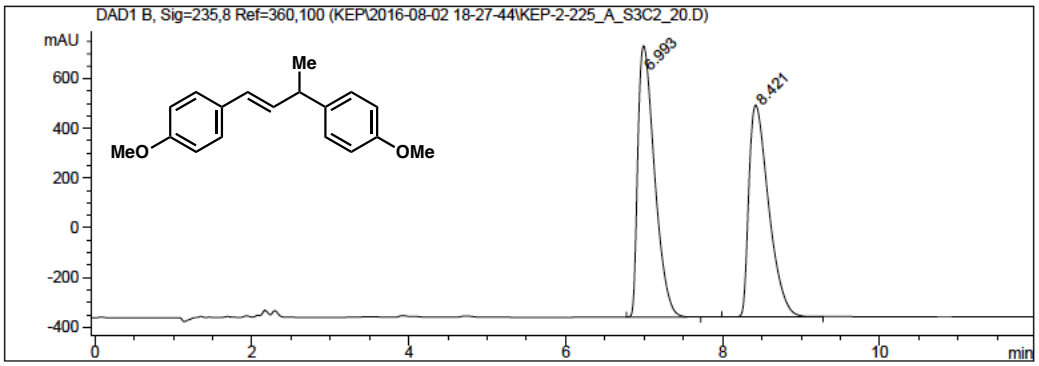

Peak #	RetTime [min]	Type	Width [min]	Area [mAU*s]	Height [mAU]	Area %
1	6.993	BB	0.2288	1.61745e4	1091.89661	51.9859
2	8.421	BB	0.2727	1.49387e4	851.43549	48.0141

141a (Figure 3.4): enantioenriched, 93% ee

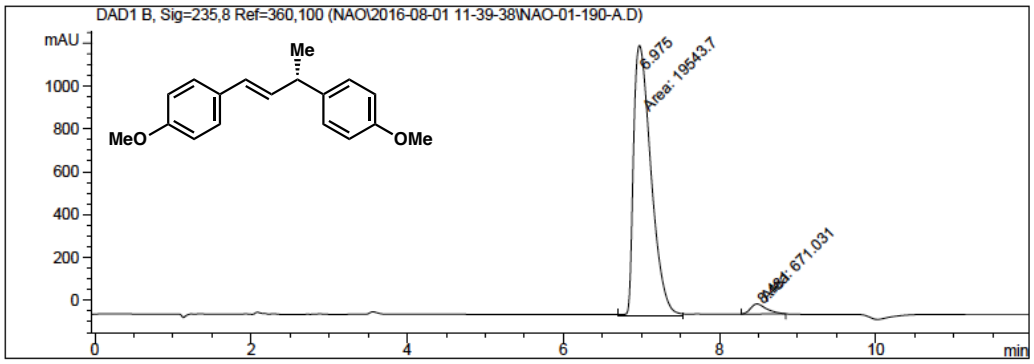

Peak #	RetTime [min]	Type	Width [min]	Area [mAU*s]	Height [mAU]	Area %
1	6.975	MM	0.2585	1.95437e4	1260.21631	96.6805
2	8.481	MM	0.2361	671.03094	47.35995	3.3195

141b (Figure 3.4): racemic

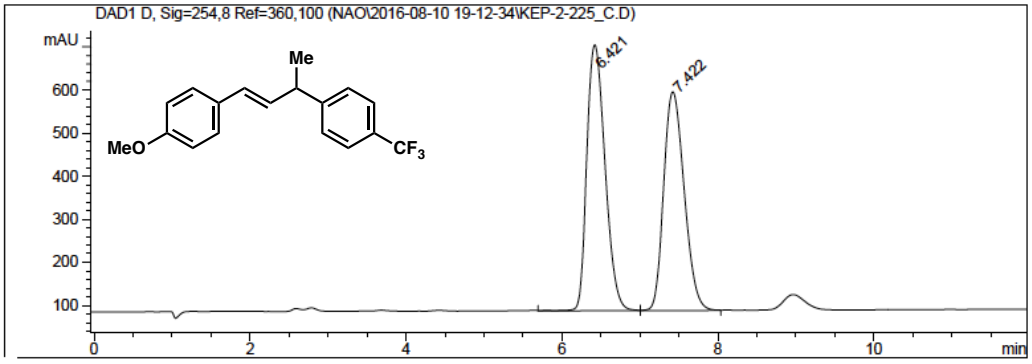

Peak #	RetTime [min]	Type	Width [min]	Area [mAU*s]	Height [mAU]	Area %
1	6.421	VV	0.2579	1.00441e4	616.96472	51.9654
2	7.422	VV	0.2894	9284.33398	507.48148	48.0346

141b (Figure 3.4): enantioenriched, 88% ee

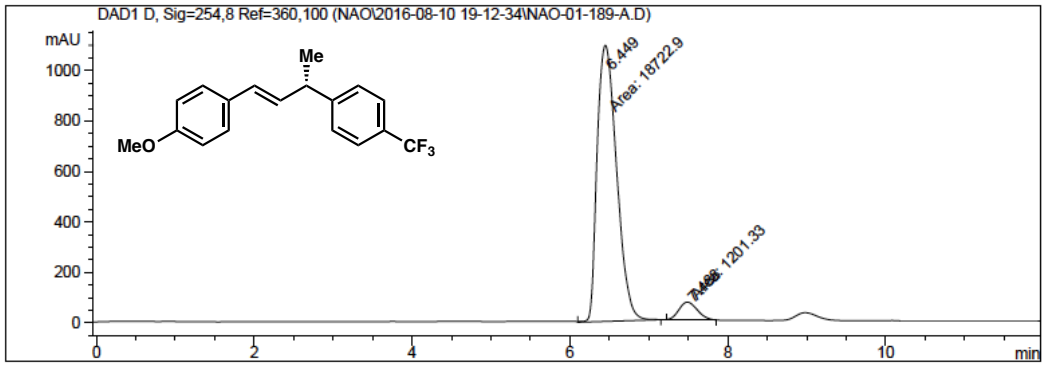

Peak #	RetTime [min]	Type	Width [min]	Area [mAU*s]	Height [mAU]	Area %
1	6.449	MM	0.2851	1.87229e4	1094.68372	93.9705
2	7.488	MM	0.2774	1201.33252	72.18948	6.0295

141c (Figure 3.4): racemic

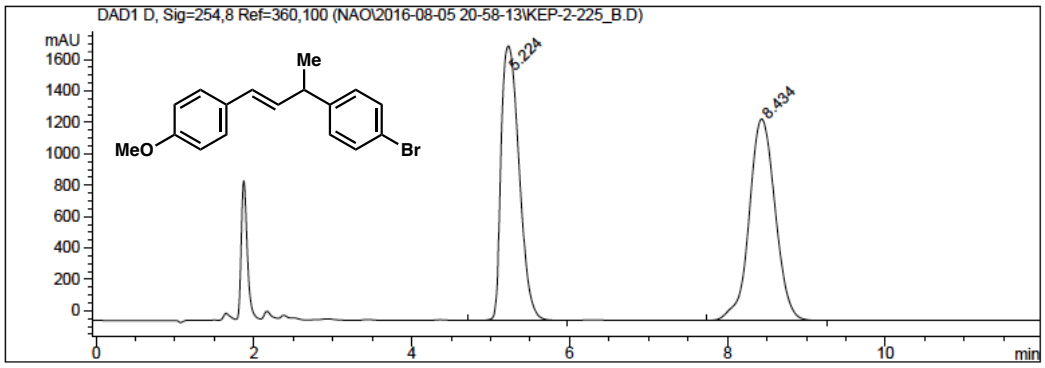

Peak #	RetTime [min]	Type	Width [min]	Area [mAU*s]	Height [mAU]	Area %
1	5.224	VV	0.2570	2.77188e4	1747.68750	48.5460
2	8.434	BB	0.3592	2.93793e4	1282.85803	51.4540

141c (Figure 3.4): enantioenriched, 90% ee

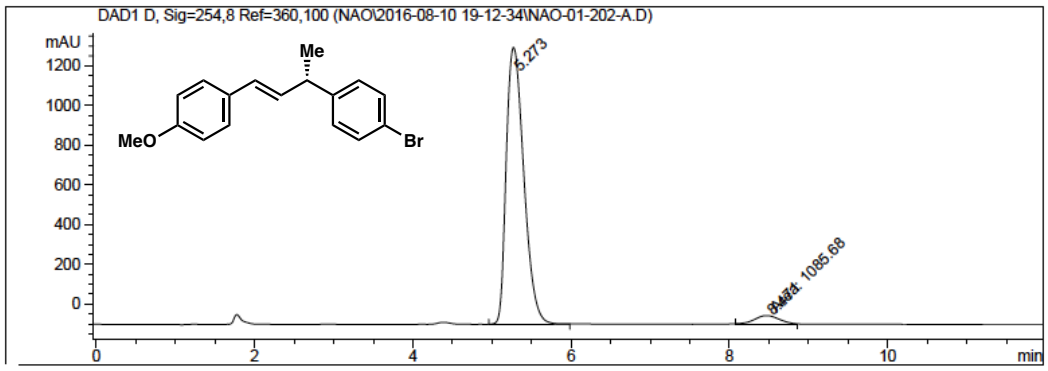

Peak #	RetTime [min]	Type	Width [min]	Area [mAU*s]	Height [mAU]	Area %
1	5.273	BB	0.2445	2.15843e4	1395.44788	95.2109
2	8.471	MM	0.3931	1085.67932	46.02574	4.7891

141d (Figure 3.4): racemic

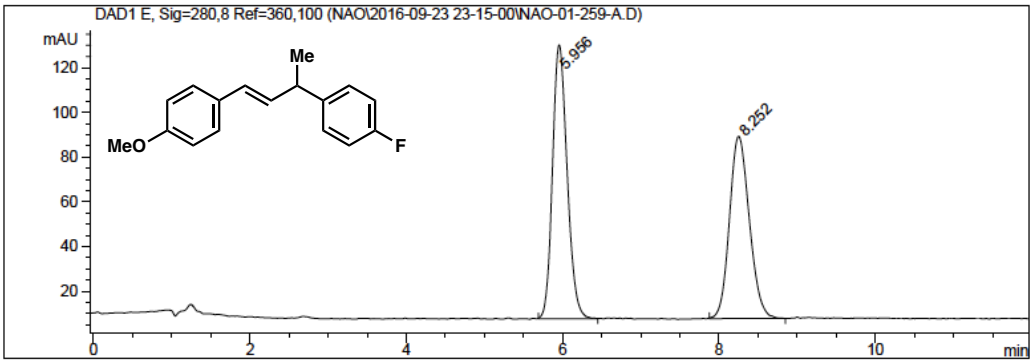

Peak #	RetTime [min]	Type	Width [min]	Area [mAU*s]	Height [mAU]	Area %
1	5.956	BB	0.2041	1597.30237	122.49622	52.5502
2	8.252	BB	0.2744	1442.27039	81.53059	47.4498

141d (Figure 3.4): enantioenriched, 92% ee

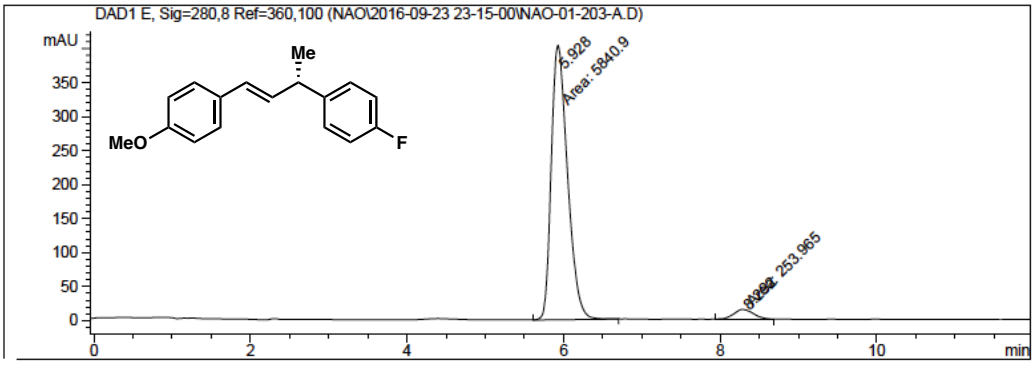

Peak #	RetTime [min]	Type	Width [min]	Area [mAU*s]	Height [mAU]	Area %
1	5.928	MM	0.2410	5840.89600	403.93130	95.8331
2	8.292	MM	0.2929	253.96486	14.45295	4.1669

141e (Figure 3.4): racemic

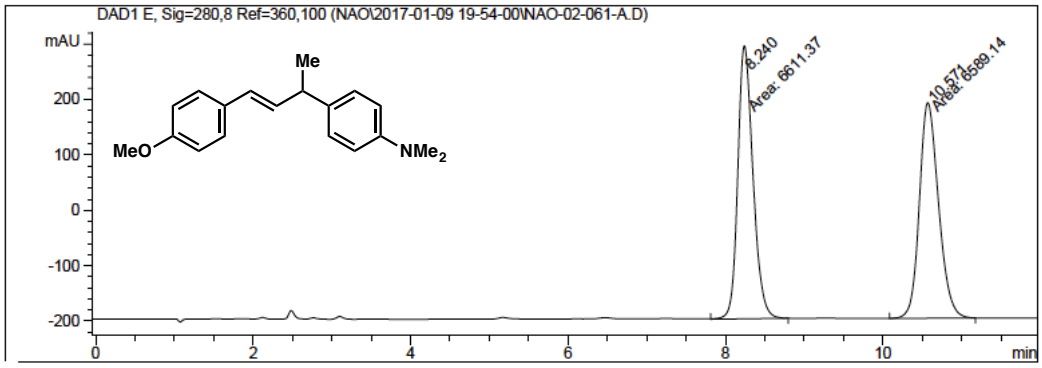

Peak #	RetTime [min]	Type	Width [min]	Area [mAU*s]	Height [mAU]	Area %
1	8.240	MM	0.2233	6611.36621	493.52872	50.0842
2	10.571	MM	0.2819	6589.13770	389.54446	49.9158

141e (Figure 3.4): enantioenriched, 94% ee

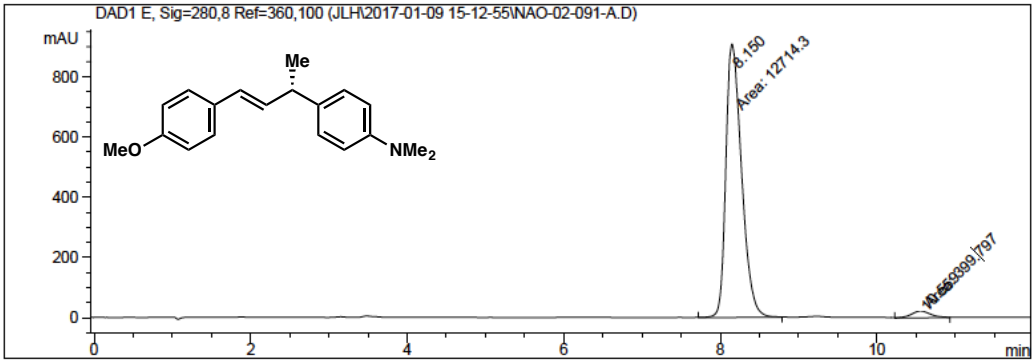

Peak #	RetTime [min]	Type	Width [min]	Area [mAU*s]	Height [mAU]	Area %
1	8.150	MM	0.2330	1.27143e4	909.57269	96.9514
2	10.559	MM	0.2917	399.79657	22.84231	3.0486

141f (Figure 3.4): racemic

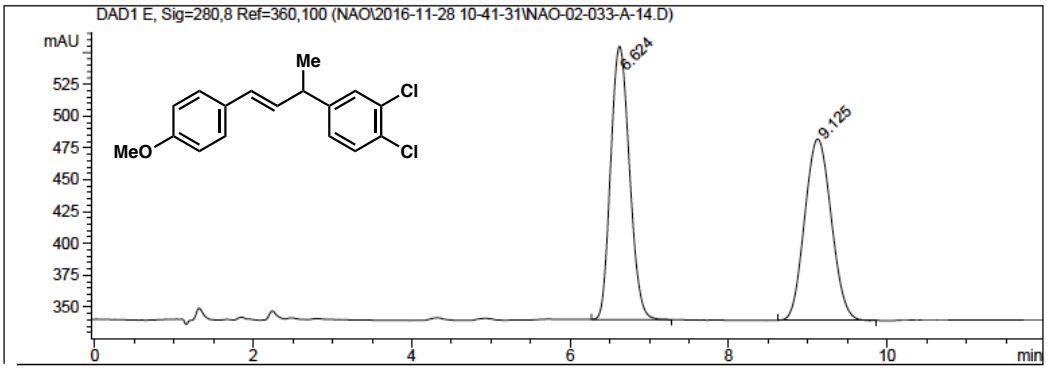

Peak #	RetTime [min]	Type	Width [min]	Area [mAU*s]	Height [mAU]	Area %
1	6.624	BB	0.2651	3551.33887	214.60269	51.6981
2	9.125	BB	0.3717	3318.03833	142.47495	48.3019

141f (Figure 3.4): enantioenriched, 82% ee

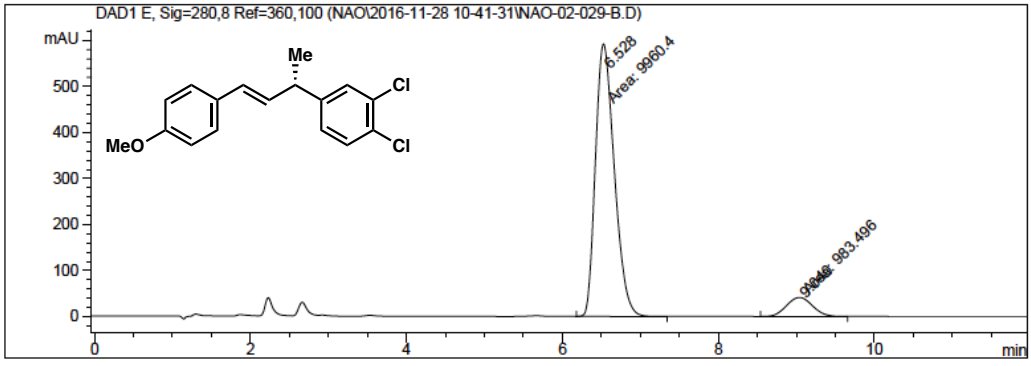

Peak #	RetTime [min]	Type	Width [min]	Area [mAU*s]	Height [mAU]	Area %
1	6.528	MM	0.2800	9960.39941	592.94763	91.0133
2	9.040	MM	0.3921	983.49628	41.80441	8.9867

141g (Figure 3.4): racemic

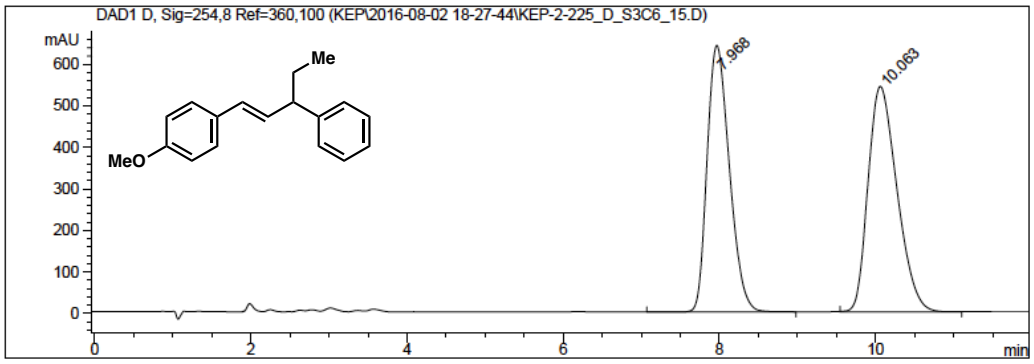

Peak #	RetTime [min]	Type	Width [min]	Area [mAU*s]	Height [mAU]	Area %
1	7.968	VB	0.3120	1.27647e4	642.02454	47.6750
2	10.063	BB	0.4049	1.40097e4	543.13721	52.3250

141g (Figure 3.4): enantioenriched, 97% ee

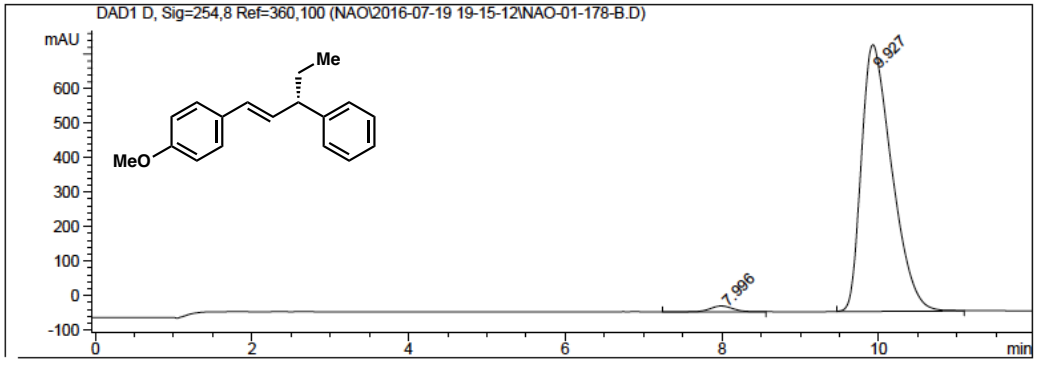

Peak #	RetTime [min]	Type	Width [min]	Area [mAU*s]	Height [mAU]	Area %
1	7.996	VB	0.3205	362.21658	17.28073	1.7024
2	9.927	BB	0.4153	2.09143e4	773.92688	98.2976

141h (Figure 3.4): racemic

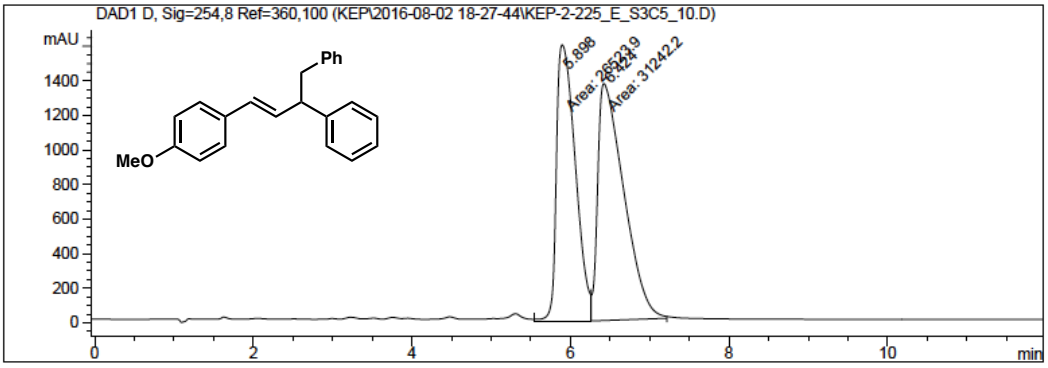

Peak #	RetTime [min]	Type	Width [min]	Area [mAU*s]	Height [mAU]	Area %
1	5.898	MM	0.2764	2.65239e4	1599.41284	45.9160
2	6.424	MM	0.3797	3.12422e4	1371.19714	54.0840

141h (Figure 3.4): enantioenriched, 95% ee

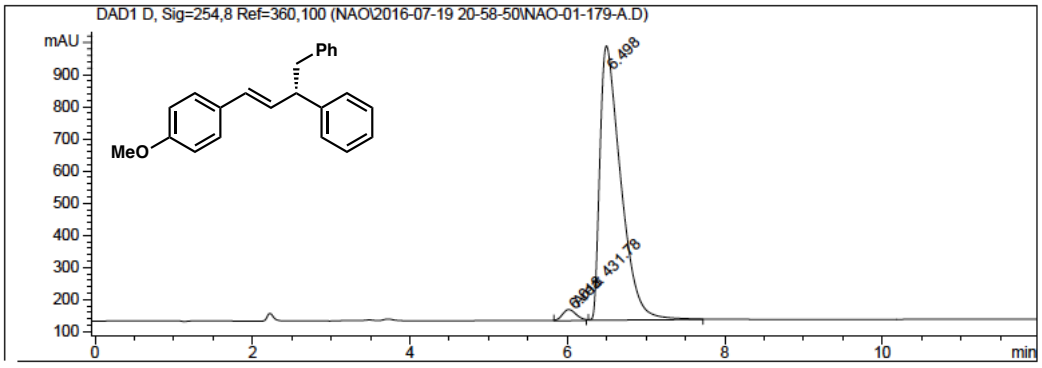

Peak #	RetTime [min]	Type	Width [min]	Area [mAU*s]	Height [mAU]	Area %
1	6.018	MM	0.2059	431.78006	34.94782	2.6714
2	6.498	VB	0.2791	1.57314e4	853.40881	97.3286

141i (Figure 3.4): racemic

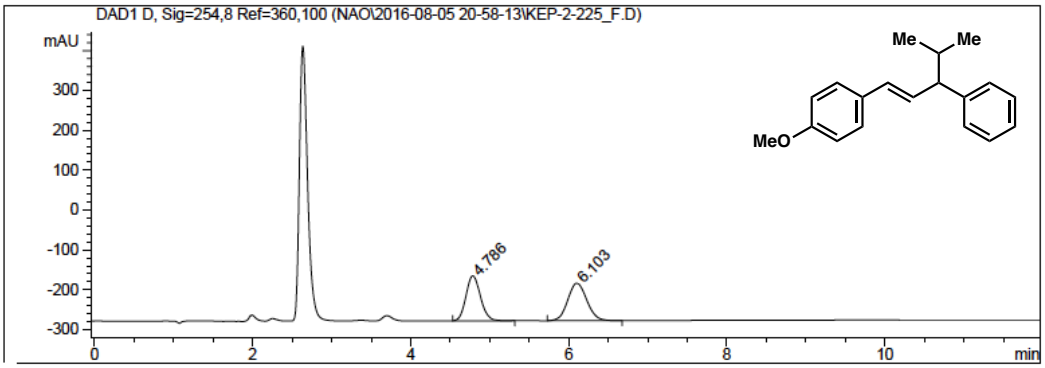

Peak #	RetTime [min]	Type	Width [min]	Area [mAU*s]	Height [mAU]	Area %
1	4.786	BB	0.2004	1430.79492	112.47615	47.8299
2	6.103	BB	0.2619	1560.63074	93.89527	52.1701

141i (Figure 3.4): enantioenriched, 97% ee

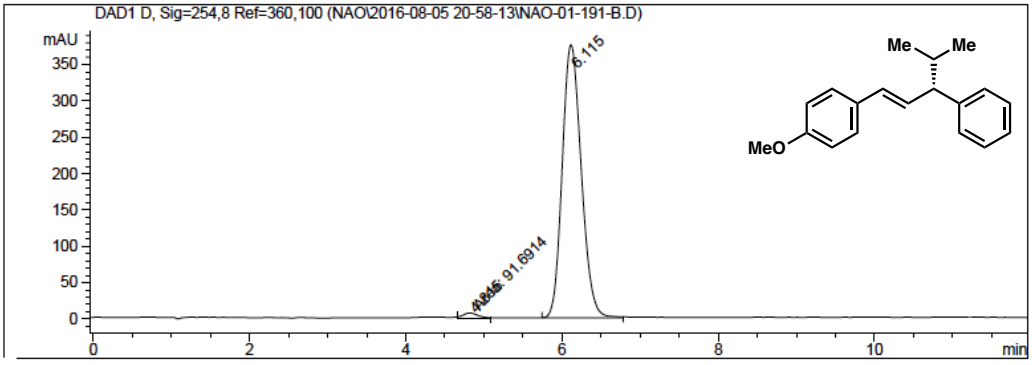

Peak #	RetTime [min]	Type	Width [min]	Area [mAU*s]	Height [mAU]	Area %
1	4.815	MM	0.2214	91.69138	6.90323	1.4194
2	6.115	BB	0.2659	6368.25781	375.46719	98.5806

141j (Figure 3.4): racemic

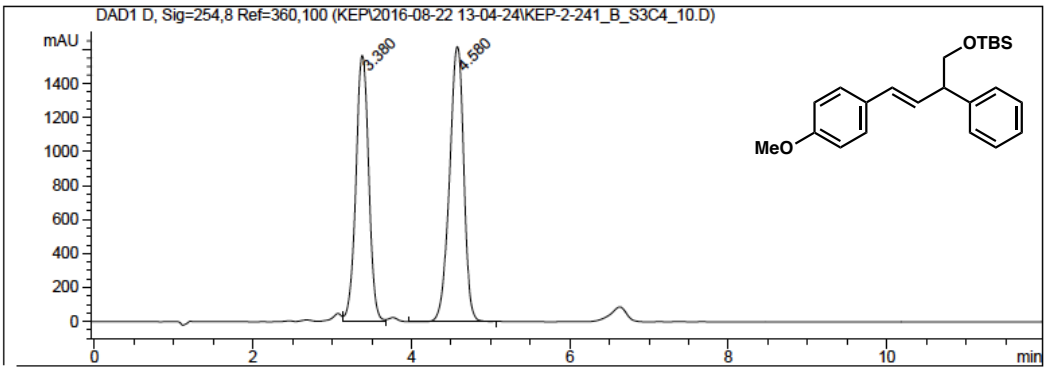

Peak #	RetTime [min]	Type	Width [min]	Area [mAU*s]	Height [mAU]	Area %
1	3.380	VV	0.1763	1.77440e4	1565.27930	46.6268
2	4.580	VB	0.1945	2.03113e4	1617.50305	53.3732

141j (Figure 3.4): enantioenriched, 98% ee

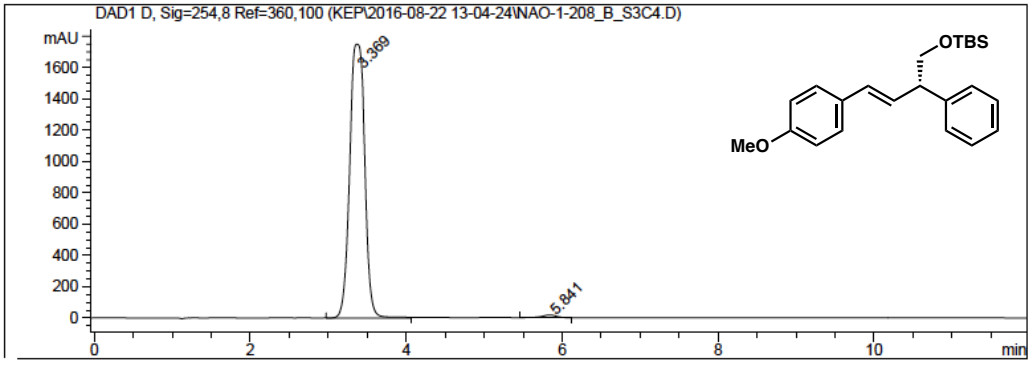

Peak #	RetTime [min]	Type	Width [min]	Area [mAU*s]	Height [mAU]	Area %
1	3.369	VV	0.2126	2.34730e4	1748.39075	98.8511
2	5.841	BV	0.2029	272.82288	19.07364	1.1489

141k (Figure 3.4): racemic

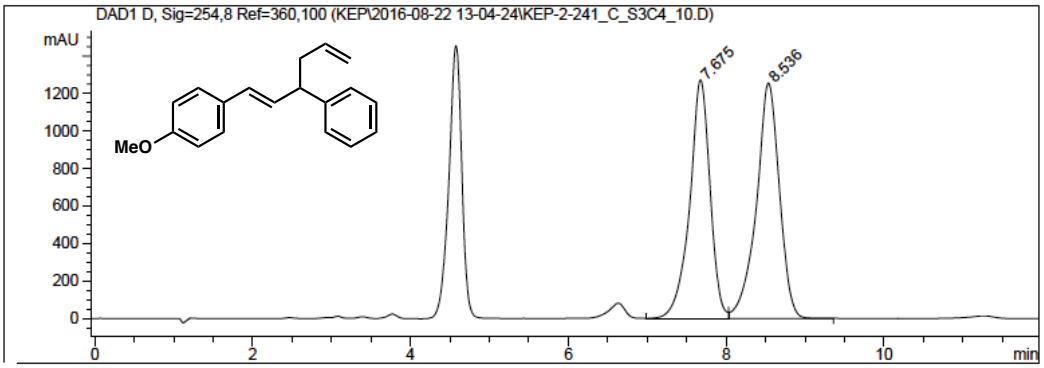

Peak #	RetTime [min]	Type	Width [min]	Area [mAU*s]	Height [mAU]	Area %
1	7.675	VV	0.2662	2.29359e4	1273.26990	47.2708
2	8.536	VB	0.3014	2.55844e4	1257.12512	52.7292

141k (Figure 3.4): enantioenriched, 96% ee

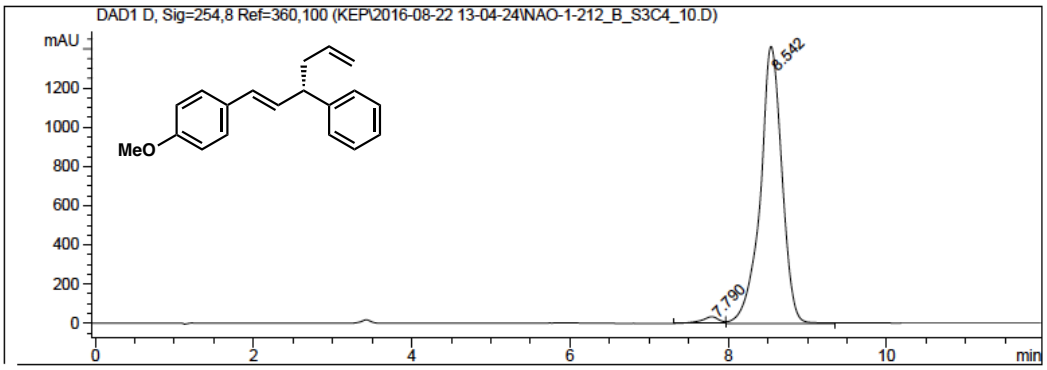

Peak #	RetTime [min]	Type	Width [min]	Area [mAU*s]	Height [mAU]	Area %
1	7.790	BV	0.2268	537.98590	34.33280	1.9596
2	8.542	VB	0.2824	2.69158e4	1411.98352	98.0404

141l (Figure 3.4): racemic

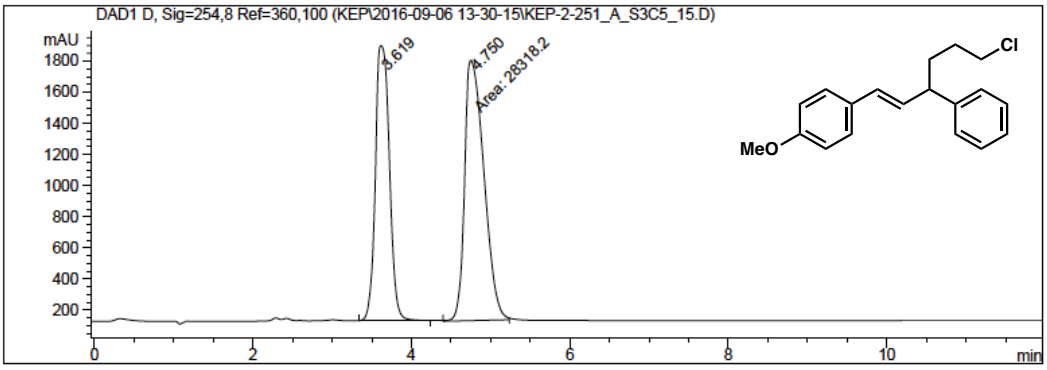

Peak #	RetTime [min]	Type	Width [min]	Area [mAU*s]	Height [mAU]	Area %
1	3.619	BV	0.1967	2.19414e4	1769.60486	43.6562
2	4.750	MM	0.2819	2.83182e4	1673.98267	56.3438

141l (Figure 3.4): enantioenriched, 93% ee

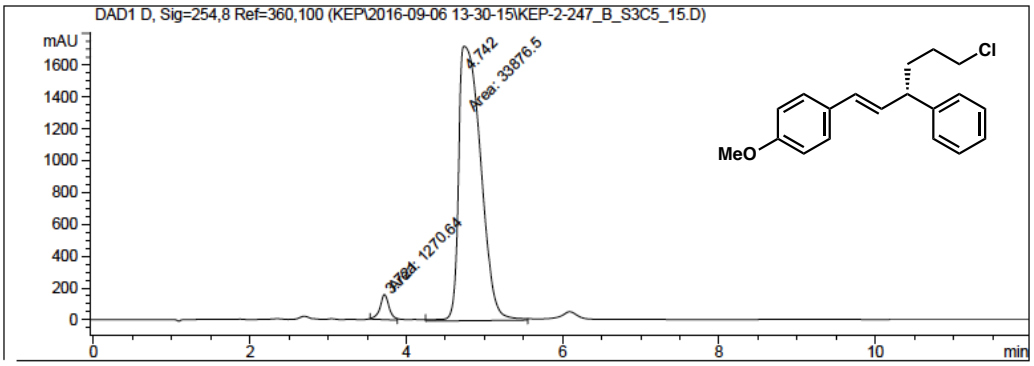

Peak #	RetTime [min]	Type	Width [min]	Area [mAU*s]	Height [mAU]	Area %
1	3.721	MM	0.1339	1270.64075	158.21689	3.6152
2	4.742	MM	0.3274	3.38765e4	1724.49841	96.3848

146 (Scheme 3.2): racemic

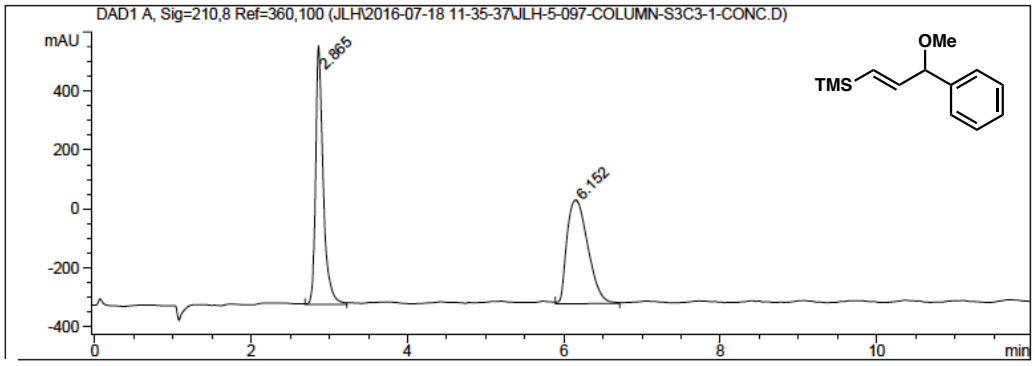

Peak #	RetTime [min]	Type	Width [min]	Area [mAU*s]	Height [mAU]	Area %
1	2.865	VV	0.1036	5942.20703	870.57599	47.5931
2	6.152	VV	0.2969	6543.22803	351.95050	52.4069

146 (Scheme 3.2): enantioenriched, 91% ee

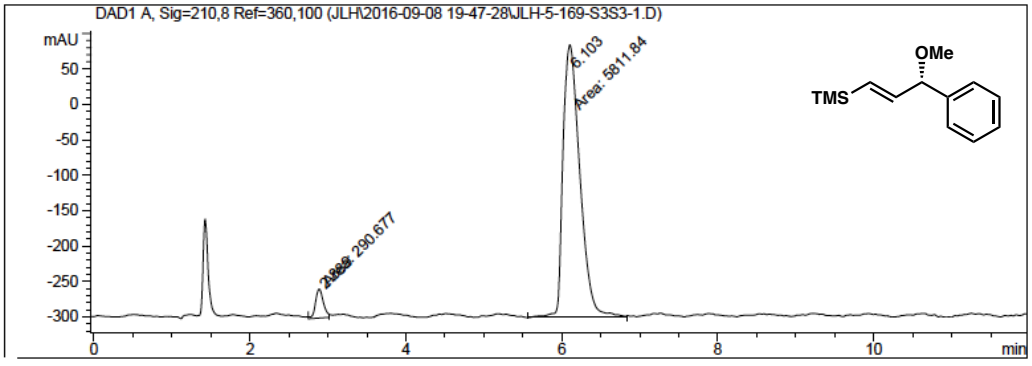

Peak #	RetTime [min]	Type	Width [min]	Area [mAU*s]	Height [mAU]	Area %
1	2.889	MM	0.1180	290.67731	41.05857	4.7632
2	6.103	MM	0.2515	5811.83789	385.08493	95.2368

3.7 REFERENCES

(1) Jana, R.; Pathak, T. P.; Sigman, M. S. *Chem. Rev.* **2011**, *111*, 1417.

(2) Hu, X. *Chem. Sci.* **2011**, *2*, 1867.

(3) Tasker, S. Z.; Standley, E. A.; Jamison, T. F. *Nature* **2014**, *509*, 299.

(4) Ananikov, V. P. *ACS Catal.* **2015**, *5*, 1964.

(5) Netherton, M. R.; Fu, G. C. *Adv. Synth. Catal.* **2004**, *346*, 1525.

(6) Park, K.; Yuan, K.; Scott, W. J. *J. Org. Chem.* **1993**, *58*, 4866.

(7) Devasagayaraj, A.; Stüdemann, T.; Knochel, P. *Angew. Chem. Int. Ed.* **1996**, *34*, 2723.

(8) Giovannini, R.; Stüdemann, T.; Dussin, G.; Knochel, P. *Angew. Chem. Int. Ed.* **1998**, *37*, 2387.

(9) Giovannini, R.; Knochel, P. *J. Am. Chem. Soc.* **1998**, *120*, 11186.

(10) Zhou, J.; Fu, G. C. *J. Am. Chem. Soc.* **2003**, *125*, 14726.

(11) Terao, J.; Todo, H.; Watanabe, H.; Ikumi, A.; Kambe, N. *Angew. Chem. Int. Ed.* **2004**, *43*, 6180.

(12) Fischer, C.; Fu, G. C. *J. Am. Chem. Soc.* **2005**, *127*, 4594.

(13) Arp, F. O.; Fu, G. C. *J. Am. Chem. Soc.* **2005**, *127*, 10482.

(14) Terao, J.; Watanabe, H.; Ikumi, A.; Kuniyasu, H.; Kambe, N. *J. Am. Chem. Soc.* **2002**, *124*, 4222.

(15) Terao, J.; Ikumi, A.; Kuniyasu, H.; Kambe, N. *J. Am. Chem. Soc.* **2003**, *125*, 5646.

(16) Vechorkin, O.; Hu, X. *Angew. Chem. Int. Ed.* **2009**, *48*, 2937.

(17) Vechorkin, O.; Proust, V.; Hu, X. *J. Am. Chem. Soc.* **2009**, *131*, 9756.

(18) Lou, S.; Fu, G. C. *J. Am. Chem. Soc.* **2010**, *132*, 1264.

(19) Zhou, J.; Fu, G. C. *J. Am. Chem. Soc.* **2004**, *126*, 1340.

(20) González-Bobes, F.; Fu, G. C. *J. Am. Chem. Soc.* **2006**, *128*, 5360.

(21) Saito, B.; Fu, G. C. *J. Am. Chem. Soc.* **2007**, *129*, 9602.

(22) Saito, B.; Fu, G. C. *J. Am. Chem. Soc.* **2008**, *130*, 6694.

(23) Lundin, P. M.; Fu, G. C. *J. Am. Chem. Soc.* **2010**, *132*, 11027.

(24) Durandetti, M.; Gosmini, C.; Périchon, J. *Tetrahedron* **2007**, *63*, 1146.

(25) Everson, D. A.; Shrestha, R.; Weix, D. J. *J. Am. Chem. Soc.* **2010**, *132*, 920.

(26) Yu, X.; Yang, T.; Wang, S.; Xu, H.; Gong, H. *Org. Lett.* **2011**, *13*, 2138.

(27) Everson, D. A.; Weix, D. J. *J. Org. Chem.* **2014**, *79*, 4793.

(28) Knappke, C. E. I.; Grupe, S.; Gärtner, D.; Corpet, M.; Gosmini, C.; Jacobi von Wangelin, A. *Chem. Eur. J.* **2014**, *20*, 6828.

(29) Moragas, T.; Correa, A.; Martin, R. *Chem. Eur. J.* **2014**, *20*, 8242.

(30) Weix, D. J. *Acc. Chem. Res.* **2015**, *48*, 1767.

(31) Gu, J.; Wang, X.; Xue, W.; Gong, H. *Org. Chem. Front.* **2015**, *2*, 1411.

(32) Wang, X.; Dai, Y.; Gong, H. *Top. Curr. Chem.* **2016**, *374*, 43.

(33) Tellis, J. C.; Primer, D. N.; Molander, G. A. *Science* **2014**, *345*, 433.

(34) Zuo, Z.; Ahneman, D. T.; Chu, L.; Terrett, J. A.; Doyle, A. G.; MacMillan, D. W. C. *Science* **2014**, *345*, 437.

(35) Noble, A.; McCarver, S. J.; MacMillan, D. W. C. *J. Am. Chem. Soc.* **2015**, *137*, 624.

(36) Primer, D. N.; Karakaya, I.; Tellis, J. C.; Molander, G. A. *J. Am. Chem. Soc.* **2015**, *137*, 2195.

(37) Jouffroy, M.; Primer, D. N.; Molander, G. A. *J. Am. Chem. Soc.* **2016**, *138*, 475.

(38) Joe, C. L.; Doyle, A. G. *Angew. Chem. Int. Ed.* **2016**, *55*, 4040.

(39) Zuo, Z.; Cong, H.; Li, W.; Choi, J.; Fu, G. C.; MacMillan, D. W. C. *J. Am. Chem. Soc.* **2016**, *138*, 1832.

(40) Cavalcanti, L. N.; Molander, G. A. *Top. Curr. Chem.* **2016**, *374*, 39.

(41) Swift, E. C.; Jarvo, E. R. *Tetrahedron* **2013**, *69*, 5799.

(42) Cherney, A. H.; Kadunce, N. T.; Reisman, S. E. *Chem. Rev.* **2015**, *115*, 9587.

(43) Cherney, A. H.; Kadunce, N. T.; Reisman, S. E. *J. Am. Chem. Soc.* **2013**, *135*, 7442.

(44) Cherney, A. H.; Reisman, S. E. *J. Am. Chem. Soc.* **2014**, *136*, 14365.

(45) Hofstra, J. L.; Cherney, A. H.; Ordner, C. M.; Reisman, S. E. *J. Am. Chem. Soc.* **2018**, *140*, 139.

(46) Kadunce, N. T.; Reisman, S. E. *J. Am. Chem. Soc.* **2015**, *137*, 10480.

(47) Okada, Keiji.; Okamoto, Kazushige.; Oda, Masaji. *J. Am. Chem. Soc.* **1988**, *110*, 8736.

(48) Okada, K.; Okamoto, K.; Morita, N.; Okubo, K.; Oda, M. *J. Am. Chem. Soc.* **1991**, *113*, 9401.

(49) Konev, M. O.; Jarvo, E. R. *Angew. Chem. Int. Ed.* **2016**, *55*, 11340.

(50) Murarka, S. *Adv. Synth. Catal.* **2018**, *360*, 1735.

(51) Qin, T.; Cornella, J.; Li, C.; Malins, L. R.; Edwards, J. T.; Kawamura, S.; Maxwell, B. D.; Eastgate, M. D.; Baran, P. S. *Science* **2016**, *352*, 801.

(52) Cornella, J.; Edwards, J. T.; Qin, T.; Kawamura, S.; Wang, J.; Pan, C.-M.; Gianatassio, R.; Schmidt, M.; Eastgate, M. D.; Baran, P. S. *J. Am. Chem. Soc.* **2016**, *138*, 2174.

(53) Edwards, J. T.; Merchant, R. R.; McClymont, K. S.; Knouse, K. W.; Qin, T.; Malins, L. R.; Vokits, B.; Shaw, S. A.; Bao, D.-H.; Wei, F.-L.; Zhou, T.; Eastgate, M. D.; Baran, P. S. *Nature* **2017**, *545*, 213.

(54) Smith, J. M.; Qin, T.; Merchant, R. R.; Edwards, J. T.; Malins, L. R.; Liu, Z.; Che, G.; Shen, Z.; Shaw, S. A.; Eastgate, M. D.; Baran, P. S. *Angew. Chem. Int. Ed.* **2017**, *56*, 11906.

(55) Sandfort, F.; O'Neill, M. J.; Cornella, J.; Wimmer, L.; Baran, P. S. *Angew. Chem. Int. Ed.* **2017**, *56*, 3319.

(56) Chen, T.-G.; Zhang, H.; Mykhailiuk, P. K.; Merchant, R. R.; Smith, C. A.; Qin, T.; Baran, P. S. *Angew. Chem. Int. Ed.* **2019**, *58*, 2454.

(57) deGruyter, J. N.; Malins, L. R.; Wimmer, L.; Clay, K. J.; Lopez-Ogalla, J.; Qin, T.; Cornella, J.; Liu, Z.; Che, G.; Bao, D.; Stevens, J. M.; Qiao, J. X.; Allen, M. P.; Poss, M. A.; Baran, P. S. *Org. Lett.* **2017**, *19*, 6196.

(58) Wang, J.; Qin, T.; Chen, T.-G.; Wimmer, L.; Edwards, J. T.; Cornella, J.; Vokits, B.; Shaw, S. A.; Baran, P. S. *Angew. Chem. Int. Ed.* **2016**, *55*, 9676.

(59) Huihui, K. M. M.; Caputo, J. A.; Melchor, Z.; Olivares, A. M.; Spiewak, A. M.; Johnson, K. A.; DiBenedetto, T. A.; Kim, S.; Ackerman, L. K. G.; Weix, D. J. *J. Am. Chem. Soc.* **2016**, *138*, 5016.

(60) Li, H.; Breen, C. P.; Seo, H.; Jamison, T. F.; Fang, Y.-Q.; Bio, M. M. *Org. Lett.* **2018**, *20*, 1338.

(61) Huang, L.; Olivares, A. M.; Weix, D. J. *Angew. Chem. Int. Ed.* **2017**, *56*, 11901.

(62) Koyanagi, T.; Herath, A.; Chong, A.; Ratnikov, M.; Valiere, A.; Chang, J.; Molteni, V.; Loren, J. *Org. Lett.* **2019**, *21*, 816.

(63) Qin, T.; Malins, L. R.; Edwards, J. T.; Merchant, R. R.; Novak, A. J. E.; Zhong, J. Z.; Mills, R. B.; Yan, M.; Yuan, C.; Eastgate, M. D.; Baran, P. S. *Angew. Chem. Int. Ed.* **2017**, *56*, 260.

(64) Ni, S.; Garrido-Castro, A. F.; Merchant, R. R.; de Gruyter, J. N.; Schmitt, D. C.; Mousseau, J. J.; Gallego, G. M.; Yang, S.; Collins, M. R.; Qiao, J. X.; Yeung, K.-S.; Langley, D. R.; Poss, M. A.; Scola, P. M.; Qin, T.; Baran, P. S. *Angew. Chem. Int. Ed.* **2018**, *57*, 14560.

(65) Lu, X.; Xiao, B.; Liu, L.; Fu, Y. *Chem. Eur. J.* **2016**, *22*, 11161.

(66) Li, C.; Wang, J.; Barton, L. M.; Yu, S.; Tian, M.; Peters, D. S.; Kumar, M.; Yu, A. W.; Johnson, K. A.; Chatterjee, A. K.; Yan, M.; Baran, P. S. *Science* **2017**, *356*, 7355.

(67) Everson, D. A.; Jones, B. A.; Weix, D. J. *J. Am. Chem. Soc.* **2012**, *134*, 6146.

(68) Johnson, K. A.; Biswas, S.; Weix, D. J. *Chem. Eur. J.* **2016**, *22*, 7399.

(69) Poremba, K. E.; Kadunce, N. T.; Suzuki, N.; Cherney, A. H.; Reisman, S. E. *J. Am. Chem. Soc.* **2017**, *139*, 5684.

(70) Biswas, S.; Weix, D. J. *J. Am. Chem. Soc.* **2013**, *135*, 16192.

(71) Broggi, J.; Terme, T.; Vanelle, P. *Angew. Chem. Int. Ed.* **2014**, *53*, 384.

(72) Anka-Lufford, L. L.; Huihui, K. M. M.; Gower, N. J.; Ackerman, L. K. G.; Weix, D. J. *Chem. Eur. J.* **2016**, *22*, 11564.

(73) Takagi, K.; Hayama, N.; Inokawa, S. *Chem. Lett.* **1978**, 1435.

(74) Tsou, T. T.; Kochi, J. K. *J. Org. Chem.* **1980**, *45*, 1930.

(75) Hofstra, J. L.; Cherney, A. H.; Ordner, C. M.; Reisman, S. E. *J. Am. Chem. Soc.* **2018**, *140*, 139.

(76) Beckwith, A. L. J.; Bowry, V. W. *J. Am. Chem. Soc.* **1994**, *116*, 2710.

(77) Halgren, T. A.; Roberts, J. D.; Horner, J. H.; Martinez, F. N.; Tronche, C.; Newcomb, M. *J. Am. Chem. Soc.* **2000**, *122*, 2988.

(78) Gutierrez, O.; Tellis, J. C.; Primer, D. N.; Molander, G. A.; Kozlowski, M. C. *J. Am. Chem. Soc.* **2015**, *137*, 4896.

(79) Still, W. C.; Kahn, M.; Mitra, A. *J. Org. Chem.* **1978**, *43*, 2923.

(80) Evans, D. A.; Downey, C. W.; Hubbs, J. L. *J. Am. Chem. Soc.* **2003**, *125*, 8706.

(81) Bestmann, H. J.; Schmid, G.; Oechsner, H.; Ermann, P. *Chem. Ber.* **1984**, *117*, 1561.

(82) Wasserman, H. H.; Ives, J. L. *J. Org. Chem.* **1985**, *50*, 3573.

(83) Mahesh, M.; Murphy, J. A.; LeStrat, F.; Wessel, H. P. *Beilstein J. Org. Chem.* **2009**, *5*, 1.

(84) Müller, D.; Alexakis, A. *Org. Lett.* **2012**, *14*, 1842.

(85) Qian, M.; Huang, Z.; Negishi, E. *Org. Lett.* **2004**, *6*, 1531.

(86) Kuang, C.; Senboku, H.; Tokuda, M. *Tetrahedron* **2005**, *61*, 637.

(87) Li, D.-R.; Zhang, D.-H.; Sun, C.-Y.; Zhang, J.-W.; Yang, L.; Chen, J.; Liu, B.; Su, C.; Zhou, W.-S.; Lin, G.-Q. *Chem. Eur. J.* **2006**, *12*, 1185.

(88) Brown, H. C.; Larock, R. C.; Gupta, S. K.; Rajagopalan, S.; Bhat, N. G. *J. Org. Chem.* **1989**, *54*, 6079.

(89) Ney, J. E.; Hay, M. B.; Yang, Q.; Wolfe, J. P. *Adv. Synth. Catal.* **2005**, *347*, 1614.

(90) Wu, H.-B.; Ma, X.-T.; Tian, S.-K. *Chem. Commun.* **2014**, *50*, 219.

(91) Ye, J.; Zhao, J.; Xu, J.; Mao, Y.; Zhang, Y. J. *Chem. Commun.* **2013**, *49*, 9761.

(92) Srinivas, H. D.; Zhou, Q.; Watson, M. P. *Org. Lett.* **2014**, *16*, 3596.

Appendix 3

Spectra Relevant to Chapter 3:

Decarboxylative Asymmetric Ni-Catalyzed Cross-Coupling of Benzylic N-Hydroxyphthalimide Esters and Alkenyl Bromides

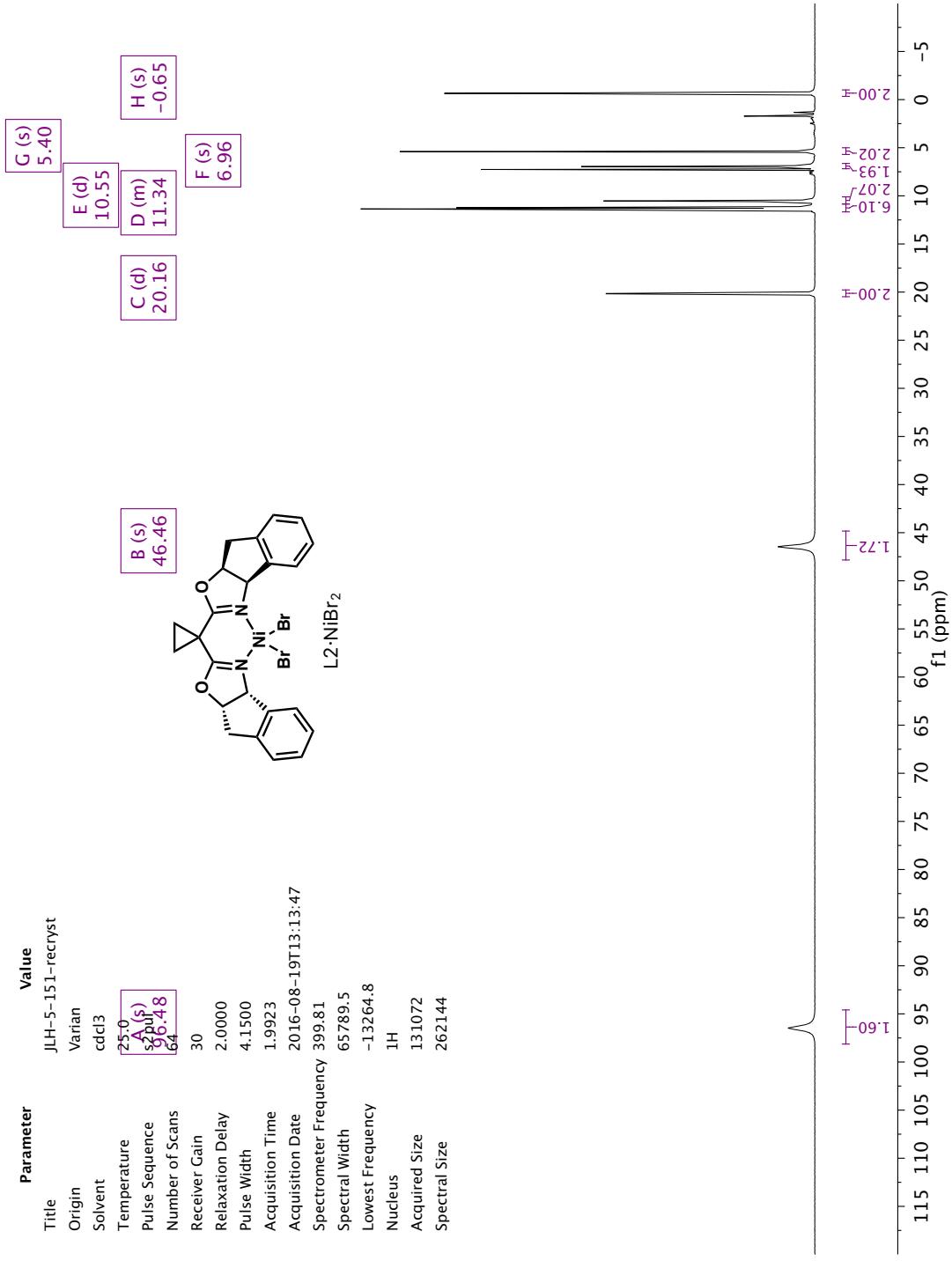
A (s) 96.48
B (s) 46.46
C (d) 20.16
D (m) 11.34
E (d) 10.55
F (s) 6.96
G (s) 5.40
H (s) -0.65
L2·NiBr2
Parameter Value
Title JLH-5-151-recryst
Origin Varian
Solvent cdcl3
Temperature 25.0
Pulse Sequence s2pul
Number of Scans 64
Receiver Gain 30
Relaxation Delay 2.0000
Pulse Width 4.1500
Acquisition Time 1.9923
Acquisition Date 2016-08-19T13:13:47
Spectrometer Frequency 399.81
Spectral Width 65789.5
Lowest Frequency -13264.8
Nucleus 1H
Acquired Size 131072
Spectral Size 262144
1.60
1.72
2.00
6.10
2.07
1.93
2.02
2.00
f1 (ppm)

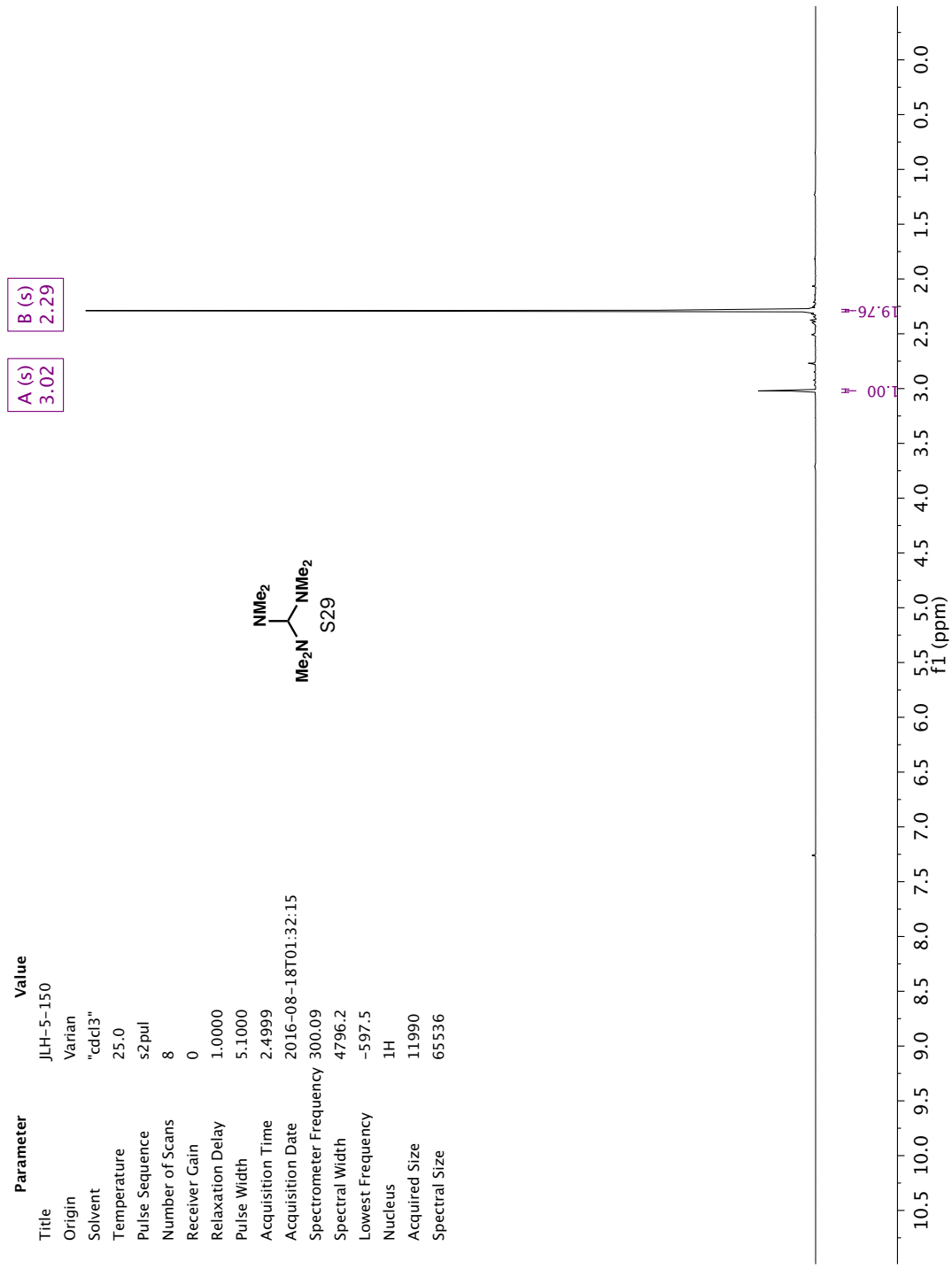

Parameter	Value
Title	JLH-5-150
Origin	Varian
Solvent	"cdcl3"
Temperature	25.0
Pulse Sequence	s2pul
Number of Scans	8
Receiver Gain	0
Relaxation Delay	1.0000
Pulse Width	5.1000
Acquisition Time	2.4999
Acquisition Date	2016-08-18T01:32:15
Spectrometer Frequency	300.09
Spectral Width	4796.2
Lowest Frequency	-597.5
Nucleus	1H
Acquired Size	11990
Spectral Size	65536

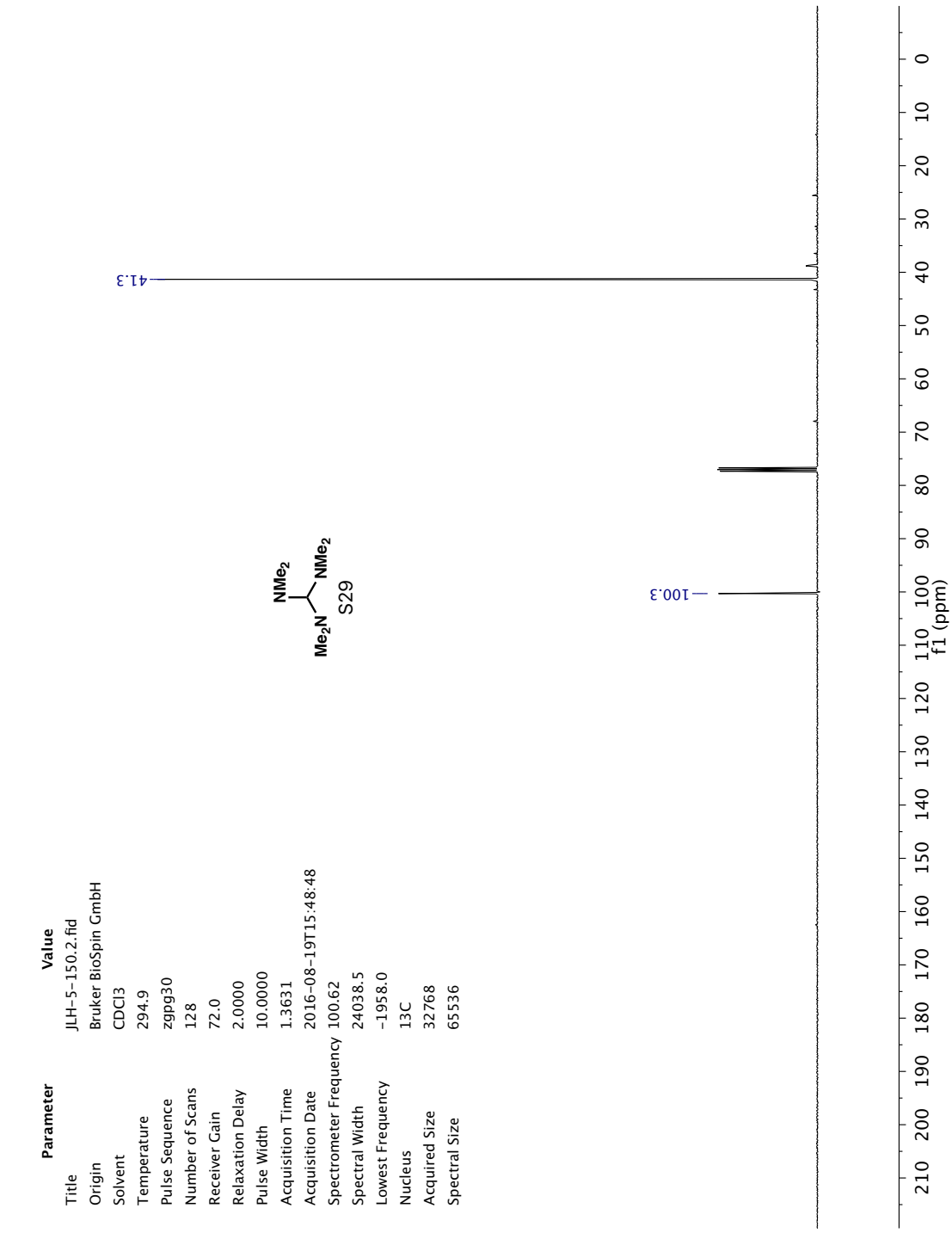
Parameter Value
Title JLH-5-150.2.fid
Origin Bruker BioSpin GmbH
Solvent CDCl3
Temperature 294.9
Pulse Sequence zgpg30
Number of Scans 128
Receiver Gain 72.0
Relaxation Delay 2.0000
Pulse Width 10.0000
Acquisition Time 1.3631
Acquisition Date 2016-08-19T15:48:48
Spectrometer Frequency 100.62
Spectral Width 24038.5
Lowest Frequency -1958.0
Nucleus 13C
Acquired Size 32768
Spectral Size 65536
41.3
100.3
NMe2
Me2N
NMe2
S29
210 200 190 180 170 160 150 140 130 120 110 100 90 80 70 60 50 40 30 20 10 0
f1 (ppm)

Parameter	Value
Title	JLH-5-168-D2F3
Origin	Varian
Solvent	cdcl3
Temperature	24.0
Pulse Sequence	s2pul
Number of Scans	1
Receiver Gain	20
Relaxation Delay	1.0000
Pulse Width	4.1500
Acquisition Time	20.4472
Acquisition Date	2016-08-30T22:06:00
Spectrometer Frequency	399.80
Spectral Width	6410.3
Lowest Frequency	-808.0
Nucleus	1H
Acquired Size	131072
Spectral Size	262144

TDAE

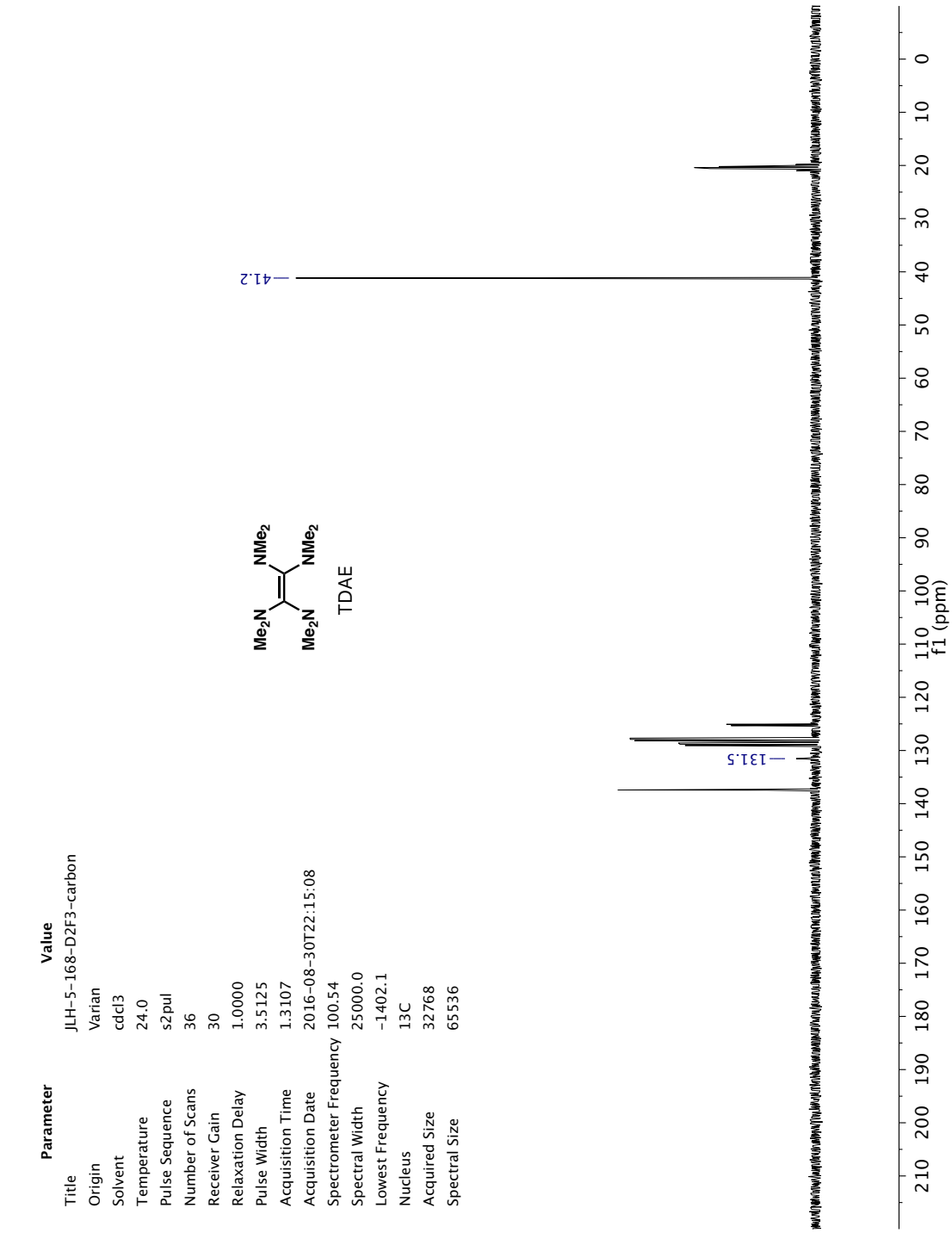
Parameter Value
Title JLH-5-168-D2F3-carbon
Origin Varian
Solvent cdcl3
Temperature 24.0
Pulse Sequence s2pul
Number of Scans 36
Receiver Gain 30
Relaxation Delay 1.0000
Pulse Width 3.5125
Acquisition Time 1.3107
Acquisition Date 2016-08-30T22:15:08
Spectrometer Frequency 100.54
Spectral Width 25000.0
Lowest Frequency -1402.1
Nucleus 13C
Acquired Size 32768
Spectral Size 65536
41.2
131.5
NMe2
Me2N
Me2N
NMe2
TDAE
210 200 190 180 170 160 150 140 130 120 110 100 90 80 70 60 50 40 30 20 10 0
f1 (ppm)

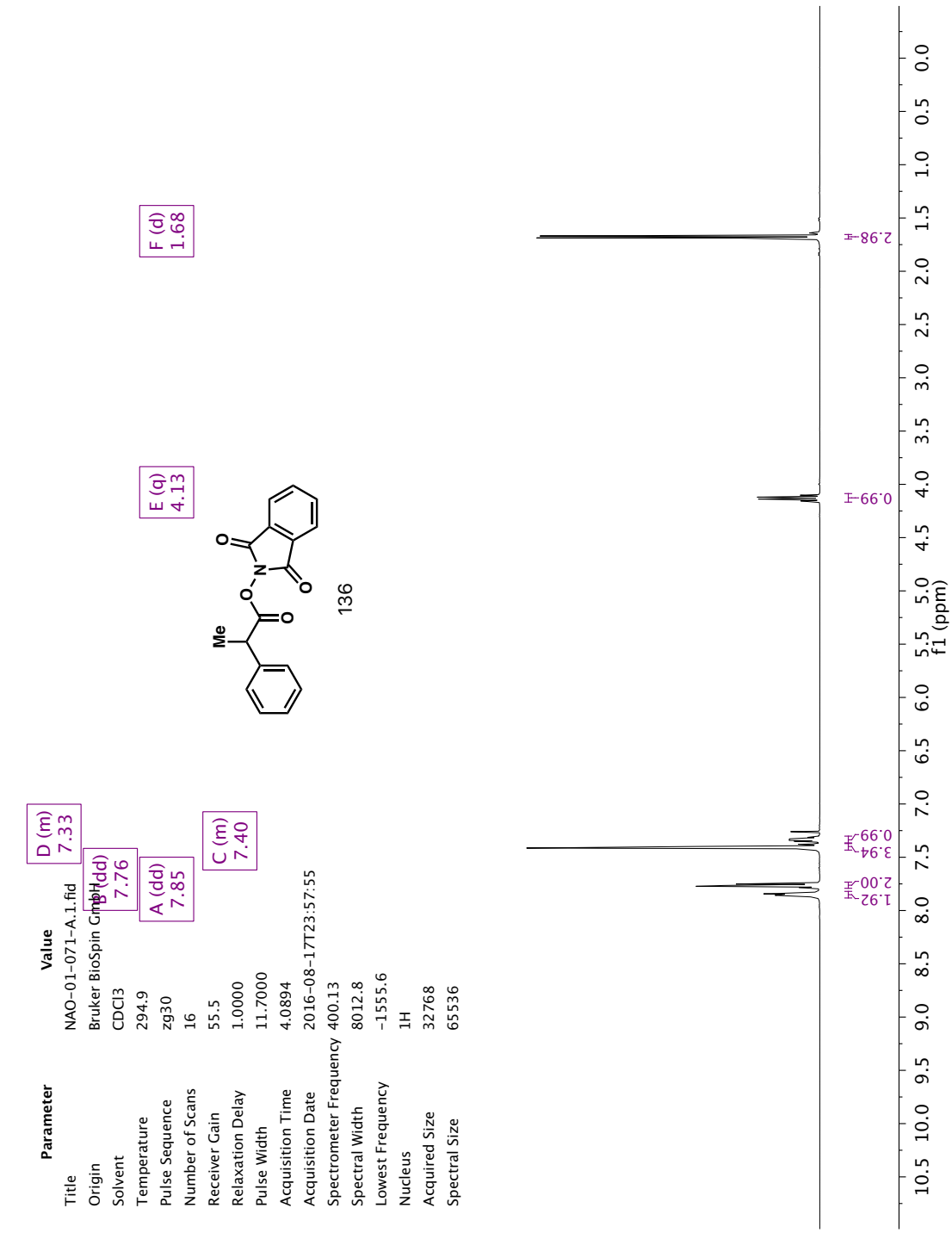
Parameter
Value
Title
NAO-01-071-A.1.fid
Origin
Bruker BioSpin GmbH
Solvent
CDCl3
Temperature
294.9
Pulse Sequence
zg30
Number of Scans
16
Receiver Gain
55.5
Relaxation Delay
1.0000
Pulse Width
11.7000
Acquisition Time
4.0894
Acquisition Date
2016-08-17T23:57:55
Spectrometer Frequency
400.13
Spectral Width
8012.8
Lowest Frequency
-1555.6
Nucleus
1H
Acquired Size
32768
Spectral Size
65536
D (m) 7.33
B (dd) 7.76
A (dd) 7.85
C (m) 7.40
E (q) 4.13
F (d) 1.68
Me
136
1.92
2.00
3.94
0.99
0.99
2.98
f1 (ppm)

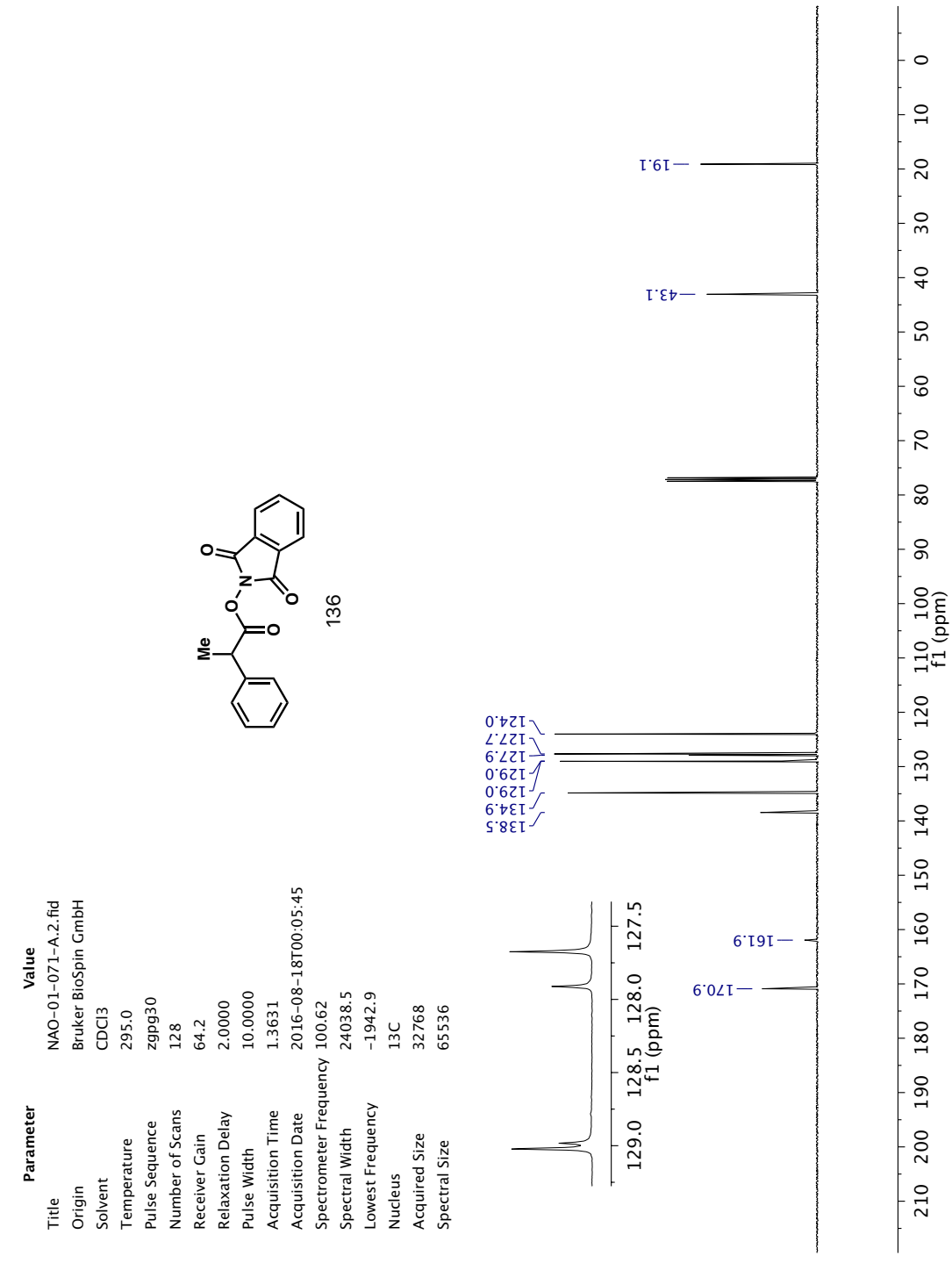
Parameter Value
Title NAO-01-071-A.2.fid
Origin Bruker BioSpin GmbH
Solvent CDCl3
Temperature 295.0
Pulse Sequence zgpg30
Number of Scans 128
Receiver Gain 64.2
Relaxation Delay 2.0000
Pulse Width 10.0000
Acquisition Time 1.3631
Acquisition Date 2016-08-18T00:05:45
Spectrometer Frequency 100.62
Spectral Width 24038.5
Lowest Frequency -1942.9
Nucleus 13C
Acquired Size 32768
Spectral Size 65536
Me
136
138.5
134.9
129.0
129.0
127.9
127.7
124.0
170.9
161.9
43.1
19.1
129.0 128.5 128.0 127.5
f1 (ppm)
210 200 190 180 170 160 150 140 130 120 110 100 90 80 70 60 50 40 30 20 10 0
f1 (ppm)

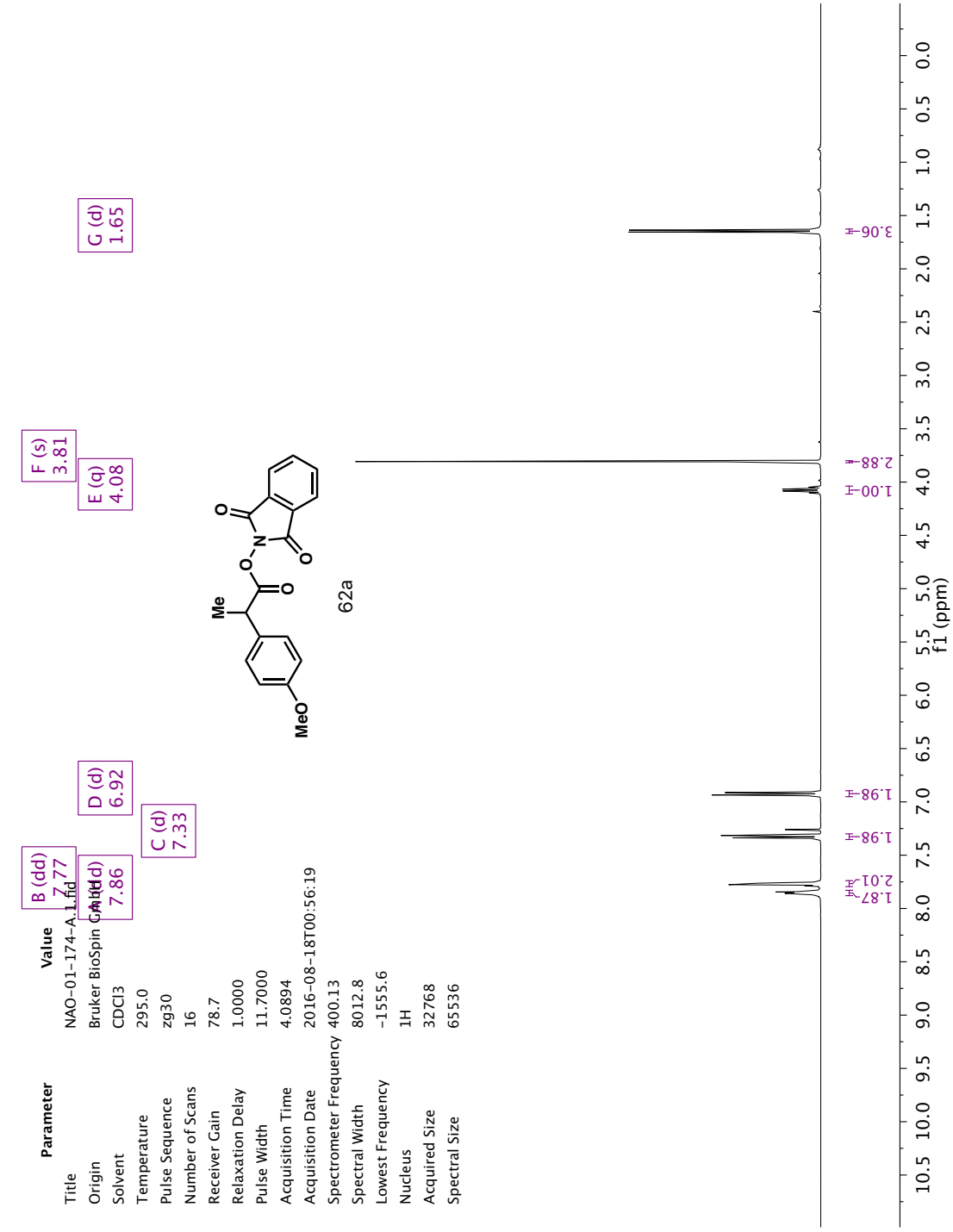
Parameter
Value
Title
NAO-01-174-A.1.fid
Origin
Bruker BioSpin GmbH
Solvent
CDCl3
Temperature
295.0
Pulse Sequence
zg30
Number of Scans
16
Receiver Gain
78.7
Relaxation Delay
1.0000
Pulse Width
11.7000
Acquisition Time
4.0894
Acquisition Date
2016-08-18T00:56:19
Spectrometer Frequency
400.13
Spectral Width
8012.8
Lowest Frequency
-1555.6
Nucleus
1H
Acquired Size
32768
Spectral Size
65536
B (dd) 7.77
A (dd) 7.86
D (d) 6.92
C (d) 7.33
F (s) 3.81
E (q) 4.08
G (d) 1.65
Me
MeO
62a
1.87
2.01
1.98
1.98
1.98
3.06
2.88
1.00
f1 (ppm)

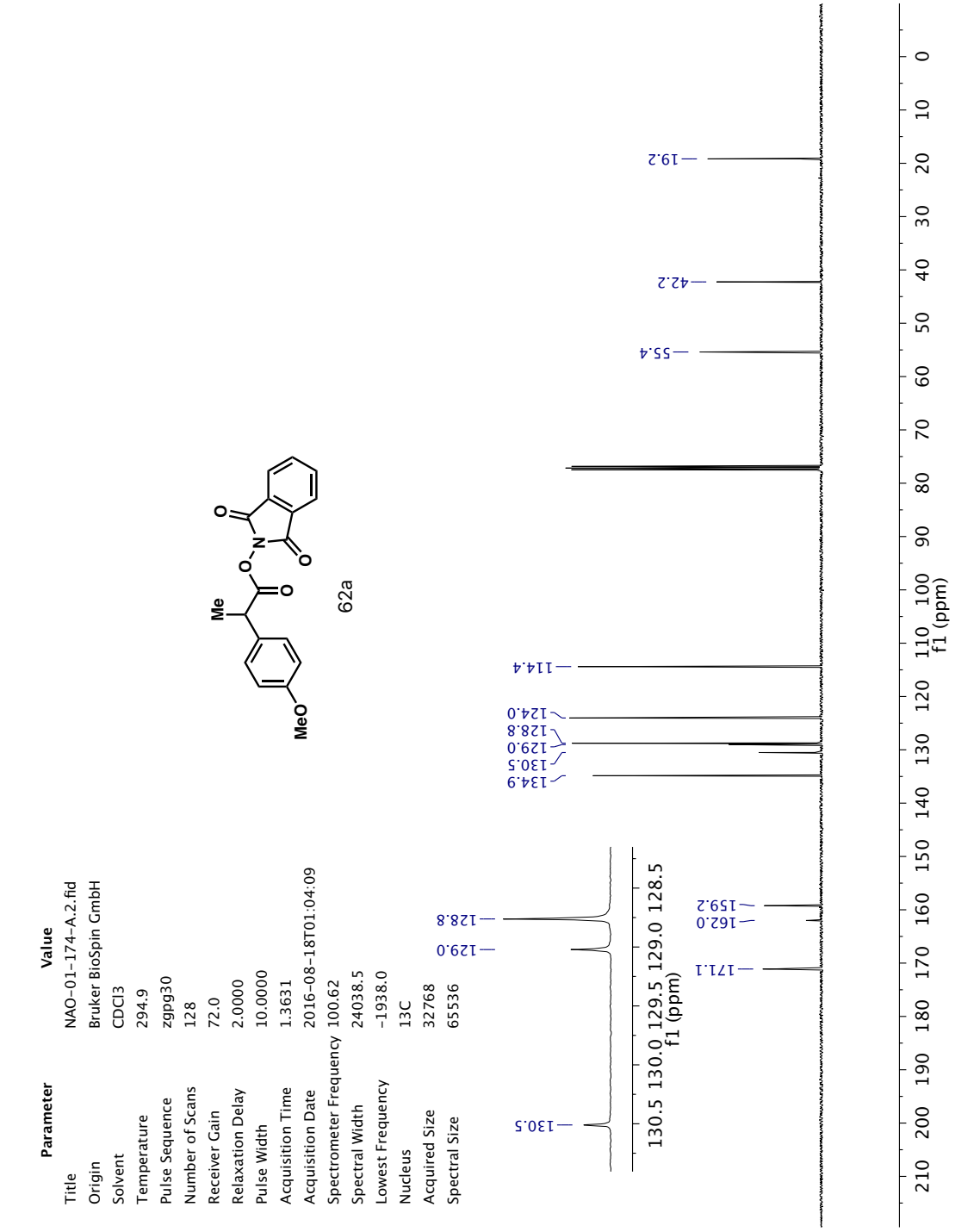
Parameter Value
Title NAO-01-174-A.2.fid
Origin Bruker BioSpin GmbH
Solvent CDCl3
Temperature 294.9
Pulse Sequence zgpg30
Number of Scans 128
Receiver Gain 72.0
Relaxation Delay 2.0000
Pulse Width 10.0000
Acquisition Time 1.3631
Acquisition Date 2016-08-18T01:04:09
Spectrometer Frequency 100.62
Spectral Width 24038.5
Lowest Frequency -1938.0
Nucleus 13C
Acquired Size 32768
Spectral Size 65536
Me
MeO
62a
114.4
124.0
128.8
129.0
130.5
134.9
19.2
42.2
55.4
130.5
129.0
128.8
171.1
162.0
159.2
130.5 130.0 129.5 129.0 128.5
f1 (ppm)
f1 (ppm)

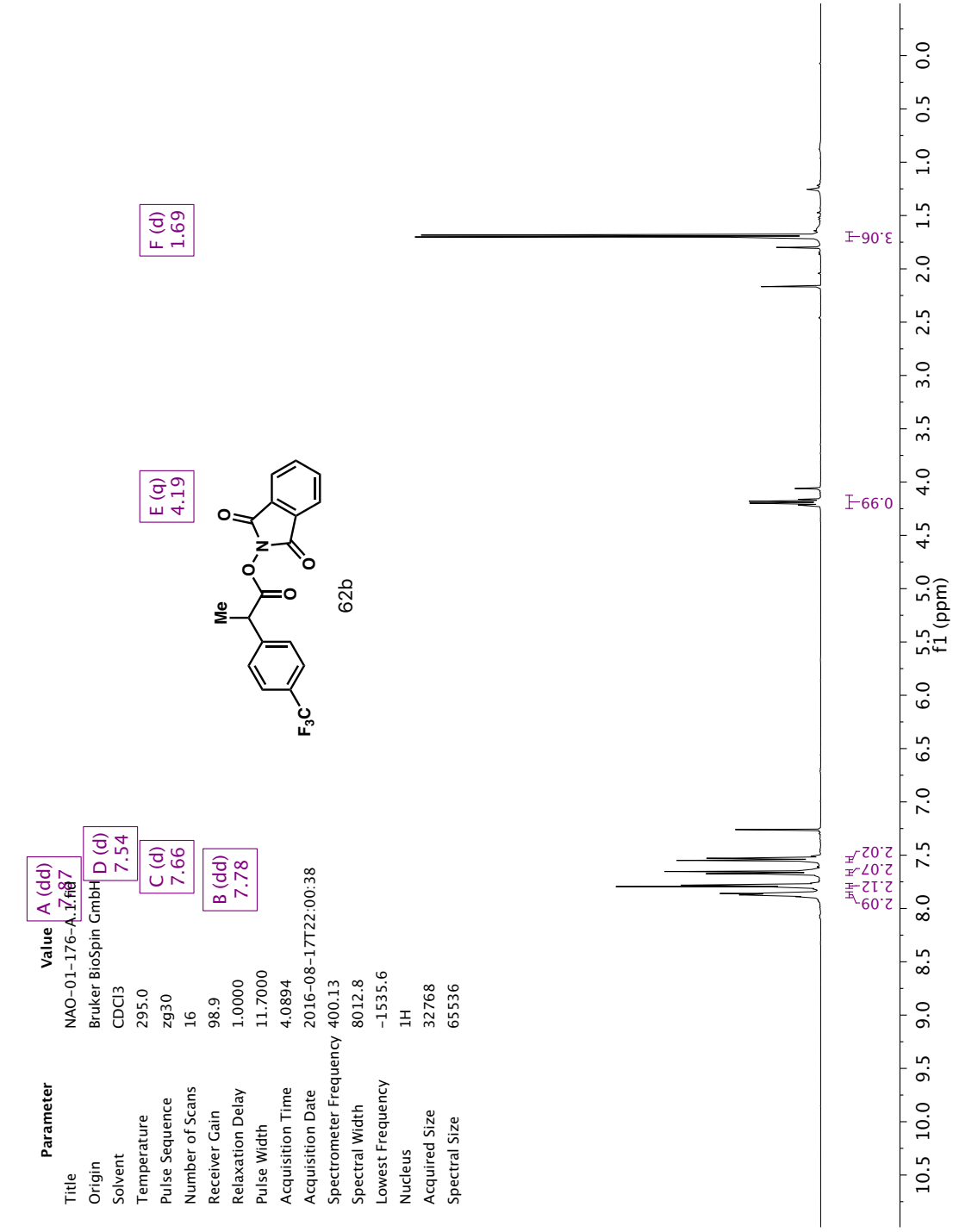
A (dd) 7.87
D (d) 7.54
C (d) 7.66
B (dd) 7.78
E (q) 4.19
F (d) 1.69
Me
F3C
62b
Parameter Value
Title NAO-01-176-A.1.fid
Origin Bruker BioSpin GmbH
Solvent CDCl3
Temperature 295.0
Pulse Sequence zg30
Number of Scans 16
Receiver Gain 98.9
Relaxation Delay 1.0000
Pulse Width 11.7000
Acquisition Time 4.0894
Acquisition Date 2016-08-17T22:00:38
Spectrometer Frequency 400.13
Spectral Width 8012.8
Lowest Frequency -1535.6
Nucleus 1H
Acquired Size 32768
Spectral Size 65536
2.09
2.12
2.07
2.02
0.99
3.06
f1 (ppm)

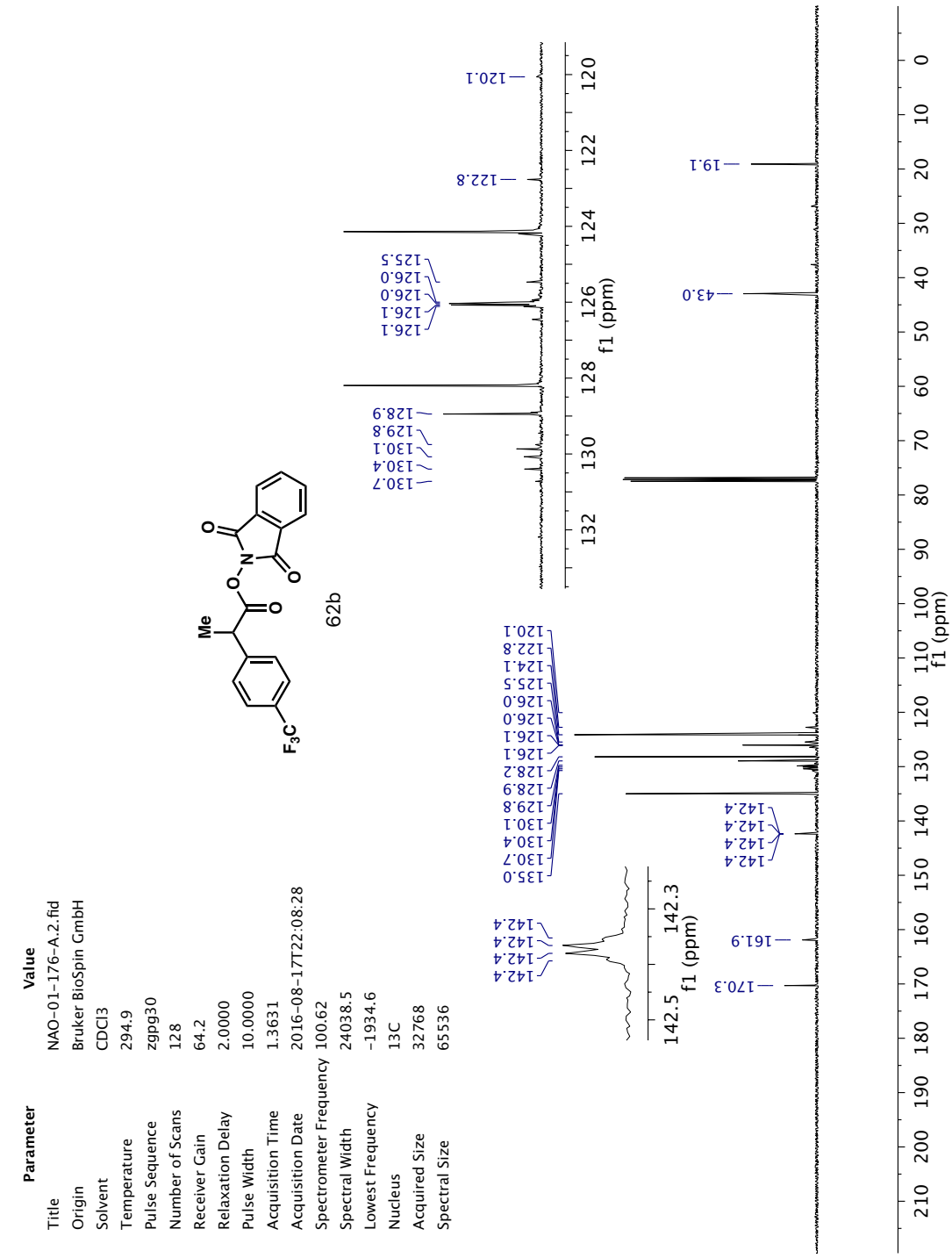
Parameter Value
Title NAO-01-176-A.2.fid
Origin Bruker BioSpin GmbH
Solvent CDCl3
Temperature 294.9
Pulse Sequence zgpg30
Number of Scans 128
Receiver Gain 64.2
Relaxation Delay 2.0000
Pulse Width 10.0000
Acquisition Time 1.3631
Acquisition Date 2016-08-17T22:08:28
Spectrometer Frequency 100.62
Spectral Width 24038.5
Lowest Frequency -1934.6
Nucleus 13C
Acquired Size 32768
Spectral Size 65536
Me
F3C
62b
f1 (ppm)

Parameter	Value
Title	NAO-01-176A
Origin	Varian
Solvent	"cdcl3"
Temperature	25.0
Pulse Sequence	s2pul
Number of Scans	16
Receiver Gain	30
Relaxation Delay	1.0000
Pulse Width	6.3333
Acquisition Time	0.9856
Acquisition Date	2016-08-31T23:19:24
Spectrometer Frequency	282.34
Spectral Width	64935.1
Lowest Frequency	-58259.3
Nucleus	19F
Acquired Size	64000
Spectral Size	131072

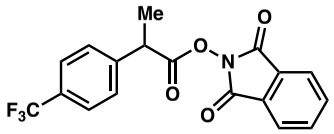

62b

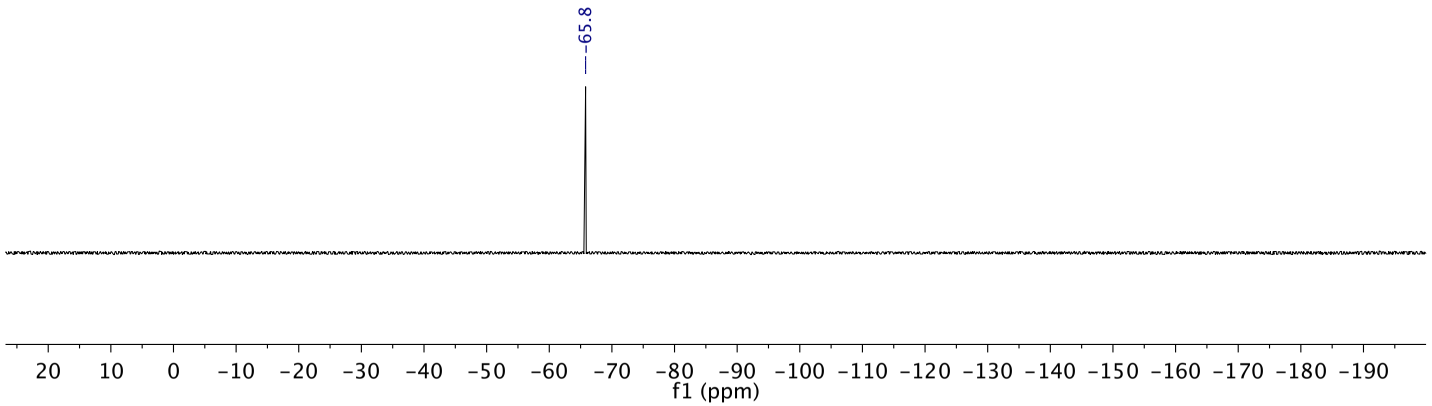

Parameter	Value
Title	NAO-01-176A-C6F6
Origin	Varian
Solvent	"cdcl3"
Temperature	25.0
Pulse Sequence	s2pul
Number of Scans	16
Receiver Gain	30
Relaxation Delay	1.0000
Pulse Width	6.3333
Acquisition Time	0.9856
Acquisition Date	2016-08-31T23:23:38
Spectrometer Frequency	282.34
Spectral Width	64935.1
Lowest Frequency	-58249.7
Nucleus	19F
Acquired Size	64000
Spectral Size	131072

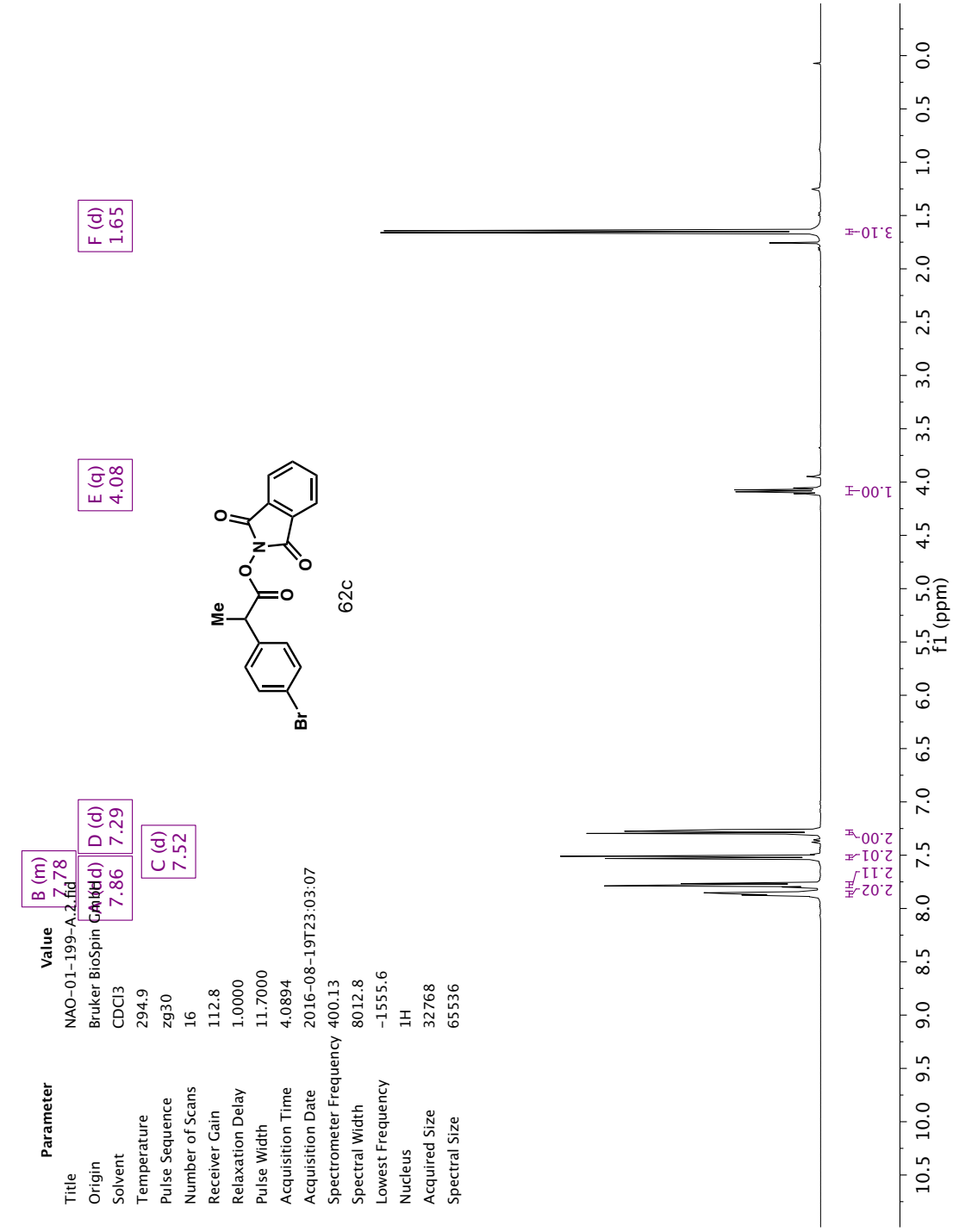
Parameter
Value
Title
NAO-01-199-A.2.fid
Origin
Bruker BioSpin GmbH
Solvent
CDCl3
Temperature
294.9
Pulse Sequence
zg30
Number of Scans
16
Receiver Gain
112.8
Relaxation Delay
1.0000
Pulse Width
11.7000
Acquisition Time
4.0894
Acquisition Date
2016-08-19T23:03:07
Spectrometer Frequency
400.13
Spectral Width
8012.8
Lowest Frequency
-1555.6
Nucleus
1H
Acquired Size
32768
Spectral Size
65536
B (m) 7.78
A (dd) 7.86
D (d) 7.29
C (d) 7.52
E (q) 4.08
F (d) 1.65
Me
O
N
O
O
O
O
Br
62c
2.02
2.11
2.01
2.00
1.00
3.10
10.5 10.0 9.5 9.0 8.5 8.0 7.5 7.0 6.5 6.0 5.5 5.0 4.5 4.0 3.5 3.0 2.5 2.0 1.5 1.0 0.5 0.0
f1 (ppm)

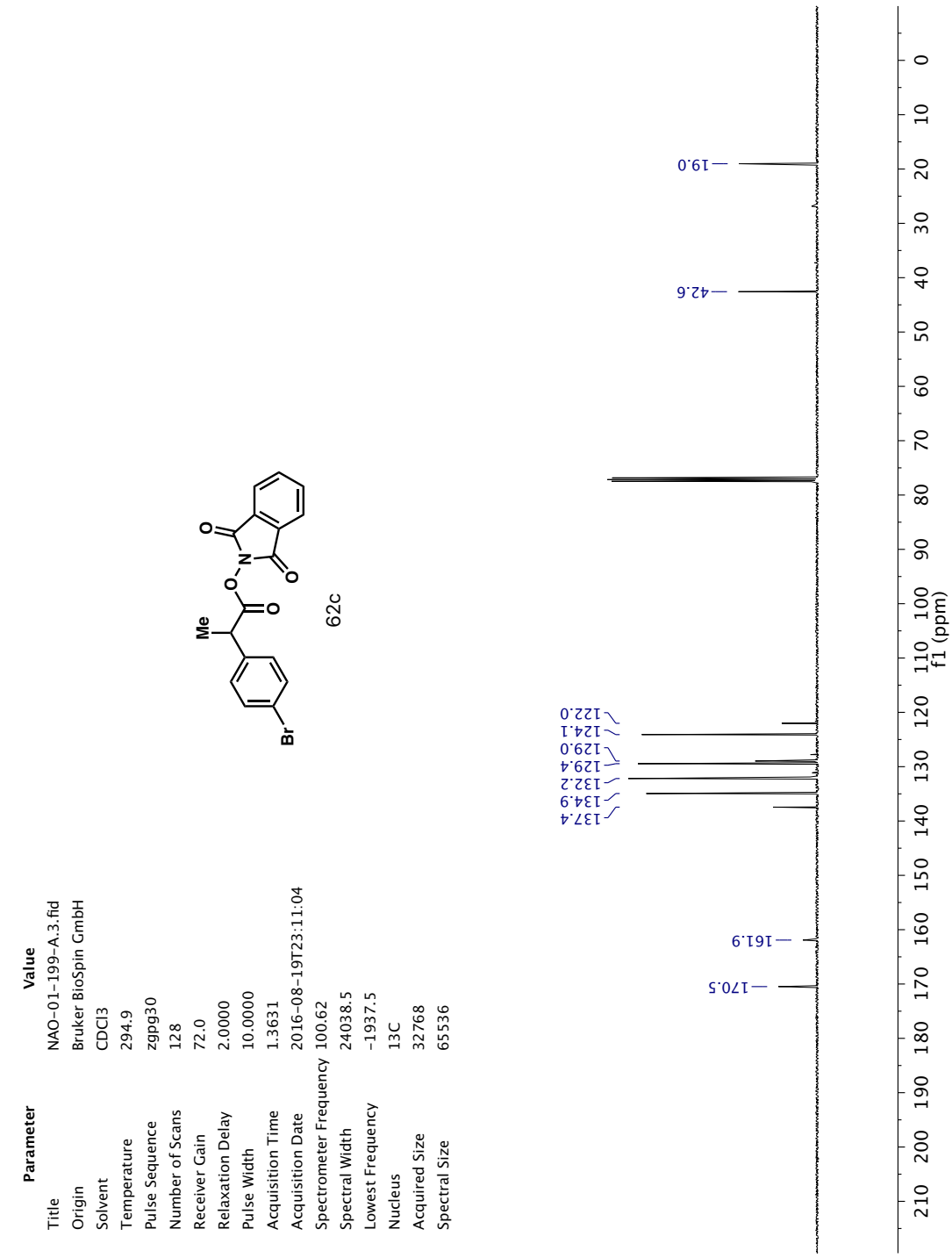
Parameter Value
Title NAO-01-199-A.3.fid
Origin Bruker BioSpin GmbH
Solvent CDCl3
Temperature 294.9
Pulse Sequence zgpg30
Number of Scans 128
Receiver Gain 72.0
Relaxation Delay 2.0000
Pulse Width 10.0000
Acquisition Time 1.3631
Acquisition Date 2016-08-19T23:11:04
Spectrometer Frequency 100.62
Spectral Width 24038.5
Lowest Frequency -1937.5
Nucleus 13C
Acquired Size 32768
Spectral Size 65536
Me
Br
62c
170.5
161.9
137.4
134.9
132.2
129.4
129.0
124.1
122.0
42.6
19.0
f1 (ppm)

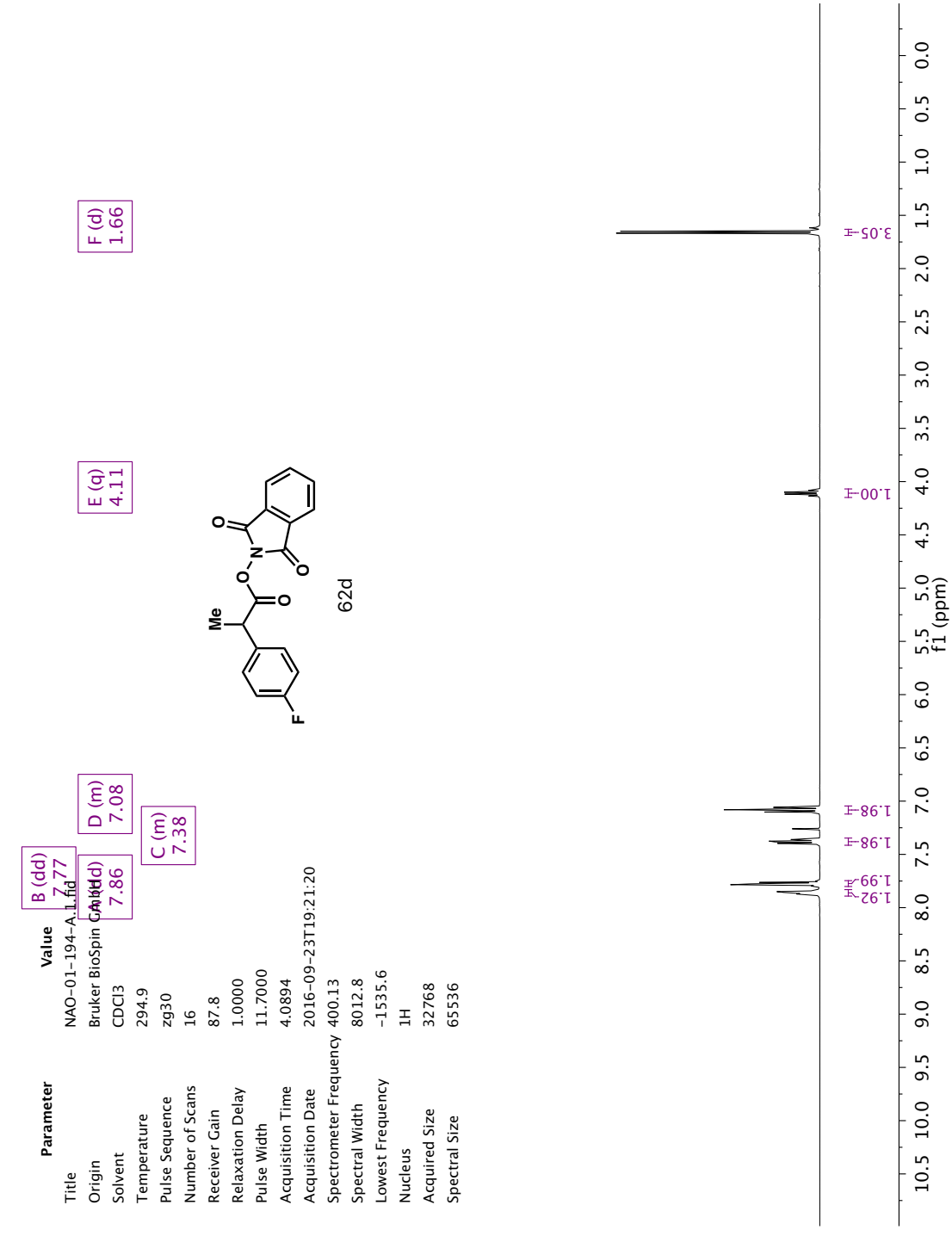
Parameter Value
Title NAO-01-194-A.1.fid
Origin Bruker BioSpin GmbH
Solvent CDCl3
Temperature 294.9
Pulse Sequence zg30
Number of Scans 16
Receiver Gain 87.8
Relaxation Delay 1.0000
Pulse Width 11.7000
Acquisition Time 4.0894
Acquisition Date 2016-09-23T19:21:20
Spectrometer Frequency 400.13
Spectral Width 8012.8
Lowest Frequency -1535.6
Nucleus 1H
Acquired Size 32768
Spectral Size 65536
B (dd) 7.77
A (dd) 7.86
D (m) 7.08
C (m) 7.38
E (q) 4.11
F (d) 1.66
Me
O
N
O
O
O
F
62d
1.92
1.99
1.98
1.98
1.00
3.05
10.5 10.0 9.5 9.0 8.5 8.0 7.5 7.0 6.5 6.0 5.5 5.0 4.5 4.0 3.5 3.0 2.5 2.0 1.5 1.0 0.5 0.0
f1 (ppm)

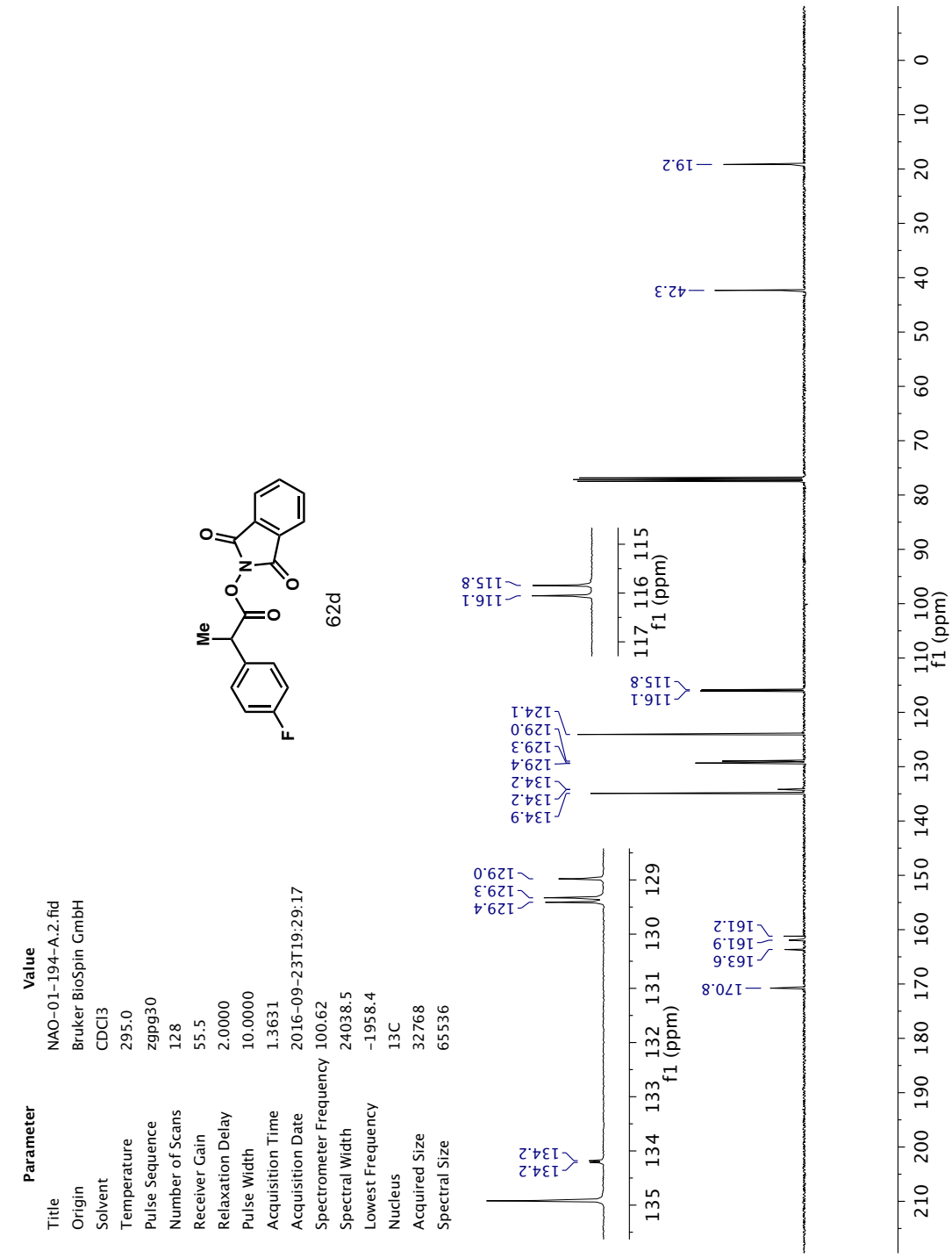
Parameter Value
Title NAO-01-194-A.2.fid
Origin Bruker BioSpin GmbH
Solvent CDCl3
Temperature 295.0
Pulse Sequence zgpg30
Number of Scans 128
Receiver Gain 55.5
Relaxation Delay 2.0000
Pulse Width 10.0000
Acquisition Time 1.3631
Acquisition Date 2016-09-23T19:29:17
Spectrometer Frequency 100.62
Spectral Width 24038.5
Lowest Frequency -1958.4
Nucleus 13C
Acquired Size 32768
Spectral Size 65536
Me
O
N
O
O
O
O
F
62d
f1 (ppm)

Parameter	Value
Title	NAO-1-194A
Origin	Varian
Solvent	"cdcl3"
Temperature	25.0
Pulse Sequence	s2pul
Number of Scans	16
Receiver Gain	30
Relaxation Delay	1.0000
Pulse Width	6.3333
Acquisition Time	0.9856
Acquisition Date	2017-01-09T22:18:30
Spectrometer Frequency	282.34
Spectral Width	64935.1
Lowest Frequency	-56468.7
Nucleus	19F
Acquired Size	64000
Spectral Size	131072

A (tt)
-117.64

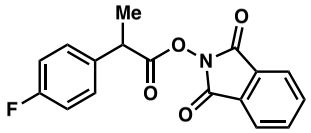

62d

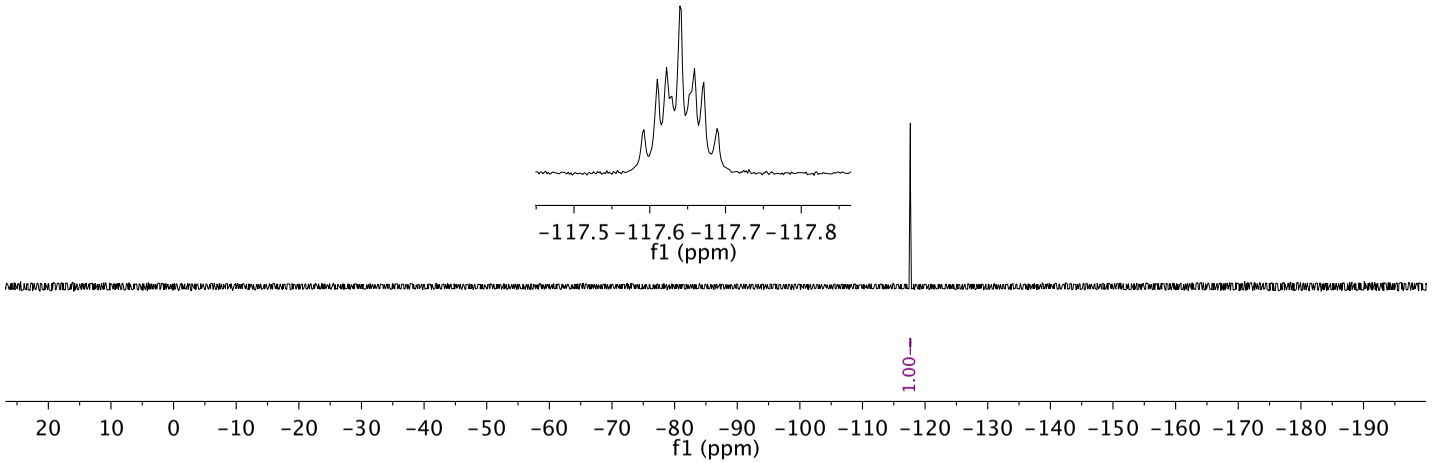

A (tt)
−117.64
Parameter Value
Title NAO-1-194A-C6F6
Origin Varian
Solvent "cdcl3"
Temperature 25.0
Pulse Sequence s2pul
Number of Scans 16
Receiver Gain 30
Relaxation Delay 1.0000
Pulse Width 6.3333
Acquisition Time 0.9856
Acquisition Date 2017-01-09T22:35:50
Spectrometer Frequency 282.34
Spectral Width 64935.1
Lowest Frequency -56468.7
Nucleus 19F
Acquired Size 64000
Spectral Size 131072
Me
O
N
O
F
62d
with C_6F_6
−117.5–117.6–117.7–117.8
f1 (ppm)
1.00
20 10 0 -10 -20 -30 -40 -50 -60 -70 -80 -90 -100 -110 -120 -130 -140 -150 -160 -170 -180 -190
f1 (ppm)

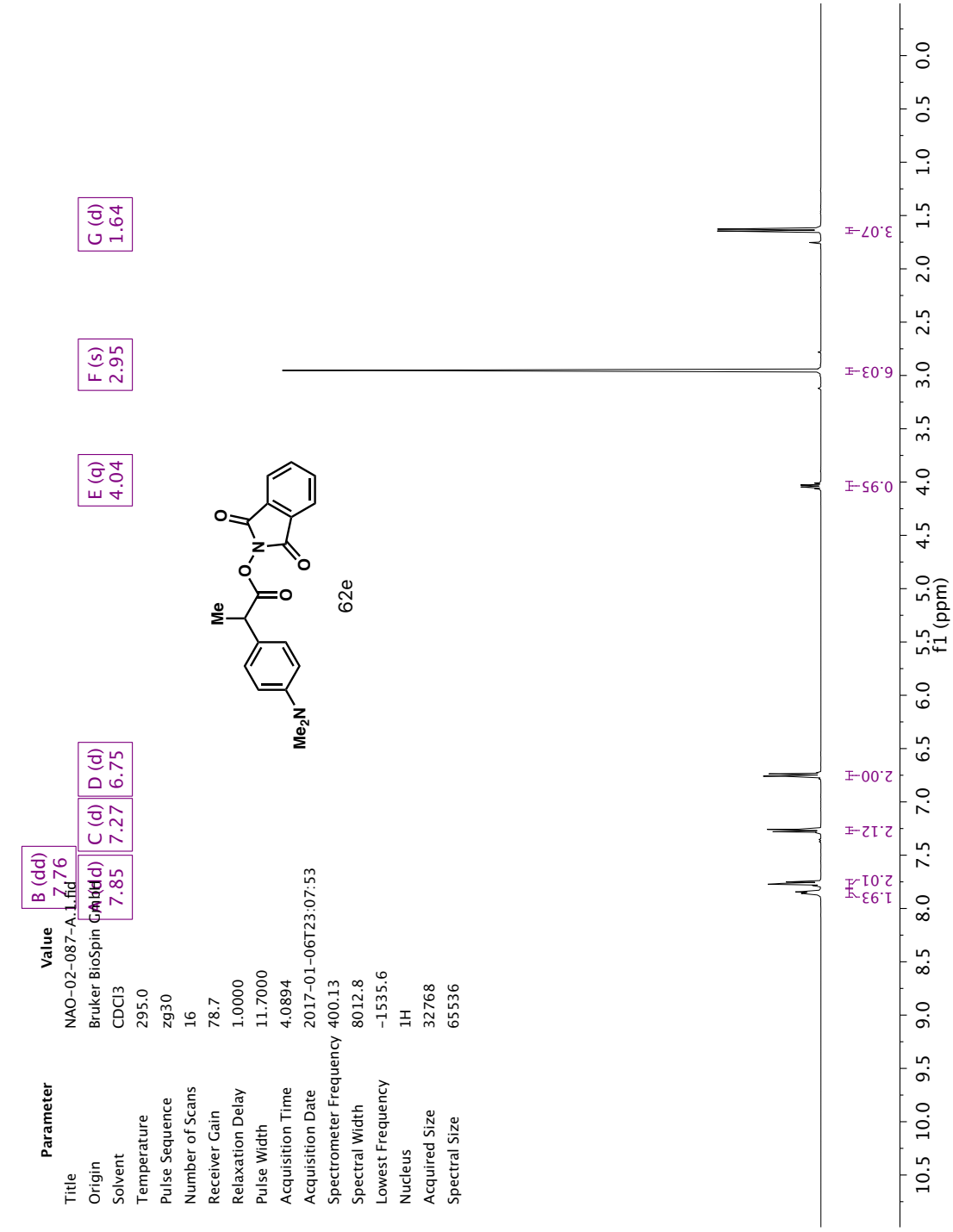
Parameter
Value
Title
NAO-02-087-A.1.fid
Origin
Bruker BioSpin GmbH
Solvent
CDCl3
Temperature
295.0
Pulse Sequence
zg30
Number of Scans
16
Receiver Gain
78.7
Relaxation Delay
1.0000
Pulse Width
11.7000
Acquisition Time
4.0894
Acquisition Date
2017-01-06T23:07:53
Spectrometer Frequency
400.13
Spectral Width
8012.8
Lowest Frequency
-1535.6
Nucleus
1H
Acquired Size
32768
Spectral Size
65536
B (dd) 7.76
A (dd) 7.85
C (d) 7.27
D (d) 6.75
E (q) 4.04
F (s) 2.95
G (d) 1.64
Me
Me2N
62e
1.93
2.01
2.12
2.00
0.95
6.03
3.07
10.5 10.0 9.5 9.0 8.5 8.0 7.5 7.0 6.5 6.0 5.5 5.0 4.5 4.0 3.5 3.0 2.5 2.0 1.5 1.0 0.5 0.0
f1 (ppm)

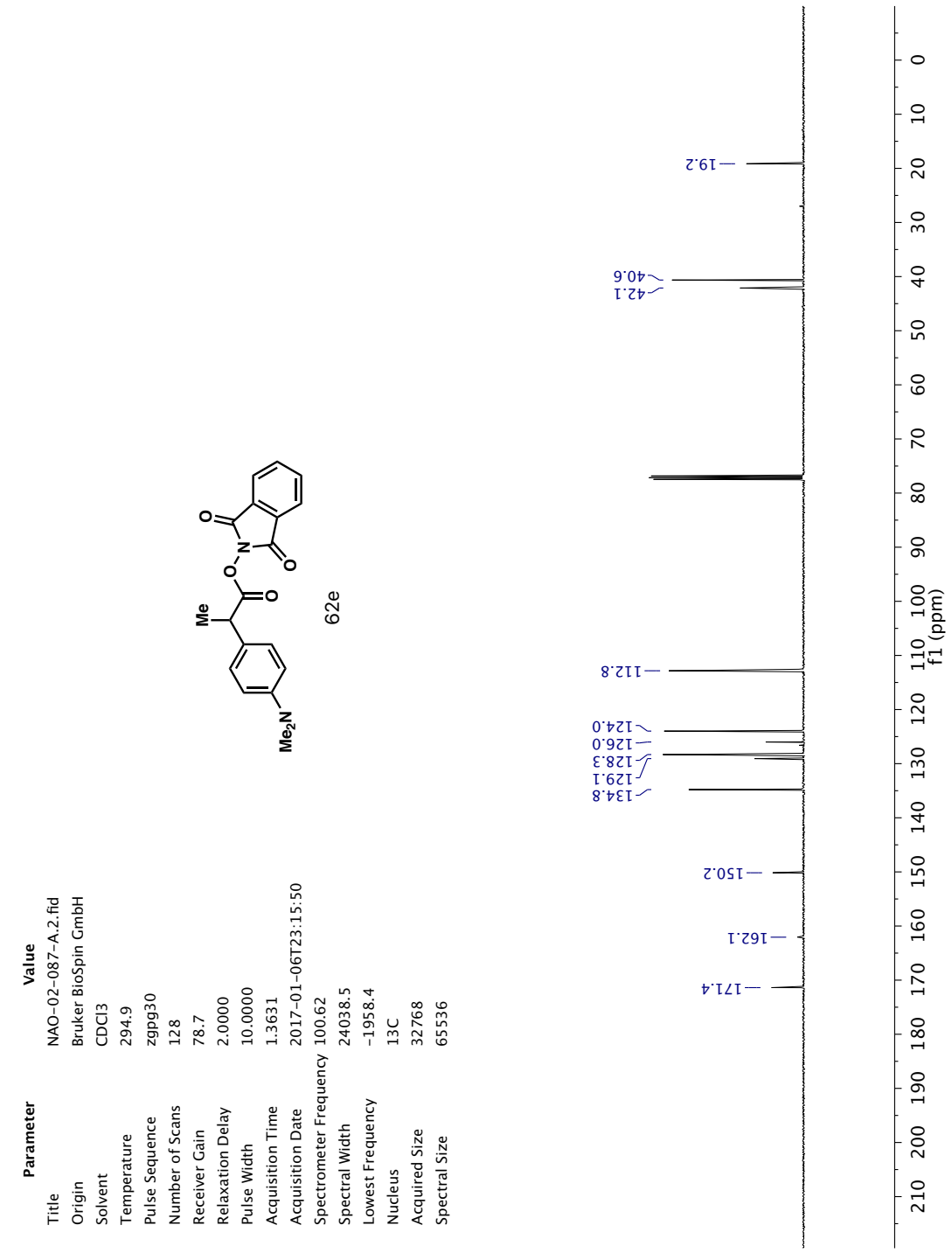
Parameter Value
Title NAO-02-087-A.2.fid
Origin Bruker BioSpin GmbH
Solvent CDCl3
Temperature 294.9
Pulse Sequence zgpg30
Number of Scans 128
Receiver Gain 78.7
Relaxation Delay 2.0000
Pulse Width 10.0000
Acquisition Time 1.3631
Acquisition Date 2017-01-06T23:15:50
Spectrometer Frequency 100.62
Spectral Width 24038.5
Lowest Frequency -1958.4
Nucleus 13C
Acquired Size 32768
Spectral Size 65536
Me
Me2N
62e
19.2
40.6
42.1
112.8
124.0
126.0
128.3
129.1
134.8
150.2
162.1
171.4
f1 (ppm)

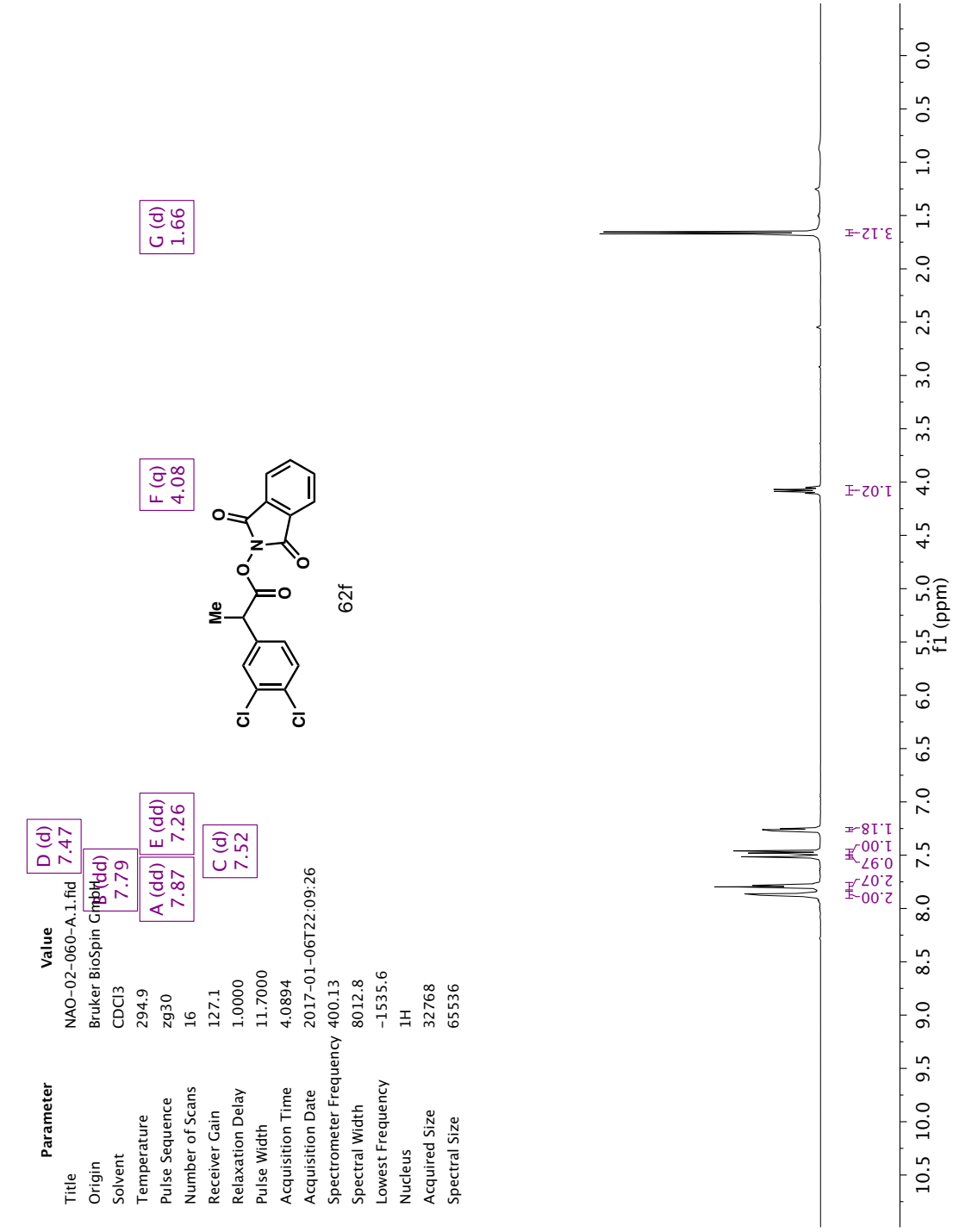
Parameter
Value
Title
NAO-02-060-A.1.fid
Origin
Bruker BioSpin GmbH
Solvent
CDCl3
Temperature
294.9
Pulse Sequence
zg30
Number of Scans
16
Receiver Gain
127.1
Relaxation Delay
1.0000
Pulse Width
11.7000
Acquisition Time
4.0894
Acquisition Date
2017-01-06T22:09:26
Spectrometer Frequency
400.13
Spectral Width
8012.8
Lowest Frequency
-1535.6
Nucleus
1H
Acquired Size
32768
Spectral Size
65536
D (d) 7.47
B (dd) 7.79
A (dd) 7.87
E (dd) 7.26
C (d) 7.52
F (q) 4.08
G (d) 1.66
Me
Cl
Cl
62f
3.12
1.02
2.00
2.07
0.97
1.00
1.18
f1 (ppm)

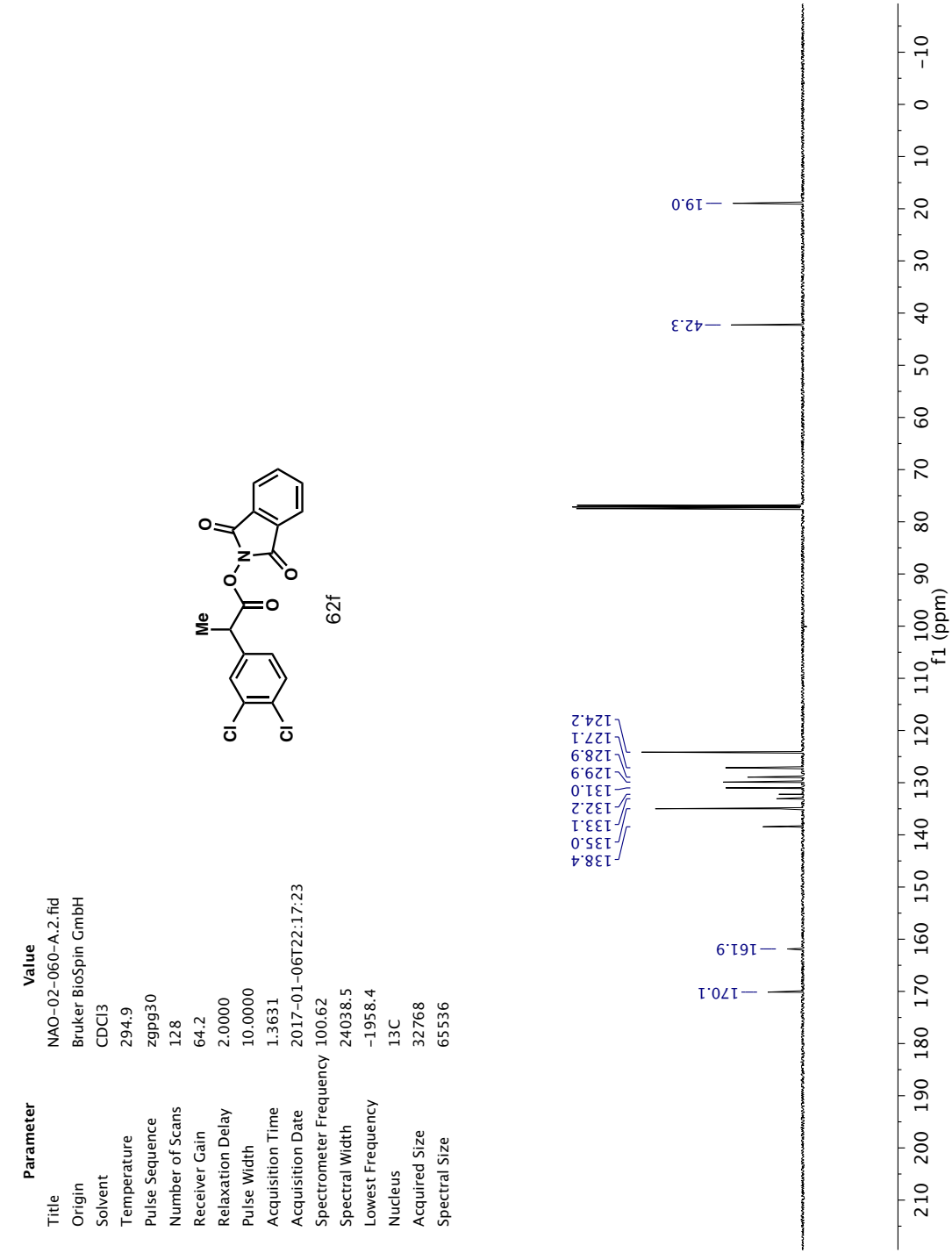
Parameter Value
Title NAO-02-060-A.2.fid
Origin Bruker BioSpin GmbH
Solvent CDCl3
Temperature 294.9
Pulse Sequence zgpg30
Number of Scans 128
Receiver Gain 64.2
Relaxation Delay 2.0000
Pulse Width 10.0000
Acquisition Time 1.3631
Acquisition Date 2017-01-06T22:17:23
Spectrometer Frequency 100.62
Spectral Width 24038.5
Lowest Frequency -1958.4
Nucleus 13C
Acquired Size 32768
Spectral Size 65536
Me
Cl
Cl
62f
170.1
161.9
138.4
135.0
133.1
132.2
131.0
129.9
128.9
127.1
124.2
42.3
19.0
f1 (ppm)

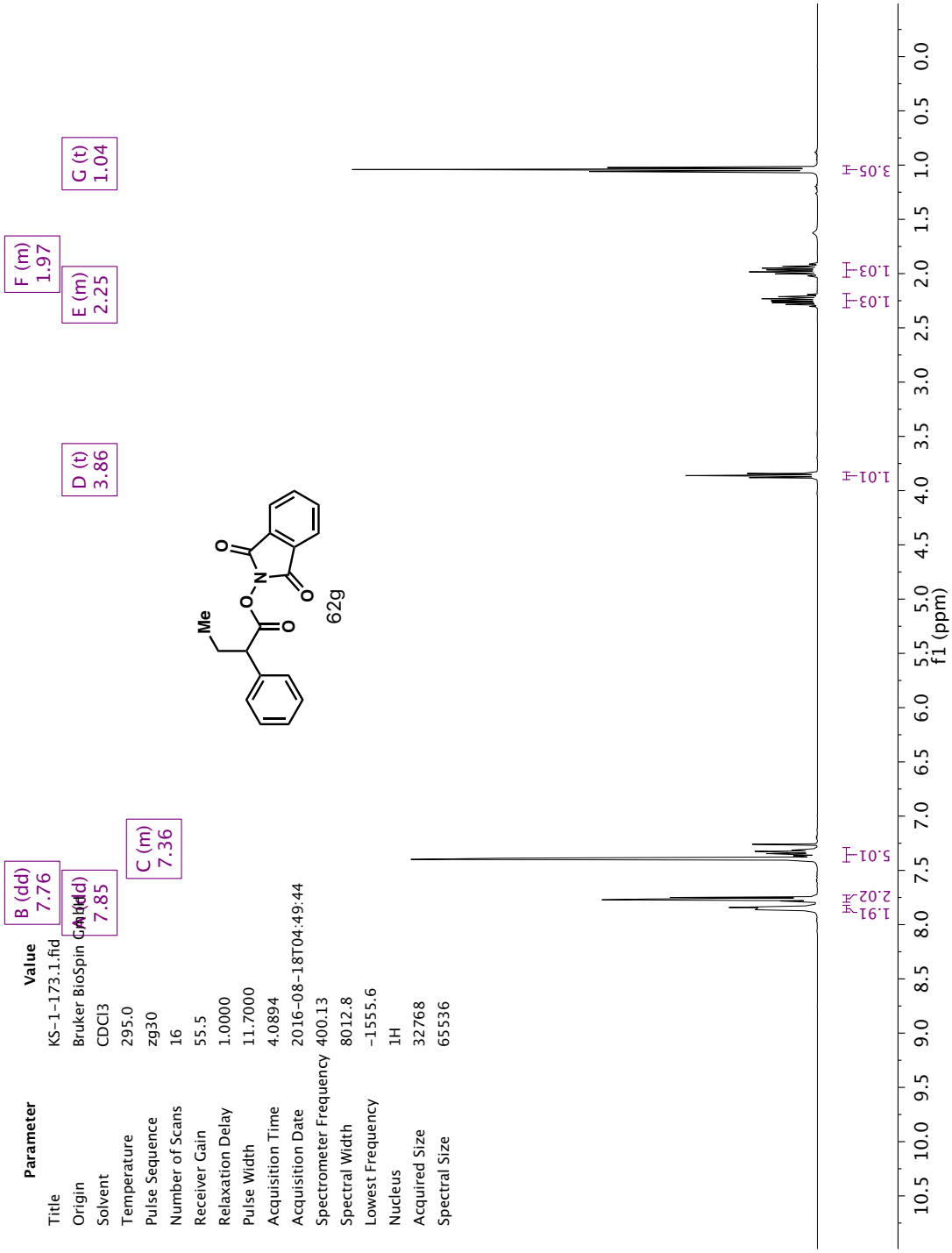
B (dd) 7.76
A (dd) 7.85
C (m) 7.36
D (t) 3.86
E (m) 2.25
F (m) 1.97
G (t) 1.04
Me
62g
Parameter Value
Title KS-1-173.1.fid
Origin Bruker BioSpin GmbH
Solvent CDCl3
Temperature 295.0
Pulse Sequence zg30
Number of Scans 16
Receiver Gain 55.5
Relaxation Delay 1.0000
Pulse Width 11.7000
Acquisition Time 4.0894
Acquisition Date 2016-08-18T04:49:44
Spectrometer Frequency 400.13
Spectral Width 8012.8
Lowest Frequency -1555.6
Nucleus 1H
Acquired Size 32768
Spectral Size 65536
1.91
2.02
5.01
1.01
1.03
1.03
3.05
f1 (ppm)

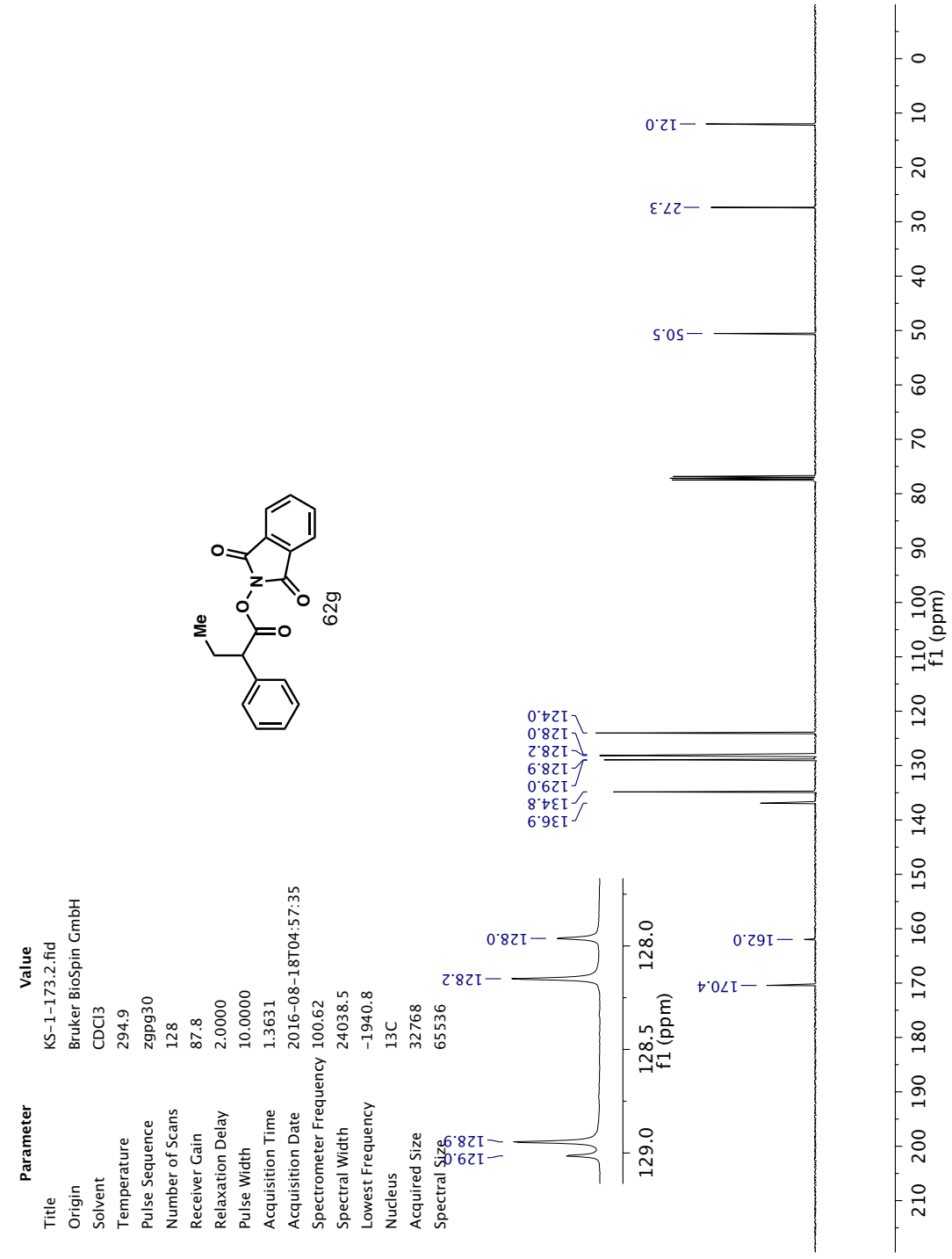
Parameter Value
Title KS-1-173.2.fid
Origin Bruker BioSpin GmbH
Solvent CDCl3
Temperature 294.9
Pulse Sequence zgpg30
Number of Scans 128
Receiver Gain 87.8
Relaxation Delay 2.0000
Pulse Width 10.0000
Acquisition Time 1.3631
Acquisition Date 2016-08-18T04:57:35
Spectrometer Frequency 100.62
Spectral Width 24038.5
Lowest Frequency -1940.8
Nucleus 13C
Acquired Size 32768
Spectral Size 65536
Me
62g
12.0
27.3
50.5
77.0
128.2
128.9
129.0
128.0
136.9
134.8
129.0
128.9
128.2
128.0
124.0
162.0
170.4
f1 (ppm)

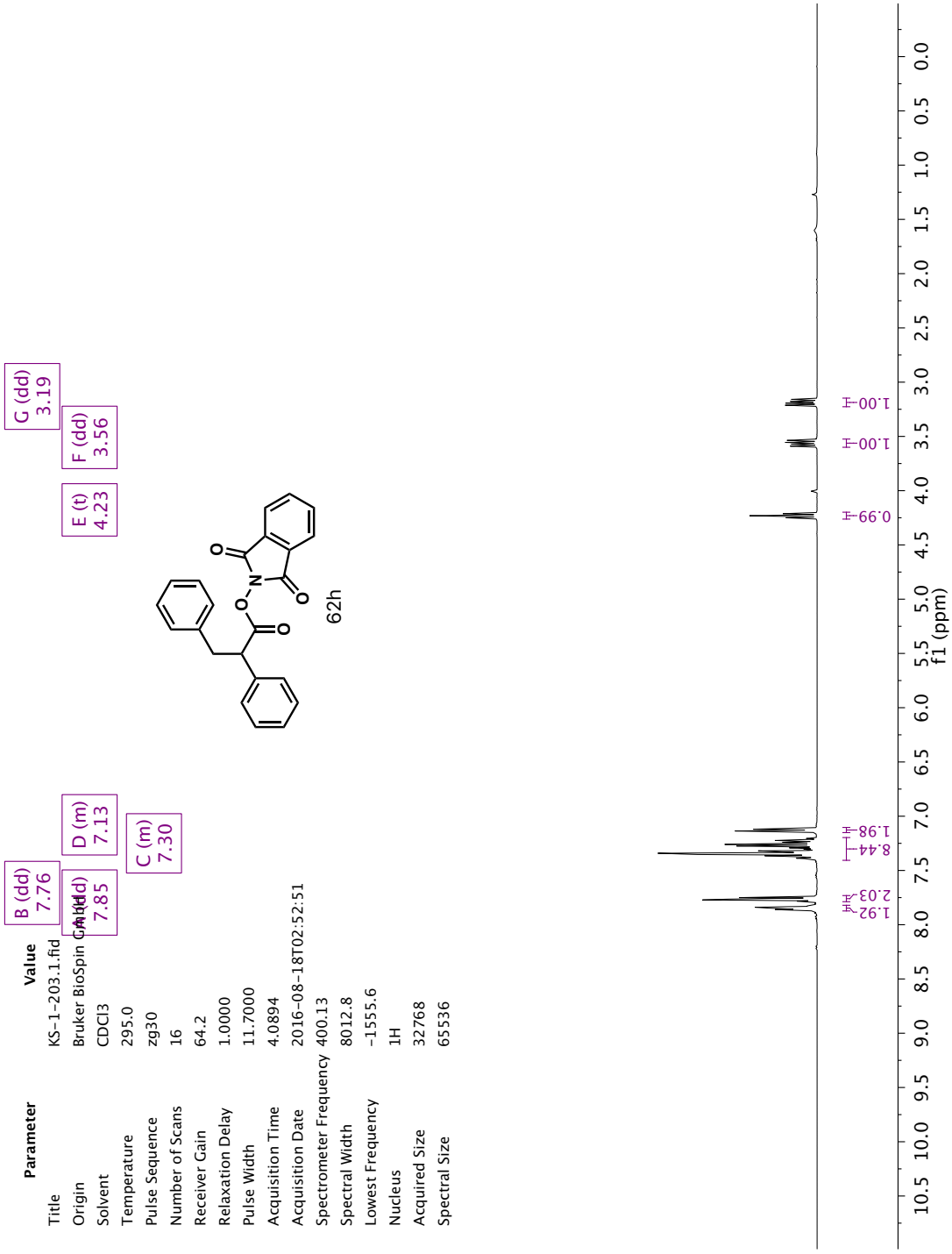
B (dd) 7.76
A (dd) 7.85
D (m) 7.13
C (m) 7.30
E (t) 4.23
F (dd) 3.56
G (dd) 3.19
62h
Parameter Value
Title KS-1-203.1.fid
Origin Bruker BioSpin GmbH
Solvent CDCl3
Temperature 295.0
Pulse Sequence zg30
Number of Scans 16
Receiver Gain 64.2
Relaxation Delay 1.0000
Pulse Width 11.7000
Acquisition Time 4.0894
Acquisition Date 2016-08-18T02:52:51
Spectrometer Frequency 400.13
Spectral Width 8012.8
Lowest Frequency -1555.6
Nucleus 1H
Acquired Size 32768
Spectral Size 65536
1.92
2.03
8.44
1.98
0.99
1.00
1.00
f1 (ppm)

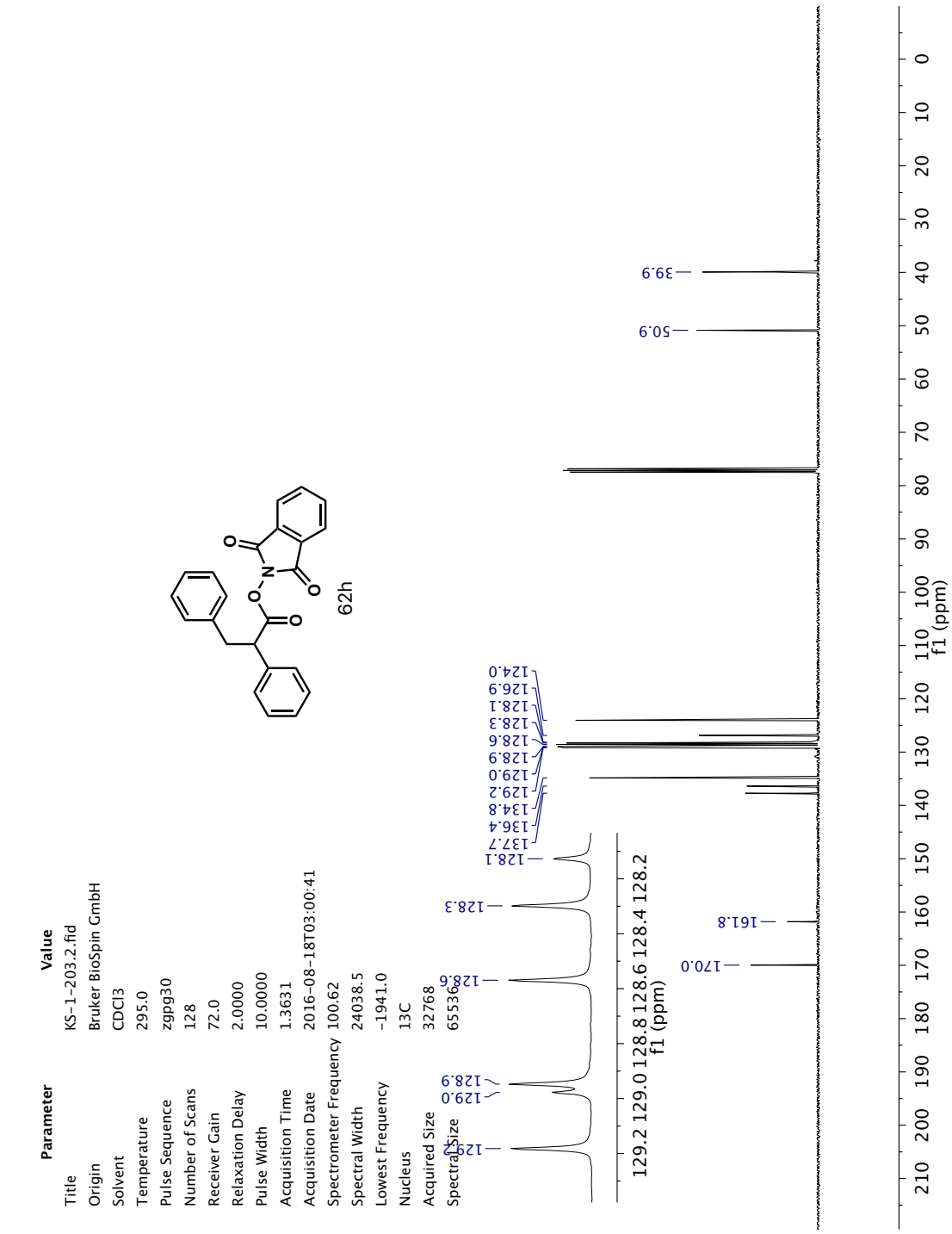
Parameter Value
Title KS-1-203.2.fid
Origin Bruker BioSpin GmbH
Solvent CDCl3
Temperature 295.0
Pulse Sequence zgpg30
Number of Scans 128
Receiver Gain 72.0
Relaxation Delay 2.0000
Pulse Width 10.0000
Acquisition Time 1.3631
Acquisition Date 2016-08-18T03:00:41
Spectrometer Frequency 100.62
Spectral Width 24038.5
Lowest Frequency -1941.0
Nucleus 13C
Acquired Size 32768
Spectral Size 65536
62h
170.0
161.8
137.7
136.4
134.8
129.2
129.0
128.9
128.6
128.3
128.1
126.9
124.0
50.9
39.9
129.2 129.0 128.8 128.6 128.4 128.2
f1 (ppm)
f1 (ppm)

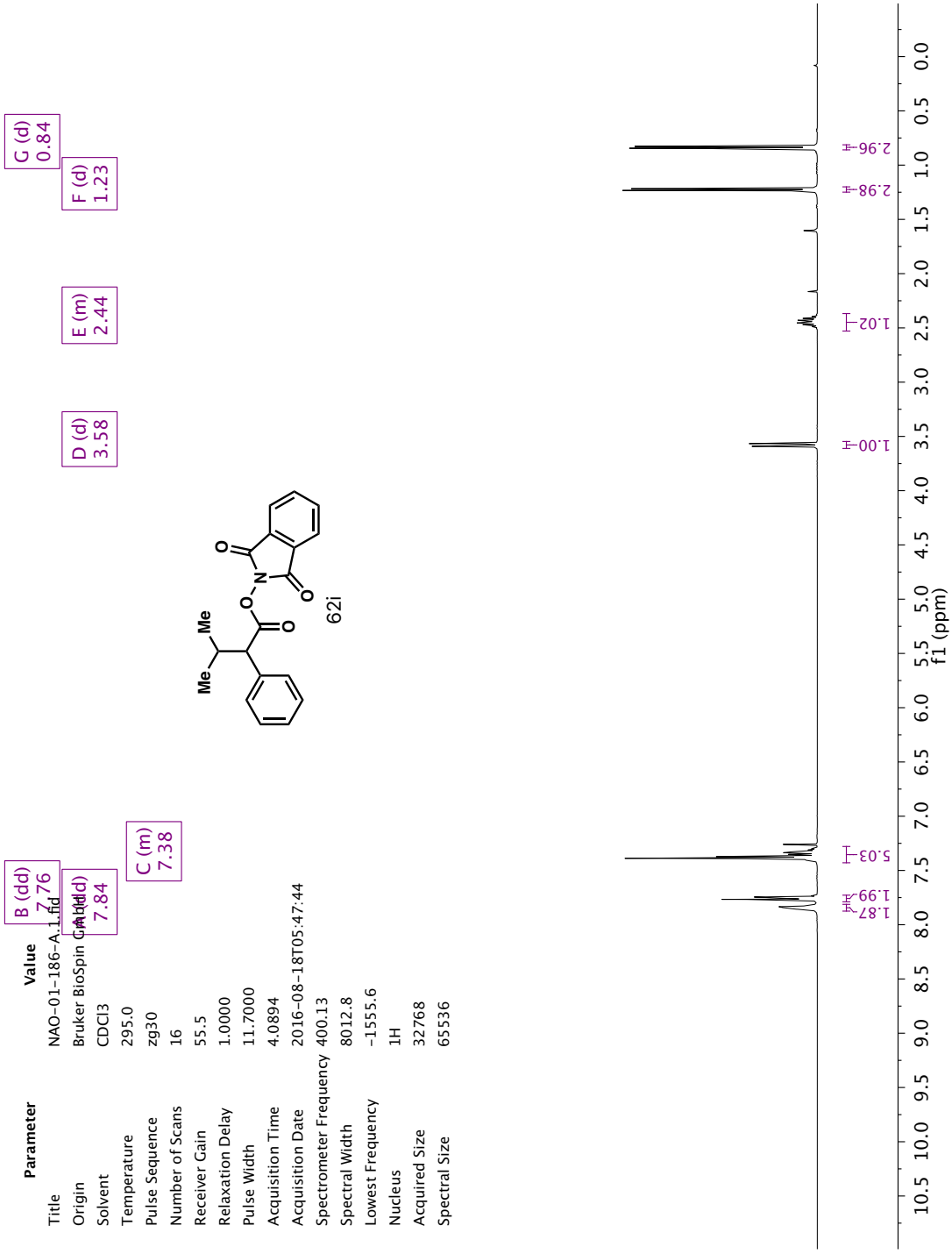
B (dd)
7.76
A (dd)
7.84
C (m)
7.38
D (d)
3.58
E (m)
2.44
F (d)
1.23
G (d)
0.84
Me
Me
62i
Parameter Value
Title NAO-01-186-A.1.fid
Origin Bruker BioSpin GmbH
Solvent CDCl3
Temperature 295.0
Pulse Sequence zg30
Number of Scans 16
Receiver Gain 55.5
Relaxation Delay 1.0000
Pulse Width 11.7000
Acquisition Time 4.0894
Acquisition Date 2016-08-18T05:47:44
Spectrometer Frequency 400.13
Spectral Width 8012.8
Lowest Frequency -1555.6
Nucleus 1H
Acquired Size 32768
Spectral Size 65536
1.87
1.99
5.03
1.00
1.02
2.98
2.96
10.5 10.0 9.5 9.0 8.5 8.0 7.5 7.0 6.5 6.0 5.5 5.0 4.5 4.0 3.5 3.0 2.5 2.0 1.5 1.0 0.5 0.0
f1 (ppm)

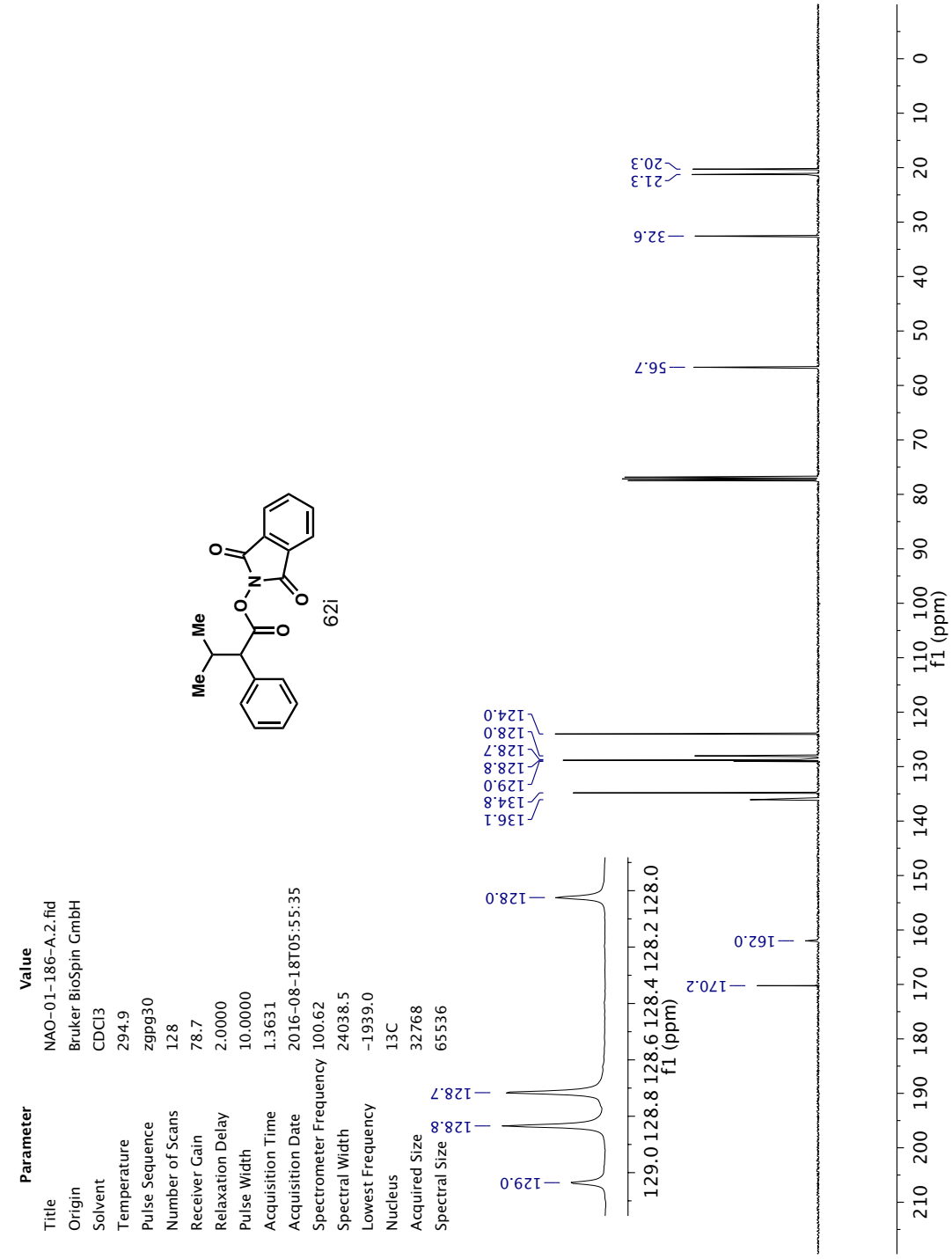
Parameter Value
Title NAO-01-186-A.2.fid
Origin Bruker BioSpin GmbH
Solvent CDCl3
Temperature 294.9
Pulse Sequence zgpg30
Number of Scans 128
Receiver Gain 78.7
Relaxation Delay 2.0000
Pulse Width 10.0000
Acquisition Time 1.3631
Acquisition Date 2016-08-18T05:55:35
Spectrometer Frequency 100.62
Spectral Width 24038.5
Lowest Frequency -1939.0
Nucleus 13C
Acquired Size 32768
Spectral Size 65536
62i
Me
Me
O
O
N
O
O
O
136.1
134.8
129.0
128.8
128.7
128.0
124.0
170.2
162.0
56.7
32.6
21.3
20.3
128.8
128.7
129.0
128.0
129.0 128.8 128.6 128.4 128.2 128.0
f1 (ppm)
210 200 190 180 170 160 150 140 130 120 110 100 90 80 70 60 50 40 30 20 10 0
f1 (ppm)

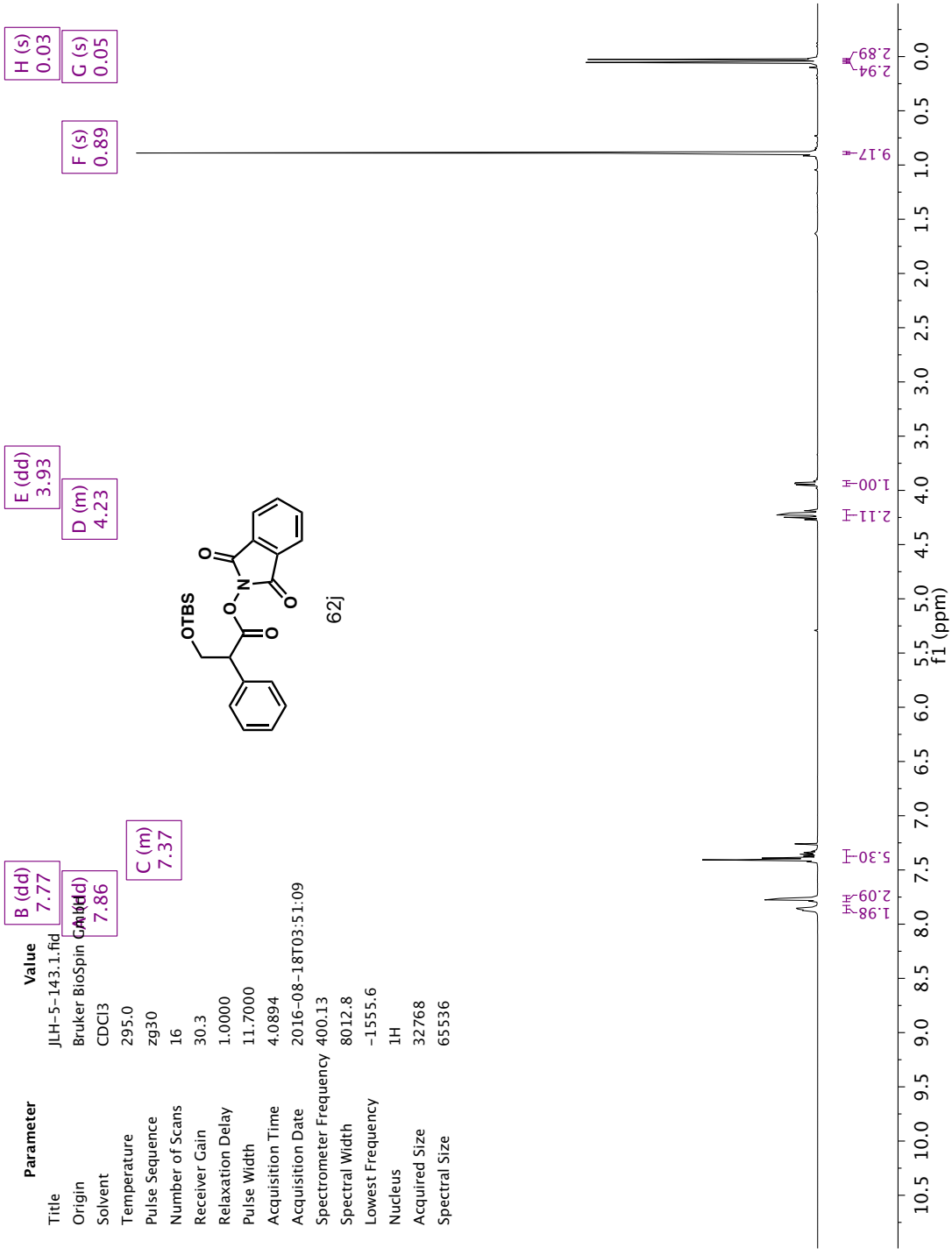
B (dd) 7.77
A (dd) 7.86
C (m) 7.37
E (dd) 3.93
D (m) 4.23
F (s) 0.89
H (s) 0.03
G (s) 0.05
OTBS
62j
Parameter Value
Title JLH-5-143.1.fid
Origin Bruker BioSpin GmbH
Solvent CDCl3
Temperature 295.0
Pulse Sequence zg30
Number of Scans 16
Receiver Gain 30.3
Relaxation Delay 1.0000
Pulse Width 11.7000
Acquisition Time 4.0894
Acquisition Date 2016-08-18T03:51:09
Spectrometer Frequency 400.13
Spectral Width 8012.8
Lowest Frequency -1555.6
Nucleus 1H
Acquired Size 32768
Spectral Size 65536
1.98
2.09
5.30
2.11
1.00
9.17
2.89
2.94
f1 (ppm)

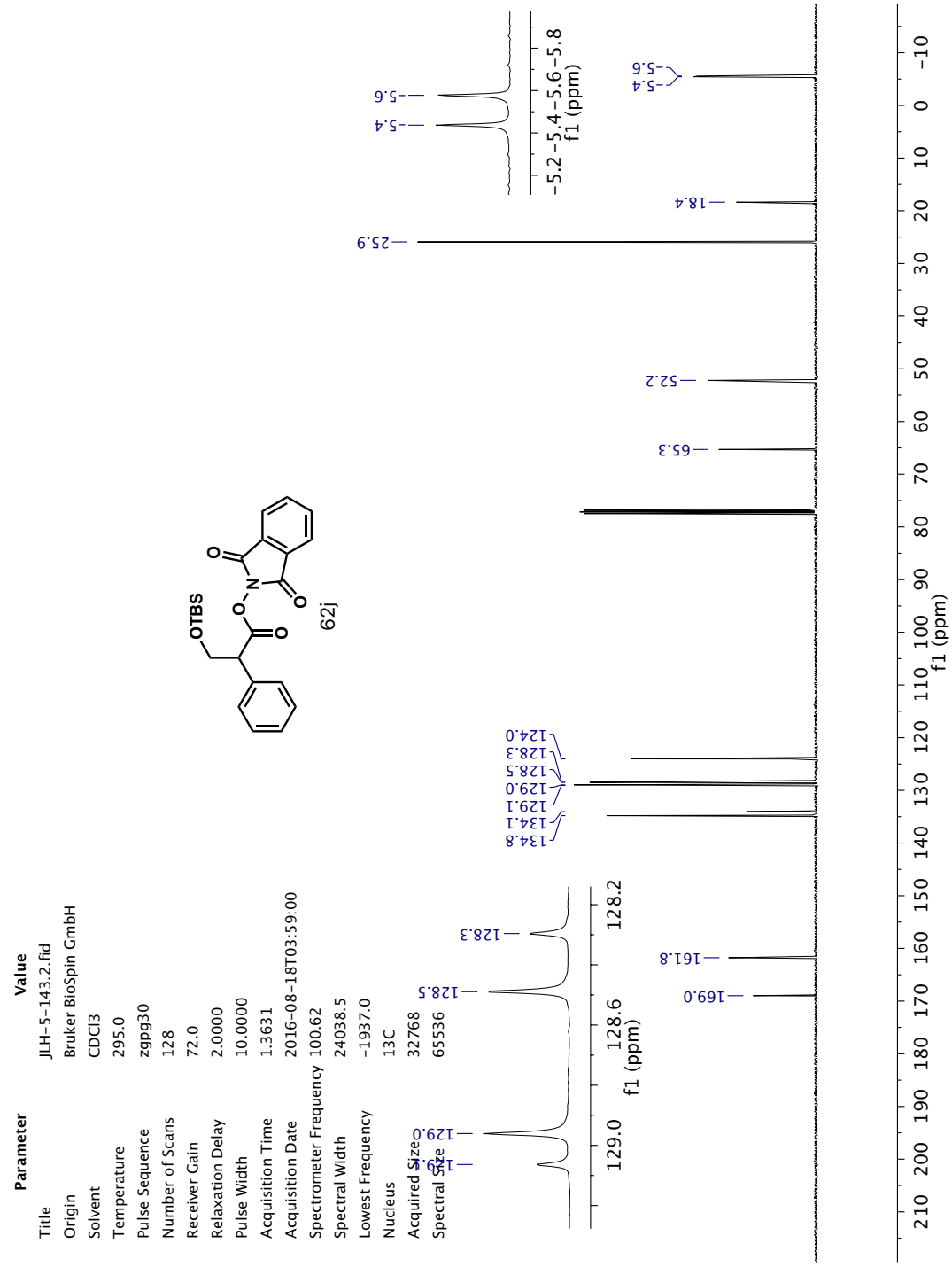
Parameter Value
Title JLH-5-143.2.fid
Origin Bruker BioSpin GmbH
Solvent CDCl3
Temperature 295.0
Pulse Sequence zgpg30
Number of Scans 128
Receiver Gain 72.0
Relaxation Delay 2.0000
Pulse Width 10.0000
Acquisition Time 1.3631
Acquisition Date 2016-08-18T03:59:00
Spectrometer Frequency 100.62
Spectral Width 24038.5
Lowest Frequency -1937.0
Nucleus 13C
Acquired Size 32768
Spectral Size 65536
OTBS
62j
f1 (ppm)
f1 (ppm)
f1 (ppm)

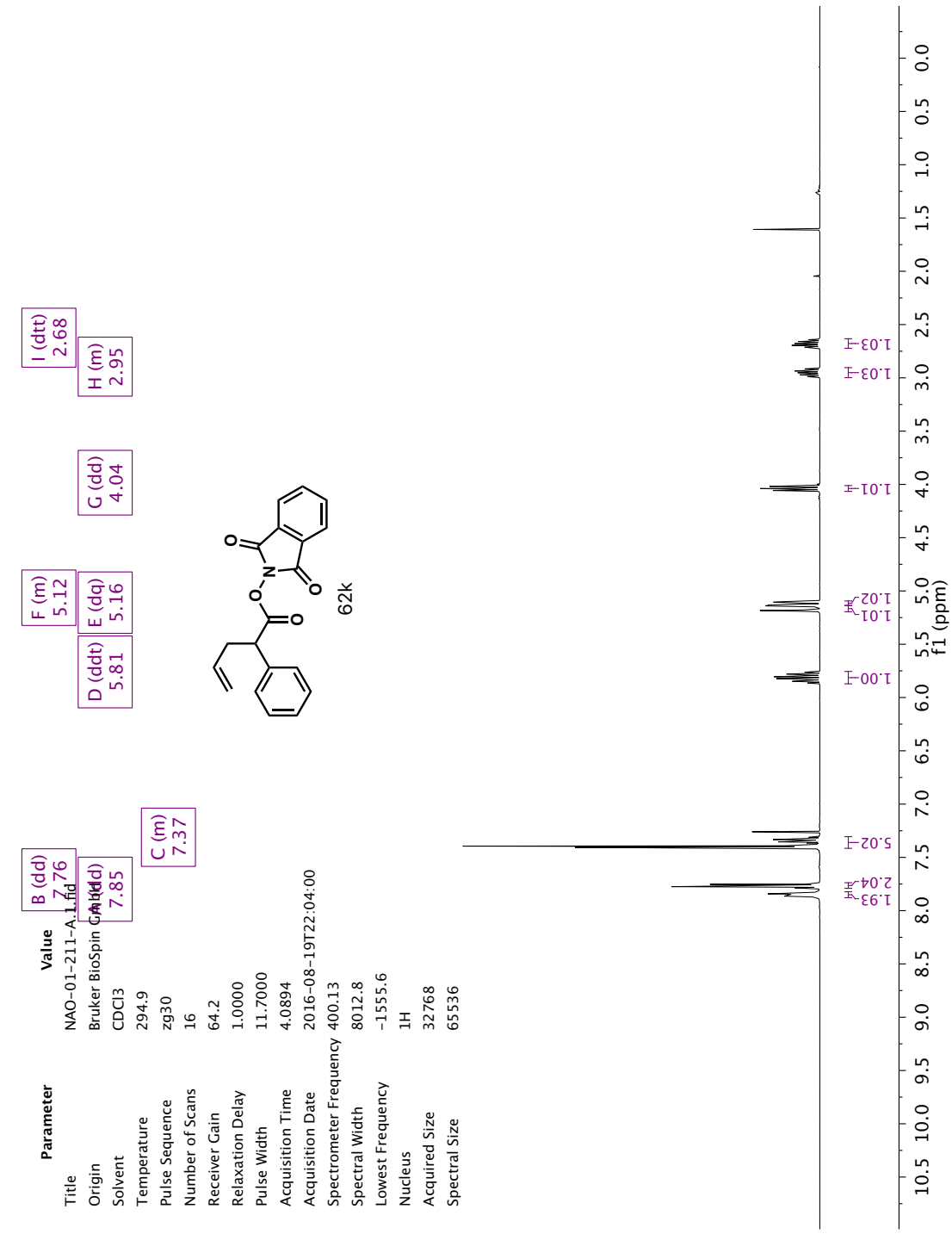
Parameter
Value
Title
NAO-01-211-A.1.fid
Origin
Bruker BioSpin GmbH
Solvent
CDCl3
Temperature
294.9
Pulse Sequence
zg30
Number of Scans
16
Receiver Gain
64.2
Relaxation Delay
1.0000
Pulse Width
11.7000
Acquisition Time
4.0894
Acquisition Date
2016-08-19T22:04:00
Spectrometer Frequency
400.13
Spectral Width
8012.8
Lowest Frequency
-1555.6
Nucleus
1H
Acquired Size
32768
Spectral Size
65536
B (dd) 7.76
A (dd) 7.85
C (m) 7.37
D (ddt) 5.81
E (dq) 5.16
F (m) 5.12
G (dd) 4.04
H (m) 2.95
I (dtt) 2.68
62k
1.93
2.04
5.02
1.00
1.01
1.02
1.01
1.03
1.03
f1 (ppm)

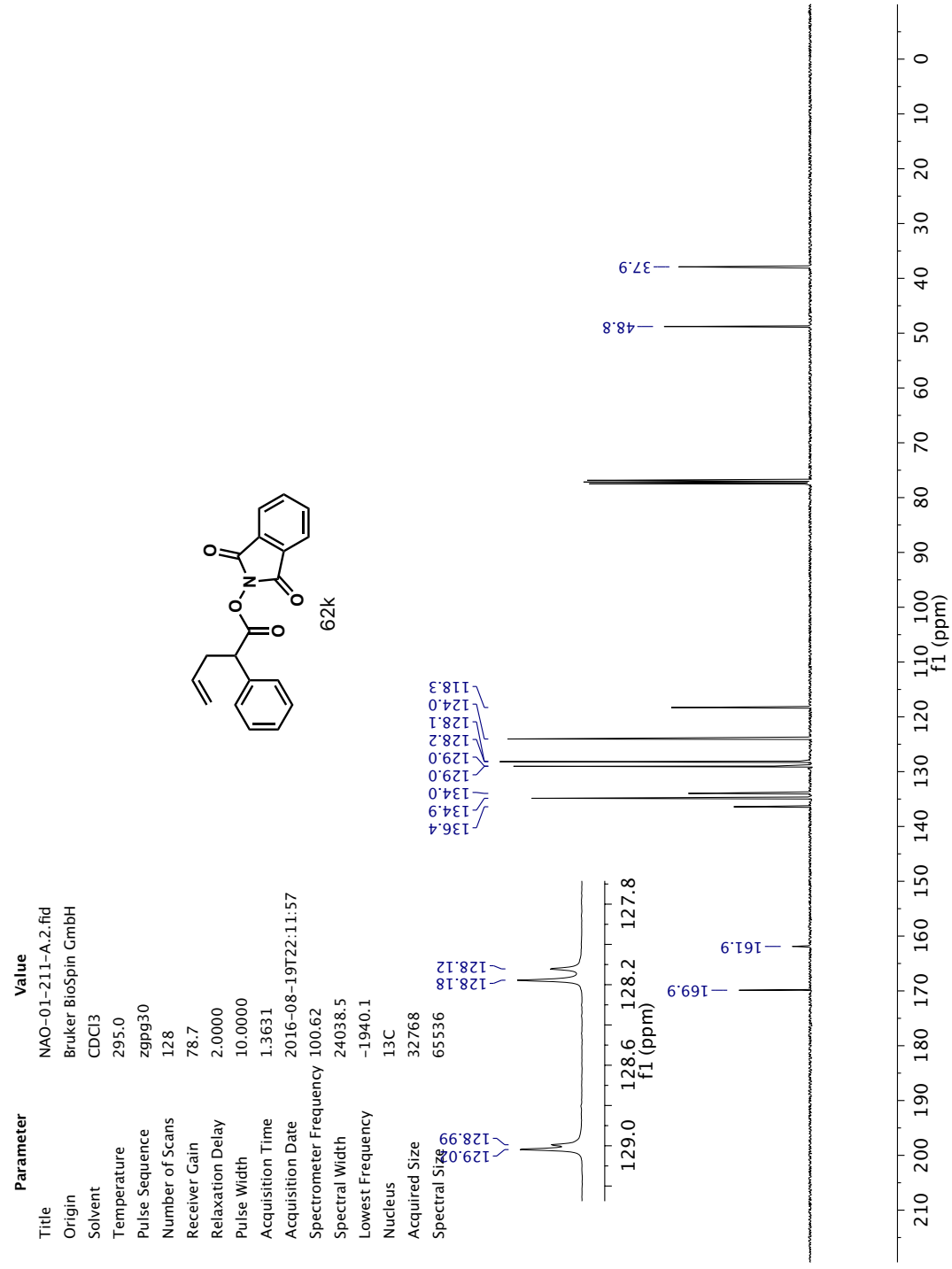
Parameter Value
Title NAO-01-211-A.2.fid
Origin Bruker BioSpin GmbH
Solvent CDCl3
Temperature 295.0
Pulse Sequence zgpg30
Number of Scans 128
Receiver Gain 78.7
Relaxation Delay 2.0000
Pulse Width 10.0000
Acquisition Time 1.3631
Acquisition Date 2016-08-19T22:11:57
Spectrometer Frequency 100.62
Spectral Width 24038.5
Lowest Frequency -1940.1
Nucleus 13C
Acquired Size 32768
Spectral Size 65536
62k
136.4
134.9
134.0
129.0
129.0
129.0
128.2
128.1
124.0
118.3
169.9
161.9
48.8
37.9
128.99
129.02
128.18
128.12
129.0
128.6
128.2
127.8
f1 (ppm)
f1 (ppm)

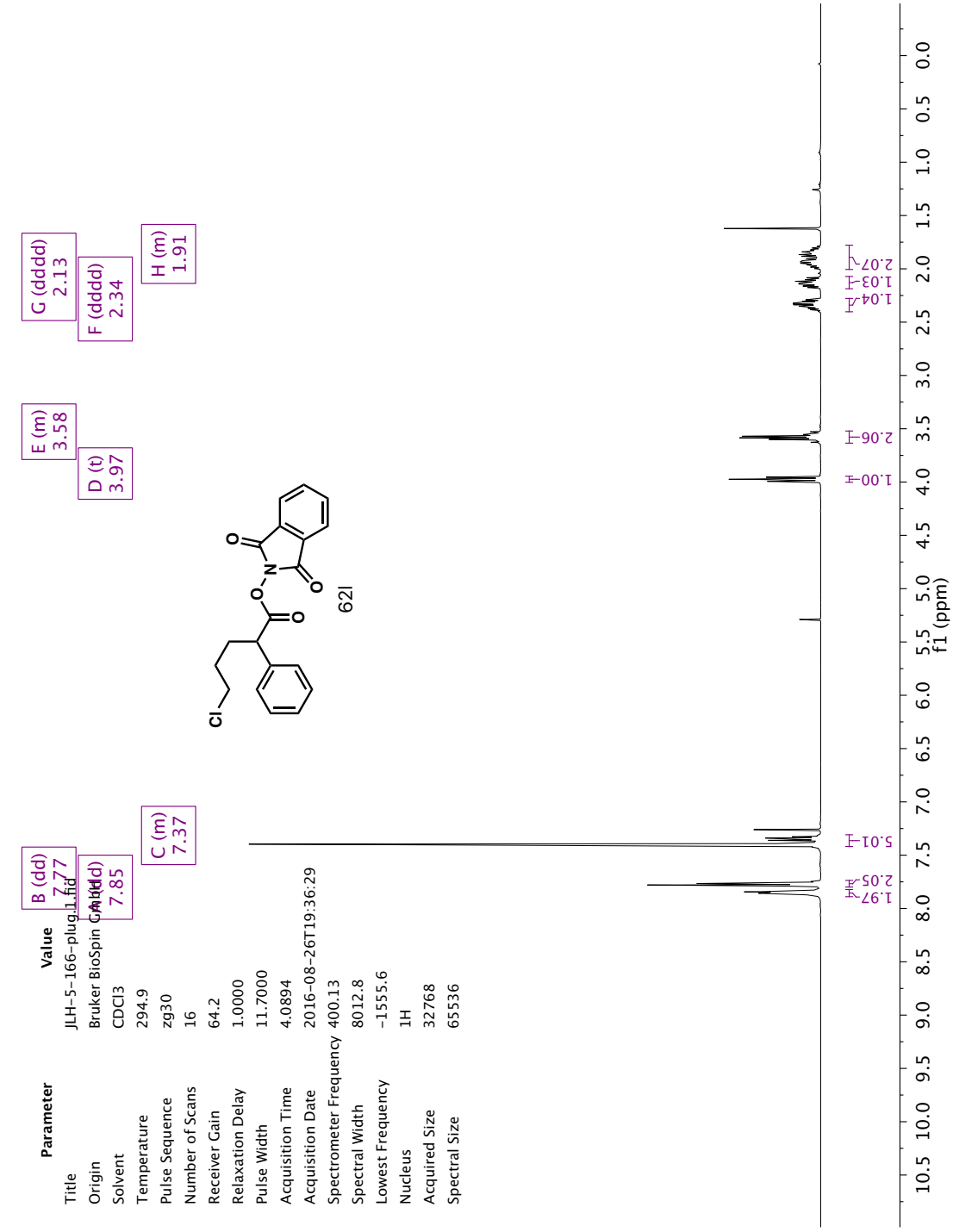

Parameter	Value
Title	JLH-5-166-plug.1.fid
Origin	Bruker BioSpin GmbH
Solvent	CDCl3
Temperature	294.9
Pulse Sequence	zg30
Number of Scans	16
Receiver Gain	64.2
Relaxation Delay	1.0000
Pulse Width	11.7000
Acquisition Time	4.0894
Acquisition Date	2016-08-26T19:36:29
Spectrometer Frequency	400.13
Spectral Width	8012.8
Lowest Frequency	-1555.6
Nucleus	1H
Acquired Size	32768
Spectral Size	65536

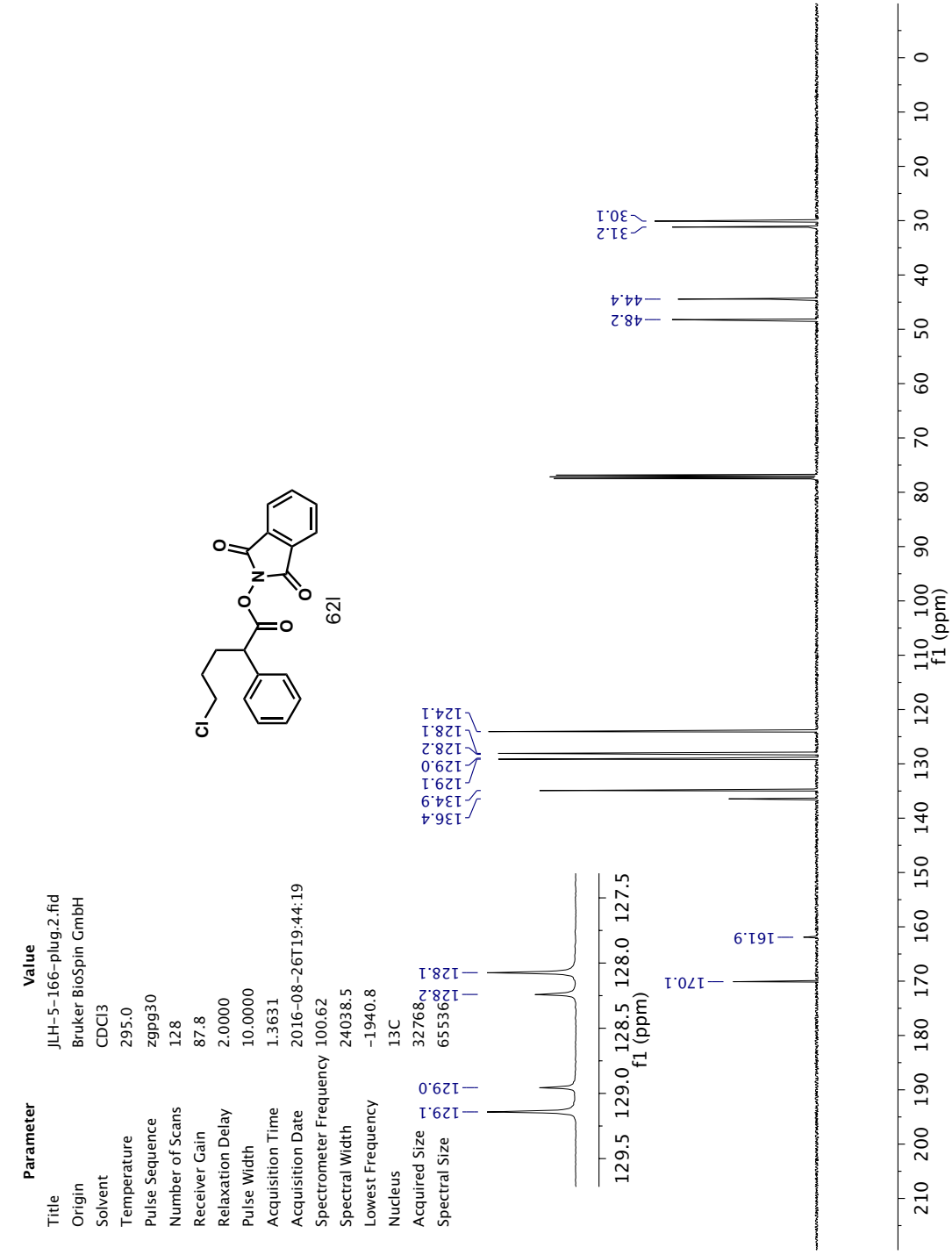
Parameter Value
Title JLH-5-166-plug.2.fid
Origin Bruker BioSpin GmbH
Solvent CDCl3
Temperature 295.0
Pulse Sequence zgpg30
Number of Scans 128
Receiver Gain 87.8
Relaxation Delay 2.0000
Pulse Width 10.0000
Acquisition Time 1.3631
Acquisition Date 2016-08-26T19:44:19
Spectrometer Frequency 100.62
Spectral Width 24038.5
Lowest Frequency -1940.8
Nucleus 13C
Acquired Size 32768
Spectral Size 65536
62l
136.4
134.9
129.1
129.0
128.2
128.1
124.1
170.1
161.9
48.2
44.4
31.2
30.1
f1 (ppm)

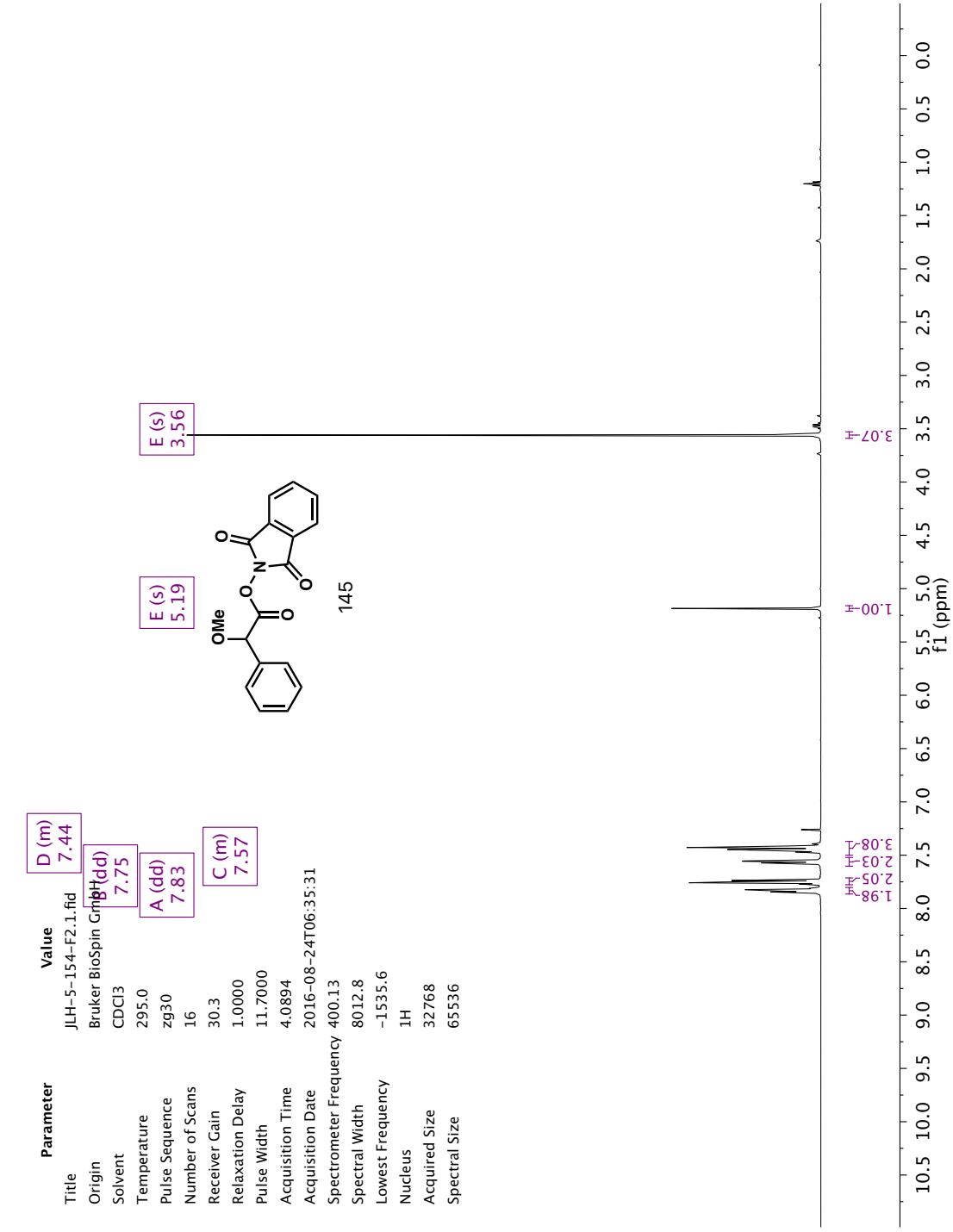
Parameter Value
Title JLH-5-154-F2.1.fid
Origin Bruker BioSpin GmbH
Solvent CDCl3
Temperature 295.0
Pulse Sequence zg30
Number of Scans 16
Receiver Gain 30.3
Relaxation Delay 1.0000
Pulse Width 11.7000
Acquisition Time 4.0894
Acquisition Date 2016-08-24T06:35:31
Spectrometer Frequency 400.13
Spectral Width 8012.8
Lowest Frequency -1535.6
Nucleus 1H
Acquired Size 32768
Spectral Size 65536
D (m) 7.44
B (dd) 7.75
A (dd) 7.83
C (m) 7.57
E (s) 5.19
E (s) 3.56
OMe
145
1.98
2.05
2.03
3.08
1.00
3.07
f1 (ppm)

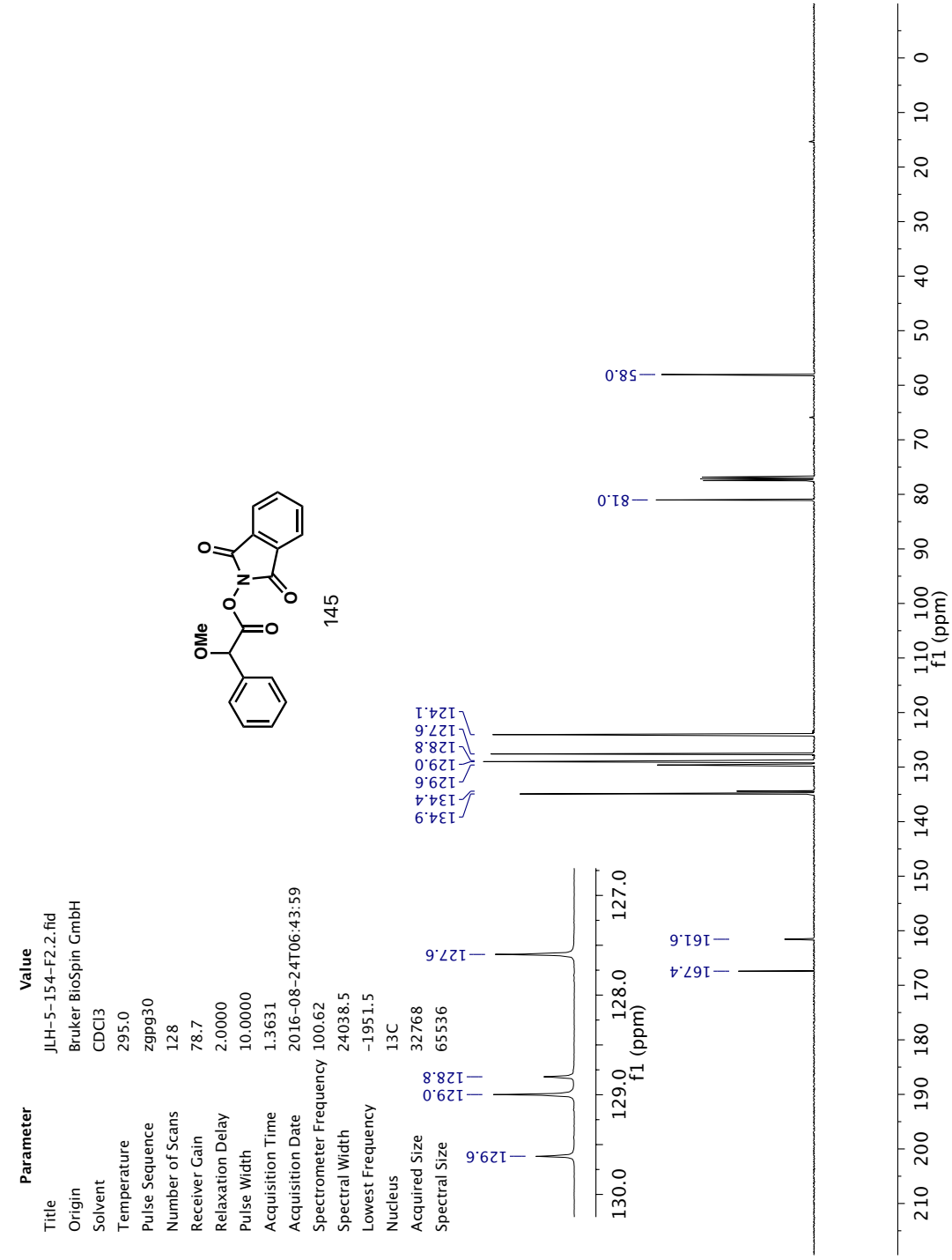
Parameter Value
Title JLH-5-154-F2.2.fid
Origin Bruker BioSpin GmbH
Solvent CDCl3
Temperature 295.0
Pulse Sequence zgpg30
Number of Scans 128
Receiver Gain 78.7
Relaxation Delay 2.0000
Pulse Width 10.0000
Acquisition Time 1.3631
Acquisition Date 2016-08-24T06:43:59
Spectrometer Frequency 100.62
Spectral Width 24038.5
Lowest Frequency -1951.5
Nucleus 13C
Acquired Size 32768
Spectral Size 65536
OMe
145
134.9
134.4
129.6
129.0
128.8
127.6
124.1
81.0
58.0
167.4
161.6
f1 (ppm)

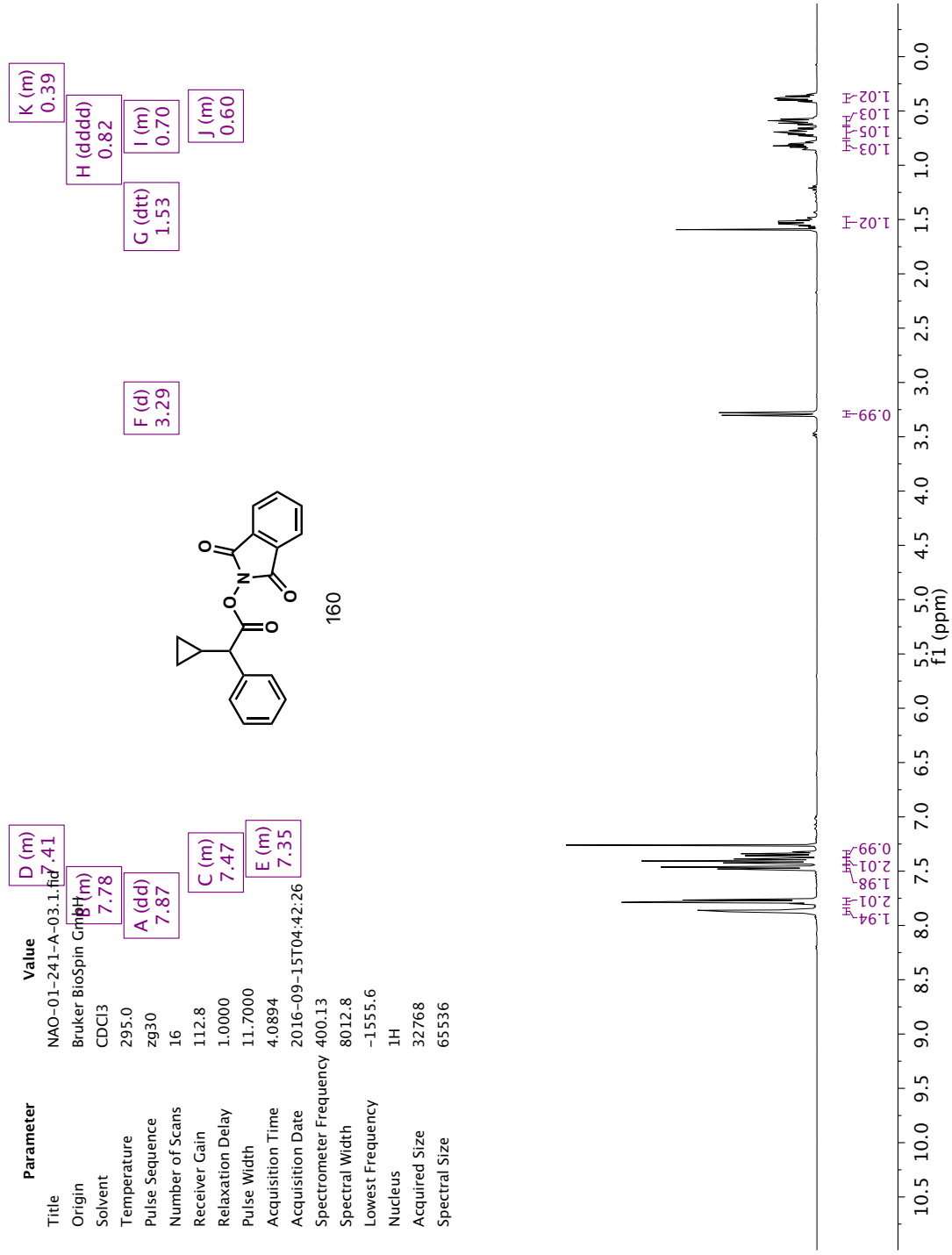
K (m) 0.39
H (dddd) 0.82
I (m) 0.70
J (m) 0.60
G (dtt) 1.53
F (d) 3.29
D (m) 7.41
B (m) 7.78
A (dd) 7.87
C (m) 7.47
E (m) 7.35
160
Parameter
Value
Title NAO-01-241-A-03.1.fid
Origin Bruker BioSpin GmbH
Solvent CDCl3
Temperature 295.0
Pulse Sequence zg30
Number of Scans 16
Receiver Gain 112.8
Relaxation Delay 1.0000
Pulse Width 11.7000
Acquisition Time 4.0894
Acquisition Date 2016-09-15T04:42:26
Spectrometer Frequency 400.13
Spectral Width 8012.8
Lowest Frequency -1555.6
Nucleus 1H
Acquired Size 32768
Spectral Size 65536
1.94
2.01
1.98
0.99
2.01
0.99
1.02
1.03
1.05
1.03
1.02
f1 (ppm)

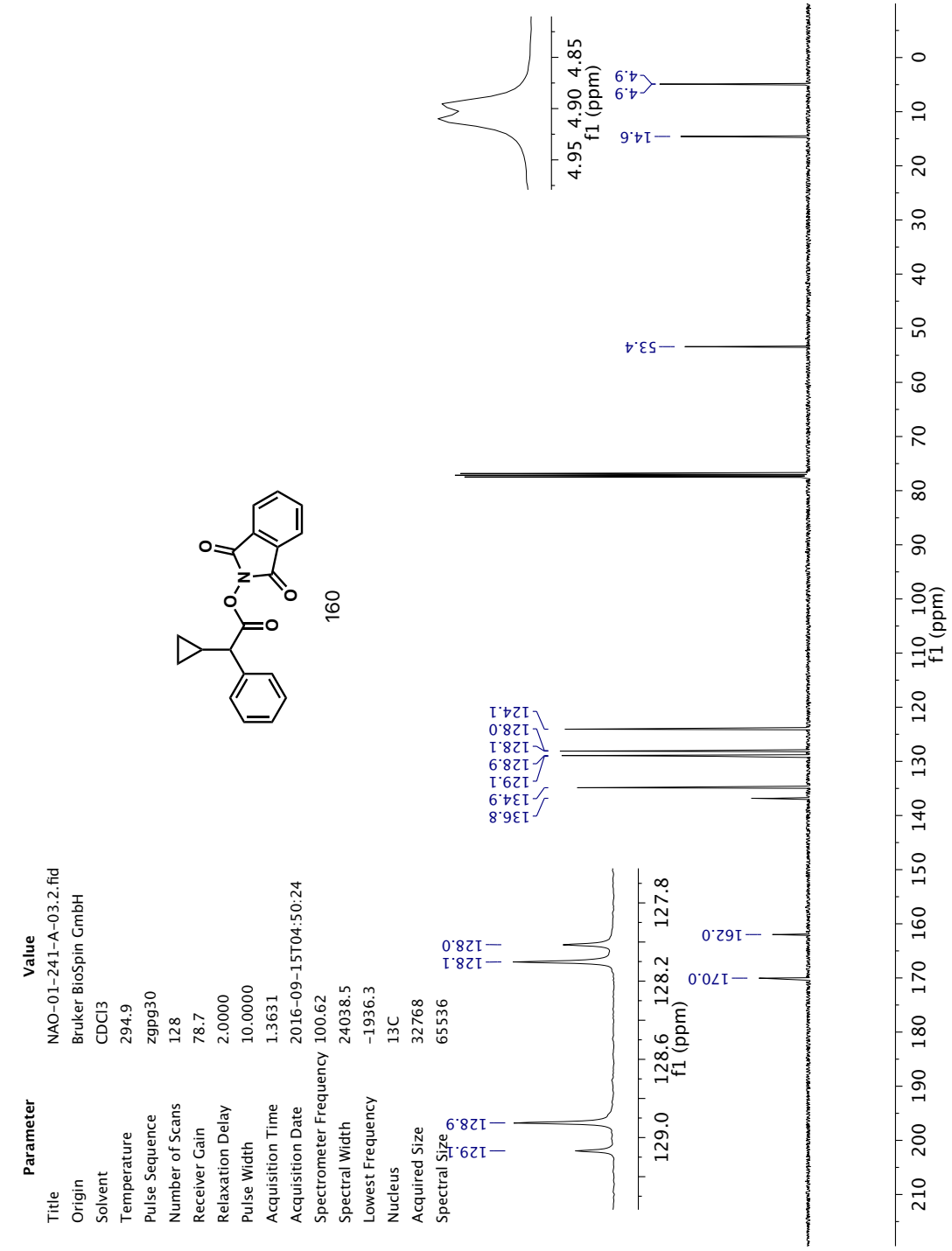
Parameter Value
Title NAO-01-241-A-03.2.fid
Origin Bruker BioSpin GmbH
Solvent CDCl3
Temperature 294.9
Pulse Sequence zgpg30
Number of Scans 128
Receiver Gain 78.7
Relaxation Delay 2.0000
Pulse Width 10.0000
Acquisition Time 1.3631
Acquisition Date 2016-09-15T04:50:24
Spectrometer Frequency 100.62
Spectral Width 24038.5
Lowest Frequency -1936.3
Nucleus 13C
Acquired Size 32768
Spectral Size 65536
160
f1 (ppm)

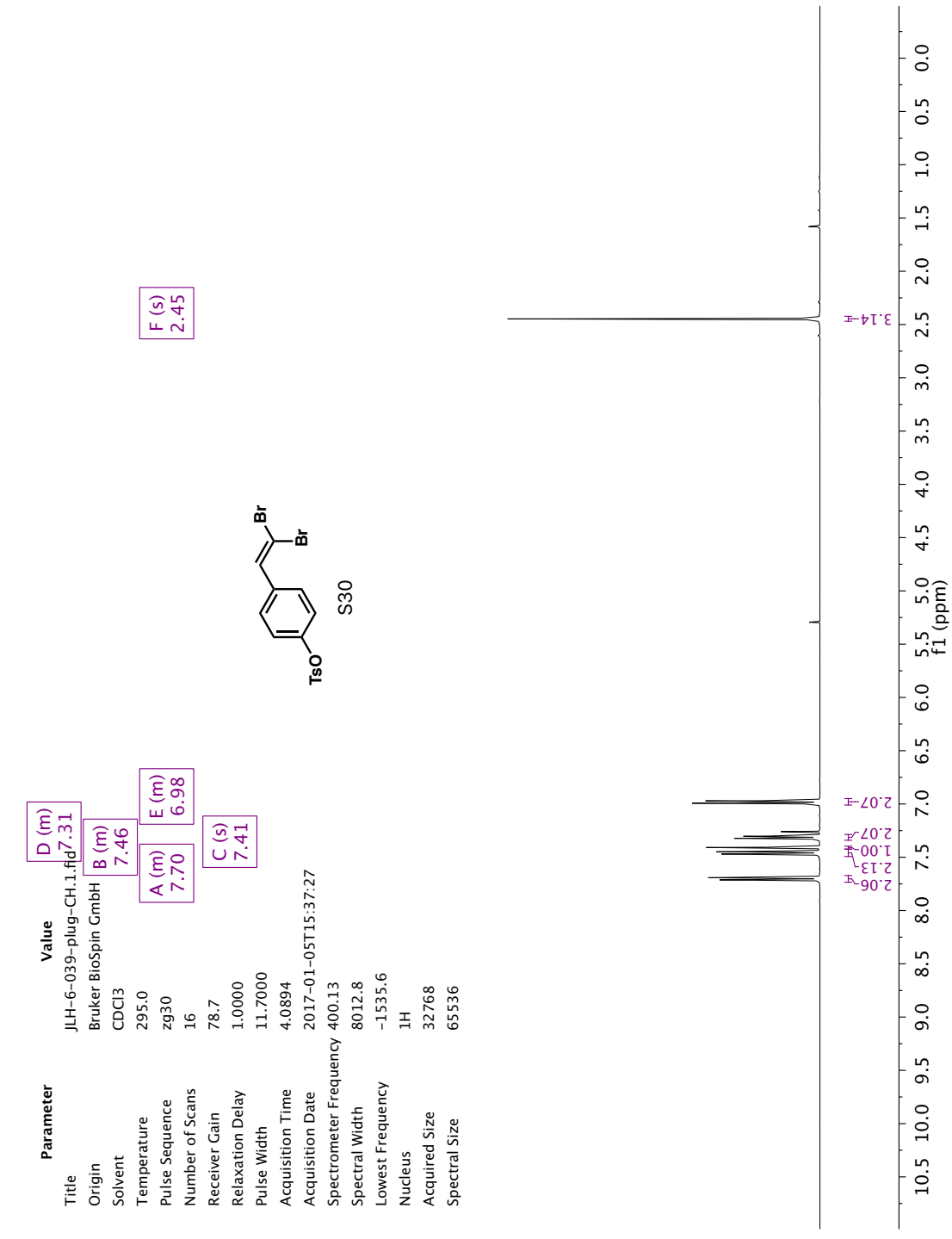
Parameter
Value
Title
JLH-6-039-plug-CH.1.fid
Origin
Bruker BioSpin GmbH
Solvent
CDCl3
Temperature
295.0
Pulse Sequence
zg30
Number of Scans
16
Receiver Gain
78.7
Relaxation Delay
1.0000
Pulse Width
11.7000
Acquisition Time
4.0894
Acquisition Date
2017-01-05T15:37:27
Spectrometer Frequency
400.13
Spectral Width
8012.8
Lowest Frequency
-1535.6
Nucleus
1H
Acquired Size
32768
Spectral Size
65536
D (m) 7.31
B (m) 7.46
A (m) 7.70
E (m) 6.98
C (s) 7.41
F (s) 2.45
Br
Br
TsO
S30
3.14
2.07
2.07
1.00
2.13
2.06
10.5 10.0 9.5 9.0 8.5 8.0 7.5 7.0 6.5 6.0 5.5 5.0 4.5 4.0 3.5 3.0 2.5 2.0 1.5 1.0 0.5 0.0
f1 (ppm)

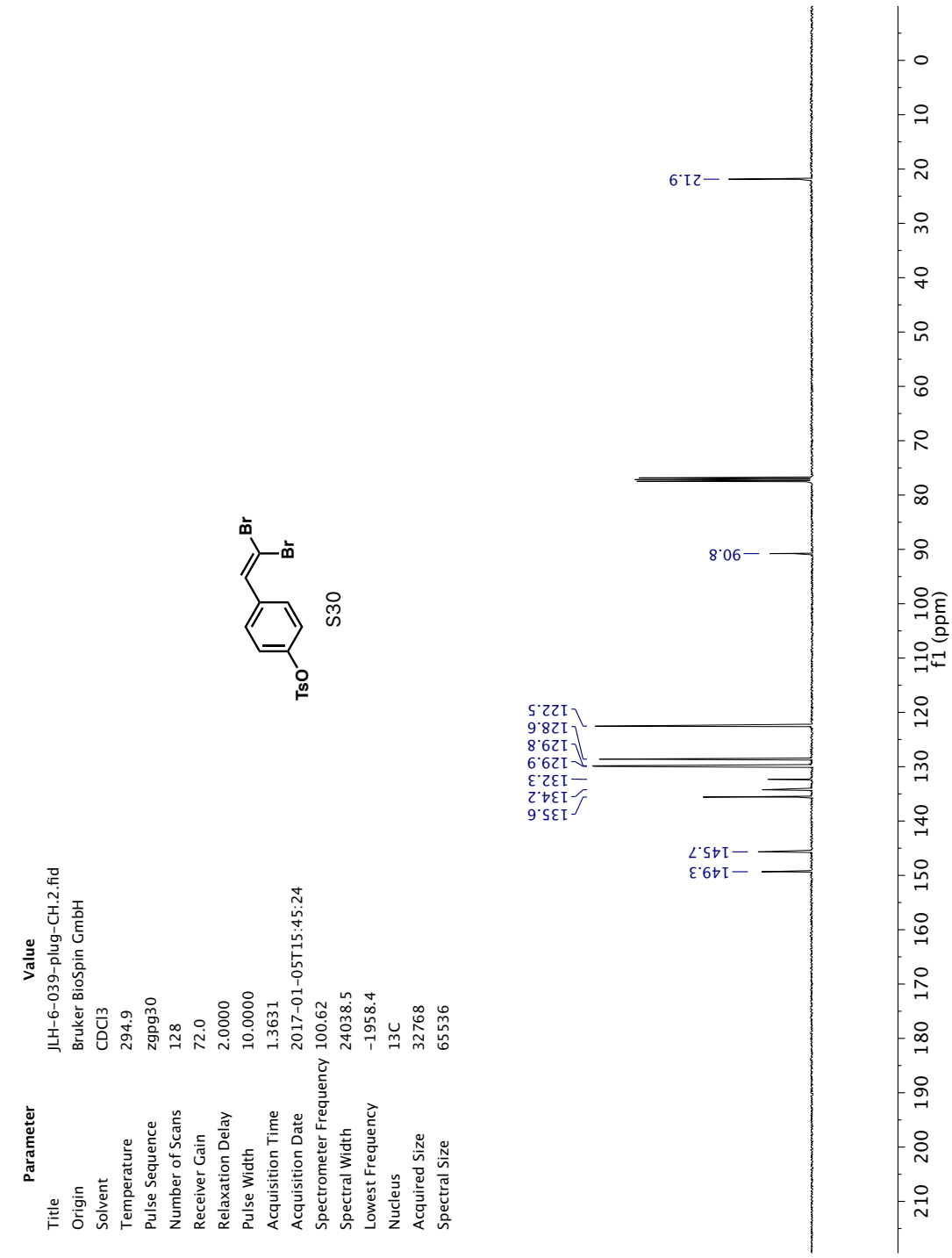
Parameter Value
Title JLH-6-039-plug-CH.2.fid
Origin Bruker BioSpin GmbH
Solvent CDCl3
Temperature 294.9
Pulse Sequence zgpg30
Number of Scans 128
Receiver Gain 72.0
Relaxation Delay 2.0000
Pulse Width 10.0000
Acquisition Time 1.3631
Acquisition Date 2017-01-05T15:45:24
Spectrometer Frequency 100.62
Spectral Width 24038.5
Lowest Frequency -1958.4
Nucleus 13C
Acquired Size 32768
Spectral Size 65536
Br
Br
TsO
S30
21.9
90.8
122.5
128.6
129.8
129.9
132.3
134.2
135.6
145.7
149.3
f1 (ppm)

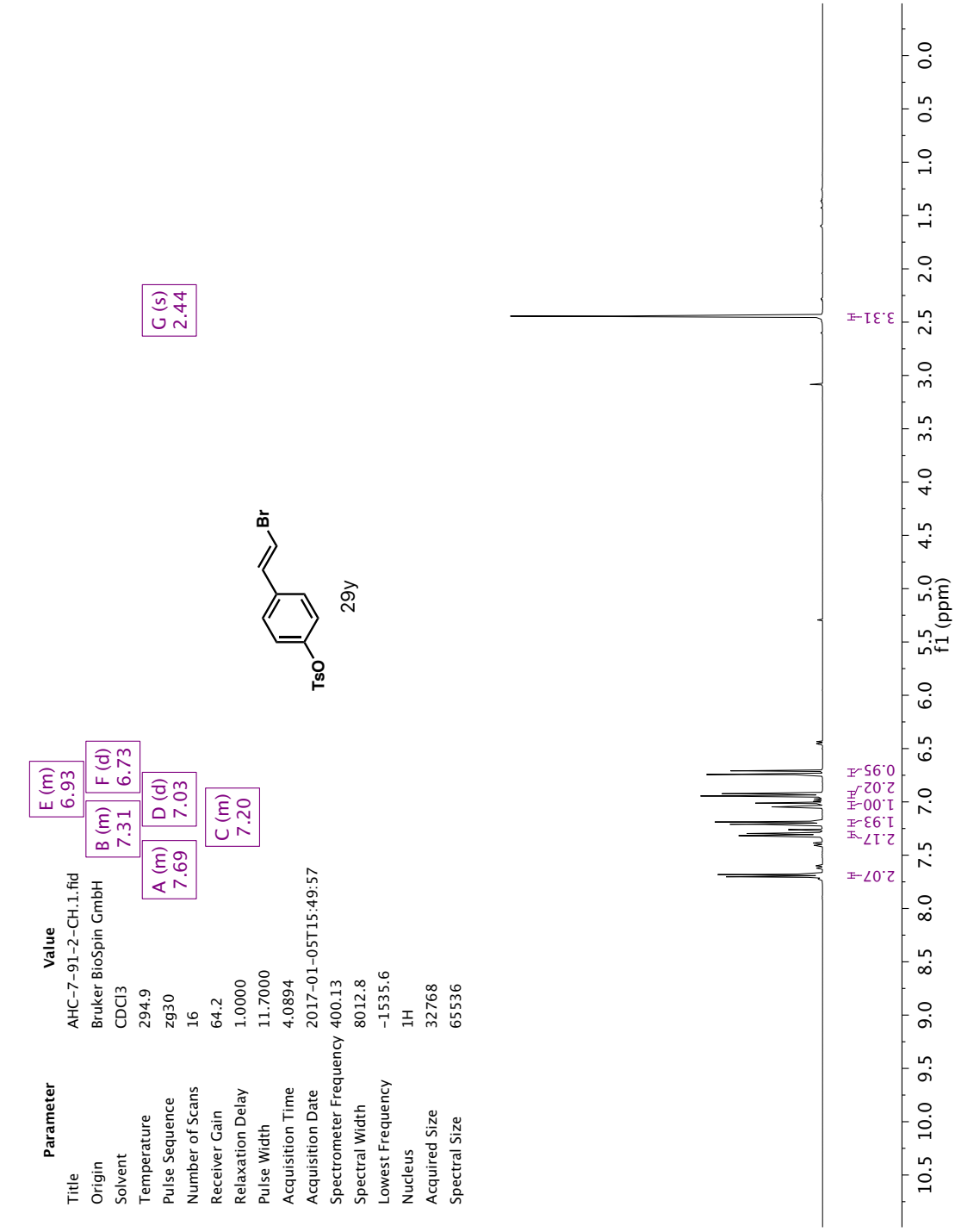
Parameter
Value
Title
AHC-7-91-2-CH.1.fid
Origin
Bruker BioSpin GmbH
Solvent
CDCl3
Temperature
294.9
Pulse Sequence
zg30
Number of Scans
16
Receiver Gain
64.2
Relaxation Delay
1.0000
Pulse Width
11.7000
Acquisition Time
4.0894
Acquisition Date
2017-01-05T15:49:57
Spectrometer Frequency
400.13
Spectral Width
8012.8
Lowest Frequency
-1535.6
Nucleus
1H
Acquired Size
32768
Spectral Size
65536
A (m) 7.69
B (m) 7.31
C (m) 7.20
D (d) 7.03
E (m) 6.93
F (d) 6.73
G (s) 2.44
TsO
Br
29y
2.07
2.17
1.93
1.00
2.02
0.95
3.31
f1 (ppm)

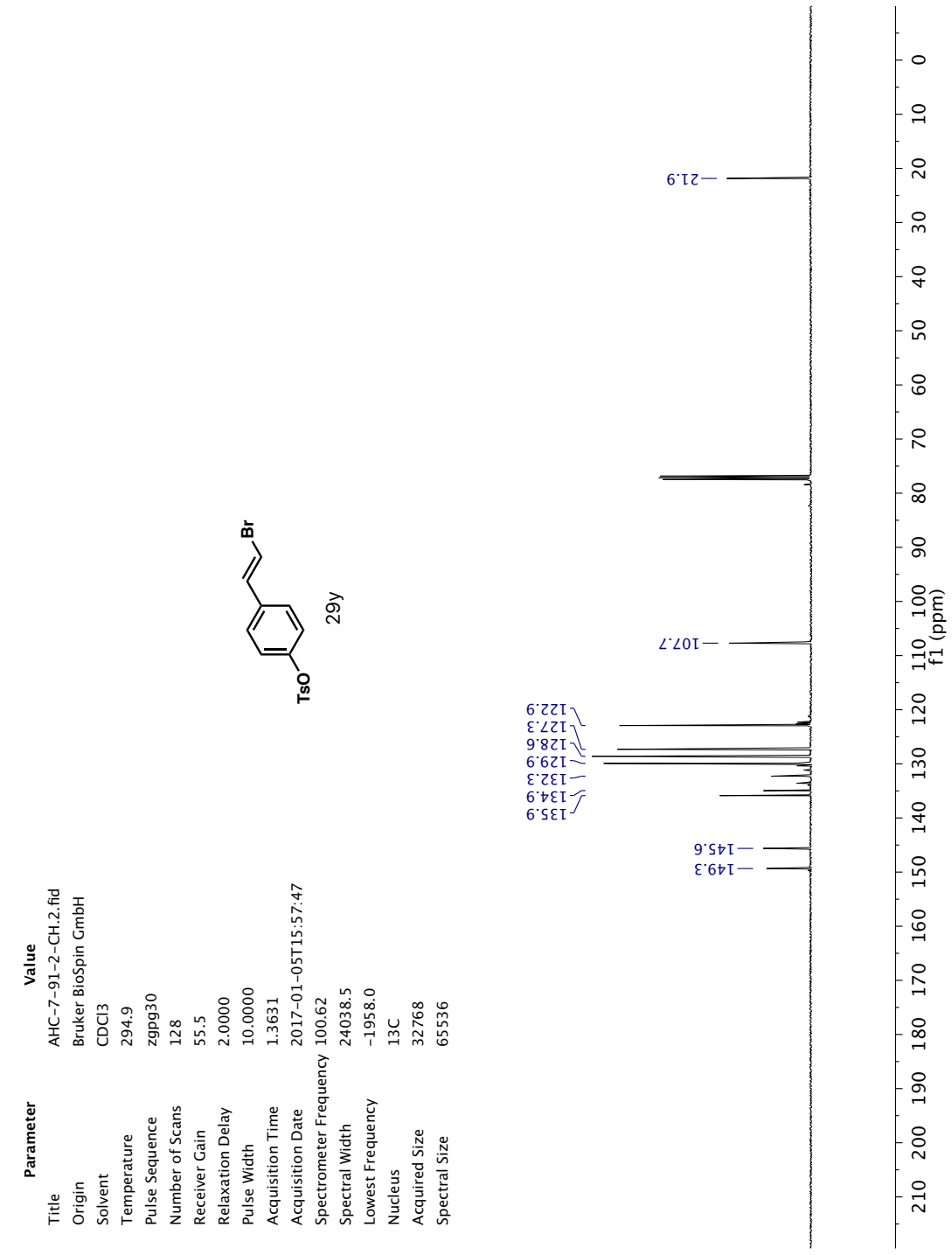
Parameter Value
Title AHC-7-91-2-CH.2.fid
Origin Bruker BioSpin GmbH
Solvent CDCl3
Temperature 294.9
Pulse Sequence zgpg30
Number of Scans 128
Receiver Gain 55.5
Relaxation Delay 2.0000
Pulse Width 10.0000
Acquisition Time 1.3631
Acquisition Date 2017-01-05T15:57:47
Spectrometer Frequency 100.62
Spectral Width 24038.5
Lowest Frequency -1958.0
Nucleus 13C
Acquired Size 32768
Spectral Size 65536
Br
TsO
29y
21.9
107.7
122.9
127.3
128.6
129.9
132.3
134.9
135.9
145.6
149.3
f1 (ppm)

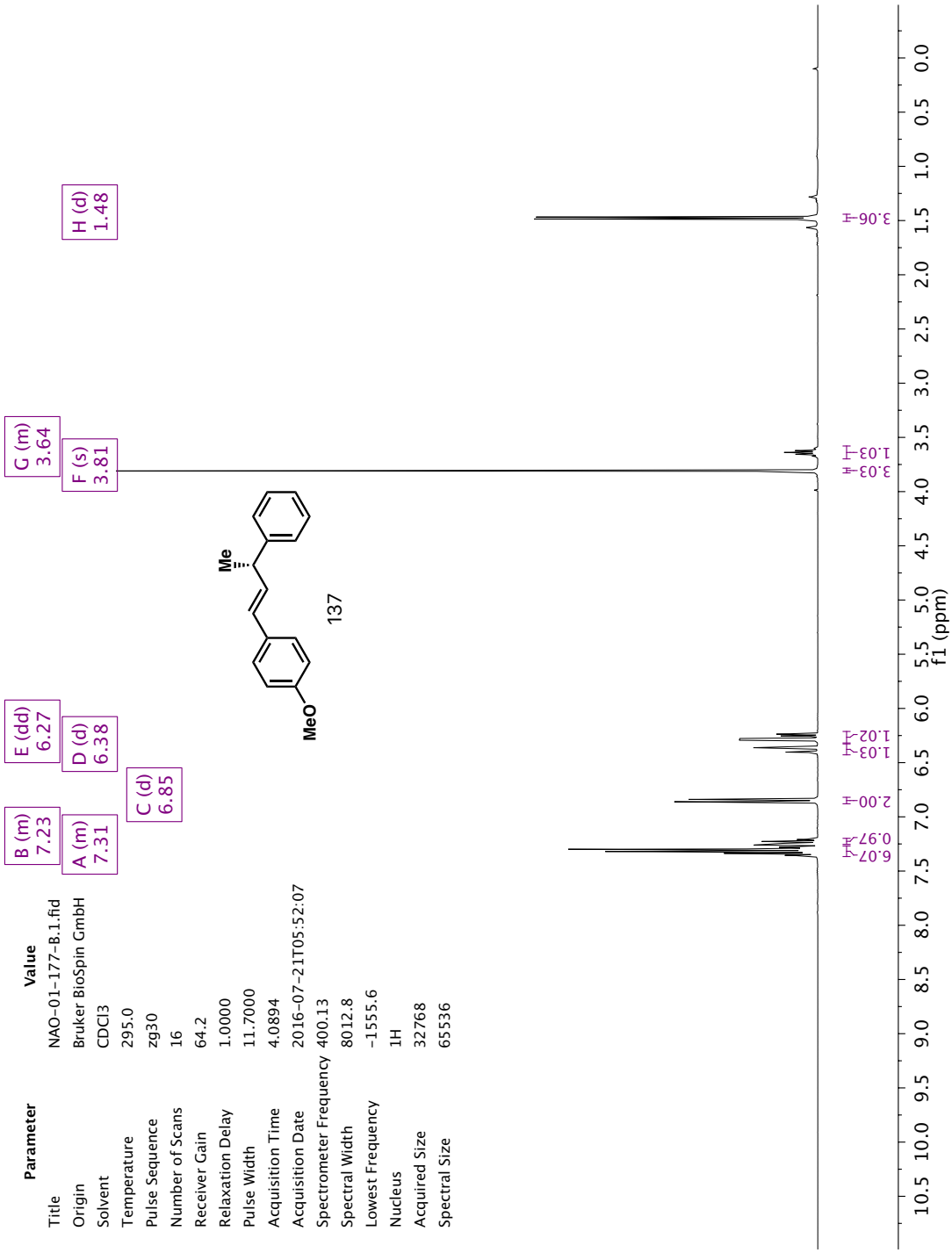
Parameter Value
Title NAO-01-177-B.1.fid
Origin Bruker BioSpin GmbH
Solvent CDCl3
Temperature 295.0
Pulse Sequence zg30
Number of Scans 16
Receiver Gain 64.2
Relaxation Delay 1.0000
Pulse Width 11.7000
Acquisition Time 4.0894
Acquisition Date 2016-07-21T05:52:07
Spectrometer Frequency 400.13
Spectral Width 8012.8
Lowest Frequency -1555.6
Nucleus 1H
Acquired Size 32768
Spectral Size 65536
B (m) 7.23
A (m) 7.31
E (dd) 6.27
D (d) 6.38
C (d) 6.85
G (m) 3.64
F (s) 3.81
H (d) 1.48
Me
MeO
137
6.07
0.97
2.00
1.03
1.02
1.03
3.03
3.06
f1 (ppm)

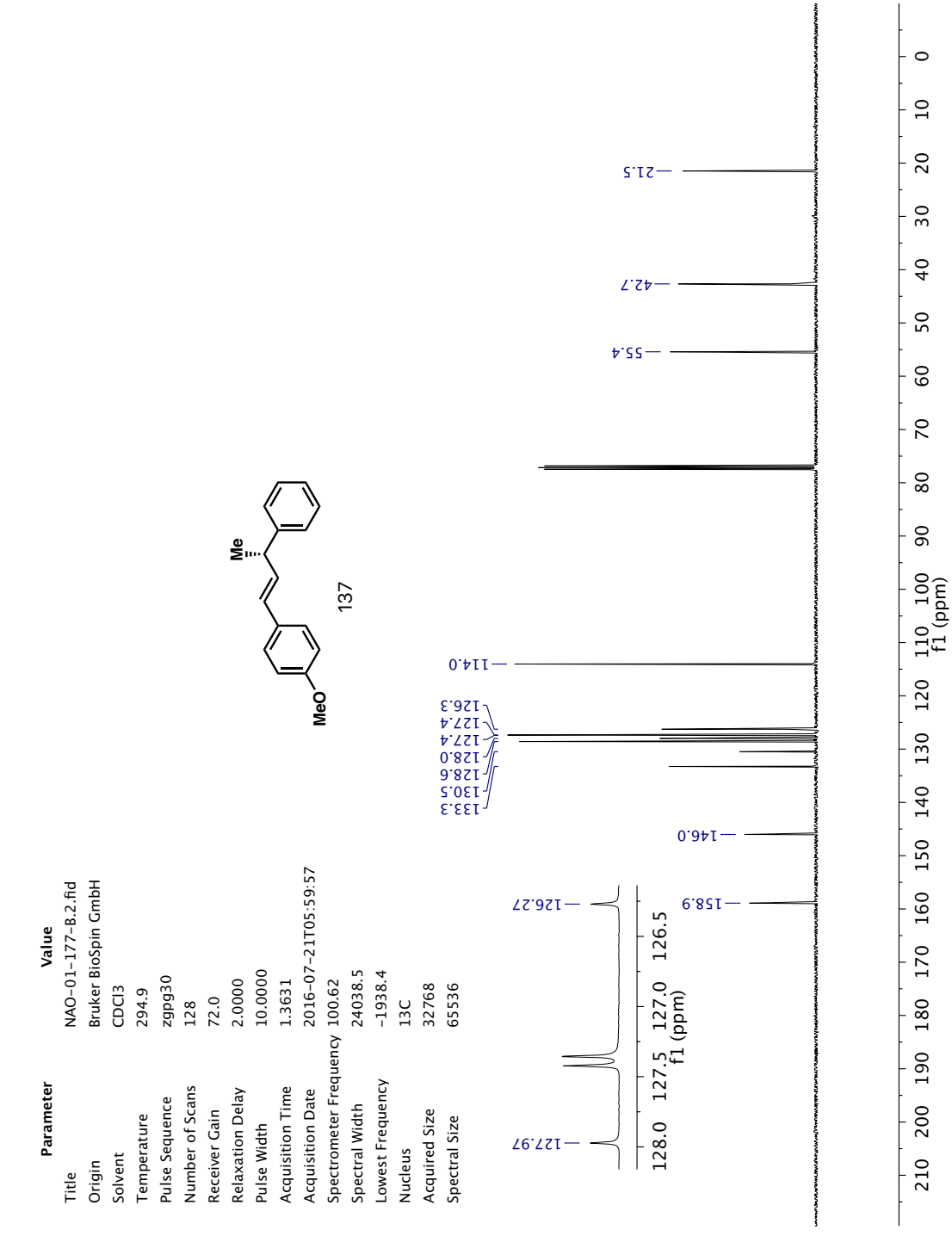
Parameter Value
Title NAO-01-177-B.2.fid
Origin Bruker BioSpin GmbH
Solvent CDCl3
Temperature 294.9
Pulse Sequence zgpg30
Number of Scans 128
Receiver Gain 72.0
Relaxation Delay 2.0000
Pulse Width 10.0000
Acquisition Time 1.3631
Acquisition Date 2016-07-21T05:59:57
Spectrometer Frequency 100.62
Spectral Width 24038.5
Lowest Frequency -1938.4
Nucleus 13C
Acquired Size 32768
Spectral Size 65536
Me
MeO
137
158.9
146.0
133.3
130.5
128.6
128.0
127.4
127.4
126.3
114.0
55.4
42.7
21.5
127.97
126.27
128.0 127.5 127.0 126.5
f1 (ppm)
210 200 190 180 170 160 150 140 130 120 110 100 90 80 70 60 50 40 30 20 10 0
f1 (ppm)

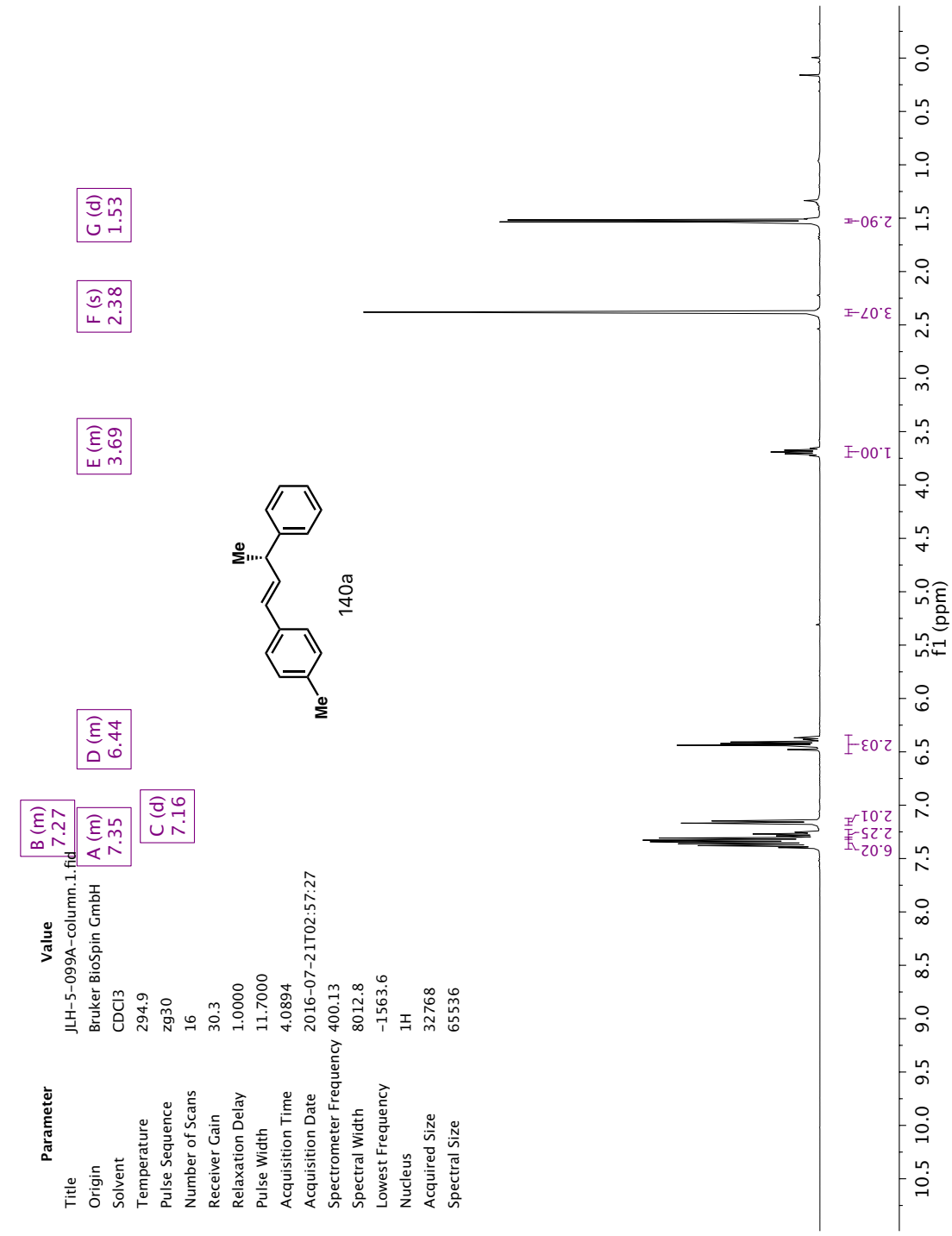
Parameter
Value
Title JLH-5-099A-column.1.fid
Origin Bruker BioSpin GmbH
Solvent CDCl3
Temperature 294.9
Pulse Sequence zg30
Number of Scans 16
Receiver Gain 30.3
Relaxation Delay 1.0000
Pulse Width 11.7000
Acquisition Time 4.0894
Acquisition Date 2016-07-21T02:57:27
Spectrometer Frequency 400.13
Spectral Width 8012.8
Lowest Frequency -1563.6
Nucleus 1H
Acquired Size 32768
Spectral Size 65536
B (m) 7.27
A (m) 7.35
C (d) 7.16
D (m) 6.44
E (m) 3.69
F (s) 2.38
G (d) 1.53
Me
Me
140a
6.02
2.25
2.01
2.03
1.00
3.07
2.90
f1 (ppm)

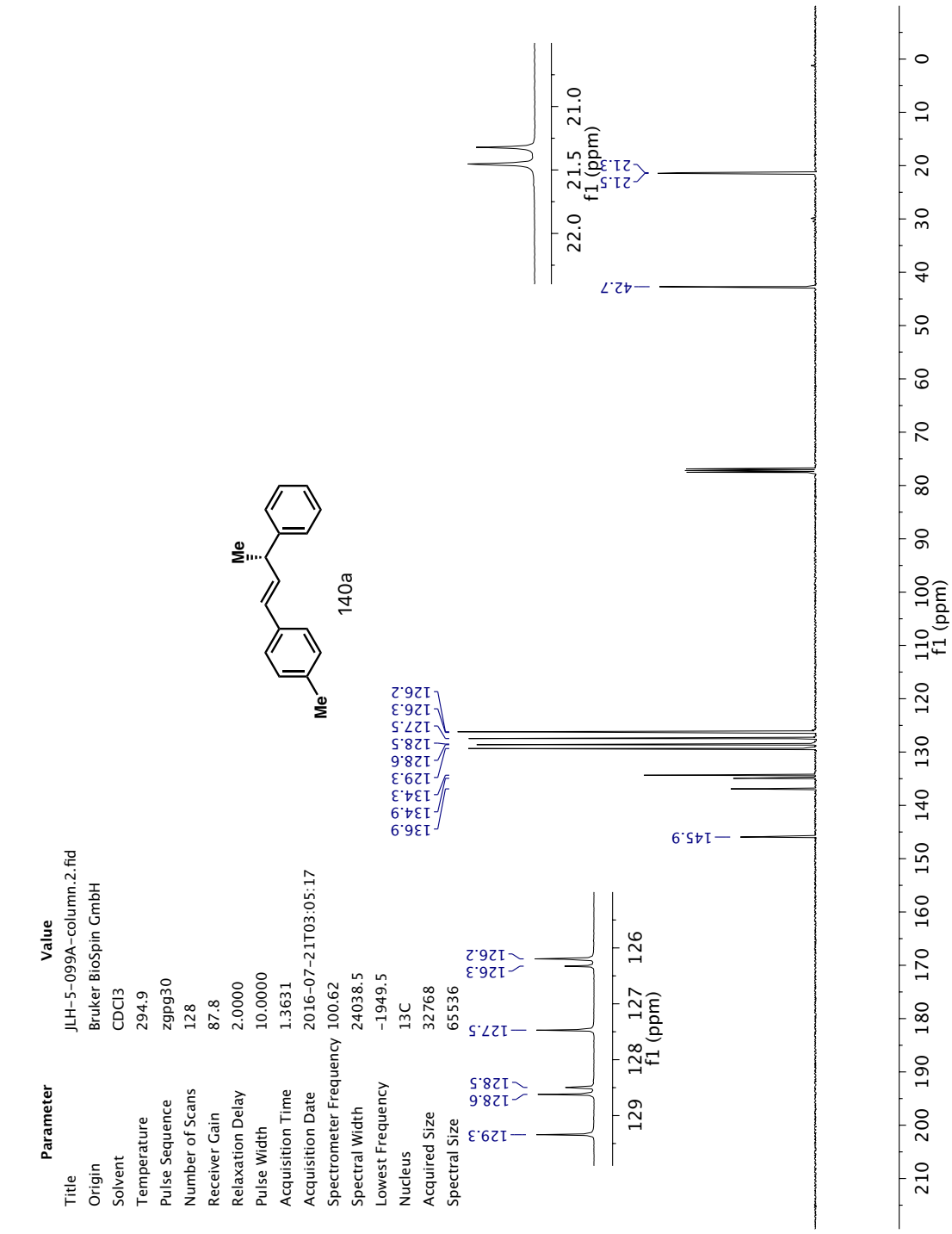
Parameter Value
Title JLH-5-099A-column.2.fid
Origin Bruker BioSpin GmbH
Solvent CDCl3
Temperature 294.9
Pulse Sequence zgpg30
Number of Scans 128
Receiver Gain 87.8
Relaxation Delay 2.0000
Pulse Width 10.0000
Acquisition Time 1.3631
Acquisition Date 2016-07-21T03:05:17
Spectrometer Frequency 100.62
Spectral Width 24038.5
Lowest Frequency -1949.5
Nucleus 13C
Acquired Size 32768
Spectral Size 65536
Me
Me
140a
145.9
136.9
134.9
134.3
129.3
128.6
128.5
127.5
126.3
126.2
42.7
21.5
21.3
f1 (ppm)

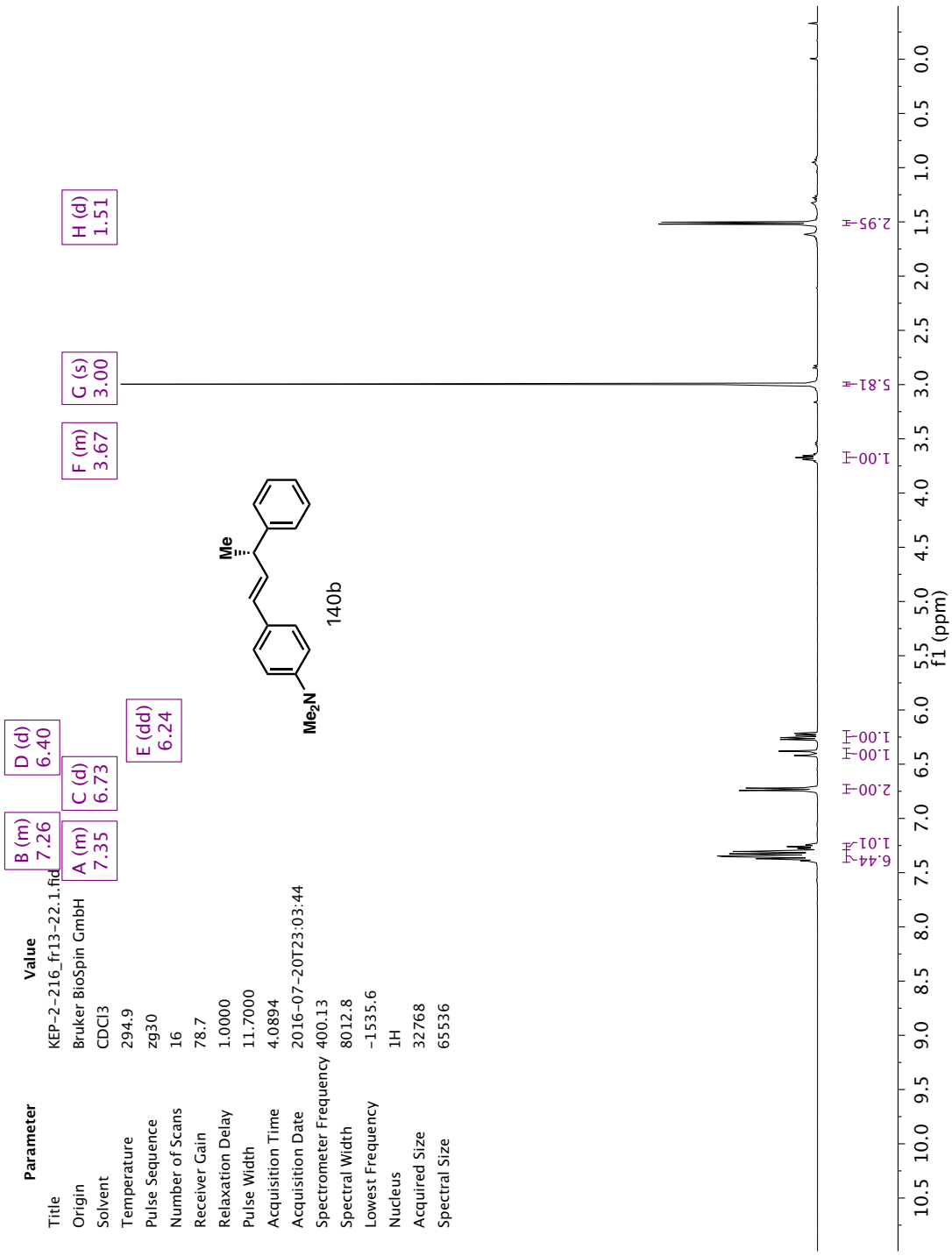
Parameter
Value
Title KEP-2-216_fr13-22.1.fid
Origin Bruker BioSpin GmbH
Solvent CDCl3
Temperature 294.9
Pulse Sequence zg30
Number of Scans 16
Receiver Gain 78.7
Relaxation Delay 1.0000
Pulse Width 11.7000
Acquisition Time 4.0894
Acquisition Date 2016-07-20T23:03:44
Spectrometer Frequency 400.13
Spectral Width 8012.8
Lowest Frequency -1535.6
Nucleus 1H
Acquired Size 32768
Spectral Size 65536
B (m) 7.26
A (m) 7.35
D (d) 6.40
C (d) 6.73
E (dd) 6.24
F (m) 3.67
G (s) 3.00
H (d) 1.51
Me
Me2N
140b
6.44
1.01
2.00
1.00
1.00
1.00
5.81
2.95
10.5 10.0 9.5 9.0 8.5 8.0 7.5 7.0 6.5 6.0 5.5 5.0 4.5 4.0 3.5 3.0 2.5 2.0 1.5 1.0 0.5 0.0
f1 (ppm)

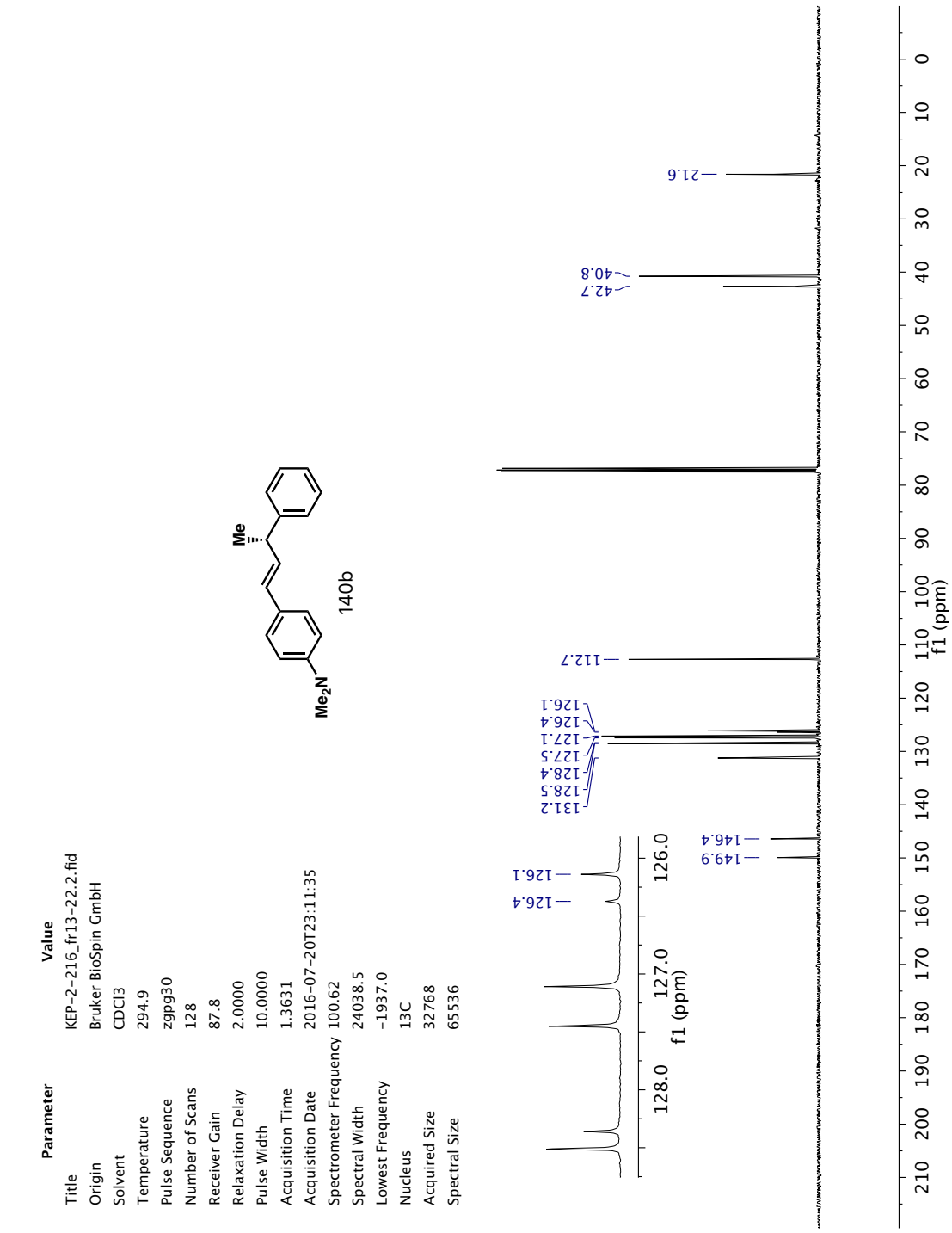
Me
Me2N
140b
Parameter Value
Title KEP-2-216_fr13-22.2.fid
Origin Bruker BioSpin GmbH
Solvent CDCl3
Temperature 294.9
Pulse Sequence zgpg30
Number of Scans 128
Receiver Gain 87.8
Relaxation Delay 2.0000
Pulse Width 10.0000
Acquisition Time 1.3631
Acquisition Date 2016-07-20T23:11:35
Spectrometer Frequency 100.62
Spectral Width 24038.5
Lowest Frequency -1937.0
Nucleus 13C
Acquired Size 32768
Spectral Size 65536
126.1
126.4
128.0
127.0
126.0
f1 (ppm)
131.2
128.5
128.4
127.5
127.1
126.4
126.1
112.7
42.7
40.8
21.6
149.9
146.4
210 200 190 180 170 160 150 140 130 120 110 100 90 80 70 60 50 40 30 20 10 0
f1 (ppm)

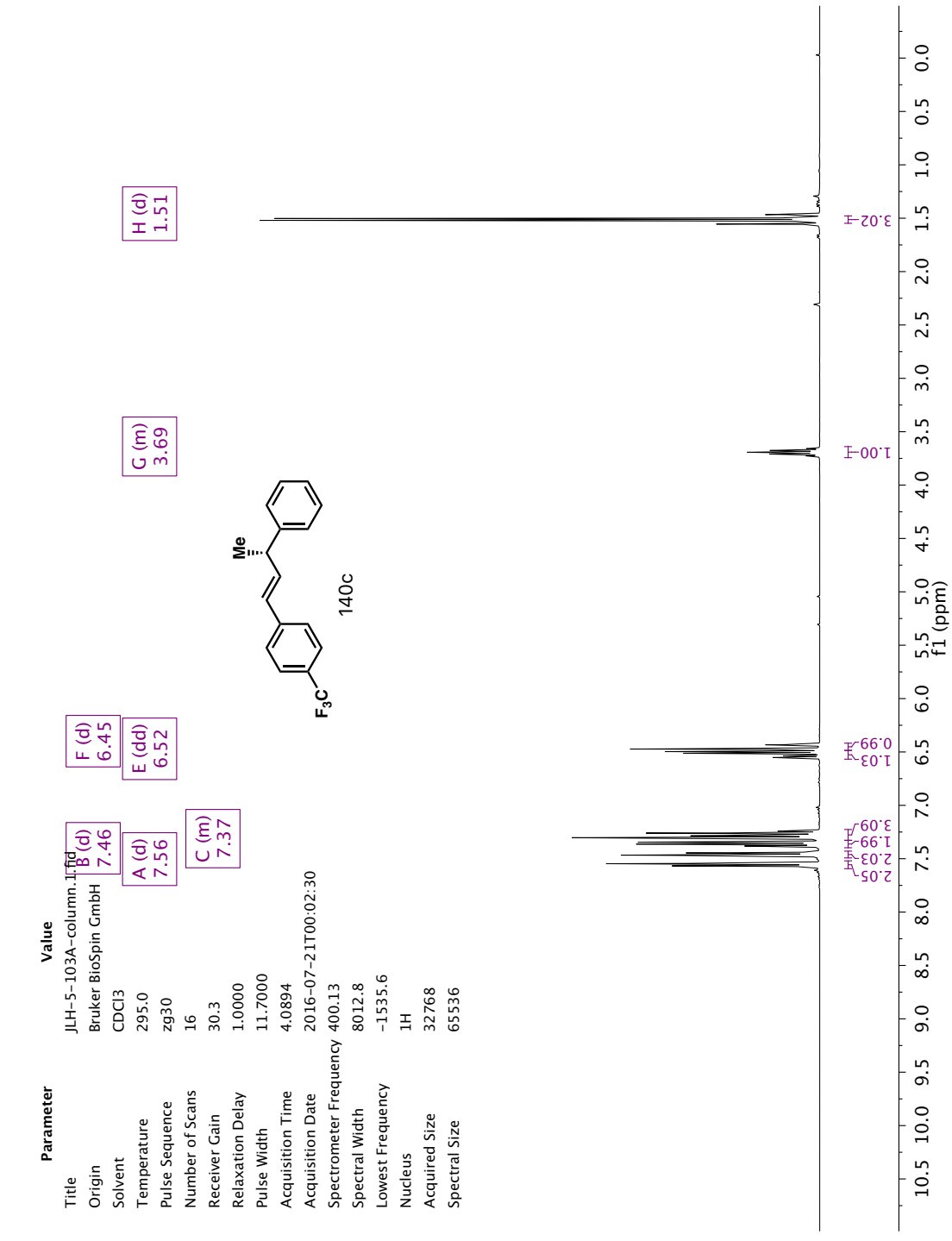
Parameter
Value
Title JLH-5-103A-column.1.fid
Origin Bruker BioSpin GmbH
Solvent CDCl3
Temperature 295.0
Pulse Sequence zg30
Number of Scans 16
Receiver Gain 30.3
Relaxation Delay 1.0000
Pulse Width 11.7000
Acquisition Time 4.0894
Acquisition Date 2016-07-21T00:02:30
Spectrometer Frequency 400.13
Spectral Width 8012.8
Lowest Frequency -1535.6
Nucleus 1H
Acquired Size 32768
Spectral Size 65536
B (d) 7.46
A (d) 7.56
C (m) 7.37
F (d) 6.45
E (dd) 6.52
G (m) 3.69
H (d) 1.51
Me
F3C
140c
2.05
2.03
1.99
3.09
1.03
0.99
1.00
3.02
f1 (ppm)

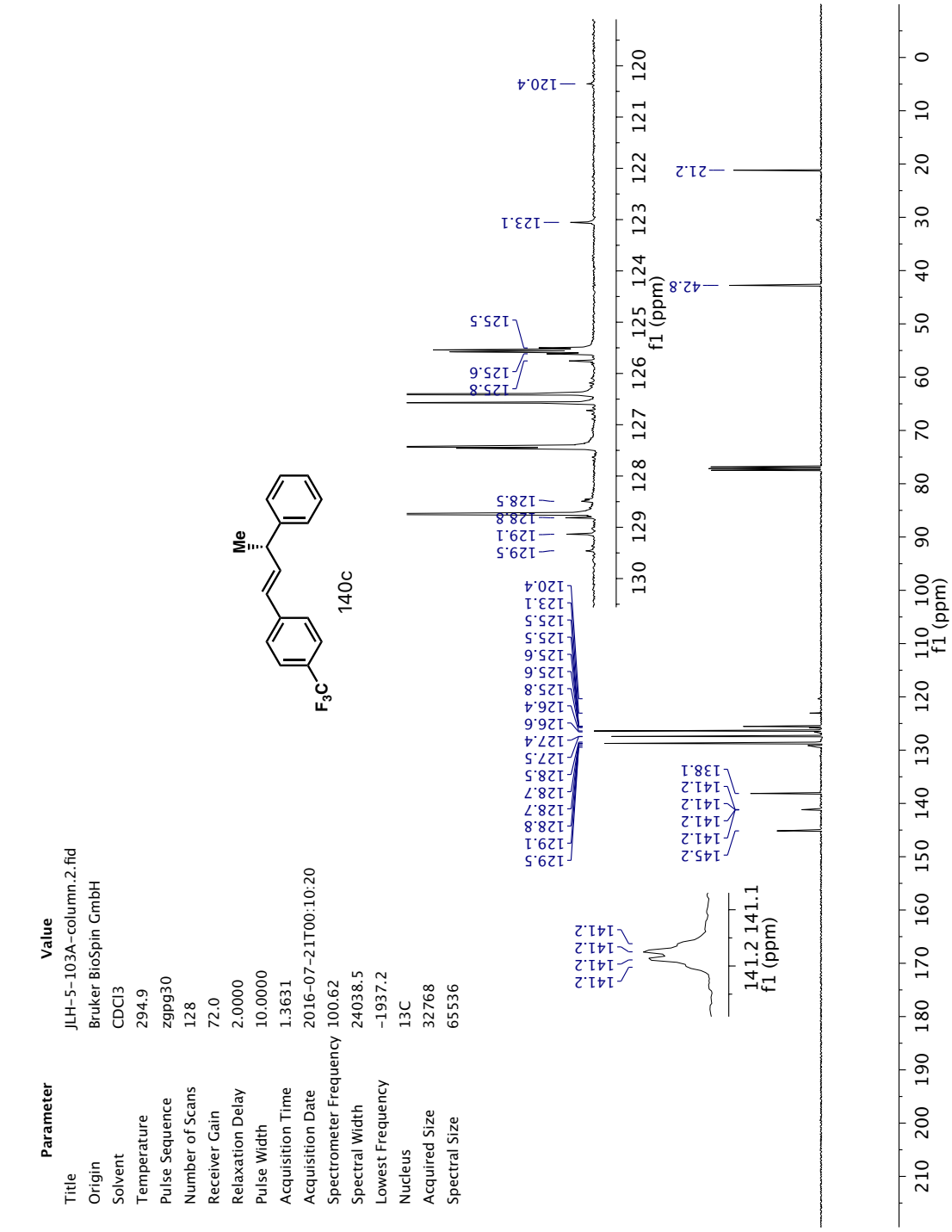
Parameter Value
Title JLH-5-103A-column.2.fid
Origin Bruker BioSpin GmbH
Solvent CDCl3
Temperature 294.9
Pulse Sequence zgpg30
Number of Scans 128
Receiver Gain 72.0
Relaxation Delay 2.0000
Pulse Width 10.0000
Acquisition Time 1.3631
Acquisition Date 2016-07-21T00:10:20
Spectrometer Frequency 100.62
Spectral Width 24038.5
Lowest Frequency -1937.2
Nucleus 13C
Acquired Size 32768
Spectral Size 65536
Me
F3C
140c
f1 (ppm)

Parameter	Value
Title	JLH-5-103A
Origin	Varian
Solvent	"cdcl3"
Temperature	25.0
Pulse Sequence	s2pul
Number of Scans	16
Receiver Gain	30
Relaxation Delay	1.0000
Pulse Width	6.3333
Acquisition Time	0.9856
Acquisition Date	2016-08-31T23:36:19
Spectrometer Frequency	282.34
Spectral Width	64935.1
Lowest Frequency	-58252.6
Nucleus	19F
Acquired Size	64000
Spectral Size	131072
Absolute Reference	

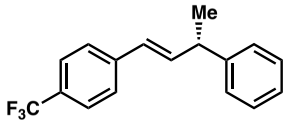

140c

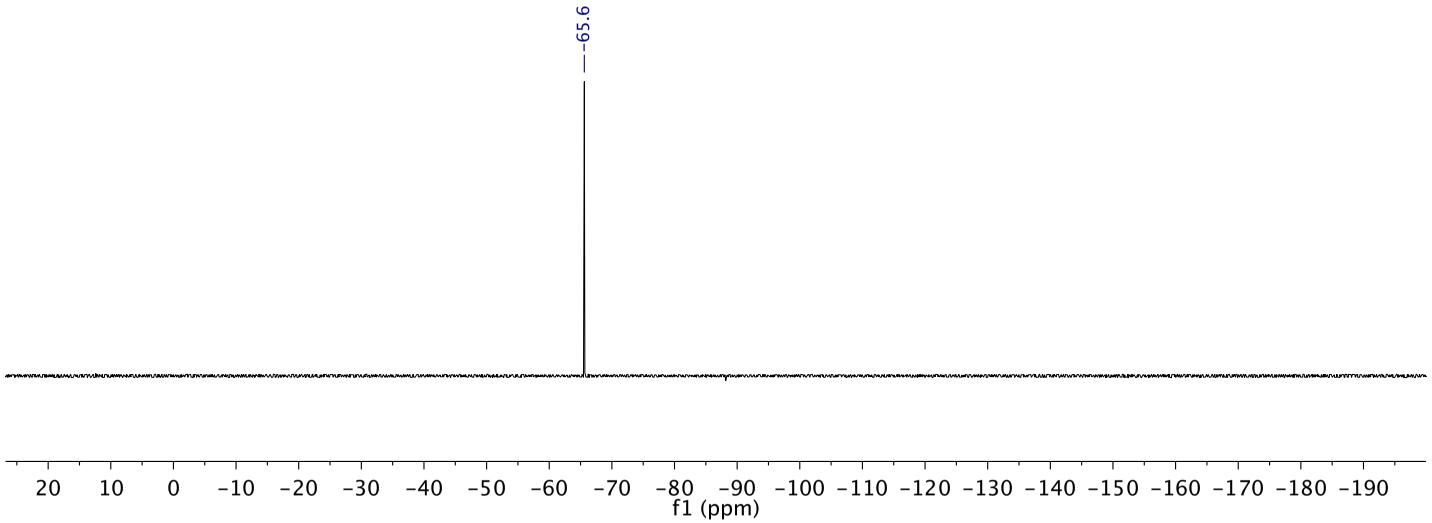

Parameter	Value
Title	JLH-5-103A-C6F6
Origin	Varian
Solvent	"cdcl3"
Temperature	25.0
Pulse Sequence	s2pul
Number of Scans	16
Receiver Gain	30
Relaxation Delay	1.0000
Pulse Width	6.3333
Acquisition Time	0.9856
Acquisition Date	2016-08-31T23:40:31
Spectrometer Frequency	282.34
Spectral Width	64935.1
Lowest Frequency	-58228.3
Nucleus	19F
Acquired Size	64000
Spectral Size	131072

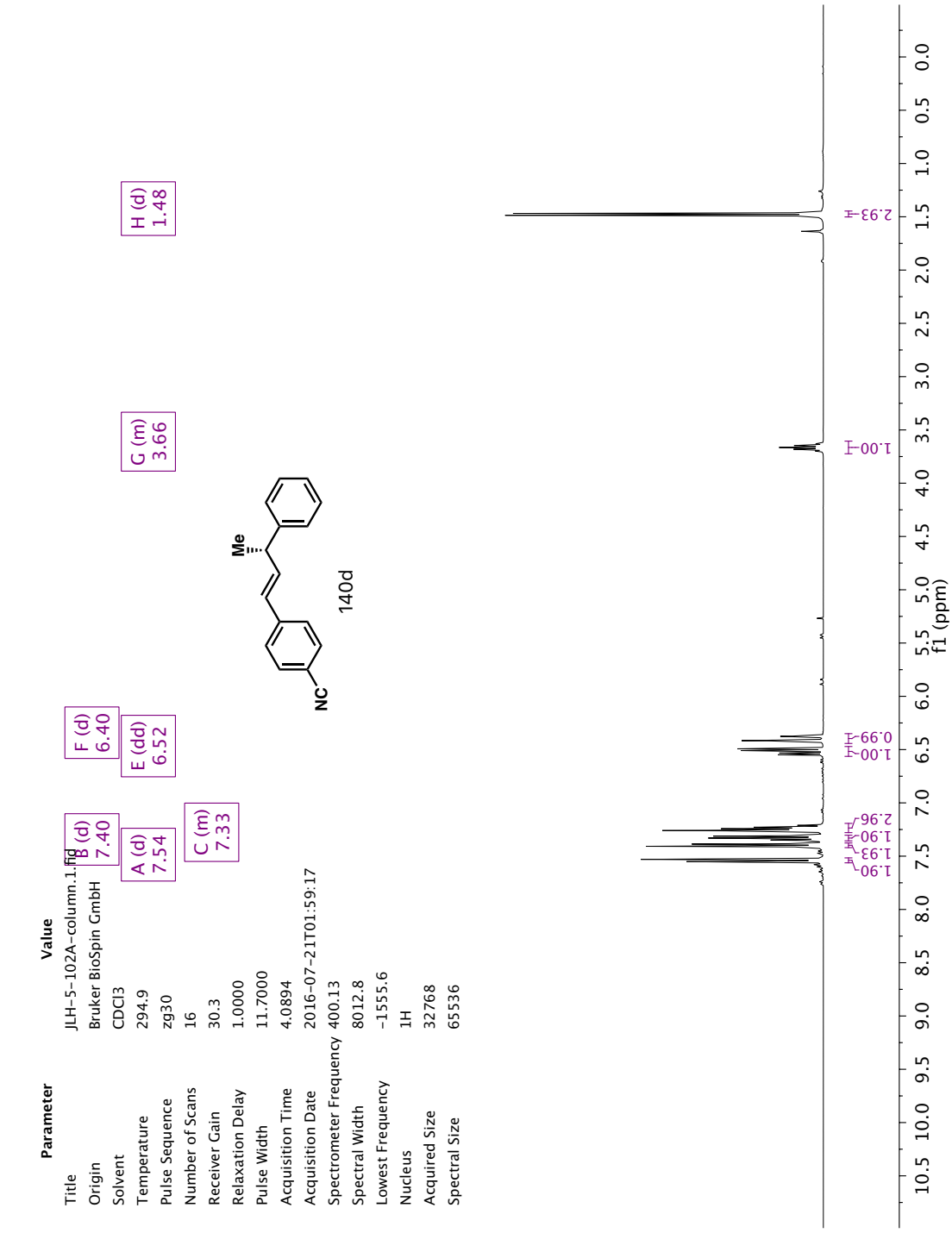
Parameter
Value
Title JLH-5-102A-column.1.fid
Origin Bruker BioSpin GmbH
Solvent CDCl3
Temperature 294.9
Pulse Sequence zg30
Number of Scans 16
Receiver Gain 30.3
Relaxation Delay 1.0000
Pulse Width 11.7000
Acquisition Time 4.0894
Acquisition Date 2016-07-21T01:59:17
Spectrometer Frequency 400.13
Spectral Width 8012.8
Lowest Frequency -1555.6
Nucleus 1H
Acquired Size 32768
Spectral Size 65536
B (d) 7.40
A (d) 7.54
C (m) 7.33
F (d) 6.40
E (dd) 6.52
G (m) 3.66
H (d) 1.48
Me
NC
140d
1.90
1.93
2.96
1.90
1.00
0.99
1.00
2.93
f1 (ppm)

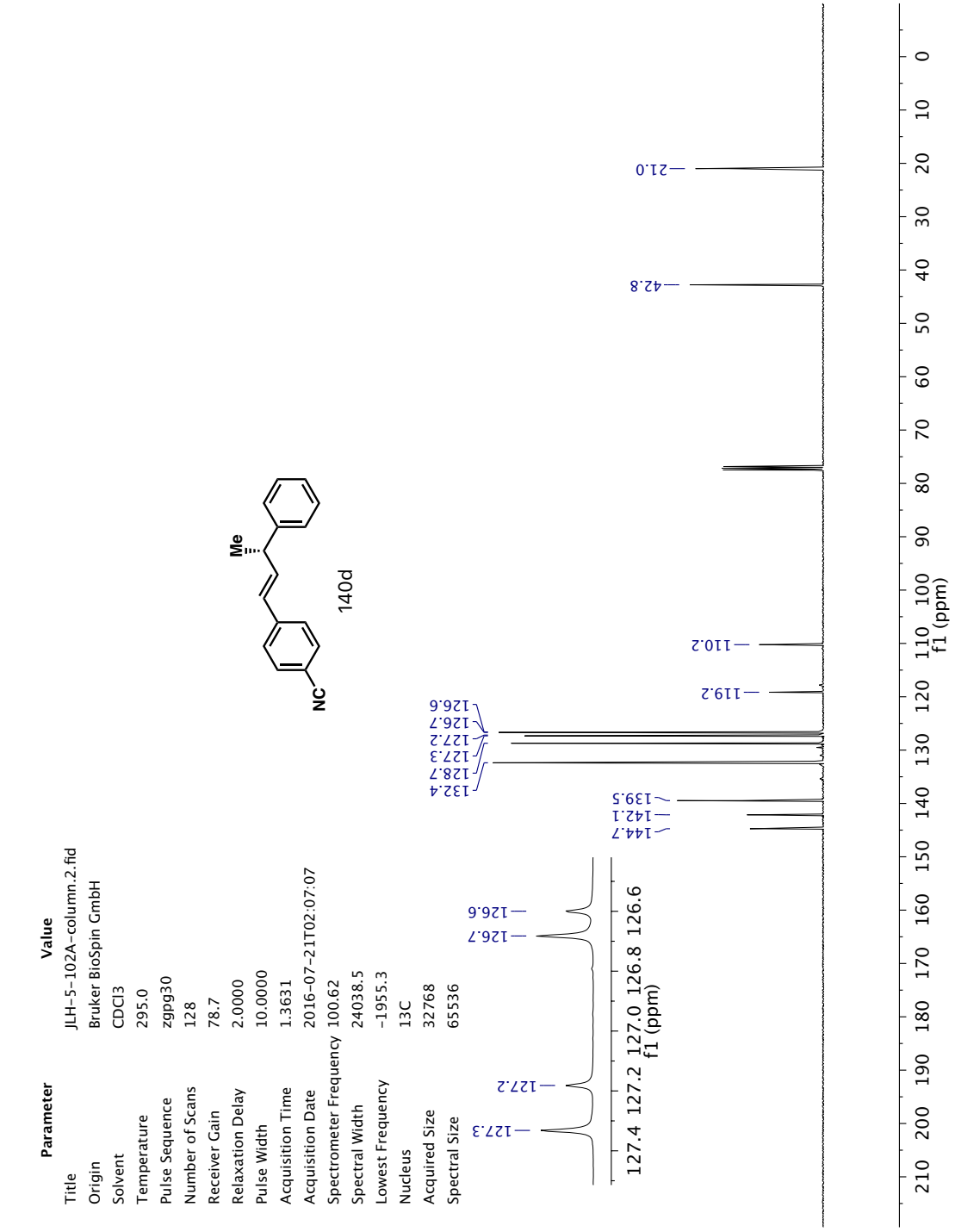
Parameter Value
Title JLH-5-102A-column.2.fid
Origin Bruker BioSpin GmbH
Solvent CDCl3
Temperature 295.0
Pulse Sequence zgpg30
Number of Scans 128
Receiver Gain 78.7
Relaxation Delay 2.0000
Pulse Width 10.0000
Acquisition Time 1.3631
Acquisition Date 2016-07-21T02:07:07
Spectrometer Frequency 100.62
Spectral Width 24038.5
Lowest Frequency -1955.3
Nucleus 13C
Acquired Size 32768
Spectral Size 65536
Me
NC
140d
144.7
142.1
139.5
132.4
128.7
127.3
127.2
126.7
126.6
119.2
110.2
42.8
21.0
f1 (ppm)

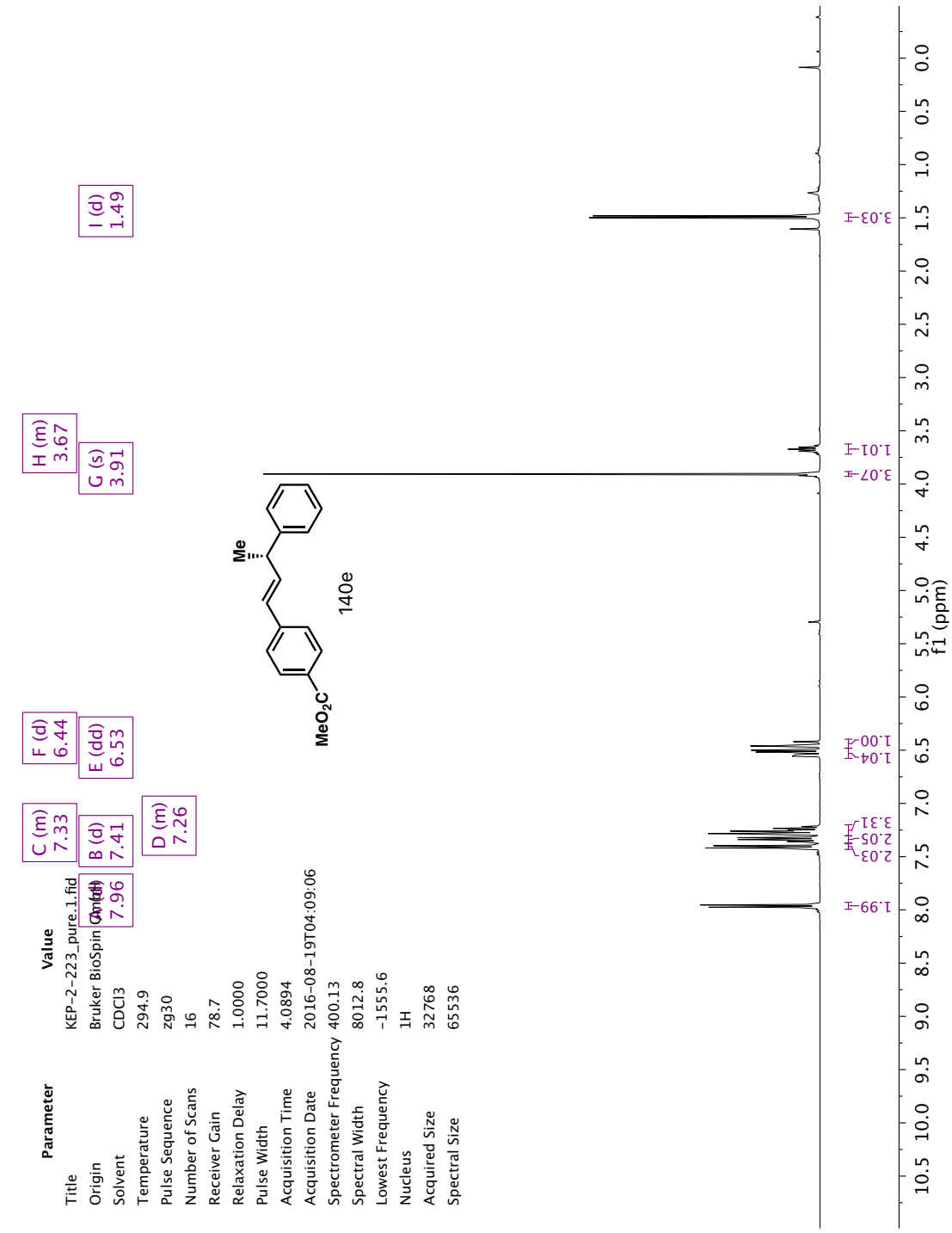
Parameter
Value
Title
KEP-2-223_pure.1.fid
Origin
Bruker BioSpin GmbH
Solvent
CDCl3
Temperature
294.9
Pulse Sequence
zg30
Number of Scans
16
Receiver Gain
78.7
Relaxation Delay
1.0000
Pulse Width
11.7000
Acquisition Time
4.0894
Acquisition Date
2016-08-19T04:09:06
Spectrometer Frequency
400.13
Spectral Width
8012.8
Lowest Frequency
-1555.6
Nucleus
1H
Acquired Size
32768
Spectral Size
65536
C (m) 7.33
B (d) 7.41
A (d) 7.96
F (d) 6.44
E (dd) 6.53
D (m) 7.26
H (m) 3.67
G (s) 3.91
I (d) 1.49
Me
MeO2C
140e
1.99
2.03
2.05
3.31
1.04
1.00
3.07
1.01
3.03
10.5 10.0 9.5 9.0 8.5 8.0 7.5 7.0 6.5 6.0 5.5 5.0 4.5 4.0 3.5 3.0 2.5 2.0 1.5 1.0 0.5 0.0
f1 (ppm)

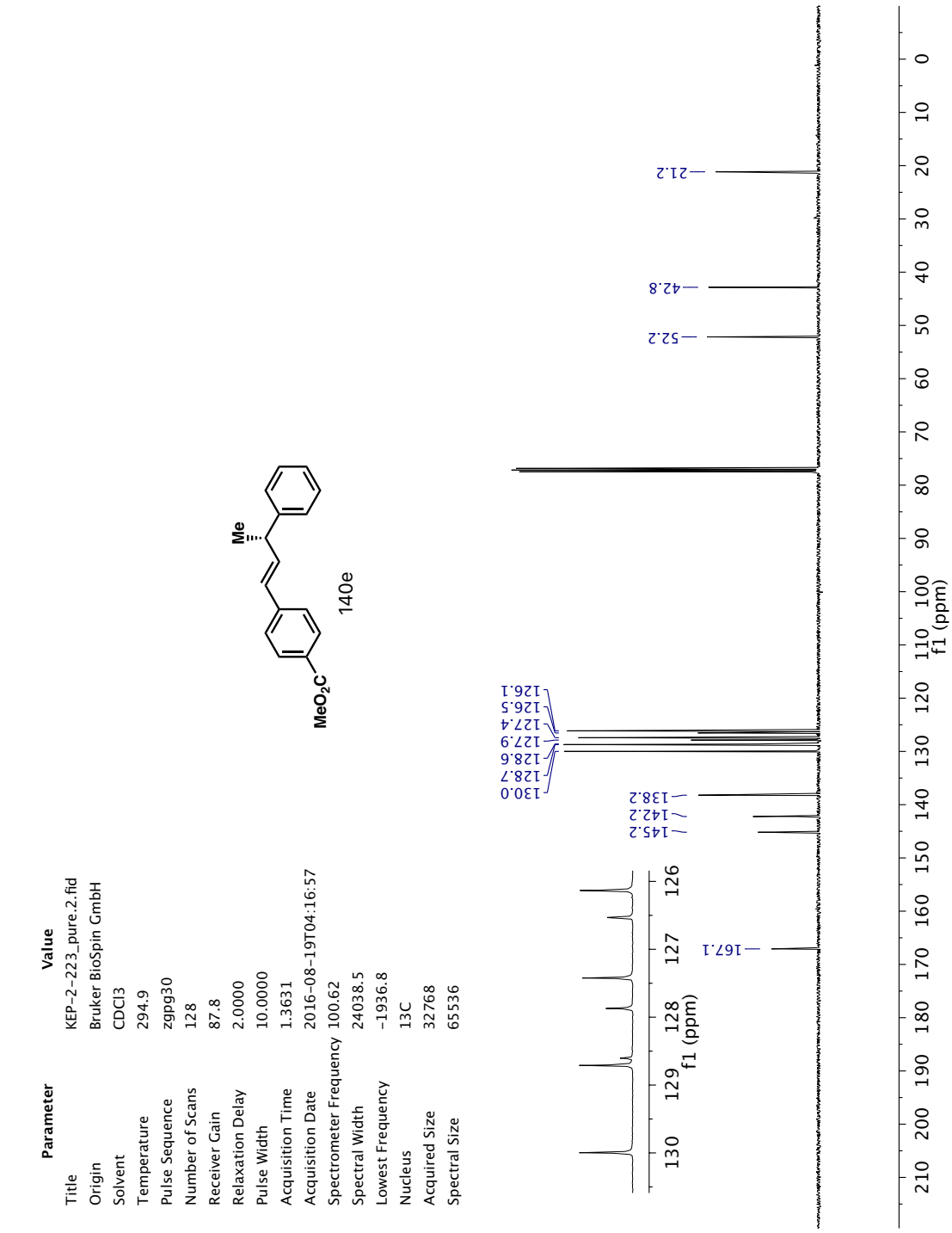
Me
MeO2C
140e
Parameter Value
Title KEP-2-223_pure.2.fid
Origin Bruker BioSpin GmbH
Solvent CDCl3
Temperature 294.9
Pulse Sequence zgpg30
Number of Scans 128
Receiver Gain 87.8
Relaxation Delay 2.0000
Pulse Width 10.0000
Acquisition Time 1.3631
Acquisition Date 2016-08-19T04:16:57
Spectrometer Frequency 100.62
Spectral Width 24038.5
Lowest Frequency -1936.8
Nucleus 13C
Acquired Size 32768
Spectral Size 65536
167.1
145.2
142.2
138.2
130.0
128.7
128.6
127.9
127.4
126.5
126.1
52.2
42.8
21.2
f1 (ppm)

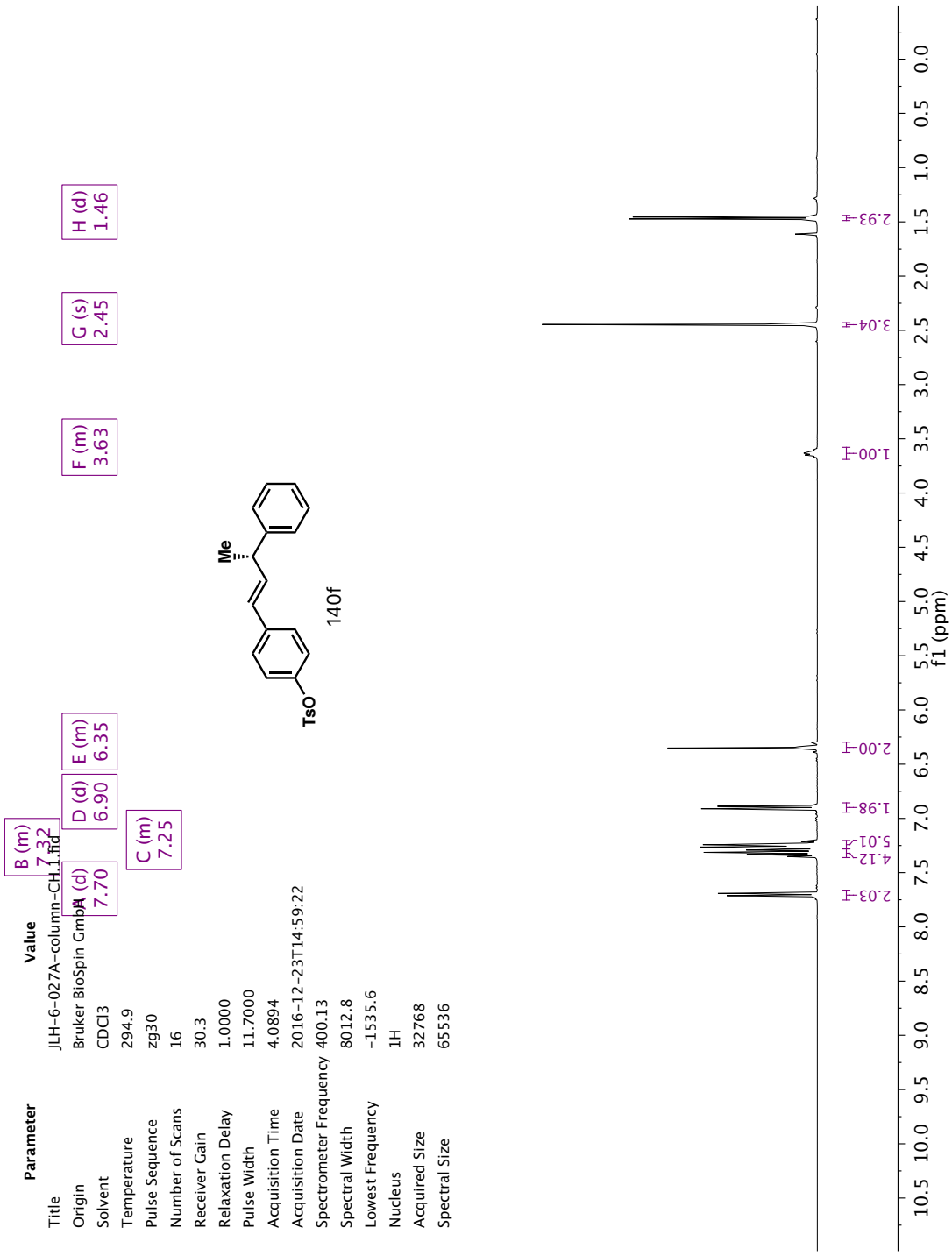
Parameter
Value
Title
JLH-6-027A-column-CH.1.fid
Origin
Bruker BioSpin GmbH
Solvent
CDCl3
Temperature
294.9
Pulse Sequence
zg30
Number of Scans
16
Receiver Gain
30.3
Relaxation Delay
1.0000
Pulse Width
11.7000
Acquisition Time
4.0894
Acquisition Date
2016-12-23T14:59:22
Spectrometer Frequency
400.13
Spectral Width
8012.8
Lowest Frequency
-1535.6
Nucleus
1H
Acquired Size
32768
Spectral Size
65536
A (d) 7.70
B (m) 7.32
C (m) 7.25
D (d) 6.90
E (m) 6.35
F (m) 3.63
G (s) 2.45
H (d) 1.46
Me
TsO
140f
2.03
4.12
5.01
1.98
2.00
1.00
3.04
2.93
10.5 10.0 9.5 9.0 8.5 8.0 7.5 7.0 6.5 6.0 5.5 5.0 4.5 4.0 3.5 3.0 2.5 2.0 1.5 1.0 0.5 0.0
f1 (ppm)

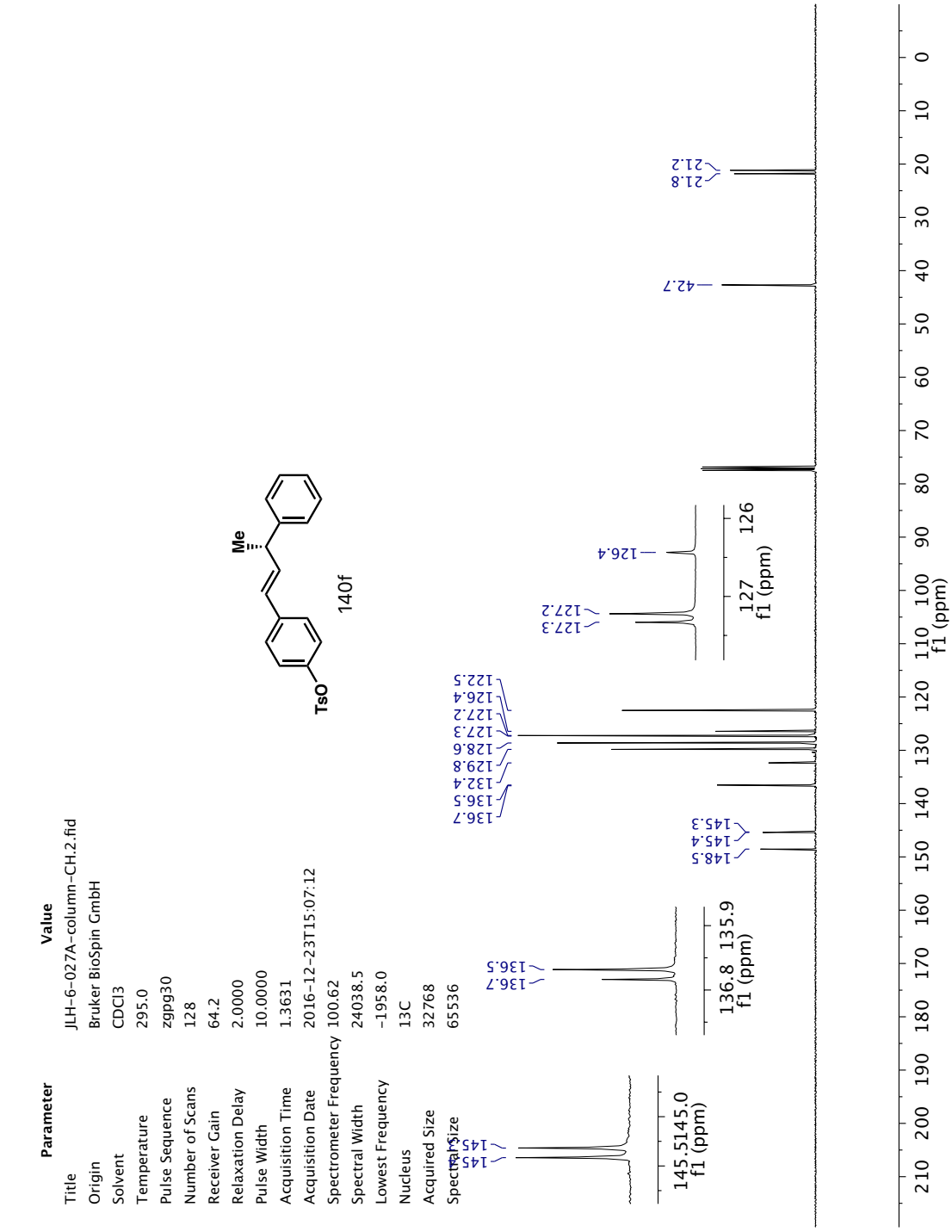
Parameter Value
Title JLH-6-027A-column-CH.2.fid
Origin Bruker BioSpin GmbH
Solvent CDCl3
Temperature 295.0
Pulse Sequence zgpg30
Number of Scans 128
Receiver Gain 64.2
Relaxation Delay 2.0000
Pulse Width 10.0000
Acquisition Time 1.3631
Acquisition Date 2016-12-23T15:07:12
Spectrometer Frequency 100.62
Spectral Width 24038.5
Lowest Frequency -1958.0
Nucleus 13C
Acquired Size 32768
Spectral Size 65536
Me
TsO
140f
145.5
145.0
f1 (ppm)
136.8 135.9
f1 (ppm)
127
126
f1 (ppm)
f1 (ppm)

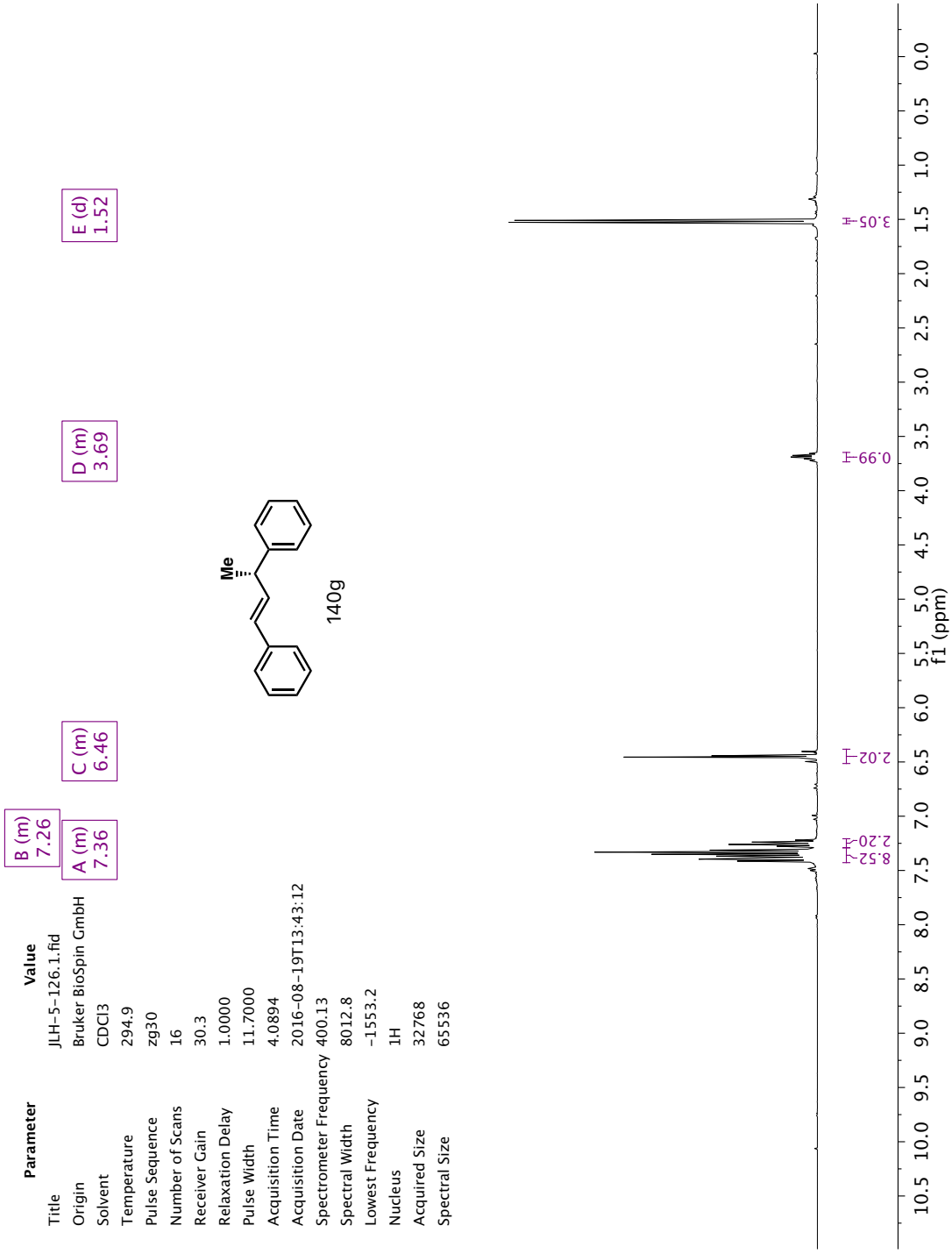
Parameter
Value
Title
JLH-5-126.1.fid
Origin
Bruker BioSpin GmbH
Solvent
CDCl3
Temperature
294.9
Pulse Sequence
zg30
Number of Scans
16
Receiver Gain
30.3
Relaxation Delay
1.0000
Pulse Width
11.7000
Acquisition Time
4.0894
Acquisition Date
2016-08-19T13:43:12
Spectrometer Frequency
400.13
Spectral Width
8012.8
Lowest Frequency
-1553.2
Nucleus
1H
Acquired Size
32768
Spectral Size
65536
B (m) 7.26
A (m) 7.36
C (m) 6.46
D (m) 3.69
E (d) 1.52
Me
140g
8.52
2.20
2.02
0.99
3.05
10.5 10.0 9.5 9.0 8.5 8.0 7.5 7.0 6.5 6.0 5.5 5.0 4.5 4.0 3.5 3.0 2.5 2.0 1.5 1.0 0.5 0.0
f1 (ppm)

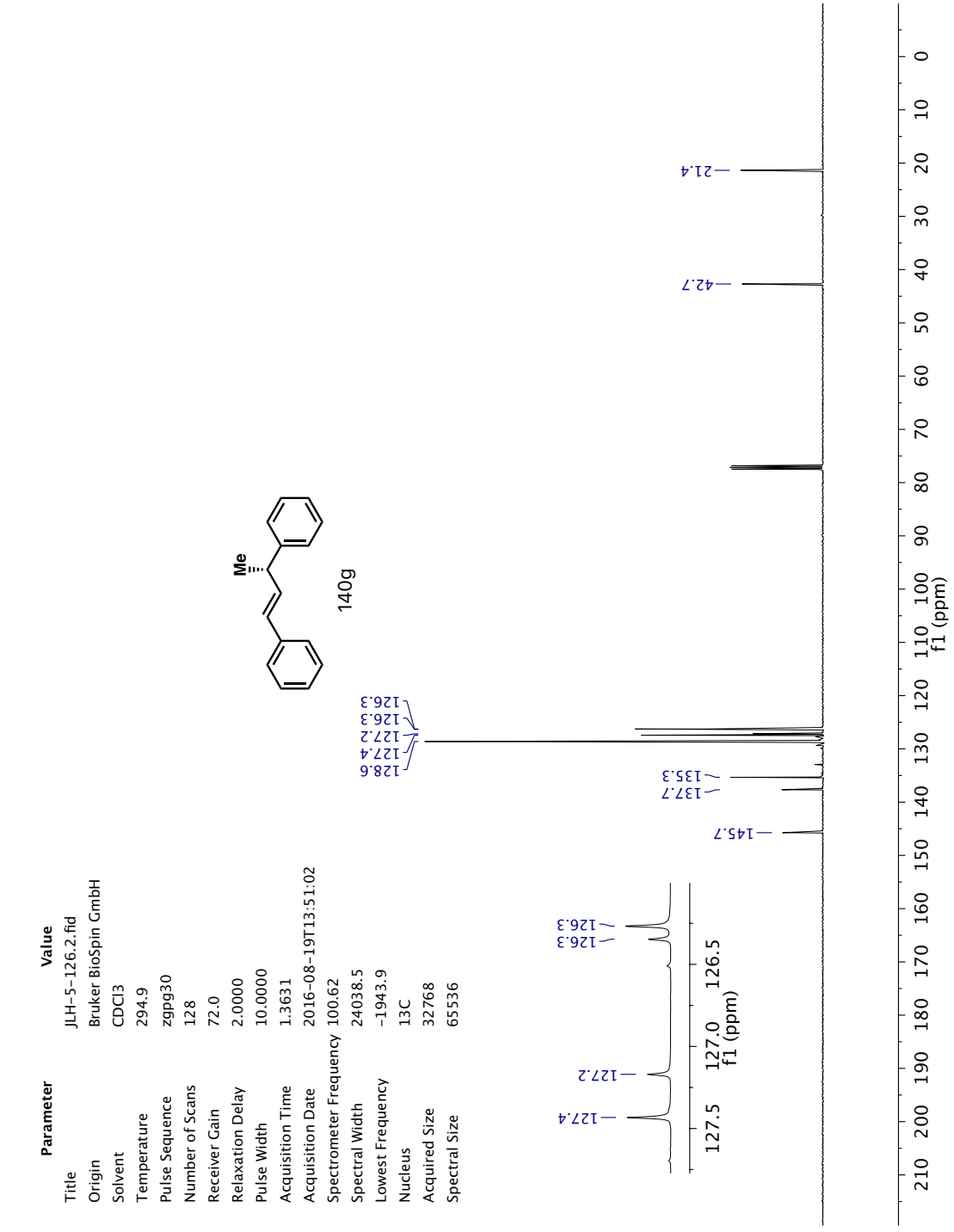
Parameter Value
Title JLH-5-126.2.fid
Origin Bruker BioSpin GmbH
Solvent CDCl3
Temperature 294.9
Pulse Sequence zgpg30
Number of Scans 128
Receiver Gain 72.0
Relaxation Delay 2.0000
Pulse Width 10.0000
Acquisition Time 1.3631
Acquisition Date 2016-08-19T13:51:02
Spectrometer Frequency 100.62
Spectral Width 24038.5
Lowest Frequency -1943.9
Nucleus 13C
Acquired Size 32768
Spectral Size 65536
Me
140g
126.3
126.3
127.2
127.4
128.6
135.3
137.7
145.7
42.7
21.4
127.4
127.2
126.3
126.3
127.5
127.0
126.5
f1 (ppm)
f1 (ppm)

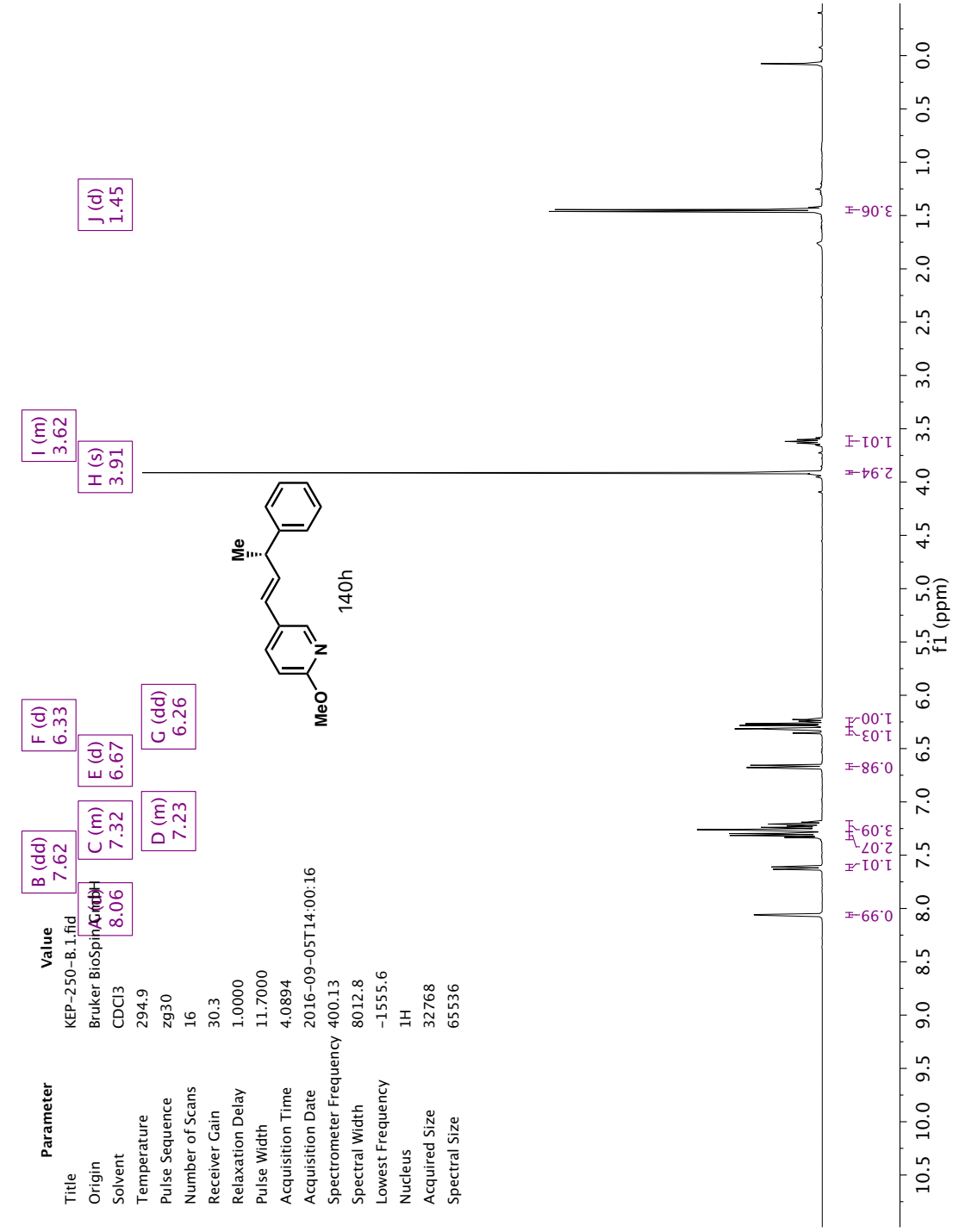
Parameter
Value
Title
KEP-250-B.1.fid
Origin
Bruker BioSpin GmbH
Solvent
CDCl3
Temperature
294.9
Pulse Sequence
zg30
Number of Scans
16
Receiver Gain
30.3
Relaxation Delay
1.0000
Pulse Width
11.7000
Acquisition Time
4.0894
Acquisition Date
2016-09-05T14:00:16
Spectrometer Frequency
400.13
Spectral Width
8012.8
Lowest Frequency
-1555.6
Nucleus
1H
Acquired Size
32768
Spectral Size
65536
A (d) 8.06
B (dd) 7.62
C (m) 7.32
D (m) 7.23
E (d) 6.67
F (d) 6.33
G (dd) 6.26
H (s) 3.91
I (m) 3.62
J (d) 1.45
Me
MeO
N
140h
0.99
1.01
2.07
3.09
0.98
1.03
1.00
1.01
2.94
3.06
f1 (ppm)

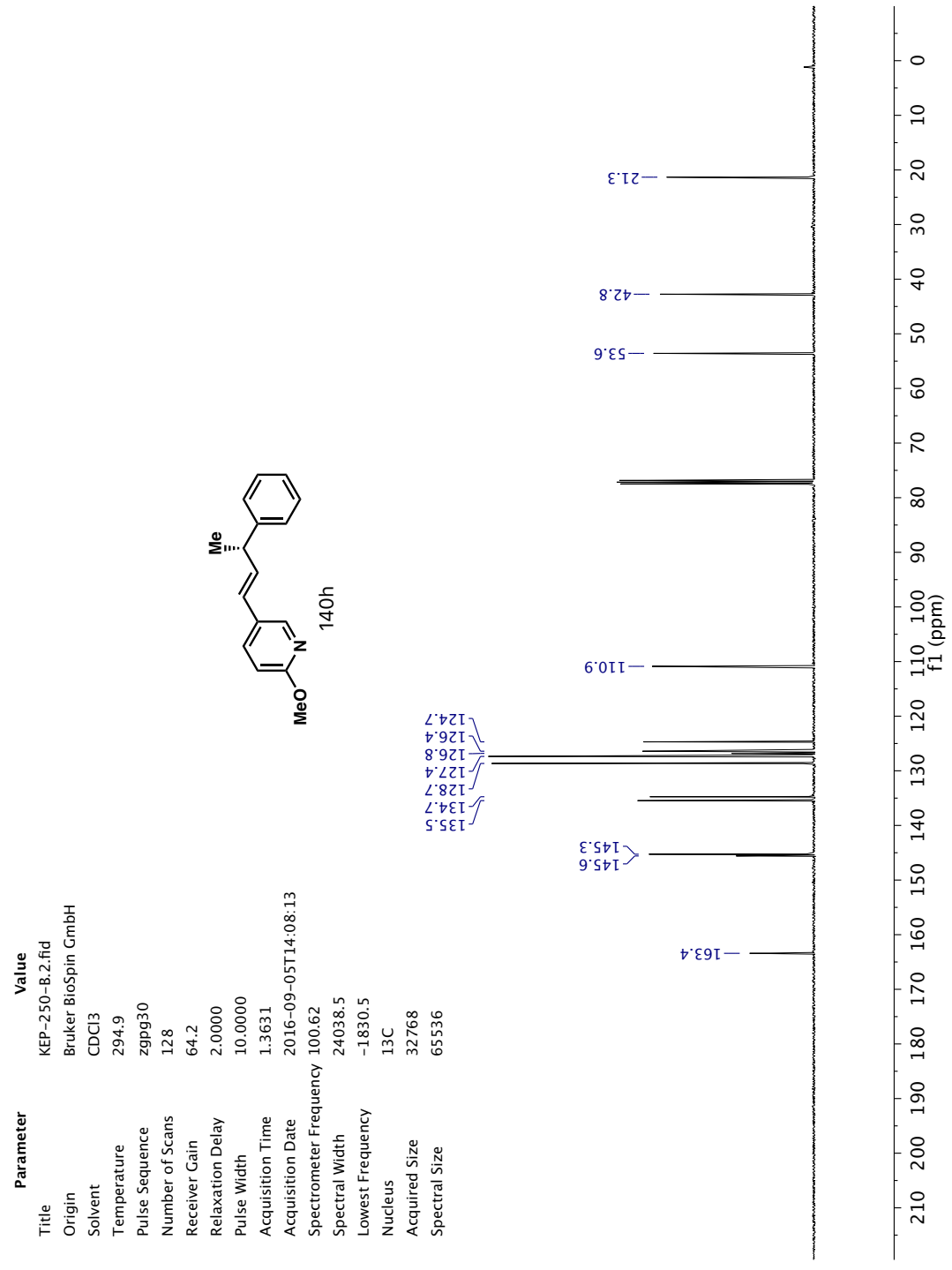

Parameter	Value
Title	KEP-250-B.2.fid
Origin	Bruker BioSpin GmbH
Solvent	CDCl3
Temperature	294.9
Pulse Sequence	zgpg30
Number of Scans	128
Receiver Gain	64.2
Relaxation Delay	2.0000
Pulse Width	10.0000
Acquisition Time	1.3631
Acquisition Date	2016-09-05T14:08:13
Spectrometer Frequency	100.62
Spectral Width	24038.5
Lowest Frequency	-1830.5
Nucleus	13C
Acquired Size	32768
Spectral Size	65536

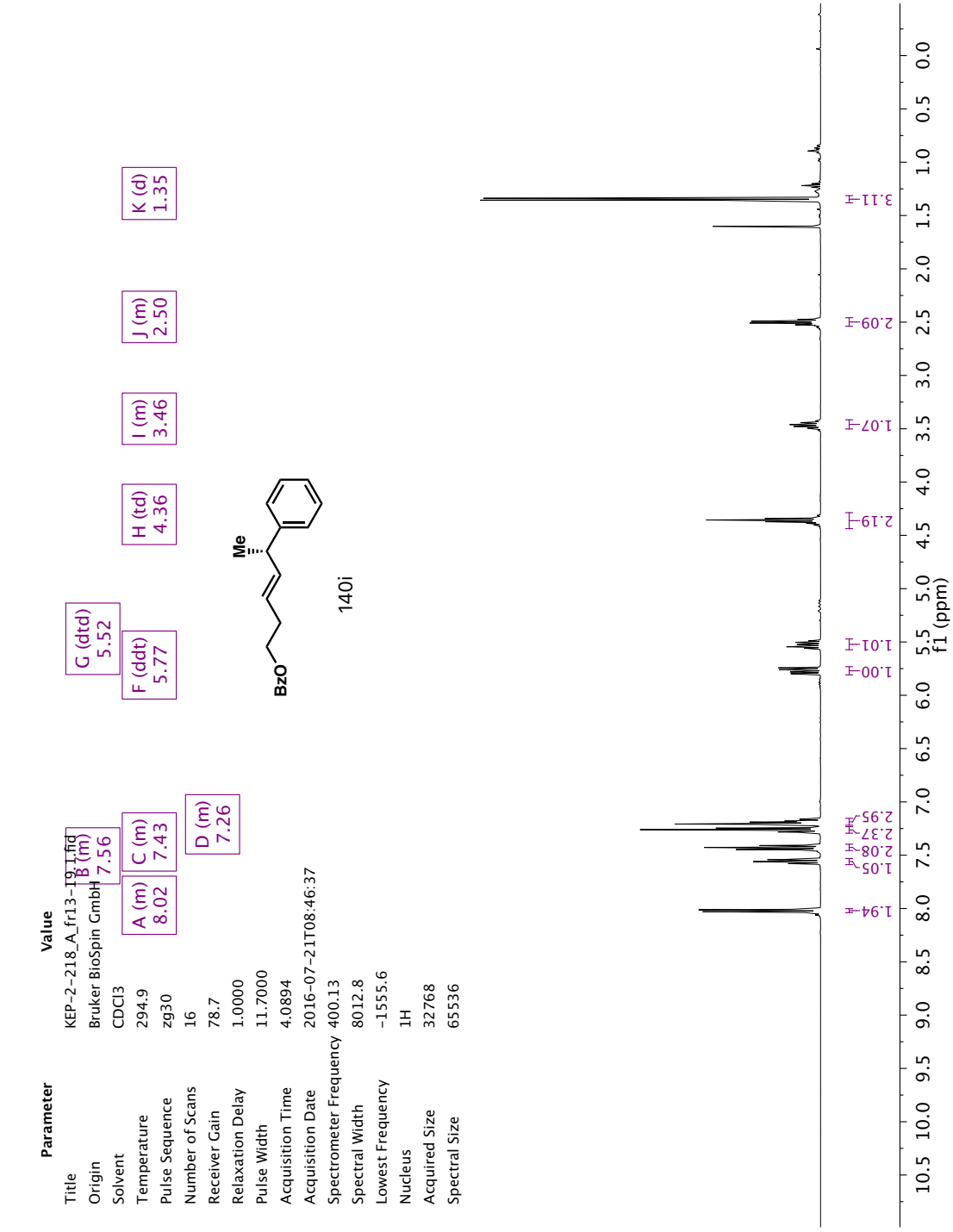
Parameter
Value
Title KEP-2-218_A_fr13-19_1.fid
Origin Bruker BioSpin GmbH
Solvent CDCl3
Temperature 294.9
Pulse Sequence zg30
Number of Scans 16
Receiver Gain 78.7
Relaxation Delay 1.0000
Pulse Width 11.7000
Acquisition Time 4.0894
Acquisition Date 2016-07-21T08:46:37
Spectrometer Frequency 400.13
Spectral Width 8012.8
Lowest Frequency -1555.6
Nucleus 1H
Acquired Size 32768
Spectral Size 65536
A (m) 8.02
B (m) 7.56
C (m) 7.43
D (m) 7.26
F (ddt) 5.77
G (dtd) 5.52
H (td) 4.36
I (m) 3.46
J (m) 2.50
K (d) 1.35
Me
BzO
140i
1.94
1.05
2.08
2.37
2.95
1.00
1.01
2.19
1.07
2.09
3.11
f1 (ppm)

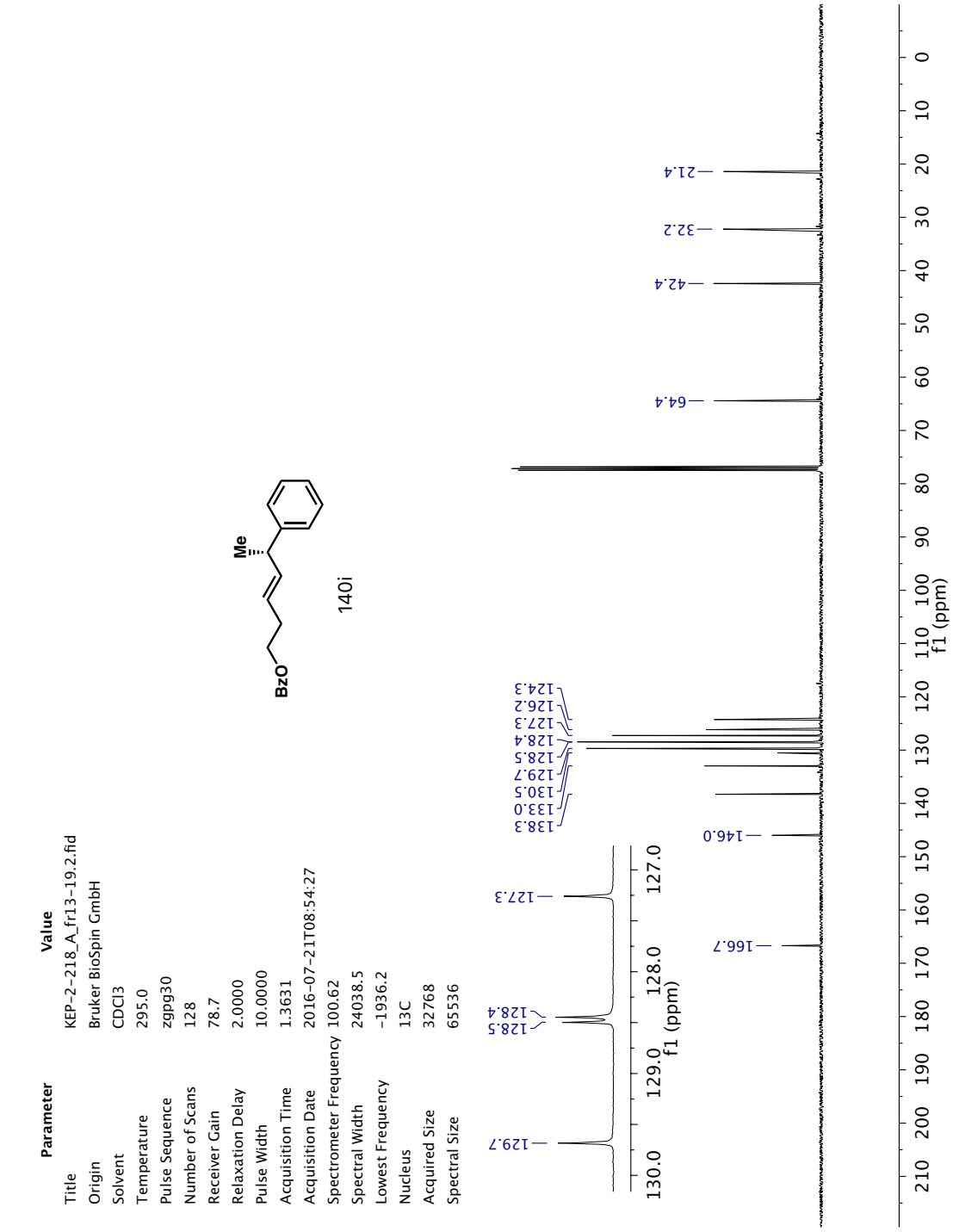
Parameter Value
Title KEP-2-218_A_fr13-19.2.fid
Origin Bruker BioSpin GmbH
Solvent CDCl3
Temperature 295.0
Pulse Sequence zgpg30
Number of Scans 128
Receiver Gain 78.7
Relaxation Delay 2.0000
Pulse Width 10.0000
Acquisition Time 1.3631
Acquisition Date 2016-07-21T08:54:27
Spectrometer Frequency 100.62
Spectral Width 24038.5
Lowest Frequency -1936.2
Nucleus 13C
Acquired Size 32768
Spectral Size 65536
Me
BzO
140i
138.3
133.0
130.5
129.7
128.5
128.4
127.3
126.2
124.3
166.7
146.0
64.4
42.4
32.2
21.4
f1 (ppm)

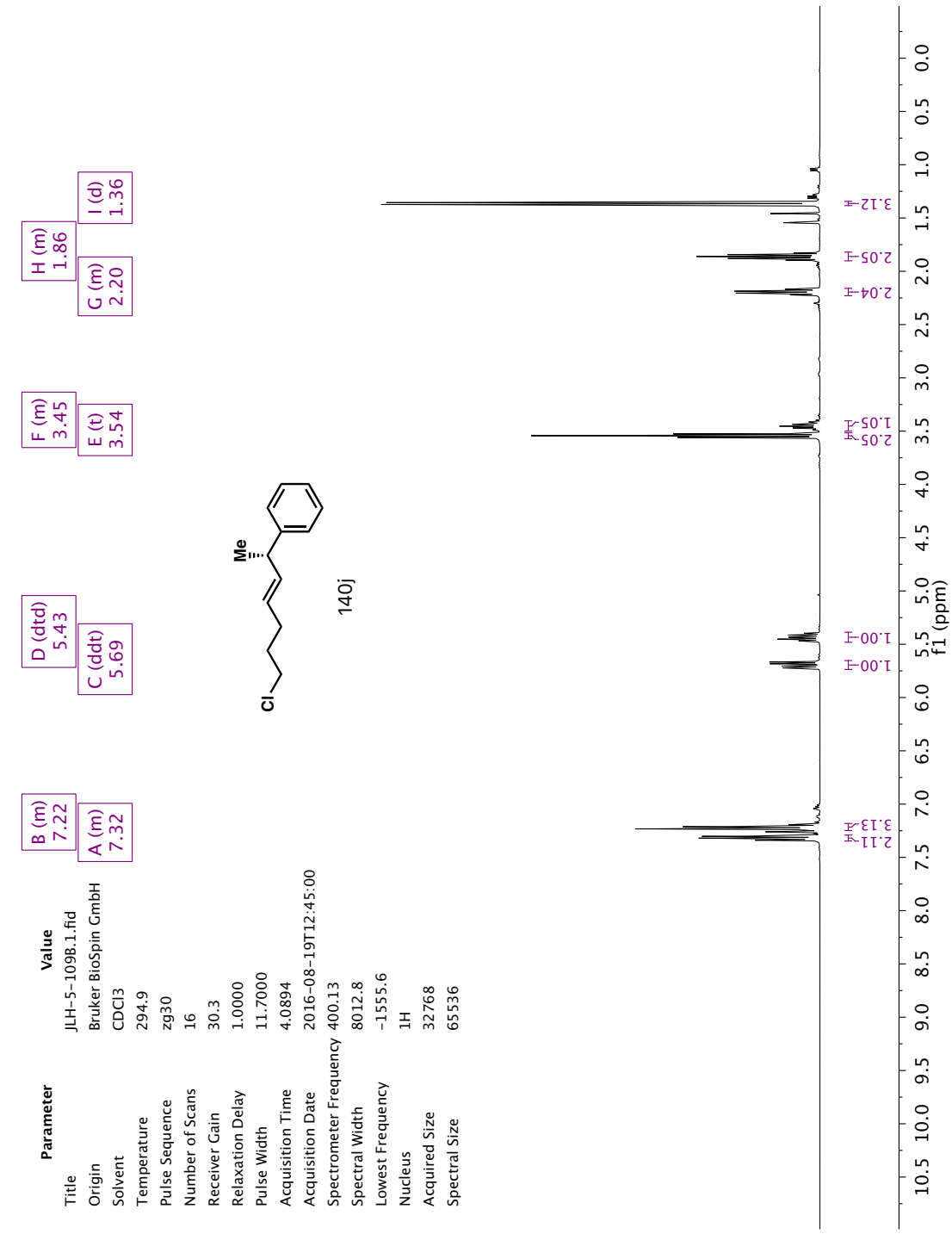
Parameter
Value
Title
JLH-5-109B.1.fid
Origin
Bruker BioSpin GmbH
Solvent
CDCl3
Temperature
294.9
Pulse Sequence
zg30
Number of Scans
16
Receiver Gain
30.3
Relaxation Delay
1.0000
Pulse Width
11.7000
Acquisition Time
4.0894
Acquisition Date
2016-08-19T12:45:00
Spectrometer Frequency
400.13
Spectral Width
8012.8
Lowest Frequency
-1555.6
Nucleus
1H
Acquired Size
32768
Spectral Size
65536
B (m) 7.22
A (m) 7.32
D (dtd) 5.43
C (ddt) 5.69
F (m) 3.45
E (t) 3.54
H (m) 1.86
G (m) 2.20
I (d) 1.36
Me
Cl
140j
2.11
3.13
1.00
1.00
2.05
1.05
2.04
2.05
3.12
10.5 10.0 9.5 9.0 8.5 8.0 7.5 7.0 6.5 6.0 5.5 5.0 4.5 4.0 3.5 3.0 2.5 2.0 1.5 1.0 0.5 0.0
f1 (ppm)

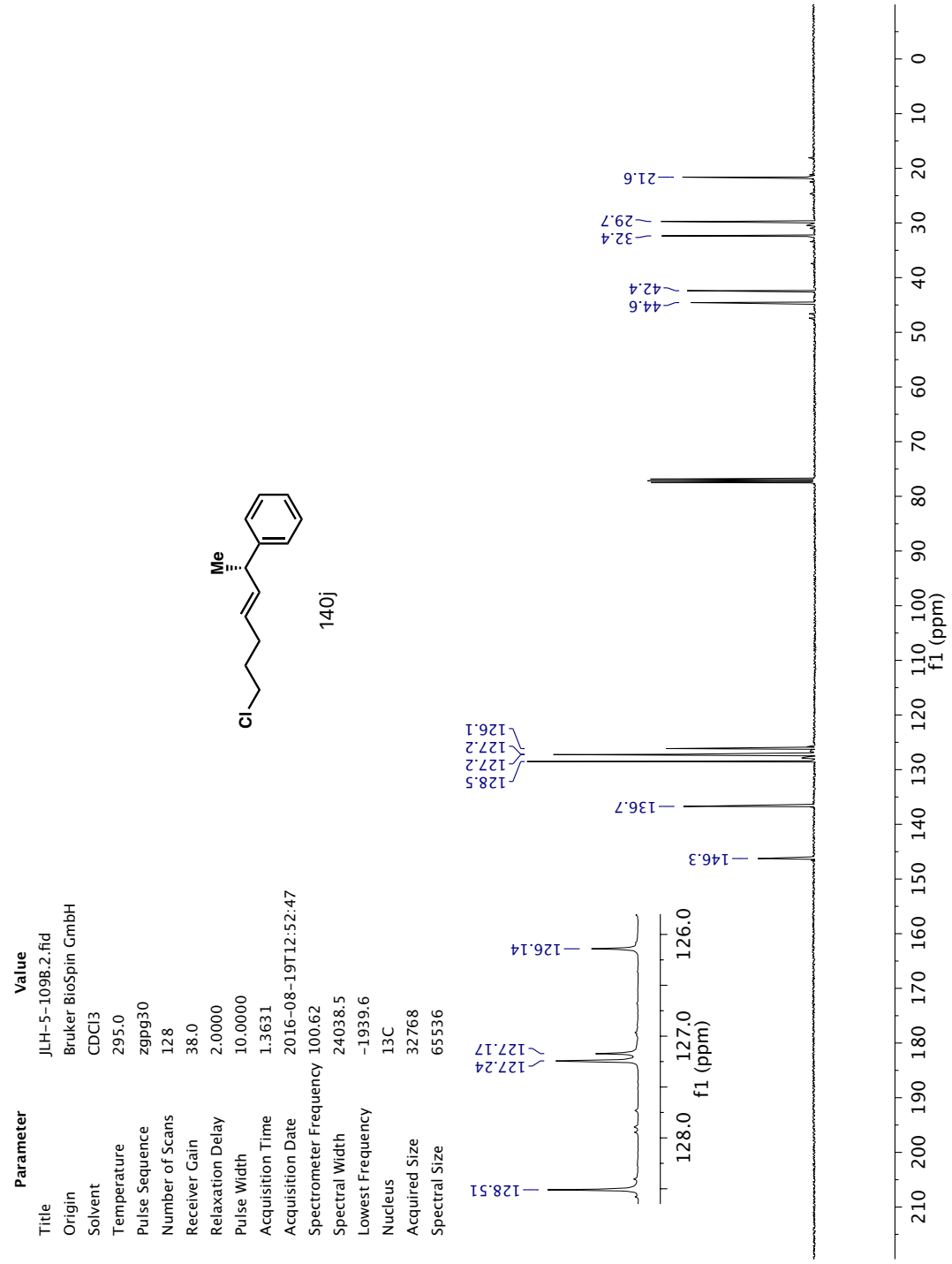
Parameter Value
Title JLH-5-109B.2.fid
Origin Bruker BioSpin GmbH
Solvent CDCl3
Temperature 295.0
Pulse Sequence zgpg30
Number of Scans 128
Receiver Gain 38.0
Relaxation Delay 2.0000
Pulse Width 10.0000
Acquisition Time 1.3631
Acquisition Date 2016-08-19T12:52:47
Spectrometer Frequency 100.62
Spectral Width 24038.5
Lowest Frequency -1939.6
Nucleus 13C
Acquired Size 32768
Spectral Size 65536
Me
Cl
140j
128.51
127.24
127.17
126.14
128.0
127.0
126.0
f1 (ppm)
146.3
136.7
128.5
127.2
127.2
126.1
44.6
42.4
32.4
29.7
21.6
210 200 190 180 170 160 150 140 130 120 110 100 90 80 70 60 50 40 30 20 10 0
f1 (ppm)

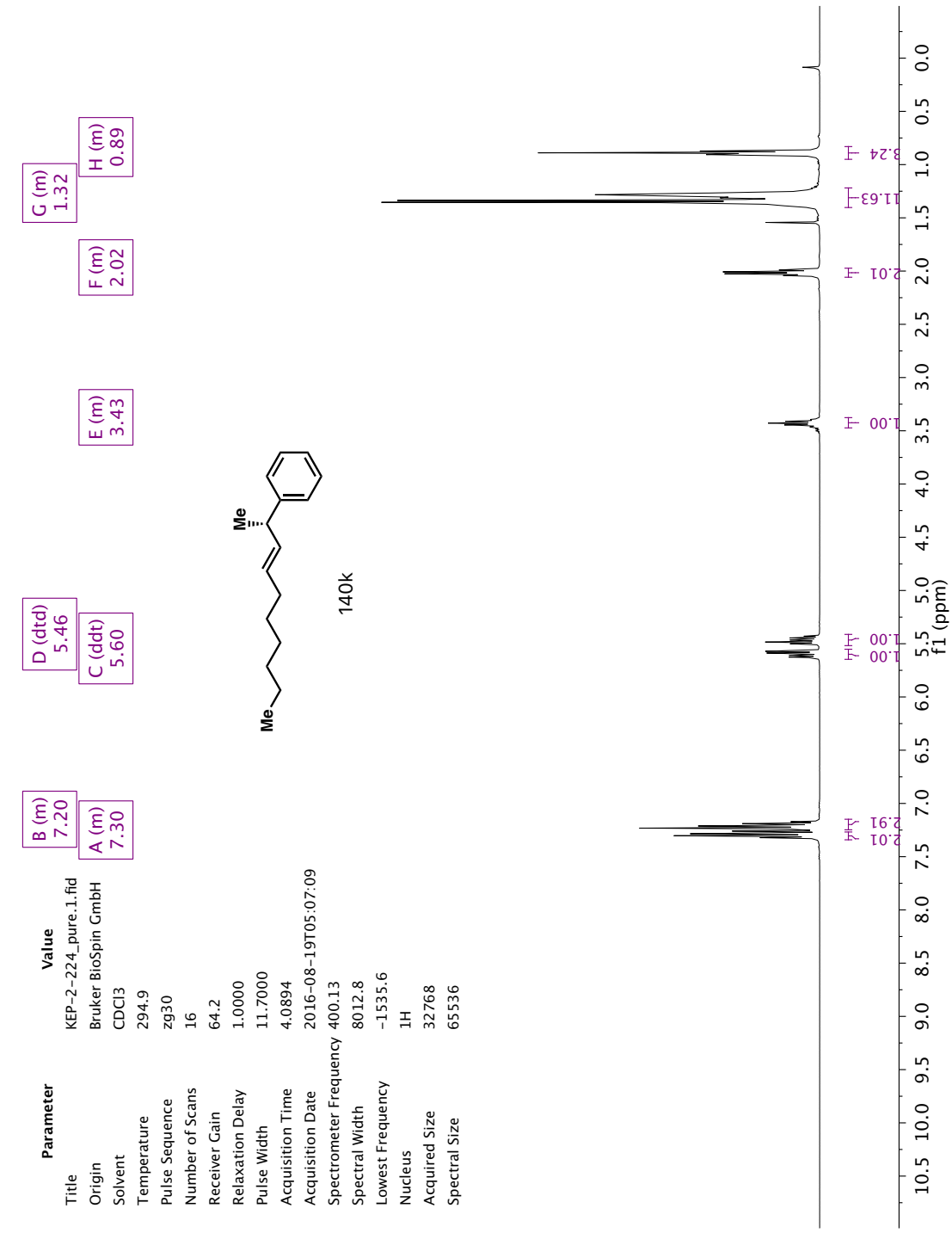
Parameter
Value
Title KEP-2-224_pure.1.fid
Origin Bruker BioSpin GmbH
Solvent CDCl3
Temperature 294.9
Pulse Sequence zg30
Number of Scans 16
Receiver Gain 64.2
Relaxation Delay 1.0000
Pulse Width 11.7000
Acquisition Time 4.0894
Acquisition Date 2016-08-19T05:07:09
Spectrometer Frequency 400.13
Spectral Width 8012.8
Lowest Frequency -1535.6
Nucleus 1H
Acquired Size 32768
Spectral Size 65536
B (m) 7.20
A (m) 7.30
D (dtd) 5.46
C (ddt) 5.60
E (m) 3.43
F (m) 2.02
G (m) 1.32
H (m) 0.89
Me
Me
140k
2.01
2.91
1.00
1.00
1.00
2.01
11.63
3.24
f1 (ppm)

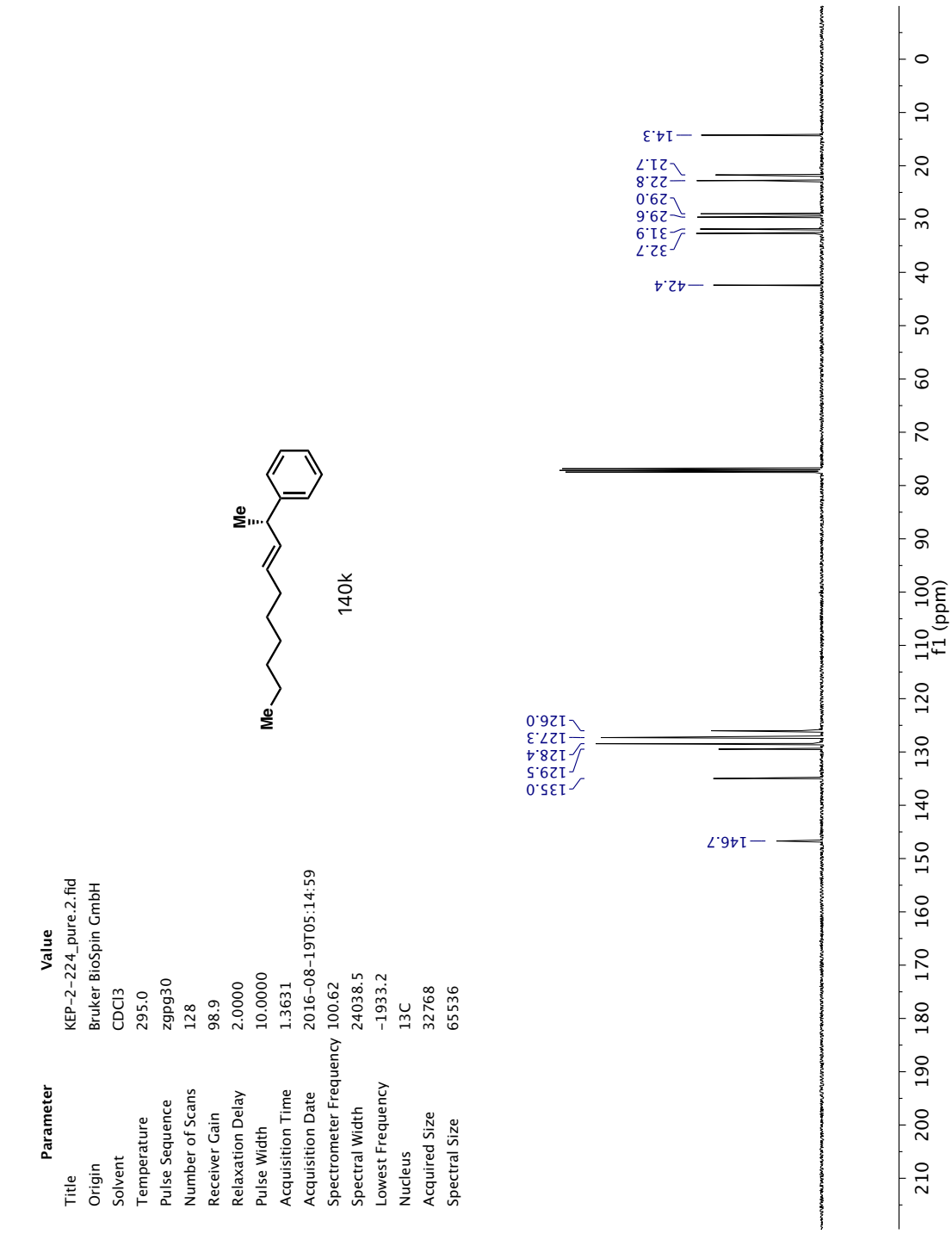
Parameter Value
Title KEP-2-224_pure.2.fid
Origin Bruker BioSpin GmbH
Solvent CDCl3
Temperature 295.0
Pulse Sequence zgpg30
Number of Scans 128
Receiver Gain 98.9
Relaxation Delay 2.0000
Pulse Width 10.0000
Acquisition Time 1.3631
Acquisition Date 2016-08-19T05:14:59
Spectrometer Frequency 100.62
Spectral Width 24038.5
Lowest Frequency -1933.2
Nucleus 13C
Acquired Size 32768
Spectral Size 65536
Me
Me
140k
146.7
135.0
129.5
128.4
127.3
126.0
42.4
32.7
31.9
29.6
29.0
22.8
21.7
14.3
f1 (ppm)

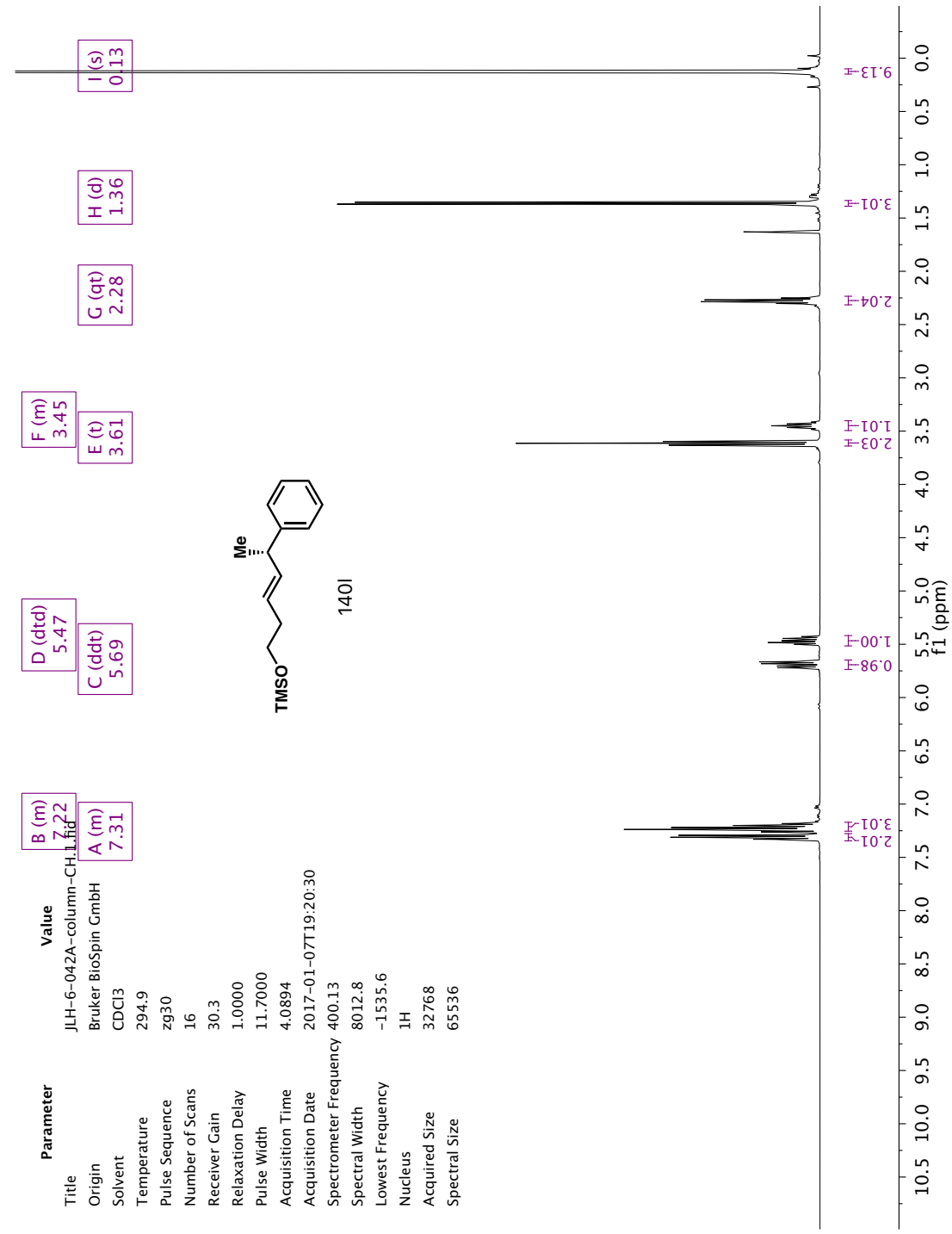
Parameter
Value
Title
JLH-6-042A-column-CH.1.fid
Origin
Bruker BioSpin GmbH
Solvent
CDCl3
Temperature
294.9
Pulse Sequence
zg30
Number of Scans
16
Receiver Gain
30.3
Relaxation Delay
1.0000
Pulse Width
11.7000
Acquisition Time
4.0894
Acquisition Date
2017-01-07T19:20:30
Spectrometer Frequency
400.13
Spectral Width
8012.8
Lowest Frequency
-1535.6
Nucleus
1H
Acquired Size
32768
Spectral Size
65536
B (m) 7.22
A (m) 7.31
D (dtd) 5.47
C (ddt) 5.69
F (m) 3.45
E (t) 3.61
G (qt) 2.28
H (d) 1.36
I (s) 0.13
Me
TMSO
140I
2.01
3.01
0.98
1.00
2.03
1.01
2.04
3.01
9.13
f1 (ppm)

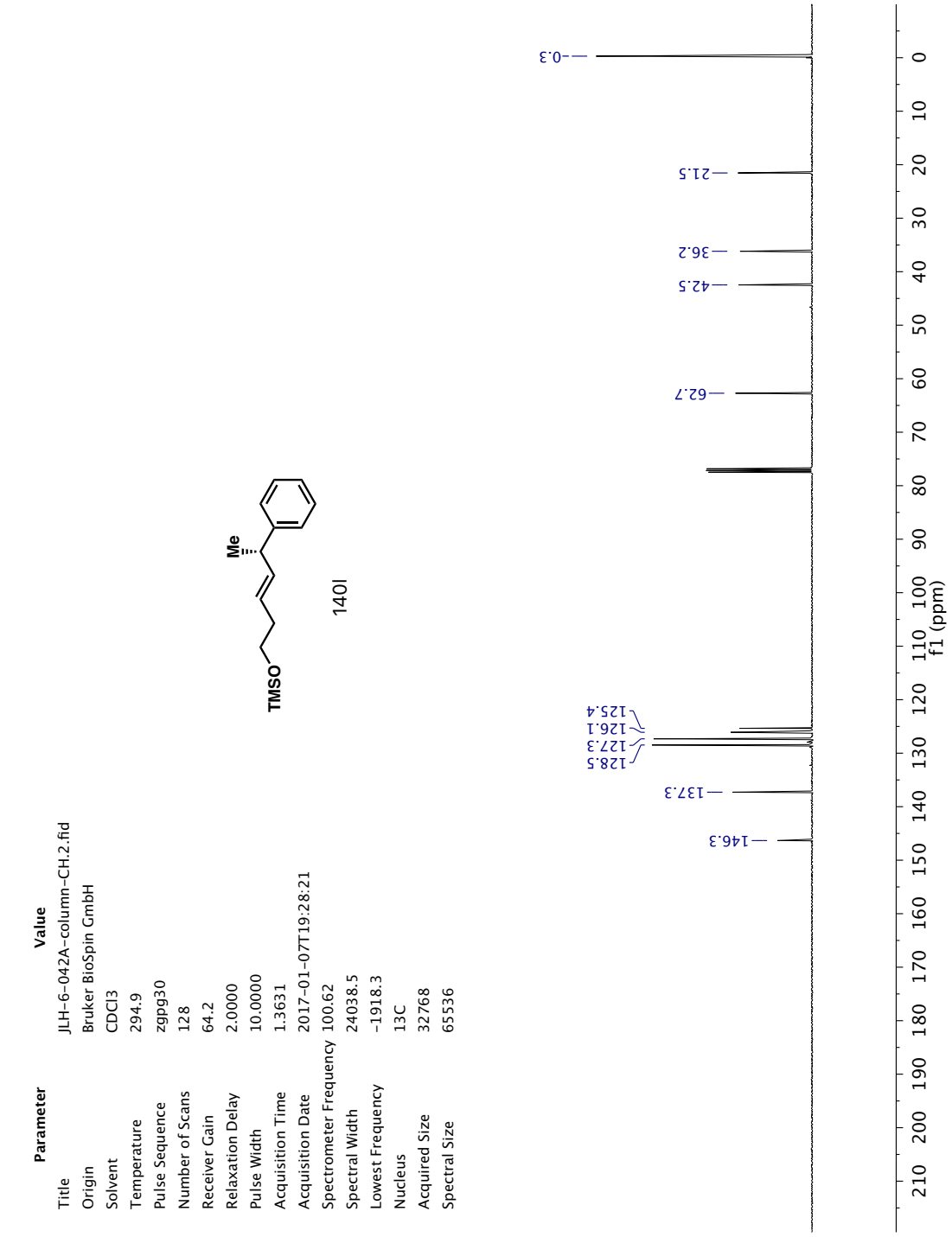

Parameter	Value
Title	JLH-6-042A-column-CH.2.fid
Origin	Bruker BioSpin GmbH
Solvent	CDCl3
Temperature	294.9
Pulse Sequence	zgpg30
Number of Scans	128
Receiver Gain	64.2
Relaxation Delay	2.0000
Pulse Width	10.0000
Acquisition Time	1.3631
Acquisition Date	2017-01-07T19:28:21
Spectrometer Frequency	100.62
Spectral Width	24038.5
Lowest Frequency	-1918.3
Nucleus	13C
Acquired Size	32768
Spectral Size	65536

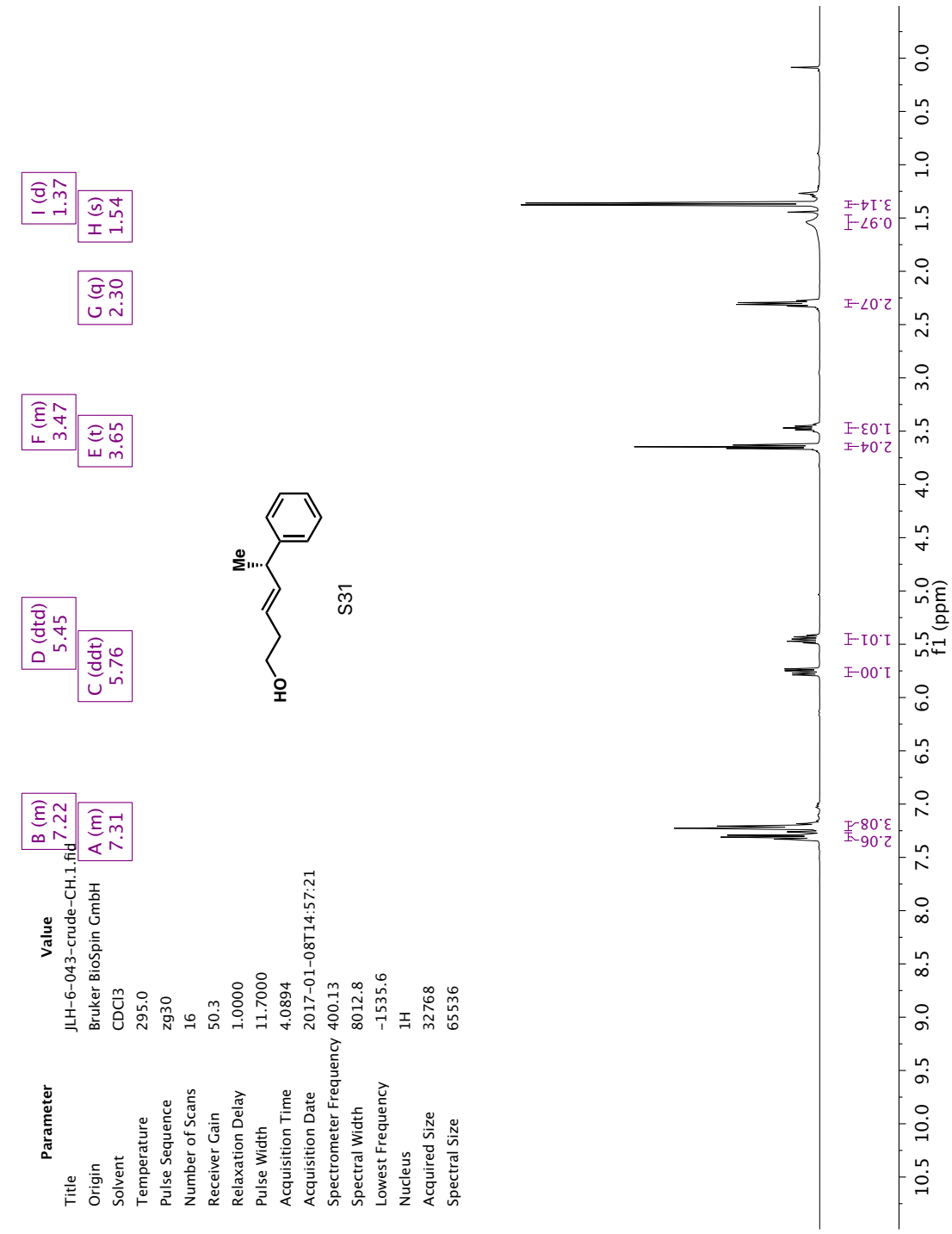
Parameter
Value
Title
JLH-6-043-crude-CH.1.fid
Origin
Bruker BioSpin GmbH
Solvent
CDCl3
Temperature
295.0
Pulse Sequence
zg30
Number of Scans
16
Receiver Gain
50.3
Relaxation Delay
1.0000
Pulse Width
11.7000
Acquisition Time
4.0894
Acquisition Date
2017-01-08T14:57:21
Spectrometer Frequency
400.13
Spectral Width
8012.8
Lowest Frequency
-1535.6
Nucleus
1H
Acquired Size
32768
Spectral Size
65536
B (m) 7.22
A (m) 7.31
D (dtd) 5.45
C (ddt) 5.76
F (m) 3.47
E (t) 3.65
G (q) 2.30
H (s) 1.54
I (d) 1.37
Me
HO
S31
2.06
3.08
1.00
1.01
2.07
2.04
1.03
3.14
0.97
f1 (ppm)

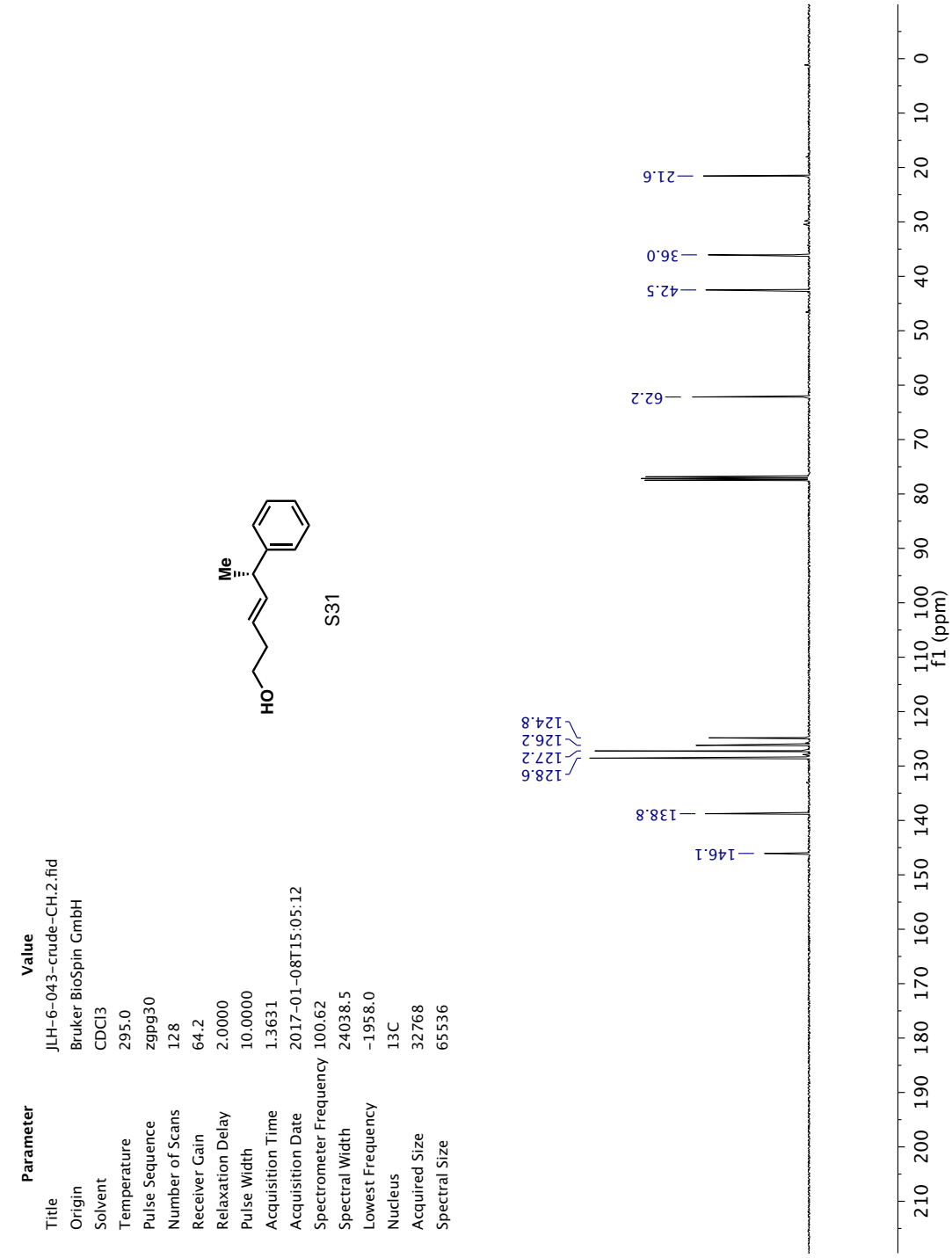
Parameter Value
Title JLH-6-043-crude-CH.2.fid
Origin Bruker BioSpin GmbH
Solvent CDCl3
Temperature 295.0
Pulse Sequence zgpg30
Number of Scans 128
Receiver Gain 64.2
Relaxation Delay 2.0000
Pulse Width 10.0000
Acquisition Time 1.3631
Acquisition Date 2017-01-08T15:05:12
Spectrometer Frequency 100.62
Spectral Width 24038.5
Lowest Frequency -1958.0
Nucleus 13C
Acquired Size 32768
Spectral Size 65536
Me
HO
S31
146.1
138.8
128.6
127.2
126.2
124.8
62.2
42.5
36.0
21.6
f1 (ppm)

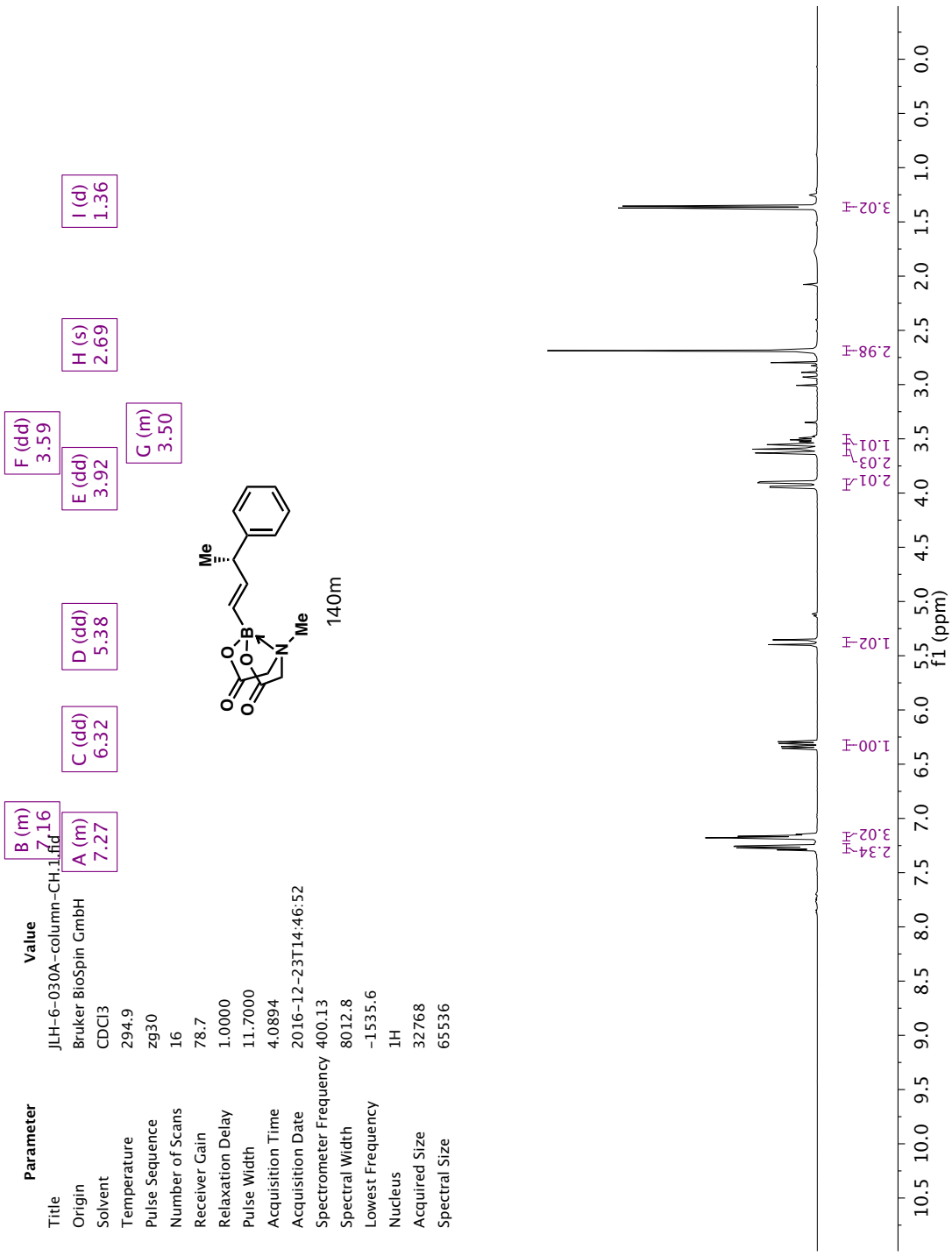
Parameter
Value
Title JLH-6-030A-column-CH.1.fid
Origin Bruker BioSpin GmbH
Solvent CDCl3
Temperature 294.9
Pulse Sequence zg30
Number of Scans 16
Receiver Gain 78.7
Relaxation Delay 1.0000
Pulse Width 11.7000
Acquisition Time 4.0894
Acquisition Date 2016-12-23T14:46:52
Spectrometer Frequency 400.13
Spectral Width 8012.8
Lowest Frequency -1535.6
Nucleus 1H
Acquired Size 32768
Spectral Size 65536
A (m) 7.27
B (m) 7.16
C (dd) 6.32
D (dd) 5.38
E (dd) 3.92
F (dd) 3.59
G (m) 3.50
H (s) 2.69
I (d) 1.36
Me
Me
140m
2.34
3.02
1.00
1.02
2.01
2.03
1.01
2.98
3.02
10.5 10.0 9.5 9.0 8.5 8.0 7.5 7.0 6.5 6.0 5.5 5.0 4.5 4.0 3.5 3.0 2.5 2.0 1.5 1.0 0.5 0.0
f1 (ppm)

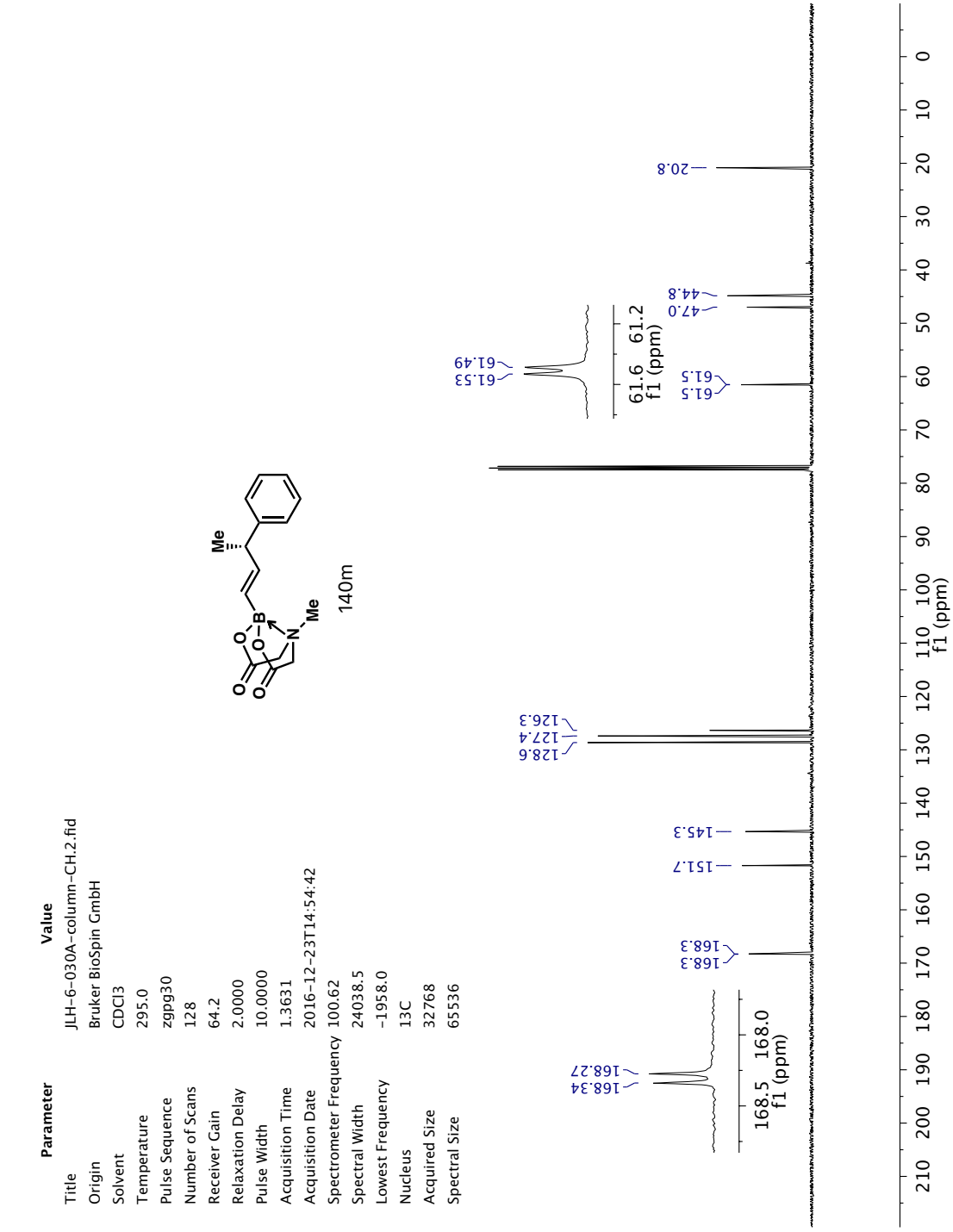
Parameter Value
Title JLH-6-030A-column-CH.2.fid
Origin Bruker BioSpin GmbH
Solvent CDCl3
Temperature 295.0
Pulse Sequence zgpg30
Number of Scans 128
Receiver Gain 64.2
Relaxation Delay 2.0000
Pulse Width 10.0000
Acquisition Time 1.3631
Acquisition Date 2016-12-23T14:54:42
Spectrometer Frequency 100.62
Spectral Width 24038.5
Lowest Frequency -1958.0
Nucleus 13C
Acquired Size 32768
Spectral Size 65536
Me
Me
140m
168.34
168.27
168.3
168.3
151.7
145.3
128.6
127.4
126.3
61.53
61.49
61.5
61.5
47.0
44.8
20.8
168.5 168.0
f1 (ppm)
61.6 61.2
f1 (ppm)
f1 (ppm)

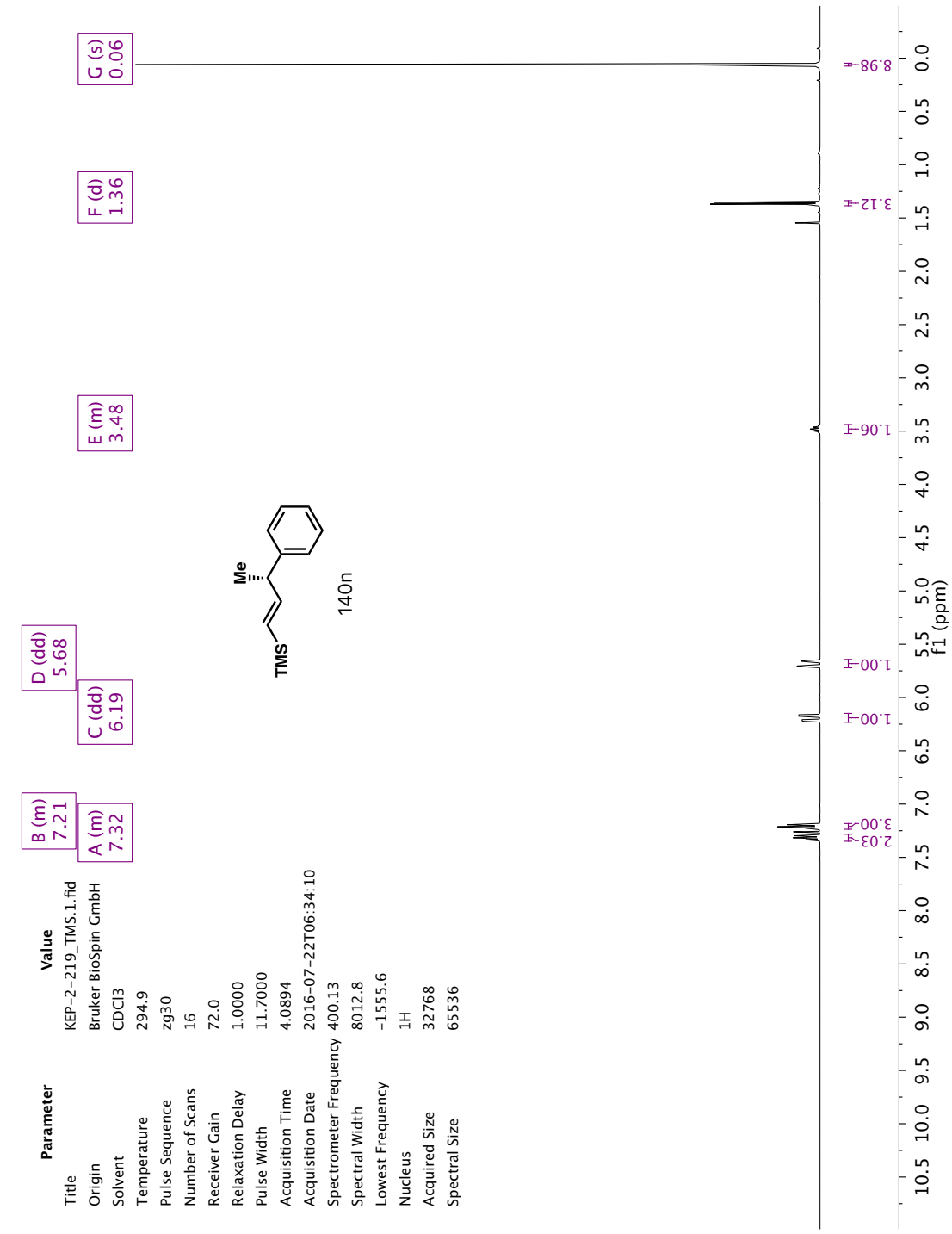
Parameter
Value
Title
KEP-2-219_TMS.1.fid
Origin
Bruker BioSpin GmbH
Solvent
CDCl3
Temperature
294.9
Pulse Sequence
zg30
Number of Scans
16
Receiver Gain
72.0
Relaxation Delay
1.0000
Pulse Width
11.7000
Acquisition Time
4.0894
Acquisition Date
2016-07-22T06:34:10
Spectrometer Frequency
400.13
Spectral Width
8012.8
Lowest Frequency
-1555.6
Nucleus
1H
Acquired Size
32768
Spectral Size
65536
B (m) 7.21
A (m) 7.32
D (dd) 5.68
C (dd) 6.19
E (m) 3.48
F (d) 1.36
G (s) 0.06
Me
TMS
140n
2.03
3.00
1.00
1.00
1.06
3.12
8.98
f1 (ppm)

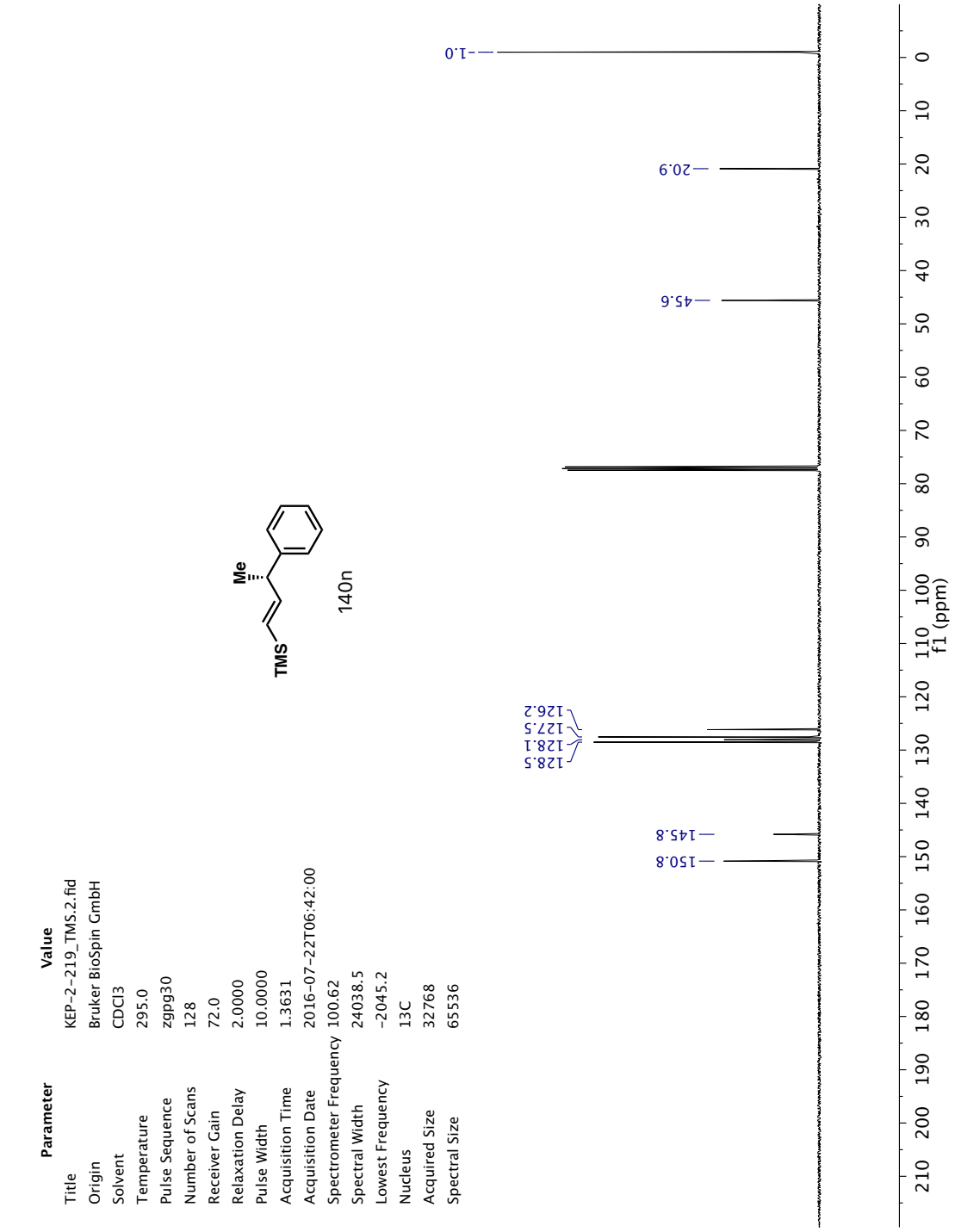

Parameter	Value
Title	KEP-2-219_TMS.2.fid
Origin	Bruker BioSpin GmbH
Solvent	CDCl3
Temperature	295.0
Pulse Sequence	zgpg30
Number of Scans	128
Receiver Gain	72.0
Relaxation Delay	2.0000
Pulse Width	10.0000
Acquisition Time	1.3631
Acquisition Date	2016-07-22T06:42:00
Spectrometer Frequency	100.62
Spectral Width	24038.5
Lowest Frequency	-2045.2
Nucleus	13C
Acquired Size	32768
Spectral Size	65536

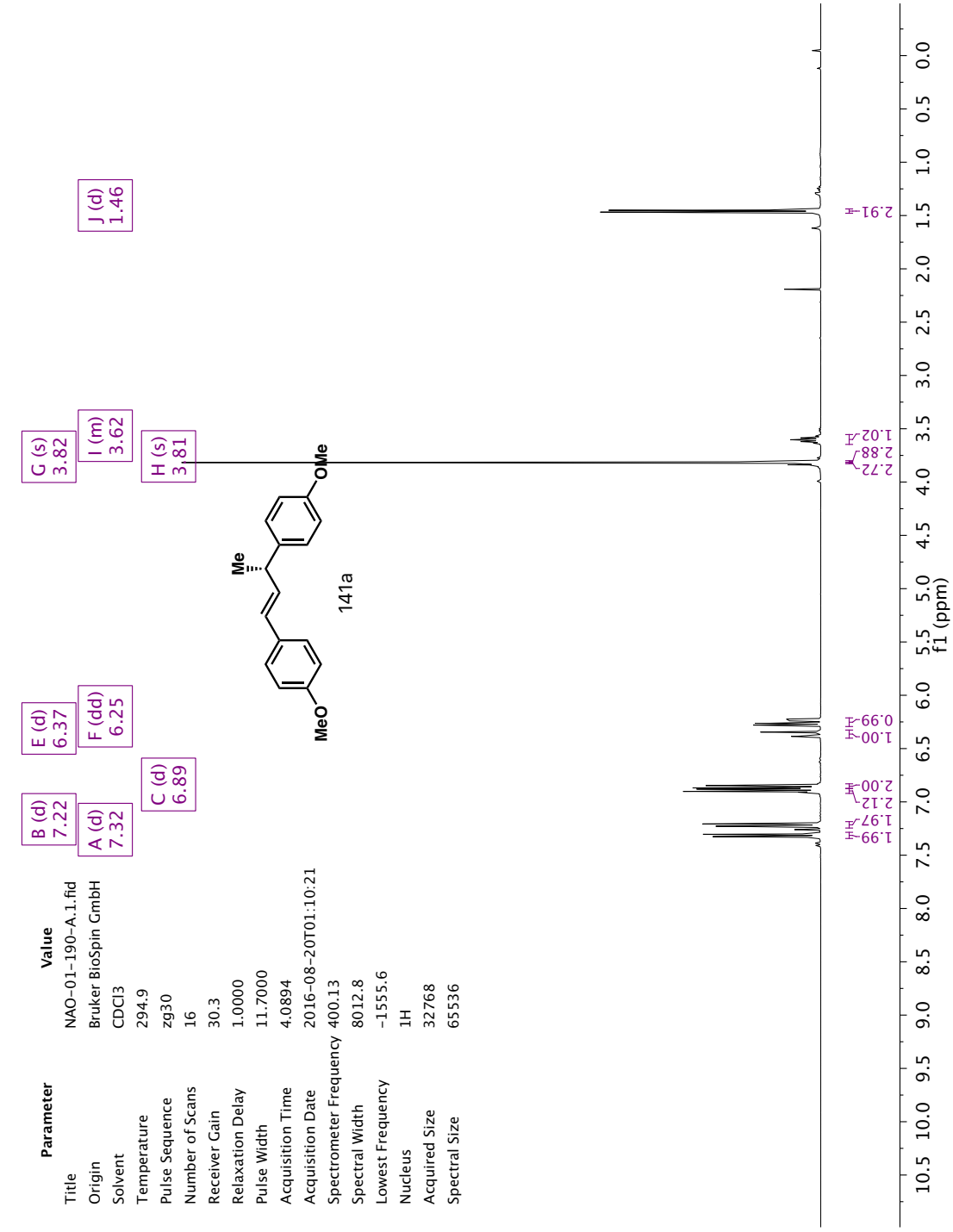
Parameter Value
Title NAO-01-190-A.1.fid
Origin Bruker BioSpin GmbH
Solvent CDCl3
Temperature 294.9
Pulse Sequence zg30
Number of Scans 16
Receiver Gain 30.3
Relaxation Delay 1.0000
Pulse Width 11.7000
Acquisition Time 4.0894
Acquisition Date 2016-08-20T01:10:21
Spectrometer Frequency 400.13
Spectral Width 8012.8
Lowest Frequency -1555.6
Nucleus 1H
Acquired Size 32768
Spectral Size 65536
B (d) 7.22
A (d) 7.32
C (d) 6.89
E (d) 6.37
F (dd) 6.25
G (s) 3.82
I (m) 3.62
H (s) 3.81
J (d) 1.46
Me
OMe
MeO
141a
1.99
1.97
2.00
2.12
1.00
0.99
1.02
2.88
2.72
2.91
f1 (ppm)

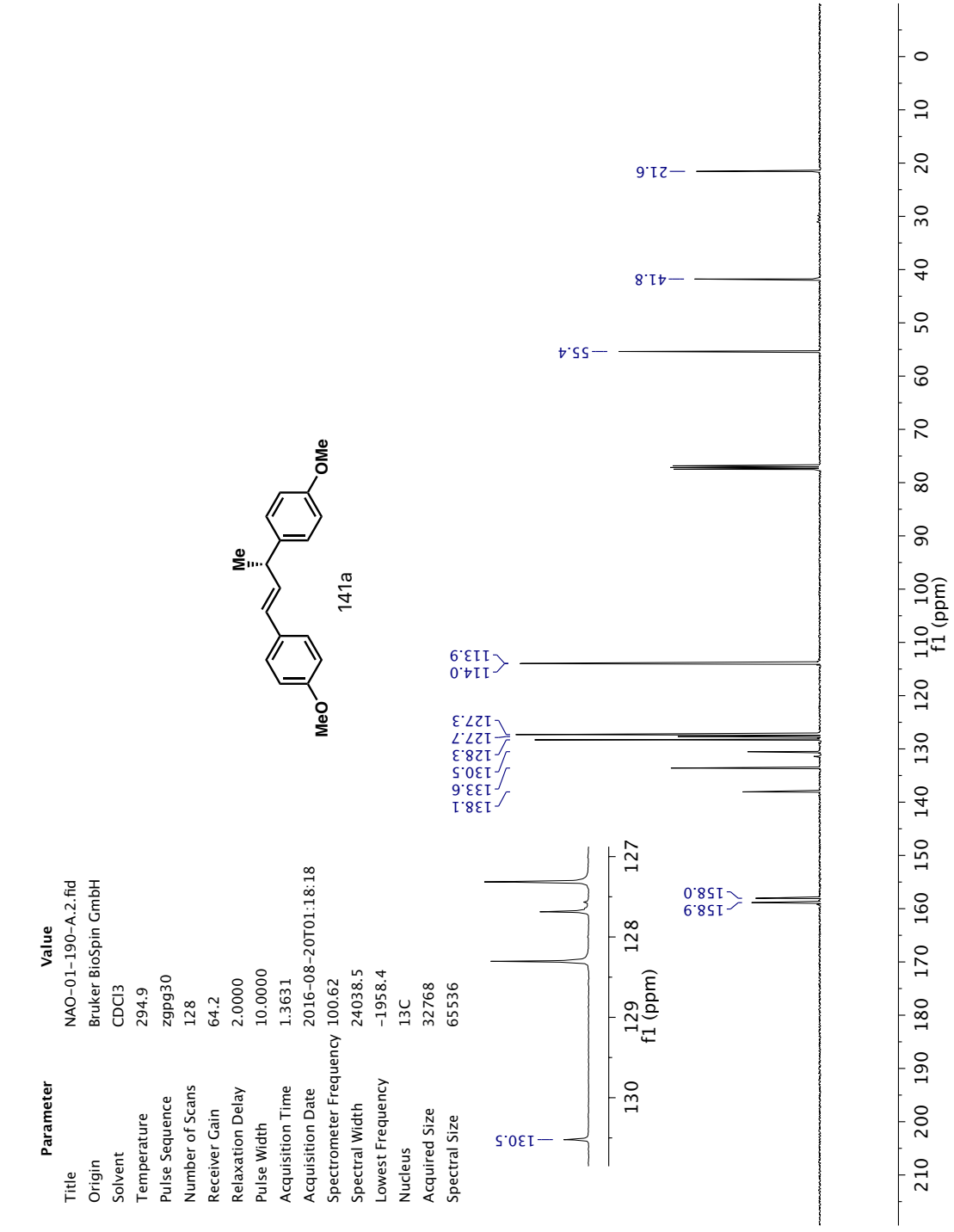
Parameter Value
Title NAO-01-190-A.2.fid
Origin Bruker BioSpin GmbH
Solvent CDCl3
Temperature 294.9
Pulse Sequence zgpg30
Number of Scans 128
Receiver Gain 64.2
Relaxation Delay 2.0000
Pulse Width 10.0000
Acquisition Time 1.3631
Acquisition Date 2016-08-20T01:18:18
Spectrometer Frequency 100.62
Spectral Width 24038.5
Lowest Frequency -1958.4
Nucleus 13C
Acquired Size 32768
Spectral Size 65536
Me
OMe
MeO
141a
158.9
158.0
138.1
133.6
130.5
128.3
127.7
127.3
114.0
113.9
55.4
41.8
21.6
130.5
f1 (ppm)

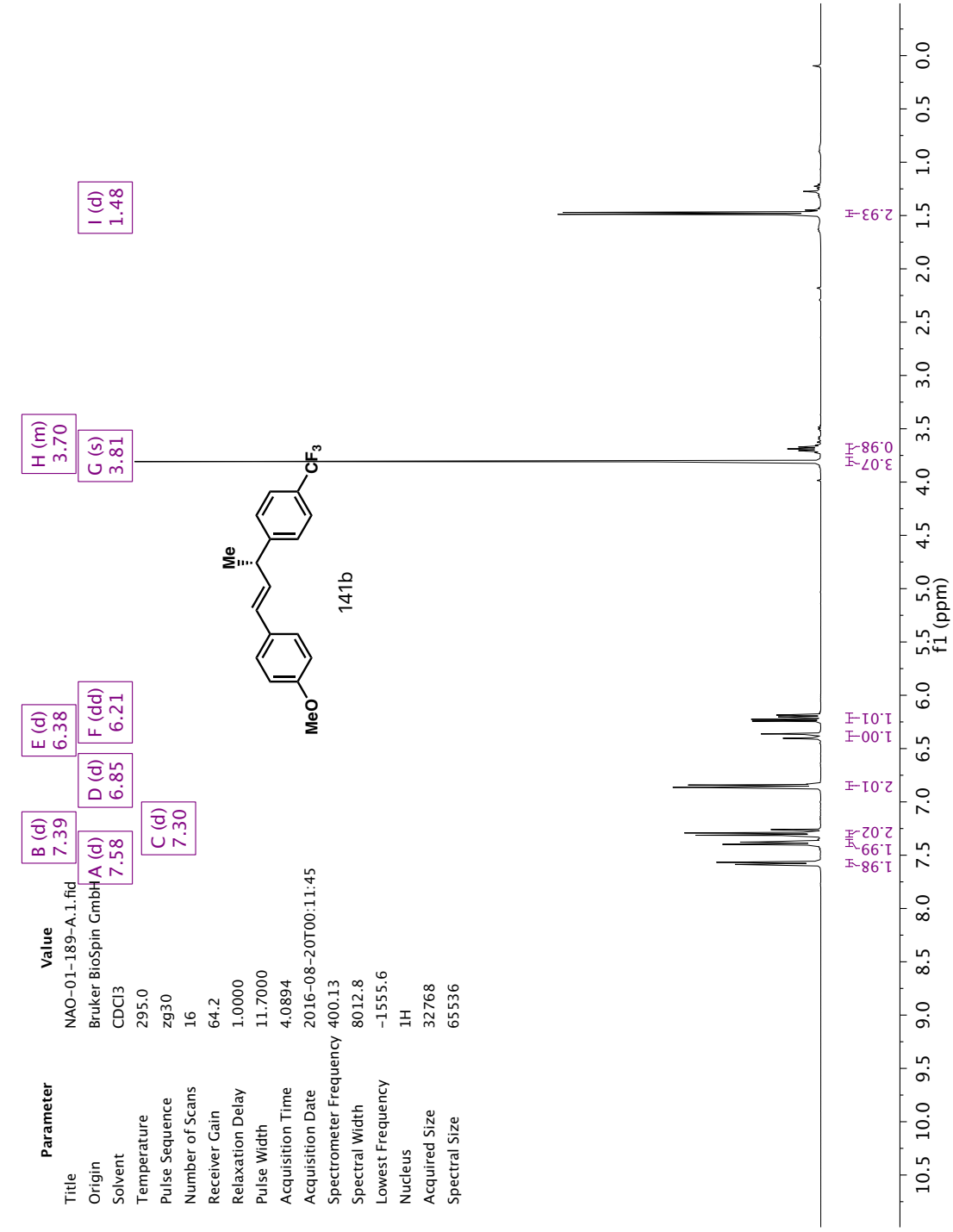
Parameter
Value
Title NAO-01-189-A.1.fid
Origin Bruker BioSpin GmbH
Solvent CDCl3
Temperature 295.0
Pulse Sequence zg30
Number of Scans 16
Receiver Gain 64.2
Relaxation Delay 1.0000
Pulse Width 11.7000
Acquisition Time 4.0894
Acquisition Date 2016-08-20T00:11:45
Spectrometer Frequency 400.13
Spectral Width 8012.8
Lowest Frequency -1555.6
Nucleus 1H
Acquired Size 32768
Spectral Size 65536
A (d) 7.58
B (d) 7.39
C (d) 7.30
D (d) 6.85
E (d) 6.38
F (dd) 6.21
G (s) 3.81
H (m) 3.70
I (d) 1.48
Me
MeO
CF3
141b
1.98
1.99
2.02
2.01
1.00
1.01
3.07
0.98
2.93
f1 (ppm)

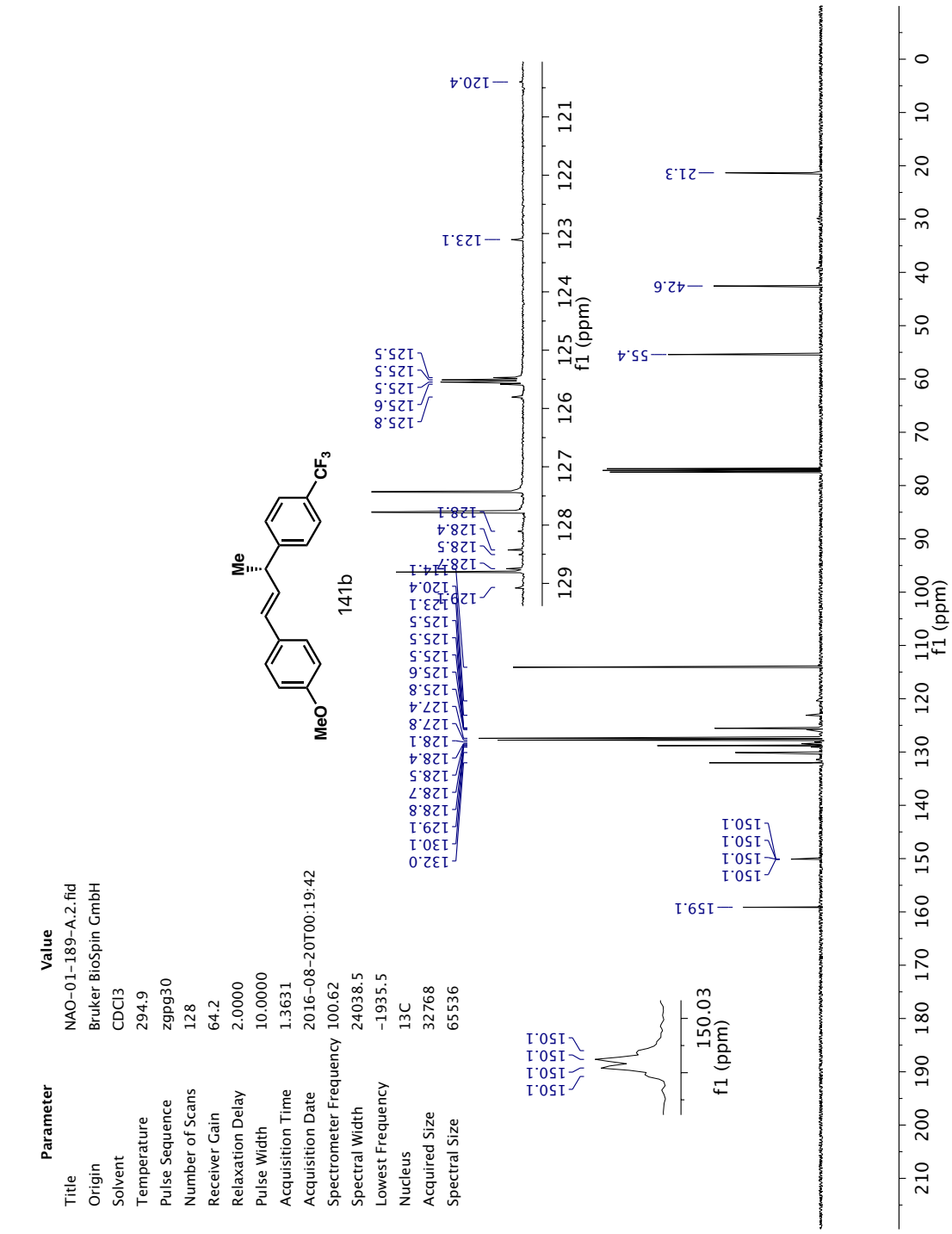
Parameter Value
Title NAO-01-189-A.2.fid
Origin Bruker BioSpin GmbH
Solvent CDCl3
Temperature 294.9
Pulse Sequence zgpg30
Number of Scans 128
Receiver Gain 64.2
Relaxation Delay 2.0000
Pulse Width 10.0000
Acquisition Time 1.3631
Acquisition Date 2016-08-20T00:19:42
Spectrometer Frequency 100.62
Spectral Width 24038.5
Lowest Frequency -1935.5
Nucleus 13C
Acquired Size 32768
Spectral Size 65536
Me
CF3
MeO
141b
f1 (ppm)
150.03

Parameter	Value
Title	NAO-01-189A
Origin	Varian
Solvent	"cdcl3"
Temperature	25.0
Pulse Sequence	s2pul
Number of Scans	16
Receiver Gain	30
Relaxation Delay	1.0000
Pulse Width	6.3333
Acquisition Time	0.9856
Acquisition Date	2016-08-31T23:27:51
Spectrometer Frequency	282.34
Spectral Width	64935.1
Lowest Frequency	-57338.6
Nucleus	19F
Acquired Size	64000
Spectral Size	131072

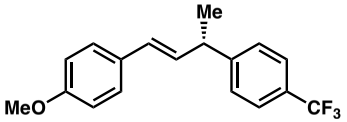

141b

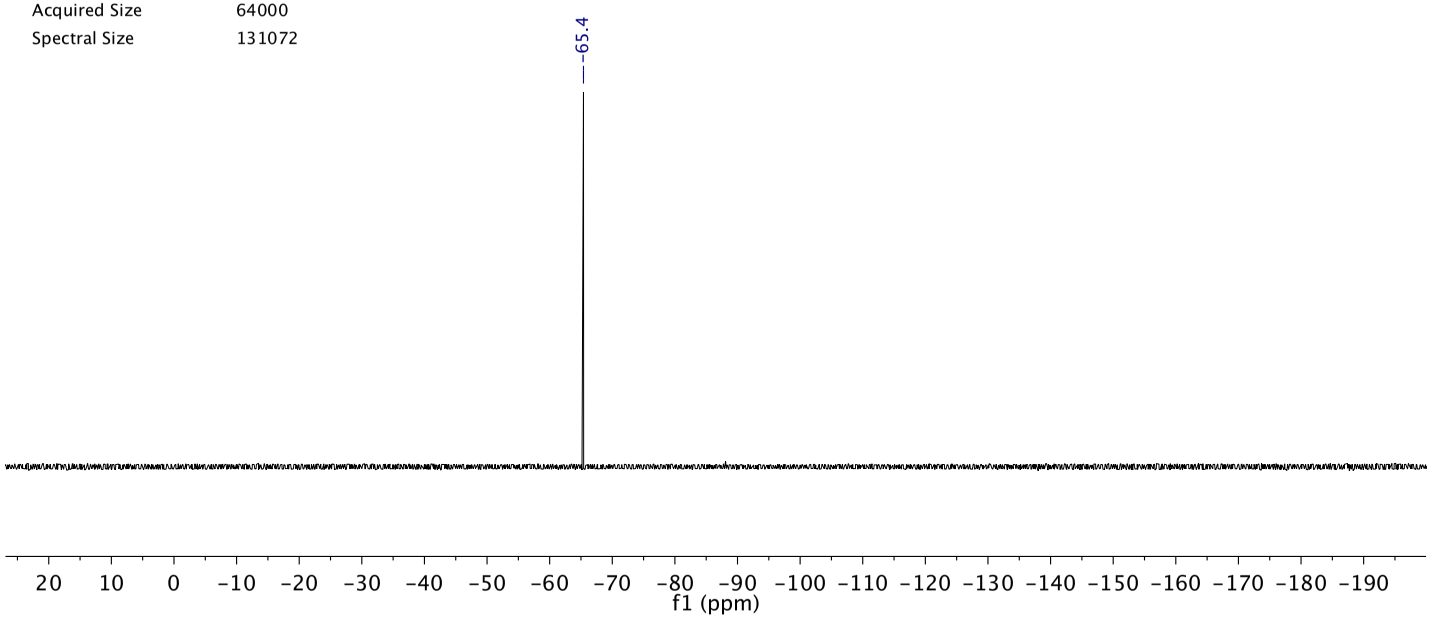

Parameter Value
Title NAO-01-189A-C6F6
Origin Varian
Solvent "cdcl3"
Temperature 25.0
Pulse Sequence s2pul
Number of Scans 16
Receiver Gain 30
Relaxation Delay 1.0000
Pulse Width 6.3333
Acquisition Time 0.9856
Acquisition Date 2016-08-31T23:32:04
Spectrometer Frequency 282.34
Spectral Width 64935.1
Lowest Frequency -58230.0
Nucleus 19F
Acquired Size 64000
Spectral Size 131072
Me
CF3
MeO
141b
with C6F6
-65.4
20 10 0 -10 -20 -30 -40 -50 -60 -70 -80 -90 -100 -110 -120 -130 -140 -150 -160 -170 -180 -190
f1 (ppm)

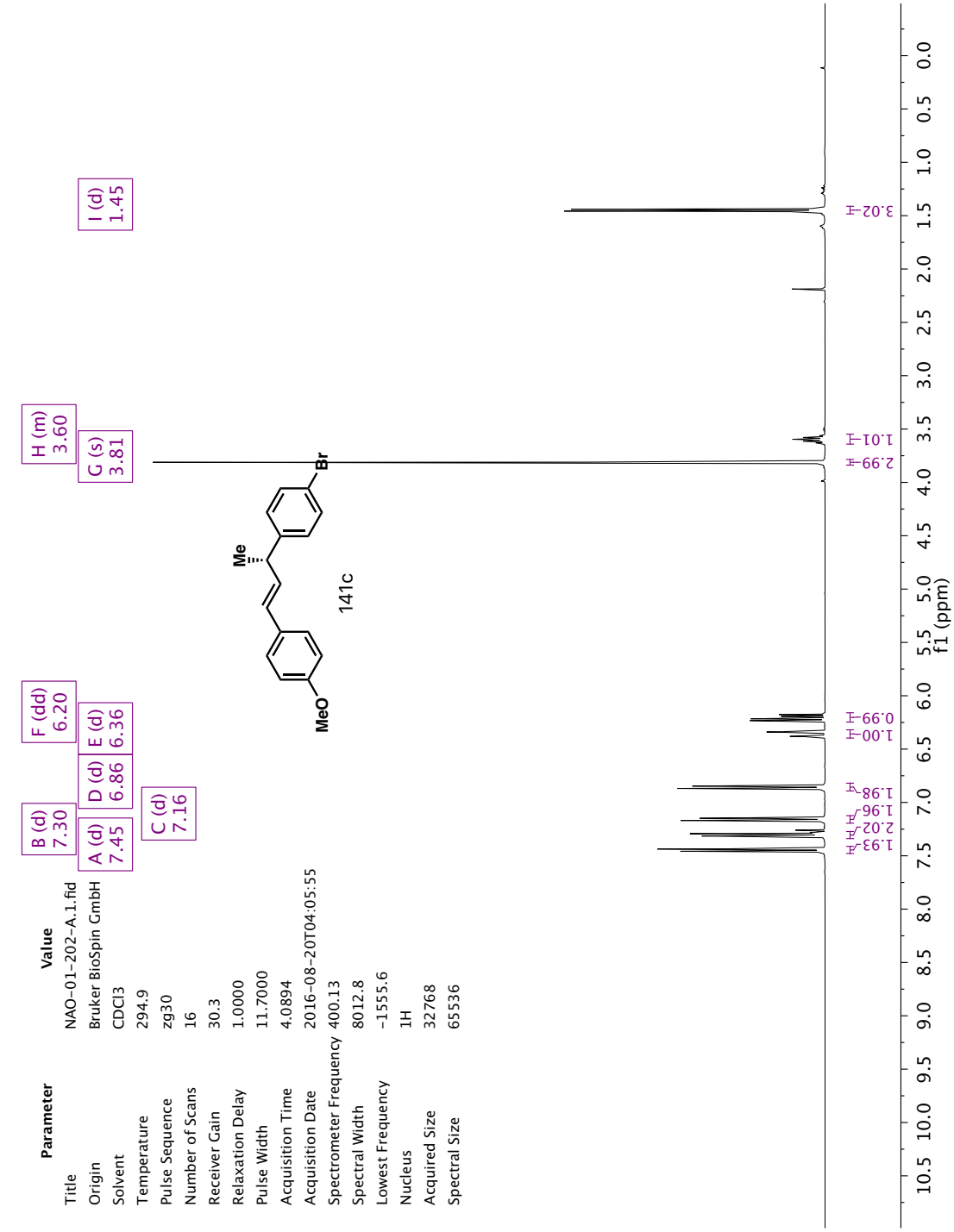
Parameter
Value
Title NAO-01-202-A.1.fid
Origin Bruker BioSpin GmbH
Solvent CDCl3
Temperature 294.9
Pulse Sequence zg30
Number of Scans 16
Receiver Gain 30.3
Relaxation Delay 1.0000
Pulse Width 11.7000
Acquisition Time 4.0894
Acquisition Date 2016-08-20T04:05:55
Spectrometer Frequency 400.13
Spectral Width 8012.8
Lowest Frequency -1555.6
Nucleus 1H
Acquired Size 32768
Spectral Size 65536
B (d) 7.30
A (d) 7.45
D (d) 6.86
E (d) 6.36
F (dd) 6.20
C (d) 7.16
H (m) 3.60
G (s) 3.81
I (d) 1.45
Me
Br
MeO
141c
3.02
2.99
1.01
1.00
0.99
1.98
1.96
2.02
1.93
f1 (ppm)

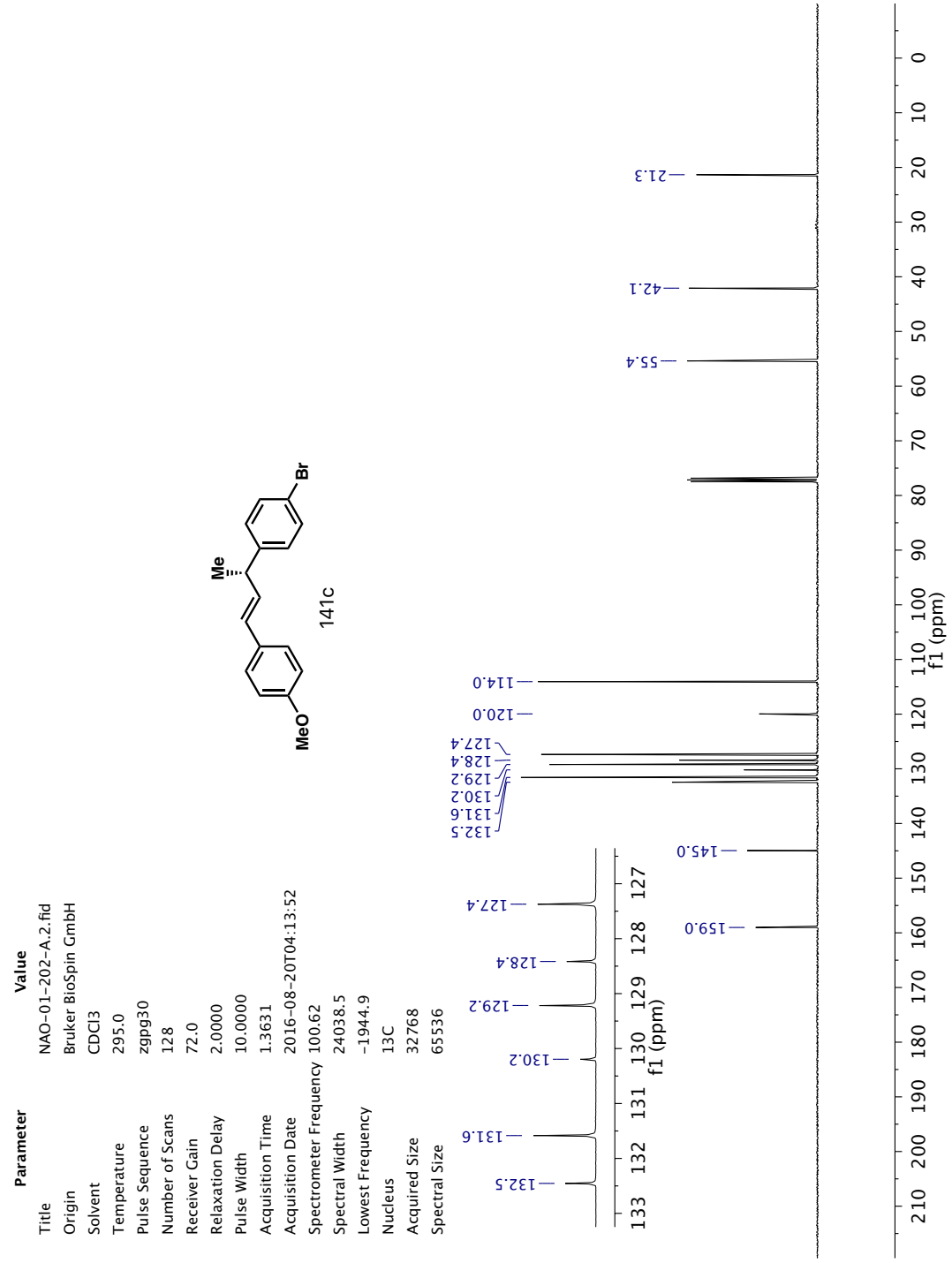
Parameter Value
Title NAO-01-202-A.2.fid
Origin Bruker BioSpin GmbH
Solvent CDCl3
Temperature 295.0
Pulse Sequence zgpg30
Number of Scans 128
Receiver Gain 72.0
Relaxation Delay 2.0000
Pulse Width 10.0000
Acquisition Time 1.3631
Acquisition Date 2016-08-20T04:13:52
Spectrometer Frequency 100.62
Spectral Width 24038.5
Lowest Frequency -1944.9
Nucleus 13C
Acquired Size 32768
Spectral Size 65536
Me
Br
MeO
141c
132.5
131.6
130.2
129.2
128.4
127.4
120.0
114.0
55.4
42.1
21.3
159.0
145.0
f1 (ppm)

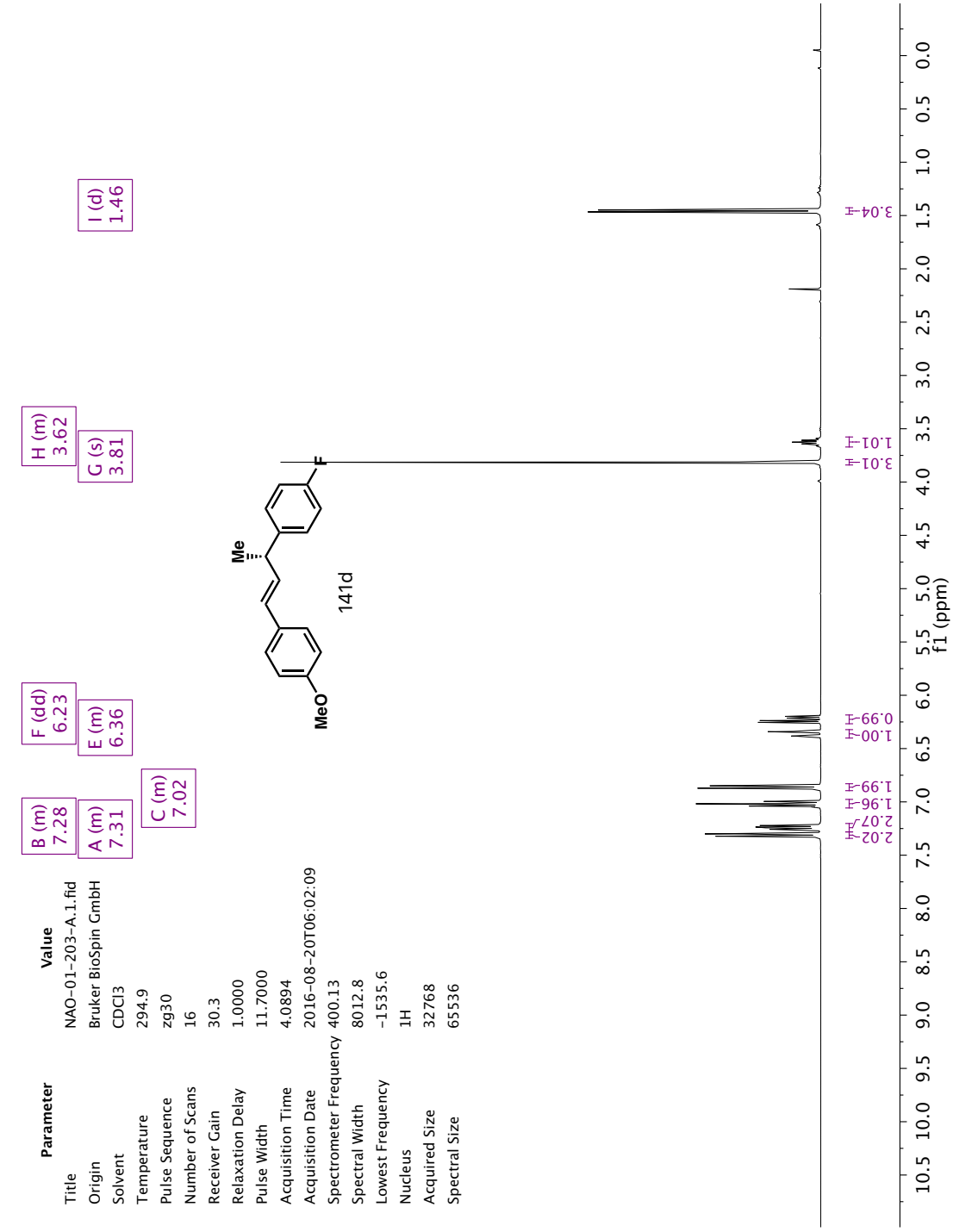
Parameter
Value
Title NAO-01-203-A.1.fid
Origin Bruker BioSpin GmbH
Solvent CDCl3
Temperature 294.9
Pulse Sequence zg30
Number of Scans 16
Receiver Gain 30.3
Relaxation Delay 1.0000
Pulse Width 11.7000
Acquisition Time 4.0894
Acquisition Date 2016-08-20T06:02:09
Spectrometer Frequency 400.13
Spectral Width 8012.8
Lowest Frequency -1535.6
Nucleus 1H
Acquired Size 32768
Spectral Size 65536
B (m) 7.28
A (m) 7.31
C (m) 7.02
F (dd) 6.23
E (m) 6.36
H (m) 3.62
G (s) 3.81
I (d) 1.46
Me
MeO
F
141d
2.02
2.07
1.96
1.99
1.00
0.99
3.01
1.01
3.04
f1 (ppm)

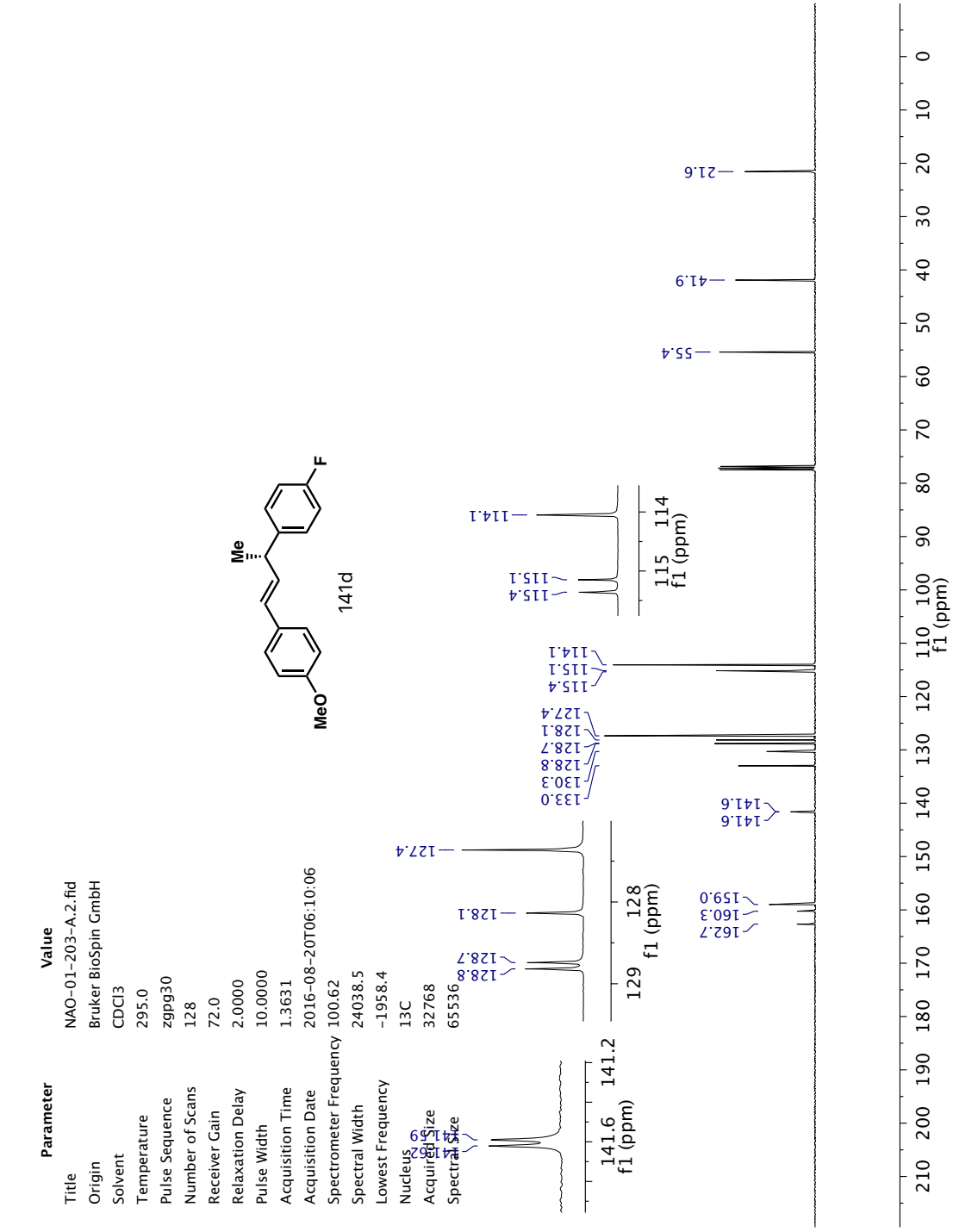
Parameter Value
Title NAO-01-203-A.2.fid
Origin Bruker BioSpin GmbH
Solvent CDCl3
Temperature 295.0
Pulse Sequence zgpg30
Number of Scans 128
Receiver Gain 72.0
Relaxation Delay 2.0000
Pulse Width 10.0000
Acquisition Time 1.3631
Acquisition Date 2016-08-20T06:10:06
Spectrometer Frequency 100.62
Spectral Width 24038.5
Lowest Frequency -1958.4
Nucleus 13C
Acquired Size 32768
Spectral Size 65536
Me
F
MeO
141d
f1 (ppm)

Parameter	Value
Title	JLH-6-040B
Origin	Varian
Solvent	"cdcl3"
Temperature	25.0
Pulse Sequence	s2pul
Number of Scans	16
Receiver Gain	30
Relaxation Delay	1.0000
Pulse Width	6.3333
Acquisition Time	0.9856
Acquisition Date	2017-01-09T23:50:23
Spectrometer Frequency	282.34
Spectral Width	64935.1
Lowest Frequency	-56468.7
Nucleus	19F
Acquired Size	64000
Spectral Size	131072

A (tt)
-123.56

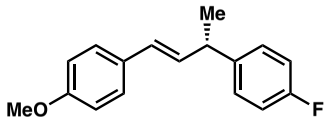

141d

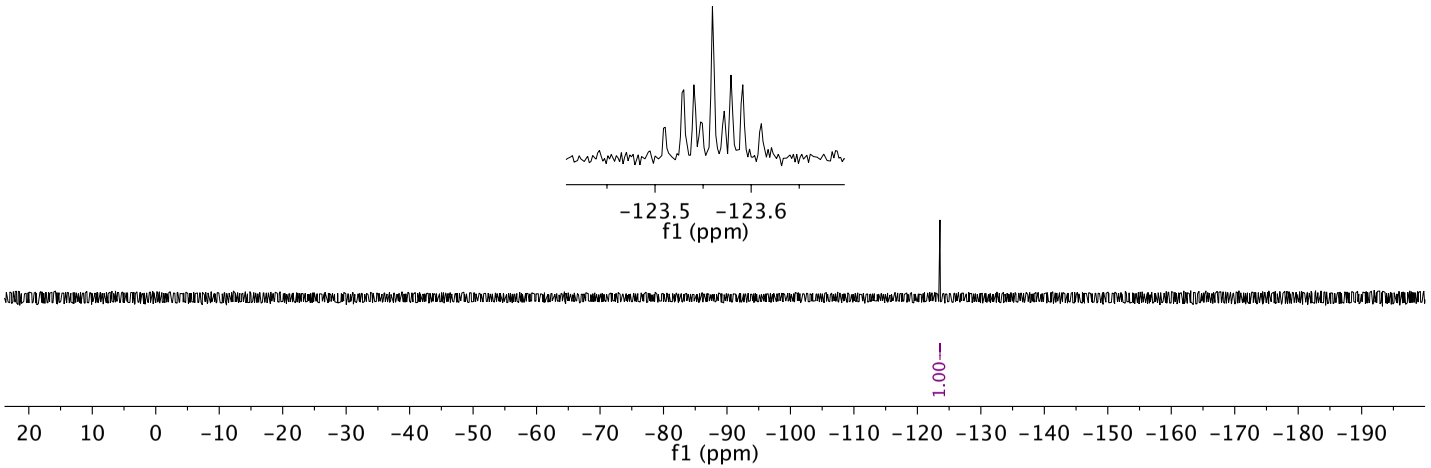

Parameter	Value
Title	JLH-6-040B-C6F6
Origin	Varian
Solvent	"cdcl3"
Temperature	25.0
Pulse Sequence	s2pul
Number of Scans	16
Receiver Gain	30
Relaxation Delay	1.0000
Pulse Width	6.3333
Acquisition Time	0.9856
Acquisition Date	2017-01-09T23:53:59
Spectrometer Frequency	282.34
Spectral Width	64935.1
Lowest Frequency	-56468.7
Nucleus	19F
Acquired Size	64000
Spectral Size	131072

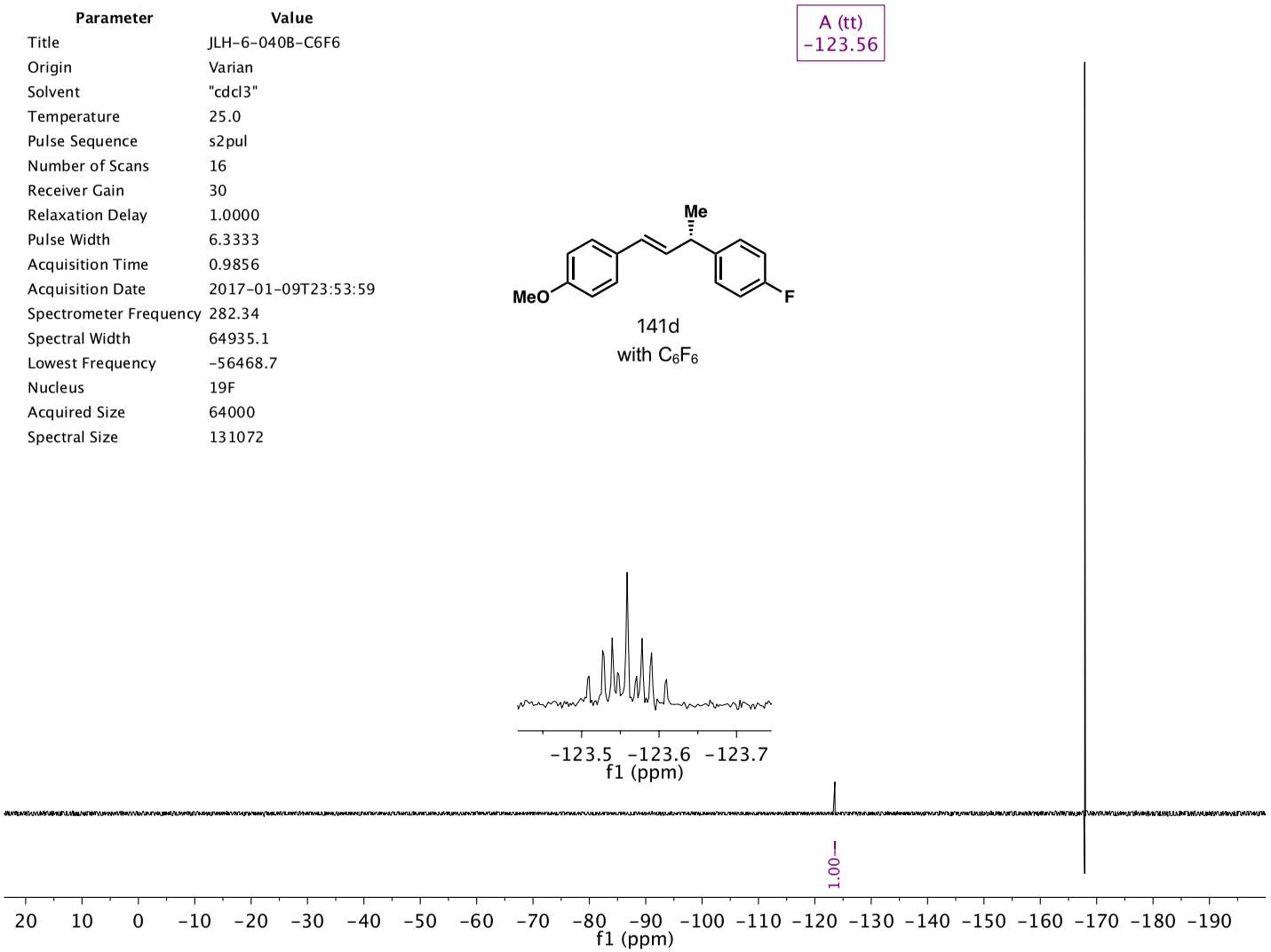

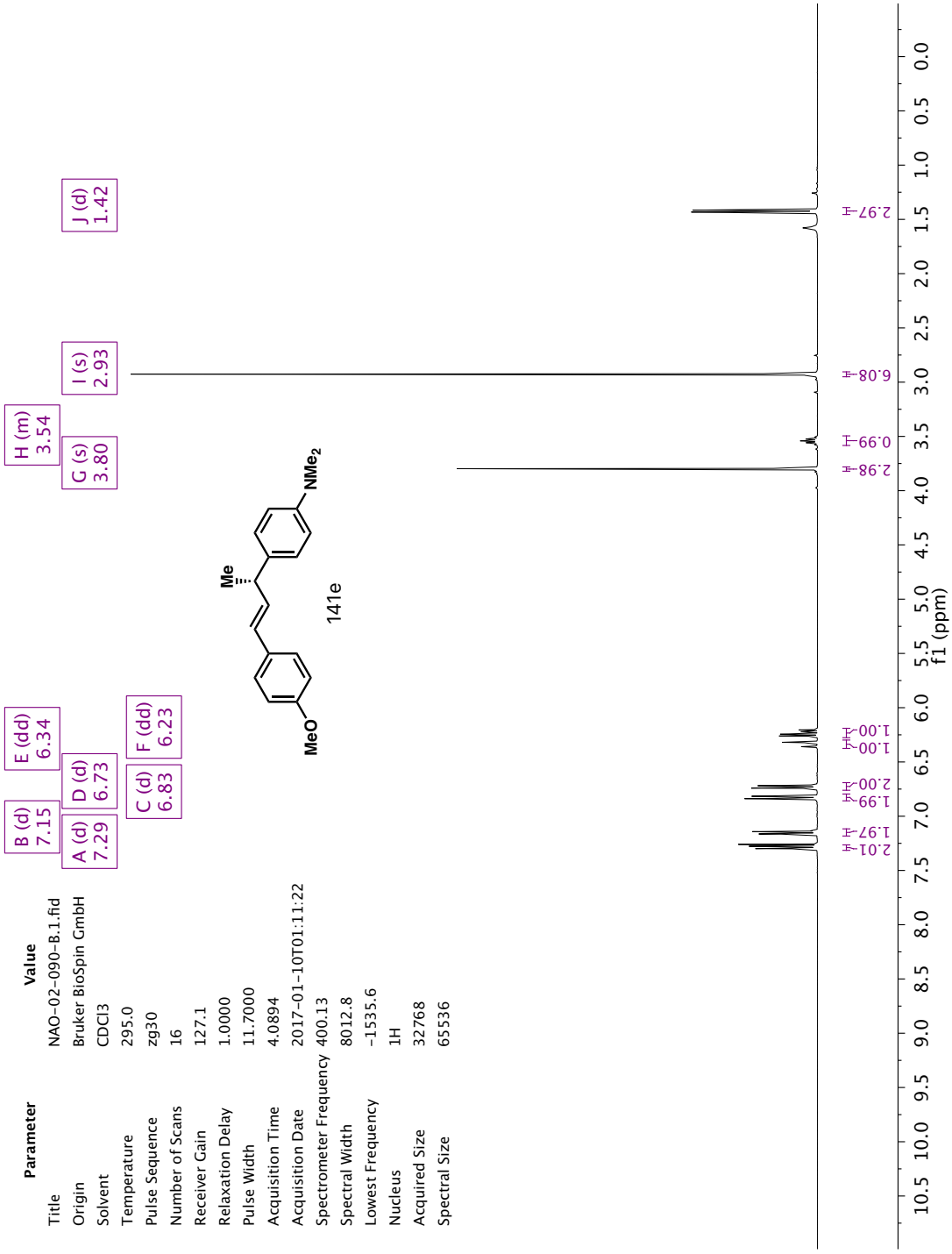
Parameter
Value
Title
NAO-02-090-B.1.fid
Origin
Bruker BioSpin GmbH
Solvent
CDCl3
Temperature
295.0
Pulse Sequence
zg30
Number of Scans
16
Receiver Gain
127.1
Relaxation Delay
1.0000
Pulse Width
11.7000
Acquisition Time
4.0894
Acquisition Date
2017-01-10T01:11:22
Spectrometer Frequency
400.13
Spectral Width
8012.8
Lowest Frequency
-1535.6
Nucleus
1H
Acquired Size
32768
Spectral Size
65536
A (d) 7.29
B (d) 7.15
C (d) 6.83
D (d) 6.73
E (dd) 6.34
F (dd) 6.23
G (s) 3.80
H (m) 3.54
I (s) 2.93
J (d) 1.42
Me
NMe2
MeO
141e
2.01
1.97
1.99
2.00
1.00
1.00
2.98
0.99
6.08
2.97
f1 (ppm)

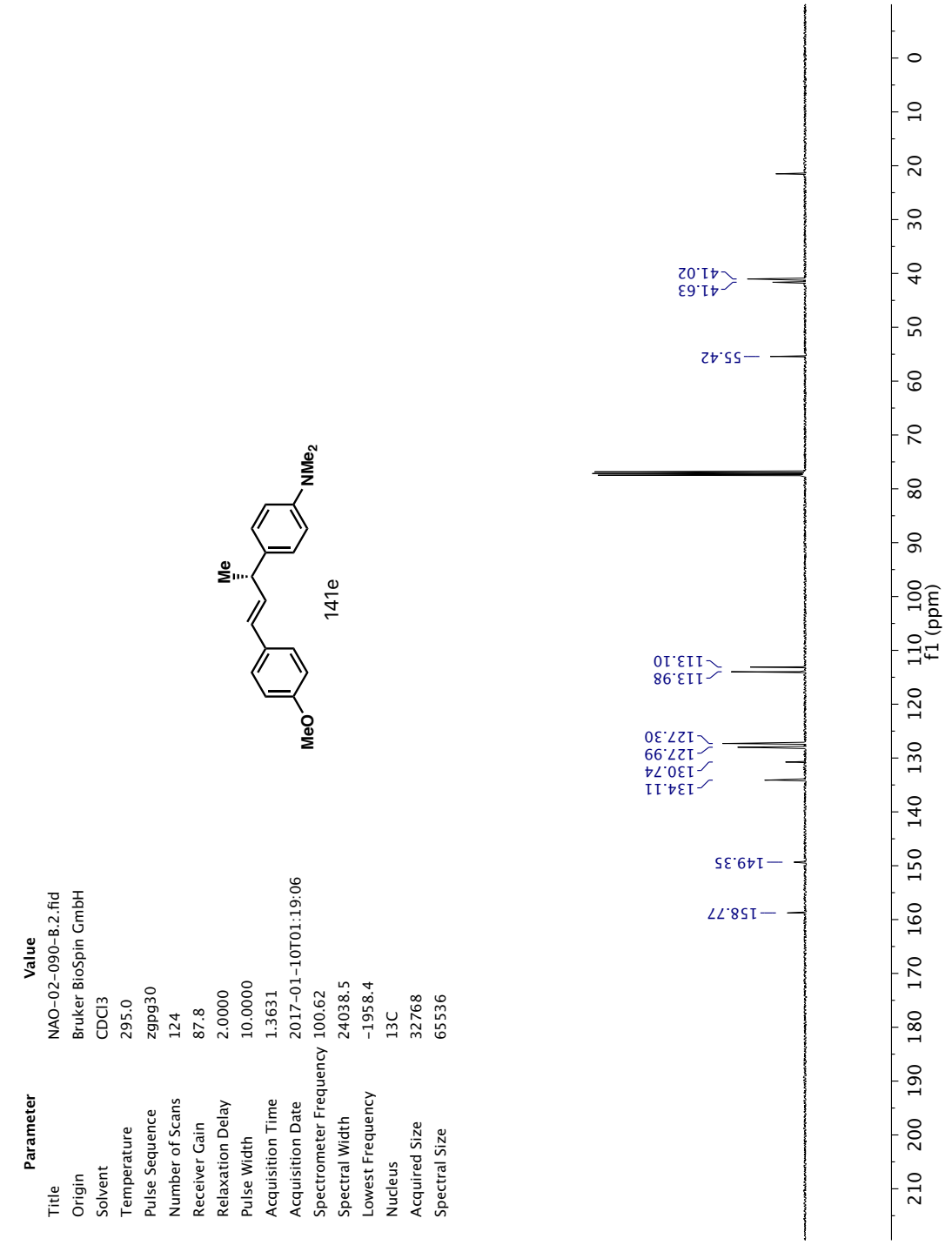
Parameter Value
Title NAO-02-090-B.2.fid
Origin Bruker BioSpin GmbH
Solvent CDCl3
Temperature 295.0
Pulse Sequence zgpg30
Number of Scans 124
Receiver Gain 87.8
Relaxation Delay 2.0000
Pulse Width 10.0000
Acquisition Time 1.3631
Acquisition Date 2017-01-10T01:19:06
Spectrometer Frequency 100.62
Spectral Width 24038.5
Lowest Frequency -1958.4
Nucleus 13C
Acquired Size 32768
Spectral Size 65536
Me
NMe2
MeO
141e
158.77
149.35
134.11
130.74
127.99
127.30
113.98
113.10
55.42
41.63
41.02
f1 (ppm)

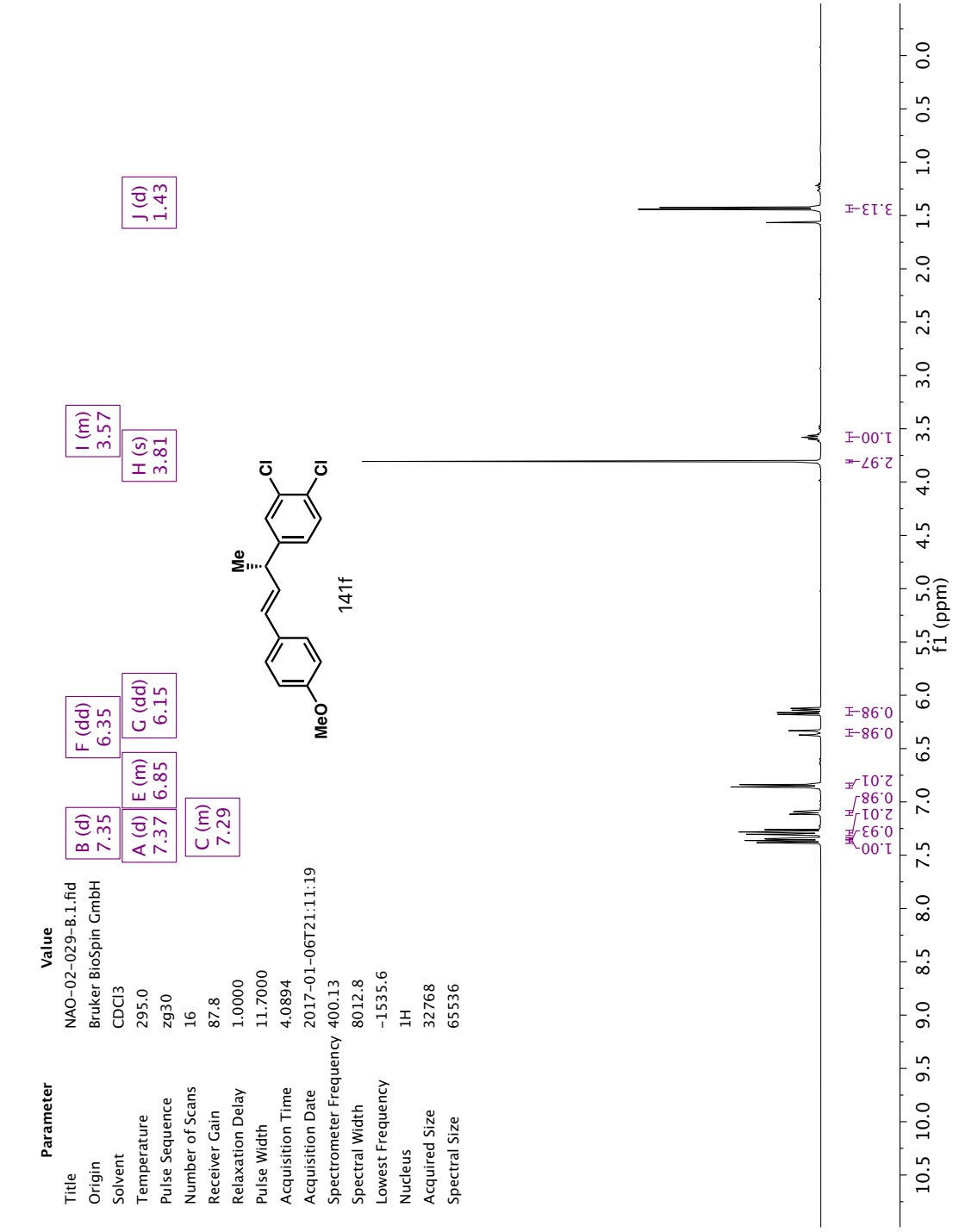
Parameter
Value
Title
NAO-02-029-B.1.fid
Origin
Bruker BioSpin GmbH
Solvent
CDCl3
Temperature
295.0
Pulse Sequence
zg30
Number of Scans
16
Receiver Gain
87.8
Relaxation Delay
1.0000
Pulse Width
11.7000
Acquisition Time
4.0894
Acquisition Date
2017-01-06T21:11:19
Spectrometer Frequency
400.13
Spectral Width
8012.8
Lowest Frequency
-1535.6
Nucleus
1H
Acquired Size
32768
Spectral Size
65536
B (d) 7.35
A (d) 7.37
E (m) 6.85
C (m) 7.29
F (dd) 6.35
G (dd) 6.15
I (m) 3.57
H (s) 3.81
J (d) 1.43
Cl
Cl
Me
MeO
141f
1.00
0.93
2.01
0.98
2.01
0.98
0.98
2.97
1.00
3.13
10.5 10.0 9.5 9.0 8.5 8.0 7.5 7.0 6.5 6.0 5.5 5.0 4.5 4.0 3.5 3.0 2.5 2.0 1.5 1.0 0.5 0.0
f1 (ppm)

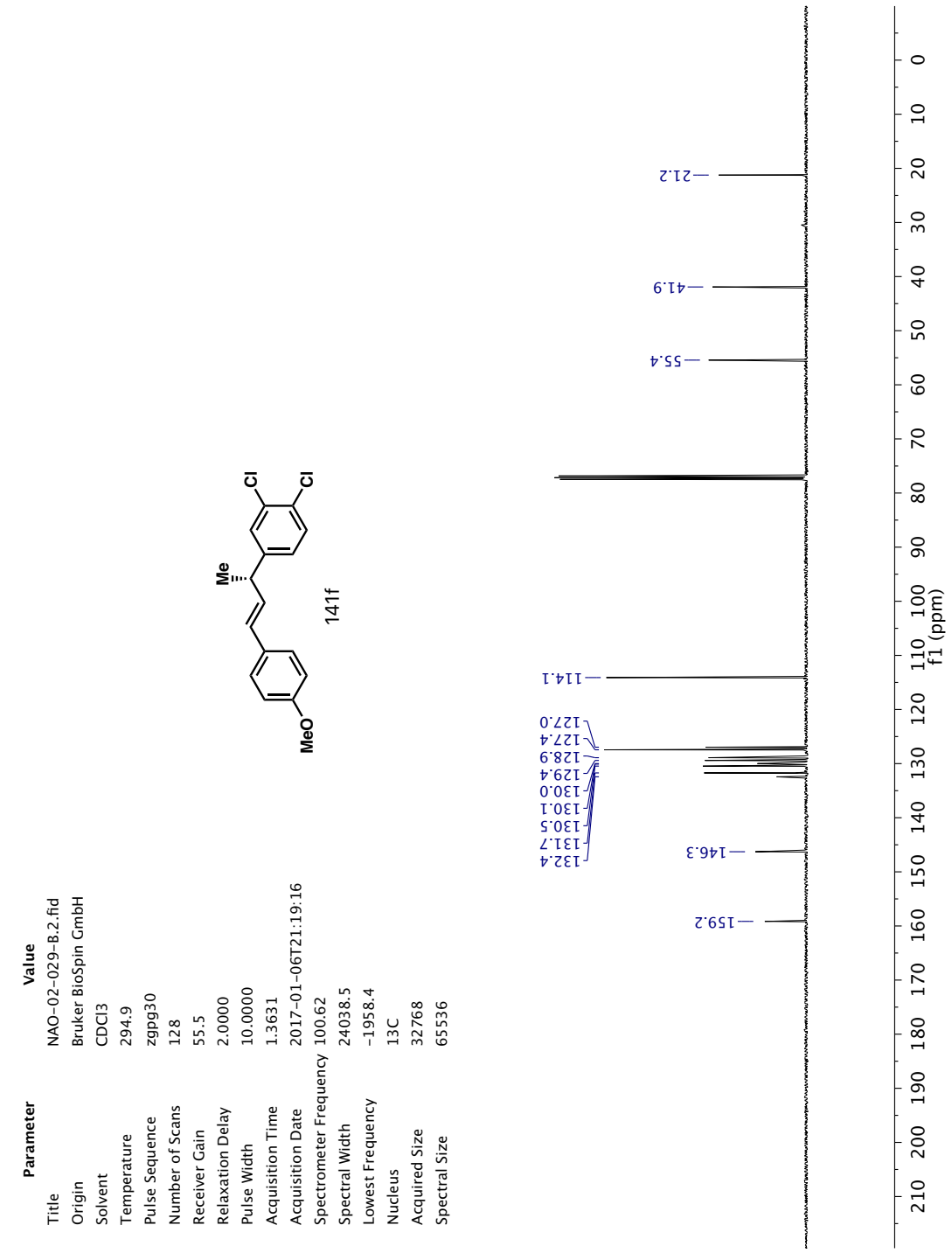

Parameter	Value
Title	NAO-02-029-B.2.fid
Origin	Bruker BioSpin GmbH
Solvent	CDCl3
Temperature	294.9
Pulse Sequence	zgpg30
Number of Scans	128
Receiver Gain	55.5
Relaxation Delay	2.0000
Pulse Width	10.0000
Acquisition Time	1.3631
Acquisition Date	2017-01-06T21:19:16
Spectrometer Frequency	100.62
Spectral Width	24038.5
Lowest Frequency	-1958.4
Nucleus	13C
Acquired Size	32768
Spectral Size	65536

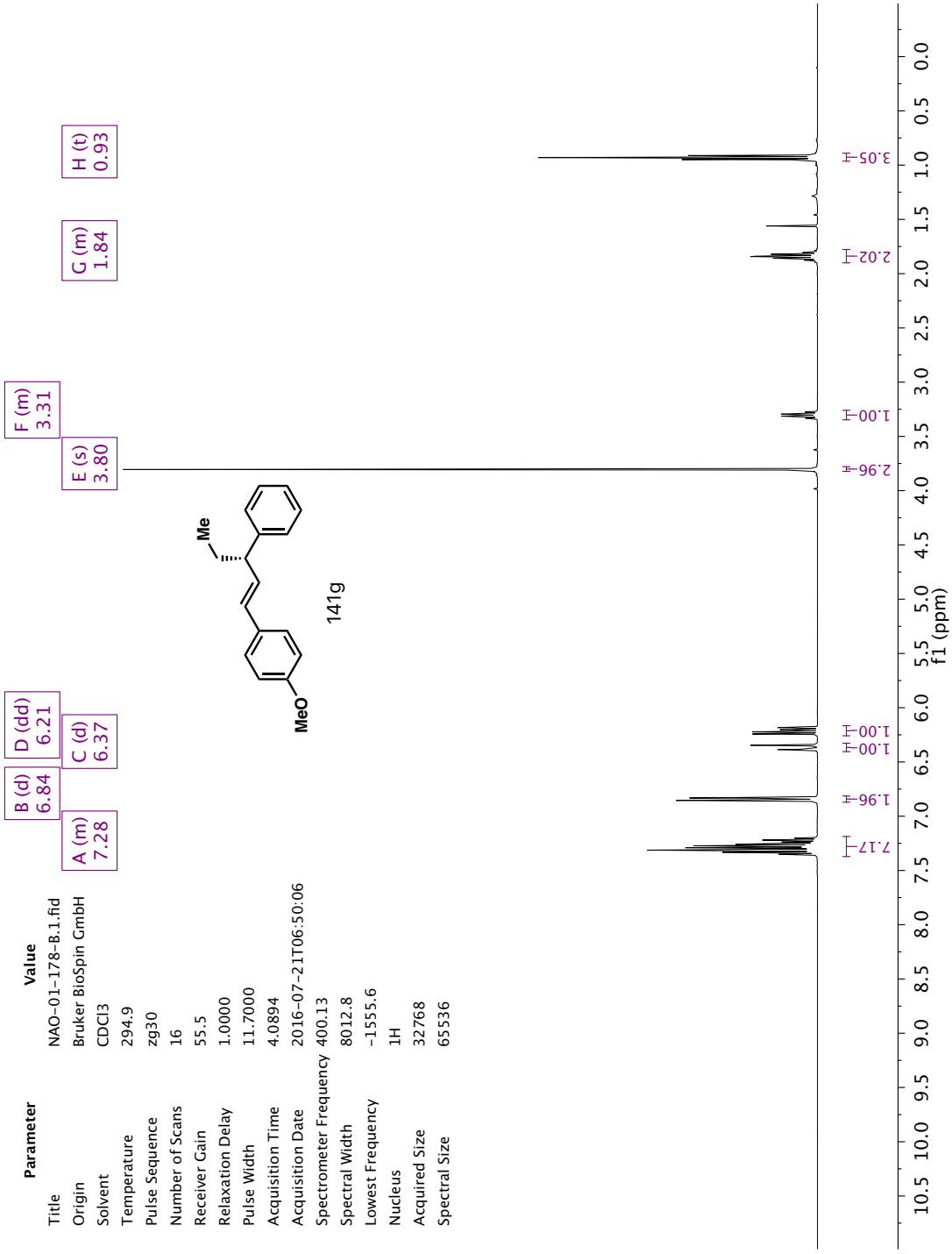
Parameter
Value
Title
NAO-01-178-B.1.fid
Origin
Bruker BioSpin GmbH
Solvent
CDCl3
Temperature
294.9
Pulse Sequence
zg30
Number of Scans
16
Receiver Gain
55.5
Relaxation Delay
1.0000
Pulse Width
11.7000
Acquisition Time
4.0894
Acquisition Date
2016-07-21T06:50:06
Spectrometer Frequency
400.13
Spectral Width
8012.8
Lowest Frequency
-1555.6
Nucleus
1H
Acquired Size
32768
Spectral Size
65536
A (m) 7.28
B (d) 6.84
C (d) 6.37
D (dd) 6.21
E (s) 3.80
F (m) 3.31
G (m) 1.84
H (t) 0.93
Me
MeO
141g
7.17
1.96
1.00
1.00
1.00
2.96
2.02
3.05
10.5 10.0 9.5 9.0 8.5 8.0 7.5 7.0 6.5 6.0 5.5 5.0 4.5 4.0 3.5 3.0 2.5 2.0 1.5 1.0 0.5 0.0
f1 (ppm)

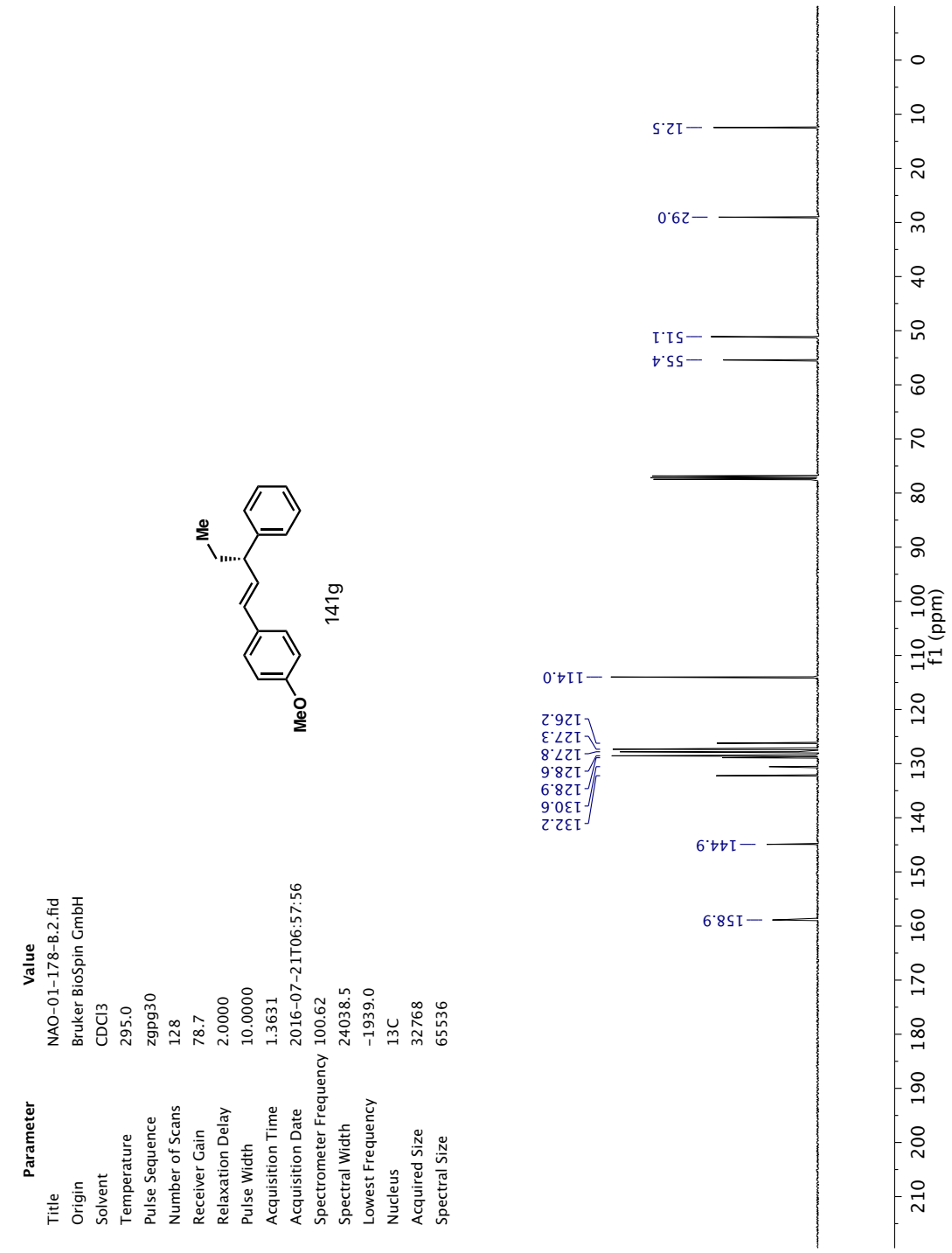

Parameter	Value
Title	NAO-01-178-B.2.fid
Origin	Bruker BioSpin GmbH
Solvent	CDCl3
Temperature	295.0
Pulse Sequence	zgpg30
Number of Scans	128
Receiver Gain	78.7
Relaxation Delay	2.0000
Pulse Width	10.0000
Acquisition Time	1.3631
Acquisition Date	2016-07-21T06:57:56
Spectrometer Frequency	100.62
Spectral Width	24038.5
Lowest Frequency	-1939.0
Nucleus	13C
Acquired Size	32768
Spectral Size	65536

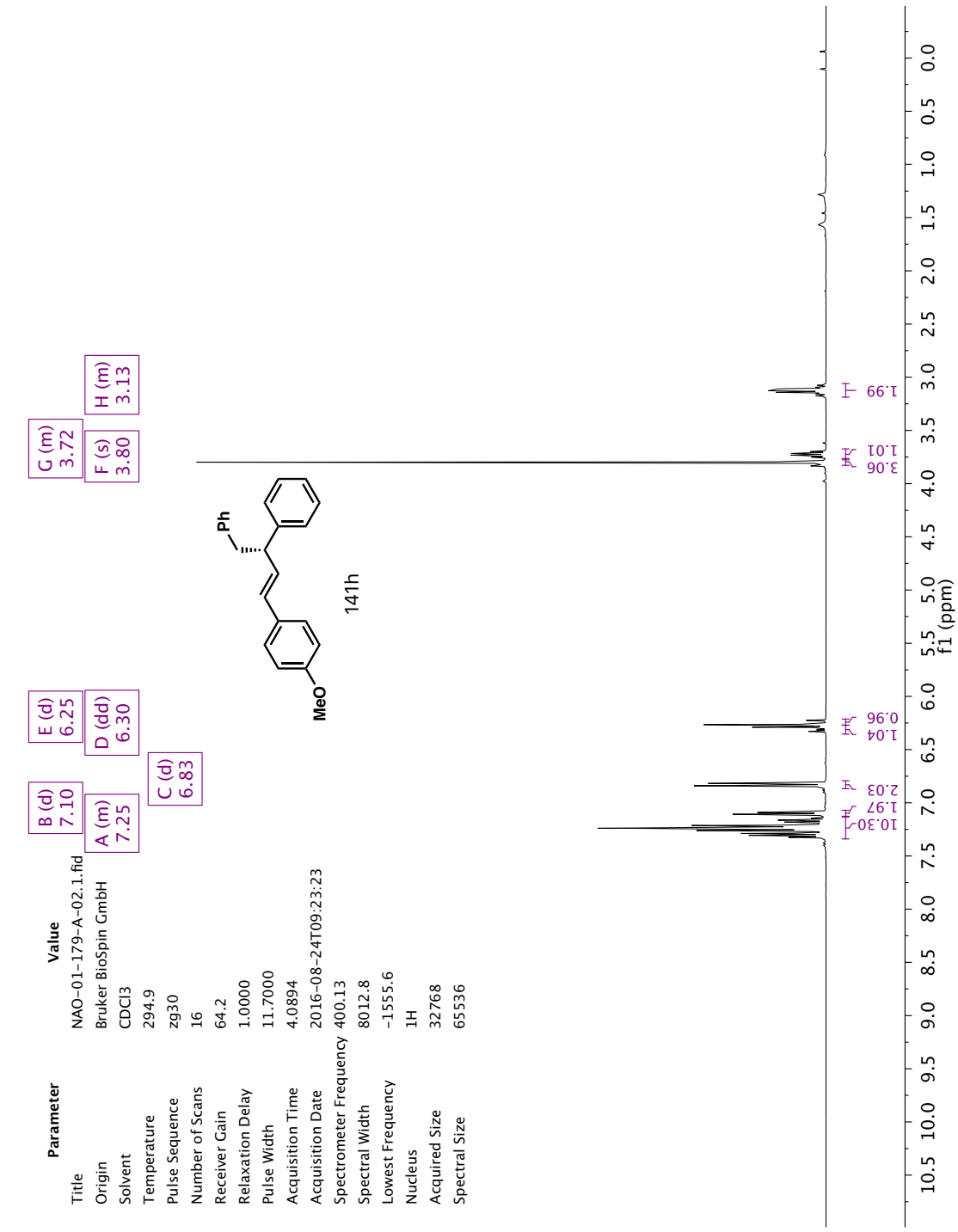
Parameter
Value
Title NAO-01-179-A-02.1.fid
Origin Bruker BioSpin GmbH
Solvent CDCl3
Temperature 294.9
Pulse Sequence zg30
Number of Scans 16
Receiver Gain 64.2
Relaxation Delay 1.0000
Pulse Width 11.7000
Acquisition Time 4.0894
Acquisition Date 2016-08-24T09:23:23
Spectrometer Frequency 400.13
Spectral Width 8012.8
Lowest Frequency -1555.6
Nucleus 1H
Acquired Size 32768
Spectral Size 65536
B (d) 7.10
A (m) 7.25
E (d) 6.25
D (dd) 6.30
C (d) 6.83
G (m) 3.72
F (s) 3.80
H (m) 3.13
Ph
MeO
141h
10.30
1.97
2.03
1.04
0.96
3.06
1.01
1.99
f1 (ppm)

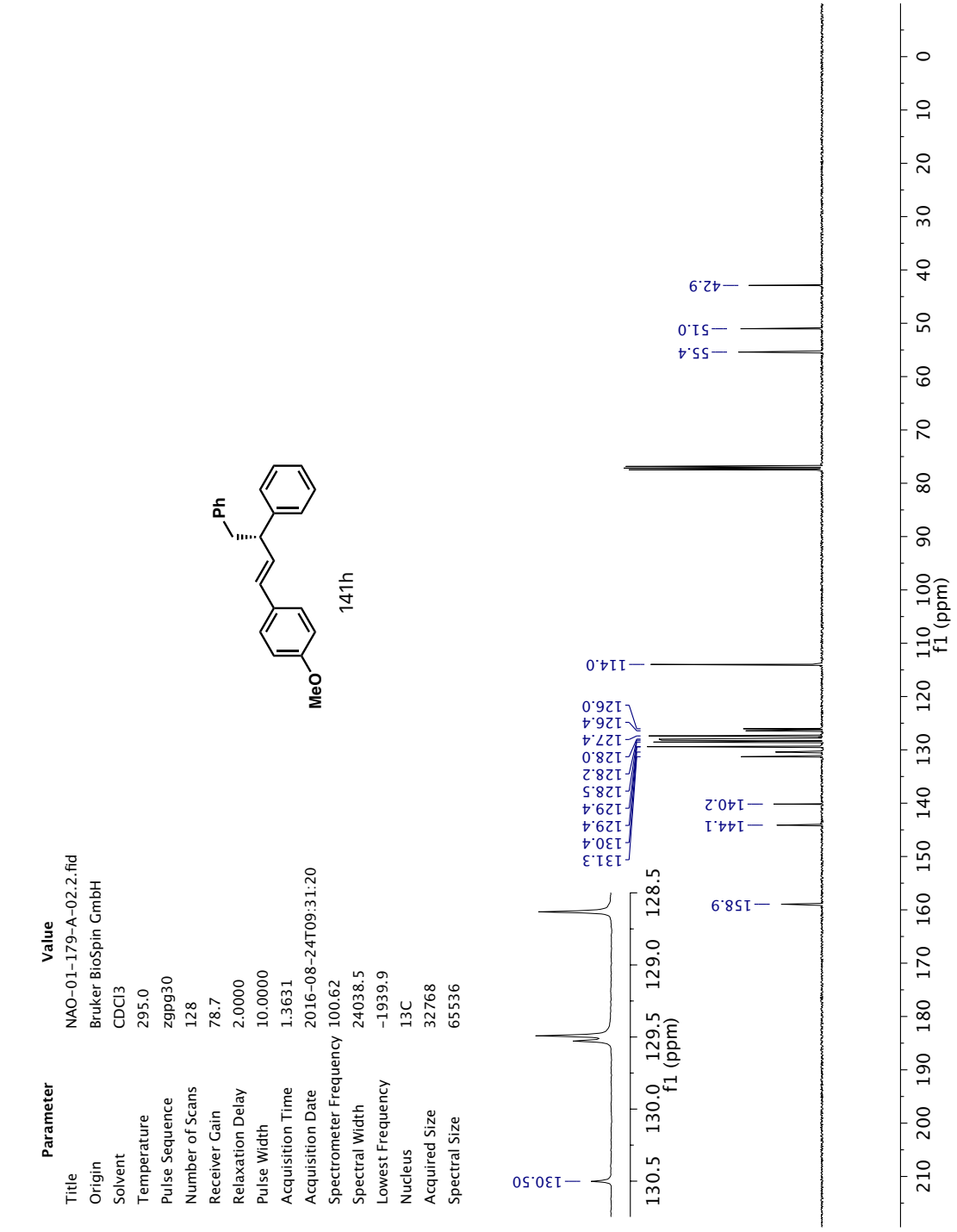
Parameter Value
Title NAO-01-179-A-02.2.fid
Origin Bruker BioSpin GmbH
Solvent CDCl3
Temperature 295.0
Pulse Sequence zgpg30
Number of Scans 128
Receiver Gain 78.7
Relaxation Delay 2.0000
Pulse Width 10.0000
Acquisition Time 1.3631
Acquisition Date 2016-08-24T09:31:20
Spectrometer Frequency 100.62
Spectral Width 24038.5
Lowest Frequency -1939.9
Nucleus 13C
Acquired Size 32768
Spectral Size 65536
Ph
MeO
141h
130.50
131.3
130.4
129.4
129.4
129.4
128.5
128.2
128.0
127.4
126.4
126.0
114.0
158.9
144.1
140.2
55.4
51.0
42.9
130.5 130.0 129.5 129.0 128.5
f1 (ppm)
210 200 190 180 170 160 150 140 130 120 110 100 90 80 70 60 50 40 30 20 10 0
f1 (ppm)

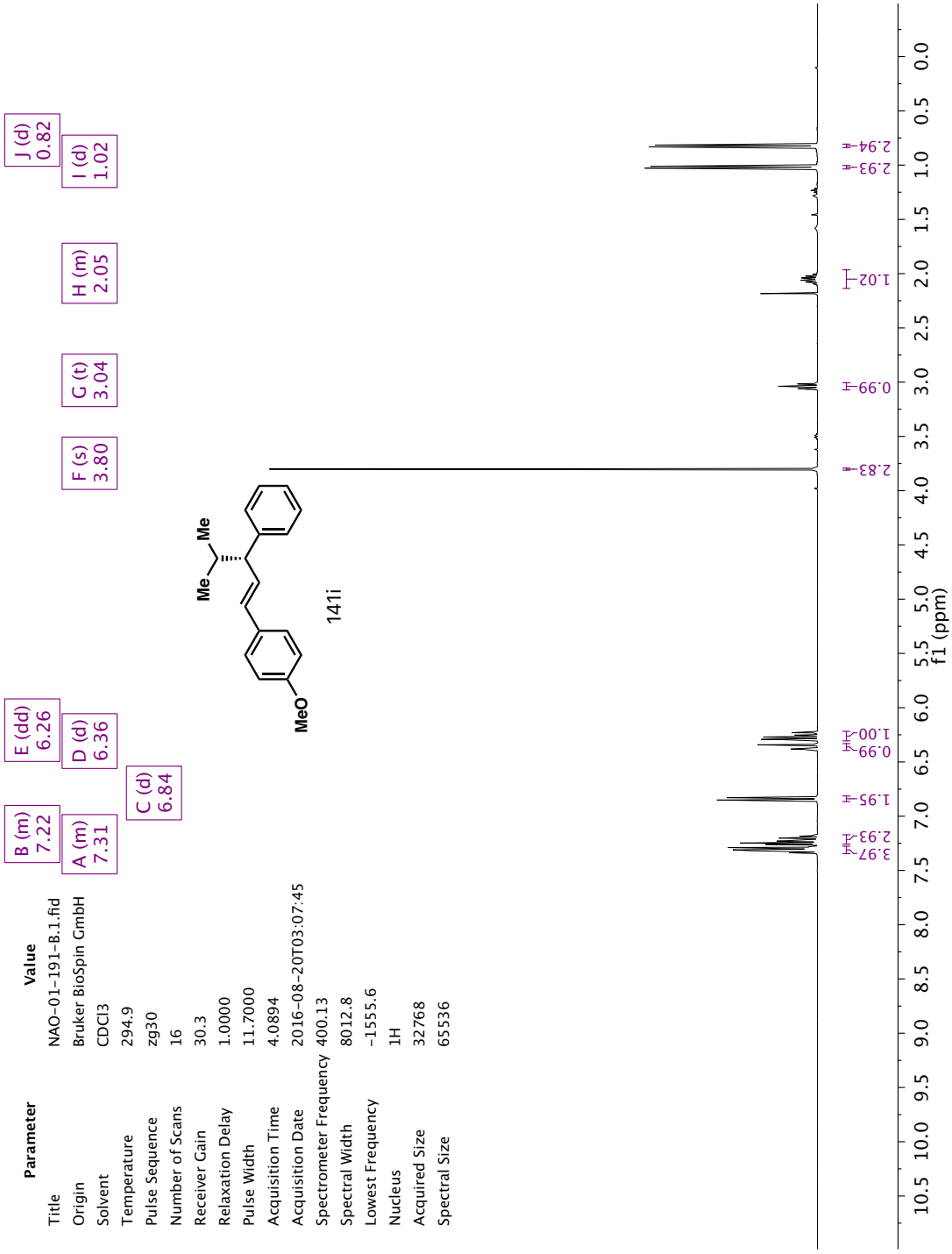
Parameter
Value
Title
NAO-01-191-B.1.fid
Origin
Bruker BioSpin GmbH
Solvent
CDCl3
Temperature
294.9
Pulse Sequence
zg30
Number of Scans
16
Receiver Gain
30.3
Relaxation Delay
1.0000
Pulse Width
11.7000
Acquisition Time
4.0894
Acquisition Date
2016-08-20T03:07:45
Spectrometer Frequency
400.13
Spectral Width
8012.8
Lowest Frequency
-1555.6
Nucleus
1H
Acquired Size
32768
Spectral Size
65536
B (m) 7.22
A (m) 7.31
E (dd) 6.26
D (d) 6.36
C (d) 6.84
F (s) 3.80
G (t) 3.04
H (m) 2.05
I (d) 1.02
J (d) 0.82
Me
Me
MeO
141i
3.97
2.93
1.95
0.99
1.00
2.83
0.99
1.02
2.93
2.94
10.5 10.0 9.5 9.0 8.5 8.0 7.5 7.0 6.5 6.0 5.5 5.0 4.5 4.0 3.5 3.0 2.5 2.0 1.5 1.0 0.5 0.0
f1 (ppm)

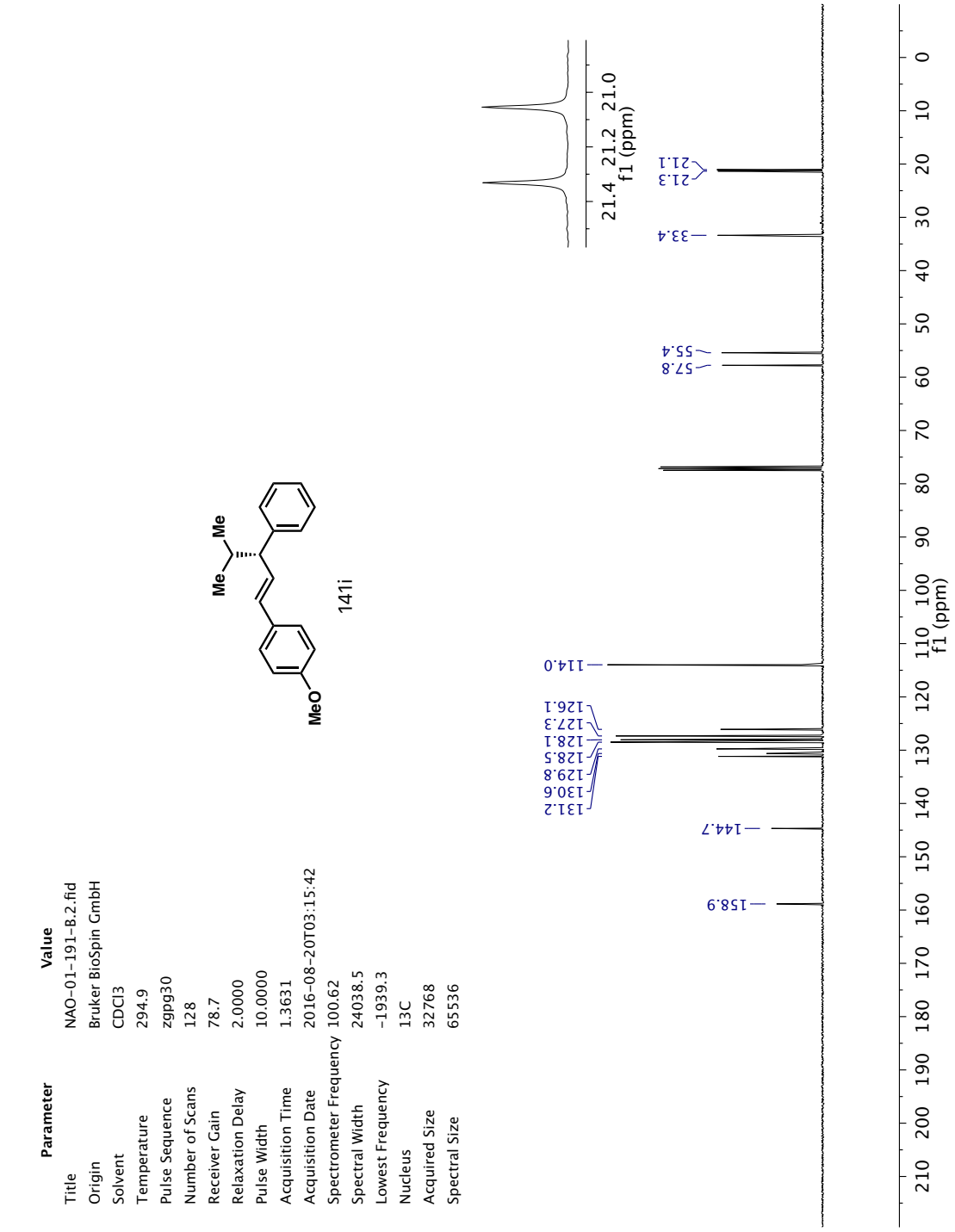
Parameter Value
Title NAO-01-191-B.2.fid
Origin Bruker BioSpin GmbH
Solvent CDCl3
Temperature 294.9
Pulse Sequence zgpg30
Number of Scans 128
Receiver Gain 78.7
Relaxation Delay 2.0000
Pulse Width 10.0000
Acquisition Time 1.3631
Acquisition Date 2016-08-20T03:15:42
Spectrometer Frequency 100.62
Spectral Width 24038.5
Lowest Frequency -1939.3
Nucleus 13C
Acquired Size 32768
Spectral Size 65536
Me
Me
MeO
141i
158.9
144.7
131.2
130.6
129.8
128.5
128.1
127.3
126.1
114.0
57.8
55.4
33.4
21.3
21.1
21.4 21.2 21.0
f1 (ppm)
f1 (ppm)

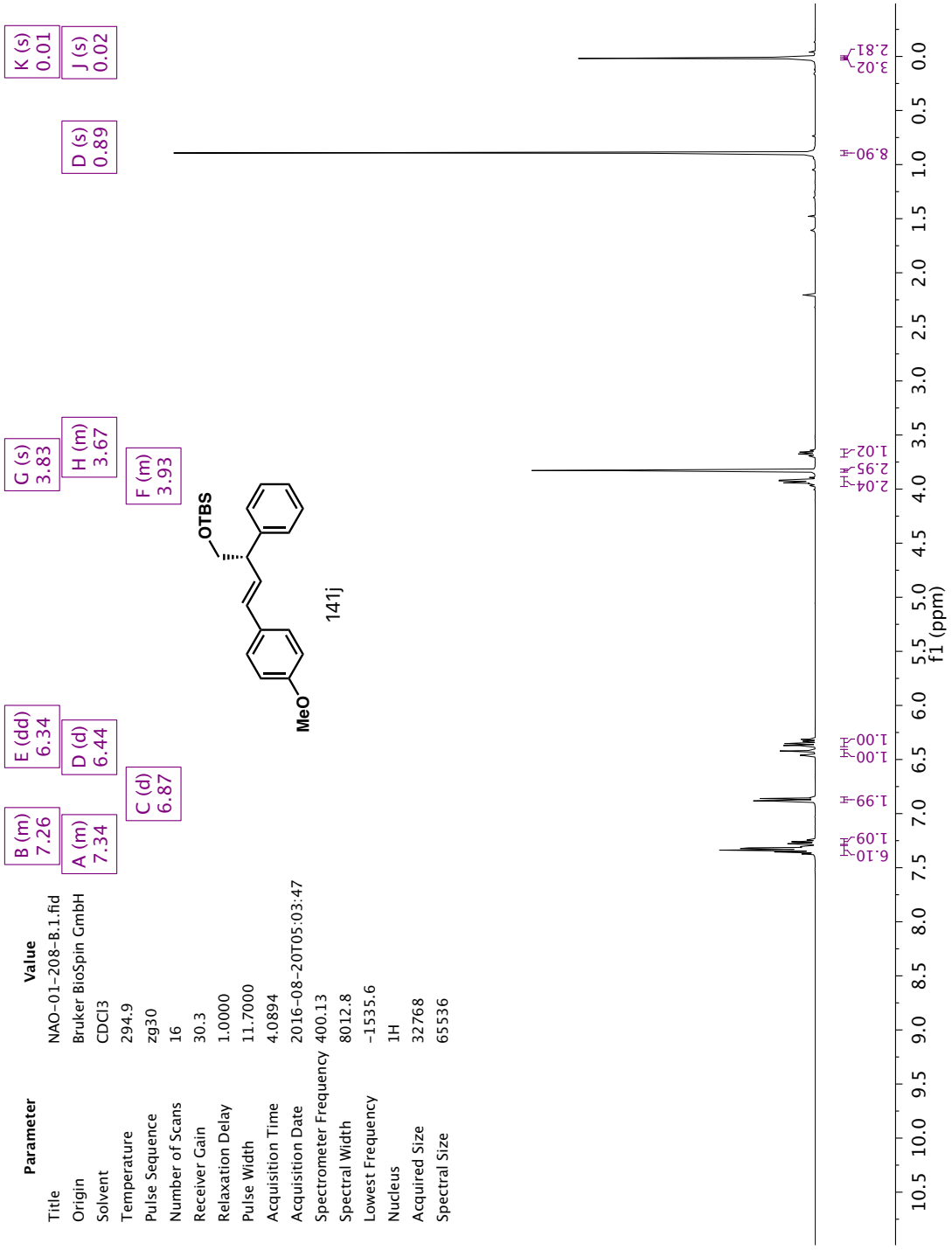
Parameter
Value
Title NAO-01-208-B.1.fid
Origin Bruker BioSpin GmbH
Solvent CDCl3
Temperature 294.9
Pulse Sequence zg30
Number of Scans 16
Receiver Gain 30.3
Relaxation Delay 1.0000
Pulse Width 11.7000
Acquisition Time 4.0894
Acquisition Date 2016-08-20T05:03:47
Spectrometer Frequency 400.13
Spectral Width 8012.8
Lowest Frequency -1535.6
Nucleus 1H
Acquired Size 32768
Spectral Size 65536
B (m) 7.26
A (m) 7.34
E (dd) 6.34
D (d) 6.44
C (d) 6.87
G (s) 3.83
H (m) 3.67
F (m) 3.93
D (s) 0.89
K (s) 0.01
J (s) 0.02
OTBS
MeO
141j
6.10
1.09
1.99
1.00
1.00
2.04
2.95
1.02
8.90
3.02
2.81
f1 (ppm)

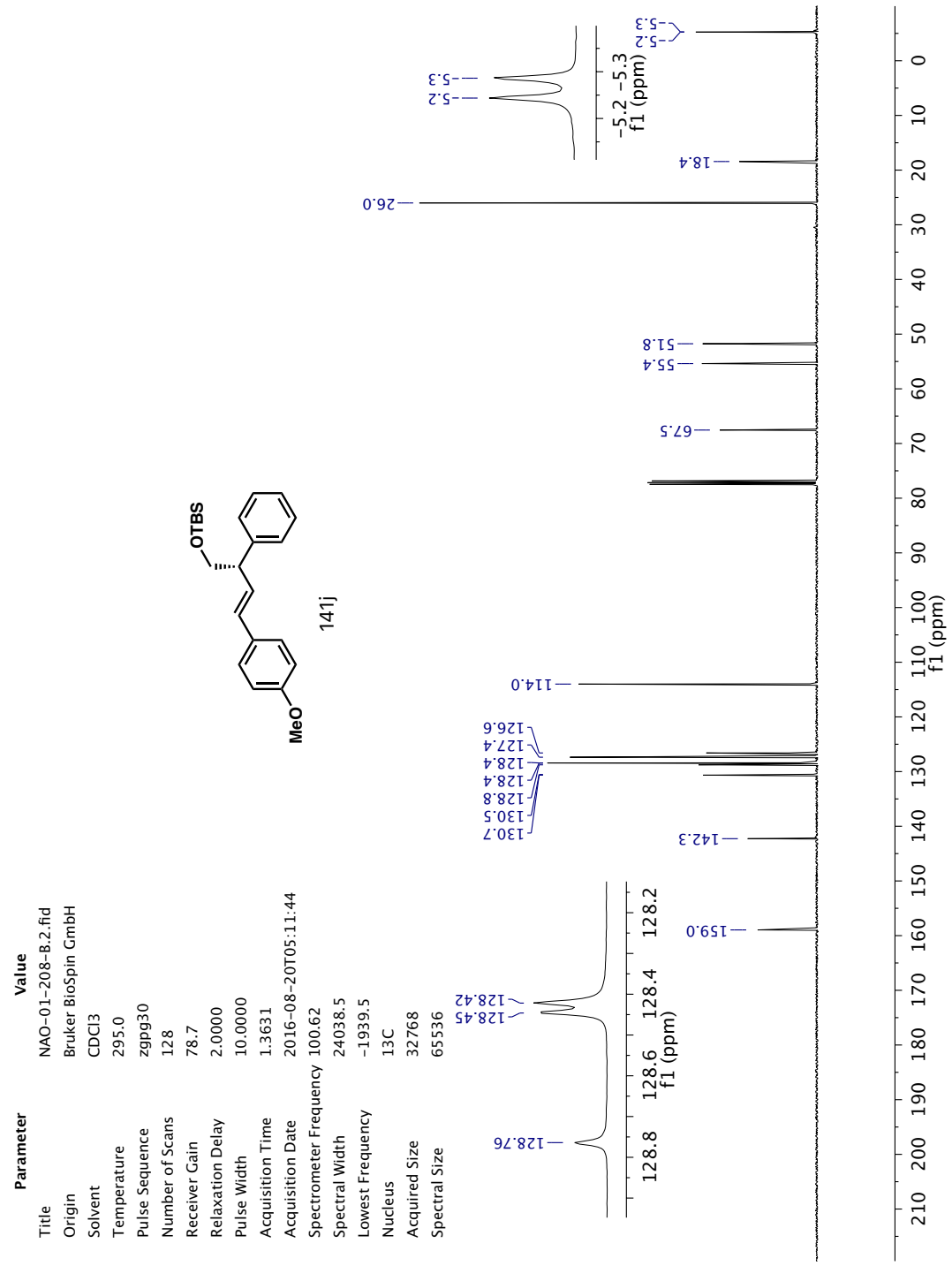
OTBS
MeO
141j
Parameter Value
Title NAO-01-208-B.2.fid
Origin Bruker BioSpin GmbH
Solvent CDCl3
Temperature 295.0
Pulse Sequence zgpg30
Number of Scans 128
Receiver Gain 78.7
Relaxation Delay 2.0000
Pulse Width 10.0000
Acquisition Time 1.3631
Acquisition Date 2016-08-20T05:11:44
Spectrometer Frequency 100.62
Spectral Width 24038.5
Lowest Frequency -1939.5
Nucleus 13C
Acquired Size 32768
Spectral Size 65536
159.0
142.3
130.7
130.5
128.8
128.4
128.4
127.4
126.6
114.0
67.5
55.4
51.8
26.0
18.4
-5.2
-5.3
128.76
128.45
128.42
f1 (ppm)

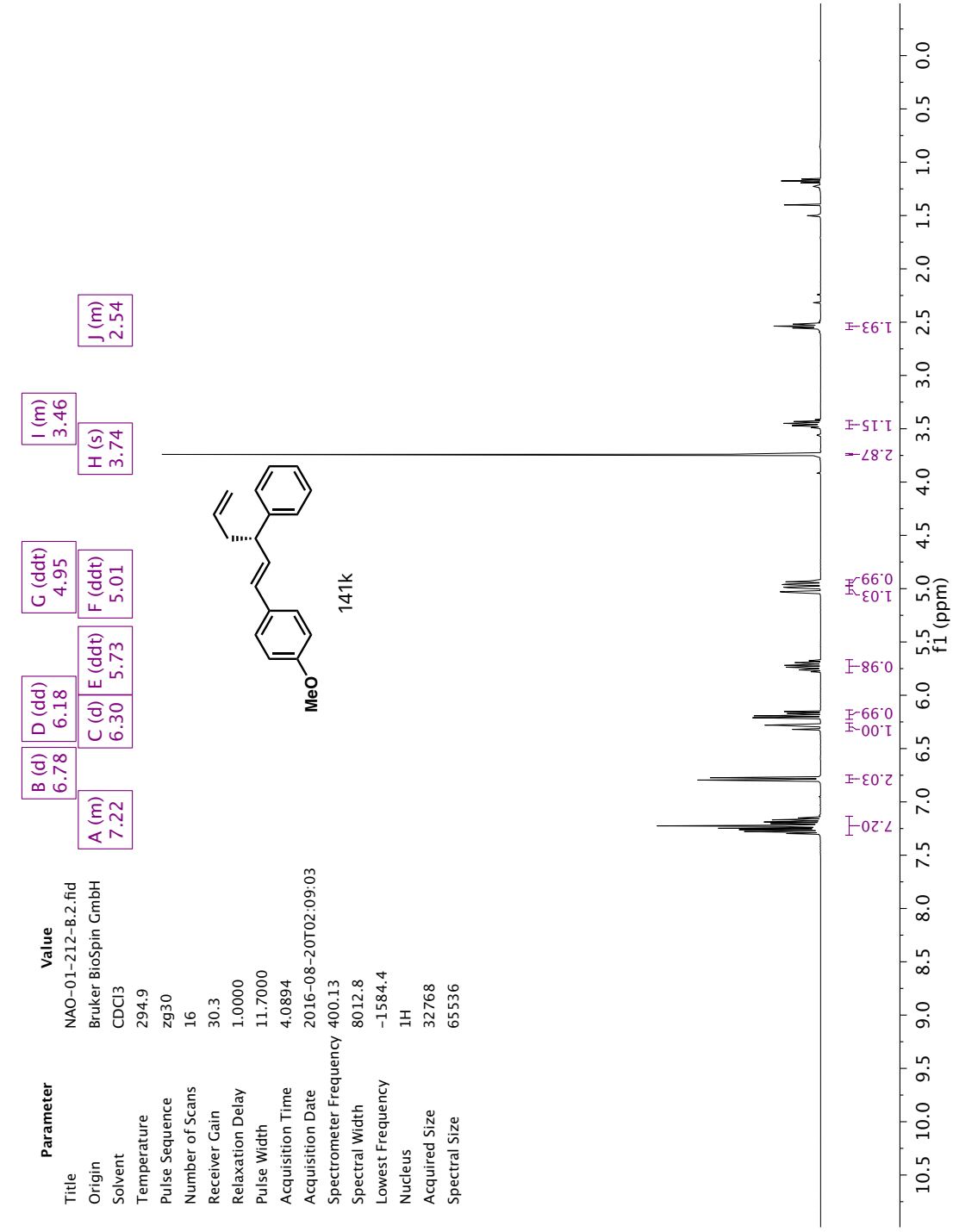
Parameter
Value
Title NAO-01-212-B.2.fid
Origin Bruker BioSpin GmbH
Solvent CDCl3
Temperature 294.9
Pulse Sequence zg30
Number of Scans 16
Receiver Gain 30.3
Relaxation Delay 1.0000
Pulse Width 11.7000
Acquisition Time 4.0894
Acquisition Date 2016-08-20T02:09:03
Spectrometer Frequency 400.13
Spectral Width 8012.8
Lowest Frequency -1584.4
Nucleus 1H
Acquired Size 32768
Spectral Size 65536
A (m) 7.22
B (d) 6.78
C (d) 6.30
D (dd) 6.18
E (ddt) 5.73
F (ddt) 5.01
G (ddt) 4.95
H (s) 3.74
I (m) 3.46
J (m) 2.54
MeO
141k
7.20
2.03
1.00
0.99
0.98
1.03
0.99
2.87
1.15
1.93
f1 (ppm)

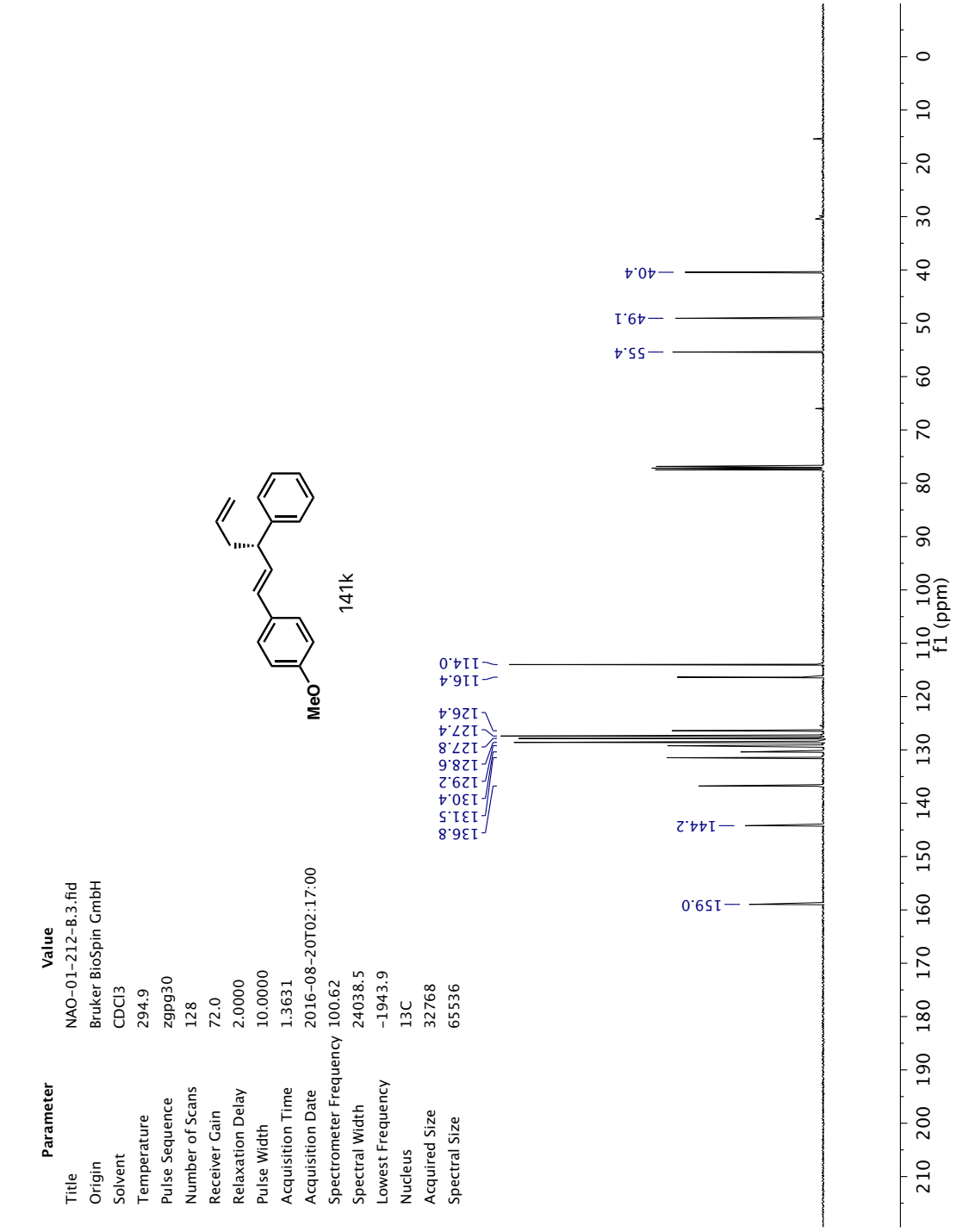
Parameter Value
Title NAO-01-212-B.3.fid
Origin Bruker BioSpin GmbH
Solvent CDCl3
Temperature 294.9
Pulse Sequence zgpg30
Number of Scans 128
Receiver Gain 72.0
Relaxation Delay 2.0000
Pulse Width 10.0000
Acquisition Time 1.3631
Acquisition Date 2016-08-20T02:17:00
Spectrometer Frequency 100.62
Spectral Width 24038.5
Lowest Frequency -1943.9
Nucleus 13C
Acquired Size 32768
Spectral Size 65536
MeO
141k
159.0
144.2
136.8
131.5
130.4
129.2
128.6
127.8
127.4
126.4
116.4
114.0
55.4
49.1
40.4
f1 (ppm)

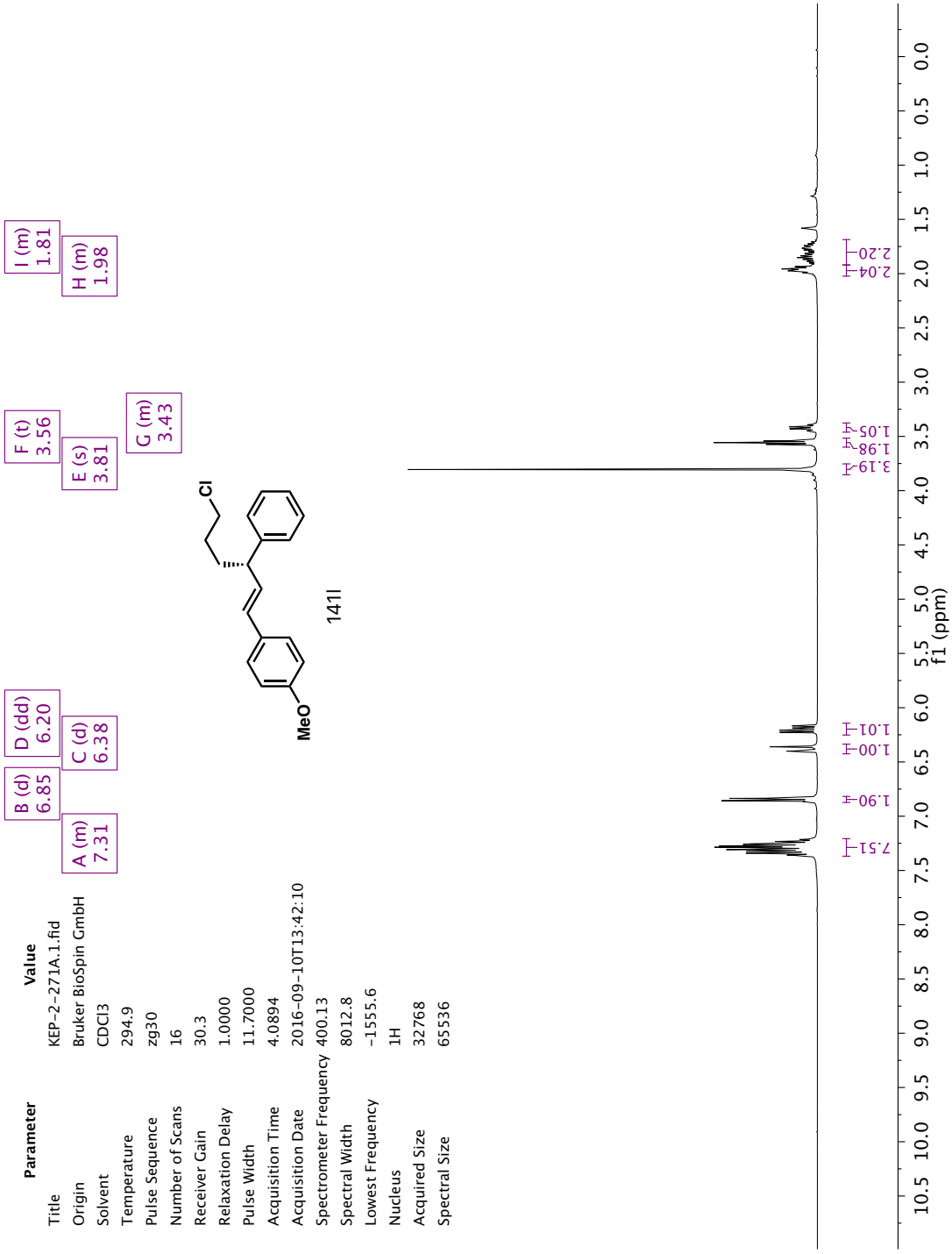

Parameter	Value
Title	KEP-2-271A.1.fid
Origin	Bruker BioSpin GmbH
Solvent	CDCl3
Temperature	294.9
Pulse Sequence	zg30
Number of Scans	16
Receiver Gain	30.3
Relaxation Delay	1.0000
Pulse Width	11.7000
Acquisition Time	4.0894
Acquisition Date	2016-09-10T13:42:10
Spectrometer Frequency	400.13
Spectral Width	8012.8
Lowest Frequency	-1555.6
Nucleus	1H
Acquired Size	32768
Spectral Size	65536

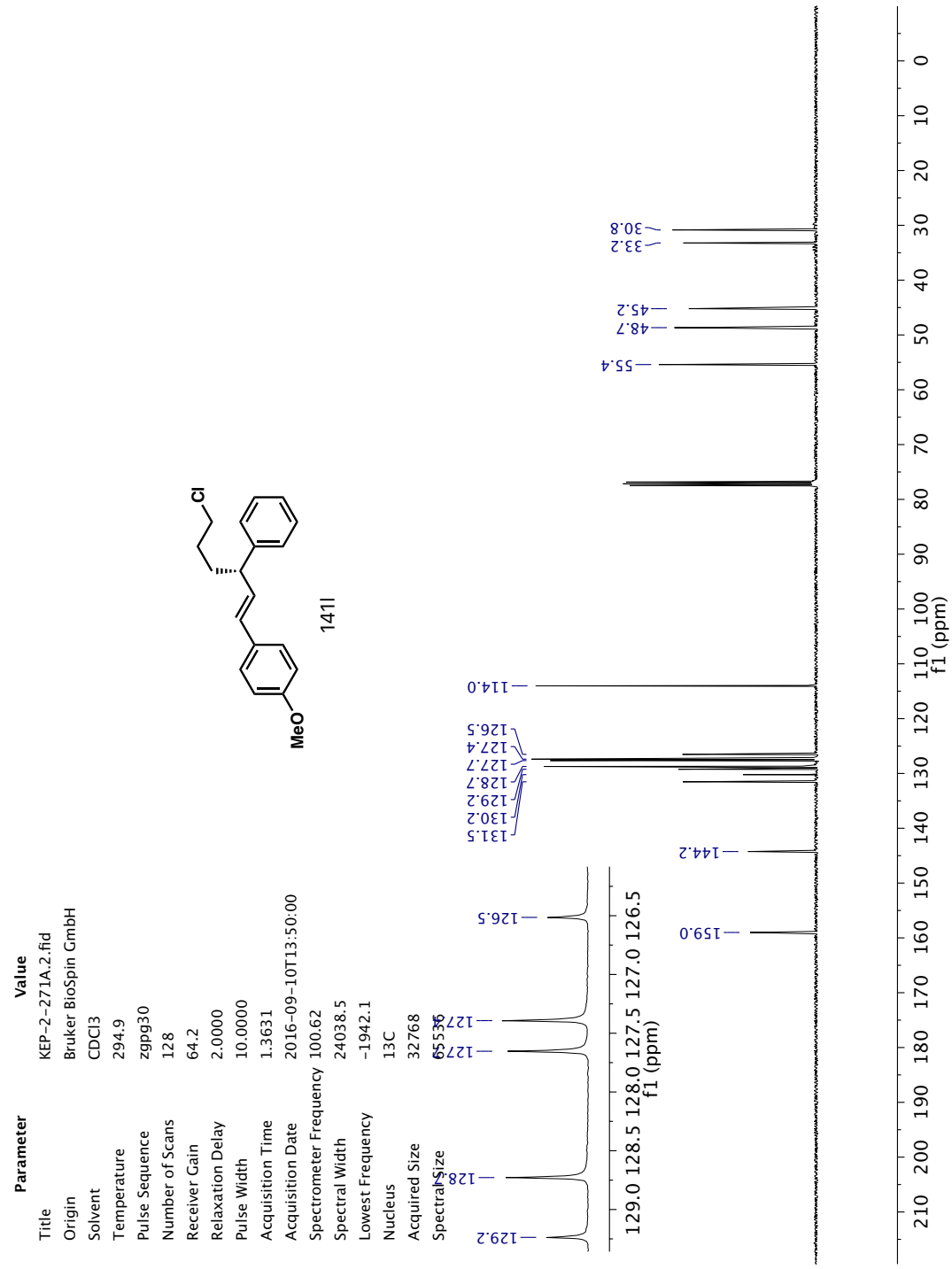
Parameter Value
Title KEP-2-271A.2.fid
Origin Bruker BioSpin GmbH
Solvent CDCl3
Temperature 294.9
Pulse Sequence zgpg30
Number of Scans 128
Receiver Gain 64.2
Relaxation Delay 2.0000
Pulse Width 10.0000
Acquisition Time 1.3631
Acquisition Date 2016-09-10T13:50:00
Spectrometer Frequency 100.62
Spectral Width 24038.5
Lowest Frequency -1942.1
Nucleus 13C
Acquired Size 32768
Spectral Size 65536
Cl
MeO
141l
114.0
126.5
127.4
127.7
128.7
129.2
130.2
131.5
144.2
159.0
55.4
48.7
45.2
33.2
30.8
129.2
128.7
127.9
127.2
126.5
129.0 128.5 128.0 127.5 127.0 126.5
f1 (ppm)
f1 (ppm)

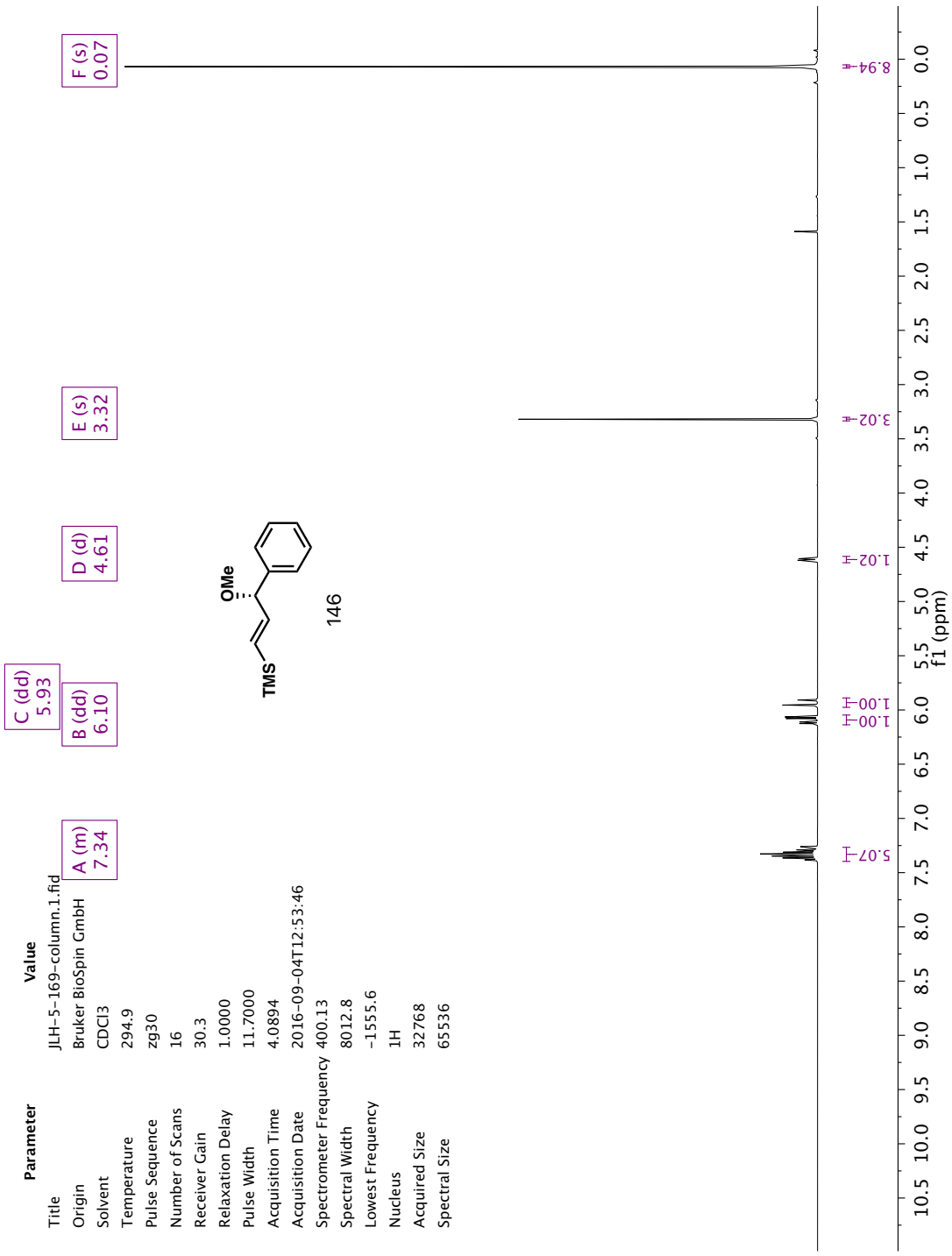
Parameter
Value
Title
JLH-5-169-column.1.fid
Origin
Bruker BioSpin GmbH
Solvent
CDCl3
Temperature
294.9
Pulse Sequence
zg30
Number of Scans
16
Receiver Gain
30.3
Relaxation Delay
1.0000
Pulse Width
11.7000
Acquisition Time
4.0894
Acquisition Date
2016-09-04T12:53:46
Spectrometer Frequency
400.13
Spectral Width
8012.8
Lowest Frequency
-1555.6
Nucleus
1H
Acquired Size
32768
Spectral Size
65536
A (m) 7.34
B (dd) 6.10
C (dd) 5.93
D (d) 4.61
E (s) 3.32
F (s) 0.07
OMe
TMS
146
5.07
1.00
1.00
1.02
3.02
8.94
f1 (ppm)

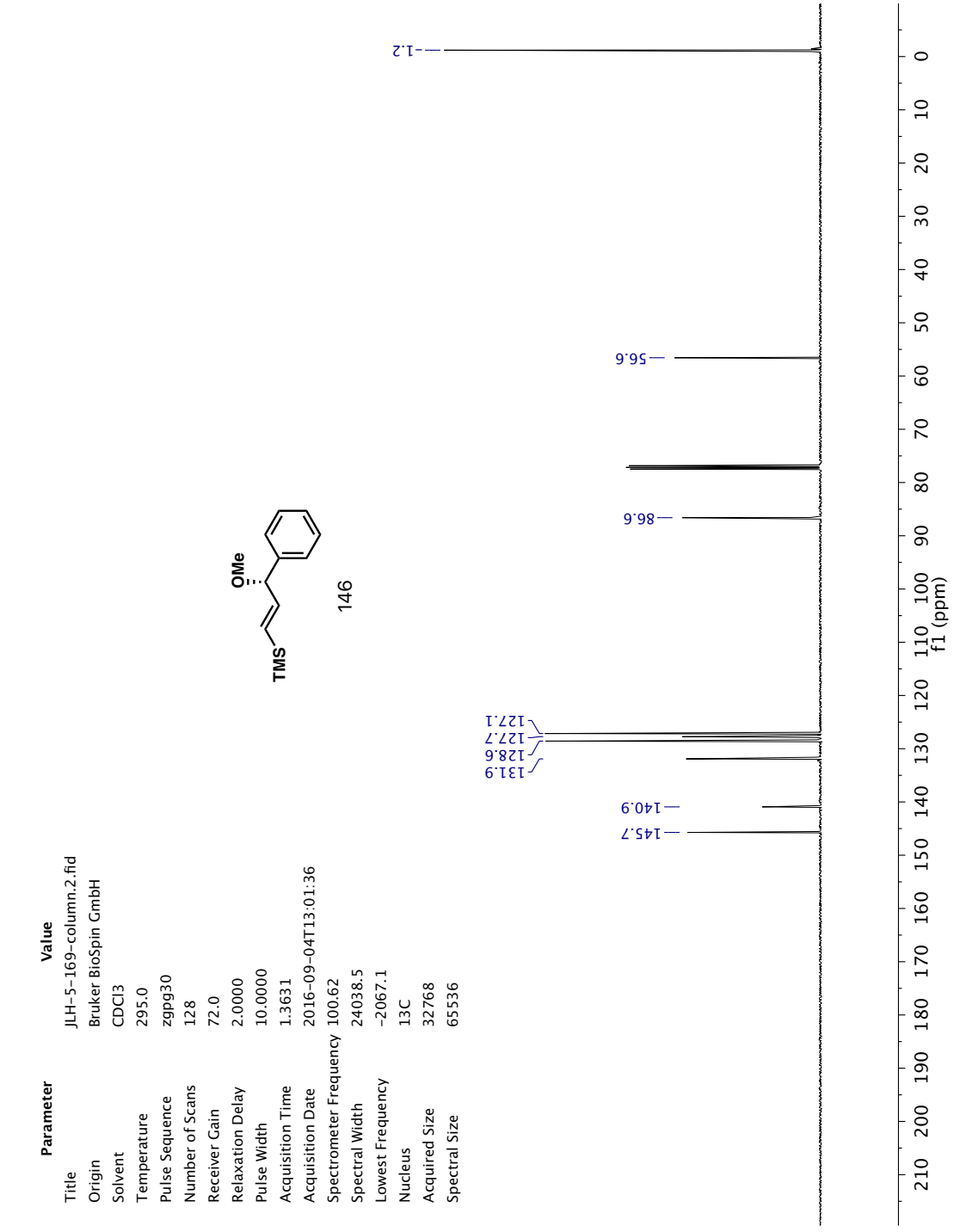

Parameter	Value
Title	JLH-5-169-column.2.fid
Origin	Bruker BioSpin GmbH
Solvent	CDCl3
Temperature	295.0
Pulse Sequence	zgpg30
Number of Scans	128
Receiver Gain	72.0
Relaxation Delay	2.0000
Pulse Width	10.0000
Acquisition Time	1.3631
Acquisition Date	2016-09-04T13:01:36
Spectrometer Frequency	100.62
Spectral Width	24038.5
Lowest Frequency	-2067.1
Nucleus	13C
Acquired Size	32768
Spectral Size	65536

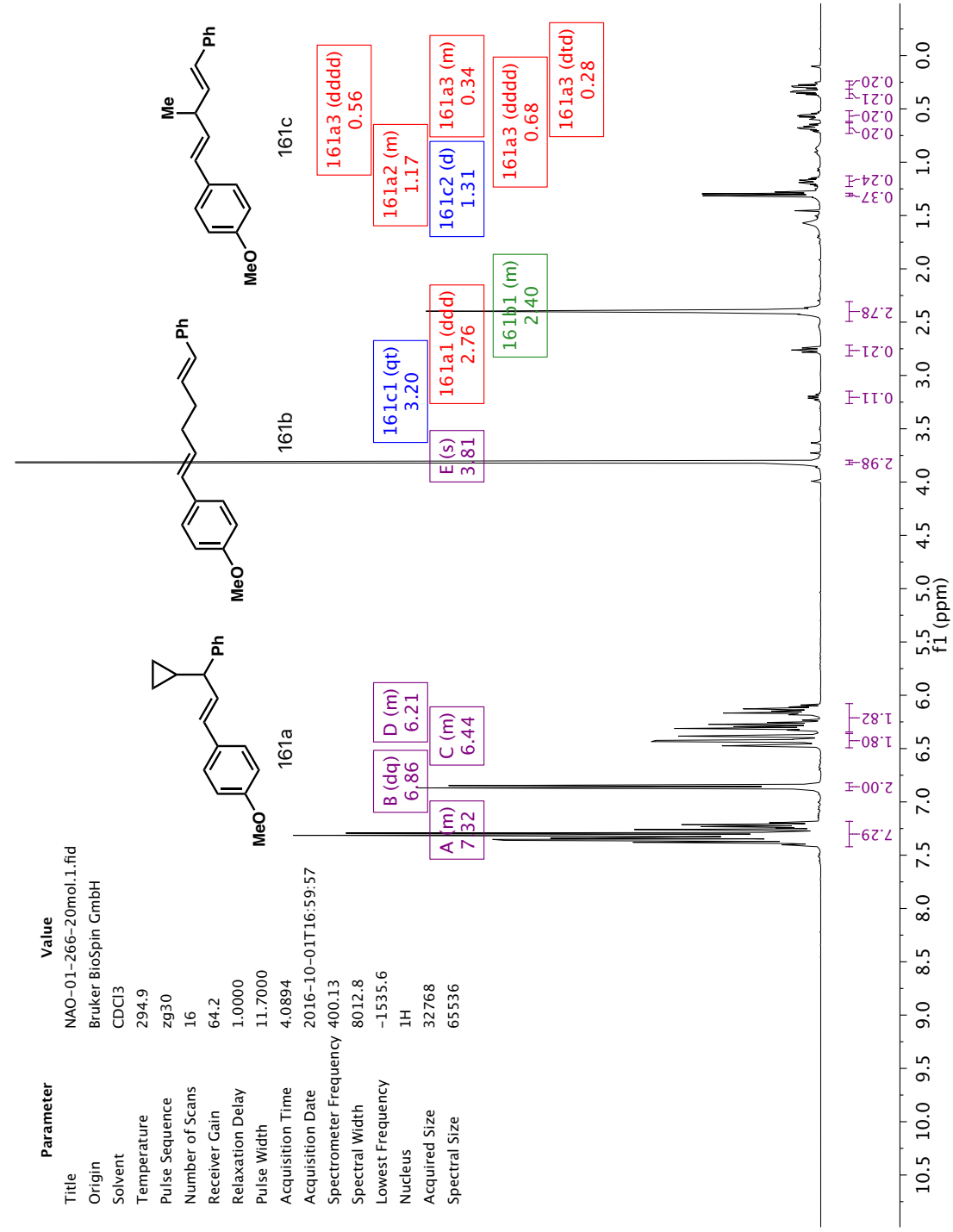
Parameter Value
Title NAO-01-266-20mol.1.fid
Origin Bruker BioSpin GmbH
Solvent CDCl3
Temperature 294.9
Pulse Sequence zg30
Number of Scans 16
Receiver Gain 64.2
Relaxation Delay 1.0000
Pulse Width 11.7000
Acquisition Time 4.0894
Acquisition Date 2016-10-01T16:59:57
Spectrometer Frequency 400.13
Spectral Width 8012.8
Lowest Frequency -1535.6
Nucleus 1H
Acquired Size 32768
Spectral Size 65536
MeO
Ph
161a
MeO
Ph
161b
MeO
Me
Ph
161c
A (m) 7.32
B (dq) 6.86
C (m) 6.44
D (m) 6.21
E (s) 3.81
161c1 (qt) 3.20
161a1 (ddd) 2.76
161b1 (m) 2.40
161c2 (d) 1.31
161a2 (m) 1.17
161a3 (dddd) 0.56
161a3 (dddd) 0.68
161a3 (dtd) 0.28
161a3 (m) 0.34
7.29
2.00
1.82
1.80
2.98
0.11
2.78
0.21
0.37
0.24
0.20
0.20
0.21
0.20
f1 (ppm)

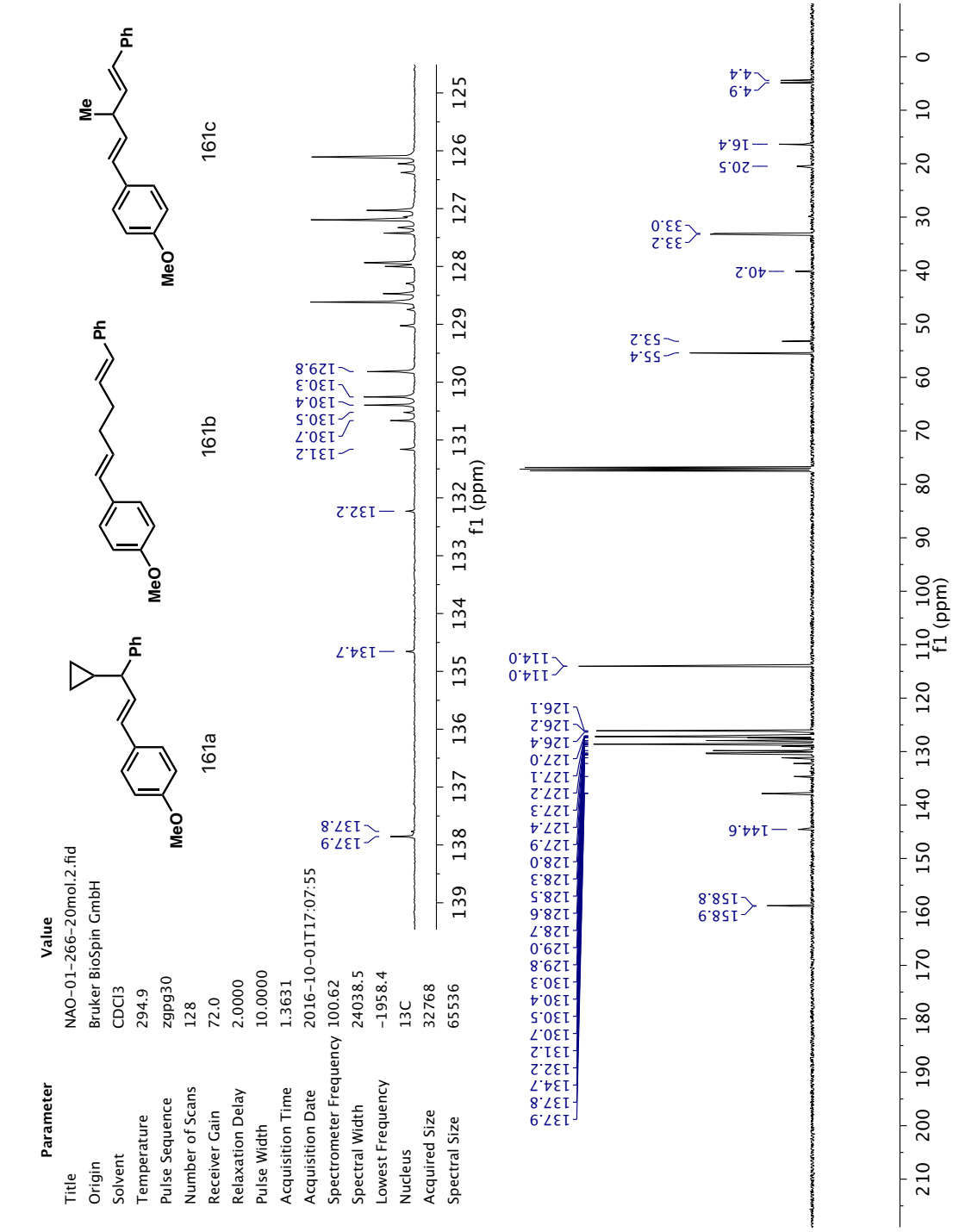
Parameter Value
Title NAO-01-266-20mol.2.fid
Origin Bruker BioSpin GmbH
Solvent CDCl3
Temperature 294.9
Pulse Sequence zgpg30
Number of Scans 128
Receiver Gain 72.0
Relaxation Delay 2.0000
Pulse Width 10.0000
Acquisition Time 1.3631
Acquisition Date 2016-10-01T17:07:55
Spectrometer Frequency 100.62
Spectral Width 24038.5
Lowest Frequency -1958.4
Nucleus 13C
Acquired Size 32768
Spectral Size 65536
MeO
Ph
161a
161b
161c
Me
f1 (ppm)

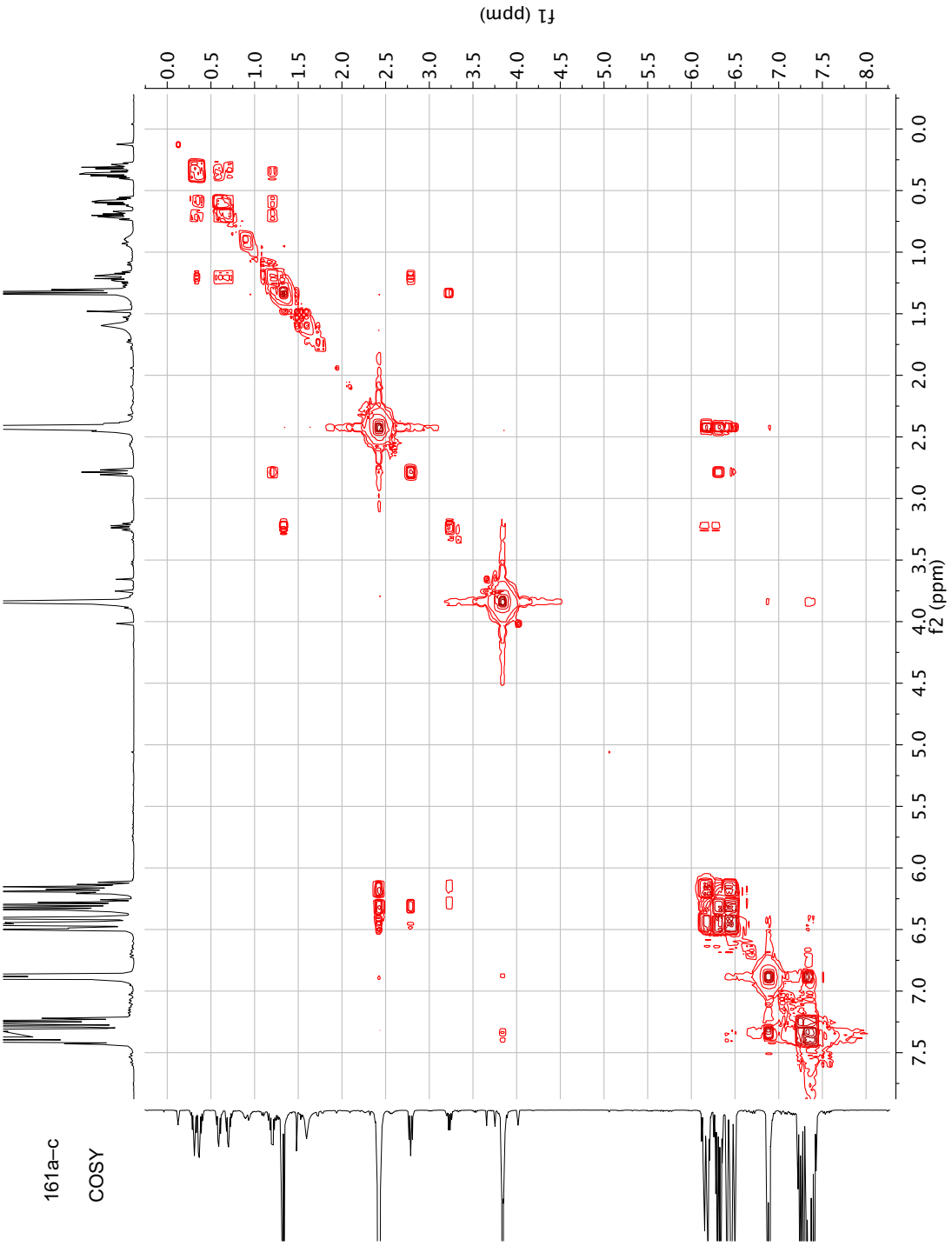
161a–c
COSY
f1 (ppm)
f2 (ppm)

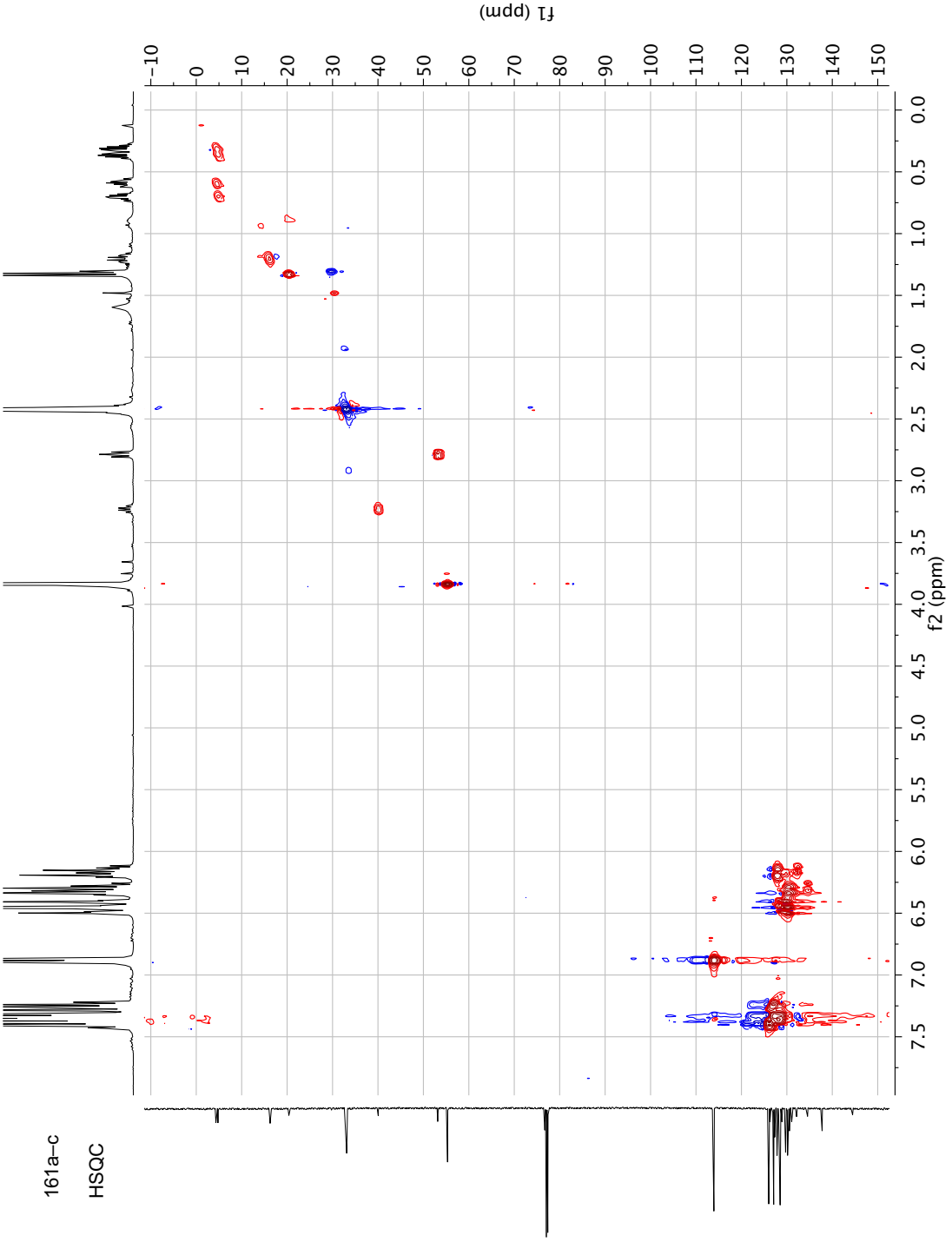
161a–c
HSQC
f1 (ppm)
f2 (ppm)

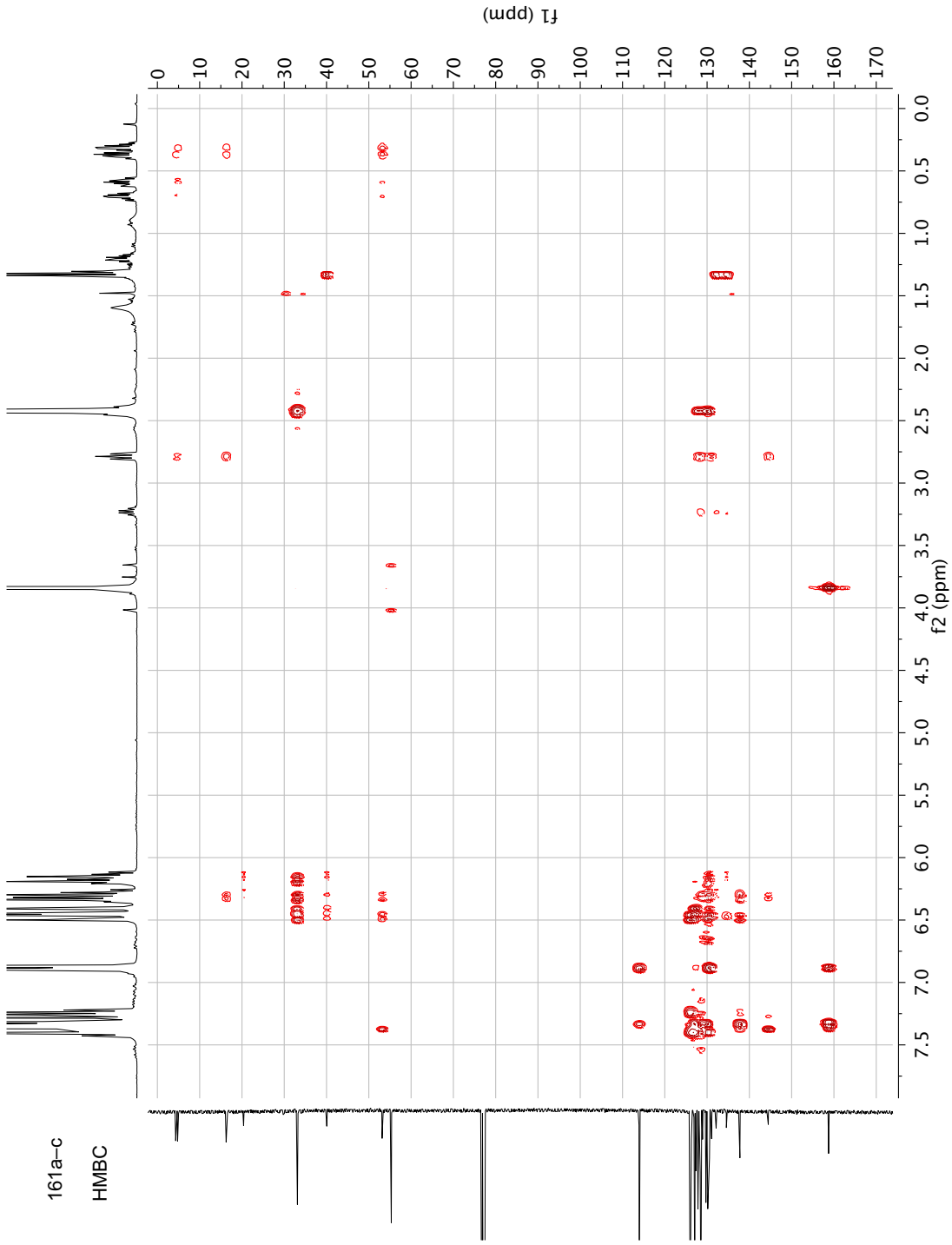
161a–c
HMBC
f1 (ppm)
f2 (ppm)

Appendix 4

X-Ray Crystallography Reports Relevant to Chapter 3:

Decarboxylative Asymmetric Ni-Catalyzed Cross-Coupling of Benzylic N-Hydroxyphthalimide Esters and Alkenyl Bromides

A4.1 STRUCTURAL DETERMINATION AND REFINEMENT DETAILS

Low-temperature diffraction data (ϕ- and ω-scans) were collected on a Bruker AXS KAPPA APEXII diffractometer coupled to a PHOTON 100 CMOS detector with Mo-$K\alpha$ radiation (λ = 0.71073 Å) from an I$_\mu$S HB micro-focused X-ray tube. All diffractometer manipulations, including data collection integration, and scaling were carried out using the Bruker APEXII software.[1] Absorption corrections were applied using SADABS.[2] The structure was solved by intrinsic phasing using SHELXT[3] and refined against F^2 on all data by full-matrix least squares with SHELXL-2014[4] using established refinement techniques.[5] All non-hydrogen atoms were refined anisotropically. All hydrogen atoms were included into the model at geometrically calculated positions and refined using a riding model. The isotropic displacement parameters of all hydrogen atoms were fixed to 1.2 times the U value of the atoms they are linked to. Absolute configuration was determined by anomalous dispersion.[6] Graphical representation of the structure with 50% probability thermal ellipsoids was generated using Mercury visualization software.

A4.2 CRYSTALLOGRAPHIC ANALYSIS OF L2·$NiBr_2$

A4.2.1 Special Refinement Details

Figure A4.1 *Rendering of Ni-complex* ***L2***·$NiBr_2$.

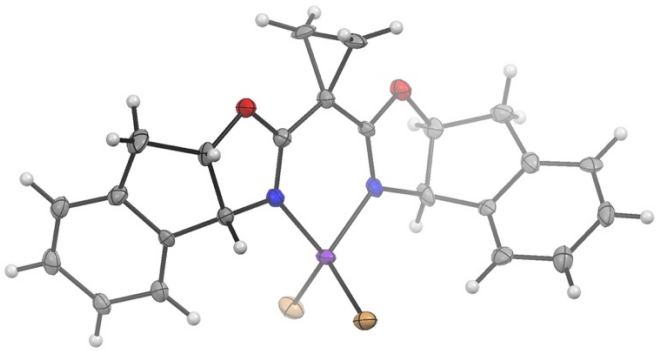

Compound **L2**·$NiBr_2$ crystallizes in the tetragonal space group $P4_1$ with one molecule in the asymmetric unit. Data was collected with Mo-$K\alpha$ radiation (λ = 0.71073 Å) at 100 K. The structure was solved as a merohedral twin with rotation around an axis 45° between a and b. The twin law was defined as the matrix (0.0, 1.0, 0.0, 1.0, 0.0, 0.0, 0.0, 0.0, -1.0). The BASF parameter [0.4980(14)] gave the twin ratio as 0.50:0.50. Absolute configuration was determined by anomalous dispersion (Flack = 0.011(2)).[6]

A4.2.2 Crystallographic Tables

Table A4.1. *Crystal data and structure refinement for* ***L2***·$NiBr_2$.

Identification code	A15178	
CCDC Deposition Number	1501744	
Empirical formula	$C_{23}H_{20}Br_2N_2NiO_2$	
Formula weight	574.94	
Temperature	100 K	
Wavelength	0.71073 Å	
Crystal system	Tetragonal	
Space group	$P4_1$	
Unit cell dimensions	a = 9.4823(6) Å	α = 90°.
	b = 9.4823(6) Å	β = 90°.
	c = 24.418(2) Å	γ = 90°.
Volume	2195.5(3) $Å^3$	
Z	4	
Density (calculated)	1.739 Mg/m^3	
Absorption coefficient	4.546 mm^{-1}	
F(000)	1144	
Crystal size	0.31 x 0.27 x 0.14 mm^3	
Theta range for data collection	0.834 to 38.918°.	
Index ranges	-16<=h<=16, -16<=k<=16, -42<=l<=43	
Reflections collected	113308	
Independent reflections	12464 [R(int) = 0.0431]	
Completeness to theta = 25.242°	100.0 %	
Absorption correction	Semi-empirical from equivalents	
Max. and min. transmission	0.7476 and 0.5466	
Refinement method	Full-matrix least-squares on F^2	
Data / restraints / parameters	12464 / 1 / 272	
Goodness-of-fit on F^2	1.056	
Final R indices [I>2sigma(I)]	R1 = 0.0470, wR2 = 0.1114	
R indices (all data)	R1 = 0.0580, wR2 = 0.1168	
Absolute structure parameter	0.011(2)	
Extinction coefficient	n/a	
Largest diff. peak and hole	2.381 and -1.019 $e.Å^{-3}$	

A4.3 REFERENCES

(1) *APEX2, Version 2 User Manual, M86-E01078, Bruker Analytical X-ray Systems*, Madison, WI, **2006**.

(2) Sheldrick, G.M. *SADABS (version 2008/1): Program for Absorption Correction for Data from Area Detector Frames*, University of Göttingen, **2008**.

(3) Sheldrick, G. *Acta Crystallogr., Sect. A: Found. Crystallogr*. **2008**, *64*, 112.

(4) Sheldrick, G. M. *Acta Crystallogr., Sect. C: Struct. Chem.* **2015**, *C71*, 3.

(5) Müller, P. *Crystallogr. Rev.* **2009**, *15*, 57.

(6) Parsons, S.; Flack, H. D.; Wagner, T. *Acta Crystallogr., Sect. B: Struct. Sci. Cryst. Eng. Mater.* **2013**, *B69*, 249.

Chapter 4

Mechanistic Investigations of Ni-Catalyzed Asymmetric Reductive Cross-Couplings with Alkenyl Bromide Electrophiles[‡]

4.1 INTRODUCTION

4.1.1 Recent Advances in Reductive Cross-Couplings

Nickel-catalyzed reductive cross-couplings have recently gained prominence as mild methods for the construction of C–C bonds. These cross-electrophile couplings use a stoichiometric reductant (typically Zn or Mn) to turn over the Ni catalyst, and commonly employ two electrophiles that are distinguished by their hybridization to afford good levels of cross-selectivity.[1] The Durandetti, Weix, and Gong groups have reported cross-couplings between a variety of different electrophile classes, including α-ester–aryl,[2]

[‡]The research presented in this chapter was completed in collaboration with: 1) Alan H. Cherney (graudate student) and Raymond Turro (graduate student) in the Reisman group, as well as Yunfang Yang (postdoctoral scholar) and Xin Hong (graduate student) in the Houk group.

alkyl–aryl,[3,4] alkyl–acyl,[5] and alkyl–alkyl[6] cross-couplings (Scheme 4.1). The mild reaction conditions allow for excellent functional group tolerance and eliminate the need to form air sensitive and highly reactive organometallic reagents typically employed in conventional cross-coupling reactions.

Scheme 4.1 *Select examples of reductive cross-couplings of organic electrophiles.*

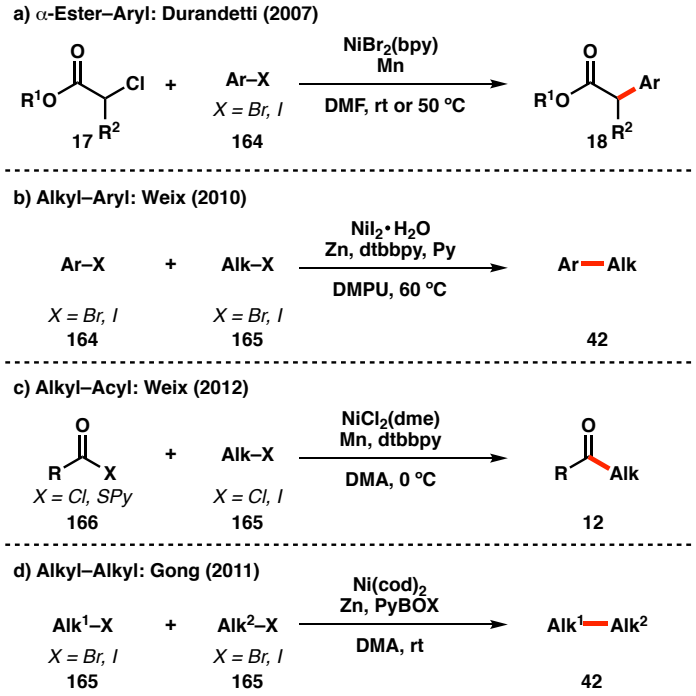

The ability to utilize C(sp^3)-hybridized electrophiles in reductive cross-couplings has also allowed for the design of asymmetric approaches. Our laboratory has recently developed a variety of asymmetric cross-couplings between C(sp^2)-hybridized (acyl chlorides,[7] alkenyl bromides,[8–10] and (hetero)aryl iodides[11,12]) and C(sp^3)-hybridized (benzyl chlorides, α-chloronitriles) electrophiles (Scheme 4.2). These reactions typically proceed in good yield and provide the desired products with good to excellent enantioselectivities when chiral BOX, BiOX, or PHOX ligands are used.

Scheme 4.2 *Asymmetric reductive cross-couplings of organic electrophiles.*

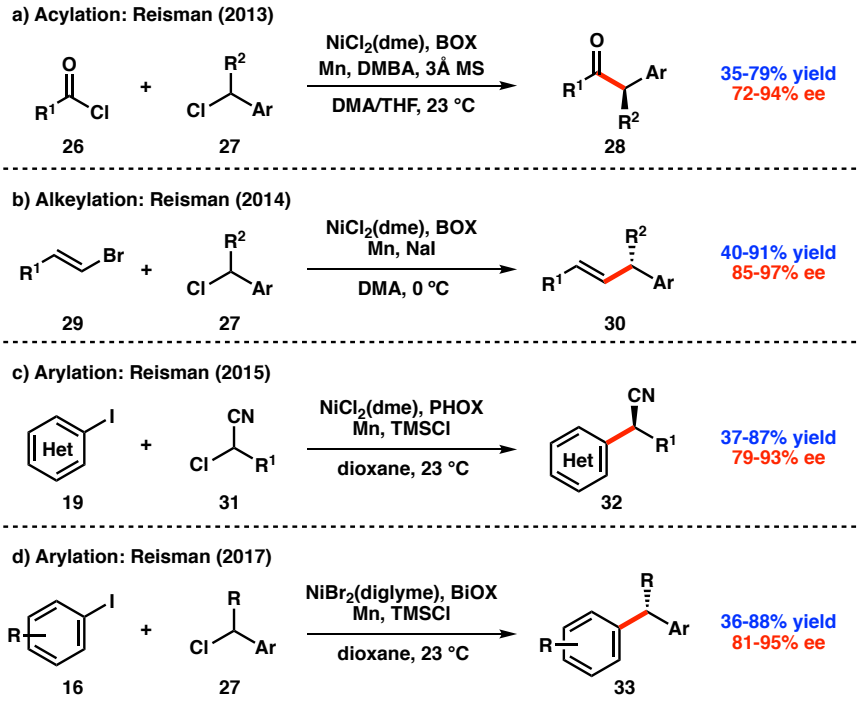

While a wide variety of electrophiles and methods have been reported, there are only a few in-depth mechanistic studies regarding these types of transformations, most of which focus on achiral reactivity.[4,13,14] In order to better understand the origins of cross-selectivity and enantioselectivity in asymmetric reductive cross-couplings, we set out to conduct a mechanistic study on the asymmetric Ni-catalyzed alkenylation reaction between alkenyl bromide **86** and benzyl chloride **167** which was previously disclosed from our laboratory in 2014 (Scheme 4.3).[8] The Ni-catalyzed cross-coupling reaction proceeds in good yields and with excellent enantioselectivities when chiral BOX ligand **L2** is used in conjunction with $NiCl_2$(dme) as a precatalyst. During the optimization of this reaction, DMA was found to be the most optimal solvent. The use of Mn affords turnover of the Ni catalyst, while the addition of NaI and low reaction temperature afford higher yields of the

desired cross-coupled product. In order to obtain a more holistic mechanistic study, we not only conducted experimental work in our laboratory, but also collaborated with Prof. Kendall Houk at UCLA in order to conduct computational studies. Herein, we describe the results of these studies and provide additional insight into the likelihood of potential reaction mechanisms.

Scheme 4.3 *Ni-catalyzed alkenylation reaction as the subject of our studies.*

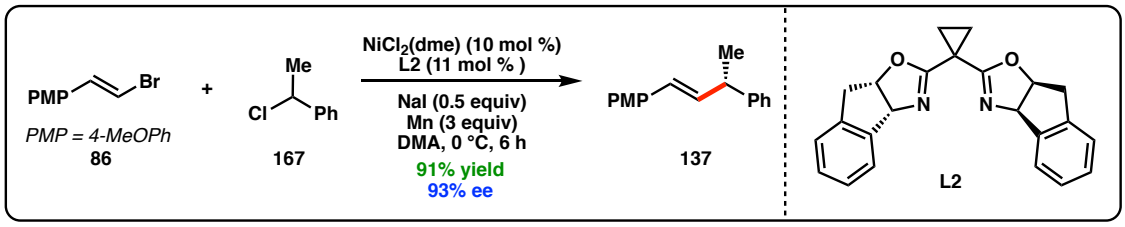

4.2 PROPOSED REACTION MECHANISMS

Weix and co-workers were the first to conduct an in-depth mechanistic study on the Ni-catalyzed reductive cross-coupling between C(sp^2)-hybridized and C(sp^3)-hybridized electrophiles.[1,4,13] They initially proposed four possible reaction mechanisms for the reductive cross-coupling of aryl iodides and alkyl iodides (Scheme 4.1b): 1) *in situ* organometallic formation, 2) disproportionation/transmetalation, 3) intermediate reduction, and 4) radical chain (Figure 4.1).[4] A series of experimental mechanistic studies revealed the reductive cross-coupling between aryl halides and alkyl halides was most consistent with a radical chain mechanism.[13] Gong and co-workers, however, further studied the intermediate reduction and radical chain mechanisms via computational studies, and found both to be thermodynamically feasible when the C(sp^2)-hybridized

electrophile was the first to undergo oxidative addition.[14] These studies were conducted on the reductive aryl–alkyl coupling, however it is possible that the reaction mechanism varies for the other nickel-catalyzed reductive cross-coupling reactions, given the differences in electrophile identity, reported ligands, and reaction conditions. The four mechanistic proposals outlined by Weix and coworkers will be discussed in greater detail in the following sections, however in order to maintain clarity throughout the duration of this chapter, analogous ligands and electrophiles consistent with the alkenylation reaction in Scheme 4.3 will be used.

Figure 4.1 *Proposed mechanisms for Ni-catalyzed reductive cross-coupling.*

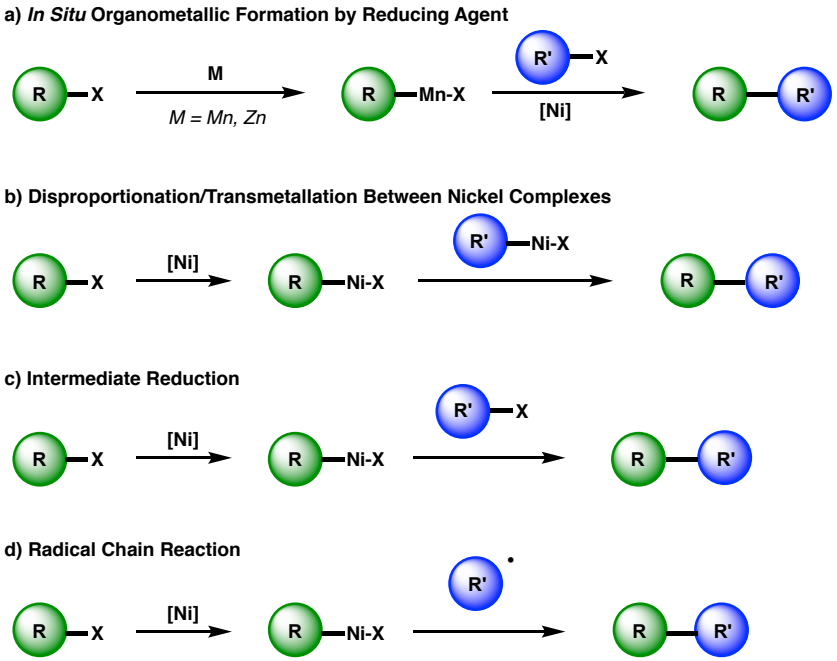

4.2.1 In Situ Organometallic Formation

One possible reaction mechanism is the *in situ* formation of organometallic species **168** from Zn or Mn insertion into the benzyl halide bond (Figure 4.2). The remaining steps in this mechanism involve oxidative addition (**169** to **170**), transmetalation (**170** to **171**),

and reductive elimination (**171** to **169**), similar to conventional redox neutral cross-coupling. While Zn or Mn can be used as heterogeneous reductants to shuttle electrons to the Ni catalyst, a variety of reductive cross-couplings have been shown to proceed with soluble organic reductants (i.e. tetrakis(dimethylamino)ethylene, TDAE).[8,10,15] Although a number of published methods depict examples describing the feasibility of forming benzylic organomanganese species,[16–19] Weix and co-workers demonstrated that the formation of organozinc was low under their reaction conditions.[13] Taken together, while this mechanism may be operable, if not in some level, in Ni-catalyzed reductive-cross couplings, it is typically disregarded when potential mechanisms are proposed for this class of reactions.

Figure 4.2 *In-situ organometallic formation mechanism.*

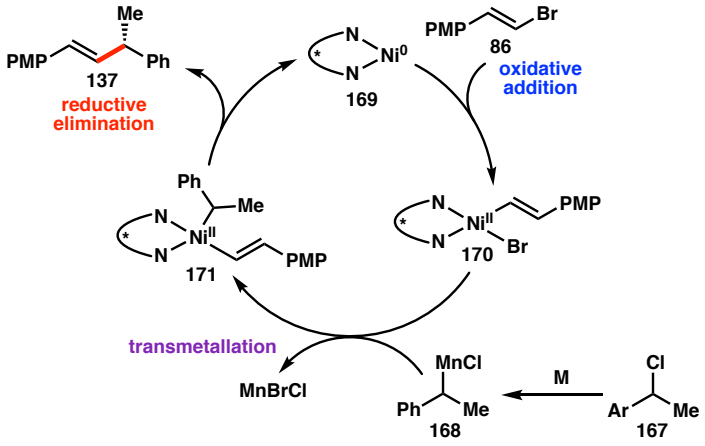

4.2.2 Disproportionation/Transmetalation

A second possible mechanism is the transmetalation and ligand exchange between two distinct Ni(II) oxidative addition complexes (Figure 4.3). Each electrophile (**86** and **167**) undergoes oxidative addition to Ni(0) complex **169** to afford **170** and **173**, which then

disproportionate to afford Ni(II) complex **171** containing both the aryl and alkenyl groups. The desired product **137** is formed by reductive elimination from complex **171**. If ligand exchange is the rate-determining step in the reaction (which is likely, given that this step is bimolecular between two catalytically generated species), one would expect to see a kinetic second order dependence on nickel.[20] In the case of an asymmetric reductive cross-coupling, a non-linear effect in the product enantioselectivity would also be observed if ligand exchange (from **170** and **173** to **172** and **171**) were the enantiodetermining step. Finally, this disproportion/transmetalation mechanism forms **137** via reductive elimination form a Ni(II) species, which is significantly harder to achieve compared to reductive elimination from a Ni(III) species.

Figure 4.3 *Disproportionation/transmetalation mechanism.*

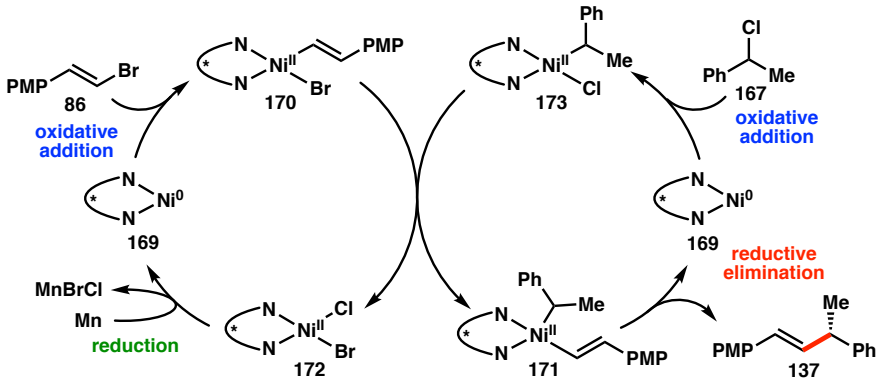

4.2.3 Intermediate Reduction

A third possible mechanism is the intermediate reduction mechanism (Figure 4.4). Aryl halide **86** undergoes a concerted oxidative addition to Ni(0) complex **169**, followed by an intermediate reduction step. The resultant Ni(I) species **174** can undergo a second, single-electron oxidative addition with alkyl halide **167** to afford Ni(III) complex

Figure 4.4 *Sequential oxidative addition mechanism.*

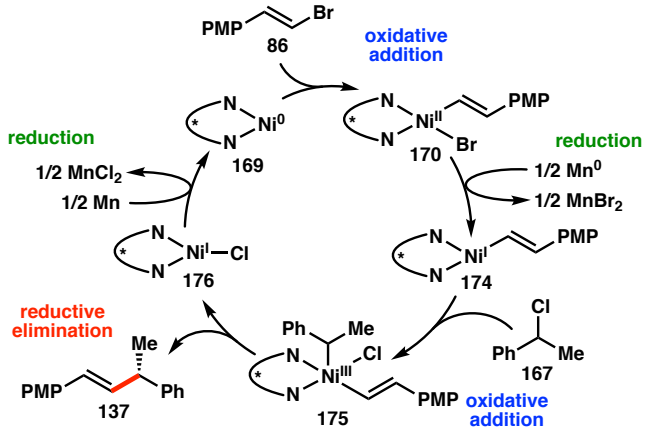

175, which can produce cross-coupled product **86** following reductive elimination. A two-step oxidative addition of the alkyl chloride, first by halide abstraction followed by recombination of alkyl radical **178** to Ni(II) center **177**, allows for stereoconvergence in the mechanism (Figure 4.5).

Figure 4.5 *Two-step radical-type oxidative addition of the alkyl halide.*

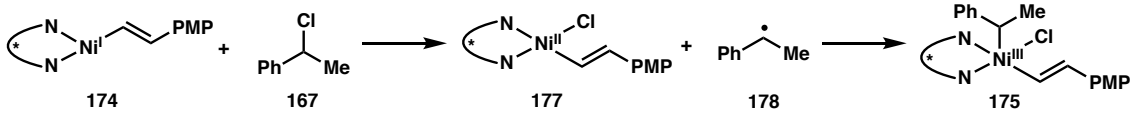

4.2.4 Radical Chain

The fourth possible mechanism for consideration, through a radical chain type processes (Figure 4.6), is distinctive from the sequential oxidative addition mechanism by the lifetime of alkyl radical **178**. Instead of the alkyl radical adding to the same Ni(II) center (**172**) that abstracted the halide atom, the alkyl radical can undergo cage escape and intercept a different Ni(II) center (**170**) to afford Ni(III) complex **175** that can provide cross-coupled product **86** following reductive elimination. This mechanism is often

distinguished from sequential oxidative addition by the use of a radical clock probe. The rearrangement of a radical clock substrate under the reaction conditions is simply used to identify the presence of a radical species. However, a difference in the ratio of rearranged to unarranged products at varying concentrations of Ni provides evidence for radical chain mechanism when rearranged products dominate at lower Ni loadings.

Figure 4.6 *Radical chain mechanism.*

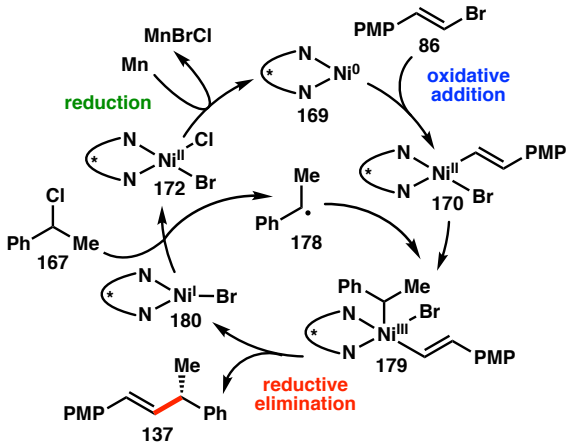

4.3 EXPERIMENTAL STUDIES: NICKEL COMPLEXES

4.3.1 Synthesis and Characterization of Ni(II) Complexes

We began our investigations by preparing **L2**·$NiCl_2$ (Scheme 4.4). Condensation of (*1R*,*2S*)-(+)-cis-1-amino-2-indanol (**181**) with diethyl malonimidate dihydrochloride (**182**) provided BOX ligand **L22** in 67% yield. Deprotonation of the methylene linker with sodium hydride and substitution with 1,2-dibromoethane afforded desired BOX ligand **L2** in 82% yield. Finally, metalation with $NiCl_2$ in acetonitrile and water at elevated temperatures provided the purple **L2**·$NiCl_2$ complex in 89% yield, and following

recrystallization we were able to confirm its structure via X-ray crystallography. The monomeric **L2**·$NiCl_2$ complex crystallized in the orthorhombic $P2_12_12_1$ space group as a distorted tetrahedral complex. Analysis by ^1H NMR reveals broad proton signals, including two resonances at 56 and –109 ppm which confirm the structure as a high-spin paramagnetic complex.

Scheme 4.4 *Synthesis of* ***L2***·$NiCl_2$ *complex.*

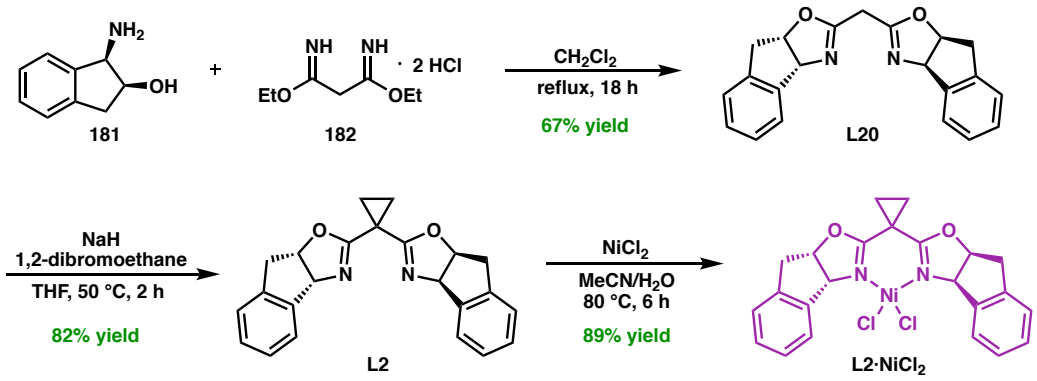

Recrystallization of **L2**·$NiCl_2$ occasionally provided orange crystals instead of purple crystals. Analysis by X-ray crystallography revealed that **L2**·$NiCl_2$ could also crystallize as a trimeric complex containing two pentavalent Ni centers and one hexavalent Ni center bridged by the chloride ligands. A series of other Ni dihalide complexes were also prepared and analyzed by X-ray crystallography (Figure 4.7). Depending on the identity of the linker, halide, and chiral pocket (indanyl vs. phenyl), a variety of Ni geometries could be obtained upon crystallization (monomer, hydrated dimer, or trimer). Typically purple or pink crystals were monomeric complexes, green crystals were hydrated dimeric complexes, and either orange or red crystals were trimeric complexes. When trimeric **L2**·$NiCl_2$ was dissolved and recrystallized, the monomeric species was often afforded, indicating the aggregation state is an artifact of the crystallization conditions.

Figure 4.7 *Prepared Ni dihalide complexes and their corresponding geometries.*

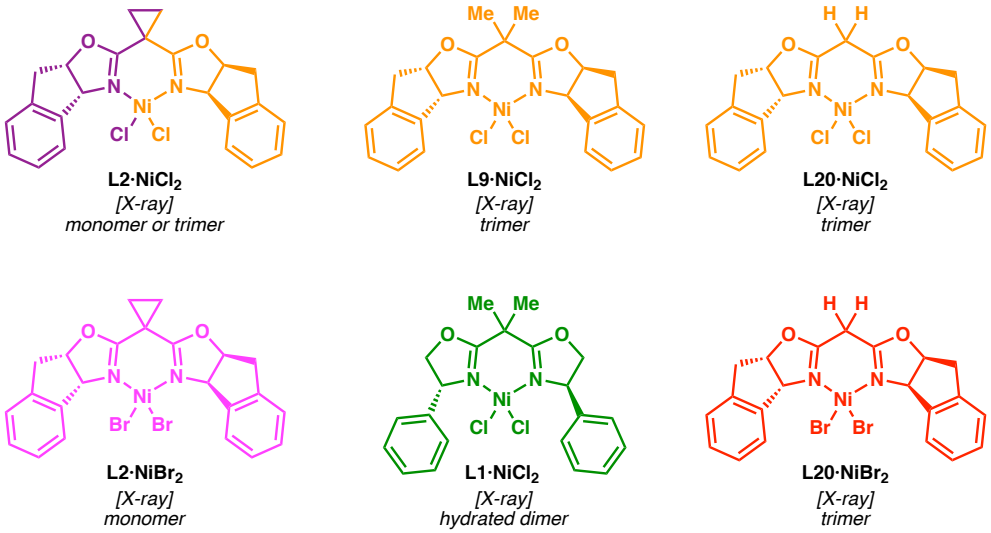

4.3.2 UV-Vis Spectroscopy

With **L2**·$NiCl_2$ in hand, we turned our attention to studying its properties. Dissolving complex **L2**·$NiCl_2$ in a variety of solvents at a concentration of 1 mg/mL revealed a chromatic solvent effect, which ranged from pink to orange to colorless solutions. Both the monomeric and trimeric **L2**·$NiCl_2$ complexes provided the same results, demonstrating they converge to the same species while in solution. Electronic absorption spectra were collected in a variety of solvents as shown in Figure 4.8. The extinction coefficient ($M^{-1}cm^{-1}$) reaches a maximum at 500 nm and 670 nm when **L2**·$NiCl_2$ is dissolved in DCM, MeCN, and acetone. Switching to more polar solvents such as DMPU (a urea), DMA, and NMP (both amides), absorption decreases in the 500 nm and 670 nm bands and a new absorption band forms at 360 nm, indicating the observation is not due to solvatochromism.[21] This may potentially be an indication of solvent binding to the Ni center. Other solvents such as DMF, DMSO, and H_2O lose nearly all absorption in the

visible spectrum as evidenced by colorless solutions. While the origin of this solvent effect is not yet understood, it may provide insight into the solvent effects realized upon initial reaction optimization (DMA provided the highest product yield, while NMP and DMPU provided the second highest yields).[8]

Figure 4.8 *Electronic absorption spectra of* ***L2***·$NiCl_2$.

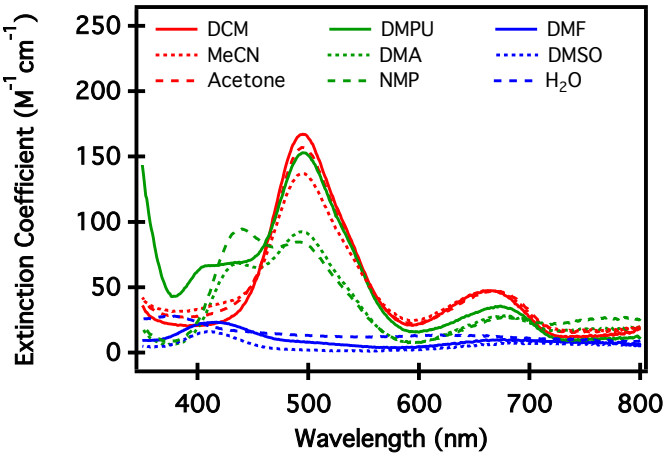

4.3.3 Cyclic Voltammetry

We then set out to analyze **L2**·$NiCl_2$ by cyclic voltammetry (CV) (Figure 4.9). When **L2**·$NiCl_2$ was analyzed at a concentration of 1.0 mM in DMA with 0.1 M Bu_4NPF_6 as the supporting electrolyte, we observed a quasi-reversible redox couple with the cathodic peak reaching a maximum at –1.60 V, as well as an irreversible redox process with a maximum cathodic peak at –3.30 V vs. the ferrocene/ferrocenium redox couple (Fc/Fc^+). This concentration corresponds to a 0.1 mol % loading of Ni under the published reaction conditions. Amperometry measurements for the first reduction peak are most consistent with a one-electron reduction process, therefore we have assigned these two reduction peaks as the Ni^{II}/Ni^{I} and Ni^{I}/Ni^{0} redox couples, respectively. The cathodic peak at –1.60 V

Figure 4.9 *Cyclic voltammetry of* ***L2***·$NiCl_2$.

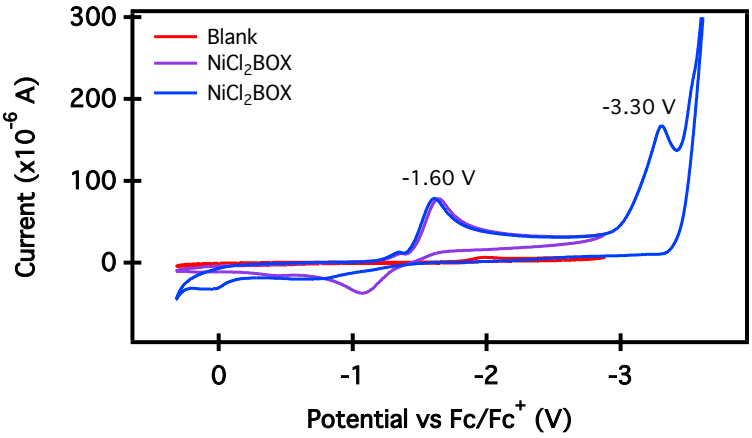

happens to also be the same reduction potential for the two-electron oxidation of Mn.[22] In contrast to bipyridine ligands which show redox activity in the absence of bound metal species, cyclic voltammetry of the free bis(oxazoline) ligand **L2** shows no redox activity, indicating **L2** may be innocent in the reduction process. The one-electron reduction potentials were converted relative to standard calomel electrode (SCE) and compared to known reduction potentials of other Ni(II) complexes containing pyridine-containing ligands (Figure 4.10).[23–26] The **L2**·$NiCl_2$ complex displays a significantly stronger Ni^I/Ni^0 redox couple compared to **L2** and **L2**, however bipyridine complex **L2** displays a weaker

Figure 4.10 *Reported reduction potentials of bidentate and tridentate N-bound Ni complexes used in cross-coupling reactions.*

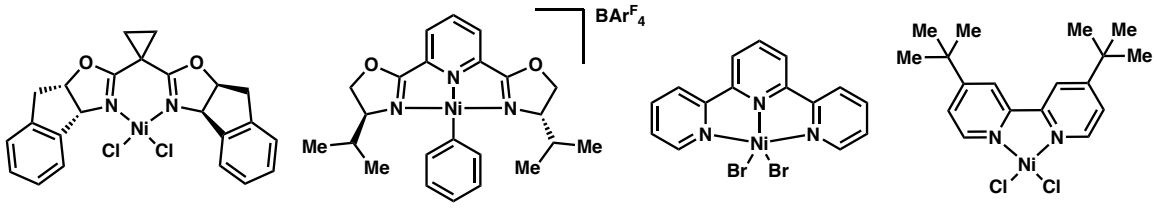

L2·$NiCl_2$
Ni^{II}/Ni^I = −1.08 V
Ni^I/Ni^0 = −2.78 V

183
Ni^{II}/Ni^I = −0.84 V
Ni^I/Ni^0 = −1.83 V

184
Ni^{II}/Ni^I = −0.72 V
Ni^I/Ni^0 = −1.30 V

185
Ni^{II}/Ni^0 = −1.34 V
$Ni^0/Ni^{0\cdot-}$ = −1.88 V

reduction potential to access Ni(0), however it proceeds via a two-electron reduction from Ni(II) to Ni(0). No reduction potentials of other bis(oxazoline) or bi(oxazoline) Ni dihalide complexes have been reported in literature.

4.3.4 EPR Spectroscopy

Further studies by electron paramagnetic resonance (EPR) spectroscopy probed the oxidation state of nickel following the reduction process at –1.6 V. A 10 mM solution of **L2** in DMA was reduced with 10 equivalents of Zn, Mn, or Mg under inert atmosphere for >12 hours to afford a dark orange solution. The reduction potentials for these three metals are shown in Equations 1–3.[22] Subsequent filtering and analysis by EPR affords a Ni(I) spectrum (Figure 4.11) when Zn and Mg are used as the reductants, which we have

$$Zn^0 \rightarrow Zn^{2+} + 2e^- = -1.2 \text{ V vs. } Fc/Fc^+ \quad (1)$$

$$Mn^0 \rightarrow Mn^{2+} + 2e^- = -1.6 \text{ V vs. } Fc/Fc^+ \quad (2)$$

$$Mg^0 \rightarrow Mg^{2+} + 2e^- = -3.1 \text{ V vs. } Fc/Fc^+ \quad (3)$$

assigned as a **L2**·NiCl complex, however with an unknown geometry (monomeric or dimeric bridged species). When Mn is used as the reductant, the Ni(I) signal is obscured by $MnCl_2$, which is consequently EPR active. Attempts to remove background absorption by $MnCl_2$ reveals the presence of the same **L2**·NiCl complex.

The obtained Ni(I) spectrum has rhombic anisotropy, and simulations afford g values of 2.4879, 2.1588, and 2.1092 that correspond to a metal-centered radical.[27] This is in contrast to PyBOX and Tpy coordinated Ni(I) complexes that display a ligand-centered radical containing contributions from ^{14}N hyperfine coupling.[23,24] Interestingly, the same

reduction reaction plates out Ni mirror with no observable Ni(I) signal when conducted with Zn as the reductant in either THF or a mixture of DCM and toluene.

Figure 4.11 *EPR spectra for reduction of* ***L2***·$NiCl_2$ *at 10 mM.*

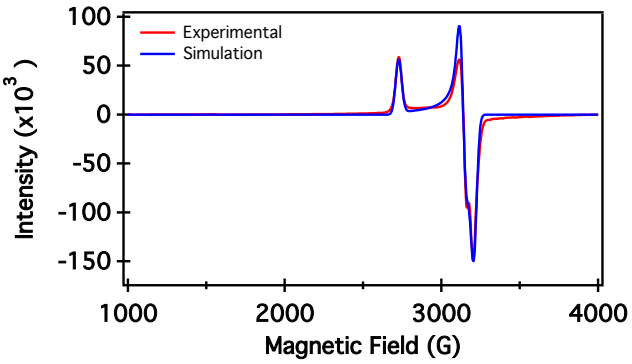

We then reduced **L2**·$NiCl_2$ for 9 hours at a concentration of 100 mM in DMA, which represents the concentration of Ni species in solution relevant to the catalytic system (10 mol % loading). When either Mg or Zn were used as the reductant, Ni(I) species were formed; however, the resulting EPR spectra were different than when conducted at 10 mM (Figure 4.12). With Zn, two Ni(I) species are formed in ~2:1 ratio with the major species being the previously observed Ni(I) complex. When Mg was used as the reductant, the previous Ni(I) complex was present, however only in trace quantities. A third Ni(I) complex becomes the major species in this reduction. Notably, there is more Ni(I) present in solution when Mg, the stronger reductant, is used; however, quantification of the signal in Figure 4.12b provides an approximate measurement which determines the signal accounts for only 10% of the available Ni species; the remaining 90% is either Ni(II), Ni(0), or a ferromagnetically coupled Ni(I) dimer. Nevertheless, these results demonstrate the possibility Ni(I) speciation at varying concentrations, and may indicate dimerization or aggregation of the catalyst. Further studies to elucidate these structures are necessary.

Figure 4.12 *EPR spectra for reduction of* ***L2***·$NiCl_2$ *at 100 mM.*

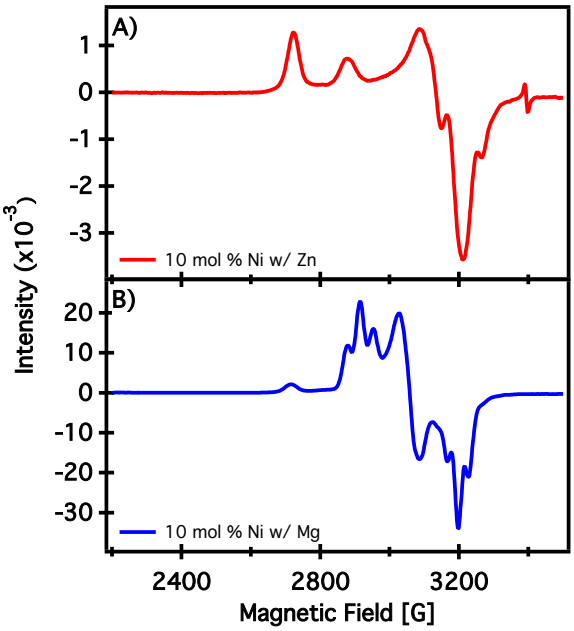

4.3.5 Oxidative Addition Complexes

In addition to synthesizing **L2**·NiX_2 complexes, we also attempted to synthesize and characterize oxidative addition complexes (Scheme 4.5). Three different approaches were taken to generate these intermediates. We first tried to metalate BOX ligand **L2** with $Ni(cod)_2$, followed by the addition of a stoichiometric amount of alkenyl halide **L2** for oxidative addition. Unfortunately, a large amount of homocoupled diene product was observed in this reaction. Our second approach involved the addition of a styrenyl Grignard reagent to **L2**·$NiCl_2$ to form the product through salt metathesis. While the crude sample was partially fractionated and analyzed by ^{1}H NMR and EPR spectroscopy, the resulting fractions were not clean. However, the identification of paramagnetic species suggests that the desired oxidative addition complex and undesired dialkenyl complex were possibly formed under the reaction conditions. Attempts to crystallize the Ni complexes provided

Scheme 4.5 *Attempts at forming oxidative addition complexes.*

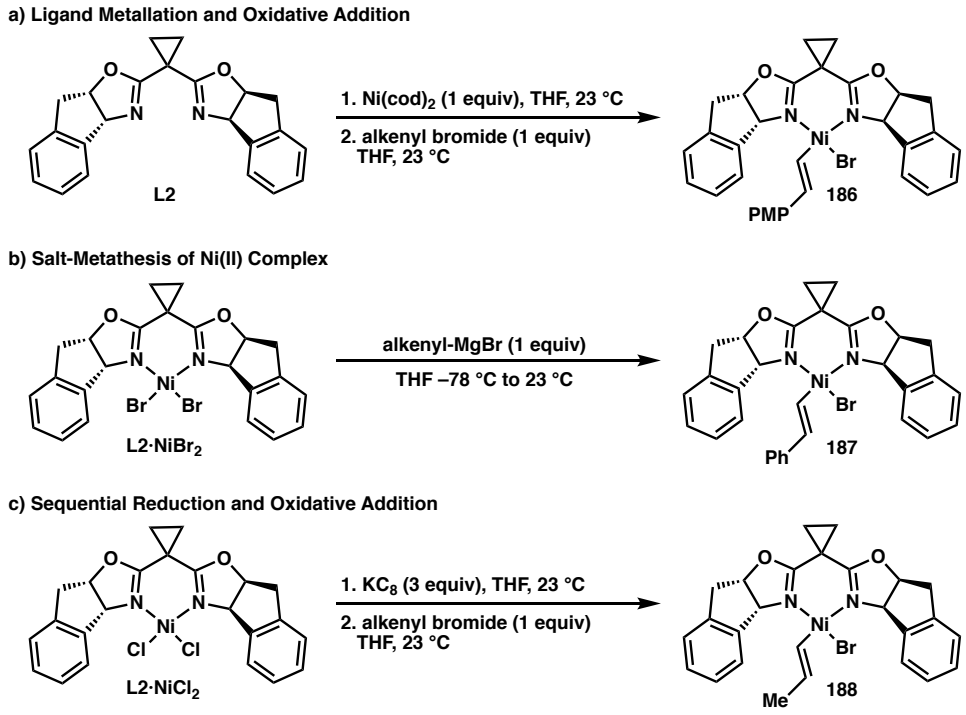

solids that unfortunately powder diffracted when analyzed by X-ray diffraction. Lastly, we attempted to reduce **L2**·$NiCl_2$ with a reductant (KC_8 used in excess), then filtered the solution and added alkenyl halide via an inverse addition protocol (Ni(0) added to electrophile). In all these approaches, we observed promising reactivity, however we were unsuccessful in purifying and crystallizing the Ni(II) oxidative addition complexes for X-ray crystallography. These reactions are by no means exhaustive, and future work dedicated to conducting similar transformations while carefully controlling cryogenic reaction and isolation temperatures may be more profitable.

4.3.6 Analysis of Ni(I) Intermediates

Since we were unable to isolate Ni(II) oxidative addition complexes, we turned our attention to analyzing in-situ generated Ni(I) intermediates by EPR spectroscopy. By

mixing a solution of **L2**·Ni(cod), $Ni(cod)_2$, and alkenyl bromide **L2** for 15 minutes in DMA under inert atmosphere, we were able to observe a mixture of Ni(I) signals by EPR spectroscopy (Figure 4.13a). Some of the resulting EPR signals corresponded to the **L2**·NiBr intermediate prepared by Mg reduction of **L2**·$NiBr_2$ (Figure 4.13c), indicating the feasibility of oxidative addition of the alkenyl bromide to Ni(0) followed by subsequent reduction via a comproportionation type mechanism.

To further confirm the likelihood of comproportionation, an equimolar mixture of **L2**·Ni(cod) and **L2**·NiBr was prepared and observed by EPR (Figure 4.13b). A mixture of two Ni(I) species are detected, one of which is the **L2**·NiBr complex. The other Ni(I) species may be a cod ligated Ni(I) halide complex. In summary, Ni(0) is capable of reducing putative **L2**·$NiBrR_{alkenyl}$ intermediates, thus indicating the feasibility of this

Figure 4.13 *EPR spectra demonstrating the feasibility of comproportionation.*

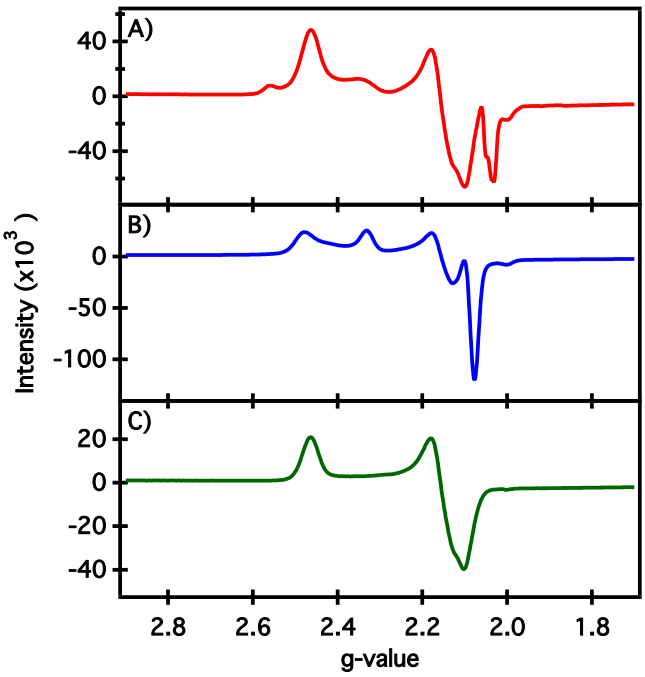

reduction step in the mechanism. These studies suggest that the reduction of **L2**·$NiBrR_{alkenyl}$ and **L2**·$NiBr_2$ complexes occurs readily, while reduction of the **L2**·NiBr occurs more slowly. However, under the catalytic conditions, in which there is an excess of Mn or Zn, it seems likely that **L2**·$NiBrR_{alkenyl}$ would be reduced by the heterogeneous reductant rather than **L2**·Ni(0).

Finally, although we have observed Ni(I) signals by EPR, analysis of the catalytic cross-coupling reaction at 50% conversion with Zn as the reductant shows no EPR active intermediates, indicating that Ni(II) may be the resting state in the transformation. Therefore, if Ni(I) intermediates are formed in the reaction, they are not long-lived species.

4.4 EXPERIMENTAL STUDIES: REACTION PROFILE

After conducting experimental studies on Ni intermediates, we turned our attention to studying the reaction process as a whole. These studies attempt to gain insight into factors that influence reaction yield and enantioselectivity.

4.4.1 Stoichiometric Ni(0) Studies

Since proposed mechanisms hypothesize that the $C(sp^2)$-hybridized electrophile undergoes oxidative addition to a ligated Ni(0) complex, we decided to analyze the cross-coupling reaction in a system using stoichiometric Ni(0) in the form of $Ni(cod)_2$ (Table 4.1). By using an equimolar mixture of alkenyl bromide **86**, benzyl chloride **167**, $Ni(cod)_2$, and ligand **L2** in the absence of a heterogeneous metal reductant, we were able to produce the desired cross-coupled product in 48% yield and 97% ee after 6 hours (entry 1). Adding radical scavengers such as 9,10-dihydroanthracene (DHA) or butylated hydroxytoluene

Table 4.1. *Alkenyl–benzyl cross-coupling with stoichiometric Ni(cod)$_2$.*

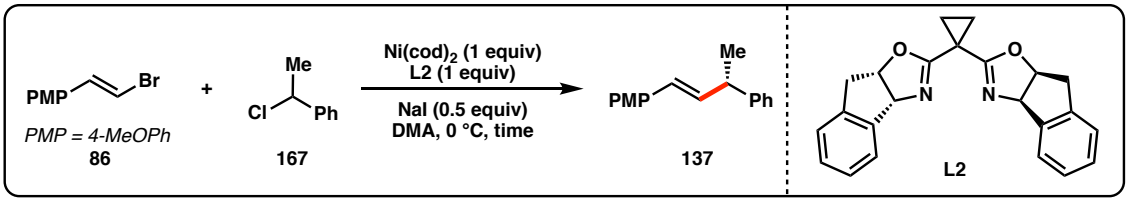

Entry	Additive	Deviation from Conditions	Time (h)	Conv. (%)[a]	Yield (%)	ee (%)
1	—	—	6	98	48	97
2	DHA	—	6	52	49	96
3	BHT	—	6	91	54	96
4	CNB	—	6	48	0	—
5	—	no ligand	6	85	2	3
6[b]	—	no NaI, premix 1 equiv Ni/L, then 86 and 167	6	47	28	83
7[c,d]	—	no NaI, premix 2 equiv Ni/L, then 86, then 167	6	50	36	94
8[c,d,e]	—	no NaI, premix 2 equiv Ni/L, then 167, then 86	6	88	5	91
9	—	—	24	100	78	96
10	DHA	—	24	100	79	96
11	BHT	—	24	100	77	96
12	galvinoxyl	—	24	60	57	96
13[f]	TEMPO	—	24	86	42	96

[a]Based off benzyl chloride. [b]Ni and ligand prestired for 24 hours. [c]first electrophile stirred for 20 min. [d]Ni and ligand prestired for 15 hours. [e]47% yield homocouplng of **167** observed. [f]benzyl–TEMPO adduct detected by ^{1}H NMR.

(BHT) did not affect the reaction yield (entries 2 and 3), however adding an electron transfer inhibitor, 1-chloro-2,4-dinitrobenzene (CNB), completely shut down productive reactivity (entry 4). These results are similar to those obtained in the catalytic nickel coupling,[8] and may be indicative of a similar reaction pathway. Interestingly, the reaction does not proceed in the absence of ligand, indicating that Ni(cod)$_2$ is not a sufficient "catalyst" to perform the cross-coupling (entry 5). During these reactions we visually observed slow dissolution of Ni(cod)$_2$ which may be critical for obtaining high ee of **137**. If Ni(cod)$_2$ and **L2** are premixed, the ee of **137** is slightly diminished (entry 6).

Since we were unsuccessful at isolating Ni(II) oxidative addition complexes, we set out to make the corresponding Ni(II) complexes in-situ. Forming the Ni(0) complex in-

situ, followed by the addition of each electrophile to the reaction sequentially, affords 36% yield of the desired cross-coupled product when the alkenyl bromide is added 20 minutes before the benzyl chloride (entry 7). Conversely, when the benzyl chloride is added to the reaction 20 minutes prior to the addition of the alkenyl bromide, only a 5% yield of product is observed and the majority of the benzyl chloride reacts to form the benzyl homocoupling product (entry 8). These observations are analogous to the stoichiometric Ni(II) oxidative addition study conducted by Weix and co-workers and suggest that the C(sp^2) partner is the first electrophile to undergo oxidative addition.[13]

In order to improve the yield of **137**, we found that better conversion and higher yields could be obtained by running the reaction for 24 hours instead of 6 hours, affording 78% yield of the product in 96% ee. Again, the addition of radical inhibitors such as DHA or BHT did not shut down reactivity, however the addition of free radicals such as galvinoxyl and TEMPO decreased the yield of **137**, partially due to decreased conversion of the electrophiles. When TEMPO was added to the reaction, the TEMPO–benzyl adduct was detected by ^{1}H NMR spectroscopy, providing evidence for the formation of a discrete benzyl radical intermediate. Given these results, again we propose a comproportionation mechanism between the alkenyl bromide oxidative addition complex and exogenous Ni(0) to afford the Ni(I) alkenyl intermediate. Subsequent oxidative addition of the benzyl chloride, followed by reductive elimination, could afford the desired product.

4.4.2 Scalemic Ligand Study

Next we investigated how the product ee changed upon altering the ee of the ligand through the systematic preparation of scalemic mixtures of both ligand enantiomers (Figure

4.14). As the ee of **L2** increases from 0 to 100% ee, the ee of **137** also increases linearly. This not only shows that one ligand is bound to Ni during the enantiodetermining step of the reaction, but also likely eliminates the possibility that the reaction proceeds via the disproportionation/transmetalation mechanism.

Figure 4.14 *Scalemic ligand study.*

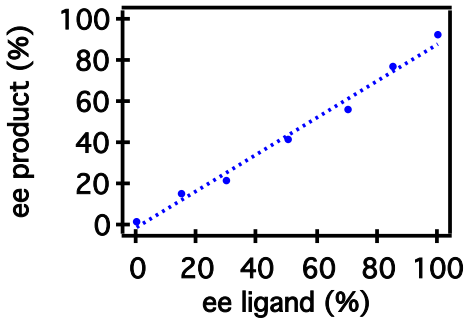

4.4.3 Reaction Progress by ^{19}F NMR

We briefly investigated the catalytic reaction with Zn as the reductant by analyzing aliquots by ^{19}F NMR. A fluorine atom was added to either the benzylic chloride electrophile (**189**) or the alkenyl bromide electrophile (**190**) to easily visualize the product distribution (Scheme 4.6). When **141d** was analyzed, rapid decrease of the starting material

Scheme 4.6 *Cross-coupling reactions with fluorinated electrophiles.*

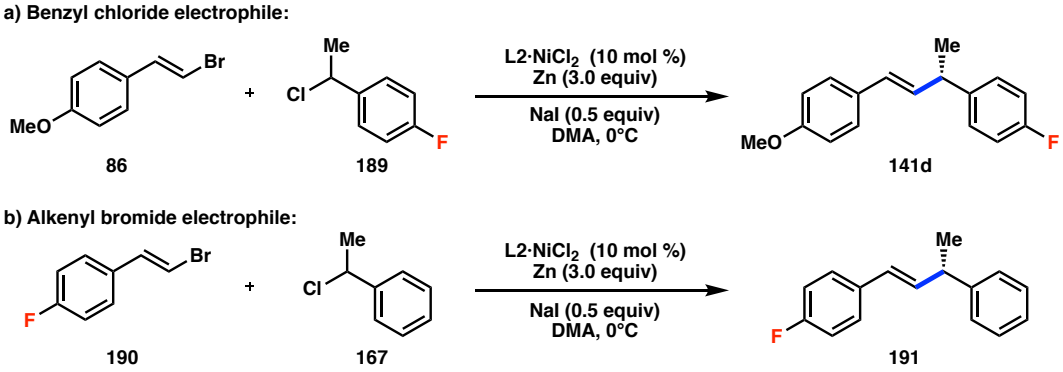

was met with concomitant formation of the desired product. Side products that could be visualized included both diastereomers of the benzylic homocoupling product (Figure 4.15). In contrast, when **191** was analyzed, the alkenyl bromide converted to the desired product and also formed halide exchange products resulting in the corresponding alkenyl chloride and alkenyl iodide. While alkenyl iodide was consumed, alkenyl chloride persisted, indicating it is not catalytically reactive under the reaction conditions.

Figure 4.15 *Benzyl chloride (left) and alkenyl bromide (right) probes by ^{19}F NMR.*

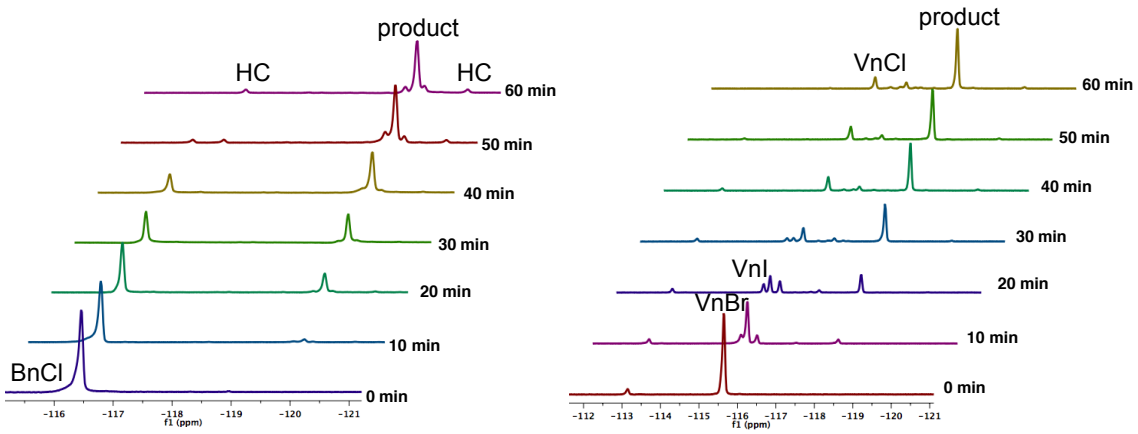

4.4.4 Reaction Kinetics

We then turned our attention towards reaction kinetics to determine how the equivalents of each reagent effected the observed rate of product formation (Scheme 4.7). By conducting the cross-coupling reaction on a larger scale at a more dilute concentration (0.2 M compared to 1 M in the original report),[8] we could effectively analyze aliquots of

Scheme 4.7 *Standard reaction conditions for kinetic analysis.*

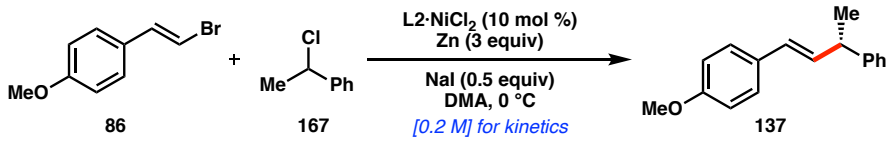

the reaction by gas chromatography (GC-FID) and quantify the concentration of product by comparison against an internal standard (dodecane).

4.4.4.1 Mn and Zn Reductants

Initial investigations revealed that the use of Mn as the reductant resulted in long induction periods (90 minutes) and long reaction times (up to 6 hours). Either activating the Mn with HCl, or using Mn stored under inert atmosphere in the glovebox shortened both the induction period and the reaction time, but only to 30 min and 100 min, respectively. We found that the use of a fine suspension of activated Zn dust began providing the product after a 5–10 min induction period, and the reaction was complete within 40 min. Altering the reductant identity did not significantly affect the overall yield and enantioselectivity of **137**: 96% yield and 96% ee with Mn versus 91% yield and 90% ee with Zn. Doubling the amount of Zn to 6 equivalents increased the reaction rate by a factor of 1.2, results similar to those observed by Weix and coworkers in analogous studies.[4] We hypothesized that the reduction of Ni(II) by Zn was no longer significantly rate-limiting, allowing us to probe the next rate-determining step in the catalytic cycle.

4.4.4.2 Observation of Side Products

In addition to looking at the concentration of the cross-coupled product over time, we also analyzed the concentration profiles of side products present in the reaction: alkenyl iodide **192**, alkenyl chloride **193**, and benzyl homocoupling **194** (Figure 4.16). Once the induction period terminates, alkenyl iodide and alkenyl chloride are observed in the reaction when monitored by GC (Figure 4.17). Although we observe halide scrambling on the akenyl C(sp^2)-hybridized electrophile, we do not observe halide scrambling on the

Figure 4.16 *Side products observed in the catalytic alkenyl–benzyl cross-coupling.*

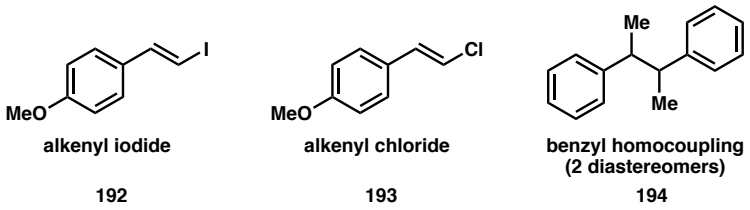

benzylic C(sp^3)-hybridized electrophile (no benzyl iodide or benzyl bromide are formed). While alkenyl iodide **192** is a competent electrophile and is consumed by the end of the reaction, alkenyl chloride **193** remains in the reaction mixture. This may explain why the addition of NaI afforded higher reaction yields during the initial reaction optimization[8]– more of the alkenyl electrophile remains a competent electrophile. Furthermore, we also observe the formation of benzyl homocoupling **194** over the course of the reaction. The side product is slowly formed during the reaction, and once full conversion of alkenyl bromide electrophile **86** is achieved, the remaining benzyl chloride **167** rapidly dimerizes.

Figure 4.17 *Concentration profiles of side products.*

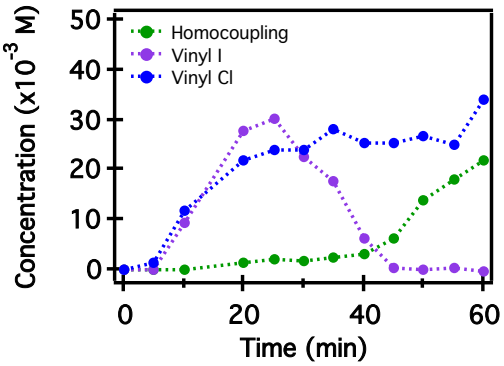

4.4.4.3 Nickel Loading

We then analyzed the observed rate of product formation as a function of reaction time with varying catalyst loadings of **L2**·$NiCl_2$. As we sequentially doubled the

concentration of the catalyst, the observed rate of product formation also doubled (Figure 4.18). After fitting the reaction traces by linear regression, and subsequently graphing the natural log (ln) of the linear slopes versus the ln of the concentration of nickel, we obtained a secondary plot as shown in Figure 4.19. The data points appear to have a linear trend,

Figure 4.18 *Concentration of* ***137*** *as a function of time at various Ni loadings.*

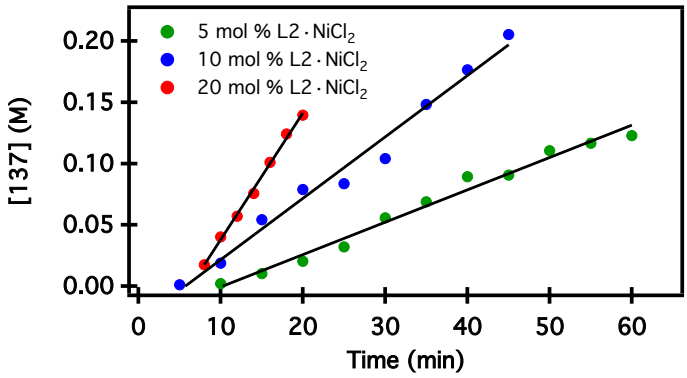

and are best fit by a regression line with an equation of $y = 1.1x - 0.96$ and an R^2 of 0.97. Interestingly the enantioselectivity of the reaction decreases as the concentration of nickel increases. With 5 mol % **L2**·$NiCl_2$, **137** is formed in 93% ee, however with 20 mol % **L2**·$NiCl_2$, **137** is formed in 84% ee. This data suggests that although the reaction appears

Figure 4.19 *Rate dependence on Ni loading.*

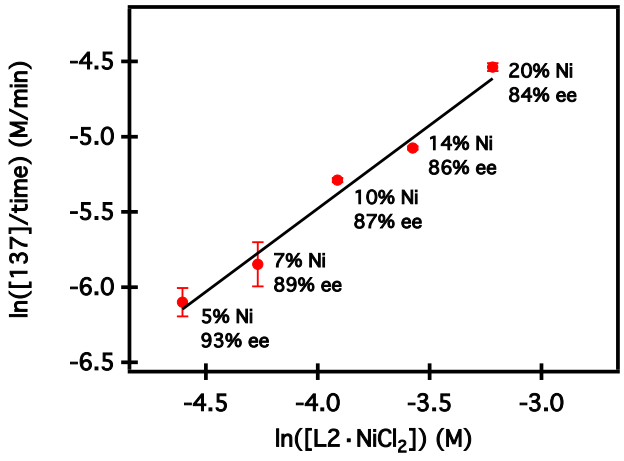

to be first order in nickel for the rate-determining step, there may be a secondary mechanism (with lower enantioselectivity) coexisting with the major pathway at higher catalyst loadings.

4.4.4.4 Electrophile Equivalents

We then analyzed the observed rate of product formation as a function of time when varying the electrophile equivalents (Figure 4.20). With two equivalents of benzyl chloride **167**, the rate of product formation increased by a factor of 1.7. In contrast, when two equivalents of alkenyl bromide **86** were added, the rate of product formation decreased by a factor of 0.5. To determine if the reduction in rate was due to alkenyl bromide coordination to nickel, we added one equivalent of 4-methoxystyrene to the reaction and found no reduction in rate. Therefore, it seems that the inverse dependence due to the alkenyl bromide is not attributable to nickel complexation. These trends are similar to those reported by Weix and co-workers in the reductive cross-coupling of aryl and alkyl iodides.[4]

Figure 4.20 *Rate of formation of* ***137*** *with increased electrophile loadings.*

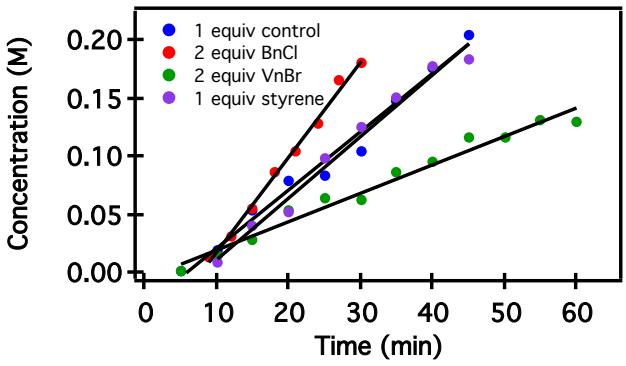

By subjecting the cross-coupling reaction to different equivalents of alkenyl bromide and benzyl chloride, we can generate natural log rate plots. As we increase the concentration of alkenyl bromide **86**, the observed rate of product formation decreases until

it reaches a saturation point at three equivalents (Figure 4.21a). A linear regression line that passes through 1–3 equivalents gives y = –1.03x – 7.01 with R^2 = 0.97. The enantioselectivity of the reaction also increases as the concentration of **137** increases. With

Figure 4.21 *The rate order of A) alkenyl bromide* ***86*** *and B) benzyl chloride* ***167****.*

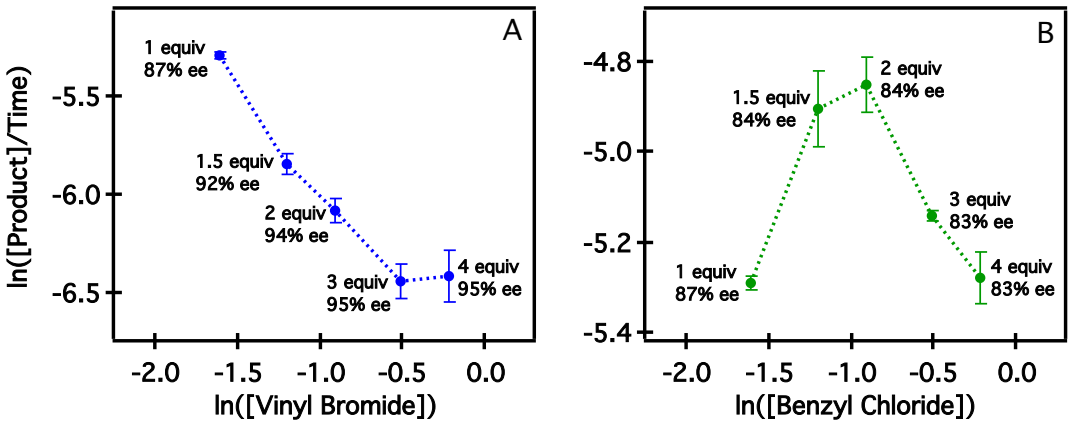

one equivalent of **86**, the product is formed in 87% ee, however with four equivalents of **86**, the product is formed in 95% ee. In contrast, as we increase the concentration of benzyl chloride **167**, the observed rate of product formation increases until two equivalents are added, and then decreases as three and four equivalents are added (Figure 4.21b).

4.4.4.5 Stirring Rate

Lastly, we evaluated the rate of product formation as a function of stir rate; all the previous studies were conducted at 1500 rpm. Figure 4.22 depicts the rate of product formation as the stirring mechanism is altered from 500 rpm to 1000 rpm to 1500 rpm. As the stir speed increases, so does the rate of product formation, which indicates our kinetic studies measure properties related to mass transfer due to the heterogeneous nature of the reaction. As the total surface area of reductant remains constant, increasing the concentration of Ni in solution also increases the number of collisions with the Zn surface.

Figure 4.22 *Product rate dependence as a function of stir rate.*

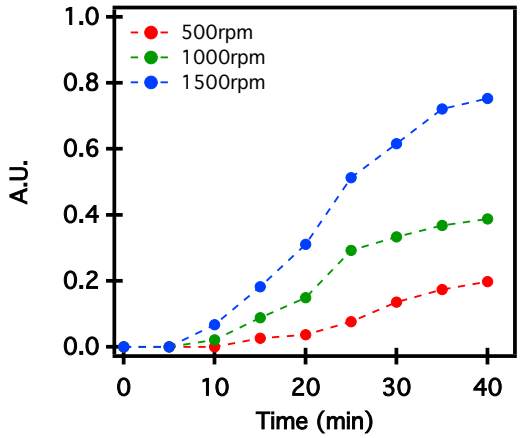

4.4.5 Radical Clock Substrates

To further analyze the probability of a radical intermediate in the mechanism, we synthesized and subjected a series of radical clock substrates to the reaction conditions. When ring closing clock **195** was used as the C(sp^3)-hybridized electrophile, a 62% yield of the uncyclized product (**196**) was formed in 96% ee. No ring closed product was observed under the reaction conditions. We then sought to use a faster cyclopropylcarbinyl radical ring opening clock similar to ones employed in our previous studies (Table 4.2).[10,12,28,29] Unfortunately the stable CF_3-substitued clock did not provide sufficient yield of the coupling products to ensure catalyst turnover;[12] instead a more reactive unsubstituted arene (**198**) had to be prepared. In order to prepare **198**, the benzyl chloride was formed

Scheme 4.8 *Evaluation of ring closing clock.*

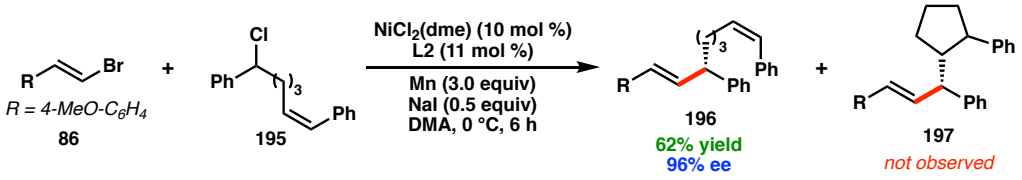

from the corresponding benzyl alcohol using thionyl chloride and immediately used due to its instability. While **198** is stable in DMA at 0 °C for the duration of the reaction (2 h), it is not stable in the presence of other reaction components (i.e. 100% recovery with

Table 4.2. *Evaluation of ring opening clock.*

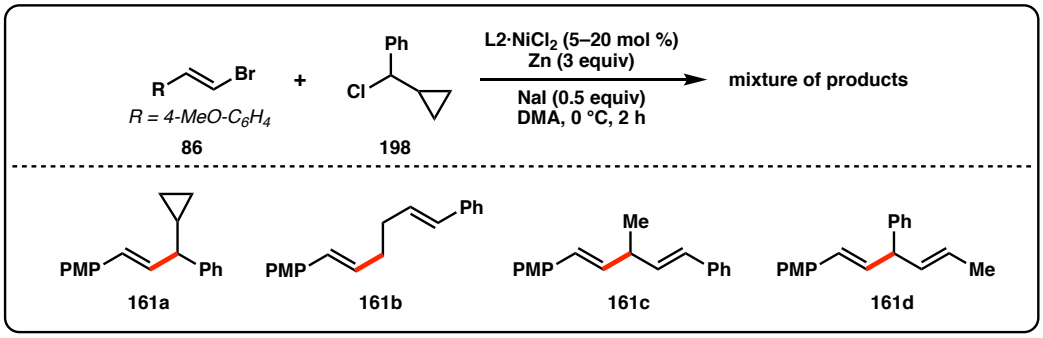

Entry	L2·$NiCl_2$ (mol %)	Total Yield (%)	161a	161b	161c	161d
1	5	33	1.7%	19%	74%	5%
2	10	34	1.2%	13%	79%	6%
3	20	33	0.7%	6%	86%	7%

L2·$NiCl_2$, 60% recovery with Zn, and 50% recovery with NaI). When **198** was subjected to the reaction, we observed a mixture of products (**161a–d**) while the major product observed was the branched ring opening product (**161c**). As the loading of catalyst increased, the ratios of the products changed, however with different trends than observed in our previous studies of NHP esters.[10]

4.5 COMPUTATIONAL STUDIES

We then sought to conduct computational studies on this transformation. To better understand the differences and compare the likelihood of the intermediate reduction and radial chain mechanisms, we collaborated with Prof. Kendall Houk at UCLA to conduct geometry optimization and energy calculations for the two reaction pathways. Geometry

optimization and frequency analysis were performed using (*E*)-1-(2-bromovinyl)-4-methoxybenzene (**86**), (1-chloroethyl)-benzene (**168**), and chiral bis(oxazoline ligand) **L2** with the B3LYP functional and a mixed basis set of LANL2DZ (for Ni and Br) and 6-31G(d) (for other atoms). Single-point energies were calculated at the M06/6-311+G(d,p) level with SDD for Ni and Br, including the SMD solvation correction (DMA solvent) on the B3LYP-optimized geometries. All calculations were performed with Gaussian 09.

4.5.1 Generation of Ni(0)

Although the generation of Ni(0) in Weix's proposed reaction mechanism (Figure 4.6) is presumed to proceed through a two-electron reduction of Ni(II) via the heterogenous metal reductant, our experimental results suggest that, for **L2**·$NiCl_2$, only a single electron reduction is viable given the measured reduction potentials of the catalyst. In order to determine an alternate reduction pathway to access Ni(0), we computed the possibility of an alkenyl bromide assisted disproportonation of a Ni(I) dimer **199** (Figure 4.23). Given the energetics of this transformation, it may be a feasible process under the given reaction

Figure 4.23 *Evaluation of Ni(I) dimer disproportionation.*

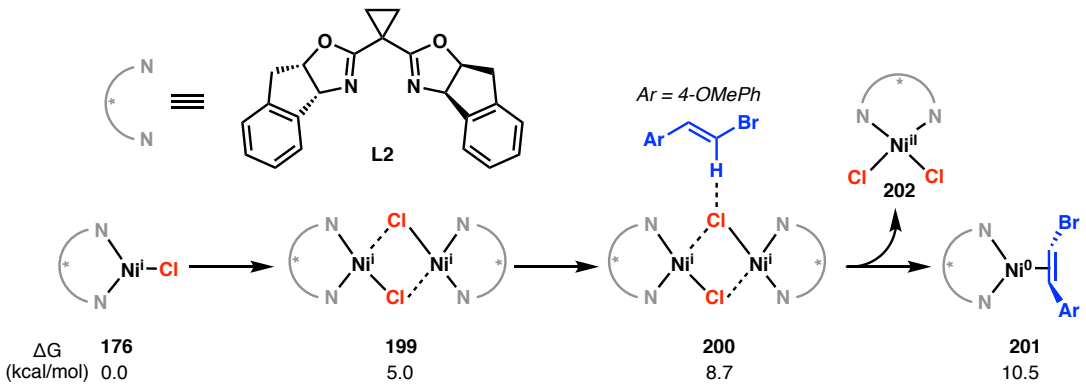

conditions. Further studies aimed at calculating the transition states for this process are ongoing and will shed additional insight into this aspect of the mechanism.

4.5.2 First Oxidative Addition

The first step in both mechanisms is the oxidative addition of alkenyl bromide **86** to Ni(0) complex **169** (Figure 4.24). We first calculated the oxidative addition of alkenyl bromide from a substrate bound Ni(0) complex **201**. Although the oxidative addition of both electrophiles is exergonic (ΔG_{rxn} = –12.1 kcal/mol for **86** and ΔG_{rxn} = –4.0 kcal/mol for **167**), comparison of the transition state energies reveals that the oxidative addition of the alkenyl bromide is more favorable by 4.0 kcal/mol ($\Delta G^{‡}$ = 16.0 kcal/mol for **86** and $\Delta G^{‡}$ = 20.0 kcal/mol for **167**). This suggests that given this set of electrophiles, the C(sp^2)-hybridized electrophile is the first to undergo oxidative addition to Ni(0) in the catalytic cycle. The oxidative addition of **86** onto Ni(I)Cl complex **176** was also calculated, which was found to be endergonic (ΔG_{rxn} = 13.2 kcal/mol) with a $\Delta G^{‡}$ = 20.2 kcal/mol.

Figure 4.24 *Gibbs free energy changes for the oxidative addition pathways of each electrophile to Ni(0) complex* ***201****.*

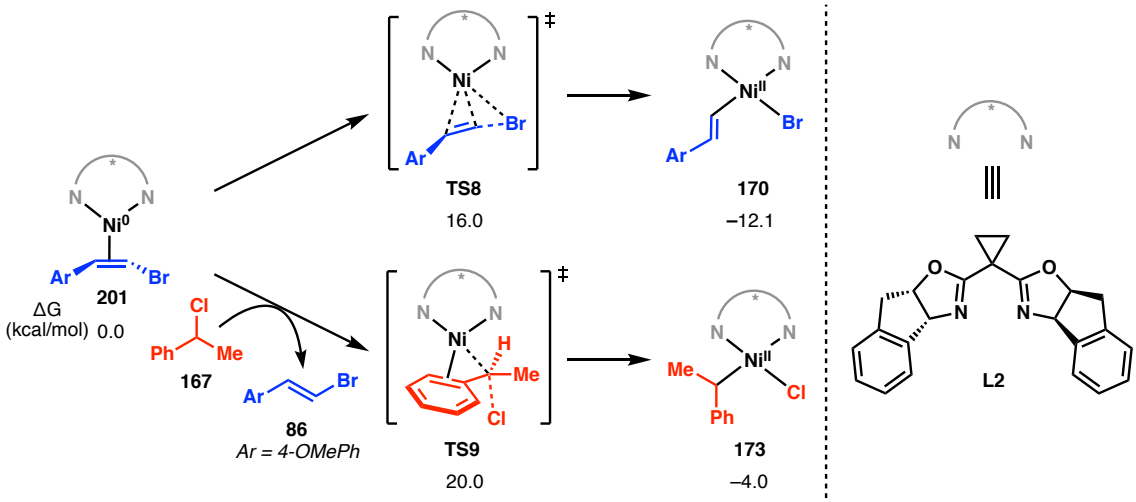

4.5.3 Preference for Cross-Coupling

From the the Ni(I) alkenyl complex, following reduction of Ni(II) complex **170** by the stoichiometric Mn reductant, we evaluated the oxidative addition of alkenyl bromide **86** through a concerted process and benzyl chloride **167** through a step-wise process which generates an intermediate benzyl radical (Figure 4.25). While the transition state energy for the chloride abstraction by Ni(I) complex **174** and the oxidative addition of alkenyl bromide **86** proceed with a difference of 1.1 kcal/mol, the overall reaction thermodynamics are quite different. Chloride abstraction from the benzyl chloride is exergonic with ΔG_{rxn} of –6.0 kcal/mol. In contrast, oxidative addition of the alkenyl bromide is endergonic with ΔG_{rxn} of 5.0 kcal/mol. These calculations may provide a basis for the high levels of cross-

Figure 4.25 *Evaluation of oxidative addition selectivity to* ***174***·$NiR_{alkenyl}$. *Energies are given in kcal/mol.*

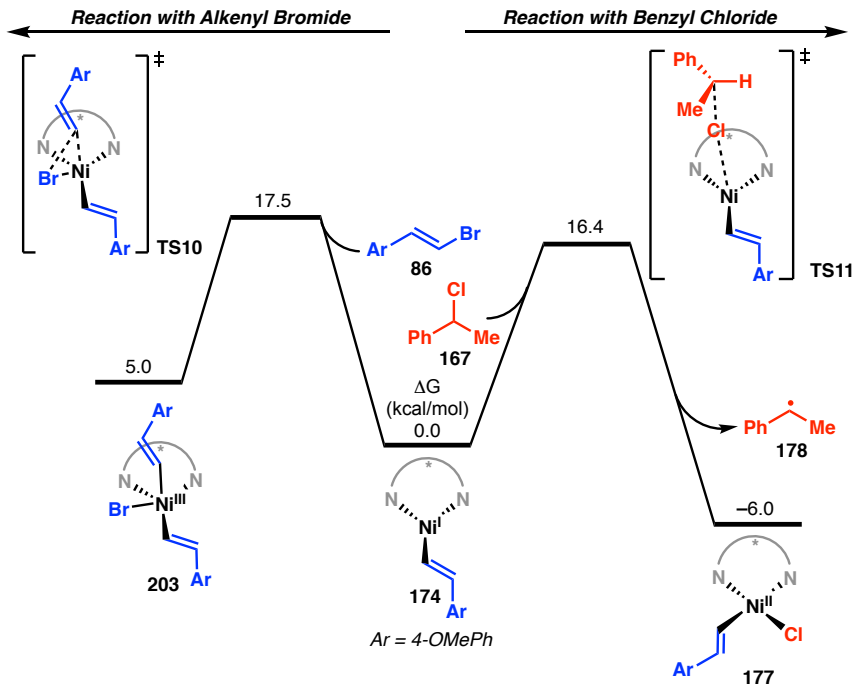

electrophile coupling, rather than homocoupling of the alkenyl bromide cross-coupling partner, particularly if the reversible oxidative addition of **86** is favored over reductive elimination to form dienyl homocoupling products.

4.5.4 Competing Mechanisms during Second Oxidative Addition

We then calculated the second oxidative addition step of benzyl chloride **168** to Ni(I) complex **174**. As shown in Figure 4.26a, there is a barrier of 16.4 kcal/mol (**TS12**) for the chloride abstraction step in the intermediate reduction mechanism. The resulting benzyl radical **178** attacks Ni(II) complex **177** and forms Ni(III) complex **175**. The cross-coupled product (**137**) is formed following reductive elimination. The radical chain mechanism was also calculated and found to be thermodynamically disfavored by 19.4 kcal/mol (Figure 4.26b). While the chlorine atom transfer step is 6.0 kcal/mol exergonic in the sequential oxidative addition mechanism, it is 13.4 kcal/mol endergonic in the radical chain mechanism. This 19.4 kcal/mol difference leads to the significant preference for the intermediate reduction mechanism.

4.5.5 Alternative Reduction

Given our experimental findings that suggest Ni(0) is a competent reductant to reduce **L2**·$NiBrR_{alkenyl}$ when stoichiometric $Ni(cod)_2$ is used, we calculated the $\Delta\Delta G_{rxn}$ for the corresponding comproportionation mechanism between **201** and **170** (Figure 4.27). Alkenyl bromide bound Ni(0) complex **201** and oxidative addition complex **170** are found to form Ni(I) complexes **174** and **180** thorough a net exergonic reaction, confirming the possibility this process may be feasible. However, under the catalytic reaction conditions, the concentration of Ni(0) in solution is likely very low compared to the amount of

Figure 4.26 *Gibbs free energy profile of the benzyl chloride oxidative addition.*

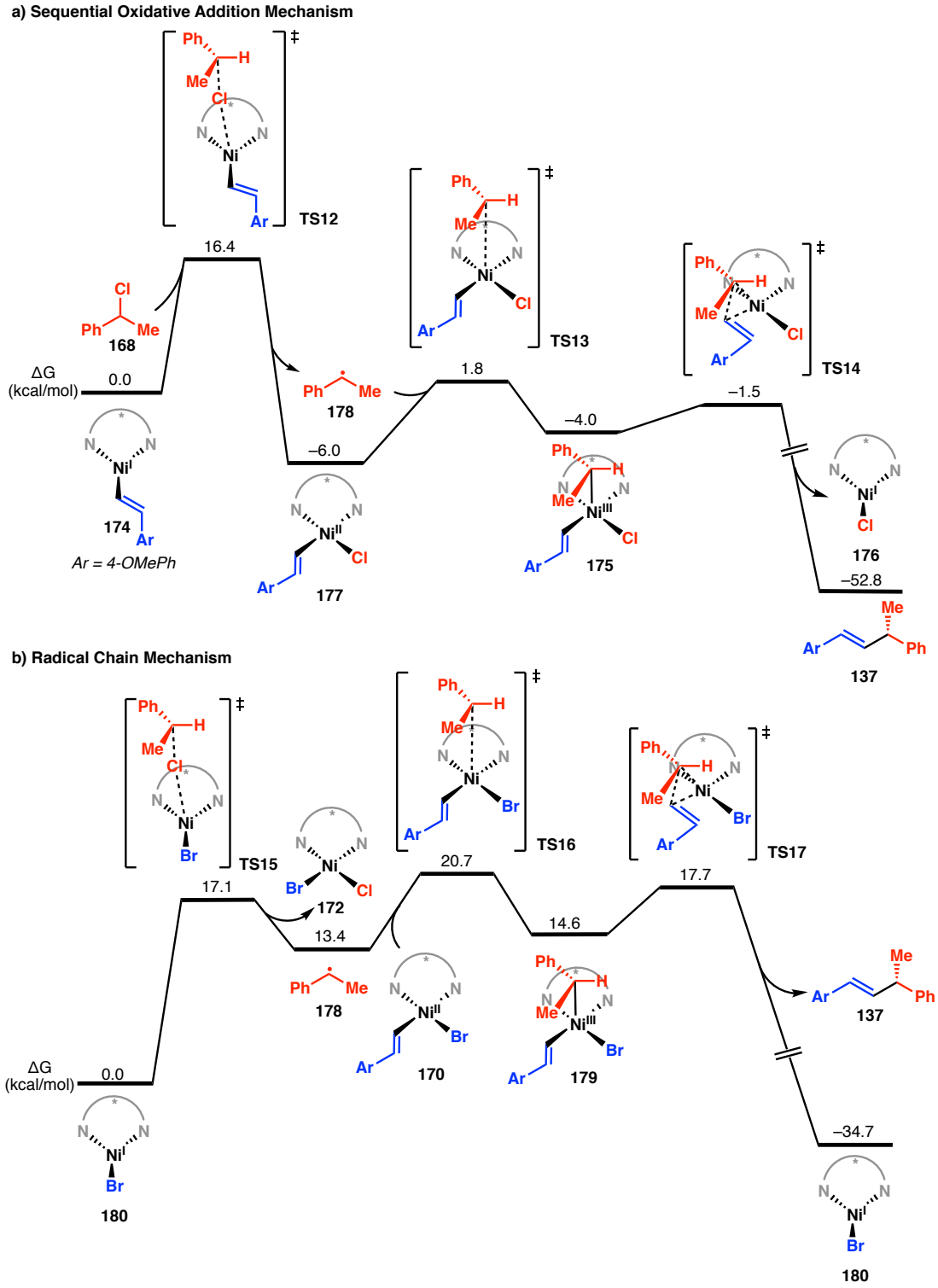

heterogeneous reductant available. Aside from kinetic limitations surrounding heterogeneous aspects of the reaction, we speculate that the metal reductant is the most likely source of electrons for the reduction of Ni complex **176**.

Figure 4.27 *Comproportionation to form* ***L2***·*NiR*$_{vinyl}$.

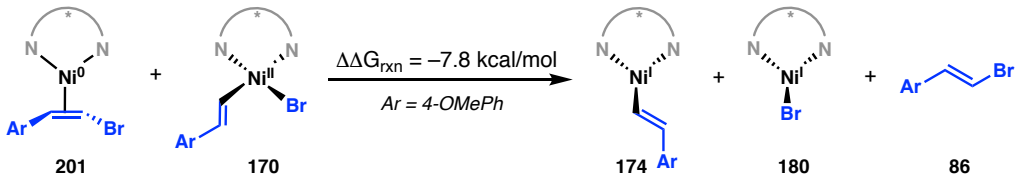

4.5.6 Radical Clock Substrate

We previously reported the use of benzyl chloride radical clock **195** in our alkenyl–benzyl cross-coupling reaction, however only the uncyclized product was afforded. By calculating the reorganization energy needed for cyclization (Figure 4.28), we determined that a 10.7 kcal/mol barrier is required, which is higher than the 7.8 kcal/mol barrier needed for the addition of benzyl radical **178** to Ni(II) intermediate **170**. Therefore, these studies suggest the radical clock used in the reaction was too slow for cyclization to occur.

Figure 4.28 *Calculated Gibbs free energy reorganization energy of the radical cyclization clock.*

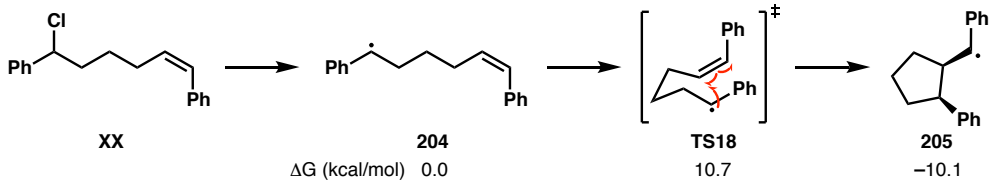

4.5.7 Enantioinduction

The reported cross-coupling reaction not only provides the cross-coupling product **137** in excellent yield (91%) but also in excellent enantioselectivity (93% ee). The

calculated reaction profile (Figure 4.26a) identifies the addition of benzyl radical **178** to Ni(II) intermediate **177** as the enantiodetermining step ($\Delta\Delta G^{\ddagger}$ = 3.3 kcal/mol between reversible benzyl radical addition and reductive elimination). To explore the origins of enantioinduction, the structures and relative Gibbs free energies of the competing transition states for radical addition were computed (Figure 4.29).

Figure 4.29 *Relative Gibbs free energy of the transition states for the enantiodetermining step.*

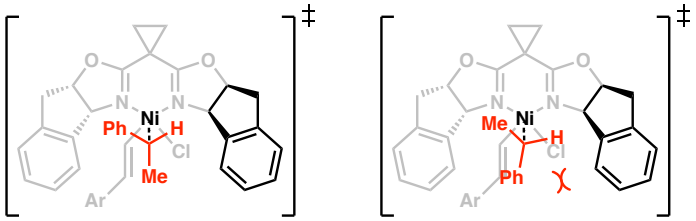

In both transition states, the smallest substituent of the approaching benzyl radical, hydrogen, is pointing towards the bulky indanyl group on the ligand. This allows the largest substituent, the phenyl group, to project away from the bulky region of the ligand in the favored transition state **TS19**. In the disfavored transition state, **TS19'**, the phenyl group is proximal to the bulky region of the ligand. This results in an almost perfectly staggered approach of the benzyl radical with respect to the Ni ligands in **TS19**, while steric repulsion from the ligand forces the benzyl radical to adopt a more eclipsed conformation in **TS19'**.

The free energy difference between **TS19** and **TS19'** is computed to be 3.3 kcal/mol, which suggests the reaction should proceed with a 547 ratio of major to minor enantiomers according to Equation 4, or an enantioselectivity of 99.8% ee. However, the computed $\Delta\Delta G^{\ddagger}$ overestimates the ee of the reaction. One possible explanation for the

overcompensation of ee may be due to competing mechanisms in the reaction, whereby background reactivity accounts via a racemic or less selective pathway accounts for the diminished ee. Nevertheless, **TS19** does lead to the formation of the major enantiomer and is consistent with the observed enantioselectivity. This stereochemical model also provides insight as to why a variety of alkyl substituents are tolerated at the benzylic position, since it projects the medium sized group away from the metal/ligand framework.

$$\frac{x_{major}}{x_{minor}} = 10^{\frac{\Delta\Delta G^{\ddagger}}{T\times(1.98\times10^{-3})\times2.3}} \tag{4}$$

The free energy difference between the major and minor transition states for a series of substituted benzylic chlorides was calculated (Table 4.3). Equation 4 can be rearranged to form Equation 5, allowing for experimental $\Delta\Delta G^{\ddagger}$ values to be determined from the ratio of major and minor enantiomers used in the calculation of %ee. The calculated $\Delta\Delta G^{\ddagger}$ values

$$\Delta\Delta G^{\ddagger} = T\times(1.98\times10^{-3})\times2.3\times\log_{10}\left(\frac{x_{major}}{x_{minor}}\right) \tag{5}$$

for an α-ethyl group are larger than the values calculated for an α-methyl group, which is consistent with the observed results (entries 1–2). However, when evaluating different aryl

Table 4.3. *Evaluation of $\Delta\Delta G^{\ddagger}$ from major and minor transition states.*

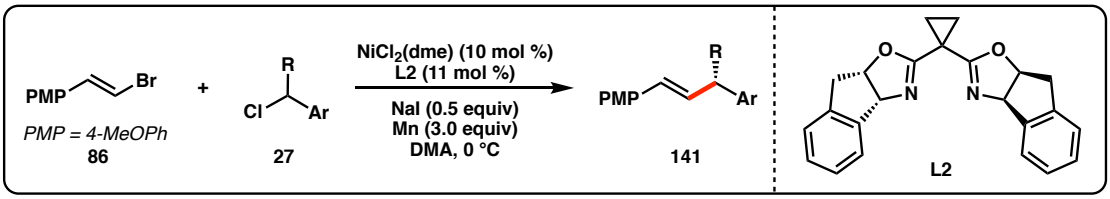

Entry	Ar	R	ee (%) *experimental*	ΔΔG (kcal/mol) *experimental*	ΔΔG (kcal/mol) *compuational*
1	Ph	Me	96	2.1	3.3
2	Ph	Et	97	2.3	4.3
3	4-OMePh	Me	93	1.8	3.2
4	4-ClPh	Me	88	1.5	3.4

substituents, the trend is unclear. Both an electron-donating group (OMe, entry 3) and an electron-withdrawing group (Cl, entry 4) were found to decrease the experimental $\Delta\Delta G^{\ddagger}$ however only the methoxy substituent was found to decrease the calculated $\Delta\Delta G^{\ddagger}$. The calculated $\Delta\Delta G^{\ddagger}$ for the chloride substituent was found to be higher than the parent compound. Further studies are ongoing to probe the $\Delta\Delta G^{\ddagger}$ for additional substrates.

4.6 CONCLUSIONS AND FUTURE DIRECTIONS

In summary, we have conducted a variety of experiments to probe the mechanism of the asymmetric Ni-catalyzed reductive cross-coupling of alkenyl bromides and benzyl chlorides. A series of stoichiometric nickel studies probed each step in the catalytic cycle (Figure 4.30). The **L2**·$NiCl_2$ complex reduces to afford **L2**·NiCl complex as determined by CV and EPR, however there is no evidence for the direct reduction of Ni(I) to form **L2**·Ni(0) in DMA under the reactions conditions. The cross-coupling reaction does proceed to afford **137** with high levels of enantioselectivity when stoichiometric $Ni(cod)_2$

Figure 4.30 *Evidence supporting sequential oxidative addition mechanism.*

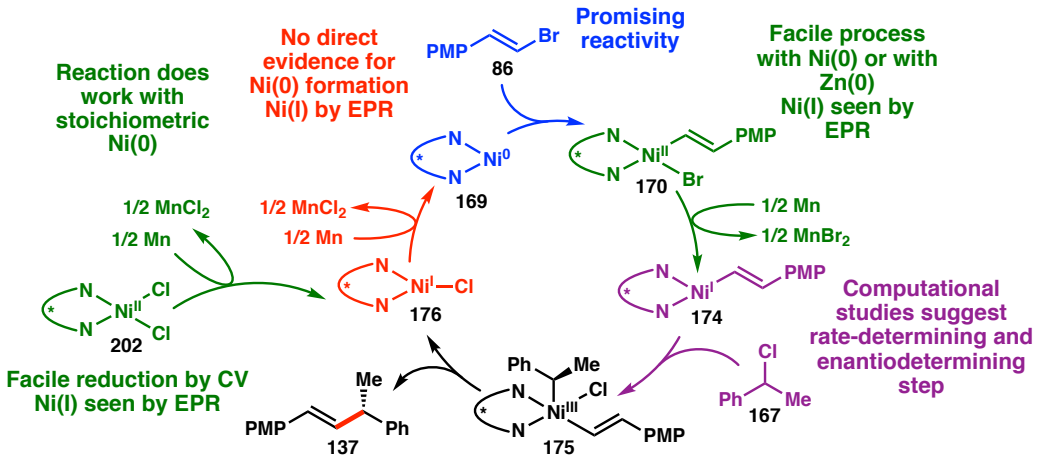

is used, and analysis by EPR further demonstrates the feasibility of both a Ni(0) and Zn mediated reduction of **L2**·$NiBrR_{alkenyl}$.

Computational studies suggest that the intermediate reduction mechanism is favored over the radical chain mechanism by $\Delta\Delta G_{rxn}$ of 19.4 kcal/mol in the chlorine atom transfer step. Comparison of the highest barrier between the two mechanisms shows sequential oxidative addition mechanism is lower by 4.3 kcal/mol. These computational studies also suggest that a Ni(I) dimer could potentially undergo a disproportionation reaction to afford a Ni(II) species as well as the requisite Ni(0) needed for oxidative addition of the alkenyl bromide electrophile. An updated mechanistic understanding including this process is depicted in Figure 4.31.

Future studies are needed to obtain a better understanding of the speciation of Ni following reduction of **L2**·$NiCl_2$ by Zn. In addition, the isolation and characterization of oxidative addition complexes would prove valuable to this study. Additional kinetic analysis on a homogeneous variant of the reaction (NHP esters with TDAE) may shed additional insight into the rate-limiting step of the reaction and help identify the resting

Figure 4.31 *Hypothesis on reaction mechanism.*

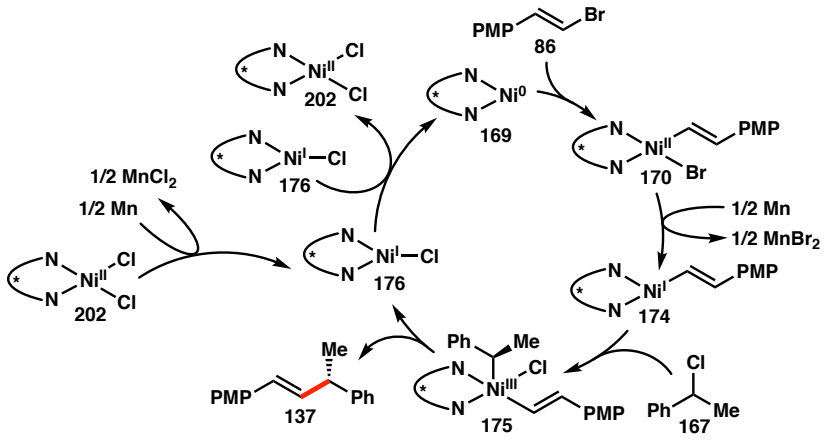

state of the catalyst. Finally, additional computational studies would provide valuable insight into chemoselectivity of the proposed mechanism. Currently, the addition of alkenyl bromide decreases the rate of product formation when Zn is used as a heterogeneous reductant. Additional computational studies aimed at identifying the energetics of the pathway for the formation of alkenyl dimer, as well as both alkenyl bromide and benzyl chloride oxidative addition and subsequent elimination form a Ni(I)-benzyl complex would be insightful.

It is often said that a mechanism can never be proven, it can only be disproven.[30] While concrete, irrefutable data to pin down the reaction mechanism is not yet obtained (if such is even possible), these studies highlight the difficulties and challenges associated with mechanistic studies of asymmetric Ni catalysis occurring in heterogeneous systems. Nevertheless, we predict that future studies on the mechanisms of Ni-catalyzed reductive cross-couplings will not only shed insight into previously developed reactions, but also serve as a basis to develop new reactions and enrich the field of organic synthesis.

4.7 EXPERIMENTAL SECTION

4.7.1 Materials and Methods

Unless otherwise stated, reactions were performed under a nitrogen atmosphere using freshly dried solvents. Tetrahydrofuran (THF) was dried by passing through activated alumina columns. Anhydrous *N*,*N*-dimethylacetamide (DMA) was purchased from Aldrich and stored under inert atmosphere. Manganese powder (~325 mesh, 99.3%) was purchased from Alfa Aesar. Zinc dust (97.5%) was purchased from Strem. Unless otherwise stated,

chemicals and reagents were used as received. All reactions were monitored by thin layer chromatography using EMD/Merck silica gel 60 F254 pre-coated plates (0.25 mm) and were visualized by UV, CAM, or $KMnO_4$ staining. Flash column chromatography was performed as described by Still et al.[31] using silica gel (particle size 0.032–0.063) purchased from Silicycle. Optical rotations were measured on a Jasco P-2000 polarimeter using a 100 mm path-length cell at 589 nm. ^1H and ^{13}C NMR spectra were recorded on a Varian Inova 300 (at 300 MHz and 75 MHz, respectively), Varian 400 MR (at 400 MHz and 101 MHz, respectively) or a Varian Inova 500 (at 500 MHz and 126 MHz, respectively), and are reported relative to internal chloroform (^1H, $\delta = 7.26$, ^{13}C, $\delta = 77.0$). ^{19}F NMR spectra were recorded on a Varian 400 MR (at 376 MHz). Data for ^1H NMR spectra are reported as follows: chemical shift (δ ppm) (multiplicity, coupling constant (Hz), integration). Multiplicity and qualifier abbreviations are as follows: s = singlet, d = doublet, t = triplet, q = quartet, p = pentet, m = multiplet, br = broad. IR spectra were recorded on a Perkin Elmer Paragon 1000 spectrometer and are reported in frequency of absorption (cm^{-1}). Analytical chiral SFC was performed with a Mettler SFC supercritical CO_2 analytical chromatography system with Chiralcel AD-H, OD-H, AS-H, OB-H, and OJ-H columns (4.6 mm x 25 cm). Analytical achiral GC was performed with an Agilent 6850 GC utilizing an HP-1 capillary column (methyl siloxane, 30.0 m x 320 μm x 0.25 μm, Agilent) column with a splitless injection and a helium flow of 7.3 mL/min. The temperature program began at 50 °C and was held for 2 min, increased to 250 °C at 25 °C/min and then held at 250 °C for 3 min. X-band EPR spectra were recorded on a Bruker EMX spectrometer. Electrochemical measurements were conducted under an N_2

atmosphere in a one compartment cell using a Bio-Logic SP300 potentiostat/galvanostat. A glassy carbon disk working electrode, silver wire pseudo-reference electrode, and graphite auxiliary electrode were used. Electronic absorbance spectra were recorded with a Varian Cary Bio 50 spectrophotometer.

4.7.2 Nickel(II) Complex Preparation

For the synthesis of ligand **L2**, see Chapter 2.

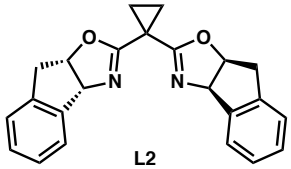

General Procedure 1: L·NiX$_2$ Complex Synthesis

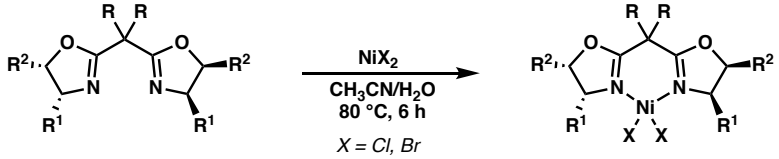

Similar to a procedure reported by Evans and co-workers,[32] the bis(oxazoline) ligand (1.2 mmol, 1 equiv) and either anhydrous nickel(II) chloride (1.2 mmol, 1 equiv) or anhydrous nickel(II) bromide (1.2 mmol, 1 equiv) were added to a round bottom flask equipped with a magnetic stirring rod and dissolved in a mixture of MeCN (26 mL) and water (340 μL). The solution was heated to 80 °C for 6 hours to afford a dark purple solution. The reaction was concentrated under reduced pressure and the obtained solid was recrystallized by vapor diffusion (DCM/pentanes) to afford crystals suitable for X-ray diffraction. For quantitative isolation of **L**·NiX_2, hexanes was vigorously added by pipet to suspend any residual solid that had not crystallized, and then was subsequently removed. The washed crystals were

then removed with a spatula, transferred to a new vial, and crushed to provide a fine powder. The resulting complex was dried under vacuum to afford the desired product.

Nickel(II) bis(chloride) (3a*R*,3a'*R*,8a*S*,8a'*S*)-2,2'-(cyclopropane-1,1-diyl)bis(3a,8a-dihydro-8*H*-indeno[1,2-*d*]oxazole) (L2·$NiCl_2$)

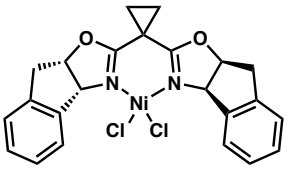

Prepared from bis(oxazoline) **L2** (428 mg, 1.2 mmol) and nickel(II) chloride (156 mg, 24 mmol) following General Procedure 1. The crude residue was recrystallized by vapor diffusion (DCM/pentane) to yield purple crystals of **L2·$NiCl_2$** as the monomeric complex. See Chapter 2 for characterization.

Nickel(II) bis(bromide) (3a*R*,3a'*R*,8a*S*,8a'*S*)-2,2'-(cyclopropane-1,1-diyl)bis(3a,8a-dihydro-8*H*-indeno[1,2-*d*]oxazole) (L2·$NiBr_2$)

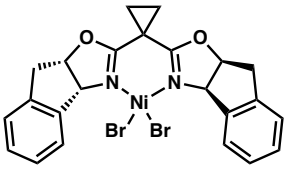

Prepared from bis(oxazoline) **L2** (73 mg, 0.2 mmol) and nickel(II) bromide (45 mg, 0.2 mmol) following General Procedure 1. The crude residue was recrystallized by vapor diffusion (DCM/pentane) to yield purple crystals of **L2·$NiBr_2$** as the monomeric complex. See Chapter 3 for characterization.

Nickel(II) bis(chloride) (3a*R*,3a'*R*,8a*S*,8a'*S*)-2,2'-(propane-2,2-diyl)bis(3a,8a-dihydro-8*H*-indeno[1,2-*d*]oxazole) (L9·$NiCl_2$)

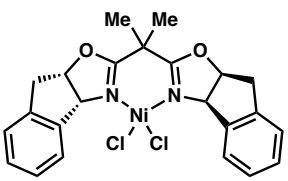

Prepared from bis(oxazoline) **L9** (71 mg, 0.2 mmol) and nickel(II) chloride (26 mg, 0.2 mmol) following General Procedure 1. The crude residue was recrystallized by vapor diffusion

(DCM/pentane) to yield orange crystals of **L9·NiCl$_2$** as the chloride bridged trimer complex.

Nickel(II) bis(chloride) bis((3a*R*,8a*S*)-3a,8a-dihydro-8*H*-indeno[1,2-*d*]oxazol-2-yl)methane (L20·NiCl$_2$)

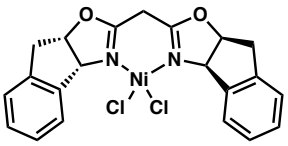

Prepared from bis(oxazoline) **L20** (66 mg, 0.2 mmol) and nickel(II) chloride (26 mg, 0.2 mmol) following General Procedure 1. The crude residue was recrystallized by vapor diffusion (DCM/pentane) to yield orange crystals of **L20·NiCl$_2$** as the chloride bridged trimer complex.

Nickel(II) bis(bromide) bis((3a*R*,8a*S*)-3a,8a-dihydro-8*H*-indeno[1,2-*d*]oxazol-2-yl)methane (L20·NiBr$_2$)

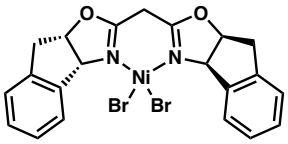

Prepared from bis(oxazoline) **L20** (66 mg, 0.2 mmol) and nickel(II) bromide (45 mg, 0.2 mmol) following General Procedure 1. The crude residue was recrystallized by vapor diffusion (CH_2Cl_2/pentane) to yield orange crystals of **L20·NiBr$_2$** as the bromide bridged trimer complex.

Nickel(II) bis(chloride) (4*R*,4'*R*)-2,2'-(propane-2,2-diyl)bis(4-phenyl-4,5-dihydrooxazole) (L1·NiCl$_2$)

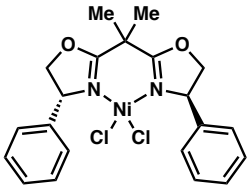

Prepared from bis(oxazoline) **L1** (67 mg, 0.2 mmol) and nickel(II) chloride (26 mg, 0.2 mmol) following General Procedure 1. The crude residue was recrystallized from DCM/pentane by slow

evaporation to yield green crystals of **L1**·$\mathbf{NiCl_2}$ as the hydrated chloride bridged dimer complex.

4.7.3 Electronic Absorption

A series of 20 mL scintillation vials were charged with the **L2**·$NiCl_2$ complex (4.4 – 5.0 mg) and desired solvent (5 mL of CH_2Cl_2, MeCN, acetone, EtOAc, DMA, NMP, DMF, DMPU, DMSO, or water). The solutions were analyzed with a UV/Visible spectrometer after collecting blank samples of each solvent. Absorbance data was converted to extinction coefficients (M^{-1} cm^{-1}) by using the measured mass, volume of solvent, and the path length of the quartz cuvette (1 cm).

4.7.4 Cyclic Voltammetry

A 20 mL scintillation vial was charged with the **L2**·$NiCl_2$ complex (5.9 mg, 0.012 mmol) and Bu_4NPF_6 (387.6 mg, 10 mmol). Then anhydrous DMA (10 mL) was added and the solution was stirred to ensure homogeneity. The final concentration of each compound was 1.2 mM **L2**·$NiCl_2$ and 0.1 M Bu_4NPF_6. To a second 20 mL scintillation vial was added **L2**·$NiCl_2$ (10.2 mg, 0.021 mmol), ferrocene (3.8 mg, 0.02 mmol), and Bu_4NPF_6 (774.9 mg, 20 mmol). Then anhydrous DMA (20 mL) was added and the solution was stirred to ensure homogeneity. The final concentration of each compound was 1.1 mM **L2**·$NiCl_2$, 1 mM, ferrocene, and 0.1 M Bu_4NPF_6. A three electrode cell with a glassy carbon disk working electrode, a silver wire pseudo-reference electrode, and a graphite rod auxillary electrode was connected to the potentiostat and the electrodes were placed in the solution. Cyclic voltammetry was used to determine the reduction potential of **L2**·$NiCl_2$ while scanning at

a rate of 0.1 V/s against the Ag wire reference electrode. The potential was normalized by setting the Fc/Fc^+ redox couple to 0.0 V.

4.7.5 EPR Spectroscopy

EPR of L2·NiX Complexes

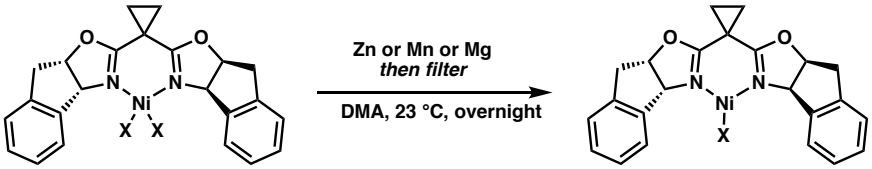

To a 2 dram vial in the glovebox was added **L2**·$NiCl_2$ or **L2**·$NiBr_2$ (0.01–0.10 mmol, 1 equiv), the metal reductant (0.1–1.0 mmol, 10 equiv), and anhydrous DMA (1 mL). The solution was stirred at room temperature overnight to produce a dark orange solution. The reaction mixture was filtered through a Kimwipe plug in a glass pipet to remove excess reductant, added to a quartz EPR tube, and sealed. The sample was brought out of the glovebox and immediately frozen in liquid nitrogen. EPR spectra were collected at 77 K. EPR simulations of 0.01 mM **L2**·NiCl were conducted using EasySpin in MATLAB. The simulated parameters were defined as follows: g_1: 2.4879, g_2: 2.1588, g_3: 2.1092, A_{Cl}: 1.2 MHz, Line Width: 4.4773, Microwave Frequency: 9.5 GHz, Range: 1000 G - 4000 G, Temperature: 77 K, RMSD: 0.0288.

EPR of L2·$NiR_{alkenyl}$ from $Ni(cod)_2$

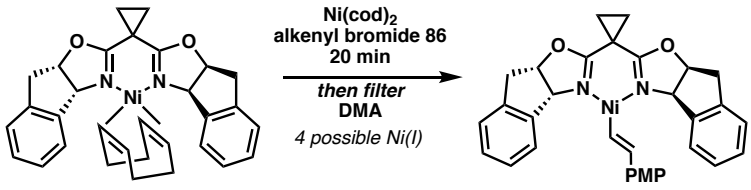

The $Ni(cod)_2$ (5.6 mg, 0.02 mmol, 2 equiv) and bis(oxazoline) ligand **L2** (3.7 mg, 0.01 mmol, 1 equiv) were added to a 2 dram vial in the glovebox and dissolved in DMA (1 mL). The solution was stirred for 14 hours and turned an orange-red color. The alkenyl bromide **86** (2.2 mg, 0.01 mmol, 1 equiv) was added and stirred for 20 minutes before being filtered through a Kimwipe plug in a glass pipet. The solution was added to a quartz EPR tube, sealed, brought out of the glovebox, and immediately frozen in liquid nitrogen. EPR spectra were collected at 77 K. Upon continued stirring (> 1 day), the solution turned purple, plated out Ni^0, contained no Ni(I) signal by EPR, and alkenyl dimer was detected by GCMS.

EPR of L2·NiR$_{alkenyl}$ complex from L2·NiCl$_2$

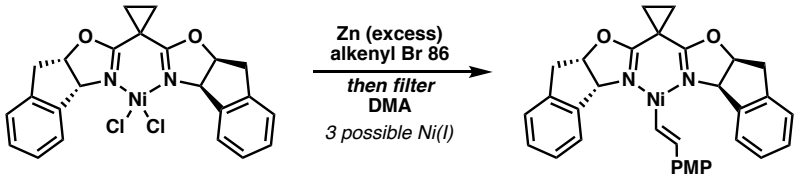

The **L2**·$NiCl_2$ complex (4.7 mg, 0.01 mmol, 1 equiv) and zinc dust (6.9 mg, 0.1 mmol, 10 equiv) were added to a 2 dram vial in the glovebox and dissolved in DMA (1 mL). The solution was stirred for 10 minutes. The alkenyl bromide **86** (2.2 mg, 0.01 mmol, 1 equiv) was added and stirred for an additional 20 minutes before being filtered through a Kimwipe plug in a glass pipet. The solution was added to a quartz EPR tube, sealed, brought out of the glovebox, and immediately frozen in liquid nitrogen. EPR spectra were collected at 77 K. Upon continued stirring (> 1 day), the solution turned a brown/orange, contained trace Ni(I) signal by EPR, and alkenyl dimer was visible by GC-MS analysis.

Figure 4.32 *EPR spectra of* ***L2***·$NiCl_2$ *reduction in the presence of alkenyl bromide.*

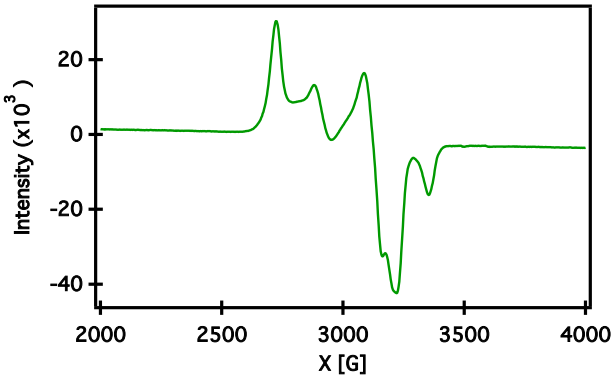

4.7.6 Stoichiometric Ni(0) Studies

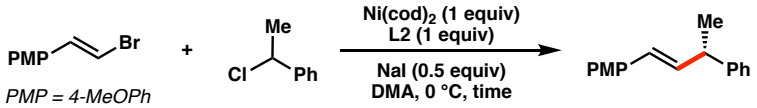

To a 10 mL round bottom flask (6 h reactions) or a 20 mL scintillation vial (24 h reactions) equipped with a magnetic stir bar was added alkenyl bromide **86** (42.9 mg, 0.2 mmol, 1 equiv), NaI (15.4 mg, 0.1 mmol, 0.5 equiv), and ligand **L2** (71.7 mg, 0.2 mmol, 1 equiv). The vial was brought into the glovebox and the $Ni(cod)_2$ (55.4 mg, 0.2 mmol, 1 equiv) was added followed by 2 mL of anhydrous DMA. The reaction was cooled to 0 °C before benzyl chloride **167** (26 μL, 0.2 mmol, 1 equiv) was added. The reaction was warmed to room temperature before an internal standard (25 μL benzyl ether) was added. The reaction was quenched with 5 mL of 1 M HCl followed by 5 mL of water. The organic material was extracted with diethyl ether (3 x 10 mL), washed with brine (10 mL) and dried with $MgSO_4$ before being filtered and concentrated. The crude mixture was analyzed by ^1H NMR and chiral SFC to obtain the product yield and ee.

4.7.7 Scalemic Ligand Study

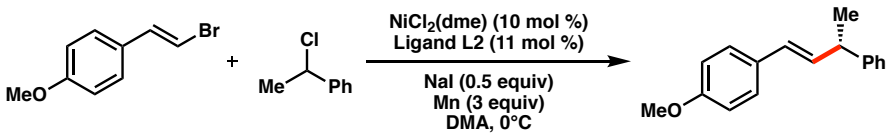

The reaction was conducted under the reported reaction conditions,[8] however a mixture of the two enantiomers of the ligand was made to conduct the reaction with scalemic ligand. The ee of the ligand used was 0, 15, 30, 50, 75, 90, and 100% ee. The measured % ee of the product was graphed as a function of the % ee of the ligand to give a linear trend of $y = 0.90x - 0.99$ with an $R^2 = 0.99$.

4.7.8 Analysis of Reaction by ^{19}F NMR

Benzyl Chloride ^{19}F Label

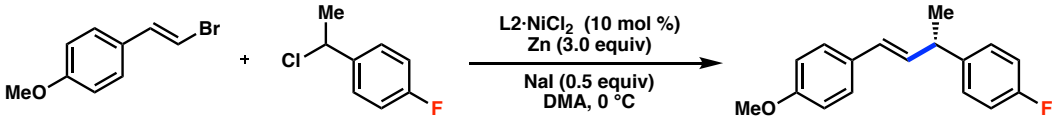

The reaction was conducted as described in literature with the exception of Zn as the reductant.[8] A fluorine tag was incorporated on the benzyl chloride electrophile. The reaction products were monitored by ^{19}F NMR over the course of the reaction by analyzing aliquots with C_6F_6 as an internal standard.

Alkenyl Bromide ^{19}F Label

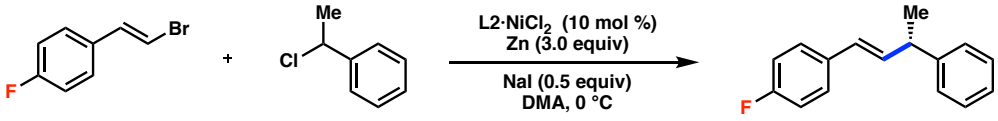

The reaction was conducted as described in literature with the exception of Zn as the reductant.[8] A fluorine tag was incorporated on the alkenyl bromide electrophile. The reaction products were monitored by ^{19}F NMR over the course of the reaction by analyzing aliquots with C_6F_6 as an internal standard.

4.7.9 Kinetics Procedures, Standards, and GC-FID Fits

Standard Reaction with Zinc Powder

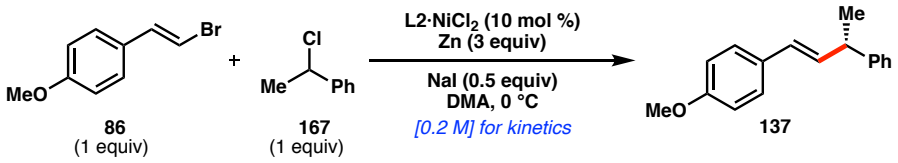

A 10 mL round bottom flask with a small magnetic stirring rod was charged with the sodium iodide (22.5 mg, 0.15 mmol, 0.5 equiv) and zinc dust (58.8 mg, 0.9 mmol, 3 equiv). The flask was sealed with a rubber septum, purged with N_2, and cooled to 0 °C by being placed in an ice water bath. Alkenyl bromide **86** (85.2 mg, 0.4 mmol) and **L2**·$NiCl_2$ (19.4 mg, 0.04 mmol) were added to a 2 mL volumetric flask, sealed with a rubber septum, and purged with N_2. Benzyl chloride **167** (53 μL, 0.4 mmol) and dodecane (48 μL) as an internal standard were added via syringe to the volumetric flask. Then anhydrous DMA was added to the volumetric flask until it reached the 2 mL line. A small stir bar was added to the volumetric flask and the solution was stirred until all of the reagents dissolved. The solution was taken up into a 2 mL syringe to ensure homogeneity, and then 1.5 mL of the solution was added to the round bottom flask. The reaction was stirred under a positive N_2 flow by using an IKA stir plate set to a stirring speed of 1500 rpm. At appropriate time points, approximately 50 μL of the solution was removed by syringe (syringe and needle

were pre-flushed with N_2), loaded onto a short silica plug (1 cm) in a glass pipette packed with cotton. The crude mixture was flushed through the silica plug with 2 mL of 10% EtOAc/hexane directly into GC vials and analyzed by GC-FID. Upon the completion of data collection, the remaining volume of the reaction in the round bottom flask was also analyzed by chiral phase SFC to obtain the enantioselectivity (% ee) of the cross-coupled product.

All data runs obtained from the GC-FID instrument were appropriately integrated for the product and the dodecane standard. The integrated data points were further processed by normalizing each product area value by its corresponding standard area value. The normalized areas were then converted to concentration by using calculated response factors obtained from preparing known mixtures of the standard and purified reaction product. Each reaction was analyzed and graphed to show the product concentration (M) as a function of reaction time (min). All data points were plotted with blue markers (•) as shown below, while only the data points included in the linear fit are shown with red markers (•). The best-fit linear regression line is also shown and the y=mx+b equation is given. Each reaction was run in duplicates as indicated by Trial 1 and Trial 2.

Figure 4.33 *Standard reaction conditions.*

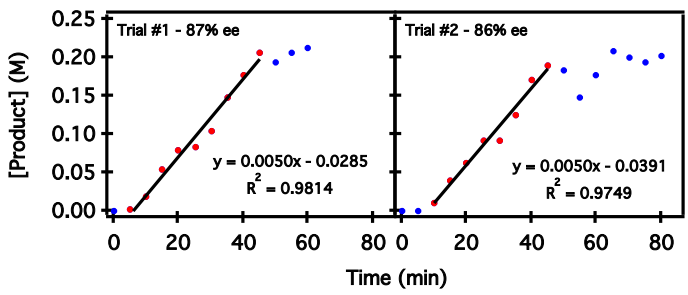

Effect of Changing Ni Loading

The standard reaction procedure was followed, except varying amounts of **L2**·$NiCl_2$ were added to give final loadings of 5%, 7%, 14%, and 20% nickel.

Figure 4.34 *Reaction conditions with 5% **L2**·$NiCl_2$.*

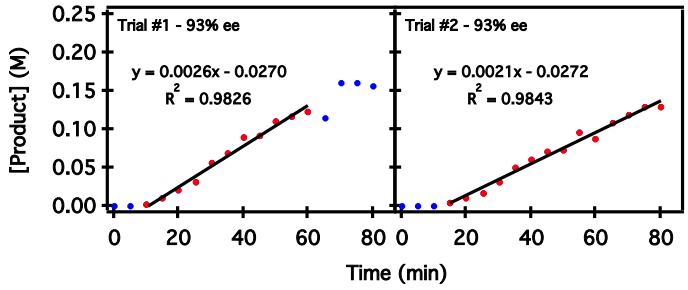

Figure 4.35 *Reaction conditions with 7% **L2**·$NiCl_2$.*

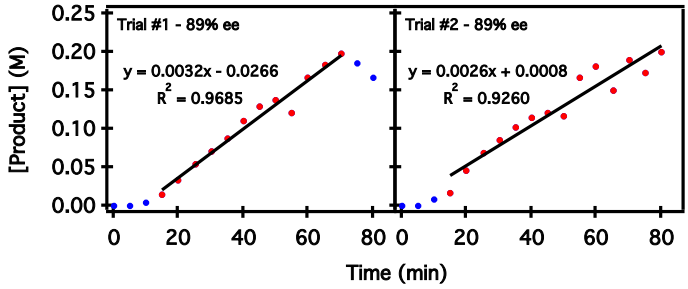

Figure 4.36 *Reaction conditions with 14% **L2**·$NiCl_2$.*

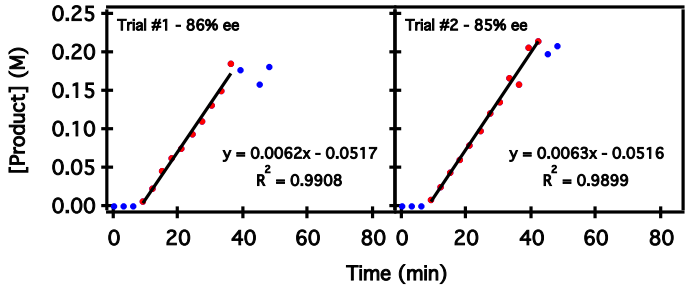

Figure 4.37 *Reaction conditions with 20% **L2**·$NiCl_2$.*

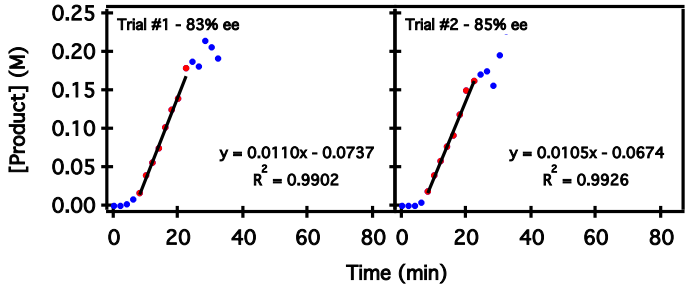

4.7.9.1 Effect of Changing Alkenyl Bromide Equivalents

The general reaction procedure was followed, except varying amounts of alkenyl bromide **86** were added to give final amounts of 1.5, 2, 3, and 4 equivalents.

Figure 4.38 *Reaction conditions with 1.5 equivalents of alkenyl bromide **86**.*

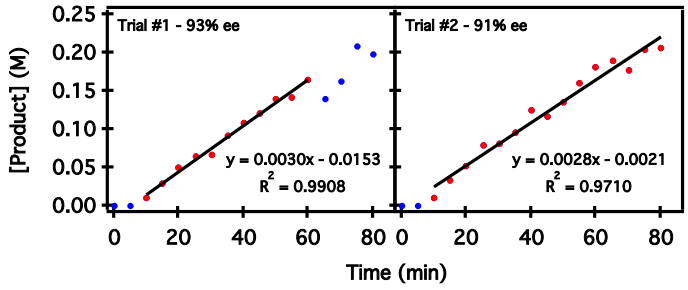

Figure 4.39 *Reaction conditions with 2.0 equivalents of alkenyl bromide **86**.*

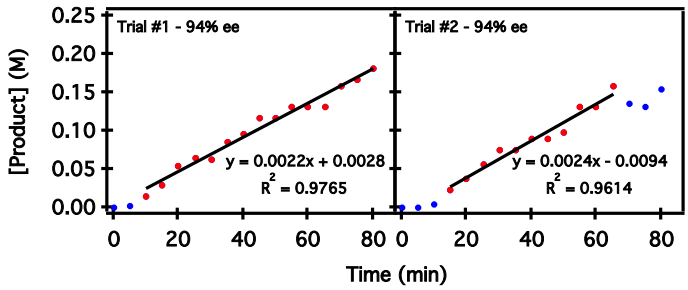

Figure 4.40 *Reaction conditions with 3.0 equivalents of alkenyl bromide* ***86***.

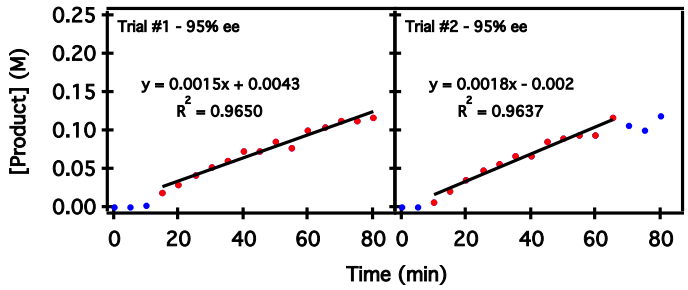

Figure 4.41 *Reaction conditions with 4.0 equivalents of alkenyl bromide* ***86***.

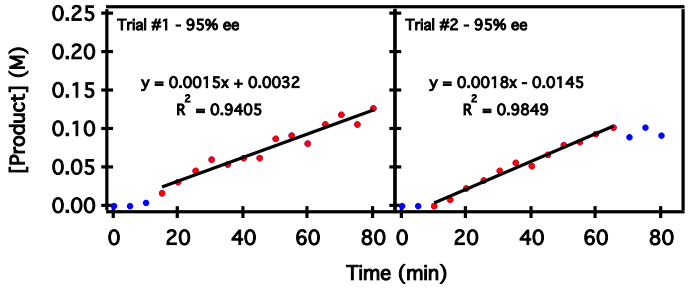

Effect of Changing Benzyl Chloride Equivalents

The general reaction procedure was followed, except varying amounts of benzyl chloride **167** were added to give final amounts of 1.5, 2, 3, and 4 equivalents.

Figure 4.42 *Reaction conditions with 1.5 equivalents of benzyl chloride* ***167***.

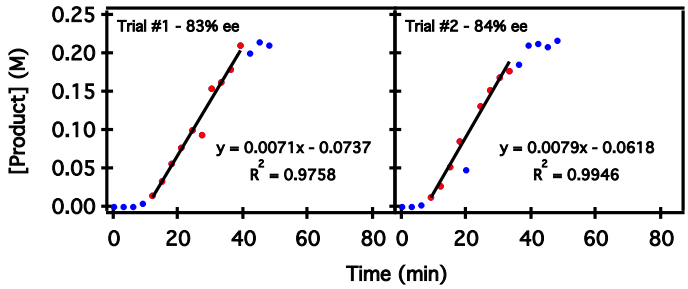

Figure 4.43 *Reaction conditions with 2.0 equivalents of benzyl chloride* ***167****.*

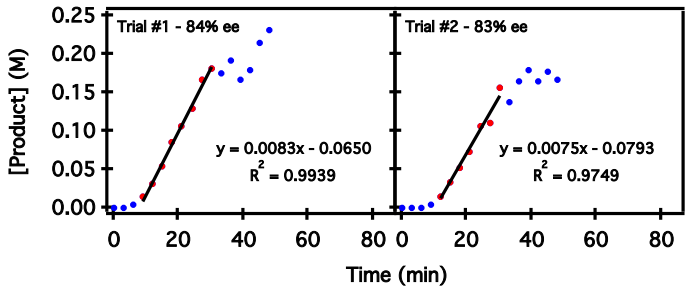

Figure 4.44 *Reaction conditions with 3.0 equivalents of benzyl chloride* ***167****.*

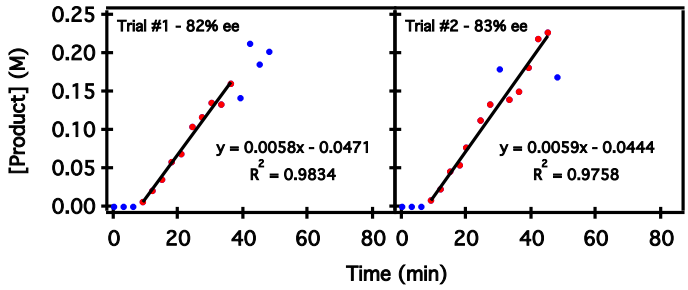

Figure 4.45 *Reaction conditions with 4.0 equivalents of benzyl chloride* ***167****.*

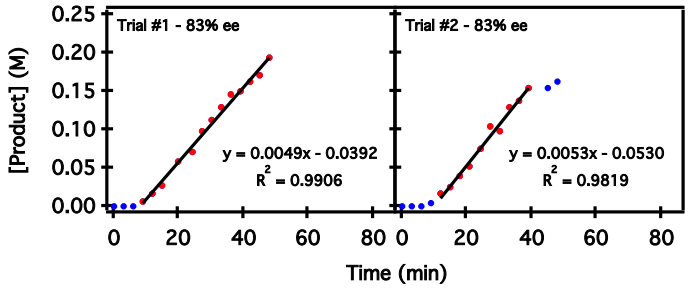

Effect of Other Reagent Equivalents

The general reaction procedure was followed, except the sodium iodide and zinc dust equivalents were varied. Furthermore, the general reaction was conducted in the presence of 4-methoxystyrene.

Figure 4.46 *Reaction conditions with 6 equivalents of zinc.*

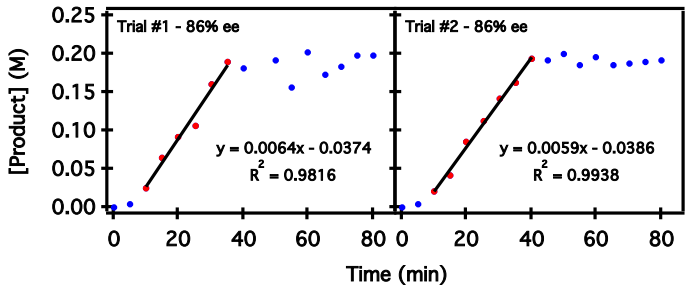

Figure 4.47 *Reaction conditions without NaI.*

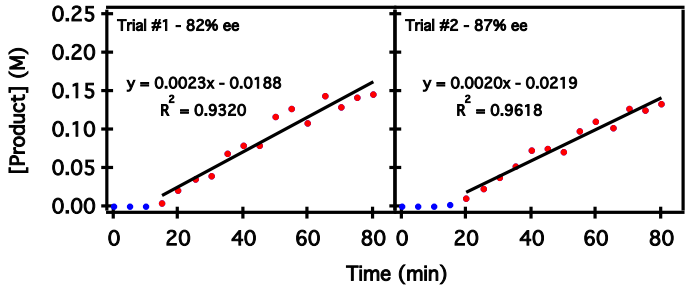

Figure 4.48 *Reaction conditions with with an added equivalent of 4-methoxystyrene.*

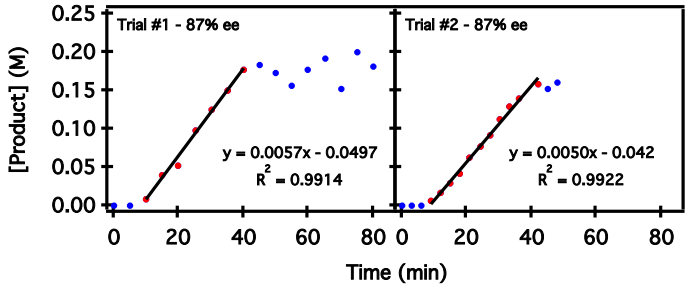

GC-FID Standards

Three standards were made to normalize the GC-FID area counts and convert the obtained data into reaction concentration (M) values. The purified reaction product and dodecane standard were each added to a 20 mL vial and massed on a balance. The mixture was

dissolved in 2 mL of ether and transferred to a GC vial for analysis. The density of dodecane (0.75 g/mL) was also used to convert the area values to concentration.

Table S5: *GC-FID standards and response factors.*

Trial	Mass PDT (mg)	Mass STD (mg)	PDT MW (g/mol)	STD MW (g/mol)	PDT Area	STD Area	Response Factor
A	3.6	4.6	238.33	170.33	17586	50259	0.626
B	7.0	7.1	238.33	170.33	42861	81360	0.748
C	3.7	5.5	238.33	170.33	20735	66615	0.647
						AVG	**0.674**

4.7.10 Radical Clock Experiments

(chloro(cyclopropyl)methyl)benzene (198)

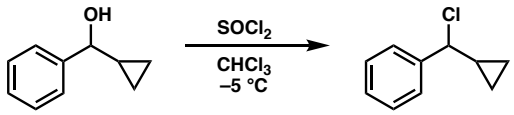

The benzyl alcohol **198** (237 mg, 1.6 mmol, 1 equiv) was dissolved in 5.3 mL of $CHCl_3$ (purified by filtering through a plug of dried basic alumina) in a flame-dried flask under N_2. The reaction was cooled to –5 °C and $SOCl_2$ (139 μL, 1.92 mmol, 1.2 equiv) was added. Reaction was allowed to stir for 10 minutes before being concentrated. A separate reaction sample was analyzed by ^1H and ^{13}C NMR in $CDCl_3$. For the cross-coupling experiments, the concentrated sample was dissolved in anhydrous DMA to prepare **198** as a 0.2 M solution and added to the reaction without further purification. **^{1}H NMR (300 MHz, $CDCl_3$):** δ 7.52 – 7.45 (m, 2H), 7.44 – 7.29 (m, 3H), 4.33 (d, *J* = 9.2 Hz, 1H), 1.70 – 1.50 (m, 1H), 0.85 (dddd, *J* = 8.8, 7.9, 5.9, 4.4 Hz, 1H), 0.78 – 0.66 (m, 1H), 0.66 – 0.56 (m,

1H), 0.46 (ddt, J = 9.1, 5.6, 4.6 Hz, 1H). **^{13}C NMR (75 MHz, $CDCl_3$):** δ 141.7, 128.6, 128.3, 127.2, 69.1, 20.0, 6.6, 6.4.

(*R*,*E*)-1-(3-cyclopropyl-3-phenylprop-1-en-1-yl)-4-methoxybenzene (161a)

1-methoxy-4-((1*E*,5*E*)-6-phenylhexa-1,5-dien-1-yl)benzene (161b)

1-methoxy-4-((*S*,1*E*,4*E*)-3-methyl-5-phenylpenta-1,4-dien-1-yl)benzene (161c)

1-methoxy-4-((*S*,1*E*,4*E*)-3-phenylhexa-1,4-dien-1-yl)benzene (161d)

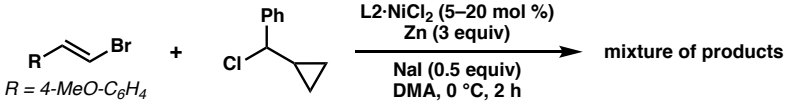

The reaction was conducted as described in literature (0.2 mmol scale) with the exception of Zn as the reductant and the benzyl chloride **198** being added as a solution in DMA.[8] The alkenyl bromide **86** (42.6 mg, 0.2 mmol, 1 equiv), **L2**·$NiCl_2$ (4.8–19.4 mg, 0.01–0.04 mmol, 0.05–0.20 equiv), Zn (39.2 mg, 0.6 mmol, 3 equiv), and NaI (15.0 mg, 0.1 mmol, 0.5 equiv) were added to a round bottom flask, sealed with a septa, and purged with N_2. The flask was cooled to 0 °C before the benzyl chloride (0.2 mmol) in DMA (0.2 mL) was added. The reactions were stirred for 2 hours, then quenched with aq. 1 M HCl (10 mL), extracted with Et_2O (3 x 10 mL), and purified by column chromatography to isolate 17.3 mg (5 mol % Ni), 17.6 mg (10 mol % Ni), and 17.4 mg (20 mol % Ni) of the product mixture (**161a**–**d**).

4.8 REFERENCES

(1) Weix, D. J. *Acc. Chem. Res.* **2015**, *48*, 1767.

(2) Durandetti, M.; Gosmini, C.; Périchon, J. *Tetrahedron* **2007**, *63*, 1146.

(3) Everson, D. A.; Shrestha, R.; Weix, D. J. *J. Am. Chem. Soc.* **2010**, *132*, 920.

(4) Everson, D. A.; Jones, B. A.; Weix, D. J. *J. Am. Chem. Soc.* **2012**, *134*, 6146.

(5) Wotal, A. C.; Weix, D. J. *Org. Lett.* **2012**, *14*, 1476.

(6) Yu, X.; Yang, T.; Wang, S.; Xu, H.; Gong, H. *Org. Lett.* **2011**, *13*, 2138.

(7) Cherney, A. H.; Kadunce, N. T.; Reisman, S. E. *J. Am. Chem. Soc.* **2013**, *135*, 7442.

(8) Cherney, A. H.; Reisman, S. E. *J. Am. Chem. Soc.* **2014**, *136*, 14365.

(9) Hofstra, J. L.; Cherney, A. H.; Ordner, C. M.; Reisman, S. E. *J. Am. Chem. Soc.* **2018**, *140*, 139.

(10) Suzuki, N.; Hofstra, J. L.; Poremba, K. E.; Reisman, S. E. *Org. Lett.* **2017**, *19*, 2150.

(11) Kadunce, N. T.; Reisman, S. E. *J. Am. Chem. Soc.* **2015**, *137*, 10480.

(12) Poremba, K. E.; Kadunce, N. T.; Suzuki, N.; Cherney, A. H.; Reisman, S. E. *J. Am. Chem. Soc.* **2017**, *139*, 5684.

(13) Biswas, S.; Weix, D. J. *J. Am. Chem. Soc.* **2013**, *135*, 16192.

(14) Ren, Q.; Jiang, F.; Gong, H. *J. Organomet. Chem.* **2014**, *770*, 130.

(15) Anka-Lufford, L. L.; Huihui, K. M. M.; Gower, N. J.; Ackerman, L. K. G.; Weix, D. J. *Chem. Eur. J.* **2016**, *22*, 11564.

(16) Suh, Y.; Lee, J.; Kim, S.-H.; Rieke, R. D. *J. Organomet. Chem.* **2003**, *684*, 20.

(17) Peng, Z.; Knochel, P. *Org. Lett.* **2011**, *13*, 3198.

(18) Benischke, A. D.; Breuillac, A. J. A.; Moyeux, A.; Cahiez, G.; Knochel, P. *Synlett* **2016**, *27*, 471.

(19) Benischke, A. D.; Desaintjean, A.; Juli, T.; Cahiez, G.; Knochel, P. *Synthesis* **2017**, *49*, 5396.

(20) Breitenfeld, J.; Wodrich, M. D.; Hu, X. *Organometallics* **2014**, *33*, 5708.

(21) Chen, C.-T.; Liao, S.-Y.; Lin, K.-J.; Chen, C.-H.; Lin, T.-Y. J. *Inorg. Chem.* **1999**, *38*, 2734.

(22) Vanýsek, P. *Handbook of Chemistry and Physics*, 93rd ed.; 2012.

(23) Jones, G. D.; Martin, J. L.; McFarland, C.; Allen, O. R.; Hall, R. E.; Haley, A. D.; Brandon, R. J.; Konovalova, T.; Desrochers, P. J.; Pulay, P.; Vicic, D. A. *J. Am. Chem. Soc.* **2006**, *128*, 13175.

(24) Schley, N. D.; Fu, G. C. *J. Am. Chem. Soc.* **2014**, *136*, 16588.

(25) Oderinde, M. S.; Frenette, M.; Robbins, D. W.; Aquila, B.; Johannes, J. W. *J. Am. Chem. Soc.* **2016**, *138*, 1760.

(26) Zhao, P.; Luo, Y.-W.; Xue, T.; Zhang, A.-J.; Lu, J.-X. *Chinese J. Chem.* **2006**, *24*, 877.

(27) Ge, P.; Riordan, C. G.; Yap, G. P. A.; Rheingold, A. L. *Inorg. Chem.* **1996**, *35*, 5408.

(28) Halgren, T. A.; Roberts, J. D.; Horner, J. H.; Martinez, F. N.; Tronche, C.; Newcomb, M. *J. Am. Chem. Soc.* **2000**, *122*, 2988.

(29) *Encyclopedia of Radicals in Chemistry, Biology and Materials*; John Wiley & Sons, Ltd., 2012.

(30) Buskirk, A.; Baradaran, H. *J. Chem. Educ.* **2009**, *86*, 551.

(31) Still, W. C.; Kahn, M.; Mitra, A. *J. Org. Chem.* **1978**, *43*, 2923.

(32) Evans, D. A.; Downey, C. W.; Hubbs, J. L. *J. Am. Chem. Soc.* **2003**, *125*, 8706.

Appendix 5

Spectra Relevant to Chapter 4:

Mechanistic Investigations of Ni-Catalyzed Asymmetric

Reductive Cross-Couplings with Alkenyl Bromide Electrophiles

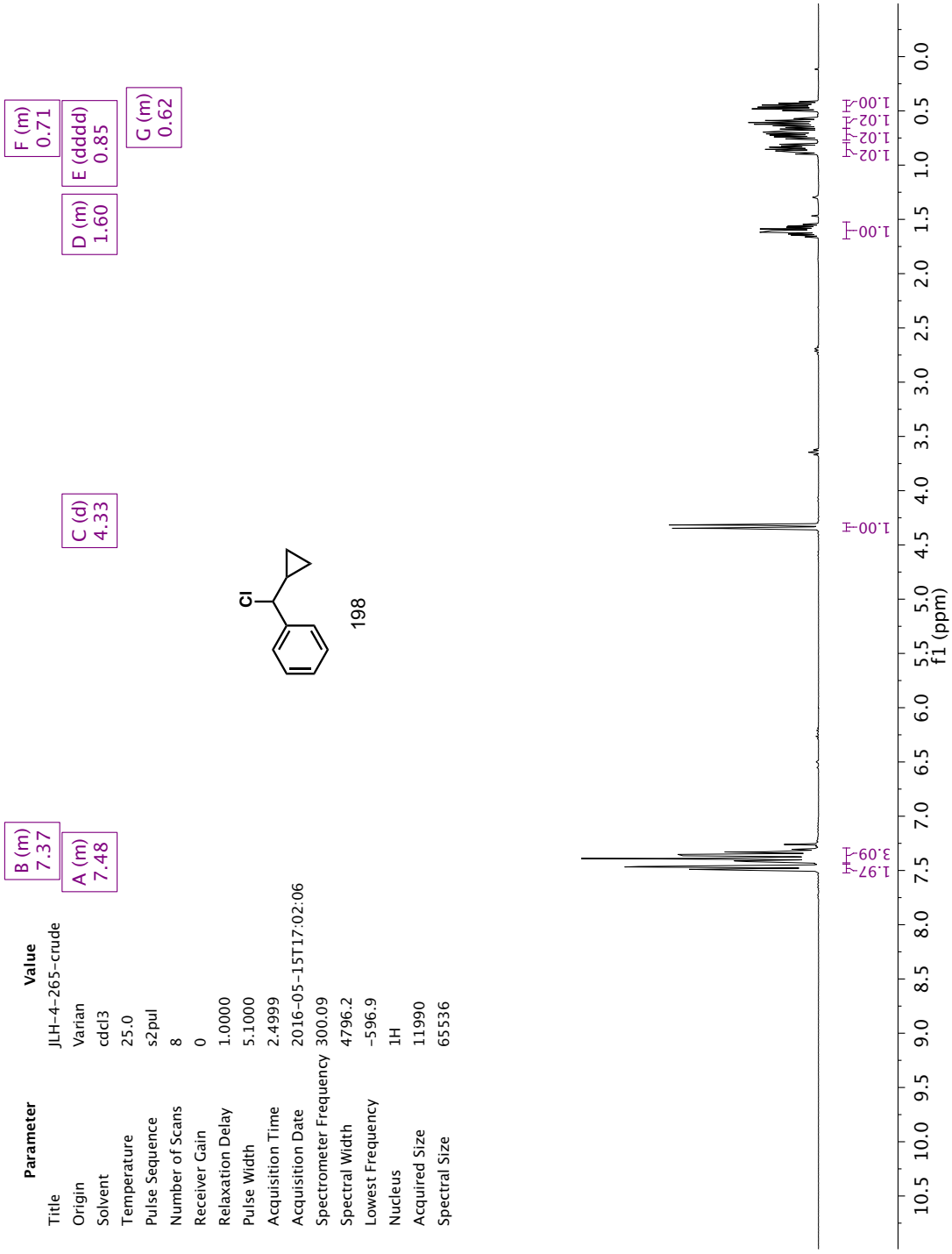

Parameter	Value
Title	JLH-4-265-crude
Origin	Varian
Solvent	cdcl3
Temperature	25.0
Pulse Sequence	s2pul
Number of Scans	8
Receiver Gain	0
Relaxation Delay	1.0000
Pulse Width	5.1000
Acquisition Time	2.4999
Acquisition Date	2016-05-15T17:02:06
Spectrometer Frequency	300.09
Spectral Width	4796.2
Lowest Frequency	-596.9
Nucleus	1H
Acquired Size	11990
Spectral Size	65536

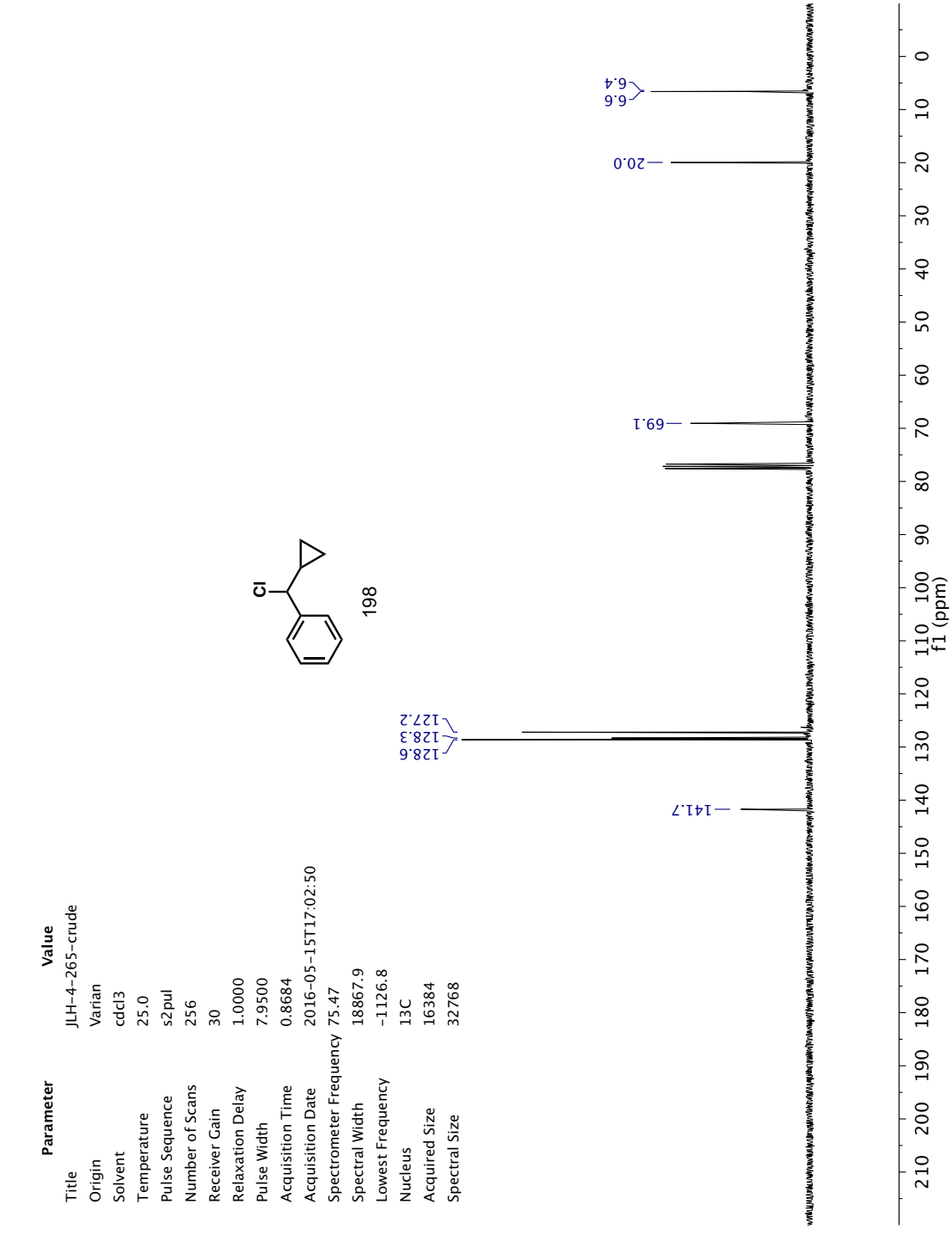
Parameter Value
Title JLH-4-265-crude
Origin Varian
Solvent cdcl3
Temperature 25.0
Pulse Sequence s2pul
Number of Scans 256
Receiver Gain 30
Relaxation Delay 1.0000
Pulse Width 7.9500
Acquisition Time 0.8684
Acquisition Date 2016-05-15T17:02:50
Spectrometer Frequency 75.47
Spectral Width 18867.9
Lowest Frequency -1126.8
Nucleus 13C
Acquired Size 16384
Spectral Size 32768
Cl
198
141.7
128.6
128.3
127.2
69.1
20.0
6.6
6.4
f1 (ppm)

Appendix 6

X-Ray Crystallography Reports Relevant to Chapter 4:

Mechanistic Investigations of Ni-Catalyzed Asymmetric

Reductive Cross-Couplings with Alkenyl Bromide Electrophiles

A6.1 STRUCTURAL DETERMINATION AND REFINEMENT DETAILS

Low-temperature diffraction data (ϕ- and ω-scans) were collected on either a Bruker AXS D8 VENTURE KAPPA diffractometer or Bruker AXS KAPPA APEXII diffractometer coupled to a PHOTON 100 CMOS detector with either Mo-$K\alpha$ radiation (λ = 0.71073 Å) or Cu-$K\alpha$ radiation (λ = 1.54178 Å) from an $I_\mu S$ HB micro-focused X-ray tube. All diffractometer manipulations, including data collection integration, and scaling were carried out using the Bruker APEXII software.[1] Absorption corrections were applied using SADABS.[2] The structure was solved by intrinsic phasing using SHELXT[3] and refined against F^2 on all data by full-matrix least squares with SHELXL-2014[4] using established refinement techniques.[5] All non-hydrogen atoms were refined anisotropically. All hydrogen atoms were included in the model at geometrically calculated positions and refined using a riding model. The isotropic displacement parameters of all hydrogen atoms were fixed to 1.2 times the U value of the atoms they are linked to (1.5 times for methyl groups). Absolute configuration was determined by anomalous dispersion.[6] Graphical representation of the structure with 50% probability thermal ellipsoids was generated using Mercury visualization software.

A6.2 CRYSTALLOGRAPHIC ANALYSIS OF L9·$NiCl_2$

A6.2.1 Special Refinement Details

Figure A6.1 *Rendering of Ni-complex* ***L9***·$NiCl_2$.

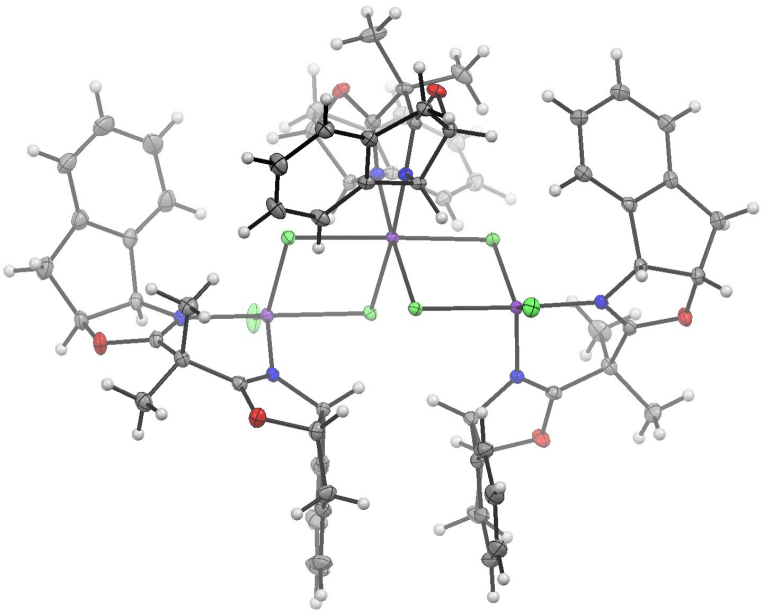

L9·$NiCl_2$ crystallizes in the monoclinic space group $P2_1$ with one molecule (consisting of three ligand·nickel subunits) in the asymmetric unit. Data was collected with Mo-$K\alpha$ radiation (λ = 0.71073 Å) at 100 K. Two molecules of dichloromethane (one disordered over two positions) and 0.299 molecules of water are co-crystallized in the unit cell. One chloride atom bound to nickel was disordered over two positions (Cl1, Cl1A), which was refined with the help of a similarity restraint on the Ni-Cl distance. The highest electron density maxima was modeled as a partially occupied water, 0.299(9). The hydrogen atoms for this water could not be located in the difference Fourier synthesis and were not included in the model. Solvent and disorder is omitted for clarity in the graphical representation. Absolute configuration was determined by anomalous dispersion (Flack = 0.004(4)).[6]

A6.2.2 Crystallographic Tables

Table A6.1. *Crystal data and structure refinement for* ***L9***·$NiCl_2$.

Identification code	A15003	
Empirical formula	$C_{69}H_{66}Cl_6N_6Ni_3O_6$, $2(CH_2Cl_2)$, $0.30(H_2O)$	
Formula weight	1639.36	
Temperature	100 K	
Wavelength	0.71073 Å	
Crystal system	Monoclinic	
Space group	$P2_1$	
Unit cell dimensions	a = 14.8865(7) Å	α = 90°.
	b = 15.8024(8) Å	β = 112.892(3)°.
	c = 16.5046(8) Å	γ = 90°.
Volume	3576.8(3) $Å^3$	
Z	2	
Density (calculated)	1.522 Mg/m^3	
Absorption coefficient	1.212 mm^{-1}	
F(000)	1686	
Crystal size	0.300 x 0.300 x 0.150 mm^3	
Theta range for data collection	1.485 to 36.533°.	
Index ranges	-24<=h<=24, -26<=k<=26, -27<=l<=27	
Reflections collected	118450	
Independent reflections	34801 [R(int) = 0.0572]	
Completeness to theta = 25.242°	100.0 %	
Absorption correction	Semi-empirical from equivalents	
Max. and min. transmission	0.7471 and 0.6710	
Refinement method	Full-matrix least-squares on F^2	
Data / restraints / parameters	34801 / 2 / 919	
Goodness-of-fit on F^2	0.984	
Final R indices [I>2sigma(I)]	R1 = 0.0410, wR2 = 0.0779	
R indices (all data)	R1 = 0.0604, wR2 = 0.0843	
Absolute structure parameter	0.004(4)	
Extinction coefficient	n/a	
Largest diff. peak and hole	1.023 and -0.795 $e.Å^{-3}$	

A6.3 CRYSTALLOGRAPHIC ANALYSIS OF L20·$NiCl_2$

A6.3.1 Special Refinement Details

Figure A6.2 *Rendering of Ni-complex* ***L20***·$NiCl_2$.

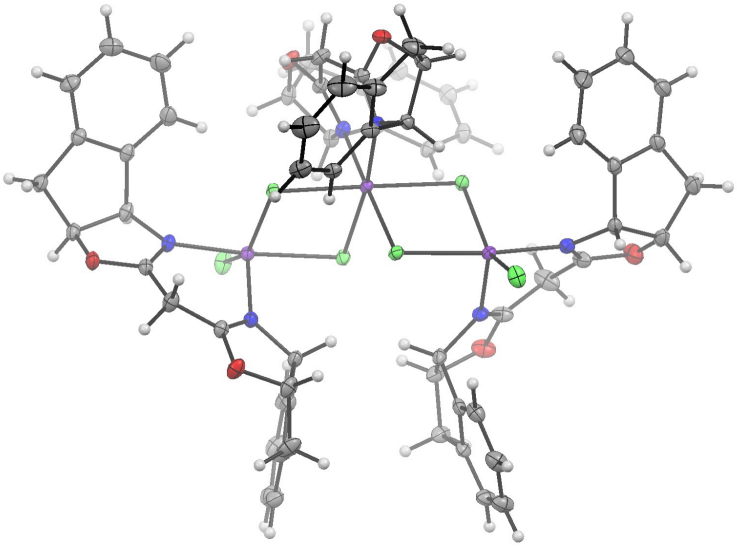

L20·$NiCl_2$ crystallizes in the monoclinic space group $P2_1$ with one molecule (consisting of three ligand·nickel subunits) in the asymmetric unit. Data was collected with Mo-$K\alpha$ radiation (λ = 0.71073 Å) at 100 K. Three molecules of dichloromethane (one was disordered over two positions) are co-crystallized in the unit cell. Solvent is omitted for clarity in the graphical representation. Absolute configuration was determined by anomalous dispersion (Flack = 0.0158(16)).[6]

A6.3.2 Crystallographic Tables

Table A6.2. *Crystal data and structure refinement for* ***L20***·$NiCl_2$.

Identification code	A15002	
Empirical formula	$C_{63}H_{54}Cl_6N_6Ni_3O_6$, $3(CH_2Cl_2)$	
Formula weight	1634.73	
Temperature	100 K	
Wavelength	0.71073 Å	
Crystal system	Orthorhombic	
Space group	$P2_12_12_1$	
Unit cell dimensions	a = 14.7835(6) Å	α = 90°.
	b = 17.8882(7) Å	β = 90°.
	c = 25.4545(11) Å	γ = 90°.
Volume	6731.4(5) $Å^3$	
Z	4	
Density (calculated)	1.613 Mg/m^3	
Absorption coefficient	1.364 mm^{-1}	
F(000)	3336	
Crystal size	0.45 x 0.34 x 0.22 mm^3	
Theta range for data collection	1.391 to 46.357°.	
Index ranges	-29<=h<=29, -36<=k<=36, -51<=l<=51	
Reflections collected	460634	
Independent reflections	58243 [R(int) = 0.0568]	
Completeness to theta = 25.000°	100.0 %	
Absorption correction	Semi-empirical from equivalents	
Max. and min. transmission	1.0000 and 0.9071	
Refinement method	Full-matrix least-squares on F^2	
Data / restraints / parameters	58243 / 0 / 851	
Goodness-of-fit on F^2	1.025	
Final R indices [I>2sigma(I)]	R1 = 0.0418, wR2 = 0.0937	
R indices (all data)	R1 = 0.0619, wR2 = 0.1025	
Absolute structure parameter	0.0158(16)	
Extinction coefficient	n/a	
Largest diff. peak and hole	1.741 and -1.330 e.$Å^{-3}$	

A6.4 CRYSTALLOGRAPHIC ANALYSIS OF L1·$NiCl_2$

A6.4.1 Special Refinement Details

Figure A6.3 *Rendering of Ni-complex* ***L1***·$NiCl_2$.

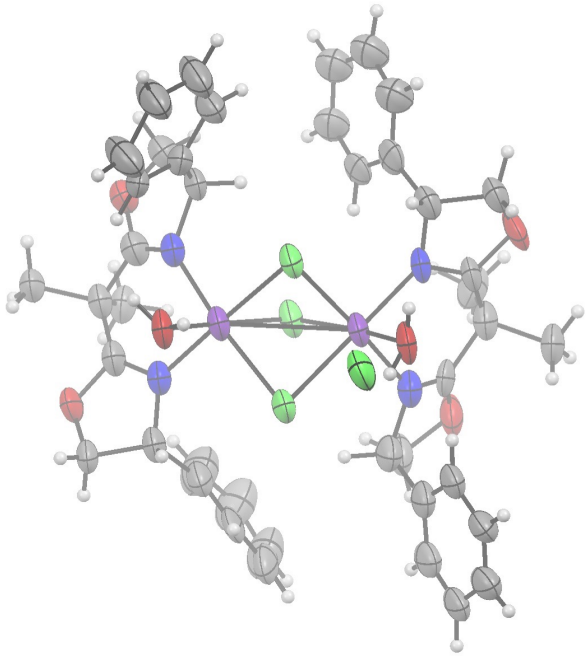

L1·$NiCl_2$ hydrate crystallizes in the orthorhombic space group $P2_12_12_1$ with one molecule (consisting of two ligand·nickel subunits) in the asymmetric unit. Data was collected with Cu-$K\alpha$ radiation (λ = 1.54178 Å) at 100 K. The sample was not stable once removed from the crystallization environment, thus resulting in poor data quality. The structure was refined to R1=13.82% with the aid of enhanced rigid bond restraints. The absolute configuration was determined by anomalous dispersion (Flack = –0.01(5)).[6]

A6.4.2 Crystallographic Tables

Table A6.3. *Crystal data and structure refinement for* ***L1***·$NiCl_2$.

Identification code	P15389	
Empirical formula	$C_{42}H_{48}C_{l4}N_4Ni_2O_6$	
Formula weight	964.06	
Temperature	100 K	
Wavelength	1.54178 Å	
Crystal system	Orthorhombic	
Space group	$P2_12_12_1$	
Unit cell dimensions	a = 21.3526(8) Å	α = 90°.
	b = 25.2721(10) Å	β = 90°.
	c = 43.5886(14) Å	γ = 90°.
Volume	23521.5(15) $Å^3$	
Z	16	
Density (calculated)	1.089 Mg/m^3	
Absorption coefficient	2.776 mm^{-1}	
F(000)	8000	
Theta range for data collection	2.304 to 70.265°.	
Index ranges	-18<=h<=25, -30<=k<=27, -27<=l<=52	
Reflections collected	79490	
Independent reflections	38321 [R(int) = 0.3120]	
Completeness to theta = 25.000°	99.9 %	
Absorption correction	Semi-empirical from equivalents	
Max. and min. transmission	0.9962 and 0.7879	
Refinement method	Full-matrix least-squares on F^2	
Data / restraints / parameters	38321 / 2208 / 2113	
Goodness-of-fit on F^2	1.025	
Final R indices [I>2sigma(I)]	R1 = 0.1382, wR2 = 0.3314	
R indices (all data)	R1 = 0.2751, wR2 = 0.4221	
Absolute structure parameter	-0.01(5)	
Extinction coefficient	n/a	
Largest diff. peak and hole	0.734 and -0.918 $e.Å^{-3}$	

A6.5 CRYSTALLOGRAPHIC ANALYSIS OF L20·$NiBr_2$

A6.5.1 Special Refinement Details

Figure A6.4 *Rendering of Ni-complex* ***L20***·$NiBr_2$.

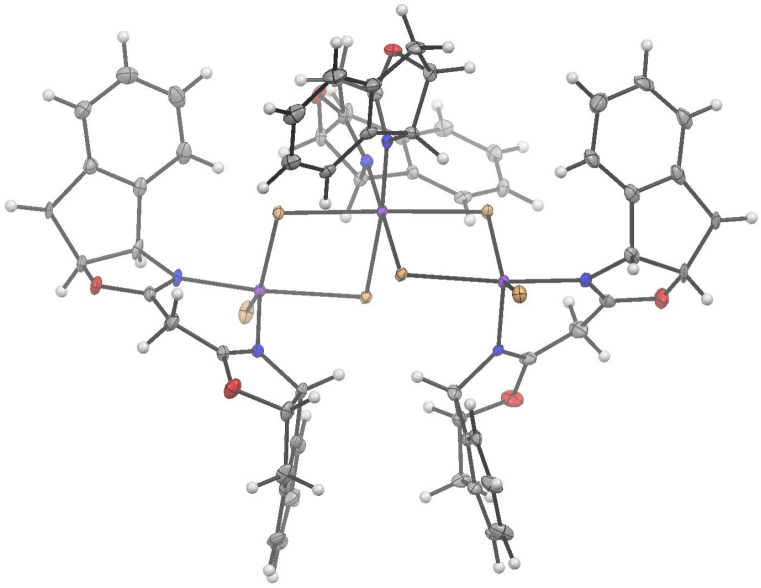

L20·$NiBr_2$ crystallizes in the monoclinic space group $P2_12_12_1$ with one molecule (consisting of three ligand·nickel subunits) in the asymmetric unit. Data was collected with Mo-$K\alpha$ radiation (λ = 0.71073 Å) at 100 K. Three molecules of dichloromethane are co-crystallized in the unit cell. Solvent is omitted for clarity in the graphical representation. Absolute configuration was determined by anomalous dispersion (Flack = -0.011(5)).[6]

A6.5.2 Crystallographic Tables

Table A6.4. *Crystal data and structure refinement for* ***L20***·$NiBr_2$.

Identification code	P15477	
Empirical formula	$C_{21}H_{17}Br_2N_2NiO_2$, CH_2Cl_2	
Formula weight	632.82	
Temperature	100 K	
Wavelength	0.71073 Å	
Crystal system	Orthorhombic	
Space group	$P2_12_12_1$	
Unit cell dimensions	a = 15.012(2) Å	α = 90°.
	b = 18.064(4) Å	β = 90°.
	c = 25.537(5) Å	γ = 90°.
Volume	6925(2) $Å^3$	
Z	12	
Density (calculated)	1.821 Mg/m^3	
Absorption coefficient	4.557 mm^{-1}	
F(000)	3756	
Crystal size	0.16 x 0.12 x 0.09 mm^3	
Theta range for data collection	2.255 to 41.217°.	
Index ranges	-18<=h<=27, -24<=k<=28, -46<=l<=29	
Reflections collected	67889	
Independent reflections	32678 [R(int) = 0.1370]	
Completeness to theta = 26.000°	99.3 %	
Absorption correction	Semi-empirical from equivalents	
Refinement method	Full-matrix least-squares on F^2	
Data / restraints / parameters	32678 / 0 / 838	
Goodness-of-fit on F^2	0.885	
Final R indices [I>2sigma(I)]	R1 = 0.0520, wR2 = 0.0642	
R indices (all data)	R1 = 0.1243, wR2 = 0.0780	
Absolute structure parameter	-0.011(5)	
Extinction coefficient	n/a	
Largest diff. peak and hole	0.961 and -1.014 $e.Å^{-3}$	

A6.6 REFERENCES

(1) *APEX2, Version 2 User Manual, M86-E01078, Bruker Analytical X-ray Systems*, Madison, WI, **2006**.

(2) Sheldrick, G.M. *SADABS (version 2008/1): Program for Absorption Correction for Data from Area Detector Frames*, University of Göttingen, **2008**.

(3) Sheldrick, G. *Acta Crystallogr., Sect. A: Found. Crystallogr*. **2008**, *64*, 112.

(4) Sheldrick, G. M. *Acta Crystallogr., Sect. C: Struct. Chem.* **2015**, *C71*, 3.

(5) Müller, P. *Crystallogr. Rev.* **2009**, *15*, 57.

(6) Parsons, S.; Flack, H. D.; Wagner, T. *Acta Crystallogr., Sect. B: Struct. Sci. Cryst. Eng. Mater.* **2013**, *B69*, 249.

Chapter 5

Ni-Catalyzed Halogenation of Alkenyl Triflates[‡]

5.1 INTRODUCTION

Alkenyl halides are versatile functional groups that can be used in various carbon–carbon and carbon–heteroatom bond-forming reactions. For example, alkenyl halides are commonly used in transition metal-catalyzed cross-coupling reactions,[1,2] or are converted via metal-halogen exchange to nucleophiles for 1,2-additions to carbonyl compounds (Figure 5.1).[3] Furthermore, the alkenyl halide moiety also appears in some natural products and bioactive molecules.[4–6] Whereas acyclic alkenyl halides are easily prepared from the corresponding alkyne[7–11] or aldehyde,[12,13] most cyclic alkenyl halides are synthesized from

[‡]The research presented in this chapter was completed in collaboration with Kelsey E. Poremba (graduate student) and Alexander M. Shimozono (graduate student) in the Reisman group. Portions of this chapter are reproduced from a manuscript which was currently under peer review at the time of thesis publication.

the corresponding ketone. The most direct method for alkenyl halide synthesis is the Barton reaction (and variations thereof),[14–20] which proceeds through an intermediate hydrazone. These reactions are notoriously capricious: the formation of the requisite hydrazone can be challenging on sterically encumbered substrates and the halogenation step often produces mixtures of alkenyl halide isomers or dihalide side products.[13]

Figure 5.1 *Strategies to access alkenyl halides and their utility in organic synthesis.*

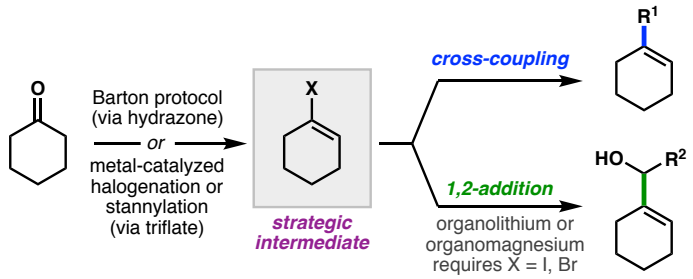

As a result, alkenyl triflates, which can be prepared directly from cyclic ketones under either kinetic or thermodynamic control, have emerged as attractive "pseudohalides" for transition metal-catalyzed cross-coupling processes. Unfortunately, alkenyl triflates cannot be directly converted to the corresponding alkenyllithium or alkenylmagnesium species commonly employed in 1,2-addition reactions. In cases where the Barton procedure to prepare the alkenyl halide is poor yielding, a multistep alternative is frequently employed: 1) conversion of the ketone to alkenyl triflate, 2) conversion of the triflate to the alkenyl stannane, and 3) conversion of the stannane to the alkenyl halide (Scheme 5.1).[21] This process uses stoichiometric quantities of hexamethylditin, which is a volatile, toxic substance. The ability to develop direct, mild methods to convert alkenyl triflates to alkenyl halides that proceed without the need for organostannane reagents (Sn_2Me_6) would improve and streamline the preparation of valuable alkenyl halide intermediates.

Scheme 5.1 *Preparation of alkenyl halides through organostannane intermediates.*

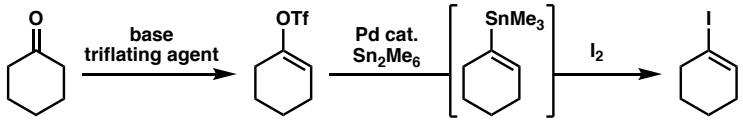

Towards this end, Buchwald and coworkers reported a Pd-catalyzed reaction to convert alkenyl triflates to alkenyl bromides and chlorides;[22,23] however, there are no examples of alkenyl iodide formation, and the reaction requires an expensive ligand, temperatures greater than 100 °C, or additives such as fluoride salts or *i*-Bu_3Al (Scheme 5.2a). These additives limit the functional group compatibility of the reaction, particularly with common groups such as silyl ethers. More recently, Hayashi and coworkers reported a Ru-catalyzed method to convert alkenyl triflates to iodides, bromides, or chlorides that proceeds at ambient temperature (Scheme 5.2b); however, the requisite ruthenium catalyst is not commercially available and only three examples of alkenyl iodide formation are reported.[23,24] An example of a Ni-catalyzed bromination of a dihydropyranyl triflate was reported by Kocienski and coworkers (Scheme 5c),[25] which proceeds with an active Ni(0) catalyst generated via DIBAL–H reduction of $Ni(acac)_2$ in the presence of PPh_3. While the authors note that the corresponding iodide, bromide, chloride, and nitrile can be obtained, only moderate yields of the bromide and nitrile are reported; no yields for the iodide and chloride are disclosed. In our hands, application of these conditions to a simple cyclic alkenyl triflate derived from menthone provided <10% yield of product (iodide, bromide, and chloride). Given the reported literature conditions, it is well-precedented that a general Ni-catalyzed alkenyl triflate halogenation could be developed; however, mild reaction conditions are required to render the reaction permissive of sensitive functional groups.

Scheme 5.2 *Metal-catalyzed alkenyl triflate halogenations.*

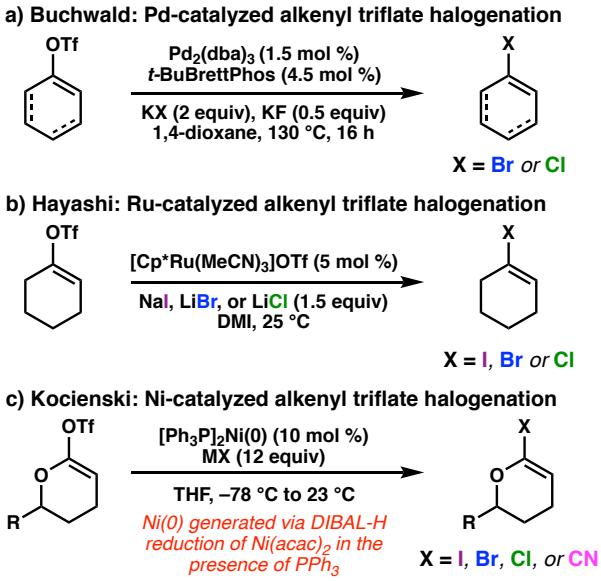

During our investigations of Ni-catalyzed asymmetric reductive coupling reactions of alkenyl bromides, we observed an off-pathway halide exchange process that generated alkenyl chlorides and iodides (see Chapter 4, Figure 4.16–17).[26,27] Whereas Ni-catalyzed aryl[28,29] and alkenyl[29–33] halide exchange processes have been previously reported and extensively investigated, the corresponding reactions of alkenyl triflates have not been developed.[25,34] Having observed promising reactivity with styrenyl triflates in a related cross-coupling reaction (see Chapter 2, Scheme 2.3),[35] we hypothesized that an appropriate Ni catalyst and inexpensive halide salts might enable the direct conversion of alkenyl triflates to alkenyl halides under mild conditions. Herein, we report the development of a simple procedure where commercially available $Ni(cod)_2$ catalyzes the conversion of alkenyl triflates to alkenyl iodides, bromides, and chlorides in good to excellent yields (Scheme 5.3). Mechanistic studies of the reaction are conducted and development of conditions that proceed with Ni(II) and a metal reductant are discussed.

Scheme 5.3 *Mild Ni-catalyzed halogenation of alkenyl triflates.*

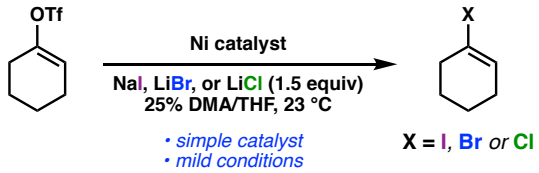

5.2 REACTION OPTIMIZATION

5.2.1 Initial Hit

Given our observation of alkenyl halide exchange during previously developed reductive cross-couplings with alkenyl bromides, we set out to test conditions that could afford alkenyl triflate halogenation in the presence of ligands used for reductive cross-couplings (Figure 5.2). When catalytic $Ni(cod)_2$ and either BOX ligand **L2** or BiOX

Figure 5.2 *Initial observation of Ni(0)-mediated alkenyl triflate halogenation.*

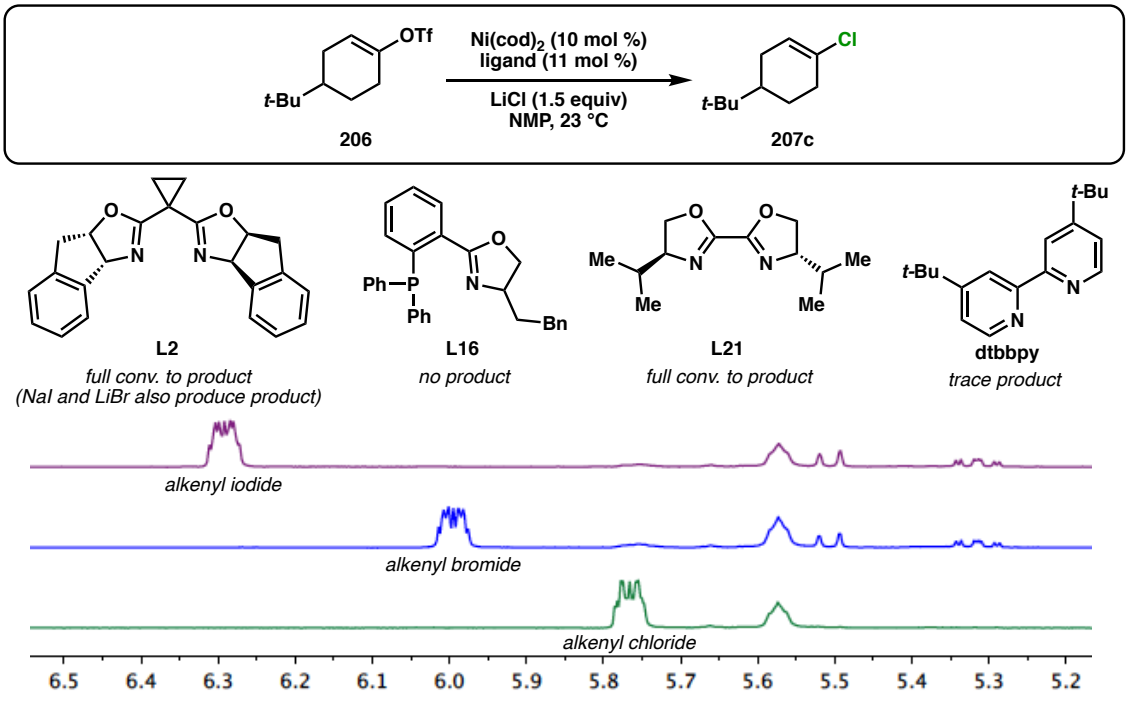

ligand **L21** were used with LiCl in NMP at room temperature (conditions used to mimic Hayashi's Ru-catalyzed reaction), the desired alkenyl chloride was formed with full consumption of starting material. PHOX ligand **L16** and bipyridine ligand dtbbpy failed to provide the desired alkenyl chloride product. When NaI and LiBr were used as the halide source in combination with BOX ligand **L2**, the desired alkenyl bromide and iodide were formed with full consumption of the alkenyl triflate. The β-alkenyl proton relative to the alkenyl halide is observed to shift downfield in the ^{1}H NMR spectrum as the halide increases in size and polarizability. Interestingly, a control experiment showed the alkenyl halide product was formed in the absence of ligand, indicating that added ligand is not required to promote the transformation.

5.2.2 Solvents

We set out to quantify and optimize the desired halogenation reaction with alkenyl triflate **208**, which is prepared in one step from commercially available menthone. Our goal was to identify general conditions that could provide the alkenyl iodide, bromide, or chloride simply by changing the halide salt. A variety of solvents were evaluated in the presence of 10 mol % $Ni(cod)_2$ and 1.5 equiv of halide salt (either NaI, LiBr, or LiCl) (Table 5.1). These initial experiments showed that alkenyl iodide formation proved most sensitive to the solvent: for example, while the bromination and chlorination worked comparably well in DMA, THF, and DMF, the yield of the alkenyl iodide was significantly better in DMA than both THF and DMF (entries 1–3). Due to improved physical properties of the reaction mixture and work-up, mixtures of DMA and THF were evaluated, and a 1:3 mixture of DMA and THF was selected as the optimal solvent system (entries 5–7).

Table 5.1. *Evaluation of solvents.*

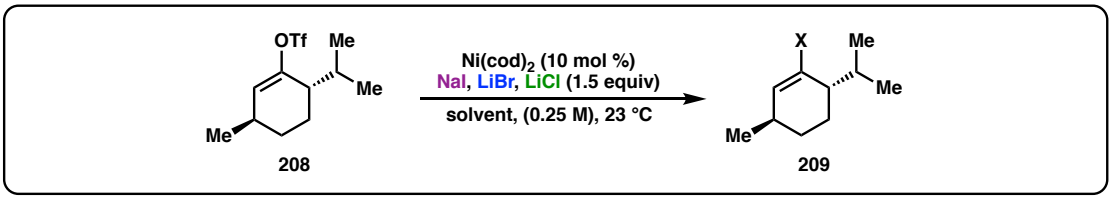

		Iodination		Bromination		Chlorination	
Entry	Solvent	Yield (%)	Triflate (%)	Yield (%)	Triflate (%)	Yield (%)	Triflate (%)
1	DMA	72	0	75	0	70	0
2	THF	35	43	75	0	61	5
3	DMF	34	47	74	0	70	3
4	MeCN	4	85	52	36	7	81
5	10% DMA/THF	68	30	68	0	77	0
6	25% DMA/THF	74	3	74	0	74	0
7	40% DMA/THF	68	0	71	0	64	0

5.2.3 Halide Source

We then investigated a variety of salts used as the halide source (Table 5.2). While K^+ salts provided poor results for all halides (entry 3), Na^+ salts only provided poor yields for bromination and chlorination (entry 1). The iodination with NaI proceeded in good yield. In contrast to K^+ and Na^+, both Li^+ salts and tetrabutylammonium salts worked well for all halides providing the alkenyl halide products in comparable yields (entries 2 and 4).

Table 5.2. *Evaluation of halide salts.*

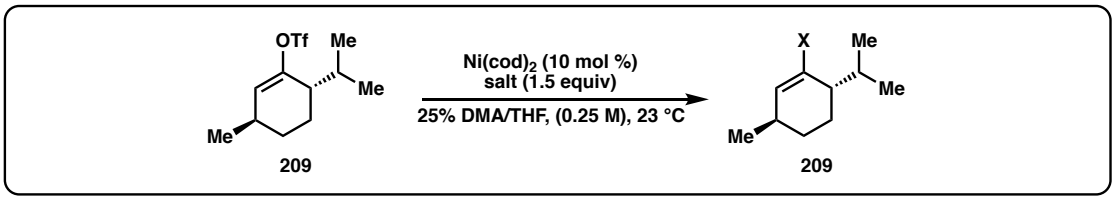

		Iodination		Bromination		Chlorination	
Entry	Salt	Yield (%)	Triflate (%)	Yield (%)	Triflate (%)	Yield (%)	Triflate (%)
1	NaX	74	3	58	6	10	69
2	LiX	70	0	74	0	74	0
3	KX	36	43	8	61	13	75
4	TBAX	71	5	84	0	80	10

5.2.4 Catalyst Loading

The catalyst loading of $Ni(cod)_2$ was evaluated and shown to provide the alkenyl iodide **209a** with the highest yield at 10 mol % Ni, whereas alkenyl bromide **209b** and alkenyl chloride **209c** were formed with the highest yield at 5 mol % Ni. Typically, higher Ni loadings resulted in decreased yield due to the increased formation of alkene homodimer. Overall, 10 mol % $Ni(cod)_2$ was selected for further optimization and used to evaluate the substrate scope because it proved most robust over a broad range of substrates. However, for highly reactive substrates, lower catalyst loadings can be beneficial to reduce formation of homodimer.

Table 5.3. *Evaluation of catalyst loading.*

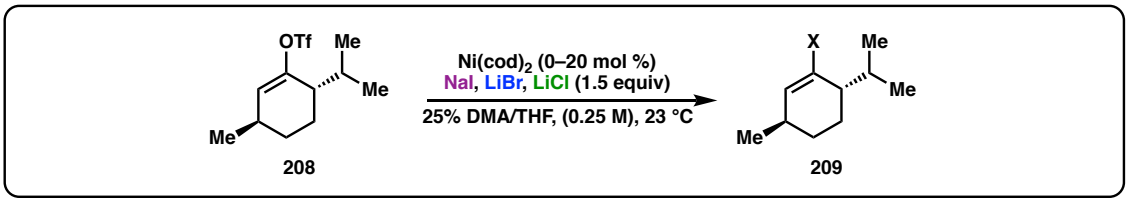

		Iodination		Bromination		Chlorination	
Entry	Ni (mol %)	Yield (%)	Triflate (%)	Yield (%)	Triflate (%)	Yield (%)	Triflate (%)
1	0	0	82	0	96	0	94
2	5	68	4	83	0	77	0
3	10	74	3	74	0	74	0
4	20	70	0	55	0	67	0

5.2.5 Concentration and Temperature

The concentration and temperature of the reaction were evaluated to determine if alternate conditions could increase the yield of product (Table 5.4). When the halogenation reaction was conducted at 0 °C (entry 1), the yield was suppressed compared to room temperature (entry 3). Increasing the temperature to 60 °C only provided slight

improvement of yield (entry 5). The concentration was also investigated, and the desired alkenyl halide products were formed in comparable yields across a range of conditions (0.1–0.4 M).

Table 5.4. *Evaluation of temperature and solvents.*

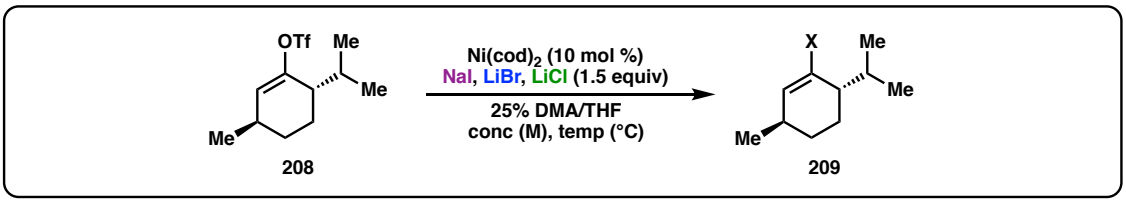

			Iodination		Bromination		Chlorination	
Entry	Temp (°C)	Conc (M)	Yield (%)	Triflate (%)	Yield (%)	Triflate (%)	Yield (%)	Triflate (%)
1	0	0.2	12	74	61	26	61	0
2	23	0.1	67	0	71	0	63	0
3	23	0.2	74	3	74	0	74	0
4	23	0.4	62	30	82	0	72	0
5	60	0.2	77	10	80	0	72	0

5.2.6 Other Alkenyl Electrophiles

Other alkenyl electrophiles were evaluated given that Hayashi and coworkers successfully employed alkenyl nonaflates, tosylates, and phosphonates in their Ru-catalyzed alkenyl triflate halogenation halogenation.[23] When $Ni(cod)_2$ was used as the catalyst, indeed both the alkenyl triflate **206** and alkenyl nonaflate **210a** were competent substrates to form desired alkenyl iodide **207a** (Figure 5.3). However, alkenyl tosylate **210b** and alkenyl phosphonate **210c** did not react under the optimized conditions. Although this diminishes the scope of the Ni-catalyzed transformation, it enables a divergent approach where substrates containing both an alkenyl triflate and alkenyl tosylate moiety could potentially be differentiated using a Ni-catalyzed approach in contrast to the Ru-catalyzed method.

Figure 5.3 *Evaluation of alkenyl electrophiles.*

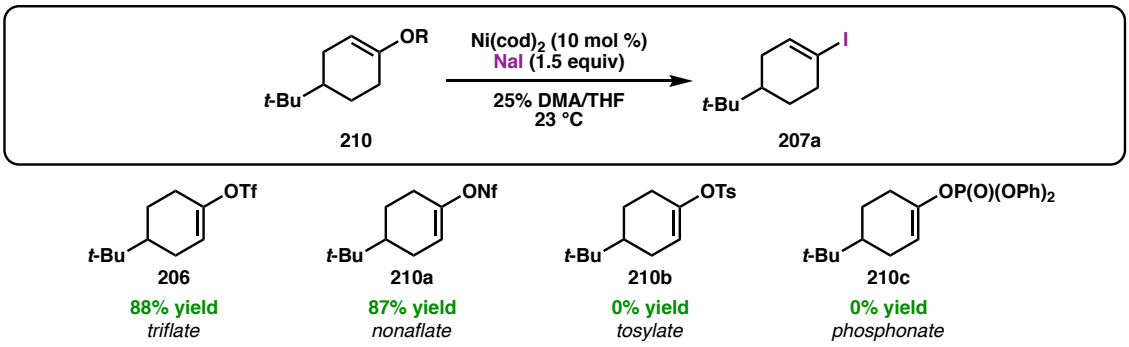

5.3 SUBSTRATE SCOPE

Having identified optimal reaction conditions with the $Ni(cod)_2$ catalyst, the substrate scope of the transformation was investigated (Figure 5.4). The halide exchange was found to be compatible with a variety of common functional groups, including amines (**213**), carbamates (**214**, **222**), pyridines (**229**), alkenes (**219**, **221**), esters (**228**), ketals (**215**, **223**), and enones (**220**). Dienyl bromides and chlorides could also be prepared in good yields; the yields of the corresponding iodides were typically lower (**219, 223**). Chemoselective halogenation of the alkenyl triflate was observed in preference to aryl triflates (**224**, **229**), aryl chlorides (**218**, **230**), and aryl boronates (**231**); however, competitive halide exchange was observed in the presence of aryl bromides and iodides. To demonstrate synthetic utility and scalability, the iodination of **208** was conducted on gram scale to afford 1.1 g of alkenyl iodide **209a** in 71% yield.

Although the Ni-catalyzed halogenation exhibits good functional group tolerance, the iodination, bromination, and chlorination did not perform equally well on all substrates. With the exception of the 1-arylvinyl triflates, the formation of the alkenyl chlorides

Figure 5.4 *Evaluation of substrate scope.*

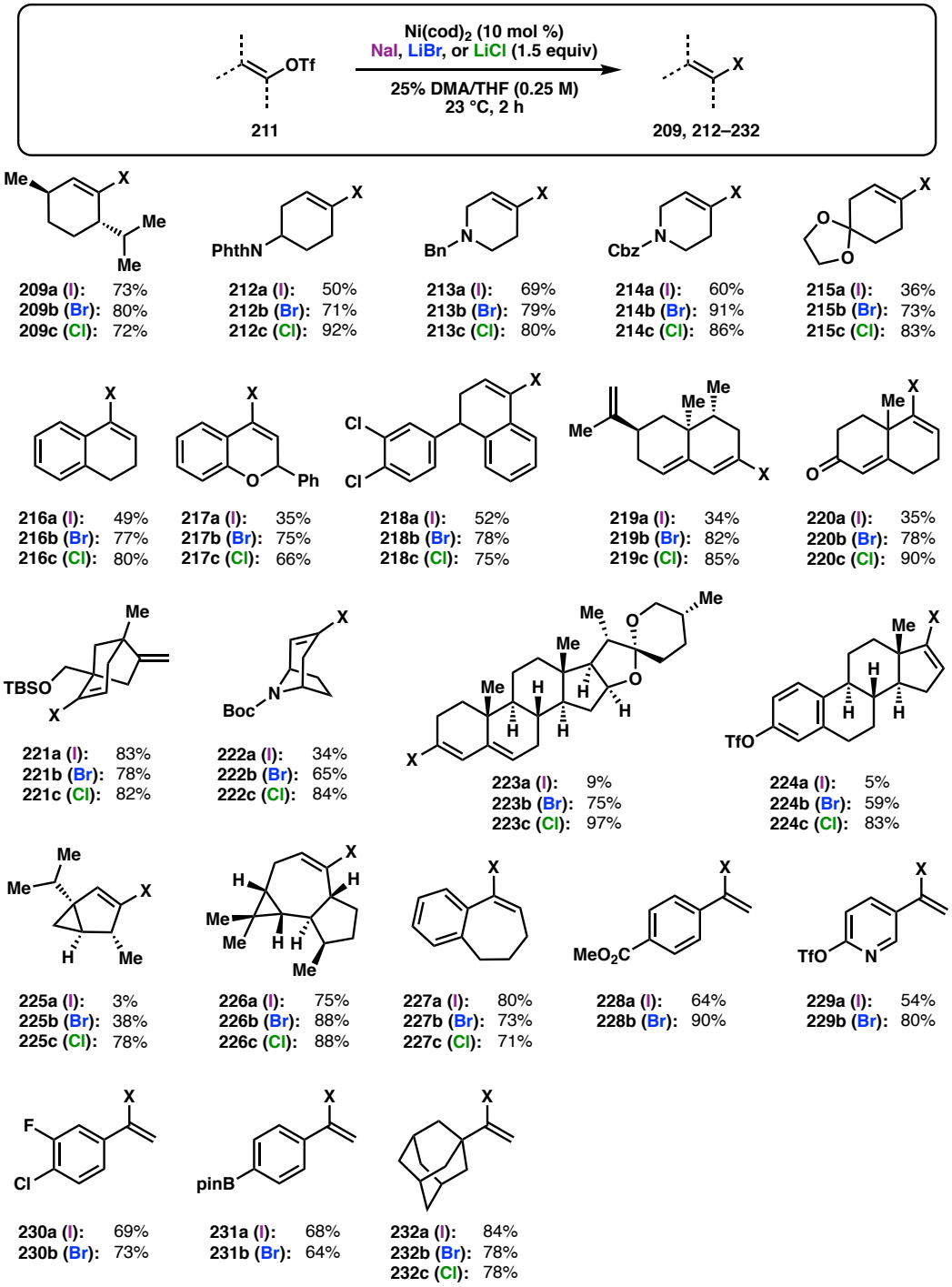

Reactions are conducted on 0.3 mmol scale under N_2. Isolated yields are provided. **225b** was conducted with 5 mol % $Ni(cod)_2$. **221b** and **221c** were conducted on 0.1 mmol scale. Yields for **217a**, **223a**, **224a**, and **225a** were determined by NMR on 0.1 mmol scale.

proceeded with the most consistently high yields across different substrate classes. Under these conditions, 1-arylvinyl triflates (**228**–**231**) provided the corresponding bromides and iodides in good yields; however, in the presence of chloride salts, elimination of the triflate by LiCl to give the aryl acetylenes outcompeted chlorination, a process previously reported by Li and coworkers.[36] The use of tetrabutylammonium salts did not improve the desired transformation. For non-styrenyl triflates, the yield of alkenyl iodide was most substrate-dependent. For example, cyclopentenyl triflates (**224**, **225**) were poor substrates for alkenyl iodide formation, but gave good yields of the alkenyl chlorides. The alkenyl iodide formation typically worked best for unactivated cyclohexenyl and cycloheptenyl triflates.

For several substrates, alkenyl iodide formation from the triflate was poor yielding (**215**, **219**, **220**, and **222**). Schoenebeck and coworkers recently reported a Ni-catalyzed trifluoromethyltiolation of alkenyl triflates and found lower yielding substrates could be rescued via the use of the corresponding alkenyl nonaflates.[34] Alkenyl nonaflates are not only more stable than their corresponding alkenyl triflates, but the calculated $\Delta G^{\ddagger}$ suggests a 0.4 kcal/mol decrease in the barrier for oxidative addition.[34,37] We were pleased to find that the use of alkenyl nonaflates could be used to improve the yield of lower yielding substrates with nearly a 20% increase in product yield (Figure 5.5).

Although the alkenyl triflate halogenation tolerates a variety of functional groups, the reaction does possess some limitations (Figure 5.6). For instance, a variety of fused bicycles were evaluated and the alkenyl halide products were formed in moderate to low yields. The alkenyl triflate derived from camphor provided the desired bromide (**234b**) and chloride (**234c**) in good yields; however, the formation of the iodide (**234a**) was low

Figure 5.5 *Evaluation of alkenyl nonaflate iodination.*

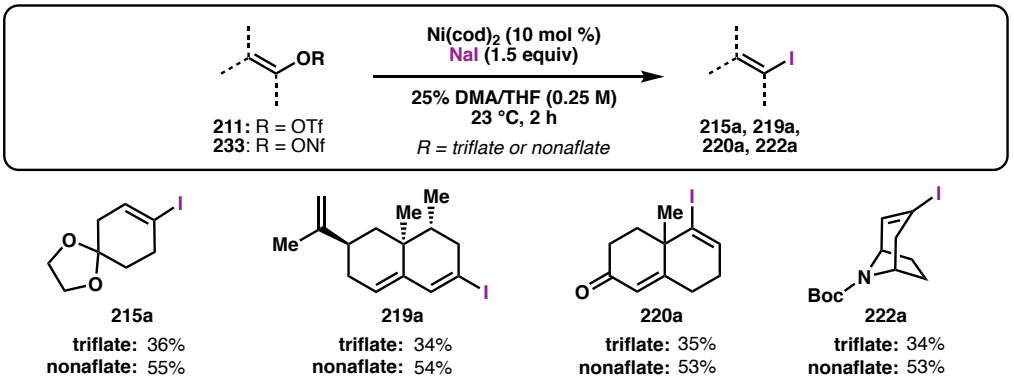

yielding. Furthermore, isolation of the bicyclic compounds was difficult due to purification difficulties (coelution with homocoupling) and product volatility. Dienyl halide **240** was formed in excellent yield; however, the product isomerized to **219** upon standing and during purification. Other substrates provided geometric constraints. Typically, five-

Figure 5.6 *Substrates possessing purification difficulties and diminished yields.*

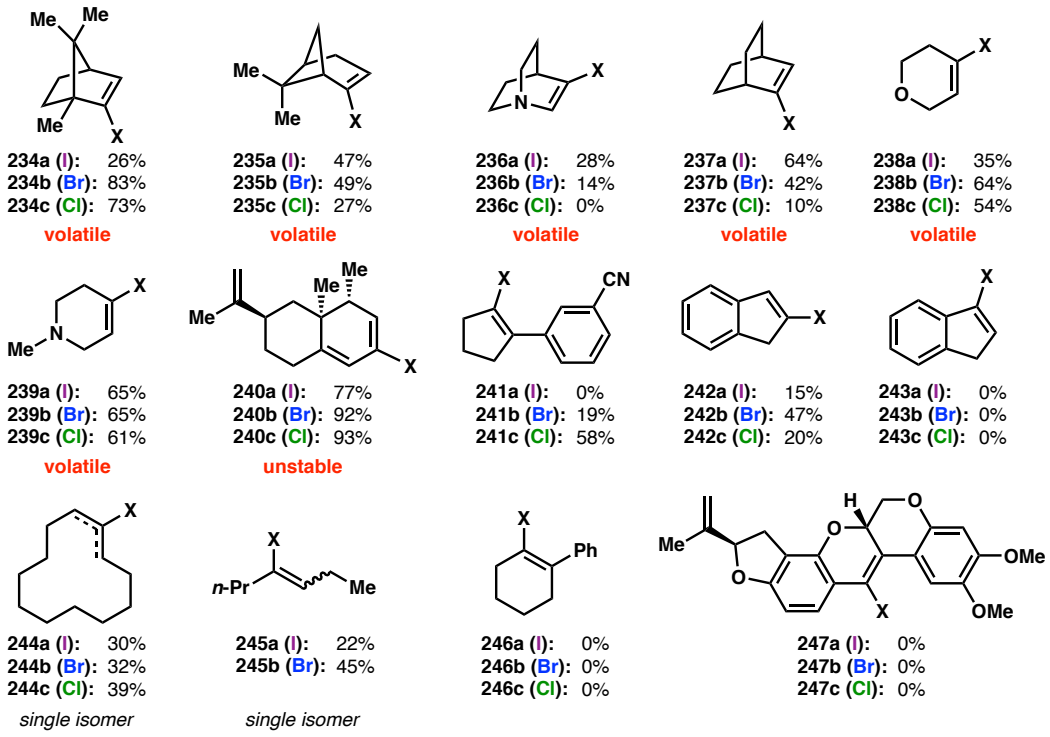

membered rings did not undergo full conversion (**241**, **242**, and **243**). Linear alkenyl triflates that were added as a mixture of isomers converged to a single isomer during the reaction; however, the yield was still fairly low (**244** and **245**). Finally, tetrasubstituted alkenes failed to provide the desired alkenyl halide product (**246** and **247**).

Lastly, given the observation of competitive halide exchange, we conducted a robustness screen to determine what coupling handles could be tolerated (Figure 5.7). When a variety of additives were added to the reaction, some were fully recovered while others were consumed. Competitive halide exchange was observed for alkyl bromides (including activated benzylic bromides) in addition to aryl bromides and aryl iodides. Aryl chlorides, aryl triflates, aryl boronic esters, and benzylic chlorides were tolerated under the reaction conditions, although the yield of **209a** was diminished in some cases.

Figure 5.7 *Evaluation of added coupling handles.*

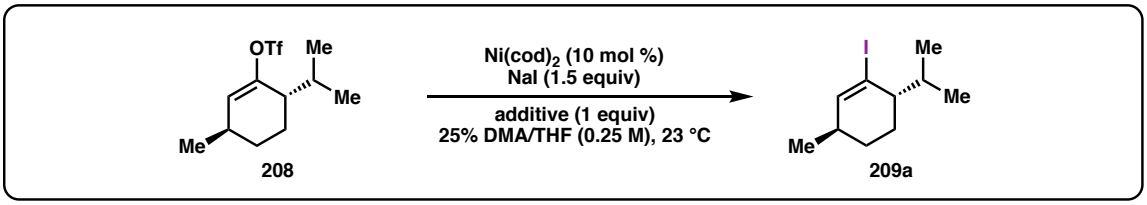

Additive	none	I, OMe	Br, OMe	Cl, OMe	OTf, OMe	Bpin	*n*-Pr, Br, *n*-Pr	Me, Br	Me, Cl
Recovery of Additive	–	19%	37%	65%	100%	100%	47%	32%	87%
Yield of Alkenyl Iodide	77%	31%*	37%	72%	29%	73%	31%	0%	59%
Other Products from Additive	–	71% ArBr	25% ArI	–	–	–	13% alkyl I	76% BnI	–

*LiBr in place of NaI, yield is of alkenyl bromide

Fluoride and cyanide salts were also evaluated in addition to the reported halogenations (X = I, Br, Cl). In all cases, fluorination failed to provide the desired product (F^- sources included NaF, LiF, and TBAF). However, the use of NaCN and TBACN provided the desired alkenyl nitrile **248** under the optimized reaction conditions (Table 5.5), albeit in trace yield (<5%). A variety of solvents were then screened, and alkenyl nitrile **248** was obtained in 18% yield when the reaction was run in DMSO (entries 1–6); the reactions, however, exhibited poor conversion. When stoichiometric $Ni(cod)_2$ was used, **248** was formed in 50% yield (entry 7). The use of tetrabutylammonium cyanide, which eliminated possible metal cation effects, also produced **248** in low yield (entry 8).

Table 5.5. *Evaluation of conditions for alkenyl nitrile formation.*

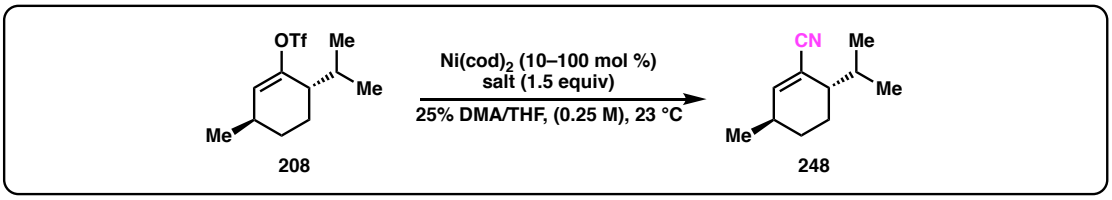

				Cyanation	
Entry	Ni (%)	Salt	Solvent	Yield (%)	Triflate (%)
1	10	NaCN	DMA	15	46
2	10	NaCN	DMF	2	77
3	10	NaCN	MeOH	0	82
4	10	NaCN	DMSO	18	33
5	10	NaCN	MeCN	2	75
6	10	NaCN	DMPU	16	16
7	100	NaCN	25% DMA/THF	50	6
8	10	TBACN	25% DMA/THF	16	16

5.4 MECHANISTIC INVESTIGATIONS

To better understand the Ni-catalyzed halogenation of alkenyl triflates, and the iodination in particular, a series of mechanistic experiments were performed.

5.4.1 Kinetics

We began by studying the kinetics of the iodination reaction with $Ni(cod)_2$. The reaction was first conducted at a variety of Ni loadings (5–20 mol % $Ni(cod)_2$) which all displayed identical reaction profiles, suggesting a zero-order rate dependence on Ni. However, further lowering the catalyst loading (0.5–5 mol %) revealed a positive rate dependence on Ni (Figure 5.8a). Excitingly, the iodination of **208** could be run with loadings as low as 0.5 mol % $Ni(cod)_2$, which provided a comparable yield of **209a** as long as the reaction was given sufficient time to obtain full conversion. At low catalyst loadings (e.g. 0.5 mol %) the reaction also exhibited a prominent induction period, which complicated initial rate kinetic analysis. Blackmond and coworkers have demonstrated the use of sigmoidal fits to extract V_{max} data from reactions exhibiting induction periods.[38] In

Figure 5.8 *Analysis of alkenyl iodide as a function of time, determination of V_{max}, and observation of positive order rate on [Ni].*

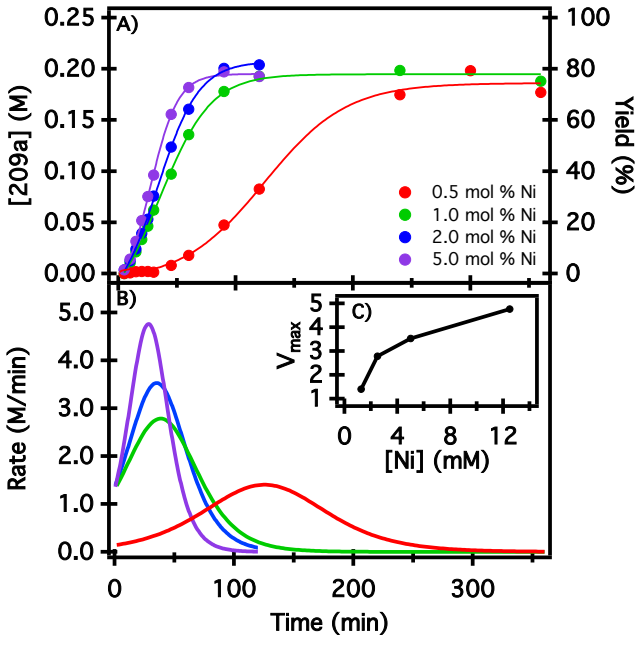

order to process our data, each run in Figure 5.8a was fit with a sigmoid fit in Igor Pro software, which were subsequently plotted over the existing data points. The derivative of each fit was calculated in Excel to give the rate of the product formation as a function of time (Figure 5.8b). The maximum rate was extracted from the respective plots (V_{max}). PlottingV_{max} vs. [Ni] revealed that the reaction has a positive-order dependence on [Ni] that negatively deviates from first order at higher [Ni] (Figure 5.8c), suggesting the formation of dimeric (or higher order) off-cycle species at higher [Ni].

We also evaluated the kinetic profile of the reaction while altering a number of other parameters (Figure 5.9). No change in the rate of iodination of **208** was observed when the amount of NaI was increased beyond 1 equivalent when conducted at 1 mol % $Ni(cod)_2$ (Figure 5.9a). Altering the stir rate of the reaction (stirring vs. no stirring) also displayed no rate dependence on the iodination of **208**, suggesting that the reaction does not proceed via a hetereogenous process (Figure 5.9b). When the concentration of alkenyl

Figure 5.9 *Kinetic profile of alkenyl iodide with a series of reaction variations.*

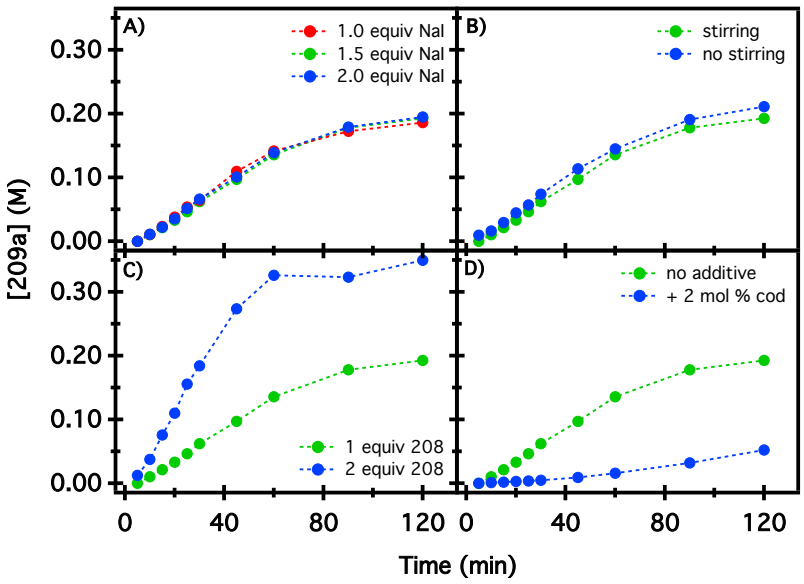

triflate was doubled (from 0.25 M to 0.5 M) while maintaining the concentration of NaI (0.375 M), the rate of product formation over time (reported as M/min) approximately doubled, indicating that substrate is present in the rate determining step of the reaction (Figure 5.9c). Finally, the addition of exogenous cyclooctadiene was found to inhibit the reaction rate, therefore we speculate that ligand dissociation could be the source of the induction period (Figure 5.9d). When the reaction with exogenous cyclooctadiene was run for 14 hours, **209a** was formed in 80% yield, indicating that cyclooctadiene does not inhibit overall reactivity.

5.4.2 Radical Inhibitors

A variety of radical inhibitors and free radicals were added to the reaction (Figure 5.10). With the addition of radical inhibitors such as DHA and BHT, alkenyl iodide **209a** was produced in slightly diminished yield. However, when free radicals such as TEMPO and galvinoxyl were added, reaction conversion ceased. Given these results, it is possible that a radical species is present in the mechanism or that added free radicals are able to bind to the active Ni catalyst and shut down productive reactivity.

Figure 5.10 *Evaluation of radical inhibitors.*

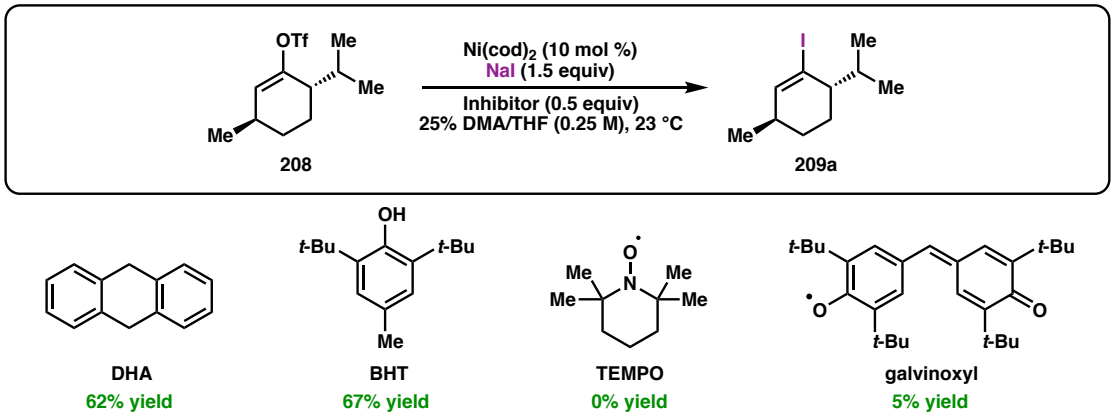

5.4.3 Investigating Catalyst Inhibition

During the evaluation of substrate scope, typically products which were formed in low yield were typically met with poor conversion of the starting material. In order to investigate whether catalyst deactivation was occurring, a series of batch experiments and kinetic studies were conducted. A series of alkenyl triflates were converted to the desired alkenyl halides for 2 hours before an additional alkenyl triflate and added NaI was added to the reaction (Scheme 5.4). In some cases, the second triflate underwent full conversion and provided the alkenyl iodide (Scheme 5.4a–b); however, in some cases reactivity had ceased (Scheme 5.4c).

Scheme 5.4 *Investigation of catalyst deactivation by sequential substrate addition.*

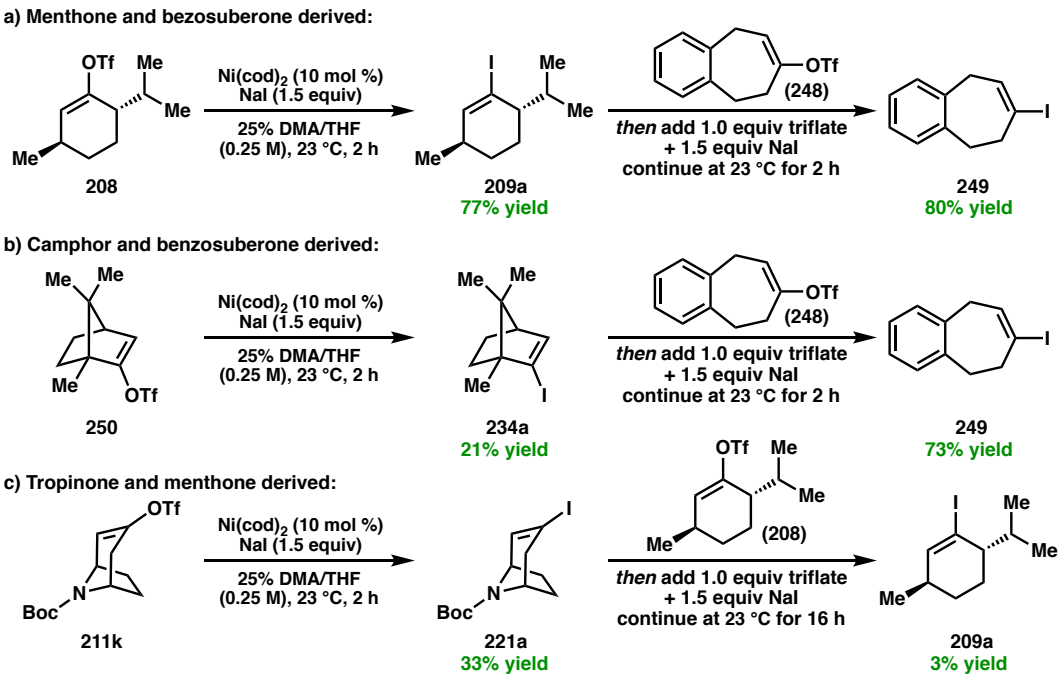

Further experimental conditions were evaluated to improve the conversion of alkenyl triflate **211k** (Table 5.6). Unfortunately, attempts to improve the yield of low-

yielding reactions (due to incomplete conversion of starting material) with $Ni(cod)_2$ as the catalyst were ultimately unsuccessful: addition of excess $Ni(cod)_2$ did not improve the yield of **222a** and instead afforded additional diene side product (entry 2). The homocoupled diene product was isolated and added to the halogenation reactions; however, it did not inhibit product formation when included at 5 mol % and 10 mol % loadings (entries 3–4). Finally, added NaI or increased reaction time also showed no improvement (entries 5–6).

Table 5.6. *Evaluation of conditions to improve low yielding substrates.*

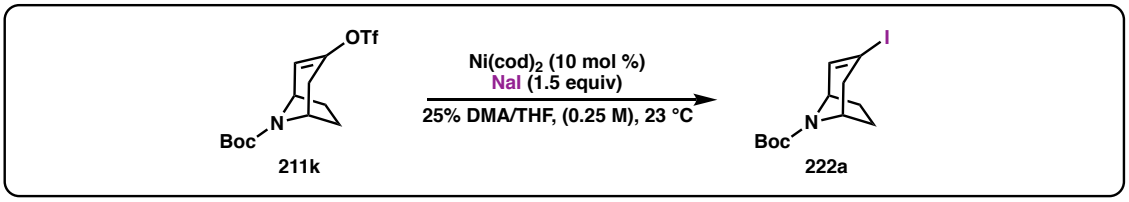

		Iodination		
Entry	Conditions	Yield (%)	Triflate (%)	Diene (%)
1	2 h	38	31	9
2	2 h, then add $Ni(cod)_2$ for 16 h	40	20	12
3	+ 5 mol % diene	35	41	11
4	+ 10 mol % diene	37	42	15
5	2 h, then add NaI for 16 h	36	39	8
7	18 h	37	38	8

We then turned back to kinetics to study the possibility of catalyst inhibition by reaction progress kinetics analysis, a method recently described by Blackmond and coworkers, where a "same excess" reaction was conducted and analyzed (Figure 5.11).[38,39] Only 0.1 mmol of **208** was added instead of 0.2 mmol, and the data was offset by the time it required the 0.2 mmol reaction to have 0.1 mmol of remaining starting material. The kinetic traces overlay nicely for the remainder of the reaction, indicating that no catalyst is decomposing during the course of the reaction.

Figure 5.11 *Same excess kinetic profile indicating no catalyst decomposition.*

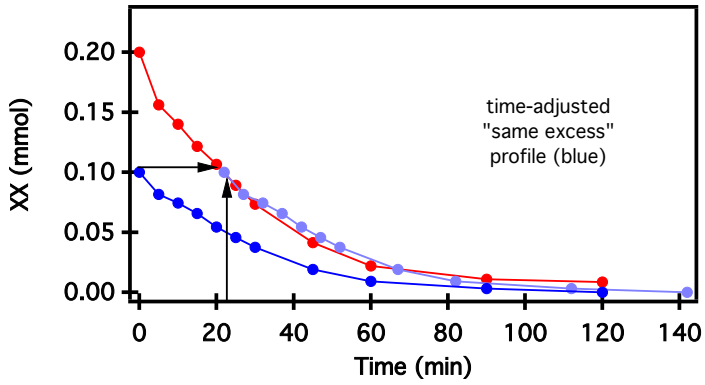

5.4.4 EPR Spectroscopy

Given the likelihood that radical species may be present during the course of the reaction, we decided to analyze the crude reaction by EPR spectroscopy (Figure 5.12).

Figure 5.12 *EPR spectra of Ni(I) halides*

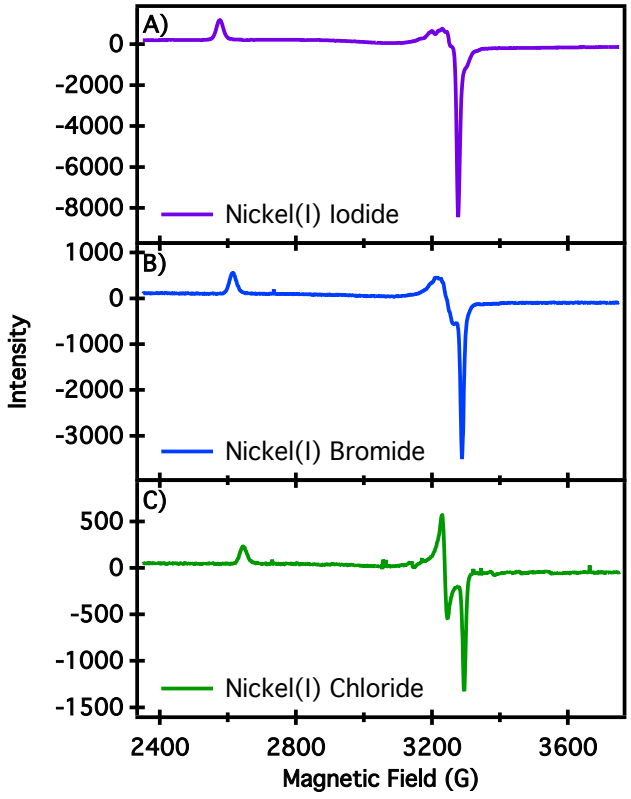

When the iodination reaction of **208** was monitored by EPR with 5 mol % $Ni(cod)_2$, a Ni(I) signal grew in over the course of the reaction, reaching a maximum concentration at 30 minutes before disappearing (Figure 5.12a). When the reaction was instead conducted with LiBr or LiCl, the EPR signal was present as well, albeit with decreased intensity and alterations in the spectral features, both in the observed hyperfine coupling and shift in g-value (Figure 5.12b–c). This suggests that the observed Ni(I) species contains the halogen nucleus. Differences in the electronegativity and polarizability of the halogens could result in differences in spin-orbit coupling and alter the level of hyperfine coupling observed (most prominent for iodide). Furthermore, the observation that increased Δg occurs as the halide size increases could possibly be due to different HOMO–LUMO spacings in the molecular orbital energy levels. The Ni(I) signals shown in Figure 5.12 were then successfully reproduced by mixing a solution of $Ni(cod)_2$ with the corresponding alkenyl halide, resulting in oxidative addition to form the Ni(I) halide complexes and alkenyl homocoupling which was observed by ^1H NMR. While this observed Ni(I) signal could potentially be active in the catalytic cycle, quantification of this species with an external standard of $CuSO_4$ in 1:9 ethylene glycol/H_2O provided the result that only 2% of the total Ni content (i.e. 2% x 5% = 0.1 mol % Ni(I)) resided as this particular Ni(I) species.

5.4.5 Crossover Experiments

Finally, a crossover experiment was designed to evaluate the reversibility of alkenyl halide formation (Figure 5.13). Treatment of a 1:1 mixture of **251** and **207b** with $Ni(cod)_2$ (10 mol %) in 1:3 DMA/THF at 23 °C resulted in complete recovery of **251** and **207b**, without detection of crossover products **252** or **206** (Figure 5.13a). Addition of 0.1 or 1.0

equivalents LiBr resulted in conversion of **251** to **252** in 10% and 90% yield, respectively. No **206** was detected at any point in either reaction. Furthermore, the subjection of alkenyl iodide **207a** to $Ni(cod)_2$ (10 mol %) and metal triflate salts (e.g. NaOTf) did not result in alkenyl triflate formation (Figure 5.13b).

Figure 5.13 *Crossover experiments to probe reversible alkenyl triflate formation.*

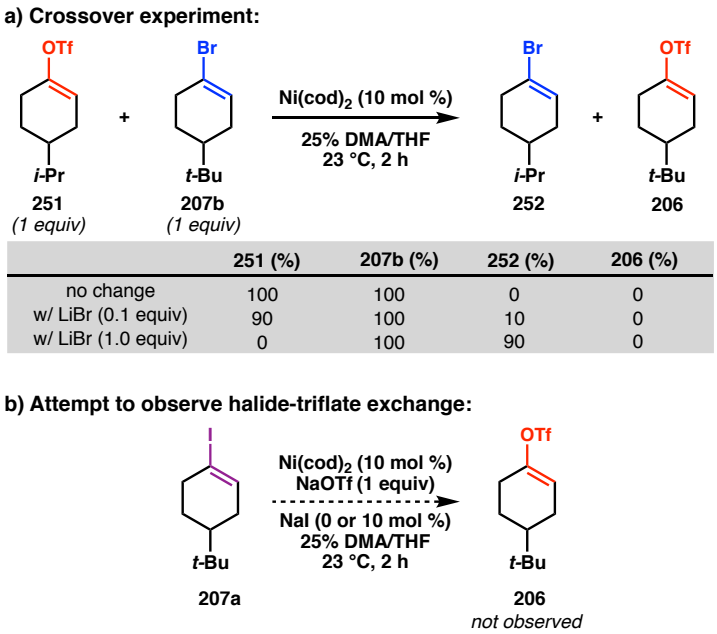

	251 (%)	207b (%)	252 (%)	206 (%)
no change	100	100	0	0
w/ LiBr (0.1 equiv)	90	100	10	0
w/ LiBr (1.0 equiv)	0	100	90	0

Interestingly, no evidence of oxidative addition was observed by ^1H NMR when alkenyl triflate **208** and $Ni(cod)_2$ (5 mol %) were mixed in the presence or absence of NaOTf. However, upon addition of a metal halide salt, conversion of **208** to alkenyl halide **209a** was observed. This is in contrast to the oxidative addition of aryl triflates which have previously been shown undergo oxidative addition to (dppf)Ni(cod) to form Ni(I) complexes.[40,41] Taken together, these results suggest that oxidative addition of the alkenyl triflate is irreversible, or that halide exchange for triflate in the oxidative addition complex is rapid and irreversible. In either scenario, the fact that the enol triflate is irreversibly

consumed enables the reaction to proceed in good yield to the respective alkenyl halides. This is in contrast to Ni-catalyzed halide exchange reactions, which are thermodynamically driven equilibrium processes (Figure 5.14).[29] For example, after 2 h, an 85:15 mixture of **207a**:**207b** is obtained for both the Ni-catalyzed reactions of **207b** with LiI, or **207a** with LiBr (Figure 5.14a–b). Although the formation of alkenyl chloride **207c** appears to be the

Figure 5.14 *Ratios in terms of percentages for halide cross-over experiments:* ***A)*** *alkenyl iodide + LiBr,* ***B)*** *alkenyl bromide + LiI,* ***C)*** *alkenyl iodide + LiCl,* ***D)*** *alkenyl chloride + LiI,* ***E)*** *alkenyl bromide + LiCl, and* ***F)*** *alkenyl chloride + LiBr.*

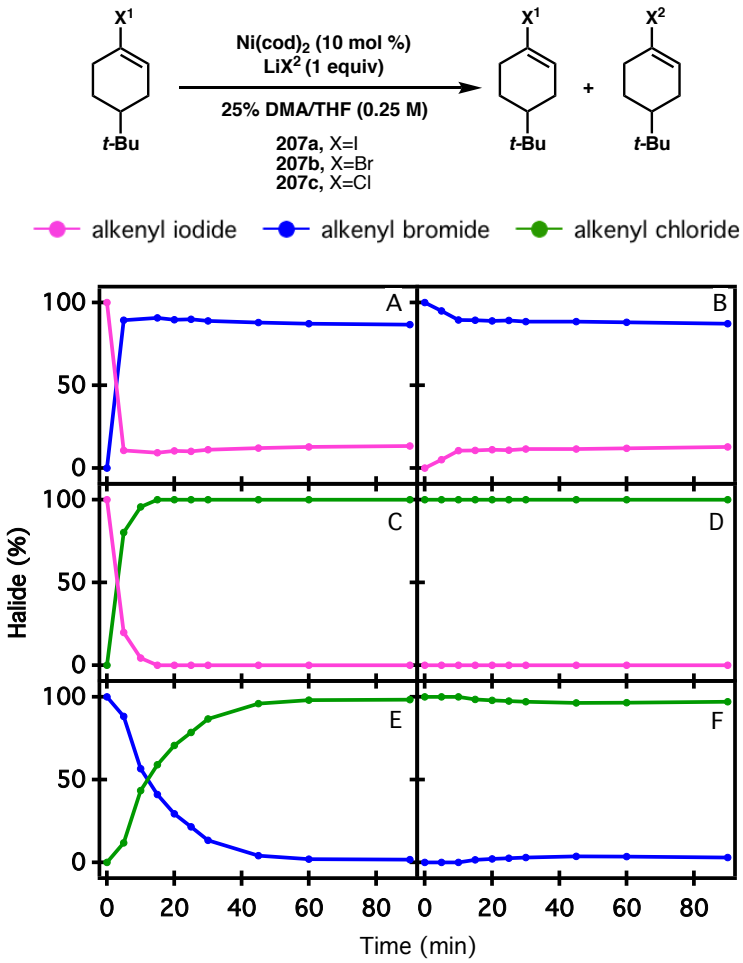

most thermodynamically favorable, when a mixture of alkenyl chloride **207c** and LiBr is monitored by GC, trace amounts of alkenyl bromide **207b** are formed, indicating that alkenyl chloride can undergo oxidative addition with Ni(0) (Figure 5.14f).

5.4.6 Potential Reaction Mechanisms

Given the experimental mechanistic results, we hypothesize three different mechanisms may be operative for the conversion of alkenyl triflates to alkenyl halides (Figure 5.15). In all cases, the formation of L–Ni(0) (**255**) proceeds via cod dissociation, owing to the observed induction period. One mechanistic possibility is a Ni(0)/Ni(II)

Figure 5.15 *Possible mechanisms for the Ni-catalyzed alkenyl triflate halogenation.*

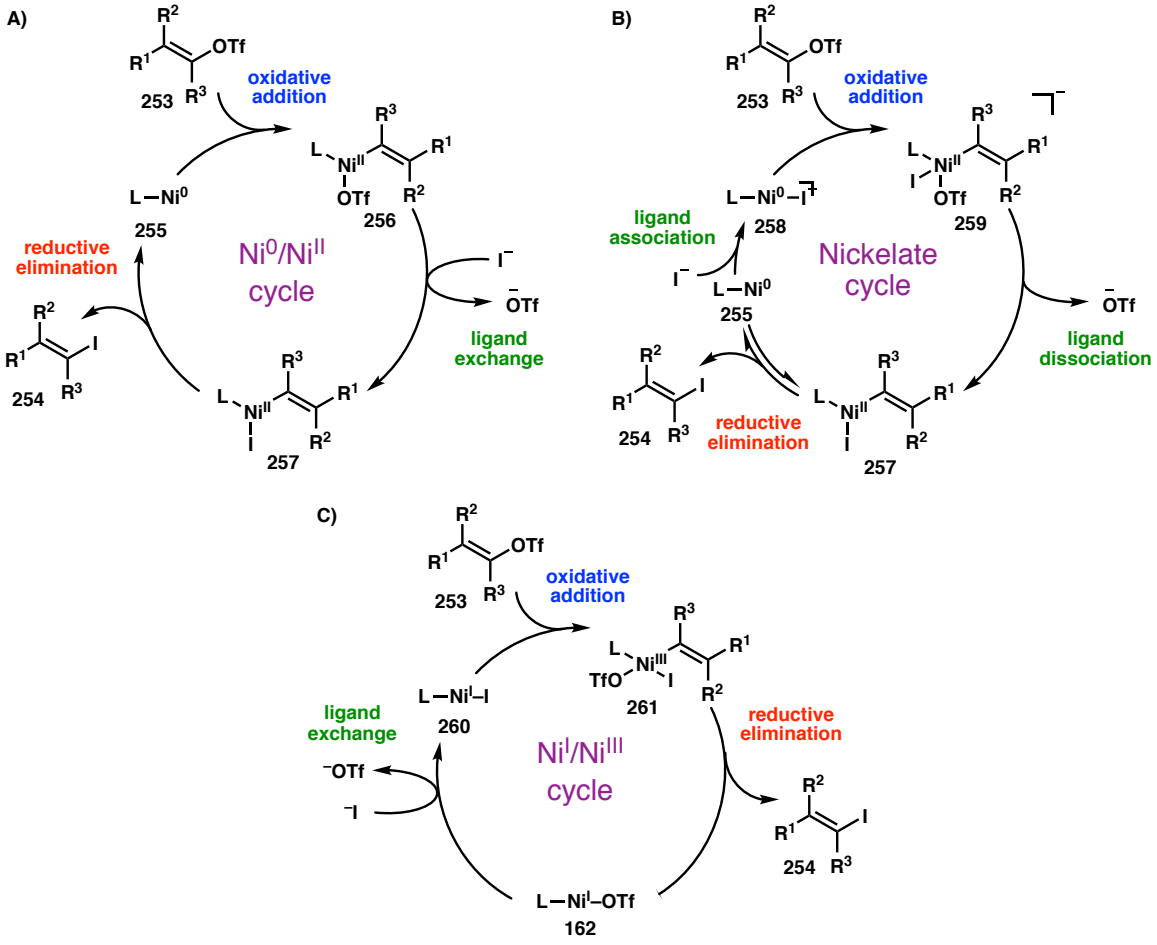

catalytic cycle which has been previously proposed for the cyanation of phenol derivatives (Figure 5.15a).[42] Monoligated Ni(0) complex **255** may undergo oxidative addition to the alkenyl triflate to form Ni(II) complex **256**. Ligand exchanged followed by reductive elimination from Ni(II) complex **257** can then afford the desired alkenyl iodide **254**. However, one shortcoming of this mechanism is that it does not account for the observation that alkenyl triflate oxidative addition does not occur in the absence of iodide. Consequently, a mechanism proceeding through a nickelate intermediates could be at play (Figure 5.15b). Kochi and coworkers previously assigned EPR spectra to a phosphine bound Ni(I) species that formed a nickelate complex upon addition of iodide.[29] It is possible that a Ni(0) nickelate complex **258** could form upon the addition of iodide via ligand association. Oxidative addition, ligand dissociation, and reductive elimination may form the desired alkenyl iodide (**254**). Lastly, given the observation of Ni(I) by EPR spectroscopy, a Ni(I)/Ni(III) catalytic cycle may be operative as well (Figure 5.15c). While our mechanistic investigations have not resulted in conclusive evidence for a particular pathway, these results shed light onto the complex and enigmatic reactivity of Ni-catalyzed halogenation reactions.

5.5 EVALUATION OF NI(II) PRECATALYSTS

5.5.1 Optimization

At this stage, we had successfully developed the $Ni(cod)_2$-catalyzed conversion of alkenyl triflates and nonaflates to alkenyl chlorides, bromides, and iodides. A broad substrate scope and good functional group tolerance were demonstrated, and a number of

mechanistic studies were performed in order to probe the reaction mechanism. However, $Ni(cod)_2$ is not bench stable and rather expensive compared to Ni(II) sources.[43] Therefore, we also investigated the use of Ni(II) salts with *in situ* reduction by Mn or Zn in order to prepare the alkenyl halides investigated in our earlier studies (Table 5.7). Reports by Inokawa and Brandsma previously demonstrated that active catalysts in Ni-mediated halogen exchange reactions of alkenyl halides were successfully prepared with the use of NiX_2 salts (anhydrous or hydrated) and Zn dust as the reductant[30,31] When NiX_2 salts were pre-reduced in the presence of excess Mn followed by filtration of the reduced catalyst, no conversion of **208** was observed (entry 1). However, upon the addition of 20 mol % cod, both Mn and Zn delivered the alkenyl halide products, albeit in variable yields (entries 2–3). In order to streamline the reaction process, Zn was directly added to the reactions in substoichiometric quantities (entry 4–6). Notably, the chlorination did not proceed to

Table 5.7. *Evaluation of Ni(II) halide salts for the halogenation of alkenyl triflates.*

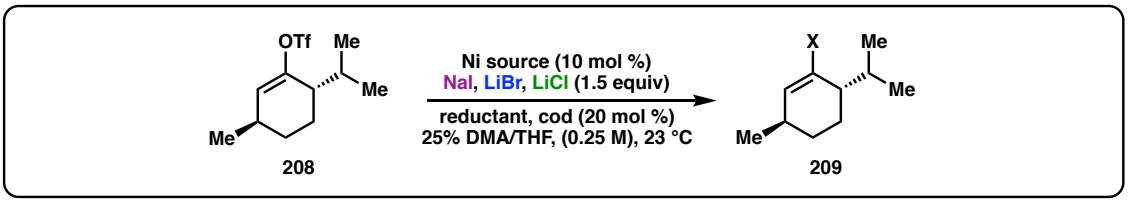

				Iodination	Bromination	Chlorination
Entry	Solvent	Ni Source	reductant	Yield (%)	Yield (%)	Yield (%)
1[a,b]	25% DMA/THF	NiX_2	excess Mn	0	0	0
2[a]	25% DMA/THF	NiX_2	excess Mn	4	41	63
3[a]	25% DMA/THF	NiX_2	excess Zn	4	37	57
4	25% DMA/THF	NiX_2	10 mol % Zn	28	84	0
5	25% DMA/THF	NiX_2	20 mol % Zn	25	85	0
6	25% DMA/THF	NiX_2	100 mol % Zn	14	24	0
7	DMA	NiX_2	20 mol % Zn	62	83	0
8	25% DMA/THF	NiX_2(dme)	20 mol % Zn	—	87	87

[a]Ni catalyst is pre-reduced with 3 equiv Zn, then filtered and added to the reaction. [b]No cod added.

provide the desired product due to insoluble nature of $NiCl_2$. In order to address the low solubility, DMA was evaluated as a solvent. While the chlorination still did not proceed, the iodination reaction improved under these conditions (entry 7). Changing the Ni halide source to the use of $NiX_2(dme)$, which is inherently much more soluble in organic solvents, provided the alkenyl bromide and chloride in 87% yield. Unfortunately, $NiI_2(dme)$ is not commercially available, although it can be made in the laboratory and was not investigated in this study.[44,45]

A series of other non-halide Ni precatalyst were evaluated, which could potentially provide for a more general reaction system (Table 5.8). While reduced $Ni(acac)_2$ successfully formed the alkenyl bromide **216b**, iodination failed under these conditions. Neither the bromination or iodination worked with $Ni(OTf)_2$, likely due to its poor solubility. Finally, the use of $Ni(OAc)_2{\cdot}4H_2O$ successfully provided alkenyl bromide **216b**

Table 5.8. *Evaluation of additional Ni(II) sources.*

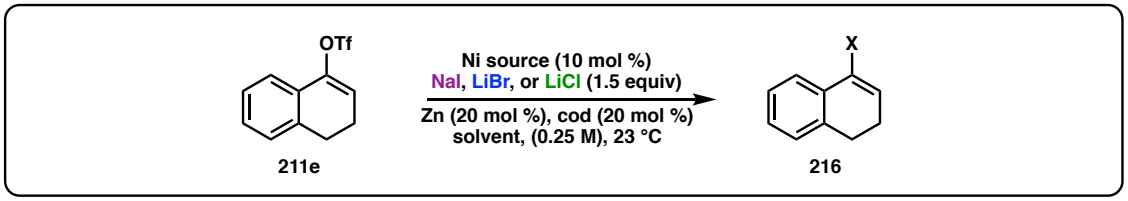

				Iodination	Bromination	Chlorination
Entry	Solvent	Ni Source	Time (h)	Yield (%)	Yield (%)	Yield (%)
1	DMA	$Ni(acac)_2$	2	4	97	—
2	25% DMA/THF	$Ni(acac)_2$	2	4	91	—
3	DMA	$Ni(OTf)_2$	2	5	0	—
4	DMA	$Ni(OAc)_2{\cdot}4H_2O$	2	0	39	—
5	25% DMA/THF	$Ni(OAc)_2{\cdot}4H_2O$	2	33	95	99
6[a]	25% DMA/THF	$Ni(OAc)_2{\cdot}4H_2O$	2	57	—	—
7[a]	25% DMA/THF	$Ni(OAc)_2{\cdot}4H_2O$	5	83	—	—
8[a]	25% DMA/THF	$Ni(OAc)_2{\cdot}4H_2O$	16	95	—	—

[a]20 mol % DMAP added.

in 95% yield and alkenyl iodide **216a** in a promising 33% yield (entry 5). The addition of 20 mol % DMAP, a ligand employed in reductive cross-couplings by Gong and coworkers,[46,47] afforded a higher yield of the **216a** (entry 6). Finally, running the reaction for an extended period of time furnished alkenyl iodide **216a** in 95% yield (entry 8).

5.5.2 Substrate Scope

With the Ni(II) conditions in hand, the scope was reevaluated (Figure 5.16). Most substrates saw an increase in yield over the Ni(0) conditions, in part due to improvements

Figure 5.16 *Evaluation of substrate scope with Ni(II).*

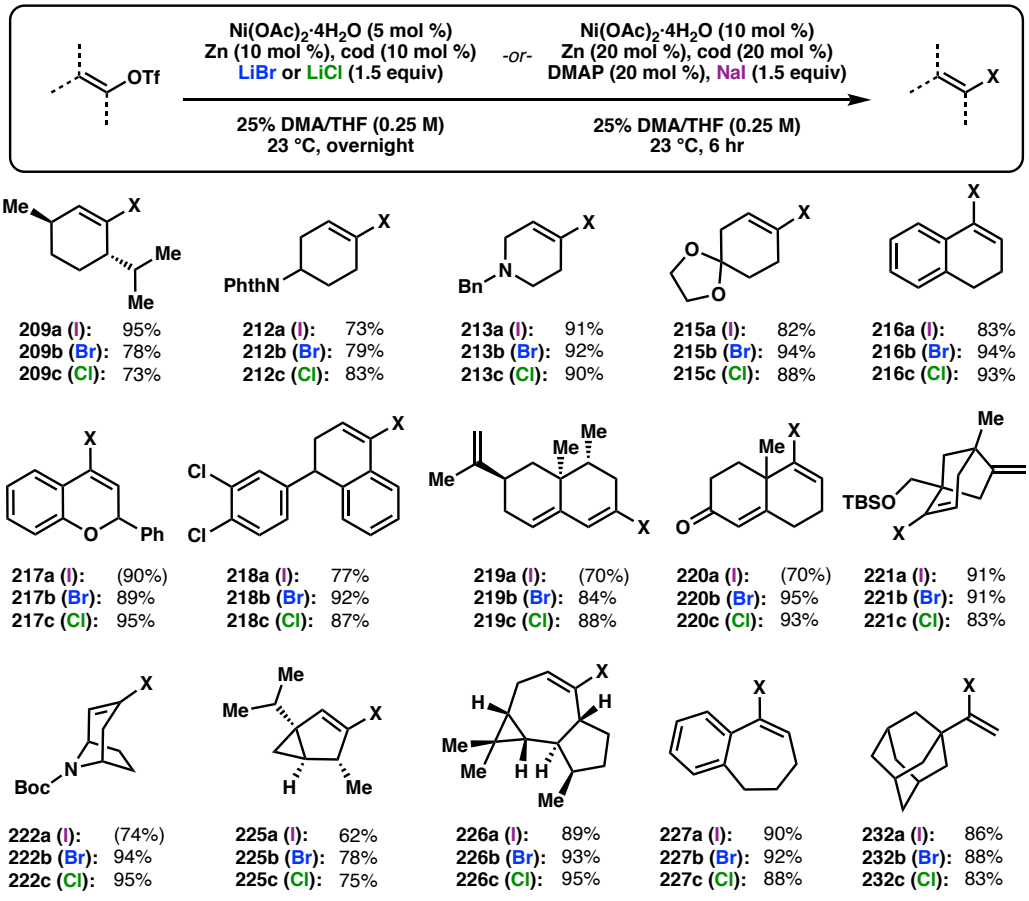

Reactions are conducted on 0.3 mmol scale under N_2. Isolated yields are provided; yields in parenthesis are ^{1}H NMR yields for substrates who could not be purified to >95% purity. Iodinations for **215a**, **217a**, **219a**, **220a**, **222a**, and **225a** conducted with 5 equiv NaI for 36 h in the absence of cod. Bromination and chlorination for **225b** and **225c** were conducted with 10 mol % DMAP instead of 10 mol % cod.

in conversion and increased recovery of mass balance. Under the Ni(II) conditions, the iodination reactions unfortunately were more prone towards the production of protodetriflation/protodehalogenation products (alkene) and some alkenyl halides could not be purified to >95% purity (**217a**, **219a**, **220a**, and **222a**); instead NMR yields are reported. Styrenyl bromides and iodides also produced significant quantities of alkene side products as well as the rearranged α-halo ketones under these reaction conditions.

5.6 CONCLUSION

In conclusion, a mild Ni-catalyzed halogenation of alkenyl triflates and alkenyl nonaflates has been developed with the use of commercially available $Ni(cod)_2$ and simple halide salts. By modifying the halide salt, alkenyl iodides, bromides, and chlorides can be readily obtained. The reaction proceeds at room temperature with the use of cod as the ancillary ligand, is amenable to gram scale preparation, and exhibits good functional group tolerance. Nevertheless, the reaction was still remarkably sensitive and required a glovebox to obtain reproducible and consistent yields. Attempts to translate the reaction to a benchtop setup were successful when $Ni(cod)_2$ was briefly exposed to air; however, the reaction was extremely sensitive to trace oxygen content in the reaction flask which inhibited the active catalyst and resulted in diminished yields. Further development of conditions that employ Ni(II) and a stoichiometric Zn reductant also successfully delivered the desired alkenyl halide products; however, in some cases product purification was challenging due to inseparable alkene byproducts. The analogous Ni(II) reactions also exhibited comparable high sensitivity to trace oxygen. A series of mechanistic experiments,

including evaluation via EPR, indicated the presence of a Ni(I) radical intermediate in the reaction; however, additional studies are required to fully elucidate the mechanism of this transformation.

5.7 EXPERIMENTAL SECTION

5.7.1 Materials and Methods

Unless otherwise stated, reactions were performed under a N_2 atmosphere using freshly dried solvents. Tetrahydrofuran (THF) and methylene chloride (CH_2Cl_2) were dried by passing through activated alumina columns. Diisopropylamine (*i*-Pr_2NH) was distilled over calcium hydride prior to use. Anhydrous dimethylacetamide (DMA), sodium iodide (NaI), lithium bromide (LiBr), and lithium chloride (LiCl) were purchased from Aldrich and stored under N_2. $Ni(cod)_2$ was purchased from Strem and stored in the glovebox at –20 °C. Unless otherwise stated, chemicals and reagents were used as received. All reactions were monitored by thin-layer chromatography using EMD/Merck silica gel 60 F254 pre-coated plates (0.25 mm) and were visualized by UV, CAM, or $KMnO_4$ staining. Flash column chromatography was performed as described by Still et al.[48] using silica gel (230-400 mesh, Silicycle). Purified compounds were dried on a high vacuum line (0.2 torr) to remove trace solvent. Optical rotations were measured on a Jasco P-2000 polarimeter using a 100 mm path-length cell at 589 nm. ^1H and ^{13}C NMR spectra were recorded on a Bruker Avance III HD with Prodigy cyroprobe (at 400 MHz and 101 MHz, respectively), a Varian 400 MR (at 400 MHz and 101 MHz, respectively), or a Varian Inova 500 (at 500 MHz and 126 MHz, respectively). ^1H and ^{19}F NMR spectra were also recorded on a Varian Inova 300 (at

300 MHz and 282 MHz, respectively). NMR data is reported relative to internal $CHCl_3$ (^1H, δ = 7.26), $CDCl_3$ (^{13}C, δ = 77.0), CD_3CN (^1H, δ = 1.94), CD_3CN (^{13}C, δ = 1.32), and C_6F_6 (^{19}F, δ = -161.64). Data for ^1H NMR spectra are reported as follows: chemical shift (δ ppm) (multiplicity, coupling constant (Hz), integration). Multiplicity and qualifier abbreviations are as follows: s = singlet, d = doublet, t = triplet, q = quartet, m = multiplet, br = broad. IR spectra were recorded on a Perkin Elmer Paragon 1000 spectrometer and are reported in frequency of absorption (cm^{-1}). HRMS were acquired from the Caltech Mass Spectral Facility using fast-atom bombardment (FAB), electrospray ionization (ESI-TOF), or electron impact (EI).

5.7.2 Optimization of Reaction Parameters

A 1-dram vial equipped with a stir bar was brought into a N_2-filled glovebox. The vial was charged with NaI, LiBr, or LiCl (0.15 mmol, 1.5 equiv) and $Ni(cod)_2$ (2.8 mg, 0.01 mmol, 0.1 equiv). Anhydrous DMA (0.1 mL) and THF (0.3 mL) were added, resulting in a clear yellow solution. Enol triflate (0.1 mmol, 1 equiv) was added neat, turning the reaction dark red (NaI) or aqua blue (LiBr or LiCl) over several minutes. The vial was sealed with a Teflon cap and brought out of the glovebox to stir on the bench (480 rpm) for two hours at room temperature. The reaction was quenched by eluting through a small plug of silica gel (5 cm of silica in a large glass pipette) with 40% Et_2O/pentane (10 mL collected). The crude reaction mixture was concentrated under reduced pressure and analyzed by NMR with tetrachloronitrobenzene as an external standard.

5.7.3 Substrate Preparation

5.7.3.1 Alkenyl Triflates

4-(1,3-dioxoisoindolin-2-yl)cyclohex-1-en-1-yl trifluoromethanesulfonate (211a)

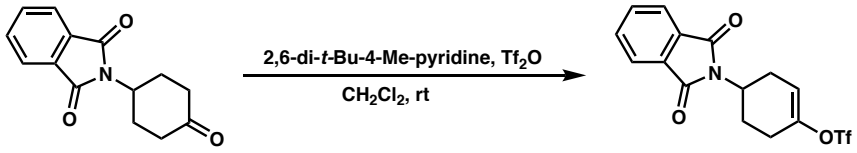

To a round bottom flask was added 2-(4-oxocyclohexyl)isoindoline-1,3-dione (730 mg, 3.0 mmol, 1.0 equiv), 2,6-di-*tert*-butyl-4-methylpyridine (924 mg, 4.5 mmol, 1.5 equiv), CH_2Cl_2 (10 mL), and trifluoromethanesulfonic anhydride (757 μL, 4.5 mmol, 1.5 equiv). The reaction was stirred overnight, then diluted with hexanes, filtered over Celite, and eluted with CH_2Cl_2. The organic filtrate was washed with H_2O and brine, and the aqueous layer was extracted with CH_2Cl_2. The combined organic layers were dried with $MgSO_4$, filtered, and concentrated. The product was purified by column chromatography (silica, 30% EtOAc/hexanes) to yield 752 mg (67% yield) of **211a** as a white solid. $\mathbf{R_f}$ = 0.30 (silica, 30% Et_2O/hexanes, $KMnO_4$). **^{1}H NMR (400 MHz, $CDCl_3$):** δ 7.83 (dd, *J* = 5.5, 3.0 Hz, 2H), 7.77 – 7.66 (m, 2H), 5.78 (dt, *J* = 5.9, 2.3 Hz, 1H), 4.43 (dddd, *J* = 12.7, 10.8, 5.5, 3.1 Hz, 1H), 3.07 (dddt, *J* = 17.3, 10.7, 4.3, 2.3 Hz, 1H), 2.81 – 2.68 (m, 1H), 2.68 – 2.54 (m, 1H), 2.52 – 2.40 (m, 1H), 2.39 – 2.26 (m, 1H), 1.92 (dddd, *J* = 12.5, 5.9, 3.8, 1.8 Hz, 1H). **^{13}C NMR (101 MHz, $CDCl_3$):** δ 168.2, 148.2, 134.3, 131.9, 123.4, 118.6 (q, $J_{C\text{-}F}$ = 320.2 Hz), 116.9, 45.6, 27.7, 26.7, 26.1. **^{19}F NMR (282 MHz, $CDCl_3$):** δ -73.7. **FTIR (NaCl, thin film, cm^{-1}):** 1704, 1698, 1418, 1385, 1249, 1196, 1139, 1112, 876, 718. **HRMS (TOF-ESI, *m/z*):** calc'd for $C_{15}H_{13}F_3O_5NS$ $[M+H]^+$: 376.0467; found: 376.0467.

Benzyl 4-(((trifluoromethyl)sulfonyl)oxy)-3,6-dihydropyridine-1(2*H*)-carboxylate (211c)

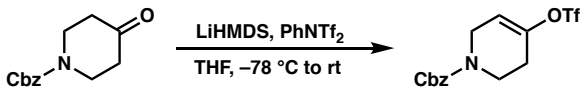

Benzyl 4-oxopiperidine-1-carboxylate (1.17 g, 5.0 mmol, 1.0 equiv) was added to a round-bottom flask and placed under an atmosphere of N_2. THF (25 mL) was added and the reaction was cooled to –78 °C. LiHMDS (5.5 mL, 1 M in THF, 5.5 mmol, 1.1 equiv) was added dropwise and allowed to stir for 30 minutes before N-phenyl-bis(trifluoromethanesulfonimide) (1.88 g, 5.25 mmol, 1.05 equiv) was added in one portion. The reaction was allowed to reach room temperature and stir overnight. The reaction was then quenched with saturated aq. NH_4Cl (50 mL) and extracted with Et_2O (2 x 50 mL). The combined organic layers were dried with $MgSO_4$, filtered, and concentrated. The product was purified by column chromatography (silica, 20% Et_2O/hexanes) to yield 901 mg (49% yield) of **211c** as a colorless oil. $\mathbf{R_f}$ = 0.30 (silica, 30% Et_2O/hexanes, $KMnO_4$). **^{1}H NMR (400 MHz, d_3-MeCN, 65 °C):** δ 7.39 (s, 1H), 7.38 (s, 2H), 7.37 – 7.30 (m, 1H), 5.91 – 5.85 (m, 1H), 5.18 – 5.14 (m, 2H), 4.14 – 4.06 (m, 2H), 3.69 (t, J = 5.8 Hz, 2H), 2.47 (ttt, J = 5.7, 2.8, 1.3 Hz, 2H). **^{13}C NMR (101 MHz, d_3-MeCN, 65 °C):** δ 156.2, 148.4, 138.5, 129.7, 129.2, 129.0, 117.4, 68.3, 43.1, 41.9, 29.0. **^{19}F NMR (282 MHz, $CDCl_3$):** δ -71.7. **FTIR (NaCl, thin film, cm^{-1}):** 3035, 2953, 1714, 1418, 1366, 1281, 1211, 1142, 1116, 1065, 872, 766, 698, 611. **HRMS (TOF-ESI, *m/z*):** calc'd for $C_{14}H_{14}F_3NO_5S$ $[M+H]^+$: 366.0623; found: 366.0613.

2-phenyl-2*H*-chromen-4-yl trifluoromethanesulfonate (211f)

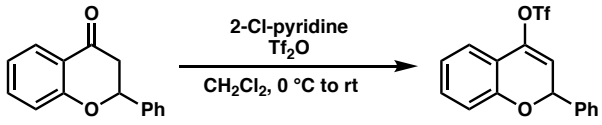

To a flame dried, N_2-filled round bottom flask was added 2-phenylchroman-4-one (500 mg, 2.9 mmol, 1.0 equiv), 2-chloropyridine (304 mg, 2.7 mmol, 1.2 equiv), and CH_2Cl_2 (8 mL). The reaction was cooled to 0 °C before trifluoromethanesulfonic anhydride (0.45 mL, 2.7 mmol, 1.2 equiv) was added. The reaction was allowed to reach room temperature and continued to stir overnight. The reaction was then cooled to 0 °C, saturated aq. $NaHCO_3$ was slowly added until gas evolution ceased, and then H_2O (25 mL) was added. The crude mixture was extracted with CH_2Cl_2 (2 x 50 mL). The combined organic layers were dried with $MgSO_4$, filtered, and concentrated. The product was purified by column chromatography (silica, 4% EtOAc/hexanes) to yield 421 mg (53% yield) of **211f** as a pale solid. $\mathbf{R_f}$ = 0.60 (silica, 10% Et_2O/hexanes, $KMnO_4$) **^{1}H NMR (400 MHz, $CDCl_3$):** δ 7.49 – 7.44 (m, 2H), 7.44 – 7.35 (m, 3H), 7.30 (dd, *J* = 7.7, 1.6 Hz, 1H), 7.26 (td, *J* = 8.1, 7.7, 1.6 Hz, 1H), 6.99 (td, *J* = 7.6, 1.1 Hz, 1H), 6.86 (dd, *J* = 8.1, 1.0 Hz, 1H), 6.12 (d, *J* = 3.8 Hz, 1H), 5.85 (d, *J* = 3.8 Hz, 1H). **^{13}C NMR (101 MHz, $CDCl_3$):** δ 153.9, 143.2, 138.8, 131.9, 129.2, 129.0, 127.1, 121.70, 121.67, 118.5 (q, $J_{C\text{-}F}$ = 320.5 Hz), 116.6, 116.4, 113.1, 77.4 **^{19}F NMR (282 MHz, $CDCl_3$):** δ -73.4. **FTIR (NaCl, thin film, cm^{-1}):** 3068, 3036, 1667, 1607, 1485, 1455, 1428, 1354, 1248, 1222, 1139, 1032, 935, 883, 858, 758, 698. **HRMS (FAB, *m/z*):** calc'd for $C_{16}H_{11}F_3O_4S$ $[M+\cdot]^+$: 356.0330; found: 356.0304.

4-(3,4-dichlorophenyl)-3,4-dihydronaphthalen-1-yl trifluoromethanesulfonate (211g)

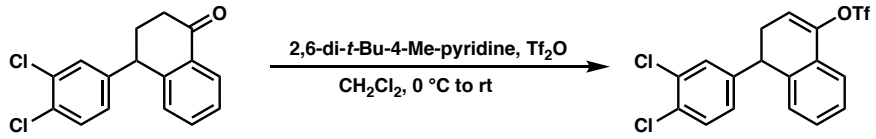

To a round bottom flask was added 4-(3,4-dichlorophenyl)-3,4-dihydronaphthalen-1(2*H*)-one (1.46 g, 5.0 mmol, 1.0 equiv), 2,6-di-*tert*-butyl-4-methylpyridine (1.13 g, 5.5 mmol, 1.1 equiv), and CH_2Cl_2 (15 mL). The reaction was cooled to 0 °C before trifluoromethanesulfonic anhydride (1.0 mL, 6.0 mmol, 1.2 equiv) was added. The reaction was allowed to reach room temperature and stirred for 30 minutes before being concentrated. The reaction mixture was then suspended in hexanes, filtered over a plug of Celite, and eluted with additional hexanes. The solution was concentrated and the product was purified by column chromatography (silica, 2% Et_2O/hexanes) to yield 2.09 g (99% yield) of **211g** as a colorless oil. $\mathbf{R_f}$ = 0.23 (silica, hexanes, $KMnO_4$). **^{1}H NMR (400 MHz, $CDCl_3$):** δ 7.47 (dd, *J* = 7.6, 1.3 Hz, 1H), 7.39 (d, *J* = 8.3 Hz, 1H), 7.35 (tdd, *J* = 7.7, 1.4, 0.6 Hz, 1H), 7.32 – 7.26 (m, 2H), 7.03 (ddd, *J* = 8.3, 2.2, 0.5 Hz, 1H), 6.94 – 6.89 (m, 1H), 5.97 (t, *J* = 4.8 Hz, 1H), 4.18 (t, *J* = 7.9 Hz, 1H), 2.89 (ddd, *J* = 17.4, 7.4, 4.8 Hz, 1H), 2.72 (ddd, *J* = 17.3, 8.6, 4.9 Hz, 1H). **^{13}C NMR (101 MHz, $CDCl_3$):** δ 146.2, 143.2, 137.4, 132.8, 131.2, 130.8, 130.3, 130.0, 128.7, 128.4, 127.9, 127.7, 121.9, 118.7 (q, $J_{C\text{-}F}$ = 320.4 Hz), 116.0, 42.4, 30.8 **^{19}F NMR (282 MHz, $CDCl_3$):** δ -73.5. **FTIR (NaCl, thin film, cm^{-1}):** 1658, 1470, 1422, 1249, 1213, 1140, 1066, 1019, 895, 765, 612. **HRMS (EI, *m/z*):** calc'd for $C_{17}H_{11}Cl_2F_3O_3S$ $[M+\cdot]^+$: 421.9758; found: 421.9755.

Methyl (1*s*,5*r*)-5-methyl-6-methylene-2-(((trifluoromethyl)sulfonyl)oxy)bicycle-[3.2.1]oct-2-ene-1-carboxylate (S31)

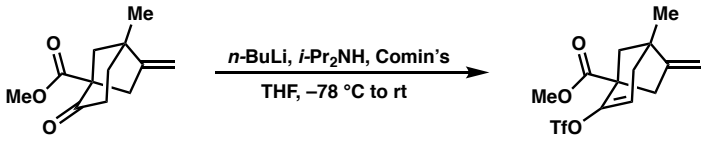

To a flame dried, N_2 filled round bottom flask was added methyl (1*s*,5*r*)-5-methyl-6-methylene-2-oxobicyclo[3.2.1]octane-1-carboxylate (670 mg, 3.0 mmol, 1 equiv) and THF (15 mL). The reaction was cooled to –78 °C (dry ice/acetone) before LDA (0.75M in THF, 4.8 mL, 3.6 mmol, 1.2 equiv) was added via cannula. The reaction mixture was stirred for 30 minutes before Comin's reagent (1M in THF, 3.45 mL, 3.45 mmol, 1.15 equiv) was added via cannula. After 1 hour, the reaction was quenched by addition of saturated aq. $NaHCO_3$ (20 mL) and warmed to room temperature. The crude mixture was extracted with Et_2O (3 x 15 mL) and the combined organic layers were dried over $MgSO_4$, filtered and concentrated. The product was purified by column chromatography (silica, 5% EtOAc/hexanes) to yield 865 mg (81% yield) of **S31** as a clear oil. $\mathbf{R_f}$ = 0.54 (silica, 10% EtOAc/hexanes, $KMnO_4$). **^{1}H NMR (400 MHz, $CDCl_3$):** δ 5.63 (dd, *J* = 4.9, 2.6 Hz, 1H), 5.02 (ddd, *J* = 2.5, 1.7, 0.8 Hz, 1H), 4.96 (dd, *J* = 3.0, 1.9 Hz, 1H), 3.76 (s, 3H), 3.11 – 2.92 (m, 2H), 2.37 (dd, *J* = 17.3, 2.7 Hz, 1H), 2.17 (ddd, *J* = 11.0, 2.7, 0.8 Hz, 1H), 2.11 – 2.02 (m, 1H), 1.96 (dd, *J* = 11.0, 1.5 Hz, 1H), 1.26 (s, 3H). **^{13}C NMR (101 MHz, $CDCl_3$):** δ 171.1, 155.2, 149.6, 120.0 (q, $J_{C\text{-}F}$ = 319.9 Hz), 116.5, 107.7, 52.8, 52.6, 48.2, 44.7, 42.9, 41.9, 23.9. **^{19}F NMR (282 MHz, $CDCl_3$):** δ -74.4. **FTIR (NaCl, thin film, cm^{-1}):** 2959, 1744, 1420, 1299, 1249, 1209, 1142, 1071, 1029, 265, 623. **HRMS (FAB, *m/z*):** calc'd for $C_{13}H_{15}F_3O_3S$ $[M+NH_4]^+$: 358.0931; found: 358.0924.

(1*r*,5*r*)-1-(hydroxymethyl)-5-methyl-6-methylenebicyclo[3.2.1]oct-2-en-2-yl trifluoromethanesulfonate (S32)

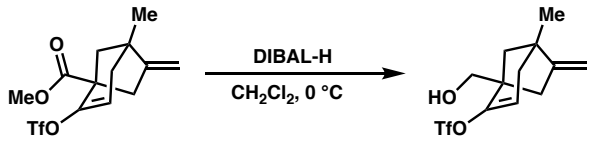

To a flame dried, N_2 filled round bottom flask was added **S31** (783 mg, 2.3 mmol, 1 equiv) and CH_2Cl_2 (23 mL). The reaction was cooled to 0 °C before DIBAL (1.23 mL, 6.9 mmol, 3 equiv) was added slowly. After 45 minutes, the reaction was quenched by addition of 1M HCl (6 mL) and warmed to room temperature. The crude mixture was diluted with water (20 mL) and extracted with CH_2Cl_2 (3 x 15 mL). The combined organic layers were washed with saturated aq. $NaHCO_3$ (30 mL), then brine (30 mL), and dried over $MgSO_4$, filtered and concentrated. The product was purified by column chromatography (silica, 10% to 20% EtOAc/hexanes) to yield 670 mg (93% yield) of **S32** as a clear oil. $\mathbf{R_f}$ = 0.36 (silica, 20% EtOAc/hexanes, $KMnO_4$). **^{1}H NMR (400 MHz, $CDCl_3$):** δ 5.61 (dd, *J* = 4.7, 2.7 Hz, 1H), 4.97 (ddd, *J* = 2.4, 1.4, 0.7 Hz, 1H), 4.94 (dd, *J* = 3.0, 1.7 Hz, 1H), 3.99 (dd, *J* = 11.3, 5.3 Hz, 1H), 3.59 (dd, *J* = 11.3, 5.7 Hz, 1H), 2.78 (ddt, *J* = 15.8, 3.2, 1.7 Hz, 1H), 2.41 – 2.29 (m, 2H), 2.08 – 1.98 (m, 2H), 1.74 – 1.67 (m, 2H), 1.25 (s, 3H). **^{13}C NMR (101 MHz, $CDCl_3$):** δ 156.6, 153.1, 118.7 (q, $J_{C\text{-}F}$ = 319.8 Hz), 117.2, 107.1, 64.5, 48.4, 47.4, 44.3, 43.1, 42.3, 24.4. **^{19}F NMR (282 MHz, $CDCl_3$):** δ -74.2. **FTIR (NaCl, thin film, cm^{-1}):** 3390 (br), 3076, 2959, 2880, 1668, 1416, 1211, 1142, 1030, 871, 621. **HRMS (FAB, *m/z*):** calc'd for $C_{11}H_{11}F_3O_3S$ $[M+H]^+$: 330.0981; found: 330.0981.

(1*r*,5*r*)-1-(((*tert*-butyldimethylsilyl)oxy)methyl)-5-methyl-6-methylenebicyclo[3.2.1]oct-2-en-2-yl trifluoromethanesulfonate (211j)

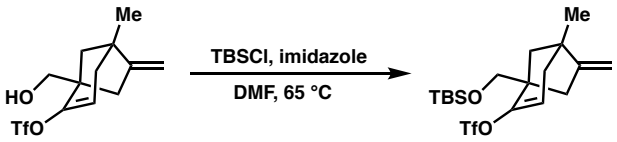

To a round bottom flask was added **211j** (576 mg, 1.8 mmol, 1 equiv), imidazole (251 mg, 3.7 mmol, 2 equiv), DMF (18 mL), and TBSCl (333 mg, 2.2 mmol, 1.2) equiv). The reaction was heated to 65 °C for 12 hours, cooled to room temperature and quenched by addition of saturated aq. NH_4Cl (20 mL). The crude mixture was extracted with EtOAc (3 x 20 mL, then the combined organic layers were washed with saturated aq. $NaHCO_3$ (30 mL), then saturated aq. NH_4Cl (3 x 30 mL), dried over $MgSO_4$, filtered and concentrated. The product was purified by column chromatography (silica, hexanes to 3% EtOAc/Hexanes) to yield 738 mg (94% yield) of **211j** as a white solid. $\mathbf{R_f}$ = 0.27 (silica, hexanes, $KMnO_4$). **^{1}H NMR (400 MHz, $CDCl_3$):** δ 5.55 (dd, *J* = 4.7, 2.7 Hz, 1H), 4.95 (ddd, *J* = 2.5, 1.5, 0.8 Hz, 1H), 4.92 (dd, *J* = 3.1, 1.7 Hz, 1H), 3.90 (d, *J* = 10.1 Hz, 1H), 3.51 (d, *J* = 10.1 Hz, 1H), 2.69 (ddt, *J* = 15.8, 3.1, 1.6 Hz, 1H), 2.43 – 2.35 (m, 1H), 2.32 (dd, *J* = 17.1, 2.7 Hz, 1H), 2.06 – 1.97 (m, 1H), 1.91 (dd, *J* = 11.0, 2.8 Hz, 1H), 1.69 (dd, *J* = 10.9, 1.5 Hz, 1H), 1.24 (s, 3H), 0.89 (s, 9H), 0.05 (s, 6H). **^{13}C NMR (101 MHz, $CDCl_3$):** δ 157.3, 153.6, 120.1 (q, $J_{C\text{-}F}$ = 319.3 Hz), 116.3, 106.7, 64.0, 48.4, 47.6, 43.8, 43.0, 42.4, 26.0, 24.5, 18.5, -5.5. **^{19}F NMR (282 MHz, $CDCl_3$):** δ -74.4. **FTIR (NaCl, thin film, cm^{-1}):** 3076, 2957, 2860, 1668, 1473, 1418, 1246, 1211, 1144, 1101, 1031, 874, 840, 778, 620. **HRMS (FAB, *m/z*):** calc'd for $C_{18}H_{29}F_3O_4S$ $[M+H]^+$: 427.1581; found: 427.1568.

(5'*R*,6a*R*,6b*S*,8a*S*,8b*R*,9*S*,10*R*,11a*S*,12a*S*,12b*S*)-5',6a,8a,9-tetramethyl-1,3',4',5,5',6,6a,6b,-6',7,8,8a,8b,9,11a,12,12a,12b-octadecahydrospiro[naphtho[2',1':4,5]indeno[2,1-*b*]furan-10,2'-pyran]-4-yl trifluoromethanesulfonate (211l)

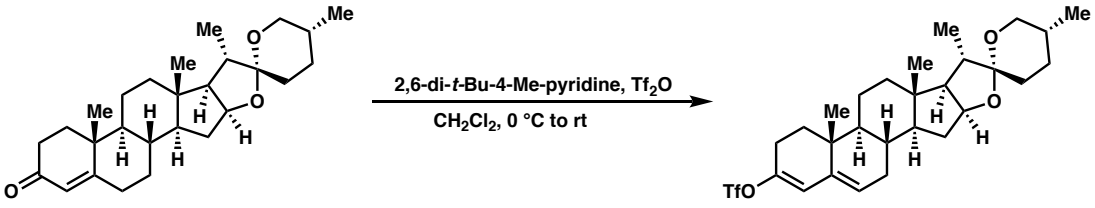

To a round bottom flask was added (5'*R*,6a*R*,6b*S*,8a*S*,8b*R*,9*S*,10*R*,11a*S*,12a*S*,12b*S*)-5',6a,8a,9-tetramethyl-1,3',4',5,5',6,6a,6b,6',7,8,8a,8b,9,11a,12,12a,12b-octadecahydro-spiro-[naphtha[2',1':4-,5]indeno[2,1-*b*]furan-10,2'-pyran]-4(3*H*)-one (661 mg, 1.8 mmol, 1.0 equiv), 2,6-di-*tert*-butyl-4-methylpyridine (395 mg, 2.16 mmol, 1.2 equiv), and CH_2Cl_2 (5.0 mL). The reaction was cooled to 0 °C and trifluoromethanesulfonic anhydride (296 μL, 1.98 mmol, 1.1 equiv) was added. The reaction was stirred at room temperature overnight, then washed with saturated aq. $NaHCO_3$ (50 mL) and extracted with CH_2Cl_2 (2 x 100 mL). The combined organic layers were dried with $MgSO_4$, filtered, and concentrated. The product was purified by column chromatography (silica, 5 to 10% Et_2O/hexanes) to yield 488 mg (50% yield) of **211l** as a white solid. $\mathbf{R_f}$ = 0.40 (silica, 10% Et_2O/hexanes, $KMnO_4$). $[\boldsymbol{a}]_D^{25}$ = –125° (c = 1.0, $CHCl_3$). **^{1}H NMR (400 MHz, $CDCl_3$):** δ 5.99 (d, *J* = 2.2 Hz, 1H), 5.57 (dd, *J* = 5.1, 2.9 Hz, 1H), 4.42 (ddd, *J* = 8.6, 7.5, 6.3 Hz, 1H), 3.47 (ddd, *J* = 10.8, 4.6, 2.0 Hz, 1H), 3.37 (t, *J* = 10.9 Hz, 1H), 2.63 – 2.48 (m, 1H), 2.40 – 2.30 (m, 1H), 2.23 (dt, *J* = 18.8, 5.2 Hz, 1H), 1.99 (ddd, *J* = 11.8, 7.5, 5.4 Hz, 1H), 1.95 – 1.51 (m, 11H), 1.51 – 1.39 (m, 2H), 1.32 (ddd, *J* = 13.7, 11.9, 6.4 Hz, 2H), 1.26 – 1.11

(m, 2H), 1.09 – 0.99 (m, 1H), 0.99 (s, 6H), 0.81 (s, 3H), 0.79 (d, J = 6.3 Hz, 3H). **^{13}C NMR (101 MHz, $CDCl_3$):** δ 147.1, 138.2, 128.1, 120.6, 118.7 (q, $J_{C\text{-}F}$ = 319.9 Hz), 109.5, 80.9, 67.0, 62.2, 56.6, 47.8, 41.8, 40.5, 39.8, 35.0, 33.9, 32.2, 31.9, 31.5, 31.3, 30.4, 28.9, 25.7, 21.2, 18.8, 17.3, 16.5, 14.7. **^{19}F NMR (282 MHz, $CDCl_3$):** δ -73.8. **FTIR (NaCl, thin film, cm^{-1}):** 3054, 2947, 2306, 1640, 1456, 1380, 1266, 1214, 1140, 1051, 919, 829, 740. **HRMS (FAB, *m/z*):** calc'd for $C_{28}H_{40}F_3O_5S$ $[M+H]^+$: 545.2549; found: 545.2536.

(1a*R*,4a*R*,7*R*,7a*S*,7b*S*)-1,1,7-trimethyl-1a,2,4a,5,6,7,7a,7b-octahydro-1*H*-cyclopropa[*e*]azulen-4-yl trifluoromethanesulfonate (211m)

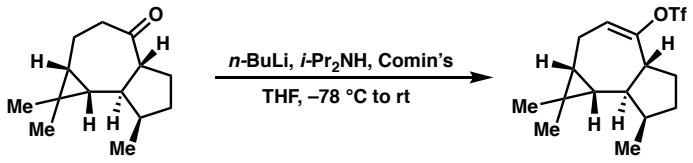

To a round bottom flask was added diisopropyl amine (337 μL, 2.4 mmol, 1.2 equiv) and THF (6 mL). The solution was cooled to 0 °C, then *n*-butyllithium (960 μL, 2.5 M in hexanes, 2.4 mmol, 1.2 equiv) was added and stirred for 30 minutes before being cooled to –78 °C. (1a*R*,4a*R*,7*R*,7a*S*,7b*S*)-1,1,7-Trimethyldecahydro-4*H*-cyclopropa[*e*]azulen-4-one (412 mg, 2.0 mmol, 1.0 equiv) was added and stirred for 30 minutes before N-(5-chloro-2-pyridyl)bis(trifluoromethanesulfonimide) (942 mg, 2.4 mmol, 1.2 equiv) was added in one portion. The reaction was allowed to reach room temperature and stir overnight. The reaction was quenched with H_2O and extracted with Et_2O (2 x 50 mL). The combined organic layers were dried with $MgSO_4$, filtered, and concentrated. The product was purified by column chromatography (silica, hexanes) to yield 386 mg (57% yield) of **211m** as a colorless oil which solidified in the freezer. $\mathbf{R}_f$ = 0.49 (silica, hexanes, $KMnO_4$)

$[\alpha]_D^{25}$ = –93° (c = 1.0, $CHCl_3$). **^{1}H NMR (400 MHz, $CDCl_3$):** δ 5.74 (ddd, *J* = 9.3, 2.9, 2.1 Hz, 1H), 2.79 (tdd, *J* = 11.3, 5.4, 2.0 Hz, 1H), 2.29 (dddd, *J* = 17.3, 9.3, 7.0, 0.8 Hz, 1H), 2.24 – 2.11 (m, 1H), 2.11 – 1.90 (m, 3H), 1.70 (td, *J* = 11.7, 8.4 Hz, 1H), 1.56 – 1.41 (m, 1H), 1.24 (dtd, *J* = 13.1, 8.5, 4.3 Hz, 1H), 1.05 (d, *J* = 1.1 Hz, 6H), 0.97 (ddd, *J* = 10.1, 9.3, 7.0 Hz, 1H), 0.92 (d, *J* = 7.2 Hz, 3H), 0.65 (dd, *J* = 11.5, 9.2 Hz, 1H). **^{13}C NMR (101 MHz, $CDCl_3$):** δ 154.6, 120.1, 118.7 (q, $J_{C\text{-}F}$ = 319.9 Hz), 48.0, 43.1, 34.4, 32.0, 29.8, 28.5, 25.7, 25.6, 20.3, 18.7, 18.0, 15.3. **^{19}F NMR (282 MHz, $CDCl_3$):** δ -74.3. **FTIR (NaCl, thin film, cm^{-1}):** 2957, 2872, 1672, 1457, 1415, 1246, 1208, 1145, 984, 941, 865. **HRMS (FAB, *m/z*):** calc'd for $C_{15}H_{21}F_3O_3S$ $[M+\cdot]^+$: 338.1164; found: 338.1164.

1-(6-(((trifluoromethyl)sulfonyl)oxy)pyridin-3-yl)vinyl trifluoromethanesulfonate (211p)

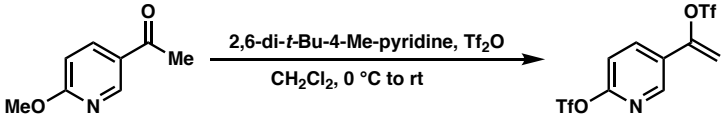

To a round bottom flask was added 1-(6-methoxypyridin-3-yl)ethan-1-one (756 mg, 5.0 mmol, 1.0 equiv), 2,6-di-*tert*-butyl-4-methylpyridine (2.26 g, 11 mmol, 2.2 equiv), and CH_2Cl_2 (15 mL). The reaction was cooled to 0 °C before trifluoromethanesulfonic anhydride (2.0 mL, 12.0 mmol, 2.4 equiv) was added. The reaction was allowed to reach room temperature and stir overnight. The reaction was then cooled to 0 °C and saturated aq. $NaHCO_3$ was added slowly until gas evolution ceased, then H_2O (25 mL) was added. The crude mixture was extracted with Et_2O (2 x 50 mL). The combined organic layers were dried with $MgSO_4$, filtered, and concentrated. The product was purified by column chromatography (silica, 20% Et_2O/hexanes) to yield 544 mg (27% yield) of **211p** as a light

orange oil. $\mathbf{R_f}$ = 0.33 (silica, 30% Et_2O/hexanes, $KMnO_4$). **^{1}H NMR (400 MHz, $CDCl_3$):** δ 8.59 (dd, *J* = 2.6, 0.7 Hz, 1H), 8.03 (dd, *J* = 8.6, 2.6 Hz, 1H), 7.30 – 7.23 (m, 1H), 5.75 (d, *J* = 4.5 Hz, 1H), 5.61 (d, *J* = 4.6 Hz, 1H). **^{13}C NMR (101 MHz, $CDCl_3$):** δ 156.6, 149.0, 145.9, 138.0, 129.3, 118.7 (q, J_{C-F} = 320.6 Hz), 118.6 (q, J_{C-F} = 320.4 Hz), 115.4, 108.0. **^{19}F NMR (282 MHz, $CDCl_3$):** δ -72.8, -73.3. **FTIR (NaCl, thin film, cm^{-1}):** 1648, 1588, 1474, 1427, 1212, 1138, 943, 890, 819. **HRMS (TOF-ESI, *m/z*):** calc'd for $C_9H_5F_6O_6NS_2$ $[M+H]^+$: 401.9541; found: 401.9551.

1-(4-chloro-3-fluorophenyl)vinyl trifluoromethanesulfonate (211q)

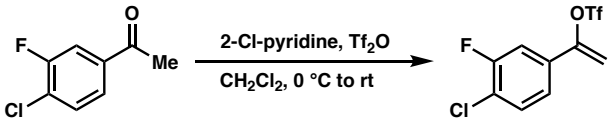

To a flame dried, N_2 filled round bottom flask was added 1-(4-chloro-3-fluorophenyl)vinyl trifluoromethanesulfonate (500 mg, 2.9 mmol, 1.0 equiv), 2-chloropyridine (428 mg, 3.8 mmol, 1.3 equiv), and CH_2Cl_2 (10 mL). The reaction was cooled to 0 °C before trifluoromethanesulfonic anhydride (0.58 mL, 3.5 mmol, 1.2 equiv) was added. The reaction was allowed to reach room temperature and continued to stir overnight. The reaction was then cooled to 0 °C and saturated aq. $NaHCO_3$ was added slowly until gas evolution ceased, then H_2O (25 mL) was added. The crude mixture was extracted with CH_2Cl_2 (2 x 50 mL). The combined organic layers were dried with $MgSO_4$, filtered, and concentrated. The product was purified by column chromatography (silica, hexanes) to yield 434 mg (49% yield) of **211q** as a light yellow oil. $\mathbf{R_f}$ = 0.31 (silica, hexanes, UV). **^{1}H NMR (400 MHz, $CDCl_3$):** δ 7.46 (dd, *J* = 8.4, 7.3 Hz, 1H), 7.32 (dd, *J* = 9.6, 2.1 Hz, 1H), 7.29 (ddd, *J* = 8.4, 2.1, 0.9 Hz, 1H), 5.64 (d, *J* = 4.3 Hz, 1H), 5.47 (d, *J* = 4.3 Hz, 1H). **^{13}C**

NMR (101 MHz, $CDCl_3$): 158.3 (d, J_{C-F} = 250.3 Hz), 151.3 (d, J_{C-F} = 2.7 Hz), 132.6 (d, J_{C-F} = 7.2 Hz), 131.4, 123.5 (d, J_{C-F} = 17.7 Hz), 121.8 (d, J_{C-F} = 3.9 Hz), 118.6 (q, J_{C-F} = 320.3 Hz), 113.8 (d, J_{C-F} = 23.7 Hz), 106.0. **^{19}F NMR (282 MHz, $CDCl_3$):** δ -73.5, -113.2 (dd, J_{F-H} = 9.3, 7.3 Hz). **FTIR (NaCl, thin film, cm^{-1}):** 1647, 1575, 1492, 1423, 1296, 1244, 1216, 1141, 1080, 955, 916, 803, 607. **HRMS (FAB, *m/z*):** calc'd for $C_9H_5ClF_4O_3S$ $[M+\cdot]^+$: 303.9584; found: 303.9592.

1-(4-(4,4,5,5-tetramethyl-1,3,2-dioxaborolan-2-yl)phenyl)vinyl trifluoromethanesulfonate (211r)

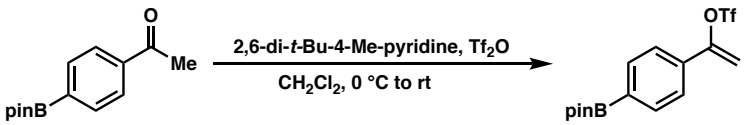

To a round bottom flask was added 1-(4-(4,4,5,5-tetramethyl-1,3,2-dioxaborolan-2-yl)phenyl)ethan-1-one (984 mg, 4.0 mmol, 1.0 equiv), 2,6-di-*tert*-butyl-4-methylpyridine (904 mg, 4.4 mmol, 1.1 equiv), and CH_2Cl_2 (12 mL). The reaction was cooled to 0 °C before trifluoromethanesulfonic anhydride (808 μL, 4.8 mmol, 1.2 equiv) was added. The reaction was allowed to reach room temperature and continued to stir overnight. The reaction was concentrated and the product was purified by column chromatography (silica, 5% EtOAc/hexanes) to yield 742 mg (49% yield) of **211r** as a blue oil. $\mathbf{R_f}$ = 0.51 (silica, 10% Et_2O/hexanes, $KMnO_4$). **^{1}H NMR (400 MHz, $CDCl_3$):** δ 7.89 – 7.81 (m, 2H), 7.56 – 7.51 (m, 2H), 5.67 (d, *J* = 4.0 Hz, 1H), 5.41 (d, *J* = 4.0 Hz, 1H), 1.35 (s, 12H). **^{13}C NMR (101 MHz, $CDCl_3$):** δ 153.6, 135.3, 134.4, 124.5, 118.6 (q, J_{C-F} = 320.2 Hz), 105.1, 84.3, 25.0. *(Note: carbon bonded to boron not observed.)* **^{19}F NMR (282 MHz, $CDCl_3$):** δ -73.7.

FTIR (NaCl, thin film, cm^{-1}): 2981, 1646, 1612, 1423, 1402, 1362, 1225, 1143, 1096, 939, 829, 660, 605. **HRMS (FAB, *m/z*):** calc'd for $C_{15}H_{15}BF_3O_5S$ $[M+\cdot]^+$: 378.0920; found: 378.0946.

4-isopropylcyclohex-1-en-1-yl trifluoromethanesulfonate (251)

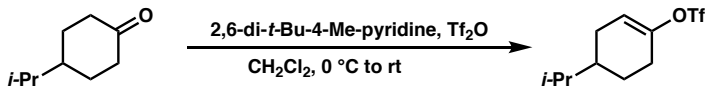

To a flame dried, N_2-filled round bottom flask was added 4-isopropylcyclohexan-1-one (1.8 g, 12.5 mmol, 1.0 equiv), 2,6-di-*tert*-butyl-4-methylpyridine (3.0 g, 14.4 mmol, 1.15 equiv), and CH_2Cl_2 (83 mL). The reaction was cooled to 0 °C before trifluoromethanesulfonic anhydride (2.3 mL, 2.7 mmol, 1.2 equiv) was added. The reaction was warmed to room temperature and continued overnight. The reaction was cooled to 0 °C, saturated aq. $NaHCO_3$ was slowly added until gas evolution ceased, and then H_2O (25 mL) was added. The crude mixture was extracted with CH_2Cl_2 (2 x 50 mL). The combined organic layers were dried with $MgSO_4$, filtered, and concentrated. The product was purified by column chromatography (silica, hexanes) to yield 2.3 g (68% yield) of **251** as a clear oil. $\mathbf{R_f}$ = 0.49 (silica, hexanes, $KMnO_4$). **^{1}H NMR (400 MHz, $CDCl_3$):** δ 5.74 (dt, J = 5.2, 2.6 Hz, 1H), 2.46 – 2.34 (m, 1H), 2.34 – 2.25 (m, 1H), 2.25 – 2.14 (m, 1H), 1.98 – 1.84 (m, 2H), 1.61 – 1.49 (m, 1H), 1.49 – 1.29 (m, 2H), 0.91 (d, J = 3.0 Hz, 3H), 0.90 (d, J = 3.0 Hz, 3H). **^{13}C NMR (101 MHz, $CDCl_3$):** δ 149.4, 118.6 (q, $J_{C\text{-}F}$ = 320.1 Hz), 118.3, 39.0, 31.7, 28.1, 27.4, 26.2, 20.0, 19.7. **^{19}F NMR (282 MHz, $CDCl_3$):** δ -73.9. **FTIR (NaCl, thin film, cm^{-1}):** 2962, 2933, 2876, 1693, 1418, 1248, 1209, 1144, 1053, 1022, 879, 853, 615. **HRMS (EI, *m/z*):** calc'd for $C_{10}H_{15}F_3O_3S$ $[M+\cdot]^+$: 272.0694; found: 272.0681.

Other Alkeny Triflates Prepared from Literature

Alkenyl triflate **208** was prepared according to a literature procedure reported by Paquette and coworkers.[49]

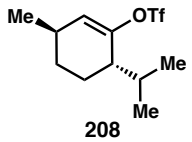

208

Alkenyl triflate **211b** was prepared according to a literature procedure reported by Stadler and coworkers.[50]

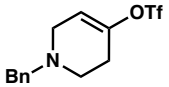

211b

Alkenyl triflates **211d**, **211e**, and **211u** were prepared according to a literature procedure reported by Yuan, Yi, and coworkers.[51]

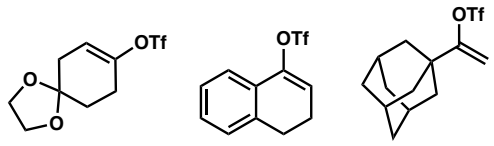

211d **211e** **211u**

Alkenyl triflate **211h** was prepared according to a literature procedure reported by Buchwald and coworkers.[52]

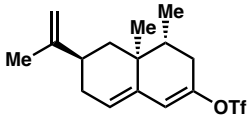

211h

Alkenyl triflate **211i** was prepared according to a literature procedure reported by Lett and coworkers.[53]

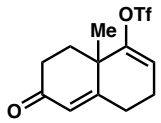

211i

Alkenyl triflate **211k** was prepared according to a literature procedure reported by Takahashi and coworkers.[54]

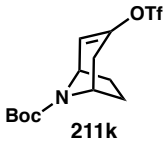

211k

Alkenyl triflate **211m** was prepared according to a literature procedure reported by Wang and coworkers.[55]

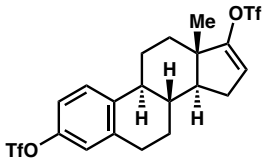

211m

Alkenyl triflate **211n** was prepared according to a literature procedure reported by Wada and coworkers.[56]

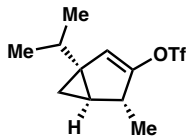

211n

Alkenyl triflate **211p** was prepared according to a literature procedure reported by Xu, Tang, and coworkers.[57]

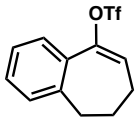

211p

Alkenyl triflate **211q** was prepared according to a literature procedure reported by Kamimura and coworkers.[58]

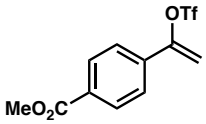

211q

5.7.3.2 Alkenyl Nonaflates

1,4-dioxaspiro[4.5]dec-7-en-8-yl 1,1,2,2,3,3,4,4,4-nonafluorobutane-1-sulfonate (233a)

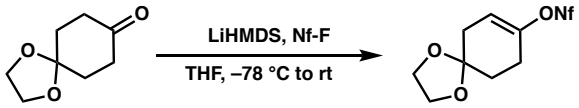

1,4-dioxaspiro[4.5]decan-8-one (1.0 g, 6.4 mmol, 1.0 equiv) was added to a flame dried round-bottom flask and placed under an atmosphere of N_2. THF (13 mL) was added and the reaction was cooled to –78 °C. LiHMDS (8.3 mL, 1 M in THF, 5.5 mmol, 1.3 equiv) was added dropwise and allowed to stir for 30 minutes before perfluorobutanesulfonylfluoride (1.27 mL, 7.0 mmol, 1.1 equiv) was added in one portion. The reaction was allowed to reach room temperature and stir overnight. The reaction was then quenched with saturated aq. NH_4Cl (50 mL) and extracted with Et_2O (2 x 50 mL). The

combined organic layers were dried with $MgSO_4$, filtered, and concentrated. The product was purified by column chromatography (silica, 10% EtOAc/hexanes) to yield 1.3 g (45 % yield) of **233a** as a colorless oil. $\mathbf{R_f}$ = 0.66 (silica, 20% Et_2O/hexanes, anisaldehyde (blue)). **^{1}H NMR (400 MHz, $CDCl_3$):** δ 5.68 (tt, *J* = 4.1, 1.4 Hz, 1H), 3.98 (p, *J* = 1.7 Hz, 4H), 2.54 (dtd, *J* = 6.6, 3.4, 2.6, 1.4 Hz, 2H), 2.41 (dt, *J* = 4.8, 2.6 Hz, 2H), 1.91 (t, *J* = 6.6 Hz, 2H). **^{13}C NMR (101 MHz, $CDCl_3$):** δ 148.4, 116.1, 106.3, 64.8, 34.3, 31.2, 26.6. (*Note: nonaflate carbons omitted due to low intensity resulting from C-F splitting*). **^{19}F NMR (282 MHz, $CDCl_3$):** δ -80.55 (tt, *J* = 9.7, 2.3 Hz), -109.78 – -109.95 (m), -120.87 (dddd, *J* = 14.9, 9.8, 6.4, 2.4 Hz), -125.66 – -125.90 (m). **FTIR (NaCl, thin film, cm^{-1}):** 2965, 2890, 1691, 1422, 1240, 1144, 1070, 883. **HRMS (EI, *m/z*):** calc'd for $C_{12}H_{12}F_9O_5S$ $[M+H]^+$: 439.0261; found: 439.0276.

(4*R*,4a*S*,6*R*)-4,4a-dimethyl-6-(prop-1-en-2-yl)-3,4,4a,5,6,7-hexahydronaphthalen-2-yl 1,1,2,2,3,3,4,4,4-nonafluorobutane-1-sulfonate (233b)

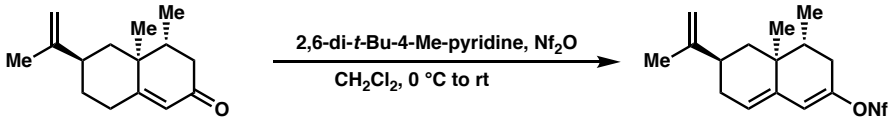

To a round bottom flask was added (4*S*,4a*R*,6*S*)-4,4a-dimethyl-6-(prop-1-en-2-yl)-4,4a,5,6,7,8-hexahydronaphthalen-2(3*H*)-one (174 mg, 0.8 mmol, 1.0 equiv), 2,6-di-*tert*-butyl-4-methylpyridine (312 mg, 0.9 mmol, 1.1 equiv), and CH_2Cl_2 (4 mL). The reaction was cooled to 0 °C before nonafluorobutanesulfonic anhydride (465 mg, 0.8 mmol, 1.0 equiv) was added. The reaction was allowed to reach room temperature and continued to stir for 2 hours. The reaction was diluted with hexanes, filtered, and concentrated. The product was purified by column chromatography (silica, hexanes) to yield 226 mg (56%

yield) of **233b** as a colorless oil. $\mathbf{R_f}$ = 0.22 (silica, hexanes, UV). $[\boldsymbol{\alpha}]_D^{25}$ = –66° (c = 0.5, $CHCl_3$). **^{1}H NMR (400 MHz, $CDCl_3$):** δ 6.04 (s, 1H), 5.63 (dd, *J* = 5.3, 2.7 Hz, 1H), 4.76 (pd, *J* = 1.9, 1.3 Hz, 2H), 2.50 – 2.36 (m, 1H), 2.36 – 2.29 (m, 3H), 2.26 (td, *J* = 5.4, 1.4 Hz, 1H), 1.98 (ddd, *J* = 18.9, 11.4, 2.3 Hz, 1H), 1.79 – 1.65 (m, 5H), 1.18 (t, *J* = 12.7 Hz, 1H), 0.96 (d, *J* = 6.8 Hz, 3H), 0.93 (s, 3H). **^{13}C NMR (101 MHz, $CDCl_3$):** δ 149.6, 147.1, 138.5, 128.2, 120.5, 109.3, 39.7, 39.3, 37.1, 35.9, 34.3, 31.4, 30.3, 20.8, 17.3, 14.5. (*Note: nonaflate carbons omitted due to low intensity resulting from C-F splitting*). **^{19}F NMR (282 MHz, $CDCl_3$):** δ -80.57 (tt, *J* = 9.8, 2.3 Hz), -109.77 – -109.94 (m), -120.90 (dddt, *J* = 15.8, 9.7, 6.3, 3.3 Hz), -125.69 – -125.92 (m). **FTIR (NaCl, thin film, cm^{-1}):** 2969, 1644, 1416, 1238, 1142, 1058, 912. **HRMS (EI, *m/z*):** calc'd for $C_{19}H_{20}F_9O_3S$ $[M–H]^+$: 499.0989; found: 499.0965.

8a-methyl-6-oxo-3,4,6,7,8,8a-hexahydronaphthalen-1-yl 1,1,2,2,3,3,4,4,4-nonafluoro-butane-1-sulfonate (233c)

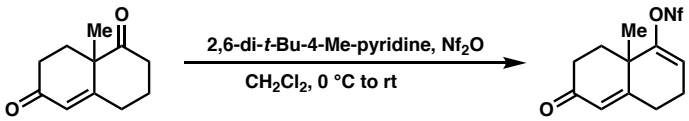

To a round bottom flask was added 8a-methyl-3,4,8,8a-tetrahydronaphthalene-1,6(2*H*,7*H*)-dione (142 mg, 0.8 mmol, 1.0 equiv), 2,6-di-tert-butyl-4-methylpyridine (312 mg, 0.9 mmol, 1.1 equiv), and CH_2Cl_2 (4 mL). The reaction was cooled to 0 °C before nonafluorobutansulfonic anhydride (465 mg, 0.8 mmol, 1.0 equiv) was added. The reaction was allowed to reach room temperature and continued to stir for 2 hours. The reaction was diluted with hexanes, filtered, and concentrated. The product was purified by column chromatography (silica, 10% Et_2O/hexanes) to yield 270 mg (73% yield) of **233c** as a white

solid. $\mathbf{R_f}$ = 0.32 (silica, 25% Et_2O/hexanes, UV). **^{1}H NMR (400 MHz, $CDCl_3$)**: δ 6.15 (d, *J* = 2.3 Hz, 1H), 5.89 – 5.82 (m, 1H), 2.81 (ddd, *J* = 15.4, 7.3, 6.2 Hz, 1H), 2.74 – 2.35 (m, 5H), 2.07 (ddd, *J* = 13.6, 5.9, 1.6 Hz, 1H), 1.75 – 1.61 (m, 1H), 1.25 (s, 3H). **^{13}C NMR (101 MHz, $CDCl_3$):** δ 213.0, 148.2, 136.4, 127.4, 119.4, 44.7, 35.2, 28.9, 25.1, 24.9, 22.7. (*Note: nonaflate carbons omitted due to low intensity resulting from C-F splitting*) **^{19}F NMR (282 MHz, $CDCl_3$):** δ -80.57 (tt, *J* = 9.8, 2.3 Hz), -109.67 – -109.85 (m), -120.88 (dtd, *J* = 14.8, 7.1, 6.5, 4.2 Hz), -125.68 – -125.92 (m). **FTIR (NaCl, thin film, cm^{-1}):** 2969, 2936, 1715, 1664, 1420, 1353, 1203, 1144, 1061, 880. **HRMS (EI, *m/z*):** calc'd for $C_{15}H_{13}F_9O_4S$ $[M+\cdot]^+$: 460.0391; found: 460.0375.

tert-butyl (1_r_,5_s_)-3-(((perfluorobutyl)sulfonyl)oxy)-8-azabicyclo[3.2.1]oct-2-ene-8-carboxylate (233d)

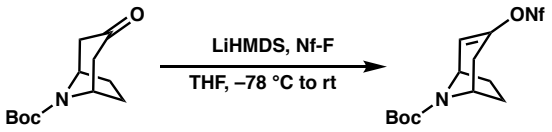

To a flame dried round-bottom flask under an inert atmosphere was added *tert*-butyl (1*R*,5*S*)-3-oxo-8-azabicyclo[3.2.1]octane-8-carboxylate (1.17 g, 5.0 mmol, 1.0 equiv). THF (9 mL) was added and the reaction was cooled to –78 °C. LiHMDS (5.5 mL, 1 M in THF, 5.5 mmol, 1.1 equiv) was added dropwise and allowed to stir for 30 minutes before perfluorobutanesulfonylfluoride (1.88 g, 5.25 mmol, 1.05 equiv) was added in one portion. The reaction was allowed to reach room temperature and stir overnight. The reaction was then quenched with saturated aq. NH_4Cl (50 mL) and extracted with Et_2O (2 x 50 mL). The combined organic layers were dried with $MgSO_4$, filtered, and concentrated. The product

was purified by column chromatography (silica, 10-20% Et_2O/hexanes) to yield 2.1 g (95% yield) of **233d** as an off white solid. $\mathbf{R_f}$ = 0.59 (silica, 75% Et_2O/hexanes, anisaldehyde (blue)). **^{1}H NMR (400 MHz, d_3-MeCN, 65 °C):** δ 6.19 (ddd, *J* = 5.8, 1.9, 1.1 Hz, 1H), 4.53 – 4.45 (m, 1H), 4.44 – 4.36 (m, 1H), 3.08 – 2.95 (m, 1H), 2.23 (dddd, *J* = 13.6, 7.4, 6.3, 1.7 Hz, 1H), 2.16 (dt, *J* = 17.0, 1.2 Hz, 1H), 2.04 – 1.96 (m, 2H), 1.81 – 1.69 (m, 1H), 1.45 (s, 9H). **^{13}C NMR (101 MHz, d_3-MeCN, 65 °C):** δ 154.9, 149.1, 125.3, 80.9, 53.6, 53.5, 37.6, 35.2, 30.4, 28.7. (*Note: nonaflate carbons omitted due to low intensity resulting from C-F splitting*) **^{19}F NMR (376 MHz, d_3-MeCN, 65 °C):** δ -81.46 (tt, *J* = 9.7, 2.8 Hz), -109.99 (ddp, *J* = 16.8, 10.7, 2.7 Hz), -121.10 – -121.26 (m), -125.91 – -126.07 (m). (*Note: not standardized with internal C_6F_6*). **FTIR (NaCl, thin film, cm^{-1}):** 3188, 3076, 2981, 1697, 1416, 1326, 1243, 1064, 875. **HRMS (EI, *m/z*):** calc'd for $C_{16}H_{19}F_9O_5SN$ $[M+H]^+$: 508.0843; found: 508.0840.

5.7.4 Ni-Catalyzed Halogenation

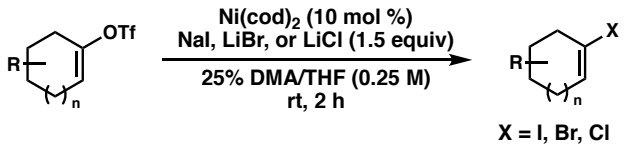

General Procedure 1: Enol Triflate Halogenation on 0.3 mmol scale.

A 2-dram vial was equipped with a stir bar and brought into a N_2-filled glovebox. The vial was charged with NaI, LiBr, or LiCl (0.45 mmol, 1.5 equiv) and $Ni(cod)_2$ (8.3 mg, 0.03 mmol, 0.1 equiv). Anhydrous DMA (0.3 mL) and THF (0.9 mL) were added, resulting in a clear yellow solution. Enol triflate (0.3 mmol, 1 equiv) was added in one portion, turning the reaction dark red (NaI) or aqua blue (LiBr or LiCl) over several minutes. The vial was

sealed with Teflon cap and brought out of the glovebox. The reaction was allowed to stir on the bench (480 rpm) for two hours at room temperature. Reaction was quenched by addition of water and Et_2O. The organic layer was separated and extracted with 2 x 10 mL Et_2O, then washed once with brine (20 mL). The combined organic layers were dried with $MgSO_4$, filtered, and concentrated under reduced pressure. The crude reaction was purified by silica gel chromatography to afford the desired product.

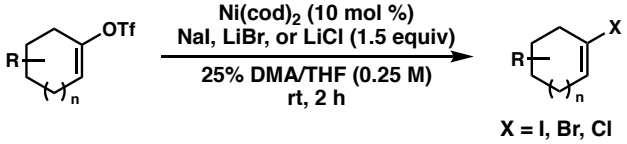

General Procedure 2: Enol Triflate Halogenation on 6.0 mmol scale.

A 100 mL Schlenk flask was equipped with a stir bar and brought into a N_2-filled glovebox. The vial was charged with NaI, LiBr, or LiCl (9.0 mmol, 1.5 equiv) and $Ni(cod)_2$ (166 mg, 0.6 mmol, 0.1 equiv). Anhydrous DMA (6 mL) and THF (18 mL) were added, resulting in a clear yellow solution. Enol triflate (6.0 mmol, 1 equiv) was added in one portion, turning the reaction dark red (NaI) or aqua blue (LiBr or LiCl) over several minutes. The Schlenk flask was sealed with a Kontes valve and brought out of the glovebox. The reaction was allowed to stir on the bench (480 rpm) for two hours at room temperature. Reaction was quenched by addition of water and Et_2O. The organic layer was separated and extracted with 2 x 200 mL Et_2O, then washed once with brine (400 mL). The combined organic layers were dried with $MgSO_4$, filtered, and concentrated under reduced pressure. The crude reaction was purified by silica gel chromatography to afford the desired product.

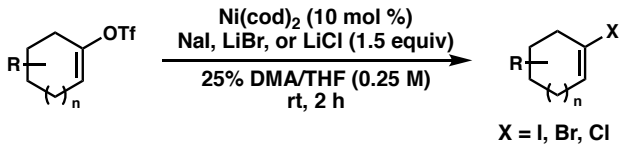

General Procedure 3: Enol Nonaflate Halogenation on 0.3 mmol scale.

A 2-dram vial was equipped with a stir bar and brought into a N_2-filled glovebox. The vial was charged with NaI, LiBr, or LiCl (0.45 mmol, 1.5 equiv) and $Ni(cod)_2$ (8.3 mg, 0.03 mmol, 0.1 equiv). Anhydrous DMA (0.3 mL) and THF (0.9 mL) were added, resulting in a clear yellow solution. Enol nonaflate (0.3 mmol, 1 equiv) was added in one portion, turning the reaction dark red (NaI) or aqua blue (LiBr or LiCl) over several minutes. The vial was sealed with Teflon cap and brought out of the glovebox. The reaction was allowed to stir on the bench (480 rpm) for two hours at room temperature. Reaction was quenched by addition of water and Et_2O. The organic layer was separated and extracted with 2 x 10 mL Et_2O, then washed once with brine (20 mL). The combined organic layers were dried with $MgSO_4$, filtered, and concentrated under reduced pressure. The crude reaction was purified by silica gel chromatography to afford the desired product.

5.7.5 Characterization of Reaction Products

(3*R*,6*S*)-1-iodo-6-isopropyl-3-methylcyclohex-1-ene (209a)

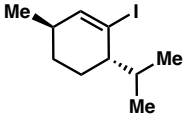

Prepared from (3*R*,6*S*)-6-isopropyl-3-methylcyclohex-1-en-1-yl trifluoromethanesulfonate (**208**, 143.2 mg, 0.3 mmol) and sodium iodide (112.5 mg, 0.75 mmol) according to General Procedure 1. The crude residue was purified by column chromatography (silica, pentane) to yield **209a** (96 mg, 73% yield) as a colorless oil. $\mathbf{R}_f = 0.79$ (silica, pentane, $KMnO_4$). $[\alpha]_D^{25} = -47°$ (c = 0.5, $CHCl_3$). **^{1}H NMR (400 MHz,**

$CDCl_3$): δ 6.36 (d, *J* = 1.2 Hz, 1H), 2.35 – 2.14 (m, 3H), 1.89 – 1.79 (m, 1H), 1.68 (dddd, *J* = 13.3, 5.9, 4.5, 3.0 Hz, 1H), 1.54 – 1.42 (m, 1H), 1.18 (tdd, *J* = 13.1, 10.2, 3.1 Hz, 1H), 0.97 (d, *J* = 7.0 Hz, 3H), 0.94 (d, *J* = 6.8 Hz, 3H), 0.72 (d, *J* = 6.7 Hz, 3H). **^{13}C NMR (101 MHz, $CDCl_3$):** δ 146.8, 109.2, 48.7, 35.7, 32.4, 30.9, 23.0, 21.5, 20.5, 15.1. **FTIR (NaCl, thin film, cm^{-1}):** 2958, 2868, 1617, 1457, 1367, 1314, 944, 852, 782, 703. **HRMS (EI, *m/z*):** calc'd for $C_{10}H_{17}I$ $[M+\cdot]^+$: 264.0375; found: 264.0392.

Prepared from (3*R*,6*S*)-6-isopropyl-3-methylcyclohex-1-en-1-yl trifluoromethanesulfonate (**208**, 1.70 g, 6.0 mmol) and sodium iodide (1.3 g, 9.0 mmol) according to General Procedure 2. The crude residue was purified by column chromatography (silica, pentane) to yield **209a** (1.12 g, 71% yield) as a colorless oil.

(3*R*,6*S*)-1-bromo-6-isopropyl-3-methylcyclohex-1-ene (209b)

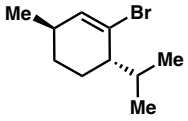

Prepared from (3*R*,6*S*)-6-isopropyl-3-methylcyclohex-1-en-1-yl trifluoromethanesulfonate (**208**, 85.9 mg, 0.3 mmol) and lithium bromide (39.1 mg, 0.45 mmol) according to General Procedure 1. The crude residue was purified by column chromatography (silica, pentane) to yield **209b** (52 mg, 80% yield) as a colorless oil. $\mathbf{R}_f$ = 0.77 (silica, hexanes, $KMnO_4$). $[\alpha]_D^{25}$ = –26° (c = 1.0, $CHCl_3$). **^{1}H NMR (400 MHz, $CDCl_3$):** δ 5.99 (td, *J* = 2.0, 1.0 Hz, 1H), 2.39 (ddt, *J* = 13.7, 6.8, 3.4 Hz, 1H), 2.32 (ddtd, *J* = 9.8, 5.8, 3.8, 1.8 Hz, 1H), 2.24 – 2.12 (m, 1H), 1.85 – 1.71 (m, 2H), 1.51 – 1.39 (m, 1H), 1.14 (tdd, *J* = 12.4, 10.1, 2.6 Hz, 1H), 0.98 (d, *J* = 7.1 Hz, 3H), 0.93 (d, *J* = 7.0 Hz, 3H), 0.75 (d, *J* = 6.8 Hz, 3H). **^{13}C NMR (101 MHz, $CDCl_3$):** δ 137.8, 129.5, 47.0, 33.9, 30.8, 29.6, 23.2, 21.6, 20.3, 15.4. **FTIR (NaCl, thin film, cm^{-1}):** 2959, 2930, 2870,

2854, 1634, 1458, 1387, 1318, 949, 851, 791. **HRMS (EI, *m/z*):** calc'd for $C_{10}H_{17}Br$ $[M+\cdot]^+$: 216.0514; found: 216.0532.

(3*R*,6*S*)-1-chloro-6-isopropyl-3-methylcyclohex-1-ene (209c)

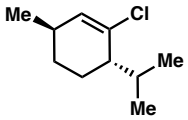

Prepared from (3*R*,6*S*)-6-isopropyl-3-methylcyclohex-1-en-1-yl trifluoromethanesulfonate (**208**, 85.9 mg, 0.3 mmol) and lithium chloride (19.1 mg, 0.45 mmol) according to General Procedure 1. The crude residue was purified by column chromatography (silica, pentane) to yield **209c** (37 mg, 72% yield) as a colorless oil. $\mathbf{R_f}$ = 0.87 (silica, hexanes, $KMnO_4$). $[\alpha]_D^{25} = -11°$ (c = 0.5, $CHCl_3$). **^{1}H NMR (400 MHz, $CDCl_3$):** δ 5.73 (td, *J* = 2.0, 1.0 Hz, 1H), 2.37 (m, 1H), 2.27 (ddtd, *J* = 9.7, 5.7, 3.8, 1.9 Hz, 1H), 2.23 – 2.14 (m, 1H), 1.84 – 1.71 (m, 2H), 1.48 – 1.35 (m, 1H), 1.16 – 1.04 (m, 1H), 0.98 (d, *J* = 7.0 Hz, 3H), 0.93 (d, *J* = 7.0 Hz, 3H), 0.76 (d, *J* = 6.8 Hz, 3H). **^{13}C NMR (101 MHz, $CDCl_3$):** δ 136.5, 133.3, 45.8, 32.5, 30.8, 28.2, 22.8, 21.8, 20.3, 15.7. **FTIR (NaCl, thin film, cm^{-1}):** 2960, 2870, 1642, 1454, 1368, 957, 851, 812, 727. **HRMS (EI, *m/z*):** calc'd for $C_{10}H_{17}Cl$ $[M+\cdot]^+$: 172.1019; found: 172.1032.

2-(4-iodocyclohex-3-en-1-yl)isoindoline-1,3-dione (212a)

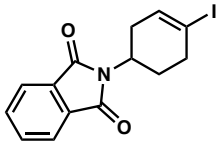

Prepared from 4-(1,3-dioxoisoindolin-2-yl)cyclohex-1-en-1-yl trifluoromethanesulfonate (**211a**, 113 mg, 0.3 mmol) and sodium iodide (67.5 mg, 0.45 mmol) according to General Procedure 1. The crude residue was purified by column chromatography (silica, 10 to 25% Et_2O/hexanes) to yield **212a** (53 mg, 50% yield) as a white solid. $\mathbf{R_f}$ = 0.40 (silica, 30% Et_2O/hexanes, $KMnO_4$). **^{1}H NMR (400 MHz, $CDCl_3$):** δ 7.81 (tt, *J* = 5.1, 2.4 Hz, 2H), 7.76 – 7.66 (m, 2H), 6.29 (dq, *J* = 5.7,

1.9 Hz, 1H), 4.44 (dqd, *J* = 11.5, 5.5, 3.1 Hz, 1H), 3.06 – 2.92 (m, 1H), 2.82 – 2.61 (m, 3H), 2.19 (dtd, *J* = 16.8, 5.7, 5.0, 3.0 Hz, 1H), 1.78 – 1.66 (m, 1H). **^{13}C NMR (101 MHz, $CDCl_3$):** δ 168.3, 135.5, 134.1, 132.0, 123.3, 95.1, 45.7, 39.9, 32.3, 28.9. **FTIR (NaCl, thin film, cm^{-1}):** 1700, 1458, 1395, 1380, 1109, 990, 874, 716. **HRMS (FAB, *m/z*):** calc'd for $C_{14}H_{12}NO_2I$ $[M+H]^+$: 353.9991; found: 353.9979.

2-(4-bromocyclohex-3-en-1-yl)isoindoline-1,3-dione (212b)

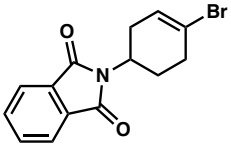

Prepared from 4-(1,3-dioxoisoindolin-2-yl)cyclohex-1-en-1-yl trifluoromethanesulfonate (**211a**, 113 mg, 0.3 mmol) and lithium bromide (39.1 mg, 0.45 mmol) according to General Procedure 1. The crude residue was purified by column chromatography (silica, 10 to 25% Et_2O/hexanes) to yield **212b** (65 mg, 71% yield) as a white solid. $\mathbf{R}_f$ = 0.36 (silica, 30% Et_2O/hexanes, $KMnO_4$). **^{1}H NMR (400 MHz, $CDCl_3$):** δ 7.86 – 7.78 (m, 2H), 7.75 – 7.67 (m, 2H), 6.01 (dtd, *J* = 5.9, 2.3, 0.9 Hz, 1H), 4.42 (dddd, *J* = 12.6, 11.1, 5.5, 3.2 Hz, 1H), 3.01 – 2.89 (m, 1H), 2.79 – 2.63 (m, 2H), 2.63 – 2.51 (m, 1H), 2.25 – 2.14 (m, 1H), 1.88 – 1.76 (m, 1H). **^{13}C NMR (101 MHz, $CDCl_3$):** δ 168.3, 134.1, 132.0, 127.0, 123.3, 121.3, 46.0, 35.4, 30.4, 27.9. **FTIR (NaCl, thin film, cm^{-1}):** 1695, 1464, 1396, 1111, 992, 919, 875, 717. **HRMS (TOF-ESI, *m/z*):** calc'd for $C_{14}H_{12}NO_2Br$ $[M+H]^+$: 306.0130; found: 306.0121.

2-(4-chlorocyclohex-3-en-1-yl)isoindoline-1,3-dione (212c)

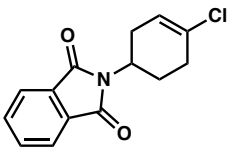

Prepared from 4-(1,3-dioxoisoindolin-2-yl)cyclohex-1-en-1-yl trifluoromethanesulfonate (**211a**, 113 mg, 0.3 mmol) and lithium chloride (19.1 mg, 0.45 mmol) according to General Procedure 1. The crude residue was

purified by column chromatography (silica, 10 to 25% Et_2O/hexanes) to yield **212c** (72 mg, 92% yield) as a white solid. $\mathbf{R_f}$ = 0.36 (silica, 30% Et_2O/hexanes, $KMnO_4$). **^{1}H NMR (500 MHz, $CDCl_3$):** δ 7.85 – 7.79 (m, 2H), 7.74 – 7.68 (m, 2H), 5.80 (dtt, *J* = 5.9, 2.4, 0.7 Hz, 1H), 4.46 – 4.36 (m, 1H), 2.97 (dddt, *J* = 16.6, 11.0, 4.4, 2.3 Hz, 1H), 2.72 (tdd, *J* = 12.5, 11.8, 5.8 Hz, 1H), 2.66 – 2.55 (m, 1H), 2.49 – 2.40 (m, 1H), 2.27 – 2.18 (m, 1H), 1.90 – 1.82 (m, 1H). **^{13}C NMR (126 MHz, $CDCl_3$):** δ 168.3, 134.1, 132.0, 131.4, 123.3, 122.7, 46.2, 33.0, 29.1, 27.1. **FTIR (NaCl, thin film, cm^{-1}):** 1700, 1465, 1378, 1112, 995, 920, 876, 717. **HRMS (FAB, *m/z*):** calc'd for $C_{14}H_{12}NO_2Cl$ $[M+H]^+$: 262.0635; found: 262.0636.

1-benzyl-4-iodo-1,2,3,6-tetrahydropyridine (213a)

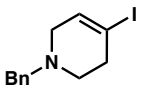

Prepared from 1-benzyl-1,2,3,6-tetrahydropyridin-4-yl trifluoromethanesulfonate (**211b**, 96 mg, 0.3 mmol) and sodium iodide (67.5 mg, 0.45 mmol) according to General Procedure 1. The crude residue was purified by column chromatography (silica, 10% Et_2O/hexanes) to yield **213a** (62 mg, 69% yield) as a light yellow oil. $\mathbf{R_f}$ = 0.31 (silica, 10% Et_2O/hexanes, $KMnO_4$). **^{1}H NMR (400 MHz, $CDCl_3$):** δ 7.35 – 7.22 (m, 5H), 6.26 (td, *J* = 3.5, 1.7 Hz, 1H), 3.56 (s, 2H), 3.04 – 3.00 (m, 2H), 2.61 (m, 4H). **^{13}C NMR (101 MHz, $CDCl_3$):** δ 138.0, 135.3, 129.2, 128.5, 127.4, 93.2, 62.3, 55.7, 51.7, 39.8. **FTIR (NaCl, thin film, cm^{-1}):** 2920, 2800, 2752, 1494, 1454, 1363, 1340, 1054, 960, 729, 698. **HRMS (FAB, *m/z*):** calc'd for $C_{12}H_{14}IN$ $[M+H–H_2]^+$: 298.0093; found: 298.0081.

1-benzyl-4-bromo-1,2,3,6-tetrahydropyridine (213b)

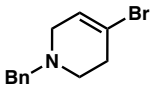

Prepared from 1-benzyl-1,2,3,6-tetrahydropyridin-4-yl trifluoromethanesulfonate (**211b**, 96 mg, 0.3 mmol) and lithium bromide (39.1 mg, 0.45 mmol) according to General Procedure 1. The crude residue was purified by column chromatography (silica, 5% to 10 Et_2O/hexanes) to yield **213b** (60 mg, 79% yield) as a light yellow oil. $\mathbf{R_f}$ = 0.60 (silica, 20% Et_2O/hexanes, $KMnO_4$). **^{1}H NMR (400 MHz, $CDCl_3$):** δ 7.37 – 7.24 (m, 5H), 5.99 (tt, *J* = 3.5, 1.6 Hz, 1H), 3.59 (s, 2H), 3.01 (dt, *J* = 3.7, 2.8 Hz, 2H), 2.66 (td, *J* = 5.7, 0.6 Hz, 2H), 2.58 – 2.52 (m, 2H). **^{13}C NMR (101 MHz, $CDCl_3$):** δ 138.0, 129.1, 128.4, 127.4, 126.8, 119.9, 62.0, 54.1, 50.9, 35.8. **FTIR (NaCl, thin film, cm^{-1}):** 3062, 3027, 2924, 2802, 2756, 1659, 1493, 1454, 1365, 1346, 1056, 995, 965, 822, 732, 698. **HRMS (TOF-ESI, *m/z*):** calc'd for $C_{12}H_{14}BrN$ $[M+H]^+$: 252.0388; found: 252.0404.

1-benzyl-4-chloro-1,2,3,6-tetrahydropyridine (213c)

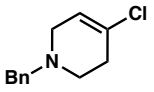

Prepared from 1-benzyl-1,2,3,6-tetrahydropyridin-4-yl trifluoromethanesulfonate (**211b**, 96 mg, 0.3 mmol) and lithium chloride (19.1 mg, 0.45 mmol) according to General Procedure 1. The crude residue was purified by column chromatography (silica, 5 to 10% Et_2O/hexanes) to yield **213c** (50 mg, 80% yield) as a light yellow oil. $\mathbf{R_f}$ = 0.56 (silica, 20% Et_2O/hexanes, $KMnO_4$). **^{1}H NMR (400 MHz, $CDCl_3$):** δ 7.36 – 7.25 (m, 5H), 5.76 (tt, *J* = 3.5, 1.6 Hz, 1H), 3.60 (s, 2H), 3.03 (dt, *J* = 3.6, 2.8 Hz, 2H), 2.67 (t, *J* = 5.7 Hz, 2H), 2.43 (ttd, *J* = 5.7, 2.8, 1.5 Hz, 2H). **^{13}C NMR (101 MHz, $CDCl_3$):** δ 138.1, 130.3, 129.1, 128.4, 127.4, 122.5, 62.0, 52.9, 50.2, 33.5. **FTIR (NaCl, thin film, cm^{-1}):** 3062, 6027, 2925, 2801, 2759, 1666, 1494, 1454, 1365, 1350,

1059, 998, 972, 824, 735, 698. **HRMS (TOF-ESI, *m/z*):** calc'd for $C_{12}H_{14}ClN$ $[M+H]^+$: 208.0893; found: 208.0881.

benzyl 4-iodo-3,6-dihydropyridine-1(2*H*)-carboxylate (214a)

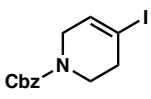

Prepared from benzyl 4-(((trifluoromethyl)sulfonyl)oxy)-3,6-dihydro-pyridine-1(2*H*)-carboxylate (**211c**, 110 mg, 0.3 mmol) and sodium iodide (67.5 mg, 0.45 mmol) according to General Procedure 1. The crude residue was purified by column chromatography (silica, 10% Et_2O/hexanes) to yield **214a** (61 mg, 60% yield) as a colorless oil. $\mathbf{R_f}$ = 0.25 (silica, 10% EtOAc/hexanes, $KMnO_4$). **^{1}H NMR (400 MHz, *d*$_3$-MeCN, 65 °C):** δ 7.61 – 7.11 (m, 5H), 6.38 – 6.30 (m, 1H), 5.13 (s, 2H), 3.97 (q, *J* = 3.0 Hz, 2H), 3.58 (t, *J* = 5.7 Hz, 2H), 2.69 – 2.49 (m, 2H). **^{13}C NMR (101 MHz, *d*$_3$-MeCN, 65 °C):** δ 156.4, 138.6, 135.5, 129.7, 129.1, 128.9, 92.7, 68.1, 47.7, 43.7, 39.9. **FTIR (NaCl, thin film, cm^{-1}):** 3032, 2932, 2838, 1704, 1428, 1361, 1335, 1273, 1231, 1108, 1044, 1027, 964, 697. **HRMS (TOF-ESI, *m/z*):** calc'd for $C_{13}H_{14}INO_2$ $[M+H]^+$: 344.0148; found: 344.0154.

benzyl 4-bromo-3,6-dihydropyridine-1(2*H*)-carboxylate (214b)

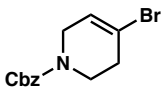

Prepared from benzyl 4-(((trifluoromethyl)sulfonyl)oxy)-3,6-dihydro-pyridine-1(2*H*)-carboxylate (**211c**, 110 mg, 0.3 mmol) and lithium bromide (39.1 mg, 0.45 mmol) according to General Procedure 1. The crude residue was purified by column chromatography (silica, 10% Et_2O/hexanes) to yield **214b** (81 mg, 91% yield) as a colorless oil. $\mathbf{R_f}$ = 0.36 (silica, 30% EtOAc/hexanes, $KMnO_4$). **^{1}H NMR (400 MHz, *d*$_3$-MeCN, 65 °C):** δ 7.38 (m, 4H), 7.33 (m, 1H), 6.06 (tt, *J* = 3.4, 1.7 Hz, 1H), 5.14 (s,

2H), 3.96 (q, *J* = 3.0 Hz, 2H), 3.63 (t, *J* = 5.8 Hz, 2H), 2.53 (ttd, *J* = 5.6, 2.7, 1.6 Hz, 2H). **^{13}C NMR (101 MHz, *d*$_3$-MeCN, 65 °C):** δ 156.2, 138.5, 129.6, 129.1, 128.9, 127.1, 120.2, 68.0, 46.1, 43.0, 35.9. **FTIR (NaCl, thin film, cm^{-1}):** 2934, 1698, 1428, 1361, 1336, 1274, 1230, 1111, 1027, 964, 757, 698. **HRMS (FAB, *m/z*):** calc'd for $C_{13}H_{14}BrNO_2$ $[M+H]^+$: 296.0286; found: 296.0285.

benzyl 4-chloro-3,6-dihydropyridine-1(2*H*)-carboxylate (214c)

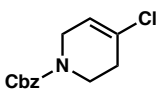

Prepared from benzyl 4-(((trifluoromethyl)sulfonyl)oxy)-3,6-dihydropyridine-1(2*H*)-carboxylate (**211c**, 110 mg, 0.3 mmol) and lithium chloride (19.1 mg, 0.45 mmol) according to General Procedure 1. The crude residue was purified by column chromatography (silica, 10% Et_2O/hexanes) to yield **214c** (65 mg, 86% yield) as a colorless oil. **R$_f$** = 0.36 (silica, 30% EtOAc/hexanes, $KMnO_4$). **^{1}H NMR (400 MHz, *d*$_3$-MeCN, 65 °C):** δ 7.41 – 7.36 (m, 4H), 7.36 – 7.31 (m, 1H), 5.84 (tt, *J* = 3.4, 1.6 Hz, 1H), 5.14 (s, 2H), 3.99 (q, *J* = 2.9 Hz, 2H), 3.64 (t, *J* = 5.8 Hz, 2H), 2.41 (ttd, *J* = 5.7, 2.7, 1.5 Hz, 2H). **^{13}C NMR (101 MHz, *d*$_3$-MeCN, 65 °C):** δ 156.2, 138.5, 131.0, 129.7, 129.1, 128.9, 122.9, 68.0, 44.9, 42.4, 33.6. **FTIR (NaCl, thin film, cm^{-1}):** 3033, 2940, 1698, 1497, 1428, 1362, 1276, 1233, 1112, 1049, 971, 813, 764, 699. **HRMS (TOF-ESI, *m/z*):** calc'd for $C_{13}H_{14}ClNO_2$ $[M+H]^+$: 252.0791; found: 252.0807.

8-iodo-1,4-dioxaspiro[4.5]dec-7-ene (215a)

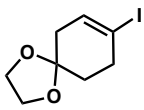

Prepared from 1,4-dioxaspiro[4.5]dec-7-en-8-yl trifluoromethanesulfonate (**211d**, 86.5 mg, 0.3 mmol) and sodium iodide (67.5 mg, 0.45 mmol) according to General Procedure 1. The crude residue was purified by column

chromatography (silica, 10% Et_2O/pentane) to yield **215a** (29 mg, 36% yield) as a colorless oil.

Prepared from 1,4-dioxaspiro[4.5]dec-7-en-8-yl 1,1,2,2,3,3,4,4,4-nonafluorobutane-1-sulfonate (**233a**, 131.4 mg, 0.3 mmol) and sodium iodide (67.5 mg, 0.45 mmol) according to General Procedure 3. The crude residue was purified by column chromatography (silica, 0.5% trimethylamine/10% EtOAc/pentane) to yield **215a** (44 mg, 55% yield) as a colorless oil. $\mathbf{R_f}$ = 0.45 (silica, 10% EtOAc/hexanes, $KMnO_4$). **^{1}H NMR (400 MHz, $CDCl_3$):** δ 6.18 (tt, *J* = 3.9, 1.7 Hz, 1H), 3.97 (s, 4H), 2.70 (tq, *J* = 6.5, 2.2 Hz, 2H), 2.30 (dddd, *J* = 4.0, 3.3, 2.3, 1.2 Hz, 2H), 1.80 (tt, *J* = 6.5, 0.9 Hz, 2H). **^{13}C NMR (101 MHz, $CDCl_3$):** δ 134.7, 106.1, 95.0, 64.6, 39.6, 38.7, 33.8. **FTIR (NaCl, thin film, cm^{-1}):** 2882, 1651, 1429, 1366, 1252, 1114, 1059, 1022, 914, 860, 650. **HRMS (FAB, *m/z*):** calc'd for $C_8H_{11}IO_2$ $[M+H]^+$: 266.9882; found: 266.9885.

8-bromo-1,4-dioxaspiro[4.5]dec-7-ene (215b)

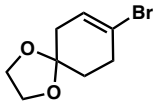

Prepared from 1,4-dioxaspiro[4.5]dec-7-en-8-yl trifluoromethanesulfonate (**211d**, 86.5 mg, 0.3 mmol) and lithium bromide (39.1 mg, 0.45 mmol) according to General Procedure 1. The crude residue was purified by column chromatography (silica, 10% Et_2O/pentane) to yield **251b** (48 mg, 73% yield) as a colorless oil. $\mathbf{R_f}$ = 0.41 (silica, 10% EtOAc/hexanes, $KMnO_4$). **^{1}H NMR (400 MHz, $CDCl_3$):** δ 5.90 (tt, *J* = 4.0, 1.6 Hz, 1H), 3.97 (s, 4H), 2.62 (ttd, *J* = 6.5, 2.4, 1.6 Hz, 2H), 2.29 (dtt, *J* = 4.1, 2.4, 0.9 Hz, 2H), 1.84 (tt, *J* = 6.6, 0.9 Hz, 2H). **^{13}C NMR (101 MHz, $CDCl_3$):** δ 126.2, 121.2, 106.4, 64.7, 37.7, 34.3, 32.8. **FTIR (NaCl, thin film, cm^{-1}):** 2883, 1652, 1430,

1368, 1255, 1117, 1060, 1024, 929, 862, 654. **HRMS (EI, *m/z*):** calc'd for $C_8H_{11}BrO_2$ $[M+\cdot]^+$: 217.9942; found: 217.9933.

8-chloro-1,4-dioxaspiro[4.5]dec-7-ene (215c)

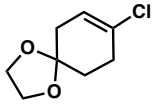

Prepared from 1,4-dioxaspiro[4.5]dec-7-en-8-yl trifluoromethanesulfonate (**211d**, 86.5 mg, 0.3 mmol) and lithium chloride (19.1 mg, 0.45 mmol) according to General Procedure 1. The crude residue was purified by column chromatography (silica, 10% Et_2O/pentane) to yield **215c** (44 mg, 83% yield) as a colorless oil. $\mathbf{R_f}$ = 0.38 (silica, 10% EtOAc/hexanes, $KMnO_4$). **^{1}H NMR (400 MHz, $CDCl_3$):** δ 5.69 (tt, *J* = 4.1, 1.6 Hz, 1H), 3.98 (s, 4H), 2.51 (tq, *J* = 6.5, 2.0 Hz, 2H), 2.36 – 2.29 (m, 2H), 1.91 – 1.81 (m, 2H). **^{13}C NMR (101 MHz, $CDCl_3$):** δ 131.4, 121.8, 106.8, 64.7, 36.4, 32.0, 31.9. **FTIR (NaCl, thin film, cm^{-1}):** 2933, 2884, 1659, 1433, 1370, 1336, 1251, 1203, 1119, 1062, 1028, 985, 944, 864, 666. **HRMS (TOF-ESI, *m/z*):** calc'd for $C_8H_{11}ClO_2$ $[M+H]^+$: 175.0526; found: 175.0521.

4-iodo-1,2-dihydronaphthalene (216a)

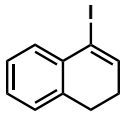

Prepared from 3,4-dihydronaphthalen-1-yl trifluoromethanesulfonate (**211e**, 93.5 mg, 0.3 mmol) and sodium iodide (67.5 mg, 0.45 mmol) according to General Procedure 1. The crude residue was purified by column chromatography (silica, pentane) to yield **216a** (38 mg, 49% yield) as a colorless oil. $\mathbf{R_f}$ = 0.65 (silica, hexanes, UV). **^{1}H NMR (400 MHz, $CDCl_3$):** δ 7.43 (dd, *J* = 7.5, 1.3 Hz, 1H), 7.27 – 7.20 (m, 1H), 7.17 (td, *J* = 7.4, 1.4 Hz, 1H), 7.05 – 7.00 (m, 1H), 6.83 (t, *J* = 4.8 Hz, 1H), 2.85 (t, *J* = 8.0 Hz, 2H), 2.36 (ddd, *J* = 9.1, 7.4, 4.9 Hz, 2H). **^{13}C NMR (101 MHz, $CDCl_3$):** δ 140.2,

135.9, 134.4, 130.9, 128.4, 127.4, 127.1, 98.1, 27.9, 27.2. **FTIR (NaCl, thin film, cm^{-1}):** 3059, 2934, 2882, 2827, 1604, 1476, 1448, 1314, 1276, 938, 805, 756, 727. **HRMS (EI, *m/z*):** calc'd for $C_{10}H_9I$ $[M+\cdot]^+$: 255.9749; found: 255.9744.

4-bromo-1,2-dihydronaphthalene (216b)

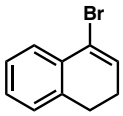

Prepared from 3,4-dihydronaphthalen-1-yl trifluoromethanesulfonate (**211e**, 93.5 mg, 0.3 mmol) and lithium bromide (39.1 mg, 0.45 mmol) according to General Procedure 1. The crude residue was purified by column chromatography (silica, pentane) to yield **216b** (48 mg, 77% yield) as a colorless oil. $\mathbf{R_f}$ = 0.62 (silica, hexanes, UV). **^{1}H NMR (400 MHz, $CDCl_3$):** δ 7.57 (dd, *J* = 7.5, 1.4 Hz, 1H), 7.26 (td, *J* = 7.6, 1.5 Hz, 1H), 7.21 (td, *J* = 7.4, 1.5 Hz, 1H), 7.11 (dq, *J* = 7.8, 1.2 Hz, 1H), 6.46 (t, *J* = 4.8 Hz, 1H), 2.85 (t, *J* = 8.1 Hz, 2H), 2.38 (ddd, *J* = 9.1, 7.4, 4.9 Hz, 2H). **^{13}C NMR (101 MHz, $CDCl_3$):** δ 136.4, 133.2, 130.8, 128.4, 127.4, 126.9, 126.6, 121.5, 27.7, 25.6. **FTIR (NaCl, thin film, cm^{-1}):** 3059, 2937, 2884, 2831, 1690, 1615, 1479, 1450, 1316, 1169, 948, 809, 758, 730. **HRMS (EI, *m/z*):** calc'd for $C_{10}H_9Br$ $[M+\cdot]^+$: 207.9888; found: 207.9876.

4-chloro-1,2-dihydronaphthalene (216c)

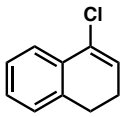

Prepared from 3,4-dihydronaphthalen-1-yl trifluoromethanesulfonate (**211e**, 93.5 mg, 0.3 mmol) and lithium chloride (19.1 mg, 0.45 mmol) according to General Procedure 1. The crude residue was purified by column chromatography (silica, pentane) to yield **216c** (39 mg, 80% yield) as a colorless oil. $\mathbf{R_f}$ = 0.56 (silica, hexanes, $KMnO_4$). **^{1}H NMR (400 MHz, $CDCl_3$):** δ 7.57 (dd, *J* = 7.5, 1.5 Hz, 1H), 7.28 – 7.23 (m, 1H), 7.21 (td, *J* = 7.4, 1.6 Hz, 1H), 7.16 – 7.11 (m, 1H), 6.18 (t, *J* = 4.8 Hz, 1H), 2.84 (t, *J*

= 8.0 Hz, 2H), 2.40 (ddd, *J* = 9.1, 7.5, 4.8 Hz, 2H). **^{13}C NMR (101 MHz, $CDCl_3$):** δ 136.5, 132.5, 130.6, 128.3, 127.4, 126.8, 126.1, 124.2, 27.7, 24.3. **FTIR (NaCl, thin film, cm^{-1}):** 3063, 2938, 2887, 2832, 1621, 1482, 1451, 1319, 1172, 964, 814, 760, 732. **HRMS (EI, *m/z*):** calc'd for $C_{10}H_9Cl$ $[M+\cdot]^+$: 164.0393; found: 164.0382.

4-bromo-2-phenyl-2*H*-chromene (217b)

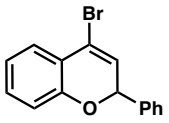

Prepared from 2-phenyl-2*H*-chromen-4-yl trifluoromethanesulfonate (**211f**, 107 mg, 0.3 mmol) and lithium bromide (39.1 mg, 0.45 mmol) according to General Procedure 1. The crude residue was purified by column chromatography (silica, 10% PhMe/hexanes) to yield **217b** (65 mg, 75% yield) as a yellow oil. *Note: This compound decomposes readily at room temperature.* $\mathbf{R_f}$ = 0.69 (silica, 10% Et_2O/hexanes, $KMnO_4$). **^{1}H NMR (400 MHz, $CDCl_3$):** δ 7.46 (ddd, *J* = 7.7, 2.6, 1.5 Hz, 3H), 7.43 – 7.33 (m, 3H), 7.23 – 7.17 (m, 1H), 6.97 (td, *J* = 7.6, 1.2 Hz, 1H), 6.81 (dd, *J* = 8.1, 1.2 Hz, 1H), 6.21 (d, *J* = 3.7 Hz, 1H), 5.91 (d, *J* = 3.7 Hz, 1H). **^{13}C NMR (101 MHz, $CDCl_3$):** δ 153.4, 139.6, 131.1, 128.9, 128.9, 127.2, 127.1, 126.5, 121.7, 121.1, 118.4, 116.2, 78.8. **FTIR (NaCl, thin film, cm^{-1}):** 1645, 1605, 1478, 1464, 1450, 1374, 1223, 1116, 1062, 756, 697. **HRMS (FAB, *m/z*):** calc'd for $C_{15}H_{11}BrO$ $[M+H-H_2]^+$: 284.9915; found: 284.9917.

4-chloro-2-phenyl-2*H*-chromene (217c)

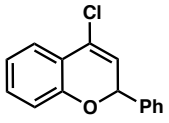

Prepared from 2-phenyl-2*H*-chromen-4-yl trifluoromethanesulfonate (**211f**, 107 mg, 0.3 mmol) and lithium chloride (19.1 mg, 0.45 mmol) according to General Procedure 1. The crude residue was purified by column

chromatography (silica, 10% PhMe/hexanes) to yield **217c** (48 mg, 66% yield) as a colorless oil. *Note: This compound decomposes readily at room temperature.* $\mathbf{R_f}$ = 0.68 (silica, 10% Et_2O/hexanes, $KMnO_4$). **^{1}H NMR (400 MHz, $CDCl_3$):** δ 7.52 – 7.47 (m, 1H), 7.47 – 7.43 (m, 2H), 7.42 – 7.35 (m, 3H), 7.21 (ddd, *J* = 8.1, 7.4, 1.6 Hz, 1H), 6.98 (td, *J* = 7.6, 1.2 Hz, 1H), 6.84 (dd, *J* = 8.1, 1.1 Hz, 1H), 5.97 (s, 2H). **^{13}C NMR (101 MHz, $CDCl_3$):** δ 153.6, 139.8, 131.0, 128.9, 128.9, 128.3, 127.2, 124.7, 122.0, 121.6, 120.4, 116.2, 78.1. **FTIR (NaCl, thin film, cm^{-1}):** 1634, 1605, 1481, 1451, 1328, 1224, 1118, 1064, 981, 914, 852, 754, 697. **HRMS (FAB, *m/z*):** calc'd for $C_{15}H_{11}ClO$ $[M+\cdot]^+$: 242.0498; found: 242.0518.

4-iodo-1-(3,4-dichlorophenyl)-1,2-dihydronaphthalene (218a)

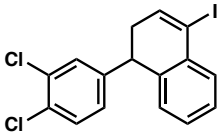

Prepared from 4-(3,4-dichlorophenyl)-3,4-dihydronaphthalen-1-yl trifluoromethanesulfonate (**211g**, 127.0 mg, 0.3 mmol) and sodium iodide (67.5 mg, 0.45 mmol) according to General Procedure 1. The crude residue was purified by column chromatography (silica, pentane) to yield **218a** (63 mg, 52% yield) as a white solid. $\mathbf{R_f}$ = 0.44 (silica, hexanes, UV). **^{1}H NMR (400 MHz, $CDCl_3$):** δ 7.54 (dd, *J* = 7.8, 1.2 Hz, 1H), 7.37 (d, *J* = 8.3 Hz, 1H), 7.33 – 7.26 (m, 2H), 7.17 (td, *J* = 7.5, 1.3 Hz, 1H), 6.98 (ddd, *J* = 8.3, 2.2, 0.5 Hz, 1H), 6.77 – 6.72 (m, 2H), 4.16 – 4.09 (m, 1H), 2.70 (ddd, *J* = 16.8, 7.0, 4.9 Hz, 1H), 2.59 (ddd, *J* = 16.8, 8.9, 4.8 Hz, 1H). **^{13}C NMR (101 MHz, $CDCl_3$):** δ 143.6, 137.9, 136.8, 134.2, 132.6, 131.5, 130.9, 130.6, 130.3, 129.0, 127.9, 127.8, 127.6, 98.0, 43.1, 35.2. **FTIR (NaCl, thin film, cm^{-1}):** 3059, 2932, 2876, 2827, 1603, 1561, 1470, 1447, 1396, 1132, 1030, 910, 862, 822, 879, 730. **HRMS (FAB, *m/z*):** calc'd for $C_{16}H_{11}ICl_2$ $[M+\cdot]^+$: 399.9283; found: 399.9279.

4-bromo-1-(3,4-dichlorophenyl)-1,2-dihydronaphthalene (218b)

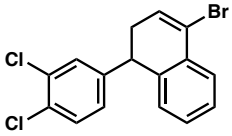

Prepared from 4-(3,4-dichlorophenyl)-3,4-dihydronaphthalen-1-yl trifluoromethanesulfonate (**211g**, 127.0 mg, 0.3 mmol) and lithium bromide (39.1 mg, 0.45 mmol) according to General Procedure 1. The crude residue was purified by column chromatography (silica, pentane) to yield **218b** (83 mg, 78% yield) as a white solid. $\mathbf{R_f}$ = 0.35 (silica, hexanes, $KMnO_4$). **^{1}H NMR (400 MHz, $CDCl_3$):** δ 7.67 (dd, *J* = 7.7, 1.3 Hz, 1H), 7.37 (d, *J* = 8.3 Hz, 1H), 7.31 (tdd, *J* = 7.7, 1.3, 0.6 Hz, 1H), 7.28 (d, *J* = 2.1 Hz, 1H), 7.20 (td, *J* = 7.5, 1.3 Hz, 1H), 7.00 (ddd, *J* = 8.3, 2.2, 0.5 Hz, 1H), 6.81 (dt, *J* = 7.4, 1.2 Hz, 1H), 6.38 (t, *J* = 4.8 Hz, 1H), 4.18 – 4.09 (m, 1H), 2.72 (ddd, *J* = 16.9, 7.1, 4.9 Hz, 1H), 2.60 (ddd, *J* = 16.9, 9.0, 4.8 Hz, 1H). **^{13}C NMR (101 MHz, $CDCl_3$):** δ 143.7, 137.4, 133.0, 132.7, 130.9, 130.7, 130.4, 129.0, 128.7, 127.82, 127.75, 127.70, 127.2, 121.5, 43.0, 33.7. **FTIR (NaCl, thin film, cm^{-1}):** 3062, 2879, 1618, 1468, 1448, 1397, 1132, 1030, 871, 822, 760. **HRMS (TOF-ESI, *m/z*):** calc'd for $C_{16}H_{11}BrCl_2$ $[M+H]^+$: 352.9499; found: 352.9485.

4-chloro-1-(3,4-dichlorophenyl)-1,2-dihydronaphthalene (218c)

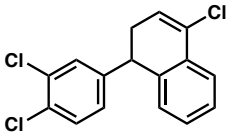

Prepared from 4-(3,4-dichlorophenyl)-3,4-dihydronaphthalen-1-yl trifluoromethanesulfonate (**211g**, 127.0 mg, 0.3 mmol) and lithium chloride (19.1 mg, 0.45 mmol) according to General Procedure 1. The crude residue was purified by column chromatography (silica, pentane) to yield **218c** (69 mg, 75% yield) as a white solid. $\mathbf{R_f}$ = 0.55 (silica, hexanes, UV). **^{1}H NMR (400 MHz, $CDCl_3$):** δ 7.70 (dd, *J* = 7.7, 1.3 Hz, 1H), 7.38 (d, *J* = 8.3 Hz, 1H), 7.33 (tdd, *J* = 7.7, 1.4, 0.6 Hz, 1H), 7.30 – 7.28 (m, 1H), 7.22 (td, *J* = 7.5, 1.4 Hz, 1H), 7.01 (ddd, *J* = 8.3, 2.2, 0.5 Hz, 1H), 6.85 (dt, *J* =

7.6, 1.2 Hz, 1H), 6.13 (t, *J* = 4.8 Hz, 1H), 4.17 – 4.09 (m, 1H), 2.76 (ddd, *J* = 17.0, 7.2, 4.9 Hz, 1H), 2.64 (ddd, *J* = 16.9, 9.0, 4.7 Hz, 1H). **^{13}C NMR (101 MHz, $CDCl_3$):** δ 143.8, 137.4, 132.6, 132.3, 130.9, 130.7, 130.6, 130.3, 129.0, 127.8, 127.7, 127.6, 124.7, 124.0, 43.0, 32.5. **FTIR (NaCl, thin film, cm^{-1}):** 3063, 2880, 1625, 1559, 1468, 1449, 1398, 1133, 1030, 980, 878, 814, 762, 735. **HRMS (TOF-ESI, *m/z*):** calc'd for $C_{16}H_{11}Cl_3$ $[M+H]^+$: 309.0005; found: 309.0005.

(2*R*,8*R*,8a*S*)-6-iodo-8,8a-dimethyl-2-(prop-1-en-2-yl)-1,2,3,7,8,8a-hexahydronaphthalene (219a)

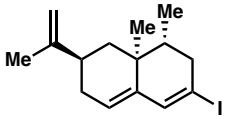

Prepared from (4*R*,4a*S*,6*R*)-4,4a-dimethyl-6-(prop-1-en-2-yl)-3,4,4a,5,6,7-hexahydronaphthalen-2-yl trifluoromethanesulfonate (**211h**, 105.1 mg, 0.3 mmol) and sodium iodide (67.5 mg, 0.45 mmol) according to General Procedure 1. The crude residue was purified by column chromatography (silica, pentane) to yield **219a** (34 mg, 34% yield) as a colorless oil. *Note: This compound decomposes readily at room temperature.*

Prepared from (4*R*,4a*S*,6*R*)-4,4a-dimethyl-6-(prop-1-en-2-yl)-3,4,4a,5,6,7-hexahydronaphthalen-2-yl 1,1,2,2,3,3,4,4,4-nonafluorobutane-1-sulfonate (**233b**, 150 mg, 0.3 mmol) and sodium iodide (67.5 mg, 0.45 mmol) according to General Procedure 3. The crude residue was purified by column chromatography (silica, pentane) to yield **219a** (54 mg, 54% yield) as a colorless oil. $\mathbf{R_f}$ = 0.63 (silica, hexanes, $KMnO_4$). $[\boldsymbol{\alpha}]_D^{25}$ = –155° (c = 1.0, $CHCl_3$). **^{1}H NMR (500 MHz, $CDCl_3$):** δ 6.58 (d, *J* = 2.4 Hz, 1H), 5.41 (dd, *J* = 5.4, 2.8 Hz, 1H), 4.80 – 4.70 (m, 2H), 2.54 (dd, *J* = 18.4, 5.2 Hz, 1H), 2.40 (dddd, *J* = 16.9, 8.5,

4.3, 2.4 Hz, 2H), 2.23 (dddd, *J* = 20.0, 6.8, 5.1, 2.3 Hz, 1H), 2.01 – 1.85 (m, 1H), 1.79 – 1.65 (m, 5H), 1.20 – 1.11 (m, 1H), 0.92 (d, *J* = 0.7 Hz, 3H), 0.86 (d, *J* = 6.9 Hz, 3H). **^{13}C NMR (126 MHz, $CDCl_3$):** δ 150.0, 142.8, 139.1, 124.4, 109.0, 95.1, 46.1, 41.5, 40.0, 37.1, 35.5, 31.1, 20.8, 17.6, 14.2. **FTIR (NaCl, thin film, cm^{-1}):** 3079, 2967, 2912, 1644, 1615, 1441, 1372, 1157, 888, 783. **HRMS (FAB, *m/z*):** calc'd for $C_{15}H_{21}I$ $[M+H-H_2]^+$: 327.0610; found: 327.0598.

(2*R*,8*R*,8a*S*)-6-bromo-8,8a-dimethyl-2-(prop-1-en-2-yl)-1,2,3,7,8,8a-hexahydronaphthalene (219b)

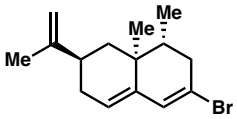

Prepared from (4*R*,4a*S*,6*R*)-4,4a-dimethyl-6-(prop-1-en-2-yl)-3,4,4a,5,6,7-hexahydronaphthalen-2-yl trifluoromethanesulfonate (**211h**, 105.1 mg, 0.3 mmol) and lithium bromide (39.1 mg, 0.45 mmol) according to General Procedure 1. The crude residue was purified by column chromatography (silica, pentane) to yield **219b** (55 mg, 82% yield) as a colorless oil which solidified in the freezer to give a white solid. *Note: This compound decomposes readily at room temperature.* $\mathbf{R_f}$ = 0.57 (silica, hexanes, $KMnO_4$). $[\alpha]_D^{25}$ = –172° (c = 1.0, $CHCl_3$). **^{1}H NMR (400 MHz, $CDCl_3$):** δ 6.30 (d, *J* = 2.3 Hz, 1H), 5.45 (dd, *J* = 5.3, 2.8 Hz, 1H), 4.79 – 4.71 (m, 2H), 2.48 – 2.29 (m, 3H), 2.22 (dt, *J* = 18.6, 5.3 Hz, 1H), 1.99 – 1.87 (m, 1H), 1.75 (t, *J* = 1.1 Hz, 3H), 1.74 – 1.67 (m, 2H), 1.21 – 1.10 (m, 1H), 0.92 (d, *J* = 0.7 Hz, 3H), 0.90 (d, *J* = 6.8 Hz, 3H). **^{13}C NMR (101 MHz, $CDCl_3$):** δ 150.0, 141.7, 131.0, 124.3, 121.0, 109.0, 41.9, 40.8, 40.0, 37.2, 35.6, 31.2, 20.8, 17.6, 14.4. **FTIR (NaCl, thin film, cm^{-1}):** 2959, 2914, 1643, 1620, 1442, 1376, 1349, 1154, 1005, 902, 888, 792, 632. **HRMS (FAB, *m/z*):** calc'd for $C_{15}H_{21}Br$ $[M+H-H_2]^+$: 279.0748; found: 279.0744.

(2*R*,8*R*,8a*S*)-6-chloro-8,8a-dimethyl-2-(prop-1-en-2-yl)-1,2,3,7,8,8a-hexahydronaphthalene (219c)

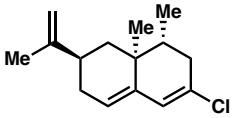

Prepared from (4*R*,4a*S*,6*R*)-4,4a-dimethyl-6-(prop-1-en-2-yl)-3,4,4a,5,6,7-hexahydronaphthalen-2-yl trifluoromethanesulfonate (**211h**, 105.1 mg, 0.3 mmol) and lithium chloride (19.1 mg, 0.45 mmol) according to General Procedure 1. The crude residue was purified by column chromatography (silica, pentane) to yield **219c** (60 mg, 85% yield) as a colorless oil. *Note: This compound decomposes readily at room temperature.* $\mathbf{R_f}$ = 0.63 (silica, hexanes, $KMnO_4$). $[\boldsymbol{\alpha}]_D^{25}$ = –165° (c = 1.0, $CHCl_3$). **^{1}H NMR (500 MHz, $CDCl_3$):** δ 6.09 (dt, *J* = 1.7, 0.9 Hz, 1H), 5.44 (ddd, *J* = 5.2, 2.1, 0.8 Hz, 1H), 4.75 (p, *J* = 1.1 Hz, 2H), 2.47 – 2.37 (m, 1H), 2.29 – 2.21 (m, 3H), 2.00 – 1.92 (m, 1H), 1.76 (t, *J* = 1.2 Hz, 3H), 1.75 – 1.71 (m, 1H), 1.71 (s, 1H), 1.17 (td, *J* = 12.7, 0.8 Hz, 1H), 0.93 – 0.90 (m, 6H). **^{13}C NMR (126 MHz, $CDCl_3$):** δ 150.0, 141.0, 130.5, 126.9, 124.0, 109.0, 40.0, 39.9, 39.5, 37.2, 35.7, 31.3, 20.8, 17.6, 14.5. **FTIR (NaCl, thin film, cm^{-1}):** 3080, 2967, 2912, 1644, 1618, 1442, 1373, 1155, 1014, 888, 824, 635. **HRMS (EI, *m/z*):** calc'd for $C_{15}H_{21}Cl$ $[M+\cdot]^+$: 236.1332; found: 236.1356.

5-iodo-4a-methyl-4,4a,7,8-tetrahydronaphthalen-2(3*H*)-one (220a)

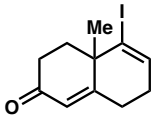

Prepared from 8a-methyl-6-oxo-3,4,6,7,8,8a-hexahydronaphthalen-1-yl trifluoromethanesulfonate (**211i**, 93.1 mg, 0.3 mmol) and sodium iodide (67.5 mg, 0.45 mmol) according to General Procedure 1. The crude residue was purified by column chromatography (silica, 5% Et_2O/hexanes) to yield **220a** (30 mg, 35% yield) as a colorless oil. *Note: This compound decomposes readily at room temperature.*

Prepared from 8a-methyl-6-oxo-3,4,6,7,8,8a-hexahydronaphthalen-1-yl 1,1,2,2,3,3,4,4,4-nonafluorobutane-1-sulfonate (**233c**, 138 mg, 0.3 mmol) and sodium iodide (67.5 mg, 0.45 mmol) according to General Procedure 3. The crude residue was purified by column chromatography (silica, 5-10% Et_2O/hexanes) to yield **220a** (46 mg, 53% yield) as a colorless oil. $\mathbf{R_f}$ = 0.24 (silica, 10% Et_2O/hexanes, $KMnO_4$). **^{1}H NMR (500 MHz, $CDCl_3$):** δ 6.68 (dt, *J* = 2.6, 0.8 Hz, 1H), 5.66 – 5.58 (m, 1H), 2.76 (ddd, *J* = 15.5, 7.3, 5.9 Hz, 1H), 2.72 (s, 2H), 2.63 – 2.53 (m, 1H), 2.49 – 2.40 (m, 1H), 2.36 (ddd, *J* = 15.5, 7.3, 6.7 Hz, 1H), 1.87 – 1.80 (m, 1H), 1.71 (dddd, *J* = 13.5, 11.5, 6.5, 0.8 Hz, 1H), 1.22 (d, *J* = 0.6 Hz, 3H). **^{13}C NMR (126 MHz, $CDCl_3$):** δ 214.3, 140.3, 137.7, 123.7, 96.8, 44.3, 36.6, 35.4, 31.3, 24.2, 22.8. **FTIR (NaCl, thin film, cm^{-1}):** 2926, 1711, 1443, 1322, 1047, 884. **HRMS (FAB, *m/z*):** calc'd for $C_{11}H_{13}OI$ $[M+\cdot]^+$: 288.0011 found: 287.9997.

5-bromo-4a-methyl-4,4a,7,8-tetrahydronaphthalen-2(3*H*)-one (220b)

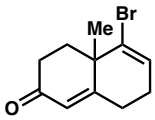

Prepared from 8a-methyl-6-oxo-3,4,6,7,8,8a-hexahydronaphthalen-1-yl trifluoromethanesulfonate (**211i**, 93.1 mg, 0.3 mmol) and lithium bromide (39.1 mg, 0.45 mmol) according to General Procedure 1. The crude residue was purified by column chromatography (silica, 5% Et_2O/hexanes) to yield **220b** (56 mg, 78% yield) as a colorless oil. *Note: This compound decomposes readily at room temperature.* $\mathbf{R_f}$ = 0.24 (silica, 10% Et_2O/hexanes, $KMnO_4$). **^{1}H NMR (400 MHz, $CDCl_3$):** δ 6.43 – 6.38 (m, 1H), 5.70 – 5.63 (m, 1H), 2.81 – 2.73 (m, 1H), 2.73 (s, 3H), 2.54 – 2.40 (m, 1H), 2.40 – 2.32 (m, 1H), 1.99 – 1.90 (m, 1H), 1.68 (dddd, *J* = 13.6, 12.2, 6.0, 0.7 Hz, 1H), 1.22 (d, *J* = 0.7 Hz, 3H). **^{13}C NMR (101 MHz, $CDCl_3$):** δ 214.1, 139.4, 129.7, 123.6, 122.8, 44.4, 35.4,

32.4, 30.5, 24.4, 22.8. **FTIR (NaCl, thin film, cm^{-1}):** 2930, 1713, 1611, 1445, 1348, 1048, 884, 750. **HRMS (FAB, *m/z*):** calc'd for $C_{11}H_{13}OBr$ $[M+\cdot]^+$: 240.0150; found: 240.0153.

5-chloro-4a-methyl-4,4a,7,8-tetrahydronaphthalen-2(3*H*)-one (220c)

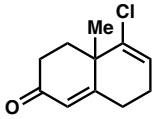

Prepared from 8a-methyl-6-oxo-3,4,6,7,8,8a-hexahydronaphthalen-1-yl trifluoromethanesulfonate (**211i**, 93.1 mg, 0.3 mmol) and lithium chloride (19.1 mg, 0.45 mmol) according to General Procedure 1. The crude residue was purified by column chromatography (silica, 5% Et_2O/hexanes) to yield **220c** (53 mg, 90% yield) as a colorless oil. *Note: This compound decomposes readily at room temperature.* $\mathbf{R_f}$ = 0.13 (silica, 10% EtOAc/hexanes, $KMnO_4$). **^{1}H NMR (400 MHz, $CDCl_3$):** δ 6.19 (dt, *J* = 2.4, 0.7 Hz, 1H), 5.68 – 5.63 (m, 1H), 2.77 (ddd, *J* = 15.4, 7.3, 5.9 Hz, 1H), 2.68 – 2.52 (m, 2H), 2.52 – 2.45 (m, 1H), 2.45 – 2.32 (m, 2H), 1.98 (dddd, *J* = 13.6, 5.7, 1.7, 0.6 Hz, 1H), 1.72 – 1.63 (m, 1H), 1.22 (d, *J* = 0.7 Hz, 3H). **^{13}C NMR (101 MHz, $CDCl_3$):** δ 214.1, 138.8, 132.4, 125.6, 123.4, 44.6, 35.5, 30.1, 29.8, 24.5, 22.8. **FTIR (NaCl, thin film, cm^{-1}):** 3549, 2938, 1714, 1682, 1652, 1446, 1424, 1253, 1155, 1080, 916, 733. **HRMS (EI, *m/z*):** calc'd for $C_{11}H_{13}OCl$ $[M+\cdot]^+$: 196.0655; found: 196.0663.

***tert*-butyl(((1*r*,5*r*)-2-iodo-5-methyl-6-methylenebicyclo[3.2.1]oct-2-en-1-yl)methoxy)-dimethylsilane (221a)**

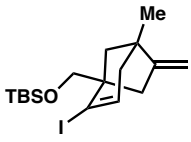

Prepared from (1*r*,5*r*)-1-(((*tert*-butyldimethylsilyl)oxy)methyl)-5-methyl-6-methylenebicyclo[3.2.1]oct-2-en-2-yl trifluoromethanesulfonate (**211j**, 128 mg, 0.3 mmol) and sodium iodide (67.5 mg, 0.45 mmol) according to General Procedure 1. The crude residue was purified by column chromatography (silica,

pentane) to yield **221a** (101 mg, 83% yield) as a colorless oil. $\mathbf{R_f}$ = 0.60 (silica, hexanes, $KMnO_4$). **^{1}H NMR (400 MHz, $CDCl_3$):** δ 6.23 (dd, *J* = 4.8, 2.5 Hz, 1H), 4.90 (td, *J* = 1.8, 0.9 Hz, 1H), 4.88 (dd, *J* = 2.9, 1.9 Hz, 1H), 3.70 (d, *J* = 9.9 Hz, 1H), 3.49 (d, *J* = 9.9 Hz, 1H), 2.41 – 2.23 (m, 3H), 1.94 – 1.77 (m, 3H), 1.17 (s, 3H), 0.91 (s, 9H), 0.08 (s, 3H), 0.07 (s, 3H). **^{13}C NMR (101 MHz, $CDCl_3$):** δ 158.7, 137.8, 107.3, 106.1, 71.1, 50.0, 49.0, 46.8, 43.4, 43.3, 26.1, 24.9, 18.5, -5.1, -5.3. **FTIR (NaCl, thin film, cm^{-1}):** 2954, 2929, 2857, 1655, 1471, 1464, 1251, 1156, 1097, 1007, 879, 851, 838, 808, 776. **HRMS (FAB, *m/z*):** calc'd for $C_{17}H_{29}OISi$ $[M+H-H_2]^+$: 403.0955; found: 403.0969.

***tert*-butyl(((1*r*,5*r*)-2-bromo-5-methyl-6-methylenebicyclo[3.2.1]oct-2-en-1-yl)-methoxy)-dimethylsilane (221b)**

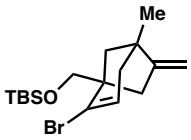

Prepared from (1*r*,5*r*)-1-(((*tert*-butyldimethylsilyl)oxy)methyl)-5-methyl-6-methylenebicyclo[3.2.1]oct-2-en-2-yl trifluoromethanesulfonate (**211j**, 36 mg, 0.1 mmol) and lithium bromide (13.0 mg, 0.15 mmol) according to General Procedure 1. The crude residue was purified by column chromatography (silica, pentane) to yield **221b** (28 mg, 78% yield) as a colorless oil. $\mathbf{R_f}$ = 0.58 (silica, hexanes, $KMnO_4$). **^{1}H NMR (500 MHz, $CDCl_3$):** δ 5.86 (dd, *J* = 4.9, 2.5 Hz, 1H), 4.91 (t, *J* = 2.1 Hz, 1H), 4.89 – 4.86 (m, 1H), 3.82 (d, *J* = 9.9 Hz, 1H), 3.57 (d, *J* = 9.9 Hz, 1H), 2.50 – 2.43 (m, 1H), 2.42 – 2.36 (m, 1H), 2.24 (dd, *J* = 16.9, 2.5 Hz, 1H), 1.94 – 1.87 (m, 1H), 1.82 (d, *J* = 1.5 Hz, 2H), 1.19 (s, 3H), 0.90 (s, 9H), 0.07 (s, 3H), 0.06 (s, 3H). **^{13}C NMR (126 MHz, $CDCl_3$):** δ 158.8, 129.8, 128.7, 106.1, 67.2, 50.0, 47.3, 46.8, 43.7, 43.2, 26.1, 24.8, 18.5, -5.26, -5.33. **FTIR (NaCl, thin film, cm^{-1}):** 2954, 2857, 1652, 1463, 1251,

1097, 1010, 880, 839, 811, 775. **HRMS (FAB, *m/z*):** calc'd for $C_{17}H_{29}OBrSi$ $[M+H-H_2]^+$: 357.1072; found: 357.1085.

***tert*-butyl(((1*r*,5*r*)-2-chloro-5-methyl-6-methylenebicyclo[3.2.1]oct-2-en-1-yl)methoxy)-dimethylsilane (221c)**

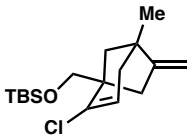

Prepared from (1*r*,5*r*)-1-(((*tert*-butyldimethylsilyl)oxy)methyl)-5-methyl-6-methylenebicyclo[3.2.1]oct-2-en-2-yl trifluoromethanesulfonate (**211j**, 36 mg, 0.1 mmol) and lithium chloride (6.4 mg, 0.15 mmol) according to General Procedure 1. The crude residue was purified by column chromatography (silica, pentane) to yield **221c** (27 mg, 82% yield) as a colorless oil. $\mathbf{R_f}$ = 0.56 (silica, hexanes, $KMnO_4$). **^{1}H NMR (400 MHz, $CDCl_3$):** δ 5.61 (dd, *J* = 4.8, 2.5 Hz, 1H), 4.89 (ddd, *J* = 7.2, 2.7, 1.8 Hz, 2H), 3.88 (d, *J* = 9.9 Hz, 1H), 3.59 (d, *J* = 9.9 Hz, 1H), 2.54 – 2.38 (m, 2H), 2.26 (dd, *J* = 16.9, 2.6 Hz, 1H), 1.97 – 1.88 (m, 1H), 1.84 – 1.73 (m, 2H), 1.20 (s, 3H), 0.90 (s, 9H), 0.06 (s, 3H), 0.06 (s, 3H). **^{13}C NMR (101 MHz, $CDCl_3$):** δ 158.9, 138.3, 124.0, 106.0, 65.4, 49.5, 47.2, 45.2, 43.9, 43.2, 26.0, 24.8, 18.5, -5.33, -5.34. **FTIR (NaCl, thin film, cm^{-1}):** 2954, 2858, 1656, 1471, 1252, 1098, 880, 838, 812, 776 **HRMS (TOF-ESI, *m/z*):** calc'd for $C_{17}H_{29}OClSi$ $[M+H]^+$: 313.1754; found: 313.1732.

***tert*-butyl (1*r*,5*s*)-3-iodo-8-azabicyclo[3.2.1]oct-2-ene-8-carboxylate (222a)**

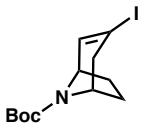

Prepared from *tert*-butyl (1*r*,5*s*)-3-(((trifluoromethyl)sulfonyl)oxy)-8-azabicyclo[3.2.1]oct-2-ene-8-carboxylate (**211k**, 402 mg, 1.2 mmol) and sodium iodide (270 mg, 1.8 mmol) according to General Procedure 1. The crude residue

was purified by column chromatography (silica, 10 to 20% Et_2O/hexanes) to yield **222a** (143 mg, 34% yield) as a colorless oil.

Prepared from *tert*-butyl (1*r*,5*s*)-3-(((perfluorobutyl)sulfonyl)oxy)-8-azabicyclo[3.2.1]oct-2-ene-8-carboxylate (**233d**, 152 mg, 0.3 mmol) and sodium iodide (67.5 mg, 0.45 mmol) according to General Procedure 3. The crude residue was purified by column chromatography (silica, 10 to 6% acetone/hexanes) to yield **222a** (53 mg, 53% yield) as a colorless oil. $\mathbf{R_f}$ = 0.55 (silica, 30% Et_2O/hexanes, $KMnO_4$). **^{1}H NMR (400 MHz, d_3-MeCN, 65 °C):** δ 6.70 – 6.65 (m, 1H), 4.23 (t, *J* = 5.6 Hz, 1H), 4.17 – 4.11 (m, 1H), 3.16 – 3.06 (m, 1H), 2.31 (dt, *J* = 17.5, 1.4 Hz, 1H), 2.26 – 2.12 (m, 1H), 1.98 – 1.81 (m, 2H), 1.76 (ddt, *J* = 15.6, 9.8, 3.8 Hz, 1H), 1.44 (d, *J* = 0.6 Hz, 9H). **^{13}C NMR (101 MHz, d_3-MeCN, 65 °C):** δ 6.70 – 6.65 (m, 1H), 4.23 (t, *J* = 5.6 Hz, 1H), 4.17 – 4.11 (m, 1H), 3.16 – 3.06 (m, 1H), 2.31 (dt, *J* = 17.5, 1.4 Hz, 1H), 2.26 – 2.12 (m, 1H), 1.98 – 1.81 (m, 2H), 1.76 (ddt, *J* = 15.6, 9.8, 3.8 Hz, 1H), 1.44 (d, *J* = 0.6 Hz, 9H). **FTIR (NaCl, thin film, cm^{-1}):** 2975, 1698, 1392, 1347, 1312, 1172, 1103, 1101, 973. **HRMS (FAB, *m/z*):** calc'd for $C_{12}H_{18}INO_2$ $[M+H]^+$: 336.0461; found: 336.0454.

tert-butyl (1*r*,5*s*)-3-bromo-8-azabicyclo[3.2.1]oct-2-ene-8-carboxylate (222b)

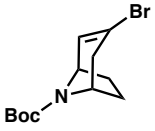

Prepared from *tert*-butyl (1*r*,5*s*)-3-(((trifluoromethyl)sulfonyl)oxy)-8-azabicyclo[3.2.1]oct-2-ene-8-carboxylate (**211k**, 107 mg, 0.3 mmol) and lithium bromide (39.1 mg, 0.45 mmol) according to General Procedure 1. The crude residue was purified by column chromatography (silica, 10 to 20% Et_2O/hexanes) to yield **222b** (56 mg, 65% yield) as a colorless oil. $\mathbf{R_f}$ = 0.55 (silica, 30% Et_2O/hexanes, $KMnO_4$).

^{1}H NMR (400 MHz, d_3-MeCN, 65 °C): δ 6.38 (ddd, *J* = 5.5, 2.0, 1.4 Hz, 1H), 4.32 (td, *J* = 5.5, 1.2 Hz, 1H), 4.29 – 4.22 (m, 1H), 3.06 (ddt, *J* = 17.3, 4.3, 2.0 Hz, 1H), 2.26 – 2.13 (m, 2H), 1.99 – 1.85 (m, 2H), 1.74 (dddd, *J* = 12.9, 9.6, 6.7, 1.2 Hz, 1H), 1.45 (s, 9H). **^{13}C NMR (101 MHz, d_3-MeCN, 65 °C):** δ 155.0, 135.7, 121.0, 80.5, 56.2, 54.8, 44.8, 35.0, 30.5, 28.8. **FTIR (NaCl, thin film, cm^{-1}):** 2976, 1698, 1392, 1367, 1350, 1320, 1171, 1103, 1107, 975. **HRMS (FAB, *m/z*):** calc'd for $C_{12}H_{18}BrNO_2$ $[M+H]^+$: 288.0599; found: 288.0593.

***tert*-butyl (1r,5*s*)-3-chloro-8-azabicyclo[3.2.1]oct-2-ene-8-carboxylate (222c)**

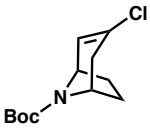

Prepared from *tert*-butyl (1*r*,5*s*)-3-(((trifluoromethyl)sulfonyl)oxy)-8-azabicyclo[3.2.1]oct-2-ene-8-carboxylate (**211k**, 107 mg, 0.3 mmol) and lithium chloride (19.1 mg, 0.45 mmol) according to General Procedure 1. The crude residue was purified by column chromatography (silica, 10 to 20% Et_2O/hexanes) to yield **222c** (61 mg, 84% yield) as a colorless oil. $\mathbf{R_f}$ = 0.55 (silica, 30% Et_2O/hexanes, $KMnO_4$). **^{1}H NMR (400 MHz, d_3-MeCN, 65 °C):** δ 6.16 (ddd, *J* = 5.6, 2.0, 1.3 Hz, 1H), 4.47 – 4.35 (m, 1H), 4.35 – 4.28 (m, 1H), 2.96 (ddt, *J* = 17.2, 3.9, 1.8 Hz, 1H), 2.26 – 2.14 (m, 1H), 2.09 (dt, *J* = 17.3, 1.4 Hz, 1H), 1.99 – 1.89 (m, 2H), 1.79 – 1.67 (m, 1H), 1.46 (s, 9H). **^{13}C NMR (101 MHz, d_3-MeCN, 65 °C):** δ 154.9, 131.4, 80.4, 55.0, 53.9, 42.5, 35.1, 30.5, 28.8. (*Note: one carbon under solvent*). **FTIR (NaCl, thin film, cm^{-1}):** 2976, 1694, 1638, 1392, 1323, 1256, 1168, 1103, 1015, 978, 888, 874, 775, 724. **HRMS (TOF-ESI, *m/z*):** calc'd for $C_{12}H_{18}ClNO_2$ $[M+H]^+$: 244.1104; found: 244.1098.

(5'*R*,6a*R*,6b*S*,8a*S*,8b*R*,9*S*,10*R*,11a*S*,12a*S*,12b*S*)-4-bromo-5',6a,8a,9-tetramethyl-1,3',4',5,5',6,6a,6b,6',7,8,8a,8b,9,11a,12,12a,12b-octadecahydrospiro[naphtha-[2',1':4,5]indeno[2,1-*b*]furan-10,2'-pyran] (223b)

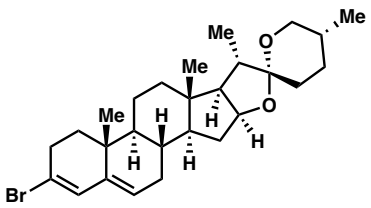

Prepared from (5'*R*,6a*R*,6b*S*,8a*S*,8b*R*,9*S*,10*R*,11a*S*,12a*S*,-12b*S*)-5',6a,8a,9-tetramethyl-1,3',4',5,5',6,6a,6b,6',7,8,8a,-8b,9,11a,12,12a,12b-octadecahydrospiro[naphtha-[2',1':4,5]indeno[2,1-*b*]furan-10,2'-pyran]-4-yl trifluoromethanesulfonate (**211l**, 163.4 mg, 0.3 mmol) and lithium bromide (39.1 mg, 0.45 mmol) according to General Procedure 1. The crude residue was purified by column chromatography (silica, 40% Et_2O/hexanes) to yield **223b** (107 mg, 75% yield) as a white solid. $\mathbf{R_f}$ = 0.56 (silica, 10% Et_2O/hexanes, $KMnO_4$). $[\boldsymbol{a}]_D^{25}$ = –176° (c = 1.0, $CHCl_3$). **^{1}H NMR (400 MHz, $CDCl_3$):** δ 6.26 (d, *J* = 2.3 Hz, 1H), 5.39 (dd, *J* = 5.1, 2.9 Hz, 1H), 4.41 (ddd, *J* = 8.6, 7.5, 6.3 Hz, 1H), 3.47 (ddd, *J* = 10.9, 4.6, 2.0 Hz, 1H), 3.36 (t, *J* = 10.8 Hz, 1H), 2.67 – 2.53 (m, 1H), 2.46 (ddd, *J* = 18.4, 5.9, 1.6 Hz, 1H), 2.17 (dt, *J* = 18.7, 5.3 Hz, 1H), 1.98 (ddd, *J* = 11.8, 7.5, 5.4 Hz, 1H), 1.91 – 1.10 (m, 17H), 1.05 – 0.92 (m, 7H), 0.84 – 0.74 (m, 6H). **^{13}C NMR (101 MHz, $CDCl_3$):** δ 141.3, 131.2, 124.4, 120.9, 109.4, 80.9, 67.0, 62.2, 56.7, 48.0, 41.7, 40.5, 39.8, 35.6, 34.6, 33.2, 32.0, 31.9, 31.5, 31.3, 30.4, 28.9, 21.0, 19.1, 17.3, 16.5, 14.7. **FTIR (NaCl, thin film, cm^{-1}):** 2949, 1616, 1455, 1377, 1241, 1173, 1051, 980, 899, 734. **HRMS (FAB, *m/z*):** calc'd for $C_{27}H_{39}BrO_2$ $[M+H]^+$: 475.2035; found: 475.2049.

(5'*R*,6a*R*,6b*S*,8a*S*,8b*R*,9*S*,10*R*,11a*S*,12a*S*,12b*S*)-4-chloro-5',6a,8a,9-tetramethyl-1,3',4',5,5',6,6a,6b,6',7,8,8a,8b,9,11a,12,12a,12b-octadecahydrospiro[naphtha-[2',1':4,5]indeno[2,1-*b*]furan-10,2'-pyran] (223c)

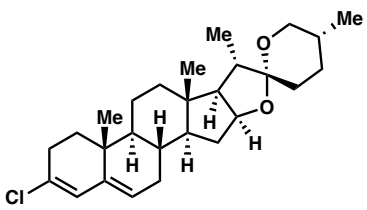

Prepared from (5'*R*,6a*R*,6b*S*,8a*S*,8b*R*,9*S*,10*R*,11a*S*,-12a*S*,12b*S*)-5',6a,8a,9-tetramethyl-1,3',4',5,5',6,6a,6b,6',7,--8,8a,8b,9,11a,12,12a,12b-octadecahydrospiro[naphtha-[2',1':4,5]indeno[2,1-*b*]furan-10,2'-pyran]-4-yl trifluoromethanesulfonate (**211l**, 163.4 mg, 0.3 mmol) and lithium chloride (19.1 mg, 0.45 mmol) according to General Procedure 1. The crude residue was purified by column chromatography (silica, 40% Et_2O/hexanes) to yield **223c** (125 mg, 97% yield) as a white solid. $\mathbf{R_f}$ = 0.57 (silica, 10% EtOAc/hexanes, $KMnO_4$). $[\boldsymbol{a}]_D^{25}$ = –183° (c = 1.0, $CHCl_3$). **^{1}H NMR (400 MHz, $CDCl_3$):** δ 6.05 (d, *J* = 2.3 Hz, 1H), 5.38 (dd, *J* = 5.0, 2.9 Hz, 1H), 4.41 (ddd, *J* = 8.6, 7.6, 6.4 Hz, 1H), 3.47 (ddd, *J* = 10.9, 4.5, 2.0 Hz, 1H), 3.37 (t, *J* = 10.9 Hz, 1H), 2.50 (ddd, *J* = 17.8, 12.0, 5.8 Hz, 1H), 2.31 (ddd, *J* = 18.3, 5.9, 1.5 Hz, 1H), 2.19 (dt, *J* = 18.7, 5.3 Hz, 1H), 1.99 (ddd, *J* = 11.7, 7.5, 5.4 Hz, 1H), 1.93 – 1.50 (m, 11H), 1.50 – 1.39 (m, 2H), 1.31 (ddd, *J* = 13.5, 11.8, 6.3 Hz, 2H), 1.24 – 1.09 (m, 2H), 1.06 – 1.00 (m, 1H), 0.97 (t, *J* = 3.5 Hz, 6H), 0.84 – 0.75 (m, 6H). **^{13}C NMR (101 MHz, $CDCl_3$):** δ 140.6, 130.4, 127.1, 124.0, 109.4, 80.9, 67.0, 62.2, 56.7, 48.0, 41.7, 40.5, 39.8, 34.9, 34.7, 32.1, 31.9, 31.5, 31.4, 30.8, 30.4, 28.9, 21.1, 19.0, 17.3, 16.5, 14.7. **FTIR (NaCl, thin film, cm^{-1}):** 2950, 2906, 1622, 1450, 1380, 1350, 1240, 1170, 1070, 1050, 981, 900, 868, 734. **HRMS (TOF-ESI, *m/z*):** calc'd for $C_{27}H_{39}ClO_2$ $[M+H]^+$: 431.2717; found: 431.2716.

(8*R*,9*S*,13*S*,14*S*)-17-bromo-13-methyl-7,8,9,11,12,13,14,15-octahydro-6*H*-cyclopenta[*a*]phenanthren-3-yl trifluoromethanesulfonate (224b)

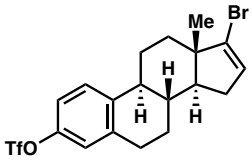

Prepared from (8*R*,9*S*,13*S*,14*S*)-13-methyl-7,8,9,11,12,13,14,15-octahydro-6*H*-cyclopenta[*a*]phenanthrene-3,17-diyl bis(trifluoromethanesulfonate) (**211m**, 160.3 mg, 0.3 mmol) and lithium bromide (39.1 mg, 0.45 mmol) according to General Procedure 1. The crude residue was purified by column chromatography (silica, 5% to 15% PhMe/hexanes) to yield **224b** (82 mg, 59% yield) as a colorless, tacky oil. $\mathbf{R_f}$ = 0.38 (silica, 10% PhMe/hexanes, $KMnO_4$). $[\boldsymbol{a}]_D^{25}$ = 39° (c = 1.0, $CHCl_3$). **^{1}H NMR (400 MHz, $CDCl_3$):** δ 7.33 (dd, *J* = 8.7, 1.1 Hz, 1H), 7.03 (dd, *J* = 8.6, 2.8 Hz, 1H), 6.99 (d, *J* = 2.6 Hz, 1H), 5.88 (dd, *J* = 3.3, 1.7 Hz, 1H), 2.97 – 2.91 (m, 2H), 2.45 – 2.36 (m, 1H), 2.36 – 2.29 (m, 1H), 2.25 (ddd, *J* = 14.8, 6.3, 3.2 Hz, 1H), 2.02 (ddd, *J* = 14.8, 11.1, 1.8 Hz, 1H), 1.99 – 1.93 (m, 1H), 1.90 (ddd, *J* = 12.3, 3.7, 2.1 Hz, 1H), 1.73 (td, *J* = 11.2, 6.2 Hz, 1H), 1.69 – 1.41 (m, 4H), 0.88 (s, 3H). **^{13}C NMR (101 MHz, $CDCl_3$):** δ 147.7, 140.8, 139.5, 135.6, 129.1, 127.0, 121.3, 118.9 (q, $J_{C\text{-}F}$ = 320.7 Hz), 118.3, 54.9, 48.9, 44.4, 37.0, 34.6, 31.7, 29.5, 27.0, 26.2, 15.3. **^{19}F NMR (282 MHz, $CDCl_3$):** δ -72.9. **FTIR (NaCl, thin film, cm^{-1}):** 2932, 1592, 1490, 1422, 1247, 1210, 1142, 996, 919, 882, 846. **HRMS (FAB, *m/z*):** calc'd for $C_{19}H_{20}BrF_3O_3S$ $[M+H-H_2]^+$: 465.0170; found: 465.0165.

(8*R*,9*S*,13*S*,14*S*)-17-chloro-13-methyl-7,8,9,11,12,13,14,15-octahydro-6*H*-cyclopenta[*a*]phenanthren-3-yl trifluoromethanesulfonate (224c)

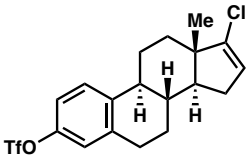

Prepared from (8*R*,9*S*,13*S*,14*S*)-13-methyl-7,8,9,11,12,13,14,15-octahydro-6*H*-cyclopenta[*a*]phenanthrene-3,17-diylbis(trifluoromethanesulfonate) (**211m**, 160.3 mg, 0.3 mmol) and lithium chloride (19.1 mg, 0.45 mmol) according to General Procedure 1. The crude residue was purified by column chromatography (silica, 1.5% EtOAc/hexanes) to yield **224c** (109 mg, 83% yield) as a colorless, tacky oil. $\mathbf{R_f}$ = 0.67 (silica, 10% EtOAc/hexanes, $KMnO_4$). $[\boldsymbol{a}]_D^{25}$ = +67° (c = 1.0, $CHCl_3$). **^{1}H NMR (400 MHz, $CDCl_3$):** δ 7.33 (dd, *J* = 8.8, 1.2 Hz, 1H), 7.03 (dd, *J* = 8.6, 2.8 Hz, 1H), 7.00 – 6.94 (m, 1H), 5.67 (dd, *J* = 3.3, 1.7 Hz, 1H), 2.99 – 2.88 (m, 2H), 2.46 – 2.30 (m, 2H), 2.27 (ddd, *J* = 14.7, 6.3, 3.2 Hz, 1H), 2.05 (ddd, *J* = 14.8, 11.0, 1.8 Hz, 1H), 2.00 – 1.89 (m, 2H), 1.73 (td, *J* = 11.2, 6.3 Hz, 1H), 1.68 – 1.42 (m, 4H), 0.91 (s, 3H). **^{13}C NMR (101 MHz, $CDCl_3$):** δ 147.7, 144.7, 140.9, 139.5, 127.0, 124.7, 121.3, 118.9 (q, $J_{C\text{-}F}$ = 320.7 Hz), 118.3, 55.1, 47.9, 44.5, 36.9, 33.8, 30.5, 29.5, 26.9, 26.1, 15.2. **^{19}F NMR (282 MHz, $CDCl_3$):** δ -72.9. **FTIR (NaCl, thin film, cm^{-1}):** 2934, 2859, 1598, 1490, 1417, 1248, 1211, 1142, 1007, 919, 851, 822, 701, 608. **HRMS (TOF-ESI, *m/z*):** calc'd for $C_{19}H_{20}ClF_3O_3S$ $[M+H]^+$: 421.0852; found: 421.0845.

(1*S*,4*R*,5*R*)-3-bromo-1-isopropyl-4-methylbicyclo[3.1.0]hex-2-ene (225b)

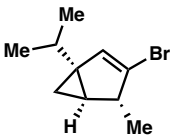

Prepared from (1*S*,4*R*,5*R*)-1-isopropyl-4-methylbicyclo[3.1.0]hex-2-en-3-yl trifluoromethanesulfonate (**211n**, 85.3 mg, 0.3 mmol) and lithium bromide (39.1 mg, 0.45 mmol) according to General Procedure 1 with the exception of 5 mol % Ni used instead of 10 mol % Ni. The crude residue was purified by column

chromatography (silica, pentane) to yield **225b** (27 mg, 42% yield, 92% purity by mass) as a colorless oil. Product was determined to be 92% pure by NMR (impurity is homocoupling product) therefore the yield is adjusted 42% x 0.92 = 38% yield. $\mathbf{R_f}$ = 0.88 (silica, hexanes, $KMnO_4$). $[\boldsymbol{\alpha}]_D^{25}$ = –13° (c = 0.5, $CHCl_3$). **^{1}H NMR (500 MHz, $CDCl_3$):** δ 5.93 (t, *J* = 1.3 Hz, 1H), 2.59 – 2.52 (m, 1H), 1.38 (p, *J* = 6.9 Hz, 1H), 1.15 – 1.11 (m, 4H), 0.99 (d, *J* = 6.8 Hz, 3H), 0.89 (d, *J* = 6.8 Hz, 3H), 0.81 – 0.78 (m, 1H), 0.28 (t, *J* = 4.2 Hz, 1H). **^{13}C NMR (126 MHz, $CDCl_3$):** δ 133.9, 123.9, 48.5, 40.9, 31.0, 26.5, 21.5, 20.9, 20.8, 20.8. **FTIR (NaCl, thin film, cm^{-1}):** 2958, 2870, 1602, 1453, 1366, 1056, 973, 867, 832, 796, 754. **HRMS (EI, *m/z*):** calc'd for $C_{10}H_{15}Br$ $[M+\cdot]^+$: 214.0357; found: 214.0358.

(1*S*,4*R*,5*R*)-3-chloro-1-isopropyl-4-methylbicyclo[3.1.0]hex-2-ene (225c)

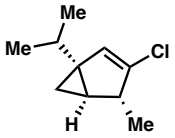

Prepared from (1*S*,4*R*,5*R*)-1-isopropyl-4-methylbicyclo[3.1.0]hex-2-en-3-yl trifluoromethanesulfonate (**211n**, 85.3 mg, 0.3 mmol) and lithium chloride (19.1 mg, 0.45 mmol) according to General Procedure 1. The crude residue was purified by column chromatography (silica, pentane) to yield **225c** (40 mg, 78% yield) as a colorless oil. $\mathbf{R_f}$ = 0.85 (silica, hexanes, $KMnO_4$). $[\boldsymbol{\alpha}]_D^{25}$ = +17° (c = 1.0, $CHCl_3$). **^{1}H NMR (400 MHz, $CDCl_3$):** δ 5.75 (t, *J* = 1.3 Hz, 1H), 2.51 (tdd, *J* = 8.0, 6.0, 0.9 Hz, 1H), 1.36 (p, *J* = 6.8 Hz, 1H), 1.14 (d, *J* = 7.1 Hz, 3H), 1.12 – 1.06 (m, 1H), 0.99 (d, *J* = 6.9 Hz, 3H), 0.89 (d, *J* = 6.8 Hz, 3H), 0.78 (dd, *J* = 7.8, 4.3 Hz, 1H), 0.27 (t, *J* = 4.2 Hz, 1H). **^{13}C NMR (101 MHz, $CDCl_3$):** δ 134.6, 129.4, 46.8, 39.5, 31.1, 26.1, 21.6, 20.9, 20.8, 20.2. **FTIR (NaCl, thin film, cm^{-1}):** 2956, 2924, 2854, 1458, 1364, 1057, 1026. **HRMS (EI, *m/z*):** calc'd for $C_{10}H_{15}Cl$ $[M+\cdot]^+$: 170.0862; found: 170.0888.

(1a*R*,4a*R*,7*R*,7a*S*,7b*S*)-4-iodo-1,1,7-trimethyl-1a,2,4a,5,6,7,7a,7b-octahydro-1*H*-cyclopropa[*e*]azulene (226a)

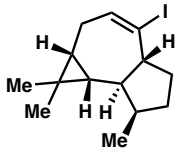

Prepared from (1a*R*,4a*R*,7*R*,7a*S*,7b*S*)-1,1,7-trimethyl-1a,2,4a,5,6,7,7a,7b-octahydro-1*H*-cyclopropa[*e*]azulen-4-yl trifluoromethanesulfonate (**211o**, 101.5 mg, 0.3 mmol) and sodium iodide (67.5 mg, 0.45 mmol) according to General Procedure 1. The crude residue was purified by column chromatography (silica, pentane) to yield **226a** (48 mg, 75% yield) as a colorless oil. $\mathbf{R_f}$ = 0.72 (silica, hexanes, $KMnO_4$). $[\alpha]_D^{25}$ = –184° (c = 1.0, $CHCl_3$). **^{1}H NMR (400 MHz, $CDCl_3$):** δ 6.43 (ddd, *J* = 8.8, 3.6, 2.2 Hz, 1H), 2.77 (tdd, *J* = 11.3, 7.4, 3.3 Hz, 1H), 2.37 – 2.22 (m, 1H), 2.18 – 2.02 (m, 3H), 1.89 (dddd, *J* = 13.0, 9.8, 8.2, 3.1 Hz, 1H), 1.77 (td, *J* = 11.6, 8.4 Hz, 1H), 1.44 (dddd, *J* = 12.5, 11.4, 9.8, 8.8 Hz, 1H), 1.16 (dtd, *J* = 13.1, 8.7, 4.5 Hz, 1H), 1.03 (s, 3H), 1.02 (s, 3H), 0.97 – 0.87 (m, 4H), 0.60 (dd, *J* = 11.5, 9.3 Hz, 1H). **^{13}C NMR (101 MHz, $CDCl_3$):** δ 138.5, 109.1, 56.7, 43.5, 36.6, 36.3, 30.9, 28.7, 26.8, 26.2, 25.8, 19.3, 18.3, 15.3. **FTIR (NaCl, thin film, cm^{-1}):** 2953, 2866, 1455, 1376, 1216, 909, 723. **HRMS (FAB, *m/z*):** calc'd for $C_{14}H_{21}I$ $[M+H–H_2]^+$: 315.0610; found: 315.0609.

(1a*R*,4a*R*,7*R*,7a*S*,7b*S*)-4-bromo-1,1,7-trimethyl-1a,2,4a,5,6,7,7a,7b-octahydro-1*H*-cyclopropa[*e*]azulene (226b)

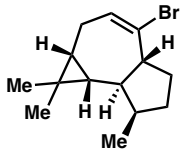

Prepared from (1a*R*,4a*R*,7*R*,7a*S*,7b*S*)-1,1,7-trimethyl-1a,2,4a,5,6,7,7a,7b-octahydro-1*H*-cyclopropa[*e*]azulen-4-yl trifluoromethanesulfonate (**211o**, 101.5 mg, 0.3 mmol) and lithium bromide (39.1 mg, 0.45 mmol) according to General Procedure 1. The crude residue was purified by column chromatography (silica, pentane) to yield **226b** (73 mg, 88% yield) as a colorless oil. $\mathbf{R_f}$ = 0.68 (silica, hexanes, $KMnO_4$).

$[\alpha]_D^{25}$ = –152° (c = 1.0, $CHCl_3$). **^{1}H NMR (400 MHz, $CDCl_3$):** δ 6.10 (ddd, *J* = 9.3, 3.3, 2.1 Hz, 1H), 2.77 (dddd, *J* = 18.2, 9.2, 3.7, 2.1 Hz, 1H), 2.29 – 2.10 (m, 3H), 2.04 – 1.85 (m, 2H), 1.76 (td, *J* = 11.7, 8.3 Hz, 1H), 1.46 (dddd, *J* = 12.6, 11.4, 9.8, 8.8 Hz, 1H), 1.18 (dtd, *J* = 13.1, 8.6, 4.3 Hz, 1H), 1.03 (d, *J* = 3.8 Hz, 6H), 0.97 – 0.88 (m, 4H), 0.60 (dd, *J* = 11.5, 9.3 Hz, 1H). **^{13}C NMR (101 MHz, $CDCl_3$):** δ 130.8, 129.8, 53.7, 43.5, 35.5, 33.7, 31.3, 28.6, 26.0, 25.7, 24.5, 18.9, 18.2, 15.3. **FTIR (NaCl, thin film, cm^{-1}):** 2953, 2867, 1633, 1455, 1376, 1251, 1064, 913, 860, 732. **HRMS (TOF-ESI, *m/z*):** calc'd for $C_{14}H_{21}Br$ $[M+H–H_2]^+$: 267.0748; found: 267.0737.

(1a*R*,4a*R*,7*R*,7a*S*,7b*S*)-4-chloro-1,1,7-trimethyl-1a,2,4a,5,6,7,7a,7b-octahydro-1*H*-cyclopropa[*e*]azulene (226c)

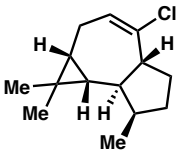

Prepared from (1a*R*,4a*R*,7*R*,7a*S*,7b*S*)-1,1,7-trimethyl-1a,2,4a,5,6,7,-7a,7b-octahydro-1*H*-cyclopropa[*e*]azulen-4-yltrifluoro-methanesulfonate (**211o**, 101.5 mg, 0.3 mmol) and lithium chloride (19.1 mg, 0.45 mmol) according to General Procedure 1. The crude residue was purified by column chromatography (silica, pentane) to yield **226c** (40 mg, 88% yield) as a colorless oil. $\mathbf{R}_f$ = 0.78 (silica, hexanes, $KMnO_4$). $[\alpha]_D^{25}$ = –174° (c = 1.0, $CHCl_3$). **^{1}H NMR (400 MHz, $CDCl_3$):** δ 5.84 (ddd, *J* = 9.3, 3.3, 2.1 Hz, 1H), 2.68 (dddd, *J* = 18.1, 9.2, 3.8, 2.1 Hz, 1H), 2.26 – 2.09 (m, 3H), 2.01 (ddt, *J* = 16.8, 10.4, 3.6 Hz, 1H), 1.90 (dddd, *J* = 13.1, 9.9, 8.2, 3.1 Hz, 1H), 1.75 (td, *J* = 11.7, 8.3 Hz, 1H), 1.44 (dddd, *J* = 12.6, 11.3, 9.8, 8.8 Hz, 1H), 1.19 (dtd, *J* = 13.0, 8.6, 4.3 Hz, 1H), 1.04 (s, 3H), 1.03 (s, 3H), 0.95 – 0.87 (m, 4H), 0.60 (dd, *J* = 11.5, 9.3 Hz, 1H). **^{13}C NMR (101 MHz, $CDCl_3$):** δ 138.6, 125.6, 51.9, 43.2, 35.0, 32.1, 31.6, 28.7, 26.1, 25.8,

23.0, 18.8, 18.1, 15.3. **FTIR (NaCl, thin film, cm^{-1}):** 2952, 2866, 1453, 1376, 921, 748. **HRMS (EI, *m/z*):** calc'd for $C_{14}H_{21}Cl$ $[M+\cdot]^+$: 224.1332; found: 224.1306.

9-iodo-6,7-dihydro-5*H*-benzo[7]annulene (227a)

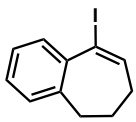

Prepared from 6,7-dihydro-5*H*-benzo[7]annulen-9-yl trifluoromethanesulfonate (**211p**, 87.7 mg, 0.3 mmol) and sodium iodide (67.5 mg, 0.45 mmol) according to General Procedure 1. The crude residue was purified by column chromatography (silica, hexanes) to yield **227a** (65 mg, 80% yield) as a light yellow oil. $\mathbf{R_f}$ = 0.66 (silica, hexanes, $KMnO_4$). **^{1}H NMR (400 MHz, $CDCl_3$):** δ 7.49 (dd, *J* = 7.7, 1.3 Hz, 1H), 7.31 – 7.25 (m, 1H), 7.18 (td, *J* = 7.4, 1.4 Hz, 1H), 7.12 (dd, *J* = 7.6, 1.4 Hz, 1H), 6.95 (t, *J* = 7.5 Hz, 1H), 2.66 (t, *J* = 7.0 Hz, 2H), 2.14 (p, *J* = 7.1 Hz, 2H), 1.83 (q, *J* = 7.3 Hz, 2H). **^{13}C NMR (101 MHz, $CDCl_3$):** δ 142.1, 141.3, 139.8, 131.1, 128.5, 128.2, 126.4, 95.8, 34.8, 32.6, 28.2. **FTIR (NaCl, thin film, cm^{-1}):** 2928, 2854, 1478, 1447, 1195, 887, 763, 742, 662. **HRMS (FAB, *m/z*):** calc'd for $C_{11}H_{11}I$ $[M+\cdot]^+$: 269.9906; found: 269.9910.

9-bromo-6,7-dihydro-5*H*-benzo[7]annulene (227b)

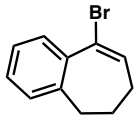

Prepared from 6,7-dihydro-5*H*-benzo[7]annulen-9-yl trifluoromethanesulfonate (**211p**, 87.7 mg, 0.3 mmol) and lithium bromide (39.1 mg, 0.45 mmol) according to General Procedure 1. The crude residue was purified by column chromatography (silica, hexanes) to yield **227b** (49 mg, 73% yield) as a light yellow oil. $\mathbf{R_f}$ = 0.51 (silica, hexanes, $KMnO_4$). **^{1}H NMR (400 MHz, $CDCl_3$):** δ 7.58 (dd, *J* = 7.7, 1.4 Hz, 1H), 7.30 (td, *J* = 7.5, 1.6 Hz, 1H), 7.25 – 7.15 (m, 2H), 6.64 (t, *J* = 7.4 Hz, 1H), 2.68 (t, *J* = 6.9 Hz, 2H), 2.14 (p, *J* = 7.1 Hz, 2H), 1.92 (q, *J* = 7.0 Hz, 2H). **^{13}C NMR (101 MHz,**

$CDCl_3$): δ 140.7, 138.8, 133.3, 129.5, 128.7, 128.4, 126.4, 120.7, 34.3, 32.7, 26.9. **FTIR (NaCl, thin film, cm^{-1}):** 3062, 2930, 2856, 1614, 1480, 1448, 1303, 1197, 897, 765, 745, 668. **HRMS (EI, *m/z*):** calc'd for $C_{11}H_{11}Br$ $[M+\cdot]^+$: 222.0044; found: 222.0042.

9-chloro-6,7-dihydro-5*H*-benzo[7]annulene (227c)

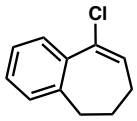

Prepared from 6,7-dihydro-5*H*-benzo[7]annulen-9-yl trifluoromethanesulfonate **211p**, 87.7 mg, 0.3 mmol) and lithium chloride (19.1 mg, 0.45 mmol) according to General Procedure 1. The crude residue was purified by column chromatography (silica, hexanes) to yield **227c** (38 mg, 71% yield) as a light yellow oil. $\mathbf{R_f}$ = 0.54 (silica, hexanes, $KMnO_4$). **^{1}H NMR (400 MHz, $CDCl_3$):** δ 7.60 (dd, *J* = 7.6, 1.5 Hz, 1H), 7.30 (td, *J* = 7.5, 1.7 Hz, 1H), 7.27 – 7.22 (m, 1H), 7.20 (dd, *J* = 7.5, 1.6 Hz, 1H), 6.40 (t, *J* = 7.1 Hz, 1H), 2.69 (t, *J* = 6.7 Hz, 2H), 2.17 – 2.09 (m, 2H), 1.99 (qd, *J* = 7.1, 0.9 Hz, 2H). **^{13}C NMR (101 MHz, $CDCl_3$):** δ 141.1, 137.6, 130.7, 129.0, 128.9, 128.4, 128.3, 126.4, 33.8, 32.9, 26.0. **FTIR (NaCl, thin film, cm^{-1}):** 3059, 2934, 2858, 1620, 1483, 1449, 1322, 1304, 1201, 1169, 916, 830, 766, 748, 676. **HRMS (EI, *m/z*):** calc'd for $C_{11}H_{11}Cl$ $[M+\cdot]^+$: 178.0549; found: 178.0547.

methyl 4-(1-iodovinyl)benzoate (228a)

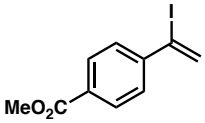

Prepared from methyl 4-(1-(((trifluoromethyl)sulfonyl)oxy)vinyl)-benzoate (**211q**, 93.1 mg, 0.3 mmol) and sodium iodide (67.5 mg, 0.45 mmol) according to General Procedure 1. The crude residue was purified by column chromatography (silica, 5 to 20% Et_2O/hexanes) to yield **228a** (56 mg, 64% yield) as a white solid. *Note: This compound slowly oxidizes to the α-bromo acetophenone under*

ambient conditions.[59] **R_f** = 0.25 (silica, 10% Et_2O/hexanes, UV). **^{1}H NMR (500 MHz, $CDCl_3$):** δ 7.99 – 7.95 (m, 2H), 7.59 – 7.54 (m, 2H), 6.56 (d, *J* = 1.9 Hz, 1H), 6.17 (d, *J* = 1.9 Hz, 1H), 3.92 (s, 3H). **^{13}C NMR (126 MHz, $CDCl_3$):** δ 166.5, 145.8, 130.4, 129.6, 129.2, 128.2, 105.8, 52.4. **FTIR (NaCl, thin film, cm^{-1}):** 2948, 1720, 1593, 1433, 1403, 1284, 1191, 1111, 1050, 902, 861, 777, 710. **HRMS (FAB, *m/z*):** calc'd for $C_{10}H_8IO_2$ $[M+H]^+$: 288.9726; found: 288.9740.

methyl 4-(1-bromovinyl)benzoate (228b)

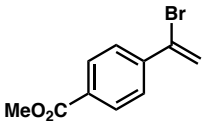

Prepared from methyl 4-(1-(((trifluoromethyl)sulfonyl)oxy)-vinyl)benzoate (**211q**, 93.1 mg, 0.3 mmol) and lithium bromide (39.1 mg, 0.45 mmol) according to General Procedure 1. The crude residue was purified by column chromatography (silica, 1 to 2% Et_2O/hexanes) to yield **228b** (69 mg, 90% yield) as a white solid. *Note: This compound slowly oxidizes to the α-bromo acetophenone under ambient conditions.*[59] **R_f** = 0.47 (silica, 10% EtOAc/hexanes, $KMnO_4$). **^{1}H NMR (400 MHz, $CDCl_3$):** δ 8.03 – 7.98 (m, 2H), 7.68 – 7.62 (m, 2H), 6.22 (d, *J* = 2.2 Hz, 1H), 5.88 (d, *J* = 2.2 Hz, 1H), 3.92 (s, 3H). **^{13}C NMR (101 MHz, $CDCl_3$):** δ 166.5, 142.7, 130.6, 129.9, 129.7, 127.4, 119.7, 52.4. **FTIR (NaCl, thin film, cm^{-1}):** 3429, 2952, 1727, 1606, 1436, 1406, 1281, 1191, 1110, 1016, 860, 776, 710. **HRMS (TOF-ESI, *m/z*):** calc'd for $C_{10}H_8BrO_2$ $[M+H]^+$: 240.9864; found: 240.9888.

5-(1-iodovinyl)pyridin-2-yl trifluoromethanesulfonate (229a)

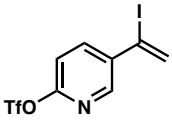

Prepared from 1-(6-(((trifluoromethyl)sulfonyl)oxy)pyridin-3-yl)vinyl trifluoromethanesulfonate (**211r**, 120 mg, 0.3 mmol) and sodium iodide

(67.5 mg, 0.45 mmol) according to General Procedure 1. The crude residue was purified by column chromatography (silica, 10% Et_2O/hexanes) to yield **229a** (62 mg, 54% yield) as a colorless oil. *Note: This compound slowly oxidizes to the α-bromo acetophenone under ambient conditions.*[59] **R_f** = 0.74 (silica, 30% EtOAc/hexanes, $KMnO_4$). **^{1}H NMR (400 MHz, $CDCl_3$):** δ 8.51 (dd, *J* = 2.6, 0.7 Hz, 1H), 8.00 (dd, *J* = 8.5, 2.6 Hz, 1H), 7.13 (dd, *J* = 8.5, 0.7 Hz, 1H), 6.58 (d, *J* = 2.2 Hz, 1H), 6.25 (d, *J* = 2.1 Hz, 1H). **^{13}C NMR (101 MHz, $CDCl_3$):** δ 155.6, 147.0, 141.0, 138.6, 130.9, 118.7 (q, J_{C-F} = 320.6 Hz), 114.6, 99.3. **^{19}F NMR (282 MHz, $CDCl_3$):** δ -72.9. **FTIR (NaCl, thin film, cm^{-1}):** 1604, 1579, 1469, 1428, 1370, 1215, 1171, 1137, 1020, 891, 842, 717, 647. **HRMS (TOF-ESI, *m/z*):** calc'd for $C_8H_5F_3INO_3S$ $[M+H]^+$: 379.9065; found: 379.9076.

5-(1-bromovinyl)pyridin-2-yl trifluoromethanesulfonate (229b)

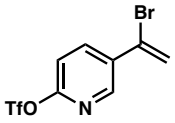

Prepared from 1-(6-(((trifluoromethyl)sulfonyl)oxy)pyridin-3-yl)vinyl trifluoromethanesulfonate (**211r**, 120 mg, 0.3 mmol) and lithium bromide (39.1 mg, 0.45 mmol) according to General Procedure 1. The crude residue was purified by column chromatography (silica, 10% Et_2O/hexanes) to yield **229b** (80 mg, 80% yield) as a colorless oil. *Note: This compound slowly oxidizes to the α-bromo acetophenone under ambient conditions.*[59] **R_f** = 0.70 (silica, 30% EtOAc/hexanes, UV). **^{1}H NMR (500 MHz, $CDCl_3$):** δ 8.58 (dd, *J* = 2.6, 0.7 Hz, 1H), 8.08 (dd, *J* = 8.5, 2.6 Hz, 1H), 7.18 (dd, *J* = 8.5, 0.6 Hz, 1H), 6.24 (d, *J* = 2.6 Hz, 1H), 5.96 (d, *J* = 2.6 Hz, 1H). **^{13}C NMR (126 MHz, $CDCl_3$):** δ 155.8, 146.9, 140.1, 135.5, 124.9, 121.3, 118.7 (q, J_{C-F} = 320.7 Hz), 114.7. **^{19}F NMR (282 MHz, $CDCl_3$):** δ -72.9. **FTIR (NaCl, thin film, cm^{-1}):** 3105, 1615, 1582, 1470,

1426, 1370, 1215, 1173, 1137, 1020, 891, 621. **HRMS (TOF-ESI, *m/z*):** calc'd for $C_8H_5F_3BrNO_3S$ $[M+H]^+$: 331.9204; found: 331.9195.

1-chloro-2-fluoro-4-(1-iodovinyl)benzene (230a)

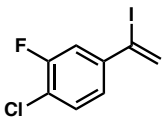

Prepared from 1-(4-chloro-3-fluorophenyl)vinyl trifluoromethanesulfonate (**211s**, 91.4 mg, 0.3 mmol) and sodium iodide (67.5 mg, 0.45 mmol) according to General Procedure 1. The crude residue was purified by column chromatography (silica, pentane) to yield **230a** (58 mg, 69% yield) as a yellow oil. *Note: This compound slowly oxidizes to the α-iodo acetophenone derivative under ambient conditions.*[59] **R_f** = 0.57 (silica, hexanes, $KMnO_4$). **^{1}H NMR (400 MHz, $CDCl_3$):** δ 7.31 – 7.23 (m, 2H), 7.21 – 7.16 (m, 1H), 6.43 (d, *J* = 2.0 Hz, 1H), 6.06 (d, *J* = 2.0 Hz, 1H). **^{13}C NMR (101 MHz, $CDCl_3$):** δ 157.5 (d, J_{C-F} = 249.4 Hz), 142.3 (d, J_{C-F} = 6.9 Hz), 130.3, 128.9, 124.4 (d, J_{C-F} = 3.5 Hz), 121.6 (d, J_{C-F} = 17.9 Hz), 116.5 (d, J_{C-F} = 22.8 Hz), 104.0 (d, J_{C-F} = 2.2 Hz). **^{19}F NMR (282 MHz, $CDCl_3$):** δ -114.9 (dd, J_{F-H} = 10.1, 7.4 Hz). **FTIR (NaCl, thin film, cm^{-1}):** 1598, 1484, 1414, 1402, 1285, 1244, 1070, 937, 901, 873, 818, 743, 733. **HRMS (EI, *m/z*):** calc'd for C_8H_5ClFI $[M+\cdot]^+$: 281.9109; found: 281.9124.

1-bromo-2-fluoro-4-(1-iodovinyl)benzene (230b)

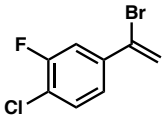

Prepared from 1-(4-chloro-3-fluorophenyl)vinyl trifluoromethanesulfonate (**211s**, 91.4 mg, 0.3 mmol) and lithium bromide (39.1 mg, 0.45 mmol) according to General Procedure 1. The crude residue was purified by column chromatography (silica, pentane) to yield **230b** (52 mg, 73% yield) as a yellow oil. *Note: This compound slowly oxidizes to the α-bromo acetophenone derivative under ambient*

conditions.[59] **R_f** = 0.65 (silica, hexanes, UV). **^{1}H NMR (500 MHz, $CDCl_3$):** δ 7.41 – 7.35 (m, 2H), 7.32 (ddd, *J* = 8.4, 2.1, 0.7 Hz, 1H), 6.15 (d, *J* = 2.3 Hz, 1H), 5.83 (d, *J* = 2.3 Hz, 1H). **^{13}C NMR (126 MHz, $CDCl_3$):** δ 157.6 (d, J_{C-F} = 249.1 Hz), 139.0 (d, J_{C-F} = 7.2 Hz), 130.3, 128.2 (d, J_{C-F} = 2.3 Hz), 123.5 (d, J_{C-F} = 3.8 Hz), 121.7 (d, J_{C-F} = 18.0 Hz), 119.2, 115.7 (d, J_{C-F} = 23.0 Hz). **^{19}F NMR (282 MHz, $CDCl_3$):** δ -114.8 (m). **FTIR (NaCl, thin film, cm^{-1}):** 1601, 1570, 1485, 1412, 1289, 1246, 1174, 1066, 937, 892, 875, 819, 738. **HRMS (EI, *m/z*):** calc'd for C_8H_5ClFBr $[M+\cdot]^+$: 233.9247; found: 233.9228.

2-(4-(1-iodovinyl)phenyl)-4,4,5,5-tetramethyl-1,3,2-dioxaborolane (231a)

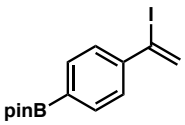

Prepared from 1-(4-(4,4,5,5-tetramethyl-1,3,2-dioxaborolan-2-yl)-phenyl)vinyl trifluoromethanesulfonate (**211t**, 113.5 mg, 0.3 mmol) and sodium iodide (68 mg, 0.45 mmol) according to General Procedure 1. The crude residue was purified by column chromatography (silica, 0 to 5% Et_2O/hexanes) to yield **231a** (72 mg, 68% yield) as a light yellow oil. **R_f** = 0.53 (silica, 10% EtOAc/hexanes, $KMnO_4$). **^{1}H NMR (400 MHz, $CDCl_3$):** δ 7.77 – 7.72 (m, 2H), 7.53 – 7.48 (m, 2H), 6.51 (d, *J* = 1.8 Hz, 1H), 6.11 (d, *J* = 1.7 Hz, 1H), 1.34 (s, 12H). **^{13}C NMR (101 MHz, $CDCl_3$):** δ 144.3, 134.8, 128.0, 127.5, 107.5, 84.1, 25.0. *(Note: carbon bonded to boron not observed.)* **FTIR (NaCl, thin film, cm^{-1}):** 2978, 2930, 1607, 1398, 1360, 1324, 1269, 1210, 1144, 1092, 1018, 859, 841, 654. **HRMS (TOF-ESI, *m/z*):** calc'd for $C_{14}H_{18}BIO_2$ $[M+H]^+$: 357.0523; found: 357.0527.

2-(4-(1-bromovinyl)phenyl)-4,4,5,5-tetramethyl-1,3,2-dioxaborolane (231b)

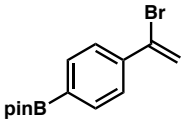

Prepared from 1-(4-(4,4,5,5-tetramethyl-1,3,2-dioxaborolan-2-yl)-phenyl)vinyl trifluoromethanesulfonate (**211t**, 113.5 mg, 0.3 mmol) and lithium bromide (39.1 mg, 0.45 mmol) according to General Procedure 1. The crude residue was purified by column chromatography (silica, 0 to 5% Et_2O/hexanes) to yield **231b** (59 mg, 64% yield) as a light yellow oil which crystallized upon standing in the freezer. $\mathbf{R_f}$ = 0.48 (silica, 10% Et_2O/hexanes, $KMnO_4$). **^{1}H NMR (400 MHz, $CDCl_3$):** δ 7.81 – 7.76 (m, 2H), 7.62 – 7.56 (m, 2H), 6.17 (d, *J* = 2.0 Hz, 1H), 5.81 (d, *J* = 2.0 Hz, 1H), 1.35 (s, 12H). **^{13}C NMR (101 MHz, $CDCl_3$):** δ 141.0, 134.8, 131.1, 126.6, 118.5, 84.1, 25.0. *(Note: carbon bonded to boron not observed.)* **FTIR (NaCl, thin film, cm^{-1}):** 2979, 1607, 1507, 160, 1326, 1270, 1216, 1143, 1092, 1018, 859, 783, 656. **HRMS (TOF-ESI, *m/z*):** calc'd for $C_{14}H_{18}BBrO_2$ $[M+H]^+$: 309.0661; found: 309.0670.

(3*r*,5*r*,7*r*)-1-(1-iodovinyl)adamantane (232a)

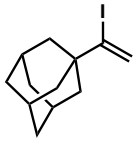

Prepared from 1-((3*r*,5*r*,7*r*)-adamantan-1-yl)vinyl trifluoromethanesulfonate (**211u**, 93.0 mg, 0.3 mmol) and sodium iodide (67.5 mg, 0.45 mmol) according to General Procedure 1. The crude residue was purified by column chromatography (silica, pentane) to yield **232a** (72 mg, 84% yield) as a colorless oil. $\mathbf{R_f}$ = 0.74 (silica, hexanes, $KMnO_4$). **^{1}H NMR (400 MHz, $CDCl_3$):** δ 6.08 (d, *J* = 2.1 Hz, 1H), 5.80 (d, *J* = 2.1 Hz, 1H), 2.04 – 1.95 (m, 3H), 1.76 – 1.71 (m, 6H), 1.71 – 1.59 (m, 6H). **^{13}C NMR (101 MHz, $CDCl_3$):** δ 131.8, 122.8, 42.4, 41.8, 36.8, 28.7. **FTIR (NaCl, thin**

film, cm^{-1}): 2903, 2849, 1611, 1600, 1450, 1343, 1257, 1184, 1142, 1055, 894, 612. **HRMS (FAB, *m/z*):** calc'd for $C_{12}H_{17}I$ $[M+H]^+$: 289.0454; found: 289.0447.

(3*r*,5*r*,7*r*)-1-(1-bromovinyl)adamantane (232b)

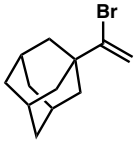

Prepared from 1-((3*r*,5*r*,7*r*)-adamantan-1-yl)vinyl trifluoromethanesulfonate (**211u**, 125 mg, 0.4 mmol) and lithium bromide (39.1 mg, 0.45 mmol) according to General Procedure 1. The crude residue was purified by column chromatography (silica, pentane) to yield **232b** (76 mg, 78% yield) as a colorless oil. $\mathbf{R_f}$ = 0.81 (silica, hexanes, $KMnO_4$). **^{1}H NMR (400 MHz, $CDCl_3$):** δ 5.56 (d, *J* = 2.0 Hz, 1H), 5.42 (d, *J* = 2.0 Hz, 1H), 2.03 (q, *J* = 3.2 Hz, 3H), 1.82 – 1.76 (m, 6H), 1.74 – 1.61 (m, 6H). **^{13}C NMR (101 MHz, $CDCl_3$):** δ 148.1, 113.7, 41.4, 41.1, 36.7, 28.5. **FTIR (NaCl, thin film, cm^{-1}):** 2905, 2850, 2678, 1622, 1453, 1344, 1152, 1057, 881, 716, 628. **HRMS (EI, *m/z*):** calc'd for $C_{12}H_{17}Br$ $[M+\cdot]^+$: 240.0514; found: 240.0510.

(3*r*,5*r*,7*r*)-1-(1-chlorovinyl)adamantane (232c)

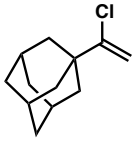

Prepared from 1-((3*r*,5*r*,7*r*)-adamantan-1-yl)vinyl trifluoromethanesulfonate (**211u**, 93.0 mg, 0.3 mmol) and lithium chloride (19.1 mg, 0.45 mmol) according to General Procedure 1. The crude residue was purified by column chromatography (silica, pentane) to yield **232c** (46 mg, 77% yield) as a colorless oil. $\mathbf{R_f}$ = 0.84 (silica, hexanes, $KMnO_4$). **^{1}H NMR (400 MHz, $CDCl_3$):** δ 5.13 (d, *J* = 1.5 Hz, 1H), 5.09 (d, *J* = 1.5 Hz, 1H), 2.04 (q, *J* = 3.2 Hz, 3H), 1.79 (d, *J* = 3.0 Hz, 6H), 1.76 – 1.62 (m, 6H). **^{13}C NMR (101 MHz, $CDCl_3$):** δ 153.5, 109.1, 40.7, 40.2, 36.7, 28.4. **FTIR (NaCl,**

thin film, cm^{-1}): 2904, 2851, 1618, 1452, 1344, 1165, 162, 877, 734, 666. **HRMS (EI, *m/z*):** calc'd for $C_{12}H_{17}Cl$ $[M+\cdot]^+$: 196.1019; found: 196.1040.

5.7.6 Mechanistic Experiments

5.7.6.1 Radical Inhibitors

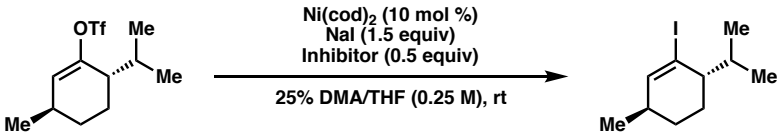

Four 1-dram vials were equipped with stir bars and brought into a N_2-filled glovebox. The vials were charged with NaI (0.15 mmol, 1.5 equiv) and $Ni(cod)_2$ (2.8 mg, 0.01 mmol, 0.1 equiv). Anhydrous DMA (0.1 mL) and THF (0.3 mL) were added, resulting in a clear yellow solution. DHA, BHT, TEMPO and Galvinoxyl were each added to one vial (0.5 equiv), then enol triflate (0.1 mmol, 1 equiv) was added in one portion. The vials were sealed with a Teflon cap and brought out of the glovebox. The reactions were allowed to stir on the bench (480 rpm) for two hours at room temperature. Reactions were quenched by filtering through a plug of silica gel, eluting with 10 mL of 40% Et_2O/Hexanes, then concentrated under reduced pressure. An NMR standard (tetrachloronitrobenzene) was added to each vial for NMR analysis.

5.7.6.2 Kinetics

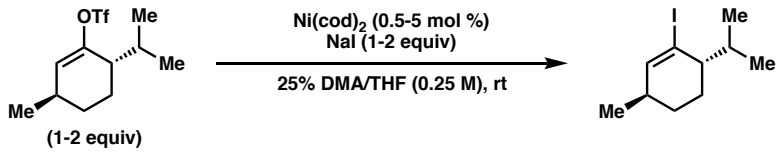

A 2-dram vial equipped with a stir bar was brought into a N_2-filled glovebox. The vial was charged with NaI and $Ni(cod)_2$. Anhydrous DMA (0.5 mL) and THF (1.5 mL) were added. Undecane (32 μL) was added as an internal analytical GC standard. Alkenyl halide (0.5 mmol, 1 equiv) was added neat. The vial was sealed with a Teflon cap and allowed to stir in the glovebox (480 rpm) at room temperature. Reaction aliquots (50 μL) were taken at various time points and were quenched by addition into 1 mL hexanes in a GC vial, giving an opaque white mixture. The reaction aliquots were analyzed by GC-FID.

5.7.6.3 EPR Studies

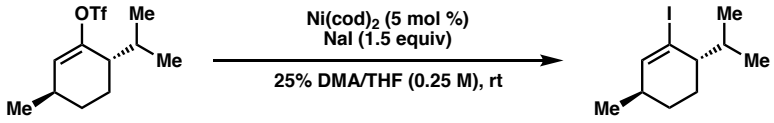

A 15 mL round-bottom flask equipped with a stir bar was brought into a N_2-filled glovebox. The vial was charged with NaI (1.2 mmol, 1.5 equiv) and $Ni(cod)_2$ (11.2 mg, 0.04 mmol, 0.05 equiv). Anhydrous DMA (0.8 mL) and THF (2.4 mL) were added. Enol triflate (0.8 mmol, 1 equiv) was added neat. The flask was sealed with a septum and allowed to stir in the glovebox (480 rpm) at room temperature. Aliquots (0.3 mL) were removed at various time points and added into EPR tubes, which were sealed and frozen at –78 ºC in a metal dewar filled with liquid nitrogen. The reaction aliquots were analyzed by EPR spectroscopy. An external standard of $CuSO_4$ in 1:9 ethylene glycol/H_2O was made and analyzed by EPR spectroscopy.

A single Ni(I) species is visible by EPR spectroscopy, which reaches a maximum concentration at 30 minutes. An additional broad Ni(II) species also forms as the reaction

proceeds, which may indicate aggregate Ni species. In order to remove contribution from the broad Ni(II) signal, baseline corrections were applied using the 'msbackadj' command in MatLab.

The spectra were processed by calculating the double integral. By comparison to the known concentration of $CuSO_4$ in Figure 5.15, the concentration of Ni(I) in the reaction was calculated to be <0.25 mM (i.e. less than 2% of all Ni added to the reaction, therefore indicating the Ni(I) species in this EPR spectrum is a trace Ni species).

Figure 5.17 *EPR of the iodination of* ***208*** *at 30 minutes compared to 12.5 mM* $CuSO_4$.

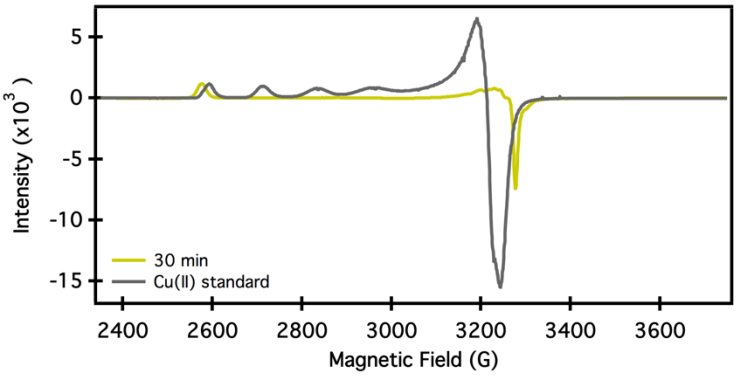

The halogenation of **208** was repeated with LiBr and LiCl to investigate the bromination and chlorination reactions. Time points were taken at 30 minutes and analyzed by EPR spectroscopy, demonstrating that the Ni(I) species observed does contain a halogen atom. The relative intensities of the spectra are I > Br > Cl.

5.7.6.4 Investigating Catalyst Death and Diene Formation

Two 1-dram vials were equipped with stir bars and brought into a N_2-filled glovebox. The vials were charged with NaI (0.15 mmol, 1.5 equiv) and $Ni(cod)_2$ (2.8 mg, 0.01 mmol, 0.1 equiv). Anhydrous DMA (0.1 mL) and THF (0.3 mL) were added, resulting in a clear

yellow solution. Enol triflate (0.1 mmol, 1 equiv) was added neat. The vials were sealed with a Teflon cap and stirred in the glovebox for two hours at room temperature. After two hours, one vial was quenched by filtering through a plug of silica gel, eluting with 10 mL of 40% Et_2O/Hexanes, then concentrated under reduced pressure. To the second vial was added an additional amount of NaI (0.15 mmol, 1.5 equiv) and a second enol triflate (0.1 mmol, 1 equiv). The vial was sealed with a Teflon cap and stirred for an additional two hours at room temperature. After two hours, the second vial was quenched by filtering through a plug of silica gel, eluting with 10 mL of 40% Et_2O/Hexanes, then concentrated under reduced pressure. An NMR standard was added to both samples for NMR analysis in order to record the yield of the first enol triflate halogenation as well as the second enol triflate halogenation. We note that in some cases, the completion of the first halogenation does not deactivate the catalyst for the second halogenation; however, in some cases the second halogenation is inhibited by the first one.

5.7.6.5 Crossover Experiments

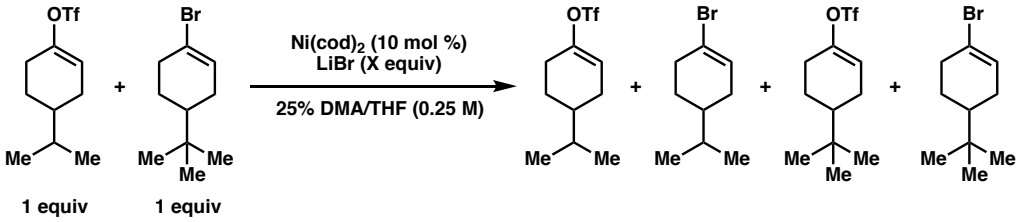

A 2-dram vial equipped with a stir bar was brought into a N_2-filled glovebox. The vial was charged with LiBr (0–1 equiv) and $Ni(cod)_2$ (5.5 mg, 0.02 mmol, 0.1 equiv). Anhydrous DMA (0.2 mL) and THF (0.6 mL) were added, resulting in a clear yellow solution. Undecane (13 μL) was added as an internal analytical GC standard. Enol triflate (0.2 mmol,

1 equiv) was added neat, followed by alkenyl bromide (0.2 mmol, 1 equiv). The vial was sealed with a Teflon cap and allowed to stir in the glovebox (480 rpm) at room temperature. Reaction aliquots (25 µL) were taken at time points and were quenched by addition into 1 mL hexanes in a GC vial, giving an opaque white mixture. The reaction aliquots were analyzed by GC-FID against the internal standard.

5.7.6.6 Halide Competition Experiments

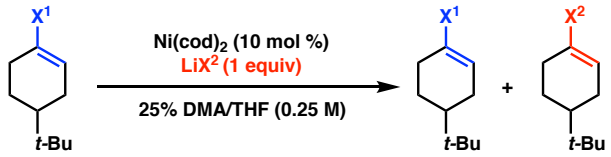

A 2-dram vial equipped with a stir bar was brought into a N_2-filled glovebox. The vial was charged with LiX^2 (0.5 mmol, 1 equiv) and $Ni(cod)_2$ (13.8 mg, 0.05 mmol, 0.1 equiv). Anhydrous DMA (0.5 mL) and THF (1.5 mL) were added. Undecane (32 µL) was added as an internal analytical GC standard. Alkenyl halide (RX^1) (0.5 mmol, 1 equiv) was added neat. The vial was sealed with a Teflon cap and allowed to stir in the glovebox (480 rpm) at room temperature. Reaction aliquots (50 µL) were taken at time points and were quenched by addition into 1 mL hexanes in a GC vial, giving an opaque white mixture. The reaction aliquots were analyzed by GC-FID against the internal standard.

5.7.6.7 NMR Experiments

A 1-dram vial equipped with a stir bar was brought into a N_2-filled glovebox. The vial was charged with $Ni(cod)_2$ (5.5 mg, 0.02 mmol, 1.0 equiv). Deuterated DMA (0.2 mL) and deuterated THF (0.6 mL) were added and solubilized, affording a yellow solution.

Trimethoxybenzene was added as an internal analytical NMR standard. Alkenyl triflate **208** (5.7 mg, 0.02 mmol, 1 equiv) was added neat and the reaction was stirred for 10 seconds, then the mixture was transferred to a J Young NMR tube. NMR analysis was performed at 10, 70, and 130 min against the internal standard. No oxidative addition of the enol triflate was observed; however, cod dissociation from $Ni(cod)_2$ was observed over time via NMR concomitant with the reaction turning brown in color.

5.8 REFERENCES

(1) De Meijer, A.; Diederich, F. *Metal-Catalyzed Cross-Coupling Reactions*; Wiley-VCH Verlag GmbH & Co. KGaA, 2004; Vol. 1 & 2.

(2) Nicolaou, K. C.; Bulger, P. G.; Sarlah, D. *Angew. Chem. Int. Ed.* **2005**, *44*, 4442.

(3) Schlosser, M. *Organometallics in Synthesis*; John Wiley & Sons, Inc., 2013.

(4) Gribble, G. W. *Naturally Occurring Organohalogen Compounds–A Comprehensive Survey*; Springer-Verlag: Wien, Austria, 1996.

(5) Gribble, G. W. *Naturally Occurring Organohalogen Compounds - A Comprehensive Update*; Springer-Verlag: Wien, Austria, 2010.

(6) Gribble, G. W. *Mar. Drugs.* **2015**, *13*, 4004.

(7) Hart, D. W.; Blackburn, T. F.; Schwartz, J. *J. Am. Chem. Soc.* **1975**, *97*, 679.

(8) Brown, H. C.; Subrahmanyam, C.; Hamaoka, T.; Ravindran, N.; Bowman, D. H.; Misumi, S.; Unni, M. K.; Somayaji, V.; Bhat, N. G. *J. Org. Chem.* **1989**, *54*, 6068.

(9) Gao, F.; Hoveyda, A. H. *J. Am. Chem. Soc.* **2010**, *132*, 10961.

(10) Uehling, M. R.; Rucker, R. P.; Lalic, G. *J. Am. Chem. Soc.* **2014**, *136*, 8799.

(11) Derosa, J.; Cantu, A. L.; Boulous, M. N.; O'Duill, M. L.; Turnbull, J. L.; Liu, Z.; De La Torre, D. M.; Engle, K. M. *J. Am. Chem. Soc.* **2017**, *139*, 5183.

(12) Takai, K.; Nitta, K.; Utimoto, K. *J. Am. Chem. Soc.* **1986**, *108*, 7408.

(13) Stork, G.; Zhao, K. *Tetrahedron Lett.* **1989**, *30*, 2173.

(14) Barton, D. H. R.; O'Brien, R. E.; Sternhell, S. *J. Chem. Soc.* **1962**, 470.

(15) Furrow, M. E.; Myers, A. G. *J. Am. Chem. Soc.* **2004**, *126*, 5436.

(16) Ojha, D. P.; Prabhu, K. R. *Org. Lett.* **2015**, *17*, 18.

(17) Spaggiari, A.; Vaccari, D.; Davoli, P.; Torre, G.; Prati, F. *J. Org. Chem.* **2007**, *72*, 2216.

(18) Stemke, J. E.; Chamberlin, A. R.; Bond, F. T. *Tetrahedron Lett.* **1976**, *34*, 2947.

(19) Chamberlin, A. R.; Stemke, J. E.; Bond, F. T. *J. Org. Chem.* **1978**, *43*, 147.

(20) Adlington, R. M.; Barrett, A. G. M. *Acc. Chem. Res.* **1983**, *16*, 55.

(21) Huters, A. D.; Quasdorf, K. W.; Styduhar, E. D.; Garg, N. K. *J. Am. Chem. Soc.* **2011**, *133*, 15797.

(22) Shen, X.; Hyde, A. M.; Buchwald, S. L. *J. Am. Chem. Soc.* **2010**, *132*, 14076.

(23) Imazaki, Y.; Shirakawa, E.; Ueno, R.; Hayashi, T. *J. Am. Chem. Soc.* **2012**, *134*, 14760.

(24) Shirakawa, E.; Imazaki, Y.; Hayashi, T. *Chem. Commun.* **2009**, *0*, 5088.

(25) Milne, J. E.; Jarowicki, K.; Kocienski, P. J. *Synlett* **2002**, *2002*, 607.

(26) Cherney, A. H.; Reisman, S. E. *J. Am. Chem. Soc.* **2014**, *136*, 14365.

(27) Suzuki, N.; Hofstra, J. L.; Poremba, K. E.; Reisman, S. E. *Org. Lett.* **2017**, *19*, 2150.

(28) Takagi, K.; Hayama, N.; Okamoto, T. *Chem. Lett.* **1978**, *7*, 191.

(29) Tsou, T. T.; Kochi, J. K. *J. Org. Chem.* **1980**, *45*, 1930.

(30) Takagi, K.; Hayama, N.; Inokawa, S. *Chem. Lett.* **1978**, *7*, 1435.

(31) Hooijdonk, M. C. J. M.; Peters, T. H. A.; Vasilevsky, S. F.; Brandsma, L. *Synth. Commun.* **1994**, *24*, 1261.

(32) Petrone, D. A.; Ye, J.; Lautens, M. *Chem. Rev.* **2016**, *116*, 8003.

(33) Evano, G.; Nitelet, A.; Thilmany, P.; Dewez, D. F. *Front. Chem.* **2018**, *6*.

(34) Dürr, A. B.; Yin, G.; Kalvet, I.; Napoly, F.; Schoenebeck, F. *Chem. Sci.* **2016**, *7*, 1076.

(35) Hofstra, J. L.; Cherney, A. H.; Ordner, C. M.; Reisman, S. E. *J. Am. Chem. Soc.* **2018**, *140*, 139.

(36) Yang, X.; Wu, D.; Lu, Z.; Sun, H.; Li, A. *Org. Biomol. Chem.* **2016**, *14*, 5591.

(37) Högermeier, J.; Reissig, H.-U. *Adv. Synth. Catal.* **2009**, *351*, 2747.

(38) Blackmond, D. G. *J. Am. Chem. Soc.* **2015**, *137*, 10852.

(39) Blackmond, D. G. *Angew. Chem. Int. Ed.* **2005**, *44*, 4302.

(40) Bajo, S.; Laidlaw, G.; Kennedy, A. R.; Sproules, S.; Nelson, D. J. *Organometallics* **2017**, *36*, 1662.

(41) Kalvet, I.; Guo, Q.; Tizzard, G. J.; Schoenebeck, F. *ACS Catal.* **2017**, *7*, 2126.

(42) Takise, R.; Itami, K.; Yamaguchi, J. *Org. Lett.* **2016**, *18*, 4428.

(43) Dander, J. E.; Weires, N. A.; Garg, N. K. *Org. Lett.* **2016**, *18*, 3934.

(44) Pfirrmann, S.; Limberg, C.; Hoppe, E. Z. *Anorg. Allg. Chem.* **2009**, *635*, 312.

(45) Gallego, D.; Brück, A.; Irran, E.; Meier, F.; Kaupp, M.; Driess, M.; Hartwig, J. F. *J. Am. Chem. Soc.* **2013**, *135*, 15617.

(46) Wang, X.; Wang, S.; Xue, W.; Gong, H. *J. Am. Chem. Soc.* **2015**, *137*, 11562.

(47) Liu, J.; Gong, H. *Org. Lett.* **2018**.

(48) Still, W. C.; Kahn, M.; Mitra, A. *J. Org. Chem.* **1978**, *43*, 2923.

(49) Paquette, L. A.; Ra, C. S.; Edmonson, S. D. *J. Org. Chem.* **1990**, *55*, 2443.

(50) Stadler, A.; von Schenck, H.; Vallin, K. S. A.; Larhed, M.; Hallberg, A. *Adv. Synth. Catal.* **2004**, *346*, 1773.

(51) Su, X.; Huang, H.; Yuan, Y.; Li, Y. *Angew. Chem. Int. Ed.* **2017**, *56*, 1338.

(52) Cho, E. J.; Buchwald, S. L. *Org. Lett.* **2011**, *13*, 6552.

(53) Zorn, N.; Lett, R. *Tetrahedron Lett.* **2006**, *47*, 4331.

(54) Takahashi, B.; Funami, H.; Iwaki, T.; Maruoka, H.; Shibata, M.; Koyama, M.; Nagahira, A.; Kamiide, Y.; Kanki, S.; Igawa, Y.; Muto, T. *Bioorg. Med. Chem.* **2015**, *23*, 4792.

(55) Sun, Q.; Jiang, C.; Xu, H.; Zhang, Z.; Liu, L.; Wang, C. *Steroids* **2010**, *75*, 936.

(56) Okitsu, T.; Sato, K.; Iwatsuka, K.; Sawada, N.; Nakagawa, K.; Okano, T.; Yamada, S.; Kakuta, H.; Wada, A. *Bioorg. Med. Chem.* **2011**, *19*, 2939.

(57) Si, T.; Li, B.; Xiong, W.; Xu, B.; Tang, W. *Org. Biomol. Chem.* **2017**, *15*, 9903.

(58) Kawamoto, T.; Sasaki, R.; Kamimura, A. *Angew. Chem. Int. Ed.* **2017**, *56*, 1342.

(59) Roman, U. V.; Ruhdorfer, J.; Knorr, R. *Synthesis* **1993**, *1993*, 985.

Appendix 7

Spectra Relevant to Chapter 5:

Ni-Catalyzed Halogenation of Alkenyl Triflates

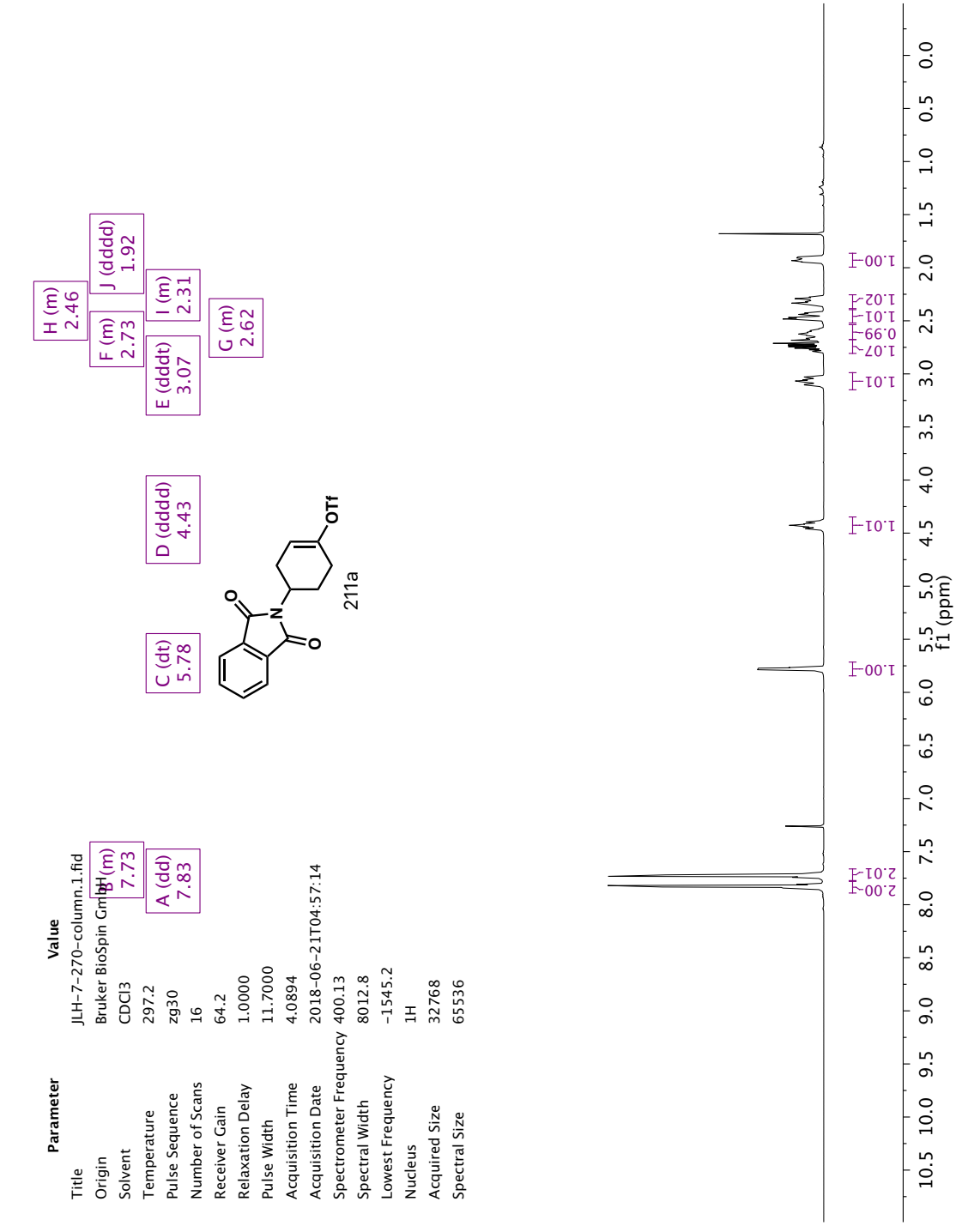
Parameter
Value
Title
JLH-7-270-column.1.fid
Origin
Bruker BioSpin GmbH
Solvent
CDCl3
Temperature
297.2
Pulse Sequence
zg30
Number of Scans
16
Receiver Gain
64.2
Relaxation Delay
1.0000
Pulse Width
11.7000
Acquisition Time
4.0894
Acquisition Date
2018-06-21T04:57:14
Spectrometer Frequency
400.13
Spectral Width
8012.8
Lowest Frequency
-1545.2
Nucleus
1H
Acquired Size
32768
Spectral Size
65536
B (m) 7.73
A (dd) 7.83
C (dt) 5.78
D (dddd) 4.43
E (dddt) 3.07
F (m) 2.73
G (m) 2.62
H (m) 2.46
I (m) 2.31
J (dddd) 1.92
OTf
211a
2.00
2.01
1.00
1.01
1.01
1.00
1.07
0.99
1.01
1.02
1.00
10.5 10.0 9.5 9.0 8.5 8.0 7.5 7.0 6.5 6.0 5.5 5.0 4.5 4.0 3.5 3.0 2.5 2.0 1.5 1.0 0.5 0.0
f1 (ppm)

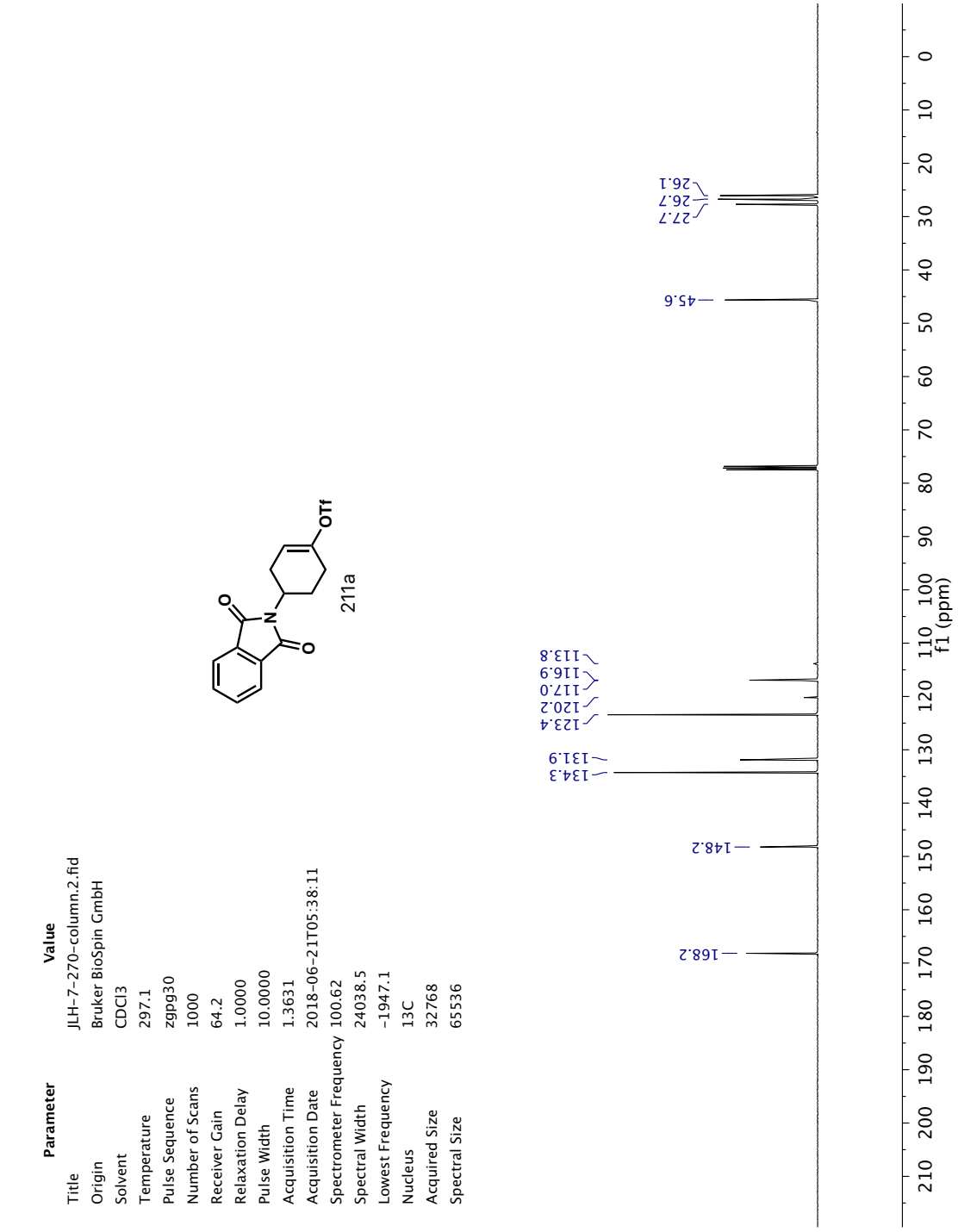

Parameter	Value
Title	JLH-7-270-column.2.fid
Origin	Bruker BioSpin GmbH
Solvent	CDCl3
Temperature	297.1
Pulse Sequence	zgpg30
Number of Scans	1000
Receiver Gain	64.2
Relaxation Delay	1.0000
Pulse Width	10.0000
Acquisition Time	1.3631
Acquisition Date	2018-06-21T05:38:11
Spectrometer Frequency	100.62
Spectral Width	24038.5
Lowest Frequency	-1947.1
Nucleus	13C
Acquired Size	32768
Spectral Size	65536

Parameter	Value
Title	JLH-7-270-F
Origin	Varian
Solvent	cdcl3
Temperature	25.0
Pulse Sequence	s2pul
Number of Scans	16
Receiver Gain	30
Relaxation Delay	1.0000
Pulse Width	6.3333
Acquisition Time	0.9856
Acquisition Date	2018-06-29T12:21:53
Spectrometer Frequency	282.34
Spectral Width	64935.1
Lowest Frequency	-56430.0
Nucleus	19F
Acquired Size	64000
Spectral Size	131072

211a

-73.7

10 0 -10 -20 -30 -40 -50 -60 -70 -80 -90 -100 -110 -120 -130 -140 -150 -160 -170 -180 -190
f1 (ppm)

Parameter	Value
Title	JLH-7-270-F-C6F6
Origin	Varian
Solvent	cdcl3
Temperature	25.0
Pulse Sequence	s2pul
Number of Scans	16
Receiver Gain	30
Relaxation Delay	1.0000
Pulse Width	6.3333
Acquisition Time	0.9856
Acquisition Date	2018-06-29T12:25:28
Spectrometer Frequency	282.34
Spectral Width	64935.1
Lowest Frequency	-56436.5
Nucleus	19F
Acquired Size	64000
Spectral Size	131072

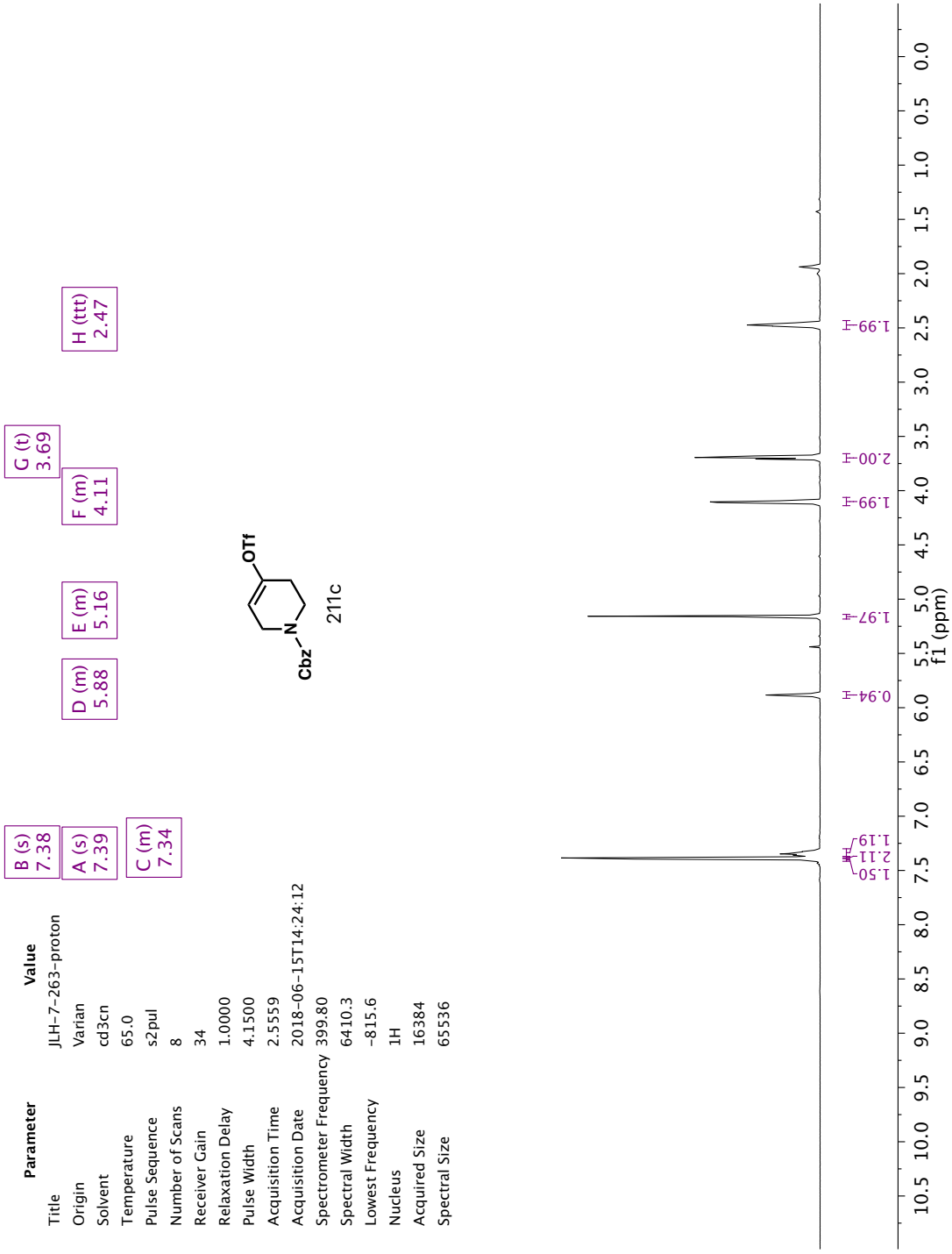

Parameter	Value
Title	JLH-7-263-proton
Origin	Varian
Solvent	cd3cn
Temperature	65.0
Pulse Sequence	s2pul
Number of Scans	8
Receiver Gain	34
Relaxation Delay	1.0000
Pulse Width	4.1500
Acquisition Time	2.5559
Acquisition Date	2018-06-15T14:24:12
Spectrometer Frequency	399.80
Spectral Width	6410.3
Lowest Frequency	-815.6
Nucleus	1H
Acquired Size	16384
Spectral Size	65536

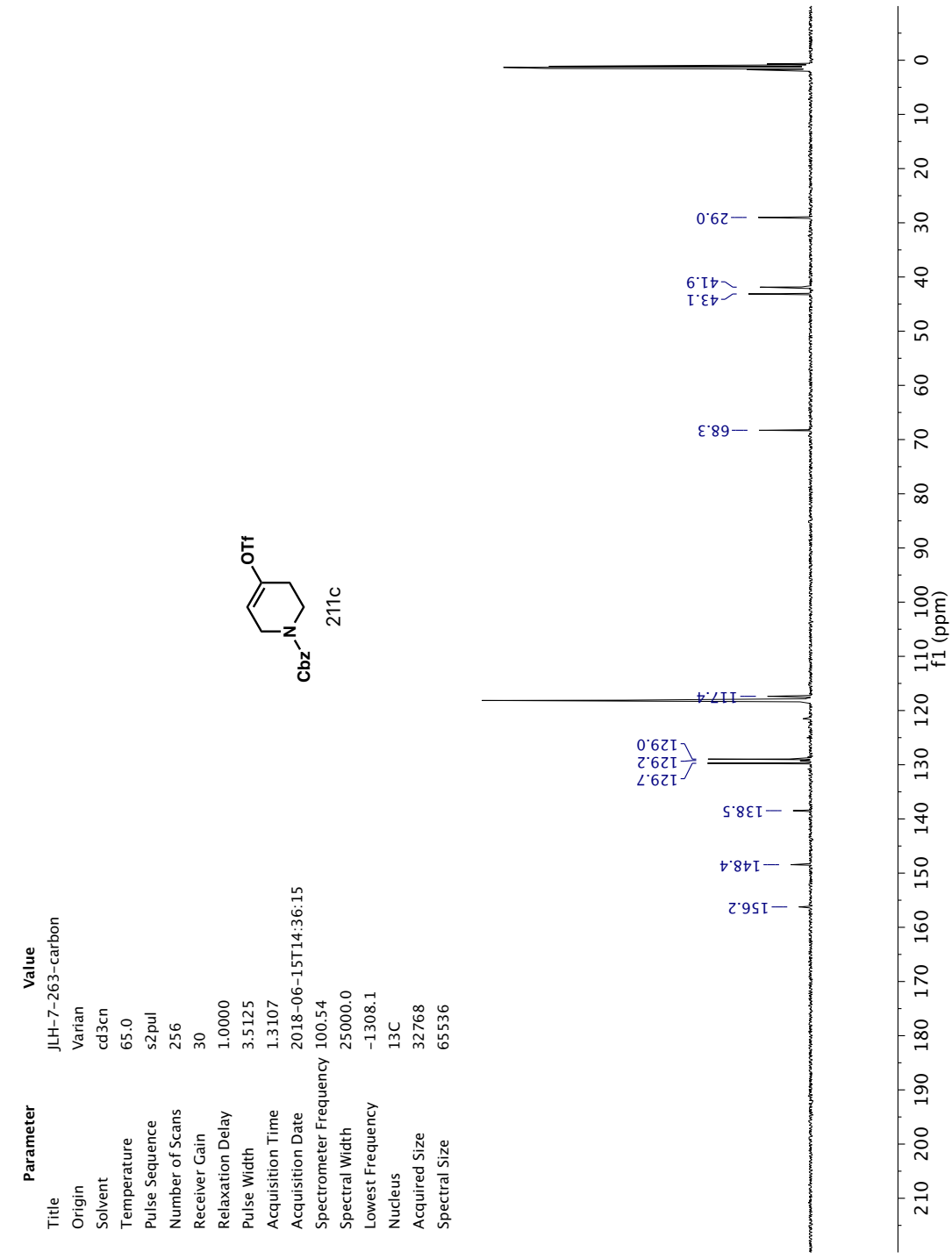

Parameter	Value
Title	JLH-7-263-carbon
Origin	Varian
Solvent	cd3cn
Temperature	65.0
Pulse Sequence	s2pul
Number of Scans	256
Receiver Gain	30
Relaxation Delay	1.0000
Pulse Width	3.5125
Acquisition Time	1.3107
Acquisition Date	2018-06-15T14:36:15
Spectrometer Frequency	100.54
Spectral Width	25000.0
Lowest Frequency	-1308.1
Nucleus	13C
Acquired Size	32768
Spectral Size	65536

Parameter	Value
Title	JLH-7-263-fluroine
Origin	Varian
Solvent	cd3cn
Temperature	65.0
Pulse Sequence	s2pul
Number of Scans	16
Receiver Gain	52
Relaxation Delay	1.0000
Pulse Width	3.2333
Acquisition Time	0.7340
Acquisition Date	2018-06-25T21:47:57
Spectrometer Frequency	376.15
Spectral Width	89285.7
Lowest Frequency	-75468.0
Nucleus	19F
Acquired Size	65536
Spectral Size	131072

211c

Parameter	Value
Title	JLH-7-263-fluroine-C6F6
Origin	Varian
Solvent	cd3cn
Temperature	65.0
Pulse Sequence	s2pul
Number of Scans	16
Receiver Gain	0
Relaxation Delay	1.0000
Pulse Width	3.2333
Acquisition Time	0.7340
Acquisition Date	2018-06-25T22:02:46
Spectrometer Frequency	376.15
Spectral Width	89285.7
Lowest Frequency	-75469.1
Nucleus	19F
Acquired Size	65536
Spectral Size	131072

211c
with C_6F_6

-71.7

10 0 -10 -20 -30 -40 -50 -60 -70 -80 -90 -100 -110 -120 -130 -140 -150 -160 -170 -180 -190
f1 (ppm)

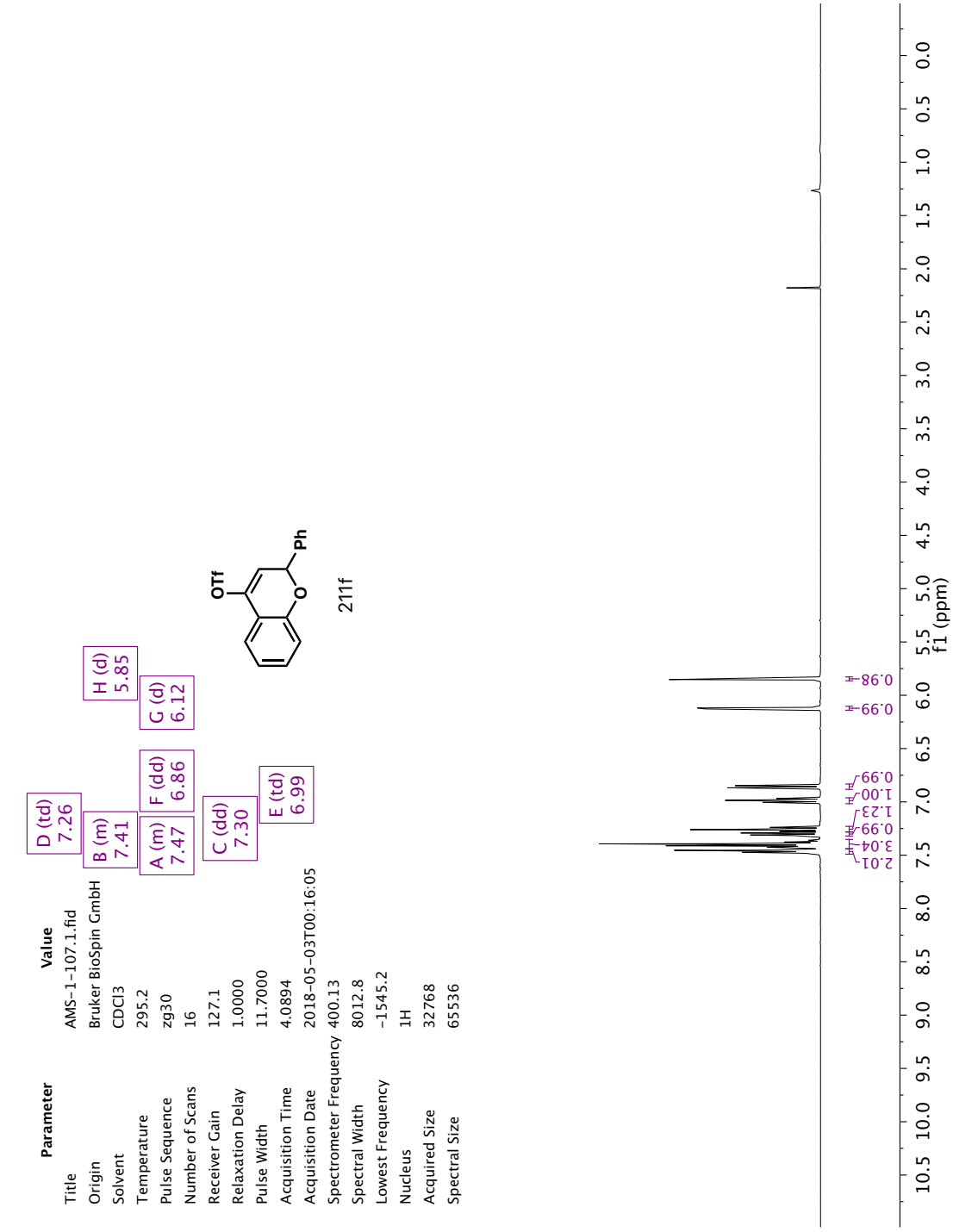
Parameter
Value
Title AMS-1-107.1.fid
Origin Bruker BioSpin GmbH
Solvent CDCl3
Temperature 295.2
Pulse Sequence zg30
Number of Scans 16
Receiver Gain 127.1
Relaxation Delay 1.0000
Pulse Width 11.7000
Acquisition Time 4.0894
Acquisition Date 2018-05-03T00:16:05
Spectrometer Frequency 400.13
Spectral Width 8012.8
Lowest Frequency -1545.2
Nucleus 1H
Acquired Size 32768
Spectral Size 65536
D (td) 7.26
B (m) 7.41
A (m) 7.47
F (dd) 6.86
C (dd) 7.30
E (td) 6.99
H (d) 5.85
G (d) 6.12
OTf
Ph
O
211f
2.01
3.04
0.99
1.23
1.00
0.99
0.99
0.98
10.5 10.0 9.5 9.0 8.5 8.0 7.5 7.0 6.5 6.0 5.5 5.0 4.5 4.0 3.5 3.0 2.5 2.0 1.5 1.0 0.5 0.0
f1 (ppm)

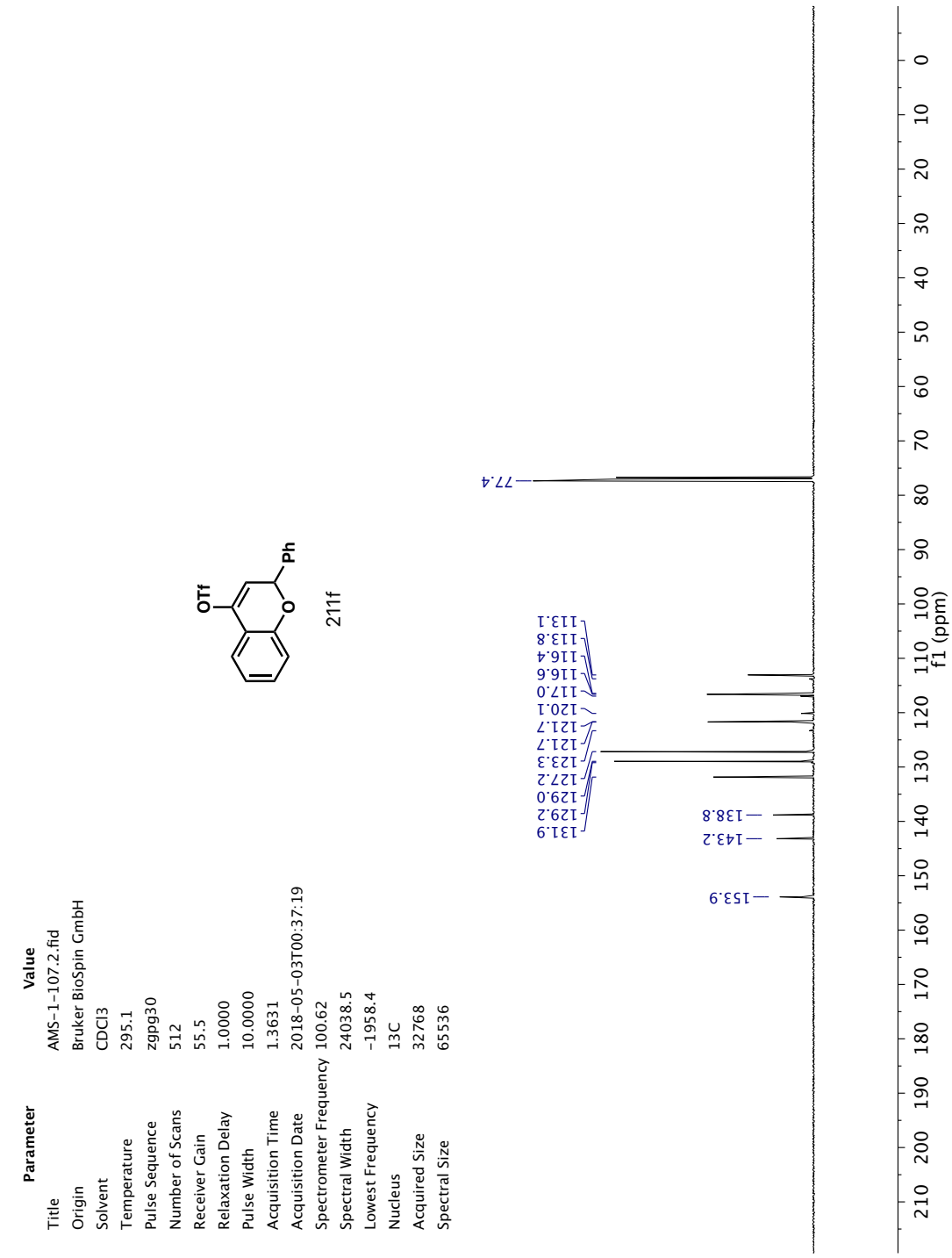

Parameter	Value
Title	AMS-1-107.2.fid
Origin	Bruker BioSpin GmbH
Solvent	CDCl3
Temperature	295.1
Pulse Sequence	zgpg30
Number of Scans	512
Receiver Gain	55.5
Relaxation Delay	1.0000
Pulse Width	10.0000
Acquisition Time	1.3631
Acquisition Date	2018-05-03T00:37:19
Spectrometer Frequency	100.62
Spectral Width	24038.5
Lowest Frequency	-1958.4
Nucleus	13C
Acquired Size	32768
Spectral Size	65536

Parameter	Value
Title	AMS-1-107-F
Origin	Varian
Solvent	cdcl3
Temperature	25.0
Pulse Sequence	s2pul
Number of Scans	16
Receiver Gain	30
Relaxation Delay	1.0000
Pulse Width	6.3333
Acquisition Time	0.9856
Acquisition Date	2018-05-03T23:05:28
Spectrometer Frequency	282.34
Spectral Width	64935.1
Lowest Frequency	-56468.7
Nucleus	19F
Acquired Size	64000
Spectral Size	131072

211f

-73.4

10 0 -10 -20 -30 -40 -50 -60 -70 -80 -90 -100 -110 -120 -130 -140 -150 -160 -170 -180 -190
f1 (ppm)

Parameter	Value
Title	AMS-1-107-F-C6F6
Origin	Varian
Solvent	cdcl3
Temperature	25.0
Pulse Sequence	s2pul
Number of Scans	16
Receiver Gain	30
Relaxation Delay	1.0000
Pulse Width	6.3333
Acquisition Time	0.9856
Acquisition Date	2018-05-23T22:51:00
Spectrometer Frequency	282.34
Spectral Width	64935.1
Lowest Frequency	-56468.7
Nucleus	19F
Acquired Size	64000
Spectral Size	131072

211f
with C_6F_6

-73.4

10 0 -10 -20 -30 -40 -50 -60 -70 -80 -90 -100 -110 -120 -130 -140 -150 -160 -170 -180 -190
f1 (ppm)

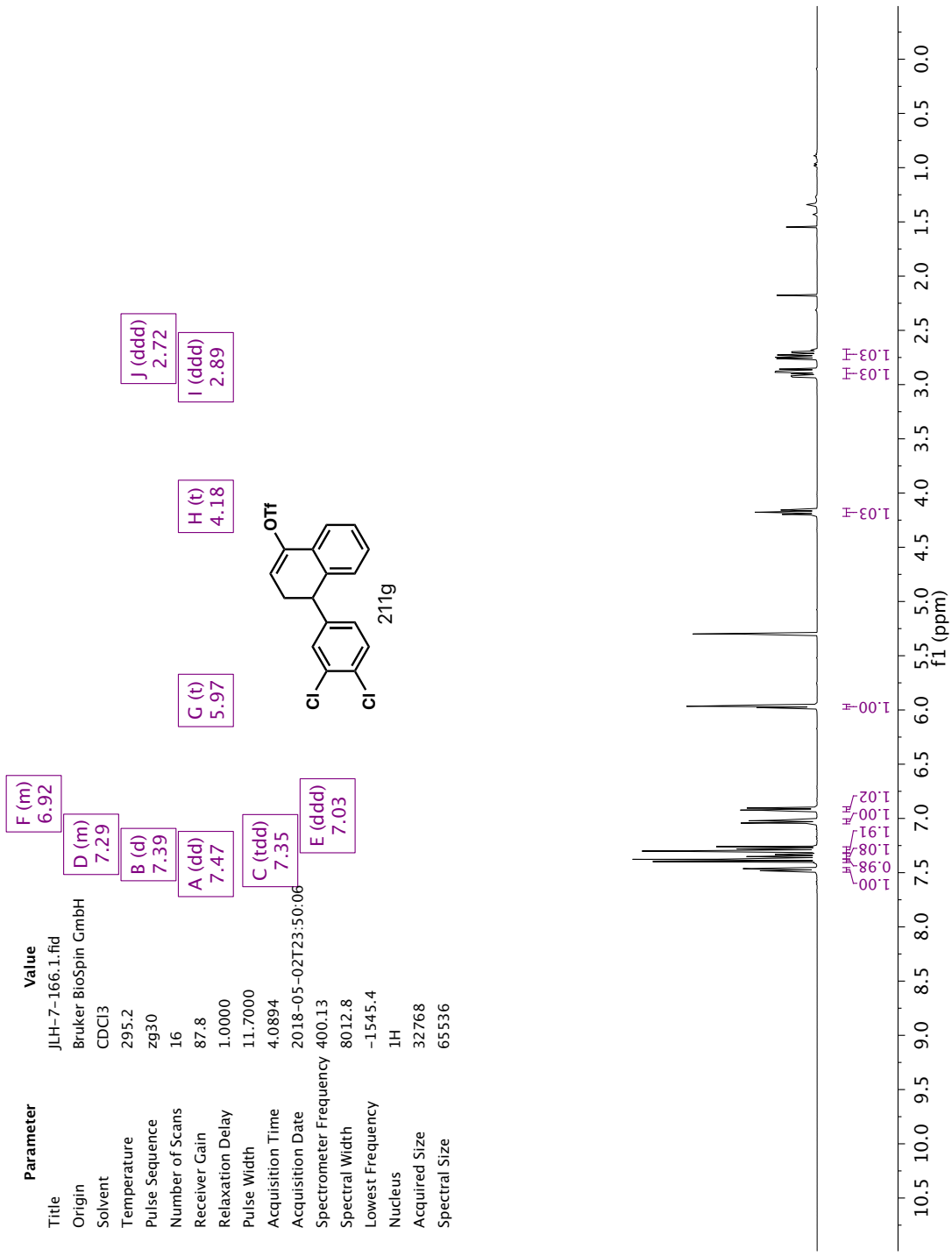
Parameter Value
Title JLH-7-166.1.fid
Origin Bruker BioSpin GmbH
Solvent CDCl3
Temperature 295.2
Pulse Sequence zg30
Number of Scans 16
Receiver Gain 87.8
Relaxation Delay 1.0000
Pulse Width 11.7000
Acquisition Time 4.0894
Acquisition Date 2018-05-02T23:50:06
Spectrometer Frequency 400.13
Spectral Width 8012.8
Lowest Frequency -1545.4
Nucleus 1H
Acquired Size 32768
Spectral Size 65536
F (m) 6.92
D (m) 7.29
B (d) 7.39
A (dd) 7.47
C (tdd) 7.35
E (ddd) 7.03
G (t) 5.97
H (t) 4.18
J (ddd) 2.72
I (ddd) 2.89
OTf
Cl
Cl
211g
1.00
0.98
1.08
1.91
1.00
1.02
1.00
1.03
1.03
1.03
10.5 10.0 9.5 9.0 8.5 8.0 7.5 7.0 6.5 6.0 5.5 5.0 4.5 4.0 3.5 3.0 2.5 2.0 1.5 1.0 0.5 0.0
f1 (ppm)

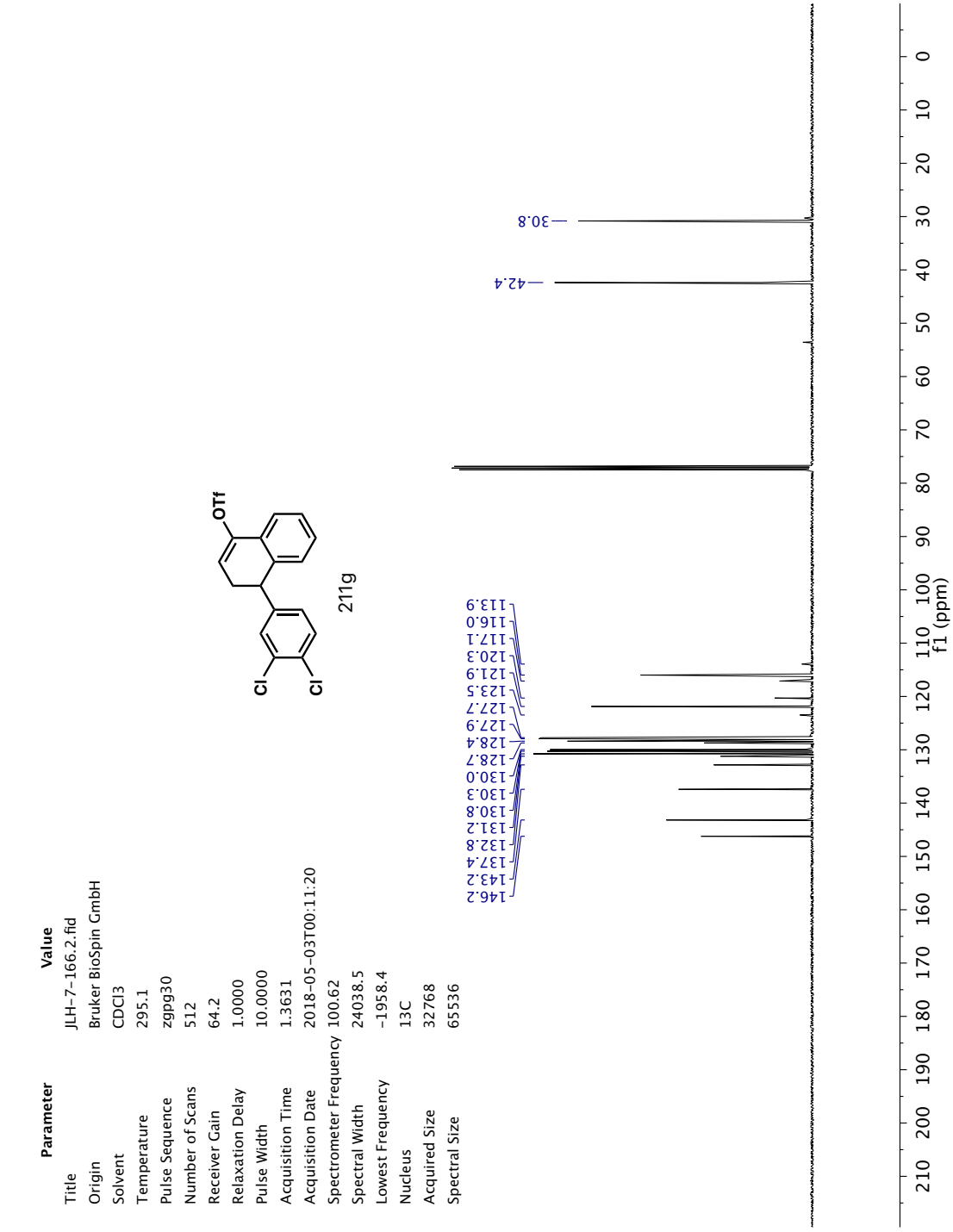
Parameter Value
Title JLH-7-166.2.fid
Origin Bruker BioSpin GmbH
Solvent CDCl3
Temperature 295.1
Pulse Sequence zgpg30
Number of Scans 512
Receiver Gain 64.2
Relaxation Delay 1.0000
Pulse Width 10.0000
Acquisition Time 1.3631
Acquisition Date 2018-05-03T00:11:20
Spectrometer Frequency 100.62
Spectral Width 24038.5
Lowest Frequency -1958.4
Nucleus 13C
Acquired Size 32768
Spectral Size 65536
OTf
Cl
Cl
211g
146.2
143.2
137.4
132.8
131.2
130.8
130.3
130.0
128.7
128.4
127.9
127.7
123.5
121.9
120.3
117.1
116.0
113.9
42.4
30.8
f1 (ppm)

Parameter	Value
Title	JLH-7-166-F
Origin	Varian
Solvent	cdcl3
Temperature	25.0
Pulse Sequence	s2pul
Number of Scans	16
Receiver Gain	30
Relaxation Delay	1.0000
Pulse Width	6.3333
Acquisition Time	0.9856
Acquisition Date	2018-05-03T22:42:22
Spectrometer Frequency	282.34
Spectral Width	64935.1
Lowest Frequency	-56468.7
Nucleus	19F
Acquired Size	64000
Spectral Size	131072

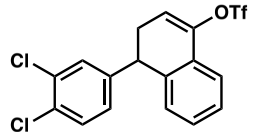

211g

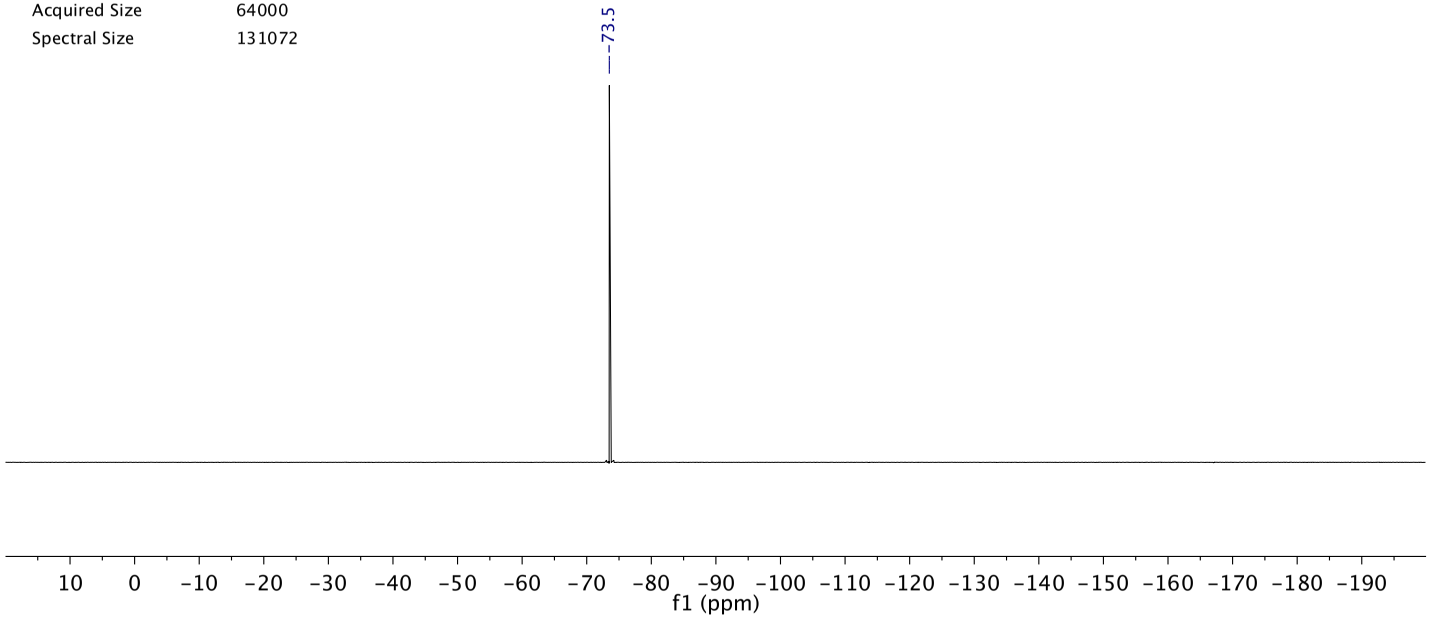

Parameter	Value
Title	JLH-7-166-F-C6F6
Origin	Varian
Solvent	cdcl3
Temperature	25.0
Pulse Sequence	s2pul
Number of Scans	16
Receiver Gain	30
Relaxation Delay	1.0000
Pulse Width	6.3333
Acquisition Time	0.9856
Acquisition Date	2018-05-23T22:38:19
Spectrometer Frequency	282.34
Spectral Width	64935.1
Lowest Frequency	-56468.7
Nucleus	19F
Acquired Size	64000
Spectral Size	131072

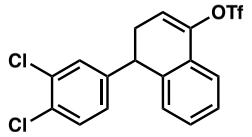

211g
with C_6F_6

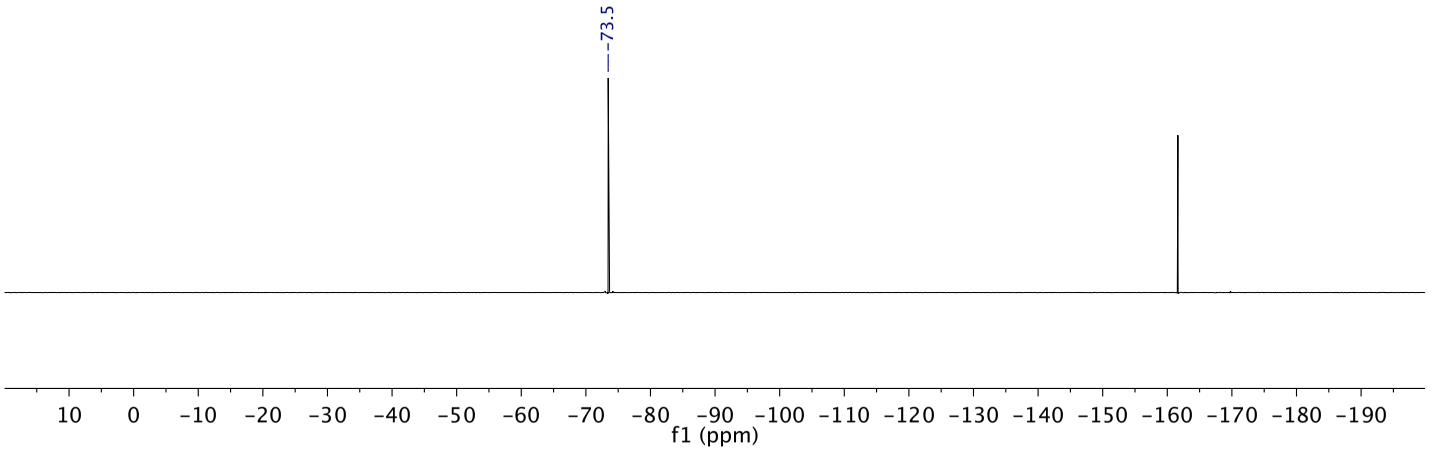

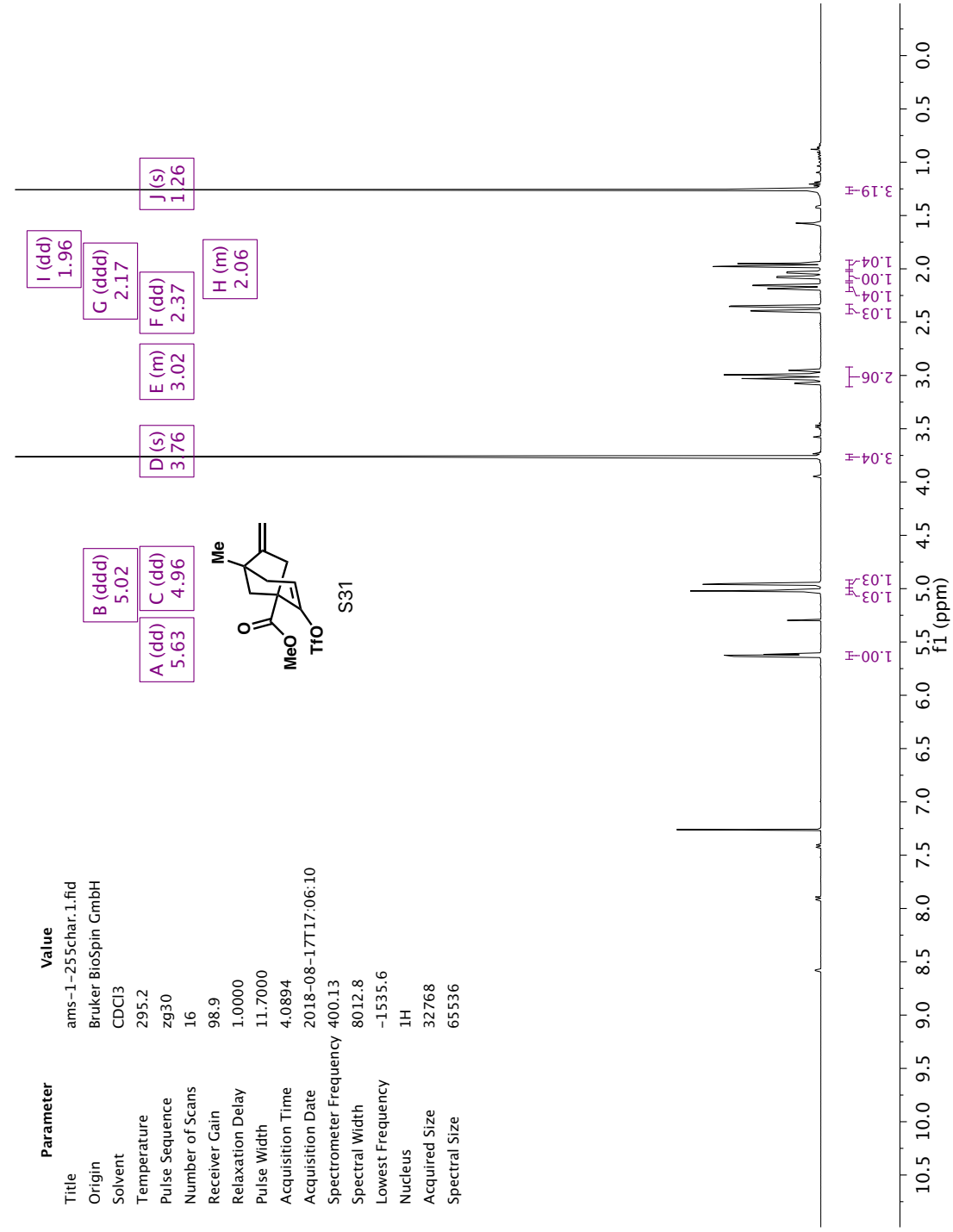
Parameter Value
Title ams-1-255char.1.fid
Origin Bruker BioSpin GmbH
Solvent CDCl3
Temperature 295.2
Pulse Sequence zg30
Number of Scans 16
Receiver Gain 98.9
Relaxation Delay 1.0000
Pulse Width 11.7000
Acquisition Time 4.0894
Acquisition Date 2018-08-17T17:06:10
Spectrometer Frequency 400.13
Spectral Width 8012.8
Lowest Frequency -1535.6
Nucleus 1H
Acquired Size 32768
Spectral Size 65536
A (dd) 5.63
B (ddd) 5.02
C (dd) 4.96
D (s) 3.76
E (m) 3.02
F (dd) 2.37
G (ddd) 2.17
H (m) 2.06
I (dd) 1.96
J (s) 1.26
Me
O
MeO
TfO
S31
1.00
1.03
1.03
3.04
2.06
1.03
1.04
1.00
1.04
3.19
f1 (ppm)

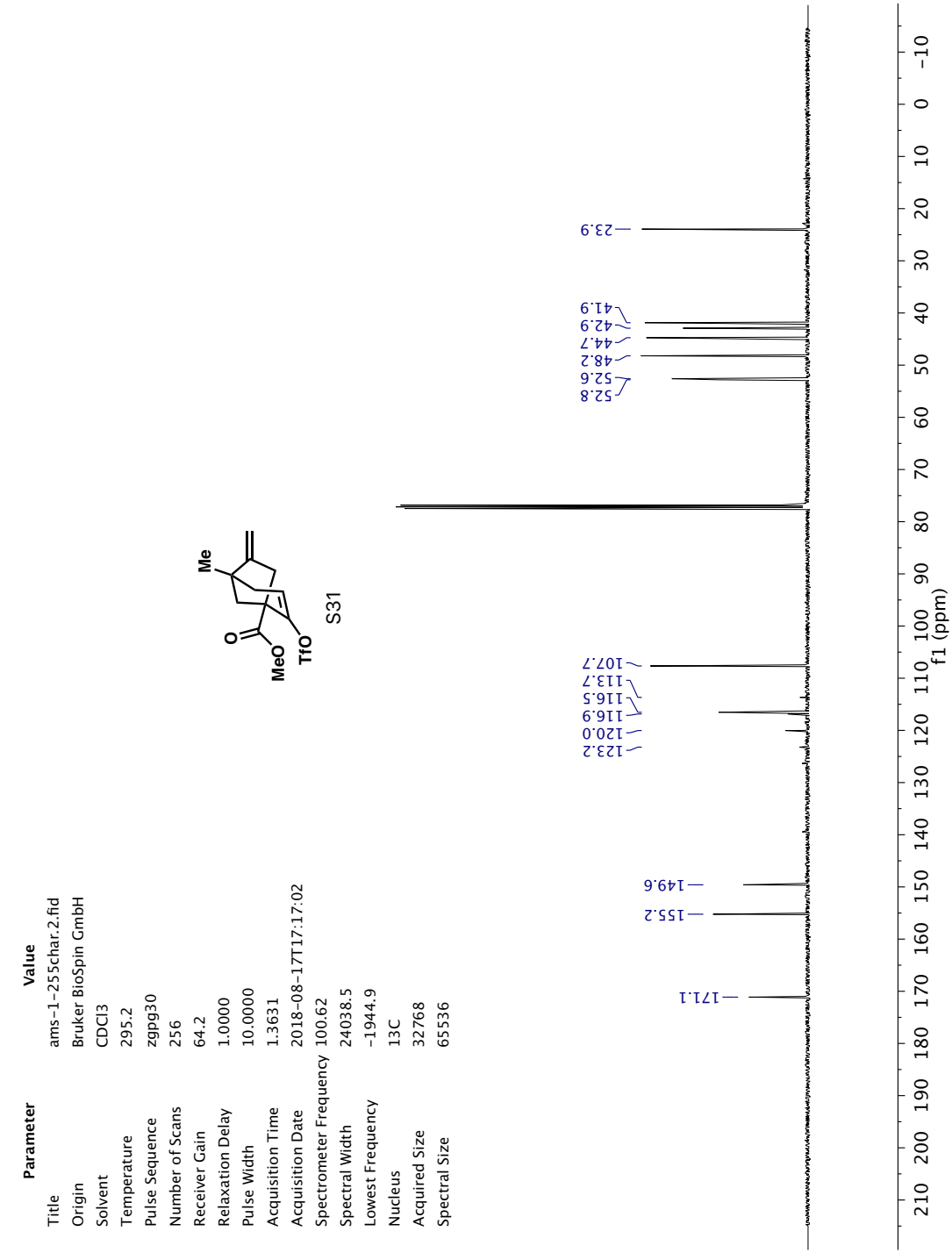

Parameter	Value
Title	ams-1-255char.2.fid
Origin	Bruker BioSpin GmbH
Solvent	CDCl3
Temperature	295.2
Pulse Sequence	zgpg30
Number of Scans	256
Receiver Gain	64.2
Relaxation Delay	1.0000
Pulse Width	10.0000
Acquisition Time	1.3631
Acquisition Date	2018-08-17T17:17:02
Spectrometer Frequency	100.62
Spectral Width	24038.5
Lowest Frequency	-1944.9
Nucleus	13C
Acquired Size	32768
Spectral Size	65536

Parameter	Value
Title	AMS-1-255-F
Origin	Varian
Solvent	cdcl3
Temperature	25.0
Pulse Sequence	s2pul
Number of Scans	16
Receiver Gain	30
Relaxation Delay	1.0000
Pulse Width	6.3333
Acquisition Time	0.9856
Acquisition Date	2018-08-14T01:17:36
Spectrometer Frequency	282.34
Spectral Width	64935.1
Lowest Frequency	-56435.4
Nucleus	19F
Acquired Size	64000
Spectral Size	131072

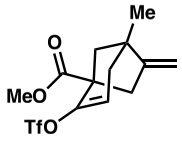

S31

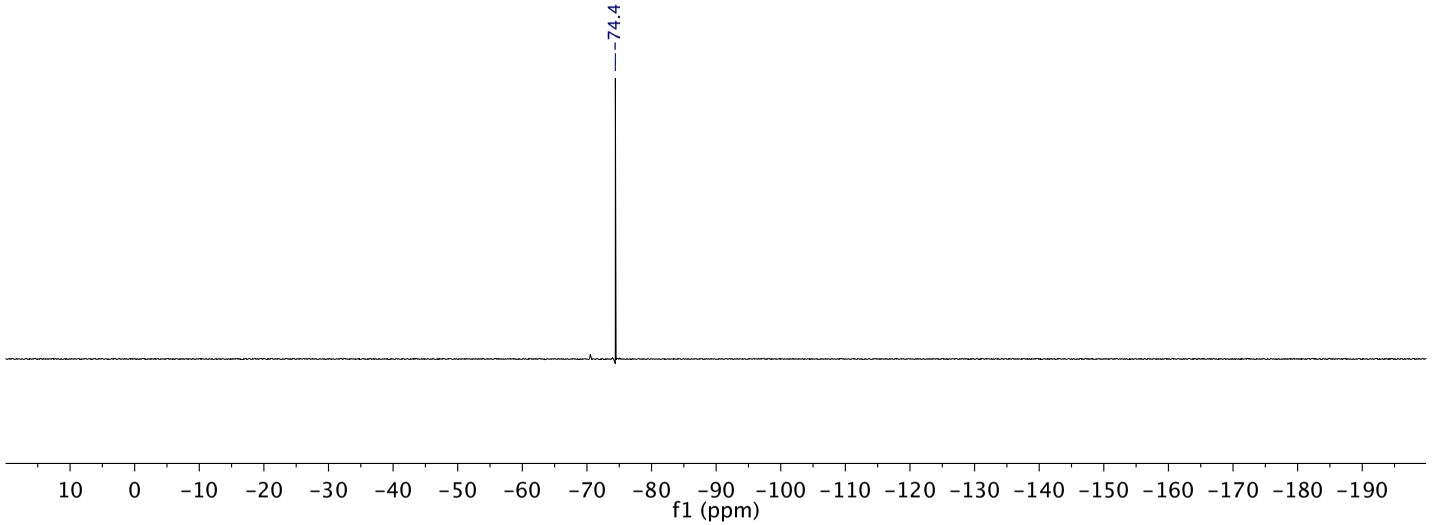

Parameter	Value
Title	AMS-1-255-F-std
Origin	Varian
Solvent	cdcl3
Temperature	25.0
Pulse Sequence	s2pul
Number of Scans	16
Receiver Gain	30
Relaxation Delay	1.0000
Pulse Width	6.3333
Acquisition Time	0.9856
Acquisition Date	2018-09-23T19:52:39
Spectrometer Frequency	282.34
Spectral Width	64935.1
Lowest Frequency	-56435.1
Nucleus	19F
Acquired Size	64000
Spectral Size	131072

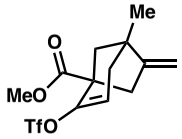

S31
with C_6F_6

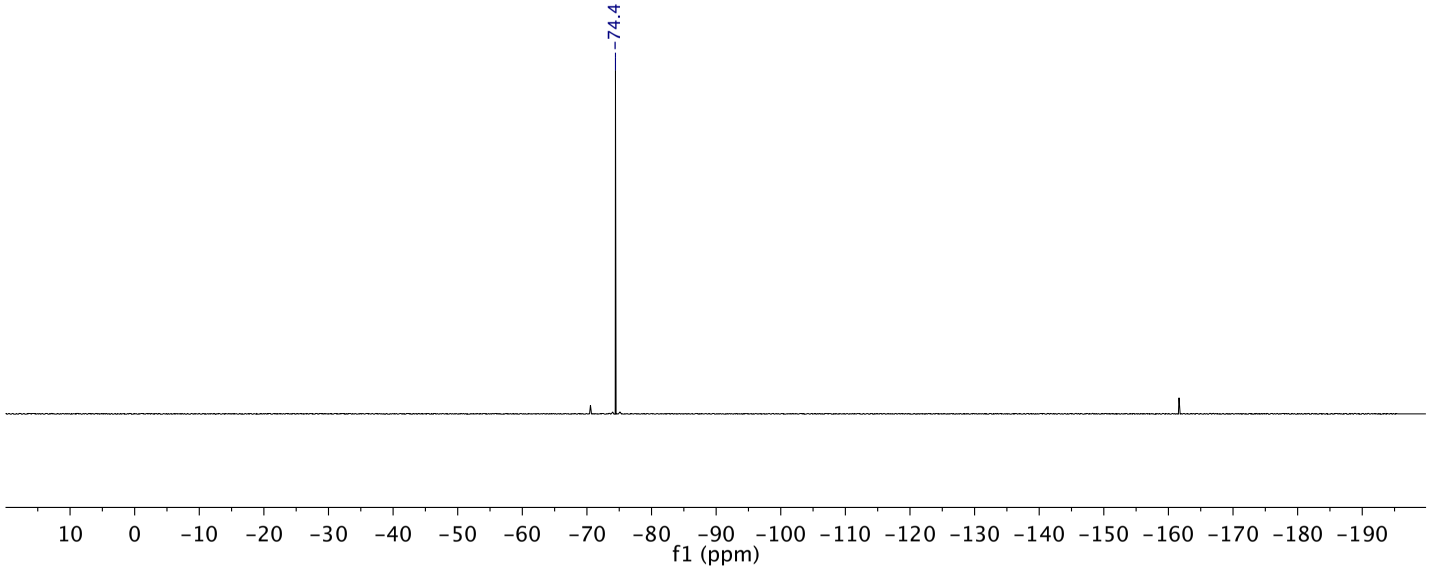

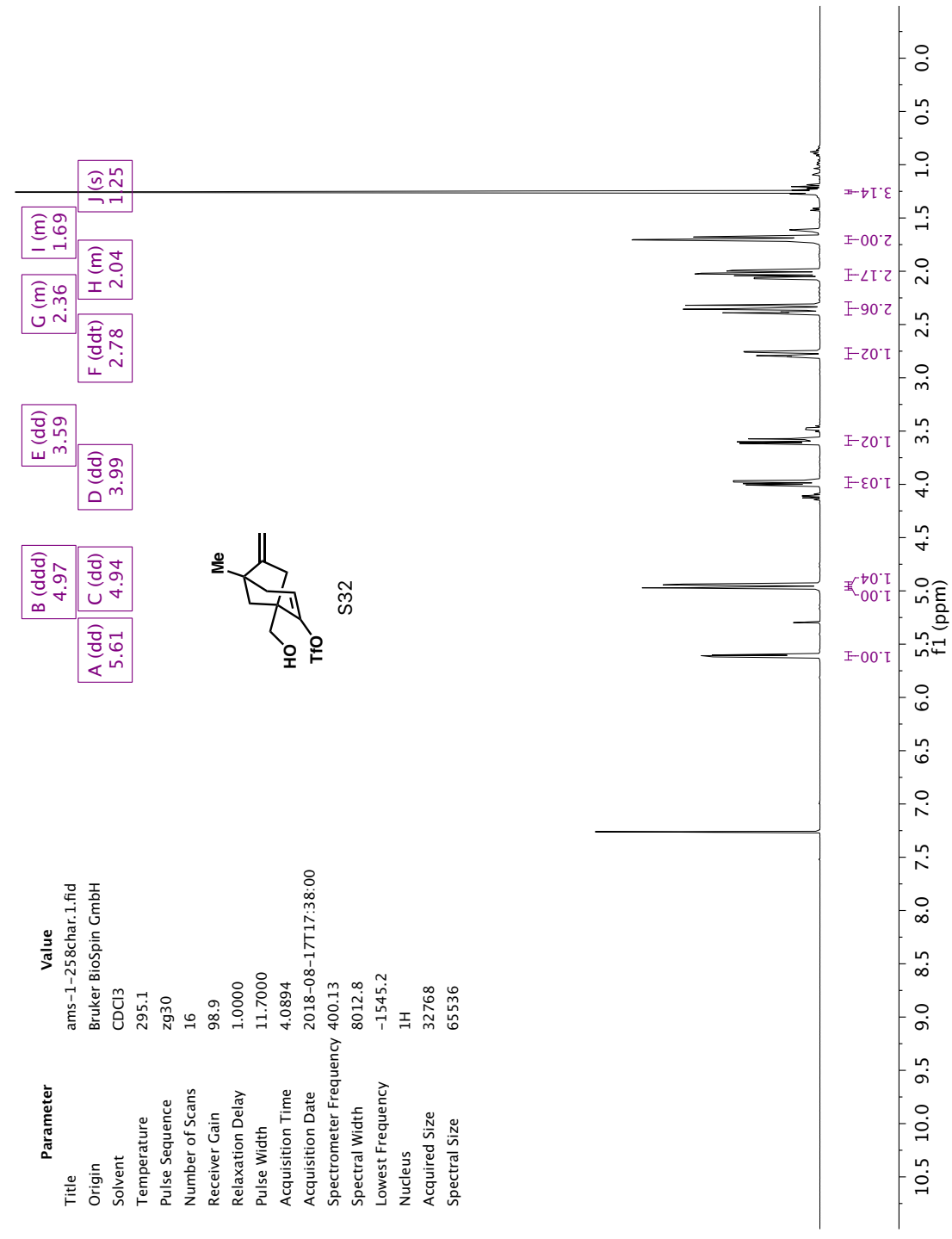

Parameter	Value
Title	ams-1-258char.1.fid
Origin	Bruker BioSpin GmbH
Solvent	CDCl3
Temperature	295.1
Pulse Sequence	zg30
Number of Scans	16
Receiver Gain	98.9
Relaxation Delay	1.0000
Pulse Width	11.7000
Acquisition Time	4.0894
Acquisition Date	2018-08-17T17:38:00
Spectrometer Frequency	400.13
Spectral Width	8012.8
Lowest Frequency	-1545.2
Nucleus	1H
Acquired Size	32768
Spectral Size	65536

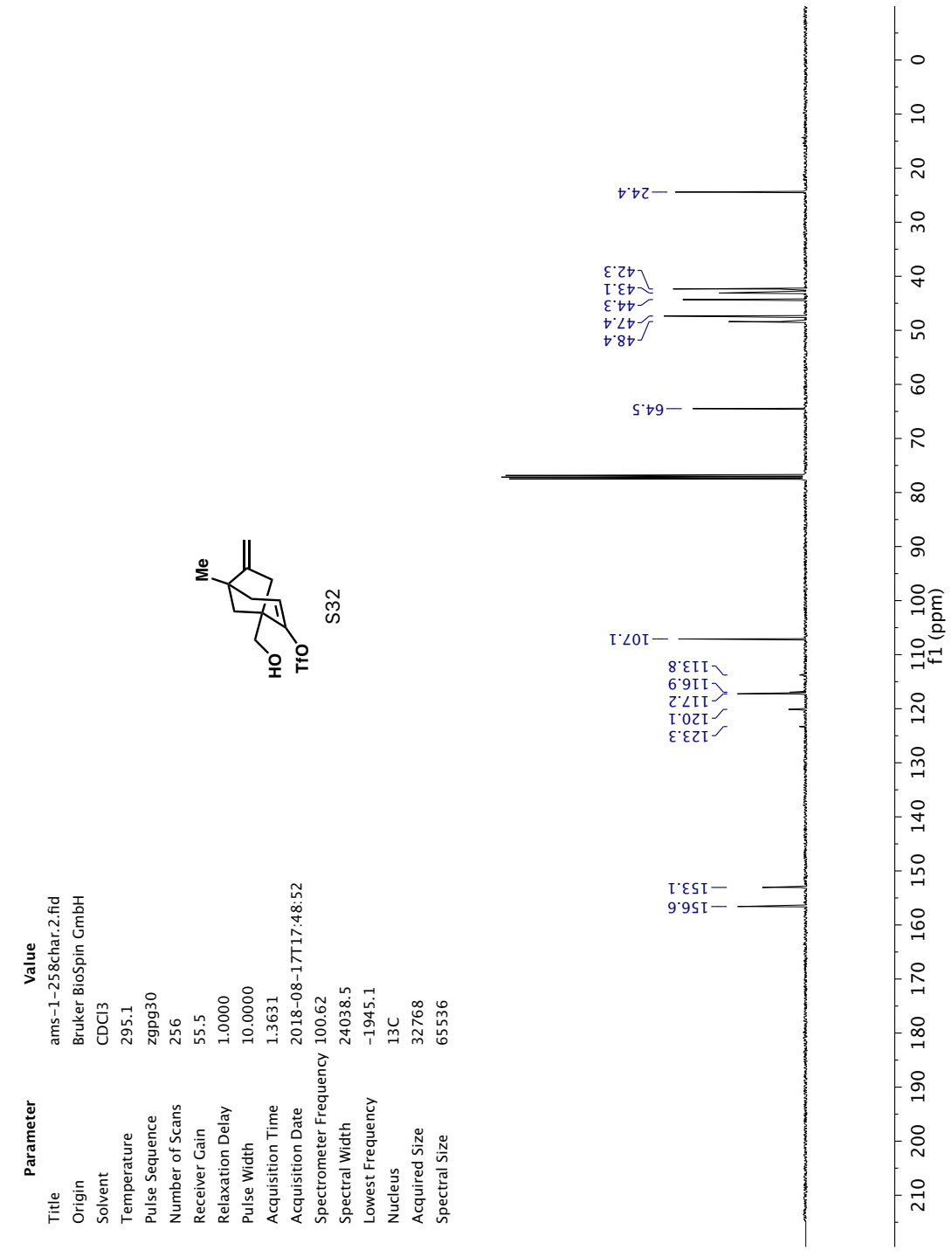

Parameter	Value
Title	ams-1-258char.2.fid
Origin	Bruker BioSpin GmbH
Solvent	CDCl3
Temperature	295.1
Pulse Sequence	zgpg30
Number of Scans	256
Receiver Gain	55.5
Relaxation Delay	1.0000
Pulse Width	10.0000
Acquisition Time	1.3631
Acquisition Date	2018-08-17T17:48:52
Spectrometer Frequency	100.62
Spectral Width	24038.5
Lowest Frequency	-1945.1
Nucleus	13C
Acquired Size	32768
Spectral Size	65536

Parameter	Value
Title	AMS-1-258-F
Origin	Varian
Solvent	cdcl3
Temperature	25.0
Pulse Sequence	s2pul
Number of Scans	16
Receiver Gain	30
Relaxation Delay	1.0000
Pulse Width	6.3333
Acquisition Time	0.9856
Acquisition Date	2018-08-19T23:06:01
Spectrometer Frequency	282.34
Spectral Width	64935.1
Lowest Frequency	-56444.7
Nucleus	19F
Acquired Size	64000
Spectral Size	131072

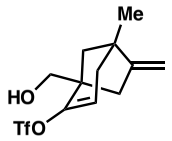

S32

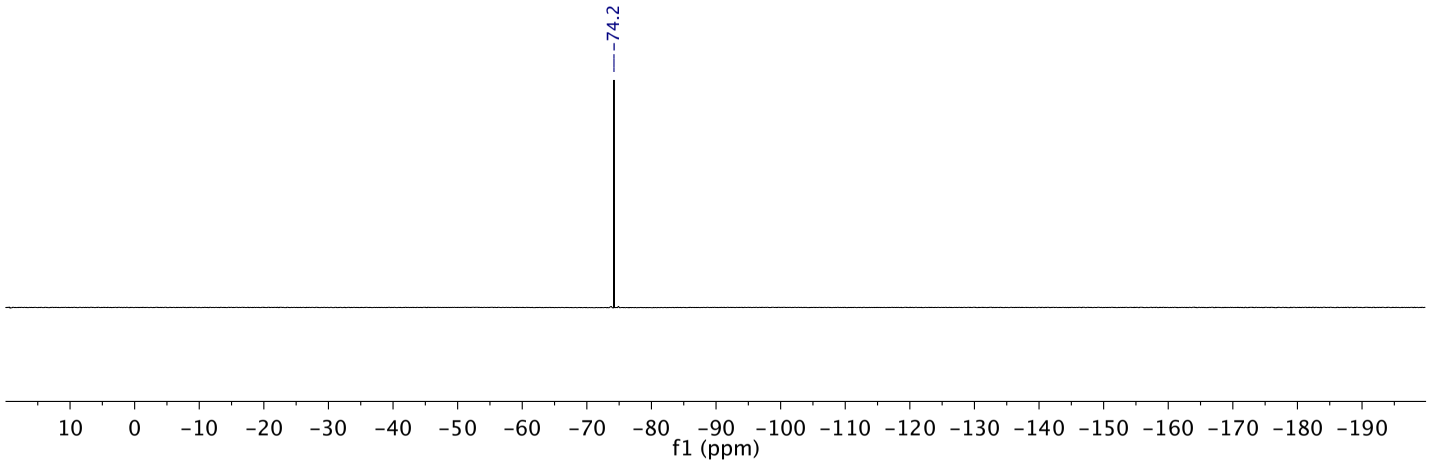

Parameter	Value
Title	AMS-1-258-F-C6F6
Origin	Varian
Solvent	cdcl3
Temperature	25.0
Pulse Sequence	s2pul
Number of Scans	16
Receiver Gain	30
Relaxation Delay	1.0000
Pulse Width	6.3333
Acquisition Time	0.9856
Acquisition Date	2018-10-01T14:38:13
Spectrometer Frequency	282.34
Spectral Width	64935.1
Lowest Frequency	-56430.6
Nucleus	19F
Acquired Size	64000
Spectral Size	131072

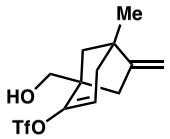

S32

with C_6F_6

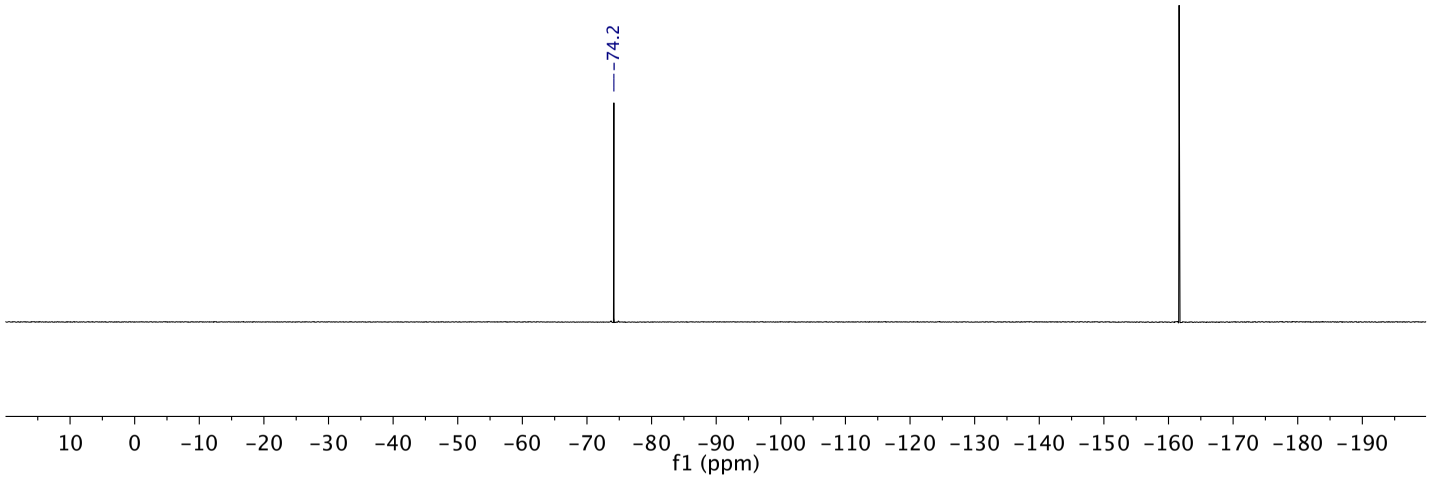

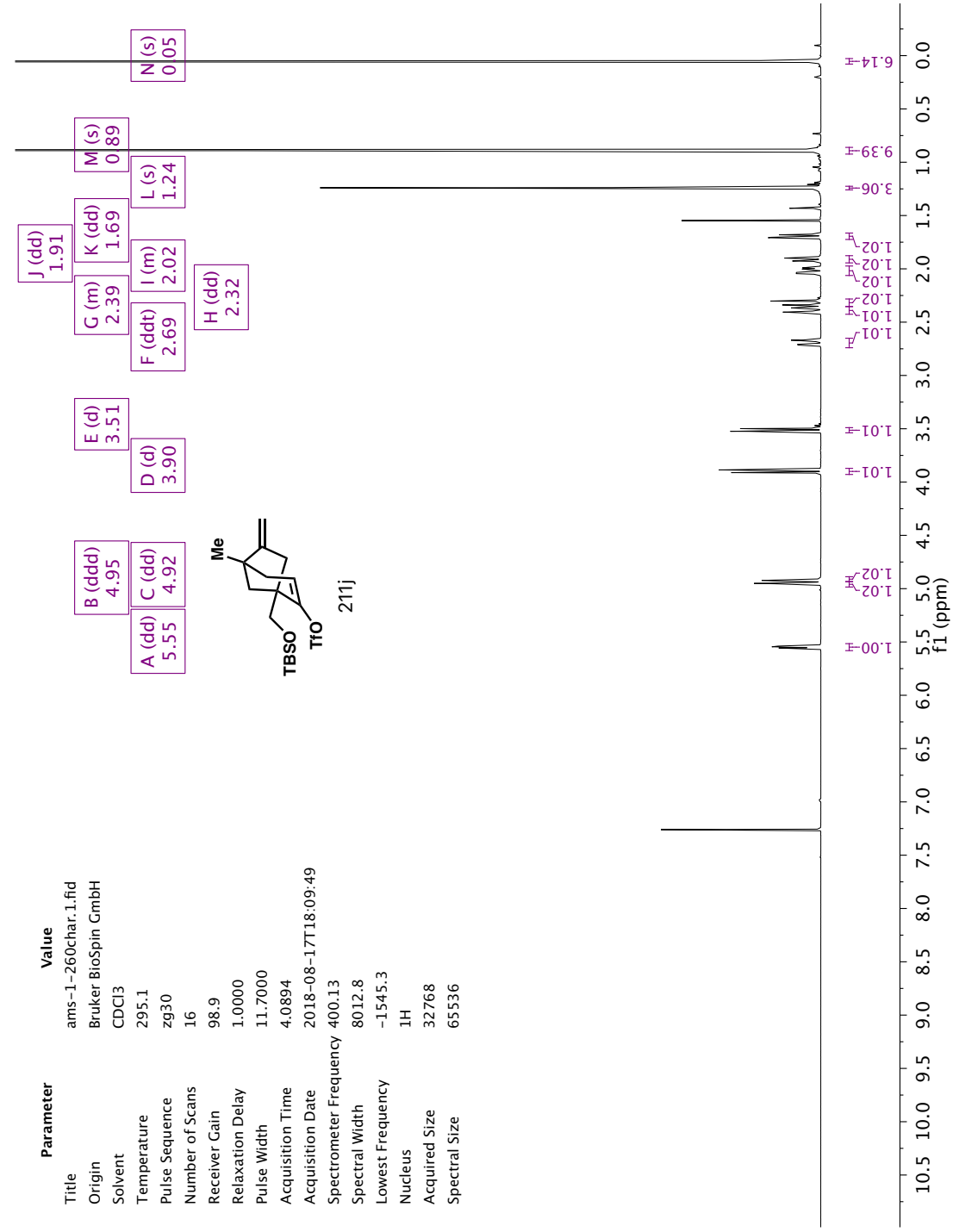
Parameter Value
Title ams-1-260char.1.fid
Origin Bruker BioSpin GmbH
Solvent CDCl3
Temperature 295.1
Pulse Sequence zg30
Number of Scans 16
Receiver Gain 98.9
Relaxation Delay 1.0000
Pulse Width 11.7000
Acquisition Time 4.0894
Acquisition Date 2018-08-17T18:09:49
Spectrometer Frequency 400.13
Spectral Width 8012.8
Lowest Frequency -1545.3
Nucleus 1H
Acquired Size 32768
Spectral Size 65536
A (dd) 5.55
B (ddd) 4.95
C (dd) 4.92
D (d) 3.90
E (d) 3.51
F (ddt) 2.69
G (m) 2.39
H (dd) 2.32
I (m) 2.02
J (dd) 1.91
K (dd) 1.69
L (s) 1.24
M (s) 0.89
N (s) 0.05
Me
TBSO
TfO
211j
f1 (ppm)

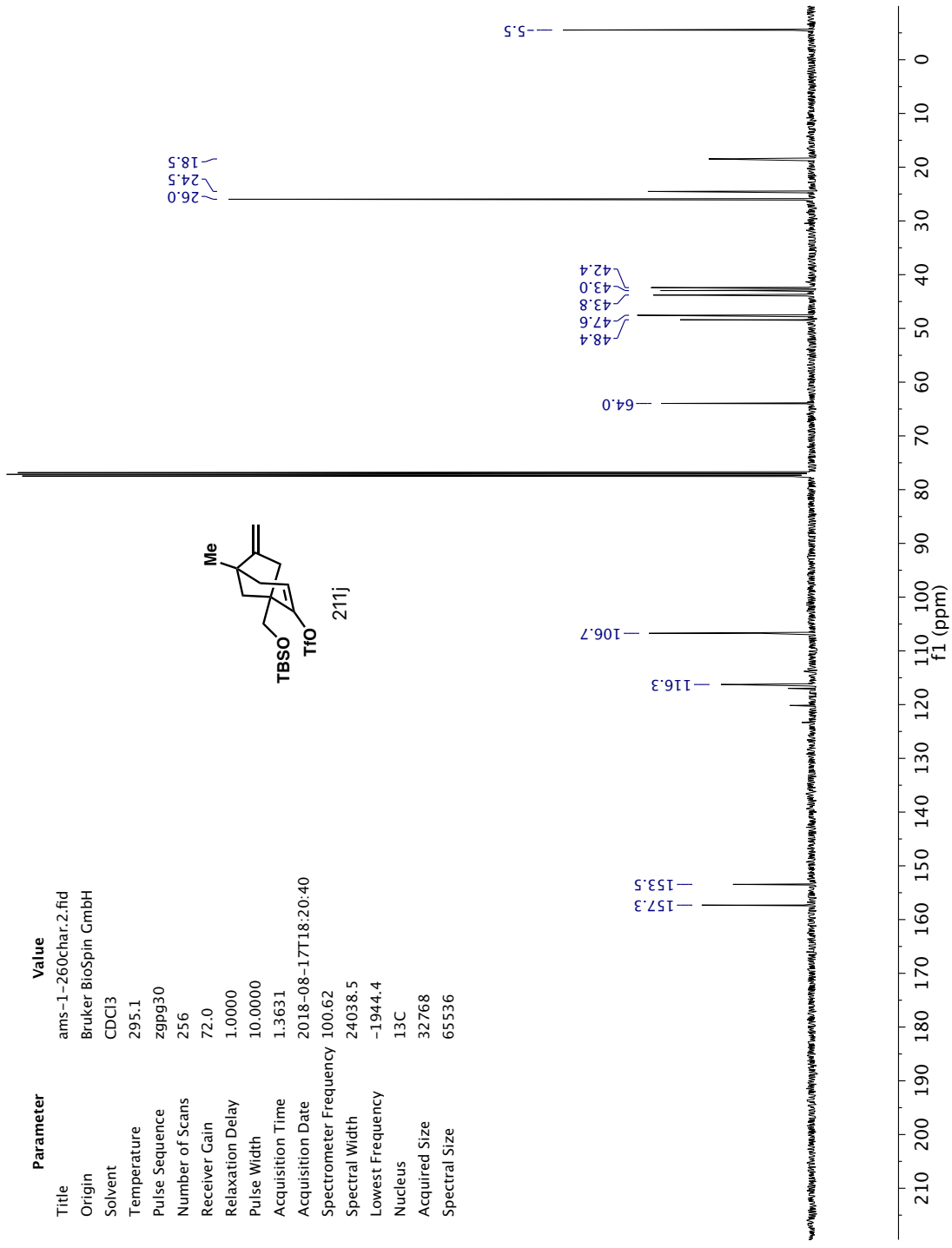
Parameter Value
Title ams-1-260char.2.fid
Origin Bruker BioSpin GmbH
Solvent CDCl3
Temperature 295.1
Pulse Sequence zgpg30
Number of Scans 256
Receiver Gain 72.0
Relaxation Delay 1.0000
Pulse Width 10.0000
Acquisition Time 1.3631
Acquisition Date 2018-08-17T18:20:40
Spectrometer Frequency 100.62
Spectral Width 24038.5
Lowest Frequency -1944.4
Nucleus 13C
Acquired Size 32768
Spectral Size 65536
Me
TBSO
TfO
211j
157.3
153.5
116.3
106.7
64.0
48.4
47.6
43.8
43.0
42.4
26.0
24.5
18.5
-5.5
f1 (ppm)

Parameter	Value
Title	AMS-1-260-F
Origin	Varian
Solvent	cdcl3
Temperature	25.0
Pulse Sequence	s2pul
Number of Scans	16
Receiver Gain	30
Relaxation Delay	1.0000
Pulse Width	6.3333
Acquisition Time	0.9856
Acquisition Date	2018-08-19T23:14:03
Spectrometer Frequency	282.34
Spectral Width	64935.1
Lowest Frequency	-56449.5
Nucleus	19F
Acquired Size	64000
Spectral Size	131072

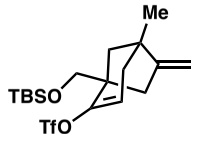

211j

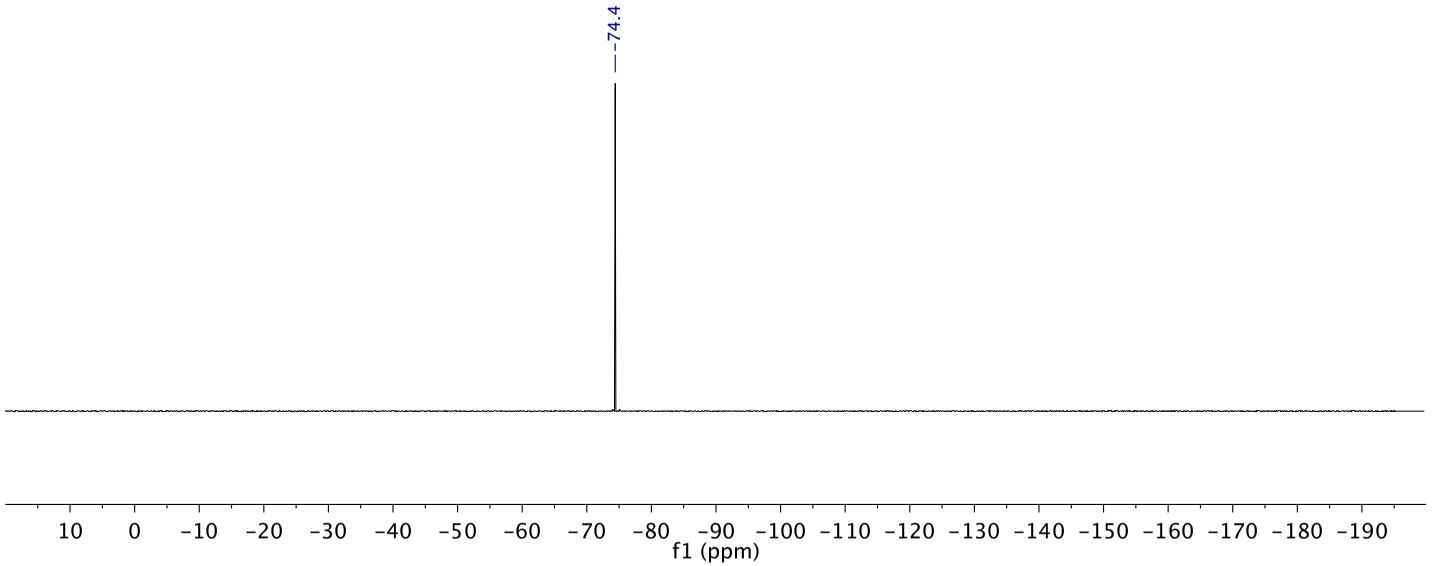

Parameter	Value
Title	AMS-1-260-F-std
Origin	Varian
Solvent	cdcl3
Temperature	25.0
Pulse Sequence	s2pul
Number of Scans	16
Receiver Gain	30
Relaxation Delay	1.0000
Pulse Width	6.3333
Acquisition Time	0.9856
Acquisition Date	2018-09-23T20:01:28
Spectrometer Frequency	282.34
Spectral Width	64935.1
Lowest Frequency	-56442.2
Nucleus	19F
Acquired Size	64000
Spectral Size	131072

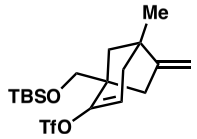

211j
with C_6F_6

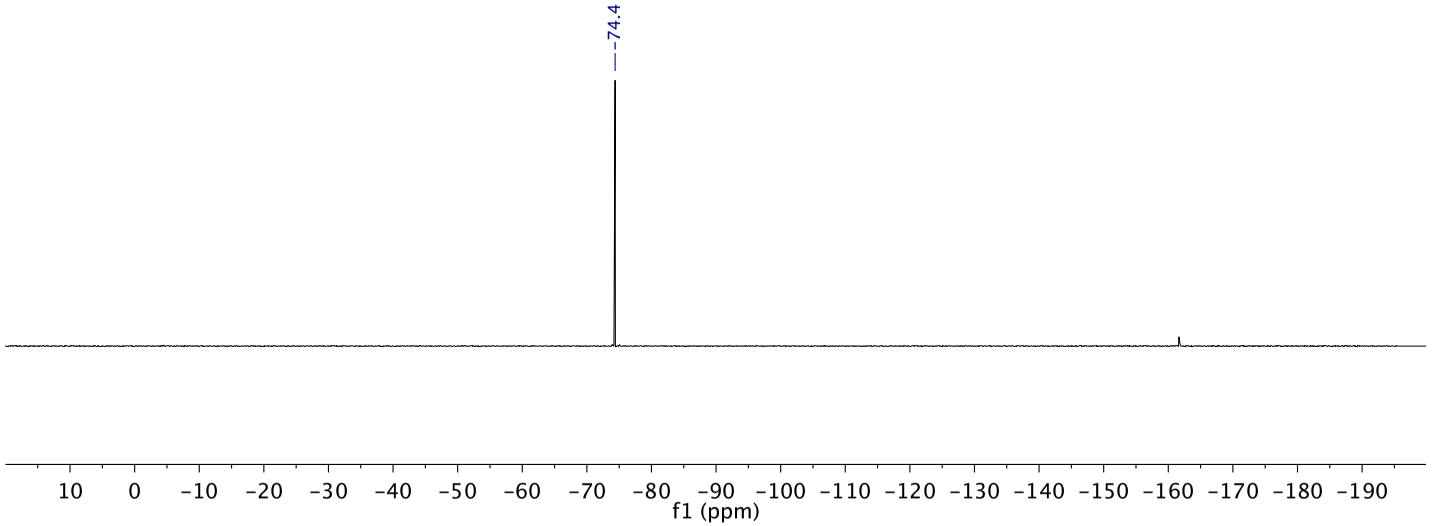

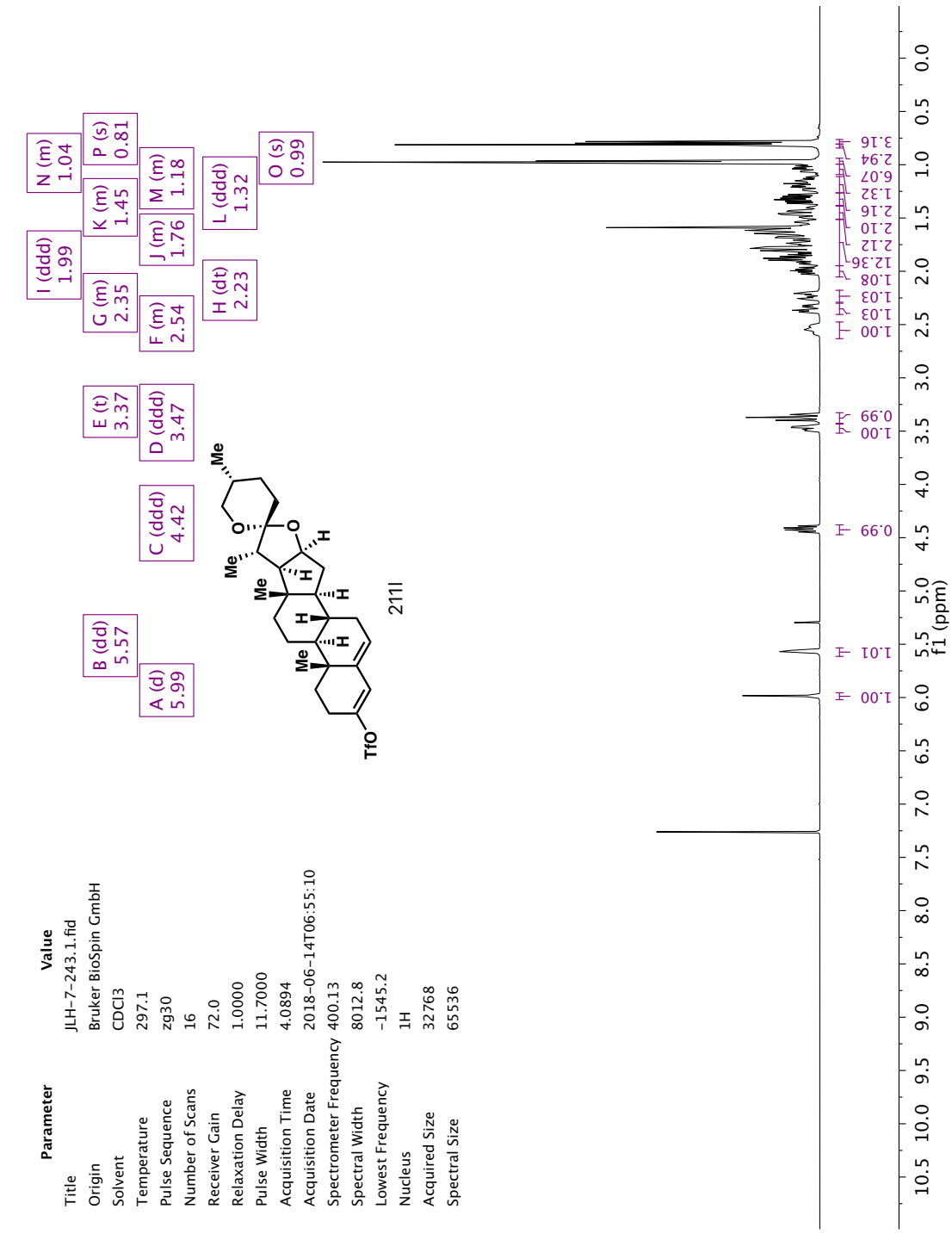

Parameter	Value
Title	JLH-7-243.1.fid
Origin	Bruker BioSpin GmbH
Solvent	CDCl3
Temperature	297.1
Pulse Sequence	zg30
Number of Scans	16
Receiver Gain	72.0
Relaxation Delay	1.0000
Pulse Width	11.7000
Acquisition Time	4.0894
Acquisition Date	2018-06-14T06:55:10
Spectrometer Frequency	400.13
Spectral Width	8012.8
Lowest Frequency	-1545.2
Nucleus	1H
Acquired Size	32768
Spectral Size	65536

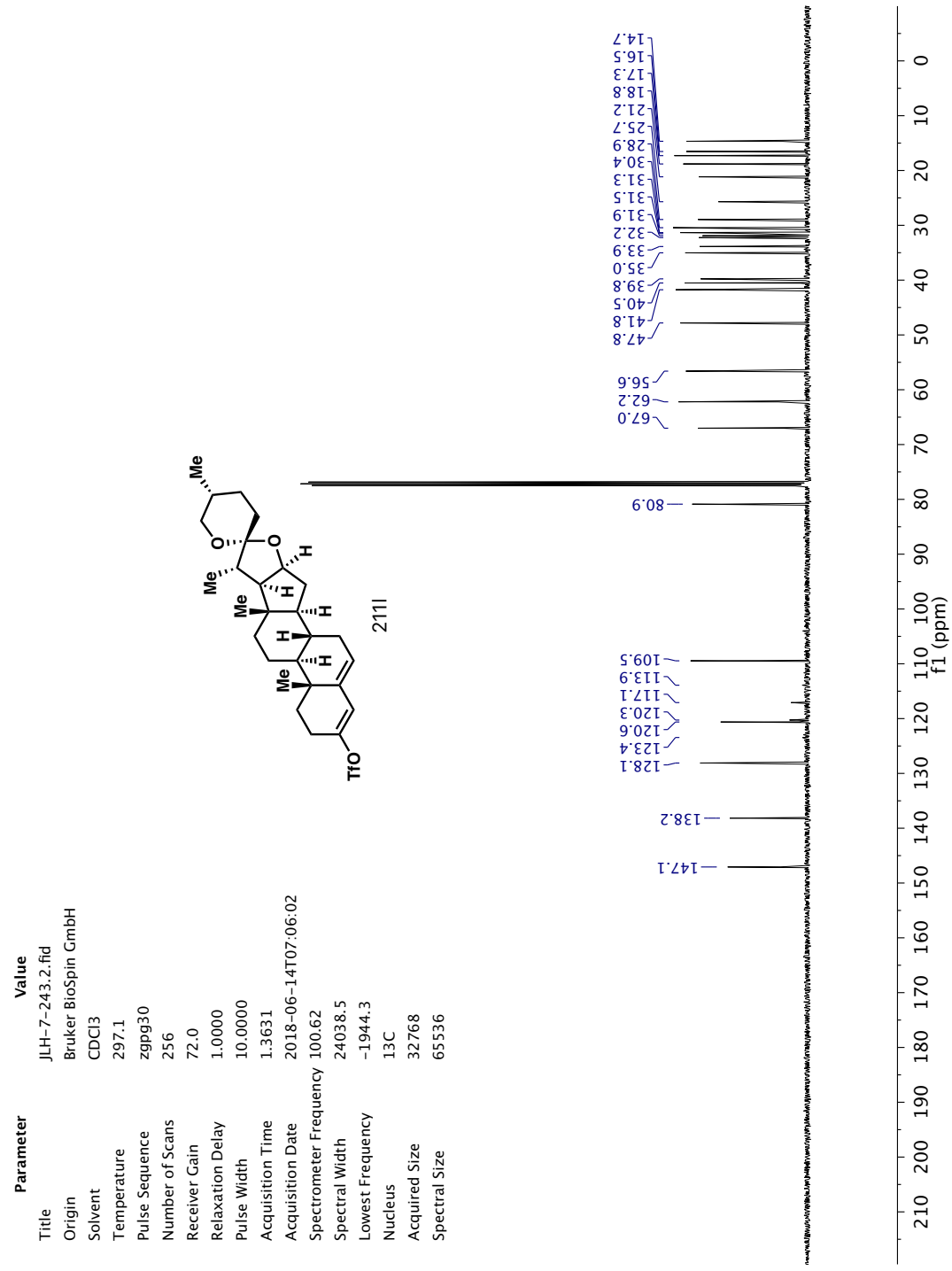
Parameter Value
Title JLH-7-243.2.fid
Origin Bruker BioSpin GmbH
Solvent CDCl3
Temperature 297.1
Pulse Sequence zgpg30
Number of Scans 256
Receiver Gain 72.0
Relaxation Delay 1.0000
Pulse Width 10.0000
Acquisition Time 1.3631
Acquisition Date 2018-06-14T07:06:02
Spectrometer Frequency 100.62
Spectral Width 24038.5
Lowest Frequency -1944.3
Nucleus 13C
Acquired Size 32768
Spectral Size 65536
Me
O
O
H
Me
Me
H
H
H
H
Me
TfO
2111
147.1
138.2
128.1
123.4
120.6
120.3
117.1
113.9
109.5
80.9
67.0
62.2
56.6
47.8
41.8
40.5
39.8
35.0
33.9
32.2
31.9
31.5
31.3
30.4
28.9
25.7
21.2
18.8
17.3
16.5
14.7
f1 (ppm)

Parameter	Value
Title	JLH-7-243-F
Origin	Varian
Solvent	cdcl3
Temperature	25.0
Pulse Sequence	s2pul
Number of Scans	16
Receiver Gain	30
Relaxation Delay	1.0000
Pulse Width	6.3333
Acquisition Time	0.9856
Acquisition Date	2018-06-14T01:19:18
Spectrometer Frequency	282.34
Spectral Width	64935.1
Lowest Frequency	-56453.2
Nucleus	19F
Acquired Size	64000
Spectral Size	131072

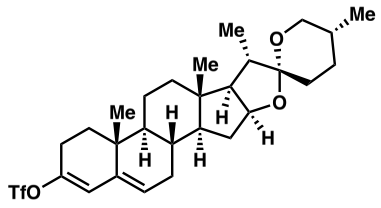

211l

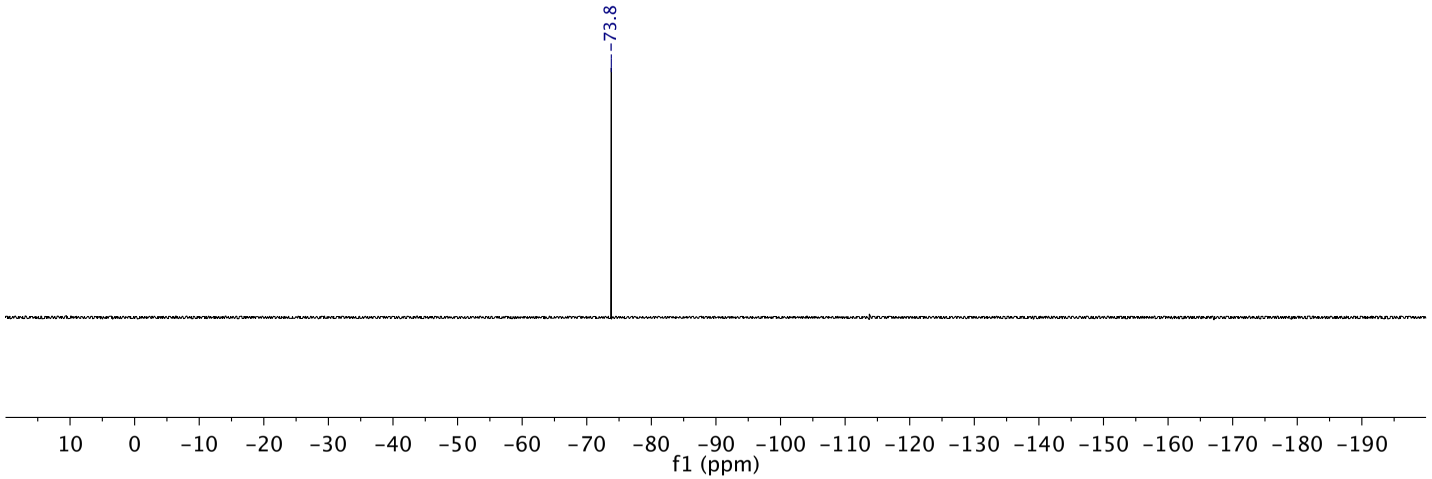

Parameter	Value
Title	JLH-7-243-F-C6F6
Origin	Varian
Solvent	cdcl3
Temperature	25.0
Pulse Sequence	s2pul
Number of Scans	16
Receiver Gain	30
Relaxation Delay	1.0000
Pulse Width	6.3333
Acquisition Time	0.9856
Acquisition Date	2018-06-14T01:24:03
Spectrometer Frequency	282.34
Spectral Width	64935.1
Lowest Frequency	-56437.9
Nucleus	19F
Acquired Size	64000
Spectral Size	131072

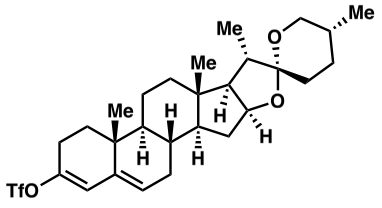

211l
with C_6F_6

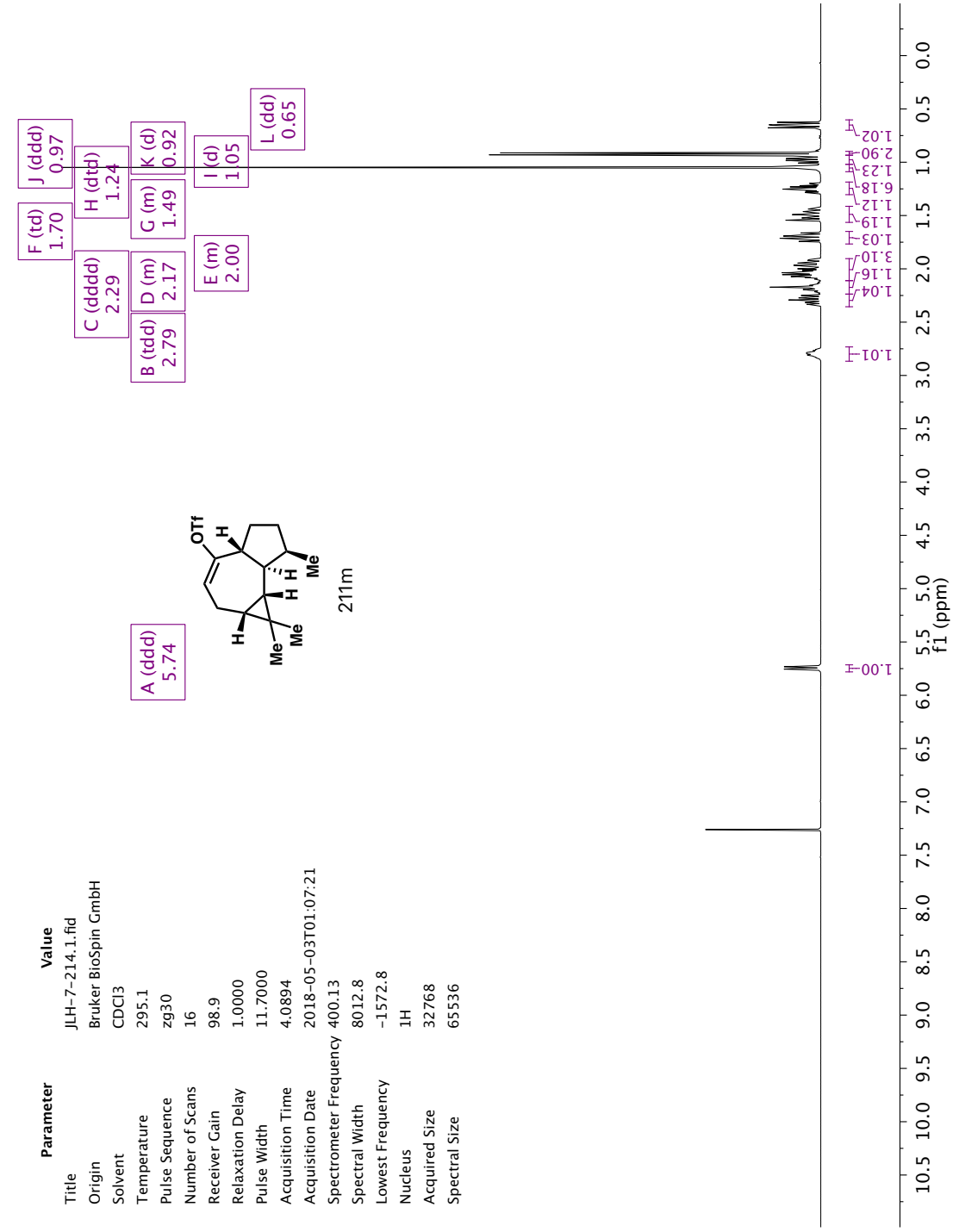

Parameter	Value
Title	JLH-7-214.1.fid
Origin	Bruker BioSpin GmbH
Solvent	CDCl3
Temperature	295.1
Pulse Sequence	zg30
Number of Scans	16
Receiver Gain	98.9
Relaxation Delay	1.0000
Pulse Width	11.7000
Acquisition Time	4.0894
Acquisition Date	2018-05-03T01:07:21
Spectrometer Frequency	400.13
Spectral Width	8012.8
Lowest Frequency	-1572.8
Nucleus	1H
Acquired Size	32768
Spectral Size	65536

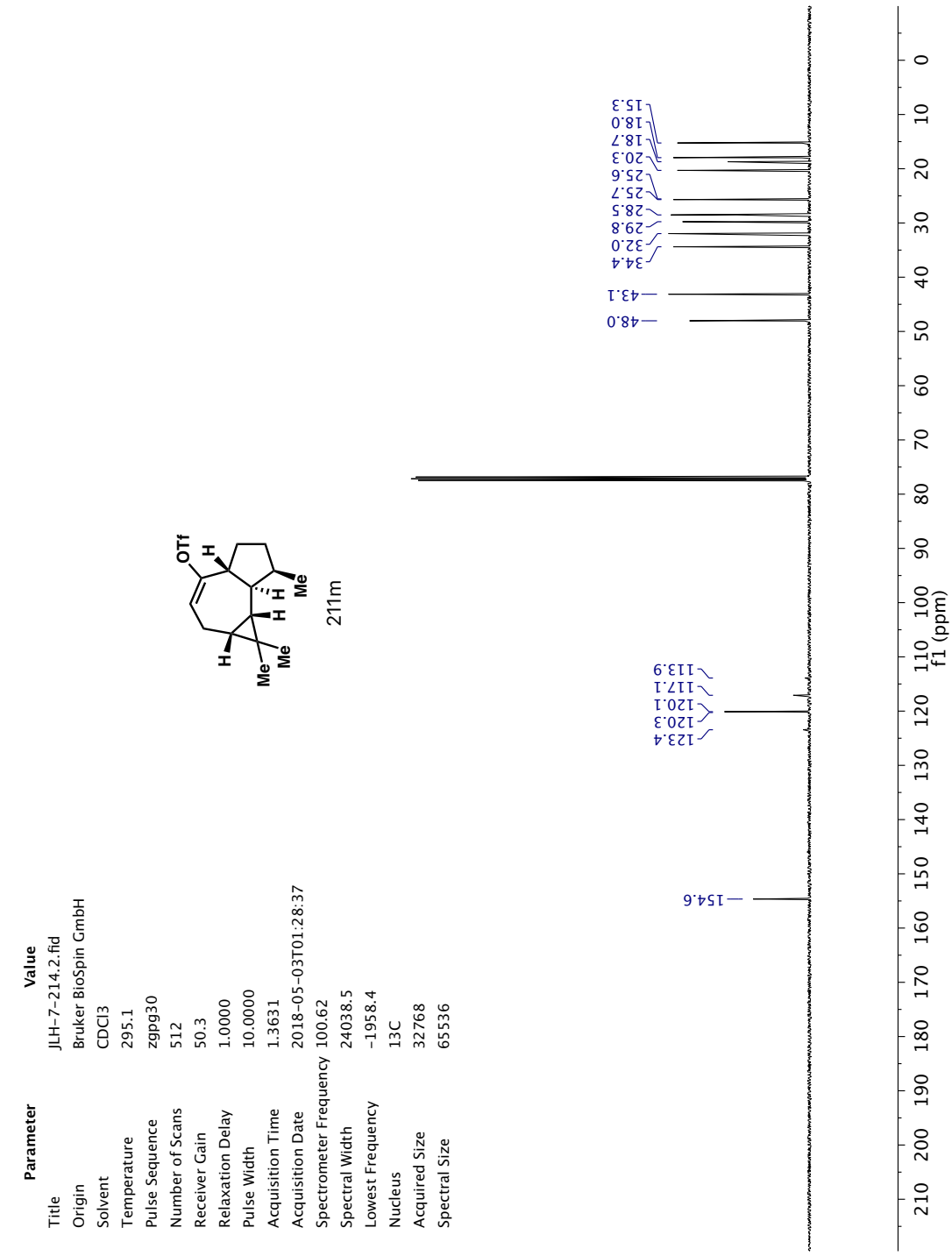
Parameter Value
Title JLH-7-214.2.fid
Origin Bruker BioSpin GmbH
Solvent CDCl3
Temperature 295.1
Pulse Sequence zgpg30
Number of Scans 512
Receiver Gain 50.3
Relaxation Delay 1.0000
Pulse Width 10.0000
Acquisition Time 1.3631
Acquisition Date 2018-05-03T01:28:37
Spectrometer Frequency 100.62
Spectral Width 24038.5
Lowest Frequency -1958.4
Nucleus 13C
Acquired Size 32768
Spectral Size 65536
OTf
H
H
Me
Me
Me
211m
154.6
123.4
120.3
120.1
117.1
113.9
48.0
43.1
34.4
32.0
29.8
28.5
25.7
25.6
20.3
18.7
18.0
15.3
f1 (ppm)

Parameter Value
Title JLH-7-214-F
Origin Varian
Solvent cdcl3
Temperature 25.0
Pulse Sequence s2pul
Number of Scans 16
Receiver Gain 30
Relaxation Delay 1.0000
Pulse Width 6.3333
Acquisition Time 0.9856
Acquisition Date 2018-05-03T23:01:13
Spectrometer Frequency 282.34
Spectral Width 64935.1
Lowest Frequency -56468.7
Nucleus 19F
Acquired Size 64000
Spectral Size 131072
OTf
H
Me
H H
Me
Me
H
211m
-74.3
10 0 -10 -20 -30 -40 -50 -60 -70 -80 -90 -100 -110 -120 -130 -140 -150 -160 -170 -180 -190
f1 (ppm)

Parameter	Value
Title	JLH-7-214-F-C6F6
Origin	Varian
Solvent	cdcl3
Temperature	25.0
Pulse Sequence	s2pul
Number of Scans	16
Receiver Gain	30
Relaxation Delay	1.0000
Pulse Width	6.3333
Acquisition Time	0.9856
Acquisition Date	2018-05-23T22:28:36
Spectrometer Frequency	282.34
Spectral Width	64935.1
Lowest Frequency	-56468.7
Nucleus	19F
Acquired Size	64000
Spectral Size	131072

211m
with C_6F_6

-74.3

10 0 -10 -20 -30 -40 -50 -60 -70 -80 -90 -100 -110 -120 -130 -140 -150 -160 -170 -180 -190
f1 (ppm)

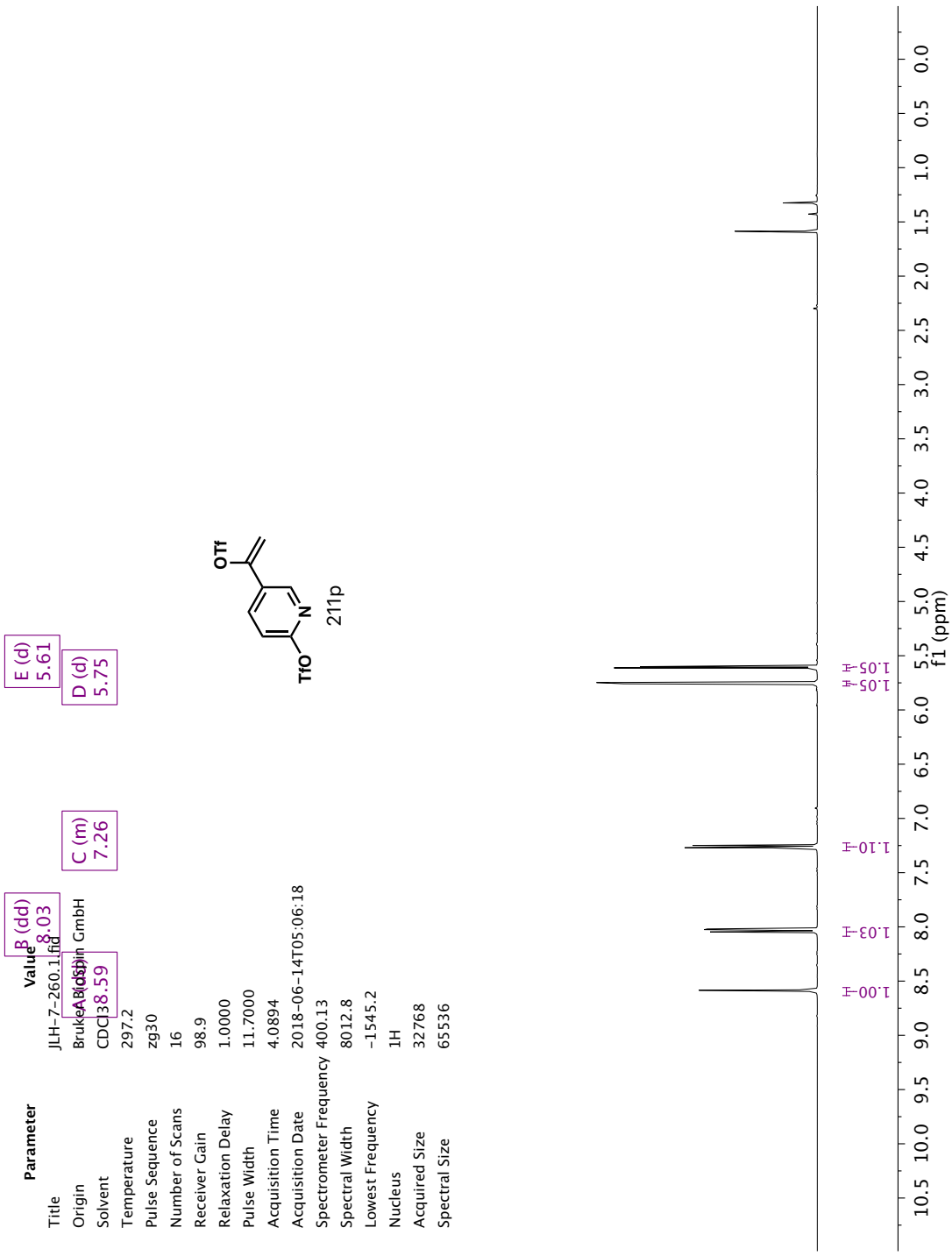
Parameter
Value
Title
JLH-7-260.1.fid
Origin
Bruker BioSpin GmbH
Solvent
CDCl3
Temperature
297.2
Pulse Sequence
zg30
Number of Scans
16
Receiver Gain
98.9
Relaxation Delay
1.0000
Pulse Width
11.7000
Acquisition Time
4.0894
Acquisition Date
2018-06-14T05:06:18
Spectrometer Frequency
400.13
Spectral Width
8012.8
Lowest Frequency
-1545.2
Nucleus
1H
Acquired Size
32768
Spectral Size
65536
B (dd) 8.03
A (dd) 8.59
C (m) 7.26
D (d) 5.75
E (d) 5.61
OTf
TfO
N
211p
1.00
1.03
1.10
1.05
1.05
10.5 10.0 9.5 9.0 8.5 8.0 7.5 7.0 6.5 6.0 5.5 5.0 4.5 4.0 3.5 3.0 2.5 2.0 1.5 1.0 0.5 0.0
f1 (ppm)

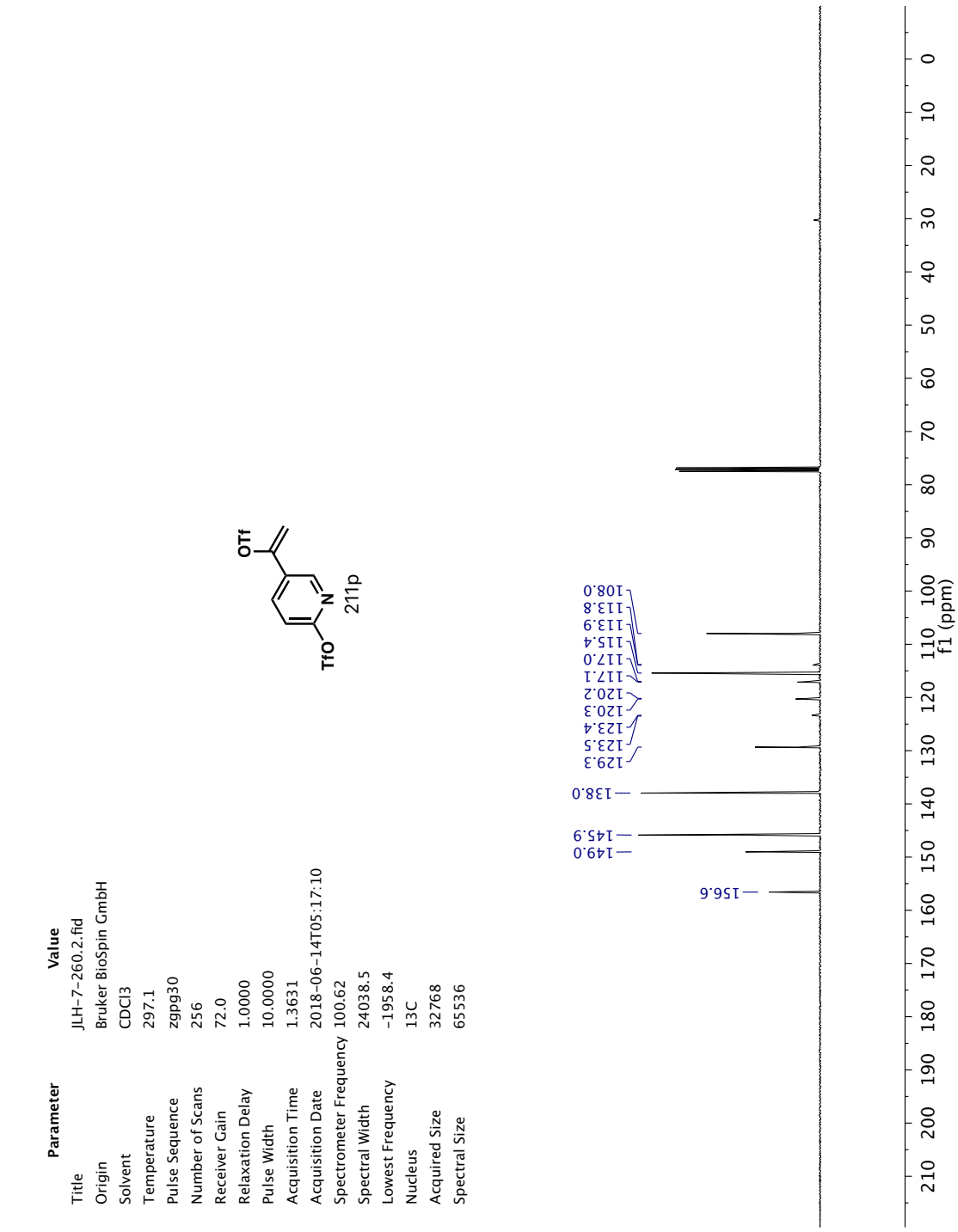

Parameter	Value
Title	JLH-7-260.2.fid
Origin	Bruker BioSpin GmbH
Solvent	CDCl3
Temperature	297.1
Pulse Sequence	zgpg30
Number of Scans	256
Receiver Gain	72.0
Relaxation Delay	1.0000
Pulse Width	10.0000
Acquisition Time	1.3631
Acquisition Date	2018-06-14T05:17:10
Spectrometer Frequency	100.62
Spectral Width	24038.5
Lowest Frequency	-1958.4
Nucleus	13C
Acquired Size	32768
Spectral Size	65536

Parameter	Value
Title	JLH-7-260-F
Origin	Varian
Solvent	cdcl3
Temperature	25.0
Pulse Sequence	s2pul
Number of Scans	16
Receiver Gain	30
Relaxation Delay	1.0000
Pulse Width	6.3333
Acquisition Time	0.9856
Acquisition Date	2018-06-14T01:00:14
Spectrometer Frequency	282.34
Spectral Width	64935.1
Lowest Frequency	-56431.2
Nucleus	19F
Acquired Size	64000
Spectral Size	131072

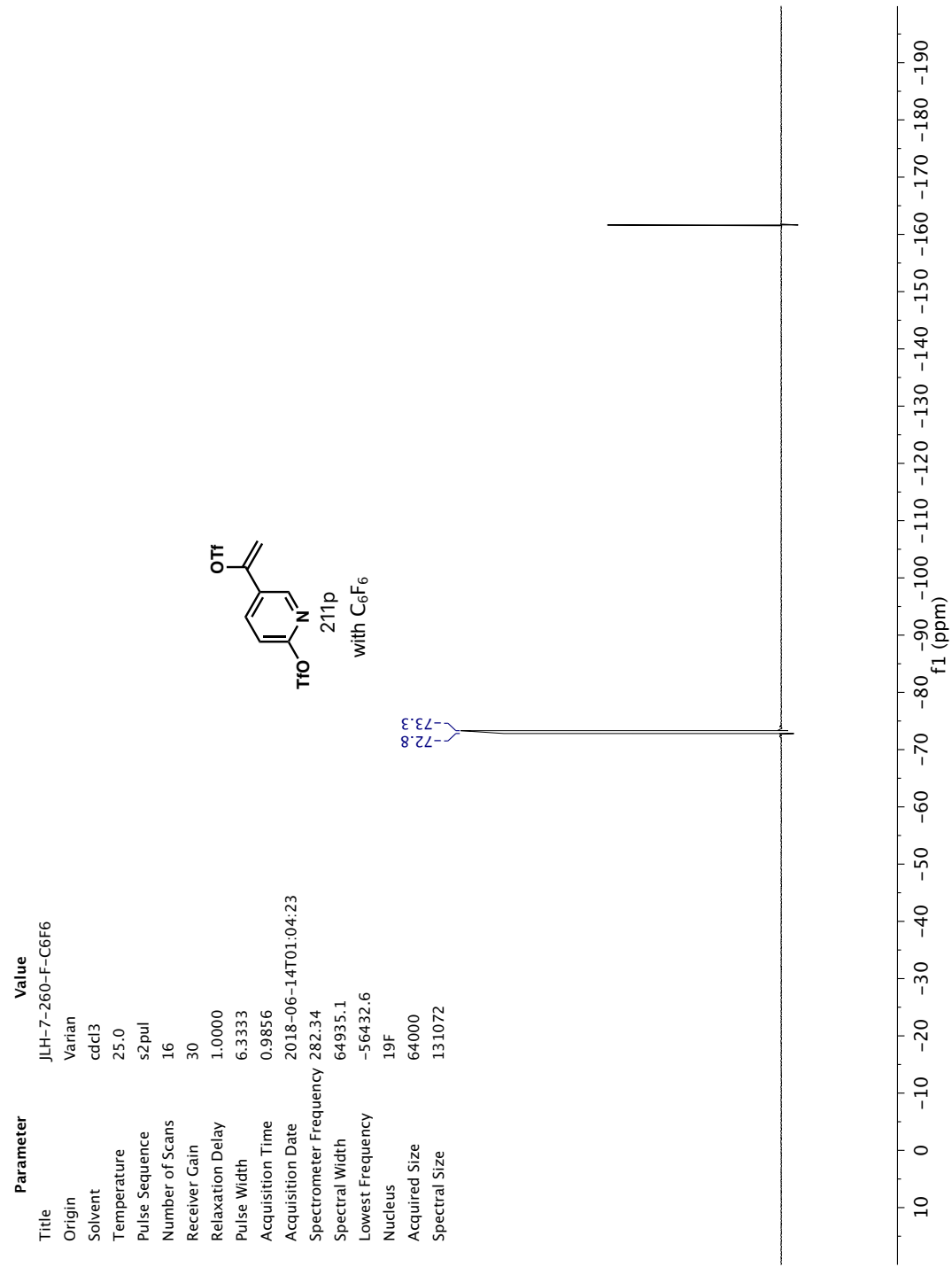
Parameter Value
Title JLH-7-260-F-C6F6
Origin Varian
Solvent cdcl3
Temperature 25.0
Pulse Sequence s2pul
Number of Scans 16
Receiver Gain 30
Relaxation Delay 1.0000
Pulse Width 6.3333
Acquisition Time 0.9856
Acquisition Date 2018-06-14T01:04:23
Spectrometer Frequency 282.34
Spectral Width 64935.1
Lowest Frequency -56432.6
Nucleus 19F
Acquired Size 64000
Spectral Size 131072
OTf
TfO
N
211p
with C6F6
-72.8
-73.3
10 0 -10 -20 -30 -40 -50 -60 -70 -80 -90 -100 -110 -120 -130 -140 -150 -160 -170 -180 -190
f1 (ppm)

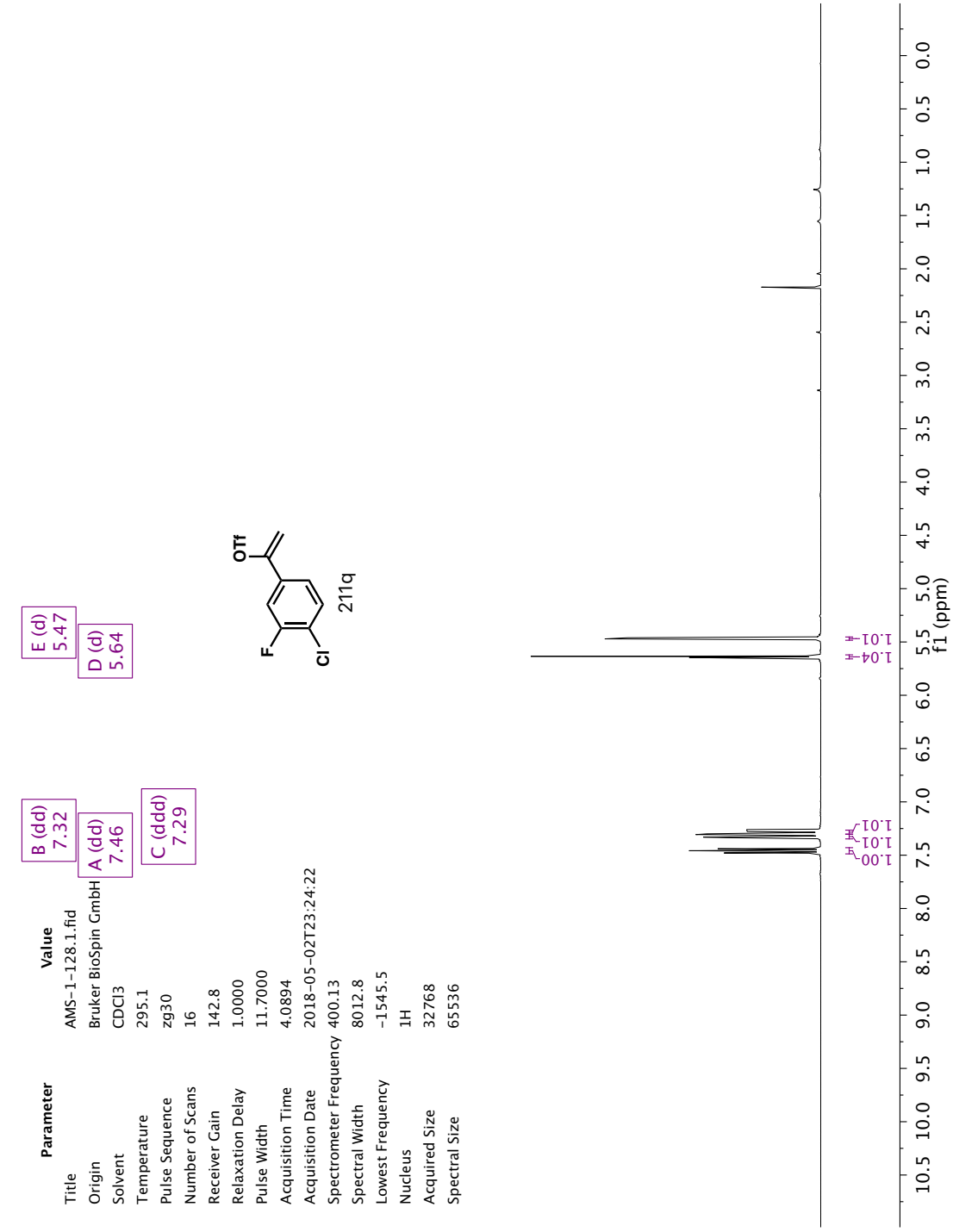

Parameter	Value
Title	AMS-1-128.1.fid
Origin	Bruker BioSpin GmbH
Solvent	CDCl3
Temperature	295.1
Pulse Sequence	zg30
Number of Scans	16
Receiver Gain	142.8
Relaxation Delay	1.0000
Pulse Width	11.7000
Acquisition Time	4.0894
Acquisition Date	2018-05-02T23:24:22
Spectrometer Frequency	400.13
Spectral Width	8012.8
Lowest Frequency	-1545.5
Nucleus	1H
Acquired Size	32768
Spectral Size	65536

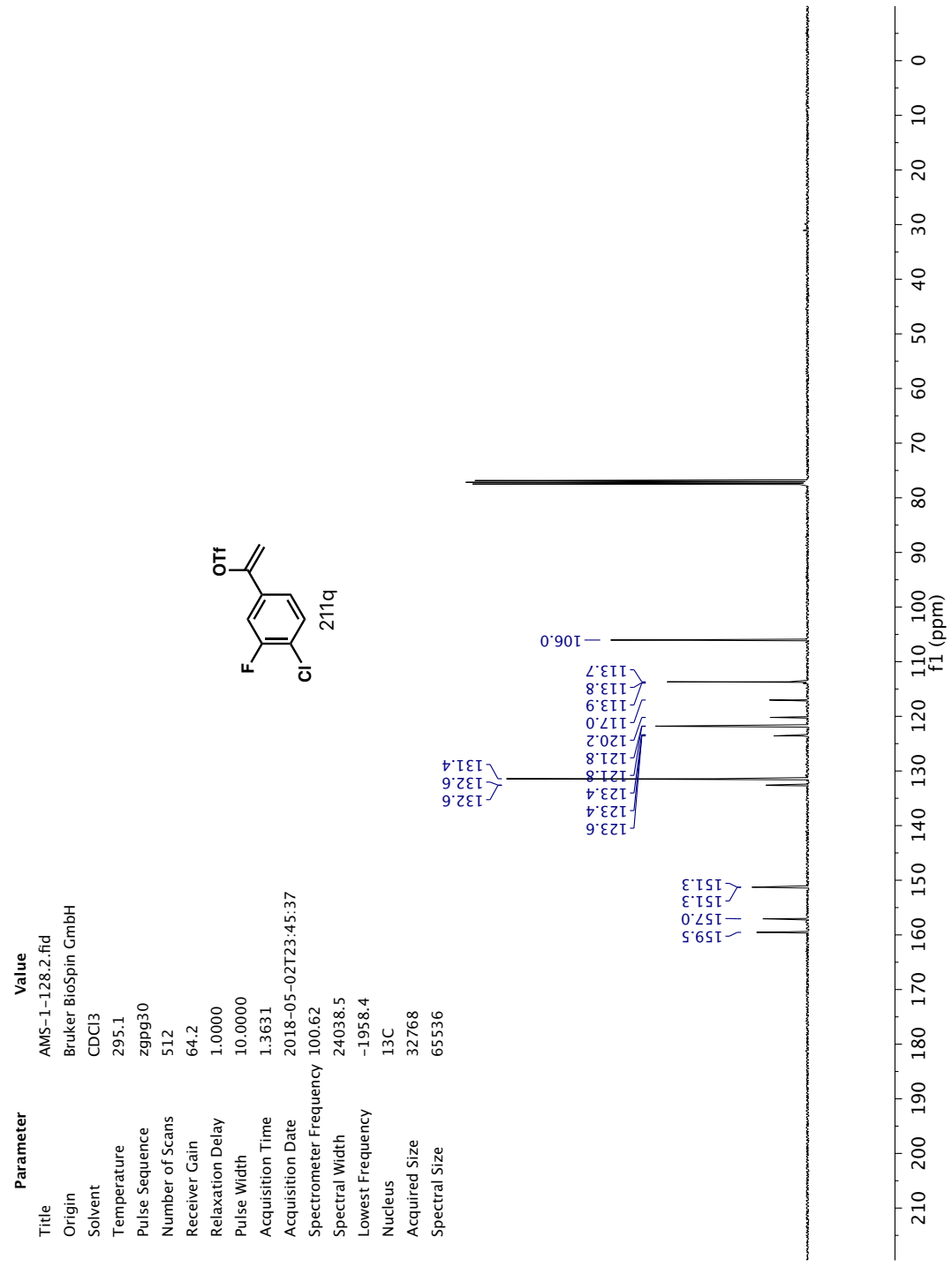

Parameter	Value
Title	AMS-1-128.2.fid
Origin	Bruker BioSpin GmbH
Solvent	CDCl3
Temperature	295.1
Pulse Sequence	zgpg30
Number of Scans	512
Receiver Gain	64.2
Relaxation Delay	1.0000
Pulse Width	10.0000
Acquisition Time	1.3631
Acquisition Date	2018-05-02T23:45:37
Spectrometer Frequency	100.62
Spectral Width	24038.5
Lowest Frequency	-1958.4
Nucleus	13C
Acquired Size	32768
Spectral Size	65536

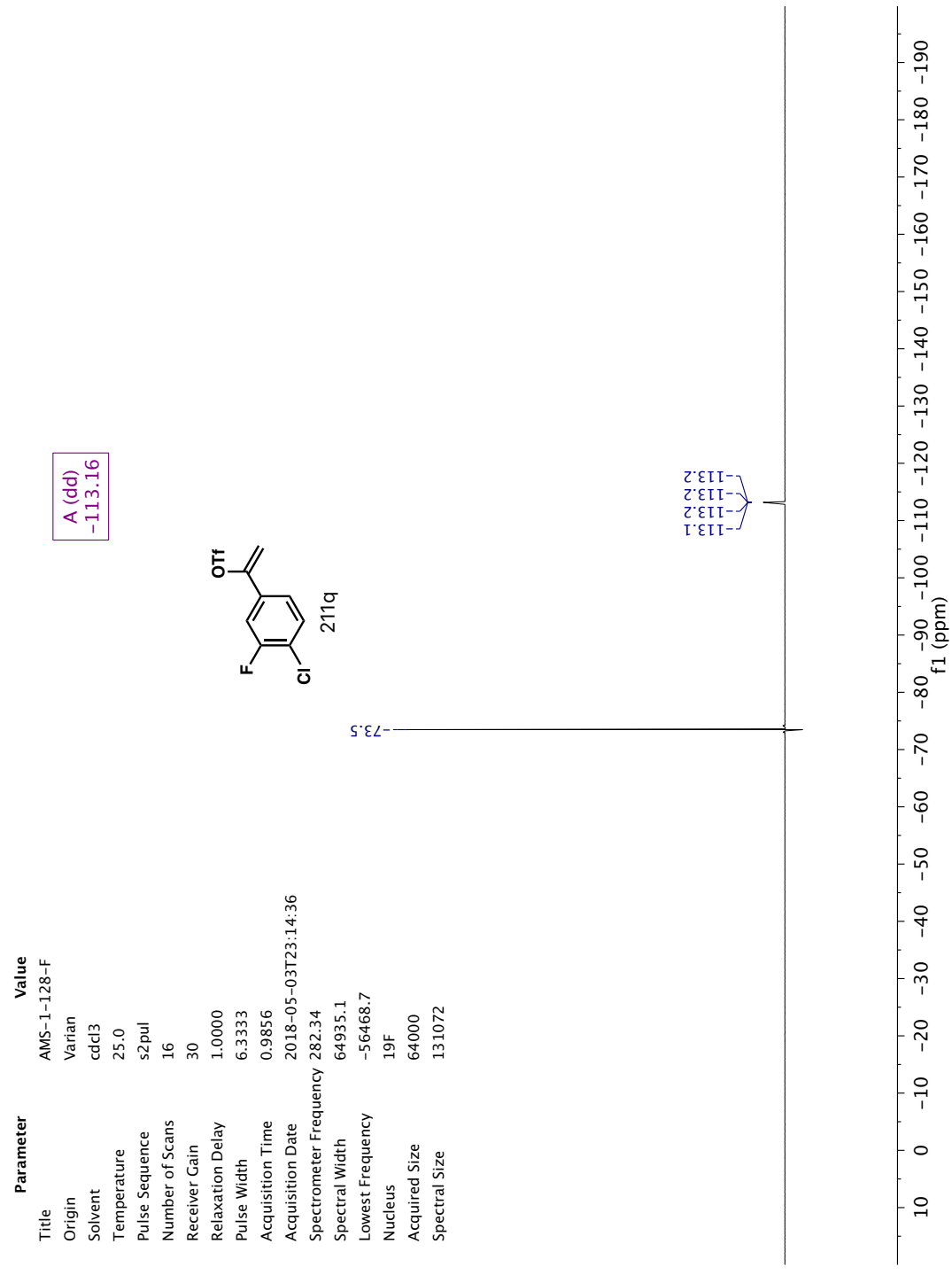

Parameter	Value
Title	AMS-1-128-F
Origin	Varian
Solvent	cdcl3
Temperature	25.0
Pulse Sequence	s2pul
Number of Scans	16
Receiver Gain	30
Relaxation Delay	1.0000
Pulse Width	6.3333
Acquisition Time	0.9856
Acquisition Date	2018-05-03T23:14:36
Spectrometer Frequency	282.34
Spectral Width	64935.1
Lowest Frequency	-56468.7
Nucleus	19F
Acquired Size	64000
Spectral Size	131072

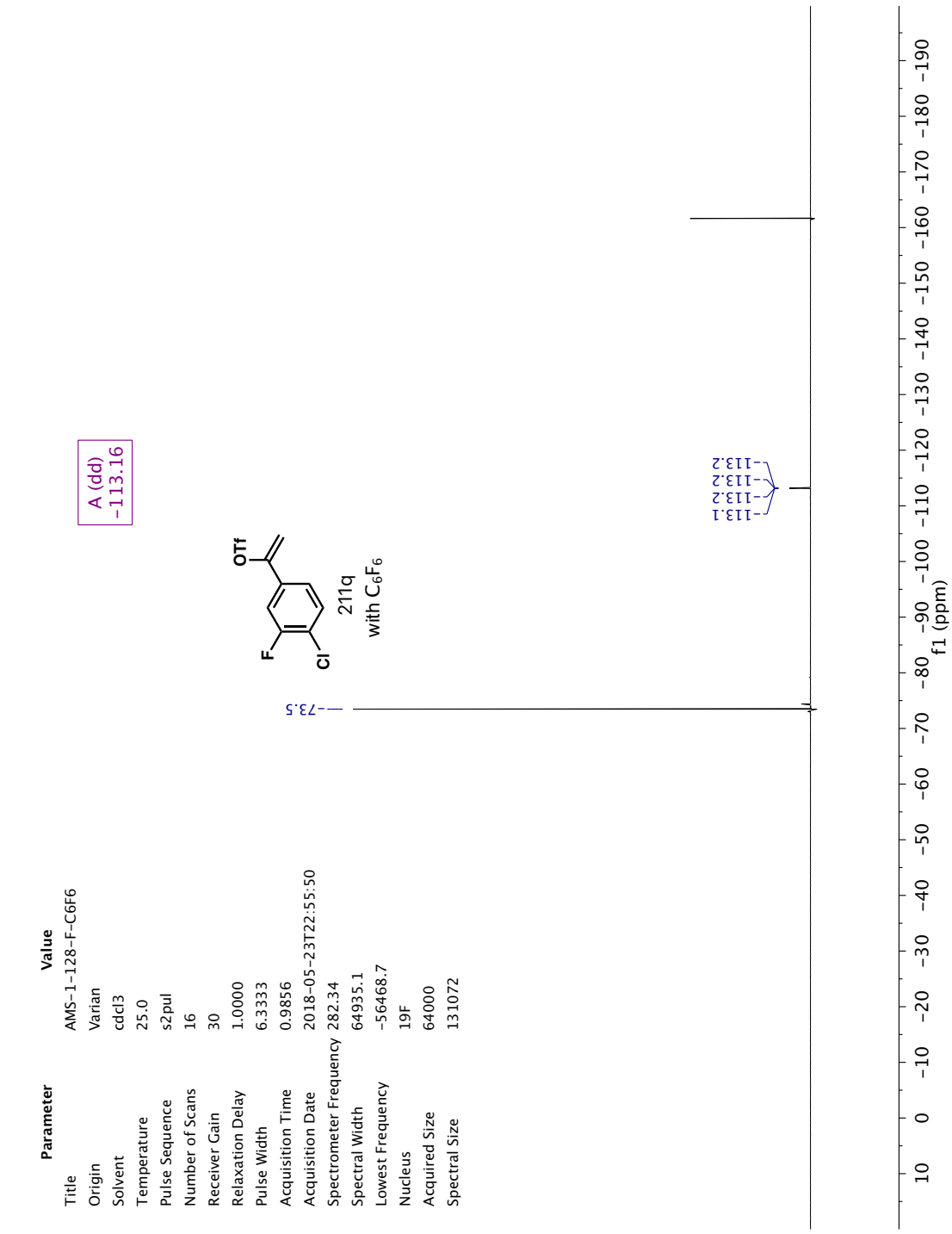

Parameter	Value
Title	AMS-1-128-F-C6F6
Origin	Varian
Solvent	cdcl3
Temperature	25.0
Pulse Sequence	s2pul
Number of Scans	16
Receiver Gain	30
Relaxation Delay	1.0000
Pulse Width	6.3333
Acquisition Time	0.9856
Acquisition Date	2018-05-23T22:55:50
Spectrometer Frequency	282.34
Spectral Width	64935.1
Lowest Frequency	-56468.7
Nucleus	19F
Acquired Size	64000
Spectral Size	131072

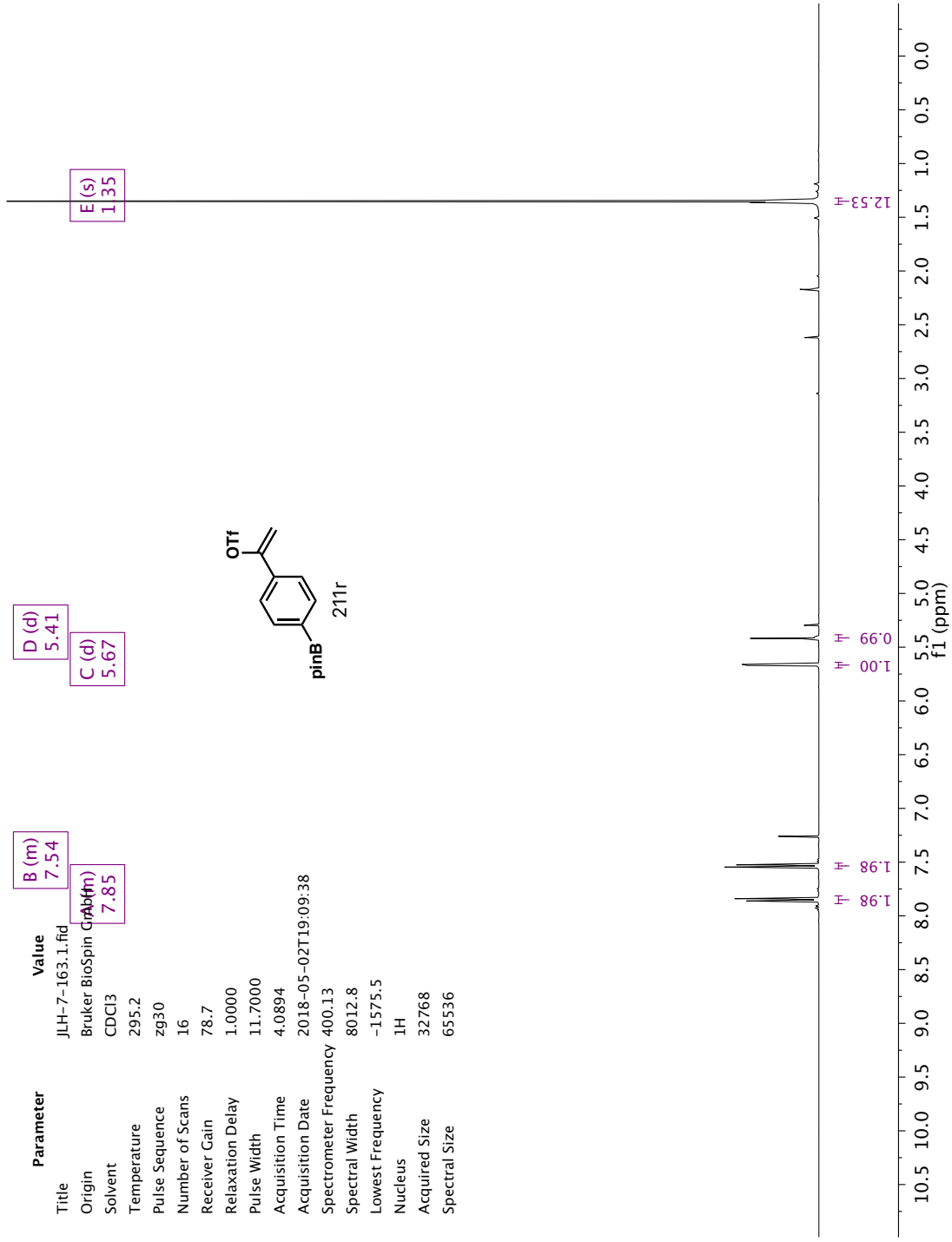
Parameter
Value
Title
JLH-7-163.1.fid
Origin
Bruker BioSpin GmbH
Solvent
CDCl3
Temperature
295.2
Pulse Sequence
zg30
Number of Scans
16
Receiver Gain
78.7
Relaxation Delay
1.0000
Pulse Width
11.7000
Acquisition Time
4.0894
Acquisition Date
2018-05-02T19:09:38
Spectrometer Frequency
400.13
Spectral Width
8012.8
Lowest Frequency
-1575.5
Nucleus
1H
Acquired Size
32768
Spectral Size
65536
B (m) 7.54
A (m) 7.85
D (d) 5.41
C (d) 5.67
E (s) 1.35
OTf
pinB
211r
12.53
1.98
1.98
1.00
0.99
f1 (ppm)

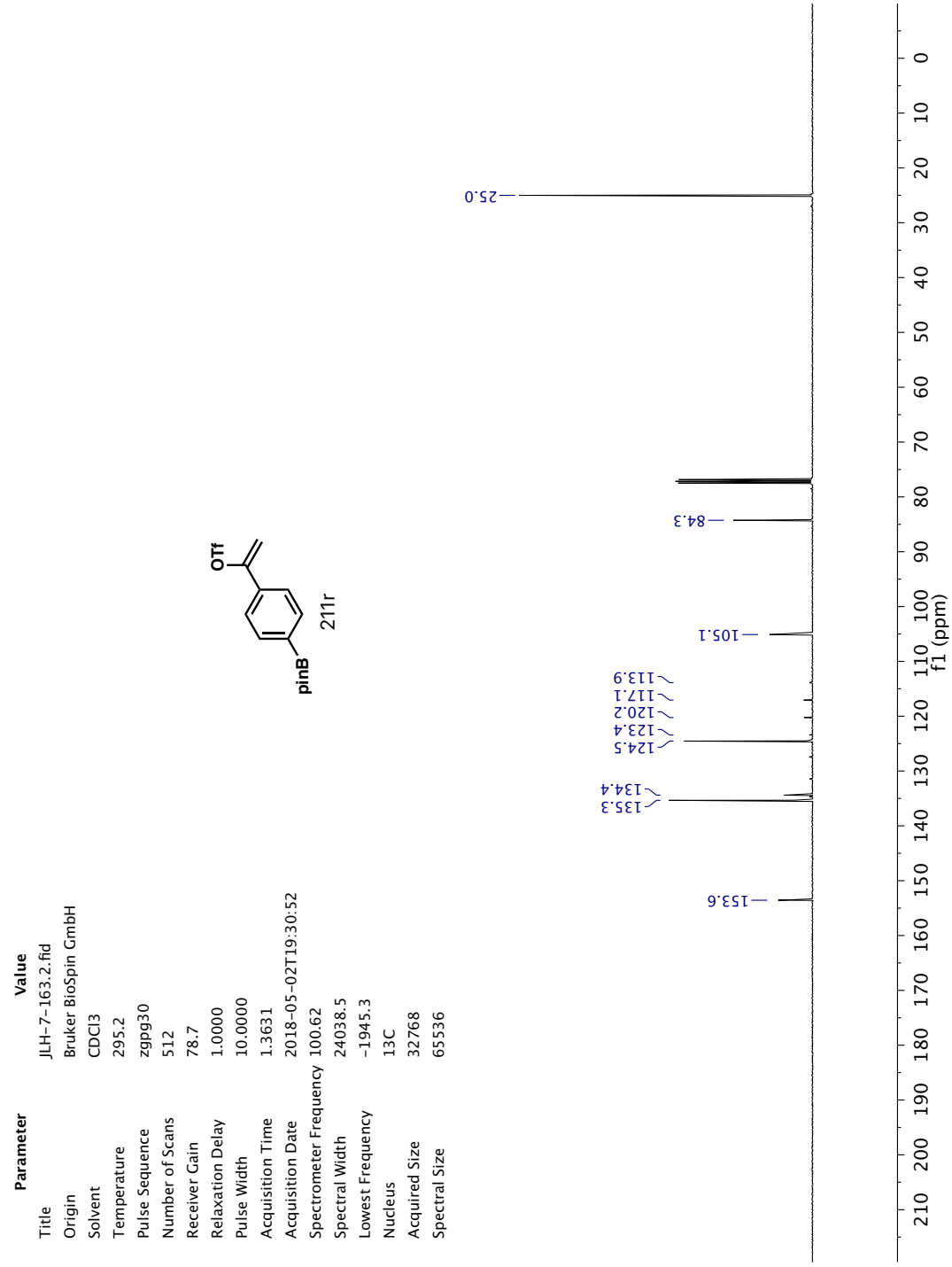

Parameter	Value
Title	JLH-7-163.2.fid
Origin	Bruker BioSpin GmbH
Solvent	CDCl3
Temperature	295.2
Pulse Sequence	zgpg30
Number of Scans	512
Receiver Gain	78.7
Relaxation Delay	1.0000
Pulse Width	10.0000
Acquisition Time	1.3631
Acquisition Date	2018-05-02T19:30:52
Spectrometer Frequency	100.62
Spectral Width	24038.5
Lowest Frequency	-1945.3
Nucleus	13C
Acquired Size	32768
Spectral Size	65536

Parameter	Value
Title	JLH-7-163-F
Origin	Varian
Solvent	cdcl3
Temperature	25.0
Pulse Sequence	s2pul
Number of Scans	16
Receiver Gain	30
Relaxation Delay	1.0000
Pulse Width	6.3333
Acquisition Time	0.9856
Acquisition Date	2018-05-03T23:10:20
Spectrometer Frequency	282.34
Spectral Width	64935.1
Lowest Frequency	-56468.7
Nucleus	19F
Acquired Size	64000
Spectral Size	131072

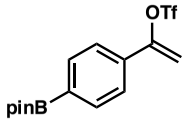

211r

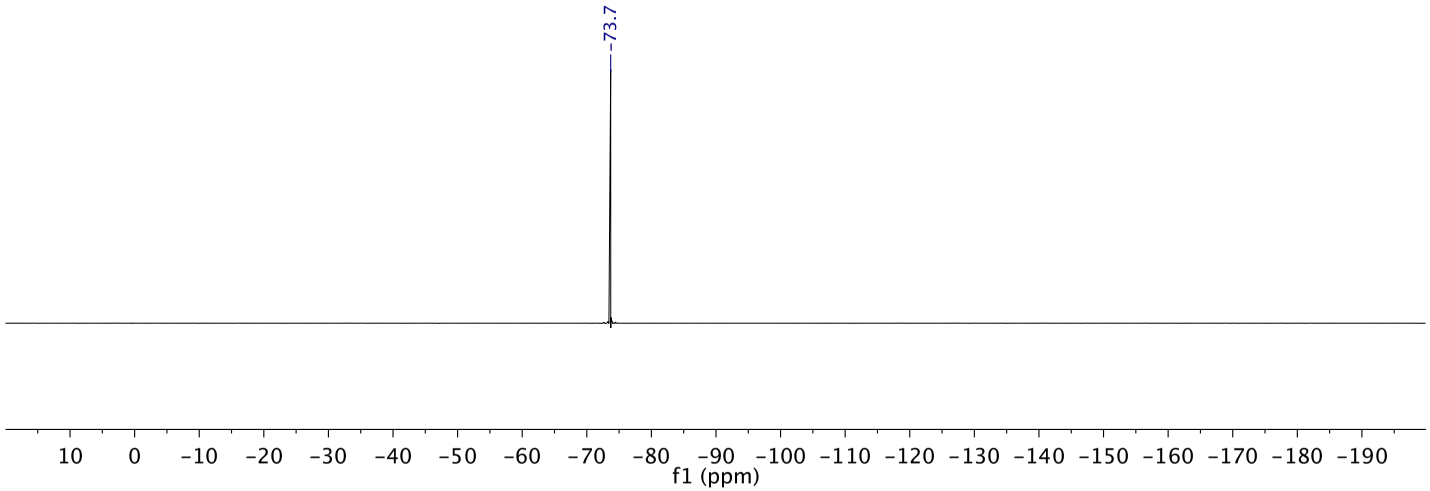

Parameter	Value
Title	JLH-7-163-F-C6F6
Origin	Varian
Solvent	cdcl3
Temperature	25.0
Pulse Sequence	s2pul
Number of Scans	16
Receiver Gain	30
Relaxation Delay	1.0000
Pulse Width	6.3333
Acquisition Time	0.9856
Acquisition Date	2018-05-23T22:23:44
Spectrometer Frequency	282.34
Spectral Width	64935.1
Lowest Frequency	-56434.5
Nucleus	19F
Acquired Size	64000
Spectral Size	131072

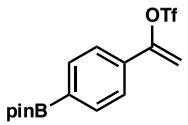

211r
with C_6F_6

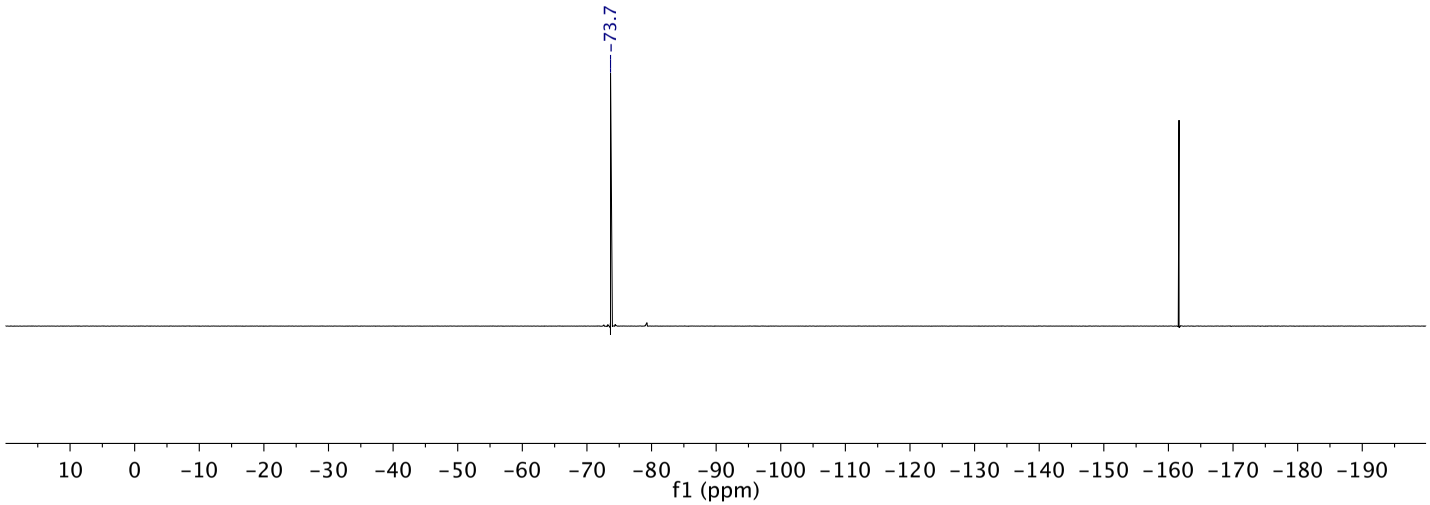

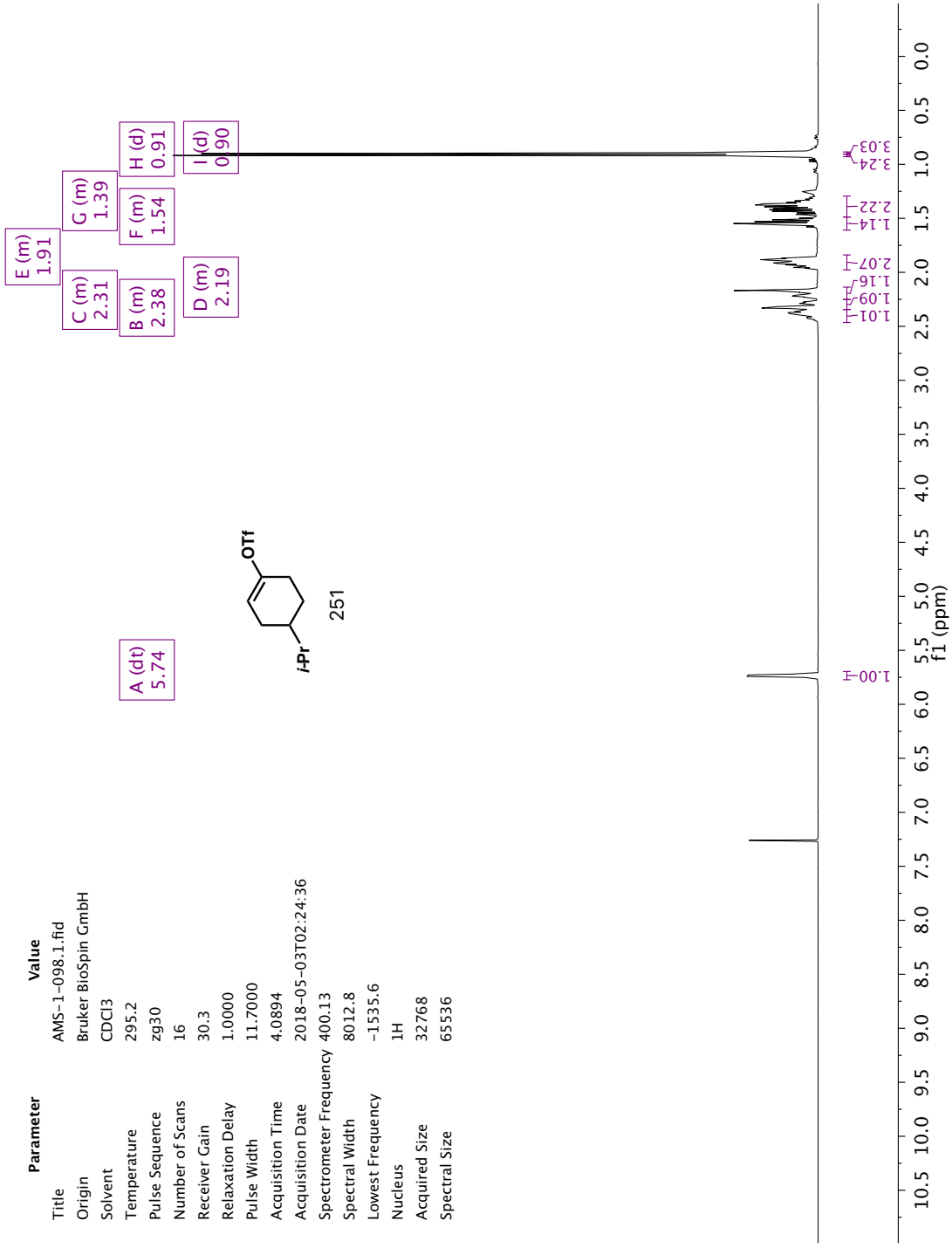

Parameter	Value
Title	AMS-1-098.1.fid
Origin	Bruker BioSpin GmbH
Solvent	CDCl3
Temperature	295.2
Pulse Sequence	zg30
Number of Scans	16
Receiver Gain	30.3
Relaxation Delay	1.0000
Pulse Width	11.7000
Acquisition Time	4.0894
Acquisition Date	2018-05-03T02:24:36
Spectrometer Frequency	400.13
Spectral Width	8012.8
Lowest Frequency	-1535.6
Nucleus	1H
Acquired Size	32768
Spectral Size	65536

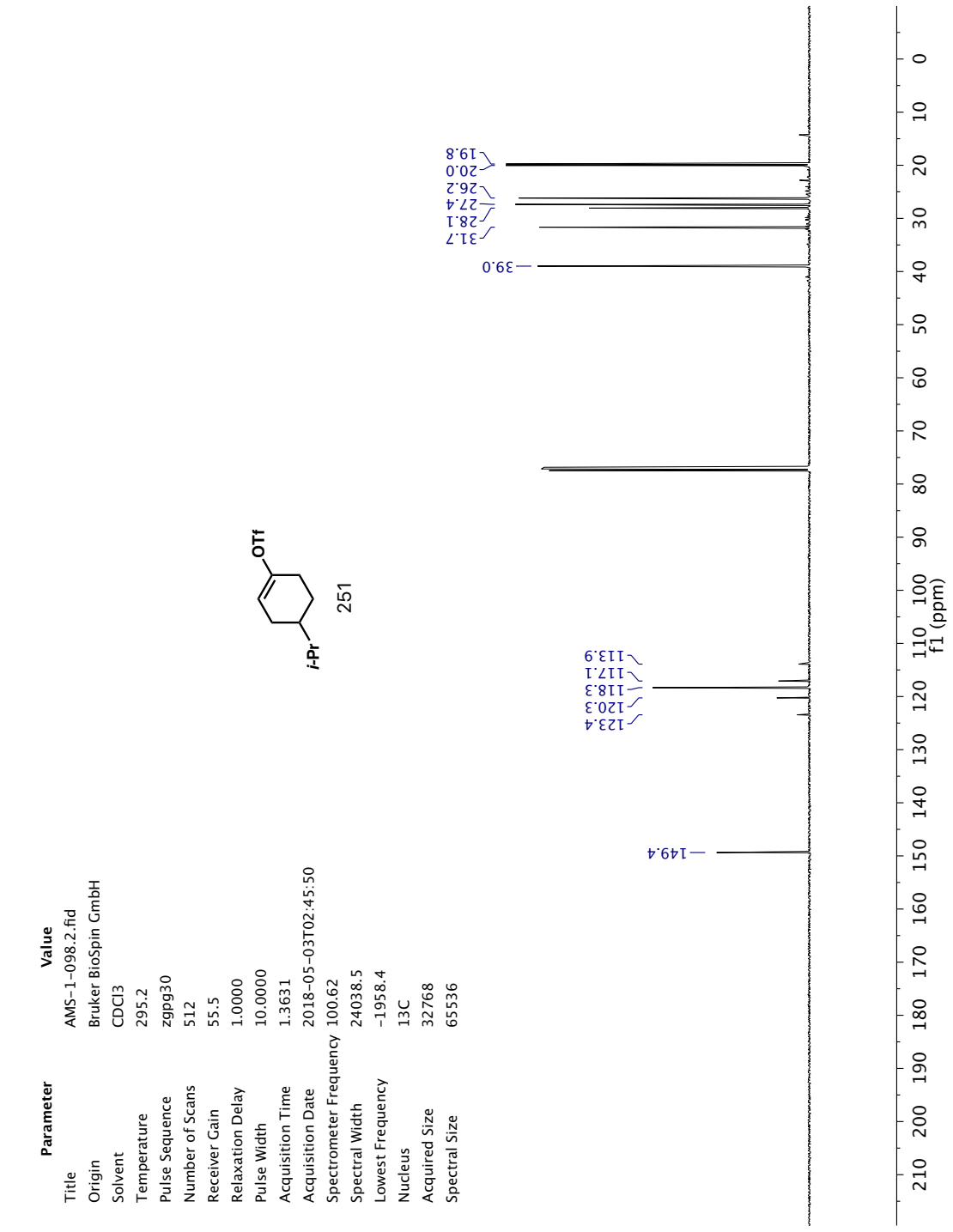
Parameter Value
Title AMS-1-098.2.fid
Origin Bruker BioSpin GmbH
Solvent CDCl3
Temperature 295.2
Pulse Sequence zgpg30
Number of Scans 512
Receiver Gain 55.5
Relaxation Delay 1.0000
Pulse Width 10.0000
Acquisition Time 1.3631
Acquisition Date 2018-05-03T02:45:50
Spectrometer Frequency 100.62
Spectral Width 24038.5
Lowest Frequency -1958.4
Nucleus 13C
Acquired Size 32768
Spectral Size 65536
OTf
i-Pr
251
149.4
123.4
120.3
118.3
117.1
113.9
39.0
31.7
28.1
27.4
26.2
20.0
19.8
f1 (ppm)

Parameter	Value
Title	AMS-1-098-F
Origin	Varian
Solvent	cdcl3
Temperature	25.0
Pulse Sequence	s2pul
Number of Scans	16
Receiver Gain	30
Relaxation Delay	1.0000
Pulse Width	6.3333
Acquisition Time	0.9856
Acquisition Date	2018-05-03T22:47:15
Spectrometer Frequency	282.34
Spectral Width	64935.1
Lowest Frequency	-56468.7
Nucleus	19F
Acquired Size	64000
Spectral Size	131072

251

-73.9

10 0 -10 -20 -30 -40 -50 -60 -70 -80 -90 -100 -110 -120 -130 -140 -150 -160 -170 -180 -190
f1 (ppm)

Parameter	Value
Title	AMS-1-098-F-C6F6
Origin	Varian
Solvent	cdcl3
Temperature	25.0
Pulse Sequence	s2pul
Number of Scans	16
Receiver Gain	30
Relaxation Delay	1.0000
Pulse Width	6.3333
Acquisition Time	0.9856
Acquisition Date	2018-05-23T22:46:47
Spectrometer Frequency	282.34
Spectral Width	64935.1
Lowest Frequency	-56468.7
Nucleus	19F
Acquired Size	64000
Spectral Size	131072

251
with C_6F_6

-73.9

10 0 -10 -20 -30 -40 -50 -60 -70 -80 -90 -100 -110 -120 -130 -140 -150 -160 -170 -180 -190
f1 (ppm)

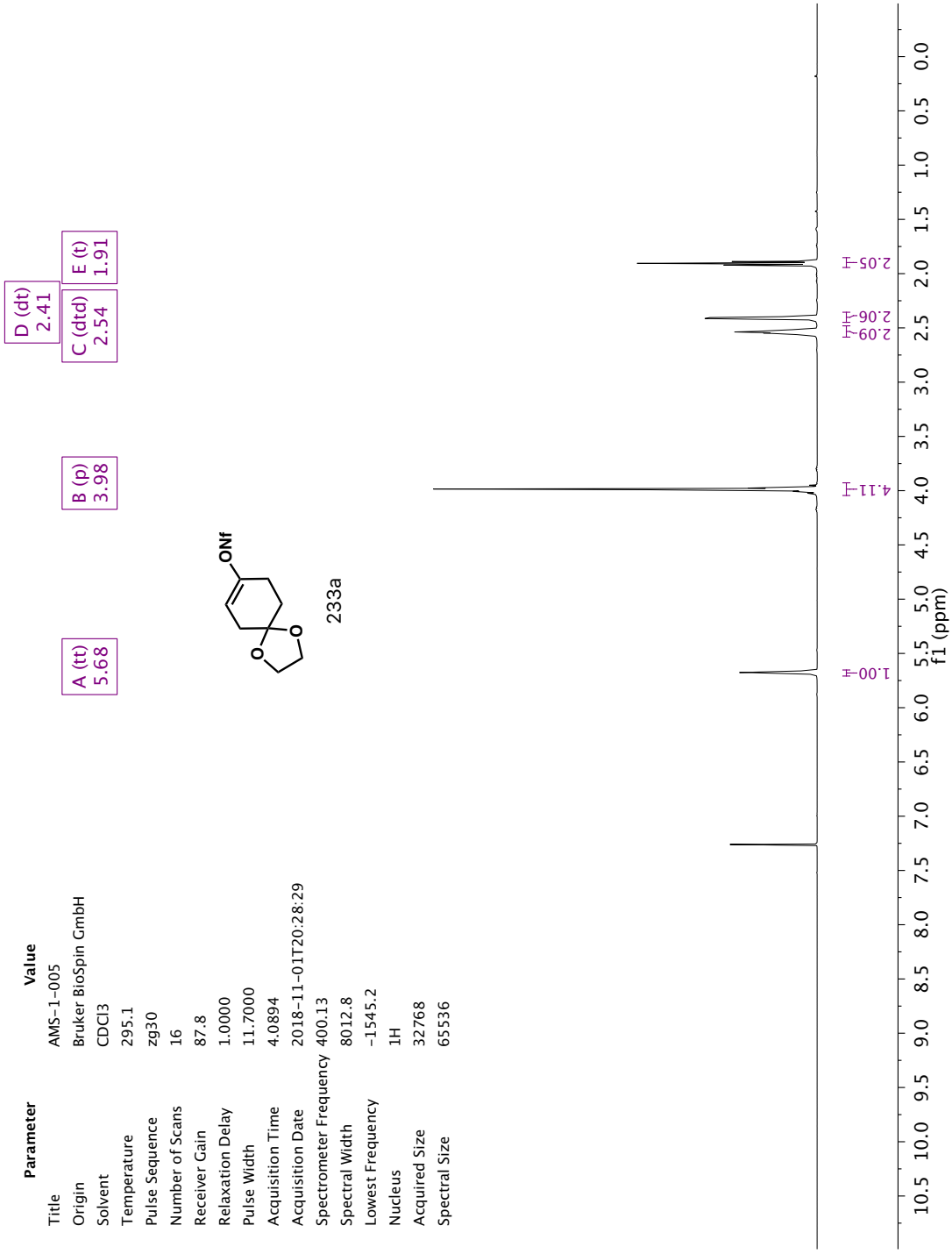
Parameter Value
Title AMS-1-005
Origin Bruker BioSpin GmbH
Solvent CDCl3
Temperature 295.1
Pulse Sequence zg30
Number of Scans 16
Receiver Gain 87.8
Relaxation Delay 1.0000
Pulse Width 11.7000
Acquisition Time 4.0894
Acquisition Date 2018-11-01T20:28:29
Spectrometer Frequency 400.13
Spectral Width 8012.8
Lowest Frequency -1545.2
Nucleus 1H
Acquired Size 32768
Spectral Size 65536
A (tt) 5.68
B (p) 3.98
C (dtd) 2.54
D (dt) 2.41
E (t) 1.91
ONf
233a
1.00
4.11
2.09
2.06
2.05
f1 (ppm)

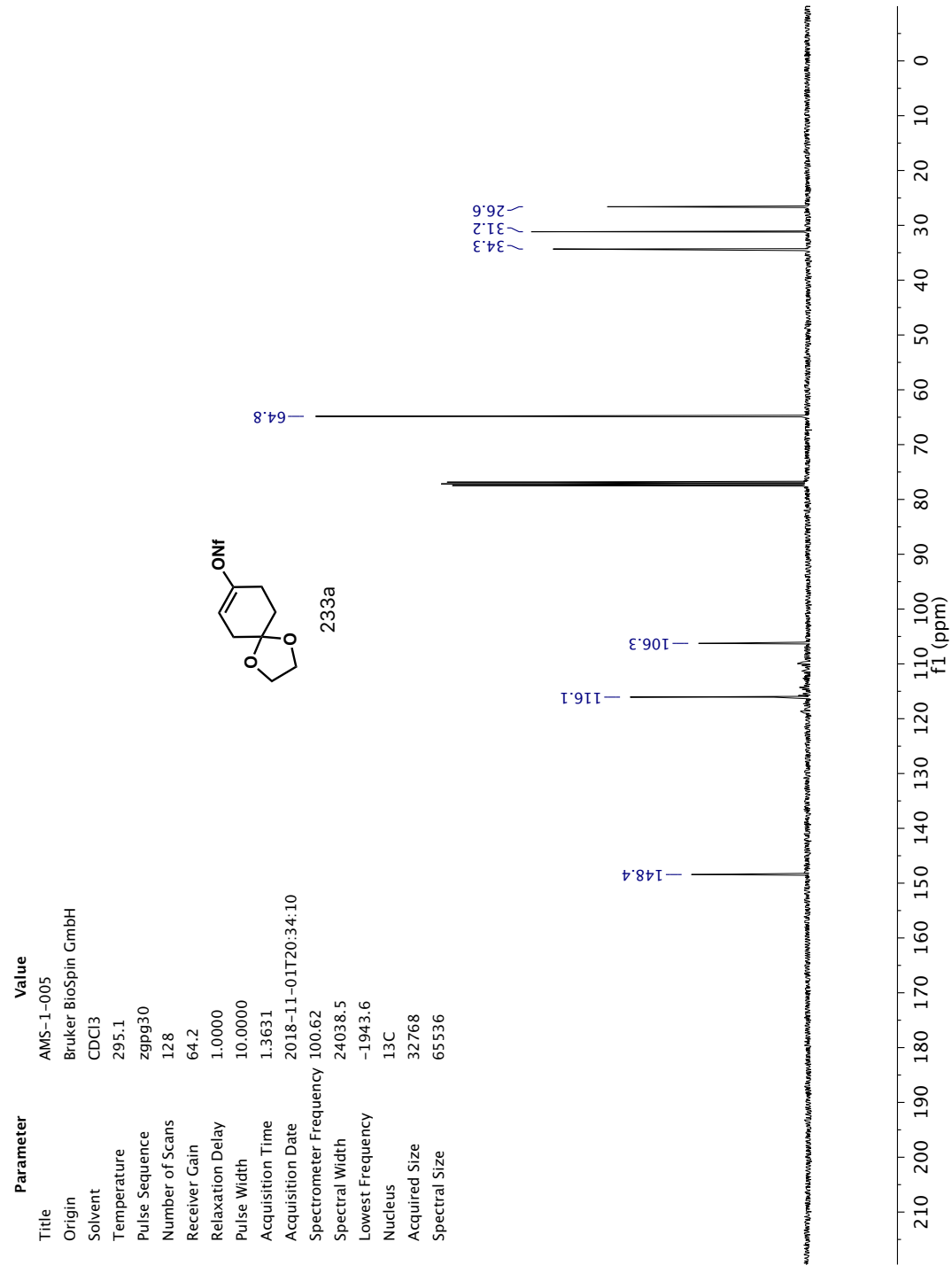
Parameter Value
Title AMS-1-005
Origin Bruker BioSpin GmbH
Solvent CDCl3
Temperature 295.1
Pulse Sequence zgpg30
Number of Scans 128
Receiver Gain 64.2
Relaxation Delay 1.0000
Pulse Width 10.0000
Acquisition Time 1.3631
Acquisition Date 2018-11-01T20:34:10
Spectrometer Frequency 100.62
Spectral Width 24038.5
Lowest Frequency -1943.6
Nucleus 13C
Acquired Size 32768
Spectral Size 65536
ONf
233a
64.8
34.3
31.2
26.6
106.3
116.1
148.4
f1 (ppm)

Parameter	Value
Title	AMS-1-005
Origin	Varian
Solvent	cdcl3
Temperature	25.0
Pulse Sequence	s2pul
Number of Scans	16
Receiver Gain	30
Relaxation Delay	1.0000
Pulse Width	6.3333
Acquisition Time	0.9856
Acquisition Date	2018-11-01T21:17:44
Spectrometer Frequency	282.34
Spectral Width	64935.1
Lowest Frequency	-56468.7
Nucleus	19F
Acquired Size	64000
Spectral Size	131072

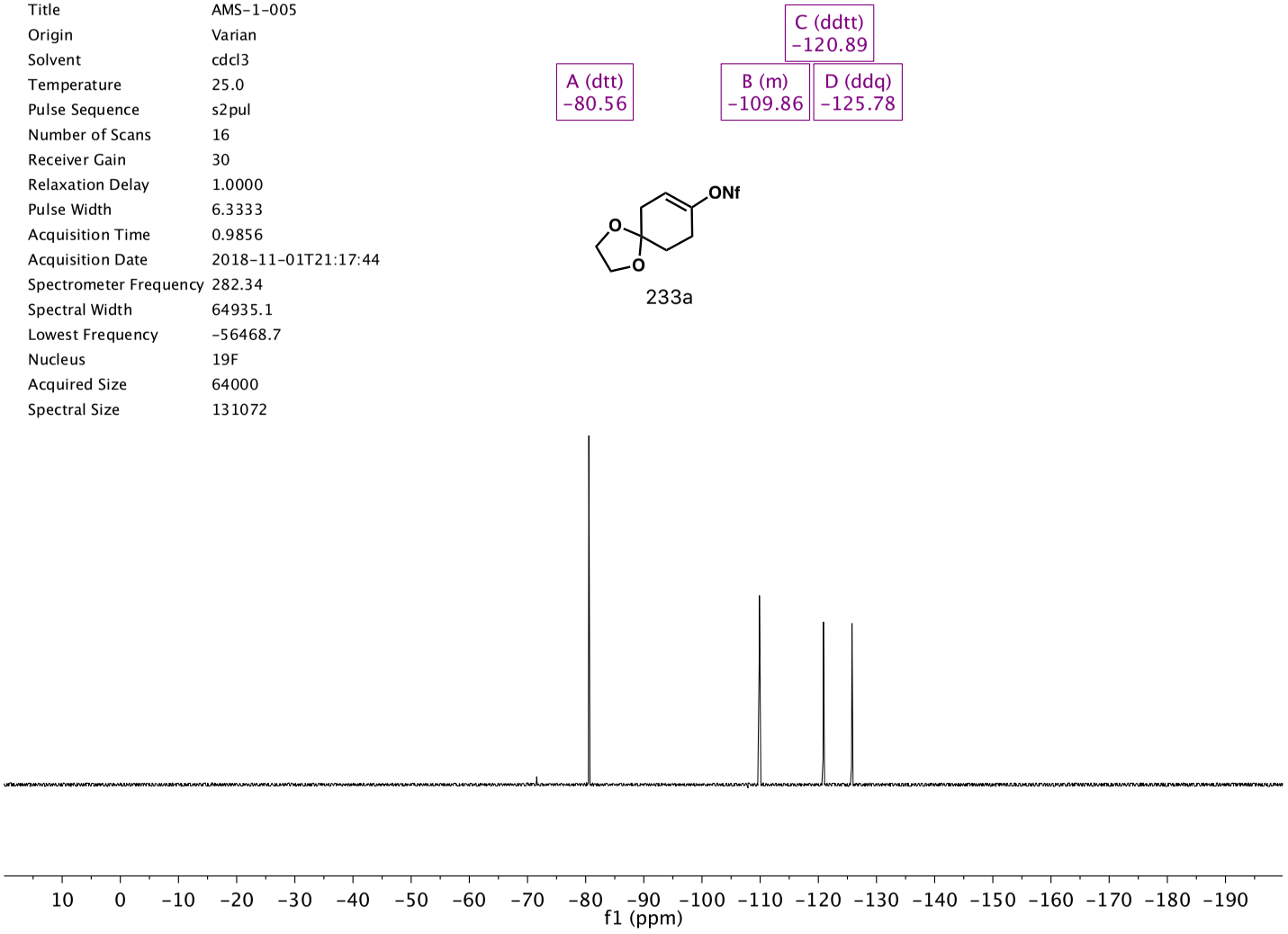

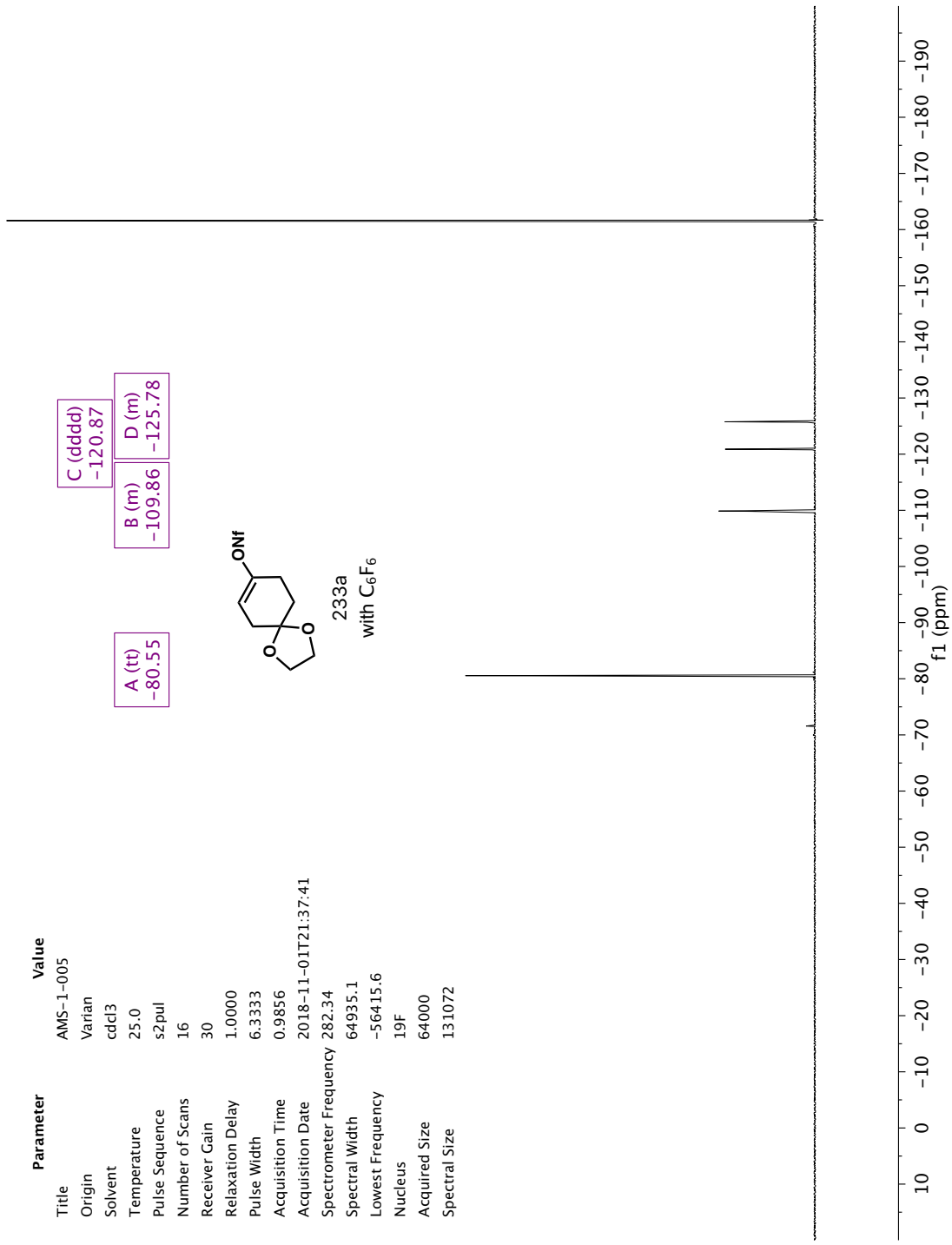

Parameter	Value
Title	AMS-1-005
Origin	Varian
Solvent	cdcl3
Temperature	25.0
Pulse Sequence	s2pul
Number of Scans	16
Receiver Gain	30
Relaxation Delay	1.0000
Pulse Width	6.3333
Acquisition Time	0.9856
Acquisition Date	2018-11-01T21:37:41
Spectrometer Frequency	282.34
Spectral Width	64935.1
Lowest Frequency	-56415.6
Nucleus	19F
Acquired Size	64000
Spectral Size	131072

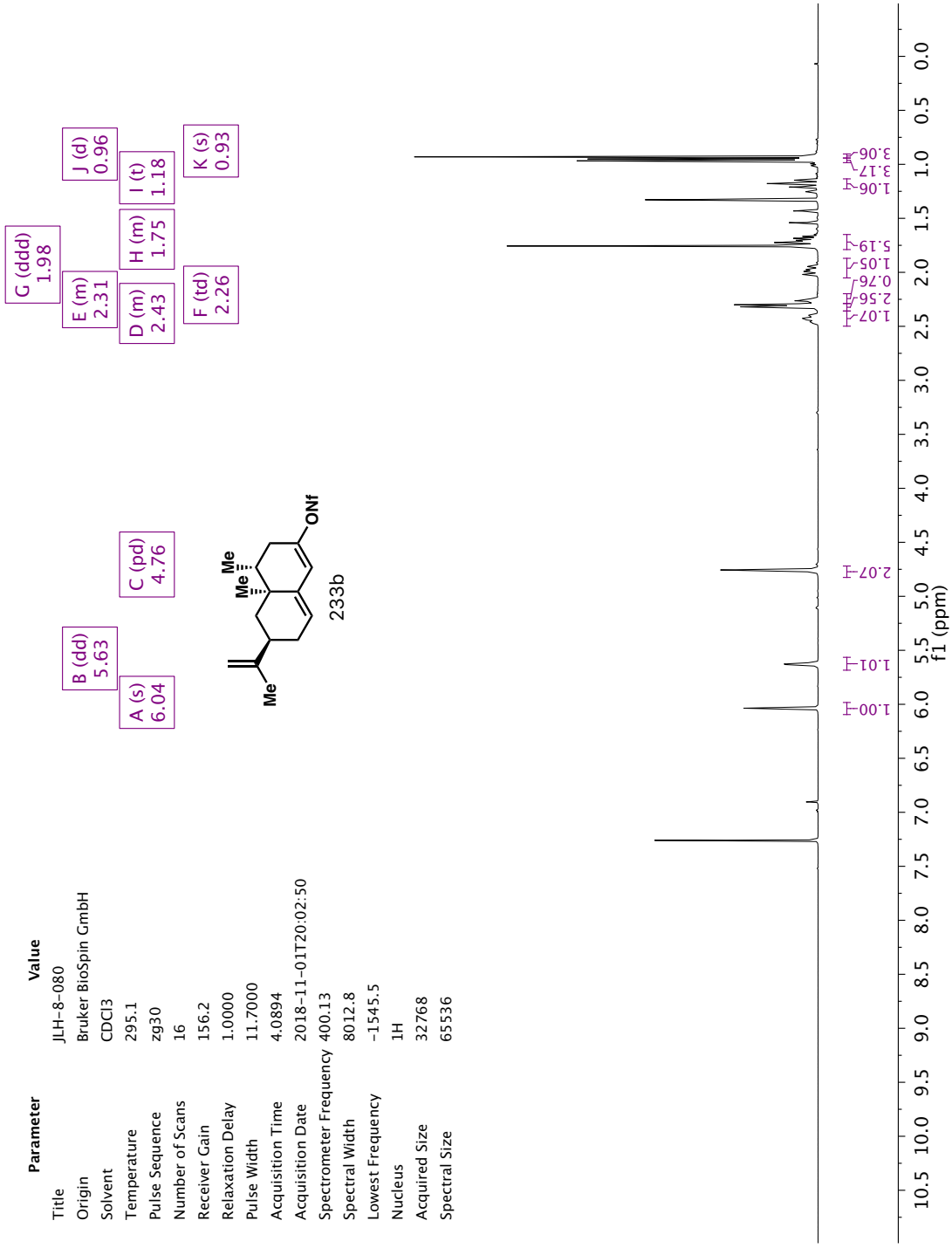

Parameter	Value
Title	JLH-8-080
Origin	Bruker BioSpin GmbH
Solvent	CDCl3
Temperature	295.1
Pulse Sequence	zg30
Number of Scans	16
Receiver Gain	156.2
Relaxation Delay	1.0000
Pulse Width	11.7000
Acquisition Time	4.0894
Acquisition Date	2018-11-01T20:02:50
Spectrometer Frequency	400.13
Spectral Width	8012.8
Lowest Frequency	-1545.5
Nucleus	1H
Acquired Size	32768
Spectral Size	65536

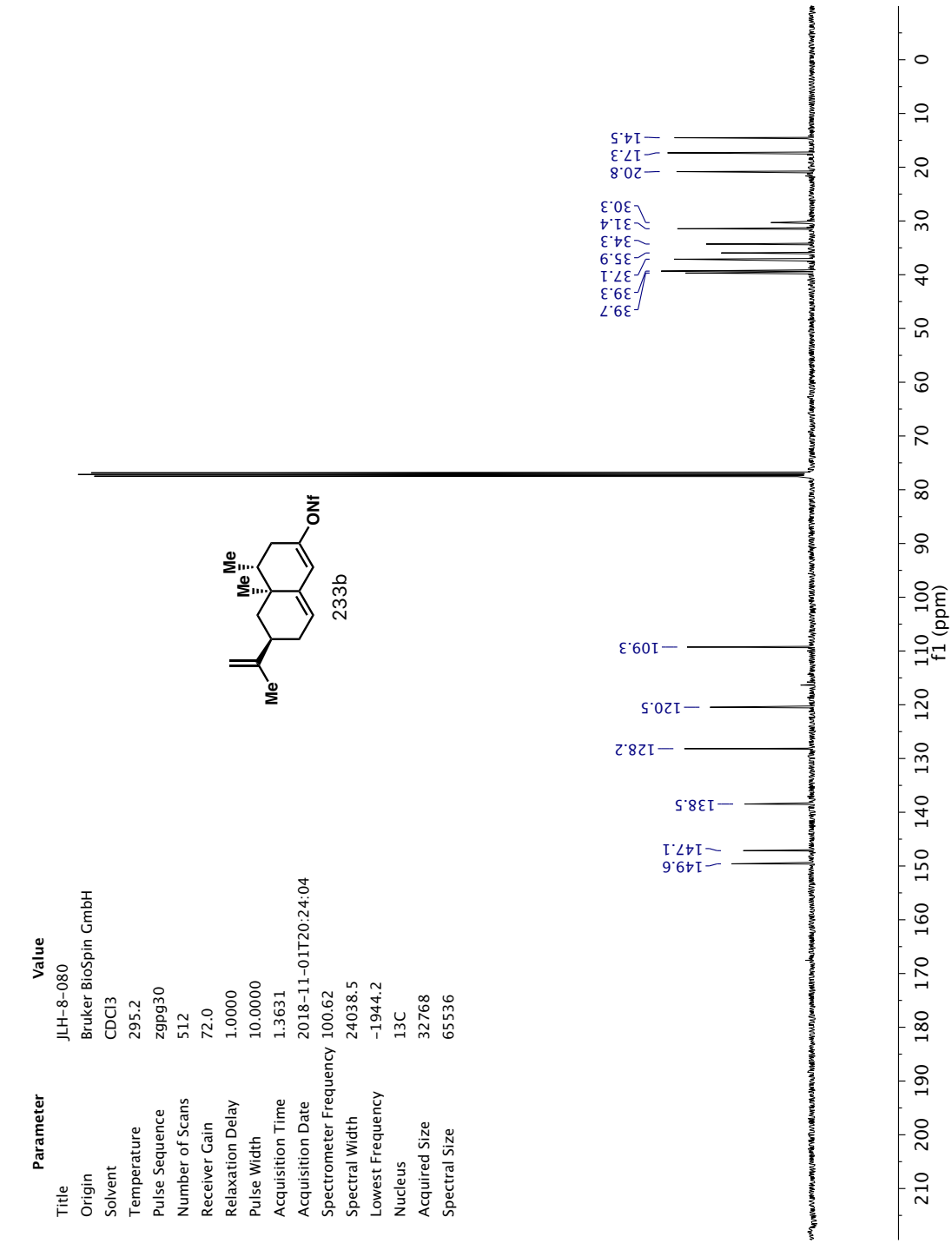
Parameter Value
Title JLH-8-080
Origin Bruker BioSpin GmbH
Solvent CDCl3
Temperature 295.2
Pulse Sequence zgpg30
Number of Scans 512
Receiver Gain 72.0
Relaxation Delay 1.0000
Pulse Width 10.0000
Acquisition Time 1.3631
Acquisition Date 2018-11-01T20:24:04
Spectrometer Frequency 100.62
Spectral Width 24038.5
Lowest Frequency -1944.2
Nucleus 13C
Acquired Size 32768
Spectral Size 65536
Me
Me
Me
ONf
233b
149.6
147.1
138.5
128.2
120.5
109.3
39.7
39.3
37.1
35.9
34.3
31.4
30.3
20.8
17.3
14.5
f1 (ppm)

Parameter	Value
Title	JLH-8-080
Origin	Varian
Solvent	cdcl3
Temperature	25.0
Pulse Sequence	s2pul
Number of Scans	16
Receiver Gain	30
Relaxation Delay	1.0000
Pulse Width	6.3333
Acquisition Time	0.9856
Acquisition Date	2018-11-01T21:12:54
Spectrometer Frequency	282.34
Spectral Width	64935.1
Lowest Frequency	-56468.7
Nucleus	19F
Acquired Size	64000
Spectral Size	131072

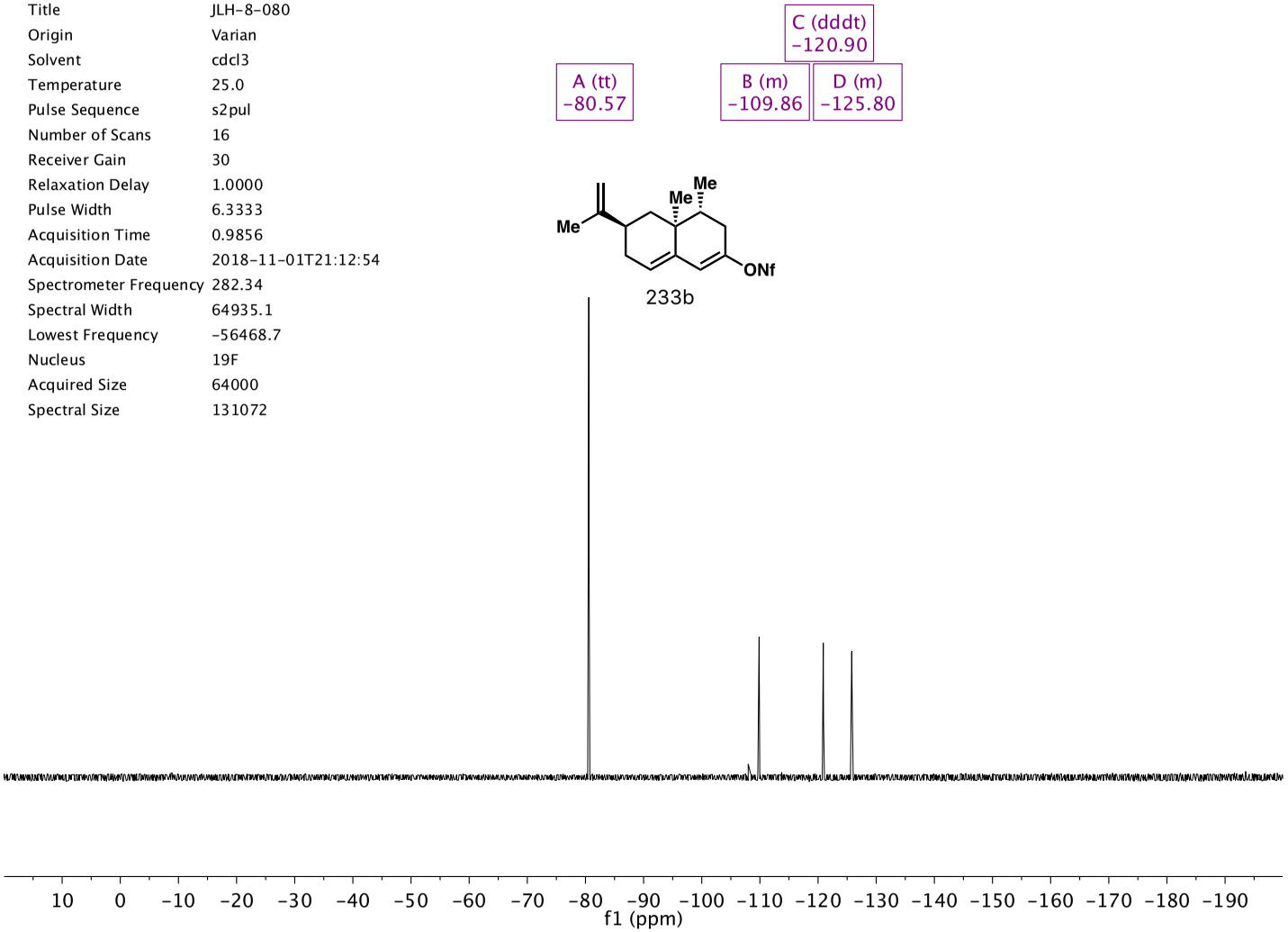

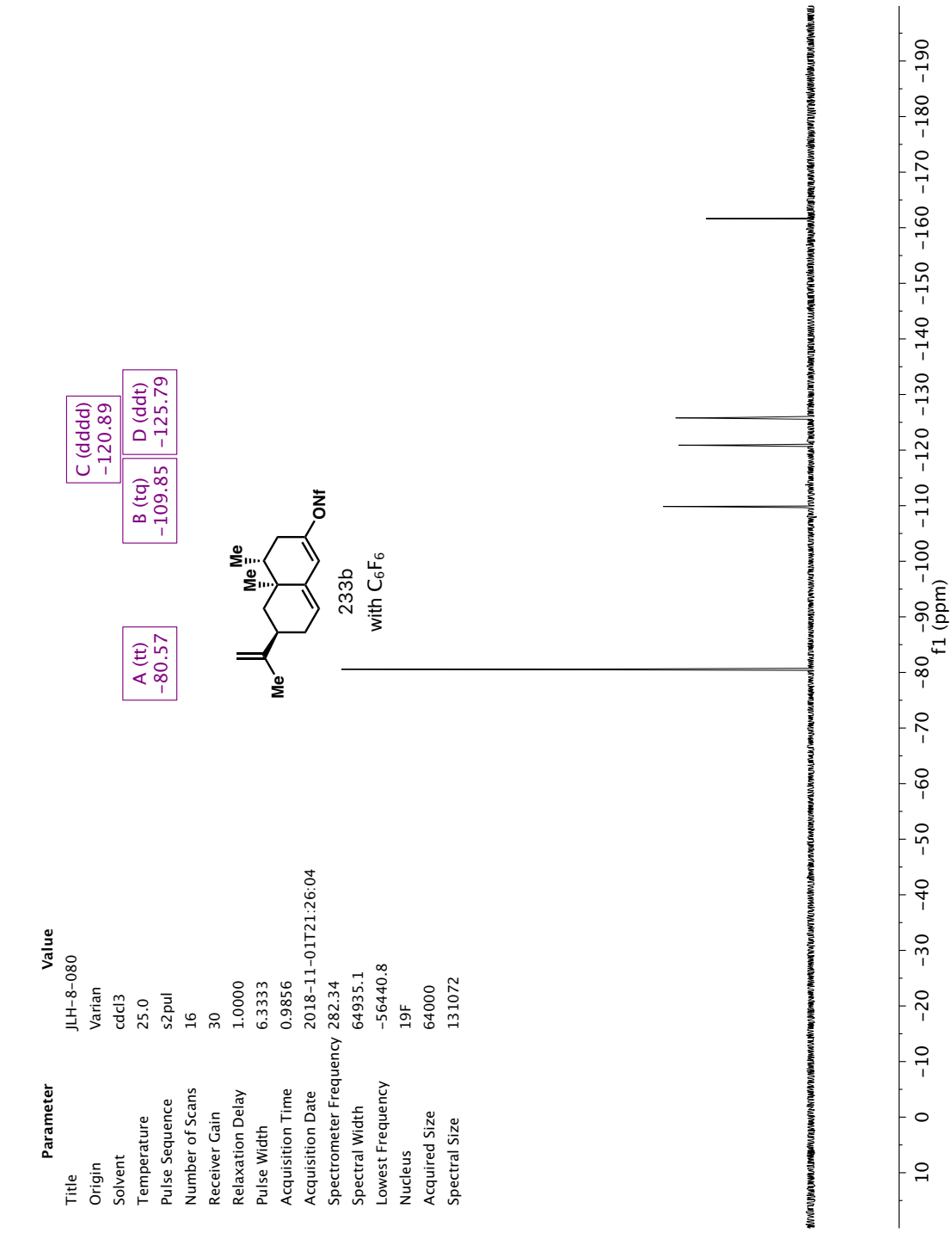

Parameter	Value
Title	JLH-8-080
Origin	Varian
Solvent	cdcl3
Temperature	25.0
Pulse Sequence	s2pul
Number of Scans	16
Receiver Gain	30
Relaxation Delay	1.0000
Pulse Width	6.3333
Acquisition Time	0.9856
Acquisition Date	2018-11-01T21:26:04
Spectrometer Frequency	282.34
Spectral Width	64935.1
Lowest Frequency	-56440.8
Nucleus	19F
Acquired Size	64000
Spectral Size	131072

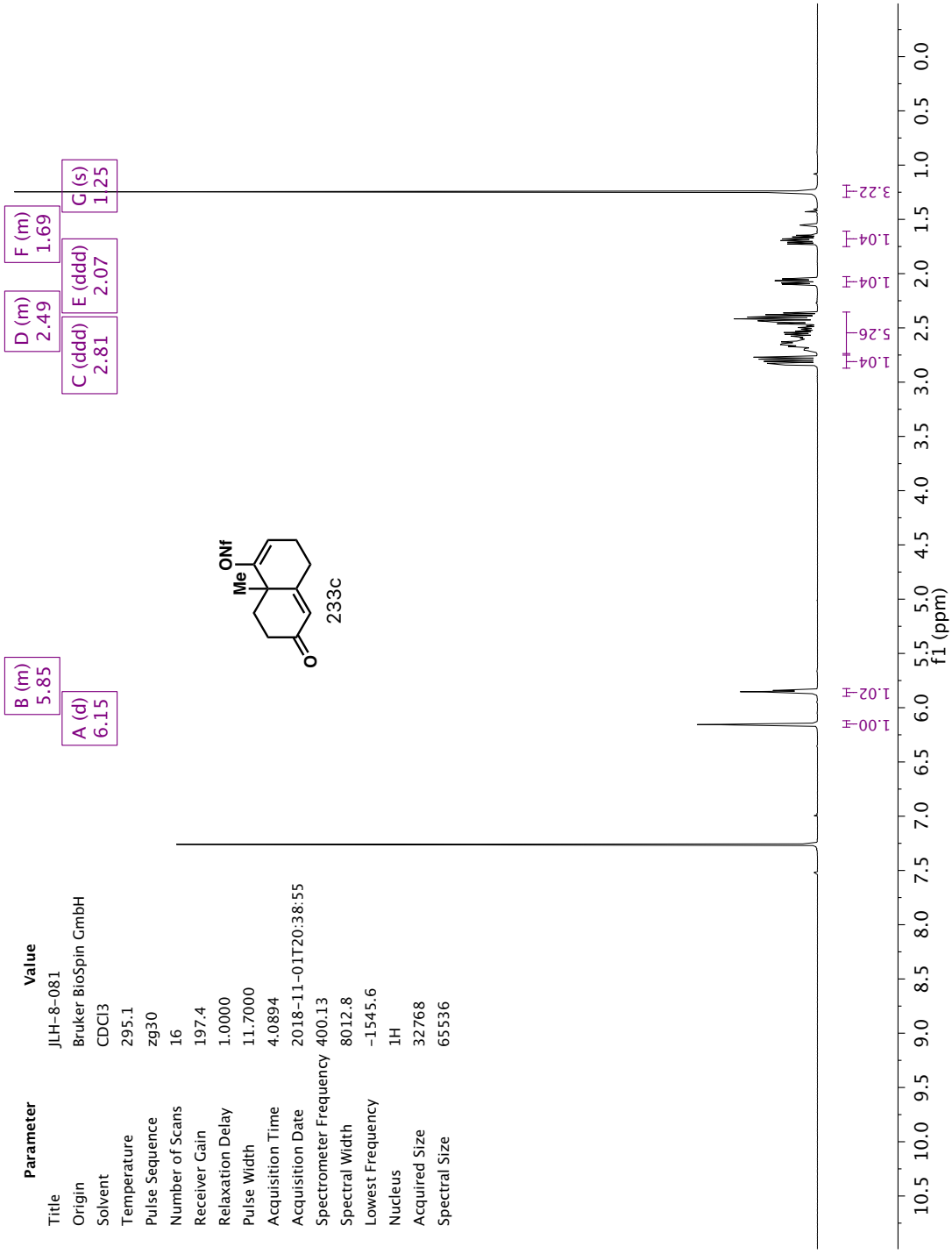

Parameter	Value
Title	JLH-8-081
Origin	Bruker BioSpin GmbH
Solvent	CDCl3
Temperature	295.1
Pulse Sequence	zg30
Number of Scans	16
Receiver Gain	197.4
Relaxation Delay	1.0000
Pulse Width	11.7000
Acquisition Time	4.0894
Acquisition Date	2018-11-01T20:38:55
Spectrometer Frequency	400.13
Spectral Width	8012.8
Lowest Frequency	-1545.6
Nucleus	1H
Acquired Size	32768
Spectral Size	65536

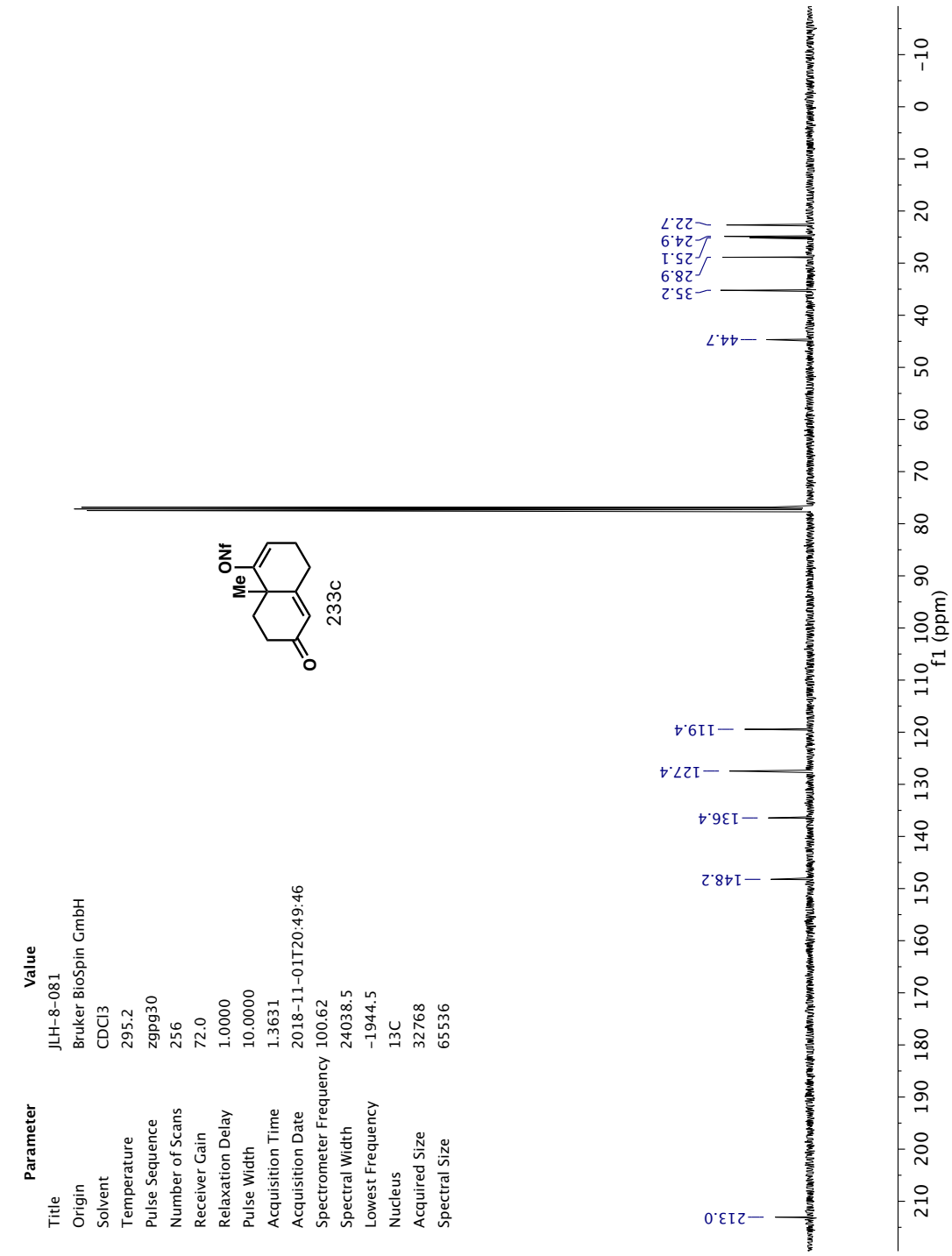
Parameter Value
Title JLH-8-081
Origin Bruker BioSpin GmbH
Solvent CDCl3
Temperature 295.2
Pulse Sequence zgpg30
Number of Scans 256
Receiver Gain 72.0
Relaxation Delay 1.0000
Pulse Width 10.0000
Acquisition Time 1.3631
Acquisition Date 2018-11-01T20:49:46
Spectrometer Frequency 100.62
Spectral Width 24038.5
Lowest Frequency -1944.5
Nucleus 13C
Acquired Size 32768
Spectral Size 65536
ONf
Me
O
233c
213.0
148.2
136.4
127.4
119.4
44.7
35.2
28.9
25.1
24.9
22.7
f1 (ppm)

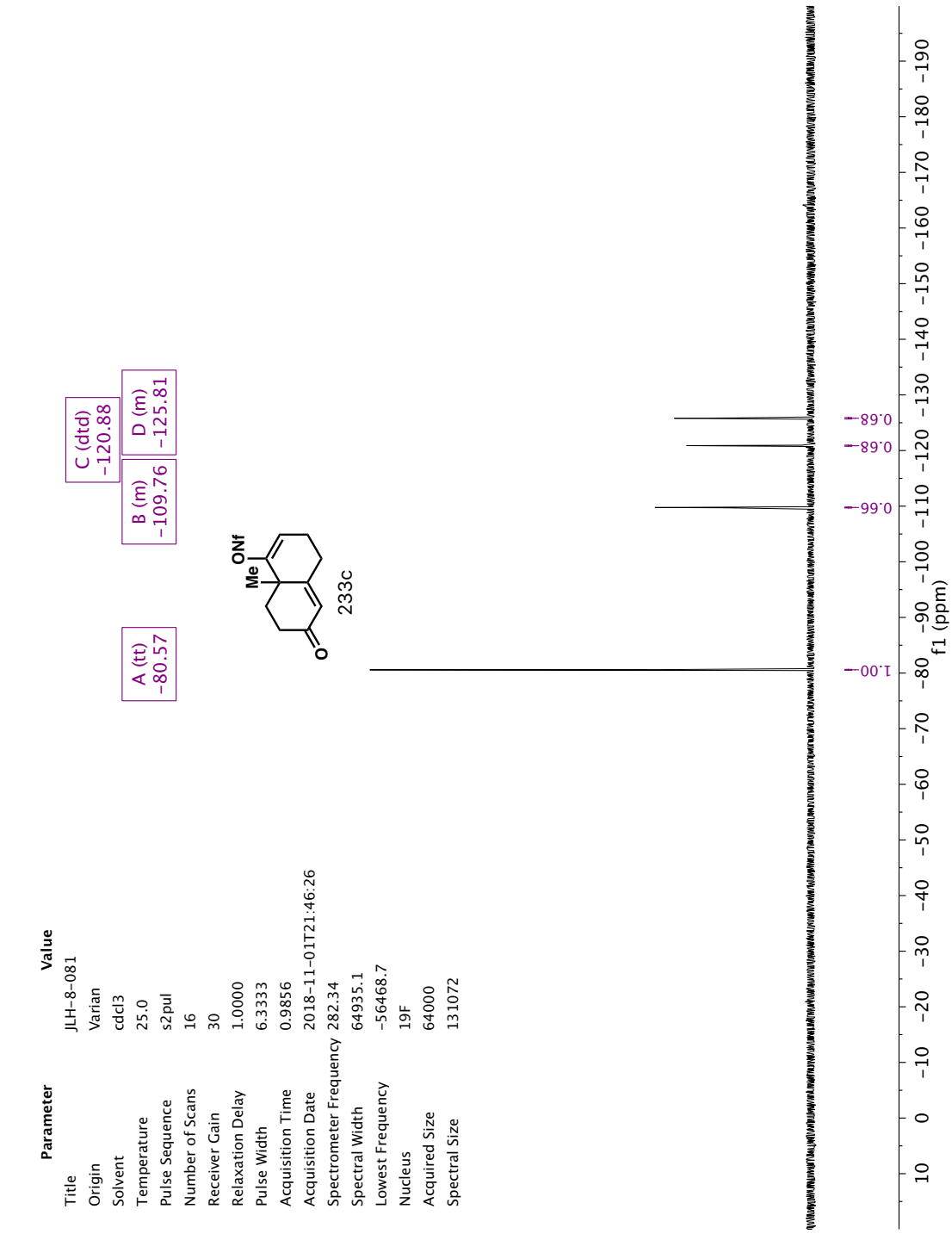

Parameter	Value
Title	JLH-8-081
Origin	Varian
Solvent	cdcl3
Temperature	25.0
Pulse Sequence	s2pul
Number of Scans	16
Receiver Gain	30
Relaxation Delay	1.0000
Pulse Width	6.3333
Acquisition Time	0.9856
Acquisition Date	2018-11-01T21:46:26
Spectrometer Frequency	282.34
Spectral Width	64935.1
Lowest Frequency	-56468.7
Nucleus	19F
Acquired Size	64000
Spectral Size	131072

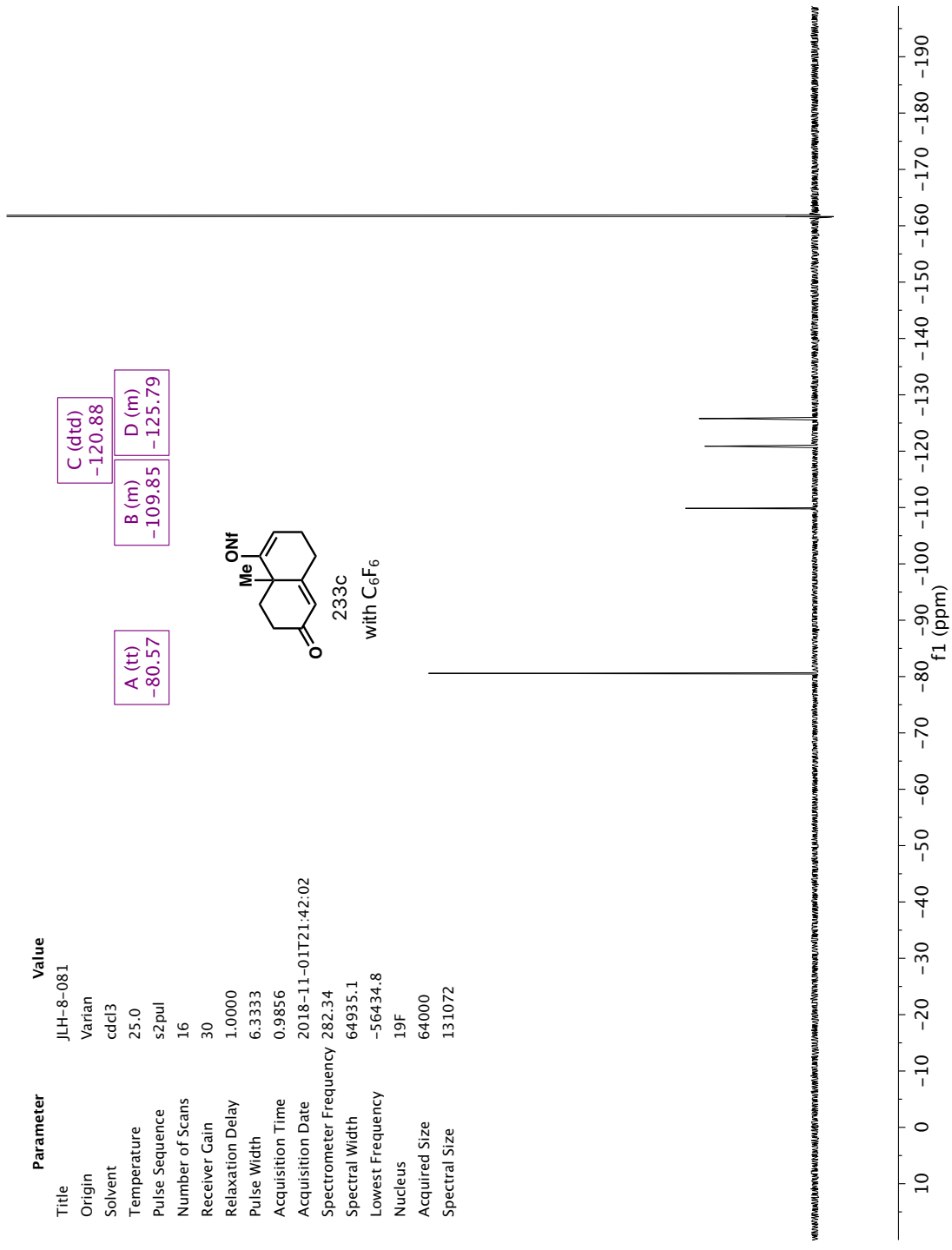

Parameter	Value
Title	JLH-8-081
Origin	Varian
Solvent	cdcl3
Temperature	25.0
Pulse Sequence	s2pul
Number of Scans	16
Receiver Gain	30
Relaxation Delay	1.0000
Pulse Width	6.3333
Acquisition Time	0.9856
Acquisition Date	2018-11-01T21:42:02
Spectrometer Frequency	282.34
Spectral Width	64935.1
Lowest Frequency	-56434.8
Nucleus	19F
Acquired Size	64000
Spectral Size	131072

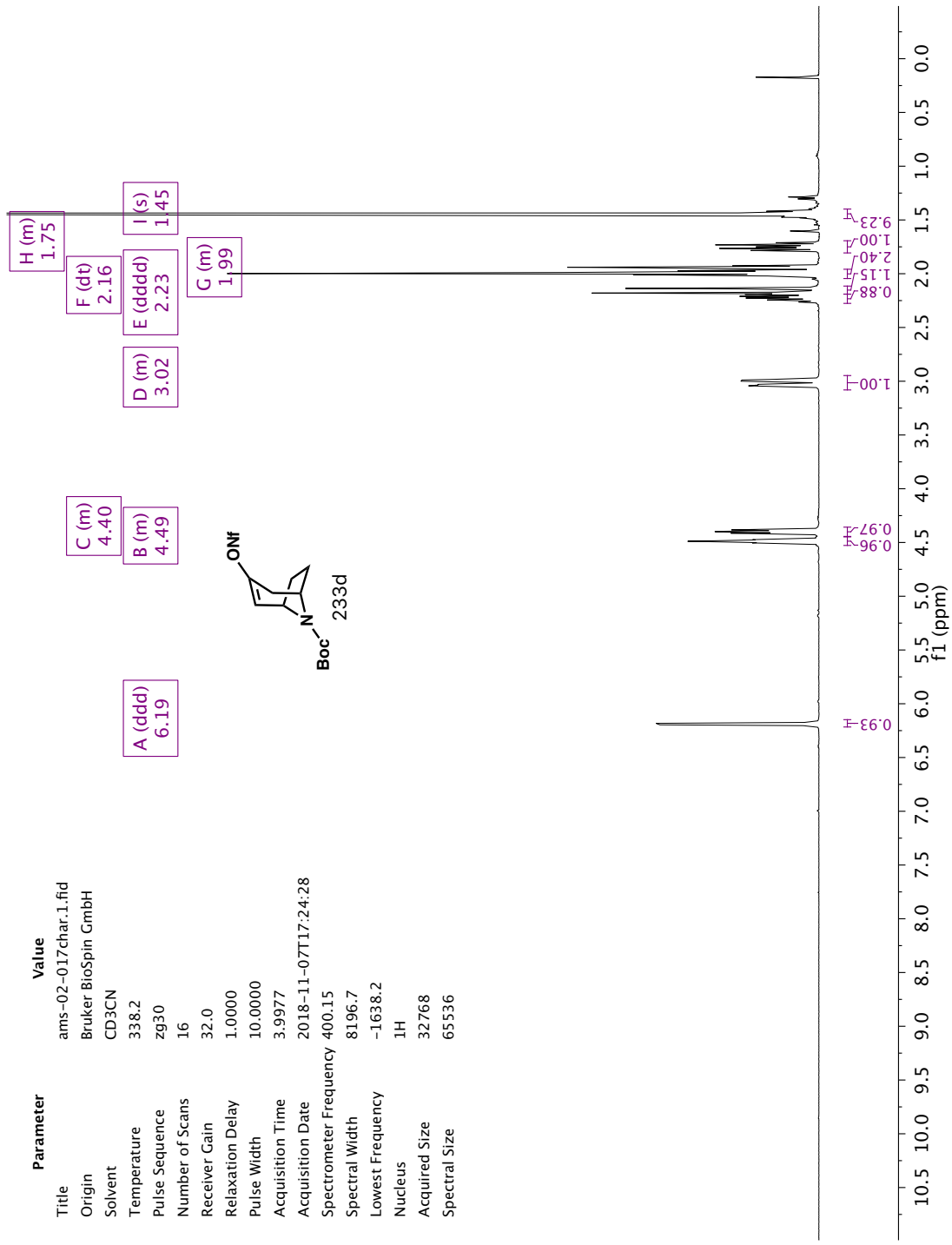
Parameter Value
Title ams-02-017char.1.fid
Origin Bruker BioSpin GmbH
Solvent CD3CN
Temperature 338.2
Pulse Sequence zg30
Number of Scans 16
Receiver Gain 32.0
Relaxation Delay 1.0000
Pulse Width 10.0000
Acquisition Time 3.9977
Acquisition Date 2018-11-07T17:24:28
Spectrometer Frequency 400.15
Spectral Width 8196.7
Lowest Frequency -1638.2
Nucleus 1H
Acquired Size 32768
Spectral Size 65536
A (ddd) 6.19
B (m) 4.49
C (m) 4.40
D (m) 3.02
E (dddd) 2.23
F (dt) 2.16
G (m) 1.99
H (m) 1.75
I (s) 1.45
ONf
N
Boc
233d
0.93
0.97
0.96
1.00
0.88
1.15
2.40
1.00
9.23
f1 (ppm)

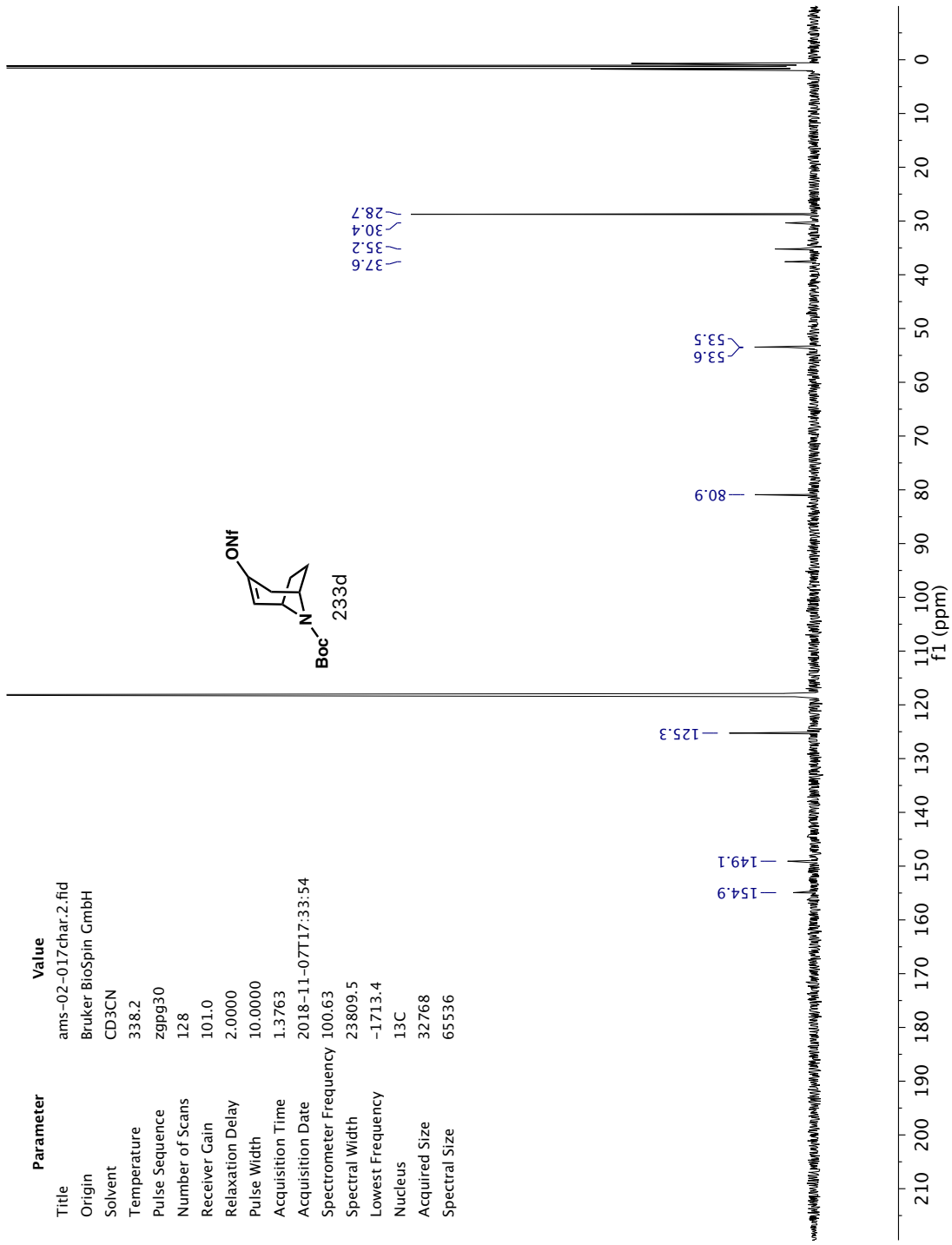

Parameter	Value
Title	ams-02-017char.2.fid
Origin	Bruker BioSpin GmbH
Solvent	CD3CN
Temperature	338.2
Pulse Sequence	zgpg30
Number of Scans	128
Receiver Gain	101.0
Relaxation Delay	2.0000
Pulse Width	10.0000
Acquisition Time	1.3763
Acquisition Date	2018-11-07T17:33:54
Spectrometer Frequency	100.63
Spectral Width	23809.5
Lowest Frequency	-1713.4
Nucleus	13C
Acquired Size	32768
Spectral Size	65536

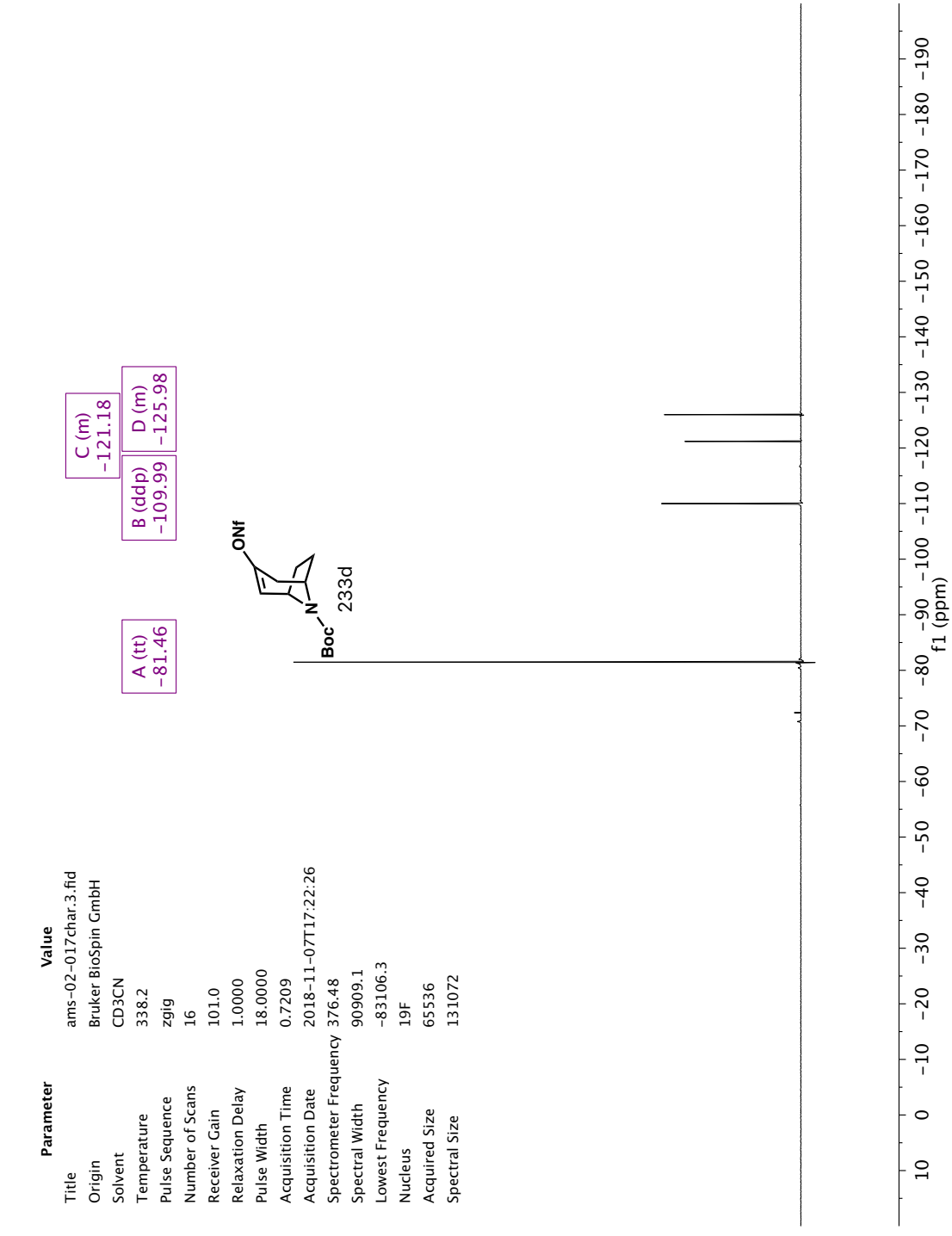
Parameter Value
Title ams-02-017char.3.fid
Origin Bruker BioSpin GmbH
Solvent CD3CN
Temperature 338.2
Pulse Sequence zgig
Number of Scans 16
Receiver Gain 101.0
Relaxation Delay 1.0000
Pulse Width 18.0000
Acquisition Time 0.7209
Acquisition Date 2018-11-07T17:22:26
Spectrometer Frequency 376.48
Spectral Width 90909.1
Lowest Frequency -83106.3
Nucleus 19F
Acquired Size 65536
Spectral Size 131072
A (tt) -81.46
B (ddp) -109.99
C (m) -121.18
D (m) -125.98
ONf
N
Boc
233d
10 0 -10 -20 -30 -40 -50 -60 -70 -80 -90 -100 -110 -120 -130 -140 -150 -160 -170 -180 -190
f1 (ppm)

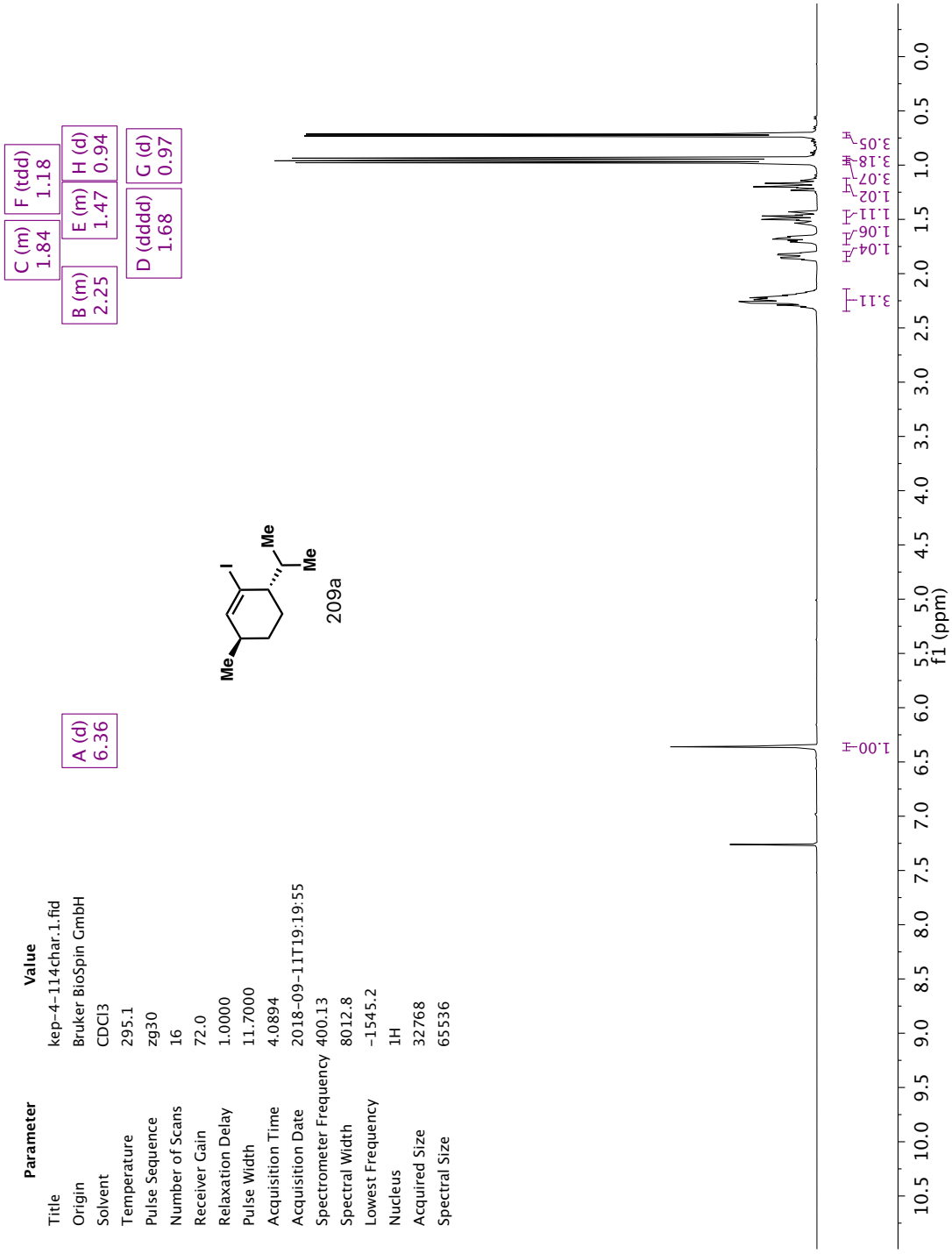

Parameter	Value
Title	kep-4-114char.1.fid
Origin	Bruker BioSpin GmbH
Solvent	CDCl3
Temperature	295.1
Pulse Sequence	zg30
Number of Scans	16
Receiver Gain	72.0
Relaxation Delay	1.0000
Pulse Width	11.7000
Acquisition Time	4.0894
Acquisition Date	2018-09-11T19:19:55
Spectrometer Frequency	400.13
Spectral Width	8012.8
Lowest Frequency	-1545.2
Nucleus	1H
Acquired Size	32768
Spectral Size	65536

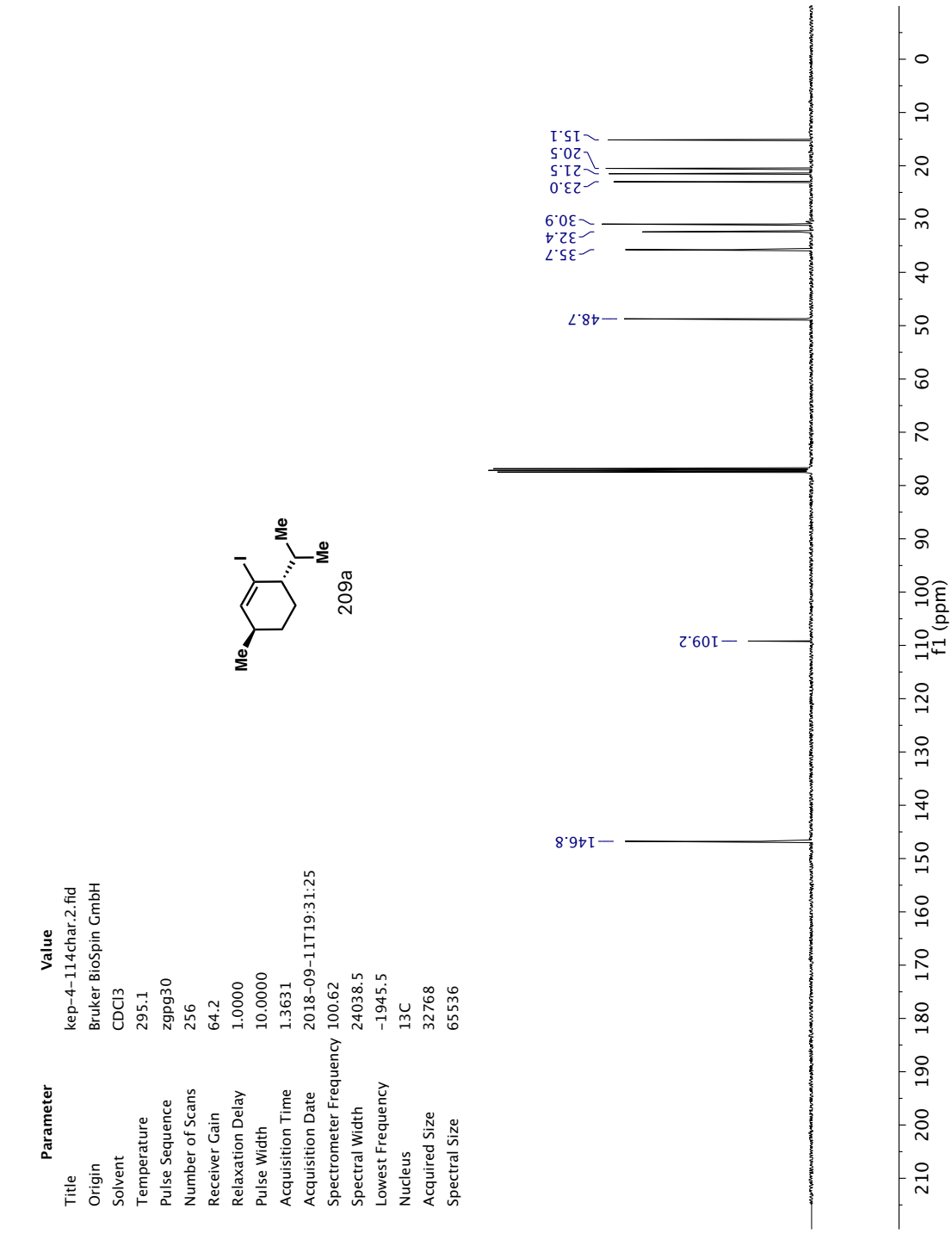
Parameter Value
Title kep-4-114char.2.fid
Origin Bruker BioSpin GmbH
Solvent CDCl3
Temperature 295.1
Pulse Sequence zgpg30
Number of Scans 256
Receiver Gain 64.2
Relaxation Delay 1.0000
Pulse Width 10.0000
Acquisition Time 1.3631
Acquisition Date 2018-09-11T19:31:25
Spectrometer Frequency 100.62
Spectral Width 24038.5
Lowest Frequency -1945.5
Nucleus 13C
Acquired Size 32768
Spectral Size 65536
I
Me
Me
Me
209a
146.8
109.2
48.7
35.7
32.4
30.9
23.0
21.5
20.5
15.1
210 200 190 180 170 160 150 140 130 120 110 100 90 80 70 60 50 40 30 20 10 0
f1 (ppm)

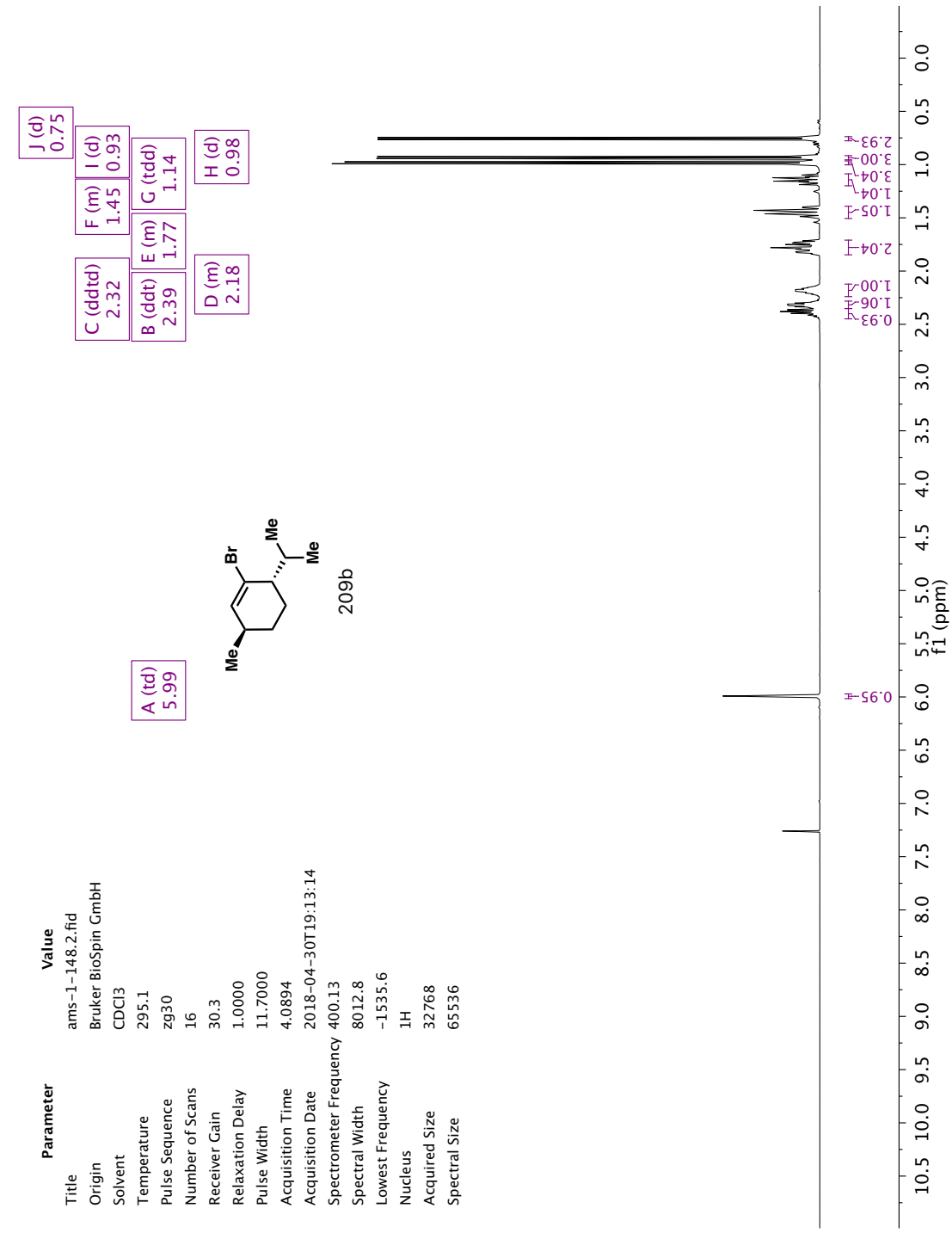

Parameter	Value
Title	ams-1-148.2.fid
Origin	Bruker BioSpin GmbH
Solvent	CDCl3
Temperature	295.1
Pulse Sequence	zg30
Number of Scans	16
Receiver Gain	30.3
Relaxation Delay	1.0000
Pulse Width	11.7000
Acquisition Time	4.0894
Acquisition Date	2018-04-30T19:13:14
Spectrometer Frequency	400.13
Spectral Width	8012.8
Lowest Frequency	-1535.6
Nucleus	1H
Acquired Size	32768
Spectral Size	65536

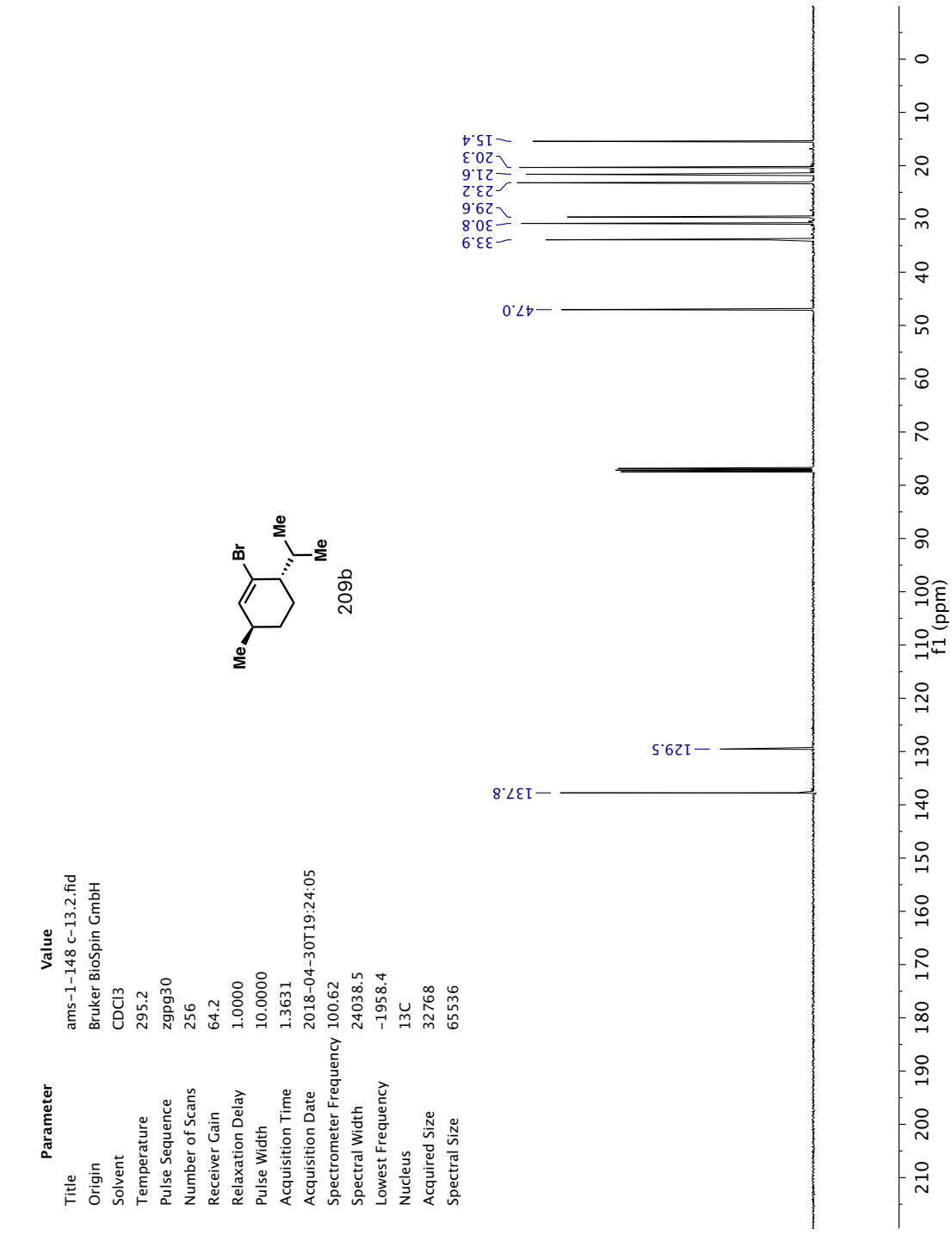
Parameter Value
Title ams-1-148 c-13.2.fid
Origin Bruker BioSpin GmbH
Solvent CDCl3
Temperature 295.2
Pulse Sequence zgpg30
Number of Scans 256
Receiver Gain 64.2
Relaxation Delay 1.0000
Pulse Width 10.0000
Acquisition Time 1.3631
Acquisition Date 2018-04-30T19:24:05
Spectrometer Frequency 100.62
Spectral Width 24038.5
Lowest Frequency -1958.4
Nucleus 13C
Acquired Size 32768
Spectral Size 65536
Br
Me
Me
Me
209b
137.8
129.5
47.0
33.9
30.8
29.6
23.2
21.6
20.3
15.4
f1 (ppm)

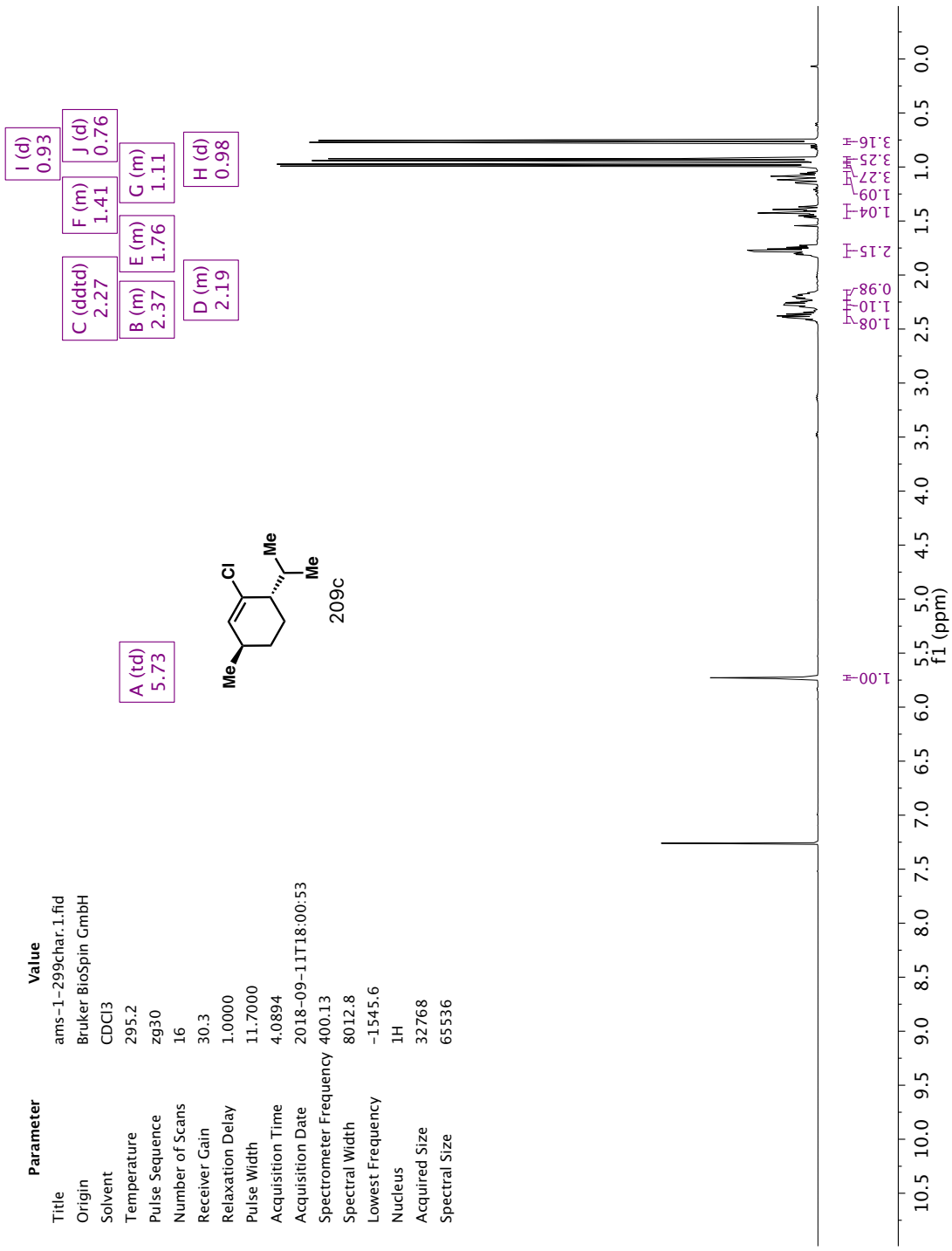
Parameter Value
Title ams-1-299char.1.fid
Origin Bruker BioSpin GmbH
Solvent CDCl3
Temperature 295.2
Pulse Sequence zg30
Number of Scans 16
Receiver Gain 30.3
Relaxation Delay 1.0000
Pulse Width 11.7000
Acquisition Time 4.0894
Acquisition Date 2018-09-11T18:00:53
Spectrometer Frequency 400.13
Spectral Width 8012.8
Lowest Frequency -1545.6
Nucleus 1H
Acquired Size 32768
Spectral Size 65536
A (td) 5.73
B (m) 2.37
C (ddtd) 2.27
D (m) 2.19
E (m) 1.76
F (m) 1.41
G (m) 1.11
H (d) 0.98
I (d) 0.93
J (d) 0.76
Me
Cl
Me
Me
209c
1.00
1.08
1.10
0.98
2.15
1.04
1.09
3.27
3.25
3.16
f1 (ppm)

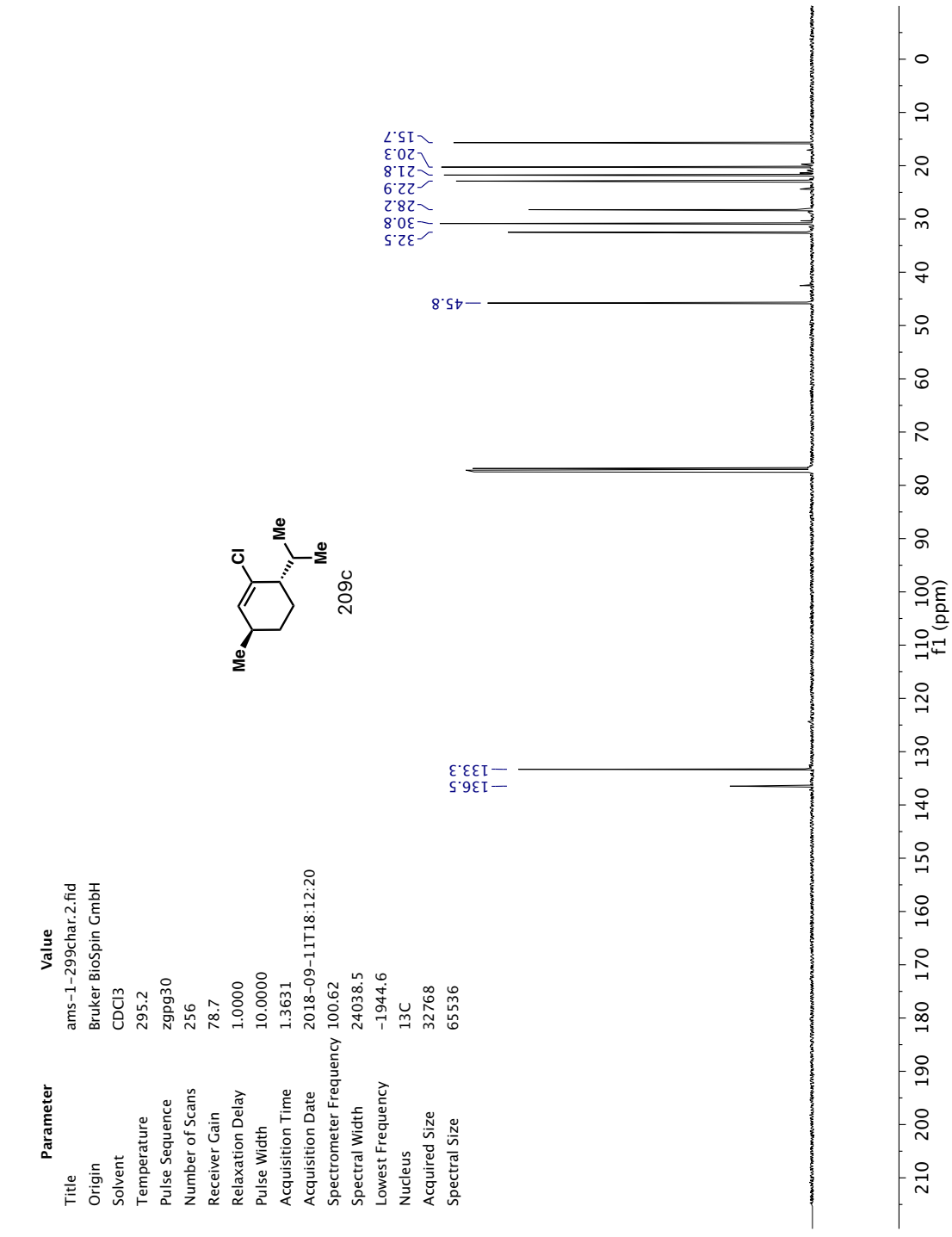
Parameter Value
Title ams-1-299char.2.fid
Origin Bruker BioSpin GmbH
Solvent CDCl3
Temperature 295.2
Pulse Sequence zgpg30
Number of Scans 256
Receiver Gain 78.7
Relaxation Delay 1.0000
Pulse Width 10.0000
Acquisition Time 1.3631
Acquisition Date 2018-09-11T18:12:20
Spectrometer Frequency 100.62
Spectral Width 24038.5
Lowest Frequency -1944.6
Nucleus 13C
Acquired Size 32768
Spectral Size 65536
Cl
Me
Me
Me
209c
133.3
136.5
45.8
32.5
30.8
28.2
22.9
21.8
20.3
15.7
f1 (ppm)

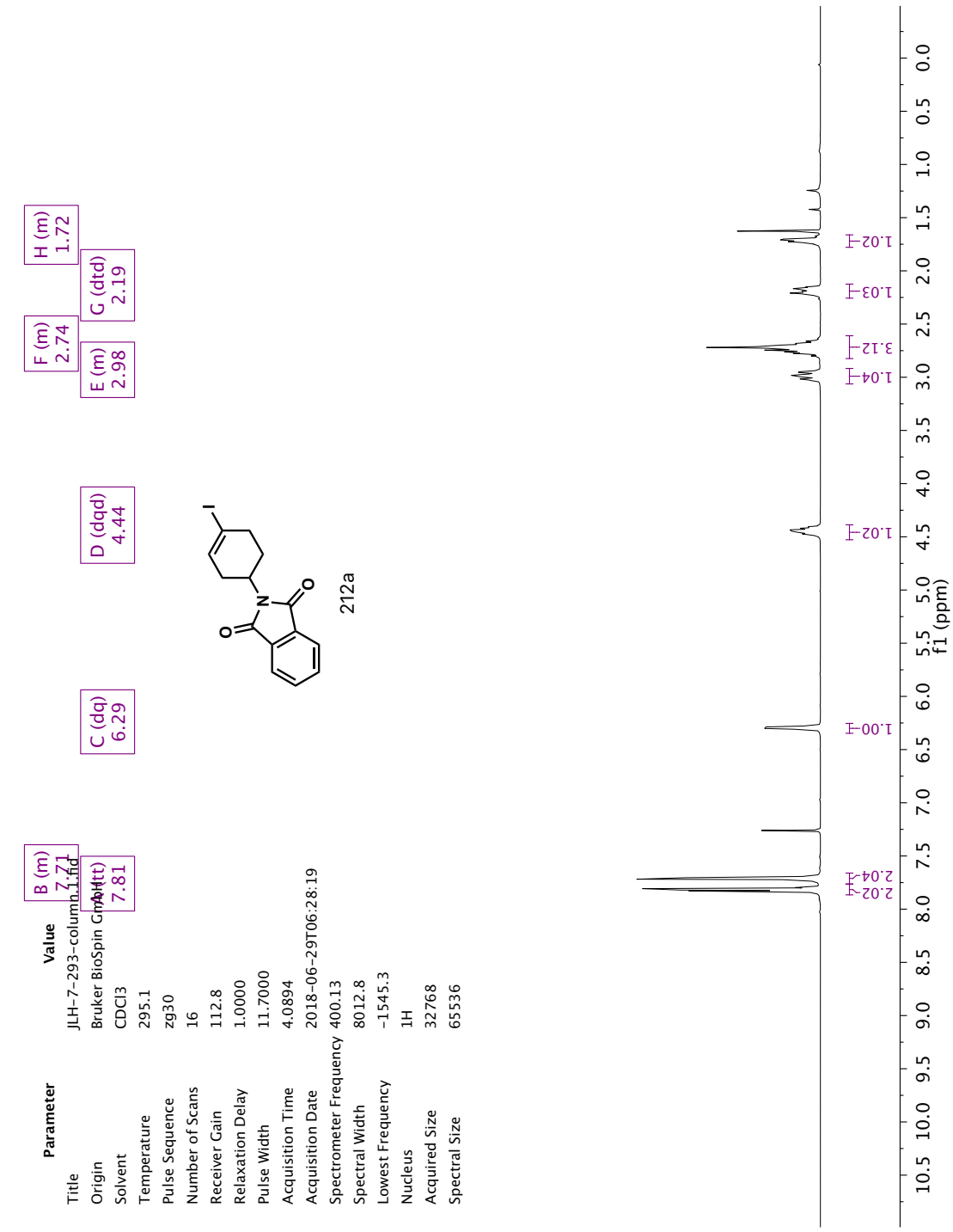

Parameter	Value
Title	JLH-7-293-column1.fid
Origin	Bruker BioSpin GmbH
Solvent	CDCl3
Temperature	295.1
Pulse Sequence	zg30
Number of Scans	16
Receiver Gain	112.8
Relaxation Delay	1.0000
Pulse Width	11.7000
Acquisition Time	4.0894
Acquisition Date	2018-06-29T06:28:19
Spectrometer Frequency	400.13
Spectral Width	8012.8
Lowest Frequency	-1545.3
Nucleus	1H
Acquired Size	32768
Spectral Size	65536

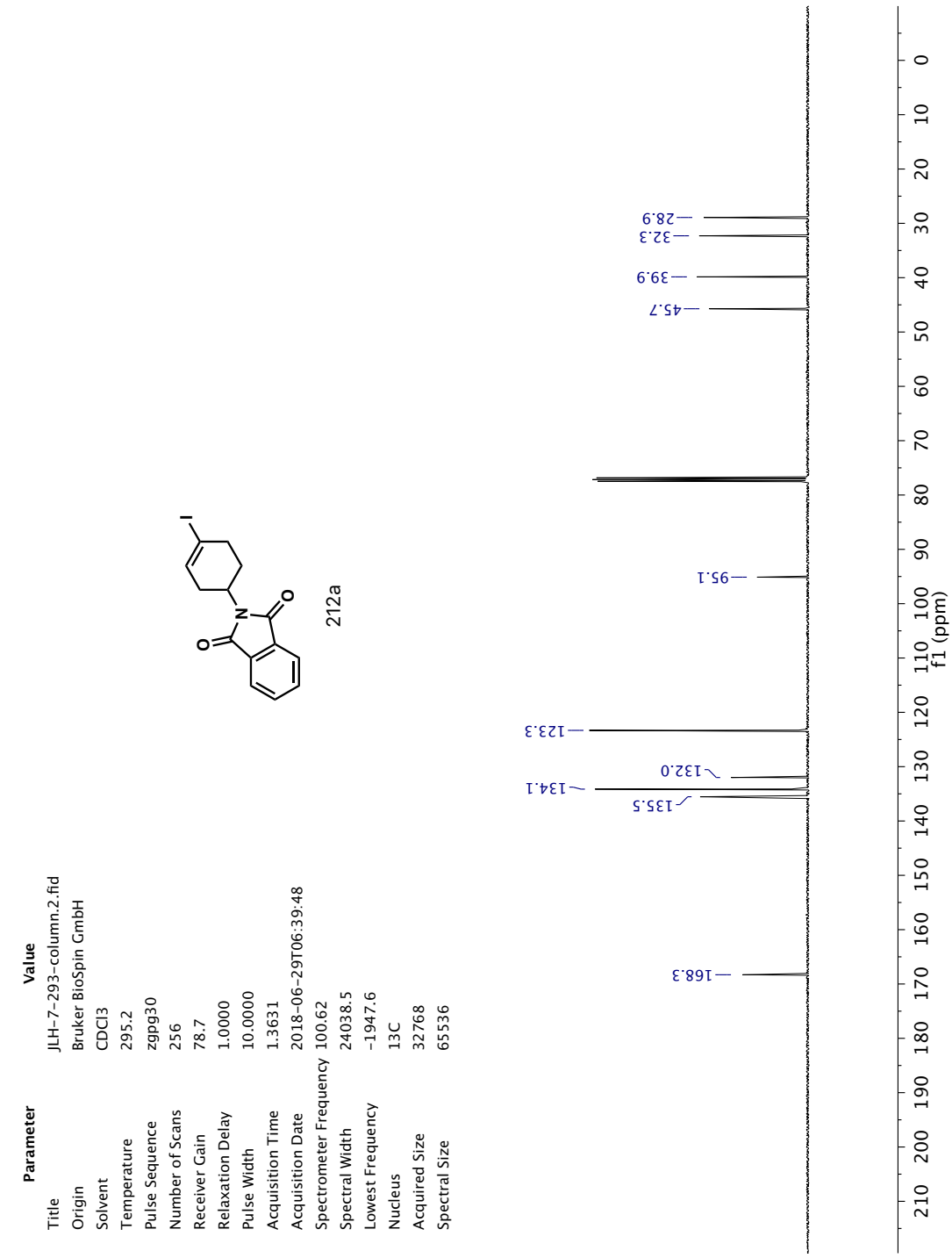
Parameter Value
Title JLH-7-293-column.2.fid
Origin Bruker BioSpin GmbH
Solvent CDCl3
Temperature 295.2
Pulse Sequence zgpg30
Number of Scans 256
Receiver Gain 78.7
Relaxation Delay 1.0000
Pulse Width 10.0000
Acquisition Time 1.3631
Acquisition Date 2018-06-29T06:39:48
Spectrometer Frequency 100.62
Spectral Width 24038.5
Lowest Frequency -1947.6
Nucleus 13C
Acquired Size 32768
Spectral Size 65536
I
O
N
O
212a
168.3
135.5
134.1
132.0
123.3
95.1
45.7
39.9
32.3
28.9
f1 (ppm)

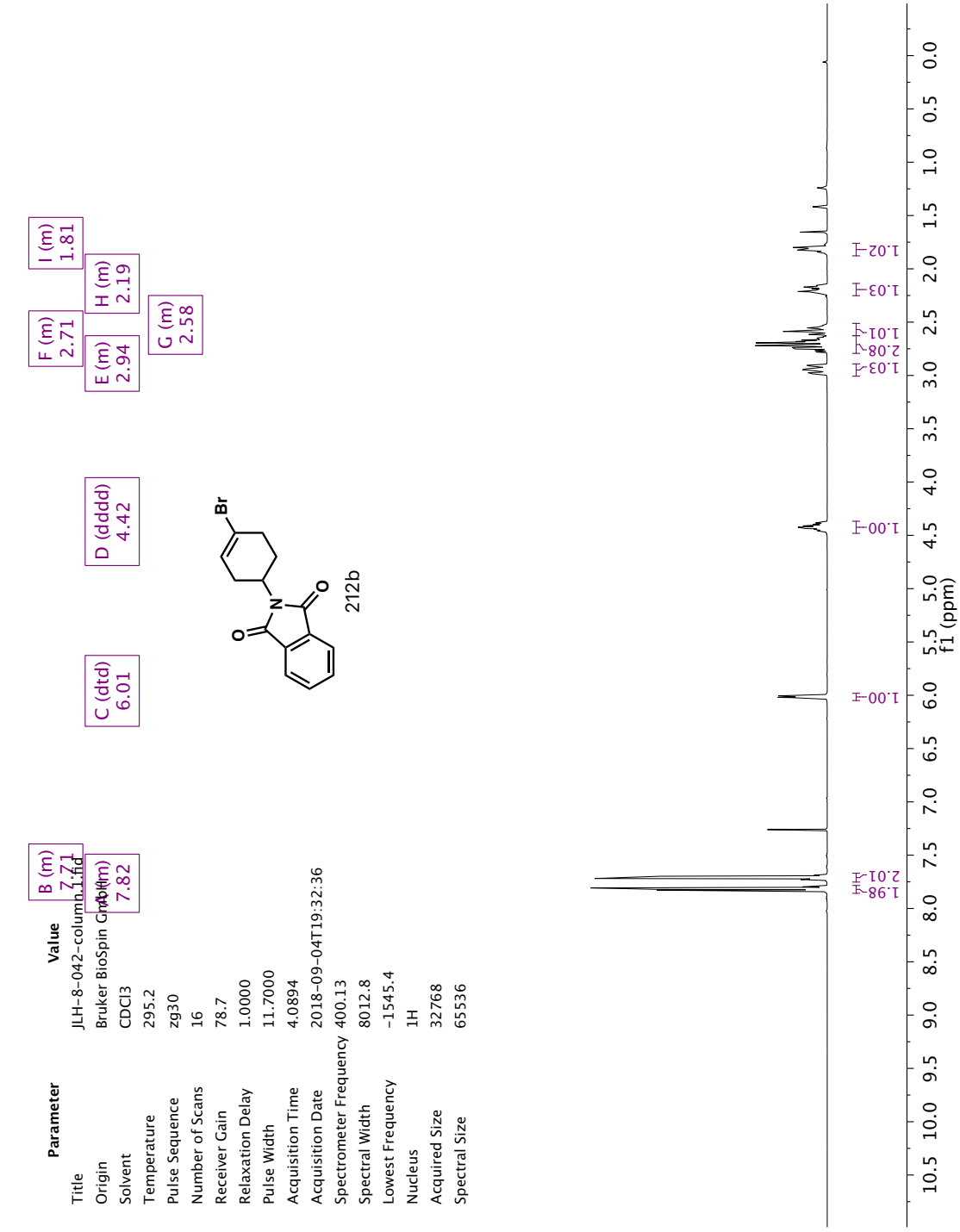
B (m) 7.71
7.74
7.82
C (dtd) 6.01
D (dddd) 4.42
F (m) 2.71
E (m) 2.94
H (m) 2.19
I (m) 1.81
G (m) 2.58
Br
O
N
O
212b
Parameter Value
Title JLH-8-042-column,1:fid
Origin Bruker BioSpin GmbH
Solvent CDCl3
Temperature 295.2
Pulse Sequence zg30
Number of Scans 16
Receiver Gain 78.7
Relaxation Delay 1.0000
Pulse Width 11.7000
Acquisition Time 4.0894
Acquisition Date 2018-09-04T19:32:36
Spectrometer Frequency 400.13
Spectral Width 8012.8
Lowest Frequency -1545.4
Nucleus 1H
Acquired Size 32768
Spectral Size 65536
1.98
2.01
1.00
1.00
1.00
2.08
1.03
1.01
1.03
1.02
10.5 10.0 9.5 9.0 8.5 8.0 7.5 7.0 6.5 6.0 5.5 5.0 4.5 4.0 3.5 3.0 2.5 2.0 1.5 1.0 0.5 0.0
f1 (ppm)

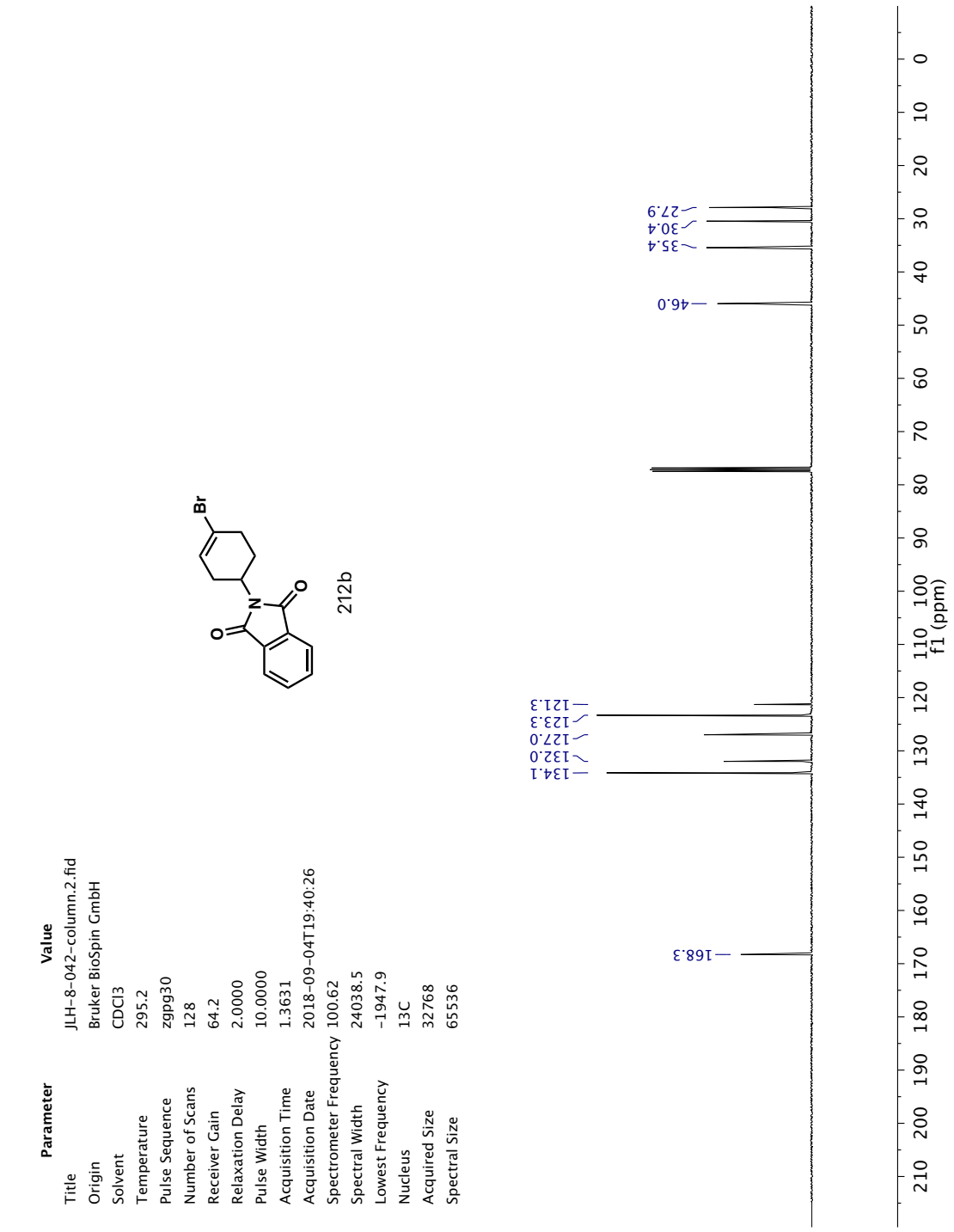
Parameter Value
Title JLH-8-042-column.2.fid
Origin Bruker BioSpin GmbH
Solvent CDCl3
Temperature 295.2
Pulse Sequence zgpg30
Number of Scans 128
Receiver Gain 64.2
Relaxation Delay 2.0000
Pulse Width 10.0000
Acquisition Time 1.3631
Acquisition Date 2018-09-04T19:40:26
Spectrometer Frequency 100.62
Spectral Width 24038.5
Lowest Frequency -1947.9
Nucleus 13C
Acquired Size 32768
Spectral Size 65536
Br
O
N
O
212b
168.3
134.1
132.0
127.0
123.3
121.3
46.0
35.4
30.4
27.9
f1 (ppm)

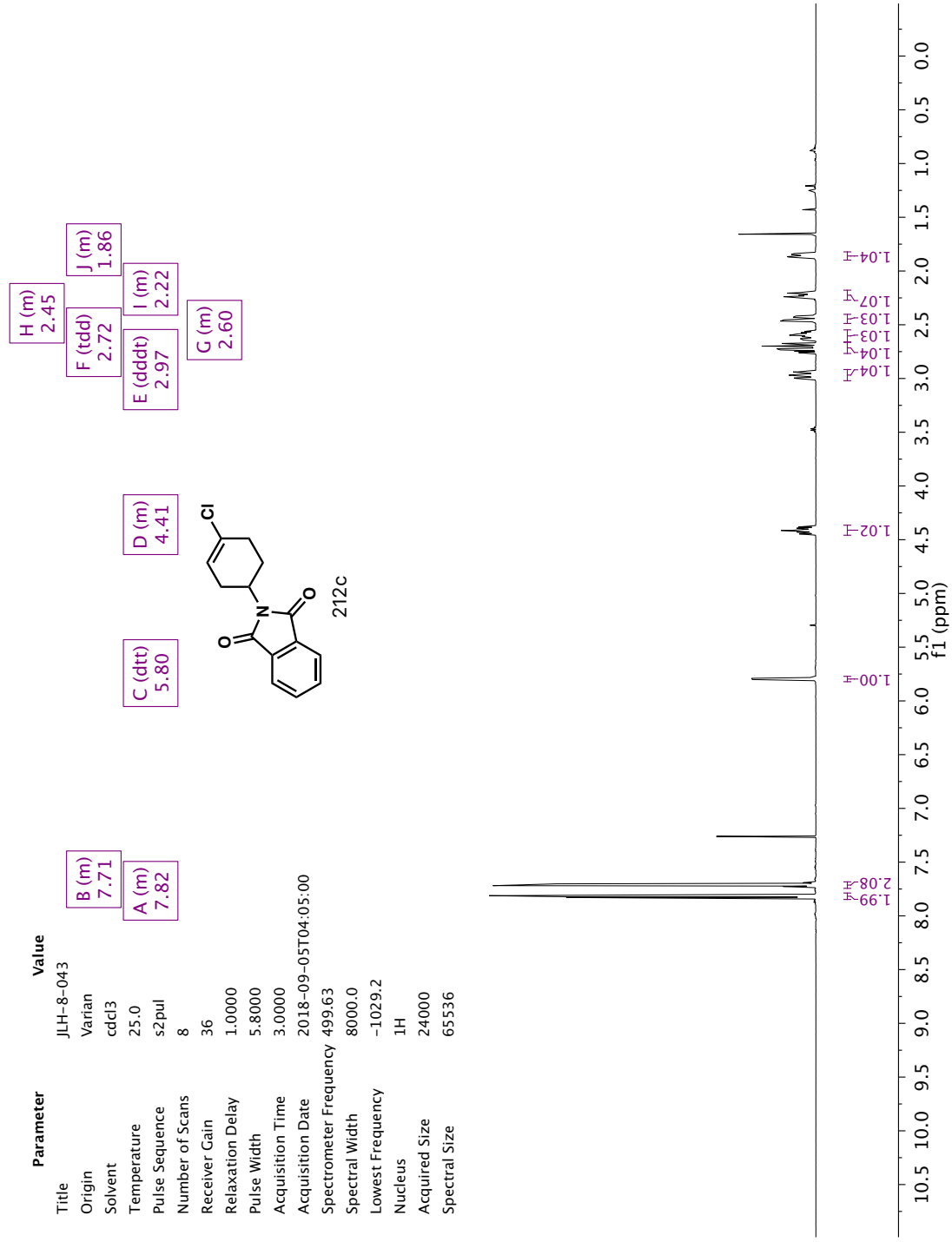
Parameter Value
Title JLH-8-043
Origin Varian
Solvent cdcl3
Temperature 25.0
Pulse Sequence s2pul
Number of Scans 8
Receiver Gain 36
Relaxation Delay 1.0000
Pulse Width 5.8000
Acquisition Time 3.0000
Acquisition Date 2018-09-05T04:05:00
Spectrometer Frequency 499.63
Spectral Width 8000.0
Lowest Frequency -1029.2
Nucleus 1H
Acquired Size 24000
Spectral Size 65536
B (m) 7.71
A (m) 7.82
C (dtt) 5.80
D (m) 4.41
E (dddt) 2.97
F (tdd) 2.72
G (m) 2.60
H (m) 2.45
I (m) 2.22
J (m) 1.86
212c
1.99
2.08
1.00
1.02
1.04
1.04
1.04
1.03
1.03
1.07
1.04
f1 (ppm)

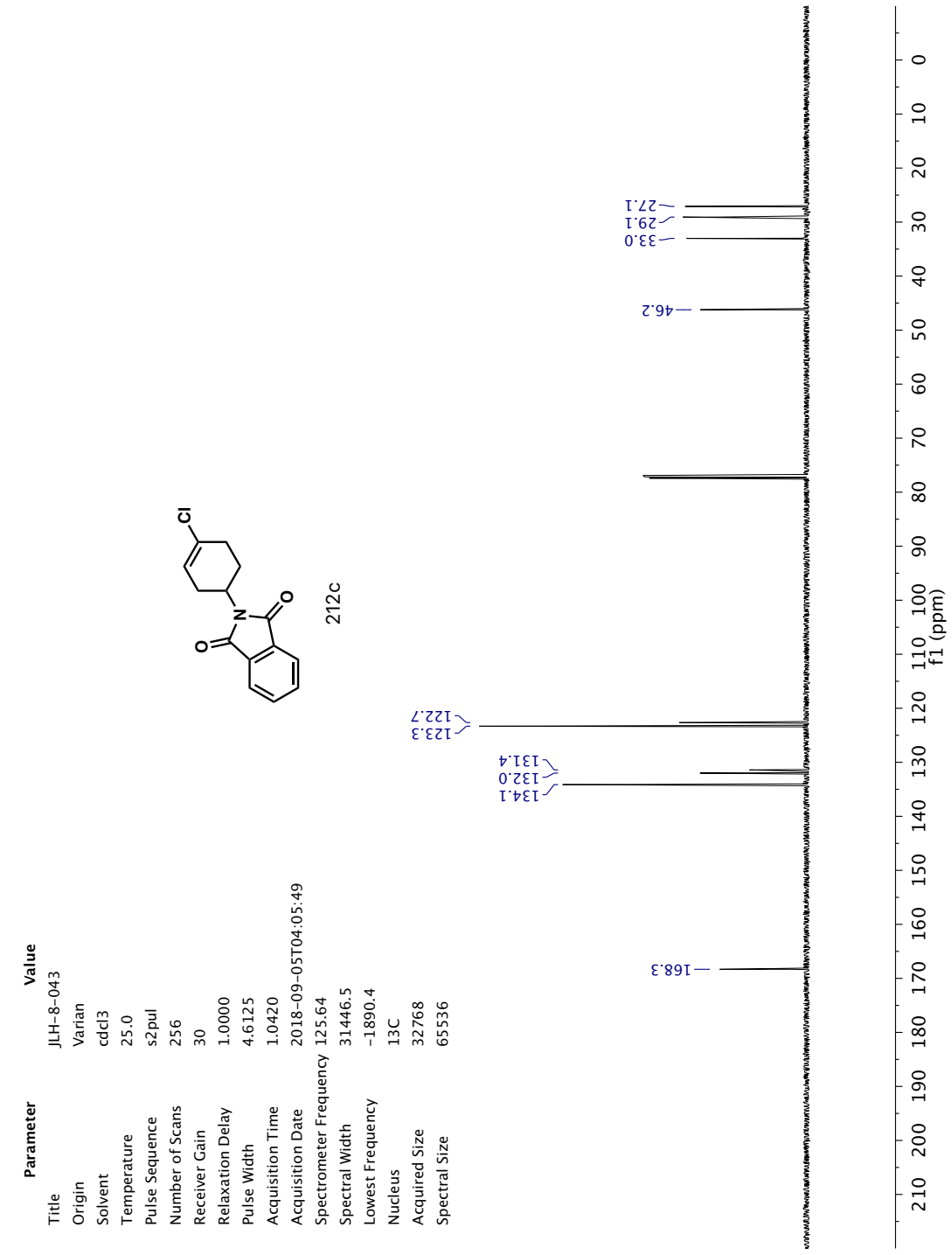
Parameter Value
Title JLH-8-043
Origin Varian
Solvent cdcl3
Temperature 25.0
Pulse Sequence s2pul
Number of Scans 256
Receiver Gain 30
Relaxation Delay 1.0000
Pulse Width 4.6125
Acquisition Time 1.0420
Acquisition Date 2018-09-05T04:05:49
Spectrometer Frequency 125.64
Spectral Width 31446.5
Lowest Frequency -1890.4
Nucleus 13C
Acquired Size 32768
Spectral Size 65536
Cl
O
N
O
212c
168.3
134.1
132.0
131.4
123.3
122.7
46.2
33.0
29.1
27.1
f1 (ppm)

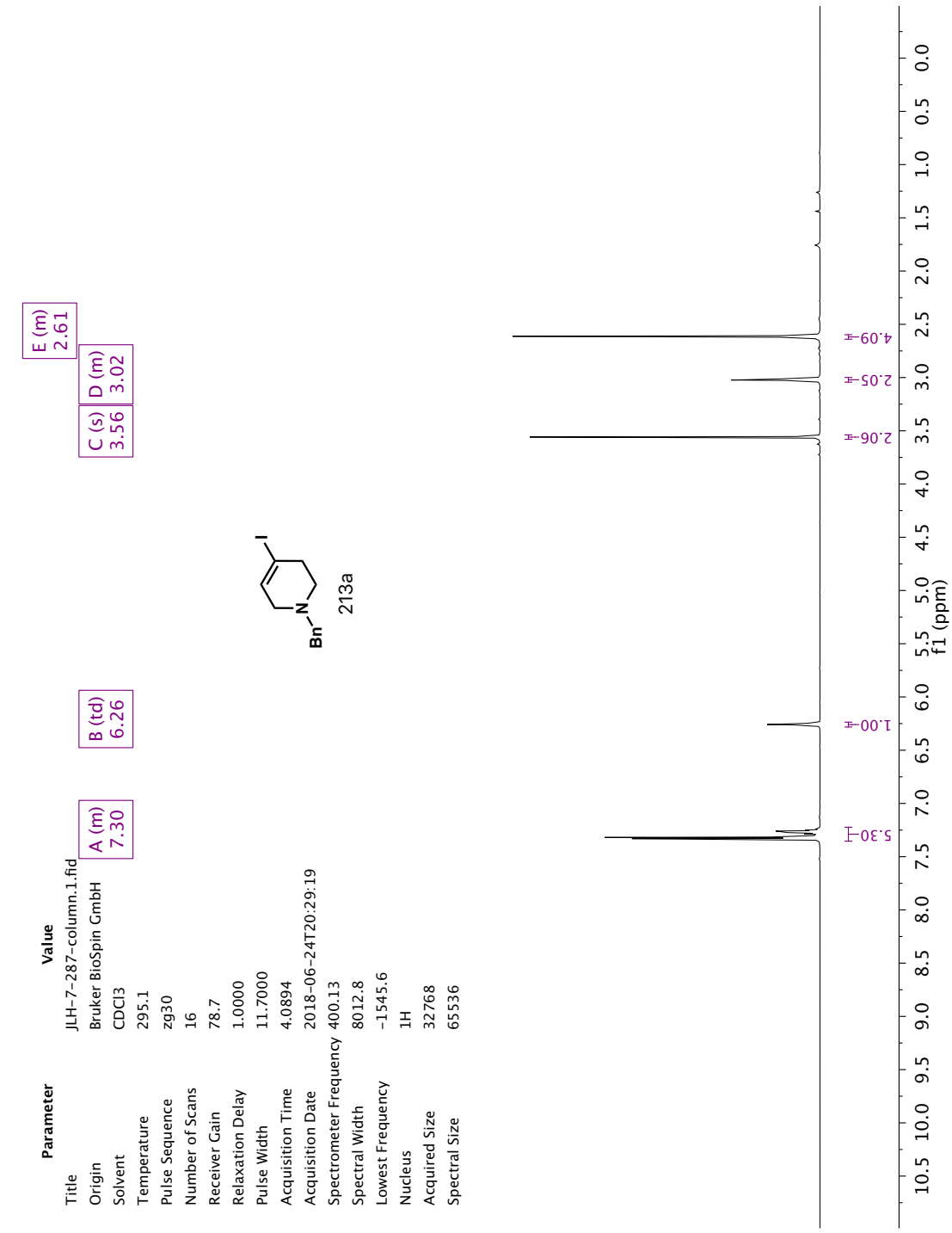
Parameter
Value
Title
JLH-7-287-column.1.fid
Origin
Bruker BioSpin GmbH
Solvent
CDCl3
Temperature
295.1
Pulse Sequence
zg30
Number of Scans
16
Receiver Gain
78.7
Relaxation Delay
1.0000
Pulse Width
11.7000
Acquisition Time
4.0894
Acquisition Date
2018-06-24T20:29:19
Spectrometer Frequency
400.13
Spectral Width
8012.8
Lowest Frequency
-1545.6
Nucleus
1H
Acquired Size
32768
Spectral Size
65536
A (m) 7.30
B (td) 6.26
C (s) 3.56
D (m) 3.02
E (m) 2.61
Bn
N
213a
5.30
1.00
2.06
2.05
4.09
10.5 10.0 9.5 9.0 8.5 8.0 7.5 7.0 6.5 6.0 5.5 5.0 4.5 4.0 3.5 3.0 2.5 2.0 1.5 1.0 0.5 0.0
f1 (ppm)

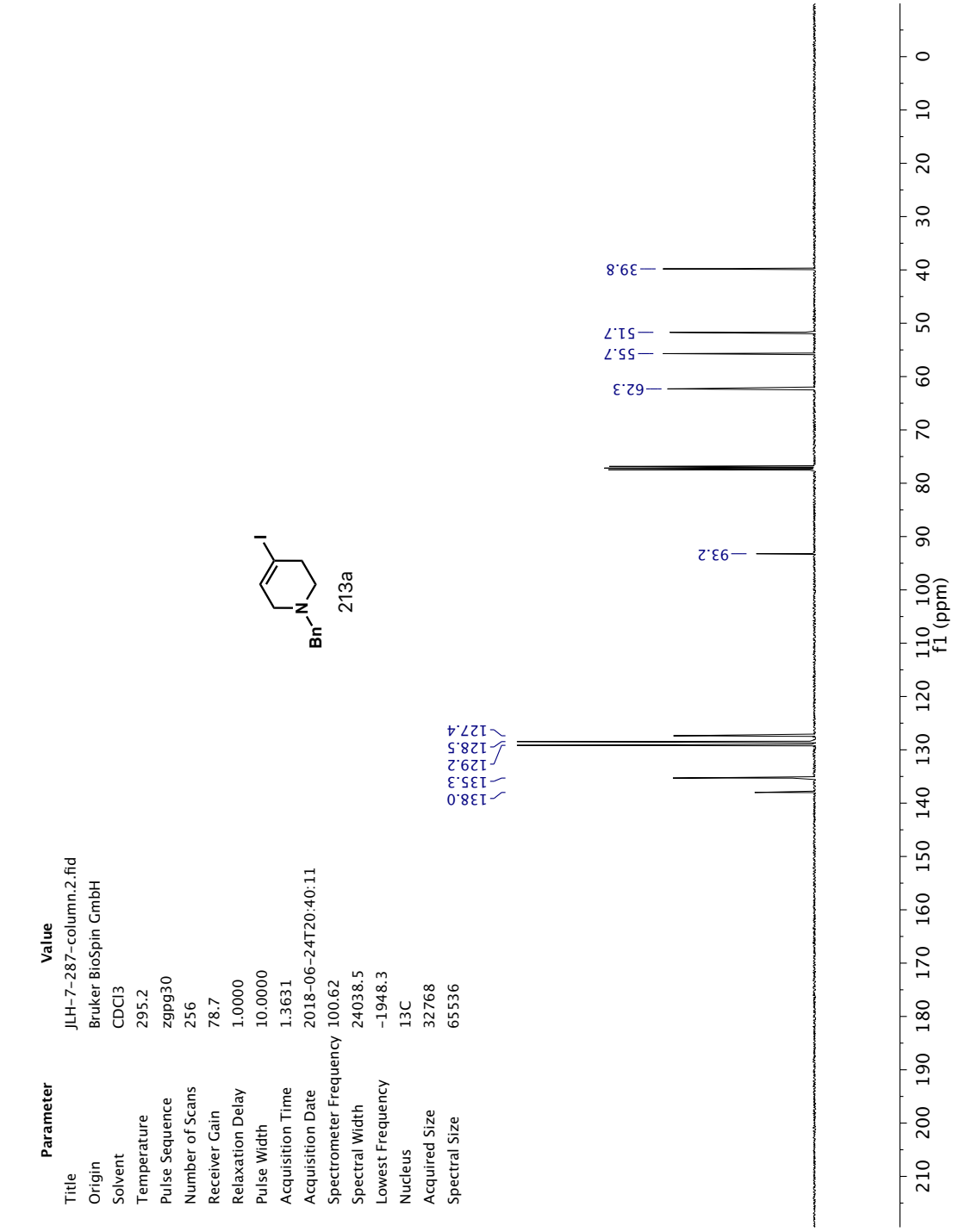
Parameter Value
Title JLH-7-287-column.2.fid
Origin Bruker BioSpin GmbH
Solvent CDCl3
Temperature 295.2
Pulse Sequence zgpg30
Number of Scans 256
Receiver Gain 78.7
Relaxation Delay 1.0000
Pulse Width 10.0000
Acquisition Time 1.3631
Acquisition Date 2018-06-24T20:40:11
Spectrometer Frequency 100.62
Spectral Width 24038.5
Lowest Frequency -1948.3
Nucleus 13C
Acquired Size 32768
Spectral Size 65536
I
N
Bn
213a
138.0
135.3
129.2
128.5
127.4
93.2
62.3
55.7
51.7
39.8
f1 (ppm)

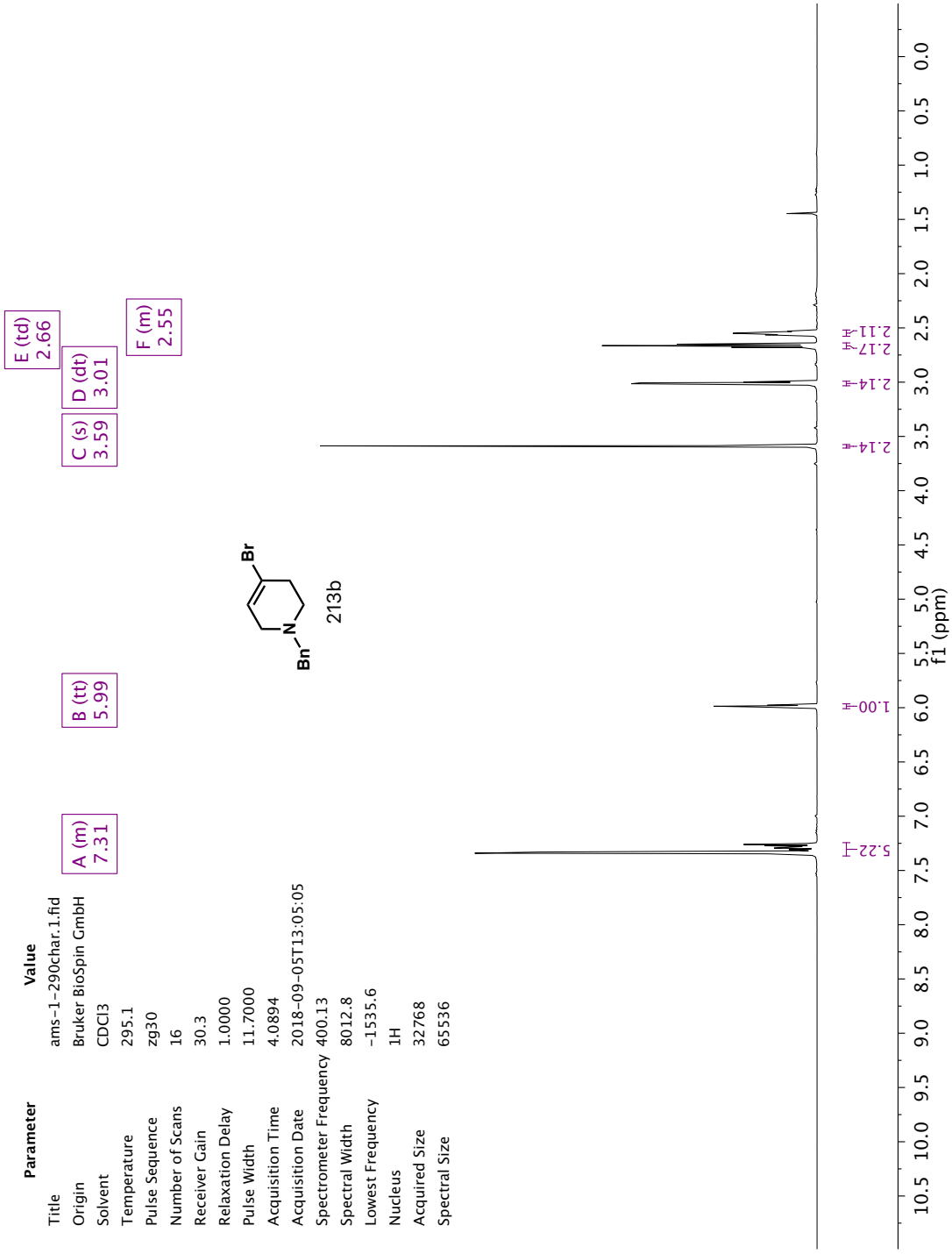
Parameter
Value
Title ams-1-290char.1.fid
Origin Bruker BioSpin GmbH
Solvent CDCl3
Temperature 295.1
Pulse Sequence zg30
Number of Scans 16
Receiver Gain 30.3
Relaxation Delay 1.0000
Pulse Width 11.7000
Acquisition Time 4.0894
Acquisition Date 2018-09-05T13:05:05
Spectrometer Frequency 400.13
Spectral Width 8012.8
Lowest Frequency -1535.6
Nucleus 1H
Acquired Size 32768
Spectral Size 65536
A (m) 7.31
B (tt) 5.99
C (s) 3.59
D (dt) 3.01
E (td) 2.66
F (m) 2.55
Br
N
Bn
213b
5.22
1.00
2.14
2.14
2.17
2.11
10.5 10.0 9.5 9.0 8.5 8.0 7.5 7.0 6.5 6.0 5.5 5.0 4.5 4.0 3.5 3.0 2.5 2.0 1.5 1.0 0.5 0.0
f1 (ppm)

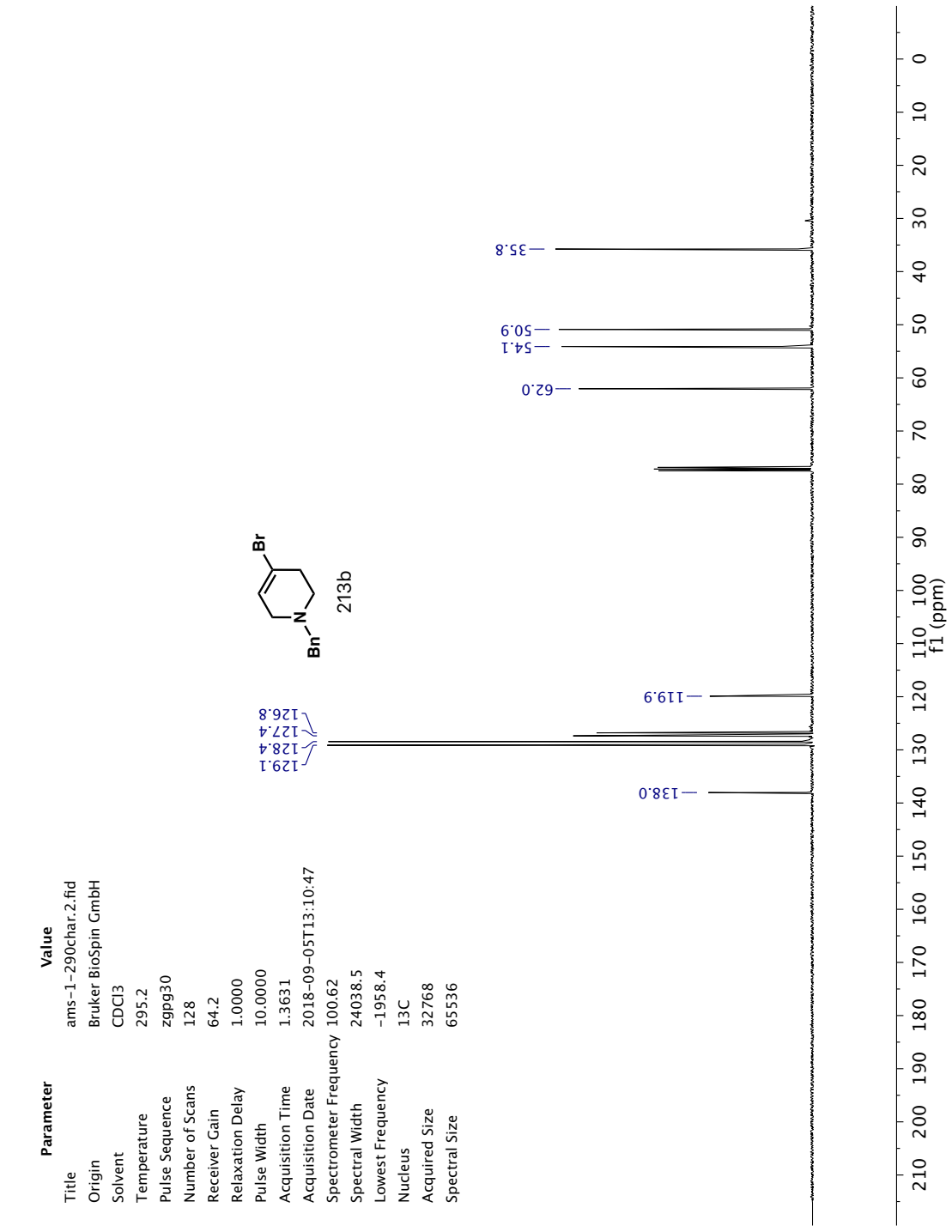
Parameter Value
Title ams-1-290char.2.fid
Origin Bruker BioSpin GmbH
Solvent CDCl3
Temperature 295.2
Pulse Sequence zgpg30
Number of Scans 128
Receiver Gain 64.2
Relaxation Delay 1.0000
Pulse Width 10.0000
Acquisition Time 1.3631
Acquisition Date 2018-09-05T13:10:47
Spectrometer Frequency 100.62
Spectral Width 24038.5
Lowest Frequency -1958.4
Nucleus 13C
Acquired Size 32768
Spectral Size 65536
Br
N
Bn
213b
138.0
129.1
128.4
127.4
126.8
119.9
62.0
54.1
50.9
35.8
f1 (ppm)

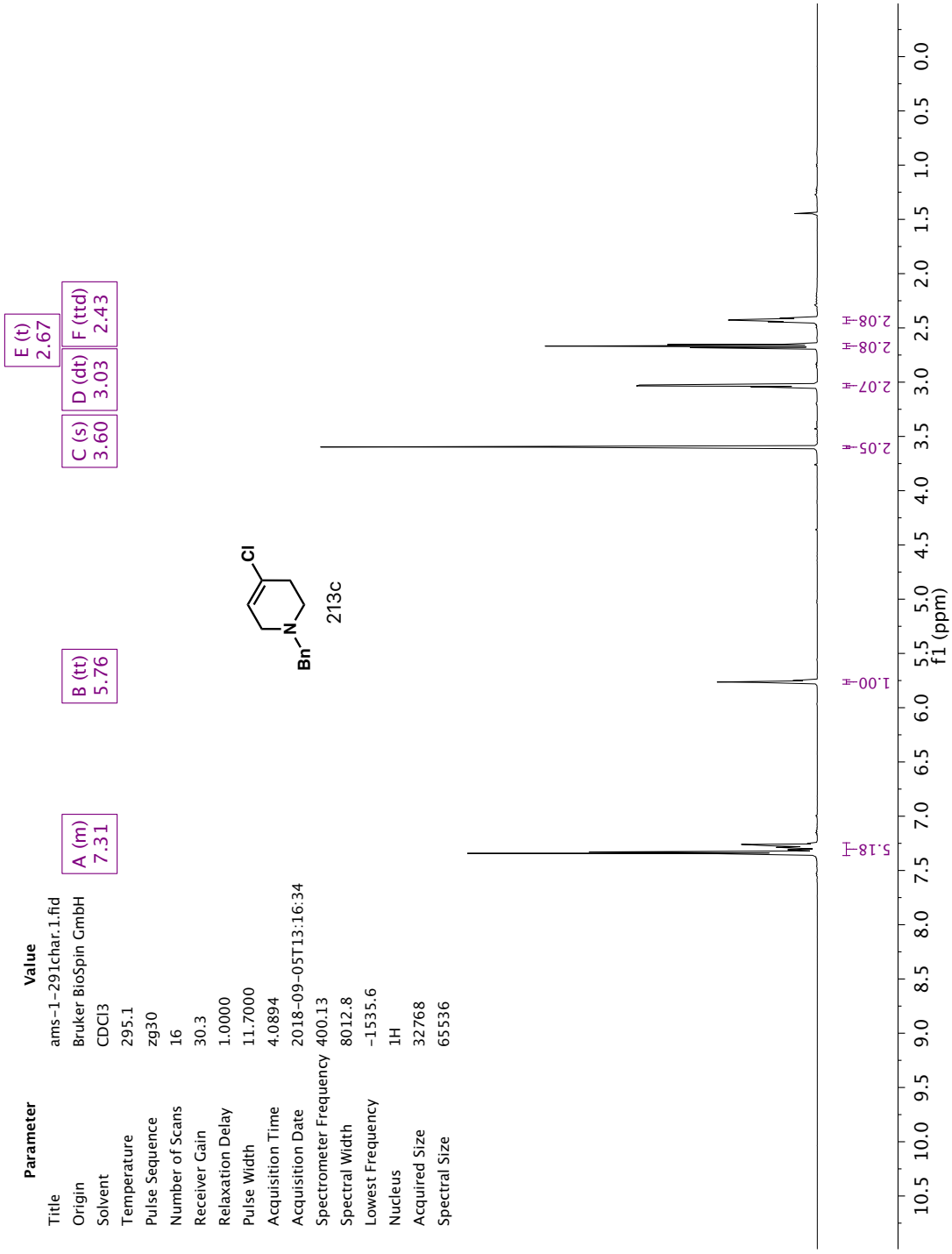
Parameter
Value
Title ams-1-291char.1.fid
Origin Bruker BioSpin GmbH
Solvent CDCl3
Temperature 295.1
Pulse Sequence zg30
Number of Scans 16
Receiver Gain 30.3
Relaxation Delay 1.0000
Pulse Width 11.7000
Acquisition Time 4.0894
Acquisition Date 2018-09-05T13:16:34
Spectrometer Frequency 400.13
Spectral Width 8012.8
Lowest Frequency -1535.6
Nucleus 1H
Acquired Size 32768
Spectral Size 65536
A (m) 7.31
B (tt) 5.76
C (s) 3.60
D (dt) 3.03
E (t) 2.67
F (ttd) 2.43
Cl
N
Bn
213c
5.18
1.00
2.05
2.07
2.08
2.08
10.5 10.0 9.5 9.0 8.5 8.0 7.5 7.0 6.5 6.0 5.5 5.0 4.5 4.0 3.5 3.0 2.5 2.0 1.5 1.0 0.5 0.0
f1 (ppm)

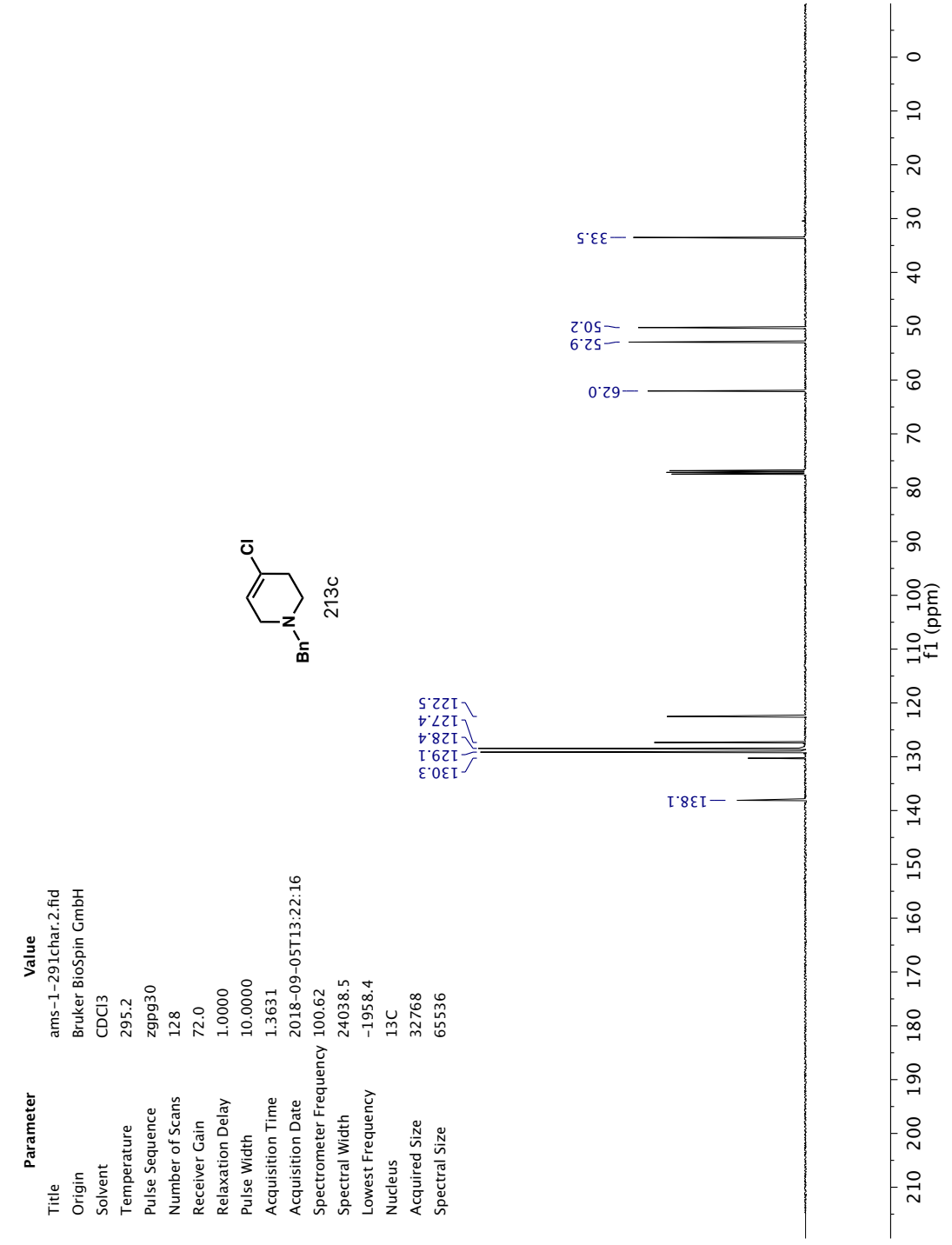
Parameter Value
Title ams-1-291char.2.fid
Origin Bruker BioSpin GmbH
Solvent CDCl3
Temperature 295.2
Pulse Sequence zgpg30
Number of Scans 128
Receiver Gain 72.0
Relaxation Delay 1.0000
Pulse Width 10.0000
Acquisition Time 1.3631
Acquisition Date 2018-09-05T13:22:16
Spectrometer Frequency 100.62
Spectral Width 24038.5
Lowest Frequency -1958.4
Nucleus 13C
Acquired Size 32768
Spectral Size 65536
Cl
N
Bn
213c
138.1
130.3
129.1
128.4
127.4
122.5
62.0
52.9
50.2
33.5
f1 (ppm)

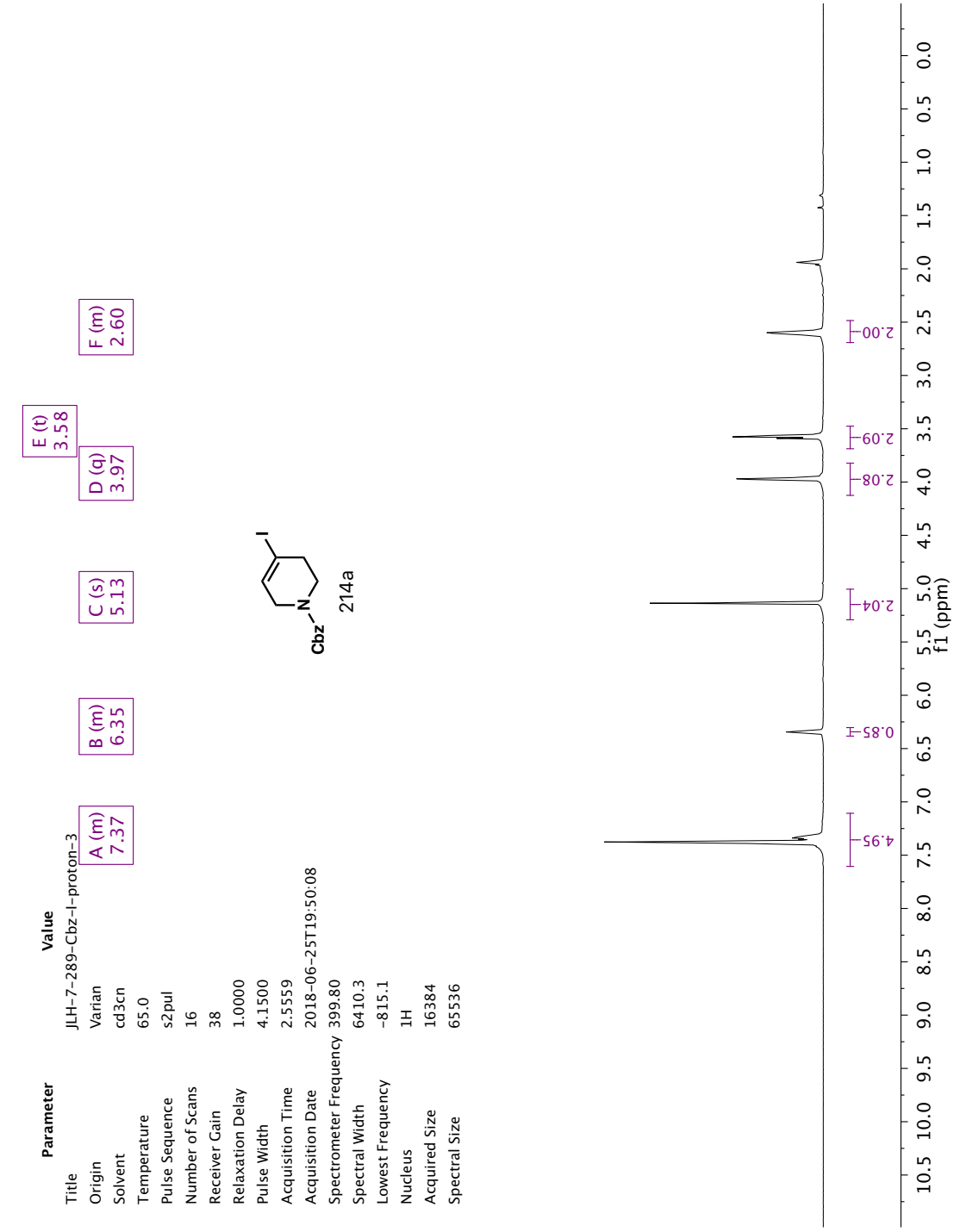
Parameter
Value
Title JLH-7-289-Cbz-I-proton-3
Origin Varian
Solvent cd3cn
Temperature 65.0
Pulse Sequence s2pul
Number of Scans 16
Receiver Gain 38
Relaxation Delay 1.0000
Pulse Width 4.1500
Acquisition Time 2.5559
Acquisition Date 2018-06-25T19:50:08
Spectrometer Frequency 399.80
Spectral Width 6410.3
Lowest Frequency -815.1
Nucleus 1H
Acquired Size 16384
Spectral Size 65536
A (m) 7.37
B (m) 6.35
C (s) 5.13
D (q) 3.97
E (t) 3.58
F (m) 2.60
Cbz
214a
4.95
0.85
2.04
2.08
2.09
2.00
10.5 10.0 9.5 9.0 8.5 8.0 7.5 7.0 6.5 6.0 5.5 5.0 4.5 4.0 3.5 3.0 2.5 2.0 1.5 1.0 0.5 0.0
f1 (ppm)

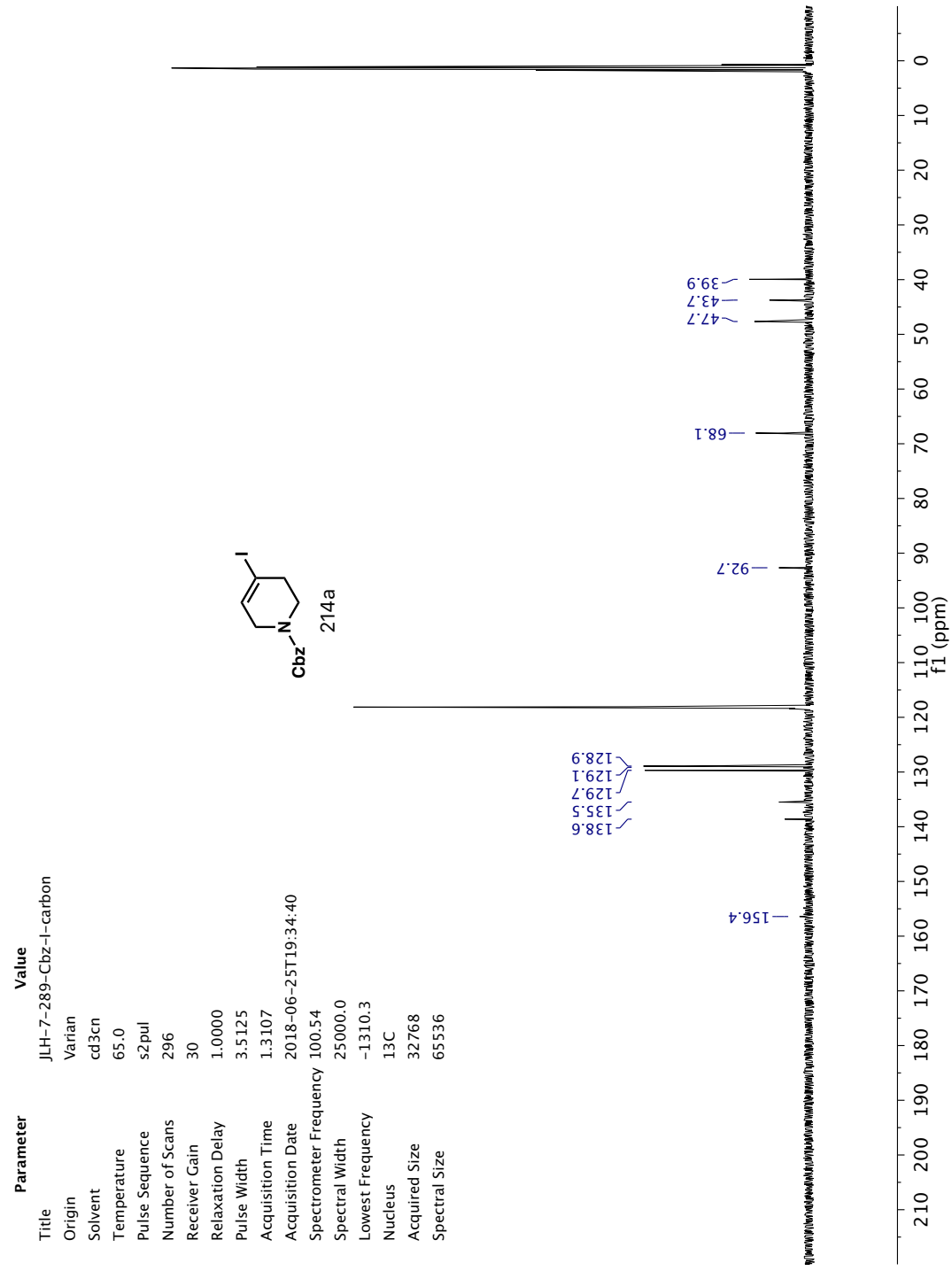
Parameter Value
Title JLH-7-289-Cbz-I-carbon
Origin Varian
Solvent cd3cn
Temperature 65.0
Pulse Sequence s2pul
Number of Scans 296
Receiver Gain 30
Relaxation Delay 1.0000
Pulse Width 3.5125
Acquisition Time 1.3107
Acquisition Date 2018-06-25T19:34:40
Spectrometer Frequency 100.54
Spectral Width 25000.0
Lowest Frequency -1310.3
Nucleus 13C
Acquired Size 32768
Spectral Size 65536
I
N
Cbz
214a
156.4
138.6
135.5
129.7
129.1
128.9
92.7
68.1
47.7
43.7
39.9
f1 (ppm)

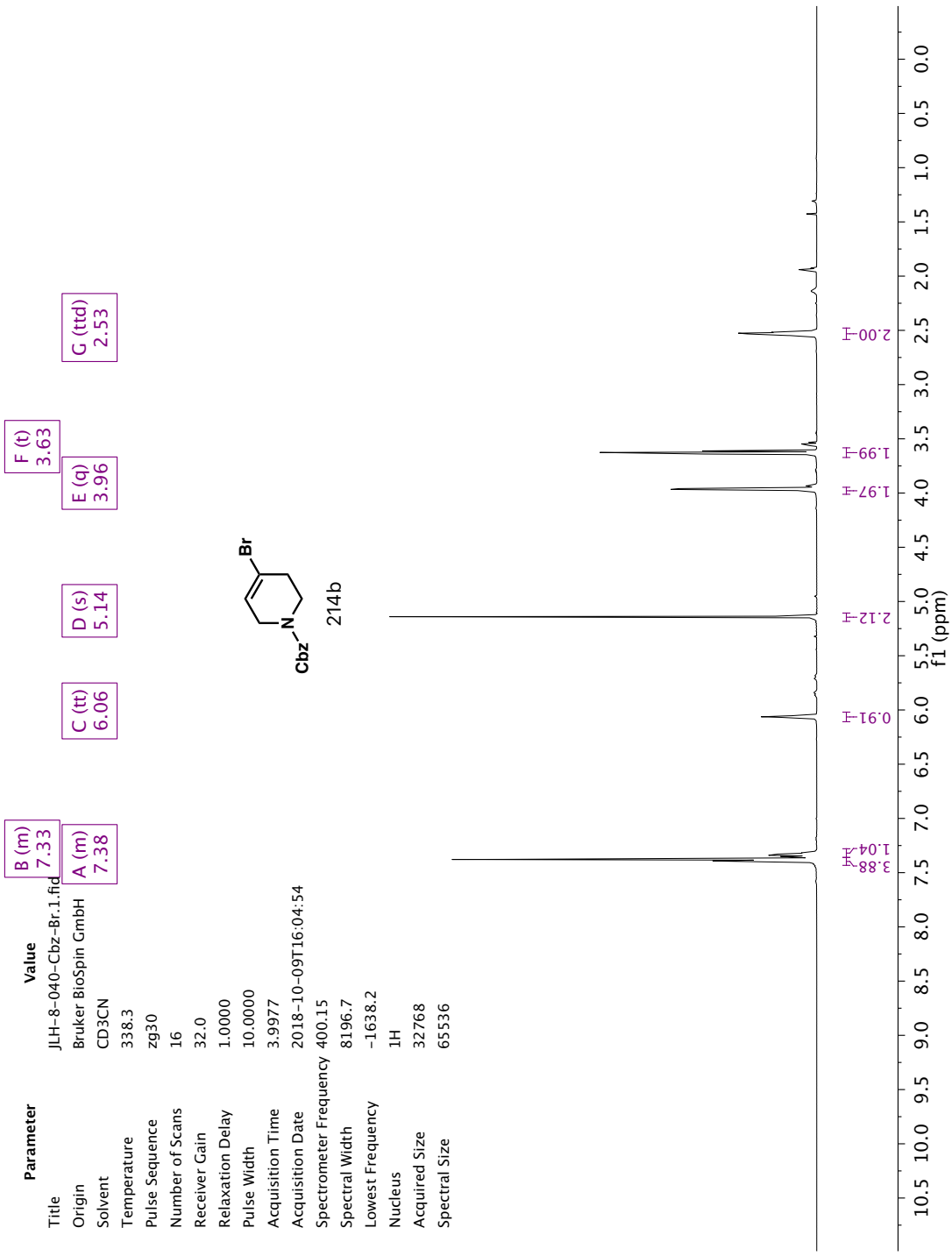
Parameter
Value
Title JLH-8-040-Cbz-Br.1.fid
Origin Bruker BioSpin GmbH
Solvent CD3CN
Temperature 338.3
Pulse Sequence zg30
Number of Scans 16
Receiver Gain 32.0
Relaxation Delay 1.0000
Pulse Width 10.0000
Acquisition Time 3.9977
Acquisition Date 2018-10-09T16:04:54
Spectrometer Frequency 400.15
Spectral Width 8196.7
Lowest Frequency -1638.2
Nucleus 1H
Acquired Size 32768
Spectral Size 65536
B (m) 7.33
A (m) 7.38
C (tt) 6.06
D (s) 5.14
F (t) 3.63
E (q) 3.96
G (ttd) 2.53
Br
Cbz
N
214b
3.88
1.04
0.91
2.12
1.97
1.99
2.00
10.5 10.0 9.5 9.0 8.5 8.0 7.5 7.0 6.5 6.0 5.5 5.0 4.5 4.0 3.5 3.0 2.5 2.0 1.5 1.0 0.5 0.0
f1 (ppm)

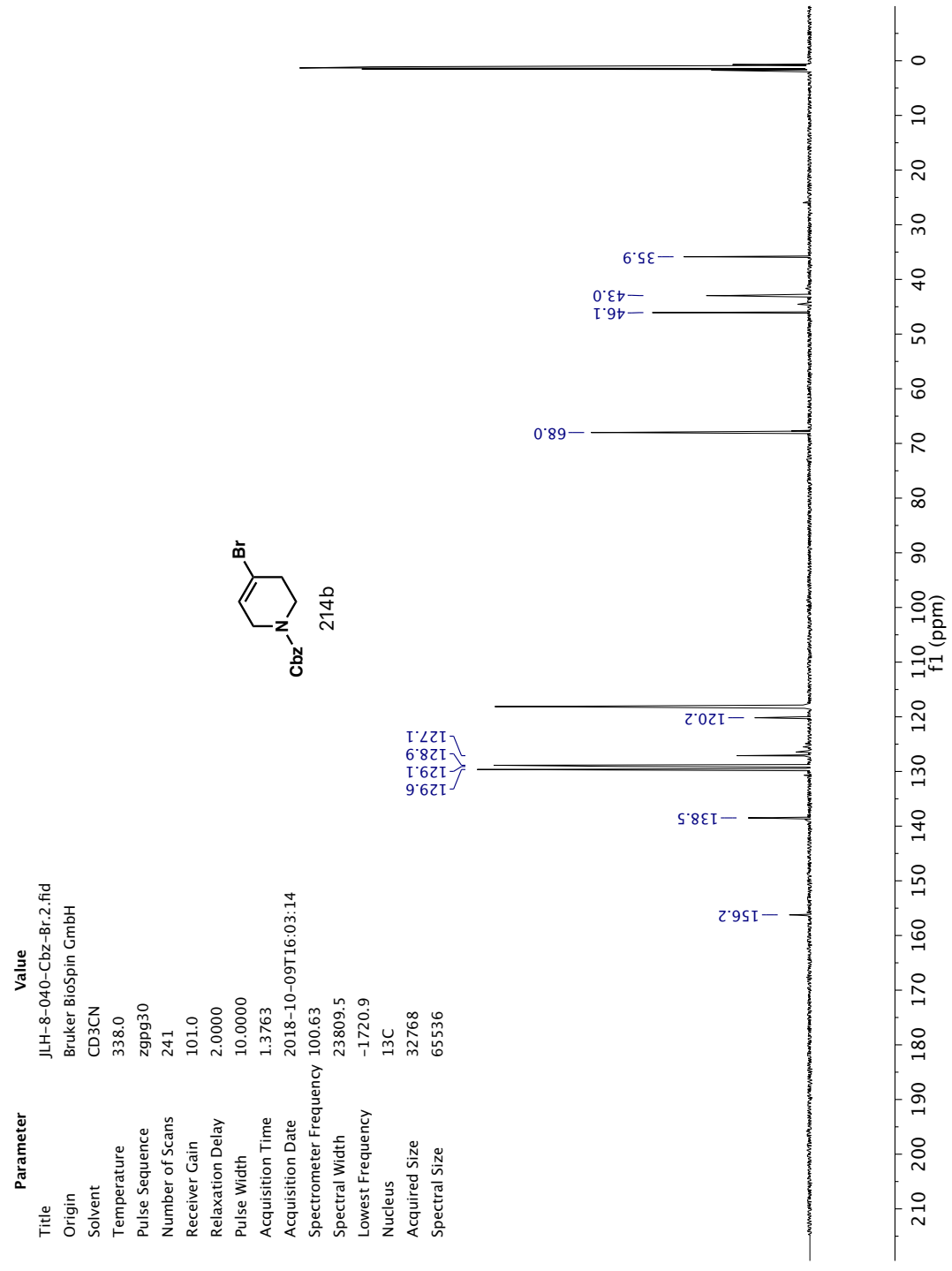
Parameter Value
Title JLH-8-040-Cbz-Br.2.fid
Origin Bruker BioSpin GmbH
Solvent CD3CN
Temperature 338.0
Pulse Sequence zgpg30
Number of Scans 241
Receiver Gain 101.0
Relaxation Delay 2.0000
Pulse Width 10.0000
Acquisition Time 1.3763
Acquisition Date 2018-10-09T16:03:14
Spectrometer Frequency 100.63
Spectral Width 23809.5
Lowest Frequency -1720.9
Nucleus 13C
Acquired Size 32768
Spectral Size 65536
Br
N
Cbz
214b
156.2
138.5
129.6
129.1
128.9
127.1
120.2
68.0
46.1
43.0
35.9
f1 (ppm)

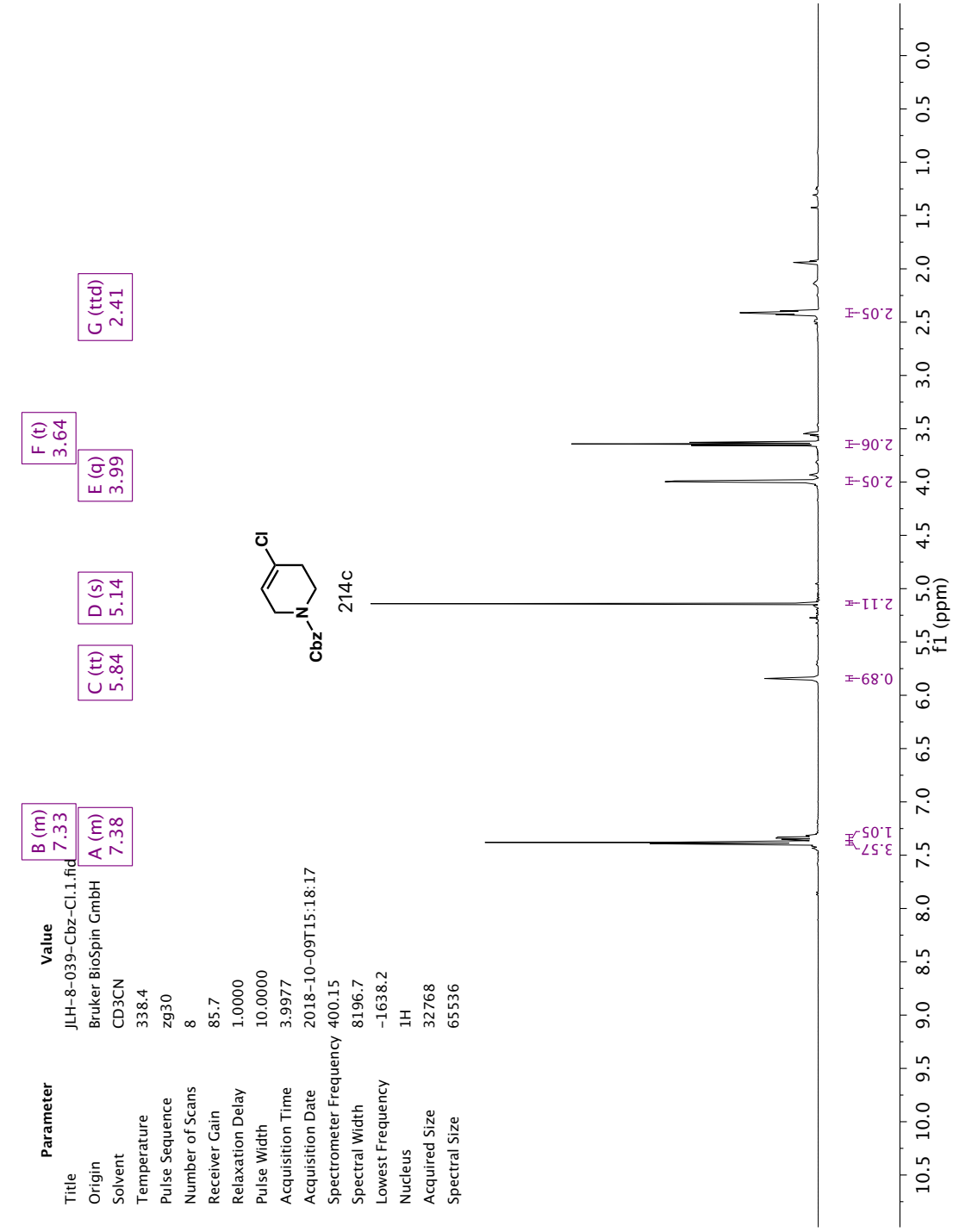
Parameter
Value
Title JLH-8-039-Cbz-Cl.1.fid
Origin Bruker BioSpin GmbH
Solvent CD3CN
Temperature 338.4
Pulse Sequence zg30
Number of Scans 8
Receiver Gain 85.7
Relaxation Delay 1.0000
Pulse Width 10.0000
Acquisition Time 3.9977
Acquisition Date 2018-10-09T15:18:17
Spectrometer Frequency 400.15
Spectral Width 8196.7
Lowest Frequency -1638.2
Nucleus 1H
Acquired Size 32768
Spectral Size 65536
B (m) 7.33
A (m) 7.38
C (tt) 5.84
D (s) 5.14
F (t) 3.64
E (q) 3.99
G (ttd) 2.41
Cl
N
Cbz
214c
3.57
1.05
0.89
2.11
2.05
2.06
2.05
2.05
10.5 10.0 9.5 9.0 8.5 8.0 7.5 7.0 6.5 6.0 5.5 5.0 4.5 4.0 3.5 3.0 2.5 2.0 1.5 1.0 0.5 0.0
f1 (ppm)

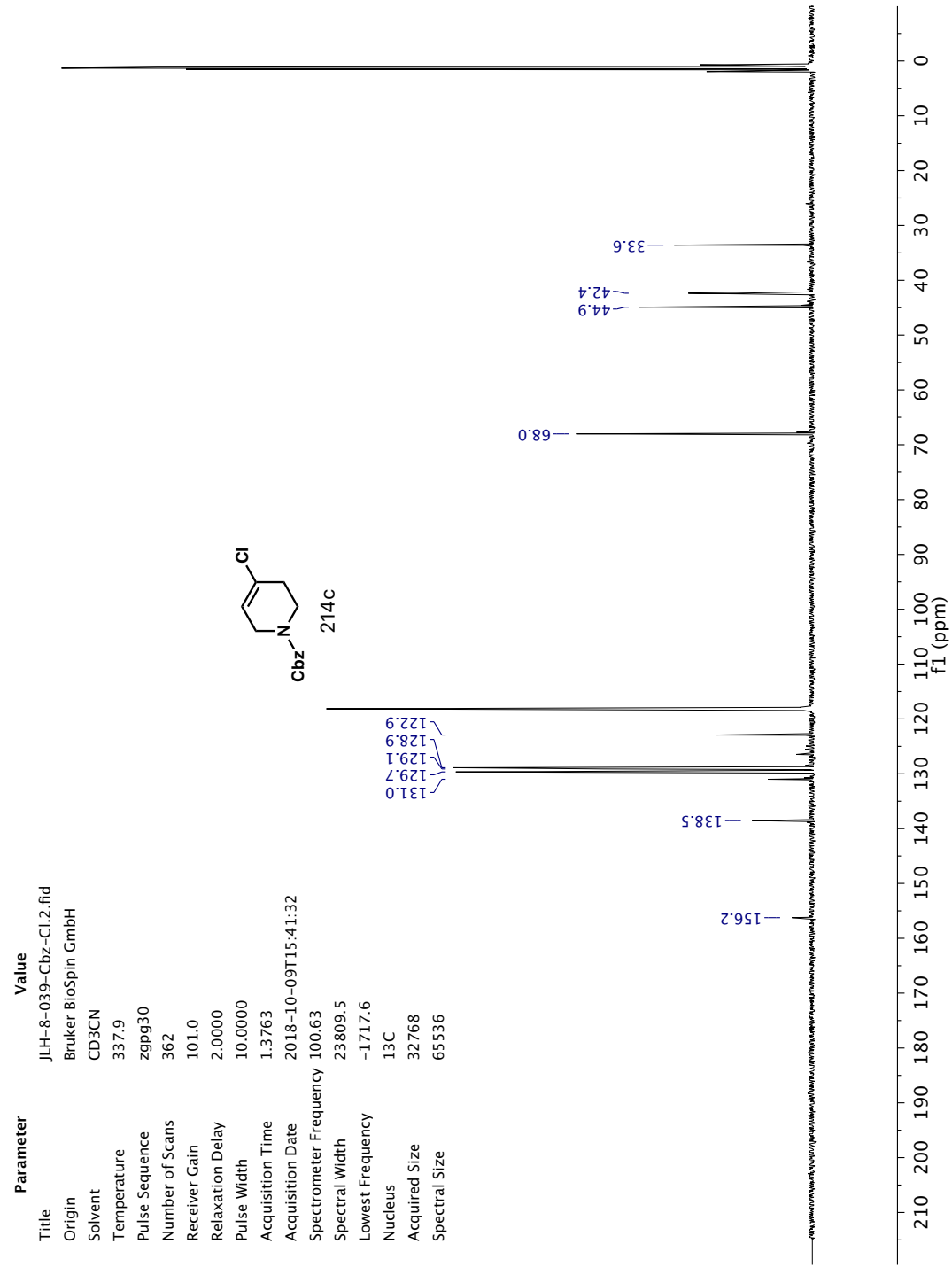

Parameter	Value
Title	JLH-8-039-Cbz-Cl.2.fid
Origin	Bruker BioSpin GmbH
Solvent	CD3CN
Temperature	337.9
Pulse Sequence	zgpg30
Number of Scans	362
Receiver Gain	101.0
Relaxation Delay	2.0000
Pulse Width	10.0000
Acquisition Time	1.3763
Acquisition Date	2018-10-09T15:41:32
Spectrometer Frequency	100.63
Spectral Width	23809.5
Lowest Frequency	-1717.6
Nucleus	13C
Acquired Size	32768
Spectral Size	65536

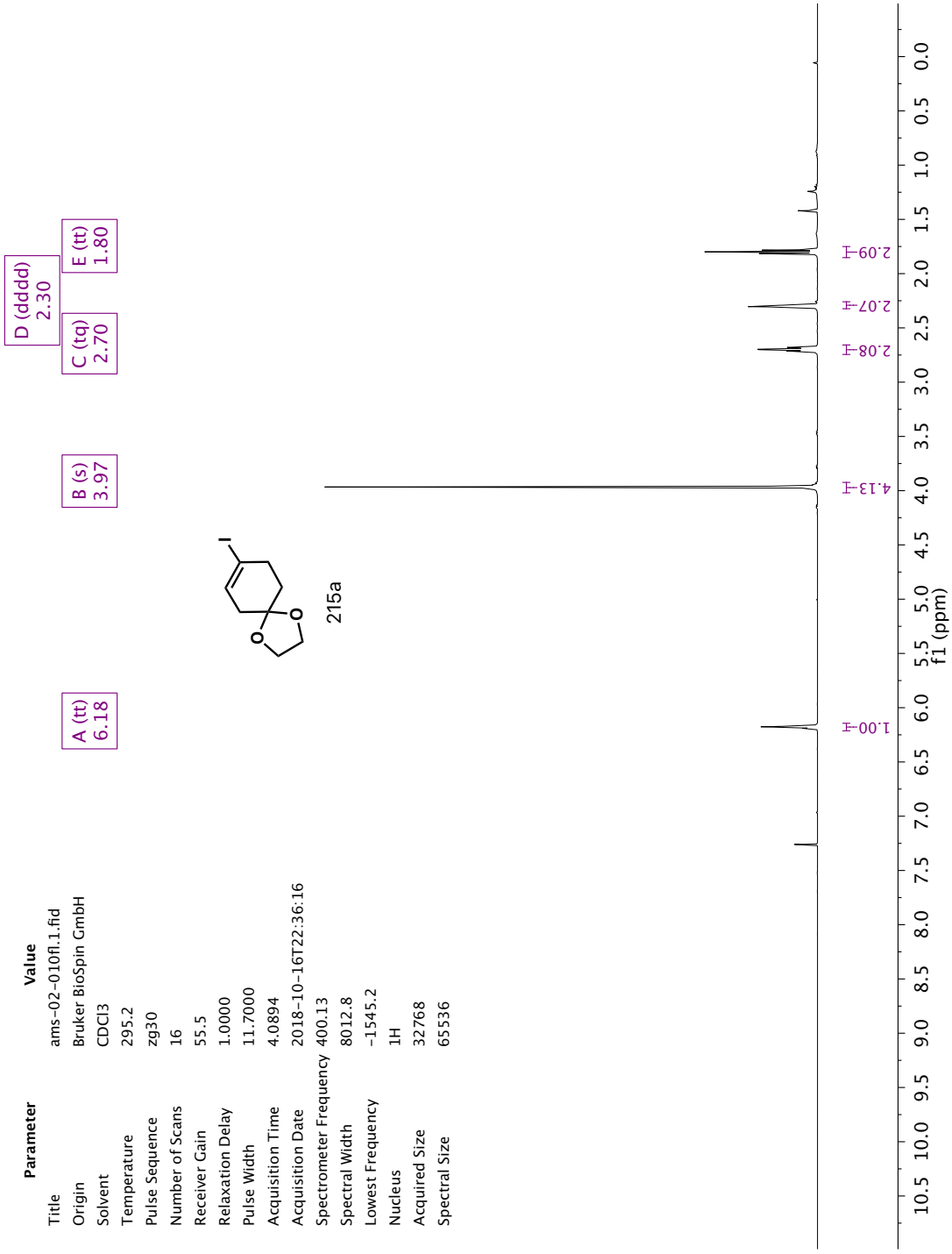
Parameter Value
Title ams-02-010fl.1.fid
Origin Bruker BioSpin GmbH
Solvent CDCl3
Temperature 295.2
Pulse Sequence zg30
Number of Scans 16
Receiver Gain 55.5
Relaxation Delay 1.0000
Pulse Width 11.7000
Acquisition Time 4.0894
Acquisition Date 2018-10-16T22:36:16
Spectrometer Frequency 400.13
Spectral Width 8012.8
Lowest Frequency -1545.2
Nucleus 1H
Acquired Size 32768
Spectral Size 65536
A (tt) 6.18
B (s) 3.97
C (tq) 2.70
D (dddd) 2.30
E (tt) 1.80
215a
1.00
4.13
2.08
2.07
2.09
10.5 10.0 9.5 9.0 8.5 8.0 7.5 7.0 6.5 6.0 5.5 5.0 4.5 4.0 3.5 3.0 2.5 2.0 1.5 1.0 0.5 0.0
f1 (ppm)

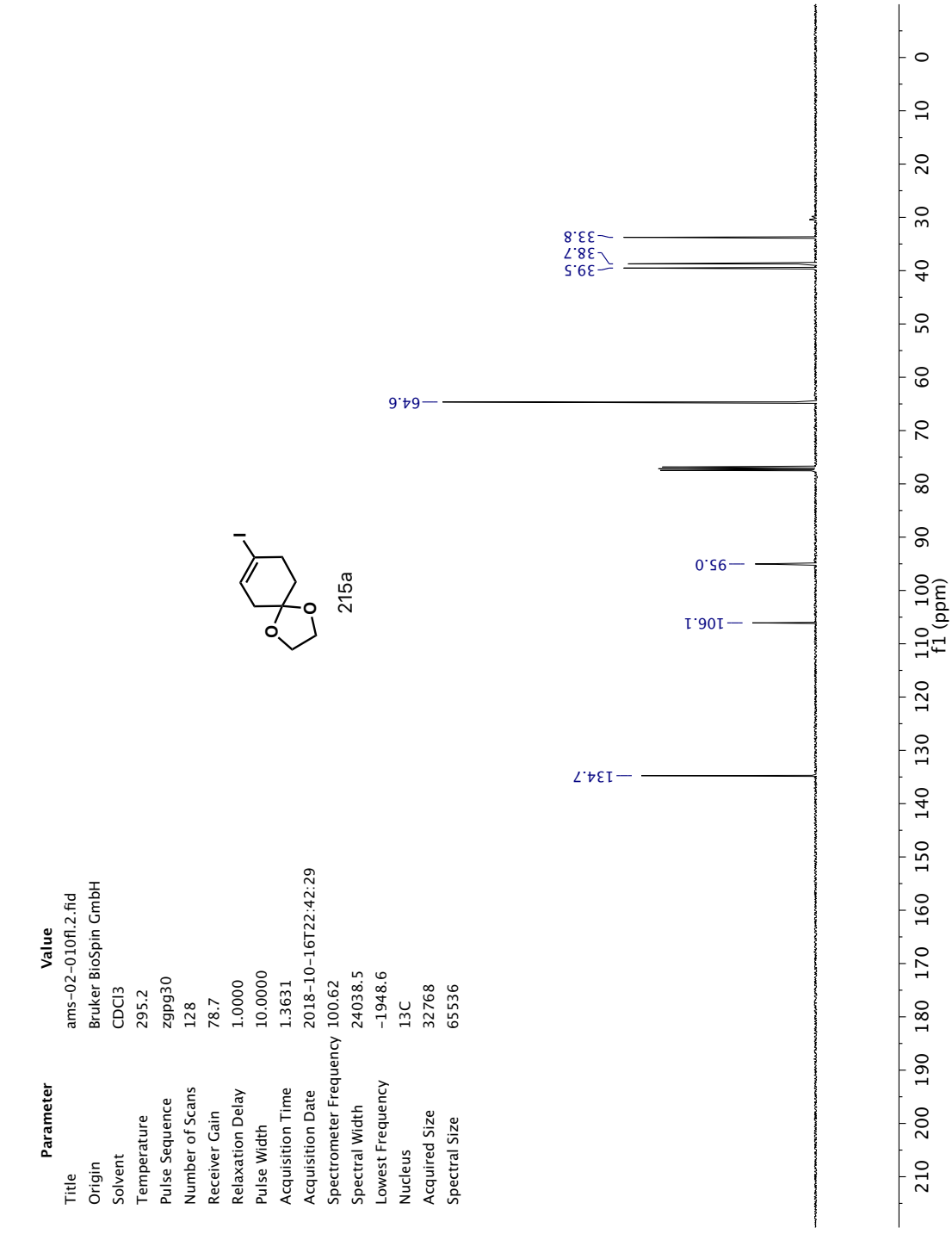
Parameter Value
Title ams-02-010fl.2.fid
Origin Bruker BioSpin GmbH
Solvent CDCl3
Temperature 295.2
Pulse Sequence zgpg30
Number of Scans 128
Receiver Gain 78.7
Relaxation Delay 1.0000
Pulse Width 10.0000
Acquisition Time 1.3631
Acquisition Date 2018-10-16T22:42:29
Spectrometer Frequency 100.62
Spectral Width 24038.5
Lowest Frequency -1948.6
Nucleus 13C
Acquired Size 32768
Spectral Size 65536
215a
134.7
106.1
95.0
64.6
39.5
38.7
33.8
f1 (ppm)

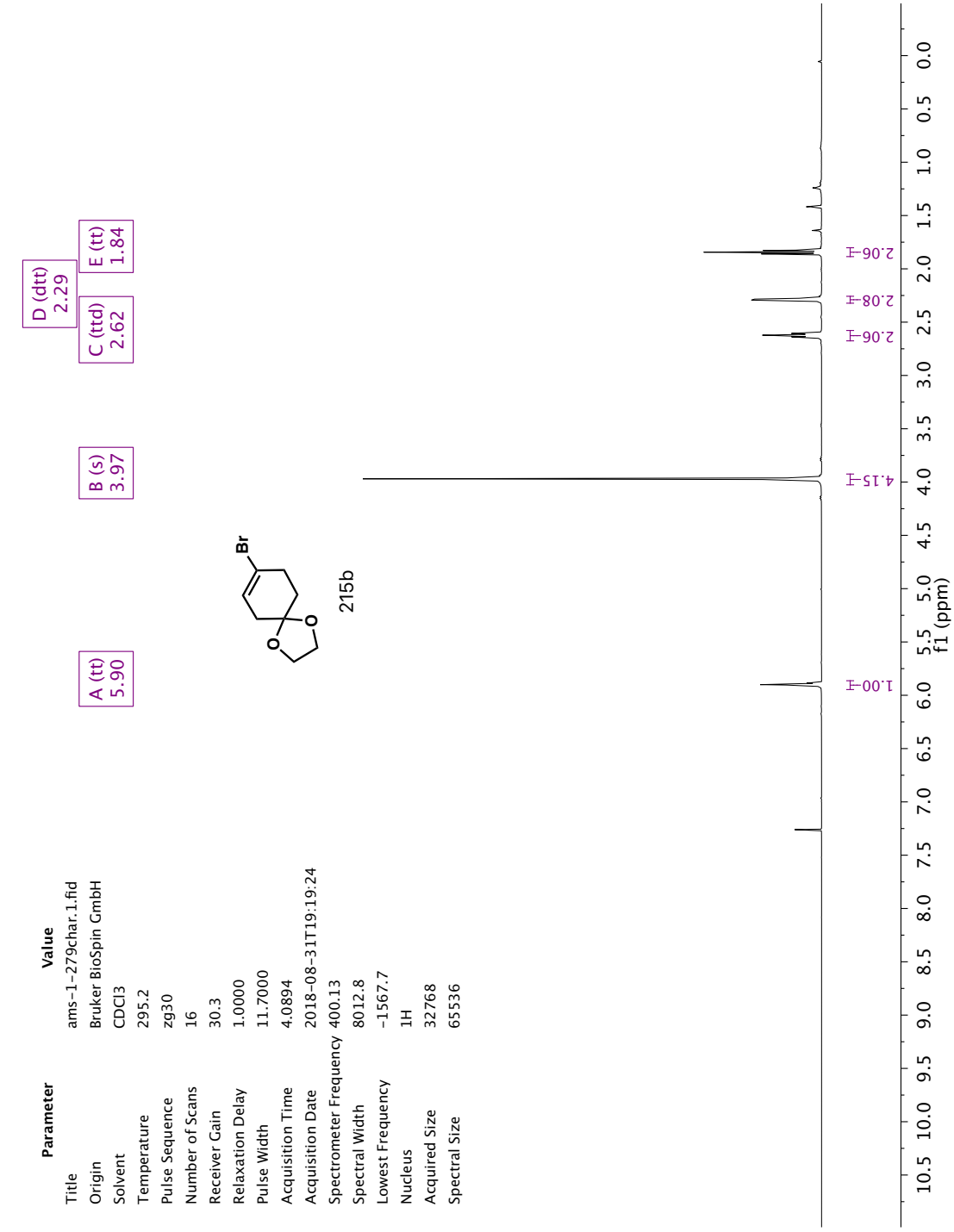
Parameter
Value
Title ams-1-279char.1.fid
Origin Bruker BioSpin GmbH
Solvent CDCl3
Temperature 295.2
Pulse Sequence zg30
Number of Scans 16
Receiver Gain 30.3
Relaxation Delay 1.0000
Pulse Width 11.7000
Acquisition Time 4.0894
Acquisition Date 2018-08-31T19:19:24
Spectrometer Frequency 400.13
Spectral Width 8012.8
Lowest Frequency -1567.7
Nucleus 1H
Acquired Size 32768
Spectral Size 65536
A (tt) 5.90
B (s) 3.97
C (ttd) 2.62
D (dtt) 2.29
E (tt) 1.84
Br
O
O
215b
1.00
4.15
2.06
2.08
2.06
10.5 10.0 9.5 9.0 8.5 8.0 7.5 7.0 6.5 6.0 5.5 5.0 4.5 4.0 3.5 3.0 2.5 2.0 1.5 1.0 0.5 0.0
f1 (ppm)

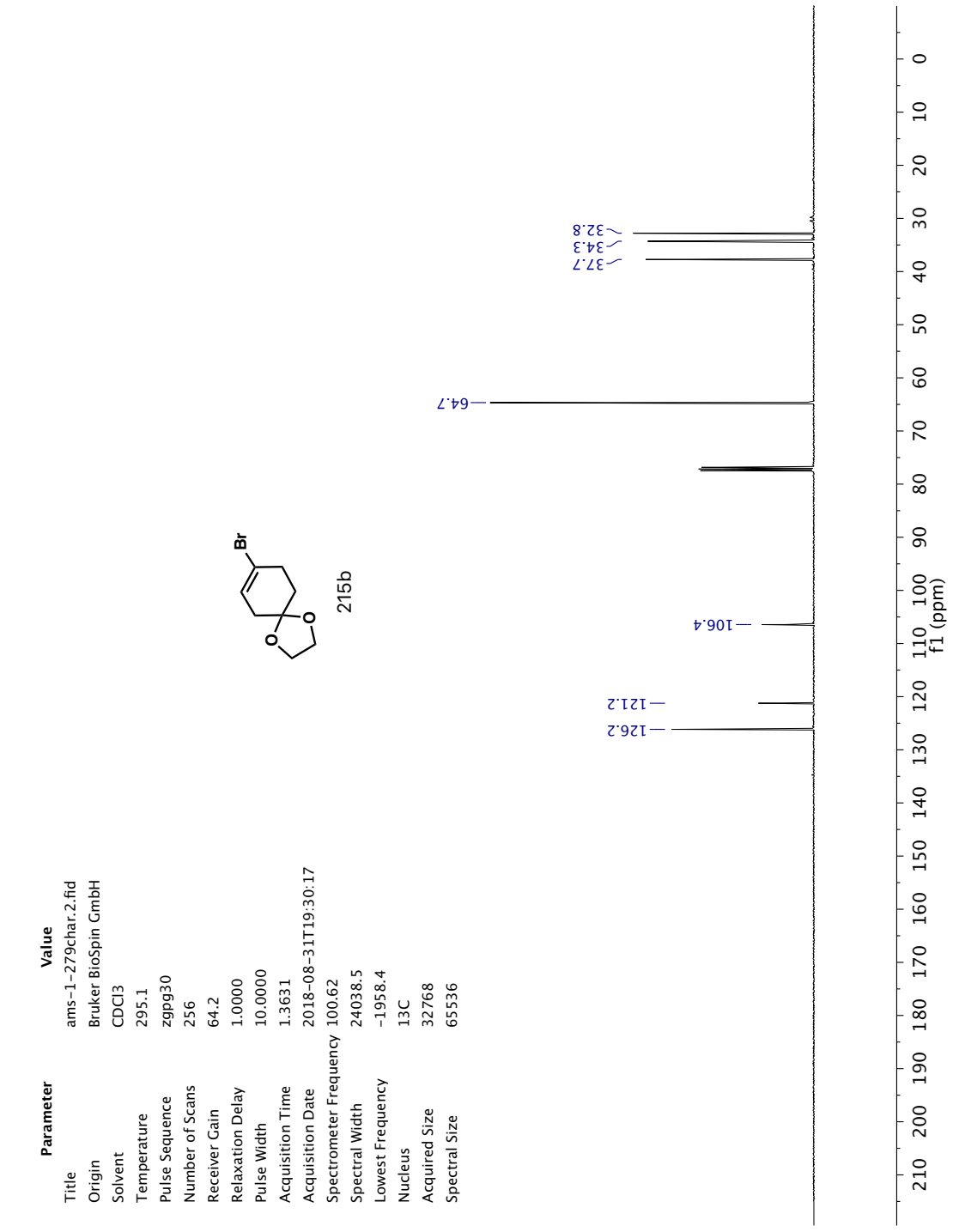
Parameter Value
Title ams-1-279char.2.fid
Origin Bruker BioSpin GmbH
Solvent CDCl3
Temperature 295.1
Pulse Sequence zgpg30
Number of Scans 256
Receiver Gain 64.2
Relaxation Delay 1.0000
Pulse Width 10.0000
Acquisition Time 1.3631
Acquisition Date 2018-08-31T19:30:17
Spectrometer Frequency 100.62
Spectral Width 24038.5
Lowest Frequency -1958.4
Nucleus 13C
Acquired Size 32768
Spectral Size 65536
Br
O
O
215b
64.7
106.4
126.2
121.2
37.7
34.3
32.8
f1 (ppm)

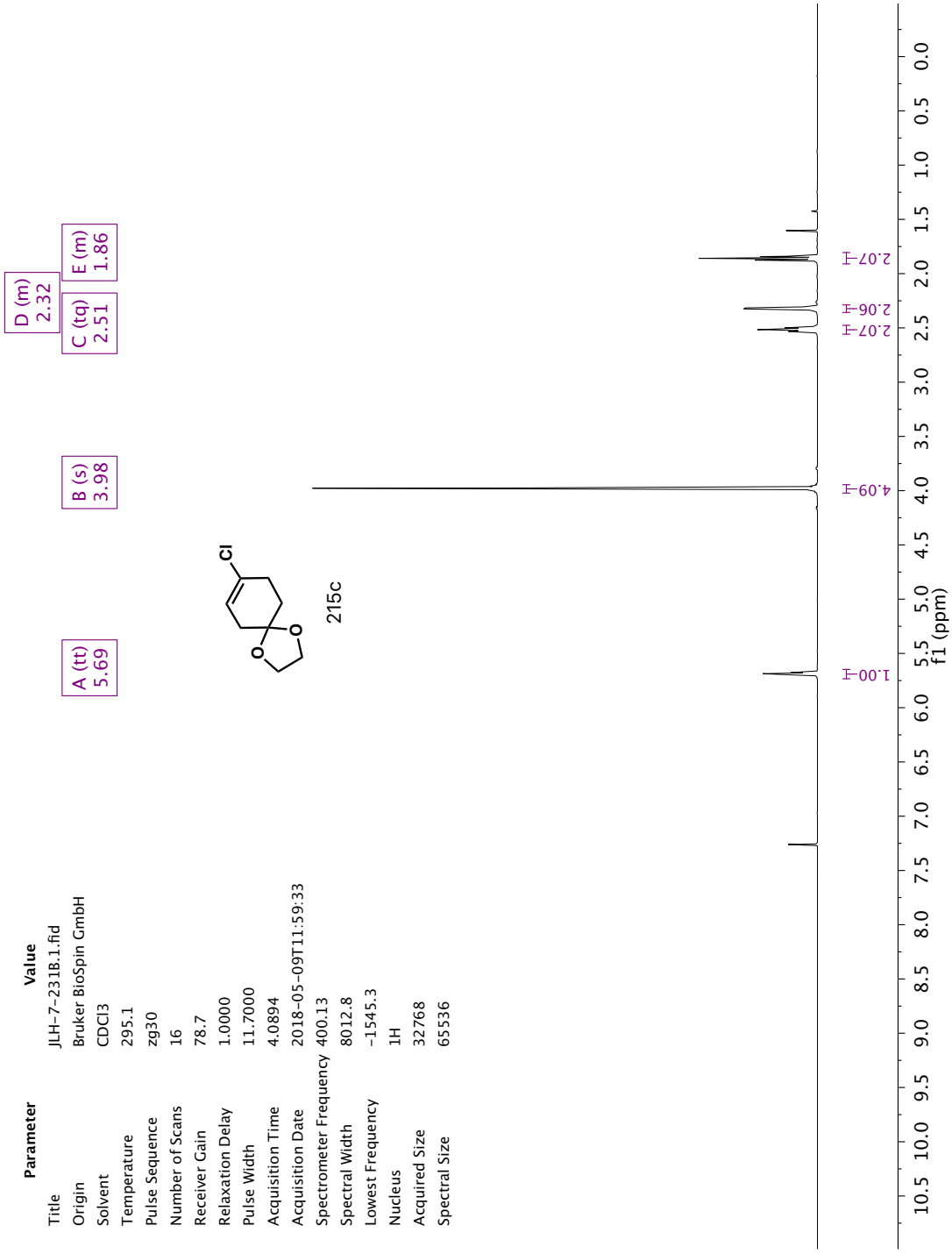
Parameter Value
Title JLH-7-231B.1.fid
Origin Bruker BioSpin GmbH
Solvent CDCl3
Temperature 295.1
Pulse Sequence zg30
Number of Scans 16
Receiver Gain 78.7
Relaxation Delay 1.0000
Pulse Width 11.7000
Acquisition Time 4.0894
Acquisition Date 2018-05-09T11:59:33
Spectrometer Frequency 400.13
Spectral Width 8012.8
Lowest Frequency -1545.3
Nucleus 1H
Acquired Size 32768
Spectral Size 65536
A (tt) 5.69
B (s) 3.98
C (tq) 2.51
D (m) 2.32
E (m) 1.86
Cl
O
O
215c
1.00
4.09
2.07
2.06
2.07
10.5 10.0 9.5 9.0 8.5 8.0 7.5 7.0 6.5 6.0 5.5 5.0 4.5 4.0 3.5 3.0 2.5 2.0 1.5 1.0 0.5 0.0
f1 (ppm)

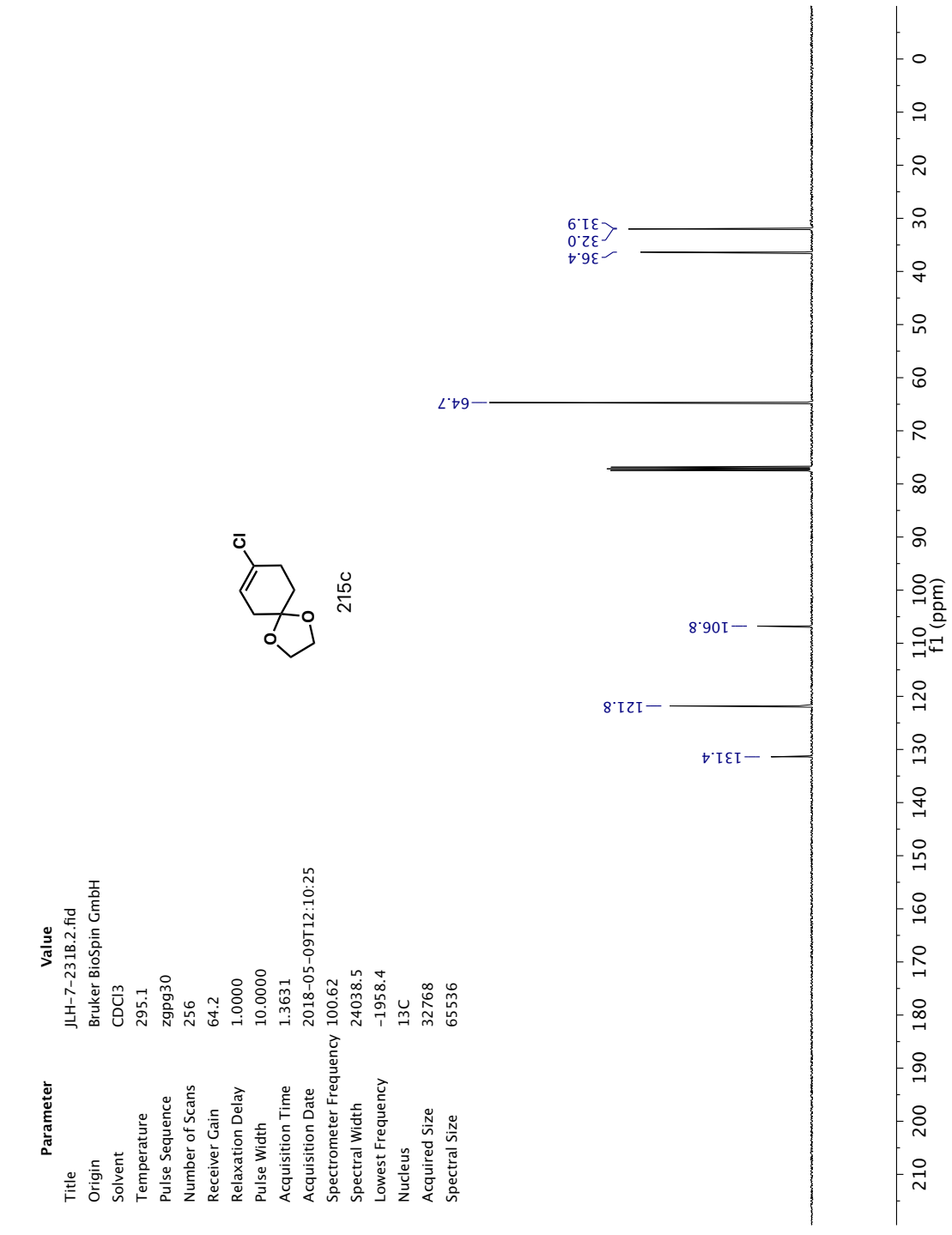
Parameter Value
Title JLH-7-231B.2.fid
Origin Bruker BioSpin GmbH
Solvent CDCl3
Temperature 295.1
Pulse Sequence zgpg30
Number of Scans 256
Receiver Gain 64.2
Relaxation Delay 1.0000
Pulse Width 10.0000
Acquisition Time 1.3631
Acquisition Date 2018-05-09T12:10:25
Spectrometer Frequency 100.62
Spectral Width 24038.5
Lowest Frequency -1958.4
Nucleus 13C
Acquired Size 32768
Spectral Size 65536
Cl
O
O
215c
64.7
36.4
32.0
31.9
106.8
121.8
131.4
f1 (ppm)

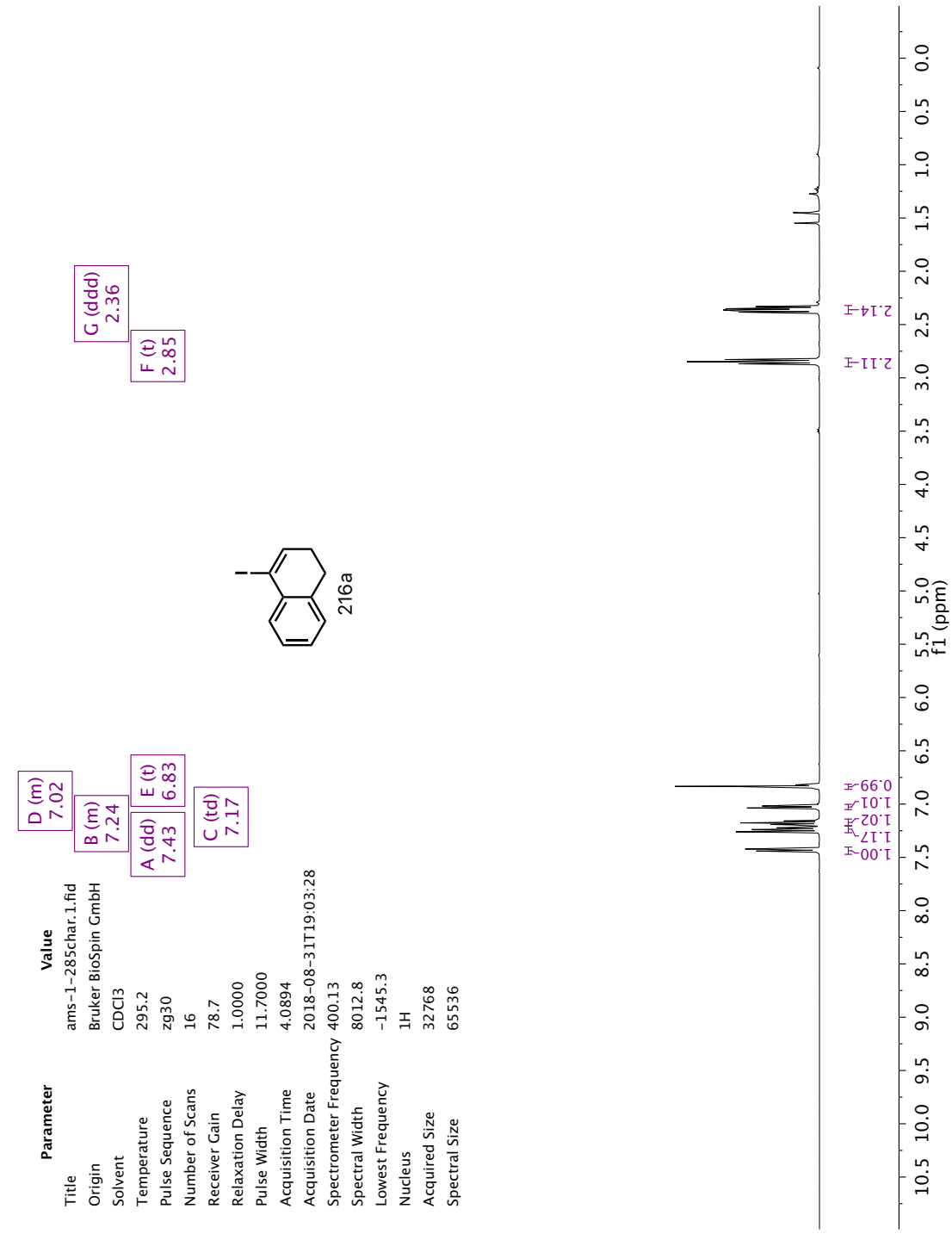
D (m) 7.02
B (m) 7.24
A (dd) 7.43
E (t) 6.83
C (td) 7.17
G (ddd) 2.36
F (t) 2.85
216a
Parameter Value
Title ams-1-285char.1.fid
Origin Bruker BioSpin GmbH
Solvent CDCl3
Temperature 295.2
Pulse Sequence zg30
Number of Scans 16
Receiver Gain 78.7
Relaxation Delay 1.0000
Pulse Width 11.7000
Acquisition Time 4.0894
Acquisition Date 2018-08-31T19:03:28
Spectrometer Frequency 400.13
Spectral Width 8012.8
Lowest Frequency -1545.3
Nucleus 1H
Acquired Size 32768
Spectral Size 65536
1.00
1.17
1.02
1.01
0.99
2.14
2.11
f1 (ppm)

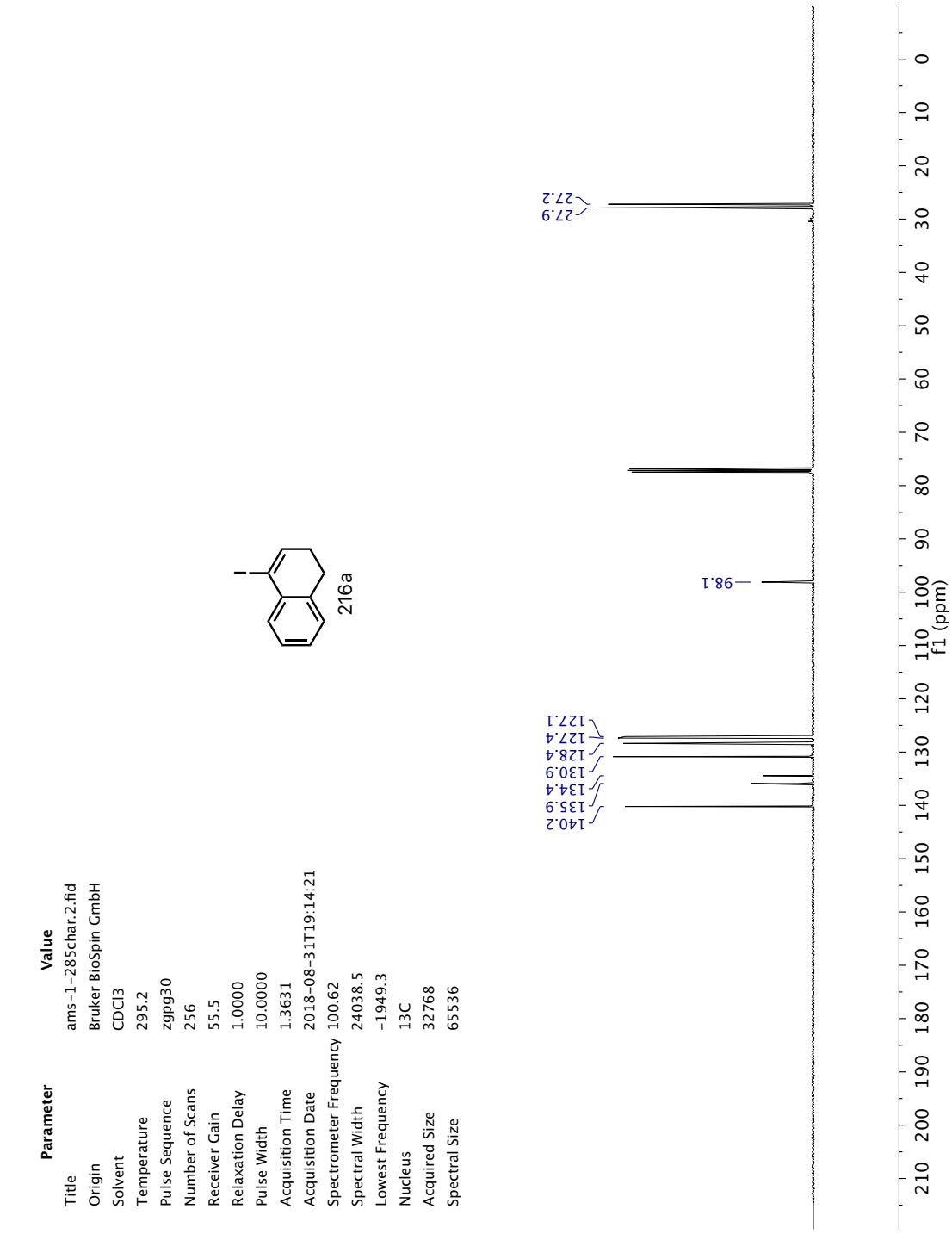
Parameter Value
Title ams-1-285char.2.fid
Origin Bruker BioSpin GmbH
Solvent CDCl3
Temperature 295.2
Pulse Sequence zgpg30
Number of Scans 256
Receiver Gain 55.5
Relaxation Delay 1.0000
Pulse Width 10.0000
Acquisition Time 1.3631
Acquisition Date 2018-08-31T19:14:21
Spectrometer Frequency 100.62
Spectral Width 24038.5
Lowest Frequency -1949.3
Nucleus 13C
Acquired Size 32768
Spectral Size 65536
216a
140.2
135.9
134.4
130.9
128.4
127.4
127.1
98.1
27.9
27.2
f1 (ppm)

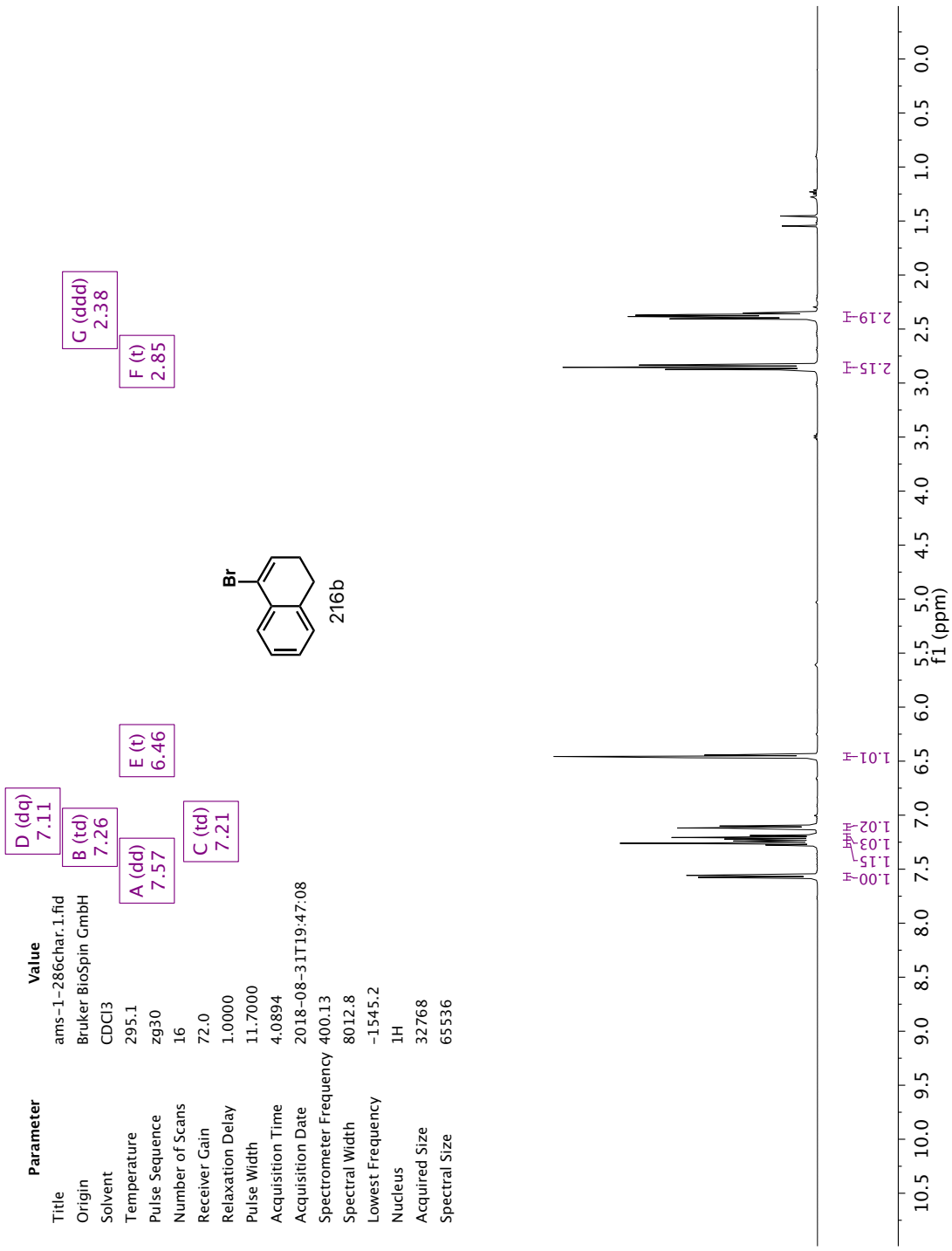
D (dq)
7.11
B (td)
7.26
A (dd)
7.57
E (t)
6.46
C (td)
7.21
G (ddd)
2.38
F (t)
2.85
Br
216b
Parameter Value
Title ams-1-286char.1.fid
Origin Bruker BioSpin GmbH
Solvent CDCl3
Temperature 295.1
Pulse Sequence zg30
Number of Scans 16
Receiver Gain 72.0
Relaxation Delay 1.0000
Pulse Width 11.7000
Acquisition Time 4.0894
Acquisition Date 2018-08-31T19:47:08
Spectrometer Frequency 400.13
Spectral Width 8012.8
Lowest Frequency -1545.2
Nucleus 1H
Acquired Size 32768
Spectral Size 65536
1.00
1.15
1.03
1.02
1.01
2.15
2.19
10.5 10.0 9.5 9.0 8.5 8.0 7.5 7.0 6.5 6.0 5.5 5.0 4.5 4.0 3.5 3.0 2.5 2.0 1.5 1.0 0.5 0.0
f1 (ppm)

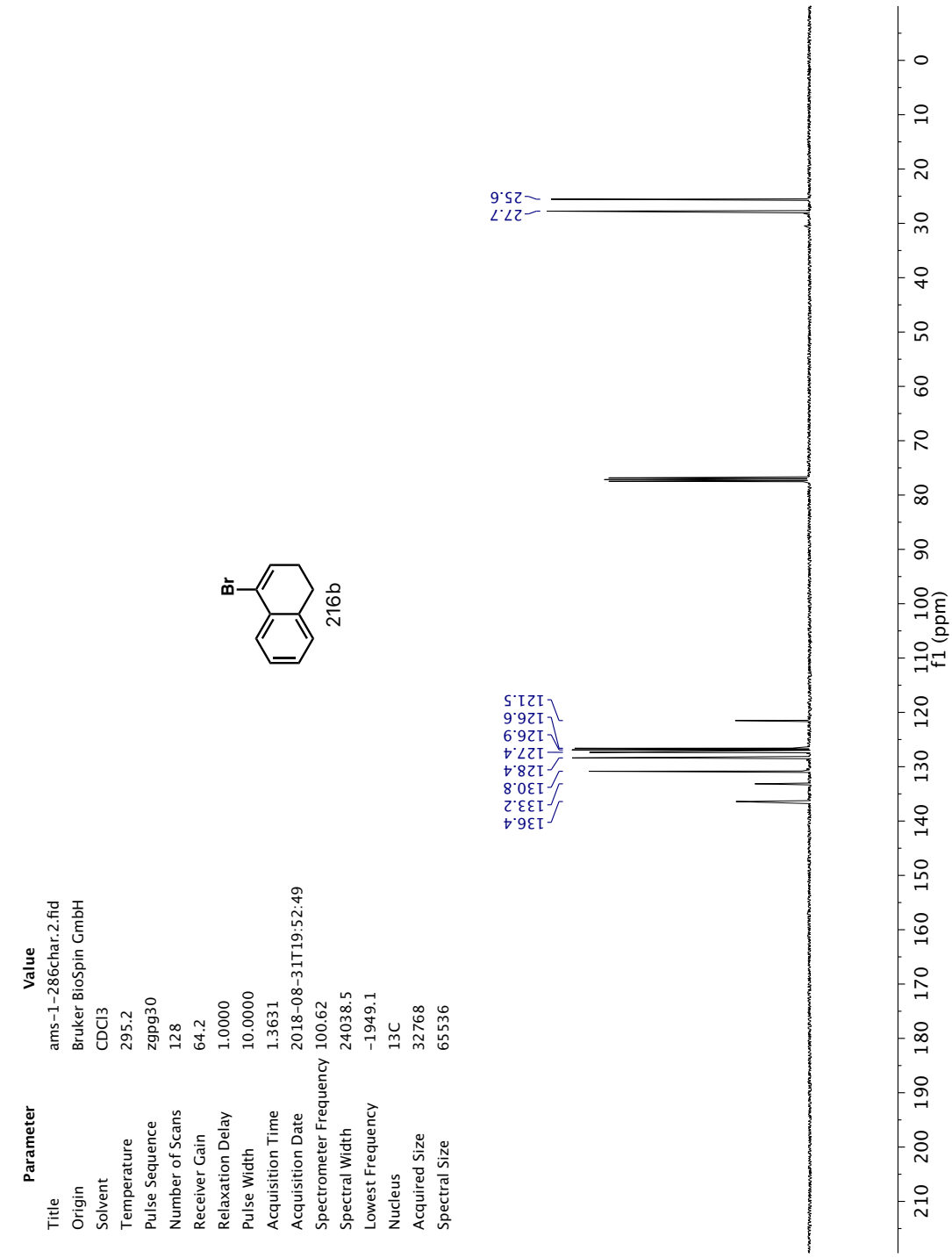

Parameter	Value
Title	ams-1-286char.2.fid
Origin	Bruker BioSpin GmbH
Solvent	CDCl3
Temperature	295.2
Pulse Sequence	zgpg30
Number of Scans	128
Receiver Gain	64.2
Relaxation Delay	1.0000
Pulse Width	10.0000
Acquisition Time	1.3631
Acquisition Date	2018-08-31T19:52:49
Spectrometer Frequency	100.62
Spectral Width	24038.5
Lowest Frequency	-1949.1
Nucleus	13C
Acquired Size	32768
Spectral Size	65536

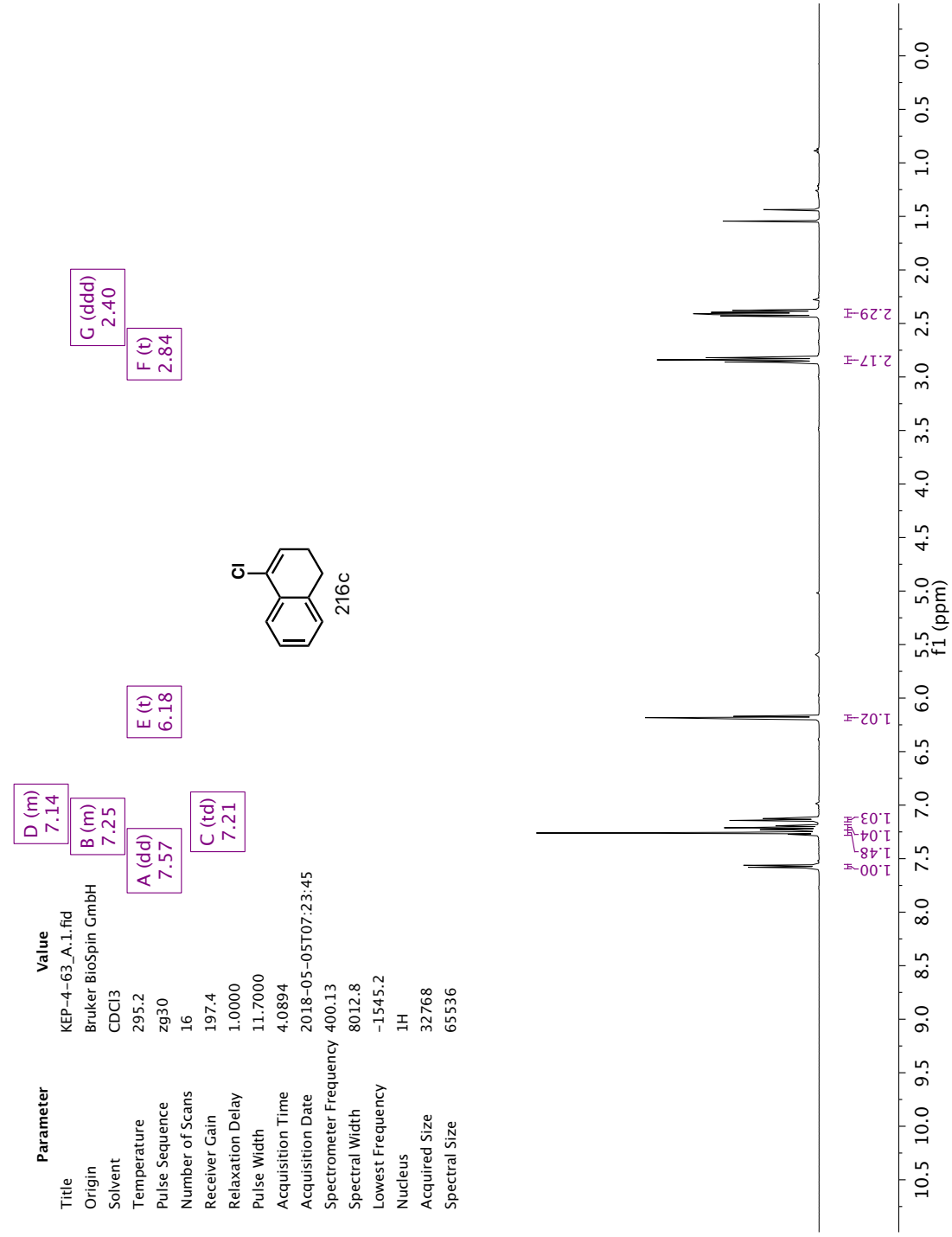

Parameter	Value
Title	KEP-4-63_A.1.fid
Origin	Bruker BioSpin GmbH
Solvent	CDCl3
Temperature	295.2
Pulse Sequence	zg30
Number of Scans	16
Receiver Gain	197.4
Relaxation Delay	1.0000
Pulse Width	11.7000
Acquisition Time	4.0894
Acquisition Date	2018-05-05T07:23:45
Spectrometer Frequency	400.13
Spectral Width	8012.8
Lowest Frequency	-1545.2
Nucleus	1H
Acquired Size	32768
Spectral Size	65536

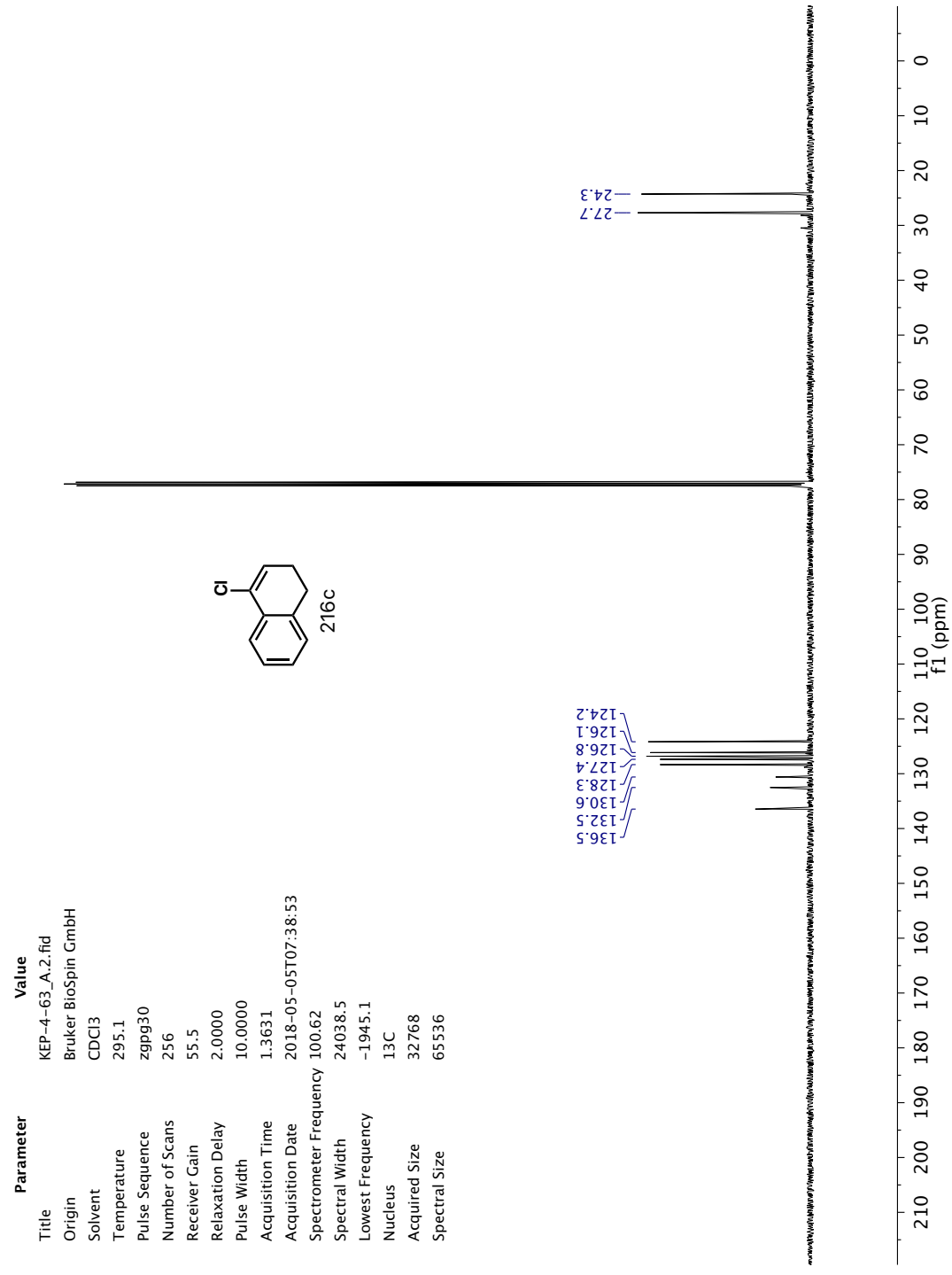
Parameter Value
Title KEP-4-63_A.2.fid
Origin Bruker BioSpin GmbH
Solvent CDCl3
Temperature 295.1
Pulse Sequence zgpg30
Number of Scans 256
Receiver Gain 55.5
Relaxation Delay 2.0000
Pulse Width 10.0000
Acquisition Time 1.3631
Acquisition Date 2018-05-05T07:38:53
Spectrometer Frequency 100.62
Spectral Width 24038.5
Lowest Frequency -1945.1
Nucleus 13C
Acquired Size 32768
Spectral Size 65536
Cl
216c
136.5
132.5
130.6
128.3
127.4
126.8
126.1
124.2
27.7
24.3
f1 (ppm)

Parameter	Value
Title	JLH-7-284-column-2.1.fid
Origin	Bruker BioSpin GmbH
Solvent	CDCl3
Temperature	295.2
Pulse Sequence	zg30
Number of Scans	16
Receiver Gain	98.9
Relaxation Delay	1.0000
Pulse Width	11.7000
Acquisition Time	4.0894
Acquisition Date	2018-06-23T15:52:10
Spectrometer Frequency	400.13
Spectral Width	8012.8
Lowest Frequency	-1545.2
Nucleus	1H
Acquired Size	32768
Spectral Size	65536

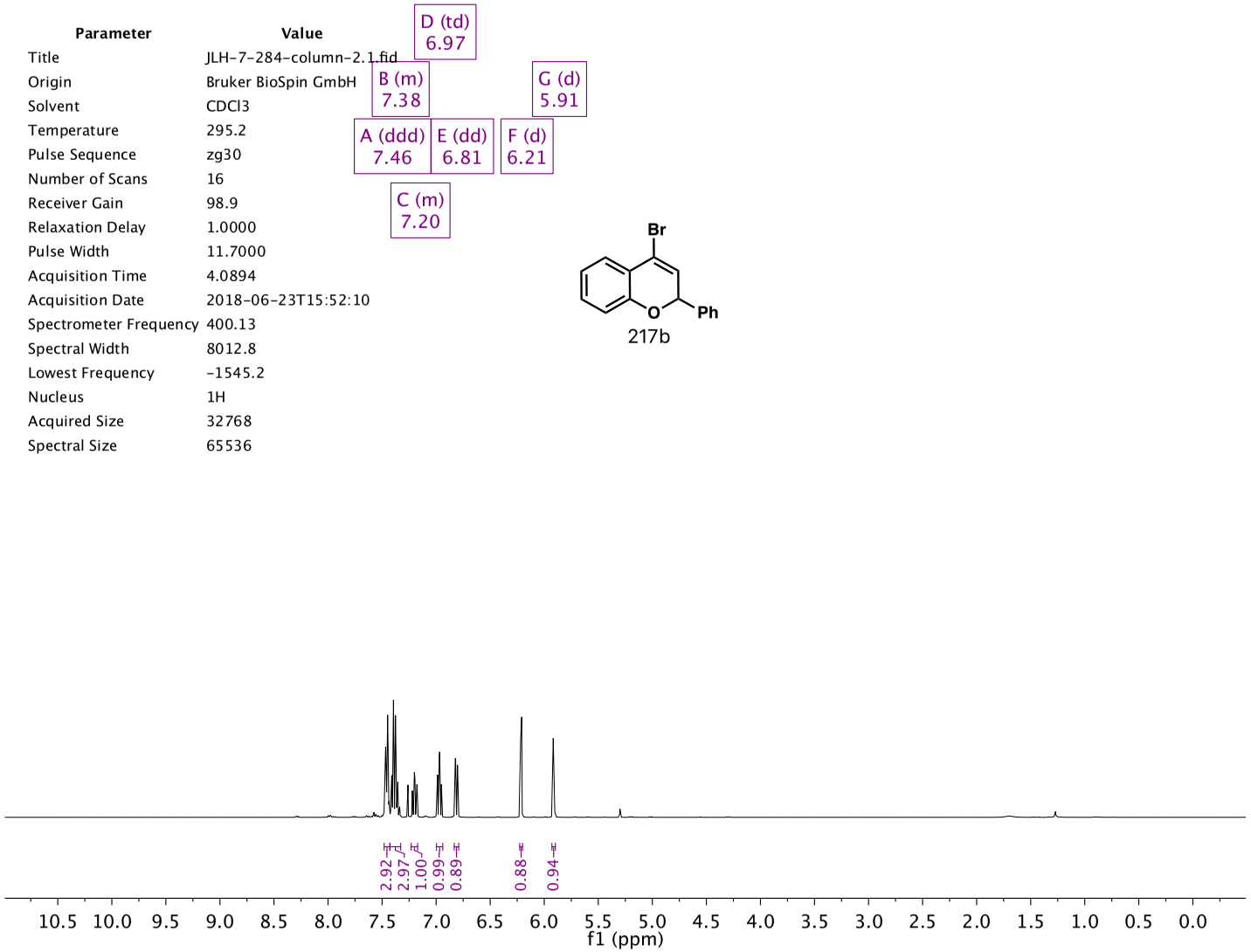

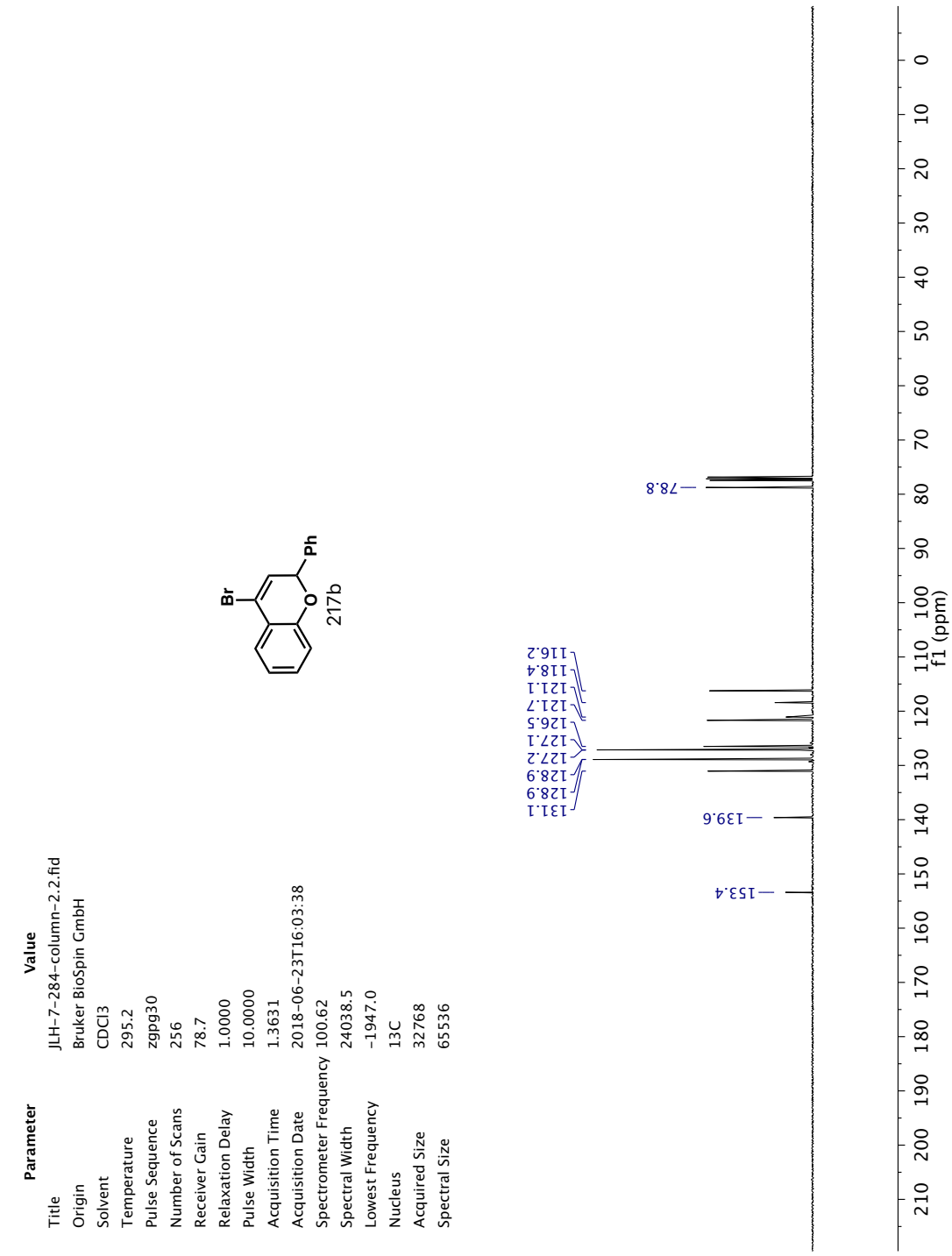

Parameter	Value
Title	JLH-7-284-column-2.2.fid
Origin	Bruker BioSpin GmbH
Solvent	CDCl3
Temperature	295.2
Pulse Sequence	zgpg30
Number of Scans	256
Receiver Gain	78.7
Relaxation Delay	1.0000
Pulse Width	10.0000
Acquisition Time	1.3631
Acquisition Date	2018-06-23T16:03:38
Spectrometer Frequency	100.62
Spectral Width	24038.5
Lowest Frequency	-1947.0
Nucleus	13C
Acquired Size	32768
Spectral Size	65536

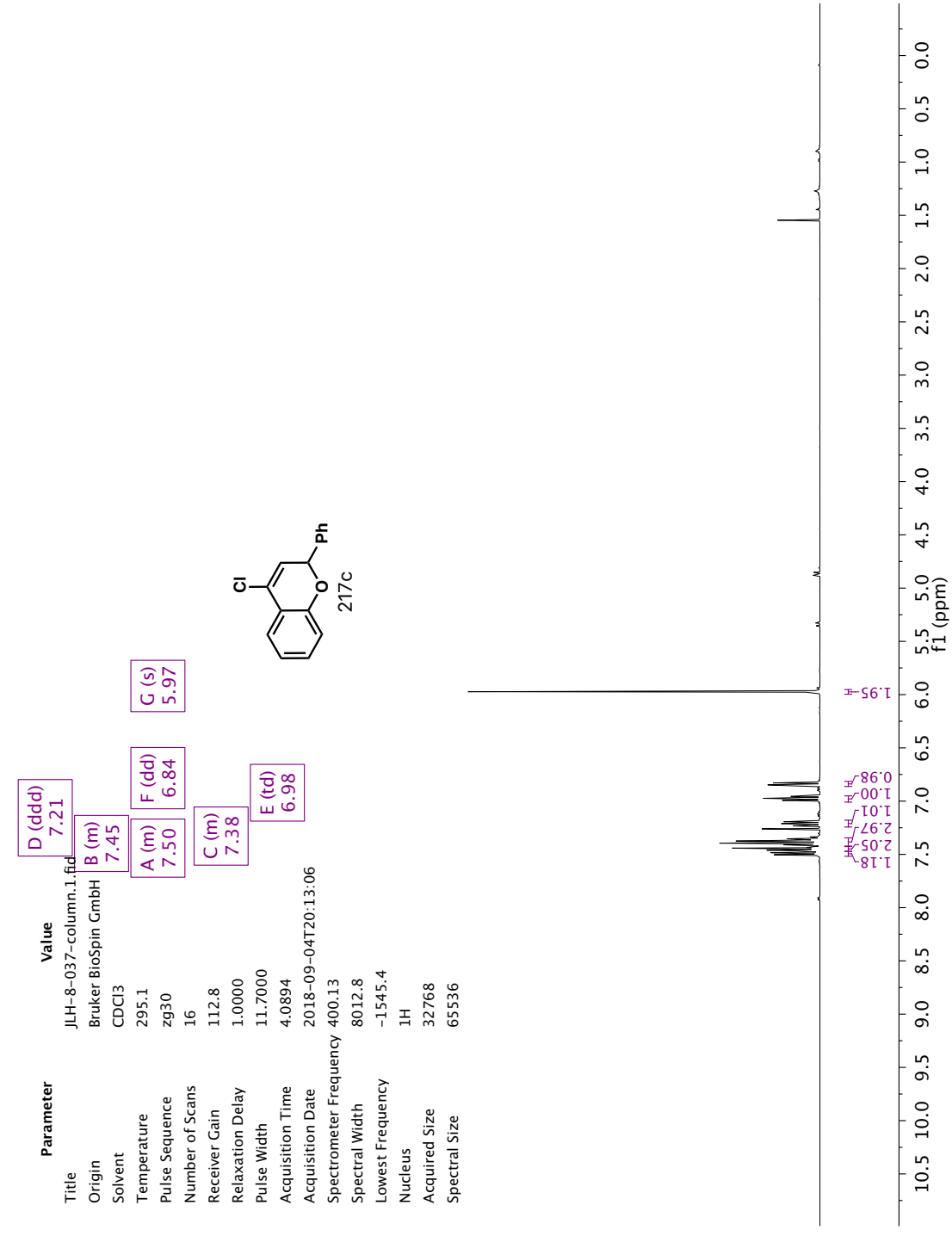
Parameter
Value
Title
JLH-8-037-column.1.fid
Origin
Bruker BioSpin GmbH
Solvent
CDCl3
Temperature
295.1
Pulse Sequence
zg30
Number of Scans
16
Receiver Gain
112.8
Relaxation Delay
1.0000
Pulse Width
11.7000
Acquisition Time
4.0894
Acquisition Date
2018-09-04T20:13:06
Spectrometer Frequency
400.13
Spectral Width
8012.8
Lowest Frequency
-1545.4
Nucleus
1H
Acquired Size
32768
Spectral Size
65536
D (ddd) 7.21
B (m) 7.45
A (m) 7.50
F (dd) 6.84
G (s) 5.97
C (m) 7.38
E (td) 6.98
Cl
O
Ph
217c
1.95
1.18
2.05
2.97
1.01
1.00
0.98
10.5 10.0 9.5 9.0 8.5 8.0 7.5 7.0 6.5 6.0 5.5 5.0 4.5 4.0 3.5 3.0 2.5 2.0 1.5 1.0 0.5 0.0
f1 (ppm)

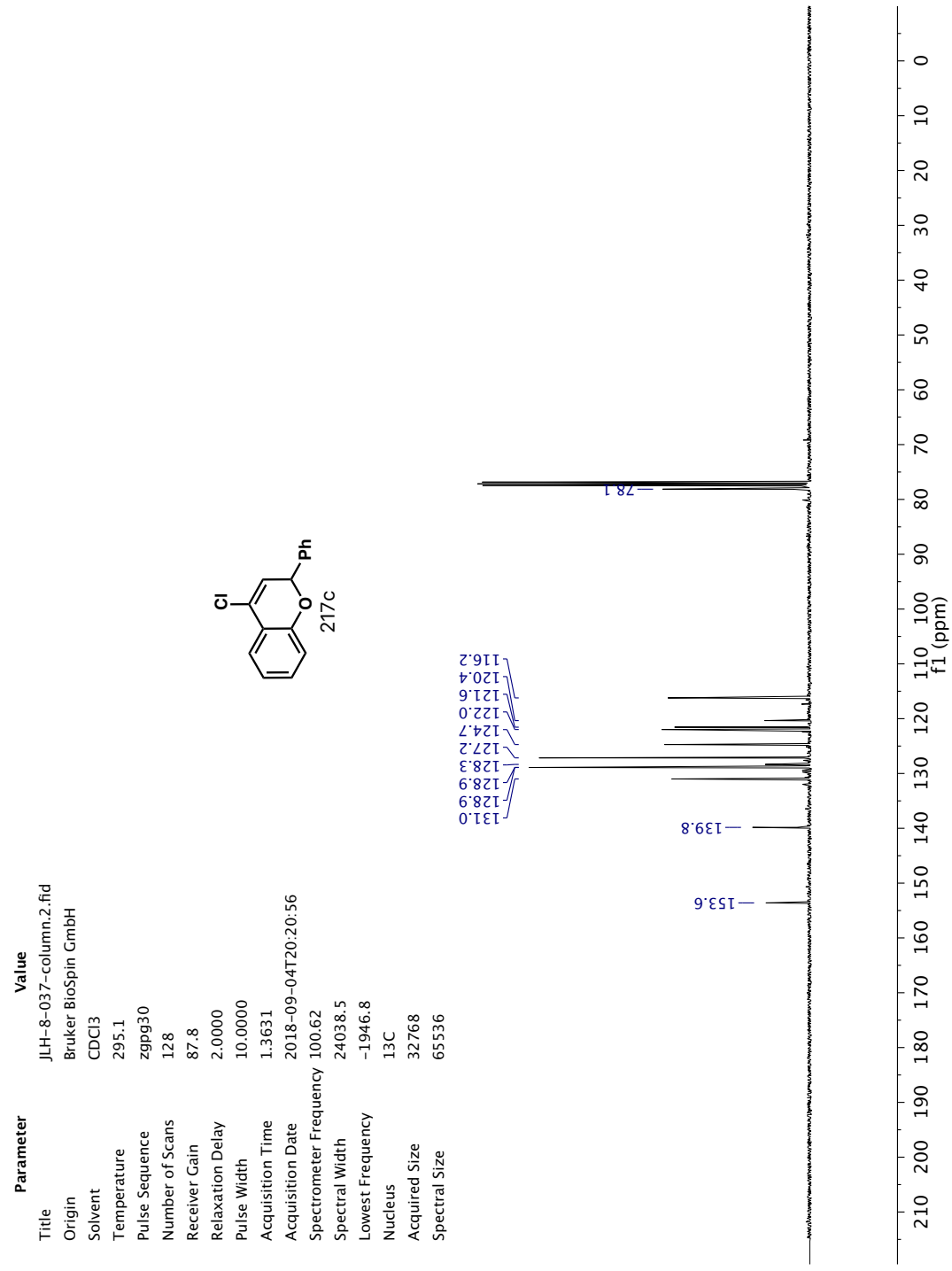
Parameter Value
Title JLH-8-037-column.2.fid
Origin Bruker BioSpin GmbH
Solvent CDCl3
Temperature 295.1
Pulse Sequence zgpg30
Number of Scans 128
Receiver Gain 87.8
Relaxation Delay 2.0000
Pulse Width 10.0000
Acquisition Time 1.3631
Acquisition Date 2018-09-04T20:20:56
Spectrometer Frequency 100.62
Spectral Width 24038.5
Lowest Frequency -1946.8
Nucleus 13C
Acquired Size 32768
Spectral Size 65536
Cl
O
Ph
217c
78.1
116.2
120.4
121.6
122.0
124.7
127.2
128.3
128.9
128.9
131.0
139.8
153.6
f1 (ppm)

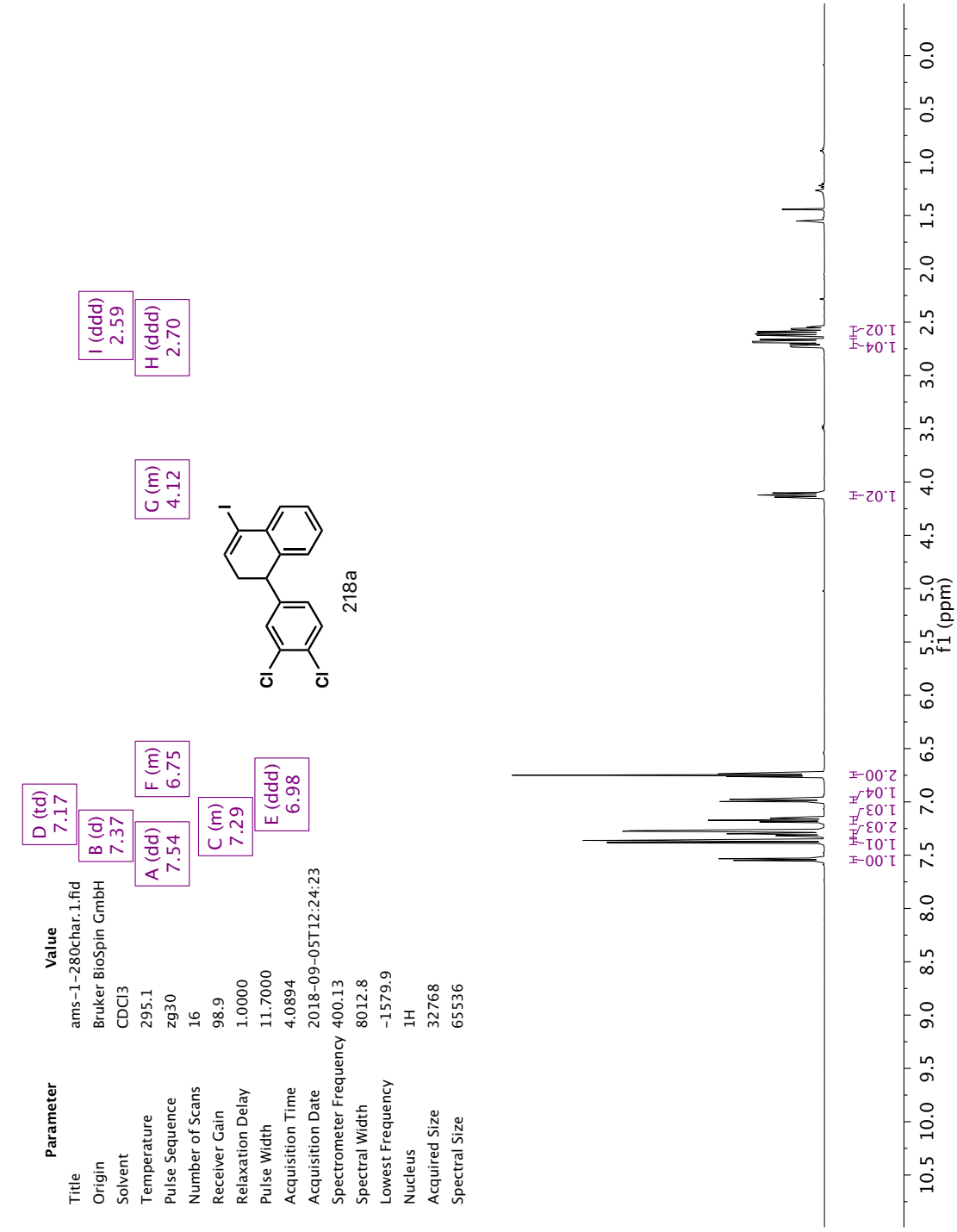
Parameter
Value
Title
ams-1-280char.1.fid
Origin
Bruker BioSpin GmbH
Solvent
CDCl3
Temperature
295.1
Pulse Sequence
zg30
Number of Scans
16
Receiver Gain
98.9
Relaxation Delay
1.0000
Pulse Width
11.7000
Acquisition Time
4.0894
Acquisition Date
2018-09-05T12:24:23
Spectrometer Frequency
400.13
Spectral Width
8012.8
Lowest Frequency
-1579.9
Nucleus
1H
Acquired Size
32768
Spectral Size
65536
D (td) 7.17
B (d) 7.37
A (dd) 7.54
F (m) 6.75
C (m) 7.29
E (ddd) 6.98
G (m) 4.12
I (ddd) 2.59
H (ddd) 2.70
I
Cl
Cl
218a
1.00
1.01
2.03
1.03
1.04
2.00
1.02
1.02
1.04
10.5 10.0 9.5 9.0 8.5 8.0 7.5 7.0 6.5 6.0 5.5 5.0 4.5 4.0 3.5 3.0 2.5 2.0 1.5 1.0 0.5 0.0
f1 (ppm)

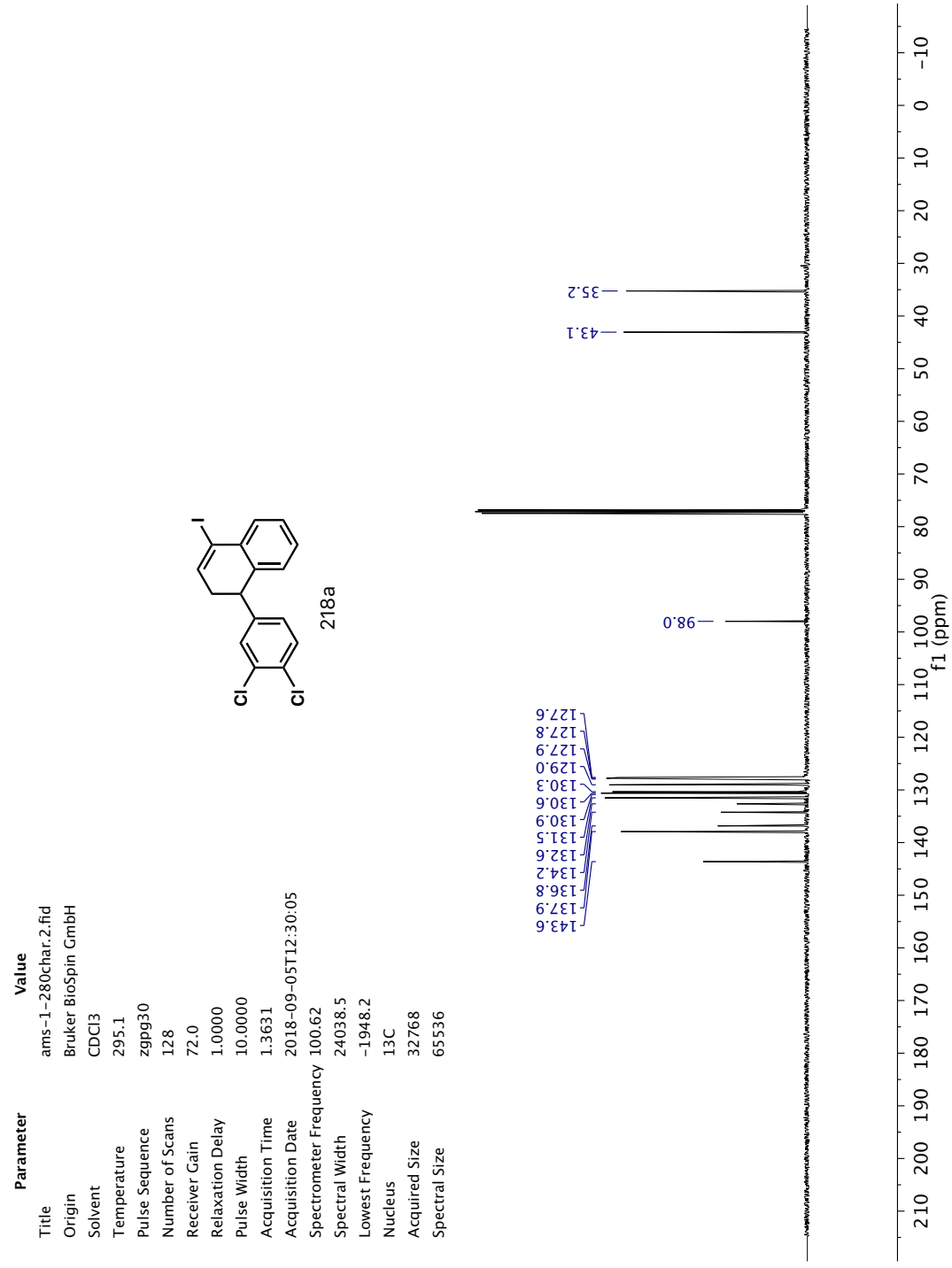
Parameter Value
Title ams-1-280char.2.fid
Origin Bruker BioSpin GmbH
Solvent CDCl3
Temperature 295.1
Pulse Sequence zgpg30
Number of Scans 128
Receiver Gain 72.0
Relaxation Delay 1.0000
Pulse Width 10.0000
Acquisition Time 1.3631
Acquisition Date 2018-09-05T12:30:05
Spectrometer Frequency 100.62
Spectral Width 24038.5
Lowest Frequency -1948.2
Nucleus 13C
Acquired Size 32768
Spectral Size 65536
I
Cl
Cl
218a
143.6
137.9
136.8
134.2
132.6
131.5
130.9
130.6
130.3
129.0
127.9
127.8
127.6
98.0
43.1
35.2
f1 (ppm)

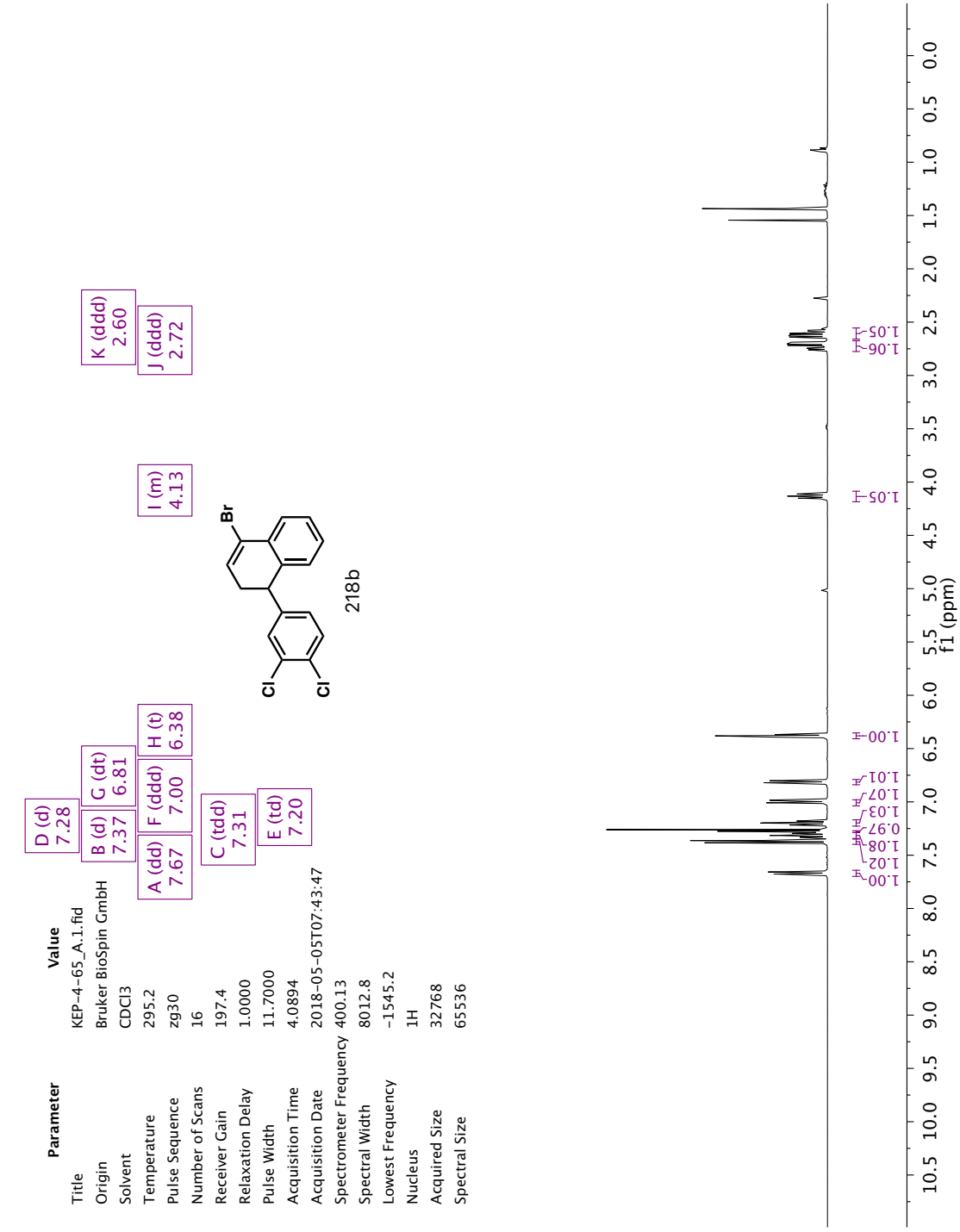
Parameter
Value
Title
KEP-4-65_A.1.fid
Origin
Bruker BioSpin GmbH
Solvent
CDCl3
Temperature
295.2
Pulse Sequence
zg30
Number of Scans
16
Receiver Gain
197.4
Relaxation Delay
1.0000
Pulse Width
11.7000
Acquisition Time
4.0894
Acquisition Date
2018-05-05T07:43:47
Spectrometer Frequency
400.13
Spectral Width
8012.8
Lowest Frequency
-1545.2
Nucleus
1H
Acquired Size
32768
Spectral Size
65536
D (d) 7.28
B (d) 7.37
G (dt) 6.81
A (dd) 7.67
F (ddd) 7.00
H (t) 6.38
C (tdd) 7.31
E (td) 7.20
I (m) 4.13
K (ddd) 2.60
J (ddd) 2.72
Br
Cl
Cl
218b
1.00
1.02
1.08
0.97
1.03
1.07
1.01
1.00
1.05
1.06
1.05
10.5 10.0 9.5 9.0 8.5 8.0 7.5 7.0 6.5 6.0 5.5 5.0 4.5 4.0 3.5 3.0 2.5 2.0 1.5 1.0 0.5 0.0
f1 (ppm)

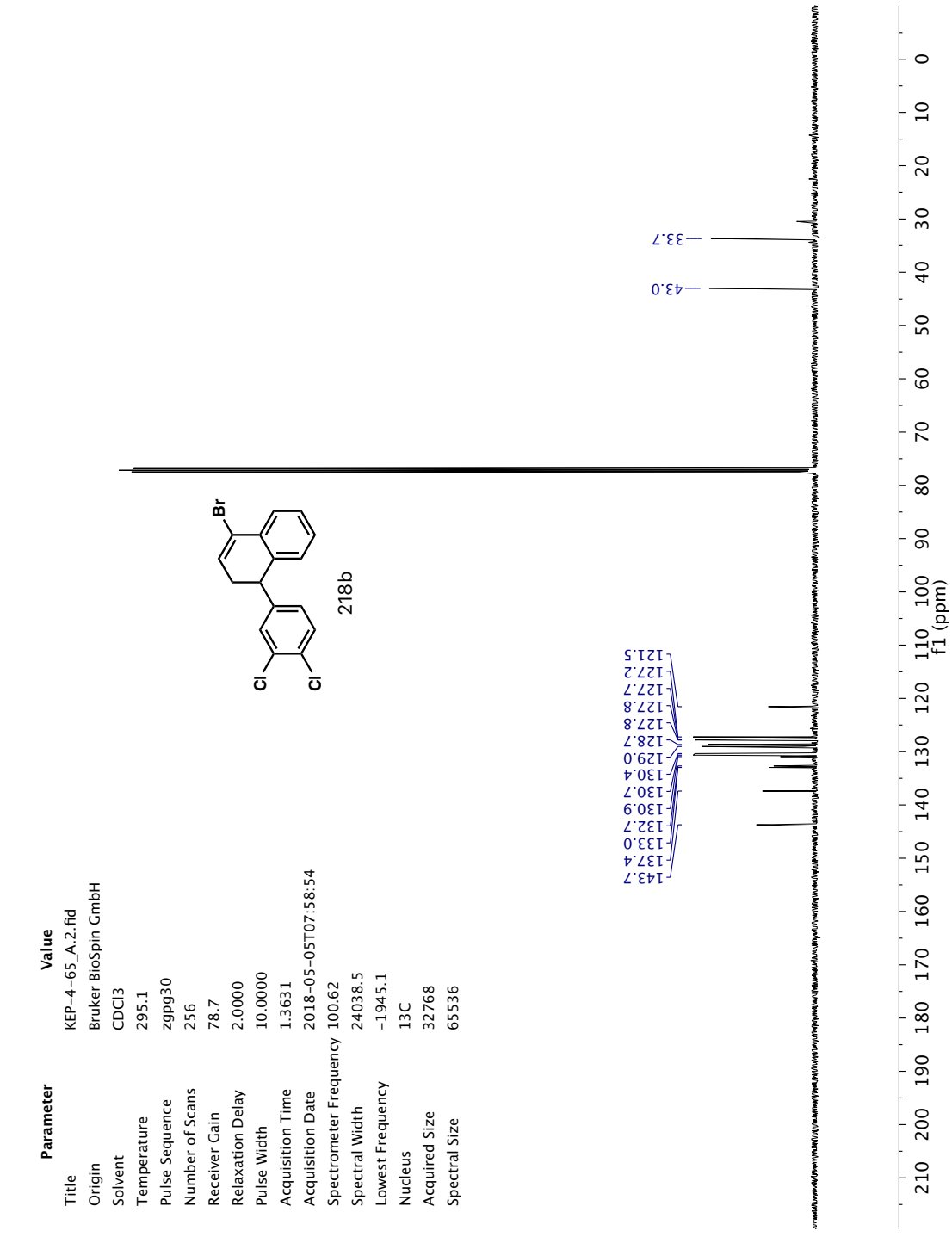
Parameter Value
Title KEP-4-65_A.2.fid
Origin Bruker BioSpin GmbH
Solvent CDCl3
Temperature 295.1
Pulse Sequence zgpg30
Number of Scans 256
Receiver Gain 78.7
Relaxation Delay 2.0000
Pulse Width 10.0000
Acquisition Time 1.3631
Acquisition Date 2018-05-05T07:58:54
Spectrometer Frequency 100.62
Spectral Width 24038.5
Lowest Frequency -1945.1
Nucleus 13C
Acquired Size 32768
Spectral Size 65536
Br
Cl
Cl
218b
33.7
43.0
121.5
127.2
127.7
127.8
127.8
128.7
129.0
130.4
130.7
130.9
132.7
133.0
137.4
143.7
f1 (ppm)

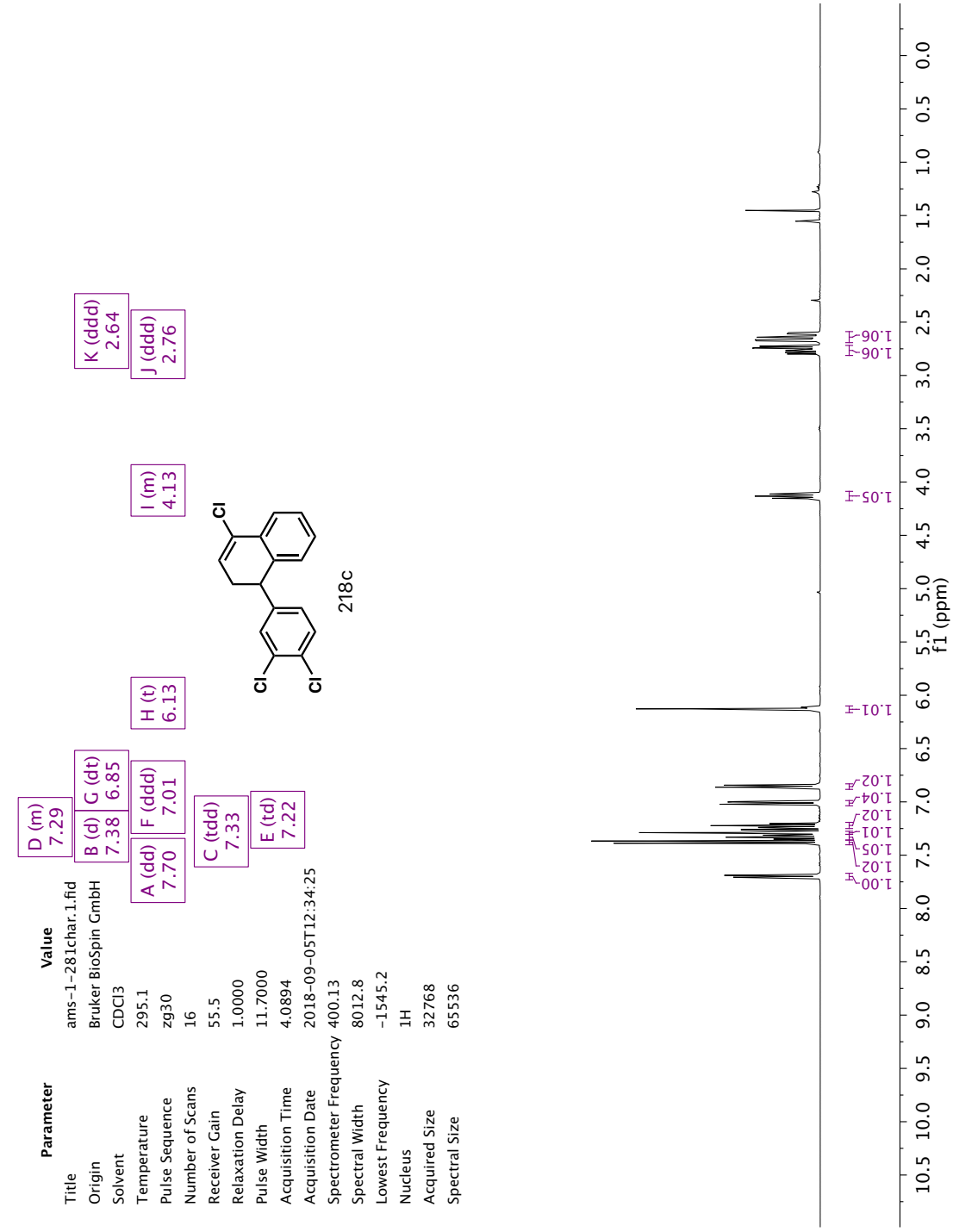

Parameter	Value
Title	ams-1-281char.1.fid
Origin	Bruker BioSpin GmbH
Solvent	CDCl3
Temperature	295.1
Pulse Sequence	zg30
Number of Scans	16
Receiver Gain	55.5
Relaxation Delay	1.0000
Pulse Width	11.7000
Acquisition Time	4.0894
Acquisition Date	2018-09-05T12:34:25
Spectrometer Frequency	400.13
Spectral Width	8012.8
Lowest Frequency	-1545.2
Nucleus	1H
Acquired Size	32768
Spectral Size	65536

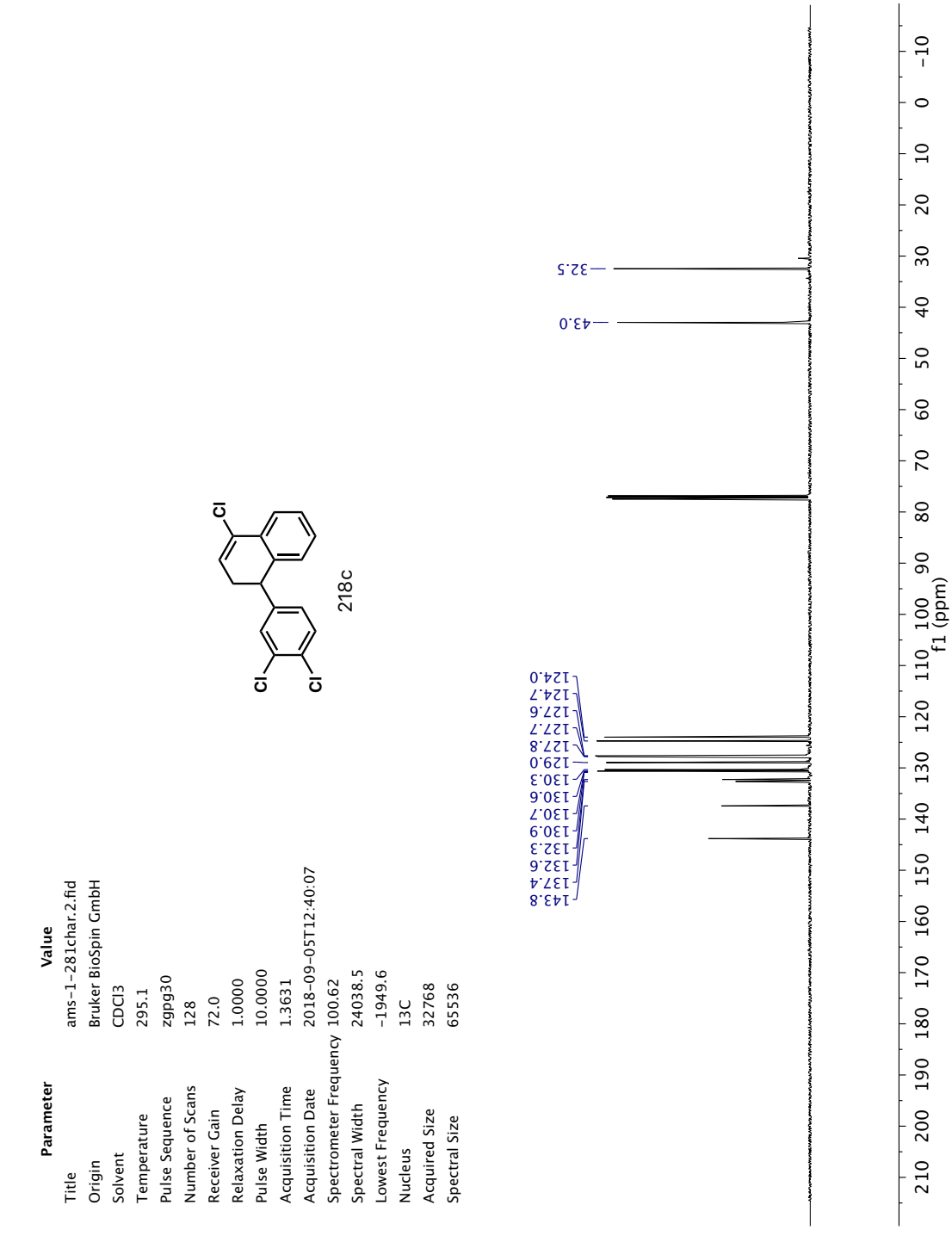
Parameter Value
Title ams-1-281char.2.fid
Origin Bruker BioSpin GmbH
Solvent CDCl3
Temperature 295.1
Pulse Sequence zgpg30
Number of Scans 128
Receiver Gain 72.0
Relaxation Delay 1.0000
Pulse Width 10.0000
Acquisition Time 1.3631
Acquisition Date 2018-09-05T12:40:07
Spectrometer Frequency 100.62
Spectral Width 24038.5
Lowest Frequency -1949.6
Nucleus 13C
Acquired Size 32768
Spectral Size 65536
Cl
Cl
Cl
218c
143.8
137.4
132.6
132.3
130.9
130.7
130.6
130.3
129.0
127.8
127.7
127.6
124.7
124.0
43.0
32.5
f1 (ppm)

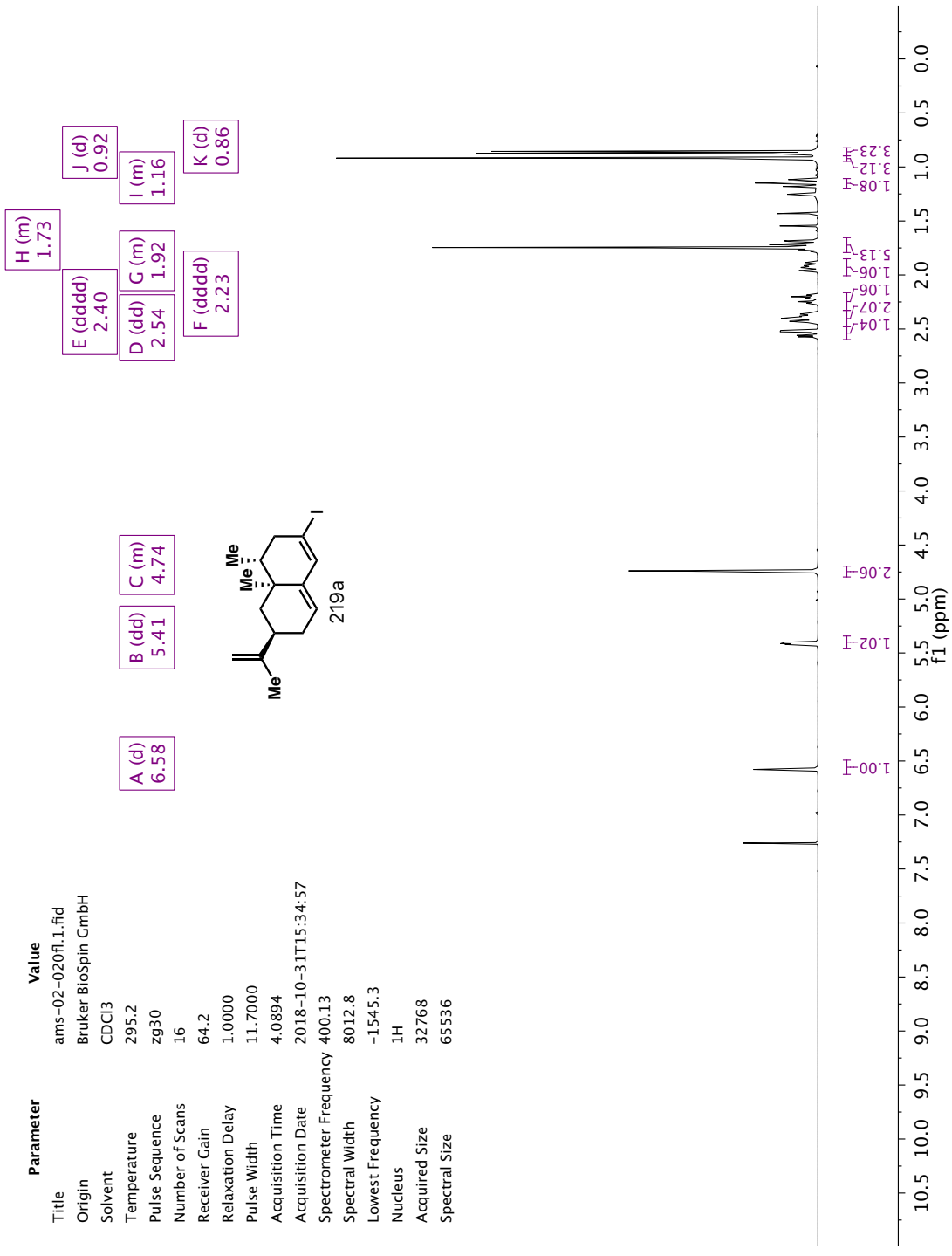
A (d) 6.58
B (dd) 5.41
C (m) 4.74
D (dd) 2.54
E (dddd) 2.40
F (dddd) 2.23
G (m) 1.92
H (m) 1.73
I (m) 1.16
J (d) 0.92
K (d) 0.86
Me
Me
Me
I
219a
Parameter Value
Title ams-02-020fl.1.fid
Origin Bruker BioSpin GmbH
Solvent CDCl3
Temperature 295.2
Pulse Sequence zg30
Number of Scans 16
Receiver Gain 64.2
Relaxation Delay 1.0000
Pulse Width 11.7000
Acquisition Time 4.0894
Acquisition Date 2018-10-31T15:34:57
Spectrometer Frequency 400.13
Spectral Width 8012.8
Lowest Frequency -1545.3
Nucleus 1H
Acquired Size 32768
Spectral Size 65536
1.00
1.02
2.06
1.04
2.07
1.06
1.06
5.13
1.08
3.12
3.23
10.5 10.0 9.5 9.0 8.5 8.0 7.5 7.0 6.5 6.0 5.5 5.0 4.5 4.0 3.5 3.0 2.5 2.0 1.5 1.0 0.5 0.0
f1 (ppm)

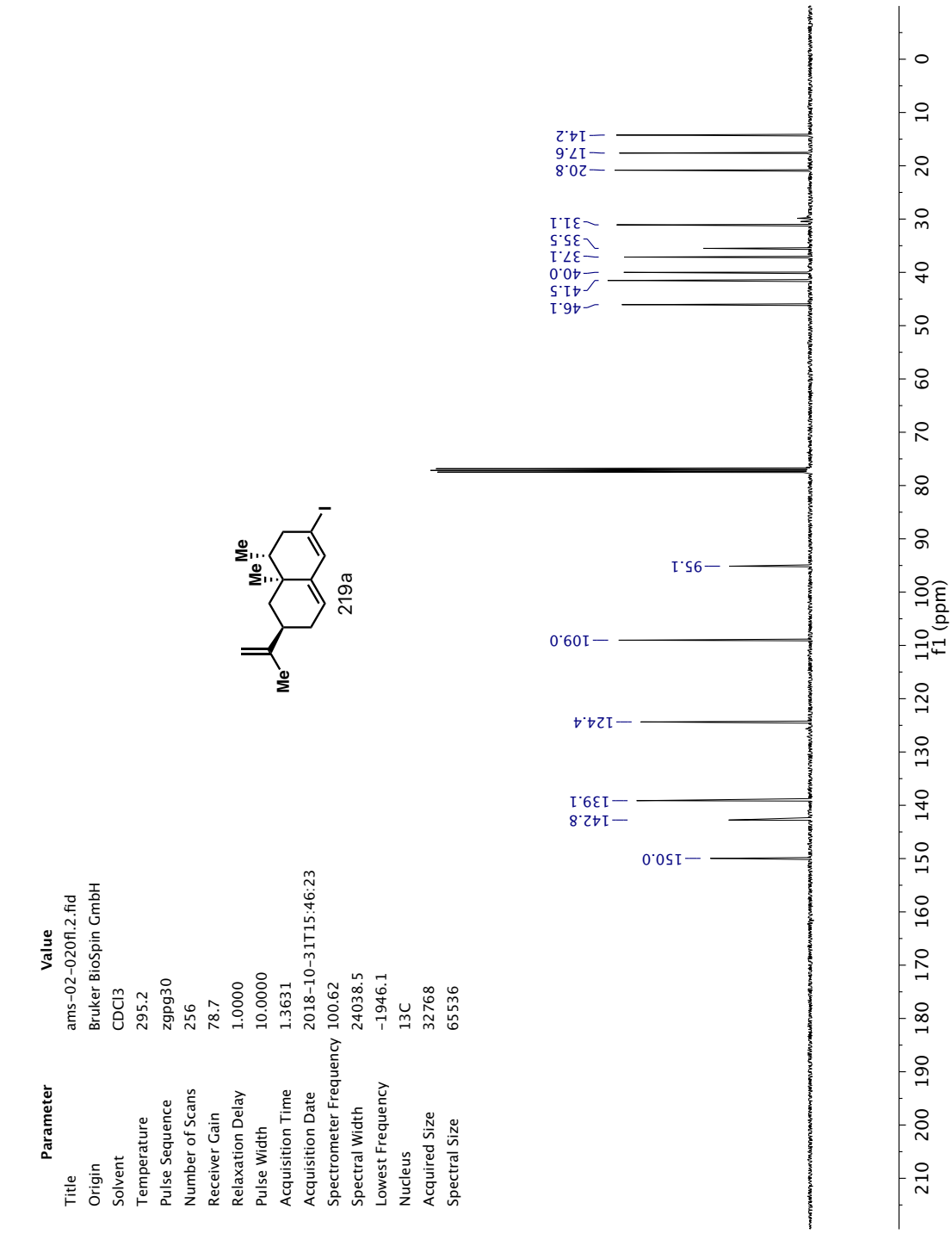
Parameter Value
Title ams-02-020fl.2.fid
Origin Bruker BioSpin GmbH
Solvent CDCl3
Temperature 295.2
Pulse Sequence zgpg30
Number of Scans 256
Receiver Gain 78.7
Relaxation Delay 1.0000
Pulse Width 10.0000
Acquisition Time 1.3631
Acquisition Date 2018-10-31T15:46:23
Spectrometer Frequency 100.62
Spectral Width 24038.5
Lowest Frequency -1946.1
Nucleus 13C
Acquired Size 32768
Spectral Size 65536
Me
Me
Me
I
219a
150.0
142.8
139.1
124.4
109.0
95.1
46.1
41.5
40.0
37.1
35.5
31.1
20.8
17.6
14.2
f1 (ppm)

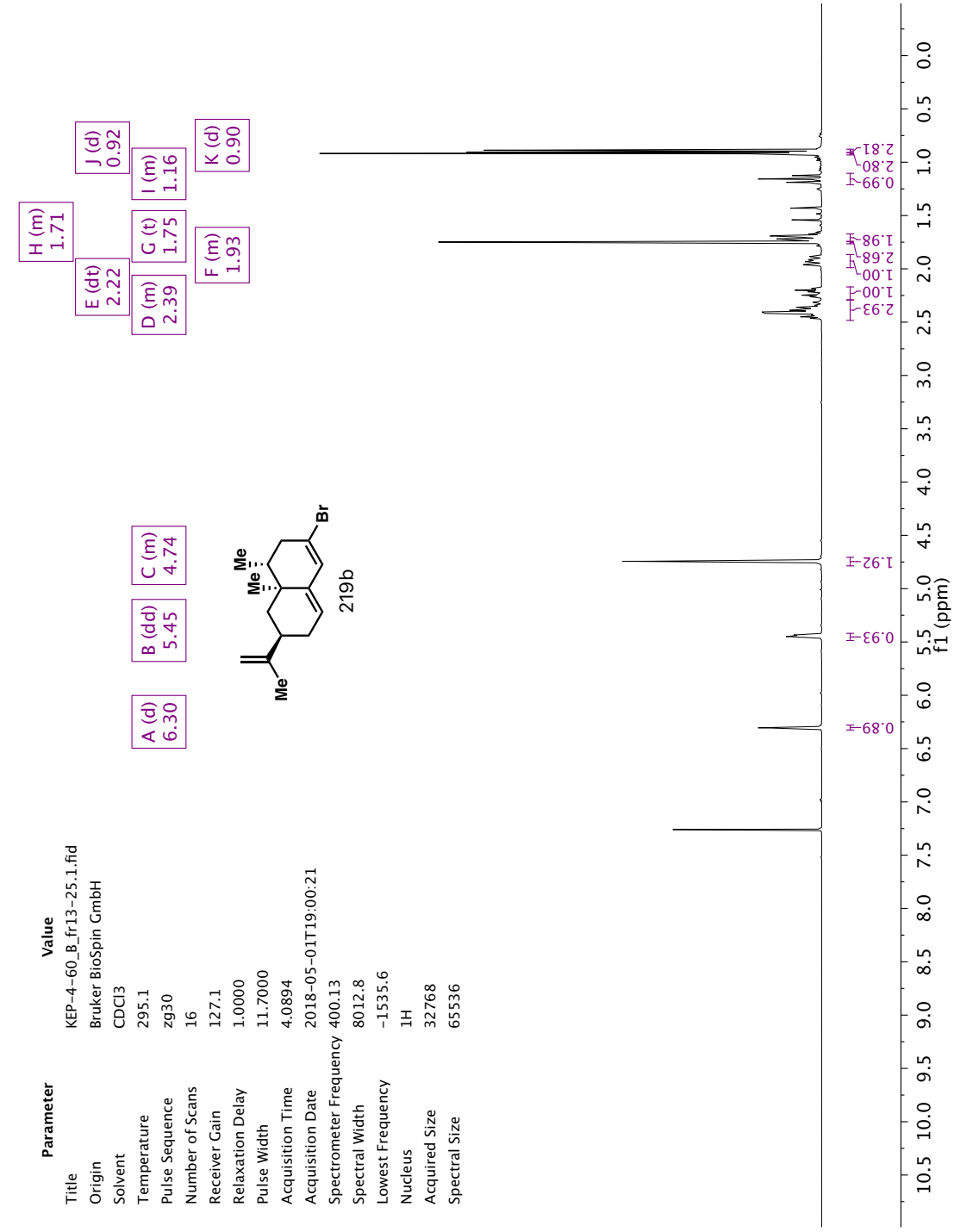
Parameter Value
Title KEP-4-60_B_fr13-25.1.fid
Origin Bruker BioSpin GmbH
Solvent CDCl3
Temperature 295.1
Pulse Sequence zg30
Number of Scans 16
Receiver Gain 127.1
Relaxation Delay 1.0000
Pulse Width 11.7000
Acquisition Time 4.0894
Acquisition Date 2018-05-01T19:00:21
Spectrometer Frequency 400.13
Spectral Width 8012.8
Lowest Frequency -1535.6
Nucleus 1H
Acquired Size 32768
Spectral Size 65536
A (d) 6.30
B (dd) 5.45
C (m) 4.74
D (m) 2.39
E (dt) 2.22
F (m) 1.93
G (t) 1.75
H (m) 1.71
I (m) 1.16
J (d) 0.92
K (d) 0.90
Me
Me
Me
Br
219b
0.89
1.92
0.93
2.93
1.00
1.00
2.68
1.00
1.98
0.99
2.80
2.81
f1 (ppm)

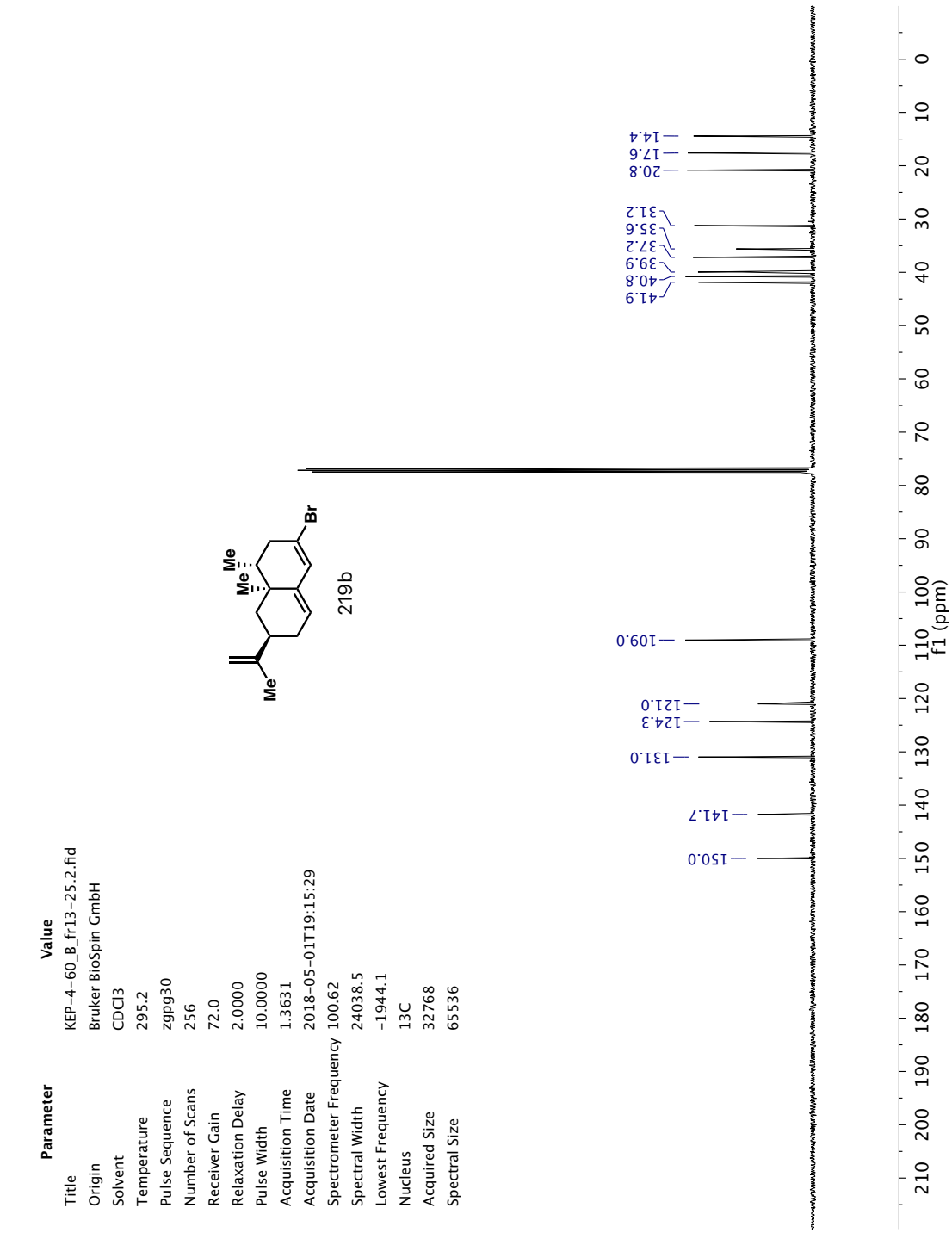
Parameter Value
Title KEP-4-60_B_fr13-25.2.fid
Origin Bruker BioSpin GmbH
Solvent CDCl3
Temperature 295.2
Pulse Sequence zgpg30
Number of Scans 256
Receiver Gain 72.0
Relaxation Delay 2.0000
Pulse Width 10.0000
Acquisition Time 1.3631
Acquisition Date 2018-05-01T19:15:29
Spectrometer Frequency 100.62
Spectral Width 24038.5
Lowest Frequency -1944.1
Nucleus 13C
Acquired Size 32768
Spectral Size 65536
Me
Me
Me
Br
219b
150.0
141.7
131.0
124.3
121.0
109.0
41.9
40.8
39.9
37.2
35.6
31.2
20.8
17.6
14.4
f1 (ppm)

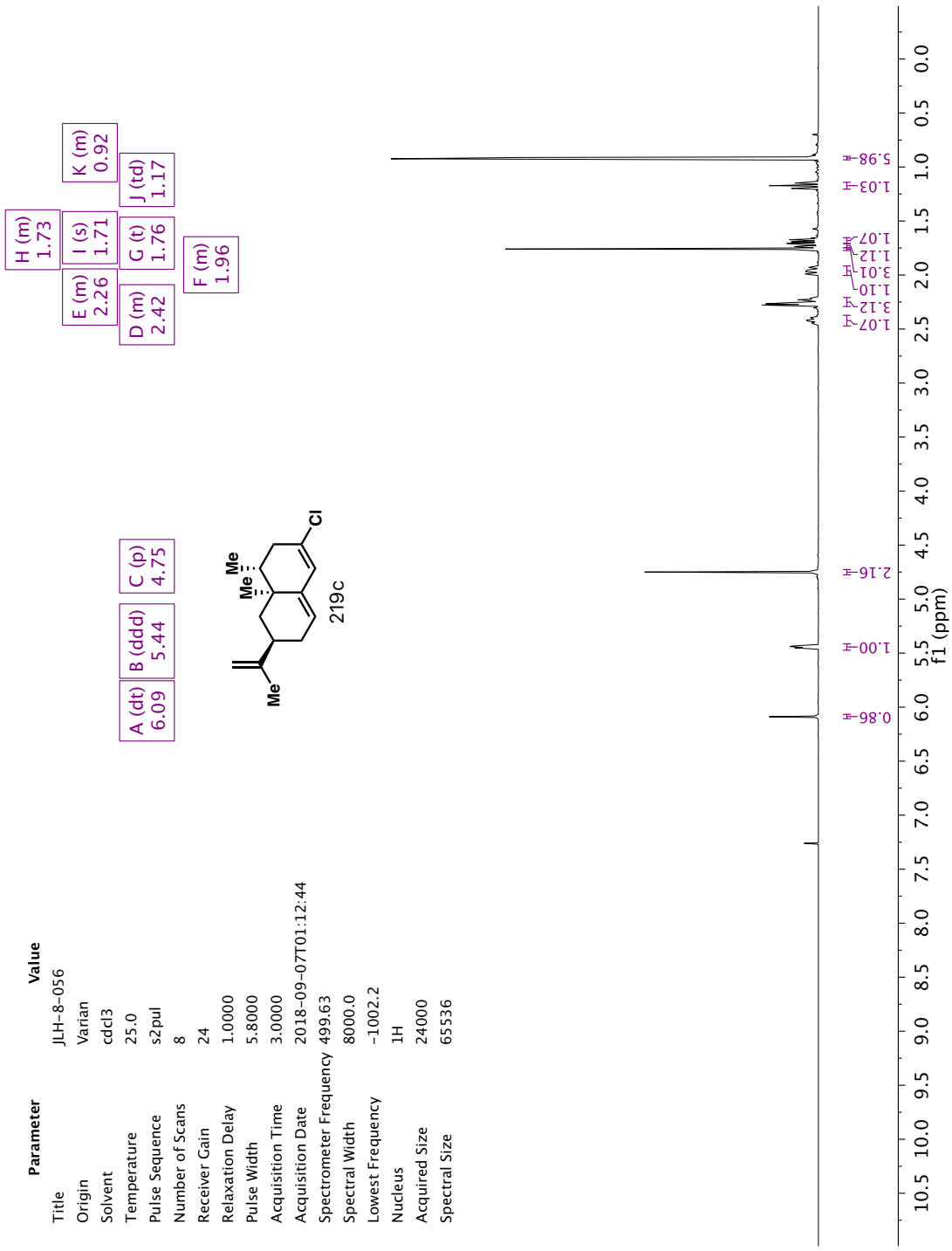
A (dt) 6.09
B (ddd) 5.44
C (p) 4.75
D (m) 2.42
E (m) 2.26
F (m) 1.96
G (t) 1.76
H (m) 1.73
I (s) 1.71
J (td) 1.17
K (m) 0.92
Me
Me
Me
Cl
219c
Parameter Value
Title JLH-8-056
Origin Varian
Solvent cdcl3
Temperature 25.0
Pulse Sequence s2pul
Number of Scans 8
Receiver Gain 24
Relaxation Delay 1.0000
Pulse Width 5.8000
Acquisition Time 3.0000
Acquisition Date 2018-09-07T01:12:44
Spectrometer Frequency 499.63
Spectral Width 8000.0
Lowest Frequency -1002.2
Nucleus 1H
Acquired Size 24000
Spectral Size 65536
0.86
1.00
2.16
1.07
3.12
1.10
3.01
1.12
1.07
1.03
5.98
f1 (ppm)

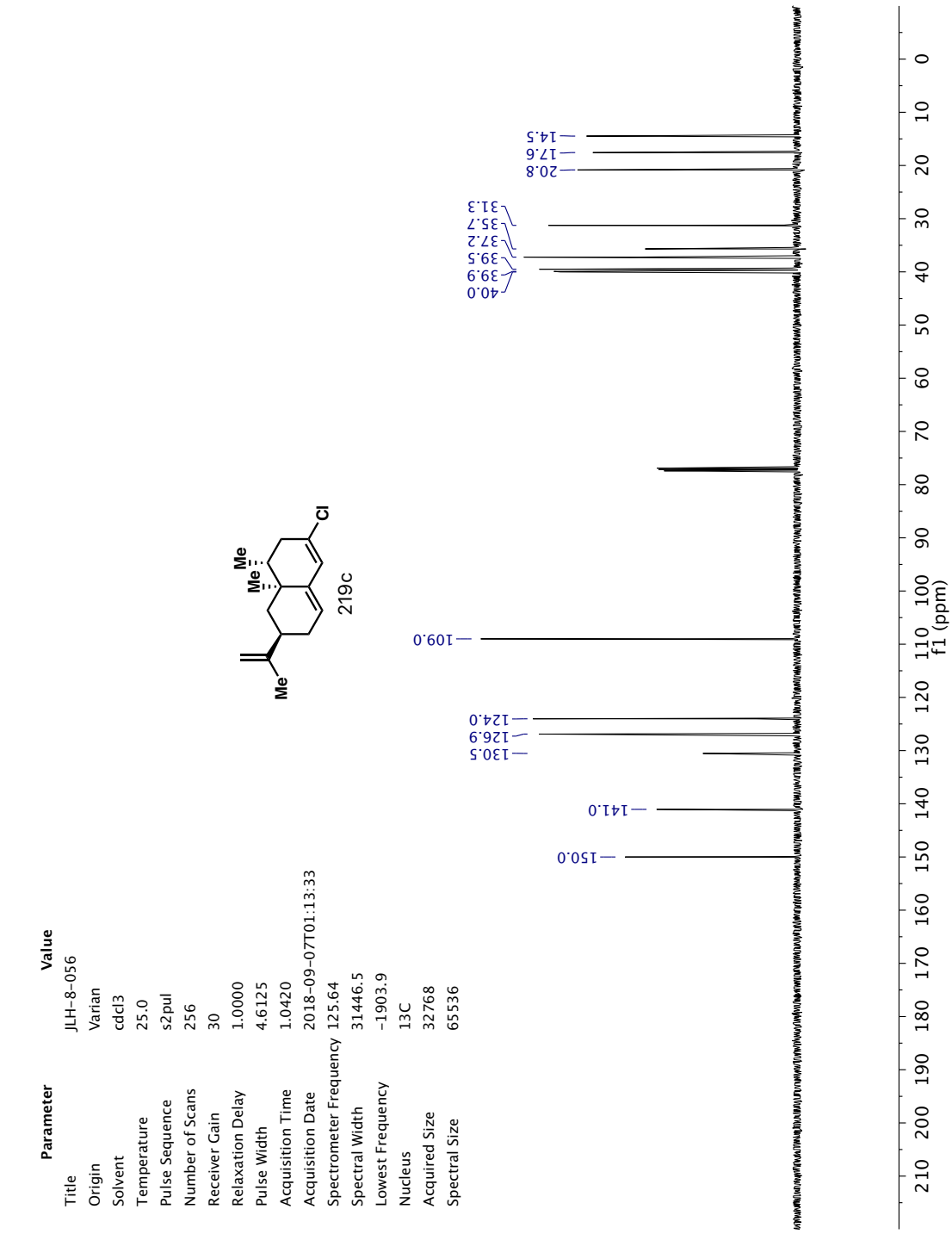
Parameter Value
Title JLH-8-056
Origin Varian
Solvent cdcl3
Temperature 25.0
Pulse Sequence s2pul
Number of Scans 256
Receiver Gain 30
Relaxation Delay 1.0000
Pulse Width 4.6125
Acquisition Time 1.0420
Acquisition Date 2018-09-07T01:13:33
Spectrometer Frequency 125.64
Spectral Width 31446.5
Lowest Frequency -1903.9
Nucleus 13C
Acquired Size 32768
Spectral Size 65536
Me
Me
Cl
Me
219c
150.0
141.0
130.5
126.9
124.0
109.0
40.0
39.9
39.5
37.2
35.7
31.3
20.8
17.6
14.5
f1 (ppm)

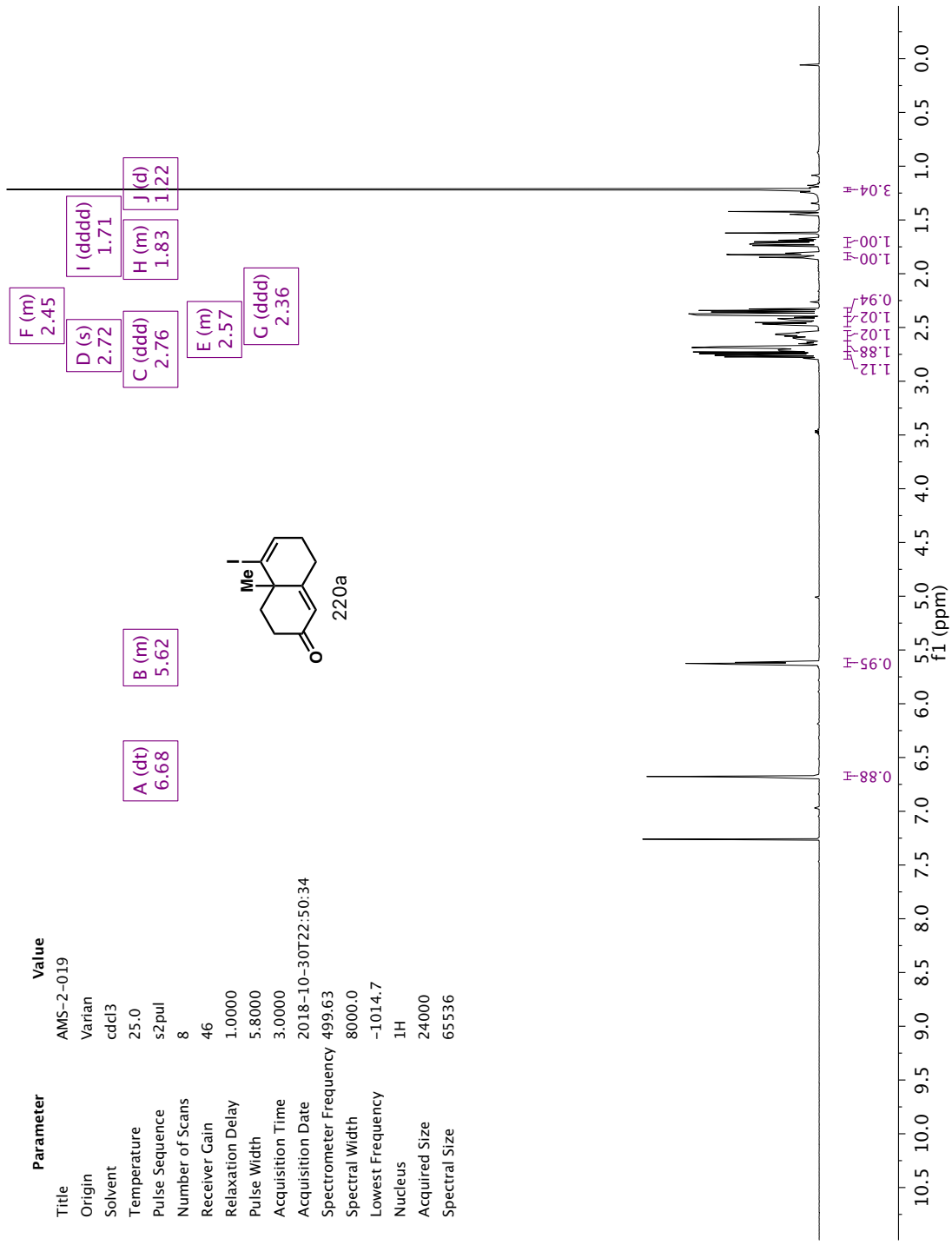

Parameter	Value
Title	AMS-2-019
Origin	Varian
Solvent	cdcl3
Temperature	25.0
Pulse Sequence	s2pul
Number of Scans	8
Receiver Gain	46
Relaxation Delay	1.0000
Pulse Width	5.8000
Acquisition Time	3.0000
Acquisition Date	2018-10-30T22:50:34
Spectrometer Frequency	499.63
Spectral Width	8000.0
Lowest Frequency	-1014.7
Nucleus	1H
Acquired Size	24000
Spectral Size	65536

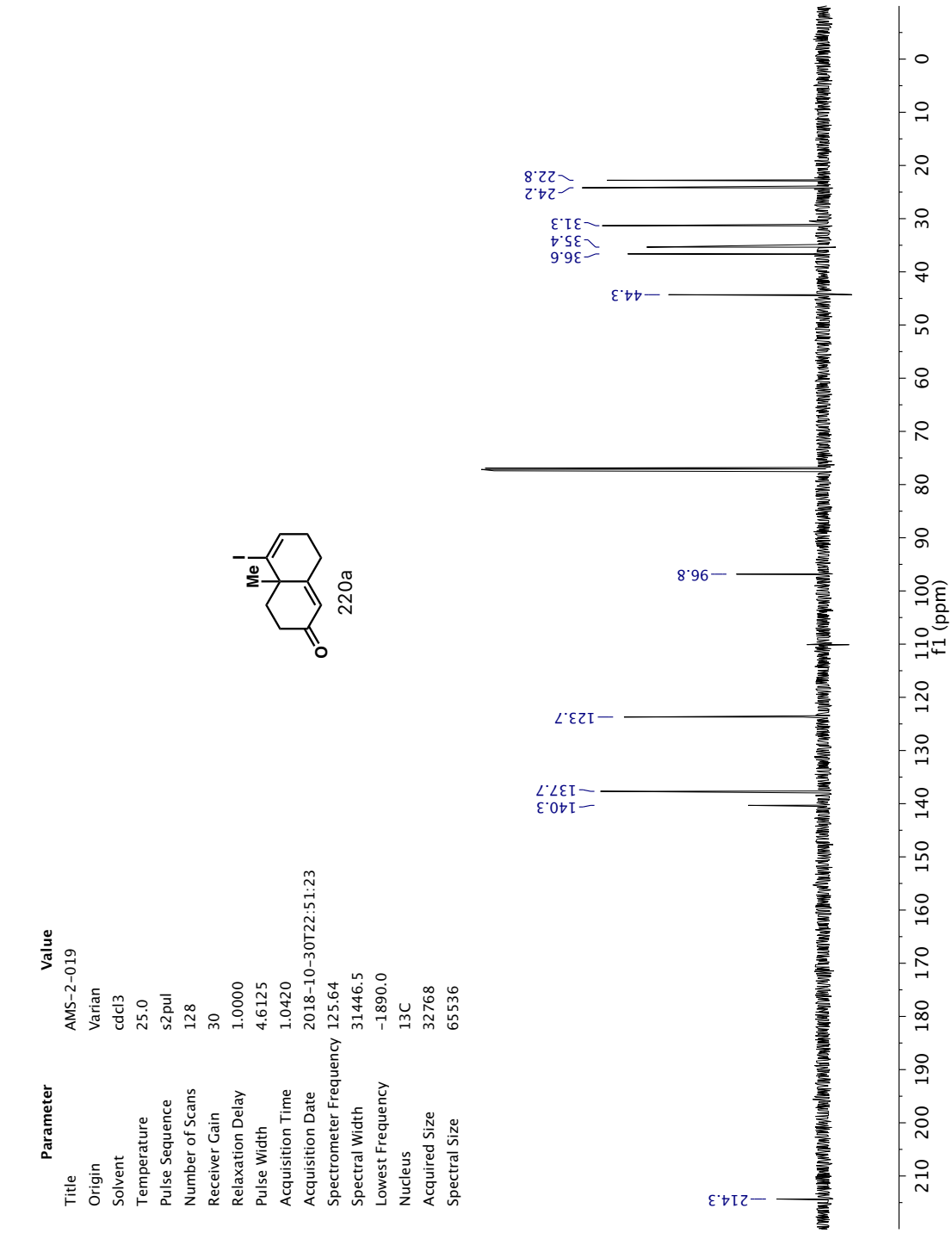
Parameter Value
Title AMS-2-019
Origin Varian
Solvent cdcl3
Temperature 25.0
Pulse Sequence s2pul
Number of Scans 128
Receiver Gain 30
Relaxation Delay 1.0000
Pulse Width 4.6125
Acquisition Time 1.0420
Acquisition Date 2018-10-30T22:51:23
Spectrometer Frequency 125.64
Spectral Width 31446.5
Lowest Frequency -1890.0
Nucleus 13C
Acquired Size 32768
Spectral Size 65536
Me
O
220a
214.3
140.3
137.7
123.7
96.8
44.3
36.6
35.4
31.3
24.2
22.8
f1 (ppm)

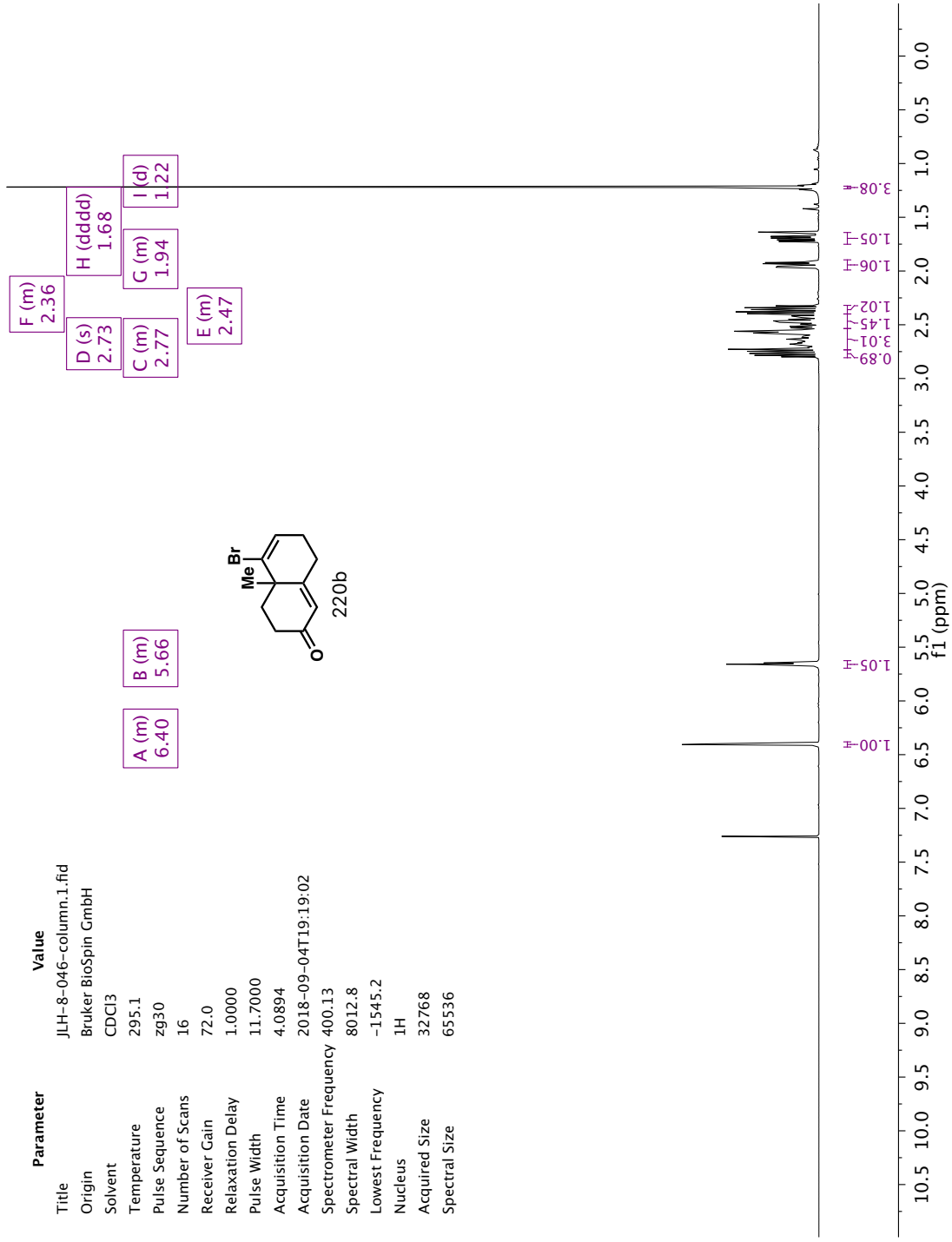

Parameter	Value
Title	JLH-8-046-column.1.fid
Origin	Bruker BioSpin GmbH
Solvent	CDCl3
Temperature	295.1
Pulse Sequence	zg30
Number of Scans	16
Receiver Gain	72.0
Relaxation Delay	1.0000
Pulse Width	11.7000
Acquisition Time	4.0894
Acquisition Date	2018-09-04T19:19:02
Spectrometer Frequency	400.13
Spectral Width	8012.8
Lowest Frequency	-1545.2
Nucleus	1H
Acquired Size	32768
Spectral Size	65536

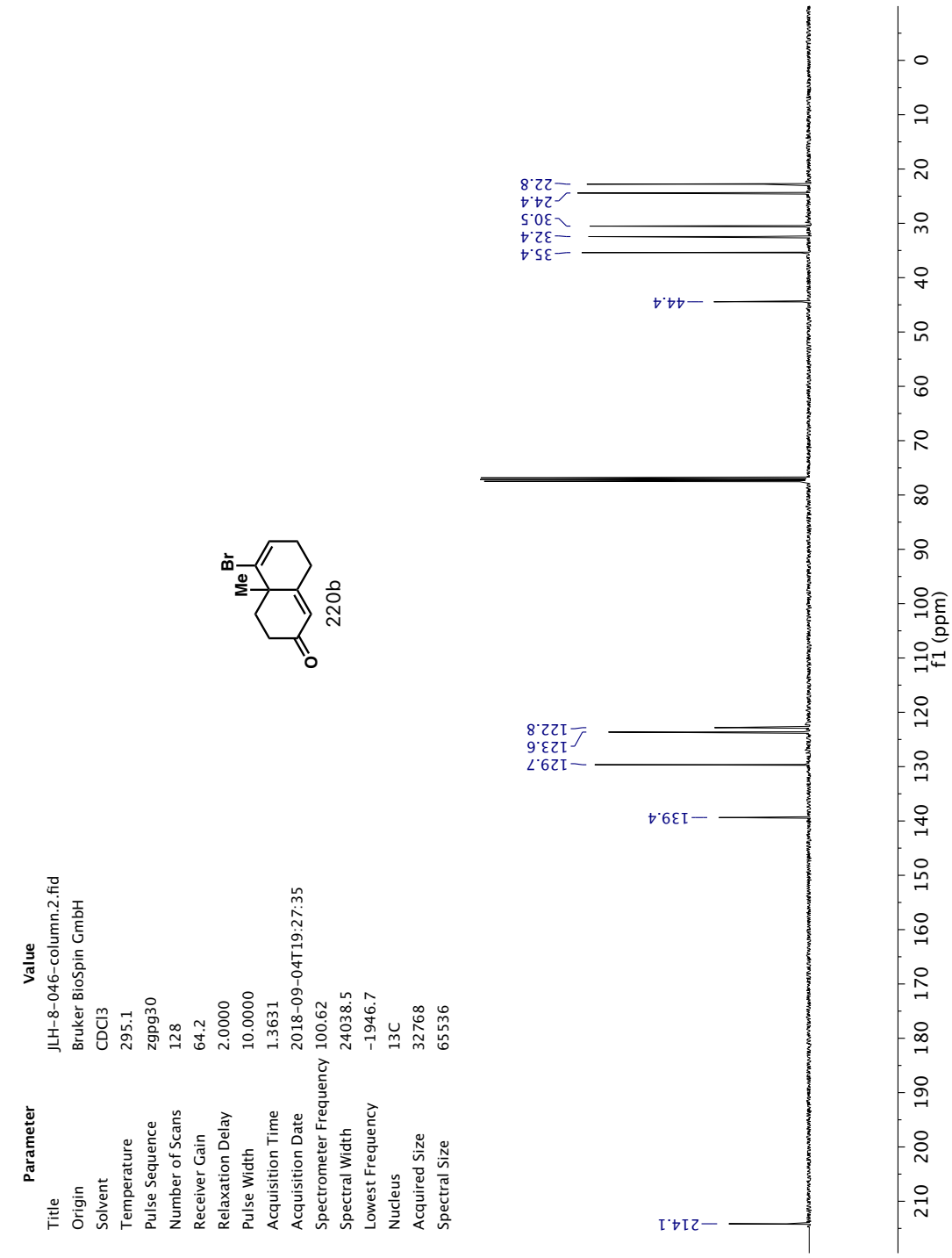

Parameter	Value
Title	JLH-8-046-column.2.fid
Origin	Bruker BioSpin GmbH
Solvent	CDCl3
Temperature	295.1
Pulse Sequence	zgpg30
Number of Scans	128
Receiver Gain	64.2
Relaxation Delay	2.0000
Pulse Width	10.0000
Acquisition Time	1.3631
Acquisition Date	2018-09-04T19:27:35
Spectrometer Frequency	100.62
Spectral Width	24038.5
Lowest Frequency	-1946.7
Nucleus	13C
Acquired Size	32768
Spectral Size	65536

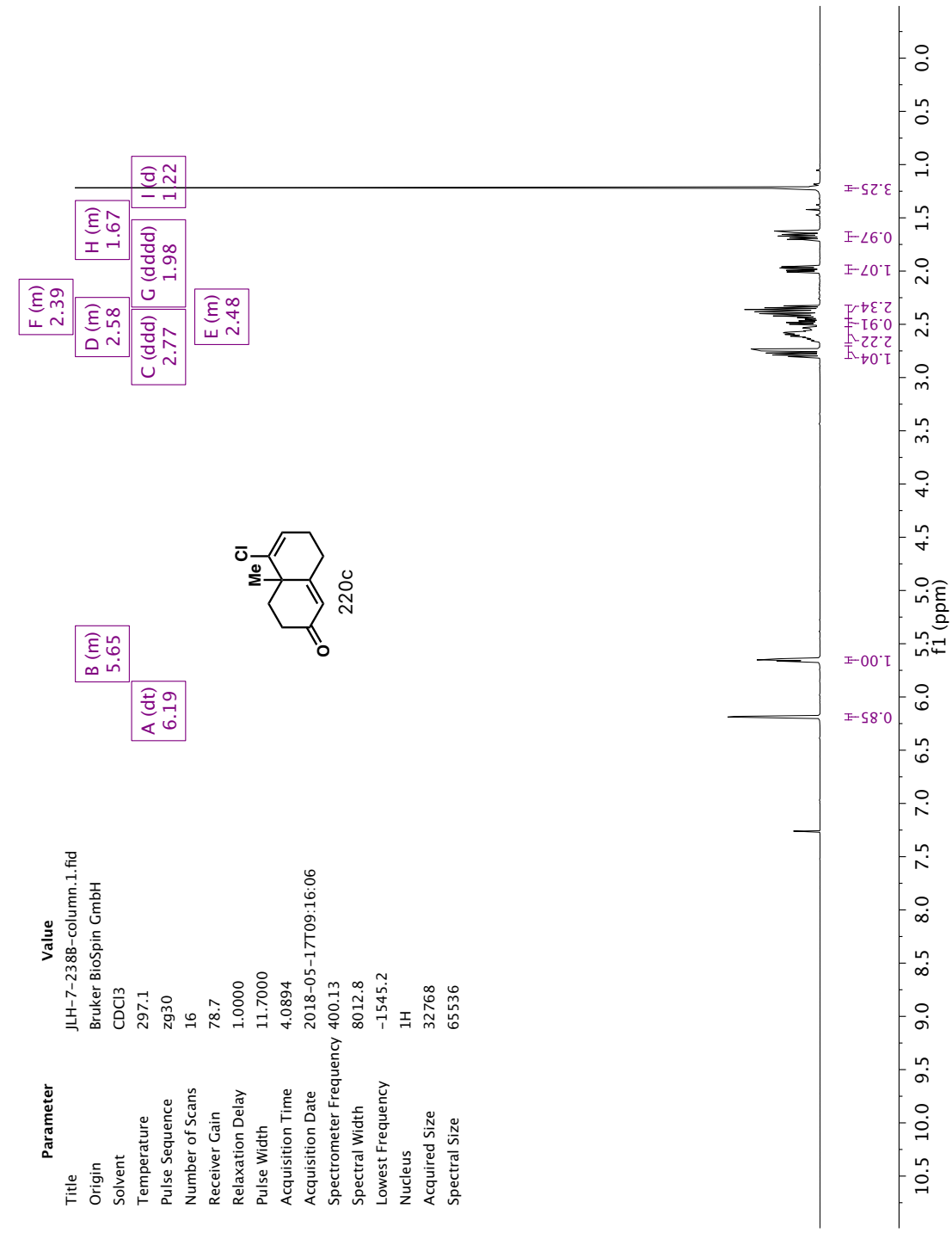

Parameter	Value
Title	JLH-7-238B-column.1.fid
Origin	Bruker BioSpin GmbH
Solvent	CDCl3
Temperature	297.1
Pulse Sequence	zg30
Number of Scans	16
Receiver Gain	78.7
Relaxation Delay	1.0000
Pulse Width	11.7000
Acquisition Time	4.0894
Acquisition Date	2018-05-17T09:16:06
Spectrometer Frequency	400.13
Spectral Width	8012.8
Lowest Frequency	-1545.2
Nucleus	1H
Acquired Size	32768
Spectral Size	65536

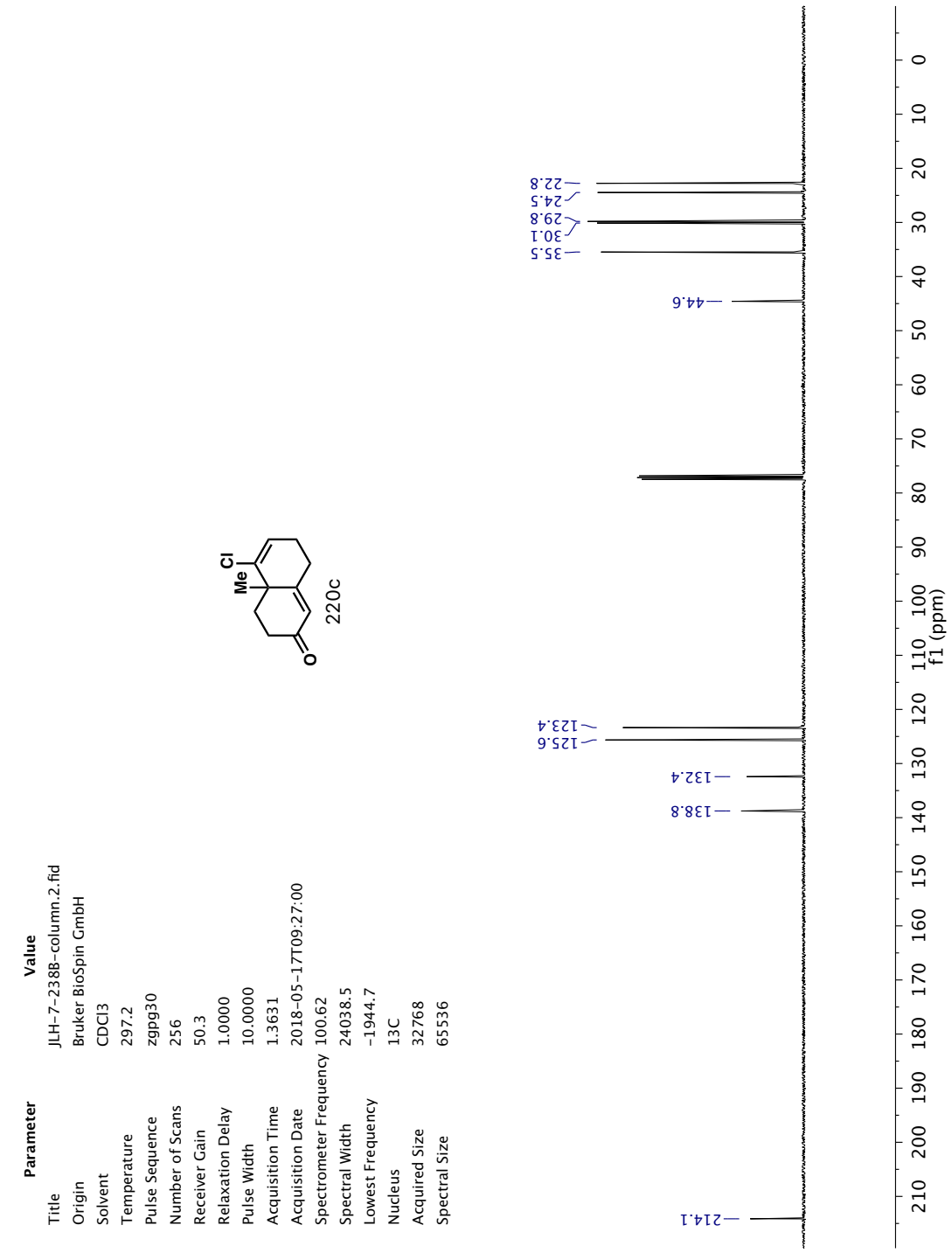
Parameter Value
Title JLH-7-238B-column.2.fid
Origin Bruker BioSpin GmbH
Solvent CDCl3
Temperature 297.2
Pulse Sequence zgpg30
Number of Scans 256
Receiver Gain 50.3
Relaxation Delay 1.0000
Pulse Width 10.0000
Acquisition Time 1.3631
Acquisition Date 2018-05-17T09:27:00
Spectrometer Frequency 100.62
Spectral Width 24038.5
Lowest Frequency -1944.7
Nucleus 13C
Acquired Size 32768
Spectral Size 65536
Cl
Me
O
220c
214.1
138.8
132.4
125.6
123.4
44.6
35.5
30.1
29.8
24.5
22.8
f1 (ppm)

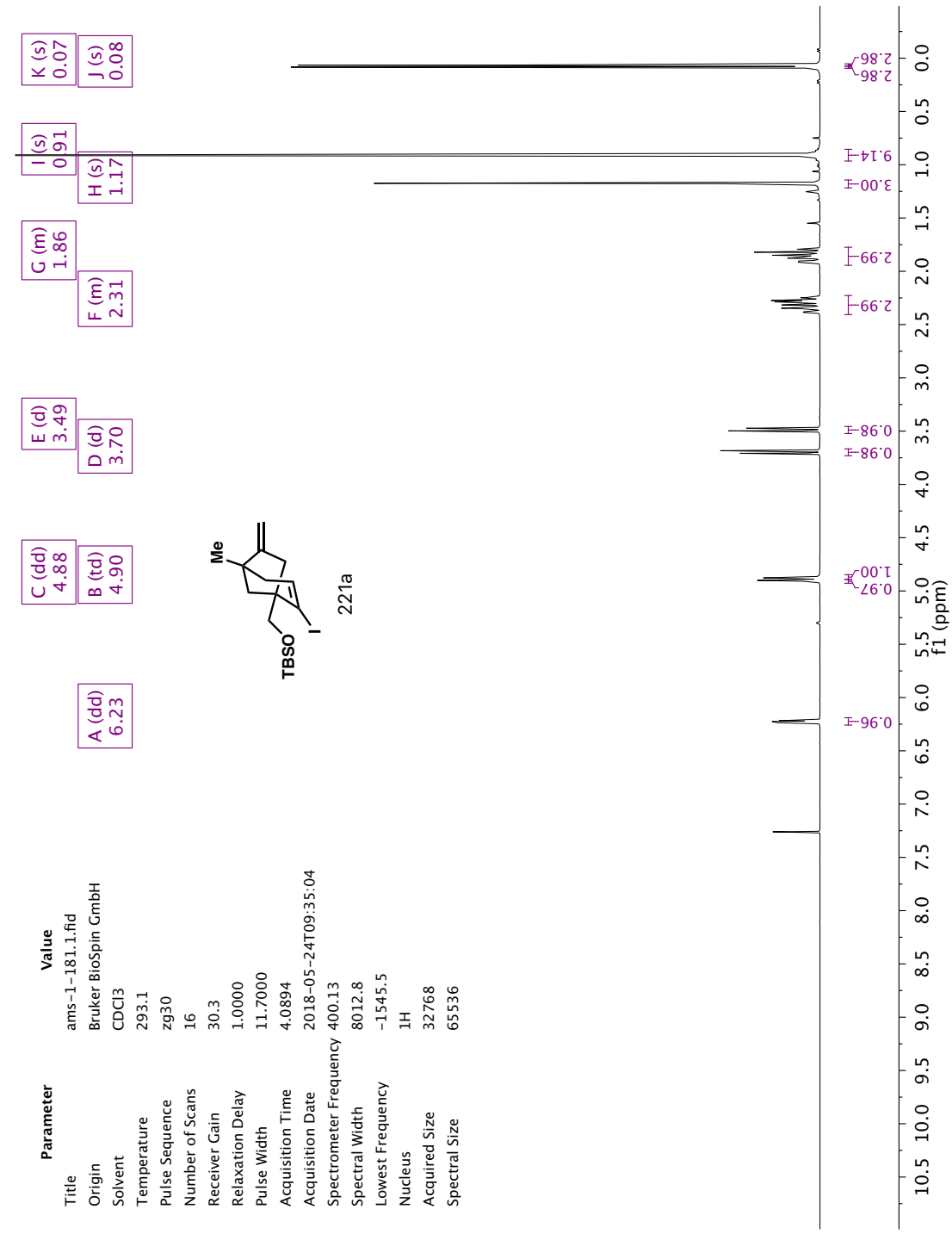
Parameter
Value
Title
ams-1-181.1.fid
Origin
Bruker BioSpin GmbH
Solvent
CDCl3
Temperature
293.1
Pulse Sequence
zg30
Number of Scans
16
Receiver Gain
30.3
Relaxation Delay
1.0000
Pulse Width
11.7000
Acquisition Time
4.0894
Acquisition Date
2018-05-24T09:35:04
Spectrometer Frequency
400.13
Spectral Width
8012.8
Lowest Frequency
-1545.5
Nucleus
1H
Acquired Size
32768
Spectral Size
65536
A (dd) 6.23
B (td) 4.90
C (dd) 4.88
D (d) 3.70
E (d) 3.49
F (m) 2.31
G (m) 1.86
H (s) 1.17
I (s) 0.91
J (s) 0.08
K (s) 0.07
Me
TBSO
I
221a
0.96
1.00
0.97
0.98
0.98
2.99
2.99
3.00
9.14
2.86
2.86
f1 (ppm)

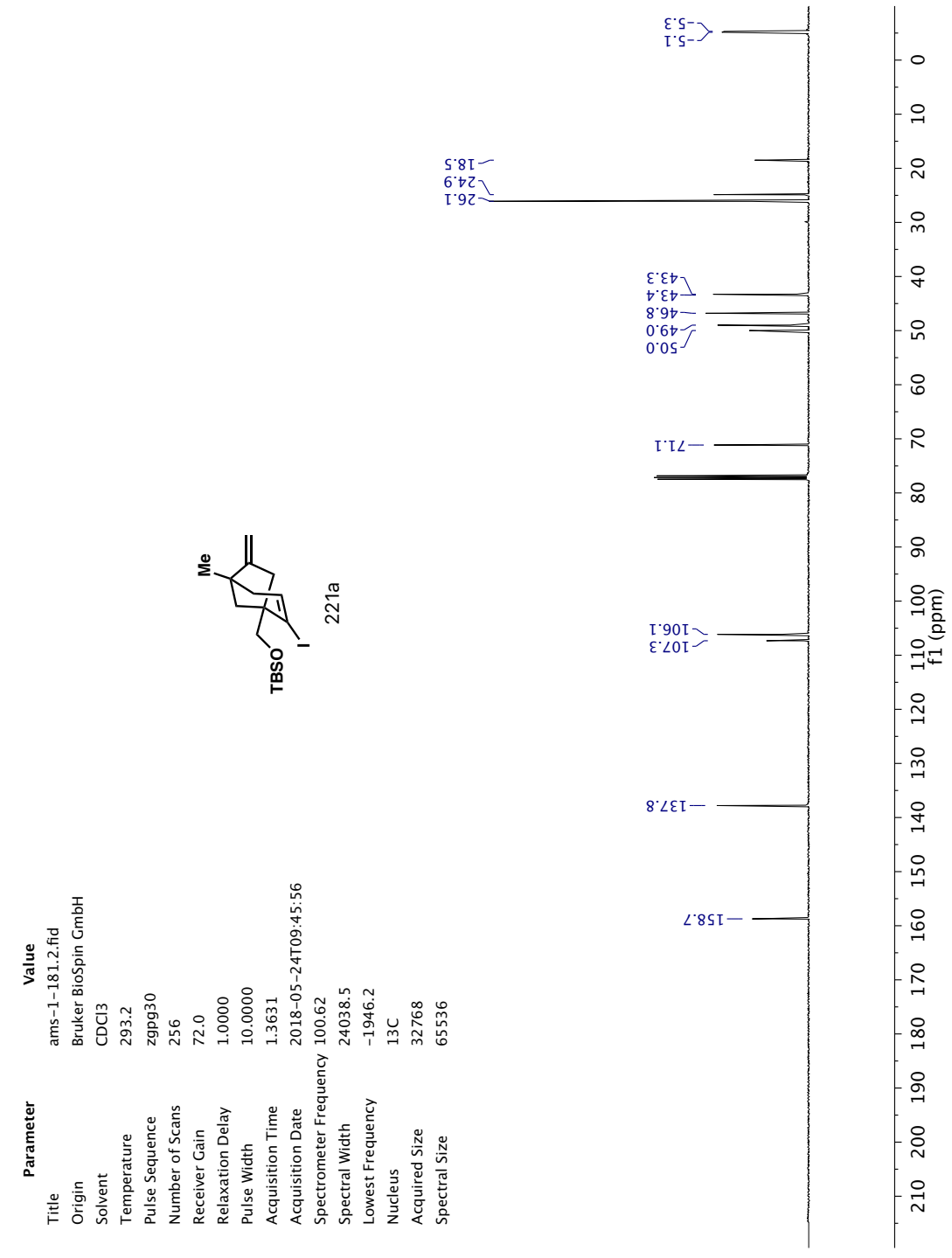
Parameter Value
Title ams-1-181.2.fid
Origin Bruker BioSpin GmbH
Solvent CDCl3
Temperature 293.2
Pulse Sequence zgpg30
Number of Scans 256
Receiver Gain 72.0
Relaxation Delay 1.0000
Pulse Width 10.0000
Acquisition Time 1.3631
Acquisition Date 2018-05-24T09:45:56
Spectrometer Frequency 100.62
Spectral Width 24038.5
Lowest Frequency -1946.2
Nucleus 13C
Acquired Size 32768
Spectral Size 65536
Me
TBSO
I
221a
158.7
137.8
107.3
106.1
71.1
50.0
49.0
46.8
43.4
43.3
26.1
24.9
18.5
-5.1
-5.3
f1 (ppm)

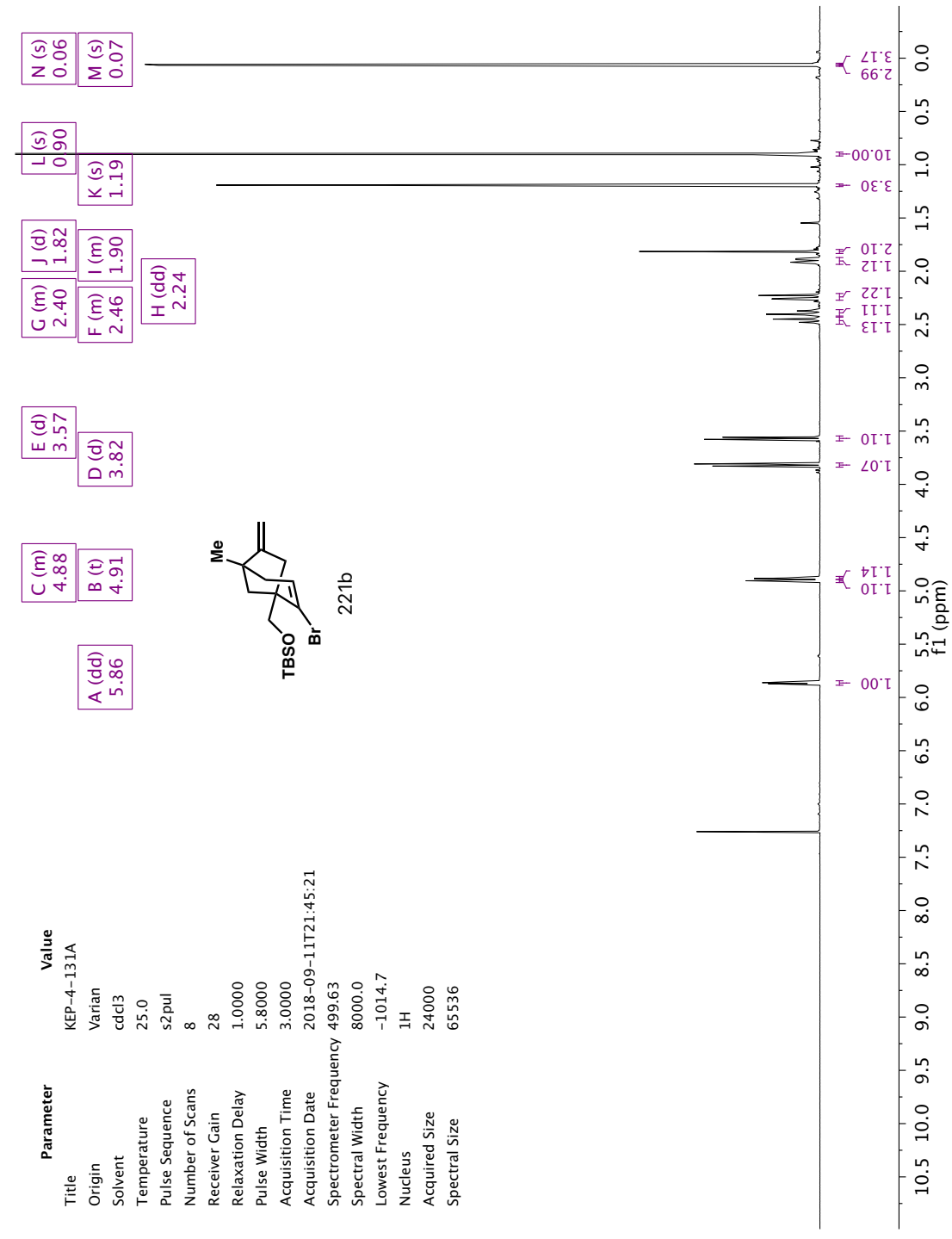

Parameter	Value
Title	KEP-4-131A
Origin	Varian
Solvent	cdcl3
Temperature	25.0
Pulse Sequence	s2pul
Number of Scans	8
Receiver Gain	28
Relaxation Delay	1.0000
Pulse Width	5.8000
Acquisition Time	3.0000
Acquisition Date	2018-09-11T21:45:21
Spectrometer Frequency	499.63
Spectral Width	8000.0
Lowest Frequency	-1014.7
Nucleus	1H
Acquired Size	24000
Spectral Size	65536

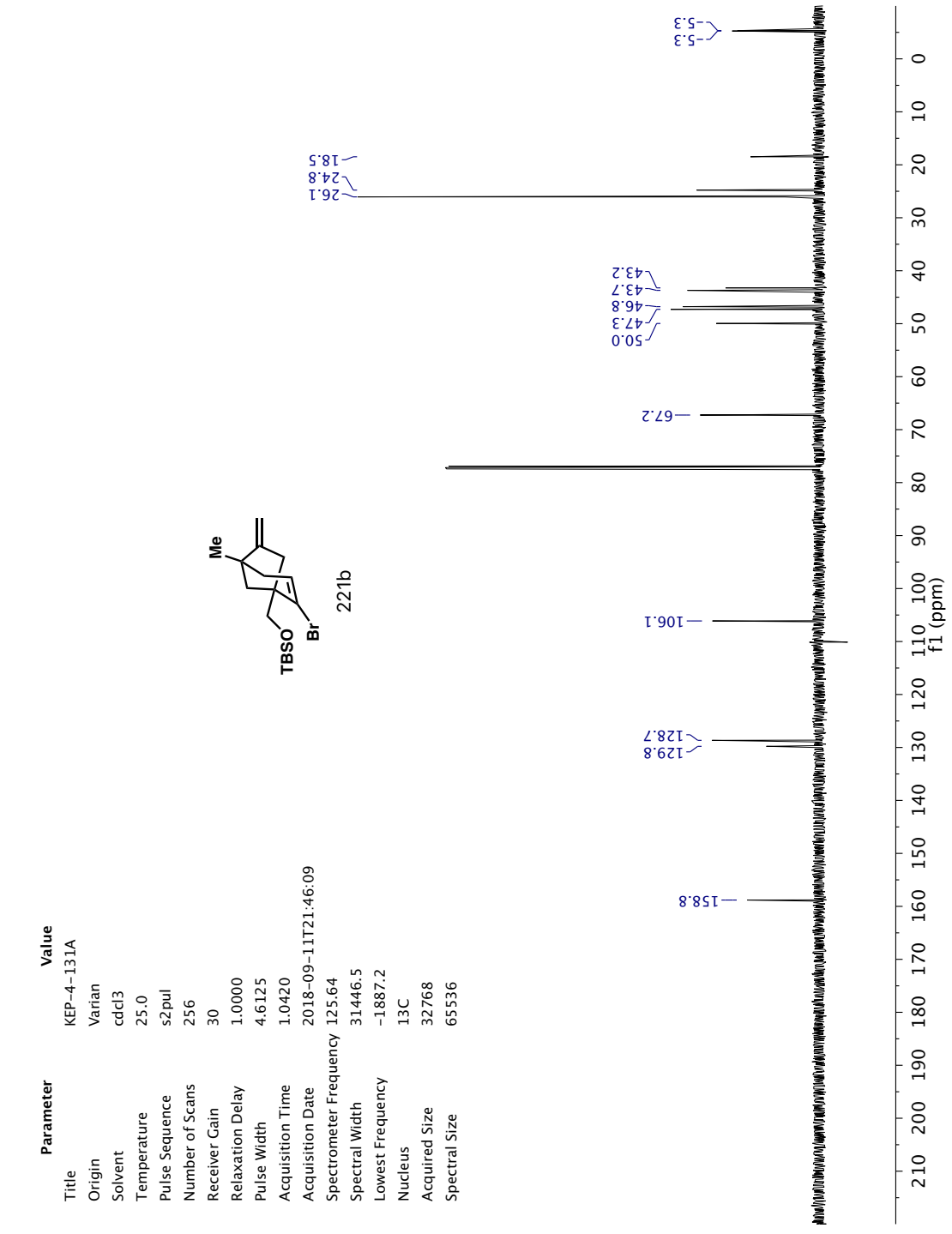
Parameter Value
Title KEP-4-131A
Origin Varian
Solvent cdcl3
Temperature 25.0
Pulse Sequence s2pul
Number of Scans 256
Receiver Gain 30
Relaxation Delay 1.0000
Pulse Width 4.6125
Acquisition Time 1.0420
Acquisition Date 2018-09-11T21:46:09
Spectrometer Frequency 125.64
Spectral Width 31446.5
Lowest Frequency -1887.2
Nucleus 13C
Acquired Size 32768
Spectral Size 65536
Me
TBSO
Br
221b
-5.3
-5.3
18.5
24.8
26.1
43.2
43.7
46.8
47.3
50.0
67.2
106.1
128.7
129.8
158.8
f1 (ppm)

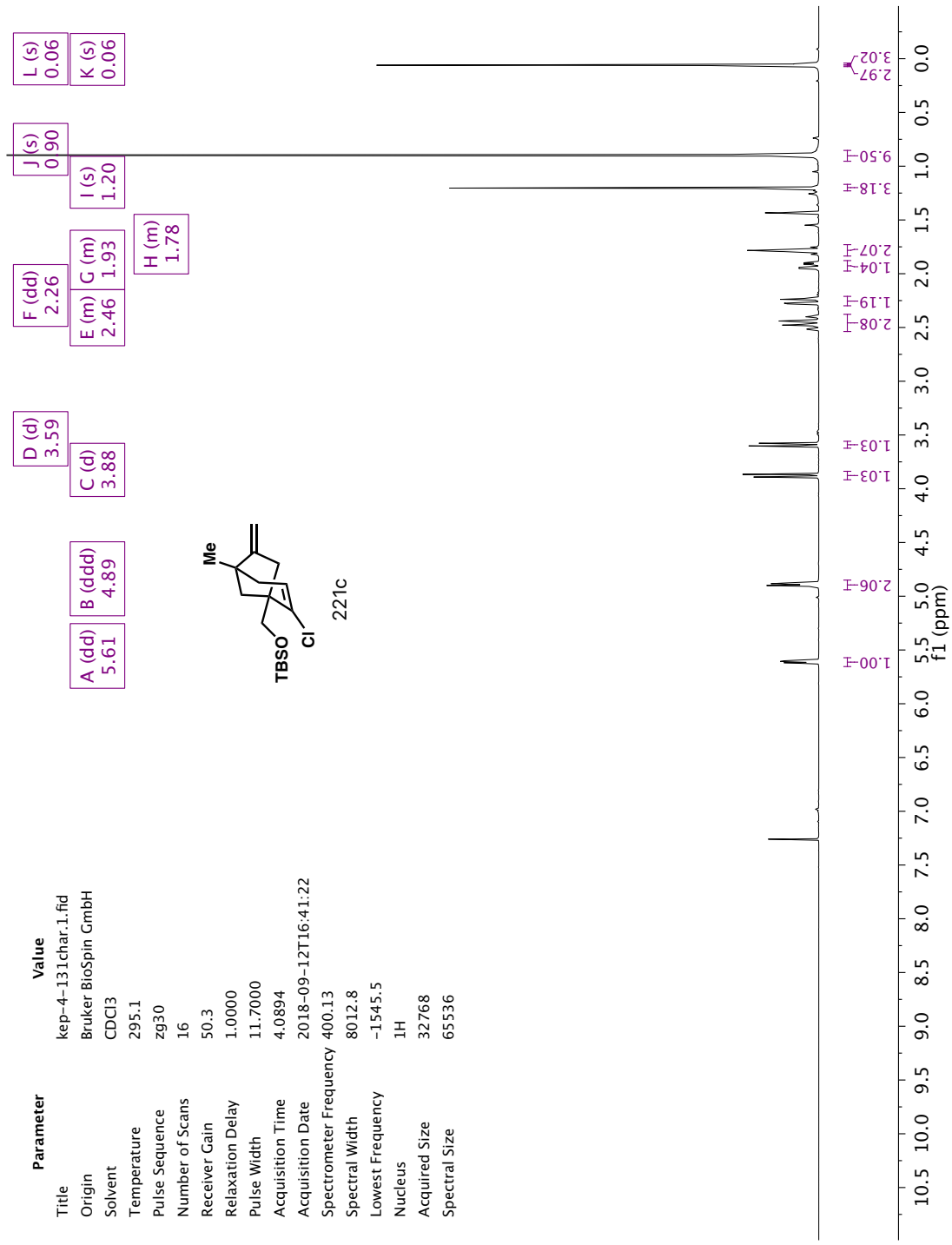
Parameter
Value
Title
kep-4-131char.1.fid
Origin
Bruker BioSpin GmbH
Solvent
CDCl3
Temperature
295.1
Pulse Sequence
zg30
Number of Scans
16
Receiver Gain
50.3
Relaxation Delay
1.0000
Pulse Width
11.7000
Acquisition Time
4.0894
Acquisition Date
2018-09-12T16:41:22
Spectrometer Frequency
400.13
Spectral Width
8012.8
Lowest Frequency
-1545.5
Nucleus
1H
Acquired Size
32768
Spectral Size
65536
A (dd) 5.61
B (ddd) 4.89
C (d) 3.88
D (d) 3.59
E (m) 2.46
F (dd) 2.26
G (m) 1.93
H (m) 1.78
I (s) 1.20
J (s) 0.90
K (s) 0.06
L (s) 0.06
Me
TBSO
Cl
221c
1.00
2.06
1.03
1.03
1.03
2.08
1.19
1.04
2.07
9.50
3.18
2.97
3.02
f1 (ppm)

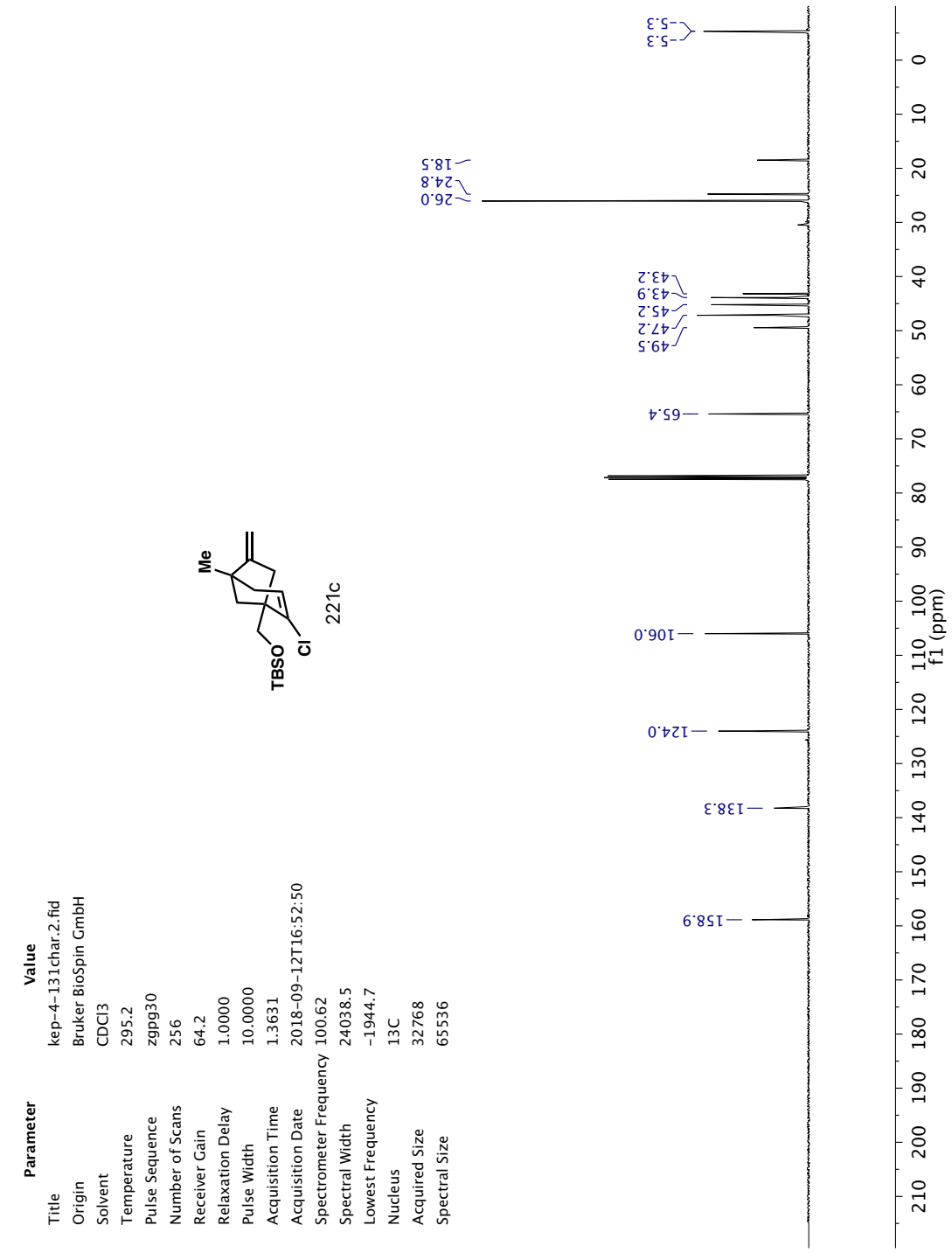

Parameter	Value
Title	kep-4-131char.2.fid
Origin	Bruker BioSpin GmbH
Solvent	CDCl3
Temperature	295.2
Pulse Sequence	zgpg30
Number of Scans	256
Receiver Gain	64.2
Relaxation Delay	1.0000
Pulse Width	10.0000
Acquisition Time	1.3631
Acquisition Date	2018-09-12T16:52:50
Spectrometer Frequency	100.62
Spectral Width	24038.5
Lowest Frequency	-1944.7
Nucleus	13C
Acquired Size	32768
Spectral Size	65536

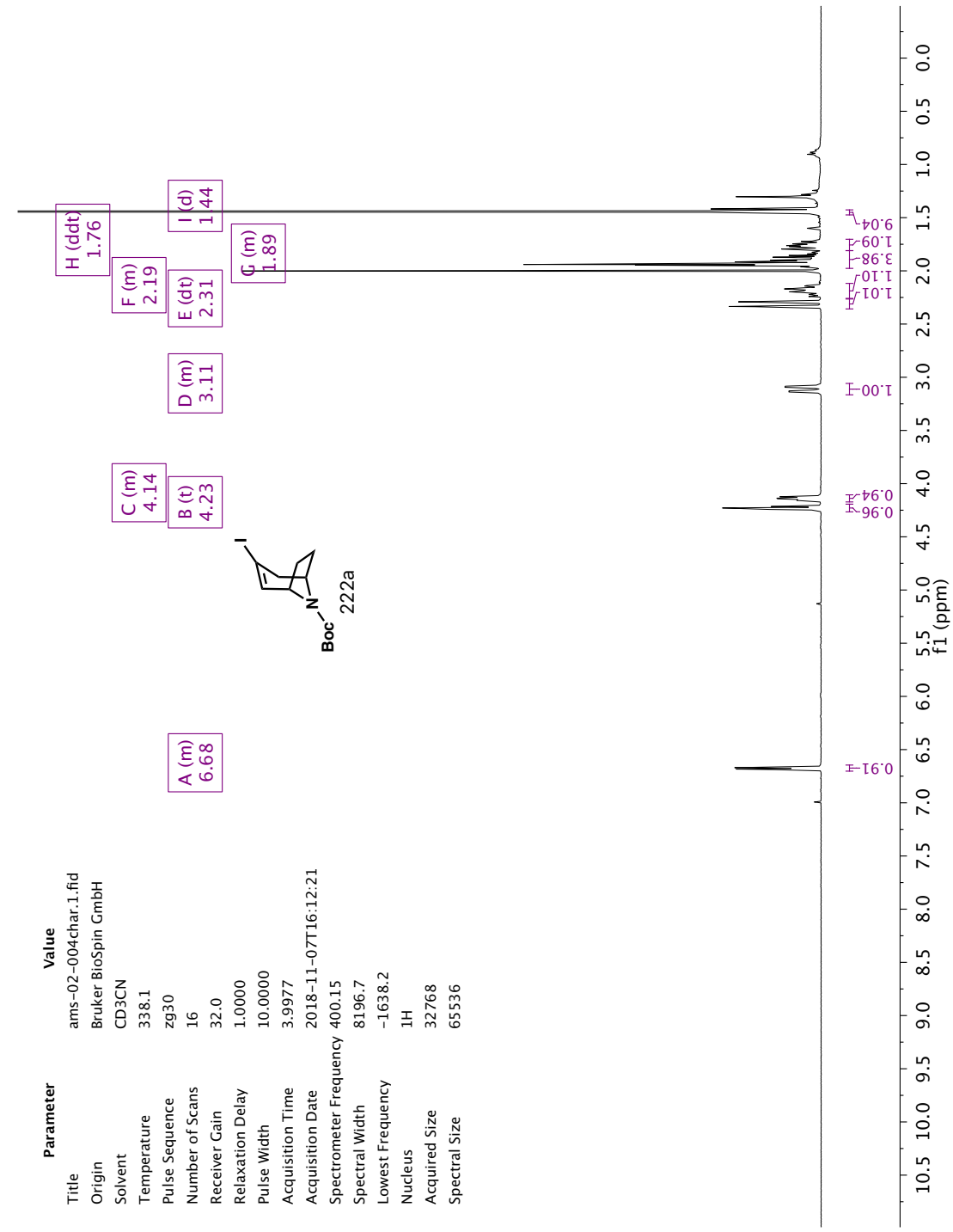
Parameter Value
Title ams-02-004char.1.fid
Origin Bruker BioSpin GmbH
Solvent CD3CN
Temperature 338.1
Pulse Sequence zg30
Number of Scans 16
Receiver Gain 32.0
Relaxation Delay 1.0000
Pulse Width 10.0000
Acquisition Time 3.9977
Acquisition Date 2018-11-07T16:12:21
Spectrometer Frequency 400.15
Spectral Width 8196.7
Lowest Frequency -1638.2
Nucleus 1H
Acquired Size 32768
Spectral Size 65536
A (m) 6.68
B (t) 4.23
C (m) 4.14
D (m) 3.11
E (dt) 2.31
F (m) 2.19
G (m) 1.89
H (ddt) 1.76
I (d) 1.44
Boc
N
I
222a
0.91
1.00
0.94
0.96
1.01
1.10
3.98
1.09
9.04
f1 (ppm)

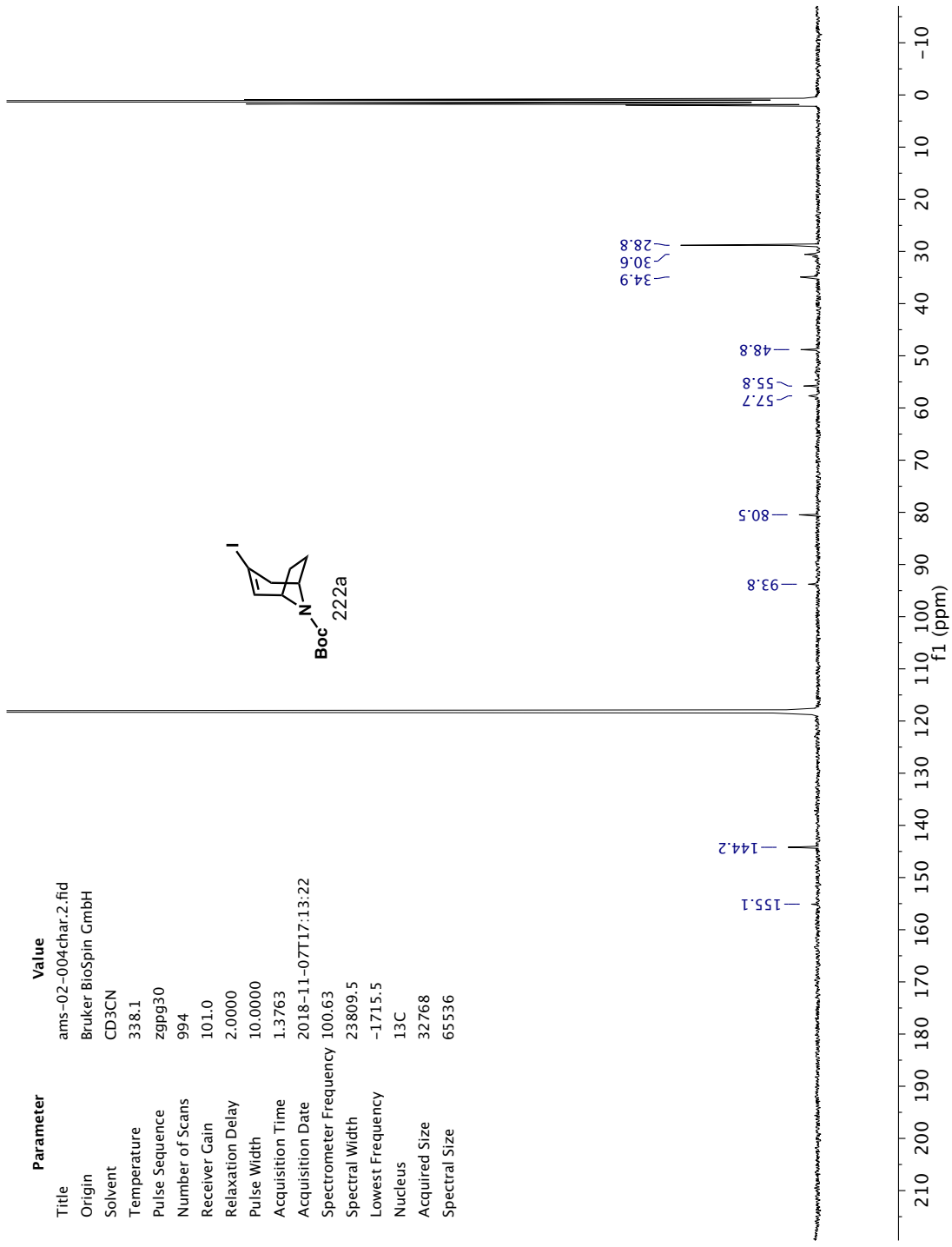
Parameter Value
Title ams-02-004char.2.fid
Origin Bruker BioSpin GmbH
Solvent CD3CN
Temperature 338.1
Pulse Sequence zgpg30
Number of Scans 994
Receiver Gain 101.0
Relaxation Delay 2.0000
Pulse Width 10.0000
Acquisition Time 1.3763
Acquisition Date 2018-11-07T17:13:22
Spectrometer Frequency 100.63
Spectral Width 23809.5
Lowest Frequency -1715.5
Nucleus 13C
Acquired Size 32768
Spectral Size 65536
I
N
Boc
222a
155.1
144.2
93.8
80.5
57.7
55.8
48.8
34.9
30.6
28.8
f1 (ppm)

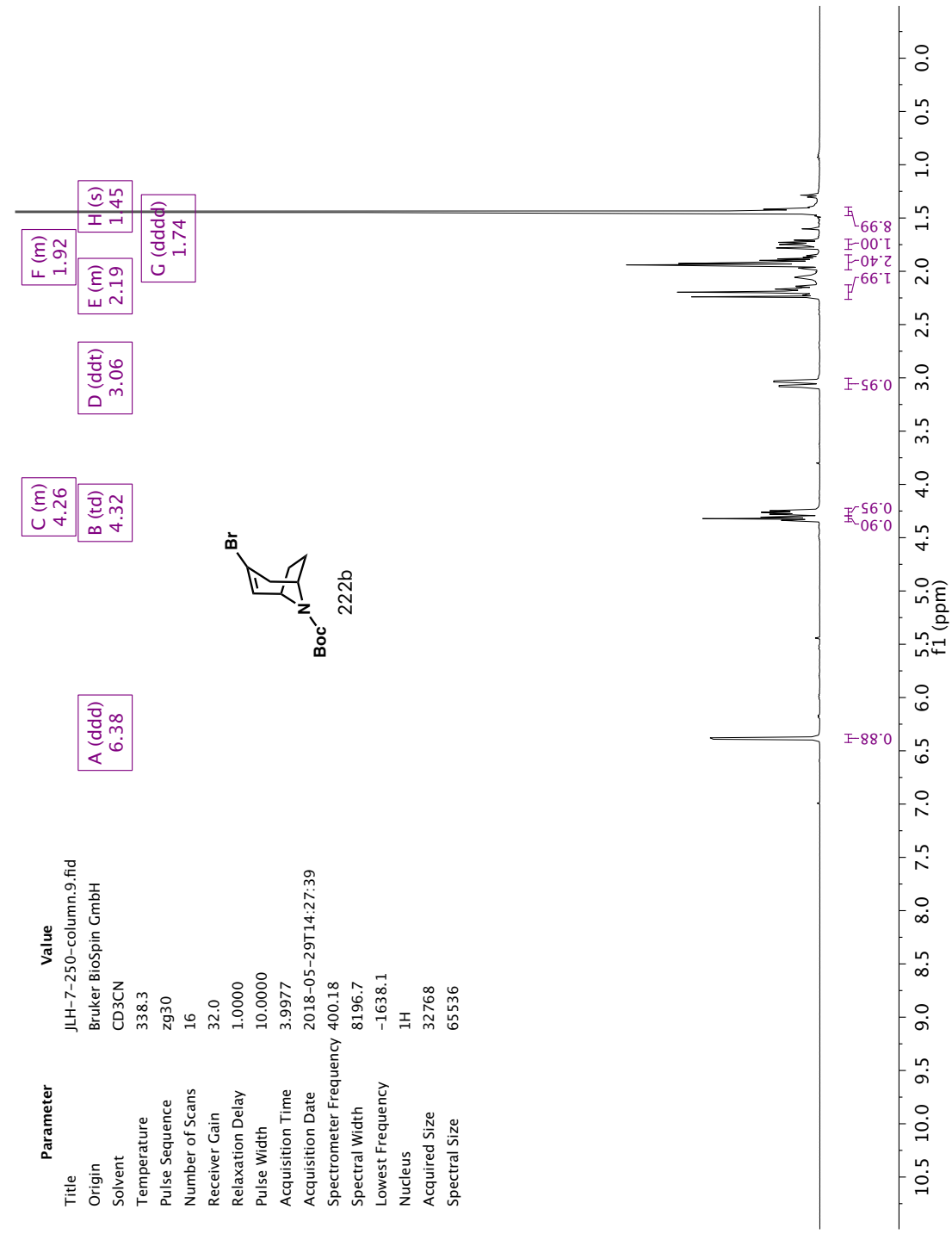
Parameter
Value
Title
JLH-7-250-column.9.fid
Origin
Bruker BioSpin GmbH
Solvent
CD3CN
Temperature
338.3
Pulse Sequence
zg30
Number of Scans
16
Receiver Gain
32.0
Relaxation Delay
1.0000
Pulse Width
10.0000
Acquisition Time
3.9977
Acquisition Date
2018-05-29T14:27:39
Spectrometer Frequency
400.18
Spectral Width
8196.7
Lowest Frequency
-1638.1
Nucleus
1H
Acquired Size
32768
Spectral Size
65536
A (ddd) 6.38
B (td) 4.32
C (m) 4.26
D (ddt) 3.06
E (m) 2.19
F (m) 1.92
G (dddd) 1.74
H (s) 1.45
Br
N
Boc
222b
0.88
0.90
0.95
0.95
1.99
2.40
1.00
8.99
f1 (ppm)

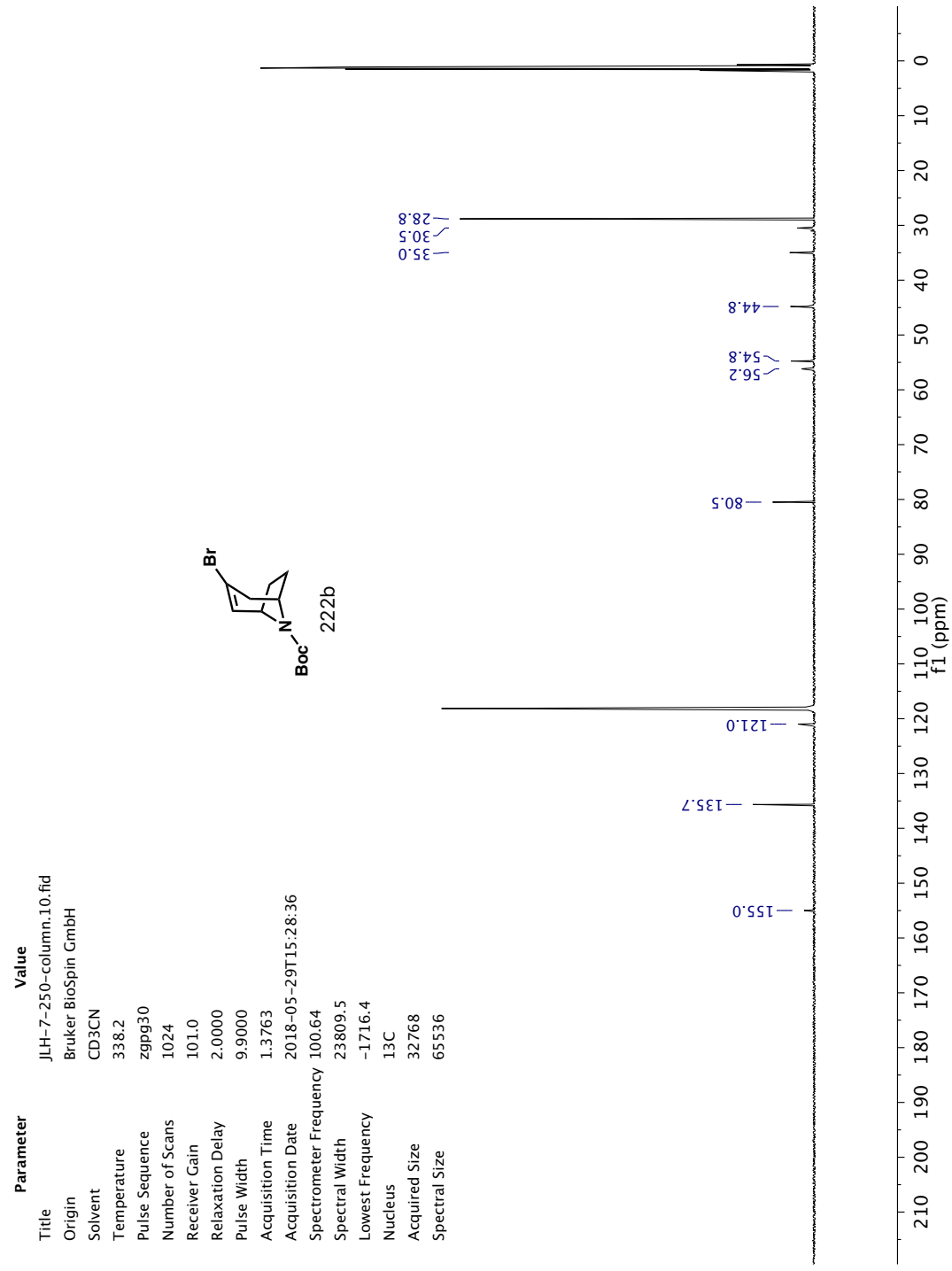
Parameter Value
Title JLH-7-250-column.10.fid
Origin Bruker BioSpin GmbH
Solvent CD3CN
Temperature 338.2
Pulse Sequence zgpg30
Number of Scans 1024
Receiver Gain 101.0
Relaxation Delay 2.0000
Pulse Width 9.9000
Acquisition Time 1.3763
Acquisition Date 2018-05-29T15:28:36
Spectrometer Frequency 100.64
Spectral Width 23809.5
Lowest Frequency -1716.4
Nucleus 13C
Acquired Size 32768
Spectral Size 65536
Br
N
Boc
222b
155.0
135.7
121.0
80.5
56.2
54.8
44.8
35.0
30.5
28.8
f1 (ppm)

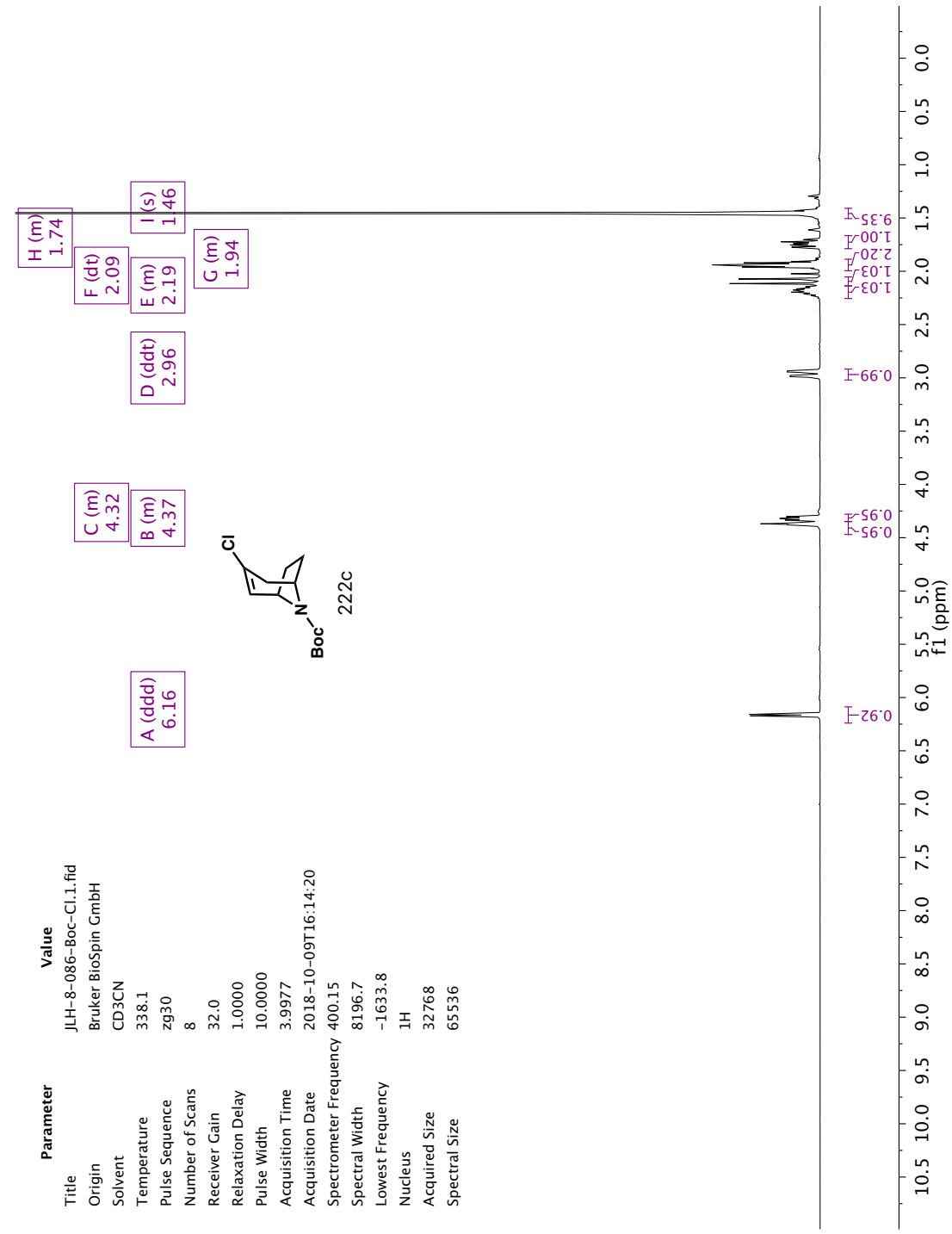

Parameter	Value
Title	JLH-8-086-Boc-Cl.1.fid
Origin	Bruker BioSpin GmbH
Solvent	CD3CN
Temperature	338.1
Pulse Sequence	zg30
Number of Scans	8
Receiver Gain	32.0
Relaxation Delay	1.0000
Pulse Width	10.0000
Acquisition Time	3.9977
Acquisition Date	2018-10-09T16:14:20
Spectrometer Frequency	400.15
Spectral Width	8196.7
Lowest Frequency	-1633.8
Nucleus	1H
Acquired Size	32768
Spectral Size	65536

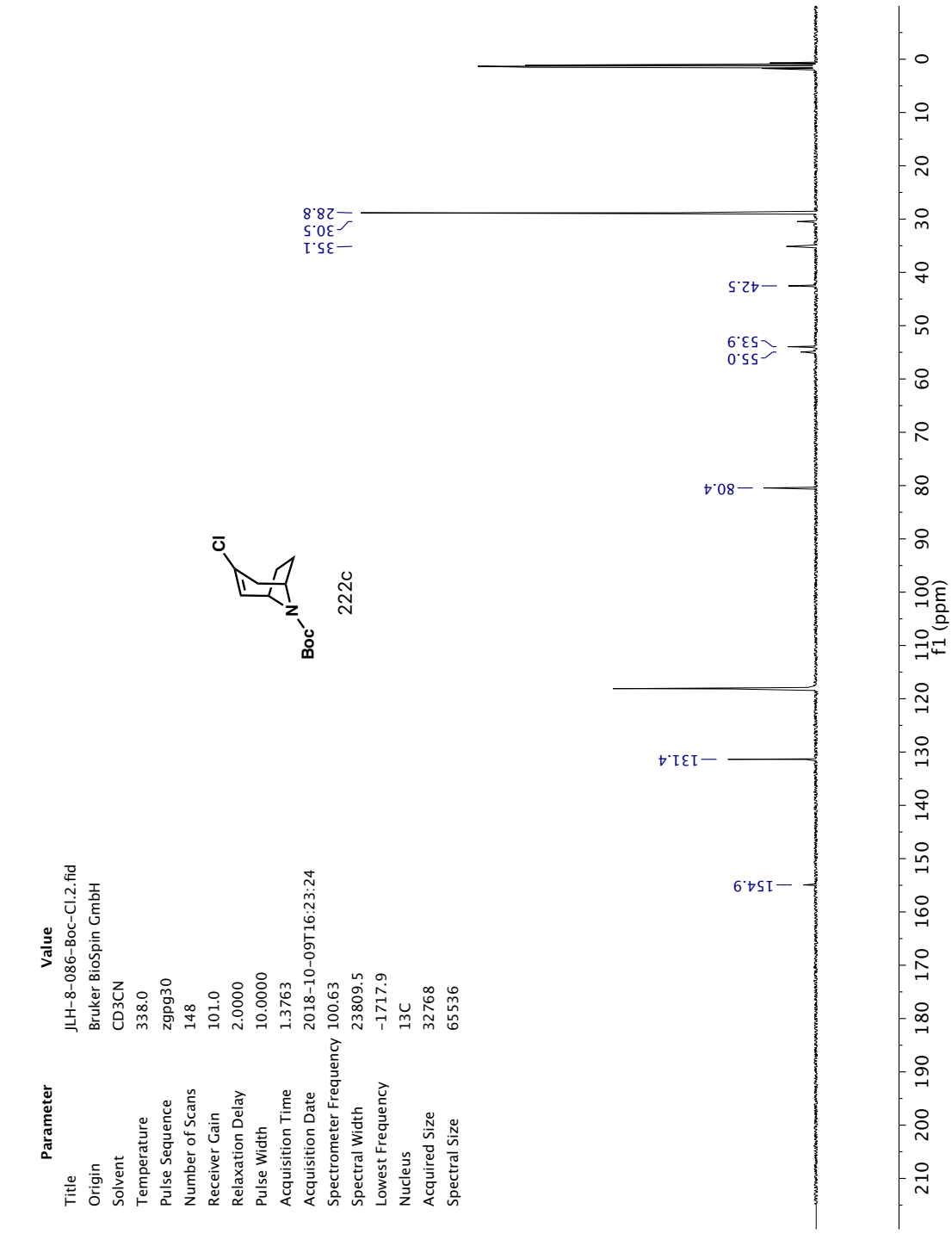
Parameter Value
Title JLH-8-086-Boc-Cl.2.fid
Origin Bruker BioSpin GmbH
Solvent CD3CN
Temperature 338.0
Pulse Sequence zgpg30
Number of Scans 148
Receiver Gain 101.0
Relaxation Delay 2.0000
Pulse Width 10.0000
Acquisition Time 1.3763
Acquisition Date 2018-10-09T16:23:24
Spectrometer Frequency 100.63
Spectral Width 23809.5
Lowest Frequency -1717.9
Nucleus 13C
Acquired Size 32768
Spectral Size 65536
Cl
N
Boc
222c
154.9
131.4
80.4
55.0
53.9
42.5
35.1
30.5
28.8
f1 (ppm)

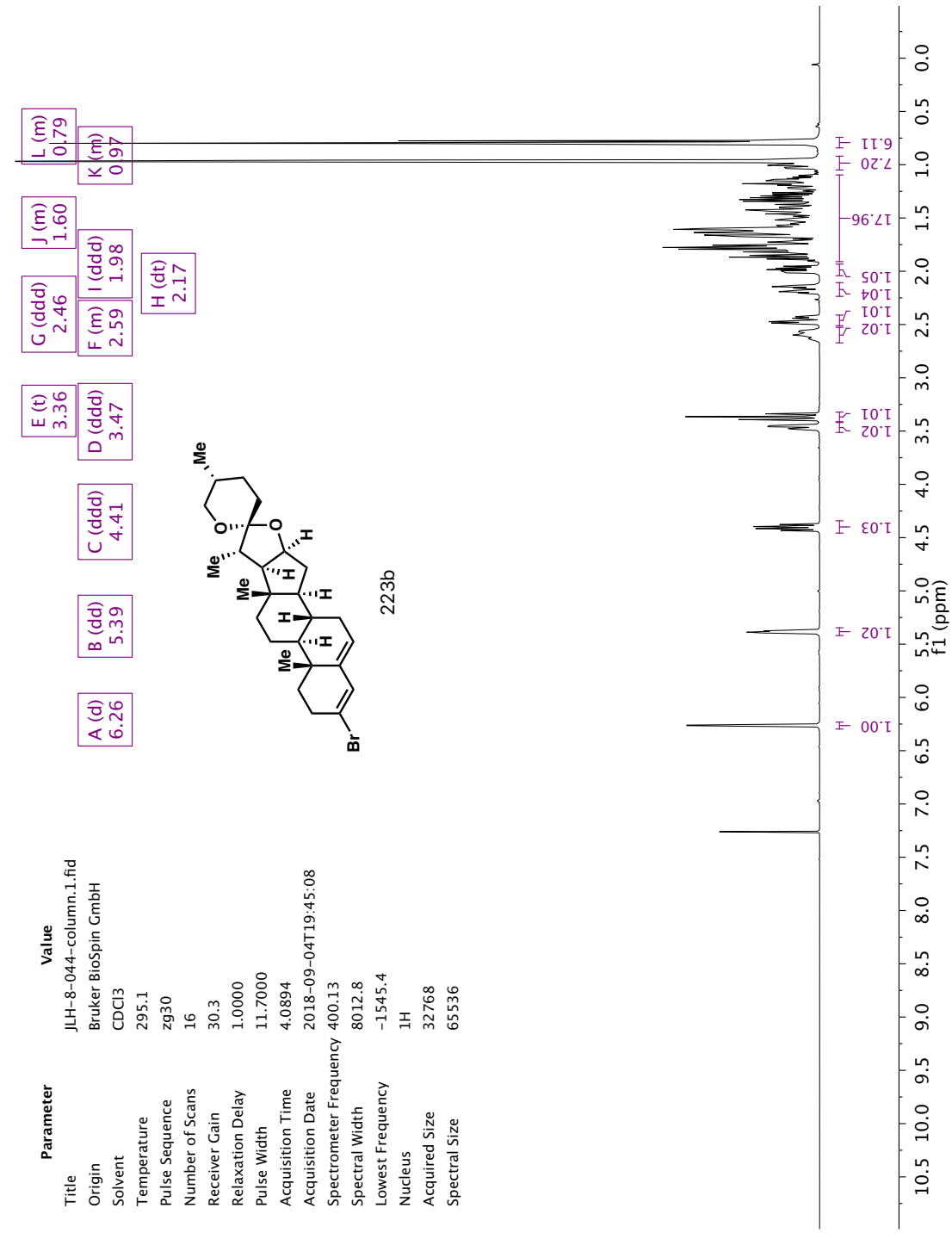

Parameter	Value
Title	JLH-8-044-column.1.fid
Origin	Bruker BioSpin GmbH
Solvent	CDCl3
Temperature	295.1
Pulse Sequence	zg30
Number of Scans	16
Receiver Gain	30.3
Relaxation Delay	1.0000
Pulse Width	11.7000
Acquisition Time	4.0894
Acquisition Date	2018-09-04T19:45:08
Spectrometer Frequency	400.13
Spectral Width	8012.8
Lowest Frequency	-1545.4
Nucleus	1H
Acquired Size	32768
Spectral Size	65536

Parameter	Value
Title	JLH-8-044-column.2.fid
Origin	Bruker BioSpin GmbH
Solvent	CDCl3
Temperature	295.2
Pulse Sequence	zgpg30
Number of Scans	128
Receiver Gain	72.0
Relaxation Delay	2.0000
Pulse Width	10.0000
Acquisition Time	1.3631
Acquisition Date	2018-09-04T19:52:59
Spectrometer Frequency	100.62
Spectral Width	24038.5
Lowest Frequency	-1947.0
Nucleus	13C
Acquired Size	32768
Spectral Size	65536

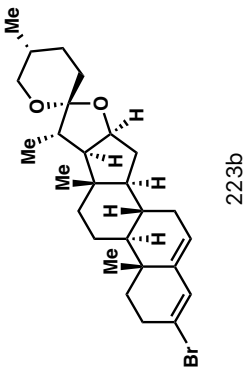

223b

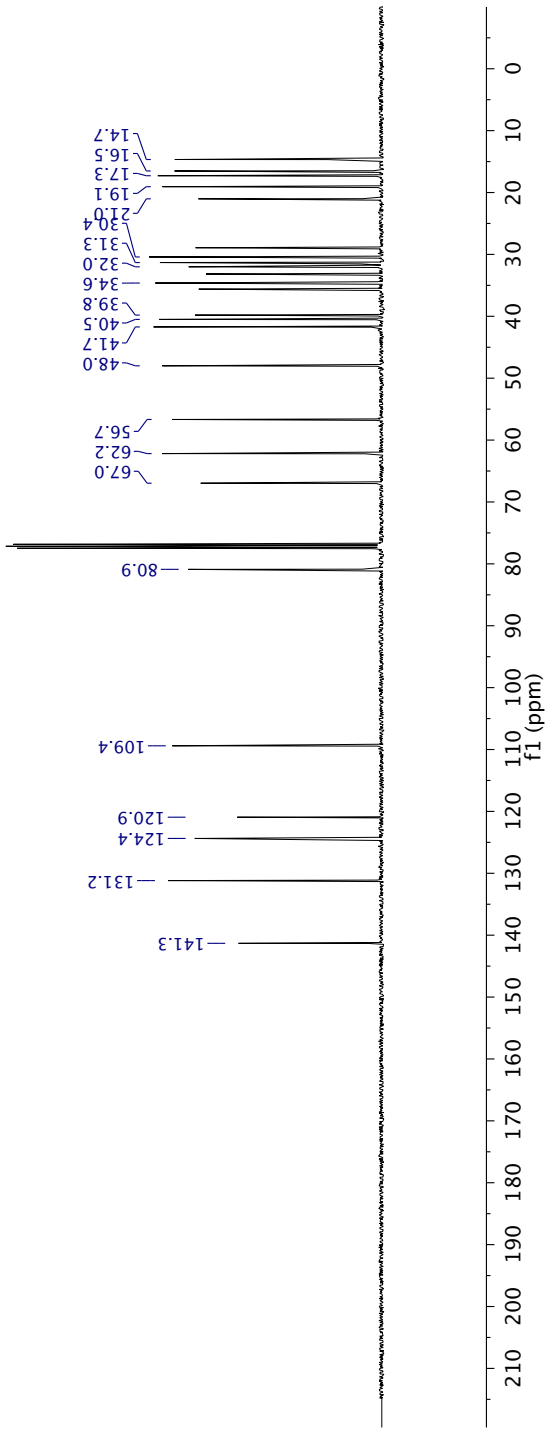

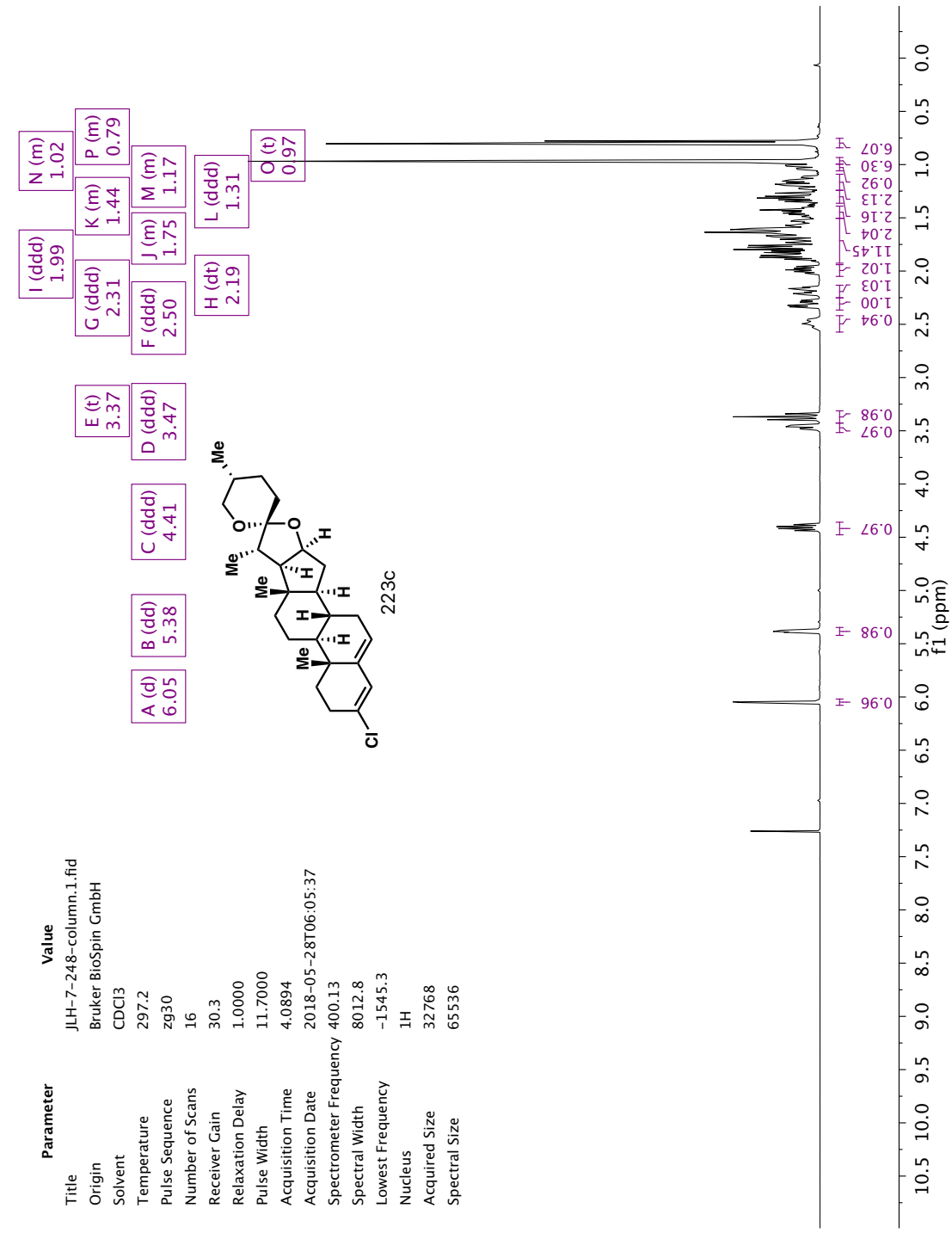

Parameter	Value
Title	JLH-7-248-column.1.fid
Origin	Bruker BioSpin GmbH
Solvent	CDCl3
Temperature	297.2
Pulse Sequence	zg30
Number of Scans	16
Receiver Gain	30.3
Relaxation Delay	1.0000
Pulse Width	11.7000
Acquisition Time	4.0894
Acquisition Date	2018-05-28T06:05:37
Spectrometer Frequency	400.13
Spectral Width	8012.8
Lowest Frequency	-1545.3
Nucleus	1H
Acquired Size	32768
Spectral Size	65536

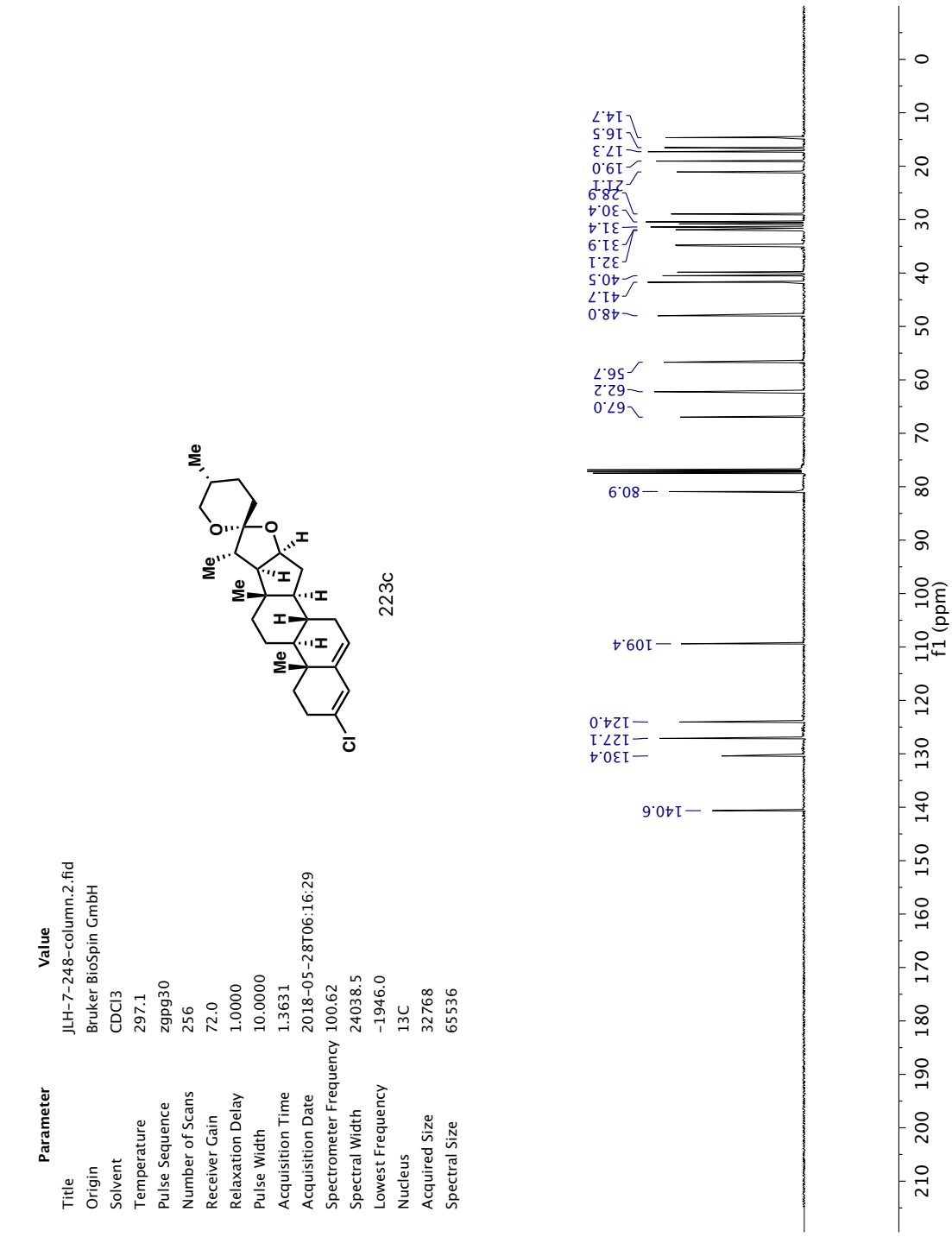

Parameter	Value
Title	JLH-7-248-column.2.fid
Origin	Bruker BioSpin GmbH
Solvent	CDCl3
Temperature	297.1
Pulse Sequence	zgpg30
Number of Scans	256
Receiver Gain	72.0
Relaxation Delay	1.0000
Pulse Width	10.0000
Acquisition Time	1.3631
Acquisition Date	2018-05-28T06:16:29
Spectrometer Frequency	100.62
Spectral Width	24038.5
Lowest Frequency	-1946.0
Nucleus	13C
Acquired Size	32768
Spectral Size	65536

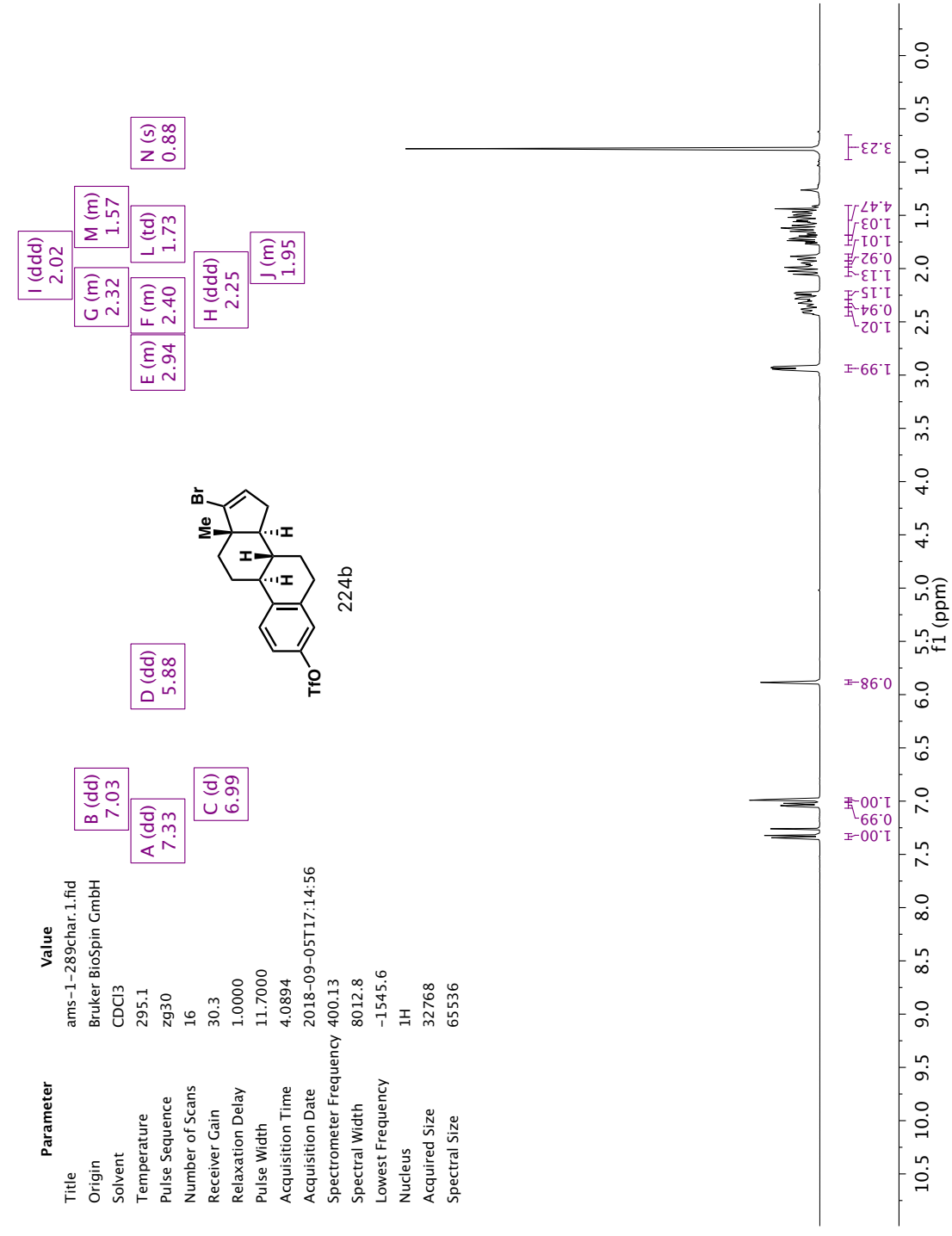
Parameter
Value
Title ams-1-289char.1.fid
Origin Bruker BioSpin GmbH
Solvent CDCl3
Temperature 295.1
Pulse Sequence zg30
Number of Scans 16
Receiver Gain 30.3
Relaxation Delay 1.0000
Pulse Width 11.7000
Acquisition Time 4.0894
Acquisition Date 2018-09-05T17:14:56
Spectrometer Frequency 400.13
Spectral Width 8012.8
Lowest Frequency -1545.6
Nucleus 1H
Acquired Size 32768
Spectral Size 65536
A (dd) 7.33
B (dd) 7.03
C (d) 6.99
D (dd) 5.88
E (m) 2.94
F (m) 2.40
G (m) 2.32
H (ddd) 2.25
I (ddd) 2.02
J (m) 1.95
L (td) 1.73
M (m) 1.57
N (s) 0.88
Br
Me
H
H
H
TfO
224b
1.00
0.99
1.00
0.98
1.99
1.02
0.94
1.15
1.13
0.92
1.01
1.03
4.47
3.23
f1 (ppm)

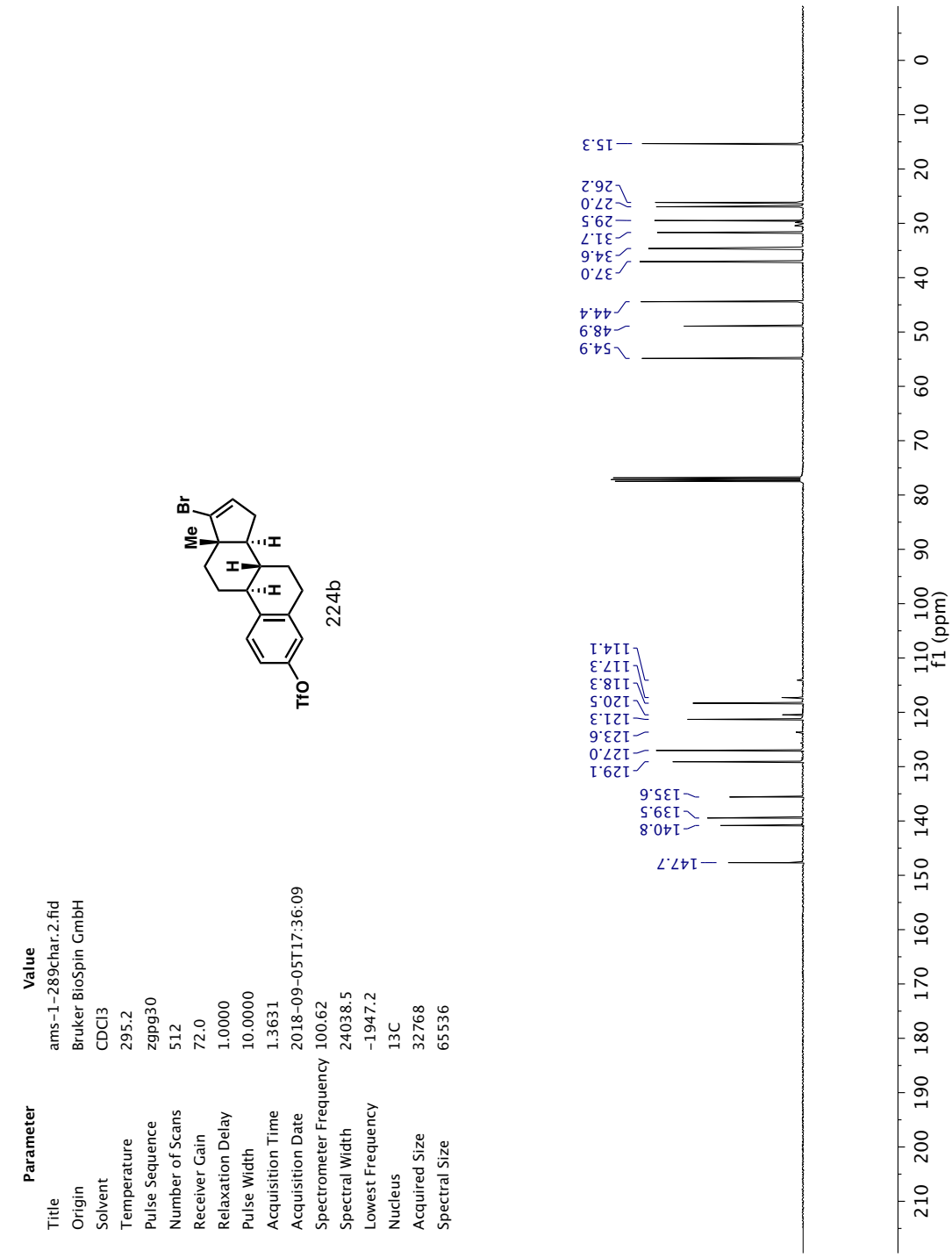

Parameter	Value
Title	ams-1-289char.2.fid
Origin	Bruker BioSpin GmbH
Solvent	CDCl3
Temperature	295.2
Pulse Sequence	zgpg30
Number of Scans	512
Receiver Gain	72.0
Relaxation Delay	1.0000
Pulse Width	10.0000
Acquisition Time	1.3631
Acquisition Date	2018-09-05T17:36:09
Spectrometer Frequency	100.62
Spectral Width	24038.5
Lowest Frequency	-1947.2
Nucleus	13C
Acquired Size	32768
Spectral Size	65536

Parameter	Value
Title	AMS-1-289-F
Origin	Varian
Solvent	cdcl3
Temperature	25.0
Pulse Sequence	s2pul
Number of Scans	16
Receiver Gain	30
Relaxation Delay	1.0000
Pulse Width	6.3333
Acquisition Time	0.9856
Acquisition Date	2018-09-05T15:27:01
Spectrometer Frequency	282.34
Spectral Width	64935.1
Lowest Frequency	-56444.7
Nucleus	19F
Acquired Size	64000
Spectral Size	131072

224b

-72.9

10 0 -10 -20 -30 -40 -50 -60 -70 -80 -90 -100 -110 -120 -130 -140 -150 -160 -170 -180 -190
f1 (ppm)

Parameter	Value
Title	AMS-1-289-F-std
Origin	Varian
Solvent	cdcl3
Temperature	25.0
Pulse Sequence	s2pul
Number of Scans	16
Receiver Gain	30
Relaxation Delay	1.0000
Pulse Width	6.3333
Acquisition Time	0.9856
Acquisition Date	2018-09-10T23:58:01
Spectrometer Frequency	282.34
Spectral Width	64935.1
Lowest Frequency	-56442.5
Nucleus	19F
Acquired Size	64000
Spectral Size	131072

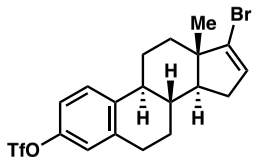

224b
with C_6F_6

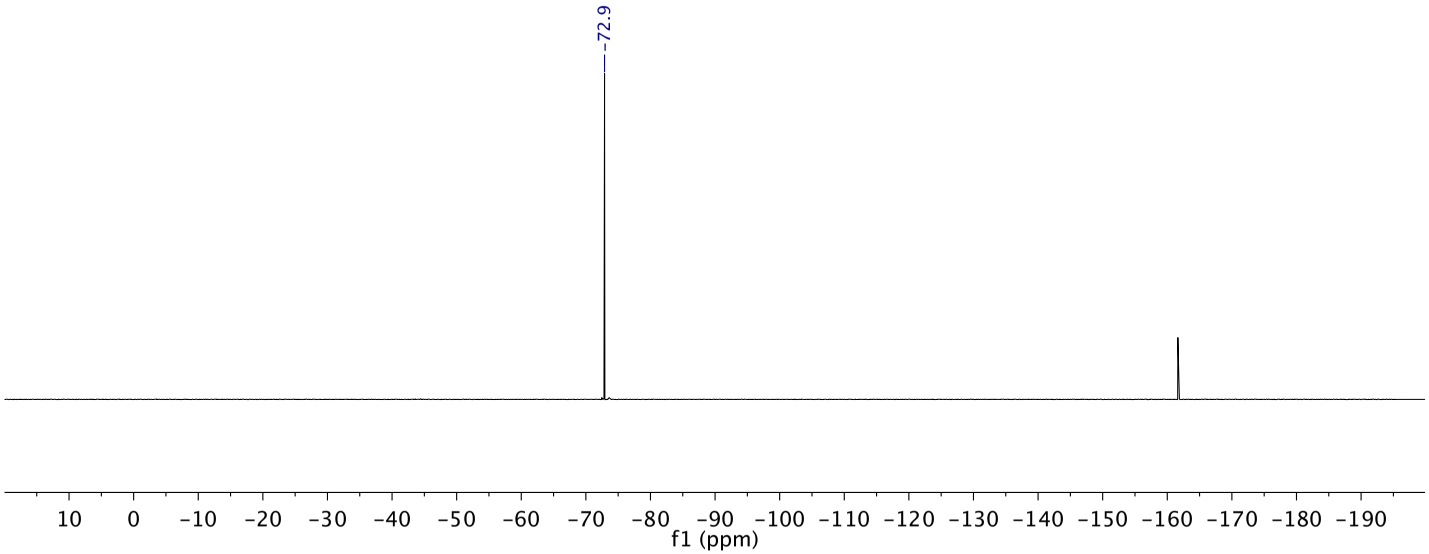

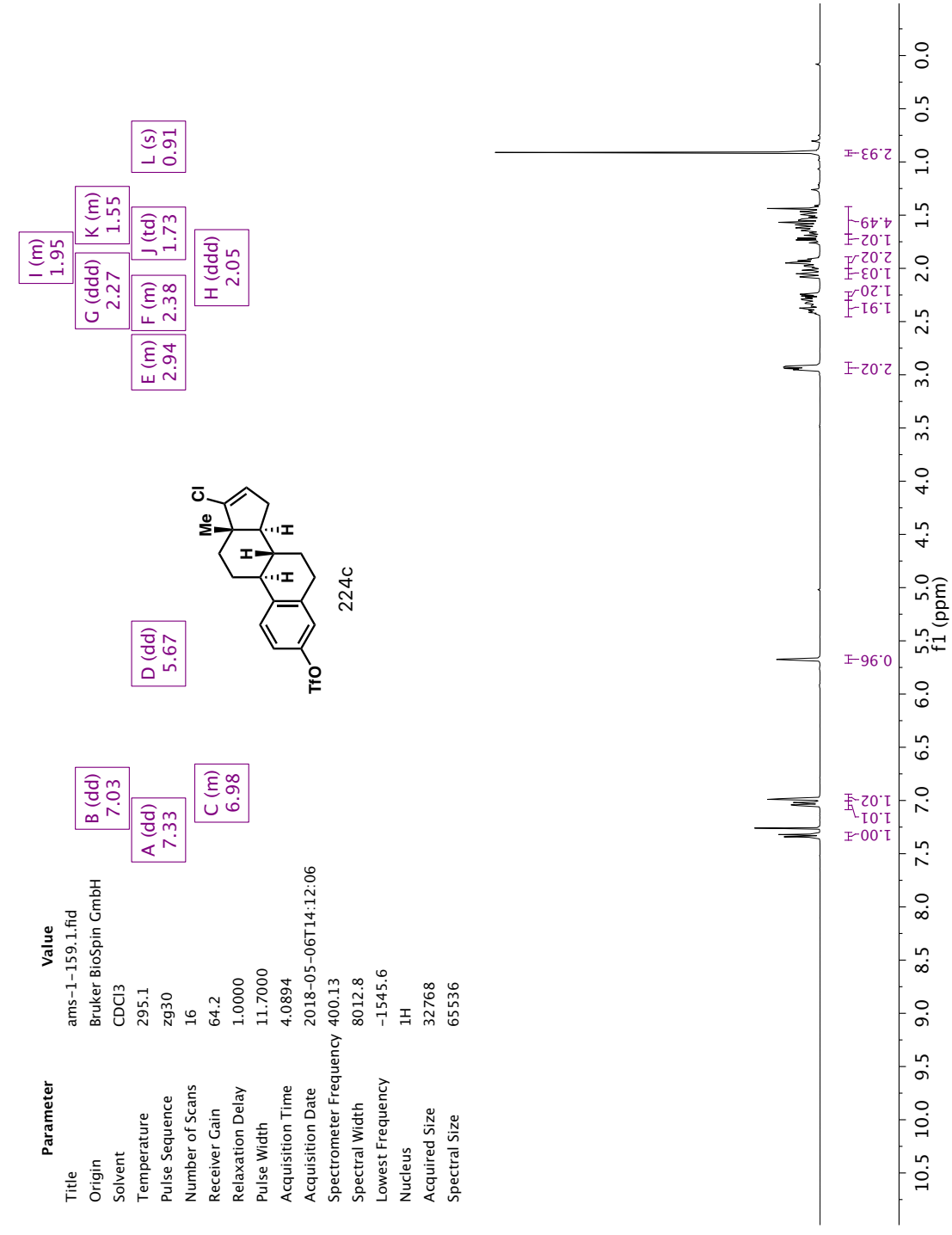
Parameter Value
Title ams-1-159.1.fid
Origin Bruker BioSpin GmbH
Solvent CDCl3
Temperature 295.1
Pulse Sequence zg30
Number of Scans 16
Receiver Gain 64.2
Relaxation Delay 1.0000
Pulse Width 11.7000
Acquisition Time 4.0894
Acquisition Date 2018-05-06T14:12:06
Spectrometer Frequency 400.13
Spectral Width 8012.8
Lowest Frequency -1545.6
Nucleus 1H
Acquired Size 32768
Spectral Size 65536
A (dd) 7.33
B (dd) 7.03
C (m) 6.98
D (dd) 5.67
E (m) 2.94
F (m) 2.38
G (ddd) 2.27
H (ddd) 2.05
I (m) 1.95
J (td) 1.73
K (m) 1.55
L (s) 0.91
Me
Cl
H
H
H
TfO
224c
1.00
1.01
1.02
0.96
2.02
1.91
1.20
1.03
2.02
1.02
4.49
2.93
10.5 10.0 9.5 9.0 8.5 8.0 7.5 7.0 6.5 6.0 5.5 5.0 4.5 4.0 3.5 3.0 2.5 2.0 1.5 1.0 0.5 0.0
f1 (ppm)

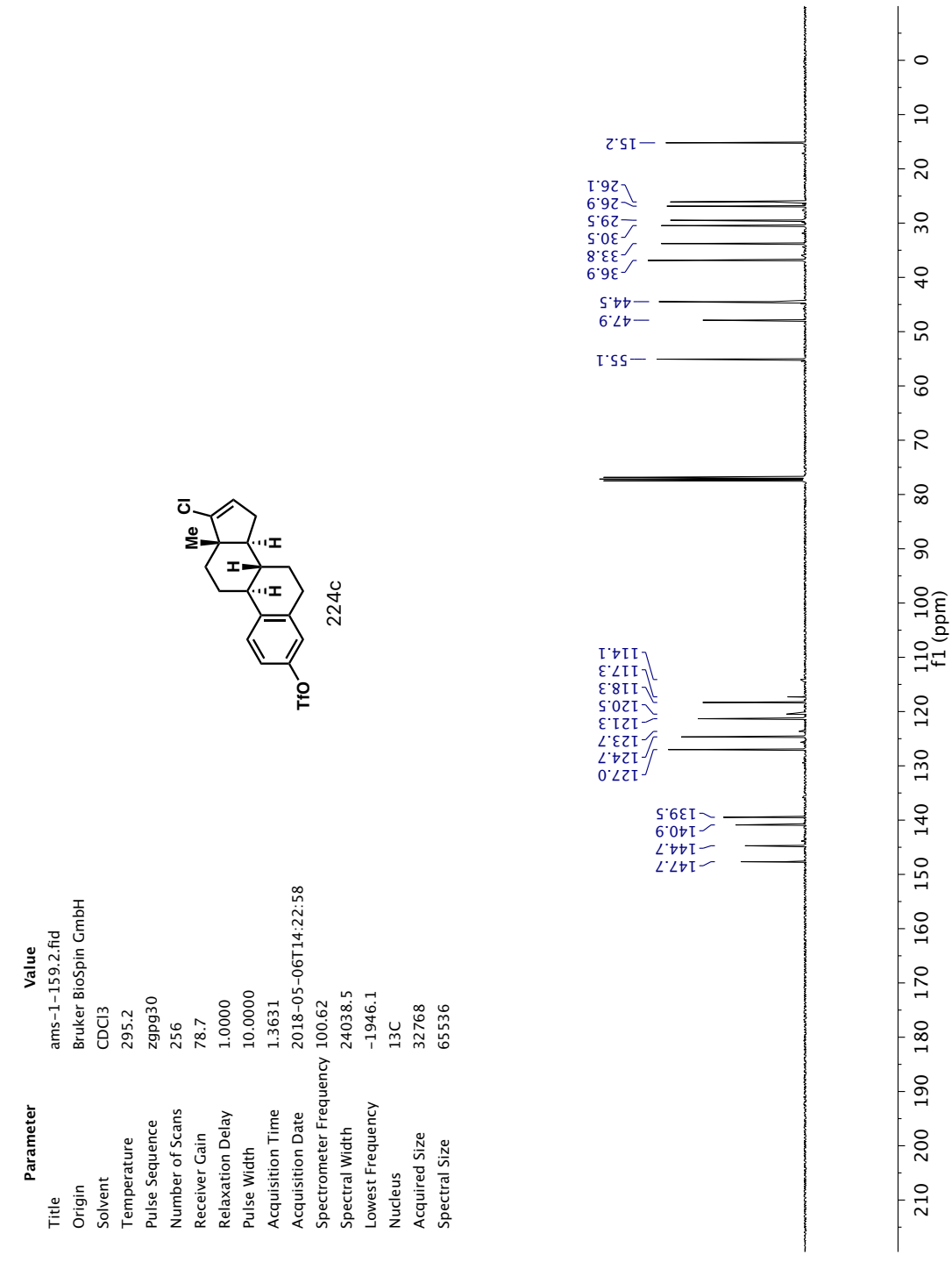

Parameter	Value
Title	ams-1-159.2.fid
Origin	Bruker BioSpin GmbH
Solvent	CDCl3
Temperature	295.2
Pulse Sequence	zgpg30
Number of Scans	256
Receiver Gain	78.7
Relaxation Delay	1.0000
Pulse Width	10.0000
Acquisition Time	1.3631
Acquisition Date	2018-05-06T14:22:58
Spectrometer Frequency	100.62
Spectral Width	24038.5
Lowest Frequency	-1946.1
Nucleus	13C
Acquired Size	32768
Spectral Size	65536

Parameter	Value
Title	AMS-1-159-F
Origin	Varian
Solvent	cdcl3
Temperature	25.0
Pulse Sequence	s2pul
Number of Scans	16
Receiver Gain	30
Relaxation Delay	1.0000
Pulse Width	6.3333
Acquisition Time	0.9856
Acquisition Date	2018-06-14T01:56:19
Spectrometer Frequency	282.34
Spectral Width	64935.1
Lowest Frequency	-56468.7
Nucleus	19F
Acquired Size	64000
Spectral Size	131072

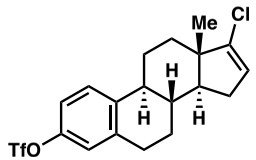

224c

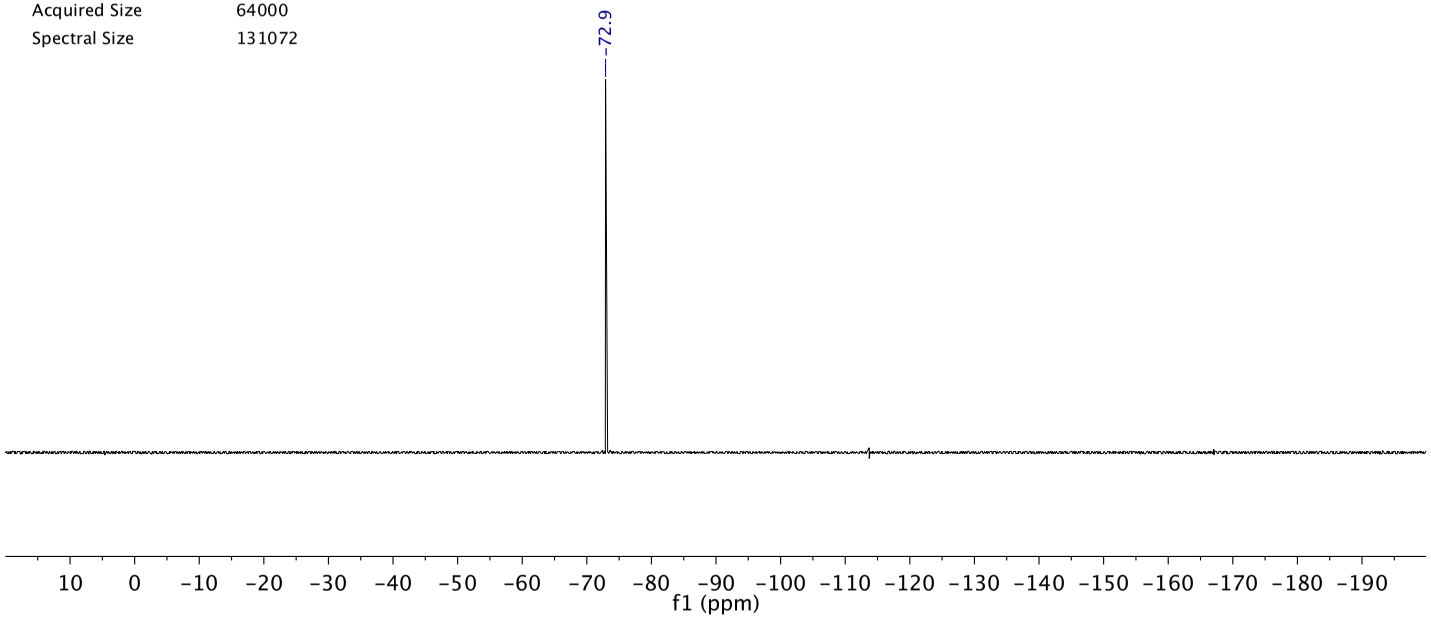

Parameter	Value
Title	AMS-1-159-F-C6F6
Origin	Varian
Solvent	cdcl3
Temperature	25.0
Pulse Sequence	s2pul
Number of Scans	16
Receiver Gain	30
Relaxation Delay	1.0000
Pulse Width	6.3333
Acquisition Time	0.9856
Acquisition Date	2018-06-14T02:00:32
Spectrometer Frequency	282.34
Spectral Width	64935.1
Lowest Frequency	-56468.7
Nucleus	19F
Acquired Size	64000
Spectral Size	131072

224c
with C_6F_6

-72.9

10 0 -10 -20 -30 -40 -50 -60 -70 -80 -90 -100 -110 -120 -130 -140 -150 -160 -170 -180 -190
f1 (ppm)

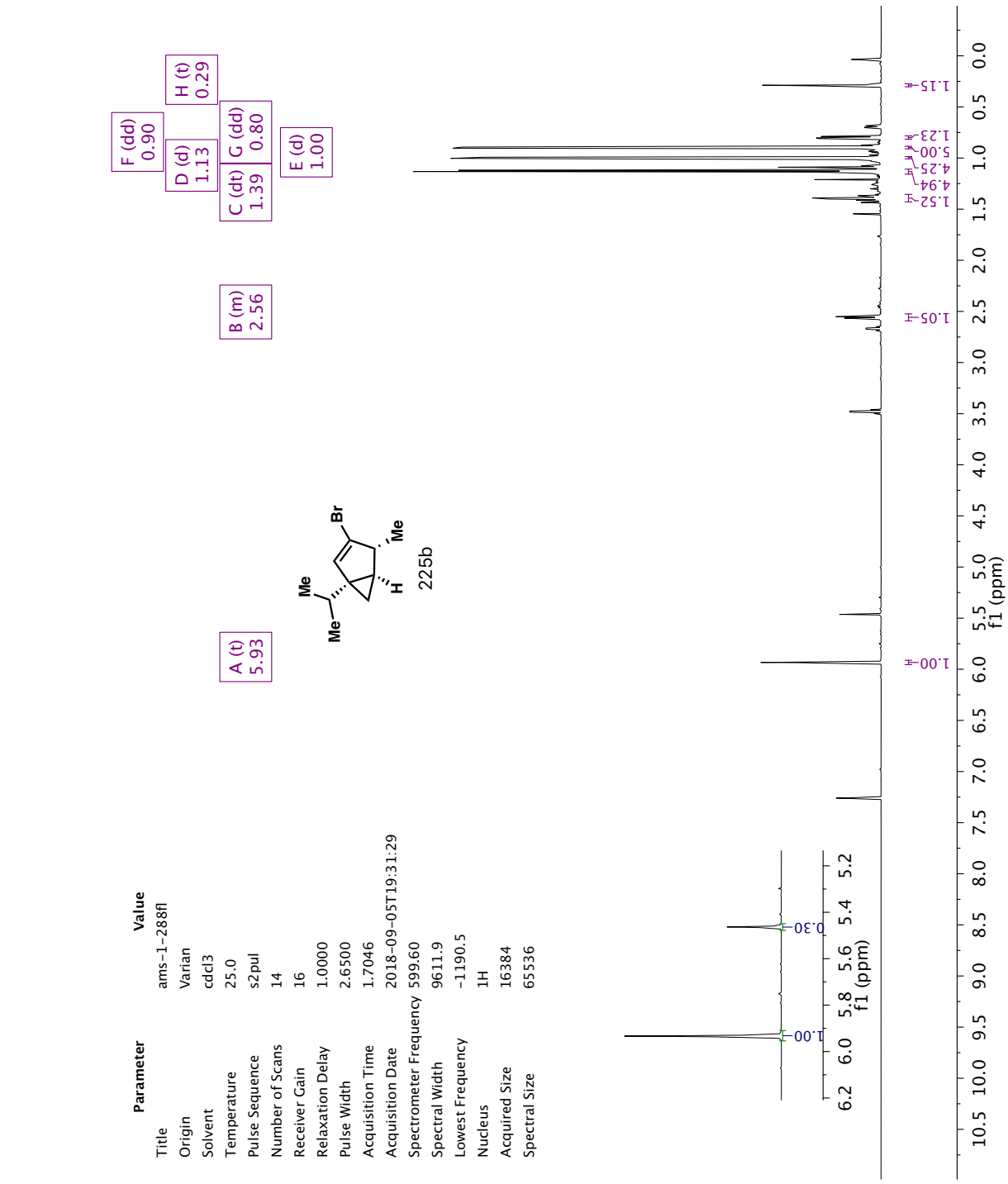

Parameter	Value
Title	ams-1-288fl
Origin	Varian
Solvent	cdcl3
Temperature	25.0
Pulse Sequence	s2pul
Number of Scans	14
Receiver Gain	16
Relaxation Delay	1.0000
Pulse Width	2.6500
Acquisition Time	1.7046
Acquisition Date	2018-09-05T19:31:29
Spectrometer Frequency	599.60
Spectral Width	9611.9
Lowest Frequency	-1190.5
Nucleus	1H
Acquired Size	16384
Spectral Size	65536

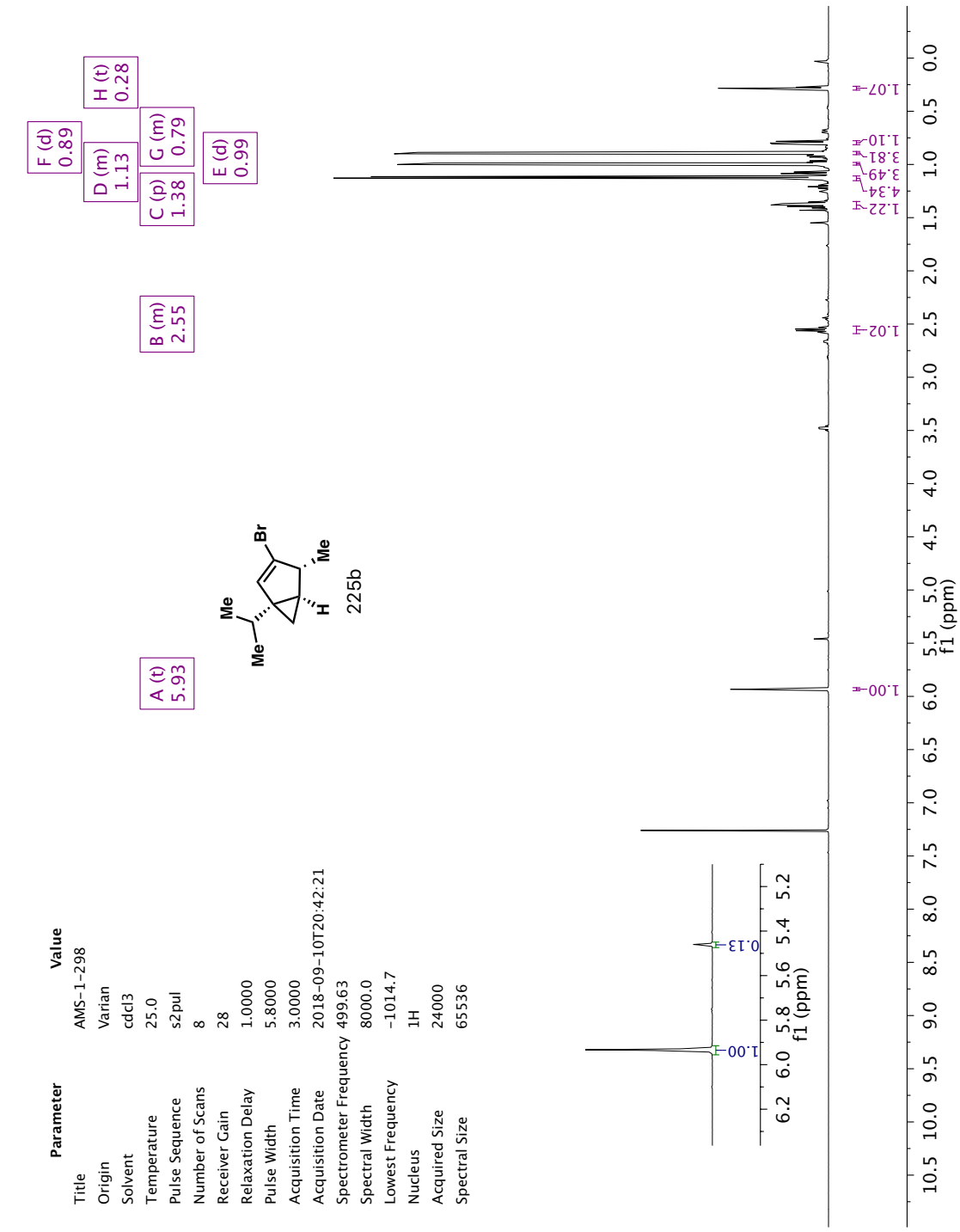

Parameter	Value
Title	AMS-1-298
Origin	Varian
Solvent	cdcl3
Temperature	25.0
Pulse Sequence	s2pul
Number of Scans	8
Receiver Gain	28
Relaxation Delay	1.0000
Pulse Width	5.8000
Acquisition Time	3.0000
Acquisition Date	2018-09-10T20:42:21
Spectrometer Frequency	499.63
Spectral Width	8000.0
Lowest Frequency	-1014.7
Nucleus	1H
Acquired Size	24000
Spectral Size	65536

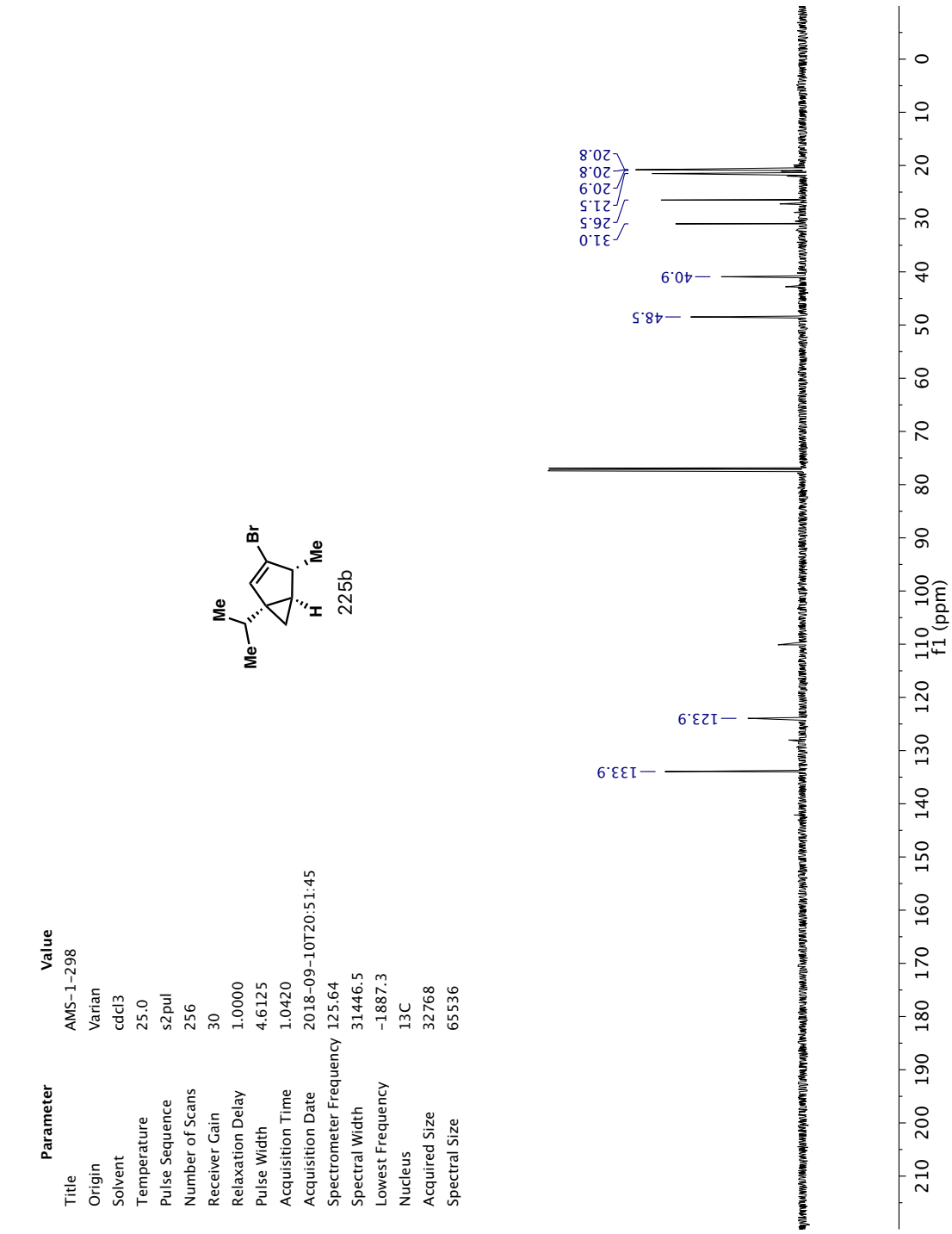
Parameter Value
Title AMS-1-298
Origin Varian
Solvent cdcl3
Temperature 25.0
Pulse Sequence s2pul
Number of Scans 256
Receiver Gain 30
Relaxation Delay 1.0000
Pulse Width 4.6125
Acquisition Time 1.0420
Acquisition Date 2018-09-10T20:51:45
Spectrometer Frequency 125.64
Spectral Width 31446.5
Lowest Frequency -1887.3
Nucleus 13C
Acquired Size 32768
Spectral Size 65536
Me
Me
H
Me
Br
225b
133.9
123.9
48.5
40.9
31.0
26.5
21.5
20.9
20.8
20.8
f1 (ppm)

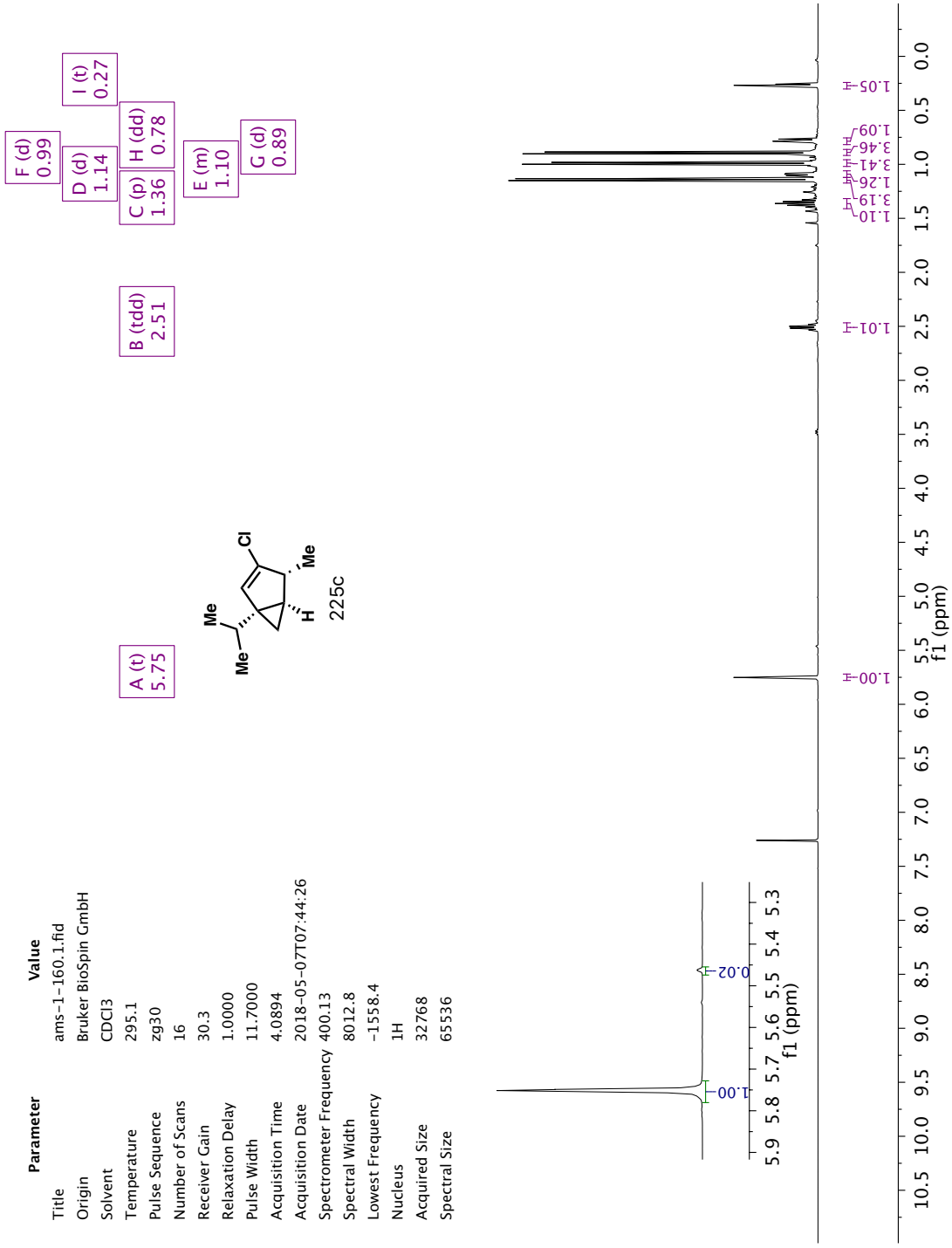

Parameter	Value
Title	ams-1-160.1.fid
Origin	Bruker BioSpin GmbH
Solvent	CDCl3
Temperature	295.1
Pulse Sequence	zg30
Number of Scans	16
Receiver Gain	30.3
Relaxation Delay	1.0000
Pulse Width	11.7000
Acquisition Time	4.0894
Acquisition Date	2018-05-07T07:44:26
Spectrometer Frequency	400.13
Spectral Width	8012.8
Lowest Frequency	-1558.4
Nucleus	1H
Acquired Size	32768
Spectral Size	65536

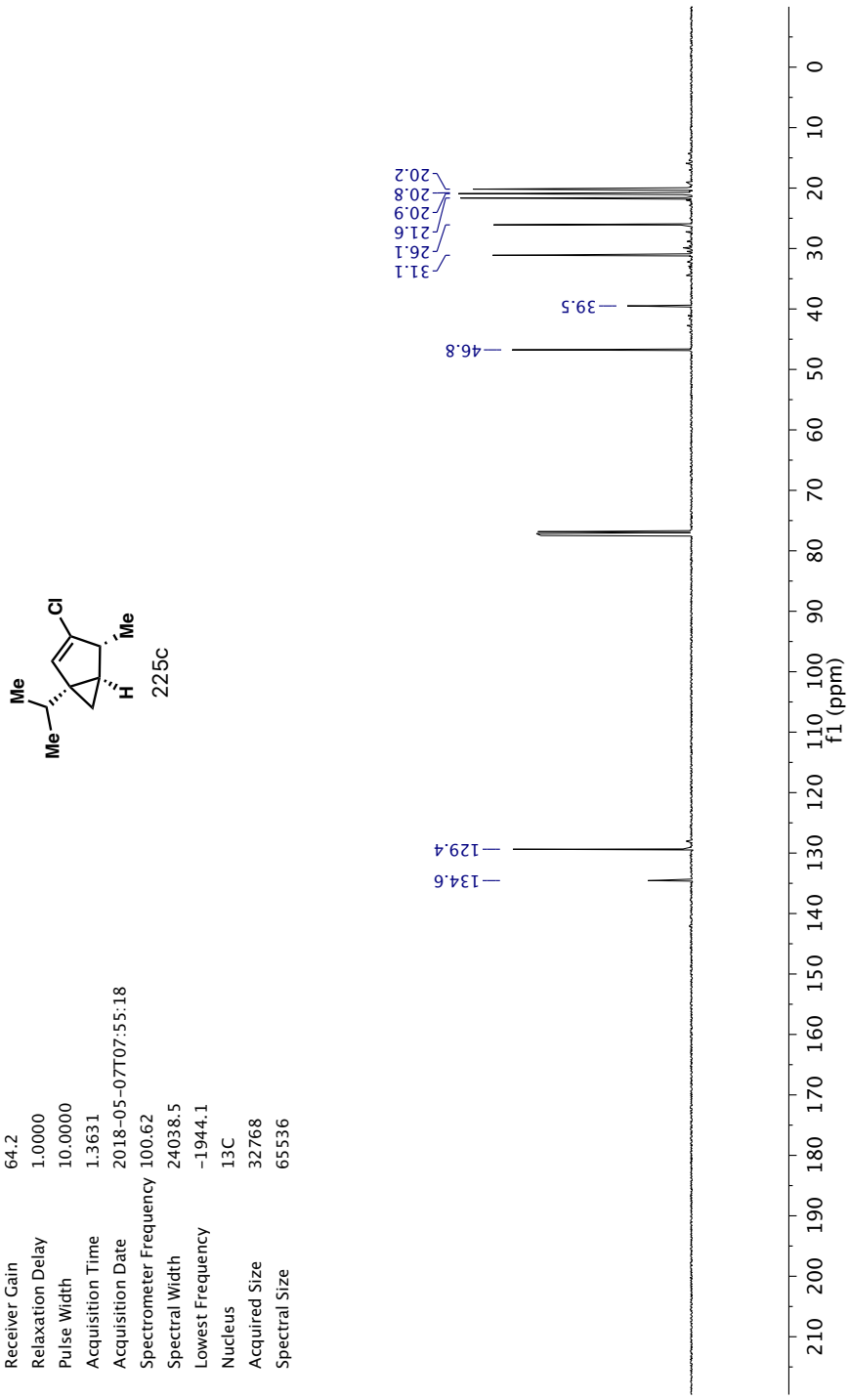

Parameter	Value
Title	ams-1-160.2.fid
Origin	Bruker BioSpin GmbH
Solvent	CDCl3
Temperature	295.2
Pulse Sequence	zgpg30
Number of Scans	256
Receiver Gain	64.2
Relaxation Delay	1.0000
Pulse Width	10.0000
Acquisition Time	1.3631
Acquisition Date	2018-05-07T07:55:18
Spectrometer Frequency	100.62
Spectral Width	24038.5
Lowest Frequency	-1944.1
Nucleus	13C
Acquired Size	32768
Spectral Size	65536

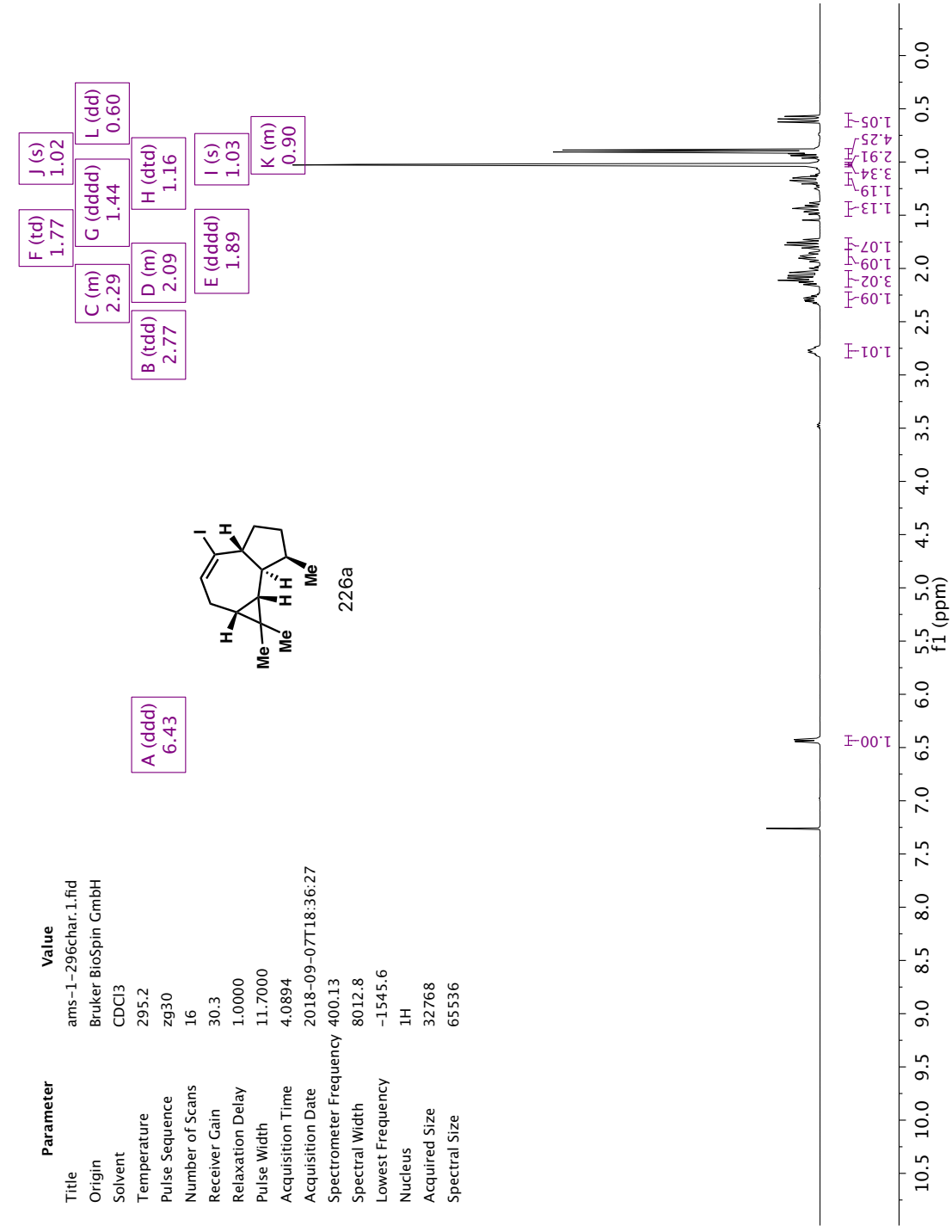
A (ddd) 6.43
B (tdd) 2.77
C (m) 2.29
D (m) 2.09
E (dddd) 1.89
F (td) 1.77
G (dddd) 1.44
H (dtd) 1.16
I (s) 1.03
J (s) 1.02
K (m) 0.90
L (dd) 0.60
226a
Parameter Value
Title ams-1-296char.1.fid
Origin Bruker BioSpin GmbH
Solvent CDCl3
Temperature 295.2
Pulse Sequence zg30
Number of Scans 16
Receiver Gain 30.3
Relaxation Delay 1.0000
Pulse Width 11.7000
Acquisition Time 4.0894
Acquisition Date 2018-09-07T18:36:27
Spectrometer Frequency 400.13
Spectral Width 8012.8
Lowest Frequency -1545.6
Nucleus 1H
Acquired Size 32768
Spectral Size 65536
1.00
1.01
1.09
3.02
1.09
1.07
1.13
1.19
3.34
2.91
4.25
1.05
f1 (ppm)

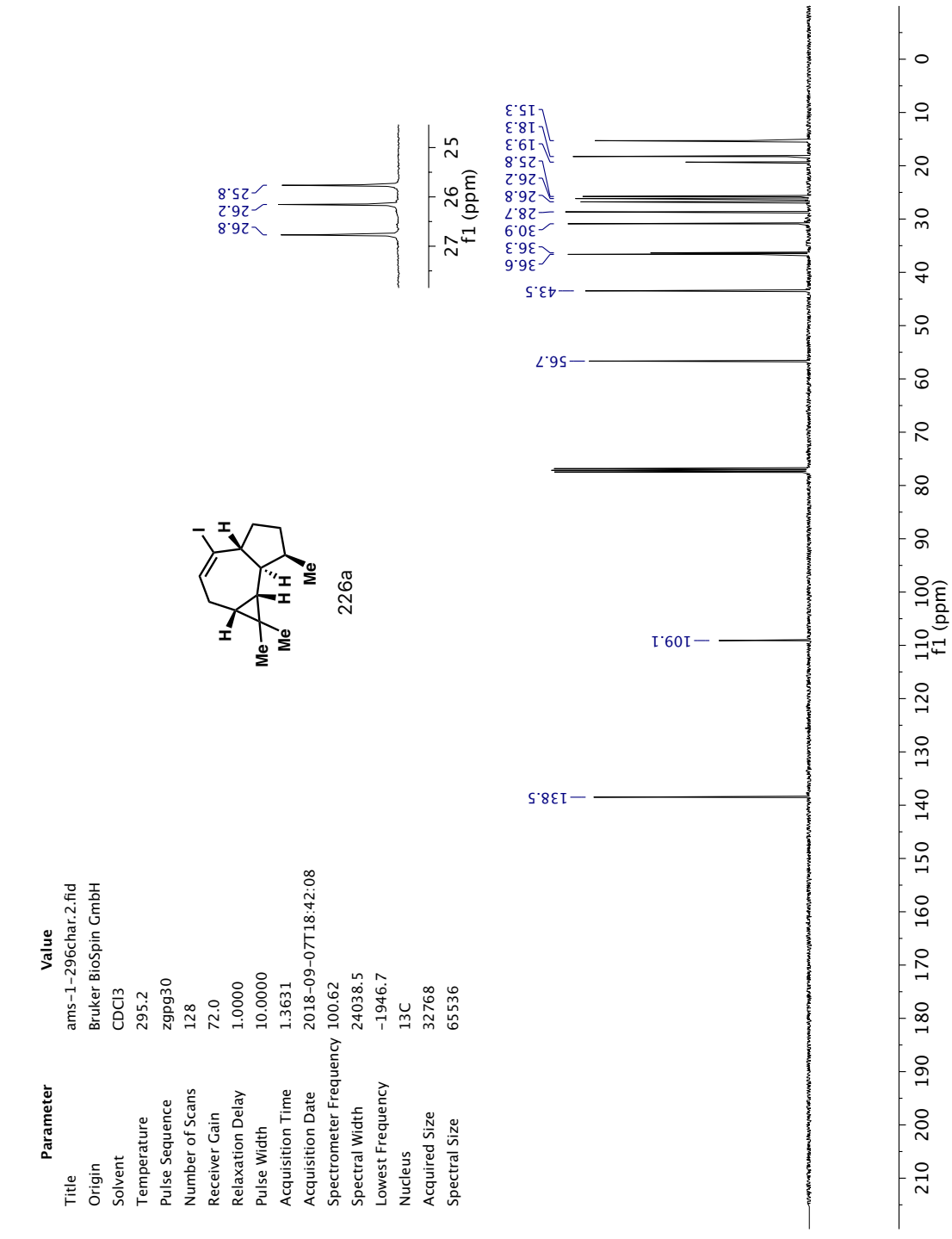
Parameter Value
Title ams-1-296char.2.fid
Origin Bruker BioSpin GmbH
Solvent CDCl3
Temperature 295.2
Pulse Sequence zgpg30
Number of Scans 128
Receiver Gain 72.0
Relaxation Delay 1.0000
Pulse Width 10.0000
Acquisition Time 1.3631
Acquisition Date 2018-09-07T18:42:08
Spectrometer Frequency 100.62
Spectral Width 24038.5
Lowest Frequency -1946.7
Nucleus 13C
Acquired Size 32768
Spectral Size 65536
226a
138.5
109.1
56.7
43.5
36.6
36.3
30.9
28.7
26.8
26.2
25.8
19.3
18.3
15.3
f1 (ppm)

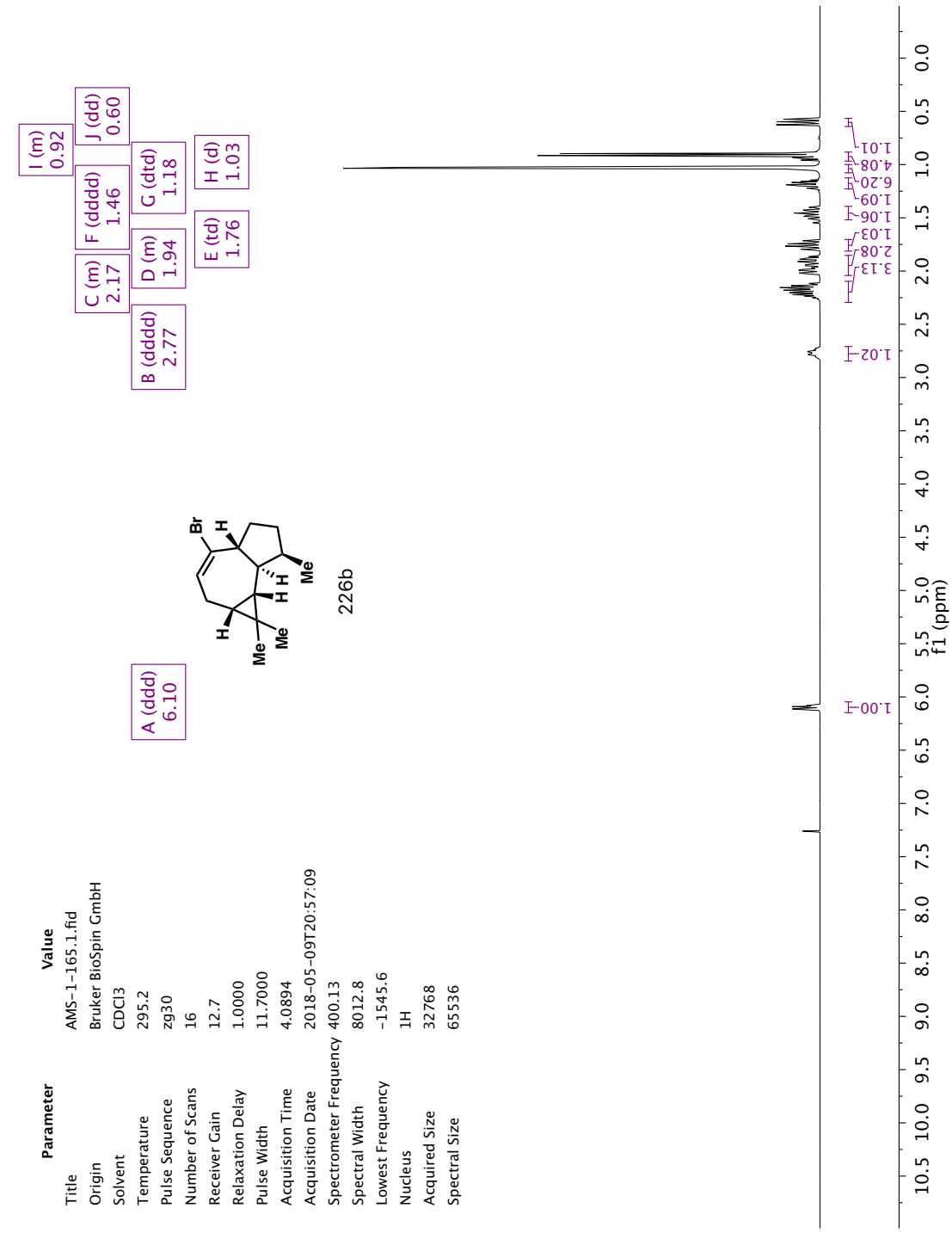

Parameter	Value
Title	AMS-1-165.1.fid
Origin	Bruker BioSpin GmbH
Solvent	CDCl3
Temperature	295.2
Pulse Sequence	zg30
Number of Scans	16
Receiver Gain	12.7
Relaxation Delay	1.0000
Pulse Width	11.7000
Acquisition Time	4.0894
Acquisition Date	2018-05-09T20:57:09
Spectrometer Frequency	400.13
Spectral Width	8012.8
Lowest Frequency	-1545.6
Nucleus	1H
Acquired Size	32768
Spectral Size	65536

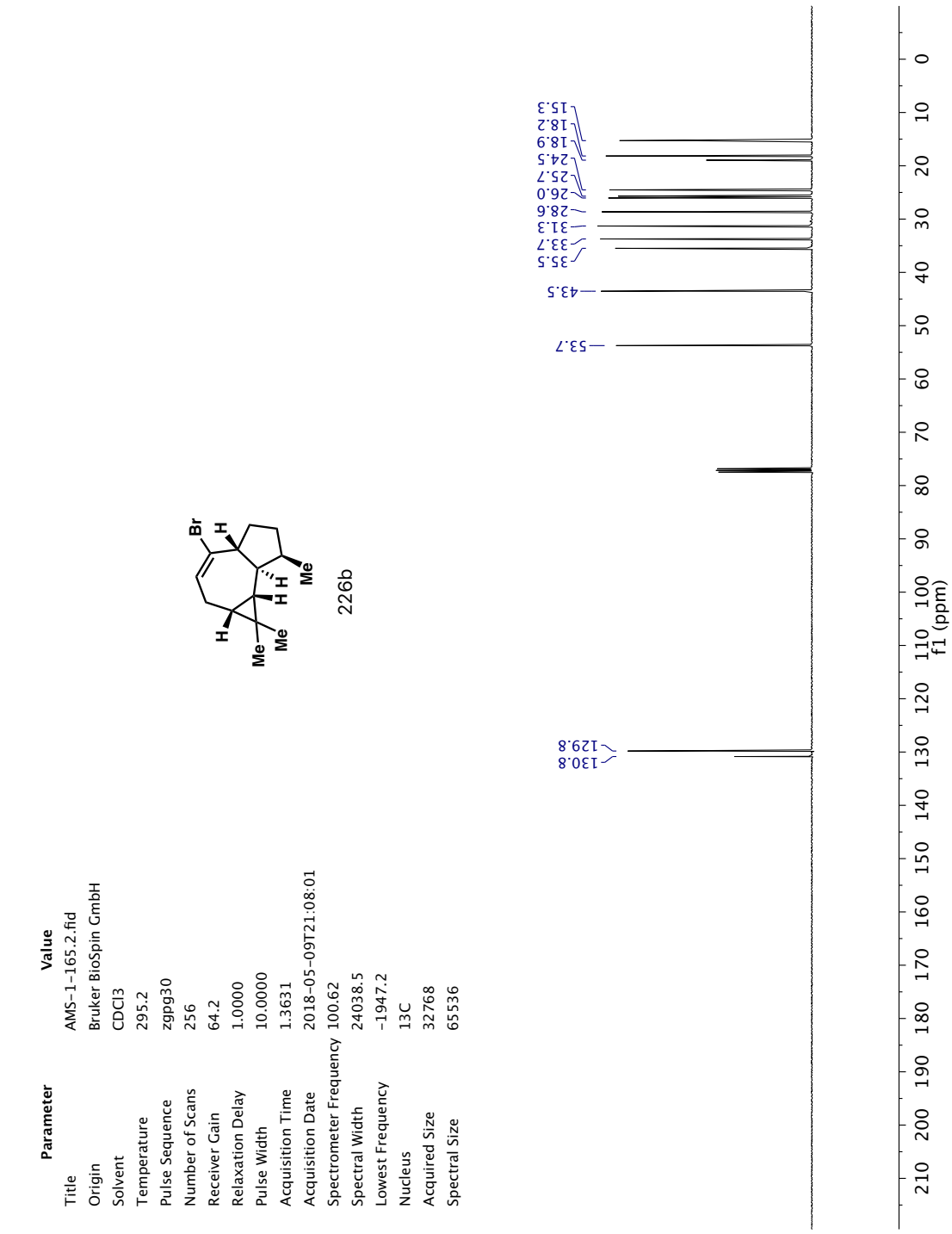

Parameter	Value
Title	AMS-1-165.2.fid
Origin	Bruker BioSpin GmbH
Solvent	CDCl3
Temperature	295.2
Pulse Sequence	zgpg30
Number of Scans	256
Receiver Gain	64.2
Relaxation Delay	1.0000
Pulse Width	10.0000
Acquisition Time	1.3631
Acquisition Date	2018-05-09T21:08:01
Spectrometer Frequency	100.62
Spectral Width	24038.5
Lowest Frequency	-1947.2
Nucleus	13C
Acquired Size	32768
Spectral Size	65536

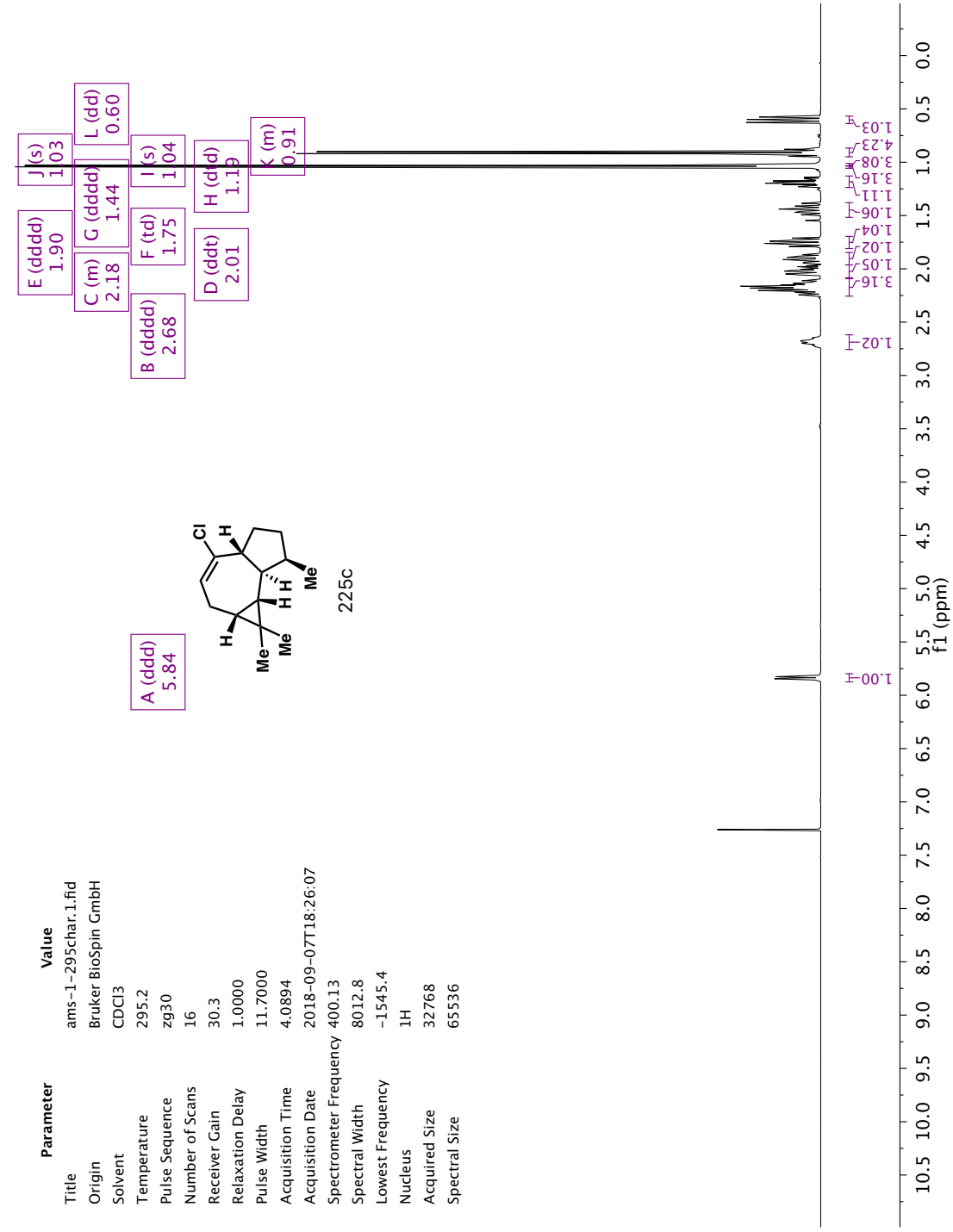

Parameter	Value
Title	ams-1-295char.1.fid
Origin	Bruker BioSpin GmbH
Solvent	CDCl3
Temperature	295.2
Pulse Sequence	zg30
Number of Scans	16
Receiver Gain	30.3
Relaxation Delay	1.0000
Pulse Width	11.7000
Acquisition Time	4.0894
Acquisition Date	2018-09-07T18:26:07
Spectrometer Frequency	400.13
Spectral Width	8012.8
Lowest Frequency	-1545.4
Nucleus	1H
Acquired Size	32768
Spectral Size	65536

Parameter	Value
Title	ams-1-295char.2.fid
Origin	Bruker BioSpin GmbH
Solvent	CDCl3
Temperature	295.2
Pulse Sequence	zgpg30
Number of Scans	128
Receiver Gain	78.7
Relaxation Delay	1.0000
Pulse Width	10.0000
Acquisition Time	1.3631
Acquisition Date	2018-09-07T18:31:49
Spectrometer Frequency	100.62
Spectral Width	24038.5
Lowest Frequency	-1945.3
Nucleus	13C
Acquired Size	32768
Spectral Size	65536

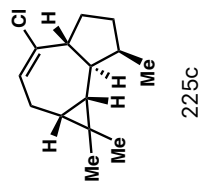

225c

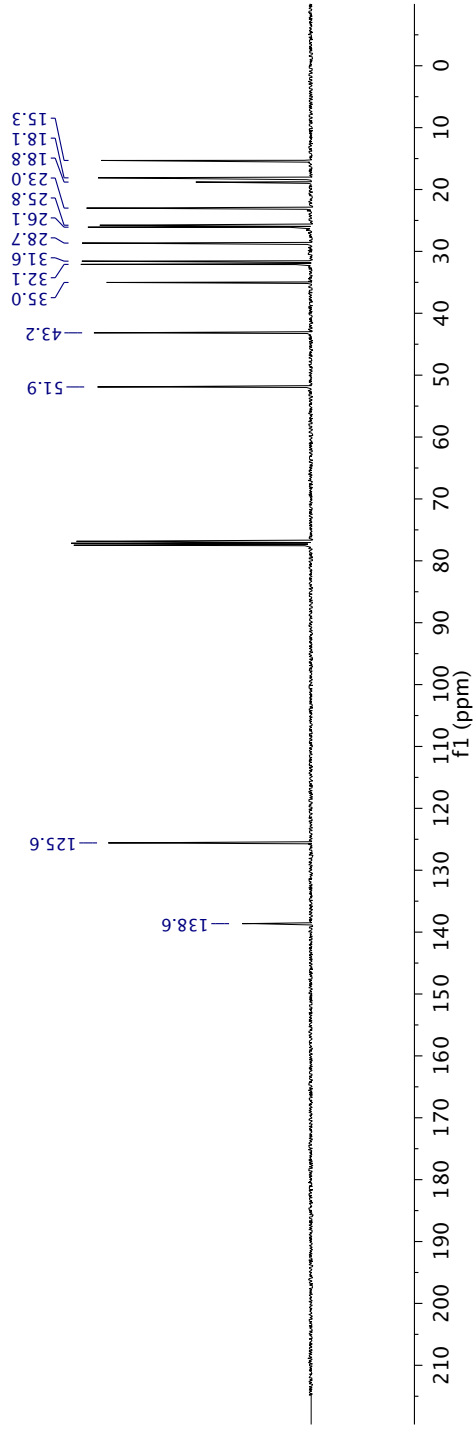

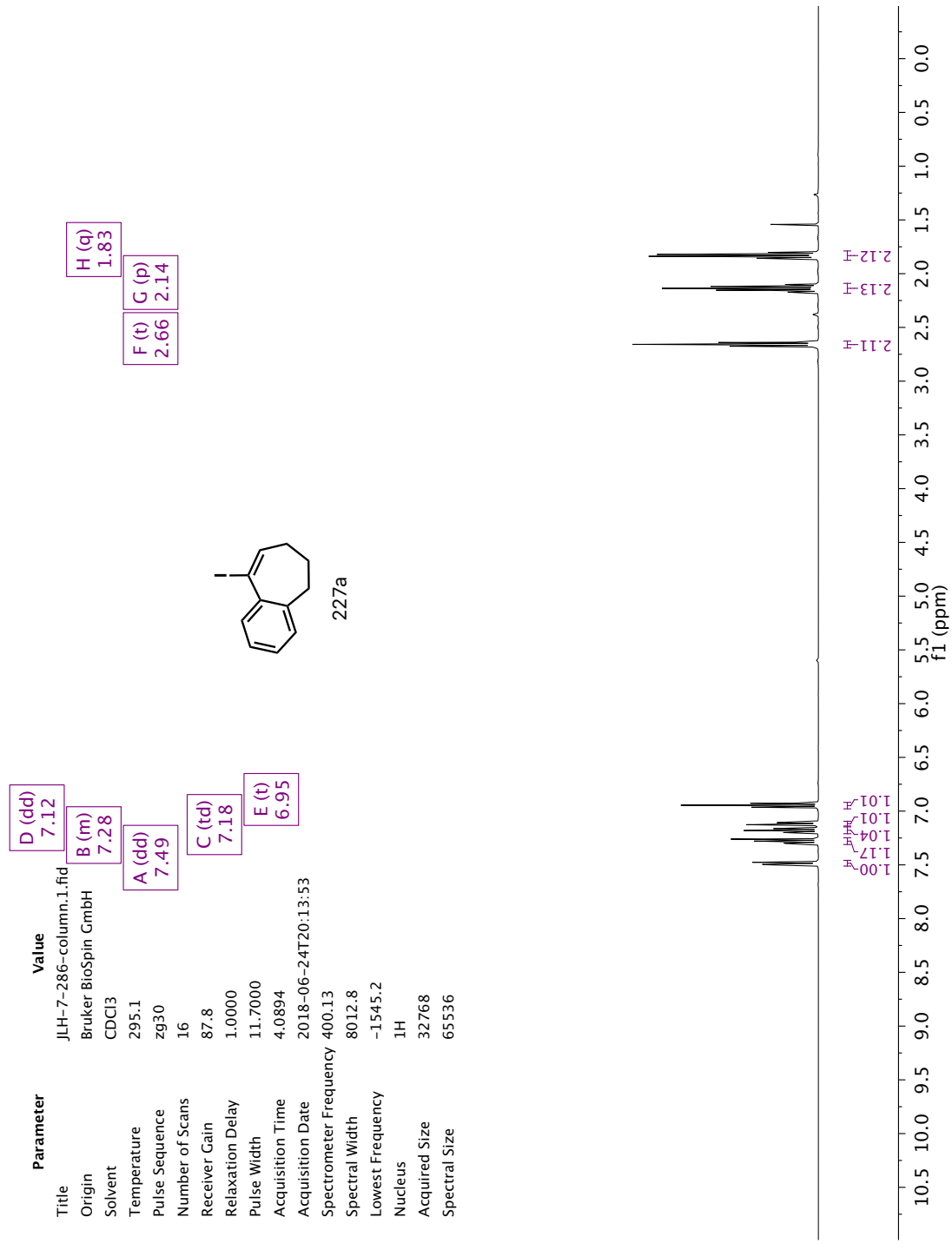
Parameter
Value
Title
JLH-7-286-column.1.fid
Origin
Bruker BioSpin GmbH
Solvent
CDCl3
Temperature
295.1
Pulse Sequence
zg30
Number of Scans
16
Receiver Gain
87.8
Relaxation Delay
1.0000
Pulse Width
11.7000
Acquisition Time
4.0894
Acquisition Date
2018-06-24T20:13:53
Spectrometer Frequency
400.13
Spectral Width
8012.8
Lowest Frequency
-1545.2
Nucleus
1H
Acquired Size
32768
Spectral Size
65536
D (dd) 7.12
B (m) 7.28
A (dd) 7.49
C (td) 7.18
E (t) 6.95
H (q) 1.83
F (t) 2.66
G (p) 2.14
227a
1.00
1.17
1.04
1.01
1.01
2.11
2.13
2.12
f1 (ppm)

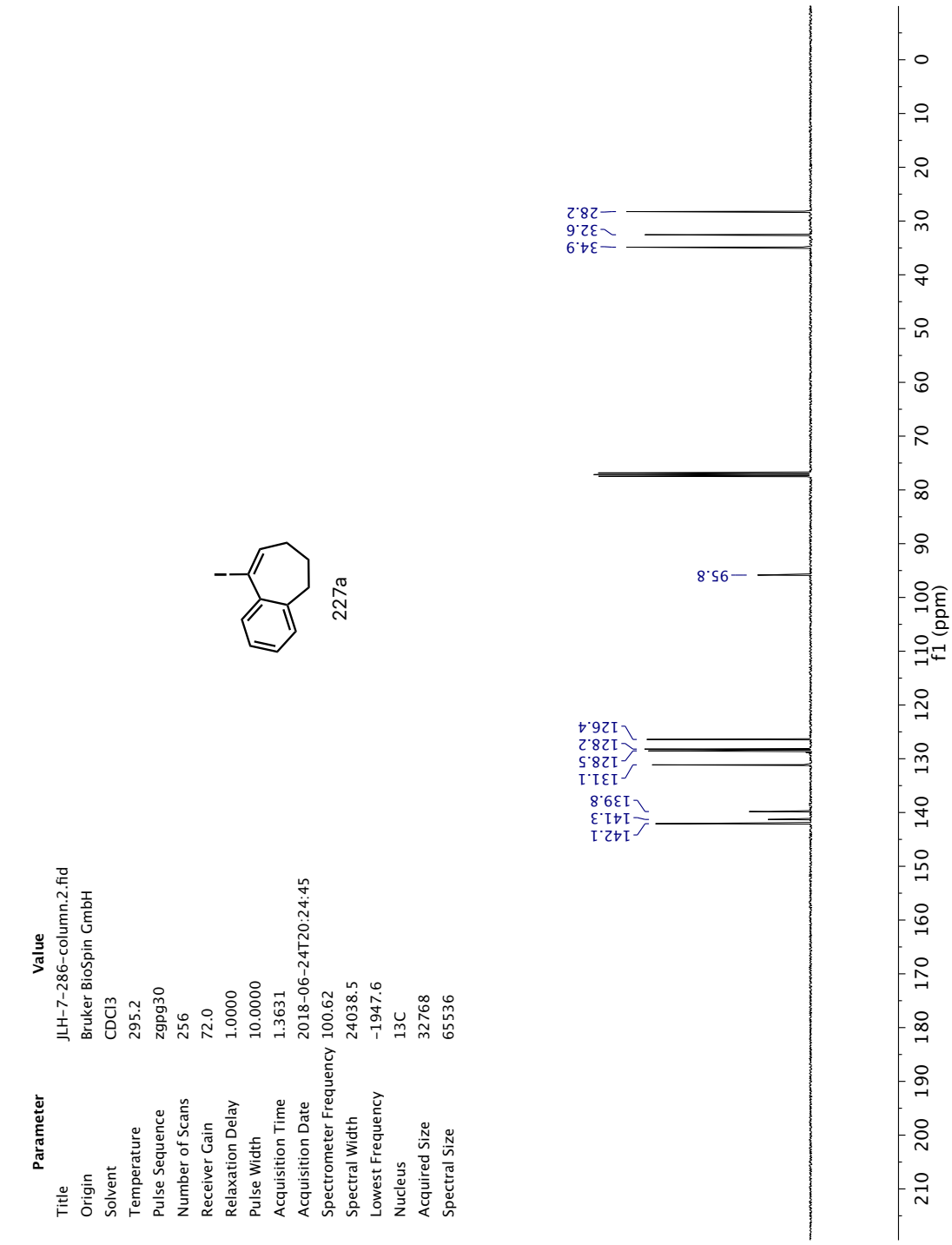
Parameter Value
Title JLH-7-286-column.2.fid
Origin Bruker BioSpin GmbH
Solvent CDCl3
Temperature 295.2
Pulse Sequence zgpg30
Number of Scans 256
Receiver Gain 72.0
Relaxation Delay 1.0000
Pulse Width 10.0000
Acquisition Time 1.3631
Acquisition Date 2018-06-24T20:24:45
Spectrometer Frequency 100.62
Spectral Width 24038.5
Lowest Frequency -1947.6
Nucleus 13C
Acquired Size 32768
Spectral Size 65536
227a
142.1
141.3
139.8
131.1
128.5
128.2
126.4
95.8
34.9
32.6
28.2
f1 (ppm)

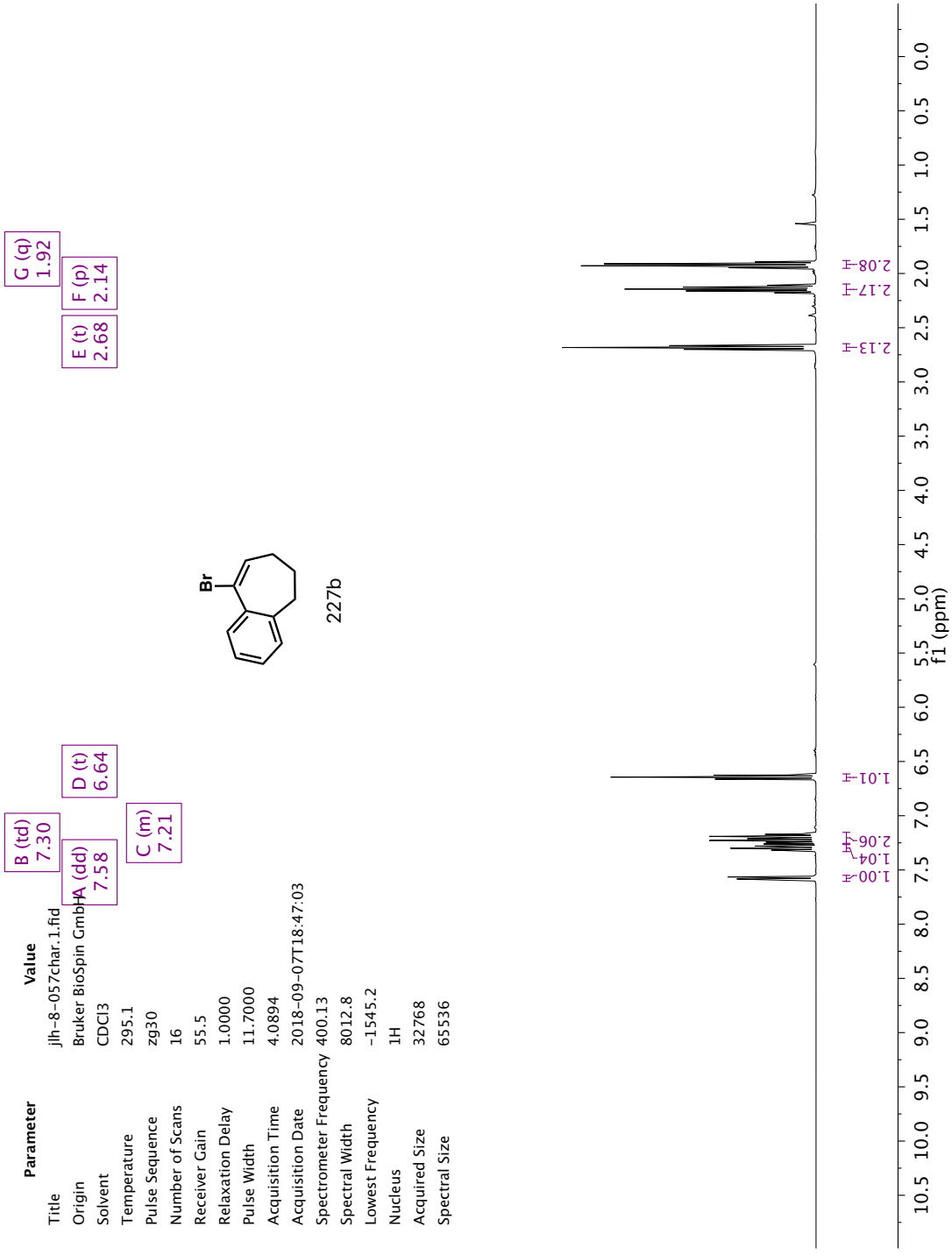
G (q) 1.92
F (p) 2.14
E (t) 2.68
D (t) 6.64
C (m) 7.21
B (td) 7.30
A (dd) 7.58
Br
227b
Parameter Value
Title jlh-8-057char.1.fid
Origin Bruker BioSpin GmbH
Solvent CDCl3
Temperature 295.1
Pulse Sequence zg30
Number of Scans 16
Receiver Gain 55.5
Relaxation Delay 1.0000
Pulse Width 11.7000
Acquisition Time 4.0894
Acquisition Date 2018-09-07T18:47:03
Spectrometer Frequency 400.13
Spectral Width 8012.8
Lowest Frequency -1545.2
Nucleus 1H
Acquired Size 32768
Spectral Size 65536
1.00
1.04
2.06
1.01
2.13
2.17
2.08
10.5 10.0 9.5 9.0 8.5 8.0 7.5 7.0 6.5 6.0 5.5 5.0 4.5 4.0 3.5 3.0 2.5 2.0 1.5 1.0 0.5 0.0
f1 (ppm)

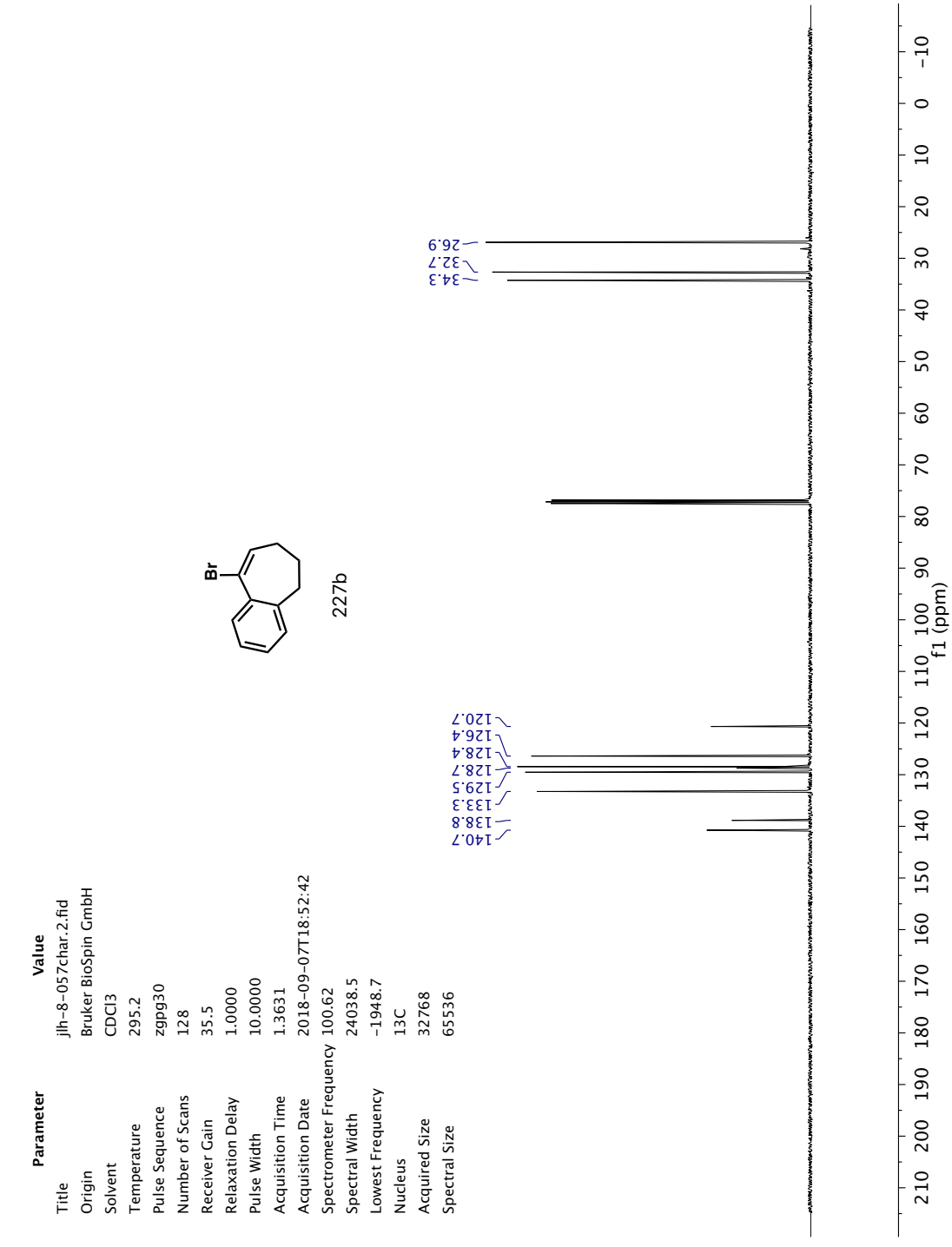

Parameter	Value
Title	jlh-8-057char.2.fid
Origin	Bruker BioSpin GmbH
Solvent	CDCl3
Temperature	295.2
Pulse Sequence	zgpg30
Number of Scans	128
Receiver Gain	35.5
Relaxation Delay	1.0000
Pulse Width	10.0000
Acquisition Time	1.3631
Acquisition Date	2018-09-07T18:52:42
Spectrometer Frequency	100.62
Spectral Width	24038.5
Lowest Frequency	-1948.7
Nucleus	13C
Acquired Size	32768
Spectral Size	65536

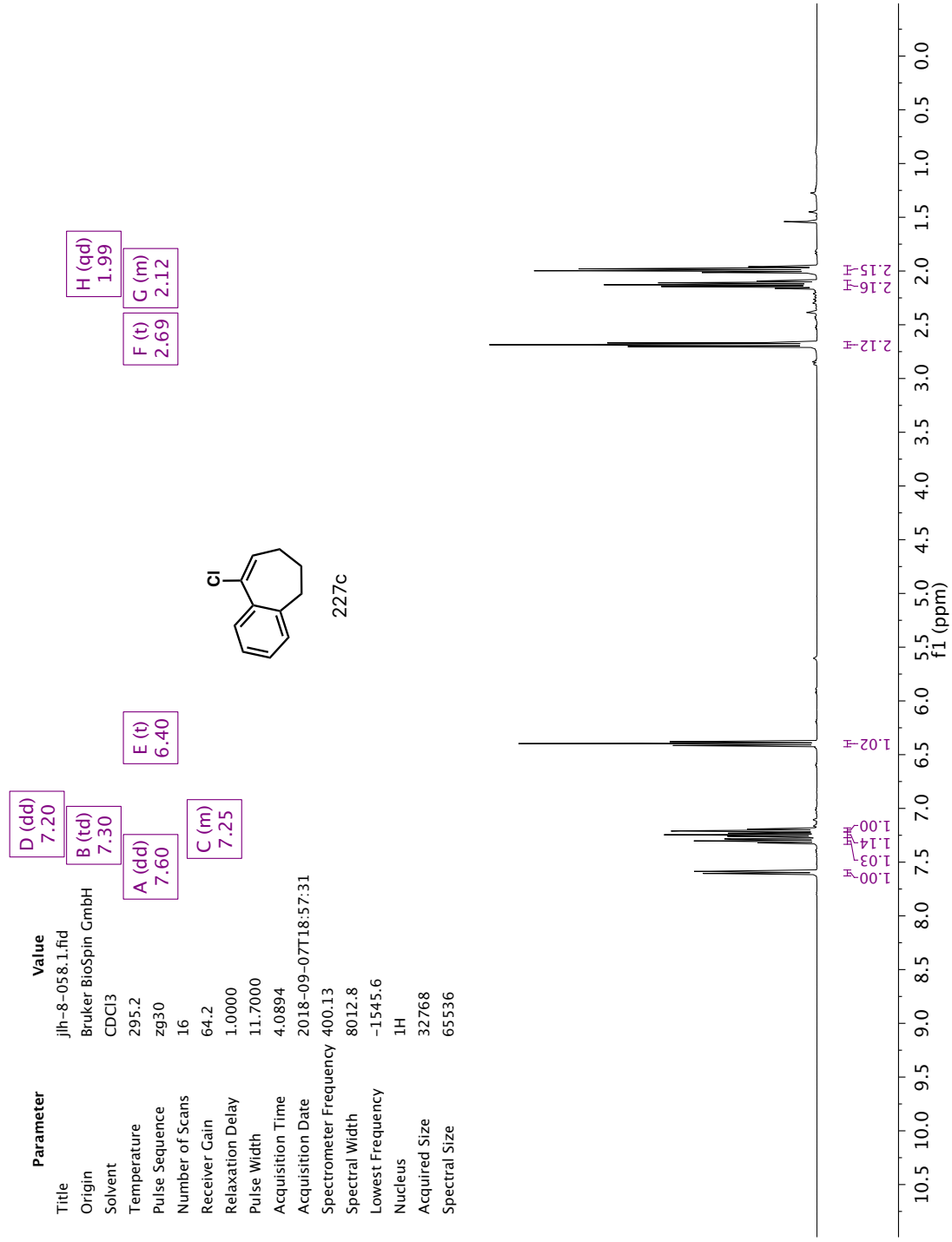
D (dd) 7.20
B (td) 7.30
A (dd) 7.60
C (m) 7.25
E (t) 6.40
H (qd) 1.99
F (t) 2.69
G (m) 2.12
Cl
227c
Parameter Value
Title jlh-8-058.1.fid
Origin Bruker BioSpin GmbH
Solvent CDCl3
Temperature 295.2
Pulse Sequence zg30
Number of Scans 16
Receiver Gain 64.2
Relaxation Delay 1.0000
Pulse Width 11.7000
Acquisition Time 4.0894
Acquisition Date 2018-09-07T18:57:31
Spectrometer Frequency 400.13
Spectral Width 8012.8
Lowest Frequency -1545.6
Nucleus 1H
Acquired Size 32768
Spectral Size 65536
1.00
1.03
1.14
1.00
1.02
2.12
2.16
2.15
f1 (ppm)

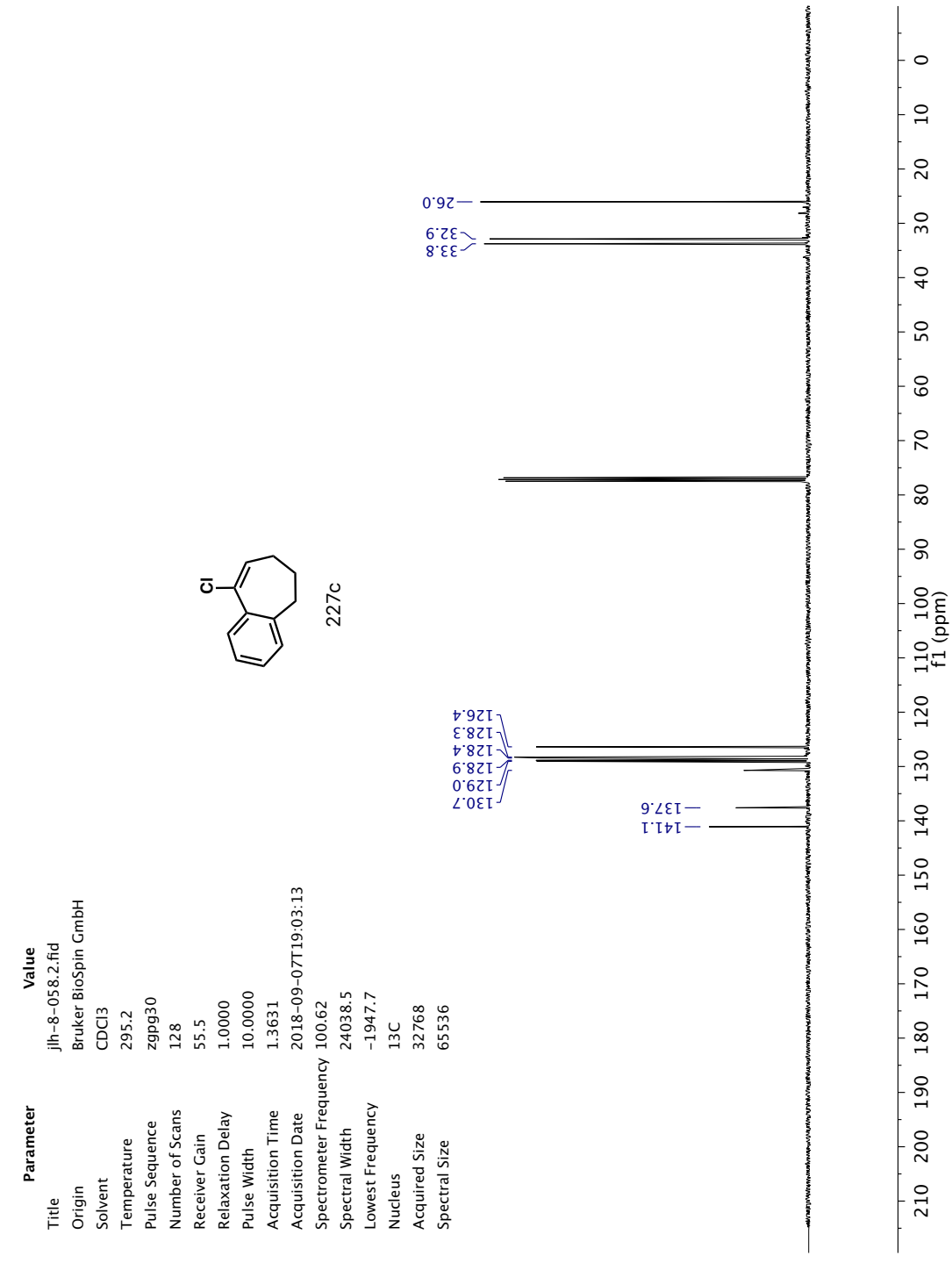
Parameter Value
Title jlh-8-058.2.fid
Origin Bruker BioSpin GmbH
Solvent CDCl3
Temperature 295.2
Pulse Sequence zgpg30
Number of Scans 128
Receiver Gain 55.5
Relaxation Delay 1.0000
Pulse Width 10.0000
Acquisition Time 1.3631
Acquisition Date 2018-09-07T19:03:13
Spectrometer Frequency 100.62
Spectral Width 24038.5
Lowest Frequency -1947.7
Nucleus 13C
Acquired Size 32768
Spectral Size 65536
Cl
227c
26.0
32.9
33.8
126.4
128.3
128.4
128.9
129.0
130.7
137.6
141.1
f1 (ppm)

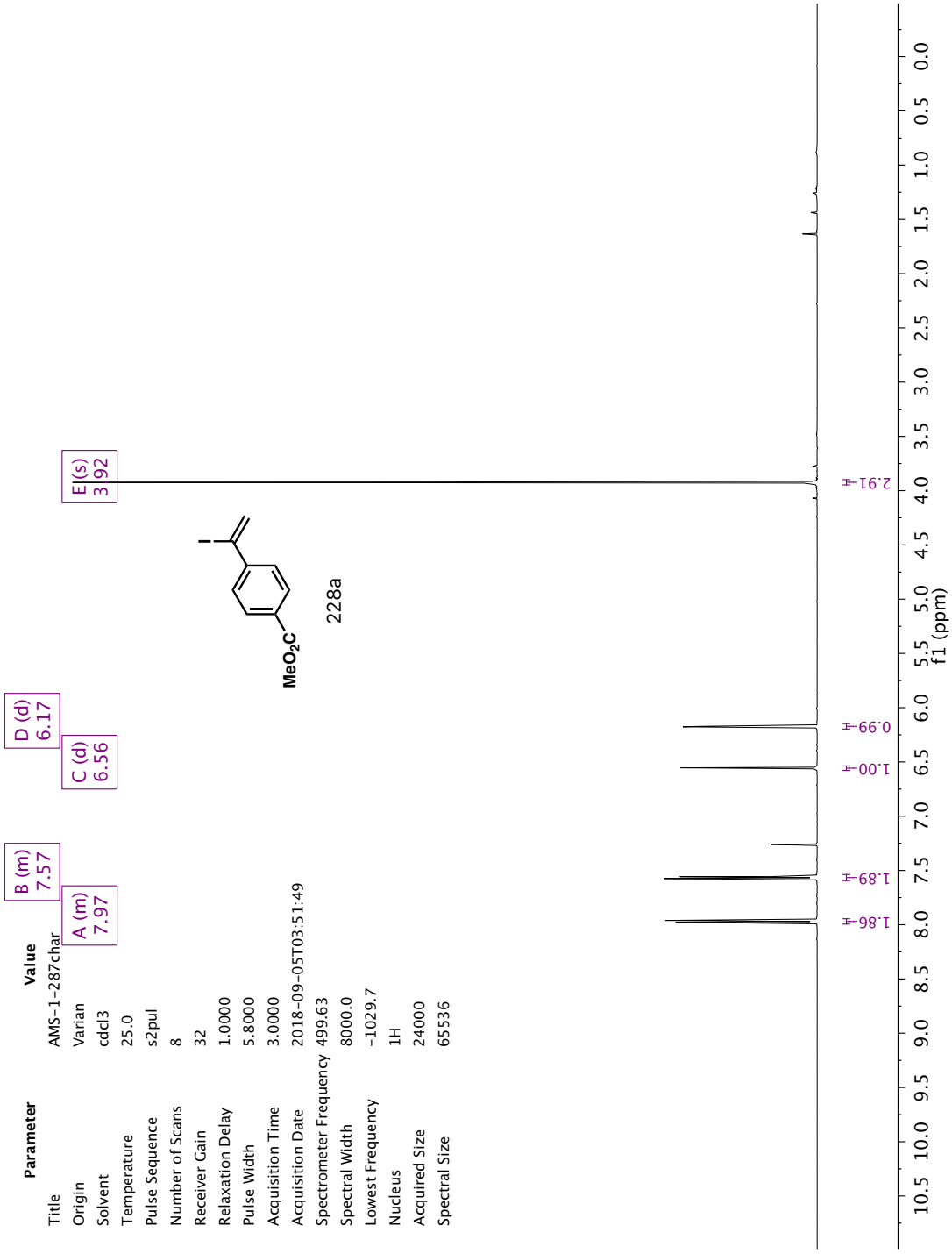
Parameter
Value
Title AMS-1-287char
Origin Varian
Solvent cdcl3
Temperature 25.0
Pulse Sequence s2pul
Number of Scans 8
Receiver Gain 32
Relaxation Delay 1.0000
Pulse Width 5.8000
Acquisition Time 3.0000
Acquisition Date 2018-09-05T03:51:49
Spectrometer Frequency 499.63
Spectral Width 8000.0
Lowest Frequency -1029.7
Nucleus 1H
Acquired Size 24000
Spectral Size 65536
A (m) 7.97
B (m) 7.57
C (d) 6.56
D (d) 6.17
E(s) 3.92
MeO2C
228a
1.86
1.89
1.00
0.99
2.91
10.5 10.0 9.5 9.0 8.5 8.0 7.5 7.0 6.5 6.0 5.5 5.0 4.5 4.0 3.5 3.0 2.5 2.0 1.5 1.0 0.5 0.0
f1 (ppm)

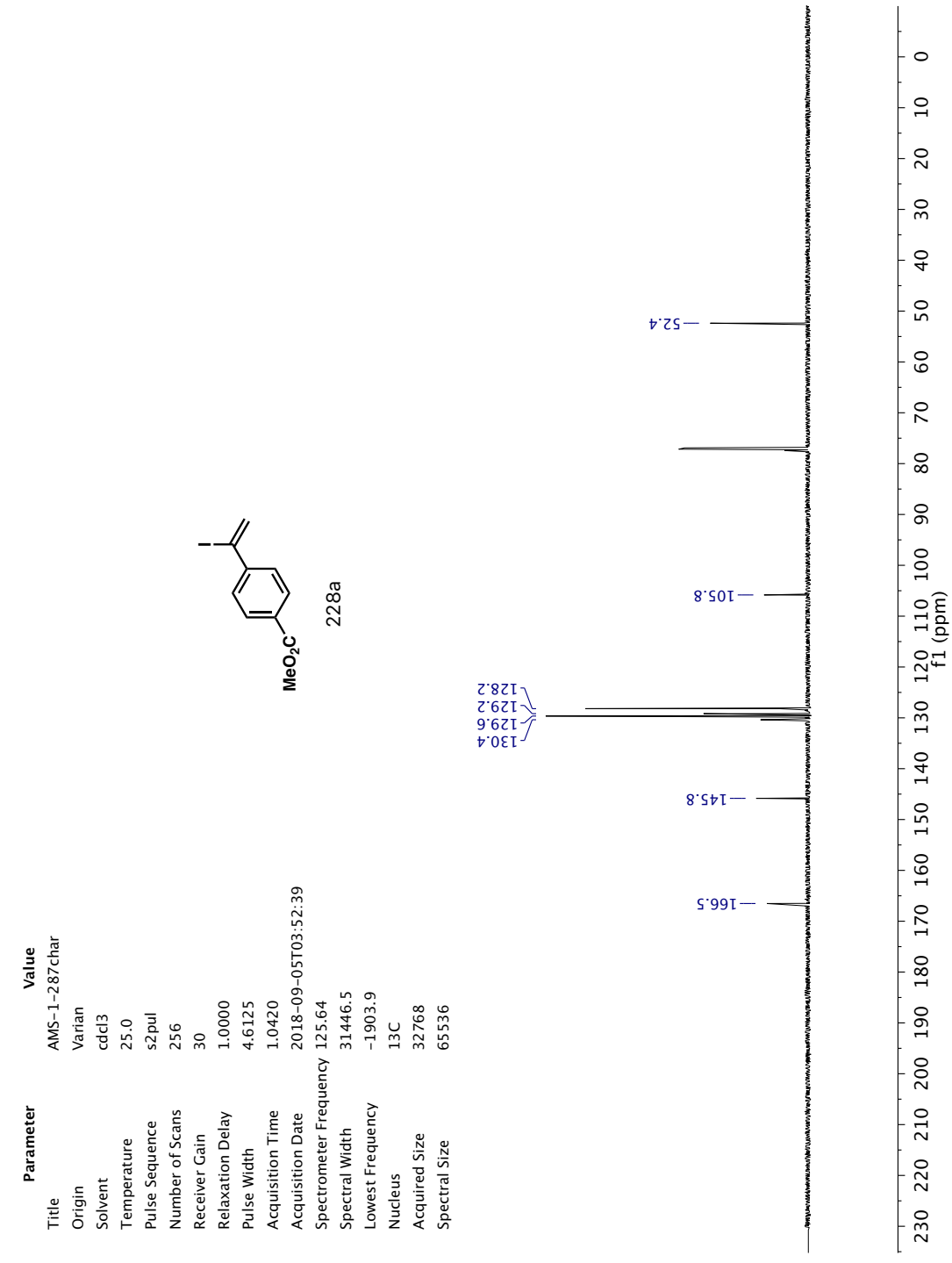
Parameter Value
Title AMS-1-287char
Origin Varian
Solvent cdcl3
Temperature 25.0
Pulse Sequence s2pul
Number of Scans 256
Receiver Gain 30
Relaxation Delay 1.0000
Pulse Width 4.6125
Acquisition Time 1.0420
Acquisition Date 2018-09-05T03:52:39
Spectrometer Frequency 125.64
Spectral Width 31446.5
Lowest Frequency -1903.9
Nucleus 13C
Acquired Size 32768
Spectral Size 65536
MeO2C
228a
166.5
145.8
130.4
129.6
129.2
128.2
105.8
52.4
f1 (ppm)

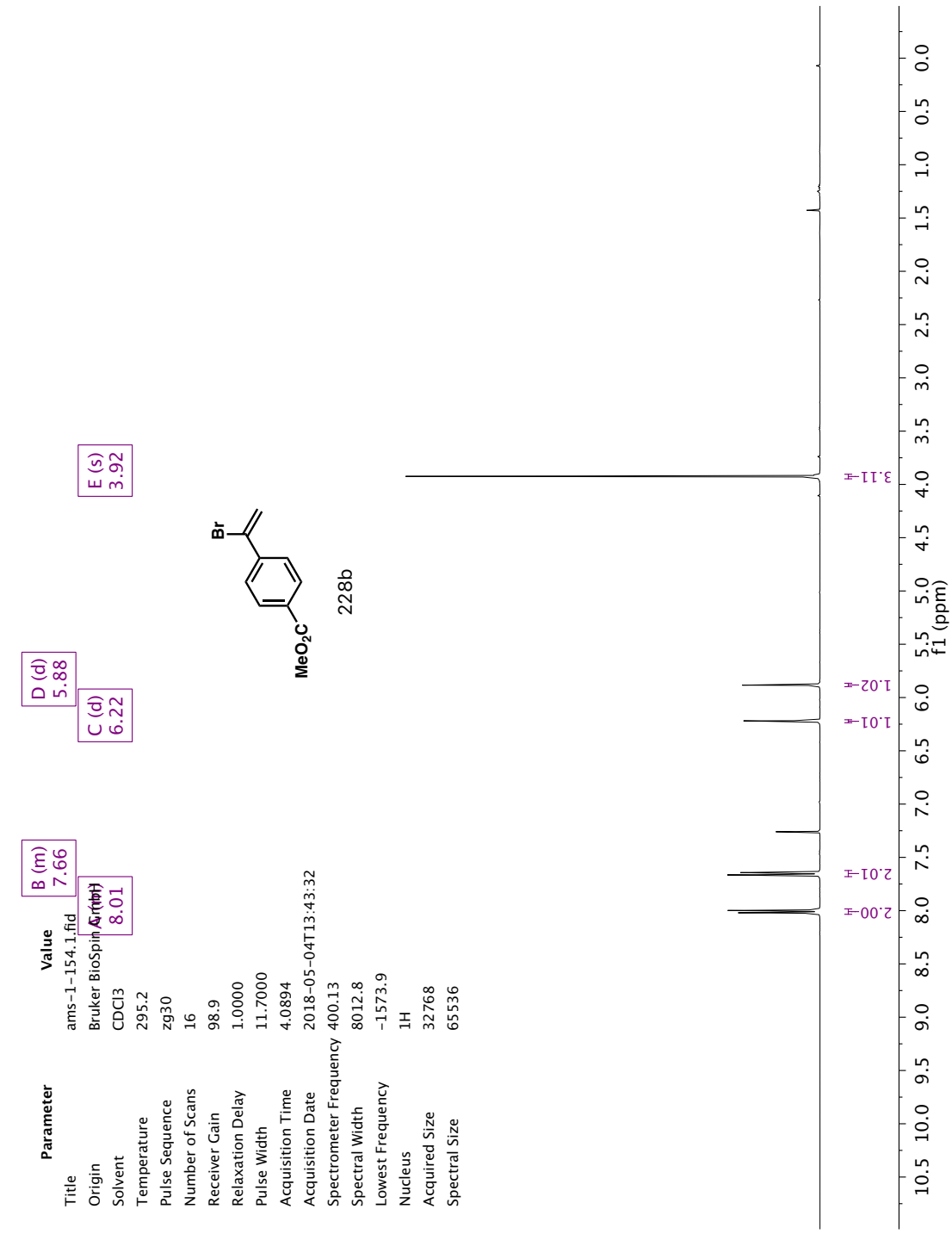
Parameter
Value
Title
ams-1-154.1.fid
Origin
Bruker BioSpin GmbH
Solvent
CDCl3
Temperature
295.2
Pulse Sequence
zg30
Number of Scans
16
Receiver Gain
98.9
Relaxation Delay
1.0000
Pulse Width
11.7000
Acquisition Time
4.0894
Acquisition Date
2018-05-04T13:43:32
Spectrometer Frequency
400.13
Spectral Width
8012.8
Lowest Frequency
-1573.9
Nucleus
1H
Acquired Size
32768
Spectral Size
65536
B (m) 7.66
A (dd) 8.01
D (d) 5.88
C (d) 6.22
E (s) 3.92
Br
MeO2C
228b
2.00
2.01
1.01
1.02
3.11
10.5 10.0 9.5 9.0 8.5 8.0 7.5 7.0 6.5 6.0 5.5 5.0 4.5 4.0 3.5 3.0 2.5 2.0 1.5 1.0 0.5 0.0
f1 (ppm)

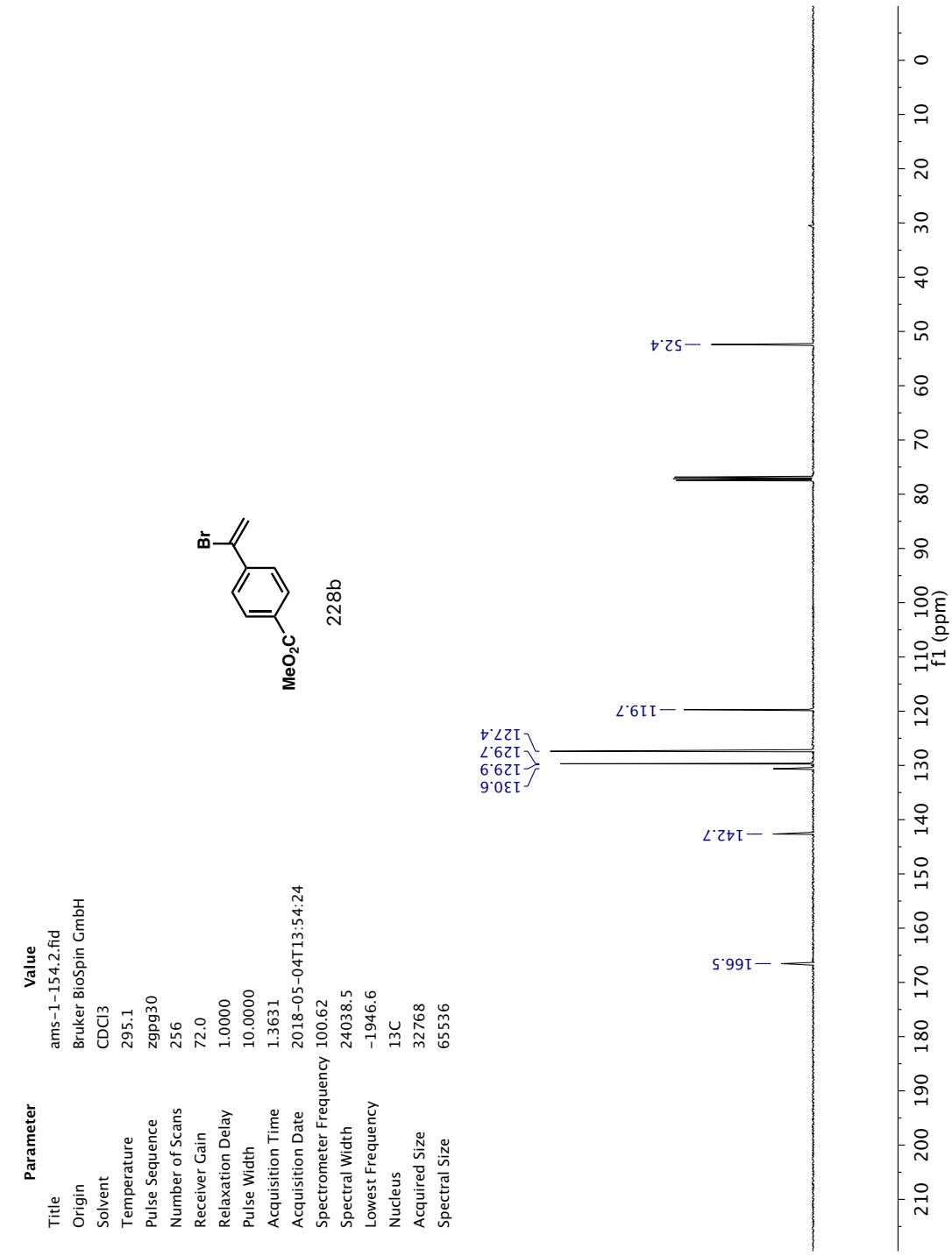
Parameter Value
Title ams-1-154.2.fid
Origin Bruker BioSpin GmbH
Solvent CDCl3
Temperature 295.1
Pulse Sequence zgpg30
Number of Scans 256
Receiver Gain 72.0
Relaxation Delay 1.0000
Pulse Width 10.0000
Acquisition Time 1.3631
Acquisition Date 2018-05-04T13:54:24
Spectrometer Frequency 100.62
Spectral Width 24038.5
Lowest Frequency -1946.6
Nucleus 13C
Acquired Size 32768
Spectral Size 65536
Br
MeO2C
228b
166.5
142.7
130.6
129.9
129.7
127.4
119.7
52.4
f1 (ppm)

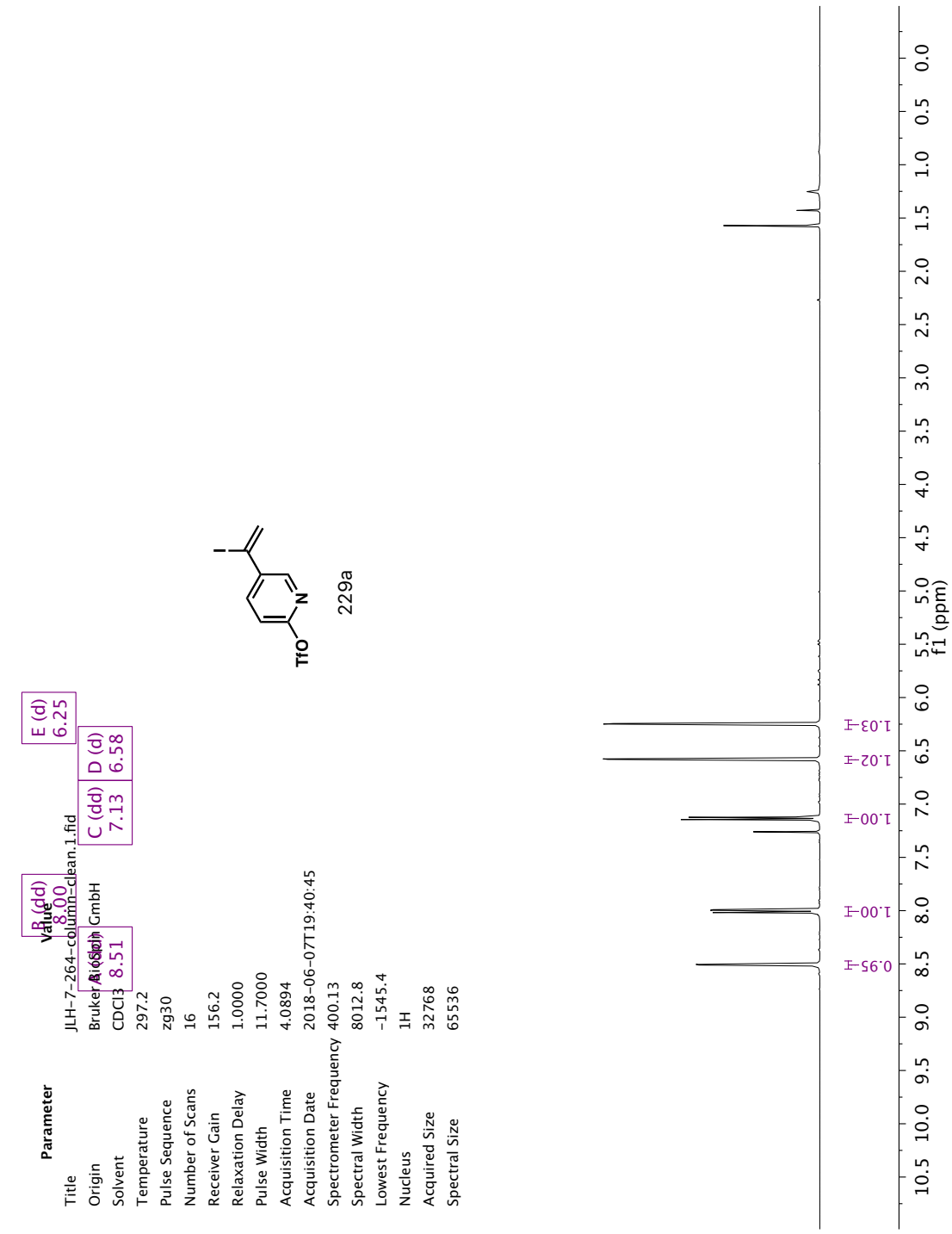

Parameter	Value
Title	JLH-7-264-column-clean.1.fid
Origin	Bruker Biospin GmbH
Solvent	CDCl3
Temperature	297.2
Pulse Sequence	zg30
Number of Scans	16
Receiver Gain	156.2
Relaxation Delay	1.0000
Pulse Width	11.7000
Acquisition Time	4.0894
Acquisition Date	2018-06-07T19:40:45
Spectrometer Frequency	400.13
Spectral Width	8012.8
Lowest Frequency	-1545.4
Nucleus	1H
Acquired Size	32768
Spectral Size	65536

Parameter	Value
Title	JLH-7-264-column-clean.2.fid
Origin	Bruker BioSpin GmbH
Solvent	CDCl3
Temperature	297.2
Pulse Sequence	zgpg30
Number of Scans	512
Receiver Gain	72.0
Relaxation Delay	1.0000
Pulse Width	10.0000
Acquisition Time	1.3631
Acquisition Date	2018-06-07T20:03:25
Spectrometer Frequency	100.62
Spectral Width	24038.5
Lowest Frequency	-1945.2
Nucleus	13C
Acquired Size	32768
Spectral Size	65536

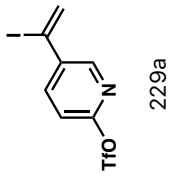

229a

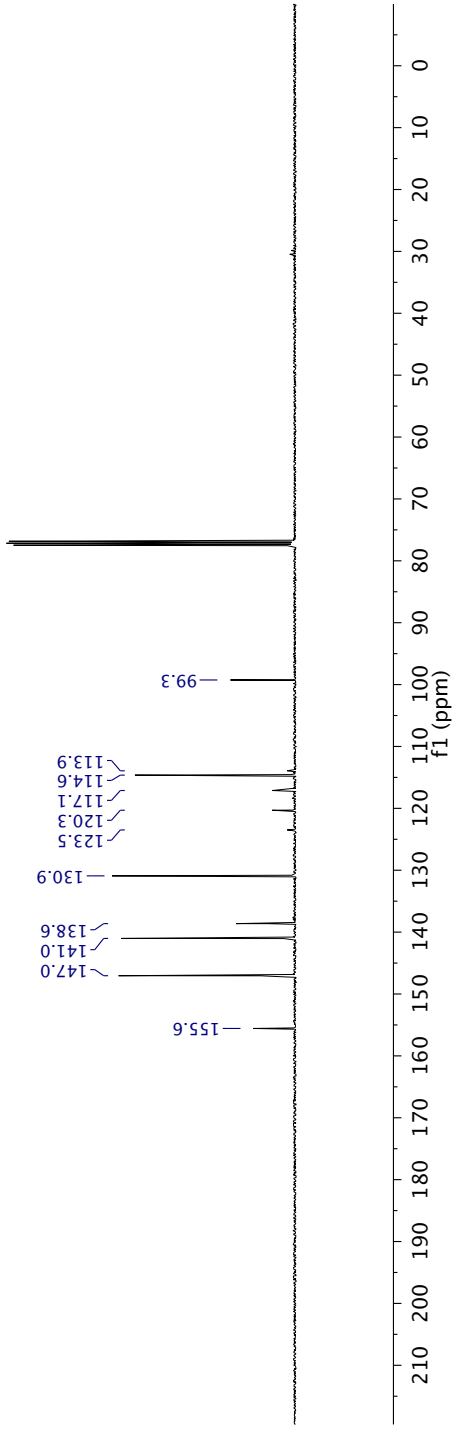

Parameter	Value
Title	JLH-7-264-F
Origin	Varian
Solvent	cdcl3
Temperature	25.0
Pulse Sequence	s2pul
Number of Scans	16
Receiver Gain	30
Relaxation Delay	1.0000
Pulse Width	6.3333
Acquisition Time	0.9856
Acquisition Date	2018-06-14T01:09:09
Spectrometer Frequency	282.34
Spectral Width	64935.1
Lowest Frequency	-56468.7
Nucleus	19F
Acquired Size	64000
Spectral Size	131072

229a

Parameter	Value
Title	JLH-7-264-F-C6F6
Origin	Varian
Solvent	cdcl3
Temperature	25.0
Pulse Sequence	s2pul
Number of Scans	16
Receiver Gain	30
Relaxation Delay	1.0000
Pulse Width	6.3333
Acquisition Time	0.9856
Acquisition Date	2018-06-14T01:14:32
Spectrometer Frequency	282.34
Spectral Width	64935.1
Lowest Frequency	-56468.7
Nucleus	19F
Acquired Size	64000
Spectral Size	131072

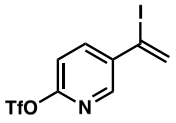

229a
with C_6F_6

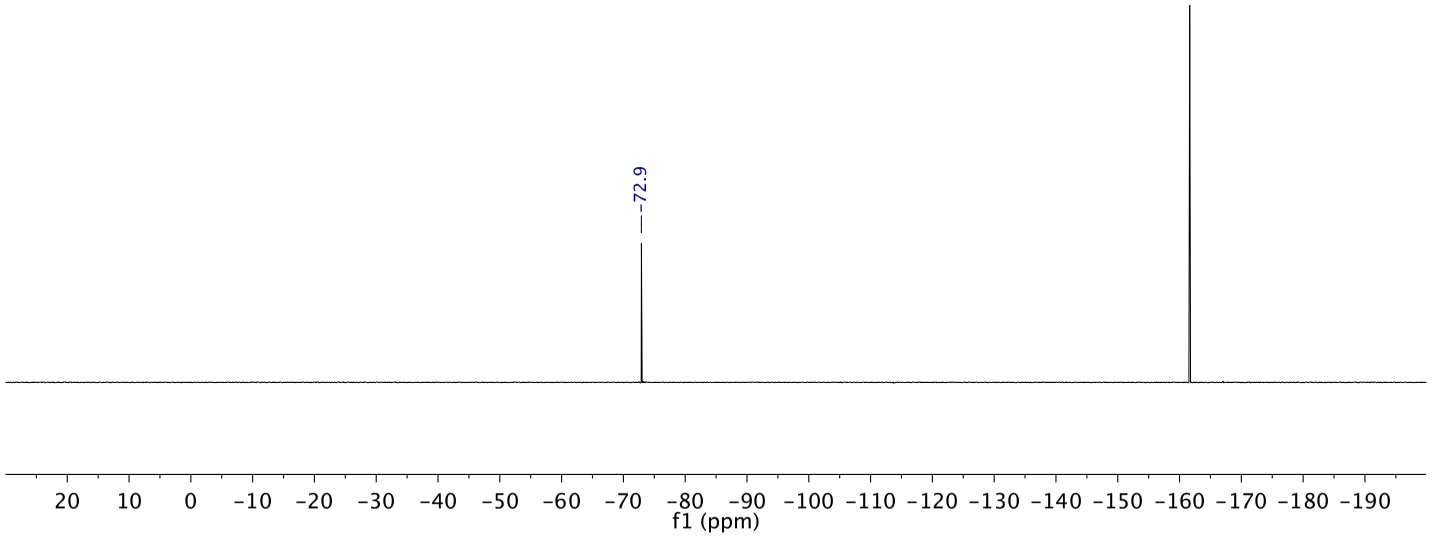

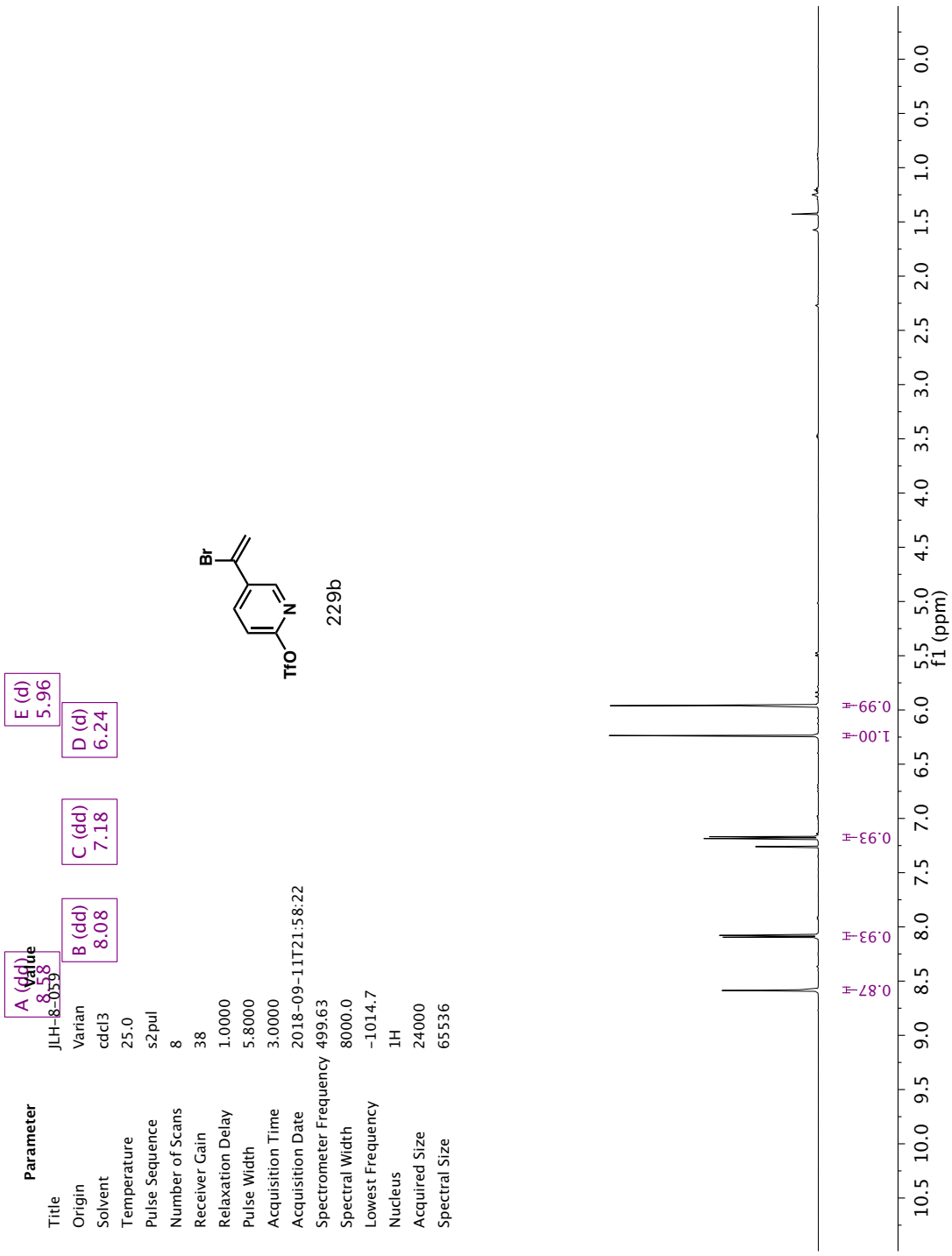

Parameter	Value
Title	JLH-8-059
Origin	Varian
Solvent	cdcl3
Temperature	25.0
Pulse Sequence	s2pul
Number of Scans	8
Receiver Gain	38
Relaxation Delay	1.0000
Pulse Width	5.8000
Acquisition Time	3.0000
Acquisition Date	2018-09-11T21:58:22
Spectrometer Frequency	499.63
Spectral Width	8000.0
Lowest Frequency	-1014.7
Nucleus	1H
Acquired Size	24000
Spectral Size	65536

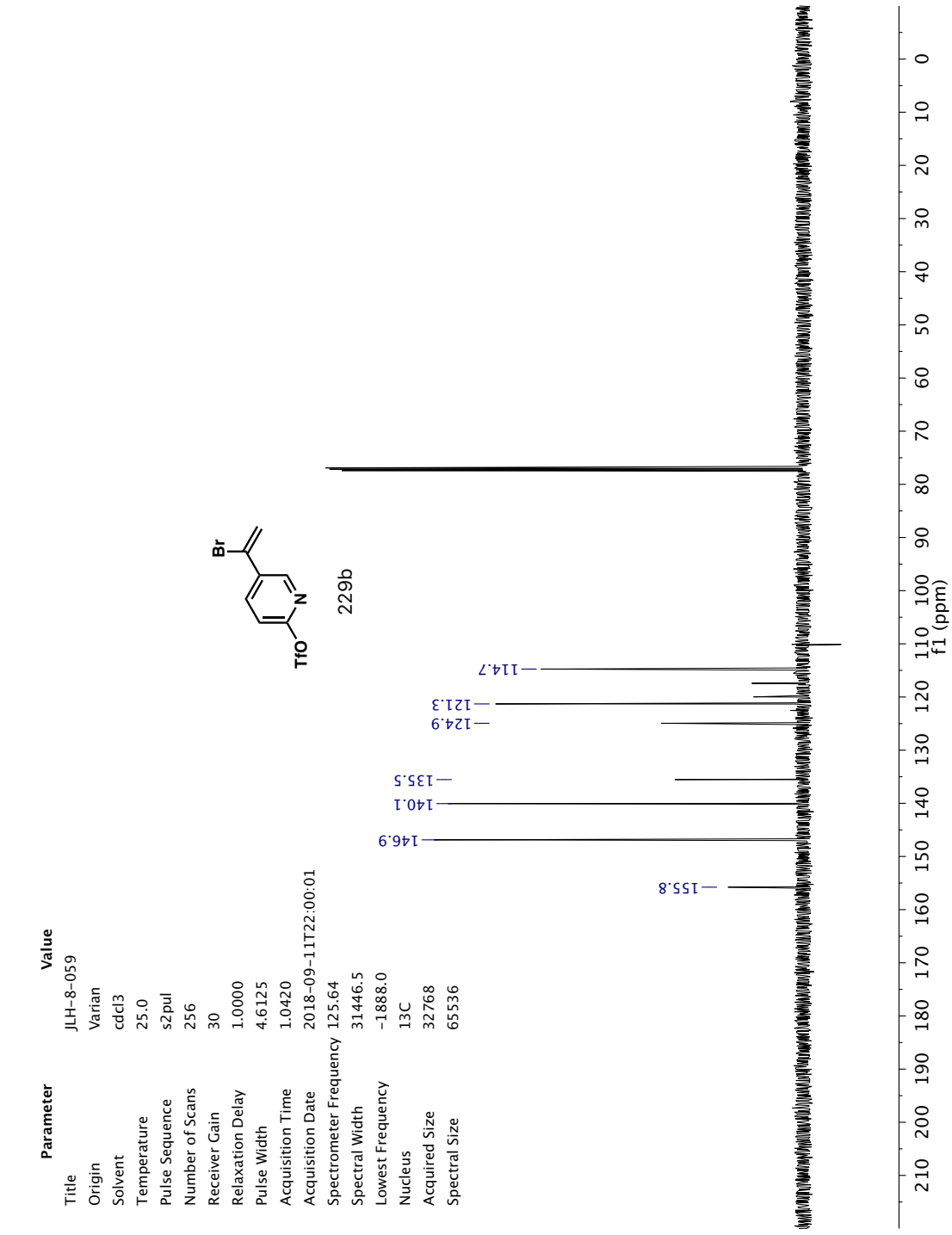
Parameter Value
Title JLH-8-059
Origin Varian
Solvent cdcl3
Temperature 25.0
Pulse Sequence s2pul
Number of Scans 256
Receiver Gain 30
Relaxation Delay 1.0000
Pulse Width 4.6125
Acquisition Time 1.0420
Acquisition Date 2018-09-11T22:00:01
Spectrometer Frequency 125.64
Spectral Width 31446.5
Lowest Frequency -1888.0
Nucleus 13C
Acquired Size 32768
Spectral Size 65536
Br
N
TfO
229b
155.8
146.9
140.1
135.5
124.9
121.3
114.7
f1 (ppm)

Parameter	Value
Title	JLH-8-059-F
Origin	Varian
Solvent	cdcl3
Temperature	25.0
Pulse Sequence	s2pul
Number of Scans	16
Receiver Gain	30
Relaxation Delay	1.0000
Pulse Width	6.3333
Acquisition Time	0.9856
Acquisition Date	2018-09-11T21:25:01
Spectrometer Frequency	282.34
Spectral Width	64935.1
Lowest Frequency	-56435.1
Nucleus	19F
Acquired Size	64000
Spectral Size	131072

229b

Parameter Value
Title JLH-8-059-F-C6F6
Origin Varian
Solvent cdcl3
Temperature 25.0
Pulse Sequence s2pul
Number of Scans 16
Receiver Gain 30
Relaxation Delay 1.0000
Pulse Width 6.3333
Acquisition Time 0.9856
Acquisition Date 2018-09-11T23:04:10
Spectrometer Frequency 282.34
Spectral Width 64935.1
Lowest Frequency -56431.7
Nucleus 19F
Acquired Size 64000
Spectral Size 131072
72.9
Br
N
TfO
229b
with C6F6
10 0 -10 -20 -30 -40 -50 -60 -70 -80 -90 -100 -110 -120 -130 -140 -150 -160 -170 -180 -190
f1 (ppm)

Parameter	Value
Title	ams-1-162 hivac.1.fid
Origin	Bruker BioSpin GmbH
Solvent	CDCl3
Temperature	295.1
Pulse Sequence	zg30
Number of Scans	16
Receiver Gain	112.8
Relaxation Delay	1.0000
Pulse Width	11.7000
Acquisition Time	4.0894
Acquisition Date	2018-05-08T20:21:54
Spectrometer Frequency	400.13
Spectral Width	8012.8
Lowest Frequency	-1576.2
Nucleus	1H
Acquired Size	32768
Spectral Size	65536

B (m) 7.18

D (d) 6.06

A (m) 7.26

C (d) 6.43

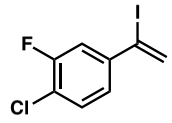

230a

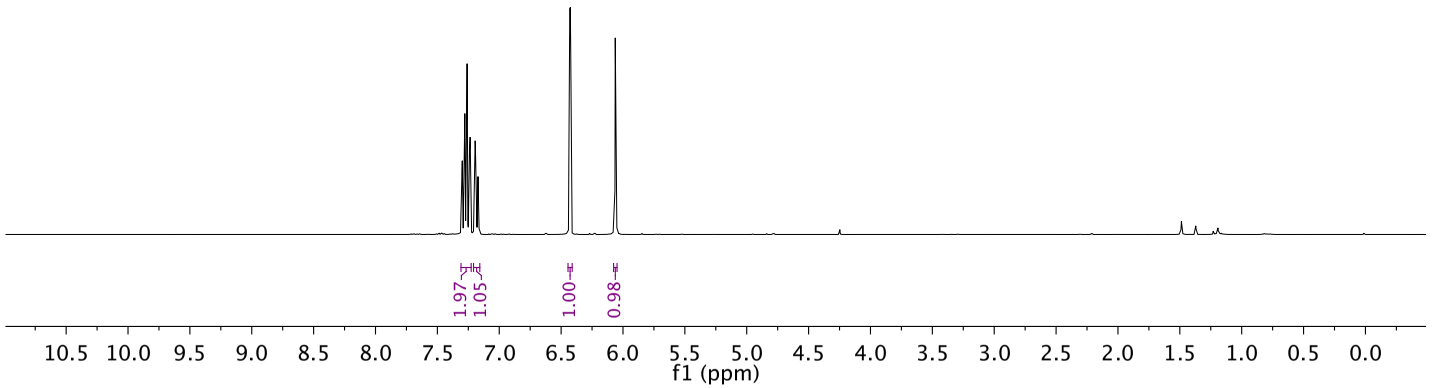

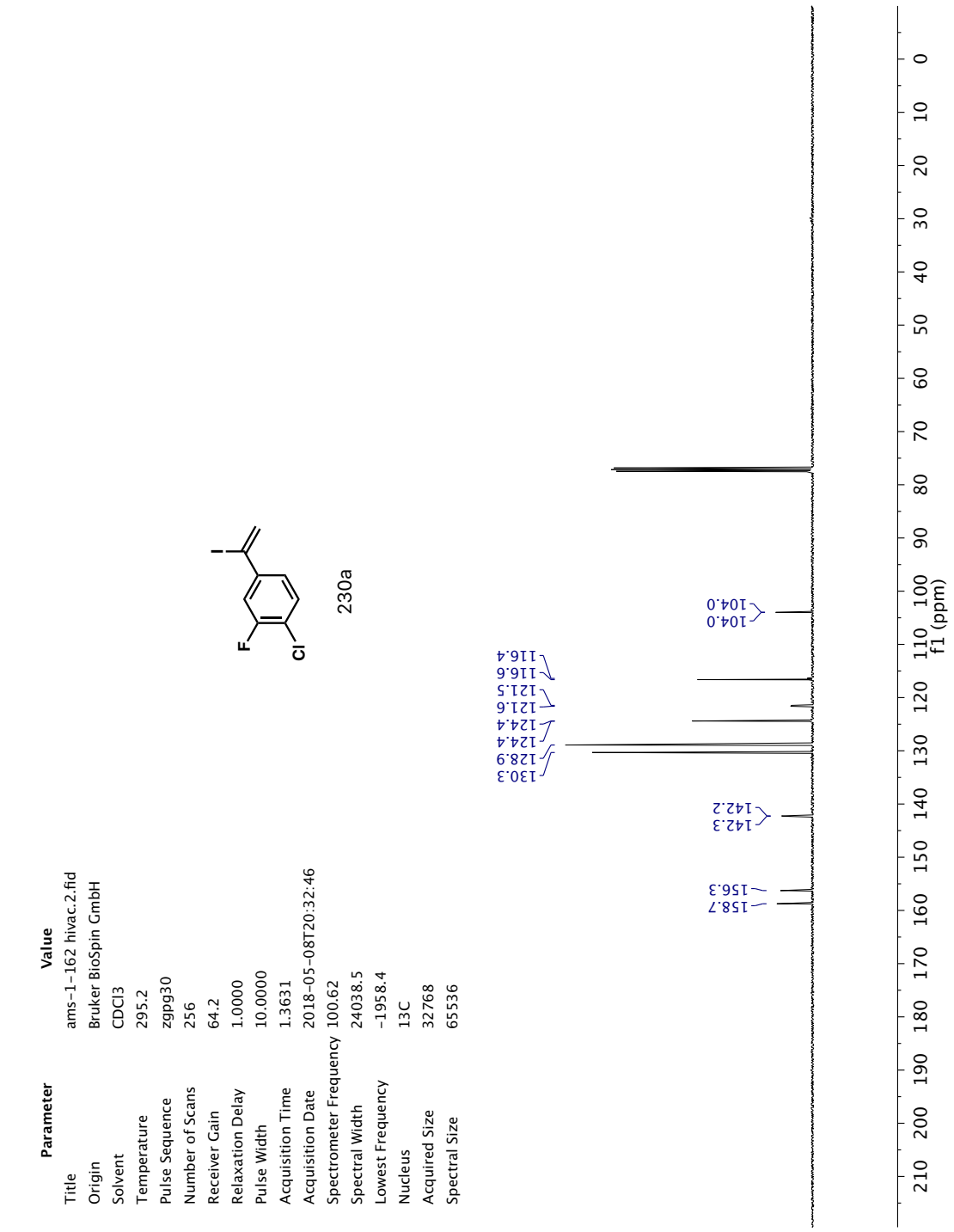
Parameter Value
Title ams-1-162 hivac.2.fid
Origin Bruker BioSpin GmbH
Solvent CDCl3
Temperature 295.2
Pulse Sequence zgpg30
Number of Scans 256
Receiver Gain 64.2
Relaxation Delay 1.0000
Pulse Width 10.0000
Acquisition Time 1.3631
Acquisition Date 2018-05-08T20:32:46
Spectrometer Frequency 100.62
Spectral Width 24038.5
Lowest Frequency -1958.4
Nucleus 13C
Acquired Size 32768
Spectral Size 65536
I
F
Cl
230a
158.7
156.3
142.3
142.2
130.3
128.9
124.4
124.4
121.6
121.5
116.6
116.4
104.0
104.0
f1 (ppm)

Parameter	Value
Title	AMS-1-162-F
Origin	Varian
Solvent	cdcl3
Temperature	25.0
Pulse Sequence	s2pul
Number of Scans	16
Receiver Gain	30
Relaxation Delay	1.0000
Pulse Width	6.3333
Acquisition Time	0.9856
Acquisition Date	2018-06-14T02:05:22
Spectrometer Frequency	282.34
Spectral Width	64935.1
Lowest Frequency	-56468.7
Nucleus	19F
Acquired Size	64000
Spectral Size	131072

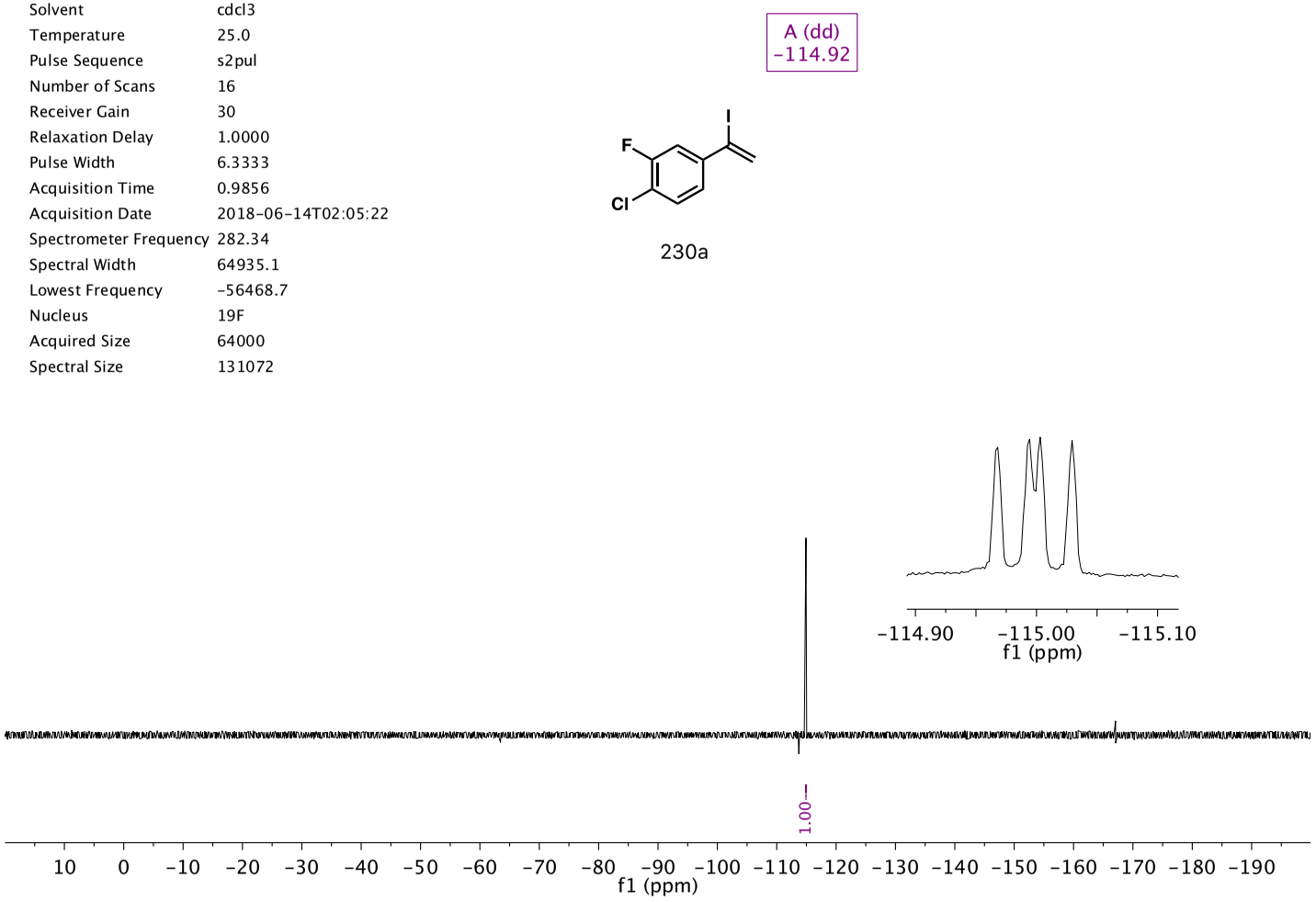

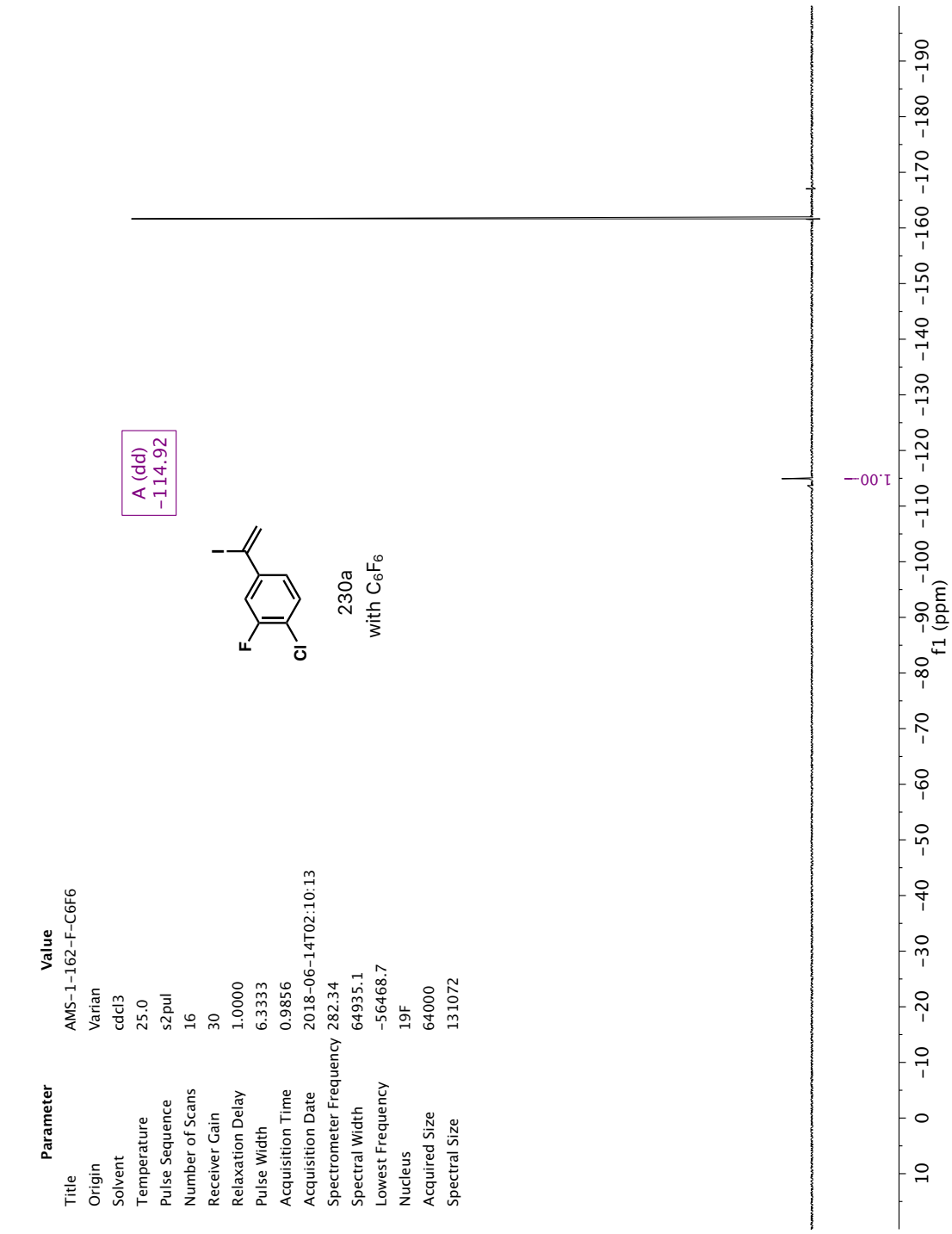
Parameter Value
Title AMS-1-162-F-C6F6
Origin Varian
Solvent cdcl3
Temperature 25.0
Pulse Sequence s2pul
Number of Scans 16
Receiver Gain 30
Relaxation Delay 1.0000
Pulse Width 6.3333
Acquisition Time 0.9856
Acquisition Date 2018-06-14T02:10:13
Spectrometer Frequency 282.34
Spectral Width 64935.1
Lowest Frequency -56468.7
Nucleus 19F
Acquired Size 64000
Spectral Size 131072
A (dd)
-114.92
F
Cl
230a
with C_6F_6
1.00
10 0 -10 -20 -30 -40 -50 -60 -70 -80 -90 -100 -110 -120 -130 -140 -150 -160 -170 -180 -190
f1 (ppm)

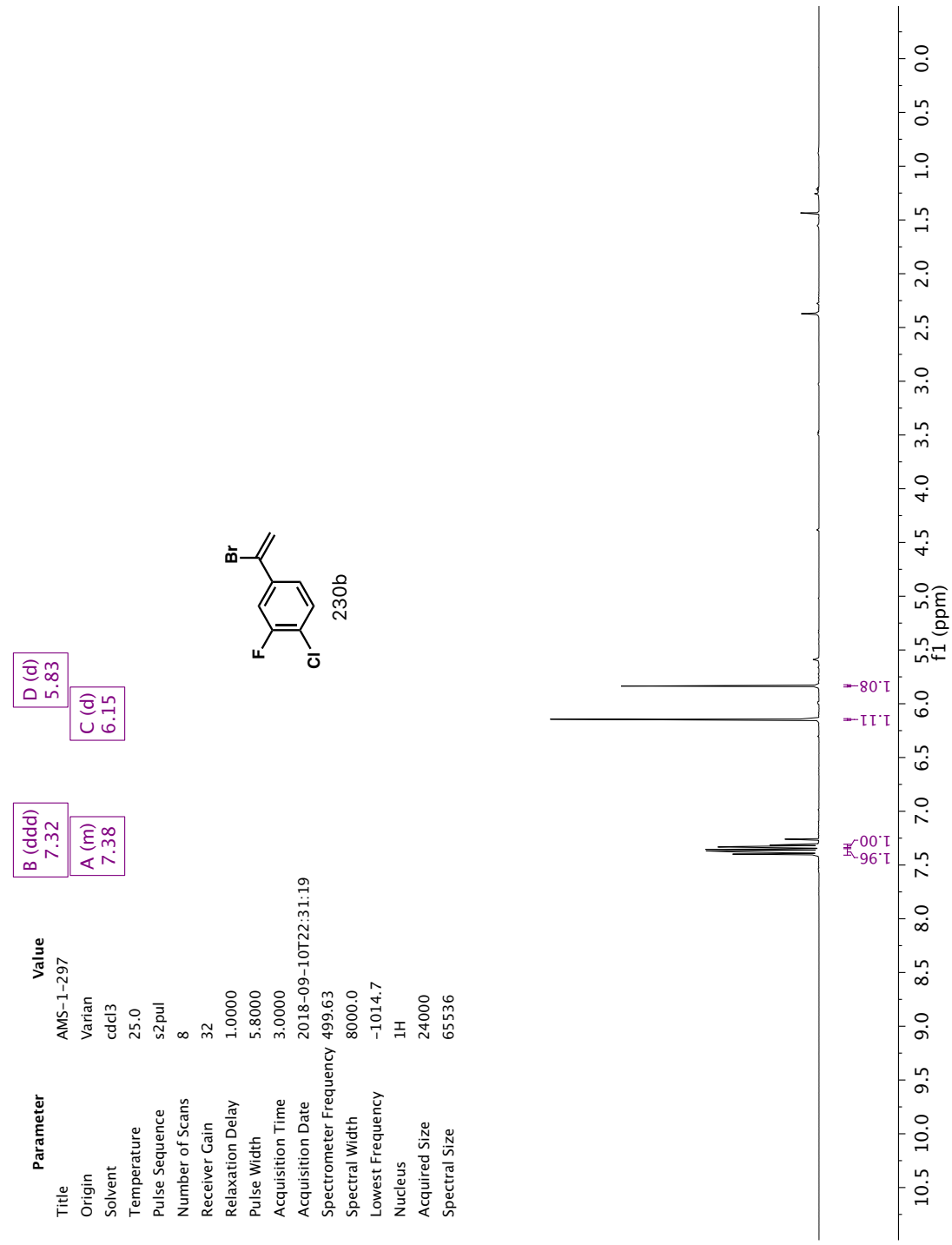

Parameter	Value
Title	AMS-1-297
Origin	Varian
Solvent	cdcl3
Temperature	25.0
Pulse Sequence	s2pul
Number of Scans	8
Receiver Gain	32
Relaxation Delay	1.0000
Pulse Width	5.8000
Acquisition Time	3.0000
Acquisition Date	2018-09-10T22:31:19
Spectrometer Frequency	499.63
Spectral Width	8000.0
Lowest Frequency	-1014.7
Nucleus	1H
Acquired Size	24000
Spectral Size	65536

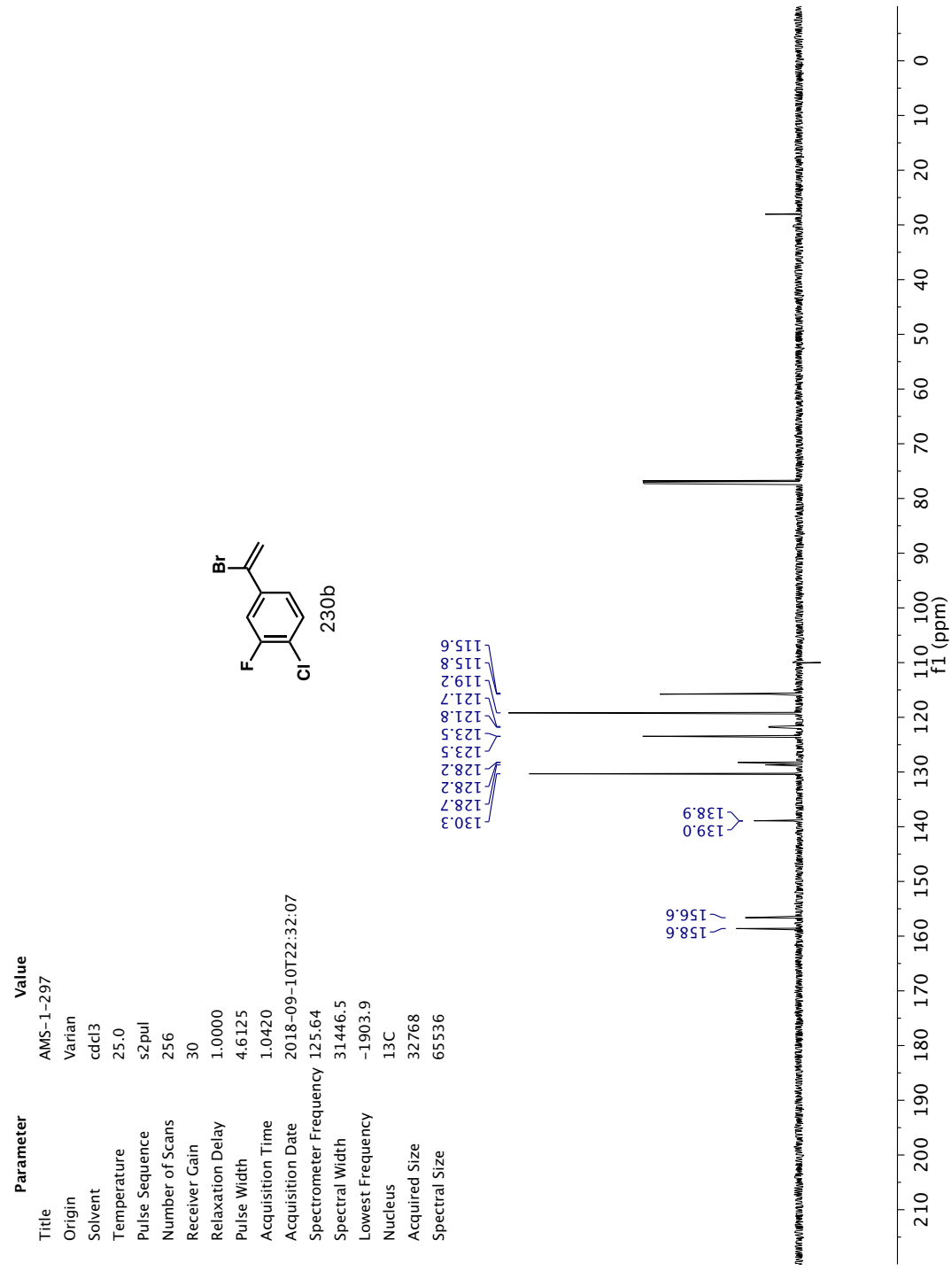
Parameter Value
Title AMS-1-297
Origin Varian
Solvent cdcl3
Temperature 25.0
Pulse Sequence s2pul
Number of Scans 256
Receiver Gain 30
Relaxation Delay 1.0000
Pulse Width 4.6125
Acquisition Time 1.0420
Acquisition Date 2018-09-10T22:32:07
Spectrometer Frequency 125.64
Spectral Width 31446.5
Lowest Frequency -1903.9
Nucleus 13C
Acquired Size 32768
Spectral Size 65536
Br
F
Cl
230b
158.6
156.6
139.0
138.9
130.3
128.7
128.2
128.2
123.5
123.5
123.3
121.8
121.7
119.2
115.8
115.6
f1 (ppm)

Parameter	Value
Title	AMS-1-297-F
Origin	Varian
Solvent	cdcl3
Temperature	25.0
Pulse Sequence	s2pul
Number of Scans	16
Receiver Gain	30
Relaxation Delay	1.0000
Pulse Width	6.3333
Acquisition Time	0.9856
Acquisition Date	2018-09-10T23:53:00
Spectrometer Frequency	282.34
Spectral Width	64935.1
Lowest Frequency	-56450.9
Nucleus	19F
Acquired Size	64000
Spectral Size	131072

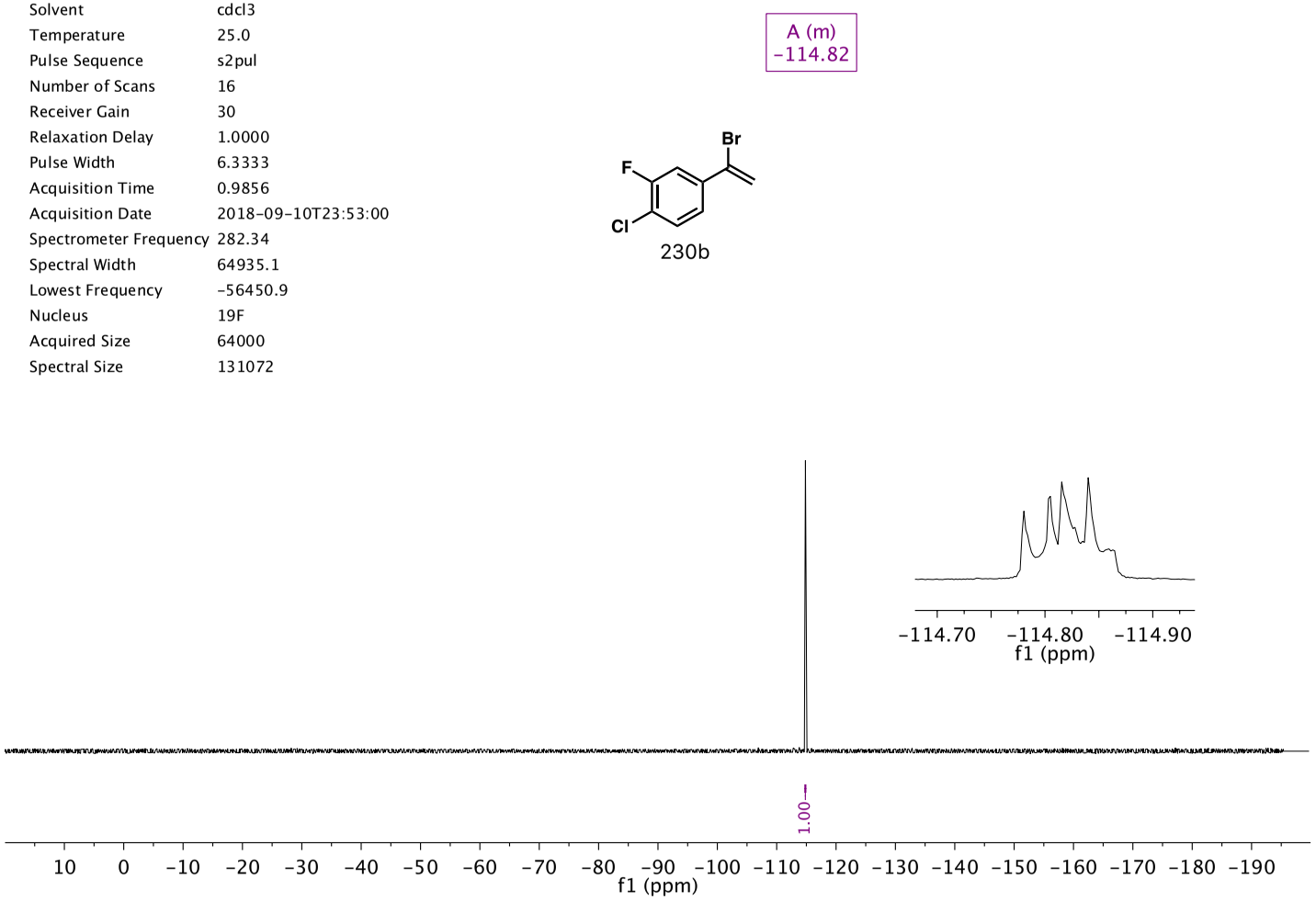

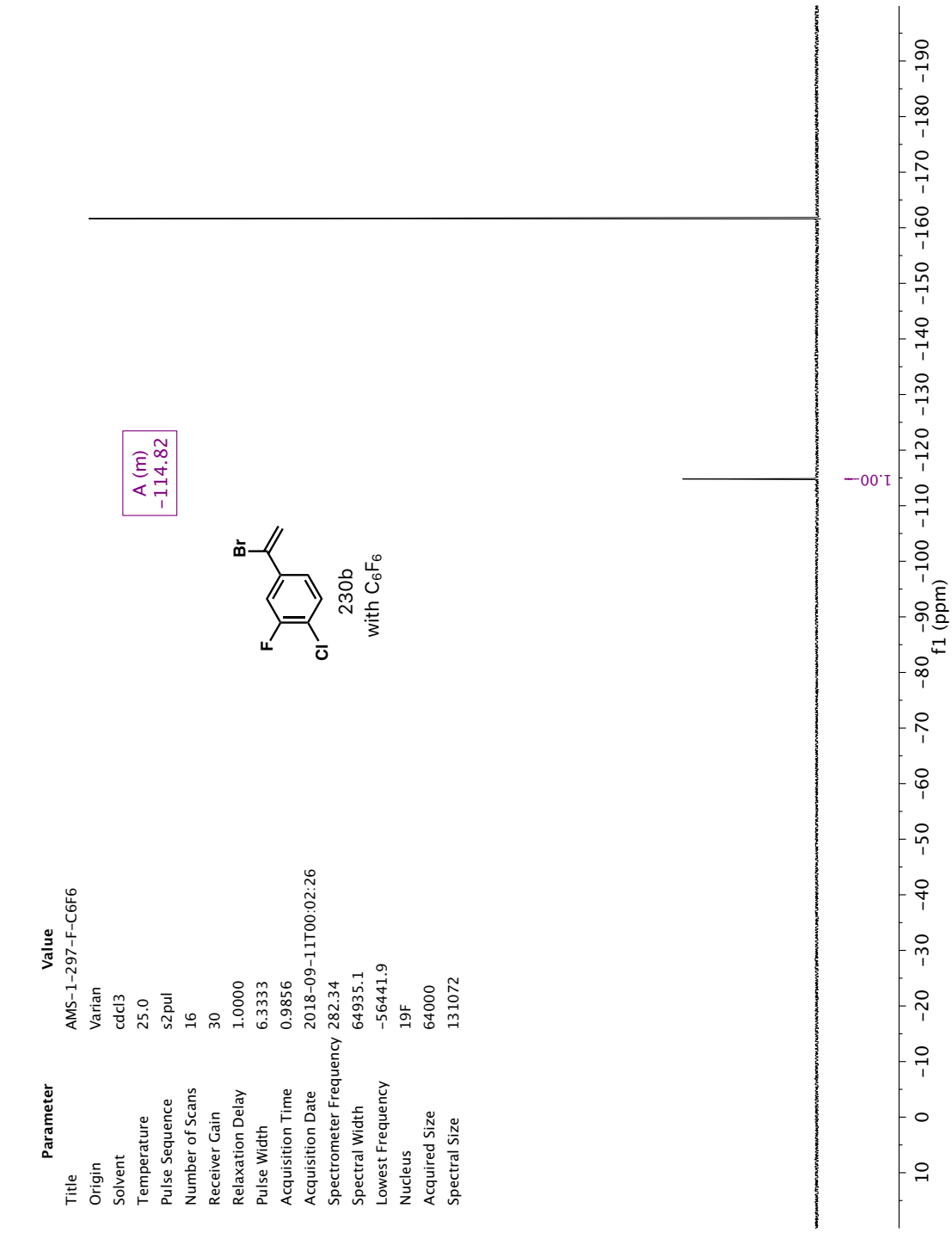

Parameter	Value
Title	AMS-1-297-F-C6F6
Origin	Varian
Solvent	cdcl3
Temperature	25.0
Pulse Sequence	s2pul
Number of Scans	16
Receiver Gain	30
Relaxation Delay	1.0000
Pulse Width	6.3333
Acquisition Time	0.9856
Acquisition Date	2018-09-11T00:02:26
Spectrometer Frequency	282.34
Spectral Width	64935.1
Lowest Frequency	-56441.9
Nucleus	19F
Acquired Size	64000
Spectral Size	131072

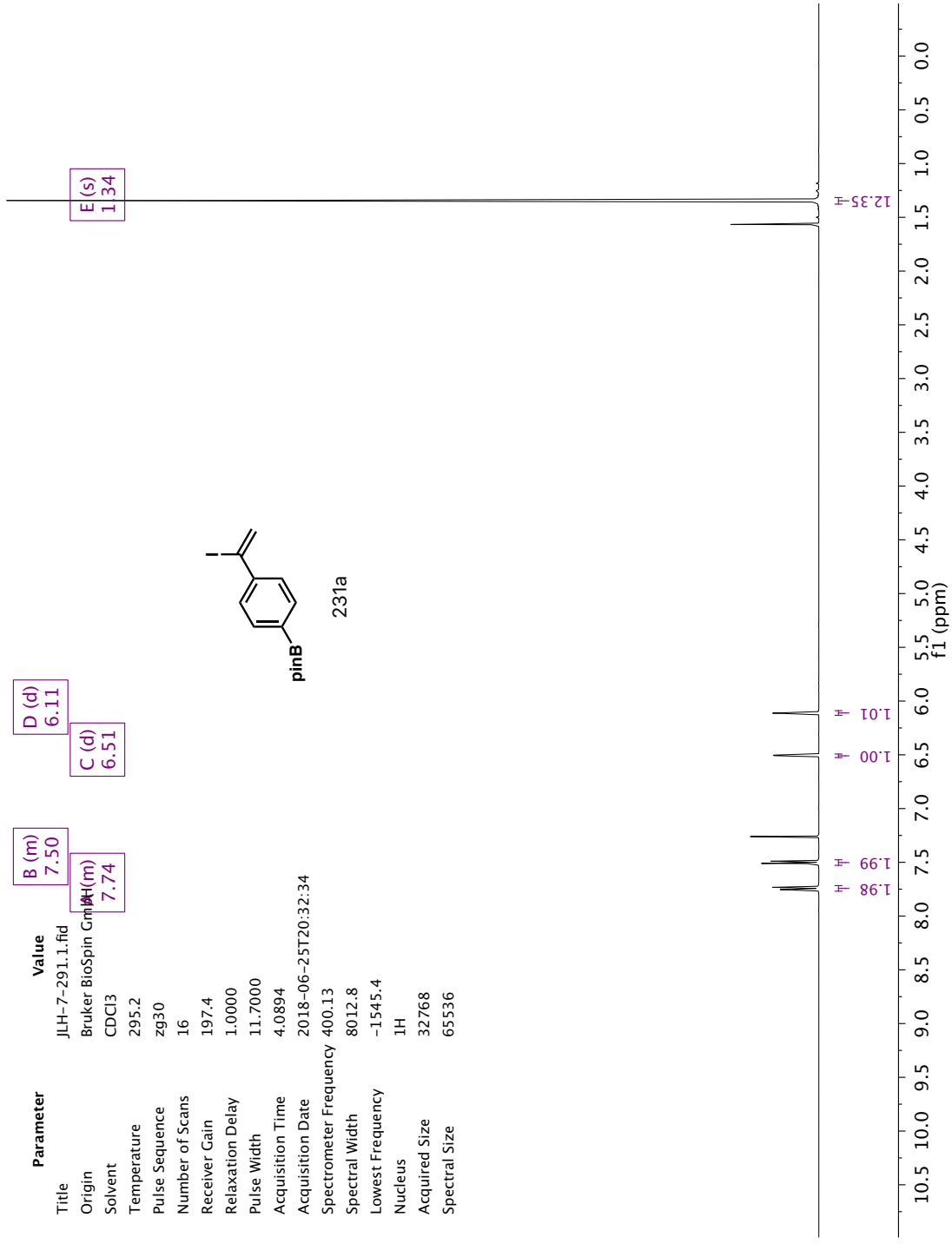
Parameter
Value
Title
JLH-7-291.1.fid
Origin
Bruker BioSpin GmbH
Solvent
CDCl3
Temperature
295.2
Pulse Sequence
zg30
Number of Scans
16
Receiver Gain
197.4
Relaxation Delay
1.0000
Pulse Width
11.7000
Acquisition Time
4.0894
Acquisition Date
2018-06-25T20:32:34
Spectrometer Frequency
400.13
Spectral Width
8012.8
Lowest Frequency
-1545.4
Nucleus
1H
Acquired Size
32768
Spectral Size
65536
B (m) 7.50
A (m) 7.74
D (d) 6.11
C (d) 6.51
E (s) 1.34
pinB
231a
12.35
1.01
1.00
1.99
1.98
f1 (ppm)

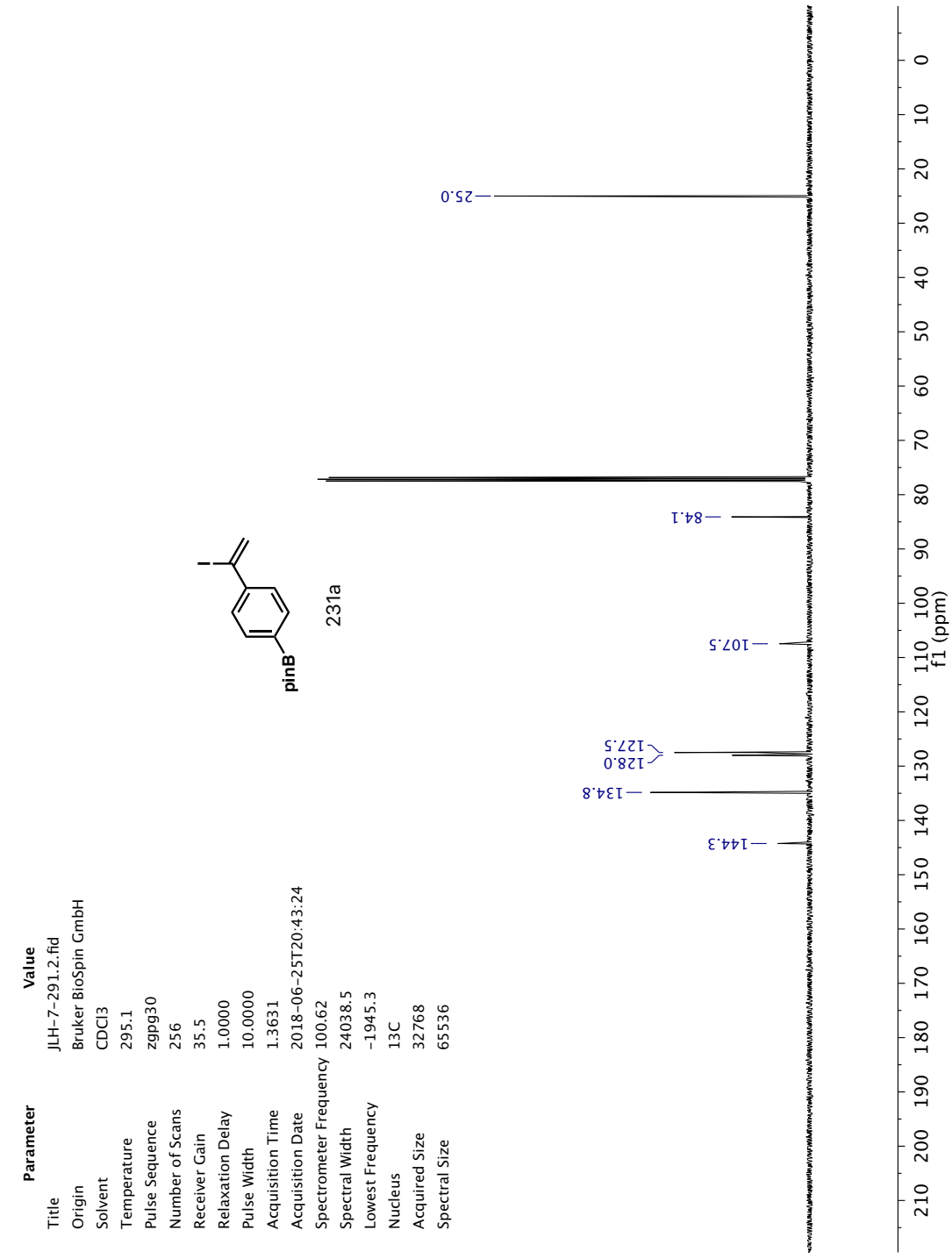
Parameter Value
Title JLH-7-291.2.fid
Origin Bruker BioSpin GmbH
Solvent CDCl3
Temperature 295.1
Pulse Sequence zgpg30
Number of Scans 256
Receiver Gain 35.5
Relaxation Delay 1.0000
Pulse Width 10.0000
Acquisition Time 1.3631
Acquisition Date 2018-06-25T20:43:24
Spectrometer Frequency 100.62
Spectral Width 24038.5
Lowest Frequency -1945.3
Nucleus 13C
Acquired Size 32768
Spectral Size 65536
pinB
231a
25.0
84.1
107.5
127.5
128.0
134.8
144.3
f1 (ppm)

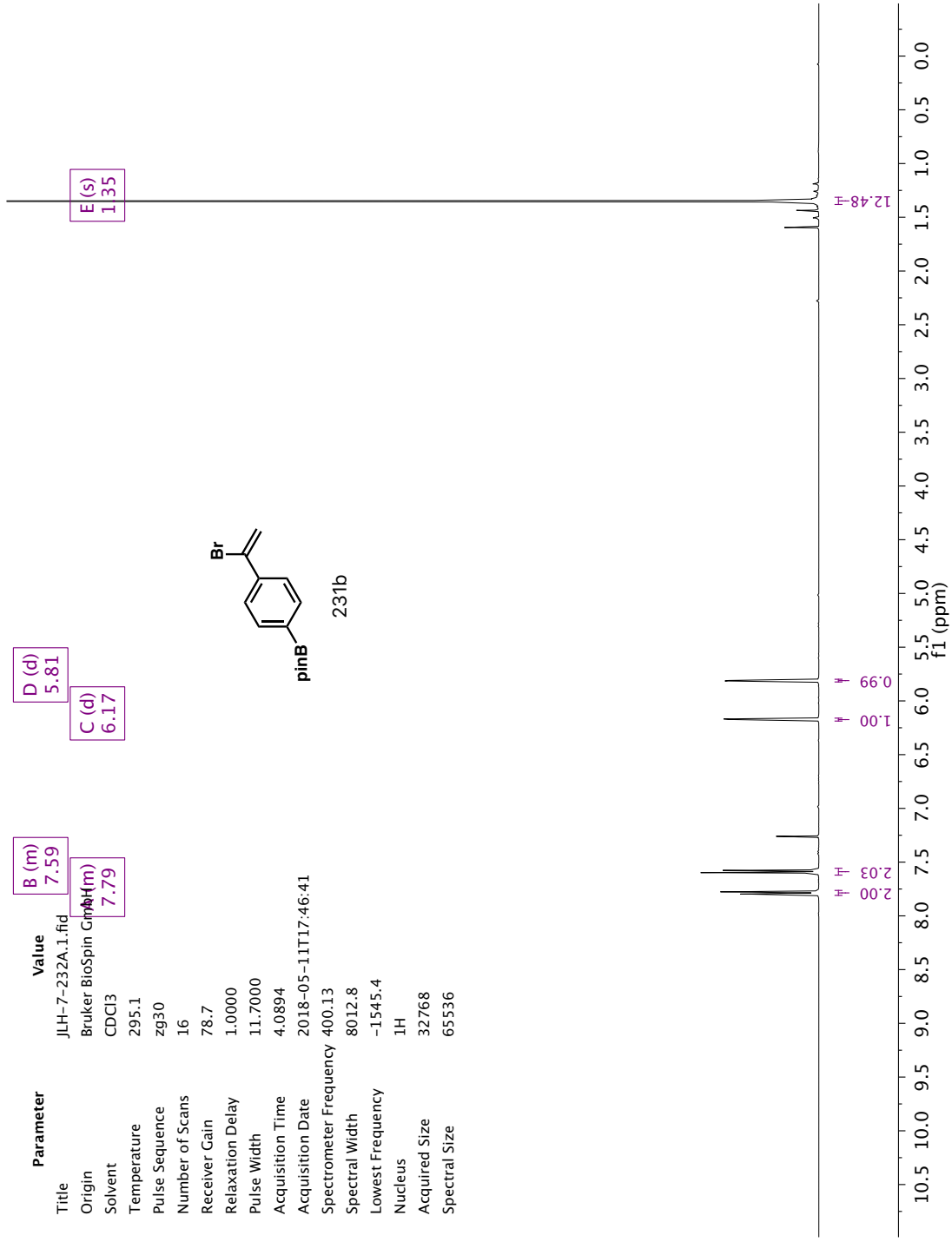
Parameter
Value
Title
JLH-7-232A.1.fid
Origin
Bruker BioSpin GmbH
Solvent
CDCl3
Temperature
295.1
Pulse Sequence
zg30
Number of Scans
16
Receiver Gain
78.7
Relaxation Delay
1.0000
Pulse Width
11.7000
Acquisition Time
4.0894
Acquisition Date
2018-05-11T17:46:41
Spectrometer Frequency
400.13
Spectral Width
8012.8
Lowest Frequency
-1545.4
Nucleus
1H
Acquired Size
32768
Spectral Size
65536
B (m) 7.59
A (m) 7.79
D (d) 5.81
C (d) 6.17
E (s) 1.35
Br
pinB
231b
12.48
2.00
2.03
1.00
0.99
f1 (ppm)

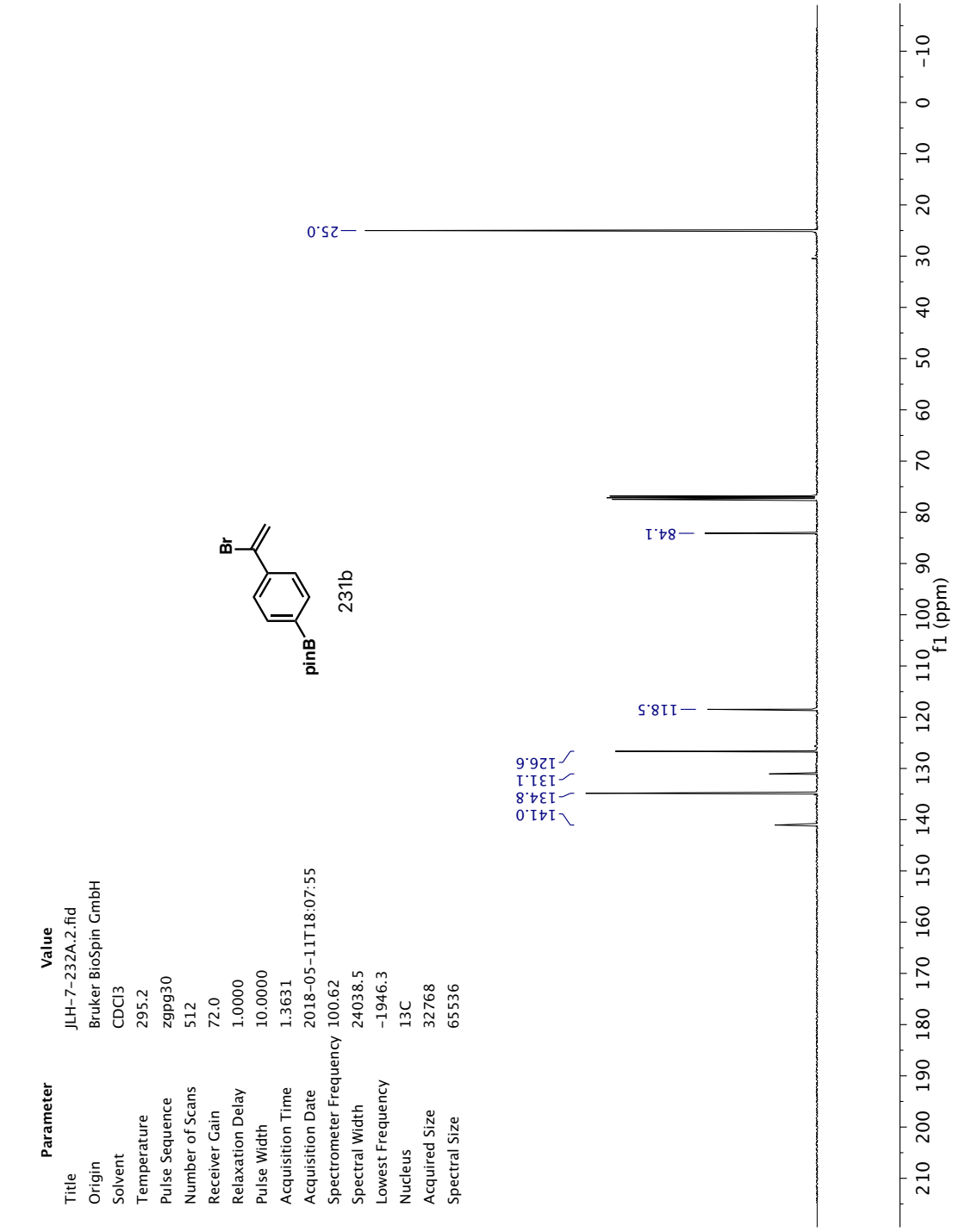
Parameter Value
Title JLH-7-232A.2.fid
Origin Bruker BioSpin GmbH
Solvent CDCl3
Temperature 295.2
Pulse Sequence zgpg30
Number of Scans 512
Receiver Gain 72.0
Relaxation Delay 1.0000
Pulse Width 10.0000
Acquisition Time 1.3631
Acquisition Date 2018-05-11T18:07:55
Spectrometer Frequency 100.62
Spectral Width 24038.5
Lowest Frequency -1946.3
Nucleus 13C
Acquired Size 32768
Spectral Size 65536
Br
pinB
231b
25.0
84.1
118.5
126.6
131.1
134.8
141.0
f1 (ppm)

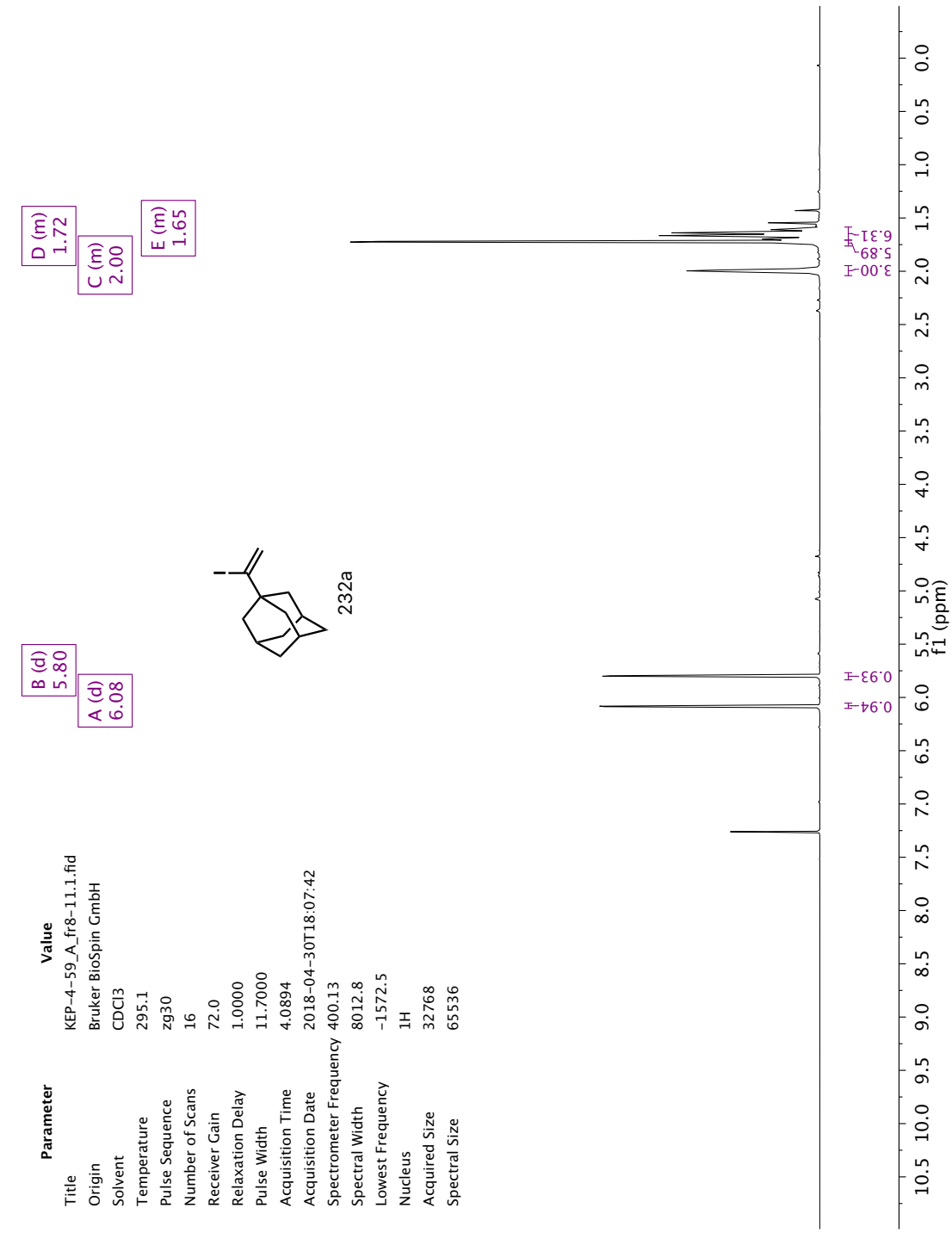

Parameter	Value
Title	KEP-4-59_A_fr8-11.1.fid
Origin	Bruker BioSpin GmbH
Solvent	CDCl3
Temperature	295.1
Pulse Sequence	zg30
Number of Scans	16
Receiver Gain	72.0
Relaxation Delay	1.0000
Pulse Width	11.7000
Acquisition Time	4.0894
Acquisition Date	2018-04-30T18:07:42
Spectrometer Frequency	400.13
Spectral Width	8012.8
Lowest Frequency	-1572.5
Nucleus	1H
Acquired Size	32768
Spectral Size	65536

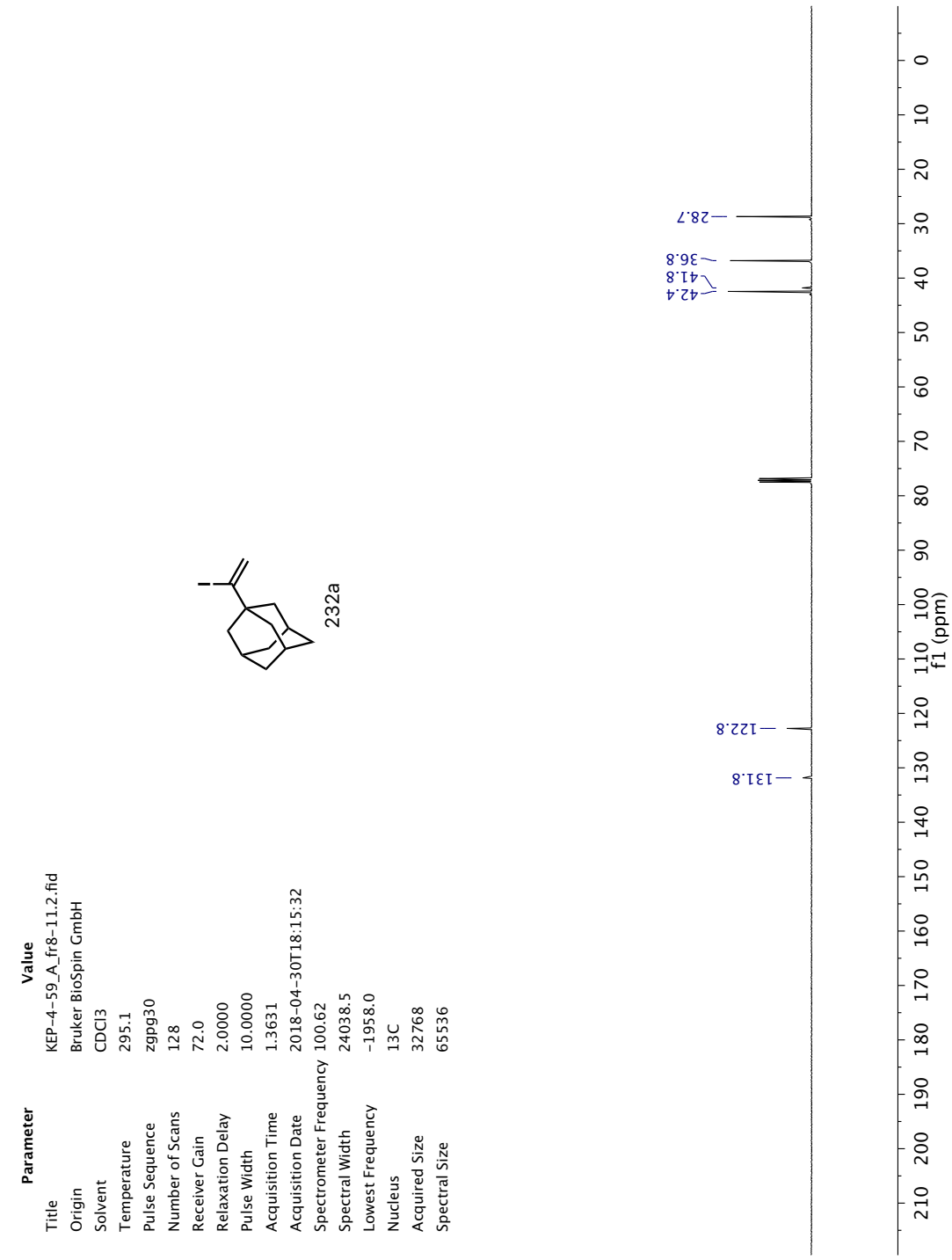
Parameter Value
Title KEP-4-59_A_fr8-11.2.fid
Origin Bruker BioSpin GmbH
Solvent CDCl3
Temperature 295.1
Pulse Sequence zgpg30
Number of Scans 128
Receiver Gain 72.0
Relaxation Delay 2.0000
Pulse Width 10.0000
Acquisition Time 1.3631
Acquisition Date 2018-04-30T18:15:32
Spectrometer Frequency 100.62
Spectral Width 24038.5
Lowest Frequency -1958.0
Nucleus 13C
Acquired Size 32768
Spectral Size 65536
232a
131.8
122.8
42.4
41.8
36.8
28.7
f1 (ppm)

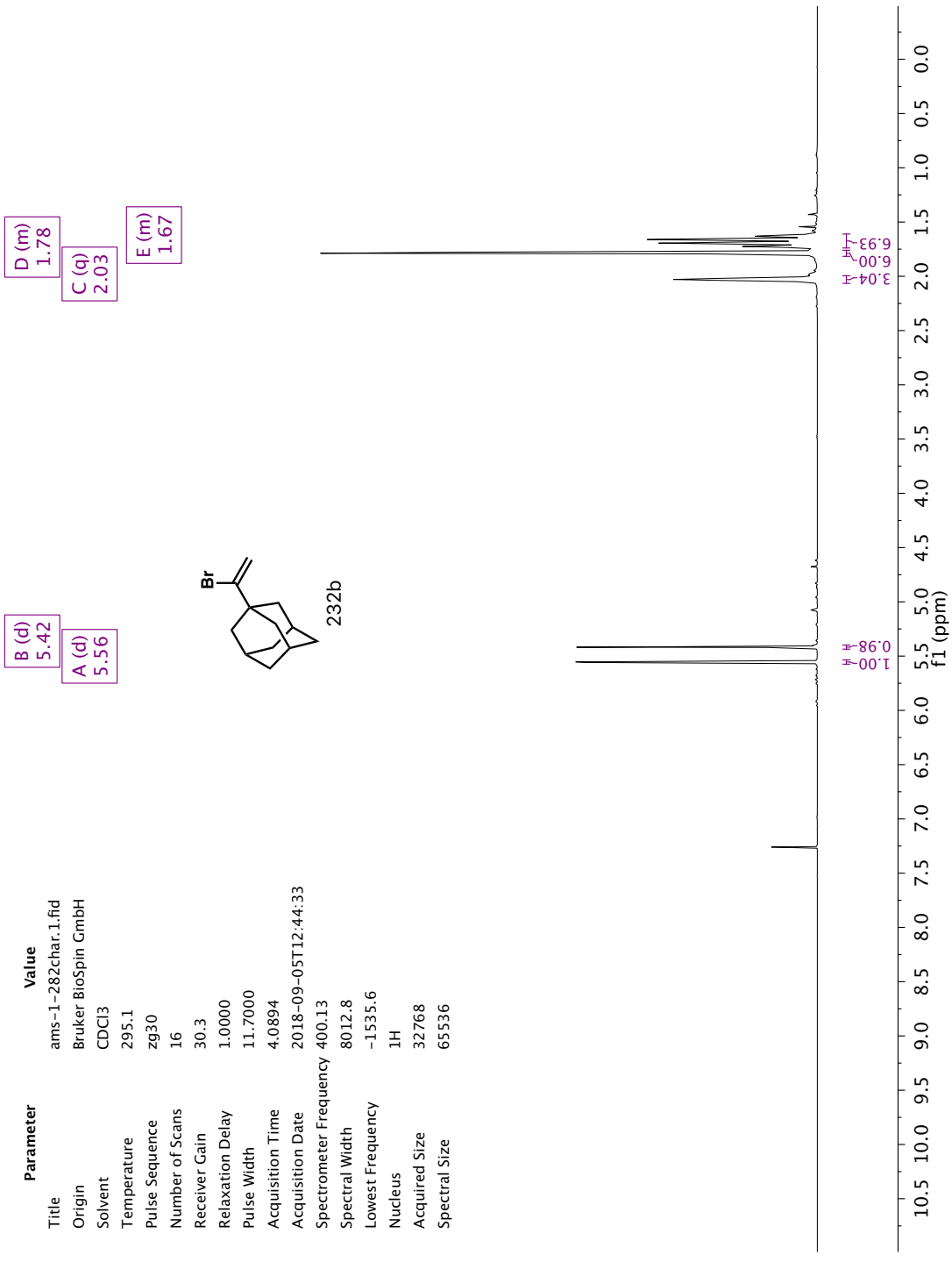

Parameter	Value
Title	ams-1-282char.1.fid
Origin	Bruker BioSpin GmbH
Solvent	CDCl3
Temperature	295.1
Pulse Sequence	zg30
Number of Scans	16
Receiver Gain	30.3
Relaxation Delay	1.0000
Pulse Width	11.7000
Acquisition Time	4.0894
Acquisition Date	2018-09-05T12:44:33
Spectrometer Frequency	400.13
Spectral Width	8012.8
Lowest Frequency	-1535.6
Nucleus	1H
Acquired Size	32768
Spectral Size	65536

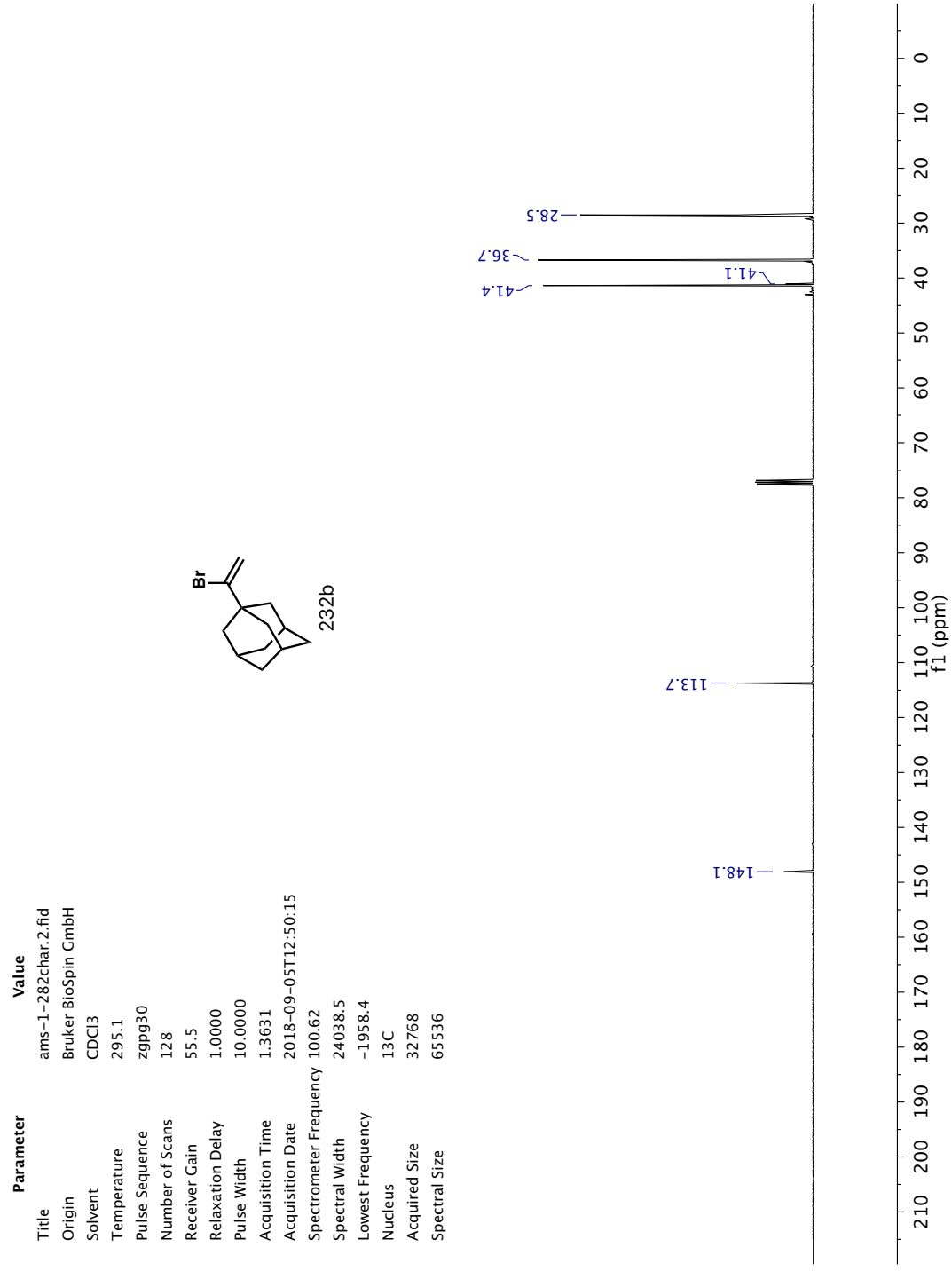
Parameter Value
Title ams-1-282char.2.fid
Origin Bruker BioSpin GmbH
Solvent CDCl3
Temperature 295.1
Pulse Sequence zgpg30
Number of Scans 128
Receiver Gain 55.5
Relaxation Delay 1.0000
Pulse Width 10.0000
Acquisition Time 1.3631
Acquisition Date 2018-09-05T12:50:15
Spectrometer Frequency 100.62
Spectral Width 24038.5
Lowest Frequency -1958.4
Nucleus 13C
Acquired Size 32768
Spectral Size 65536
Br
232b
148.1
113.7
41.4
41.1
36.7
28.5
f1 (ppm)

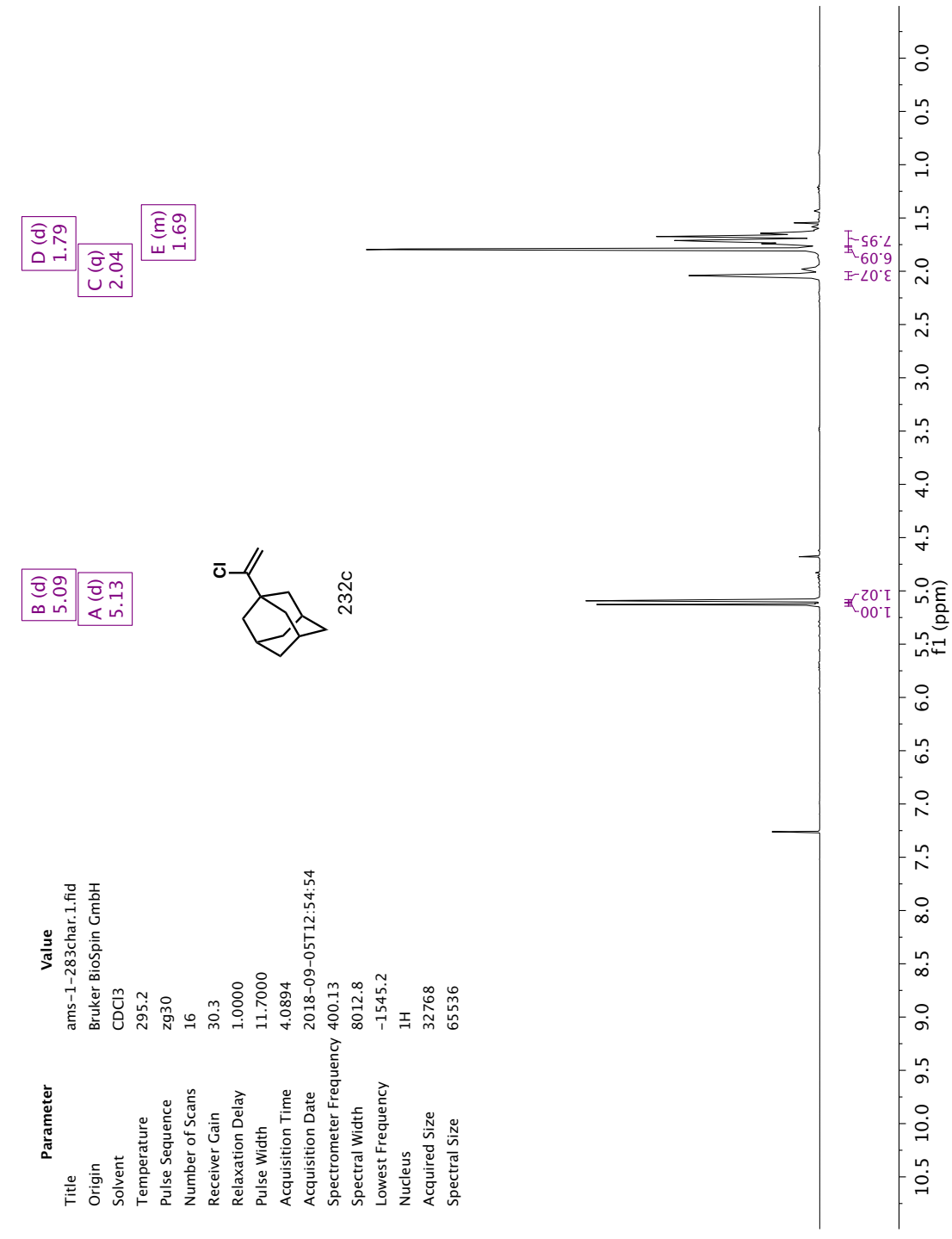

Parameter	Value
Title	ams-1-283char.1.fid
Origin	Bruker BioSpin GmbH
Solvent	CDCl3
Temperature	295.2
Pulse Sequence	zg30
Number of Scans	16
Receiver Gain	30.3
Relaxation Delay	1.0000
Pulse Width	11.7000
Acquisition Time	4.0894
Acquisition Date	2018-09-05T12:54:54
Spectrometer Frequency	400.13
Spectral Width	8012.8
Lowest Frequency	-1545.2
Nucleus	1H
Acquired Size	32768
Spectral Size	65536

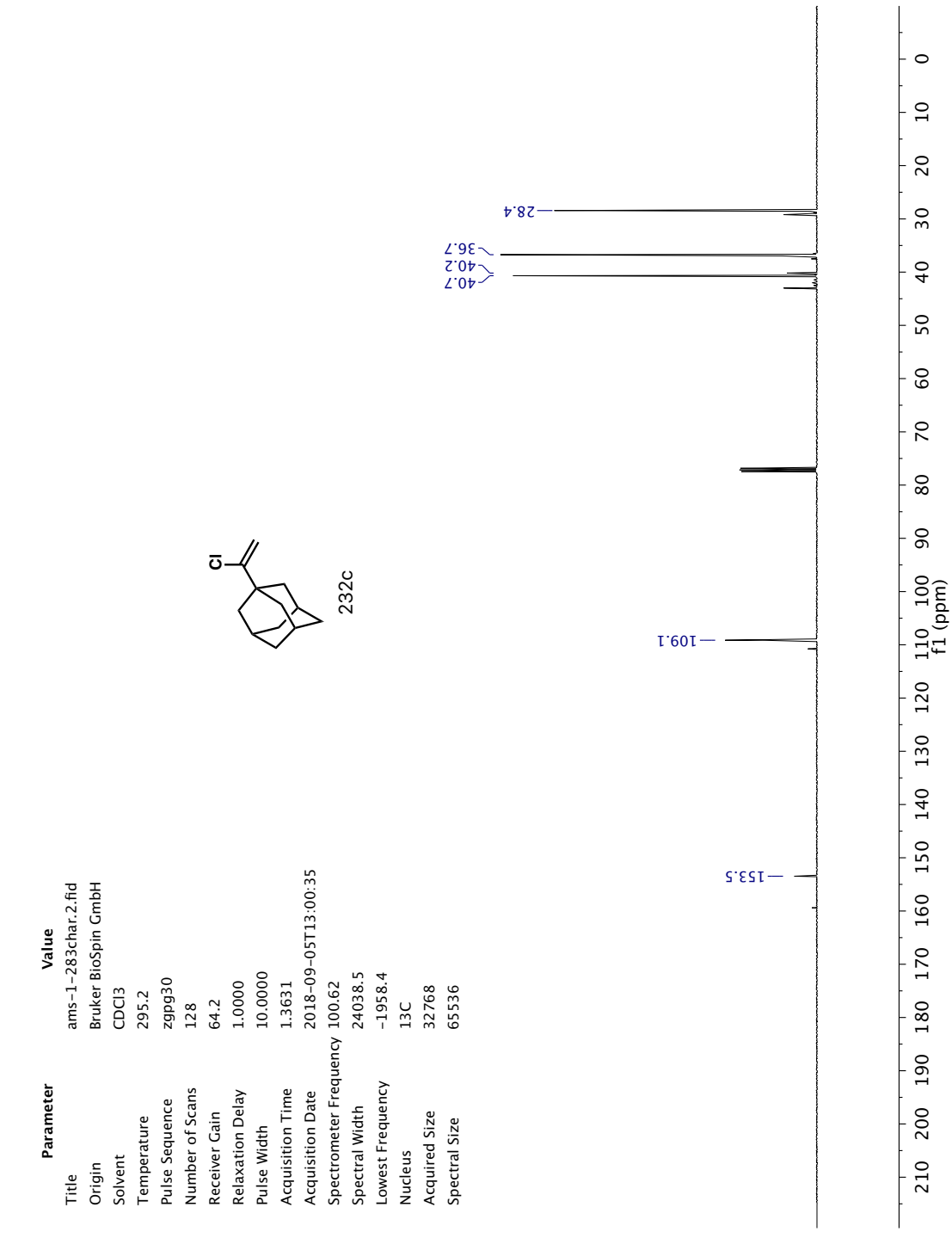
Parameter Value
Title ams-1-283char.2.fid
Origin Bruker BioSpin GmbH
Solvent CDCl3
Temperature 295.2
Pulse Sequence zgpg30
Number of Scans 128
Receiver Gain 64.2
Relaxation Delay 1.0000
Pulse Width 10.0000
Acquisition Time 1.3631
Acquisition Date 2018-09-05T13:00:35
Spectrometer Frequency 100.62
Spectral Width 24038.5
Lowest Frequency -1958.4
Nucleus 13C
Acquired Size 32768
Spectral Size 65536
Cl
232c
153.5
109.1
40.7
40.2
36.7
28.4
f1 (ppm)

Appendix 8

Phosphino(oxazoline)Ligand Parameterization for Ni-Catalyzed Reductive Cross-Coupling of Aryl Iodides and α-Chloronitriles[‡]

A8.1 INTRODUCTION

The ability to efficiently synthesize enantiopure small molecules is an important and ongoing synthetic challenge not only in academic research but also in the pharmaceutical industry as over 60% of FDA-approved medications contain C(sp^3)-hybridized stereocenters,[1] some of which are commercialized as a single enantiomer. Chiral benzylic stereocenters are a common structural motif found in a variety of drug molecules, some of which also contain β-disposed functional groups (Figure A8.1). When developing synthetic approaches to access enantioenriched pharmaceuticals, it is often

[‡]The research presented in this chapter was completed in collaboration with: 1) Nathaniel Kadunce (graudate student) and Raymond Turro (graduate student) in the Reisman group, as well as Iris Guo (graduate student) in the Sigman group.

imperative to dictate the absolute chirality of these stereocenters as opposite enantiomers of drug molecules often display drastically different efficacy.[2,3] Furthermore, increased C(sp^3) content has been correlated with improved aqueous solubility and clinical success.[1] In order to synthesize a broad range of target drug molecules, the need for a diverse set of reactions to form C–C bonds continues to drive the development of new synthetic methods.

Figure A8.1 *Pharmaceuticals containing chiral benzylic stereocenters.*

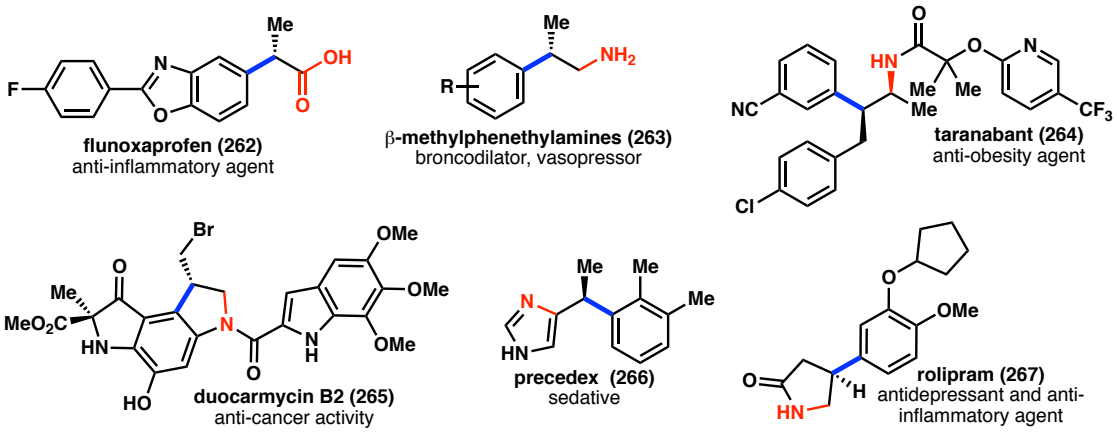

A8.1.1 Origins of Stereoinduction

In the context of organic synthesis, the introduction of enantioenriched C(sp^3)-hybridized stereocenters often relies on one of three different approaches: 1) substrate control, 2) appendage and removal of chiral auxillaries, or 3) the use of chiral catalysts (Scheme A8.1).[4–6] In each case, a diastereoselective approach is utilized to transfer chiral information to the newly formed stereogenic center, either from an existing chiral handle on the substrate or through coordination to a chiral catalyst. In cases where a reaction takes place on an existing C(sp^3)-hybridized carbon atom, the utility of stereospecific and stereoconvergent approaches, either through the use of organocatalysts or metal catalysts,[7] proves particularly useful. Asymmetric catalysis, unlike substrate control and chiral

auxillaries, does not require pre-installation of stereochemical information that may need to be removed downstream in a synthetic sequence. Furthermore, asymmetric catalysis allows one to finely tune the electronic and structural parameters of a catalyst, which at times can even override inherent substrate controlled diastereoselectivity.

Scheme A8.1 *Approaches to synthesize chiral C(sp³) stereocenters.*

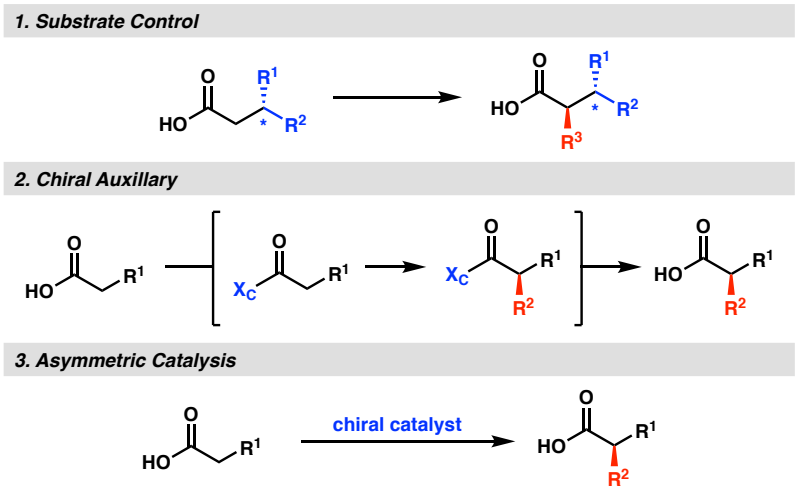

A8.1.2 Asymmetric Reductive Cross-Couplings

Our laboratory has recently published a number of asymmetric nickel-catalyzed cross-electrophile couplings using a broad scope of C(sp^2)-hybridized electrophiles (e.g. aryl iodides, alkenyl bromides, and acid chlorides) (Scheme A8.2).[8–13] Thus far we have discovered that diversifying the C(sp^3)-hybridized electrophile has proven challenging; in order to obtain high levels of reactivity and enantioselectivity, the C(sp^3)-hybridized electrophile requires the use of a radical stabilizing functional group adjacent to the electrophilic carbon, which has shown success when included as either an aromatic ring or nitrile moiety. For each new set of coupling partners, reactions were extensively reoptimized. To obtain high selectivity in the benzylic systems, the use of BOX ligands **L1**

or **L2**, or BiOX ligand **L4**, provided the products in up to 98% ee. In contrast, the α-chloronitrile reaction proceeded in poor yield when BOX and BiOX ligands were used, and it was found during initial optimization that PHOX ligands improved reactivity. A series of BnPHOX ligands were evaluated, and the use of an electron-rich PHOX ligand **L4** provided the products in up to 93% ee.

Scheme A8.2 *Asymmetric Reductive Cross-Coupling Reactions*

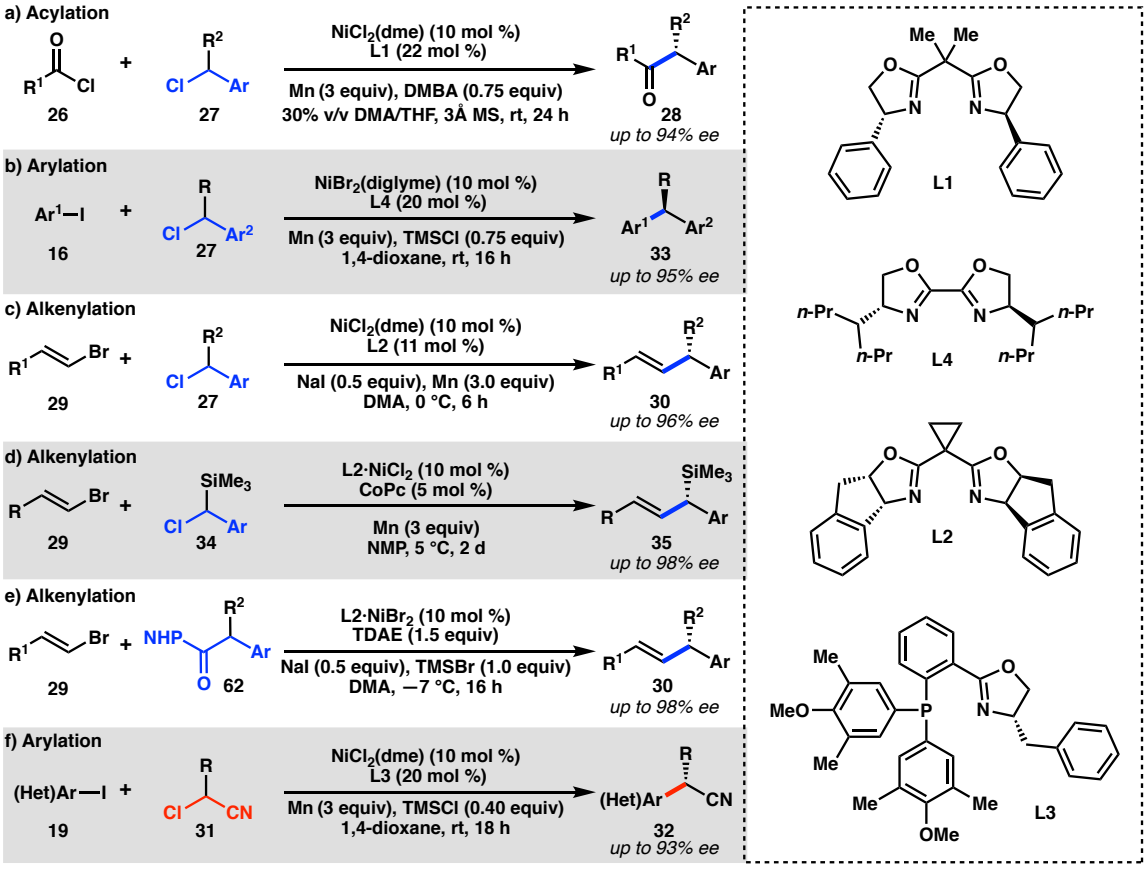

It is evident from these results that the PHOX ligand possess unique electronic and structural characteristics that promote good reactivity and selectivity for the α-chloronitrile system. In order to more efficiently develop novel asymmetric cross-coupling reactions, we became interested in studies that advance our understanding of reaction mechanisms.

In particular, we became interested in studying the PHOX ligand scaffold in the context of a ligand parameterization study in collaboration with the Sigman laboratory. A systematic study that probes how steric and electronic factors of the ligand perturb the yield and selectivity of this reductive cross-coupling reaction will allow for the future development of new cross-coupling reactions that proceed through α-nitrile radical intermediates. Furthermore, this study may also provide insight as we ask questions on how to utilize other radical stabilizing groups (e.g. esters, ketones, amides, alkenes, alkynes) as well as unactivated electrophiles in Ni-catalyzed asymmetric cross-couplings.

A8.1.3 Ligand Parameterization

The fine tuning of chiral catalysts, either by exploiting stabilizing or destabilizing interactions, can lead to highly enantiopure products as selectivity is governed by the reaction temperature and the Gibbs free energy difference ($\Delta\Delta G^{\ddagger}$) between the major and minor transition states (Figure A8.2). While the key principles of asymmetric catalysis are rooted in fundamental physical organic chemistry, they are often overlooked in reaction development and optimization. Although asymmetric catalysis has undeniably become a powerful approach to introduce chirality in target molecules, the straightforward

Figure A8.2 *Gibbs free energy difference for a given transition state.*

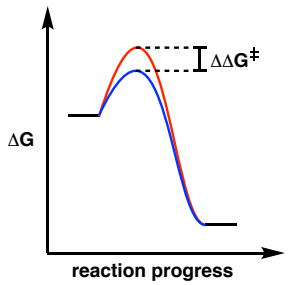

construction of stereogenic centers remains an ongoing challenge as success is often achieved through extensive screening processes. This empirical approach requires a significant amount of time and resources in order to fully optimize a given reaction.

In order to address these challenges, the Sigman laboratory has studied catalyst optimization through a data-driven approach that focuses on understanding the fundamental physical principles of transition state stabilization by studying how structural parameters, electronic parameters, and non-covalent interactions between the catalyst and substrate impacts enantioselectivity. To study these interactions, the laboratory turns to the use of multi-variable linear free energy relationships and modern statistical analysis techniques in order to probe multiple components that affect the overall transition state energy.[14–19] This approach is particularly useful, as it also allows one to study catalyst effects without knowledge of the reaction mechanism; often ligand parameters can be used as catalyst surrogates.

The workflow of this analytical technique consists of four main parts: 1) data collection, 2) computational parameterization, 3) mathematical modeling, and 4) testing and evaluating hypotheses (Figure A8.3). The mathematical equation obtained through this process can be used to help predict better catalysts through virtual screening but perhaps of more importance it can allow one to glean insight into the reaction mechanism. This information can be further utilized in the development of novel reactivity. This research area fosters an innovative and collaborative environment where the overall goal is to develop a universal understanding of asymmetric catalysis from a physical organic perspective.

Figure A8.3 *Sigman parameterization workflow.*

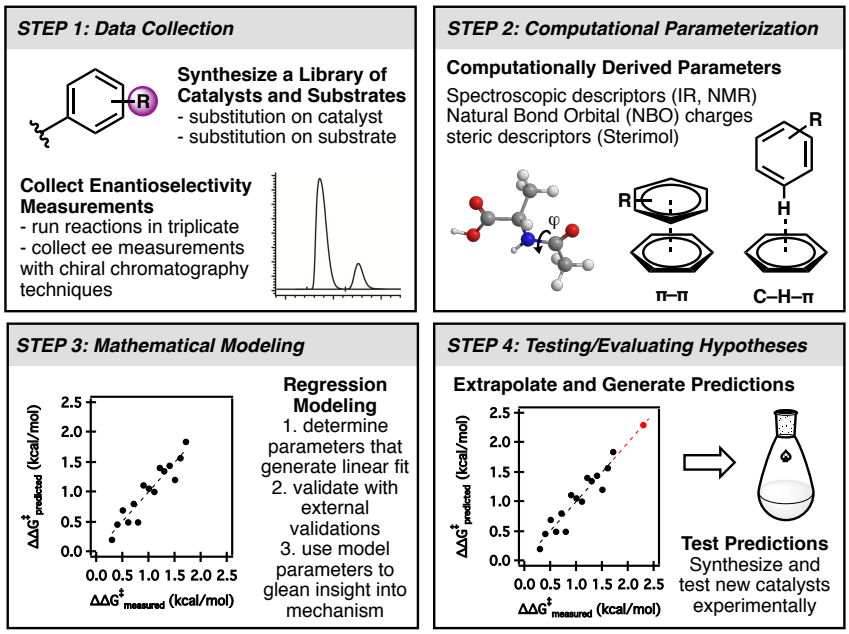

A8.2 PRELIMINARY RESULTS

A8.2.1 Cross-Coupling of α-Chloronitriles and Aryl Iodides

We set out to initiate a collaboration with the Sigman laboratory to better understand how different components of the PHOX ligand impacted the enantioselectivity of the α-arylated nitrile products (**32**). For the cross-coupling of α-chloronitriles (**31**) and aryl iodides (**16**) to generate chiral α-arylated nitriles (**32**), the developed reaction proceeded in good yield and enantioselectivity for a range of different substrates, which included heterocycles such as thiophenes (**32a**), pyridines (**32b**), pyrimidines (**32c**), and quinolines (**32e–g**) (Figure A8.4).[12] Although optimized, these conditions did possess some pitfalls. Typically, good yields and lower ee were observed for smaller α-substituents (i.e.

32e) while poorer yields and better ee are observed with bulkier substrates (i.e. **32f**). Furthermore, aryl iodides lacking a heterocyclic motif typically resulted in lower ee (**32h)**, and substrates containing 2-aryl pyrimidines provided racemic products (**32d**). Although the published method evaluated heteroaromatic iodides for the substrate scope, these reactions typically proceeded with higher levels of enantioselectivity. Therefore, we elected to pursue parameterization studies with a non-heteroaromatic aryl iodide (i.e. 4-bromobenzonitrile) in hopes to discover second-generation conditions to access a variety of new chiral products in synthetically tractable enantiopurities.

Figure A8.4 *Representative scope of α-chloronitrile and aryl iodide cross-coupling.*

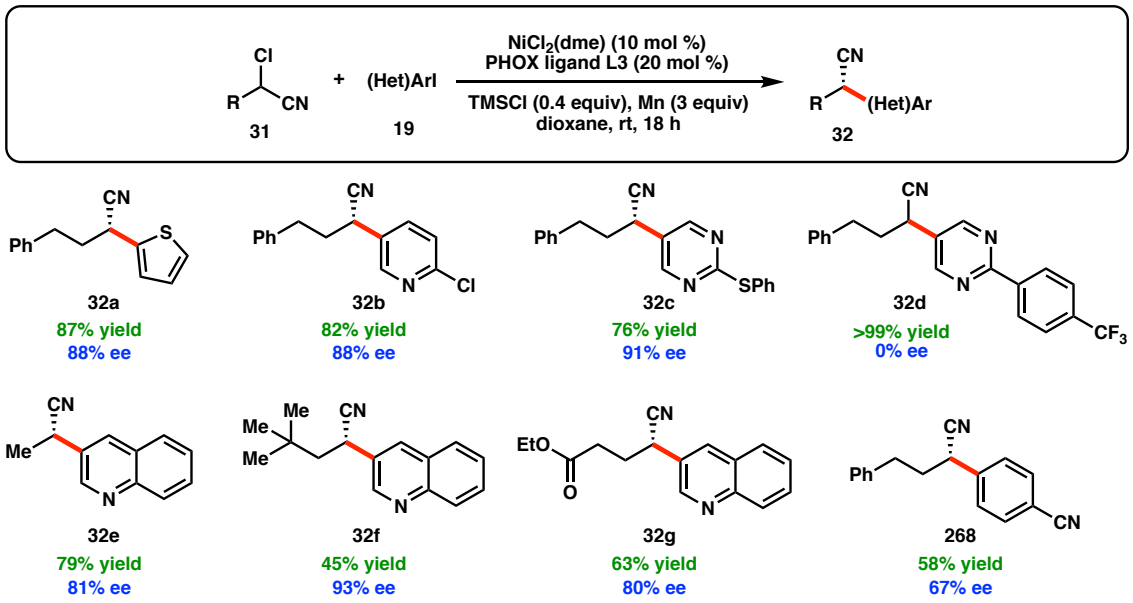

A8.2.2 Initial Data Set

During the initial optimization of the cross-coupling between α-chloronitrile **269** and aryl iodide **270**, an expansive ligand screen revealed that the benzyl PHOX ligand **L16** (readily synthesized from L-phenylalanine) was found to form the product (**268**) in high

yield (86%), albeit in a modest 69% ee. In contrast, the use of other commercially available PHOX ligands (i.e. *i*-Pr, *t*-Bu, Ph) provided the desired product with poor selectivity, and the use of BOX or BiOX ligands delivered **268** in trace yield (Figure A8.5). We hypothesized that the electron-rich nature of the PHOX ligand might be more strongly bound to the nickel center due to the softer nature of the P-donor and accelerate the rate of oxidative addition of aryl iodide **270** to an **L16**·Ni(0) complex.

Figure A8.5 *Effect of chiral PHOX ligand on enantioselectivity.*

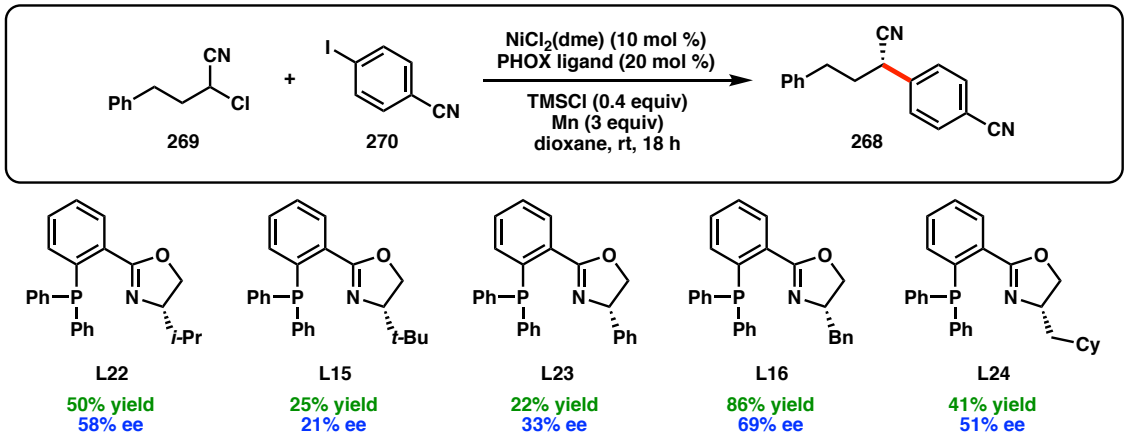

In order to optimize the ee of **268**, a series of 40 novel BnPHOX ligands were synthesized and evaluated in the cross-coupling between **269** and **270** (Figure A8.6). Ultimately, an electron rich phosphine was found to improve the enantioselectivity of **268**. Nevertheless, a significant amount of data was collected during this screening process which was used as the starting point for our parameterization study. With the exception of *ortho*-substitution, tuning arene substitution on the benzyl ring resulted in minimal effects in the observed enantioselectivity, however, altering the electronic nature of the core aryl ring or the phosphine aromatic groups proved more detrimental to enantioselectivity. Empirical observations show that the ee of **268** increases with more electron-rich

phosphines, although steric interactions (e.g. *t*-Bu) might also contribute to selectivity. A Hammett plot of the core substitution provides no correlation, indicating that selectivity is likely due to a complex function of parameters, and thus difficult to predict using empirical observations. Final evaluation of these ligands provided **268** across a significant range of enantioselectivities, a requirement for ligand parameterization studies.

Figure A8.6 *Representative scope of α-chloronitrile and aryl iodide cross-coupling.*

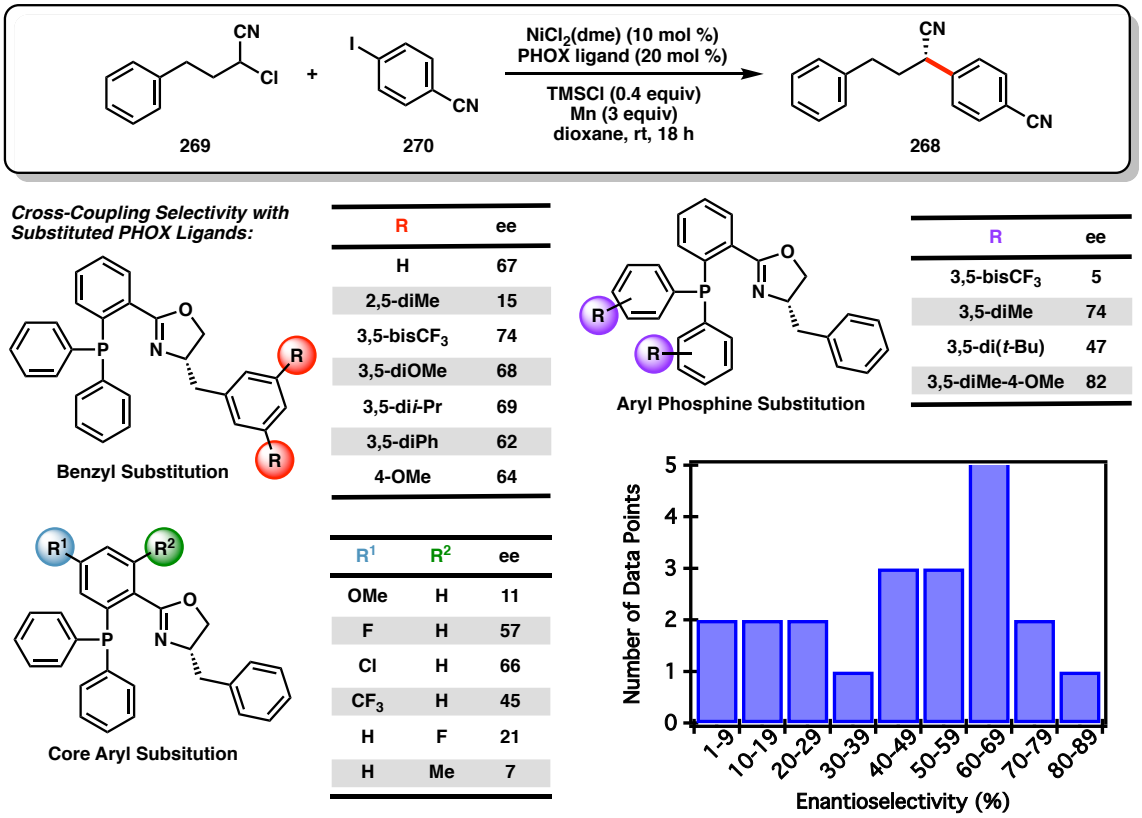

R	ee
H	67
2,5-diMe	15
3,5-bisCF$_3$	74
3,5-diOMe	68
3,5-di*i*-Pr	69
3,5-diPh	62
4-OMe	64

R^1	R^2	ee
OMe	H	11
F	H	57
Cl	H	66
CF$_3$	H	45
H	F	21
H	Me	7

R	ee
3,5-bisCF$_3$	5
3,5-diMe	74
3,5-di(*t*-Bu)	47
3,5-diMe-4-OMe	82

A8.3 EXPERIMENTAL RESULTS

Based on the results in the initial data set, arene substitution studies can be broken down into three categories: 1) benzyl substitution, 2) core aryl substitution, and 3) aryl

phosphine substitution (Figure A8.7). Given the seemingly minimal effects on benzyl substitution, we first elected to study the other two parts of the ligand. Our plan for this project was for first synthesize the electrophiles and ligands necessary to repeat our enantioselectivity measurements in triplicate. Geometry optimizations of the PHOX ligands would then be obtained to conduct single point calculations. Various electronic and structural parameters can be extracted from these calculations and correlated to the enantioselectivity data. Finally, correlations between experimental data and calculated features of the catalyst will allow us to develop a model that can potentially identify features important to the enantioselectivity of this reaction, shed insight into the reaction mechanism, and allow us to predict a more selective PHOX ligand.

Figure A8.7 *Types of substitution on the BnPHOX ligand.*

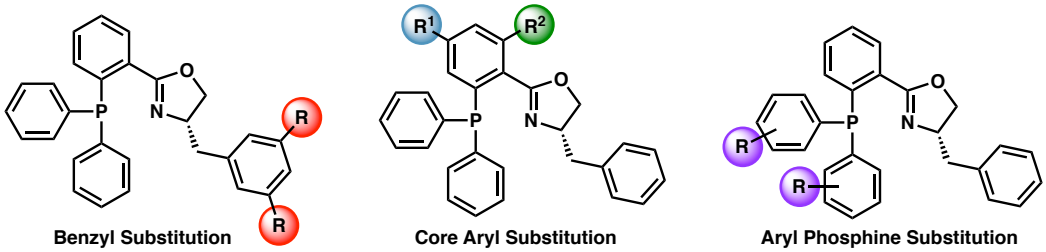

A8.3.1 Ligand Synthesis

We set out to synthesize and characterize a systematic scope of BnPHOX ligands. The PHOX ligand synthesis can be carried out via a number of different routes (Scheme A8.3). *Ortho*-lithiation of the arene (**271**, X=H) followed by substitution with chlorodiphenylphosphine[20] or the substitution of aryl fluorides (**271**, X=F) with a diarylphosphine anion[21] provides the desired ligands (**272**). The most common way PHOX ligands are synthesized is from the aryl bromide (**273**), either through a Grignard addition

into chlorodiarylphosphine,[22] Cu-catalyzed coupling with diarylphosphine,[23] or Cu-catalyzed coupling of diarylphosphine oxide followed by reduction with diphenylsilane.[24]

Scheme A8.3 *Synthesis of PHOX ligands.*

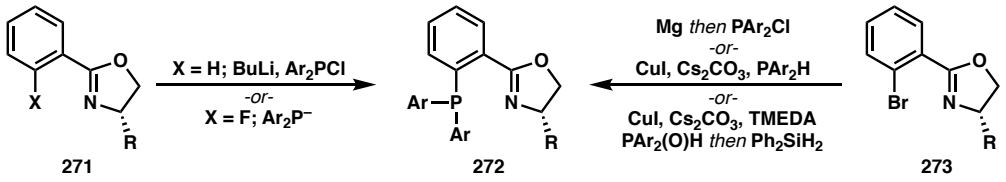

Although the synthesis of aryl bromide core **271** has been previously developed, it required isolation of the intermediate amide or alkyl electrophile. In order to streamline the ligand synthesis, we discovered alternate one-pot conditions (Table 8.1). When amide bond formation was conducted in the presence of NEt_3, the addition of MsCl not only induced

Table A8.1 *Synthesis of PHOX ligands with core substituents.*

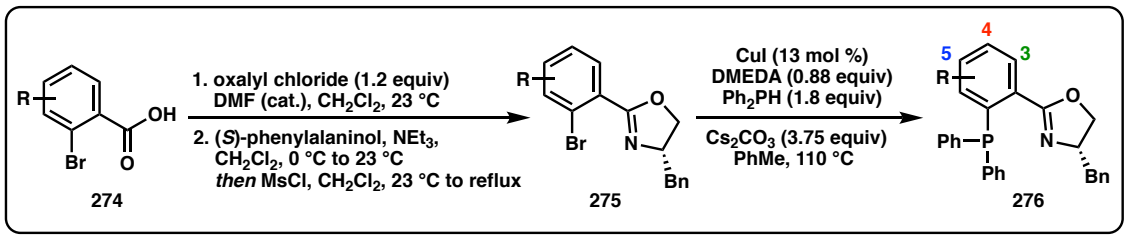

Entry	R	275 yield (g)	275 yield (%)	276 yield (mg)	276 yield (%)	276 = L
1	H	43.0	91	620	49	L16
2	3-Me	4.7	72	830	64	L25
3[a]	3-F	4.8	72	840	64	L26
4	4-OMe	5.1	74	580	43	L27
5	4-Me	5.9	89	410	32	L28
6[a]	4-F	5.3	79	860	66	L29
7[a,b]	4-Cl	3.9	56	620	45	L30
8	4-CF_3	5.2	75	460	31	L31
9	5-OMe	5.6	82	1050	78	L32
10	5-Me	4.7	72	1090	83	L33
11[a]	5-F	5.0	72	510	39	L34
12[a,b]	5-Cl	3.4	49	740	54	L35
13	5-CF_3	4.3	63	600	41	L36

[a]1 equiv Ph_2PH, [b]3.6 equiv $(COCl)_2$

mesylation but also produced the oxazoline product upon heating. Subsequent Cu-catalyzed coupling of diphenyl phosphine proceeded smoothly to afforded a variety of substituted PHOX ligands.

In order to prepare PHOX ligands with various aryl substitution on the phosphine, the corresponding diaryl phosphine oxides were instead coupled to aryl bromide core **274** with the same Cu-catalyzed conditions (Table A8.2). This alleviated the need to prepare the necessary air sensitive diaryl phosphine reagents. Reduction of the triaryl phosphine oxide was achieved by heating **277** in neat diphenyl silane at 140 °C.

Table A8.2 *Synthesis of PHOX ligands with phosphine aryl substituents.*

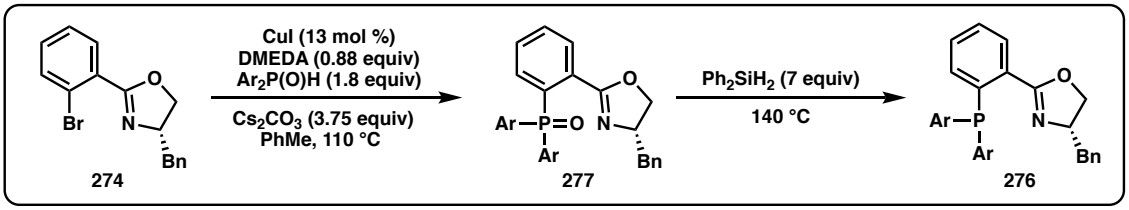

Entry	Ar	277 yield (mg)	277 yield (%)	276 yield (mg)	276 yield (%)	276 = L
1	*p*-Me	330	72	640	78	L37
2	*p*-*t*-Bu	1320	64	600	77	L38
3	*p*-Cl	1550	52	370	76	L39
4	*p*-F	1076	39	410	91	L40
5	*p*-CF_3	770	43	450	81	L41
6	*p*-OMe	950	70	—	—	L42

A8.3.2 Cyclic Voltammetry Studies

With a range of synthesized PHOX ligands, we set out to measure electrochemical properties of synthetic PHOX·$NiCl_2$ complexes to compare their redox properties to the observed enantioselectivity of **268**.[20] Complexation of **L3** with $NiCl_2$(dme) in CH_2Cl_2 at room temperature provides **L3**·$NiCl_2$ complex, which can be characterized by nuclear magnetic resonance (NMR) spectroscopy (Scheme A8.4). The broad ^{1}H NMR signals and

lack of ^{31}P resonance demonstrates the paramagnetic nature of the complex, thus confirming a distorted tetrahedral geometry when in solution. In contrast to **L2**·$NiCl_2$,

Scheme A8.4 *Synthesis of* ***L3***·$NiCl_2$ *complex.*

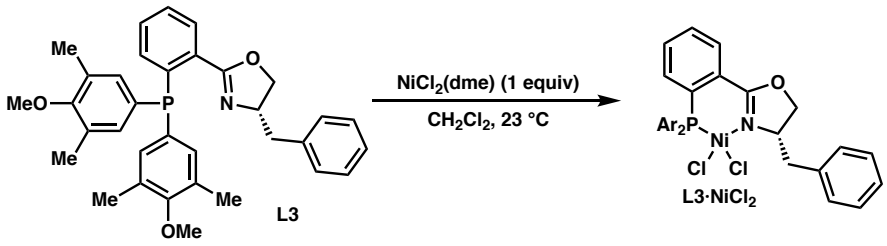

where a square planar geometry would position the chloride anion directly into the ligand arm, **L3**·$NiCl_2$ is not C_2 symmetric and has more rotational freedom to position halides. Although attempts to crystallize **L3**·$NiCl_2$ to obtain solid state geometries were unsuccessful, analogous Ni(II) achiral complexes have been synthesized and reported by X-ray crystallography, which also dictate a tetrahedral geometry.[22] With **L3**·$NiCl_2$ in hand, we sought to analyze its electrochemical properties (Figure A8.8). While the reduction of BOX complex **L2**·$NiCl_2$ demonstrates two one-electron reductions at E_{pc} = –1.60 V (Ni^{II}/Ni^{I}) and E_{pc} = –3.30 V (Ni^{I}/Ni^{0}) vs. Fc/Fc^{+}, the reduction of **L3**·$NiCl_2$ does

Figure A8.8 *Cyclic voltammetry traces for the reduction of Ni complexes.*

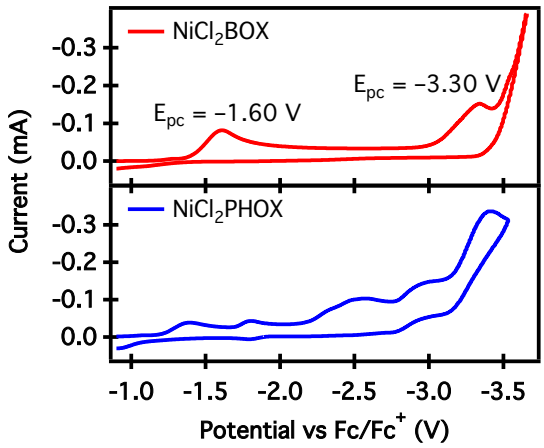

not proceed cleanly. These results support the notion to pursue ligand parametrization studies with computational data given the challenges of obtaining clean redox potentials.

A8.3.3 Iodobenzonitrile Aryl Electrophile

We then investigated the enantioselectivity of **268** with the PHOX ligand series containing core aryl substitution at both the 4-position and the 5-position (**L25**–**L36**). Ligands were evaluated in the cross-coupling reaction until n=5 data points were obtained (Table A8.3); any outliers were removed via the t-test at 95% confidence interval. Although the variation between subsequent runs in the data set was still quite large, we decided to move forward and analyze the results relative to reported Hammett coefficients to determine any trends. Since core aryl substitutions and the ligand are both in *meta* and *para* positions depending if they are in reference to the phosphine or oxazoline, Hammett plot

Table A8.3 *Evaluation of core substitution.*

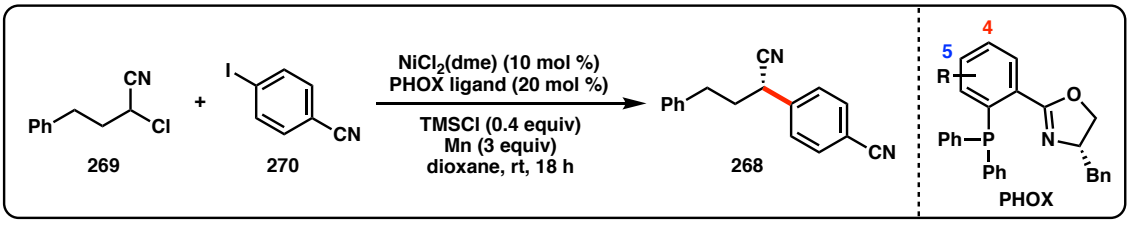

Entry	R	PHOX	ee (%)	ee (%)	ee (%)	ee (%)	ee (%)
1	H	L16	64	64	65	64	63
2	4-OMe	L27	65	66	69	68	67
3	4-Me	L28	65	68	63	65	62
4	4-F	L29	61	60	61	64	64
5	4-Cl	L30	59	57	51	51	56
6	4-CF_3	L31	61	61	61	60	60
7	5-OMe	L32	67	68	69	67	69
8	5-Me	L33	65	68	64	61	62
9	5-F	L34	60	59	63	62	59
10	5-Cl	L35	51	50	54	58	58
11	5-CF_3	L36	35	49	56	44	49

correlations for each combination was plotted (Figure A8.9). Data points collected with 4-position substitution (red data) showed poor Hammett plot correlations when analyzed with respect to the oxazoline (circles, A), however a better trend is observed with respect to the phosphine (triangles, C). In contrast, data points collected with 5-position substitution (blue data) showed poor Hammett plot correlations when analyzed with respect to the phosphine (triangles, D), however a linear trend is observed with respect to the oxazoline (circles, B).

Figure A8.9 *Hammett plot correlations for core aryl substitution.*

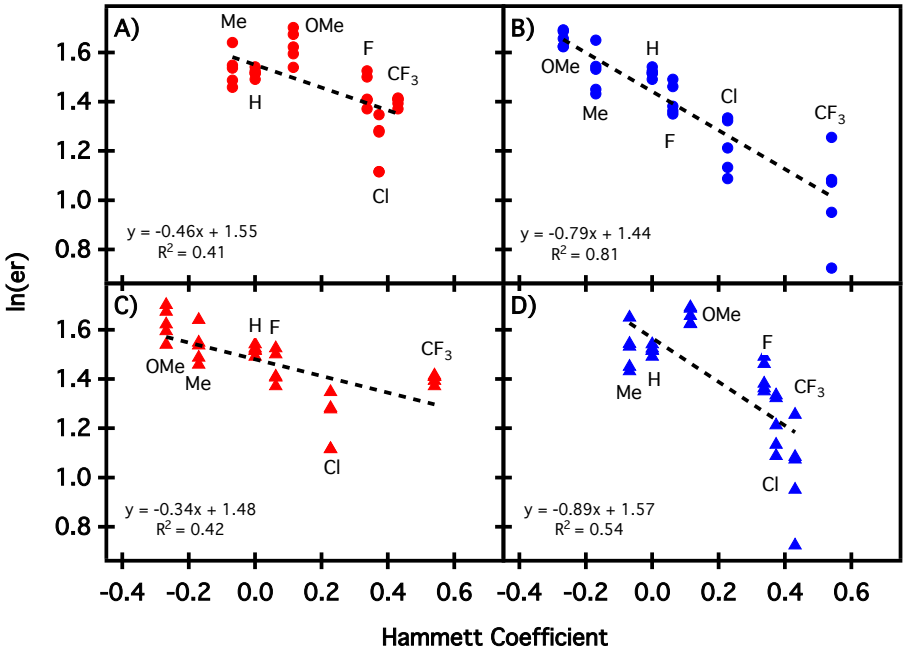

Further attempts to improve the variability in the data, either by pre-stirring the reaction prior to the addition of the α-chloronitrile or by pre-complexing the PHOX ligand with $NiCl_2$(dme) proved unfruitful. After screening a wide variety of reaction conditions we serendipitously discovered the root cause to ee variability: the cross-coupled product **268** is not configurationally stable and racemizes over time in solution, sometimes providing racemic product after 24 hours. This begs the question on the origin of the

observed Hammett trend in Figure A8.9b. *Is the ee variation due to the cross-coupling or due to a racemization process?* A variety of workup conditions were evaluated, yet no solution was found to consistently prevent racemization of **268**. In order to circumvent this issue, other aryl halide electrophiles were used to evaluated their corresponding benzylic nitrile coupling products (**271a–c**) (Figure A8.10). Gratifyingly, pyrimidine **271c,** which is a crystalline product, was found to be configurationally stable in solution over the course of 24 hours.

Figure A8.10 *Racemization studies with various aryl iodide coupling partners.*

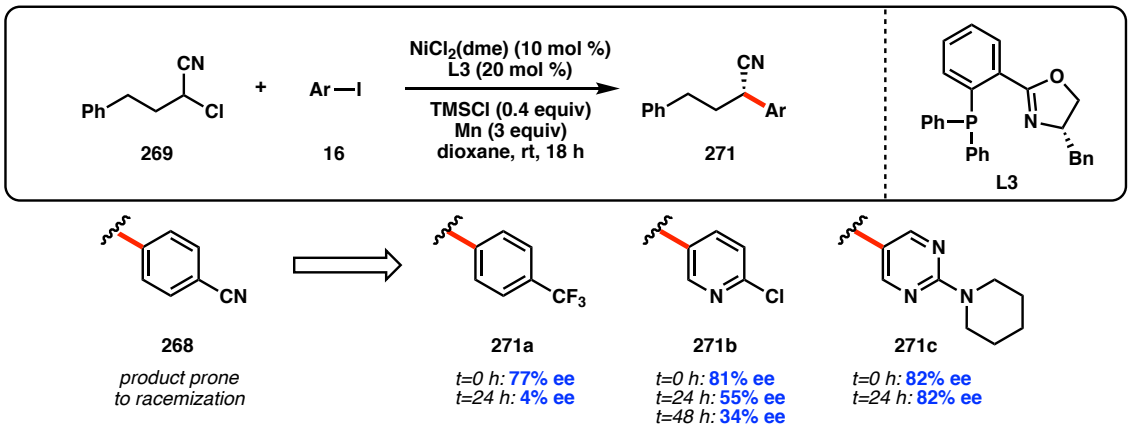

A8.3.4 Pyrimidine Heteroaryl Iodide Electrophile

With a configurationally stable product in hand, we turned to evaluate substitution effects on the diaryl phosphine motif (Table A8.4). In contrast to our initial data set, which showed drastic variability on the ee of **268** when 3,5-disubstituted aryl groups were evaluated on the phosphine portion of the PHOX ligand, *para*-substitution on the arene shows minimal effect on the enantioselectivity of **271c**. Of notable importance is the reproducible enantioselectivity measurements of cross-coupled product **271c**, which provides promising results to utilize this substrate in further screening efforts. However, if

electronic and conformational effects are to be parsed out when combining our experimental results to the computational studies conducted by the Sigman laboratory, larger differences in ee measurements between different ligands are necessary. Further studies are needed to evaluate additional 3,5-disubstituted arenes. Additionally, other parameters need to be evaluated with the new substrate: revisiting the core substitution and investigate other structural groups in the chiral pocket besides benzyl (i.e. Ph, *i*-Pr, *t*-Bu).

Table A8.4 *Evaluation of phosphine aryl substitution.*

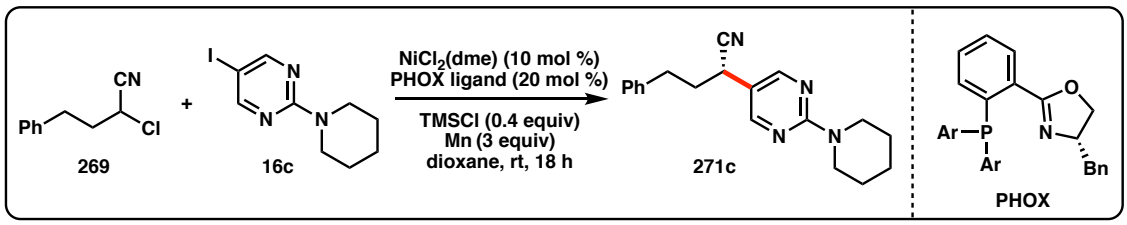

Entry	Ar	ee (%)	ee (%)	ee (%)
1	*p-H*	82	82	82
2	*p*-Me	82	82	82
3	*p-t*-Bu	80	80	81
4	*p*-Cl	83	83	83
5	*p*-F	83	83	83
6	*p*-CF_3	81	81	81

A8.4 CONCLUSIONS AND FUTURE DIRECTIONS

In summary, we have shown that arene substitution on the BnPHOX ligand scaffold effects the enantioselectivity of the cross-coupling reaction between α-chloronitriles and aryl iodides, however the stability of the product plays a critical role in the ability to obtain statistically significant data to conduct a ligand parameterization study. For electron deficient aryl iodides, racemization of the cross-coupling product occurred following reaction workup. Whether or not substitution on the PHOX ligand contributes to the enantioselectivity of the product formation during the cross-coupling or effects

racemization processes has yet to be determined. These results highlight the importance of choosing the appropriate substrate in mechanistic investigations as the use of different substrates may render such studies intractable and probe different aspects of the catalytic cycle. Future studies are ongoing in order to further elucidate the role of the catalyst in altering product racemization as well as determine other ligand parameters that influence the enantiodetermining step for the cross-coupling with configurationally stable pyrimidine products formed with heteroaryl iodides.

A8.5 EXPERIMENTAL SECTION

A8.5.1 Materials and Methods

Unless otherwise stated, reactions were performed under a nitrogen atmosphere using freshly dried solvents. Toluene (PhMe) was dried by passing through activated alumina columns. Trimethylsilyl chloride (TMSCl) and anhydrous dioxane were purchased from Sigma Aldrich and stored in the glovebox. Manganese powder (–325 mesh, 99.3%) was purchased from Alfa Aesar. Nickel(II) chloride dimethoxyethane adduct ($NiCl_2$(dme)) was purchased from Strem. Unless otherwise stated, chemicals were used as received. All reactions were monitored by thin-layer chromatography (TLC) using EMD/Merck silica gel 60 F254 pre-coated plates (0.25 mm) and were visualized by ultraviolet (UV) light or with cerium ammonium molybdate (CAM) staining. Flash column chromatography was performed as described by Still et al.[25] using silica gel (230-400 mesh) purchased from Silicycle. Optical rotations were measured on a Jasco P-2000 polarimeter using a 100 mm path-length cell at 589 nm. ^{1}H and ^{13}C and NMR spectra were recorded on a Bruker Avance

III HD with Prodigy cyroprobe (at 400 MHz and 101 MHz, respectively). NMR data is reported relative to internal $CHCl_3$ (^1H, δ = 7.26), $CDCl_3$ (^{13}C, δ = 77.1), Data for ^1H NMR spectra are reported as follows: chemical shift (δ ppm) (multiplicity, coupling constant (Hz), integration). Multiplicity and qualifier abbreviations are as follows: s = singlet, d = doublet, t = triplet, q = quartet, m = multiplet. IR spectra were recorded on a Perkin Elmer Paragon 1000 spectrometer and are reported in frequency of absorption (cm^{-1}). Analytical chiral SFC was performed with a Mettler SFC supercritical CO_2 chromatography system with Chiralcel AD-H, OD-H, AS-H, OB-H, and OJ-H columns (4.6 mm x 25 cm).

A8.5.2 PHOX Ligand Synthesis

Note: Not all synthesized PHOX ligands are characterized in the following section. The project remains ongoing at the time of thesis submission and current work is being carried out by graduate student Raymond Turro.

General Procedure 1: Oxazoline Formation

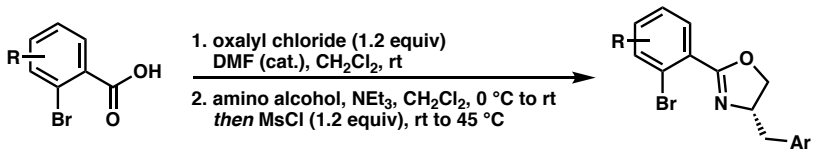

The following procedure was conducted using benchtop solvents and under an air atmosphere. The benzoic acid (1.0 equiv, 20 mmol) was added to a 100 mL round bottom flask equipped with a stir bar and suspended in 35 mL CH_2Cl_2 and 8 drops of DMF. The oxalyl chloride (2 mL, 1.2 equiv, 24 mmol) was added and the reaction was stirred at room temperature until the acid had completely dissolved *and* gas evolution ceased (ca. 1 hour). The reaction was concentrated under reduced pressure to afford the crude acid chloride,

which was used without further purification. The amino alcohol (1.0 equiv, 20 mmol) was added to a 200 mL round bottom flask equipped with a stir bar and dissolved in 35 mL CH_2Cl_2. The triethylamine (11.1 mL, 4.0 equiv, 80 mmol) was added and the solution was cooled to 0 °C. The acid chloride was dissolved in 35 mL CH_2Cl_2 and slowly added to the amino alcohol. The reaction was warmed to room temperature and stirred for 15 minutes before the addition of methanesulfonyl chloride (1.9 mL, 1.2 equiv, 24 mmol). The reaction stirred at room temperature for 15 minutes before being heated to reflux (45 °C) and continued to stir overnight. The reaction was cooled to room temperature before being quenched with aq. NH_4Cl (20 mL) and water (60 mL). The layers were separated and the aqueous layer was extracted with CH_2Cl_2 (2 x 50 mL). The combined organic layers were dried with Na_2SO_4, filtered, and concentrated under reduced pressure. The crude residue was purified by column chromatography (silica, EtOAc/hexane) to afford the desired product.

(*S*)-4-benzyl-2-(2-bromophenyl)-4,5-dihydrooxazole (275a)

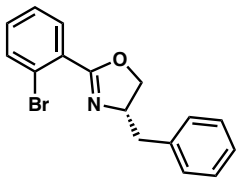

Prepared from 2-bromobenzoic acid (30.15 g, 150 mmol) and (*S*)-phenylalaninol (22.68 g, 150 mmol) following General Procedure 1 except 1.1 equiv (14.15 mL, 165 mmol) of oxalyl chloride was used. The crude residue was purified filtering over a plug of silica and eluting with 40% EtOAc/hexane to yield 43.04 g (91% yield) of **275a** as a light yellow-green oil. $[\boldsymbol{a}]_{\boldsymbol{D}}^{\mathbf{25}}$ = –11° (c = 1.0, $CHCl_3$). **^{1}H NMR (400 MHz, $CDCl_3$):** δ 7.69 – 7.61 (m, 2H), 7.36 – 7.22 (m, 7H), 4.65 (dddd, *J* = 9.4, 8.4, 7.3, 5.4 Hz, 1H), 4.38 (dd, *J* = 9.4, 8.5 Hz, 1H), 4.18 (dd, *J* = 8.5, 7.3 Hz, 1H), 3.25 (dd, *J* = 13.8, 5.3 Hz, 1H), 2.82 (dd, *J* = 13.7, 8.4 Hz, 1H). **^{13}C NMR**

(101 MHz, $CDCl_3$): δ 163.4, 137.8, 133.8, 131.7, 131.3, 129.8, 129.4, 128.6, 127.1, 126.6, 121.9, 71.9, 68.2, 41.6.

(*S*)-4-benzyl-2-(2-bromo-6-methylphenyl)-4,5-dihydrooxazole (275b)

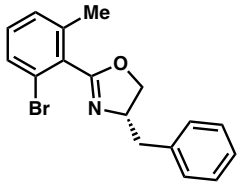

Prepared from 2-bromo-6-methylbenzoic acid (4.30 g, 20 mmol) and (*S*)-phenylalaninol (3.02 g, 20 mmol) following General Procedure 1. The crude residue was purified by column chromatography (silica, 5 to 20% EtOAc/hexane) to yield 4.05 g (72% yield) of **275b** as a light yellow oil. $[\boldsymbol{\alpha}]_{\boldsymbol{D}}^{\mathbf{25}}$ = –19° (c = 1.0, $CHCl_3$). **^{1}H NMR (400 MHz, $CDCl_3$):** δ 7.45 – 7.39 (m, 1H), 7.37 – 7.27 (m, 4H), 7.27 – 7.21 (m, 1H), 7.19 – 7.12 (m, 2H), 4.67 (dddd, *J* = 9.4, 8.4, 7.4, 5.8 Hz, 1H), 4.41 (dd, *J* = 9.4, 8.5 Hz, 1H), 4.20 (dd, *J* = 8.5, 7.4 Hz, 1H), 3.27 (dd, *J* = 13.8, 5.8 Hz, 1H), 2.85 (dd, *J* = 13.8, 8.4 Hz, 1H), 2.34 (d, *J* = 0.6 Hz, 3H). **^{13}C NMR (101 MHz, $CDCl_3$):** δ 163.1, 139.4, 138.0, 130.9, 130.8, 130.0, 129.4, 129.0, 128.7, 126.6, 122.4, 72.1, 68.4, 41.8, 20.0.

(*S*)-4-benzyl-2-(2-bromo-6-fluorophenyl)-4,5-dihydrooxazole (275c)

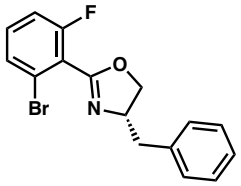

Prepared from 2-bromo-6-fluorobenzoic acid (4.36 g, 20 mmol) and (*S*)-phenylalaninol (3.02 g, 20 mmol) following General Procedure 1. The crude residue was purified by column chromatography (silica, 5 to 20% EtOAc/hexane) to yield 4.81 g (72% yield) of **275c** as a light yellow oil. $[\boldsymbol{\alpha}]_{\boldsymbol{D}}^{\mathbf{25}}$ = –21° (c = 1.0, $CHCl_3$). **^{1}H NMR (400 MHz, $CDCl_3$):** δ 7.41 (dt, *J* = 8.1, 1.0 Hz, 1H), 7.37 – 7.21 (m, 6H), 7.09 (td, *J* = 8.6, 1.1 Hz, 1H), 4.67 (dddd, *J* = 9.5, 8.4, 7.3, 5.9 Hz, 1H), 4.43 (dd, *J* = 9.4, 8.4 Hz, 1H), 4.21 (dd, *J* = 8.5, 7.4 Hz, 1H), 3.26 (dd, *J* = 13.8, 5.9 Hz,

1H), 2.84 (dd, J = 13.8, 8.3 Hz, 1H). **^{13}C NMR (101 MHz, $CDCl_3$):** δ 160.8 (d, J_{C-F} = 254.9 Hz), 159.1, 137.8, 132.2 (d, J_{C-F} = 9.1 Hz), 129.3, 128.7, 128.6 (d, J_{C-F} = 3.6 Hz), 126.6, 123.1 (d, J_{C-F} = 3.3 Hz), 120.2 (d, J_{C-F} = 18.6 Hz), 114.9 (d, J_{C-F} = 21.5 Hz), 72.4, 68.5, 41.7.

(*S*)-4-benzyl-2-(2-bromo-4-methoxyphenyl)-4,5-dihydrooxazole (275d)

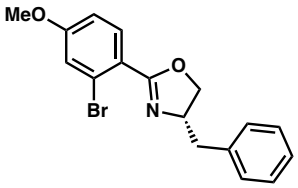

Prepared from 2-bromo-4-methoxybenzoic acid (4.62 g, 20 mmol) and (*S*)-phenylalaninol (3.02 g, 20 mmol) following General Procedure 1. The crude residue was purified by column chromatography (silica, 5 to 20% EtOAc/hexane) to yield 5.65 g (82% yield) of **275d** as a light yellow oil which solidified in the freezer to give a white waxy solid. $[\boldsymbol{a}]_{\boldsymbol{D}}^{\mathbf{25}}$ = +3° (c = 1.0, $CHCl_3$) (*Note: This aryl bromide core has + optical rotation*). **^{1}H NMR (400 MHz, $CDCl_3$):** δ 7.65 (d, J = 8.7 Hz, 1H), 7.35 – 7.20 (m, 5H), 7.18 (d, J = 2.5 Hz, 1H), 6.86 (dd, J = 8.7, 2.6 Hz, 1H), 4.61 (dddd, J = 9.3, 8.5, 7.1, 5.2 Hz, 1H), 4.33 (dd, J = 9.3, 8.5 Hz, 1H), 4.14 (dd, J = 8.5, 7.2 Hz, 1H), 3.82 (s, 3H), 3.24 (dd, J = 13.7, 5.2 Hz, 1H), 2.78 (dd, J = 13.7, 8.6 Hz, 1H). **^{13}C NMR (101 MHz, $CDCl_3$):** δ 163.2, 161.5, 138.0, 132.5, 129.4, 128.6, 126.6, 122.8, 121.8, 119.3, 113.2, 71.7, 68.2, 55.7, 41.8.

(*S*)-4-benzyl-2-(2-bromo-4-methylphenyl)-4,5-dihydrooxazole (275e)

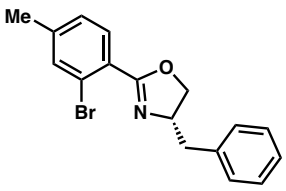

Prepared from 2-bromo-4-methylbenzoic acid (4.30 g, 20 mmol) and (*S*)-phenylalaninol (3.02 g, 20 mmol) following General Procedure 1. The crude residue was purified by column chromatography (silica, 5 to 20% EtOAc/hexane) to yield 4.72 g (72% yield) of **275e** as a

light yellow oil. $[a]_D^{25}$ = –3° (c = 1.0, $CHCl_3$). **^{1}H NMR (400 MHz, $CDCl_3$):** δ 7.57 (d, *J* = 7.9 Hz, 1H), 7.47 (dd, *J* = 1.7, 0.8 Hz, 1H), 7.35 – 7.21 (m, 5H), 7.13 (ddd, *J* = 8.0, 1.7, 0.8 Hz, 1H), 4.63 (dddd, *J* = 9.4, 8.5, 7.2, 5.2 Hz, 1H), 4.35 (dd, *J* = 9.4, 8.5 Hz, 1H), 4.16 (dd, *J* = 8.5, 7.2 Hz, 1H), 3.25 (dd, *J* = 13.7, 5.2 Hz, 1H), 2.79 (dd, *J* = 13.7, 8.5 Hz, 1H), 2.35 (d, *J* = 0.7 Hz, 3H). **^{13}C NMR (101 MHz, $CDCl_3$):** δ 163.4, 142.4, 137.9, 134.4, 131.2, 129.4, 128.6, 128.0, 126.8, 126.6, 121.7, 71.8, 68.2, 41.7, 21.1.

(*S*)-4-benzyl-2-(2-bromo-4-fluorophenyl)-4,5-dihydrooxazole (275f)

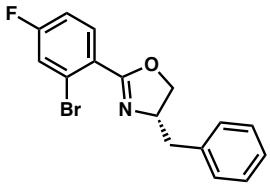

Prepared from 2-bromo-4-fluorobenzoic acid (4.36 g, 20 mmol) and (*S*)-phenylalaninol (3.02 g, 20 mmol) following General Procedure 1. The crude residue was purified by column chromatography (silica, 5 to 20% EtOAc/hexane) to yield 4.76 g (71% yield) of **275f** as a light yellow oil. $[a]_D^{25}$ = –13° (c = 1.0, $CHCl_3$). **^{1}H NMR (400 MHz, $CDCl_3$):** δ 7.69 (dd, *J* = 8.7, 6.0 Hz, 1H), 7.39 (dd, *J* = 8.3, 2.6 Hz, 1H), 7.35 – 7.21 (m, 5H), 7.06 (ddd, *J* = 8.7, 7.8, 2.6 Hz, 1H), 4.64 (dddd, *J* = 9.4, 8.4, 7.3, 5.4 Hz, 1H), 4.37 (dd, *J* = 9.4, 8.5 Hz, 1H), 4.17 (dd, *J* = 8.5, 7.3 Hz, 1H), 3.23 (dd, *J* = 13.7, 5.3 Hz, 1H), 2.80 (dd, *J* = 13.8, 8.4 Hz, 1H). **^{13}C NMR (101 MHz, $CDCl_3$):** δ 163.3 (d, $J_{C\text{-}F}$ = 255.2 Hz), 162.6, 137.7, 132.9 (d, $J_{C\text{-}F}$ = 9.1 Hz), 129.4, 128.7, 126.69, 126.1 (d, $J_{C\text{-}F}$ = 3.6 Hz), 122.7 (d, $J_{C\text{-}F}$ = 9.8 Hz), 121.4 (d, $J_{C\text{-}F}$ = 24.6 Hz), 114.6 (d, $J_{C\text{-}F}$ = 21.3 Hz), 72.0, 68.3, 41.7.

(*S*)-4-benzyl-2-(2-bromo-4-chlorophenyl)-4,5-dihydrooxazole (275g)

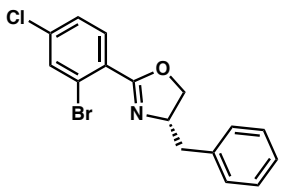

Prepared from 2-bromo-4-chlorobenzoic acid (4.71 g, 20 mmol) and (*S*)-phenylalaninol (3.02 g, 20 mmol) following General Procedure 1 except 3.6 equiv (6.2 mL, 72 mmol) of oxalyl

chloride was used. The crude residue was purified by column chromatography (silica, 5 to 20% EtOAc/hexane) to yield 3.45 g (49% yield) of **275g** as a light yellow oil. $[\boldsymbol{a}]_D^{25}$ = –3° (c = 1.0, $CHCl_3$). **^{1}H NMR (400 MHz, $CDCl_3$):** δ 7.67 (d, *J* = 2.1 Hz, 1H), 7.62 (d, *J* = 8.4 Hz, 1H), 7.35 – 7.22 (m, 6H), 4.64 (dddd, *J* = 9.4, 8.3, 7.2, 5.3 Hz, 1H), 4.37 (dd, *J* = 9.4, 8.5 Hz, 1H), 4.17 (dd, *J* = 8.5, 7.3 Hz, 1H), 3.23 (dd, *J* = 13.8, 5.3 Hz, 1H), 2.80 (dd, *J* = 13.8, 8.3 Hz, 1H). **^{13}C NMR (101 MHz, $CDCl_3$):** δ 162.6, 137.7, 137.1, 133.7, 132.2, 129.5, 128.7, 128.2, 127.5, 126.7, 122.5, 72.0, 68.3, 41.6.

(*S*)-4-benzyl-2-(2-bromo-4-(trifluoromethyl)phenyl)-4,5-dihydrooxazole (275h)

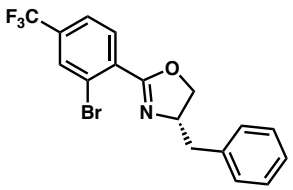

Prepared from 2-bromo-4-(trifluoromethyl)benzoic acid (4.84 g, 18 mmol) and (*S*)-phenylalaninol (2.72 g, 18 mmol) following General Procedure 1. The crude residue was purified by column chromatography (silica, 5 to 20% EtOAc/hexane) to yield 3.34 g (48% yield) of **275h** as a light yellow oil which solidified in the freezer to give a white crystalline solid. $[\boldsymbol{a}]_D^{25}$ = –14° (c = 1.0, $CHCl_3$). **^{1}H NMR (400 MHz, $CDCl_3$):** δ 7.91 (dd, *J* = 1.6, 0.8 Hz, 1H), 7.78 (dd, *J* = 8.2, 1.0 Hz, 1H), 7.60 (ddd, *J* = 8.1, 1.7, 0.8 Hz, 1H), 7.36 – 7.22 (m, 6H), 4.68 (dddd, *J* = 9.4, 8.2, 7.3, 5.4 Hz, 1H), 4.42 (dd, *J* = 9.5, 8.5 Hz, 1H), 4.21 (dd, *J* = 8.5, 7.3 Hz, 1H), 3.23 (dd, *J* = 13.8, 5.4 Hz, 1H), 2.84 (dd, *J* = 13.8, 8.2 Hz, 1H). **^{13}C NMR (101 MHz, $CDCl_3$):** δ 162.4, 137.6, 133.6 (q, $J_{C\text{-}F}$ = 33.4 Hz), 133.3 (q, $J_{C\text{-}F}$ = 1.1 Hz), 131.9, 130.9 (q, $J_{C\text{-}F}$ = 3.9 Hz), 129.5, 128.7, 126.8, 124.1 (q, $J_{C\text{-}F}$ = 3.6 Hz), 122.9 (q, $J_{C\text{-}F}$ = 273.1 Hz), 122.4, 72.2, 68.4, 41.6.

(*S*)-4-benzyl-2-(2-bromo-5-methoxyphenyl)-4,5-dihydrooxazole (275i)

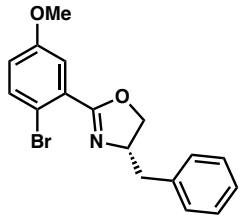

Prepared from 2-bromo-5-methoxybenzoic acid (4.62 g, 20 mmol) and (*S*)-phenylalaninol (3.02 g, 20 mmol) following General Procedure 1. The crude residue was purified by column chromatography (silica, 5 to 20% EtOAc/hexane) to yield 5.05 g (73% yield) of **275i** as a light yellow oil. $[\boldsymbol{a}]_{\boldsymbol{D}}^{\mathbf{25}}$ = –4° (c = 1.0, $CHCl_3$). **^{1}H NMR (400 MHz, $CDCl_3$):** δ 7.50 (d, *J* = 8.8 Hz, 1H), 7.36 – 7.21 (m, 5H), 7.18 (d, *J* = 3.1 Hz, 1H), 6.85 (dd, *J* = 8.9, 3.1 Hz, 1H), 4.64 (dddd, *J* = 9.4, 8.4, 7.2, 5.2 Hz, 1H), 4.38 (dd, *J* = 9.4, 8.5 Hz, 1H), 4.18 (dd, *J* = 8.5, 7.3 Hz, 1H), 3.80 (s, 3H), 3.25 (dd, *J* = 13.8, 5.2 Hz, 1H), 2.81 (dd, *J* = 13.8, 8.4 Hz, 1H). **^{13}C NMR (101 MHz, $CDCl_3$):** δ 163.4, 158.6, 137.8, 134.7, 130.5, 129.5, 128.7, 126.7, 118.5, 116.1, 112.3, 72.0, 68.3, 55.7, 41.7.

(*S*)-4-benzyl-2-(2-bromo-5-methylphenyl)-4,5-dihydrooxazole (275j)

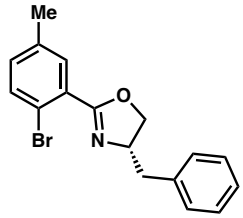

Prepared from 2-bromo-5-methylbenzoic acid (4.30 g, 20 mmol) and (*S*)-phenylalaninol (3.02 g, 20 mmol) following General Procedure 1. The crude residue was purified by column chromatography (silica, 5 to 20% EtOAc/hexane) to yield 5.43 g (82% yield) of **275j** as a light yellow oil. $[\boldsymbol{a}]_{\boldsymbol{D}}^{\mathbf{25}}$ = –5° (c = 1.0, $CHCl_3$). **^{1}H NMR (400 MHz, $CDCl_3$):** δ 7.50 (d, *J* = 8.2 Hz, 1H), 7.49 – 7.47 (m, 1H), 7.35 – 7.21 (m, 5H), 7.11 – 7.07 (m, 1H), 4.63 (dddd, *J* = 9.4, 8.5, 7.3, 5.2 Hz, 1H), 4.37 (dd, *J* = 9.4, 8.5 Hz, 1H), 4.18 (dd, *J* = 8.5, 7.3 Hz, 1H), 3.25 (dd, *J* = 13.7, 5.2 Hz, 1H), 2.80 (dd, *J* = 13.8, 8.5 Hz, 1H), 2.31 (d, *J* = 0.8 Hz, 3H). **^{13}C NMR (101 MHz, $CDCl_3$):** δ 163.7, 137.9, 137.2, 133.6, 132.6, 132.0, 129.5, 129.4, 128.7, 126.6, 118.4, 72.0, 68.2, 41.7, 20.8.

(*S*)-4-benzyl-2-(2-bromo-5-fluorophenyl)-4,5-dihydrooxazole (275k)

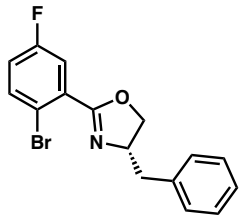

Prepared from 2-bromo-5-fluorobenzoic acid (4.36 g, 20 mmol) and (*S*)-phenylalaninol (3.02 g, 20 mmol) following General Procedure 1. The crude residue was purified by column chromatography (silica, 5 to 20% EtOAc/hexane) to yield 5.10 g (76% yield) of **275k** as a light yellow oil. $[\boldsymbol{\alpha}]_{\boldsymbol{D}}^{\mathbf{25}}$ = –13° (c = 1.0, $CHCl_3$). **^{1}H NMR (400 MHz, $CDCl_3$):** δ 7.60 (dd, *J* = 8.9, 5.1 Hz, 1H), 7.41 (dd, *J* = 8.9, 3.1 Hz, 1H), 7.36 – 7.22 (m, 5H), 7.02 (ddd, *J* = 8.8, 7.7, 3.1 Hz, 1H), 4.66 (dddd, *J* = 9.4, 8.3, 7.3, 5.4 Hz, 1H), 4.39 (dd, *J* = 9.4, 8.5 Hz, 1H), 4.19 (dd, *J* = 8.5, 7.3 Hz, 1H), 3.23 (dd, *J* = 13.7, 5.4 Hz, 1H), 2.82 (dd, *J* = 13.8, 8.3 Hz, 1H). **^{13}C NMR (101 MHz, $CDCl_3$):** δ 162.3 (d, $J_{C\text{-}F}$ = 2.3 Hz), 161.4 (d, $J_{C\text{-}F}$ = 248.1 Hz), 137.6, 135.4 (d, $J_{C\text{-}F}$ = 7.8 Hz), 131.3 (d, $J_{C\text{-}F}$ = 8.1 Hz), 129.4, 128.7, 126.7, 119.0 (d, $J_{C\text{-}F}$ = 22.3 Hz), 118.6 (d, $J_{C\text{-}F}$ *J* = 24.7 Hz), 116.3 (d, $J_{C\text{-}F}$ = 3.6 Hz), 72.1, 68.3, 41.6.

(*S*)-4-benzyl-2-(2-bromo-5-chlorophenyl)-4,5-dihydrooxazole (275l)

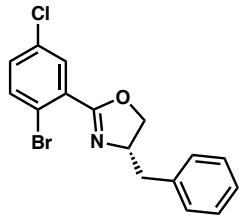

Prepared from 2-bromo-5-chlorobenzoic acid (4.71 g, 20 mmol) and (*S*)-phenylalaninol (3.02 g, 20 mmol) following General Procedure 1 except 3.6 equiv (6.2 mL, 72 mmol) of oxalyl chloride was used. The crude residue was purified by column chromatography (silica, 5 to 20% EtOAc/hexane) to yield 3.89 g (56% yield) of **275l** as a light yellow oil. $[\boldsymbol{\alpha}]_{\boldsymbol{D}}^{\mathbf{25}}$ = –8° (c = 1.0, $CHCl_3$). **^{1}H NMR (400 MHz, $CDCl_3$):** δ 7.66 (d, *J* = 2.6 Hz, 1H), 7.56 (d, *J* = 8.6 Hz, 1H), 7.36 – 7.30 (m, 2H), 7.29 – 7.22 (m, 4H), 4.65 (dddd, *J* = 9.4, 8.2, 7.3, 5.3 Hz, 1H), 4.39 (dd, *J* = 9.4, 8.5 Hz, 1H), 4.18 (dd, *J* = 8.5, 7.3 Hz, 1H), 3.23 (dd, *J* = 13.7, 5.3 Hz, 1H), 2.81 (dd, *J* =

13.8, 8.3 Hz, 1H). **^{13}C NMR (101 MHz, $CDCl_3$):** δ 162.3, 137.6, 135.1, 133.4, 131.8, 131.4, 131.2, 129.5, 128.7, 126.8, 119.9, 72.2, 68.4, 41.6.

(*S*)-4-benzyl-2-(2-bromo-5-(trifluoromethyl)phenyl)-4,5-dihydrooxazole (275m)

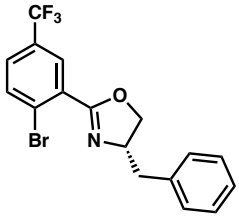

Prepared from 2-bromo-5-(trifluoromethyl)benzoic acid (4.84 g, 18 mmol) and (*S*)-phenylalaninol (2.72 g, 18 mmol) following General Procedure 1. The crude residue was purified by column chromatography (silica, 5 to 20% EtOAc/hexane) to yield 5.20 g (75% yield) of **275m** as a light yellow oil. $[\boldsymbol{a}]_D^{25}$ = –12° (c = 1.0, $CHCl_3$). **^{1}H NMR (400 MHz, $CDCl_3$):** δ 7.93 (d, *J* = 2.3 Hz, 1H), 7.78 (dd, *J* = 8.4, 1.0 Hz, 1H), 7.52 (ddt, *J* = 8.4, 2.4, 0.7 Hz, 1H), 7.36 – 7.23 (m, 5H), 4.69 (dddd, *J* = 9.4, 8.2, 7.3, 5.3 Hz, 1H), 4.42 (dd, *J* = 9.5, 8.5 Hz, 1H), 4.22 (dd, *J* = 8.6, 7.3 Hz, 1H), 3.24 (dd, *J* = 13.8, 5.3 Hz, 1H), 2.85 (dd, *J* = 13.8, 8.2 Hz, 1H). **^{13}C NMR (101 MHz, $CDCl_3$):** δ 162.2, 137.5, 134.7, 130.7, 129.9 (q, J_{C-F} = 33.5 Hz), 129.5, 128.7, 128.4 (q, J_{C-F} = 3.9 Hz), 128.1 (q, J_{C-F} = 3.6 Hz), 126.8, 126.0 (q, J_{C-F} = 1.6 Hz), 123.5 (q, J_{C-F} = 272.4 Hz), 72.2, 68.4, 41.5.

General Procedure 2: Ullman Coupling with Phosphine

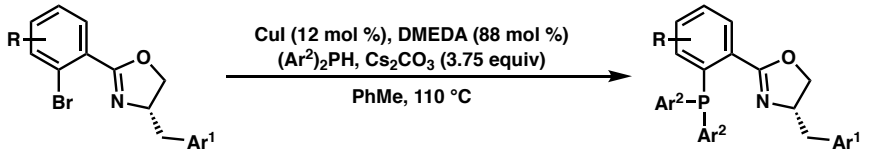

The following procedure was conducted under an N_2 atmosphere in a glovebox. The CuI (74 mg, 0.39 mmol, 0.13 equiv) was added to a 150 mL heavy wall pressure flask equipped with a stir bar and dissolved in 20 mL of anhydrous toluene. The DMEDA (375 μL, 2.64

mmol, 0.88 equiv) and diarylphosphine (3.0-5.4 mmol, 1.0-1.8 equiv) was added and stirred for 10 minutes. The Cs_2CO_3 (3.66 g, 11.25 mmol, 3.75 equiv) was added, followed by the aryl bromide (3.0 mmol, 1.0 equiv) dissolved in 10 mL of toluene. The flask was sealed with a screw cap fitted with a viton o-ring, removed from the glovebox, and stirred overnight at 110 °C. The reaction was then cooled to room temperature and filtered over a pad of celite, eluting with CH_2Cl_2. The crude mixture was concentrated under reduced pressure and purified by column chromatography under a flow of N_2 to afford the desired product.

(*S*)-4-benzyl-2-(2-(diphenylphosphaneyl)phenyl)-4,5-dihydrooxazole (L16)

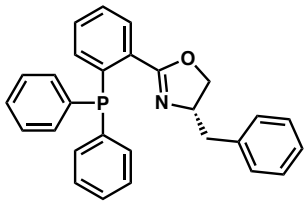

Prepared from (*S*)-4-benzyl-2-(2-bromophenyl)-4,5-dihydro-oxazole **275a** (949 mg, 3.0 mmol, 1.0 equiv) and diphenylphosphine (940 μL, 1.00 g, 5.4 mmol, 1.8 equiv) following General Procedure 2. The reaction stirred overnight for 24 hours. The crude residue was purified by column chromatography (silica, 0 to 3% Et_2O/DCM) under a flow of N_2 to yield 622 mg (49% yield) of **L16** as a sticky white solid. $[\boldsymbol{a}]_{\boldsymbol{D}}^{\mathbf{25}}$ = +28° (c = 1.0, $CHCl_3$). **^{1}H NMR (400 MHz, $CDCl_3$):** δ 7.88 (ddd, *J* = 7.5, 3.5, 1.5 Hz, 1H), 7.42 – 7.23 (m, 14H), 7.22 – 7.16 (m, 1H), 7.12 – 7.05 (m, 2H), 6.87 (ddd, *J* = 7.6, 4.3, 1.3 Hz, 1H), 4.36 (tdd, *J* = 9.3, 7.4, 5.1 Hz, 1H), 4.04 (dd, *J* = 9.3, 8.4 Hz, 1H), 3.78 (dd, *J* = 8.4, 7.4 Hz, 1H), 2.93 (dd, *J* = 13.8, 5.1 Hz, 1H), 2.11 (dd, *J* = 13.8, 9.2 Hz, 1H). **^{13}C NMR (101 MHz, $CDCl_3$):** δ 163.9 (d, $J_{C\text{-}P}$ = 2.9 Hz), [Ar region: 139.02, 138.77, 138.18, 137.94, 137.90, 137.82, 137.81, 134.54, 134.33, 133.98, 133.78, 133.55, 133.53, 131.61, 131.43,

130.52, 129.96, 129.94, 129.09, 128.77, 128.61, 128.56, 128.48, 128.45, 128.40, 127.96, 126.31], 71.5, 68.0, 41.1.

(*S*)-4-benzyl-2-(2-(diphenylphosphaneyl)-6-methylphenyl)-4,5-dihydrooxazole (L25)

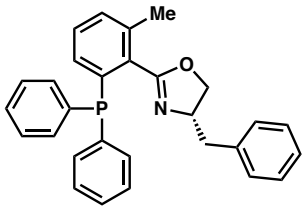

Prepared from (*S*)-4-benzyl-2-(2-bromo-6-methylphenyl)-4,5-dihydrooxazole **275b** (991 mg, 3.0 mmol, 1.0 equiv) and diphenylphosphine (940 μL, 1.00 g, 5.4 mmol, 1.8 equiv) following General Procedure 2. The reaction stirred overnight for 24 hours. The crude residue was purified by column chromatography (silica, 0 to 3% Et_2O/DCM) under a flow of N_2 to yield 834 mg (64% yield) of **L25** as a sticky white solid. $[\boldsymbol{a}]_{\boldsymbol{D}}^{\mathbf{25}}$ = +8° (c = 1.0, $CHCl_3$). **^{1}H NMR (400 MHz, $CDCl_3$):** δ 7.42 – 7.30 (m, 10H), 7.30 – 7.24 (m, 2H), 7.24 – 7.12 (m, 5H), 6.88 – 6.79 (m, 1H), 4.47 (ddddd, *J* = 9.4, 8.5, 7.5, 5.7, 0.9 Hz, 1H), 4.10 (dd, *J* = 9.4, 8.4 Hz, 1H), 3.95 (dd, *J* = 8.4, 7.5 Hz, 1H), 3.16 (dd, *J* = 13.8, 5.7 Hz, 1H), 2.65 (dd, *J* = 13.8, 8.6 Hz, 1H), 2.37 (s, 3H). **^{13}C NMR (101 MHz, $CDCl_3$):** δ 163.8 (d, $J_{C\text{-}P}$ = 2.5 Hz), [Ar region: 138.45, 137.73, 137.57, 137.55, 137.50, 137.43, 137.40, 137.29, 134.60, 134.32, 134.11, 134.05, 133.91, 133.85, 131.30, 130.72, 129.63, 129.29, 128.71, 128.60, 128.56, 128.49, 126.44], 71.6, 68.5, 41.7, 20.0 (d, $J_{C\text{-}P}$ = 1.6 Hz).

(*S*)-4-benzyl-2-(2-(diphenylphosphaneyl)-6-fluorophenyl)-4,5-dihydrooxazole (L26)

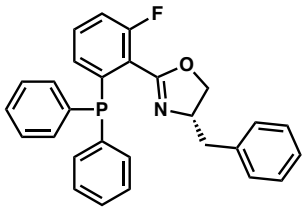

Prepared from (*S*)-4-benzyl-2-(2-bromo-6-fluorophenyl)-4,5-dihydrooxazole **275c** (1.00 g, 3.0 mmol, 1.0 equiv) and diphenylphosphine (522 μL, 559 mg, 3.0 mmol, 1.0 equiv) following General Procedure 2. The reaction stirred overnight for 12 hours. The crude

residue was purified by column chromatography (silica, 5 to 15% EtOAc/hexane) under a flow of N_2 to yield 840 mg (64% yield) of **L26** as a white solid. $[\boldsymbol{a}]_{\boldsymbol{D}}^{\mathbf{25}}$ = +20° (c = 1.0, $CHCl_3$). **^{1}H NMR (400 MHz, $CDCl_3$):** δ 7.40 – 7.33 (m, 10H), 7.31 – 7.24 (m, 3H), 7.23 – 7.17 (m, 1H), 7.16 – 7.12 (m, 2H), 7.09 (ddt, *J* = 9.3, 8.4, 0.9 Hz, 1H), 6.71 (ddd, *J* = 7.7, 3.7, 1.1 Hz, 1H), 4.38 (tdd, *J* = 9.2, 7.7, 5.5 Hz, 1H), 4.02 (dd, *J* = 9.4, 8.4 Hz, 1H), 3.82 (dd, *J* = 8.4, 7.7 Hz, 1H), 3.09 (dd, *J* = 13.8, 5.5 Hz, 1H), 2.38 (dd, *J* = 13.8, 9.0 Hz, 1H). **^{13}C NMR (101 MHz, $CDCl_3$):** δ 159.9, [Ar region: 162.37, 162.30, 159.84, 159.77, 141.48, 141.25, 138.25, 136.72, 136.65, 136.60, 136.54, 134.35, 134.32, 134.14, 134.12, 131.48, 131.40, 129.21, 129.18, 129.15, 129.13, 129.12, 129.10, 128.78, 128.76, 128.70, 128.69, 128.62, 126.48, 121.71, 121.57, 121.46, 121.32, 116.21, 115.99], 71.8, 68.3, 41.4.

(*S*)-4-benzyl-2-(2-(diphenylphosphaneyl)-5-methoxyphenyl)-4,5-dihydrooxazole (L27)

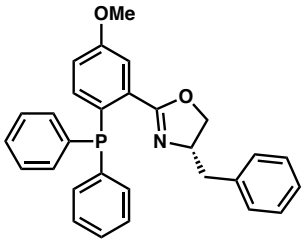

Prepared from (*S*)-4-benzyl-2-(2-bromo-5-methoxyphenyl)-4,5-dihydrooxazole **275d** (1.04 g, 3.0 mmol, 1.0 equiv) and diphenylphosphine (940 μL, 1.00 g, 5.4 mmol, 1.8 equiv) following General Procedure 2. The reaction stirred overnight for 24 hours. The crude residue was purified by column chromatography (silica, 0 to 3% Et_2O/DCM) under a flow of N_2 to yield 579 mg (43% yield) of **L27** as a sticky white solid. $[\boldsymbol{a}]_{\boldsymbol{D}}^{\mathbf{25}}$ = +28° (c = 1.0, $CHCl_3$). **^{1}H NMR (400 MHz, $CDCl_3$):** δ 7.43 (t, *J* = 2.9 Hz, 1H), 7.39 – 7.29 (m, 10H), 7.29 – 7.23 (m, 2H), 7.23 – 7.16 (m, 1H), 7.11 – 7.06 (m, 2H), 6.86 (dd, *J* = 8.6, 2.7 Hz, 1H), 6.79 (dd, *J* = 8.6, 3.9 Hz, 1H), 4.40 (tdd, *J* = 9.2, 7.4, 5.1 Hz, 1H), 4.09 (dd, *J* = 9.3, 8.4 Hz, 1H), 3.88 – 3.79 (m, 4H), 2.95 (dd, *J* = 13.8, 5.1 Hz, 1H),

2.19 (dd, *J* = 13.8, 9.1 Hz, 1H). **^{13}C NMR (101 MHz, $CDCl_3$):** δ 163.9 (d, J_{C-P} = 2.6 Hz), [Ar region: 159.52, 138.58, 138.54, 138.46, 138.44, 138.26, 135.36, 135.34, 134.44, 134.23, 133.92, 133.72, 133.30, 133.09, 129.61, 129.39, 129.24, 128.70, 128.60, 128.55, 128.53, 128.51, 128.44, 126.43, 116.99, 115.06, 115.03], 71.7, 68.1, 55.5, 41.3.

(*S*)-4-benzyl-2-(2-(diphenylphosphaneyl)-5-methylphenyl)-4,5-dihydrooxazole (L28)

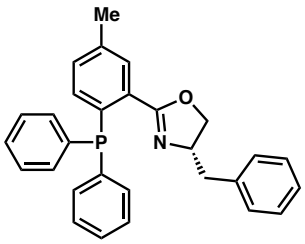

Prepared from (*S*)-4-benzyl-2-(2-bromo-5-methylphenyl)-4,5-dihydrooxazole **275e** (991 mg, 3.0 mmol, 1.0 equiv) and diphenylphosphine (940 μL, 1.00 g, 5.4 mmol, 1.8 equiv) following General Procedure 2. The reaction stirred overnight for 19 hours. The crude residue was purified by column chromatography (silica, 0 to 3% Et_2O/DCM) under a flow of N_2 to yield 416 mg (32% yield) of **L28** as a white solid. $[\boldsymbol{\alpha}]_D^{25}$ = +38° (c = 1.0, $CHCl_3$). **^{1}H NMR (400 MHz, $CDCl_3$):** δ 7.76 – 7.69 (m, 1H), 7.41 – 7.29 (m, 10H), 7.29 – 7.22 (m, 2H), 7.22 – 7.15 (m, 1H), 7.14 – 7.10 (m, 1H), 7.10 – 7.05 (m, 2H), 6.76 (dd, *J* = 7.9, 4.3 Hz, 1H), 4.36 (tdd, *J* = 9.3, 7.5, 5.1 Hz, 1H), 4.04 (dd, *J* = 9.3, 8.4 Hz, 1H), 3.77 (dd, *J* = 8.4, 7.5 Hz, 1H), 2.95 (dd, *J* = 13.8, 5.0 Hz, 1H), 2.36 (s, 3H), 2.11 (dd, *J* = 13.8, 9.3 Hz, 1H). **^{13}C NMR (101 MHz, $CDCl_3$):** δ 164.3 (d, J_{C-P} = 2.8 Hz), [Ar region: 138.32, 138.30, 138.23, 138.18, 138.16, 138.13, 135.45, 135.22, 134.55, 134.34, 134.08, 133.88, 133.79, 133.77, 131.66, 131.51, 131.47, 130.81, 130.78, 129.20, 128.79, 128.65, 128.63, 128.57, 128.55, 128.47, 126.42], 71.6, 68.0, 41.3, 21.0.

(*S*)-4-benzyl-2-(2-(diphenylphosphaneyl)-5-fluorophenyl)-4,5-dihydrooxazole (L29)

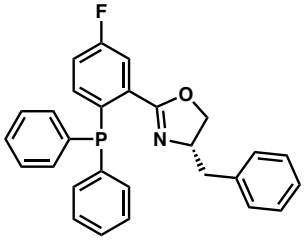

Prepared from (*S*)-4-benzyl-2-(2-bromo-5-fluorophenyl)-4,5-dihydrooxazole **275f** (1.00 g, 3.0 mmol, 1 equiv) and diphenylphosphine (522 μL, 559 mg, 3.0 mmol, 1.0 equiv) following General Procedure 2. The reaction stirred overnight for 12 hours. The crude residue was purified by column chromatography (silica, 5 to 15% EtOAc/hexane) under a flow of N_2 to yield 860 mg (65% yield) of **L29** as a sticky colorless semi-solid. $[\boldsymbol{a}]_{\boldsymbol{D}}^{\mathbf{25}}$ = +21° (c = 1.0, $CHCl_3$). **^{1}H NMR (400 MHz, $CDCl_3$):** δ 7.60 (dt, *J* = 9.5, 2.8 Hz, 1H), 7.40 – 7.29 (m, 10H), 7.29 – 7.23 (m, 2H), 7.23 – 7.17 (m, 1H), 7.10 – 7.05 (m, 2H), 7.01 (td, *J* = 8.3, 2.8 Hz, 1H), 6.85 (ddd, *J* = 8.7, 5.9, 3.7 Hz, 1H), 4.40 (tdd, *J* = 9.2, 7.4, 5.2 Hz, 1H), 4.08 (dd, *J* = 9.3, 8.4 Hz, 1H), 3.82 (dd, *J* = 8.4, 7.5 Hz, 1H), 2.91 (dd, *J* = 13.8, 5.2 Hz, 1H), 2.16 (dd, *J* = 13.9, 8.9 Hz, 1H). **^{13}C NMR (101 MHz, $CDCl_3$):** δ 162.8 (dd, $J_{C\text{-}P}$ = 3.0 Hz, $J_{C\text{-}F}$ = 3.0 Hz), [Ar region: 163.71, 161.23, 138.10, 137.97, 137.94, 137.84, 135.90, 135.88, 135.82, 135.80, 134.75, 134.71, 134.54, 134.49, 134.45, 134.33, 133.93, 133.75, 133.73, 133.67, 133.55, 133.48, 129.22, 128.98, 128.80, 128.75, 128.68, 128.66, 128.59, 126.50, 117.75, 117.55, 117.39, 117.36, 117.16, 117.13], 71.7, 68.2, 41.2.

(*S*)-4-benzyl-2-(5-chloro-2-(diphenylphosphaneyl)phenyl)-4,5-dihydrooxazole (L30)

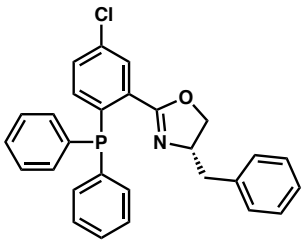

Prepared from (*S*)-4-benzyl-2-(2-bromo-5-chlorophenyl)-4,5-dihydrooxazole **275g** (1.05 g, 3.0 mmol, 1.0 equiv) and diphenylphosphine (522 μL, 559 mg, 3.0 mmol, 1.0 equiv) following General Procedure 2. The reaction stirred overnight

for 12 hours. The crude residue was purified by column chromatography (silica, 5 to 15% EtOAc/hexane) under a flow of N_2 to yield 621 mg (45% yield) of **L30** as a white solid. $[\alpha]_D^{25}$ = +27° (c = 1.0, $CHCl_3$). **^{1}H NMR (400 MHz, $CDCl_3$):** δ 7.88 (dd, *J* = 3.1, 2.3 Hz, 1H), 7.41 – 7.29 (m, 10H), 7.29 – 7.23 (m, 3H), 7.23 – 7.16 (m, 1H), 7.10 – 7.04 (m, 2H), 6.79 (dd, *J* = 8.4, 3.8 Hz, 1H), 4.37 (tdd, *J* = 9.2, 7.5, 5.1 Hz, 1H), 4.06 (dd, *J* = 9.3, 8.4 Hz, 1H), 3.79 (dd, *J* = 8.4, 7.5 Hz, 1H), 2.90 (dd, *J* = 13.9, 5.2 Hz, 1H), 2.12 (dd, *J* = 13.9, 9.1 Hz, 1H). **^{13}C NMR (101 MHz, $CDCl_3$):** δ 162.8 (d, *J* = 3.3 Hz), [Ar region: 138.08, 137.88, 137.63, 137.61, 137.59, 137.51, 137.49, 135.12, 135.09, 134.59, 134.40, 134.37, 134.01, 133.80, 133.11, 132.93, 130.59, 130.04, 130.01, 129.20, 129.09, 128.91, 128.79, 128.72, 128.64, 128.60, 126.51], 71.8, 68.2, 41.2.

(*S*)-4-benzyl-2-(2-(diphenylphosphaneyl)-5-(trifluoromethyl)phenyl)-4,5-dihydro-oxazole (L31)

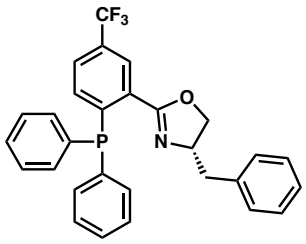

Prepared from (*S*)-4-benzyl-2-(2-bromo-5-(trifluoromethyl)-phenyl)-4,5-dihydrooxazole **275h** (1.15 g, 3.0 mmol, 1.0 equiv) and diphenylphosphine (940 μL, 1.00 g, 5.4 mmol, 1.8 equiv) following General Procedure 2. The reaction stirred overnight for 19 hours. The crude residue was purified by column chromatography (silica, 0 to 3% Et_2O/DCM) under a flow of N_2 to yield 457 mg (31% yield) of **L31** as a sticky white solid. $[\alpha]_D^{25}$ = +27° (c = 1.0, $CHCl_3$). **^{1}H NMR (400 MHz, $CDCl_3$):** δ 8.13 (t, *J* = 2.6 Hz, 1H), 7.52 (dd, *J* = 8.2, 2.0 Hz, 1H), 7.43 – 7.30 (m, 10H), 7.30 – 7.23 (m, 2H), 7.23 – 7.17 (m, 1H), 7.10 – 7.04 (m, 2H), 6.99 (dd, *J* = 8.2, 3.8 Hz, 1H), 4.37 (tdd, *J* = 9.2, 7.5, 5.1 Hz,

1H), 4.06 (dd, *J* = 9.3, 8.5 Hz, 1H), 3.80 (dd, *J* = 8.5, 7.5 Hz, 1H), 2.91 (dd, *J* = 13.8, 5.1 Hz, 1H), 2.09 (dd, *J* = 13.9, 9.1 Hz, 1H).

(*S*)-4-benzyl-2-(2-(diphenylphosphaneyl)-4-methoxyphenyl)-4,5-dihydrooxazole (L32)

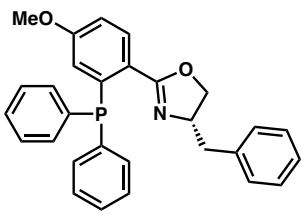

Prepared from (*S*)-4-benzyl-2-(2-bromo-4-methoxyphenyl)-4,5-dihydrooxazole **275i** (1.04 g, 3.0 mmol, 1.0 equiv) and diphenylphosphine (940 μL, 1.00 g, 5.4 mmol, 1.8 equiv) following General Procedure 2. The reaction stirred overnight for 19 hours. The crude residue was purified by column chromatography (silica, 0 to 5% Et_2O/DCM) under a flow of N_2 to yield 1055 mg (78% yield) of **L32** as a sticky white solid. $[\alpha]_D^{25}$ = +45° (c = 1.0, $CHCl_3$). **^{1}H NMR (400 MHz, $CDCl_3$):** δ 7.87 (dd, *J* = 8.6, 3.8 Hz, 1H), 7.40 – 7.30 (m, 10H), 7.28 – 7.22 (m, 2H), 7.22 – 7.15 (m, 1H), 7.09 – 7.03 (m, 2H), 6.85 (ddd, *J* = 8.6, 2.7, 0.6 Hz, 1H), 6.36 (dd, *J* = 4.4, 2.6 Hz, 1H), 4.33 (tdd, *J* = 9.3, 7.3, 5.0 Hz, 1H), 4.00 (dd, *J* = 9.2, 8.4 Hz, 1H), 3.73 (dd, *J* = 8.4, 7.3 Hz, 1H), 3.60 (s, 3H), 2.88 (dd, *J* = 13.8, 5.0 Hz, 1H), 2.03 (dd, *J* = 13.8, 9.4 Hz, 1H). **^{13}C NMR (101 MHz, $CDCl_3$):** δ 163.6 (d, J_{C-P} = 3.6 Hz), [Ar region: 161.03, 141.48, 141.21, 138.44, 138.06, 138.01, 137.93, 137.91, 134.76, 134.54, 134.05, 133.84, 131.89, 131.86, 129.19, 128.96, 128.73, 128.67, 128.60, 128.57, 128.54, 128.50, 126.37, 123.84, 123.68, 119.74, 119.70, 112.78], 71.3, 68.0, 55.1, 41.3.

(*S*)-4-benzyl-2-(2-(diphenylphosphaneyl)-4-methylphenyl)-4,5-dihydrooxazole (L33)

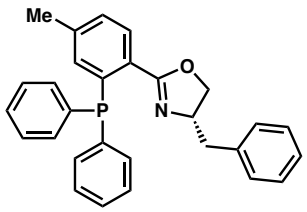

Prepared from (*S*)-4-benzyl-2-(2-bromo-4-methylphenyl)-4,5-dihydrooxazol **275j** (1.09 g, 3.0 mmol, 1.0 equiv) and diphenylphosphine (940 μL, 1.00 g, 5.4 mmol, 1.8 equiv) following General Procedure 2. The reaction stirred overnight for 24 hours. The crude residue was purified by column chromatography (silica, 0 to 3% Et_2O/DCM) under a flow of N_2 to yield 1088 mg (83% yield) of **L33** as a white solid. $[\alpha]_D^{25}$ = +35° (c = 1.0, $CHCl_3$) **^{1}H NMR (400 MHz, $CDCl_3$):** δ 7.78 (dd, *J* = 7.8, 3.7 Hz, 1H), 7.41 – 7.29 (m, 10H), 7.29 – 7.22 (m, 2H), 7.22 – 7.14 (m, 2H), 7.10 – 7.04 (m, 2H), 6.65 (dd, *J* = 4.7, 1.7 Hz, 1H), 4.34 (tdd, *J* = 9.3, 7.4, 5.0 Hz, 1H), 4.01 (dd, *J* = 9.3, 8.4 Hz, 1H), 3.75 (dd, *J* = 8.4, 7.4 Hz, 1H), 2.91 (dd, *J* = 13.8, 5.0 Hz, 1H), 2.20 (s, 3H), 2.07 (dd, *J* = 13.8, 9.3 Hz, 1H). **^{13}C NMR (101 MHz, $CDCl_3$):** δ 164.03 (d, $J_{C\text{-}P}$ = 3.0 Hz), [Ar region: 140.75, 138.91, 138.66, 138.39, 138.19, 138.18, 138.08, 138.07, 134.69, 134.48, 134.28, 134.26, 134.08, 133.88, 130.12, 130.10, 129.21, 128.88, 128.84, 128.82, 128.70, 128.65, 128.62, 128.55, 128.47, 126.39], 71.5, 68.0, 41.3, 21.8.

(*S*)-4-benzyl-2-(2-(diphenylphosphaneyl)-4-fluorophenyl)-4,5-dihydrooxazole (L34)

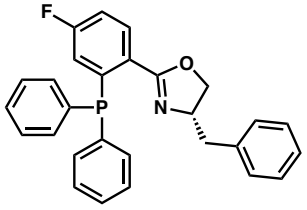

Prepared from (S)-4-benzyl-2-(2-bromo-4-fluorophenyl)-4,5-dihydrooxazole **275k** (1.00 g, 3.0 mmol, 1.0 equiv) and diphenylphosphine (522 μL, 559 mg, 3.0 mmol, 1.0 equiv) following General Procedure 2. The reaction stirred overnight for 13 hours. The crude residue was purified by column chromatography (silica, 5 to 15% EtOAc/hexane) under a

flow of N_2 to yield 515 mg (39% yield) of **L34** as a sticky colorless semi-solid. $[\boldsymbol{\alpha}]_{\boldsymbol{D}}^{\mathbf{25}}$ = +29° (c = 1.0, $CHCl_3$). **^{1}H NMR (400 MHz, $CDCl_3$):** δ 7.89 (ddd, *J* = 8.6, 5.7, 3.6 Hz, 1H), 7.42 – 7.30 (m, 10H), 7.30 – 7.23 (m, 2H), 7.23 – 7.17 (m, 1H), 7.10 – 7.05 (m, 2H), 7.05 – 6.99 (m, 1H), 6.55 (ddd, *J* = 9.8, 3.5, 2.6 Hz, 1H), 4.35 (tdd, *J* = 9.2, 7.4, 5.1 Hz, 1H), 4.03 (dd, *J* = 9.3, 8.4 Hz, 1H), 3.76 (dd, *J* = 8.4, 7.4 Hz, 1H), 2.89 (dd, *J* = 13.8, 5.1 Hz, 1H), 2.08 (dd, *J* = 13.8, 9.2 Hz, 1H). **^{13}C NMR (101 MHz, $CDCl_3$):** δ 163.0 ($J_{C\text{-}P}$, *J* = 3.5 Hz), [Ar region: 165.14, 162.62, 143.29, 143.23, 143.00, 142.94, 138.21, 137.37, 137.36, 137.26, 137.25, 134.66, 134.45, 134.04, 133.83, 132.37, 132.35, 132.29, 132.26, 129.22, 129.19, 129.00, 128.85, 128.77, 128.75, 128.68, 128.57, 127.59, 127.56, 127.42, 127.39, 126.46, 120.72, 120.69, 120.49, 120.46, 115.11, 114.89], 71.6, 68.1, 41.2.

(*S*)-4-benzyl-2-(4-chloro-2-(diphenylphosphaneyl)phenyl)-4,5-dihydrooxazole (L35)

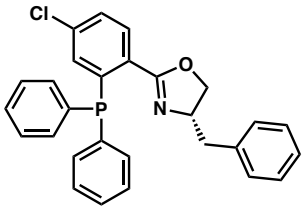

Prepared from (*S*)-4-benzyl-2-(2-bromo-4-chlorophenyl)-4,5-dihydrooxazole **275l** (1.05 g, 3.0 mmol, 1.0 equiv) and diphenylphosphine (522 μL, 559 mg, 3.0 mmol, 1.0 equiv) following General Procedure 2. The reaction stirred overnight for 18 hours. The crude residue was purified by column chromatography (silica, 5 to 15% EtOAc/hexane) under a flow of N_2 to yield 742 mg (54% yield) of **L35** as a white solid. $[\boldsymbol{\alpha}]_{\boldsymbol{D}}^{\mathbf{25}}$ = +40° (c = 1.0, $CHCl_3$). **^{1}H NMR (400 MHz, $CDCl_3$):** δ 7.81 (dd, *J* = 8.3, 3.5 Hz, 1H), 7.41 – 7.30 (m, 11H), 7.26 (tt, *J* = 6.6, 1.1 Hz, 2H), 7.22 – 7.16 (m, 1H), 7.09 – 7.03 (m, 2H), 6.80 (dd, *J* = 3.5, 2.1 Hz, 1H), 4.35 (tdd, *J* = 9.2, 7.4, 5.1 Hz, 1H), 4.03 (dd, *J* = 9.3, 8.4 Hz, 1H), 3.77 (dd, *J* = 8.4, 7.5 Hz, 1H), 2.89 (dd, *J* = 13.8, 5.1 Hz, 1H), 2.09 (dd, *J* = 13.9, 9.1 Hz, 1H).

^{13}C NMR (101 MHz, $CDCl_3$): δ 163.08 (d, J_{C-P} = 3.4 Hz), [Ar region: 142.14, 141.84, 138.14, 137.26, 137.16, 137.13, 134.65, 134.44, 134.05, 133.84, 133.37, 133.34, 131.43, 131.40, 129.88, 129.71, 129.25, 129.20, 129.04, 128.86, 128.79, 128.77, 128.69, 128.59, 128.19, 128.18, 126.49], 71.6, 68.1, 41.2.

(*S*)-4-benzyl-2-(2-(diphenylphosphaneyl)-4-(trifluoromethyl)phenyl)-4,5-dihydro-oxazole (L36)

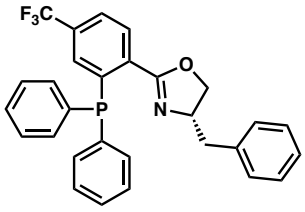

Prepared from (*S*)-4-benzyl-2-(2-bromo-4-(trifluoromethyl)-phenyl)-4,5-dihydrooxazole **275m** (1.15 g, 3.0 mmol, 1.0 equiv) and diphenylphosphine (940 μL, 1.00 g, 5.4 mmol, 1.8 equiv) following General Procedure 2. The reaction stirred overnight for 19 hours. The crude residue was purified by column chromatography (silica, 0 to 2% Et_2O/DCM) under a flow of N_2 to yield 602 mg (41% yield) of **L36** as a faint yellow oil. $[\alpha]_D^{25}$ = +24° (c = 1.0, $CHCl_3$). **^{1}H NMR (400 MHz, $CDCl_3$):** δ 7.97 (dd, *J* = 8.1, 3.3 Hz, 1H), 7.60 (ddt, *J* = 8.1, 1.7, 0.8 Hz, 1H), 7.44 – 7.30 (m, 10H), 7.30 – 7.23 (m, 2H), 7.23 – 7.17 (m, 1H), 7.13 – 7.09 (m, 1H), 7.09 – 7.05 (m, 2H), 4.38 (tdd, *J* = 9.2, 7.5, 5.2 Hz, 1H), 4.06 (dd, *J* = 9.4, 8.5 Hz, 1H), 3.80 (dd, *J* = 8.5, 7.5 Hz, 1H), 2.91 (dd, *J* = 13.8, 5.2 Hz, 1H), 2.12 (dd, *J* = 13.9, 9.1 Hz, 1H).

General Procedure 3: Ullman Coupling with Phosphine Oxide

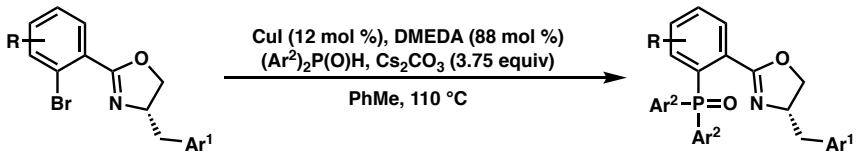

The following procedure was conducted under an N_2 atmosphere in a glovebox. The CuI (74 mg, 0.39 mmol, 0.13 equiv) was added to a 150 mL heavy wall pressure flask equipped with a stir bar and dissolved in 20 mL of anhydrous toluene. The DMEDA (375 μL, 2.64 mmol, 0.88 equiv) and diarylphosphine oxide (1.8 mmol, 1.8 equiv) was added and stirred for 10 minutes. The Cs_2CO_3 (3.66 g, 11.25 mmol, 3.75 equiv) was added, followed by the aryl bromide (1 mmol, 1.0 equiv) dissolved in 10 mL of toluene. The flask was sealed with a screw cap fitted with a viton o-ring, removed from the glovebox, and stirred overnight at 110 °C. The reaction was then cooled to room temperature and filtered over a pad of celite, eluting with CH_2Cl_2. The crude mixture was concentrated under reduced pressure and purified by column chromatography to afford the desired product.

General Procedure 4: Phosphine Oxide Reduction

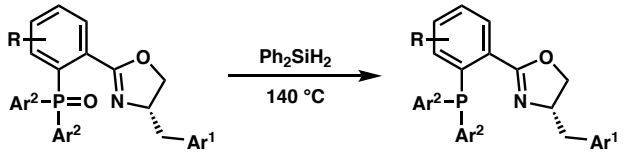

On a bench-top, the tertiary phosphine oxide (1.0–1.8 mmol, 1.0 equiv) was added to a 2-dram vial and equipped with a stir bar. The vial was then brought into the glovebox and diphenylsilane (7.0–12.60 mmol, 7.0 equiv) was added. The vial was sealed with a Teflon cap and electrical tape and brought out of the box. The reaction mixture was then added to an oil bath preheated to 140 ºC and stirred for 48 hours. After completion of the reaction, the vial cap was removed and replaced with a rubber septum. The oil bath was cooled to 65 ºC and the vial was placed under high vacuum and stirred overnight. The crude mixture was then further purified by column chromatography under a flow of Argon to afford the

desired product in the third fraction. Eluents for chromatography were sparged with argon for 3 hours prior to purification.

A8.5.3 Cross-Coupling Reactions

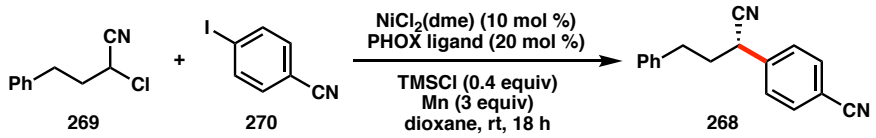

On a bench-top, the phosphine ligand (0.04 mmol, 0.2 equiv), manganese (0.6 mmol, 3 equiv), and aryl iodide **270** (0.2 mmol, 1 equiv) were added to a 1 dram vial equipped with a stir bar. The vial was then brought into the glovebox and sequentially charged with $NiCl_2$(dme) (0.01 mmol, 0.1 equiv), dioxane (0.35 mL), α-chloronitrile **269** (0.2 mmol, 1 equiv), benzyl ether internal standard, and TMSCl (0.08 mmol, 0.4 equiv). The vial was sealed with a Teflon cap and stirred at 700 rpm for 18 hours. The reaction was then dissolved in 20% EtOAc/hexane, loaded onto a silica plug, and flushed through with additional 20% EtOAc/hexane. The samples were concentrated to obtain yield by ^{1}H NMR spectroscopy. The crude samples were then purified by preparatory TLC and analyzed by chiral SFC in order to obtain the enantioselectivity of the product.

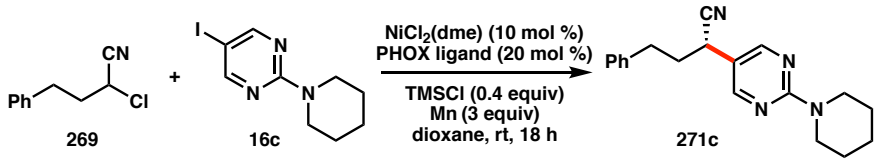

On a bench-top manganese (0.6 mmol, 3 equiv), and aryl iodide **16c** (0.2 mmol, 1 equiv) were added to a 1 dram vial equipped with a stir bar. The phosphine ligand (0.04 mmol,

0.2 equiv) was added to a separate 1 dram vial with a stir bar. The vials were then brought into the glovebox where $NiCl_2$(dme) (0.01 mmol, 0.1 equiv) was added to the vial containing the phosphine ligand. Then dioxane (0.35 mL) was added to the vial containing the catalyst and was stirred for 10 minutes to allow for complexation. The solution was then transferred to the vial containing manganese and the aryl iodide followed by α-chloronitrile **271c** (0.2 mmol, 1 equiv), benzyl ether internal standard, and TMSCl (0.08 mmol, 0.4 equiv). The vial was sealed with a Teflon cap and stirred at 1000 rpm for 18 hours. The reaction was then dissolved in 30% EtOAc/hexane, loaded onto a silica plug, and flushed through with additional 30% EtOAc/hexane. The samples were concentrated to obtain yield by ^{1}H NMR spectroscopy. The crude samples were then purified by preparatory TLC and analyzed by chiral SFC in order to obtain the enantioselectivity of the product.

A8.6 REFERENCES

(1) Lovering, F.; Bikker, J.; Humblet, C. *J. Med. Chem.* **2009**, *52*, 6752.

(2) Nguyen, L. A.; He, H.; Pham-Huy, C. *Int. J. Biomed. Sci.* **2006**, *2*, 85.

(3) McConathy, J.; Owens, M. J. *Prim. Care Companion J. Clin. Psychiatry* **2003**, *5*, 70.

(4) Seyden-Penne, J. *Chiral Auxiliaries and Ligands in Asymmetric Synthesis*, 1st ed.; Wiley-Interscience, 1995.

(5) Cruz, A.; Padilla-Martínez, I. I.; Bautista-Ramirez, M. E. *Curr. Org. Synth.* **2018**, *15*, 38.

(6) Bhadra, S.; Yamamoto, H. *Chem. Rev.* **2018**.

(7) Cherney, A. H.; Kadunce, N. T.; Reisman, S. E. *Chem. Rev.* **2015**, *115*, 9587.

(8) Cherney, A. H.; Kadunce, N. T.; Reisman, S. E. *J. Am. Chem. Soc.* **2013**, *135*, 7442.

(9) Cherney, A. H.; Reisman, S. E. *J. Am. Chem. Soc.* **2014**, *136*, 14365.

(10) Hofstra, J. L.; Cherney, A. H.; Ordner, C. M.; Reisman, S. E. *J. Am. Chem. Soc.* **2018**, *140*, 139.

(11) Suzuki, N.; Hofstra, J. L.; Poremba, K. E.; Reisman, S. E. *Org. Lett.* **2017**, *19*, 2150.

(12) Kadunce, N. T.; Reisman, S. E. *J. Am. Chem. Soc.* **2015**, *137*, 10480.

(13) Poremba, K. E.; Kadunce, N. T.; Suzuki, N.; Cherney, A. H.; Reisman, S. E. *J. Am. Chem. Soc.* **2017**, *139*, 5684.

(14) Sigman, M. S.; Harper, K. C.; Bess, E. N.; Milo, A. *Acc. Chem. Res.* **2016**, *49*, 1292.

(15) Orlandi, M.; Coelho, J. A. S.; Hilton, M. J.; Toste, F. D.; Sigman, M. S. *J. Am. Chem. Soc.* **2017**, *139*, 6803.

(16) Santiago, C. B.; Guo, J.-Y.; Sigman, M. S. *Chem. Sci.* **2018**, *9*, 2398.

(17) Guo, J.-Y.; Minko, Y.; Santiago, C. B.; Sigman, M. S. *ACS Catal.* **2017**, *7*, 4144.

(18) Neel, A. J.; Hilton, M. J.; Sigman, M. S.; Toste, F. D. *Nature* **2017**, *543*, 637.

(19) Milo, A.; Neel, A. J.; Toste, F. D.; Sigman, M. S. *Science* **2015**, *347*, 737.

(20) Liu, D.; Dai, Q.; Zhang, X. *Tetrahedron* **2005**, *61*, 6460.

(21) Peer, M.; de Jong, J. C.; Kiefer, M.; Langer, T.; Rieck, H.; Schell, H.; Sennhenn, P.; Sprinz, J.; Steinhagen, H.; Wiese, B.; Helmchen, G. *Tetrahedron* **1996**, *52*, 7547.

(22) Sprinz, J.; Helmchen, G. *Tetrahedron Lett.* **1993**, *34*, 1769.

(23) Krout, M. R.; Mohr, J. T.; Stoltz, B. M. *Org. Synth.* **2009**, No. 86, 181.

(24) McDougal, N. T.; Streuff, J.; Mukherjee, H.; Virgil, S. C.; Stoltz, B. M. *Tetrahedron Lett.* **2010**, *51*, 5550.

(25) Still, W. C.; Kahn, M.; Mitra, A. *J. Org. Chem.* **1978**, *43*, 2923.

ABOUT THE AUTHOR

Julie Lyn Hofstra was born on February 19, 1991 to Andrew S. Hofstra and Patricia L. Hofstra in Lakewood, California. She grew up in the neighboring city of Bellflower alongside her brother James, yet frequented many places along the west coast given her family's interest in camping and fishing. Julie's delight in science and nature was always evident, but it was during her studies at Downey High School where she became fascinated by chemistry, largely due to the enthusiasm of her high school chemistry teacher.

In 2009, Julie began her post-secondary education at Cerritos College, earning an A.A. in General Natural Science and an A.A. in Mathematics in 2011. She then transferred to California State University, Fullerton (CSUF) where she earned her B.S. in Chemistry in 2014. During her time at CSUF, Julie had the privilege of conducting research in the laboratories of Professor Paula K. Hudson and Professor H. J. Peter de Lijser where she studied analytical atmospheric chemistry and physical organic chemistry. Julie also completed a summer internship through the MIT Summer Research Program while working in the laboratory of Professor Stephen L. Buchwald. It was there she had her first taste of Pd-catalyzed cross-coupling while working under the direction of Dr. Thomas Barton, which ultimately led her to pursue her graduate studies in organometallics.

Following her graduation from CSUF, Julie made the short trip across Los Angeles to pursue her graduate studies under the direction of Professor Sarah E. Reisman at the California Institute of Technology. Her graduate work has focused on the development and mechanistic studies of asymmetric Ni-catalyzed reductive cross-coupling reactions. Following the completion of her Ph.D., Julie will move to Salt Lake City to continue pursuing her love for outdoor adventures while conducting postdoctoral studies under the direction of Professor Matthew S. Sigman at the University of Utah.